VISUAL INSPECTION AND EVALUATION REPORT

Rockwall-Forney Dam
Dallas Water Utilities
Dallas/Kaufman Counties, Texas

Schnabel Reference #20C22001.00
July 30, 2021

Schnabel ENGINEERING

Schnabel ENGINEERING
T 770.781.8008 / F 770.781.8003
6445 Shiloh Road, Suite A / Alpharetta, GA 30005
schnabel-eng.com

July 30, 2021

Randall G. McIntyre, PE
Vice President
Garver, LLC
14160 N. Dallas Parkway, Suite 850
Dallas, TX 75254

Subject: **Visual Inspection and Evaluation Report, Rockwall-Forney Dam, Dallas Water Utilities, Dallas/Kaufman Counties, Texas (Schnabel Reference 20C22001.00)**

Dear Mr. McIntyre:

SCHNABEL ENGINEERING, LLC (Schnabel) has completed the authorized visual inspection and evaluation of the Rockwall-Forney Dam. This report includes a summary of our understanding of the project, a description of the work performed by Schnabel to evaluate the existing structure, observations and opinions based upon the results of the work performed, and recommendations for future work. Supporting documentation is provided in the appendices.

We appreciate the opportunity to be of service for this project. Please call us if you have any questions regarding this report.

Sincerely,

SCHNABEL ENGINEERING, LLC

Brett W. Dodd, PE (Georgia only)
Project Engineer

Robert T. Indri, PE
Senior Associate

Joseph S. Monroe, PE
Principal

BWD:JSM:RTI

CC: Ikram Sayed (Garver, LLC)
Tommy Lyvers (Garver, LLC)
Kevin Flynn (Garver, LLC)

VISUAL INSPECTION AND EVALUATION REPORT
ROCKWALL-FORNEY DAM
DALLAS WATER UTILITIES
DALLAS/KAUFMAN COUNTIES, TEXAS

TABLE OF CONTENTS

 ©2021 All Rights Reserved

LIST OF FIGURES

LIST OF TABLES

APPENDICES

©2021 All Rights Reserved

1.0 EXECUTIVE SUMMARY

Due to recommendations provided in a 2016 dam safety inspection report, Schnabel was engaged as a subconsultant to Garver, LLC to perform a visual inspection and evaluation of the Rockwall-Forney Dam located in Dallas and Kaufman Counties, Texas. The scope of services generally consisted of a review of record documents and available data, a visual inspection of the dam and spillway, a structure analysis of the Tainter gates, a review of the current flood operation procedures, and the preparation of safety procedures for drainage gallery inspections. In addition, Schnabel facilitated a Potential Failure Mode Assessment (PFMA) workshop and presented the results in a report under a separate cover. The results of the visual inspection and evaluation are documented in this report and summarized below. This summary should not be used in lieu of reading the entire report, to include the appendices.

- Record documents indicate that the soil shear strength parameters utilized for the stability analysis of the embankment slopes and spillway gravity structures rely on cohesion values higher than generally acceptable by current standards. Stability analyses of the gravity dam and embankment should be reviewed and updated based upon current engineering criteria. (See Section 4.0)
- The embankment is maintained with no visual indications of distress or instability. While no areas of wetness or seepage were observed on the dam during Schnabel's visual inspection, DWU personnel have indicated past wetness near the abutment contacts. In addition, areas of dampness were noted by representatives of Schnabel and have been documented by DWU in the floodplain downstream of the dam. These areas should continue to be monitored. (See Sections 6.1 and 6.2, and Appendix B).
- The asphaltic concrete service road on the crest of the dam was noted to have some deterioration, such as cracking and potholes. The service road should be repaired and consideration should be given to replacing/repaving this road in the near future. (See Section 6.1 and Appendix B).
- Three areas of remedial repair, designated as 'Work Areas', were constructed to address ongoing or historic seepage issues associated with the dam, foundation, and downstream areas. The Work Areas contain pumped relief wells which operate automatically. Pressure relief well operations should be integrated in the SCADA system so that flow rates and run times can be documented, and an operational log for the pressure relief wells should be maintained. In addition, two unlined drainage channels are located downstream from the embankment to collect surface water and seepage discharges from the relief wells. Water was observed to be elevated in these channels, resulting the inundation of several relief well outlets. Appropriate measures should be implemented to promote drainage from these channels. (See Section 6.1 and Appendix B).
- The presence of a significant "void" or eroded area has been documented by DWU beneath the grouted riprap revetment along the left side slope of the spillway upstream of the left non-overflow section. Due to the elevation of the water at the time of the site reconnaissance by Schnabel personnel, the "void" could not be observed. The presence of this "void" or eroded area should be evaluated with respect to seepage observed on the left side of the stilling basin side wall and appropriate measures should be designed and implemented to address the void. (See Section 6.3 and Appendix B).

©2021 All Rights Reserved

- The concrete comprising the spillway is exhibiting visual signs of weathering and physical deterioration. The observed cracks in the spillway concrete appear to be surficial and not indicative of overstressing of the structures. However, the cracks and spalls should continue to be monitored. In particular, the large spall observed between spillway monoliths Q and R, and the longitudinal crack observed in spillway monolith Q should continue to be monitored for future degradation. (See Section 6.4 and Appendix B).
- Significant vegetative growth and iron ochre were observed in the upper drain outlets located along the left spillway outlet sidewall, which should be removed. According to the record documents, drain fill material placed on the outside face of the sidewalls was specified as ¾" to 1" stone, which may be susceptible to piping of backfill material through the drains or clogging. The utilized drainage material should be evaluated for compatibility with backfill material and appropriate modifications be incorporated. (See Section 6.4 and Appendix B).
- Visual observations of the Tainter gates indicated the presence of deterioration and corrosion of the gate members. Fractured welds or welds of poor quality should be repaired. In addition, a significant fracture was observed on Gate 6. This weld should be repaired and other gates should be further evaluated for possible similar fractures that may be obscured. (See Section 6.5 and Appendix E).
- The drainage gallery is generally well lit, well ventilated, and does not appear to collect significant amounts of seepage. The concrete was observed to be in adequate condition with relatively minor visual signs of deterioration. However, some corrosion of the steel conduits located within the foundation drain holes was observed and should be routinely cleaned. In addition, Schnabel recommends providing a means to activate the drainage gallery ventilation fan without having to enter the adit. (See Section 6.6 and Appendix B).
- A dive inspection was performed by American Underwater Services, Inc. within the stilling basin, and generally indicated an adequate condition of the concrete with limited evidence of concrete degradation or spalling noted. Some debris was noted in the stilling basin and should be removed when the stilling basin is dewatered. The area immediately downstream of the stilling basin has gradually increased over the life of the structure due to erosion resulting from spillway discharges. Additional armoring of the outlet channel should be provided to limit the potential for continued erosion. (See Section 6.7, Appendix B, and Appendix C).
- A significant amount of flowing water was observed discharging from the left side slope immediately downstream from the riprap at the end of the left stilling basin sidewall. The source of this flowing water should be evaluated, particularly considering the "void" or eroded area observed near the spillway entrance channel. (See Section 6.7 and Appendix B).
- Based on a review of instrumentation data provided, widely varying piezometric levels exist within the structure and foundation. Importantly, piezometric levels near the ground surface were noted in several of the piezometers. Additional piezometers are recommended for comprehensive monitoring and evaluation of the structure. (See Section 7.0 and Appendix D).
- Given the length of the dam, a registered land surveyor should be utilized to install station along the dam in order to provide horizontal control for future observations/inspections. In addition, monuments should be install across the crest of the dam to measure and document vertical and horizontal movement. (See Section 7.0).

©2021 All Rights Reserved

- A structural analysis of the Tainter gates was performed. The results of the analysis indicated that structural members on each gate are deficient based on the current Tainter gate design guidelines. Continued use, without proper modification, could result in overstressing and failure of the structurally deficient members. Development of a plan to modify the gates is recommended. (See Section 8.0 and Appendix E).
- An evaluation of the current flood operation procedures was performed. The procedures are well presented, but rely on the ability to obtain the necessary flood data in a timely manner. Upgrades to the procedures and implementation into a SCADA system are recommended. In addition, an updated hydrologic and hydraulic analysis should be performed to evaluate the Texas statewide Probable Maximum Precipitation (PMP) study, as well as to account for additional development within the watershed. (See Section 9.0 and Appendix F).
- In order to mitigate or limit potential risks, a Site Safety and Health Plan (SSHP) has been developed for future inspections of the drainage gallery adit. The SSHP was developed in general conformance with Occupational Safety and Health Administration (OSHA) guidelines. (See Section 10.0 and Appendix G).

©2021 All Rights Reserved

2.0 BACKGROUND

The Rockwall-Forney Dam (Forney Dam) is a combination earthen embankment and concrete gravity structure located on the East Fork Trinity River in Dallas and Kaufman Counties, Texas. More specifically, the dam is located approximately 15 miles east of Dallas, Texas at approximate 32°48'06"N Latitude and approximate 96°30'24"W Longitude. The dam impounds Lake Ray Hubbard, which serves as a water supply reservoir for the City of Dallas. Lavon Dam, which is owned and operated by the U.S. Army Corps of Engineers (USACE), is located within the watershed and immediately upstream of Lake Ray Hubbard. Site vicinity maps are included in Appendix A.

Based upon historic records, construction of the dam was completed circa 1967, with the reservoir first reaching the normal operating pool elevation of 435.5 feet in 1969. While the City of Dallas owns the dam, operation and maintenance of the structure is performed by the Dallas Water Utilities (DWU) department. The dam is regulated by the Texas Commission on Environmental Quality (TCEQ) as a large, high-hazard structure. The dam is also listed in the National Inventory of Dams (NID) with an inventory number of TX00837.

Throughout this report, standardized nomenclature is used in describing the dam that is typical in the dam engineering profession. Orientations provided in the text are based on one facing in the direction of stream flow with one's back to the impoundment. "Right" and "left" are referenced in this manner. The face or side next to the lake is the "upstream face/side" and the opposite face is the "downstream face/side". The top of the dam is the "crest." The base of the dam where contact with natural ground is made is referred to as the "toe". The side of the natural valley against which the dam is constructed are known as the "abutments". The structures which discharge water either through, around, under, or over the dam are "spillways" or "outlet works".

Elevations referenced in this report are based on the "as-built" plans by Forrest and Cotton, Inc. (1967). The vertical datum used to establish vertical control for the project was not indicated in the Forrest and Cotton, Inc. record documents. However, Schnabel is of the opinion that the National Geodetic Vertical Datum of 1929 (NGVD 29) was likely used. The North American Vertical Datum of 1988 (NAVD 88), which superseded NGVD 29, is the current vertical datum used to establish vertical control in the United States. We note that orthometric heights between NGVD 29 and NAVD 88 typically vary. However, based upon the VERTCON datum conversion tool on the National Oceanic and Atmospheric Administration (NOAA) website, the orthometric difference between NGVD 29 and NAVD 88 at the subject dam is on the order of 0.06 feet, with NAVD 88 being lower. Given that the datums are similar, no effort was made by Schnabel to establish the datum upon which the project was designed.

The earthen embankment, comprising about 10,500 feet of the total crest length and a maximum height on the order of 60 feet, is a rolled or compacted earthen structure spanning from the right abutment to non-overflow concrete gravity section located near the left abutment. The crest of the earthen embankment, with a design elevation of 450.0 feet, is approximately 22 feet in width to accommodate a paved, asphaltic-concrete service roadway. The upstream and downstream slopes vary from a grade of 3 feet horizontal to 1 foot vertical (3H:1V) near the crest to 7H:1V near the toe. Based on provided record documents, the embankment is "zoned" with more impervious core earthfill materials being located in the upstream areas and a more pervious earthfill materials being located in the downstream areas. A cutoff trench extending into the foundation of the embankment at the centerline of the dam and extending not less than 8 feet below

 ©2021 All Rights Reserved

natural ground line is detailed on the provided construction documents. Schnabel notes that the cutoff trench was designed to extend to a substantially deeper depth near the spillway. Riprap is present on the upstream slope from elevation 420.0 feet to the crest of the dam for protection against wave action erosion.

A general layout of Forney Dam and appurtenant structures is presented in Figure 2-1.

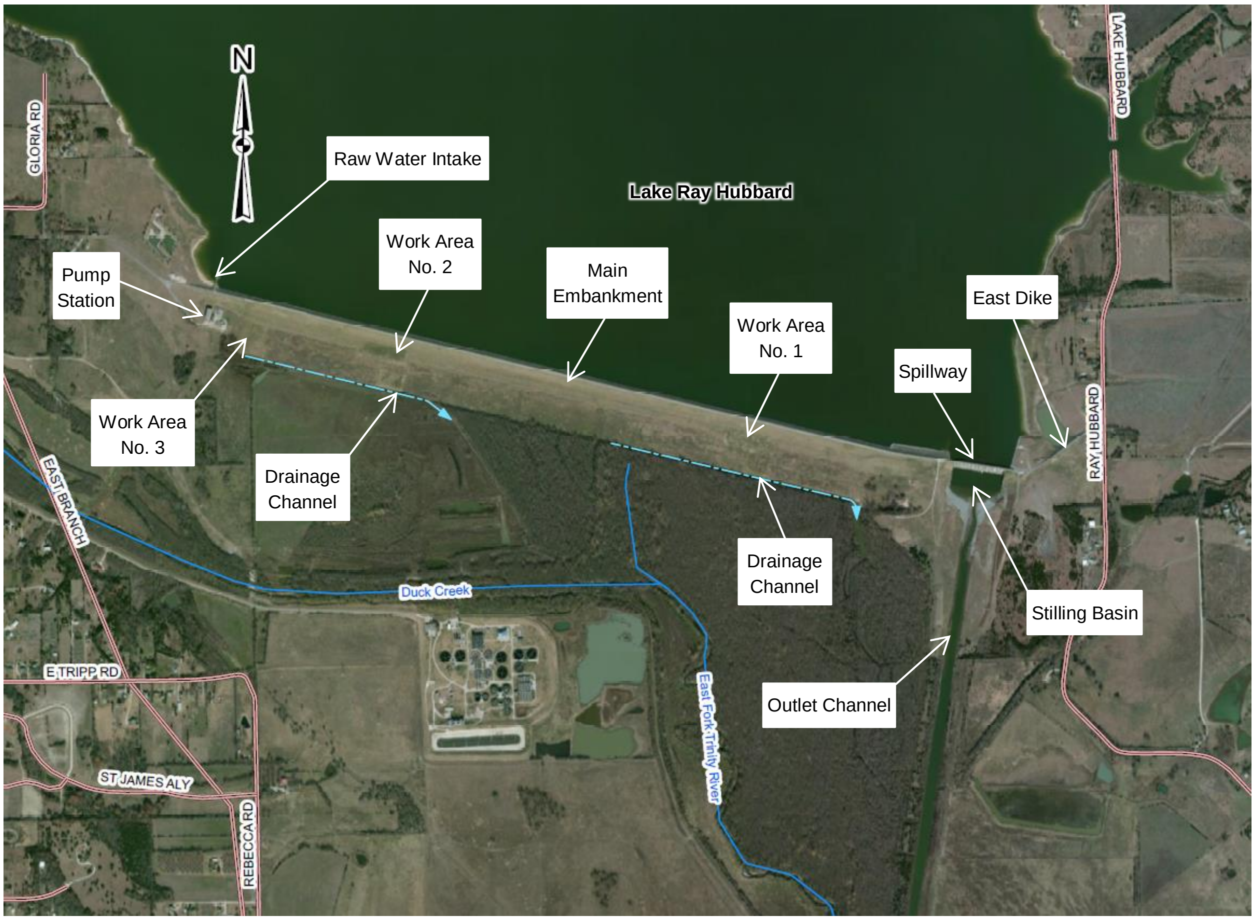

Figure 2-1: General Site Layout

A limited internal drainage system was originally constructed within the embankment to collect seepage. The internal drainage system consists of a sand and gravel trench drain having cross sectional dimensions of 2-feet by 4-feet. Lateral drain outlets, designated as “finger drains” on the “as-built” plans, are provided every 20 feet. The lateral drain outlets have a 2-foot by 2-foot cross section and are sloped at 1 percent to the downstream toe. The “as-built” plans do not indicate that piping was installed with the internal drainage system. In addition, no information regarding drain fill material or “as-built” locations were indicated in the available record documents.

Three areas of remedial repair, designated as ‘Work Areas’, were constructed circa 1995 to address ongoing or historic seepage issues associated with the dam, foundation, and downstream areas. Work Areas 1 and 2 generally consist of earthen berms with pumped relief wells, while Work Area 3 consists of an earthen berm and vertical sand wells.

 ©2021 All Rights Reserved

The concrete dam consists of a 904-foot wide gravity section that is founded on shale. From right to left the concrete gravity structure consists of the right non-overflow, 664-foot wide spillway consisting of 14 radial gates seating on ogee crests, and left non-overflow. The crest elevation of the ogee weir is labeled on the "as-built" documents to be 409.5 feet. The 14 radial gates each have horizontal and vertical dimensions of 40-feet and 28-feet, respectively. Within this report, radial gate and Tainter gate may be used interchangeably. The gate bays are separated by thirteen (13) 8-foot wide piers resulting in an effective spillway width of 560 feet. A reinforced-concrete chute conveys spillway discharges at a grade of 3H:1V to the stilling basin with a top of concrete elevation of 367.0 feet. The stilling basin is 125 feet in length, and contains staggered baffle blocks and an end sill. Three low-level sluiceways, each 4.5-feet by 6.75-feet, are located in the central spillway piers. A vertical intake tower is located on the upstream end of each central pier, with sluice gates provided at varying elevations to release water. A general layout of the spillway is presented in Figure 2-2.

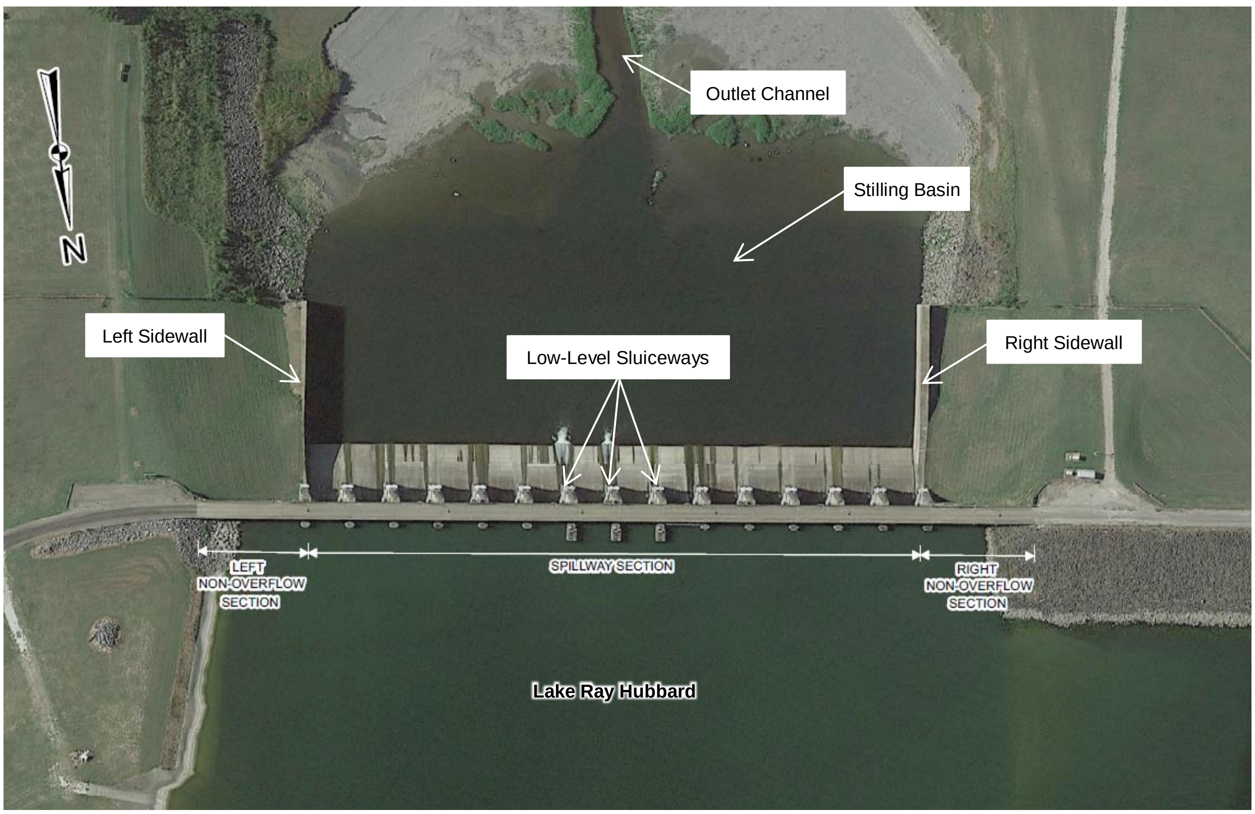

Figure 2-2: Spillway Layout

Each concrete non-overflow structure has a crest length of 120-feet, with crest elevations varying from 450.0 feet to 452.0 feet. The upstream face of the non-overflow structures is vertical from the crest to elevation 423.3 feet, and 1H:1.5V thereafter to the upstream toe. The downstream face of the non-overflow structures is vertical from the crest to elevation 423.3 feet, and 1H:3V thereafter to the downstream toe. A drainage gallery is located within the concrete gravity dam for drainage collection and internal observations of the structure. Access into the drainage gallery is via a spiral staircase located in the right non-overflow structure. Discharges from foundation drains are collected in two sumps within the drainage gallery, where 6-inch diameter cast iron pipes (CIPs) convey flows through the spillway training walls on each side of the chute.

 ©2021 All Rights Reserved

A saddle embankment, referred to as the "East Dike" in previous inspection reports and other record documents, spans a low-lying area to the left of the concrete gravity spillway structure. The East Dike is a rolled or compacted earthen structure on the order of 20 feet in height and 1,000 feet in length. The crest is approximately 30 feet in width to accommodate a paved, asphaltic-concrete service roadway. The upstream slope is approximately 3H:1V and the downstream slope is approximately 4H:1V. We note that the downstream slope of the East Dike was originally constructed at 3H:1V but was flattened to the current grade in 2011 to address slope stability issues. The available record documents do not indicate whether the saddle embankment was constructed with "zoned" earthfill or an internal drainage system.

A raw water intake tower is located near the right abutment of the dam. The intake tower is irregularly shaped; however, the total width from left-to-right is about 77 feet and the total length in the upstream-to-downstream direction is about 41 feet. A bridge spans from the crest of the dam to the top of the intake tower for access. Six 8-foot by 8-foot sluice gates are located at varying elevations on the intake tower to provide a means to withdraw water from the reservoir. Water is conveyed to a pump station located at the downstream toe via two 8-foot diameter conduits located at the base of the intake tower. According to the "as-built" plans, the intake conduits are located within a vertical shale excavation and were backfilled with impervious material. Concrete collars were provide every 20 feet along the conduit for seepage control.

Pertinent data for Lake Ray Hubbard and Forney Dam is presented in Table 2.1 below.

©2021 All Rights Reserved

Table 2-1: Pertinent Data for Lake Ray Hubbard and Forney Dam

General	
Dam Type	Earthen and Concrete Gravity
Year Constructed	1967
Purpose	Water Supply
Owner	City of Dallas
Reservoir	
Normal Pool Elevation (ft.)	435.5
Surface Area (ac.)	20,947 (Normal Pool) 28,644 (Top of Dam)
Impoundment Volume (ac.-ft.)	439,559 (Normal Pool) 810,247 (Top of Dam)
Dam	
Watershed (sq. mi.)	1,074 (Total) 777 (Upstream of Lavon Dam) 297 (Downstream of Lavon Dam)
Top of Dam Elevation (ft.)	450.0
Maximum Height (ft.)	60
Crest Length (ft.)	12,500
Crest Width (ft.)	22
Upstream Slope	Varies 3H:1V to 7H:1V
Downstream Slope	Varies 3H:1V to 7H:1V
Spillway	
Type	Concrete Ogee-crested Overflow
Control	14 Tainter Gates (40’ x 28’ Each)
Crest Elevation (ft.)	409.5 (Ogee Control Section) 437.5 (Top of Gates)
Crest Length (ft.)	560 (Effective)
Outlet Works	
Type	3 Intake Towers & Sluiceways through Center Spillway Piers
Control	3 Sluice Gates Each Pier (Size Varies)
Control Elevation (ft.)	388.0 (4’ x 6’ Gate) 409.0 (2’ x 3’ Gate) 409.0 (1.5’ x 2’ Gate)
Conduit Size	4.5’ x 6.75’ Each
Water Supply Intake	
Type	Concrete Intake Structure & 2 Conduits
Control	6 Sluice Gates (8’ x 8’ Each)
Control Elevation (ft.)	392.0 (2 Gates) 406.0 (2 Gates) 420.0 (2 Gates)
Conduit Size	8’ Diameter Each

©2021 All Rights Reserved

3.0 TEXAS DAM SAFETY

TCEQ regulates both public and private dams within the state via the Dam Safety Program. Texas Administrative Code Title 30, Part 1, Chapter 299, titled 'Dams and Reservoirs', provides the framework and requirements for structures regulated by the Dam Safety Program. TCEQ regulates dams that have a height equal to, or greater than, 25 feet and a maximum storage capacity of not less than 15 acre-feet. In addition, TCEQ provides for the regulation of smaller dams (6 feet in height or greater) impounding large storage volumes (50 acre-feet and greater). Figure 3-1 below summarizes the structures that are regulated by TCEQ based upon height and/or volume.

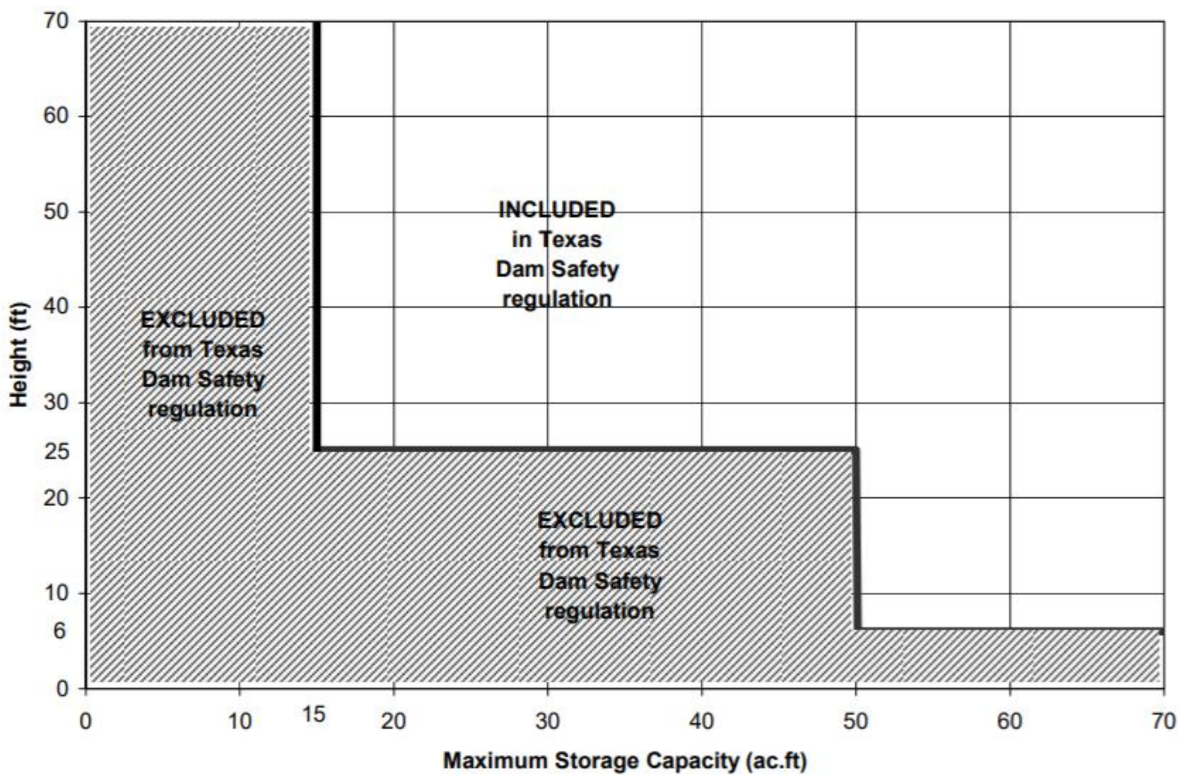

Figure 3-1: Texas Dam Safety Regulation

Once a dam has been identified based on a height and/or maximum storage volume large enough to be regulated by TCEQ, the referenced regulations separate the dams into size categories as shown in Table 3-1.

Table 3-1: Texas Dam Size Classification

Category	Impoundment Maximum Storage (acre-feet)	Height (feet)
Small	≥15 and <1,000 ≥50 and <1,000	≥25 and <40 ≥6 and <40
Intermediate	≥1,000 and <50,000	≥40 and <100
Large	≥50,000	≥100

©2021 All Rights Reserved

Additionally, TCEQ classifies dams based upon their hazard potential should the structure fail catastrophically. Summarized below are the three hazard classifications for dams regulated by TCEQ.

- Low hazard potential
    - No loss of human life expected (no permanent habitable structures in the breach inundation area downstream of the dam)
    - Minimal economic loss (located primarily in rural areas where failure may damage occasional farm buildings, limited agricultural improvements, and minor highways)
- Significant hazard potential
    - Loss of human life possible (one to six lives or one or two habitable structures in the breach inundation area downstream of the dam)
    - Appreciable economic loss, located primarily in rural areas where failure may cause damage to isolated homes, damage to secondary highways, damage to minor railroads; or interruption of service or use of public utilities
- High hazard potential
    - Loss of life expected (seven or more lives or three or more habitable structures in the breach inundation area downstream of the dam)
    - Excessive economic loss, located primarily in or near urban areas where failure would be expected to cause extensive damage to public facilities, agricultural, industrial, or commercial facilities, public utilities, including the design purpose of the utility, main highways or railroads used as a major transportation system

The minimum design flood hydrograph for dams regulated by TCEQ is established based upon the size and hazard classification of the dam and calculated using the criteria in the most current version of the agency's *Hydrologic and Hydraulic Guidelines for Dams in Texas* (Guidelines).

Based upon the height of Forney Dam (60 feet) and the maximum potential storage volume of the impounded reservoir (810,247 acre-feet), the dam is classified as being a large, high hazard potential structure and is subject to the requirements set forth in Chapter 299 of the Texas Administrative Code and the TCEQ Guidelines. Based on the large, high hazard classification, the corresponding design storm is the full Probable Maximum Flood (PMF). The most recent hydrologic and hydraulic analysis of Forney Dam was performed in 2014 by Freese and Nichols in support of the development of an Emergency Action Plan (EAP). The results of that study indicated that Forney Dam is capable of passing the full PMF with freeboard. Schnabel notes that PMP depths utilized for development of the PMF in the Freese and Nichols report were computed utilizing Hydrometeorlogical Report 52 (HMR52) developed by the USACE. A statewide PMP study was completed for Texas in 2017 and updated PMP depths were provided. The TCEQ Guidelines have recently been updated to specify the use of this study for future analyses. Schnabel recommends that an updated hydrologic and hydraulic analysis be performed utilizing precipitation depths from the 2017 statewide PMP study.

©2021 All Rights Reserved

4.0 CONSTRUCTION HISTORY

The Forney Dam and reservoir was constructed under authorization of the Texas State Board of Water Engineers (Permit No. 1923 dated March 6, 1959) to provide municipal water supply for the City of Dallas and surrounding communities. Design of the dam, spillway, and appurtenant structures was performed by Forrest and Cotton, Inc. As previously mentioned, construction of the dam was completed circa 1967, with first full reservoir impoundment obtained or achieved circa 1969. Construction of the raw water pump station at the outlet end of the intake conduits was completed circa 1972.

According to record documents, construction of the dam was completed in phases. Phase I consisted of excavations for the spillway and associated stilling basin, intake structure, and intake conduits, as well as the construction of portions of the embankment. The spillway was excavated to the approximate concrete subgrade in this phase. Material from the spillway excavation was utilized to construct the embankment to approximate elevation of 404.0 feet. The embankment was then raised to elevation 413.0 feet utilizing additional borrow material. Pore water pressures and settlement of the initial embankment section were monitored during Phase I construction. A 500-foot section, termed the "closure section", remained open in the embankment during this time for normal stream flow and flood diversion. This closure section was located near the center of the embankment in the original location of the East Fork Trinity River. Phase II consisted of the construction of portions of the spillway, intake structure, and conduit during the normal low-flow months of August through November. The spillway weir was constructed with the low-level sluiceways for re-routing of the stream diversion. After diversion of stream flows through the sluiceways, the embankment across the 500-foot closure section was constructed. Phase III consisted of the completion of the remaining portions of the embankment and spillway. Diversion of stream flow through the low-level sluiceways continued until deliberate impoundment of the reservoir commenced.

An inspection of the dam was performed by Jones & Boyd, Inc. in 1987. A report titled 'Inspection of Forney Dam and Appurtenances at Lake Ray Hubbard' (1987) was prepared. The report contained several recommendations to address observed deficiencies. In response, piezometers were installed within the embankment circa 1989 in general accordance with the proposed instrumentation plan provided in the inspection report, clearing was performed up to approximately 500 feet downstream of the toe of the embankment, and downstream drainage channels were regraded. In addition, slurry walls were constructed in the left and right abutment areas in general accordance with recommendations from the inspection report, and the riprap located on the upstream slope of the embankment was replaced. No record documents for the design of aforementioned remedial measures and limited construction records were provided to Schnabel for the above described work.

Subsequent to the installation of the recommended piezometers, measurements recorded in the years following indicated the presence of artesian conditions near the downstream toe. In 1993, Jones & Boyd prepared a report titled 'Design Report for Abatement of Excessive Hydrostatic Pressures at Forney Dam' which contained alternatives developed to address excessive hydrostatic pressures, as well as other deficiencies identified during recent inspections. The other noted deficiencies include slope failures along the downstream slope of the saddle embankment and behind the spillway sidewalls, as well as undermining of the revetment mat behind the left side of the spillway entrance channel.

A geotechnical investigation of Forney Dam was performed by TEAM Consultants, Inc. in support of the design of alternatives. The results of the geotechnical investigation were presented in a report titled 'Geotechnical Evaluation, Lake Ray Hubbard Dam' dated January 1993, and contained in the appendix of

©2021 All Rights Reserved

the Jones & Boyd design report. Alternatives to address excessive hydrostatic pressures were developed in three areas along the downstream slope and toe, designated as Work Areas 1, 2, and 3. Work Areas 1 and 2 consist of pumped relief wells, earthfill buttresses, and sand blankets located at the toe of the embankment. Discharges from the relief wells and sand blankets are piped to the drainage channels downstream of the dam. Work Area 3 consists of a trench drain and vertical sand wells, supplemented with an earthen berm. Construction of the proposed measures to relieve hydrostatic pressures, as well as remedial repairs to address the other identified deficiencies, was completed circa 1995. No record documents for the final design or construction of these remedial measures were provided to Schnabel.

In 2011, construction plans were prepared by Freese and Nichols for repairs to Work Areas 1 and 2. The 2011 construction plans also indicate other remedial repairs to include the replacement of the trunnion pins for Tainter Gate 14 (left most gate), the placement of earthfill to repair a slope failure along the left bank of the spillway outlet channel, the excavation and reconstruction of the downstream slope of the saddle embankment, the construction of a subsurface drain and retaining wall behind the stilling basin left training wall, the placement of grout overlay to repair the existing riprap revetment along the left slope of the spillway entrance channel, construction of a new reinforced-concrete boat ramp, replacement of the sluice gates located on the intake towers of the low-flow release piers, and the replacement of miscellaneous electrical appurtenances.

Record documents were available for the original design of the dam and spillway structures. A review of the design documents indicated that the soil shear strength parameters utilized for the stability analysis of the embankment slopes and spillway gravity structures rely on cohesion values higher than generally acceptable by current standards. In addition, past seepage observations indicate that pore water pressures within the embankment may be higher than the design assumptions. Therefore, Schnabel recommends that the gravity dam and embankment stability analyses be reviewed and updated based upon current engineering criteria.

 ©2021 All Rights Reserved

5.0 SCOPE OF SERVICES

In 2016, Arcadis performed a dam safety inspection of the Forney Dam. The dam safety inspection included a visual evaluation of the structure and review of available record documents. A report titled "Rockwell-Forney Dam Safety Inspection Report" dated December 2016 was prepared to document the findings and provide recommendations. Schnabel was engaged as a subconsultant to Garver, LLC to address several of the recommended items in the report, which are summarized below:

- Develop safety procedures for the inspection and drainage gallery that are compliant with OSHA standards for signage and ventilation. Because the gallery is a non-permitted confined space, at a minimum, the oxygen levels should be checked prior to entry and during occupation with operation of the ventilation fan to provide good air exchange.

- Facilitate a Potential Failure Mode Assessment (PFMA) to evaluate the potential mechanisms most likely to impact the performance of the dam project and lead to failure. The PFMA is used to focus surveillance and monitoring activities on the failure modes that are of significant risk to the dam.

- Review the Flood Release Manual. Site and loading conditions have changed significantly since the effective update from 1989, and reportedly based on 1981 stream loading for inflow calculations. The SCADA system used to determine inflow and release rates should be evaluated and updated to a current data management system.

- Conduct a detailed inspection of the Tainter gates, equipment and structural components. This should include dewatering the gates and also conducting a climbing inspection of Tainter gates to evaluate structural members and connections. Operating components of the gate hoist, the spillway bridge and all other structural or operational features should be evaluated routinely with reports as defined in O&M Manual. Such inspections should then be made on a 10-year frequency.

- Review a dive inspection of the stilling basin to evaluate concrete damage or deterioration, sediment accumulation, drain clogging and other factors. The initial inspection may be performed by divers, with the need for a dewatered inspection evaluated at that time, based on the findings of the inspection.

In addition, an evaluation of Forney Dam, to include archival research and a visual evaluation, was included in the scope of services. This work was performed in accordance with the subcontractor agreement between Garver, LLC and Schnabel dated March 18, 2020.

Schnabel facilitated a PFMA workshop with individuals from Garver and DWU with critical knowledge of the dam and operations. The findings from this workshop and recommendations are presented in a report provided under a separate cover titled "Potential Failure Mode Analysis Report, Rockwall-Forney Dam".

©2021 All Rights Reserved

6.0 VISUAL EVALUATION

As authorized, Schnabel personnel performed visual evaluations of the Forney Dam, spillway outlet works, and appurtenant structures between March 2020 and July 2020. A detailed physical inspection of the Tainter gates and the trunnion friction testing were performed between March 30, 2020 and April 14, 2020. Visual inspections of the dam embankment, concrete gravity sections, chute, stilling basin (above the tailwater elevation), and saddle embankment were performed on July 8, 2020 and July 9, 2020. No topographic surveying, subsurface exploration, non-destructive testing, instrumentation measurements, or engineering analyses were performed during the visual evaluation. Selected photographs from the inspection are included in Appendix B.

6.1 Embankment

On July 9, 2020, Schnabel personnel visually inspected the embankment, to include the upstream slope visible above the operating water level, the crest, and the downstream slope. In addition, Schnabel personnel visually inspected the drainage channel downstream of the toe. Temperatures on the day of the inspection varied from 76° Fahrenheit (F) to 94° F. In addition, no precipitation occurred on the date of the visual inspection or for 10 days preceding the inspection. During the inspection of the embankment, stations were marked on the crest every 500 feet in general accordance with the “as-built” plans (1967) using a measurement wheel. Approximate stations of observations are indicated accordingly.

Observations of the upstream slope were made from the crest of the embankment, as well as from the lake utilizing a boat operated by DWU personnel. The upstream slope was observed to be generally uniform in grade with no visual indications of movement or instability. Although not measured, the upstream slope visible above the water line appears to be a grade of approximately 3H:1V, which would be in accordance with the “as-built” plans (1967). Riprap was observed from the crest of the embankment to the waterline. The riprap slope protection is adequate with no observed areas of sparse riprap coverage, excessive vegetation, or sloughs noted. We note that two abandoned piezometers from the original construction were observed on the upstream slope of the dam.

The crest of the dam is generally uniform except in areas of pavement distress. Pavement distress can be a sign of structure movement or simply a soft subgrade due to poor drainage from the roadway. A paved asphaltic-concrete roadway traverses the length of the crest. The pavement width is about 20 feet with grassed shoulders on each side. In general, the pavement is in adequate condition with some deterioration, such as cracking and potholes noted. This observed deterioration does not appear to be indicative of instability as recent construction activities appear to have occurred to provide electrical service across the dam. The grassed shoulders are well maintained with a good stand of grass. No depressions or cracks, other than surficial pavement cracking, were observed on the crest. Electrical manholes were noted at multiple locations along the crest. In addition, about 4 feet of pavement on the upstream side of the roadway has been recently re-paved. This new pavement was reportedly placed following the installation of new electrical duct banks within the crest, as indicated in the Freese and Nichols construction plans (2011).

The downstream slope was observed to have generally uniform slopes to the ‘designed’ breaks in grade. Based upon visual observations, the downstream slope and toe appeared to be in general conformance with the “as-built” plans (1967) except where modified by the above referenced work areas. No evidence of sloughs or slides were noted. In addition, no depressions, bulges, cracks, or other visual signs of instability were observed. A good stand of maintained turf grass is generally present with few bare areas

 ©2021 All Rights Reserved

noted. Schnabel was unable to identify locations of the lateral subsurface drain outlets, or “finger drains” that reportedly convey collected seepage to the toe of the structure. No wet areas or obvious areas of seepage were noted on the embankment or immediately downstream of the toe. However, DWU personnel indicated two areas near the abutment contacts where seepage has been observed in the past. In addition, Schnabel noted and DWU personnel concurred that areas of wetness are present, from time to time, in the floodplain downstream of the dam. The first area of seepage indicated by DWU personnel is located at the right downstream abutment contact near approximate station 4+00 and piezometer EP-3. Previous inspection reports have identified perennial seepage in in this area. No active seepage was noted during Schnabel’s visual inspection; however, tire ruts and displaced soil are indicative of past wetness. The second apparent area of seepage is located at the left downstream abutment contact and to the right of the spillway near approximate station 100+00. Similarly, while no evidence of active seepage was noted during Schnabel’s visual inspection, indications of past wetness were observed. The areas where embankment seepage has been observed by DWU personnel are indicated in Figure 6-1.

Figure 6-1: Locations of Embankment Seepage Observed by DWU

The three Work Areas constructed to address excessive hydrostatic pressures at the toe of the embankment were observed during the visual inspection of the downstream slope. Work Areas 1 and 2, located at approximate stations 78+50 and 29+00, respectively, consist of earthen berms approximately 15 feet in height with pressure relief wells and sand blankets to collect and discharge seepage and alleviate excess pore pressures. Work Area 2 has an additional earthen berm approximately 5 feet in height with a sand blanket located downstream of the toe near the drainage channel. The pressure relief wells operate automatically and discharges are conveyed to the drainage channels downstream from the dam. The downstream ends of the discharge conduits are situated on concrete outlet supports along the edge of the channel. Schnabel notes that substantial erosion capable of undermining or destabilizing the concrete outlets was noted adjacent to several of the outlets. The pressure relief wells did not operate at the time of the inspection; however, DWU personnel indicated that the pressure relief wells are operational. A general layout of Work Area 2 is presented in Figure 6-2. Work Area 1 is similar.

©2021 All Rights Reserved

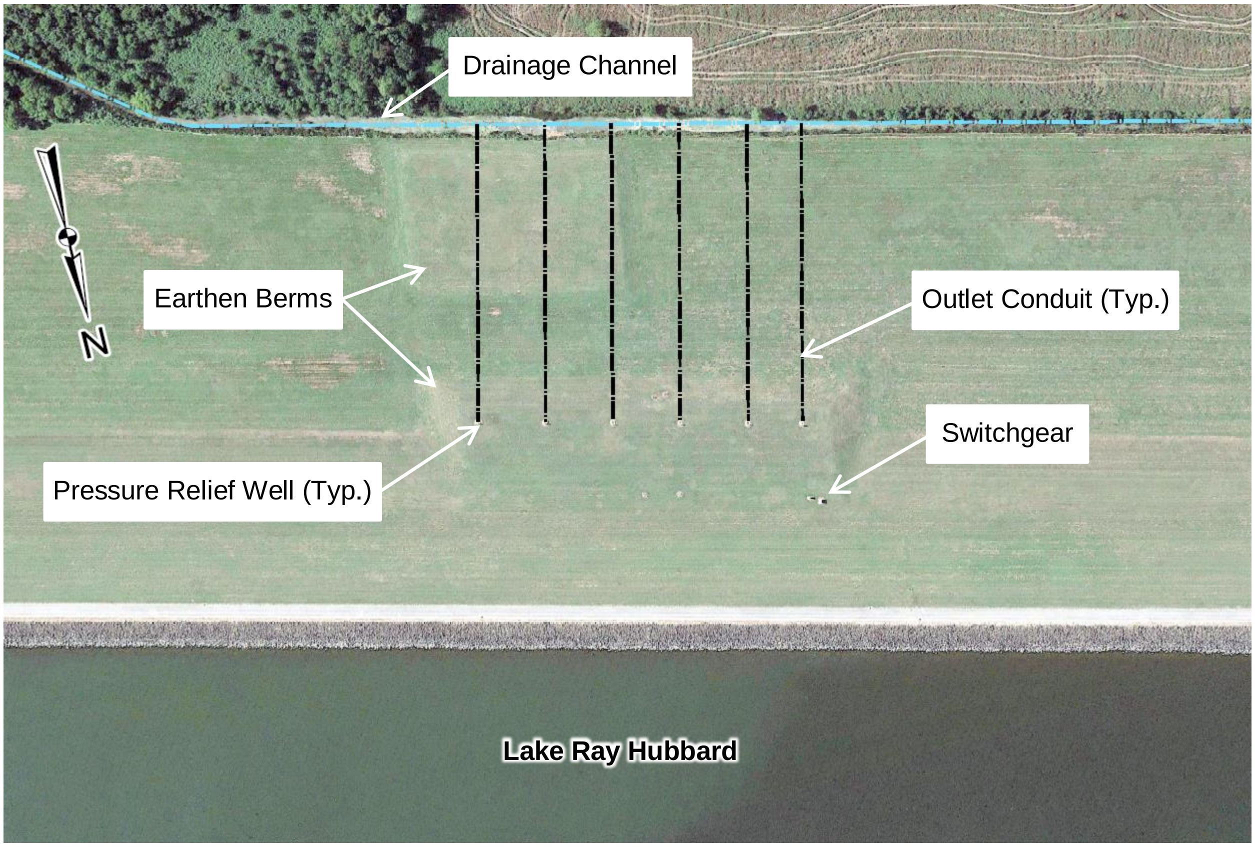

Figure 6-2: Work Area 2 Layout

Work Area 3 is located at approximate station 12+00, and consists of an earthen berm with a sand trench drain and vertical sand wells. The earthen berm for Work Area 3 is approximately 5 feet in height and does not contain pressure relief wells. No evidence of seepage was observed near the Work Areas.

Two unlined drainage channels are located approximately 500 feet downstream from the downstream toe of the embankment. These channels collect surface water and seepage discharges. At the time of the inspection, water was elevated to the approximate top of bank the both channels, resulting in the inundation of several of the pressure relief well outlets. The causes of elevated water surfaces were not evaluated during the visual inspection; however, the elevated water is reportedly caused by poor drainage (mild slopes) and beaver activity. Schnabel recommends that appropriate measures be implemented to promote drainage from these channels.

6.2 East Dike

On July 8, 2020, the saddle embankment, or East Dike, was visually inspected by Schnabel personnel. Temperatures on the day of the inspection varied from 73° F to 92° F. In addition, no precipitation occurred on the date of the visual inspection or for 9 days preceding the inspection. Observations were made of the upstream slope visible above the water line, the crest, and the downstream slope.

The upstream slope visible above the water line appears to have a uniform grade of approximately 3H:1V in general accordance with the "as-built" plans (1967). No visual signs of instability were noted. Similar to

©2021 All Rights Reserved

the dam embankment, riprap was observed from the crest of the embankment to the waterline. The riprap slope protection is adequate with no observed areas of sparse coverage or sloughs.

The crest of the saddle embankment is generally uniform and flat with a paved asphaltic-concrete roadway on the crest. The pavement, with a width of about 20 feet, is in adequate condition. The grassed shoulders are well maintained with a good stand of grass. No depressions or cracks, other than surficial pavement cracking, were observed on the crest.

The downstream slope is generally uniform in grade with no visual indications of movement or instability. In addition, no wet areas or flowing seepage were observed. According to the record documents, modifications were made to the saddle embankment in 2011 to include the widening of the crest, reconstruction of the downstream portion of the embankment, and flattening of the downstream slope. Based on observations, the downstream slope has a generally uniform grade of approximately 4H:1V in general accordance with the Freese and Nichols construction plans (2011). No indications of a subsurface drainage system were observed. A good stand of well-maintained turf grass was observed on the East Dike at the time of the site reconnaissance.

6.3 Non-Overflow Sections

On July 8, 2020, Schnabel personnel visually inspected the left and right concrete non-overflow sections located on each side of the spillway. Observations were made of the exposed upstream and downstream faces, as well as the crest. The upstream faces were observed from the lake utilizing a boat operated by DWU personnel. During the inspection, no visual and obvious signs of structural integrity or instability were observed. Minor deterioration and surficial cracking of the concrete, generally consistent with the age of the structure, was noted. Clear and defined horizontal construction joint lines are discernable along the upstream and downstream faces. In addition, clear and defined vertical contraction joints are also discernable. No visual signs of significant seepage was observed through the joints. DWU personnel indicated the presence of a significant “void” or eroded area beneath the grouted riprap revetment along the left side slope near the left non-overflow spillway. Based on conversations, the void is only observable during periods of low water levels in the reservoir. Due to the water level at the time of the inspection, Schnabel was unable to visually inspect the indicated void area. However, this void should be evaluated further and proper mitigation measures should be designed and implemented.

6.4 Spillway Section

On July 8, 2020, the spillway section was visually inspected by Schnabel personnel. Observations of the concrete were made on the chute sections, ogee sections, and piers. The upstream sides of the piers above the water level were observed from the lake utilizing a boat operated by DWU personnel. During the inspection of the downstream side of the spillway, the two left sluiceways were discharging. Due to elevated water level within the stilling basin, only the two upper chute slab rows were visible during the inspection. Observation locations are indicated based on the spillway monolith, chute slab, and stilling basin slab numbering and nomenclature found in the “as-built” plans (1967). Figure 6-3 indicates the numbering and nomenclature for the right side of the spillway. The left side of the spillway is similar.

©2021 All Rights Reserved

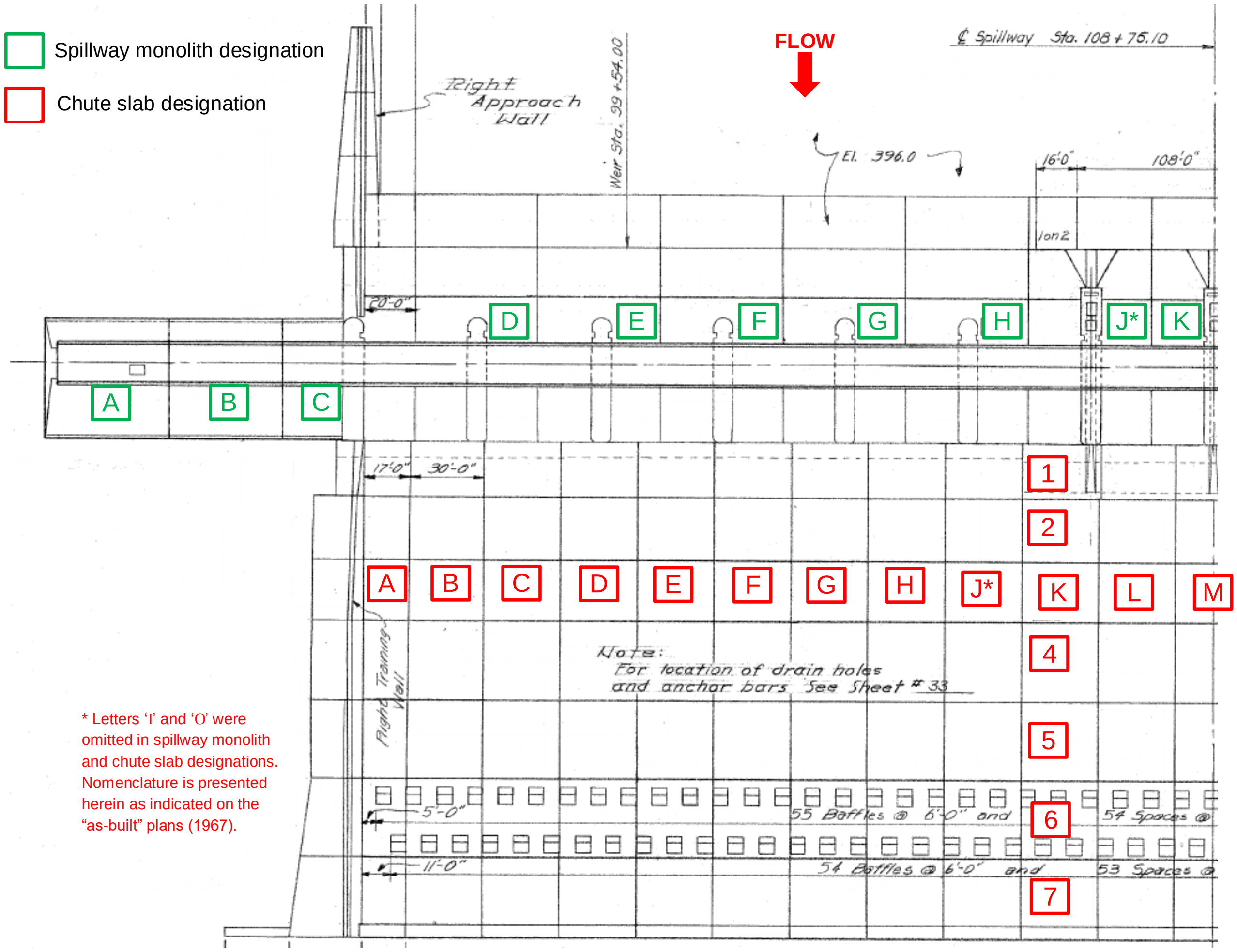

Figure 6-3: Spillway Numbering and Nomenclature

In addition, the Tainter gate numbering system shown in Figure 6-4 is referenced throughout the report.

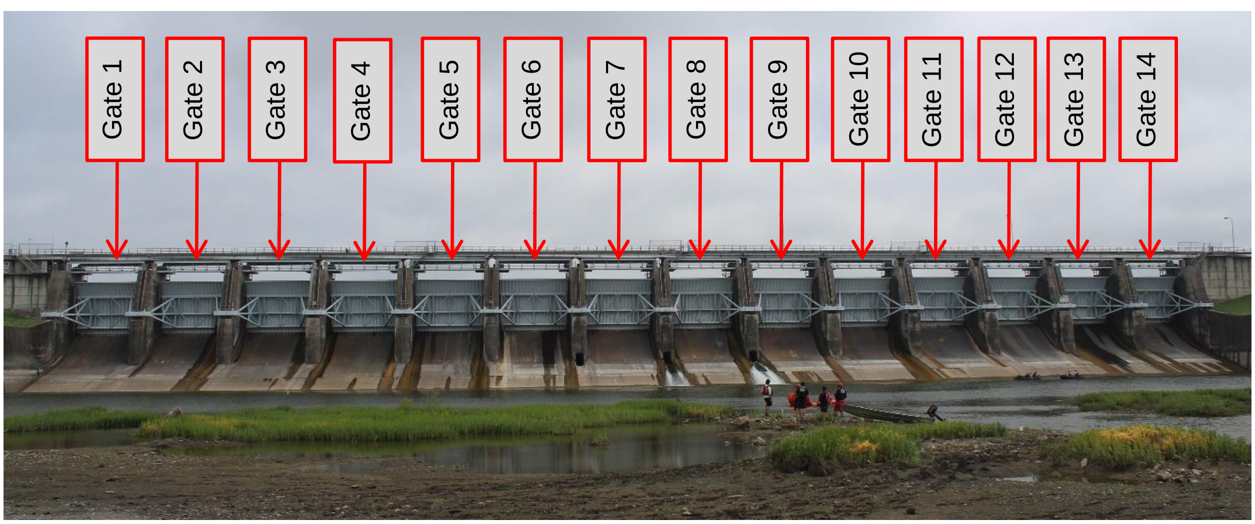

Figure 6-4: Tainter Gate Numbering

©2021 All Rights Reserved

In general, some deterioration of the concrete, generally consistent with the age of the structure, was observed throughout the spillway section with some surficial cracking and spalls. Most observed spalls were located along contraction joints. Small spalls and some degradation were noted along the vertical joints between spillway monoliths. Water, possibly seepage or water from leaking gates being conveyed in construction joints, was observed discharging from some of the cracks and joints within the chute, as well through the left sidewall drain outlets. No visual signs of structural integrity or instability were observed. The sidewalls are generally straight and uniform, with some weathering and hairline cracks observed. During the detailed inspection of the spillway concrete, specific items of note include:

- Gate 1 Bay
    - Small spalls observed along a vertical lift joint on spillway monolith D.
    - Small spalls observed along longitudinal joint between chute slabs A1 and B1, as well as A2 and B2.
- Gate 2 Bay
    - Small spalls observed along longitudinal joint between spillway monoliths D and E. In addition, small spall observed along a vertical lift joint on spillway monolith E.
    - Small spalls observed along longitudinal joint between chute slabs C2 and D2.
- Gate 3 Bay
    - Spalls observed along longitudinal joint between spillway monoliths E and F. In addition, small spalls observed along downstream transverse joint on spillway monolith E.
    - Small spalls observed along longitudinal joint between chute slabs E1 and F1, as well as E2 and F2.
- Gate 4 Bay
    - Small spall observed along a vertical lift joint on spillway monolith G. In addition, seepage observed flowing from a vertical lift joint near the crest.
    - Small spalls observed along longitudinal joint between chute slabs F1 and G1.
    - Spall with flowing seepage observed along longitudinal joint between chute slabs F2 and G2.
- Gate 5 Bay
    - Small spalls observed along vertical lift joints on spillway monoliths G and H.
    - Small spall observed along longitudinal joint between chute slabs G1 and H1.
- Gate 6 Bay
    - Spall observed along longitudinal joint between spillway monoliths H and J. In addition, small spalls observed along vertical lift joints.
- Gate 7 Bay
    - Small spall observed along a vertical lift joints on spillway monolith K.
    - Small spalls observed along longitudinal joint between chute slabs L2 and M2.
- Gate 8 Bay
    - Small spalls observed along vertical lift joints on spillway monolith K.
    - Small spalls observed along longitudinal joint between chute slabs M2 and K2. In addition, seepage observed flowing from this joint.
- Gate 9 Bay
    - Seepage observed flowing from transverse joint between chute slabs P1 and P2, as well as from longitudinal joint between chute slabs P2 and Q2.
- Gate 10 Bay

 ©2021 All Rights Reserved

    - Spall observed along longitudinal joint between chute slabs Q1 and R1. The observed spall is likely concrete that was placed as part of past repair efforts.
- Gate 11 Bay
    - Small spall observed along longitudinal joint between spillway monoliths N and P.
    - Spall observed along longitudinal joint between between chute slabs S1 and T1.
    - Aggregate pop-out observed on right pier.
- Gate 12 Bay
    - Small spalls observed along transverse joint between chute slab V1 and spillway monolith Q.
- Gate 13 Bay
    - Large spall observed along longitudinal joint between spillway monoliths Q and R.
    - Flowing seepage observed along longitudinal joint between spillway monoliths Q and R near chute.
    - Longitudinal crack extending through the bottom two lifts observed in spillway monolith Q.
    - Small aggregate pop-outs observed in chute slab W1.
- Gate 14 Bay
    - Spall observed along longitudinal joint between spillway monoliths R and S. The observed spall is likely concrete that was placed as part of past repair efforts.
    - Spall observed along vertical lift joint in spillway monolith S. In addition, seepage was observed flowing from a vertical lift joint near the crest of this monolith.
    - Small aggregate pop-out observed in chute slab Y1.
    - Seepage observed flowing from transverse joint between chute slab X1 and X2, as well as Y1 and Y2. Some areas of joint seepage have vegetative growth.
    - Small aggregate pop-out observed in chute sidewall Y1.
    - Seepage observed flowing from vertical joints between chute sidewalls Y1 and Y2, as well as sidewalls Y3 and Y4.

Significant vegetative growth and iron ochre were observed in the upper drain outlets located along the left spillway outlet sidewall. According to the record documents, these drains are located above the shale excavation and serve to relieve hydrostatic pressures from within the backfill material placed behind the wall. This vegetative growth, which was observed in most, if not all, of upper drain outlets on the left side, is impeding drain discharges. In addition, the record documents also indicate that the drain fill material was specified as ¾” to 1” stone. Based on Schnabel’s experience, an aggregate of this size is likely not an adequate filter for the backfill material, and piping of backfill material may be occurring through the drains or clogging of the drainage material may have occurred. Therefore, Schnabel recommends that the utilized drainage material be evaluated for compatibility with backfill material and appropriate modifications be incorporated.

The lower drain outlets are provided on the sidewall where shale was excavated to construct the stilling basin and also serve to relieve hydrostatic pressures behind the wall. No evidence of discharge was noted from the lower drain outlets at the time of the inspection. In addition, the drain outlets located along the right stilling basin sidewall were dry at the time of the inspection, and no vegetation was observed.

©2021 All Rights Reserved

6.5 Tainter Gates

A detailed inspection of the Tainter gates was performed between March 30, 2020 and April 3, 2020. A comprehensive description of the findings from the inspection is presented in the report titled 'Rockwall-Forney Dam Visual Gate Inspection, Trunnion Friction Testing and Structural Evaluation Report' prepared by Schnabel and dated July 23, 2021. A copy of this report is included in Appendix E. In general, evidence of deterioration was noted on each of the Tainter gates. The coating on the gates is deteriorated, with areas of corrosion noted. Inadequately sized, poorly located, or clogged drain holes have also resulted in trapped water, increasing the potential for corrosion. In addition, section loss at the bottom of the gate leaf was observed.

The welded connections of the gate members was observed during the inspection. Welds were generally observed to be of poor quality, and many fractured welds were noted. During the inspection of Gate 6, a significant fracture was observed between the web and flange of one of the struts.

6.6 Drainage Gallery

On July 8, 2020, Schnabel personnel visually inspected the interior of the drainage gallery within the concrete gravity sections. During the inspection, the ventilation system was operational and the drainage gallery was well lit. However, DWU indicated that personnel must enter the adit in order to access the control panel utilized to activate the ventilation system. In general, the drainage gallery is in adequate condition with minor concrete deterioration, consistent with the age of the structure, noted. Concrete spalls were noted in a few locations. Little seepage through the concrete was observed. Foundation drain outlets located near the bottom of the upstream side of the drainage gallery were not flowing at the time of the inspection. Some corrosion of the steel conduits located within the foundation drain holes was observed. This corrosion does not appear to impact the ability of the foundation drains to discharge water. However, routine cleaning of the foundation drain holes is recommended. The upstream end of the sump outlet conduits, which convey flows from foundations drains to the stilling basin, have been retrofitted with gate valves to prevent potential backwater within the stilling basin from flooding the gallery. Based on conversations with DWU personnel, the gate valves have been recently operated. Flap valves are located on the outlet end of the CIP outlet conduits protruding through the stilling basin sidewall. The flap valves were closed at the time of the inspection and unobstructed.

6.7 Stilling Basin and Outlet Channel

An underwater inspection of the stilling basin was performed by American Underwater Services, Inc. on July 8, 2020. During the inspection, about 10 feet of water was present in the stilling basin. The results of the inspection were presented in a report titled 'Inspection of Forney Dam Stilling Basin and Tawakoni Balancing Reservoir Pipe Line, Inspections performed on July 8^{th}, 9^{th}, and 10, 2020' and dated July 14, 2020. A copy of this report is included in Appendix C. In addition, two video files of the dive inspection were provided to Schnabel for review. The videos contain the portion of the inspection performed near the right training wall in the stilling basin. Low visibility, and/or poor video quality, prevented a thorough review of the inspection videos by Schnabel personnel. However, audio containing dialog between the dive personnel was provided. We note that video and audio were not provided for the entire stilling basin inspection.

Based upon Schnabel's review of the provided information, the underwater portions of the Forney Dam stilling basin are in adequate condition with limited evidence of concrete degradation or spalling noted. Based upon the audio from the recorded portions of the dive inspection, the presence of organic growth

 ©2021 All Rights Reserved

was noted on most concrete surfaces. However, one area of spalling, having a depth of 1-½ inches and located near the right sidewall, was identified. In addition to the noted limited spalling, minor concrete degradation with some exposed aggregate was observed in portions of the inspection video at/above the water surface. Various debris ranging from soil to rock to metal to wood were also noted in the stilling basin inspection report.

Subsequent to the underwater inspection of the stilling basin, the outlet channel above the tailwater elevation located immediately downstream was observed by Schnabel personnel. Observations were made of the outlet channel, floodplain, and side slopes adjacent to the floodplain. The outlet channel and floodplain immediately downstream from the stilling basin are generally uniform and free from obstructions. No excessive surficial erosion was observed; however, based upon a comparison of the design documents to the current condition, the general overall extent of the stilling basin has gradually increased over the life of the structure due to erosion resulting from spillway discharges. This expansion suggests that additional armoring of the outlet channel would be prudent to limit the potential for continued erosion to negatively impact the stability of the spillway structure. The side slopes adjacent to the floodplain are generally uniform in grade. No visual and obvious signs of instability were noted. According to the Freese and Nichols construction plans (2011), repairs were made to a failed portion of the left side slope located about 500 feet downstream of the end of the left stilling basin sidewall. The slope was reconstructed utilizing earthfill to a grade of 2.5H:1V, and sand blanket drain was installed at the bottom. No visual signs of instability were noted with the repaired portion of the left side slope.

A significant amount of flowing water was observed discharging from the left side slope immediately downstream from the riprap at the end of the left stilling basin sidewall. This area is indicated in Figure 6-5. The water was observed to be clear, and discharging from between the shale and soil at the bottom of the left side slope. No water was observed flowing from the slope at higher elevations; however, riprap coverage in this area hindered observations. A determination could not be made as to whether the origin of the flowing water is seepage or groundwater. Previous inspection reports have identified perennial flowing water in in this area. Given the presence of the void upstream of the gravity structure, the potential for drainage material to not be compatible with soil materials, and the presence of historic seepage, Schnabel recommends that this seepage be evaluated and, if needed, appropriate remedial measures be designed and implemented to address the source and impact of the seepage.

©2021 All Rights Reserved

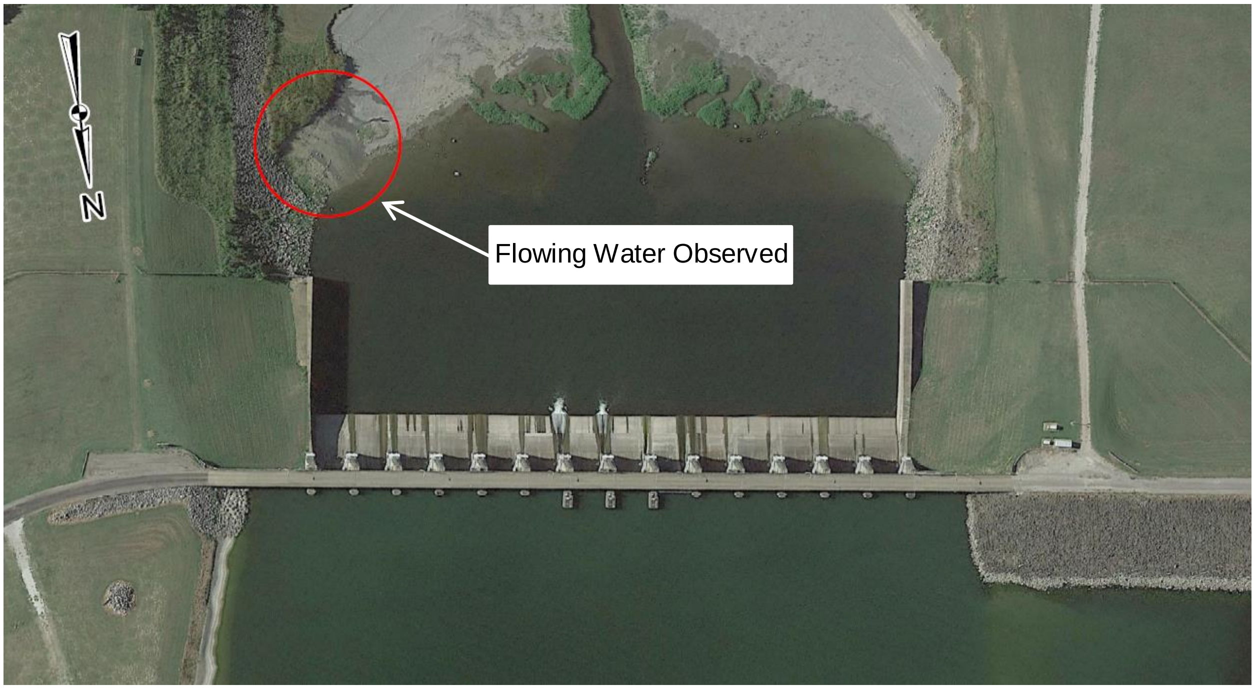

Figure 6-5: Potential Seepage Area near Stilling Basin

In addition, DWU personnel indicated an area at the toe of the left side slope along the floodplain where wetness has been observed in the past. No evidence of wetness was observed by Schnabel personnel in this area, which is located approximately 1,000 feet downstream from the end of the left stilling basin sidewall, during Schnabel's visual inspection; however, indications of past wetness were observed. Given the location of this area with respect to the dam, the wetness is likely not the result of seepage flows.

©2021 All Rights Reserved

7.0 INSTRUMENTATION DATA

The instrumentation for Forney Dam consists of forty-two (42) piezometers located within the embankment, abutments, and downstream area. Twenty-three (23) piezometers were installed circa 1989 based on recommendations in an inspection report prepared by Jones & Boyd, Inc. (1987). Measurements of these piezometers during ensuing inspections indicated excess hydrostatic pressures and artesian conditions in portions of the embankment and downstream toe. During the construction of remedial repairs to address the excesses hydrostatic pressures, an additional nineteen (19) piezometers were installed. An instrumentation plan indicating the piezometer locations is included in Appendix D.

Pressure relief wells were installed in the berms at Work Areas 1 and 2 circa 1995 to address hydrostatic pressures within the embankment. The pressure relief wells operate automatically and discharges are pumped into conduits to convey flows to the drainage channels downstream from the dam. The downstream ends of each conduit is situated on a concrete outlet support in the channel. Each Work Area contains six (6) pressure relief wells. No data regarding the operational frequency of the pressure relief wells located in the Work Areas was provided.

The record documents indicate that piezometers, pore pressure cells, and settlement plates were installed within the embankment during Phase I construction. Past inspections indicate that the original piezometers, which were constructed utilizing galvanized steel pipes, have corroded and are no longer functional. Some abandoned steel pipe piezometers were observed along the upstream slope. What is likely an abandoned pore pressure cell recording tower was also observed near the downstream toe of the embankment. No record documents were available indicating the abandonment of the original piezometers and none of the original piezometers were observed on the crest and downstream slope during the site reconnaissance. In addition, no indications of the pore pressure cells, other than the one indicated, and settlement plates were observed during the site reconnaissance. Schnabel also notes that no survey monuments were observed to monitor horizontal and vertical movements of the dam.

DWU provided Schnabel with piezometer and tailwater measurements obtained from January 2014 to August 2020, as well as coordinates of piezometer locations. Graphs were generated by Schnabel to display the recorded water elevation versus time for each piezometer, and several cross section were generated to display the measured phreatic surface through the embankment at convenient locations where piezometers are in a row. In addition, a profile of the piezometers located in the crest of the embankment was generated. The water level of Lake Ray Hubbard was not provided with the data. Lake water surface elevations for the same period were obtained from USGS stream gauge 08061550 for use on the graphs. The piezometer graphs are presented in Appendix D.

During Schnabel's review of the piezometer data, several items were noted:

- The embankment cross sections taken along piezometers located at Work Areas 1 and 2 indicate a locally depressed phreatic surface within the embankment, likely due to a well point drawdown from the pressure relief wells. The embankment cross section at Work Area 1 indicates that the phreatic surface is also depressed in EP-12, which is located within the crest, and rebounds to a higher elevation downstream of the embankment.
- The recorded water elevations from piezometers located within the floodplain downstream of the dam indicate water near the ground surface.

©2021 All Rights Reserved

- Graphs of piezometer water elevations versus tailwater elevations indicate that the piezometers located within the floodplain downstream of the dam exhibit a rapid response to changes in tailwater. As such, the water elevations in these piezometers are likely tailwater driven. In addition, EP-4, EP-8, EP-40, and EP-44 are likely tailwater driven as well, despite being located within the embankment.
- The recorded water elevations from EP-9, which is located within the embankment immediately left of Work Area 2, were at or above the ground surface for most measurements taken in the past five years. High water levels can create destabilizing forces for the embankment.
- The graphs of piezometer measurements from EP-4, EP-14, EP-15, and EP-39 indicate an upward trend in recorded water elevations over the past 7 years.
- The graph of piezometer measurements from EP-40 indicates erratic swings of 20 or more feet in the recorded water elevation. Conversely, the graph of measurements from EP-26, which is adjacent to EP-40, indicates a relatively constant recorded water elevation over the past 7 years.
- There are relatively wide ‘gaps’ of structure that are not monitored by piezometer. Given that performance of the embankment is not monitored in these areas, Schnabel recommends that consideration be given to installing additional piezometers to document the phreatic surface within structure. While there are no hard rules regarding piezometer spacing, consideration should be given to have a row of piezometers every several hundred feet.

©2021 All Rights Reserved

8.0 TAINTER GATE ANALYSIS

A structural analysis of the Tainter gates at Forney Dam was performed based on the inspection, record documents, and the results of the trunnion friction testing. The Tainter gates were analyzed based on several load combinations outlined in the U.S. Army Corps of Engineers (USACE) Engineering Technical Letters (ETL) 1110-2-584, Design of Hydraulic Steel Structures. The load combinations include self-weight of the Tainter gate, hydrostatic load, wave load, earthquake load, side seal friction, trunnion friction and cable hoist load. Trunnion friction factors of 0.3 were utilized in the analysis based on recommendations in ETL 1110-2-584. Trunnion friction test results indicate that actual average values of trunnion friction measured at Forney Dam are less than the utilized value.

The results of the gate analysis indicate that some structural members are deficient based on the current Tainter gate design guidelines. As such, continued exposure of the gates to the load cases could result in overstressing of the members. Detailed analysis procedures and results are presented in the report titled 'Rockwall-Forney Dam Visual Gate Inspection, Trunnion Friction Testing and Structural Evaluation Report' prepared by Schnabel and dated July 23, 2021. A copy of this report is included in Appendix E.

©2021 All Rights Reserved

9.0 FLOOD OPERATION PROCEDURES EVALUATION

Schnabel completed an evaluation of the current flood operation procedures for Lake Ray Hubbard and Forney Dam. Schnabel's understanding of current procedures was based on discussions with DWU personnel and a review of available record documentation. The evaluation considered the current status of operations, as well as any changes in the watershed, downstream conditions, and availability of data since the last update to operation procedures. In addition, hydrologic data was reviewed with respect to the current operation procedures.

Based on the results of the evaluation, the current flood operation procedures are well presented and provide reasonable responses to varying conditions. However, the procedures are dependent on the ability of DWU personnel to obtain the necessary data in a timely manner. Currently, a supervisory control and data acquisition (SCADA) system, referred to as the Flood Alert System, is used to obtain current lake levels and other data. DWU personnel have identified concerns related to the general age of the Flood Alert System, stage-storage estimates of the lake above normal pool, accurate estimation of inflow rates from stream gauges, and inherent error associated with estimating the lake level during storm events with relatively high winds. In addition, Schnabel notes that development has occurred within the watershed since the most recent hydrologic and hydraulic analysis was performed in 2014, which can impact timing of runoff and peak inflows. The comprehensive evaluation of flood operation procedures is presented in the report titled 'Review of Flood Operation Procedures, Rockwall-Forney Dam' prepared by Schnabel and dated July 26, 2021. A copy of this report is included in Appendix F.

©2021 All Rights Reserved

10.0 DRAINAGE GALLERY INSPECTION SAFETY PROCEDURES

Schnabel has developed a Site Safety and Health Plan (SSHP) to mitigate or limit potential risks to personnel involved with engineering and inspection of the drainage gallery adit. The SSHP was developed in general conformance with Occupational Safety and Health Administration (OSHA) guidelines, and is presented under a separate cover titled 'Site Safety and Health Plan, Rockwall-Forney Dam Adit Investigation'. A copy of the SSHP is included in Appendix G.

©2021 All Rights Reserved

11.0 CONCLUSIONS AND RECOMMENDATIONS

11.1 Conclusions

Based on the results of the visual evaluation, instrumentation review, Tainter gate evaluation, and flood operation procedures review, as well as our experience with other dams, the Forney Dam, spillway, and appurtenant structures are generally well-maintained with the exception of a few significant issues such as the fractured web noted on one gate. However, given that the structure was design and constructed in the 1960s, improvements or upgrades are recommended.

The embankment is being maintained and no visual indications of distress or instability were noted. While no areas of wetness or seepage were observed during Schnabel's visual inspection, DWU personnel have indicated past wetness near the abutment contacts and within the floodplain downstream of the dam. Given the time of year that the inspection was performed (i.e., the summer) and lack of recent precipitation, seepage may have not been readily apparent. These areas should continue to be monitored for indications of seepage and changes in seepage rates.

A review of the provided piezometer data indicates that widely varying piezometric levels exist within the structure and foundation. Currently, distances of 2,000 feet or more exist between piezometer locations. Given the distances between piezometers, the size of the structure, and the hazard potential of the structure, additional piezometers are recommended for a comprehensive evaluation of differences in piezometer water levels. In addition, a review of the existing provided data indicated piezometric levels near the ground surface in several piezometers within the embankment and downstream area. In addition, some piezometer data indicates an upward trend in recorded water levels.

The condition of the concrete comprising the spillway and non-overflow structures is generally consistent with other structures having a similar date of construction. Some visual signs of weathering and physical deterioration were observed. Concrete cracks observed appear to be surficial and do not indicate instability of the structures. Concrete spalls were observed in the spillway section, with damage likely resulting from flowing water during spillway discharges. Some spalls were in areas where concrete was likely repaired in the past, as indicated by neat saw cut lines around the spalled area. The spalls observed were mostly minor and not a concern to the stability of the structure. However, a large spall was observed between spillway monoliths Q and R, as well as a longitudinal crack in spillway monolith Q extending through the bottom two lifts.

The results of the Tainter gate structural analysis and visual inspection did not indicate significant structural issues with the gates, with the exception of Gate 6, which require immediate attention or removing gates from service. However, some of the gates members are overstressed for the load cases analyzed. A fracture was observed on one of the Gate 6 strut arms during the visual evaluation. Due to the severity of the fracture observed on the Gate 6 member, continued operation could result in the expansion of the fracture and failure of the primary strut arm. While Gate 6 contained the only observed fracture, other strut arms may contain fractures that were not observable during the inspection.

A specific area of concern is related to the left side of the spillway section. All of the drain outlets located along the left stilling basin sidewall and above the shale excavation are blocked with vegetative growth and iron ochre. This vegetative growth indicates the presence of past seepage in this area, and the blocked drain outlets could result in excess hydrostatic pressures behind the sidewalls. In addition, flowing water

©2021 All Rights Reserved

was observed discharging from the left side slope immediately downstream from the left stilling basin sidewall. During the inspection, Schnabel personnel could not determine whether this flowing water was seepage from the reservoir and through the dam or general groundwater from the adjacent hillside. Schnabel understands that a slurry wall was constructed behind the left sidewall to address perennial flowing water observed in this area. However, based on observations made during the site reconnaissance, the slurry wall does not appear to be effective. Furthermore, DWU personnel indicated the presence of a large void beneath the grouted riprap near the upstream side of the left non-overflow section, and drain fill material behind the stilling basin sidewalls is inadequately sized to properly filter the backfill. Given the location of this void, the erosion of soil beneath the grouted riprap could be the result of wave action. However, without additional evaluations, the potential that this collective group of observations is indicative of seepage and soil piping around the left non-overflow section cannot be dismissed.

11.2 Recommendations

DWU should continue proactive maintenance of Forney Dam. Monitoring and inspections, in addition to the daily on site presence of DWU personnel, should be performed in accordance with TCEQ guidelines. Based on the visual inspections and evaluations of Forney Dam, Schnabel offers the following recommendations:

- Evaluate the potential seepage area located adjacent to the left side of the spillway.
- Evaluate the void beneath the grouted riprap revetment along the left side slope of the spillway entrance channel near the left non-overflow spillway.
- Utilizing a registered land surveyor, install monuments across the crest of the dam that can be used to measure and document vertical and horizontal movement.
- Install stationing on the dam crest corresponding to the project stationing on the “as-built” drawings to provide horizontal control for future observations/inspections. Stationing should be visible and readable from the upstream and downstream embankment slopes.
- Install additional piezometers within the embankment crest, downstream slope, and toe such that the distance between rows of piezometers is limited to several hundred feet. The locations and depths of additional piezometers should be determined by a professional engineer.
- Evaluate elevated piezometric levels near the ground surface in several piezometers within the embankment and downstream area. In addition, evaluate the cause of the upward trend in recorded water levels of some piezometers.
- Evaluate the stability of the earthen embankment dam and concrete gravity dam.
- Integrate pressure relief well operations in the SCADA system so that flow rates and run times can be documented.
- Maintain an operational log for the pressure relief wells, to include runtimes and discharges.
- Evaluate the cause for the elevated water in the drainage channels downstream of the dam. The channel blockage should be removed such that the pressure relief well outlets are not inundated.

 ©2021 All Rights Reserved

- Remove vegetation from drain outlets located along the left stilling basin sidewall. In addition, evaluate the drain fill material for filter compatibility with backfill material and incorporate appropriate modifications.

- Perform an updated hydrologic and hydraulic analysis to evaluate the Texas statewide PMP study and account for additional upstream development that has occurred since the last analysis was performed.

- Repair the asphaltic concrete service roadway on crest of the dam. In addition, develop plans to replace/repave this roadway in the near future.

- Continue to monitor the large spall observed between spillway monoliths Q and R for future degradation. In addition, the longitudinal crack observed in spillway monolith Q extending through the bottom two lifts should be monitored as well. Continued degradation may necessitate repairs in these locations.

- Perform Tainter gate recommendations provided in the 'Rockwall-Forney Dam Gate Inspection, Testing and Analysis Report'.

- Perform flood operation procedures recommendations provided in the report tilted 'Review of Flood Operation Procedures, Rockwall-Forney Dam'.

- Provide a means to activate drainage gallery ventilation fans without having to enter the adit.

- Remove various debris accumulated within the stilling basin.

- Provide additional armoring of the stilling basin to limit the potential for continued erosion to negatively impact the stability of the spillway structure.

©2021 All Rights Reserved

12.0 REFERENCES

Arcadis. (2016). "Rockwall-Forney Dam Safety Inspection Report." Contract No. 15-189E. Dallas Water Utilities. City of Dallas, Texas.

Dallas Water Utilities (1974). "Operations & Maintenance Manual for Forney Dam Lake Ray Hubbard." Dallas, Texas.

Dallas Water Utilities Personnel. (2005). "Flood Operation of Lake Ray Hubbard." Dallas Water Utilities Division. City of Dallas, Texas.

Forrest and Cotton, Inc. (1960). "Design Memorandum No. 1, Design of Floods and Freeboard Requirements." Forney Dam and Reservoir. City of Dallas, Texas.

Forrest and Cotton, Inc. (1961). "Design Memorandum No. 2, Detailed Design of Dam, Spillway and Appurtenant Works." Forney Dam and Reservoir. City of Dallas, Texas.

Forrest and Cotton, Inc. (1967). "Forney Dam and Reservoir." *As-Built Drawing.* Contract No. 64-215. City of Dallas, Texas.

Forrest and Cotton, Inc. (1972). "Plans for the Construction of the Forney Raw Water Pump Station." *As-Built Drawing.* Contract No. 70-200. City of Dallas, Texas.

Freese and Nichols. (2011). "Forney Dam Miscellaneous Improvements." *Construction Plans.* Contract No. 11-207. Dallas Water Utilities Division. City of Dallas, Texas.

Freese and Nichols. (2014). "Forney Dam (Lake Ray Hubbard) TX00837 Emergency Action Plan." Contract No. DWU08358. Dallas Water Utilities Division. City of Dallas, Texas.

Freese and Nichols. (2011). "Specifications and Forms of Contract and Bonds for Forney Dam Miscellaneous Improvements." Contract No. 11-207. Dallas Water Utilities Division. City of Dallas, Texas.

Jones and Boyd, Inc. (1993). "Design Report for Abatement of Excessive Hydrostatic Pressures at Forney Dam." Contract No. 92-033E. Dallas Water Utilities. City of Dallas, Texas.

Jones and Boyd, Inc. (1987). "Report on Inspection of Forney Dam and Appurtenances at Lake Ray Hubbard." Dallas Water Utilities. City of Dallas, Texas.

Texas Department of Water Resources (1982). "Inspection Report on Existing Dam." Rockwall-Forney Dam and Lake Ray Hubbard. July 6, 1982.

Texas Department of Water Resources (1978). "Rockwall-Forney Dam (Lake Ray Hubbard) Phase I Inspection Report." National Dam Safety Program. U.S. Army Engineer District. Fort Worth, Texas.

Texas Natural Resource Conservation Commission (1994). "Evaluation Report." Rockwall-Forney Dam / Lake Ray Hubbard. October 11, 1994.

©2021 All Rights Reserved

Texas Water Commission (1987). “Evaluation Report.” Rockwall-Forney Dam and Lake Ray Hubbard. December 7, 1987.

Texas Water Commission (1992). “Evaluation Report.” Rockwall-Forney Dam / Lake Ray Hubbard. September 3, 1992.

Texas Water Rights Commission (1970). “Inspection Report on Existing Dam.” Rockwall-Forney Dam and Lake Ray Hubbard. September 29, 1970

Texas Water Development Board (2016). “Volumetric and Sedimentation Survey of Lake Ray Hubbard, August 2015 Survey.” City of Dallas, Texas.

Texas Water Rights Commission (1973). “Inspection Report on Existing Dam.” Rockwall-Forney Dam and Lake Ray Hubbard. February 28, 1973.

©2021 All Rights Reserved

APPENDIX A

GENERAL INFORMATION

Site Vicinity Map
Overall Site Plan
Spillway Plan
Selected "As-Built" Plan Sheets
Lake Ray Hubbard Volumetric Survey

©2021 All Rights Reserved

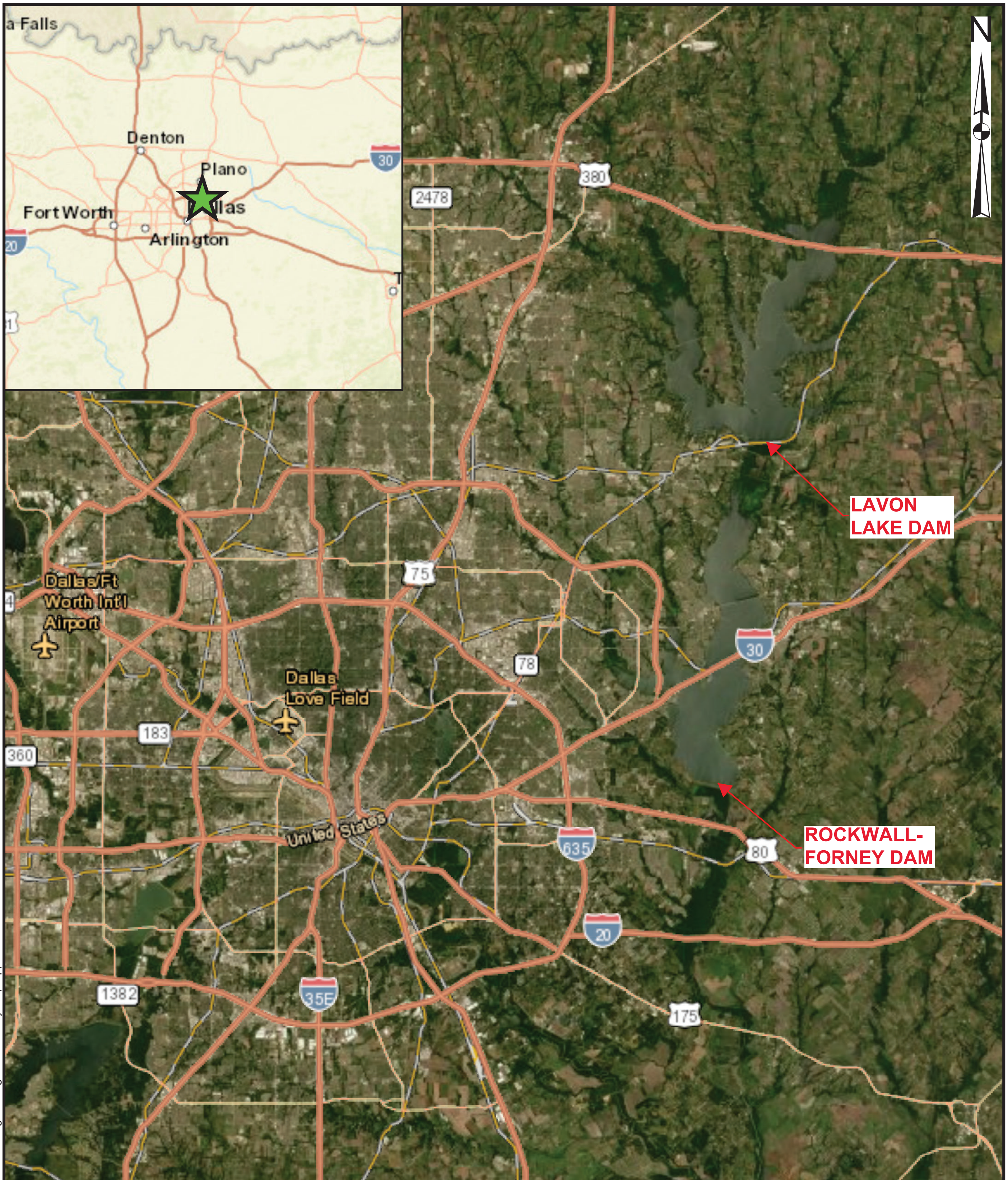

Source: Esri, Maxar, GeoEye, Earthstar Geographics, CNES/Airbus DS, USDA, USGS, AeroGRID, IGN, and the GIS User Community
Sources: Esri, HERE, Garmin, USGS, Intermap, INCREMENT P, NRCan, Esri Japan, METI, Esri China (Hong Kong), Esri Korea, Esri (Thailand), NGCC, (c) OpenStreetMap contributors, and the

NOT TO SCALE

12/7/2020 This Map was Created In Schnabel Engineerings Site Vicinity Map Application arcgis

Schnabel ENGINEERING

ROCKWALL-FORNEY DAM
DALLAS/KAUFMAN COUNTIES, TX

PROJECT NO. 20C22001.00

SITE VICINITY MAP

FIGURE 1

© Schnabel Engineering, 2020. All Rights Reserved.

8/27/2020 10:03:27 AM G:\2020\OTHER BRANCH PROJECTS\Texas\20C22001_00_DWU_Rehab_of_Raw_Water_Facilities_SA#1\03-SE\Products\07-GIS\Maps\Forney_Overall Site Plan.mxd

Legend

- Rivers
- Drainage Channels
- Roads

Source: Source: Esri, DigitalGlobe, GeoEye, Earthstar Geographics, CNES/Airbus DS, USDA, USGS, AeroGRID, IGN, and the GIS User Community
Projection: NAD 1983 StatePlane Texas North Central FIPS 4202 Feet

Scale: 1 " = 1,000 ' — 0, 500, 1,000, 2,000 Feet

Schnabel ENGINEERING

ROCKWALL-FORNEY DAM
DALLAS WATER UTILITIES SA#1
DALLAS/KAUFMAN COUNTIES, TX

PROJECT NO 20C22001.00

OVERALL SITE PLAN

© Schnabel Engineering, 2020. All Rights Reserved.

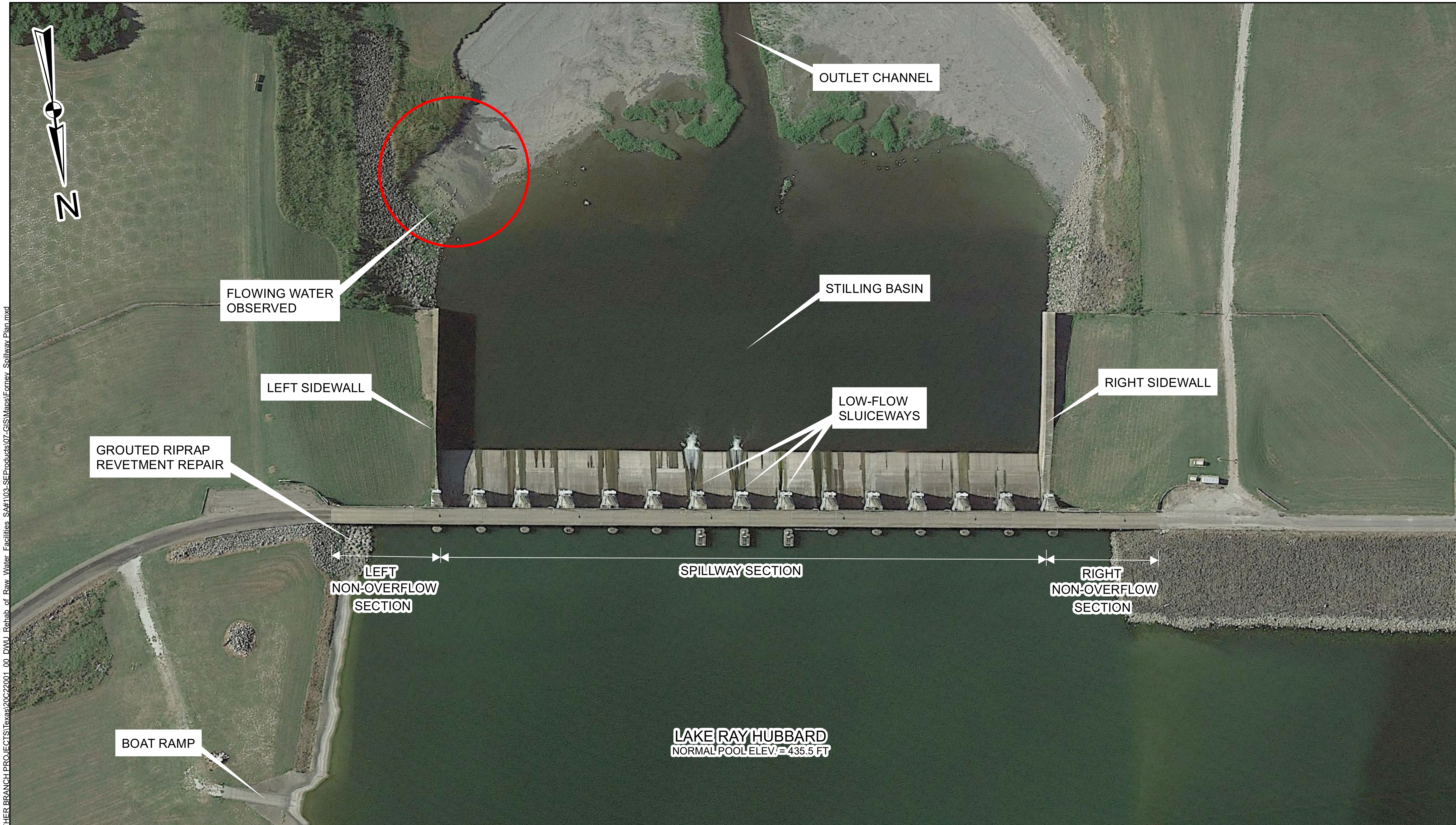

8/27/2020 1:40:34 PM G:\2020\OTHER BRANCH PROJECTS\Texas\20C22001_00_DWU_Rehab_of_Raw_Water_Facilities_SA#1\03-SEProducts\07-GIS\Maps\Forney_Spillway Plan.mxd

Source:
Projection: NAD 1983 StatePlane Texas North Central FIPS 4202 Feet

Scale: 1 " = 100 '

0 50 100 200 Feet

Schnabel ENGINEERING

ROCKWALL-FORNEY DAM
DALLAS WATER UTILITIES SA#1
DALLAS/KAUFMAN COUNTIES, TX

PROJECT NO 20C22001.00

SPILLWAY PLAN

© Schnabel Engineering, 2020. All Rights Reserved.

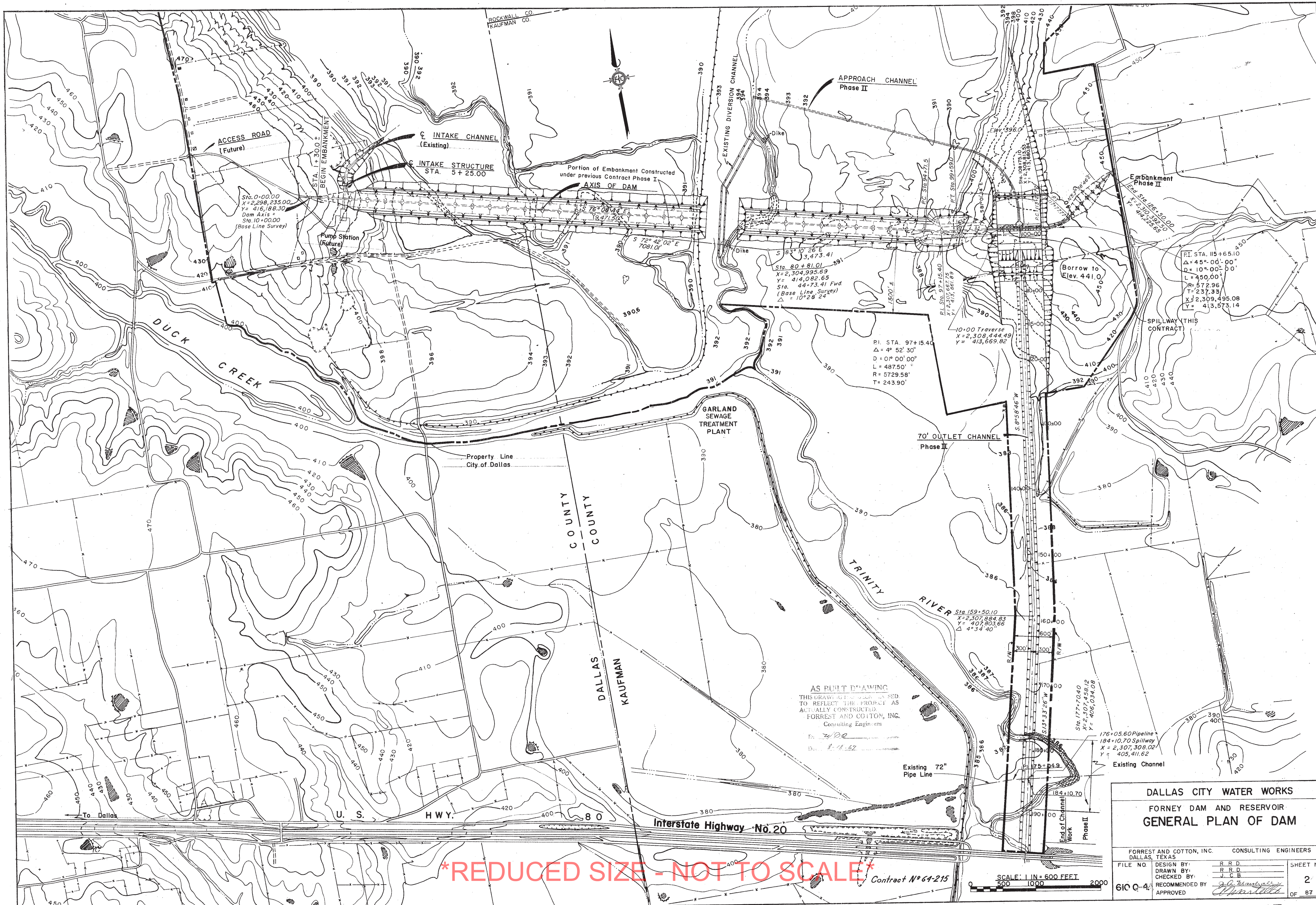

DALLAS CITY WATER WORKS
FORNEY DAM AND RESERVOIR
GENERAL PLAN OF DAM
FORREST AND COTTON, INC. CONSULTING ENGINEERS
DALLAS, TEXAS
FILE NO. 610 Q-4
DESIGN BY: R R D
DRAWN BY: R R D
CHECKED BY: J C B
RECOMMENDED BY
APPROVED
SHEET NO. 2 OF 87
SCALE: 1 IN = 600 FEET
Contract Nº 64-215
AS BUILT DRAWING
FORREST AND COTTON, INC.
Consulting Engineers
ROCKWALL CO.
KAUFMAN CO.
ACCESS ROAD (Future)
℄ INTAKE CHANNEL (Existing)
℄ INTAKE STRUCTURE STA. 5+25.00
Portion of Embankment Constructed under previous Contract Phase I
AXIS OF DAM
Pump Station (Future)
EXISTING DIVERSION CHANNEL
APPROACH CHANNEL Phase II
Embankment Phase II
Borrow to Elev. 441.0
SPILLWAY (THIS CONTRACT)
70' OUTLET CHANNEL Phase II
DUCK CREEK
GARLAND SEWAGE TREATMENT PLANT
Property Line City of Dallas
DALLAS COUNTY
KAUFMAN COUNTY
TRINITY RIVER
Existing 72" Pipe Line
Existing Channel
End of Channel Work
U. S. HWY. 80
Interstate Highway No. 20
To Dallas
REDUCED SIZE - NOT TO SCALE

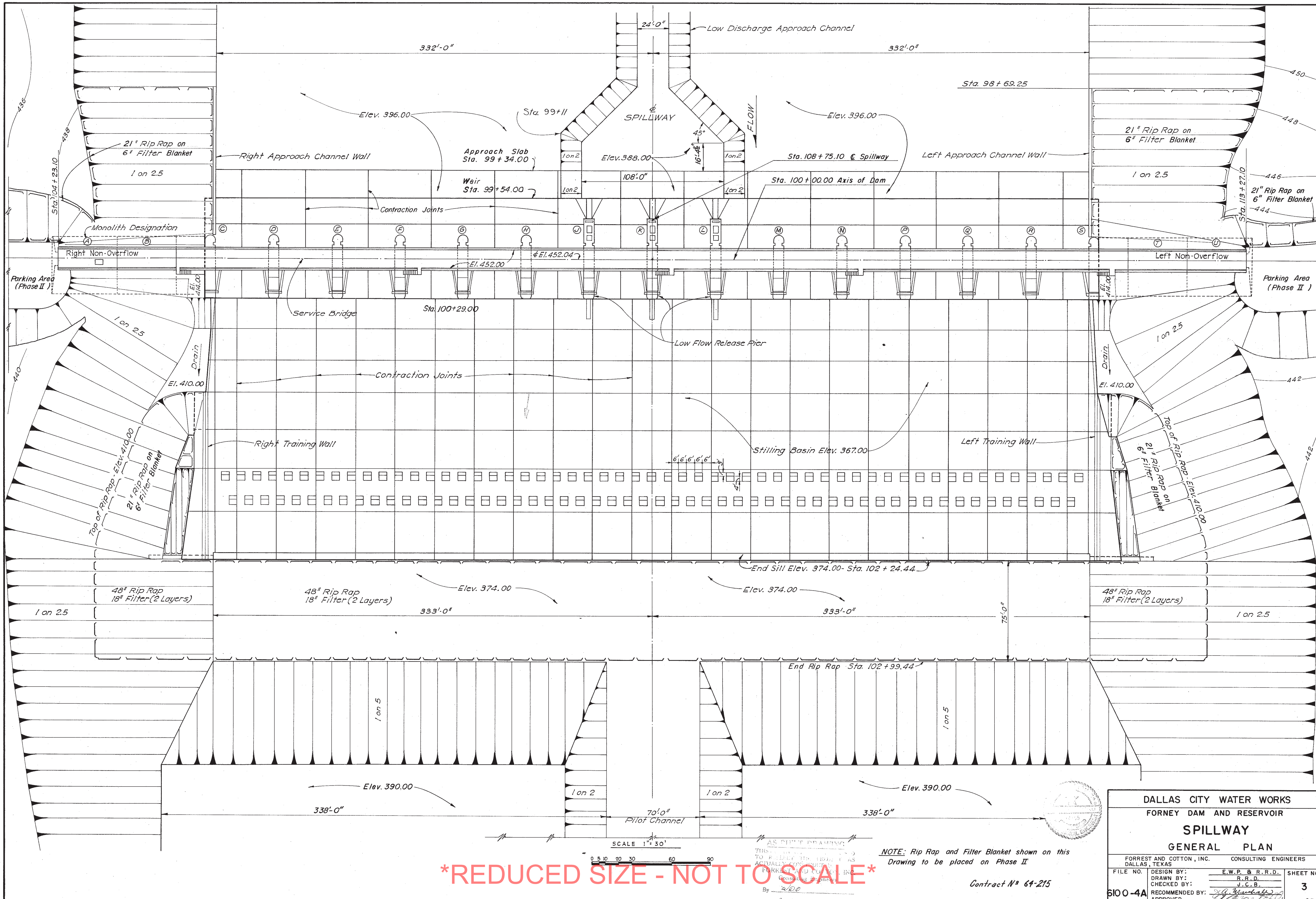

REDUCED SIZE - NOT TO SCALE

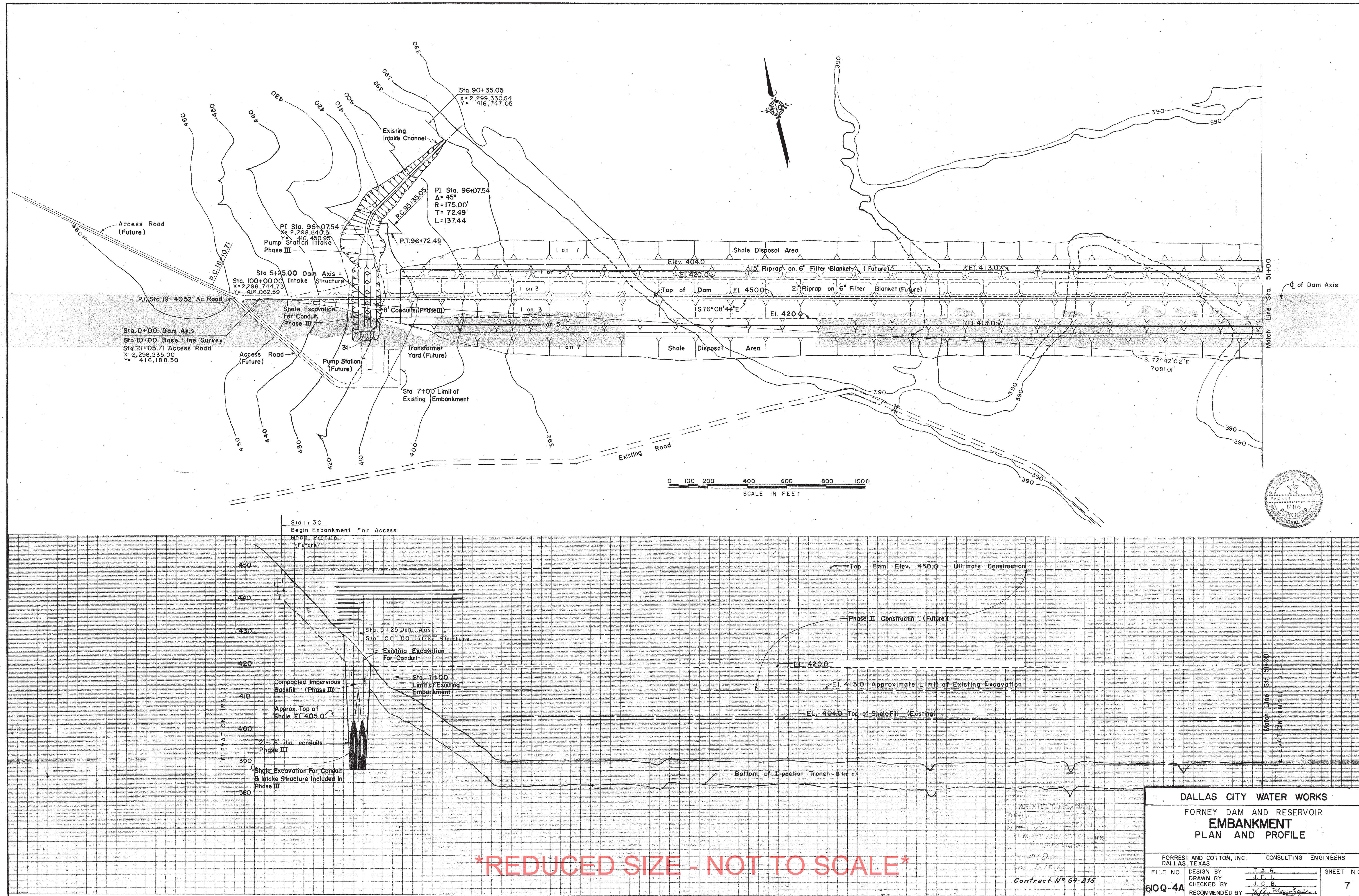

REDUCED SIZE - NOT TO SCALE

Contract Nº 64-215

DALLAS CITY WATER WORKS

FORNEY DAM AND RESERVOIR

EMBANKMENT

PLAN AND PROFILE

FORREST AND COTTON, INC. CONSULTING ENGINEERS
DALLAS, TEXAS

FILE NO.			SHEET NO.
610Q-4A	DESIGN BY	T.A.R.	7
	DRAWN BY	J.E.I.	
	CHECKED BY	J.C.B.	OF 87
	RECOMMENDED BY		
	APPROVED		

III

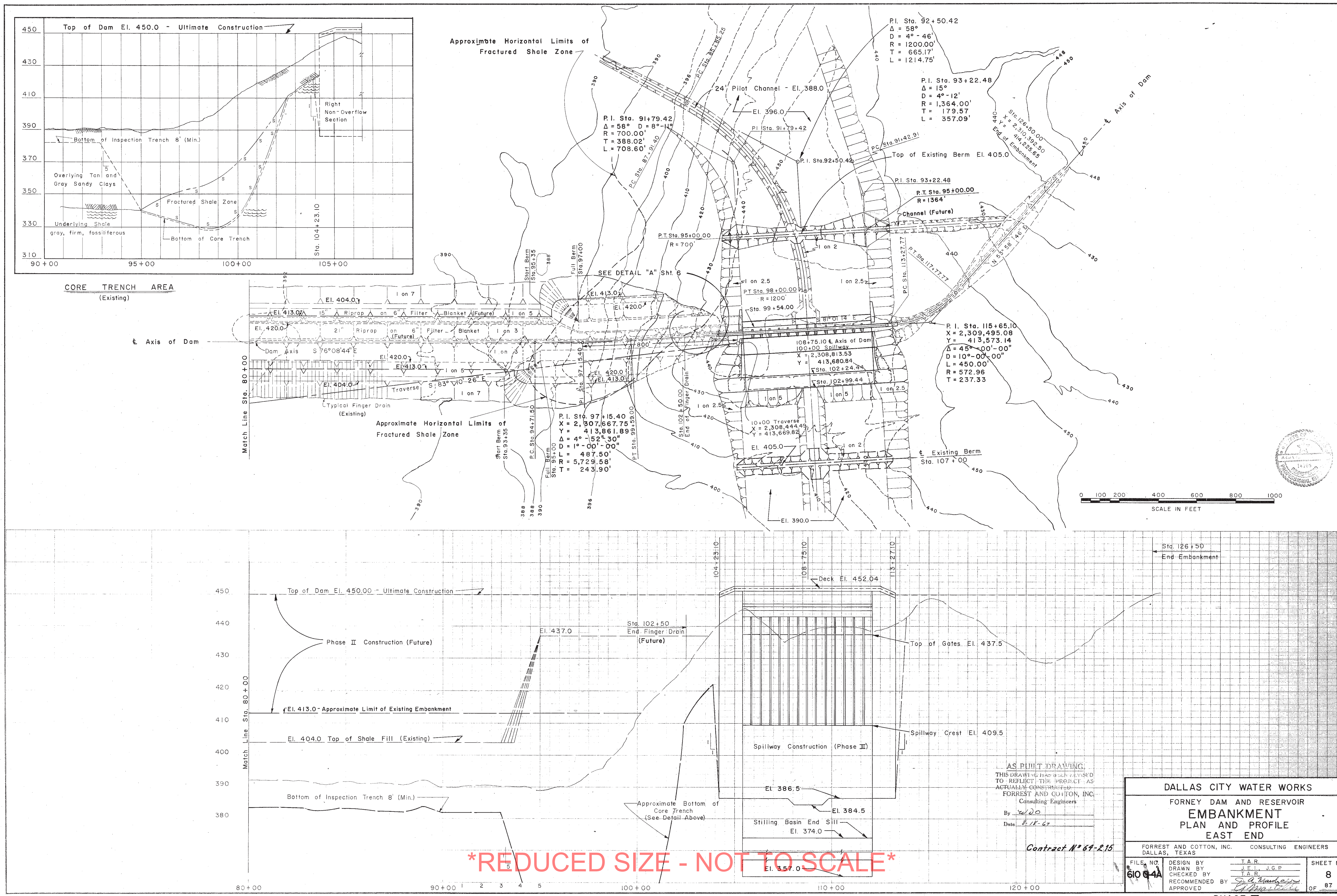

AS BUILT DRAWING
THIS DRAWING HAS BEEN REVISED TO REFLECT THE PROJECT AS ACTUALLY CONSTRUCTED
FORREST AND COTTON, INC. Consulting Engineers
By W.D.O.
Date 8-18-67

Contract № 64-215

REDUCED SIZE - NOT TO SCALE

DALLAS CITY WATER WORKS

FORNEY DAM AND RESERVOIR

EMBANKMENT
PLAN AND PROFILE
EAST END

FORREST AND COTTON, INC. DALLAS, TEXAS — CONSULTING ENGINEERS

FILE NO.			SHEET NO.
610 G-4A	DESIGN BY	T.A.R.	8
	DRAWN BY	J.E.T., J.G.P.	OF 87
	CHECKED BY	T.A.R.	
	RECOMMENDED BY	[signature]	
	APPROVED	[signature]	

PHASE III

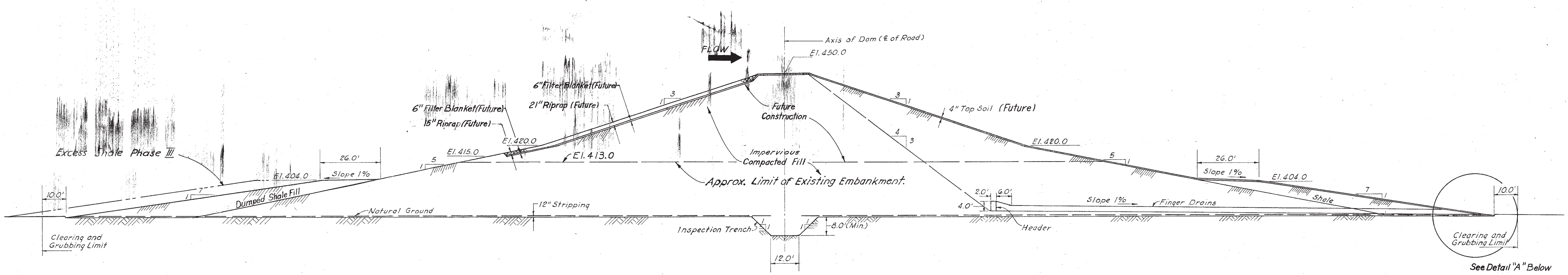

MAXIMUM SECTION

10 0 10 20 30 40 50

SCALE 1 INCH = 20 FEET

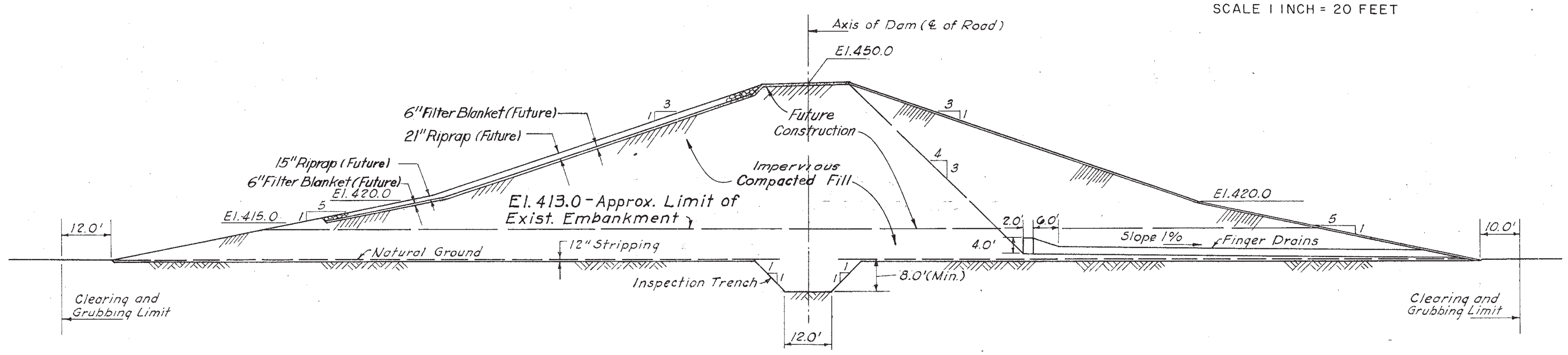

SECTION ABOVE ELEV. 404.0

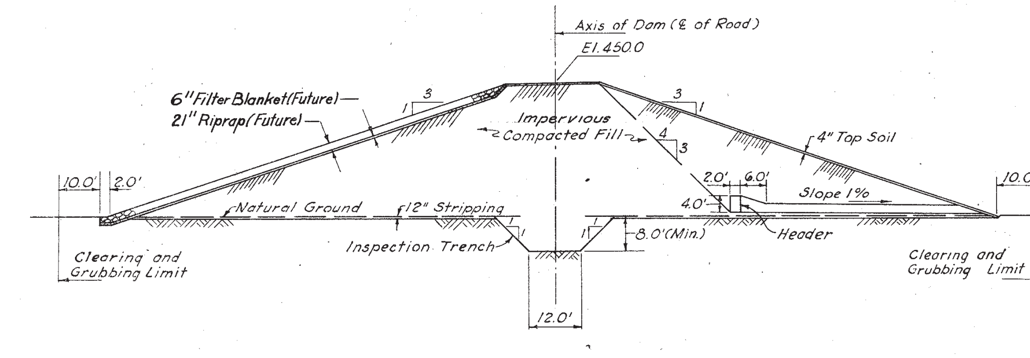

SECTION ABOVE ELEV. 420.0

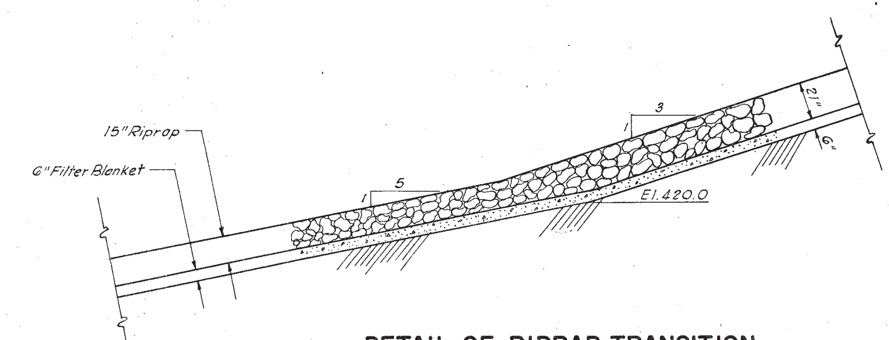

DETAIL OF RIPRAP TRANSITION

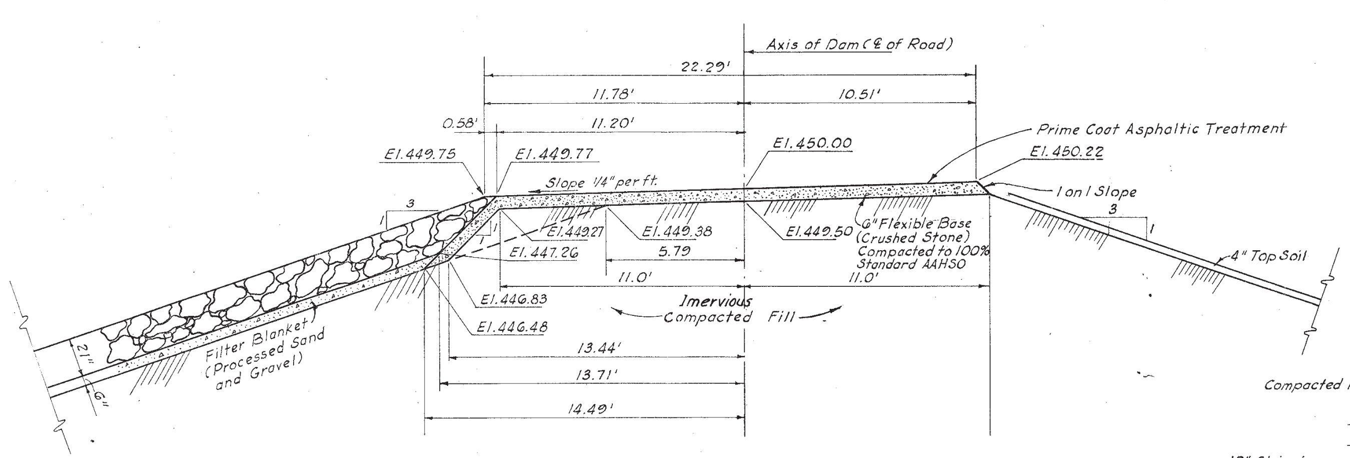

DETAIL OF TOP OF EMBANKMENT

(FUTURE)

1 0 1 2 3 4 5 6 7 8 9 10 11 12

SCALE 1/4 INCH = 1 FOOT

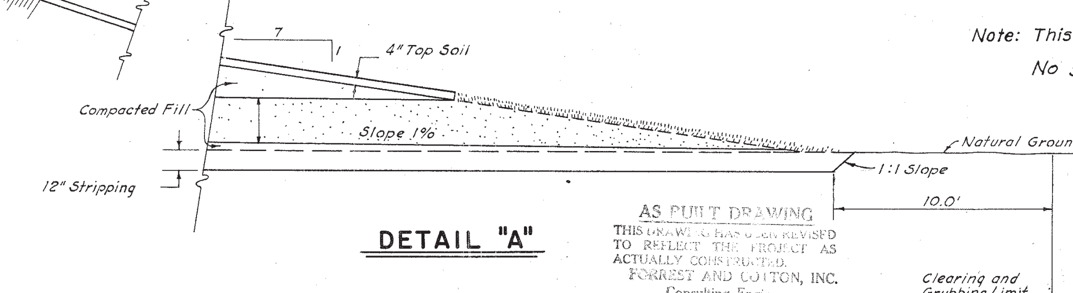

DETAIL "A"

Note: This sheet included for general information only.
No shale shall be used as fill unless noted.

AS BUILT DRAWING
THIS DRAWING HAS BEEN REVISED TO REFLECT THE PROJECT AS ACTUALLY CONSTRUCTED.
FORREST AND COTTON, INC.
Consulting Engineers
By W.D.O.
Date 8-18-67

Contract Nº 64-215

REDUCED SIZE - NOT TO SCALE

DALLAS CITY WATER WORKS

FORNEY DAM AND RESERVOIR

EMBANKMENT

TYPICAL SECTIONS

FORREST AND COTTON, INC. DALLAS, TEXAS — CONSULTING ENGINEERS

FILE NO.			SHEET NO.
6100-4	DESIGN BY:	T.A.R.	9
	DRAWN BY:	L.B.	
	CHECKED BY:	T.A.R.	
	RECOMMENDED BY:	[signature]	
	APPROVED	[signature]	OF 87

III

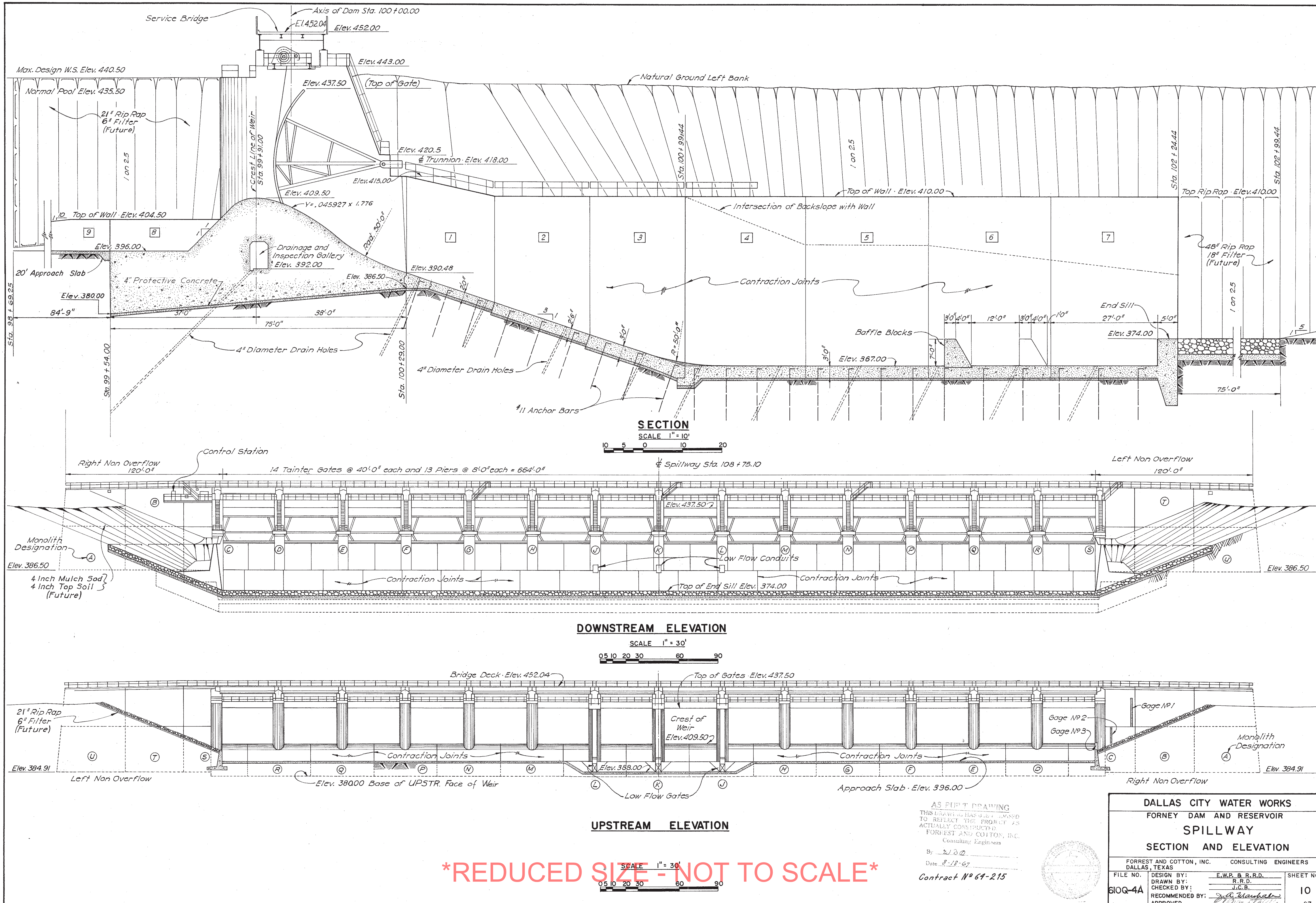

DALLAS CITY WATER WORKS
FORNEY DAM AND RESERVOIR
SPILLWAY
SECTION AND ELEVATION

FORREST AND COTTON, INC. CONSULTING ENGINEERS
DALLAS, TEXAS

FILE NO.			SHEET NO.
610Q-4A	DESIGN BY:	E.W.P. & R.R.D.	10
	DRAWN BY:	R.R.D.	
	CHECKED BY:	J.C.B.	
	RECOMMENDED BY:		
	APPROVED		OF 87

AS BUILT - 8-10-67

III

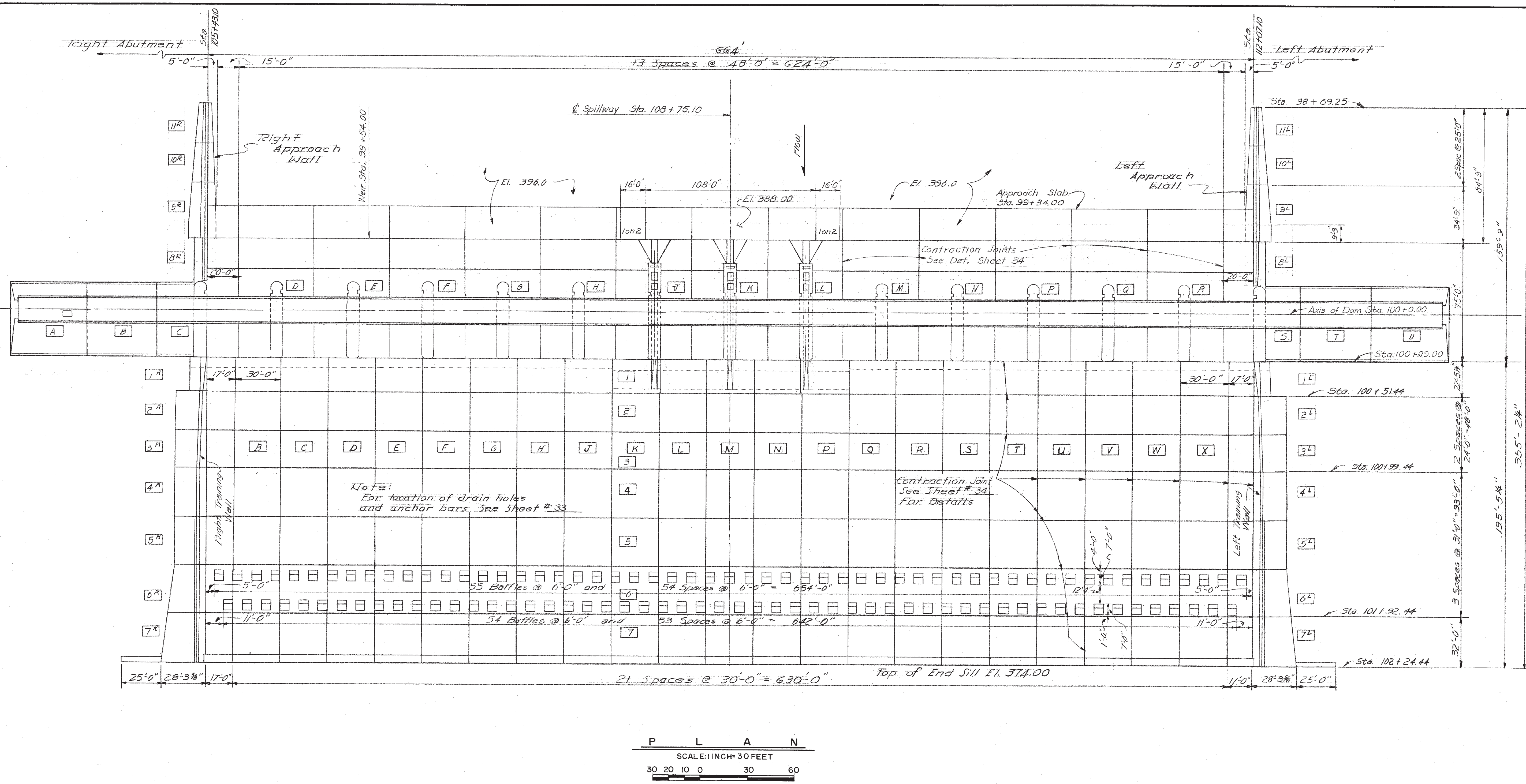

Contract № 64-215

REDUCED SIZE - NOT TO SCALE

By W.D.O.
Date 8-18-67

DALLAS CITY WATER WORKS

FORNEY DAM AND RESERVOIR

SPILLWAY

TRAINING WALLS, PAVING PLAN AND APPROACH WALLS

FORREST AND COTTON, INC. CONSULTING ENGINEERS
DALLAS, TEXAS

FILE NO.			SHEET NO.
610Q-4A	DESIGN BY:	R.R.D.	29
	DRAWN BY:	J.W.P.	OF 87
	CHECKED BY:	J.C.B.	
	RECOMMENDED BY:		
	APPROVED		

III

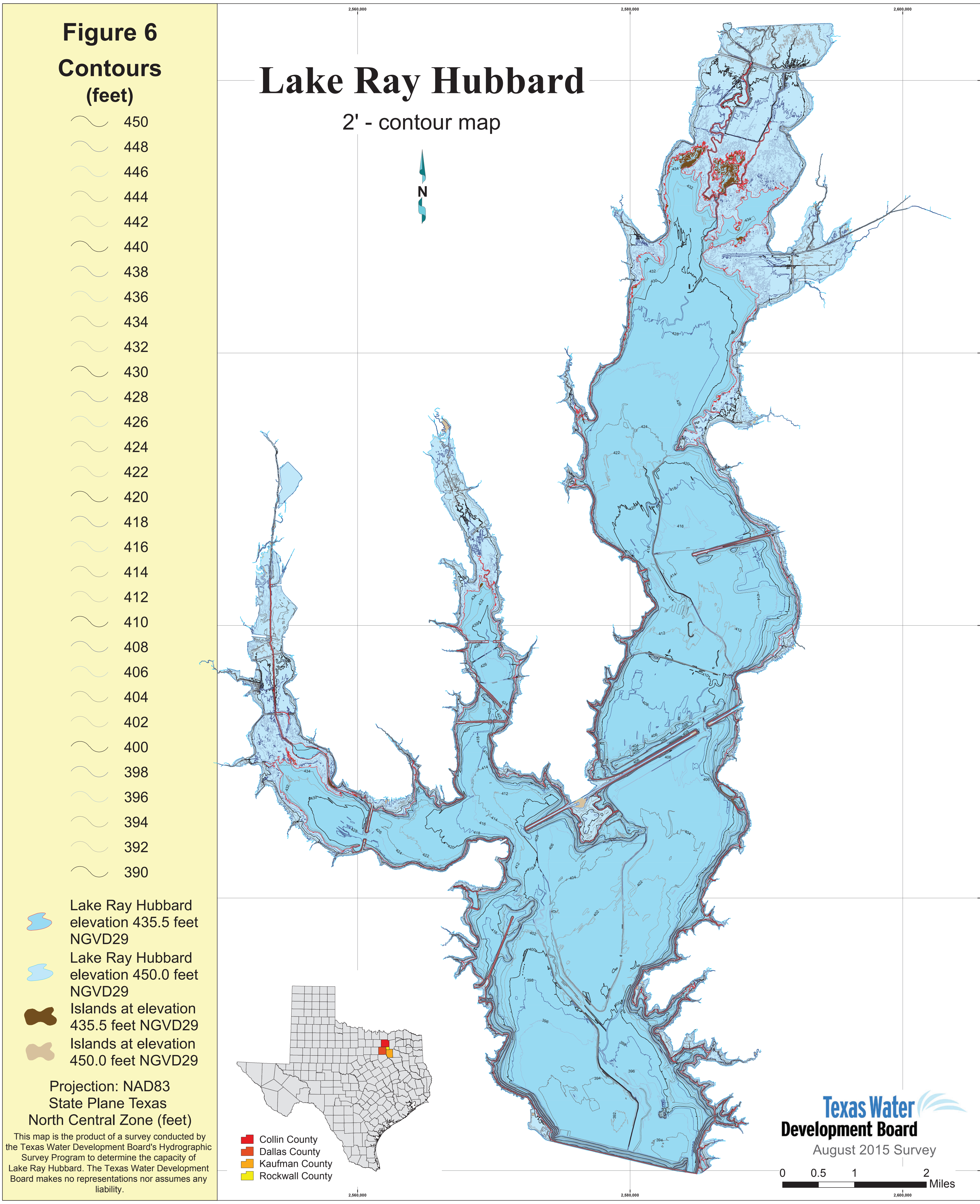

REDUCED SIZE - NOT TO SCALE

APPENDIX B

INSPECTION PHOTOGRAPHS

Photograph Log

©2021 All Rights Reserved

PHOTOGRAPH No.: 1

Photo Taken: 7/9/2020

LOCATION: Sta 4+00, upstream slope of main embankment, looking left

COMMENTS: Riprap is adequate. No visual indication of instability.

PHOTOGRAPH No.: 2

Photo Taken: 7/9/2020

LOCATION: Sta 4+00, downstream slope of main embankment, looking left

COMMENTS: Slope is uniform and well-maintained.

Schnabel ENGINEERING

ROCKWALL-FORNEY DAM
DALLAS WATER UTILITIES
DALLAS/KAUFMAN COUNTIES, TX

PROJECT NO. 20C22001.00

INSPECTION PHOTOGRAPHS

© Schnabel Engineering 2020 All Rights Reserved

PHOTOGRAPH No.: 3

Photo Taken: 7/9/2020

LOCATION: Sta 5+00, crest of main embankment, looking up-stream

COMMENTS: Raw water in-take structure is shown.

PHOTOGRAPH No.: 4

Photo Taken: 7/9/2020

LOCATION: Sta 5+00, crest of main embankment, looking downstream

COMMENTS: Pump station is shown.

© Schnabel Engineering 2020 All Rights Reserved

PHOTOGRAPH No.: 5

Photo Taken: 7/9/2020

LOCATION: Sta 24+00, upstream slope of main embankment, looking left

COMMENTS: Riprap is adequate. No visual indication of instability.

PHOTOGRAPH No.: 6

Photo Taken: 7/9/2020

LOCATION: Sta 24+00, downstream slope of main embankment, looking left

COMMENTS: Slope is uniform and well-maintained.

© Schnabel Engineering 2020 All Rights Reserved

PHOTOGRAPH No.: 7

Photo Taken: 7/9/2020

LOCATION: Sta 36+00, upstream slope of main embankment, looking downstream

COMMENTS: Abandoned piezometer is shown.

PHOTOGRAPH No.: 8

Photo Taken: 7/9/2020

LOCATION: Sta 44+00, upstream slope of main embankment, looking left

COMMENTS: Riprap is adequate. No visual indication of instability.

© Schnabel Engineering 2020 All Rights Reserved

PHOTOGRAPH No.: 9

Photo Taken: 7/9/2020

LOCATION: Sta 44+00, downstream slope of main embankment, looking left

COMMENTS: Slope is uniform and well-maintained.

PHOTOGRAPH No.: 10

Photo Taken: 7/9/2020

LOCATION: Sta 64+00, upstream slope of main embankment, looking left

COMMENTS: Riprap is adequate. No visual indication of instability.

© Schnabel Engineering 2020 All Rights Reserved

PHOTOGRAPH No.: 11

Photo Taken: 7/9/2020

LOCATION: Sta 64+00, downstream slope of main embankment, looking left

COMMENTS: Slope is uniform and well-maintained.

PHOTOGRAPH No.: 12

Photo Taken: 7/9/2020

LOCATION: Sta 84+00, upstream slope of main embankment, looking left

COMMENTS: Riprap is adequate. No visual indication of instability.

© Schnabel Engineering 2020 All Rights Reserved

PHOTOGRAPH No.: 13

Photo Taken: 7/9/2020

LOCATION: Sta 84+00, downstream slope of main embankment, looking left

COMMENTS: Slope is uniform and well-maintained.

PHOTOGRAPH No.: 14

Photo Taken: 7/9/2020

LOCATION: Sta 97+50, upstream slope of main embankment, looking left

COMMENTS: Abandoned piezometer is shown.

Schnabel ENGINEERING	ROCKWALL-FORNEY DAM DALLAS WATER UTILITIES DALLAS/KAUFMAN COUNTIES, TX PROJECT NO. 20C22001.00	INSPECTION PHOTOGRAPHS

© Schnabel Engineering 2020 All Rights Reserved

PHOTOGRAPH No.: 15

Photo Taken: 7/9/2020

LOCATION: Sta 4+00, right abutment of main embankment, looking left

COMMENTS: Piezometer EP-3 is shown.

PHOTOGRAPH No.: 16

Photo Taken: 7/9/2020

LOCATION: Sta 4+00, right abutment of main embankment

COMMENTS: Historic wet area indicated by DWU personnel. No wetness was present at time of inspection.

© Schnabel Engineering 2020 All Rights Reserved

PHOTOGRAPH No.: 17

Photo Taken: 7/9/2020

LOCATION: Sta 10+00, downstream toe of main embankment, looking right

COMMENTS: Concrete channel collecting surface water was dry at the time of inspection.

PHOTOGRAPH No.: 18

Photo Taken: 7/9/2020

LOCATION: Sta 78+50, crest of main embankment, looking downstream

COMMENTS: Work Area 1 is shown.

© Schnabel Engineering 2020 All Rights Reserved

PHOTOGRAPH No.: 19

Photo Taken: 7/9/2020

LOCATION: Sta 78+50, drainage channel downstream of Work Area 1

COMMENTS: Pressure relief well outlet is shown.

PHOTOGRAPH No.: 20

Photo Taken: 7/9/2020

LOCATION: Sta 29+00, crest of main embankment, looking downstream

COMMENTS: Work Area 2 is shown.

© Schnabel Engineering 2020 All Rights Reserved

PHOTOGRAPH No.: 21

Photo Taken: 7/9/2020

LOCATION: Sta 29+00, downstream slope main embankment, looking left

COMMENTS: Relief well for Work Area 2 is shown.

PHOTOGRAPH No.: 22

Photo Taken: 7/9/2020

LOCATION: Sta 29+00, drainage channel downstream of Work Area 2

COMMENTS: Pressure relief well outlet is shown. Note elevated water surface has inundated the outlet.

© Schnabel Engineering 2020 All Rights Reserved

PHOTOGRAPH No.: 23

Photo Taken: 7/9/2020

LOCATION: Sta 83+00, drain-age channel downstream of main embankment

COMMENTS: Note elevated water surface.

PHOTOGRAPH No.: 24

Photo Taken: 7/9/2020

LOCATION: Sta. 84+00, down-stream toe of main embank-ment

COMMENTS: Abandoned pore pressure cell recording tower is shown.

© Schnabel Engineering 2020 All Rights Reserved

PHOTOGRAPH No.: 25

Photo Taken: 7/9/2020

LOCATION: Sta. 115+00, downstream slope of saddle embankment, looking left

COMMENTS: Slope is uniform and well-maintained.

PHOTOGRAPH No.: 26

Photo Taken: 7/9/2020

LOCATION: Sta. 126+00, crest of saddle embankment, looking right

COMMENTS: Crest is uniform and flat.

© Schnabel Engineering 2020 All Rights Reserved

PHOTOGRAPH No.: 27

Photo Taken: 7/9/2020

LOCATION: Sta. 125+50, upstream slope of saddle embankment, looking right

COMMENTS: Riprap is adequate. No visual indication of instability.

PHOTOGRAPH No.: 28

Photo Taken: 7/9/2020

LOCATION: Upstream side of left non-overflow section

COMMENTS: No visual and obvious signs of structural instability.

© Schnabel Engineering 2020 All Rights Reserved

PHOTOGRAPH No.: 29

Photo Taken: 7/9/2020

LOCATION: Upstream side of left non-overflow section, looking left

COMMENTS: Area of void below grouted riprap indicated by DWU personnel.

PHOTOGRAPH No.: 30

Photo Taken: 7/9/2020

LOCATION: Downstream side of left non-overflow section

COMMENTS: No visual and obvious signs of structural instability.

© Schnabel Engineering 2020 All Rights Reserved

PHOTOGRAPH No.: 31

Photo Taken: 7/9/2020

LOCATION: Upstream side of right non-overflow section

COMMENTS: No visual and obvious signs of structural in-stability.

PHOTOGRAPH No.: 32

Photo Taken: 7/9/2020

LOCATION: Downstream side of right non-overflow section

COMMENTS: No visual and obvious signs of structural in-stability.

Schnabel ENGINEERING	ROCKWALL-FORNEY DAM DALLAS WATER UTILITIES DALLAS/KAUFMAN COUNTIES, TX PROJECT NO. 20C22001.00	INSPECTION PHOTOGRAPHS

© Schnabel Engineering 2020 All Rights Reserved

PHOTOGRAPH No.: 33

Photo Taken: 7/9/2020

LOCATION: Bridge over spill-way, viewed from left side

COMMENTS: Bridge is straight and level.

PHOTOGRAPH No.: 34

Photo Taken: 7/9/2020

LOCATION: Downstream side of spillway

COMMENTS: Gates 1 through 14 shown from left to right.

© Schnabel Engineering 2020 All Rights Reserved

PHOTOGRAPH No.: 35

Photo Taken: 7/9/2020

LOCATION: Upstream side of spillway

COMMENTS: Gates 1 through 14 shown from right to left.

PHOTOGRAPH No.: 36

Photo Taken: 7/9/2020

LOCATION: Downstream side of Gate 1

COMMENTS: Some surficial cracking and spalls observed.

© Schnabel Engineering 2020 All Rights Reserved

PHOTOGRAPH No.: 37

Photo Taken: 7/9/2020

LOCATION: Downstream side of Gate 2

COMMENTS: Some surficial cracking and spalls observed.

PHOTOGRAPH No.: 38

Photo Taken: 7/9/2020

LOCATION: Downstream side of Gate 3

COMMENTS: Some surficial cracking and spalls observed.

© Schnabel Engineering 2020 All Rights Reserved

PHOTOGRAPH No.: 39

Photo Taken: 7/9/2020

LOCATION: Downstream side of Gate 4

COMMENTS: Some surficial cracking and spalls observed.

PHOTOGRAPH No.: 40

Photo Taken: 7/9/2020

LOCATION: Downstream side of Gate 5

COMMENTS: Some surficial cracking and spalls observed.

© Schnabel Engineering 2020 All Rights Reserved

PHOTOGRAPH No.: 41

Photo Taken: 7/9/2020

LOCATION: Downstream side of Gate 6

COMMENTS: Some surficial cracking and spalls observed.

PHOTOGRAPH No.: 42

Photo Taken: 7/9/2020

LOCATION: Downstream side of Gate 7

COMMENTS: Some surficial cracking and spalls observed.

© Schnabel Engineering 2020 All Rights Reserved

PHOTOGRAPH No.: 43

Photo Taken: 7/9/2020

LOCATION: Downstream side of Gate 8

COMMENTS: Some surficial cracking and spalls observed.

PHOTOGRAPH No.: 44

Photo Taken: 7/9/2020

LOCATION: Downstream side of Gate 9

COMMENTS: Some surficial cracking and spalls observed.

© Schnabel Engineering 2020 All Rights Reserved

PHOTOGRAPH No.: 45

Photo Taken: 7/9/2020

LOCATION: Downstream side of Gate 10

COMMENTS: Some surficial cracking and spalls observed.

PHOTOGRAPH No.: 46

Photo Taken: 7/9/2020

LOCATION: Downstream side of Gate 11

COMMENTS: Some surficial cracking and spalls observed.

© Schnabel Engineering 2020 All Rights Reserved

PHOTOGRAPH No.: 47

Photo Taken: 7/9/2020

LOCATION: Downstream side of Gate 12

COMMENTS: Some surficial cracking and spalls observed.

PHOTOGRAPH No.: 48

Photo Taken: 7/9/2020

LOCATION: Downstream side of Gate 13

COMMENTS: Some surficial cracking and spalls observed.

Schnabel ENGINEERING	ROCKWALL-FORNEY DAM DALLAS WATER UTILITIES DALLAS/KAUFMAN COUNTIES, TX PROJECT NO. 20C22001.00	INSPECTION PHOTOGRAPHS

© Schnabel Engineering 2020 All Rights Reserved

PHOTOGRAPH No.: 49

Photo Taken: 7/9/2020

LOCATION: Downstream side of Gate 14

COMMENTS: Some surficial cracking and spalls observed.

PHOTOGRAPH No.: 50

Photo Taken: 7/9/2020

LOCATION: Left spillway sidewall

COMMENTS: Significant vegetative growth was observed in the upper wall drain outlets.

© Schnabel Engineering 2020 All Rights Reserved

PHOTOGRAPH No.: 51

Photo Taken: 7/9/2020

LOCATION: Drainage gallery, looking left

COMMENTS: Gallery is in adequate condition with little seepage observed.

PHOTOGRAPH No.: 52

Photo Taken: 7/9/2020

LOCATION: Drainage gallery, upstream side

COMMENTS: Typical foundation drain is shown. Some corrosion of the steel conduits within the drain holes was observed.

© Schnabel Engineering 2020 All Rights Reserved

PHOTOGRAPH No.: 53

Photo Taken: 7/9/2020

LOCATION: Left drainage gallery sump, upstream side

COMMENTS: Note concrete spalling at corner.

PHOTOGRAPH No.: 54

Photo Taken: 7/9/2020

LOCATION: Stilling basin, viewed from left side

COMMENTS: Note extent of stilling basin has gradually increased over the life of the structure.

© Schnabel Engineering 2020 All Rights Reserved

PHOTOGRAPH No.: 55

Photo Taken: 7/8/2020

LOCATION: Right spillway sidewall, looking downstream

COMMENTS: Wall is level and straight. Wall drain outlets were dry at time of inspection.

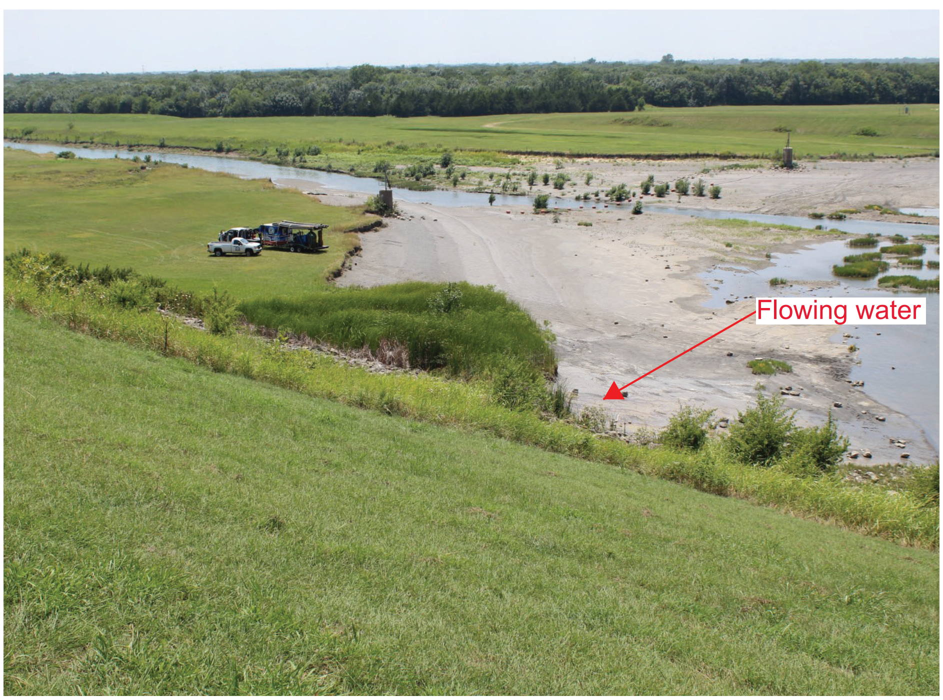

PHOTOGRAPH No.: 56

Photo Taken: 7/9/2020

LOCATION: Left side of stilling basin and outlet channel, viewed from left side

COMMENTS: Flowing water can be seen in foreground.

© Schnabel Engineering 2020 All Rights Reserved

PHOTOGRAPH No.: 57

Photo Taken: 7/9/2020

LOCATION: Left side of stilling basin, downstream of sidewall

COMMENTS: Flowing water was observed.

PHOTOGRAPH No.: 58

Photo Taken: 7/9/2020

LOCATION: Right side of outlet channel, looking upstream

COMMENTS: Historic wet area indicated by DWU personnel. No wetness was present at time of inspection.

© Schnabel Engineering 2020 All Rights Reserved

APPENDIX C

STILLING BASIN INSPECTION

Inspection of Forney Dam Stilling Basin and Tawakoni Balancing Reservoir Pipe Line, Inspections performed on July 8th, 9th, and 10, 2020

Schnabel Engineering, LLC
©2021 All Rights Reserved

Inspection of Forney Dam Stilling Basin and Tawakoni Balancing Reservoir Pipe Line

Inspections performed on July 8th, 9th and 10,2020

Report By Marty Pearce

7/14/2020

Attention: Randy McIntyre
Garver

Randy,

The divers inspected the Forney Dam Stilling Basin on July 8th and 9th 2020, and they inspected the Tawakoni Balancing Reservoir Cell 2, 84" outlet pipe on July 10, 2020.

The divers entered the water and begin a grid pattern inspection of the dam. They used a grid pattern copy of the dam to mark their findings. The pictures below are the field notes they copied the information on.

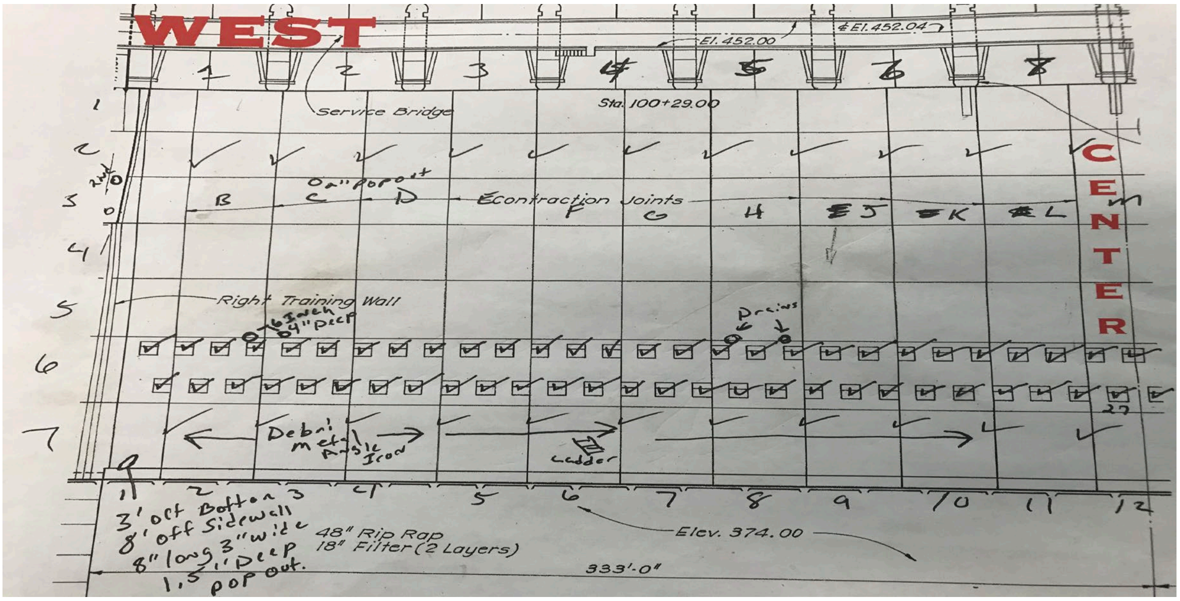

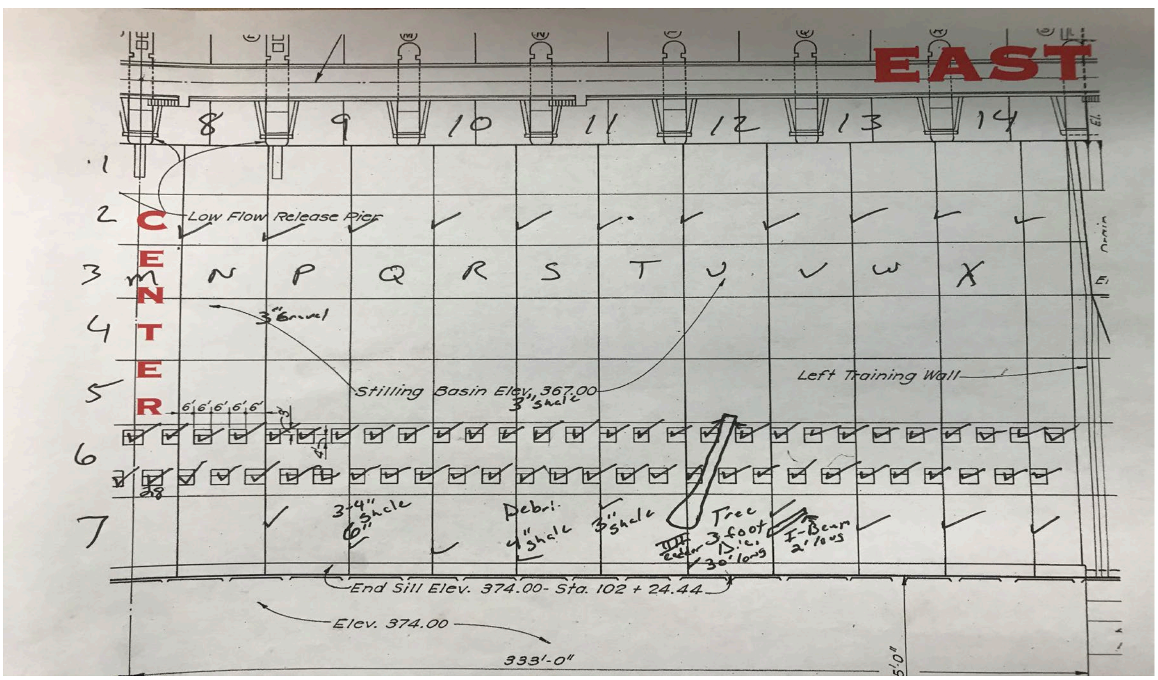

Overall, the baffle blocks, end sill and the floor are in good condition. There was some minor spalling of the concrete. The only spalling of concern was located in grid 7-A. It is located in the end sill. It is 3' off bottom and 8' off of the right training wall. It measures 8" long by 3" wide and is 1.5" deep.

The divers did find some small sediment mounds and debris. Debris included 2 ladders, some angle iron, and a 6" by 2' long piece of H-Beam. The largest debris was a 3' diameter by 30' long log. It was located wedged between the baffle blocks located in grid 6-U.

I recommend removing the log using an underwater chainsaw.


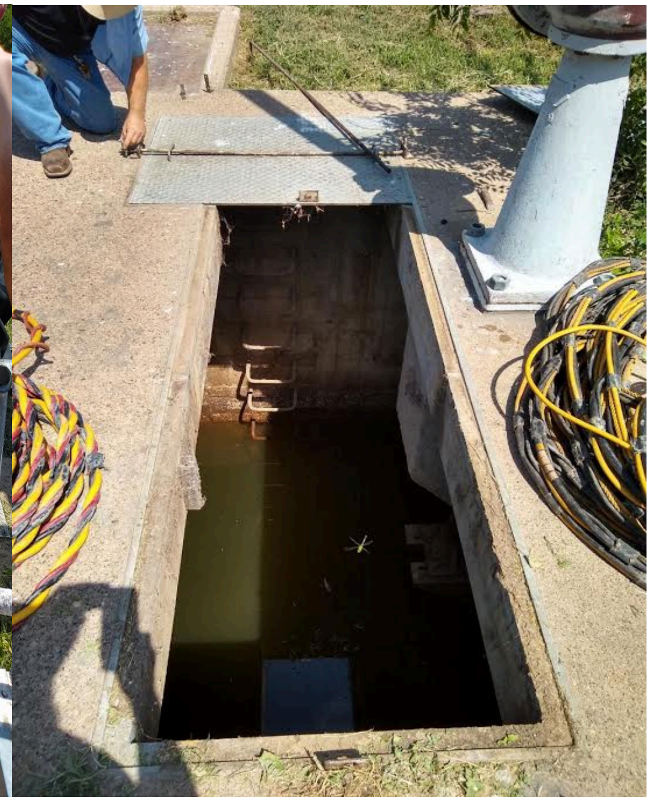

The divers inspected the 84" outlet pipe at Tawakoni Balancing reservoir cell 2. The divers penetrated the pipe 240'. The divers noted 12" of sediment and muscle shells from the start of the pipe to the 160' mark. They noted 2" of sediment from 160' to 240'. There was moderate marine growth throughout the pipe.

The divers noted a leak at the 12 o'clock position at 65'. They used a red dye to detect the leak. It seems to be a small leak that is exiting through the porous concrete.

The second leak was located at the 1 o'clock position at 103'. It is a quarter sized hole that the divers located using red dye.

The two pictures below are still shots of the video when they diver discovered the leaks. They are time stamped so that they can be located in the videos that have been provided.

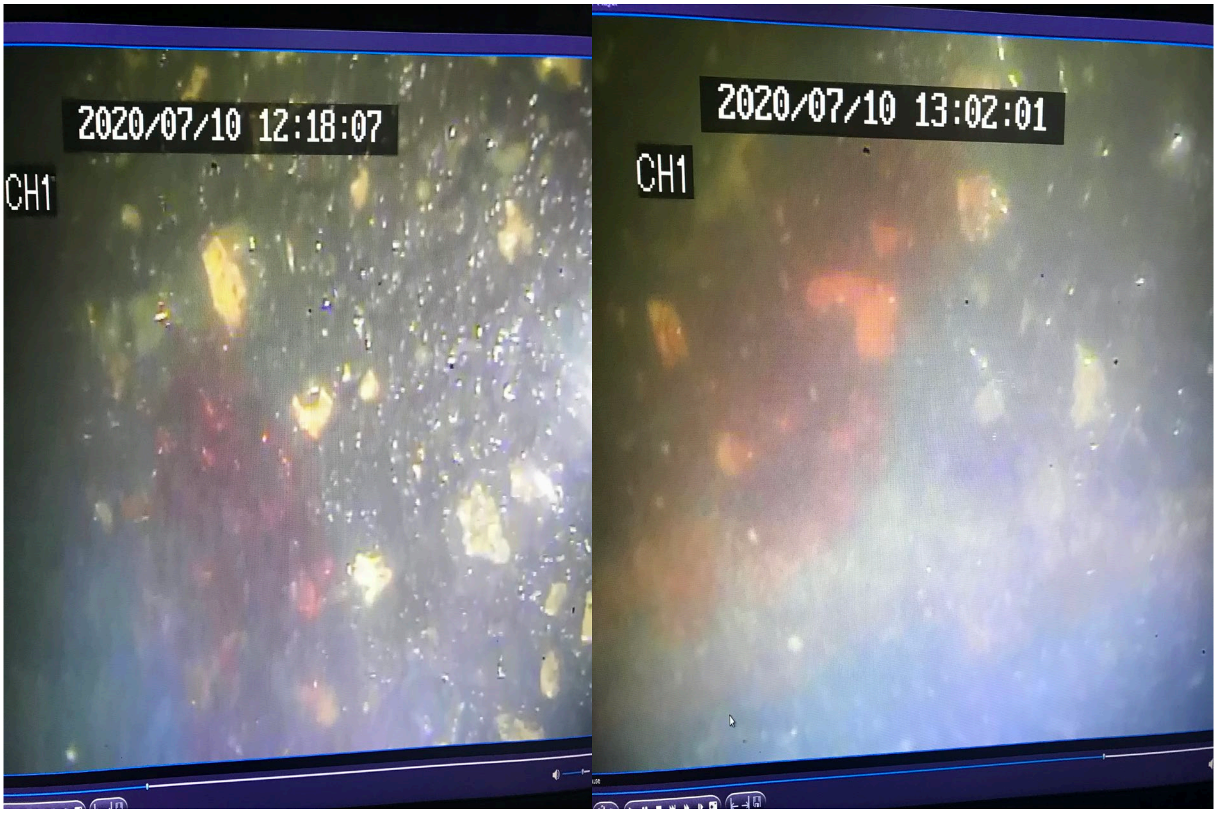

Both leaks where marked with a grease pencil inside the pipe. We recommend cleaning the concrete around the leaks and repairing the leaks with underwater epoxy.

If you have any questions please feel free to call us at (817) 377-8512.

Thank you

Marty Pearce
Sales Manager
American Underwater Services

APPENDIX D

PIEZOMETER DATA

Instrumentation Plan
Recorded Water Elevations versus Time
Embankment Cross Sections
Profile along the Crest of the Embankment

©2021 All Rights Reserved

Piezometer Table

Piezometer No.	Top Elevation (ft)*	Depth (ft)*	Northing (ft)*	Easting (ft)*
EP-9	410.0	63.4	6981213.07	2577319.36
EP-1	447.3	40.1	6982150.37	2573827.61
EP-2	450.4	36.9	6982116.53	2574210.20
EP-3	431.6	27.8	6982013.46	2574175.94
EP-4	449.9	85.8	6981927.24	2575010.20
EP-5	408.5	32.9	6981754.41	2574971.60
EP-6	399.0	16.3	6981544.90	2574842.70
EP-7	397.7	42.1	6981319.07	2574795.72
EP-8	449.8	103.8	6981370.36	2577352.22
EP-10	395.0	48.3	6980980.97	2577268.20
EP-11	393.9	48.2	6980734.98	2577221.93
EP-12	449.8	89.9	6980397.20	2581481.48
EP-13	411.9	51.0	6980229.46	2581446.44
EP-14	395.8	45.6	6979935.13	2581381.37

Piezometer Table

Piezometer No.	Top Elevation (ft)*	Depth (ft)*	Northing (ft)*	Easting (ft)*
EP-15	395.6	50.9	6979751.37	2581341.02
EP-16	449.8	54.7	6979749.44	2584951.15
EP-17	452.7	61.4	6979688.76	2584950.12
EP-18	452.3	54.0	6979630.28	2584946.85
EP-19	451.4	53.2	6979484.57	2584937.49
EP-20	451.5	55.8	6979632.41	2585177.75
EP-21	449.9	52.8	6980061.47	2585626.55
EP-22	431.6	37.9	6979903.60	2585726.40
EP-23	451.8	58.2	6980276.09	2585976.66
EP-24	428.6	24.8	6981411.17	2573914.60
EP-25	404.1	21.7	6981502.98	2574652.90
EP-26	412.2	64.5	6981378.56	2576586.48
EP-27	406.5	28.3	6981229.73	2576560.37
EP-28	407.9	56.2	6981230.50	2576581.21

Piezometer Table

Piezometer No.	Top Elevation (ft)*	Depth (ft)*	Northing (ft)*	Easting (ft)*
EP-29	399.9	52.7	6980844.16	2576720.35
EP-30	395.0	18.2	6980979.81	2577249.55
EP-32	409.9	63.0	6980864.70	2578698.88
EP-33	395.7	47.0	6980688.93	2578650.69
EP-34	395.9	18.2	6980682.48	2578675.50
EP-35	408.2	62.1	6980553.57	2580056.56
EP-36	395.7	48.7	6980374.76	2580003.93
EP-37	395.7	18.3	6980369.17	2580221.40
EP-39	395.7	18.3	6980013.70	2581445.42
EP-40	412.2	30.8	**	**
EP-41	409.5	27.7	6981200.86	2577370.21
EP-42	409.6	28.0	6980872.62	2578749.01
EP-43	407.5	27.7	6980540.15	2580107.86
EP-44	411.9	30.8	6980215.83	2581497.02

*ELEVATIONS, DEPTHS, AND COORDINATES PROVIDED BY DWU.
**COORDINATES PROVIDED FOR EP-40 NOT CORRECT BASED ON RECORD DOCUMENTS AND VISUAL OBSERVATIONS. LOCATION SHOWN IS APPROXIMATE.

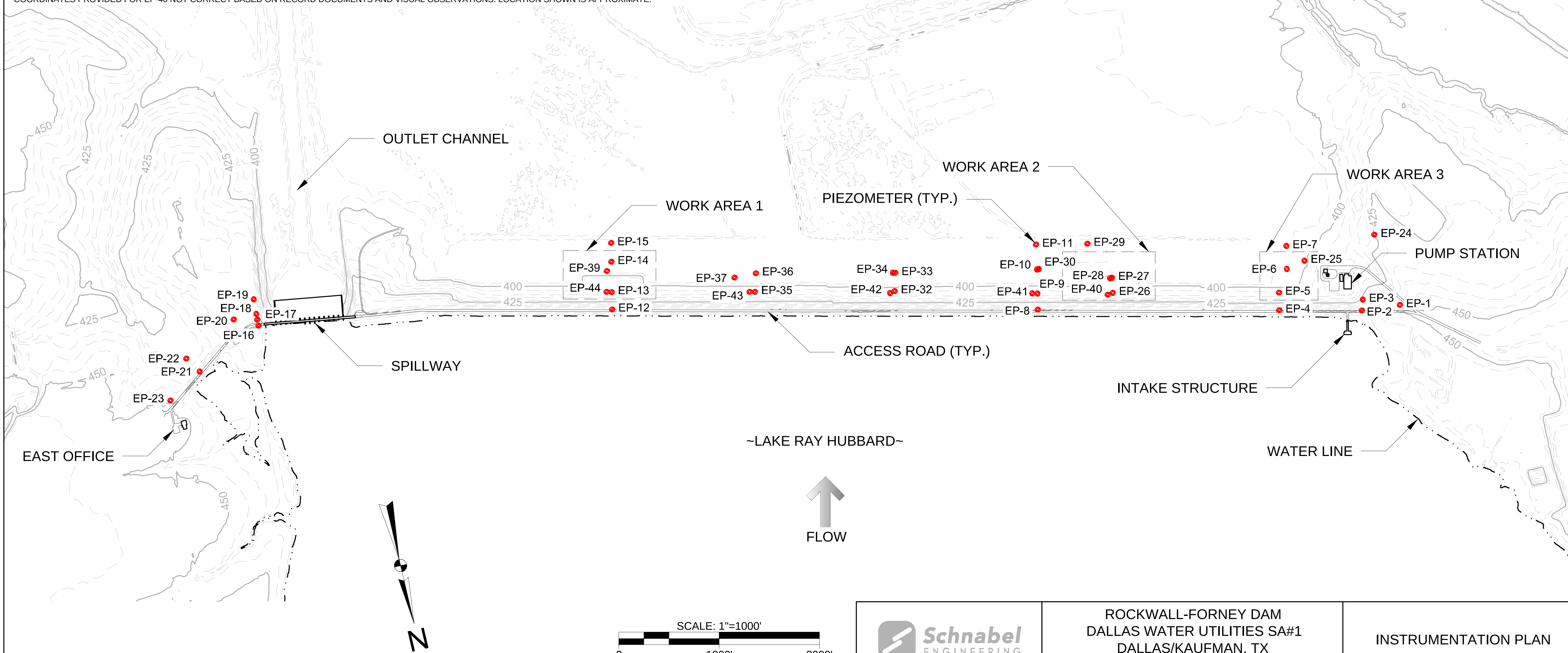

Schnabel ENGINEERING

ROCKWALL-FORNEY DAM
DALLAS WATER UTILITIES SA#1
DALLAS/KAUFMAN, TX
PROJECT NO. 20C22001.00

INSTRUMENTATION PLAN

© Schnabel Engineering 2020 All Rights Reserved

G:\2020\OTHER BRANCH PROJECTS\TEXAS\20C22001_00_DWU_REHAB_OF_RAW_WATER_FACILITIES_SA#1\03-SE\PRODUCTS\08-CAD\DRAWINGS\06-WORKING\PIEZOMETERLOCATIONS.DWG

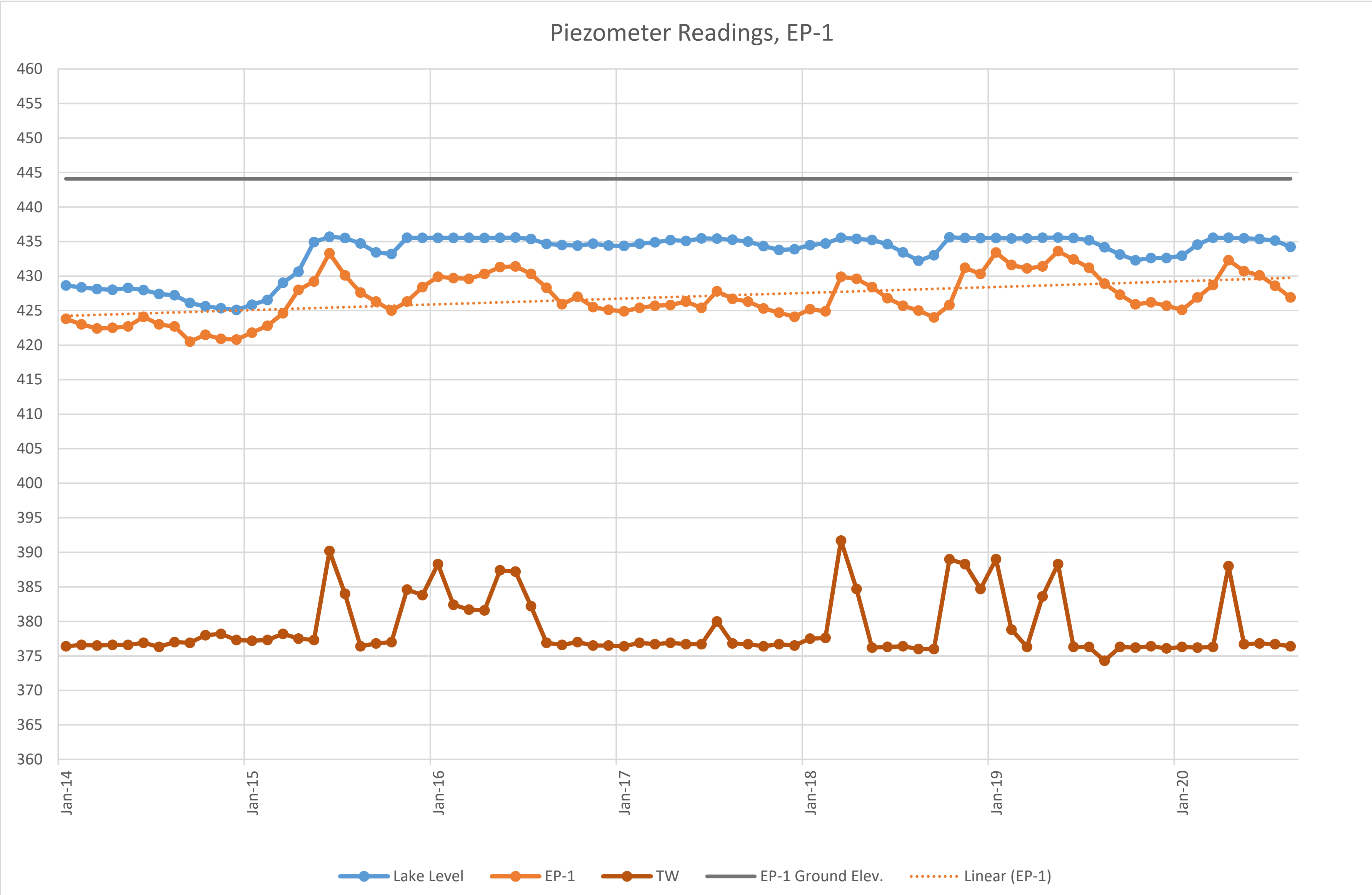
Piezometer Readings, EP-1
460
455
450
445
440
435
430
425
420
415
410
405
400
395
390
385
380
375
370
365
360
Jan-14
Jan-15
Jan-16
Jan-17
Jan-18
Jan-19
Jan-20
Lake Level
EP-1
TW
EP-1 Ground Elev.
Linear (EP-1)

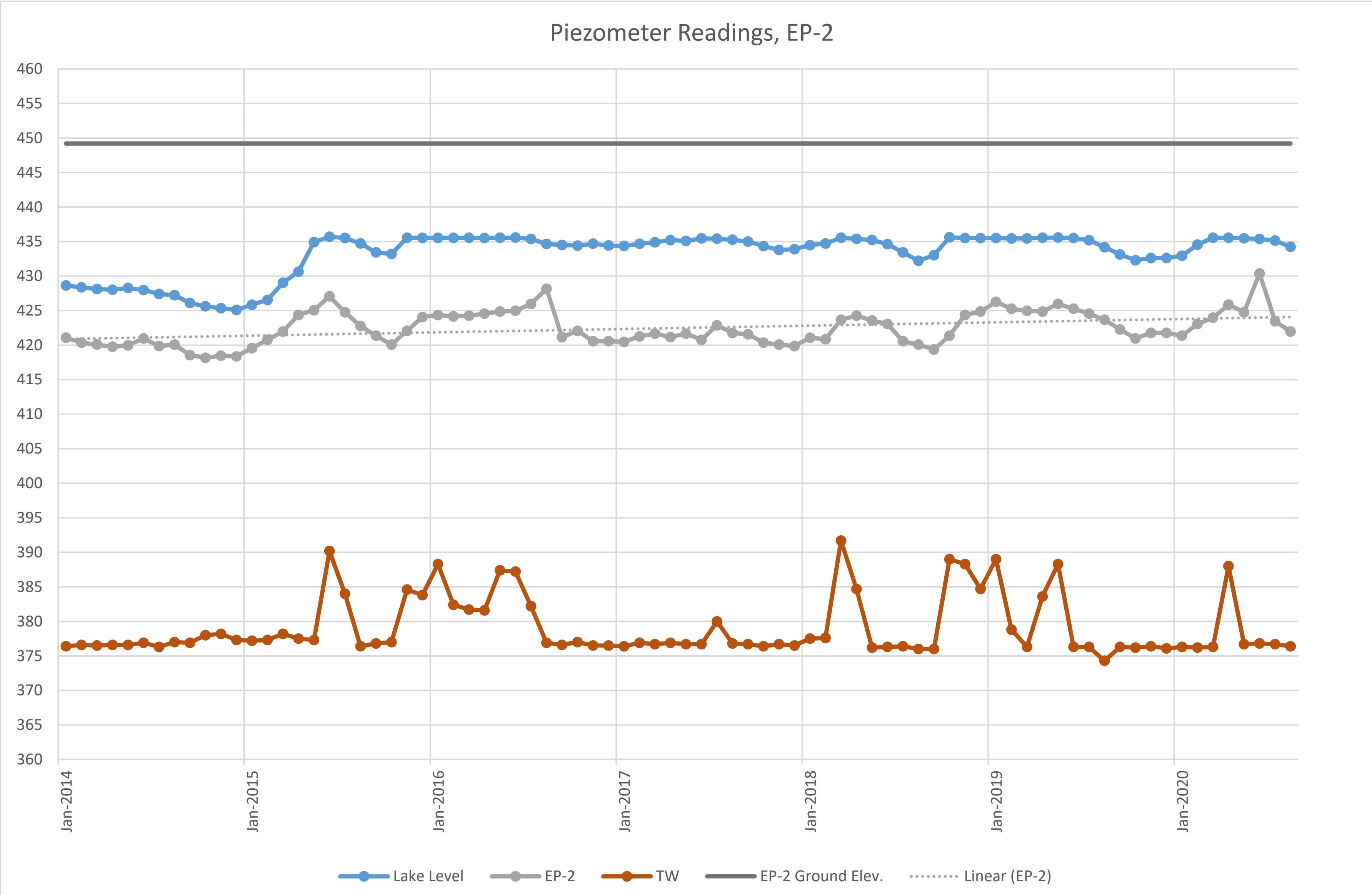

Piezometer Readings, EP-2
460
455
450
445
440
435
430
425
420
415
410
405
400
395
390
385
380
375
370
365
360
Jan-2014
Jan-2015
Jan-2016
Jan-2017
Jan-2018
Jan-2019
Jan-2020
Lake Level
EP-2
TW
EP-2 Ground Elev.
Linear (EP-2)

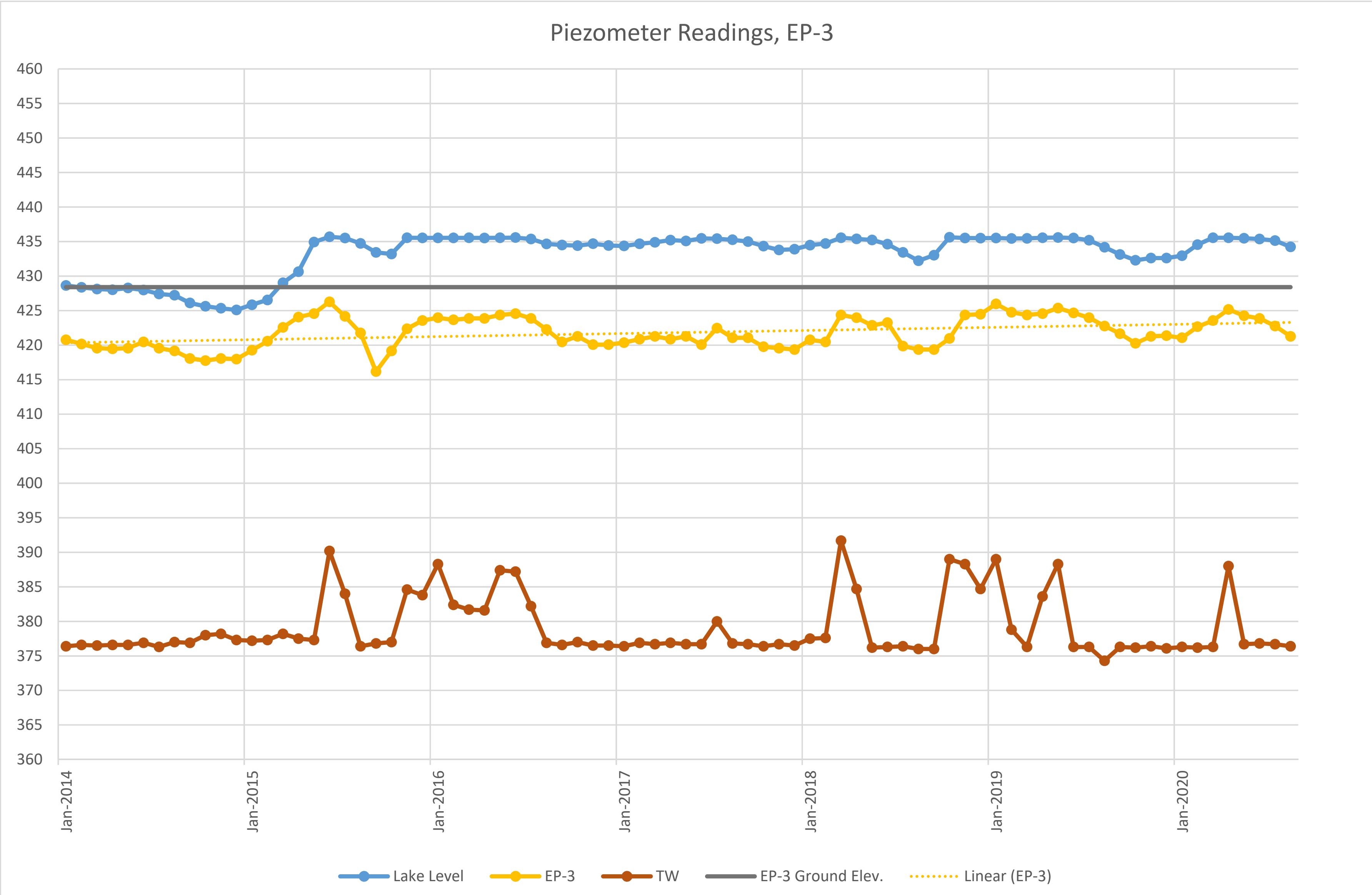
Piezometer Readings, EP-3
460
455
450
445
440
435
430
425
420
415
410
405
400
395
390
385
380
375
370
365
360
Jan-2014
Jan-2015
Jan-2016
Jan-2017
Jan-2018
Jan-2019
Jan-2020
Lake Level
EP-3
TW
EP-3 Ground Elev.
Linear (EP-3)

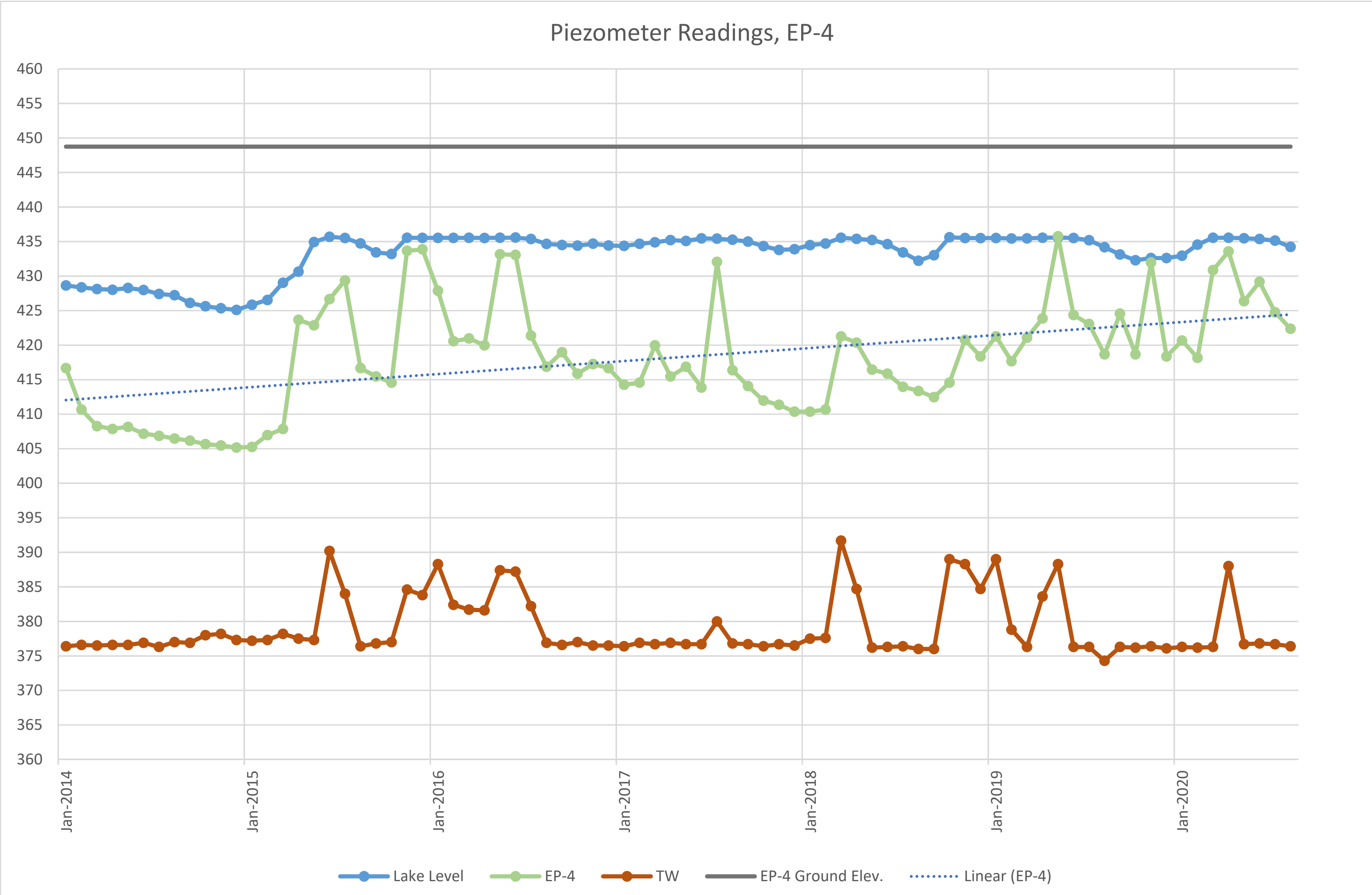

Piezometer Readings, EP-4
460
455
450
445
440
435
430
425
420
415
410
405
400
395
390
385
380
375
370
365
360
Jan-2014
Jan-2015
Jan-2016
Jan-2017
Jan-2018
Jan-2019
Jan-2020
Lake Level
EP-4
TW
EP-4 Ground Elev.
Linear (EP-4)

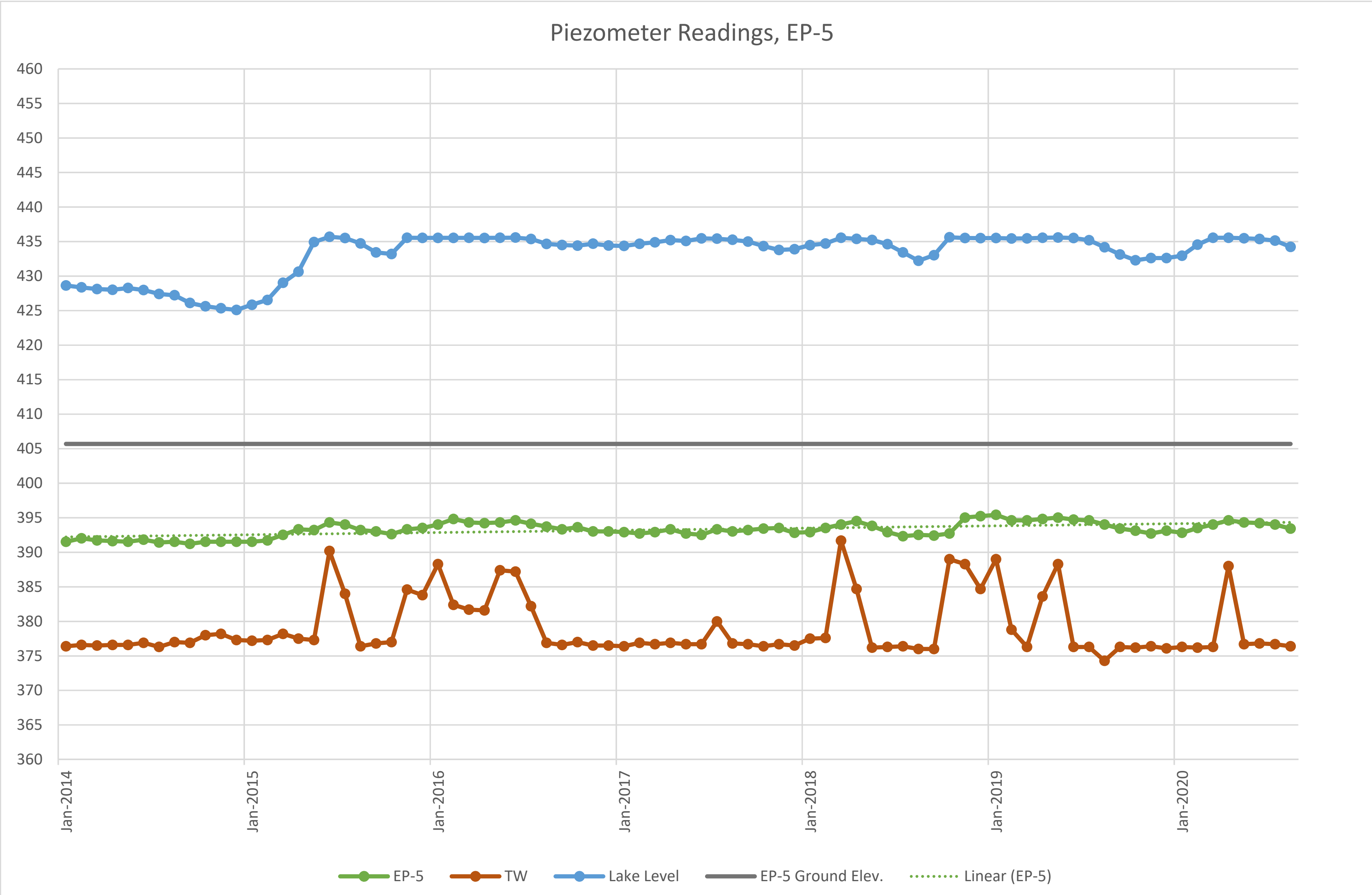
Piezometer Readings, EP-5
460
455
450
445
440
435
430
425
420
415
410
405
400
395
390
385
380
375
370
365
360
Jan-2014
Jan-2015
Jan-2016
Jan-2017
Jan-2018
Jan-2019
Jan-2020
EP-5
TW
Lake Level
EP-5 Ground Elev.
Linear (EP-5)

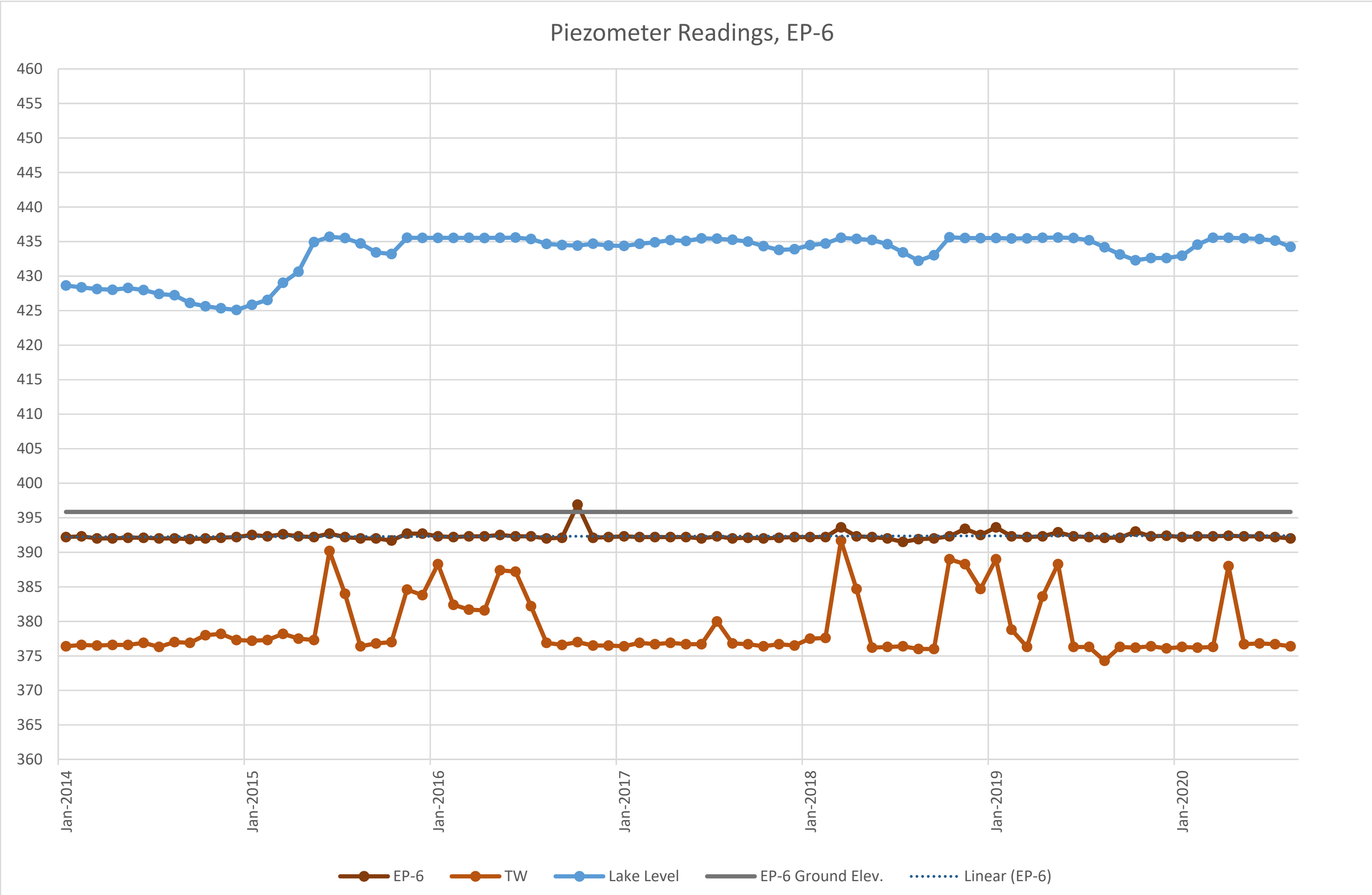

Piezometer Readings, EP-6
460
455
450
445
440
435
430
425
420
415
410
405
400
395
390
385
380
375
370
365
360
Jan-2014
Jan-2015
Jan-2016
Jan-2017
Jan-2018
Jan-2019
Jan-2020
EP-6
TW
Lake Level
EP-6 Ground Elev.
Linear (EP-6)

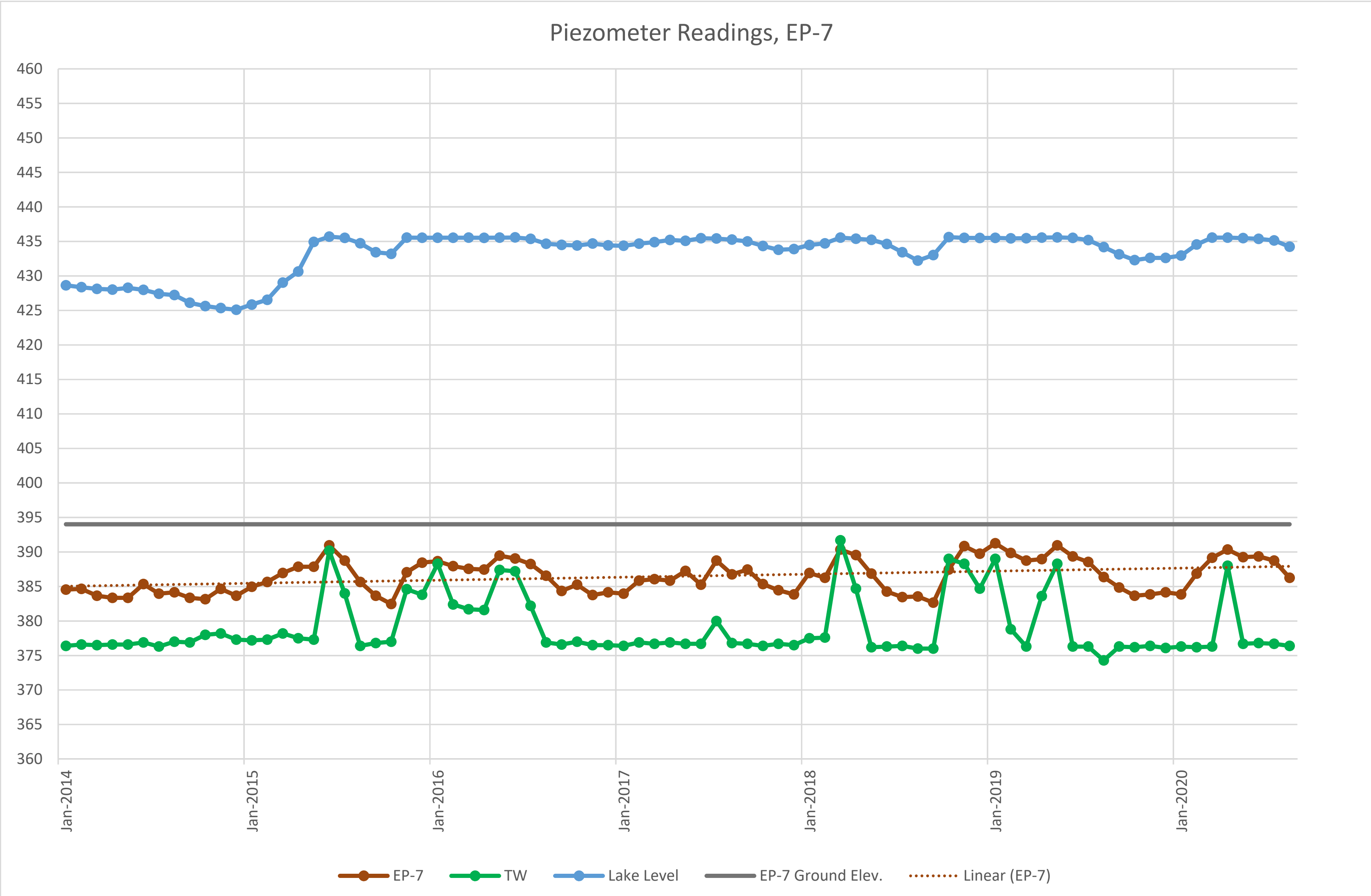

Piezometer Readings, EP-7
460
455
450
445
440
435
430
425
420
415
410
405
400
395
390
385
380
375
370
365
360
Jan-2014
Jan-2015
Jan-2016
Jan-2017
Jan-2018
Jan-2019
Jan-2020
EP-7
TW
Lake Level
EP-7 Ground Elev.
Linear (EP-7)

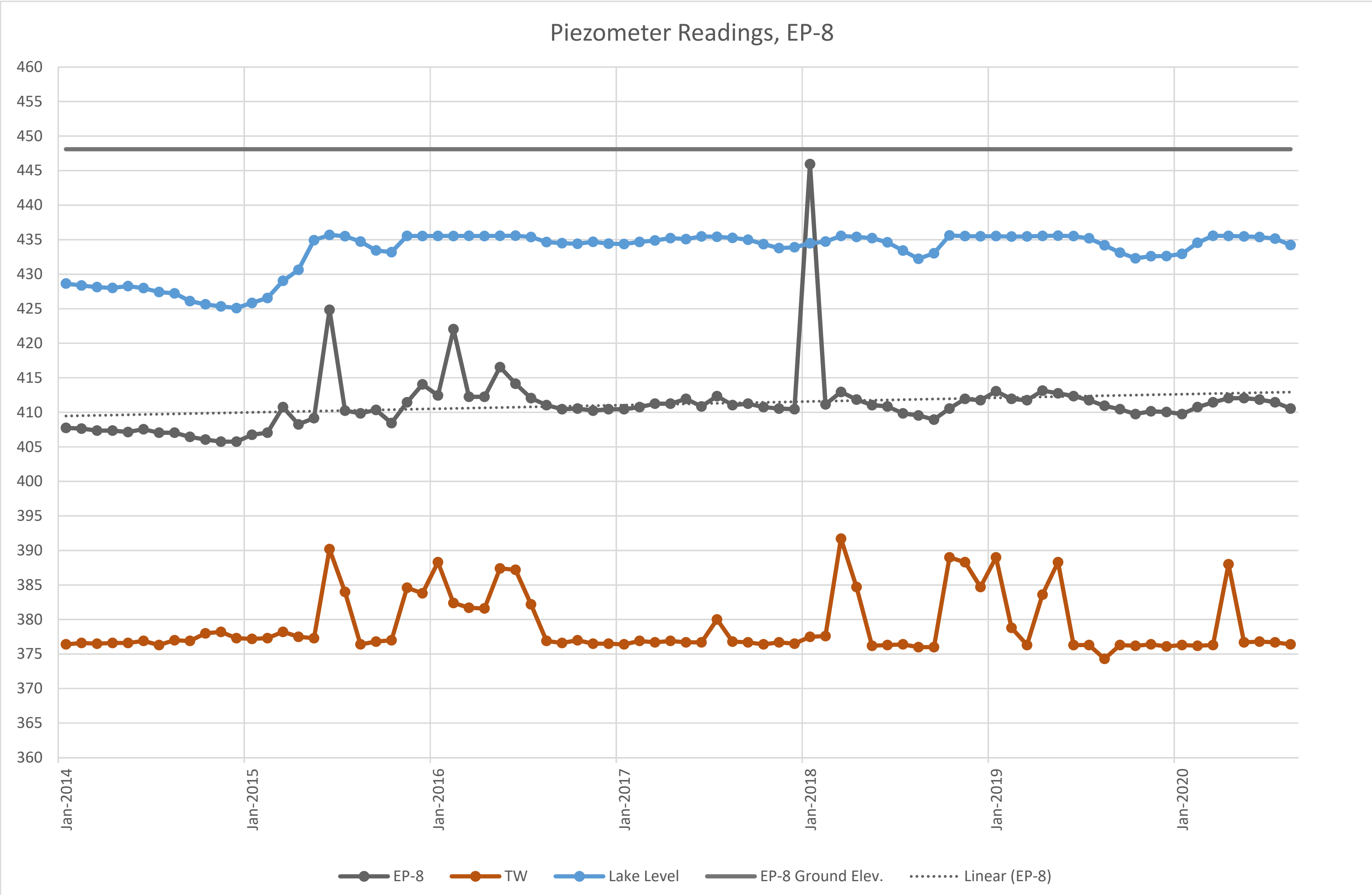
Piezometer Readings, EP-8
460
455
450
445
440
435
430
425
420
415
410
405
400
395
390
385
380
375
370
365
360
Jan-2014
Jan-2015
Jan-2016
Jan-2017
Jan-2018
Jan-2019
Jan-2020
EP-8
TW
Lake Level
EP-8 Ground Elev.
Linear (EP-8)

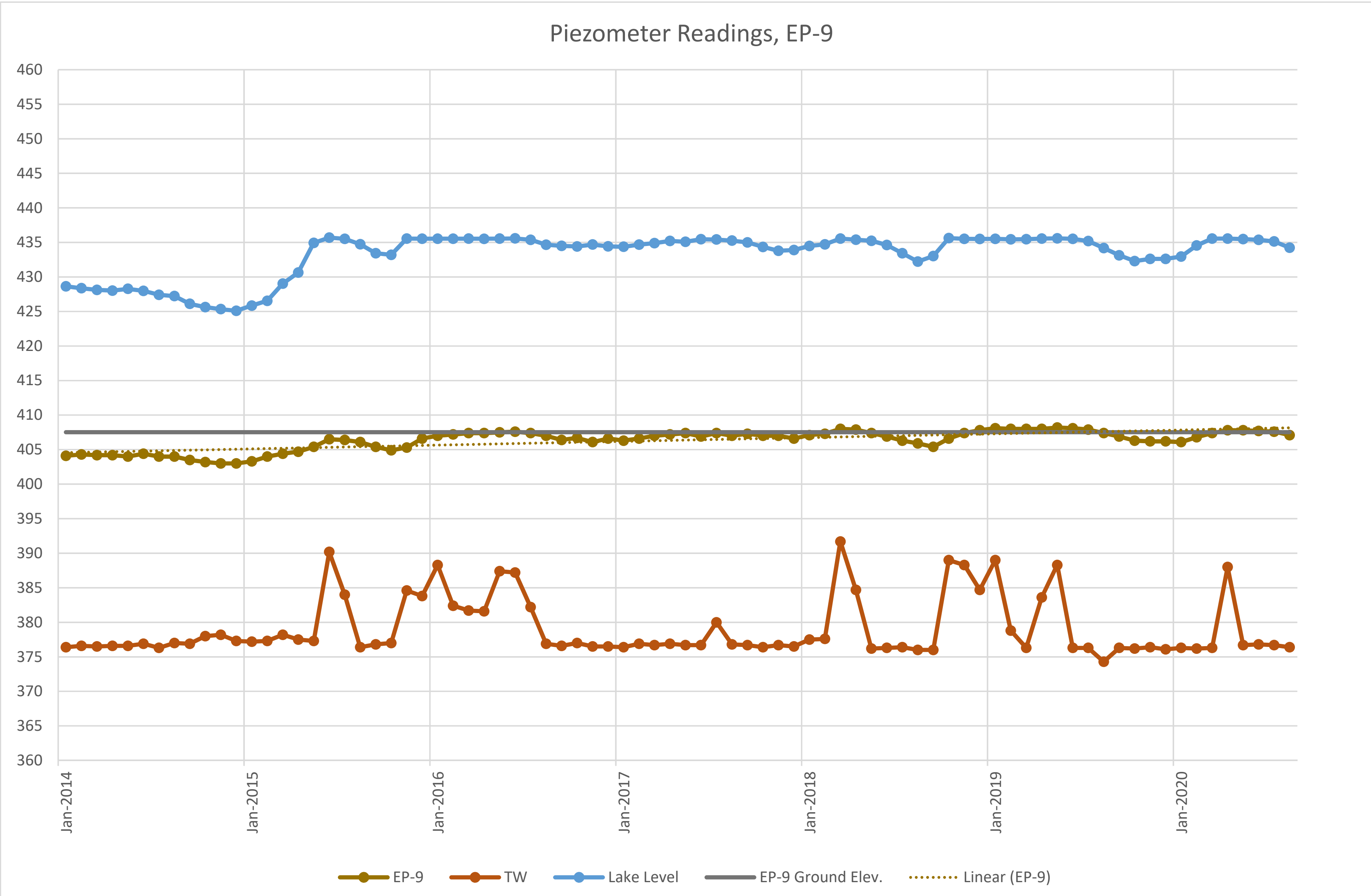
Piezometer Readings, EP-9
460
455
450
445
440
435
430
425
420
415
410
405
400
395
390
385
380
375
370
365
360
Jan-2014
Jan-2015
Jan-2016
Jan-2017
Jan-2018
Jan-2019
Jan-2020
EP-9
TW
Lake Level
EP-9 Ground Elev.
Linear (EP-9)

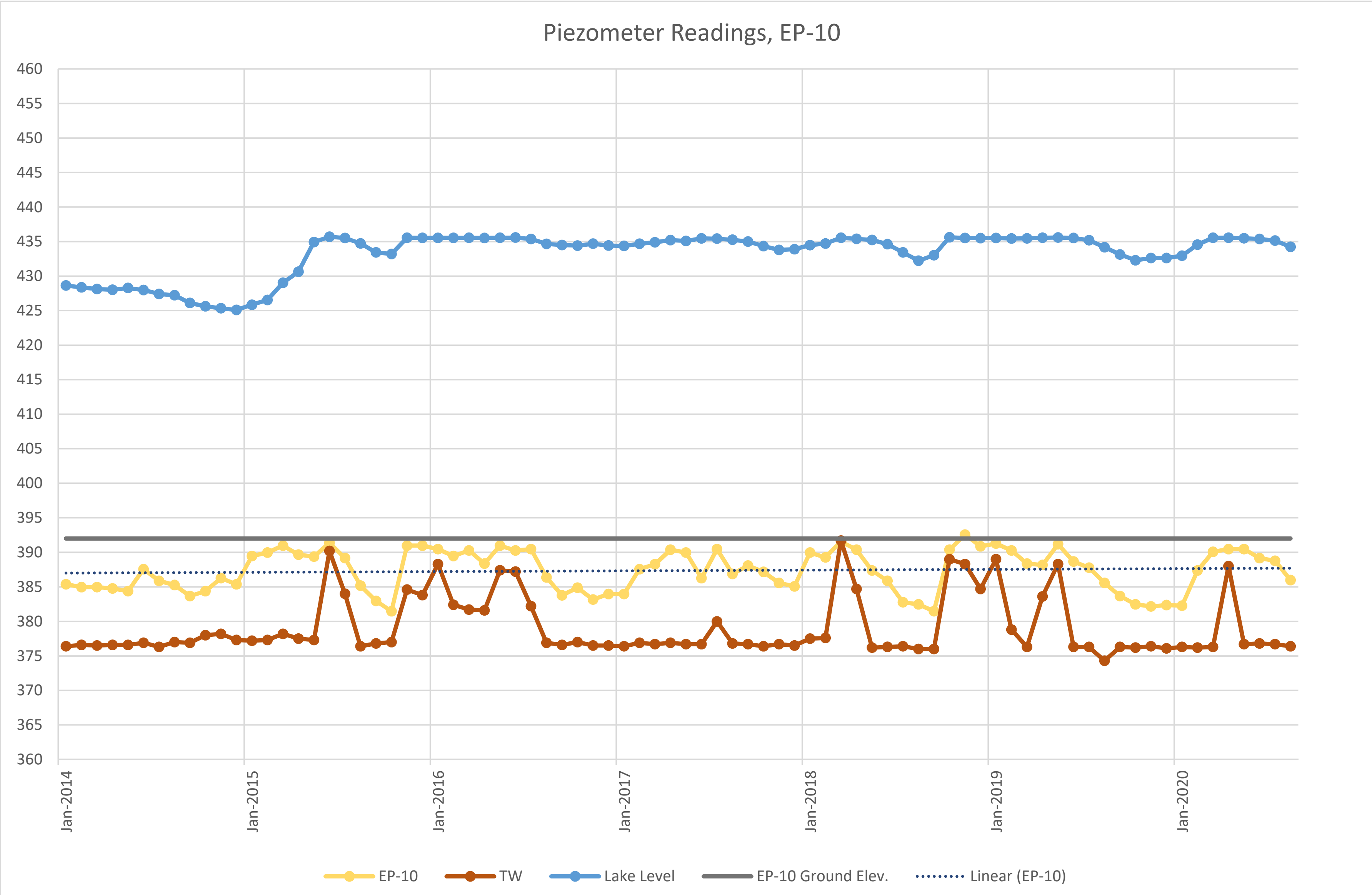

Piezometer Readings, EP-10
460
455
450
445
440
435
430
425
420
415
410
405
400
395
390
385
380
375
370
365
360
Jan-2014
Jan-2015
Jan-2016
Jan-2017
Jan-2018
Jan-2019
Jan-2020
EP-10
TW
Lake Level
EP-10 Ground Elev.
Linear (EP-10)

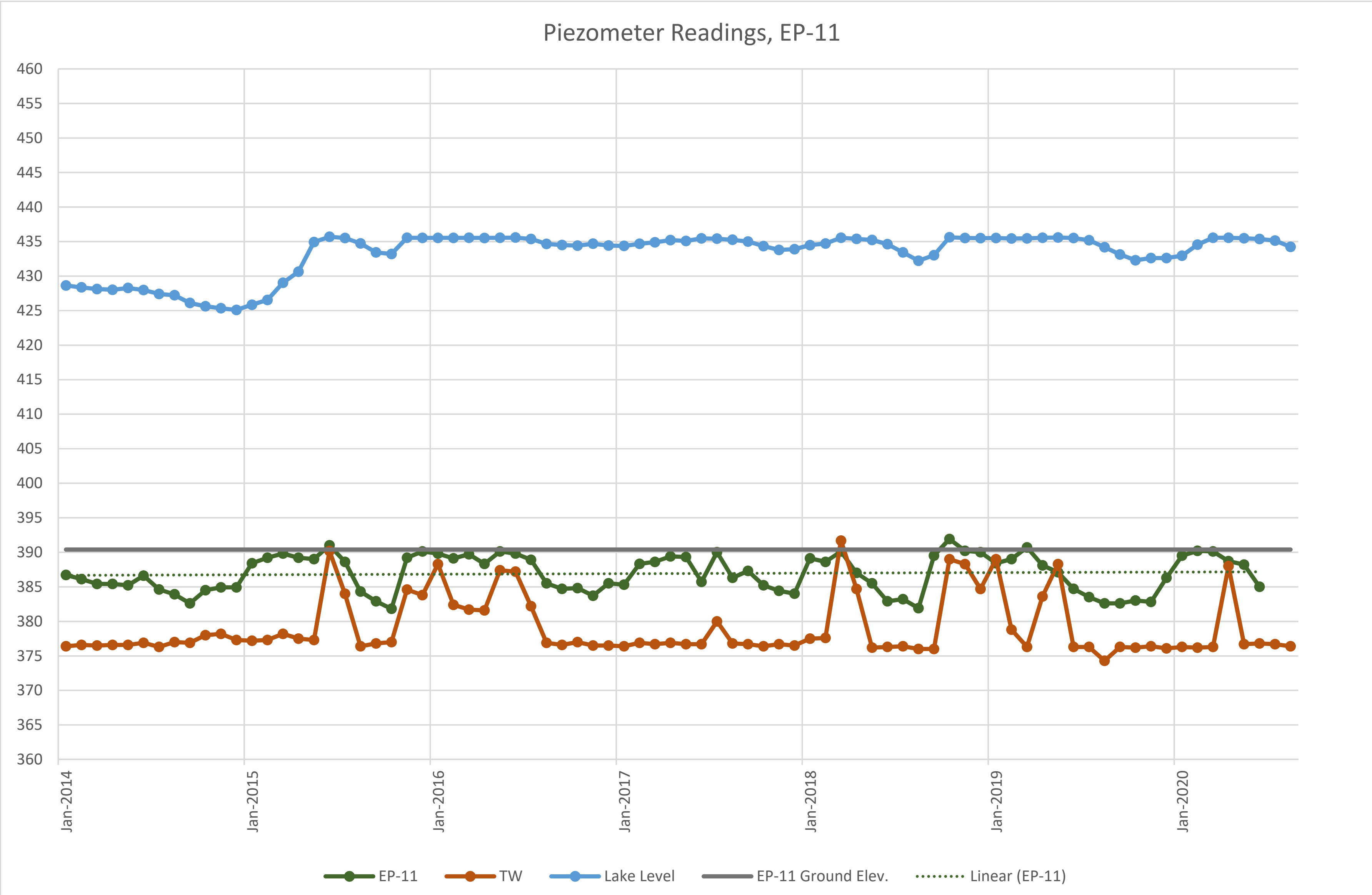
Piezometer Readings, EP-11
460
455
450
445
440
435
430
425
420
415
410
405
400
395
390
385
380
375
370
365
360
Jan-2014
Jan-2015
Jan-2016
Jan-2017
Jan-2018
Jan-2019
Jan-2020
EP-11
TW
Lake Level
EP-11 Ground Elev.
Linear (EP-11)

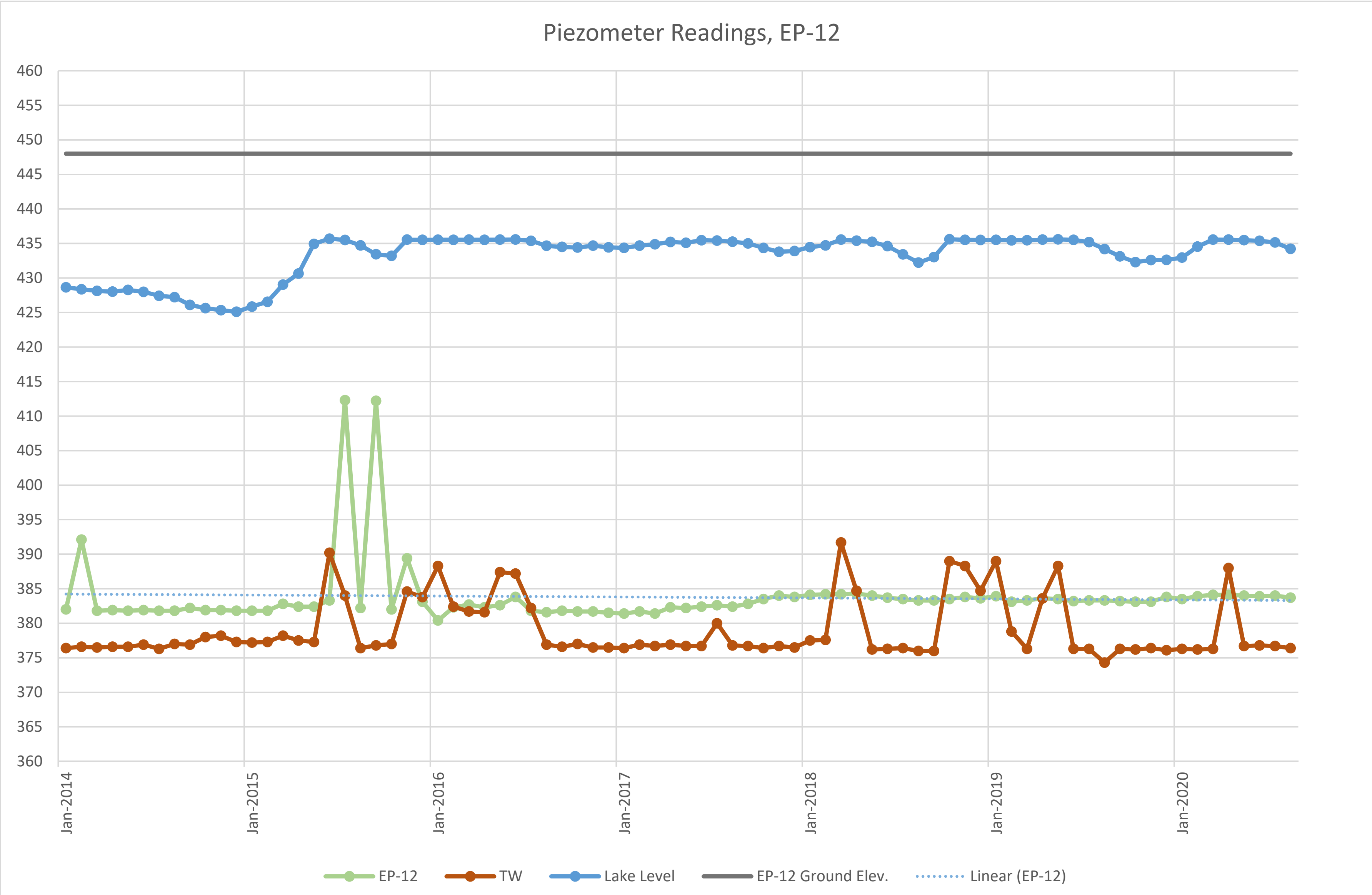
Piezometer Readings, EP-12
460
455
450
445
440
435
430
425
420
415
410
405
400
395
390
385
380
375
370
365
360
Jan-2014
Jan-2015
Jan-2016
Jan-2017
Jan-2018
Jan-2019
Jan-2020
EP-12
TW
Lake Level
EP-12 Ground Elev.
Linear (EP-12)

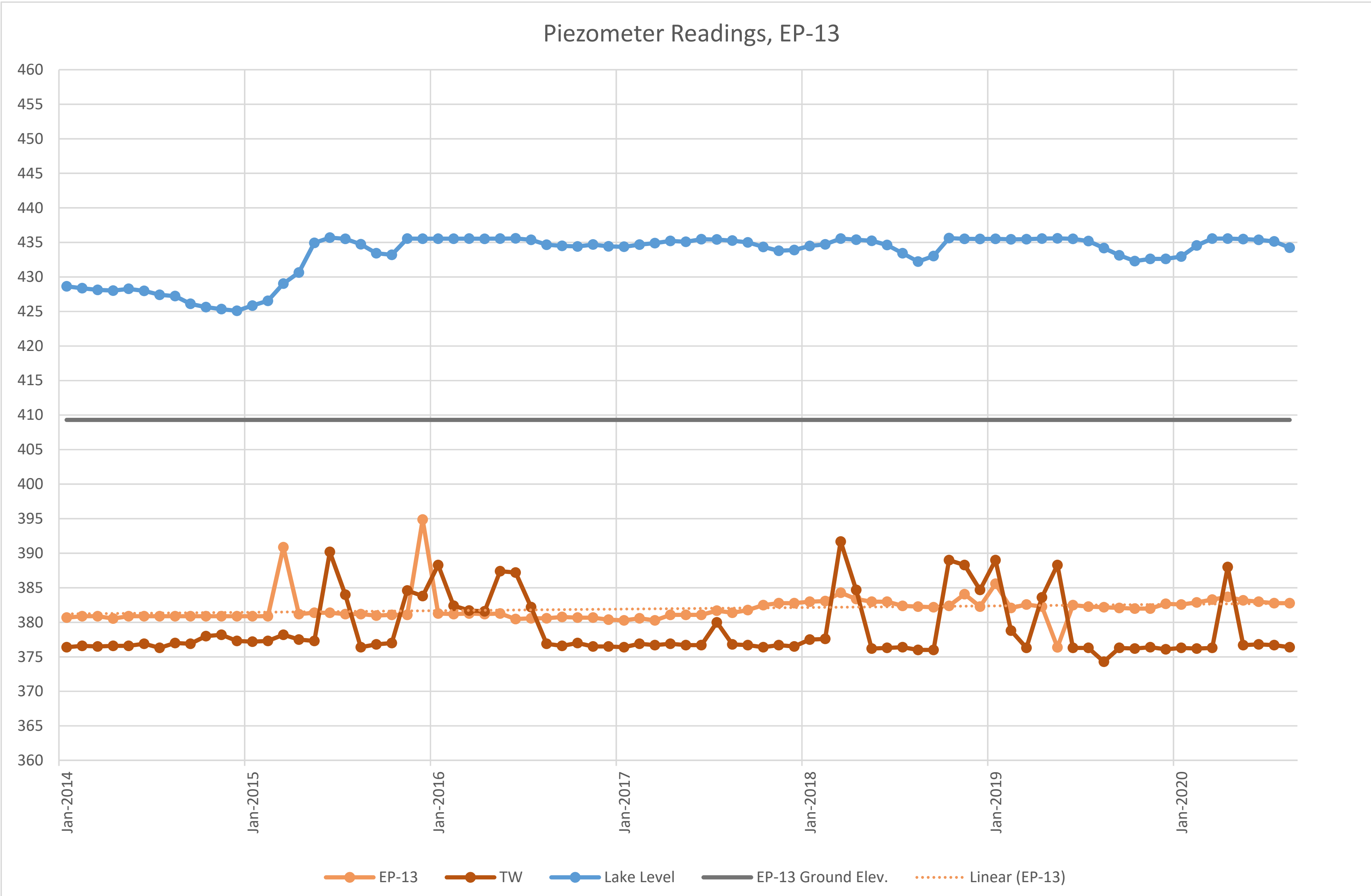

Piezometer Readings, EP-13
460
455
450
445
440
435
430
425
420
415
410
405
400
395
390
385
380
375
370
365
360
Jan-2014
Jan-2015
Jan-2016
Jan-2017
Jan-2018
Jan-2019
Jan-2020
EP-13
TW
Lake Level
EP-13 Ground Elev.
Linear (EP-13)

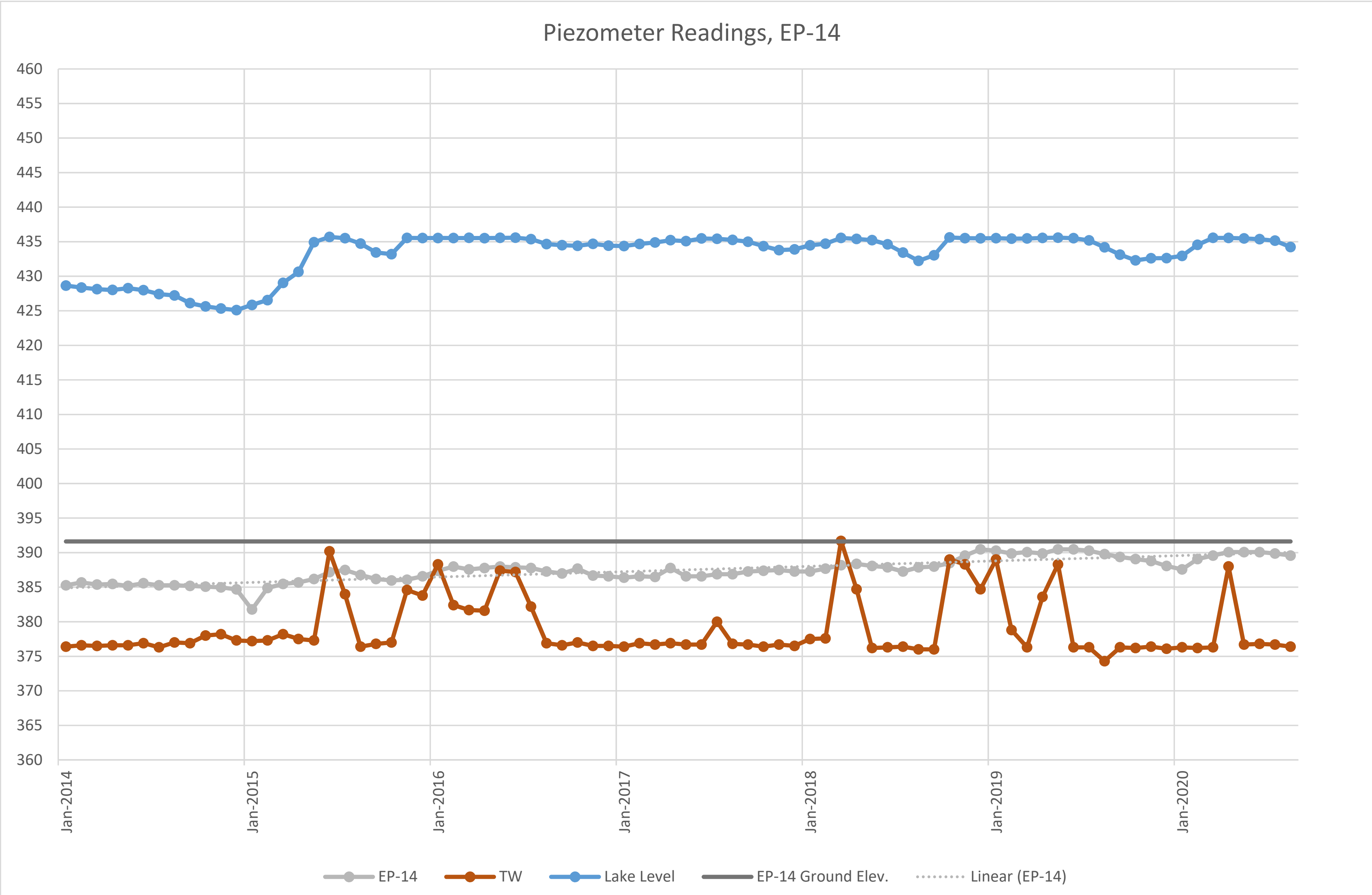

Piezometer Readings, EP-14
460
455
450
445
440
435
430
425
420
415
410
405
400
395
390
385
380
375
370
365
360
Jan-2014
Jan-2015
Jan-2016
Jan-2017
Jan-2018
Jan-2019
Jan-2020
EP-14
TW
Lake Level
EP-14 Ground Elev.
Linear (EP-14)

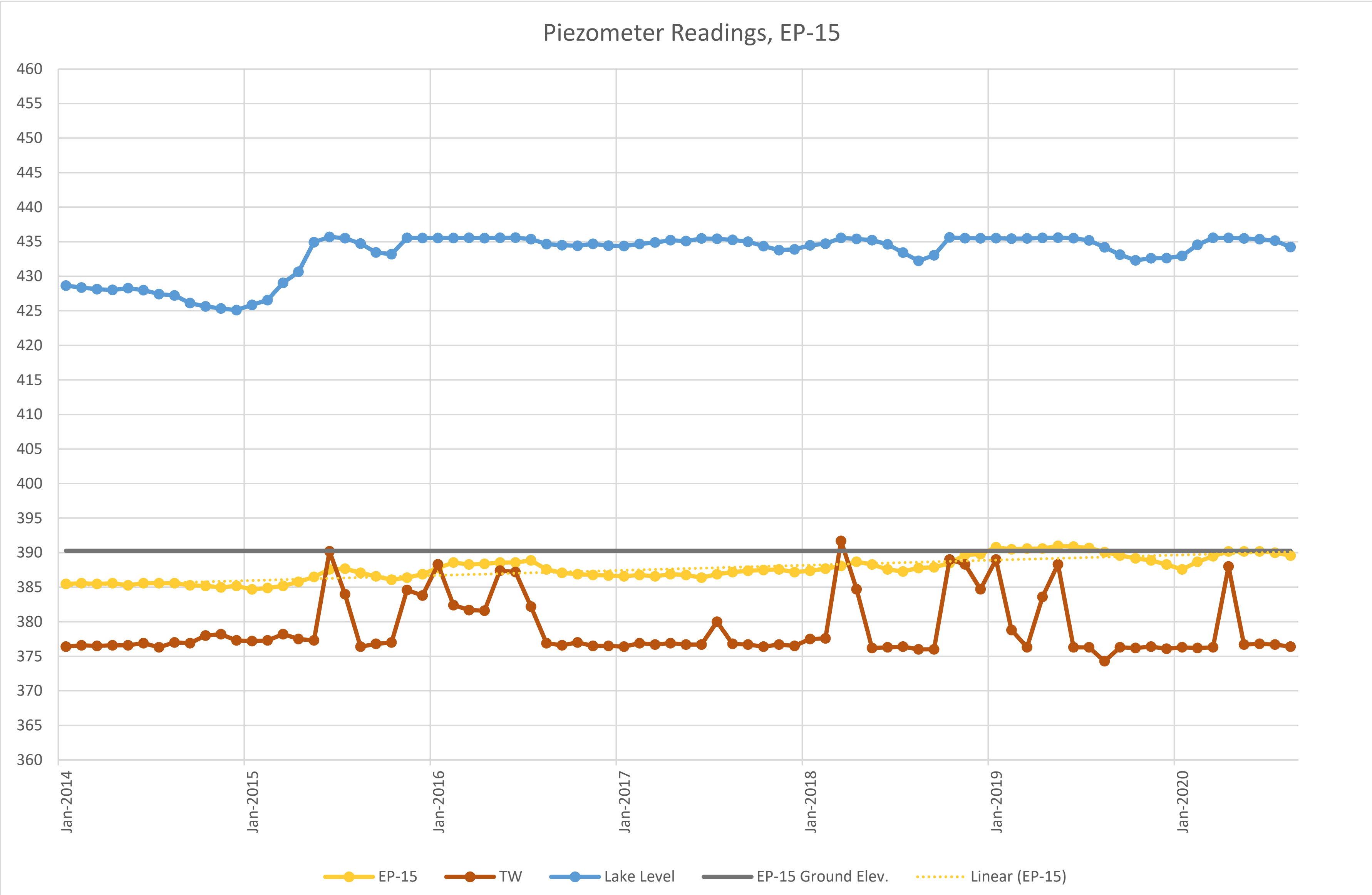
Piezometer Readings, EP-15
460
455
450
445
440
435
430
425
420
415
410
405
400
395
390
385
380
375
370
365
360
Jan-2014
Jan-2015
Jan-2016
Jan-2017
Jan-2018
Jan-2019
Jan-2020
EP-15
TW
Lake Level
EP-15 Ground Elev.
Linear (EP-15)

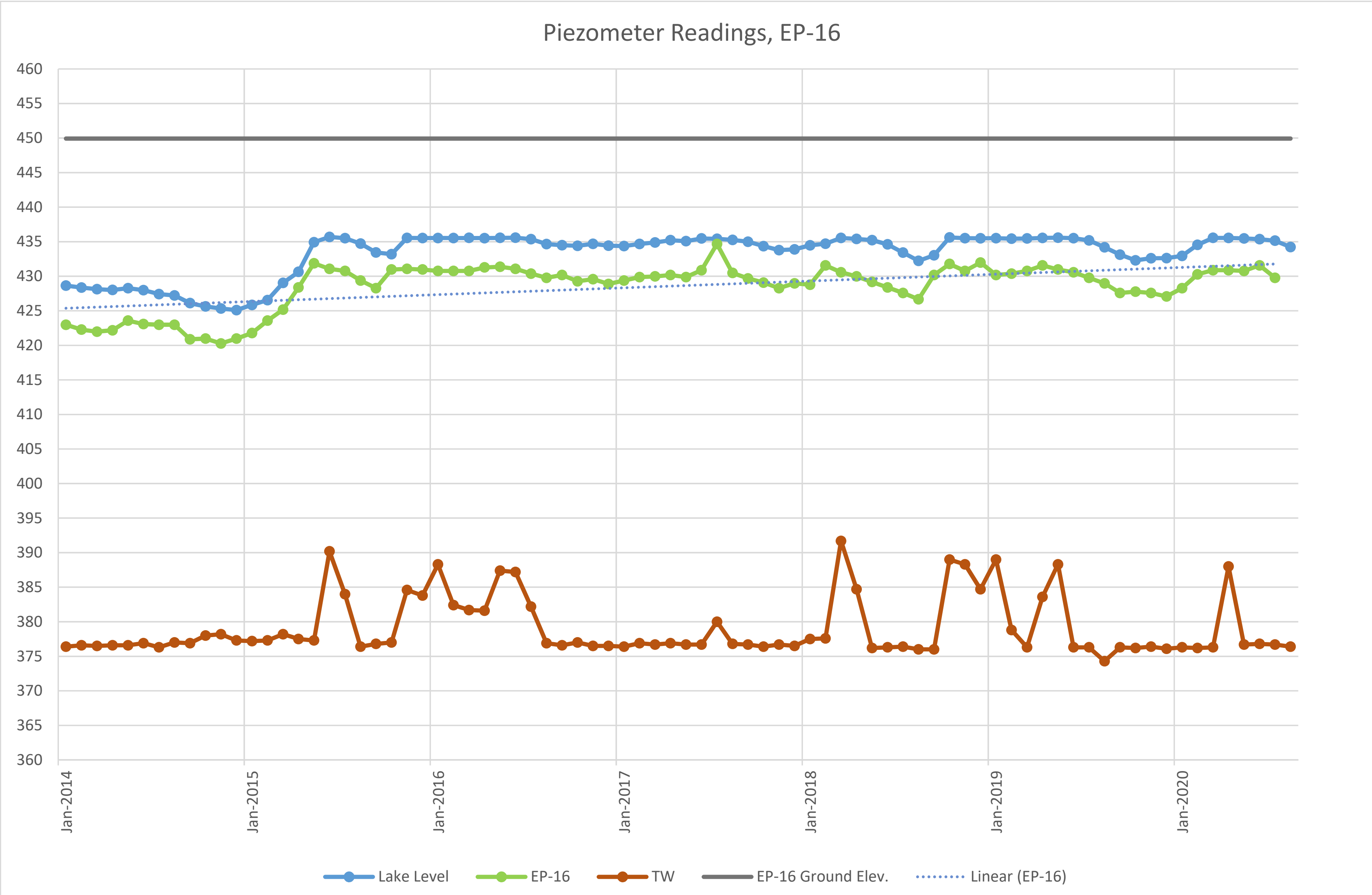
Piezometer Readings, EP-16
460
455
450
445
440
435
430
425
420
415
410
405
400
395
390
385
380
375
370
365
360
Jan-2014
Jan-2015
Jan-2016
Jan-2017
Jan-2018
Jan-2019
Jan-2020
Lake Level
EP-16
TW
EP-16 Ground Elev.
Linear (EP-16)

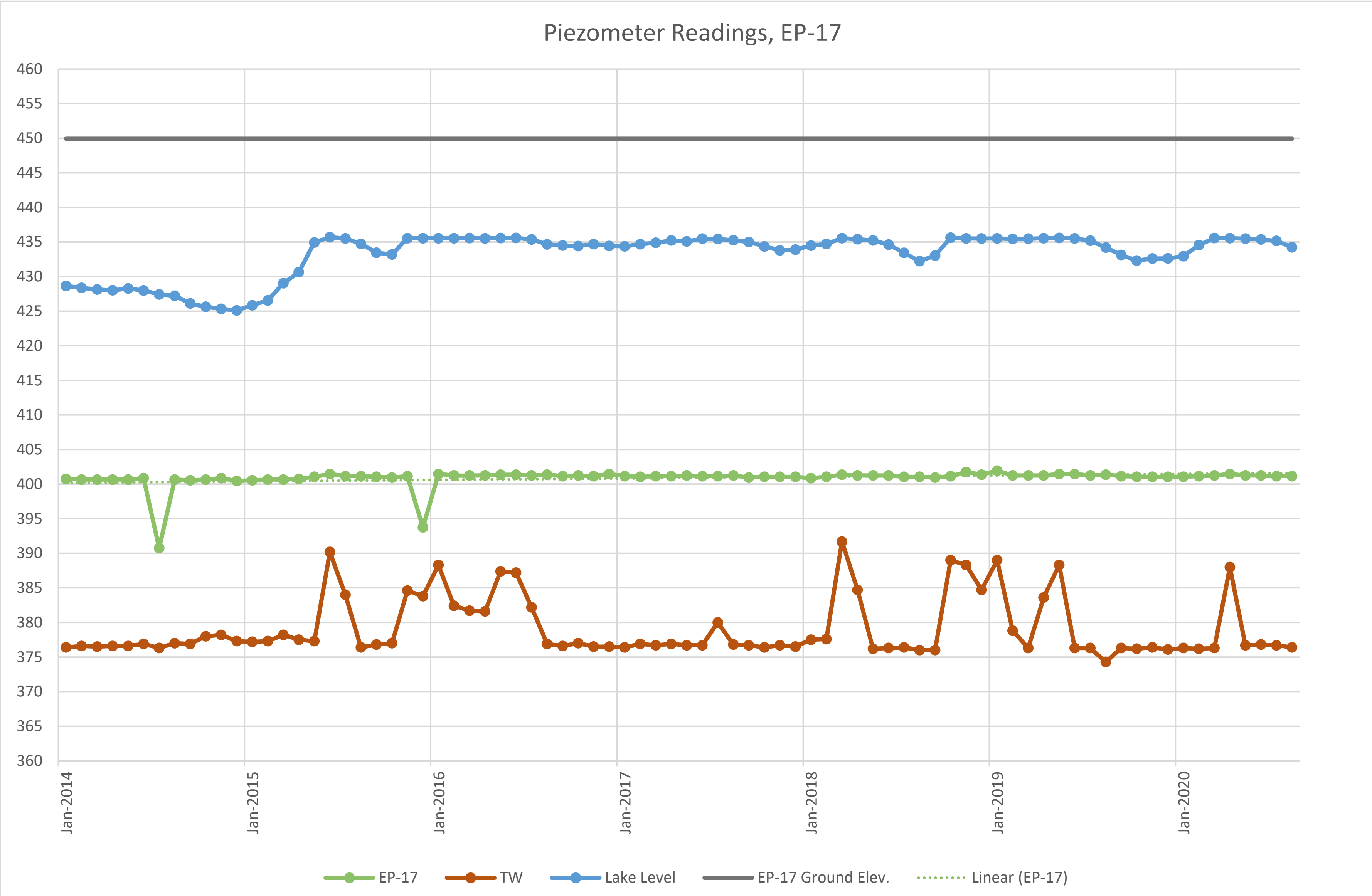
Piezometer Readings, EP-17
460
455
450
445
440
435
430
425
420
415
410
405
400
395
390
385
380
375
370
365
360
Jan-2014
Jan-2015
Jan-2016
Jan-2017
Jan-2018
Jan-2019
Jan-2020
EP-17
TW
Lake Level
EP-17 Ground Elev.
Linear (EP-17)

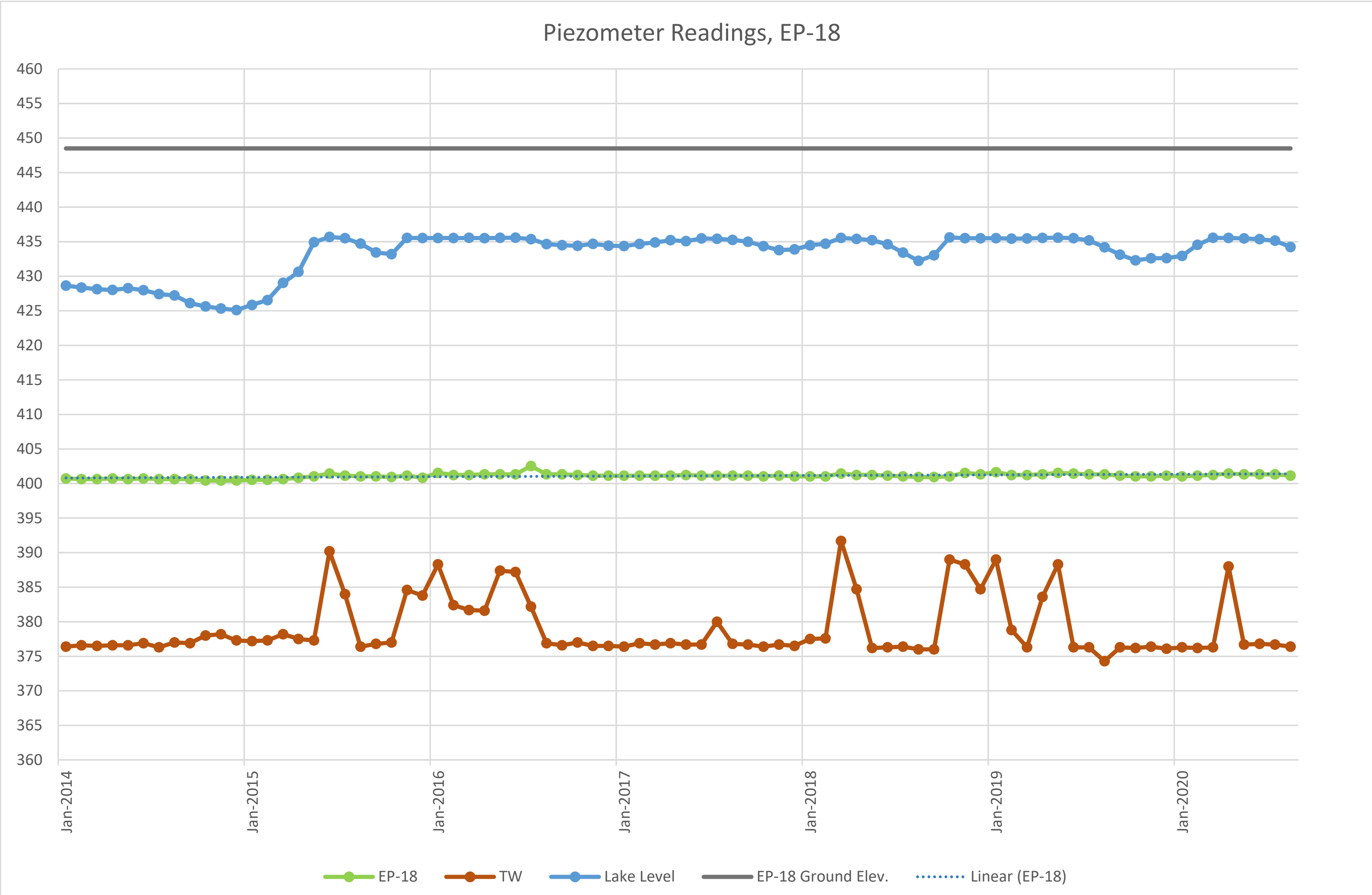

Piezometer Readings, EP-18
460
455
450
445
440
435
430
425
420
415
410
405
400
395
390
385
380
375
370
365
360
Jan-2014
Jan-2015
Jan-2016
Jan-2017
Jan-2018
Jan-2019
Jan-2020
EP-18
TW
Lake Level
EP-18 Ground Elev.
Linear (EP-18)

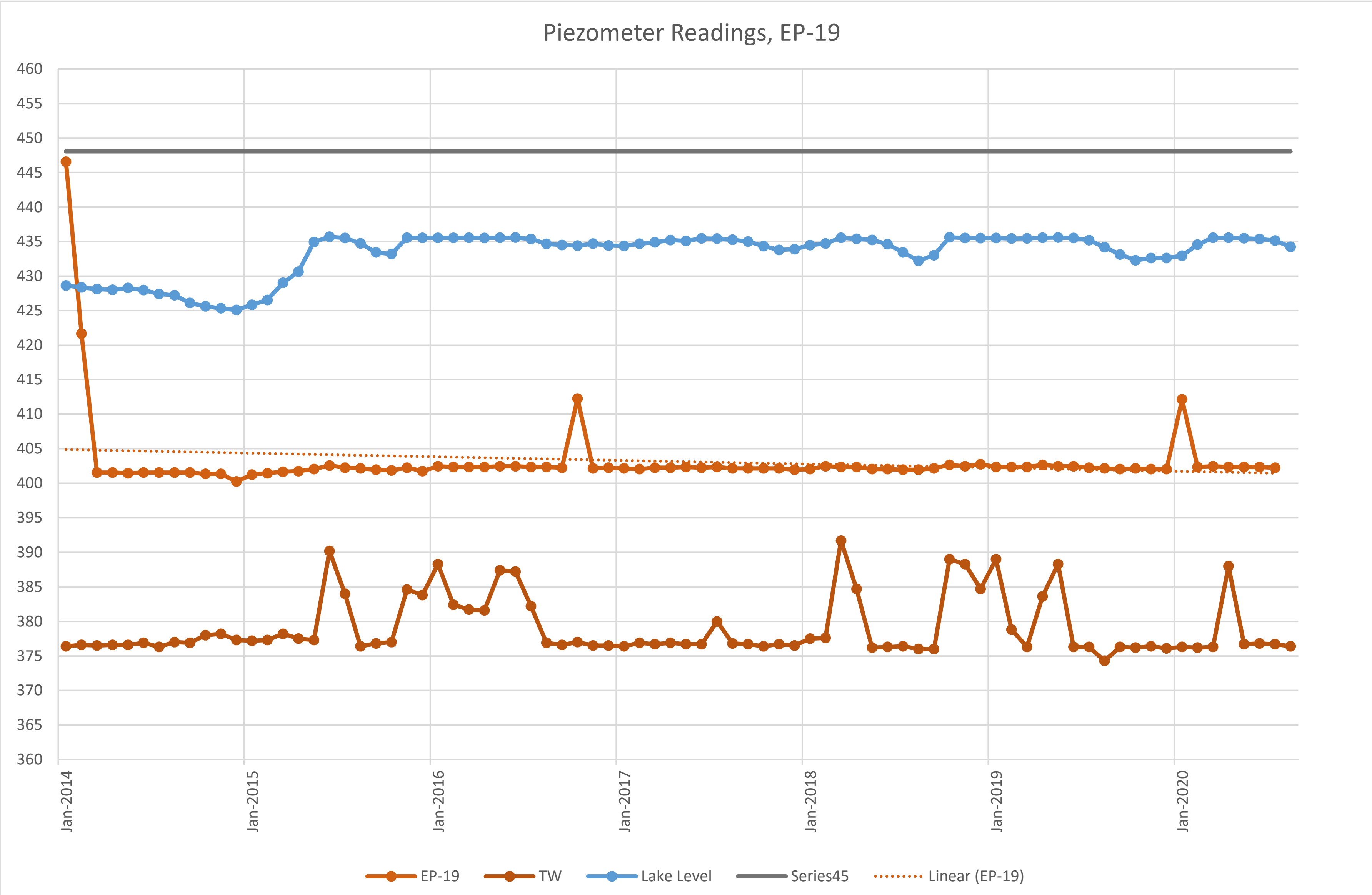

Piezometer Readings, EP-19
460
455
450
445
440
435
430
425
420
415
410
405
400
395
390
385
380
375
370
365
360
Jan-2014
Jan-2015
Jan-2016
Jan-2017
Jan-2018
Jan-2019
Jan-2020
EP-19
TW
Lake Level
Series45
Linear (EP-19)

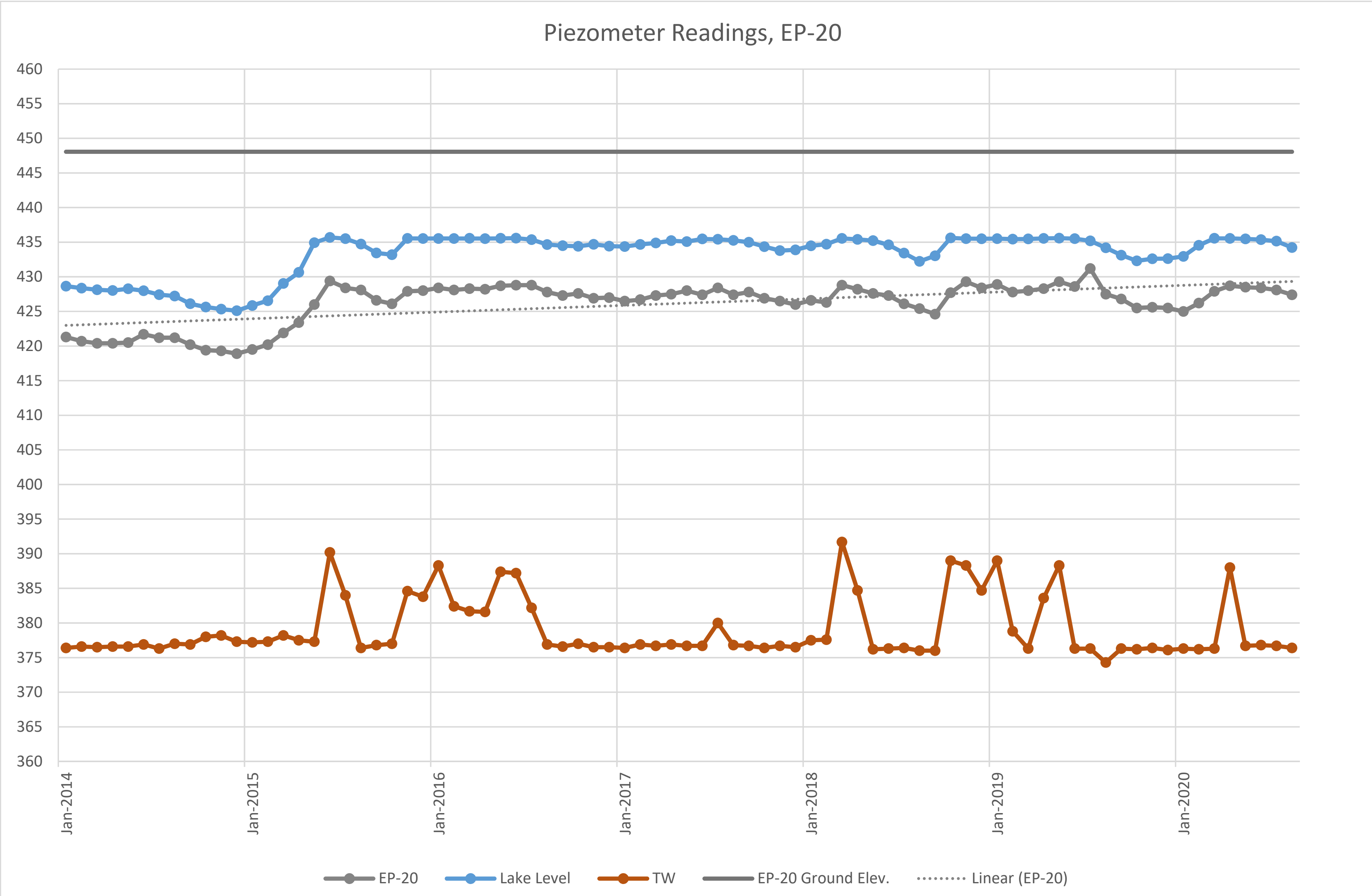

Piezometer Readings, EP-20
460
455
450
445
440
435
430
425
420
415
410
405
400
395
390
385
380
375
370
365
360
Jan-2014
Jan-2015
Jan-2016
Jan-2017
Jan-2018
Jan-2019
Jan-2020
EP-20
Lake Level
TW
EP-20 Ground Elev.
Linear (EP-20)

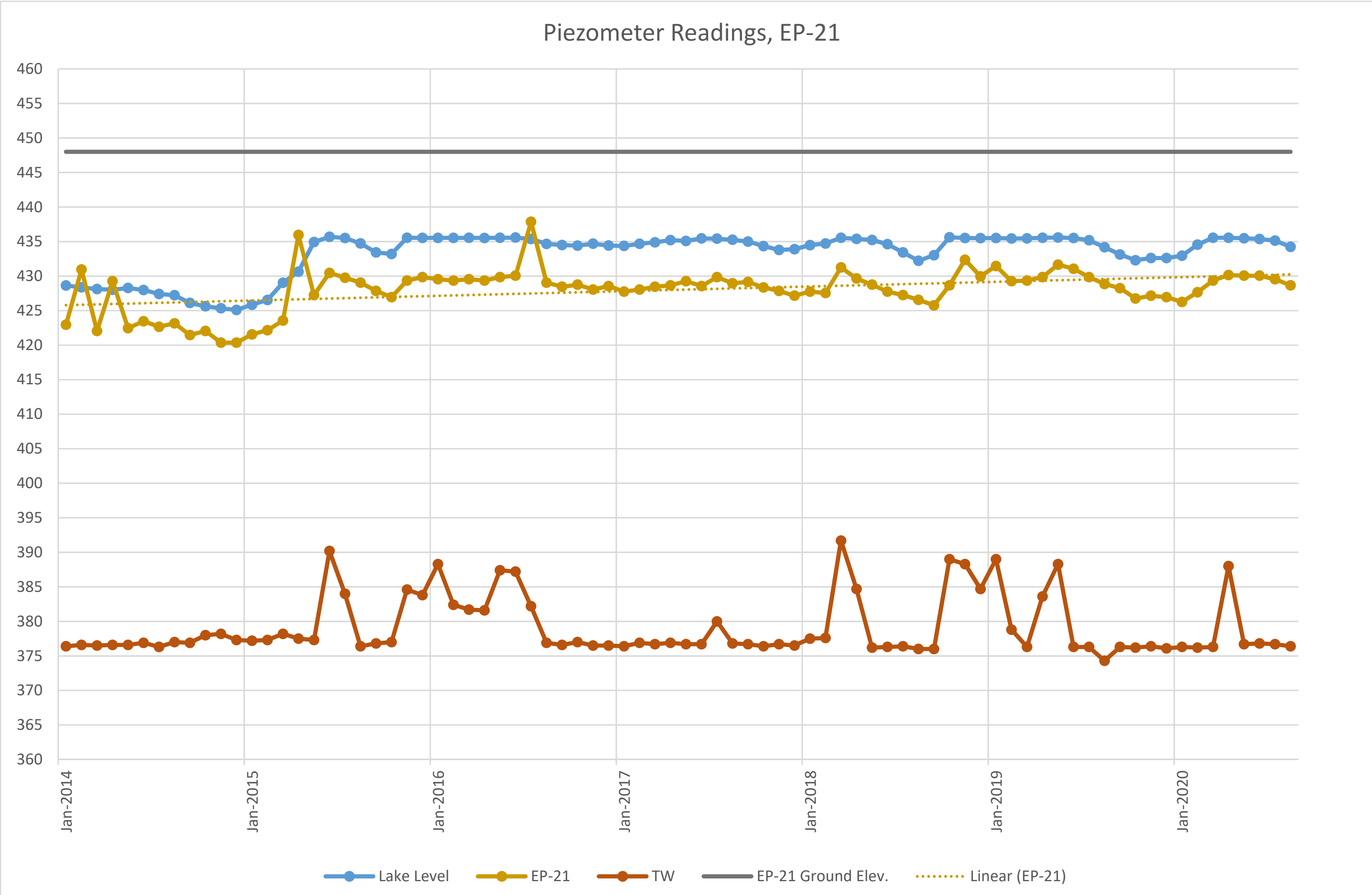

Piezometer Readings, EP-21
460
455
450
445
440
435
430
425
420
415
410
405
400
395
390
385
380
375
370
365
360
Jan-2014
Jan-2015
Jan-2016
Jan-2017
Jan-2018
Jan-2019
Jan-2020
Lake Level
EP-21
TW
EP-21 Ground Elev.
Linear (EP-21)

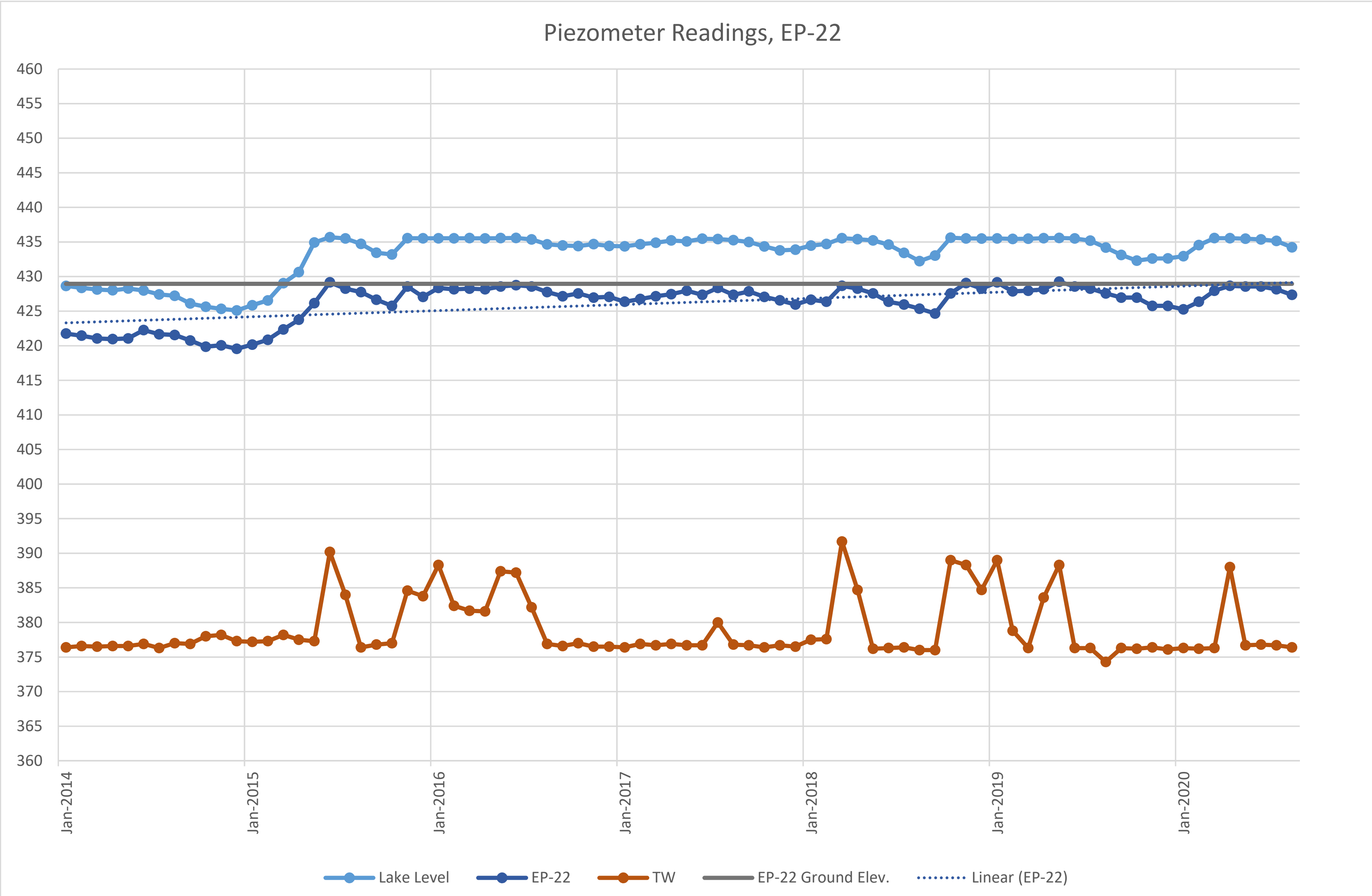

Piezometer Readings, EP-22
460
455
450
445
440
435
430
425
420
415
410
405
400
395
390
385
380
375
370
365
360
Jan-2014
Jan-2015
Jan-2016
Jan-2017
Jan-2018
Jan-2019
Jan-2020
Lake Level
EP-22
TW
EP-22 Ground Elev.
Linear (EP-22)

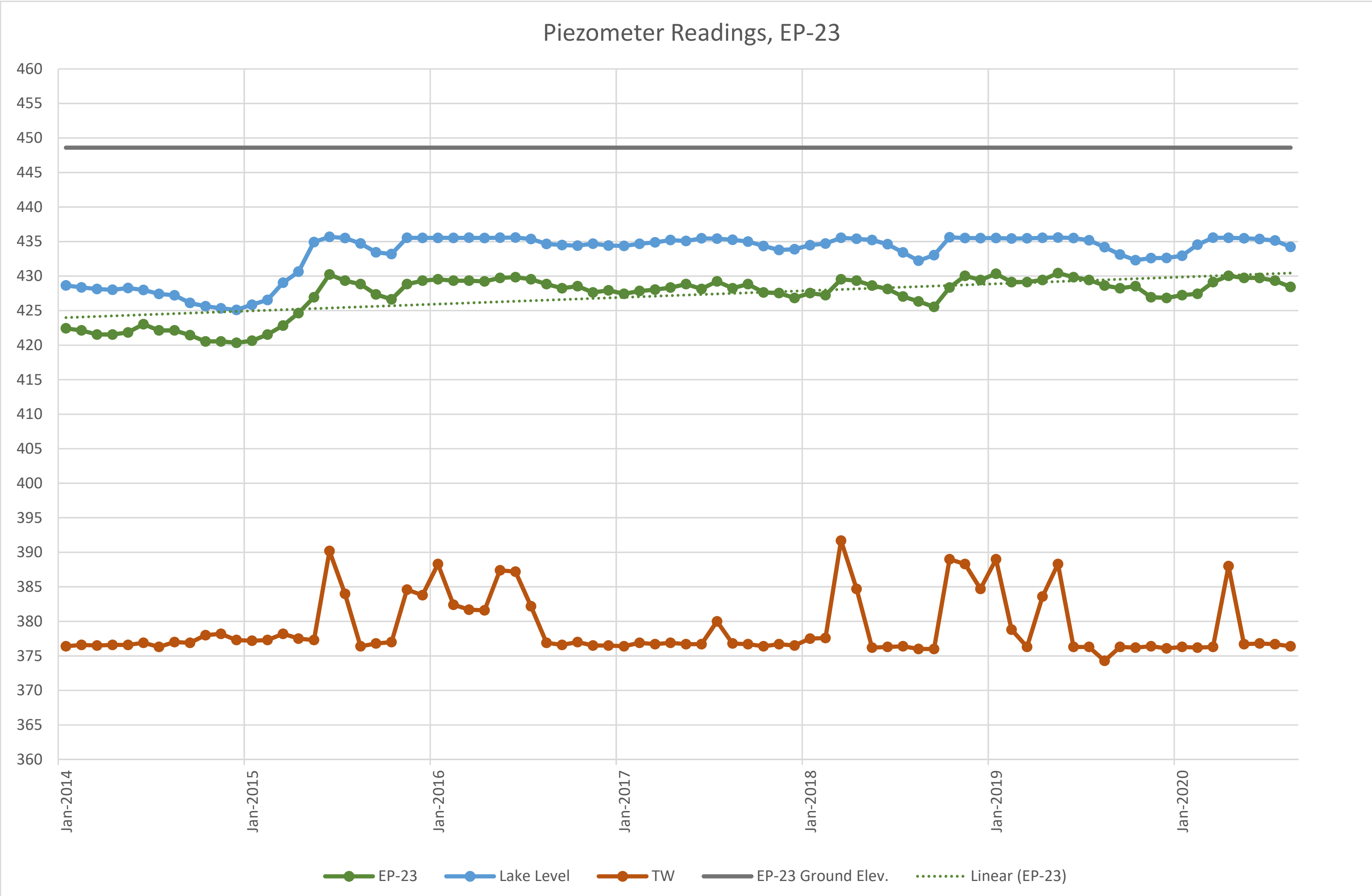
Piezometer Readings, EP-23
460
455
450
445
440
435
430
425
420
415
410
405
400
395
390
385
380
375
370
365
360
Jan-2014
Jan-2015
Jan-2016
Jan-2017
Jan-2018
Jan-2019
Jan-2020
EP-23
Lake Level
TW
EP-23 Ground Elev.
Linear (EP-23)

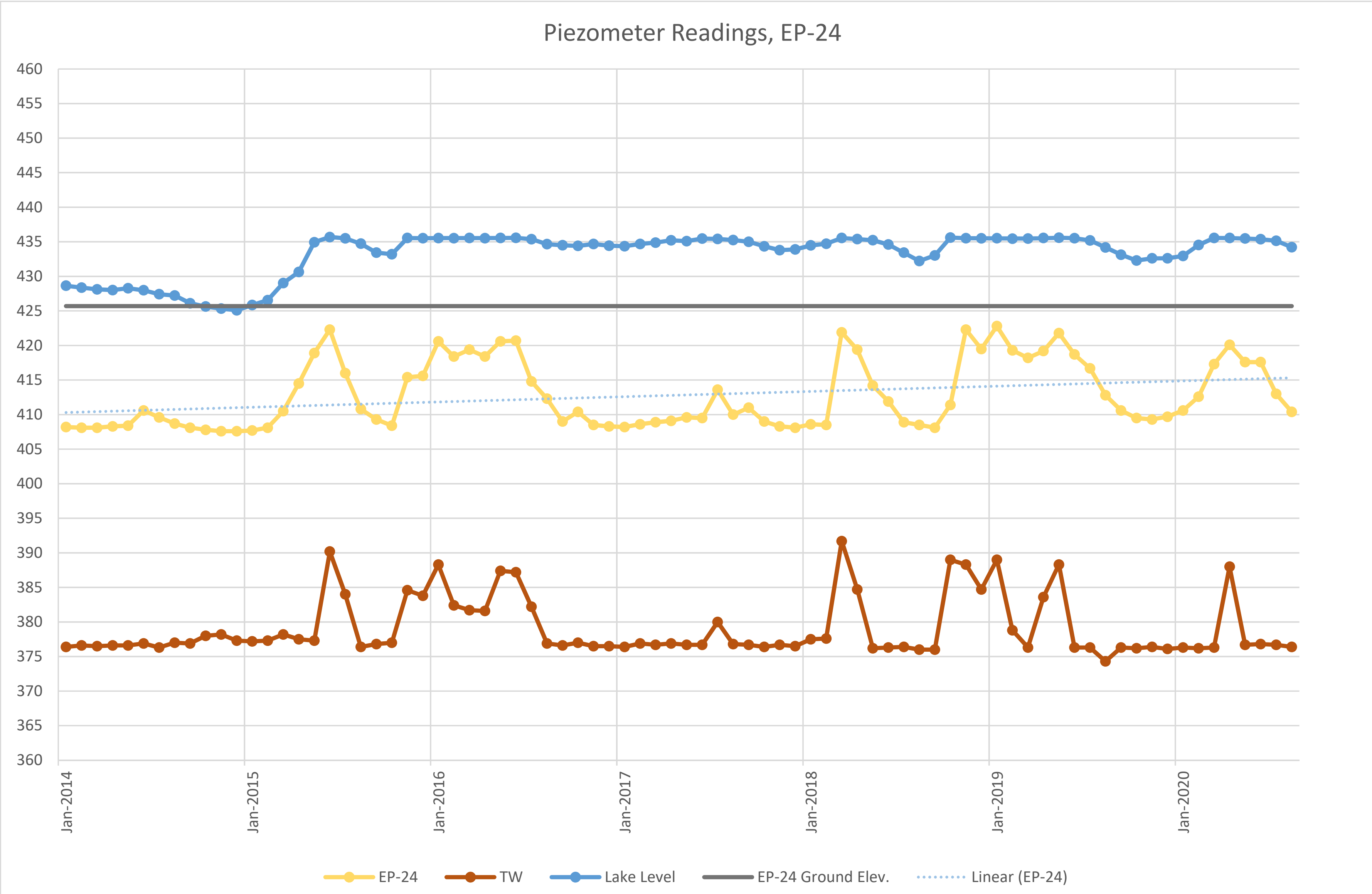
Piezometer Readings, EP-24
460
455
450
445
440
435
430
425
420
415
410
405
400
395
390
385
380
375
370
365
360
Jan-2014
Jan-2015
Jan-2016
Jan-2017
Jan-2018
Jan-2019
Jan-2020
EP-24
TW
Lake Level
EP-24 Ground Elev.
Linear (EP-24)

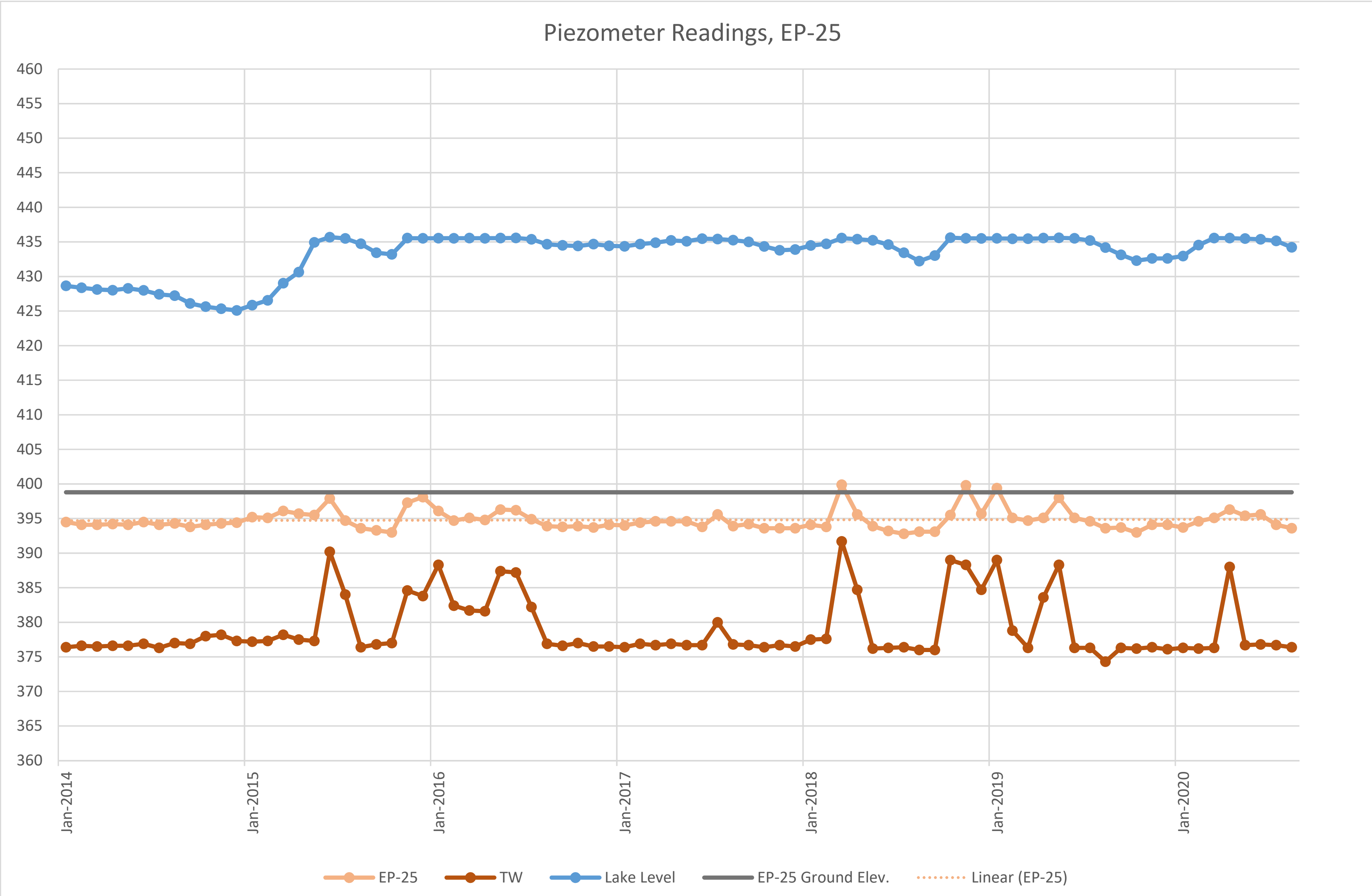
Piezometer Readings, EP-25
460
455
450
445
440
435
430
425
420
415
410
405
400
395
390
385
380
375
370
365
360
Jan-2014
Jan-2015
Jan-2016
Jan-2017
Jan-2018
Jan-2019
Jan-2020
EP-25
TW
Lake Level
EP-25 Ground Elev.
Linear (EP-25)

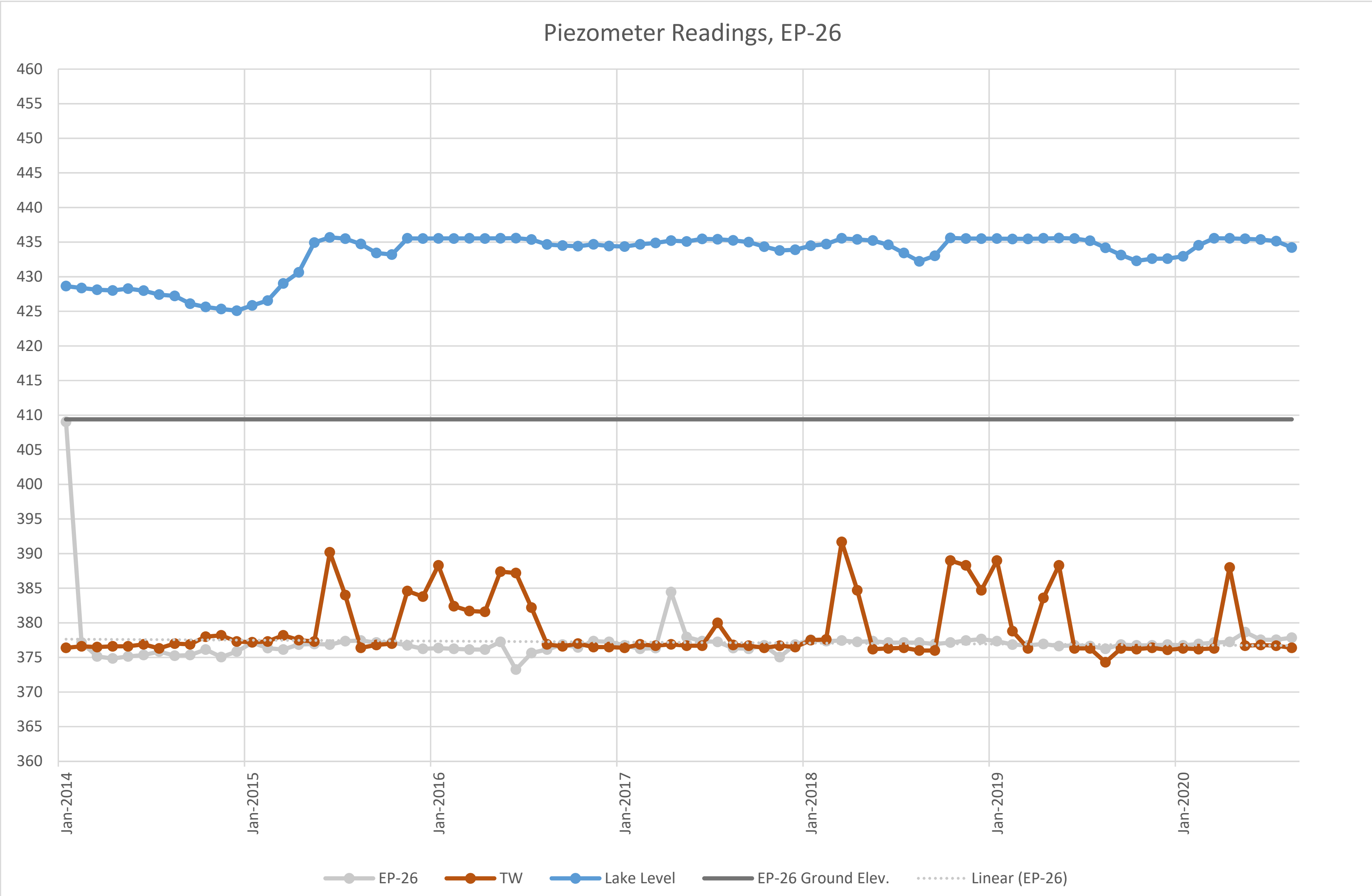
Piezometer Readings, EP-26
460
455
450
445
440
435
430
425
420
415
410
405
400
395
390
385
380
375
370
365
360
Jan-2014
Jan-2015
Jan-2016
Jan-2017
Jan-2018
Jan-2019
Jan-2020
EP-26
TW
Lake Level
EP-26 Ground Elev.
Linear (EP-26)

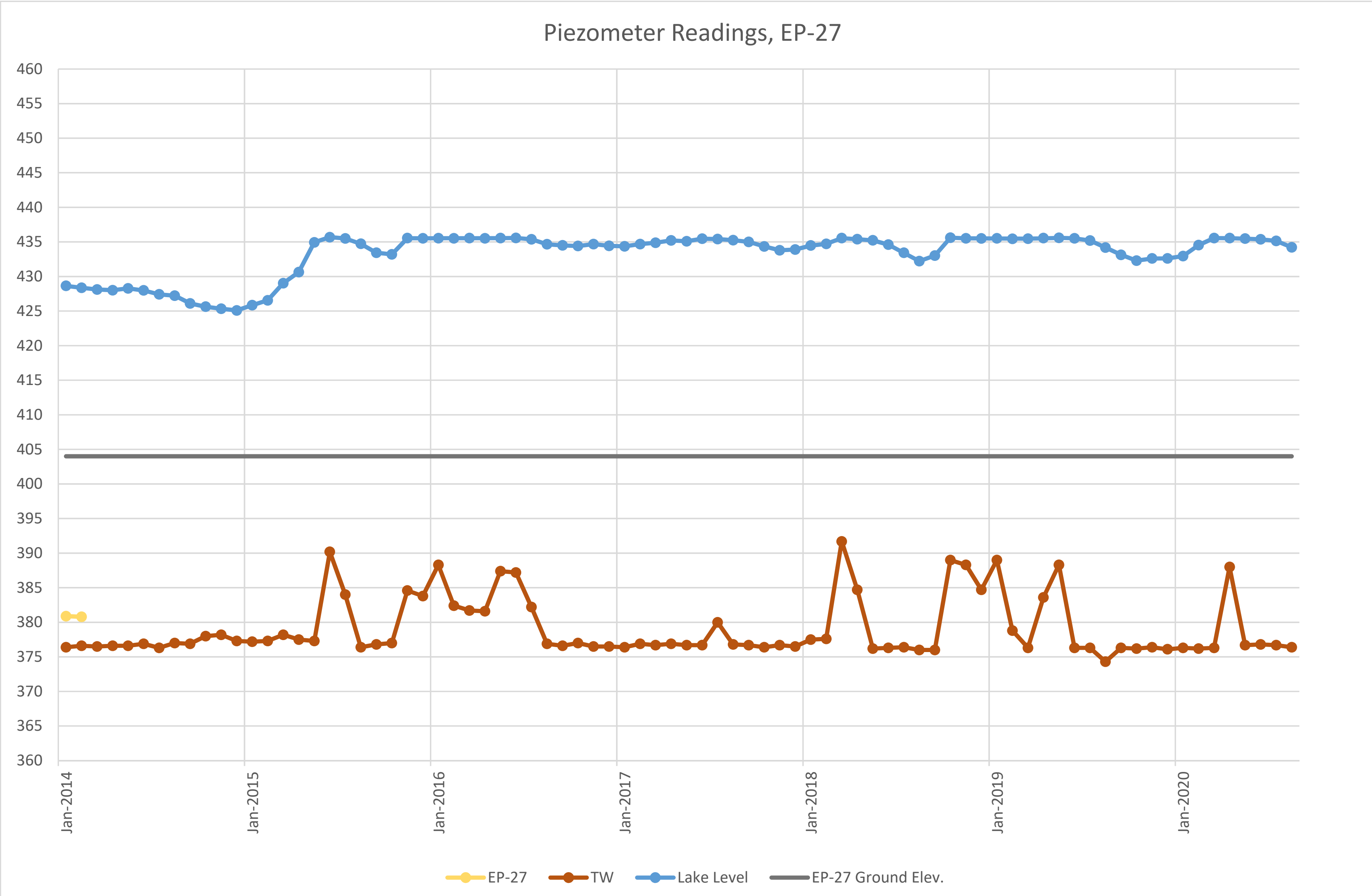
Piezometer Readings, EP-27
460
455
450
445
440
435
430
425
420
415
410
405
400
395
390
385
380
375
370
365
360
Jan-2014
Jan-2015
Jan-2016
Jan-2017
Jan-2018
Jan-2019
Jan-2020
EP-27
TW
Lake Level
EP-27 Ground Elev.

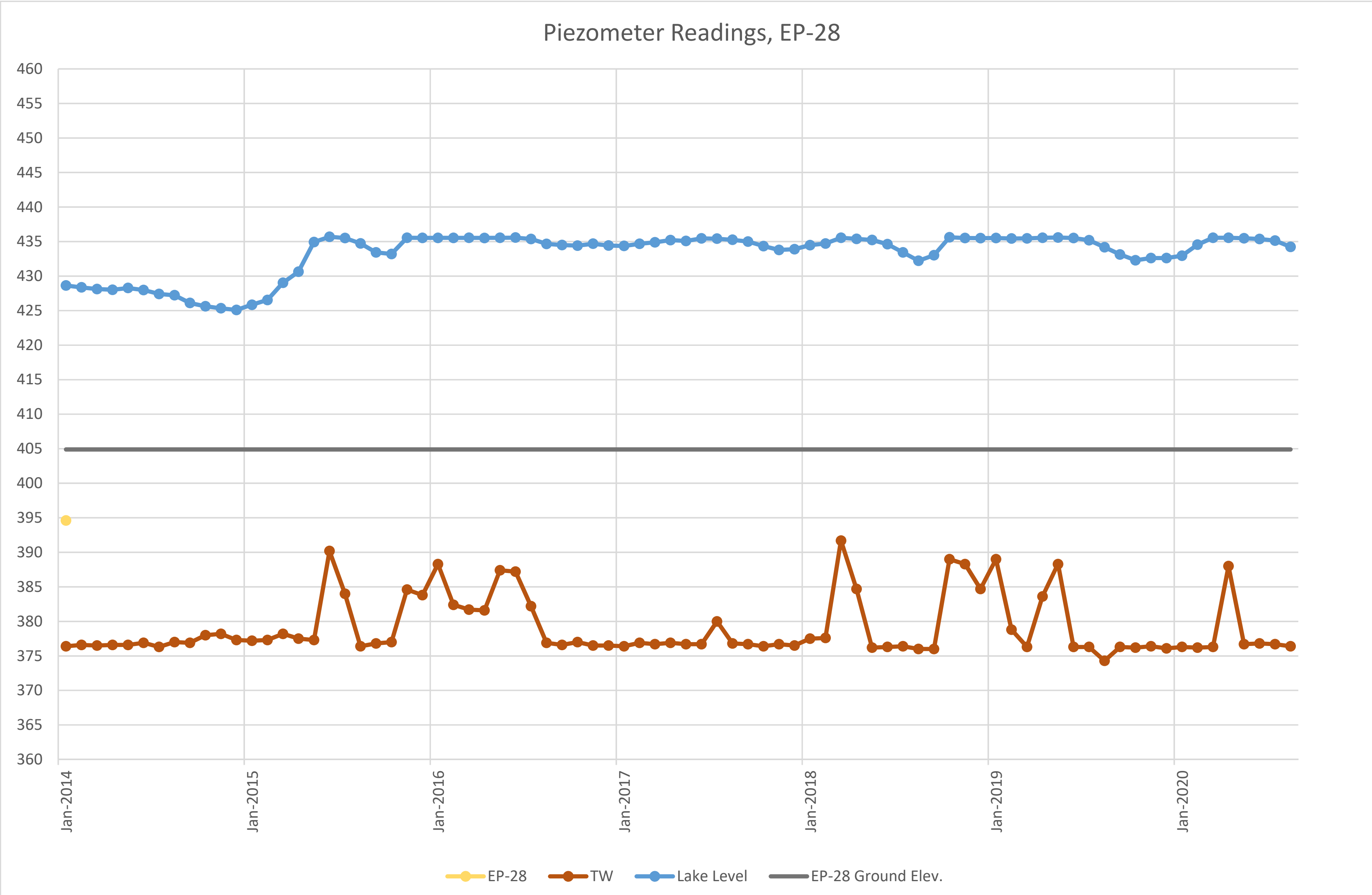
Piezometer Readings, EP-28
460
455
450
445
440
435
430
425
420
415
410
405
400
395
390
385
380
375
370
365
360
Jan-2014
Jan-2015
Jan-2016
Jan-2017
Jan-2018
Jan-2019
Jan-2020
EP-28
TW
Lake Level
EP-28 Ground Elev.

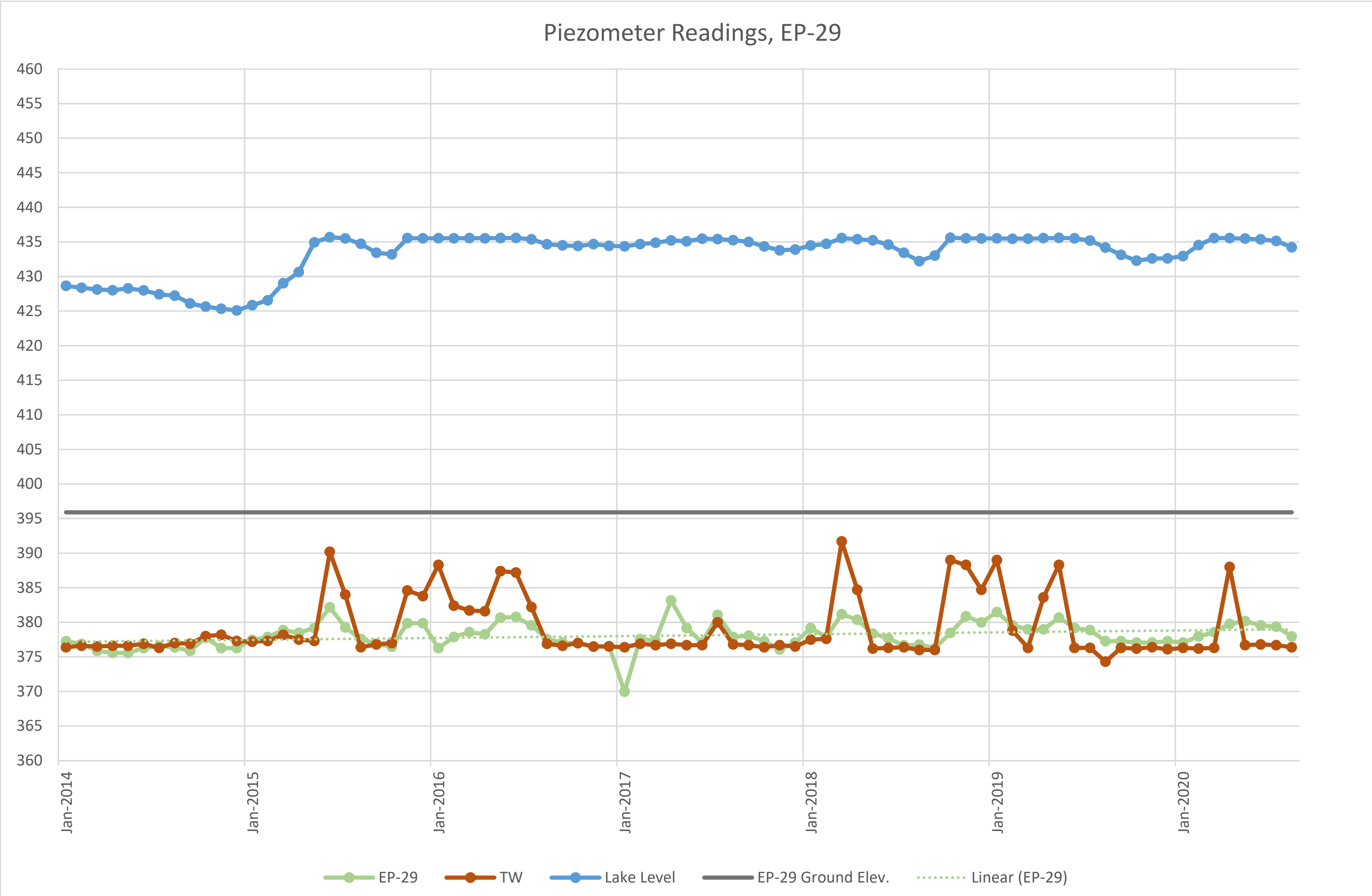

Piezometer Readings, EP-29
460
455
450
445
440
435
430
425
420
415
410
405
400
395
390
385
380
375
370
365
360
Jan-2014
Jan-2015
Jan-2016
Jan-2017
Jan-2018
Jan-2019
Jan-2020
EP-29
TW
Lake Level
EP-29 Ground Elev.
Linear (EP-29)

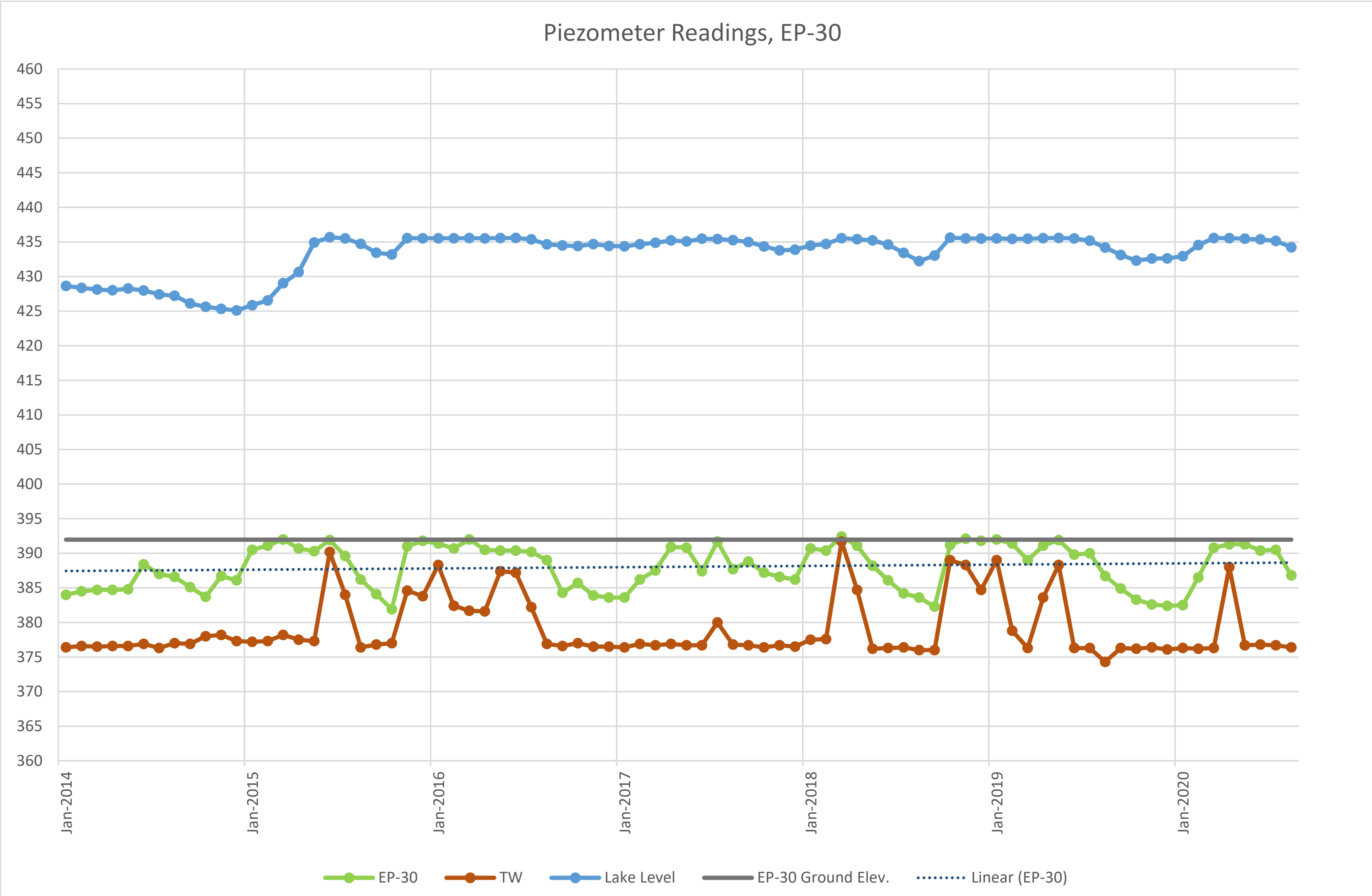

Piezometer Readings, EP-30
460
455
450
445
440
435
430
425
420
415
410
405
400
395
390
385
380
375
370
365
360
Jan-2014
Jan-2015
Jan-2016
Jan-2017
Jan-2018
Jan-2019
Jan-2020
EP-30
TW
Lake Level
EP-30 Ground Elev.
Linear (EP-30)

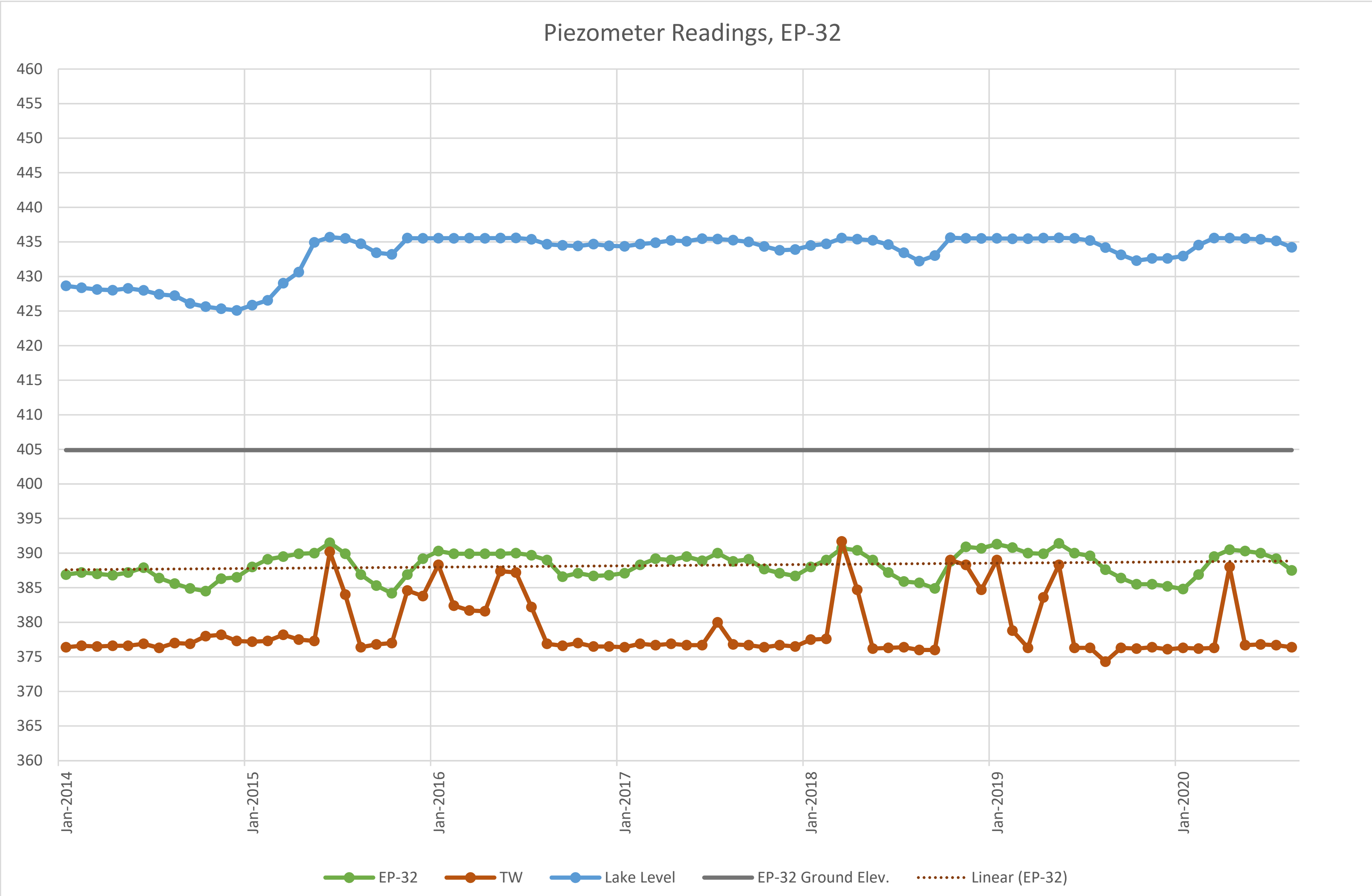

Piezometer Readings, EP-32
460
455
450
445
440
435
430
425
420
415
410
405
400
395
390
385
380
375
370
365
360
Jan-2014
Jan-2015
Jan-2016
Jan-2017
Jan-2018
Jan-2019
Jan-2020
EP-32
TW
Lake Level
EP-32 Ground Elev.
Linear (EP-32)

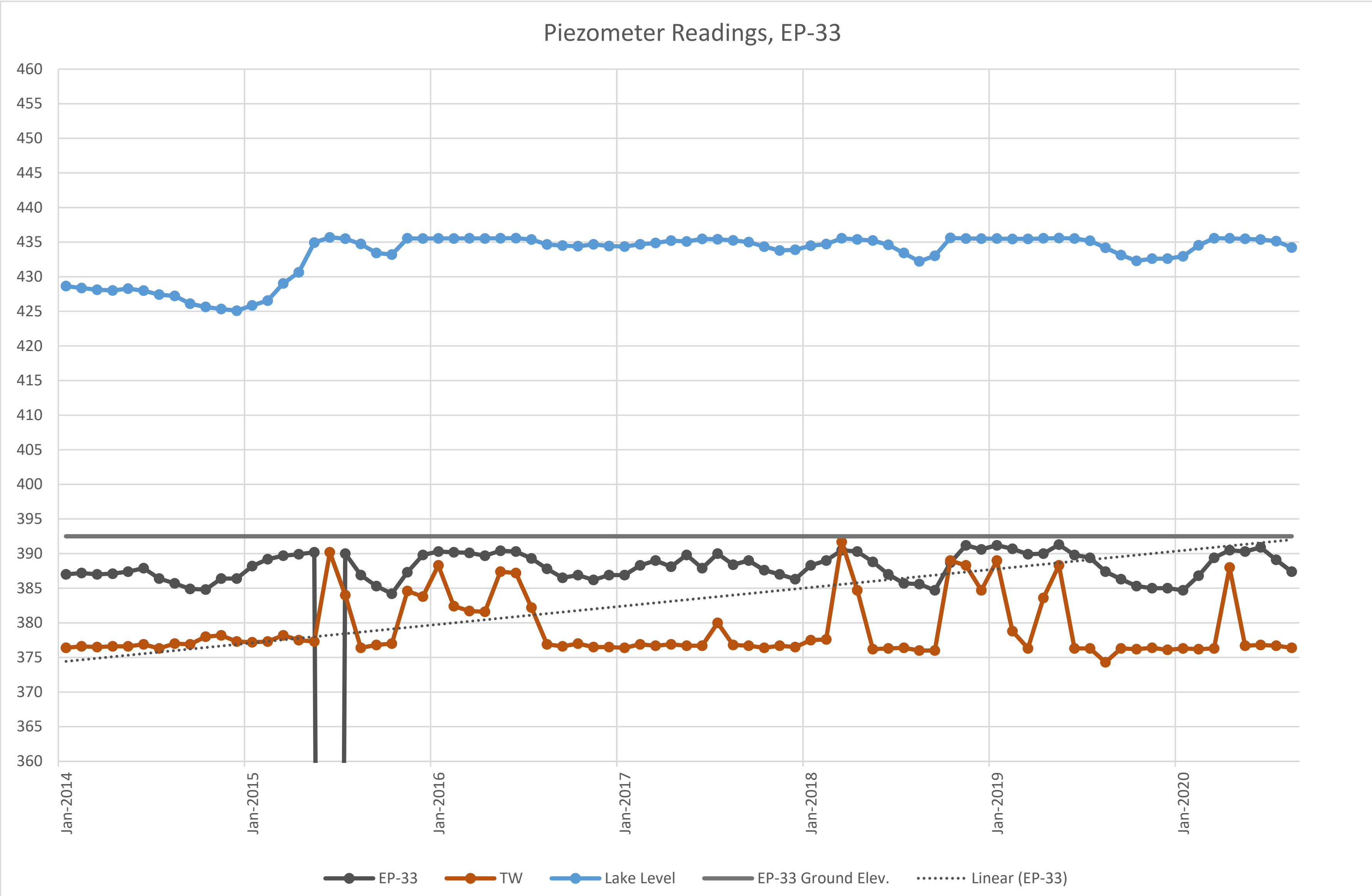
Piezometer Readings, EP-33
460
455
450
445
440
435
430
425
420
415
410
405
400
395
390
385
380
375
370
365
360
Jan-2014
Jan-2015
Jan-2016
Jan-2017
Jan-2018
Jan-2019
Jan-2020
EP-33
TW
Lake Level
EP-33 Ground Elev.
Linear (EP-33)

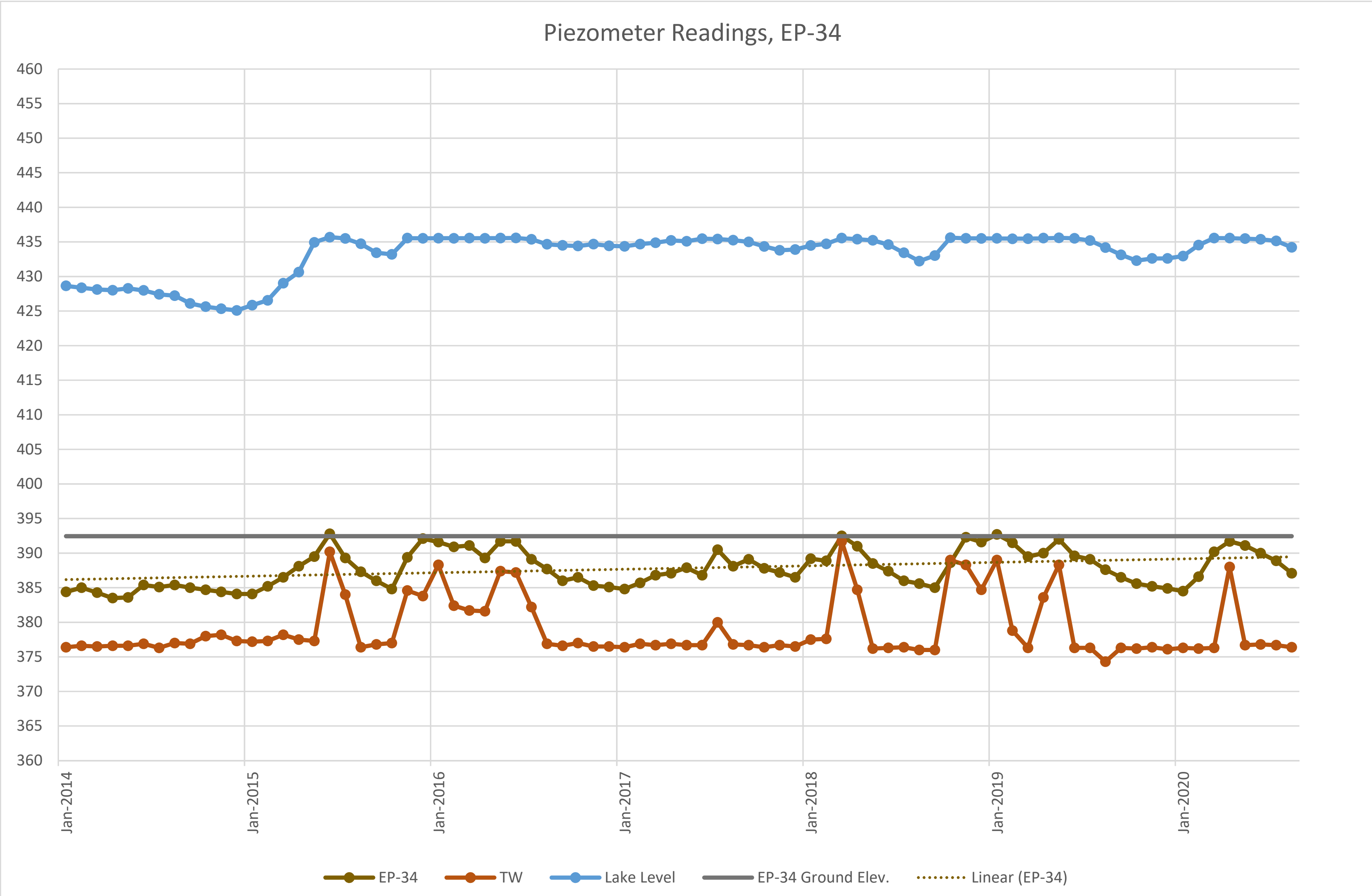

Piezometer Readings, EP-34
460
455
450
445
440
435
430
425
420
415
410
405
400
395
390
385
380
375
370
365
360
Jan-2014
Jan-2015
Jan-2016
Jan-2017
Jan-2018
Jan-2019
Jan-2020
EP-34
TW
Lake Level
EP-34 Ground Elev.
Linear (EP-34)

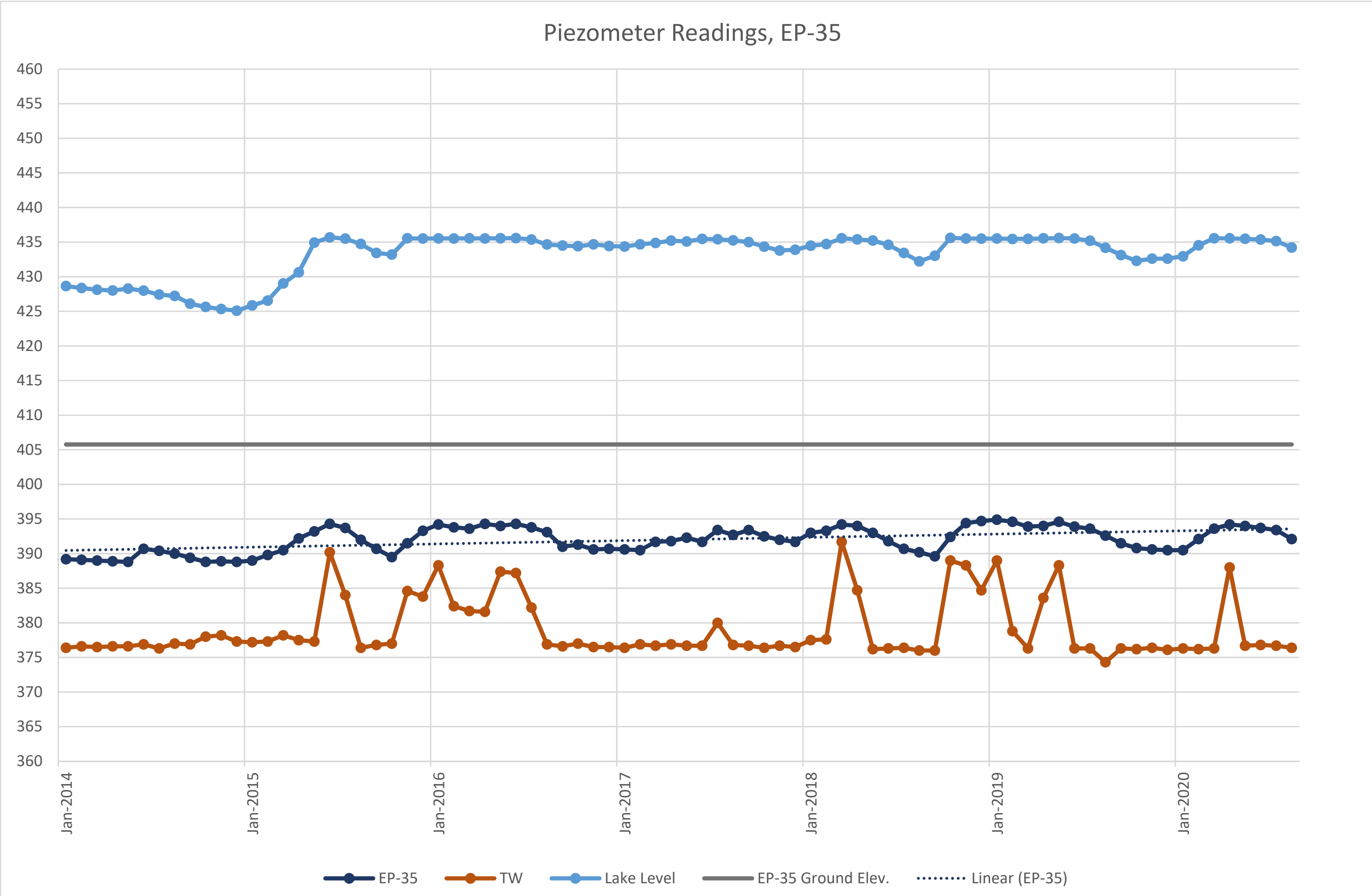
Piezometer Readings, EP-35
460
455
450
445
440
435
430
425
420
415
410
405
400
395
390
385
380
375
370
365
360
Jan-2014
Jan-2015
Jan-2016
Jan-2017
Jan-2018
Jan-2019
Jan-2020
EP-35
TW
Lake Level
EP-35 Ground Elev.
Linear (EP-35)

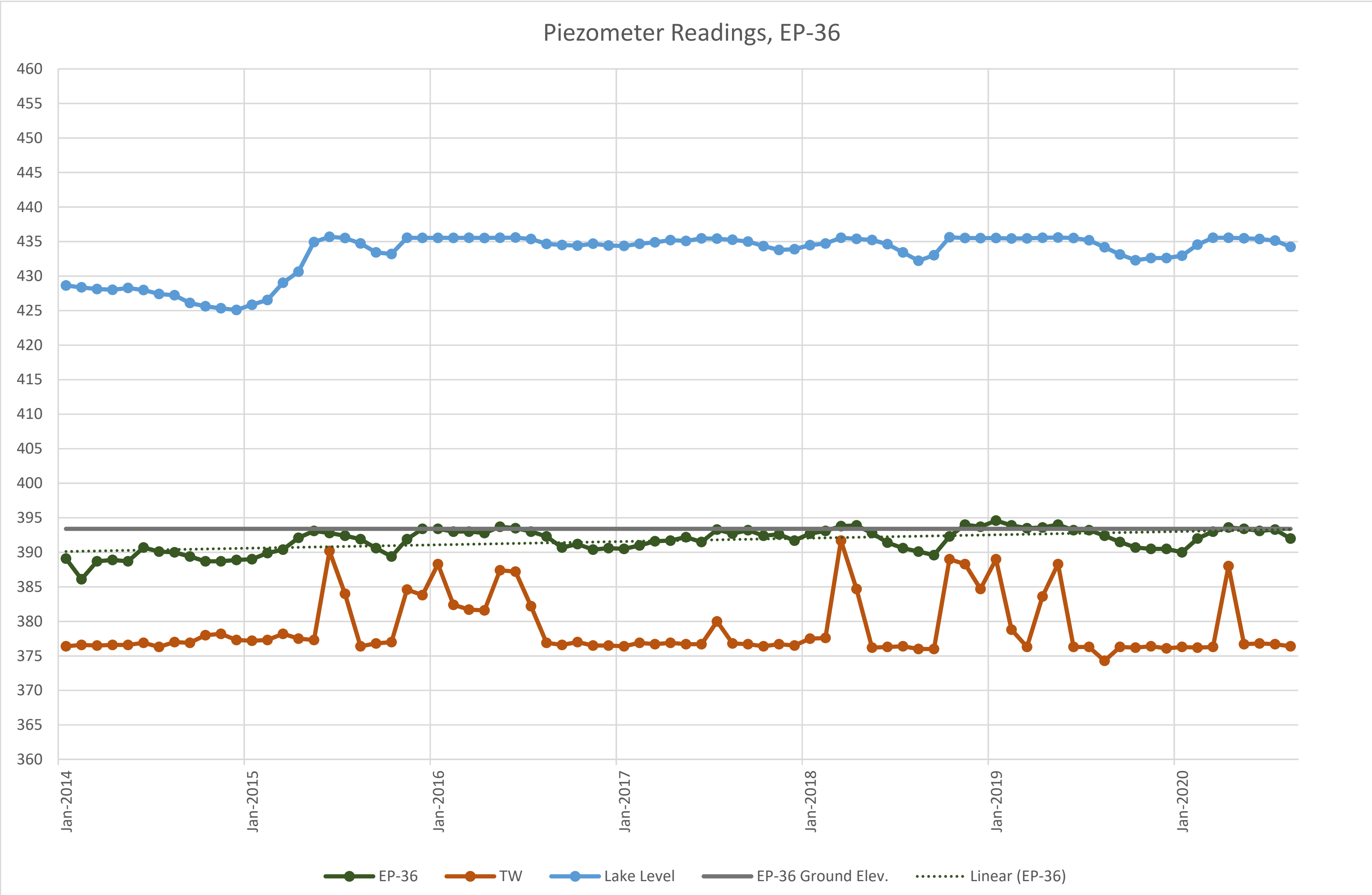
Piezometer Readings, EP-36
460
455
450
445
440
435
430
425
420
415
410
405
400
395
390
385
380
375
370
365
360
Jan-2014
Jan-2015
Jan-2016
Jan-2017
Jan-2018
Jan-2019
Jan-2020
EP-36
TW
Lake Level
EP-36 Ground Elev.
Linear (EP-36)

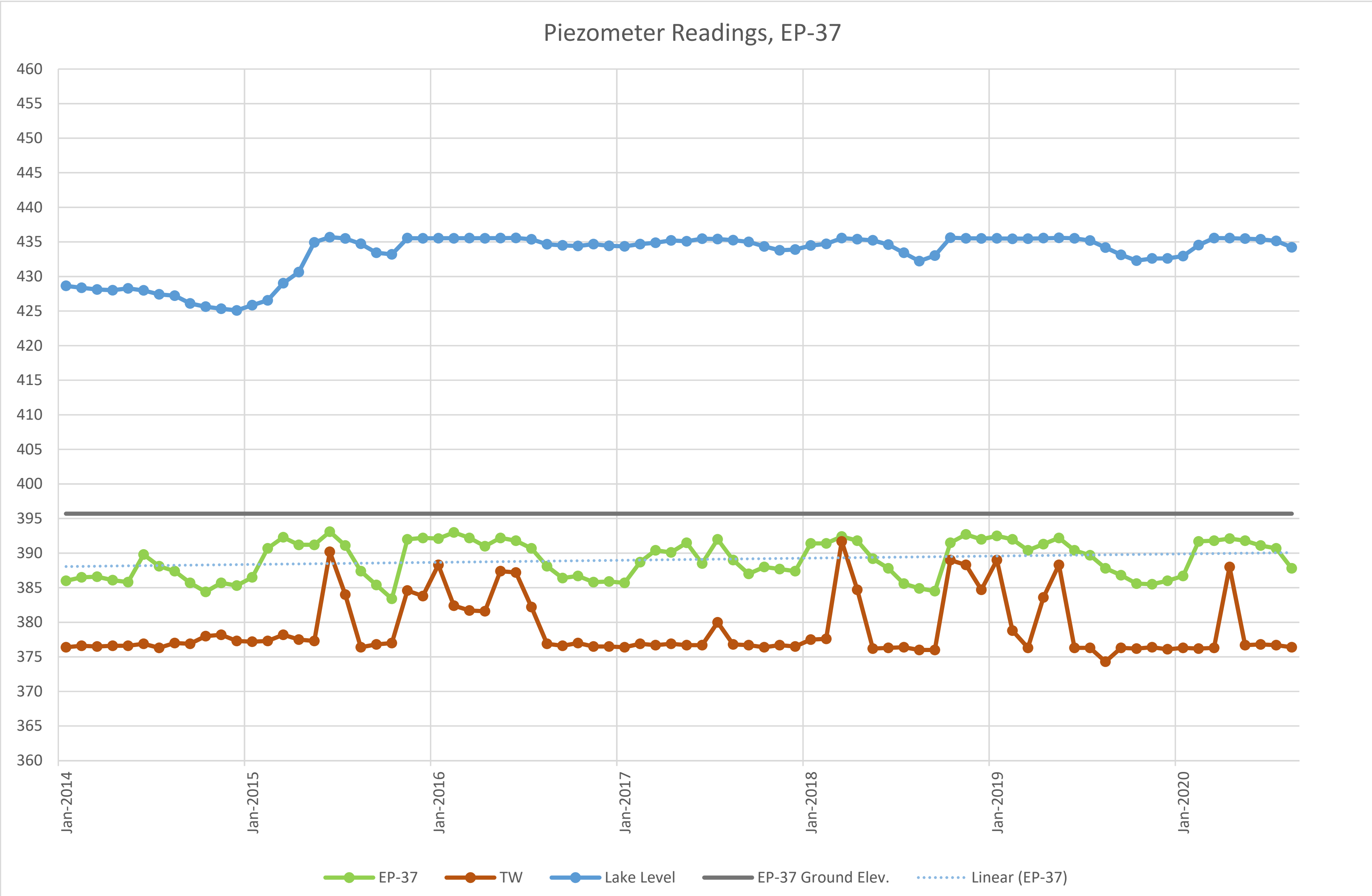

Piezometer Readings, EP-37
460
455
450
445
440
435
430
425
420
415
410
405
400
395
390
385
380
375
370
365
360
Jan-2014
Jan-2015
Jan-2016
Jan-2017
Jan-2018
Jan-2019
Jan-2020
EP-37
TW
Lake Level
EP-37 Ground Elev.
Linear (EP-37)

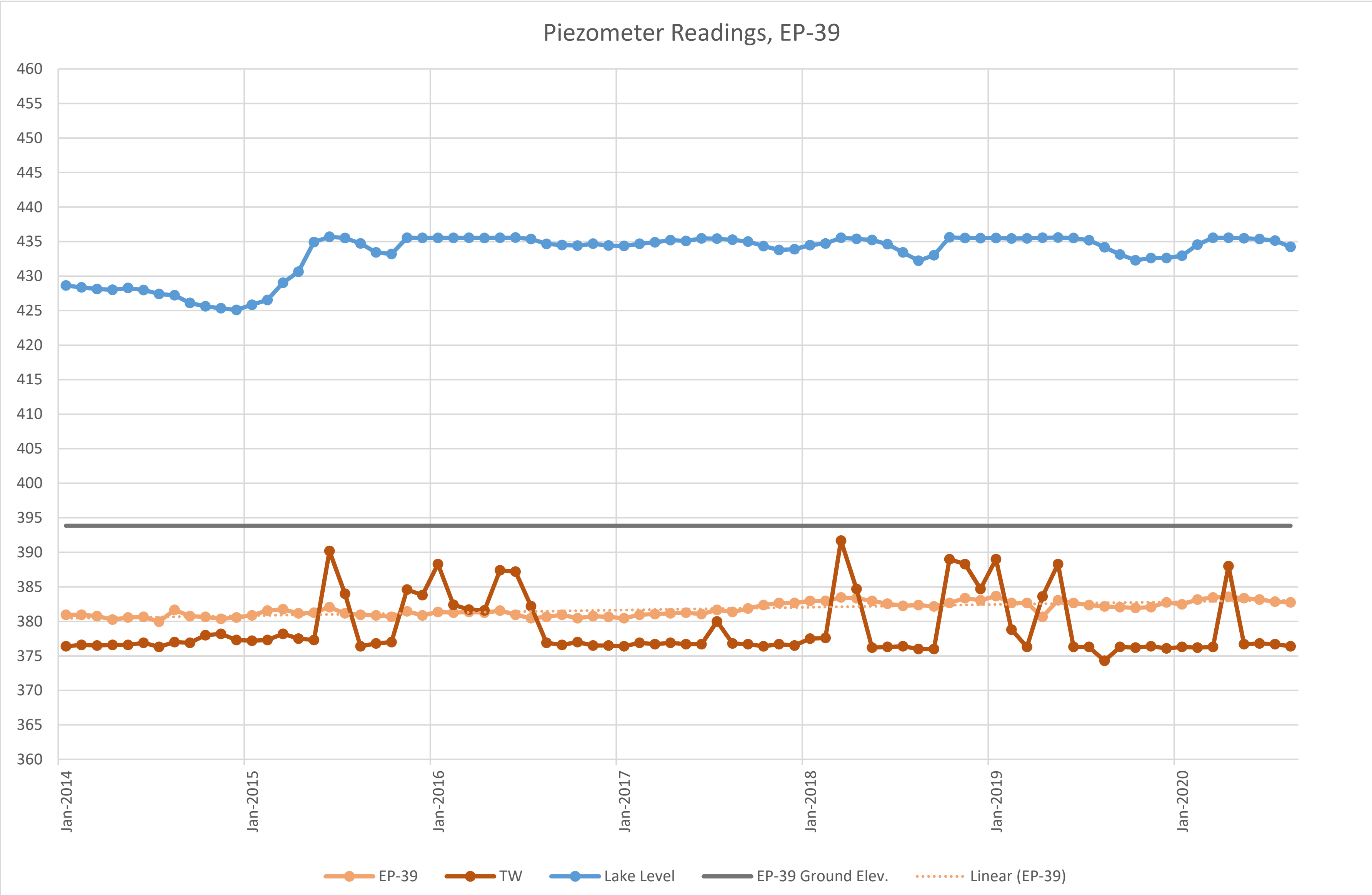

Piezometer Readings, EP-39
460
455
450
445
440
435
430
425
420
415
410
405
400
395
390
385
380
375
370
365
360
Jan-2014
Jan-2015
Jan-2016
Jan-2017
Jan-2018
Jan-2019
Jan-2020
EP-39
TW
Lake Level
EP-39 Ground Elev.
Linear (EP-39)

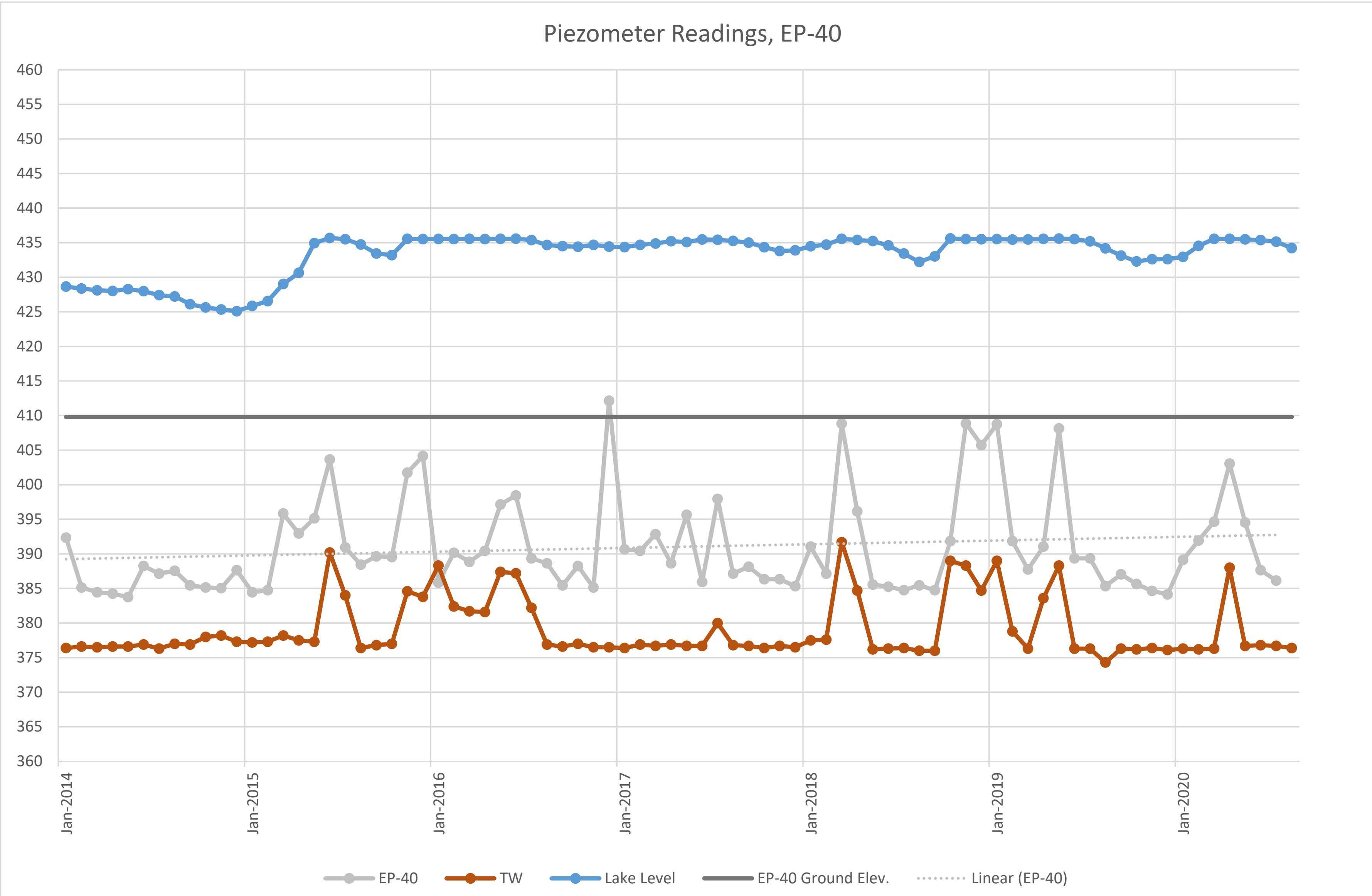

Piezometer Readings, EP-40
460
455
450
445
440
435
430
425
420
415
410
405
400
395
390
385
380
375
370
365
360
Jan-2014
Jan-2015
Jan-2016
Jan-2017
Jan-2018
Jan-2019
Jan-2020
EP-40
TW
Lake Level
EP-40 Ground Elev.
Linear (EP-40)

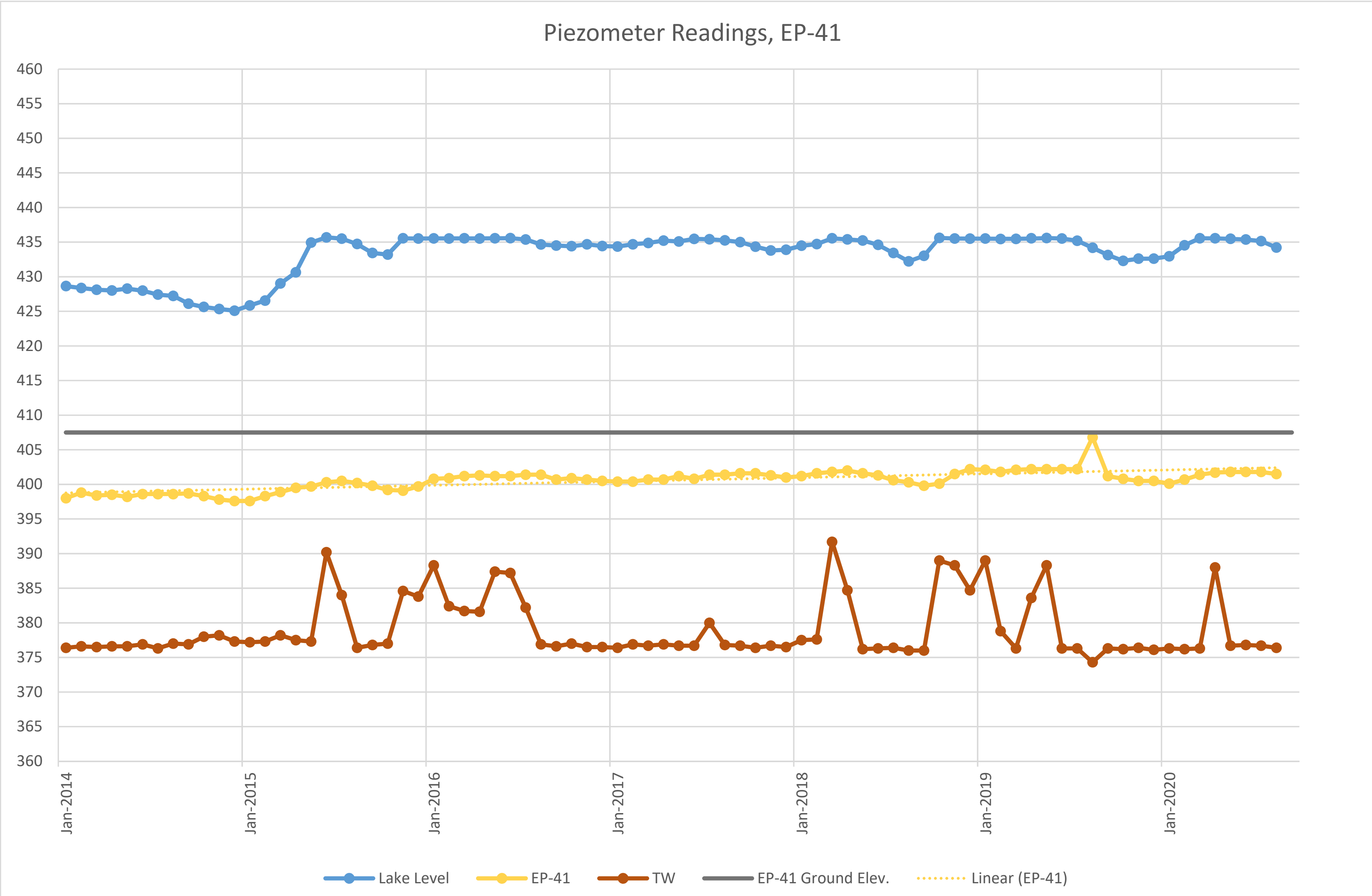
Piezometer Readings, EP-41
460
455
450
445
440
435
430
425
420
415
410
405
400
395
390
385
380
375
370
365
360
Jan-2014
Jan-2015
Jan-2016
Jan-2017
Jan-2018
Jan-2019
Jan-2020
Lake Level
EP-41
TW
EP-41 Ground Elev.
Linear (EP-41)

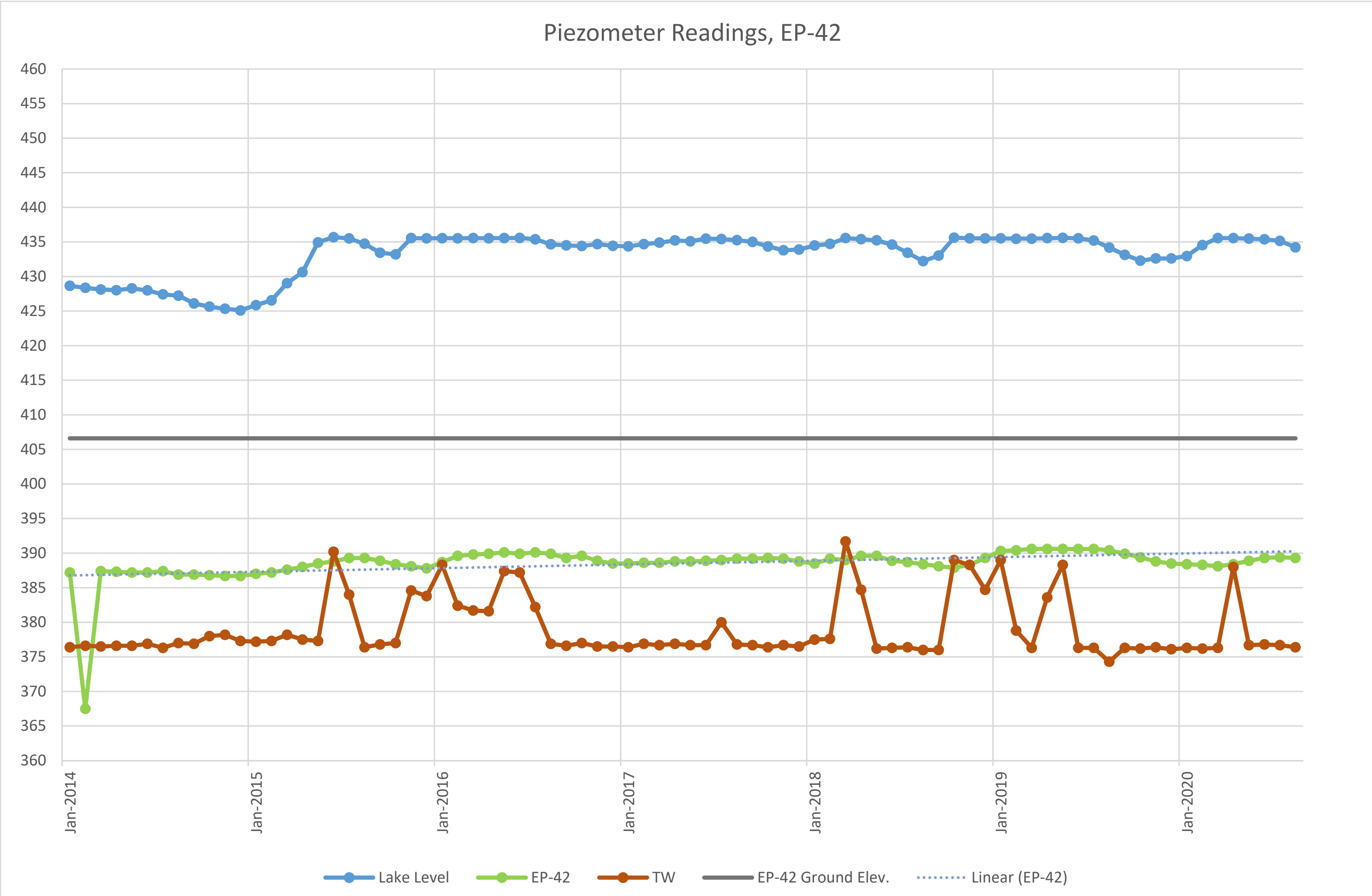
Piezometer Readings, EP-42
460
455
450
445
440
435
430
425
420
415
410
405
400
395
390
385
380
375
370
365
360
Jan-2014
Jan-2015
Jan-2016
Jan-2017
Jan-2018
Jan-2019
Jan-2020
Lake Level
EP-42
TW
EP-42 Ground Elev.
Linear (EP-42)

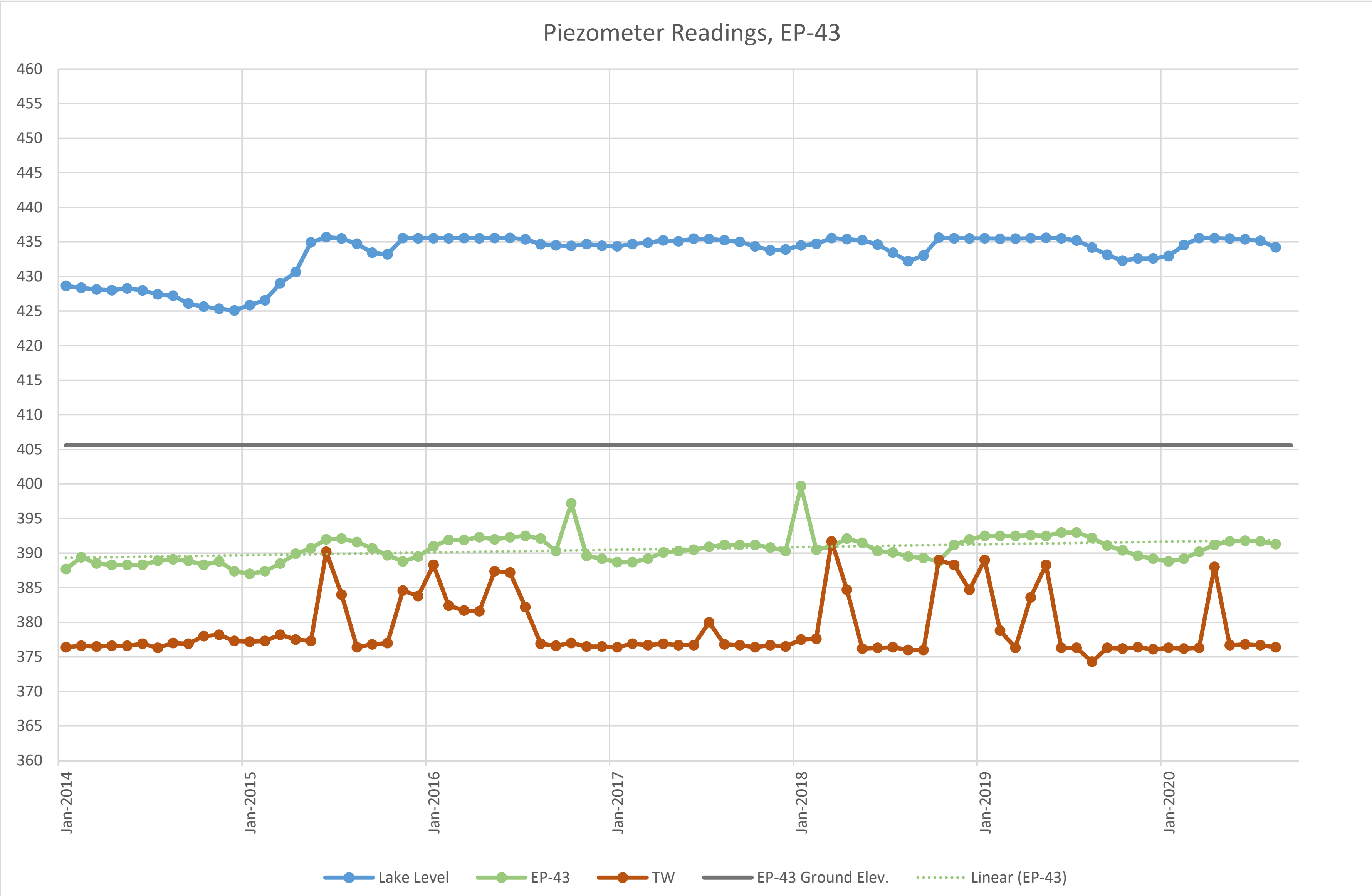
Piezometer Readings, EP-43
460
455
450
445
440
435
430
425
420
415
410
405
400
395
390
385
380
375
370
365
360
Jan-2014
Jan-2015
Jan-2016
Jan-2017
Jan-2018
Jan-2019
Jan-2020
Lake Level
EP-43
TW
EP-43 Ground Elev.
Linear (EP-43)

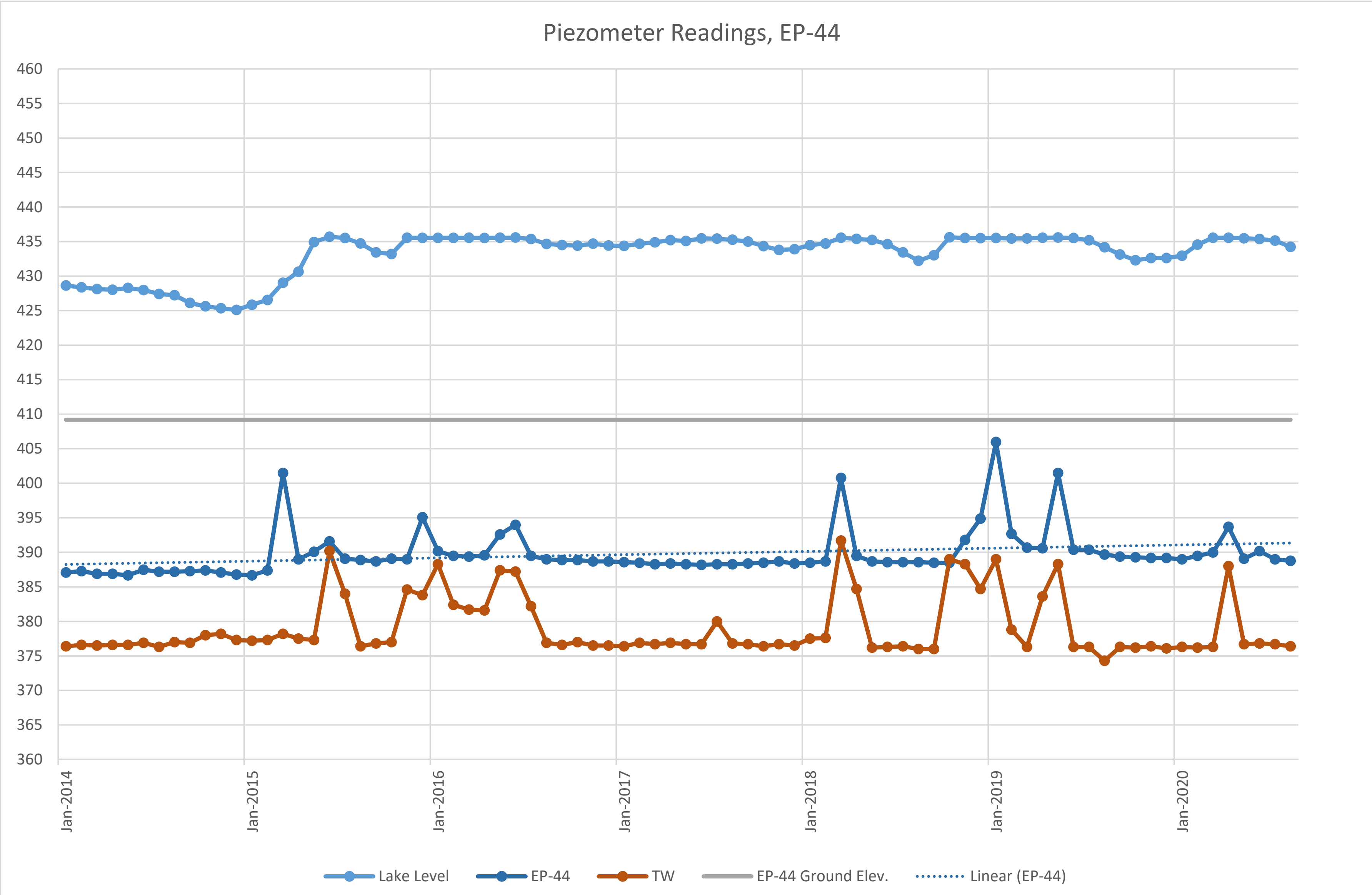

Piezometer Readings, EP-44
460
455
450
445
440
435
430
425
420
415
410
405
400
395
390
385
380
375
370
365
360
Jan-2014
Jan-2015
Jan-2016
Jan-2017
Jan-2018
Jan-2019
Jan-2020
Lake Level
EP-44
TW
EP-44 Ground Elev.
Linear (EP-44)

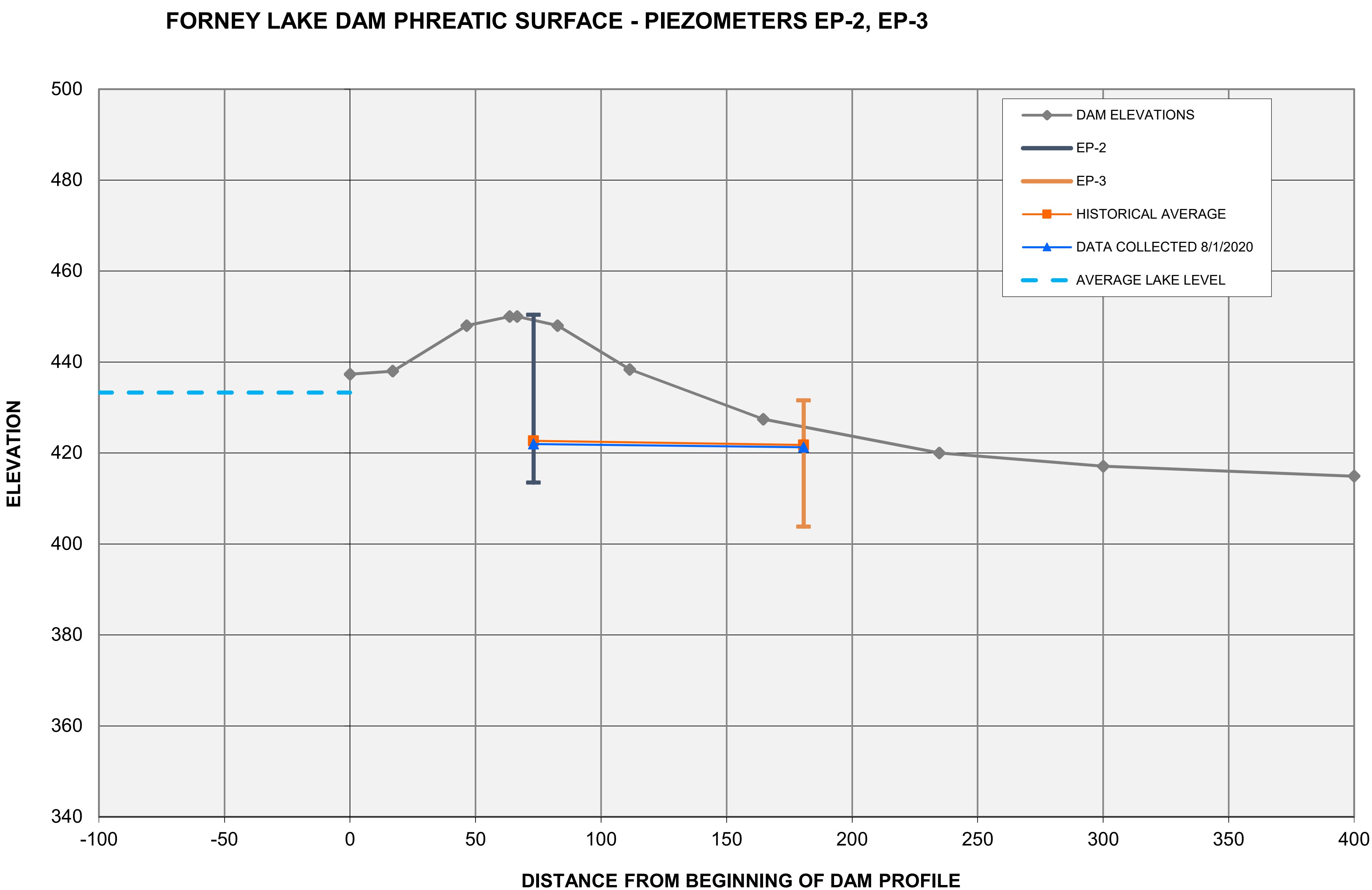
FORNEY LAKE DAM PHREATIC SURFACE - PIEZOMETERS EP-2, EP-3
ELEVATION
500
480
460
440
420
400
380
360
340
-100
-50
0
50
100
150
200
250
300
350
400
DISTANCE FROM BEGINNING OF DAM PROFILE
DAM ELEVATIONS
EP-2
EP-3
HISTORICAL AVERAGE
DATA COLLECTED 8/1/2020
AVERAGE LAKE LEVEL

FORNEY LAKE DAM PHREATIC SURFACE - PIEZOMETERS EP-4, EP-5, EP-6, EP-7

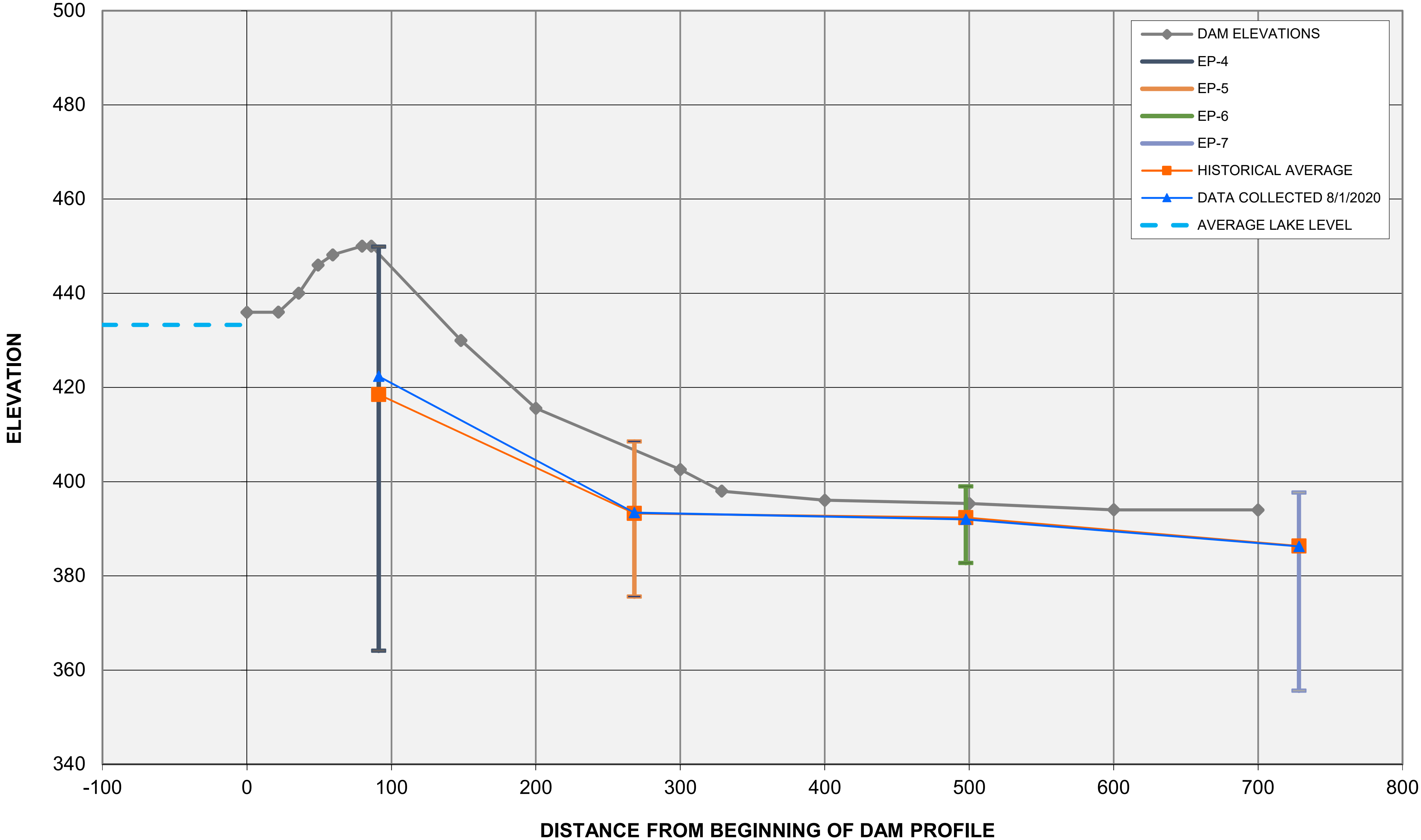

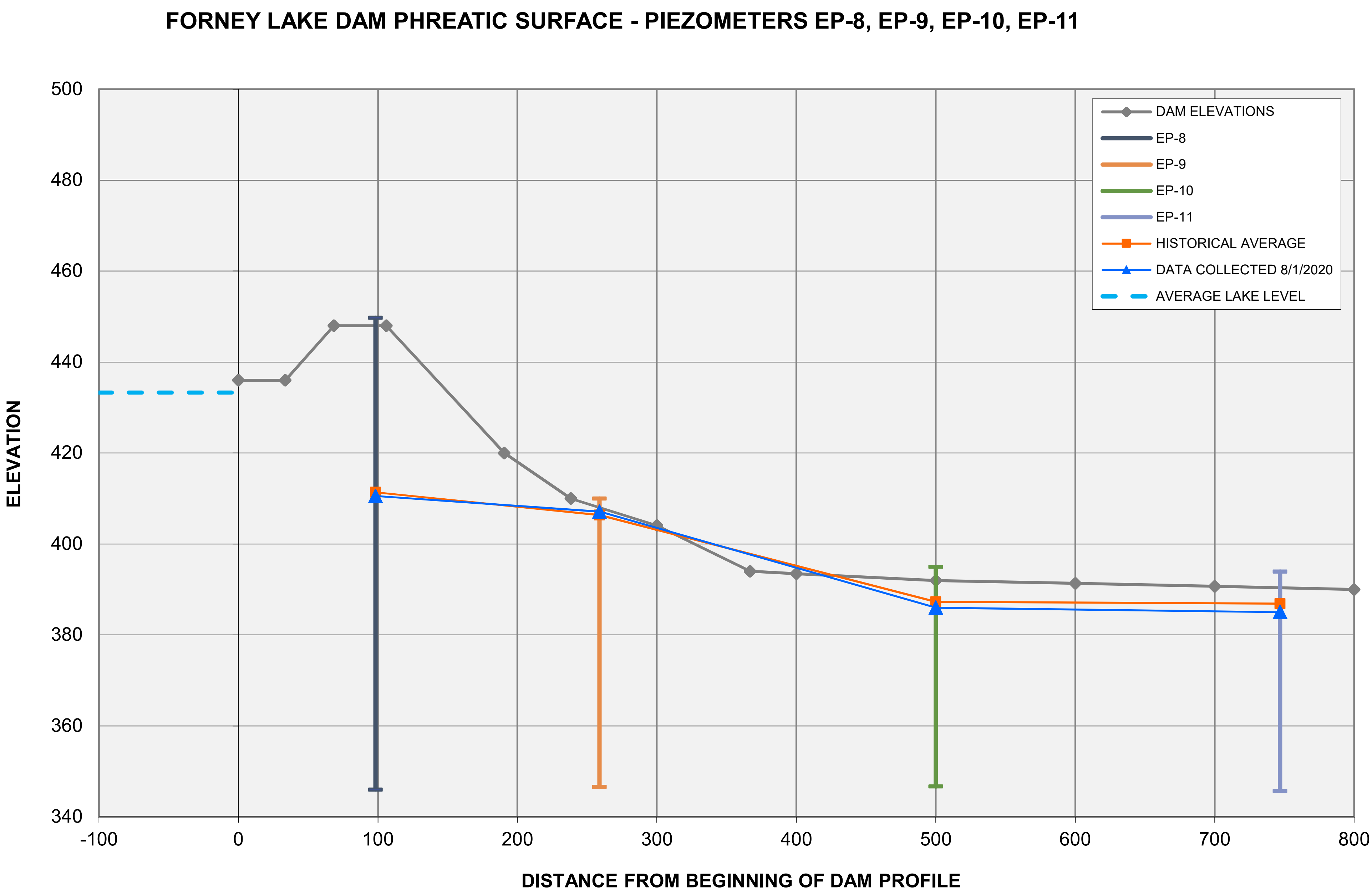
FORNEY LAKE DAM PHREATIC SURFACE - PIEZOMETERS EP-8, EP-9, EP-10, EP-11
ELEVATION
500
480
460
440
420
400
380
360
340
-100
0
100
200
300
400
500
600
700
800
DISTANCE FROM BEGINNING OF DAM PROFILE
DAM ELEVATIONS
EP-8
EP-9
EP-10
EP-11
HISTORICAL AVERAGE
DATA COLLECTED 8/1/2020
AVERAGE LAKE LEVEL

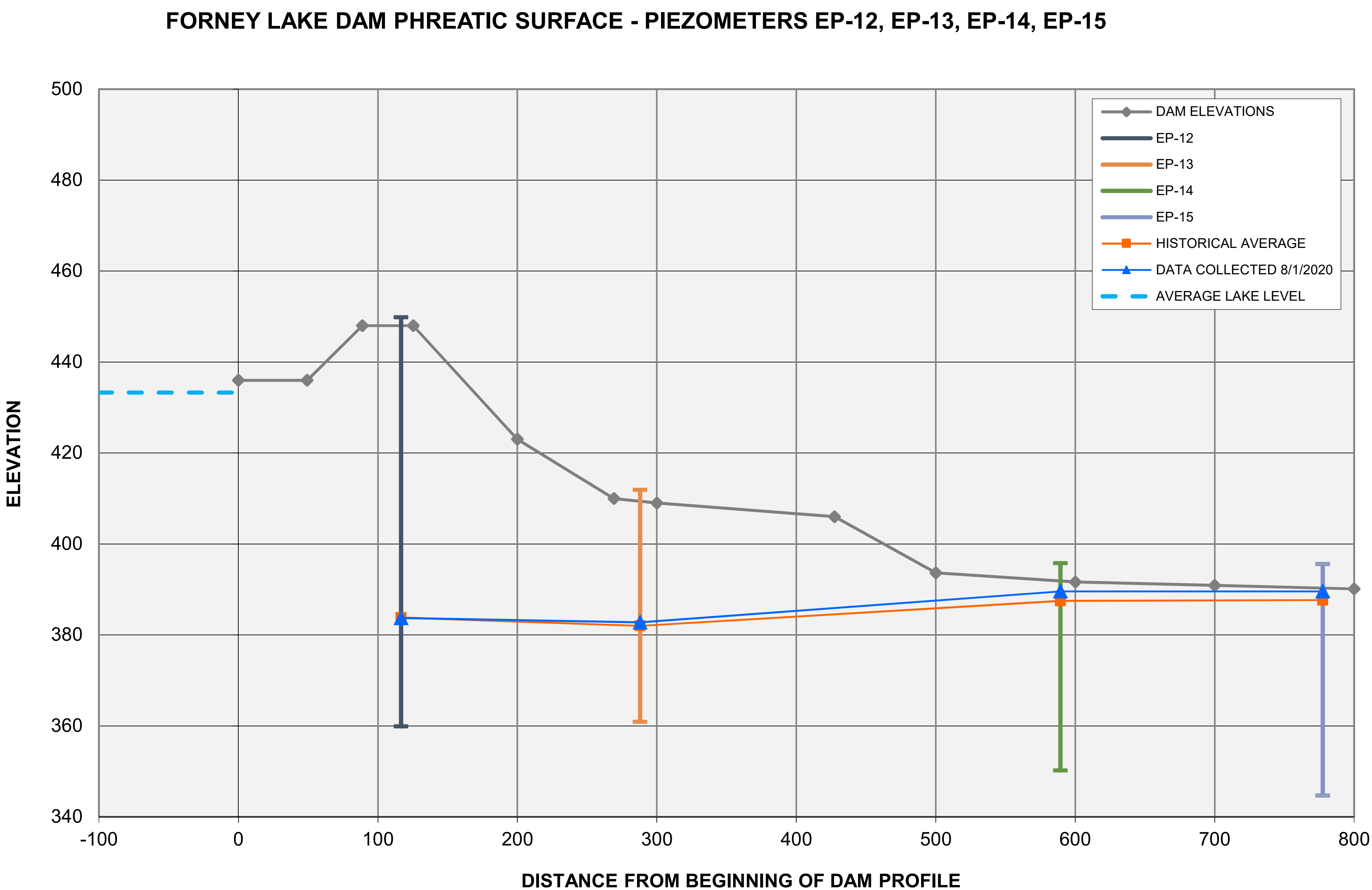
FORNEY LAKE DAM PHREATIC SURFACE - PIEZOMETERS EP-12, EP-13, EP-14, EP-15
ELEVATION
500
480
460
440
420
400
380
360
340
-100
0
100
200
300
400
500
600
700
800
DISTANCE FROM BEGINNING OF DAM PROFILE
DAM ELEVATIONS
EP-12
EP-13
EP-14
EP-15
HISTORICAL AVERAGE
DATA COLLECTED 8/1/2020
AVERAGE LAKE LEVEL

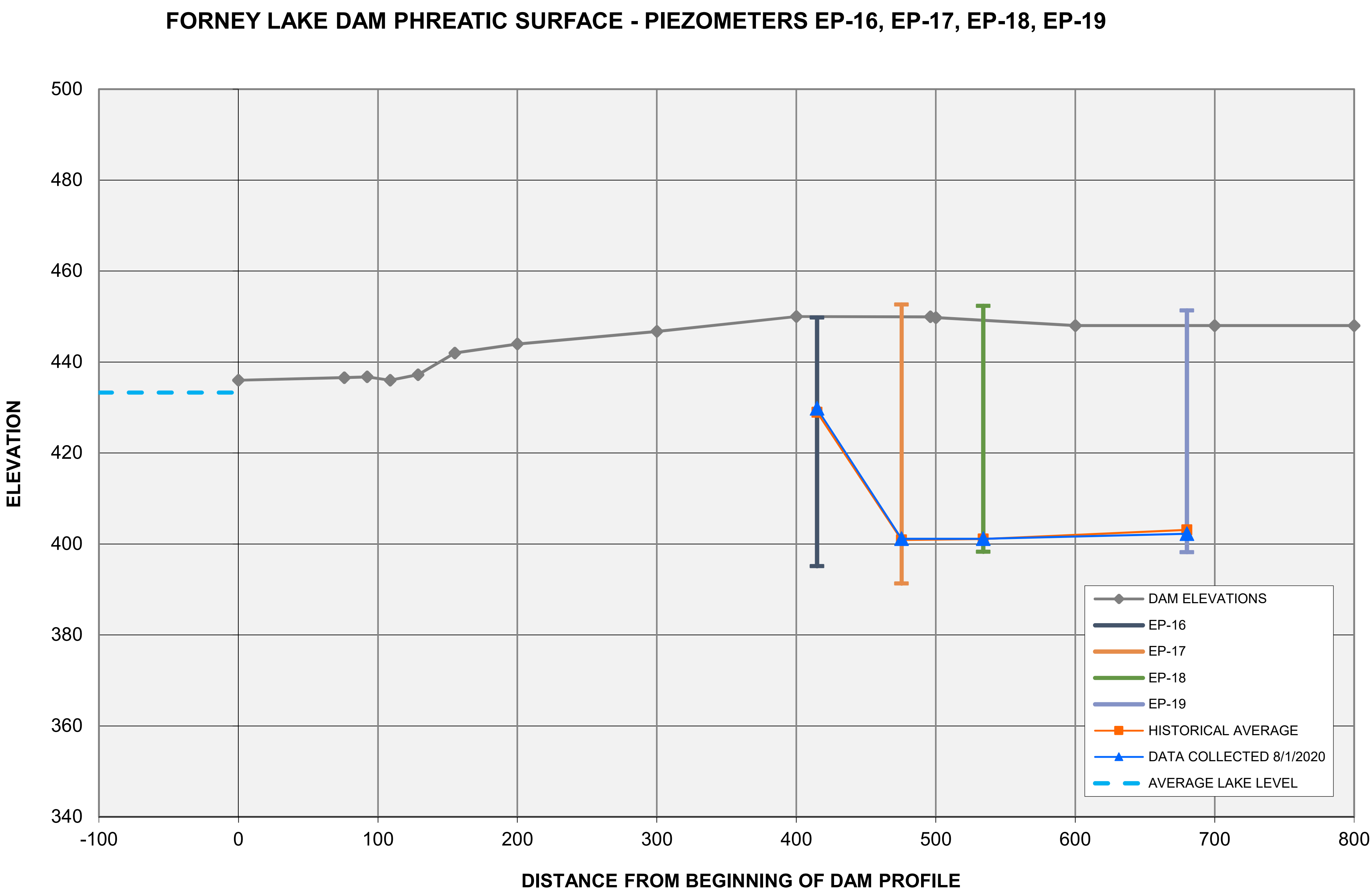
FORNEY LAKE DAM PHREATIC SURFACE - PIEZOMETERS EP-16, EP-17, EP-18, EP-19
ELEVATION
500
480
460
440
420
400
380
360
340
-100
0
100
200
300
400
500
600
700
800
DISTANCE FROM BEGINNING OF DAM PROFILE
DAM ELEVATIONS
EP-16
EP-17
EP-18
EP-19
HISTORICAL AVERAGE
DATA COLLECTED 8/1/2020
AVERAGE LAKE LEVEL

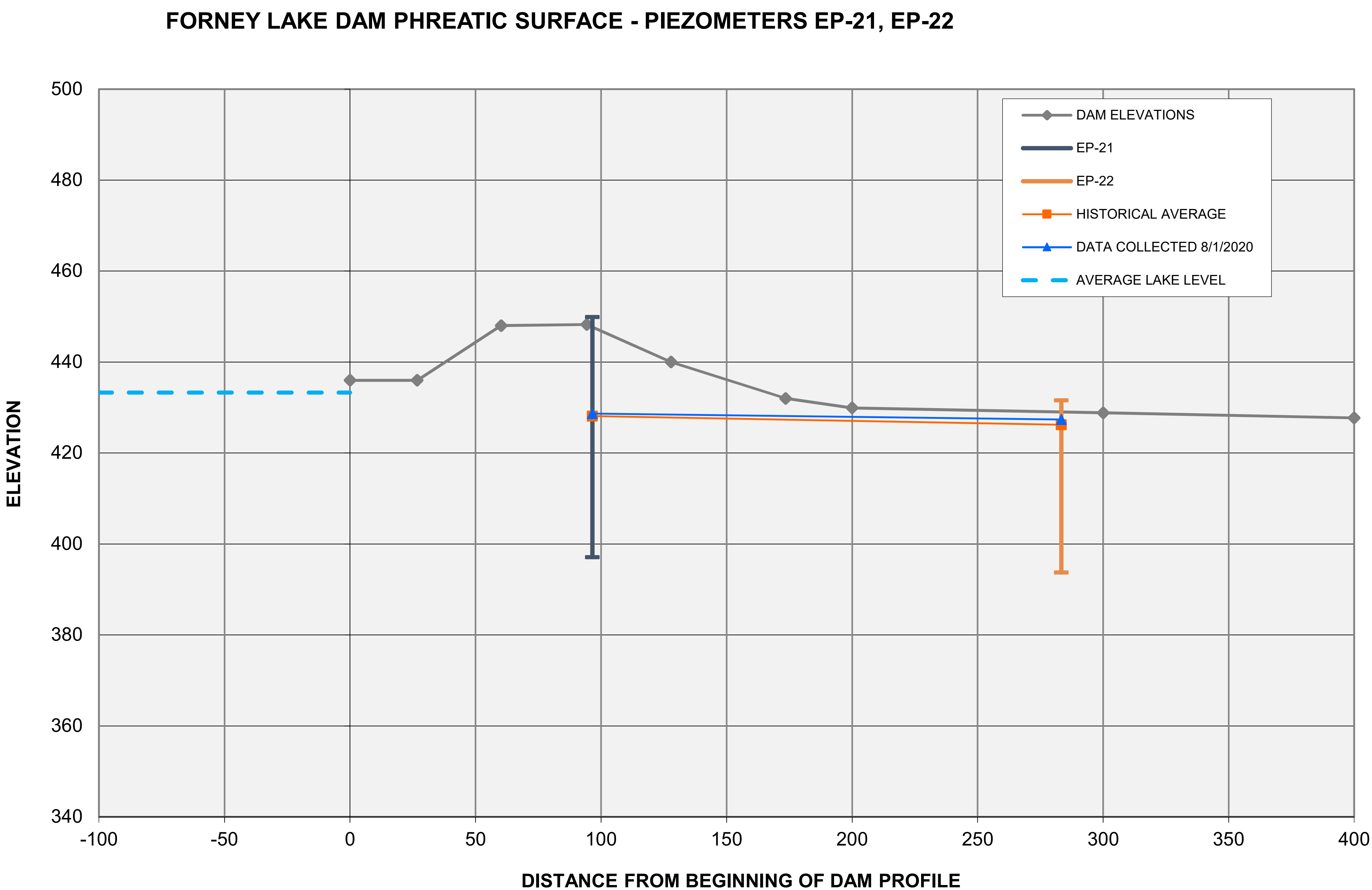
FORNEY LAKE DAM PHREATIC SURFACE - PIEZOMETERS EP-21, EP-22
DAM ELEVATIONS
EP-21
EP-22
HISTORICAL AVERAGE
DATA COLLECTED 8/1/2020
AVERAGE LAKE LEVEL
ELEVATION
500
480
460
440
420
400
380
360
340
-100
-50
0
50
100
150
200
250
300
350
400
DISTANCE FROM BEGINNING OF DAM PROFILE

FORNEY LAKE DAM PHREATIC SURFACE - PIEZOMETERS EP-26, EP-27

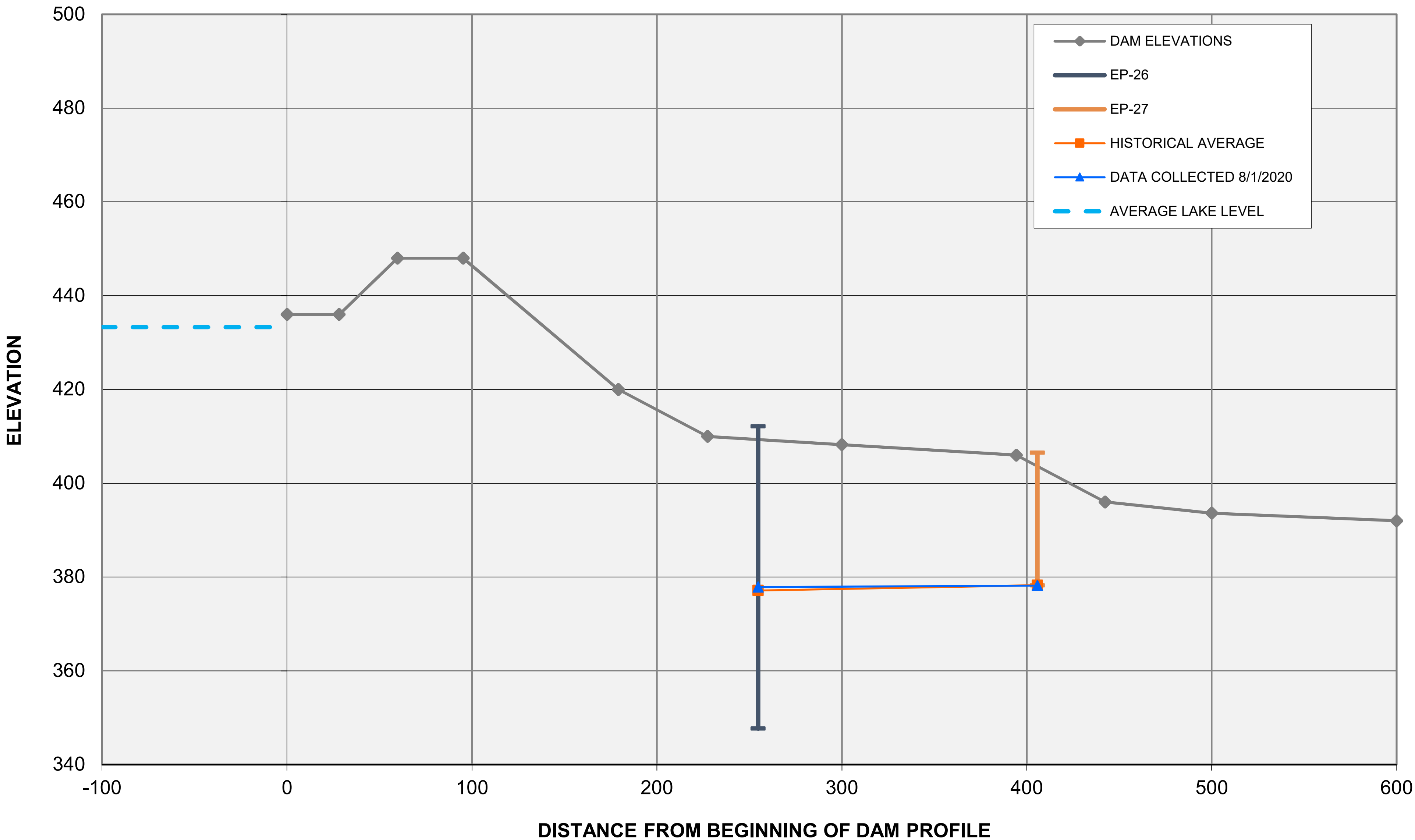

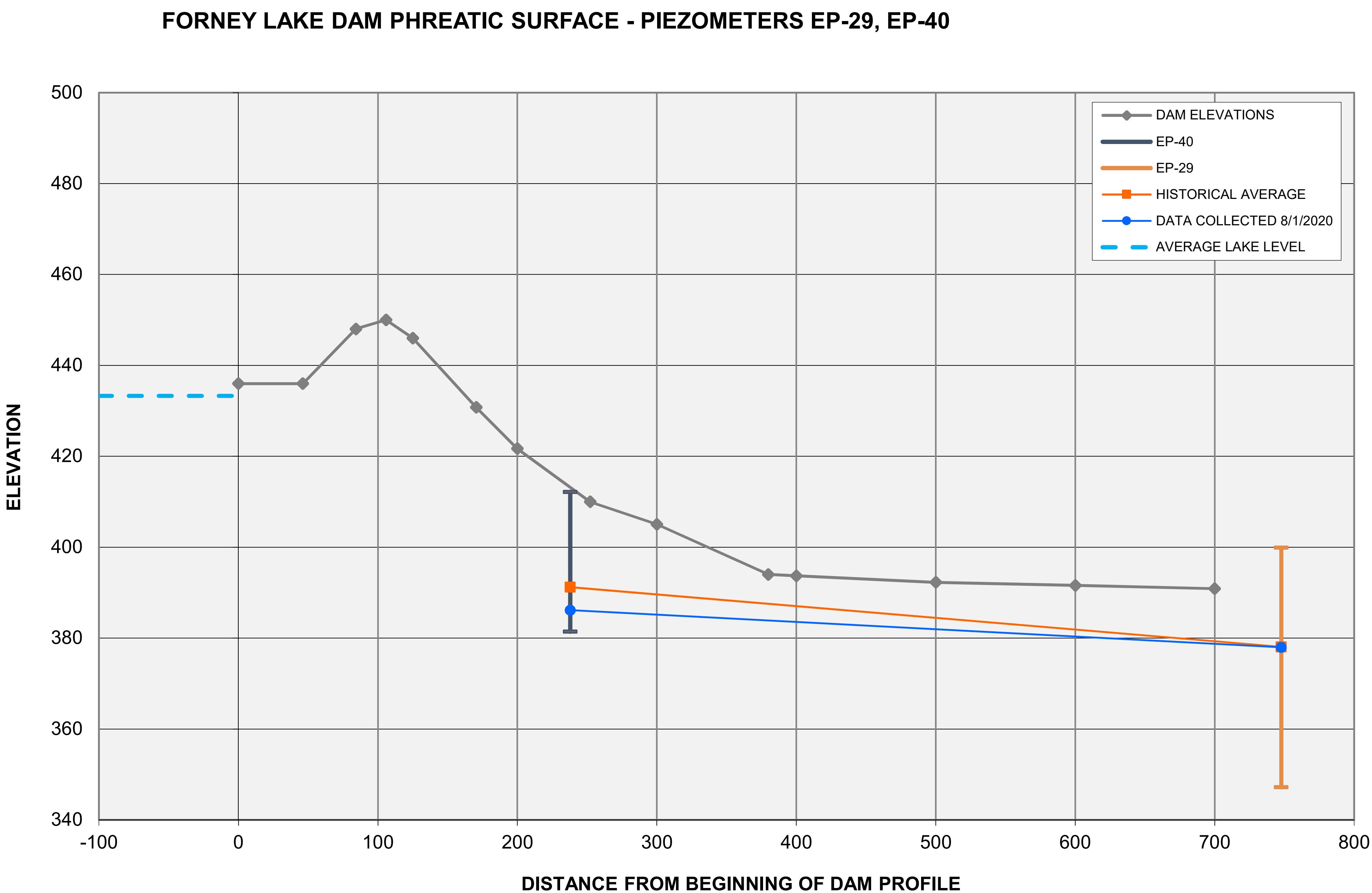
FORNEY LAKE DAM PHREATIC SURFACE - PIEZOMETERS EP-29, EP-40
ELEVATION
DISTANCE FROM BEGINNING OF DAM PROFILE
500
480
460
440
420
400
380
360
340
-100
0
100
200
300
400
500
600
700
800
DAM ELEVATIONS
EP-40
EP-29
HISTORICAL AVERAGE
DATA COLLECTED 8/1/2020
AVERAGE LAKE LEVEL

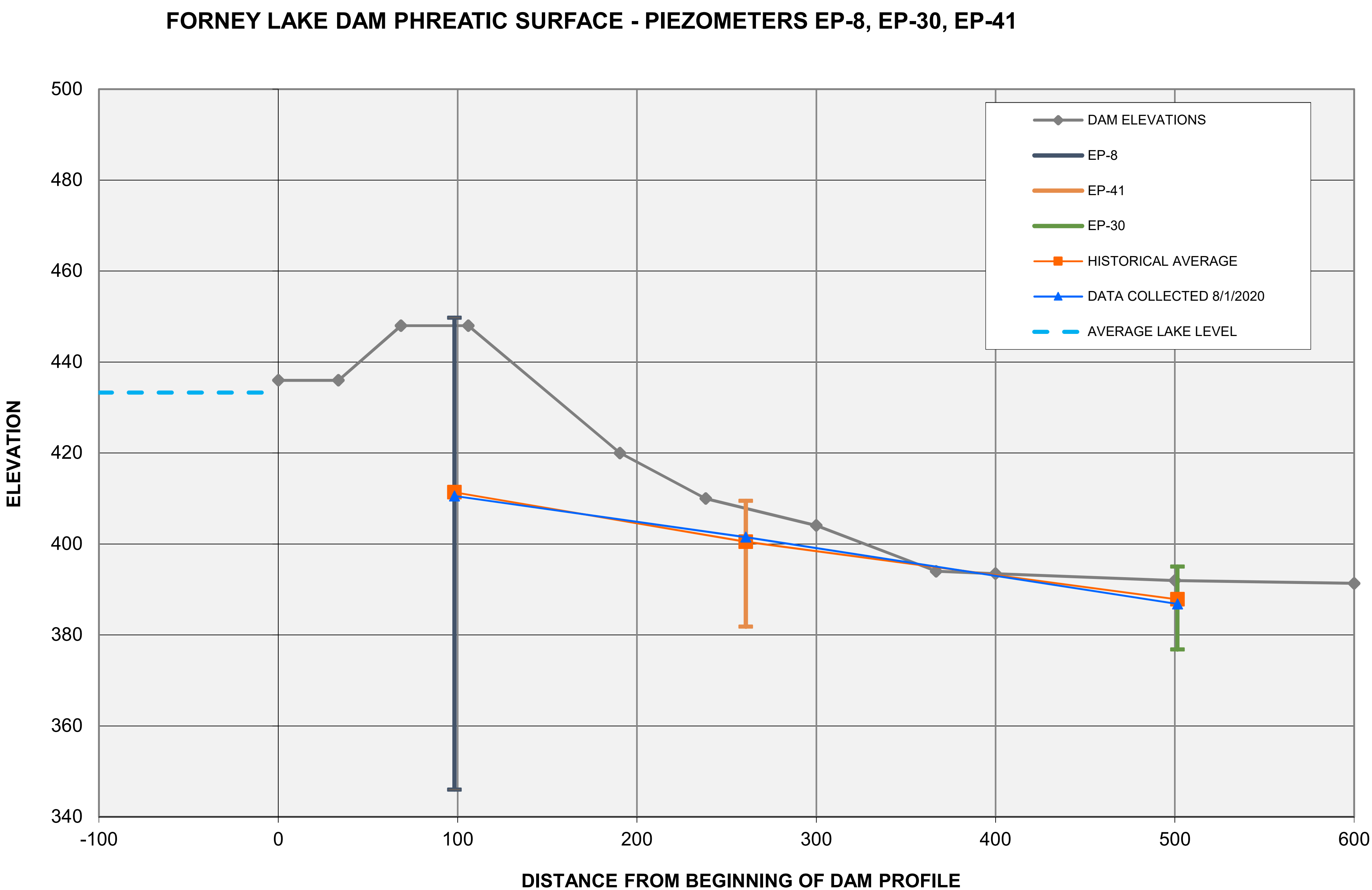
FORNEY LAKE DAM PHREATIC SURFACE - PIEZOMETERS EP-8, EP-30, EP-41
ELEVATION
500
480
460
440
420
400
380
360
340
-100
0
100
200
300
400
500
600
DISTANCE FROM BEGINNING OF DAM PROFILE
DAM ELEVATIONS
EP-8
EP-41
EP-30
HISTORICAL AVERAGE
DATA COLLECTED 8/1/2020
AVERAGE LAKE LEVEL

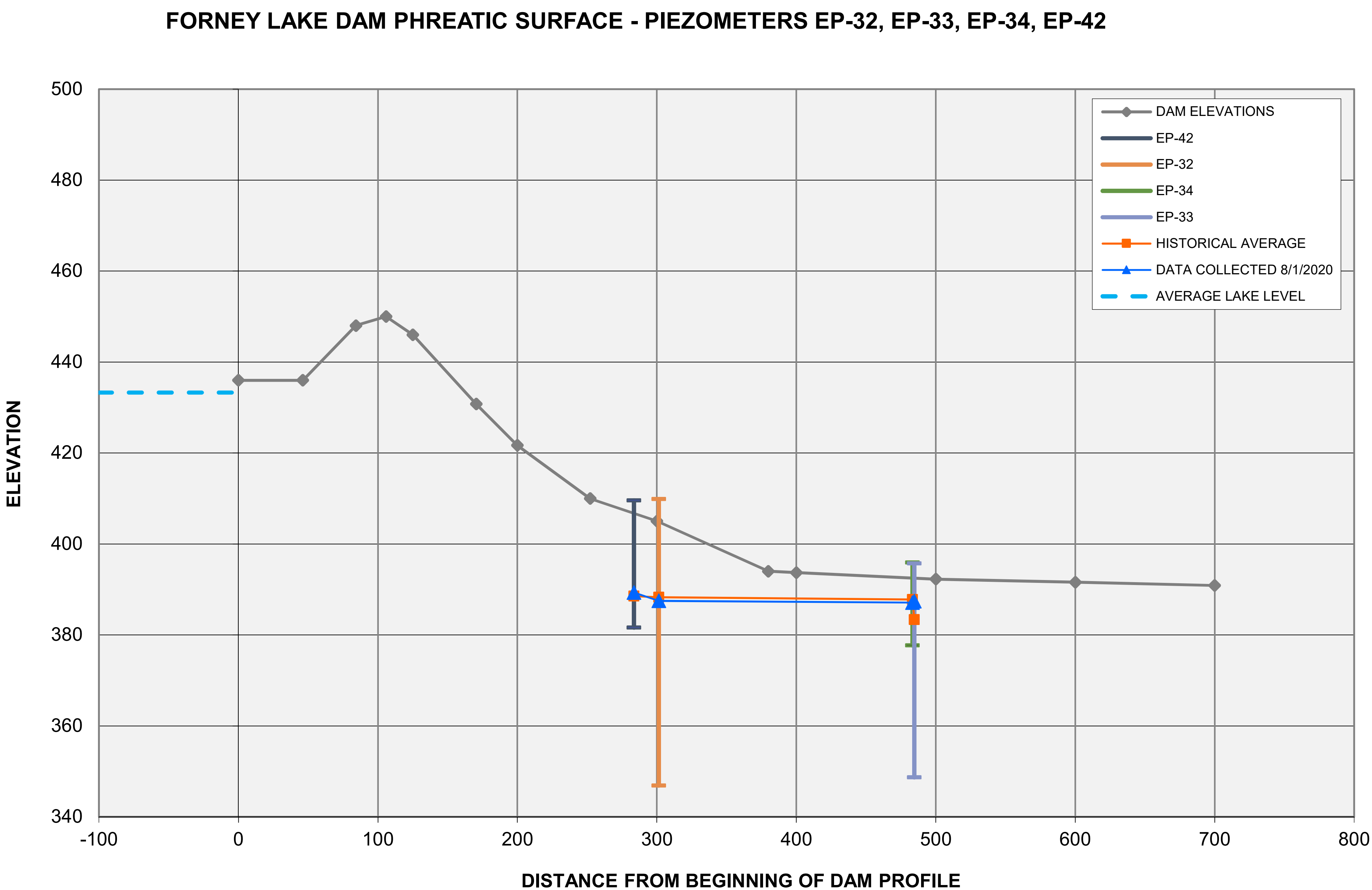
FORNEY LAKE DAM PHREATIC SURFACE - PIEZOMETERS EP-32, EP-33, EP-34, EP-42
ELEVATION
DISTANCE FROM BEGINNING OF DAM PROFILE
500
480
460
440
420
400
380
360
340
-100
0
100
200
300
400
500
600
700
800
DAM ELEVATIONS
EP-42
EP-32
EP-34
EP-33
HISTORICAL AVERAGE
DATA COLLECTED 8/1/2020
AVERAGE LAKE LEVEL

FORNEY LAKE DAM PHREATIC SURFACE - PIEZOMETERS EP-35, EP-36, EP-37

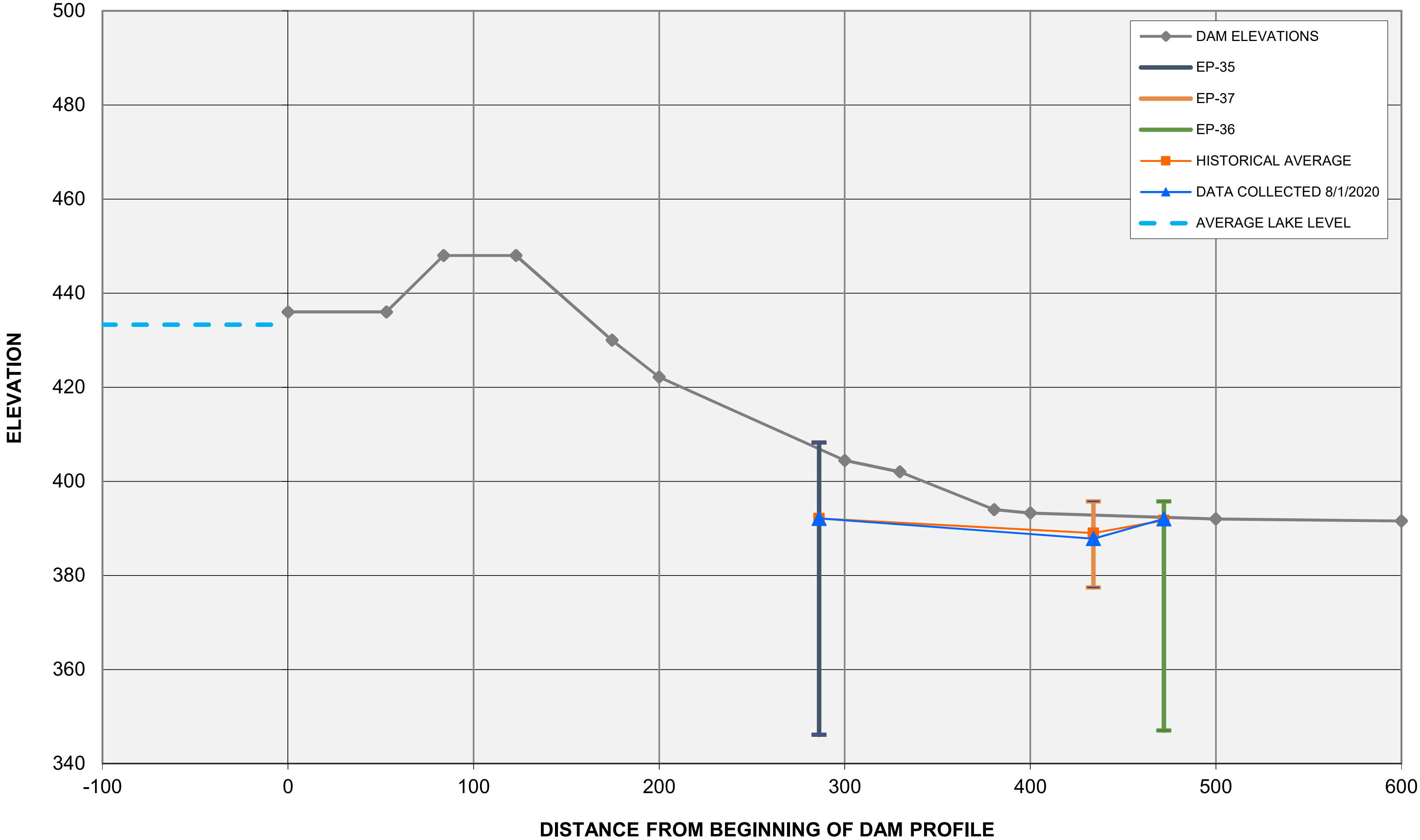

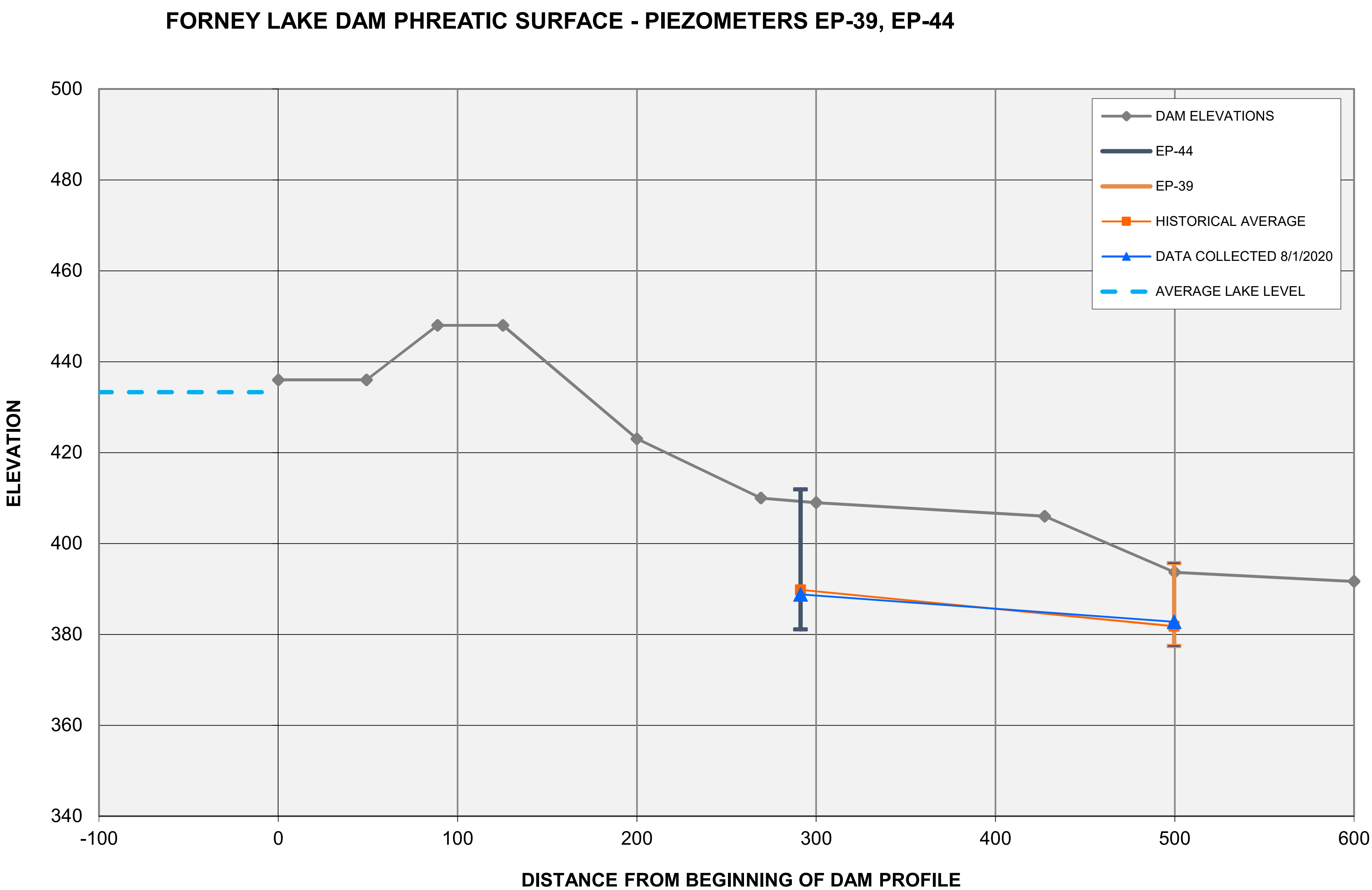
FORNEY LAKE DAM PHREATIC SURFACE - PIEZOMETERS EP-39, EP-44
ELEVATION
500
480
460
440
420
400
380
360
340
-100
0
100
200
300
400
500
600
DISTANCE FROM BEGINNING OF DAM PROFILE
DAM ELEVATIONS
EP-44
EP-39
HISTORICAL AVERAGE
DATA COLLECTED 8/1/2020
AVERAGE LAKE LEVEL

FORNEY LAKE DAM PHREATIC SURFACE - PIEZOMETERS EP-2, EP-3

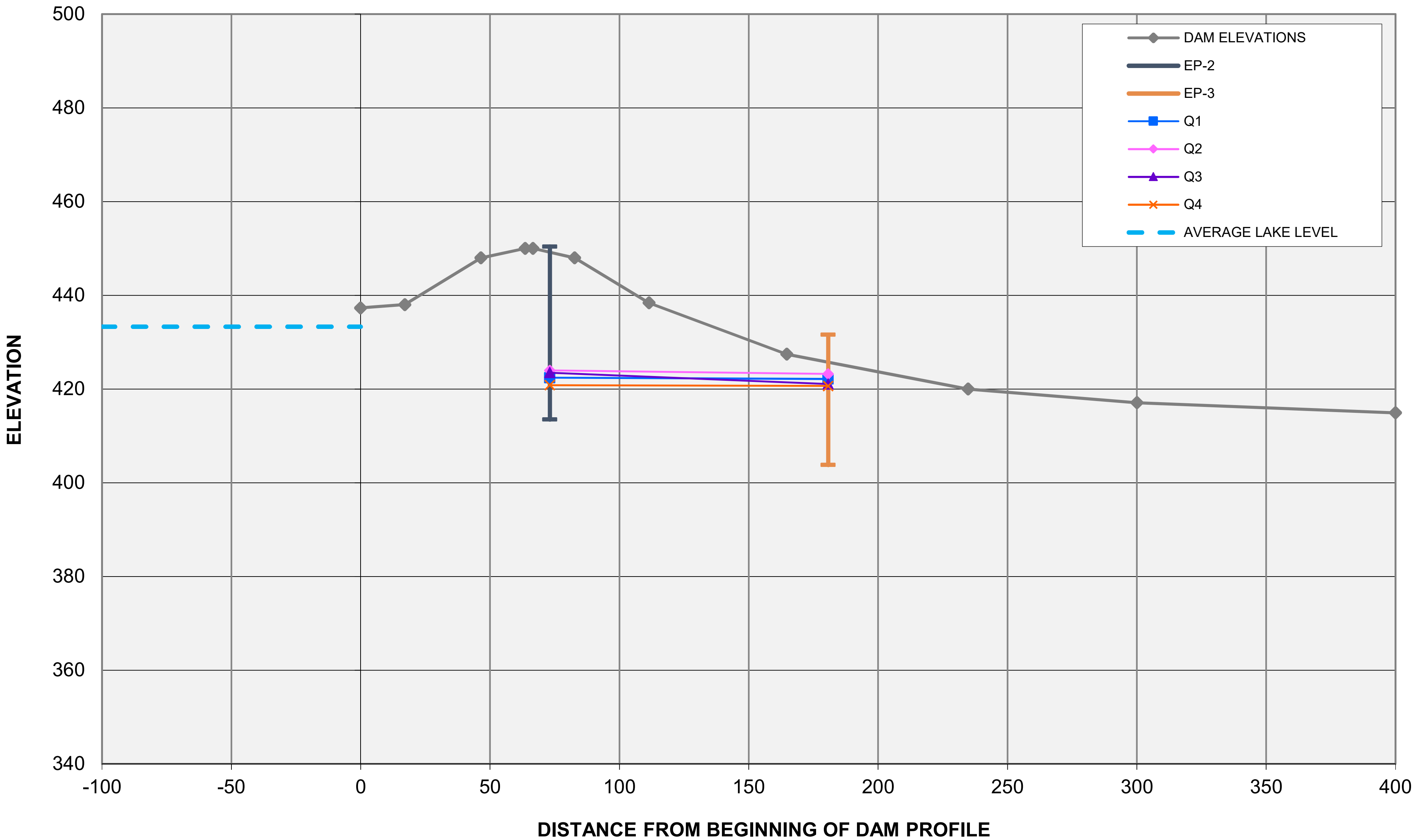

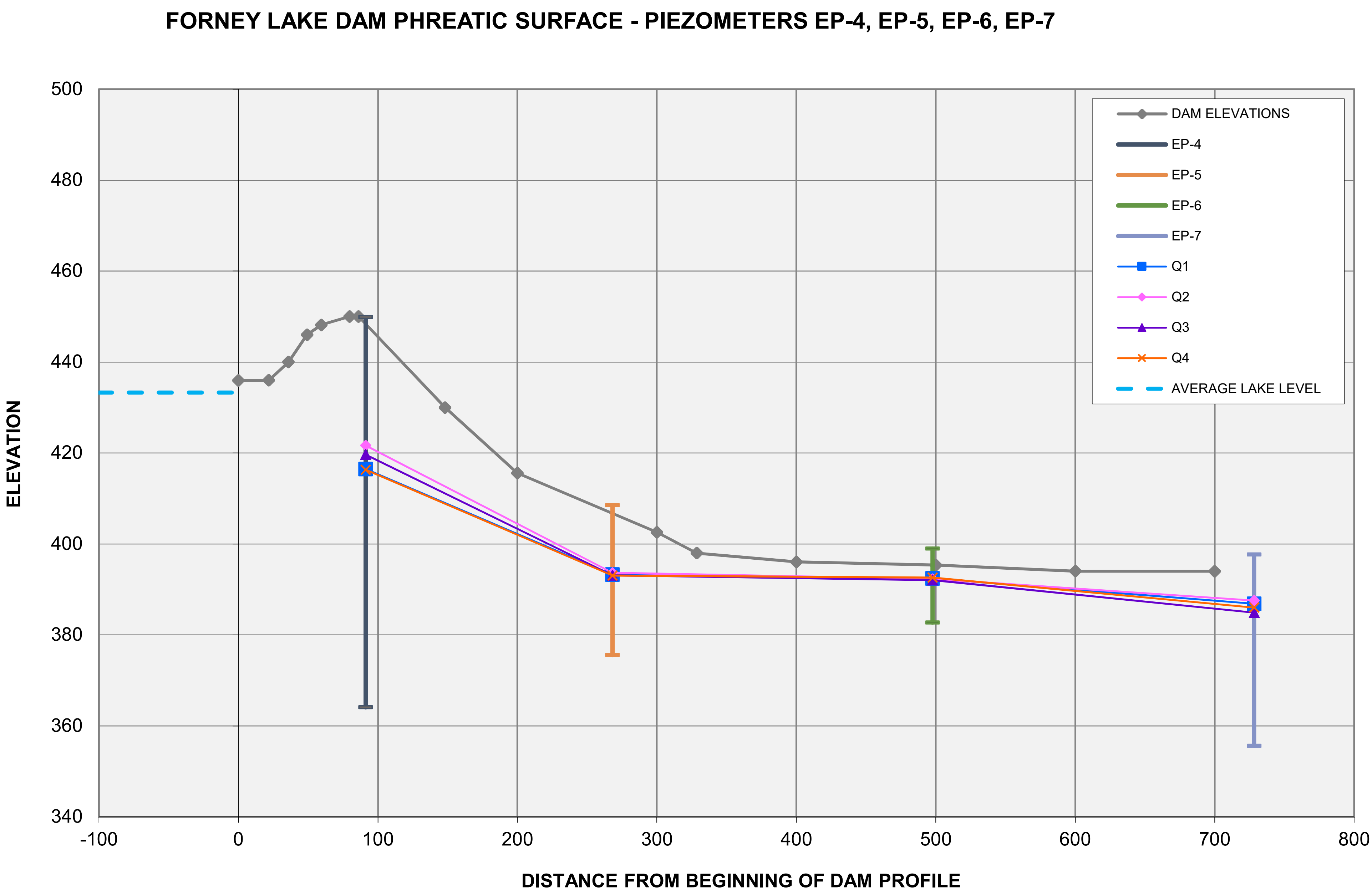
FORNEY LAKE DAM PHREATIC SURFACE - PIEZOMETERS EP-4, EP-5, EP-6, EP-7
ELEVATION
500
480
460
440
420
400
380
360
340
-100
0
100
200
300
400
500
600
700
800
DISTANCE FROM BEGINNING OF DAM PROFILE
DAM ELEVATIONS
EP-4
EP-5
EP-6
EP-7
Q1
Q2
Q3
Q4
AVERAGE LAKE LEVEL

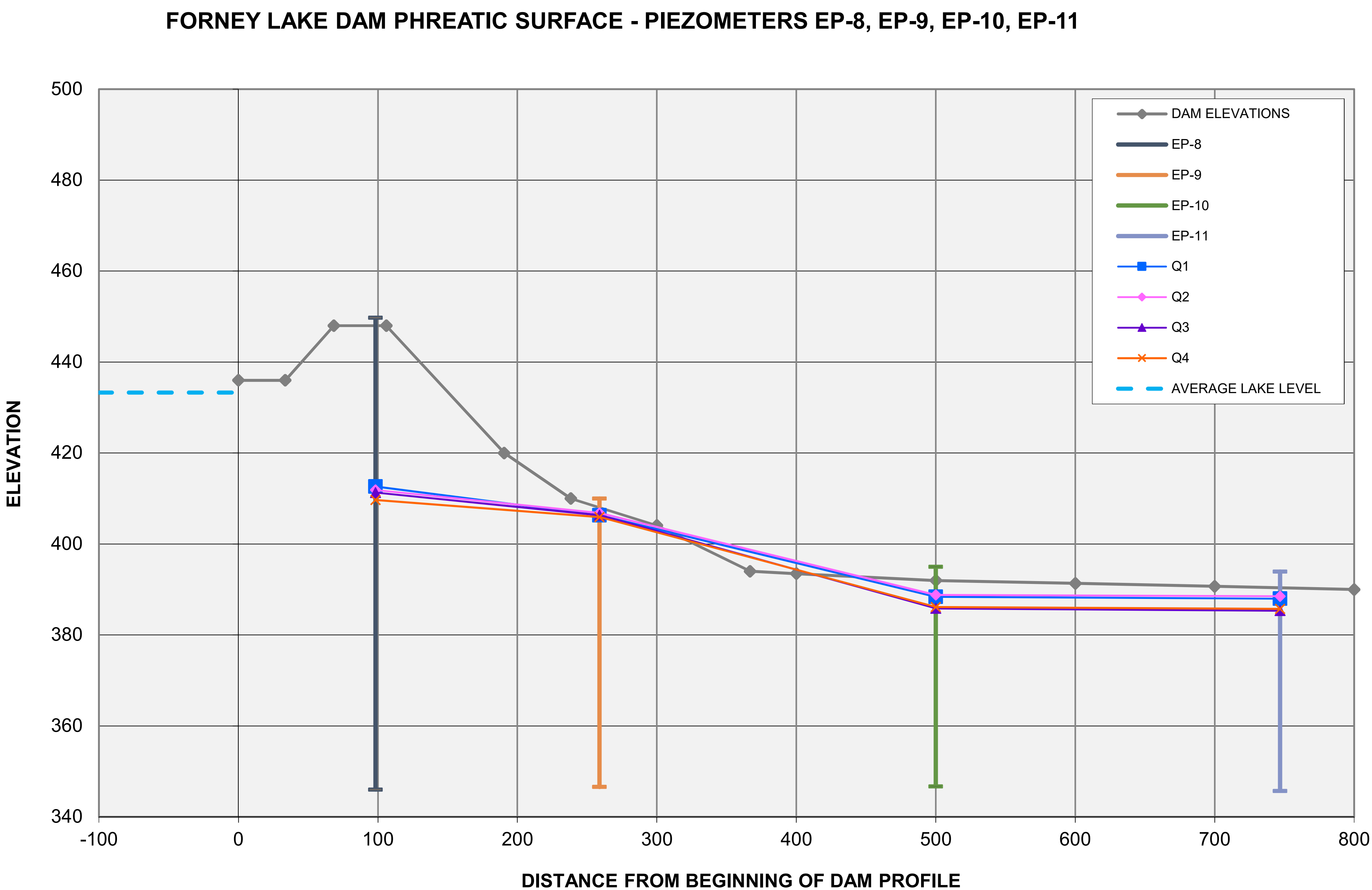
FORNEY LAKE DAM PHREATIC SURFACE - PIEZOMETERS EP-8, EP-9, EP-10, EP-11
ELEVATION
500
480
460
440
420
400
380
360
340
-100
0
100
200
300
400
500
600
700
800
DISTANCE FROM BEGINNING OF DAM PROFILE
DAM ELEVATIONS
EP-8
EP-9
EP-10
EP-11
Q1
Q2
Q3
Q4
AVERAGE LAKE LEVEL

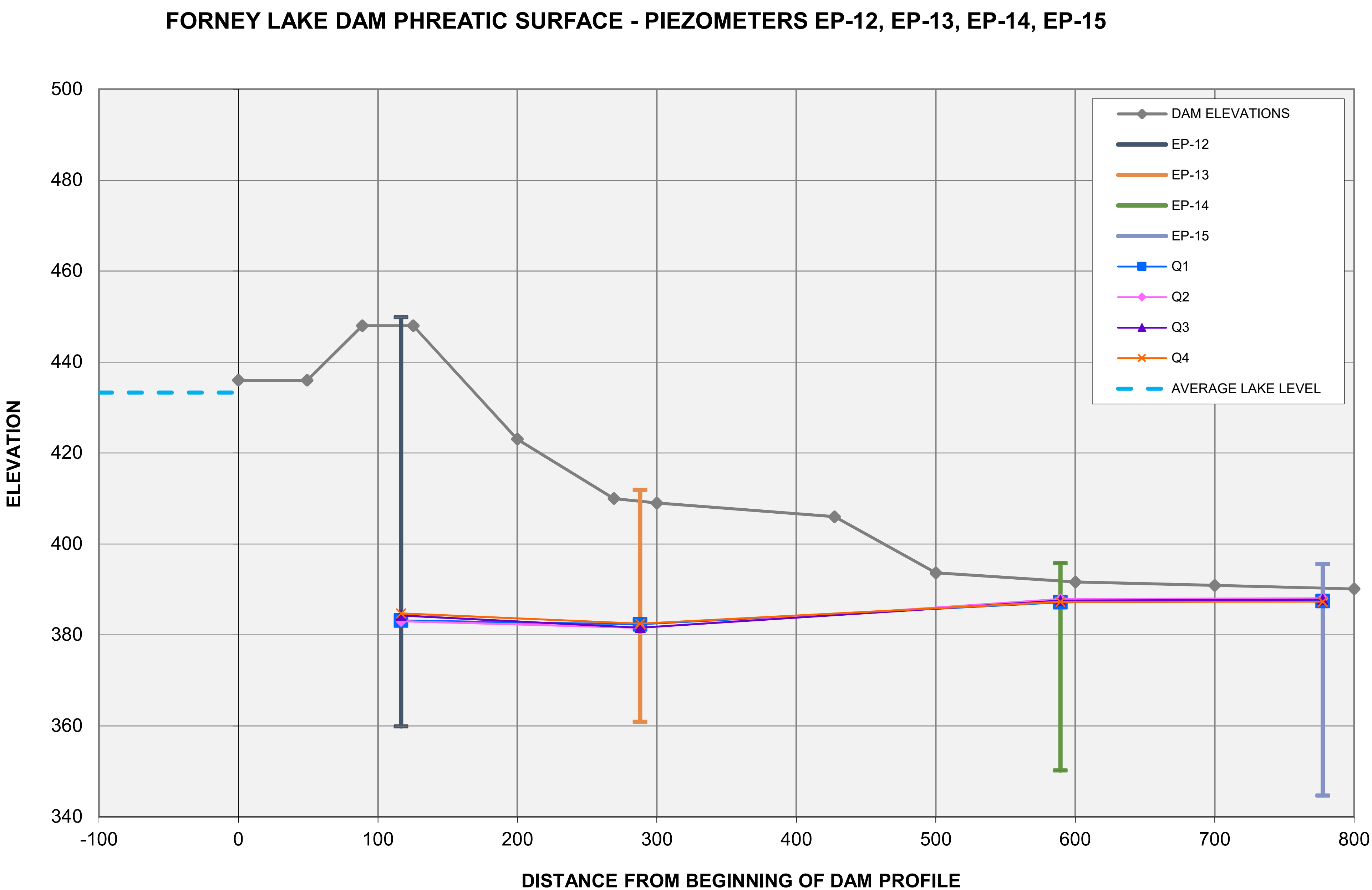
FORNEY LAKE DAM PHREATIC SURFACE - PIEZOMETERS EP-12, EP-13, EP-14, EP-15
ELEVATION
500
480
460
440
420
400
380
360
340
-100
0
100
200
300
400
500
600
700
800
DISTANCE FROM BEGINNING OF DAM PROFILE
DAM ELEVATIONS
EP-12
EP-13
EP-14
EP-15
Q1
Q2
Q3
Q4
AVERAGE LAKE LEVEL

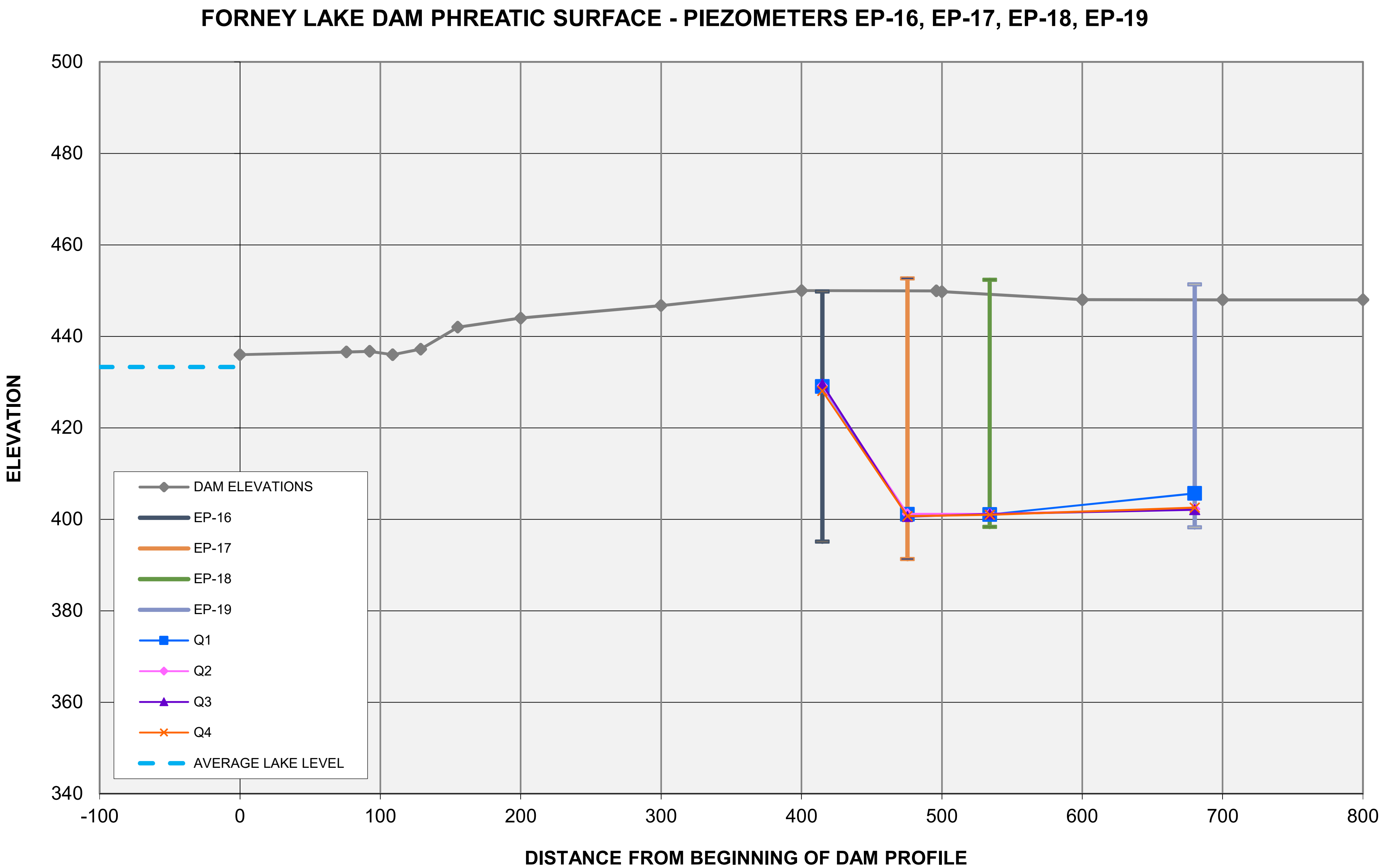
FORNEY LAKE DAM PHREATIC SURFACE - PIEZOMETERS EP-16, EP-17, EP-18, EP-19
500
480
460
440
420
400
380
360
340
ELEVATION
-100
0
100
200
300
400
500
600
700
800
DISTANCE FROM BEGINNING OF DAM PROFILE
DAM ELEVATIONS
EP-16
EP-17
EP-18
EP-19
Q1
Q2
Q3
Q4
AVERAGE LAKE LEVEL

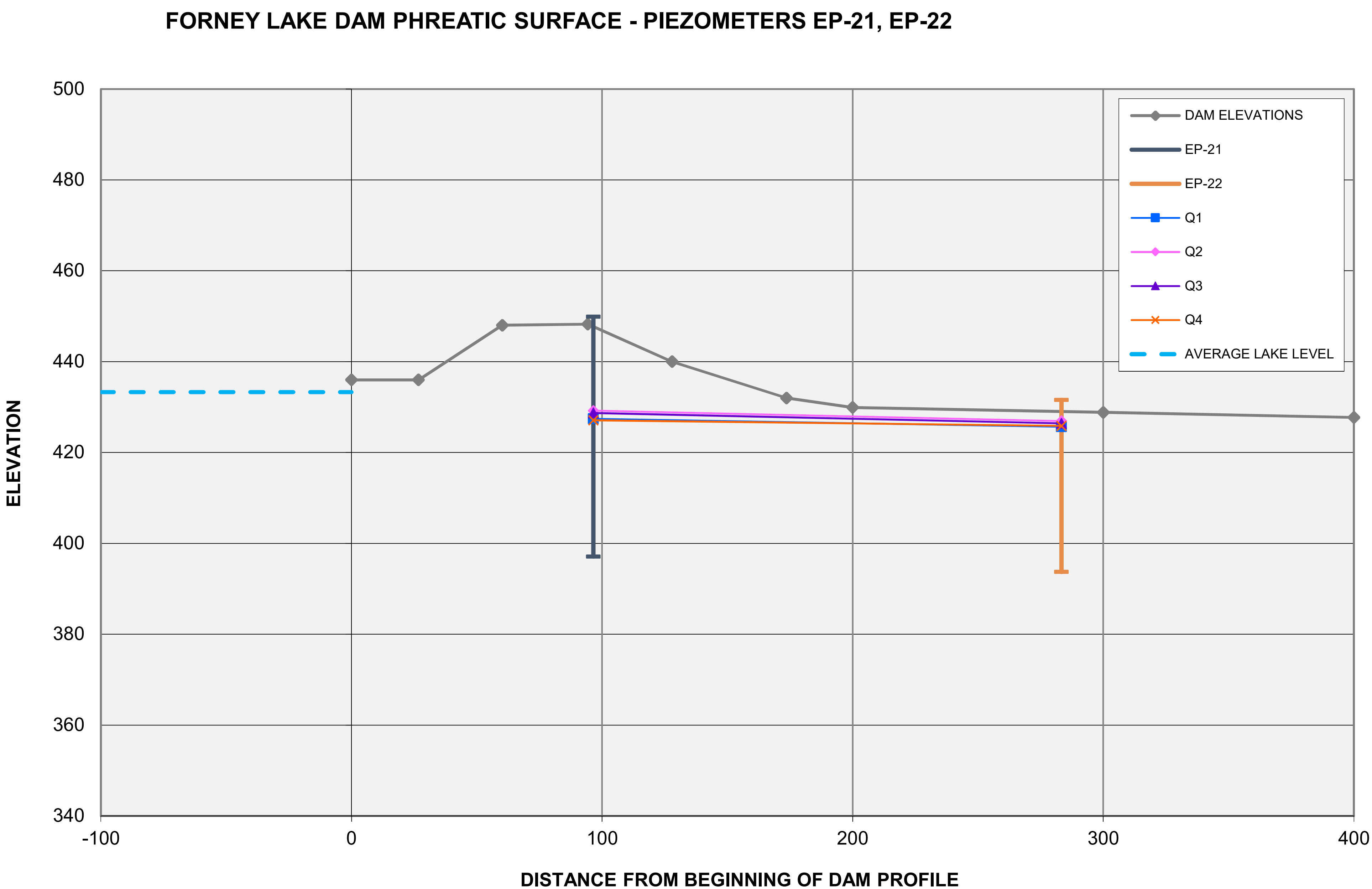

FORNEY LAKE DAM PHREATIC SURFACE - PIEZOMETERS EP-21, EP-22
500
480
460
440
420
400
380
360
340
-100
0
100
200
300
400
ELEVATION
DISTANCE FROM BEGINNING OF DAM PROFILE
DAM ELEVATIONS
EP-21
EP-22
Q1
Q2
Q3
Q4
AVERAGE LAKE LEVEL

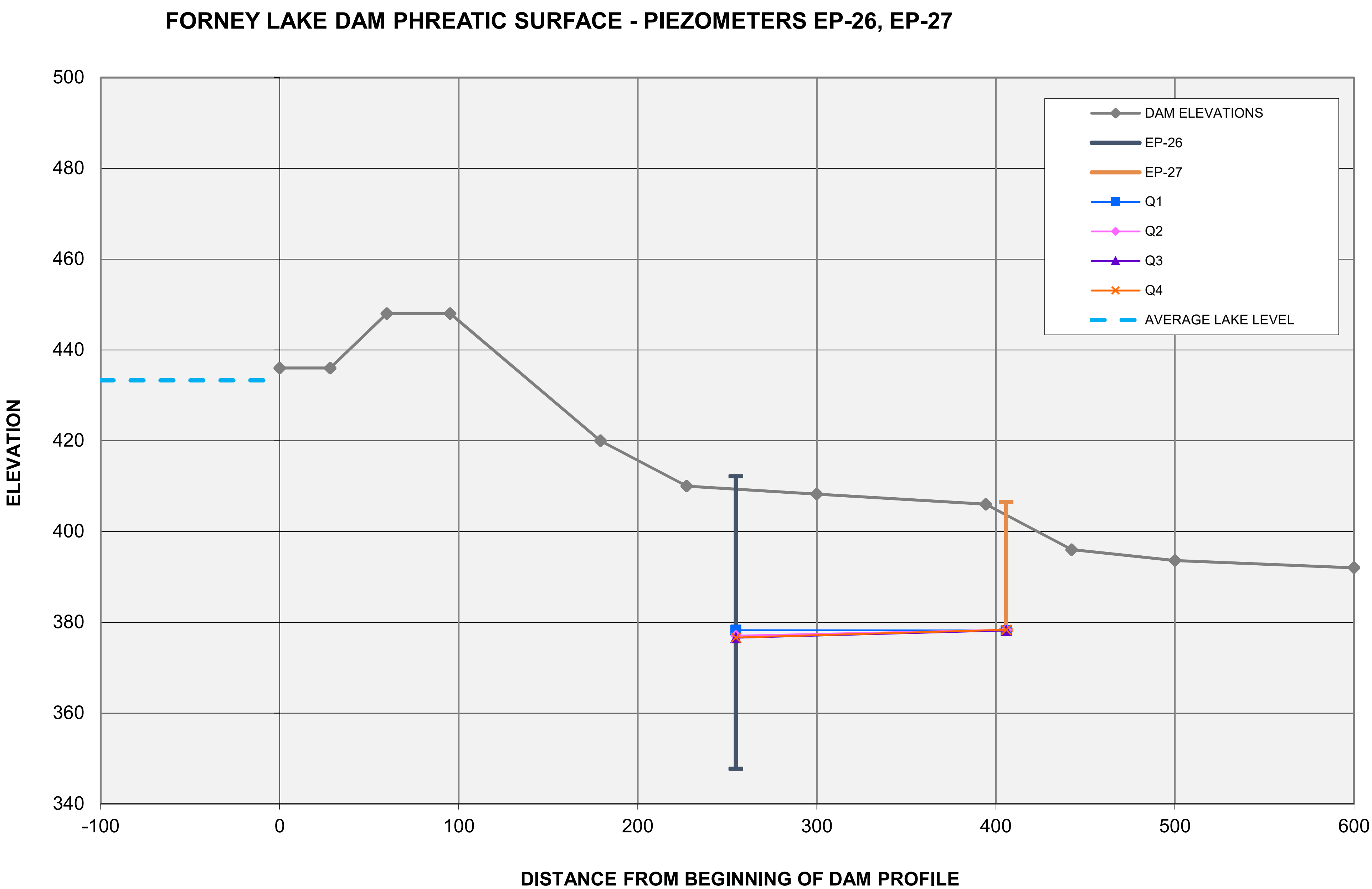
FORNEY LAKE DAM PHREATIC SURFACE - PIEZOMETERS EP-26, EP-27
500
480
460
440
420
400
380
360
340
ELEVATION
-100
0
100
200
300
400
500
600
DISTANCE FROM BEGINNING OF DAM PROFILE
DAM ELEVATIONS
EP-26
EP-27
Q1
Q2
Q3
Q4
AVERAGE LAKE LEVEL

FORNEY LAKE DAM PHREATIC SURFACE - PIEZOMETERS EP-29, EP-40

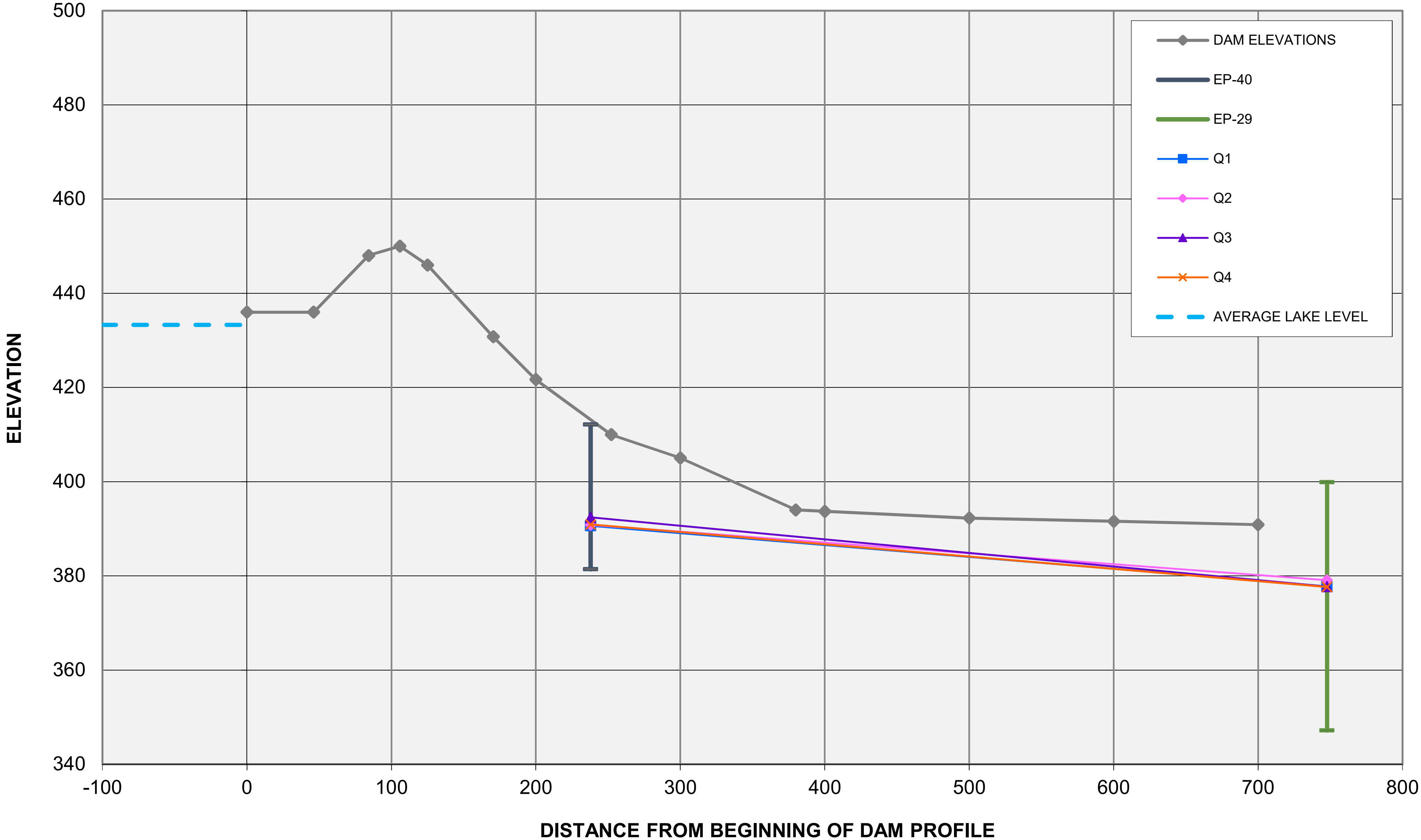

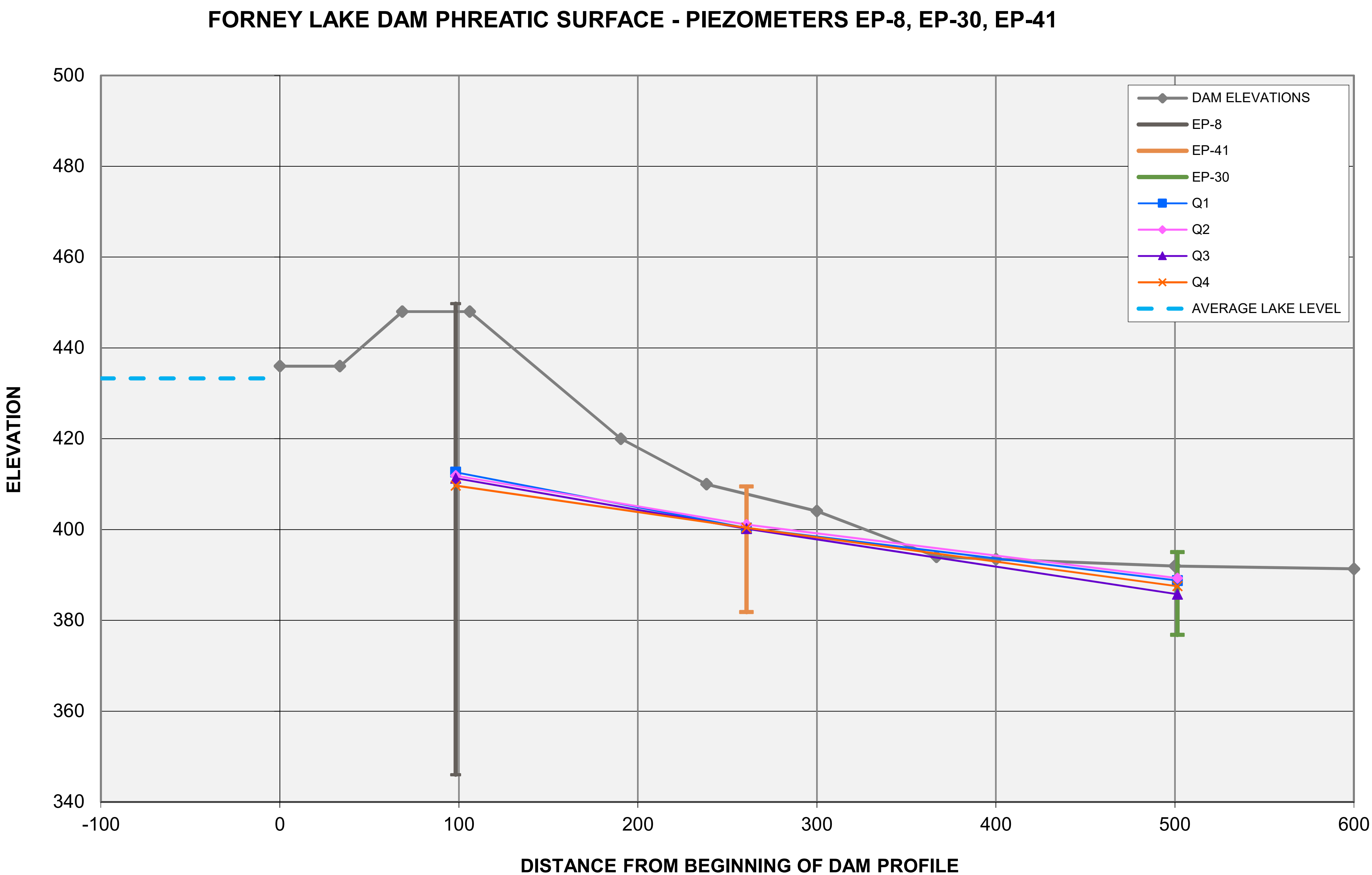
FORNEY LAKE DAM PHREATIC SURFACE - PIEZOMETERS EP-8, EP-30, EP-41
ELEVATION
500
480
460
440
420
400
380
360
340
-100
0
100
200
300
400
500
600
DISTANCE FROM BEGINNING OF DAM PROFILE
DAM ELEVATIONS
EP-8
EP-41
EP-30
Q1
Q2
Q3
Q4
AVERAGE LAKE LEVEL

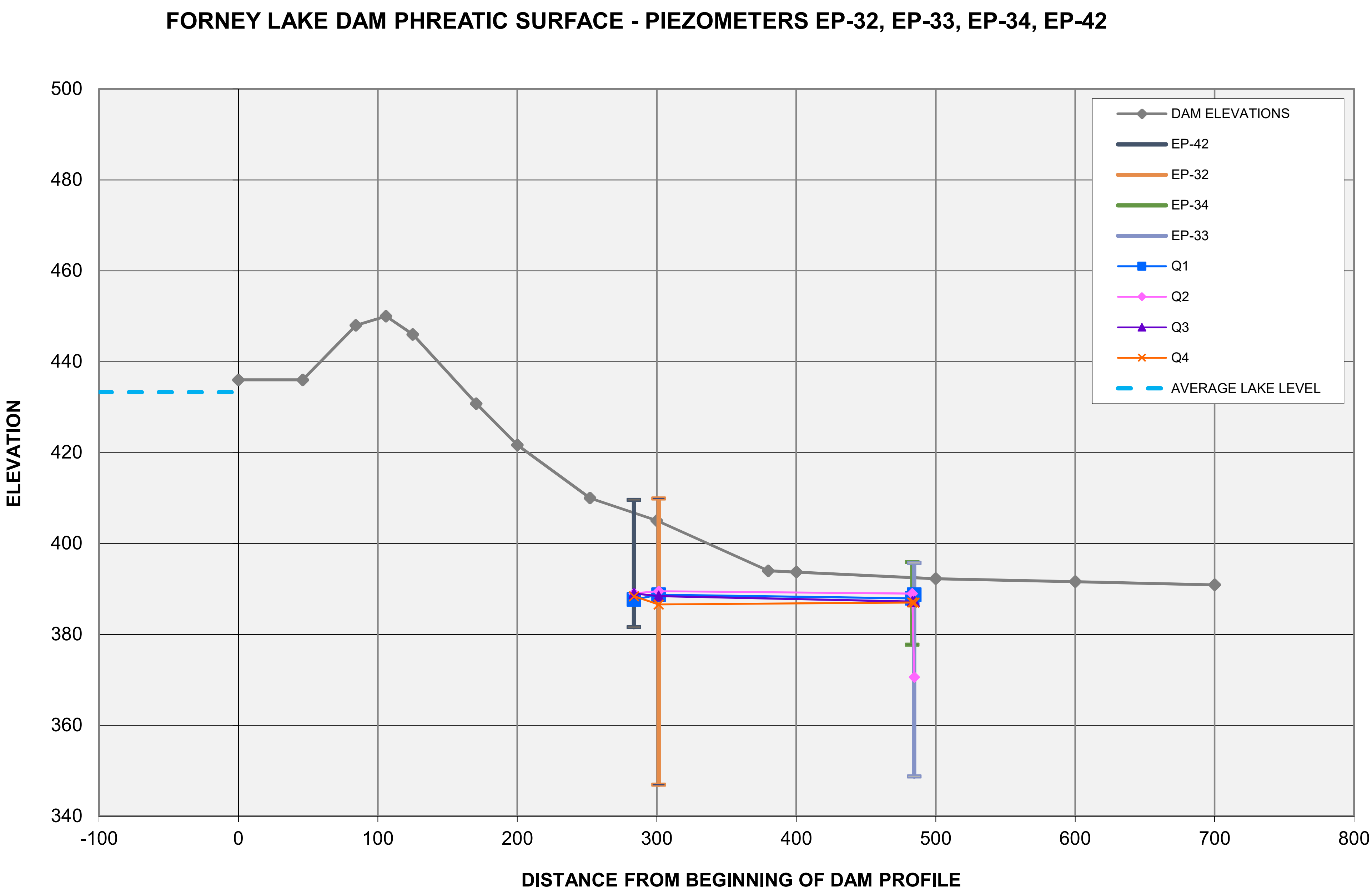
FORNEY LAKE DAM PHREATIC SURFACE - PIEZOMETERS EP-32, EP-33, EP-34, EP-42
ELEVATION
DISTANCE FROM BEGINNING OF DAM PROFILE
500
480
460
440
420
400
380
360
340
-100
0
100
200
300
400
500
600
700
800
DAM ELEVATIONS
EP-42
EP-32
EP-34
EP-33
Q1
Q2
Q3
Q4
AVERAGE LAKE LEVEL

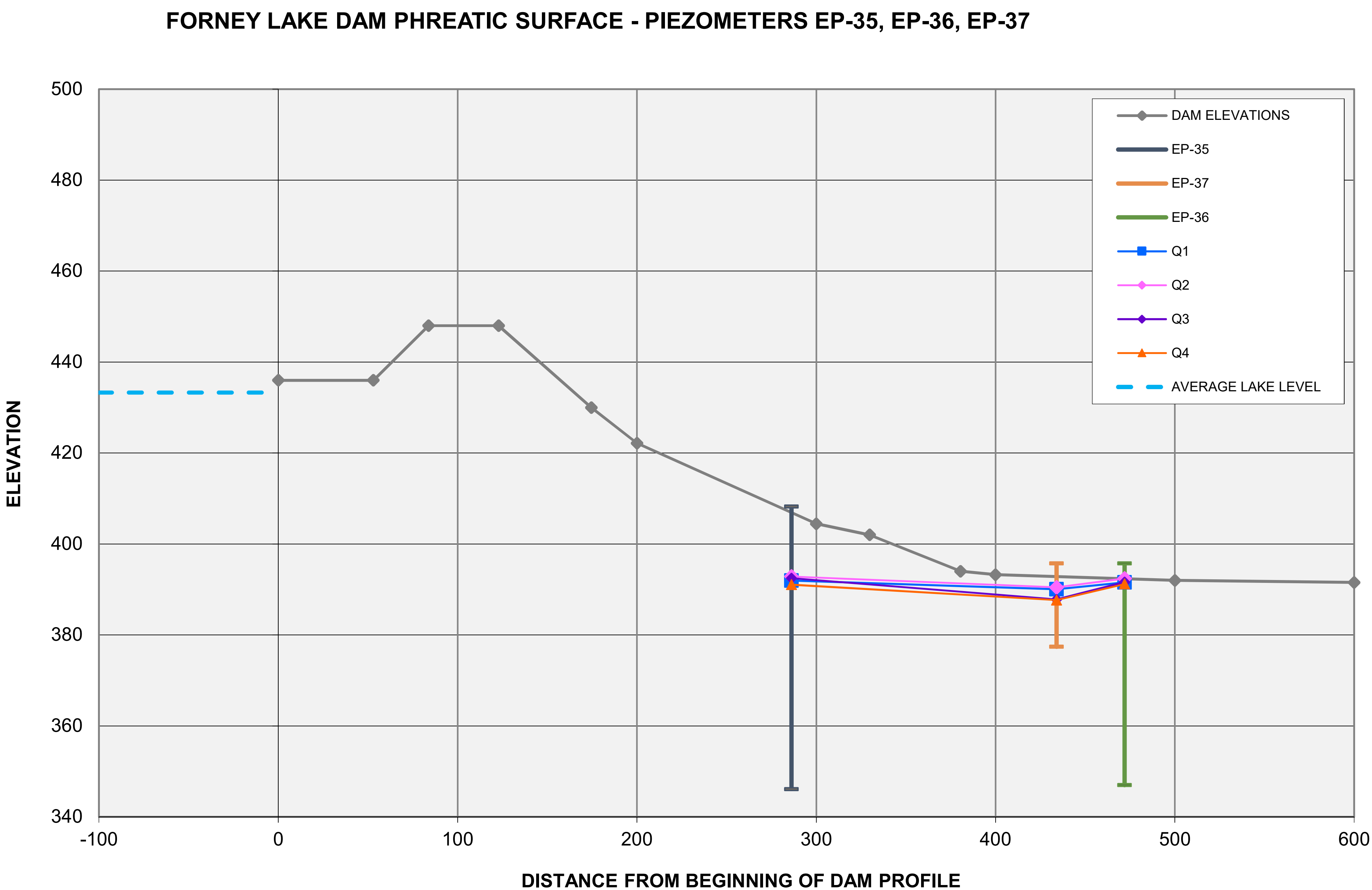
FORNEY LAKE DAM PHREATIC SURFACE - PIEZOMETERS EP-35, EP-36, EP-37
ELEVATION
500
480
460
440
420
400
380
360
340
-100
0
100
200
300
400
500
600
DISTANCE FROM BEGINNING OF DAM PROFILE
DAM ELEVATIONS
EP-35
EP-37
EP-36
Q1
Q2
Q3
Q4
AVERAGE LAKE LEVEL

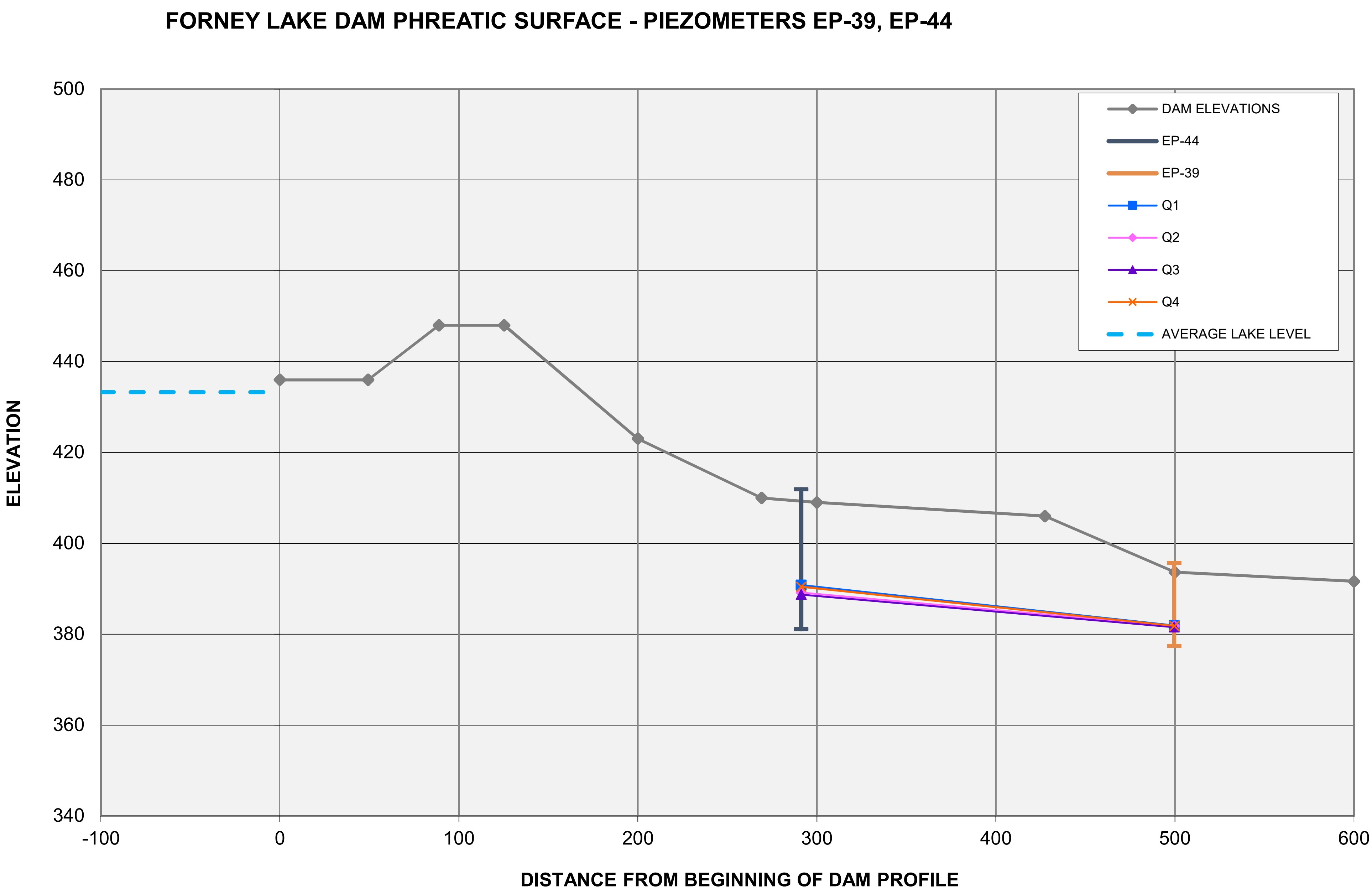
FORNEY LAKE DAM PHREATIC SURFACE - PIEZOMETERS EP-39, EP-44
ELEVATION
500
480
460
440
420
400
380
360
340
-100
0
100
200
300
400
500
600
DISTANCE FROM BEGINNING OF DAM PROFILE
DAM ELEVATIONS
EP-44
EP-39
Q1
Q2
Q3
Q4
AVERAGE LAKE LEVEL

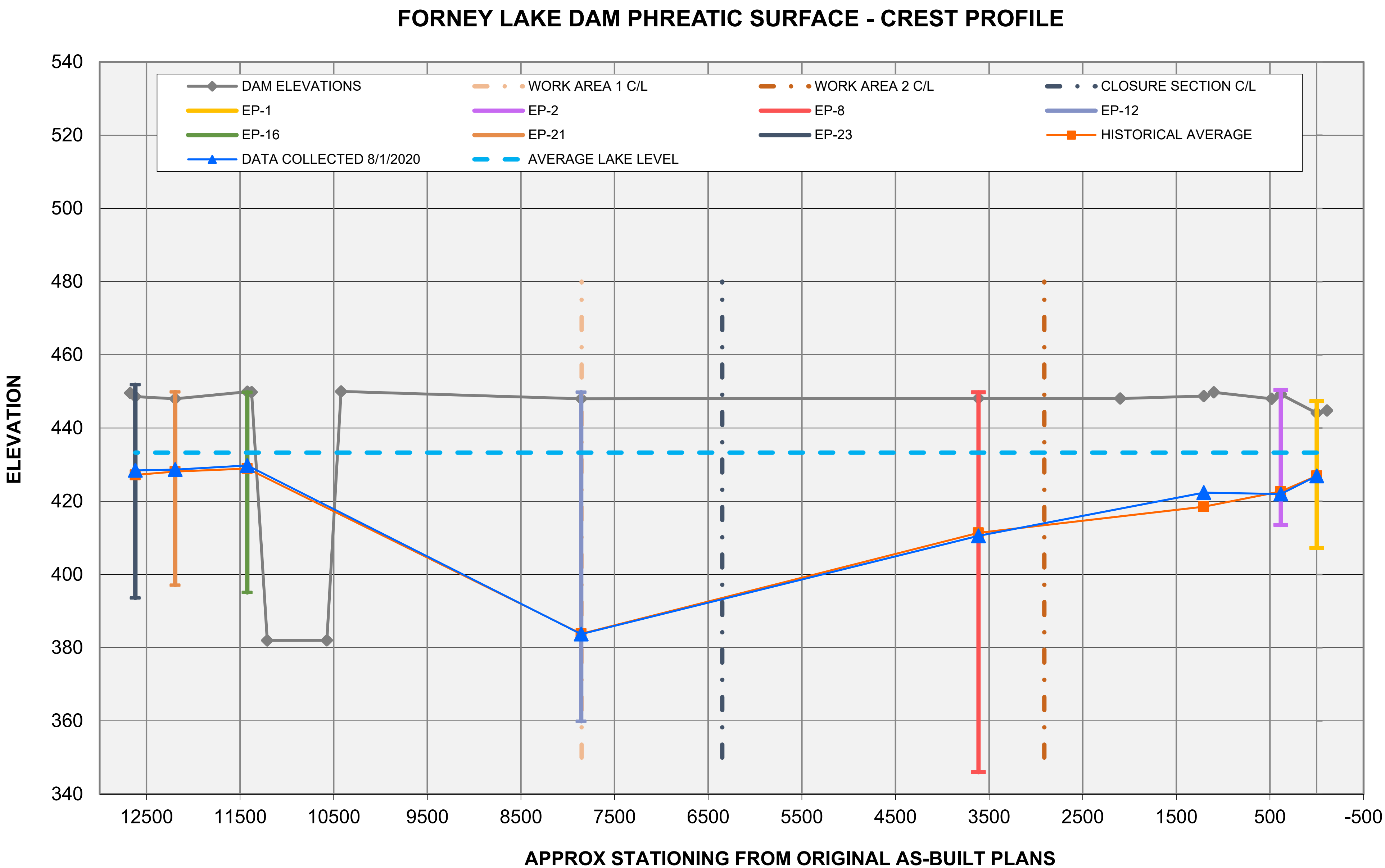

FORNEY LAKE DAM PHREATIC SURFACE - CREST PROFILE
DAM ELEVATIONS
WORK AREA 1 C/L
WORK AREA 2 C/L
CLOSURE SECTION C/L
EP-1
EP-2
EP-8
EP-12
EP-16
EP-21
EP-23
HISTORICAL AVERAGE
DATA COLLECTED 8/1/2020
AVERAGE LAKE LEVEL
ELEVATION
540
520
500
480
460
440
420
400
380
360
340
12500
11500
10500
9500
8500
7500
6500
5500
4500
3500
2500
1500
500
-500
APPROX STATIONING FROM ORIGINAL AS-BUILT PLANS

APPENDIX E

TAINTER GATE INSPECTION AND ANALYSIS

Rockwall-Forney Dam Visual Gate Inspection, Trunnion Friction Testing and Structural Evaluation Report

©2021 All Rights Reserved

ROCKWALL-FORNEY DAM VISUAL GATE INSPECTION, TRUNNION FRICTION TESTING AND STRUCTURAL EVALUATION REPORT

Rockwell-Forney Dam ID: Texas State Dam No. TX00837
Contract: Major Rehab of Raw Water Facilities – SA#1
Project Location: Kaufman County, Texas

Schnabel Project Reference #: 20C22001.00
Garver Project Reference #: 14088280.1

July 23, 2021

Schnabel ENGINEERING

Schnabel
ENGINEERING

T 206.573.5190
16000 Christensen Road, Suite 101 / Seattle, WA 98188
schnabel-eng.com

July 23, 2021

Mr. Randall McIntyre, PE
Garver, LLC
14160 N Dallas Parkway, Suite 850
Dallas, TX 75254

Subject: **Project 20C22001.00 Major Rehab of Raw Water Facilities – SA#1, Rockwall-Forney Dam Visual Gate Inspection, Trunnion Friction Testing and Structural Evaluation Report**
Kaufman County, Texas

Dear Mr. McIntyre:

SCHNABEL ENGINEERING, LLC is pleased to submit this report documenting the visual inspection, trunnion friction testing, and preliminary structural evaluation of the Tainter gates associated with the Rockwall-Forney Dam. This report includes selected supporting tables, figures, and appendices with relevant data collected for this study.

We appreciate the opportunity to be of service for this project. Please call us if you have any questions regarding this report.

Sincerely,

SCHNABEL ENGINEERING, LLC

Robert T. Indri, PE
Senior Associate

Date Signed: July 23, 2021

RTI:CD:JSM

Distribution:
Client (one electronic copy)
Attn: Randall McIntyre, PE

ROCKWALL-FORNEY DAM VISUAL GATE INSPECTION, TRUNNION FRICTION TESTING AND STRUCTURAL EVALUATION REPORT

CONTENTS

©2021 All Rights Reserved

FIGURES

TABLES

APPENDICES

©2021 All Rights Reserved

1.0 EXECUTIVE SUMMARY

This report presents the results of the visual gate inspections, trunnion friction testing and preliminary structural evaluation for the 14 Tainter spillway gates at Forney Dam. The work was performed by **Schnabel Engineering, LLC** (Schnabel) and its sub-consultants. The purpose of the work performed was to determine the current condition of the gates and asses the adequacy of the spillway gates for continued service.

The report is divided into the following sections:

- Sections 2, 3, and 4 provide background information including the scope of services, a description of the site and a description of documents reviewed during development of this report.
- Section 5 summarizes the results of the visual gate inspection.
- Section 6 summarizes the approach and result of the gate structural analysis.
- Section 7 summarizes the results of the trunnion friction testing

The appendices include detailed information used to develop the summaries listed above.

1.1 Summary of Conclusions

Structural issues with the gates that require immediate attention or removing gates from service with the exception of Gate 6 were not observed or documented during the performance of the work describe herein; however, immediate maintenance of the gates is strongly recommended to address the failing coatings and to remediate poor quality and fractured welds.

The results of the gate analysis indicate that some of the gate members are overstressed for the load cases analyzed.

The results of the gate trunnion friction testing indicate that the average values for trunnion friction for the Tainter gates at Forney Dam are below the 0.3 trunnion friction factor utilized in the analysis.

1.2 Summary of Recommendations

The following recommendations are based on the results of the visual gate inspection and the structural gate structural analysis:

Dam Safety-related:

Gate 6 fracture observed on member LS-1. Due to the severity of the crack, Schnabel recommends that the gate remain out of service until the strut is repaired or replaced. Design of the repairs should be performed by a Professional Engineer with experience in steel defects and fracture mechanics.

Overall recommendation (all gates) due to the LS-1, Gate 6 fracture, other strut arms may have similar fractures or cracks that were no observed. NDT should be performed on other gate struts to determine if the problem is widespread. Future inspectors should be aware of this issue and observant for similar fractures.

©2021 All Rights Reserved

Connections and Welds (All Gates): We recommend repairing fractured welds and repairing or reinforcing poor quality welds. Selection of welds to be repaired and methods of repair should be coordinated between an AWS Certified Weld Inspector and a Professional Engineer experienced in the design and repair of welded connections.

For overstressed members, we recommend that DWU develop a plan to modify the gates, in particular the lower diagonal strut arm braces (LB-5 and RB-5) to reduce the interaction ratios to 1.0 or less.

Maintenance:

We recommend that DWU search their archives for shop drawings and any other documentation from gate construction and subsequent modifications/repairs including photos and digitize the documents for future use.

We recommend that the gate opening indicators be re-indexed to accurately reflect actual gate opening.

We recommend that DWU develop a plan for gate operations testing. Full height opening tests are typically performed at 5 year intervals under full head to evaluate performance of the gates under these type of flow conditions; however, if reservoir operations preclude gate operations testing under full head, then full height testing under dewatered conditions should be performed. Gate amperage draw should be measured and recorded during gate testing. Additionally, the emergency generator should be used to operate a gate monthly to test the backup power system.

We recommend a close-up detailed inspection of the gates be performed on a 10-year interval.

Coatings (All Gates): We recommend recoating of the gates within the next 2 to 5 years.

Drain Holes (All Gates): In the short term (less than 2 years), we recommend that the gates be cleaned and any obstructed drain holes be cleared to allow trapped water to drain and reduce the corrosion potential associated with water accumulating on the members. In the long term (recommended to be performed during re-coating of the gates) we recommend installing new drain holes where the location of the existing drain holes still results in trapped water; and, reaming of poorly cut existing drain holes to provide smooth hole.

Section Loss (All Gates): The bottom of the gate leafs exhibited section loss. This area should be repaired/reinforced during re-coating of the gates. Other areas of section loss should be evaluated by a Professional Engineer during re-coating of the gates and documented and evaluated for repair on a case-by-case basis.

For Gate 2, we recommend that the hole in the skinplate (Ref. Photo 23, Gate 2) be plugged/repaired. The hole should be repaired prior to the gate re-coating.

For Gate 3, we recommend that the hole in the skinplate (Ref. Photo 7, Gate 3) be plugged/repaired. The hole should be repaired prior to the gate re-coating.

©2021 All Rights Reserved

For Gate 5, we recommend monitoring the skinplate patch shown (Ref. Photo 17, Gate 5). If the patch fails prior to the gate re-coating project, it should be plugged/repaired. Otherwise, the patch should be repaired during the gate re-coating work.

For Gate 14 we recommend that abrupt changes in geometry for the trunnion hub be ground down to provide a more gradual transition. This should be performed as part of the next recoating project.

For Gate 14, we recommend installing grease fittings in the threaded holes on top of the trunnion hubs to prevent moisture and debris from entering. This should be performed within the next year.

©2021 All Rights Reserved

2.0 SCOPE OF SERVICES

Schnabel's contract with Garver dated March 18, 2020 generally defines the scope of services for this project. The scope of services includes the following:

2.1 Review of Existing Documentation

The Project team will review available documentation on the gates' design, construction, operation and maintenance. Depending on availability, this may include:

- Design drawings and specifications
- Previous structural analyses
- Operating procedures
- Operational history
- Operation and Maintenance records
- Previous inspection reports

The Project team will review the structural analysis of record, if available, and comment on the assumptions (including material properties), methods and results. The results of the review will also aid the inspection team in identifying critical members and connections.

2.2 Inspection Work Plan

Schnabel will prepare a work plan for the gate inspections. Given the size and configuration of the gates, rope access techniques were utilized for the visual inspection. The Safety Plan included a hazard assessment and specific measures to be taken to help ensure personnel safety during the gate inspections.

Inspection checklists were prepared listing each element of each gate, including skin plates, structural members, seals, trunnions, trunnion anchorages, lifting attachments and hoisting equipment. The listing for each structural element covers alignment, welding, mechanical fasteners and corrosion.

2.3 Visual Gate Inspection

Schnabel provided a team of experienced structural engineers and gate inspection technicians to perform the detailed gate inspection.

During the inspection, each individual gate component was examined, with focus on:

- Bent, deformed, or missing members or connecting elements
- Weld defects: to identify any instances of cracking, problematic details, or visibly poor weld quality
- Mechanical fasteners: comparing bolts and rivets to the information shown on the drawings. Loose fasteners, those visibly cracking or deformed, and those that do not conform to the record drawings will be identified

©2021 All Rights Reserved

- Corrosion protection: covering the condition of the coating system and any cathodic protection system
- Corrosion: to clearly identify the type of corrosion (e.g., surface, pitting, etc.), the location and percent of the member affected
- Drainage and debris: to identify the location of any ponding water or accumulation of debris and excessive animal waste
- Seal condition and serviceability (including side, bottom, and top seals, as applicable)
- Condition of the gate trunnions and their lubrication systems
- Condition of lifting devices and attachments (including cables, chains, eyebolts, clevises, sheaves, etc.)
- Mechanical and electrical components of the hoist equipment.
- Observations and measurements will be supplemented by photographs of each element inspected.

2.4 Trunnion Friction Testing

In addition to the gate inspections, trunnion friction tests, as described below, were performed.

- Installation of strain gage sensors on the gate arms to monitor internal strains during the lift test. Instrumentation generally consists of groups of four strain gages mounted at selected cross sections of the struts to monitor changes in axial and bending forces during gate lift. In addition to the strain gages, two displacement measurement sensors will be placed along the skin plate to monitor gate movement during the lift test.
- Test procedure generally consists of the following steps:
    - Step 1: Install gate instrumentation.
    - Step 2: Zero sensors and begin data collection.
    - Step 3: Lift gate to approximately 1-foot off sill and hold for 10 seconds.
    - Step 4: Lower gate to approximately 6 inches off sill and hold for 10 seconds.
    - Step 5: Repeat lifting and lowering cycle two more times without bringing gate back to sill.
    - Step 6: Lower gate back to sill.
    - Step 7: Repeat Steps 3 through 6 two more times to obtain three complete sets of data.
- Preparation of trunnion friction test report and recommendations for further action, if required.

2.5 Structural Analysis/Model for One Gate

A structural model for a typical existing tainter gate was developed to aid in the evaluation of the gate for general compliance with U.S. Army Corps of Engineers guidelines for Tainter gates, dated 2014 (Reference 2). This model can be used for a future fitness-for-service evaluation based on any observations of damaged connections, member section loss, or higher then assumed trunnion friction values.

©2021 All Rights Reserved

3.0 SITE DESCRIPTION

3.1 General

Rockwall-Forney Dam (Forney Dam), with a Texas State Dam No. of TX00837 is a water supply project owned and operated by Dallas Water Utilities (DWU). Construction of the project was completed circa 1969. The dam is located near the east border of the City of Dallas at approximately river-mile 31.8 of the East Fork Trinity River. The water storage reservoir formed by the dam is known as Lake Ray Hubbard and contains approximately 452,000 acre-feet at its normal water level (EL 435.5). The project is categorized as a large, high hazard dam in accordance with Texas Dam Safety criteria.

The dam is composed of the following primary components:

- **East Dike** – Rolled earthfill embankment approximately 1,200 feet long with maximum height of 30 feet.
- **Left Non-overflow Section** – Concrete gravity section located adjacent (left) to the spillway. Approximately 120 feet long with maximum height of 65 feet with an 18-foot-wide top deck.
- **Principal Spillway** - The total length of the spillway is approximately 664 feet, including the piers that are each 8-feet wide and contains the following flow control elements:
    - Fourteen (14) 40-foot x 28-foot Tainter gates with a net length of approximately 560 feet for the weir crest at approximately EL 409.5; and,
    - Three (3) 4.5-foot x 6.75-foot gated low flow outlets.
- **Right Non-overflow Section** – Concrete gravity section located adjacent (right) to the spillway. Approximately 120 feet long with maximum height of 65 feet with an 18-foot-wide top width.
- **Main Embankment** – Compacted earthfill embankment approximately 12,500 feet long with a maximum height of 68 feet and a crest width of 22 feet. The crest elevation is at approximate EL 450.

3.2 Spillway Gates

The spillway contains 14 Tainter gates. Each gate measures approximately 40-ft wide by 28-ft high with the top of the gate at EL 437.5 providing 2-ft of freeboard with the reservoir at normal pool (EL 435.5). The gate sill is at EL 408.36. The gates have a 28-foot-radius from the center of the trunnion to the downstream face of the skinplate. The trunnions are supported by trunnion girders that are anchored into the piers with post-tensioned bar anchors. Photo 3-1 shows the downstream view of a Forney Dam Tainter gate.

The steel skin plate thicknesses varies in three sections from 1/4-in at the top to 3/8-in at the bottom in 1/8-in increments. Vertical ST6B9.5 rib members that are curved to the gate radius are welded along the webs to the skin plate downstream face at 2-ft spacing. The skin plate and the ribs, therefore, act as composite members. Three horizontal girders are welded to the rib flanges at three levels and are oriented with the web axes in the radial direction. The member sizes are 27WF84 for the top girder and 30WF116 for the middle, and 30WF124 for bottom girders. The girders are braced by ST6B9.5 members vertically and diagonally.

 ©2021 All Rights Reserved

Each girder is supported by two radial struts extending from the downstream flange of the girder to the built-up trunnion hub on each side of the gate. The three struts on each side form the left, or the right, strut arm of the gate. The member size of the three struts of each arm are 10WF39 for the top strut, 10WF60 for the middle strut, and 10WF72 for the bottom strut. The struts are welded to the girder flanges at one end and welded to the built-up hub at the other end. The struts are trussed together forming a vertical plane by vertical and diagonal 10B15 bracing members. The struts are oriented with the web laid horizontally, and the strut braces are oriented their flanges in alignment with the flanges of the struts. The built-up hub is composed of 3/8-in and 1/2-in plates for the web stiffener and 13/16-in plates for the sides. Photo 3-2 shows the left strut arm of Tainter gate at Forney Dam. Although erection bolts can be observed, all structural connections of the main structural members are welded connections. The welded connections are intended to develop the full structural capacity of the members.

The Tainter gates have dedicated electric wire cable hoists that are operated from a switch panel at each gate. There are no automated or remotely controlled gate operations. The gate hoist equipment are located on the hoist deck at El. 443, directly above the gates and underneath the spillway bridge. Each Tainter gate has dedicated wire cable hoists and electric motor that are operated from a switch panel adjacent to the gate. Per DWU staff, the hoists have limit switches set at 1-foot increments for the first 6 feet of gate operation and one set for has when the gate has reached its maximum open position. The Tainter gates are not expected to experience extreme hoist loads outside of its normal lifting range. Gates are operated regularly as part of routine operations.

Figure 3-1: Principal spillway and gate numbering nomenclature. Photo is taken looking upstream.

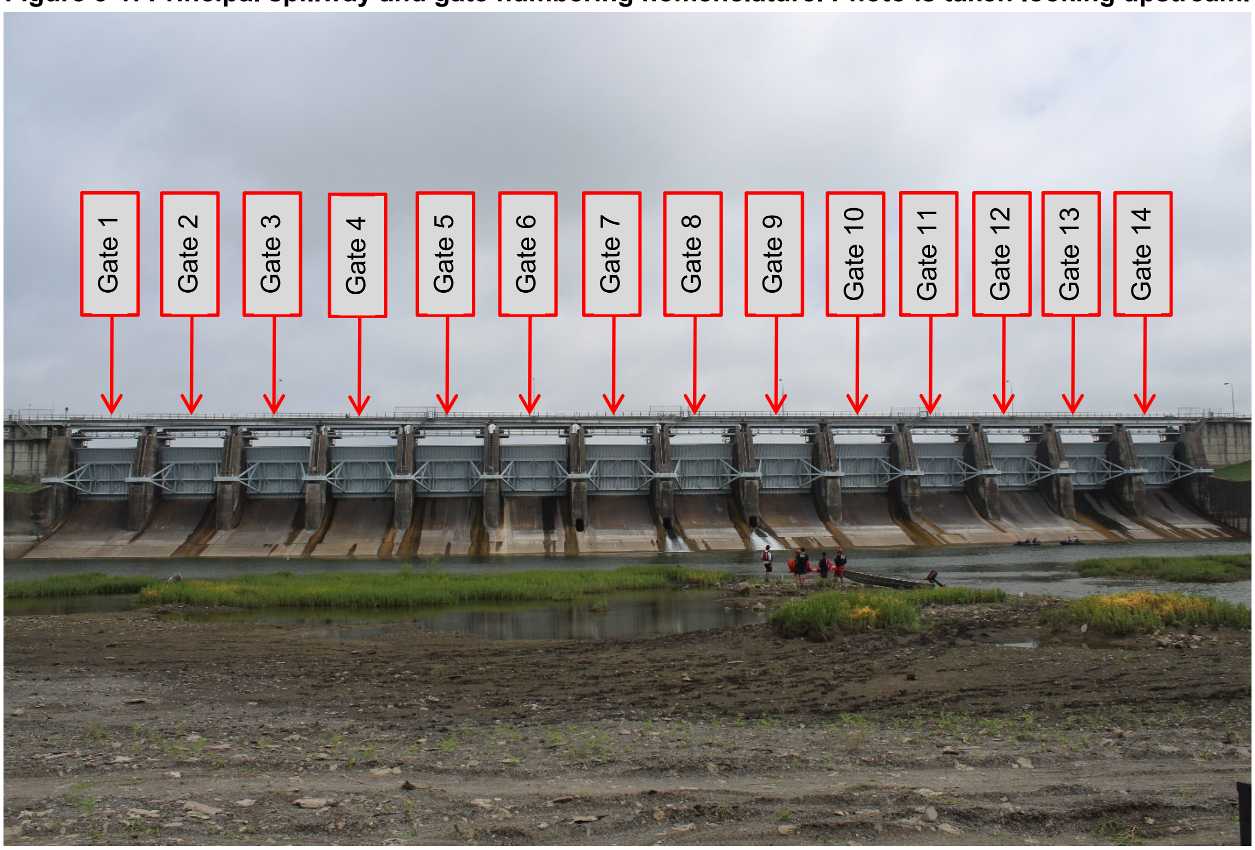

©2021 All Rights Reserved

Photo 3-1: Downstream view of a Forney Dam Tainter gate.

Photo 3-2: Left strut arm, Forney Dam (typical).

 ©2021 All Rights Reserved

3.3 Report Nomenclature

The gate numbering system as shown above in Figure 3-1 is used consistently in this report to identify individual gates and is consistent with the project gate numbering system. Left and right as used in this report are referenced to looking in the downstream direction unless otherwise noted.

©2021 All Rights Reserved

4.0 REVIEW OF EXISTING DOCUMENTATION

The original design report and asbuilt drawings were reviewed as part of the gate analysis and gate inspection. A listing of project documents reviewed and other references utilized in the development of this report are listed in Section 8.0. It is noted on the project asbuilt drawing set that shop drawings were required for the gates; however, these drawings, if actually produced, have not yet been found. It is important to maintain complete records on the project to inform future investigations, modifications and maintenance of project components. Based on this we make the following recommendation:

We recommend that DWU search their archives for shop drawings and any other documentation from gate construction and subsequent modifications/repairs including photos and digitize the documents for future use.

©2021 All Rights Reserved

5.0 SPILLWAY GATE DETAILED INSPECTION

5.1 Inspection Team Qualifications

Visual inspections of the 14 Tainter gates were performed by Schnabel and Extreme Access starting on March 30, 2020 and ending on April 3, 2020. The lead engineer for the inspection was Robert Indri, PE.

The inspection team consisted of the following personnel:

- Robert Indri, PE (RI) (Lead Engineer, EOR) (Sprat Level I)
- Mike Coleman (MC) (Lead Technician) (Sprat Level III)
- Chris Lowry (CL) (Technician) (Sprat Level III)
- Dakota Keller (DK) (Technician) (Sprat Level II)

The Lead Engineer, Robert Indri, PE, is a specialist in dam engineering, with over 15 years of dedicated dam engineering experience. Mr. Indri's primary area of expertise is in the design, inspection and construction of hydraulic structures. Mike Coleman and Chris Lowry each have over 12 years of experience in the inspection and evaluation of steel structures. Dakota Keller has over 4 years of experience in the inspection and evaluation of steel structures.

5.2 Statement of Independence

Inspection findings, conclusions, and recommendations were made independently of Dallas Water Utilities, its subsidiaries, employees, and representatives.

5.3 Inspection Nomenclature

Gate numbering is based on the numbering system as shown in Figure 3-1. The terms left and right as used in this report are based on looking downstream unless otherwise noted.

Schematics of the gate were developed for the visual inspection and each gate member was given a unique alphanumeric designation. Field observations are referenced by the member designations shown on the schematics. The schematics used during the inspection are included in Appendix A.

5.4 Inspection Findings

The gates were visually inspected in one or two person teams under the supervision of the Lead Engineer. The reservoir elevation during the inspection was at approximately normal pool (EL 435.5). The majority of the upstream face of the skin plate was below water and not visible.

The inspection was supported by onsite DWU staff; James (Jimmy) Baxter, Chief Operator; and operators Greg, Caesar, and Manuel. Schnabel discussed spillway operations with DWU staff to better understand the history of the gates. Results of the interviews are listed in Section 5.4.1 below.

Representatives from Garver and JQ Engineering were onsite during performance of portions of the fieldwork.

©2021 All Rights Reserved

Detailed inspection sheets for each gate noting specific deficiencies/observations along with a substantiating photo are included in Appendix B. A digital copy of the photos taken during the inspection are included with this report on a portable hard drive. Included on the drive are all photos used in development of the inspection sheets as well as additional gate documentation photos taken during the gate inspection and photos of the gates during a subsequent site inspection performed on July 8 and 9, 2020.

Findings for each gate are summarized below. Location, details and photos for each observed deficiency are included in the detailed inspection sheets in Appendix B. Where specific members are called out, the reader should reference the gate schematics included in Appendix A for the location of the member in reference.

A coding system was used to quantify the condition of the following:

- corrosion and coatings;
- cracking and fatigue;
- connections;
- distortion; and,
- damage.

The coding system is based on the Oregon Department of Transportation (ODOT) Bridge Inspection Coding Guide, date March 2015. A key sheet for the codes is included in Appendix B.

5.4.1 Findings from Interviews with Operations Staff

The following information was gathered during discussions with DWU staff:

- Gate position indicators were removed and re-installed as part of the 2004-2006 painting project and are no longer accurate. Operators judge gate opening by timing. 60 seconds of operation approximately equals 1 foot of gate opening.
- There are limit switches are set at 1-foot increments up to 6 feet of gate operation. There is a limit switch for full open.
- Gates have been recoated twice, with the first being performed in the late 80's/early 90's.
- Second re-coating of the gates was performed between 2004 and 2006.
    - Re-coating included the gates, operators, and bridge.
    - Components were sand blasted to bare metal and re-coated.
    - Side rollers were sent off for refurbishment and re-installed.
    - Archer Western was the contractor for the re-coating.
- Pits in the skinplate were filled with a bondo type filler during the last re-coating project.
- Gate operating cables are believed stainless steel and from original construction.
- Water chemistry; corrosion is not aggressive at the site.
- In 2012, new wiring was installed for the gate operators and new brake pads were installed for the gate operators.
- In 2006, operators first noted issues with Gate 14. A loud banging was heard coming from the trunnions during operations. The noise was described as sounding, "like someone was trying to

 ©2021 All Rights Reserved

beat their way out of the trunnion with a hammer". A bulkhead was installed and the gate was de-watered until the repair. The trunnion bearing was replaced and work was completed in 2012.

- Three significant spillway flow events were noted:
  - 1989 (~54,000 CFS) Storm of Record
  - 1990 (~40,000 CFS)
  - 1991 (~26,000 CFS)
  - During the Storm of Record, most of the gates were open approximately 4 feet. This was the highest the gates have been opened under full head, with one exception noted below.
- During the 1990's, one gate was opened under full head as a test.
- During the second re-coating the gates were opened full height to perform the work. Gates were de-watered with a bulkhead in place.
- All of the 14 spillway gates are consistently operated, i.e. no favored gates, unless a gate is out of service for maintenance.
- Operators keep records of gate operations.
- Gates are operated locally (at the gate). There are no connections to the gates for remote operations.
- Stilling basing was dewatered for inspection approximately 15 years ago (~ 2005).

Based on our interviews with DWU operations staff, we make the following recommendations:

We recommend that the gate opening indicators be re-indexed to accurately reflect actual gate opening.

We recommend that DWU develop a plan for gate operations testing. Full height opening tests are typically performed at 5 year intervals under full head to evaluate performance of the gates under these type of flow conditions; however, if reservoir operations preclude gate operations testing under full head, then full height testing under dewatered conditions should be performed. Gate amperage draw should be measured and recorded during gate testing. Additionally, the emergency generator should be used to operate a gate monthly to test the backup power system.

We recommend a close-up detailed inspection of the gates be performed on a 10-year interval.

©2021 All Rights Reserved

5.4.2 General Findings, All Gates

Coatings and Section Loss:

In general, the coatings on the gates are approaching the end of their lifespan. The majority of the coatings on the gates are presently intact; however, there are areas where the coating has failed and corrosion has initiated. Corrosion and paint failure is typical for wet areas where the drain holes are clogged resulting in trapped water or due to side and bottom seal leakage. We did not observe structurally significant section loss or corrosion of the gate members. We did observe section loss at the bottom of the gate leaf that is not structurally significant, but should be reinforced as part of re-coating. Drain holes were installed in the members to reduce the potential for trapped water on the structure; however, in many places the existing drain holes were clogged with debris. Some of the drain holes are undersized and poorly cut, resulting in an increased susceptibility for clogging.

Photo 5-1: Local coating failure.

Photo 5-2: Water trapped in between the flanges of a primary strut arm due to clogged drainage hole.

Coatings (All Gates): We recommend recoating of the gates within the next 2 to 5 years.

Drain Holes (All Gates): In the short term (less than 2 years), we recommend that the gates be cleaned and any obstructed drain holes be cleared to allow trapped water to drain and reduce the corrosion potential associated with water accumulating on the members. In the long term (recommended to be performed during re-coating of the gates) we recommend installing new drain holes where the location of the existing drain holes still results in trapped water; and, reaming of poorly cut existing drain holes to provide smooth hole.

Section Loss (All Gates): The bottom of the gate leafs exhibited section loss. This area should be repaired/reinforced during re-coating of the gates. Other areas of section loss should be evaluated by a Professional Engineer during re-coating of the gates and documented and evaluated for repair on a case-by-case basis.

©2021 All Rights Reserved

Connections:

Based upon field observations, Schnabel is of the opinion that the gates were largely assembled and field welded onsite. It is more common, in current practice, to shop assemble major components where there is greater control over the QC/QA process. In general, observed weld quality was lower than typically observed on gates of similar size and age. Better quality welds were observed at the critical connections and lower quality welds were observed at the secondary connections. Some of the connection details made field welding difficult. In particular, the welds between the vertical ribs on the skin plate and the horizontal girders were difficult access welds. We noted numerous fractured welds at that location. These fractures are not considered structurally significant at this time. Fractured welds are annotated in the detail inspection sheets for each gate.

Photo 5-3: Fractured weld between the vertical rib and horizontal girder.

The following recommendation applies to all gates:

Connections and Welds (All Gates): We recommend repairing fractured welds and repairing or reinforcing poor quality welds. Selection of welds to be repaired and methods of repair should be coordinated between an AWS Certified Weld Inspector and a Professional Engineer experienced in the design and repair of welded connections.

.

Photo 5-4: Example of a poor quality weld.

©2021 All Rights Reserved

5.4.3 Gate 1 Findings

Coatings conditions, drain hole clogging, and connection observations for Gate 1 are generally consistent with the summary. Out-of-plane bending was observed on several of the vertical skinplate stiffeners (V-X). In our opinion, the observed distortion is not structurally significant at this time and may be the result of damage during installation or during subsequent work on the gates. No repairs are recommended at this time; however, the distortion should be monitored during future inspections for change.

5.4.4 Gate 2 Findings

Coatings conditions, drain hole clogging, and connection observations for Gate 2 are generally consistent with the summary. There is a hole in the skinplate between V-19 and V-20 (Ref. Photo 23, Gate 2). Leakage through the hole is contributing to coating degradation and corrosion. We noted numerous areas of out-of-plane bending on Gate 2 members. In our opinion, the observed distortion is not structurally significant at this time and may be the result of damage during installation or during subsequent work on the gates. No repairs are recommended at this time; however, the distortion should be monitored during future inspections for change.

For Gate 2, we recommend that the hole in the skinplate (Ref. Photo 23, Gate 2) be plugged/repaired. The hole should be repaired prior to or during the gate re-coating.

5.4.5 Gate 3 Findings

Coatings conditions, drain hole clogging, and connection observations for Gate 3 are generally consistent with the summary. Similar to Gate 2, there is a hole in the skinplate between V-19 and V-20 (Ref. Photo 7, Gate 3) that is contributing to coating degradation and corrosion. We noted several areas of out-of-plane bending on Gate 3 members. In our opinion, the observed distortion is not structurally significant at this time and may be the result of damage during installation or during subsequent work on the gates. No repairs are recommended at this time; however, the distortion should be monitored during future inspections for change. The right side roller of G-2 is seized.

For Gate 3, we recommend that the hole in the skinplate (Ref. Photo 7, Gate 3) be plugged/repaired. The hole should be repaired prior to or during the gate re-coating.

5.4.6 Gate 4 Findings

Coatings conditions, drain hole clogging, and connection observations for Gate 4 are generally consistent with the summary. We noted several areas of out-of-plane bending on Gate 4 members. In our opinion, the observed distortion is not structurally significant at this time and may be the result of damage during installation or during subsequent work on the gates. No repairs are recommended at this time; however, the distortion should be monitored during future inspections for change.

5.4.7 Gate 5 Findings

Coatings conditions, drain hole clogging, and connection observations for Gate 5 are generally consistent with the summary. We noted one area of out-of-plane bending on Gate 5. In our opinion, the observed

©2021 All Rights Reserved

distortion is not structurally significant at this time and may be the result of damage during installation or during subsequent work on the gates. No repairs are recommended at this time; however, the distortion should be monitored during future inspections for change. A patch on the skinplate is failing (Ref. Photo 17, Gate 5).

For Gate 5, we recommend monitoring the skinplate patch shown (Ref. Photo 17, Gate 5). If the patch fails prior to the gate re-coating project, it should be plugged/repaired. Otherwise, the patch should be repaired during the gate re-coating work.

5.4.8 Gate 6 Findings

Coatings conditions, drain hole clogging, and connection observations for Gate 6 are generally consistent with the summary. At the time of inspection, Gate 6 was out of service due to operational concerns/issues that occurred when the gate was last opened in May 2019. This incident and the subsequent evaluation are summarized below. Additionally, a structurally significant fracture was observed on member LS-1, which is discussed in detail below. Following the May 2019 incident, a bulkhead was installed in front of the gate. The bulkhead is currently still in place due to the fracture on member LS-1.

Gate 6 Operational Issues:

Original Issue:

In May of 2019, the operator closing the gate noted several loud noises on closing. Additionally, the gate racked on closing with the right side of the gate being approximately 2+ inches above the sill plate and the left side in contact with the sill plate. DWU placed bulkheads upstream of the gate to allow dewatering and inspection of the upstream and downstream sides of the gate for debris or other issues that may explain the mis-operation. No issues were noted by DWU staff during the inspection. DWU staff left the bulkheads in front of the gate and took the gate out of service until the root cause of the issues could be determined. Over time, the racked gate closed on the sill.

Evaluation and Results:

An evaluation team consisting of engineers from Schnabel, Garver and JQ supported by DWU Operations, BDI and Extreme Access developed and executed a test operation plan to evaluate the root cause of the operational issue associated with Gate 6.

Prior to test operation, the gate was visually inspected by the gate inspection team. No structural deficiencies or anomalies that would explain the operational issues were observed. A significant fracture between the web and flange of member LS-1 was observed. Based on our engineering judgement, the fracture was not a contributing factor in the operational issues; however, the torsion of the racked gate may have been a contributing factor in development or expansion of the fracture. The gate was cleared by the inspection team and DWU management for test operation under de-watered conditions.

With the bulkheads in place, DWU staff mobilized two submersible pumps to dewater the space in front of the gate. There was significant leakage through the bulkhead. Additionally, high winds resulted in wave overtopping of the bulkhead. Two inspectors from the gate inspection team rappelled down the upstream

 ©2021 All Rights Reserved

face of the gate to inspect the condition of the operating cables and their connection to the gate and to look for any debris in front of the gate. The cables and connection were noted to be in good condition, with no anomalies noted; however due to the leakage and wave overtopping of the cofferdam, close visual inspection of the upstream side was difficult. No debris was noted.

Photo 5-5: DWU Crews placing submersible pumps to de-water in front of Gate 6.

Prior to test operation, the gate was instrumented by BDI in the same manner as the other gates with the goal of measuring stress changes in the primary strut arms during test operation. The results of the measurements are included in Appendix D. Since the gate was de-watered during the operation, the results of the measurements are not sufficient to determine trunnion friction for the gate.

With the bulkheads in place, DWU staff mobilized two submersible pumps to dewater the space in front of the gate. This was performed, though there was significant leakage through the bulkhead. Additionally, high winds resulted in wave overtopping of the bulkhead. Two inspectors from the gate inspection team rappelled down the upstream face of the gate to inspect the condition of the operating cables and their connection to the gate and to look for any debris in front of the gate. The cables and connection were noted to be in good condition, with no anomalies noted; however due to the leakage and wave overtopping of the cofferdam, close inspection was difficult. No debris was noted.

Photo 5-7: Gate inspector checking operating cables and cable connection to gate.

The test operation plan included incrementally opening and closing the gate starting with cracking the gate open and then opening and closing the gate in increasing increments. A gate opening of 1 foot was set as the upper limit for test operations. 2x4’s were attached to the top of gate on each side to measure differential in opening between the left and right side. Measurements were recorded for both sides and are included in Table 5-1. The measurements indicate an even (little to no racking) opening and closing of the gate. Observers were placed at strategic locations during test operation with instructions to call a stop to operations if any anomalous behavior was observed. Observers were stationed at each trunnion, at the top of the piers on each side, at the cables for each side and at the 2x4’s to measure gate opening. Robert

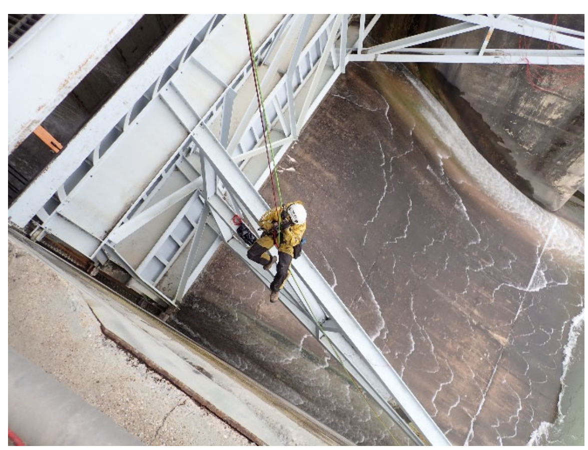

Photo 5-6: Inspector rappelling down to retrieve debris.

©2021 All Rights Reserved

Indri, Jimmy Baxter, Chris Story and Randy McIntyre conferred with the observation team and each other during each step of the test operation. During the 7.5-inch gate opening, one of the downstream observers noted a piece of debris below the gate on the right side. One of the gate inspectors rappelled down on the downstream side of the gate and the piece of debris was recovered. The debris was a short log, approximately 2-feet long and 12+ inches in diameter.

The evaluation team unanimously agreed that this piece of debris was the source of the operational issues observed in May of 2019. The piece of debris appeared to be the correct diameter to get one end of the log partially wedged between the gate and sill. On closing the weight of the gate crushed the end of the log resulting in the crimped end visible in the photos and resulting in the gate racking on closure. Since it was at the very end, the piece of debris would not be visible from the downstream side, and similarly due to the short length of the log, not visible on the upstream side. Over time the weight of the gate and the angle of the crimp allowed the log to displace upstream and for the gate to close back on the sill.

Photo 5-9: Log recovered from below the gate.

Photo 5-8: Side view of log recovered from below the gate.

Table 5-1: Gate opening measurements taken during the Gate 6 test operation.**

Operation Time (Seconds)	Right Side Measurement (Inches)**	Left Side Measurement (Inches)**
Not recorded	1/16	1/8
5	3/4	15/16
Gate Closed	--	--
10	1-5/16	1-7/16
10	2-7/8	2-7/8
10	4-1/2	4-3/8
10	5-3/4	5-7/8
Gate Closed	--	--
No time, first limit switch	7-1/2	7-1/2

** The measurements taken are not a reflection of actual gate opening because of how the 2x4's were connected to the gate and the movement of the gate in an arc. Measurements were taken to measure relative differences (potential racking) between the opposing sides of the gate.

 ©2021 All Rights Reserved

Gate 6 Strut Arm Fracture:

An anomalous fracture was observed on the left, upper strut arm for Gate 6 (member designation LS-1) (Ref. Photo 17 and18, Gate 6). An approximately 18" long fracture was noted on the flange to web connection on member LS-1 (left side, top gate arm member) for Gate #6 between the trunnion gusset plate and connection with bracing member LB-1. The fracture extended from approximately 18" upstream of connection between trunnion gusset plate and LS-1. The fracture was clearly visible on the bottom of the member, but was less visible on the top of the member.

Photo 5-10: Bottom of member LS-1 (Gate 6) showing fracture between flange and web.

LS-1 is a primary structural member. Therefore, we recommended to DWU that Gate 6 remain out of service and that the bulkheads remain in place in front of the gate until appropriate repairs can be completed.

Detailed Discussion on the fracture:

Strut LS-1 is a W10x39 I-beam that connects the Tainter gate to the trunnion on the left side of Gate 6. LS-1 exhibits longitudinal cracking between LB-1 and the gusset plate that extends through the width of the web. The crack is approximately 18 inches long and occurs in the web-to-flange connection (K-area) of the member.

The crack does not appear to be a bending, shear, or axial failure. Bending failure would result in distortion of the flanges. Shear failure would result in cracking in the web perpendicular, not longitudinally, to the beam direction. Axial failure would also cause distortion in the web and flanges from buckling. Other than the cracks along the web-flange joints, the beam does not appear to have any signs of distress or distortion. It is possible that torsion on the member due to the gate racking that occurred in May 2019 led to development and propagation of the crack; however, the rust staining on the tight crack indicates it formed prior to that incident.

Given the age of the beam and the direction of the crack, it is possible that the cracking was caused by defects that developed in the manufacturing process and was exacerbated by low-cycle fatigue under high loads. A combination of impurities in the steel, a high sulfur content, improper casting speed, uneven cooling, and high heat flux often contributes to defects such as hot tear segregations, cold shuts, and laminations in the steel blank during the casting process. Defects may not be apparent upon visual inspection of the beam blanks but can surface or intensify internally during subsequent hot rolling. In particular, concentrations of hot tear segregations formed during casting can be compressed by hot rolling into internal longitudinal cracks. During hot rolling, improperly heated, cooled, or rolled steel members can also develop longitudinal facial cracks. The K-area of hot rolled sections, along which the LS-1 crack stretches, is especially susceptible to cracking due to metallurgical changes experienced during the cold work to straighten the member and the high stress concentrations that develop in the fillet between the flange and web. Defects could take up to 48 hours after hot rolling to become apparent to

©2021 All Rights Reserved

inspection. Undetected internal cracks can go on to propagate to the surface due to fatigue under cyclic loading. As modern quality control practices had not yet been adopted when LS-1 was manufactured, it is possible that fine surficial cracking went unnoticed or that internal defects did not surface before its installation.

Gate 6 Recommendations:

Gate 6 fracture observed on member LS-1. Due to the severity of the crack, Schnabel recommends that the gate remain out of service until the strut is repaired or replaced. Design of the repairs should be performed by a Professional Engineer with experience in steel defects and fracture mechanics.

Overall recommendation (all gates) due to the LS-1, Gate 6 fracture, other strut arms may have similar fractures or cracks that were no observed. NDT should be performed on other gate struts to determine if the problem is widespread. Future inspectors should be aware of this issue and observant for similar fractures.

5.4.9 Gate 7 Findings

Coatings conditions, drain hole clogging, and connection observations for Gate 7 are generally consistent with the summary. We noted several areas of out-of-plane bending on Gate 7 members. In our opinion, the observed distortion is not structurally significant at this time and may be the result of damage during installation or during subsequent work on the gates. No repairs are recommended at this time; however, the distortion should be monitored during future inspections for change.

5.4.10 Gate 8 Findings

Coatings conditions, drain hole clogging, and connection observations for Gate 8 are generally consistent with the summary. We noted several areas of out-of-plane bending on Gate 8 members. In our opinion, the observed distortion is not structurally significant at this time and may be the result of damage during installation or during subsequent work on the gates. No repairs are recommended at this time; however, the distortion should be monitored during future inspections for change. Several welds between the vertical ribs (V-X) and the horizontal girders (G-X) were missing or incomplete, these welds should be performed/fixed during the next re-coating of the gate.

5.4.11 Gate 9 Findings

Coatings conditions, drain hole clogging, and connection observations for Gate 9 are generally consistent with the summary. We noted one area of out-of-plane bending on Gate 9. In our opinion, the observed distortion is not structurally significant at this time and may be the result of damage during installation or during subsequent work on the gates. No repairs are recommended at this time; however, the distortion should be monitored during future inspections for change.

5.4.12 Gate 10 Findings

Coatings conditions, drain hole clogging, and connection observations for Gate 10 are generally consistent with the summary. We noted several areas of out-of-plane bending on Gate 10 members. In

©2021 All Rights Reserved

our opinion, the observed distortion is not structurally significant at this time and may be the result of damage during installation or during subsequent work on the gates. No repairs are recommended at this time; however, the distortion should be monitored during future inspections for change.

5.4.13 Gate 11 Findings

Coatings conditions, drain hole clogging, and connection observations for Gate 11 are generally consistent with the summary. We noted several areas of out-of-plane bending on Gate 11 members. In our opinion, the observed distortion is not structurally significant at this time and may be the result of damage during installation or during subsequent work on the gates. No repairs are recommended at this time; however, the distortion should be monitored during future inspections for change.

5.4.14 Gate 12 Findings

Coatings conditions, drain hole clogging, and connection observations for Gate 12 are generally consistent with the summary. We noted several areas of out-of-plane bending on Gate 12 member. In our opinion, the observed distortion is not structurally significant at this time and may be the result of damage during installation or during subsequent work on the gates. No repairs are recommended at this time; however, the distortion should be monitored during future inspections for change.

5.4.15 Gate 13 Findings

Coatings conditions, drain hole clogging, and connection observations for Gate 13 are generally consistent with the summary with the exception of section loss at the bottom sill near the right side of the gate which was more advanced than observed at other gates (Ref. Photo 20, Gate 13). We noted several areas of out-of-plane bending on Gate 13 members. In our opinion, the observed distortion is not structurally significant at this time and may be the result of damage during installation or during subsequent work on the gates. No repairs are recommended at this time; however, the distortion should be monitored during future inspections for change. We noted that brace LB-5 was installed initially in the wrong direction then cut out and installed in the correct direction.

5.4.16 Gate 14 Findings

Coatings conditions, drain hole clogging, and connection observations for Gate 14 are generally consistent with the summary. We noted several areas of out-of-plane bending on Gate 14 members. In our opinion, the observed distortion is not structurally significant at this time and may be the result of damage during installation or during subsequent work on the gates. No repairs are recommended at this time; however, the distortion should be monitored during future inspections for change. We noted areas on the trunnion hubs that were ground down, likely as part of the work for the trunnion hub replacement performed on Gate 14, these abrupt changes in geometry may act as stress risers. We also observed a small tapped hole on top of the trunnion hubs; presumably, for installation of a grease fitting that was never installed.

For Gate 14 we recommend that abrupt changes in geometry for the trunnion hub be ground down to provide a more gradual transition. This should be performed as part of the next recoating project.

 ©2021 All Rights Reserved

For Gate 14, we recommend installing grease fittings in the threaded holes on top of the trunnion hubs to prevent moisture and debris from entering. This should be performed within the next year.

5.5 Gate Operations Testing

The gates were operated as part of the trunnion friction testing. Height of operation during trunnion friction testing was limited to what was required for the test (generally less than 2 feet). No anomalies were noted during operation. It is our understanding that all of the gates are operated regularly with the operator observing the operation. Other than the operational issues with Gate 6 observed in May of 2019, no recent gate operation issues were noted by DWU staff.

5.6 Conclusions – Gate Inspection

The gates are maintained and, in generally in good shape with minimal section loss observed. Observed areas of out-of-plane bending, where in our opinion, not structurally significant. The coating system is at the end of its service life and re-coating is required to reduce the corrosion potential and extend the service life of the gates. The numerous poor quality welds and weld fractures should be addressed as part of the re-coating project. The fracture in the Gate 6 arm requires attention prior to operation. This defect may be present in other strut arm members assuming they came from the same batch as LS-1. Investigation and repair of the defect should be performed as recommended below prior to returning Gate 6 to service.

5.7 Recommendations – Gate Inspection

Recommendations included in the text above are summarized in this section.

5.7.1 Dam Safety-related

Gate 6 fracture observed on member LS-1. Due to the severity of the crack, Schnabel recommends that the gate remain out of service until the strut is repaired or replaced. Design of the repairs should be performed by a Professional Engineer with experience in steel defects and fracture mechanics.

Overall recommendation (all gates) due to the LS-1, Gate 6 fracture, other strut arms may have similar fractures or cracks that were not observed. NDT should be performed on other gate struts to determine if the problem is widespread. Future inspectors should be aware of this issue and observant for similar fractures.

Connections and Welds (All Gates): We recommend repairing fractured welds and repairing or reinforcing poor quality welds. Selection of welds to be repaired and methods of repair should be coordinated between an AWS Certified Weld Inspector and a Professional Engineer experienced in the design and repair of welded connections.

©2021 All Rights Reserved

5.7.2 Maintenance

We recommend that DWU search there archives for shop drawings and any other documentation from gate construction and subsequent modifications/repairs including photos and digitize the documents for future use.

We recommend that the gate opening indicators be re-indexed to accurately reflect actual gate opening.

We recommend that DWU develop a plan for gate operations testing. Full height opening tests are typically performed at 5 year intervals under full head to evaluate performance of the gates under these type of flow conditions; however, if reservoir operations preclude gate operations testing under full head, then full height testing under dewatered conditions should be performed. Gate amperage draw should be measured and recorded during gate testing. Additionally, the emergency generator should be used to operate a gate monthly to test the backup power system.

We recommend a close-up detailed inspection of the gates be performed on a 10-year interval.

Coatings (All Gates): We recommend recoating of the gates within the next 2 to 5 years.

Drain Holes (All Gates): In the short term (less than 2 years), we recommend that the gates be cleaned and any obstructed drain holes be cleared to allow trapped water to drain and reduce the corrosion potential associated with water accumulating on the members. In the long term (recommended to be performed during re-coating of the gates) we recommend installing new drain holes where the location of the existing drain holes still results in trapped water; and, reaming of poorly cut existing drain holes to provide smooth hole.

Section Loss (All Gates): The bottom of the gate leafs exhibited section loss. This area should be repaired/reinforced during re-coating of the gates. Other areas of section loss should be evaluated by a Professional Engineer during re-coating of the gates and documented and evaluated for repair on a case-by-case basis.

For Gate 2, we recommend that the hole in the skinplate (Ref. Photo 23, Gate 2) be plugged/repaired. The hole should be repaired prior to the gate re-coating.

For Gate 3, we recommend that the hole in the skinplate (Ref. Photo 7, Gate 3) be plugged/repaired. The hole should be repaired prior to the gate re-coating

For Gate 5, we recommend monitoring the skinplate patch shown (Ref. Photo 17, Gate 5). If the patch fails prior to the gate re-coating project, it should be plugged/repaired. Otherwise, the patch should be repaired during the gate re-coating work.

For Gate 14 we recommend that abrupt changes in geometry for the trunnion hub be ground down to provide a more gradual transition. This should be performed as part of the next recoating project.

For Gate 14, we recommend installing grease fittings in the threaded holes on top of the trunnion hubs to prevent moisture and debris from entering. This should be performed within the next year.

©2021 All Rights Reserved

6.0 SPILLWAY GATE ANALYSIS

6.1 Background and Approach

In 2015, Arcadis, Inc. was retained by DWU to perform the engineering inspection of Forney Dam, as well as for the remaining inventory of Dallas City dams. The 2015 Forney Dam Inspection report presented a summary of background information and detailed the inspection findings. A list of recommendations were also provided in the 2015 Forney Dam engineering inspection report. Section 6 of the Arcadis report specifically pointed out the need of have the analyses-of-record "for those having responsibility for the Forney Dam to have a good understanding of the design and performance of the dam." The analyses of the spillway Tainter gates was specifically included on the list.

The original design analysis of the Tainter gates was concisely included in the 1961 Design Memorandum No. 2 (Reference 4) in three drawing plates. Since the Tainter gate failure at Folsom Dam in 1995, it has become standard practice to perform new structural analysis based on changes in design and safety criteria. More specifically, the analysis should include trunnion friction load combinations that were not considered in the older designs. The trunnion friction load was identified as one of the primary factors in the Folsom Tainter gate failure. For the completeness of the analysis, the wave and earthquake load combinations are also included per recent guidelines.

The work provided herein partially addresses the need for an up-to-date structural analysis of the spillway Tainter gates. The analysis is based on the design and analysis guidelines provided by the US Army Corps of Engineers (USACE) and Federal Energy Regulatory commission (FERC). Since the Tainter gates do not appear to have been structurally modified since its original design, the structural analysis is based on the Tainter gate design drawings signed and dated on August 18, 1967. The drawings are included in Appendix A of this report. The analyses assume all of the Tainter gates were fabricated and installed in general accordance with the 1969 design drawings.

The Tainter gate analysis described herein was performed based on the engineering guidelines presented in the U.S. Army Corps of Engineers (USACE) Engineering Technical Letters, ETL 1110-2-584, Design of Hydraulic Steel Structures (Reference 2). Loads and load combination were applied in general accordance with the guidelines. Load and resistance factor design (LRFD) is the recommended method of analysis by ETL 1110-2-584. American Institute of Steel Construction (AISC) Specification 360-10 included in the 14th Edition of the Steel Construction Manual (Reference 1) was used to perform the structural evaluation of members. Member adequacy is expressed as an interaction value (utilization ratio) of the required strength from the applied forces and moments on the member divided by the design strength capacity of the member. An interaction value (utilization ratio) less than 1.0 indicates the member meets strength requirements in accordance with AISC Specification 360-10. An interaction value (utilization ratio) greater than 1.0 indicates the member is overstressed per the specified criteria. However, it does not necessarily indicate a physical failure of the member due the inherent safety factors included in the load factors and the strength factors.

An additional safety factor is applied per ETL 1110-2-584, which mandates multiplication of the AISC strength resistance factors by an additional reliability (performance) factor equal to 0.9. For the Tainter gate evaluation, the 0.9 reliability factor is multiplied the strengths of the steel. Therefore, interaction value (utilization ratio) of 1.0 remains as the criteria for code compliance.

©2021 All Rights Reserved

The Tainter gate evaluation involved developing a three dimensional (3D) space frame model of the structure. STAAD Pro, a commercial 3D structural analysis software by Bentley, was used for the development of the structural model as well as checking member adequacy.

6.2 Loads and Load Combinations

The loads and load combinations used for the Forney Dam Tainter gate evaluation are selected from the load combinations recommended by ETL 1110-2-584. Each load in the load combinations has its prescribed load factor.

For comparison purposes, two additional load combinations under gate operating conditions were also evaluated with the load factors removed. The unfactored load combinations provide indicators of gate performance without the conservatism introduced by the load factors. Therefore, they provide insight into the stress conditions the gates are likely exposed to during operation. Besides allowing comparison between factored and unfactored load combinations, the unfactored load combinations also provide comparison with the results from the recent trunnion friction tests performed.

Seven load combinations were analyzed. The load combinations can be separated into to two groups: gate closed and gate operating.

<u>Gate closed load combinations</u>:

Load Combination LC1a – Gate closed:
$1.2D + 1.4\ H_2$

Load Combination LC1b – Gate closed with wave load:
$1.2D + 1.4\ H_2 + 1.2W_A$

Load Combination LC4b – Gate closed with earthquake:
$1.2D + 1.4\ H_1 + 1.0E$

<u>Gate operating with two hoists load combinations</u>:

Load Combination LC2a – Gate operating:
$1.2D + 1.4\ H_3 + 1.4\ F_s + 1.0\ F_t + Q_h$

Load Combination LC2aU – Gate operating (unfactored):
$D + H_3 + F_s + F_t + Q_h$

Load Combination LC2b – Gate operating with wave load:
$1.2D + 1.4\ H_2 + 1.4\ F_s + 1.0\ F_t + 1.4\ W_A + Q_h$

Load Combination LC2bU – Gate operating with wave load (unfactored):
$D + H_2 + F_s + F_t + W_A + Q_h$

Where

H_1 Hydrostatic load from the usual (normal) pool level
H_2 Hydrostatic load from the unusual pool level
H_3 Hydrostatic load from the extreme pool level
D Gate dead load
F_S Side seal friction load

©2021 All Rights Reserved

F_t Trunnion friction load
E Earthquake load
W_A Wave load
Q_h Wire cable hoist load

The gate opening load combinations also include the corresponding cable lifting forces applied at the cable connection with the gate and the radial cable wrap forces applied at the cable-skin plate contact areas to simulate the operating condition as described in ETL 1110-2-584. For this study, both gate opening and gate closing conditions are modeled although gate opening condition usually provides the more critical load condition for most of the gate members. **Gate full open load combinations are not considered in this study.**

When possible, loads are determined based the documents made available by DWU. Following assumptions and estimates were made in determining the loads for the Tainter gate analysis:

- Weight of the gate was not found from the documents provided by DWU. Based on the STAAD model, each Tainter gate weighs approximately 52.3 kips which includes a gate weight factor of 1.03 used to account for the weights not modeled, such as the weights of stiffeners, side seals fixtures, welds, part of trunnion hub beyond center of pin, paint and etc. The model indicates that the center of gravity of the gate in closed position is located at 23.0 ft upstream of the trunnion and 2.4 ft above the trunnion. In the original design calculation, the corresponding center of gravity location was reported to be at 22.0 ft and 2.5 ft, respectively.
- The usual pool elevation for determining hydrostatic load H_1 is defined in the ETL 1110-2-584 as having a mean return period between 1 and 10 years. For Forney Dam, this is interpreted as the normal pool at elevation 435.5 ft.
- The unusual pool elevation for determining hydrostatic load H_2 is defined in the ETL 1110-2-584 as having a mean return period between 10 and 300 years. For Forney Dam, this is interpreted as an unusual pool at elevation 436.5 ft. The interpretation is based on the “Flood Operation of Lake Ray Hubbard by Dallas Water Utilities Personnel” (Reference 5) prepared in 2005. The flood operation stated that the freeboard should not be allowed to become less than one foot on any of the gates. Therefore, all of the gates must be raised by the time the lake rises to 436.50 ft.
- The extreme pool elevation for determining hydrostatic load H_3 is defined in the ETL 1110-2-584 as having a mean return period greater than 300 years. For Forney Dam, this is interpreted as an extreme pool at elevation 437.5 ft matching the elevation at the top of the gate. This is the pool elevation reportedly used in the original design calculation.
- Side seal friction load F_s is determined based on the method described in ETL 1110-2-584 with a recommended side seal friction μ_s coefficient of 0.5. Based on project Drawing No. 37, there is no preset δ of the side seals.
- Trunnion friction load F_t is a function of the trunnion reactions from the STAAD model and the coefficient of friction of the trunnion pin and the trunnion end bearing (thrust washer). A default coefficient of friction μ_t of 0.3 is recommended by ETL 1110-2-584 for any bushing material that may be slightly worn or improperly maintained although the trunnion bushings and end bearing rings are self-lubricating. The trunnion friction force is determined based on the reactions at the trunnion support. The resultant radial reaction force about the pin and the trunnion pin friction coefficient are used to determine the trunnion pin friction force. The axial force along the pin and

 ©2021 All Rights Reserved

the end bearing friction coefficient are used to determine the trunnion end bearing friction force. Trunnion friction load F_t is the combination of these two friction forces.

- The wave pressure load W_A on the gate is assumed to have a linear distribution that decreases with depth from a static head of 4 ft (equivalent of 249.6 psf in pressure) at the top of the gate to a static head of 2 ft (equivalent of 124.8 psf in pressure) at the bottom of the gate. The 4 ft of head at the top of the gate is based on the total water rise of 5.0 ft above the unusual pool level that is at 1.0 ft below the top of the gate. The total water rise of 5.0 ft is the sum of the computed wave height of 4.5 ft and the wind tide of 0.5 ft described in Design Memorandum No. 1 (Reference 3). The wave pressure at the bottom of the gate is approximated as half of the pressure at the top of the gate, or a static head of 2 ft.
- The earthquake load E is assumed to have a peak ground acceleration a_{PGA} of 0.05g as was used in the original stability analysis of the spillway concrete structure described in Design Memorandum No. 2 (Reference 4). No additional amplification of the seismic acceleration due to dam motion is assumed. When seismic acceleration is applied in one principle direction, the orthogonal seismic acceleration is approximated as 1/3 of the principle acceleration.
- On each gate, there are two sets of wire cables connected to the cable hitch on each side of the gate as shown on project Drawing No. 39. Wire cable hoist force Q_h is needed to lift the gate. The greatest cable hoist force required is when the gate is operated near the closed position where the gate is experiencing full pool hydrostatic pressure, wave pressure, gate weight, side seal friction, and trunnion friction loads. The cable hoist force Q_h is determined when the cable lifting force balances all other loads on the gate and the gate is about to move. The cable hoist force will be different for opening and closing as friction force directions will change with the gate rotation direction. Where the wire cable bears on the skin plate, the tensioned cable exerts a contact pressure (line load) on the skin plate and normal to the skin plate. The contact pressure (wrap) force is equal to the cable tension force divided by the gate radius. The magnitude of this cable wrap force is dependent of the cable hoist force. In the STAAD model, it is applied to the gate as a part of wire cable hoist load.

Other loads such as mud weight, atmospheric ice weight, and ice impact load included in ETL 1110-2-584 are not expected to occur for the Tainter gates at Forney Dam. The load values used for the structural analysis of the Tainter gate are summarized in Table 6-1.

©2021 All Rights Reserved

Table 6-1: Forney Dam Tainter Gate Load Data Summary

Load Description	Symbol	Load Value	Definition/Source/Notes
Gravity Loads			
Gate weight	D	52.3 kip	Per STAAD Model
Hydrostatic Loads H			
Usual (normal) pool elevation	H_1	435.5 ft	ETL 1110-2-584, normal pool
Unusual pool elevation	H_2	436.5 ft	ETL 1110-2-584, Flood Operation (Reference 5)
Extreme pool elevation	H_3	437.5 ft	ETL 1110-2-584, original design calculation
Side-seal Friction Load F_s			
Coefficient of friction	μ_s	0.5	ETL 1110-2-584
Preset deflection	δ	0 in	Project Drawing No. 37
Trunnion Pin Friction F_t			
Coefficient of friction	μ_t	0.3	ETL 1110-2-584
Earthquake design load E			
Seismic acceleration	a_{PGA}	0.05g	Design Memorandum No 2 (Reference 4)
Wave Load			
Wave load	W_A	249.6 psf, top 124.8 psf, bot	Design Memorandum No 1 (Reference 3)
Wire cable hoist Load			
Wire cable hoist load	Q_h	Magnitude as required for gate operation	Based on STAAD Model for each specific gate operating condition.

6.3 Gate Analysis and Modelling Considerations

6.3.1 Material and Section Properties

Per project Drawing No. 36 included in Appendix A, the Tainter gates are primarily comprised of ASTM A-36 steel with a yield strength of 36 ksi with the exception of the skin plates and ribs which are made of ASTM A-441 steel. It is worth noting that the vertical and horizontal girder braces are made of the same steel shapes as the rib members, and therefore, they are likely to be made of A-411 steel as well. However, a strict interpretation of the project drawings is used, and the girder braces are modeled as A36 steel. A-441 steel is a high-strength low-alloy steel that is lighter and has greater durability than typical A-36 steel. For plate and bars up to 3/4 inch thick, A-441 has a yield strength of 50 ksi. All structural steel used to construct the Tainter gates are welding grade steel. The modulus of elasticity of steel is modeled as 29,000 ksi, and the Poisson’s ratio is taken as 0.3.

©2021 All Rights Reserved

The Tainter gates were fabricated circa 1969. Some of the old steel shapes used to construct the gates are no longer used today. To address the common need of analyzing older structures, STAAD has incorporated a database of these old steel shapes. When modeling the Tainter gate with discontinued steel shapes, the STAAD built-in database is utilized.

6.3.2 Structural Model

The gate structure geometry is developed to accurately represent the ribs, girders, struts, and main bracing based on the project drawings. Coordinates at some secondary bracing members and skin plate thickness transitions were adjusted to limit model complexity while maintaining a suitable representation of the gate structure for accurate load application and structural analysis. In order to model the structural integrity of the gate, the following modeling techniques are used:

- The webs of ST6B9.5 ribs are continuously welded to the skin plate. As such, the ribs and the skin plate behave interactively as skin-rib composite members. The effective width of the skin plate attributed to each skin-rib composite member is taken to the mid span on either side of the rib. These dimensions are entered into STAAD as built-up members. The section properties of the skin-rib composite members are calculated using the Section Wizard tool included in STAAD. The calculations are included in Attachment A of Appendix C. The skin plate is also modeled using plate elements to allow accurate application of hydrostatic, hydrodynamic and wave pressure loads and to retain the structural integrity of the entire skin plate. However, since the skin plate is already included in the construction of the skin-rib composites, the skin plate elements are modeled with zero density steel to not double count its weight. The plate elements are also modeled with reduced (one tenth) modulus to not double count its structural capacity.
- The built-up hub is composed of web plates and side plates. The hub tappers down towards the trunnion as shown on project Drawing No. 38. A detailed model of the trunnion is beyond the scope and level of this study. However, to take advantage of the STAAD model and the code check capability of STAAD, an approximation of the built-up hub is made by separating the hub into three generalized segments. Each segment is modeled with section properties representing the actual steel sections geometry at the middle of the segment. The most critical section with the smallest section properties is the shortest (weakest) section closest to the trunnion hub. This modeling approach allows an approximate check of the structural capacity of the built-up hub. The section properties of each segments are calculated using the Section Wizard. The calculated section properties of the built-up hub representative segments are include in Attachment A of Appendix C. STAAD master-slave node control is used to connect the ends of the three struts to the built-up hub.
- To limit the potential loss of geometrical accuracy, the horizontal girders and the skin-rib composite are modeled at their respective design locations. Weightless fictitious steel plates with thickness matching the webs of the girders are used to connect the girders to the ribs. These fictitious members span the gap between the centroid node of the girder and the centroid node of the girder members.
- For gate closed load combinations, weightless fictitious compression-only members are used to simulate compression only supports along the bottom sill. This is done to prevent the bottom support from falsely pulling the gate down when the skin plate and rib system starts to deform

 ©2021 All Rights Reserved

under loads. These compression-only support members are oriented in the same angle as the sill plate.

A schematic stick-frame view of the STAAD structural model of the Forney Dam Tainter gate is shown in Figure 6-1. Figure 6-2 shows the model with full sections of the members. The built-up hub can be seen modeled as representative segments.

Figure 6-1: Forney Dam Tainter Gate STAAD Model in Stick Frame View

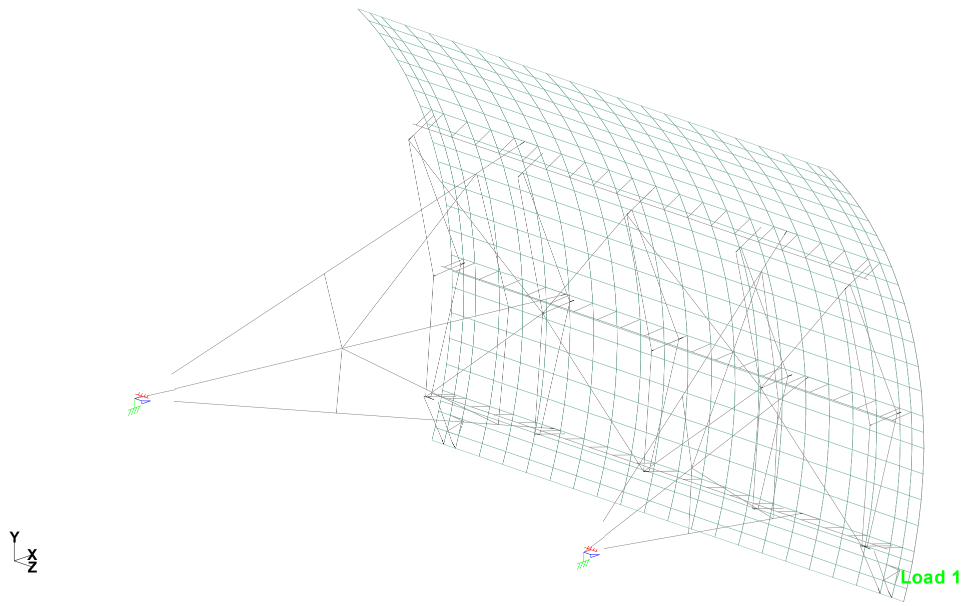

Figure 6-2: Forney Dam Tainter Gate STAAD Model in Member Full Section View

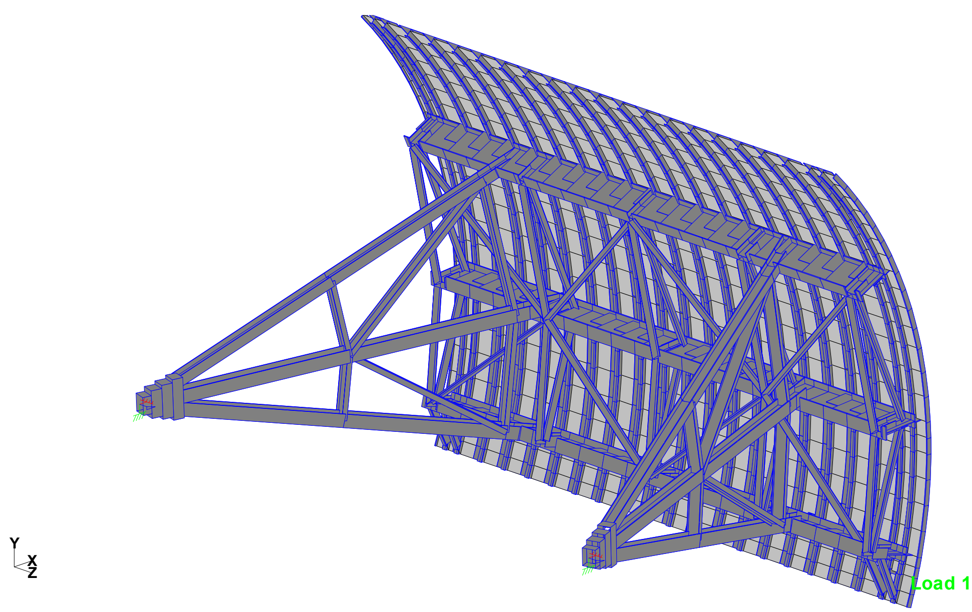

 ©2021 All Rights Reserved

The X, Y, and Z global coordinates of the STAAD model correspond to the instream (upstream-downstream), vertical, and cross-stream (left-right) directions, respectively. The STAAD member local coordinates x, y, and z correspond to member axial, member section major axis, and member section minor axis, respectively. It is important to note that the member local axis convention used in STAAD is different from the convention used in the AISC Steel Construction Manual. The member z-axis in STAAD is the x-axis in the AISC. Therefore, all sectional and structural properties about the member z-axis reported in STAAD are equivalent to the same properties about the x-axis in the AISC manual while structural properties about the member y-axis are the same for both conventions. In this Tainter gate evaluation, the STAAD global and member local coordinate convention is used unless otherwise noted. The unbraced length of each modeled member was determined based on the structural geometry and connection configuration of the member with reference to the member local coordinate system. The effective length factors for member buckling behavior check were selected based on AISC recommendations. Model members are adjusted as needed by a rotation angle about it local member x-axis to match the as designed orientation.

The Tainter gate members, steel shape, location description, and STAAD model member numbers are summarized in Table 6-2 for reference. Diagrams of STAAD model node numbers and member numbers are provided in Attachment B of Appendix C.

Table 6-2: Forney Dam Tainter Gate Member Structural Properties

Gate Member Description	Steel Shape	Location/ Description	STAAD Model Member ID #
Skin Plate (Weightless)	1/4" plate 5/16" plate 3/8" plate	Skin Plate	801 to 1328
Skin-Rib Composites	ST6B9.5 Skin Plate	Ribs	201 to 752
Horizontal Girders	27WF84	Top Girder	37 to 64
	30WF116	Middle Girder	65 to 92
	30WF124	Bottom Girder	93 to 120
Girder Lateral Bracing	ST6B9.5	DS Girder Flange Instream Diagonal	121 to 138 143 to 152
		Bottom Girder to Gate bottom	139 to 142
Strut Arms	10WF39	Top Strut	2 to 4 (20 to 22)
	10WF60	Middle Strut	6 to 8 (24 to 26)
	10WF72	Bottom Strut	10 to 12 (28 to 30)

 ©2021 All Rights Reserved

Gate Member Description	Steel Shape	Location/ Description	STAAD Model Member ID #
Strut Bracing	10B15	Vertical Brace	13 to 16 (31 to 34)
		Diagonal Brace	17 to 18 (35 to 36)
Hub	Built-up	Trunnion Hub	1332 to 1334 (1336 to 1338)

6.3.3 Analyses and Results

<u>Analyses and Results of Gate Closed Load Combinations</u>

Load combination LC1a – Gate closed – is the normal case for the Tainter Gate in the closed position resisting the hydrostatic pressure from an unusual pool level at elevation 436.5ft. Figure 6-3 shows the STAAD model structural diagram for this load case. The trunnion supports are modeled as fixed except its rotation about the trunnion pins in global Z-axis. A row of compression only fictitious members connecting to the bottom of the gate were used to simulate the sill support of the spillway dam. The compression only feature is to ensure the supporting concrete does not "pull" the gate down when the Tainter gate deflects under loads. The angles of these members are normal to the concrete surface to ensure the reaction forces are normal to the concrete surface. Load diagrams of the loads applicable to the load combinations are included in Attachment C of Appendix C.

Figure 6-3: Forney Dam Tainter Gate STAAD Model for Gate Closed Load Combinations

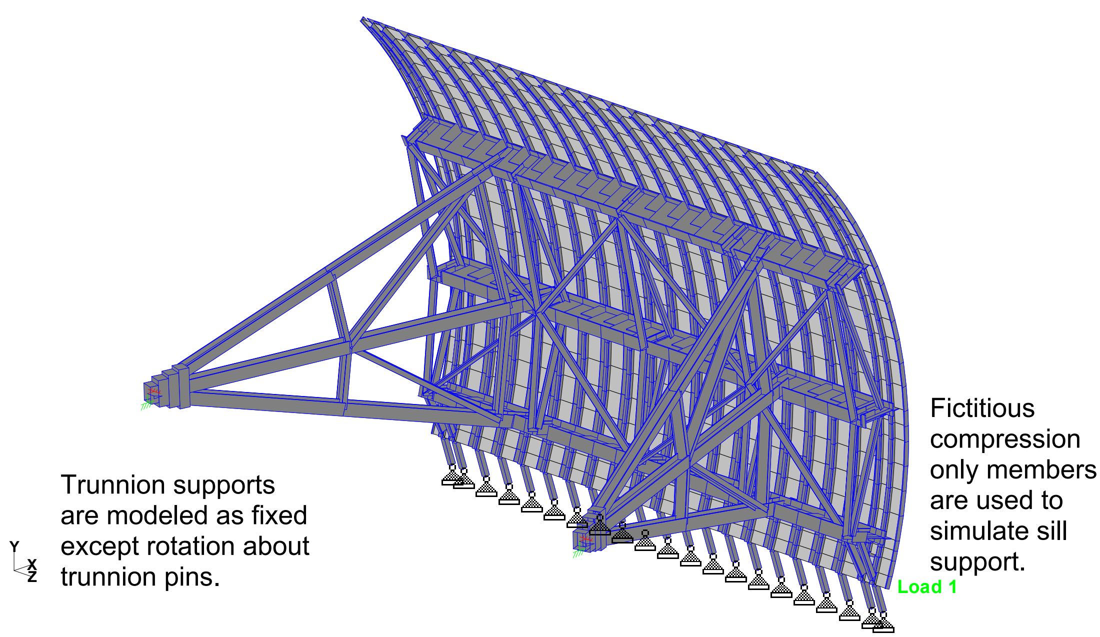

©2021 All Rights Reserved

Load combination LC1b – Gate closed with wave load – has the same loads and load factors as load combination LC1a with an additional wave load. Therefore, structural members develop higher stresses in LC1b than LC1a. Load combination LC4b – Gate closed with earthquake – has the same loads and load factors as load combination LC1a except the hydrostatic pressure load is from a normal pool level at elevation 435.5ft, and there is an additional earthquake load. By judgment, the orthogonal seismic loads are more critical if the seismic acceleration are applied in the directions that is additive to the hydrostatic and gravity loads. Thus, two different earthquake load combinations are modeled. In one load combination, the seismic acceleration is applied horizontally in the downstream direction and 1/3 of the seismic acceleration applied vertically in the direction of gravity. In the other load combination, the seismic load is applied vertically in the direction of gravity and 1/3 of the seismic load applied horizontally in the downstream direction. The corresponding hydrodynamic loads are applied and scaled accordingly.

The resultant interaction values (utilization ratios) of the structural members from the STAAD model analysis are included in Attachment D of Appendix C and summarized in Table 6-3. The analysis results of the gate closed load combinations show some members are overstressed for load combinations LC1a and LC1b. The table is color coded such that the blue color shaded cells indicate one or more members of the location group are overstressed with interaction values between 1.00 and 1.30. The red color shaded cells indicate one or more members of the location group are overstressed with interaction values greater than 1.30.

©2021 All Rights Reserved

Table 6-3: Forney Dam Tainter Gate Critical Member Interaction Values (Utilization Ratio) for Gate Closed Load Combinations

Member Description	Location	Gate Closed Load Combinations			
		LC1a (Base)	LC1b (Wave)	LC4b (Earthquake)	
				Horizontal	Vertical
Skin-Ribs Composites	Top of Gate to Top Girder	0.37	1.00	0.28	0.26
	Top Girder to Middle Girder	0.55	0.99	0.55	0.53
	Middle Girder to Bottom Girder	0.65	0.70	0.65	0.64
	Bottom Girder to Bottom of Gate	0.65	0.70	0.65	0.64
Horizontal Girders	Top	0.38	0.67	0.39	0.37
	Middle	0.54	0.57	0.53	0.52
	Bottom	0.66	0.70	0.66	0.64
Girder Bracing	Between Top and Middle Girder	0.13	0.18	0.13	0.13
	Between Middle and Bottom Girder	0.17	0.16	0.18	0.19
Strut Arms	Top	0.50	0.86	0.46	0.44
	Middle	0.74	0.84	0.73	0.71
	Bottom	0.65	0.71	0.65	0.64
Strut Bracing	Vertical	0.09	0.13	0.11	0.11
	Diagonal	1.08	1.59	0.99	0.97
Built-up Hub	Hub	0.71	0.73	0.71	0.69

The overstressed members are also indicated by the diagrams of Figure 6-4 and Figure 6-5 in blue and red with the skin plate members removed for clarity. The diagrams are color coded with blue and red indicating the different levels of overstress as the way was done with the interaction value summary table.

 ©2021 All Rights Reserved

Figure 6-4: Overstressed Members of Gate Closed Base Load Combination (LC1a)

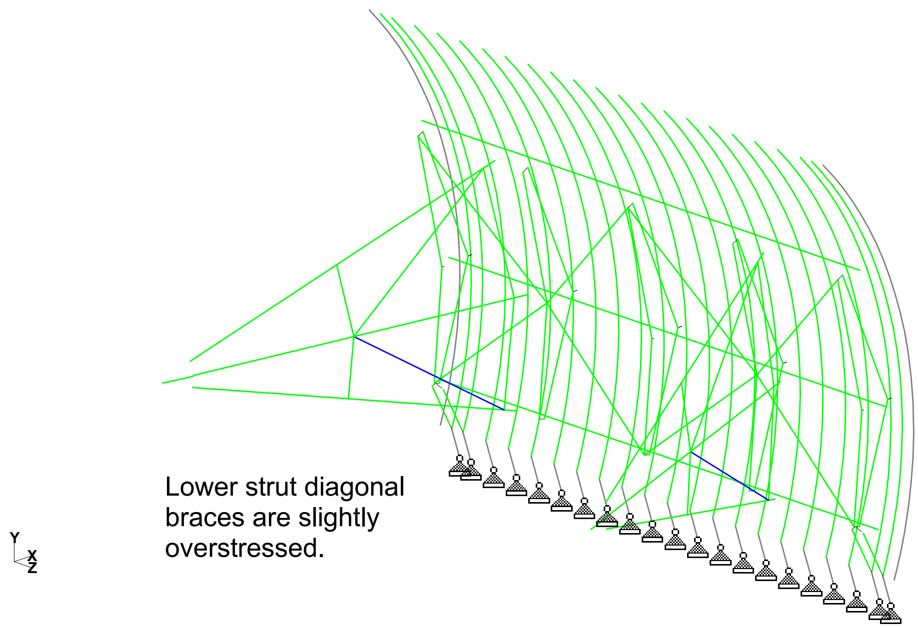

Figure 6-5: Overstressed Members of Gate Closed Wave Load Combination (LC1b)

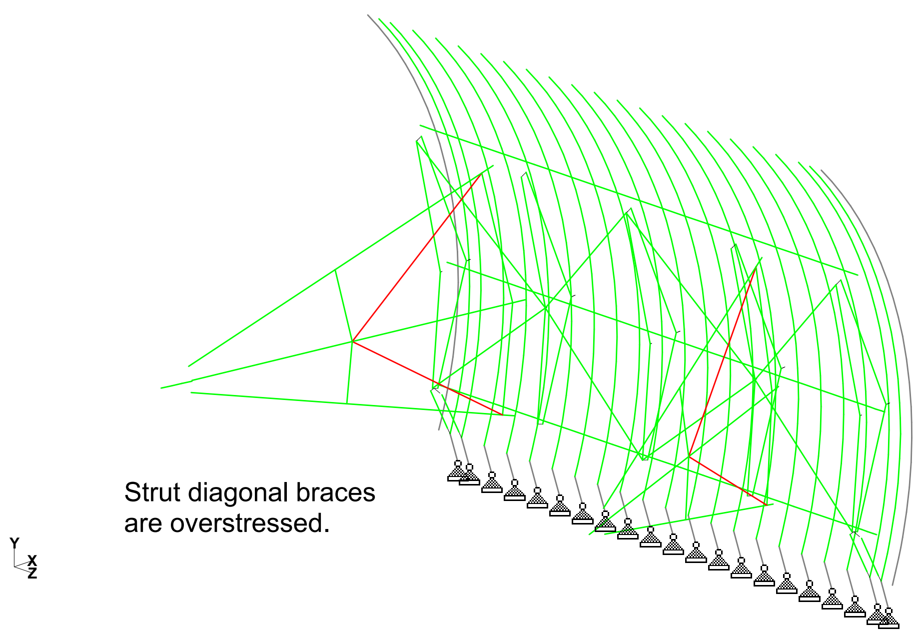

©2021 All Rights Reserved

Results of LC1a analyses indicate the strut diagonal brace is slightly overstressed with an interaction value of 1.08. This is mainly due to the configuration of the strut member allows the diagonal brace to pick more hydrostatic load from the bottom portion of the gate and transfer it to the middle strut before transferring the load to the trunnion hub. The strut diagonal brace is, therefore, undersized for this load path. This strut diagonal brace overstress is further stressed with the addition of the wave load in load combination LC1b to have an interaction value of 1.59. The skin-rib composite members are found to be overstressed in different regions, but mostly at locations close to the horizontal girder connections where the members experiences the highest bending moments. Overall, the wave load of LC1b adds additional stresses to the members leading higher interaction values for the majority of the members.

For the two seismic load combinations of LC4b, no member is found to be overstressed. The member stresses are generally slightly lower than those of LC1a. The main reason for the decrease is the reduced hydrostatic load of H_1 at reservoir elevation 435.5 ft as compared to the H_2 reservoir elevation of 346.5 ft. Although an earthquake load is included in LC4b, the seismic coefficient of 0.05g is a relatively low.

<u>Analyses and Results of Gate Operating Load Combinations</u>

Load Case LC2a – Gate operating – is for evaluating gate stresses during operation while resisting the hydrostatic pressure from an extreme pool level at elevation 437.5ft. When the gate is in operation, it will experience additional loads including side seal friction, trunnion friction, wire cable hoisting load, and cable wrap force. These loads are present in both opening and closing operations. The reactive friction loads, side seal friction and trunnion friction, exert forces on the gate in opposite direction between opening and closing.

Load combination LC2b – Gate operating with wave load – has the same loads and load factors as load combination LC2a with an additional wave load. Therefore, structural members develop higher stresses in LC2b than LC2a. As discussed previous, load combinations LC2a and LC2b were also analyzed with all the load factors removed. The unfactored load combinations provide results for the structure without the load factors. Therefore, they simulate the stress states the gates are likely to see during gate operations. Besides allowing comparison between factored and unfactored load combinations, the unfactored load combinations also provide comparison with the results from the recent trunnion friction tests performed.

Although not explicitly described in EM 1110-2-2702 (Reference 2), gate operating load case include both gate opening and gate closing conditions. Opening and closing yield different load conditions as the frictions load act in opposition direction of gate movement. Thus, in all there are eight different load combinations modeled as listed below:

Load Combination LC2a – Gate operating:

$1.2D + 1.4\ H_3 + 1.4\ F_s + 1.0\ F_t + Q_h$ (opening)

$1.2D + 1.4\ H_3 + 1.4\ F_s + 1.0\ F_t + Q_h$ (closing)

Load Combination LC2aU – Gate operating (unfactored):

$D + H_3 + F_s + F_t + Q_h$ (opening)

$D + H_3 + F_s + F_t + Q_h$ (closing)

Load Combination LC2b – Gate operating with wave load:

©2021 All Rights Reserved

$1.2D + 1.4 H_2 + 1.4 F_s + 1.0 F_t + 1.4 W_A + Q_h$ (opening)
$1.2D + 1.4 H_2 + 1.4 F_s + 1.0 F_t + 1.4 W_A + Q_h$ (closing)

Load Combination LC2bU – Gate operating with wave load (unfactored):

$D + H_2 + F_s + F_t + W_A + Q_h$ (opening)
$D + H_2 + F_s + F_t + W_A + Q_h$ (closing)

Trunnion friction load can be a significant load depending on the friction coefficient at the trunnion pin and the trunnion end bearing plate. A trunnion friction coefficient of 0.3, as recommended by ETL 1110-2-584, is used for all gate operating load combinations analyzed, although the trunnion bushings and end bearing rings are self-lubricating. The trunnion friction coefficient of 0.3 is generally higher than the trunnion friction coefficient found in the field test results range from 0.08 to 0.33. Trunnion friction adds stress to the already highly stressed strut arm members. The most critical loading conditions for gate lifting and closing occurs when the gate is operated near the closed position, just lifted off from the sill. At this instant, the full hydrostatic head is acting on the gate and generates the highest support reactions at the trunnions and thus the highest trunnion friction moments.

To determent the trunnion friction moments, the two trunnion supports are modeled as fixed supports. The gate is modeled in the near closed position without any support at the bottom of the gate. Figure 6-6 shows the STAAD model structural diagram for this load case. The cable lifting forces are applied at the modeled lifting pins of the cable hitches. The radial wrap forces are applied at the skin plate to simulate the tensioned ropes pressing against the gate.

Figure 6-6: Forney Dam Tainter Gate STAAD Model for Gate Operating Load Combinations

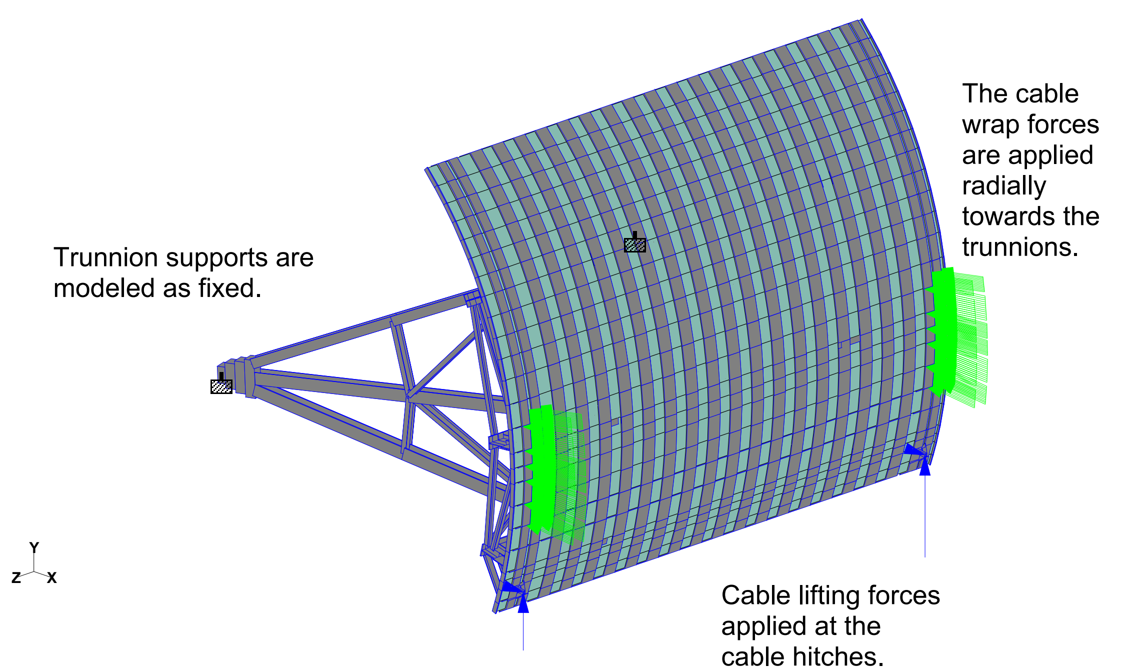

©2021 All Rights Reserved

As the hoist-lifting load is increased, the resisting moments at the fixed trunnion supports will increase, simulating the trunnion friction moments. At the same time, the trunnion friction moments can also be calculated from the axial reactions from the pin supports as discussion previously. The amount of cable lifting force for operation is determined when the fixed support moments are equal to the calculated trunnion friction moments. An iterative process with a series of STAAD model trial runs is used to reach this balance for each gate operating load combination. Table 6-4 summarizes the resultant cable hoist forces and trunnion friction moments for the eight gate operating load combinations.

The total cable hoist force ranges from 17.2 kips for an unfactored load combination to 33.7 kips for a factored load combination as compared to the hoist system's design capacity of 64.4 kips stated in Design Memorandum No 2. For each gate operating load combination, there is a difference in cable hoist force between opening and closing simulation. The difference is mainly caused by friction forces including trunnion friction and side seal friction that always act to resist the direction of movement between opening and closing. This differences ranged from 4.4 kips to 7.0 kips on each side.

Table 6-4: Wire Cable Hoist Forces and Trunnion Friction Moments for Gate Operating Load Combinations

Load Combination	Gate Operation	Cable Hoist Force (kip)		Trunnion Friction Moment (kip-ft)			
		Each Side	Total	Trunnion Pin	End Bearing	Each Side (Pin + Bearing)	Total
LC2a Gate operating	Opening	16.8	33.7	86.3	34.5	120.8	241.6
	Closing	9.9	19.8	86.2	34.4	120.7	241.3
LC2aU Gate operating (Unfactored)	Opening	13.6	27.1	61.7	24.7	86.4	172.7
	Closing	8.6	17.2	61.6	24.6	86.3	172.5
LC2b Gate operating with Wave	Opening	16.4	32.8	95.8	38.2	134.0	268.0
	Closing	10.4	20.8	95.7	38.2	133.9	267.7
LC2bU Gate operating with Wave (Unfactored)	Opening	13.3	26.6	70.3	28.1	98.4	196.7
	Closing	8.9	17.8	70.2	28.0	98.2	196.5

The resultant interaction values (utilization ratios) of the structural members from the STAAD model analysis are included in Attachment D of Appendix C and summarized in Table 6-5 for gate operating load combinations. The table is again color coded with blue and red color shaded cells indicating when the interaction values are between 1.00 and 1.30 and greater than 1.30, respectively. The analysis results of the gate operating load combinations show some members are overstressed for factored load

 ©2021 All Rights Reserved

combinations LC2a and LC2b. The interaction values are much lower for the unfactored load combinations.

When comparing the results of the gate operating load combinations in Table 6-5 with the results of the gate closed load combinations of Table 6-3, it can be concluded that gate operation condition shifts stresses from the lower part of the strut arms to upper part of the strut arms. This matches the understanding that the moment created by the cable hoist force about the trunnion supports would induce more compression in the upper part of the strut arms. Thus, with the combination of wave load and the trunnion moments all three strut arms are overstressed for LC2b.

As with the gate closed load combinations, results of LC2a show the strut diagonal brace is overstressed with an interaction value of 1.62. This is mainly due to the configuration of the strut arm that allows the diagonal brace to pick more hydrostatic load from the bottom portion of the gate and transfer it to the middle strut before transferring to the trunnion hub. The strut diagonal brace is, therefore, undersized for its role in the load path. This strut diagonal brace overstress is further stressed with the addition wave load in LC2b to have an interaction value of 2.09. The strut diagonal brace was found to be overstressed in most of the load combinations.

The skin-rib composite members are found to have interaction value of 1.0 for the load combinations that include wave load. The higher stress part is in the region near the top horizontal girder where the skin-rib composite members experience the cantilever bending moments from the wave load above the top girder.

Overall, with the wave load acting on top of the hydrostatic load, LC2b adds additional stresses that leads to higher interaction values for nearly all of the members. Figure 6-7 and Figure 6-8 show the overstressed members for opening and closing of the gate operating base load combination LC2a. Figure 6-9 and Figure 6-10 show the overstressed members for opening and closing of the gate operating with wave load combination LC2b.

©2021 All Rights Reserved

Table 6-5: Forney Dam Tainter Gate Critical Member Interaction Values (Utilization Ratio) for Gate Operating Load Combinations

Member Description	Location	Gate Operating Load Combinations							
		LC2a (Base)		LC2aU (Base) (unfactored)		LC2b (Wave)		LC2bU (Wave) (unfactored)	
		Opening	Closing	Opening	Closing	Opening	Closing	Opening	Closing
Skin-Ribs Composites	Top of Gate to Top Girder	0.55	0.54	0.39	0.39	1.00	1.00	0.79	0.79
	Top Girder to Middle Girder	0.59	0.59	0.42	0.42	0.99	0.99	0.78	0.78
	Middle Girder to Bottom Girder	0.58	0.58	0.44	0.42	0.61	0.59	0.41	0.42
	Bottom Girder to Bottom of Gate	0.56	0.56	0.42	0.42	0.58	0.59	0.44	0.44
Horizontal Girders	Top	0.52	0.46	0.33	0.33	0.66	0.67	0.51	0.51
	Middle	0.60	0.59	0.42	0.42	0.61	0.60	0.44	0.44
	Bottom	0.64	0.70	0.46	0.46	0.67	0.72	0.48	0.48
Girder Bracing	Between Top and Middle Girder	0.17	0.15	0.12	0.11	0.18	0.18	0.14	0.14
	Between Middle and Bottom Girder	0.12	0.11	0.09	0.08	0.17	0.16	0.13	0.12
Strut Arms	Top	0.95	0.84	0.68	0.60	1.23	1.10	0.93	0.84
	Middle	1.18	1.13	0.85	0.81	1.29	1.23	0.94	0.90
	Bottom	0.93	1.01	0.67	0.72	0.98	1.06	0.71	0.77
Strut Bracing	Vertical	0.30	0.41	0.21	0.30	0.32	0.43	0.23	0.31
	Diagonal	1.62	1.18	1.18	0.90	2.09	1.65	1.60	1.24
Built-up Hub	Hub	0.89	0.96	0.64	0.68	1.02	1.00	0.76	0.73

©2021 All Rights Reserved

Figure 6-7: Overstressed Members of Gate Operating Base Load Combination (LC2a), Opening

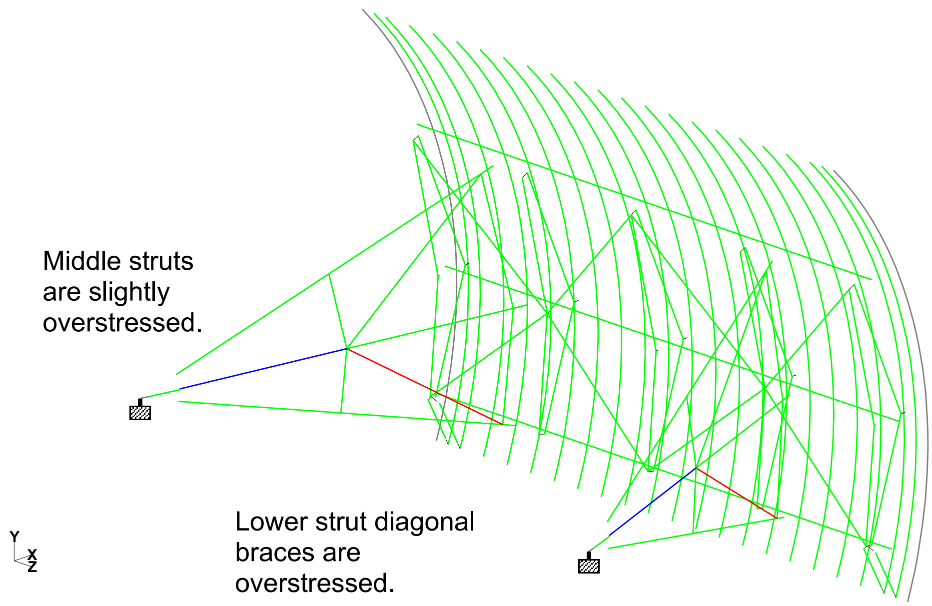

Figure 6-8: Overstressed Members of Gate Operating Base Load Combination (LC2a), Closing

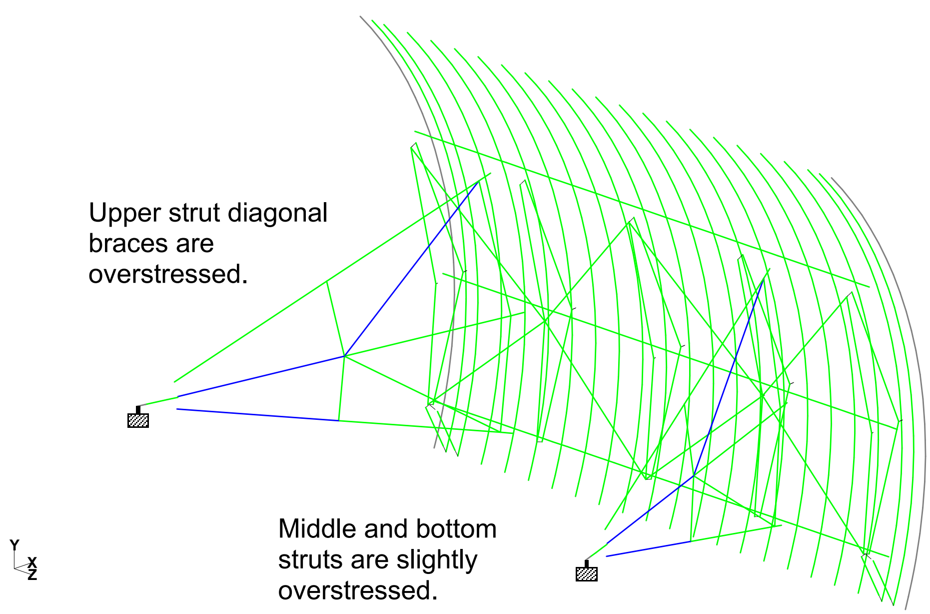

©2021 All Rights Reserved

Figure 6-9: Overstressed Members of Gate Operating Wave Load Combination (LC2b), Opening

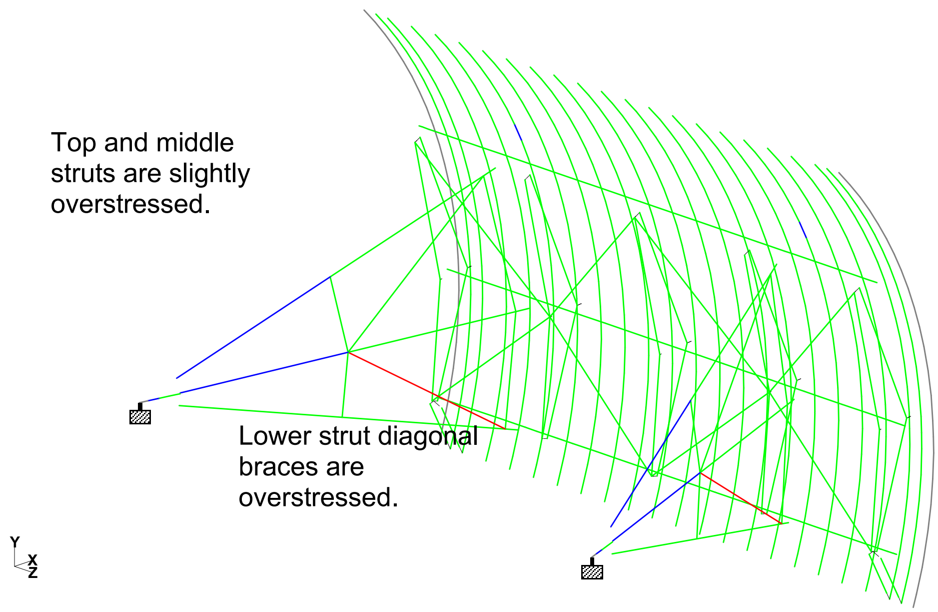

Figure 6-10: Overstressed Members of Gate Operating Wave Load Combination (LC2b), Closing

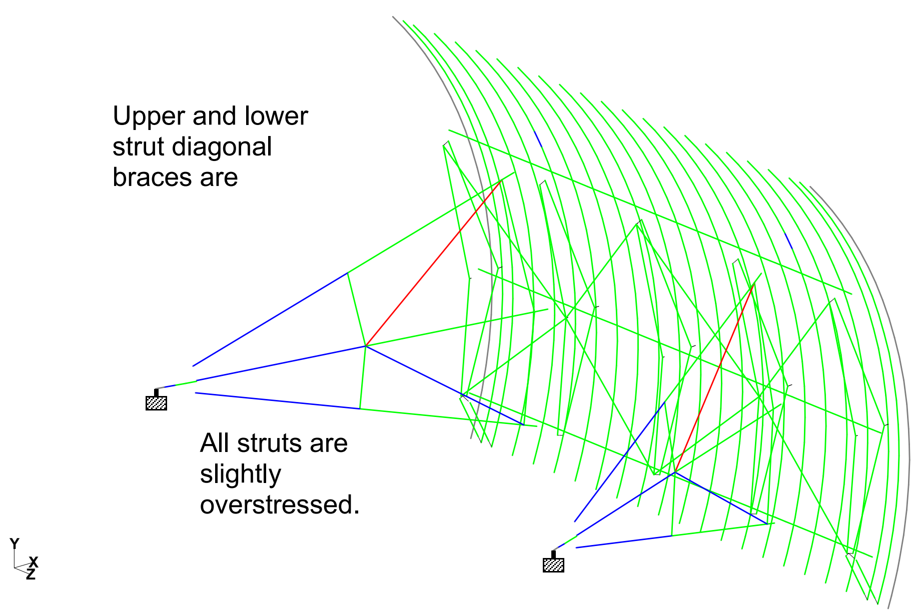

 ©2021 All Rights Reserved

6.3.4 Gate Analysis Conclusions and Recommendations

Forney Dam Tainter gates have been evaluated with gate closed and gate operating load combinations described in ETL 1110-2-584. The loads included in the load combinations include self-weight of the Tainter gate, hydrostatic load, wave load, earthquake load, side seal friction, trunnion friction and cable hoist load. ETL 1110-2-584 and project documents were used as the basis for developing the loads. Unfactored load combinations simulating the stress states of the gates during gate operation were also analyzed. The unfactored gate operating load combinations allow comparison with the results from the recent trunnion friction field tests performed. The resultant cable hoist forces and trunnion friction moments were also presented.

STAAD Pro structural analysis program was used for the Tainter Gate evaluation. Project drawings were used as the basis for the geometry of the model. The steps used to construct the analysis model are discussed in the report and the results of the analysis are summarized in the report. Some structural members of the Forney Dam Tainter gates are found to be deficient in meeting the current Tainter gate design guidelines. This is mainly due the fact that the original design did not include wave and trunnion friction loads and did not consider the more stringent load combinations of the current guidelines. Thus, there is some level of risk inherent in continued exposure of the gates to the load combinations resulting in the member overstresses.

Structural deficiencies are found in the struts and strut diagonal braces. The strut diagonal braces were found to be overstressed in the largest number of load combinations and had the highest interaction values (utilization ratios). The diagonal braces appear to be undersized during original design for the load path. The top, middle, and bottom struts were found to be slightly overstressed when subjected to the gate operation load combination with trunnion friction and with wave load. The skin-rib composite members at region near the top girder were found to have interaction values at 1.0 for the load combinations with waves. Wave pressure acting on the upper cantilever portion of the gate creates high moments about the top girder which acts as a fulcrum.

It is noted that an interaction value (utilization ratio) greater than 1.0 only indicates the member is overstressed per the specified criteria. It does not necessarily indicate a physical failure of the member. With built-in conservatism in material properties, load factors, and strength reduction factors, structural members in general are capable of taking on higher loads than what is allowed by the 1.0 interaction value criterion before seeing signs of failure. There is also some inherent, but limited ability for the structure to redistribute loads should a structure member yield. However, the importance of meeting the industry guidelines is to retain the conservatism in reducing risk.

For overstressed members, we recommend that DWU develop a plan to modify the gates, in particular the lower diagonal strut arm braces (LB-5 and RB-5) to reduce the interaction ratios to 1.0 or less.

©2021 All Rights Reserved

7.0 SPILLWAY GATE TRUNNION FRICTION TESTING

7.1 General - Gate Trunnion Friction Testing

Schnabel Engineering contracted Bridge Diagnostics, Inc. (BDI) to provide instrumentation and testing services on spillway Gates 1-14. The goal of these tests was to measure trunnion friction, hoist force, and total gage friction for 13 of the 14 gates. Gate 6 was instrumented and responses were collected during gate operation; however, trunnion friction calculations were not performed since all testing was performed in a dewatered condition. For Gates 1-5 and 7-14, the summary tables below list the values for:

- maximum trunnion friction coefficient;
- maximum pin moment due to trunnion friction;
- maximum hoist force; and,
- maximum hoist force due to total gate friction.

Detailed results of the based on the data collected as part of the trunnion friction testing is included in Appendix D.

Instrumentation and testing were performed March 31st to April 15th, 2020. The gate arms were instrumented with strain and rotation sensors and the hoist motors' pinion shafts were instrumented with torque sensors. The hoist motor control panel was instrumented with amperage sensors. Following installation of the instrumentation, a series of spill tests (lift/lower) were performed on Gates 1-5 and 7-14 to measure the structural responses resulting from trunnion pin friction. Data was also record on Gate 6 while it was dewatered and during operation in the dewatered condition. All instrumentation installation and removal was performed using BDI's rope access team.

Following demobilization from the field, the test data was examined for quality and then further processed to evaluate the gate's performance. Strain measurements were converted into axial and bending forces which were then applied to pin-strut free-body diagrams. By summing forces at each pin, friction induced moments can be computed, allowing accurate friction coefficients to be determined.

Due to restrictions caused by the hoist limit switches on closing, the hoist cables could not always be fully slacked at the beginning and end of the performed tests. Throughout testing of the Rockwell Forney gates, it was found that this limit switch restriction varied gate to gate and arm to arm. Therefore, it is not recommended to use the collected hoist force data to quantify overall hoist forces during gate operation. Rather, this hoist data can be better utilized to evaluate total friction behavior.

Amperage responses were not used to compute friction results and were collected as verification that the motor performance was not causing unexpected gate responses. These responses indicated the motor was functioning in a stable manner and should be reviewed by a licensed electrician to further evaluate the motor's performance.

©2021 All Rights Reserved

7.2 Summary of Results - Gate Trunnion Friction Testing

The results of the trunnion friction testing are summarized in the tables below:

Table 7-1 – Trunnion Friction Testing: Gate 1 test performance summary

Pin Designation	Maximum Friction Coefficient	Maximum Pin Moment due to Pin Friction (kip-in)	Maximum Hoist Force (kips)	Maximum Hoist Force due to Total Gate Friction (kips)
Right Pin	0.28	748.8	29.71	5.32
Left Pin	0.29	766.4	28.16	5.33

Table 7-2 – Trunnion Friction Testing: Gate 2 test performance summary

Pin Designation	Maximum Friction Coefficient	Maximum Pin Moment due to Pin Friction (kip-in)	Maximum Hoist Force (kips)	Maximum Hoist Force due to Total Gate Friction (kips)
Right Pin	0.14	372.0	19.73	4.50
Left Pin	0.21	557.7	24.95	4.04

Table 7-3 – Trunnion Friction Testing: Gate 3 test performance summary

Pin Designation	Maximum Friction Coefficient	Maximum Pin Moment due to Pin Friction (kip-in)	Maximum Hoist Force (kips)	Maximum Hoist Force due to Total Gate Friction (kips)
Right Pin	0.18	471.3	31.03	4.22
Left Pin	0.21	555.7	9.46	3.68

Table 7-4 – Trunnion Friction Testing: Gate 4 test performance summary

Pin Designation	Maximum Friction Coefficient	Maximum Pin Moment due to Pin Friction (kip-in)	Maximum Hoist Force (kips)	Maximum Hoist Force due to Total Gate Friction (kips)
Right Pin	0.17	462.0	29.46	3.47
Left Pin	0.18	487.5	26.06	3.60

©2021 All Rights Reserved

Table 7-5 – Trunnion Friction Testing: Gate 5 test performance summary

Pin Designation	Maximum Friction Coefficient	Maximum Pin Moment due to Pin Friction (kip-in)	Maximum Hoist Force (kips)	Maximum Hoist Force due to Total Gate Friction (kips)
Right Pin	0.21	554.4	27.26	4.38
Left Pin	0.24	648.6	28.49	4.47

Table 7-6 – Trunnion Friction Testing: Gate 7 test performance summary

Pin Designation	Maximum Friction Coefficient	Maximum Pin Moment due to Pin Friction (kip-in)	Maximum Hoist Force (kips)	Maximum Hoist Force due to Total Gate Friction (kips)
Right Pin	0.23	606.4	24.89	4.55
Left Pin	0.33	869.3	24.91	4.49

Table 7-7 – Trunnion Friction Testing: Gate 8 test performance summary

Pin Designation	Maximum Friction Coefficient	Maximum Pin Moment due to Pin Friction (kip-in)	Maximum Hoist Force (kips)	Maximum Hoist Force due to Total Gate Friction (kips)
Right Pin	0.18	486.3	32.96	4.57
Left Pin	0.28	749.9	28.07	3.89

Table 7-8 – Trunnion Friction Testing: Gate 9 test performance summary

Pin Designation	Maximum Friction Coefficient	Maximum Pin Moment due to Pin Friction (kip-in)	Maximum Hoist Force (kips)	Maximum Hoist Force due to Total Gate Friction (kips)
Right Pin	0.17	443.0	31.09	4.19
Left Pin	0.20	522.7	23.34	3.05

Table 7-9 – Trunnion Friction Testing: Gate 10 test performance summary

Pin Designation	Maximum Friction Coefficient	Maximum Pin Moment due to Pin Friction (kip-in)	Maximum Hoist Force (kips)	Maximum Hoist Force due to Total Gate Friction (kips)
Right Pin	0.15	397.4	29.08	3.71
Left Pin	0.20	512.3	27.57	3.60

©2021 All Rights Reserved

Table 7-10 – Trunnion Friction Testing: Gate 11 test performance summary

Pin Designation	Maximum Friction Coefficient	Maximum Pin Moment due to Pin Friction (kip-in)	Maximum Hoist Force (kips)	Maximum Hoist Force due to Total Gate Friction (kips)
Right Pin	0.23	604.9	35.18	4.63
Left Pin	0.20	513.7	21.35	3.11

Table 7-11 – Trunnion Friction Testing: Gate 12 test performance summary

Pin Designation	Maximum Friction Coefficient	Maximum Pin Moment due to Pin Friction (kip-in)	Maximum Hoist Force (kips)	Maximum Hoist Force due to Total Gate Friction (kips)
Right Pin	0.13	335.0	28.51	4.02
Left Pin	0.20	530.7	28.45	3.77

Table 7-12 – Trunnion Friction Testing: Gate 13 test performance summary

Pin Designation	Maximum Friction Coefficient	Maximum Pin Moment due to Pin Friction (kip-in)	Maximum Hoist Force (kips)	Maximum Hoist Force due to Total Gate Friction (kips)
Right Pin	0.16	427.0	29.07	4.16
Left Pin	0.16	432.6	28.63	3.96

Table 7-13 – Trunnion Friction Testing: Gate 14 test performance summary

Pin Designation	Maximum Friction Coefficient	Maximum Pin Moment due to Pin Friction (kip-in)	Maximum Hoist Force (kips)	Maximum Hoist Force due to Total Gate Friction (kips)
Right Pin	0.09	238.3	20.05	3.61
Left Pin	0.08	219.5	32.06	4.90

7.3 Conclusions - Gate Trunnion Friction Testing

Average values for trunnion friction for the Tainter gates at Forney Dam are below the 0.3 trunnion friction factor used in the analysis.

©2021 All Rights Reserved

8.0 REFERENCES

The following references were provided by DWU and reviewed as part of the development of this report:

Year of Publication	Title	Author	Type of Publication
2016	Rockwall-Forney Dam-Safety Inspection Report	Arcadis	Report
1960	Forney Dam Design Memorandum No. 1, Design Floods and Freeboard Requirements	Forrest and Cotton, Inc.	Report
1961	Forney Dam Design Memorandum No. 2, Detailed Design of Dam, Spillway and Appurtenant Works	Forrest and Cotton, Inc.	Report
2005	Flood Operation of Lake Ray Hubbard by Dallas Water utility Personnel	DWU	Report

The following reference was used to develop the gate inspection condition assessment coding system:

Oregon Department of Transportation (ODOT) Bridge Inspection Coding Guide, date March 2015

The following references were used as a basis for the structural analysis of the Tainter gates:

R1. *American Institute of Steel Construction (2010). "AISC Steel Construction Manual, 14^{th} Ed."*
R2. U.S. Army Corps of Engineers (2014). "Design of Hydraulic Steel Structures". ETL 1110-2-584.
R3. Forney Dam Design Memorandum No. 1, Design Floods and Freeboard Requirements, April 1960.
R4. Forney Dam Design Memorandum No. 2, Detailed Design of Dam, Spillway and Appurtenant Works, November 1961.
R5. "Flood Operation of Lake Ray Hubbard by Dallas Water utility Personnel," 2005.

The following references were used in research of the Gate 6, LS-1 fracture investigation:

Bagheri, Majid & Alizadeh, M.. (2013). The effects of hot tear segregations on the rolled product quality of continuously cast steel. International Journal of ISSI. Vol 10, pp. 11-17.

©2021 All Rights Reserved

Camisani-Calzolari, Ferdinando & Craig, Ian & Pistorius, P.. (2003). A Review on Causes of Surface Defects in Continuous Casting. IFAC Proceedings Volumes. Vol 36, pp. 113-121.

Chen, W., Yang, G., Zhu, L., Wang, X., & He, B. (2019). Reducing Surface Cracks and Improving Cleanliness of H-Beam Blanks in Continuous Casting — Improving continuous casting of H-beam blanks, High Temperature Materials and Processes, Vol 38(2019), pp. 612-620.

Chi, Brandon & Uang, Chia-Ming. (2004). Effect of straightening method on the cyclic behavior of k-area in steel rolled shapes. Engineering Journal (New York). Vol 41, pp. 15-22.

Lee, Jung-Eui & Yeo, Tae-, Usok. (2000). Prediction of cracks in continuously cast steel beam blank through fully coupled analysis of fluid flow, heat transfer, and deformation behavior of a solidifying shell. Metallurgical and Materials Transactions A. Vol 31, pp. 225-237.

Madias, Jorge & Genzano, Cristian & Oropeza, Marco & Moss, Carlos. (2017). A Review of Defects in Beam Blank Casting and the Measures Proposed for their Elimination. AISTech 2017 Proceedings.

Thornton, Charles H. (1973). Quality Control in Design and Supervision Can Eliminate Lamellar Tearing. Engineering Journal, American Institute of Steel Construction. Vol. 10, pp. 112-116.

Tide, R.H.R. (2000). Evaluation of steel properties and cracking in “k”-area of W shapes. Engineering Structures. Vol 22, pp. 128-134.

©2021 All Rights Reserved

APPENDIX A
DRAWINGS & SCHEMATICS

©2021 All Rights Reserved

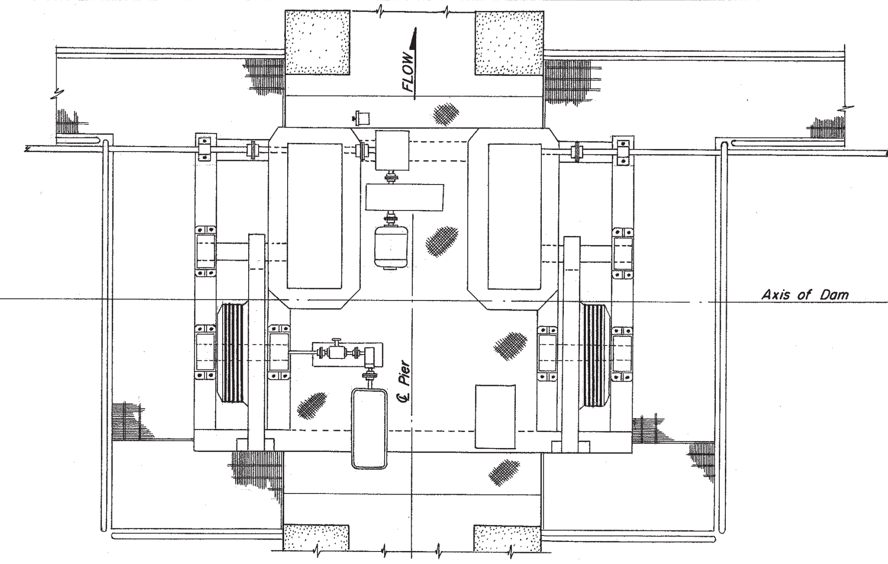

HOIST MACHINERY PLAN

SCALE: 3/8 INCH = 1 FOOT

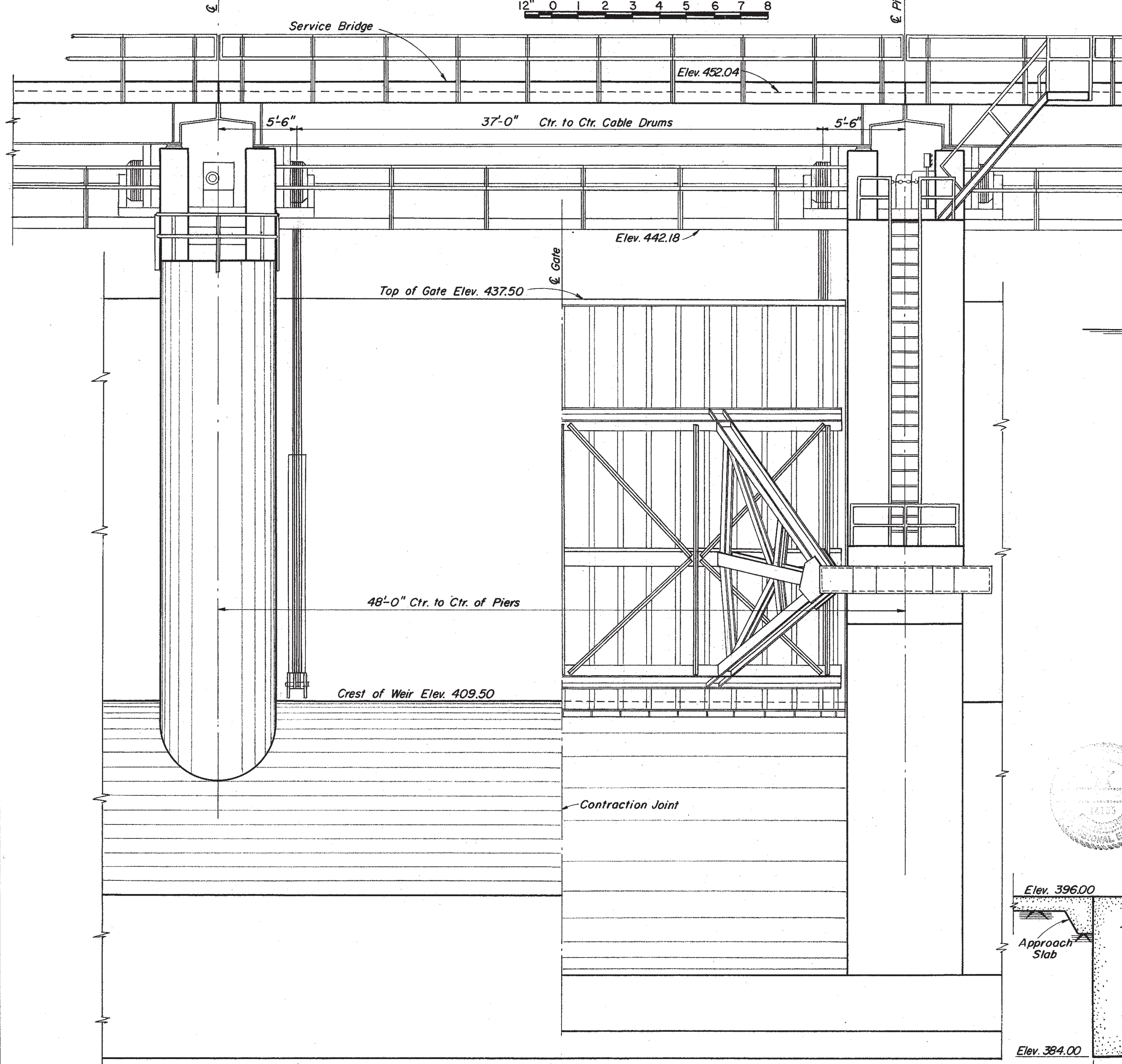

HALF UPSTREAM ELEVATION   HALF DOWNSTREAM ELEVATION

SCALE: 1 INCH = 5 FEET

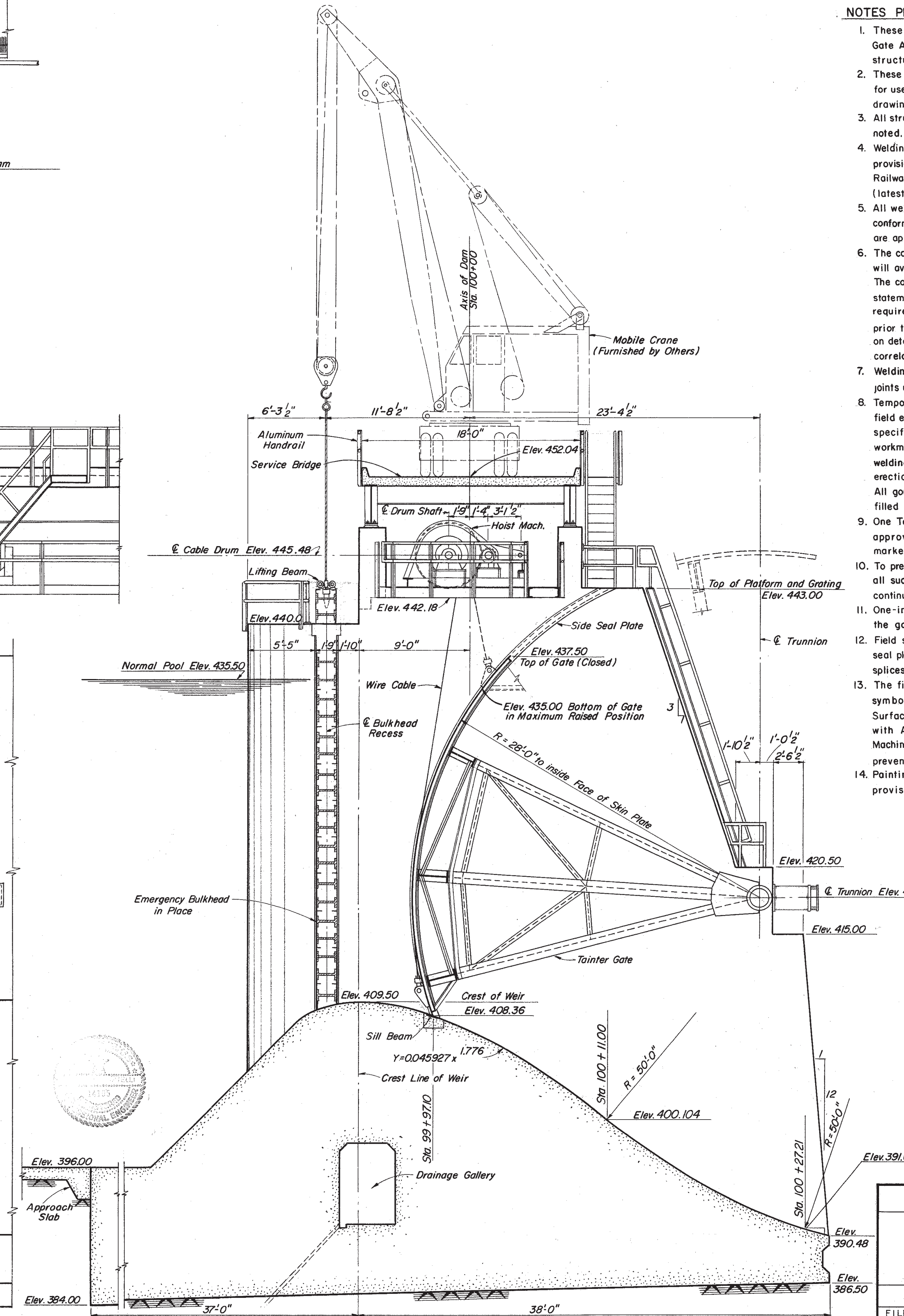

TYPICAL SECTION THROUGH WEIR

SCALE: 1 INCH = 5 FEET

Contract Nº 64-215

NOTES PERTAINING TO STRUCTURAL STEEL

1. These notes apply to structural steel for Tainter Gates, Tainter Gate Anchorages, Machinery Platform and other items where structural steel is involved.
2. These drawings shall not be traced or reproduced by any method for use as or in lieu of detail shop drawings. Do not scale these drawings; use dimensions shown.
3. All structural steel shall be welding grade steel unless otherwise noted.
4. Welding, unless otherwise specified, shall conform to the applicable provisions of the current "Specifications for Welded Highway and Railway Bridges", published by the American Welding Society, (A.W.S.) (latest issue).
5. All welding of mild steel shall be performed with electrodes conforming to the A.W.S. Type E6010 or E6011, unless other electrodes are approved by the Engineer.
6. The contractor shall adopt a Welding Sequence and Procedure which will avoid needless distortion, and minimize shrinkage stresses. The contractor shall submit with the detail shop drawings a complete statement of his proposed welding procedure and sequence, as required by the specifications, for the approval of the engineer prior to commencement of fabrication. Weld symbols shall be shown on detail shop drawings and field erection drawings and shall be correlated with the welding procedure and sequence.
7. Welding symbols shown on these drawings are typical for similar joints unless otherwise shown or noted.
8. Temporary clip angles and erection bolts may be used for shop and field erection. If clips are of new material, (conforming to specifications cited above), and are cut and welded in a neat workman-like manner, they need not be removed after the field welding is complete. Erection bolts need not be removed after erection, but must be seal welded to prevent entrance of moisture All gouges, scars, etc, regardless of how produced, shall be filled with weld metal and ground smooth.
9. One Tainter Gate shall be completely assembled in the shop. After approval of the assembly the individual pieces shall be match marked prior to disassembly for shipment.
10. To prevent corrosion by moisture between surfaces in contact all such contacts shall be sealed watertight by running a continuous 1/8" fillet along all edges of the contact.
11. One-inch drain holes shall be provided to drain all pockets with the gate in either the opened or closed position.
12. Field splices shown in the Tainter Gate skin plate, arms, side seal plates, and sill beam are suggested only; additional field splices will be permitted subject to the approval of the engineer.
13. The finish of machined surfaces is indicated by standard symbols established by the American Standards Association. Surface roughness, waviness and lay shall be in accordance with American Standards Association publication ASA.B46.1-1955. Machined surfaces shall be treated with an approved rust preventative compound prior to shipment.
14. Painting of structural steel shall conform to applicable provisions of the specifications.

AS BUILT DRAWING
THIS DRAWING HAS BEEN REVISED TO REFLECT THE PROJECT AS ACTUALLY CONSTRUCTED.
FORREST AND COTTON, INC.
Consulting Engineers
By W.D.O.
Date 8-18-67

DALLAS CITY WATER WORKS

FORNEY DAM AND RESERVOIR

SPILLWAY

TAINTER GATES

GENERAL ARRANGEMENT

FORREST AND COTTON, INC. CONSULTING ENGINEERS
DALLAS, TEXAS

FILE NO.			SHEET NO.
6LOQ-4A	DESIGN BY:	E.W.P.	35
	DRAWN BY:	P.E.N.	
	CHECKED BY:	E.W.P.	
	RECOMMENDED BY:	[signature]	
	APPROVED	[signature]	OF 87

III

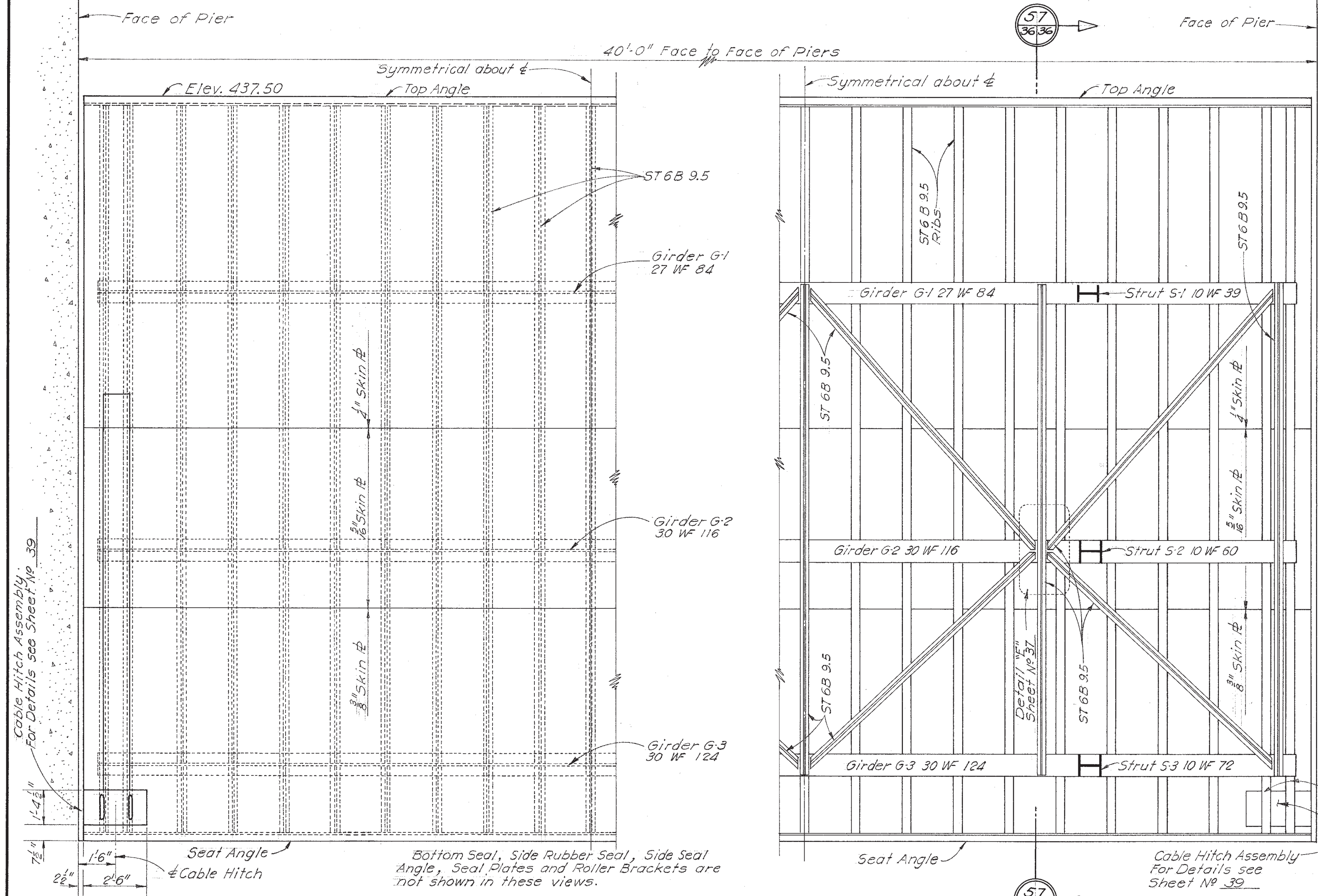

DEVELOPED ELEVATIONS

SCALE: 3/8 INCH = 1 FOOT

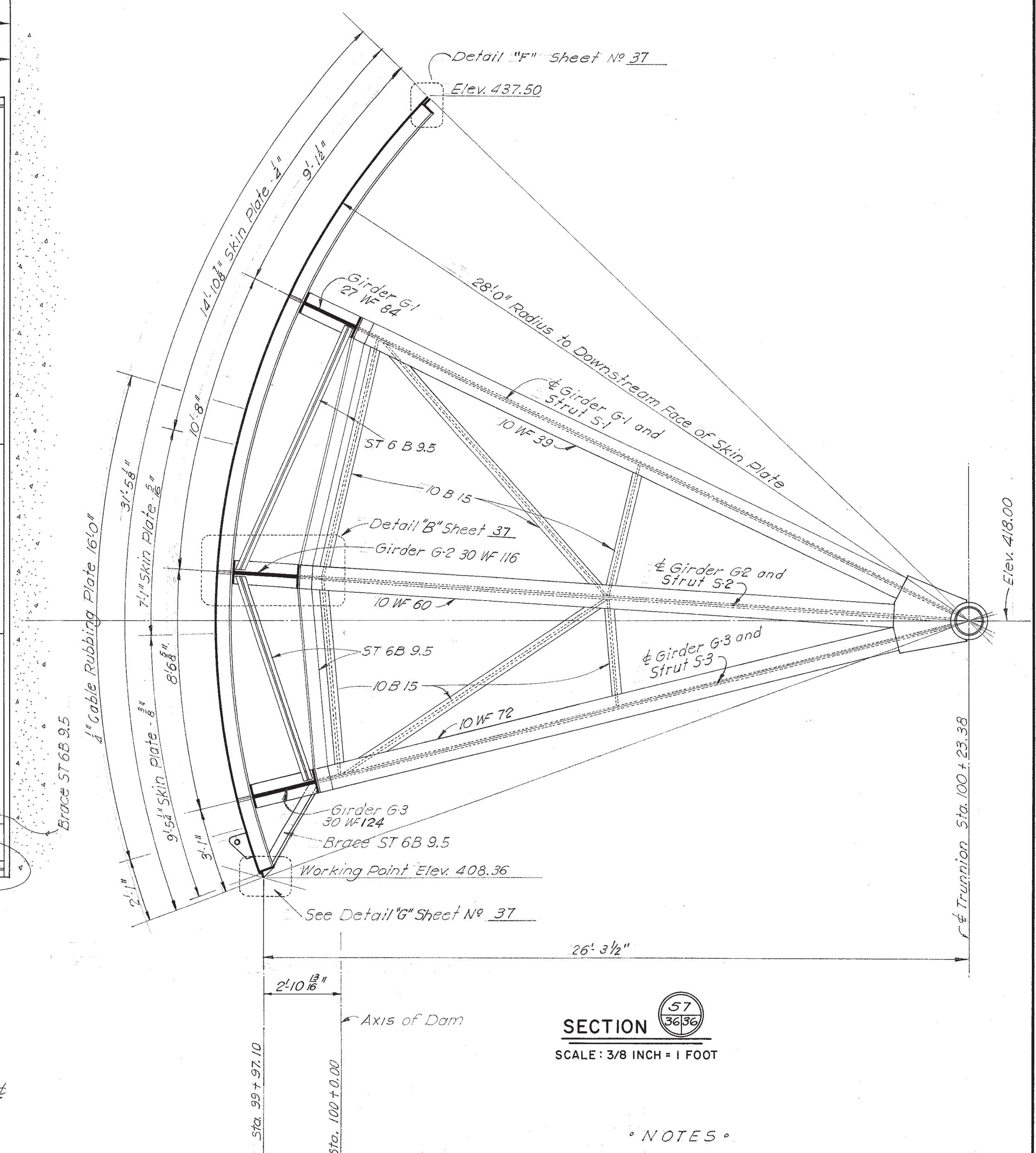

SECTION 57/36-36

SCALE: 3/8 INCH = 1 FOOT

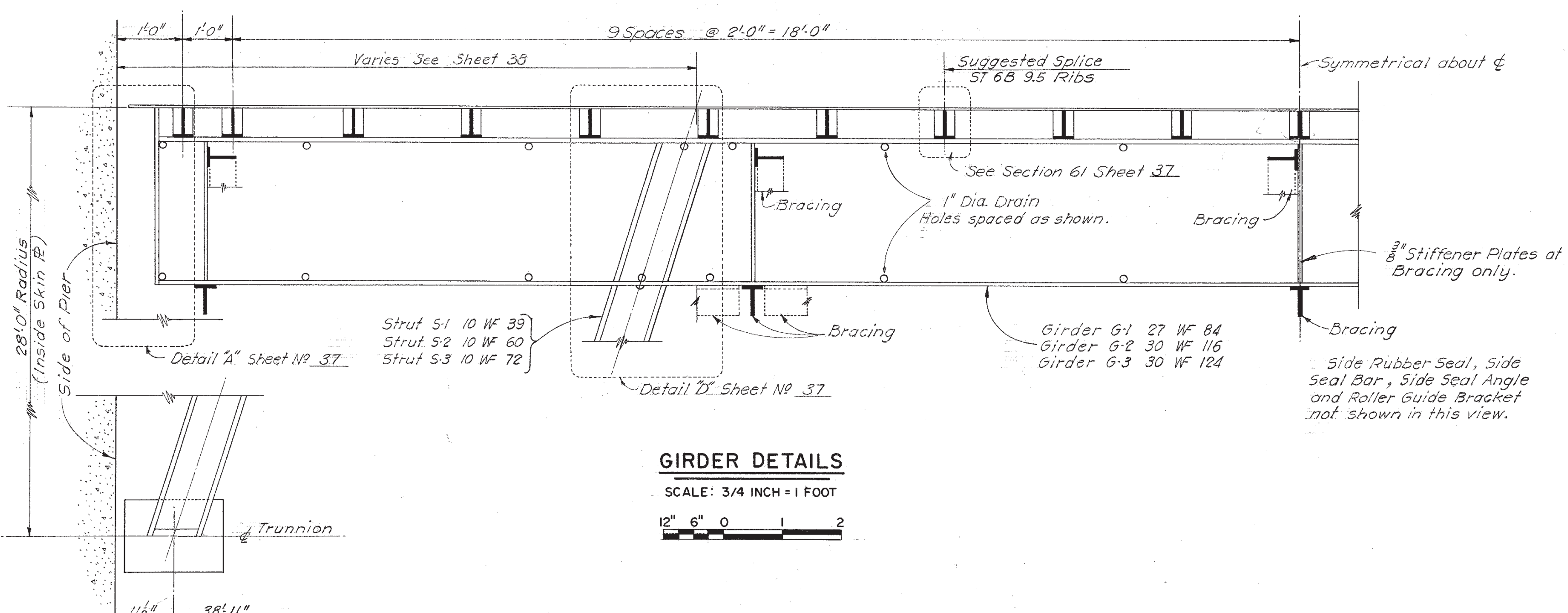

GIRDER DETAILS

SCALE: 3/4 INCH = 1 FOOT

° NOTES °

1. For General Notes see Sheet Nº 35
2. For Additional Framing Details see Sheet Nº 37
3. All Material shown on this Sheet will be paid for under Item 24.
4. All Holes used for Erection Bolts to be Plug Welded after erection.
5. Back up or beads are required.
6. All Structural Steel shown on this Sheet shall be welding Grade.
7. All Members bent to a Radius shall be Hot Formed to Radius except Skin Plate which may be Cold Rolled.
8. Skin Plates, Top & Sill Angles and ST 6B 9.5 Ribs shall be ASTM A-441 Structural Steel. All others shall be ASTM A-36 Steel unless otherwise noted.

AS BUILT DRAWING
THIS DRAWING HAS BEEN REVISED TO REFLECT THE PROJECT AS ACTUALLY CONSTRUCTED.
FORREST AND COTTON, INC.
Consulting Engineers
By W.D.C.
Date 8-18-67

Contract Nº 64-215

DALLAS CITY WATER WORKS

FORNEY DAM AND RESERVOIR

SPILLWAY

TAINTER GATES

ELEVATIONS, SECTIONS, & DETAILS

FORREST AND COTTON, INC. CONSULTING ENGINEERS
DALLAS, TEXAS

FILE NO.			SHEET NO.
610Q-4A	DESIGN BY:	J.C.C.	36
	DRAWN BY:	L.S. & J.L.H.	
	CHECKED BY:	D.W.W.	
	RECOMMENDED BY:	[signature]	
	APPROVED	[signature]	OF 87

III

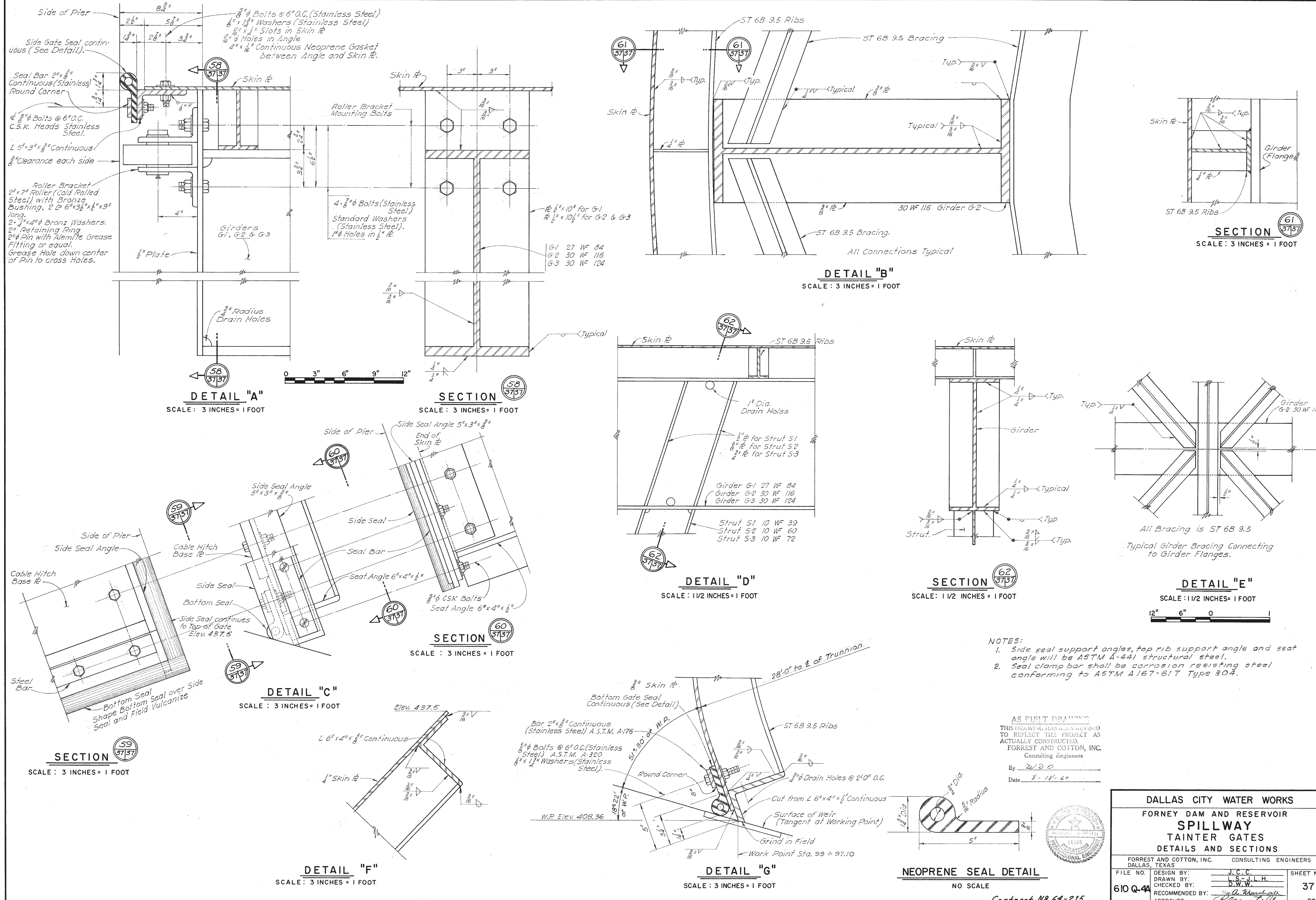

NOTES:
1. Side seal support angles, top rib support angle and seat angle will be ASTM A-441 structural steel.
2. Seal clamp bar shall be corrosion resisting steel conforming to ASTM A167-61T Type 304.

AS BUILT DRAWING
THIS DRAWING HAS BEEN REVISED TO REFLECT THE PROJECT AS ACTUALLY CONSTRUCTED.
FORREST AND COTTON, INC.
Consulting Engineers
By W.D.O.
Date 8-18-67

DALLAS CITY WATER WORKS
FORNEY DAM AND RESERVOIR
SPILLWAY
TAINTER GATES
DETAILS AND SECTIONS

FORREST AND COTTON, INC. CONSULTING ENGINEERS
DALLAS, TEXAS

FILE NO.			SHEET NO.
610 Q-4A	DESIGN BY:	J. C. C.	37
	DRAWN BY:	L. S.-J. L. H.	
	CHECKED BY:	D. W. W.	
	RECOMMENDED BY:	[signature]	
	APPROVED	[signature]	OF 87

Contract Nº 64-215

III

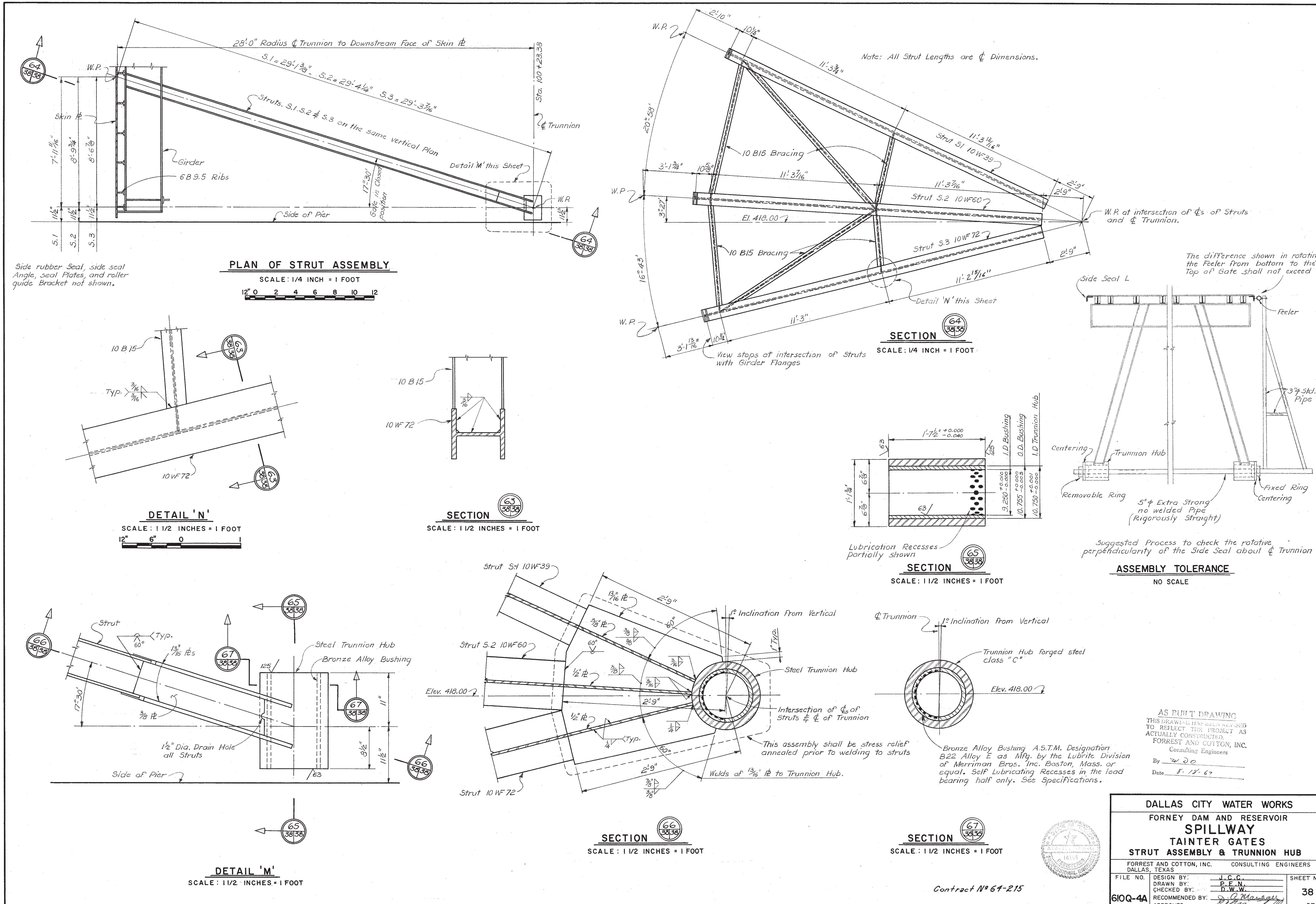

DALLAS CITY WATER WORKS

FORNEY DAM AND RESERVOIR

SPILLWAY

TAINTER GATES

STRUT ASSEMBLY & TRUNNION HUB

FORREST AND COTTON, INC. CONSULTING ENGINEERS
DALLAS, TEXAS

FILE NO.			SHEET NO.
610Q-4A	DESIGN BY:	J.C.C.	38
	DRAWN BY:	P.F.N.	
	CHECKED BY:	D.W.W.	
	RECOMMENDED BY:	[signature]	
	APPROVED	[signature]	OF 87

III

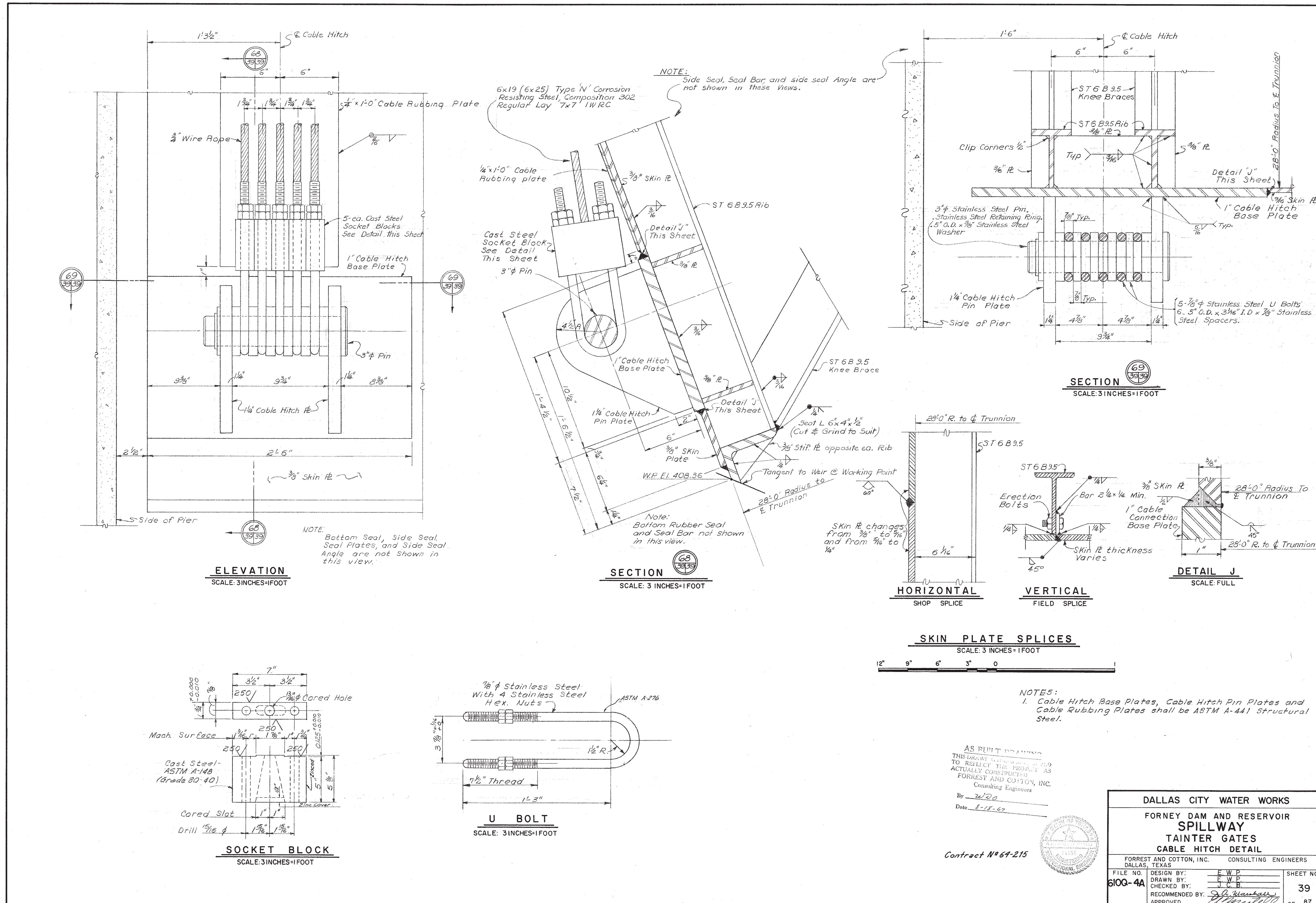
ELEVATION
SCALE: 3 INCHES=1 FOOT
NOTE: Bottom Seal, Side Seal, Seal Plates, and Side Seal Angle are not shown in this view.
SECTION 68/39 39
SCALE: 3 INCHES=1 FOOT
NOTE: Side Seal, Seal Bar, and side seal Angle are not shown in these views.
6x19 (6x25) Type 'N' Corrosion Resisting Steel, Composition 302 Regular Lay 7x7 IWRC
Note: Bottom Rubber Seal and Seal Bar not shown in this view.
SECTION 69/39 39
SCALE: 3 INCHES=1 FOOT
5-7/8" ϕ Stainless Steel U Bolts 6. 5" O.D. x 3 1/16" I.D x 7/8" Stainless Steel Spacers.
HORIZONTAL
SHOP SPLICE
VERTICAL
FIELD SPLICE
DETAIL J
SCALE: FULL
SKIN PLATE SPLICES
SCALE: 3 INCHES=1 FOOT
SOCKET BLOCK
SCALE: 3 INCHES=1 FOOT
Cast Steel- ASTM A-148 (Grade 80-40)
U BOLT
SCALE: 3 INCHES=1 FOOT
7/8" ϕ Stainless Steel With 4 Stainless Steel Hex. Nuts
NOTES:
1. Cable Hitch Base Plates, Cable Hitch Pin Plates and Cable Rubbing Plates shall be ASTM A-441 Structural Steel.
AS BUILT DRAWING
THIS DRAWING HAS BEEN REVISED TO REFLECT THE PROJECT AS ACTUALLY CONSTRUCTED.
FORREST AND COTTON, INC. Consulting Engineers
By W.D.O.
Date 8-18-67
Contract Nº 64-215
DALLAS CITY WATER WORKS
FORNEY DAM AND RESERVOIR
SPILLWAY
TAINTER GATES
CABLE HITCH DETAIL
FORREST AND COTTON, INC. CONSULTING ENGINEERS
DALLAS, TEXAS
FILE NO. 610Q-4A
DESIGN BY: E.W.P.
DRAWN BY: E.W.P.
CHECKED BY: J.C.B.
RECOMMENDED BY:
APPROVED
SHEET NO. 39 OF 87
III

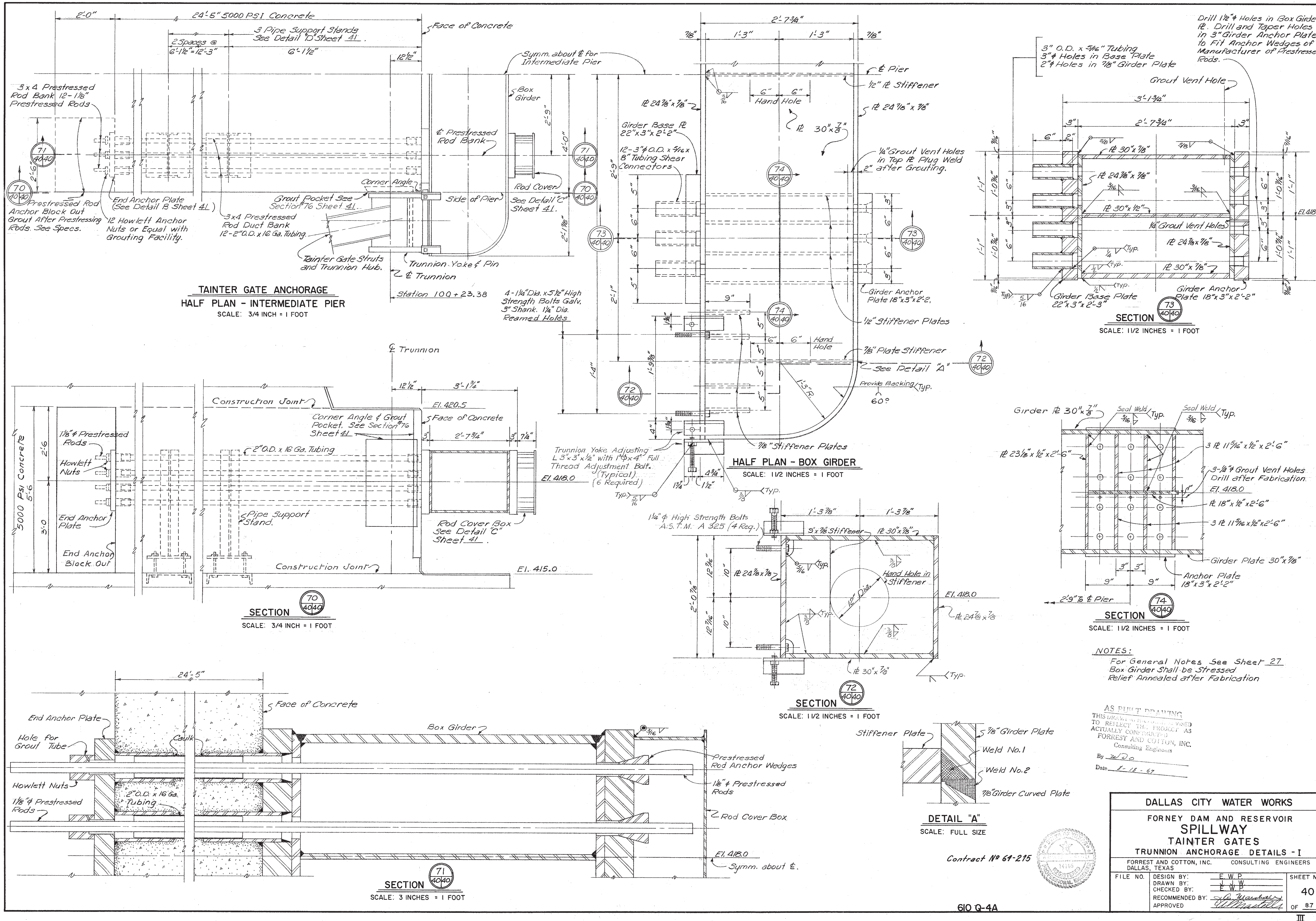
TAINTER GATE ANCHORAGE
HALF PLAN - INTERMEDIATE PIER
SCALE: 3/4 INCH = 1 FOOT
24'-5" 5000 PSI Concrete
3 Pipe Support Stands See Detail "D" Sheet 41
Face of Concrete
Symm. about ℄ for Intermediate Pier
3x4 Prestressed Rod Bank 12-1⅛" Prestressed Rods
Box Girder
℄ Prestressed Rod Bank
Prestressed Rod Anchor Block Out Grout After Prestressing Rods. See Specs.
End Anchor Plate (See Detail B Sheet 41)
12 Howlett Anchor Nuts or Equal with Grouting Facility.
3x4 Prestressed Rod Duct Bank 12-2" O.D. x 16 Ga. Tubing.
Grout Pocket See Section 76 Sheet 41.
Corner Angle
Side of Pier
Rod Cover
See Detail "C" Sheet 41.
Tainter Gate Struts and Trunnion Hub.
Trunnion Yoke & Pin
℄ Trunnion
Station 100+23.38
HALF PLAN - BOX GIRDER
SCALE: 1 1/2 INCHES = 1 FOOT
℄ Pier
½" ℄ Stiffener
Hand Hole
Girder Base ℄ 22"x3"x2'-2"
12-3"φ O.D. x 5/16 x 8" Tubing Shear Connectors
¼" Grout Vent Holes in Top ℄ Plug Weld after Grouting.
Girder Anchor Plate 18"x3"x2'-2.
½" Stiffener Plates
⅞" Plate Stiffener
See Detail "A"
Provide Backing Typ.
⅞" Stiffener Plates
4-1¼" Dia. x 5½" High Strength Bolts Galv. 3" Shank. 1¼" Dia. Reamed Holes
Trunnion Yoke Adjusting L 3"x3"x½" with 1"φx4" Full Thread Adjustment Bolt. (Typical) (6 Required)
SECTION 70
SCALE: 3/4 INCH = 1 FOOT
Construction Joint
Corner Angle & Grout Pocket. See Section 76 Sheet 41
El. 420.5
El. 418.0
El. 415.0
1⅛"φ Prestressed Rods
Howlett Nuts
End Anchor Plate
End Anchor Block Out
2" O.D. x 16 Ga. Tubing
Pipe Support Stand.
Rod Cover Box See Detail "C" Sheet 41.
5000 Psi Concrete
SECTION 73
SCALE: 1 1/2 INCHES = 1 FOOT
Drill 1½"φ Holes in Box Girder ℄. Drill and Taper Holes in 3" Girder Anchor Plate, to Fit Anchor Wedges of Manufacturer of Prestressed Rods.
3" O.D. x 5/16" Tubing
3"φ Holes in Base Plate
2"φ Holes in ⅞" Girder Plate
Grout Vent Hole
¼" Grout Vent Holes
Girder Base Plate 22"x3"x2'-3"
Girder Anchor Plate 18"x3"x2'-2"
El. 418.0
SECTION 74
SCALE: 1 1/2 INCHES = 1 FOOT
Girder ℄ 30"x⅞"
Seal Weld
3 ℄ 11 9/16"x½"x2'-6"
3-⅛"φ Grout Vent Holes Drill after Fabrication.
℄ 18"x½"x2'-6"
Girder Plate 30"x⅞"
Anchor Plate 18"x3"x2'-2"
2'-9" To ℄ Pier
SECTION 72
SCALE: 1 1/2 INCHES = 1 FOOT
1¼"φ High Strength Bolts A.S.T.M. A 325 (4 Req.)
Hand Hole in Stiffener
12" Dia.
SECTION 71
SCALE: 3 INCHES = 1 FOOT
End Anchor Plate
Hole for Grout Tube
Howlett Nuts
1⅛"φ Prestressed Rods
2" O.D. x 16 Ga. Tubing
Caulk
Box Girder
Prestressed Rod Anchor Wedges
Rod Cover Box
Symm. about ℄.
DETAIL "A"
SCALE: FULL SIZE
Stiffener Plate
⅞" Girder Plate
Weld No. 1
Weld No. 2
⅞" Girder Curved Plate
NOTES:
For General Notes See Sheet 27
Box Girder Shall be Stressed Relief Annealed after Fabrication
AS BUILT DRAWING
THIS DRAWING HAS BEEN REVISED TO REFLECT THE PROJECT AS ACTUALLY CONSTRUCTED
FORREST AND COTTON, INC. Consulting Engineers
Date 8-18-67
Contract No 61-215
DALLAS CITY WATER WORKS
FORNEY DAM AND RESERVOIR
SPILLWAY
TAINTER GATES
TRUNNION ANCHORAGE DETAILS - I
FORREST AND COTTON, INC. CONSULTING ENGINEERS
DALLAS, TEXAS
DESIGN BY: E.W.P.
DRAWN BY: J.J.W.
CHECKED BY: E.W.P.
SHEET NO. 40 OF 87
610 Q-4A

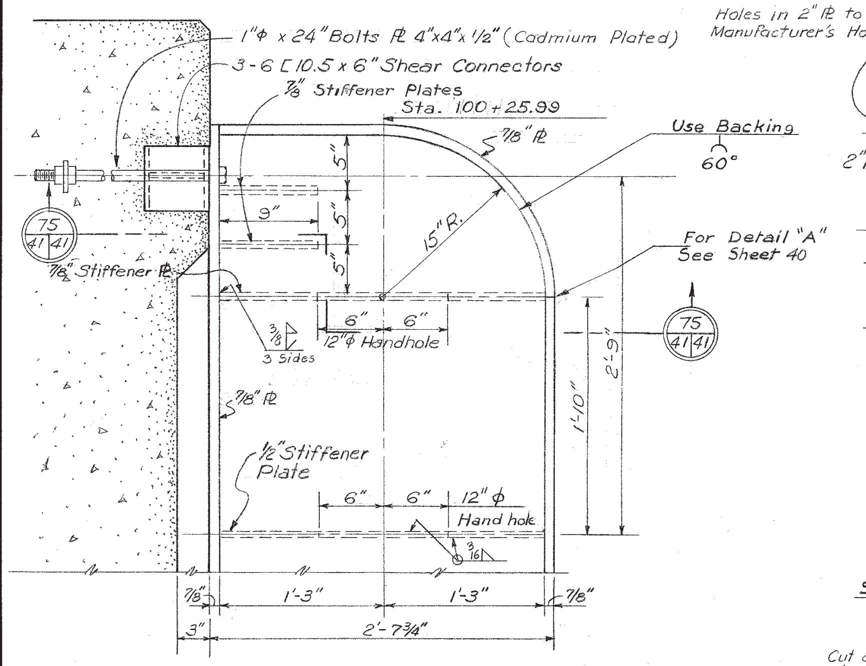

HALF PLAN - END PIER

FOR OTHER HALF SEE INTERMEDIATE PIER

SCALE: 1-1/2" = 1'-0"

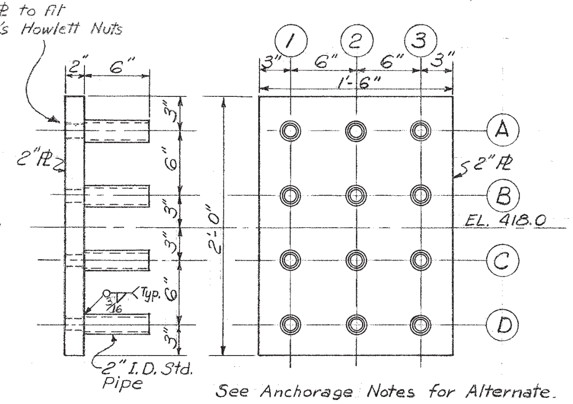

DETAIL "B" - END ANCHOR PLATE

SCALE: 1-1/2" = 1'-0"

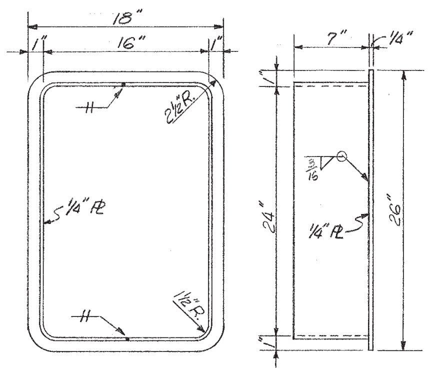

DETAIL "C" - ROD COVER BOX

SCALE: 1-1/2" = 1'-0"

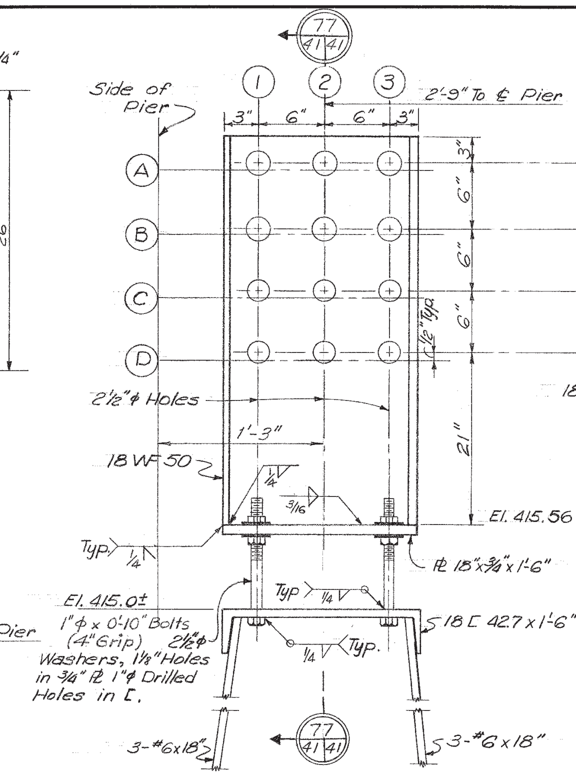

DETAIL "D" - PIPE SUPPORT STAND

SCALE: 1-1/2" = 1'-0"

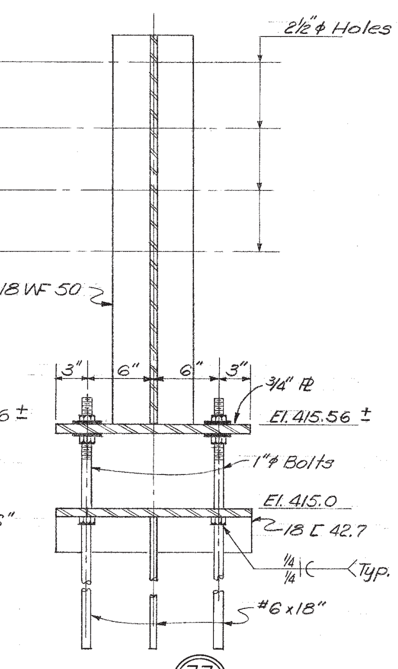

SECTION

SCALE: 1-1/2" = 1'-0"

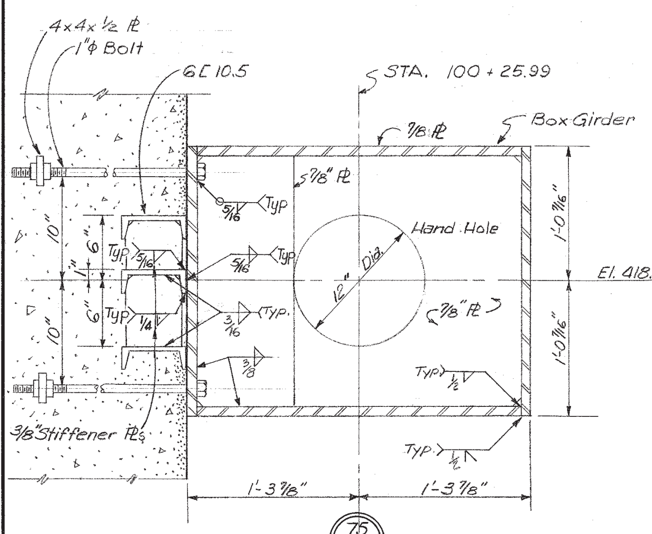

SECTION

SCALE: 1-1/2" = 1'-0"

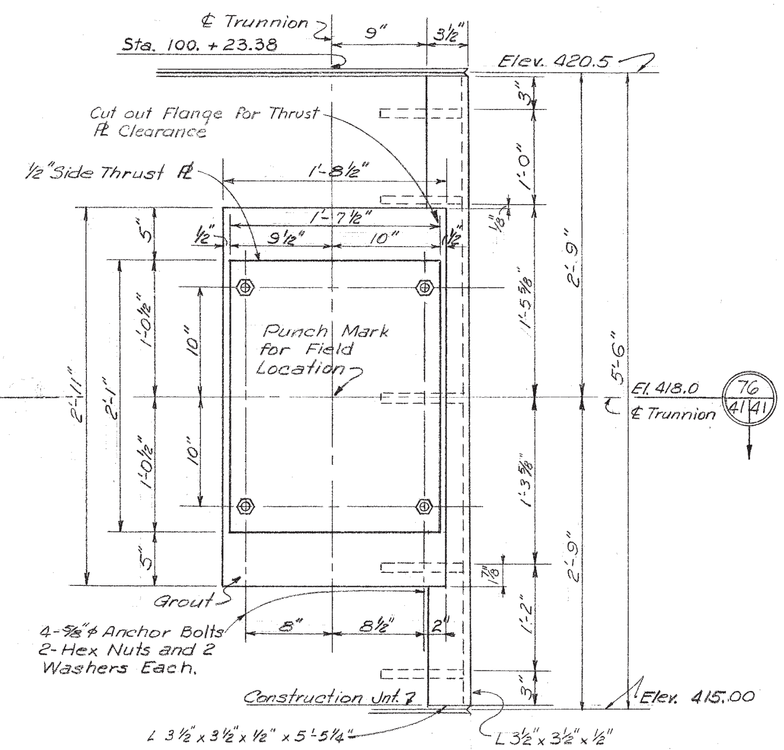

DETAIL "E" - SIDE THRUST PLATE

SCALE: 1-1/2" = 1'-0"

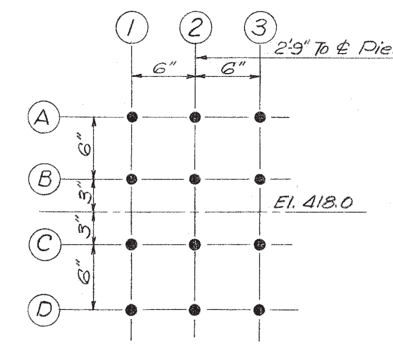

ROD PATTERN

STAGE	RODS
1	B-3 & D-3
2	A-3 & C-3
3	B-2 & D-2
4	A-2 & C-2
5	B-1 & D-1
6	A-1 & C-1

Rods will be tensioned to 115,000 pounds each (80% of ultimate). For details of stressing procedure see specifications. Prestress rods of end pier two rods at a time in the sequence listed above. For intermediate piers prestress two rods on each side simultaneously in the sequence listed above.

ROD STRESSING SEQUENCE

ANCHORAGE NOTES:

1. All groove welds for trunnion yokes and box girders shall be full penetratration welds unless otherwise shown.
2. The end anchor plates shall be provided by the prestress rod manufacturer and may consist of one plate or multiples of the manufacturer's standard plates; Subject to the approval of the Engineer.
3. All material shown on these sheets shall be structural steel unless otherwise noted and shall conform to ASTM A-36.
4. 2" O.D. Standard Pipe may be used instead of 2" O.D. X 16 Ga. Tubing.
5. After installation has been completed paint all exposed metal with Aluminum colored vinyl plastic Paint (See Specs.)
6. Box girder shall be stress relief annealed after fabrication.
7. Difference in elevation between any two pipe support stands shall not be greater than 0.06".

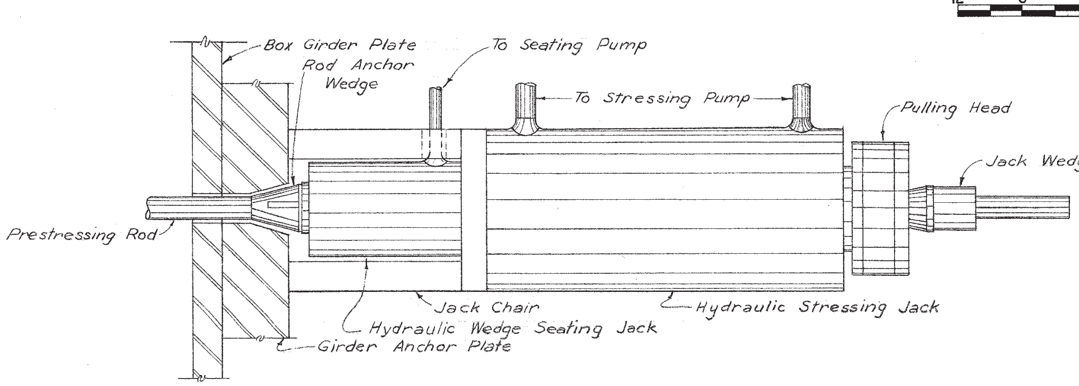

ROD JACKING FACILITY

NOT TO SCALE

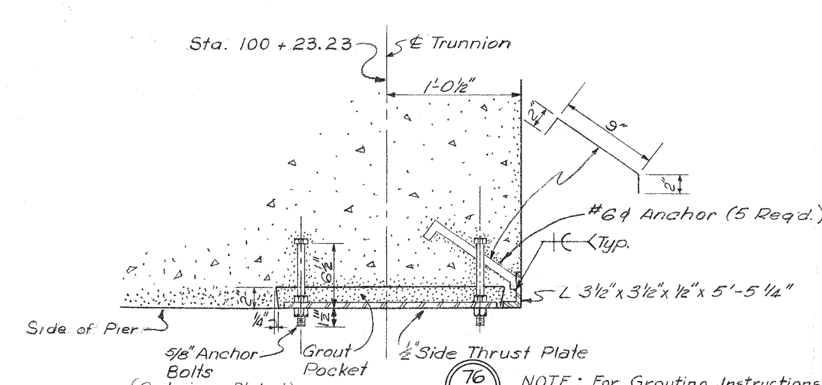

NOTE: For Grouting Instructions See Sheet 42

SECTION

SCALE: 3" = 1'-0"

AS BUILT DRAWING
FORREST AND COTTON, INC.
Consulting Engineers
By W.D.O.
Date 8-18-67

Contract No 64-215

DALLAS CITY WATER WORKS

FORNEY DAM AND RESERVOIR

SPILLWAY

TAINTER GATES

TRUNNION ANCHORAGE DETAILS-II

FORREST AND COTTON, INC. CONSULTING ENGINEERS
DALLAS, TEXAS

FILE NO.		SHEET NO.
	DESIGN BY: E.W.P.	41
	DRAWN BY: J.J.W.	
	CHECKED BY: E.W.P.	
	RECOMMENDED BY: [signature]	
	APPROVED [signature]	OF 87

6D Q-4A

III

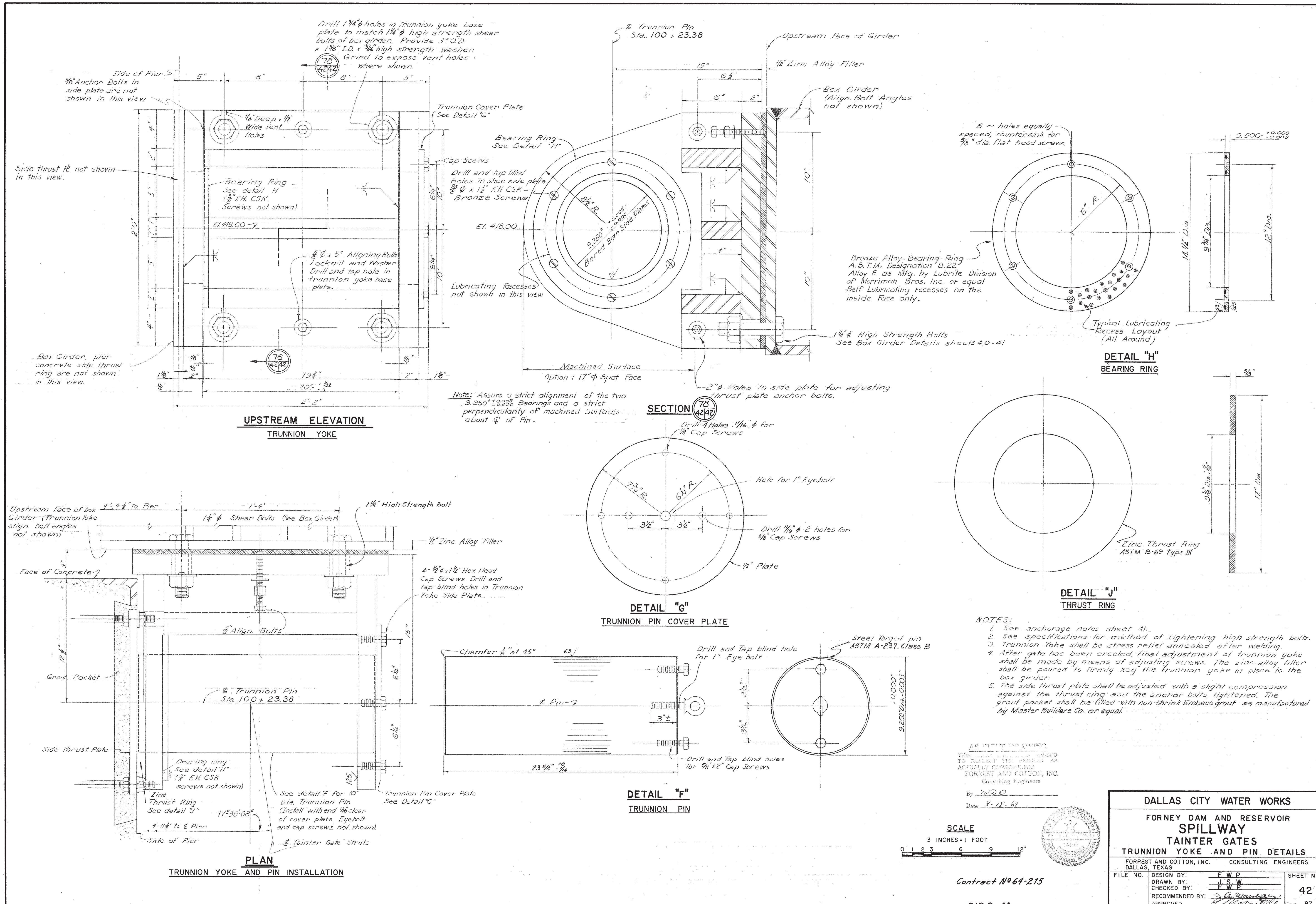
UPSTREAM ELEVATION
TRUNNION YOKE
Drill 1 3/4" ϕ holes in trunnion yoke base plate to match 1 5/8" ϕ high strength shear bolts of box girder. Provide 3" O.D. x 1 3/8" I.D. x 5/16" high strength washer. Grind to expose vent holes where shown.
Side of Pier
5/8" Anchor Bolts in side plate are not shown in this view
1/4" Deep x 1/2" Wide Vent Holes
Trunnion Cover Plate See Detail "G"
Cap Screws
Side thrust Pℓ not shown in this view.
Bearing Ring See detail H (3/8" F.H. CSK. Screws not shown)
El 418.00
5/8" ϕ x 5" Aligning Bolts Locknut and Washer Drill and tap hole in trunnion yoke base plate.
Box Girder, pier concrete side thrust ring are not shown in this view.
SECTION
℄ Trunnion Pin Sta. 100 + 23.38
Upstream Face of Girder
1/2" Zinc Alloy Filler
Box Girder (Align. Bolt Angles not shown)
Bearing Ring See Detail "H"
Drill and tap blind holes in shoe side plate 3/8" ϕ x 1 1/4" F.H. CSK Bronze Screws
El. 418.00
Bored Both Side Plates
Lubricating Recesses not shown in this view
1 5/8" ϕ High Strength Bolts See Box Girder Details sheets 40-41
Machined Surface
Option: 17" ϕ Spot Face
2" ϕ Holes in side plate for adjusting thrust plate anchor bolts.
Note: Assure a strict alignment of the two 9.250" +0.005 -0.000 Bearings and a strict perpendicularity of machined Surfaces about ℄ of Pin.
DETAIL "H"
BEARING RING
6 ~ holes equally spaced, countersink for 3/8" dia. flat head screws.
Bronze Alloy Bearing Ring A.S.T.M. Designation B.22 Alloy E as Mfg. by Lubrite Division of Merriman Bros. Inc. or equal Self Lubricating recesses on the inside Face only.
Typical Lubricating Recess Layout (All Around)
DETAIL "G"
TRUNNION PIN COVER PLATE
Drill 4 Holes 11/16" ϕ for 1/2" Cap Screws
Hole for 1" Eyebolt
Drill 11/16" ϕ 2 holes for 5/8" Cap Screws
1/2" Plate
DETAIL "J"
THRUST RING
Zinc Thrust Ring ASTM B-69 Type III
PLAN
TRUNNION YOKE AND PIN INSTALLATION
Upstream Face of box Girder (Trunnion Yoke align. bolt angles not shown)
4'-4 1/2" to Pier
1 5/8" ϕ Shear Bolts (See Box Girder)
1 1/4" High Strength Bolt
1/2" Zinc Alloy Filler
Face of Concrete
4 - 1/2" ϕ x 1 1/2" Hex Head Cap Screws. Drill and tap blind holes in Trunnion Yoke Side Plate
5/8" Align. Bolts
Grout Pocket
℄ Trunnion Pin Sta. 100 + 23.38
Side Thrust Plate
Bearing ring See detail "H" (3/8" F.H. CSK screws not shown)
Zinc Thrust Ring See detail "J"
See detail "F" for 10" Dia. Trunnion Pin (Install with end 1/16" clear of cover plate. Eyebolt and cap screws not shown)
Trunnion Pin Cover Plate See Detail "G"
4'-11 1/2" to ℄ Pier
Side of Pier
℄ Tainter Gate Struts
DETAIL "F"
TRUNNION PIN
Chamfer 1/8" at 45°
℄ Pin
Drill and Tap blind hole for 1" Eye bolt
Drill and Tap blind holes for 5/8" x 2" Cap Screws
Steel forged pin ASTM A-237 Class B
NOTES:
1. See anchorage notes sheet 41.
2. See specifications for method of tightening high strength bolts.
3. Trunnion Yoke shall be stress relief annealed after welding.
4. After gate has been erected, final adjustment of trunnion yoke shall be made by means of adjusting screws. The zinc alloy filler shall be poured to firmly key the trunnion yoke in place to the box girder.
5. The side thrust plate shall be adjusted with a slight compression against the thrust ring and the anchor bolts tightened. The grout pocket shall be filled with non-shrink Embeco grout as manufactured by Master Builders Co. or equal.
AS BUILT DRAWING
FORREST AND COTTON, INC. Consulting Engineers
By WDO
Date 8-18-67
SCALE
3 INCHES = 1 FOOT
Contract Nº 64-215
610 Q-4A
DALLAS CITY WATER WORKS
FORNEY DAM AND RESERVOIR
SPILLWAY
TAINTER GATES
TRUNNION YOKE AND PIN DETAILS
FORREST AND COTTON, INC. CONSULTING ENGINEERS DALLAS, TEXAS
FILE NO.
DESIGN BY: E.W.P.
DRAWN BY: J.S.W.
CHECKED BY: E.W.P.
RECOMMENDED BY:
APPROVED
SHEET NO. 42 OF 87
III

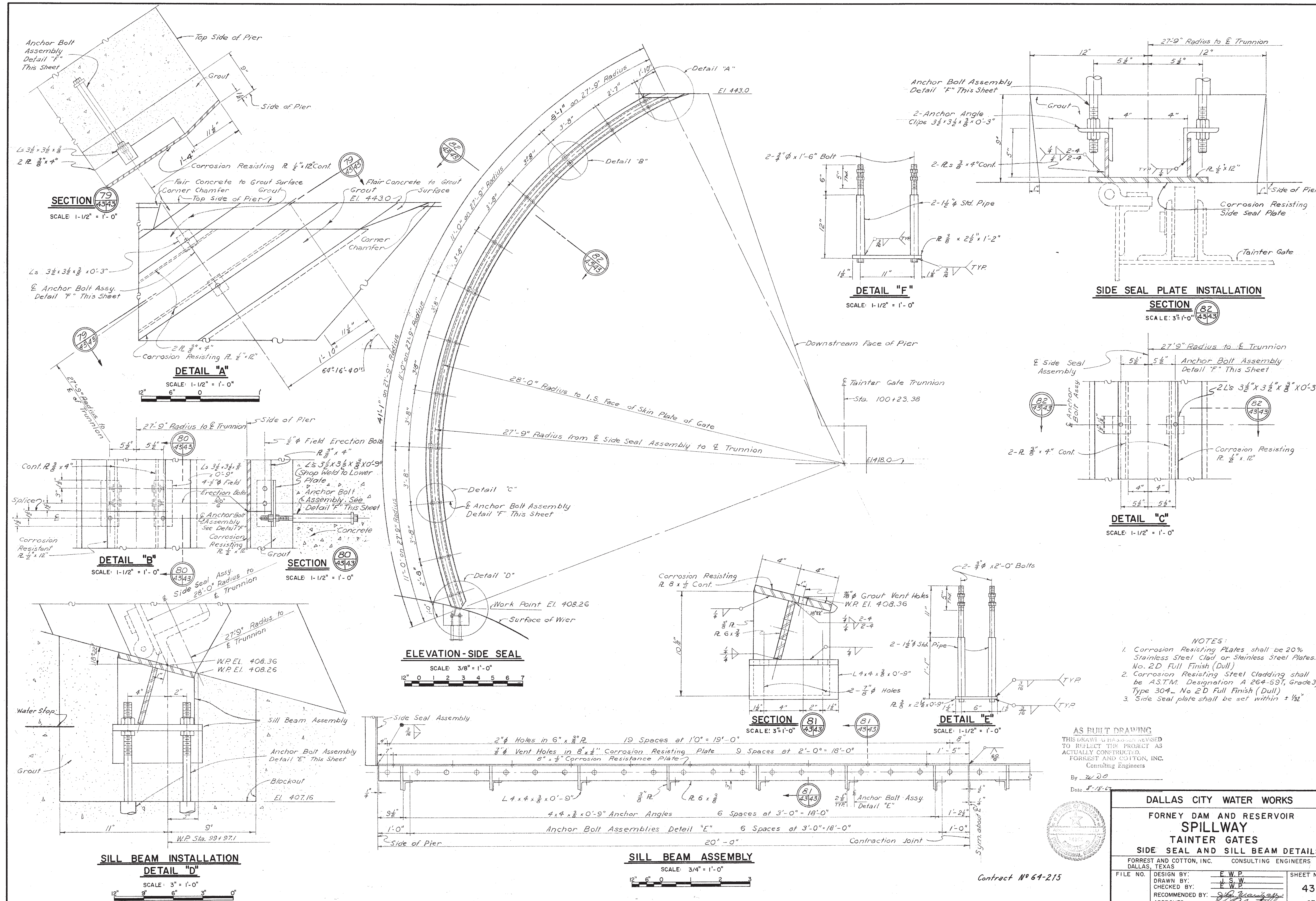

NOTES:
1. Corrosion Resisting Plates shall be 20% Stainless Steel Clad or Stainless Steel Plates. No. 2D Full Finish (Dull)
2. Corrosion Resisting Steel Cladding shall be A.S.T.M. Designation A 264-59T, Grade 3, Type 304 - No. 2D Full Finish (Dull)
3. Side Seal plate shall be set within ± 1/32"

AS BUILT DRAWING
THIS DRAWING HAS BEEN REVISED TO REFLECT THE PROJECT AS ACTUALLY CONSTRUCTED.
FORREST AND COTTON, INC.
Consulting Engineers
By W.D.O.
Date 8-18-67

DALLAS CITY WATER WORKS
FORNEY DAM AND RESERVOIR
SPILLWAY
TAINTER GATES
SIDE SEAL AND SILL BEAM DETAILS
FORREST AND COTTON, INC. CONSULTING ENGINEERS
DALLAS, TEXAS

FILE NO.			SHEET NO.
	DESIGN BY:	E.W.P.	43
	DRAWN BY:	J.S.W.	
	CHECKED BY:	E.W.P.	
	RECOMMENDED BY:	[signature]	
	APPROVED	[signature]	OF 87

III

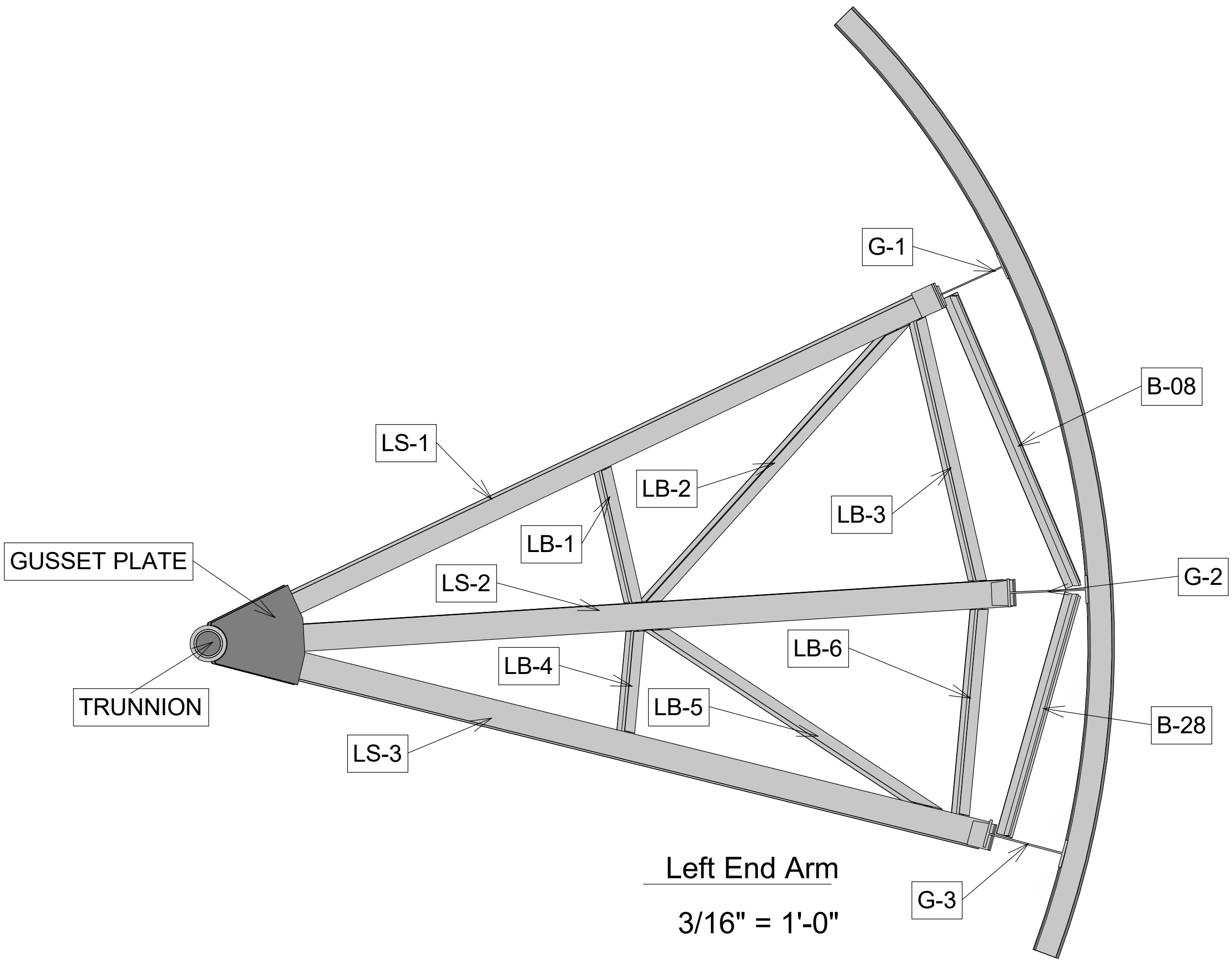

Left End Arm

3/16" = 1'-0"

© Schnabel Engineering 2020 All Rights Reserved

SHEET 01 OF 04

DRAWING #: S.1

PROJECT: 20C22001.00

FORNEY DAM TAINTER GATE
GATE INSPECTION
GARVER, LLC
DALLAS, TEXAS

LEFT RADIAL GATE SECTION

Schnabel ENGINEERING

SCHNABEL ENGINEERING
LICENSE NUMBER: C-2599

16000 Christensen Rd., Ste. 101 / Seattle, WA / 98188
T/ 206-573-5190 F/206-573-5195 / schnabel-eng.com

DESIGNED BY:	DRAWN BY:	CHECKED BY:
	CAS	RTI

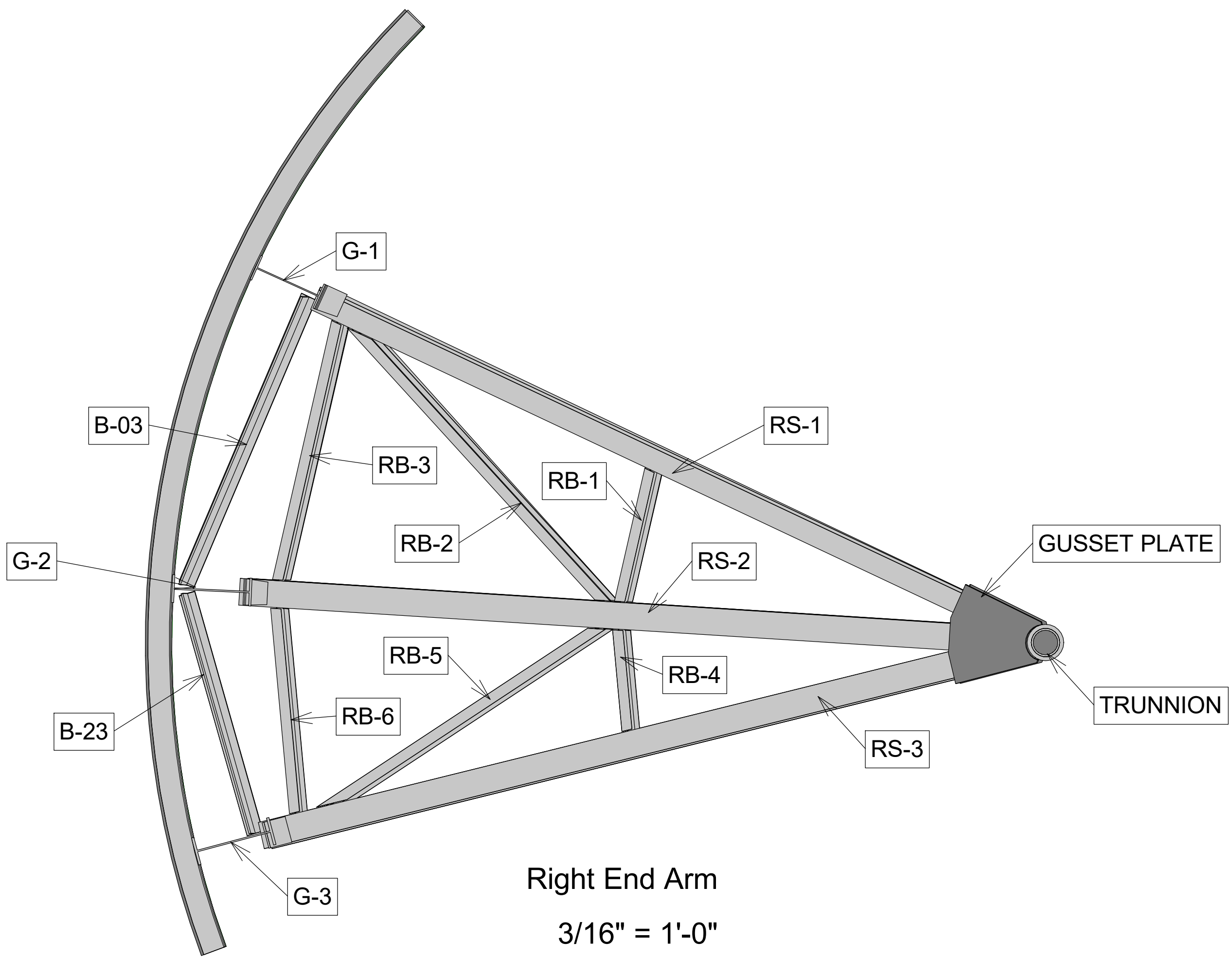

Right End Arm

3/16" = 1'-0"

© Schnabel Engineering 2020 All Rights Reserved

SHEET	DRAWING #:	PROJECT:					
02 OF 04	S.2	20C22001.00	FORNEY DAM TAINTER GATE GATE INSPECTION GARVER, LLC DALLAS, TEXAS RIGHT RADIAL GATE SECTION	Schnabel ENGINEERING SCHNABEL ENGINEERING LICENSE NUMBER: C-2599 16000 Christensen Rd., Ste. 101 / Seattle, WA / 98188 T/ 206-573-5190 F/206-573-5195 / schnabel-eng.com	DESIGNED BY:	DRAWN BY: CAS	CHECKED BY: RTI

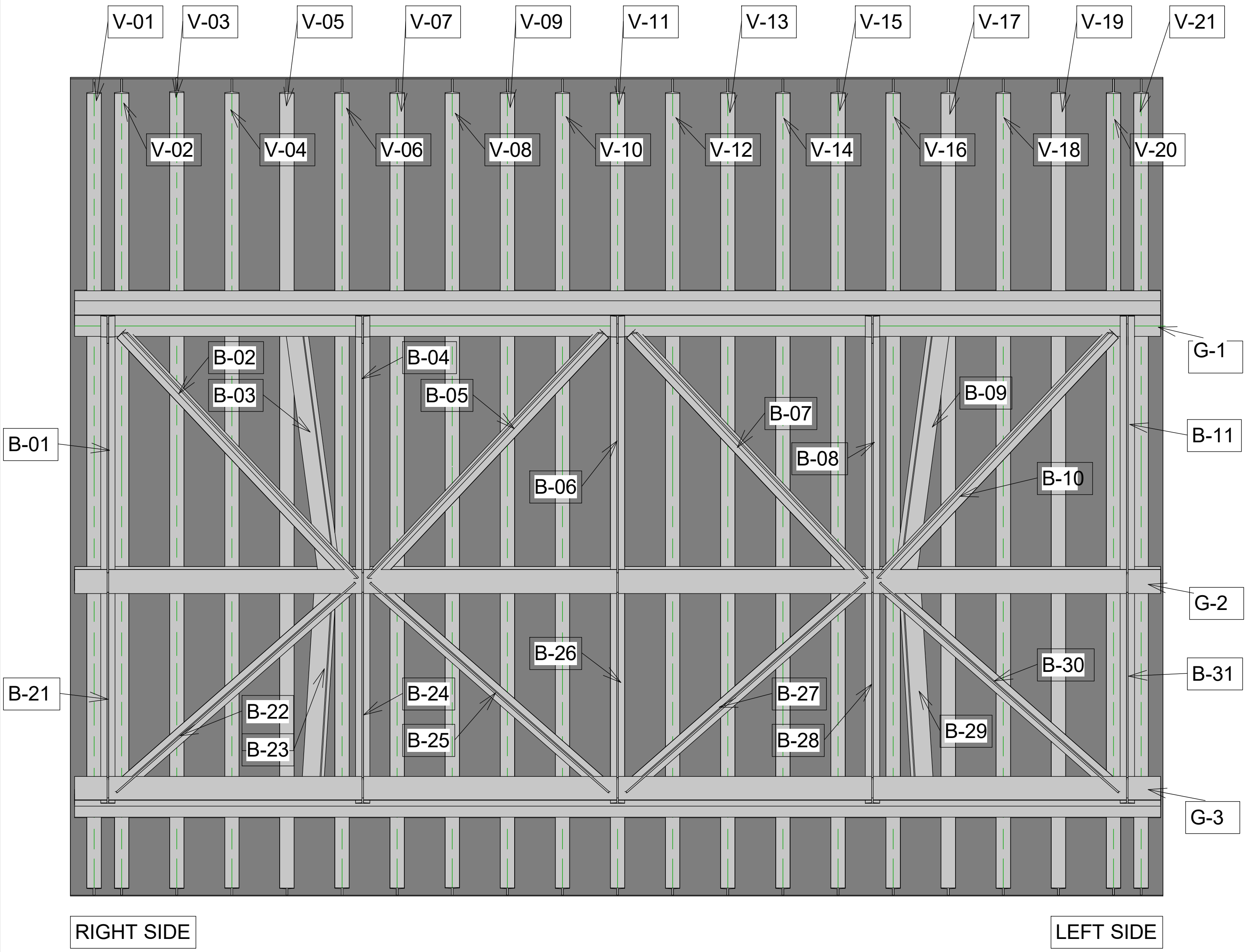

1 Downstream Elevation of Skin Plate
3/16" = 1'-0"

© Schnabel Engineering 2020 All Rights Reserved

SHEET 03 OF 04	DRAWING #: S.3	PROJECT: 20C22001.00	FORNEY DAM TAINTER GATE GATE INSPECTION GARVER, LLC DALLAS, TEXAS SOUTH ELEVATION	Schnabel ENGINEERING SCHNABEL ENGINEERING LICENSE NUMBER: C-2599 16000 Christensen Rd., Ste. 101 / Seattle, WA / 98188 T/ 206-573-5190 F/206-573-5195 / schnabel-eng.com	DESIGNED BY:	DRAWN BY: CAS	CHECKED BY: RTI

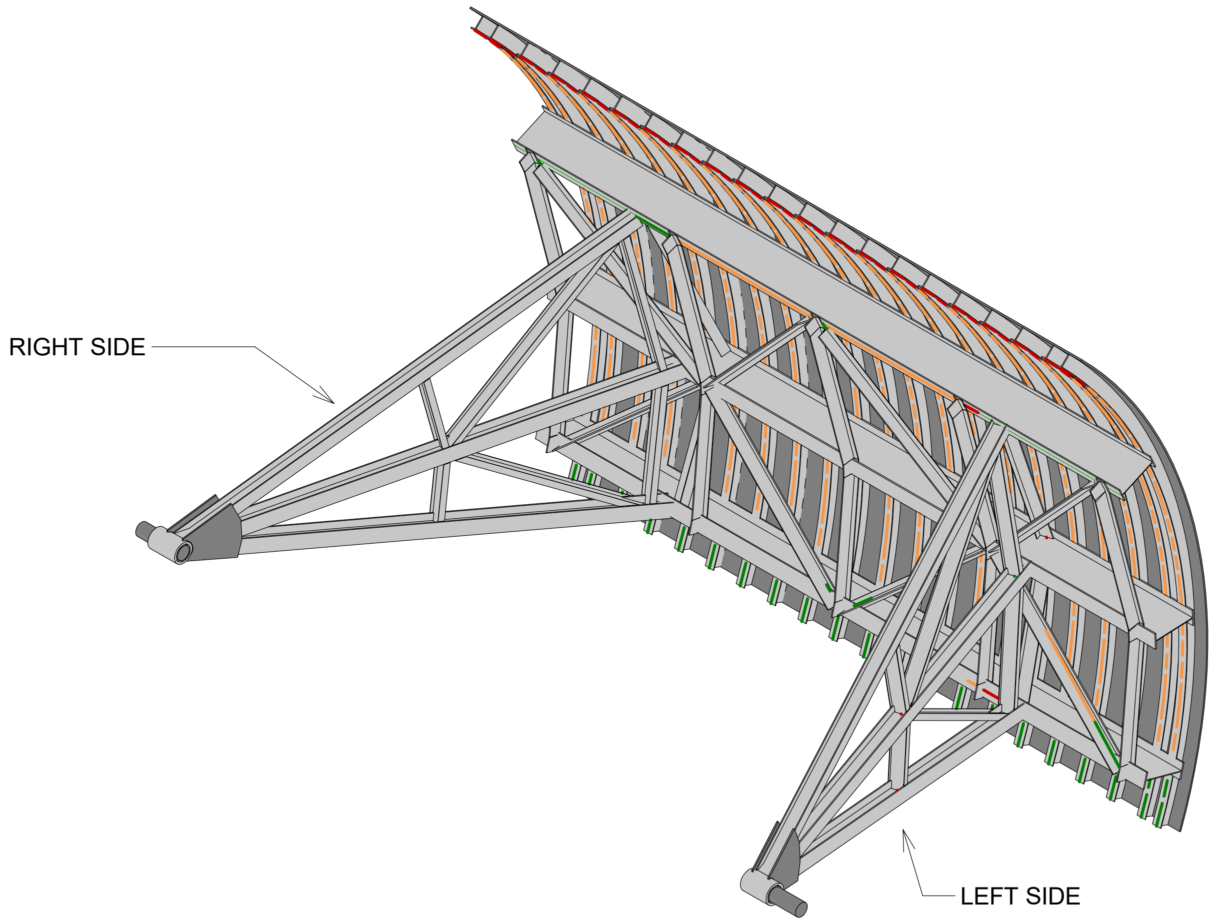

1 Typical Isometric View

© Schnabel Engineering 2020 All Rights Reserved

SHEET	DRAWING #:	PROJECT:					
04 OF 04	S.4	20C22001.00	FORNEY DAM TAINTER GATE GATE INSPECTION GARVER, LLC DALLAS, TEXAS	Schnabel ENGINEERING SCHNABEL ENGINEERING LICENSE NUMBER: C-2599	DESIGNED BY:	DRAWN BY: CAS	CHECKED BY: RTI
			TYPICAL ISOMETRIC VIEW	16000 Christensen Rd., Ste. 101 / Seattle, WA / 98188 T/ 206-573-5190 F/206-573-5195 / schnabel-eng.com			

APPENDIX B
GATE INSPECTION PHOTOGRAPHS

©2021 All Rights Reserved

PHOTOGRAPH No.: 1
GATE: Gate 1
Photo Taken: 3/30/2020
File: MC-1.jpg

LOCATION:
Right arm.

COMMENTS:

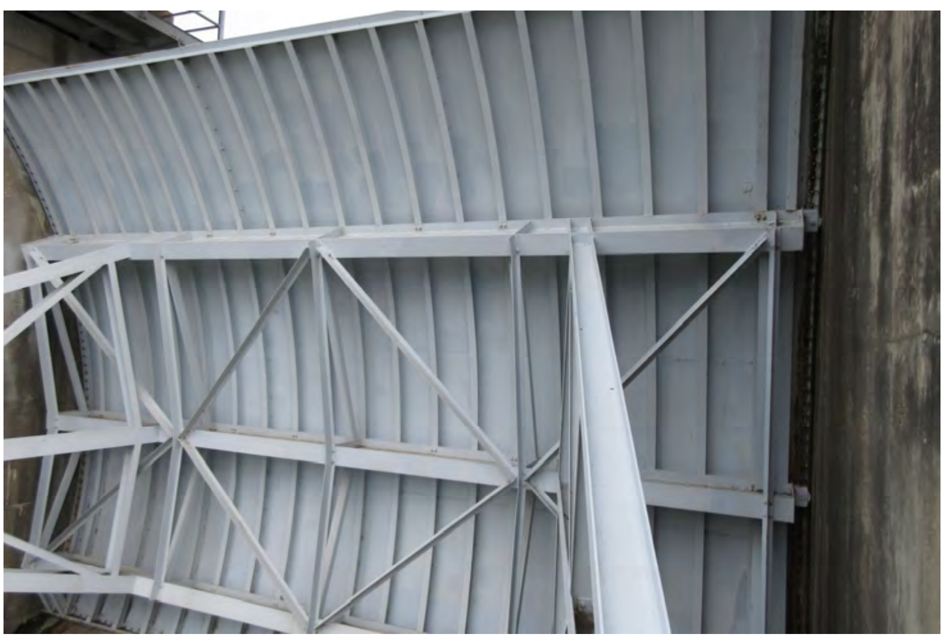

PHOTOGRAPH No.: 2
GATE: Gate 1
Photo Taken: 3/30/2020
File: MC-2.jpg

LOCATION:
Downstream face of gate.

COMMENTS:
Gate seals are effective with little seepage noted.

© Schnabel Engineering 2020 All Rights Reserved

PHOTOGRAPH No.: 3
GATE: Gate 1
Photo Taken: 3/30/2020
File: MC-4.jpg

LOCATION:
Left trunnion casting.

COMMENTS:
Light surface rust and thin paint coating. No section loss noted. CS-2

PHOTOGRAPH No.: 4
GATE: Gate 1
Photo Taken: 3/30/2020
File: MC-5.jpg

LOCATION:
Downstream face of skin between V-19 & V-20 and 1-1/2' above G-1.

COMMENTS:
4-1/2" diameter plate welded to skin with failing paint and moderate surface rust. CS-2.

© Schnabel Engineering 2020 All Rights Reserved

PHOTOGRAPH No.: 5

GATE: Gate 1

Photo Taken: 3/30/2020

File: MC-6.jpg

LOCATION:
G-1 looking right.

COMMENTS:
Minor debris buildup partially blocking drains. Typical for G-2 & G-3.

PHOTOGRAPH No.: 6

GATE: Gate 1

Photo Taken: 3/30/2020

File: MC-7.jpg

LOCATION:
V-17, left web stiffener at G-1.

COMMENTS:
Cracked weld. 100% cracked though. CS-2.

© Schnabel Engineering 2020 All Rights Reserved

PHOTOGRAPH No.: 7
GATE: Gate 1
Photo Taken: 3/30/2020
File: MC-8.jpg

LOCATION:
V-17 at G-1.

COMMENTS:
Cracked weld along G-1 flange. Potential for propagation. CS-3.

PHOTOGRAPH No.: 8
GATE: Gate 1
Photo Taken: 3/30/2020
File: MC-9.jpg

LOCATION:
V-14 at top of gate.

COMMENTS:
1-1/2" x 2" cutout of flange. Similar at V-8.

© Schnabel Engineering 2020 All Rights Reserved

PHOTOGRAPH No.: 9

GATE: Gate 1

Photo Taken: 3/30/2020

File: MC-10.jpg

LOCATION:
LS-2 at LB-2.

COMMENTS:
Light surface rust along welds and assembly bolts. CS-2.

PHOTOGRAPH No.: 10

GATE: Gate 1

Photo Taken: 3/30/2020

File: MC-11.jpg

LOCATION:
V-16 left web stiffener at G-2.

COMMENTS:
Cracked weld. Potential for propagation. CS-3. Similar condition at V-17 and V-18.

© Schnabel Engineering 2020 All Rights Reserved

PHOTOGRAPH No.: 11
GATE: Gate 1
Photo Taken: 3/30/2020
File: MC-12.jpg

LOCATION:
G-2, left side.

COMMENTS:
Arrested pitting on web and stiffener up to 1/16" deep. CS-3.

PHOTOGRAPH No.: 12
GATE: Gate 1
Photo Taken: 3/30/2020
File: MC-13.jpg

LOCATION:
V-14, 3' to 4' above G-2.

COMMENTS:
Out-of-plane bending in flange up to 1/4" over 5" long. Three locations. CS-2.

© Schnabel Engineering 2020 All Rights Reserved

PHOTOGRAPH No.: 13

GATE: Gate 1

Photo Taken: 3/30/2020

File: MC-14.jpg

LOCATION:
LS-3 at LB-6.

COMMENTS:
Failed paint and moderate surface rust. Rust along welds. Minor section loss. CS-3. Drains partly blocked.

PHOTOGRAPH No.: 14

GATE: Gate 1

Photo Taken: 3/30/2020

File: MC-15.jpg

LOCATION:
Gate skin and verticals V-1 & V-2. below G-3.

COMMENTS:
Sand buildup on stiffener up to 2" deep.

© Schnabel Engineering 2020 All Rights Reserved

PHOTOGRAPH No.: 15

GATE: Gate 1

Photo Taken: 3/30/2020

File: MC-16.jpg

LOCATION:
V-3 right web stiffener at G-3.

COMMENTS:
Cracked web. Potential for propagation. CS-3.

PHOTOGRAPH No.: 16

GATE: Gate 1

Photo Taken: 3/30/2020

File: MC-17.jpg

LOCATION:
V-5 right web stiffener at G-3.

COMMENTS:
Cracked web. Potential for propagation. CS-3.

© Schnabel Engineering 2020 All Rights Reserved

PHOTOGRAPH No.: 17

GATE: Gate 1

Photo Taken: 3/30/2020

File: MC-18.jpg

LOCATION:
V-7, between G-2 & G-3.

COMMENTS:
Out-of-plane bending in flange up to 2" over 20" long. CS-2. Also two torch cut gorges in flange up to 1/16" deep.

PHOTOGRAPH No.: 18

GATE: Gate 1

Photo Taken: 3/30/2020

File: MC-19.jpg

LOCATION:
RS-3 at RB-6.

COMMENTS:
Debris & vegetation buildup to 3". Drain holes blocked.

© Schnabel Engineering 2020 All Rights Reserved

PHOTOGRAPH No.: 19

GATE: Gate 1

Photo Taken: 3/30/2020

File: MC-20.jpg

LOCATION:
RS-3 at RB-5.

COMMENTS:
Ponding water with sand buildup.

PHOTOGRAPH No.: 20

GATE: Gate 1

Photo Taken: 3/30/2020

File: MC-21.jpg

LOCATION:
V-3 at G-2.

COMMENTS:
Cracked weld along G-2 flange. Potential for propagation as 2" of weld has not cracked, CS-3.

© Schnabel Engineering 2020 All Rights Reserved

PHOTOGRAPH No.: 21

GATE: Gate 1

Photo Taken: 3/30/2020

File: MC-22.jpg

LOCATION:
Skin plate between V-3 & V-4 between G-2 & G-3.

COMMENTS:
Hole though skin plate. Patched from upstream side of skin. No propagation potential. CS-2.

PHOTOGRAPH No.: 22

GATE: Gate 1

Photo Taken: 3/30/2020

File: MC-23.jpg

LOCATION:
V-6 at G-2.

COMMENTS:
Cracked weld along G-2 flange. Weld cracked 100%. No propagation potential CS-2.

© Schnabel Engineering 2020 All Rights Reserved

PHOTOGRAPH No.: 23
GATE: Gate 1
Photo Taken: 3/30/2020
File: MC-24.jpg

LOCATION:
RS-2 at gusset plates.

COMMENTS:
Ponding water and blocked drain.

PHOTOGRAPH No.: 24
GATE: Gate 1
Photo Taken: 3/30/2020
File: MC-25.jpg

LOCATION:
Left arm.

COMMENTS:

© Schnabel Engineering 2020 All Rights Reserved

PHOTOGRAPH No.: 25
GATE: Gate 1
Photo Taken: 3/30/2020
File: MC-26.jpg

LOCATION:
V-6 at G-1, right web stiffener.

COMMENTS:
Cracked weld. 100% cracked through CS-2.

PHOTOGRAPH No.: 26
GATE: Gate 1
Photo Taken: 3/30/2020
File: MC-27.jpg

LOCATION:
V-8 at G-1, right web stiffener .

COMMENTS:
Cracked weld. 100% cracked through CS-2.

© Schnabel Engineering 2020 All Rights Reserved

PHOTOGRAPH No.: 1
GATE: Gate 2
Photo Taken: 3/30/2020
File: CL-1.jpg

LOCATION:
Gate 2, left arm.

COMMENTS:

PHOTOGRAPH No.: 2
GATE: Gate 2
Photo Taken: 3/30/2020
File: CL-2.jpg

LOCATION:
Gate 2, right trunnion.

COMMENTS:
CS2 - rust on the inside of the coating. Common throughout.

© Schnabel Engineering 2020 All Rights Reserved

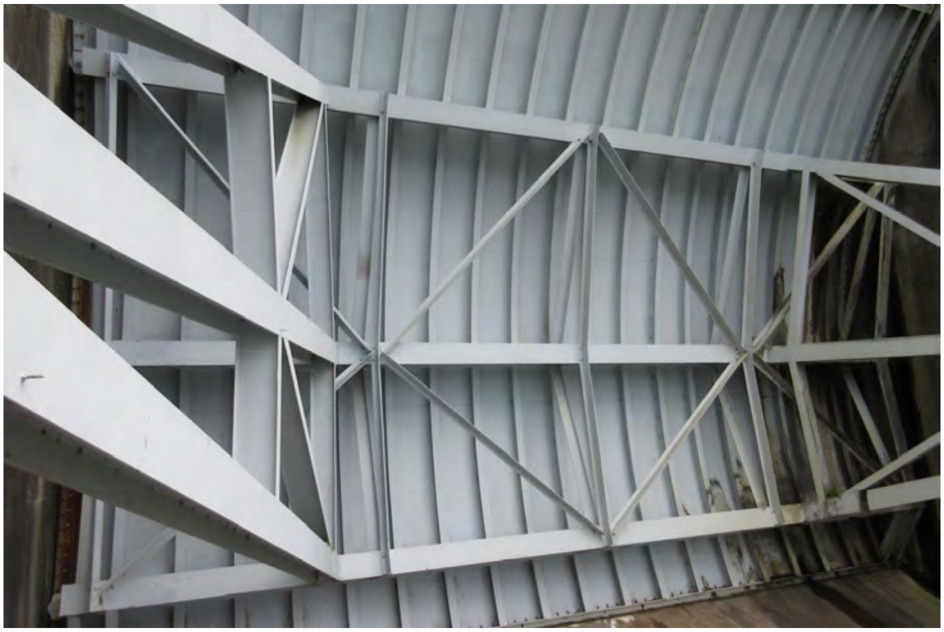

PHOTOGRAPH No.: 3
GATE: Gate 2
Photo Taken: 3/30/2020
File: CL-3.jpg

LOCATION:
Gate 2, skin and frame.

COMMENTS:

PHOTOGRAPH No.: 4
GATE: Gate 2
Photo Taken: 3/30/2020
File: CL-4.jpg

LOCATION:
Gate 2, RS-1, 5' from G-1.

COMMENTS:
Out-of-plane bending, 1/4" over 5" on flange of RS-1.

© Schnabel Engineering 2020 All Rights Reserved

PHOTOGRAPH No.: 5
GATE: Gate 2
Photo Taken: 3/30/2020
File: CL-5.jpg

LOCATION:
Gate 2, RS-2, 5' from trunnion.

COMMENTS:
CS2 on edge of flanges for 4'. Plus paint failure on web for 1'. CS2 also.

PHOTOGRAPH No.: 6
GATE: Gate 2
Photo Taken: 3/30/2020
File: CL-6.jpg

LOCATION:
Gate 2, RB-2, 6' from G-1.

COMMENTS:
Out-of-plane bending, 3/4" over 3" in flange.

© Schnabel Engineering 2020 All Rights Reserved

PHOTOGRAPH No.: 7

GATE: Gate 2

Photo Taken: 3/30/2020

File: CL-7.jpg

LOCATION:
Gate 2, skin between V-01 and V-02, 1' above G-2.

COMMENTS:
Two dimples from impact damage on upstream side paint failure with CS2 on both.

PHOTOGRAPH No.: 8

GATE: Gate 2

Photo Taken: 3/30/2020

File: CL-8.jpg

LOCATION:
Gate 2, V-04 at G-2 web stiffener.

COMMENTS:
Sand from paint job was not cleaned off and was painted over. CS2 was present after cleaning paint and sand.

© Schnabel Engineering 2020 All Rights Reserved

PHOTOGRAPH No.: 9

GATE: Gate 2

Photo Taken: 3/30/2020

File: CL-9.jpg

LOCATION:
Gate 2, V-04 at G-2 vertical weld between girder and vertical.

COMMENTS:
7" long crack in weld CS3.

PHOTOGRAPH No.: 10

GATE: Gate 2

Photo Taken: 3/30/2020

File: CL-10.jpg

LOCATION:
Gate 2, V-08, 3' above G-2.

COMMENTS:
Out-of-plane bending in flange over 2".

© Schnabel Engineering 2020 All Rights Reserved

PHOTOGRAPH No.: 11
GATE: Gate 2
Photo Taken: 3/30/2020
File: CL-11.jpg

LOCATION:
Gate 2, V-11 at G-2. Vertical weld between girder and vertical rib.

COMMENTS:
Full height crack in weld on both sides of flange.

PHOTOGRAPH No.: 12
GATE: Gate 2
Photo Taken: 3/30/2020
File: CL-12.jpg

LOCATION:
Gate 2, skin between V-01 and V-02, 6' above G-3.

COMMENTS:
1-1/2" dimple from impact on upstream side causing paint failure at CS2.

© Schnabel Engineering 2020 All Rights Reserved

PHOTOGRAPH No.: 13
GATE: Gate 2
Photo Taken: 3/30/2020
File: CL-13.jpg

LOCATION:
Gate 2, G-3 at V-01.

COMMENTS:
4" x 3" area of rust at CS3. Note debris buildup between web stiffener.

PHOTOGRAPH No.: 16
GATE: Gate 2
Photo Taken: 3/30/2020
File: CL-16.jpg

LOCATION:
Gate 2, bottom plate under V-01.

COMMENTS:
Heavy pitting up to 1/8" at CS3.

© Schnabel Engineering 2020 All Rights Reserved

PHOTOGRAPH No.: 17
GATE: Gate 2
Photo Taken: 3/30/2020
File: CL-17.jpg

LOCATION:
Gate 2, right seal.

COMMENTS:
Heavy rust staining from pack rust about half way up. Note: seal is tight with no leakage.

PHOTOGRAPH No.: 18
GATE: Gate 2
Photo Taken: 3/30/2020
File: CL-18.jpg

LOCATION:
Gate 2, RS-3 at RB-5.

COMMENTS:
Heavy debris build up in web of RS-3. Up to 4" deep. No drain hole present.

© Schnabel Engineering 2020 All Rights Reserved

PHOTOGRAPH No.: 19
GATE: Gate 2
Photo Taken: 3/30/2020
File: CL-19.jpg

LOCATION:
Gate 2, LS-3 at trunnion.

COMMENTS:
Multiple shallow gouges in flange with paint failure at CS2.

PHOTOGRAPH No.: 20
GATE: Gate 2
Photo Taken: 3/30/2020
File: CL-20.jpg

LOCATION:
Gate 2, right arm.

COMMENTS:

© Schnabel Engineering 2020 All Rights Reserved

PHOTOGRAPH No.: 21

GATE: Gate 2

Photo Taken: 3/30/2020

File: CL-21.jpg

LOCATION:
Gate 2, skin between V-15 and V-16 at G-1.

COMMENTS:
Full thickness hole that has a 4' x 4" repair patch.

PHOTOGRAPH No.: 22

GATE: Gate 2

Photo Taken: 3/30/2020

File: CL-22.jpg

LOCATION:
Gate 2, LB-2 at LS-2.

COMMENTS:
Out-of-plane bending 3/4" over 3" in flange.

© Schnabel Engineering 2020 All Rights Reserved

PHOTOGRAPH No.: 23

GATE: Gate 2

Photo Taken: 3/30/2020

File: CL-23.jpg

LOCATION:
Gate 2, skin between V-19 and V-20, 8' above G-2.

COMMENTS:
Plugged hole in skin. Wood and moss currently block hole. Evidence of moss and staining suggest a lot of water flowed at one time.

PHOTOGRAPH No.: 24

GATE: Gate 2

Photo Taken: 3/30/2020

File: CL-24.jpg

LOCATION:
Gate 2, V-14, 4' above G-2.

COMMENTS:
Out-of-plane bending in 3 spots on flange 1/4" over 1".

© Schnabel Engineering 2020 All Rights Reserved

PHOTOGRAPH No.: 25
GATE: Gate 2
Photo Taken: 3/30/2020
File: CL-25.jpg

LOCATION:
Gate 2, G-3 from V-16 to V-21.

COMMENTS:
Drain holes are plugged and there is 4" of standing water and debris.

PHOTOGRAPH No.: 26
GATE: Gate 2
Photo Taken: 3/30/2020
File: CL-26.jpg

LOCATION:
Gate 2, RB-6 at RS-3.

COMMENTS:
5" x 3" paint failure with S/L and pitting to 1/8" CS3.

© Schnabel Engineering 2020 All Rights Reserved

PHOTOGRAPH No.: 27

GATE: Gate 2

Photo Taken: 3/30/2020

File: CL-27.jpg

LOCATION:
Gate 2, bottom plate at V-08.

COMMENTS:
Arrested pitting throughout the whole plate up to 3/16" deep.

PHOTOGRAPH No.: 28

GATE: Gate 2

Photo Taken: 3/30/2020

File: CL-28.jpg

LOCATION:
Gate 2, LS-3 at LB-6 connection.

COMMENTS:
Drain hole is plugged. Debris and vegetation is filling the web.

© Schnabel Engineering 2020 All Rights Reserved

PHOTOGRAPH No.: 29
GATE: Gate 2
Photo Taken: 3/30/2020
File: CL-29.jpg

LOCATION:
Gate 2, LB-6, 1' down from LS-2.

COMMENTS:
Out-of-plane bending 1/2" over 3" on flange.

PHOTOGRAPH No.: 30
GATE: Gate 2
Photo Taken: 3/30/2020
File: CL-30.jpg

LOCATION:
Gate 2, LS-3 at LB-5.

COMMENTS:
Drain hole is plugged. 4" of water and debris.

© Schnabel Engineering 2020 All Rights Reserved

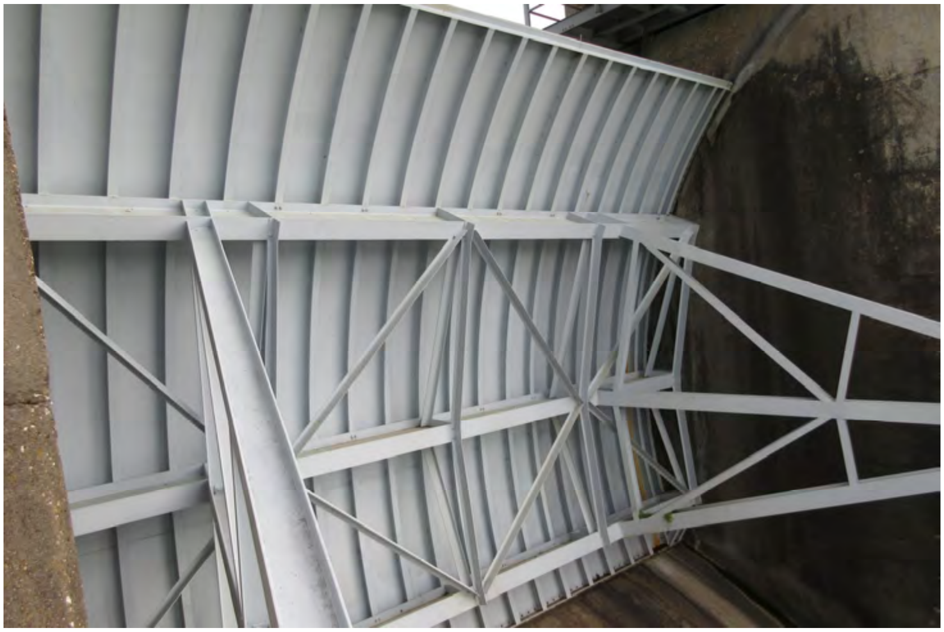

PHOTOGRAPH No.: 1
GATE: Gate 3
Photo Taken: 3/30/2020
File: DK-1.jpg

LOCATION:
Gate 3, General overview.

COMMENTS:

PHOTOGRAPH No.: 2
GATE: Gate 3
Photo Taken: 3/30/2020
File: DK-2.jpg

LOCATION:
Gate 3, right arms RS-3, under-side flanges at RB-4.

COMMENTS:
Out-of-plane bending 3/16" over 8" section CS2.

© Schnabel Engineering 2020 All Rights Reserved

PHOTOGRAPH No.: 3
GATE: Gate 3
Photo Taken: 3/30/2020
File: DK-3.jpg

LOCATION:
Gate 3, left arm overview.

COMMENTS:

PHOTOGRAPH No.: 4
GATE: Gate 3
Photo Taken: 3/30/2020
File: DK-4.jpg

LOCATION:
Gate 3, Downstream side of skin plate between V16 & V17, 1' above G-1.

COMMENTS:
A typical circular cover plate, tack welds in good condition, paint is cracked with rust bleeding, CS2.

© Schnabel Engineering 2020 All Rights Reserved

PHOTOGRAPH No.: 5
GATE: Gate 3
Photo Taken: 3/30/2020
File: DK-5.jpg

LOCATION:
Gate 3, left arm LS-1 topside inboard flange 6' from G-1.

COMMENTS:
4" scrape along flange edge with surface rust, CS2, 1/16" deep.

PHOTOGRAPH No.: 6
GATE: Gate 3
Photo Taken: 3/30/2020
File: DK-6.jpg

LOCATION:
Gate 3, right arm overview.

COMMENTS:

© Schnabel Engineering 2020 All Rights Reserved

PHOTOGRAPH No.: 7

GATE: Gate 3

Photo Taken: 3/30/2020

File: DK-7.jpg

LOCATION:
Gate 3, Downstream side of skin, between V-19 & V-20, 4' above G-2.

COMMENTS:
1/2" drill hole through skin steel, leaking 2 gpm.

PHOTOGRAPH No.: 8

GATE: Gate 3

Photo Taken: 3/30/2020

File: DK-8.jpg

LOCATION:
Gate 3, V-14, 2' above G-2.

COMMENTS:
Out-of-plane bending, 1/2" over 18" section, CS2.

© Schnabel Engineering 2020 All Rights Reserved

PHOTOGRAPH No.: 9

GATE: Gate 3

Photo Taken: 3/30/2020

File: DK-9.jpg

LOCATION:
Gate 3, V-1 & upstream flange of G-2.

COMMENTS:
Areas of failed paint with light surface rust due to paint application over sand, CS2.

PHOTOGRAPH No.: 10

GATE: Gate 3

Photo Taken: 3/30/2020

File: DK-10.jpg

LOCATION:
Gate 3, right arm RB-1 at RS-2.

COMMENTS:
Corrosion at bottom of web, pitting to 1/8" & pack rust to 1/4", CS3.

© Schnabel Engineering 2020 All Rights Reserved

PHOTOGRAPH No.: 11
GATE: Gate 3
Photo Taken: 3/30/2020
File: DK-11.jpg

LOCATION:
Gate 3, G-2 right roller.

COMMENTS:
Roller is seized, paint failure with surface rust & pitting to 1/16", CS3.

PHOTOGRAPH No.: 12
GATE: Gate 3
Photo Taken: 3/30/2020
File: DK-12.jpg

LOCATION:
Gate 3, V-12, 1' below G-1.

COMMENTS:
V-12 has field weld across flange with one end only 25% thick as normal flange thickness, CS2.

© Schnabel Engineering 2020 All Rights Reserved

PHOTOGRAPH No.: 13

GATE: Gate 3

Photo Taken: 3/30/2020

File: DK-13.jpg

LOCATION:
Gate 3, V-2 at G-3.

COMMENTS:
Vertical weld is cracked entire length, CS2.

PHOTOGRAPH No.: 14

GATE: Gate 3

Photo Taken: 3/30/2020

File: DK-14.jpg

LOCATION:
Gate 3, left arm LS-3 at LB-5 & LB-6.

COMMENTS:
Dirt & debris are clogging drain holes holding water & vegetation.

© Schnabel Engineering 2020 All Rights Reserved

PHOTOGRAPH No.: 15
GATE: Gate 3
Photo Taken: 3/30/2020
File: DK-15.jpg

LOCATION:
Gate 3, V-2 at G-3.

COMMENTS:
1/4" pack rust between rib flange & girder, CS3.

PHOTOGRAPH No.: 16
GATE: Gate 3
Photo Taken: 3/30/2020
File: DK-16.jpg

LOCATION:
Gate 3, B-22 at G-3.

COMMENTS:
Area 18" x 4" paint failure with light pitting, CS3.

© Schnabel Engineering 2020 All Rights Reserved

PHOTOGRAPH No.: 17
GATE: Gate 3
Photo Taken: 3/30/2020
File: DK-17.jpg

LOCATION:
Gate 3, right J-bulb seal, bottom corner.

COMMENTS:
Minor leak in seal, about 1 gpm.

PHOTOGRAPH No.: 18
GATE: Gate 3
Photo Taken: 3/30/2020
File: DK-18.jpg

LOCATION:
Gate 3, bottom edge of gate.

COMMENTS:
Corrosion & pack rust & pitting to 3/16" along 50% of gate, CS3.

© Schnabel Engineering 2020 All Rights Reserved

PHOTOGRAPH No.: 1
GATE: Gate 4
Photo Taken: 3/31/2020
File: CL-1.jpg

LOCATION:
Gate 4, left arm.

COMMENTS:

PHOTOGRAPH No.: 2
GATE: Gate 4
Photo Taken: 3/31/2020
File: CL-2.jpg

LOCATION:
Gate 4, right trunnion.

COMMENTS:
Paint failure on inside of trunnion CS-2. Same on left trunnion.

© Schnabel Engineering 2020 All Rights Reserved

PHOTOGRAPH No.: 3
GATE: Gate 4
Photo Taken: 3/31/2020
File: CL-3.jpg

LOCATION:
Gate 4, G-1 top right side.

COMMENTS:
Freckle rust bleeding through on bottom flange. CS2 and typical for all.

PHOTOGRAPH No.: 4
GATE: Gate 4
Photo Taken: 3/31/2020
File: CL-4.jpg

LOCATION:
Gate 4, RB-3 1' above RS-2.

COMMENTS:
Out-of-plane bending, 1" over 2" on flange .

© Schnabel Engineering 2020 All Rights Reserved

PHOTOGRAPH No.: 5
GATE: Gate 4
Photo Taken: 3/31/2020
File: CL-5.jpg

LOCATION:
Gate 4, RB-6.

COMMENTS:
Out-of-plane bending on the whole member, 1" over 6'. Due to impact, not to the member bucking.

PHOTOGRAPH No.: 6
GATE: Gate 4
Photo Taken: 3/31/2020
File: CL-6.jpg

LOCATION:
Gate 4, RB-6.

COMMENTS:
Out-of-plane bending on the whole member 1" over 6'. Due to impact, not to the member bucking.

© Schnabel Engineering 2020 All Rights Reserved

PHOTOGRAPH No.: 7

GATE: Gate 4

Photo Taken: 3/31/2020

File: CL-7.jpg

LOCATION:
Gate 4, skin plate 1' above G-2 by V-05.

COMMENTS:
2" x 2" paint failure with pitting to 1/16", CS3.

PHOTOGRAPH No.: 8

GATE: Gate 4

Photo Taken: 3/31/2020

File: CL-8.jpg

LOCATION:
Gate 4, web stiffener on V-06 by G-2.

COMMENTS:
1/2" long crack in weld on stiffener CS3.

© Schnabel Engineering 2020 All Rights Reserved

PHOTOGRAPH No.: 9
GATE: Gate 4
Photo Taken: 3/31/2020
File: CL-9.jpg

LOCATION:
Gate 4, V-08, 3' above G-2.

COMMENTS:
Out-of-plane bending 1" over 2" in flange.

PHOTOGRAPH No.: 10
GATE: Gate 4
Photo Taken: 3/31/2020
File: CL-10.jpg

LOCATION:
Gate 4, G-3 left side.

COMMENTS:
No drain hole. Water and debris collects same on right side .

© Schnabel Engineering 2020 All Rights Reserved

PHOTOGRAPH No.: 11

GATE: Gate 4

Photo Taken: 3/31/2020

File: CL-11.jpg

LOCATION:
Gate 4, G-3 & LS-3 connection.

COMMENTS:
Drain hole plugged, 5" of standing water in bays.

PHOTOGRAPH No.: 12

GATE: Gate 4

Photo Taken: 3/31/2020

File: CL-12.jpg

LOCATION:
Gate 4, skin plate between V-15 and V-16, 6" above G-3.

COMMENTS:
3" round paint failure with heavy surface rust. Similar spot between V-17 and V-16, CS2 for both.

© Schnabel Engineering 2020 All Rights Reserved

PHOTOGRAPH No.: 13
GATE: Gate 4
Photo Taken: 3/31/2020
File: CL-13.jpg

LOCATION:
Gate 4, LS-3 to LB-6 connection.

COMMENTS:
Heavy arrested pitting throughout web of both members. Note: built up repair in web of LB-5 web.

PHOTOGRAPH No.: 14
GATE: Gate 4
Photo Taken: 3/31/2020
File: CL-14.jpg

LOCATION:
Gate 4, LS-2 at trunnion.

COMMENTS:
Drain hole is plugged. Standing water to 6" deep.

© Schnabel Engineering 2020 All Rights Reserved

PHOTOGRAPH No.: 15
GATE: Gate 4
Photo Taken: 3/31/2020
File: CL-15.jpg

LOCATION:
Gate 4, LB-2, 5' from G-1.

COMMENTS:
Out-of-plane bending, 1/2" over 2" on flange.

PHOTOGRAPH No.: 16
GATE: Gate 4
Photo Taken: 3/31/2020
File: CL-16.jpg

LOCATION:
Gate 4, skin between V-16 and V-17 at G-2.

COMMENTS:
6" x 10" area of paint failure with heavy rust bleed CS2. Similar spot between V-17 and V-18 at G-2.

© Schnabel Engineering 2020 All Rights Reserved

PHOTOGRAPH No.: 17

GATE: Gate 4

Photo Taken: 3/31/2020

File: CL-17.jpg

LOCATION:
Gate 4, web stiffener in V-16 at G-2.

COMMENTS:
1/2" crack in weld of web stiffener, CS3.

PHOTOGRAPH No.: 18

GATE: Gate 4

Photo Taken: 3/31/2020

File: CL-18.jpg

LOCATION:
Gate 4, web stiffener in V-18 at G-2.

COMMENTS:
1/2" crack in weld of web stiffener, CS3.

© Schnabel Engineering 2020 All Rights Reserved

PHOTOGRAPH No.: 19
GATE: Gate 4
Photo Taken: 3/31/2020
File: CL-19.jpg

LOCATION:
Gate 4, V-14 at G-1.

COMMENTS:
1" long crack in vertical weld between vertical and girder, CS3.

PHOTOGRAPH No.: 20
GATE: Gate 4
Photo Taken: 3/31/2020
File: CL-20.jpg

LOCATION:
Gate 4, right arm.

COMMENTS:

© Schnabel Engineering 2020 All Rights Reserved

PHOTOGRAPH No.: 21
GATE: Gate 4
Photo Taken: 3/31/2020
File: CL-21.jpg

LOCATION:
Gate 4, gate and frame.

COMMENTS:

PHOTOGRAPH No.: 22
GATE: Gate 4
Photo Taken: 3/31/2020
File: CL-22.jpg

LOCATION:
Gate 4, LS-1 at trunnion.

COMMENTS:
1" bar welded between flanges top and bottom of gussets.

© Schnabel Engineering 2020 All Rights Reserved

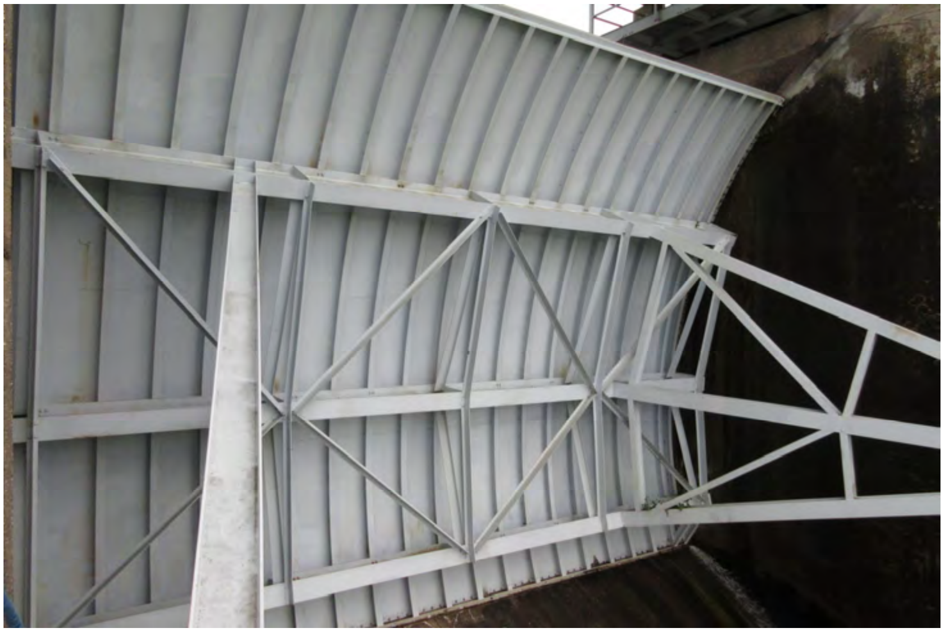

PHOTOGRAPH No.: 1
GATE: Gate 5
Photo Taken: 3/31/2020
File: DK-25.jpg

LOCATION:
Gate 5, overview.

COMMENTS:
Overview - isolated areas of freckle rust on girders & skin.

PHOTOGRAPH No.: 2
GATE: Gate 5
Photo Taken: 3/31/2020
File: DK-26.jpg

LOCATION:
Gate 5, left arm overview.

COMMENTS:

© Schnabel Engineering 2020 All Rights Reserved

PHOTOGRAPH No.: 3

GATE: Gate 5

Photo Taken: 3/31/2020

File: DK-27.jpg

LOCATION:
Gate 5, right arm trunnion, underside connection of RS-3, gusset plate & trunnion.

COMMENTS:
Areas of freckle rust, CS-2.

PHOTOGRAPH No.: 4

GATE: Gate 5

Photo Taken: 3/31/2020

File: DK-28.jpg

LOCATION:
Gate 5, interior of gusset plate between RS-1 & RS-2

COMMENTS:
Heavy freckle rust, pitting to 1/8", unarrested, CS-3.

© Schnabel Engineering 2020 All Rights Reserved

PHOTOGRAPH No.: 5
GATE: Gate 5
Photo Taken: 3/31/2020
File: DK-29.jpg

LOCATION:
Gate 5, RS-2, topside/outboard flange, 6 ft from trunnion.

COMMENTS:
Arrested pitting to 1/8" over 3' section, CS-3.

PHOTOGRAPH No.: 6
GATE: Gate 5
Photo Taken: 3/31/2020
File: DK-30.jpg

LOCATION:
Gate 5, G-1 at stiffener at V-11 (midspan).

COMMENTS:
Topside of G-1 web and stiffener welds have paint failure with unarrested pitting to 1/8" (about 4" x 6" area) (due to dirt accumulation holding moisture), CS-3.

© Schnabel Engineering 2020 All Rights Reserved

PHOTOGRAPH No.: 7
GATE: Gate 5
Photo Taken: 3/31/2020
File: DK-31.jpg

LOCATION:
Gate 5, V-7 at G-1.

COMMENTS:
Pack rust to 1/4" between rib & girder flanges, CS-3.

PHOTOGRAPH No.: 8
GATE: Gate 5
Photo Taken: 3/31/2020
File: DK-32.jpg

LOCATION:
Gate 5, B-22 at G-2 connection.

COMMENTS:
5" x 1" area of paint failure, surface rust with light pitting, CS-3.

© Schnabel Engineering 2020 All Rights Reserved

PHOTOGRAPH No.: 9

GATE: Gate 5

Photo Taken: 3/31/2020

File: DK-33.jpg

LOCATION:
Gate 5, RB-2 & RS-2 connection.

COMMENTS:
2' x 1' area of pitting on both members to 1/8". 75% arrested, CS-3.

PHOTOGRAPH No.: 10

GATE: Gate 5

Photo Taken: 3/31/2020

File: DK-34.jpg

LOCATION:
Gate 5, V-9 - V-11 & G-3.

COMMENTS:
Areas of freckle rust (typical throughout), CS-2.

© Schnabel Engineering 2020 All Rights Reserved

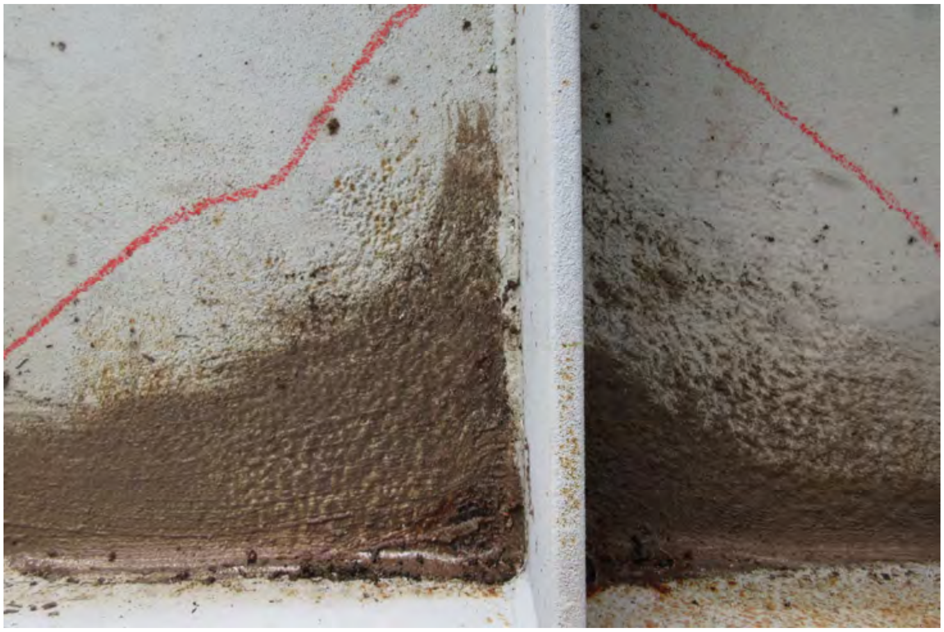

PHOTOGRAPH No.: 11
GATE: Gate 5
Photo Taken: 3/31/2020
File: DK-35.jpg

LOCATION:
Gate 5, G-3 at V-11 (midspan).

COMMENTS:
Topside web has 2' x 1' area of arrested pitting to 1/16", CS-3.

PHOTOGRAPH No.: 12
GATE: Gate 5
Photo Taken: 3/31/2020
File: DK-36.jpg

LOCATION:
Gate 5, bottom right corner.

COMMENTS:
Minor leak (about 1 gpm) typical rust staining down edges onto rollers, V1 & V2 flange edges have corrosion & section loss at bottom plate, CS-3.

© Schnabel Engineering 2020 All Rights Reserved

PHOTOGRAPH No.: 13
GATE: Gate 5
Photo Taken: 3/31/2020
File: DK-37.jpg

LOCATION:
Gate 5, Bottom 1' of skin along full width of gate.

COMMENTS:
This area has pitting to 1/8" arrested along full width of gate, bottom edge is also corroded full width with section loss, CS-3.

PHOTOGRAPH No.: 14
GATE: Gate 5
Photo Taken: 3/31/2020
File: DK-38.jpg

LOCATION:
Gate 5, G-3 left end (at V-21).

COMMENTS:
Dirt/debris is holding water between stiffeners & more significant leak in seal at the bottom left corner, about 3 gpm.

© Schnabel Engineering 2020 All Rights Reserved

PHOTOGRAPH No.: 15
GATE: Gate 5
Photo Taken: 3/31/2020
File: DK-39.jpg

LOCATION:
Gate 5, left arm LB-4.

COMMENTS:
Out-of-plane bending of in-board U/S flange, 1/2" over 6" section, CS-2.

PHOTOGRAPH No.: 16
GATE: Gate 5
Photo Taken: 3/31/2020
File: DK-40.jpg

LOCATION:
Gate 5, G-2 (between V-15 & V-16).

COMMENTS:
4" x 3" area paint failure with surface rust & light pitting, also 1' x 2' area of arrested pitting to 1/16" on topside web and typical freckle rust on girder & skin CS-3.

© Schnabel Engineering 2020 All Rights Reserved

PHOTOGRAPH No.: 17
GATE: Gate 5
Photo Taken: 3/31/2020
File: DK-41.jpg

LOCATION:
Gate 5, cover plate between V-19 & V-20, 8' above G-2.

COMMENTS:
Tack welds have failed along left side and 1" of pack rust exists between cover plate & skin plate. Skin plate is pitted to 1/16" inch behind pack rust.

PHOTOGRAPH No.: 18
GATE: Gate 5
Photo Taken: 3/31/2020
File: DK-42.jpg

LOCATION:
Gate 5, left arm (LS-2).

COMMENTS:
Member is not draining, water creating pond between flanges.

© Schnabel Engineering 2020 All Rights Reserved

PHOTOGRAPH No.: 19
GATE: Gate 5
Photo Taken: 3/31/2020
File: DK-43.jpg

LOCATION:
Gate 5, left arm LS-3 & LB-5.

COMMENTS:
Dirt & debris collected between members holding water & vegetation.

PHOTOGRAPH No.: 20
GATE: Gate 5
Photo Taken: 3/31/2020
File: DK-44.jpg

LOCATION:
Gate 5, right arm overview.

COMMENTS:

© Schnabel Engineering 2020 All Rights Reserved

PHOTOGRAPH No.: 1
GATE: Gate 6
Photo Taken: 3/31/2020
File: MC-01.jpg

LOCATION:
Gate 6, left arm.

COMMENTS:

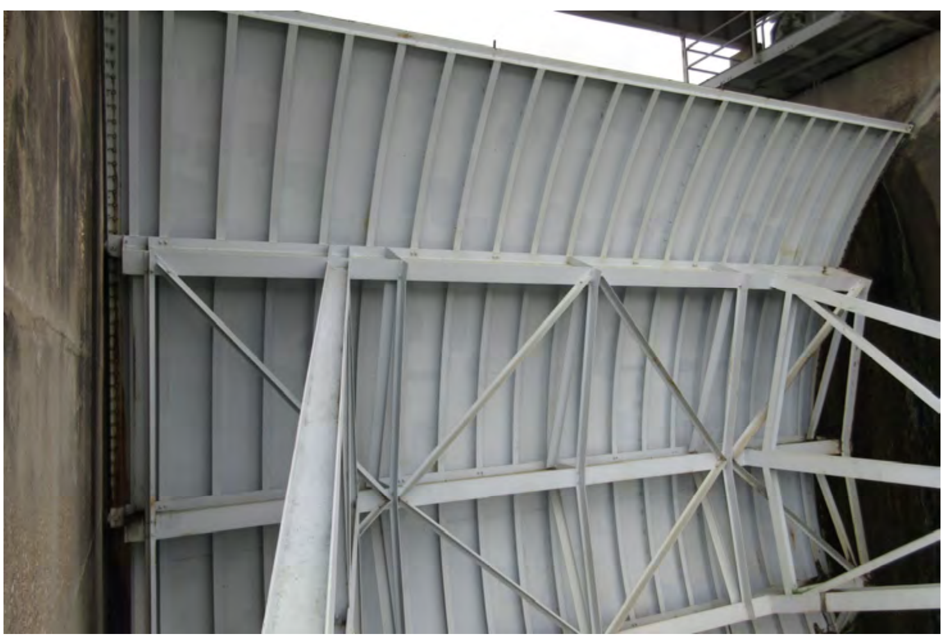

PHOTOGRAPH No.: 2
GATE: Gate 6
Photo Taken: 3/31/2020
File: MC-02.jpg

LOCATION:
Gate 6, Downstream face of gate.

COMMENTS:
Right roller guides at G-1 & G-2 spin free w/ 1/4" gap. Right roller guide at G-3 is touching buttress wall.

© Schnabel Engineering 2020 All Rights Reserved

PHOTOGRAPH No.: 3
GATE: Gate 6
Photo Taken: 3/31/2020
File: MC-03.jpg

LOCATION:
Gate 6, right trunnion.

COMMENTS:
Blocked drain and ponding water at RS-1 & RS-2. Light surface rust on trunnion and trunnion casting CS-2.

PHOTOGRAPH No.: 4
GATE: Gate 6
Photo Taken: 3/31/2020
File: MC-04.jpg

LOCATION:
Gate 6, RS-1 at gusset plate. Outboard vertical field weld.

COMMENTS:
Rust bleed along weld. Weld appears to have poor penetration along the downstream edge. CS-2.

© Schnabel Engineering 2020 All Rights Reserved

PHOTOGRAPH No.: 5
GATE: Gate 6
Photo Taken: 3/31/2020
File: MC-05.jpg

LOCATION:
Gate 6, G-1 connection to skin plate on right side of V-1.

COMMENTS:
Vertical crack. 1/2" rebar or round rod was welded in place between skin and end of G-1. Crack is 100% through. No chance of propagation. CS-2.

PHOTOGRAPH No.: 6
GATE: Gate 6
Photo Taken: 3/31/2020
File: MC-06.jpg

LOCATION:
Gate 6, V-6 at G-2, right vertical weld.

COMMENTS:
Cracked weld. Potential for propagation. CS-3.

© Schnabel Engineering 2020 All Rights Reserved

PHOTOGRAPH No.: 7
GATE: Gate 6
Photo Taken: 3/31/2020
File: MC-07.jpg

LOCATION:
Gate 6, RS-2 at G-2.

COMMENTS:
Cracked weld. Potential for propagation. CS-3.

PHOTOGRAPH No.: 8
GATE: Gate 6
Photo Taken: 3/31/2020
File: MC-08.jpg

LOCATION:
Gate 6, RB-1 at RS-1.

COMMENTS:
Void in weld 1-1/4" long w/light surface rust. CS-2.

© Schnabel Engineering 2020 All Rights Reserved

PHOTOGRAPH No.: 9
GATE: Gate 6
Photo Taken: 3/31/2020
File: MC-09.jpg

LOCATION:
Gate 6, underside of RS-2 between RB-1 & RB-3.

COMMENTS:
Light surface rust along flanges. CS-2.

PHOTOGRAPH No.: 10
GATE: Gate 6
Photo Taken: 3/31/2020
File: MC-10.jpg

LOCATION:
Gate 6, G-3 right side.

COMMENTS:
Debris build-up to 2-1/2" w/ vegetation. Similar at left side of G-3.

© Schnabel Engineering 2020 All Rights Reserved

PHOTOGRAPH No.: 11
GATE: Gate 6
Photo Taken: 3/31/2020
File: MC-11.jpg

LOCATION:
Gate 6, V-4 at G-3. Right side of V-4.

COMMENTS:
Lack of vertical weld to G-3 flange, skin plate material visible. CS-3.

PHOTOGRAPH No.: 12
GATE: Gate 6
Photo Taken: 3/31/2020
File: MC-12.jpg

LOCATION:
Gate 6, bottom seal at V-1 to V-3.

COMMENTS:
Approximately 20 gpm flow. No visible obstruction.

© Schnabel Engineering 2020 All Rights Reserved

PHOTOGRAPH No.: 13

GATE: Gate 6

Photo Taken: 3/31/2020

File: MC-13.jpg

LOCATION:
Gate 6, bottom of gate at V-5 to V-7.

COMMENTS:
Mostly arrested pitting up to 3/16" in bottom horizontal 7/16" plate and up to 1/16" in skin plate. Typical throughout gate bottom 8". CS-3.

PHOTOGRAPH No.: 14

GATE: Gate 6

Photo Taken: 3/31/2020

File: MC-14.jpg

LOCATION:
Gate 6, underside of LB-5 at LS-3.

COMMENTS:
Laminar rust w/minor section loss. Approx. 10% CS-3. Debris build-up and blocked drain.

© Schnabel Engineering 2020 All Rights Reserved

PHOTOGRAPH No.: 15
GATE: Gate 6
Photo Taken: 3/31/2020
File: MC-15.jpg

LOCATION:
Gate 6, LS-3 at LB-4.

COMMENTS:
Ponding water and blocked drain.

PHOTOGRAPH No.: 16
GATE: Gate 6
Photo Taken: 3/31/2020
File: MC-16.jpg

LOCATION:
Gate 6, LS-2 at downstream end.

COMMENTS:
Ponding water and blocked drain.

© Schnabel Engineering 2020 All Rights Reserved

PHOTOGRAPH No.: 17
GATE: Gate 6
Photo Taken: 3/31/2020
File: MC-17.jpg

LOCATION:
Gate 6, LS-1 between LB-1 & gusset plate, underside.

COMMENTS:
Cracked weld. Flange to web weld crack 18" long. Potential for propagation. CS-4.

PHOTOGRAPH No.: 18
GATE: Gate 6
Photo Taken: 3/31/2020
File: MC-18.jpg

LOCATION:
Gate 6, LS-1 between LB-1 & gusset plate, topside.

COMMENTS:
Cracked weld. Flange to web weld crack 18" long. Potential for propagation. CS-4.

© Schnabel Engineering 2020 All Rights Reserved

PHOTOGRAPH No.: 19
GATE: Gate 6
Photo Taken: 3/31/2020
File: MC-19.jpg

LOCATION:
Gate 6, LS-1.

COMMENTS:
Failing paint with light rust bleed through. CS-2.

PHOTOGRAPH No.: 20
GATE: Gate 6
Photo Taken: 3/31/2020
File: MC-20.jpg

LOCATION:
Gate 6, skin plate. Between V-19 & V-20 and between G-2 & G-3.

COMMENTS:
Minor paint chip w/moderate surface rust and rust bleed through. Typical of isolated spots throughout skin. CS-2.

© Schnabel Engineering 2020 All Rights Reserved

PHOTOGRAPH No.: 21

GATE: Gate 6

Photo Taken: 3/31/2020

File: MC-21.jpg

LOCATION:
Gate 6, left seal between G-1 & G-2.

COMMENTS:
Vegetation growth.

PHOTOGRAPH No.: 22

GATE: Gate 6

Photo Taken: 3/31/2020

File: MC-22.jpg

LOCATION:
Gate 6, B-8.

COMMENTS:
Failed paint with heavy corrosion and section loss to 1/16". CS-3.

© Schnabel Engineering 2020 All Rights Reserved

PHOTOGRAPH No.: 23

GATE: Gate 6

Photo Taken: 3/31/2020

File: MC-23.jpg

LOCATION:
Gate 6, V-19 at G-2, left side web stiffener.

COMMENTS:
Cracked weld. Partially cracked weld. Potential for propagation. CS-3.

PHOTOGRAPH No.: 24

GATE: Gate 6

Photo Taken: 3/31/2020

File: MC-24.jpg

LOCATION:
Gate 6, V-18 at G-2, left side vertical weld.

COMMENTS:
Cracked weld. 100% cracked through. No potential for propagation. CS-2.

© Schnabel Engineering 2020 All Rights Reserved

PHOTOGRAPH No.: 25
GATE: Gate 6
Photo Taken: 3/31/2020
File: MC-25.jpg

LOCATION:
Gate 6, left trunnion.

COMMENTS:
Sticks and debris build-up inside casting.

PHOTOGRAPH No.: 26
GATE: Gate 6
Photo Taken: 3/31/2020
File: MC-26.jpg

LOCATION:
Gate 6, right arm.

COMMENTS:

© Schnabel Engineering 2020 All Rights Reserved

PHOTOGRAPH No.: 1

GATE: Gate 7

Photo Taken: 3/31/2020

File: CL-23.jpg

LOCATION:
Gate 7, left arm.

COMMENTS:

PHOTOGRAPH No.: 2

GATE: Gate 7

Photo Taken: 3/31/2020

File: CL-25.jpg

LOCATION:
Gate 7, right trunnion

COMMENTS:
Inside of casting has paint failure with heavy rust bleed throughout, CS2.

© Schnabel Engineering 2020 All Rights Reserved

PHOTOGRAPH No.: 3
GATE: Gate 7
Photo Taken: 3/31/2020
File: CL-26.jpg

LOCATION:
Gate 7, trunnion girder be-tween Gates 7 & 6.

COMMENTS:
Paint failure on backside of block, CS2.

PHOTOGRAPH No.: 4
GATE: Gate 7
Photo Taken: 3/31/2020
File: CL-27.jpg

LOCATION:
Gate 7, RS-1 at RB-1.

COMMENTS:
Rust bleed throughout. Plus out-of-plane bending in flange 1/4" over 5", CS2.

© Schnabel Engineering 2020 All Rights Reserved

PHOTOGRAPH No.: 5

GATE: Gate 7

Photo Taken: 3/31/2020

File: CL-28.jpg

LOCATION:
Gate 7, skin plate 2' above G-16 at V-06.

COMMENTS:
3/4" hole in skin plate that has been patched.

PHOTOGRAPH No.: 6

GATE: Gate 7

Photo Taken: 3/31/2020

File: CL-29.jpg

LOCATION:
Gate 7, RS-2 at trunnion.

COMMENTS:
Drain hole plugged holding debris and water.

© Schnabel Engineering 2020 All Rights Reserved

PHOTOGRAPH No.: 7

GATE: Gate 7

Photo Taken: 3/31/2020

File: CL-31.jpg

LOCATION:
Gate 7, skin plate between V-04 and V-05, 9' above G-2.

COMMENTS:
Two full depth holes in skin plate that have been patched.

PHOTOGRAPH No.: 8

GATE: Gate 7

Photo Taken: 3/31/2020

File: CL-32.jpg

LOCATION:
Gate 7, V-04 at G-2 web stiffener.

COMMENTS:
3/4" long crack in weld, CS3.

© Schnabel Engineering 2020 All Rights Reserved

PHOTOGRAPH No.: 9
GATE: Gate 7
Photo Taken: 3/31/2020
File: CL-34.jpg

LOCATION:
Gate 7, V-06 at G-2 web stiffener.

COMMENTS:
3/4" long crack in weld, CS3.

PHOTOGRAPH No.: 10
GATE: Gate 7
Photo Taken: 3/31/2020
File: CL-35.jpg

LOCATION:
Gate 7, skin plate between V-05 and V-06 at G-2.

COMMENTS:
Rust bleed through paint CS2. Common on 10% of this gate.

© Schnabel Engineering 2020 All Rights Reserved

PHOTOGRAPH No.: 11
GATE: Gate 7
Photo Taken: 3/31/2020
File: CL-36.jpg

LOCATION:
Gate 7, gate and frame.

COMMENTS:
General overview.

PHOTOGRAPH No.: 12
GATE: Gate 7
Photo Taken: 3/31/2020
File: CL-37.jpg

LOCATION:
Gate 7, RB-6, 3' above RS-3.

COMMENTS:
Out-of-plane bending 1/2" over 2" on flange.

© Schnabel Engineering 2020 All Rights Reserved

PHOTOGRAPH No.: 13
GATE: Gate 7
Photo Taken: 3/31/2020
File: CL-38.jpg

LOCATION:
Gate 7, bottom plate on vertical between V-04 and V-05.

COMMENTS:
Heavy pitting up to 1/8". Common for the whole plate.

PHOTOGRAPH No.: 14
GATE: Gate 7
Photo Taken: 3/31/2020
File: CL-39.jpg

LOCATION:
Gate 7, V-10 at G-3.

COMMENTS:
Both welds on either side of the vertical are cracked, CS3.

© Schnabel Engineering 2020 All Rights Reserved

PHOTOGRAPH No.: 15
GATE: Gate 7
Photo Taken: 3/31/2020
File: CL-40.jpg

LOCATION:
Gate 7, V-10 at G-3.

COMMENTS:
Both welds on either side of the vertical are cracked, CS3.

PHOTOGRAPH No.: 16
GATE: Gate 7
Photo Taken: 3/31/2020
File: CL-41.jpg

LOCATION:
Gate 7, G-3 left side.

COMMENTS:
No drain hole in left section allows for standing water and debris in web.

© Schnabel Engineering 2020 All Rights Reserved

PHOTOGRAPH No.: 17
GATE: Gate 7
Photo Taken: 3/31/2020
File: CL-42.jpg

LOCATION:
Gate 7, V-19 at G-3.

COMMENTS:
Weld in web stiffener is cracked clean through, CS2.

PHOTOGRAPH No.: 18
GATE: Gate 7
Photo Taken: 3/31/2020
File: CL-43.jpg

LOCATION:
Gate 7, skin plate between V-16 and V-17 at G-2.

COMMENTS:
Hole in skin plate 1/2" round has been repaired 10" x 20" area of paint failure with heavy surface rust, CS2.

© Schnabel Engineering 2020 All Rights Reserved

PHOTOGRAPH No.: 19

GATE: Gate 7

Photo Taken: 3/31/2020

File: CL-44.jpg

LOCATION:
Gate 7. LS3 to LB-6 connection.

COMMENTS:
Heavy pitting in LB-6 web rust bleed through most recent paint job. Note: Out-of-plane bending in flange 1/2" over 2".

PHOTOGRAPH No.: 20

GATE: Gate 7

Photo Taken: 3/31/2020

File: CL-45.jpg

LOCATION:
Gate 7, LS2 to LB-5 connection.

COMMENTS:
Paint failure with moderate rust bleed 1' x 1', CS2.

© Schnabel Engineering 2020 All Rights Reserved

PHOTOGRAPH No.: 21
GATE: Gate 7
Photo Taken: 3/31/2020
File: CL-46.jpg

LOCATION:
Gate 7, V-18 at G-2.

COMMENTS:
1 1/2" crack in vertical weld, CS3.

PHOTOGRAPH No.: 22
GATE: Gate 7
Photo Taken: 3/31/2020
File: CL-47.jpg

LOCATION:
Gate 7, LS-2 to G-2 connection.

COMMENTS:
Angle bracket and flange have heavy surface rust and some minor section loss, CS3.

© Schnabel Engineering 2020 All Rights Reserved

PHOTOGRAPH No.: 23
GATE: Gate 7
Photo Taken: 3/31/2020
File: CL-48.jpg

LOCATION:
Gate 7, left seal.

COMMENTS:
Minor leaks are causing mold and constant moisture.

PHOTOGRAPH No.: 24
GATE: Gate 7
Photo Taken: 3/31/2020
File: CL-49.jpg

LOCATION:
Gate 7, right arm.

COMMENTS:

© Schnabel Engineering 2020 All Rights Reserved

PHOTOGRAPH No.: 1
GATE: Gate 8
Photo Taken: 3/31/2020
File: MC-27.jpg

LOCATION:
Gate 8, left arm.

COMMENTS:

PHOTOGRAPH No.: 2
GATE: Gate 8
Photo Taken: 3/31/2020
File: MC-28.jpg

LOCATION:
Gate 8, RS-1 & RS-2 at gusset plate.

COMMENTS:
Ponding water and blocked drains.

© Schnabel Engineering 2020 All Rights Reserved

PHOTOGRAPH No.: 3
GATE: Gate 8
Photo Taken: 3/31/2020
File: MC-29.jpg

LOCATION:
Gate 8, right seal above G-1.

COMMENTS:
Rust staining from seal plate. Roller guide is in contact with buttress, CS-2.

PHOTOGRAPH No.: 4
GATE: Gate 8
Photo Taken: 3/31/2020
File: MC-30.jpg

LOCATION:
Gate 8, V-3 at G-1, right side.

COMMENTS:
Lack of vertical weld to G-1 flange, CS-3.

© Schnabel Engineering 2020 All Rights Reserved

PHOTOGRAPH No.: 5

GATE: Gate 8

Photo Taken: 3/31/2020

File: MC-31.jpg

LOCATION:
Gate 8, G-2 right side.

COMMENTS:
Light debris build-up on girder. Drain holes are clear. 4" x 6" area of flaking paint and moderate surface rust. CS-2. Roller guide spins freely and is 1/4" from buttress.

PHOTOGRAPH No.: 6

GATE: Gate 8

Photo Taken: 3/31/2020

File: MC-32.jpg

LOCATION:
Gate 8, V8 between G-1 & G-2.

COMMENTS:
Out-of-plane bending in flange. Two locations up to 3/4" over 6" long each. CS-2.

© Schnabel Engineering 2020 All Rights Reserved

PHOTOGRAPH No.: 7

GATE: Gate 8

Photo Taken: 3/31/2020

File: MC-33.jpg

LOCATION:
Gate 8, V-3 at G-3, right side.

COMMENTS:
Lack of vertical weld to G-3 flange. 1/4" shim visible. Light pack rust. CS-3. Similar at V-4.

PHOTOGRAPH No.: 8

GATE: Gate 8

Photo Taken: 3/31/2020

File: MC-34.jpg

LOCATION:
Gate 8, V-6 at G-3, right ride.

COMMENTS:
4" long area without vertical weld to G-1 flange. 1/4" shim visible. No significant deficien-cy. CS-2.

© Schnabel Engineering 2020 All Rights Reserved

PHOTOGRAPH No.: 9

GATE: Gate 8

Photo Taken: 3/31/2020

File: MC-35.jpg

LOCATION:
Gate 8, RS-3 at G-3.

COMMENTS:
Pitting area on underside of web. 1 1/4" x 2 1/2" x 3/16" deep. Light surface rust. CS-3.

PHOTOGRAPH No.: 10

GATE: Gate 8

Photo Taken: 3/31/2020

File: MC-36.jpg

LOCATION:
Gate 8, bottom of gate at V-12 to V-15 and 7/16" thick bottom plate.

COMMENTS:
Mostly arrested pitting up to 1/8" deep along the bottom 6" of skin and bottom plate. Typical throughout.

© Schnabel Engineering 2020 All Rights Reserved

PHOTOGRAPH No.: 11
GATE: Gate 8
Photo Taken: 3/31/2020
File: MC-37.jpg

LOCATION:
Gate 8, RS-3 at RB-5.

COMMENTS:
Ponding water and debris w/ blocked drains.

PHOTOGRAPH No.: 12
GATE: Gate 8
Photo Taken: 3/31/2020
File: DK-45.jpg

LOCATION:
Gate 8 overview.

COMMENTS:

© Schnabel Engineering 2020 All Rights Reserved

PHOTOGRAPH No.: 13
GATE: Gate 8
Photo Taken: 3/31/2020
File: DK-46.jpg

LOCATION:
Gate 8, right arm overview.

COMMENTS:

PHOTOGRAPH No.: 14
GATE: Gate 8
Photo Taken: 3/31/2020
File: DK-47.jpg

LOCATION:
Gate 8, left trunnion.

COMMENTS:
Heavy freckle rust inside trunnion casting, this trunnion has its pick-point eyebolt torched off. CS-2.

© Schnabel Engineering 2020 All Rights Reserved

PHOTOGRAPH No.: 15

GATE: Gate 8

Photo Taken: 3/31/2020

File: DK-48.jpg

LOCATION:
Gate 8, B-11.

COMMENTS:
Typical area of freckle rusting, CS-2.

PHOTOGRAPH No.: 16

GATE: Gate 8

Photo Taken: 3/31/2020

File: DK-49.jpg

LOCATION:
Gate 8, skin between V-13 & V-14, 5' above G-2.

COMMENTS:
8'x4" and 2"x1" areas of paint failure with surface rust and light pitting, CS-3.

© Schnabel Engineering 2020 All Rights Reserved

PHOTOGRAPH No.: 17
GATE: Gate 8
Photo Taken: 3/31/2020
File: DK-50.jpg

LOCATION:
Gate 8, V-14, 3' above G-2.

COMMENTS:
Three points of out of plane bending up to 1/2" over an 18" section, CS-2.

PHOTOGRAPH No.: 18
GATE: Gate 8
Photo Taken: 3/31/2020
File: DK-51.jpg

LOCATION:
Gate 8, G-2 underside, left arm.

COMMENTS:
Areas of moderate freckle rust, CS-2.

© Schnabel Engineering 2020 All Rights Reserved

PHOTOGRAPH No.: 19

GATE: Gate 8

Photo Taken: 3/31/2020

File: DK-52.jpg

LOCATION:
Gate 8, G-3 topside of web.

COMMENTS:
Arrested pitting to 1/8" through-out, CS-3.

PHOTOGRAPH No.: 20

GATE: Gate 8

Photo Taken: 3/31/2020

File: DK-53.jpg

LOCATION:
Gate 8, bottom left corner.

COMMENTS:
Left seal has minor leaks throughout resulting in a buildup of organic matter on G-3 left end.

© Schnabel Engineering 2020 All Rights Reserved

PHOTOGRAPH No.: 21
GATE: Gate 8
Photo Taken: 3/31/2020
File: DK-54.jpg

LOCATION:
Gate 8, left arm LB-5 & LS-3.

COMMENTS:
Build up of dirt/debris between members holding water and vegetation.

PHOTOGRAPH No.: 22
GATE: Gate 8
Photo Taken: 3/31/2020
File: DK-55.jpg

LOCATION:
Gate 8, Left arm interior of gusset plate between L-S1 & LS-2.

COMMENTS:
Paint failure with pitting to 1/8". 50% of pitting is arrested, CS-3.

© Schnabel Engineering 2020 All Rights Reserved

PHOTOGRAPH No.: 1
GATE: Gate 9
Photo Taken: 4/1/2020
File: MC-01.jpg

LOCATION:
Gate 9, left arm.

COMMENTS:

PHOTOGRAPH No.: 2
GATE: Gate 9
Photo Taken: 4/1/2020
File: MC-02.jpg

LOCATION:
Gate 9, D/S face of gate.

COMMENTS:

© Schnabel Engineering 2020 All Rights Reserved

PHOTOGRAPH No.: 3
GATE: Gate 9
Photo Taken: 4/1/2020
File: MC-03.jpg

LOCATION:
Gate 9, right trunnion casting.

COMMENTS:
Light surface rust. CS-2.

PHOTOGRAPH No.: 4
GATE: Gate 9
Photo Taken: 4/1/2020
File: MC-04.jpg

LOCATION:
Gate 9, right trunnion casting.

COMMENTS:
Light surface rust. CS-2.

© Schnabel Engineering 2020 All Rights Reserved

PHOTOGRAPH No.: 5
GATE: Gate 9
Photo Taken: 4/1/2020
File: MC-05.jpg

LOCATION:
Gate 9, V-3 at G-1.

COMMENTS:
Low quality, built up field weld.

PHOTOGRAPH No.: 6
GATE: Gate 9
Photo Taken: 4/1/2020
File: MC-06.jpg

LOCATION:
Gate 9, V-6 at G-1, right side stiffener.

COMMENTS:
Cracked weld. Not fully cracked. Potential for propagation. CS-3.

© Schnabel Engineering 2020 All Rights Reserved

PHOTOGRAPH No.: 7
GATE: Gate 9
Photo Taken: 4/1/2020
File: MC-07.jpg

LOCATION:
Gate 9, V-8 above G-1. V-8 vertical weld to skin.

COMMENTS:
12" of flaking paint with light surface rust. CS-2.

PHOTOGRAPH No.: 8
GATE: Gate 9
Photo Taken: 4/1/2020
File: MC-08.jpg

LOCATION:
Gate 9, RS-1 & RS-2 at gusset plates.

COMMENTS:
Ponding water and blocked drains.

© Schnabel Engineering 2020 All Rights Reserved

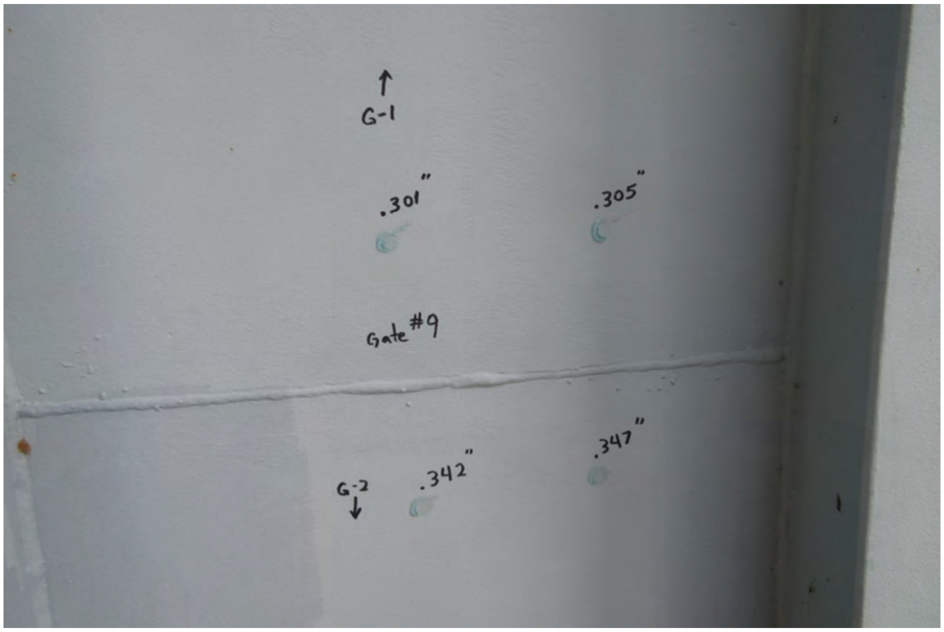

PHOTOGRAPH No.: 9
GATE: Gate 9
Photo Taken: 4/1/2020
File: MC-10.jpg

LOCATION:
Gate 9, skin plate UT reading between V-3 & V-4, and between G-1 & G-2. Above & below horizontal skin plate weld.

COMMENTS:
Above weld measurements:
.301" & .305"
Below weld measurements:
.342 & .347"

PHOTOGRAPH No.: 10
GATE: Gate 9
Photo Taken: 4/1/2020
File: MC-11.jpg

LOCATION:
Gate 9, RS-2 at RB-2.

COMMENTS:
Moderate surface rust and low quality field welds. CS-2

© Schnabel Engineering 2020 All Rights Reserved

PHOTOGRAPH No.: 11
GATE: Gate 9
Photo Taken: 4/1/2020
File: MC-12.jpg

LOCATION:
Gate 9, RS-3 at RB-6.

COMMENTS:
Debris & vegetation buildup. Drains are blocked.

PHOTOGRAPH No.: 12
GATE: Gate 9
Photo Taken: 4/1/2020
File: MC-13.jpg

LOCATION:
Gate 9, G-3, left side.

COMMENTS:
Debris buildup up to 4".

© Schnabel Engineering 2020 All Rights Reserved

PHOTOGRAPH No.: 13
GATE: Gate 9
Photo Taken: 4/1/2020
File: MC-14.jpg

LOCATION:
Gate 9, left seal at bottom corner of gate.

COMMENTS:
Approximately 10 gpm leak.

PHOTOGRAPH No.: 14
GATE: Gate 9
Photo Taken: 4/1/2020
File: MC-15.jpg

LOCATION:
Gate 9, V-14 to V-15, skin plate and bottom 7/16" plate.

COMMENTS:
Typical. Mostly arrested pitting up to 1/8" deep along the bottom 6" of skin and the 7/16" bottom plate. CS-3.

© Schnabel Engineering 2020 All Rights Reserved

PHOTOGRAPH No.: 15
GATE: Gate 9
Photo Taken: 4/1/2020
File: MC-16.jpg

LOCATION:
Gate 9, RS-2 & RS-3 at gusset plate.

COMMENTS:
Light surface rust. CS-2.

PHOTOGRAPH No.: 16
GATE: Gate 9
Photo Taken: 4/1/2020
File: MC-17.jpg

LOCATION:
Gate 9, right arm.

COMMENTS:

© Schnabel Engineering 2020 All Rights Reserved

PHOTOGRAPH No.: 17

GATE: Gate 9

Photo Taken: 4/1/2020

File: MC-18.jpg

LOCATION:
Gate 9, left trunnion casting.

COMMENTS:
Moderate surface rust. CS-2.

PHOTOGRAPH No.: 18

GATE: Gate 9

Photo Taken: 4/1/2020

File: MC-19.jpg

LOCATION:
Gate 9, LS-1 & LS-2 at gusset plates.

COMMENTS:
Ponding water and debris with blocked drains.

© Schnabel Engineering 2020 All Rights Reserved

PHOTOGRAPH No.: 19
GATE: Gate 9
Photo Taken: 4/1/2020
File: MC-20.jpg

LOCATION:
Gate 9, left side.

COMMENTS:
Cracked weld in left stiffener.
Potential for propagation. CS-3.

PHOTOGRAPH No.: 20
GATE: Gate 9
Photo Taken: 4/1/2020
File: MC-21.jpg

LOCATION:
Gate 9, right side.

COMMENTS:
Cracked weld in right stiffener.
No potential for propagation.
Cracked 100% through. CS-2

© Schnabel Engineering 2020 All Rights Reserved

PHOTOGRAPH No.: 21
GATE: Gate 9
Photo Taken: 4/1/2020
File: MC-22.jpg

LOCATION:
Gate 9, V-18 at G-2, right side.

COMMENTS:
Cracked weld in stiffener. No chance for propagation. Weld cracked clear through. CS-2.

PHOTOGRAPH No.: 22
GATE: Gate 9
Photo Taken: 4/1/2020
File: MC-23.jpg

LOCATION:
Gate 9, LB-2, inboard flange.

COMMENTS:
Three areas of out of plane bending up to 9" x 1". CS-2.

© Schnabel Engineering 2020 All Rights Reserved

PHOTOGRAPH No.: 23
GATE: Gate 9
Photo Taken: 4/1/2020
File: MC-24.jpg

LOCATION:
Gate 9, LS-3 at LB-6.

COMMENTS:
Debris build-up w/vegetation. Drains blocked.

PHOTOGRAPH No.: 24
GATE: Gate 9
Photo Taken: 4/1/2020
File: MC-25.jpg

LOCATION:
Gate 9, underside of LB-5 at LS-3.

COMMENTS:
Debris buildup and ponding water. Drains blocked. Laminar rust on web of LB-5 end with approximately 10% section loss. CS-3.

© Schnabel Engineering 2020 All Rights Reserved

PHOTOGRAPH No.: 1
GATE: Gate 10
Photo Taken: 4/1/2020
File: CL-1.jpg

LOCATION:
Gate 10, left arm.

COMMENTS:

PHOTOGRAPH No.: 2
GATE: Gate 10
Photo Taken: 4/1/2020
File: CL-2.jpg

LOCATION:
Gate 10, right trunnion.

COMMENTS:
Inside of trunnion cast has moderate surface rust.

© Schnabel Engineering 2020 All Rights Reserved

PHOTOGRAPH No.: 3
GATE: Gate 10
Photo Taken: 4/1/2020
File: CL-3.jpg

LOCATION:
Gate 10, RB-2.

COMMENTS:
Out-of-plane bending, 1" over 5' in the beam itself.

PHOTOGRAPH No.: 4
GATE: Gate 10
Photo Taken: 4/1/2020
File: CL-4.jpg

LOCATION:
Gate 10, V-03 at G-2.

COMMENTS:
6" long crack in vertical weld, CS3.

© Schnabel Engineering 2020 All Rights Reserved

PHOTOGRAPH No.: 5
GATE: Gate 10
Photo Taken: 4/1/2020
File: CL-5.jpg

LOCATION:
Gate 10, skin plate between V-02 and V-03 at G-2.

COMMENTS:
Light rust bleed 8" x 30", CS2.

PHOTOGRAPH No.: 6
GATE: Gate 10
Photo Taken: 4/1/2020
File: CL-6.jpg

LOCATION:
Gate 10, V-05 at G-2 connection.

COMMENTS:
1" long crack in weld of web stiffener, CS3.

© Schnabel Engineering 2020 All Rights Reserved

PHOTOGRAPH No.: 7

GATE: Gate 10

Photo Taken: 4/1/2020

File: CL-7.jpg

LOCATION:
Gate 10, V-06 at G-2 connection.

COMMENTS:
1-1/2" long crack in vertical weld, CS3.

PHOTOGRAPH No.: 8

GATE: Gate 10

Photo Taken: 4/1/2020

File: CL-8.jpg

LOCATION:
Gate 10, RS-2 at G-2 connection.

COMMENTS:
4" long crack in angle bracket weld, CS3.

© Schnabel Engineering 2020 All Rights Reserved

PHOTOGRAPH No.: 9

GATE: Gate 10

Photo Taken: 4/1/2020

File: CL-9.jpg

LOCATION:
Gate 10, RB-6 1' down from RS -2.

COMMENTS:
Out-of-plane bending 1" over 3" in flange.

PHOTOGRAPH No.: 10

GATE: Gate 10

Photo Taken: 4/1/2020

File: CL-10.jpg

LOCATION:
Gate 10, RS-3 at RB-5 connection.

COMMENTS:
Drain plug is plugged and 5" of water and debris collected. Note: heavy arrested pitting up to 1/8".

© Schnabel Engineering 2020 All Rights Reserved

PHOTOGRAPH No.: 11
GATE: Gate 10
Photo Taken: 4/1/2020
File: CL-11.jpg

LOCATION:
Gate 10, V-03 at G-7.

COMMENTS:
3" long crack in vertical weld. Note: 1/8" pack rust starting in between vertical rib and G-1 flange.

PHOTOGRAPH No.: 12
GATE: Gate 10
Photo Taken: 4/1/2020
File: CL-12.jpg

LOCATION:
Gate 10, V-01 at bottom plate.

COMMENTS:
Up to 100% section loss on flange of rib coming to a knife edge. Similar condition on V-02.

© Schnabel Engineering 2020 All Rights Reserved

PHOTOGRAPH No.: 13

GATE: Gate 10

Photo Taken: 4/1/2020

File: CL-13.jpg

LOCATION:
Gate 10, bottom plate between V-02 & V-03.

COMMENTS:
Heavy arrested pitting throughout plate up to 1/8" deep. Similar condition across whole gate.

PHOTOGRAPH No.: 14

GATE: Gate 10

Photo Taken: 4/1/2020

File: CL-14.jpg

LOCATION:
Gate 10, G-3 web at V-10.

COMMENTS:
Heavy arrested pitting the whole length of girder up to 6" wide and 1/8" deep.

© Schnabel Engineering 2020 All Rights Reserved

PHOTOGRAPH No.: 15
GATE: Gate 10
Photo Taken: 4/1/2020
File: CL-15.jpg

LOCATION:
Gate 10, G-3 left side.

COMMENTS:
Leak in seal is keeping buttress wall and end of girder constantly wet. Heavy debris and growth along with standing water are present. CS2.

PHOTOGRAPH No.: 16
GATE: Gate 10
Photo Taken: 4/1/2020
File: CL-16.jpg

LOCATION:
Gate 10, LS-3 at LB-6 connection.

COMMENTS:
Drain hole is plugged and 5" of water and debris has collected.

© Schnabel Engineering 2020 All Rights Reserved

PHOTOGRAPH No.: 17

GATE: Gate 10

Photo Taken: 4/1/2020

File: CL-17.jpg

LOCATION:
Gate 10, LB-5 4' down from LS-2.

COMMENTS:
Out-of-plane bending 3/4" over 3" on flange.

PHOTOGRAPH No.: 18

GATE: Gate 10

Photo Taken: 4/1/2020

File: CL-18.jpg

LOCATION:
Gate 10, G-2 web stiffener at left arm connection.

COMMENTS:
3" x 2" area of paint failure with section loss and pitting to 1/8".

© Schnabel Engineering 2020 All Rights Reserved

PHOTOGRAPH No.: 19
GATE: Gate 10
Photo Taken: 4/1/2020
File: CL-19.jpg

LOCATION:
Gate 10, G-1 bottom side web on left end.

COMMENTS:
2' x 2' area of paint failure moderate rust bleed, CS2.

PHOTOGRAPH No.: 20
GATE: Gate 10
Photo Taken: 4/1/2020
File: CL-20.jpg

LOCATION:
Gate 10, V-17 at G-1.

COMMENTS:
Web stiffener has 3/8" crack in weld, CS3.

© Schnabel Engineering 2020 All Rights Reserved

PHOTOGRAPH No.: 21
GATE: Gate 10
Photo Taken: 4/1/2020
File: CL-21.jpg

LOCATION:
Gate 10, V-20 at G-1.

COMMENTS:
3" long crack in vertical weld, CS3.

PHOTOGRAPH No.: 22
GATE: Gate 10
Photo Taken: 4/1/2020
File: CL-22.jpg

LOCATION:
Gate 10, right arm.

COMMENTS:

© Schnabel Engineering 2020 All Rights Reserved

PHOTOGRAPH No.: 23
GATE: Gate 10
Photo Taken: 4/1/2020
File: CL-23.jpg

LOCATION:
Gate 10, gate and frame.

COMMENTS:

PHOTOGRAPH No.: 24
GATE: Gate 10
Photo Taken: 4/1/2020
File: CL-24.jpg

LOCATION:
Gate 10, left arm.

COMMENTS:

© Schnabel Engineering 2020 All Rights Reserved

PHOTOGRAPH No.: 25
GATE: Gate 10
Photo Taken: 4/1/2020
File: CL-25.jpg

LOCATION:
Gate 10, gate and frame.

COMMENTS:

PHOTOGRAPH No.: 26
GATE: Gate 10
Photo Taken: 4/1/2020
File: CL-26.jpg

LOCATION:
Gate 10, right trunnion.

COMMENTS:
Paint failure moderate rust bleed on inside of trunnion.

© Schnabel Engineering 2020 All Rights Reserved

PHOTOGRAPH No.: 27
GATE: Gate 10
Photo Taken: 4/1/2020
File: CL-27.jpg

LOCATION:
Gate 10, V-05 at G-1.

COMMENTS:
1" long crack in vertical weld, CS3.

PHOTOGRAPH No.: 28
GATE: Gate 10
Photo Taken: 4/1/2020
File: CL-28.jpg

LOCATION:
Gate 10, V-06 at G-1.

COMMENTS:
1/2" long crack in web stiffener, CS3.

© Schnabel Engineering 2020 All Rights Reserved

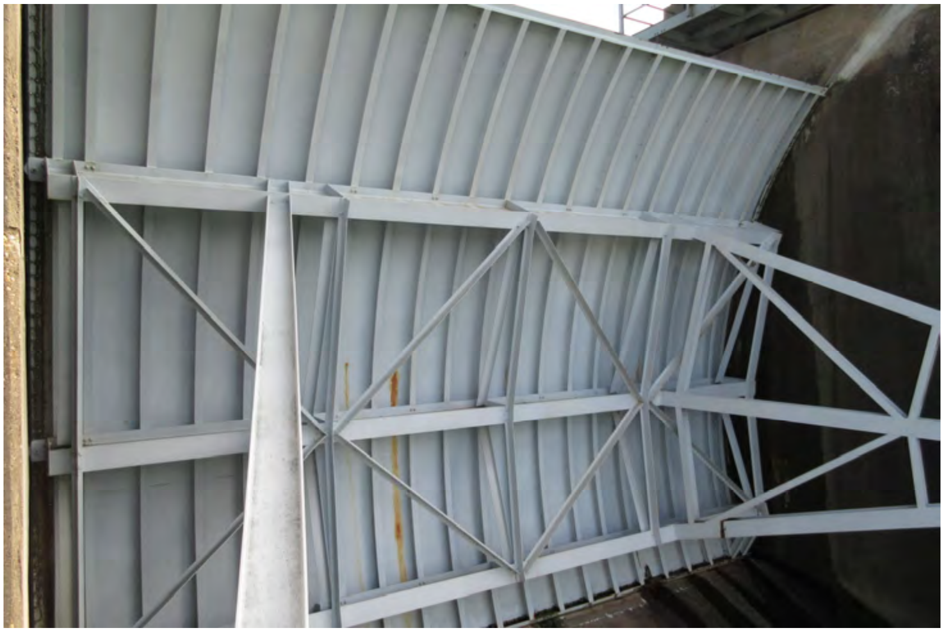

PHOTOGRAPH No.: 1
GATE: Gate 11
Photo Taken: 4/1/2020
File: DK-01.jpg

LOCATION:
Gate 11, overview.

COMMENTS:

PHOTOGRAPH No.: 2
GATE: Gate 11
Photo Taken: 4/1/2020
File: DK-02.jpg

LOCATION:
Gate 11, left arm overview.

COMMENTS:

© Schnabel Engineering 2020 All Rights Reserved

PHOTOGRAPH No.: 3

GATE: Gate 11

Photo Taken: 4/1/2020

File: DK-03.jpg

LOCATION:
Gate 11, right arm trunnion.

COMMENTS:
Downstream side of right arm trunnion has moderate surface rust due to lack of paint coating. No pitting present. CS-2.

PHOTOGRAPH No.: 4

GATE: Gate 11

Photo Taken: 4/1/2020

File: DK-04.jpg

LOCATION:
Gate 11, V-5 at G-1, vertical weld.

COMMENTS:
Vertical weld between members is cracked 80% of weld length, CS-2.

© Schnabel Engineering 2020 All Rights Reserved

PHOTOGRAPH No.: 5
GATE: Gate 11
Photo Taken: 4/1/2020
File: DK-05.jpg

LOCATION:
Gate 11, right arm, RS-2.

COMMENTS:
Member is holding water at the trunnion due to clogged drain hole.

PHOTOGRAPH No.: 6
GATE: Gate 11
Photo Taken: 4/1/2020
File: DK-06.jpg

LOCATION:
Gate 11, right arm, RB-1.

COMMENTS:
Outboard flange has two small areas of impact damage resulting in paint failure with surface rust, CS-2.

© Schnabel Engineering 2020 All Rights Reserved

PHOTOGRAPH No.: 7
GATE: Gate 11
Photo Taken: 4/1/2020
File: DK-07.jpg

LOCATION:
Gate 11, skin plate, between V-7 & V-9, 2' above G-2.

COMMENTS:
(2) Dents in skin plates (impact from upstream) resulting in paint failure downstream and rust bleeding down gate, down-stream bulges measure 3/16" out of plane from skin plate, CS-2.

PHOTOGRAPH No.: 8
GATE: Gate 11
Photo Taken: 4/1/2020
File: DK-08.jpg

LOCATION:
Gate 11, RS-3 & RB-5 & RB-6 connection.

COMMENTS:
Build-up of dirt & debris at the connection of these members holding water & vegetation.

© Schnabel Engineering 2020 All Rights Reserved

PHOTOGRAPH No.: 9

GATE: Gate 11

Photo Taken: 4/1/2020

File: DK-09.jpg

LOCATION:
Gate 11, G-3 right end & B-21/ B-22 connections.

COMMENTS:
These (3) members have isolated areas of arrested pitting to 1/8", CS-3.

PHOTOGRAPH No.: 10

GATE: Gate 11

Photo Taken: 4/1/2020

File: DK-10.jpg

LOCATION:
Gate 11, V1-V7, bottom edge of gate.

COMMENTS:
Bottom plate is holding water and organic matter between every vertical across gate, vertical flanges are corroding at bottom as a result, also noted bottom right seal has minor leak 2 gpm, left corner is similar.

© Schnabel Engineering 2020 All Rights Reserved

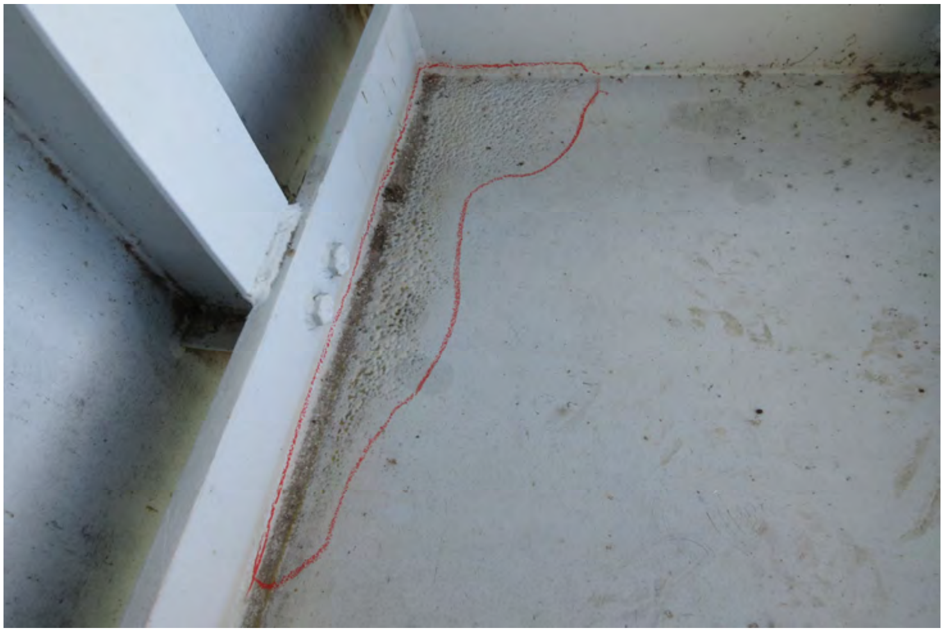

PHOTOGRAPH No.: 11
GATE: Gate 11
Photo Taken: 4/1/2020
File: DK-11.jpg

LOCATION:
Gate 11, G-3 (photo at V-15) topside of web.

COMMENTS:
Several areas of arrested pitting to 1/8" exist along G-3's topside of web, CS-3.

PHOTOGRAPH No.: 12
GATE: Gate 11
Photo Taken: 4/1/2020
File: DK-12.jpg

LOCATION:
Gate 11, G-3 between V-15 & V-16 & skin plate.

COMMENTS:
Upstream flange has moderate surface rust from failed application of paint, skin plate facing that area has a 4" circle of paint failure with surface rust, CS-2.

© Schnabel Engineering 2020 All Rights Reserved

PHOTOGRAPH No.: 13
GATE: Gate 11
Photo Taken: 4/1/2020
File: DK-13.jpg

LOCATION:
Gate 11, left arm, LB-6.

COMMENTS:
Out-of-plane bending 1/2" over 6" section, CS-2.

PHOTOGRAPH No.: 14
GATE: Gate 11
Photo Taken: 4/1/2020
File: DK-14.jpg

LOCATION:
Gate 11, left arm LS-3 & LB-5.

COMMENTS:
Ponding water at this connection, LB-5 has paint failure with heavy rust and pitting to 1/8", CS-3.

© Schnabel Engineering 2020 All Rights Reserved

PHOTOGRAPH No.: 15
GATE: Gate 11
Photo Taken: 4/1/2020
File: DK-15.jpg

LOCATION:
Gate 11, V-14, 3' above G-2.

COMMENTS:
(3) points of out-of-plane bending up to 5/16" over 18" section, CS-2.

PHOTOGRAPH No.: 16
GATE: Gate 11
Photo Taken: 4/1/2020
File: DK-16.jpg

LOCATION:
Gate 11, left arm LS-2.

COMMENTS:
Member is holding water at the trunnion.

© Schnabel Engineering 2020 All Rights Reserved

PHOTOGRAPH No.: 17
GATE: Gate 11
Photo Taken: 4/1/2020
File: DK-17.jpg

LOCATION:
Gate 11, left arm trunnion.

COMMENTS:
Areas of moderate surface rust where paint application failed, CS2.

PHOTOGRAPH No.: 18
GATE: Gate 11
Photo Taken: 4/1/2020
File: DK-18.jpg

LOCATION:
Gate 11, right arm overview.

COMMENTS:

© Schnabel Engineering 2020 All Rights Reserved

PHOTOGRAPH No.: 1
GATE: Gate 12
Photo Taken: 4/1/2020
File: CL-29.jpg

LOCATION:
Gate 12, V-06 at G-1.

COMMENTS:
2" long vertical crack in weld, CS3.

PHOTOGRAPH No.: 2
GATE: Gate 12
Photo Taken: 4/1/2020
File: CL-30.jpg

LOCATION:
Gate 12, V-07 at G-1.

COMMENTS:
1-1/2" long vertical crack in weld, CS3.

© Schnabel Engineering 2020 All Rights Reserved

PHOTOGRAPH No.: 3

GATE: Gate 12

Photo Taken: 4/1/2020

File: CL-31.jpg

LOCATION:
Gate 12, V-11 at G-1.

COMMENTS:
1" long vertical crack in weld, CS3.

PHOTOGRAPH No.: 4

GATE: Gate 12

Photo Taken: 4/1/2020

File: CL-32.jpg

LOCATION:
Gate 12, V-11 at G-1.

COMMENTS:
2-1/2" long crack in weld between the flange of the rib and the edge of the flange on the girder.

© Schnabel Engineering 2020 All Rights Reserved

PHOTOGRAPH No.: 5
GATE: Gate 12
Photo Taken: 4/1/2020
File: CL-33.jpg

LOCATION:
Gate 12, RS-2 to RS-1 connection.

COMMENTS:
Evidence of the water and debris recently being present, paint intact.

PHOTOGRAPH No.: 6
GATE: Gate 12
Photo Taken: 4/1/2020
File: CL-34.jpg

LOCATION:
Gate 12, V-04 at G-2.

COMMENTS:
Cracks on either side of vertical on the vertical welds, CS3.

© Schnabel Engineering 2020 All Rights Reserved

PHOTOGRAPH No.: 7

GATE: Gate 12

Photo Taken: 4/1/2020

File: CL-35.jpg

LOCATION:
Gate 12, V-04 at G-2.

COMMENTS:
Cracks on either side of vertical on the vertical, CS3.

PHOTOGRAPH No.: 8

GATE: Gate 12

Photo Taken: 4/1/2020

File: CL-36.jpg

LOCATION:
Gate 12, V-03 at G-2.

COMMENTS:
1/2" crack in web stiffener, CS3.

© Schnabel Engineering 2020 All Rights Reserved

PHOTOGRAPH No.: 9
GATE: Gate 12
Photo Taken: 4/1/2020
File: CL-37.jpg

LOCATION:
Gate 12, V-03 at G-2.

COMMENTS:
3" long in vertical weld, CS3.

PHOTOGRAPH No.: 10
GATE: Gate 12
Photo Taken: 4/1/2020
File: CL-38.jpg

LOCATION:
Gate 12, V-06 at G-2.

COMMENTS:
5" long crack in vertical weld, CS3.

© Schnabel Engineering 2020 All Rights Reserved

PHOTOGRAPH No.: 11

GATE: Gate 12

Photo Taken: 4/1/2020

File: CL-39.jpg

LOCATION:
Gate 12, skin plate in between V-07 & V-08.

COMMENTS:
2" round paint failure with moderate surface rust, CS2. Spots are common through out gate.

PHOTOGRAPH No.: 12

GATE: Gate 12

Photo Taken: 4/1/2020

File: CL-40.jpg

LOCATION:
Gate 12, bottom plate between V-02 and V-03.

COMMENTS:
Standing water and plant growth in plate. Area of paint failure with moderate to heavy surface rust. Common for bottom plate of gate.

© Schnabel Engineering 2020 All Rights Reserved

PHOTOGRAPH No.: 13
GATE: Gate 12
Photo Taken: 4/1/2020
File: CL-41.jpg

LOCATION:
Gate 12, RB-6, 4' up from RS-3.

COMMENTS:
Out-of-plane bending, 1" over 3" in flange.

PHOTOGRAPH No.: 14
GATE: Gate 12
Photo Taken: 4/1/2020
File: CL-42.jpg

LOCATION:
Gate 12, RS-3 to RB-5 connection.

COMMENTS:
Drain hole is plugged and 5" of water and sand are present.

© Schnabel Engineering 2020 All Rights Reserved

PHOTOGRAPH No.: 15
GATE: Gate 12
Photo Taken: 4/2/2021
File: CL-01.jpg

LOCATION:
Gate 12, right arm.

COMMENTS:

PHOTOGRAPH No.: 16
GATE: Gate 12
Photo Taken: 4/2/2021
File: CL-02.jpg

LOCATION:
Gate 12, left trunnion.

COMMENTS:
1/2" crack in alignment bolt plate. CS-3.

© Schnabel Engineering 2020 All Rights Reserved

PHOTOGRAPH No.: 17
GATE: Gate 12
Photo Taken: 4/2/2021
File: CL-03.jpg

LOCATION:
Gate 12, V-20 at G-1.

COMMENTS:
1/2" crack in weld of web stiff-ener.

PHOTOGRAPH No.: 18
GATE: Gate 12
Photo Taken: 4/2/2021
File: CL-04.jpg

LOCATION:
Gate 12, V-19 at G-1.

COMMENTS:
1/2" crack in weld of web stiff-ener.

© Schnabel Engineering 2020 All Rights Reserved

PHOTOGRAPH No.: 19
GATE: Gate 12
Photo Taken: 4/2/2021
File: CL-05.jpg

LOCATION:
Gate 12, V-19 at G-1.

COMMENTS:
2" long crack in vertical weld, CS3.

PHOTOGRAPH No.: 20
GATE: Gate 12
Photo Taken: 4/2/2021
File: CL-06.jpg

LOCATION:
Gate 12, V-17 at G-1.

COMMENTS:
2-1/2" long crack in vertical weld.

© Schnabel Engineering 2020 All Rights Reserved

PHOTOGRAPH No.: 21
GATE: Gate 12
Photo Taken: 4/2/2021
File: CL-07.jpg

LOCATION:
Gate 12, LS-1 to LS-2 connection.

COMMENTS:
Evidence of water and debris recently being present due to drain hole being plugged.

PHOTOGRAPH No.: 22
GATE: Gate 12
Photo Taken: 4/2/2021
File: CL-08.jpg

LOCATION:
Gate 12, skin plate between V-16 and V-17 at G-2.

COMMENTS:
16" x 4' area of paint failure. Moderate surface rust, CS2.

© Schnabel Engineering 2020 All Rights Reserved

PHOTOGRAPH No.: 23

GATE: Gate 12

Photo Taken: 4/2/2021

File: CL-09.jpg

LOCATION:
Gate 12, LB-6, 3" down from LS-2.

COMMENTS:
Out-of-plane bending, 1" over 3" These are two more spots of out-of-plane bending on this same member.

PHOTOGRAPH No.: 24

GATE: Gate 12

Photo Taken: 4/2/2021

File: CL-10.jpg

LOCATION:
Gate 12, left seal and the bottom.

COMMENTS:
Seal is leaking and causing moisture and moss to be present.

© Schnabel Engineering 2020 All Rights Reserved

PHOTOGRAPH No.: 1
GATE: Gate 13
Photo Taken: 4/1/2020
File: DK-19.jpg

LOCATION:
Gate 13, overview.

COMMENTS:

PHOTOGRAPH No.: 2
GATE: Gate 13
Photo Taken: 4/1/2020
File: DK-20.jpg

LOCATION:
Gate 13, left arm overview.

COMMENTS:

© Schnabel Engineering 2020 All Rights Reserved

PHOTOGRAPH No.: 3

GATE: Gate 13

Photo Taken: 4/1/2020

File: DK-21.jpg

LOCATION:
Gate 13, right arm RS-3 & gusset plate weld.

COMMENTS:
Cavity in the weld, 3/16" at opening (grows wider and deeper into the weld).

PHOTOGRAPH No.: 4

GATE: Gate 13

Photo Taken: 4/1/2020

File: DK-22.jpg

LOCATION:
Gate 13, plate capping verticals at top of gate between V6 & V7.

COMMENTS:
Out-of-plane bending, 1/4" over 5" section CS2.

© Schnabel Engineering 2020 All Rights Reserved

PHOTOGRAPH No.: 5
GATE: Gate 13
Photo Taken: 4/1/2020
File: DK-23.jpg

LOCATION:
Gate 13, right seal.

COMMENTS:
Minor leak high on right seal is pooling water of G-1, G-2, G-3 right ends.

PHOTOGRAPH No.: 6
GATE: Gate 13
Photo Taken: 4/1/2020
File: DK-24.jpg

LOCATION:
Gate 13, G-3 right end (V1 & V2).

COMMENTS:
2" pipe & hardware connected to B-21, no obvious purpose, does not touch skin plate.

© Schnabel Engineering 2020 All Rights Reserved

PHOTOGRAPH No.: 7
GATE: Gate 13
Photo Taken: 4/1/2020
File: DK-25.jpg

LOCATION:
Gate 13, G-3 right end (at V1).

COMMENTS:
Water ponding in girder from leak above.

PHOTOGRAPH No.: 8
GATE: Gate 13
Photo Taken: 4/1/2020
File: DK-26.jpg

LOCATION:
Gate 13, ogee spillway.

COMMENTS:
Spall about 7' x 3' x 4" deep, no exposed rebar.

© Schnabel Engineering 2020 All Rights Reserved

PHOTOGRAPH No.: 9
GATE: Gate 13
Photo Taken: 4/1/2020
File: DK-27.jpg

LOCATION:
Gate 13, ogee spillway.

COMMENTS:
Spall just below gate (12" long x 3/4" deep) surrounded by diagonal cracks with efflo- rescence.

PHOTOGRAPH No.: 10
GATE: Gate 13
Photo Taken: 4/1/2020
File: DK-28.jpg

LOCATION:
Gate 13, bottom right corner of gate (V-1 & V-6).

COMMENTS:
Bottom plate is holding water and organic matter corroding vertical flange edges, CS-3. Bottom right corner also has minor leak about 3 gpm.

© Schnabel Engineering 2020 All Rights Reserved

PHOTOGRAPH No.: 11
GATE: Gate 13
Photo Taken: 4/1/2020
File: DK-29.jpg

LOCATION:
Gate 13, RB-1 & RB-2 at RS-2.

COMMENTS:
Non-uniform field welds at connection (typical at most arm braces).

PHOTOGRAPH No.: 12
GATE: Gate 13
Photo Taken: 4/2/2021
File: DK-01.jpg

LOCATION:
Gate 13, right arm overview.

COMMENTS:

© Schnabel Engineering 2020 All Rights Reserved

PHOTOGRAPH No.: 13
GATE: Gate 13
Photo Taken: 4/2/2021
File: DK-02.jpg

LOCATION:
Gate 13, left arm trunnion.

COMMENTS:
Surface rust on downstream side trunnion due to failed paint application, CS-2.

PHOTOGRAPH No.: 14
GATE: Gate 13
Photo Taken: 4/2/2021
File: DK-03.jpg

LOCATION:
Gate 13, left arm, LS-1, 3' U/S from LB-1.

COMMENTS:
Out-of-plane bending on out-board/upper flange, 3/16" over 9" section, CS-2.

© Schnabel Engineering 2020 All Rights Reserved

PHOTOGRAPH No.: 15

GATE: Gate 13

Photo Taken: 4/2/2021

File: DK-04.jpg

LOCATION:
Gate 13, left seal & G-2/G-3 left ends.

COMMENTS:
Minor leak high on left seal is pooling water on G2 & G3 left ends.

PHOTOGRAPH No.: 16

GATE: Gate 13

Photo Taken: 4/2/2021

File: DK-05.jpg

LOCATION:
Gate 13, left arm LS-1 at G-1 connection.

COMMENTS:
Slight out-of-plane bending on inboard upper flange, 1/8" over 9" section, CS-2.

© Schnabel Engineering 2020 All Rights Reserved

PHOTOGRAPH No.: 17

GATE: Gate 13

Photo Taken: 4/2/2021

File: DK-06.jpg

LOCATION:
Gate 13, left arm LB-3.

COMMENTS:
(2) areas of out-of-plane bending on outboard/ downstream flange, both measures 3/16" over 5".

PHOTOGRAPH No.: 18

GATE: Gate 13

Photo Taken: 4/2/2021

File: DK-07.jpg

LOCATION:
Gate 13, left arm LB-2.

COMMENTS:
(2) areas of out-of-plane bending on inboard/upper flange, both measure 3/16" over 4".

© Schnabel Engineering 2020 All Rights Reserved

PHOTOGRAPH No.: 19

GATE: Gate 13

Photo Taken: 4/2/2021

File: DK-08.jpg

LOCATION:
Gate 13, V-18 at G-2 connection weld.

COMMENTS:
Middle 1/3 of weld is cracked, CS-2.

PHOTOGRAPH No.: 20

GATE: Gate 13

Photo Taken: 4/2/2021

File: DK-09.jpg

LOCATION:
Gate 13, V-20 at bottom plate.

COMMENTS:
100% section loss (4" x 1") in vertical web at knee brace for B-31. CS3. (V21 is similar).

© Schnabel Engineering 2020 All Rights Reserved

PHOTOGRAPH No.: 21

GATE: Gate 13

Photo Taken: 4/2/2021

File: DK-10.jpg

LOCATION:
Gate 13, left arm, LB-5 near LS -3 connection.

COMMENTS:
LB-5 appears to have installed incorrectly, cut, and installed correctly requiring this splice plate, a splice plate exists on the underside of web also.

PHOTOGRAPH No.: 22

GATE: Gate 13

Photo Taken: 4/2/2021

File: DK-11.jpg

LOCATION:
Gate 13, LB-6 at LS-2.

COMMENTS:
Remnants of LB-5 incorrect installation and being cut out.

© Schnabel Engineering 2020 All Rights Reserved

PHOTOGRAPH No.: 23
GATE: Gate 13
Photo Taken: 4/2/2021
File: DK-12.jpg

LOCATION:
Gate 13, LB-4 at LS-3.

COMMENTS:
Remnants of LB-5 incorrect installation and being cut out.

PHOTOGRAPH No.: 24
GATE: Gate 13
Photo Taken: 4/2/2021
File: DK-13.jpg

LOCATION:
Gate 13, left arm LB-6.

COMMENTS:
Multiple areas of out-of-plane bending on outboard flanges (largest being 1/4" over 3").

© Schnabel Engineering 2020 All Rights Reserved

PHOTOGRAPH No.: 1
GATE: Gate 14
Photo Taken: 4/1/2020
File: MC-26.jpg

LOCATION:
Gate 14, left arm.

COMMENTS:

PHOTOGRAPH No.: 2
GATE: Gate 14
Photo Taken: 4/1/2020
File: MC-27.jpg

LOCATION:
Gate 14, D/S face of gate.

COMMENTS:

© Schnabel Engineering 2020 All Rights Reserved

PHOTOGRAPH No.: 3
GATE: Gate 14
Photo Taken: 4/1/2020
File: MC-28.jpg

LOCATION:
Gate 14, right trunnion casting.

COMMENTS:
Moderate surface rust. CS-2.

PHOTOGRAPH No.: 4
GATE: Gate 14
Photo Taken: 4/1/2020
File: MC-29.jpg

LOCATION:
Gate 14, underside of right trunnion.

COMMENTS:
2 1/2" x 6" area of failed paint w/light surface rust. CS-2.

© Schnabel Engineering 2020 All Rights Reserved

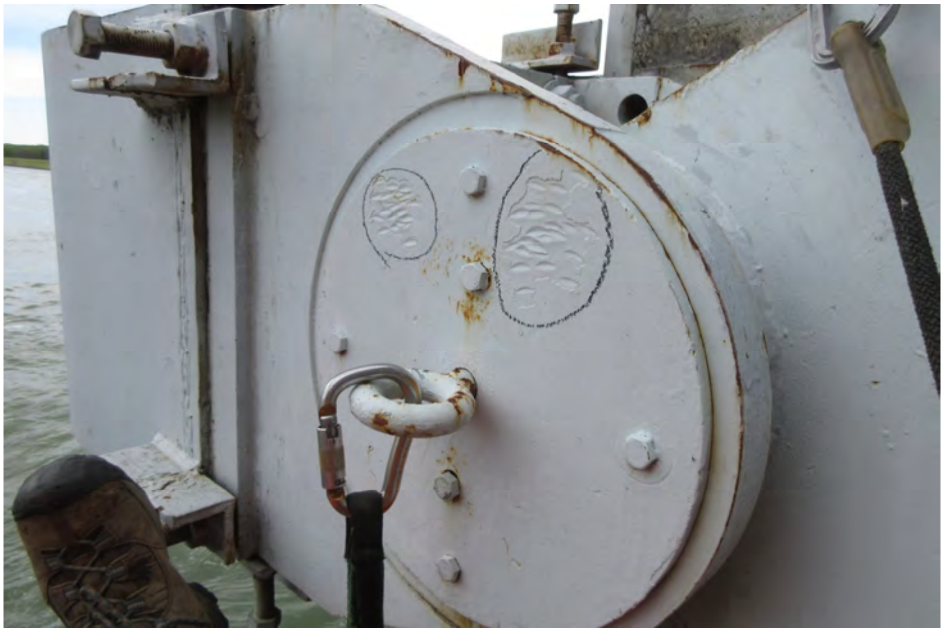

PHOTOGRAPH No.: 5
GATE: Gate 14
Photo Taken: 4/1/2020
File: MC-30.jpg

LOCATION:
Gate 14, right trunnion cover plate.

COMMENTS:
Two, 4" dia area w/hammer dents. Light surface rust on edges and eyebolt. CS-2.

PHOTOGRAPH No.: 6
GATE: Gate 14
Photo Taken: 4/1/2020
File: MC-31.jpg

LOCATION:
Gate 14, right trunnion.

COMMENTS:
Numerous paint chips and are-as with light surface rust. There is a threaded 5/16" hole in the center of the trunnion.

© Schnabel Engineering 2020 All Rights Reserved

PHOTOGRAPH No.: 7
GATE: Gate 14
Photo Taken: 4/1/2020
File: MC-32.jpg

LOCATION:
Gate 14, right trunnion, outboard side.

COMMENTS:
Saw kerf scars in casting. Potential stress riser.

PHOTOGRAPH No.: 8
GATE: Gate 14
Photo Taken: 4/1/2020
File: MC-33.jpg

LOCATION:
Gate 14, V-7 at G-1, right side.

COMMENTS:
Low quality field weld to G-1 flange. V-7 has out of plane bending up to 1/4" over 8" long. CS-2.

© Schnabel Engineering 2020 All Rights Reserved

PHOTOGRAPH No.: 9

GATE: Gate 14

Photo Taken: 4/1/2020

File: MC-34.jpg

LOCATION:
Gate 14, RS-1 & RS-2 at gusset plates.

COMMENTS:
Debris buildup and ponding water. Drains are blocked.

PHOTOGRAPH No.: 10

GATE: Gate 14

Photo Taken: 4/1/2020

File: MC-35.jpg

LOCATION:
Gate 14, RS-1 at RB-1.

COMMENTS:
Undercut weld 7" long. Web of RS-1 is undercut up to 3/32" x 7" long. CS-3.

© Schnabel Engineering 2020 All Rights Reserved

PHOTOGRAPH No.: 11
GATE: Gate 14
Photo Taken: 4/1/2020
File: MC-36.jpg

LOCATION:
Gate 14, V-4 at G-2, right side.

COMMENTS:
Partially cracked vertical weld. Potential for propagation. Low quality field weld. CS-3.

PHOTOGRAPH No.: 12
GATE: Gate 14
Photo Taken: 4/1/2020
File: MC-37.jpg

LOCATION:
Gate 14, B-6 at G-1.

COMMENTS:
Out of plane bending at top, 12" up to 4" out of plane. CS-2.

© Schnabel Engineering 2020 All Rights Reserved

PHOTOGRAPH No.: 13
GATE: Gate 14
Photo Taken: 4/1/2020
File: MC-38.jpg

LOCATION:
Gate 14, RB-5, inboard flange near midpoint.

COMMENTS:
Out of plane bending, 1" over 7" long. CS-2.

PHOTOGRAPH No.: 14
GATE: Gate 14
Photo Taken: 4/1/2020
File: MC-39.jpg

LOCATION:
Gate 14, RS-3 at RB-6.

COMMENTS:
Debris buildup with vegetation. Drains blocked.

© Schnabel Engineering 2020 All Rights Reserved

PHOTOGRAPH No.: 15

GATE: Gate 14

Photo Taken: 4/1/2020

File: MC-40.jpg

LOCATION:
Gate 14, concrete apron at midpoint and 10' below gate.

COMMENTS:
Delaminated grout patch 26" x 6".

PHOTOGRAPH No.: 16

GATE: Gate 14

Photo Taken: 4/2/2021

File: MC-01.jpg

LOCATION:
Gate 14, right arm.

COMMENTS:

© Schnabel Engineering 2020 All Rights Reserved

PHOTOGRAPH No.: 17

GATE: Gate 14

Photo Taken: 4/2/2021

File: MC-02.jpg

LOCATION:
Gate 14, left trunnion casting, right side.

COMMENTS:
Area with grinding marks. Approximately 1/2" of material has been ground away. Light surface rust. CS-4 due to section loss.

PHOTOGRAPH No.: 18

GATE: Gate 14

Photo Taken: 4/2/2021

File: MC-03.jpg

LOCATION:
Gate 14, left trunnion casting, right side.

COMMENTS:
Area with grinding marks. Approximately 1/2" of material has been ground away. Light surface rust. CS-4 due to section loss.

© Schnabel Engineering 2020 All Rights Reserved

PHOTOGRAPH No.: 19
GATE: Gate 14
Photo Taken: 4/2/2021
File: MC-04.jpg

LOCATION:
Gate 14, left trunnion, top side.

COMMENTS:
5/16" hole drilled in top of trunnion. Light surface rust. CS-2.

PHOTOGRAPH No.: 20
GATE: Gate 14
Photo Taken: 4/2/2021
File: MC-05.jpg

LOCATION:
Gate 14, left trunnion casting, right side.

COMMENTS:
Wood debris inside casting. Light surface rust. CS-2.

© Schnabel Engineering 2020 All Rights Reserved

PHOTOGRAPH No.: 21
GATE: Gate 14
Photo Taken: 4/2/2021
File: MC-06.jpg

LOCATION:
Gate 14, left gate seal, 4' from top of gate.

COMMENTS:
Leak, approximately 20 gpm.

PHOTOGRAPH No.: 22
GATE: Gate 14
Photo Taken: 4/2/2021
File: MC-07.jpg

LOCATION:
Gate 14, LS-2 at gusset plates.

COMMENTS:
Ponding water and blocked drain.

© Schnabel Engineering 2020 All Rights Reserved

PHOTOGRAPH No.: 23
GATE: Gate 14
Photo Taken: 4/2/2021
File: MC-08.jpg

LOCATION:
Gate 14, concrete apron, 26' down from gate and 15' from left buttress wall.

COMMENTS:
Spall 14" x 22" x 2 1/2" deep.

PHOTOGRAPH No.: 24
GATE: Gate 14
Photo Taken: 4/2/2021
File: MC-09.jpg

LOCATION:
Gate 14, concrete apron, 34' down from gate at midpoint.

COMMENTS:
Spall 38" x 7" x 2 1/2" deep.

© Schnabel Engineering 2020 All Rights Reserved

PHOTOGRAPH No.: 25
GATE: Gate 14
Photo Taken: 4/2/2021
File: MC-10.jpg

LOCATION:
Gate 14, G-2, left side.

COMMENTS:
Minor debris buildup with vegetation. Drains are clear.

PHOTOGRAPH No.: 26
GATE: Gate 14
Photo Taken: 4/2/2021
File: MC-11.jpg

LOCATION:
Gate 14, G-3 at V-16.

COMMENTS:
Debris buildup to 3" deep with vegetation.

© Schnabel Engineering 2020 All Rights Reserved

PHOTOGRAPH No.: 27
GATE: Gate 14
Photo Taken: 4/2/2021
File: MC-12.jpg

LOCATION:
Gate 14, G-3, left side.

COMMENTS:
Ponding water and debris buildup. Drains blocked.

PHOTOGRAPH No.: 28
GATE: Gate 14
Photo Taken: 4/2/2021
File: MC-13.jpg

LOCATION:
Gate 14, left gate seal at bottom of gate.

COMMENTS:
Leak, approximately 10 gpm.

© Schnabel Engineering 2020 All Rights Reserved

PHOTOGRAPH No.: 29
GATE: Gate 14
Photo Taken: 4/2/2021
File: MC-14.jpg

LOCATION:
Gate 14, right trunnion casting.

COMMENTS:
Trunnion casting has been thinned down with saw and grinder. Approximately 3/8" on each side. CS-4.

© Schnabel Engineering 2020 All Rights Reserved

ODOT CODING SYSTEM
BASED ON 2015 MANUAL

©2021 All Rights Reserved

Coding System: CS Definitions (Deterioration Paths & Thresholds)
Based on 2015 ODOT Bridge Inspection Manual

Defects	CS1 (Good)	CS2 (Fair)	CS3 (Poor)	CS4
Corrosion	None	Freckled rust Corrosion begun	Section loss or pack rust	**Warrants Structural Review to determine the strength or serviceability**
Cracking Fatigue	None	Crack has self-arrested or been mitigated	Un-arrested crack	
Connection	Connection in place, functional	Loose fasteners or pack rust w/o distortion, but connection in place, functional	Missing bolts, rivets or fasteners, broken or pack rust with distortion	
Distortion	None	Exists but no mitigation required or is mitigated	Exists Mitigation req'd	
Damage	None	Damage Exists is described by other CS2 defect	Damage Exists is described by other CS3 defect	

Examples for ODOT Coding System for assessment of coating loss, corrosion and section loss.

Condition State	Description	Example
Condition State 1 (CS-1)	There is no evidence of corrosion and any paint systems are sound and functioning as intended to protect the metal surface.	
Condition State 2 (CS-3)	Surface or freckled rust is moderate to heavy. There may be exposed metal, but there is no measurable loss of section.	
Condition State 3 (CS-4)	The paint system has failed. Corrosion may be present but any section loss due to active corrosion does not yet warrant a structural analysis of the element.	
Condition State 4 (CS-5)	Corrosion has caused section loss and is sufficient to warrant structural analysis to ascertain the impact on the ultimate strength and/or serviceability of either the element.	

APPENDIX C
GATE ANALYSIS COMPUTATIONS

©2021 All Rights Reserved

Attachment A

Section Properties of Skin-Rib Composites

Section Properties of Built-up Hub

Section Properties of Skin-Rib Composite
Composed of ST6B9.5 and 15.5-inch wide and 0.25-inch thick Skin Plate
Using STAAD Section Wizard

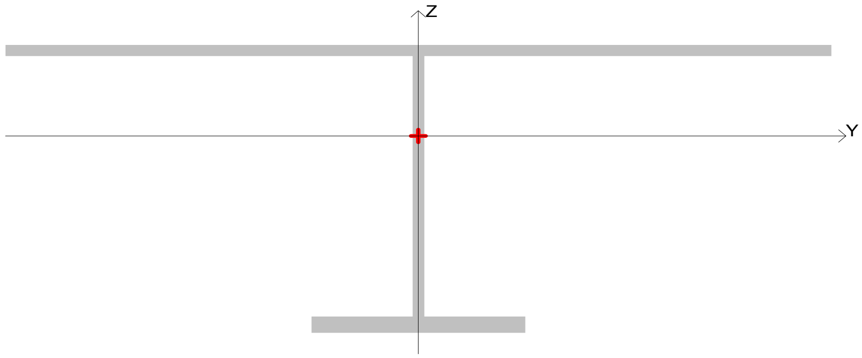

Section element	Rotation angle	Mirror	Material	E (kip/inch^2)
Sheet 4.01 x 0.349			Steel	29732.747
Sheet 5.731 x 0.24	90.0		Steel	29732.747
Sheet 15.5 x 0.25			Steel	29732.747

The overall dimensions of the section are 15 x 6 inch

Basic geometry of the section

	Parameter	Value	
A	Cross sectional area	6.65	$inch^2$
α	Angle between Y-Z and U-V axes	-90.0	deg
I_y	Moment of inertia about axis parallel to Y passing through centroid	43.3	$inch^4$
I_z	Moment of inertia about axis parallel to Z passing through centroid	79.46	$inch^4$
I_t	Torsional moment of inertia (St. Venant)	0.15	$inch^4$
i_y	Radius of gyration about axis parallel to Y passing through centroid	2.55	inch
i_z	Radius of gyration about axis parallel to Z passing through centroid	3.46	inch
W_{u+}	Elastic modulus about U-axis (+ve extreme)	10.25	$inch^3$
W_{u-}	Elastic modulus about U-axis (-ve extreme)	10.25	$inch^3$
W_{v+}	Elastic modulus about V-axis (+ve extreme)	10.03	$inch^3$
W_{v-}	Elastic modulus about V-axis (-ve extreme)	21.51	$inch^3$
$W_{pl,u}$	Plastic modulus about axis parallel to U-axis	16.61	$inch^3$
$W_{pl,v}$	Plastic modulus about axis parallel to V-axis	14.58	$inch^3$
I_u	Moment of inertia about U-axis	79.46	$inch^4$
I_v	Moment of inertia about V-axis	43.3	$inch^4$
i_u	Radius of gyration about U-axis	3.46	inch
i_v	Radius of gyration about V-axis	2.55	inch
a_{u+}	Centroid to edge of compression zone along +ve U-axis	1.51	inch
a_{u-}	Centroid to edge of compression zone along -ve U-axis	3.24	inch
a_{v+}	Centroid to edge of compression zone along +ve V-axis	1.54	inch
a_{v-}	Centroid to edge of compression zone along -ve	1.54	inch

	V-axis		
y_M	Distance to centroid along Y-axis	2.73185e-016	
z_M	Distance to centroid along Z-axis	-4.97464e-016	
y_P	Distance to equal area axis along Y-axis	2.73185e-016	
z_P	Distance to equal area axis along Z-axis	-1.8	inch
I_{yz}	Moment of inertia Iyz in the user coordinates	0.0	$inch^4$
u_P	Distance to equal area axis along U-axis	-1.8	inch
v_P	Distance to equal area axis along V-axis	0.0	inch

Section Properties of Skin-Rib Composite
Composed of ST6B9.5 and 18-inch wide and 0.25-inch thick Skin Plate
Using STAAD Section Wizard

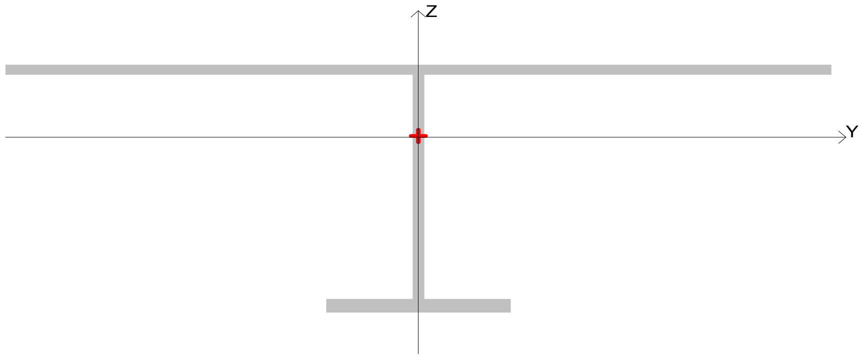

Section element	Rotation angle	Mirror	Material	E (kip/inch^2)
Sheet 4.01 x 0.349			Steel	29732.747
Sheet 5.731 x 0.24	90.0		Steel	29732.747
Sheet 18 x 0.25			Steel	29732.747

The overall dimensions of the section are 18 x 6 inch

Basic geometry of the section

	Parameter	Value	
A	Cross sectional area	7.27	$inch^2$
α	Angle between Y-Z and U-V axes	-90.0	deg
I_y	Moment of inertia about axis parallel to Y passing through centroid	45.34	$inch^4$
I_z	Moment of inertia about axis parallel to Z passing through centroid	123.38	$inch^4$
I_t	Torsional moment of inertia (St. Venant)	0.17	$inch^4$
i_y	Radius of gyration about axis parallel to Y passing through centroid	2.5	inch
i_z	Radius of gyration about axis parallel to Z passing through centroid	4.12	inch
W_{u+}	Elastic modulus about U-axis (+ve extreme)	13.71	$inch^3$
W_{u-}	Elastic modulus about U-axis (-ve extreme)	13.71	$inch^3$
W_{v+}	Elastic modulus about V-axis (+ve extreme)	10.12	$inch^3$
W_{v-}	Elastic modulus about V-axis (-ve extreme)	24.5	$inch^3$
$W_{pl,u}$	Plastic modulus about axis parallel to U-axis	21.88	$inch^3$
$W_{pl,v}$	Plastic modulus about axis parallel to V-axis	15.34	$inch^3$
I_u	Moment of inertia about U-axis	123.38	$inch^4$
I_v	Moment of inertia about V-axis	45.34	$inch^4$
i_u	Radius of gyration about U-axis	4.12	inch
i_v	Radius of gyration about V-axis	2.5	inch
a_{u+}	Centroid to edge of compression zone along +ve U-axis	1.39	inch
a_{u-}	Centroid to edge of compression zone along -ve U-axis	3.37	inch
a_{v+}	Centroid to edge of compression zone along +ve V-axis	1.88	inch
a_{v-}	Centroid to edge of compression zone along -ve	1.88	inch

	V-axis		
y_M	Distance to centroid along Y-axis	0.0	inch
z_M	Distance to centroid along Z-axis	2.27363e-016	
y_P	Distance to equal area axis along Y-axis	0.0	inch
z_P	Distance to equal area axis along Z-axis	-1.65	inch
I_{yz}	Moment of inertia Iyz in the user coordinates	0.0	$inch^4$
u_P	Distance to equal area axis along U-axis	-1.65	inch
v_P	Distance to equal area axis along V-axis	0.0	inch

Section Properties of Skin-Rib Composite
Composed of ST6B9.5 and 24-inch wide and 0.25-inch thick Skin Plate
Using STAAD Section Wizard

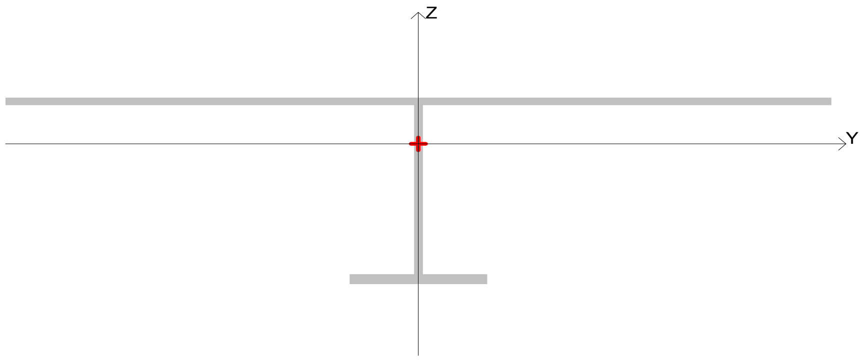

Section element	Rotation angle	Mirror	Material	E (kip/inch^2)
Sheet 4.01 x 0.349			Steel	29732.747
Sheet 5.731 x 0.24	90.0		Steel	29732.747
Sheet 24 x 0.25			Steel	29732.747

The overall dimensions of the section are 24 x 6 inch

Basic geometry of the section

	Parameter	Value	
A	Cross sectional area	8.77	$inch^2$
α	Angle between Y-Z and U-V axes	-90.0	deg
I_y	Moment of inertia about axis parallel to Y passing through centroid	49.05	$inch^4$
I_z	Moment of inertia about axis parallel to Z passing through centroid	289.88	$inch^4$
I_t	Torsional moment of inertia (St. Venant)	0.2	$inch^4$
i_y	Radius of gyration about axis parallel to Y passing through centroid	2.36	inch
i_z	Radius of gyration about axis parallel to Z passing through centroid	5.75	inch
W_{u+}	Elastic modulus about U-axis (+ve extreme)	24.16	$inch^3$
W_{u-}	Elastic modulus about U-axis (-ve extreme)	24.16	$inch^3$
W_{v+}	Elastic modulus about V-axis (+ve extreme)	10.27	$inch^3$
W_{v-}	Elastic modulus about V-axis (-ve extreme)	31.53	$inch^3$
$W_{pl,u}$	Plastic modulus about axis parallel to U-axis	37.73	$inch^3$
$W_{pl,v}$	Plastic modulus about axis parallel to V-axis	16.95	$inch^3$
I_u	Moment of inertia about U-axis	289.88	$inch^4$
I_v	Moment of inertia about V-axis	49.05	$inch^4$
i_u	Radius of gyration about U-axis	5.75	inch
i_v	Radius of gyration about V-axis	2.36	inch
a_{u+}	Centroid to edge of compression zone along +ve U-axis	1.17	inch
a_{u-}	Centroid to edge of compression zone along -ve U-axis	3.59	inch
a_{v+}	Centroid to edge of compression zone along +ve V-axis	2.75	inch
a_{v-}	Centroid to edge of compression zone along -ve	2.75	inch

	V-axis		
y_M	Distance to centroid along Y-axis	0.0	inch
z_M	Distance to centroid along Z-axis	-1.88497e-016	
y_P	Distance to equal area axis along Y-axis	0.0	inch
z_P	Distance to equal area axis along Z-axis	-1.37	inch
I_{yz}	Moment of inertia Iyz in the user coordinates	0.0	$inch^4$
u_P	Distance to equal area axis along U-axis	-1.37	inch
v_P	Distance to equal area axis along V-axis	0.0	inch

File: D:\Projects\Dallas Water Utility\2020_03_Forney Dam Tainter Gate\5_Calcs\RibTop2.sec

Section Properties of Skin-Rib Composite
Composed of ST6B9.5 and 15.5-inch wide and 0.3125-inch thick Skin Plate
Using STAAD Section Wizard

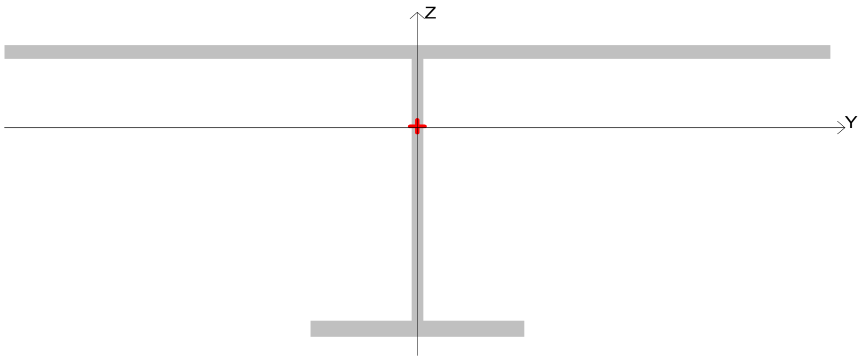

Section element	Rotation angle	Mirror	Material	E (kip/inch^2)
Sheet 4.01 x 0.349			Steel	29732.747
Sheet 5.731 x 0.24	90.0		Steel	29732.747
Sheet 15.5 x 0.3125			Steel	29732.747

The overall dimensions of the section are 15 x 6 inch

Basic geometry of the section

	Parameter	Value	
A	Cross sectional area	7.62	inch^2
α	Angle between Y-Z and U-V axes	-90.0	deg
I_y	Moment of inertia about axis parallel to Y passing through centroid	46.83	inch^4
I_z	Moment of inertia about axis parallel to Z passing through centroid	98.86	inch^4
I_t	Torsional moment of inertia (St. Venant)	0.23	inch^4
i_y	Radius of gyration about axis parallel to Y passing through centroid	2.48	inch
i_z	Radius of gyration about axis parallel to Z passing through centroid	3.6	inch
W_{u+}	Elastic modulus about U-axis (+ve extreme)	12.76	inch^3
W_{u-}	Elastic modulus about U-axis (-ve extreme)	12.76	inch^3
W_{v+}	Elastic modulus about V-axis (+ve extreme)	10.23	inch^3
W_{v-}	Elastic modulus about V-axis (-ve extreme)	25.8	inch^3
$W_{pl,u}$	Plastic modulus about axis parallel to U-axis	20.39	inch^3
$W_{pl,v}$	Plastic modulus about axis parallel to V-axis	15.99	inch^3
I_u	Moment of inertia about U-axis	98.86	inch^4
I_v	Moment of inertia about V-axis	46.83	inch^4
i_u	Radius of gyration about U-axis	3.6	inch
i_v	Radius of gyration about V-axis	2.48	inch
a_{u+}	Centroid to edge of compression zone along +ve U-axis	1.34	inch
a_{u-}	Centroid to edge of compression zone along -ve U-axis	3.39	inch
a_{v+}	Centroid to edge of compression zone along +ve V-axis	1.67	inch
a_{v-}	Centroid to edge of compression zone along -ve	1.67	inch

	V-axis		
y_M	Distance to centroid along Y-axis	0.0	inch
z_M	Distance to centroid along Z-axis	2.17105e-016	
y_P	Distance to equal area axis along Y-axis	0.0	inch
z_P	Distance to equal area axis along Z-axis	-1.57	inch
I_{yz}	Moment of inertia Iyz in the user coordinates	0.0	$inch^4$
u_P	Distance to equal area axis along U-axis	-1.57	inch
v_P	Distance to equal area axis along V-axis	0.0	inch

Section Properties of Skin-Rib Composite
Composed of ST6B9.5 and 18-inch wide and 0.3125-inch thick Skin Plate
Using STAAD Section Wizard

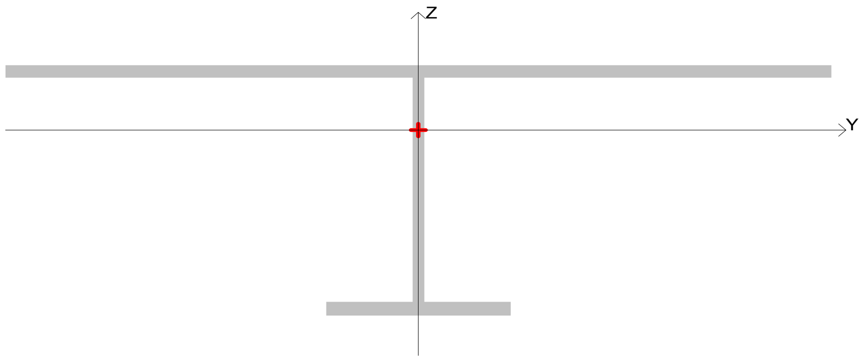

Section element	Rotation angle	Mirror	Material	E (kip/inch^2)
Sheet 4.01 x 0.349			Steel	29732.747
Sheet 5.731 x 0.24	90.0		Steel	29732.747
Sheet 18 x 0.3125			Steel	29732.747

The overall dimensions of the section are 18 x 6 inch

Basic geometry of the section

	Parameter	Value	
A	Cross sectional area	8.4	$inch^2$
α	Angle between Y-Z and U-V axes	-90.0	deg
I_y	Moment of inertia about axis parallel to Y passing through centroid	48.79	$inch^4$
I_z	Moment of inertia about axis parallel to Z passing through centroid	153.76	$inch^4$
I_t	Torsional moment of inertia (St. Venant)	0.25	$inch^4$
i_y	Radius of gyration about axis parallel to Y passing through centroid	2.41	inch
i_z	Radius of gyration about axis parallel to Z passing through centroid	4.28	inch
W_{u+}	Elastic modulus about U-axis (+ve extreme)	17.08	$inch^3$
W_{u-}	Elastic modulus about U-axis (-ve extreme)	17.08	$inch^3$
W_{v+}	Elastic modulus about V-axis (+ve extreme)	10.31	$inch^3$
W_{v-}	Elastic modulus about V-axis (-ve extreme)	29.37	$inch^3$
$W_{pl,u}$	Plastic modulus about axis parallel to U-axis	26.66	$inch^3$
$W_{pl,v}$	Plastic modulus about axis parallel to V-axis	16.71	$inch^3$
I_u	Moment of inertia about U-axis	153.76	$inch^4$
I_v	Moment of inertia about V-axis	48.79	$inch^4$
i_u	Radius of gyration about U-axis	4.28	inch
i_v	Radius of gyration about V-axis	2.41	inch
a_{u+}	Centroid to edge of compression zone along +ve U-axis	1.23	inch
a_{u-}	Centroid to edge of compression zone along -ve U-axis	3.5	inch
a_{v+}	Centroid to edge of compression zone along +ve V-axis	2.03	inch
a_{v-}	Centroid to edge of compression zone along -ve	2.03	inch

	V-axis		
y_M	Distance to centroid along Y-axis	0.0	inch
z_M	Distance to centroid along Z-axis	1.96913e-016	
y_P	Distance to equal area axis along Y-axis	0.0	inch
z_P	Distance to equal area axis along Z-axis	-1.43	inch
I_{yz}	Moment of inertia Iyz in the user coordinates	0.0	$inch^4$
u_P	Distance to equal area axis along U-axis	-1.43	inch
v_P	Distance to equal area axis along V-axis	0.0	inch

Section Properties of Skin-Rib Composite
Composed of ST6B9.5 and 24-inch wide and 0.3125-inch thick Skin Plate
Using STAAD Section Wizard

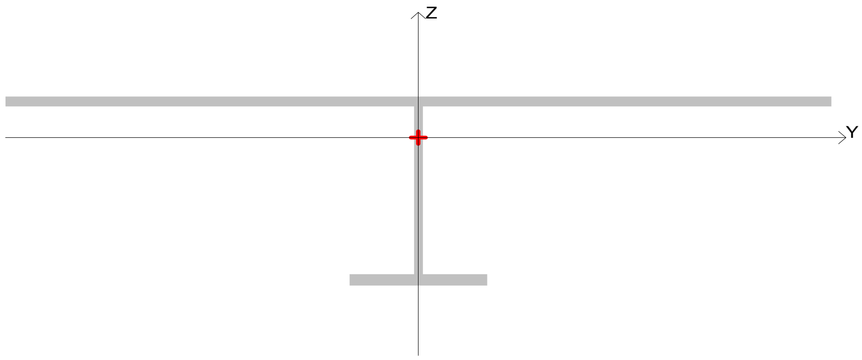

Section element	Rotation angle	Mirror	Material	E (kip/inch^2)
Sheet 4.01 x 0.349			Steel	29732.747
Sheet 5.731 x 0.24	90.0		Steel	29732.747
Sheet 24 x 0.3125			Steel	29732.747

The overall dimensions of the section are 24 x 6 inch

Basic geometry of the section

	Parameter	Value	
A	Cross sectional area	10.27	$inch^2$
α	Angle between Y-Z and U-V axes	-90.0	deg
I_y	Moment of inertia about axis parallel to Y passing through centroid	52.27	$inch^4$
I_z	Moment of inertia about axis parallel to Z passing through centroid	361.88	$inch^4$
I_t	Torsional moment of inertia (St. Venant)	0.31	$inch^4$
i_y	Radius of gyration about axis parallel to Y passing through centroid	2.26	inch
i_z	Radius of gyration about axis parallel to Z passing through centroid	5.93	inch
W_{u+}	Elastic modulus about U-axis (+ve extreme)	30.16	$inch^3$
W_{u-}	Elastic modulus about U-axis (-ve extreme)	30.16	$inch^3$
W_{v+}	Elastic modulus about V-axis (+ve extreme)	10.44	$inch^3$
W_{v-}	Elastic modulus about V-axis (-ve extreme)	37.71	$inch^3$
$W_{pl,u}$	Plastic modulus about axis parallel to U-axis	46.81	$inch^3$
$W_{pl,v}$	Plastic modulus about axis parallel to V-axis	18.35	$inch^3$
I_u	Moment of inertia about U-axis	361.88	$inch^4$
I_v	Moment of inertia about V-axis	52.27	$inch^4$
i_u	Radius of gyration about U-axis	5.93	inch
i_v	Radius of gyration about V-axis	2.26	inch
a_{u+}	Centroid to edge of compression zone along +ve U-axis	1.02	inch
a_{u-}	Centroid to edge of compression zone along -ve U-axis	3.67	inch
a_{v+}	Centroid to edge of compression zone along +ve V-axis	2.93	inch
a_{v-}	Centroid to edge of compression zone along -ve	2.93	inch

	V-axis		
y_M	Distance to centroid along Y-axis	0.0	inch
z_M	Distance to centroid along Z-axis	-0.0	inch
y_P	Distance to equal area axis along Y-axis	0.0	inch
z_P	Distance to equal area axis along Z-axis	-1.17	inch
I_{yz}	Moment of inertia Iyz in the user coordinates	0.0	$inch^4$
u_P	Distance to equal area axis along U-axis	-1.17	inch
v_P	Distance to equal area axis along V-axis	0.0	inch

Section Properties of Skin-Rib Composite
Composed of ST6B9.5 and 15.5-inch wide and 0.375-inch thick Skin Plate
Using STAAD Section Wizard

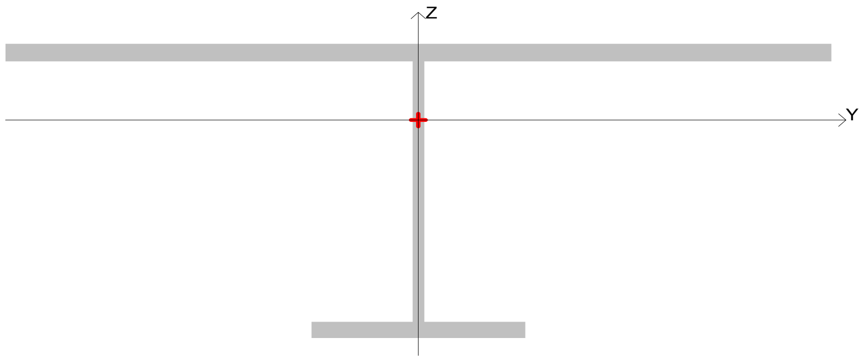

Section element	Rotation angle	Mirror	Material	E (kip/inch^2)
Sheet 4.01 x 0.349			Steel	29732.747
Sheet 5.731 x 0.24	90.0		Steel	29732.747
Sheet 15.5 x 0.375			Steel	29732.747

The overall dimensions of the section are 15 x 6 inch

Basic geometry of the section

	Parameter	Value	
A	Cross sectional area	8.59	$inch^2$
α	Angle between Y-Z and U-V axes	-90.0	deg
I_y	Moment of inertia about axis parallel to Y passing through centroid	49.76	$inch^4$
I_z	Moment of inertia about axis parallel to Z passing through centroid	118.25	$inch^4$
I_t	Torsional moment of inertia (St. Venant)	0.33	$inch^4$
i_y	Radius of gyration about axis parallel to Y passing through centroid	2.41	inch
i_z	Radius of gyration about axis parallel to Z passing through centroid	3.71	inch
W_{u+}	Elastic modulus about U-axis (+ve extreme)	15.26	$inch^3$
W_{u-}	Elastic modulus about U-axis (-ve extreme)	15.26	$inch^3$
W_{v+}	Elastic modulus about V-axis (+ve extreme)	10.4	$inch^3$
W_{v-}	Elastic modulus about V-axis (-ve extreme)	29.81	$inch^3$
$W_{pl,u}$	Plastic modulus about axis parallel to U-axis	24.18	$inch^3$
$W_{pl,v}$	Plastic modulus about axis parallel to V-axis	17.13	$inch^3$
I_u	Moment of inertia about U-axis	118.25	$inch^4$
I_v	Moment of inertia about V-axis	49.76	$inch^4$
i_u	Radius of gyration about U-axis	3.71	inch
i_v	Radius of gyration about V-axis	2.41	inch
a_{u+}	Centroid to edge of compression zone along +ve U-axis	1.21	inch
a_{u-}	Centroid to edge of compression zone along -ve U-axis	3.47	inch
a_{v+}	Centroid to edge of compression zone along +ve V-axis	1.78	inch
a_{v-}	Centroid to edge of compression zone along -ve	1.78	inch

	V-axis		
y_M	Distance to centroid along Y-axis	0.0	inch
z_M	Distance to centroid along Z-axis	-1.92613e-016	
y_P	Distance to equal area axis along Y-axis	0.0	inch
z_P	Distance to equal area axis along Z-axis	-1.39	inch
I_{yz}	Moment of inertia Iyz in the user coordinates	0.0	$inch^4$
u_P	Distance to equal area axis along U-axis	-1.39	inch
v_P	Distance to equal area axis along V-axis	0.0	inch

Section Properties of Skin-Rib Composite
Composed of ST6B9.5 and 18-inch wide and 0.375-inch thick Skin Plate
Using STAAD Section Wizard

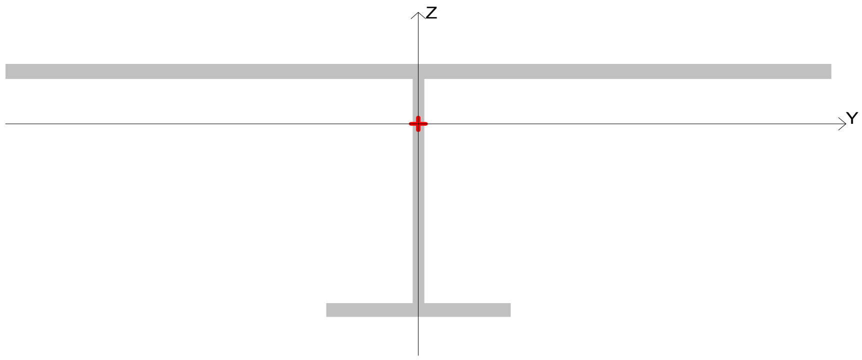

Section element	Rotation angle	Mirror	Material	E (kip/inch^2)
Sheet 4.01 x 0.349			Steel	29732.747
Sheet 5.731 x 0.24	90.0		Steel	29732.747
Sheet 18 x 0.375			Steel	29732.747

The overall dimensions of the section are 18 x 6 inch

Basic geometry of the section

	Parameter	Value	
A	Cross sectional area	9.52	$inch^2$
α	Angle between Y-Z and U-V axes	-90.0	deg
I_y	Moment of inertia about axis parallel to Y passing through centroid	51.63	$inch^4$
I_z	Moment of inertia about axis parallel to Z passing through centroid	184.13	$inch^4$
I_t	Torsional moment of inertia (St. Venant)	0.38	$inch^4$
i_y	Radius of gyration about axis parallel to Y passing through centroid	2.33	inch
i_z	Radius of gyration about axis parallel to Z passing through centroid	4.4	inch
W_{u+}	Elastic modulus about U-axis (+ve extreme)	20.46	$inch^3$
W_{u-}	Elastic modulus about U-axis (-ve extreme)	20.46	$inch^3$
W_{v+}	Elastic modulus about V-axis (+ve extreme)	10.47	$inch^3$
W_{v-}	Elastic modulus about V-axis (-ve extreme)	33.89	$inch^3$
$W_{pl,u}$	Plastic modulus about axis parallel to U-axis	31.78	$inch^3$
$W_{pl,v}$	Plastic modulus about axis parallel to V-axis	17.93	$inch^3$
I_u	Moment of inertia about U-axis	184.13	$inch^4$
I_v	Moment of inertia about V-axis	51.63	$inch^4$
i_u	Radius of gyration about U-axis	4.4	inch
i_v	Radius of gyration about V-axis	2.33	inch
a_{u+}	Centroid to edge of compression zone along +ve U-axis	1.1	inch
a_{u-}	Centroid to edge of compression zone along -ve U-axis	3.56	inch
a_{v+}	Centroid to edge of compression zone along +ve V-axis	2.15	inch
a_{v-}	Centroid to edge of compression zone along -ve	2.15	inch

	V-axis		
y_M	Distance to centroid along Y-axis	0.0	inch
z_M	Distance to centroid along Z-axis	1.73655e-016	
y_P	Distance to equal area axis along Y-axis	0.0	inch
z_P	Distance to equal area axis along Z-axis	-1.26	inch
I_{yz}	Moment of inertia Iyz in the user coordinates	0.0	$inch^4$
u_P	Distance to equal area axis along U-axis	-1.26	inch
v_P	Distance to equal area axis along V-axis	0.0	inch

Section Properties of Skin-Rib Composite
Composed of ST6B9.5 and 24-inch wide and 0.375-inch thick Skin Plate
Using STAAD Section Wizard

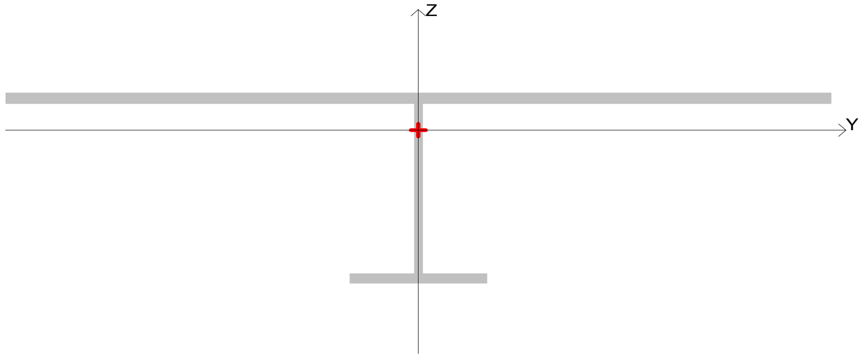

Section element	Rotation angle	Mirror	Material	E (kip/inch^2)
Sheet 4.01 x 0.349			Steel	29732.747
Sheet 5.731 x 0.24	90.0		Steel	29732.747
Sheet 24 x 0.375			Steel	29732.747

The overall dimensions of the section are 24 x 6 inch

Basic geometry of the section

	Parameter	Value	
A	Cross sectional area	11.77	$inch^2$
α	Angle between Y-Z and U-V axes	-90.0	deg
I_y	Moment of inertia about axis parallel to Y passing through centroid	54.91	$inch^4$
I_z	Moment of inertia about axis parallel to Z passing through centroid	433.88	$inch^4$
I_t	Torsional moment of inertia (St. Venant)	0.48	$inch^4$
i_y	Radius of gyration about axis parallel to Y passing through centroid	2.16	inch
i_z	Radius of gyration about axis parallel to Z passing through centroid	6.07	inch
W_{u+}	Elastic modulus about U-axis (+ve extreme)	36.16	$inch^3$
W_{u-}	Elastic modulus about U-axis (-ve extreme)	36.16	$inch^3$
W_{v+}	Elastic modulus about V-axis (+ve extreme)	10.59	$inch^3$
W_{v-}	Elastic modulus about V-axis (-ve extreme)	43.29	$inch^3$
$W_{pl,u}$	Plastic modulus about axis parallel to U-axis	55.88	$inch^3$
$W_{pl,v}$	Plastic modulus about axis parallel to V-axis	19.35	$inch^3$
I_u	Moment of inertia about U-axis	433.88	$inch^4$
I_v	Moment of inertia about V-axis	54.91	$inch^4$
i_u	Radius of gyration about U-axis	6.07	inch
i_v	Radius of gyration about V-axis	2.16	inch
a_{u+}	Centroid to edge of compression zone along +ve U-axis	0.9	inch
a_{u-}	Centroid to edge of compression zone along -ve U-axis	3.68	inch
a_{v+}	Centroid to edge of compression zone along +ve V-axis	3.07	inch
a_{v-}	Centroid to edge of compression zone along -ve V-axis	3.07	inch

y_M	Distance to centroid along Y-axis	0.0	inch
z_M	Distance to centroid along Z-axis	-0.0	inch
y_P	Distance to equal area axis along Y-axis	0.0	inch
z_P	Distance to equal area axis along Z-axis	-1.02	inch
I_{yz}	Moment of inertia Iyz in the user coordinates	0.0	$inch^4$
u_P	Distance to equal area axis along U-axis	-1.02	inch
v_P	Distance to equal area axis along V-axis	0.0	inch

Section Properties of Skin-Rib Composite
Composed of ST6B9.5 and 15.5-inch wide and 1.0-inch thick Plate at cable hitch
Using STAAD Section Wizard

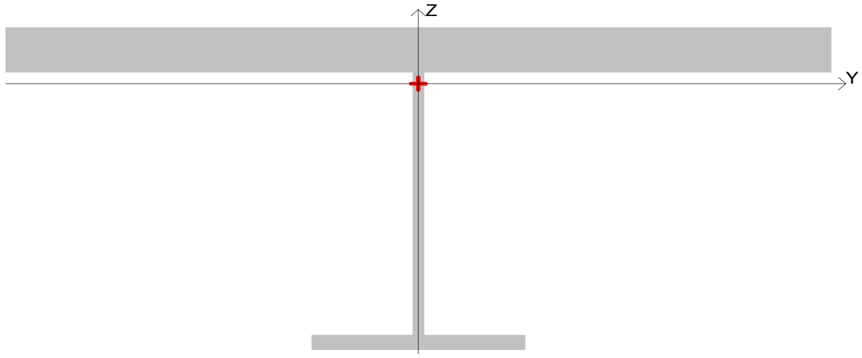

Section element	Rotation angle	Mirror	Material	E (kip/inch^2)
Sheet 4.01 x 0.349			Steel	29732.747
Sheet 5.731 x 0.24	90.0		Steel	29732.747
Sheet 15.5 x 1			Steel	29732.747

The overall dimensions of the section are 15 x 7 inch

Basic geometry of the section

	Parameter	Value	
A	Cross sectional area	18.27	$inch^2$
α	Angle between Y-Z and U-V axes	-90.0	deg
I_y	Moment of inertia about axis parallel to Y passing through centroid	67.96	$inch^4$
I_z	Moment of inertia about axis parallel to Z passing through centroid	312.2	$inch^4$
I_t	Torsional moment of inertia (St. Venant)	4.93	$inch^4$
i_y	Radius of gyration about axis parallel to Y passing through centroid	1.93	inch
i_z	Radius of gyration about axis parallel to Z passing through centroid	4.13	inch
W_{u+}	Elastic modulus about U-axis (+ve extreme)	40.28	$inch^3$
W_{u-}	Elastic modulus about U-axis (-ve extreme)	40.28	$inch^3$
W_{v+}	Elastic modulus about V-axis (+ve extreme)	11.64	$inch^3$
W_{v-}	Elastic modulus about V-axis (-ve extreme)	54.64	$inch^3$
$W_{pl,u}$	Plastic modulus about axis parallel to U-axis	61.52	$inch^3$
$W_{pl,v}$	Plastic modulus about axis parallel to V-axis	22.9	$inch^3$
I_u	Moment of inertia about U-axis	312.2	$inch^4$
I_v	Moment of inertia about V-axis	67.96	$inch^4$
i_u	Radius of gyration about U-axis	4.13	inch
i_v	Radius of gyration about V-axis	1.93	inch
a_{u+}	Centroid to edge of compression zone along +ve U-axis	0.64	inch
a_{u-}	Centroid to edge of compression zone along -ve U-axis	2.99	inch
a_{v+}	Centroid to edge of compression zone along +ve V-axis	2.2	inch
a_{v-}	Centroid to edge of compression zone along -ve V-axis	2.2	inch

y_M	Distance to centroid along Y-axis	0.0	inch
z_M	Distance to centroid along Z-axis	-0.0	inch
y_P	Distance to equal area axis along Y-axis	0.0	inch
z_P	Distance to equal area axis along Z-axis	-0.65	inch
I_{yz}	Moment of inertia Iyz in the user coordinates	0.0	$inch^4$
u_P	Distance to equal area axis along U-axis	-0.65	inch
v_P	Distance to equal area axis along V-axis	0.0	inch

Section Properties of Skin-Rib Composite
Composed of ST6B9.5 and 18-inch wide and 1.0-inch thick Plate at cable hitch
Using STAAD Section Wizard

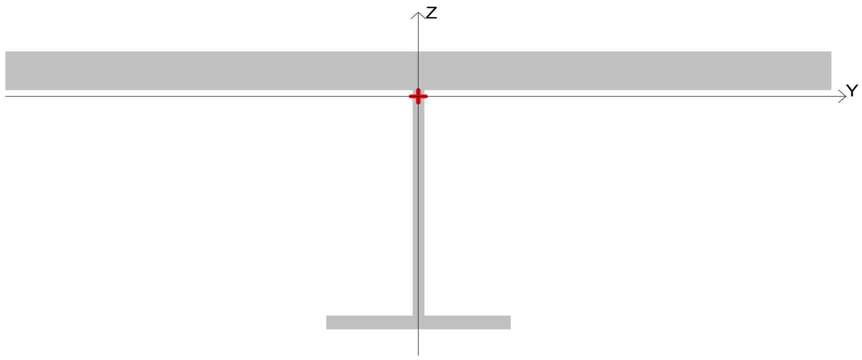

Section element	Rotation angle	Mirror	Material	E (kip/inch^2)
Sheet 4.01 x 0.349			Steel	29732.747
Sheet 5.731 x 0.24	90.0		Steel	29732.747
Sheet 18 x 1			Steel	29732.747

The overall dimensions of the section are 18 x 7 inch

Basic geometry of the section

	Parameter	Value	
A	Cross sectional area	20.77	$inch^2$
α	Angle between Y-Z and U-V axes	-90.0	deg
I_y	Moment of inertia about axis parallel to Y passing through centroid	69.39	$inch^4$
I_z	Moment of inertia about axis parallel to Z passing through centroid	487.88	$inch^4$
I_t	Torsional moment of inertia (St. Venant)	5.72	$inch^4$
i_y	Radius of gyration about axis parallel to Y passing through centroid	1.83	inch
i_z	Radius of gyration about axis parallel to Z passing through centroid	4.85	inch
W_{u+}	Elastic modulus about U-axis (+ve extreme)	54.21	$inch^3$
W_{u-}	Elastic modulus about U-axis (-ve extreme)	54.21	$inch^3$
W_{v+}	Elastic modulus about V-axis (+ve extreme)	11.71	$inch^3$
W_{v-}	Elastic modulus about V-axis (-ve extreme)	60.11	$inch^3$
$W_{pl,u}$	Plastic modulus about axis parallel to U-axis	82.49	$inch^3$
$W_{pl,v}$	Plastic modulus about axis parallel to V-axis	23.41	$inch^3$
I_u	Moment of inertia about U-axis	487.88	$inch^4$
I_v	Moment of inertia about V-axis	69.39	$inch^4$
i_u	Radius of gyration about U-axis	4.85	inch
i_v	Radius of gyration about V-axis	1.83	inch
a_{u+}	Centroid to edge of compression zone along +ve U-axis	0.56	inch
a_{u-}	Centroid to edge of compression zone along -ve U-axis	2.89	inch
a_{v+}	Centroid to edge of compression zone along +ve V-axis	2.61	inch
a_{v-}	Centroid to edge of compression zone along -ve	2.61	inch

	V-axis		
y_M	Distance to centroid along Y-axis	0.0	inch
z_M	Distance to centroid along Z-axis	-0.0	inch
y_P	Distance to equal area axis along Y-axis	0.0	inch
z_P	Distance to equal area axis along Z-axis	-0.58	inch
I_{yz}	Moment of inertia Iyz in the user coordinates	0.0	$inch^4$
u_P	Distance to equal area axis along U-axis	-0.58	inch
v_P	Distance to equal area axis along V-axis	0.0	inch

Approximate Built-up Hub Section Properties at 0.94ft from Trunnion Centerline Using STAAD Section Wizard

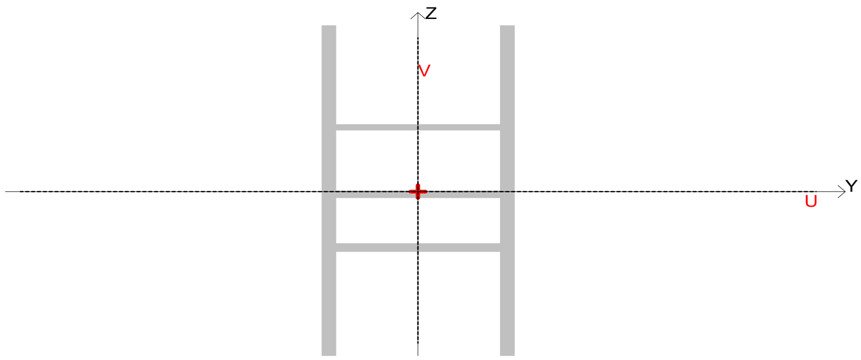

Section element	Rotation angle	Mirror	Material	E (kip/inch^2)
Sheet 21.132 x 0.8125	90.0		Steel	29732.747
Sheet 21.132 x 0.8125	90.0		Steel	29732.747
Sheet 9 x 0.375			Steel	29732.747
Sheet 9 x 0.5			Steel	29732.747
Sheet 9 x 0.5			Steel	29732.747

The overall dimensions of the section are 11 x 21 inch

Basic geometry of the section

	Parameter	Value	
A	Cross sectional area	46.71	$inch^2$
α	Angle between Y-Z and U-V axes	-0.0	deg
I_y	Moment of inertia about axis parallel to Y passing through centroid	1392.29	$inch^4$
I_z	Moment of inertia about axis parallel to Z passing through centroid	912.02	$inch^4$
I_t	Torsional moment of inertia (St. Venant)	7.96	$inch^4$,
i_y	Radius of gyration about axis parallel to Y passing through centroid	5.46	inch
i_z	Radius of gyration about axis parallel to Z passing through centroid	4.42	inch
W_{u+}	Elastic modulus about U-axis (+ve extreme)	130.76	$inch^3$
W_{u-}	Elastic modulus about U-axis (-ve extreme)	132.8	$inch^3$
W_{v+}	Elastic modulus about V-axis (+ve extreme)	171.67	$inch^3$
W_{v-}	Elastic modulus about V-axis (-ve extreme)	171.67	$inch^3$
$W_{pl,u}$	Plastic modulus about axis parallel to U-axis	211.6	$inch^3$
$W_{pl,v}$	Plastic modulus about axis parallel to V-axis	195.87	$inch^3$
I_u	Moment of inertia about U-axis	1392.29	$inch^4$
I_v	Moment of inertia about V-axis	912.02	$inch^4$
i_u	Radius of gyration about U-axis	5.46	inch
i_v	Radius of gyration about V-axis	4.42	inch
a_{u+}	Centroid to edge of compression zone along +ve U-axis	3.67	inch
a_{u-}	Centroid to edge of compression zone along -ve U-axis	3.67	inch
a_{v+}	Centroid to edge of compression zone along +ve V-axis	2.8	inch

Torsion moment of inertia is replaced by torsion property of an approximate hollow rectangular section

a_{v-}	Centroid to edge of compression zone along -ve V-axis	2.84	inch
y_M	Distance to centroid along Y-axis	0.0	inch
z_M	Distance to centroid along Z-axis	-8.49784e-016	
y_P	Distance to equal area axis along Y-axis	0.0	inch
z_P	Distance to equal area axis along Z-axis	-0.16	inch
I_{yz}	Moment of inertia Iyz in the user coordinates	0.0	$inch^4$
u_P	Distance to equal area axis along U-axis	0.0	inch
v_P	Distance to equal area axis along V-axis	-0.16	inch

Note: STAAD Section Wizard calculated Torsional moment of inertia is based on summation of the torsional moment of inertia of individual plate elements. Although conservative, this approach can dramatically underestimate the torsional properties of closed hollow sections. For this reason, torsional moment of inertia is approximated by a rectangular hollow tube instead.

Approximate Built-up Hub Section Properties at 1.67ft from Trunnion Centerline Using STAAD Section Wizard

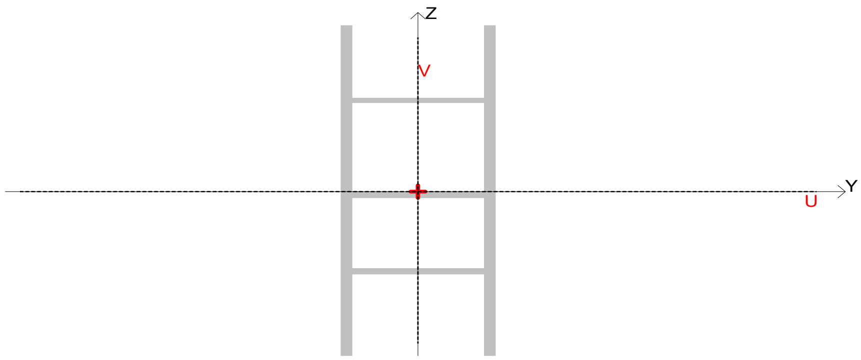

Section element	Rotation angle	Mirror	Material	E (kip/inch^2)
Sheet 26.228 x 0.8125	90.0		Steel	29732.747
Sheet 26.228 x 0.8125	90.0		Steel	29732.747
Sheet 9 x 0.375			Steel	29732.747
Sheet 9 x 0.5			Steel	29732.747
Sheet 9 x 0.5			Steel	29732.747

The overall dimensions of the section are 11 x 26 inch

Basic geometry of the section

	Parameter	Value	
A	Cross sectional area	55.0	$inch^2$
α	Angle between Y-Z and U-V axes	-0.0	deg
I_y	Moment of inertia about axis parallel to Y passing through centroid	2803.3	$inch^4$
I_z	Moment of inertia about axis parallel to Z passing through centroid	1111.81	$inch^4$
I_t	Torsional moment of inertia (St. Venant)	9.67	$inch^4$
i_y	Radius of gyration about axis parallel to Y passing through centroid	7.14	inch
i_z	Radius of gyration about axis parallel to Z passing through centroid	4.5	inch
W_{u+}	Elastic modulus about U-axis (+ve extreme)	211.86	$inch^3$
W_{u-}	Elastic modulus about U-axis (-ve extreme)	215.7	$inch^3$
W_{v+}	Elastic modulus about V-axis (+ve extreme)	209.28	$inch^3$
W_{v-}	Elastic modulus about V-axis (-ve extreme)	209.28	$inch^3$
$W_{pl,u}$	Plastic modulus about axis parallel to U-axis	334.04	$inch^3$
$W_{pl,v}$	Plastic modulus about axis parallel to V-axis	236.57	$inch^3$
I_u	Moment of inertia about U-axis	2803.3	$inch^4$
I_v	Moment of inertia about V-axis	1111.81	$inch^4$
i_u	Radius of gyration about U-axis	7.14	inch
i_v	Radius of gyration about V-axis	4.5	inch
a_{u+}	Centroid to edge of compression zone along +ve U-axis	3.81	inch
a_{u-}	Centroid to edge of compression zone along -ve U-axis	3.81	inch
a_{v+}	Centroid to edge of compression zone along +ve V-axis	3.85	inch

Torsion moment of inertia is replaced by torsion property of an approximate hollow rectangular section

a_{V-}	Centroid to edge of compression zone along -ve V-axis	3.92	inch
y_M	Distance to centroid along Y-axis	0.0	inch
z_M	Distance to centroid along Z-axis	-1.50381e-015	
y_P	Distance to equal area axis along Y-axis	0.0	inch
z_P	Distance to equal area axis along Z-axis	-0.25	inch
I_{yz}	Moment of inertia Iyz in the user coordinates	0.0	$inch^4$
u_P	Distance to equal area axis along U-axis	0.0	inch
v_P	Distance to equal area axis along V-axis	-0.25	inch

Note: STAAD Section Wizard calculated Torsional moment of inertia is based on summation of the torsional moment of inertia of individual plate elements. Although conservative, this approach can dramatically underestimate the torsional properties of closed hollow sections. For this reason, torsional moment of inertia is approximated by a rectangular hollow tube instead.

Approximate Built-up Hub Section Properties at 2.39ft from Trunnion Centerline Using STAAD Section Wizard

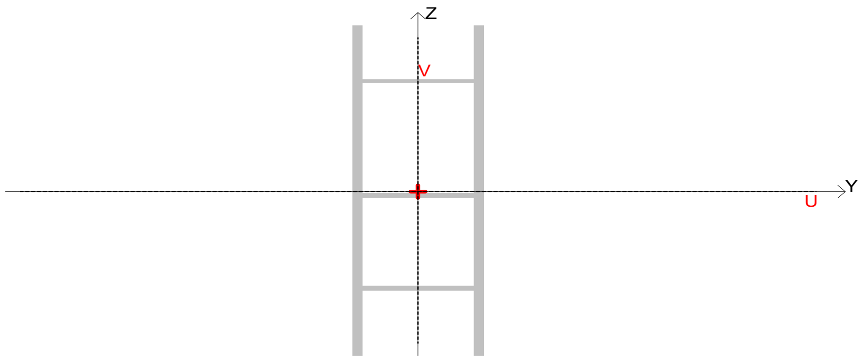

Section element	Rotation angle	Mirror	Material	E (kip/inch^2)
Sheet 31.324 x 0.8125	90.0		Steel	29732.747
Sheet 31.324 x 0.8125	90.0		Steel	29732.747
Sheet 9 x 0.375			Steel	29732.747
Sheet 9 x 0.5			Steel	29732.747
Sheet 9 x 0.5			Steel	29732.747

The overall dimensions of the section are 11 x 31 inch

Basic geometry of the section

	Parameter	Value	
A	Cross sectional area	63.28	$inch^2$
α	Angle between Y-Z and U-V axes	-0.0	deg
I_y	Moment of inertia about axis parallel to Y passing through centroid	4905.13	$inch^4$
I_z	Moment of inertia about axis parallel to Z passing through centroid	1311.6	$inch^4$
I_t	Torsional moment of inertia (St. Venant)	11.39	$inch^4$
i_y	Radius of gyration about axis parallel to Y passing through centroid	8.8	inch
i_z	Radius of gyration about axis parallel to Z passing through centroid	4.55	inch
W_{u+}	Elastic modulus about U-axis (+ve extreme)	310.33	$inch^3$
W_{u-}	Elastic modulus about U-axis (-ve extreme)	316.1	$inch^3$
W_{v+}	Elastic modulus about V-axis (+ve extreme)	246.89	$inch^3$
W_{v-}	Elastic modulus about V-axis (-ve extreme)	246.89	$inch^3$
$W_{pl,u}$	Plastic modulus about axis parallel to U-axis	476.6	$inch^3$
$W_{pl,v}$	Plastic modulus about axis parallel to V-axis	277.03	$inch^3$
I_u	Moment of inertia about U-axis	4905.13	$inch^4$
I_v	Moment of inertia about V-axis	1311.6	$inch^4$
i_u	Radius of gyration about U-axis	8.8	inch
i_v	Radius of gyration about V-axis	4.55	inch
a_{u+}	Centroid to edge of compression zone along +ve U-axis	3.9	inch
a_{u-}	Centroid to edge of compression zone along -ve U-axis	3.9	inch
a_{v+}	Centroid to edge of compression zone along +ve V-axis	4.9	inch

Torsion moment of inertia is replaced by torsion property of an approximate hollow rectangular section

a_{V-}	Centroid to edge of compression zone along -ve V-axis	5.0	inch
y_M	Distance to centroid along Y-axis	0.0	inch
z_M	Distance to centroid along Z-axis	2.09121e-016	
y_P	Distance to equal area axis along Y-axis	0.0	inch
z_P	Distance to equal area axis along Z-axis	-0.36	inch
I_{yz}	Moment of inertia Iyz in the user coordinates	0.0	$inch^4$
u_P	Distance to equal area axis along U-axis	0.0	inch
v_P	Distance to equal area axis along V-axis	-0.36	inch

Note: STAAD Section Wizard calculated Torsional moment of inertia is based on summation of the torsional moment of inertia of individual plate elements. Although conservative, this approach can dramatically underestimate the torsional properties of closed hollow sections. For this reason, torsional moment of inertia is approximated by a rectangular hollow tube instead.

Attachment B

STAAD Model Node Numbers and Member Numbers

Skin-Rib Composite Node Numbers

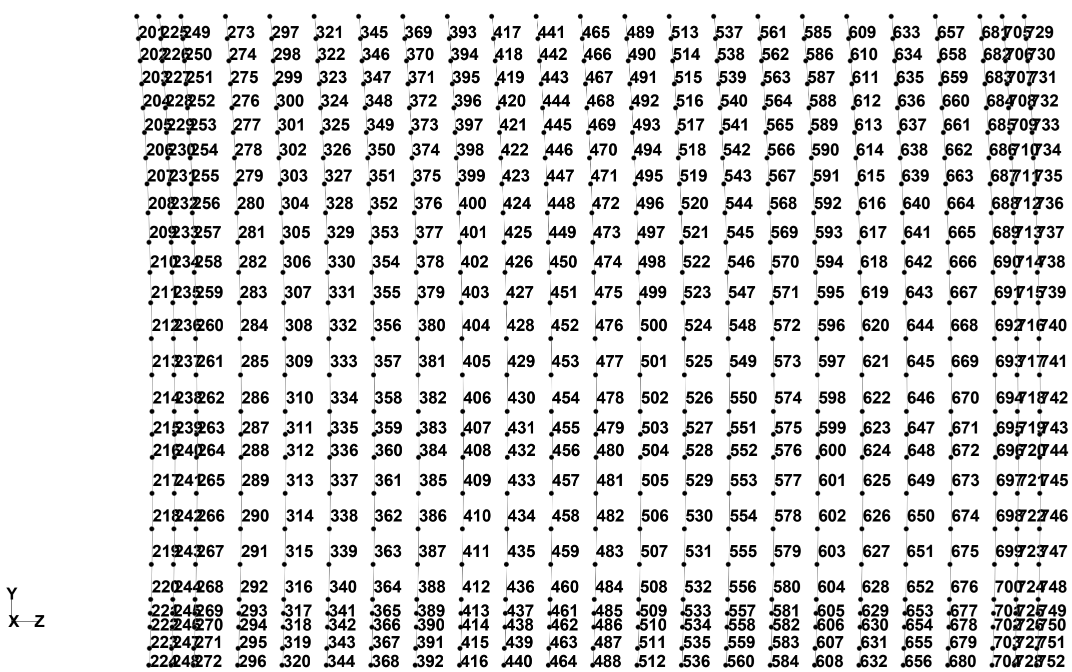

Skin-Rib Composite Member Numbers

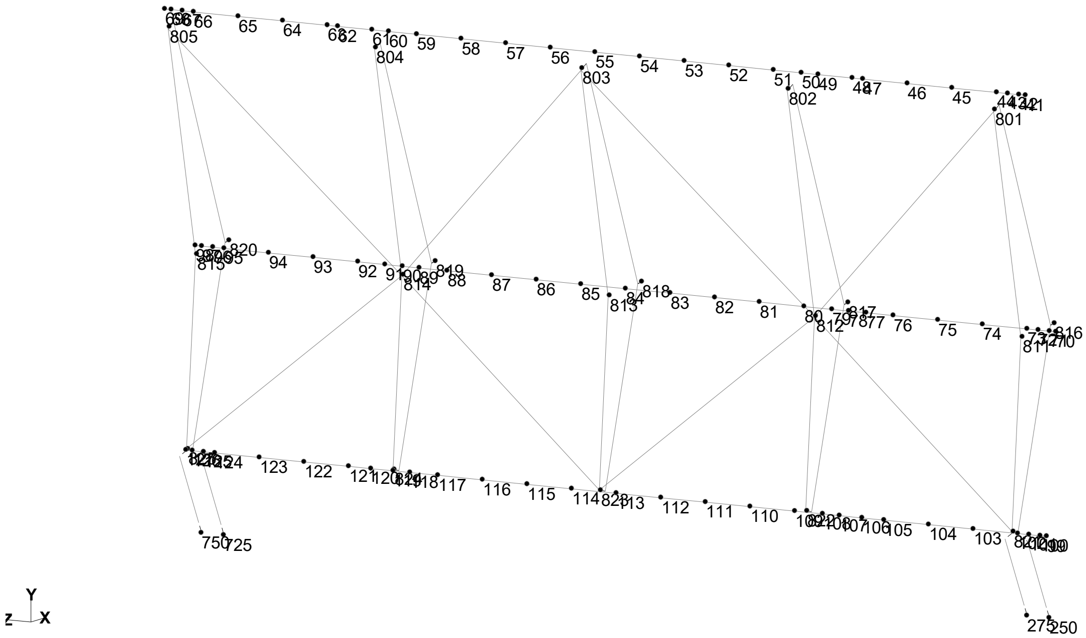

Girder and Girder Brace Node Numbers

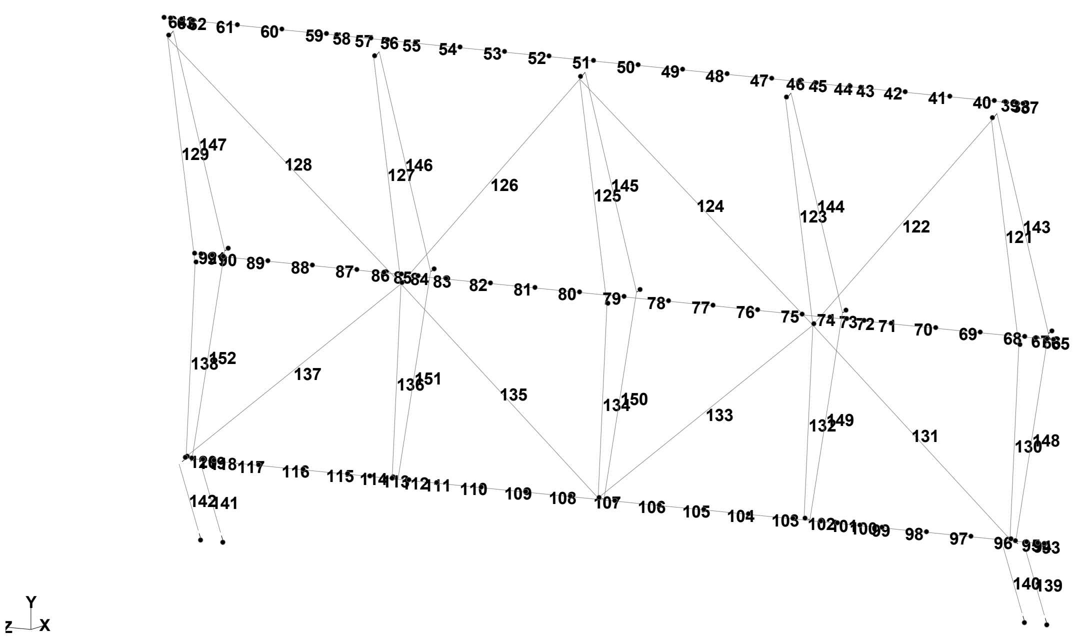

Girder and Girder Brace Member Numbers

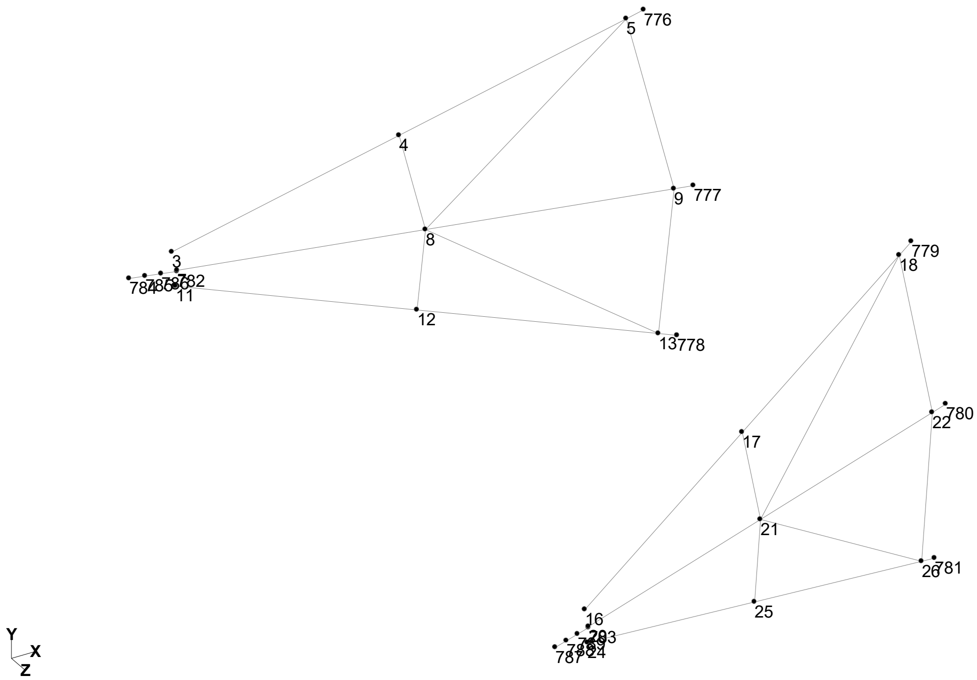

Built-up Hub, Strut, and Strut Bracing Node Numbers

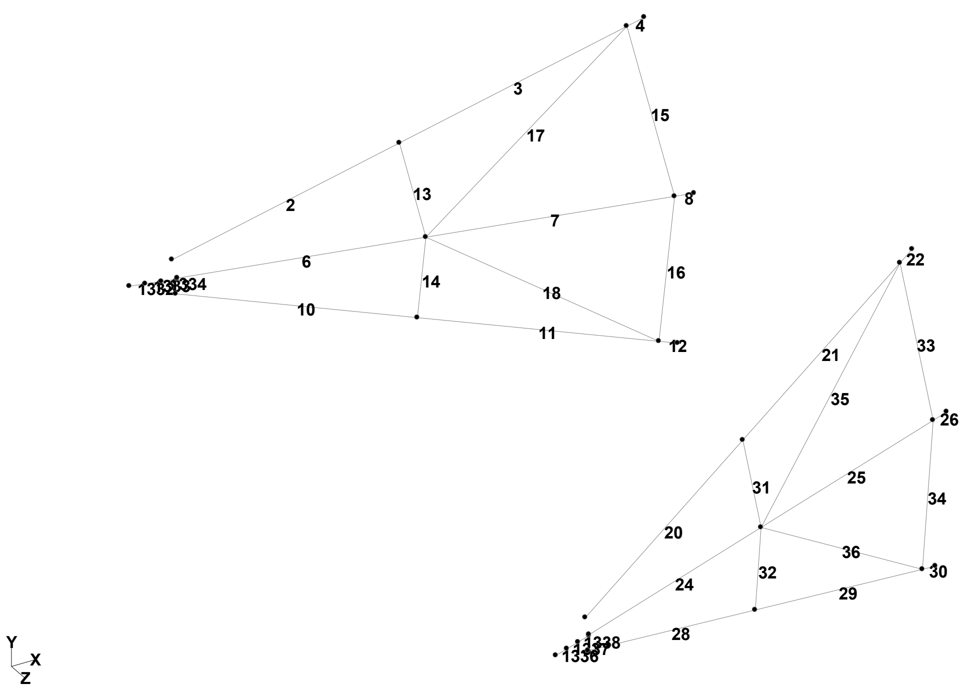

Built-up Hub, Strut, and Strut Bracing Member Numbers

Attachment C

STAAD Model Load Diagrams

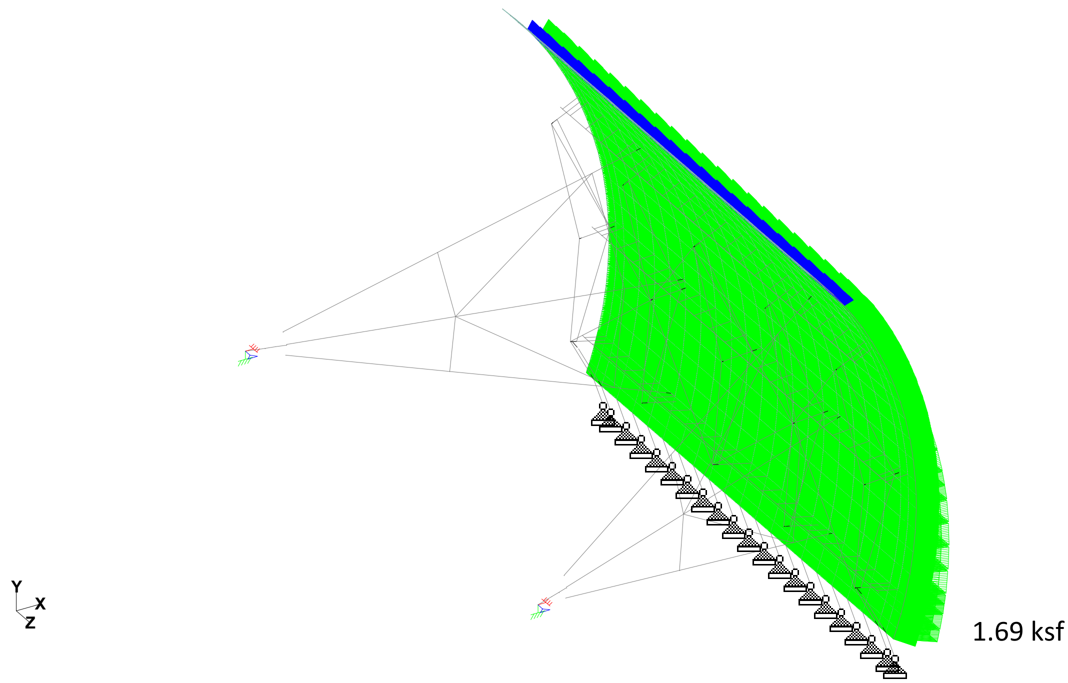

Hydrostatic Load H_1, Reservoir Elevation 435.5 ft

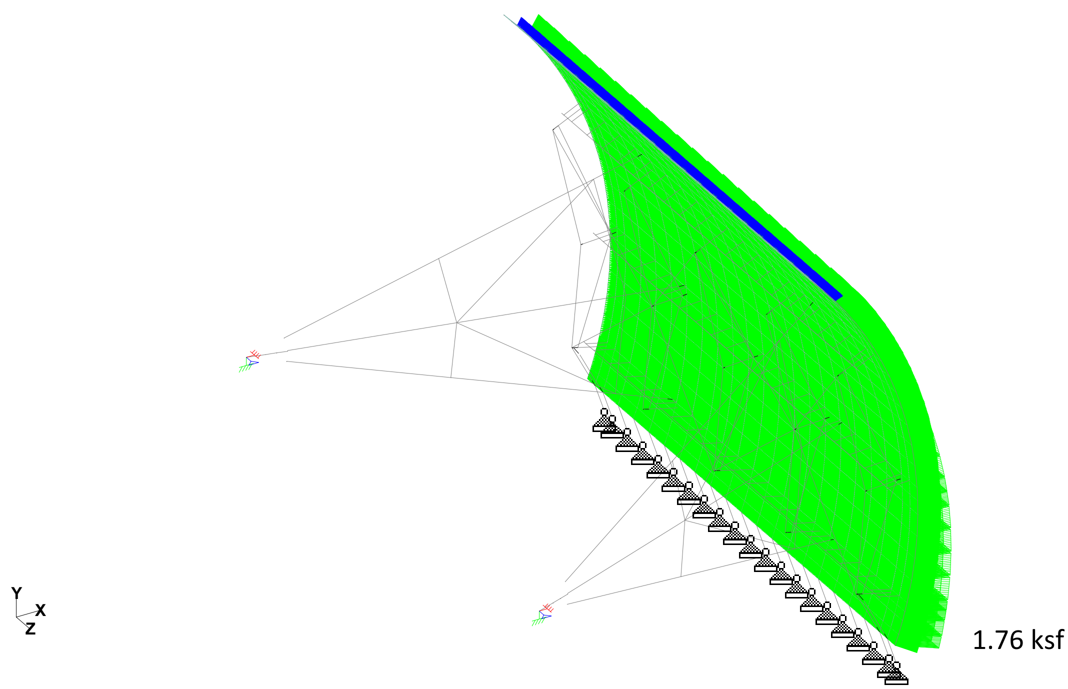

Hydrostatic Load H_2, Reservoir Elevation 436.5 ft

Notes: All load values shown are unfactored values

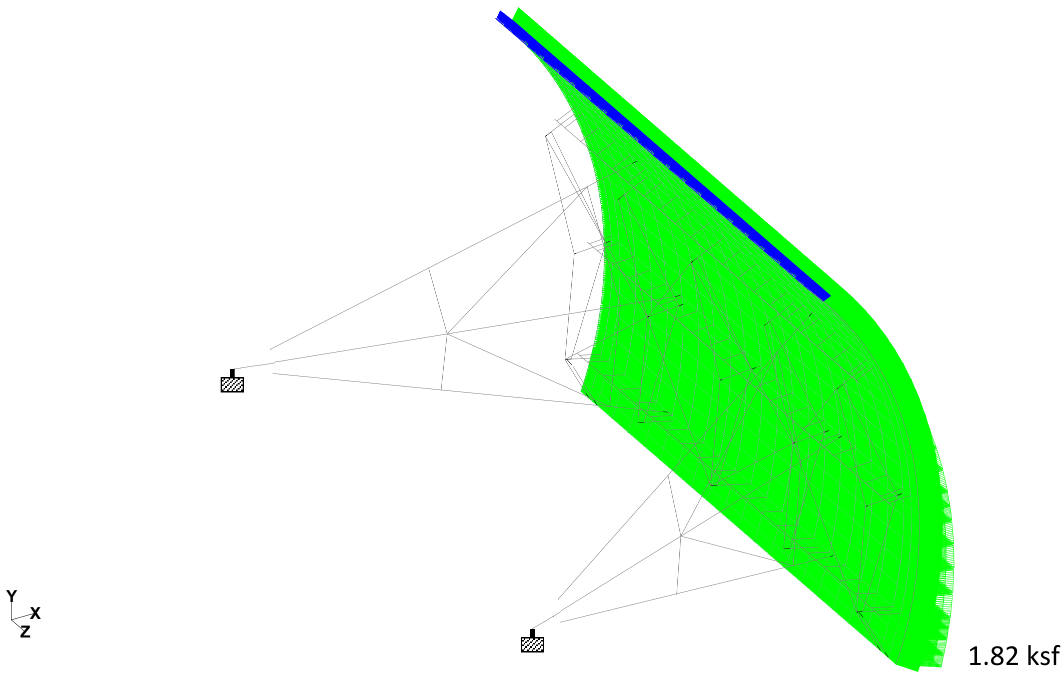

Hydrostatic Load H_3, Reservoir Elevation 437.5 ft

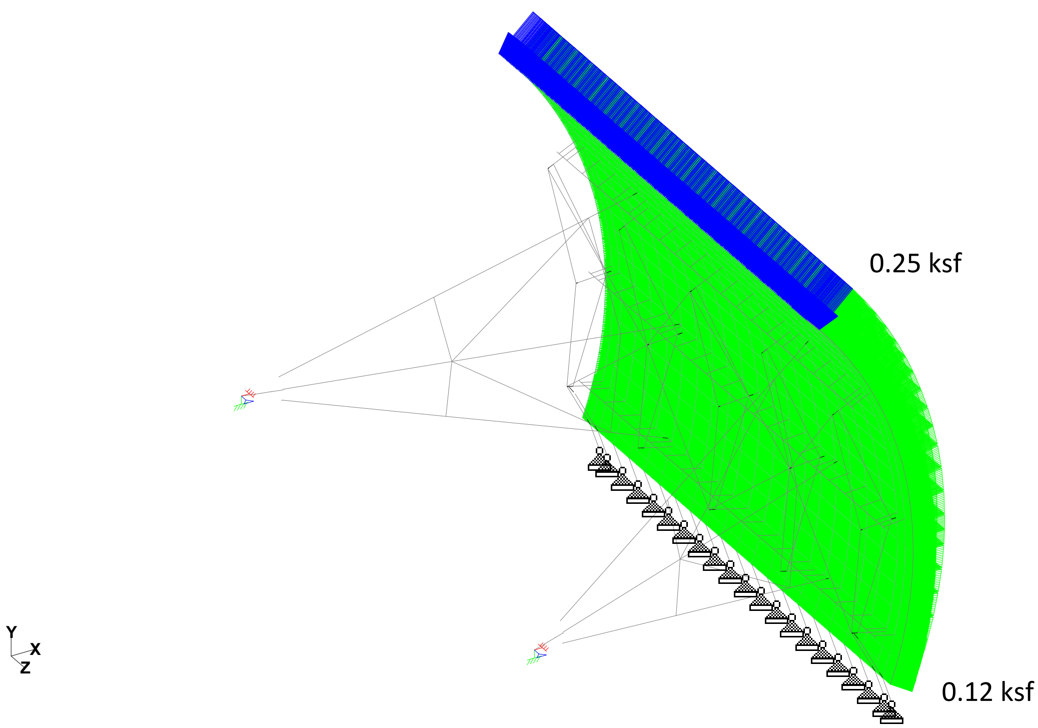

Hydrostatic Equivalent Wave Load W_A

Notes: All load values shown are unfactored values

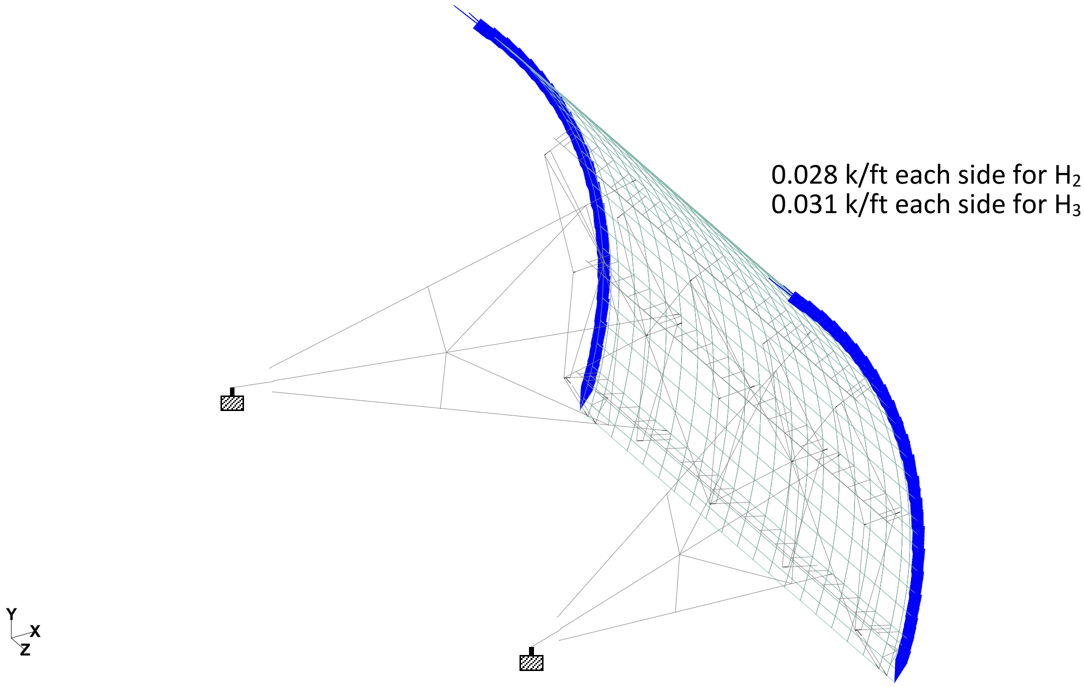

Side Seal Friction Load F_s

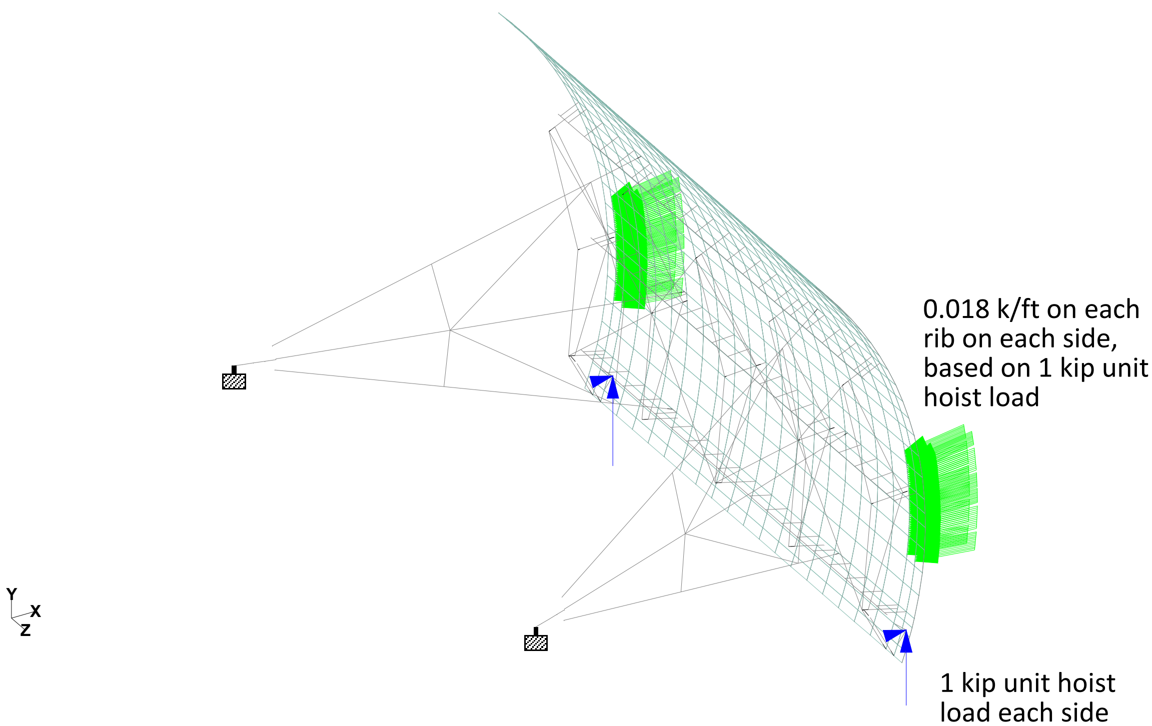

Unit Cable Hoist Lifting Load

Notes: All load values shown are unfactored values

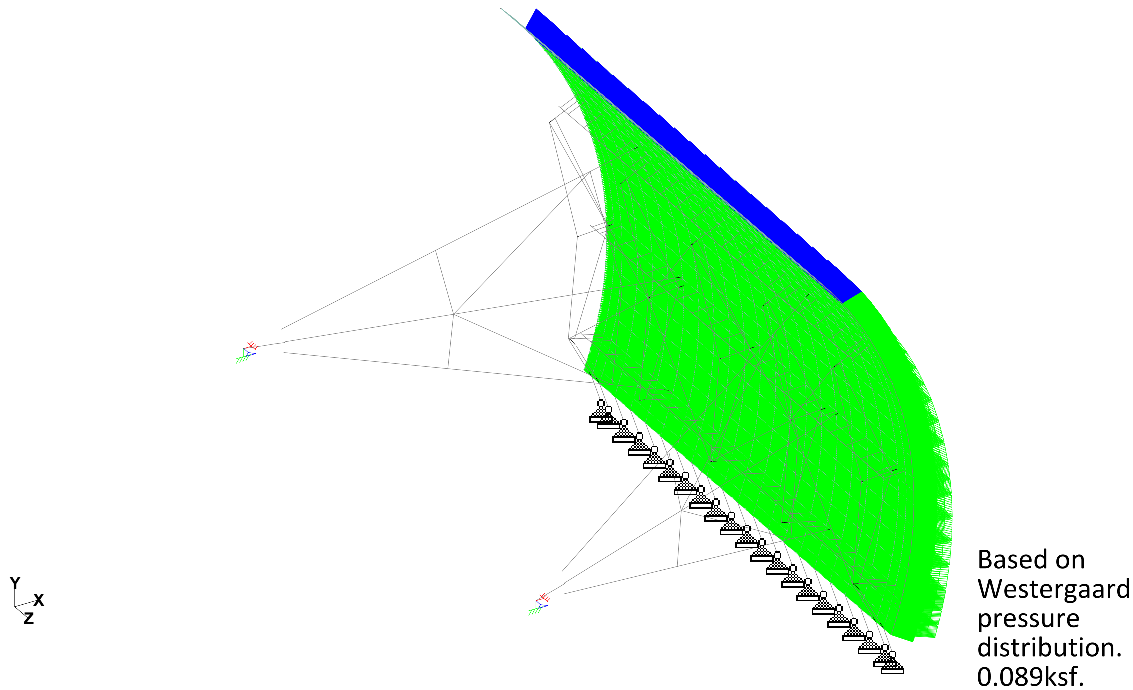

Seismic Hydrodynamic Load H_{EQ}, Reservoir Elevation 435.5 ft

Notes: All load values shown are unfactored values

Attachment D

Member Interaction Values (Utilization Ratios) for Different Load Combinations

STAAD Analysis Member Interaction Values (Utilization Ratios)

Gate Closed Load Combination LC1a – Base Case

Software licensed to Schnabel Engineering, Inc CONNECTED User: Charles Denq	Job No 20C22001.00.0	Sheet No 1	Rev 0
	Part LC1a â€“ Gate closed		
Job Title Forney Dam Tainter Gate Analysis	Ref 1.2D + 1.4 H2		
	By Charles Denq	Date 8/30/2020	Chd
Client GARVER FOR DWU	File FDLC1a.STD	Date/Time 22-Jul-2021 22:56	

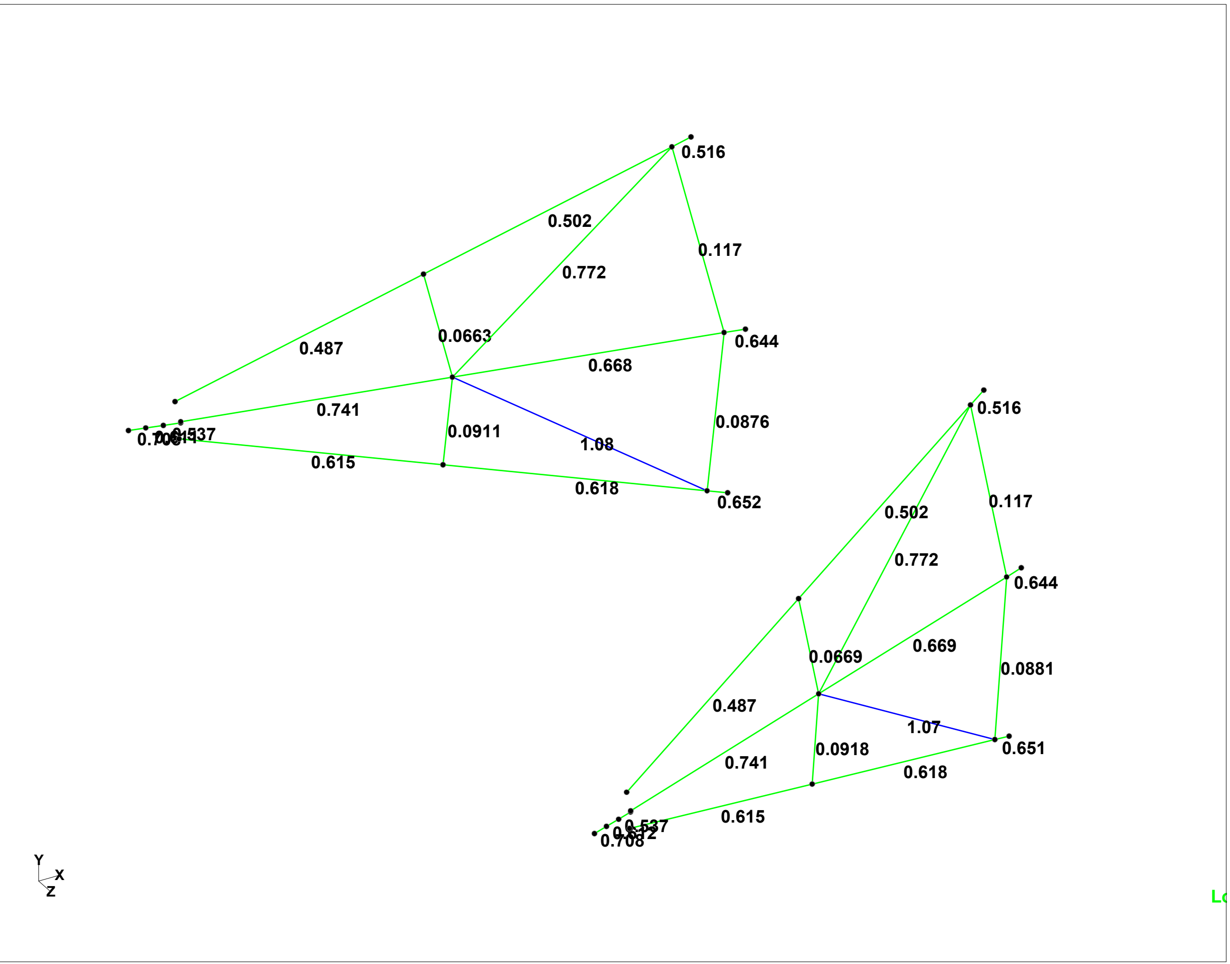

Arm Struts and Trunnion Hubs Member Utilization Ratios

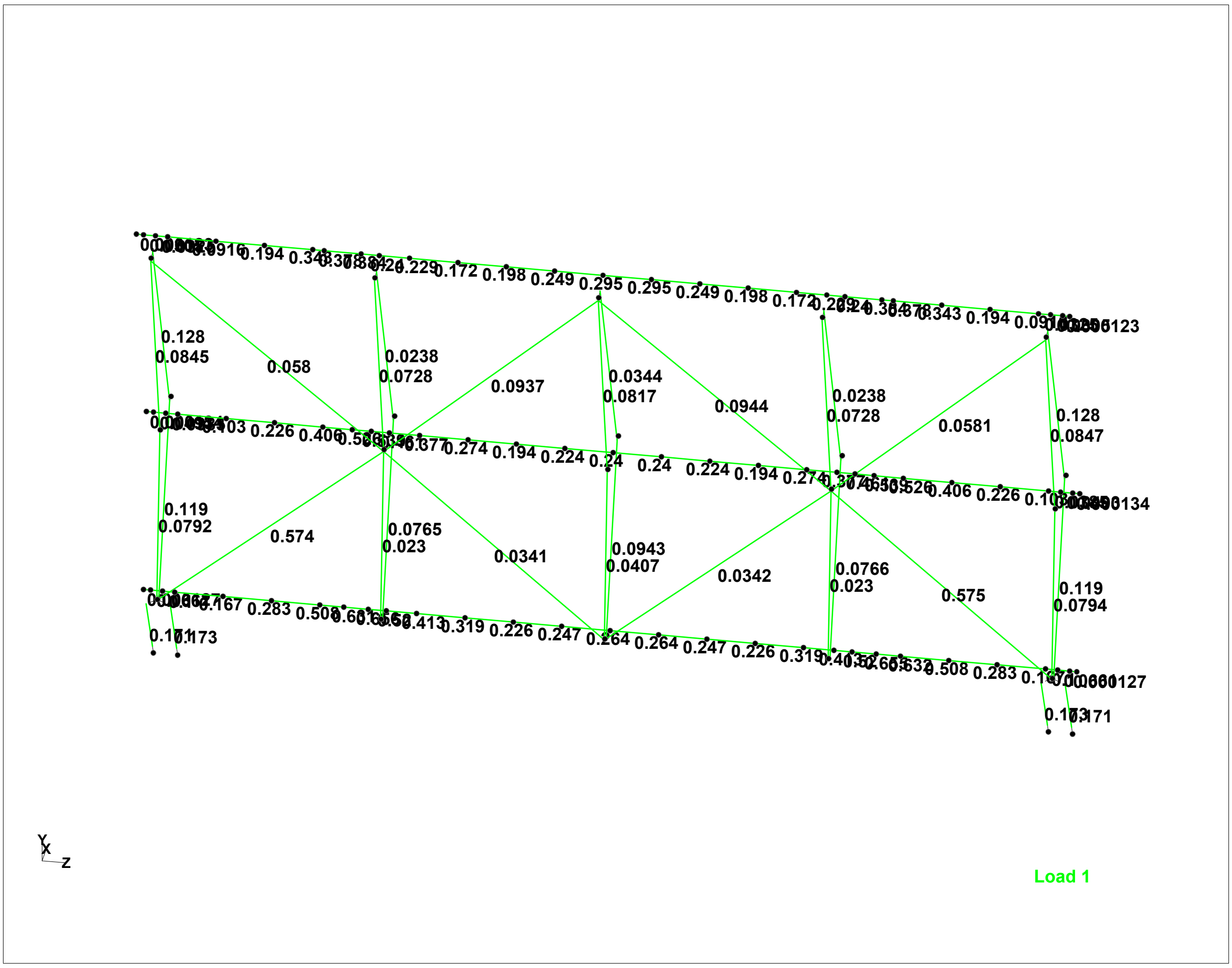

Horizontal Girders and Braces Member Utilization Ratios

	Job No	Sheet No	Rev
Software licensed to Schnabel Engineering, Inc CONNECTED User: Charles Denq	20C22001.00.0	3	0
	Part LC1a â€“ Gate closed		
Job Title Forney Dam Tainter Gate Analysis	Ref 1.2D + 1.4 H2		
	By Charles Denq	Date 8/30/2020	Chd
Client GARVER FOR DWU	File FDLC1a.STD	Date/Time 22-Jul-2021 22:56	

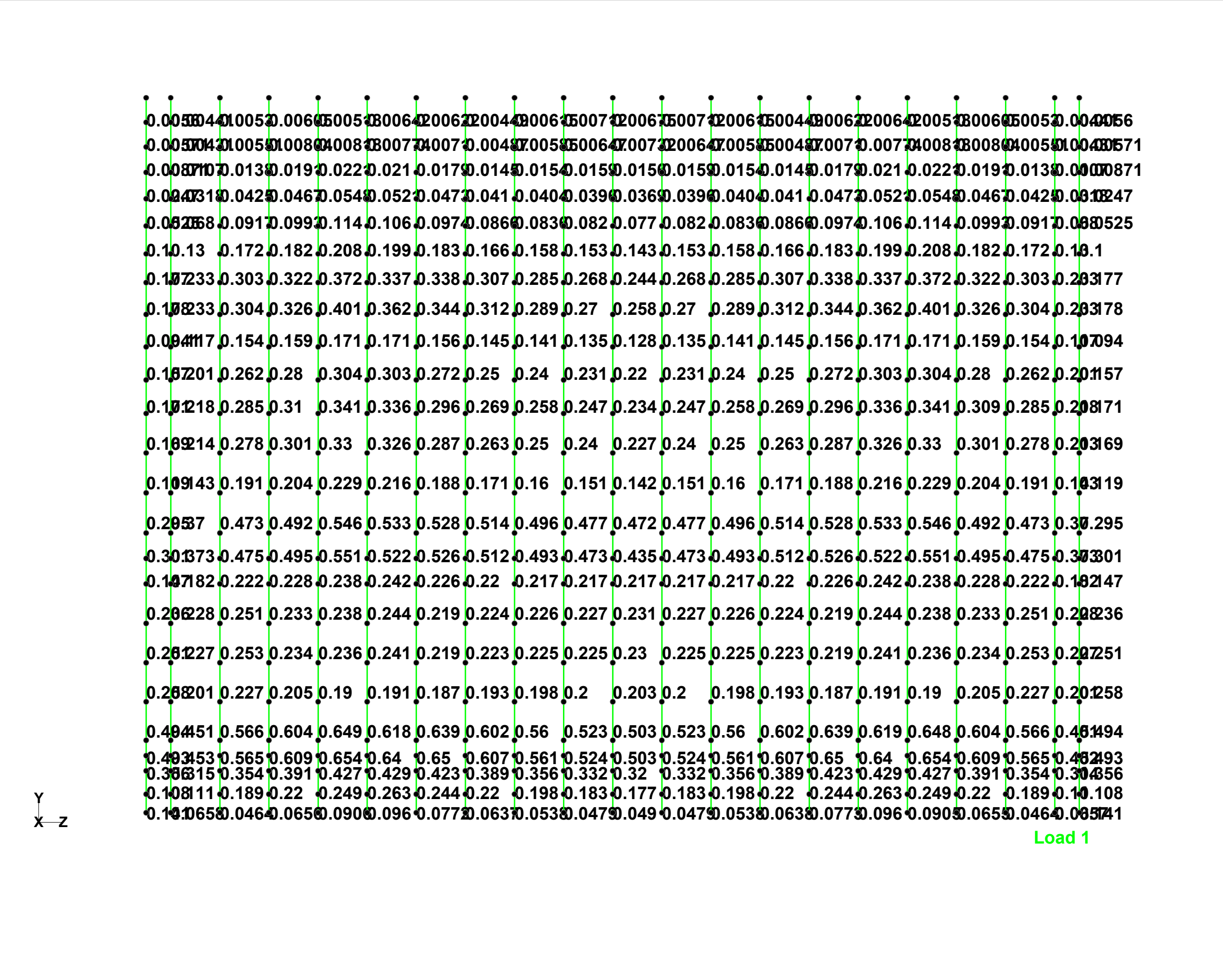

Skin-Rib Composite Member Utilization Ratios

STAAD Analysis Member Interaction Values (Utilization Ratios)

Gate Closed Load Combination LC1b – Wave

Software licensed to Schnabel Engineering, Inc CONNECTED User: Charles Denq	Job No **20C22001.00.0**	Sheet No **1**	Rev 0
	Part LC1b â€“ Gate closed with wave load		
Job Title Forney Dam Tainter Gate Analysis	Ref 1.2D + 1.4 H2 + 1.2WA		
	By Charles Denq	Date 8/30/2020	Chd
Client GARVER FOR DWU	File FDLC1b.STD	Date/Time 22-Jul-2021 23:44	

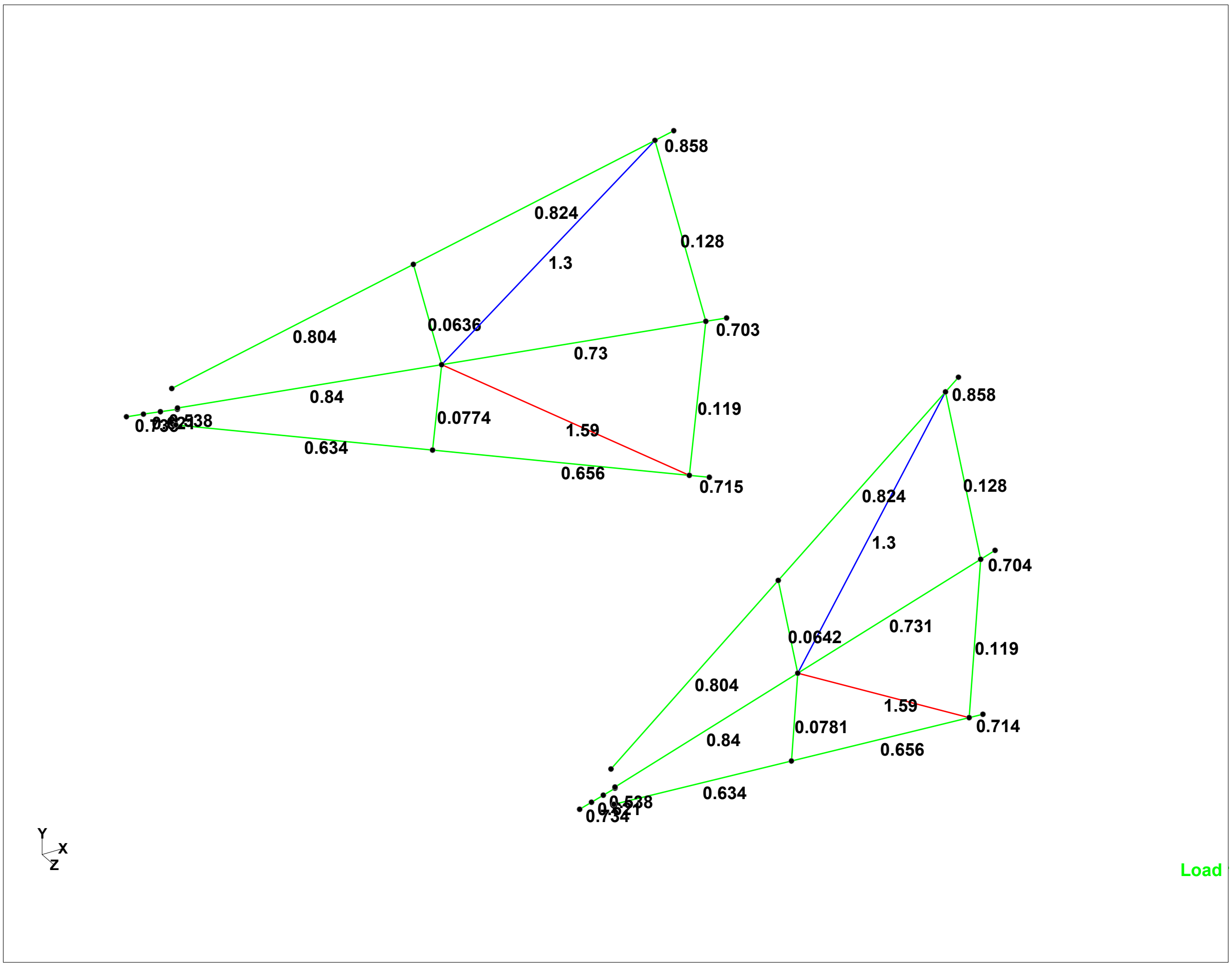

Arm Struts and Trunnion Hubs Member Utilization Ratios

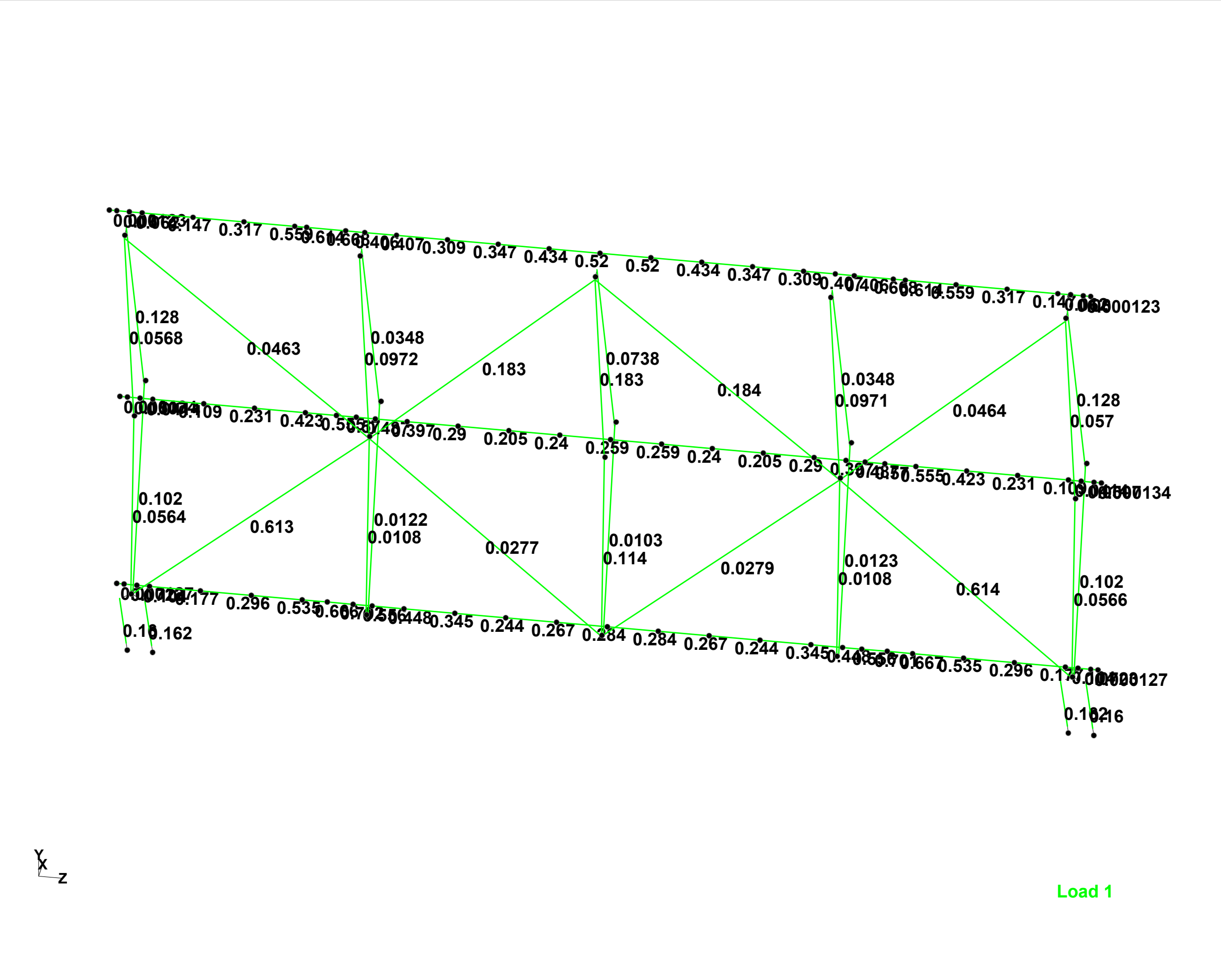

Horizontal Girders and Braces Member Utilization Ratios

Software licensed to Schnabel Engineering, Inc CONNECTED User: Charles Denq	Job No **20C22001.00.0**	Sheet No **3**	Rev 0
	Part LC1b â€“ Gate closed with wave load		
Job Title Forney Dam Tainter Gate Analysis	Ref 1.2D + 1.4 H2 + 1.2WA		
	By Charles Denq	Date 8/30/2020	Chd
Client GARVER FOR DWU	File FDLC1b.STD	Date/Time 22-Jul-2021 23:44	

Skin-Rib Composite Member Utilization Ratios

STAAD Analysis Member Interaction Values (Utilization Ratios)

Gate Closed Load Combination LC4b – Earthquake (Horizontal)

Software licensed to Schnabel Engineering, Inc CONNECTED User: Charles Denq	Job No **20C22001.00.0**	Sheet No **1**	Rev 0
	Part LC4b â€“ Gate closed with earthquake		
Job Title Forney Dam Tainter Gate Analysis	Ref 1.2D + 1.4 H1 + 1.0E		
	By Charles Denq	Date 8/30/2020	Chd
Client GARVER FOR DWU	File FDLC4b.STD	Date/Time 23-Jul-2021 01:49	

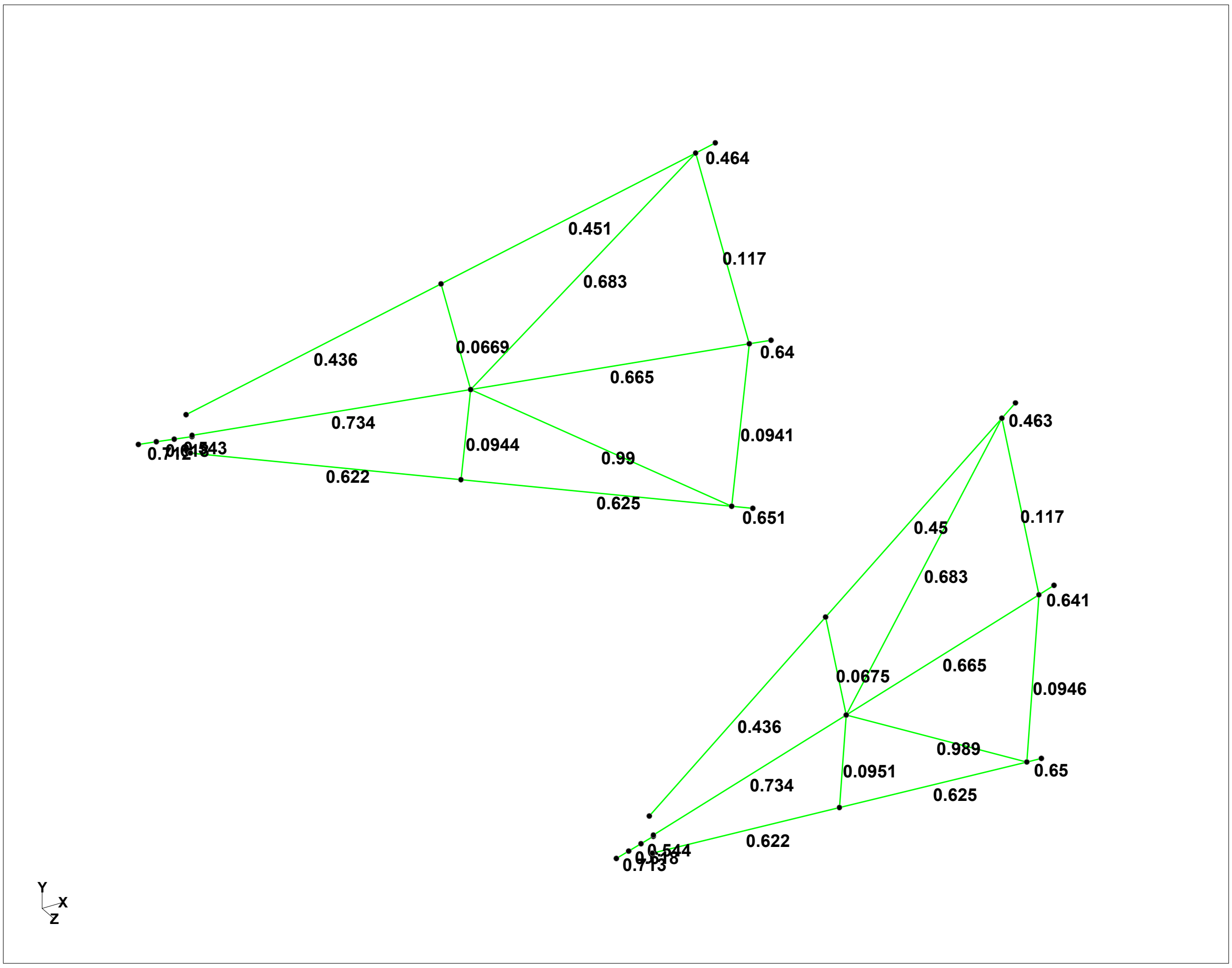

Arm Struts and Trunnion Hubs Member Utilization Ratios

Software licensed to Schnabel Engineering, Inc CONNECTED User: Charles Denq	Job No **20C22001.00.0**	Sheet No **2**	Rev 0
	Part LC4b â€“ Gate closed with earthquake		
Job Title Forney Dam Tainter Gate Analysis	Ref 1.2D + 1.4 H1 + 1.0E		
	By Charles Denq	Date 8/30/2020	Chd
Client GARVER FOR DWU	File FDLC4b.STD	Date/Time 23-Jul-2021 01:49	

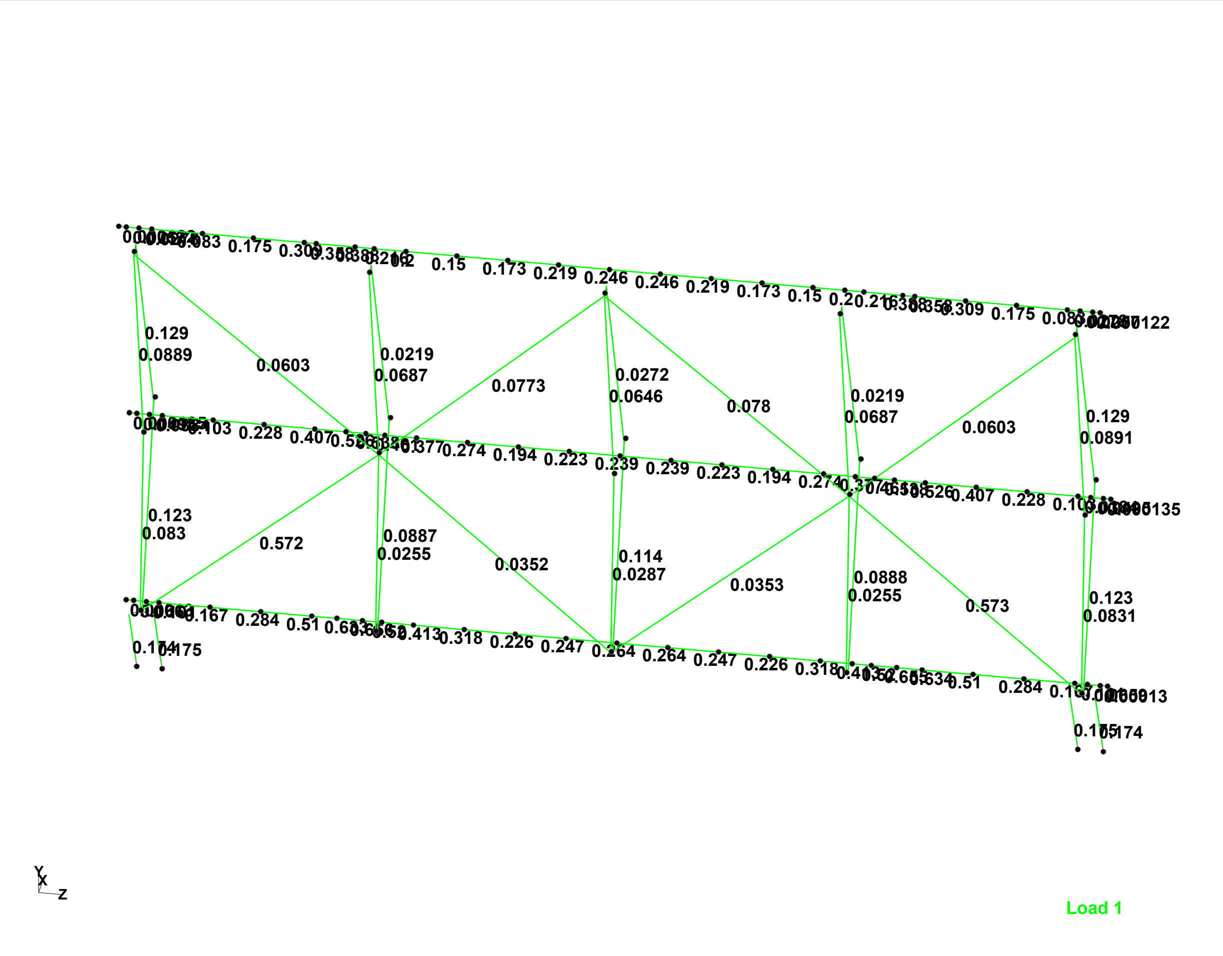

Horizontal Girders and Braces Member Utilization Ratios

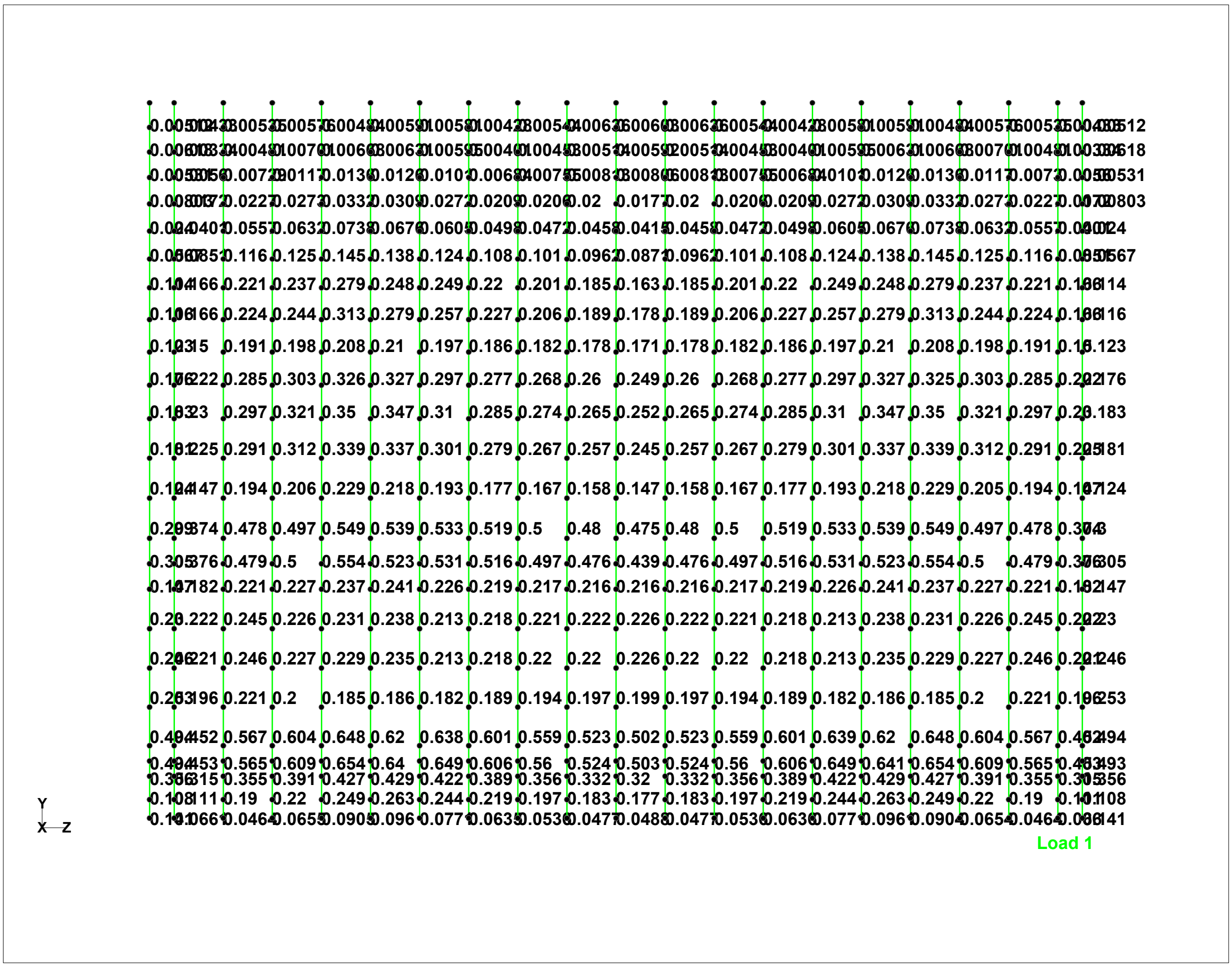

Skin-Rib Composite Member Utilization Ratios

STAAD Analysis Member Interaction Values (Utilization Ratios)

Gate Closed Load Combination LC4b – Earthquake (Vertical)

Software licensed to Schnabel Engineering, Inc CONNECTED User: Charles Denq	Job No **20C22001.00.0**	Sheet No **1**	Rev 0
	Part LC4b â€“ Gate closed with earthquake		
Job Title Forney Dam Tainter Gate Analysis	Ref 1.2D + 1.4 H1 + 1.0E		
	By Charles Denq	Date 8/30/2020	Chd
Client GARVER FOR DWU	File FDLC4b.STD	Date/Time 23-Jul-2021 01:53	

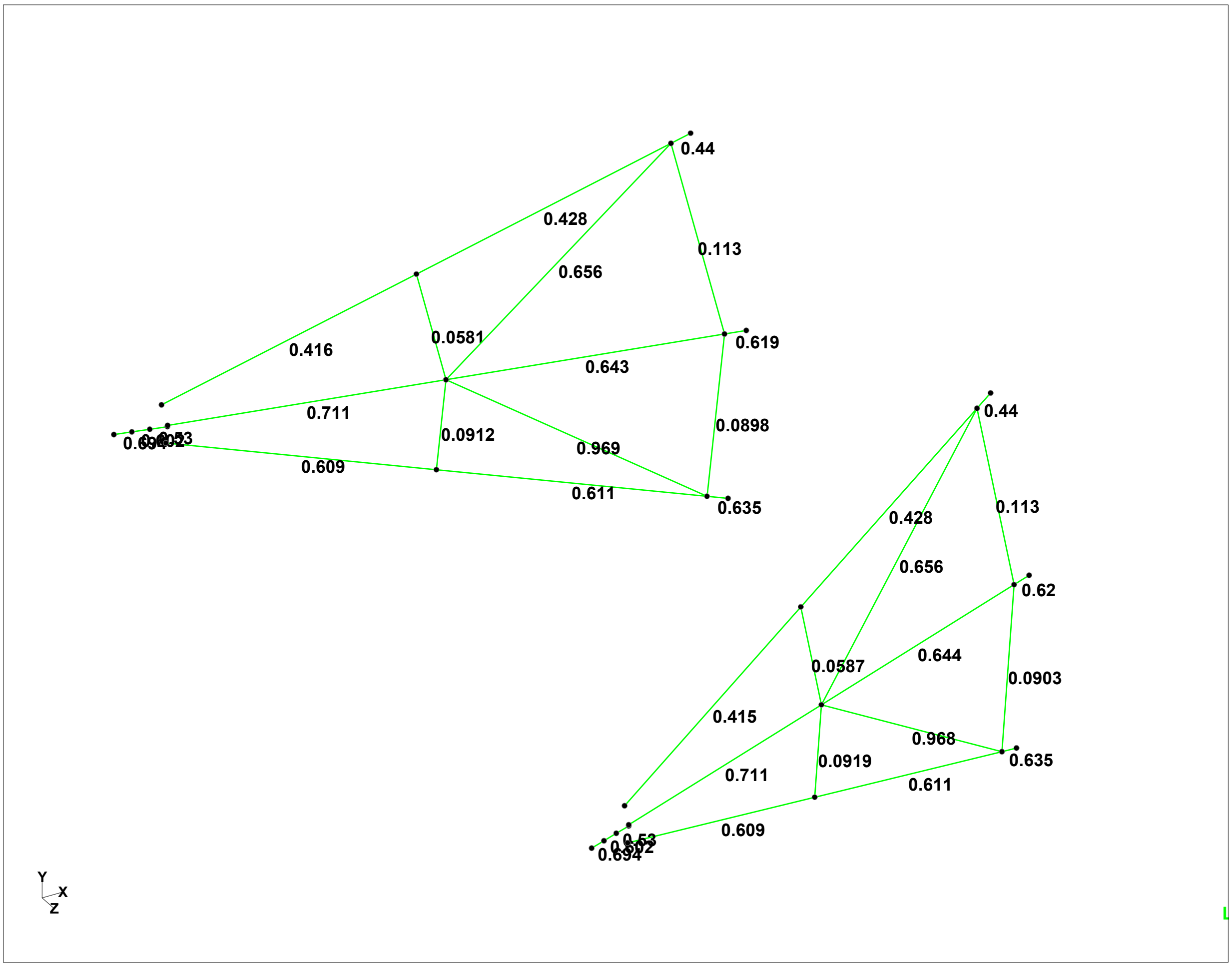

Arm Struts and Trunnion Hubs Member Utilization Ratios

Software licensed to Schnabel Engineering, Inc CONNECTED User: Charles Denq	Job No **20C22001.00.0**	Sheet No **2**	Rev 0
	Part LC4b â€“ Gate closed with earthquake		
Job Title Forney Dam Tainter Gate Analysis	Ref 1.2D + 1.4 H1 + 1.0E		
	By Charles Denq	Date 8/30/2020	Chd
Client GARVER FOR DWU	File FDLC4b.STD	Date/Time 23-Jul-2021 01:53	

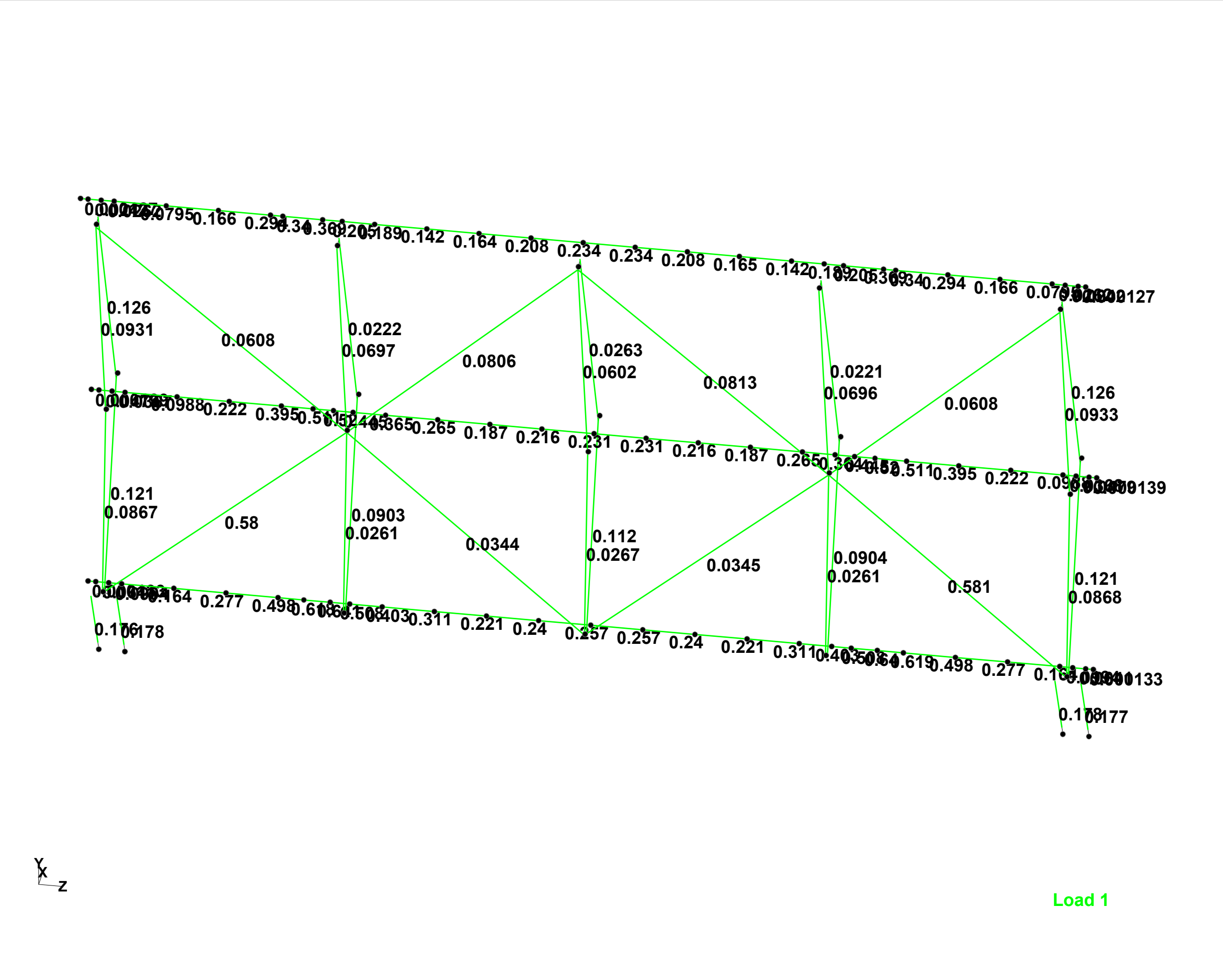

Horizontal Girders and Braces Member Utilization Ratios

	Job No	Sheet No	Rev
Software licensed to Schnabel Engineering, Inc CONNECTED User: Charles Denq	20C22001.00.0	3	0
	Part LC4b â€“ Gate closed with earthquake		
Job Title Forney Dam Tainter Gate Analysis	Ref 1.2D + 1.4 H1 + 1.0E		
	By Charles Denq	Date 8/30/2020	Chd
Client GARVER FOR DWU	File FDLC4b.STD	Date/Time 23-Jul-2021 01:53	

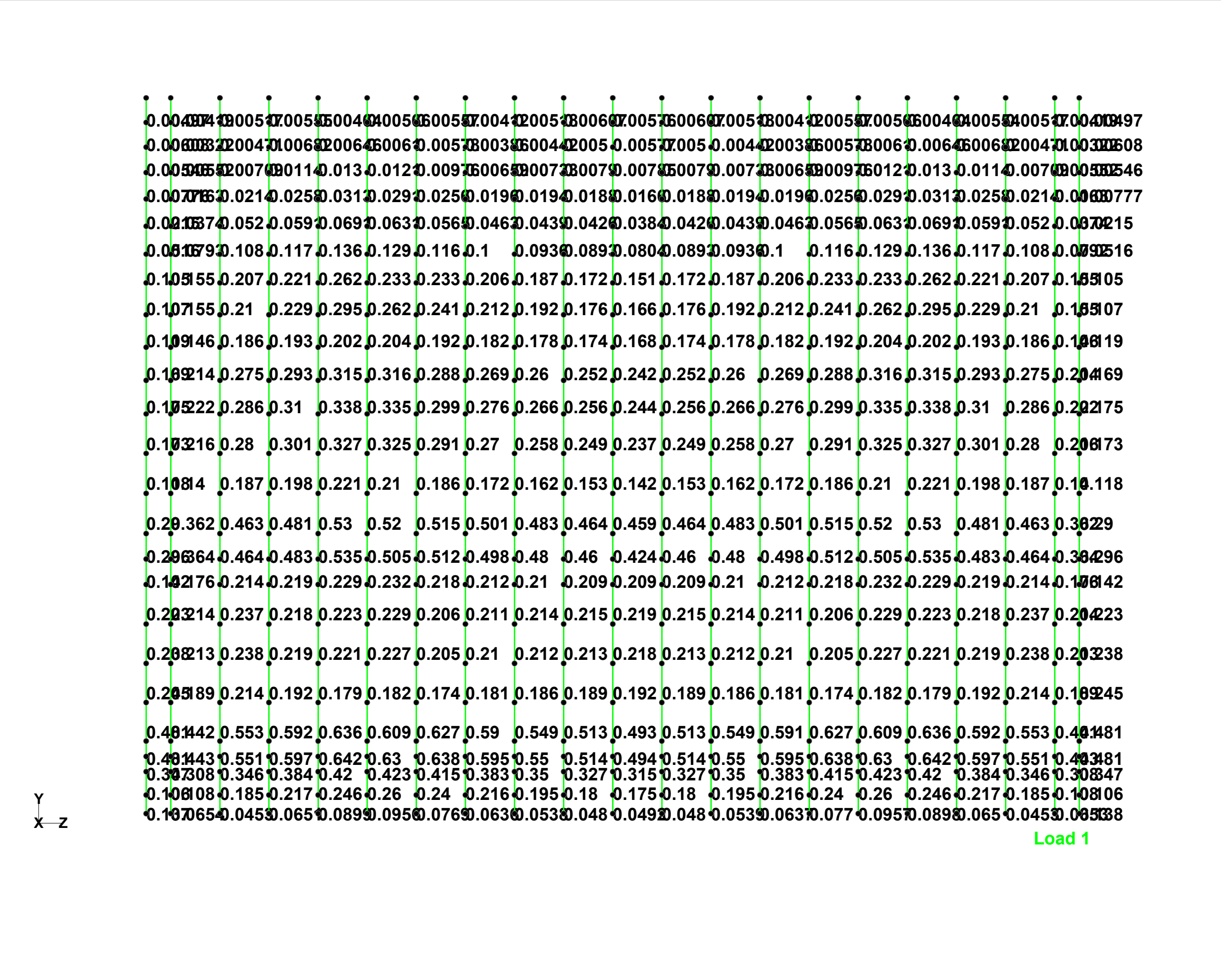

Skin-Rib Composite Member Utilization Ratios

STAAD Analysis Member Interaction Values (Utilization Ratios)

Gate Operating Load Combination LC2a – Base Case (Opening)

Software licensed to Schnabel Engineering, Inc
CONNECTED User: Charles Denq

Job No 20C22001.00.0	Sheet No 1	Rev 0	
Part LC2a â€“ Gate operating			
Job Title Forney Dam Tainter Gate Analysis	Ref 1.2D + 1.4 H3 + 1.4 Fs + 1.0 Ft + Qh		
	By Charles Denq	Date 8/30/2020	Chd
Client GARVER FOR DWU	File FDLC2a.STD	Date/Time 23-Jul-2021 00:01	

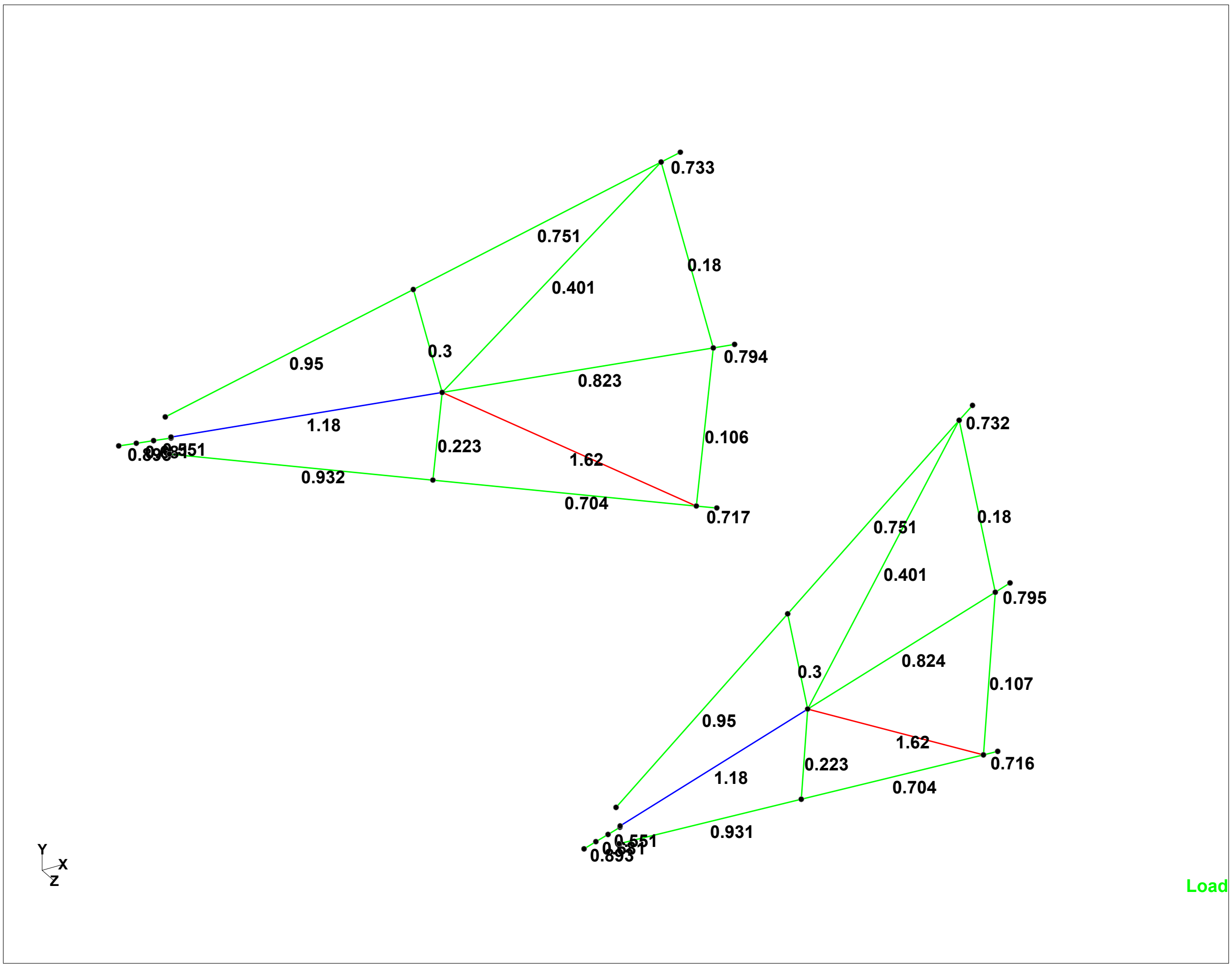

Arm Struts and Trunnion Hubs Member Utilization Ratios

Software licensed to Schnabel Engineering, Inc CONNECTED User: Charles Denq	Job No **20C22001.00.0**	Sheet No **2**	Rev 0
	Part LC2a â€" Gate operating		
Job Title Forney Dam Tainter Gate Analysis	Ref 1.2D + 1.4 H3 + 1.4 Fs + 1.0 Ft + Qh		
	By Charles Denq	Date 8/30/2020	Chd
Client GARVER FOR DWU	File FDLC2a.STD	Date/Time 23-Jul-2021 00:01	

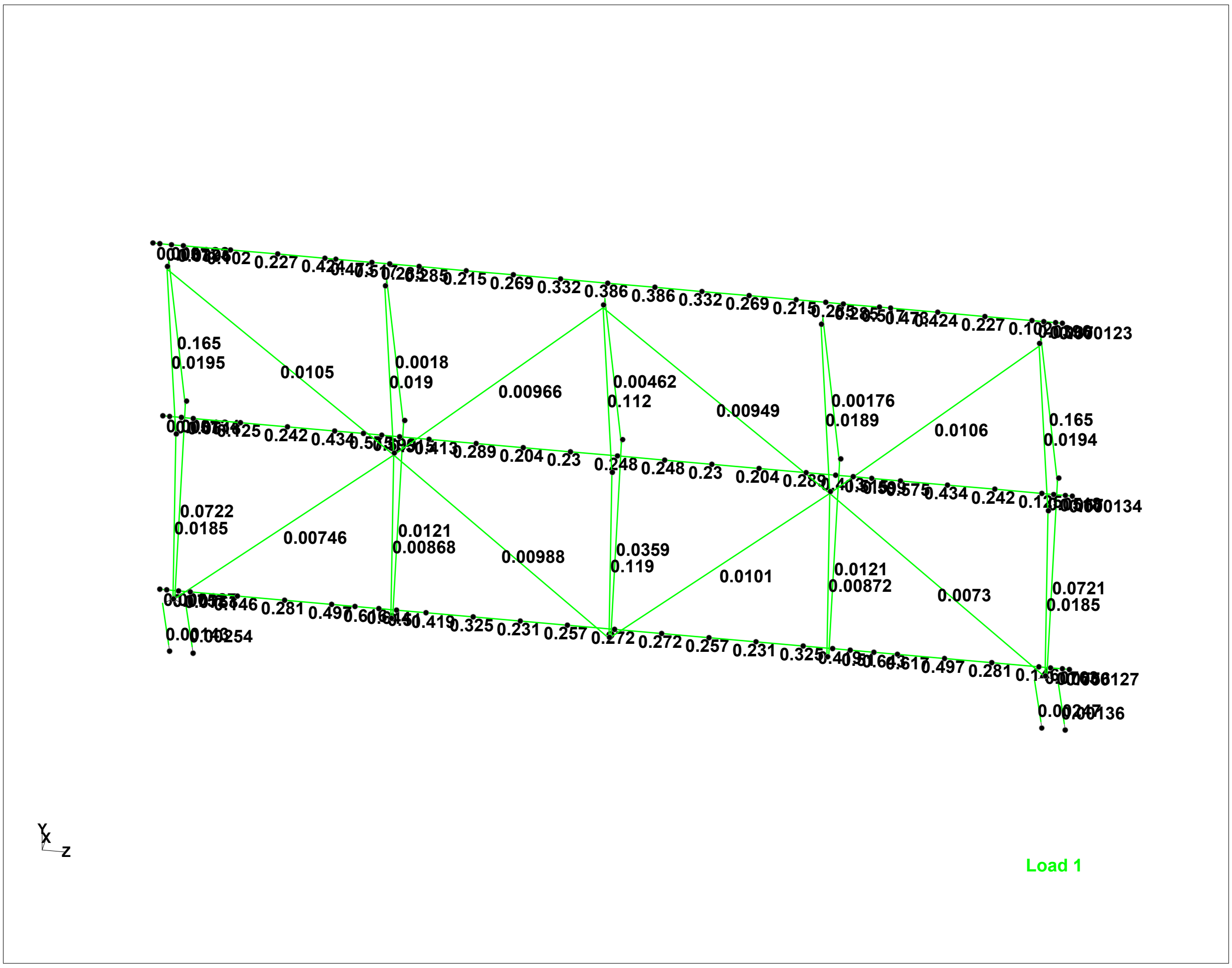

Horizontal Girders and Braces Member Utilization Ratios

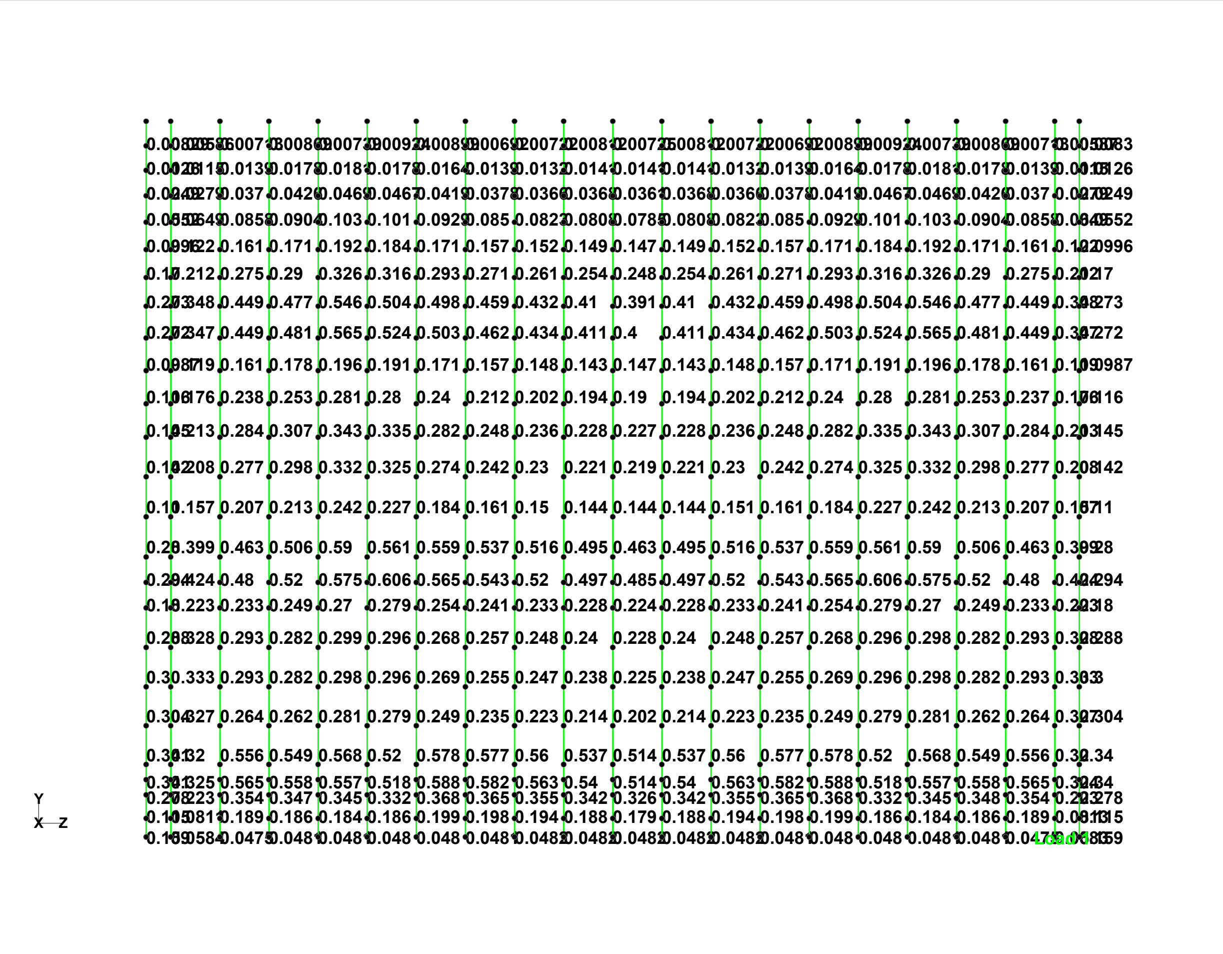

Skin-Rib Composite Member Utilization Ratios

STAAD Analysis Member Interaction Values (Utilization Ratios)

Gate Operating Load Combination LC2aU – Base Case (Closing), Unfactored

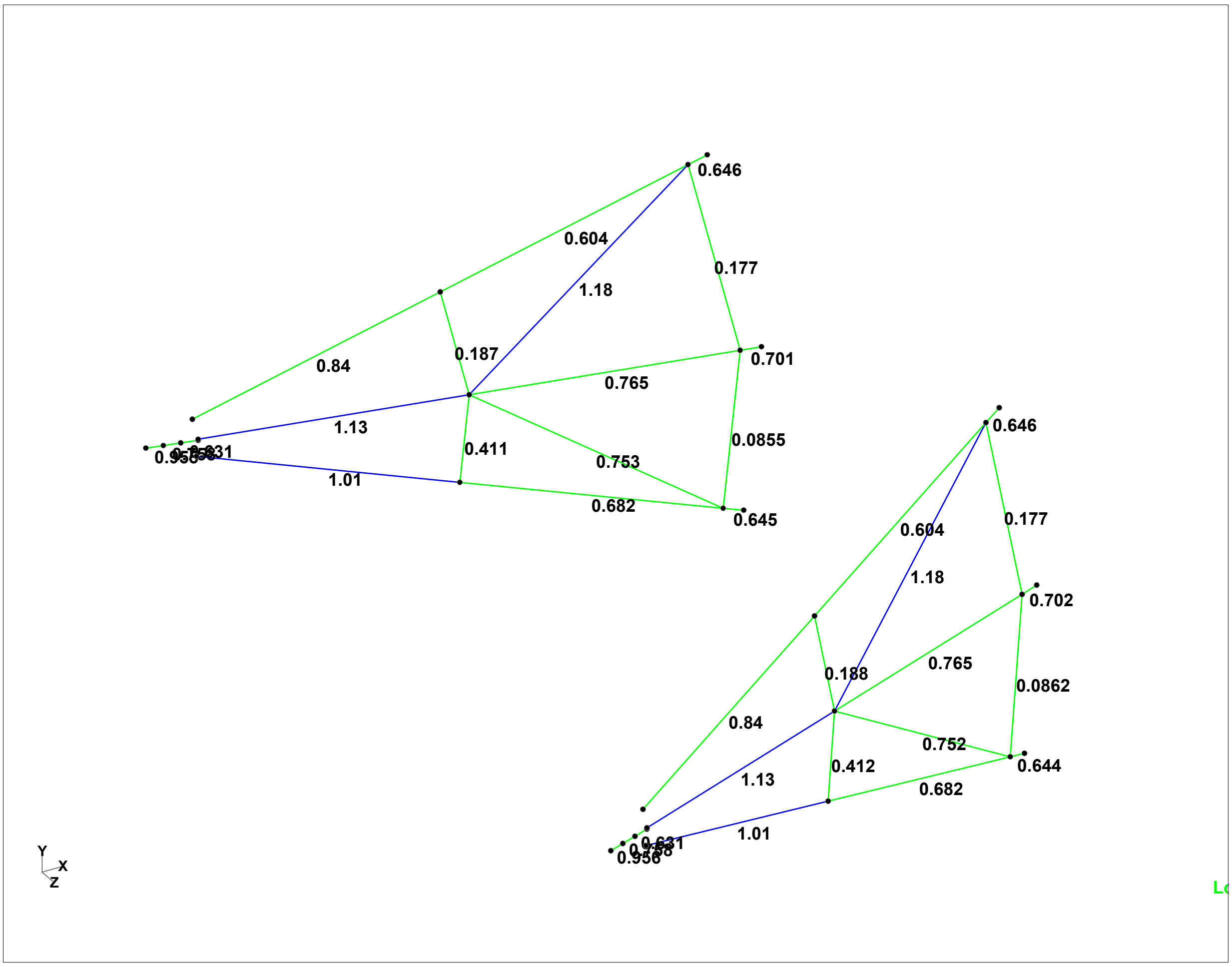

Arm Struts and Trunnion Hubs Member Utilization Ratios

Software licensed to Schnabel Engineering, Inc CONNECTED User: Charles Denq	Job No **20C22001.00.0**	Sheet No **2**	Rev 0
	Part LC2a â€“ Gate operating		
Job Title Forney Dam Tainter Gate Analysis	Ref 1.2D + 1.4 H3 + 1.4 Fs + 1.0 Ft + Qh		
	By Charles Denq	Date 8/30/2020	Chd
Client GARVER FOR DWU	File FDLC2a.STD	Date/Time 23-Jul-2021 00:07	

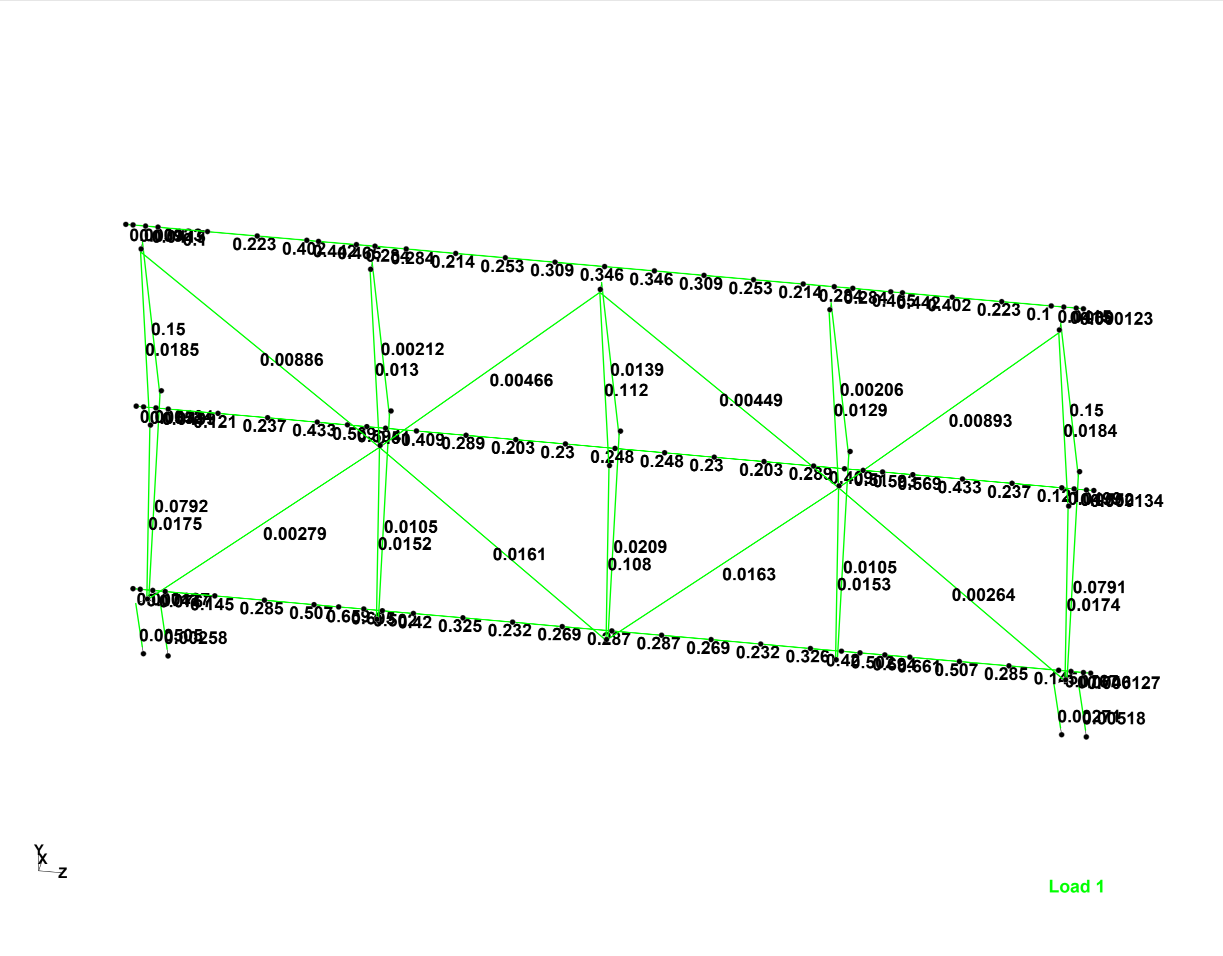

Horizontal Girders and Braces Member Utilization Ratios

Software licensed to Schnabel Engineering, Inc CONNECTED User: Charles Denq	Job No **20C22001.00.0**	Sheet No **3**	Rev 0
	Part LC2a â€“ Gate operating		
Job Title Forney Dam Tainter Gate Analysis	Ref 1.2D + 1.4 H3 + 1.4 Fs + 1.0 Ft + Qh		
	By Charles Denq	Date 8/30/2020	Chd
Client GARVER FOR DWU	File FDLC2a.STD	Date/Time 23-Jul-2021 00:07	

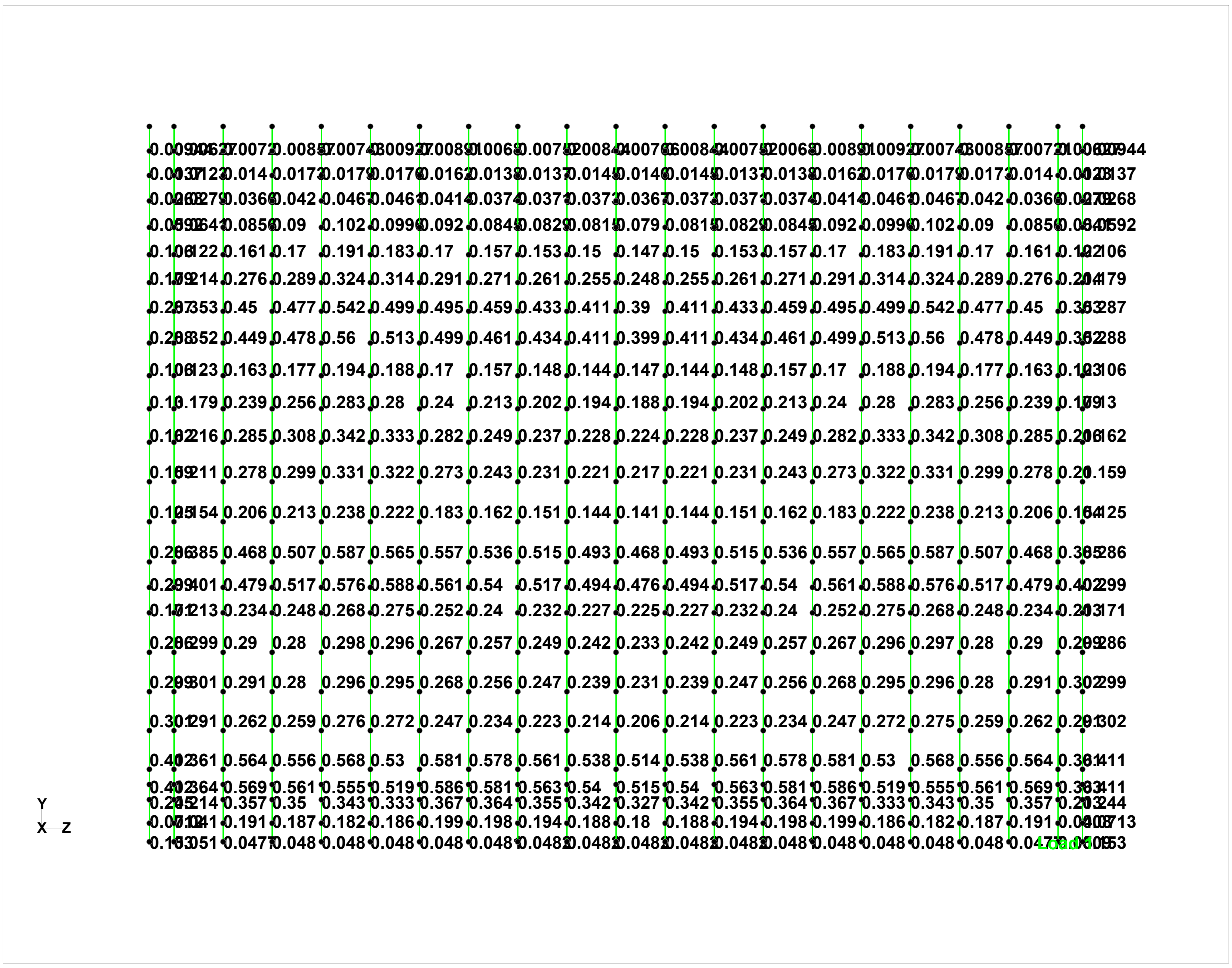

Skin-Rib Composite Member Utilization Ratios

STAAD Analysis Member Interaction Values (Utilization Ratios)

Gate Operating Load Combination LC2aU – Base Case (Opening), Unfactored

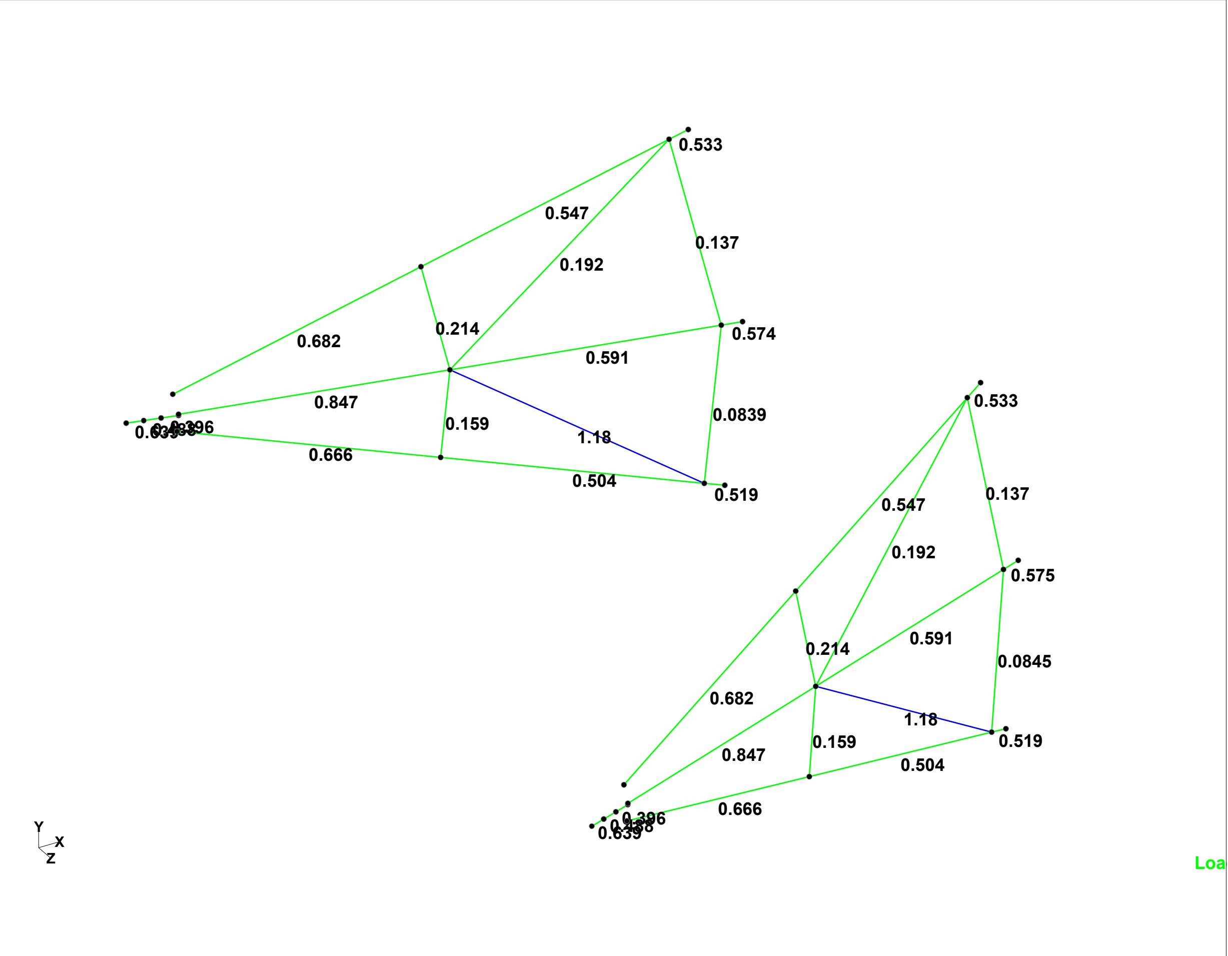

Arm Struts and Trunnion Hubs Member Utilization Ratios

Software licensed to Schnabel Engineering, Inc CONNECTED User: Charles Denq	Job No 20C22001.00.0	Sheet No 2	Rev 0
	Part LC2aU â€“ Gate operating		
Job Title Forney Dam Tainter Gate Analysis	Ref 1.2D + 1.4 H3 + 1.4 Fs + 1.0 Ft + Qh		
	By Charles Denq	Date 8/30/2020	Chd
Client GARVER FOR DWU	File FDLC2aU.STD	Date/Time 23-Jul-2021 00:58	

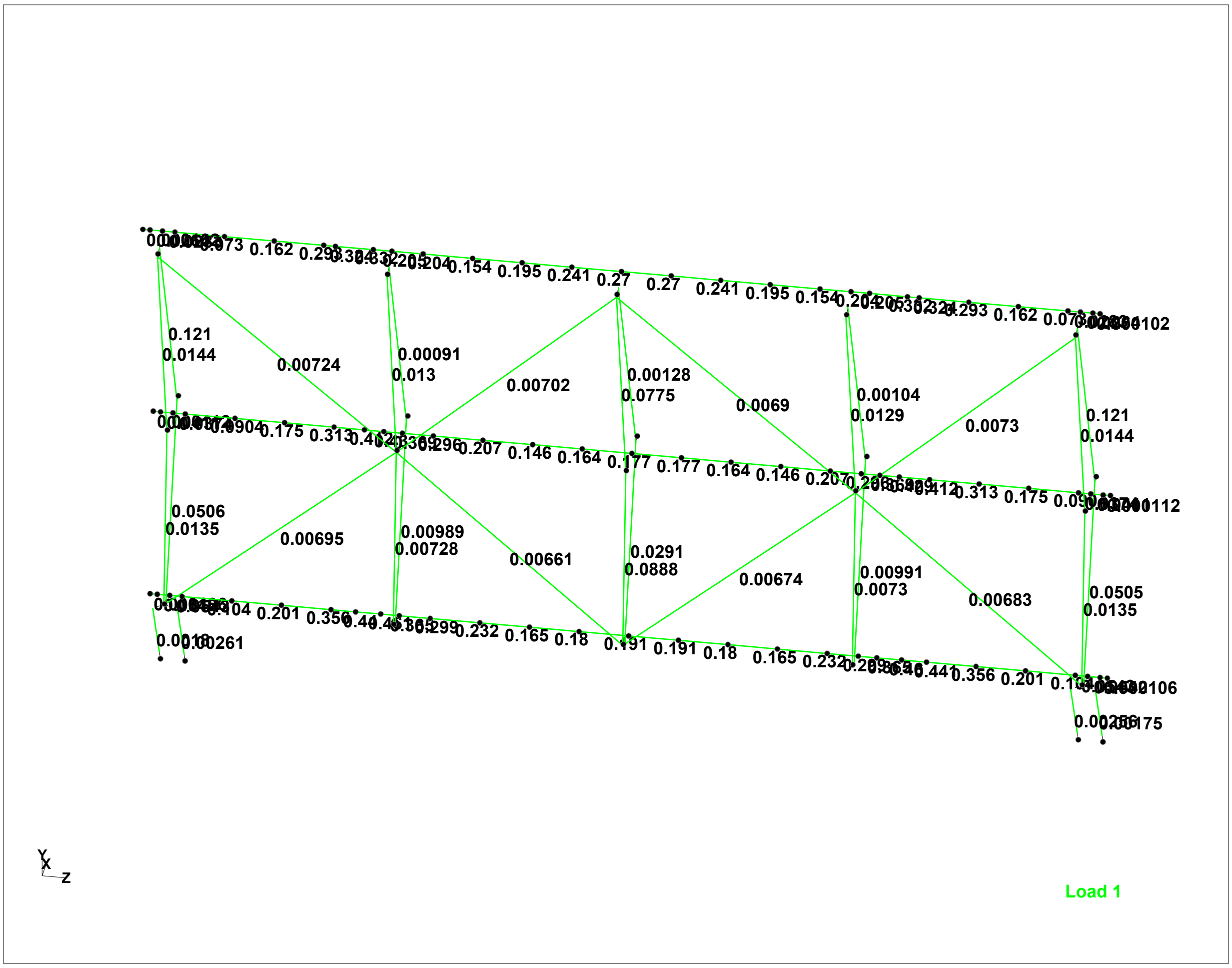

Horizontal Girders and Braces Member Utilization Ratios

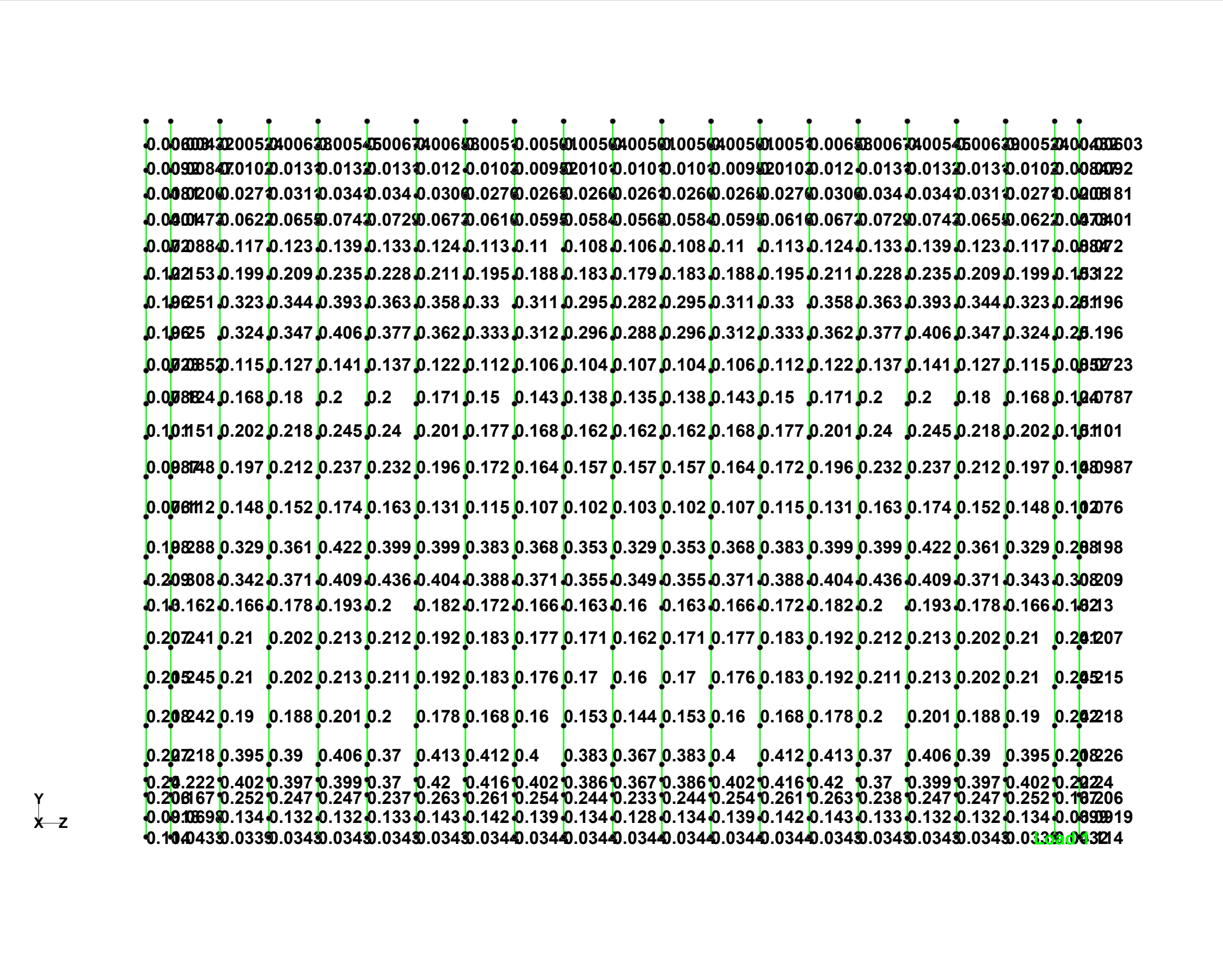

Skin-Rib Composite Member Utilization Ratios

STAAD Analysis Member Interaction Values (Utilization Ratios)

Gate Operating Load Combination LC2aU – Base Case (Closing), Unfactored

Software licensed to Schnabel Engineering, Inc CONNECTED User: Charles Denq	Job No **20C22001.00.0**	Sheet No **1**	Rev 0
	Part LC2aU â€“ Gate operating		
Job Title Forney Dam Tainter Gate Analysis	Ref 1.2D + 1.4 H3 + 1.4 Fs + 1.0 Ft + Qh		
	By Charles Denq	Date 8/30/2020	Chd
Client GARVER FOR DWU	File FDLC2aU.STD	Date/Time 23-Jul-2021 01:23	

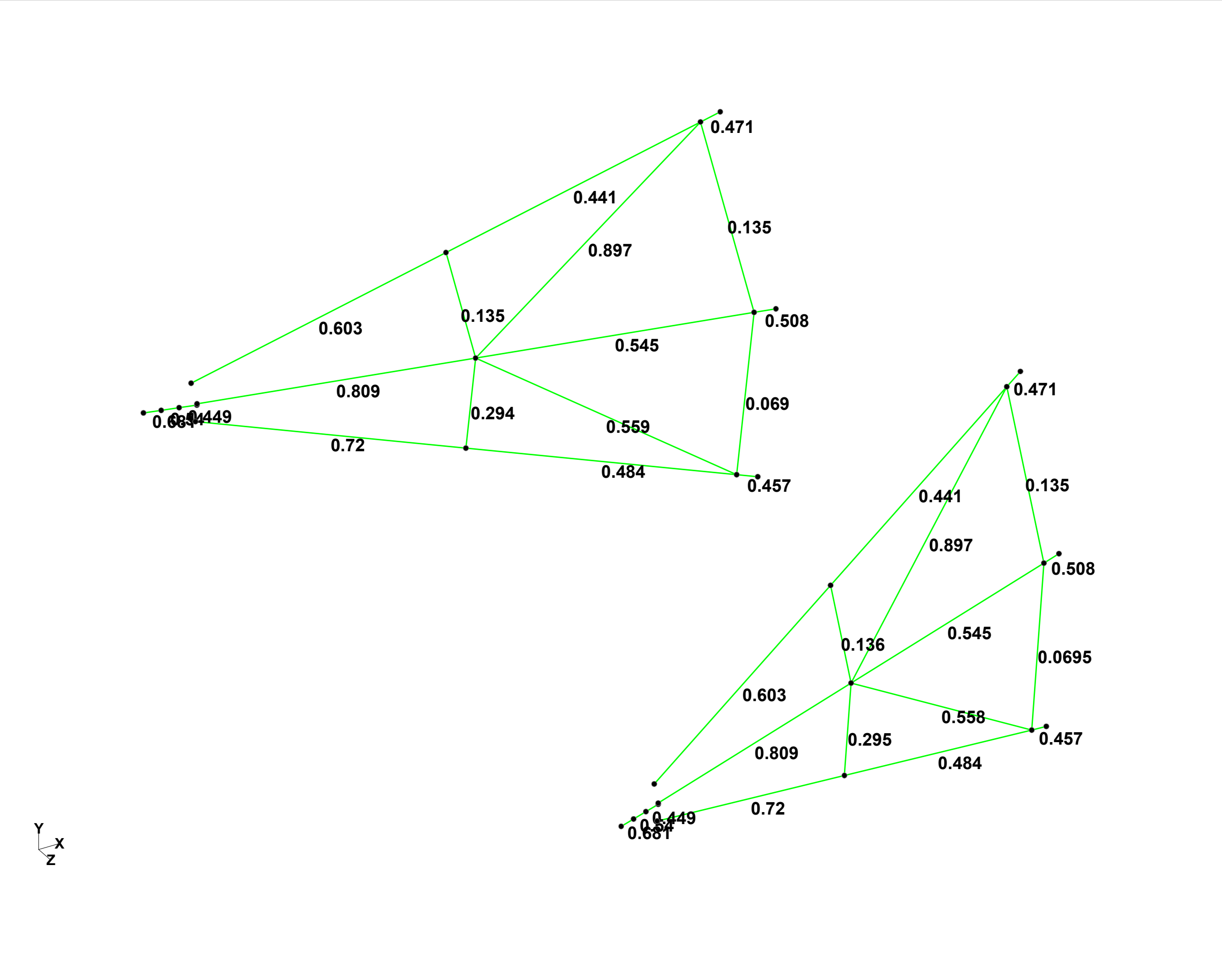

Arm Struts and Trunnion Hubs Member Utilization Ratios

Software licensed to Schnabel Engineering, Inc CONNECTED User: Charles Denq	Job No **20C22001.00.0**	Sheet No **2**	Rev 0
	Part LC2aU â€“ Gate operating		
Job Title Forney Dam Tainter Gate Analysis	Ref 1.2D + 1.4 H3 + 1.4 Fs + 1.0 Ft + Qh		
	By Charles Denq	Date 8/30/2020	Chd
Client GARVER FOR DWU	File FDLC2aU.STD	Date/Time 23-Jul-2021 01:23	

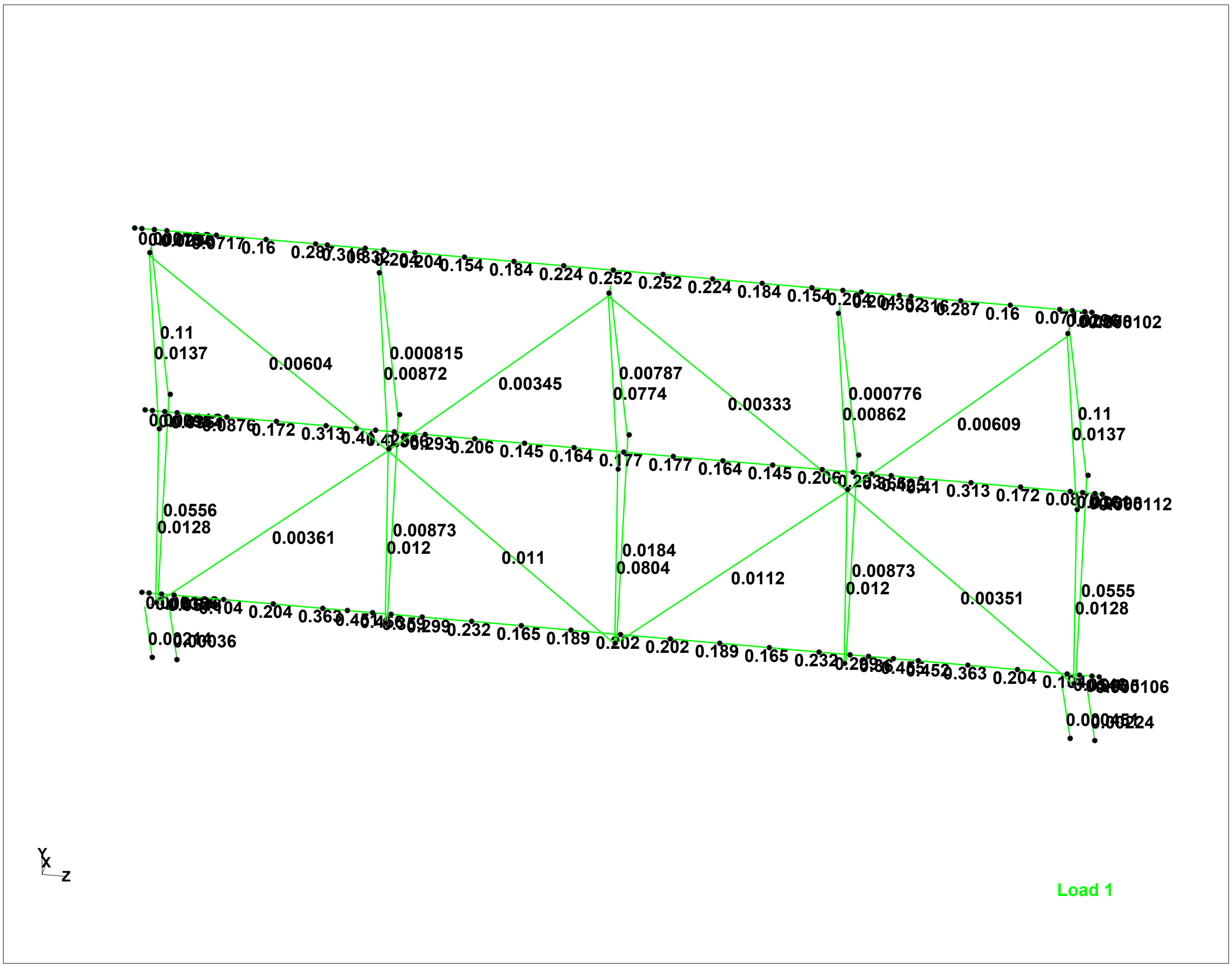

Whole Structure

Software licensed to Schnabel Engineering, Inc CONNECTED User: Charles Denq	Job No **20C22001.00.0**	Sheet No **3**	Rev 0
	Part LC2aU â€“ Gate operating		
Job Title Forney Dam Tainter Gate Analysis	Ref 1.2D + 1.4 H3 + 1.4 Fs + 1.0 Ft + Qh		
	By Charles Denq	Date 8/30/2020	Chd
Client GARVER FOR DWU	File FDLC2aU.STD	Date/Time 23-Jul-2021 01:23	

Skin-Rib Composite Member Utilization Ratios

STAAD Analysis Member Interaction Values (Utilization Ratios)

Gate Operating Load Combination LC2b – Wave (Opening)

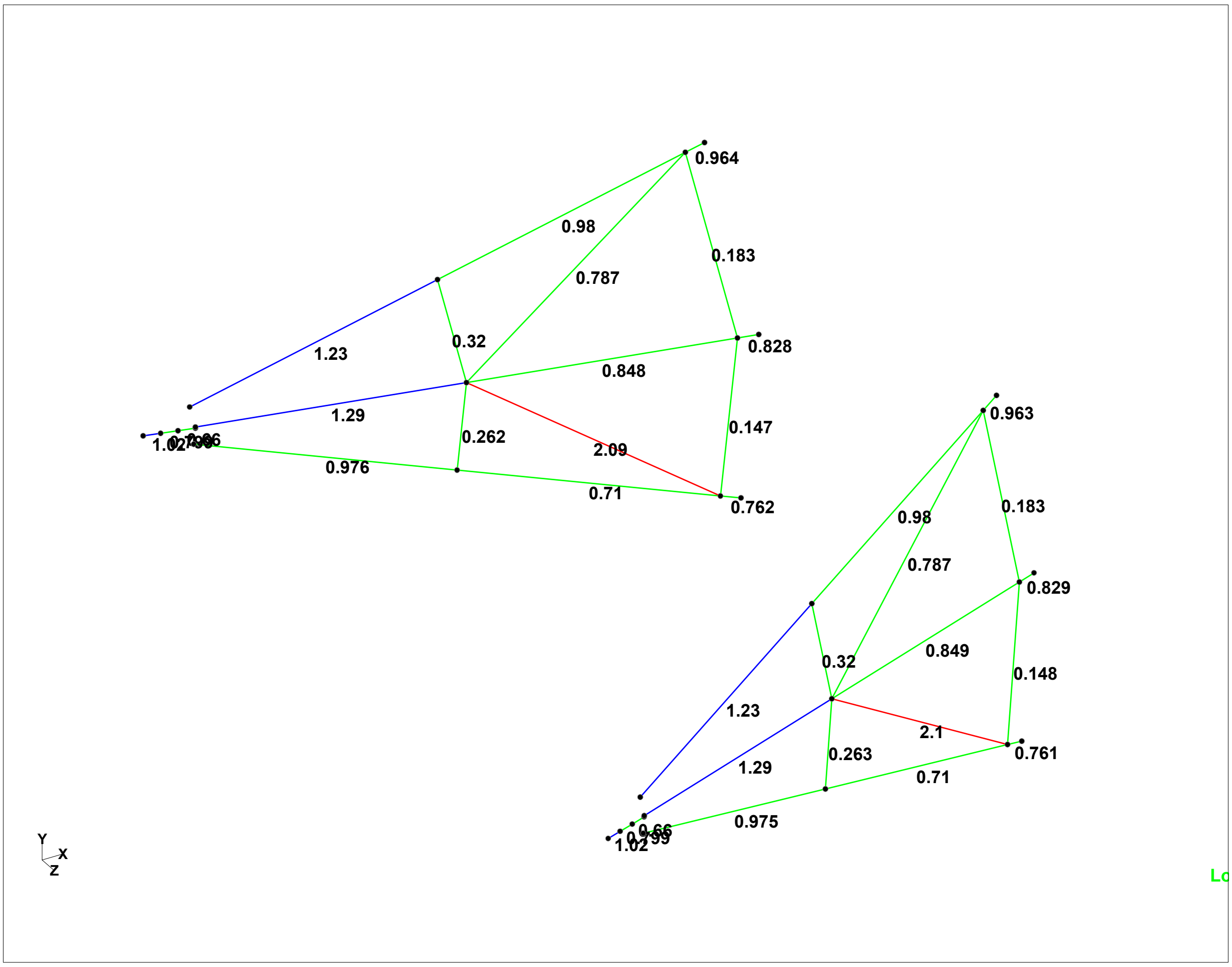

Arm Struts and Trunnion Hubs Member Utilization Ratios

Software licensed to Schnabel Engineering, Inc CONNECTED User: Charles Denq	Job No **20C22001.00.0**	Sheet No **2**	Rev 0
	Part LC2b â€“ Gate operating with wave load		
Job Title Forney Dam Tainter Gate Analysis	Ref 1.2D + 1.4 H2 + 1.4 Fs + 1.0 Ft + 1.4 WA + Qh		
	By Charles Denq	Date 8/30/2020	Chd
Client GARVER FOR DWU	File FDLC2b.STD	Date/Time 23-Jul-2021 01:28	

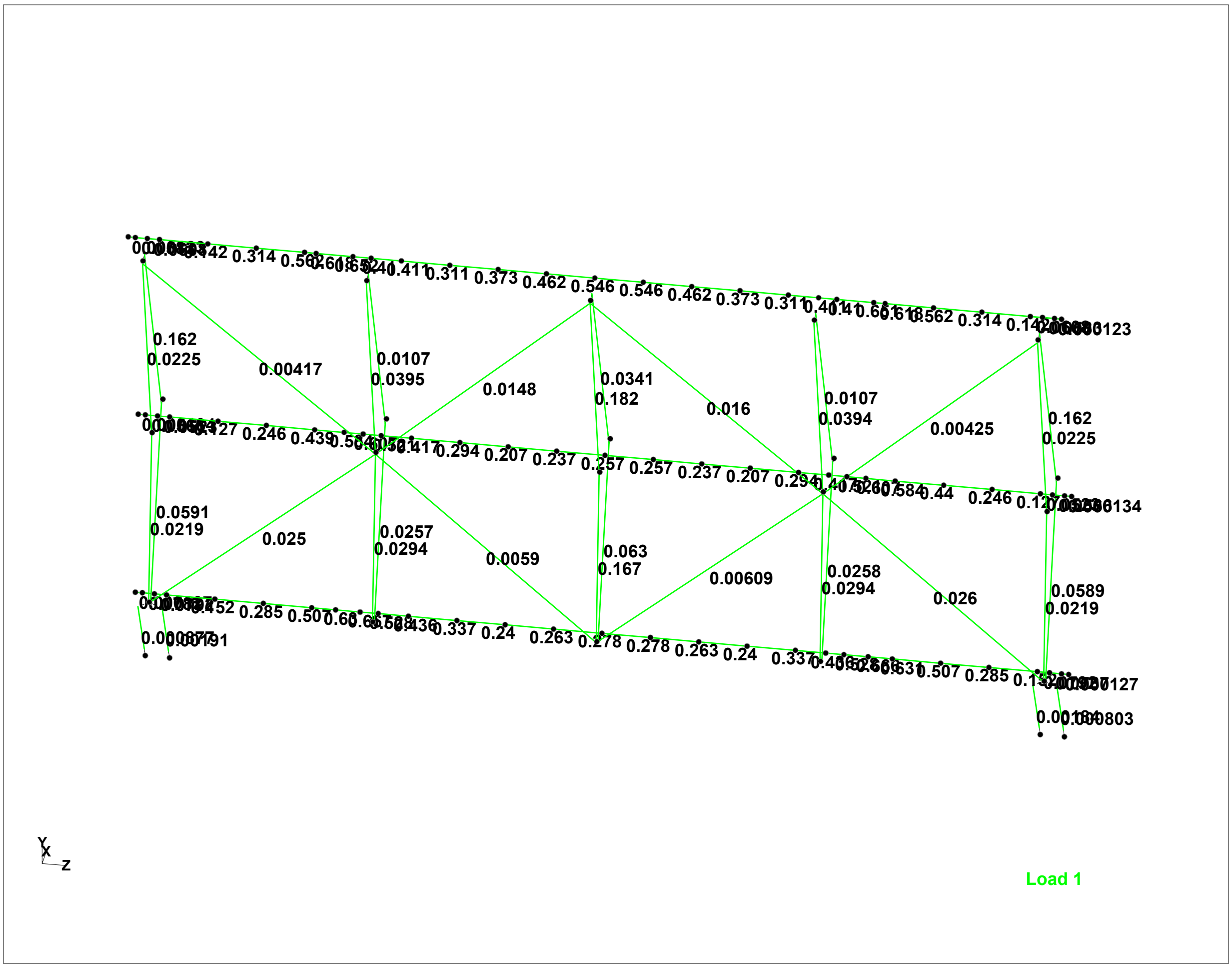

Horizontal Girders and Braces Member Utilization Ratios

Software licensed to Schnabel Engineering, Inc
CONNECTED User: Charles Denq

Job No	20C22001.00.0
Sheet No	3
Rev	0
Part	LC2b â€“ Gate operating with wave load
Job Title	Forney Dam Tainter Gate Analysis
Ref	1.2D + 1.4 H2 + 1.4 Fs + 1.0 Ft + 1.4 WA + Qh
By	Charles Denq
Date	8/30/2020
Chd	
Client	GARVER FOR DWU
File	FDLC2b.STD
Date/Time	23-Jul-2021 01:28

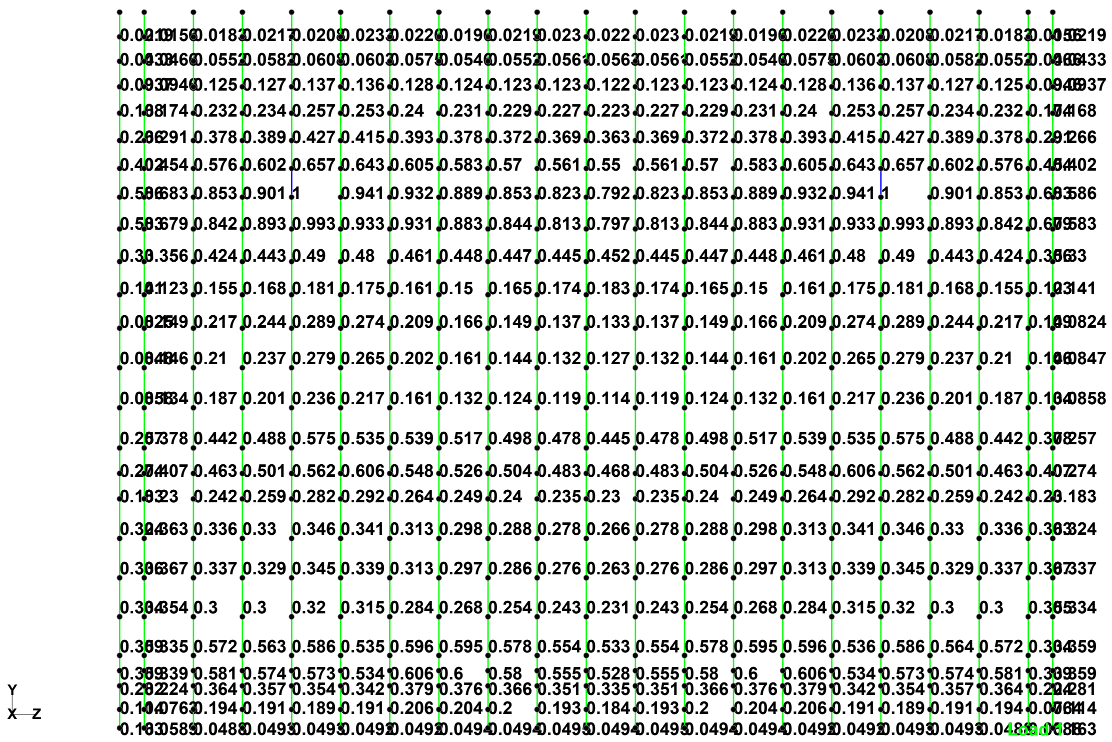

Skin-Rib Composite Member Utilization Ratios

STAAD Analysis Member Interaction Values (Utilization Ratios)

Gate Operating Load Combination LC2b – Wave (Closing)

Software licensed to Schnabel Engineering, Inc CONNECTED User: Charles Denq	Job No **20C22001.00.0**	Sheet No **1**	Rev 0
	Part LC2b â€“ Gate operating with wave load		
Job Title Forney Dam Tainter Gate Analysis	Ref 1.2D + 1.4 H2 + 1.4 Fs + 1.0 Ft + 1.4 WA + Qh		
	By Charles Denq	Date 8/30/2020	Chd
Client GARVER FOR DWU	File FDLC2b.STD	Date/Time 23-Jul-2021 01:33	

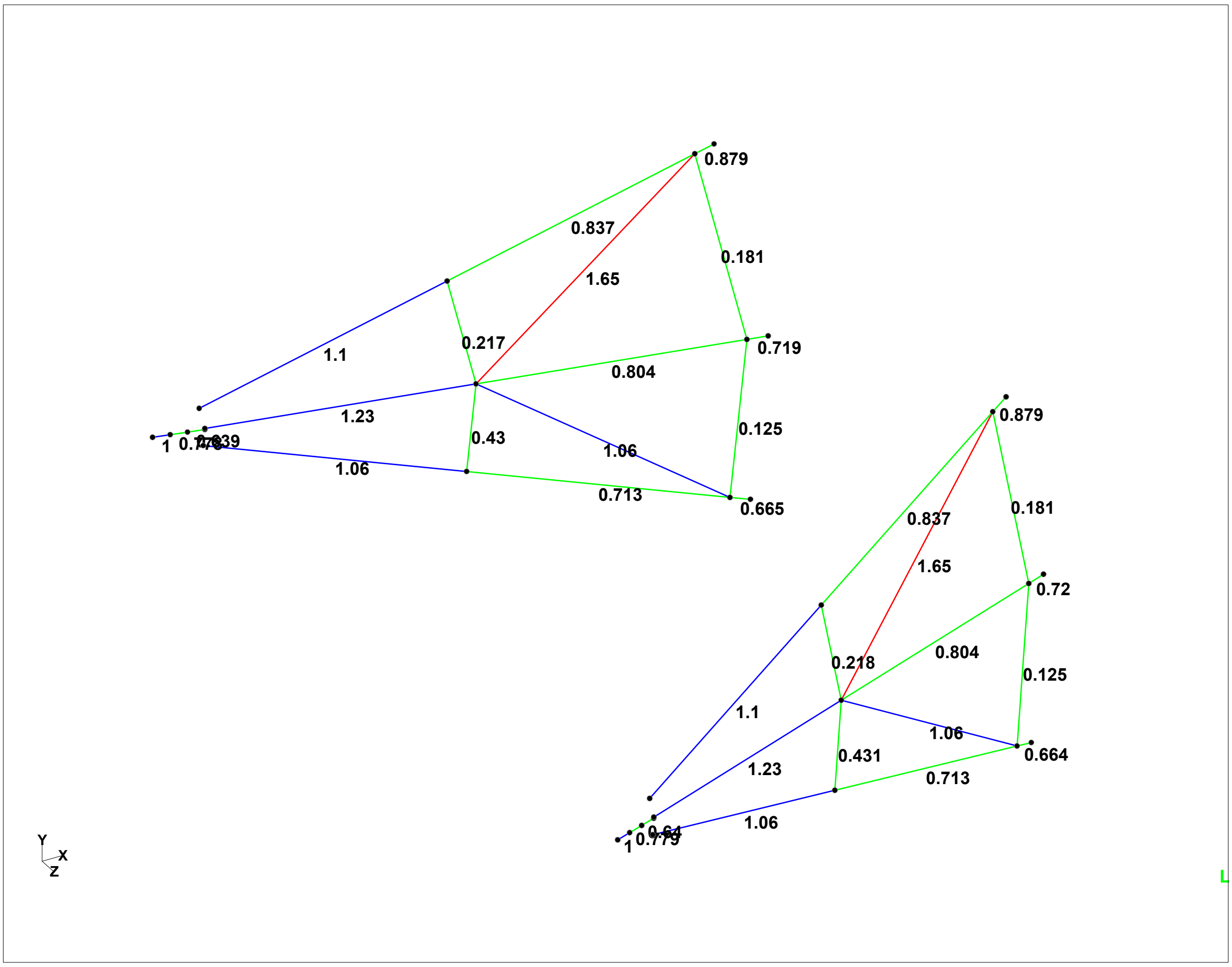

Arm Struts and Trunnion Hubs Member Utilization Ratios

Software licensed to Schnabel Engineering, Inc CONNECTED User: Charles Denq	Job No **20C22001.00.0**	Sheet No **2**	Rev 0
	Part LC2b â€“ Gate operating with wave load		
Job Title Forney Dam Tainter Gate Analysis	Ref 1.2D + 1.4 H2 + 1.4 Fs + 1.0 Ft + 1.4 WA + Qh		
	By Charles Denq	Date 8/30/2020	Chd
Client GARVER FOR DWU	File FDLC2b.STD	Date/Time 23-Jul-2021 01:33	

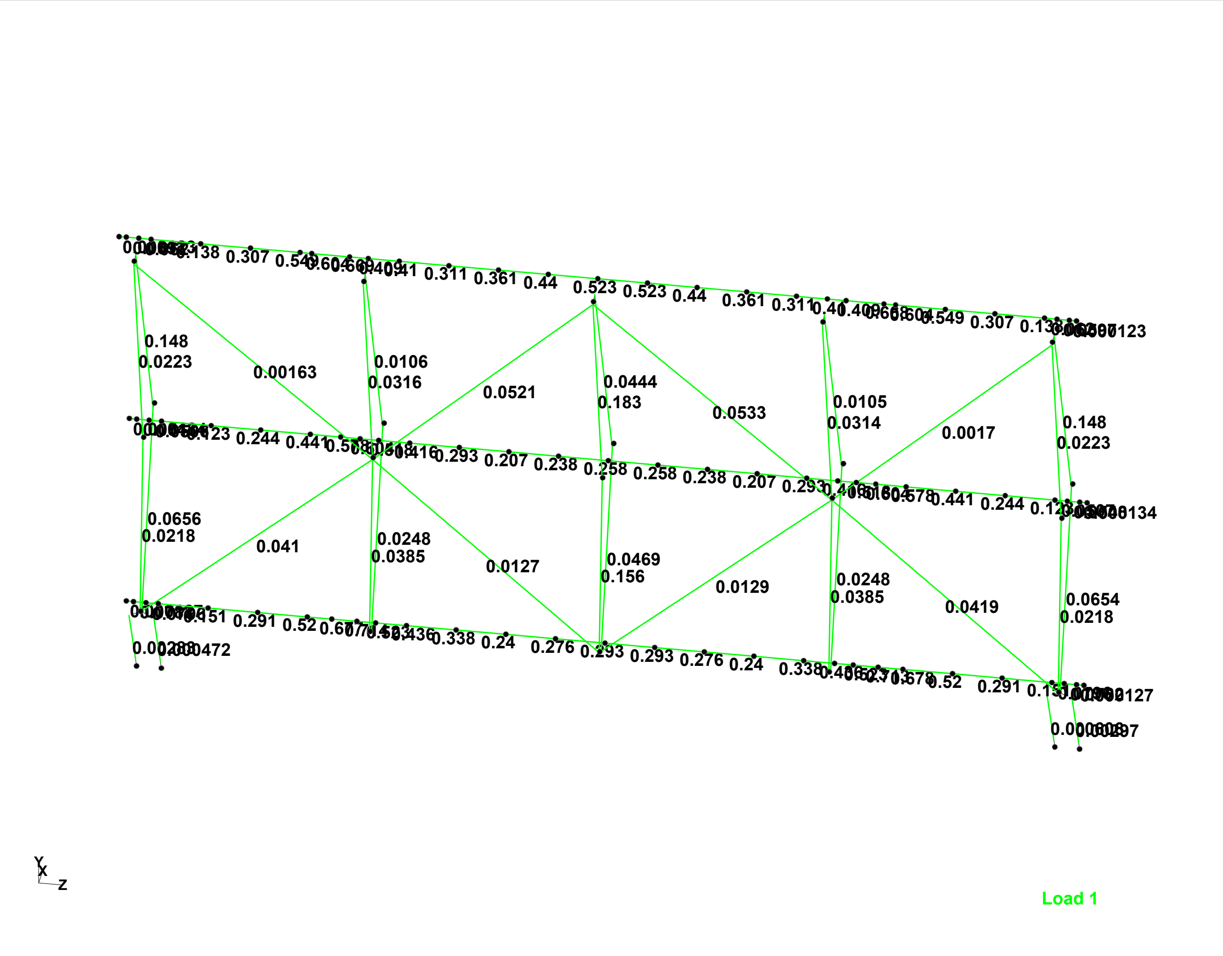

Horizontal Girders and Braces Member Utilization Ratios

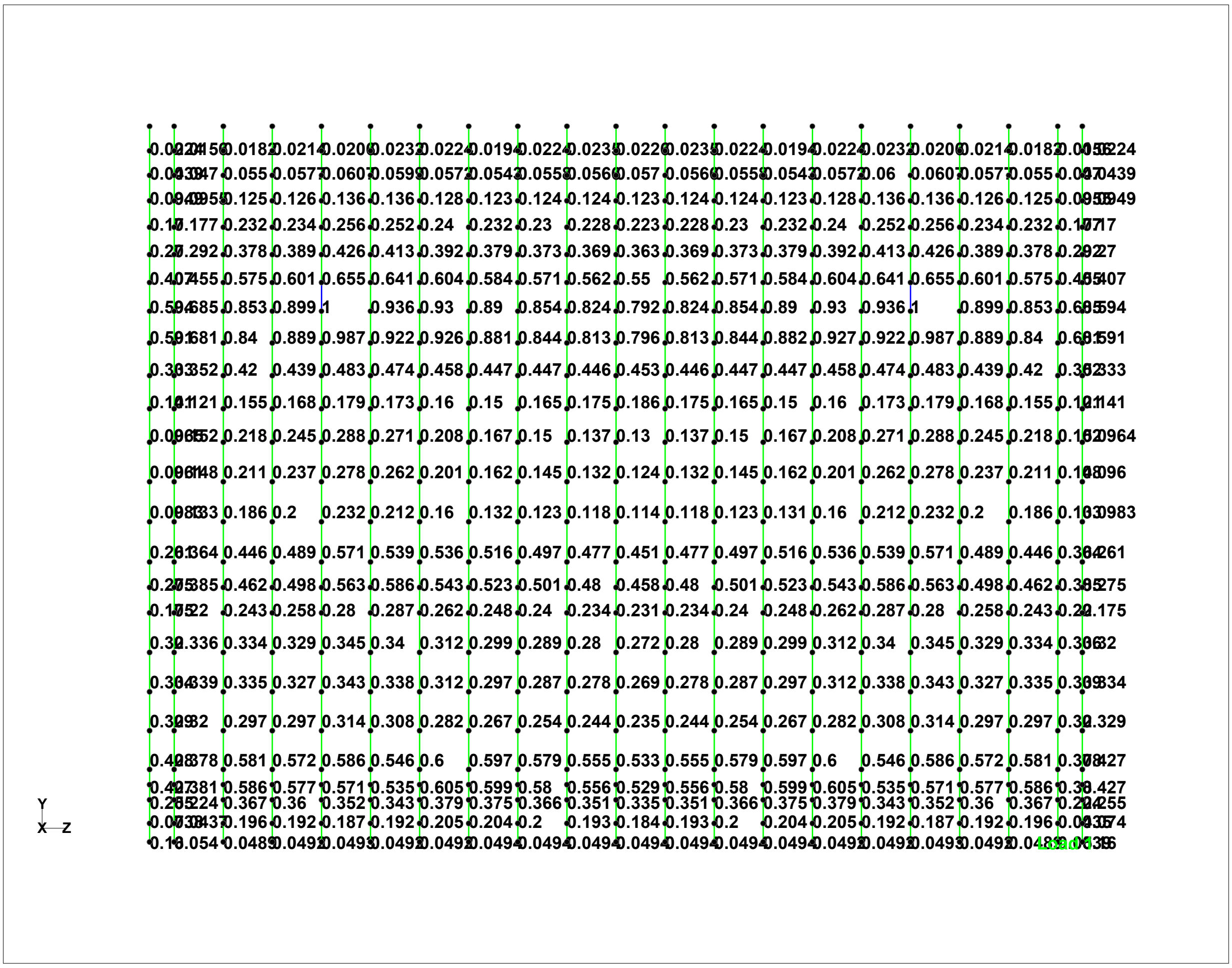

Skin-Rib Composite Member Utilization Ratios

STAAD Analysis Member Interaction Values (Utilization Ratios)

Gate Operating Load Combination LC2bU – Wave (Opening), Unfactored

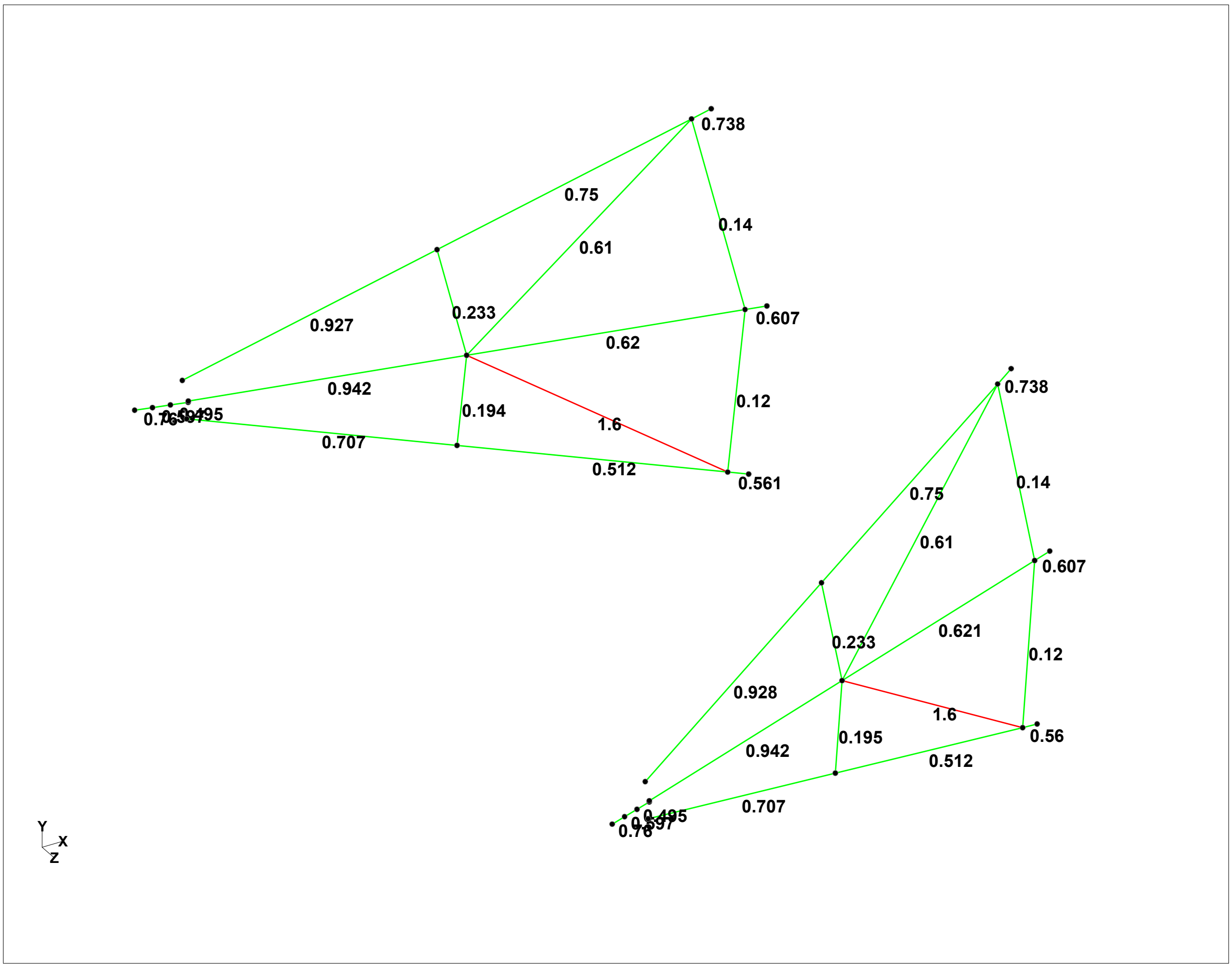

Arm Struts and Trunnion Hubs Member Utilization Ratios

Software licensed to Schnabel Engineering, Inc
CONNECTED User: Charles Denq

Job No	20C22001.00.0	Sheet No 2	Rev 0
Part	LC2bU â€“ Gate operating with wave load		
Job Title	Forney Dam Tainter Gate Analysis	Ref	1.2D + 1.4 H2 + 1.4 Fs + 1.0 Ft + 1.4 WA + Qh
		By	Charles Denq Date 8/30/2020 Chd
Client	GARVER FOR DWU	File	FDLC2bU.STD Date/Time 23-Jul-2021 01:38

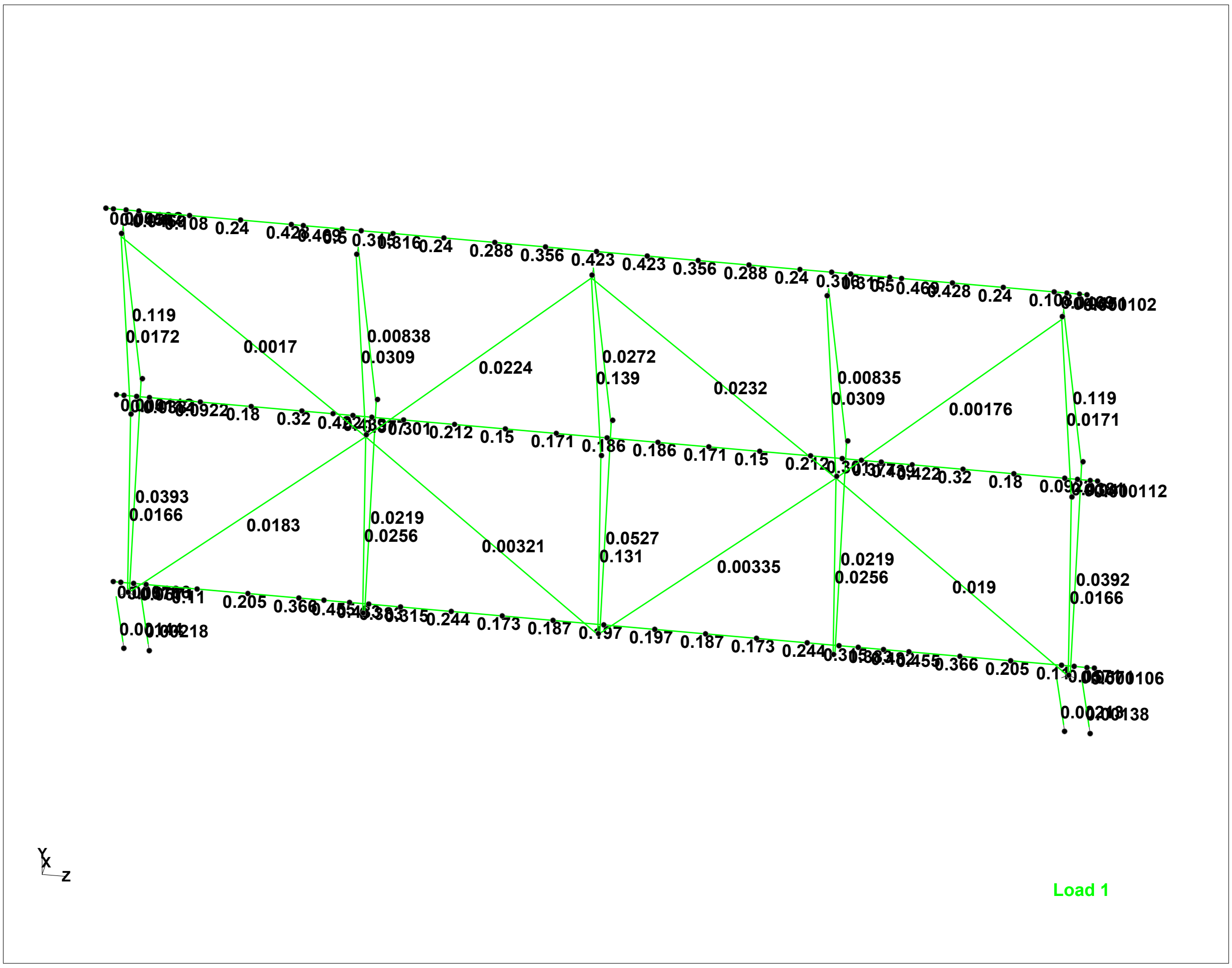

Horizontal Girders and Braces Member Utilization Ratios

Software licensed to Schnabel Engineering, Inc CONNECTED User: Charles Denq	Job No 20C22001.00.0	Sheet No 3	Rev 0
	Part LC2bU â€“ Gate operating with wave load		
Job Title Forney Dam Tainter Gate Analysis	Ref 1.2D + 1.4 H2 + 1.4 Fs + 1.0 Ft + 1.4 WA + Qh		
	By Charles Denq	Date 8/30/2020	Chd
Client GARVER FOR DWU	File FDLC2bU.STD	Date/Time 23-Jul-2021 01:38	

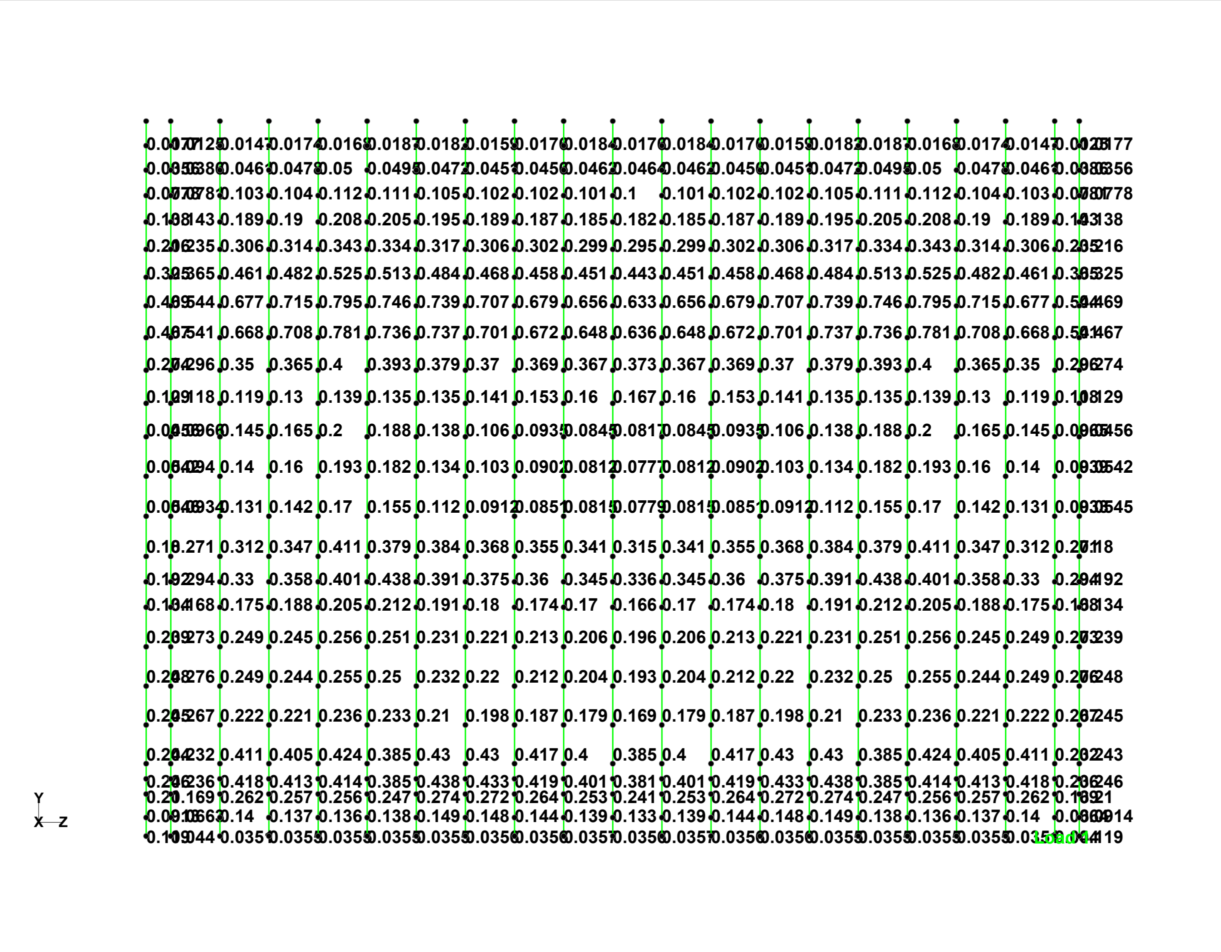

Skin-Rib Composite Member Utilization Ratios

STAAD Analysis Member Interaction Values (Utilization Ratios)

Gate Operating Load Combination LC2bU – Wave (Closing), Unfactored

Job No	Sheet No	Rev
20C22001.00.0	1	0

Software licensed to Schnabel Engineering, Inc
CONNECTED User: Charles Denq

Part LC2bU â€“ Gate operating with wave load

Job Title Forney Dam Tainter Gate Analysis

Ref 1.2D + 1.4 H2 + 1.4 Fs + 1.0 Ft + 1.4 WA + Qh

By Charles Denq Date 8/30/2020 Chd

Client GARVER FOR DWU

File FDLC2bU.STD Date/Time 23-Jul-2021 01:42

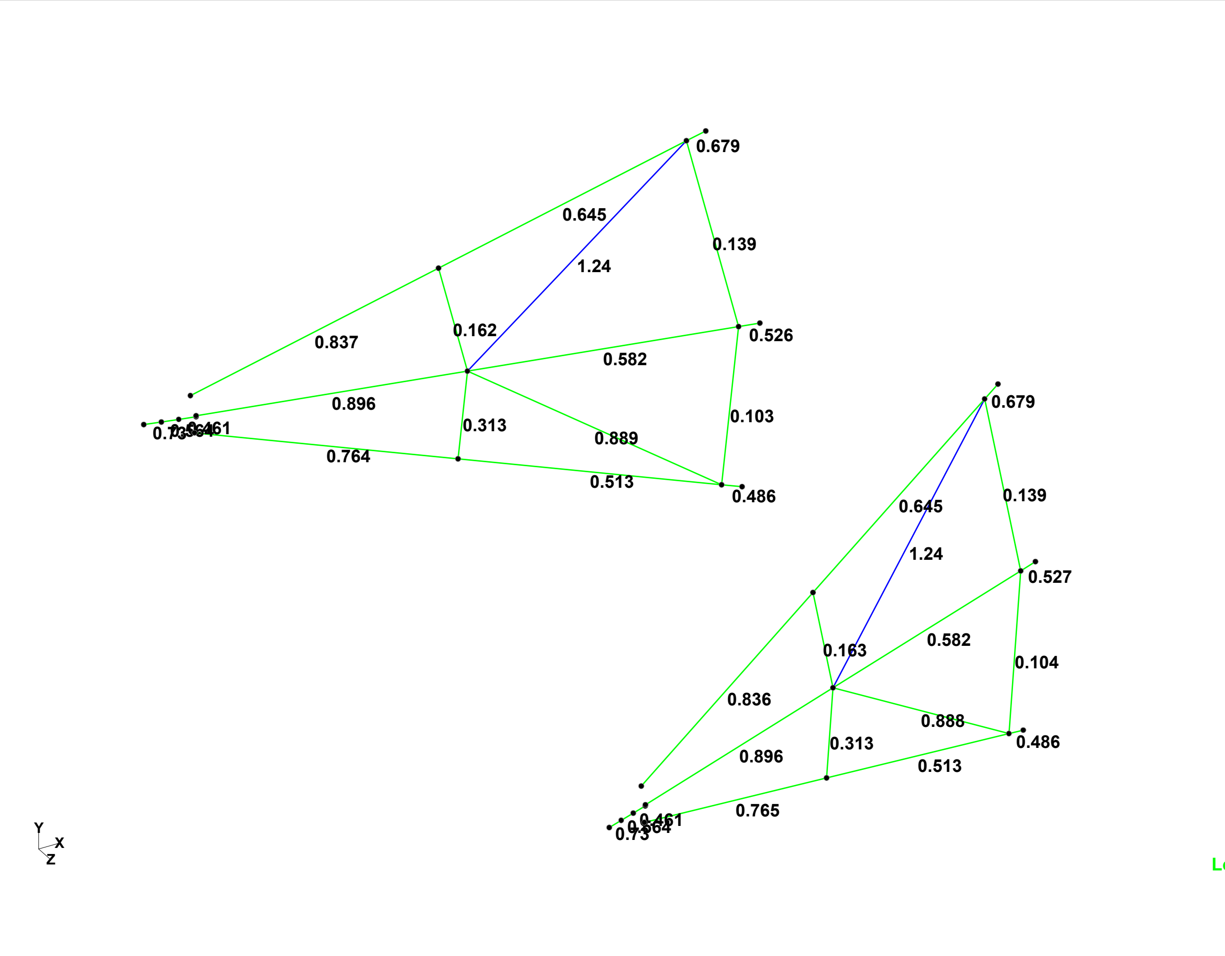

Arm Struts and Trunnion Hubs Member Utilization Ratios

Software licensed to Schnabel Engineering, Inc CONNECTED User: Charles Denq	Job No **20C22001.00.0**	Sheet No **2**	Rev 0
	Part LC2bU â€“ Gate operating with wave load		
Job Title Forney Dam Tainter Gate Analysis	Ref 1.2D + 1.4 H2 + 1.4 Fs + 1.0 Ft + 1.4 WA + Qh		
	By Charles Denq	Date 8/30/2020	Chd
Client GARVER FOR DWU	File FDLC2bU.STD	Date/Time 23-Jul-2021 01:42	

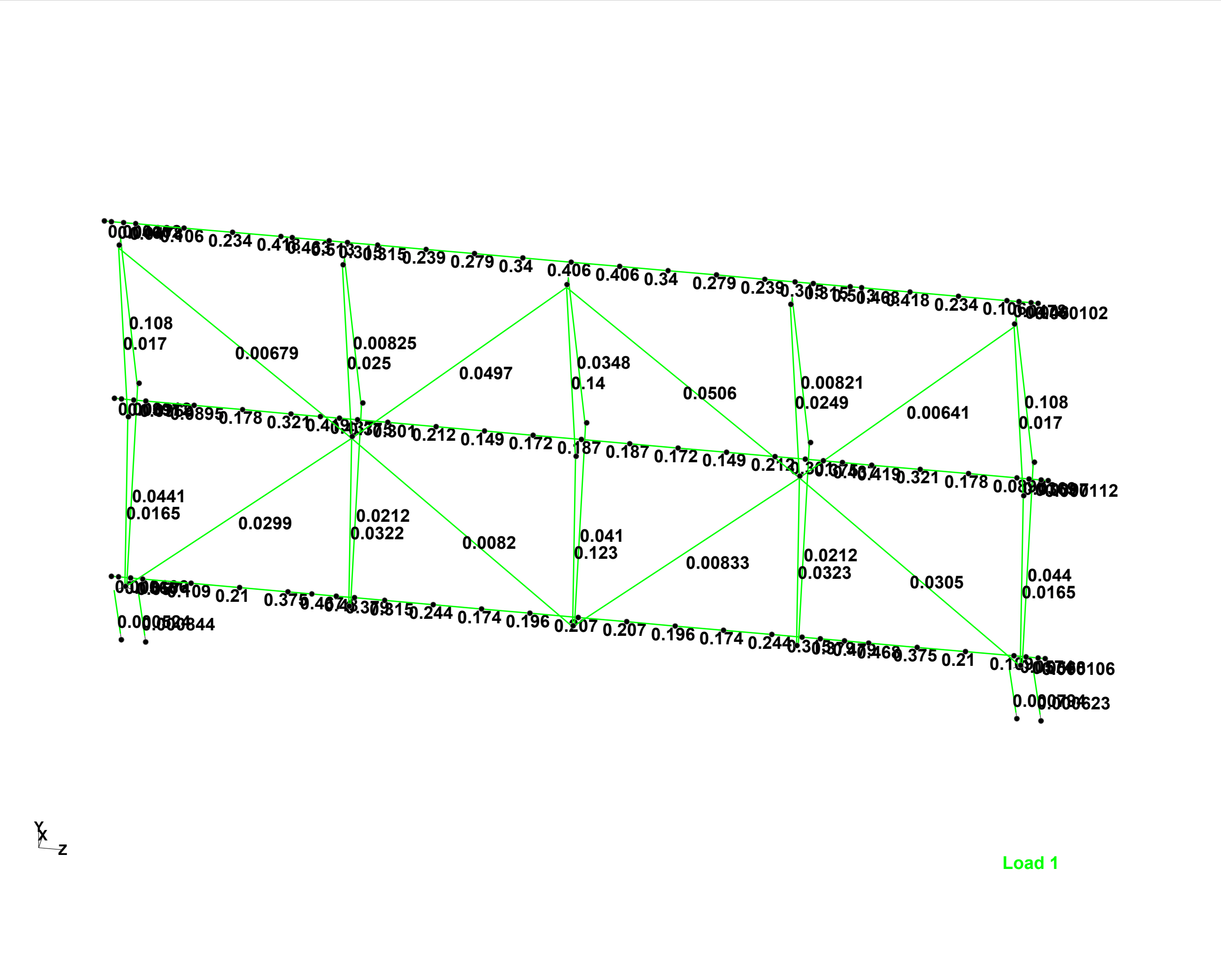

Horizontal Girders and Braces Member Utilization Ratios

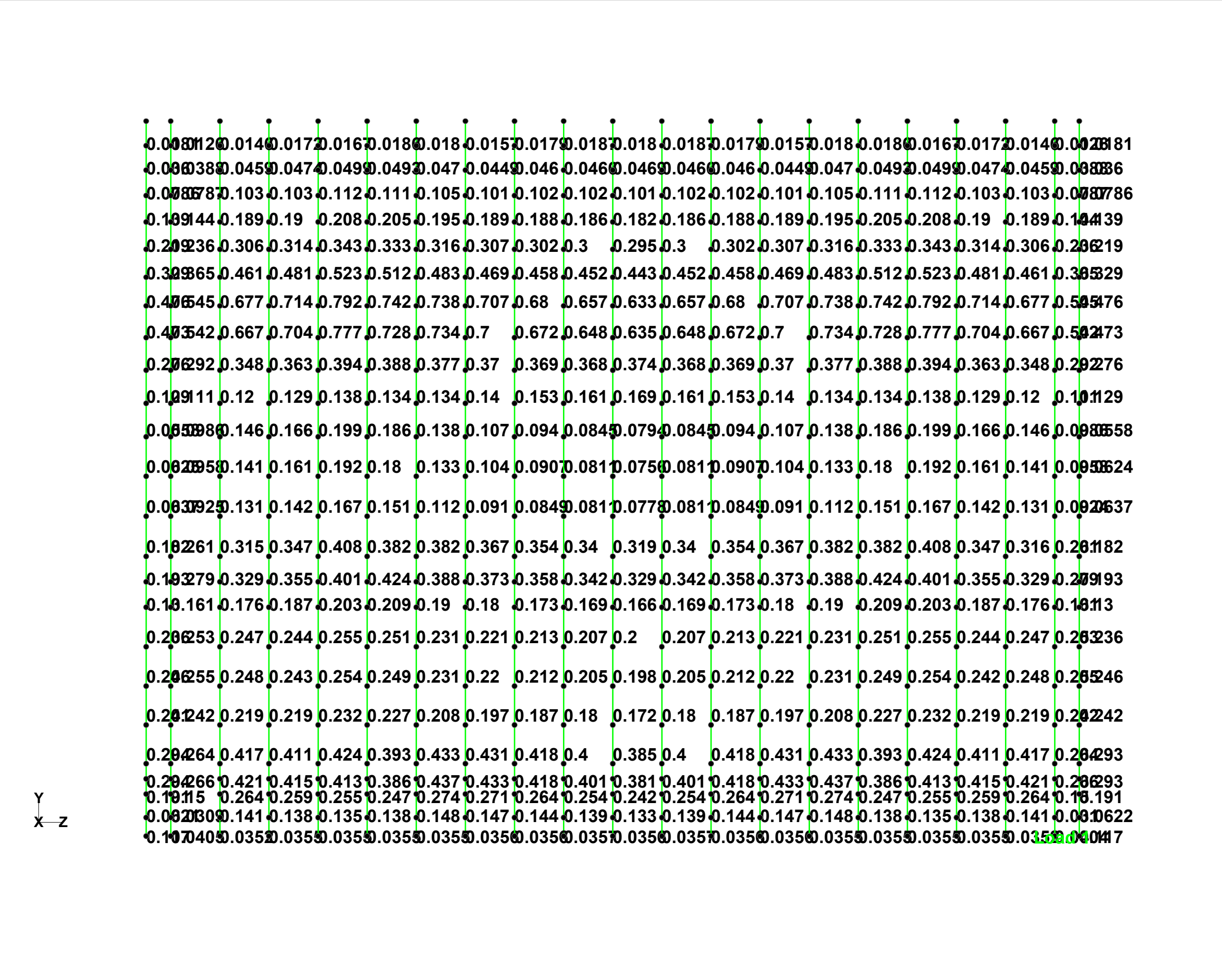

Skin-Rib Composite Member Utilization Ratios

APPENDIX D
TRUNNION FRICTION TESTING REPORTS
(GATES 1-14)

©2021 All Rights Reserved

SCHNABEL ENGINEERING

TRUNNION PIN FRICTION TESTING REPORT

ROCKWALL FORNEY DAM – GATE 1
FORNEY, TX

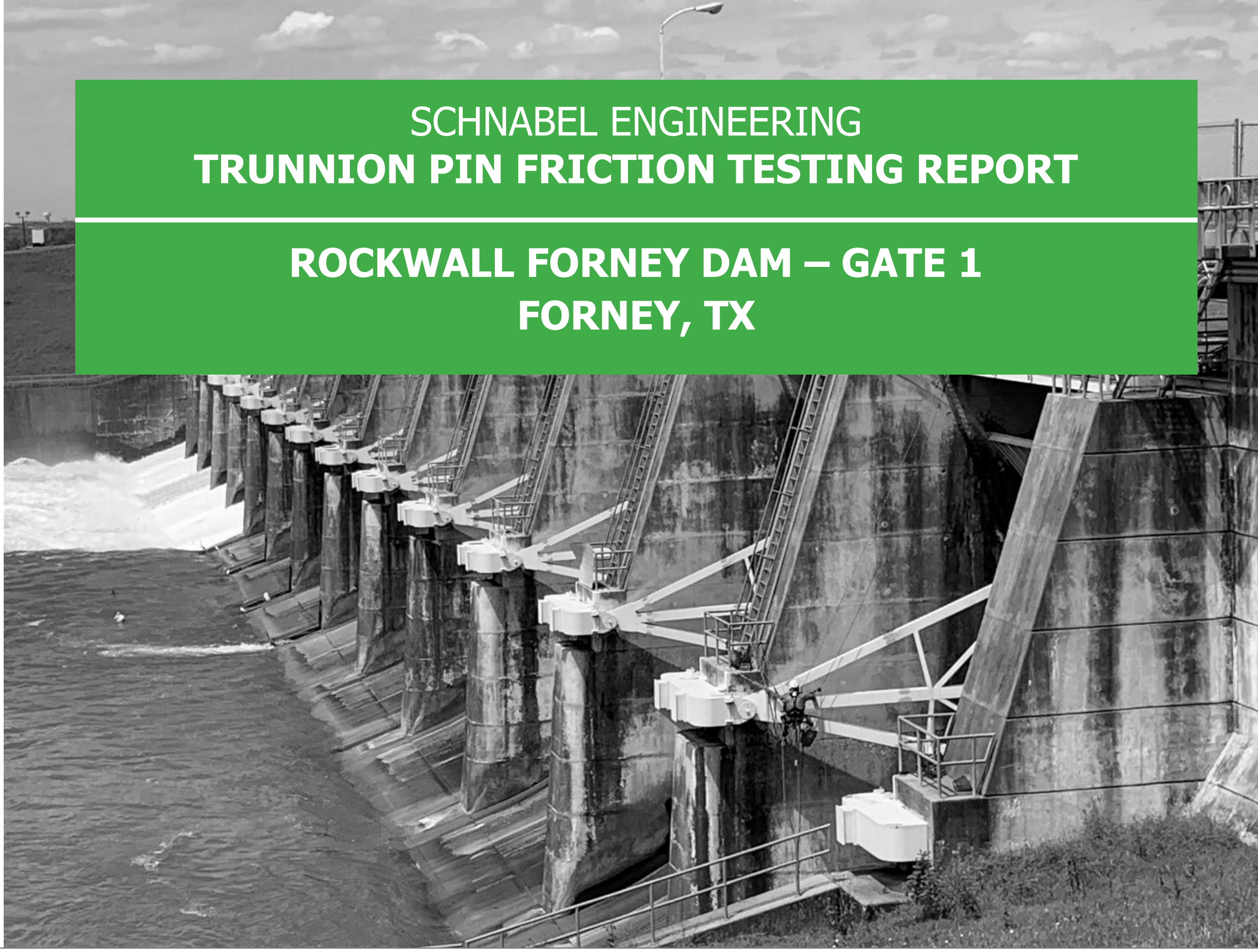

SUBMITTED TO:

SCHNABEL ENGINEERING
16000 CHRISTENSEN RD, SUITE 101
SEATTLE, WA 98188

SUBMITTED BY:

BDI – CO
740 SOUTH PIERCE AVE, UNIT 15
LOUISVILLE, CO 80027

BDI Project No.: **190701-TX**
Report Version: **V3**
Version Submitted: **August 26, 2020**

RAW DATA. REFINED RESULTS.

This document contains Confidential Information and is submitted in confidence to the customer. The submission of the information contained herein shall not be deemed to constitute public disclosure or authorization for disclosure to other parties. BDI's information and name may not be used in advertising or for promotional purposes without BDI's written consent.

TABLE OF CONTENTS

LIST OF FIGURES

LIST OF TABLES

Executive Summary

Schnabel Engineering contracted BDI to provide instrumentation and testing services on Gates 1-14 on the Rockwall Forney Dam near Dallas, Texas. The goal of these tests was to record each gate's structural responses during a series of spill tests and use the data to compute accurate coefficients of friction for each trunnion pin, cable lift force, total gate friction, and motor amperage. This report provides details on the work performed on Gate 1.

Instrumentation and testing were performed on Gate 1 at the Rockwall Forney Dam on April 1st, 2020. The gate arms were instrumented with strain and rotation sensors. The hoist motors' pinion shafts were instrumented with torque sensors and the hoist motor controls were instrumented with amperage sensors. Following the instrumentation, a series of spill tests were performed to measure the structural responses resulting from trunnion pin friction. All instrumentation setup and removal were performed using BDI's rope access team.

Following demobilization from the field, the test data was examined for quality and then further processed to evaluate the gate's performance. Strain measurements were converted into bending forces which were then applied to pin-strut free-body diagrams. By summing forces at each pin, friction induced moments could be computed, allowing accurate friction coefficients to be determined.

The resulting maximum trunnion friction coefficients and corresponding hoist forces are shown in Table 1.

Table 1 – Gate 1 performance summary

Pin Designation	Maximum Friction Coefficient	Maximum Pin Moment due to Pin Friction (kip-In)	Maximum Hoist Force (kips)	Maximum Hoist Force due to Total Gate Friction (kips)
Right Pin	0.28	748.8	29.71	5.32
Left Pin	0.29	766.4	28.16	5.33

Note: Pin designations are in reference to looking downstream

Generally, the observed gate behavior showed that Gate 1 was operating as expected and in a symmetric manner. The hoist behavior showed indications of minor racking/hoist system alignment issues but overall had no major signs of distress (seizing, etc).

Due to restrictions caused by the hoist limit switches, the hoist cables could not always be fully slacked at the beginning and end of the performed tests. Throughout testing of the Rockwell Forney gates, it was found that this limit switch restriction varied gate to gate and arm to arm. Therefore, it is not recommended to use the collected hoist force data to quantify overall hoist forces during gate operation. Rather, this hoist data can be better utilized to evaluate total friction behavior.

Amperage responses were not used to compute friction results and were collected as verification that the motor performance was not causing unexpected gate responses. These responses indicated the motor was functioning in a stable manner and should be reviewed by a licensed electrician to further evaluate the motor's performance.

All results and recommendations provided in this report were based on the structure in its current condition; therefore, any significant changes in condition must be noted as they may alter their validity. Questions regarding this report and/or data should be directed to Kyle Ramer (kyler@bditest.com) at BDI. For further information on BDI's equipment, services, and analysis methods please visit www.bditest.com

INSTRUMENTATION AND LOAD TESTING PROCEDURE

GATE INSTRUMENTATION SUMMARY

Instrumentation and testing were performed on Gate 1 at the Rockwall Forney Dam on April 1st, 2020. Instrumentation plans have been provided along with this report and include the following number of instrumented locations and sensor types:

+ **REUSABLE SURFACE MOUNTED STRAIN TRANSDUCERS:** Each gate arm was instrumented with a total of 24 strain transducers at 6 locations on each of the gate arms (48 strain sensors total). A typical strain gage installation is shown in Figure 1. Note these sensors were installed with the mounting tabs on the extreme fiber of the strut flanges, which puts the center of the gage approximately 0.66" from the extreme fiber.
+ **TILTMETER ROTATION SENSORS:** MEMS style rotation sensors were located on the middle strut of the gate arm near the skin plate and near the trunnion hub (4 rotation sensors total). The rotation responses were used to calculate vertical skin plate movement and measure pin rotation relative to skin plate rotation. Typical tiltmeter installations are shown in Figure 1 and Figure 2.
+ **TORQUE SENSORS:** Two total torque sensors were installed on the hoist's pinion shafts (QTY1 on each hoist pinion shaft) near the cable hoist motor to measure direct torque and in turn lift force (See Figure 3).
+ **AMPERAGE SENSORS:** 3 Hall-Effect amperage transducers were clamped over each phase of the hoist motor to measure the motor's current draw (See Figure 4). The purpose of these sensors was to provide additional data in case there were any issues with the hoist systems and to verify any data issues related to lifting and lowering the gates.
+ **BDI'S STS-4 WIRELESS DATA ACQUISITION SYSTEM:** BDI's STS-4 wireless data acquisition (DAQ) was used to collect and record data during testing. A group of sensors were wired to each nodal DAQ which then communicated wirelessly back to the wireless base station and was controlled by BDI's STS-Live testing software.

Complete specifications are available upon request and can be found at http://www.bditest.com.

SENSOR INSTALLATION

BDI strain transducers were installed by first sanding paint off the struts to expose bare metal at two small locations (1"x2" areas) for the sensor's mounting tabs. Each transducer was then attached using a combination of fast-setting adhesive and accelerator and applying pressure until the adhesive was fully cured. Each strain transducer took approximately five minutes to attach.

Tiltmeters were installed using the same adhesive process as the strain transducers. However, no surface preparation was necessary.

Torque sensors were installed on the pinion shafts by capacitive discharge bonding. Properly bonding to the shaft required sanding the surface to a smooth finish, clean of any paint or grease. Responses from these gages were measured using Binsfeld Torque Trak 10k wireless transmitters.

A typical installation has been shown in Figure 1 through Figure 4. Access to all the sensor locations was provided by BDI's own SPRAT certified rope access technicians and engineers as shown in Figure 5.

Once testing was completed, sensors were removed, and exposed steel areas were covered using cold galvanizing compound.

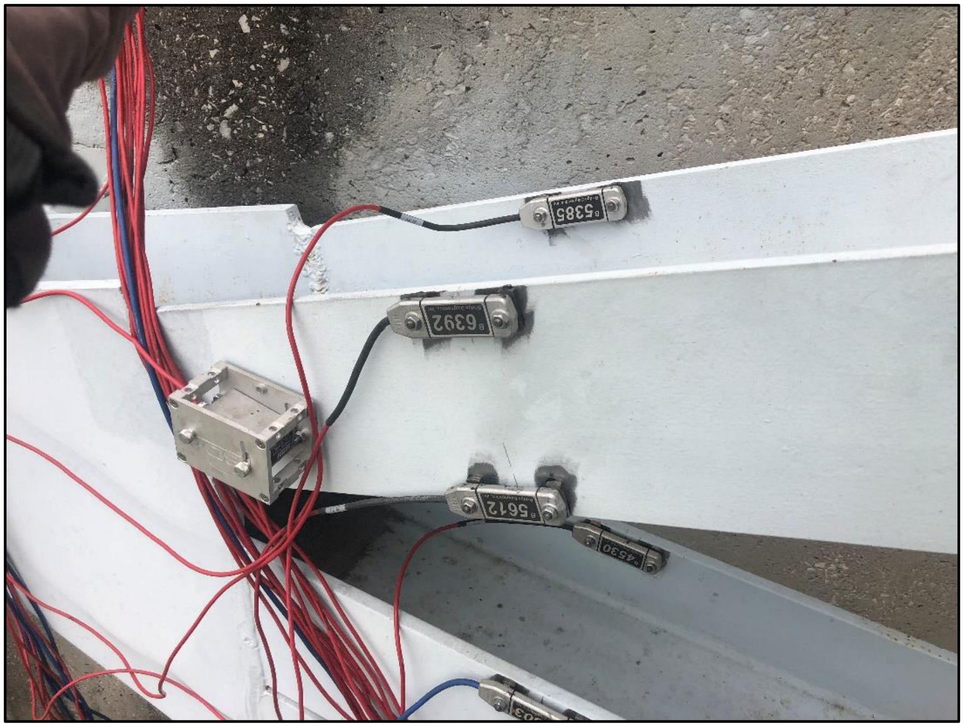

Figure 1 – BDI tiltmeter rotation sensor and reusable strain transducers installed near trunnion hub (Typical)

Figure 2 – BDI tiltmeter rotation sensor installed near skin plate (Typical)

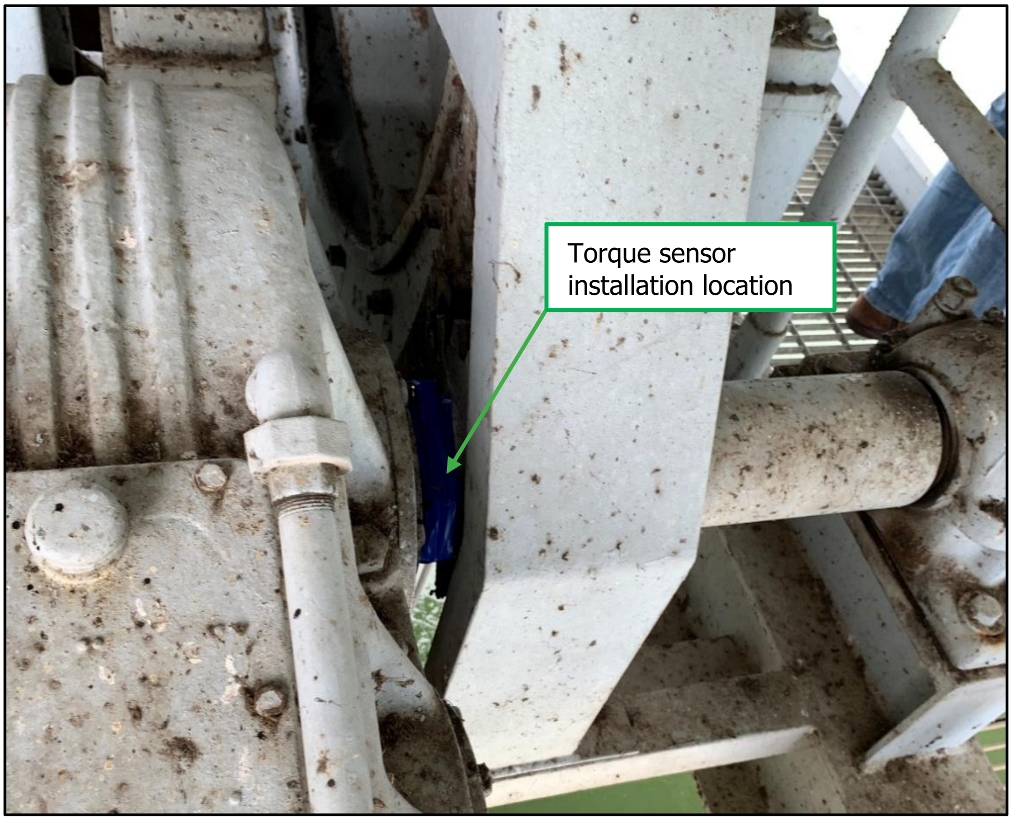

Figure 3 – Torque sensor installation on hoist pinion shaft (Typical)

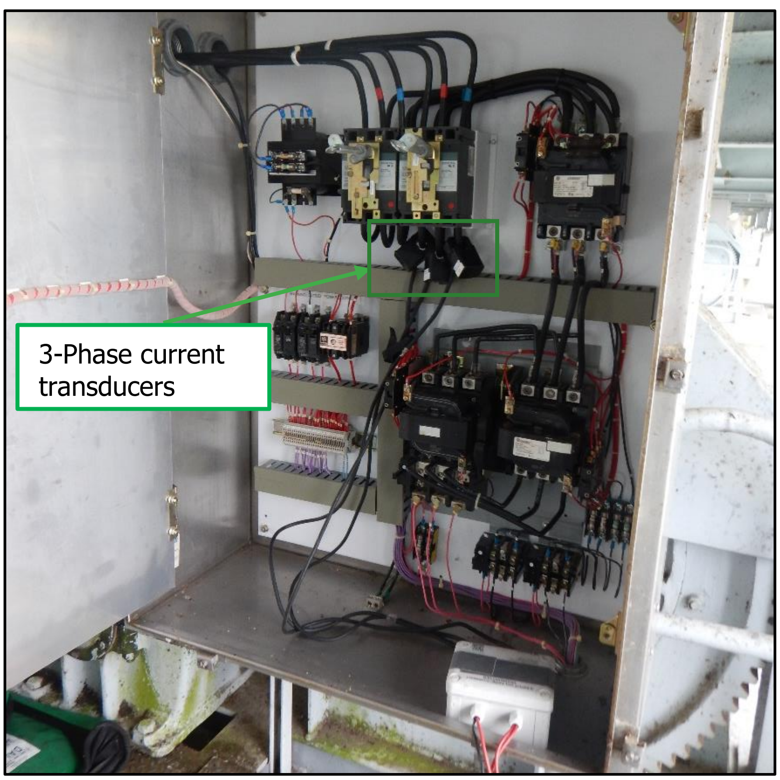

Figure 4 – Current transducers installed on hoist motor controls (Typical)

Figure 5 – BDI personnel installing instrumentation on the gate arm

TESTING PROCEDURES

Structural response data was recorded on all sensors at 50Hz while the gate was run through three spill tests. Each test consisted of three "up-down" cycles (direction reversals) without lowering the gate back to the sill. Each direction reversal consisted of lifting the gate approximately 6-12", pausing for a few seconds, and lowering the gate approximately 6", and repeating until all reversals had been completed.

RESULTS SUMMARY

GENERAL DISCUSSIONS BASED ON STRUCTURAL RESPONSES

The following outline contains general discussion points and observations that were made during the data review process. Note: Strain measurements were converted to stress for all subsequent analysis by multiplying the strain values by a steel elastic modulus of 29,000 ksi.

+ **DESCRIPTIONS OF RESPONSE MEASUREMENTS:** All sensor readings were zeroed at the end of each test (which consisted of three cycles of direction reversals) so that each measurement corresponded to response change relative to the final gate position as shown in Figure 6 (gates in the downward "closed" position with the hoist cables slacked as much as possible). It is also worth noting that the stresses did not always start and end at the same levels between tests. This variation in behavior is due to small changes in the flexed gate condition between the start and end of tests. It is common for the flex in the gate, caused by pin friction, to slowly release as it rests on the sill. The purpose of the three up-down cycles per test, prior to sitting the gate back onto the sill, is to ensure that these changes in boundary conditions, including gate flexure due to friction, did not affect BDI's trunnion friction results. ***It is important to note that the recorded measurements were changes in structural response due to gate movement, and do not include the in-situ stresses due to the dead load, cable wrap, and hydrostatic loads present prior to testing.***
+ **QUALITATIVE DATA REVIEW:** Review of the response data indicated a good level of reproducibility between the three tests. For reference, Figure 6 and Figure 7 show stress responses measured along Gate 1's right arm top strut for all three tests (Test #1-3). The data in these plots have been provided as both a function of time and the gate position as determined by the skin plate tilt sensor. Structural response behavior slightly varied during the first test's first cycle compared to subsequent lift/lower cycles and tests. After the first test's initial lift to approximately 9 inches, the gate was lifted further up to 16 inches instead of being lowered to 4 inches. This resulted in a small stress spike, followed by a continued linear increase in stress until the gate was stopped and subsequently lowered. Despite this variation in test procedures, the first test stress responses remained consistent with the two subsequent cycles and the two subsequent tests.
+ **DIRECTION/FRICTION REVERSAL IN RESPONSES:** The difference in stress during gate opening and closing for a given position is shown in Figure 8. The stress variation at any given gate position was a result of direction reversal and in turn due to trunnion friction reversal. This statement is true since all other loads such as dead-load and hydrostatic pressure were essentially constant barring small changes in hydrostatic pressure due to slight changes in head. This direction/friction reversal is depicted in Figure 9, with deflected shape renderings from a gate arm finite element model under lifting and lowering loads. Note that this figure shows an arm configuration that does not match this gate, but the concept of the direction/friction reversal still applies.
+ **MOTOR PERFORMANCE:** Current measurements taken at the hoist motor indicated steady and stable current draws during the lifting and lowering portions. An example plot of current draw and gate position is provided in Figure 10. Current draw ranges during lifting were higher than the ranges during lowering, which is common due to gravity/dead load. These results are summarized along with recorded peak in-rush current in Table 2. Note that the sample rates used during testing were set for collecting gate responses and may not have been appropriate to fully capture the in-rush current. The readings should be evaluated by a licensed electrician with knowledge of the operating parameters.
+ **TORQUE AND HOIST FORCE:** Due to restrictions caused by the hoist limit switches, the hoist cables could not always be fully slacked at the beginning and end of the performed tests. Throughout testing of the Rockwell Forney gates, it was found that this limit switch restriction varied gate to gate and arm to arm. Therefore, it is not recommended to use the collected torque and hoist force data to quantify overall hoist forces. Rather, this data was utilized to evaluate total friction behavior, which is observed as half the difference between the lifting and lowering torque/force (friction reversal). Torque measurements taken at the hoist pinion shafts, and the derived hoist forces, had a certain degree of shifting and reversals between arms as shown in Figure 23 and Figure 24. This observed behavior indicated some level of racking/hoist system alignment issues in the gate as

it was operated. Note that issues with the wireless transmitter connected to the left gate hoist gages caused intermittent loss of data. While not optimal, this data loss did not significantly affect the hoist results summarized in this report.

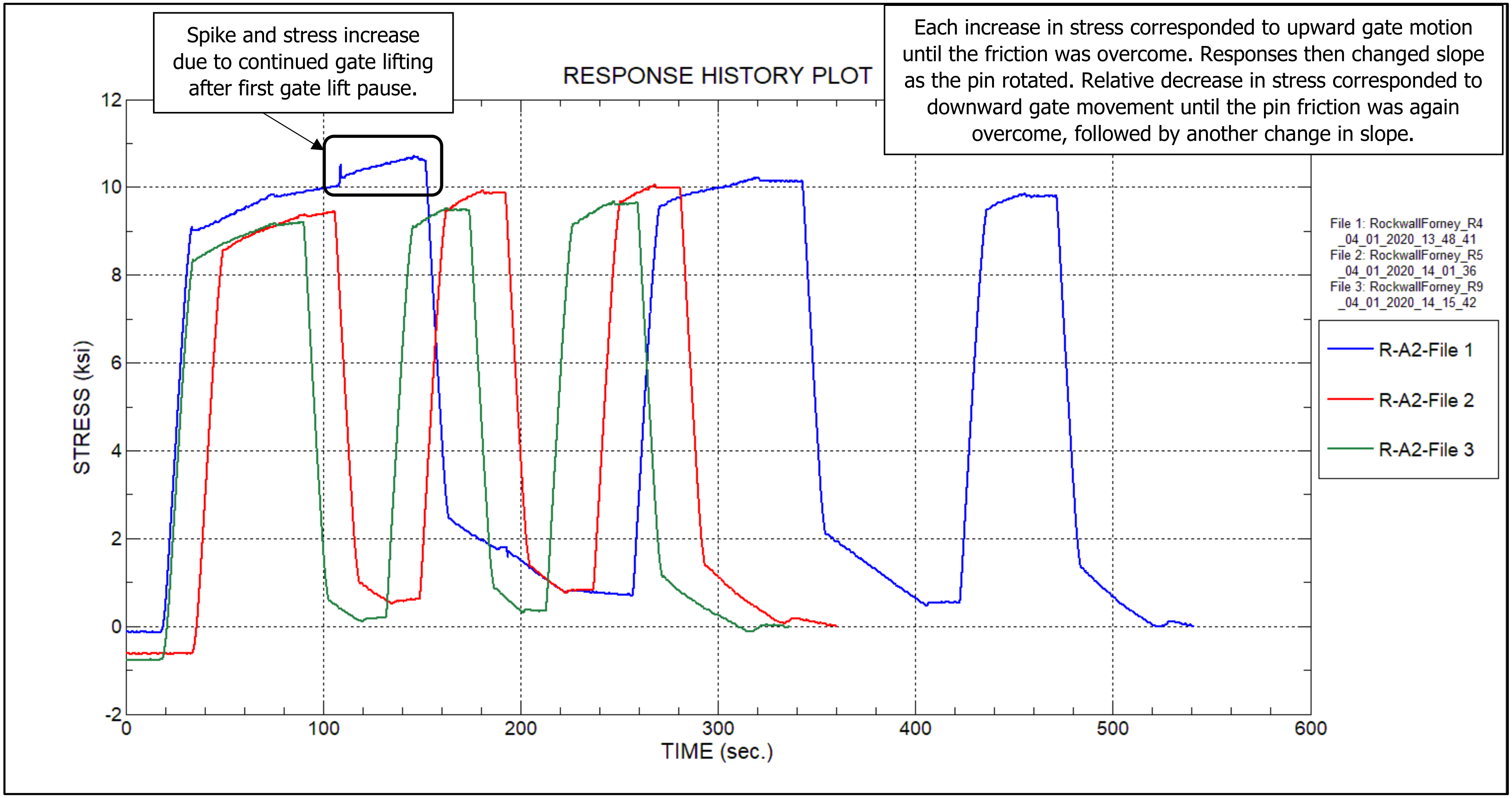

Figure 6 – Stress response history – Right arm – Gage A2 – Time based
File 1 = Test Run 1, File 2 = Test Run 2, File 3 = Test Run 3

(Section A along top strut near pin – Sensor location 2 along bottom of inner flange)

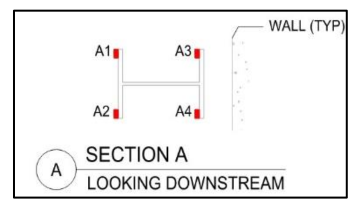

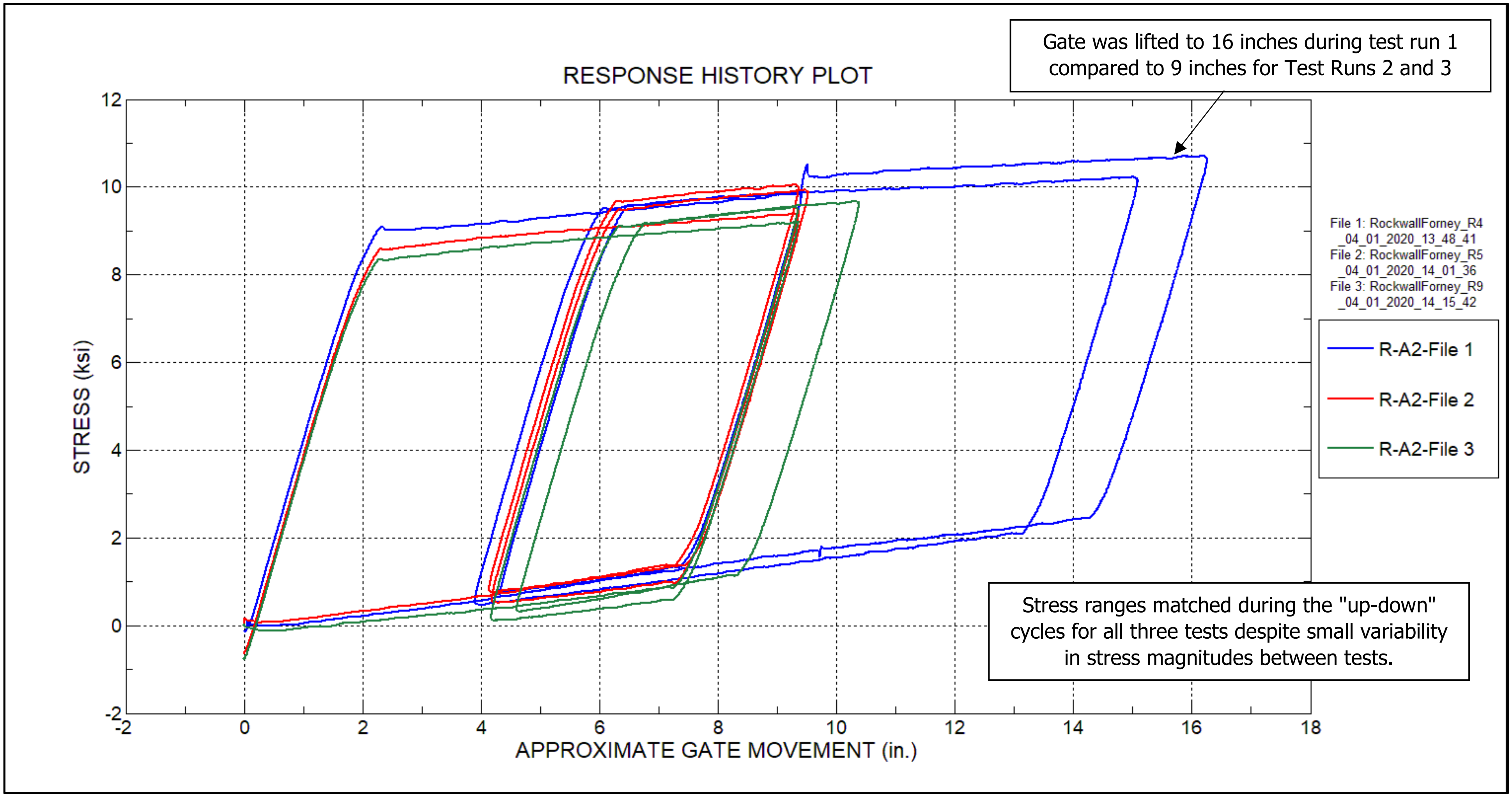

Figure 7 – Stress response history – Right arm – Gage A2 – Function of gate movement
File 1 = Test Run 1, File 2 = Test Run 2, File 3 = Test Run 3

(Section A along top strut near pin – Sensor location 2 along bottom of inner flange)

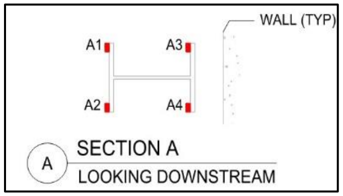

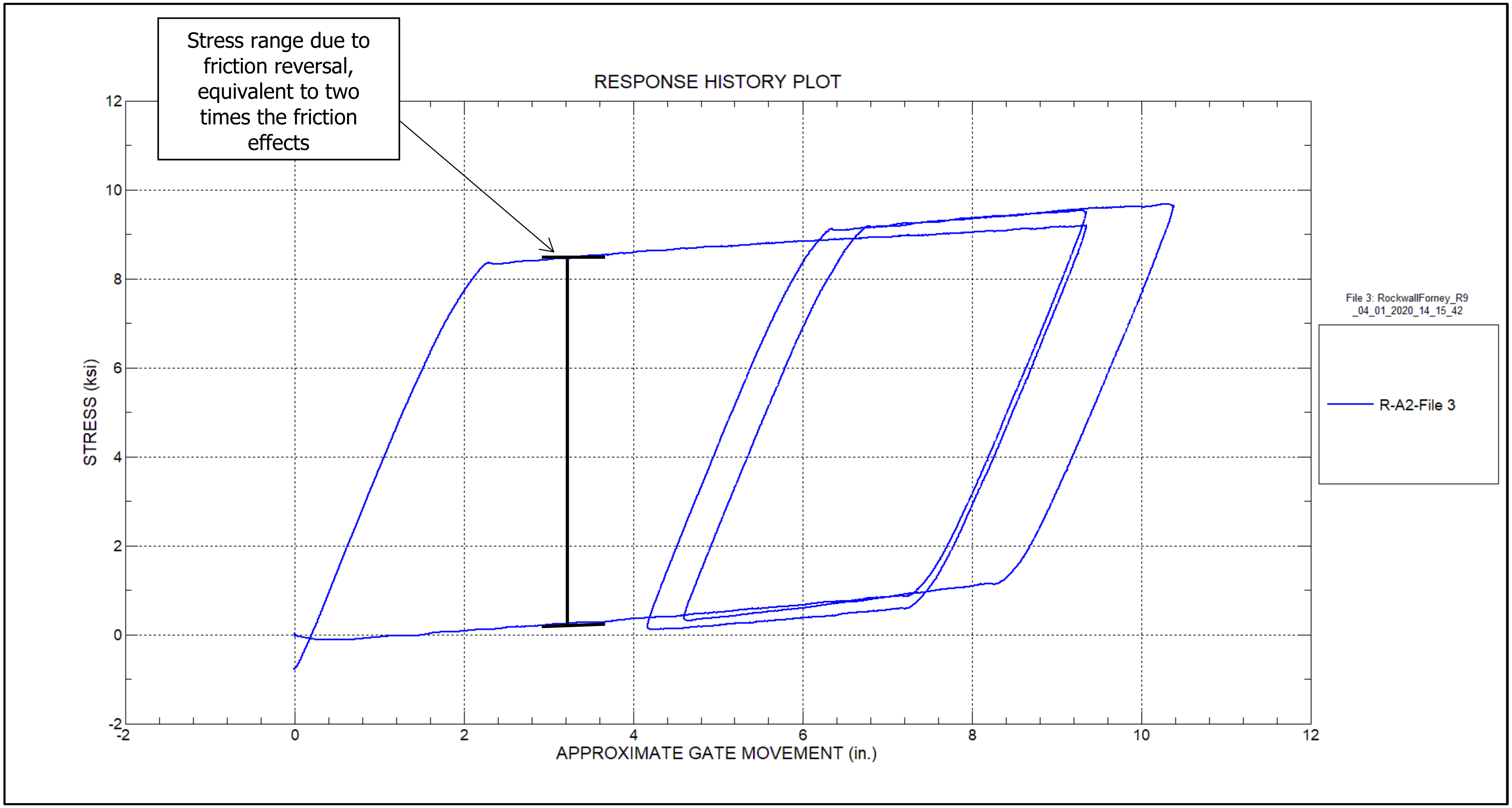

Figure 8 – Stress response history – Right arm – Gage A2 – Friction effect in stress responses

(Section A along top strut near pin – Sensor location 2 along bottom of inner flange)

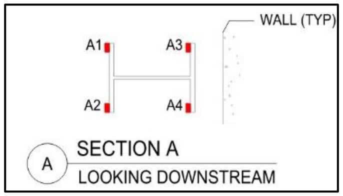

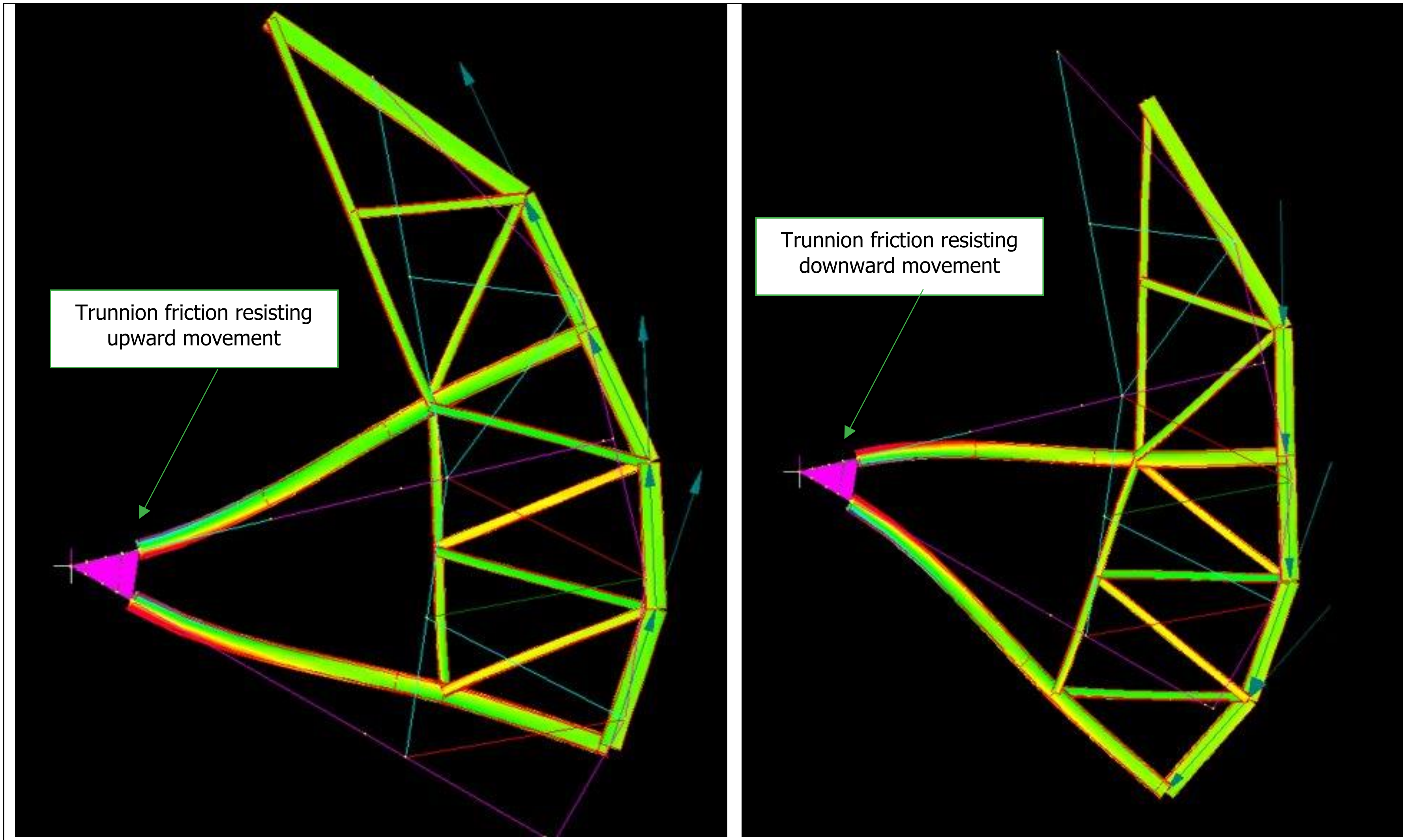

Gate traveling upward **Gate traveling downward**

Figure 9 – Deflected shapes during lifting and lowering of Gate – Visualization of direction/friction reversals

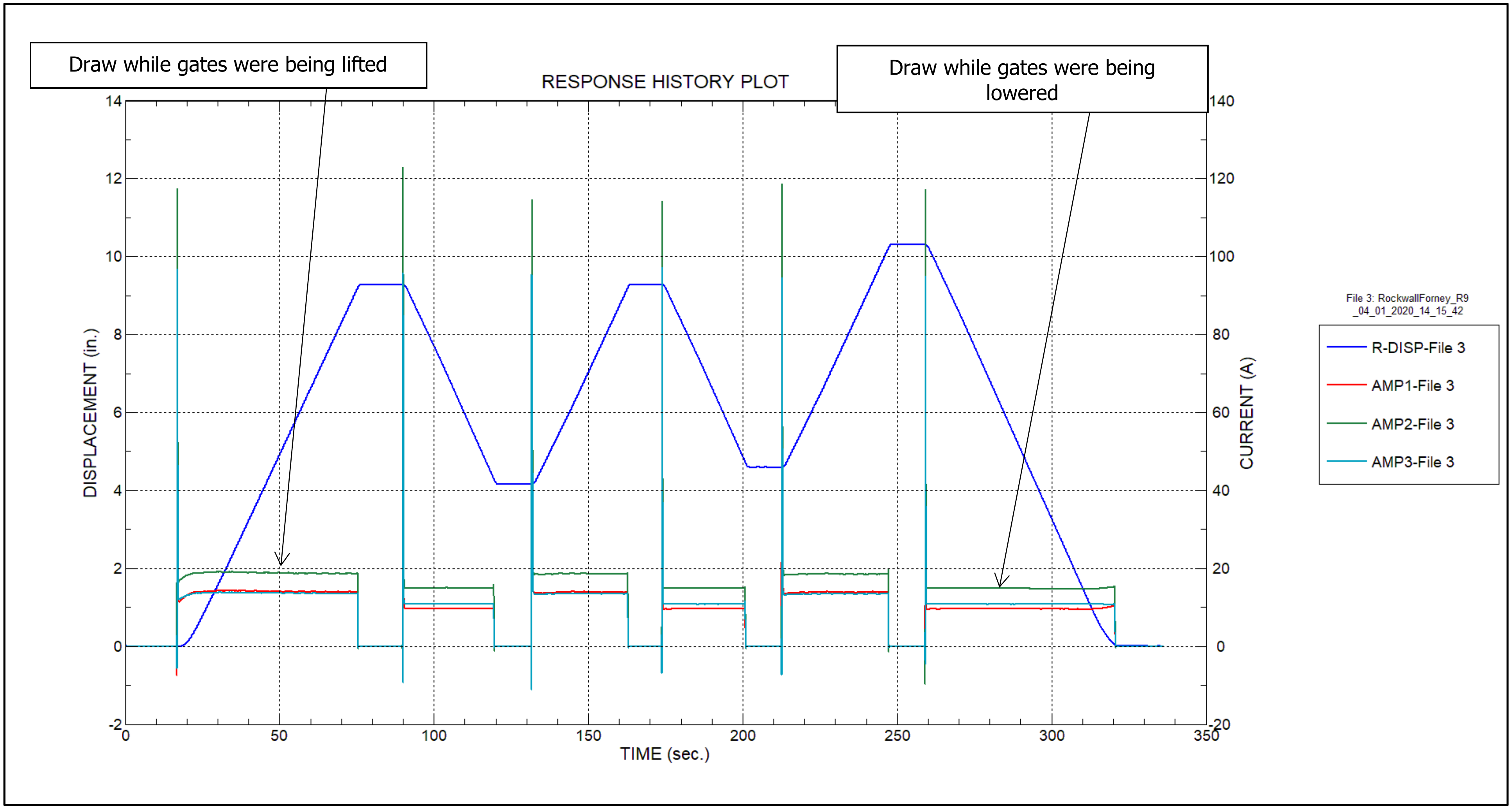

Figure 10 – Motor current & gate movement response history – Lift motor – Highlighting motor draw during lift and lower cycles

Methodology and Findings of The Strut Force and Moment Calculations

The following outline provides the methodology used to calculate the required member forces and moments.

- **CHANGE IN STRESS DUE TO GATE OPERATION:** Strain data can be viewed as a function of time starting when the gate was in the down position and was then lifted off the sill. When examining data in this manner, it is easy to see how stresses ramped up as the gate began to move and then changed slope once pin friction was overcome and the trunnion hub began to rotate with the gate. The first point in time where the friction was overcome (both lifting and lowering) has been highlighted in the stress histories shown in Figure 11. These stress histories show the response of all four sensors along the top strut of the right arm (Section A). ***It is important to note that the recorded measurements were changes in structural response due to gate movement, and do not include the in-situ stresses due to the dead load, cable wrap, and hydrostatic loads present prior to testing.***
- **CALCULATION OF STRUT CROSS-SECTIONAL MOMENTS:** The use of four strain gages per strut cross-section allowed accurate in-plane flexural bending moments to be computed from the recorded strain measurements. These moments were computed for every cross-section in each gate arm using the basic mechanics equation provided in Figure 12.

  In-plane or weak-axis flexure refers to bending about a given strut's web. This designation is consistent with typical nomenclature. In-plane bending can be observed visually from the strain response histories as a difference between the top and bottom stresses, whereas out-of-plane or strong-axis bending is visualized as the difference in stress from side to side. Figure 13 provides a visual reference for both types of strut flexure.
- **EXAMINATION OF RESPONSES AS A FUNCTION OF GATE POSITION:** Changes in cross-sectional moment related to friction becomes clearer when the responses are plotted as a function of gate position. Because the gate was operated with several up and down movements, the effects of friction associated with each direction reversal can be viewed for all measured and calculated responses. Figure 14 through Figure 17 show all cross-sectional flexural moment plots for both trunnion arms. The responses in these plots have been centered about the stress state corresponding to a zero-moment, unflexed condition. The zero-moment offset was estimated as the average moment values between up and downward movement (i.e. half the moment difference) at the gate position with the greatest pin friction moment difference (greatest difference between lifting and lowering).
- **TRUNNION FREE-BODY-DIAGRAM & PIN MOMENT CALCULATION:** Figure 18 shows the instrumented member cross-sections and shows how the measured cross-sectional flexural responses were used to compute pin moment. The in-plane moment values used in these calculations were determined directly from the strain measurements at each cross-section using the provided mechanics equations. It should be noted that the out-of-plane moments were not considered in the calculation of pin moment since they were orthogonal to the axis of the pin rotation. Total pin moment was then determined by summing all the moment components about the pin, which included the in-plane moment and the shear components at the strut cross-sections nearest the pin.
- **STRUT SHEAR CALCULATION:** From the examination of the trunnion free-body-diagram described above, the shear vectors at the three struts were a primary component in the pin moment calculation. For this type of structural element, shear vectors were calculated using the moment differential between the two cross sections along each strut. It is important to recognize that shear was constant between the two instrumented cross-sections and the applied shear was a function of the recorded change in moment ($V = dM/dX$). Subsequently, the shear vectors were calculated by dividing the difference in moment by the distance between the two instrumented cross-sections. Shear values for each strut have been plotted as a function of gate position in Figure 19 and Figure 20.

+ **CALCULATION OF PIN MOMENT DUE TO FRICTION:** Once all the trunnion arm force vectors were calculated, the equations shown in the free-body-diagram were applied to compute pin moment as a function of gate position. It is important to note that because the calculated pin moment range corresponds to a direction reversal, a reversal in friction also occurred. The effect of direction reversal on pin moment due to friction is best conceptualized by centering the moment response plots about the zero-moment axis. The moment due to lifting and the moment due to lowering can then be visualized as a change from this new zero point corresponding to the gate in an unflexed condition. Therefore, the total moment differential between lifting and lowering was twice the moment due to friction acting in a single direction. Pin-moment plots have been provided in Figure 21 and Figure 22. From these plots, it is apparent that pin moment due to friction remained relatively constant throughout the gate operation tests, with a slight decrease in pin friction moment as the gate continued to be lifted. This slight decrease in pin friction moment most likely corresponded to the change in hydrostatic load as the gate position changed. Pin-moment plots for all tests on Gate 1 are also provided for reference in Appendix B – Gate 1 Pin Moment Component Plots.

+ **SHAFT TORQUE & HOIST FORCE:** Torque measurements were taken on the pinion shafts near the hoist motor during testing, with single torque gages installed on the left and right hoist pinion shaft. Responses were recorded in units of micro-strain and converted to torque in units of kip-ft using Equation 1 thru Equation 3 and the following shaft properties.

$$d_O = 5.5\ inches, \qquad d_I = 0\ inches, \qquad E = 29000\ ksi, \qquad \nu = 0.3$$

$$G = \frac{E}{2(1+\nu)}$$

Equation 1

$$J = \frac{\pi\left({d_O}^4 - {d_I}^4\right)}{32}$$

Equation 2

$$\tau = \varepsilon * \frac{2GJ}{\frac{d_O}{2} * 1000000 * 12}$$

Equation 3

Figure 23 shows example torque measurements, recorded on the Gate 1 torque shafts. Best practices for torque measurements is to measure torque on opposite sides of the shaft so that any bending in the shaft can be removed by averaging the two responses. Due to access limitations, only one gage at each location could be installed. Therefore, any bending in the shaft may be reflected in the torque measurements and may be related to the peaks and valleys observed in the torque responses.

Torque values were converted to force in the hoist cables per gate arm using the gear ratio and drum radius, as shown in Figure 24. The gear ratio and drum radius were 5.182 and 1.086 feet respectively, as defined in the provided as-built shop drawings. It should be noted that the hoist force calculated may be smaller than the actual hoist force applied. This difference is due to the limit switch engaging the brake before the hoist cable was fully slacked, resulting in an initial force in the cable. A hoist force due to total gate friction was then calculated. This friction hoist force was equal to half the differential in force measured during the lifting and lowering of the gate (similar to the pin friction calculations). As shown in Table 3, the change in cable force due to friction was generally consistent between tests. Note that the total hoist force was due to the total friction effects, including side seal, hoist bearings, trunnion friction effects, etc. It is difficult to determine the exact proportion and composition of the total friction sources. Additional torque and hoist force plots for all collected data files are provided in Appendix A – Gate 1 Torque and Hoist Force Plots.

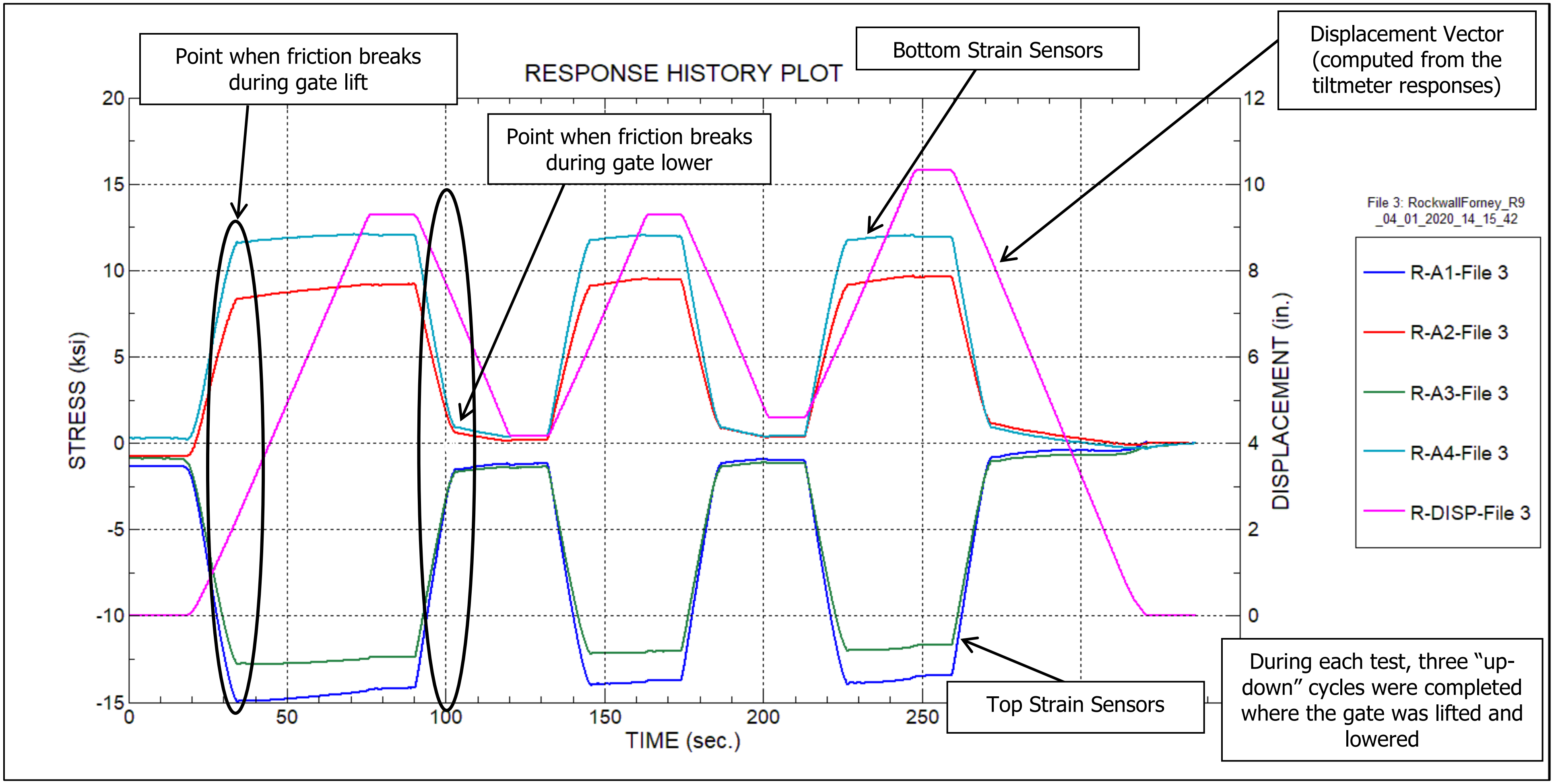

Figure 11 – Stress response & gate movement history – Right arm – Section A - Highlighting friction behavior (Section A along top strut near pin)

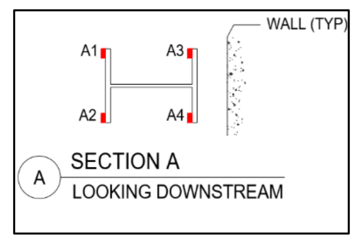

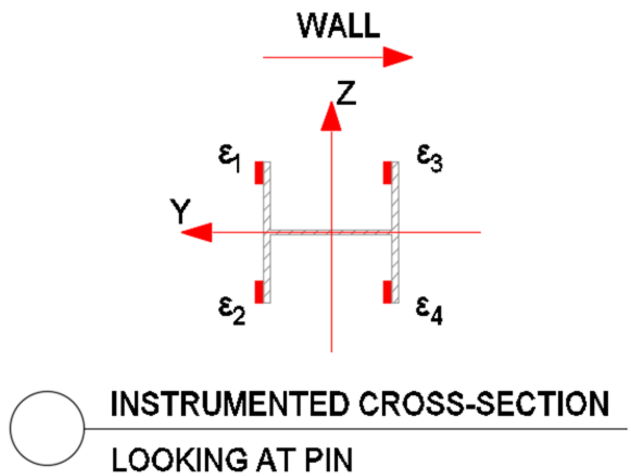

Calculation of Weak-axis (In-plane) bending

$$M_Y = \frac{E[\frac{\varepsilon_2 + \varepsilon_4}{2} - \frac{\varepsilon_1 + \varepsilon_3}{2}]S_{Y(gage)}}{2}$$

Sy(gage) = Section modulus to the center of gages (not extreme fiber of flanges)
(locations of gages were accounted for in moment computation)

Figure 12 – Basic mechanic equation used to calculate moment

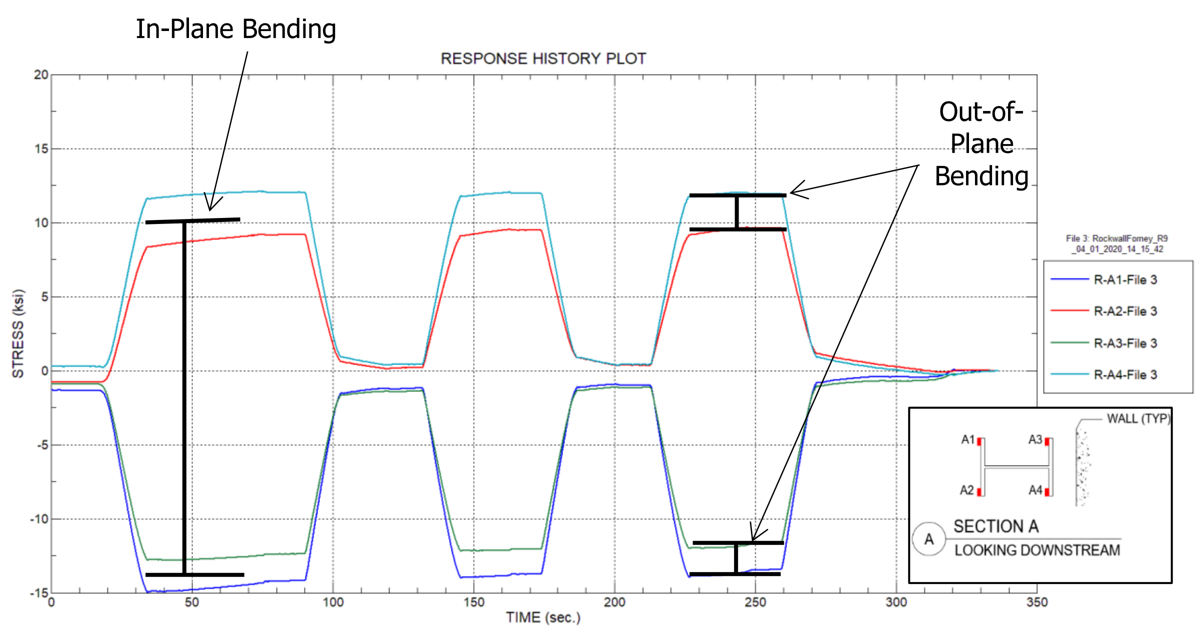

Figure 13 – Stress response history – Right arm – Section A – Bending components
(Section A along top strut near pin)

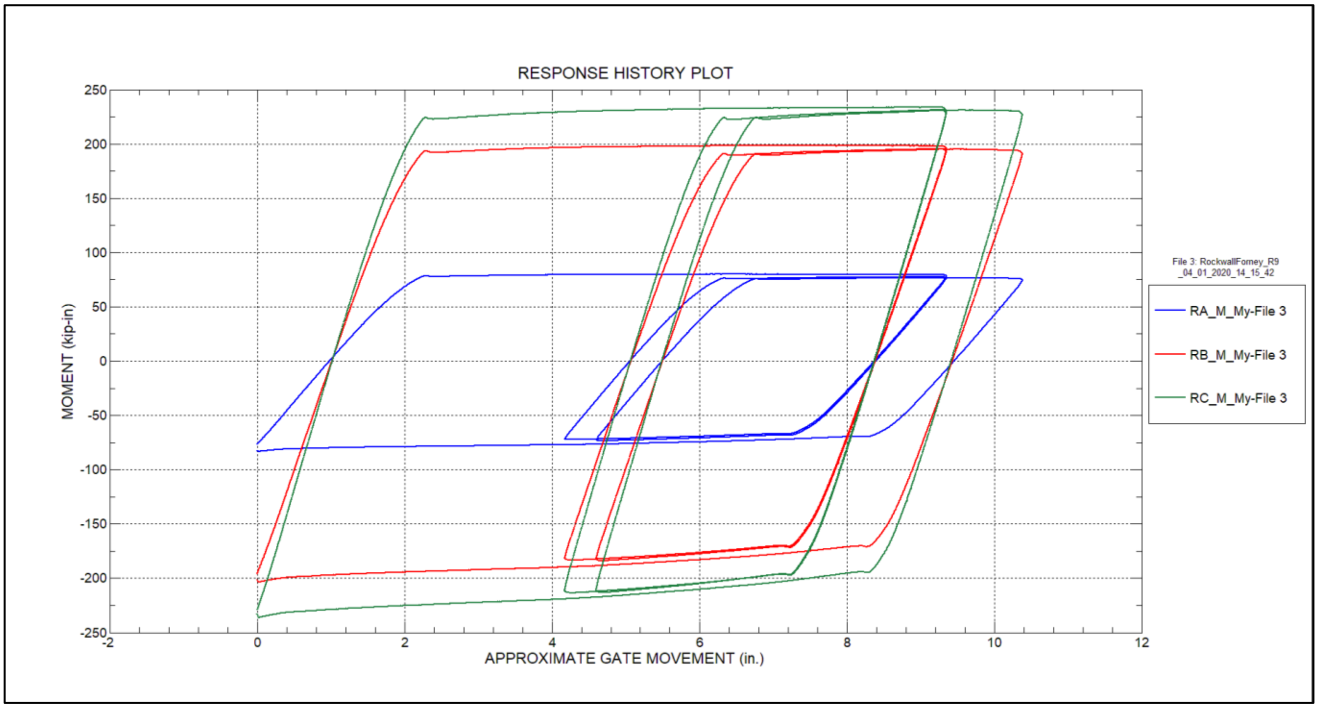

Figure 14 – In-plane moment response history – Right arm – Sections near pin

(RA = Right Arm Top Strut, RB = Right Arm Middle Strut, RC = Right Arm Bottom Strut)

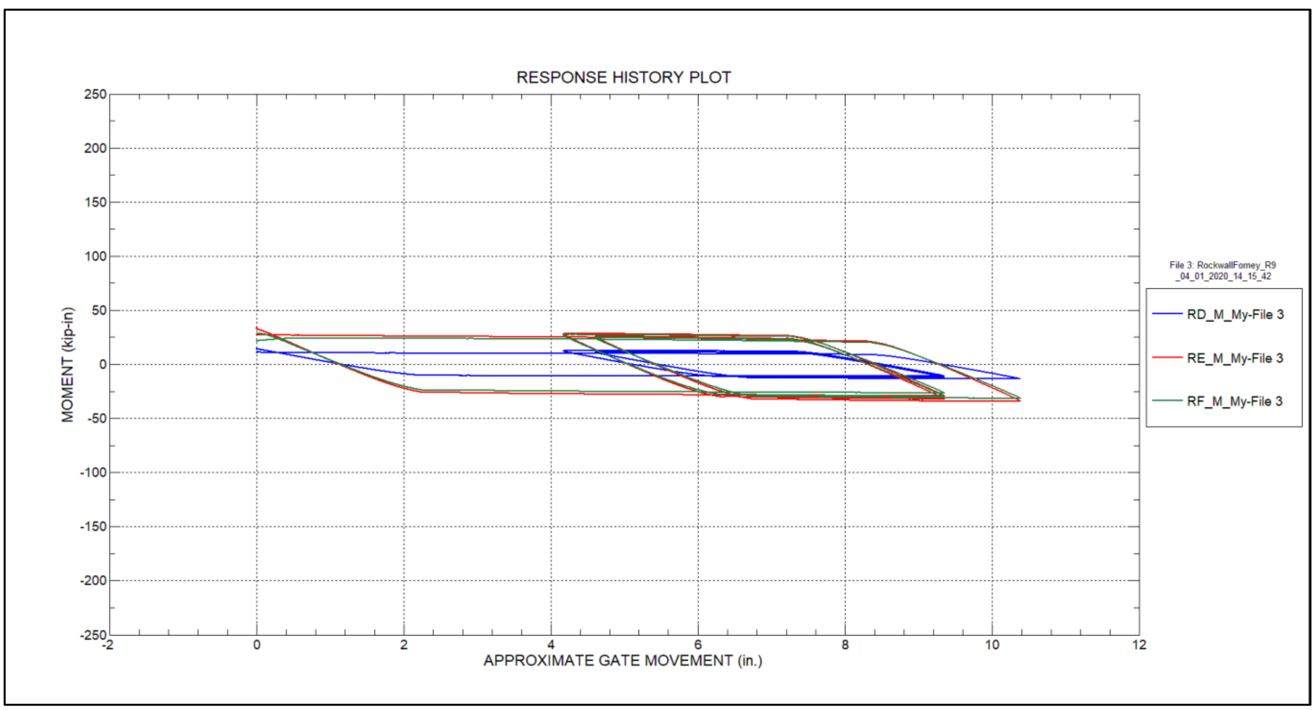

Figure 15 – In-plane moment response history – Right arm – Sections away from pin

(RD = Right Arm Top Strut, RE = Right Arm Middle Strut, RF = Right Arm Bottom Strut)

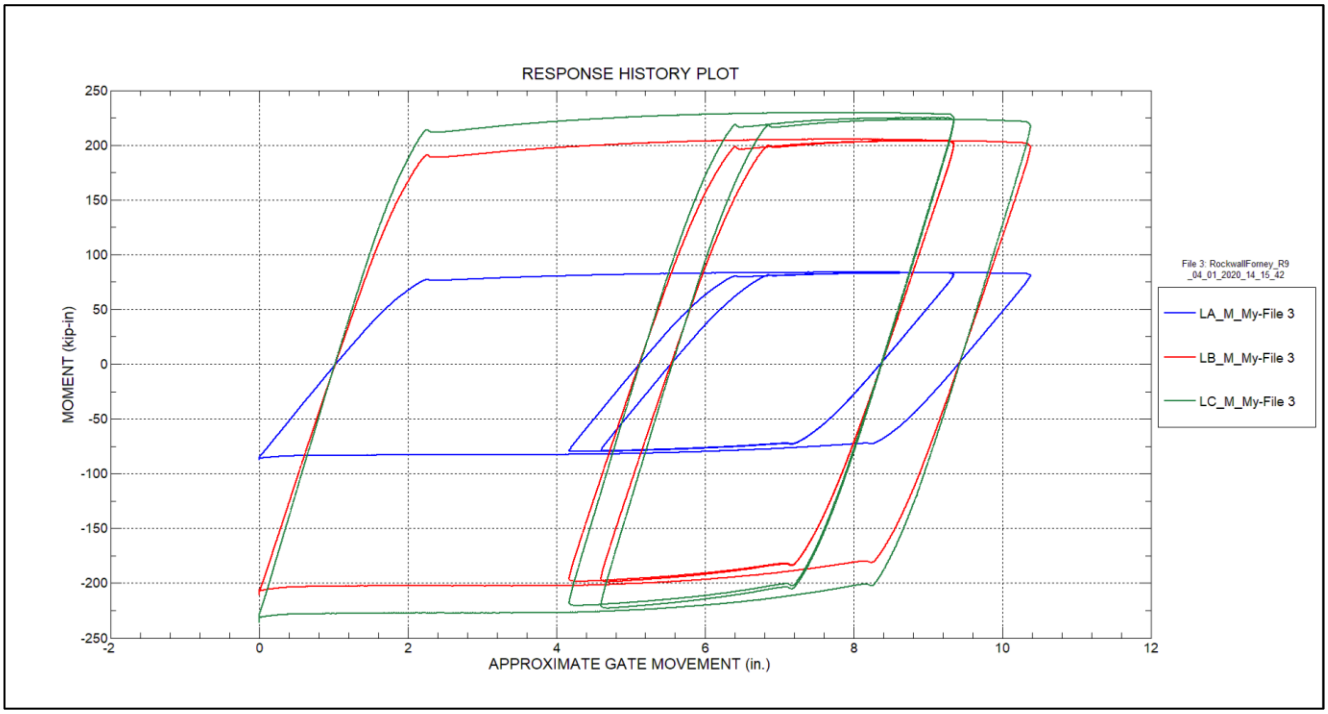

Figure 16 – In-plane moment response history – Left arm – Sections near pin

(LA = Left Arm Top Strut, LB = Left Arm Middle Strut, LC = Left Arm Bottom Strut)

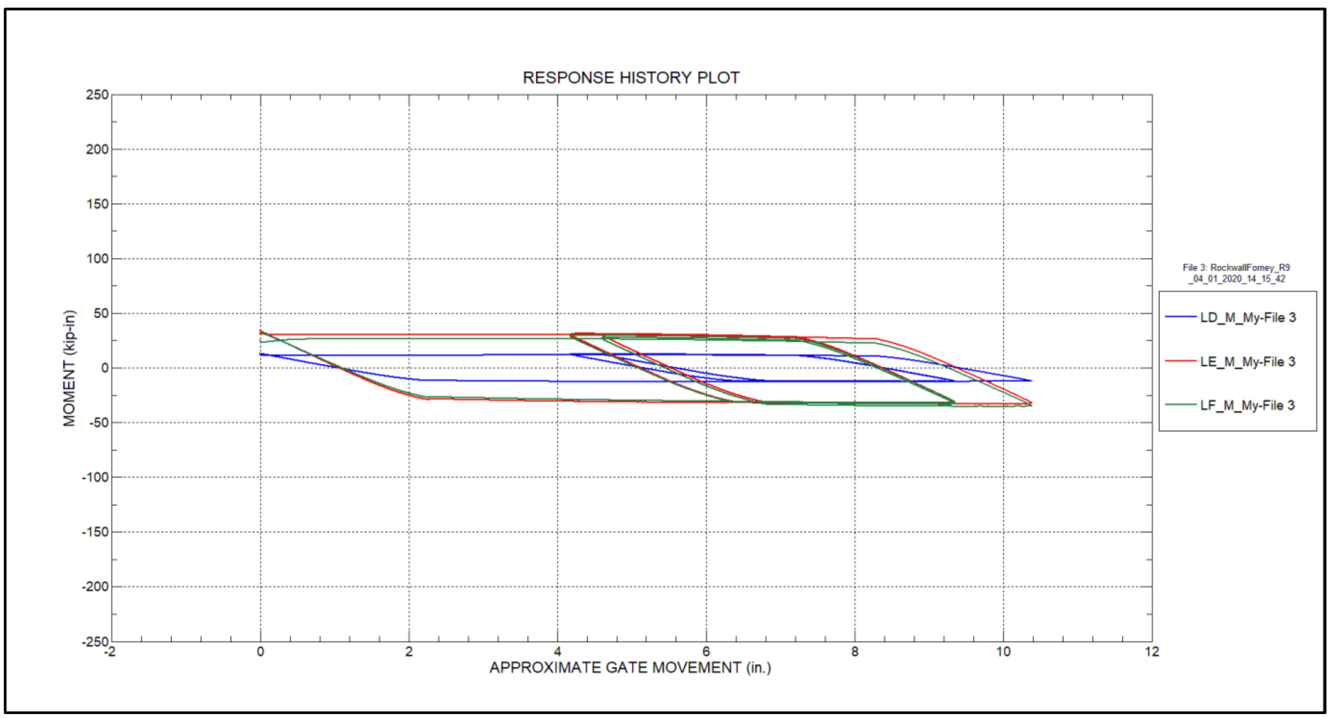

Figure 17 - In-plane moment response history – Left arm – Sections away from pin

(LD = Left Arm Top Strut, LE = Left Arm Middle Strut, LF = Left Arm Bottom Strut)

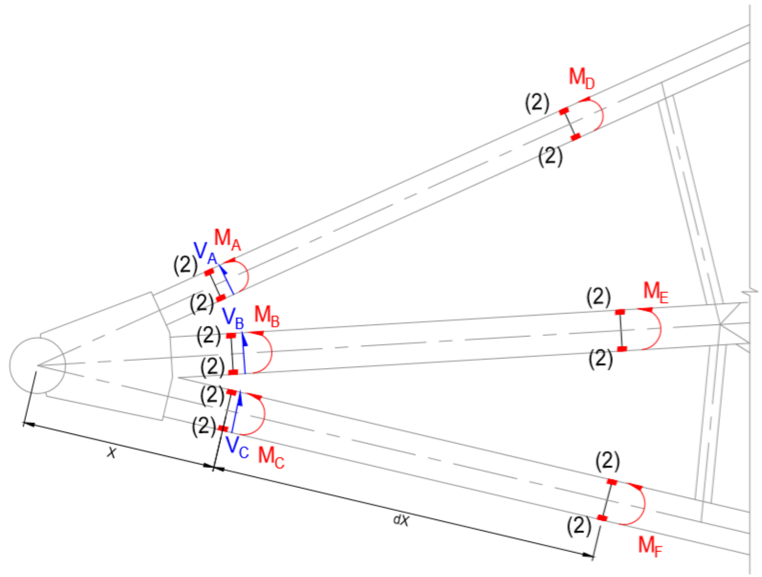

Elevation View of Gate Arm

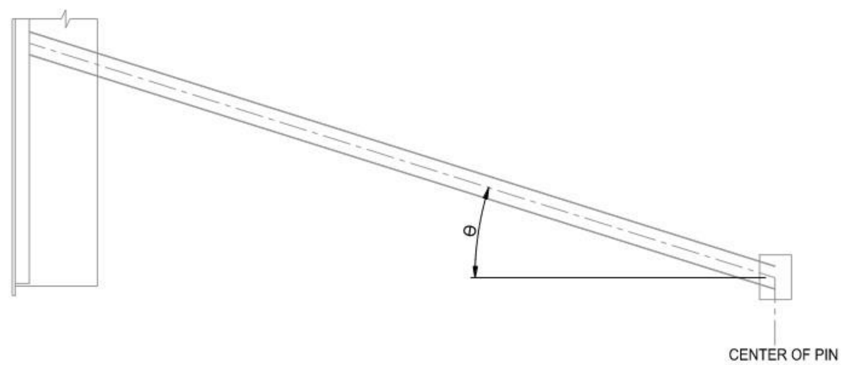

Plan View of Gate Arm

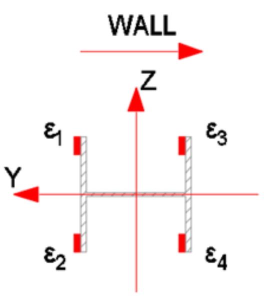

$$M_Y(M_A, M_B, M_C, M_D, M_E, M_F) = \frac{E\left[\frac{\varepsilon_2 + \varepsilon_4}{2} - \frac{\varepsilon_1 + \varepsilon_3}{2}\right] S_{Y(gage)}}{2}$$

$$V_A = \frac{M_A - M_D}{dX}$$

$$V_B = \frac{M_B - M_E}{dX}$$

$$V_C = \frac{M_C - M_F}{dX}$$

$$\sum M_o = 0$$

$$M_{PIN} = [X(V_A + V_B + V_C) + M_A + M_B + M_C]\cos\theta$$

Figure 18 – Direct calculation of pin moment from strain measurements

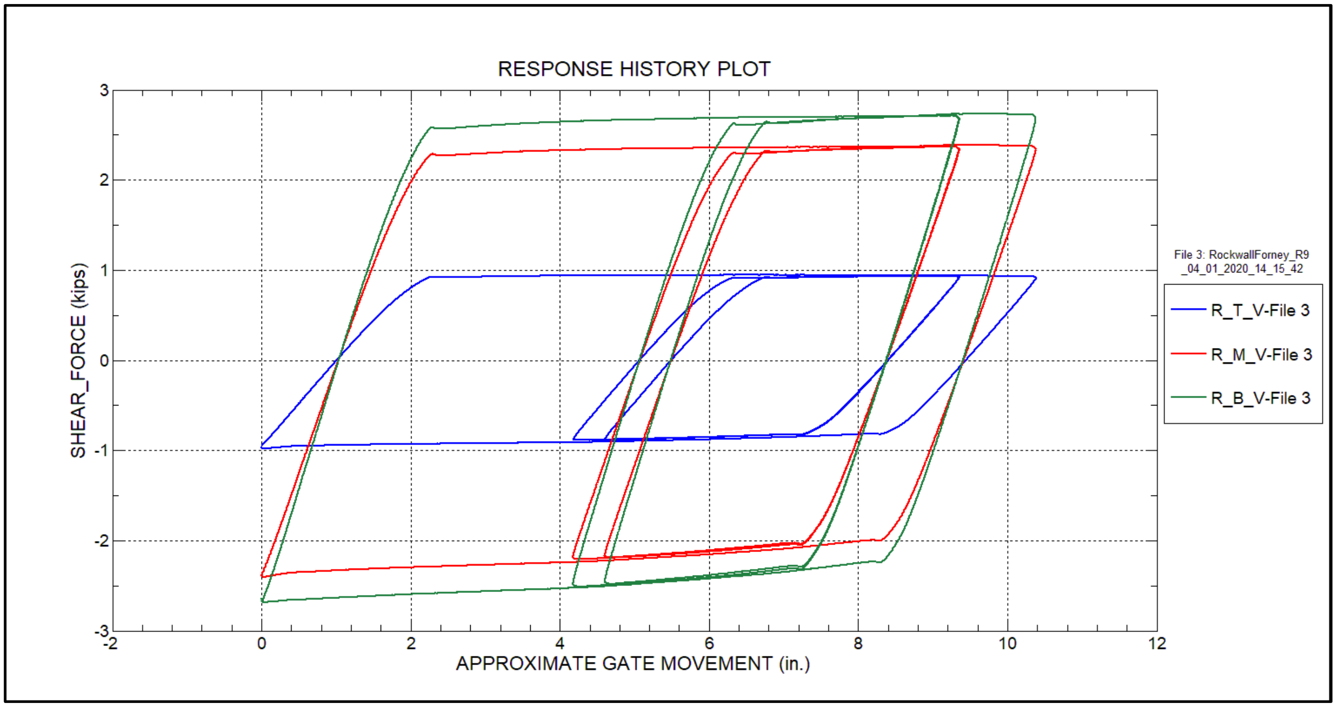

Figure 19 – Strut shear response history – Right arm

(R_T = Right Arm Top Strut, R_M = Right Arm Middle Strut, R_B = Right Arm Bottom Strut)

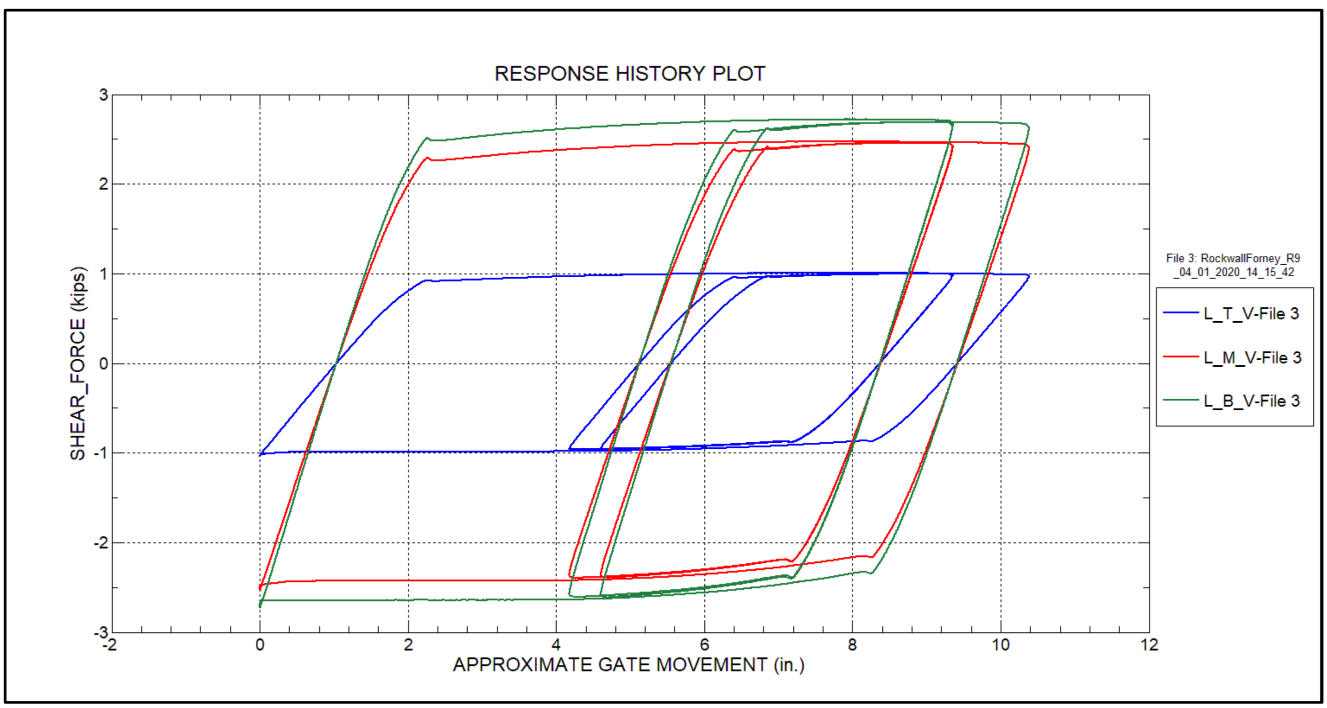

Figure 20 – Strut shear response history – Left arm

(L_T = Left Arm Top Strut, L_M = Left Arm Middle Strut, L_B = Left Arm Bottom Strut)

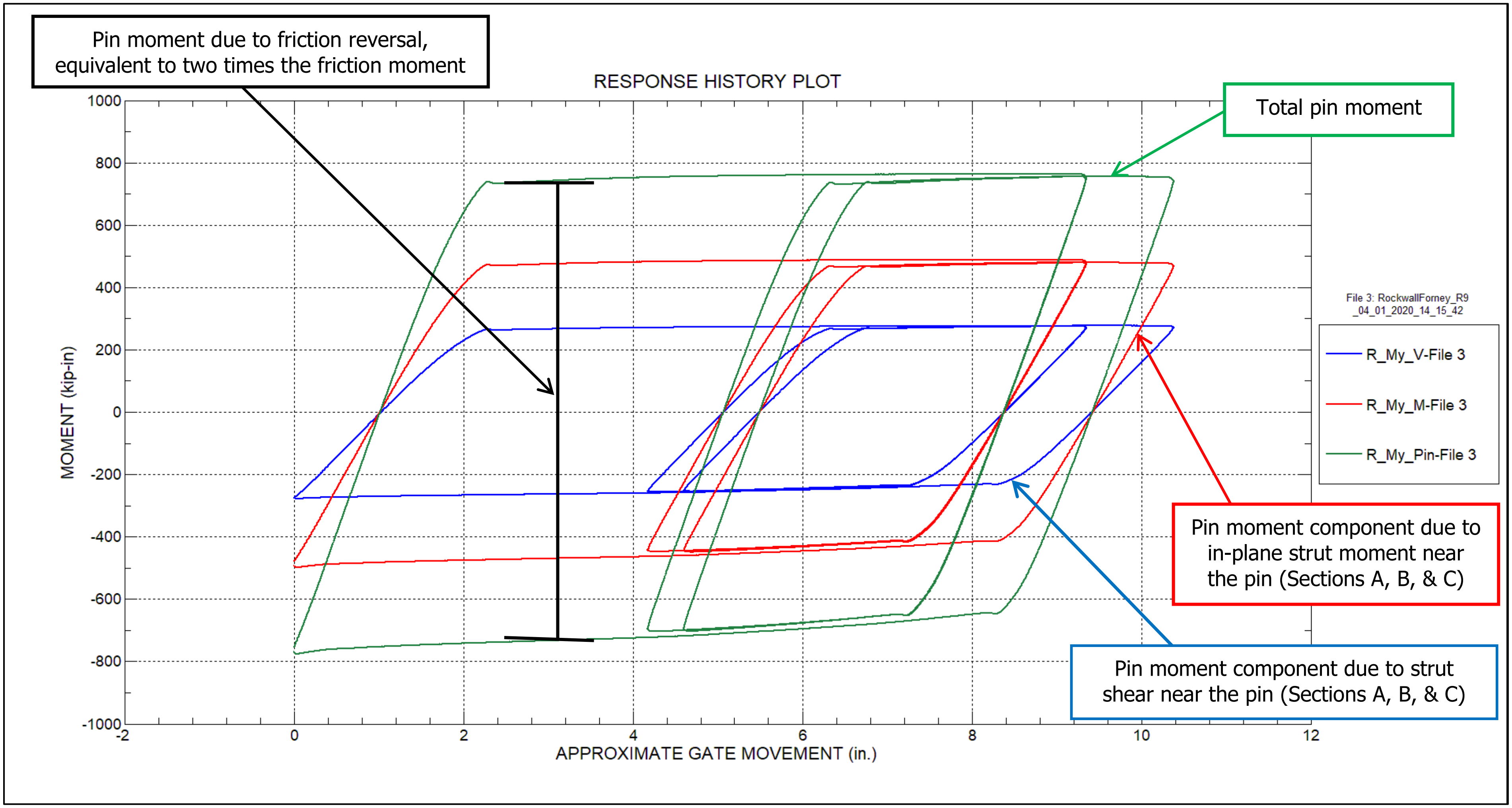

Figure 21 – Pin moment response history – Right arm

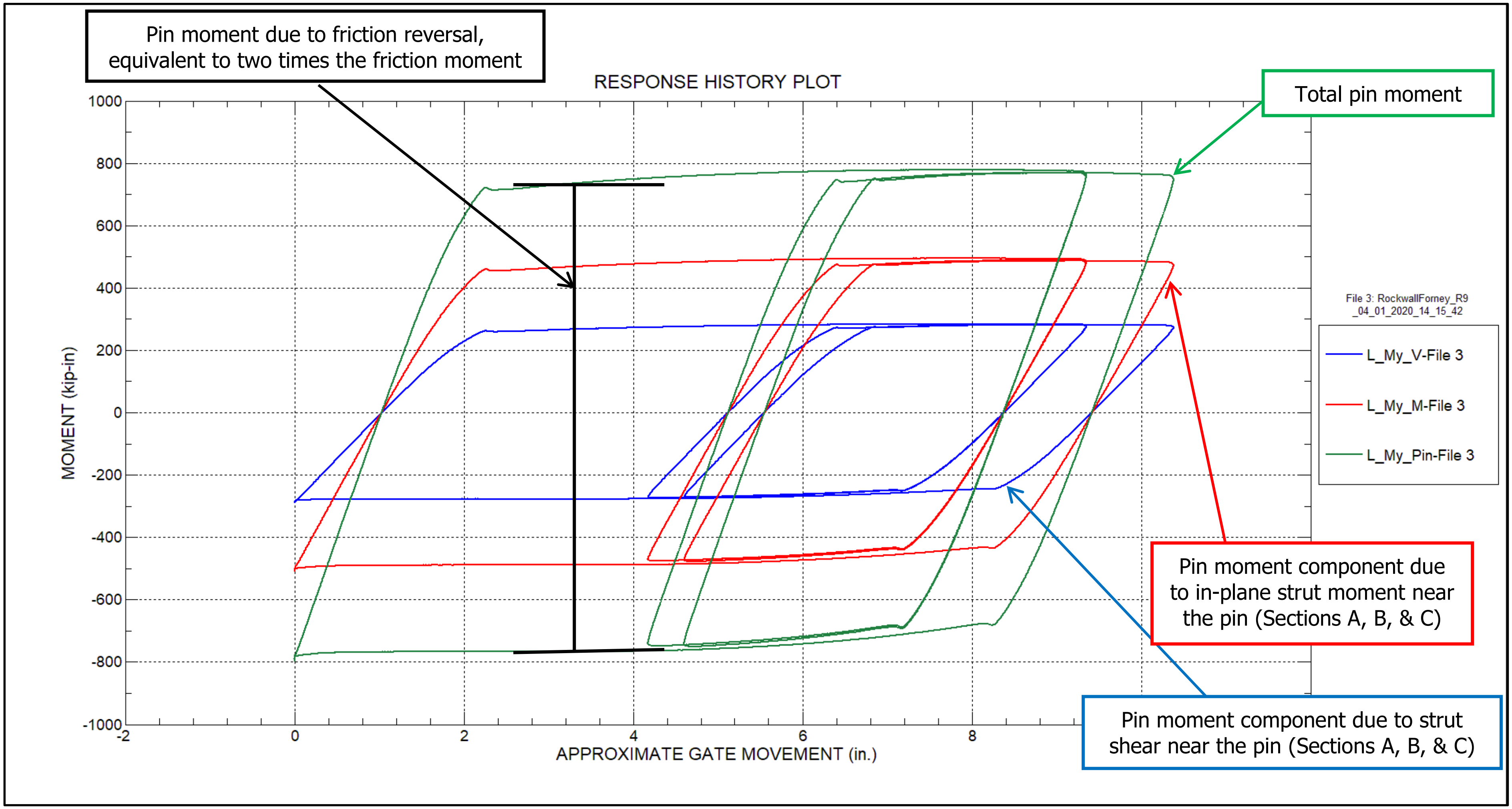

Figure 22 – Pin moment response history – Left arm

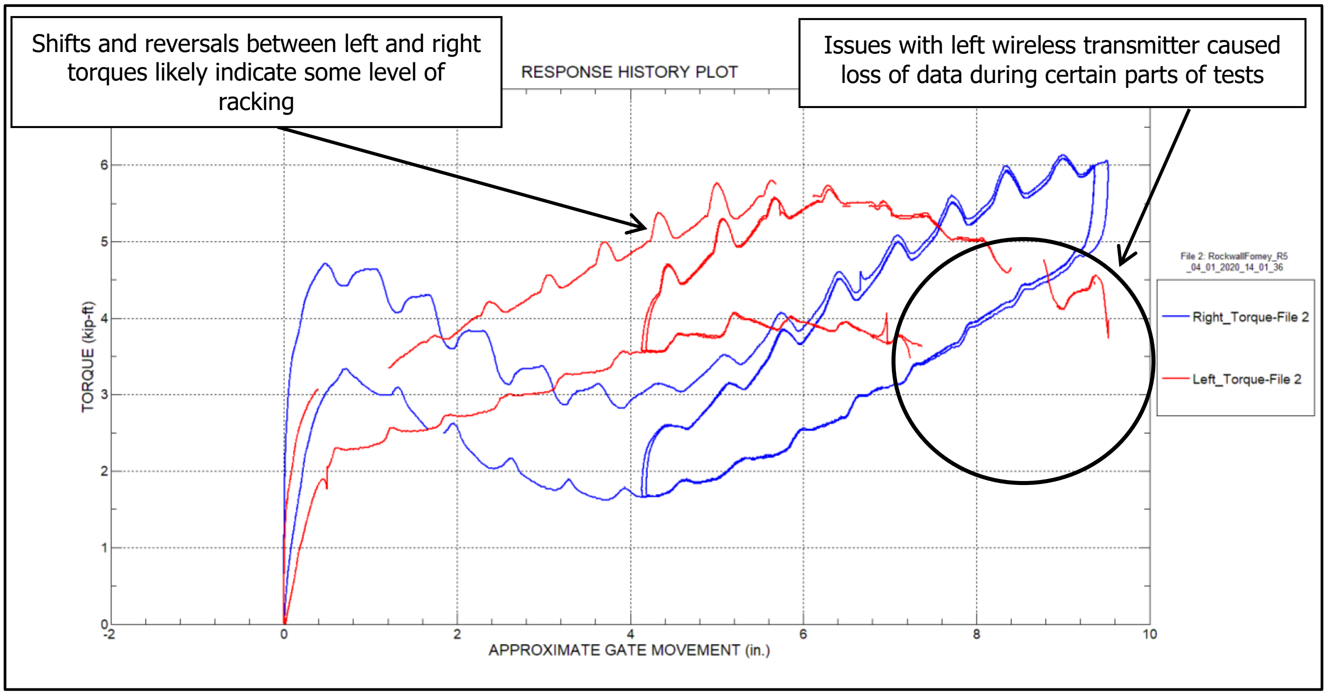

Figure 23 – Hoist torque response history – Gate 1 – Test 2
Note: missing left hoist data due to wireless connectivity issues as the sensor rotated with the pinion shaft

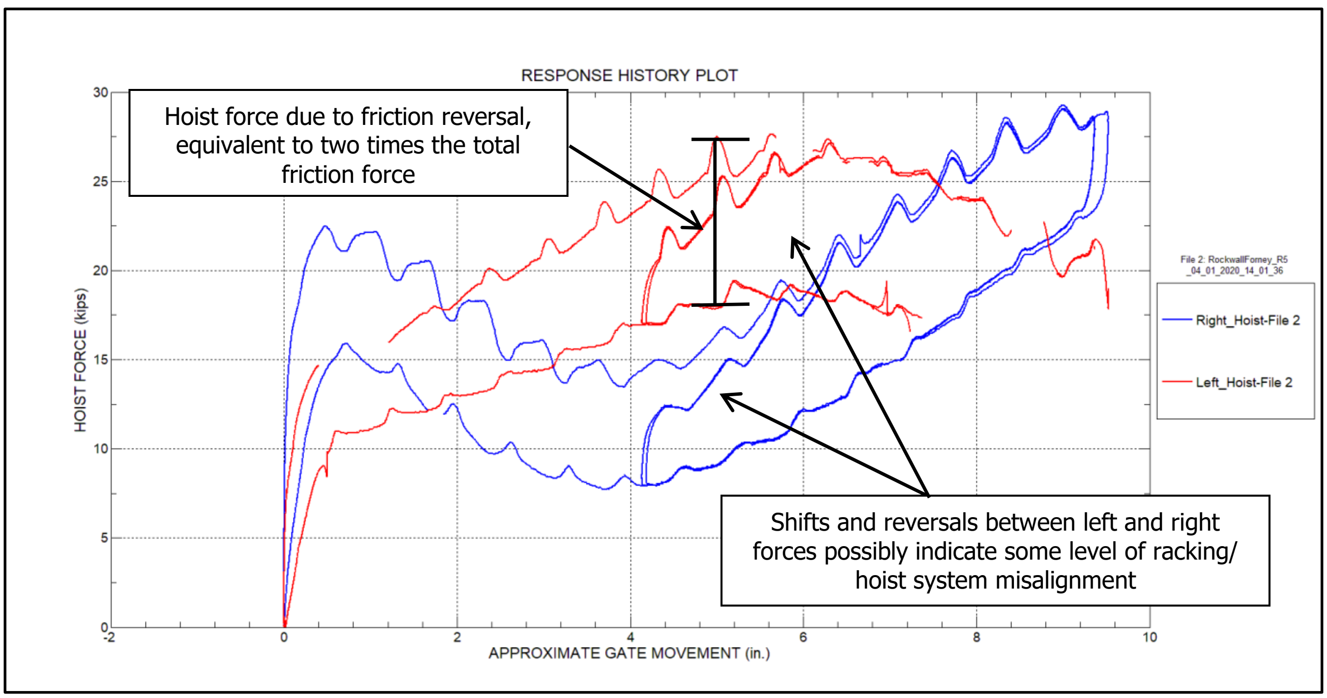

Figure 24 – Hoist force response history – Gate 1 – Test 2
Note: missing left hoist data due to wireless connectivity issues as the sensor rotated with the pinion shaft

Summary of Friction Results

The raw data files have been included in the submittal package for reference and were formatted as "tdms" files that can be opened in Microsoft Excel using a "tdms" reader extension.

Examination of the stress histories for each test was necessary to obtain a thorough understanding of the gate performance. The response shapes, variations in stress magnitudes, and timing sequences provided direct clues as to how the gate performed under typical service conditions. The following is a breakdown of the provided tabulated results:

+ Table 2 provides motor current ranges and maximum in-flow for lift and lower cycles for each test
+ Table 3 provides maximum hoist force as well as hoist force due to total friction for each test
+ Table 4 provides the maximum stress ranges measured at the sensor locations for each member
+ Table 5 provides maximum bending stress and moment ranges observed during the gate tests
+ Table 6 provides maximum friction bending stress and moment values at each of the instrumented strut locations
+ Table 7 provides the computed shear values in each strut due to friction
+ Table 8 provides calculated measured friction moments, calculated hydrostatic loads based on the measured water elevation, and coefficients of friction for each gate and gate arm during all three tests

The resulting pin friction moments were used to compute friction coefficients from Eq. 4, given the pin radius and the applied thrust. The thrust used in this calculation consisted of the calculated resultant hydrostatic load based on the measured water elevation and was adjusted to account for the loss of head as the gate was lifted. This thrust adjustment was based on the recorded gate movement and was performed in order to calculate more accurate friction coefficients. The water elevation during testing was nearly constant throughout each gate test and was documented during each "up-down" cycle. It should be noted that the minor thrust due to cable wrapping, which was minimal compared to hydrostatic thrust, was not included in the thrust calculation. This assumption resulted in slightly conservative friction coefficients.

$$\mu = \frac{M_F}{T * r} \qquad \text{Eq. 4}$$

where:

	μ	=	Friction Coefficient
	M_F	=	Friction Moment
	T	=	Thrust per Pin
	r	=	Pin Radius, 5.375"

The out-of-plane shear and moments were not considered in the pin friction calculations due to orthogonal geometry considerations (resulting pin moment associated with out-of-plane flexure being perpendicular to pin rotation).

The data was presented in a specific coordinate system applicable to both arms. Data was processed so that the positive x-axis was always pointing towards the pin and the right-hand rule applied. In-plane bending can be referred to as "bending about the horizontal or y-axis" and shows how much the beams bend up and down within the plane of the gate arms. Refer to Figure 12 above for visual reference of coordinate system and mathematical explanation of calculations. Tabulated results do not include any in-situ effects.

Table 2 – Motor current summary table – Gate 1

Test Run	Current Range due to Lifting (A)	Current Range due to Lowering (A)	Max In-rush Current (A)
1	14-20	10-15	121
2	14-19	10-15	124
3	14-19	10-15	123

Table 3 – Hoist force summary table – Gate 1

Test Run	Right Arm Peak Hoist Force (kips)	Left Arm Peak Hoist Force (kips)	Right Arm Hoist Force due to Total Gate Friction (kips)	Left Arm Hoist Force due to Total Gate Friction (kips)
1	29.17	28.02	5.32	5.33
2	29.28	27.66	4.82	4.83
3	29.71	28.16	5.24	4.94

Tabulated friction force values correspond to the response induced by friction in one direction

Table 4 – Maximum measured sensor stress range

Arm Designation	Top Strut (ksi)	Middle Strut (ksi)	Bottom Strut (ksi)
Right Arm	15.06	16.82	18.17
Left Arm	15.69	18.01	17.80

Tabulated values correspond to the total measured change in response during tests

Stress values have not been extrapolated to the extreme fibers (correspond to center of gage)

Table 5 – Maximum in-plane total bending stress & moment ranges – Total

Section Label	Section Description	Right Arm Stress (ksi)	Right Arm Moment (kip-in)	Left Arm Stress (ksi)	Left Arm Moment (kip-in)
Section A	Top Strut Near Pin	14.63	164.39	16.10	180.90
Section B	Middle Strut Near Pin	18.04	417.31	19.18	443.47
Section C	Bottom Strut Near Pin	17.61	490.95	17.46	486.75
Section D	Top Strut Away from Pin	2.61	29.29	2.59	29.12
Section E	Middle Strut Away from Pin	3.01	69.56	3.01	69.68
Section F	Bottom Strut Away from Pin	2.24	62.59	2.41	67.27

Tabulated values correspond to the total measured change in response during tests

Table 6 – In-plane frictional bending stress & moment at maximum gate friction

Section Label	Section Description	Right Arm Stress (ksi)	Right Arm Moment (kip-in)	Left Arm Stress (ksi)	Left Arm Moment (kip-in)
Section A	Top Strut Near Pin	6.99	78.57	7.28	81.84
Section B	Middle Strut Near Pin	8.48	196.09	8.76	202.69
Section C	Bottom Strut Near Pin	8.16	227.64	8.13	226.78
Section D	Top Strut Away from Pin	1.13	12.72	1.24	13.95
Section E	Middle Strut Away from Pin	1.22	28.31	1.42	32.85
Section F	Bottom Strut Away from Pin	0.94	26.26	1.14	31.79

Tabulated values correspond to the response induced by friction in one direction

Table 7 – Strut shear range summary table due to friction

Arm Designation	Top Strut Shear (kip)	Middle Strut Shear (kip)	Bottom Strut Shear (kip)
Right Arm	0.94	2.34	2.64
Left Arm	0.99	2.45	2.69

Tabulated values correspond to the response induced by friction in one direction

Table 8 – Pin friction summary table

Test Run	Average Water Elevation during testing (ft)	Approximate Thrust at time of Testing (kips per arm)	Gate/Member Designation	Pin Friction Moment (kip-in)	Friction Coefficient
1	435.60	490.00	Right Pin	748.80	0.28
			Left Pin	766.40	0.29
2	435.60	490.00	Right Pin	737.60	0.28
			Left Pin	758.50	0.29
3	435.60	490.00	Right Pin	739.50	0.28
			Left Pin	760.50	0.29

Tabulated values correspond to the response induced by friction in one direction

APPENDIX A – GATE 1 TORQUE AND HOIST FORCE PLOTS

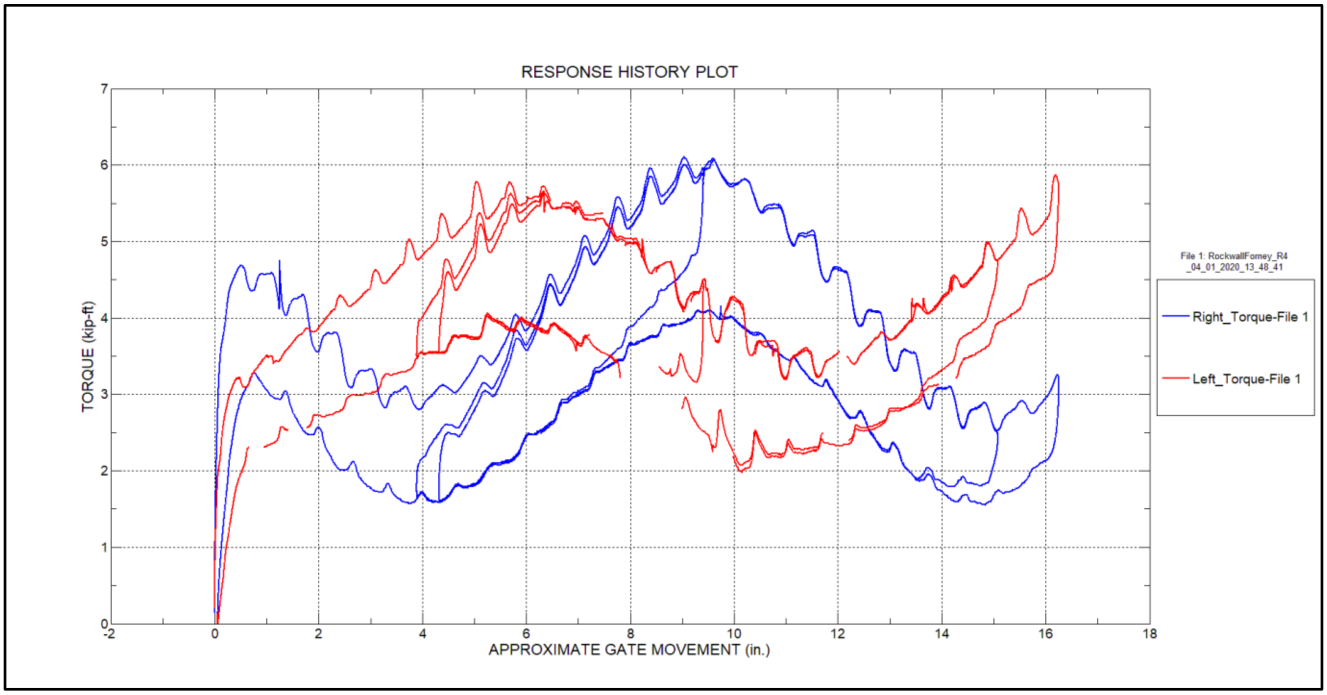

Figure 25 – Hoist torque response history – Gate 1 – Test 1

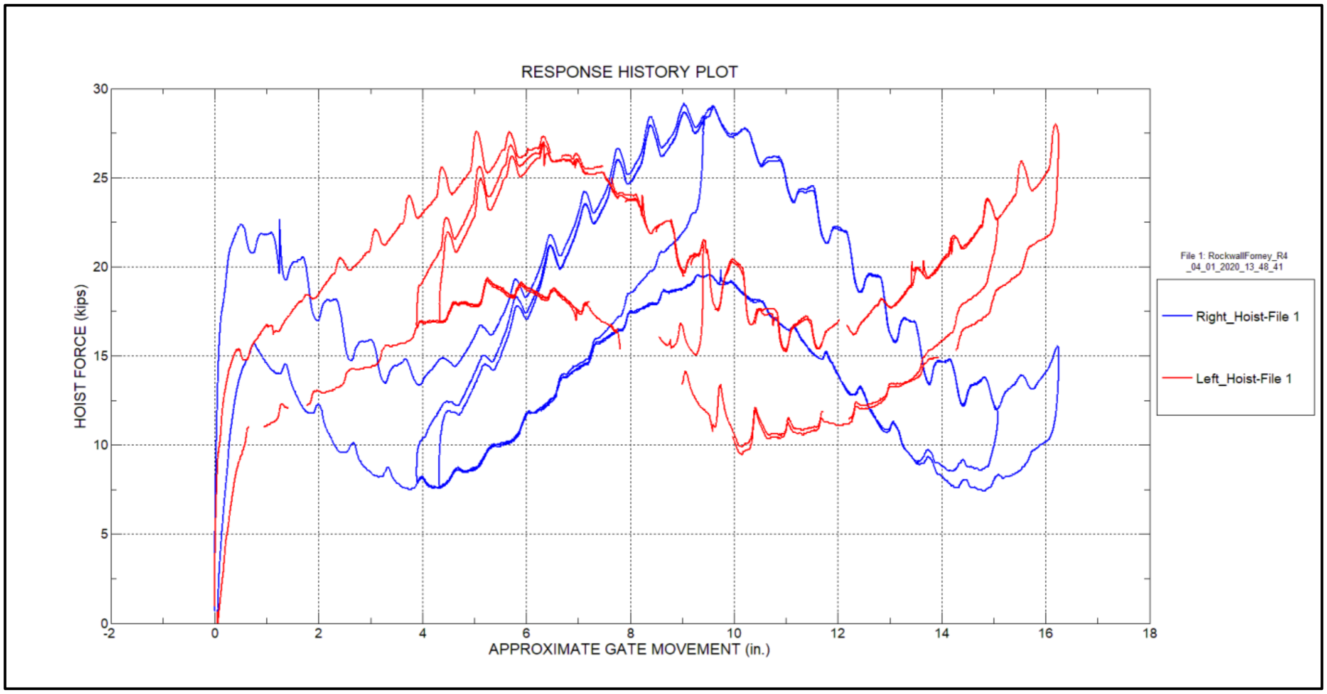

Figure 26 – Hoist force response history – Gate 1 – Test 1

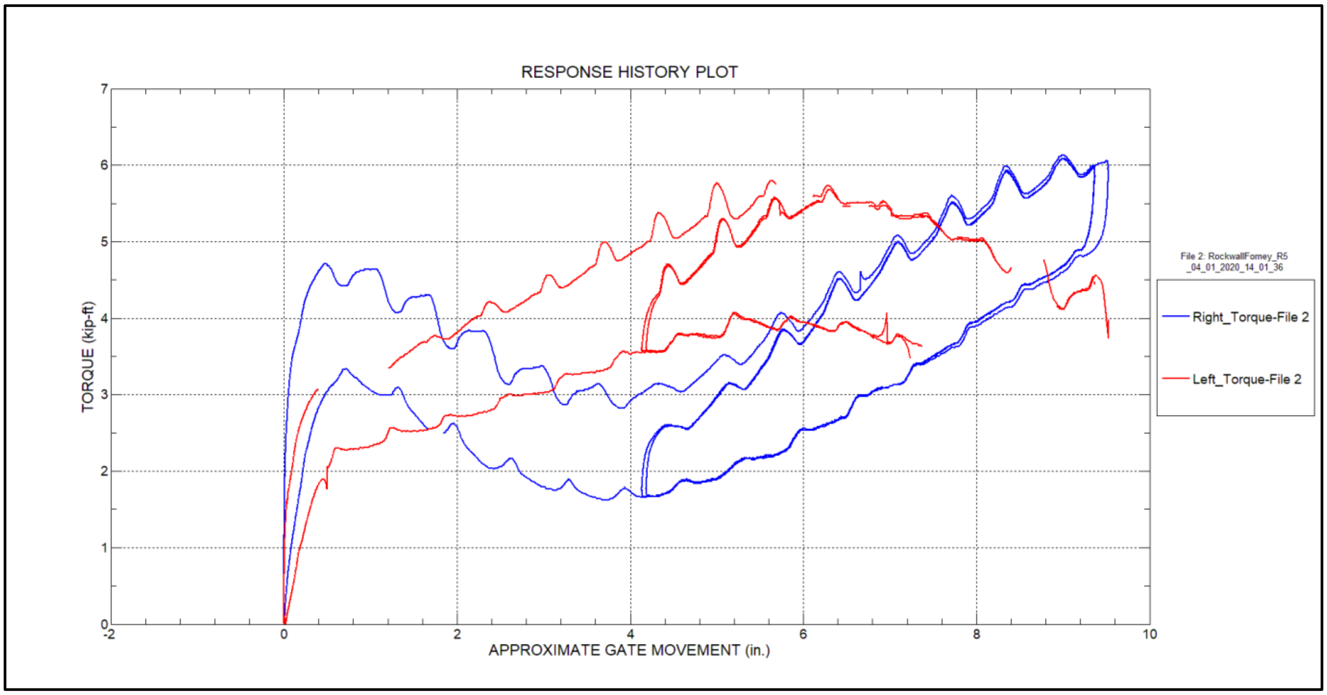

Figure 27 – Hoist torque response history – Gate 1 – Test 2

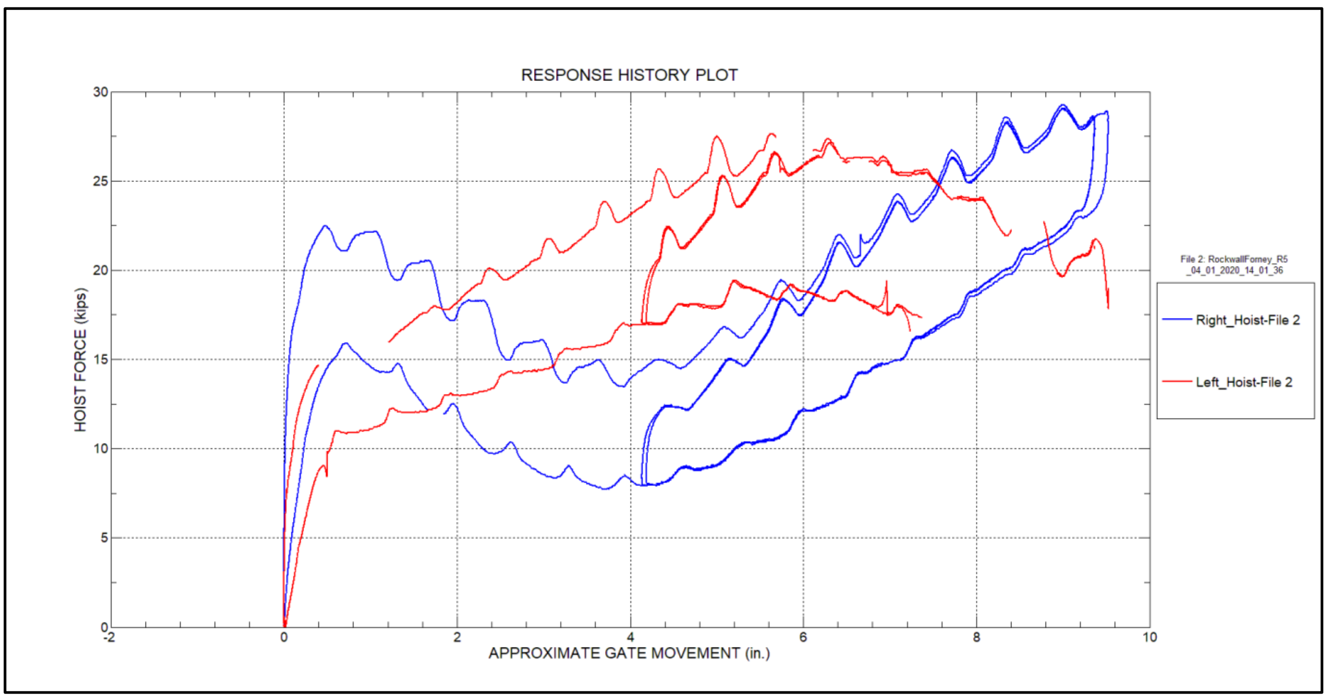

Figure 28 – Hoist force response history – Gate 1 – Test 2

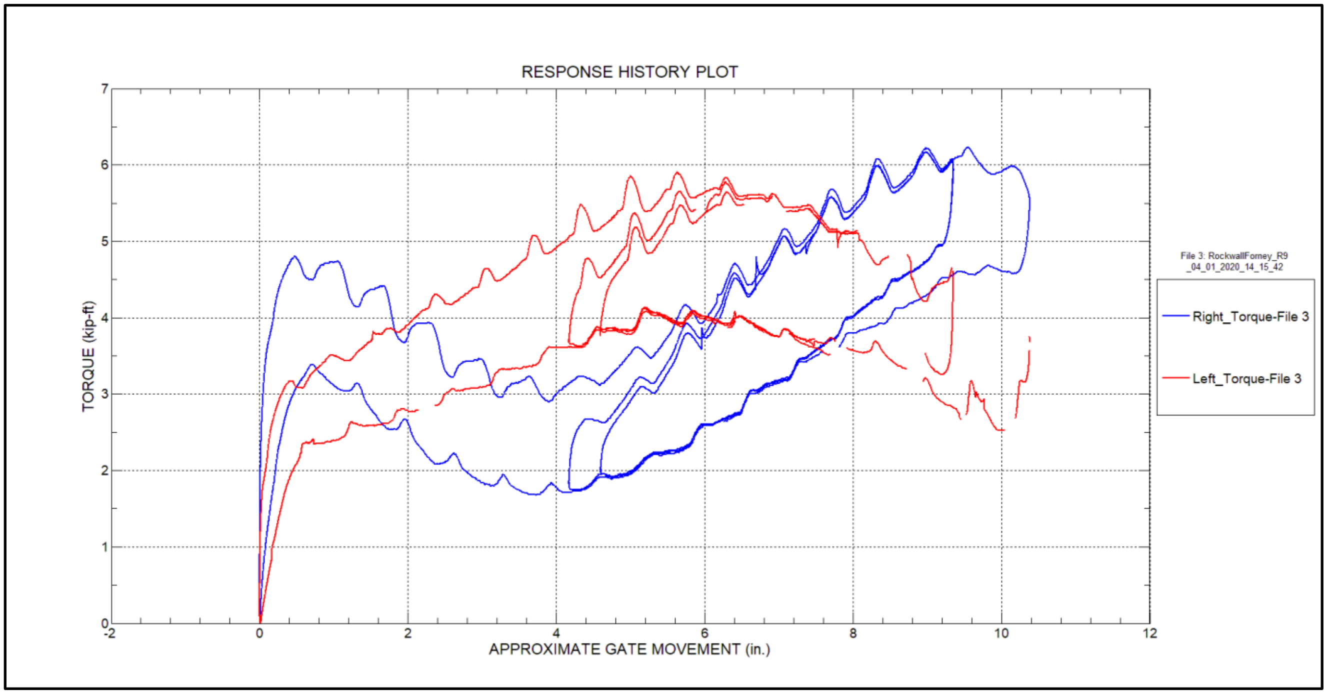

Figure 29 – Hoist torque response history – Gate 1 – Test 3

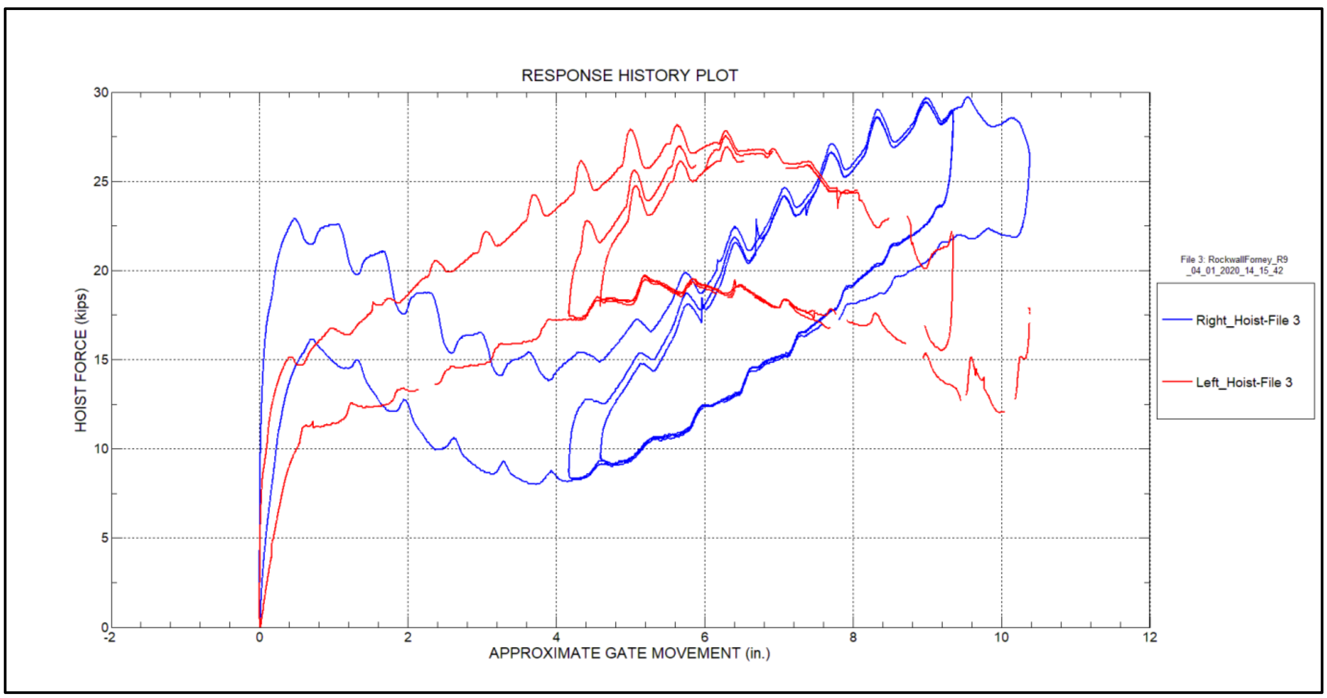

Figure 30 – Hoist force response history – Gate 1 – Test 3

Appendix B – Gate 1 Pin Moment Component Plots

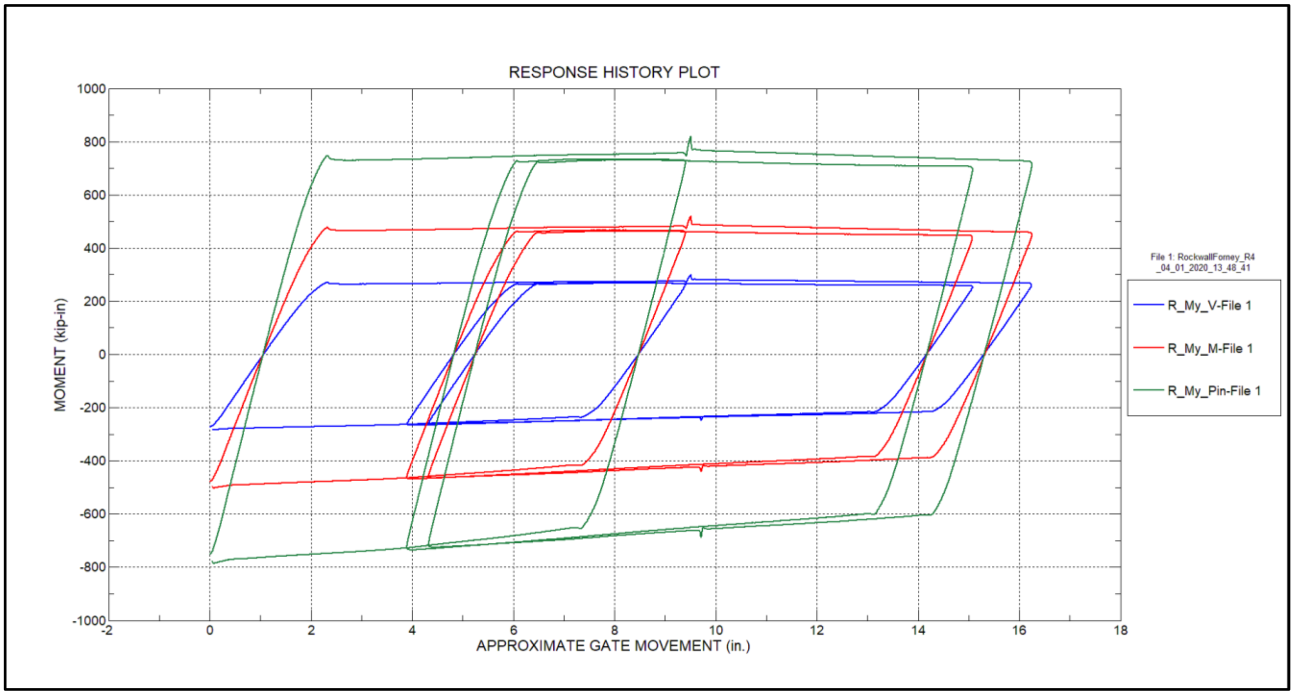

Figure 31 – Pin moment response history – Right arm – Test run 1

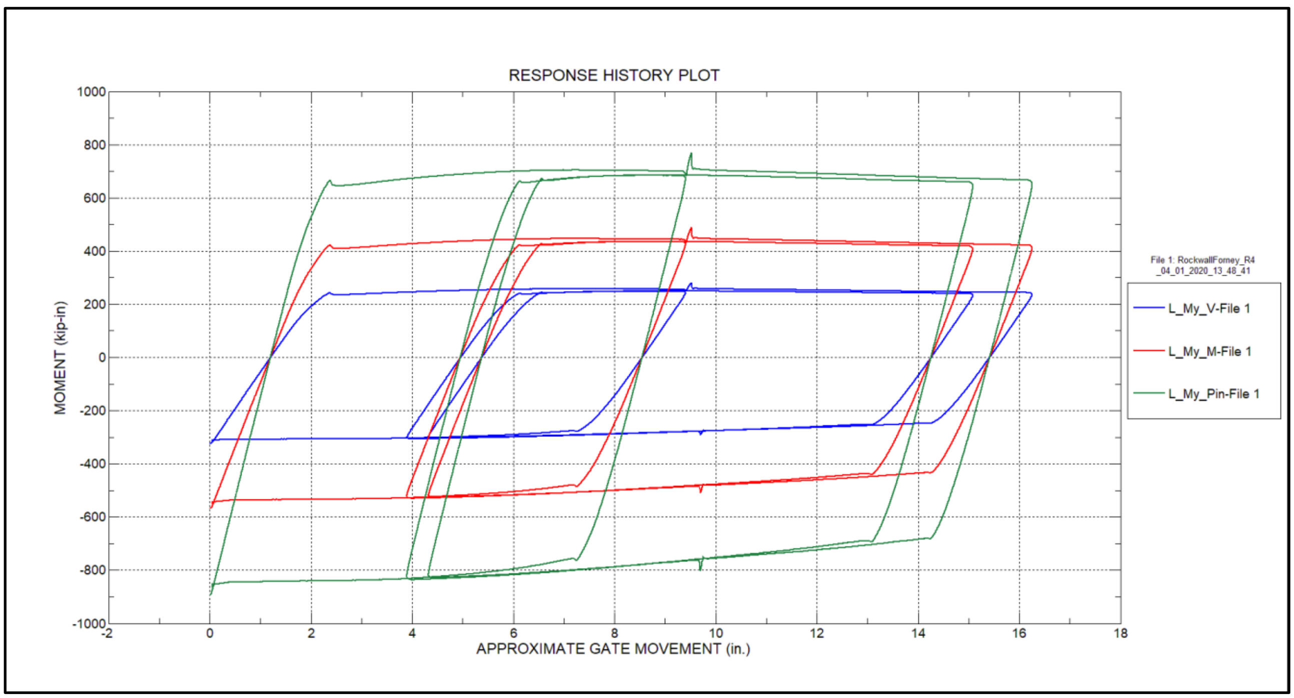

Figure 32 – Pin moment response history – Left arm – Test run 1

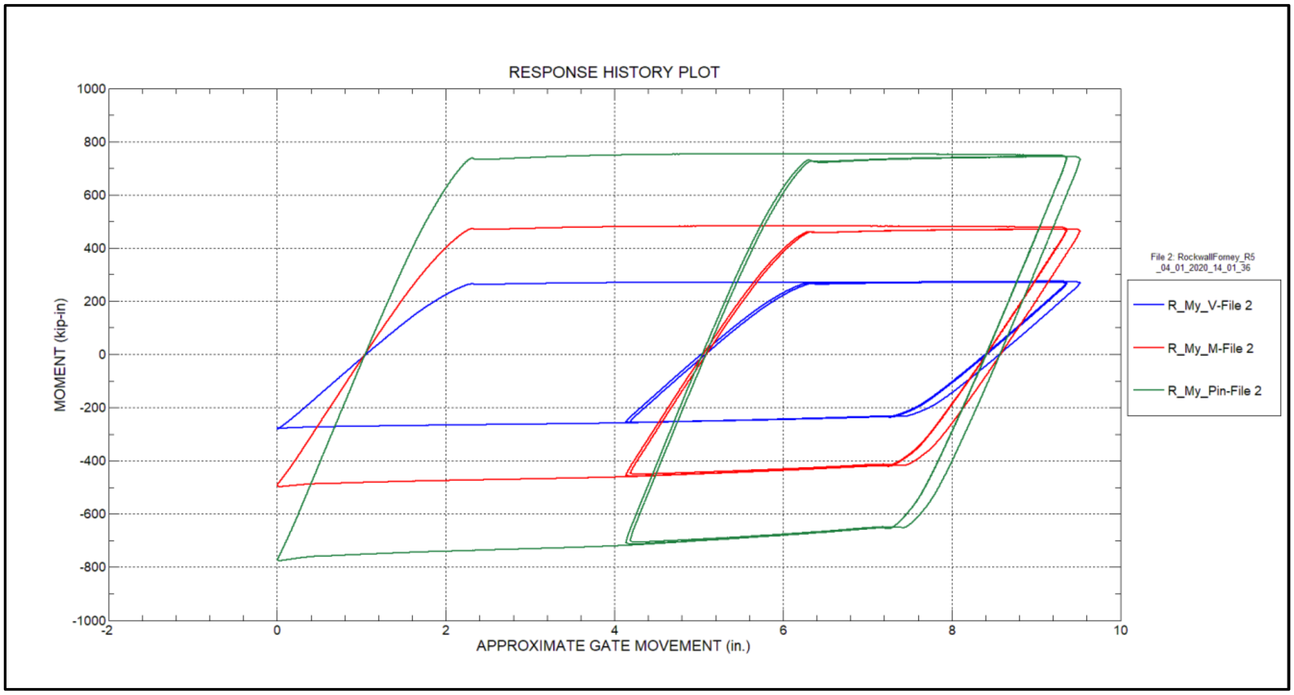

Figure 33 – Pin moment response history – Right arm – Test run 2

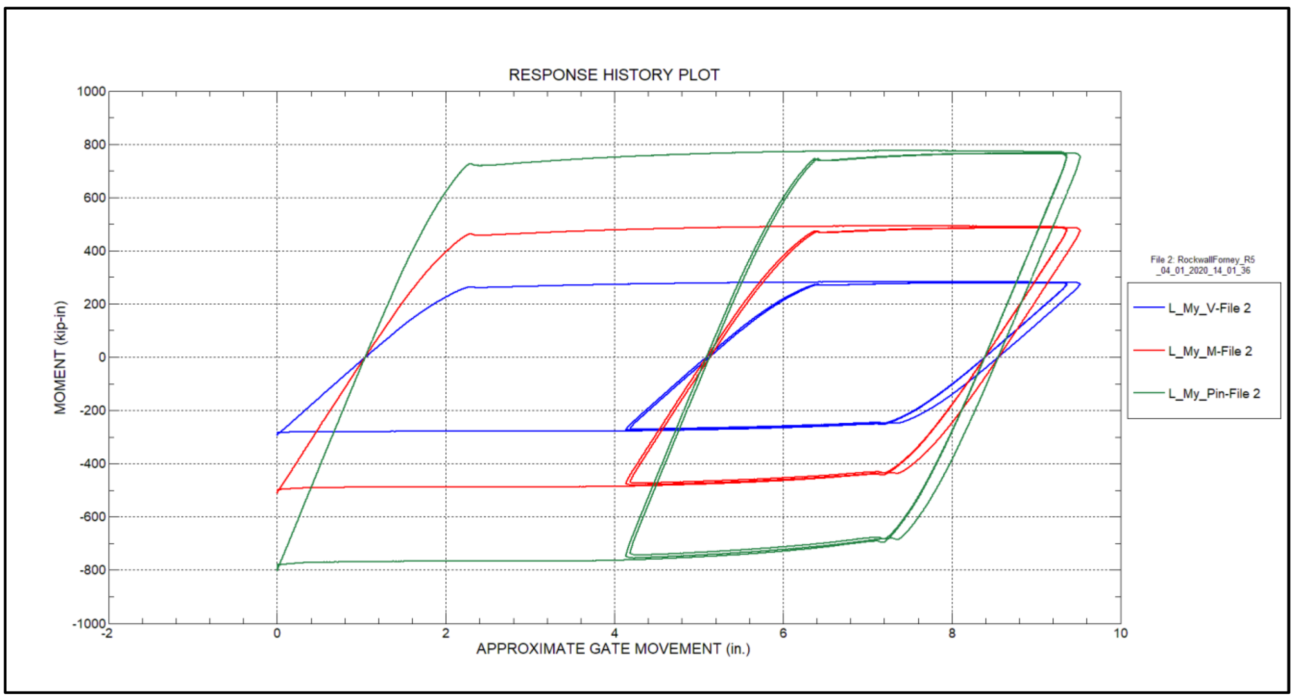

Figure 34 – Pin moment response history – Left arm – Test run 2

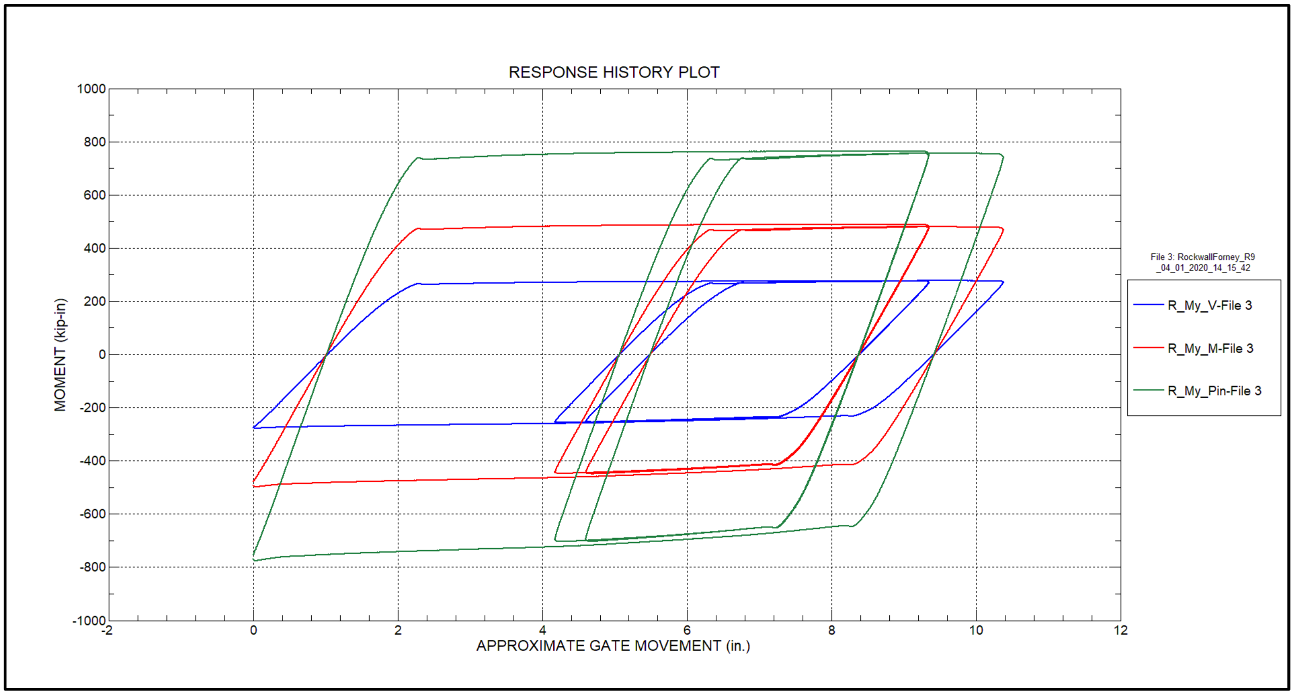

Figure 35 – Pin moment response history – Right arm – Test run 3

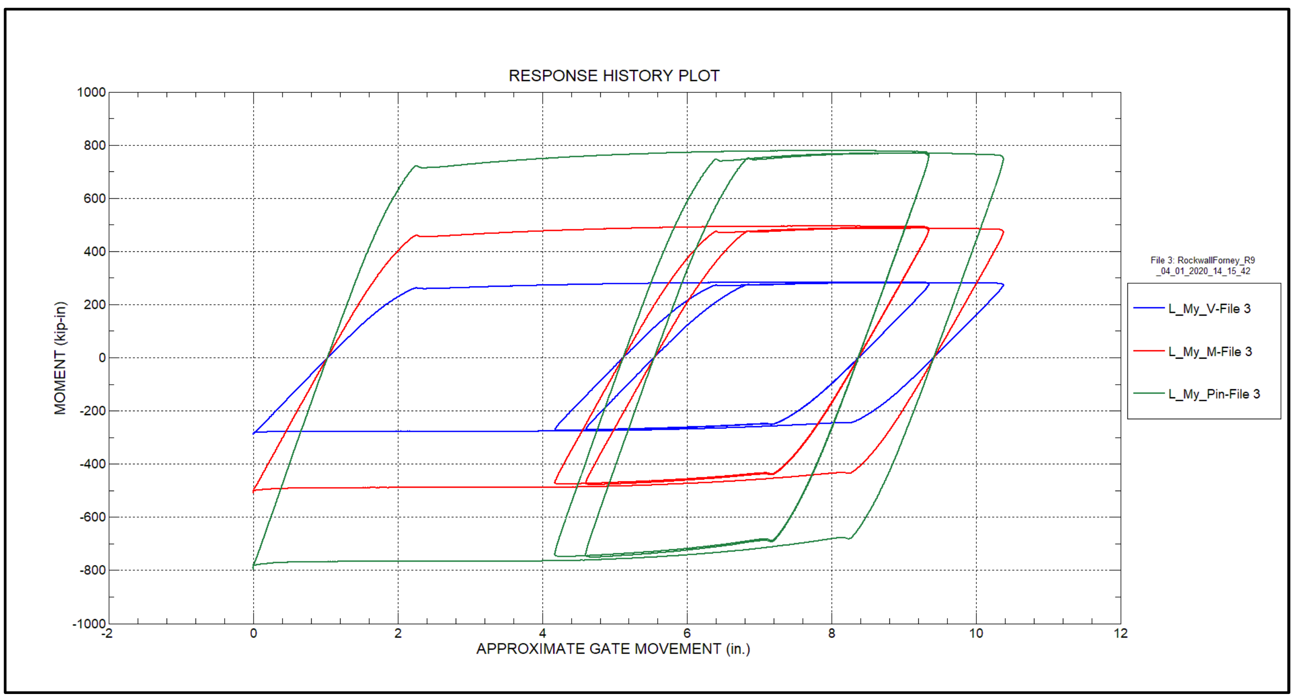

Figure 36 – Pin moment response history – Left arm – Test run 3

APPENDIX C – INSTRUMENTATION PLANS

RAW DATA. REFINED RESULTS.

SCHNABEL ENGINEERING
ROCKWALL FORNEY DAM
LIVE LOAD TESTING

The user acknowledges that these documents are instruments of professional service, and are protected by Copyright. This document and the information contained in this document are the property of Bridge Diagnostics, Inc., and shall not be reused, copied, disseminated, modified, amended or altered in any way. It is issued for information purposes only. The user agrees to hold harmless, indemnify and defend Bridge Diagnostics, Inc. against any and all damages, claims and losses, including defense costs, arising out of any use, reuse or copying of this document.

PLOT TIME: 6/12/2020 3:22 PM
FILEPATH: C:\Users\colemand\BDI\Services - Documents\Server_Remote\190701-TX_Schnabel_RockwallForneyDam\7. Instrumentation Plans\BDI_ROCKWALLFORNEY_01_GENERAL.dwg
© YYYY BRIDGE DIAGNOSTICS INC.

RAW DATA. REFINED RESULTS.
740 S PIERCE AVE, SUITE 15
LOUISVILLE, CO 80027
303.494.3230
WWW.BDITEST.COM

ISSUE

CLIENT

SCHNABEL ENGINEERING
16000 CHRISTENSEN RD, STE 101
SEATTLE, WA 98188

PROJECT NAME

SCHNABEL ENGINEERING
ROCKWALL FORNEY DAM
LIVE LOAD TESTING

Drawn By:	KNR
Checked By:	JDS
Date:	05/27/2020
Client No.:	
BDI No.:	190701-TX
SCALE:	NTS

COVER PAGE

LLT-00

The user acknowledges that these documents are instruments of professional service, and are protected by Copyright. This document and the information contained in this document are the property of Bridge Diagnostics, Inc., and shall not be reused, copied, disseminated, modified, amended or altered in any way. It is issued for information purposes only. The user agrees to hold harmless, indemnify and defend Bridge Diagnostics, Inc. against any and all damages, claims and losses, including defense costs, arising out of any use, reuse or copying of this document.

GAGE LEGEND & SPECIFICATION

SYMBOL	TYPE	BRAND	MODEL	NOTES
	STRAIN TRANSDUCER	BDI	ST350	
	TILTMETER (UNI-AXIAL)	BDI	T500-030	
	TORQUE SENSOR	HPI	-	HBWS-35-125-6-0.5VR-FB
	AMP SENSOR	CR MAGNETICS	CR42105-200	

GENERAL NOTES

- INSTRUMENTATION SHALL BEGIN ON APRIL 1ST, 2020.
- GATES 1 THRU 14 SHALL BE ACCESSED USING SPRAT ROPE ACCESS TECHNIQUES.
- BDI WILL PERFORM ALL SURFACE PREPARATION, SENSOR INSTALLATION, AND EQUIPMENT INSTALLATION.
- SEE LLT-31 FOR SENSOR INSTALLATION DETAILS.
- TWO PAIRS OF TORQUE GAGES WILL BE INSTALLED ON THE GATE MOTORS' PINION SHAFTS BETWEEN THE MOTORS AND THE HOISTS.
  - GAGE PAIRS WILL BE INSTALLED 180° APART FROM EACH OTHER.
  - EXACT POSITIONS OF THE GAGE PAIRS ON THE PINION SHAFT WILL BE DETERMINED IN THE FIELD.
- THREE PHASE AMPERAGE GAGES WILL BE INSTALLED ON THE MOTOR CONTROLS BY A QUALIFIED ELECTRICIAN PROVIDED BY GARVER.

TESTING PROCEDURE:

- TESTING SHALL BE STARTED WITH THE GATE IN THE CLOSED POSITION.
- ONCE DATA COLLECTION BEGINS, THE GATE SHALL BE RAISED TO TWO OR THREE TIMES THE HEIGHT NECESSARY FOR TRUNNION FRICTION TO BE OVERCOME, H1 (TYPICALLY 6"-12"), AND HELD THERE UNTIL DATA STABILIZES.
- THE GATE SHALL BE LOWERED APPROXIMATELY TWICE THE DISTANCE TO OVERCOME TRUNNION FRICTION, H2, AND HELD THERE UNTIL DATA STABILIZES.
- THE GATE SHALL BE RAISED TO H1 AND HELD THERE UNTIL DATA STABILIZES.
- THE GATE SHALL BE LOWERED TO H2 AND HELD THERE UNTIL DATA STABILIZES.
- THE GATE SHALL BE RAISED TO H1 AND HELD THERE UNTIL DATA STABILIZES.
- THE GATE WAS LOWERED BACK TO CLOSED POSITION AND DATA COLLECTION STOPPED.
- A MINIMUM OF 3 TESTS SHALL BE PERFORMED PER GATE.

GAGE COUNT PER GATE

SENSOR LEGEND	SENSOR COUNT	CHANNEL COUNT
STRAIN TRANSDUCER	(48)	(48)
TILTMETER (UNI-AXIAL)	(4)	(4)
TORQUE SENSOR	(4)	(4)
AMP SENSOR	(3)	(3)
TOTAL	(59)	(59)

LOCATION KEY

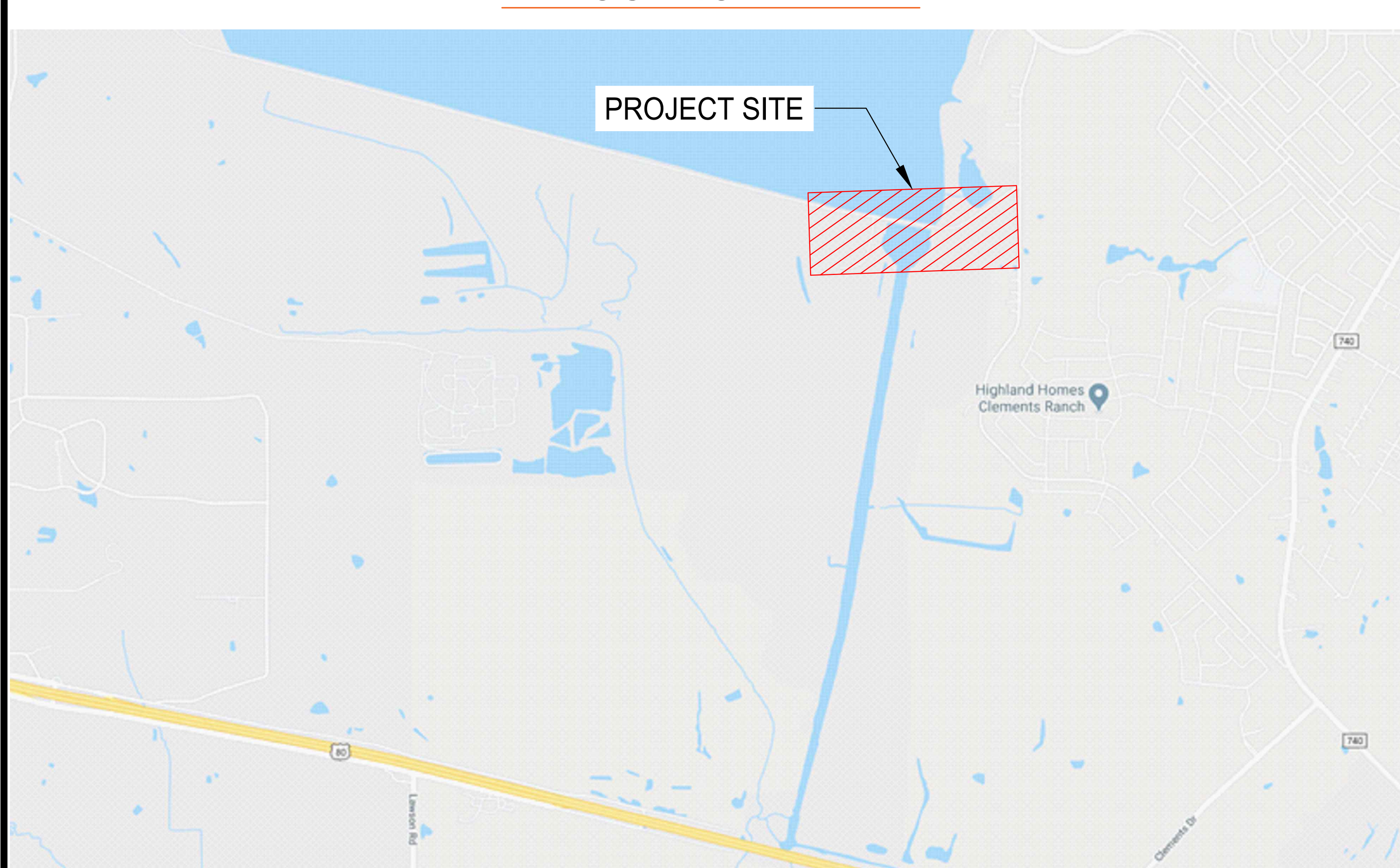

INDEX OF SHEETS

INDEX OF ISSUE

NO.	DATE	REVISION DESCRIPTION
1	3/20/2020	LIVE LOAD TESTING (LLT) INSTRUMENTATION PLAN (FOR APPROVAL)
2	5/27/2020	LIVE LOAD TESTING (LLT) INSTRUMENTATION PLAN AS BUILTS
BDI REFERENCE NUMBER: 190701-TX		

BDI
RAW DATA. REFINED RESULTS.
740 S PIERCE AVE, SUITE 15
LOUISVILLE, CO 80027
303.494.3230
WWW.BDITEST.COM

ISSUE

CLIENT

SCHABEL ENGINEERING
16000 CHRISTENSEN RD, STE 101
SEATTLE, WA 98188

PROJECT NAME

SCHNABEL ENGINEERING
ROCKWALL FORNEY DAM
LIVE LOAD TESTING

Drawn By:	KNR
Checked By:	JDS
Date:	05/27/2020
Client No.:	
BDI No.:	190701-TX
SCALE:	NTS

OVERALL LEGEND

LLT-01

PLOT TIME: 6/12/2020 3:22 PM
FILEPATH: C:\Users\coleman\BDI\Services - Documents\Server_Remote\190701-TX_Schnabel_RockwallForneyDam\7. Instrumentation Plans\BDI_ROCKWALLFORNEY_01_GENERAL.dwg
© YYYY BRIDGE DIAGNOSTICS INC.

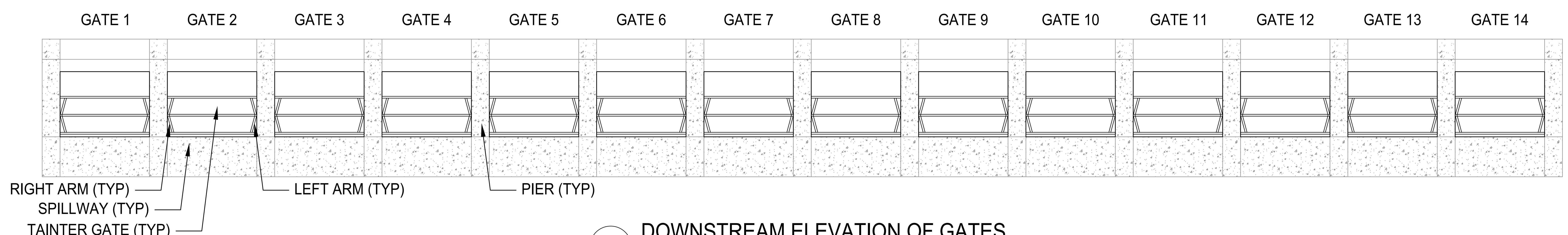

1 DOWNSTREAM ELEVATION OF GATES
LOOKING NORTH (UPSTREAM)

The user acknowledges that these documents are instruments of professional service, and are protected by Copyright. This document and the information contained in this document are the property of Bridge Diagnostics, Inc., and shall not be reused, copied, disseminated, modified, amended or altered in any way. It is issued for information purposes only. The user agrees to hold harmless, indemnify and defend Bridge Diagnostics, Inc. against any and all damages, claims and losses, including defense costs, arising out of any use, reuse or copying of this document.

PLOT TIME: 6/12/2020 3:22 PM
FILEPATH: C:\Users\colemand\BDI\Services - Documents\Server_Remote\190701-TX_Schabel_RockwallForneyDam\7. Instrumentation Plans\BDI_ROCKWALLFORNEY_01_GENERAL.dwg
© YYYY BRIDGE DIAGNOSTICS INC.

BDI
RAW DATA. REFINED RESULTS.
740 S PIERCE AVE, SUITE 15
LOUISVILLE, CO 80027
303.494.3230
WWW.BDITEST.COM

ISSUE

CLIENT

SCHABEL ENGINEERING
16000 CHRISTENSEN RD, STE 101
SEATTLE, WA 98188

PROJECT NAME

SCHNABEL ENGINEERING
ROCKWALL FORNEY DAM
LIVE LOAD TESTING

Drawn By:	KNR
Checked By:	JDS
Date:	05/27/2020
Client No.:	
BDI No.:	190701-TX
SCALE:	NTS

OVERALL STRUCTURE LAYOUT
LLT-02

The user acknowledges that these documents are instruments of professional service, and are protected by Copyright. This document and the information contained in this document are the property of Bridge Diagnostics, Inc., and shall not be reused, copied, disseminated, modified, amended or altered in any way. It is issued for information purposes only. The user agrees to hold harmless, indemnify and defend Bridge Diagnostics, Inc. against any and all damages, claims and losses, including defense costs, arising out of any use, reuse or copying of this document.

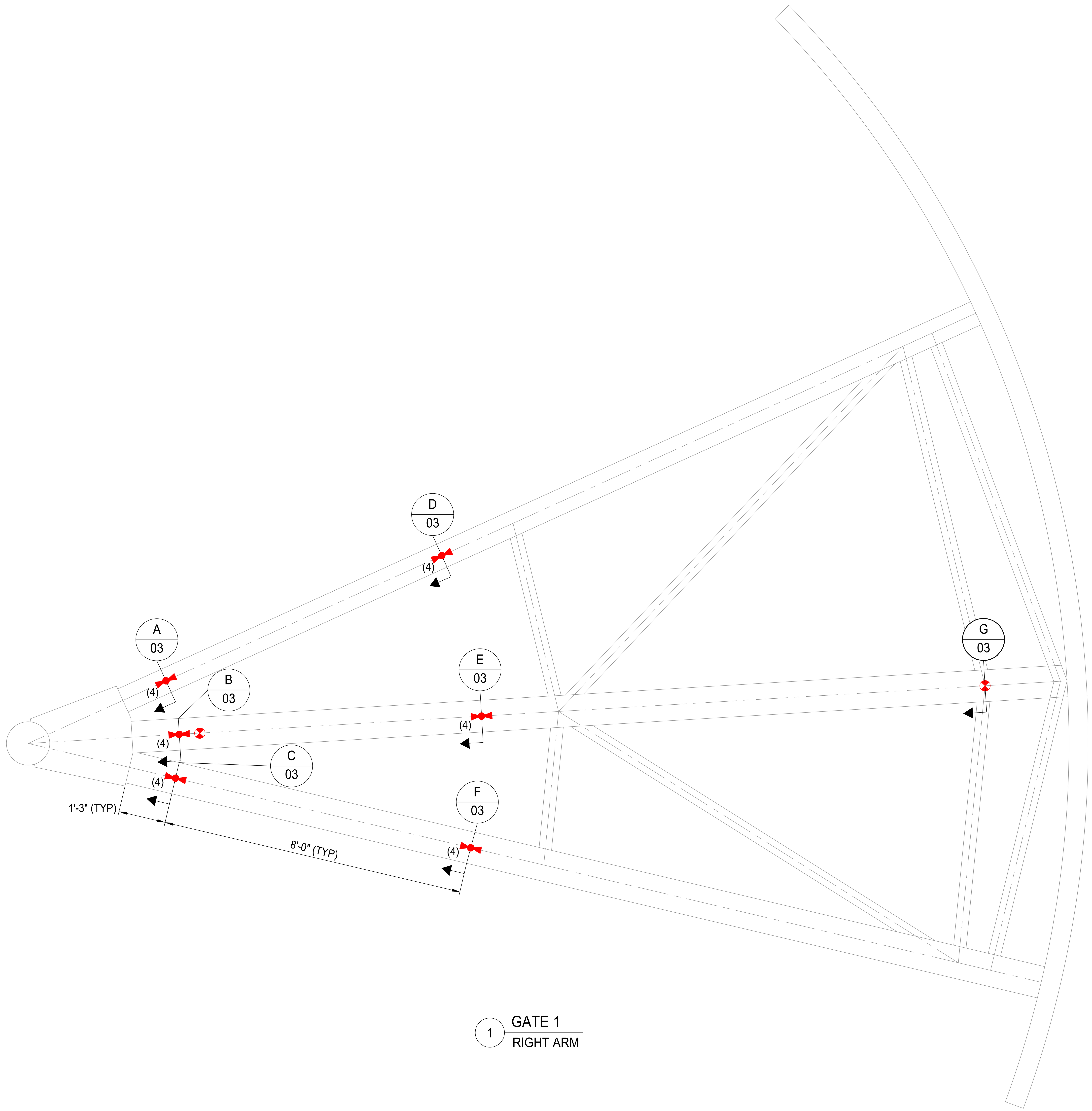

1 GATE 1
RIGHT ARM

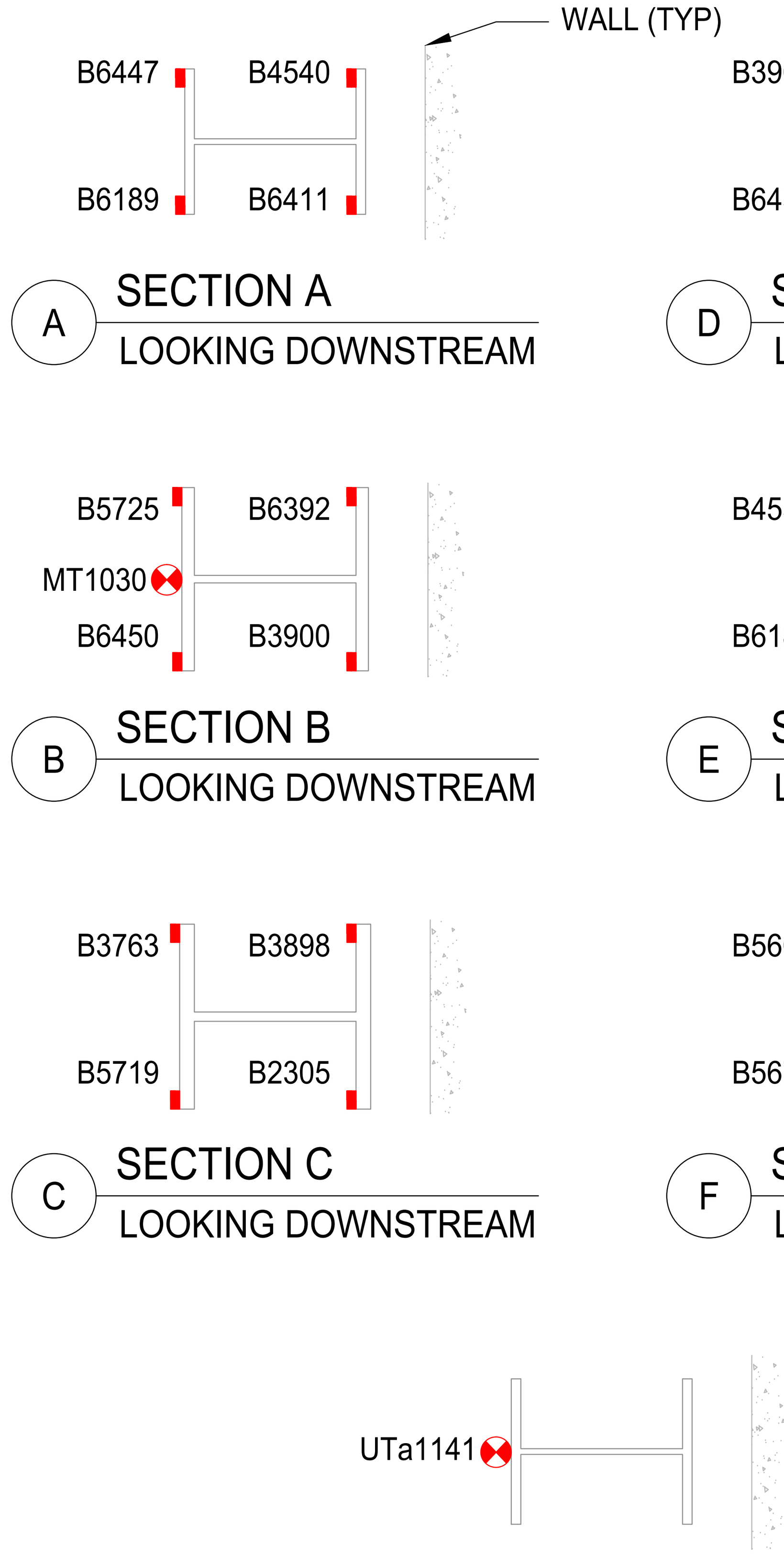

A SECTION A
LOOKING DOWNSTREAM

D SECTION D
LOOKING DOWNSTREAM

B SECTION B
LOOKING DOWNSTREAM

E SECTION E
LOOKING DOWNSTREAM

C SECTION C
LOOKING DOWNSTREAM

F SECTION F
LOOKING DOWNSTREAM

G SECTION G
LOOKING DOWNSTREAM

UNIT ID
TT-3

TORQUE GAGES
RIGHT ARM

NOTES:
1. SECTIONS A, B, & C SHALL BE INSTALLED 15 INCHES AWAY FROM TRUNNION PLATE.
2. TILTMETERS SHALL BE INSTALLED CENTERED ON THE MIDDLE STRUT FLANGE.
3. SECTION G'S TILTMETER SHALL BE INSTALLED AS CLOSE TO THE SKINPLATE AS POSSIBLE.

SENSOR LEGEND
STRAIN TRANSDUCER
TILTMETER (UNI-AXIAL)
TORQUE SENSOR

BDI
RAW DATA. REFINED RESULTS.
740 S PIERCE AVE, SUITE 15
LOUISVILLE, CO 80027
303.494.3230
WWW.BDITEST.COM

ISSUE

CLIENT
SCHABEL ENGINEERING
16000 CHRISTENSEN RD, STE 101
SEATTLE, WA 98188

PROJECT NAME
SCHABEL ENGINEERING
ROCKWALL FORNEY DAM
LIVE LOAD TESTING

Drawn By:	KNR
Checked By:	JDS
Date:	05/27/2020
Client No.:	
BDI No.:	190701-TX
SCALE:	NTS

GATE 1 - RIGHT ARM
ELEVATION
LLT-03

PLOT TIME: 6/12/2020 3:22 PM
FILEPATH: C:\Users\colemand\BDI\Services - Documents\Server_Remote\190701-TX_Schabel_RockwallForneyDam\7. Instrumentation Plans\BDI_ROCKWALLFORNEY_01_GENERAL.dwg
© YYYY BRIDGE DIAGNOSTICS INC.

The user acknowledges that these documents are instruments of professional service, and are protected by Copyright. This document and the information contained in this document are the property of Bridge Diagnostics, Inc., and shall not be reused, copied, disseminated, modified, amended or altered in any way. It is issued for information purposes only. The user agrees to hold harmless, indemnify and defend Bridge Diagnostics, Inc. against any and all damages, claims and losses, including defense costs, arising out of any use, reuse or copying of this document.

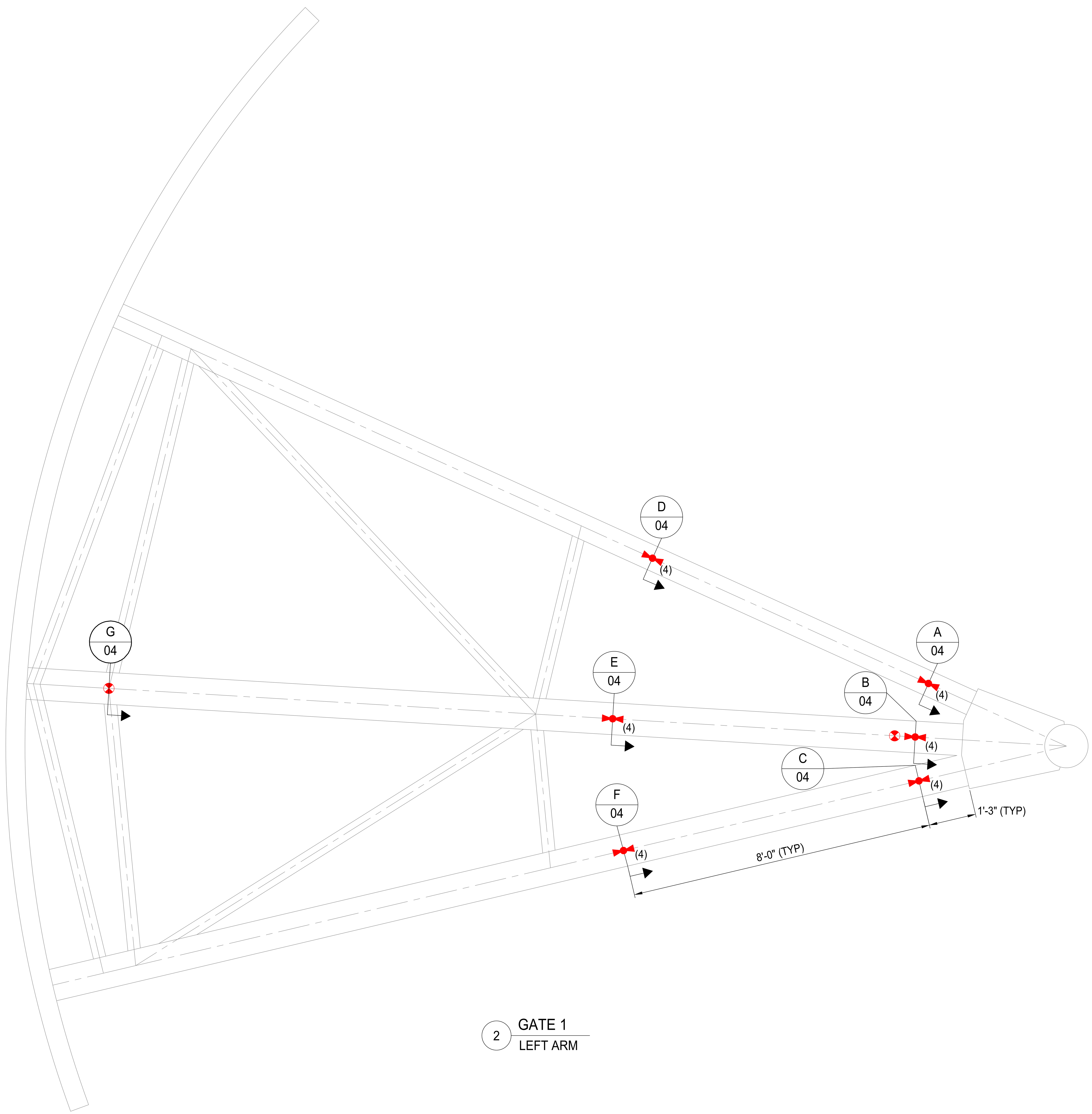

2 GATE 1
LEFT ARM

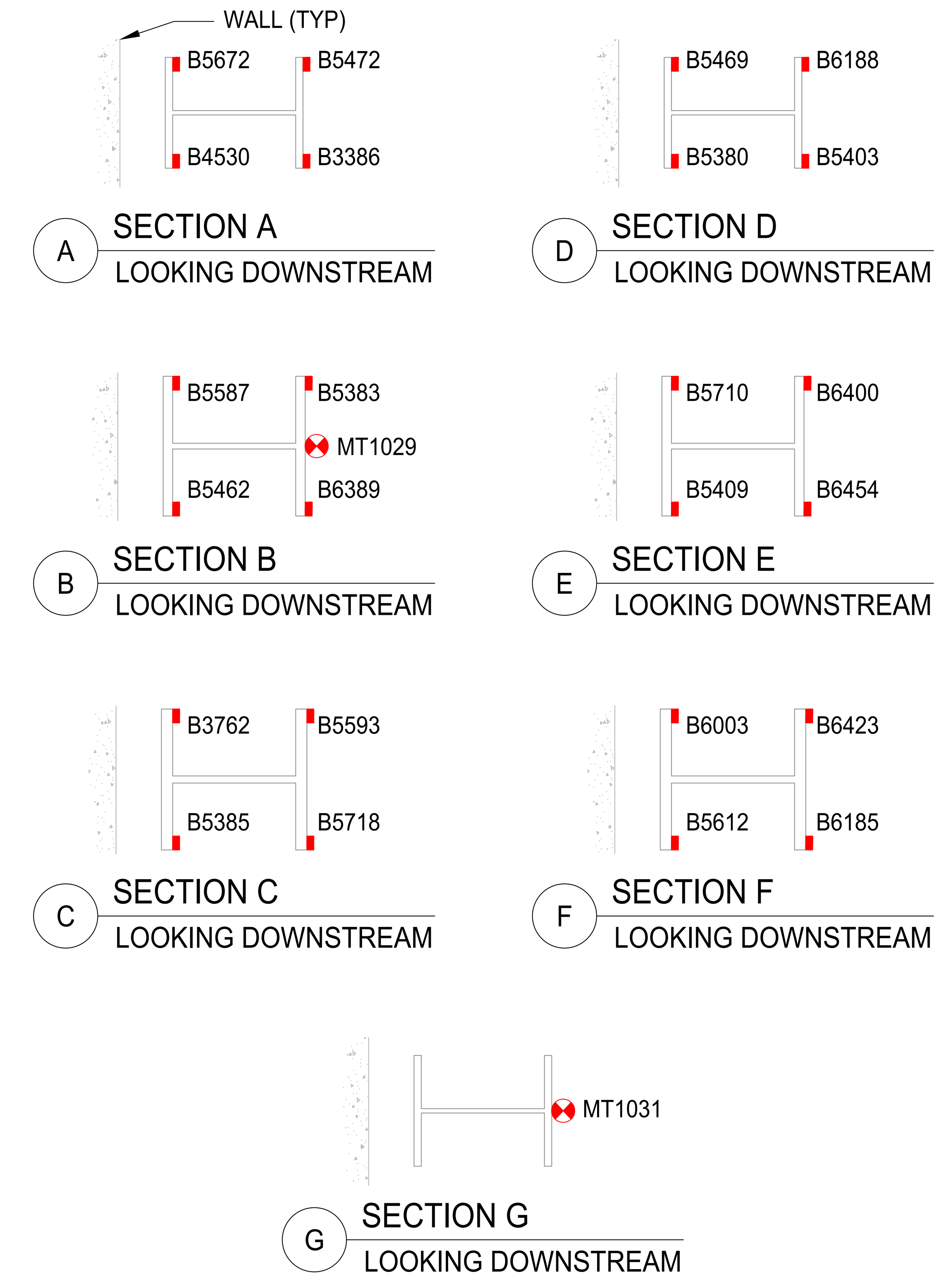

UNIT ID
TT-2

TORQUE GAGES
LEFT ARM

NOTES:
1. SECTIONS A, B, & C SHALL BE INSTALLED 15 INCHES AWAY FROM TRUNNION PLATE.
2. TILTMETERS SHALL BE INSTALLED CENTERED ON THE MIDDLE STRUT FLANGE.
3. SECTION G'S TILTMETER SHALL BE INSTALLED AS CLOSE TO THE SKINPLATE AS POSSIBLE.

SENSOR LEGEND
STRAIN TRANSDUCER
TILTMETER (UNI-AXIAL)
TORQUE SENSOR

BDI
RAW DATA. REFINED RESULTS.
740 S PIERCE AVE, SUITE 15
LOUISVILLE, CO 80027
303.494.3230
WWW.BDITEST.COM

ISSUE

CLIENT
SCHABEL ENGINEERING
16000 CHRISTENSEN RD, STE 101
SEATTLE, WA 98188

PROJECT NAME

SCHABEL ENGINEERING ROCKWALL FORNEY DAM LIVE LOAD TESTING

Drawn By:	KNR
Checked By:	JDS
Date:	05/27/2020
Client No.:	
BDI No.:	190701-TX
SCALE:	NTS

GATE 1 - LEFT ARM
ELEVATION
LLT-04

PLOT TIME: 6/12/2020 3:22 PM
FILEPATH: C:\Users\colemand\BDI\Services - Documents\Server_Remote\190701-TX_Schabel_RockwallForneyDam\7. Instrumentation Plans\BDI_ROCKWALLFORNEY_01_GENERAL.dwg
© YYYY BRIDGE DIAGNOSTICS INC.

The user acknowledges that these documents are instruments of professional service, and are protected by Copyright. This document and the information contained in this document are the property of Bridge Diagnostics, Inc., and shall not be reused, copied, disseminated, modified, amended or altered in any way. It is issued for information purposes only. The user agrees to hold harmless, indemnify and defend Bridge Diagnostics, Inc. against any and all damages, claims and losses, including defense costs, arising out of any use, reuse or copying of this document.

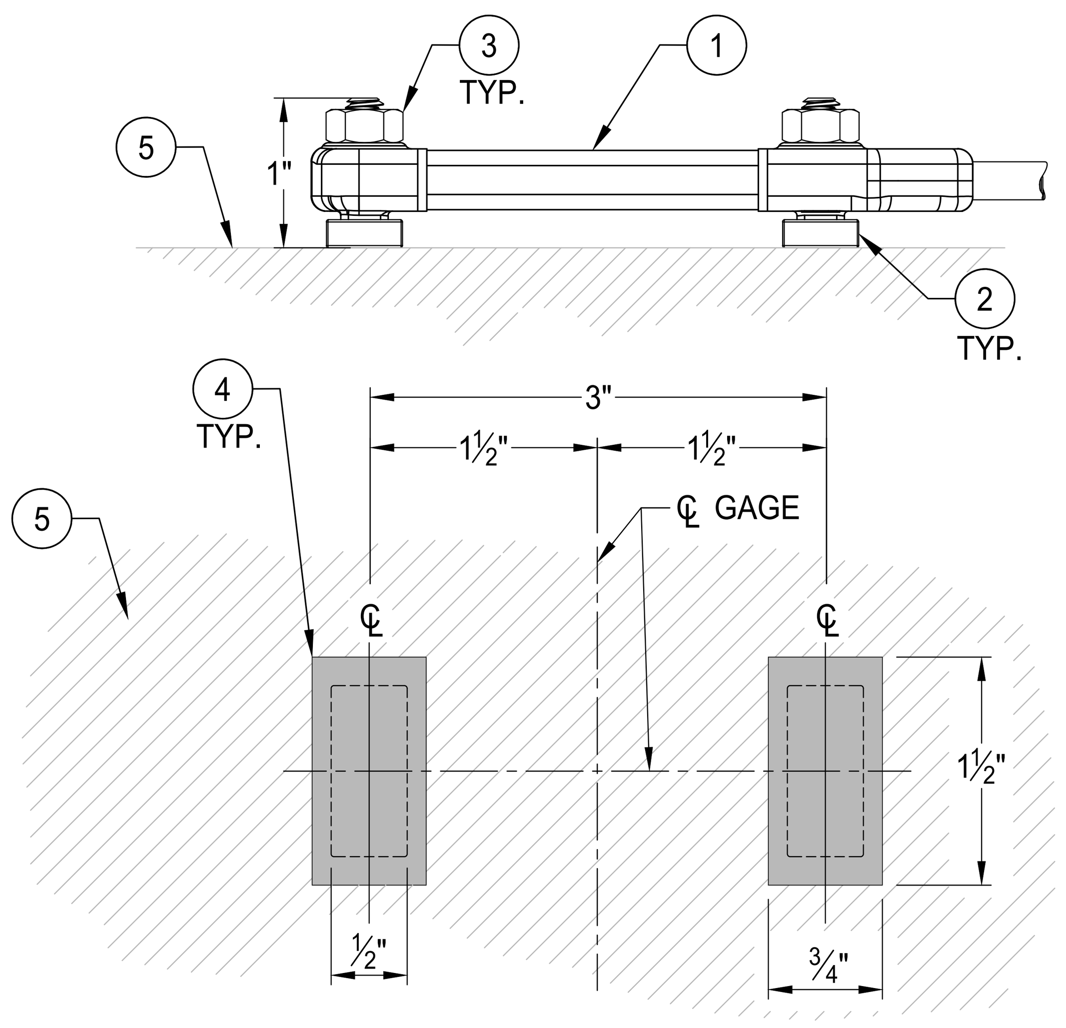

COMPONENT DESCRIPTION

1. ST350 STRAIN GAGE
2. 1/4"-20 THREADED MOUNTING TAB
3. 1/4"-20 STAINLESS STEEL NUT
4. TYPICAL SURFACE PREP REQUIRED TO MOUNT STRAIN GAGES
5. TYPICAL MOUNTING SURFACE

FOOTNOTES - INSTANT ADHESIVE
1. STRAIN GAGES SHALL BE MOUNTED WITH LOCTITE 410 INSTANT ADHESIVE AND LOCTITE 7452 ACCELERANT 2. DURING SURFACE PREP ALL PAINT AND SURFACE DEFORMATIONS MUST BE REMOVED. 3. SURFACE PREP IS REQUIRED JUST PRIOR TO GAGE INSTALLATION AS TO NOT ALLOW SURFACE CONTAMINANTS TO ACCUMULATE.

1 TYPICAL ST350 STRAIN GAGE INSTALLATION

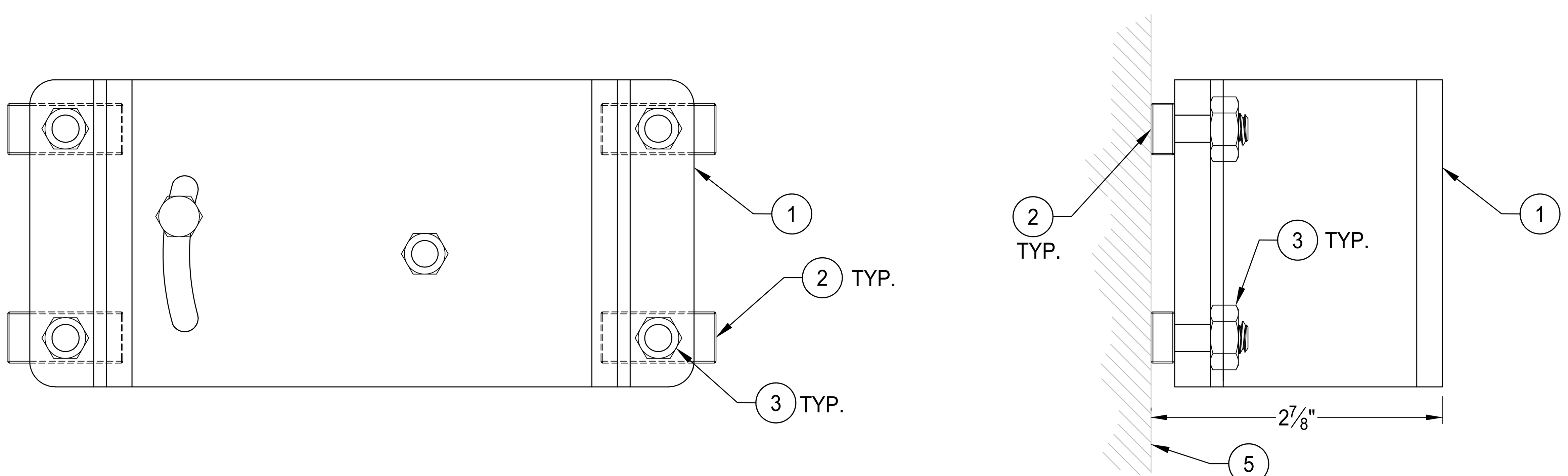

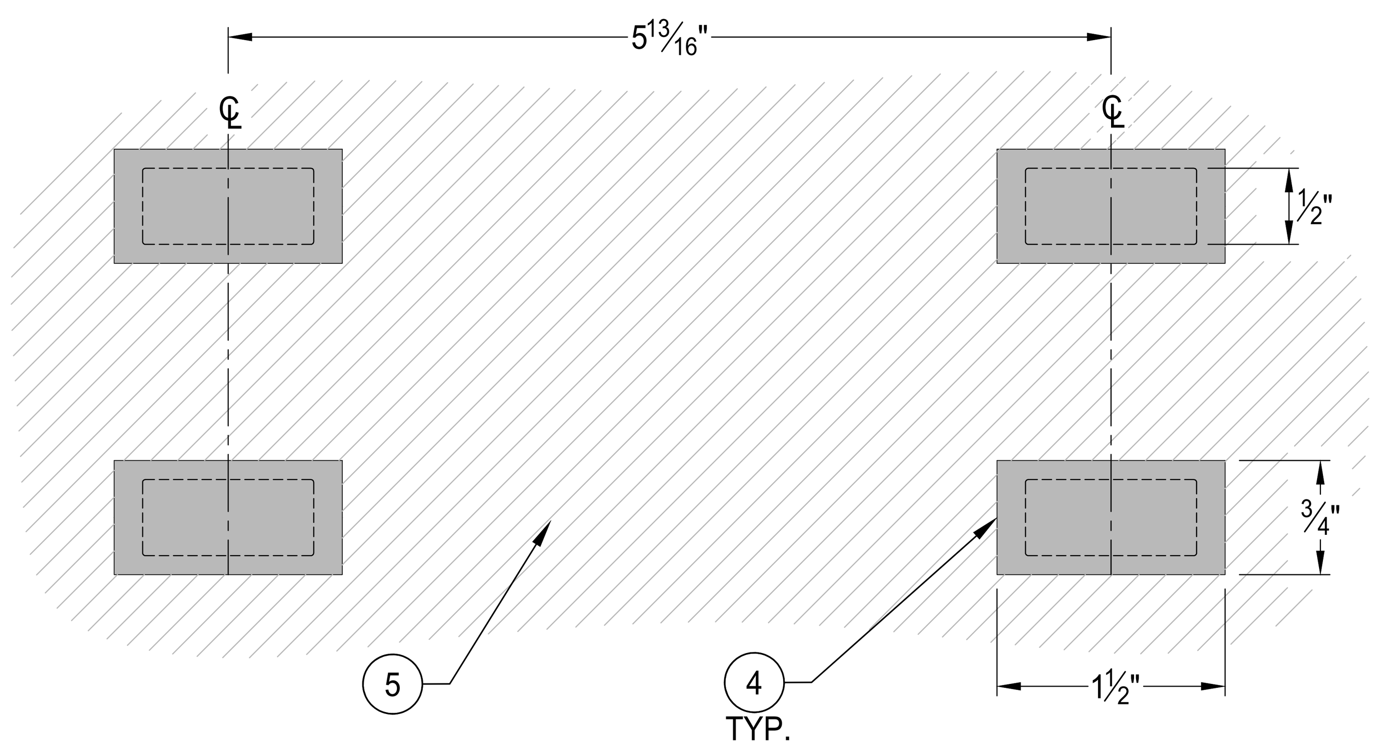

COMPONENT DESCRIPTION

1. BDI +/- 15 DEGREE TILTMETER WITH COVER AND ADJUSTMENT BOLTS
2. 1/4"-20 THREADED MOUNTING TAB
3. 1/4"-20 STAINLESS STEEL NUT
4. TYPICAL SURFACE PREP REQUIRED TO MOUNT TILTMETERS
5. TYPICAL MOUNTING SURFACE

FOOTNOTES - INSTANT ADHESIVE
1. TILTMETERS SHALL BE MOUNTED WITH LOCTITE 410 INSTANT ADHESIVE AND LOCTITE 7452 ACCELERANT 2. DURING SURFACE PREP ALL PAINT AND SURFACE DEFORMATIONS MUST BE REMOVED. 3. SURFACE PREP IS REQUIRED JUST PRIOR TO GAGE INSTALLATION AS TO NOT ALLOW SURFACE CONTAMINANTS TO ACCUMULATE.

2 TYPICAL BDI TILTMETER INSTALLATION

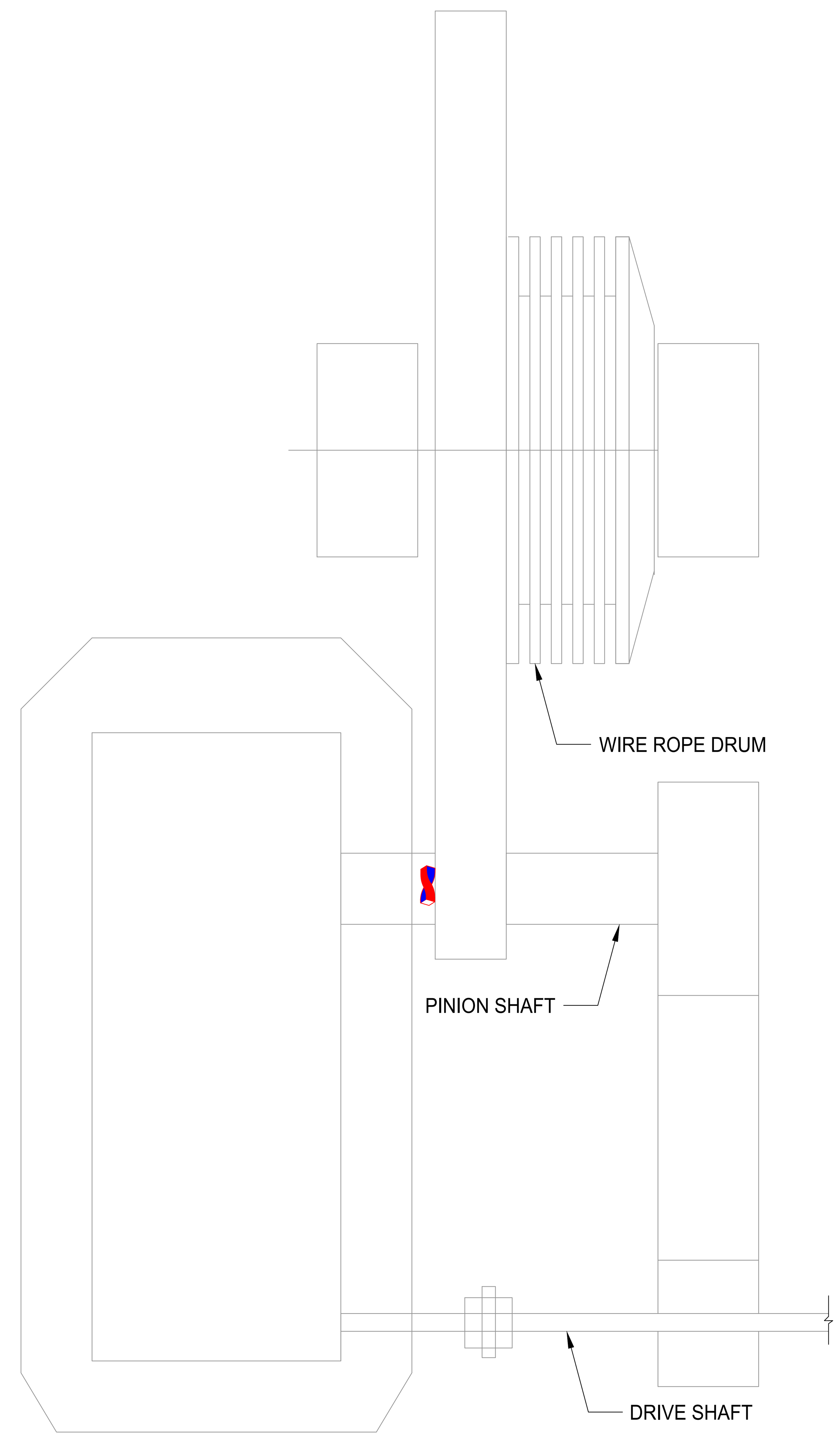

3 TYPICAL HOIST INSTRUMENTATION

TORQUE SENSOR INSTALLATION NOTES:

- TORQUE GAGES WILL BE INSTALLED ON THE PINION SHAFT ON EITHER HOIST MOTOR BETWEEN THE MOTOR AND THE HOIST DRUM
- EXACT POSITIONS OF THE GAGE PAIRS ON THE PINION SHAFT WILL BE DETERMINED IN THE FIELD

SENSOR LEGEND

TORQUE SENSOR

BDI
RAW DATA. REFINED RESULTS.
740 S PIERCE AVE, SUITE 15
LOUISVILLE, CO 80027
303.494.3230
WWW.BDITEST.COM

ISSUE

CLIENT

SCHABEL ENGINEERING
16000 CHRISTENSEN RD, STE 101
SEATTLE, WA 98188

PROJECT NAME

SCHNABEL ENGINEERING
ROCKWALL FORNEY DAM
LIVE LOAD TESTING

Drawn By:	KNR
Checked By:	JDS
Date:	05/27/2020
Client No.:	
BDI No.:	190701-TX
SCALE:	NTS

SENSOR INSTALLATION DETAILS

LLT-31

PLOT TIME: 6/12/2020 3:24 PM
FILEPATH: C:\Users\colemand\BDI\Services - Documents\Server_Remote\190701-TX_Schnabel_RockwallForneyDam\7. Instrumentation Plans\BDI_ROCKWALLFORNEY_01_GENERAL.dwg
© YYYY BRIDGE DIAGNOSTICS INC.

SCHNABEL ENGINEERING

TRUNNION PIN FRICTION TESTING REPORT

ROCKWALL FORNEY DAM – GATE 2
FORNEY, TX

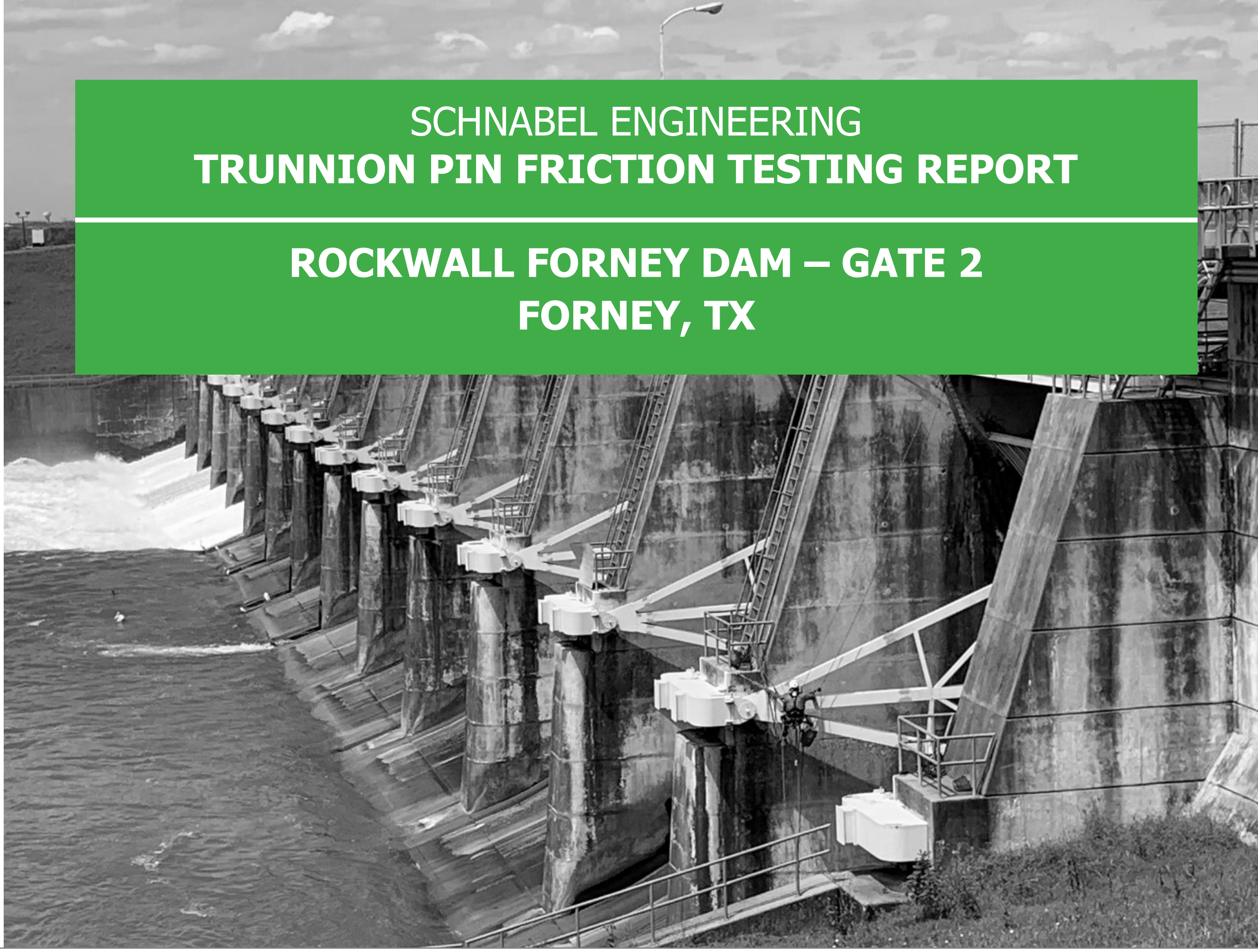

SUBMITTED TO:
SCHNABEL ENGINEERING
16000 CHRISTENSEN RD, SUITE 101
SEATTLE, WA 98188

SUBMITTED BY:
BDI – CO
740 SOUTH PIERCE AVE, UNIT 15
LOUISVILLE, CO 80027

BDI Project No.: **190701-TX**
Report Version: **V1**
Version Submitted: **August 26, 2020**

RAW DATA. REFINED RESULTS.

This document contains Confidential Information and is submitted in confidence to the customer. The submission of the information contained herein shall not be deemed to constitute public disclosure or authorization for disclosure to other parties. BDI's information and name may not be used in advertising or for promotional purposes without BDI's written consent.

BDI RAW DATA. REFINED RESULTS.

TABLE OF CONTENTS

LIST OF FIGURES

LIST OF TABLES

EXECUTIVE SUMMARY

Schnabel Engineering contracted BDI to provide instrumentation and testing services on Gates 1-14 on the Rockwall Forney Dam near Dallas, Texas. The goal of these tests was to record each gate's structural responses during a series of spill tests and use the data to compute accurate coefficients of friction for each trunnion pin, cable lift force, total gate friction, and motor amperage. This report provides details on the work performed on Gate 2.

Instrumentation and testing were performed on Gate 2 at the Rockwall Forney Dam on April 1st, 2020. The gate arms were instrumented with strain and rotation sensors. The hoist motors' pinion shafts were instrumented with torque sensors and the hoist motor controls were instrumented with amperage sensors. Following the instrumentation, a series of spill tests were performed to measure the structural responses resulting from trunnion pin friction. All instrumentation setup and removal were performed using BDI's rope access team.

Following demobilization from the field, the test data was examined for quality and then further processed to evaluate the gate's performance. Strain measurements were converted into bending forces which were then applied to pin-strut free-body diagrams. By summing forces at each pin, friction induced moments could be computed, allowing accurate friction coefficients to be determined. Generally, the observed gate behavior showed that Gate 2 was operating as expected with no major signs of distress.

The resulting maximum trunnion friction coefficients and corresponding hoist forces are shown in Table 1.

Table 1 – Gate 2 performance summary

Pin Designation	Maximum Friction Coefficient	Maximum Pin Moment due to Pin Friction (kip-In)	Maximum Hoist Force (kips)	Maximum Hoist Force due to Total Gate Friction (kips)
Right Pin	0.14	372.0	19.73	4.50
Left Pin	0.21	557.7	24.95	4.04

Note: Pin designations are in reference to looking downstream

Lower maximum hoist forces were collected in Gate 2 when compared to other gates. Due to restrictions caused by the hoist limit switches, the hoist cables could not always be fully slacked at the beginning and end of the performed tests. Throughout testing of the Rockwall Forney gates, it was found that this limit switch restriction varied gate to gate and arm to arm. Therefore, it is not recommended to use the collected hoist force data to quantify overall hoist forces during gate operation. Rather, this hoist data can be better utilized to evaluate total friction behavior.

Amperage responses were not used to compute friction results and were collected as verification that the motor performance was not causing unexpected gate responses. These responses indicated the motor was functioning in a stable manner and should be reviewed by a licensed electrician to further evaluate the motor's performance.

All results and recommendations provided in this report were based on the structure in its current condition; therefore, any significant changes in condition must be noted as they may alter their validity. Questions regarding this report and/or data should be directed to Kyle Ramer (kyler@bditest.com) at BDI. For further information on BDI's equipment, services, and analysis methods please visit www.bditest.com

INSTRUMENTATION AND LOAD TESTING PROCEDURE

GATE INSTRUMENTATION SUMMARY

Instrumentation and testing were performed on Gate 2 at the Rockwall Forney Dam on April 2nd, 2020. Instrumentation plans have been provided along with this report and include the following number of instrumented locations and sensor types:

+ **REUSABLE SURFACE MOUNTED STRAIN TRANSDUCERS:** Each gate arm was instrumented with a total of 24 strain transducers at 6 locations on each of the gate arms (48 strain sensors total). A typical strain gage installation is shown in Figure 1. Note these sensors were installed with the mounting tabs on the extreme fiber of the strut flanges, which puts the center of the gage approximately 0.66" from the extreme fiber.
+ **TILTMETER ROTATION SENSORS:** MEMS style rotation sensors were located on the middle strut of the gate arm near the skin plate and near the trunnion hub (4 rotation sensors total). The rotation responses were used to calculate vertical skin plate movement and measure pin rotation relative to skin plate rotation. Typical tiltmeter installations are shown in Figure 1 and Figure 2.
+ **TORQUE SENSORS:** Two total torque sensors were installed on the hoist's pinion shafts (QTY1 on each hoist pinion shaft) near the cable hoist motor to measure direct torque and in turn lift force (See Figure 3).
+ **AMPERAGE SENSORS:** 3 Hall-Effect amperage transducers were clamped over each phase of the hoist motor to measure the motor's current draw (See Figure 4). The purpose of these sensors was to provide additional data in case there were any issues with the hoist systems and to verify any data issues related to lifting and lowering the gates.
+ **BDI'S STS-4 WIRELESS DATA ACQUISITION SYSTEM:** BDI's STS-4 wireless data acquisition (DAQ) was used to collect and record data during testing. A group of sensors were wired to each nodal DAQ which then communicated wirelessly back to the wireless base station and was controlled by BDI's STS-Live testing software.

Complete specifications are available upon request and can be found at http://www.bditest.com.

SENSOR INSTALLATION

BDI strain transducers were installed by first sanding paint off the struts to expose bare metal at two small locations (1"x2" areas) for the sensor's mounting tabs. Each transducer was then attached using a combination of fast-setting adhesive and accelerator and applying pressure until the adhesive was fully cured. Each strain transducer took approximately five minutes to attach.

Tiltmeters were installed using the same adhesive process as the strain transducers. However, no surface preparation was necessary.

Torque sensors were installed on the pinion shafts by capacitive discharge bonding. Properly bonding to the shaft required sanding the surface to a smooth finish, clean of any paint or grease. Responses from these gages were measured using Binsfeld Torque Trak 10k wireless transmitters.

A typical installation has been shown in Figure 1 through Figure 4. Access to all the sensor locations was provided by BDI's own SPRAT certified rope access technicians and engineers as shown in Figure 5

Once testing was completed, sensors were removed, and exposed steel areas were covered using cold galvanizing compound.

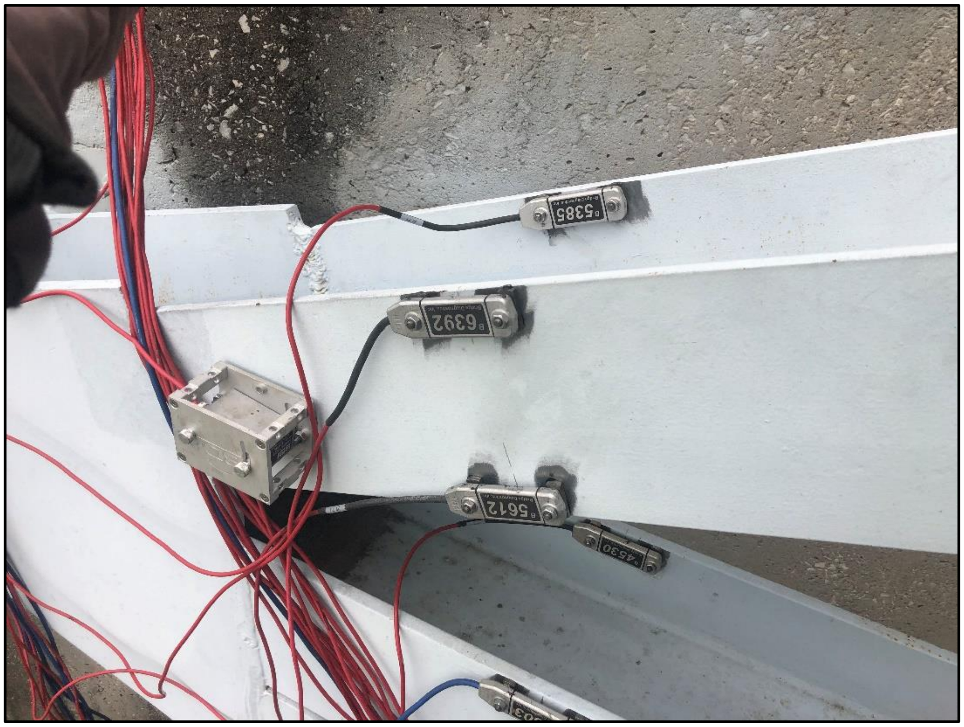

Figure 1 – BDI tiltmeter rotation sensor and reusable strain transducers installed near trunnion hub (Typical)

Figure 2 – BDI tiltmeter rotation sensor installed near skin plate (Typical)

Figure 3 – Torque sensor installation on hoist pinion shaft (Typical)

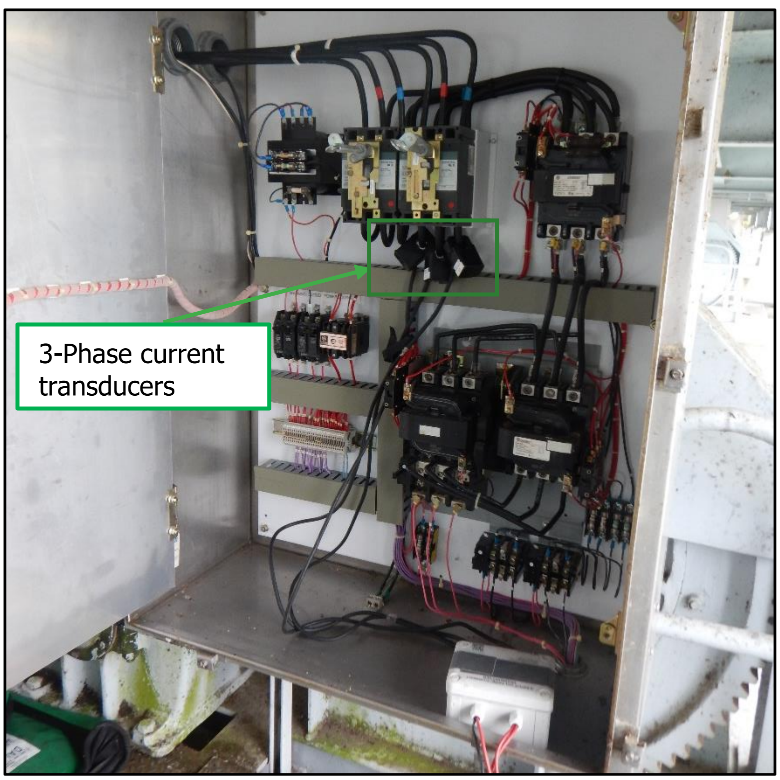

Figure 4 – Current transducers installed on hoist motor controls (Typical)

Figure 5 – BDI personnel installing instrumentation on the gate arm

TESTING PROCEDURES

Structural response data was recorded on all sensors at 50Hz while the gate was run through three spill tests. Each test consisted of three “up-down” cycles (direction reversals) without lowering the gate back to the sill. Each direction reversal consisted of lifting the gate approximately 6-12”, pausing for a few seconds, and lowering the gate approximately 6”, and repeating until all reversals had been completed.

RESULTS SUMMARY

GENERAL DISCUSSIONS BASED ON STRUCTURAL RESPONSES

The following outline contains general discussion points and observations that were made during the data review process. Note: Strain measurements were converted to stress for all subsequent analysis by multiplying the strain values by a steel elastic modulus of 29,000 ksi.

- **DESCRIPTIONS OF RESPONSE MEASUREMENTS:** All sensor readings were zeroed at the end of each test (which consisted of three cycles of direction reversals) so that each measurement corresponded to response change relative to the final gate position as shown in Figure 6 (gates in the downward "closed" position with the hoist cables slacked as much as possible). It is also worth noting that the stresses did not always start and end at the same levels between tests. This variation in behavior is due to small changes in the flexed gate condition between the start and end of tests. It is common for the flex in the gate, caused by pin friction, to slowly release as it rests on the sill. The purpose of the three up-down cycles per test, prior to sitting the gate back onto the sill, is to ensure that these changes in boundary conditions, including gate flexure due to friction, did not affect BDI's trunnion friction results. ***It is important to note that the recorded measurements were changes in structural response due to gate movement, and do not include the in-situ stresses due to the dead load, cable wrap, and hydrostatic loads present prior to testing.***
- **QUALITATIVE DATA REVIEW:** Review of the response data indicated a good level of reproducibility between the three tests. For reference, Figure 6 and Figure 7 show stress responses measured along Gate 2's right arm top strut for all three tests (Test #1-3). The data in these plots have been provided as both a function of time and the gate position as determined by the skin plate tilt sensor. Structural response behavior slightly varied during the first test's first cycle compared to subsequent lift/lower cycles and tests, with the first cycle having a slightly smaller change in stress due to pin friction. The observed variation was likely caused by a larger release of built-up pin friction as the gate rested on the sill for a longer period of time.
- **DIRECTION/FRICTION REVERSAL IN RESPONSES:** The difference in stress during gate opening and closing for a given position is shown in Figure 8. The stress variation at any given gate position was a result of direction reversal and in turn due to trunnion friction reversal. This statement is true since all other loads such as dead-load and hydrostatic pressure were essentially constant barring small changes in hydrostatic pressure due to slight changes in head. This direction/friction reversal is depicted in Figure 9, with deflected shape renderings from a gate arm finite element model under lifting and lowering loads. Note that this figure shows an arm configuration that does not match this gate, but the concept of the direction/friction reversal still applies.
- **MOTOR PERFORMANCE:** Current measurements taken at the hoist motor indicated steady and stable current draws during the lifting and lowering portions. An example plot of current draw and gate position is provided in Figure 10. Current draw ranges during lifting were higher than the ranges during lowering, which is common due to gravity/dead load. These results are summarized along with recorded peak in-rush current in Table 2. Note that the sample rates used during testing were set for collecting gate responses and may not have been appropriate to fully capture the in-rush current. The readings should be evaluated by a licensed electrician with knowledge of the operating parameters.
- **TORQUE AND HOIST FORCE:** Due to restrictions caused by the hoist limit switches, the hoist cables could not always be fully slacked at the beginning and end of the performed tests. Throughout testing of the Rockwell Forney gates, it was found that this limit switch restriction varied gate to gate and arm to arm. Therefore, it is not recommended to use the collected torque and hoist force data to quantify overall hoist forces. Rather, this data was utilized to evaluate total friction behavior, which is observed as half the difference between the lifting and lowering torque/force (friction reversal). Note that issues with the wireless transmitter connected to the left gate hoist gages caused loss of all data for test runs 1 and 2 and partial loss of data for test run 3. While not optimal, this data loss did not significantly affect the hoist results summarized in this report.

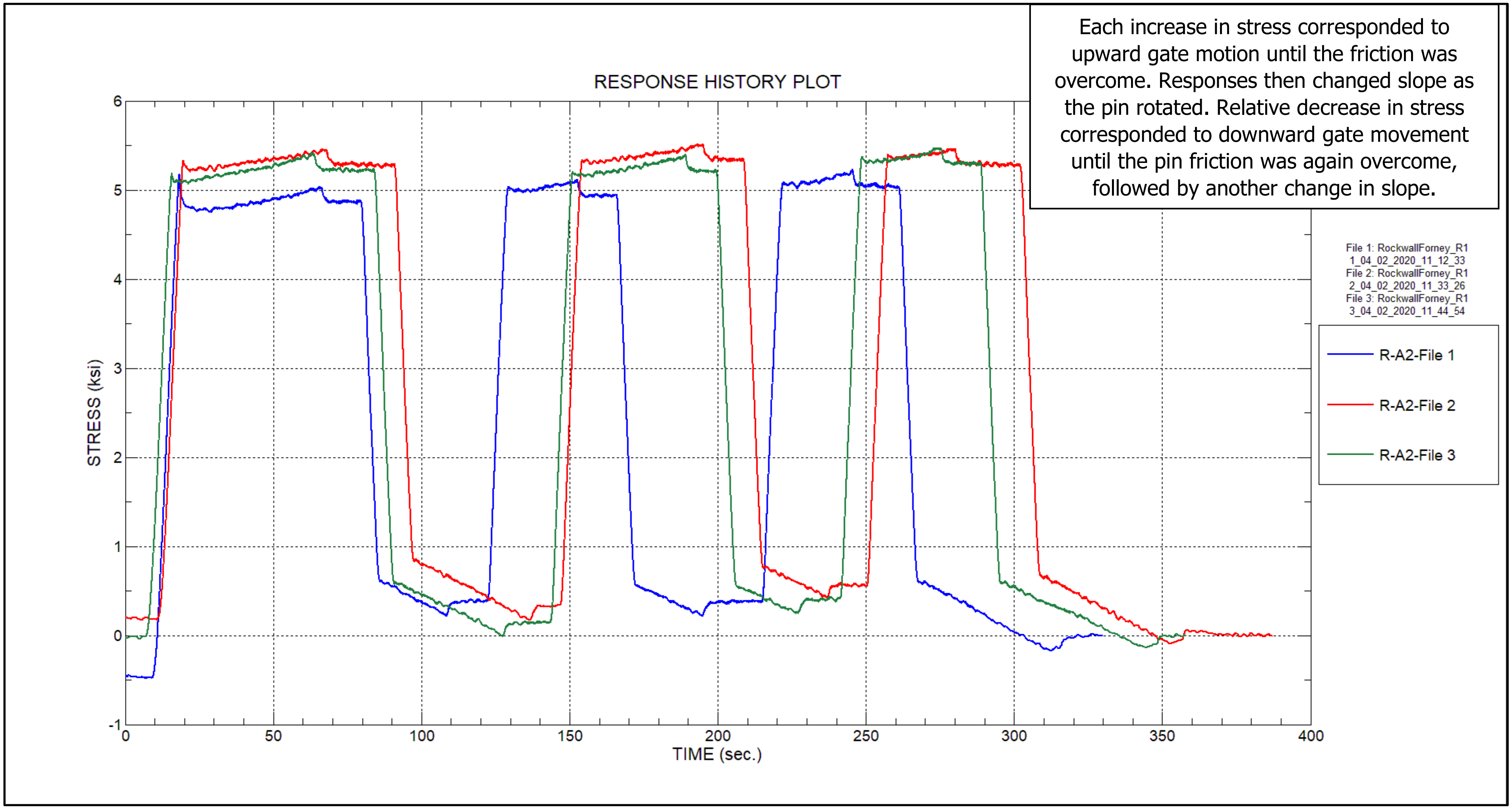

Figure 6 – Stress response history – Right arm – Gage A2 – Time based
File 1 = test run 1, File 2 = test run 2, File 3 = test run 3

(Section A along top strut near pin – Sensor location 2 along bottom of inner flange)

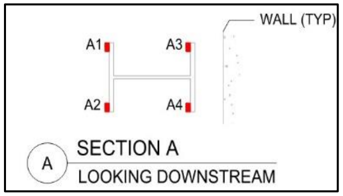

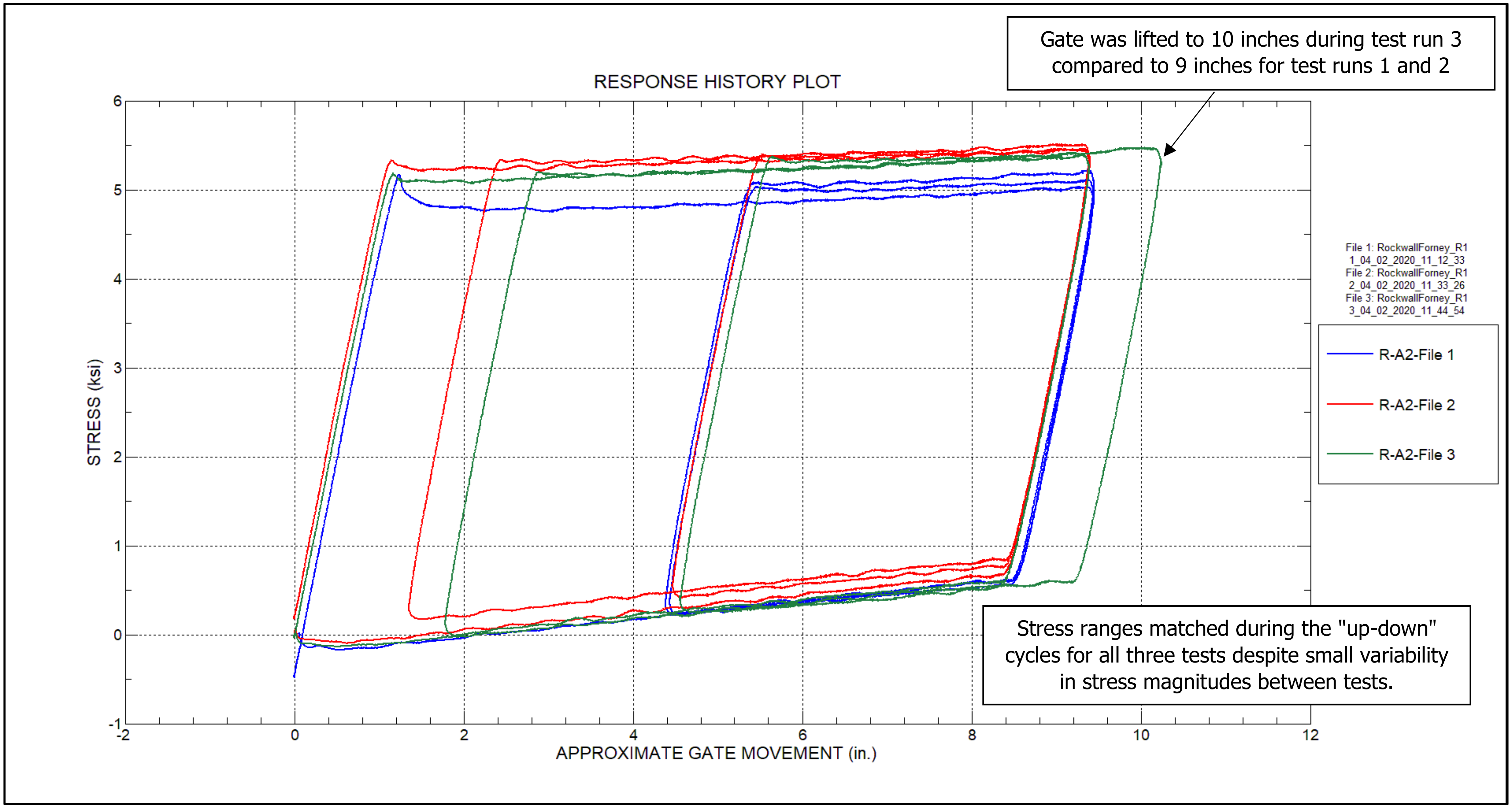

Figure 7 – Stress response history – Right arm – Gage A2 – Function of gate movement
File 1 = test run 1, File 2 = test run 2, File 3 = test run 3

(Section A along top strut near pin – Sensor location 2 along bottom of inner flange)

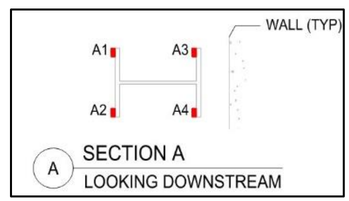

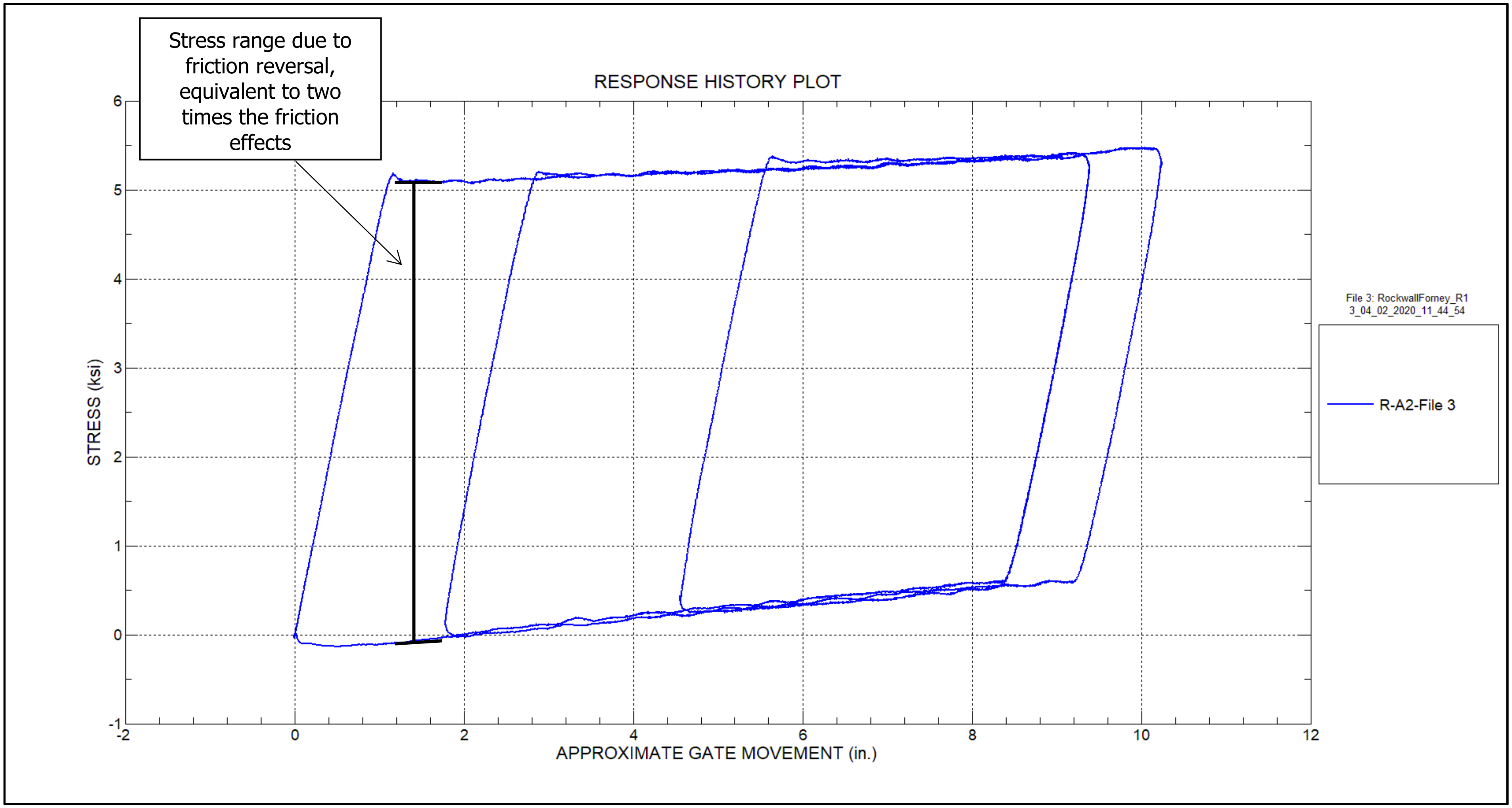

Figure 8 – Stress response history – Right arm – Gage A2 – Friction effect in stress responses

(Section A along top strut near pin – Sensor location 2 along bottom of inner flange)

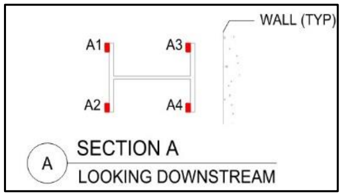

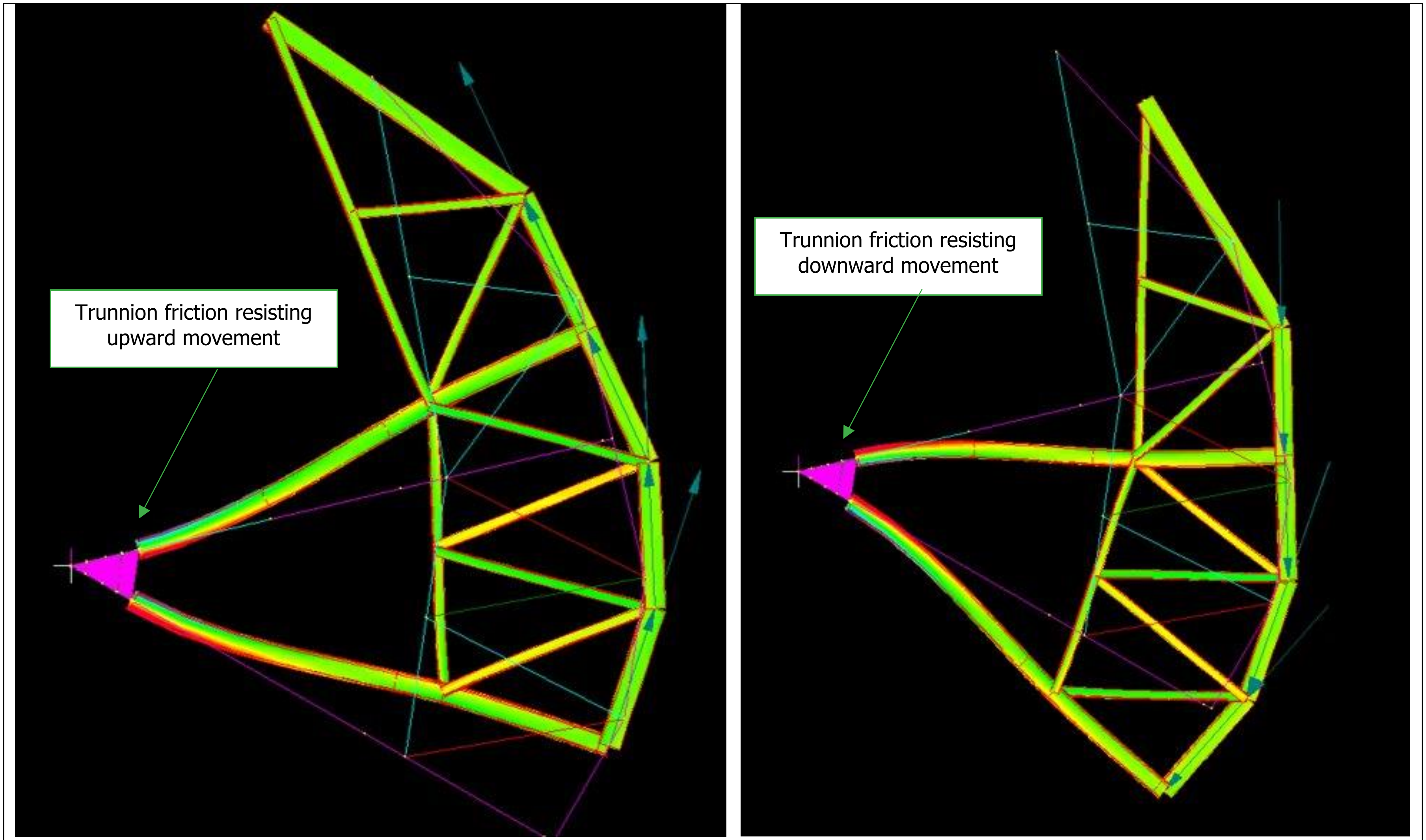

Gate traveling upward **Gate traveling downward**

Figure 9 – Deflected shapes during lifting and lowering of Gate – Visualization of direction/friction reversals

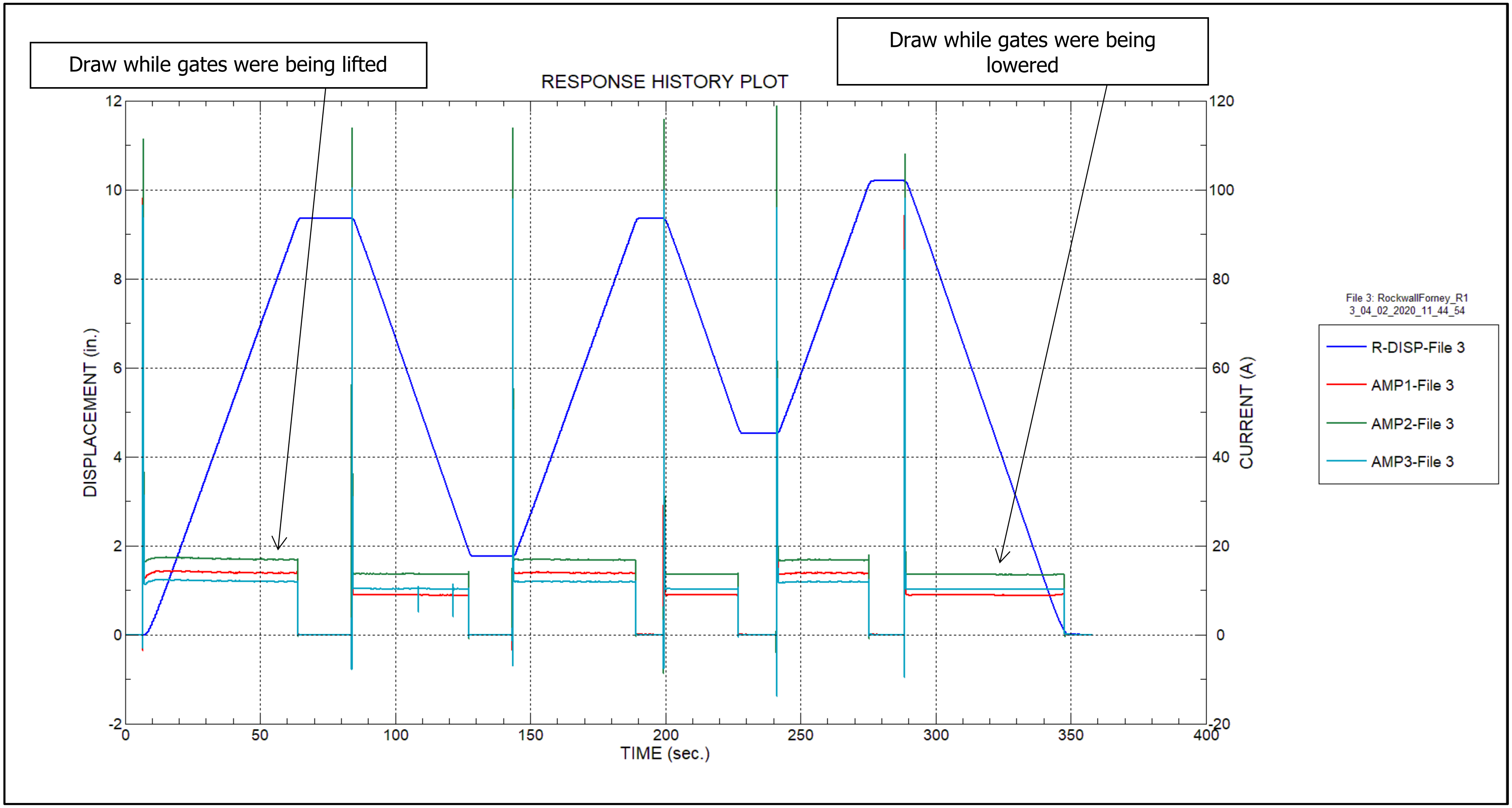

Figure 10 – Motor current & gate movement response history – Lift motor – Highlighting motor draw during lift and lower cycles

METHODOLOGY AND FINDINGS OF THE STRUT FORCE AND MOMENT CALCULATIONS

The following outline provides the methodology used to calculate the required member forces and moments.

+ **CHANGE IN STRESS DUE TO GATE OPERATION:** Strain data can be viewed as a function of time starting when the gate was in the down position and was then lifted off the sill. When examining data in this manner, it is easy to see how stresses ramped up as the gate began to move and then changed slope once pin friction was overcome and the trunnion hub began to rotate with the gate. The first point in time where the friction was overcome (both lifting and lowering) has been highlighted in the stress histories shown in Figure 11. These stress histories show the response of all four sensors along the top strut of the right arm (Section A). ***It is important to note that the recorded measurements were changes in structural response due to gate movement, and do not include the in-situ stresses due to the dead load, cable wrap, and hydrostatic loads present prior to testing.***
+ **CALCULATION OF STRUT CROSS-SECTIONAL MOMENTS:** The use of four strain gages per strut cross-section allowed accurate in-plane flexural bending moments to be computed from the recorded strain measurements. These moments were computed for every cross-section in each gate arm using the basic mechanics equation provided in Figure 12.

  In-plane or weak-axis flexure refers to bending about a given strut's web. This designation is consistent with typical nomenclature. In-plane bending can be observed visually from the strain response histories as a difference between the top and bottom stresses, whereas out-of-plane or strong-axis bending is visualized as the difference in stress from side to side. Figure 13 provides a visual reference for both types of strut flexure.
+ **EXAMINATION OF RESPONSES AS A FUNCTION OF GATE POSITION:** Changes in cross-sectional moment related to friction becomes clearer when the responses are plotted as a function of gate position. Because the gate was operated with several up and down movements, the effects of friction associated with each direction reversal can be viewed for all measured and calculated responses. Figure 14 through Figure 17 show all cross-sectional flexural moment plots for both trunnion arms. The responses in these plots have been centered about the stress state corresponding to a zero-moment, unflexed condition. The zero-moment offset was estimated as the average moment values between up and downward movement (i.e. half the moment difference) at the gate position with the greatest pin friction moment difference (greatest difference between lifting and lowering).
+ **TRUNNION FREE-BODY-DIAGRAM & PIN MOMENT CALCULATION:** Figure 18 shows the instrumented member cross-sections and shows how the measured cross-sectional flexural responses were used to compute pin moment. The in-plane moment values used in these calculations were determined directly from the strain measurements at each cross-section using the provided mechanics equations. It should be noted that the out-of-plane moments were not considered in the calculation of pin moment since they were orthogonal to the axis of the pin rotation. Total pin moment was then determined by summing all the moment components about the pin, which included the in-plane moment and the shear components at the strut cross-sections nearest the pin.
+ **STRUT SHEAR CALCULATION:** From the examination of the trunnion free-body-diagram described above, the shear vectors at the three struts were a primary component in the pin moment calculation. For this type of structural element, shear vectors were calculated using the moment differential between the two cross sections along each strut. It is important to recognize that shear was constant between the two instrumented cross-sections and the applied shear was a function of the recorded change in moment ($V = dM/dX$). Subsequently, the shear vectors were calculated by dividing the difference in moment by the distance between the two instrumented cross-sections. Shear values for each strut have been plotted as a function of gate position in Figure 19 and Figure 20.

- **CALCULATION OF PIN MOMENT DUE TO FRICTION:** Once all the trunnion arm force vectors were calculated, the equations shown in the free-body-diagram were applied to compute pin moment as a function of gate position. It is important to note that because the calculated pin moment range corresponds to a direction reversal, a reversal in friction also occurred. The effect of direction reversal on pin moment due to friction is best conceptualized by centering the moment response plots about the zero-moment axis. The moment due to lifting and the moment due to lowering can then be visualized as a change from this new zero point corresponding to the gate in an unflexed condition. Therefore, the total moment differential between lifting and lowering was twice the moment due to friction acting in a single direction. Pin-moment plots have been provided in Figure 21 and Figure 22. From these plots, it is apparent that pin moment due to friction remained relatively constant throughout the gate operation tests, with a slight decrease in pin friction moment as the gate continued to be lifted. This slight decrease in pin friction moment most likely corresponded to the change in hydrostatic load as the gate position changed. Pin-moment plots for all tests on Gate 2 are also provided for reference in Appendix B – Gate 2 Pin Moment Component Plots.
- **SHAFT TORQUE & HOIST FORCE:** Torque measurements were taken on the pinion shafts near the hoist motor during testing, with single torque gages installed on the left and right hoist pinion shaft. Responses were recorded in units of micro-strain and converted to torque in units of kip-ft using Equation 1 thru Equation 3 and the following shaft properties.

$$d_O = 5.5\ inches, \qquad d_I = 0\ inches, \qquad E = 29000\ ksi, \qquad \nu = 0.3$$

$$G = \frac{E}{2(1+\nu)}$$

Equation 1

$$J = \frac{\pi\left({d_O}^4 - {d_I}^4\right)}{32}$$

Equation 2

$$\tau = \varepsilon * \frac{2GJ}{\frac{d_O}{2} * 1000000 * 12}$$

Equation 3

Figure 23 shows example torque measurements, recorded on the Gate 2 torque shafts. Best practices for torque measurements is to measure torque on opposite sides of the shaft so that any bending in the shaft can be removed by averaging the two responses. Due to access limitations, only one gage at each location could be installed. Therefore, any bending in the shaft may be reflected in the torque measurements and may be related to the peaks and valleys observed in the torque responses.

Torque values were converted to force in the hoist cables per gate arm using the gear ratio and drum radius, as shown in Figure 24. The gear ratio and drum radius were 5.182 and 1.086 feet respectively, as defined in the provided as-built shop drawings. It should be noted that the hoist force calculated may be smaller than the actual hoist force applied. This difference is due to the limit switch engaging the brake before the hoist cable was fully slacked, resulting in an initial force in the cable. A hoist force due to total gate friction was then calculated. This friction hoist force was equal to half the differential in force measured during the lifting and lowering of the gate (similar to the pin friction calculations). As shown in Table 3, the change in cable force due to friction was generally consistent between tests. Note that the total hoist force was due to the total friction effects, including side seal, hoist bearings, trunnion friction effects, etc. It is difficult to determine the exact proportion and composition of the total friction sources. Additional torque and hoist force plots for all collected data files are provided in Appendix A – Gate 2 Torque and Hoist Force Plots.

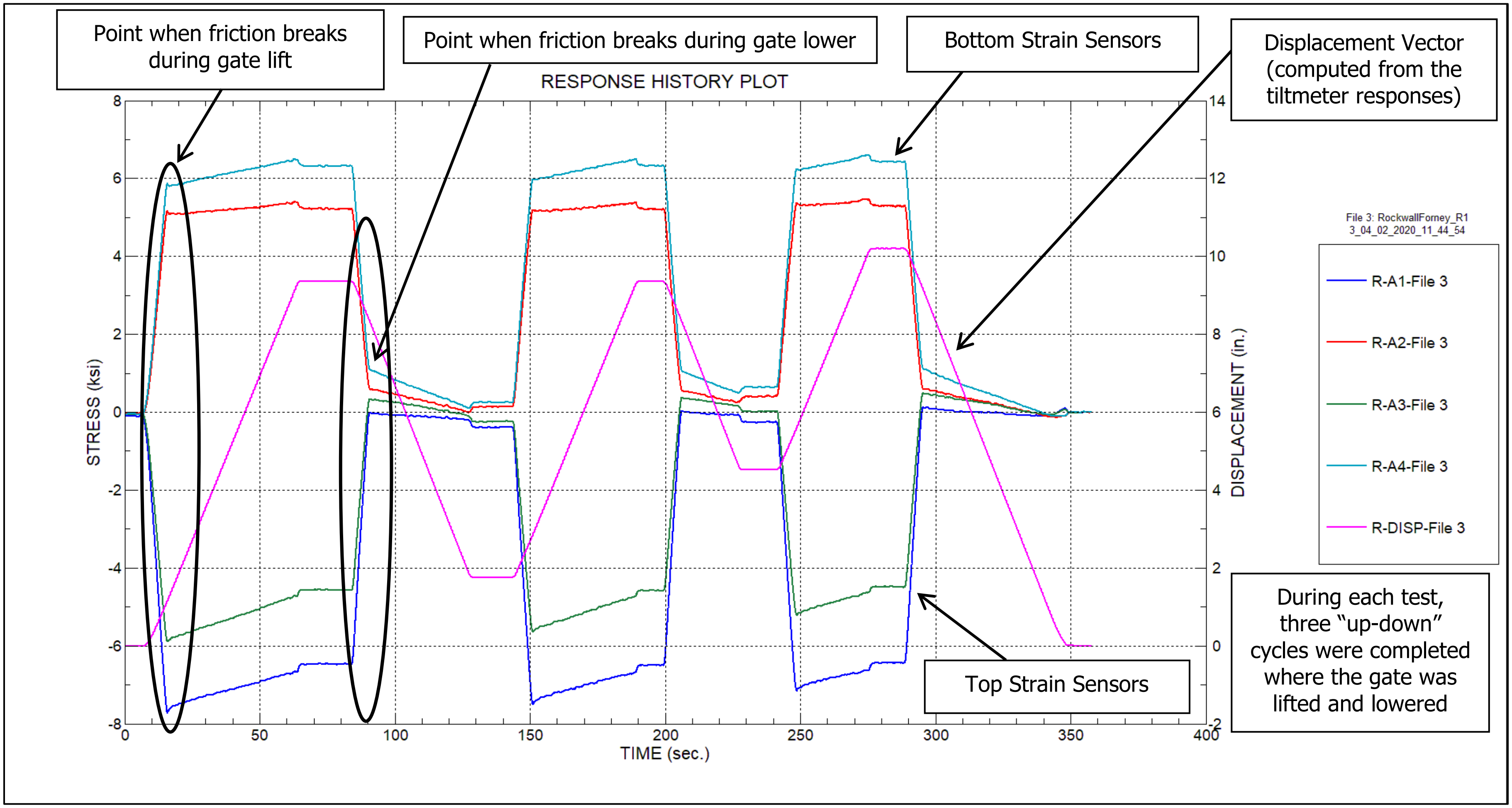

Figure 11 – Stress response & gate movement history – Right arm – Section A - Highlighting friction behavior

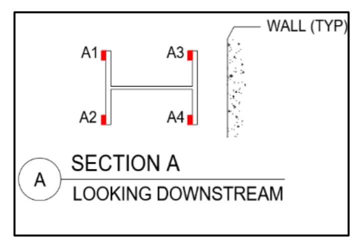

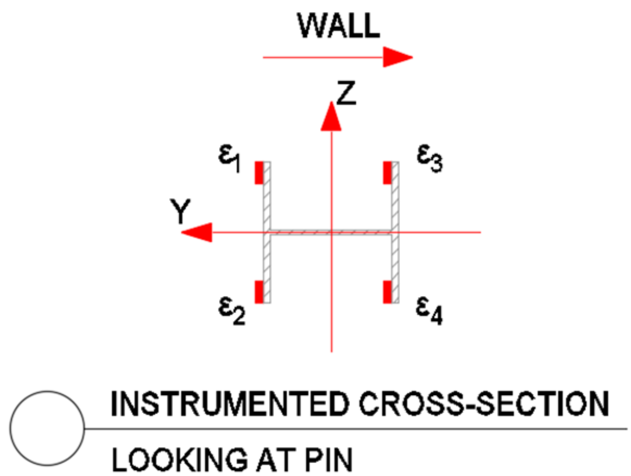

Calculation of Weak-axis (In-plane) bending

$$M_Y = \frac{E[\frac{\varepsilon_2 + \varepsilon_4}{2} - \frac{\varepsilon_1 + \varepsilon_3}{2}]S_{Y(gage)}}{2}$$

Sy(gage) = Section modulus to the center of gages (not extreme fiber of flanges)
(locations of gages were accounted for in moment computation)

Figure 12 – Basic mechanic equation used to calculate moment

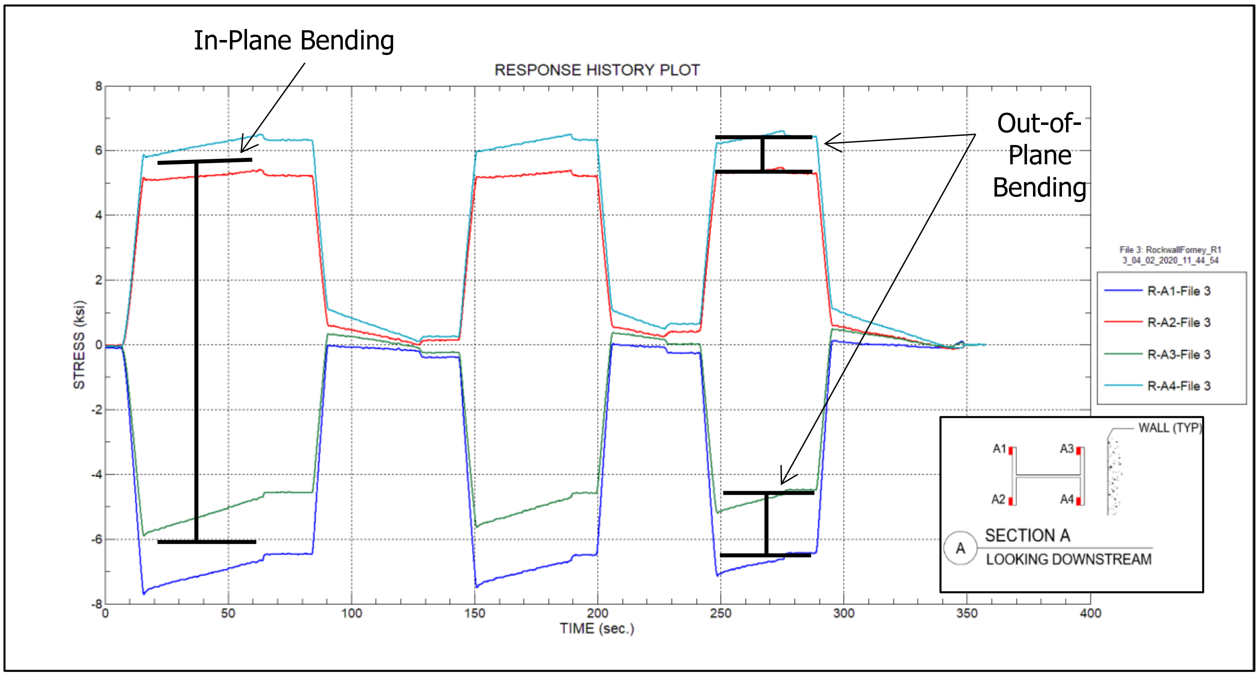

Figure 13 – Stress response history – Right arm – Section A – Bending components
(Section A along top strut near pin)

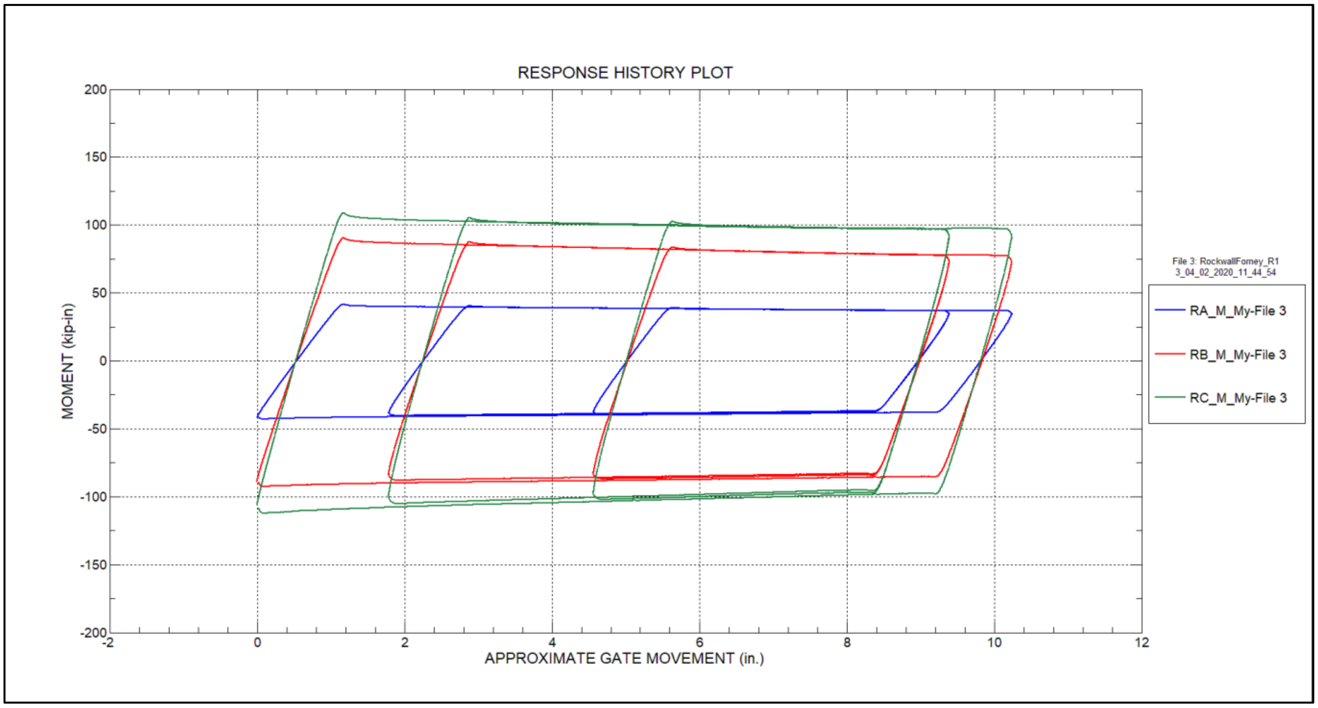

Figure 14 – In-plane moment response history – Right arm – Sections near pin

(RA = Right Arm Top Strut, RB = Right Arm Middle Strut, RC = Right Arm Bottom Strut)

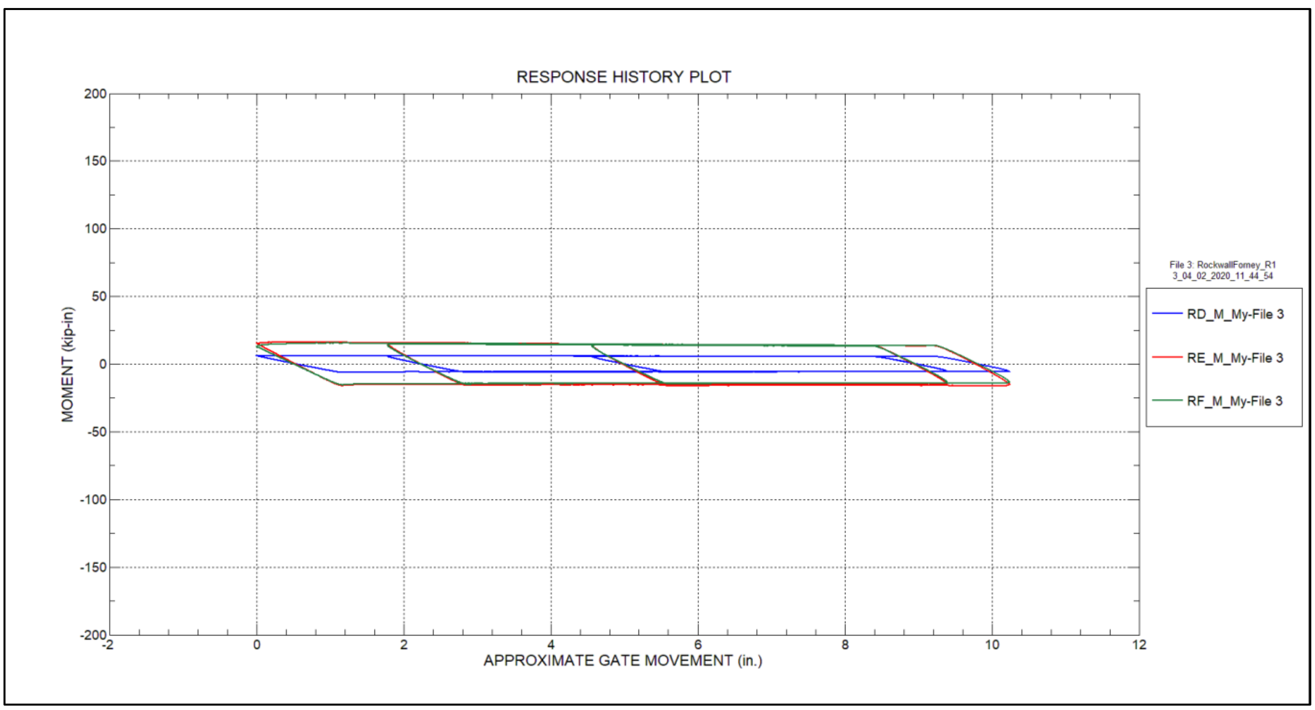

Figure 15 – In-plane moment response history – Right arm – Sections away from pin

(RD = Right Arm Top Strut, RE = Right Arm Middle Strut, RF = Right Arm Bottom Strut)

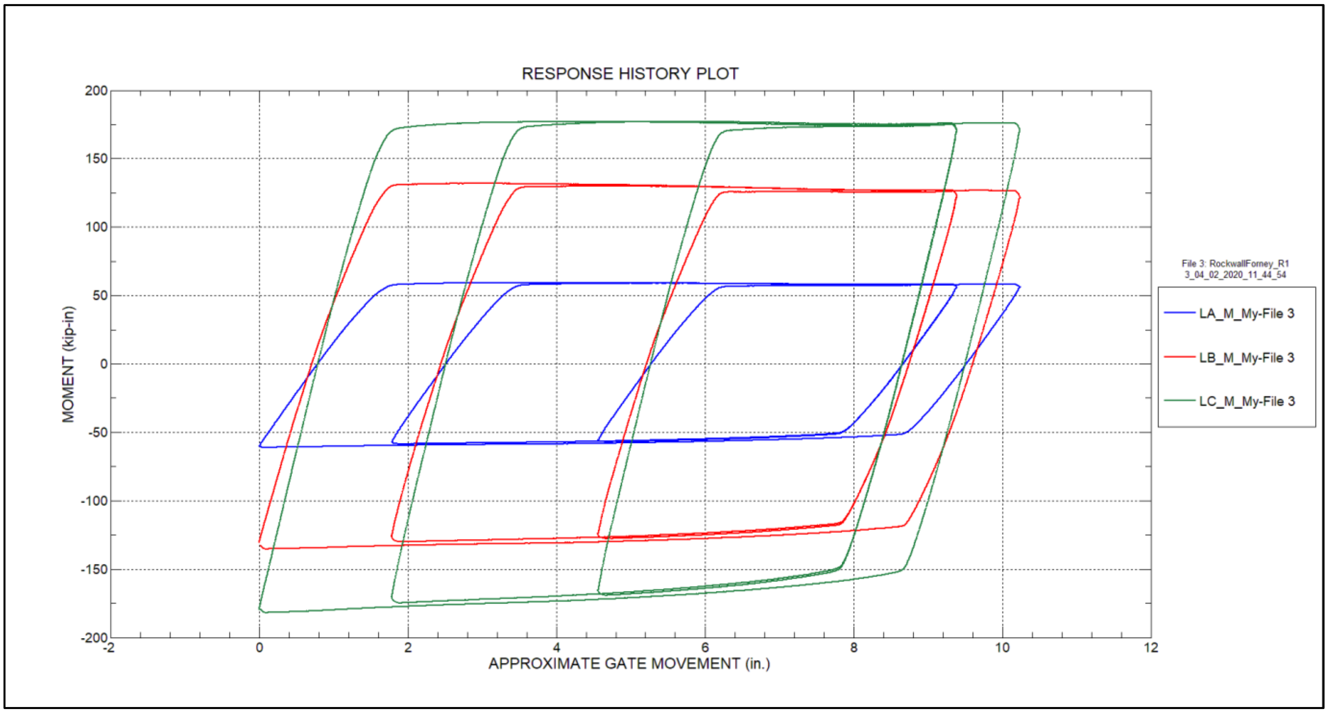

Figure 16 – In-plane moment response history – Left arm – Sections near pin

(LA = Left Arm Top Strut, LB = Left Arm Middle Strut, LC = Left Arm Bottom Strut)

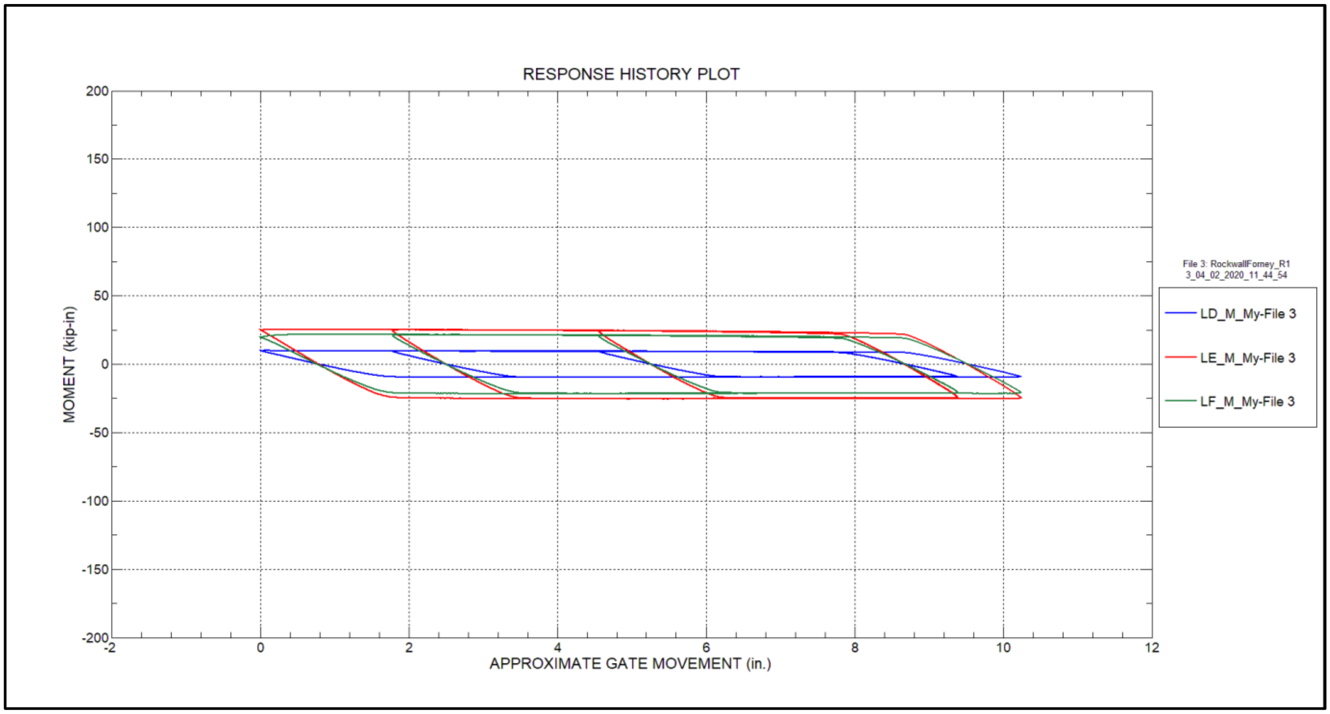

Figure 17 - In-plane moment response history – Left arm – Sections away from pin

(LD = Left Arm Top Strut, LE = Left Arm Middle Strut, LF = Left Arm Bottom Strut)

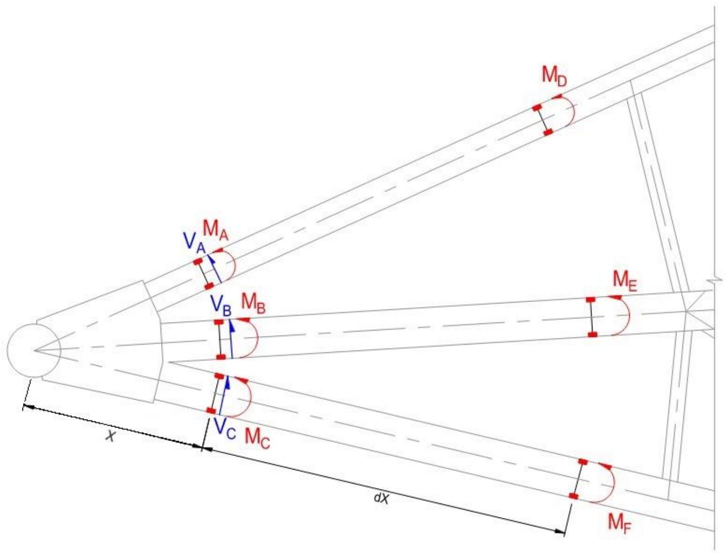

Elevation View of Gate Arm

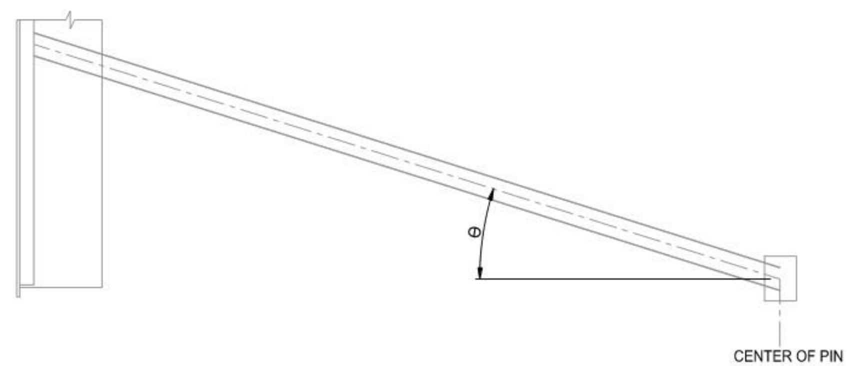

Plan View of Gate Arm

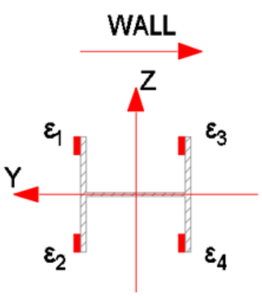

$$M_Y(M_A, M_B, M_C, M_D, M_E, M_F) = \frac{E\left[\frac{\varepsilon_2 + \varepsilon_4}{2} - \frac{\varepsilon_1 + \varepsilon_3}{2}\right] S_{Y(gage)}}{2}$$

$$V_A = \frac{M_A - M_D}{dX}$$

$$V_B = \frac{M_B - M_E}{dX}$$

$$V_C = \frac{M_C - M_F}{dX}$$

$$\sum M_o = 0$$

$$M_{PIN} = [X(V_A + V_B + V_C) + M_A + M_B + M_C] \cos\theta$$

Figure 18 – Direct calculation of pin moment from strain measurements

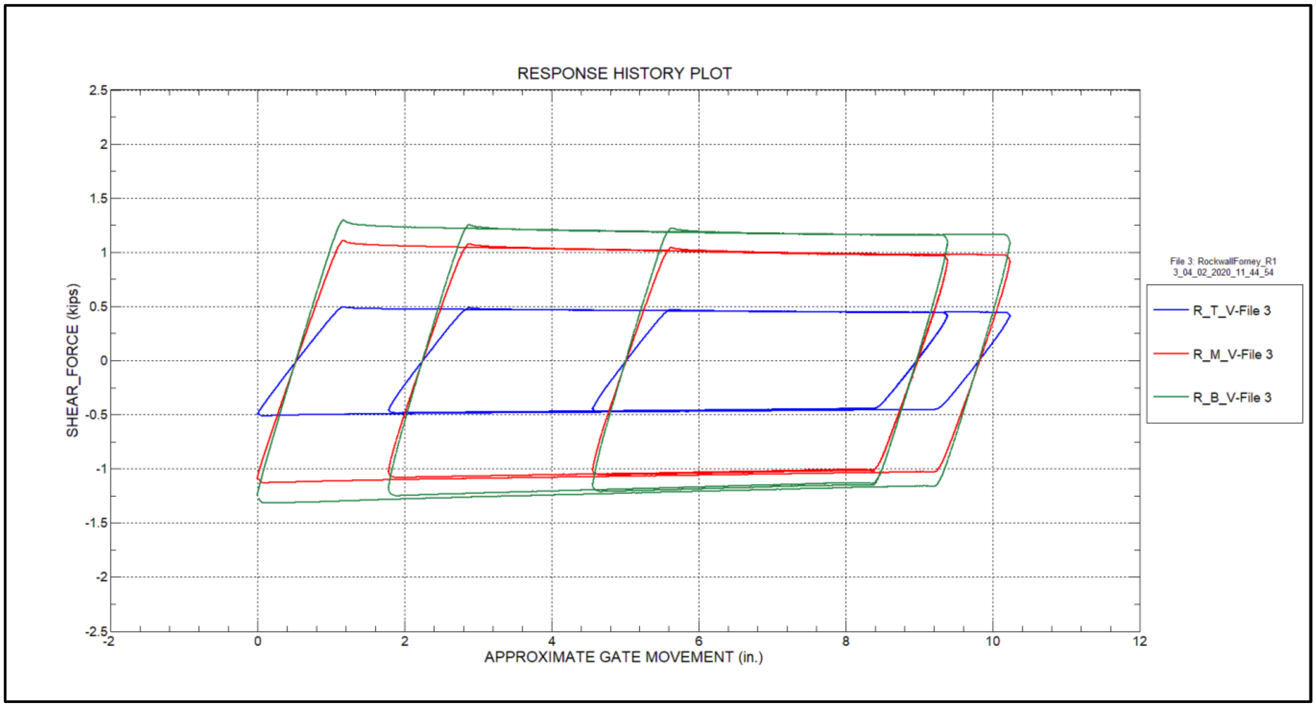

Figure 19 – Strut shear response history – Right arm

(R_T = Right Arm Top Strut, R_M = Right Arm Middle Strut, R_B = Right Arm Bottom Strut)

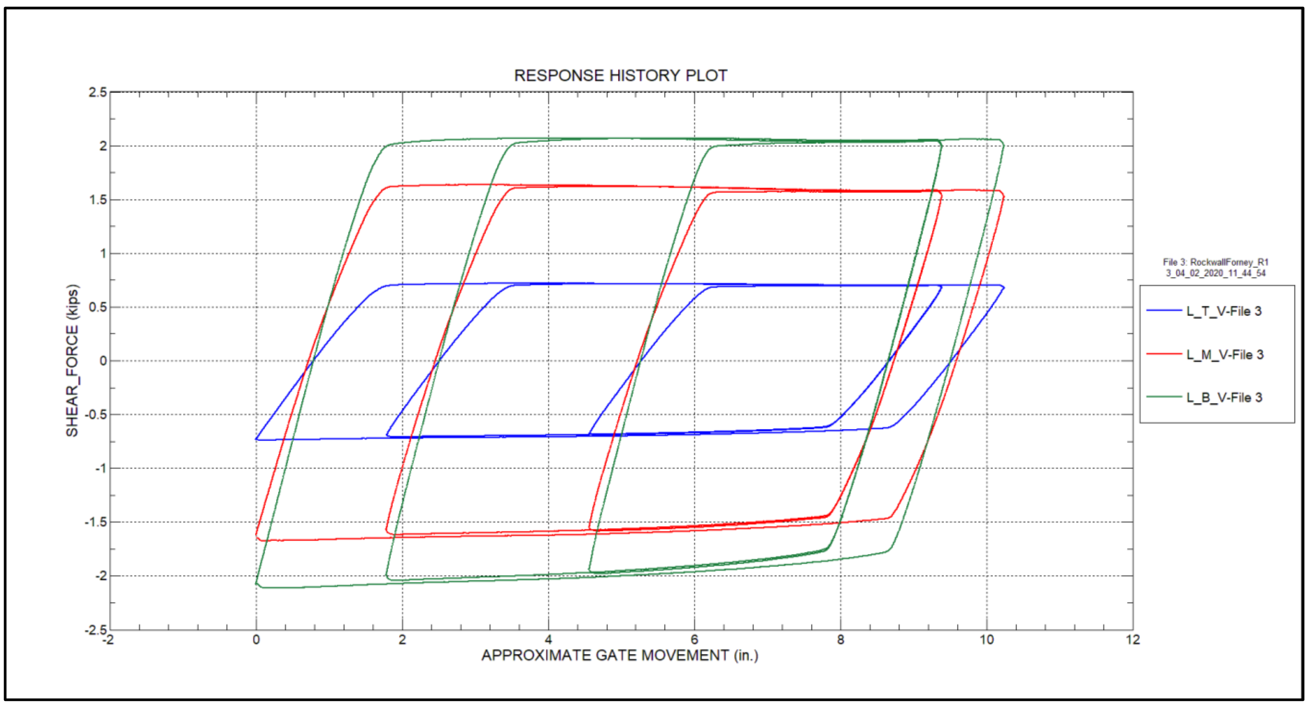

Figure 20 – Strut shear response history – Left arm

(L_T = Left Arm Top Strut, L_M = Left Arm Middle Strut, L_B = Left Arm Bottom Strut)

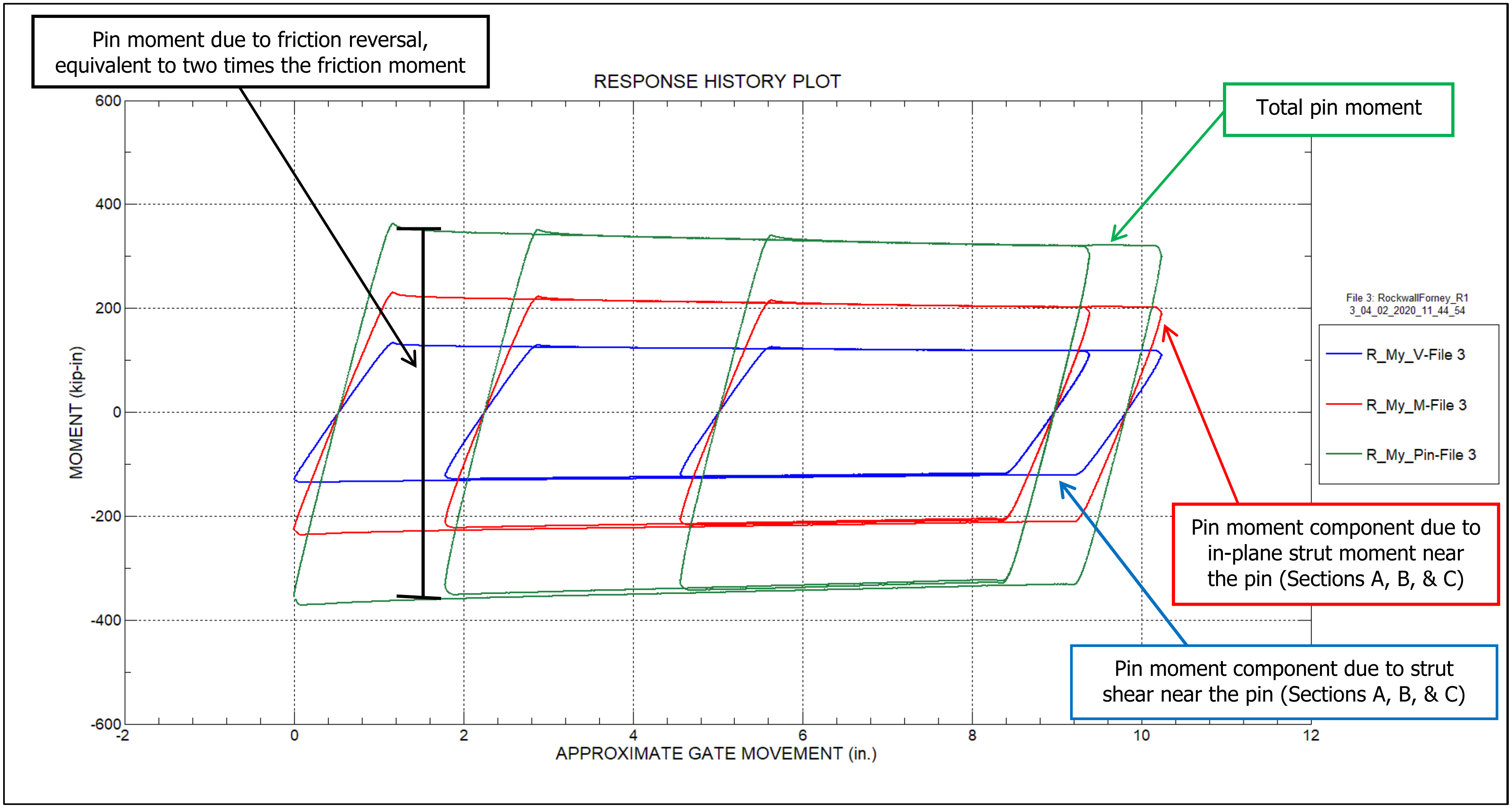

Figure 21 – Pin moment response history – Right arm

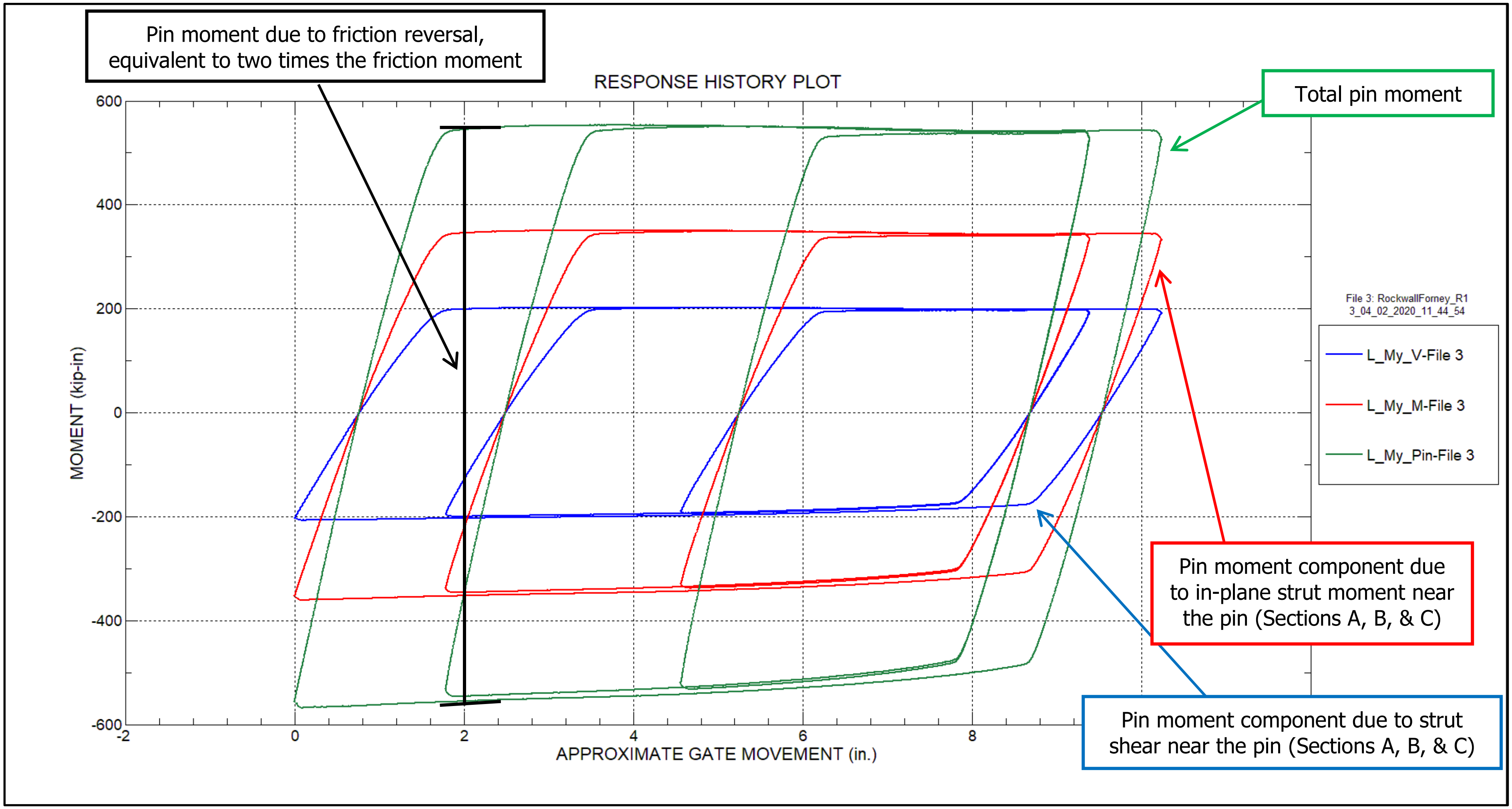

Figure 22 – Pin moment response history – Left arm

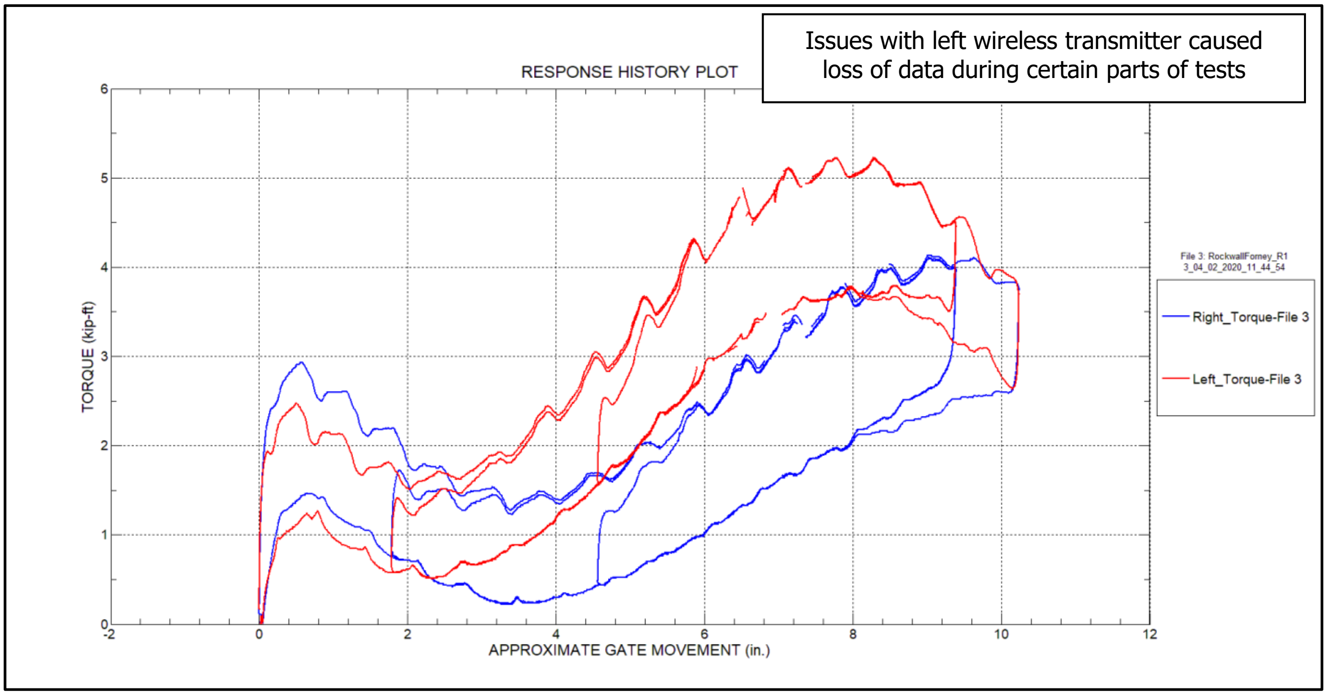

Figure 23 – Hoist torque response history – Gate 2 – Test 3
Note: missing data due to wireless connectivity issues as the sensor rotates with the pinion shaft

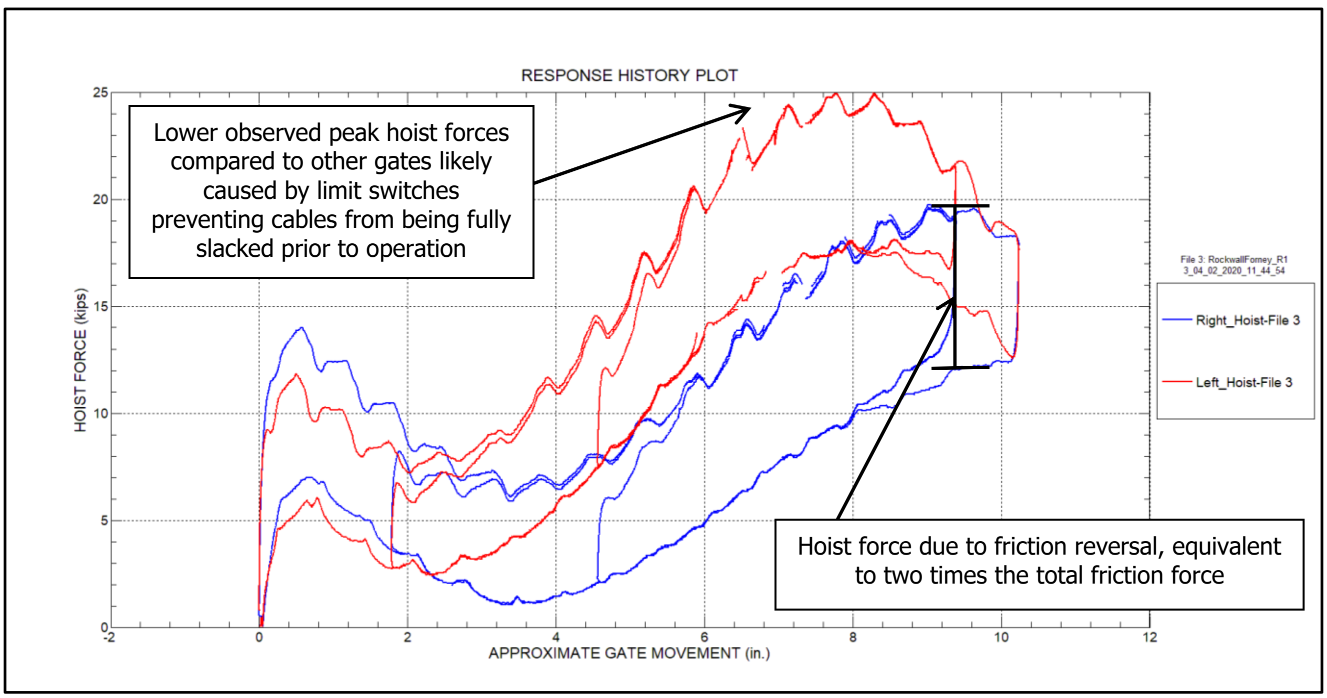

Figure 24 – Hoist force response history – Gate 2 – Test 3
Note: missing data due to wireless connectivity issues as the sensor rotated with the pinion shaft

Summary of Friction Results

The raw data files have been included in the submittal package for reference and were formatted as "tdms" files that can be opened in Microsoft Excel using a "tdms" reader extension.

Examination of the stress histories for each test was necessary to obtain a thorough understanding of the gate performance. The response shapes, variations in stress magnitudes, and timing sequences provided direct clues as to how the gate performed under typical service conditions. The following is a breakdown of the provided tabulated results:

+ Table 2 provides motor current ranges and maximum in-flow for lift and lower cycles for each test
+ Table 3 provides maximum hoist force as well as hoist force due to total friction for each test
+ Table 4 provides the maximum stress ranges measured at the sensor locations for each member
+ Table 5 provides maximum bending stress and moment ranges observed during the gate tests
+ Table 6 provides maximum friction bending stress and moment values at each of the instrumented strut locations
+ Table 7 provides the computed shear values in each strut due to friction
+ Table 8 provides calculated measured friction moments, calculated hydrostatic loads based on the measured water elevation, and coefficients of friction for each gate and gate arm during all three tests

The resulting pin friction moments were used to compute friction coefficients from Eq. 4, given the pin radius and the applied thrust. The thrust used in this calculation consisted of the calculated resultant hydrostatic load based on the measured water elevation and was adjusted to account for the loss of head as the gate was lifted. This thrust adjustment was based on the recorded gate movement and was performed in order to calculate more accurate friction coefficients. The water elevation during testing was nearly constant throughout each gate test and was documented during each "up-down" cycle. It should be noted that the minor thrust due to cable wrapping, which was minimal compared to hydrostatic thrust, was not included in the thrust calculation. This assumption resulted in slightly conservative friction coefficients.

$$\mu = \frac{M_F}{T * r} \qquad \text{Eq. 4}$$

where:

μ = Friction Coefficient

M_F = Friction Moment

T = Thrust per Pin

r = Pin Radius, 5.375"

The out-of-plane shear and moments were not considered in the pin friction calculations due to orthogonal geometry considerations (resulting pin moment associated with out-of-plane flexure being perpendicular to pin rotation).

The data was presented in a specific coordinate system applicable to both arms. Data was processed so that the positive x-axis was always pointing towards the pin and the right-hand rule applied. In-plane bending can be referred to as "bending about the horizontal or y-axis" and shows how much the beams bend up and down within the plane of the gate arms. Refer to Figure 12 above for visual reference of coordinate system and mathematical explanation of calculations. Tabulated results do not include any in-situ effects.

Table 2 – Motor current summary table – Gate 2

Test Run	Current Range due to Lifting (A)	Current Range due to Lowering (A)	Max In-rush Current (A)
1	12-19	8-15	120
2	12-18	9-14	120
3	12-18	9-14	119

Table 3 – Hoist force summary table – Gate 2

Test Run	Right Arm Peak Hoist Force (kips)	Left Arm Peak Hoist Force (kips)	Right Arm Hoist Force due to Total Gate Friction (kips)	Left Arm Hoist Force due to Total Gate Friction (kips)
1	18.43	N/A	4.40	N/A
2	19.30	N/A	4.39	N/A
3	19.73	24.95	4.50	4.04

Tabulated friction force values correspond to the response induced by friction in one direction

Table 4 – Maximum measured sensor stress range

Arm Designation	Top Strut (ksi)	Middle Strut (ksi)	Bottom Strut (ksi)
Right Arm	8.09	8.75	8.55
Left Arm	10.25	12.65	12.96

Tabulated values correspond to the total measured change in response during tests

Stress values have not been extrapolated to the extreme fibers (correspond to center of gage)

Table 5 – Maximum in-plane total bending stress & moment ranges – Total

Section Label	Section Description	Right Arm Stress (ksi)	Right Arm Moment (kip-in)	Left Arm Stress (ksi)	Left Arm Moment (kip-in)
Section A	Top Strut Near Pin	7.89	88.63	10.75	120.80
Section B	Middle Strut Near Pin	8.28	191.55	12.40	286.78
Section C	Bottom Strut Near Pin	8.24	229.66	12.88	359.19
Section D	Top Strut Away from Pin	1.19	13.37	1.76	19.83
Section E	Middle Strut Away from Pin	1.45	33.64	2.21	51.22
Section F	Bottom Strut Away from Pin	1.12	31.14	1.55	43.35

Tabulated values correspond to the total measured change in response during tests

Table 6 – In-plane frictional bending stress & moment at maximum gate friction

Section Label	Section Description	Right Arm Stress (ksi)	Right Arm Moment (kip-in)	Left Arm Stress (ksi)	Left Arm Moment (kip-in)
Section A	Top Strut Near Pin	3.78	42.51	5.26	59.11
Section B	Middle Strut Near Pin	4.00	92.55	6.14	141.92
Section C	Bottom Strut Near Pin	4.03	112.42	6.31	175.89
Section D	Top Strut Away from Pin	0.55	6.21	0.85	9.57
Section E	Middle Strut Away from Pin	0.70	16.20	1.09	25.11
Section F	Bottom Strut Away from Pin	0.56	15.52	0.77	21.54

Tabulated values correspond to the response induced by friction in one direction

Table 7 – Strut shear range summary table due to friction

Arm Designation	Top Strut Shear (kip)	Middle Strut Shear (kip)	Bottom Strut Shear (kip)
Right Arm	0.51	1.13	1.33
Left Arm	0.72	1.73	2.06

Tabulated values correspond to the response induced by friction in one direction

Table 8 – Pin friction summary table

Test Run	Average Water Elevation during testing (ft)	Approximate Thrust at time of Testing (kips per arm)	Gate/Member Designation	Pin Friction Moment (kip-in)	Friction Coefficient
1	435.52	486.90	Right Pin	372.00	0.14
			Left Pin	557.70	0.21
2	435.52	486.90	Right Pin	360.00	0.14
			Left Pin	546.10	0.21
3	435.52	486.90	Right Pin	363.30	0.14
			Left Pin	551.80	0.21

Tabulated values correspond to the response induced by friction in one direction

APPENDIX A – GATE 2 TORQUE AND HOIST FORCE PLOTS

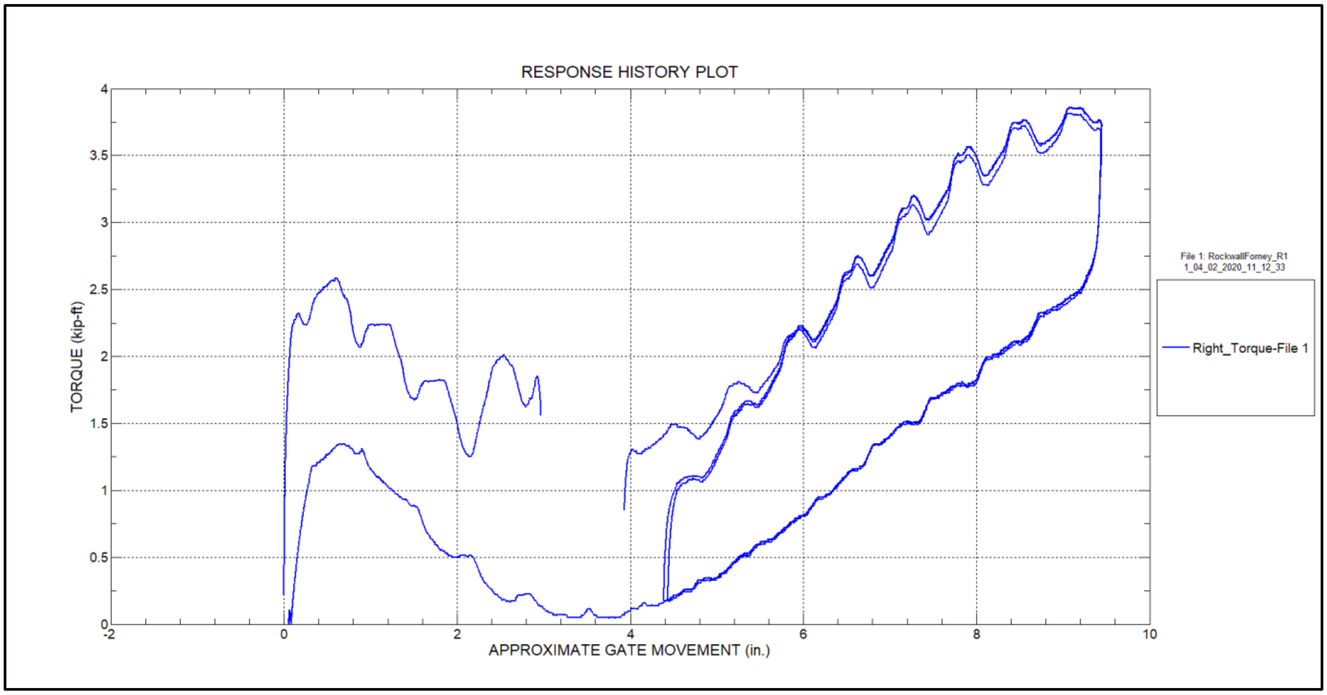

Figure 25 – Hoist torque response history – Gate 2 – Test 1

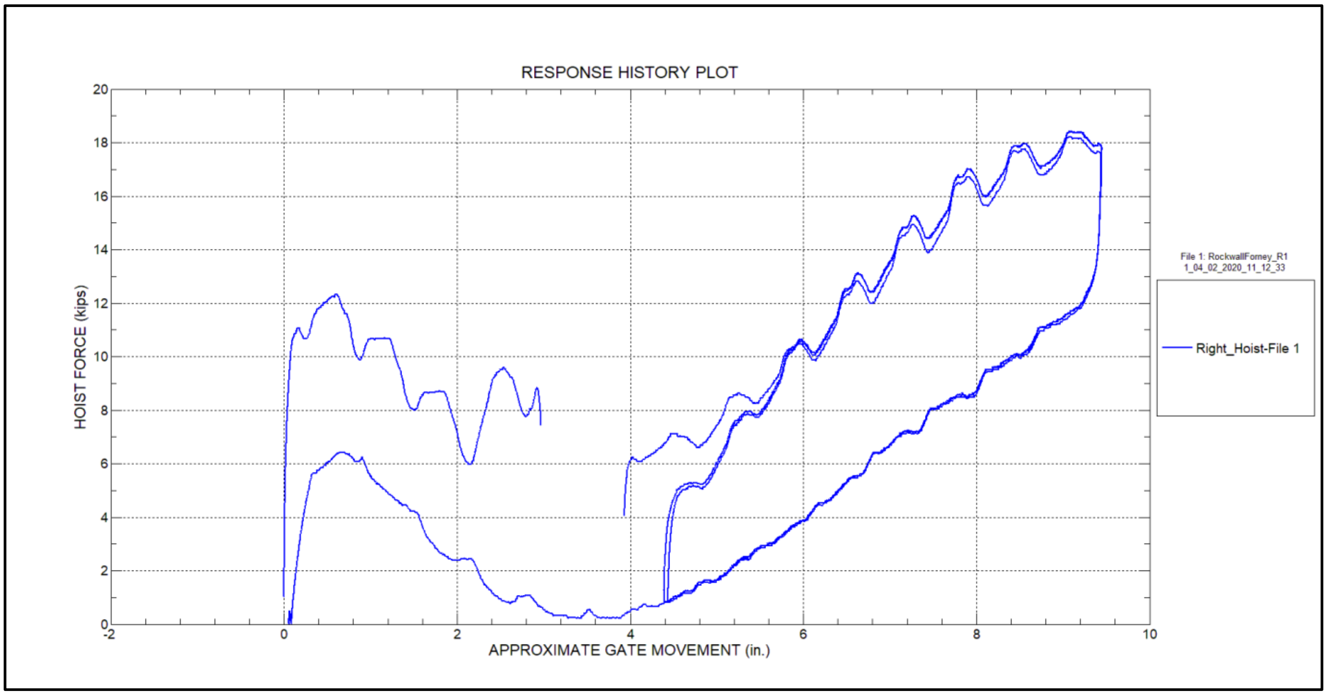

Figure 26 – Hoist force response history – Gate 2 – Test 1

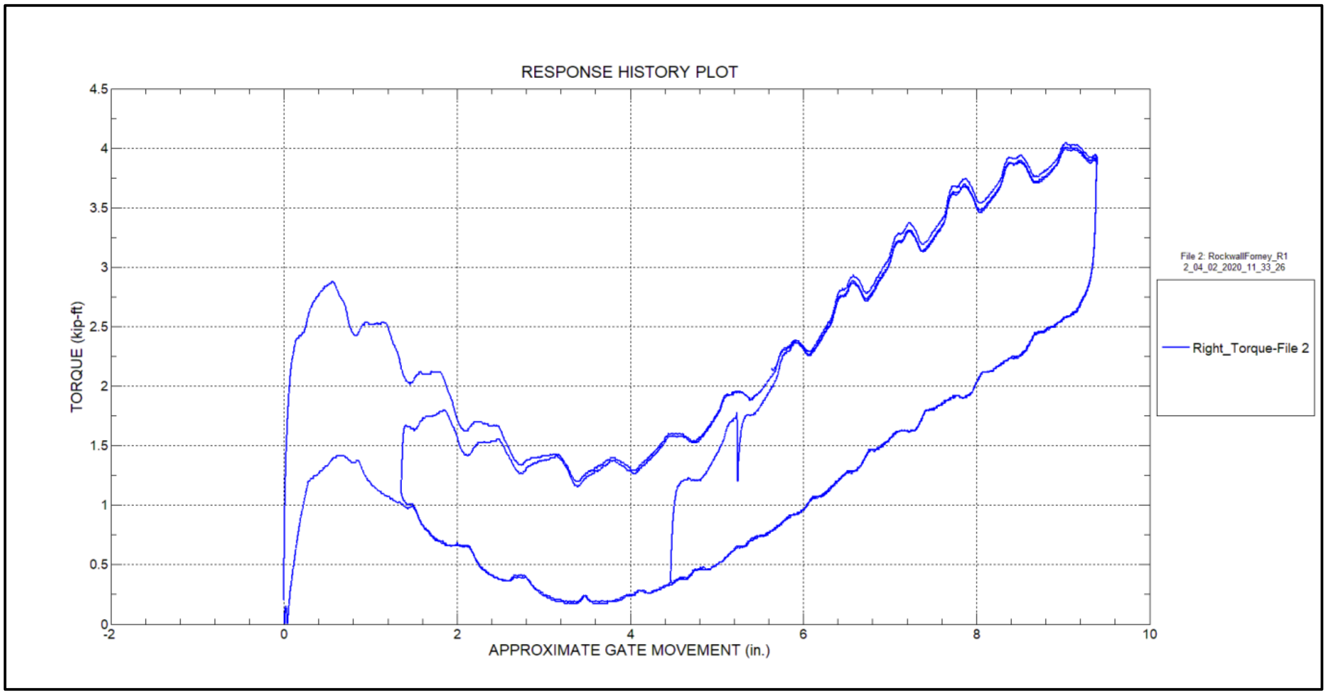

Figure 27 – Hoist torque response history – Gate 2 – Test 2

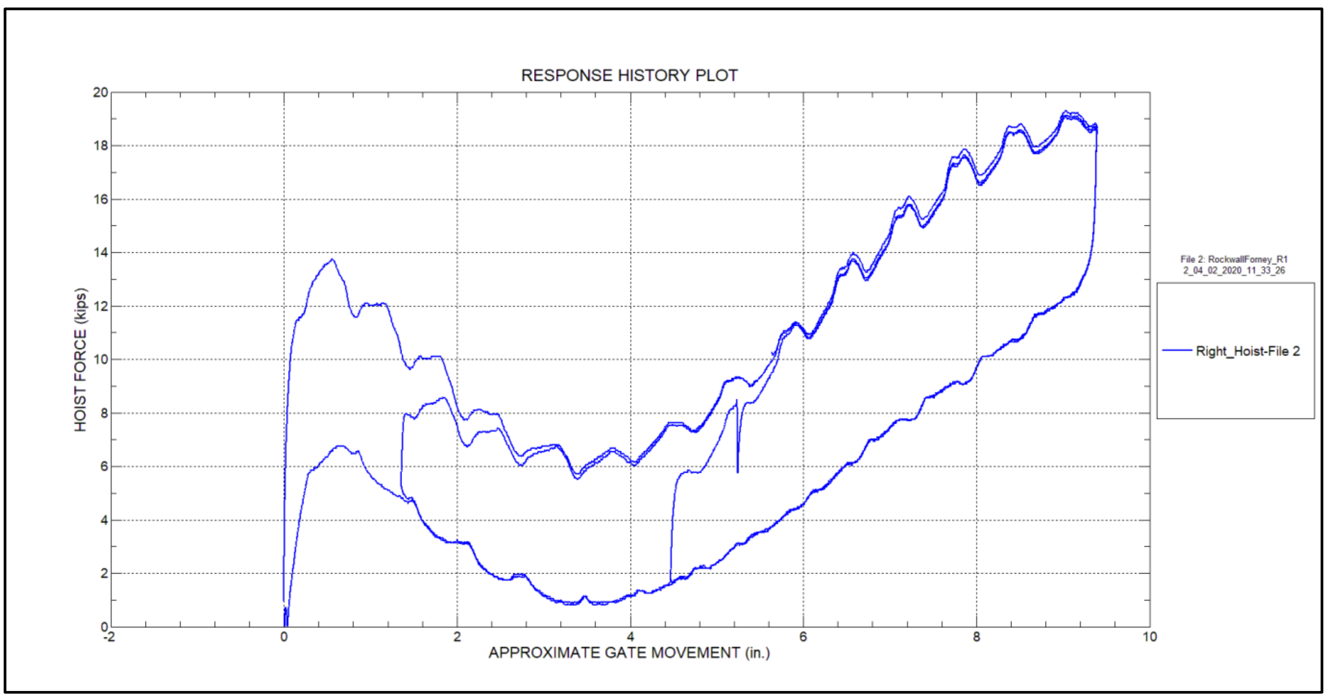

Figure 28 – Hoist force response history – Gate 2 – Test

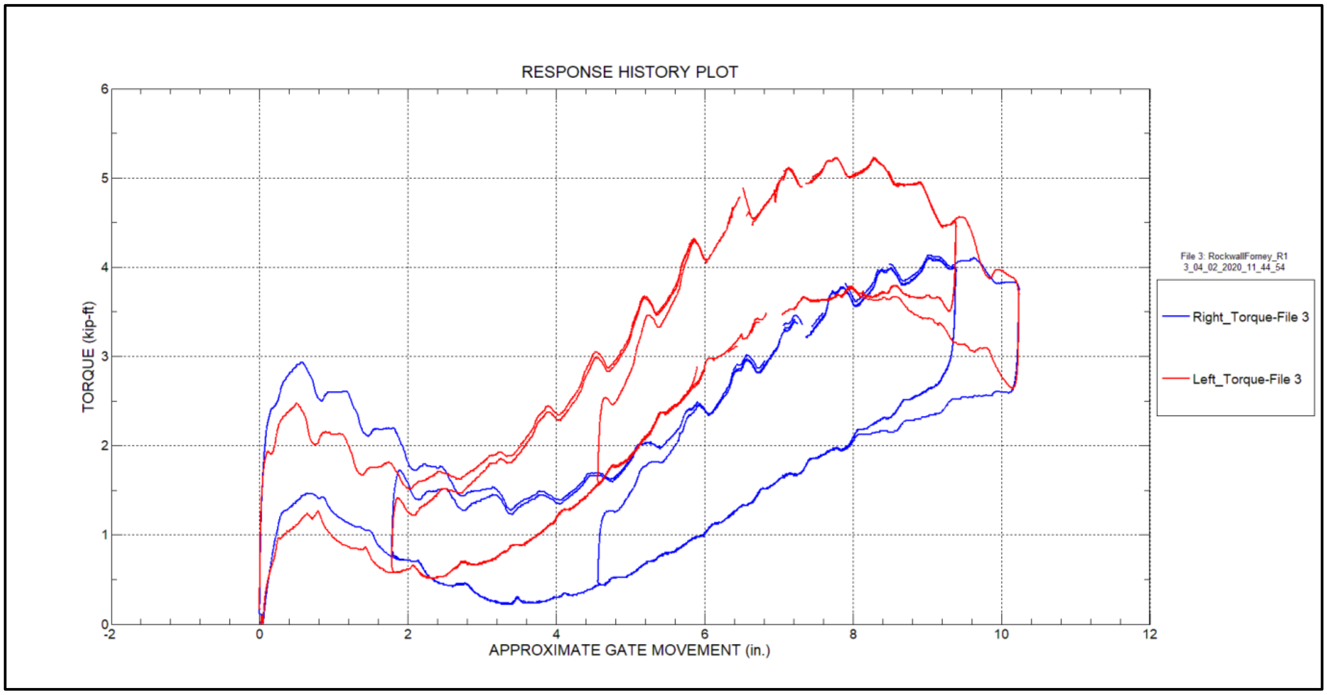

Figure 29 – Hoist torque response history – Gate 2 – Test 3

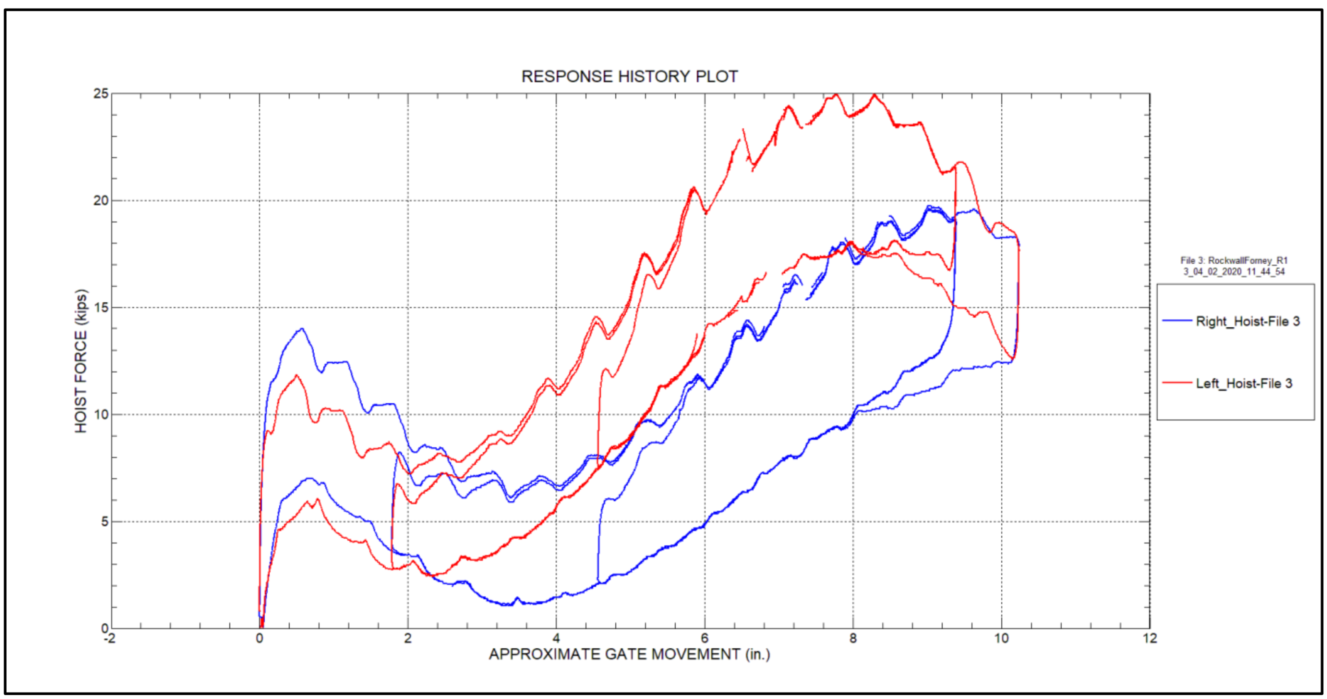

Figure 30 – Hoist force response history – Gate 2 – Test 3

APPENDIX B – GATE 2 PIN MOMENT COMPONENT PLOTS

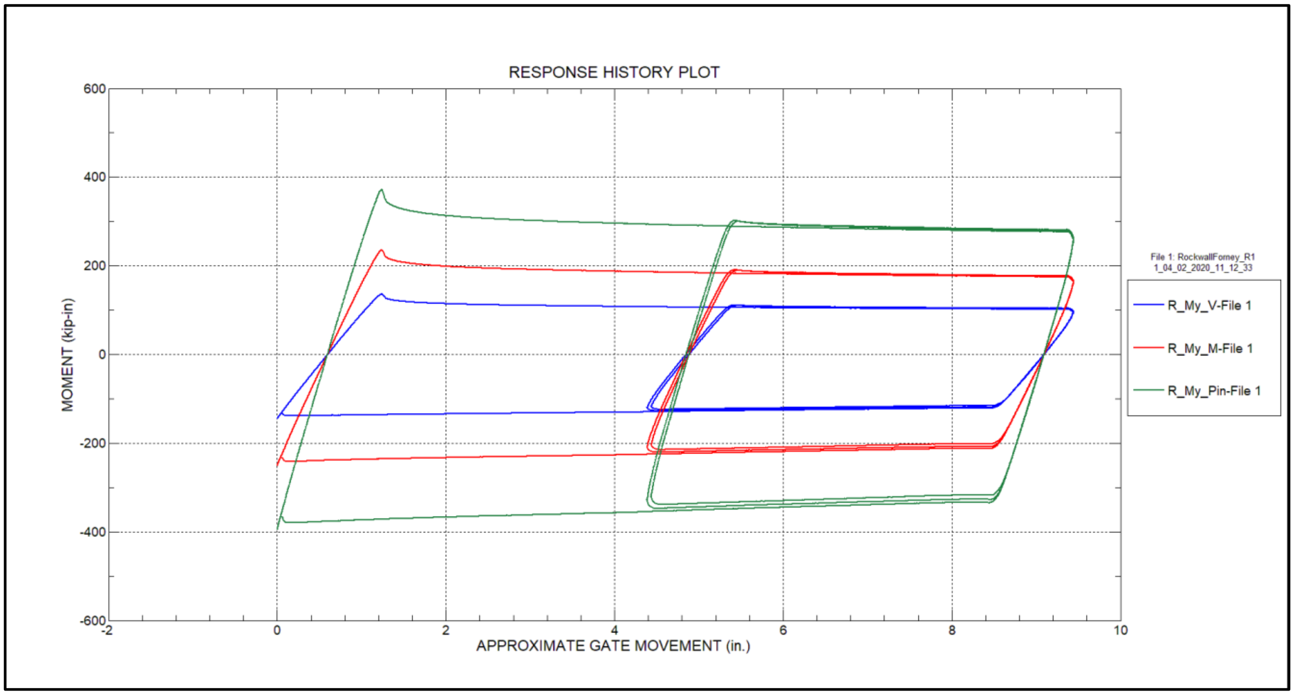

Figure 31 – Pin moment response history – Right arm – Test run 1

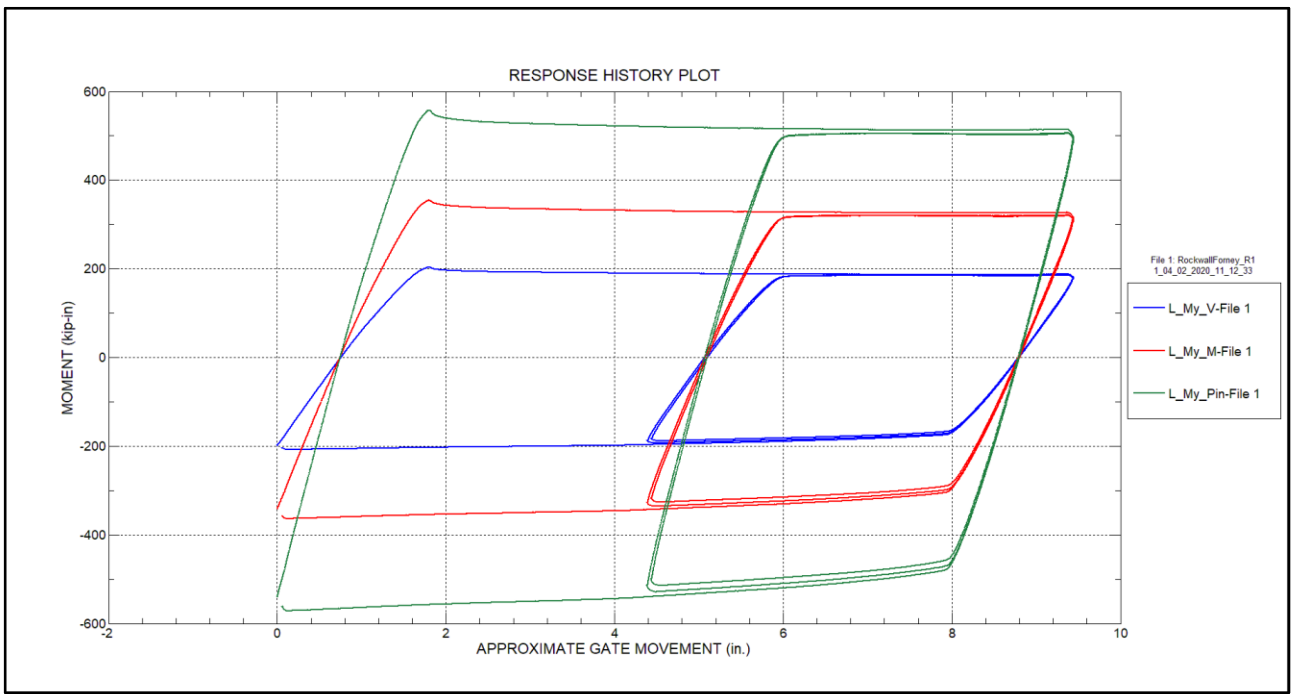

Figure 32 – Pin moment response history – Left arm – Test run 1

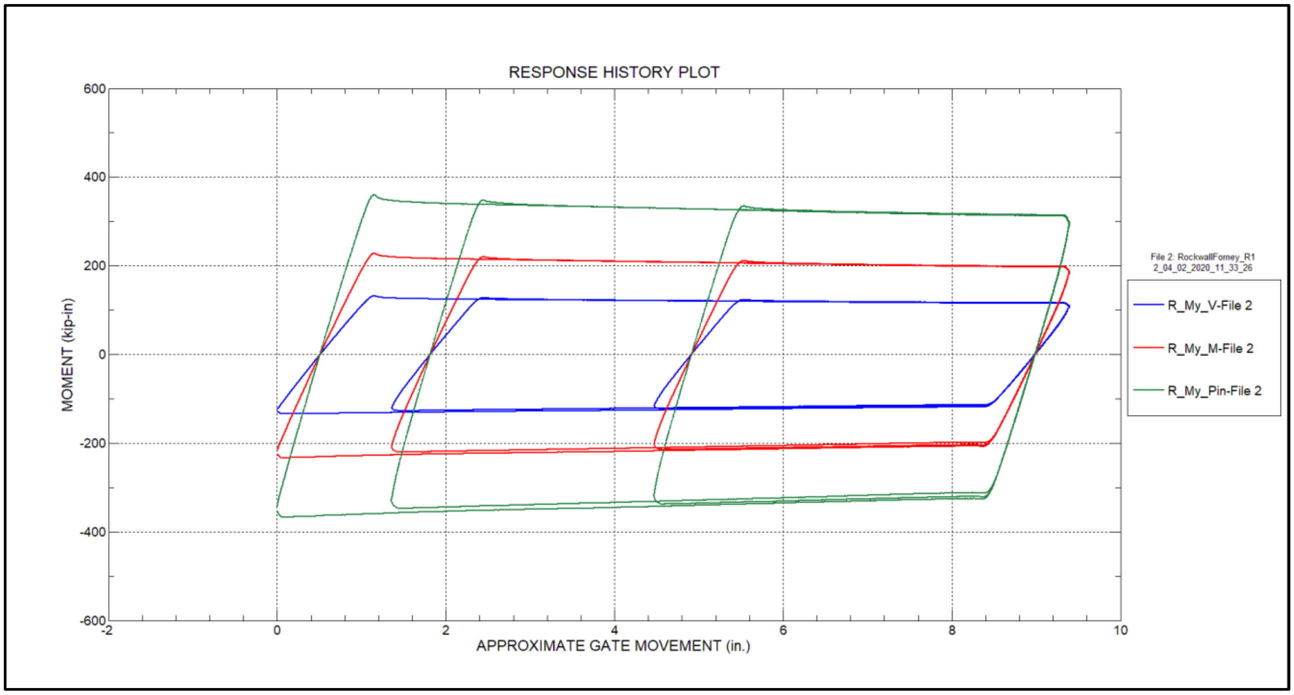

Figure 33 – Pin moment response history – Right arm – Test run 2

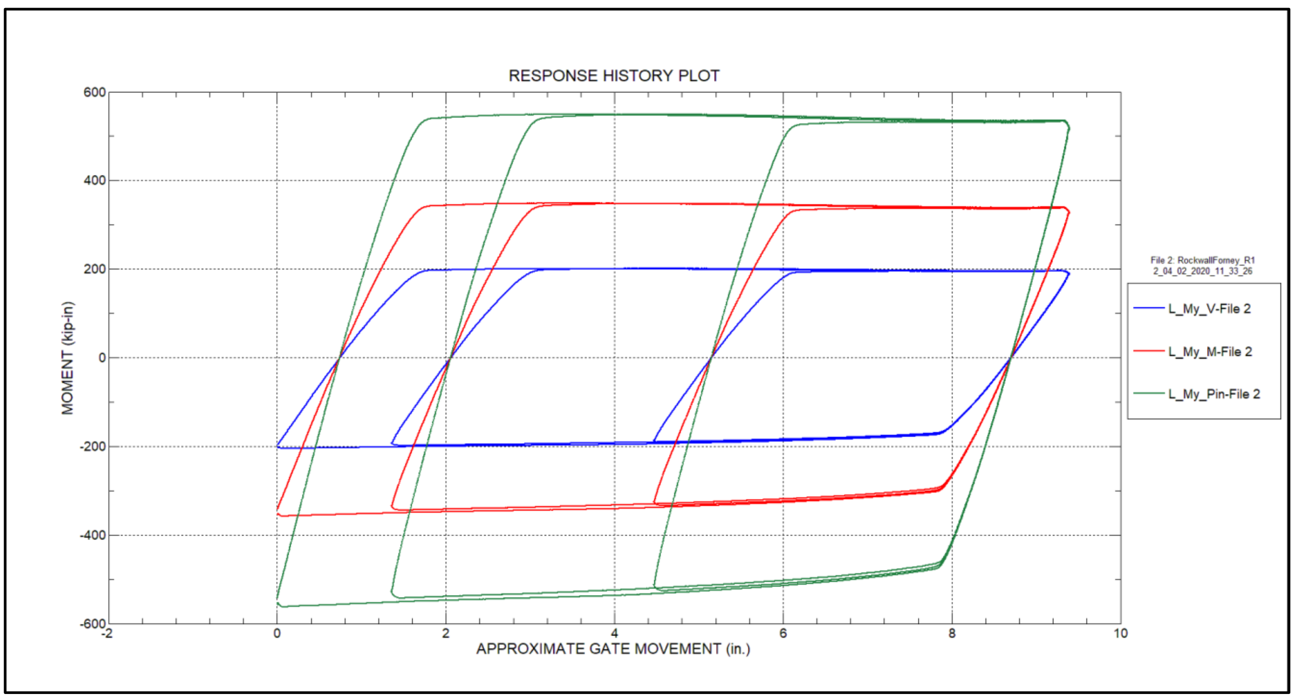

Figure 34 – Pin moment response history – Left arm – Test run 2

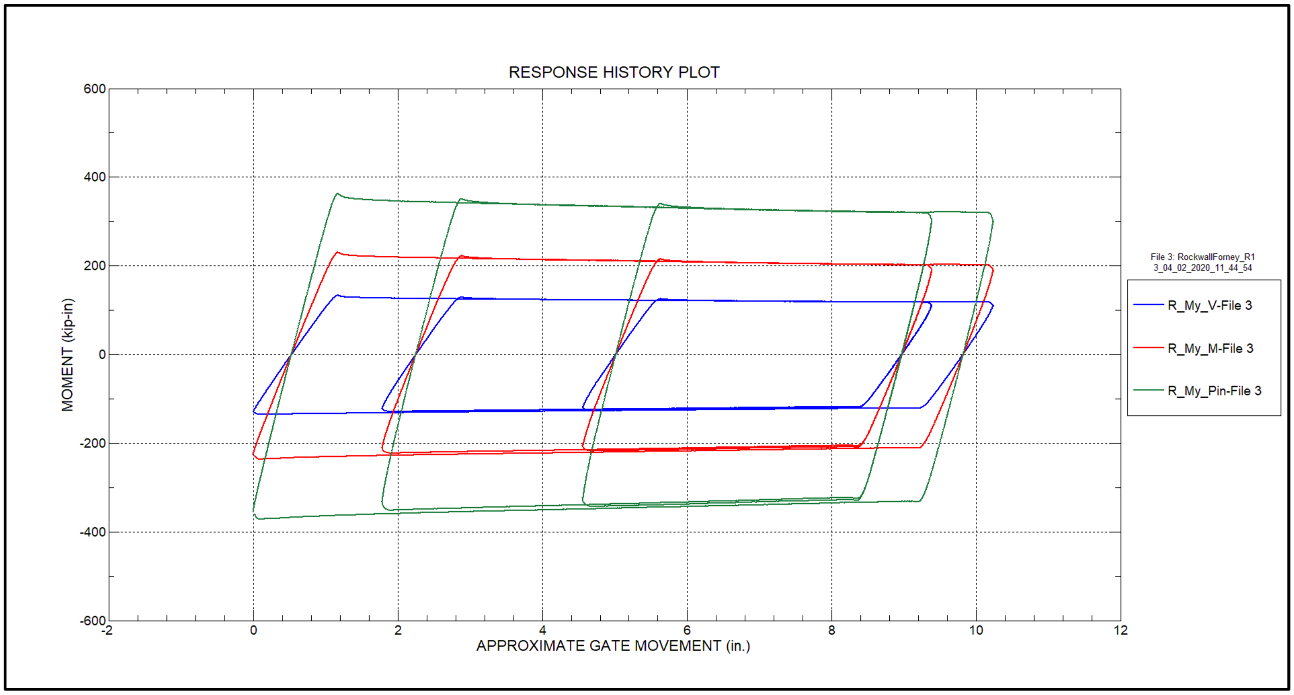

Figure 35 – Pin moment response history – Right arm – Test run 3

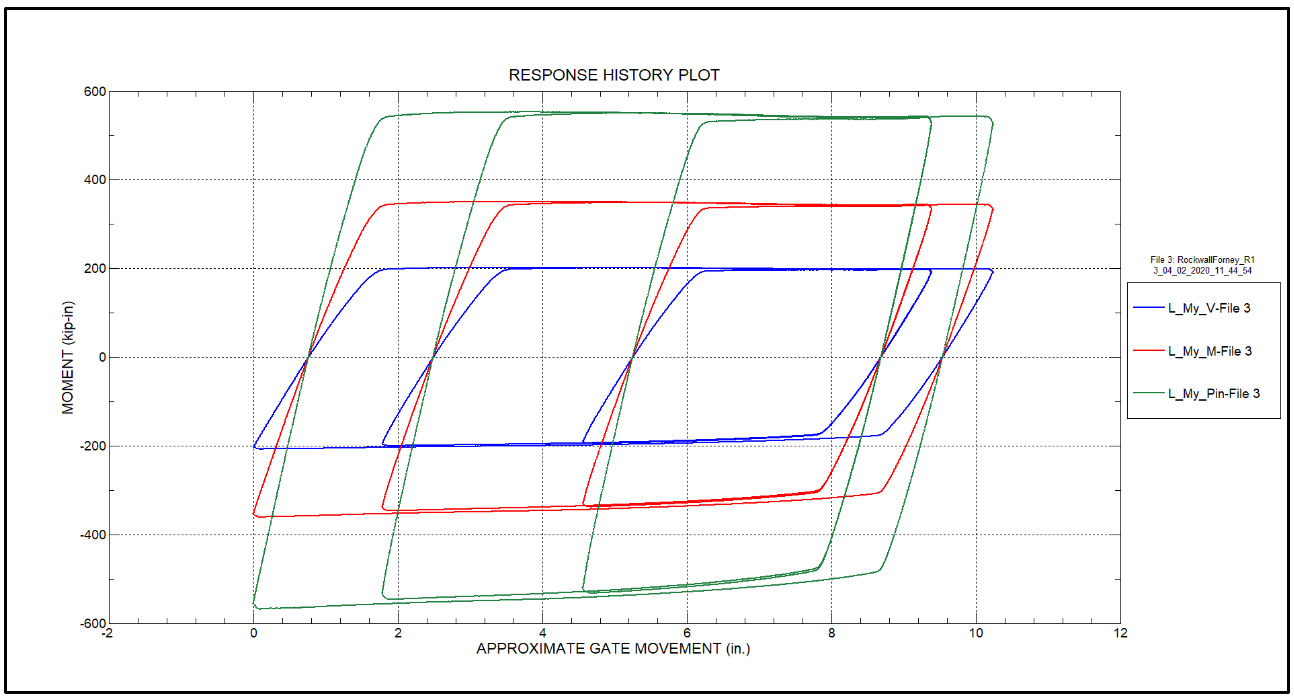

Figure 36 – Pin moment response history – Left arm – Test run 3

Appendix C – Instrumentation Plans

The user acknowledges that these documents are instruments of professional service, and are protected by Copyright. This document and the information contained in this document are the property of Bridge Diagnostics, Inc., and shall not be reused, copied, disseminated, modified, amended or altered in any way. It is issued for information purposes only. The user agrees to hold harmless, indemnify and defend Bridge Diagnostics, Inc. against any and all damages, claims and losses, including defense costs, arising out of any use, reuse or copying of this document.

RAW DATA. REFINED RESULTS.

SCHNABEL ENGINEERING
ROCKWALL FORNEY DAM
LIVE LOAD TESTING

RAW DATA. REFINED RESULTS.
740 S PIERCE AVE, SUITE 15
LOUISVILLE, CO 80027
303.494.3230
WWW.BDITEST.COM

ISSUE

CLIENT

SCHABEL ENGINEERING
16000 CHRISTENSEN RD, STE 101
SEATTLE, WA 98188

PROJECT NAME

SCHNABEL ENGINEERING
ROCKWALL FORNEY DAM
LIVE LOAD TESTING

Drawn By:	KNR
Checked By:	JDS
Date:	05/27/2020
Client No.:	
BDI No.:	190701-TX
SCALE:	NTS

COVER PAGE

LLT-00

PLOT TIME: 6/12/2020 3:22 PM
FILEPATH: C:\Users\colemand\BDI\Services - Documents\Server_Remote\190701-TX_Schnabel_RockwallForneyDam\7. Instrumentation Plans\BDI_ROCKWALLFORNEY_01_GENERAL.dwg
© YYYY BRIDGE DIAGNOSTICS INC.

GAGE LEGEND & SPECIFICATION

SYMBOL	TYPE	BRAND	MODEL	NOTES
	STRAIN TRANSDUCER	BDI	ST350	
	TILTMETER (UNI-AXIAL)	BDI	T500-030	
	TORQUE SENSOR	HPI	-	HBWS-35-125-6-0.5VR-FB
	AMP SENSOR	CR MAGNETICS	CR42105-200	

GENERAL NOTES

- INSTRUMENTATION SHALL BEGIN ON APRIL 1ST, 2020.
- GATES 1 THRU 14 SHALL BE ACCESSED USING SPRAT ROPE ACCESS TECHNIQUES.
- BDI WILL PERFORM ALL SURFACE PREPARATION, SENSOR INSTALLATION, AND EQUIPMENT INSTALLATION.
- SEE LLT-31 FOR SENSOR INSTALLATION DETAILS.
- TWO PAIRS OF TORQUE GAGES WILL BE INSTALLED ON THE GATE MOTORS' PINION SHAFTS BETWEEN THE MOTORS AND THE HOISTS.
  - GAGE PAIRS WILL BE INSTALLED 180° APART FROM EACH OTHER.
  - EXACT POSITIONS OF THE GAGE PAIRS ON THE PINION SHAFT WILL BE DETERMINED IN THE FIELD.
- THREE PHASE AMPERAGE GAGES WILL BE INSTALLED ON THE MOTOR CONTROLS BY A QUALIFIED ELECTRICIAN PROVIDED BY GARVER.

TESTING PROCEDURE:

- TESTING SHALL BE STARTED WITH THE GATE IN THE CLOSED POSITION.
- ONCE DATA COLLECTION BEGINS, THE GATE SHALL BE RAISED TO TWO OR THREE TIMES THE HEIGHT NECESSARY FOR TRUNNION FRICTION TO BE OVERCOME, H1 (TYPICALLY 6"-12"), AND HELD THERE UNTIL DATA STABILIZES.
- THE GATE SHALL BE LOWERED APPROXIMATELY TWICE THE DISTANCE TO OVERCOME TRUNNION FRICTION, H2, AND HELD THERE UNTIL DATA STABILIZES.
- THE GATE SHALL BE RAISED TO H1 AND HELD THERE UNTIL DATA STABILIZES.
- THE GATE SHALL BE LOWERED TO H2 AND HELD THERE UNTIL DATA STABILIZES.
- THE GATE SHALL BE RAISED TO H1 AND HELD THERE UNTIL DATA STABILIZES.
- THE GATE WAS LOWERED BACK TO CLOSED POSITION AND DATA COLLECTION STOPPED.
- A MINIMUM OF 3 TESTS SHALL BE PERFORMED PER GATE.

GAGE COUNT PER GATE

SENSOR LEGEND	SENSOR COUNT	CHANNEL COUNT
STRAIN TRANSDUCER	(48)	(48)
TILTMETER (UNI-AXIAL)	(4)	(4)
TORQUE SENSOR	(4)	(4)
AMP SENSOR	(3)	(3)
TOTAL	(59)	(59)

LOCATION KEY

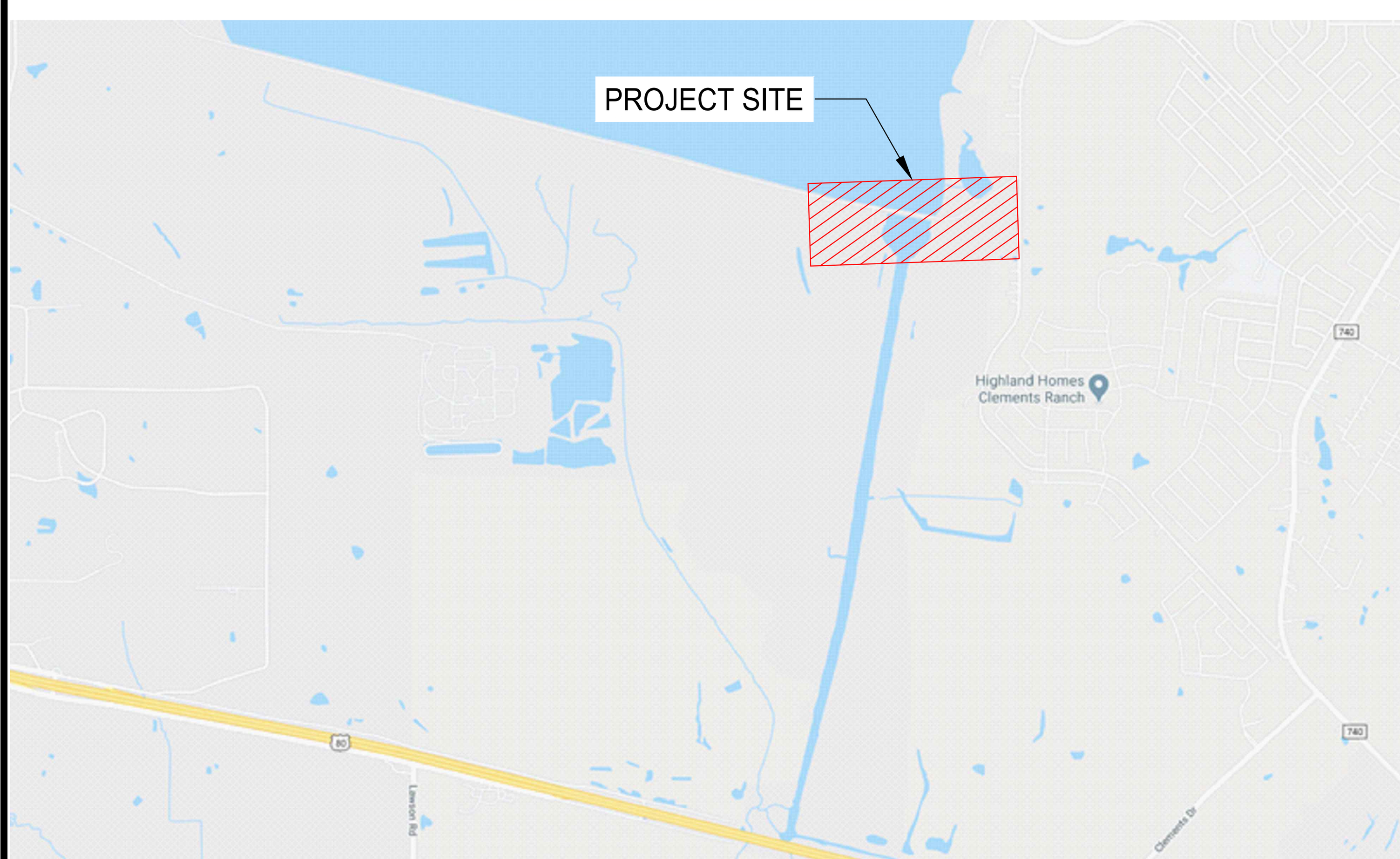

INDEX OF SHEETS

INDEX OF ISSUE

NO.	DATE	REVISION DESCRIPTION
1	3/20/2020	LIVE LOAD TESTING (LLT) INSTRUMENTATION PLAN (FOR APPROVAL)
2	5/27/2020	LIVE LOAD TESTING (LLT) INSTRUMENTATION PLAN AS BUILTS

BDI REFERENCE NUMBER: 190701-TX

BDI
RAW DATA. REFINED RESULTS.
740 S PIERCE AVE, SUITE 15
LOUISVILLE, CO 80027
303.494.3230
WWW.BDITEST.COM

ISSUE

CLIENT

SCHABEL ENGINEERING
16000 CHRISTENSEN RD, STE 101
SEATTLE, WA 98188

PROJECT NAME

SCHABEL ENGINEERING
ROCKWALL FORNEY DAM
LIVE LOAD TESTING

Drawn By:	KNR
Checked By:	JDS
Date:	05/27/2020
Client No.:	
BDI No.:	190701-TX
SCALE:	NTS

OVERALL LEGEND

LLT-01

The user acknowledges that these documents are instruments of professional service, and are protected by Copyright. This document and the information contained in this document are the property of Bridge Diagnostics, Inc., and shall not be reused, copied, disseminated, modified, amended or altered in any way. It is issued for information purposes only. The user agrees to hold harmless, indemnify and defend Bridge Diagnostics, Inc. against any and all damages, claims and losses, including defense costs, arising out of any use, reuse or copying of this document.

PLOT TIME: 6/12/2020 3:22 PM
FILEPATH: C:\Users\colemand\BDI\Services - Documents\Server_Remote\190701-TX_Schnabel_RockwallForneyDam\7. Instrumentation Plans\BDI_ROCKWALLFORNEY_01_GENERAL.dwg
© YYYY BRIDGE DIAGNOSTICS INC.

The user acknowledges that these documents are instruments of professional service, and are protected by Copyright. This document and the information contained in this document are the property of Bridge Diagnostics, Inc., and shall not be reused, copied, disseminated, modified, amended or altered in any way. It is issued for information purposes only. The user agrees to hold harmless, indemnify and defend Bridge Diagnostics, Inc. against any and all damages, claims and losses, including defense costs, arising out of any use, reuse or copying of this document.

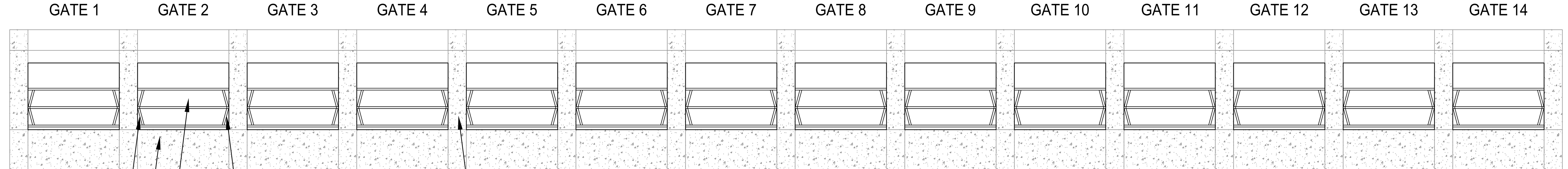

1 DOWNSTREAM ELEVATION OF GATES
LOOKING NORTH (UPSTREAM)

RAW DATA. REFINED RESULTS.
740 S PIERCE AVE, SUITE 15
LOUISVILLE, CO 80027
303.494.3230
WWW.BDITEST.COM

ISSUE

CLIENT

SCHABEL ENGINEERING
16000 CHRISTENSEN RD, STE 101
SEATTLE, WA 98188

PROJECT NAME

SCHNABEL ENGINEERING
ROCKWALL FORNEY DAM
LIVE LOAD TESTING

Drawn By:	KNR
Checked By:	JDS
Date:	05/27/2020
Client No.:	
BDI No.:	190701-TX
SCALE:	NTS

OVERALL STRUCTURE LAYOUT
LLT-02

PLOT TIME: 6/12/2020 3:22 PM
FILEPATH: C:\Users\colemand\BDI\Services - Documents\Server_Remote\190701-TX_Schnabel_RockwallForneyDam\7. Instrumentation Plans\BDI_ROCKWALLFORNEY_01_GENERAL.dwg
© YYYY BRIDGE DIAGNOSTICS INC.

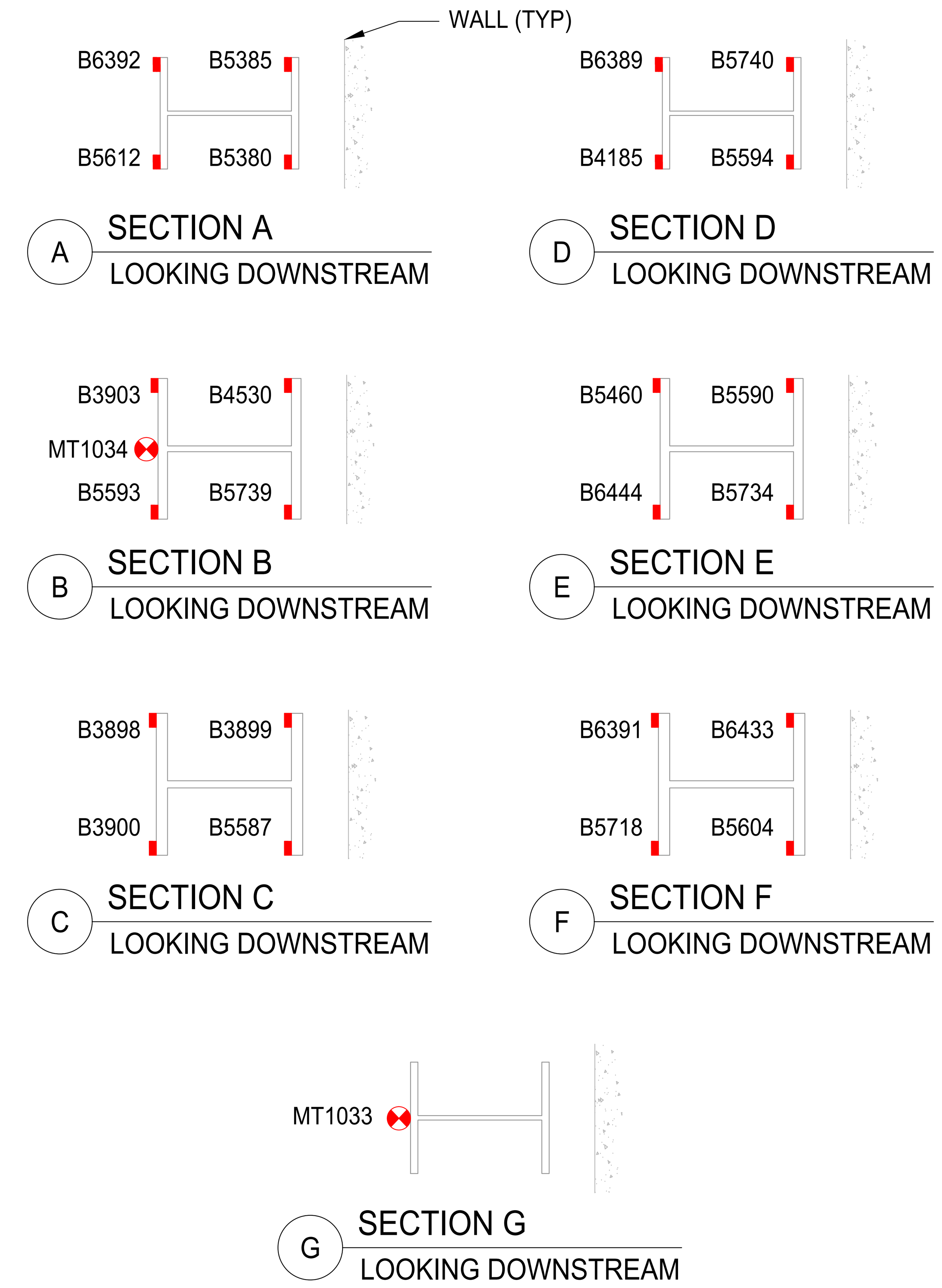

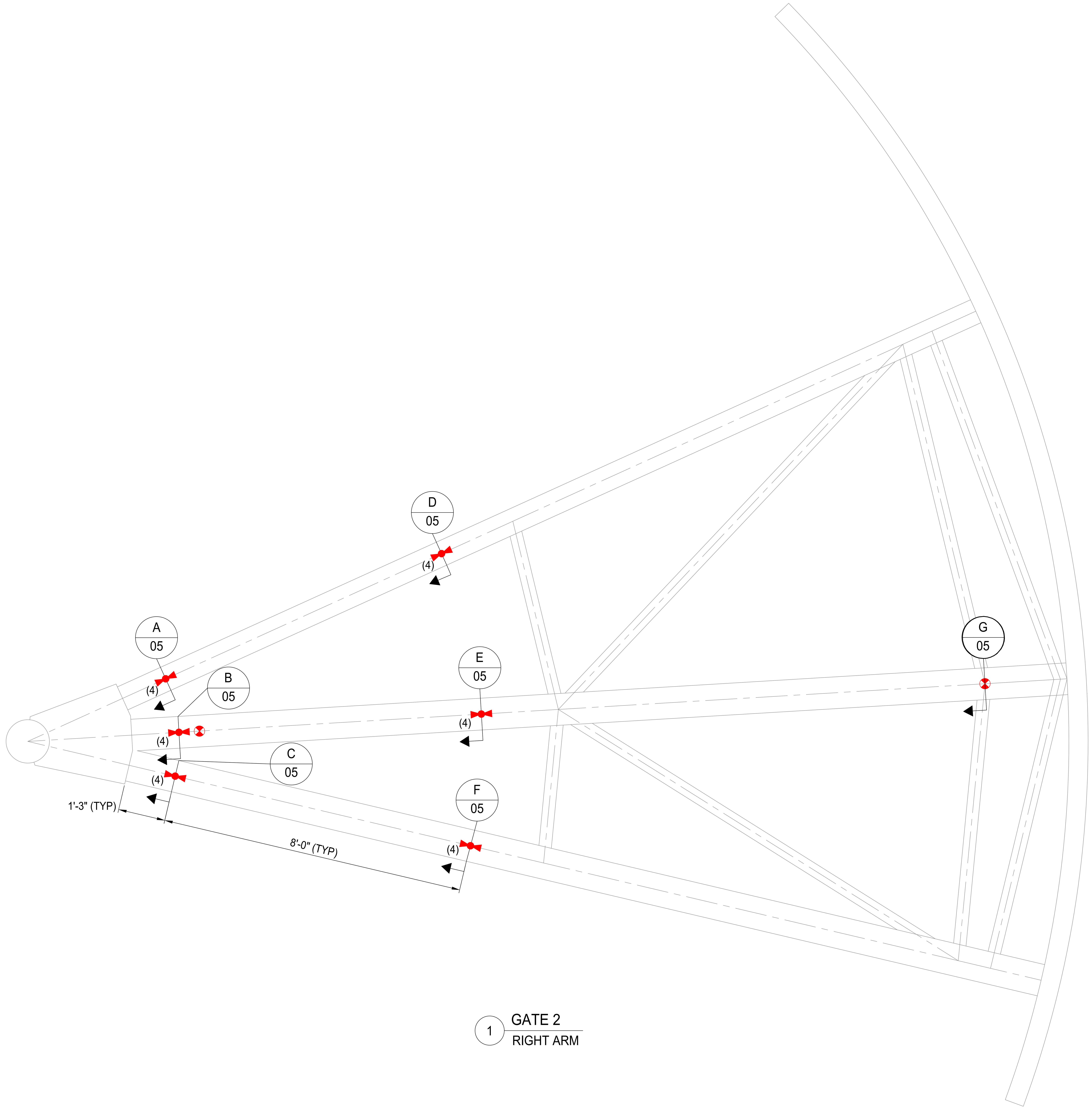

UNIT ID
TT-2

TORQUE GAGES
RIGHT ARM

NOTES:
1. SECTIONS A, B, & C SHALL BE INSTALLED 15 INCHES AWAY FROM TRUNNION PLATE.
2. TILTMETERS SHALL BE INSTALLED CENTERED ON THE MIDDLE STRUT FLANGE.
3. SECTION G'S TILTMETER SHALL BE INSTALLED AS CLOSE TO THE SKINPLATE AS POSSIBLE.

SENSOR LEGEND
- STRAIN TRANSDUCER
- TILTMETER (UNI-AXIAL)
- TORQUE SENSOR

BDI
RAW DATA. REFINED RESULTS.
740 S PIERCE AVE, SUITE 15
LOUISVILLE, CO 80027
303.494.3230
WWW.BDITEST.COM

ISSUE

CLIENT
SCHABEL ENGINEERING
16000 CHRISTENSEN RD, STE 101
SEATTLE, WA 98188

PROJECT NAME
SCHABEL ENGINEERING
ROCKWALL FORNEY DAM
LIVE LOAD TESTING

Drawn By:	KNR
Checked By:	JDS
Date:	05/27/2020
Client No.:	
BDI No.:	190701-TX
SCALE:	NTS

GATE 2 - RIGHT ARM
ELEVATION
LLT-05

The user acknowledges that these documents are instruments of professional service, and are protected by Copyright. This document and the information contained in this document are the property of Bridge Diagnostics, Inc., and shall not be reused, copied, disseminated, modified, amended or altered in any way. It is issued for information purposes only. The user agrees to hold harmless, indemnify and defend Bridge Diagnostics, Inc. against any and all damages, claims and losses, including defense costs, arising out of any use, reuse or copying of this document.

PLOT TIME: 6/12/2020 3:22 PM
FILEPATH: C:\Users\colemand\BDI\Services - Documents\Server_Remote\190701-TX_Schabel_RockwallForneyDam\7. Instrumentation Plans\BDI_ROCKWALLFORNEY_01_GENERAL.dwg
© YYYY BRIDGE DIAGNOSTICS INC.

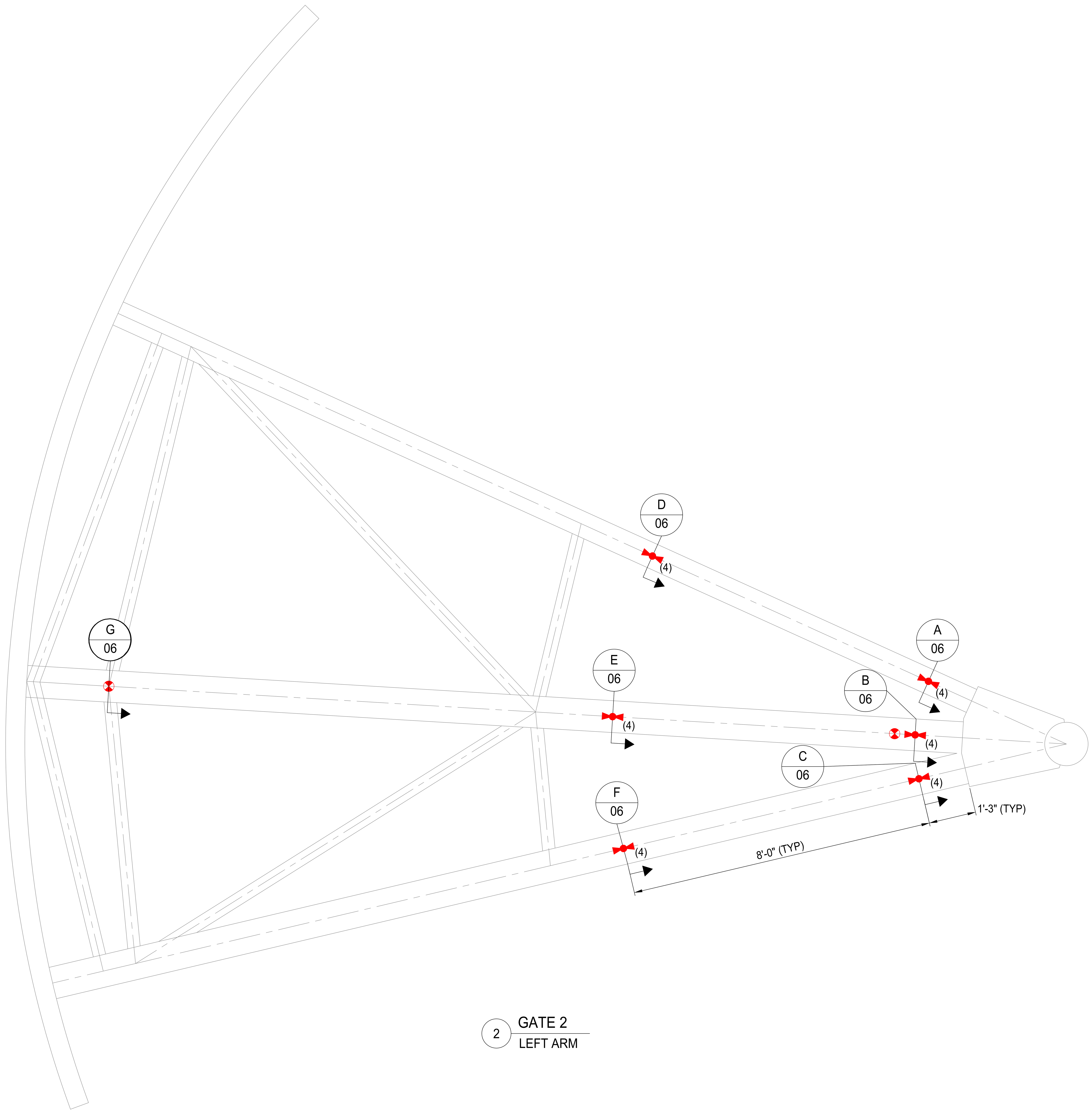

2 GATE 2
LEFT ARM

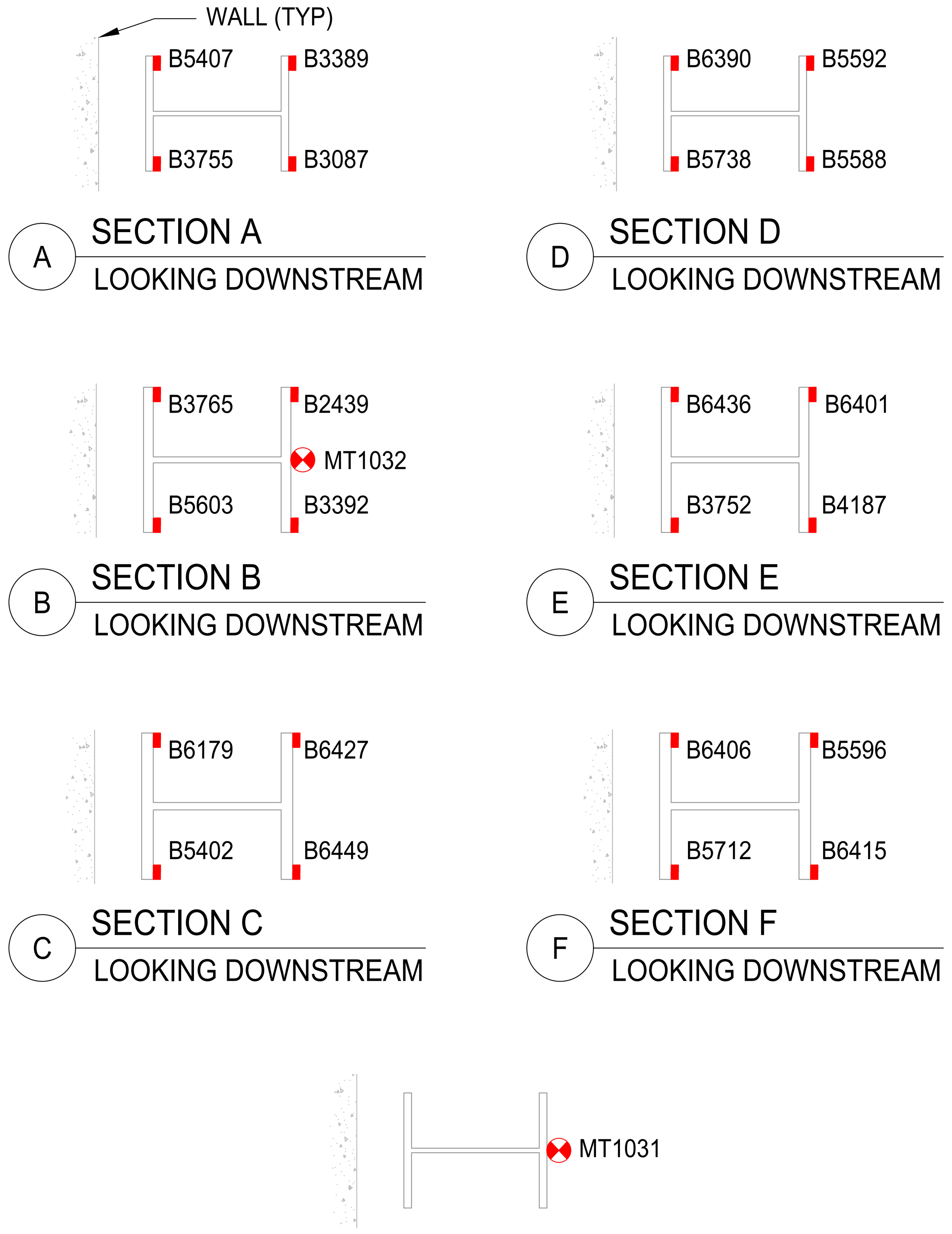

A SECTION A
LOOKING DOWNSTREAM

D SECTION D
LOOKING DOWNSTREAM

B SECTION B
LOOKING DOWNSTREAM

E SECTION E
LOOKING DOWNSTREAM

C SECTION C
LOOKING DOWNSTREAM

F SECTION F
LOOKING DOWNSTREAM

G SECTION G
LOOKING DOWNSTREAM

UNIT ID
TT-3

TORQUE GAGES
LEFT ARM

NOTES:
1. SECTIONS A, B, & C SHALL BE INSTALLED 15 INCHES AWAY FROM TRUNNION PLATE.
2. TILTMETERS SHALL BE INSTALLED CENTERED ON THE MIDDLE STRUT FLANGE.
3. SECTION G'S TILTMETER SHALL BE INSTALLED AS CLOSE TO THE SKINPLATE AS POSSIBLE.

SENSOR LEGEND
STRAIN TRANSDUCER
TILTMETER (UNI-AXIAL)
TORQUE SENSOR

BDI
RAW DATA. REFINED RESULTS.
740 S PIERCE AVE, SUITE 15
LOUISVILLE, CO 80027
303.494.3230
WWW.BDITEST.COM

ISSUE

CLIENT
SCHABEL ENGINEERING
16000 CHRISTENSEN RD, STE 101
SEATTLE, WA 98188

PROJECT NAME
SCHABEL ENGINEERING
ROCKWALL FORNEY DAM
LIVE LOAD TESTING

Drawn By:	KNR
Checked By:	JDS
Date:	05/27/2020
Client No.:	
BDI No.:	190701-TX
SCALE:	NTS

GATE 2 - LEFT ARM
ELEVATION
LLT-06

The user acknowledges that these documents are instruments of professional service, and are protected by Copyright. This document and the information contained in this document are the property of Bridge Diagnostics, Inc., and shall not be reused, copied, disseminated, modified, amended or altered in any way. It is issued for information purposes only. The user agrees to hold harmless, indemnify and defend Bridge Diagnostics, Inc. against any and all damages, claims and losses, including defense costs, arising out of any use, reuse or copying of this document.

PLOT TIME: 6/12/2020 3:22 PM
FILEPATH: C:\Users\colemand\BDI\Services - Documents\Server_Remote\190701-TX_Schabel_RockwallForneyDam\7. Instrumentation Plans\BDI_ROCKWALLFORNEY_01_GENERAL.dwg
© YYYY BRIDGE DIAGNOSTICS INC.

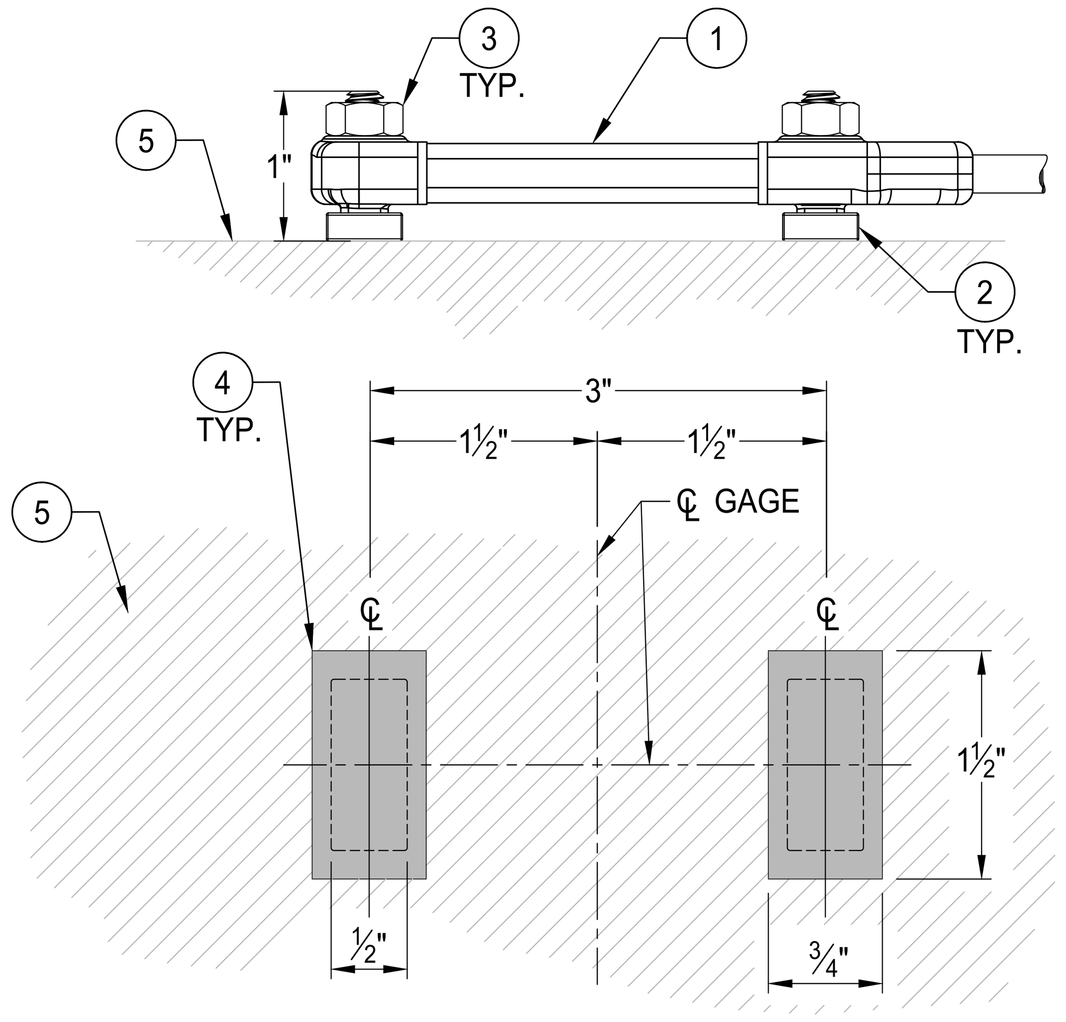

1 TYPICAL ST350 STRAIN GAGE INSTALLATION

COMPONENT DESCRIPTION

1. ST350 STRAIN GAGE
2. 1/4"-20 THREADED MOUNTING TAB
3. 1/4"-20 STAINLESS STEEL NUT
4. TYPICAL SURFACE PREP REQUIRED TO MOUNT STRAIN GAGES
5. TYPICAL MOUNTING SURFACE

FOOTNOTES - INSTANT ADHESIVE
1. STRAIN GAGES SHALL BE MOUNTED WITH LOCTITE 410 INSTANT ADHESIVE AND LOCTITE 7452 ACCELERANT 2. DURING SURFACE PREP ALL PAINT AND SURFACE DEFORMATIONS MUST BE REMOVED. 3. SURFACE PREP IS REQUIRED JUST PRIOR TO GAGE INSTALLATION AS TO NOT ALLOW SURFACE CONTAMINANTS TO ACCUMULATE.

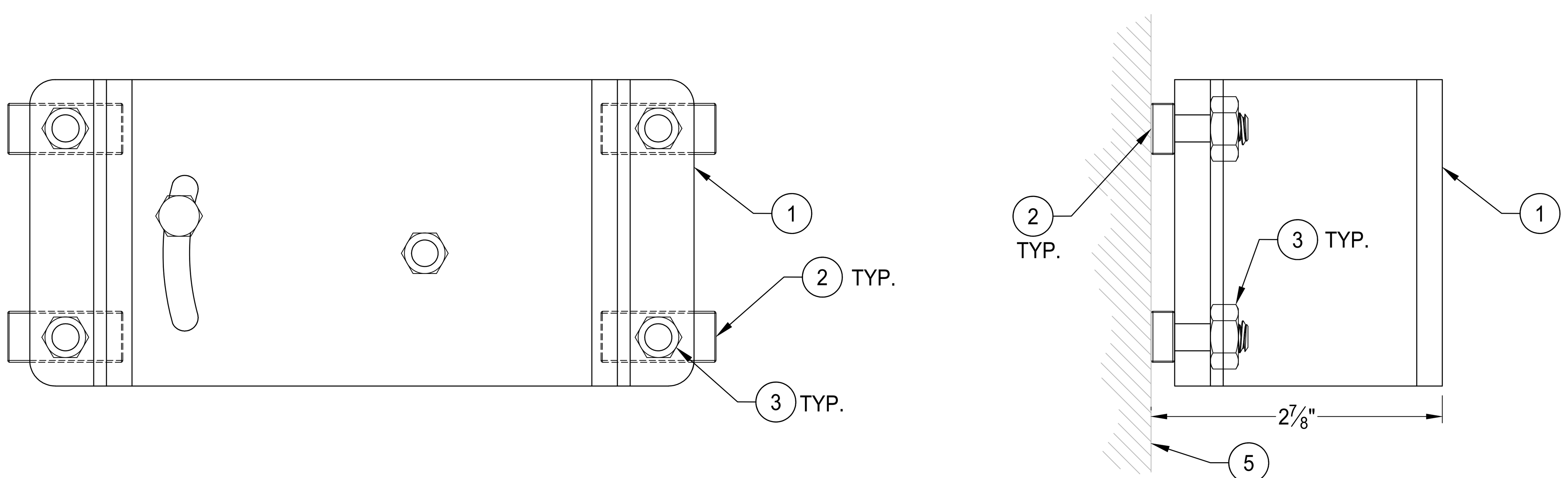

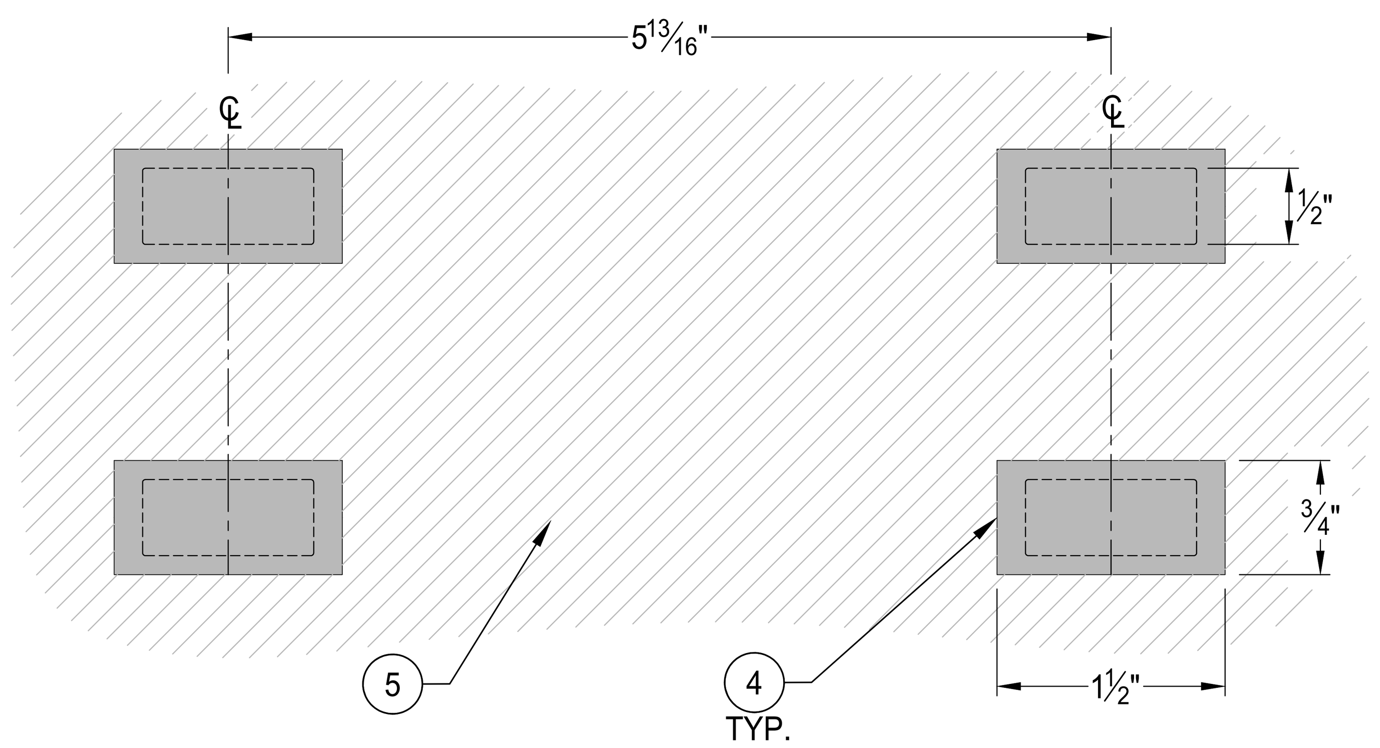

COMPONENT DESCRIPTION

1. BDI +/- 15 DEGREE TILTMETER WITH COVER AND ADJUSTMENT BOLTS
2. 1/4"-20 THREADED MOUNTING TAB
3. 1/4"-20 STAINLESS STEEL NUT
4. TYPICAL SURFACE PREP REQUIRED TO MOUNT TILTMETERS
5. TYPICAL MOUNTING SURFACE

FOOTNOTES - INSTANT ADHESIVE
1. TILTMETERS SHALL BE MOUNTED WITH LOCTITE 410 INSTANT ADHESIVE AND LOCTITE 7452 ACCELERANT 2. DURING SURFACE PREP ALL PAINT AND SURFACE DEFORMATIONS MUST BE REMOVED. 3. SURFACE PREP IS REQUIRED JUST PRIOR TO GAGE INSTALLATION AS TO NOT ALLOW SURFACE CONTAMINANTS TO ACCUMULATE.

2 TYPICAL BDI TILTMETER INSTALLATION

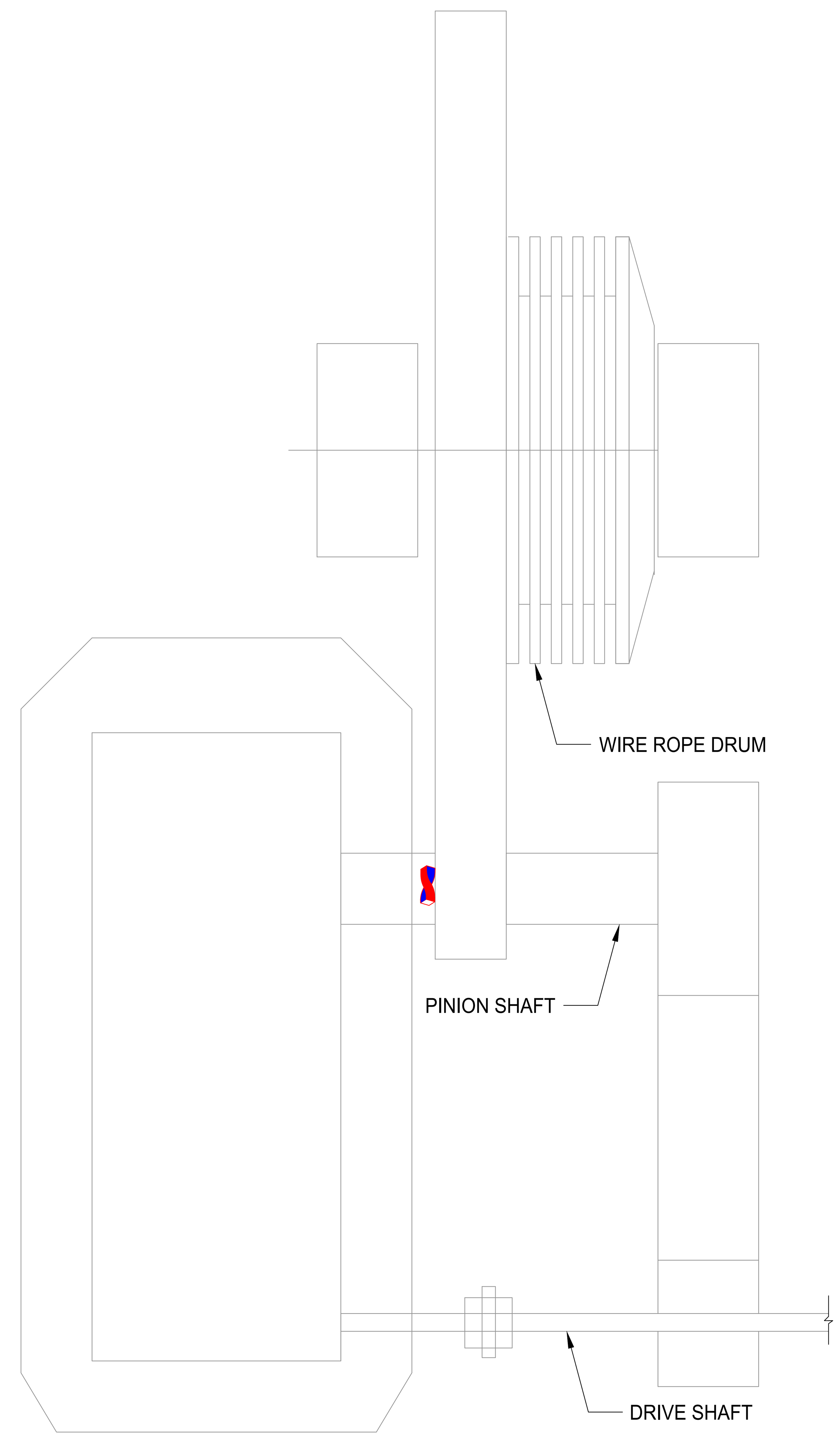

3 TYPICAL HOIST INSTRUMENTATION

TORQUE SENSOR INSTALLATION NOTES:

- TORQUE GAGES WILL BE INSTALLED ON THE PINION SHAFT ON EITHER HOIST MOTOR BETWEEN THE MOTOR AND THE HOIST DRUM
- EXACT POSITIONS OF THE GAGE PAIRS ON THE PINION SHAFT WILL BE DETERMINED IN THE FIELD

SENSOR LEGEND

TORQUE SENSOR

BDI
RAW DATA. REFINED RESULTS.
740 S PIERCE AVE, SUITE 15
LOUISVILLE, CO 80027
303.494.3230
WWW.BDITEST.COM

ISSUE

CLIENT

SCHABEL ENGINEERING
16000 CHRISTENSEN RD, STE 101
SEATTLE, WA 98188

PROJECT NAME

SCHABEL ENGINEERING
ROCKWALL FORNEY DAM
LIVE LOAD TESTING

Drawn By:	KNR
Checked By:	JDS
Date:	05/27/2020
Client No.:	
BDI No.:	190701-TX
SCALE:	NTS

SENSOR INSTALLATION DETAILS

LLT-31

The user acknowledges that these documents are instruments of professional service, and are protected by Copyright. This document and the information contained in this document are the property of Bridge Diagnostics, Inc., and shall not be reused, copied, disseminated, modified, amended or altered in any way. It is issued for information purposes only. The user agrees to hold harmless, indemnify and defend Bridge Diagnostics, Inc. against any and all damages, claims and losses, including defense costs, arising out of any use, reuse or copying of this document.

PLOT TIME: 6/12/2020 3:24 PM
FILEPATH: C:\Users\colemand\BDI\Services - Documents\Server_Remote\190701-TX_Schabel_RockwallForneyDam\7. Instrumentation Plans\BDI_ROCKWALLFORNEY_01_GENERAL.dwg
© YYYY BRIDGE DIAGNOSTICS INC.

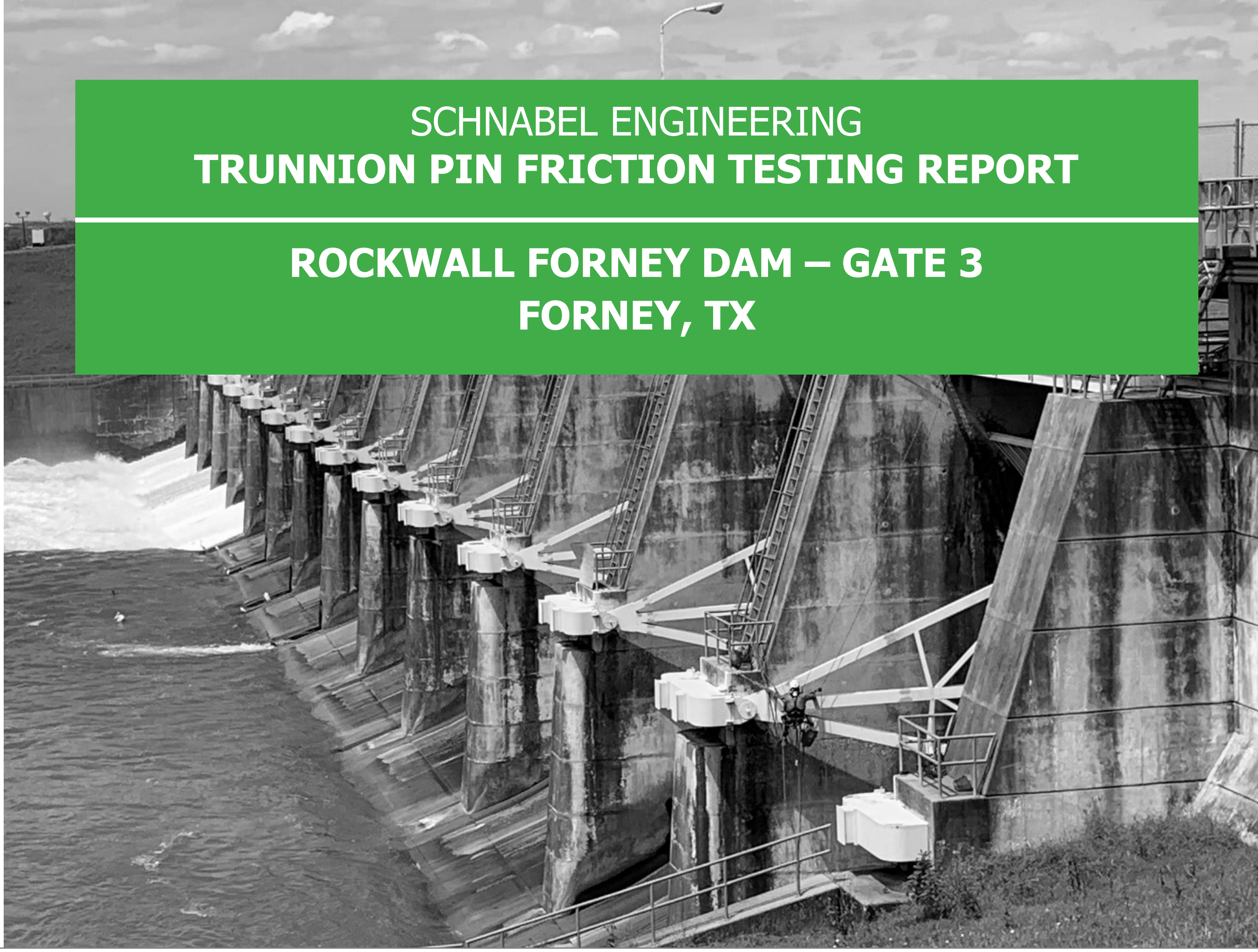

SCHNABEL ENGINEERING

TRUNNION PIN FRICTION TESTING REPORT

ROCKWALL FORNEY DAM – GATE 3
FORNEY, TX

SUBMITTED TO:
SCHNABEL ENGINEERING
16000 CHRISTENSEN RD, SUITE 101
SEATTLE, WA 98188

SUBMITTED BY:
BDI – CO
740 SOUTH PIERCE AVE, UNIT 15
LOUISVILLE, CO 80027

BDI Project No.: **190701-TX**
Report Version: **V1**
Version Submitted: **August 26, 2020**

RAW DATA. REFINED RESULTS.

This document contains Confidential Information and is submitted in confidence to the customer. The submission of the information contained herein shall not be deemed to constitute public disclosure or authorization for disclosure to other parties. BDI's information and name may not be used in advertising or for promotional purposes without BDI's written consent.

TABLE OF CONTENTS

LIST OF FIGURES

LIST OF TABLES

EXECUTIVE SUMMARY

Schnabel Engineering contracted BDI to provide instrumentation and testing services on Gates 1-14 on the Rockwall Forney Dam near Dallas, Texas. The goal of these tests was to record each gate's structural responses during a series of spill tests and use the data to compute accurate coefficients of friction for each trunnion pin, cable lift force, total gate friction, and motor amperage. This report provides details on the work performed on Gate 3.

Instrumentation and testing were performed on Gate 3 at the Rockwall Forney Dam on April 2nd, 2020. The gate arms were instrumented with strain and rotation sensors. The hoist motors' pinion shafts were instrumented with torque sensors and the hoist motor controls were instrumented with amperage sensors. Following the instrumentation, a series of spill tests were performed to measure the structural responses resulting from trunnion pin friction. All instrumentation setup and removal were performed using BDI's rope access team.

Following demobilization from the field, the test data was examined for quality and then further processed to evaluate the gate's performance. Strain measurements were converted into bending forces which were then applied to pin-strut free-body diagrams. By summing forces at each pin, friction induced moments could be computed, allowing accurate friction coefficients to be determined.

The resulting maximum trunnion friction coefficients and corresponding hoist forces are shown in Table 1.

Table 1 – Gate 3 performance summary

Pin Designation	Maximum Friction Coefficient	Maximum Pin Moment due to Pin Friction (kip-In)	Maximum Hoist Force (kips)	Maximum Hoist Force due to Total Gate Friction (kips)
Right Pin	0.18	471.3	31.03	4.22
Left Pin	0.21	555.7	9.46	3.68

Note: Pin designations are in reference to looking downstream

Generally, the observed gate behavior showed that Gate 3 was operating as expected and in a symmetric manner. The hoist behavior showed unexpected responses in the left arm but overall had no major signs of distress (seizing, etc).

Due to restrictions caused by the hoist limit switches, the hoist cables could not always be fully slacked at the beginning and end of the performed tests. Throughout testing of the Rockwell Forney gates, it was found that this limit switch restriction varied gate to gate and arm to arm. Therefore, it is not recommended to use the collected hoist force data to quantify overall hoist forces during gate operation. Rather, this hoist data can be better utilized to evaluate total friction behavior. This issue was likely caused the variation between the right and left maximum hoist forces but does not account for the varying levels of total friction observed in the left hoist responses.

Amperage responses were not used to compute friction results and were collected as verification that the motor performance was not causing unexpected gate responses. These responses indicated the motor was functioning in a stable manner and should be reviewed by a licensed electrician to further evaluate the motor's performance.

All results and recommendations provided in this report were based on the structure in its current condition; therefore, any significant changes in condition must be noted as they may alter their validity. Questions regarding this report and/or data should be directed to Kyle Ramer (kyler@bditest.com) at BDI. For further information on BDI's equipment, services, and analysis methods please visit www.bditest.com

INSTRUMENTATION AND LOAD TESTING PROCEDURE

GATE INSTRUMENTATION SUMMARY

Instrumentation and testing were performed on Gate 3 at the Rockwall Forney Dam on April 2nd, 2020. Instrumentation plans have been provided along with this report and include the following number of instrumented locations and sensor types:

+ **REUSABLE SURFACE MOUNTED STRAIN TRANSDUCERS:** Each gate arm was instrumented with a total of 24 strain transducers at 6 locations on each of the gate arms (48 strain sensors total). A typical strain gage installation is shown in Figure 1. Note these sensors were installed with the mounting tabs on the extreme fiber of the strut flanges, which puts the center of the gage approximately 0.66" from the extreme fiber.
+ **TILTMETER ROTATION SENSORS:** MEMS style rotation sensors were located on the middle strut of the gate arm near the skin plate and near the trunnion hub (4 rotation sensors total). The rotation responses were used to calculate vertical skin plate movement and measure pin rotation relative to skin plate rotation. Typical tiltmeter installations are shown in Figure 1 and Figure 2.
+ **TORQUE SENSORS:** Two total torque sensors were installed on the hoist's pinion shafts (QTY1 on each hoist pinion shaft) near the cable hoist motor to measure direct torque and in turn lift force (See Figure 3).
+ **AMPERAGE SENSORS:** 3 Hall-Effect amperage transducers were clamped over each phase of the hoist motor to measure the motor's current draw (See Figure 4). The purpose of these sensors was to provide additional data in case there were any issues with the hoist systems and to verify any data issues related to lifting and lowering the gates.
+ **BDI'S STS-4 WIRELESS DATA ACQUISITION SYSTEM:** BDI's STS-4 wireless data acquisition (DAQ) was used to collect and record data during testing. A group of sensors were wired to each nodal DAQ which then communicated wirelessly back to the wireless base station and was controlled by BDI's STS-Live testing software.

Complete specifications are available upon request and can be found at http://www.bditest.com.

SENSOR INSTALLATION

BDI strain transducers were installed by first sanding paint off the struts to expose bare metal at two small locations (1"x2" areas) for the sensor's mounting tabs. Each transducer was then attached using a combination of fast-setting adhesive and accelerator and applying pressure until the adhesive was fully cured. Each strain transducer took approximately five minutes to attach.

Tiltmeters were installed using the same adhesive process as the strain transducers. However, no surface preparation was necessary.

Torque sensors were installed on the pinion shafts by capacitive discharge bonding. Properly bonding to the shaft required sanding the surface to a smooth finish, clean of any paint or grease. Responses from these gages were measured using Binsfeld Torque Trak 10k wireless transmitters.

A typical installation has been shown in Figure 1 through Figure 4. Access to all the sensor locations was provided by BDI's own SPRAT certified rope access technicians and engineers as shown in Figure 5.

Once testing was completed, sensors were removed, and exposed steel areas were covered using cold galvanizing compound.

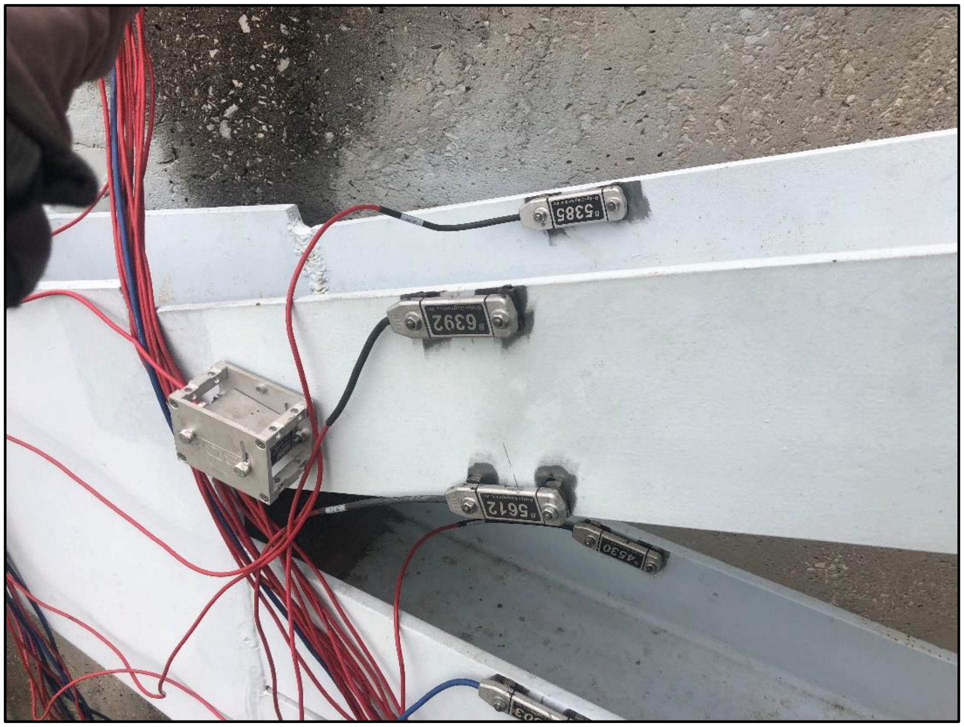

Figure 1 – BDI tiltmeter rotation sensor and reusable strain transducers installed near trunnion hub (Typical)

Figure 2 – BDI tiltmeter rotation sensor installed near skin plate (Typical)

Figure 3 – Torque sensor installation on hoist pinion shaft (Typical)

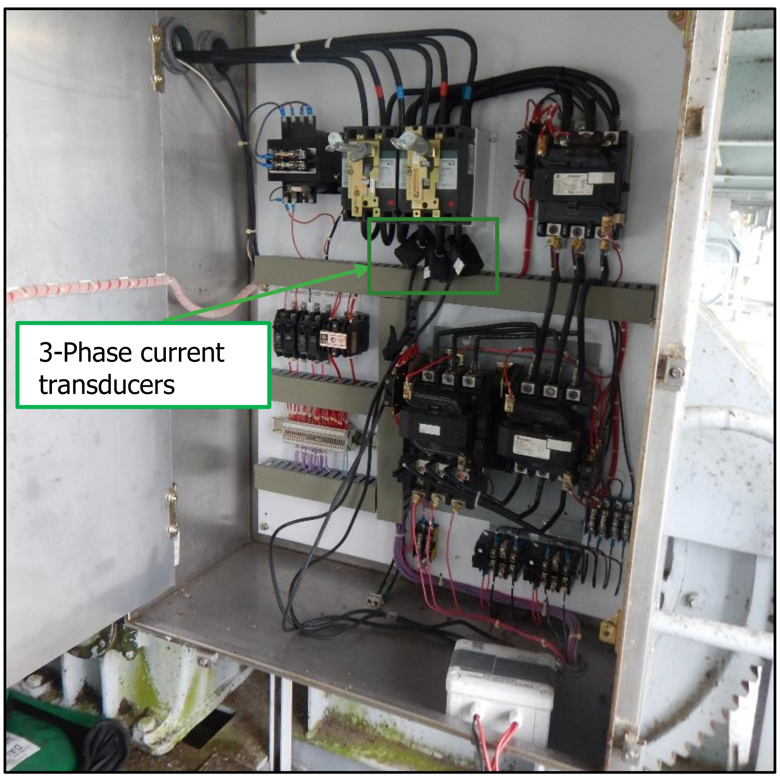

Figure 4 – Current transducers installed on hoist motor controls (Typical)

Figure 5 – BDI personnel installing instrumentation on the gate arm

TESTING PROCEDURES

Structural response data was recorded on all sensors at 50Hz while the gate was run through three spill tests. Each test consisted of three "up-down" cycles (direction reversals) without lowering the gate back to the sill. Each direction reversal consisted of lifting the gate approximately 6-12", pausing for a few seconds, and lowering the gate approximately 6", and repeating until all reversals had been completed.

RESULTS SUMMARY

GENERAL BASED ON STRUCTURAL RESPONSES

The following outline contains general discussion points and observations that were made during the data review process. Note: Strain measurements were converted to stress for all subsequent analysis by multiplying the strain values by a steel elastic modulus of 29,000 ksi.

+ **DESCRIPTIONS OF RESPONSE MEASUREMENTS:** All sensor readings were zeroed at the end of each test (which consisted of three cycles of direction reversals) so that each measurement corresponded to response change relative to the final gate position as shown in Figure 6 (gates in the downward "closed" position with the hoist cables slacked as much as possible). It is also worth noting that the stresses did not always start and end at the same levels between tests. This variation in behavior is due to small changes in the flexed gate condition between the start and end of tests. It is common for the flex in the gate, caused by pin friction, to slowly release as it rests on the sill. The purpose of the three up-down cycles per test, prior to sitting the gate back onto the sill, is to ensure that these changes in boundary conditions, including gate flexure due to friction, did not affect BDI's trunnion friction results. ***It is important to note that the recorded measurements were changes in structural response due to gate movement, and do not include the in-situ stresses due to the dead load, cable wrap, and hydrostatic loads present prior to testing.***
+ **QUALITATIVE DATA REVIEW:** Review of the response data indicated a good level of reproducibility between the three tests. For reference, Figure 6 and Figure 7 show stress responses measured along Gate 3's right arm top strut for all three tests (Test #1-3). The data in these plots have been provided as both a function of time and the gate position as determined by the skin plate tilt sensor. Structural response behavior slightly varied during the first test's first cycle compared to subsequent lift/lower cycles and tests, with the first cycle having a slightly smaller change in stress due to pin friction. The observed variation was likely caused by a larger release of built-up pin friction as the gate rested on the sill for a longer period of time.
+ **DIRECTION/FRICTION REVERSAL IN RESPONSES:** The difference in stress during gate opening and closing for a given position is shown in Figure 8. The stress variation at any given gate position was a result of direction reversal and in turn due to trunnion friction reversal. This statement is true since all other loads such as dead-load and hydrostatic pressure were essentially constant barring small changes in hydrostatic pressure due to slight changes in head. This direction/friction reversal is depicted in Figure 9, with deflected shape renderings from a gate arm finite element model under lifting and lowering loads. Note that this figure shows an arm configuration that does not match this gate, but the concept of the direction/friction reversal still applies.
+ **MOTOR PERFORMANCE:** Current measurements taken at the hoist motor indicated steady and stable current draws during the lifting and lowering portions. An example plot of current draw and gate position is provided in Figure 10. Current draw ranges during lifting were higher than the ranges during lowering, which is common due to gravity/dead load. These results are summarized along with recorded peak in-rush current in Table 2. Note that the sample rates used during testing were set for collecting gate responses and may not have been appropriate to fully capture the in-rush current. The readings should be evaluated by a licensed electrician with knowledge of the operating parameters.
+ **TORQUE AND HOIST FORCE:** Due to restrictions caused by the hoist limit switches, the hoist cables could not always be fully slacked at the beginning and end of the performed tests. Throughout testing of the Rockwell Forney gates, it was found that this limit switch restriction varied gate to gate and arm to arm. Therefore, it is not recommended to use the collected torque and hoist force data to quantify overall hoist forces. Rather, this data was utilized to evaluate total friction behavior, which is observed as half the difference between the lifting and lowering torque/force (friction reversal). The response behavior from the left hoist was found to unexpected, with varying levels of friction throughout the lift/lower tests. Note that issues with the wireless transmitter connected to the left gate hoist gages caused intermittent loss of data. While not optimal, this data loss did not significantly affect the hoist results summarized in this report.

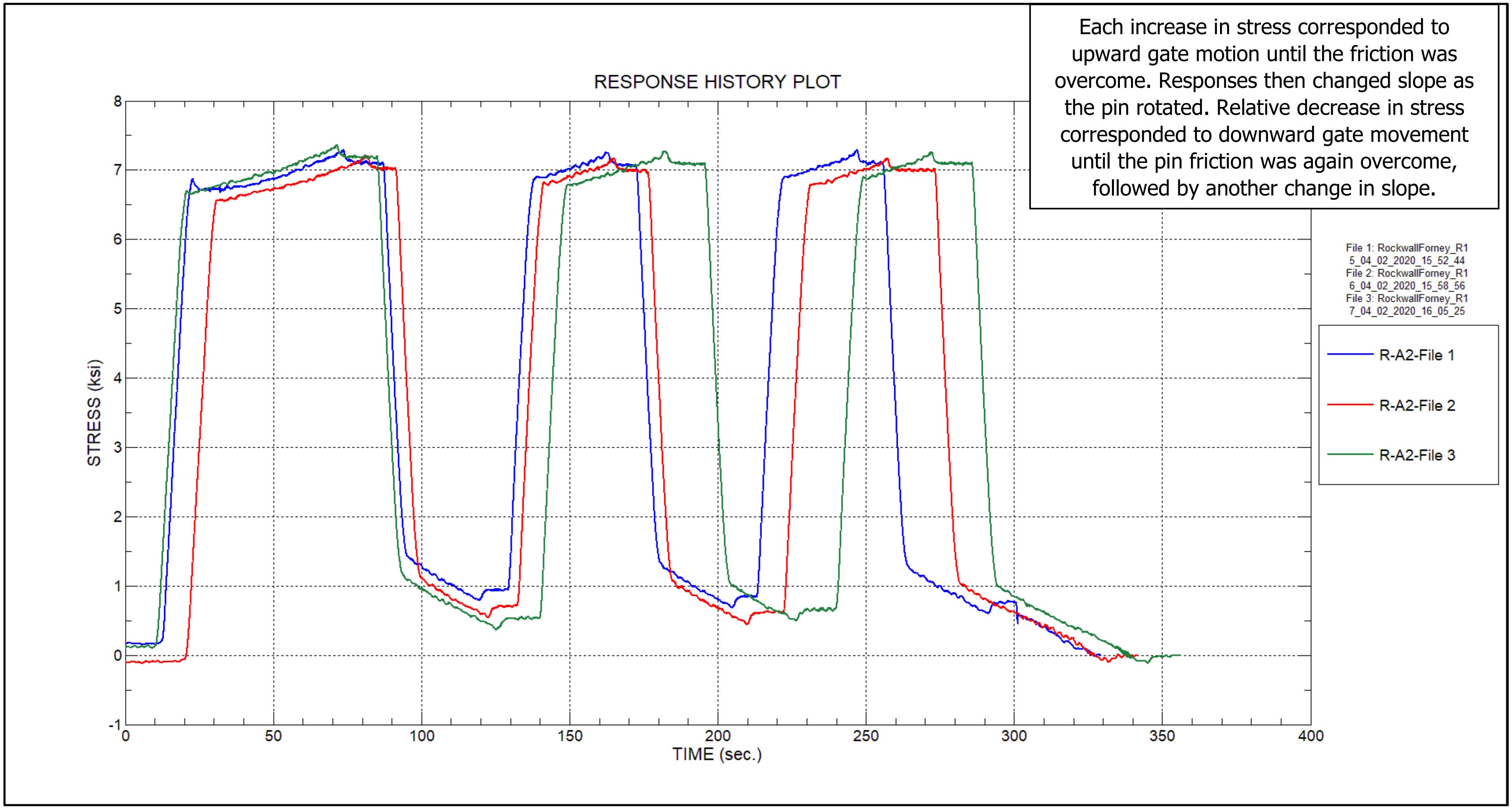

Figure 6 – Stress response history – Right arm – Gage A2 – Time based
File 1 = test run 1, File 2 = test run 2, File 3 = test run 3

(Section A along top strut near pin – Sensor location 2 along bottom of inner flange)

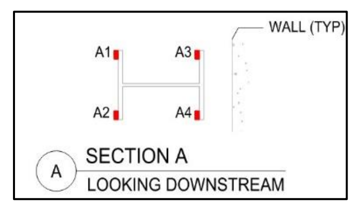

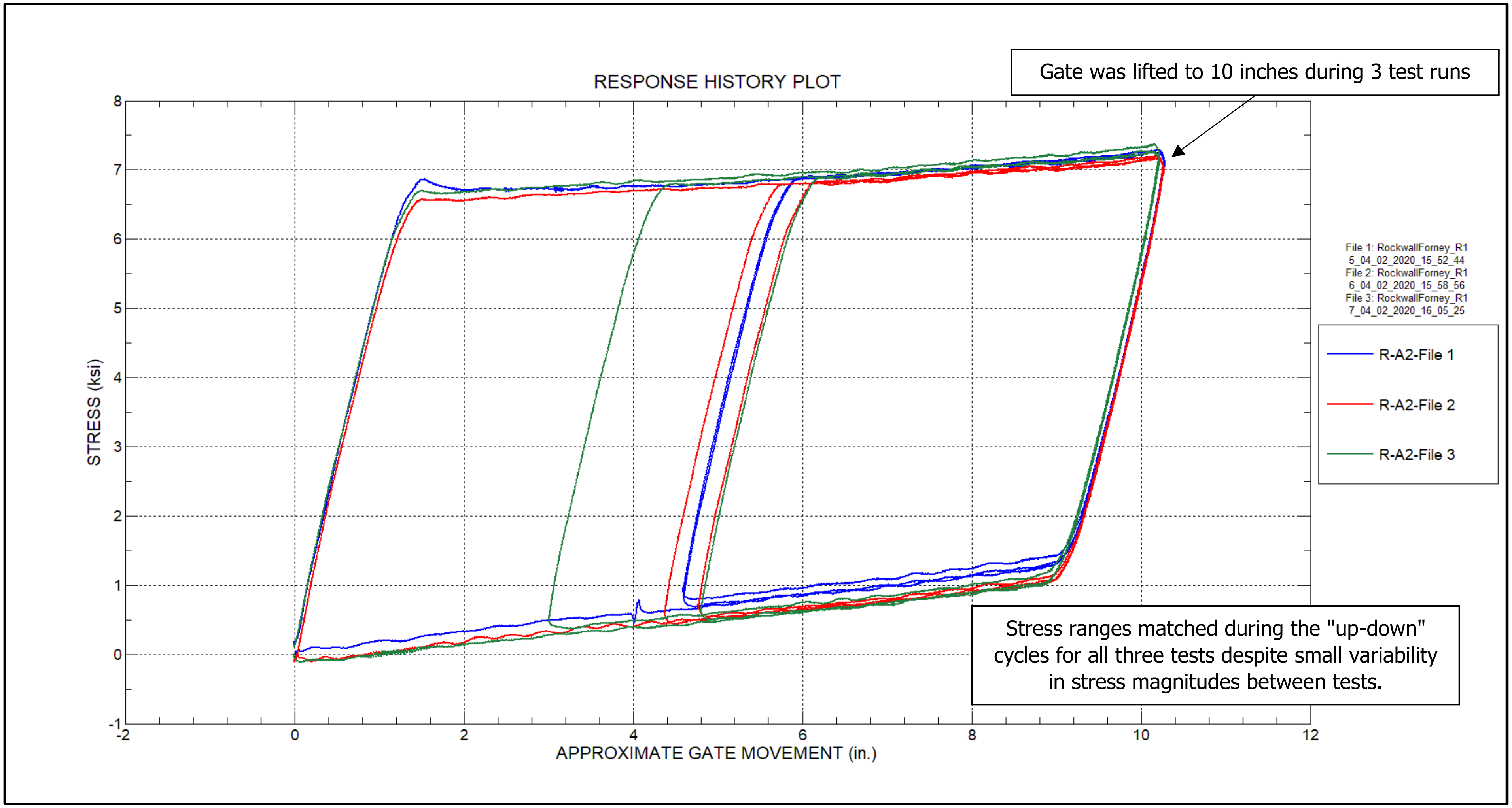

Figure 7 – Stress response history – Right arm – Gage A2 – Function of gate movement
File 1 = test run 1, File 2 = test run 2, File 3 = test run 3
(Section A along top strut near pin – Sensor location 2 along bottom of inner flange)

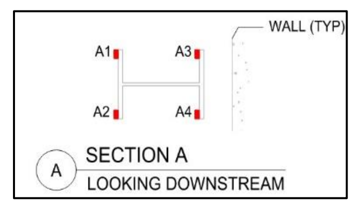

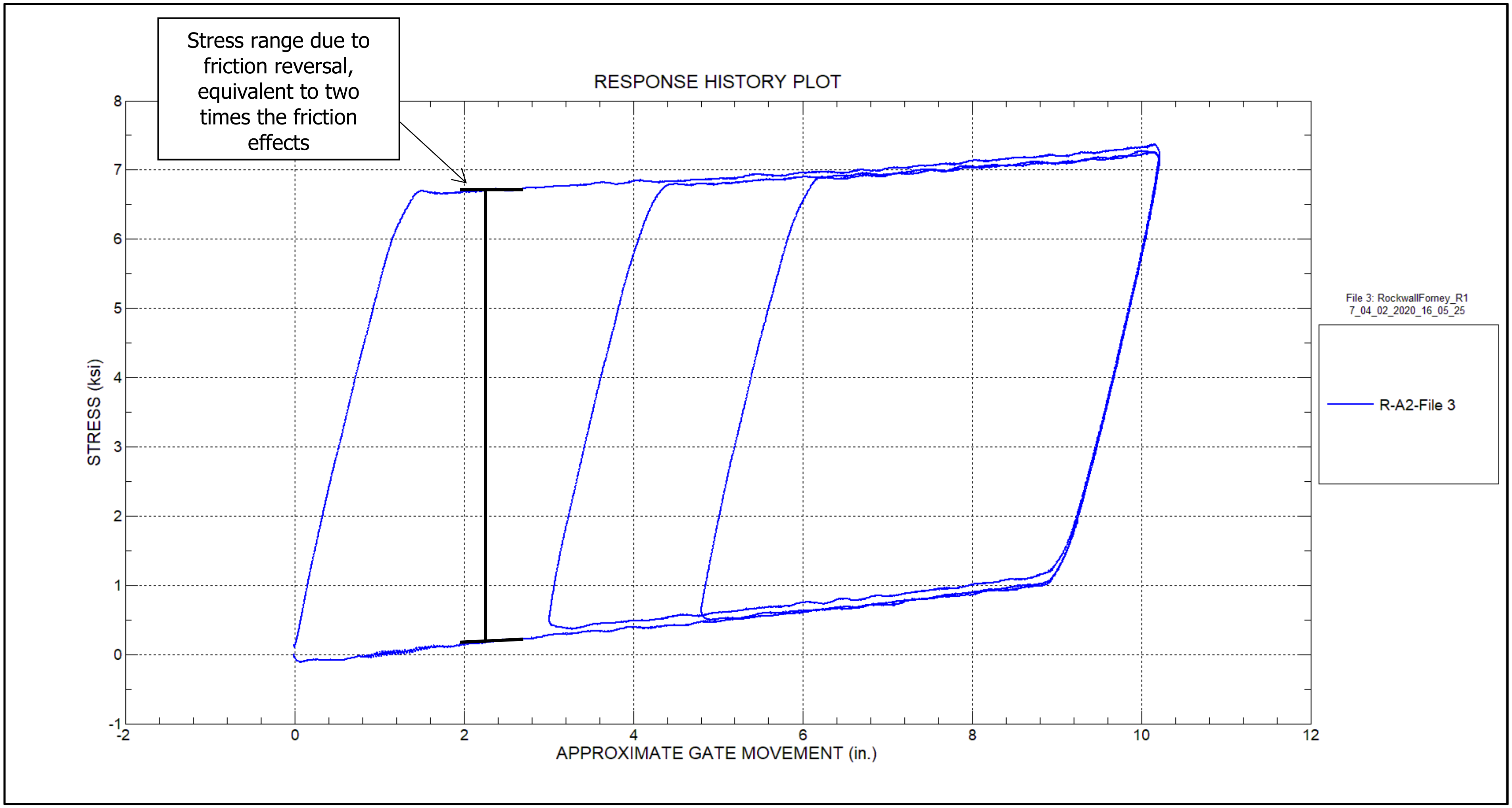

Figure 8 – Stress response history – Right arm – Gage A2 – Friction effect in stress responses

(Section A along top strut near pin – Sensor location 2 along bottom of inner flange)

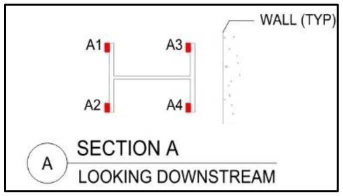

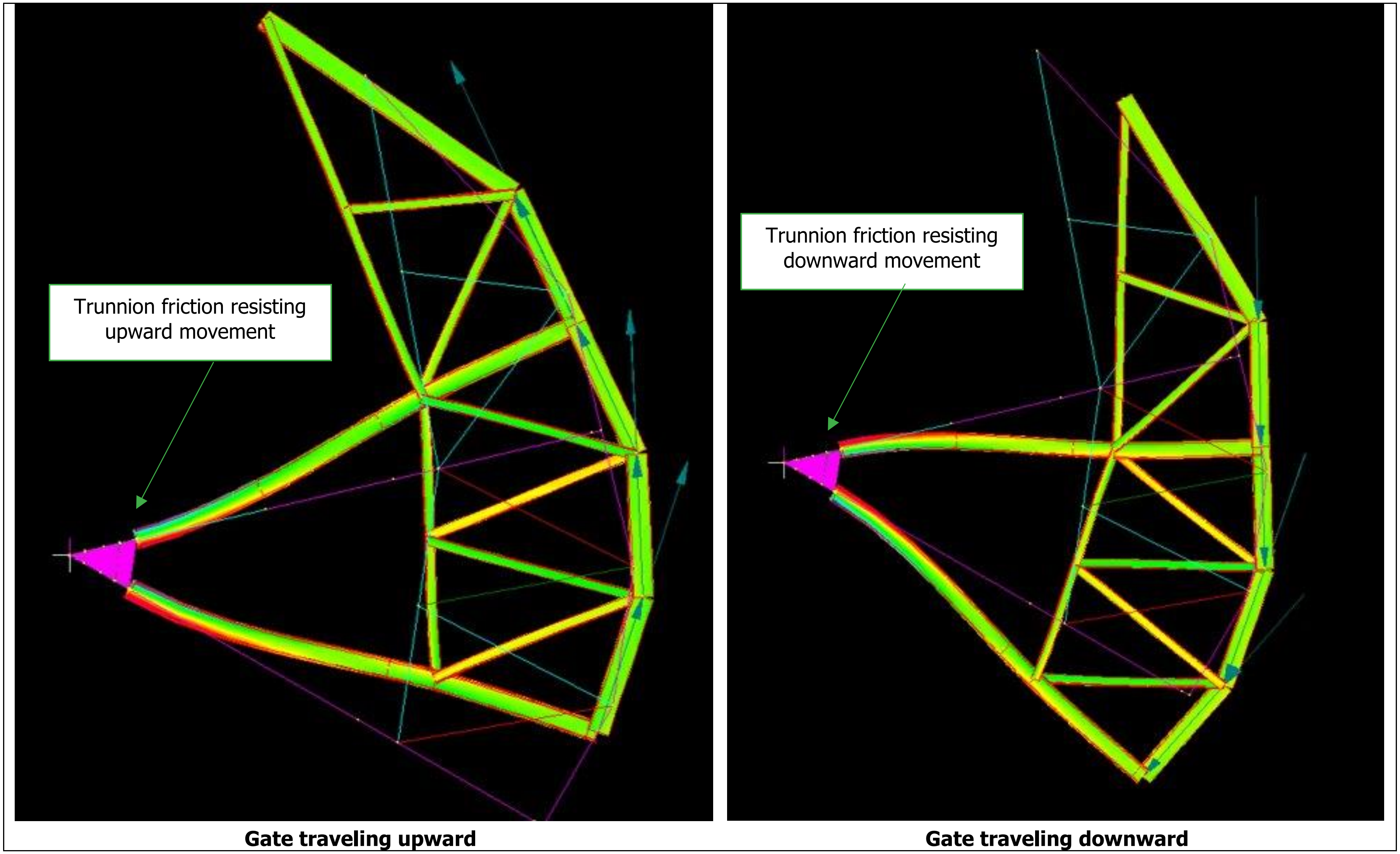

Figure 9 – Deflected shapes during lifting and lowering of Gate – Visualization of direction/friction reversals

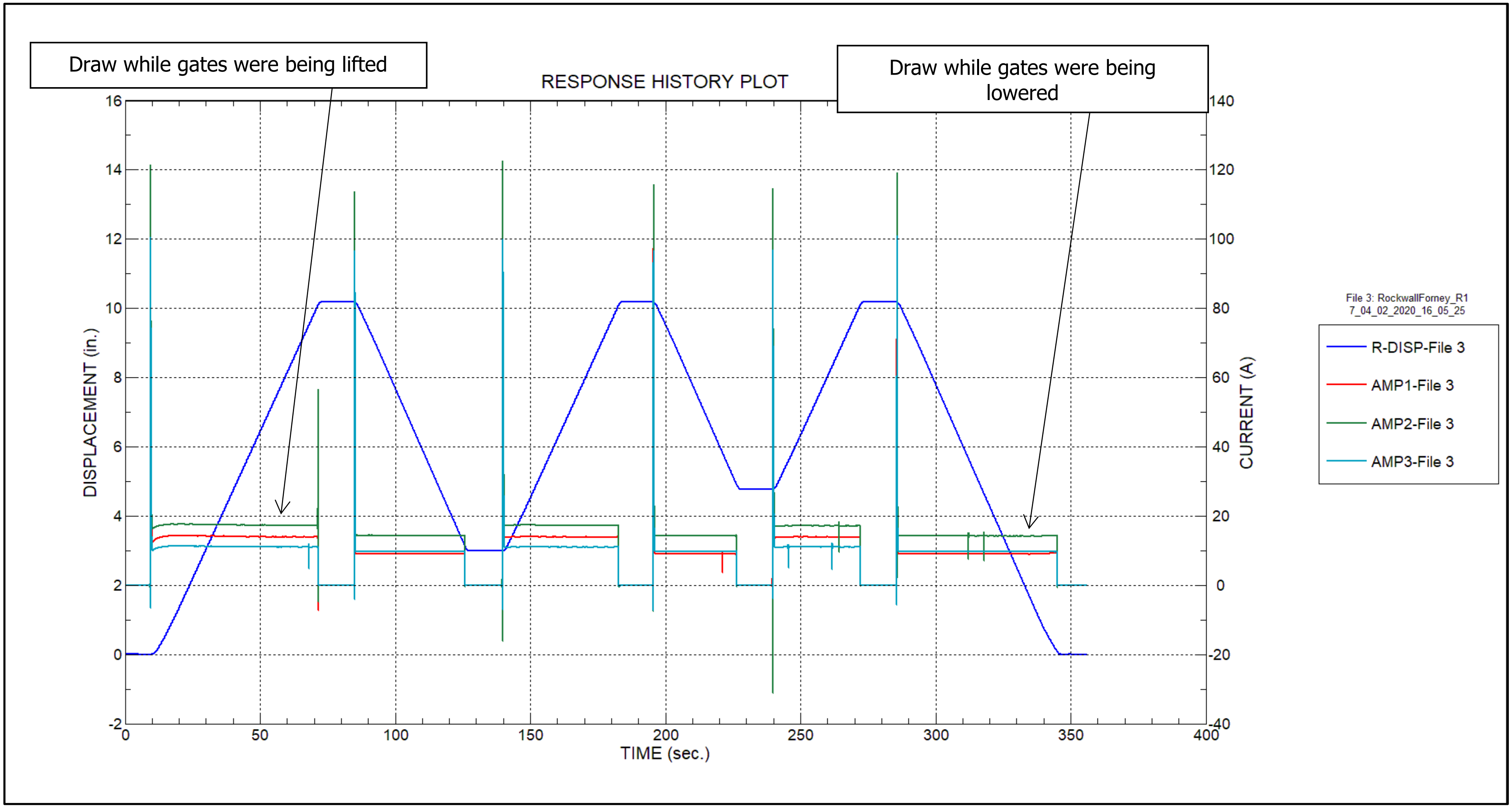

Figure 10 – Motor current & gate movement response history – Lift motor – Highlighting motor draw during lift and lower cycles

METHODOLOGY AND FINDINGS OF THE STRUT FORCE AND MOMENT CALCULATIONS

The following outline provides the methodology used to calculate the required member forces and moments.

- **CHANGE IN STRESS DUE TO GATE OPERATION:** Strain data can be viewed as a function of time starting when the gate was in the down position and was then lifted off the sill. When examining data in this manner, it is easy to see how stresses ramped up as the gate began to move and then changed slope once pin friction was overcome and the trunnion hub began to rotate with the gate. The first point in time where the friction was overcome (both lifting and lowering) has been highlighted in the stress histories shown in Figure 11. These stress histories show the response of all four sensors along the top strut of the right arm (Section A). ***It is important to note that the recorded measurements were changes in structural response due to gate movement, and do not include the in-situ stresses due to the dead load, cable wrap, and hydrostatic loads present prior to testing.***
- **CALCULATION OF STRUT CROSS-SECTIONAL MOMENTS:** The use of four strain gages per strut cross-section allowed accurate in-plane flexural bending moments to be computed from the recorded strain measurements. These moments were computed for every cross-section in each gate arm using the basic mechanics equation provided in Figure 12.

  In-plane or weak-axis flexure refers to bending about a given strut's web. This designation is consistent with typical nomenclature. In-plane bending can be observed visually from the strain response histories as a difference between the top and bottom stresses, whereas out-of-plane or strong-axis bending is visualized as the difference in stress from side to side. Figure 13 provides a visual reference for both types of strut flexure.
- **EXAMINATION OF RESPONSES AS A FUNCTION OF GATE POSITION:** Changes in cross-sectional moment related to friction becomes clearer when the responses are plotted as a function of gate position. Because the gate was operated with several up and down movements, the effects of friction associated with each direction reversal can be viewed for all measured and calculated responses. Figure 14 through Figure 17 show all cross-sectional flexural moment plots for both trunnion arms. The responses in these plots have been centered about the stress state corresponding to a zero-moment, unflexed condition. The zero-moment offset was estimated as the average moment values between up and downward movement (i.e. half the moment difference) at the gate position with the greatest pin friction moment difference (greatest difference between lifting and lowering).
- **TRUNNION FREE-BODY-DIAGRAM & PIN MOMENT CALCULATION:** Figure 18 shows the instrumented member cross-sections and shows how the measured cross-sectional flexural responses were used to compute pin moment. The in-plane moment values used in these calculations were determined directly from the strain measurements at each cross-section using the provided mechanics equations. It should be noted that the out-of-plane moments were not considered in the calculation of pin moment since they were orthogonal to the axis of the pin rotation. Total pin moment was then determined by summing all the moment components about the pin, which included the in-plane moment and the shear components at the strut cross-sections nearest the pin.
- **STRUT SHEAR CALCULATION:** From the examination of the trunnion free-body-diagram described above, the shear vectors at the three struts were a primary component in the pin moment calculation. For this type of structural element, shear vectors were calculated using the moment differential between the two cross sections along each strut. It is important to recognize that shear was constant between the two instrumented cross-sections and the applied shear was a function of the recorded change in moment ($V = dM/dX$). Subsequently, the shear vectors were calculated by dividing the difference in moment by the distance between the two instrumented cross-sections. Shear values for each strut have been plotted as a function of gate position in Figure 19 and Figure 20.

- **CALCULATION OF PIN MOMENT DUE TO FRICTION:** Once all the trunnion arm force vectors were calculated, the equations shown in the free-body-diagram were applied to compute pin moment as a function of gate position. It is important to note that because the calculated pin moment range corresponds to a direction reversal, a reversal in friction also occurred. The effect of direction reversal on pin moment due to friction is best conceptualized by centering the moment response plots about the zero-moment axis. The moment due to lifting and the moment due to lowering can then be visualized as a change from this new zero point corresponding to the gate in an unflexed condition. Therefore, the total moment differential between lifting and lowering was twice the moment due to friction acting in a single direction. Pin-moment plots have been provided in Figure 21 and Figure 22. From these plots, it is apparent that pin moment due to friction remained relatively constant throughout the gate operation tests, with a slight decrease in pin friction moment as the gate continued to be lifted. This slight decrease in pin friction moment most likely corresponded to the change in hydrostatic load as the gate position changed. Pin-moment plots for all tests on Gate 3 are also provided for reference in Appendix B – Gate 3 Pin Moment Component Plots.
- **SHAFT TORQUE & HOIST FORCE:** Torque measurements were taken on the pinion shafts near the hoist motor during testing, with single torque gages installed on the left and right hoist pinion shaft. Responses were recorded in units of micro-strain and converted to torque in units of kip-ft using Equation 1 thru Equation 3 and the following shaft properties.

$$d_O = 5.5\ inches, \qquad d_I = 0\ inches, \qquad E = 29000\ ksi, \qquad \nu = 0.3$$

$$G = \frac{E}{2(1+\nu)}$$

Equation 1

$$J = \frac{\pi\left(d_O{}^4 - d_I{}^4\right)}{32}$$

Equation 2

$$\tau = \varepsilon * \frac{2GJ}{\frac{d_O}{2} * 1000000 * 12}$$

Equation 3

Figure 23 shows example torque measurements, recorded on the Gate 3 torque shafts. Best practices for torque measurements is to measure torque on opposite sides of the shaft so that any bending in the shaft can be removed by averaging the two responses. Due to access limitations, only one gage at each location could be installed. Therefore, any bending in the shaft may be reflected in the torque measurements and may be related to the peaks and valleys observed in the torque responses.

Torque values were converted to force in the hoist cables per gate arm using the gear ratio and drum radius, as shown in Figure 24. The gear ratio and drum radius were 5.182 and 1.086 feet respectively, as defined in the provided as-built shop drawings. It should be noted that the hoist force calculated may be smaller than the actual hoist force applied. This difference is due to the limit switch engaging the brake before the hoist cable was fully slacked, resulting in an initial force in the cable. A hoist force due to total gate friction was then calculated. This friction hoist force was equal to half the differential in force measured during the lifting and lowering of the gate (similar to the pin friction calculations). As shown in Table 3, the change in cable force due to friction was generally consistent between tests. Note that the total hoist force was due to the total friction effects, including side seal, hoist bearings, trunnion friction effects, etc. It is difficult to determine the exact proportion and composition of the total friction sources. Additional torque and hoist force plots for all collected data files are provided in Appendix A – Gate 3 Torque and Hoist Force Plots.

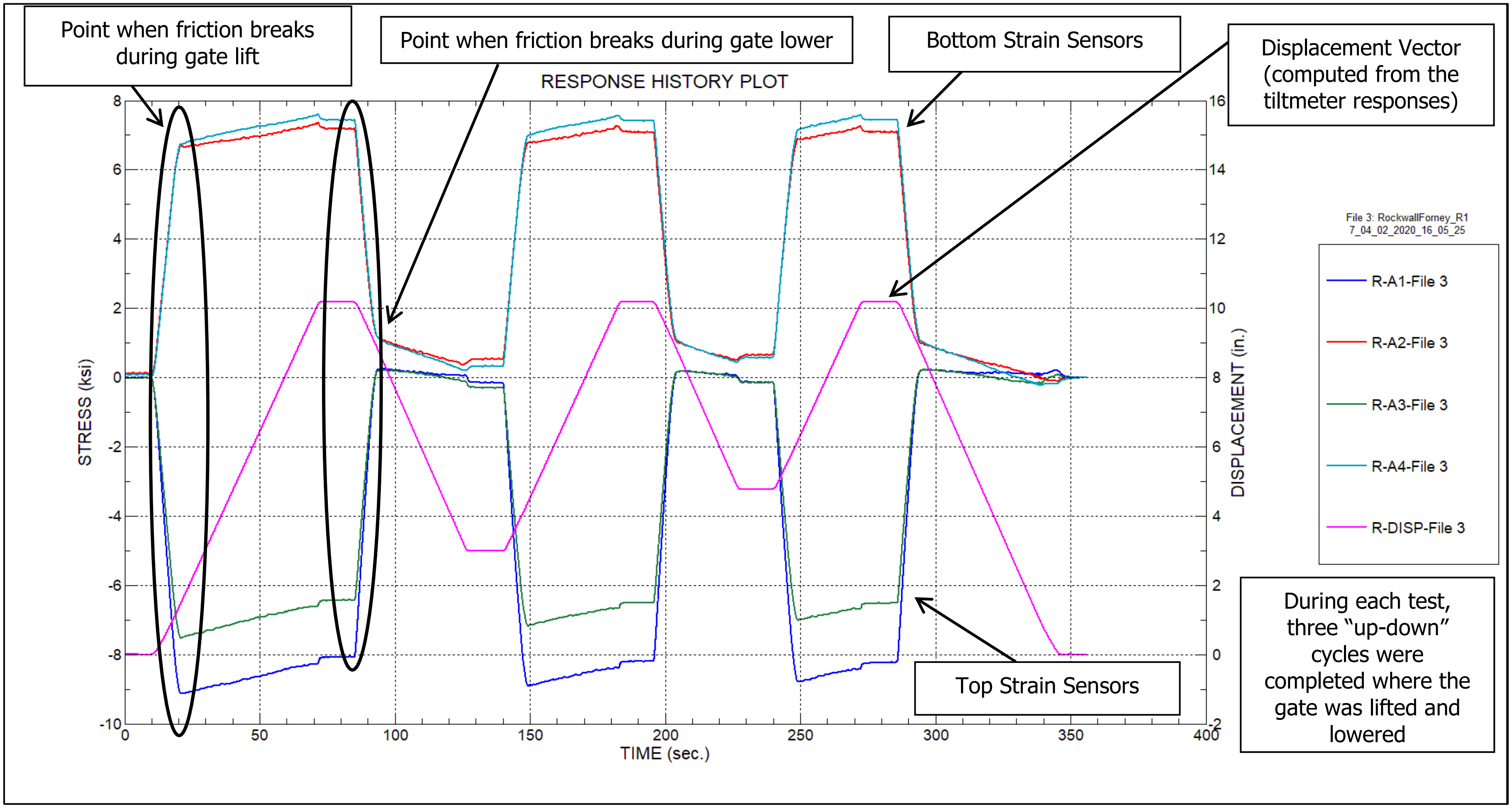

Figure 11 – Stress response & gate movement history – Right arm – Section A - Highlighting friction behavior
(Section A along top strut near pin)

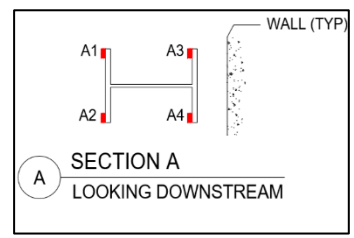

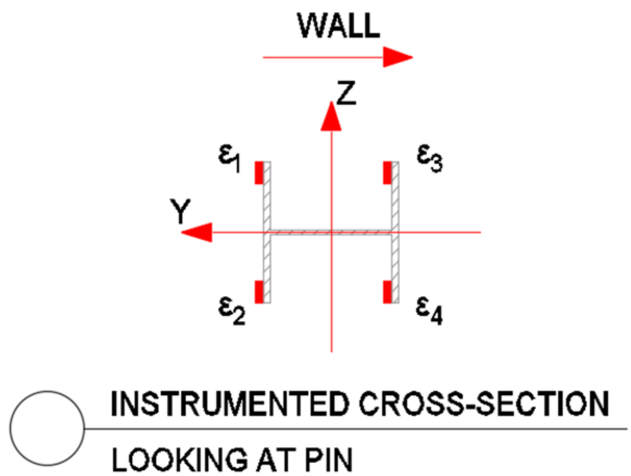

Calculation of Weak-axis (In-plane) bending

$$M_Y = \frac{E[\frac{\varepsilon_2 + \varepsilon_4}{2} - \frac{\varepsilon_1 + \varepsilon_3}{2}]S_{Y(gage)}}{2}$$

Sy(gage) = Section modulus to the center of gages (not extreme fiber of flanges)
(locations of gages were accounted for in moment computation)

Figure 12 – Basic mechanic equation used to calculate moment

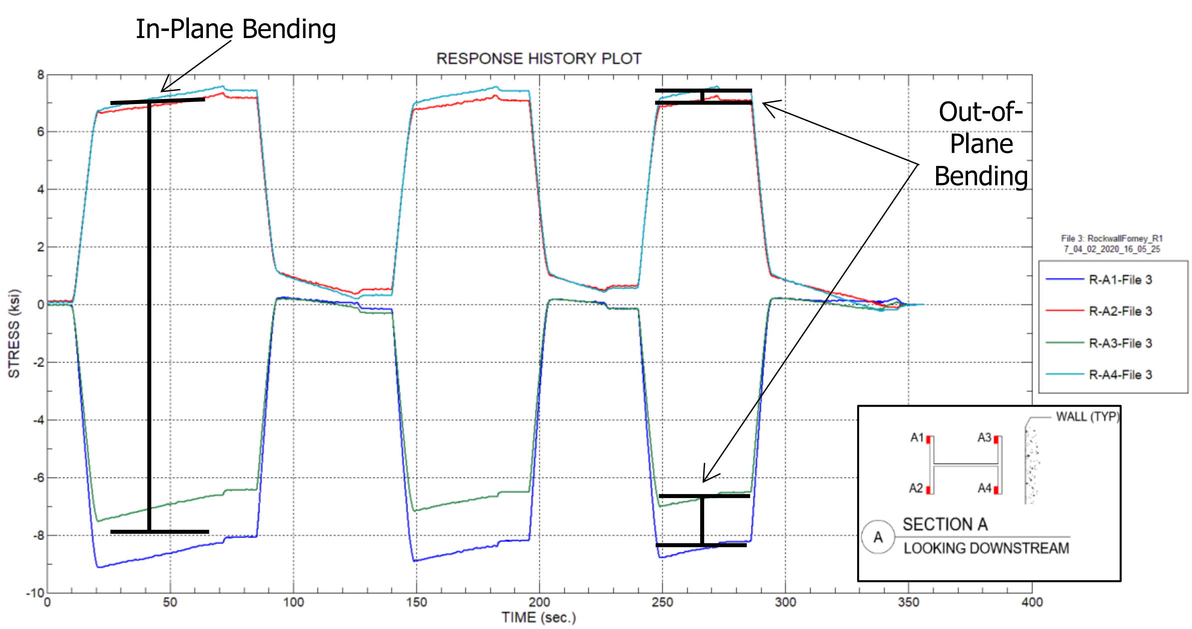

Figure 13 – Stress response history – Right arm – Section A – Bending components
(Section A along top strut near pin)

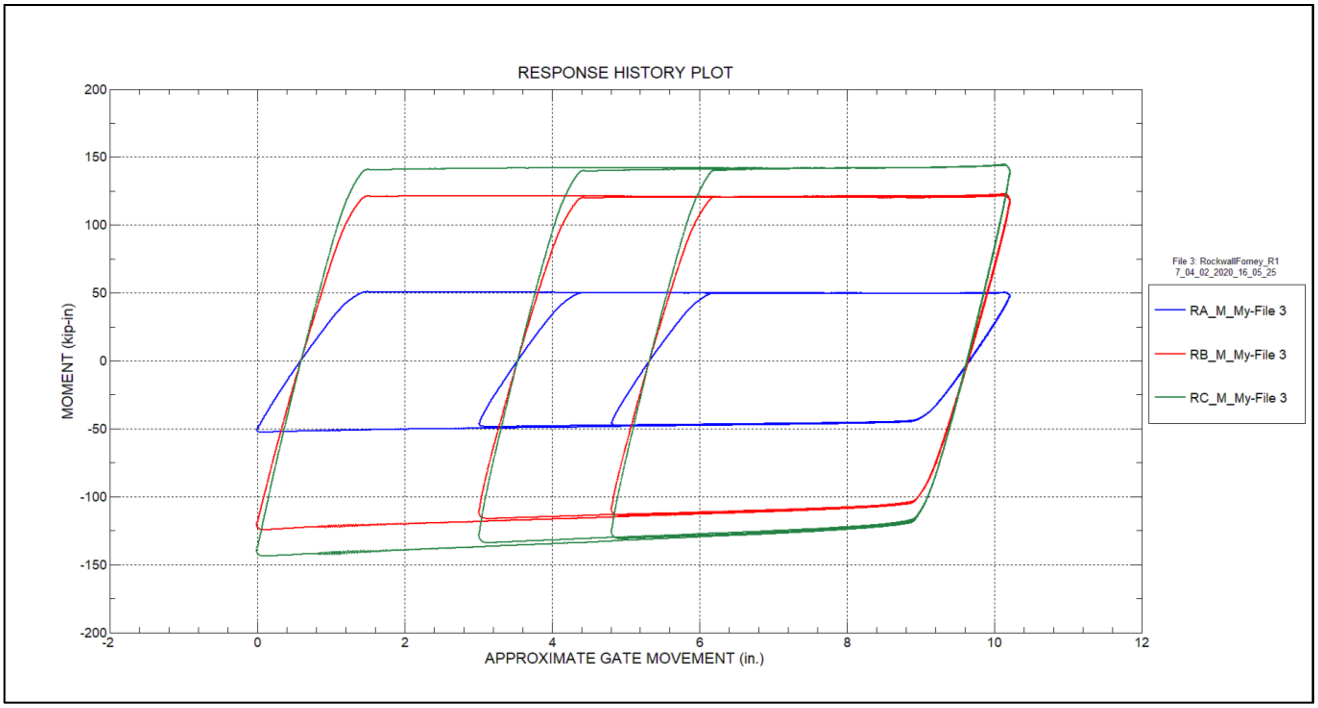

Figure 14 – In-plane moment response history – Right arm – Sections near pin

(RA = Right Arm Top Strut, RB = Right Arm Middle Strut, RC = Right Arm Bottom Strut)

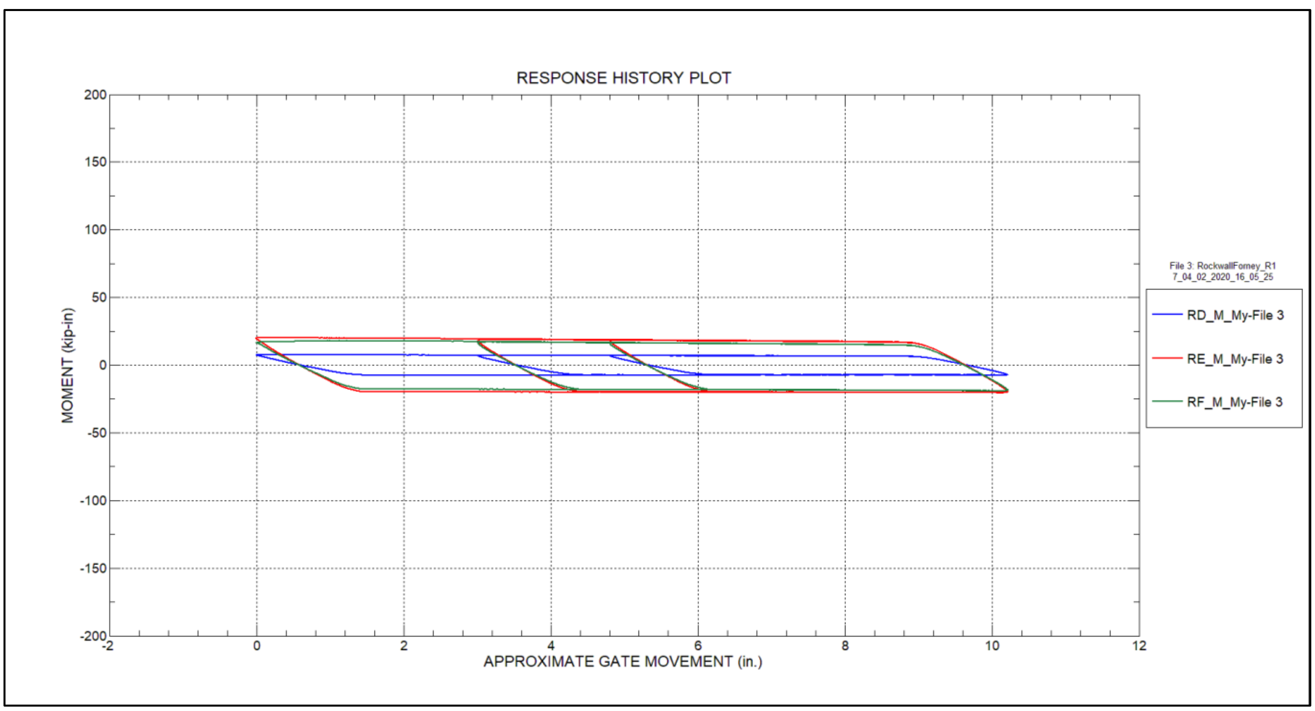

Figure 15 – In-plane moment response history – Right arm – Sections away from pin

(RD = Right Arm Top Strut, RE = Right Arm Middle Strut, RF = Right Arm Bottom Strut)

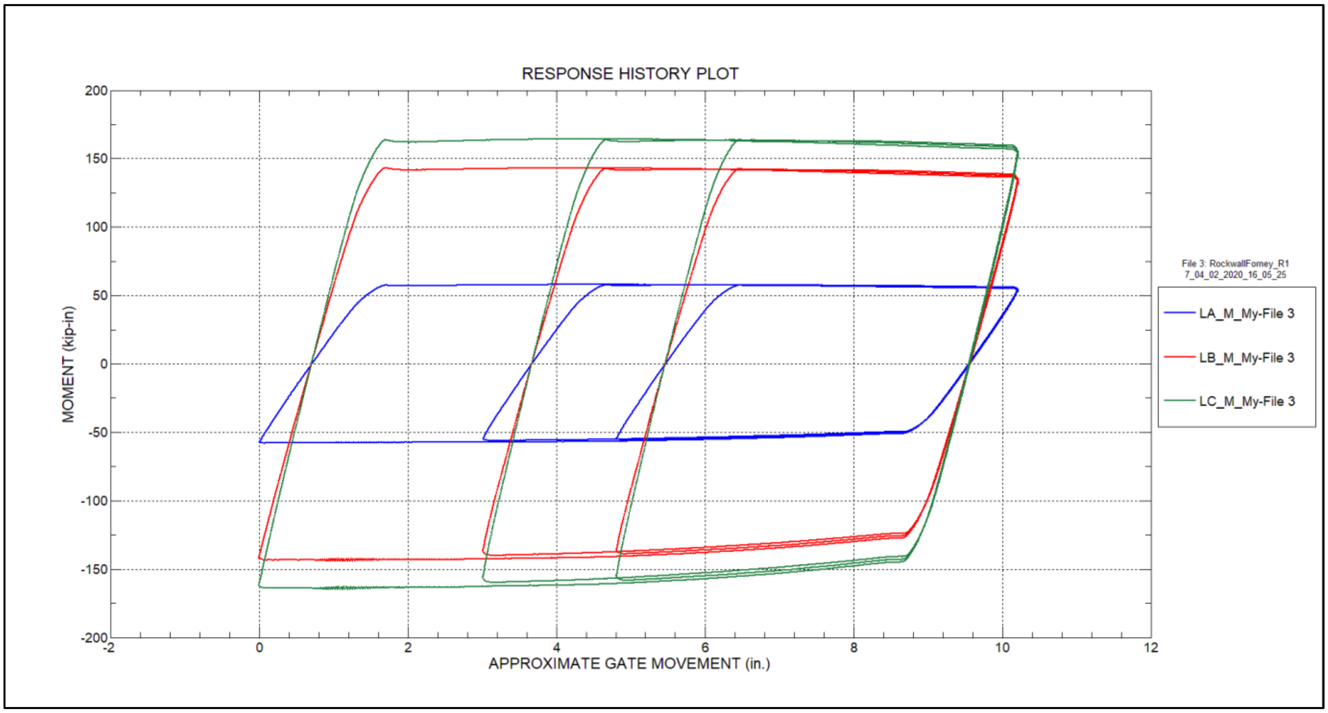

Figure 16 – In-plane moment response history – Left arm – Sections near pin

(LA = Left Arm Top Strut, LB = Left Arm Middle Strut, LC = Left Arm Bottom Strut)

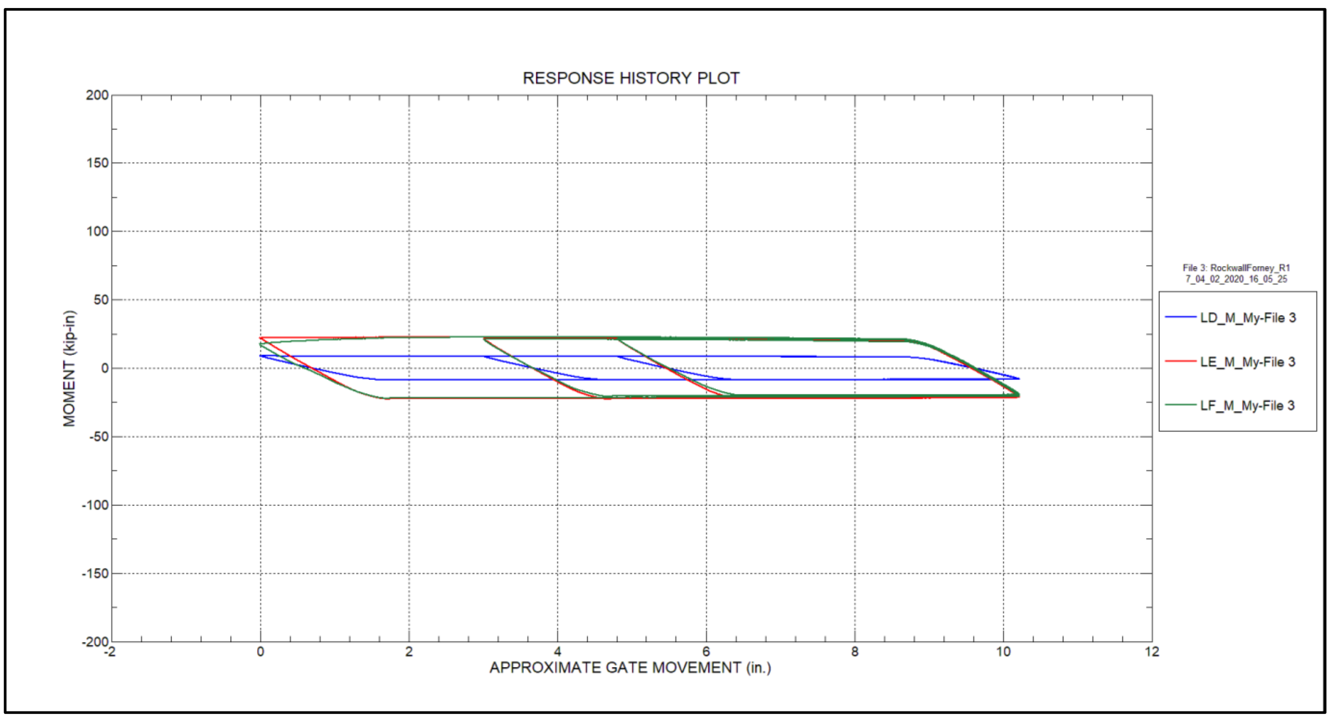

Figure 17 - In-plane moment response history – Left arm – Sections away from pin

(LD = Left Arm Top Strut, LE = Left Arm Middle Strut, LF = Left Arm Bottom Strut)

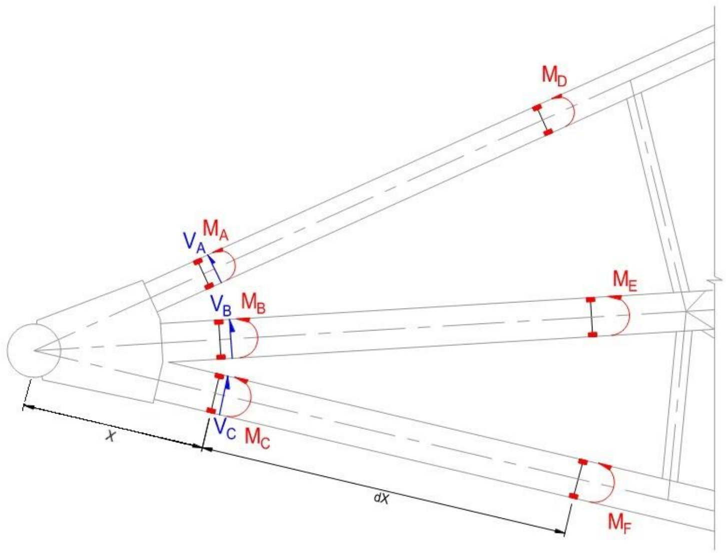

Elevation View of Gate Arm

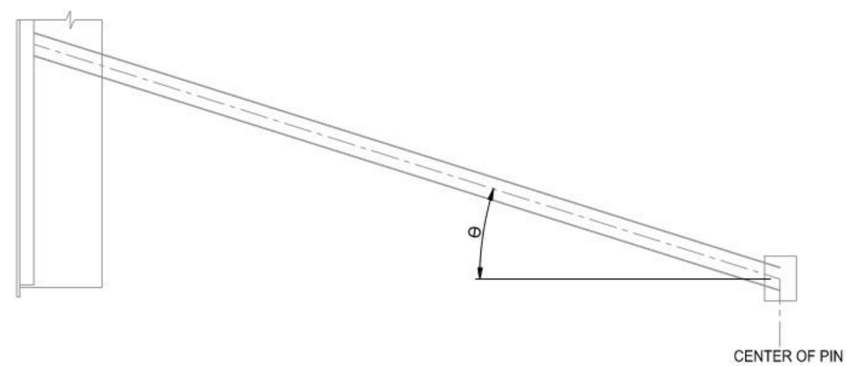

Plan View of Gate Arm

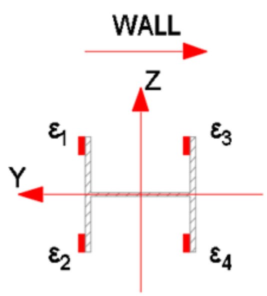

$$M_Y(M_A, M_B, M_C, M_D, M_E, M_F) = \frac{E\left[\frac{\varepsilon_2 + \varepsilon_4}{2} - \frac{\varepsilon_1 + \varepsilon_3}{2}\right] S_{Y(gage)}}{2}$$

$$V_A = \frac{M_A - M_D}{dX}$$

$$V_B = \frac{M_B - M_E}{dX}$$

$$V_C = \frac{M_C - M_F}{dX}$$

$$\sum M_o = 0$$

$$M_{PIN} = [X(V_A + V_B + V_C) + M_A + M_B + M_C]\cos\theta$$

Figure 18 – Direct calculation of pin moment from strain measurements

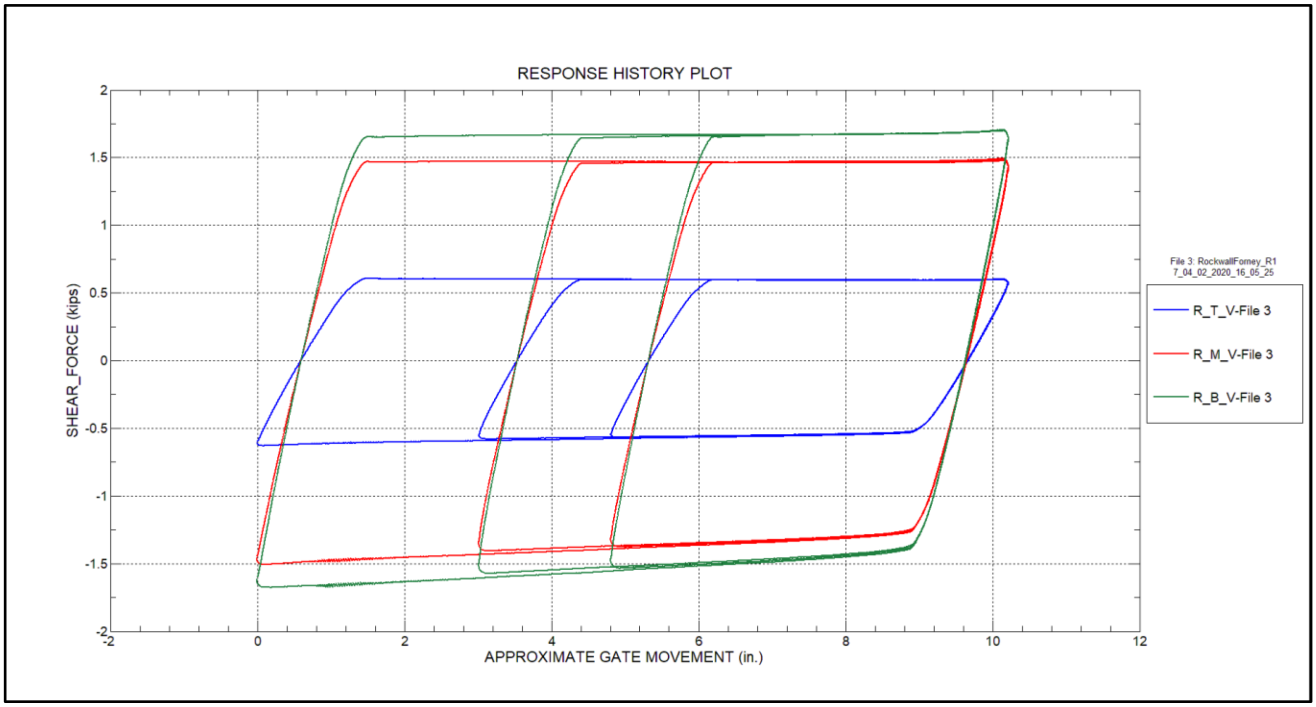

Figure 19 – Strut shear response history – Right arm

(R_T = Right Arm Top Strut, R_M = Right Arm Middle Strut, R_B = Right Arm Bottom Strut)

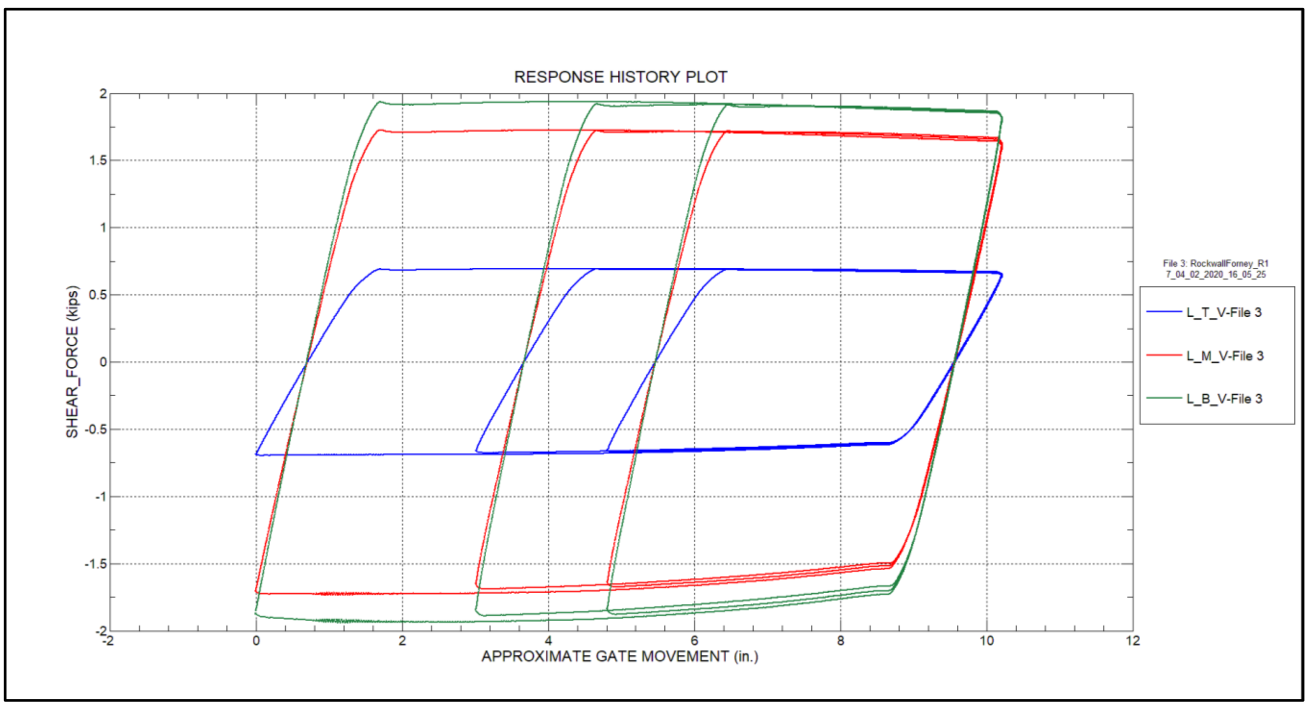

Figure 20 – Strut shear response history – Left arm

(L_T = Left Arm Top Strut, L_M = Left Arm Middle Strut, L_B = Left Arm Bottom Strut)

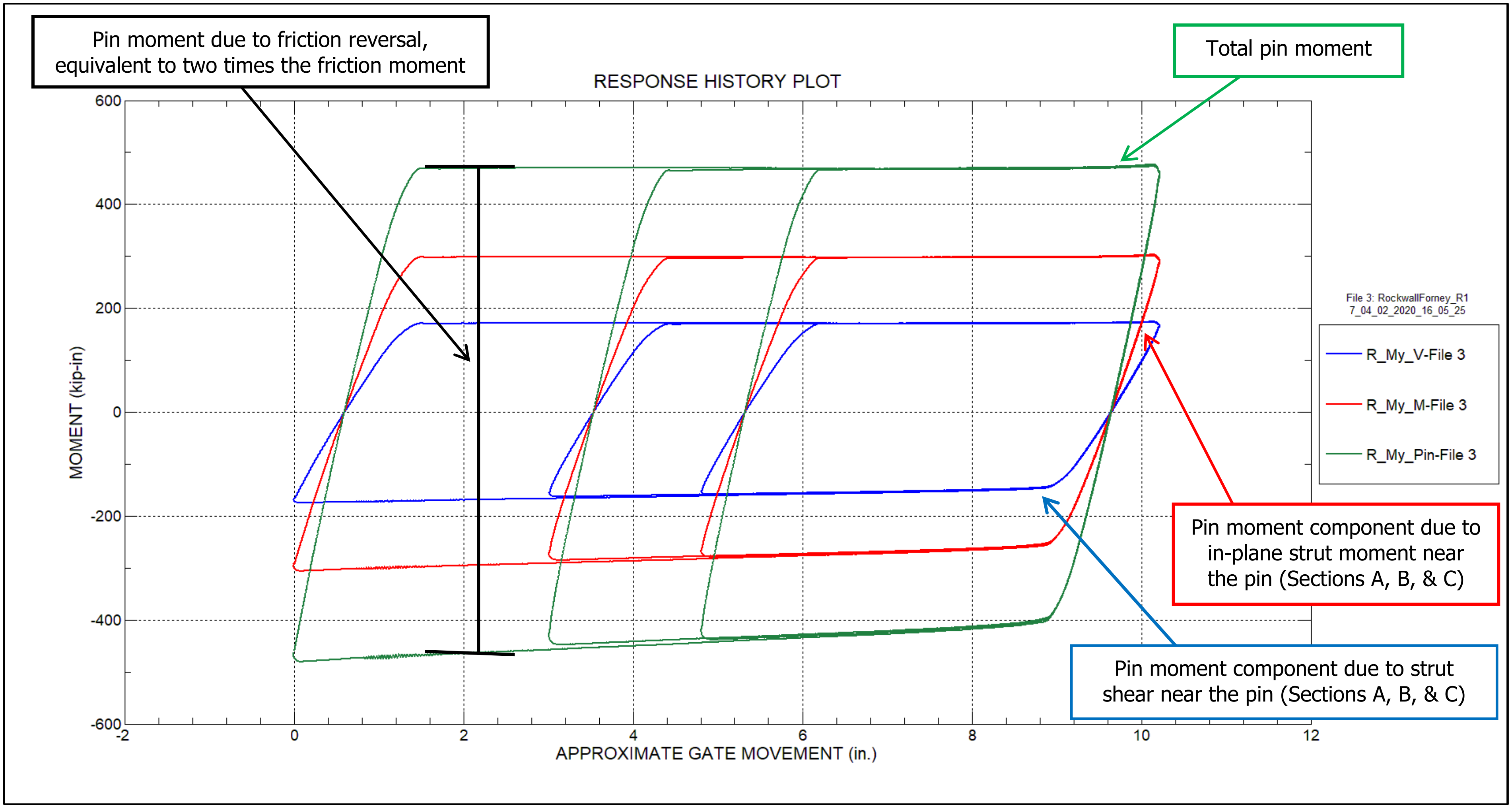

Figure 21 – Pin moment response history – Right arm

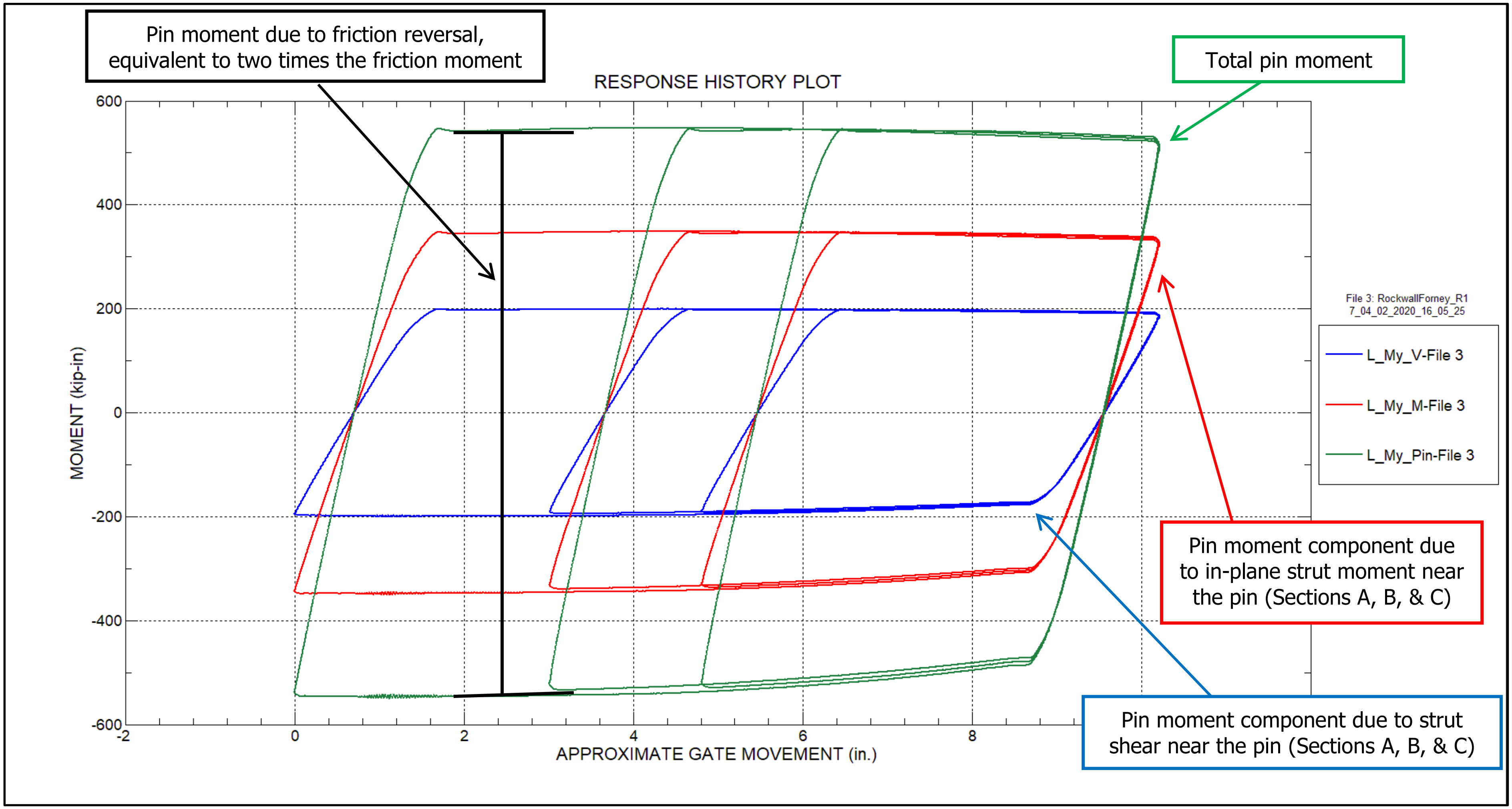

Figure 22 – Pin moment response history – Left arm

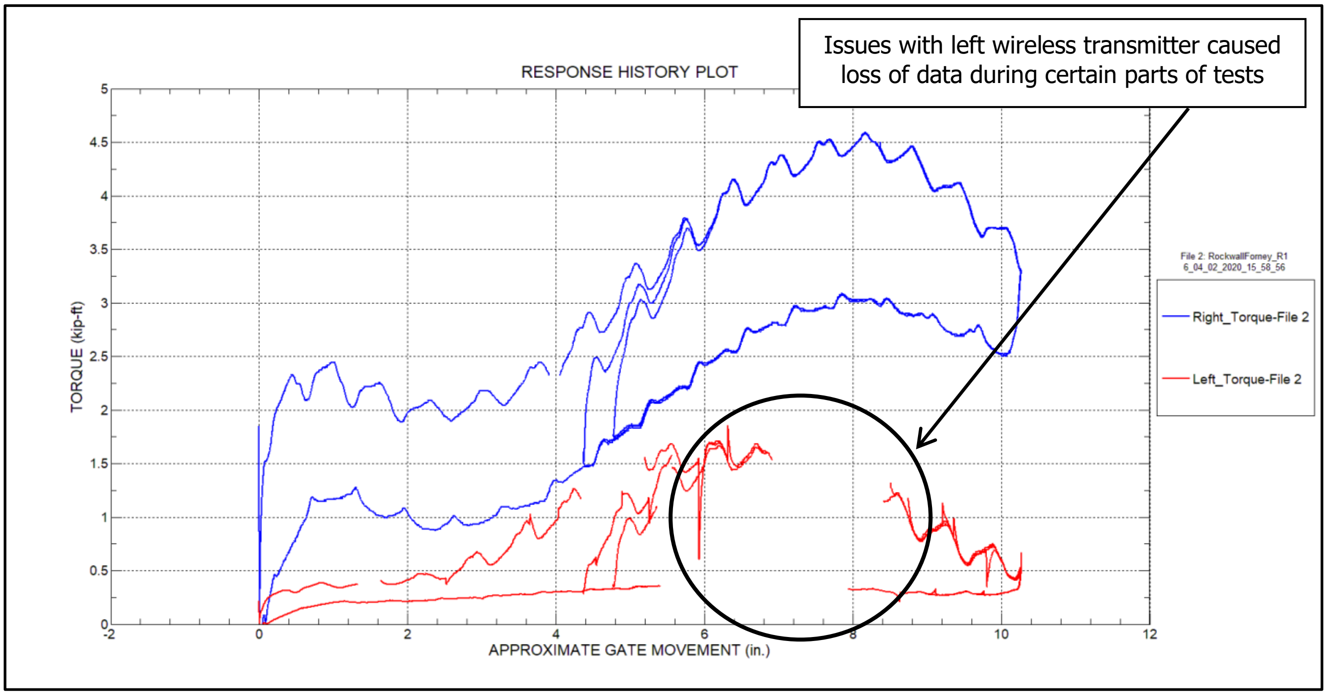

Figure 23 – Hoist torque response history – Gate 3 – Test 2
Note: missing data due to wireless connectivity issues as the sensor rotates with the pinion shaft

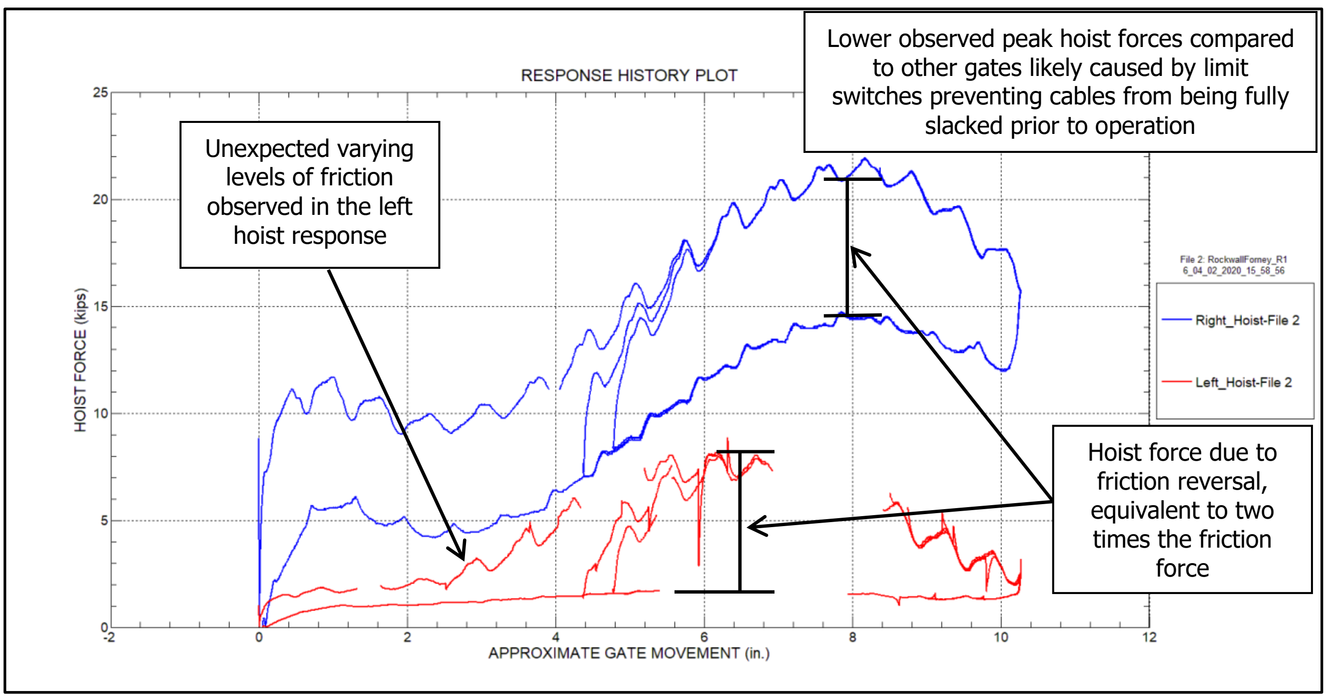

Figure 24 – Hoist force response history – Gate 3 – Test 2
Note: missing data due to wireless connectivity issues as the sensor rotated with the pinion shaft

Summary of Friction Results

The raw data files have been included in the submittal package for reference and were formatted as "tdms" files that can be opened in Microsoft Excel using a "tdms" reader extension.

Examination of the stress histories for each test was necessary to obtain a thorough understanding of the gate performance. The response shapes, variations in stress magnitudes, and timing sequences provided direct clues as to how the gate performed under typical service conditions. The following is a breakdown of the provided tabulated results:

+ Table 2 provides motor current ranges and maximum in-flow for lift and lower cycles for each test
+ Table 3 provides maximum hoist force as well as hoist force due to total friction for each test
+ Table 4 provides the maximum stress ranges measured at the sensor locations for each member
+ Table 5 provides maximum bending stress and moment ranges observed during the gate tests
+ Table 6 provides maximum friction bending stress and moment values at each of the instrumented strut locations
+ Table 7 provides the computed shear values in each strut due to friction
+ Table 8 provides calculated measured friction moments, calculated hydrostatic loads based on the measured water elevation, and coefficients of friction for each gate and gate arm during all three tests

The resulting pin friction moments were used to compute friction coefficients from Eq. 4, given the pin radius and the applied thrust. The thrust used in this calculation consisted of the calculated resultant hydrostatic load based on the measured water elevation and was adjusted to account for the loss of head as the gate was lifted. This thrust adjustment was based on the recorded gate movement and was performed in order to calculate more accurate friction coefficients. The water elevation during testing was nearly constant throughout each gate test and was documented during each "up-down" cycle. It should be noted that the minor thrust due to cable wrapping, which was minimal compared to hydrostatic thrust, was not included in the thrust calculation. This assumption resulted in slightly conservative friction coefficients.

$$\mu = \frac{M_F}{T * r} \qquad \text{Eq. 4}$$

where:

	μ	=	Friction Coefficient
	M_F	=	Friction Moment
	T	=	Thrust per Pin
	r	=	Pin Radius, 5.375"

The out-of-plane shear and moments were not considered in the pin friction calculations due to orthogonal geometry considerations (resulting pin moment associated with out-of-plane flexure being perpendicular to pin rotation).

The data was presented in a specific coordinate system applicable to both arms. Data was processed so that the positive x-axis was always pointing towards the pin and the right-hand rule applied. In-plane bending can be referred to as "bending about the horizontal or y-axis" and shows how much the beams bend up and down within the plane of the gate arms. Refer to Figure 12 above for visual reference of coordinate system and mathematical explanation of calculations. Tabulated results do not include any in-situ effects.

Table 2 – Motor current summary table – Gate 3

Test Run	Current Range due to Lifting (A)	Current Range due to Lowering (A)	Max In-rush Current (A)
1	11-18	9-15	128
2	11-18	9-15	124
3	11-18	9-14	123

Table 3 – Hoist force summary table – Gate 3

Test Run	Right Arm Peak Hoist Force (kips)	Left Arm Peak Hoist Force (kips)	Right Arm Hoist Force due to Total Gate Friction (kips)	Left Arm Hoist Force due to Total Gate Friction (kips)
1	30.73	9.46	3.90	3.38
2	21.93	8.86	3.88	3.68
3	22.23	8.38	4.22	3.41

Tabulated friction force values correspond to the response induced by friction in one direction

Table 4 – Maximum measured sensor stress range

Arm Designation	Top Strut (ksi)	Middle Strut (ksi)	Bottom Strut (ksi)
Right Arm	9.63	10.18	11.35
Left Arm	10.50	11.96	11.60

Tabulated values correspond to the total measured change in response during tests

Stress values have not been extrapolated to the extreme fibers (correspond to center of gage)

Table 5 – Maximum in-plane total bending stress & moment ranges – Total

Section Label	Section Description	Right Arm Stress (Ksi)	Right Arm Moment (Kip-In)	Left Arm Stress (Ksi)	Left Arm Moment (Kip-In)
Section A	Top Strut Near Pin	9.31	104.65	10.59	118.97
Section B	Middle Strut Near Pin	10.71	247.72	12.84	297.01
Section C	Bottom Strut Near Pin	10.35	288.51	12.14	338.62
Section D	Top Strut Away from Pin	1.36	15.33	1.62	18.17
Section E	Middle Strut Away from Pin	1.77	41.00	2.03	47.06
Section F	Bottom Strut Away from Pin	1.34	37.29	1.78	49.54

Tabulated values correspond to the total measured change in response during tests

Table 6 – In-plane frictional bending stress & moment at maximum gate friction

Section Label	Section Description	Right Arm Stress (ksi)	Right Arm Moment (kip-in)	Left Arm Stress (ksi)	Left Arm Moment (kip-in)
Section A	Top Strut Near Pin	4.56	51.26	5.19	58.29
Section B	Middle Strut Near Pin	5.27	121.93	6.29	145.50
Section C	Bottom Strut Near Pin	5.07	141.38	5.96	166.13
Section D	Top Strut Away from Pin	0.66	7.45	0.79	8.84
Section E	Middle Strut Away from Pin	0.86	19.88	0.99	22.94
Section F	Bottom Strut Away from Pin	0.64	17.94	0.85	23.82

Tabulated values correspond to the response induced by friction in one direction

Table 7 – Strut shear range summary table due to friction

Arm Designation	Top Strut Shear (Kip)	Middle Strut Shear (Kip)	Bottom Strut Shear (Kip)
Right Arm	0.61	1.48	1.66
Left Arm	0.70	1.75	1.98

Tabulated values correspond to the response induced by friction in one direction

Table 8 – Pin friction summary table

Test Run	Average Water Elevation during testing (ft)	Approximate Thrust at time of Testing (kips per arm)	Gate/Member Designation	Pin Friction Moment (kip-in)	Friction Coefficient
1	435.56	488.50	Right Pin	471.30	0.18
			Left Pin	555.70	0.21
2	435.56	488.50	Right Pin	464.00	0.18
			Left Pin	542.60	0.21
3	435.56	488.50	Right Pin	469.60	0.18
			Left Pin	547.10	0.21

Tabulated values correspond to the response induced by friction in one direction

Appendix A – Gate 3 Torque and Hoist Force Plots

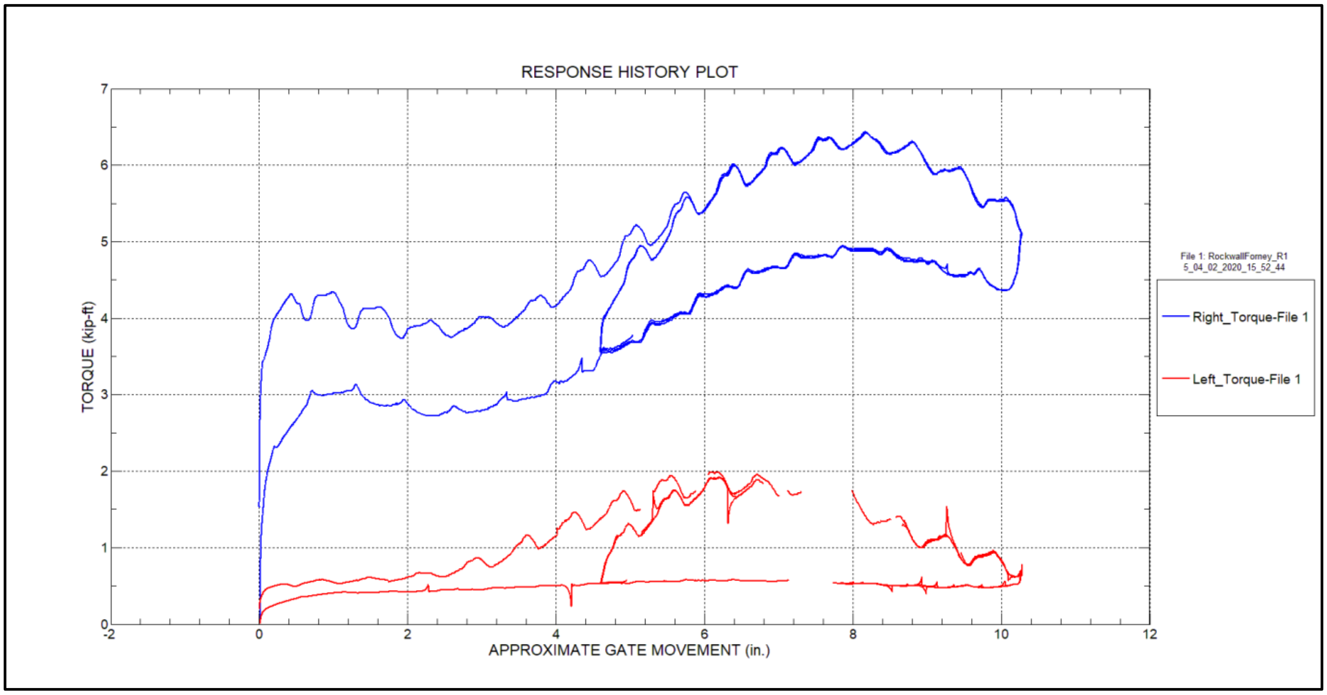

Figure 25 – Hoist torque response history – Gate 3 – Test 1

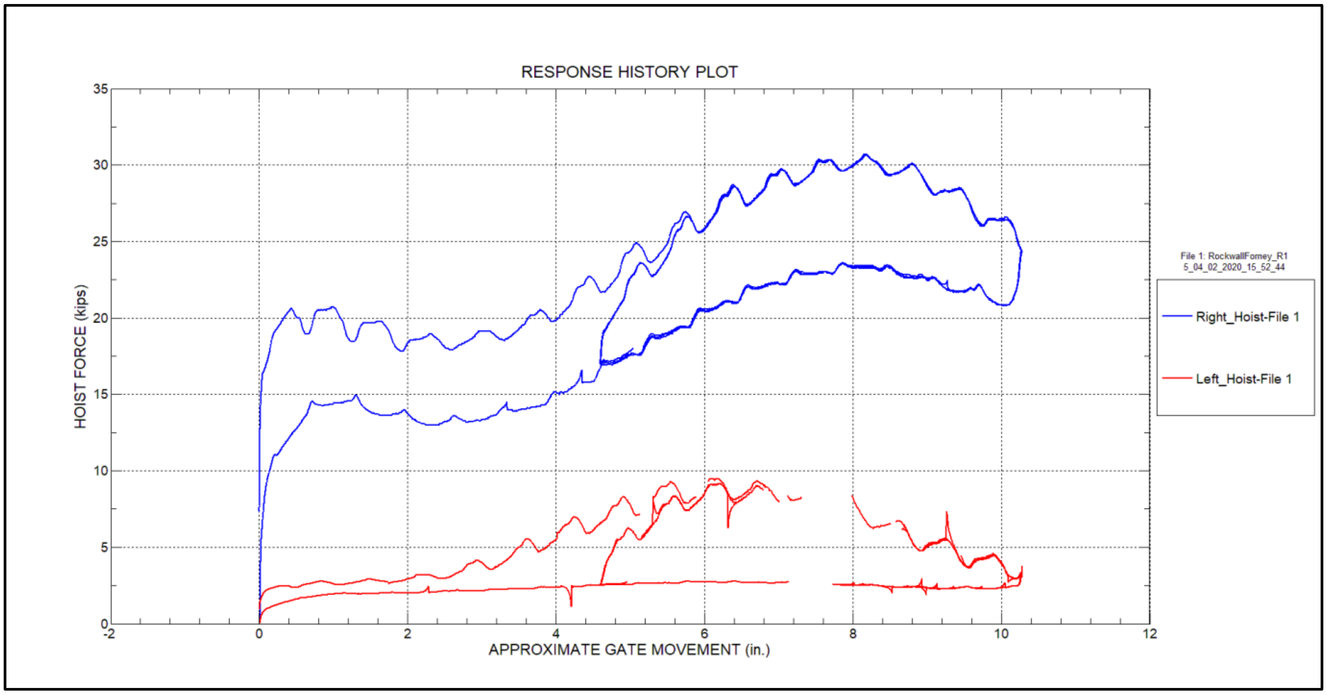

Figure 26 – Hoist force response history – Gate 3 – Test 1

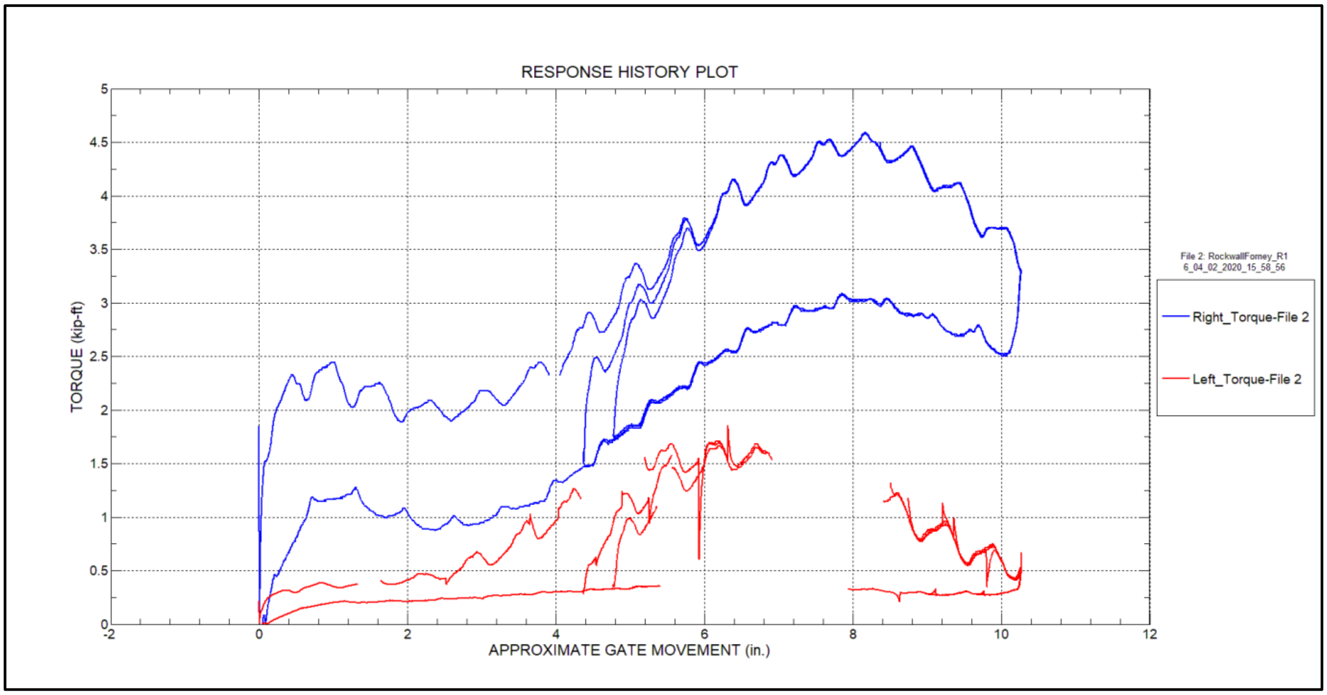

Figure 27 – Hoist torque response history – Gate 3 – Test 2

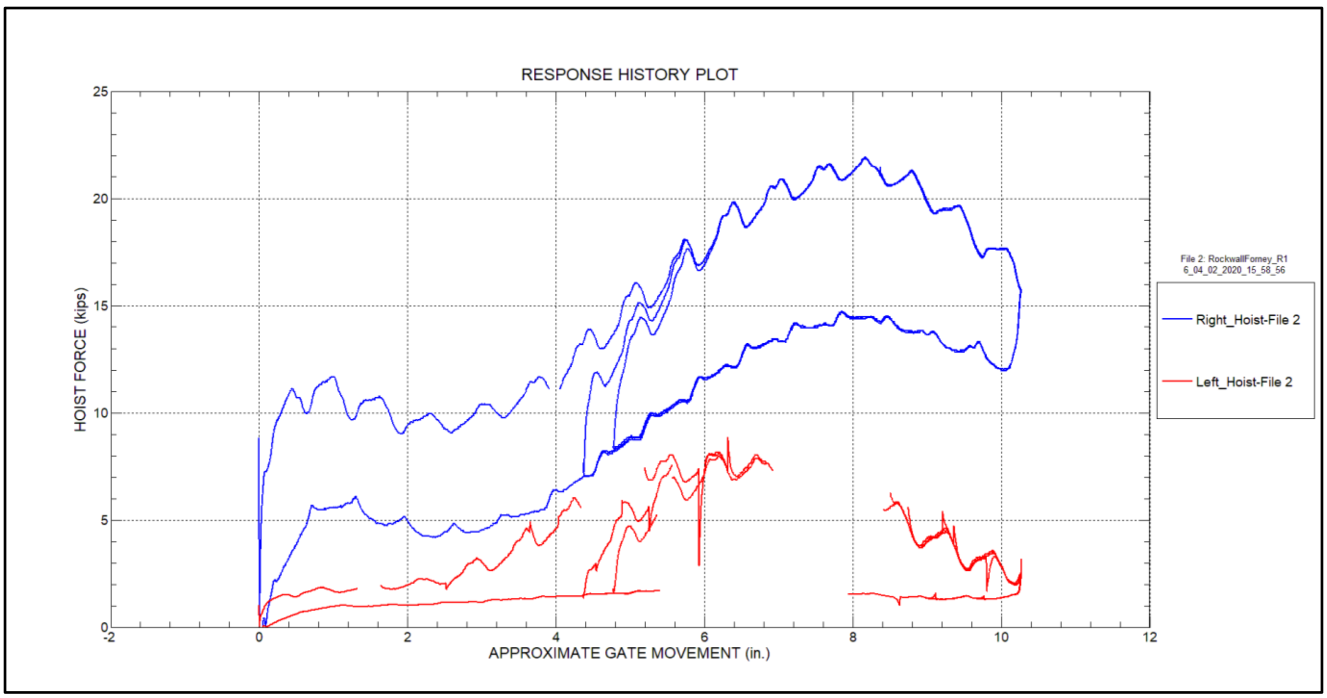

Figure 28 – Hoist force response history – Gate 3 – Test 2

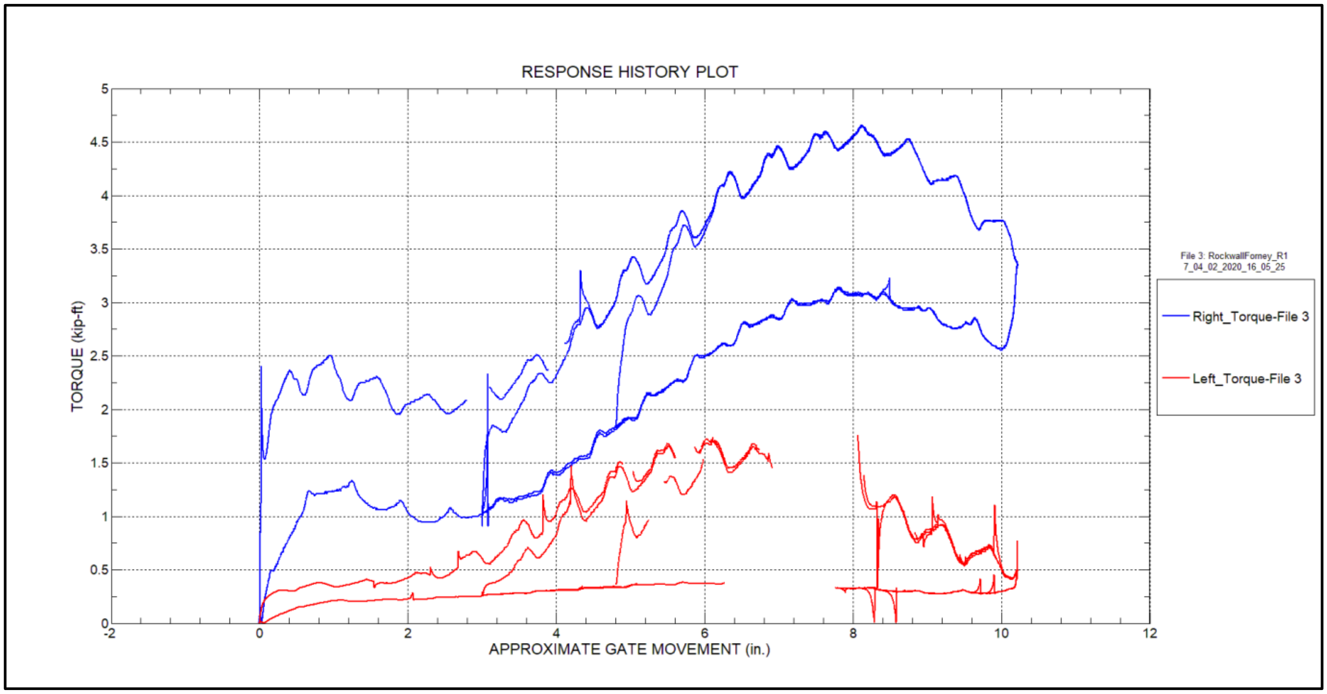

Figure 29 – Hoist torque response history – Gate 3 – Test 3

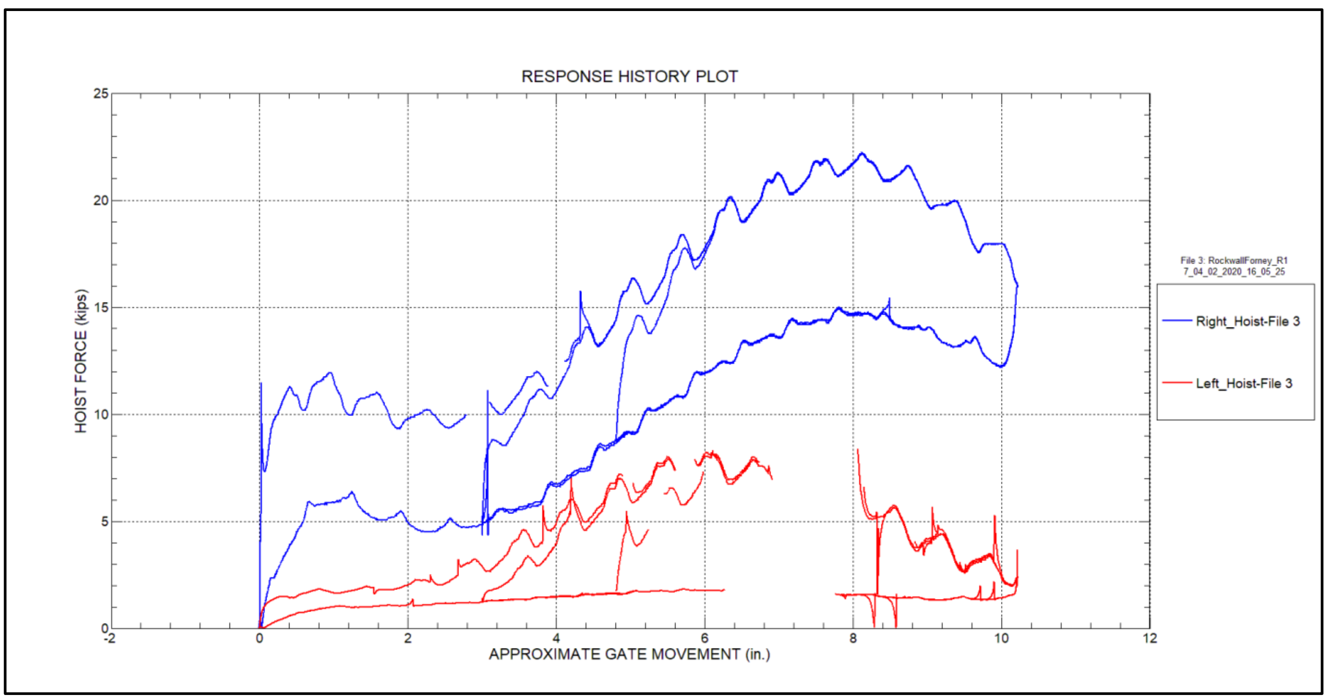

Figure 30 – Hoist force response history – Gate 3 – Test 3

APPENDIX B – GATE 3 PIN MOMENT COMPONENT PLOTS

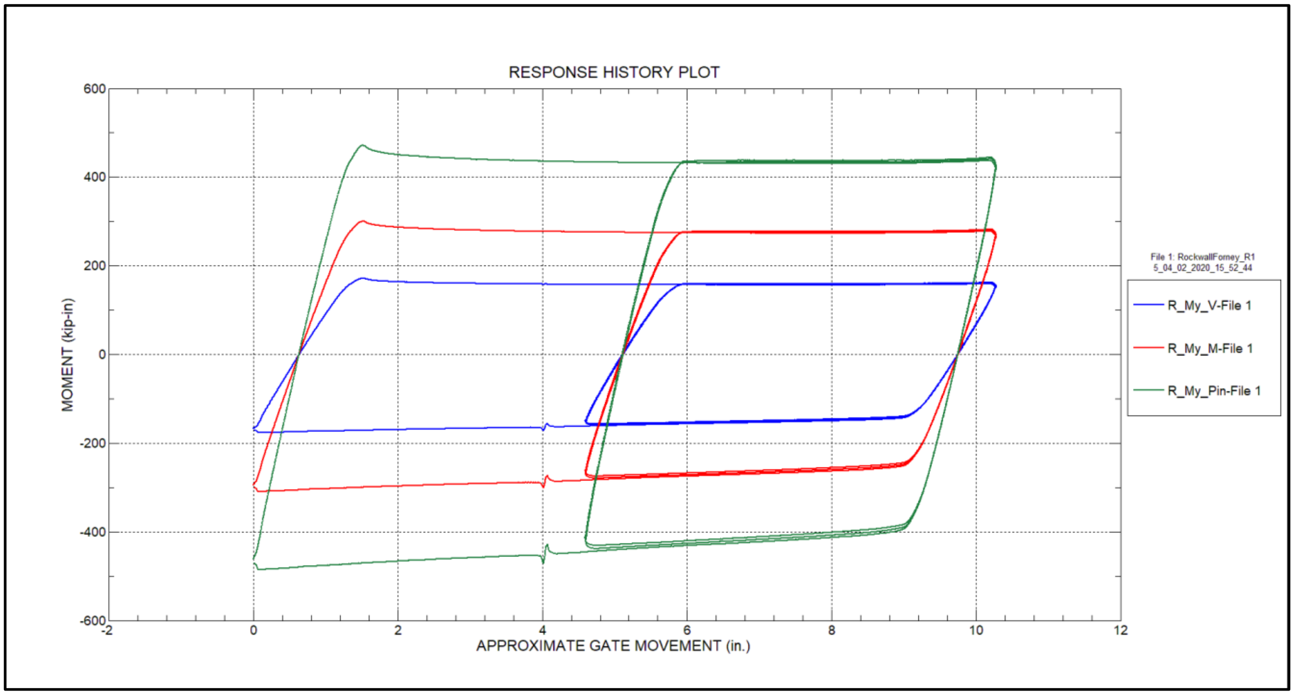

Figure 31 – Pin moment response history – Right arm – Test run 1

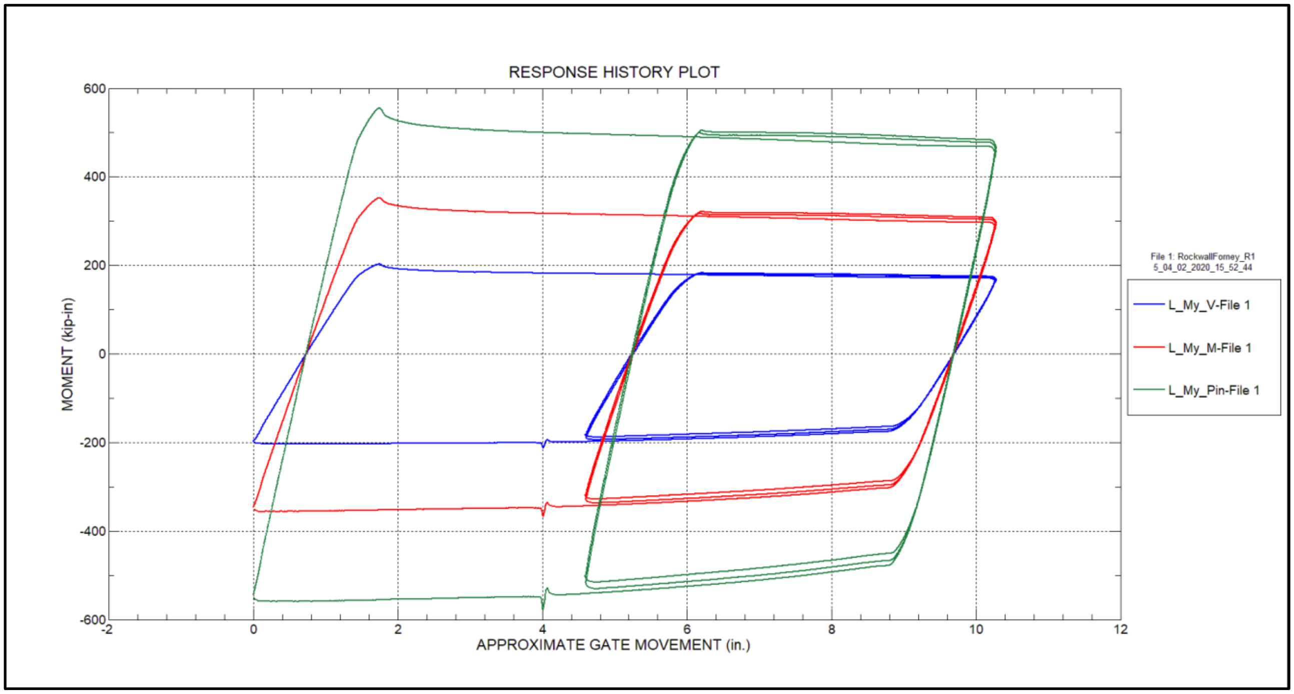

Figure 32 – Pin moment response history – Left arm – Test run 1

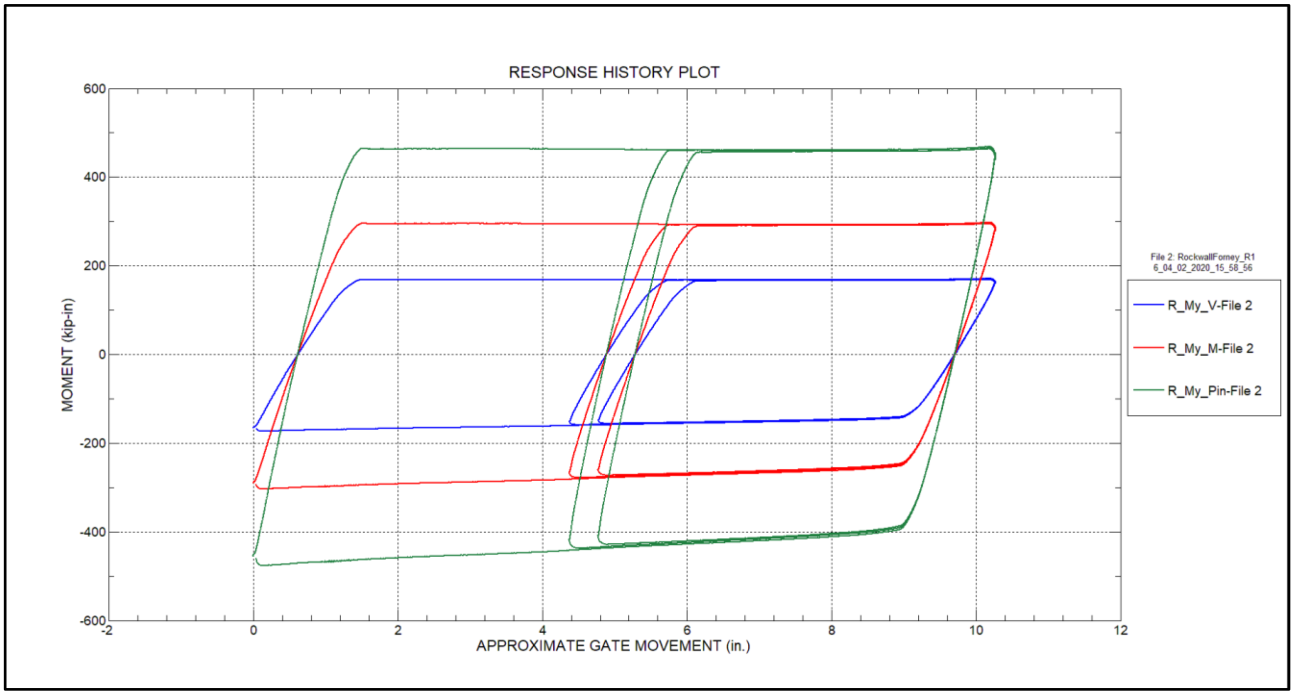

Figure 33 – Pin moment response history – Right arm – Test run 2

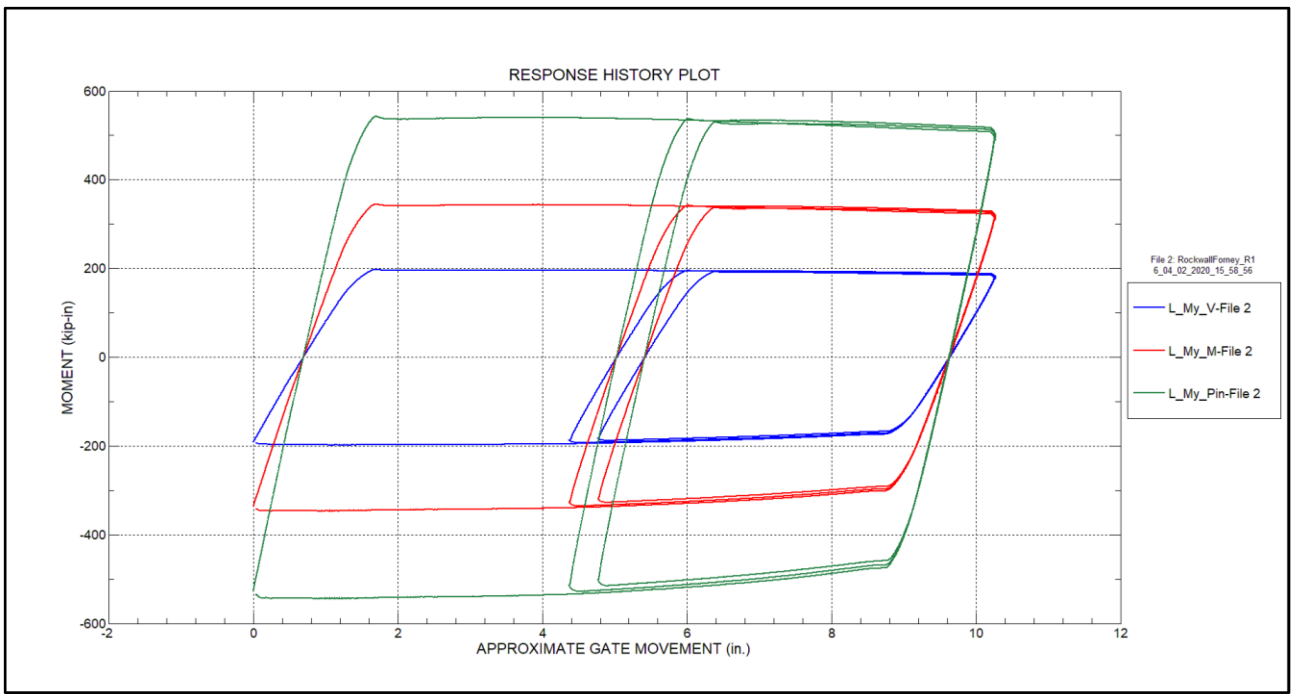

Figure 34 – Pin moment response history – Left arm – Test run 2

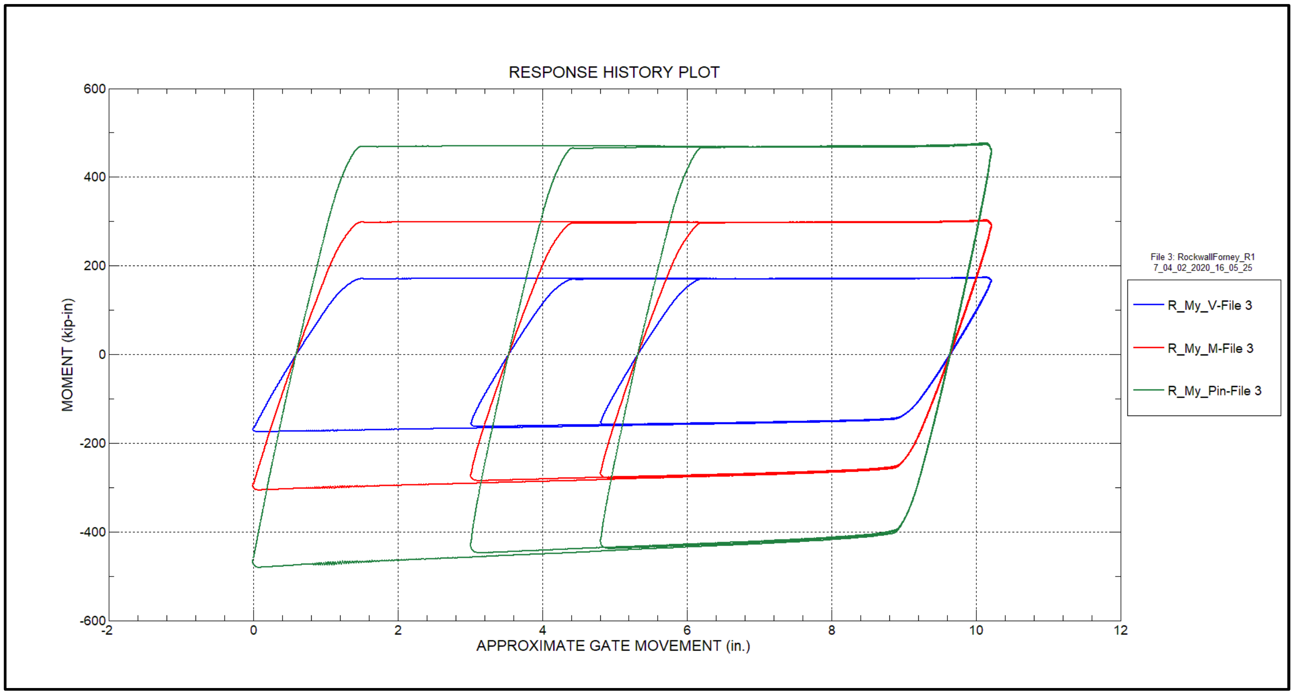

Figure 35 – Pin moment response history – Right arm – Test run 3

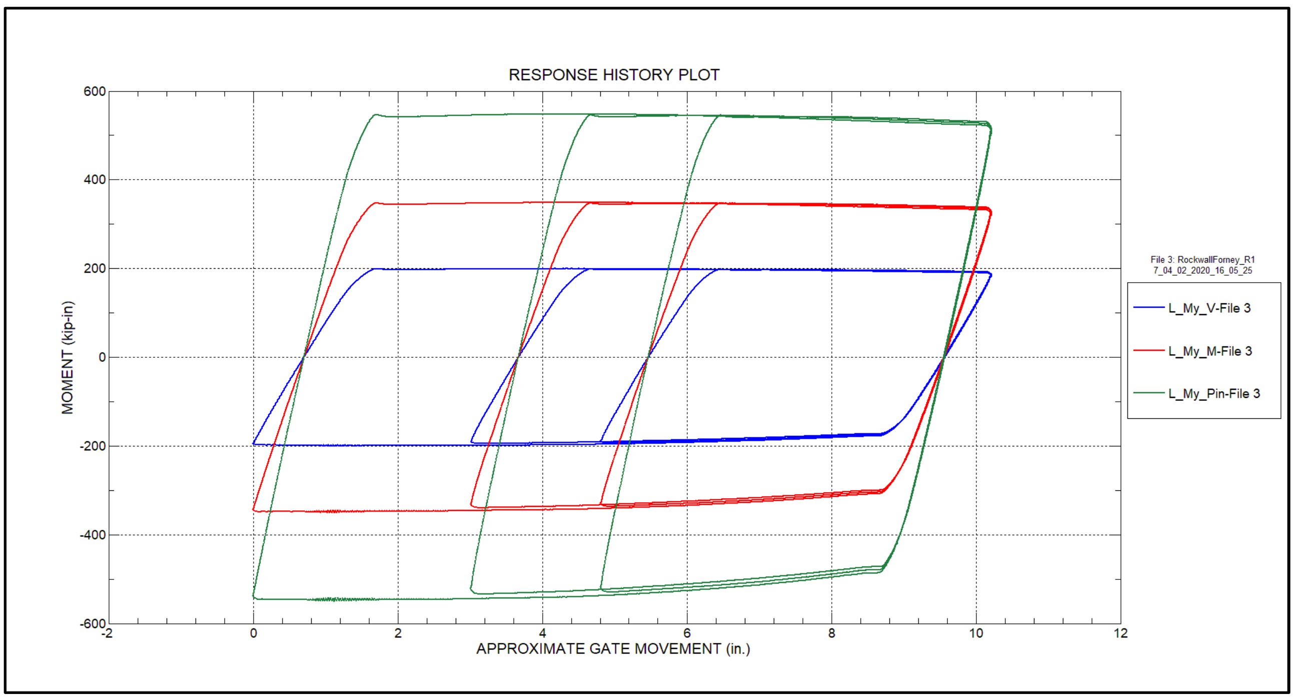

Figure 36 – Pin moment response history – Left arm – Test run 3

APPENDIX C – INSTRUMENTATION PLANS

RAW DATA. REFINED RESULTS.

SCHNABEL ENGINEERING
ROCKWALL FORNEY DAM
LIVE LOAD TESTING

RAW DATA. REFINED RESULTS.
740 S PIERCE AVE, SUITE 15
LOUISVILLE, CO 80027
303.494.3230
WWW.BDITEST.COM

ISSUE

CLIENT

SCHABEL ENGINEERING
16000 CHRISTENSEN RD, STE 101
SEATTLE, WA 98188

PROJECT NAME

SCHNABEL ENGINEERING
ROCKWALL FORNEY DAM
LIVE LOAD TESTING

Drawn By:	KNR
Checked By:	JDS
Date:	05/27/2020
Client No.:	
BDI No.:	190701-TX
SCALE:	NTS

COVER PAGE

LLT-00

The user acknowledges that these documents are instruments of professional service, and are protected by Copyright. This document and the information contained in this document are the property of Bridge Diagnostics, Inc., and shall not be reused, copied, disseminated, modified, amended or altered in any way. It is issued for information purposes only. The user agrees to hold harmless, indemnify and defend Bridge Diagnostics, Inc. against any and all damages, claims and losses, including defense costs, arising out of any use, reuse or copying of this document.

PLOT TIME: 6/12/2020 3:22 PM
FILEPATH: C:\Users\colemand\BDI\Services - Documents\Server_Remote\190701-TX_Schnabel_RockwallForneyDam\7. Instrumentation Plans\BDI_ROCKWALLFORNEY_01_GENERAL.dwg
© YYYY BRIDGE DIAGNOSTICS INC.

The user acknowledges that these documents are instruments of professional service, and are protected by Copyright. This document and the information contained in this document are the property of Bridge Diagnostics, Inc., and shall not be reused, copied, disseminated, modified, amended or altered in any way. It is issued for information purposes only. The user agrees to hold harmless, indemnify and defend Bridge Diagnostics, Inc. against any and all damages, claims and losses, including defense costs, arising out of any use, reuse or copying of this document.

GAGE LEGEND & SPECIFICATION

SYMBOL	TYPE	BRAND	MODEL	NOTES
	STRAIN TRANSDUCER	BDI	ST350	
	TILTMETER (UNI-AXIAL)	BDI	T500-030	
	TORQUE SENSOR	HPI	-	HBWS-35-125-6-0.5VR-FB
	AMP SENSOR	CR MAGNETICS	CR42105-200	

GENERAL NOTES

- INSTRUMENTATION SHALL BEGIN ON APRIL 1ST, 2020.
- GATES 1 THRU 14 SHALL BE ACCESSED USING SPRAT ROPE ACCESS TECHNIQUES.
- BDI WILL PERFORM ALL SURFACE PREPARATION, SENSOR INSTALLATION, AND EQUIPMENT INSTALLATION.
- SEE LLT-31 FOR SENSOR INSTALLATION DETAILS.
- TWO PAIRS OF TORQUE GAGES WILL BE INSTALLED ON THE GATE MOTORS' PINION SHAFTS BETWEEN THE MOTORS AND THE HOISTS.
  - GAGE PAIRS WILL BE INSTALLED 180° APART FROM EACH OTHER.
  - EXACT POSITIONS OF THE GAGE PAIRS ON THE PINION SHAFT WILL BE DETERMINED IN THE FIELD.
- THREE PHASE AMPERAGE GAGES WILL BE INSTALLED ON THE MOTOR CONTROLS BY A QUALIFIED ELECTRICIAN PROVIDED BY GARVER.

TESTING PROCEDURE:

- TESTING SHALL BE STARTED WITH THE GATE IN THE CLOSED POSITION.
- ONCE DATA COLLECTION BEGINS, THE GATE SHALL BE RAISED TO TWO OR THREE TIMES THE HEIGHT NECESSARY FOR TRUNNION FRICTION TO BE OVERCOME, H1 (TYPICALLY 6"-12"), AND HELD THERE UNTIL DATA STABILIZES.
- THE GATE SHALL BE LOWERED APPROXIMATELY TWICE THE DISTANCE TO OVERCOME TRUNNION FRICTION, H2, AND HELD THERE UNTIL DATA STABILIZES.
- THE GATE SHALL BE RAISED TO H1 AND HELD THERE UNTIL DATA STABILIZES.
- THE GATE SHALL BE LOWERED TO H2 AND HELD THERE UNTIL DATA STABILIZES.
- THE GATE SHALL BE RAISED TO H1 AND HELD THERE UNTIL DATA STABILIZES.
- THE GATE WAS LOWERED BACK TO CLOSED POSITION AND DATA COLLECTION STOPPED.
- A MINIMUM OF 3 TESTS SHALL BE PERFORMED PER GATE.

GAGE COUNT PER GATE

SENSOR LEGEND	SENSOR COUNT	CHANNEL COUNT
STRAIN TRANSDUCER	(48)	(48)
TILTMETER (UNI-AXIAL)	(4)	(4)
TORQUE SENSOR	(4)	(4)
AMP SENSOR	(3)	(3)
TOTAL	(59)	(59)

LOCATION KEY

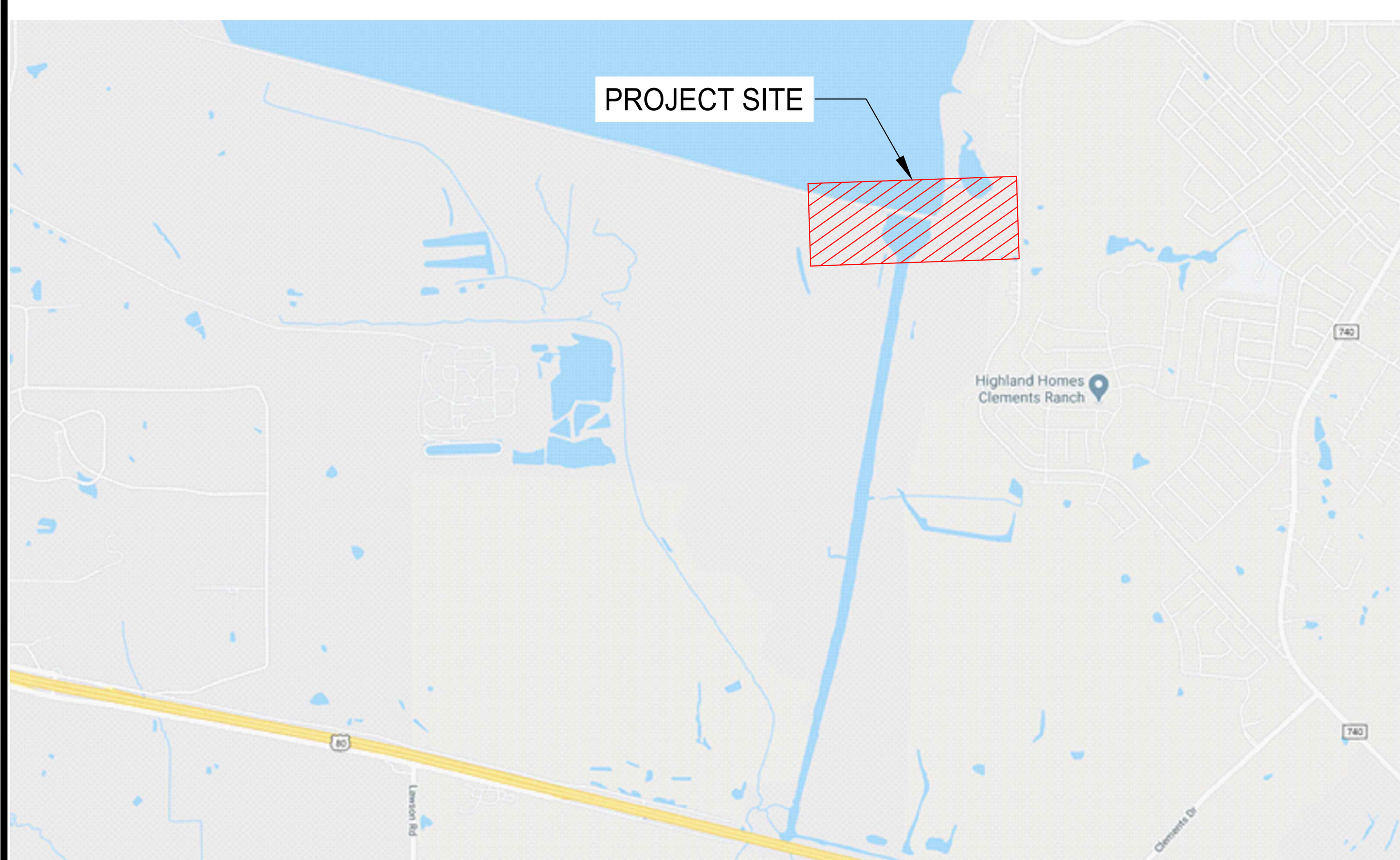

INDEX OF SHEETS

INDEX OF ISSUE

NO.	DATE	REVISION DESCRIPTION
1	3/20/2020	LIVE LOAD TESTING (LLT) INSTRUMENTATION PLAN (FOR APPROVAL)
2	5/27/2020	LIVE LOAD TESTING (LLT) INSTRUMENTATION PLAN AS BUILTS
BDI REFERENCE NUMBER: 190701-TX		

RAW DATA. REFINED RESULTS.
740 S PIERCE AVE, SUITE 15
LOUISVILLE, CO 80027
303.494.3230
WWW.BDITEST.COM

ISSUE

CLIENT

SCHABEL ENGINEERING
16000 CHRISTENSEN RD, STE 101
SEATTLE, WA 98188

PROJECT NAME

SCHABEL ENGINEERING
ROCKWALL FORNEY DAM
LIVE LOAD TESTING

Drawn By:	KNR
Checked By:	JDS
Date:	05/27/2020
Client No.:	
BDI No.:	190701-TX
SCALE:	NTS

OVERALL LEGEND

LLT-01

PLOT TIME: 6/12/2020 3:22 PM
FILEPATH: C:\Users\colemand\BDI\Services - Documents\Server_Remote\190701-TX_Schabel_RockwallForneyDam\7. Instrumentation Plans\BDI_ROCKWALLFORNEY_01_GENERAL.dwg
© YYYY BRIDGE DIAGNOSTICS INC.

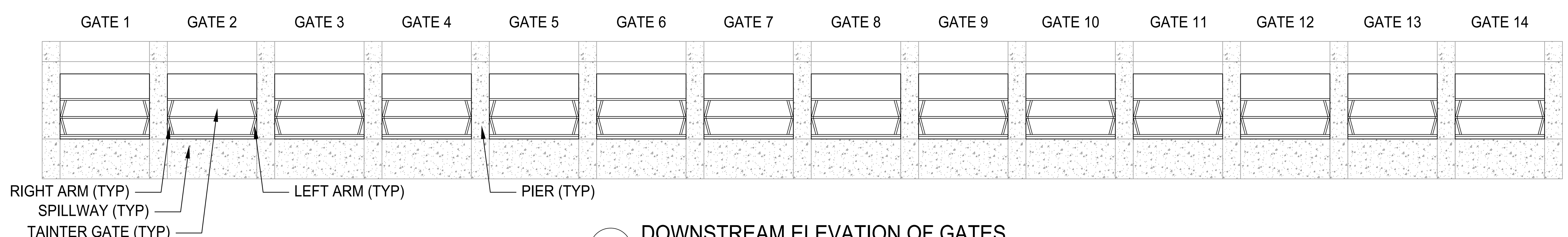

1 DOWNSTREAM ELEVATION OF GATES
LOOKING NORTH (UPSTREAM)

The user acknowledges that these documents are instruments of professional service, and are protected by Copyright. This document and the information contained in this document are the property of Bridge Diagnostics, Inc., and shall not be reused, copied, disseminated, modified, amended or altered in any way. It is issued for information purposes only. The user agrees to hold harmless, indemnify and defend Bridge Diagnostics, Inc. against any and all damages, claims and losses, including defense costs, arising out of any use, reuse or copying of this document.

PLOT TIME: 6/12/2020 3:22 PM
FILEPATH: C:\Users\colemand\BDI\Services - Documents\Server_Remote\190701-TX_Schabel_RockwallForneyDam\7. Instrumentation Plans\BDI_ROCKWALLFORNEY_01_GENERAL.dwg
© YYYY BRIDGE DIAGNOSTICS INC.

RAW DATA. REFINED RESULTS.
740 S PIERCE AVE, SUITE 15
LOUISVILLE, CO 80027
303.494.3230
WWW.BDITEST.COM

ISSUE

CLIENT

SCHABEL ENGINEERING
16000 CHRISTENSEN RD, STE 101
SEATTLE, WA 98188

PROJECT NAME

SCHNABEL ENGINEERING
ROCKWALL FORNEY DAM
LIVE LOAD TESTING

Drawn By:	KNR
Checked By:	JDS
Date:	05/27/2020
Client No.:	
BDI No.:	190701-TX
SCALE:	NTS

OVERALL STRUCTURE LAYOUT
LLT-02

The user acknowledges that these documents are instruments of professional service, and are protected by Copyright. This document and the information contained in this document are the property of Bridge Diagnostics, Inc., and shall not be reused, copied, disseminated, modified, amended or altered in any way. It is issued for information purposes only. The user agrees to hold harmless, indemnify and defend Bridge Diagnostics, Inc. against any and all damages, claims and losses, including defense costs, arising out of any use, reuse or copying of this document.

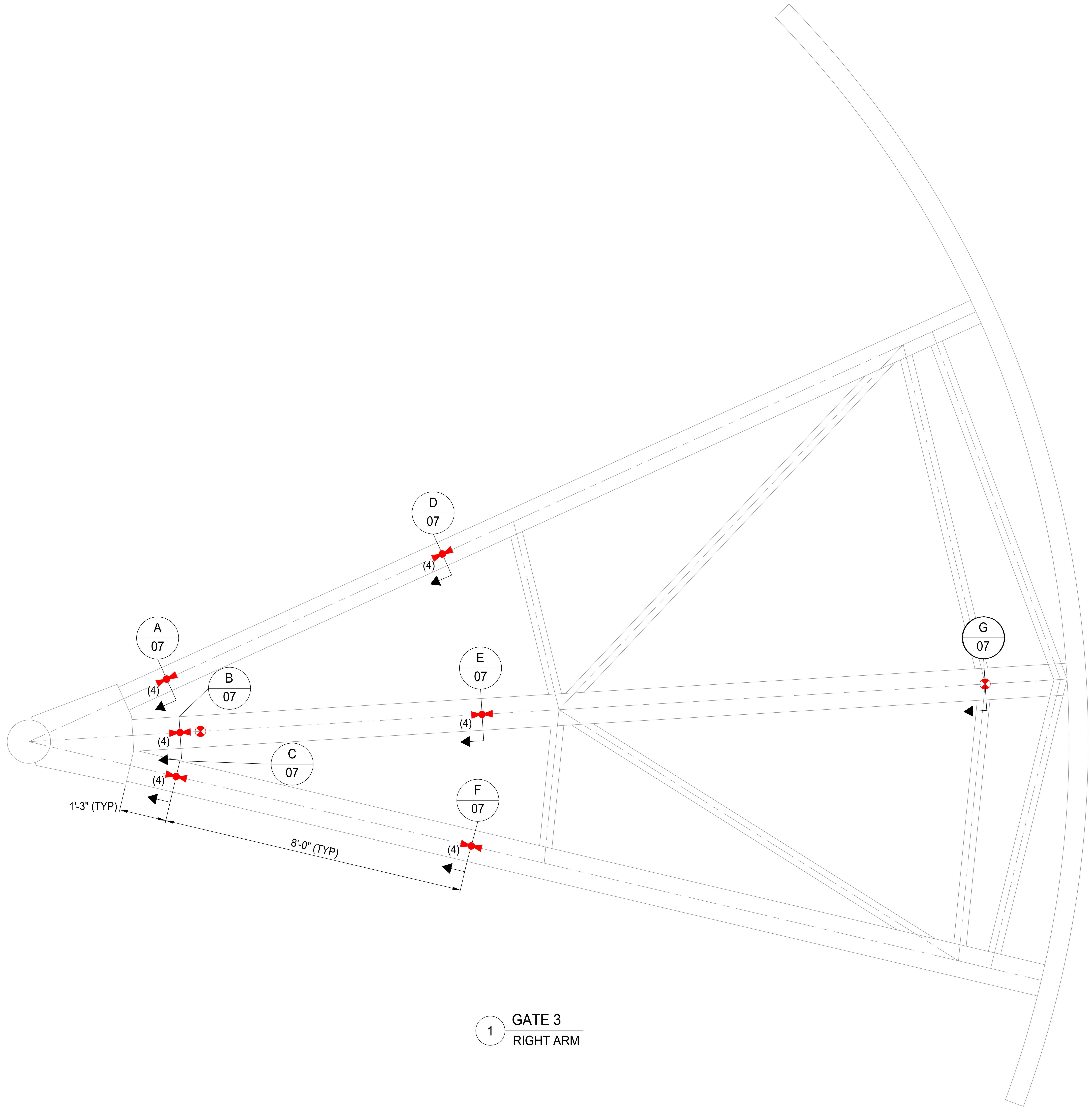

1 GATE 3
RIGHT ARM

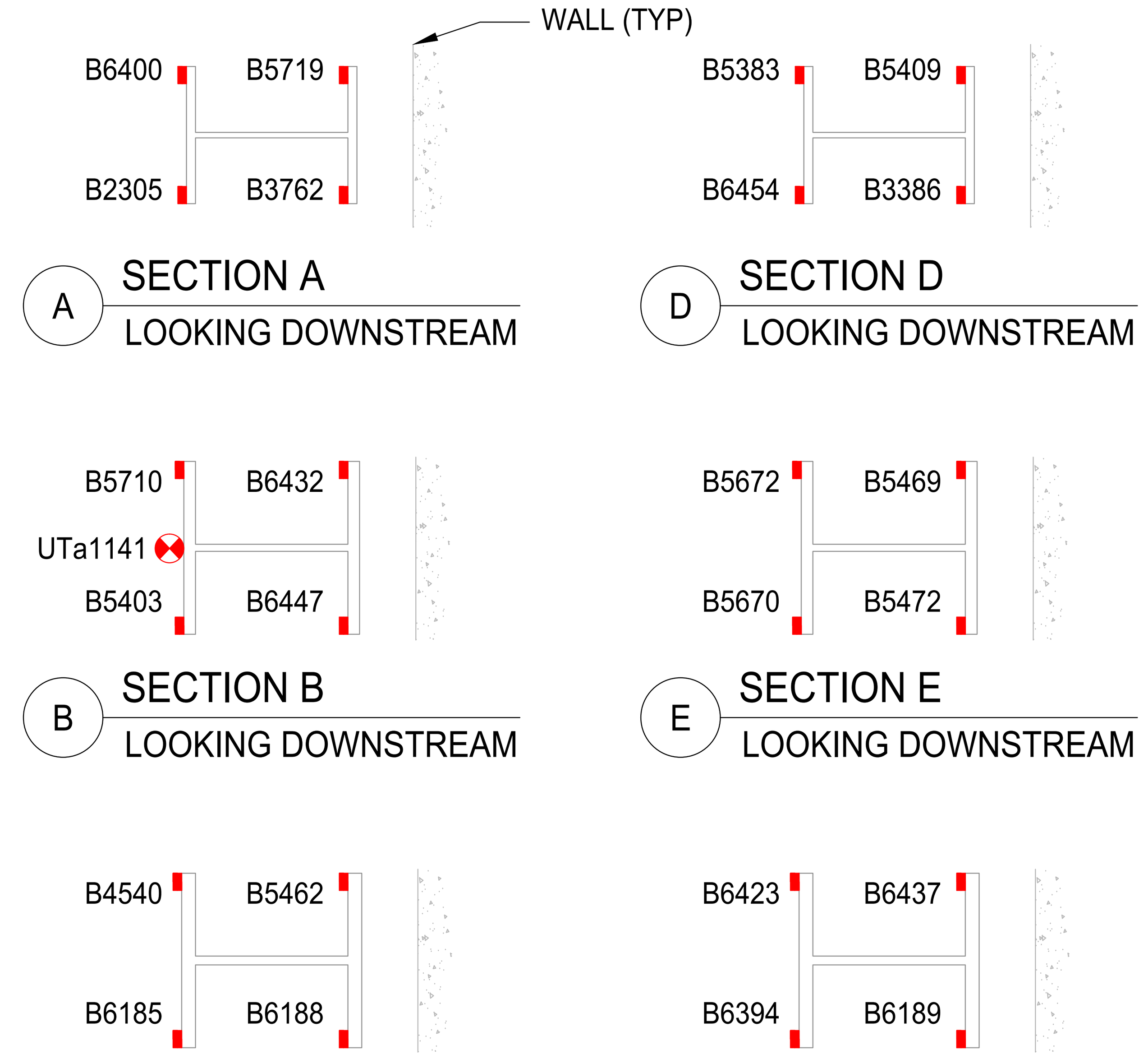

A SECTION A
LOOKING DOWNSTREAM

D SECTION D
LOOKING DOWNSTREAM

B SECTION B
LOOKING DOWNSTREAM

E SECTION E
LOOKING DOWNSTREAM

C SECTION C
LOOKING DOWNSTREAM

F SECTION F
LOOKING DOWNSTREAM

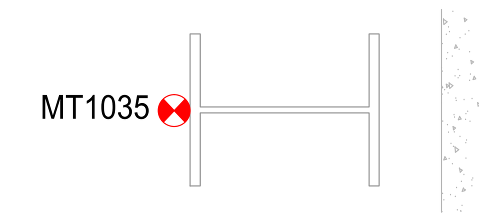

G SECTION G
LOOKING DOWNSTREAM

UNIT ID
TT-3

TORQUE GAGES
RIGHT ARM

NOTES:

1. SECTIONS A, B, & C SHALL BE INSTALLED 15 INCHES AWAY FROM TRUNNION PLATE.
2. TILTMETERS SHALL BE INSTALLED CENTERED ON THE MIDDLE STRUT FLANGE.
3. SECTION G'S TILTMETER SHALL BE INSTALLED AS CLOSE TO THE SKINPLATE AS POSSIBLE.

SENSOR LEGEND

- STRAIN TRANSDUCER
- TILTMETER (UNI-AXIAL)
- TORQUE SENSOR

BDI
RAW DATA. REFINED RESULTS.
740 S PIERCE AVE, SUITE 15
LOUISVILLE, CO 80027
303.494.3230
WWW.BDITEST.COM

ISSUE

CLIENT

SCHABEL ENGINEERING
16000 CHRISTENSEN RD, STE 101
SEATTLE, WA 98188

PROJECT NAME

SCHABEL ENGINEERING
ROCKWALL FORNEY DAM
LIVE LOAD TESTING

Drawn By:	KNR
Checked By:	JDS
Date:	05/27/2020
Client No.:	
BDI No.:	190701-TX
SCALE:	NTS

GATE 3 - RIGHT ARM
ELEVATION

LLT-07

PLOT TIME: 6/12/2020 3:22 PM
FILEPATH: C:\Users\colemand\BDI\Services - Documents\Server_Remote\190701-TX_Schabel_RockwallForneyDam\7. Instrumentation Plans\BDI_ROCKWALLFORNEY_01_GENERAL.dwg
© YYYY BRIDGE DIAGNOSTICS INC.

The user acknowledges that these documents are instruments of professional service, and are protected by Copyright. This document and the information contained in this document are the property of Bridge Diagnostics, Inc., and shall not be reused, copied, disseminated, modified, amended or altered in any way. It is issued for information purposes only. The user agrees to hold harmless, indemnify and defend Bridge Diagnostics, Inc. against any and all damages, claims and losses, including defense costs, arising out of any use, reuse or copying of this document.

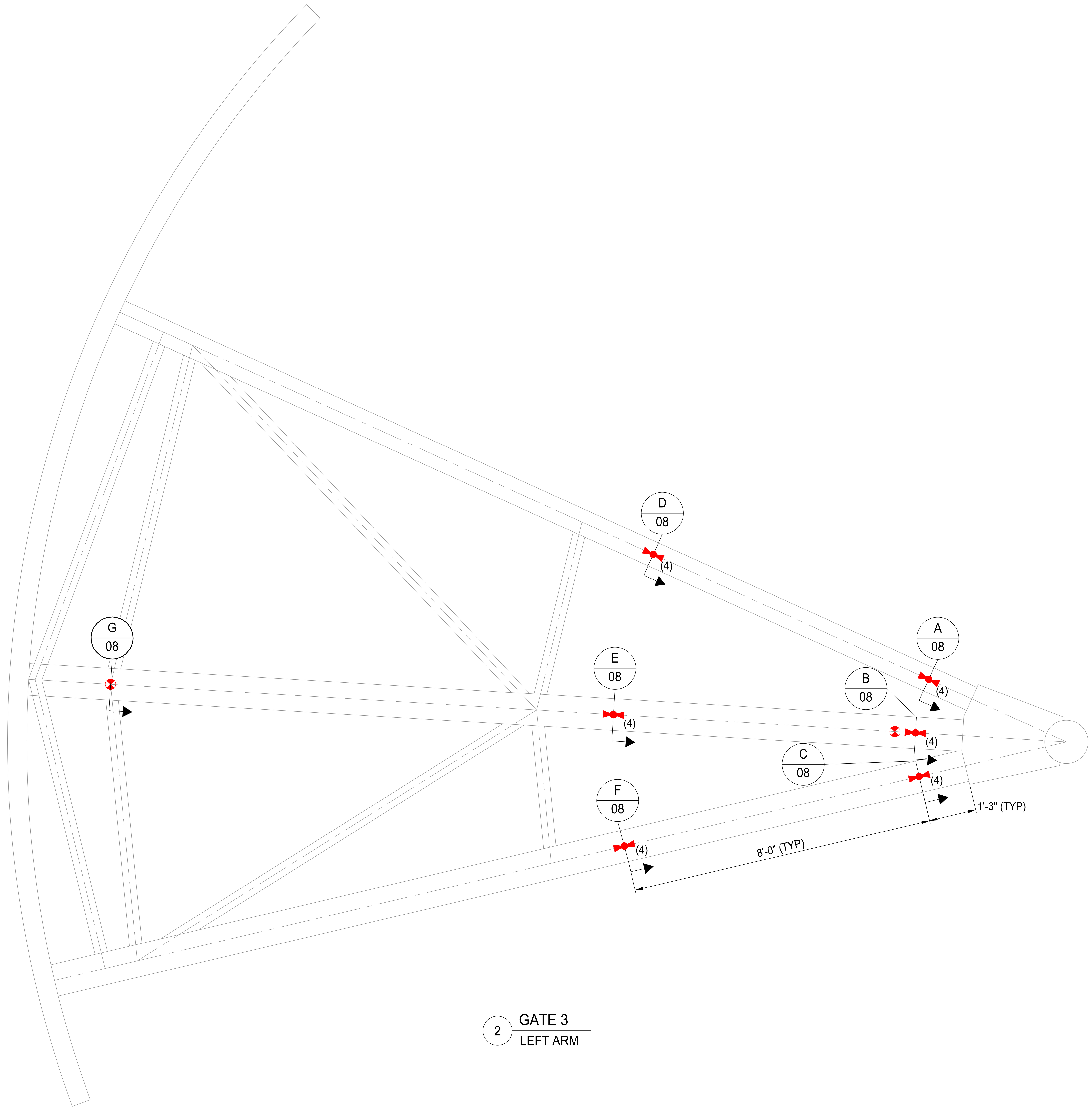

2 GATE 3
LEFT ARM

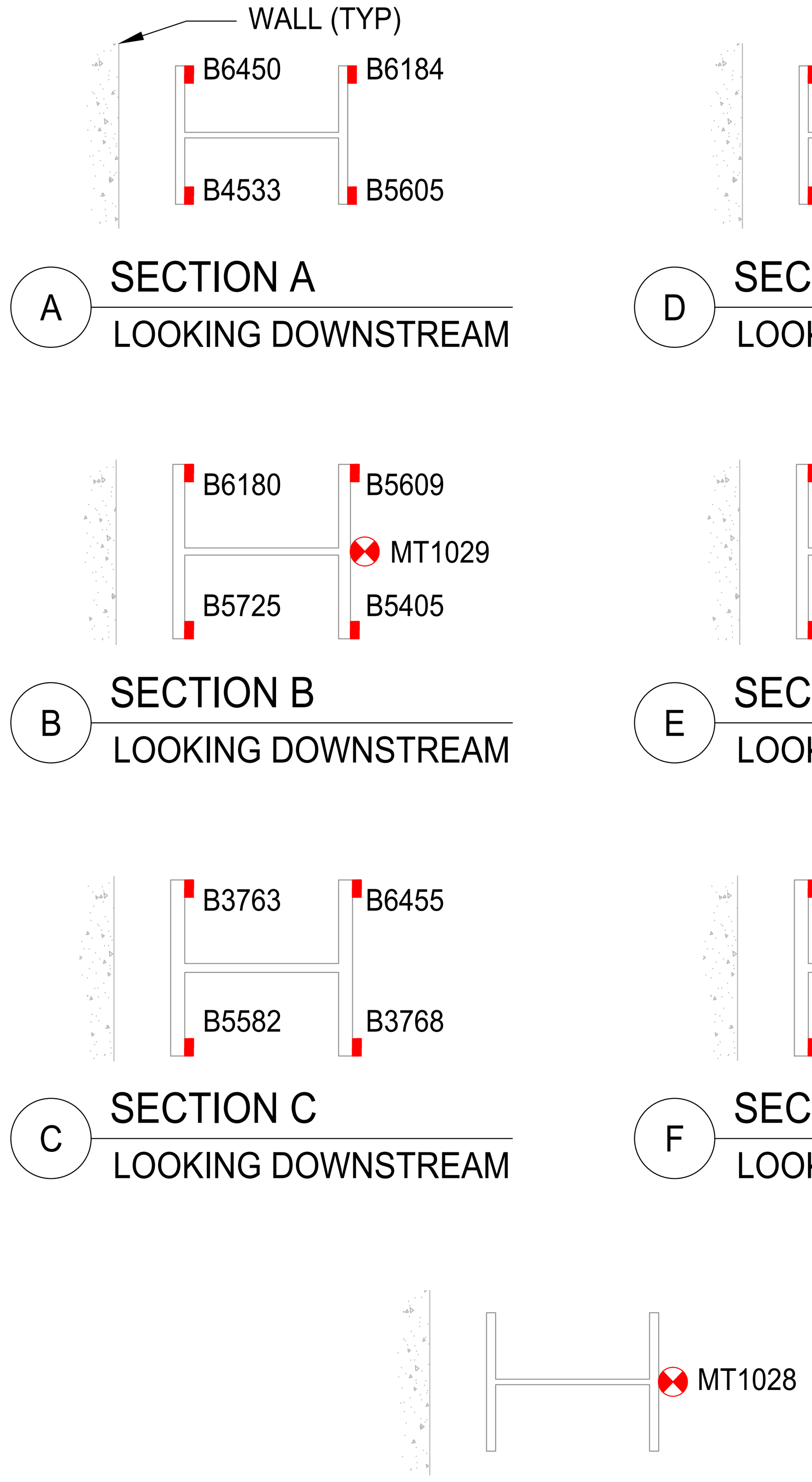

A SECTION A
LOOKING DOWNSTREAM

D SECTION D
LOOKING DOWNSTREAM

B SECTION B
LOOKING DOWNSTREAM

E SECTION E
LOOKING DOWNSTREAM

C SECTION C
LOOKING DOWNSTREAM

F SECTION F
LOOKING DOWNSTREAM

G SECTION G
LOOKING DOWNSTREAM

UNIT ID
TT-2

TORQUE GAGES
LEFT ARM

NOTES:

1. SECTIONS A, B, & C SHALL BE INSTALLED 15 INCHES AWAY FROM TRUNNION PLATE.
2. TILTMETERS SHALL BE INSTALLED CENTERED ON THE MIDDLE STRUT FLANGE.
3. SECTION G'S TILTMETER SHALL BE INSTALLED AS CLOSE TO THE SKINPLATE AS POSSIBLE.

SENSOR LEGEND

- STRAIN TRANSDUCER
- TILTMETER (UNI-AXIAL)
- TORQUE SENSOR

BDI
RAW DATA. REFINED RESULTS.
740 S PIERCE AVE, SUITE 15
LOUISVILLE, CO 80027
303.494.3230
WWW.BDITEST.COM

ISSUE

CLIENT

SCHABEL ENGINEERING
16000 CHRISTENSEN RD, STE 101
SEATTLE, WA 98188

PROJECT NAME

SCHABEL ENGINEERING
ROCKWALL FORNEY DAM
LIVE LOAD TESTING

Drawn By:	KNR
Checked By:	JDS
Date:	05/27/2020
Client No.:	
BDI No.:	190701-TX
SCALE:	NTS

GATE 3 - LEFT ARM
ELEVATION
LLT-08

PLOT TIME: 6/12/2020 3:22 PM
FILEPATH: C:\Users\colemand\BDI\Services - Documents\Server_Remote\190701-TX_Schabel_RockwallForneyDam\7. Instrumentation Plans\BDI_ROCKWALLFORNEY_01_GENERAL.dwg
© YYYY BRIDGE DIAGNOSTICS INC.

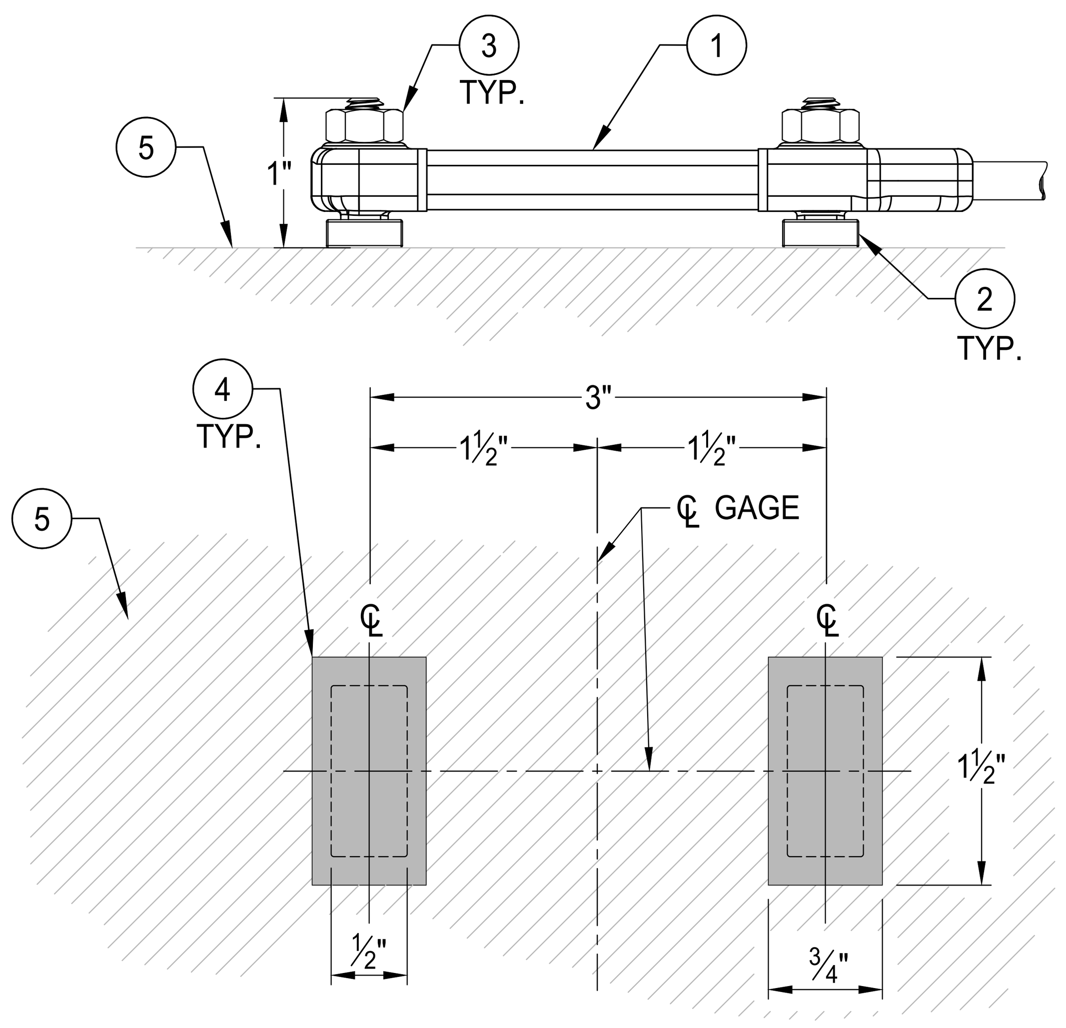

COMPONENT DESCRIPTION

1. ST350 STRAIN GAGE
2. 1/4"-20 THREADED MOUNTING TAB
3. 1/4"-20 STAINLESS STEEL NUT
4. TYPICAL SURFACE PREP REQUIRED TO MOUNT STRAIN GAGES
5. TYPICAL MOUNTING SURFACE

FOOTNOTES - INSTANT ADHESIVE
1. STRAIN GAGES SHALL BE MOUNTED WITH LOCTITE 410 INSTANT ADHESIVE AND LOCTITE 7452 ACCELERANT 2. DURING SURFACE PREP ALL PAINT AND SURFACE DEFORMATIONS MUST BE REMOVED. 3. SURFACE PREP IS REQUIRED JUST PRIOR TO GAGE INSTALLATION AS TO NOT ALLOW SURFACE CONTAMINANTS TO ACCUMULATE.

1 TYPICAL ST350 STRAIN GAGE INSTALLATION

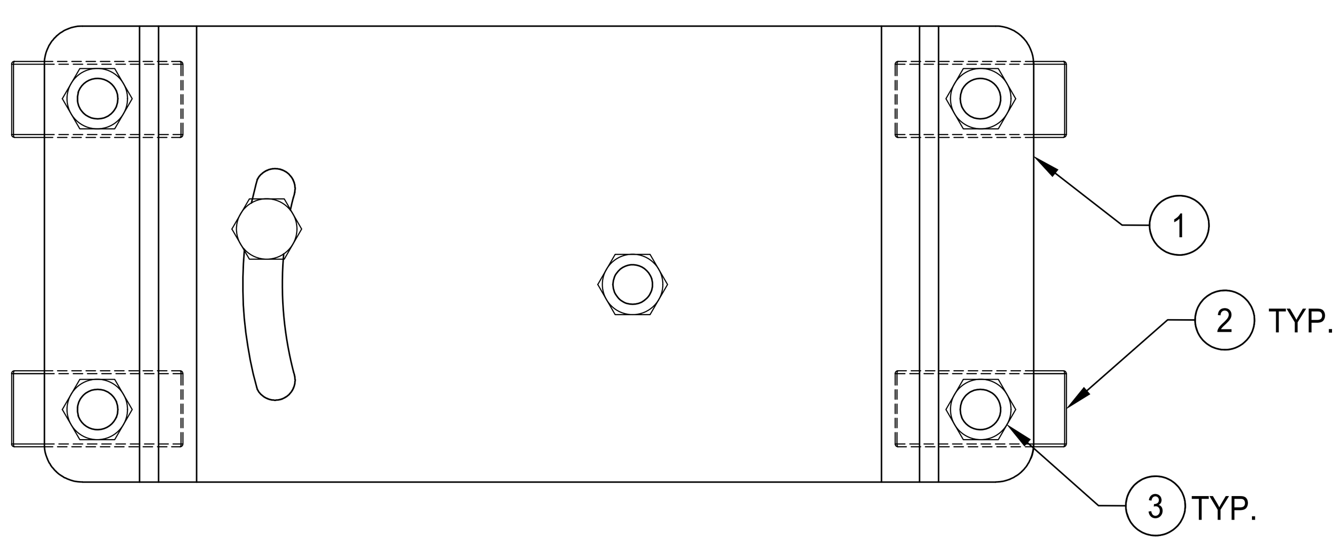

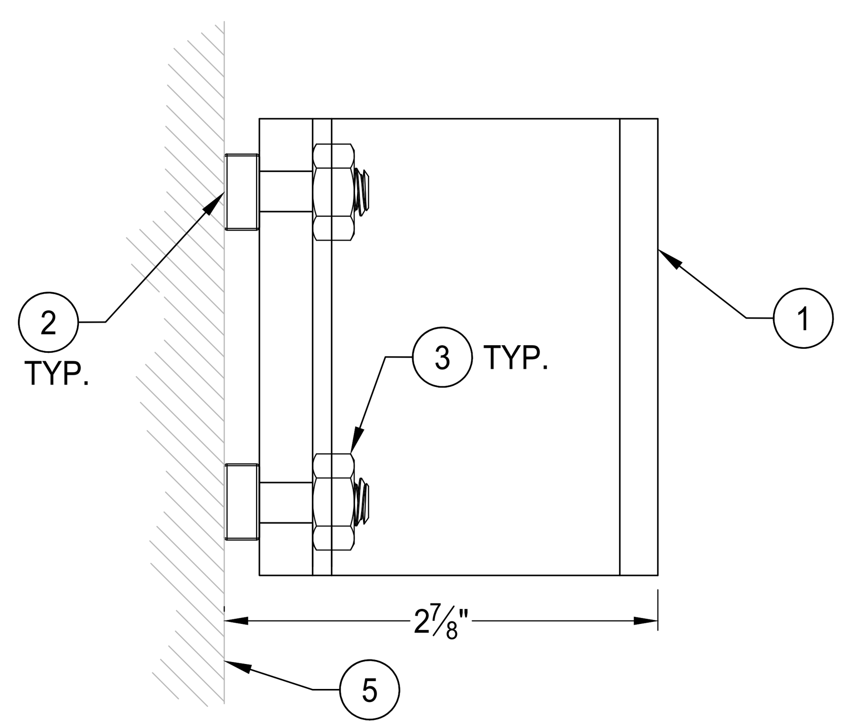

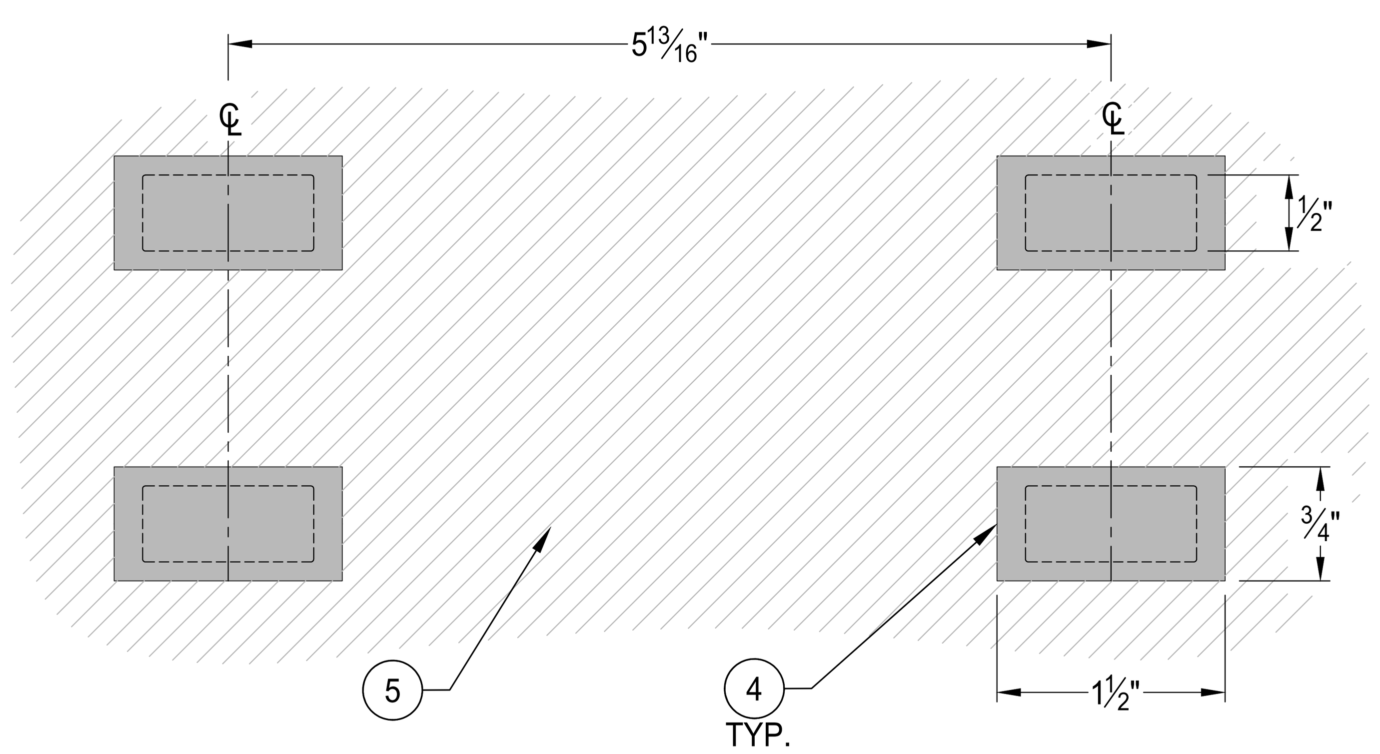

COMPONENT DESCRIPTION

1. BDI +/- 15 DEGREE TILTMETER WITH COVER AND ADJUSTMENT BOLTS
2. 1/4"-20 THREADED MOUNTING TAB
3. 1/4"-20 STAINLESS STEEL NUT
4. TYPICAL SURFACE PREP REQUIRED TO MOUNT TILTMETERS
5. TYPICAL MOUNTING SURFACE

FOOTNOTES - INSTANT ADHESIVE
1. TILTMETERS SHALL BE MOUNTED WITH LOCTITE 410 INSTANT ADHESIVE AND LOCTITE 7452 ACCELERANT 2. DURING SURFACE PREP ALL PAINT AND SURFACE DEFORMATIONS MUST BE REMOVED. 3. SURFACE PREP IS REQUIRED JUST PRIOR TO GAGE INSTALLATION AS TO NOT ALLOW SURFACE CONTAMINANTS TO ACCUMULATE.

2 TYPICAL BDI TILTMETER INSTALLATION

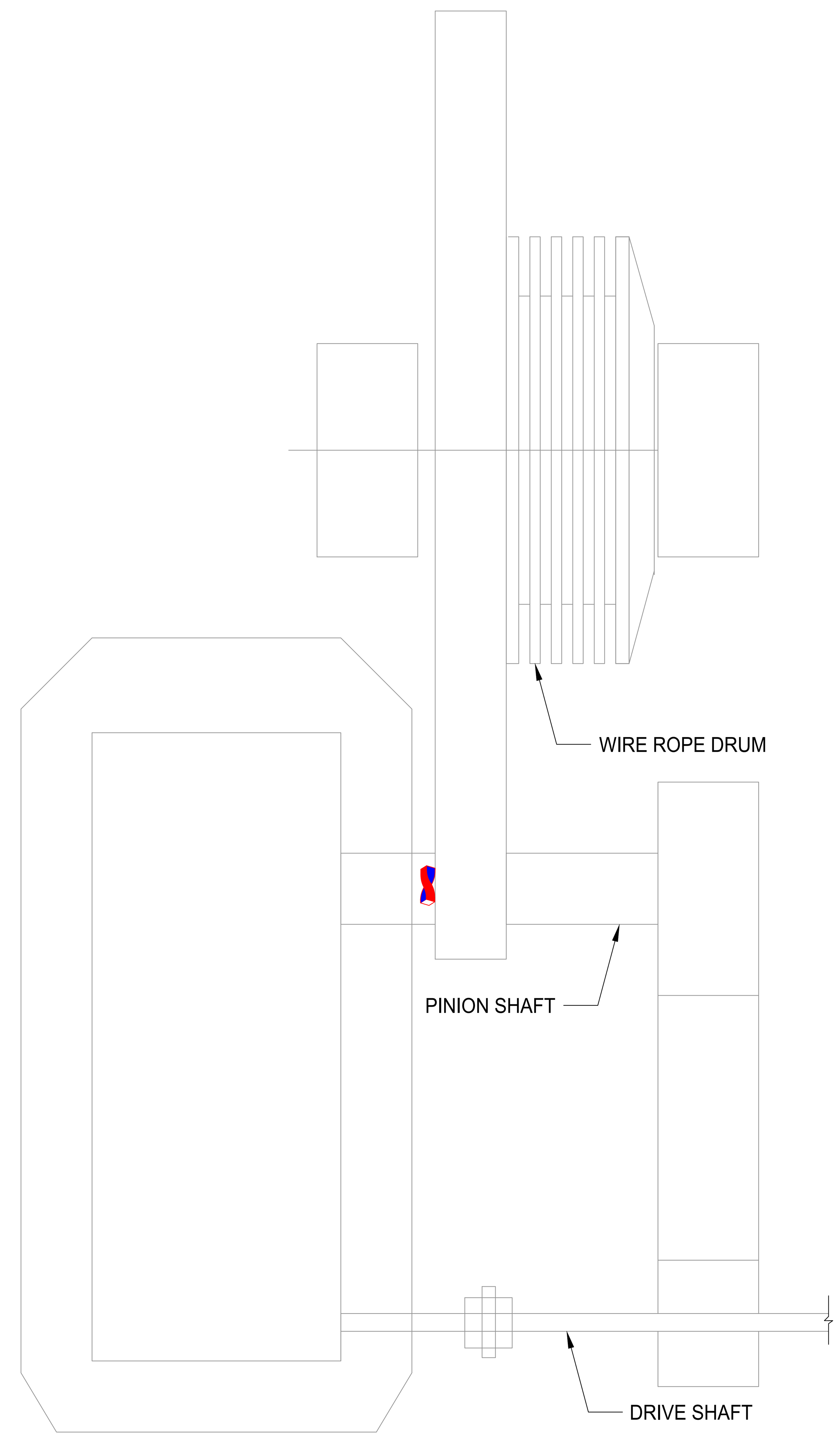

3 TYPICAL HOIST INSTRUMENTATION

TORQUE SENSOR INSTALLATION NOTES:

- TORQUE GAGES WILL BE INSTALLED ON THE PINION SHAFT ON EITHER HOIST MOTOR BETWEEN THE MOTOR AND THE HOIST DRUM
- EXACT POSITIONS OF THE GAGE PAIRS ON THE PINION SHAFT WILL BE DETERMINED IN THE FIELD

SENSOR LEGEND

TORQUE SENSOR

BDI
RAW DATA. REFINED RESULTS.
740 S PIERCE AVE, SUITE 15
LOUISVILLE, CO 80027
303.494.3230
WWW.BDITEST.COM

ISSUE

CLIENT

SCHABEL ENGINEERING
16000 CHRISTENSEN RD, STE 101
SEATTLE, WA 98188

PROJECT NAME

SCHNABEL ENGINEERING
ROCKWALL FORNEY DAM
LIVE LOAD TESTING

Drawn By:	KNR
Checked By:	JDS
Date:	05/27/2020
Client No.:	
BDI No.:	190701-TX
SCALE:	NTS

SENSOR INSTALLATION DETAILS

LLT-31

The user acknowledges that these documents are instruments of professional service, and are protected by Copyright. This document and the information contained in this document are the property of Bridge Diagnostics, Inc., and shall not be reused, copied, disseminated, modified, amended or altered in any way. It is issued for information purposes only. The user agrees to hold harmless, indemnify and defend Bridge Diagnostics, Inc. against any and all damages, claims and losses, including defense costs, arising out of any use, reuse or copying of this document.

PLOT TIME: 6/12/2020 3:24 PM
FILEPATH: C:\Users\colemand\BDI\Services - Documents\Server_Remote\190701-TX_Schnabel_RockwallForneyDam\7. Instrumentation Plans\BDI_ROCKWALLFORNEY_01_GENERAL.dwg
© YYYY BRIDGE DIAGNOSTICS INC.

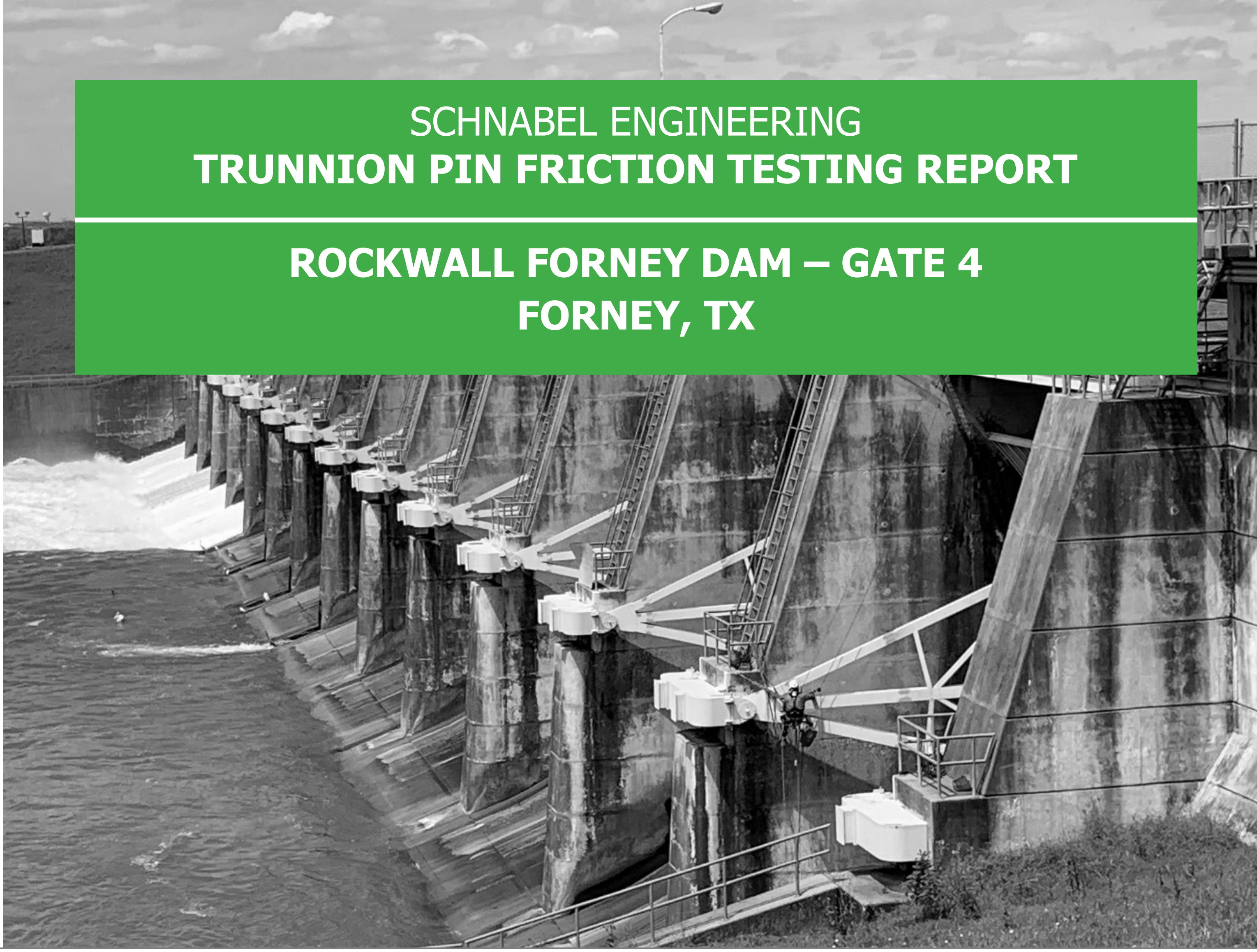

SCHNABEL ENGINEERING
TRUNNION PIN FRICTION TESTING REPORT

ROCKWALL FORNEY DAM – GATE 4
FORNEY, TX

SUBMITTED TO:
SCHNABEL ENGINEERING
16000 CHRISTENSEN RD, SUITE 101
SEATTLE, WA 98188

SUBMITTED BY:
BDI – CO
740 SOUTH PIERCE AVE, UNIT 15
LOUISVILLE, CO 80027

BDI Project No.: **190701-TX**
Report Version: **V1**
Version Submitted: **August 03, 2020**

RAW DATA. REFINED RESULTS.

This document contains Confidential Information and is submitted in confidence to the customer. The submission of the information contained herein shall not be deemed to constitute public disclosure or authorization for disclosure to other parties. BDI's information and name may not be used in advertising or for promotional purposes without BDI's written consent.

TABLE OF CONTENTS

LIST OF FIGURES

LIST OF TABLES

EXECUTIVE SUMMARY

Schnabel Engineering contracted BDI to provide instrumentation and testing services on Gates 1-14 on the Rockwall Forney Dam near Dallas, Texas. The goal of these tests was to record each gate's structural responses during a series of spill tests and use the data to compute accurate coefficients of friction for each trunnion pin, cable lift force, total gate friction, and motor amperage. This report provides details on the work performed on Gate 4.

Instrumentation and testing were performed on Gate 4 at the Rockwall Forney Dam on April 5th, 2020. The gate arms were instrumented with strain and rotation sensors. The hoist motors' pinion shafts were instrumented with torque sensors and the hoist motor controls were instrumented with amperage sensors. Following the instrumentation, a series of spill tests were performed to measure the structural responses resulting from trunnion pin friction. All instrumentation setup and removal were performed using BDI's rope access team.

Following demobilization from the field, the test data was examined for quality and then further processed to evaluate the gate's performance. Strain measurements were converted into bending forces which were then applied to pin-strut free-body diagrams. By summing forces at each pin, friction induced moments could be computed, allowing accurate friction coefficients to be determined. Generally, the observed gate behavior showed that Gate 4 was operating as expected and in a symmetric manner.

The resulting maximum trunnion friction coefficients and corresponding hoist forces are shown in Table 1.

Table 1 – Gate 4 performance summary

Pin Designation	Maximum Friction Coefficient	Maximum Pin Moment due to Pin Friction (kip-In)	Maximum Hoist Force (kips)	Maximum Hoist Force due to Total Gate Friction (kips)
Right Pin	0.17	462.0	29.46	3.47
Left Pin	0.18	487.5	26.06	3.60

Note: Pin designations are in reference to looking downstream

Due to restrictions caused by the hoist limit switches, the hoist cables could not always be fully slacked at the beginning and end of the performed tests. Throughout testing of the Rockwell Forney gates, it was found that this limit switch restriction varied gate to gate and arm to arm. Therefore, it is not recommended to use the collected hoist force data to quantify overall hoist forces during gate operation. Rather, this hoist data can be better utilized to evaluate total friction behavior.

Amperage responses were not used to compute friction results and were collected as verification that the motor performance was not causing unexpected gate responses. These responses indicated the motor was functioning in a stable manner and should be reviewed by a licensed electrician to further evaluate the motor's performance.

All results and recommendations provided in this report were based on the structure in its current condition; therefore, any significant changes in condition must be noted as they may alter their validity. Questions regarding this report and/or data should be directed to Kyle Ramer (kyler@bditest.com) at BDI. For further information on BDI's equipment, services, and analysis methods please visit www.bditest.com

INSTRUMENTATION AND LOAD TESTING PROCEDURE

GATE INSTRUMENTATION SUMMARY

Instrumentation and testing were performed on Gate 4 at the Rockwall Forney Dam on April 5th, 2020. Instrumentation plans have been provided along with this report and include the following number of instrumented locations and sensor types:

+ **REUSABLE SURFACE MOUNTED STRAIN TRANSDUCERS:** Each gate arm was instrumented with a total of 24 strain transducers at 6 locations on each of the gate arms (48 strain sensors total). A typical strain gage installation is shown in Figure 1. Note these sensors were installed with the mounting tabs on the extreme fiber of the strut flanges, which puts the center of the gage approximately 0.66” from the extreme fiber.
+ **TILTMETER ROTATION SENSORS:** MEMS style rotation sensors were located on the middle strut of the gate arm near the skin plate and near the trunnion hub (4 rotation sensors total). The rotation responses were used to calculate vertical skin plate movement and measure pin rotation relative to skin plate rotation. Typical tiltmeter installations are shown in Figure 1 and Figure 2.
+ **TORQUE SENSORS:** Two total torque sensors were installed on the hoist’s pinion shafts (QTY1 on each hoist pinion shaft) near the cable hoist motor to measure direct torque and in turn lift force (See Figure 3).
+ **AMPERAGE SENSORS:** 3 Hall-Effect amperage transducers were clamped over each phase of the hoist motor to measure the motor's current draw (See Figure 4). The purpose of these sensors was to provide additional data in case there were any issues with the hoist systems and to verify any data issues related to lifting and lowering the gates.
+ **BDI'S STS-4 WIRELESS DATA ACQUISITION SYSTEM:** BDI's STS-4 wireless data acquisition (DAQ) was used to collect and record data during testing. A group of sensors were wired to each nodal DAQ which then communicated wirelessly back to the wireless base station and was controlled by BDI's STS-Live testing software.

Complete specifications are available upon request and can be found at http://www.bditest.com.

SENSOR INSTALLATION

BDI strain transducers were installed by first sanding paint off the struts to expose bare metal at two small locations (1”x2” areas) for the sensor’s mounting tabs. Each transducer was then attached using a combination of fast-setting adhesive and accelerator and applying pressure until the adhesive was fully cured. Each strain transducer took approximately five minutes to attach.

Tiltmeters were installed using the same adhesive process as the strain transducers. However, no surface preparation was necessary.

Torque sensors were installed on the pinion shafts by capacitive discharge bonding. Properly bonding to the shaft required sanding the surface to a smooth finish, clean of any paint or grease. Responses from these gages were measured using Binsfeld Torque Trak 10k wireless transmitters.

A typical installation has been shown in Figure 1 through Figure 4. Access to all the sensor locations was provided by BDI’s own SPRAT certified rope access technicians and engineers as shown in Figure 5.

Once testing was completed, sensors were removed, and exposed steel areas were covered using cold galvanizing compound.

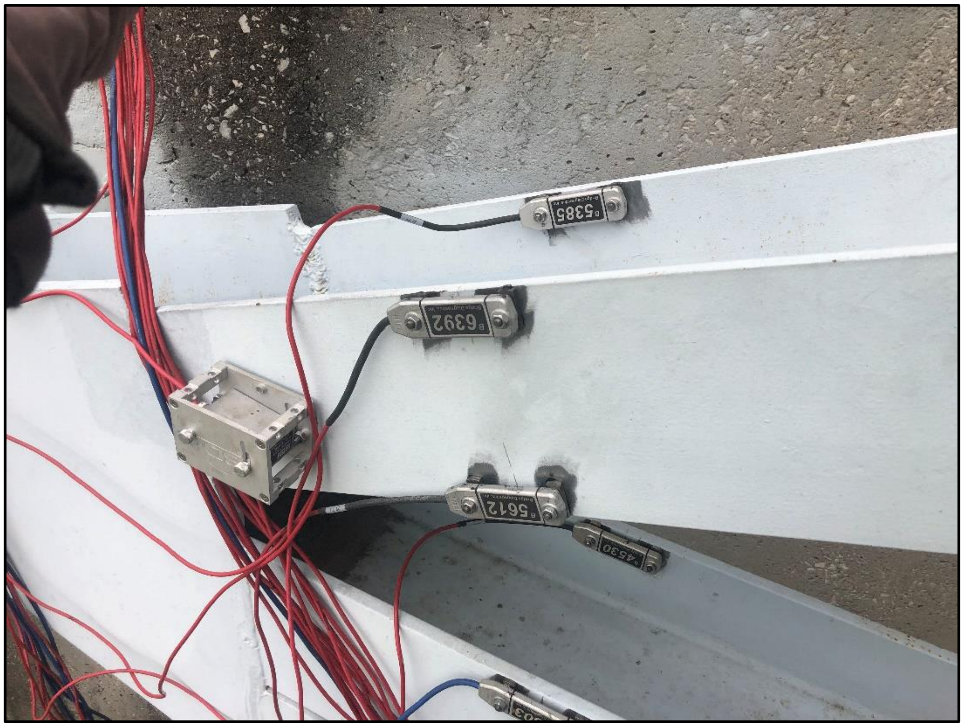

Figure 1 – BDI tiltmeter rotation sensor and reusable strain transducers installed near trunnion hub (Typical)

Figure 2 – BDI tiltmeter rotation sensor installed near skin plate (Typical)

Figure 3 – Torque sensor installation on hoist pinion shaft (Typical)

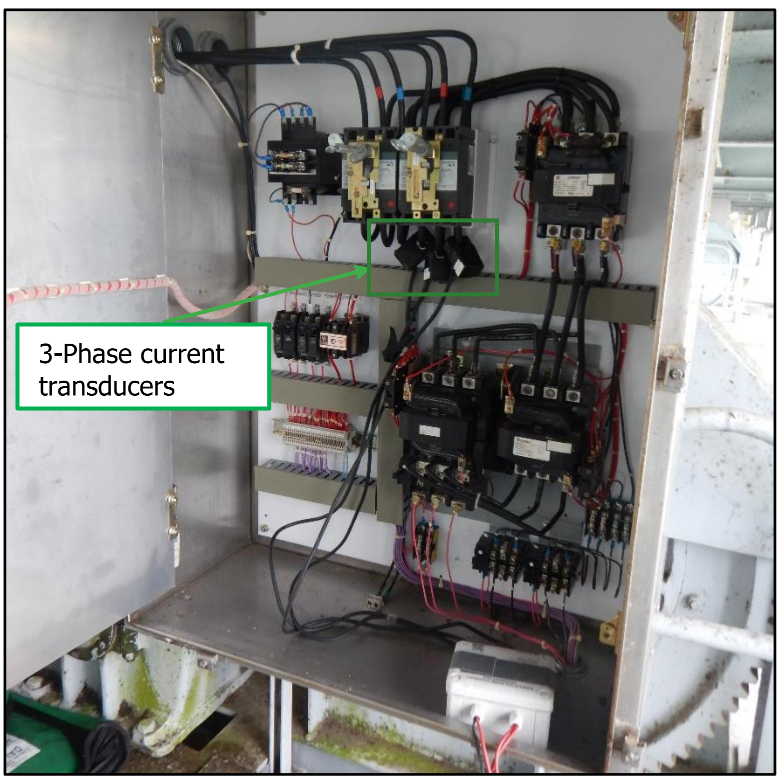

Figure 4 – Current transducers installed on hoist motor controls (Typical)

Figure 5 – BDI personnel installing instrumentation on the gate arm

TESTING PROCEDURES

Structural response data was recorded on all sensors at 50Hz while the gate was run through three spill tests. Each test consisted of three "up-down" cycles (direction reversals) without lowering the gate back to the sill. Each direction reversal consisted of lifting the gate approximately 6-12", pausing for a few seconds, and lowering the gate approximately 6", and repeating until all reversals had been completed.

Results Summary

General Based on Structural Responses

The following outline contains general discussion points and observations that were made during the data review process. Note: Strain measurements were converted to stress for all subsequent analysis by multiplying the strain values by a steel elastic modulus of 29,000 ksi.

+ **DESCRIPTIONS OF RESPONSE MEASUREMENTS:** All sensor readings were zeroed at the end of each test (which consisted of three cycles of direction reversals) so that each measurement corresponded to response change relative to the final gate position as shown in Figure 6 (gates in the downward "closed" position with the hoist cables slacked as much as possible). It is also worth noting that the stresses did not always start and end at the same levels between tests. This variation in behavior is due to small changes in the flexed gate condition between the start and end of tests. It is common for the flex in the gate, caused by pin friction, to slowly release as it rests on the sill. The purpose of the three up-down cycles per test, prior to sitting the gate back onto the sill, is to ensure that these changes in boundary conditions, including gate flexure due to friction, did not affect BDI's trunnion friction results. ***It is important to note that the recorded measurements were changes in structural response due to gate movement, and do not include the in-situ stresses due to the dead load, cable wrap, and hydrostatic loads present prior to testing.***
+ **QUALITATIVE DATA REVIEW:** Review of the response data indicated a good level of reproducibility between the three tests. For reference, Figure 6 and Figure 7 show stress responses measured along Gate 4's right arm top strut for all three tests (Test #1-3). The data in these plots have been provided as both a function of time and the gate position as determined by the skin plate tilt sensor. Structural response behavior slightly varied during the first test's first cycle compared to subsequent lift/lower cycles and tests, with the first cycle having a slightly smaller change in stress due to pin friction. The observed variation was likely caused by a larger release of built-up pin friction as the gate rested on the sill for a longer period of time.
+ **DIRECTION/FRICTION REVERSAL IN RESPONSES:** The difference in stress during gate opening and closing for a given position is shown in Figure 8. The stress variation at any given gate position was a result of direction reversal and in turn due to trunnion friction reversal. This statement is true since all other loads such as dead-load and hydrostatic pressure were essentially constant barring small changes in hydrostatic pressure due to slight changes in head. This direction/friction reversal is depicted in Figure 9, with deflected shape renderings from a gate arm finite element model under lifting and lowering loads. Note that this figure shows an arm configuration that does not match this gate, but the concept of the direction/friction reversal still applies.
+ **MOTOR PERFORMANCE:** Current measurements taken at the hoist motor indicated steady and stable current draws during the lifting and lowering portions. An example plot of current draw and gate position is provided in Figure 10. Current draw ranges during lifting were higher than the ranges during lowering, which is common due to gravity/dead load. These results are summarized along with recorded peak in-rush current in Table 2. Note that the sample rates used during testing were set for collecting gate responses and may not have been appropriate to fully capture the in-rush current. The readings should be evaluated by a licensed electrician with knowledge of the operating parameters.
+ **TORQUE AND HOIST FORCE:** Due to restrictions caused by the hoist limit switches, the hoist cables could not always be fully slacked at the beginning and end of the performed tests. Throughout testing of the Rockwell Forney gates, it was found that this limit switch restriction varied gate to gate and arm to arm. Therefore, it is not recommended to use the collected torque and hoist force data to quantify overall hoist forces. Rather, this data was utilized to evaluate total friction behavior, which is observed as half the difference between the lifting and lowering torque/force (friction reversal).

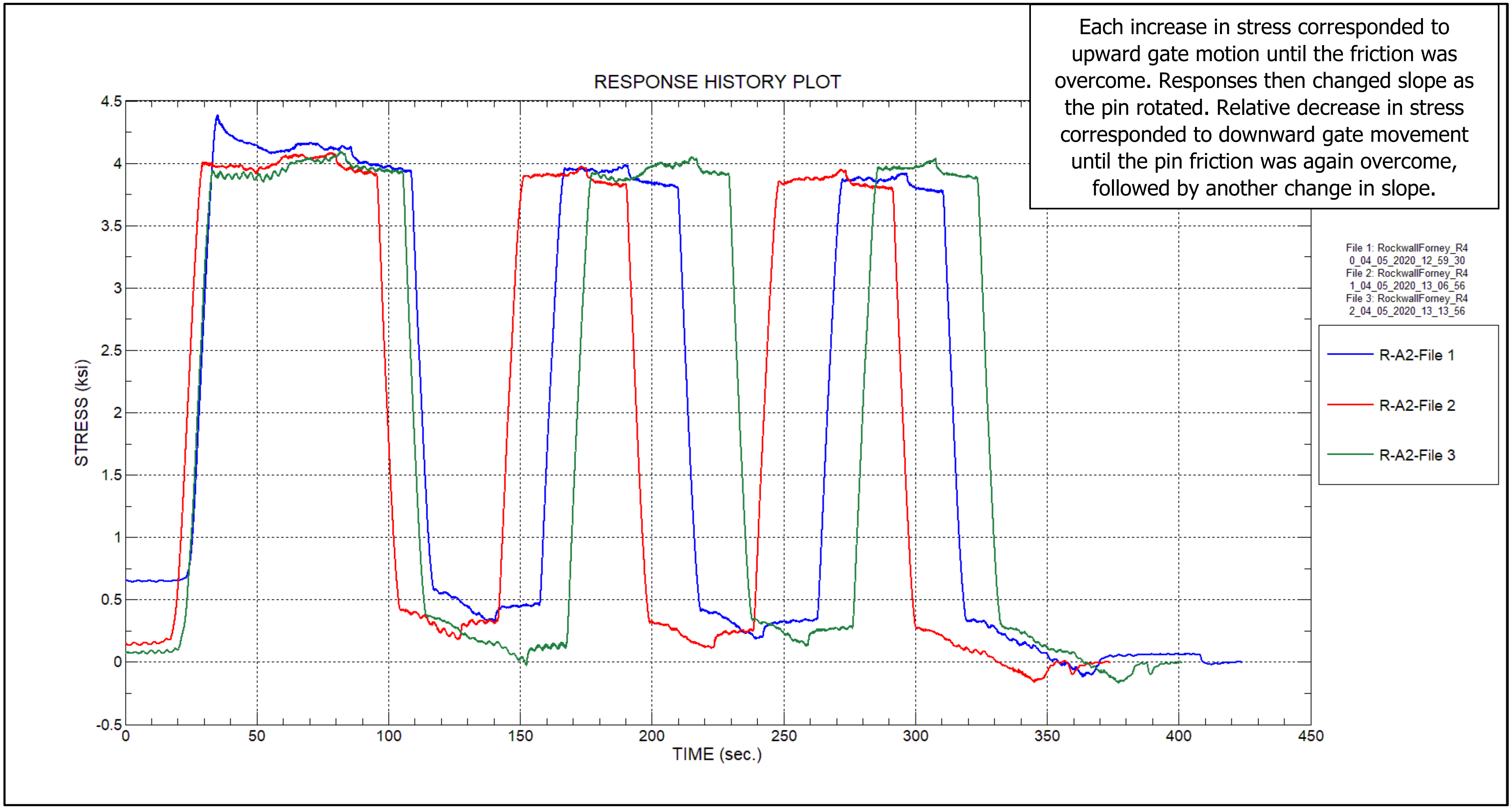

Figure 6 – Stress response history – Right arm – Gage A2 – Time based
File 1 = test run 1, File 2 = test run 2, File 3 = test run 3

(Section A along top strut near pin – Sensor location 2 along bottom of inner flange)

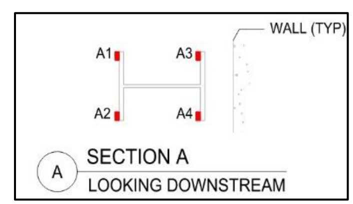

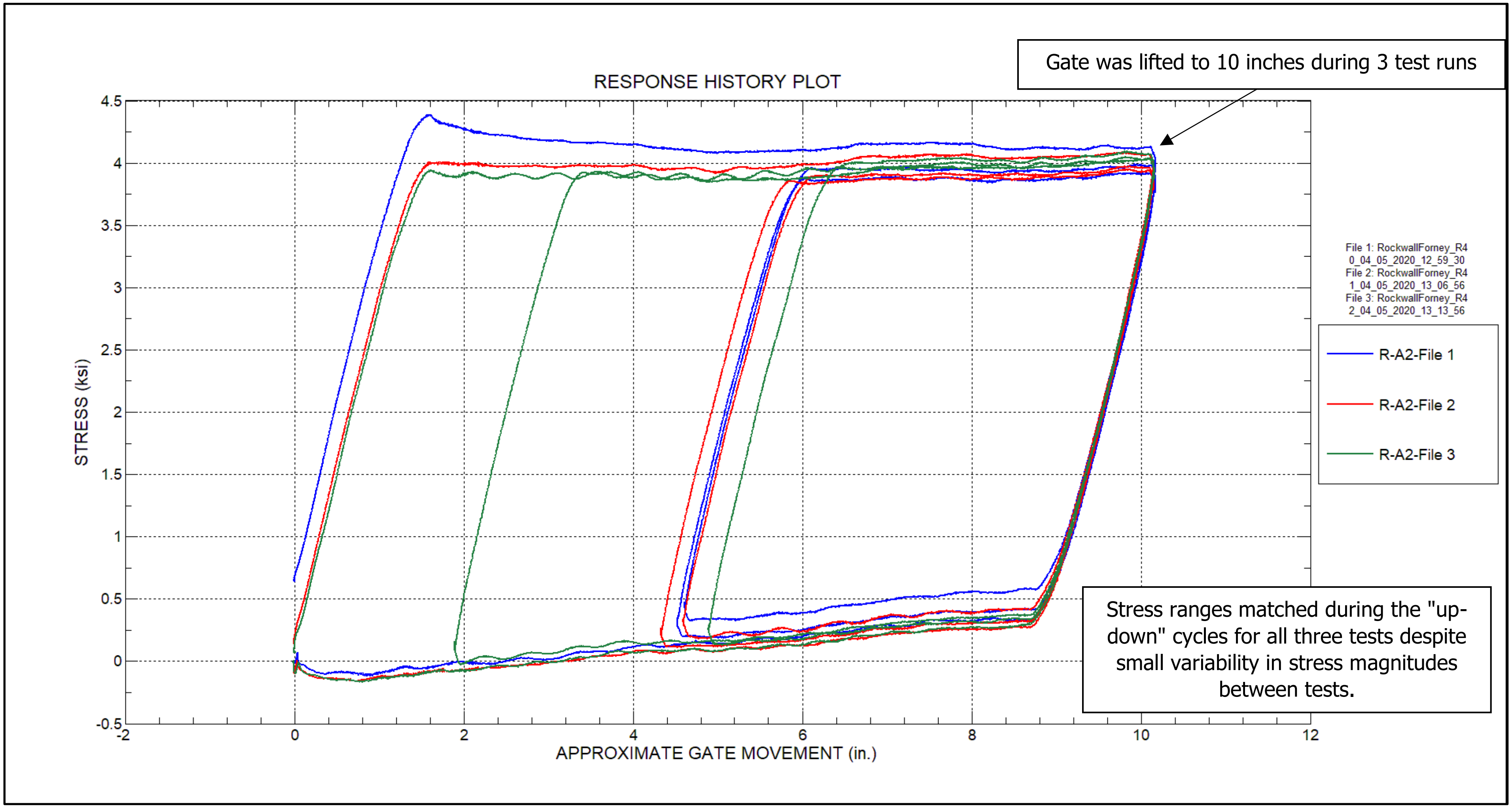

Figure 7 – Stress response history – Right arm – Gage A2 – Function of gate movement
File 1 = test run 1, File 2 = test run 2, File 3 = test run 3

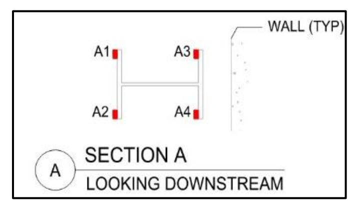

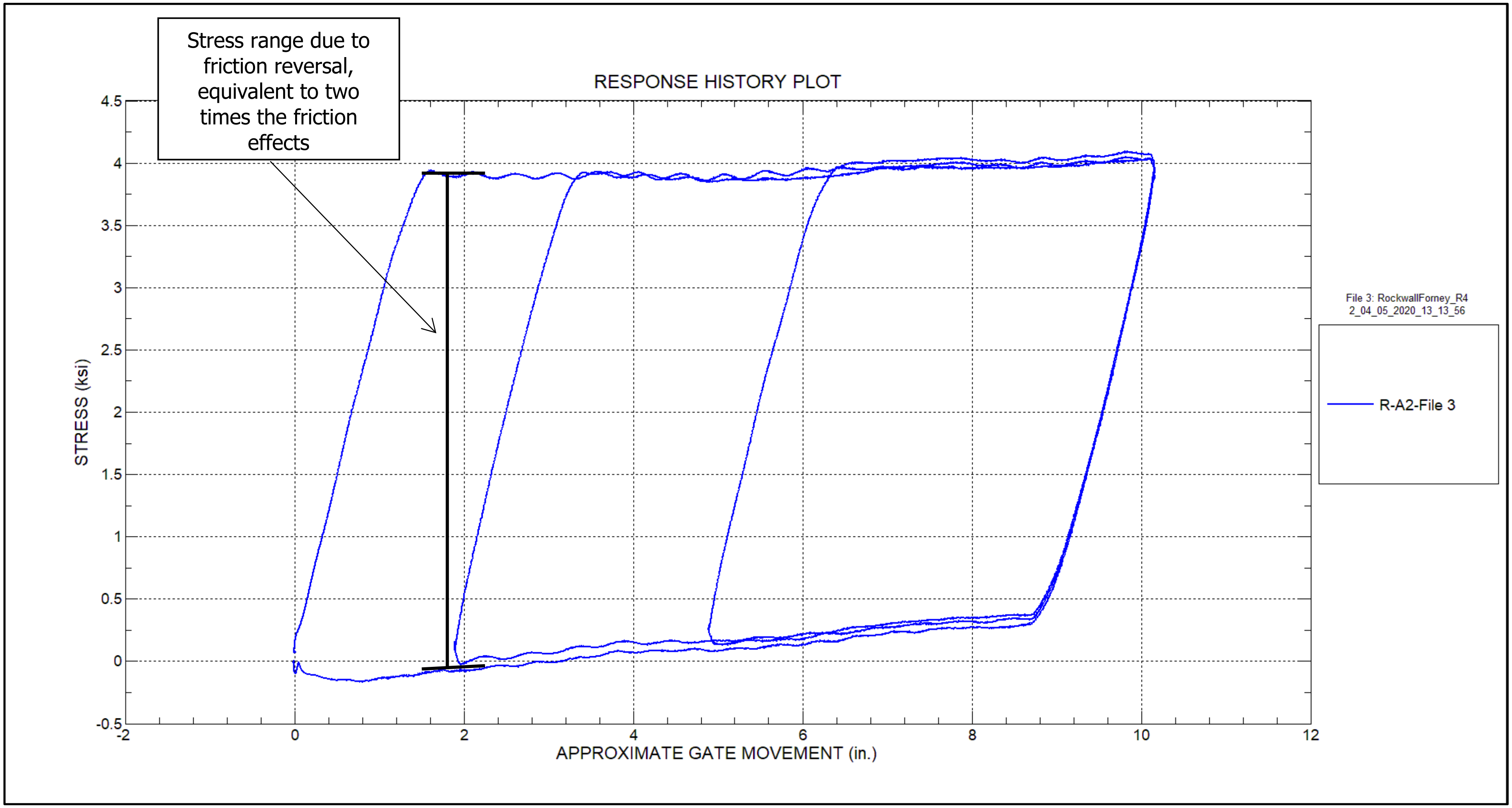

Figure 8 – Stress response history – Right arm – Gage A2 – Friction effect in stress responses

(Section A along top strut near pin – Sensor location 2 along bottom of inner flange)

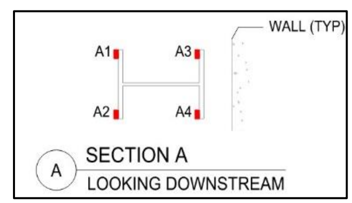

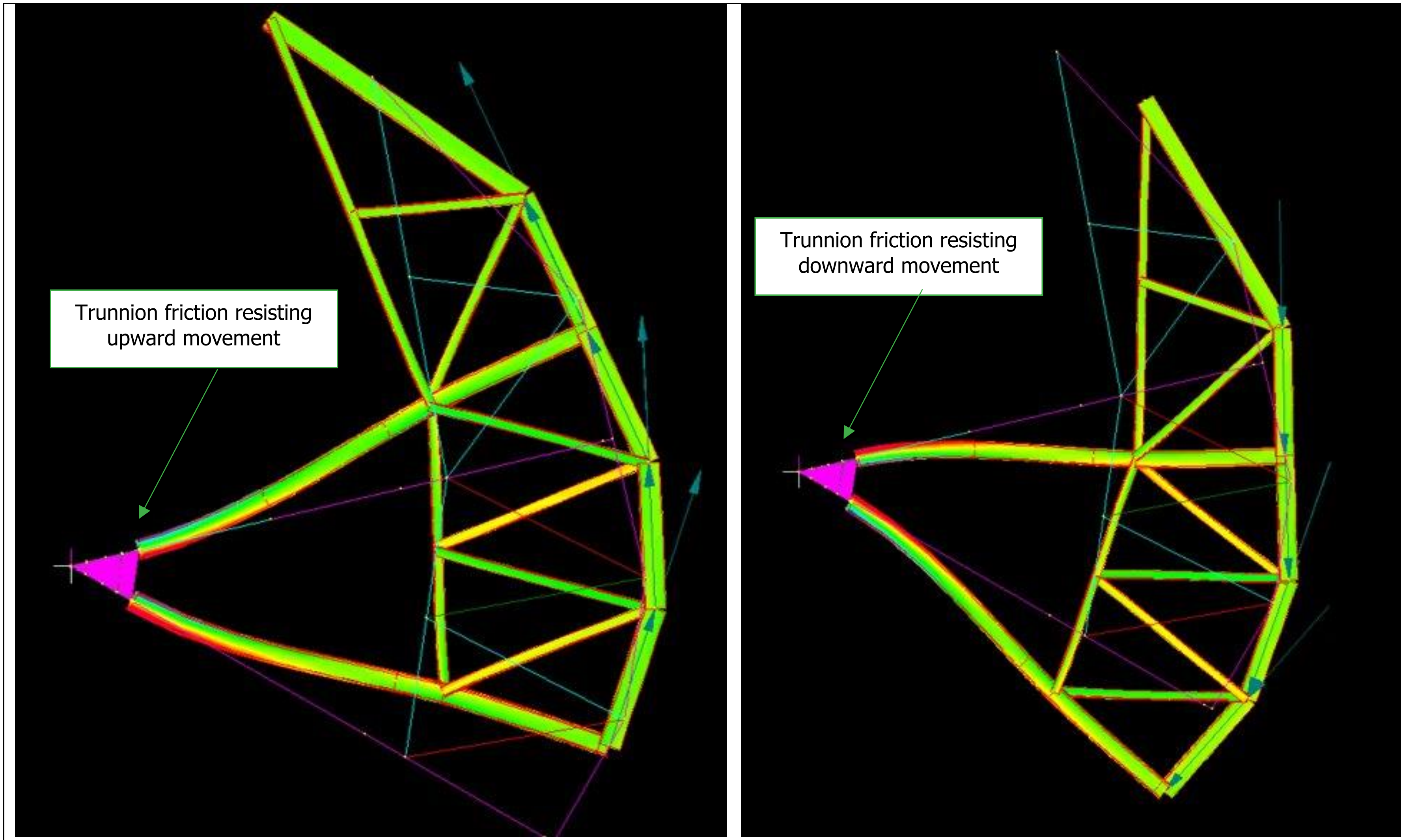

Gate traveling upward **Gate traveling downward**

Figure 9 – Deflected shapes during lifting and lowering of Gate – Visualization of direction/friction reversals

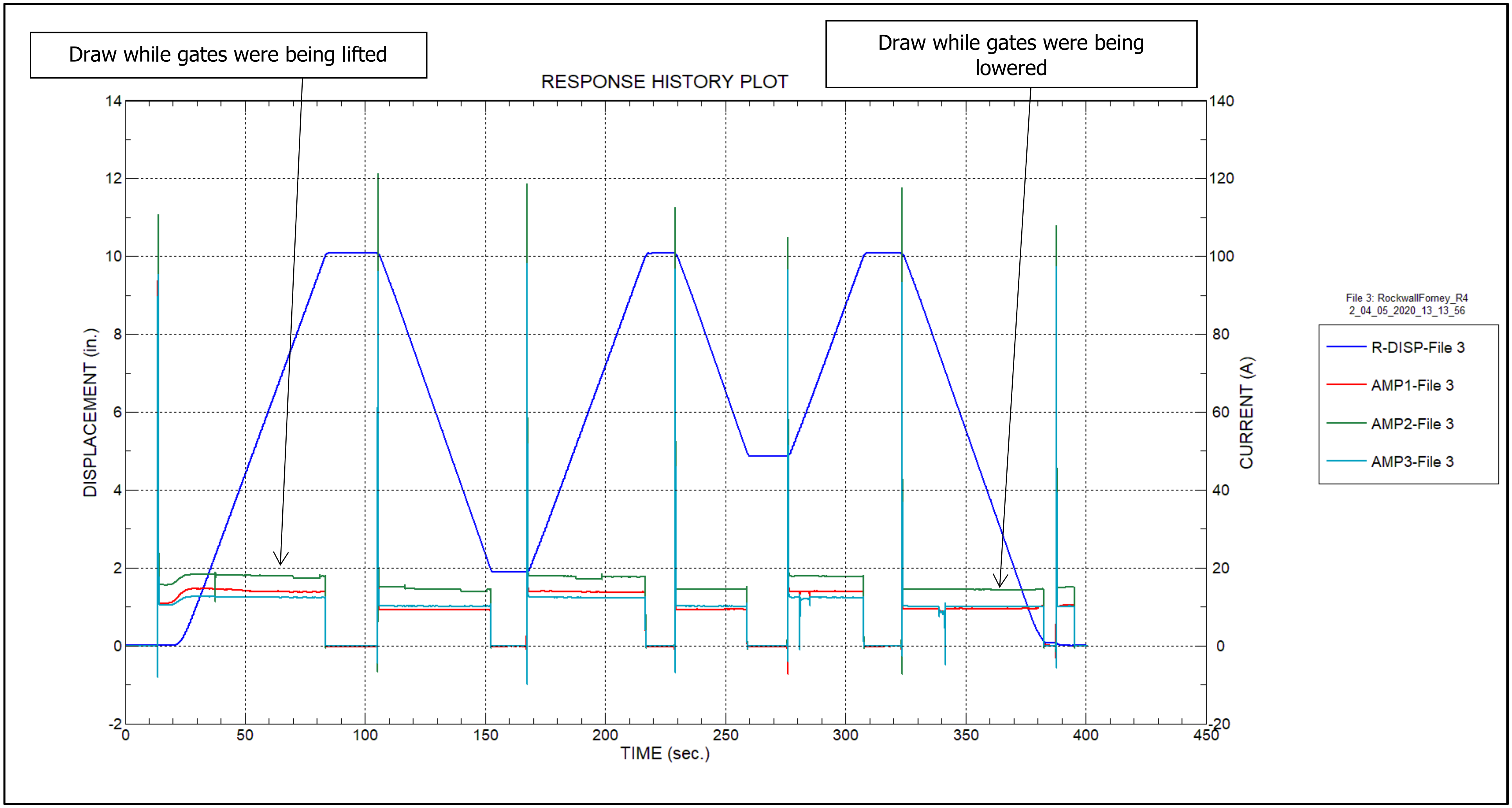

Figure 10 – Motor current & gate movement response history – Lift motor – Highlighting motor draw during lift and lower cycles

Methodology and Findings of The Strut Force and Moment Calculations

The following outline provides the methodology used to calculate the required member forces and moments.

- **CHANGE IN STRESS DUE TO GATE OPERATION:** Strain data can be viewed as a function of time starting when the gate was in the down position and was then lifted off the sill. When examining data in this manner, it is easy to see how stresses ramped up as the gate began to move and then changed slope once pin friction was overcome and the trunnion hub began to rotate with the gate. The first point in time where the friction was overcome (both lifting and lowering) has been highlighted in the stress histories shown in Figure 11. These stress histories show the response of all four sensors along the top strut of the right arm (Section A). ***It is important to note that the recorded measurements were changes in structural response due to gate movement, and do not include the in-situ stresses due to the dead load, cable wrap, and hydrostatic loads present prior to testing.***
- **CALCULATION OF STRUT CROSS-SECTIONAL MOMENTS:** The use of four strain gages per strut cross-section allowed accurate in-plane flexural bending moments to be computed from the recorded strain measurements. These moments were computed for every cross-section in each gate arm using the basic mechanics equation provided in Figure 12.

  In-plane or weak-axis flexure refers to bending about a given strut's web. This designation is consistent with typical nomenclature. In-plane bending can be observed visually from the strain response histories as a difference between the top and bottom stresses, whereas out-of-plane or strong-axis bending is visualized as the difference in stress from side to side. Figure 13 provides a visual reference for both types of strut flexure.
- **EXAMINATION OF RESPONSES AS A FUNCTION OF GATE POSITION:** Changes in cross-sectional moment related to friction becomes clearer when the responses are plotted as a function of gate position. Because the gate was operated with several up and down movements, the effects of friction associated with each direction reversal can be viewed for all measured and calculated responses. Figure 14 through Figure 17 show all cross-sectional flexural moment plots for both trunnion arms. The responses in these plots have been centered about the stress state corresponding to a zero-moment, unflexed condition. The zero-moment offset was estimated as the average moment values between up and downward movement (i.e. half the moment difference) at the gate position with the greatest pin friction moment difference (greatest difference between lifting and lowering).
- **TRUNNION FREE-BODY-DIAGRAM & PIN MOMENT CALCULATION:** Figure 18 shows the instrumented member cross-sections and shows how the measured cross-sectional flexural responses were used to compute pin moment. The in-plane moment values used in these calculations were determined directly from the strain measurements at each cross-section using the provided mechanics equations. It should be noted that the out-of-plane moments were not considered in the calculation of pin moment since they were orthogonal to the axis of the pin rotation. Total pin moment was then determined by summing all the moment components about the pin, which included the in-plane moment and the shear components at the strut cross-sections nearest the pin.
- **STRUT SHEAR CALCULATION:** From the examination of the trunnion free-body-diagram described above, the shear vectors at the three struts were a primary component in the pin moment calculation. For this type of structural element, shear vectors were calculated using the moment differential between the two cross sections along each strut. It is important to recognize that shear was constant between the two instrumented cross-sections and the applied shear was a function of the recorded change in moment ($V = dM/dX$). Subsequently, the shear vectors were calculated by dividing the difference in moment by the distance between the two instrumented cross-sections. Shear values for each strut have been plotted as a function of gate position in Figure 19 and Figure 20.

- **CALCULATION OF PIN MOMENT DUE TO FRICTION:** Once all the trunnion arm force vectors were calculated, the equations shown in the free-body-diagram were applied to compute pin moment as a function of gate position. It is important to note that because the calculated pin moment range corresponds to a direction reversal, a reversal in friction also occurred. The effect of direction reversal on pin moment due to friction is best conceptualized by centering the moment response plots about the zero-moment axis. The moment due to lifting and the moment due to lowering can then be visualized as a change from this new zero point corresponding to the gate in an unflexed condition. Therefore, the total moment differential between lifting and lowering was twice the moment due to friction acting in a single direction. Pin-moment plots have been provided in Figure 21 and Figure 22. From these plots, it is apparent that pin moment due to friction remained relatively constant throughout the gate operation tests, with a slight decrease in pin friction moment as the gate continued to be lifted. This slight decrease in pin friction moment most likely corresponded to the change in hydrostatic load as the gate position changed. Pin-moment plots for all tests on Gate 4 are also provided for reference in Appendix B – Gate 4 Pin Moment Component Plots.
- **SHAFT TORQUE & HOIST FORCE:** Torque measurements were taken on the pinion shafts near the hoist motor during testing, with single torque gages installed on the left and right hoist pinion shaft. Responses were recorded in units of micro-strain and converted to torque in units of kip-ft using Equation 1 thru Equation 3 and the following shaft properties.

$$d_O = 5.5\ inches, \qquad d_I = 0\ inches, \qquad E = 29000\ ksi, \qquad \nu = 0.3$$

$$G = \frac{E}{2(1+\nu)}$$

Equation 1

$$J = \frac{\pi\left(d_O{}^4 - d_I{}^4\right)}{32}$$

Equation 2

$$\tau = \varepsilon * \frac{2GJ}{\frac{d_O}{2} * 1000000 * 12}$$

Equation 3

Figure 23 shows example torque measurements, recorded on the Gate 4 torque shafts. Best practices for torque measurements is to measure torque on opposite sides of the shaft so that any bending in the shaft can be removed by averaging the two responses. Due to access limitations, only one gage at each location could be installed. Therefore, any bending in the shaft may be reflected in the torque measurements and may be related to the peaks and valleys observed in the torque responses.

Torque values were converted to force in the hoist cables per gate arm using the gear ratio and drum radius, as shown in Figure 24. The gear ratio and drum radius were 5.182 and 1.086 feet respectively, as defined in the provided as-built shop drawings. It should be noted that the hoist force calculated may be smaller than the actual hoist force applied. This difference is due to the limit switch engaging the brake before the hoist cable was fully slacked, resulting in an initial force in the cable. A hoist force due to total gate friction was then calculated. This friction hoist force was equal to half the differential in force measured during the lifting and lowering of the gate (similar to the pin friction calculations). As shown in Table 3, the change in cable force due to friction was generally consistent between tests. Note that the total hoist force was due to the total friction effects, including side seal, hoist bearings, trunnion friction effects, etc. It is difficult to determine the exact proportion and composition of the total friction sources. Additional torque and hoist force plots for all collected data files are provided in Appendix A – Gate 4 Torque and Hoist Force Plots.

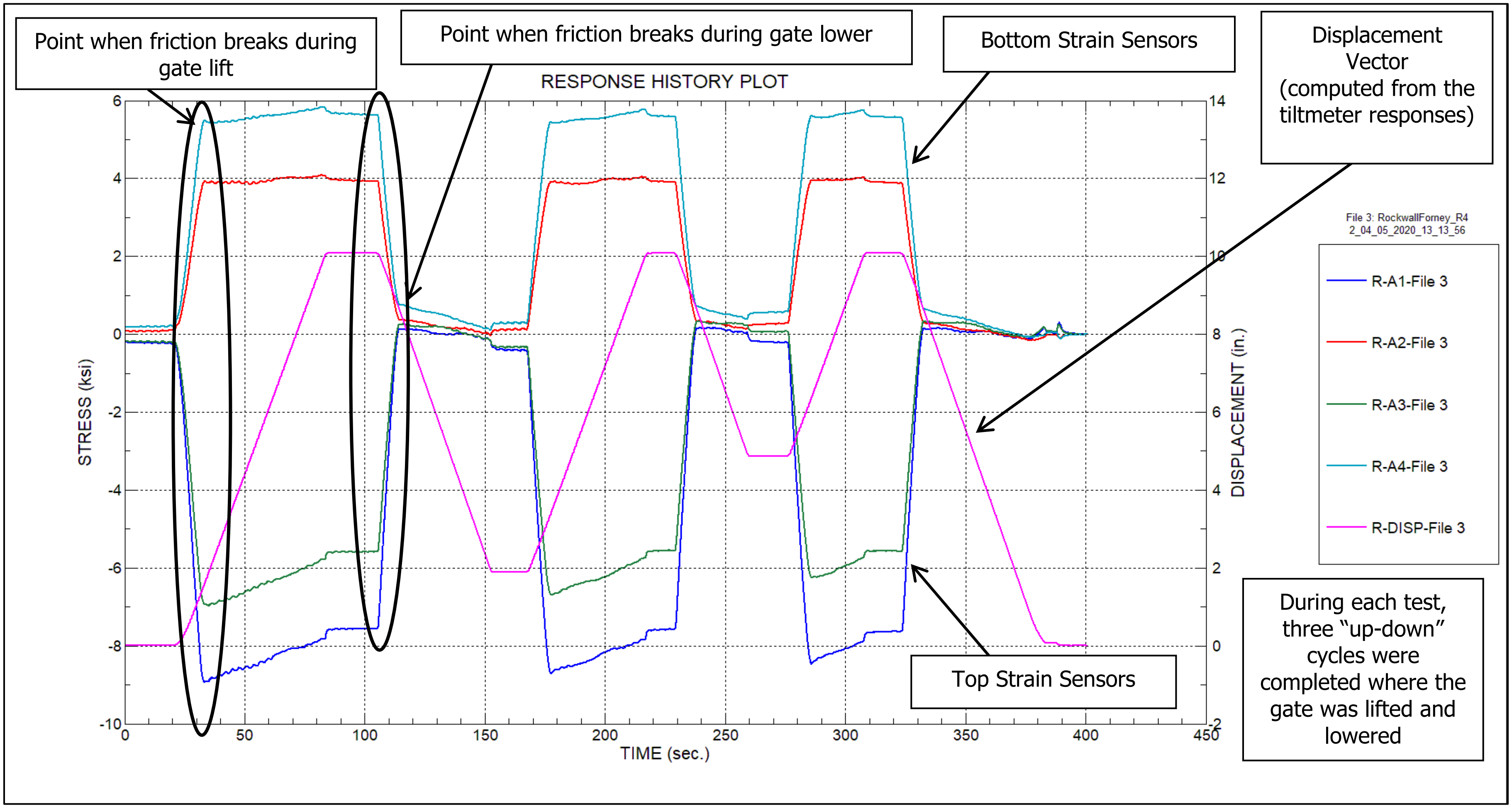

Figure 11 – Stress response & gate movement history – Right arm – Section A - Highlighting friction behavior (Section A along top strut near pin)

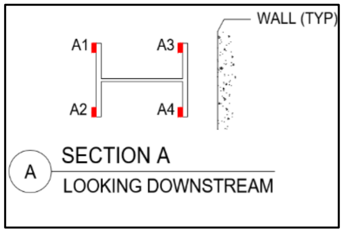

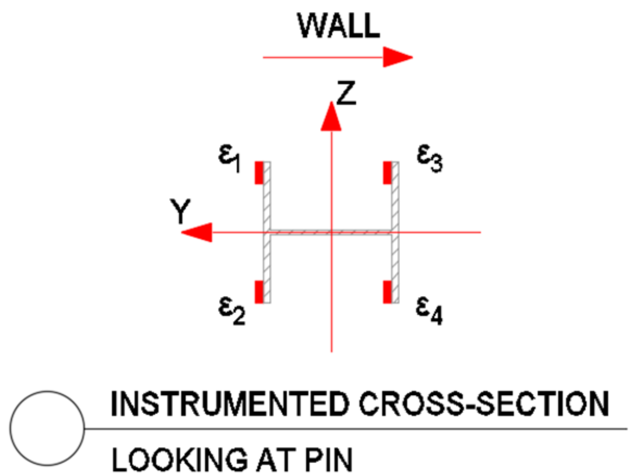

Calculation of Weak-axis (In-plane) bending

$$M_Y = \frac{E\left[\frac{\varepsilon_2 + \varepsilon_4}{2} - \frac{\varepsilon_1 + \varepsilon_3}{2}\right] S_{Y(gage)}}{2}$$

Sy(gage) = Section modulus to the center of gages (not extreme fiber of flanges)
(locations of gages were accounted for in moment computation)

Figure 12 – Basic mechanic equation used to calculate moment

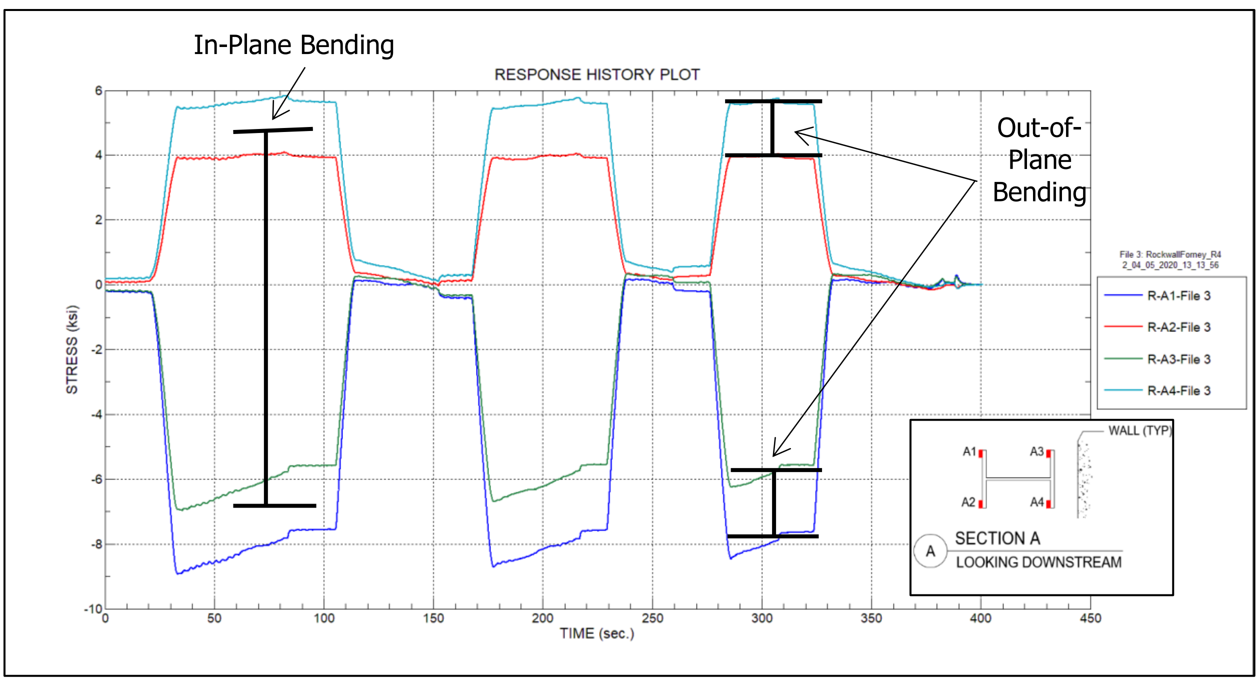

Figure 13 – Stress response history – Right arm – Section A – Bending components
(Section A along top strut near pin)

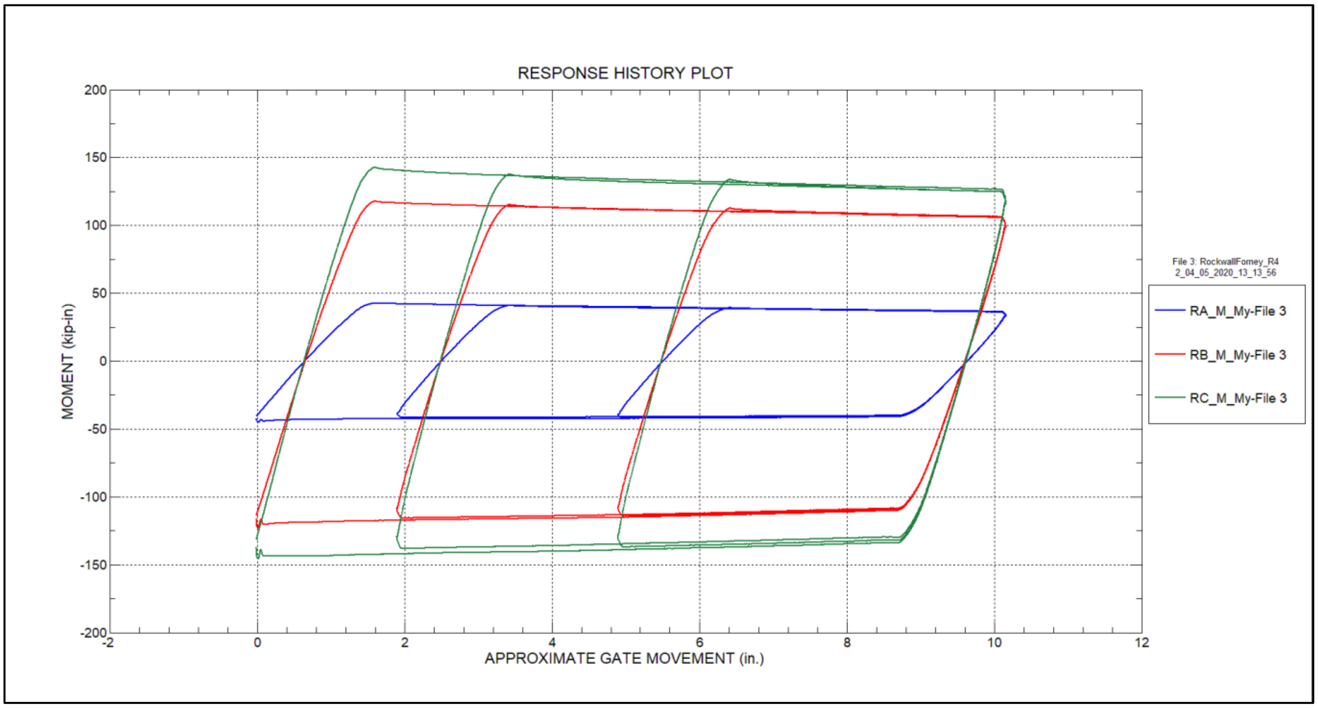

Figure 14 – In-plane moment response history – Right arm – Sections near pin

(RA = Right Arm Top Strut, RB = Right Arm Middle Strut, RC = Right Arm Bottom Strut)

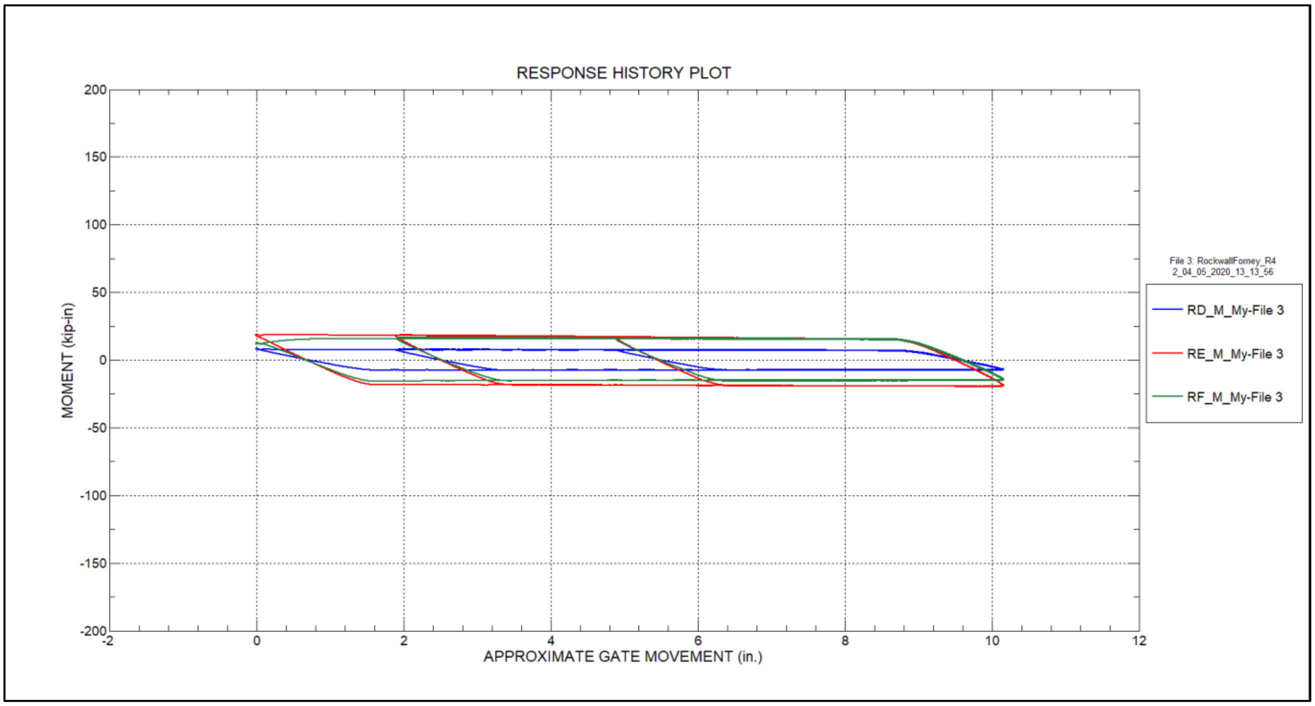

Figure 15 – In-plane moment response history – Right arm – Sections away from pin

(RD = Right Arm Top Strut, RE = Right Arm Middle Strut, RF = Right Arm Bottom Strut)

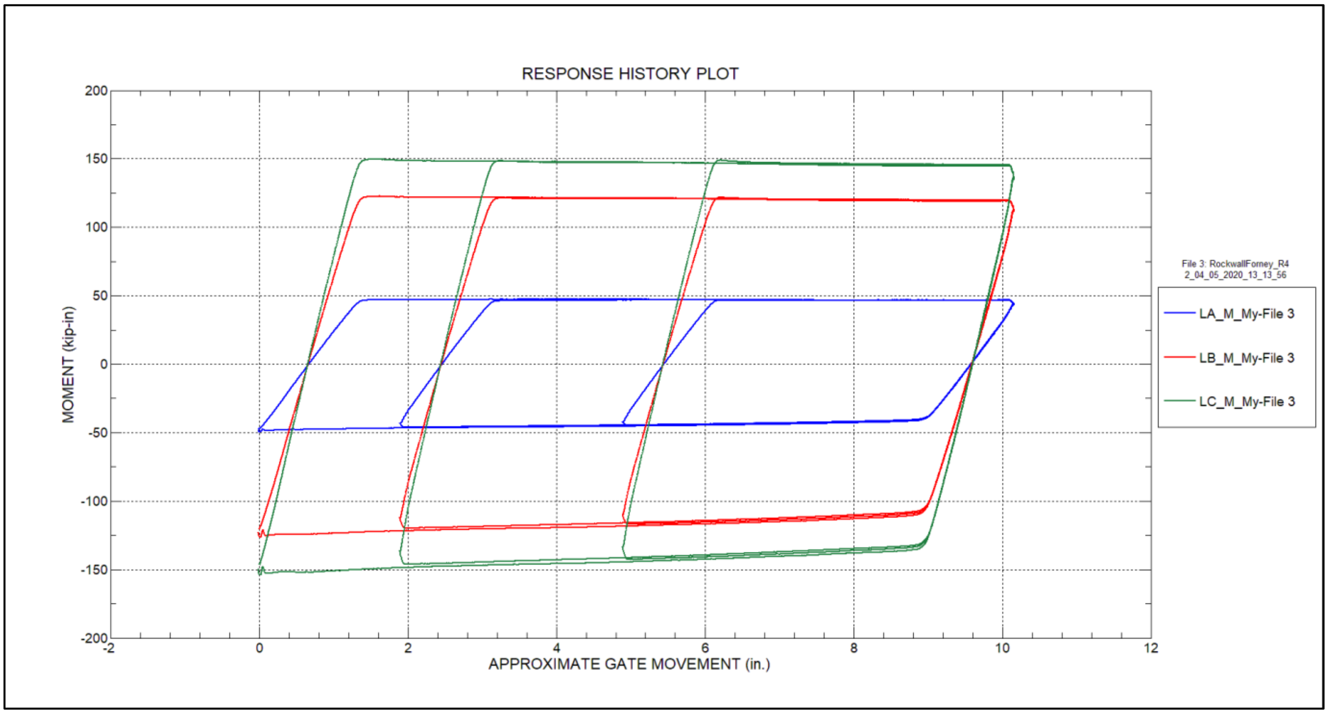

Figure 16 – In-plane moment response history – Left arm – Sections near pin

(LA = Left Arm Top Strut, LB = Left Arm Middle Strut, LC = Left Arm Bottom Strut)

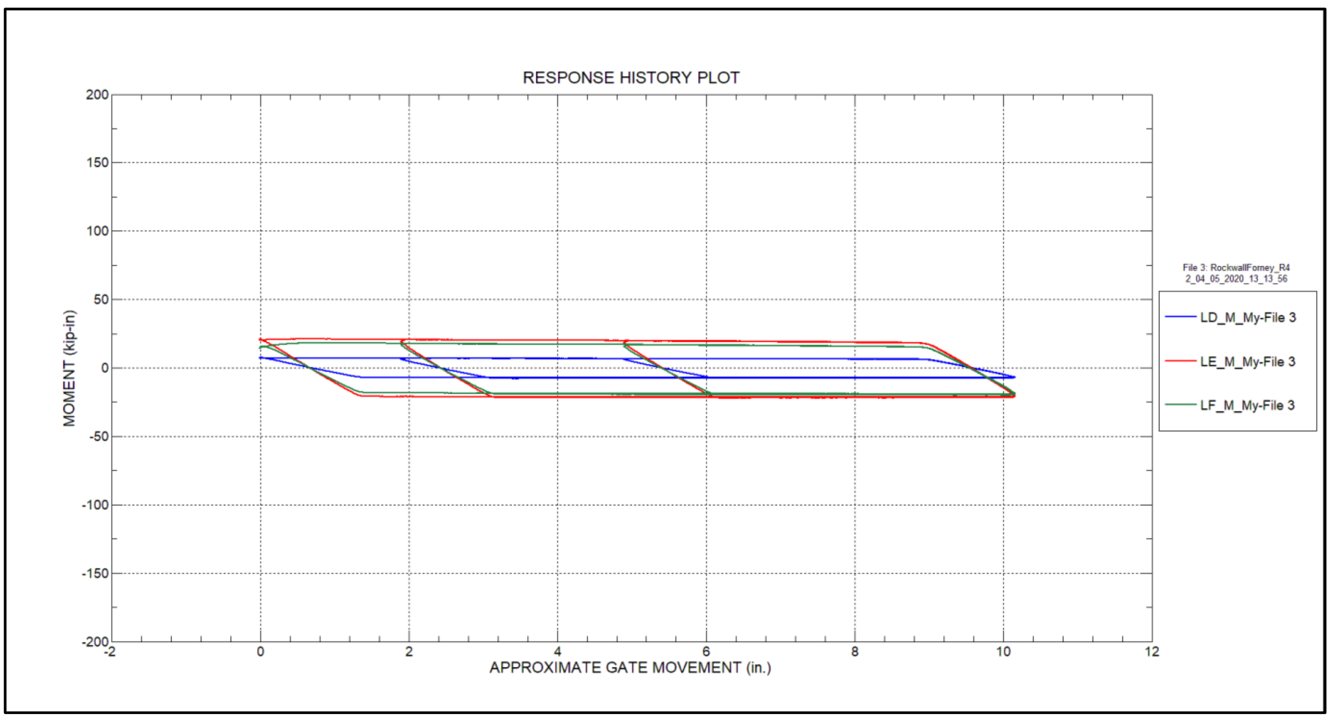

Figure 17 - In-plane moment response history – Left arm – Sections away from pin

(LD = Left Arm Top Strut, LE = Left Arm Middle Strut, LF = Left Arm Bottom Strut)

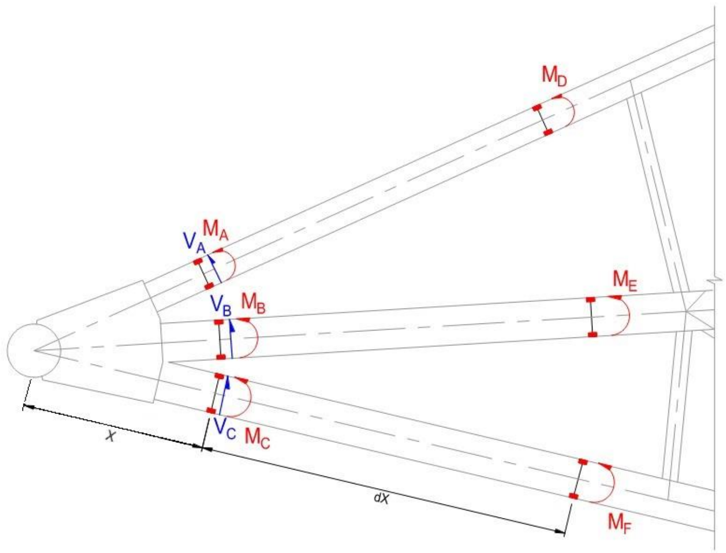

Elevation View of Gate Arm

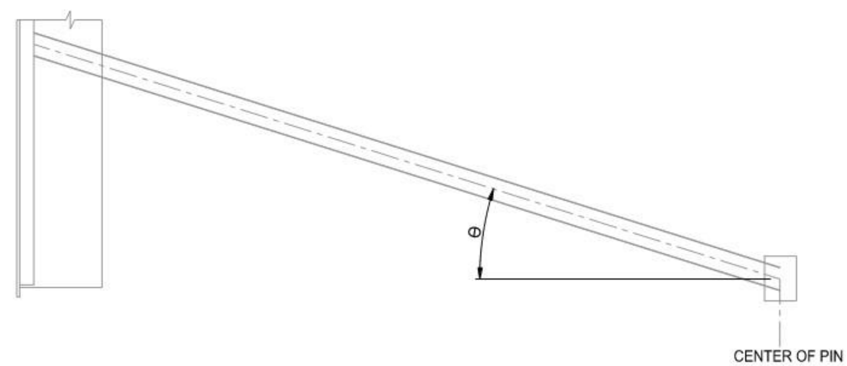

Plan View of Gate Arm

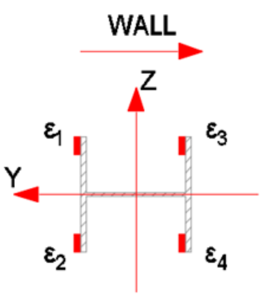

$$M_Y(M_A, M_B, M_C, M_D, M_E, M_F) = \frac{E\left[\frac{\varepsilon_2 + \varepsilon_4}{2} - \frac{\varepsilon_1 + \varepsilon_3}{2}\right] S_{Y(gage)}}{2}$$

$$V_A = \frac{M_A - M_D}{dX}$$

$$V_B = \frac{M_B - M_E}{dX}$$

$$V_C = \frac{M_C - M_F}{dX}$$

$$\sum M_o = 0$$

$$M_{PIN} = [X(V_A + V_B + V_C) + M_A + M_B + M_C]\cos\theta$$

Figure 18 – Direct calculation of pin moment from strain measurements

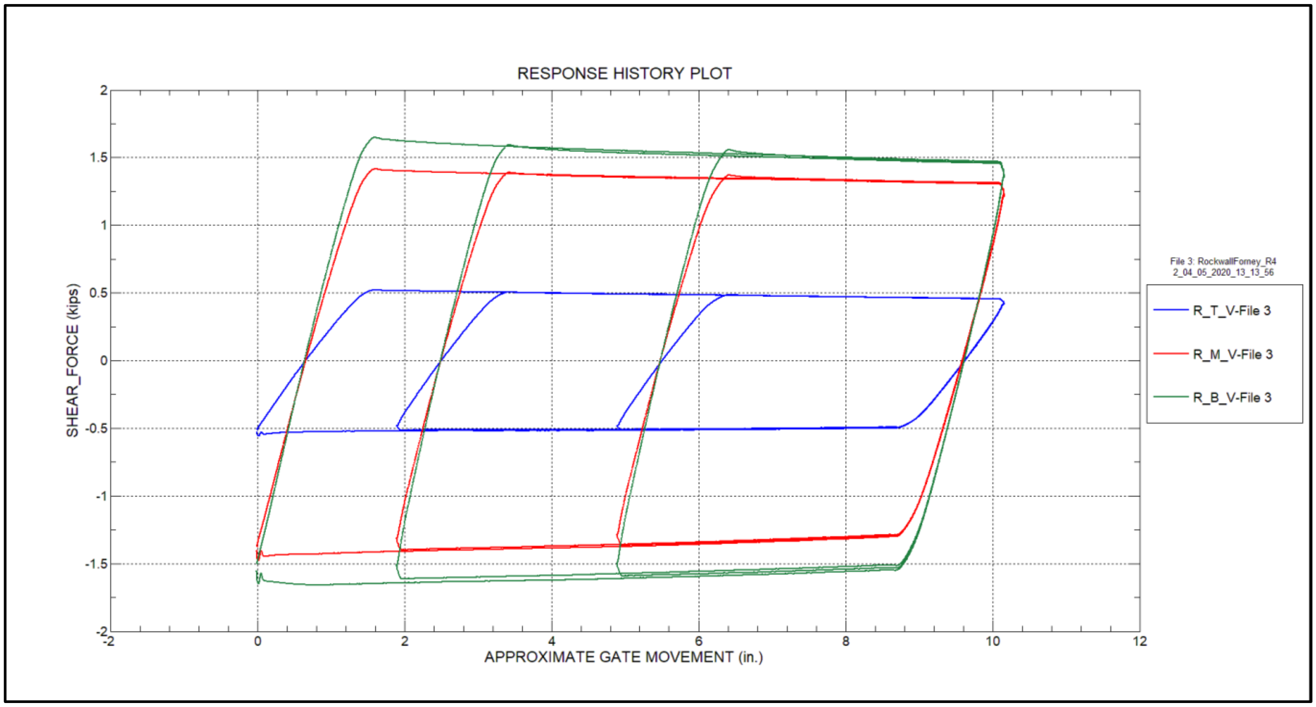

Figure 19 – Strut shear response history – Right arm

(R_T = Right Arm Top Strut, R_M = Right Arm Middle Strut, R_B = Right Arm Bottom Strut)

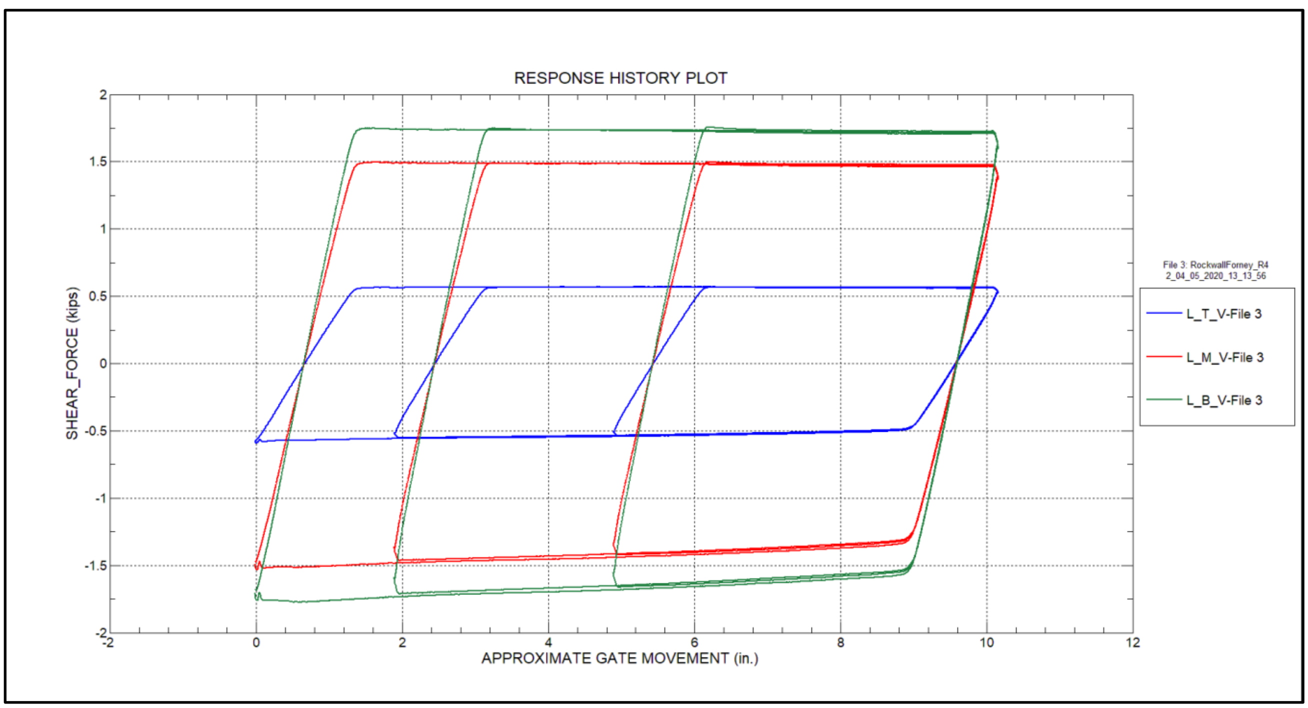

Figure 20 – Strut shear response history – Left arm

(L_T = Left Arm Top Strut, L_M = Left Arm Middle Strut, L_B = Left Arm Bottom Strut)

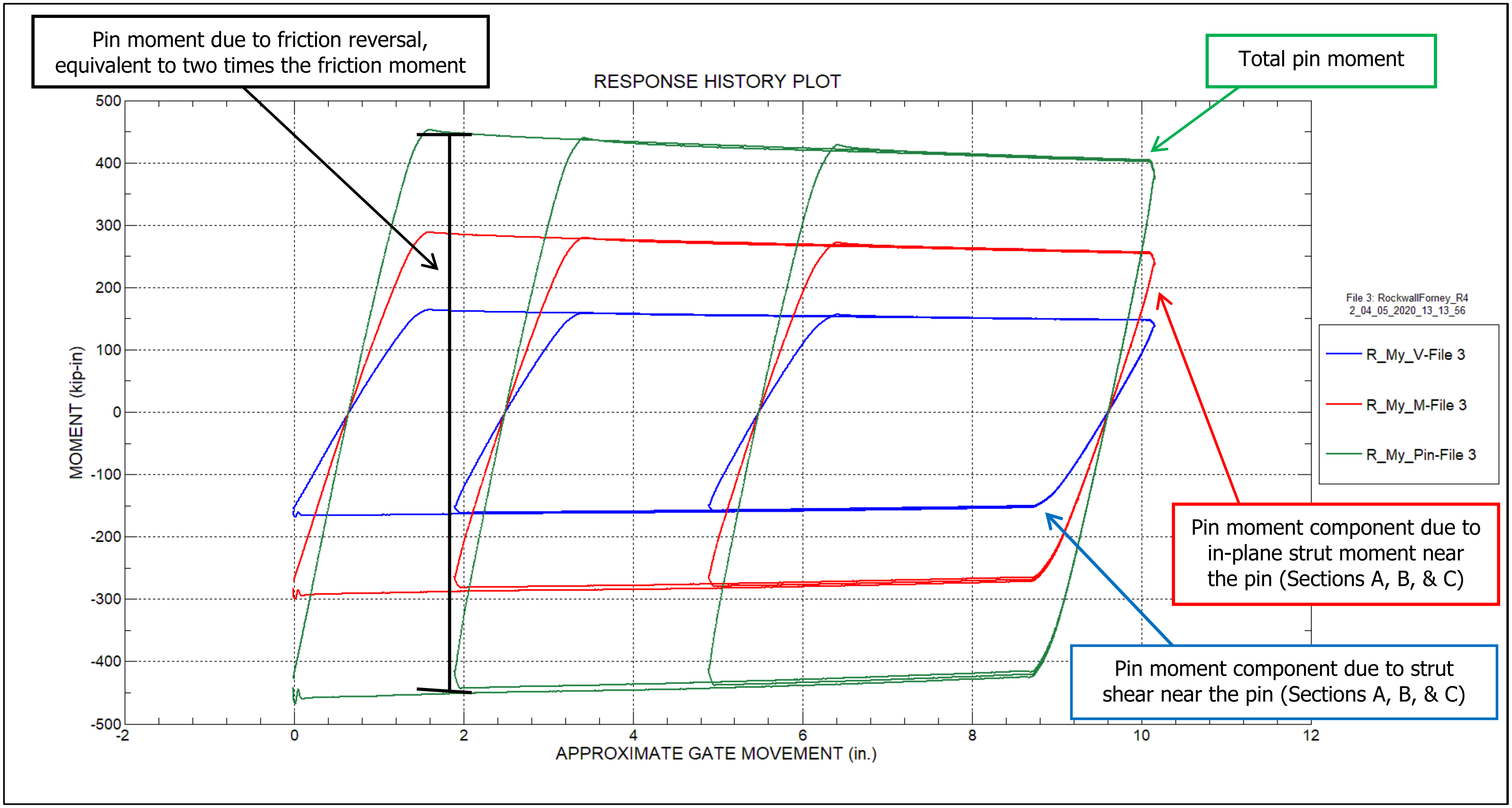

Figure 21 – Pin moment response history – Right arm

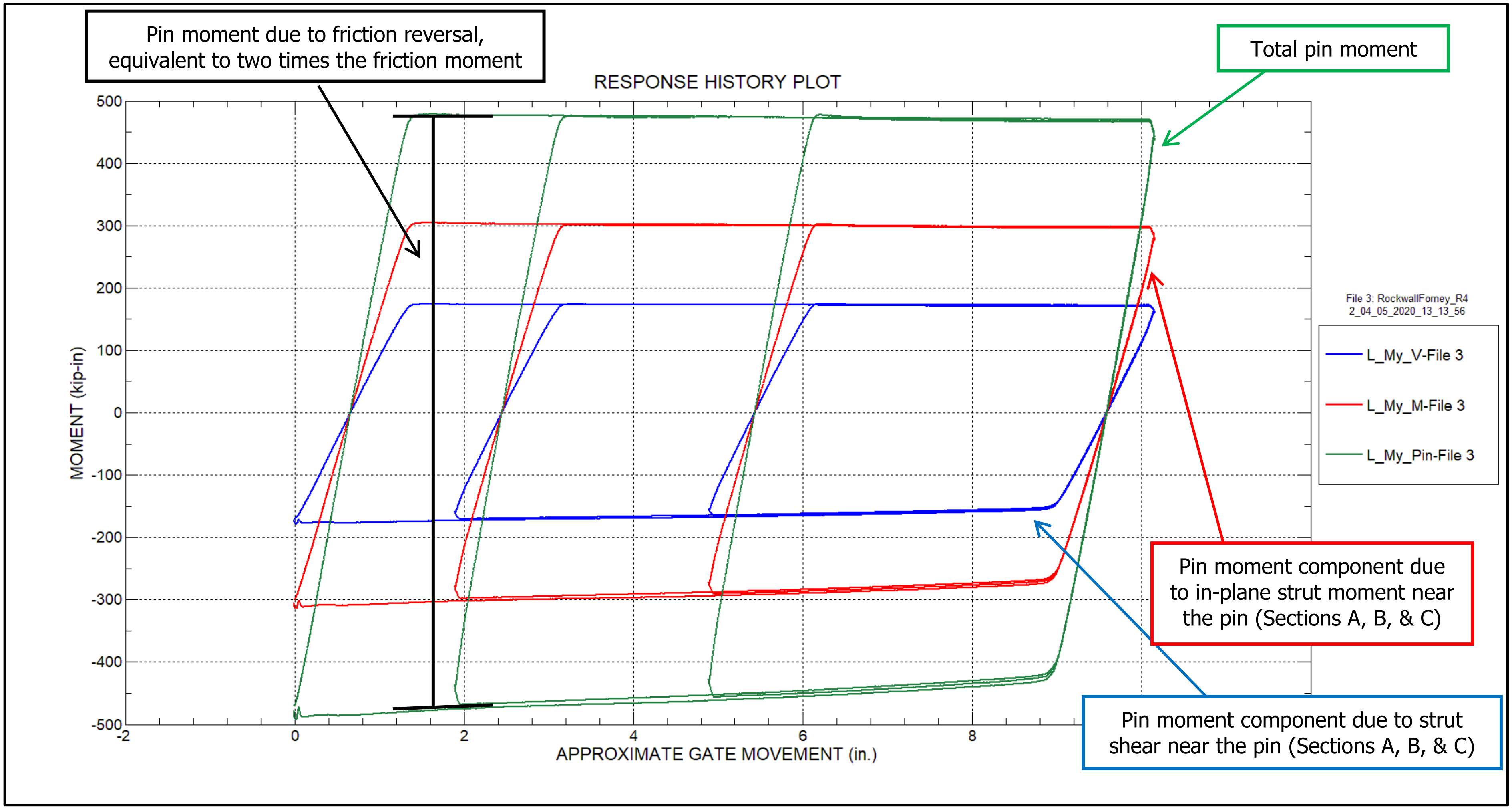

Figure 22 – Pin moment response history – Left arm

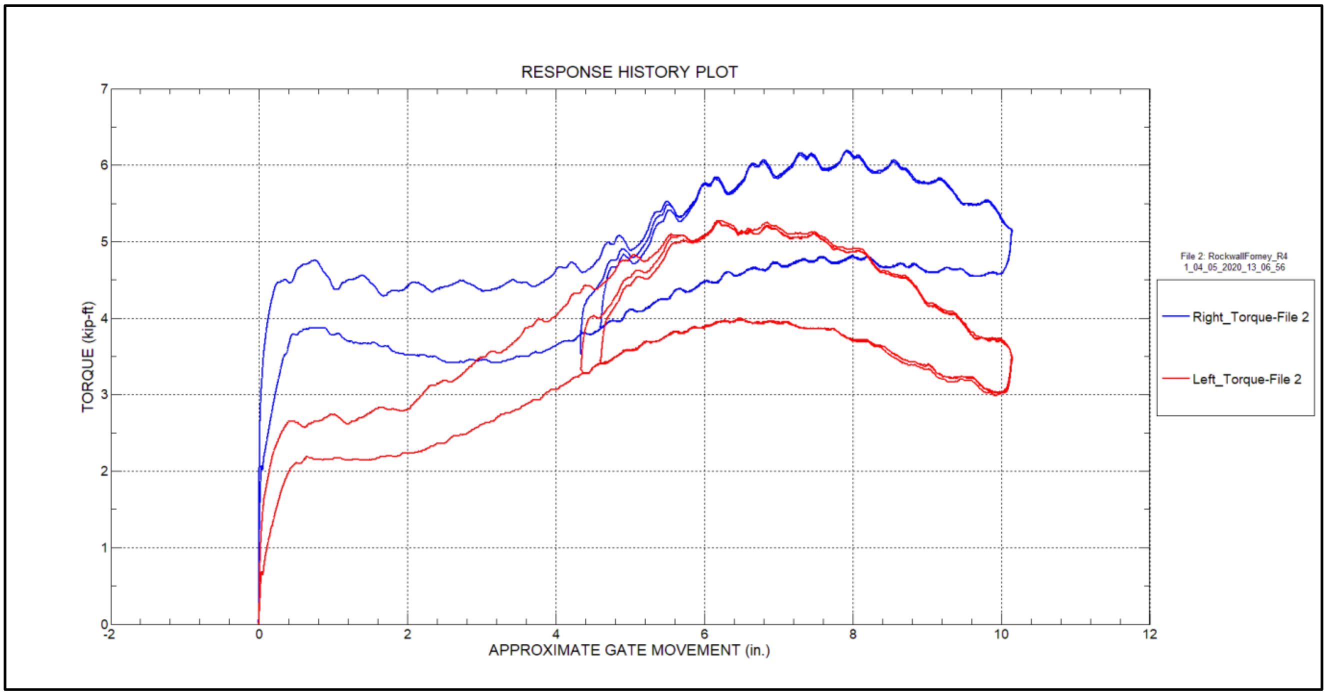

Figure 23 – Hoist torque response history – Gate 4 – Test 2

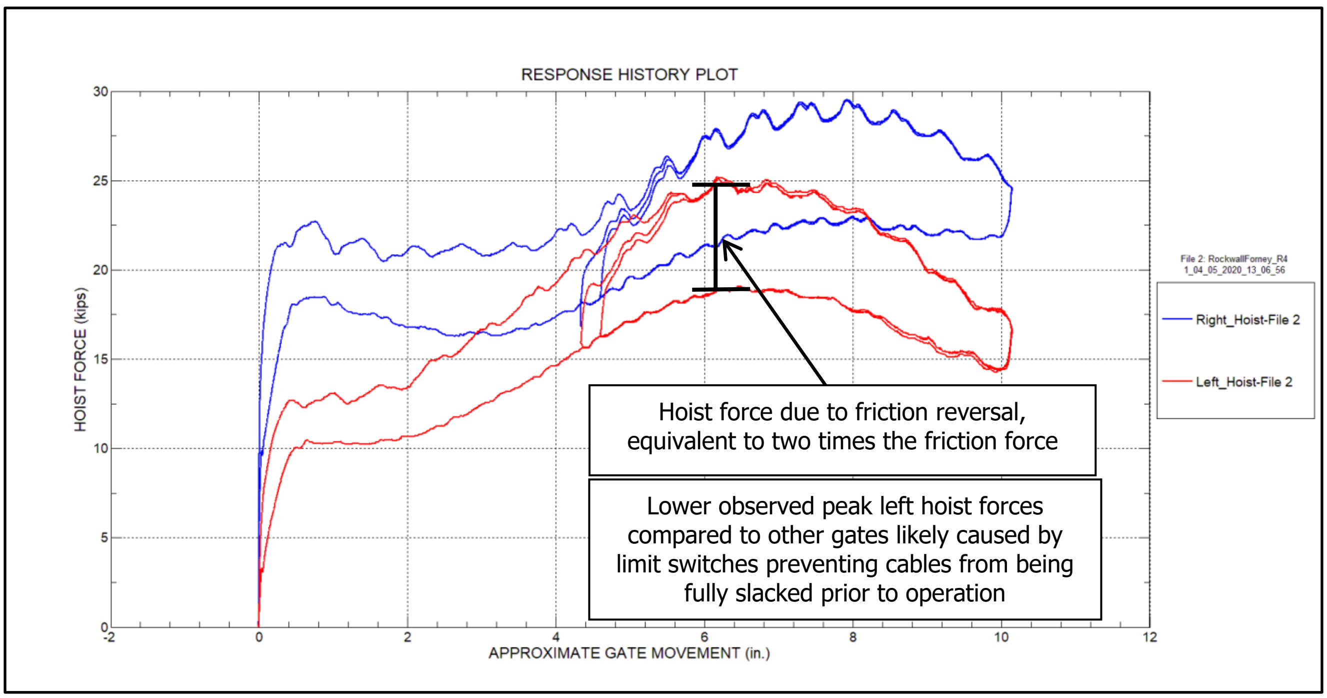

Figure 24 – Hoist force response history – Gate 4 – Test 2

Summary of Friction Results

The raw data files have been included in the submittal package for reference and were formatted as "tdms" files that can be opened in Microsoft Excel using a "tdms" reader extension.

Examination of the stress histories for each test was necessary to obtain a thorough understanding of the gate performance. The response shapes, variations in stress magnitudes, and timing sequences provided direct clues as to how the gate performed under typical service conditions. The following is a breakdown of the provided tabulated results:

- Table 2 provides motor current ranges and maximum in-flow for lift and lower cycles for each test

Table 3 provides maximum hoist force and hoist force due to friction for each testTable 3 – Hoist force summary table – Gate 4

Test Run	Right Arm Peak Hoist Force (kips)	Left Arm Peak Hoist Force (kips)	Right Arm Hoist Force due to Total Gate Friction (kips)	Left Arm Hoist Force due to Total Gate Friction (kips)
1	29.46	26.06	3.47	3.60
2	29.57	25.19	3.45	3.22
3	29.57	25.26	3.51	3.24

Tabulated friction force values correspond to the response induced by friction in one direction

- Table 4 provides the maximum stress ranges measured at the sensor locations for each member
- Table 5 provides maximum bending stress and moment ranges observed during the gate tests
- Table 6 provides maximum friction bending stress and moment values at each of the instrumented strut locations
- Table 7 provides the computed shear values in each strut due to friction
- Table 8 provides calculated measured friction moments, calculated hydrostatic loads based on the measured water elevation, and coefficients of friction for each gate and gate arm during all three tests

The resulting pin friction moments were used to compute friction coefficients from Eq. 4, given the pin radius and the applied thrust. The thrust used in this calculation consisted of the calculated resultant hydrostatic load based on the measured water elevation and was adjusted to account for the loss of head as the gate was lifted. This thrust adjustment was based on the recorded gate movement and was performed in order to calculate more accurate friction coefficients. The water elevation during testing was nearly constant throughout each gate test and was documented during each "up-down" cycle. It should be noted that the minor thrust due to cable wrapping, which was minimal compared to hydrostatic thrust, was not included in the thrust calculation. This assumption resulted in slightly conservative friction coefficients.

$$\mu = \frac{M_F}{T * r} \qquad \text{Eq. 1}$$

where:
μ = Friction Coefficient
M_F = Friction Moment
T = Thrust per Pin
r = Pin Radius, 5.375"

The out-of-plane shear and moments were not considered in the pin friction calculations due to orthogonal geometry considerations (resulting pin moment associated with out-of-plane flexure being perpendicular to pin rotation).

The data was presented in a specific coordinate system applicable to both arms. Data was processed so that the positive x-axis was always pointing towards the pin and the right-hand rule applied. In-plane bending can be referred to as "bending about the horizontal or y-axis" and shows how much the beams bend up and down within the plane of the gate arms. Refer to Figure 12 above for visual reference of coordinate system and mathematical explanation of calculations. Tabulated results do not include any in-situ effects.

Table 2 – Motor current summary table – Gate 4

Test Run	Current Range due to Lifting (A)	Current Range due to Lowering (A)	Max In-rush Current (A)
1	13-20	10-15	116
2	13-19	10-15	117
3	12-18	9-15	121

Table 3 – Hoist force summary table – Gate 4

Test Run	Right Arm Peak Hoist Force (kips)	Left Arm Peak Hoist Force (kips)	Right Arm Hoist Force due to Total Gate Friction (kips)	Left Arm Hoist Force due to Total Gate Friction (kips)
1	29.46	26.06	3.47	3.60
2	29.57	25.19	3.45	3.22
3	29.57	25.26	3.51	3.24

Tabulated friction force values correspond to the response induced by friction in one direction

Table 4 – Maximum measured sensor stress range

Arm Designation	Top Strut (ksi)	Middle Strut (ksi)	Bottom Strut (ksi)
Right Arm	9.30	9.95	10.12
Left Arm	8.77	10.26	11.94

Tabulated values correspond to the total measured change in response during tests

Stress values have not been extrapolated to the extreme fibers (correspond to center of gage)

Table 5 – Maximum in-plane total bending stress & moment ranges – Total

Section Label	Section Description	Right Arm Stress (ksi)	Right Arm Moment (kip-in)	Left Arm Stress (ksi)	Left Arm Moment (kip-in)
Section A	Top Strut Near Pin	8.00	89.94	8.604	96.70
Section B	Middle Strut Near Pin	10.40	240.45	10.82	250.31
Section C	Bottom Strut Near Pin	10.52	293.39	11.10	309.45
Section D	Top Strut Away from Pin	1.47	16.57	1.40	15.69
Section E	Middle Strut Away from Pin	1.68	38.77	1.87	43.22
Section F	Bottom Strut Away from Pin	1.17	32.59	1.37	38.22

Tabulated values correspond to the total measured change in response during tests

Table 6 – In-plane frictional bending stress & moment at maximum gate friction

Section Label	Section Description	Right Arm Stress (ksi)	Right Arm Moment (kip-in)	Left Arm Stress (ksi)	Left Arm Moment (kip-in)
Section A	Top Strut Near Pin	3.95	44.37	4.22	47.45
Section B	Middle Strut Near Pin	5.15	119.04	5.38	124.40
Section C	Bottom Strut Near Pin	5.24	146.01	5.51	153.73
Section D	Top Strut Away from Pin	0.68	7.68	0.66	7.43
Section E	Middle Strut Away from Pin	0.79	18.28	0.92	21.23
Section F	Bottom Strut Away from Pin	0.57	15.85	0.66	18.37

Tabulated values correspond to the response induced by friction in one direction

Table 7 – Strut shear range summary table due to friction

Arm Designation	Top Strut Shear (kip)	Middle Strut Shear (kip)	Bottom Strut Shear (kip)
Right Arm	0.54	1.43	1.68
Left Arm	0.57	1.51	1.79

Tabulated values correspond to the response induced by friction in one direction

Table 8 – Pin friction summary table

Test Run	Average Water Elevation during testing (ft)	Approximate Thrust at time of Testing (kips per arm)	Gate/Member Designation	Pin Friction Moment (kip-in)	Friction Coefficient
1	435.66	492.40	Right Pin	462.00	0.17
			Left Pin	487.50	0.18
2	435.66	492.40	Right Pin	451.40	0.17
			Left Pin	476.30	0.18
3	435.66	492.40	Right Pin	453.20	0.17
			Left Pin	478.90	0.18

Tabulated values correspond to the response induced by friction in one direction

APPENDIX A – GATE 4 TORQUE AND HOIST FORCE PLOTS

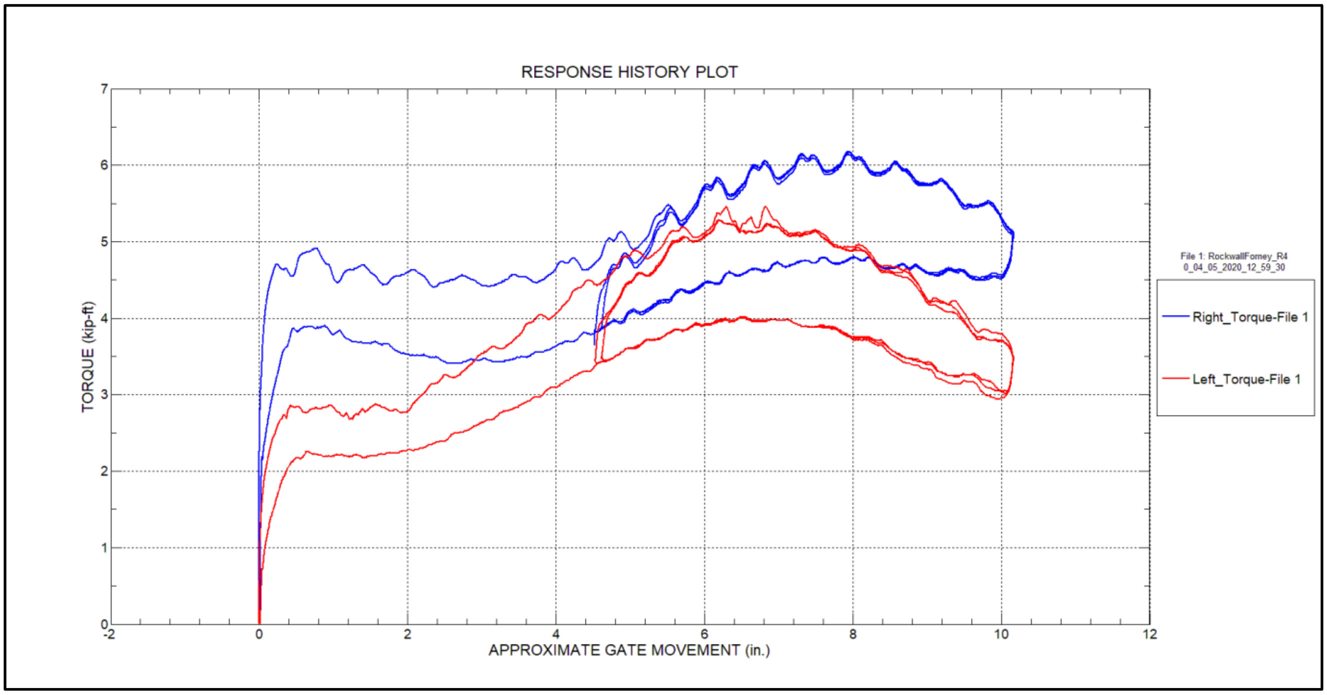

Figure 25 – Hoist torque response history – Gate 4 – Test 1

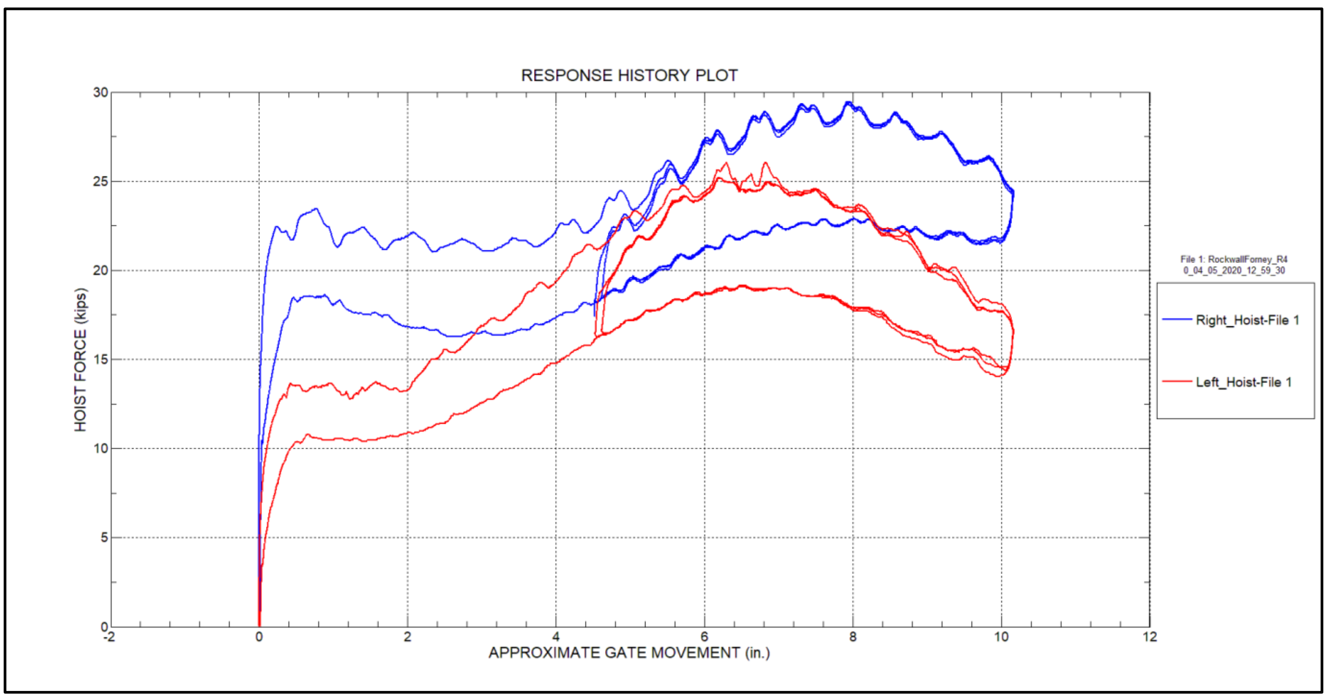

Figure 26 – Hoist force response history – Gate 4 – Test 1

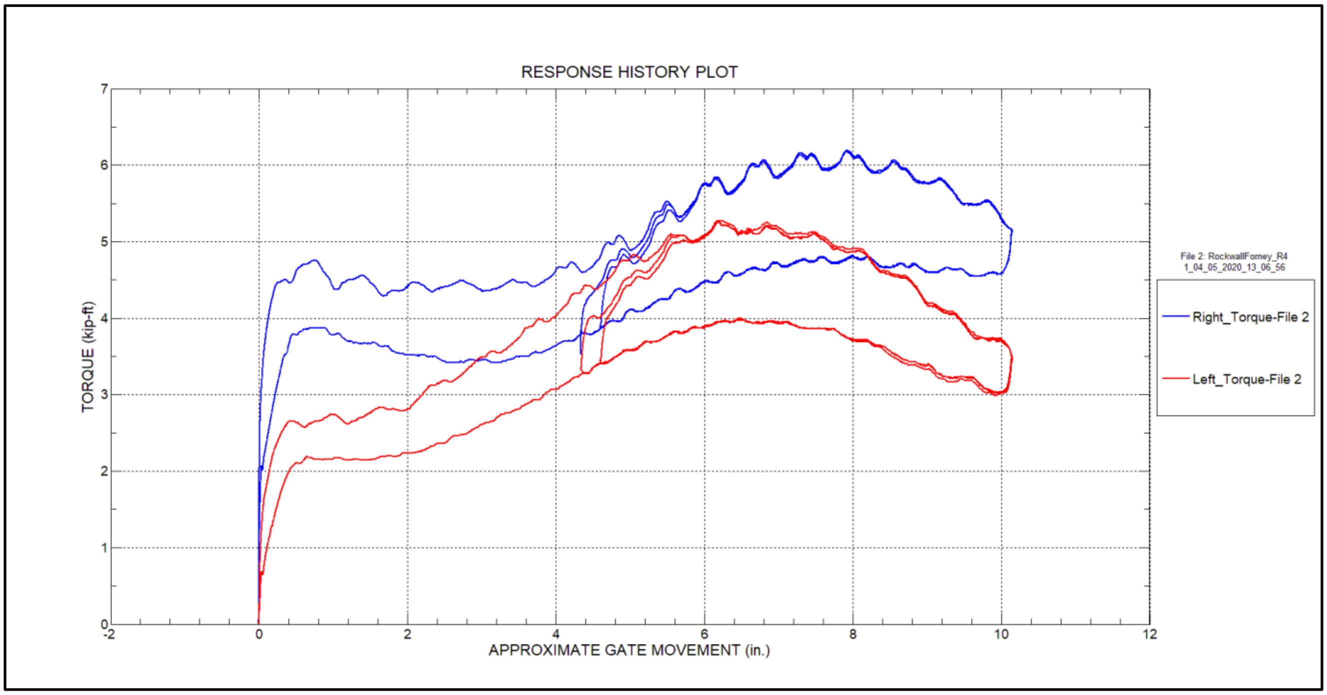

Figure 27 – Hoist torque response history – Gate 4 – Test 2

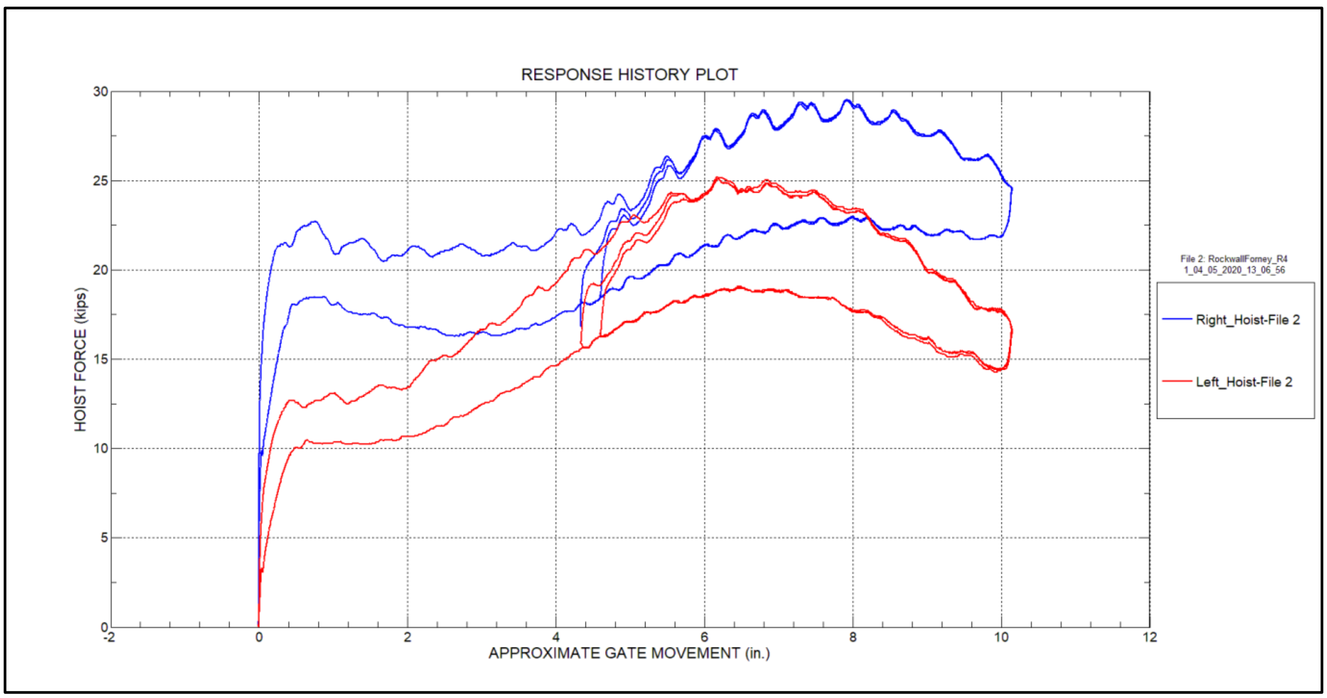

Figure 28 – Hoist force response history – Gate 4 – Test 2

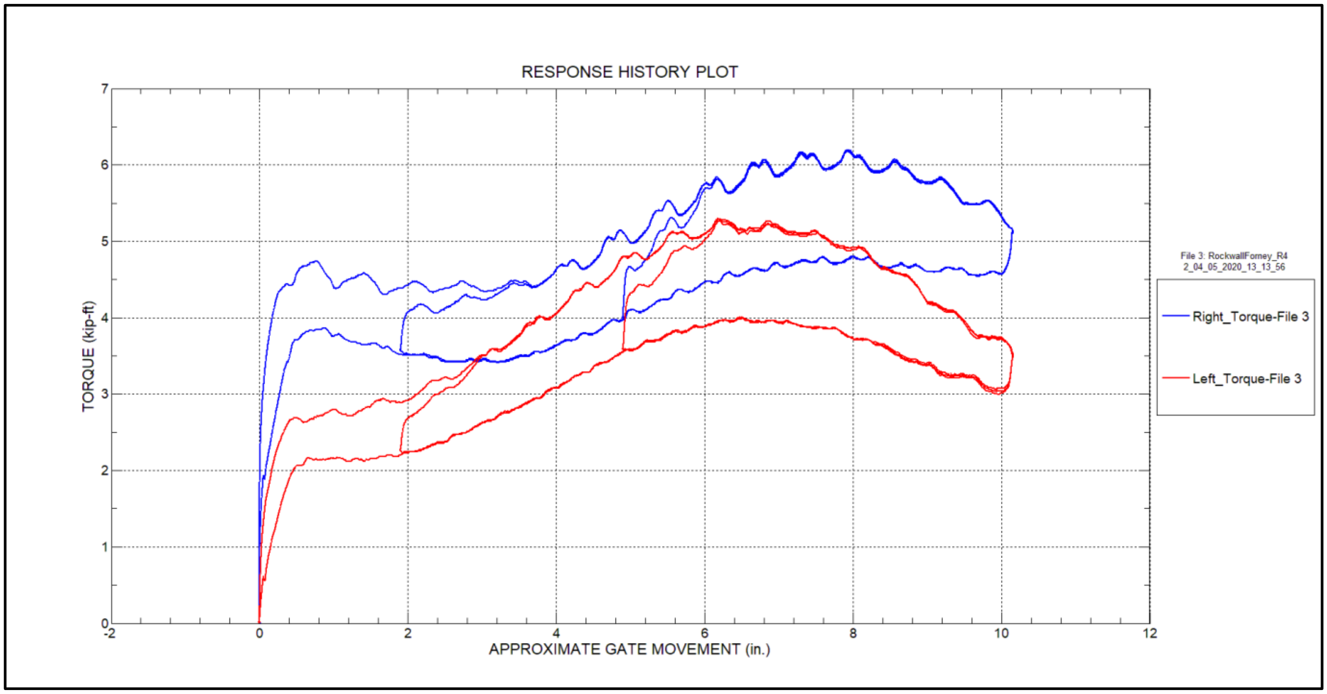

Figure 29 – Hoist torque response history – Gate 4 – Test 3

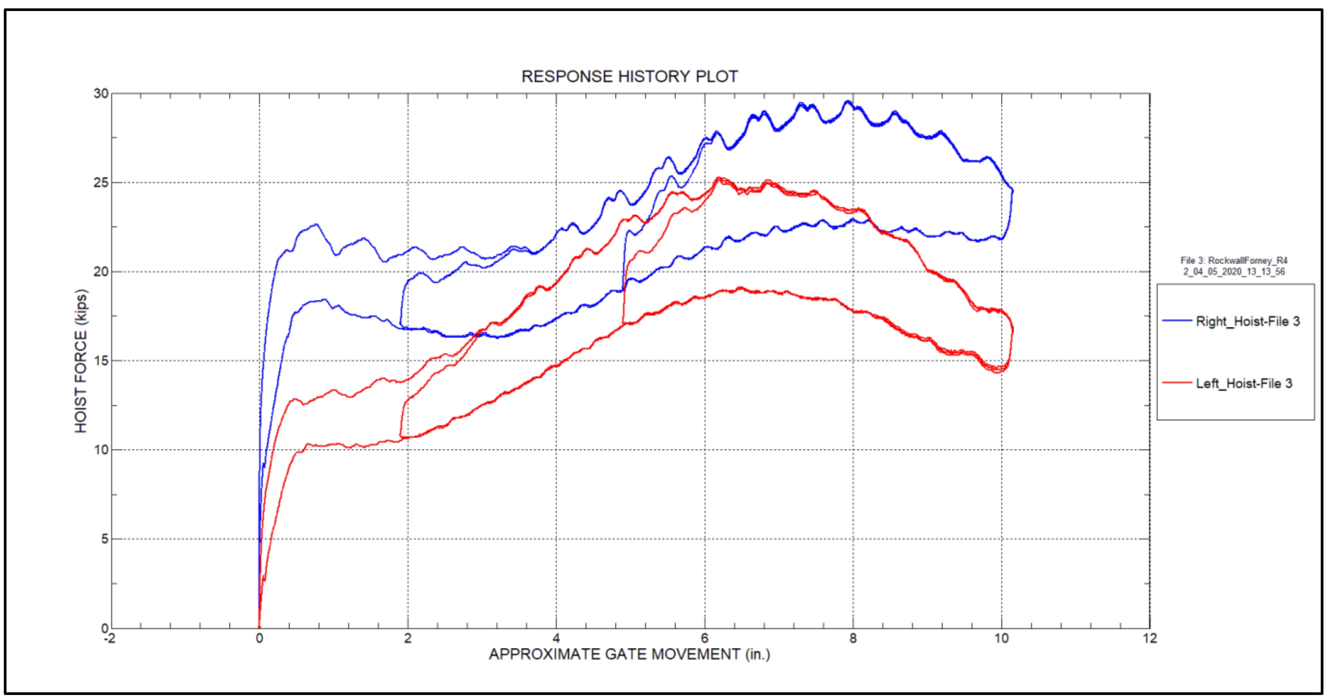

Figure 30 – Hoist force response history – Gate 4 – Test 3

APPENDIX B – GATE 4 PIN MOMENT COMPONENT PLOTS

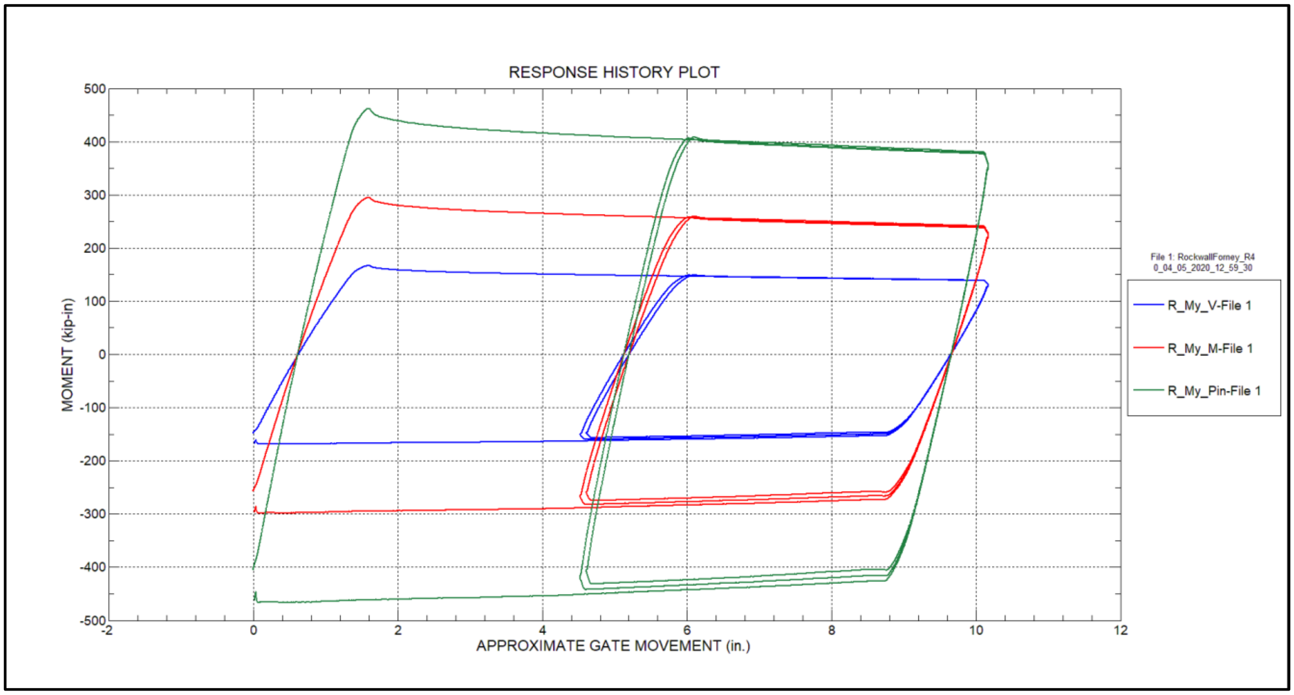

Figure 31 – Pin moment response history – Right arm – Test run 1

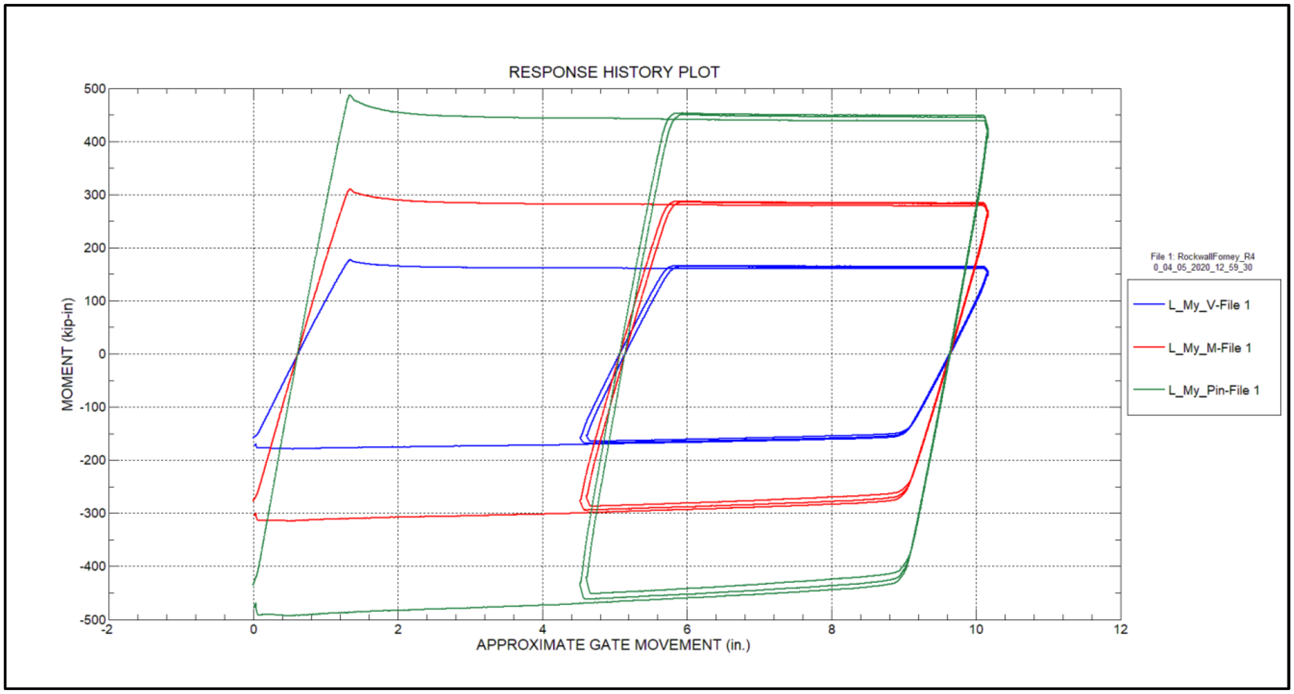

Figure 32 – Pin moment response history – Left arm – Test run 1

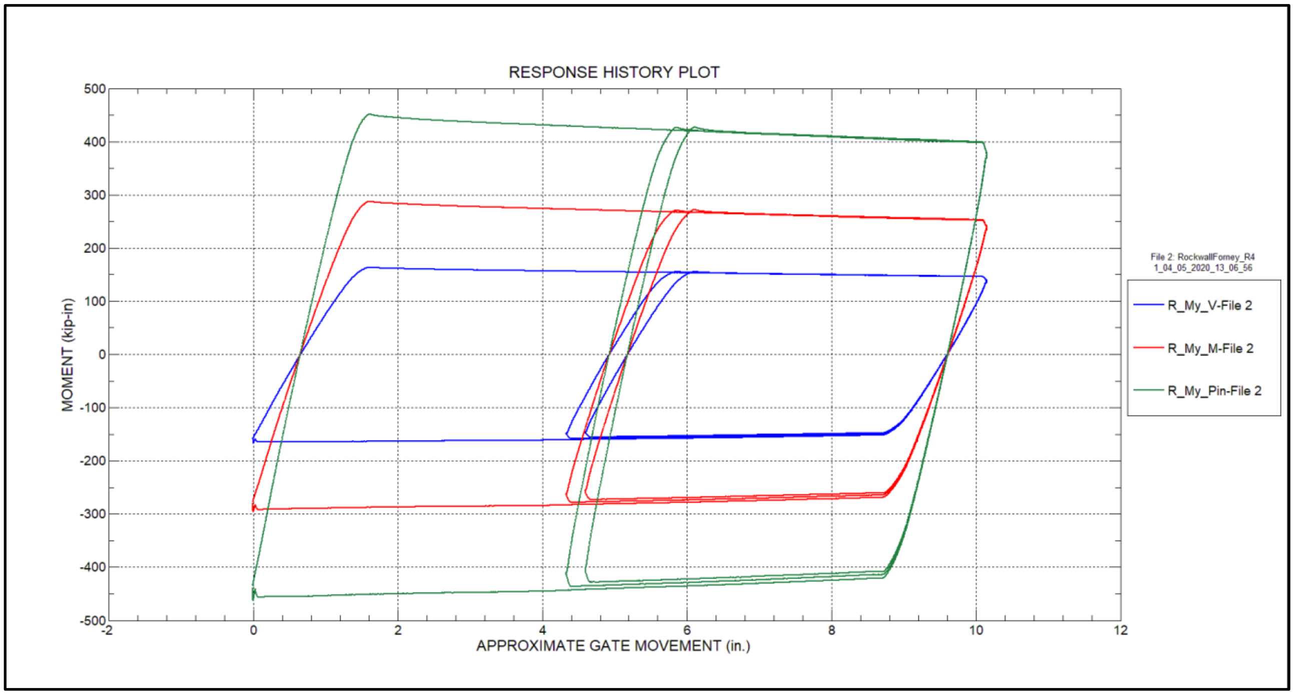

Figure 33 – Pin moment response history – Right arm – Test run 2

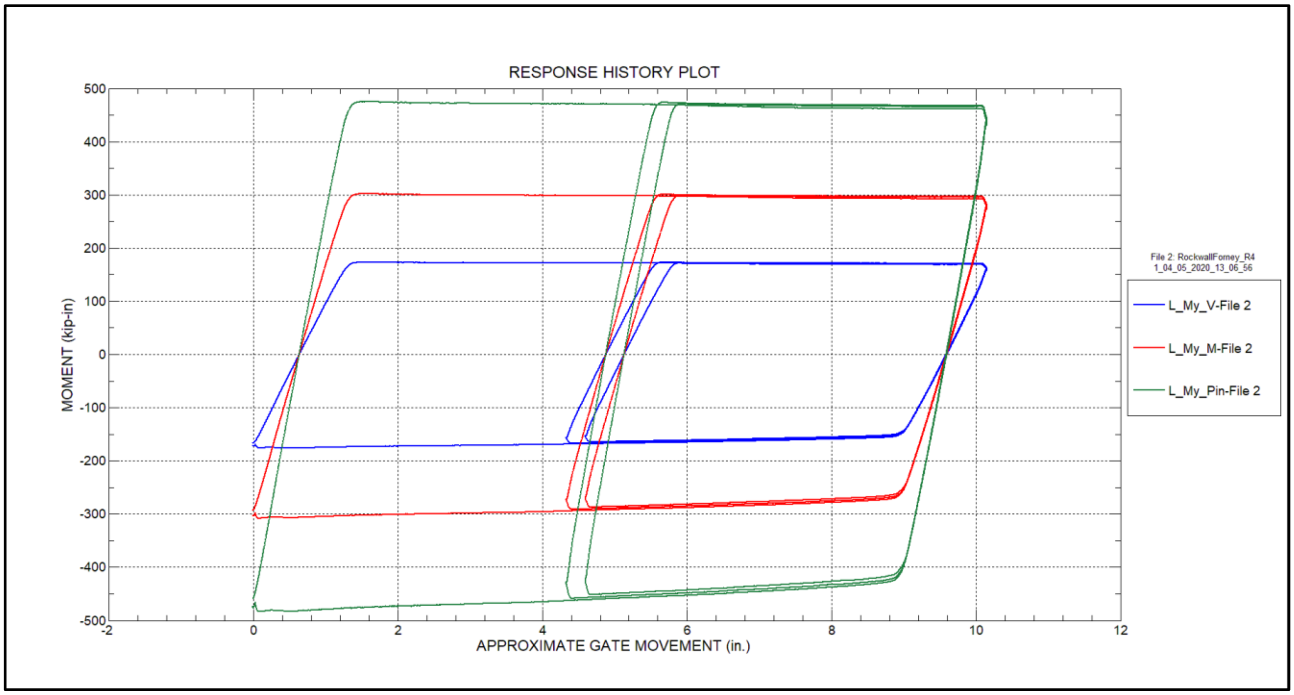

Figure 34 – Pin moment response history – Left arm – Test run 2

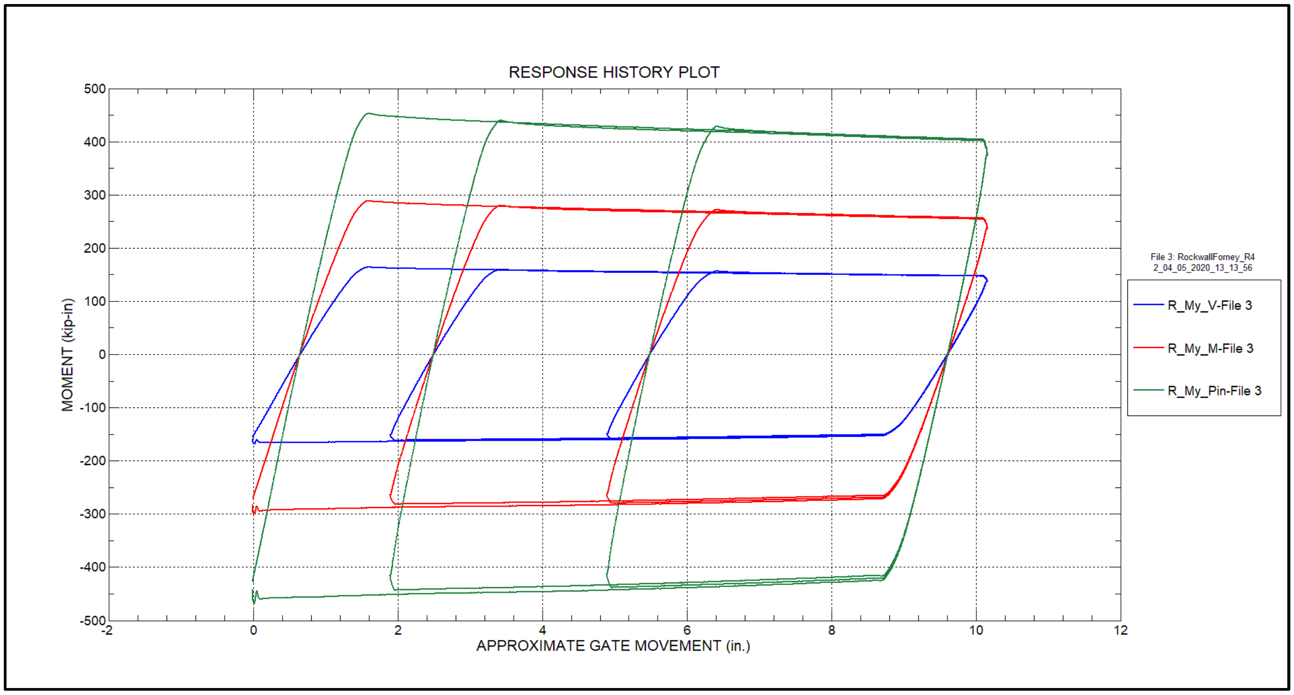

Figure 35 – Pin moment response history – Right arm – Test run 3

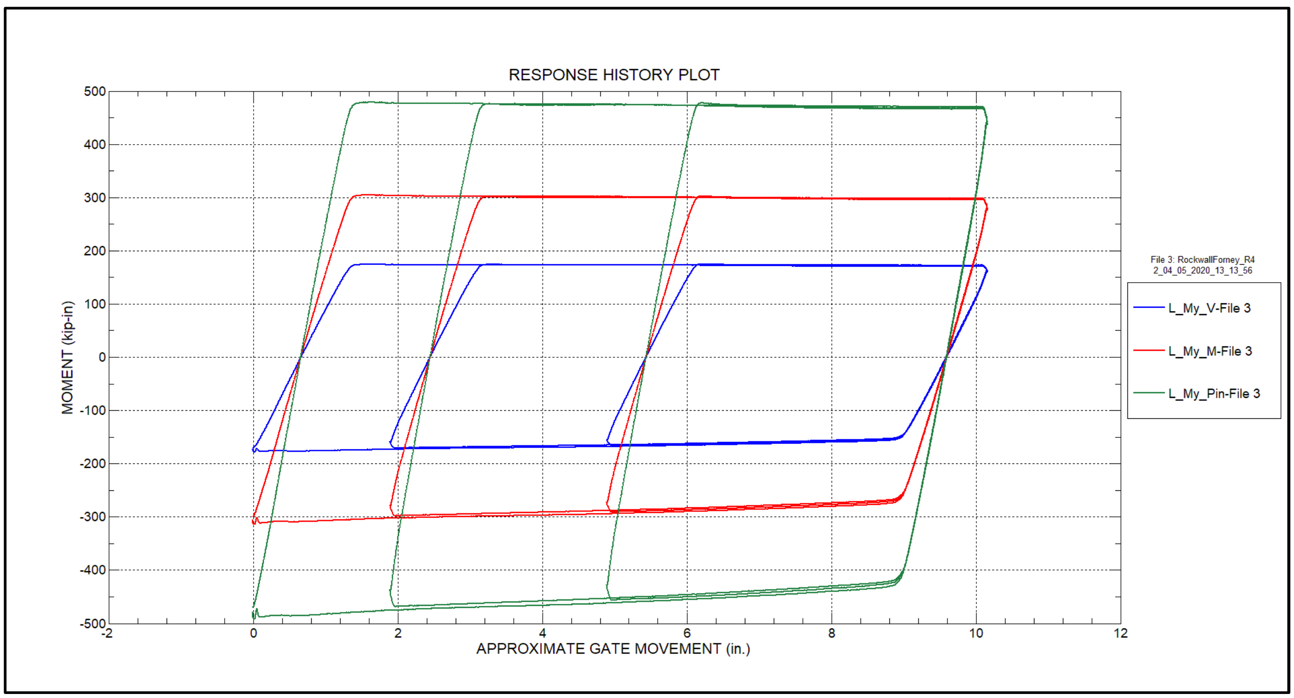

Figure 36 – Pin moment response history – Left arm – Test run 3

APPENDIX C – INSTRUMENTATION PLANS

SCHNABEL ENGINEERING
ROCKWALL FORNEY DAM
LIVE LOAD TESTING

RAW DATA. REFINED RESULTS.
740 S PIERCE AVE, SUITE 15
LOUISVILLE, CO 80027
303.494.3230
WWW.BDITEST.COM

ISSUE

CLIENT

SCHABEL ENGINEERING
16000 CHRISTENSEN RD, STE 101
SEATTLE, WA 98188

PROJECT NAME

SCHNABEL ENGINEERING
ROCKWALL FORNEY DAM
LIVE LOAD TESTING

Drawn By:	KNR
Checked By:	JDS
Date:	05/27/2020
Client No.:	
BDI No.:	190701-TX
SCALE:	NTS

COVER PAGE

LLT-00

The user acknowledges that these documents are instruments of professional service, and are protected by Copyright. This document and the information contained in this document are the property of Bridge Diagnostics, Inc., and shall not be reused, copied, disseminated, modified, amended or altered in any way. It is issued for information purposes only. The user agrees to hold harmless, indemnify and defend Bridge Diagnostics, Inc. against any and all damages, claims and losses, including defense costs, arising out of any use, reuse or copying of this document.

PLOT TIME: 6/12/2020 3:22 PM
FILEPATH: C:\Users\colemand\BDI\Services - Documents\Server_Remote\190701-TX_Schnabel_RockwallForneyDam\7. Instrumentation Plans\BDI_ROCKWALLFORNEY_01_GENERAL.dwg
© YYYY BRIDGE DIAGNOSTICS INC.

GAGE LEGEND & SPECIFICATION

SYMBOL	TYPE	BRAND	MODEL	NOTES
	STRAIN TRANSDUCER	BDI	ST350	
	TILTMETER (UNI-AXIAL)	BDI	T500-030	
	TORQUE SENSOR	HPI	-	HBWS-35-125-6-0.5VR-FB
	AMP SENSOR	CR MAGNETICS	CR42105-200	

GENERAL NOTES

- INSTRUMENTATION SHALL BEGIN ON APRIL 1ST, 2020.
- GATES 1 THRU 14 SHALL BE ACCESSED USING SPRAT ROPE ACCESS TECHNIQUES.
- BDI WILL PERFORM ALL SURFACE PREPARATION, SENSOR INSTALLATION, AND EQUIPMENT INSTALLATION.
- SEE LLT-31 FOR SENSOR INSTALLATION DETAILS.
- TWO PAIRS OF TORQUE GAGES WILL BE INSTALLED ON THE GATE MOTORS' PINION SHAFTS BETWEEN THE MOTORS AND THE HOISTS.
  - GAGE PAIRS WILL BE INSTALLED 180° APART FROM EACH OTHER.
  - EXACT POSITIONS OF THE GAGE PAIRS ON THE PINION SHAFT WILL BE DETERMINED IN THE FIELD.
- THREE PHASE AMPERAGE GAGES WILL BE INSTALLED ON THE MOTOR CONTROLS BY A QUALIFIED ELECTRICIAN PROVIDED BY GARVER.

TESTING PROCEDURE:

- TESTING SHALL BE STARTED WITH THE GATE IN THE CLOSED POSITION.
- ONCE DATA COLLECTION BEGINS, THE GATE SHALL BE RAISED TO TWO OR THREE TIMES THE HEIGHT NECESSARY FOR TRUNNION FRICTION TO BE OVERCOME, H1 (TYPICALLY 6"-12"), AND HELD THERE UNTIL DATA STABILIZES.
- THE GATE SHALL BE LOWERED APPROXIMATELY TWICE THE DISTANCE TO OVERCOME TRUNNION FRICTION, H2, AND HELD THERE UNTIL DATA STABILIZES.
- THE GATE SHALL BE RAISED TO H1 AND HELD THERE UNTIL DATA STABILIZES.
- THE GATE SHALL BE LOWERED TO H2 AND HELD THERE UNTIL DATA STABILIZES.
- THE GATE SHALL BE RAISED TO H1 AND HELD THERE UNTIL DATA STABILIZES.
- THE GATE WAS LOWERED BACK TO CLOSED POSITION AND DATA COLLECTION STOPPED.
- A MINIMUM OF 3 TESTS SHALL BE PERFORMED PER GATE.

LOCATION KEY

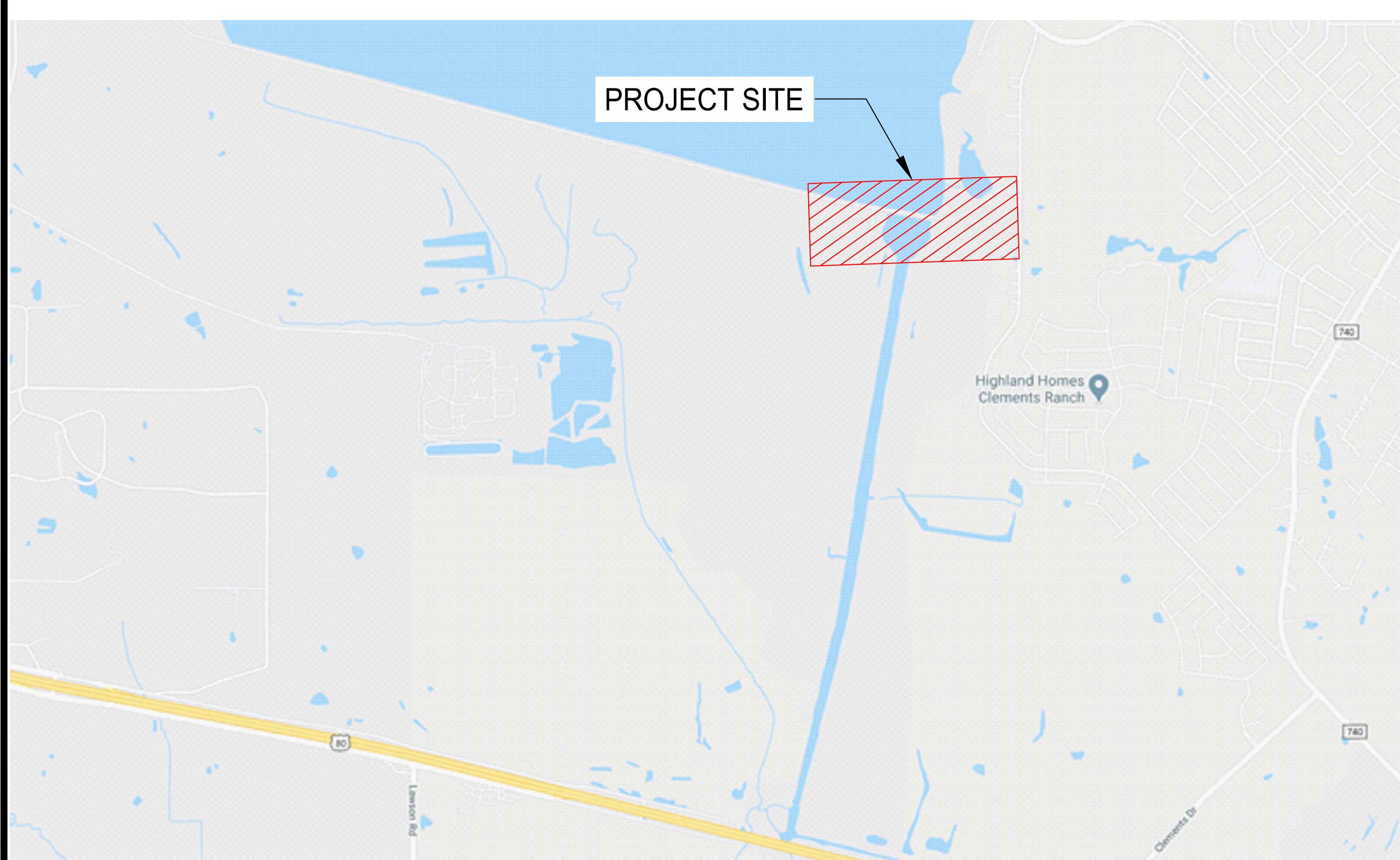

GAGE COUNT PER GATE

SENSOR LEGEND	SENSOR COUNT	CHANNEL COUNT
STRAIN TRANSDUCER	(48)	(48)
TILTMETER (UNI-AXIAL)	(4)	(4)
TORQUE SENSOR	(4)	(4)
AMP SENSOR	(3)	(3)
TOTAL	(59)	(59)

INDEX OF SHEETS

INDEX OF ISSUE

NO.	DATE	REVISION DESCRIPTION
1	3/20/2020	LIVE LOAD TESTING (LLT) INSTRUMENTATION PLAN (FOR APPROVAL)
2	5/27/2020	LIVE LOAD TESTING (LLT) INSTRUMENTATION PLAN AS BUILTS

BDI REFERENCE NUMBER: 190701-TX

RAW DATA. REFINED RESULTS.
740 S PIERCE AVE, SUITE 15
LOUISVILLE, CO 80027
303.494.3230
WWW.BDITEST.COM

ISSUE

CLIENT

SCHABEL ENGINEERING
16000 CHRISTENSEN RD, STE 101
SEATTLE, WA 98188

PROJECT NAME

SCHABEL ENGINEERING
ROCKWALL FORNEY DAM
LIVE LOAD TESTING

Drawn By:	KNR
Checked By:	JDS
Date:	05/27/2020
Client No.:	
BDI No.:	190701-TX
SCALE:	NTS

OVERALL LEGEND

LLT-01

The user acknowledges that these documents are instruments of professional service, and are protected by Copyright. This document and the information contained in this document are the property of Bridge Diagnostics, Inc., and shall not be reused, copied, disseminated, modified, amended or altered in any way. It is issued for information purposes only. The user agrees to hold harmless, indemnify and defend Bridge Diagnostics, Inc. against any and all damages, claims and losses, including defense costs, arising out of any use, reuse or copying of this document.

PLOT TIME: 6/12/2020 3:22 PM
FILEPATH: C:\Users\colemand\BDI\Services - Documents\Server_Remote\190701-TX_Schnabel_RockwallForneyDam\7. Instrumentation Plans\BDI_ROCKWALLFORNEY_01_GENERAL.dwg
© YYYY BRIDGE DIAGNOSTICS INC.

GATE 1 GATE 2 GATE 3 GATE 4 GATE 5 GATE 6 GATE 7 GATE 8 GATE 9 GATE 10 GATE 11 GATE 12 GATE 13 GATE 14

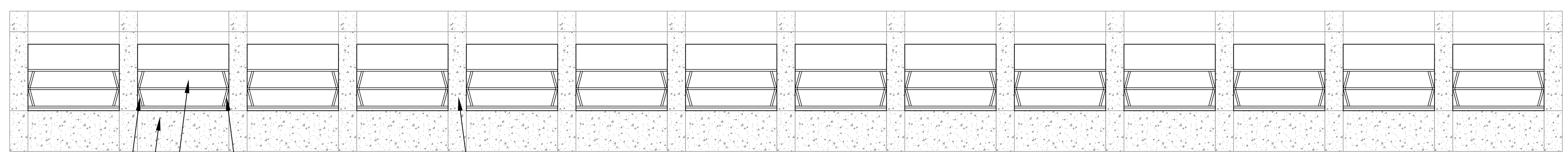

1 DOWNSTREAM ELEVATION OF GATES

LOOKING NORTH (UPSTREAM)

RAW DATA. REFINED RESULTS.
740 S PIERCE AVE, SUITE 15
LOUISVILLE, CO 80027
303.494.3230
WWW.BDITEST.COM

ISSUE

CLIENT

SCHABEL ENGINEERING
16000 CHRISTENSEN RD, STE 101
SEATTLE, WA 98188

PROJECT NAME

SCHNABEL ENGINEERING
ROCKWALL FORNEY DAM
LIVE LOAD TESTING

Drawn By:	KNR
Checked By:	JDS
Date:	05/27/2020
Client No.:	
BDI No.:	190701-TX
SCALE:	NTS

OVERALL STRUCTURE LAYOUT

LLT-02

The user acknowledges that these documents are instruments of professional service, and are protected by Copyright. This document and the information contained in this document are the property of Bridge Diagnostics, Inc., and shall not be reused, copied, disseminated, modified, amended or altered in any way. It is issued for information purposes only. The user agrees to hold harmless, indemnify and defend Bridge Diagnostics, Inc. against any and all damages, claims and losses, including defense costs, arising out of any use, reuse or copying of this document.

PLOT TIME: 6/12/2020 3:22 PM
FILEPATH: C:\Users\colemand\BDI\Services - Documents\Server_Remote\190701-TX_Schnabel_RockwallForneyDam\7. Instrumentation Plans\BDI_ROCKWALLFORNEY_01_GENERAL.dwg
© YYYY BRIDGE DIAGNOSTICS INC.

The user acknowledges that these documents are instruments of professional service, and are protected by Copyright. This document and the information contained in this document are the property of Bridge Diagnostics, Inc., and shall not be reused, copied, disseminated, modified, amended or altered in any way. It is issued for information purposes only. The user agrees to hold harmless, indemnify and defend Bridge Diagnostics, Inc. against any and all damages, claims and losses, including defense costs, arising out of any use, reuse or copying of this document.

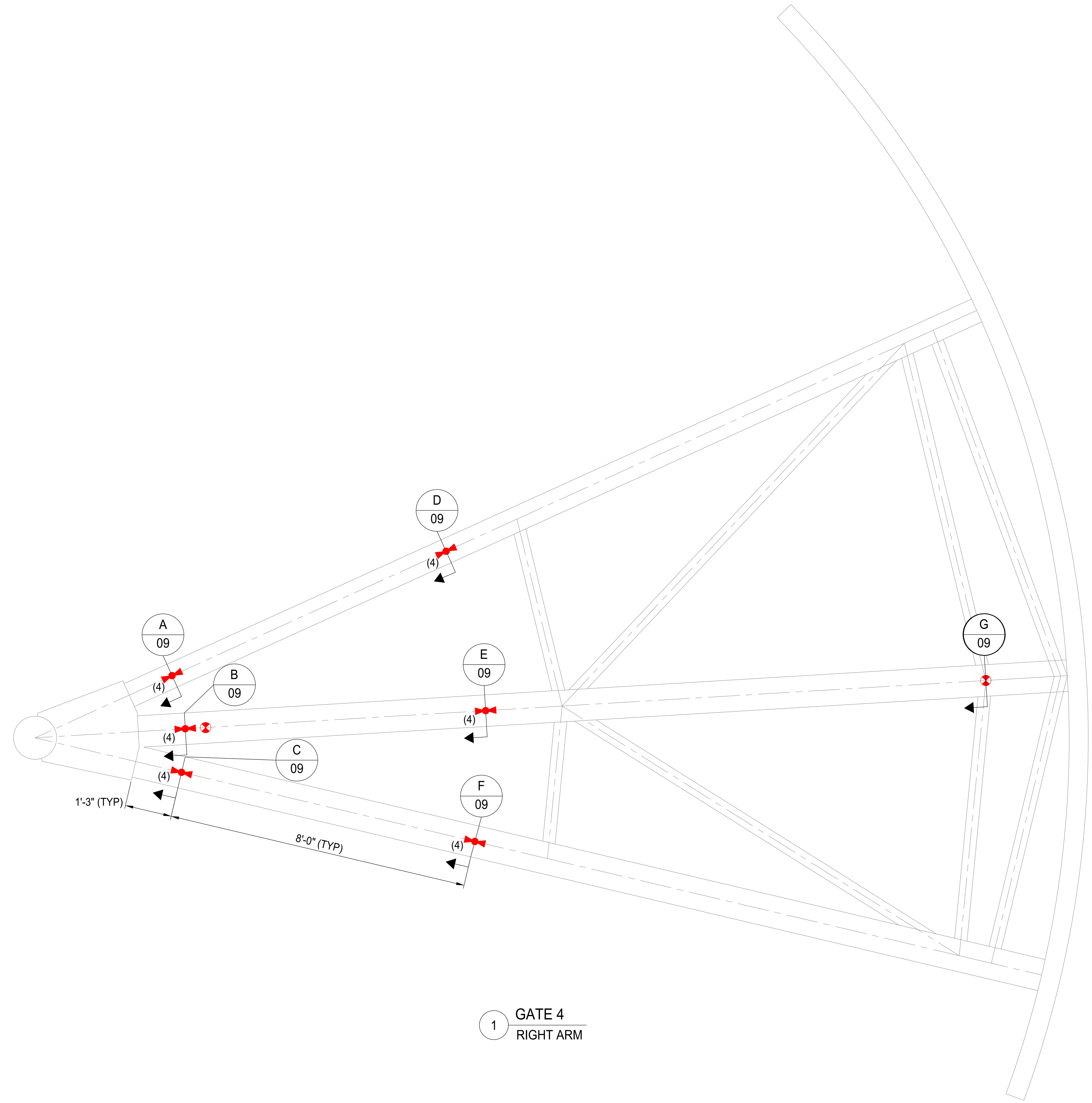

1 GATE 4
RIGHT ARM

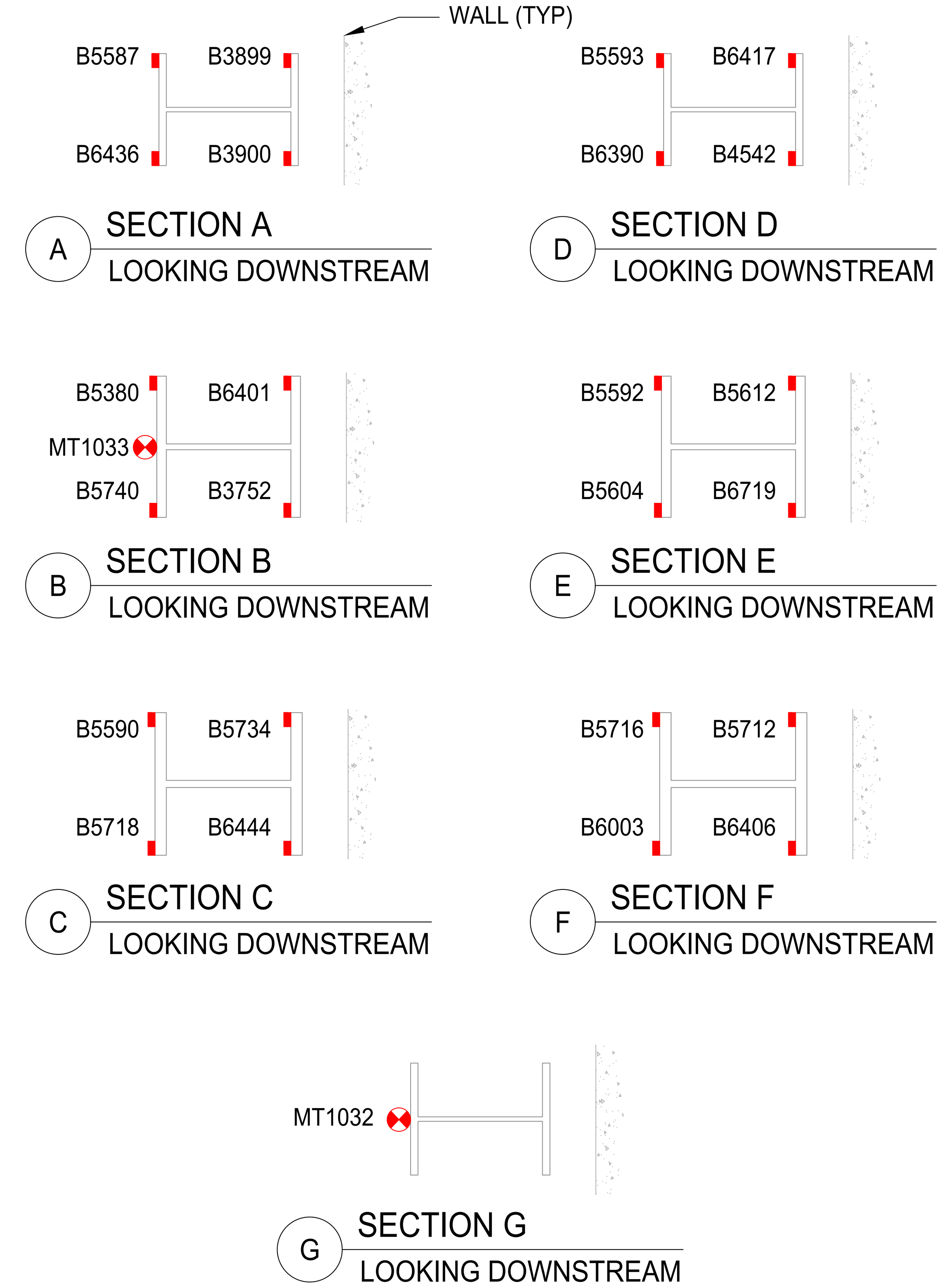

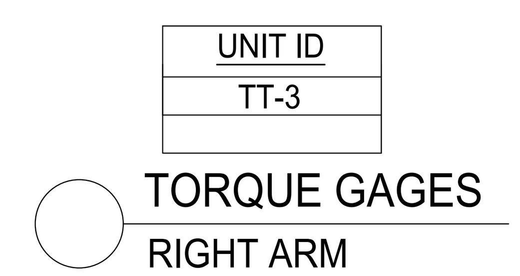

NOTES:

1. SECTIONS A, B, & C SHALL BE INSTALLED 15 INCHES AWAY FROM TRUNNION PLATE.
2. TILTMETERS SHALL BE INSTALLED CENTERED ON THE MIDDLE STRUT FLANGE.
3. SECTION G'S TILTMETER SHALL BE INSTALLED AS CLOSE TO THE SKINPLATE AS POSSIBLE.

SENSOR LEGEND

- STRAIN TRANSDUCER
- TILTMETER (UNI-AXIAL)
- TORQUE SENSOR

BDI
RAW DATA. REFINED RESULTS.
740 S PIERCE AVE, SUITE 15
LOUISVILLE, CO 80027
303.494.3230
WWW.BDITEST.COM

ISSUE

CLIENT

SCHABEL ENGINEERING
16000 CHRISTENSEN RD, STE 101
SEATTLE, WA 98188

PROJECT NAME

SCHABEL ENGINEERING
ROCKWALL FORNEY DAM
LIVE LOAD TESTING

Drawn By:	KNR
Checked By:	JDS
Date:	05/27/2020
Client No.:	
BDI No.:	190701-TX
SCALE:	NTS

GATE 4 - RIGHT ARM
ELEVATION

LLT-09

PLOT TIME: 6/12/2020 3:22 PM
FILEPATH: C:\Users\coleman\BDI\Services - Documents\Server_Remote\190701-TX_Schabel_RockwallForneyDam\7. Instrumentation Plans\BDI_ROCKWALLFORNEY_01_GENERAL.dwg
© YYYY BRIDGE DIAGNOSTICS INC.

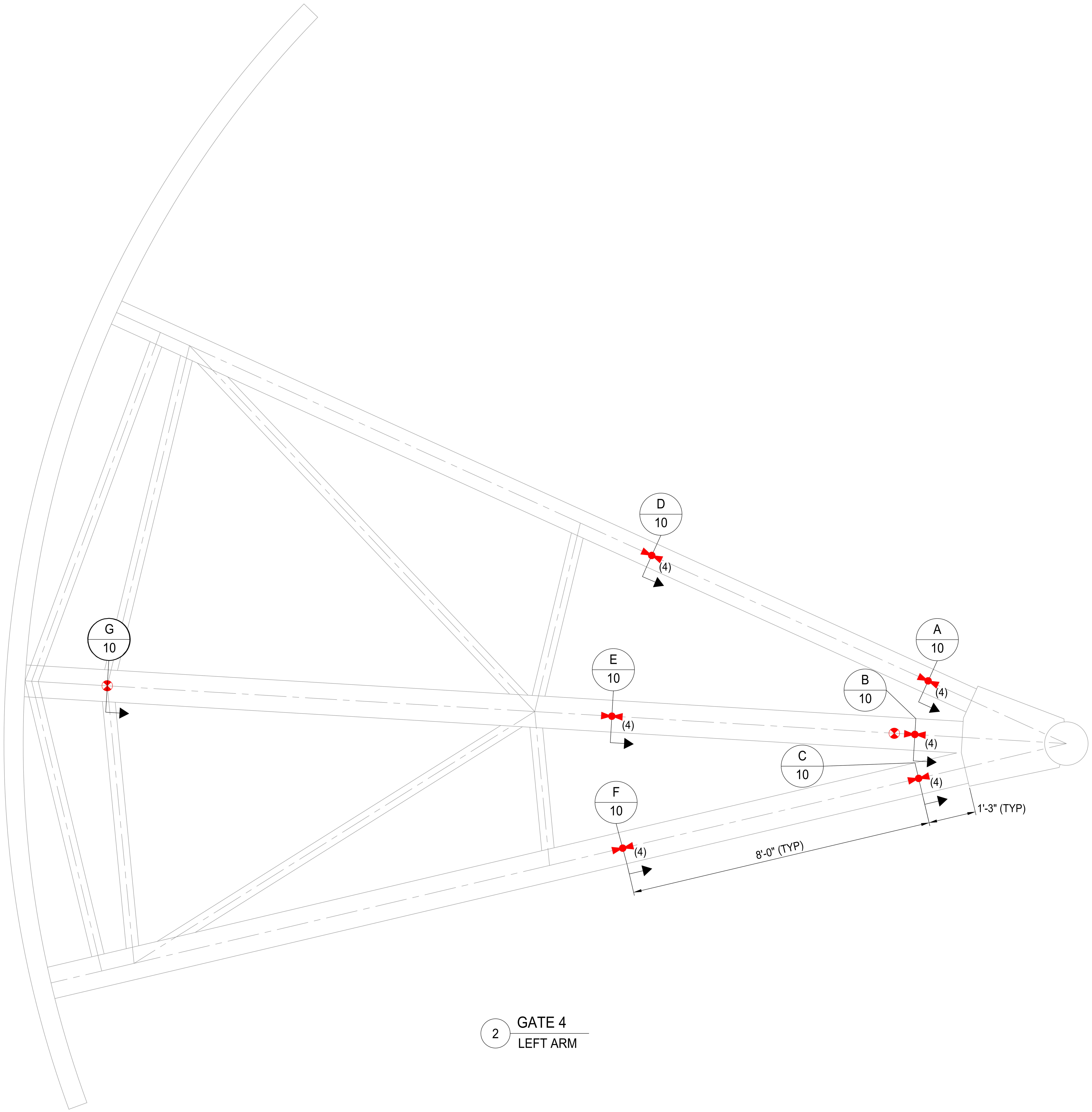

2 GATE 4
LEFT ARM

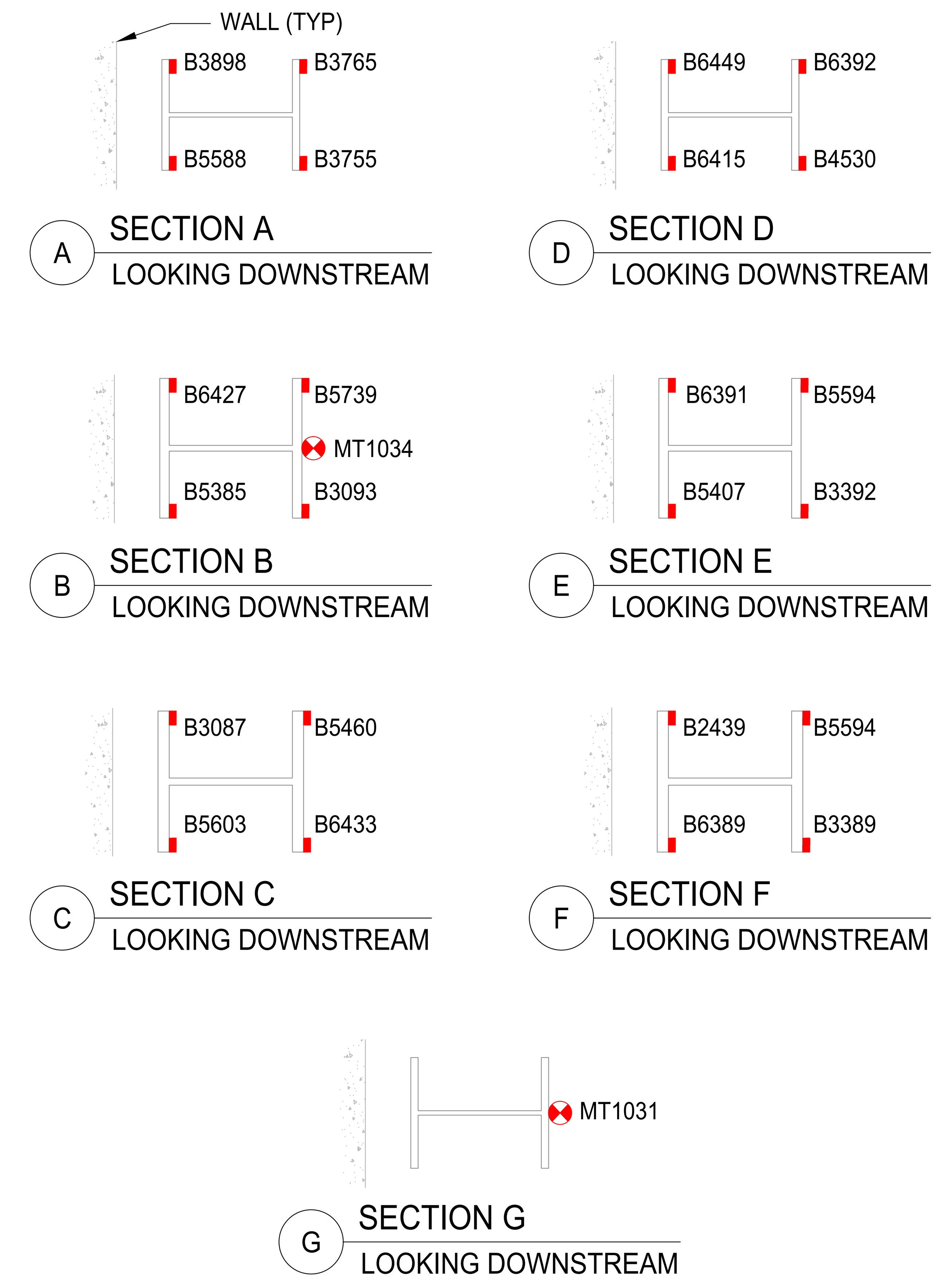

A SECTION A
LOOKING DOWNSTREAM

D SECTION D
LOOKING DOWNSTREAM

B SECTION B
LOOKING DOWNSTREAM

E SECTION E
LOOKING DOWNSTREAM

C SECTION C
LOOKING DOWNSTREAM

F SECTION F
LOOKING DOWNSTREAM

G SECTION G
LOOKING DOWNSTREAM

UNIT ID
TT-4

TORQUE GAGES
LEFT ARM

NOTES:
1. SECTIONS A, B, & C SHALL BE INSTALLED 15 INCHES AWAY FROM TRUNNION PLATE.
2. TILTMETERS SHALL BE INSTALLED CENTERED ON THE MIDDLE STRUT FLANGE.
3. SECTION G'S TILTMETER SHALL BE INSTALLED AS CLOSE TO THE SKINPLATE AS POSSIBLE.

SENSOR LEGEND
- STRAIN TRANSDUCER
- TILTMETER (UNI-AXIAL)
- TORQUE SENSOR

BDI
RAW DATA. REFINED RESULTS.
740 S PIERCE AVE, SUITE 15
LOUISVILLE, CO 80027
303.494.3230
WWW.BDITEST.COM

ISSUE

CLIENT

SCHABEL ENGINEERING
16000 CHRISTENSEN RD, STE 101
SEATTLE, WA 98188

PROJECT NAME

SCHABEL ENGINEERING ROCKWALL FORNEY DAM LIVE LOAD TESTING

Drawn By:	KNR
Checked By:	JDS
Date:	05/27/2020
Client No.:	
BDI No.:	190701-TX
SCALE:	NTS

GATE 4 - LEFT ARM
ELEVATION
LLT-10

The user acknowledges that these documents are instruments of professional service, and are protected by Copyright. This document and the information contained in this document are the property of Bridge Diagnostics, Inc., and shall not be reused, copied, disseminated, modified, amended or altered in any way. It is issued for information purposes only. The user agrees to hold harmless, indemnify and defend Bridge Diagnostics, Inc. against any and all damages, claims and losses, including defense costs, arising out of any use, reuse or copying of this document.

PLOT TIME: 6/12/2020 3:22 PM
FILEPATH: C:\Users\colemand\BDI\Services - Documents\Server_Remote\190701-TX_Schabel_RockwallForneyDam\7. Instrumentation Plans\BDI_ROCKWALLFORNEY_01_GENERAL.dwg
© YYYY BRIDGE DIAGNOSTICS INC.

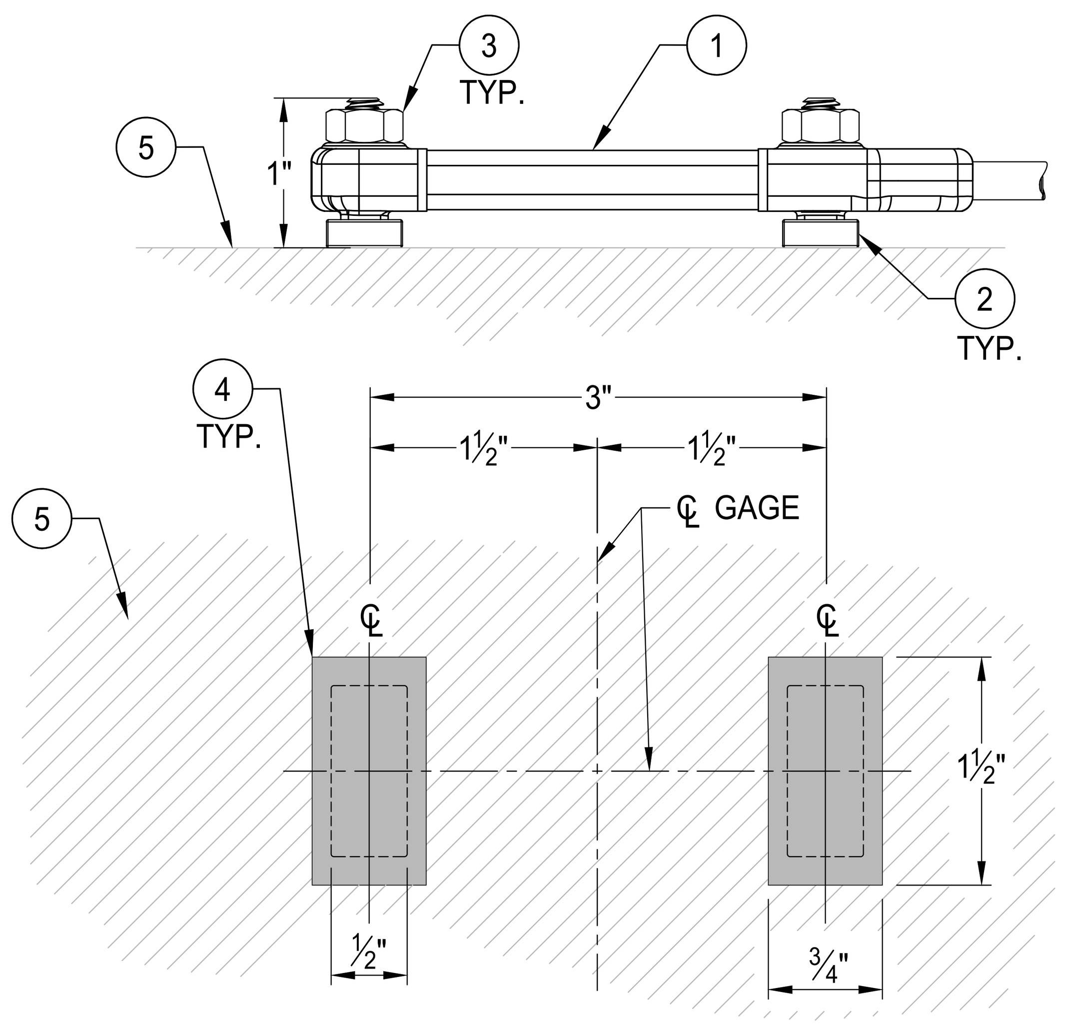

COMPONENT DESCRIPTION

1. ST350 STRAIN GAGE
2. 1/4"-20 THREADED MOUNTING TAB
3. 1/4"-20 STAINLESS STEEL NUT
4. TYPICAL SURFACE PREP REQUIRED TO MOUNT STRAIN GAGES
5. TYPICAL MOUNTING SURFACE

FOOTNOTES - INSTANT ADHESIVE
1. STRAIN GAGES SHALL BE MOUNTED WITH LOCTITE 410 INSTANT ADHESIVE AND LOCTITE 7452 ACCELERANT 2. DURING SURFACE PREP ALL PAINT AND SURFACE DEFORMATIONS MUST BE REMOVED. 3. SURFACE PREP IS REQUIRED JUST PRIOR TO GAGE INSTALLATION AS TO NOT ALLOW SURFACE CONTAMINANTS TO ACCUMULATE.

1 TYPICAL ST350 STRAIN GAGE INSTALLATION

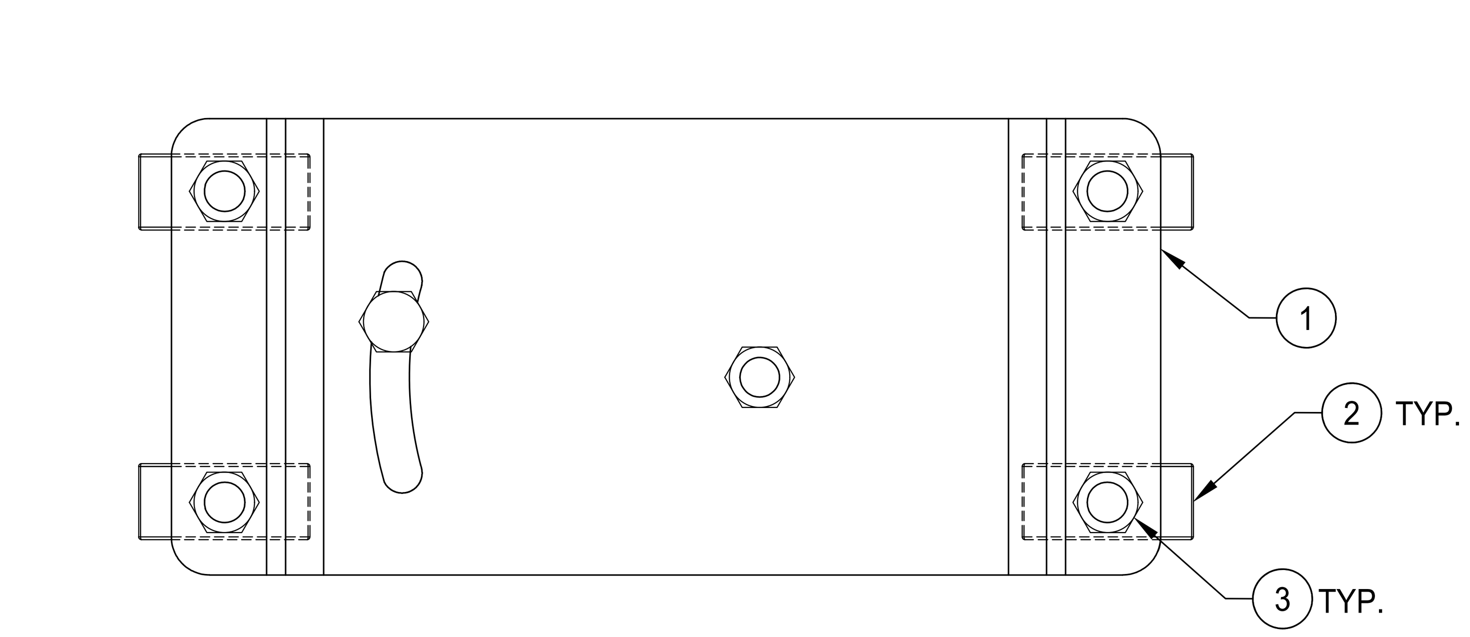

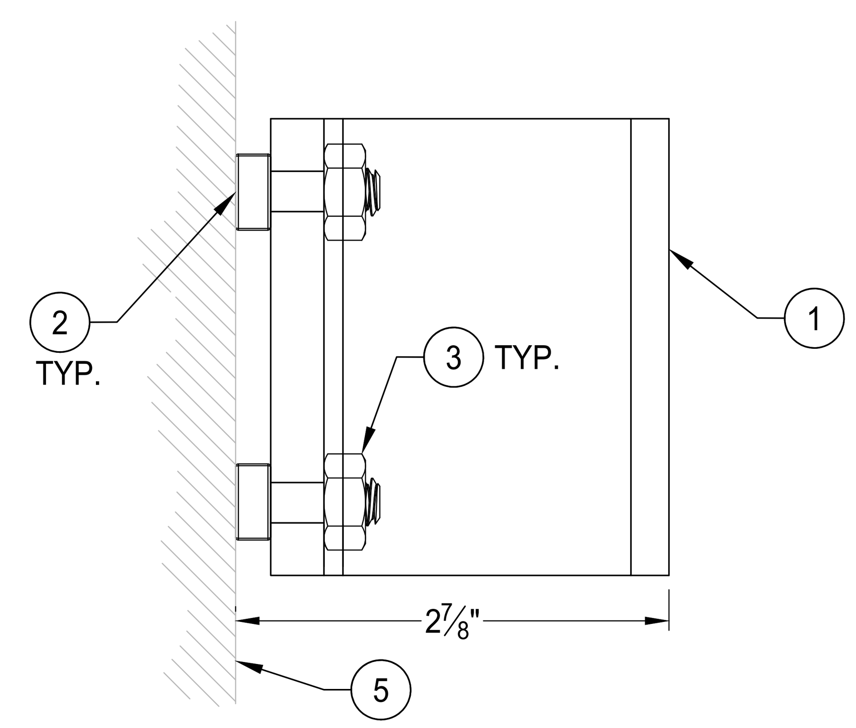

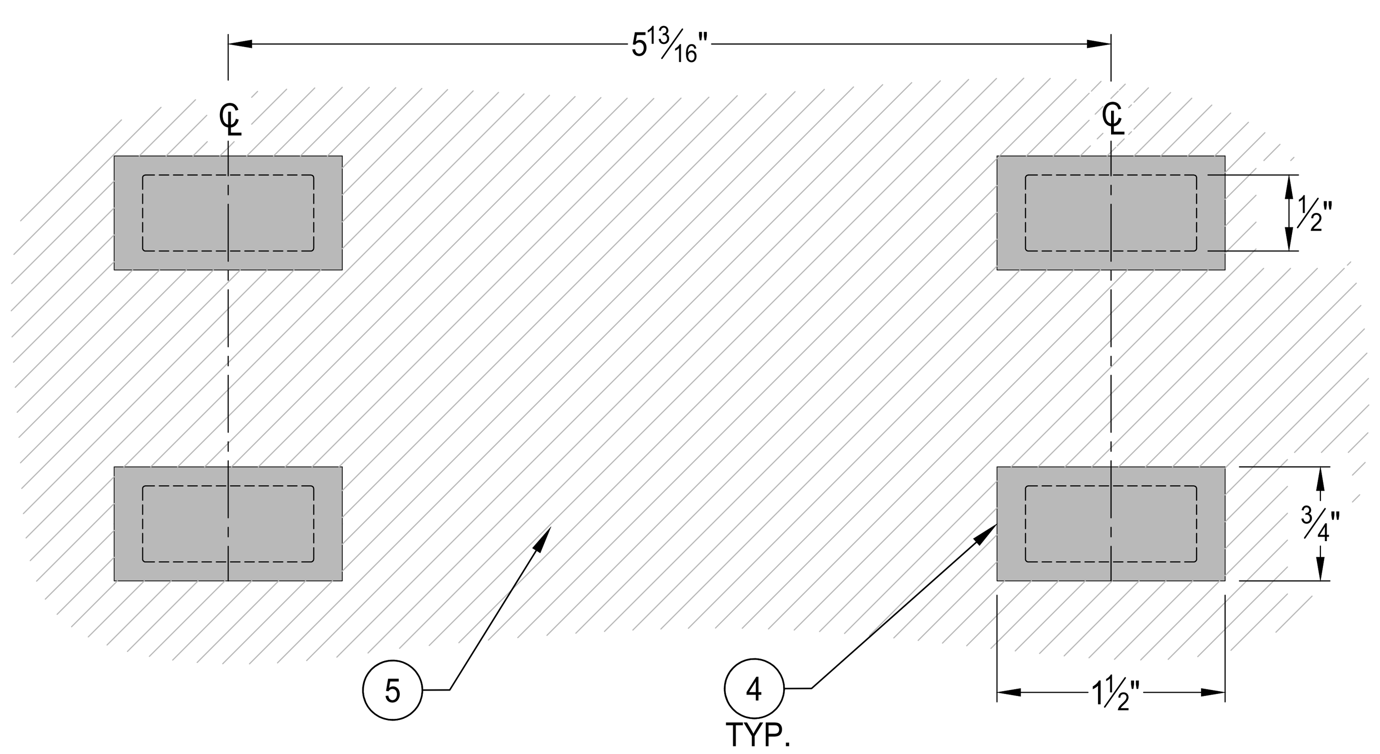

COMPONENT DESCRIPTION

1. BDI +/- 15 DEGREE TILTMETER WITH COVER AND ADJUSTMENT BOLTS
2. 1/4"-20 THREADED MOUNTING TAB
3. 1/4"-20 STAINLESS STEEL NUT
4. TYPICAL SURFACE PREP REQUIRED TO MOUNT TILTMETERS
5. TYPICAL MOUNTING SURFACE

FOOTNOTES - INSTANT ADHESIVE
1. TILTMETERS SHALL BE MOUNTED WITH LOCTITE 410 INSTANT ADHESIVE AND LOCTITE 7452 ACCELERANT 2. DURING SURFACE PREP ALL PAINT AND SURFACE DEFORMATIONS MUST BE REMOVED. 3. SURFACE PREP IS REQUIRED JUST PRIOR TO GAGE INSTALLATION AS TO NOT ALLOW SURFACE CONTAMINANTS TO ACCUMULATE.

2 TYPICAL BDI TILTMETER INSTALLATION

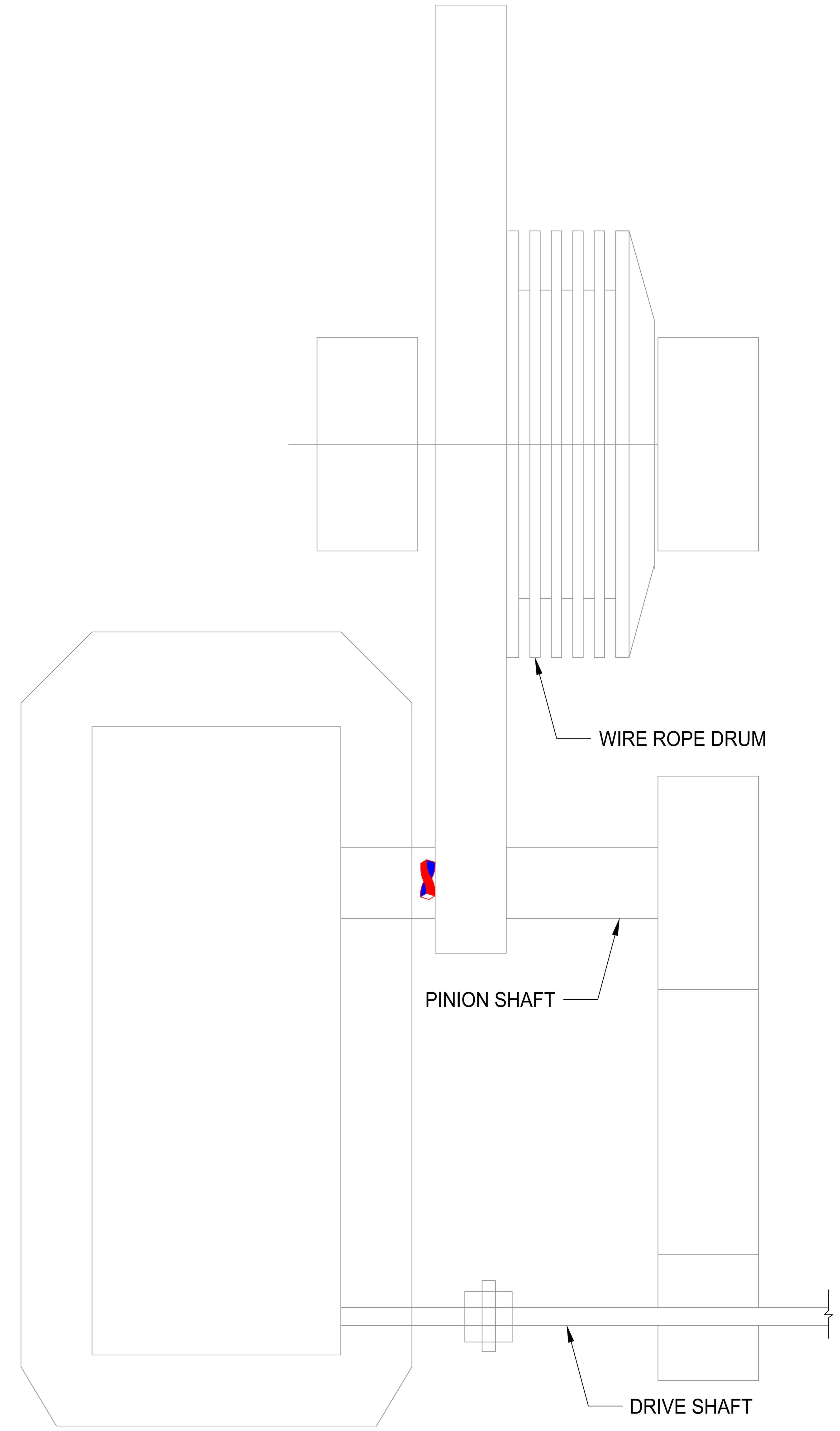

3 TYPICAL HOIST INSTRUMENTATION

TORQUE SENSOR INSTALLATION NOTES:

- TORQUE GAGES WILL BE INSTALLED ON THE PINION SHAFT ON EITHER HOIST MOTOR BETWEEN THE MOTOR AND THE HOIST DRUM
- EXACT POSITIONS OF THE GAGE PAIRS ON THE PINION SHAFT WILL BE DETERMINED IN THE FIELD

SENSOR LEGEND

TORQUE SENSOR

BDI
RAW DATA. REFINED RESULTS.
740 S PIERCE AVE, SUITE 15
LOUISVILLE, CO 80027
303.494.3230
WWW.BDITEST.COM

ISSUE

CLIENT

SCHABEL ENGINEERING
16000 CHRISTENSEN RD, STE 101
SEATTLE, WA 98188

PROJECT NAME

SCHNABEL ENGINEERING
ROCKWALL FORNEY DAM
LIVE LOAD TESTING

Drawn By:	KNR
Checked By:	JDS
Date:	05/27/2020
Client No.:	
BDI No.:	190701-TX
SCALE:	NTS

SENSOR INSTALLATION DETAILS

LLT-31

The user acknowledges that these documents are instruments of professional service, and are protected by Copyright. This document and the information contained in this document are the property of Bridge Diagnostics, Inc., and shall not be reused, copied, disseminated, modified, amended or altered in any way. It is issued for information purposes only. The user agrees to hold harmless, indemnify and defend Bridge Diagnostics, Inc. against any and all damages, claims and losses, including defense costs, arising out of any use, reuse or copying of this document.

PLOT TIME: 6/12/2020 3:24 PM
FILEPATH: C:\Users\colemand\BDI\Services - Documents\Server_Remote\190701-TX_Schabel_RockwallForneyDam\7. Instrumentation Plans\BDI_ROCKWALLFORNEY_01_GENERAL.dwg
© YYYY BRIDGE DIAGNOSTICS INC.

SCHNABEL ENGINEERING
TRUNNION PIN FRICTION TESTING REPORT

ROCKWALL FORNEY DAM – GATE 5
FORNEY, TX

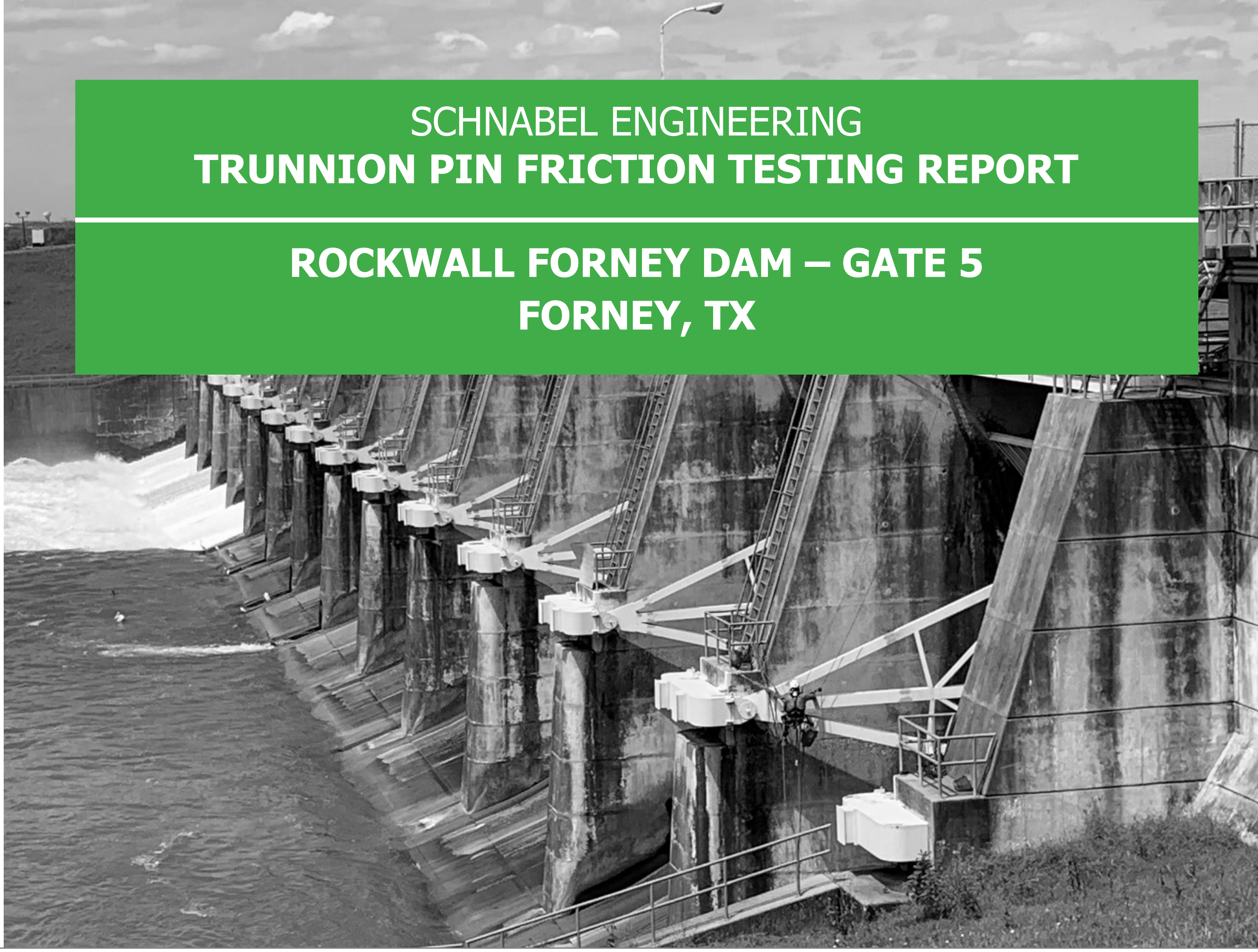

SUBMITTED TO:
SCHNABEL ENGINEERING
16000 CHRISTENSEN RD, SUITE 101
SEATTLE, WA 98188

SUBMITTED BY:
BDI – CO
740 SOUTH PIERCE AVE, UNIT 15
LOUISVILLE, CO 80027

BDI Project No.: **190701-TX**
Report Version: **V1**
Version Submitted: **August 26, 2020**

RAW DATA. REFINED RESULTS.

This document contains Confidential Information and is submitted in confidence to the customer. The submission of the information contained herein shall not be deemed to constitute public disclosure or authorization for disclosure to other parties. BDI's information and name may not be used in advertising or for promotional purposes without BDI's written consent.

TABLE OF CONTENTS

LIST OF FIGURES

LIST OF TABLES

EXECUTIVE SUMMARY

Schnabel Engineering contracted BDI to provide instrumentation and testing services on Gates 1-14 on the Rockwall Forney Dam near Dallas, Texas. The goal of these tests was to record each gate's structural responses during a series of spill tests and use the data to compute accurate coefficients of friction for each trunnion pin, cable lift force, total gate friction, and motor amperage. This report provides details on the work performed on Gate 5.

Instrumentation and testing were performed on Gate 5 at the Rockwall Forney Dam on April 4th, 2020. The gate arms were instrumented with strain and rotation sensors. The hoist motors' pinion shafts were instrumented with torque sensors and the hoist motor controls were instrumented with amperage sensors. Following the instrumentation, a series of spill tests were performed to measure the structural responses resulting from trunnion pin friction. All instrumentation setup and removal were performed using BDI's rope access team.

Following demobilization from the field, the test data was examined for quality and then further processed to evaluate the gate's performance. Strain measurements were converted into bending forces which were then applied to pin-strut free-body diagrams. By summing forces at each pin, friction induced moments could be computed, allowing accurate friction coefficients to be determined. Generally, the observed gate behavior showed that Gate 5 was operating as expected and in a symmetric manner.

The resulting maximum trunnion friction coefficients and corresponding hoist forces are shown in Table 1.

Table 1 – Gate 5 performance summary

Pin Designation	Maximum Friction Coefficient	Maximum Pin Moment due to Pin Friction (kip-In)	Maximum Hoist Force (kips)	Maximum Hoist Force due to Total Gate Friction (kips)
Right Pin	0.21	554.4	27.26	4.38
Left Pin	0.24	648.6	28.49	4.47

Note: Pin designations are in reference to looking downstream

Due to restrictions caused by the hoist limit switches, the hoist cables could not always be fully slacked at the beginning and end of the performed tests. Throughout testing of the Rockwell Forney gates, it was found that this limit switch restriction varied gate to gate and arm to arm. Therefore, it is not recommended to use the collected hoist force data to quantify overall hoist forces during gate operation. Rather, this hoist data can be better utilized to evaluate total friction behavior.

Amperage responses were not used to compute friction results and were collected as verification that the motor performance was not causing unexpected gate responses. These responses indicated the motor was functioning in a stable manner and should be reviewed by a licensed electrician to further evaluate the motor's performance.

All results and recommendations provided in this report were based on the structure in its current condition; therefore, any significant changes in condition must be noted as they may alter their validity. Questions regarding this report and/or data should be directed to Kyle Ramer (kyler@bditest.com) at BDI. For further information on BDI's equipment, services, and analysis methods please visit www.bditest.com

INSTRUMENTATION AND LOAD TESTING PROCEDURE

GATE INSTRUMENTATION SUMMARY

Instrumentation and testing were performed on Gate 5 at the Rockwall Forney Dam on April 4th, 2020. Instrumentation plans have been provided along with this report and include the following number of instrumented locations and sensor types:

+ **REUSABLE SURFACE MOUNTED STRAIN TRANSDUCERS:** Each gate arm was instrumented with a total of 24 strain transducers at 6 locations on each of the gate arms (48 strain sensors total). A typical strain gage installation is shown in Figure 1. Note these sensors were installed with the mounting tabs on the extreme fiber of the strut flanges, which puts the center of the gage approximately 0.66" from the extreme fiber.
+ **TILTMETER ROTATION SENSORS:** MEMS style rotation sensors were located on the middle strut of the gate arm near the skin plate and near the trunnion hub (4 rotation sensors total). The rotation responses were used to calculate vertical skin plate movement and measure pin rotation relative to skin plate rotation. Typical tiltmeter installations are shown in Figure 1 and Figure 2.
+ **TORQUE SENSORS:** Two total torque sensors were installed on the hoist's pinion shafts (QTY1 on each hoist pinion shaft) near the cable hoist motor to measure direct torque and in turn lift force (See Figure 3).
+ **AMPERAGE SENSORS:** 3 Hall-Effect amperage transducers were clamped over each phase of the hoist motor to measure the motor's current draw (See Figure 4). The purpose of these sensors was to provide additional data in case there were any issues with the hoist systems and to verify any data issues related to lifting and lowering the gates.
+ **BDI'S STS-4 WIRELESS DATA ACQUISITION SYSTEM:** BDI's STS-4 wireless data acquisition (DAQ) was used to collect and record data during testing. A group of sensors were wired to each nodal DAQ which then communicated wirelessly back to the wireless base station and was controlled by BDI's STS-Live testing software.

Complete specifications are available upon request and can be found at http://www.bditest.com.

SENSOR INSTALLATION

BDI strain transducers were installed by first sanding paint off the struts to expose bare metal at two small locations (1"x2" areas) for the sensor's mounting tabs. Each transducer was then attached using a combination of fast-setting adhesive and accelerator and applying pressure until the adhesive was fully cured. Each strain transducer took approximately five minutes to attach.

Tiltmeters were installed using the same adhesive process as the strain transducers. However, no surface preparation was necessary.

Torque sensors were installed on the pinion shafts by capacitive discharge bonding. Properly bonding to the shaft required sanding the surface to a smooth finish, clean of any paint or grease. Responses from these gages were measured using Binsfeld Torque Trak 10k wireless transmitters.

A typical installation has been shown in Figure 1 through Figure 4. Access to all the sensor locations was provided by BDI's own SPRAT certified rope access technicians and engineers as shown in Figure 5.

Once testing was completed, sensors were removed, and exposed steel areas were covered using cold galvanizing compound.

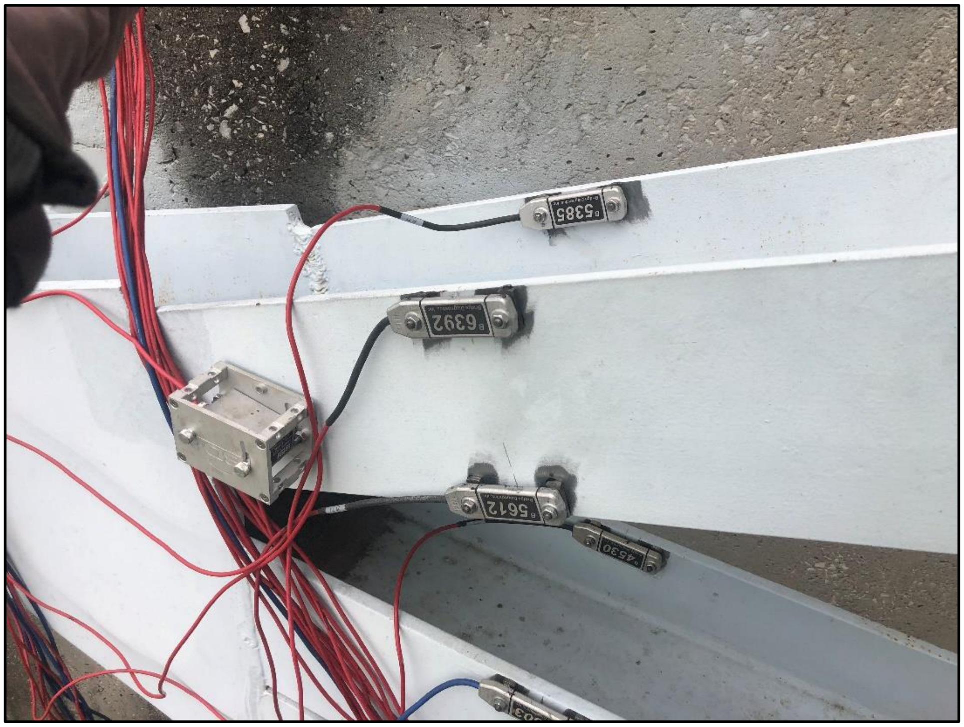

Figure 1 – BDI tiltmeter rotation sensor and reusable strain transducers installed near trunnion hub (Typical)

Figure 2 – BDI tiltmeter rotation sensor installed near skin plate (Typical)

Figure 3 – Torque sensor installation on hoist pinion shaft (Typical)

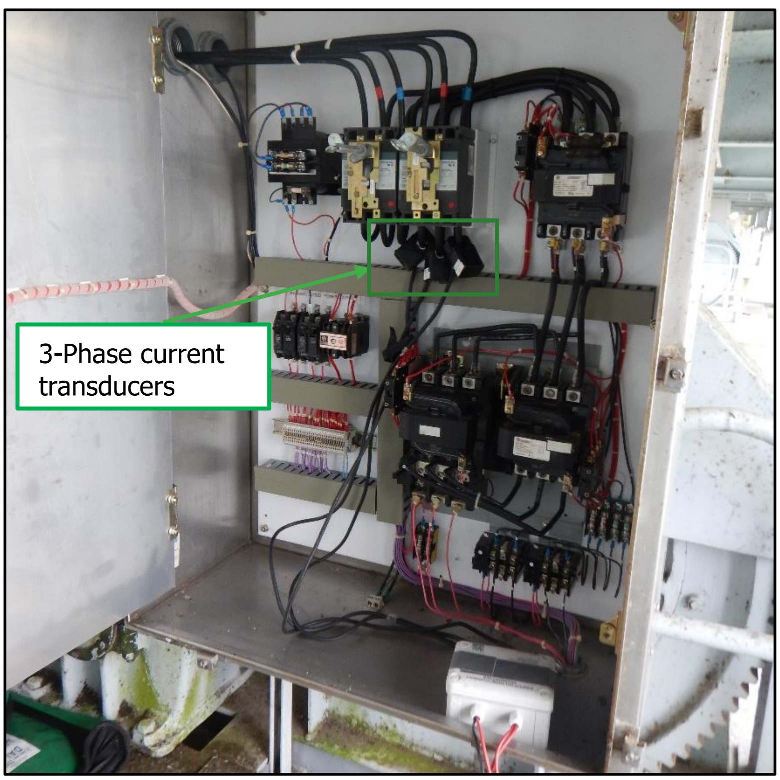

Figure 4 – Current transducers installed on hoist motor controls (Typical)

Figure 5 – BDI personnel installing instrumentation on the gate arm

Testing Procedures

Structural response data was recorded on all sensors at 50Hz while the gate was run through three spill tests. Each test consisted of three “up-down” cycles (direction reversals) without lowering the gate back to the sill. Each direction reversal consisted of lifting the gate approximately 6-12”, pausing for a few seconds, and lowering the gate approximately 6”, and repeating until all reversals had been completed.

RESULTS SUMMARY

GENERAL BASED ON STRUCTURAL RESPONSES

The following outline contains general discussion points and observations that were made during the data review process. Note: Strain measurements were converted to stress for all subsequent analysis by multiplying the strain values by a steel elastic modulus of 29,000 ksi.

+ **DESCRIPTIONS OF RESPONSE MEASUREMENTS:** All sensor readings were zeroed at the end of each test (which consisted of three cycles of direction reversals) so that each measurement corresponded to response change relative to the final gate position as shown in Figure 6 (gates in the downward "closed" position with the hoist cables slacked as much as possible). It is also worth noting that the stresses did not always start and end at the same levels between tests. This variation in behavior is due to small changes in the flexed gate condition between the start and end of tests. It is common for the flex in the gate, caused by pin friction, to slowly release as it rests on the sill. The purpose of the three up-down cycles per test, prior to sitting the gate back onto the sill, is to ensure that these changes in boundary conditions, including gate flexure due to friction, did not affect BDI's trunnion friction results. ***It is important to note that the recorded measurements were changes in structural response due to gate movement, and do not include the in-situ stresses due to the dead load, cable wrap, and hydrostatic loads present prior to testing.***
+ **QUALITATIVE DATA REVIEW:** Review of the response data indicated a good level of reproducibility between the three tests. For reference, Figure 6 and Figure 7 show stress responses measured along Gate 5's right arm top strut for all three tests (Test #1-3). The data in these plots have been provided as both a function of time and the gate position as determined by the skin plate tilt sensor. Structural response behavior slightly varied during the first test's first cycle compared to subsequent lift/lower cycles and tests, with the first cycle having a slightly smaller change in stress due to pin friction. The observed variation was likely caused by a larger release of built-up pin friction as the gate rested on the sill for a longer period of time.
+ **DIRECTION/FRICTION REVERSAL IN RESPONSES:** The difference in stress during gate opening and closing for a given position is shown in Figure 8. The stress variation at any given gate position was a result of direction reversal and in turn due to trunnion friction reversal. This statement is true since all other loads such as dead-load and hydrostatic pressure were essentially constant barring small changes in hydrostatic pressure due to slight changes in head. This direction/friction reversal is depicted in Figure 9, with deflected shape renderings from a gate arm finite element model under lifting and lowering loads. Note that this figure shows an arm configuration that does not match this gate, but the concept of the direction/friction reversal still applies.
+ **MOTOR PERFORMANCE:** Current measurements taken at the hoist motor indicated steady and stable current draws during the lifting and lowering portions. An example plot of current draw and gate position is provided in Figure 10. Current draw ranges during lifting were higher than the ranges during lowering, which is common due to gravity/dead load. These results are summarized along with recorded peak in-rush current in Table 2. Note that the sample rates used during testing were set for collecting gate responses and may not have been appropriate to fully capture the in-rush current. The readings should be evaluated by a licensed electrician with knowledge of the operating parameters.
+ **TORQUE AND HOIST FORCE:** Due to restrictions caused by the hoist limit switches, the hoist cables could not always be fully slacked at the beginning and end of the performed tests. Throughout testing of the Rockwell Forney gates, it was found that this limit switch restriction varied gate to gate and arm to arm. Therefore, it is not recommended to use the collected torque and hoist force data to quantify overall hoist forces. Rather, this data was utilized to evaluate total friction behavior, which is observed as half the difference between the lifting and lowering torque/force (friction reversal).

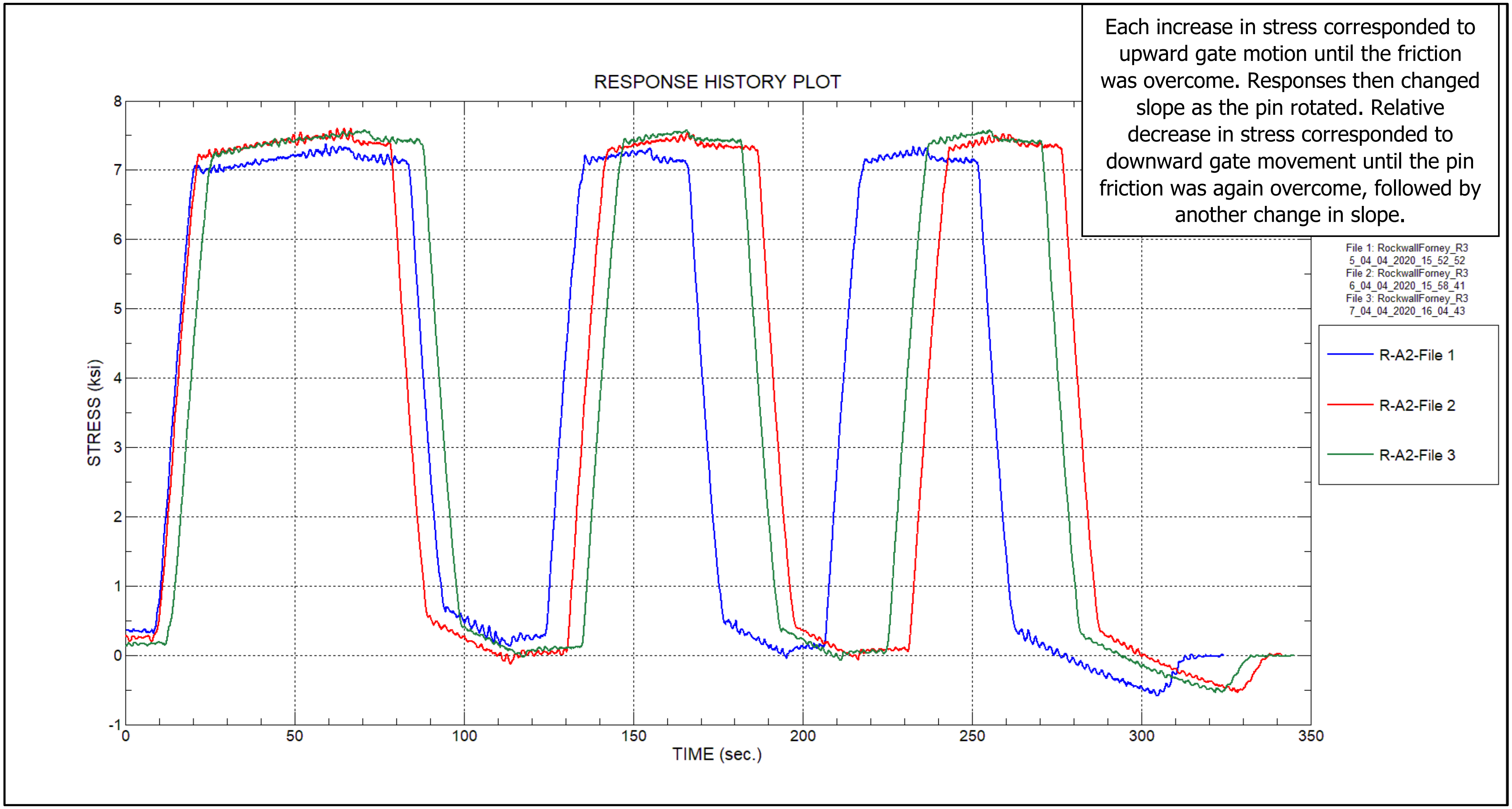

Figure 6 – Stress response history – Right arm – Gage A2 – Time based
File 1 = test run 1, File 2 = test run 2, File 3 = test run 3

(Section A along top strut near pin – Sensor location 2 along bottom of inner flange)

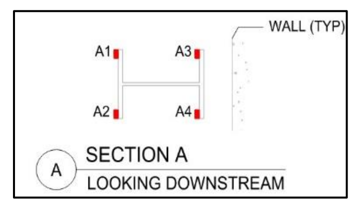

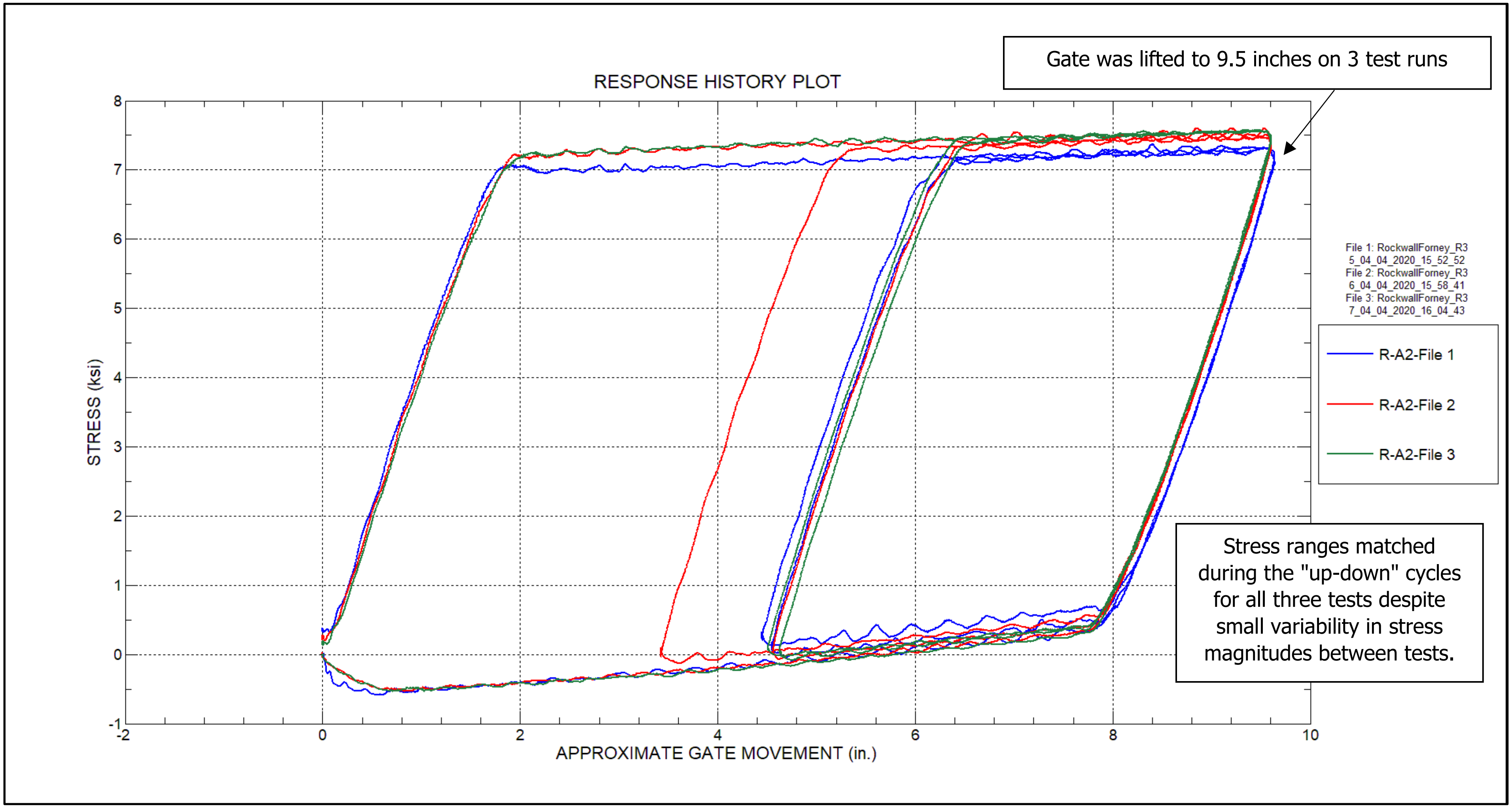

Figure 7 – Stress response history – Right arm – Gage A2 – Function of gate movement
File 1 = test run 1, File 2 = test run 2, File 3 = test run 3

(Section A along top strut near pin – Sensor location 2 along bottom of inner flange)

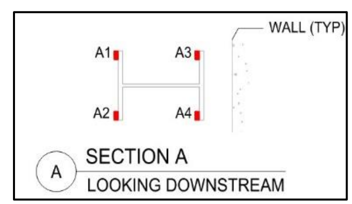

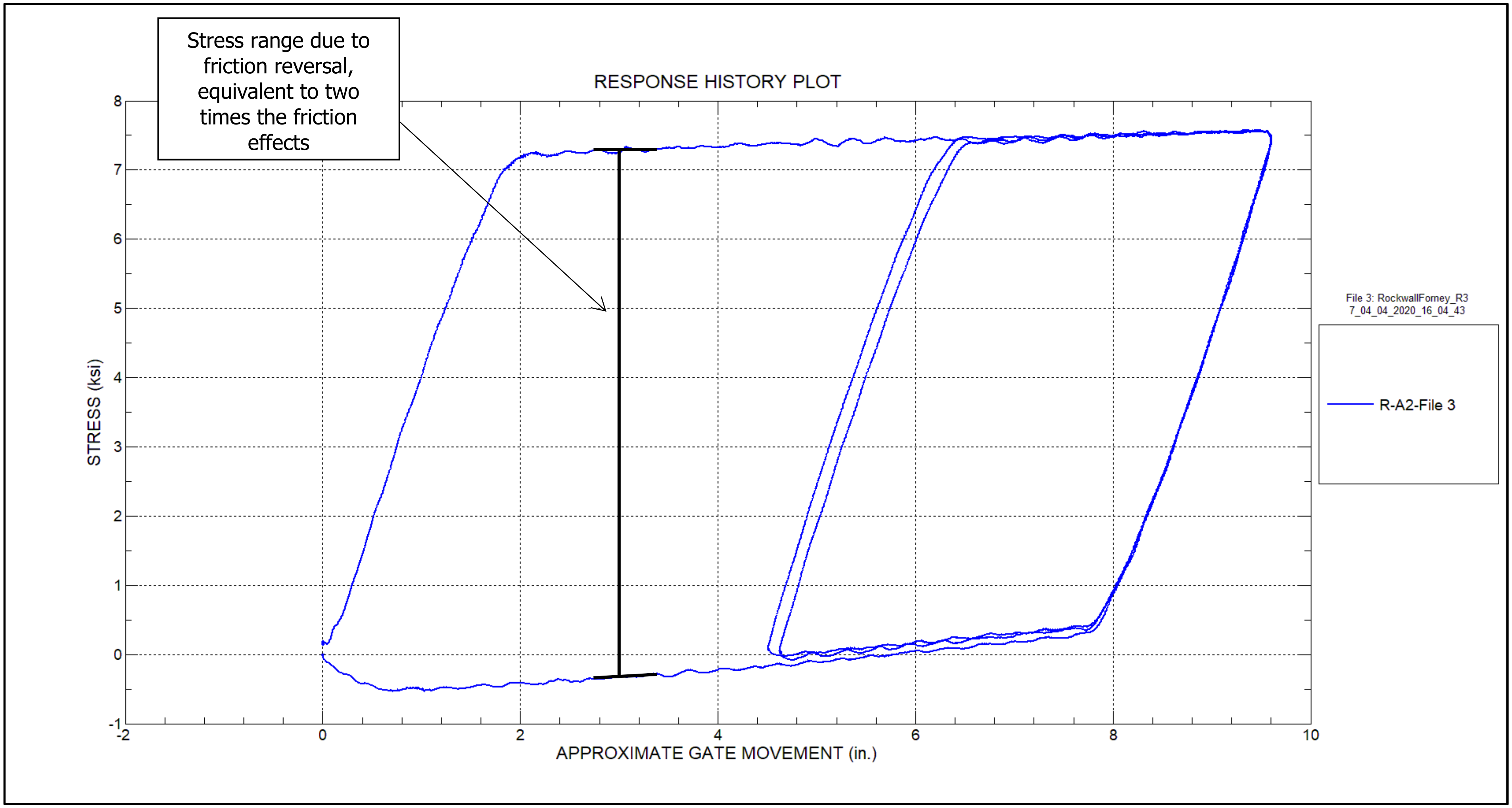

Figure 8 – Stress response history – Right arm – Gage A2 – Friction effect in stress responses

(Section A along top strut near pin – Sensor location 2 along bottom of inner flange)

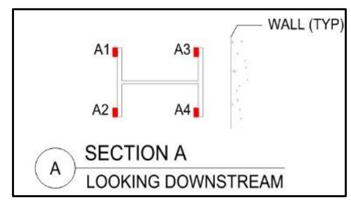

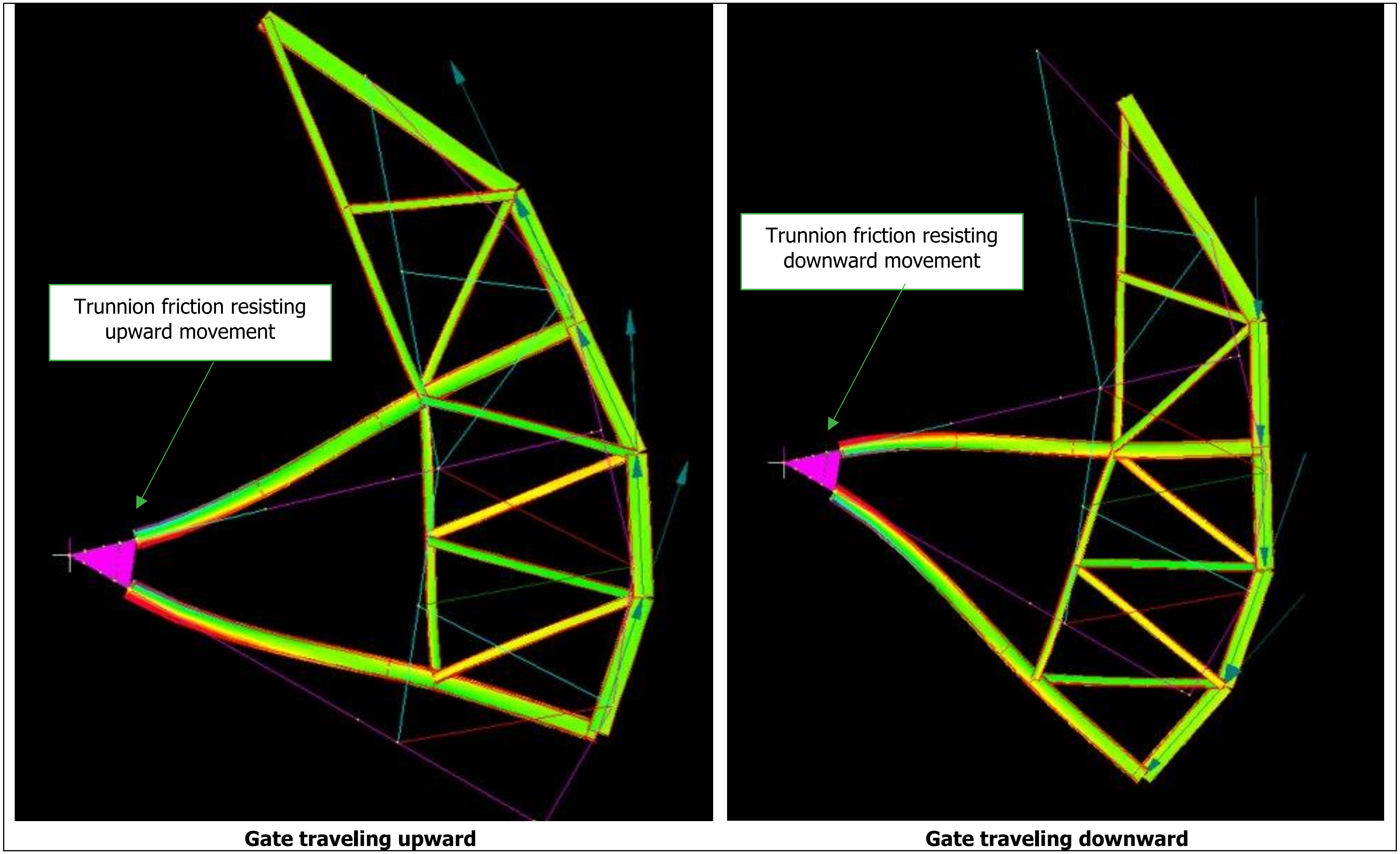

Figure 9 – Deflected shapes during lifting and lowering of Gate – Visualization of direction/friction reversals

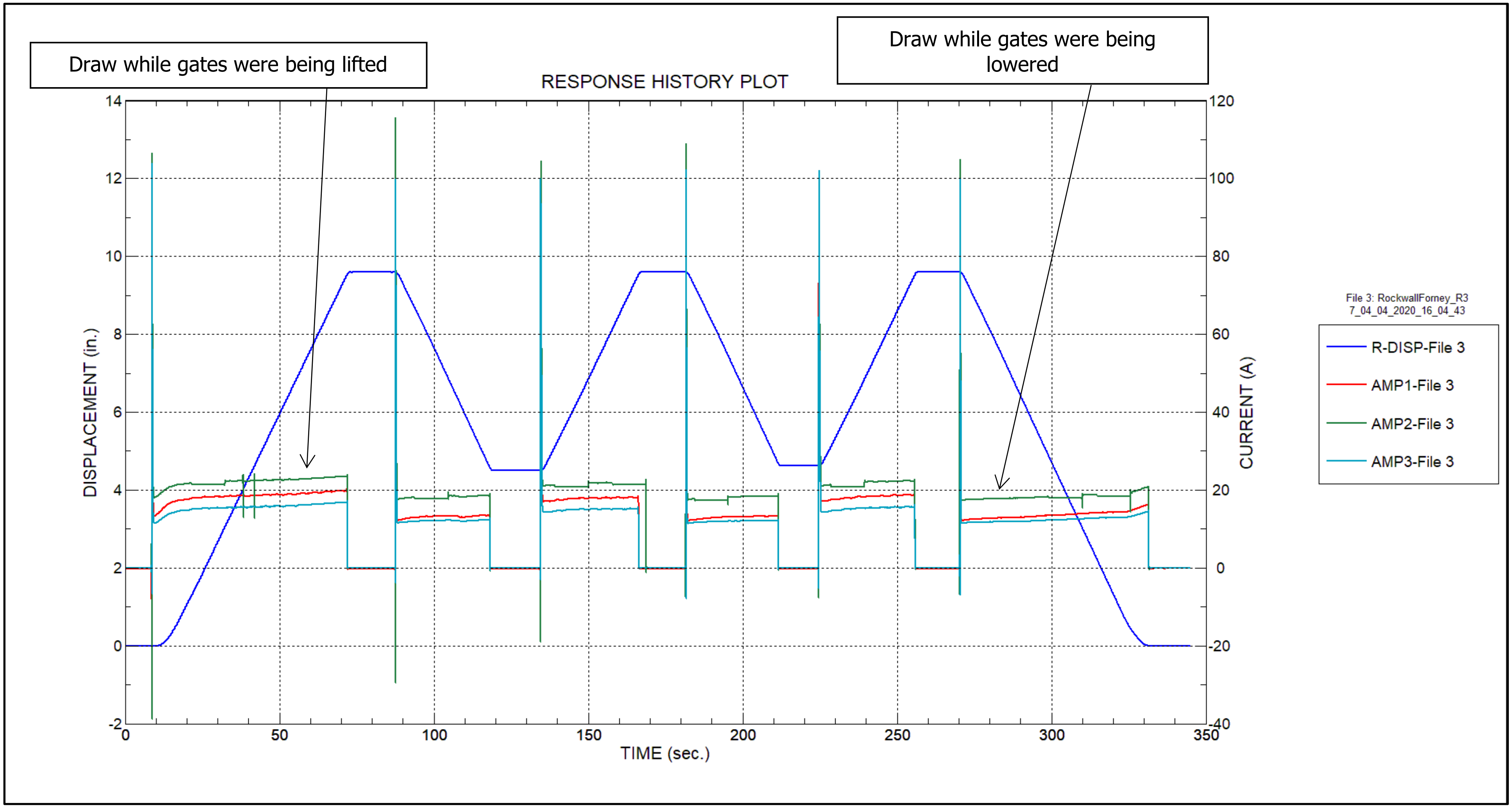

Figure 10 – Motor current & gate movement response history – Lift motor – Highlighting motor draw during lift and lower cycles

Methodology and Findings of The Strut Force and Moment Calculations

The following outline provides the methodology used to calculate the required member forces and moments.

- **CHANGE IN STRESS DUE TO GATE OPERATION:** Strain data can be viewed as a function of time starting when the gate was in the down position and was then lifted off the sill. When examining data in this manner, it is easy to see how stresses ramped up as the gate began to move and then changed slope once pin friction was overcome and the trunnion hub began to rotate with the gate. The first point in time where the friction was overcome (both lifting and lowering) has been highlighted in the stress histories shown in Figure 11. These stress histories show the response of all four sensors along the top strut of the right arm (Section A). ***It is important to note that the recorded measurements were changes in structural response due to gate movement, and do not include the in-situ stresses due to the dead load, cable wrap, and hydrostatic loads present prior to testing.***
- **CALCULATION OF STRUT CROSS-SECTIONAL MOMENTS:** The use of four strain gages per strut cross-section allowed accurate in-plane flexural bending moments to be computed from the recorded strain measurements. These moments were computed for every cross-section in each gate arm using the basic mechanics equation provided in Figure 12.

  In-plane or weak-axis flexure refers to bending about a given strut's web. This designation is consistent with typical nomenclature. In-plane bending can be observed visually from the strain response histories as a difference between the top and bottom stresses, whereas out-of-plane or strong-axis bending is visualized as the difference in stress from side to side. Figure 13 provides a visual reference for both types of strut flexure.
- **EXAMINATION OF RESPONSES AS A FUNCTION OF GATE POSITION:** Changes in cross-sectional moment related to friction becomes clearer when the responses are plotted as a function of gate position. Because the gate was operated with several up and down movements, the effects of friction associated with each direction reversal can be viewed for all measured and calculated responses. Figure 14 through Figure 17 show all cross-sectional flexural moment plots for both trunnion arms. The responses in these plots have been centered about the stress state corresponding to a zero-moment, unflexed condition. The zero-moment offset was estimated as the average moment values between up and downward movement (i.e. half the moment difference) at the gate position with the greatest pin friction moment difference (greatest difference between lifting and lowering).
- **TRUNNION FREE-BODY-DIAGRAM & PIN MOMENT CALCULATION:** Figure 18 shows the instrumented member cross-sections and shows how the measured cross-sectional flexural responses were used to compute pin moment. The in-plane moment values used in these calculations were determined directly from the strain measurements at each cross-section using the provided mechanics equations. It should be noted that the out-of-plane moments were not considered in the calculation of pin moment since they were orthogonal to the axis of the pin rotation. Total pin moment was then determined by summing all the moment components about the pin, which included the in-plane moment and the shear components at the strut cross-sections nearest the pin.
- **STRUT SHEAR CALCULATION:** From the examination of the trunnion free-body-diagram described above, the shear vectors at the three struts were a primary component in the pin moment calculation. For this type of structural element, shear vectors were calculated using the moment differential between the two cross sections along each strut. It is important to recognize that shear was constant between the two instrumented cross-sections and the applied shear was a function of the recorded change in moment ($V = dM/dX$). Subsequently, the shear vectors were calculated by dividing the difference in moment by the distance between the two instrumented cross-sections. Shear values for each strut have been plotted as a function of gate position in Figure 19 and Figure 20.

+ **CALCULATION OF PIN MOMENT DUE TO FRICTION:** Once all the trunnion arm force vectors were calculated, the equations shown in the free-body-diagram were applied to compute pin moment as a function of gate position. It is important to note that because the calculated pin moment range corresponds to a direction reversal, a reversal in friction also occurred. The effect of direction reversal on pin moment due to friction is best conceptualized by centering the moment response plots about the zero-moment axis. The moment due to lifting and the moment due to lowering can then be visualized as a change from this new zero point corresponding to the gate in an unflexed condition. Therefore, the total moment differential between lifting and lowering was twice the moment due to friction acting in a single direction. Pin-moment plots have been provided in Figure 21 and Figure 22. From these plots, it is apparent that pin moment due to friction remained relatively constant throughout the gate operation tests, with a slight decrease in pin friction moment as the gate continued to be lifted. This slight decrease in pin friction moment most likely corresponded to the change in hydrostatic load as the gate position changed. Pin-moment plots for all tests on Gate 5 are also provided for reference in Appendix B – Gate 5 Pin Moment Component Plots.

+ **SHAFT TORQUE & HOIST FORCE:** Torque measurements were taken on the pinion shafts near the hoist motor during testing, with single torque gages installed on the left and right hoist pinion shaft. Responses were recorded in units of micro-strain and converted to torque in units of kip-ft using Equation 1 thru Equation 3 and the following shaft properties.

$$d_O = 5.5\ inches, \qquad d_I = 0\ inches, \qquad E = 29000\ ksi, \qquad \nu = 0.3$$

$$G = \frac{E}{2(1+\nu)}$$

Equation 1

$$J = \frac{\pi\left({d_O}^4 - {d_I}^4\right)}{32}$$

Equation 2

$$\tau = \varepsilon * \frac{2GJ}{\frac{d_O}{2} * 1000000 * 12}$$

Equation 3

Figure 23 shows example torque measurements, recorded on the Gate 5 torque shafts. Best practices for torque measurements is to measure torque on opposite sides of the shaft so that any bending in the shaft can be removed by averaging the two responses. Due to access limitations, only one gage at each location could be installed. Therefore, any bending in the shaft may be reflected in the torque measurements and may be related to the peaks and valleys observed in the torque responses.

Torque values were converted to force in the hoist cables per gate arm using the gear ratio and drum radius, as shown in Figure 24. The gear ratio and drum radius were 5.182 and 1.086 feet respectively, as defined in the provided as-built shop drawings. It should be noted that the hoist force calculated may be smaller than the actual hoist force applied. This difference is due to the limit switch engaging the brake before the hoist cable was fully slacked, resulting in an initial force in the cable. A hoist force due to total gate friction was then calculated. This friction hoist force was equal to half the differential in force measured during the lifting and lowering of the gate (similar to the pin friction calculations). As shown in Table 3, the change in cable force due to friction was generally consistent between tests. Note that the total hoist force was due to the total friction effects, including side seal, hoist bearings, trunnion friction effects, etc. It is difficult to determine the exact proportion and composition of the total friction sources. Additional torque and hoist force plots for all collected data files are provided in Appendix A – Gate 5 Torque and Hoist Force Plots.

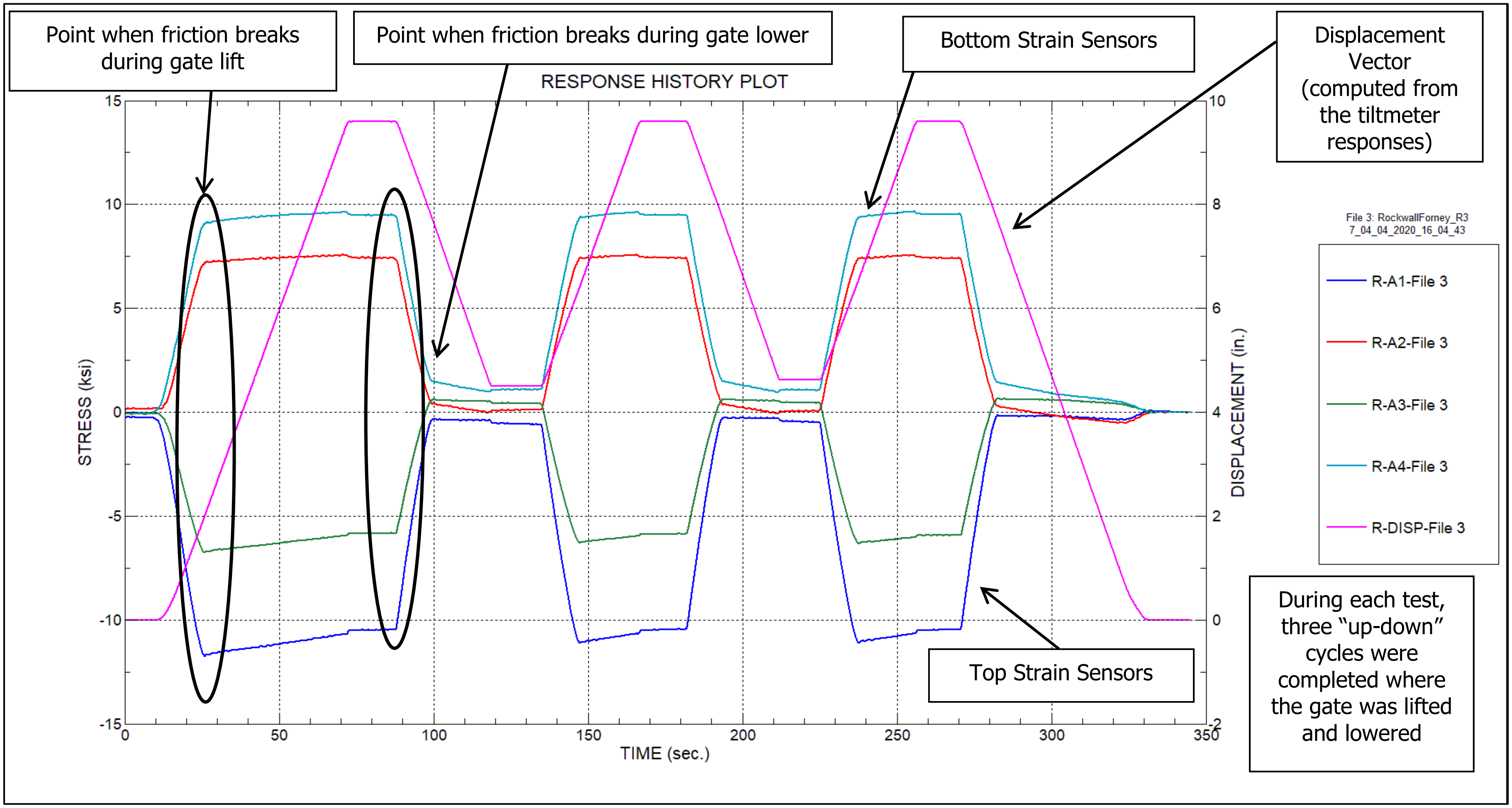

Figure 11 – Stress response & gate movement history – Right arm – Section A - Highlighting friction behavior (Section A along top strut near pin)

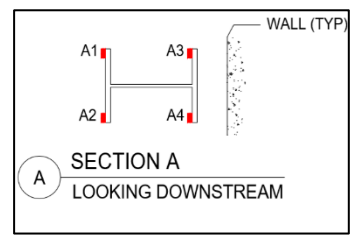

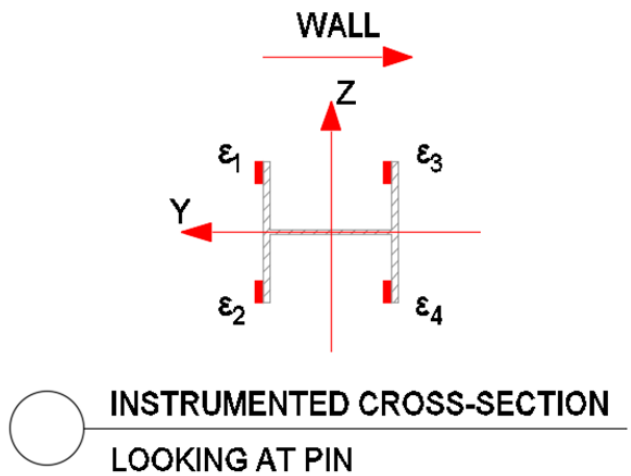

Calculation of Weak-axis (In-plane) bending

$$M_Y = \frac{E[\frac{\varepsilon_2 + \varepsilon_4}{2} - \frac{\varepsilon_1 + \varepsilon_3}{2}]S_{Y(gage)}}{2}$$

Sy(gage) = Section modulus to the center of gages (not extreme fiber of flanges)
(locations of gages were accounted for in moment computation)

Figure 12 – Basic mechanic equation used to calculate moment

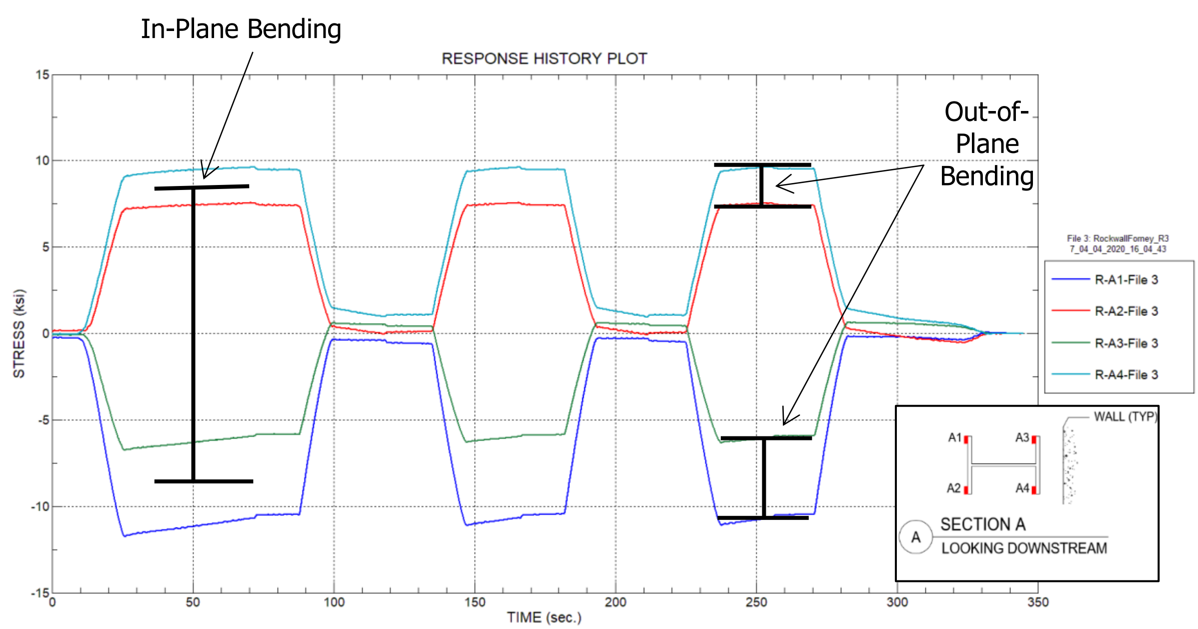

Figure 13 – Stress response history – Right arm – Section A – Bending components
(Section A along top strut near pin)

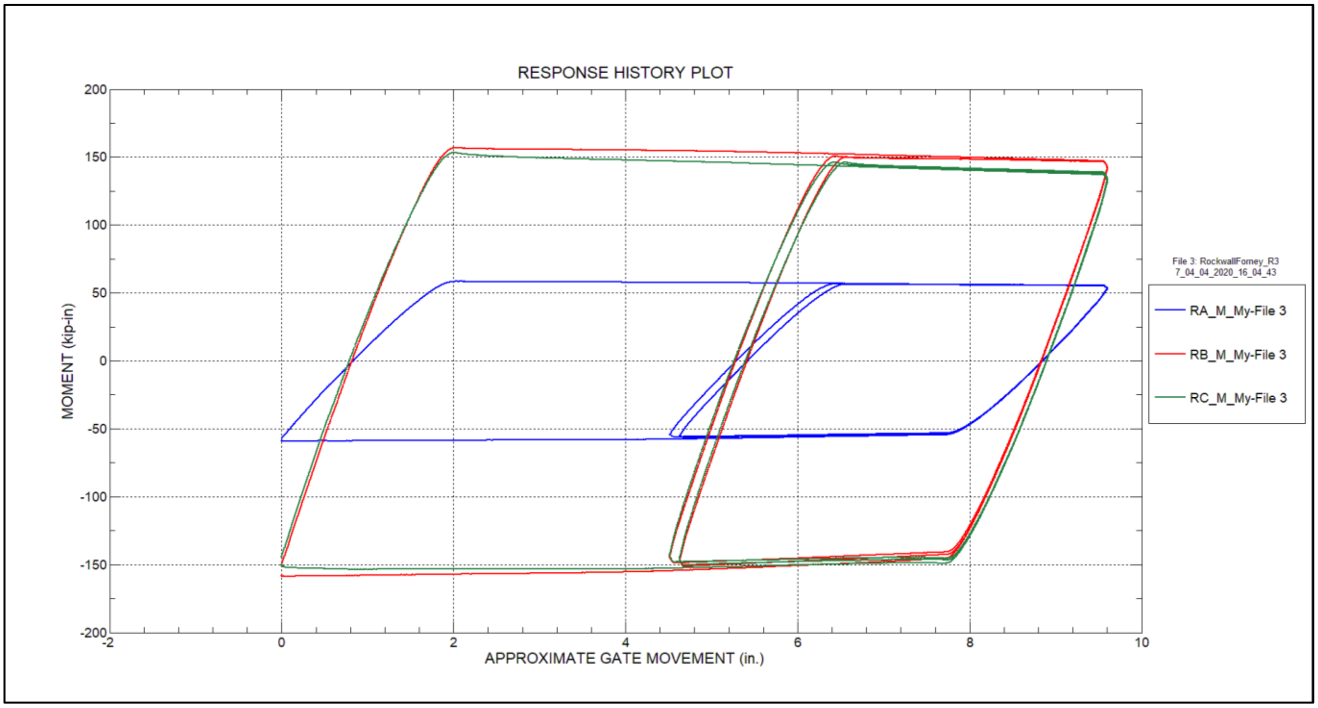

Figure 14 – In-plane moment response history – Right arm – Sections near pin

(RA = Right Arm Top Strut, RB = Right Arm Middle Strut, RC = Right Arm Bottom Strut)

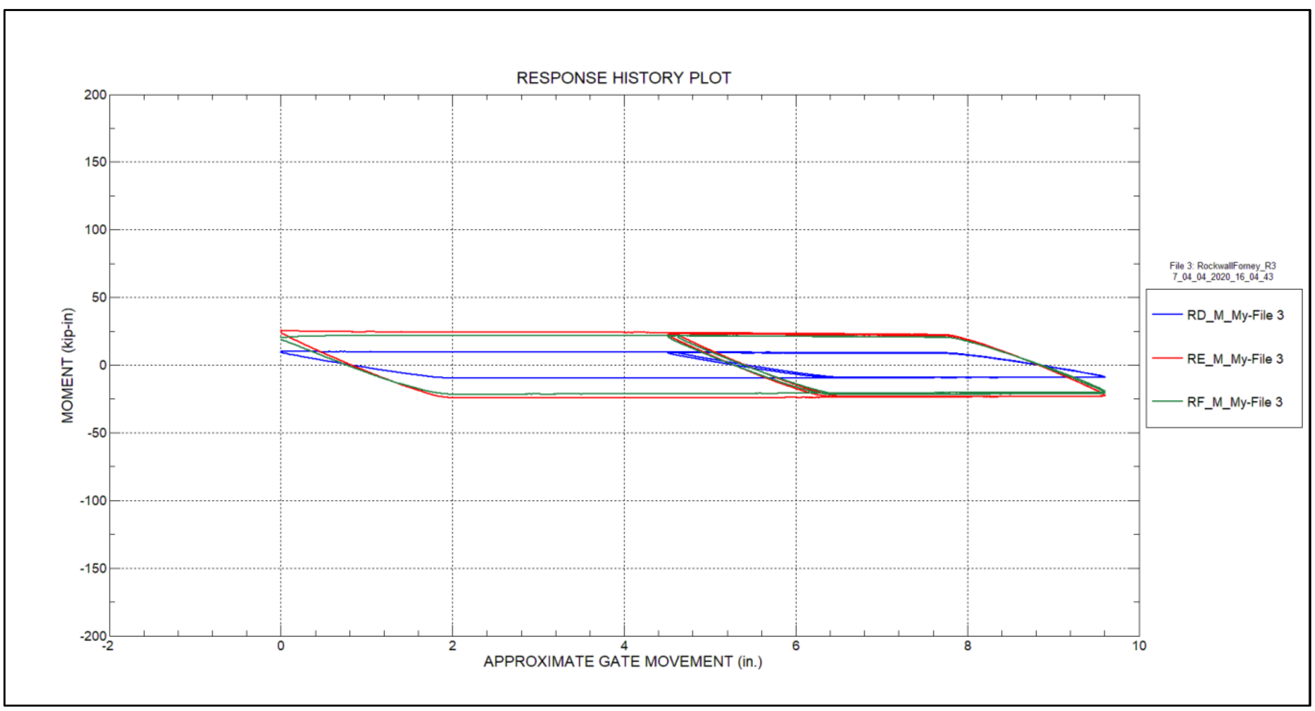

Figure 15 – In-plane moment response history – Right arm – Sections away from pin

(RD = Right Arm Top Strut, RE = Right Arm Middle Strut, RF = Right Arm Bottom Strut)

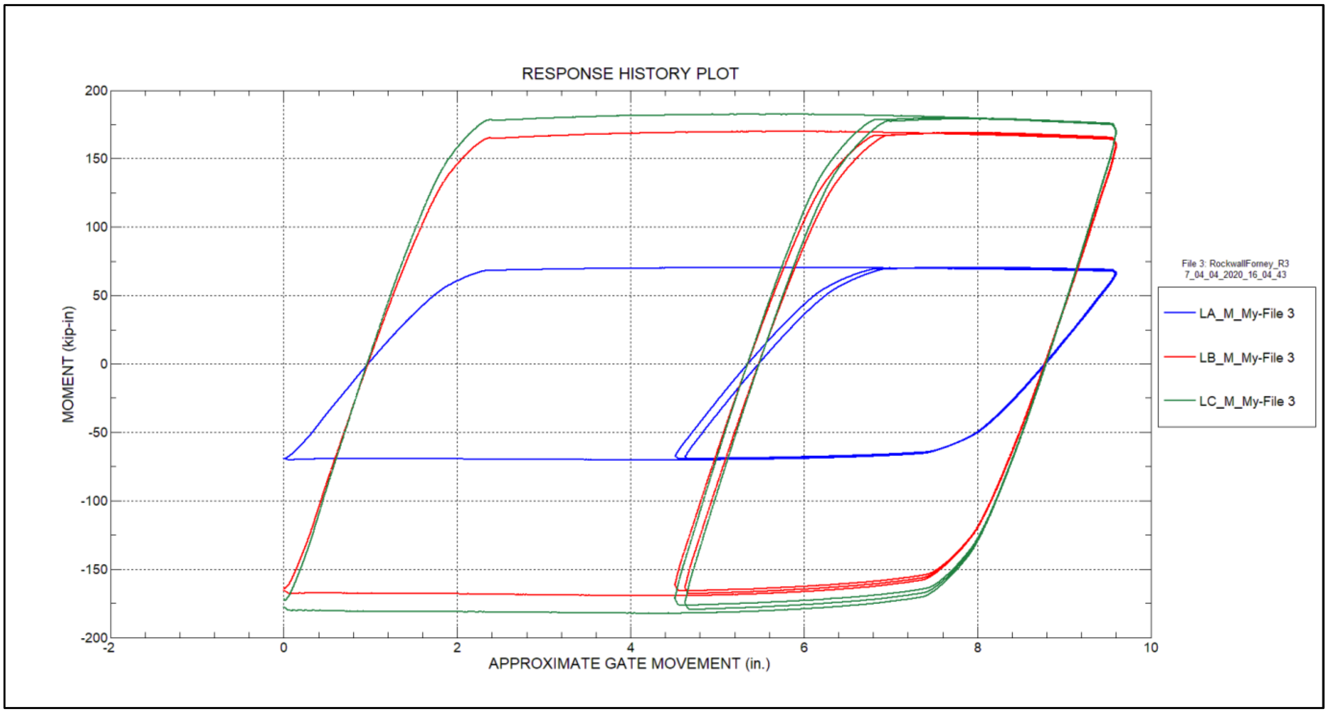

Figure 16 – In-plane moment response history – Left arm – Sections near pin

(LA = Left Arm Top Strut, LB = Left Arm Middle Strut, LC = Left Arm Bottom Strut)

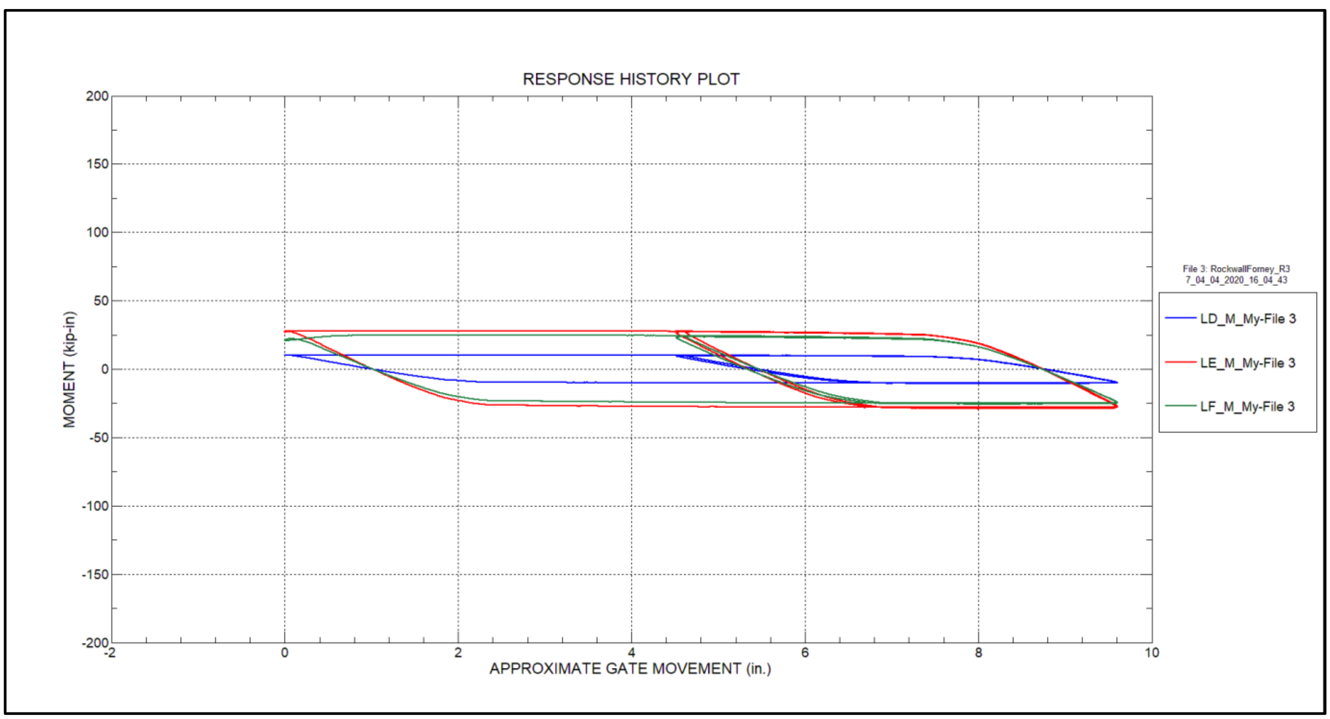

Figure 17 - In-plane moment response history – Left arm – Sections away from pin

(LD = Left Arm Top Strut, LE = Left Arm Middle Strut, LF = Left Arm Bottom Strut

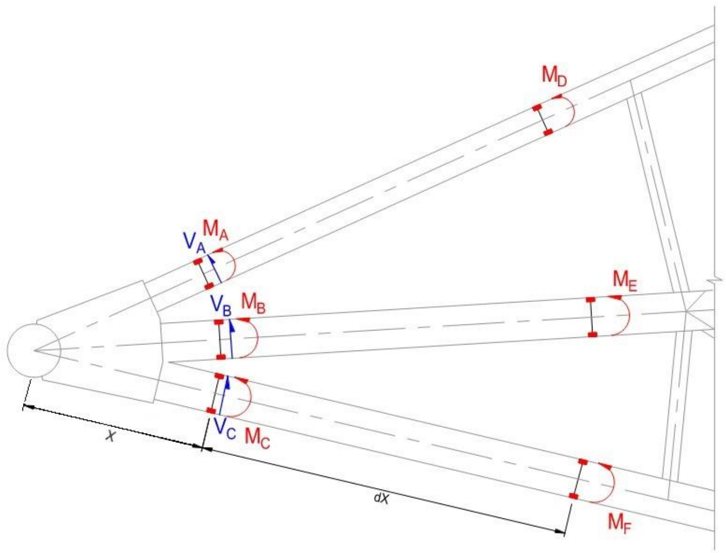

Elevation View of Gate Arm

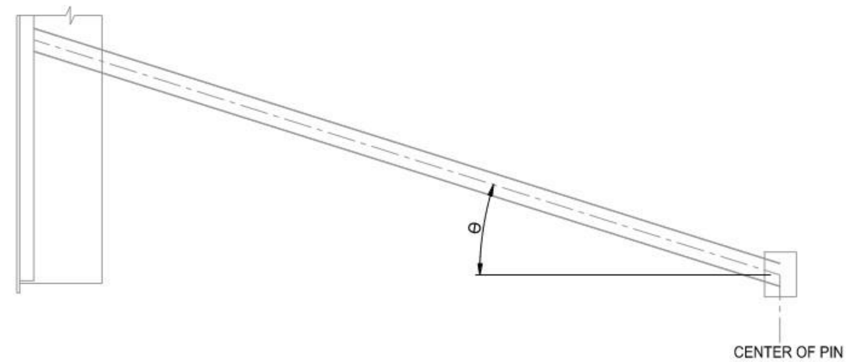

Plan View of Gate Arm

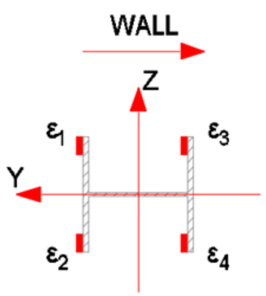

$$M_Y(M_A, M_B, M_C, M_D, M_E, M_F) = \frac{E\left[\frac{\varepsilon_2 + \varepsilon_4}{2} - \frac{\varepsilon_1 + \varepsilon_3}{2}\right] S_{Y(gage)}}{2}$$

$$V_A = \frac{M_A - M_D}{dX}$$

$$V_B = \frac{M_B - M_E}{dX}$$

$$V_C = \frac{M_C - M_F}{dX}$$

$$\sum M_o = 0$$

$$M_{PIN} = [X(V_A + V_B + V_C) + M_A + M_B + M_C] \cos\theta$$

Figure 18 – Direct calculation of pin moment from strain measurements

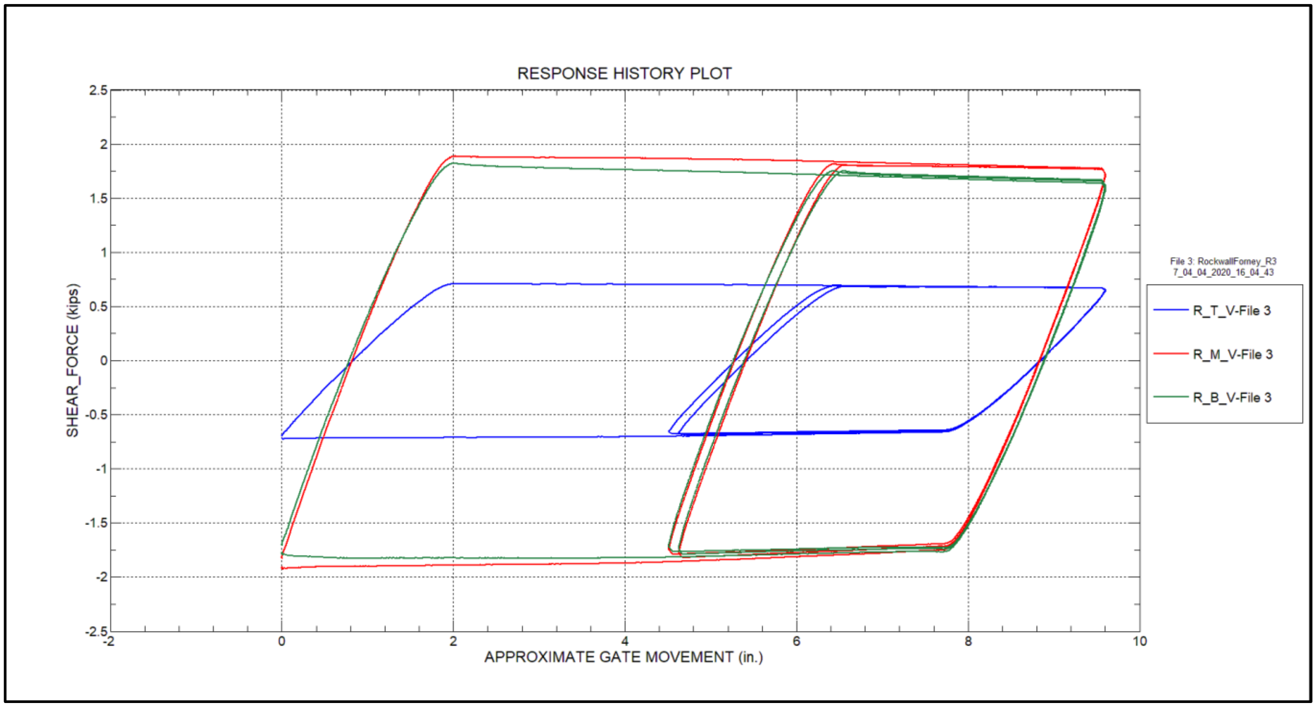

Figure 19 – Strut shear response history – Right arm

(R_T = Right Arm Top Strut, R_M = Right Arm Middle Strut, R_B = Right Arm Bottom Strut)

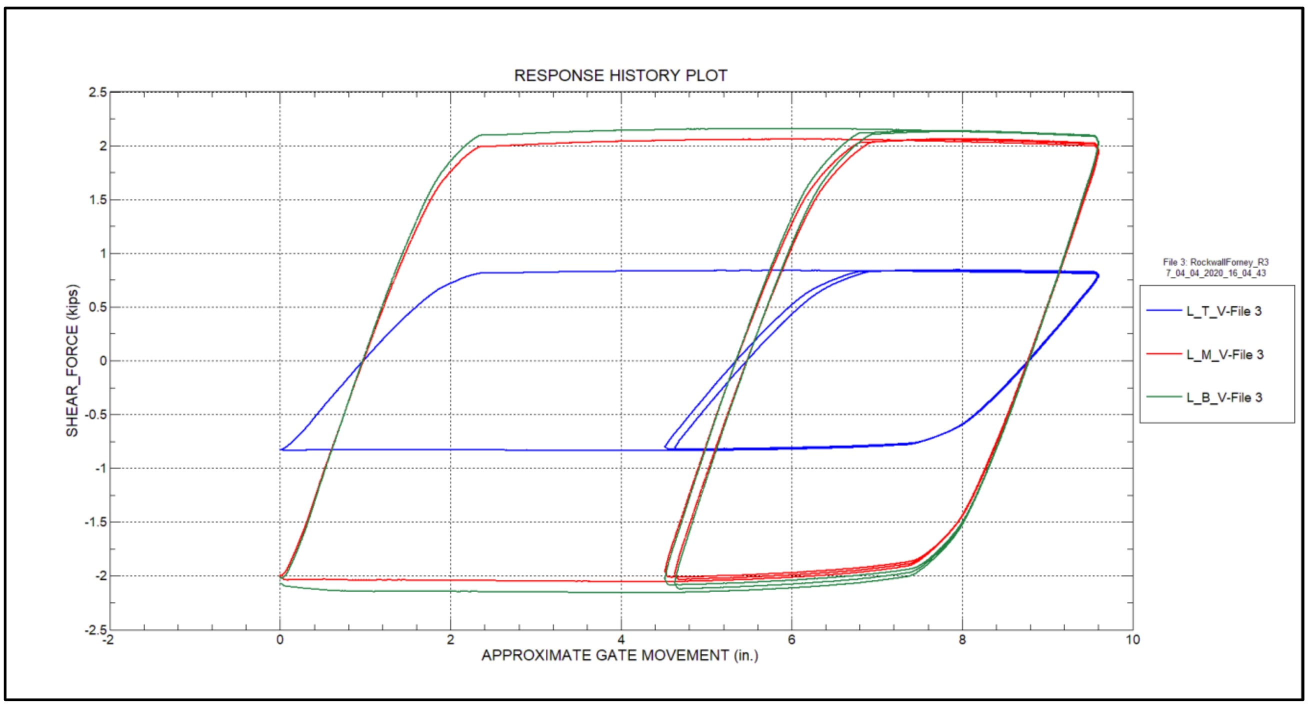

Figure 20 – Strut shear response history – Left arm

(L_T = Left Arm Top Strut, L_M = Left Arm Middle Strut, L_B = Left Arm Bottom Strut)

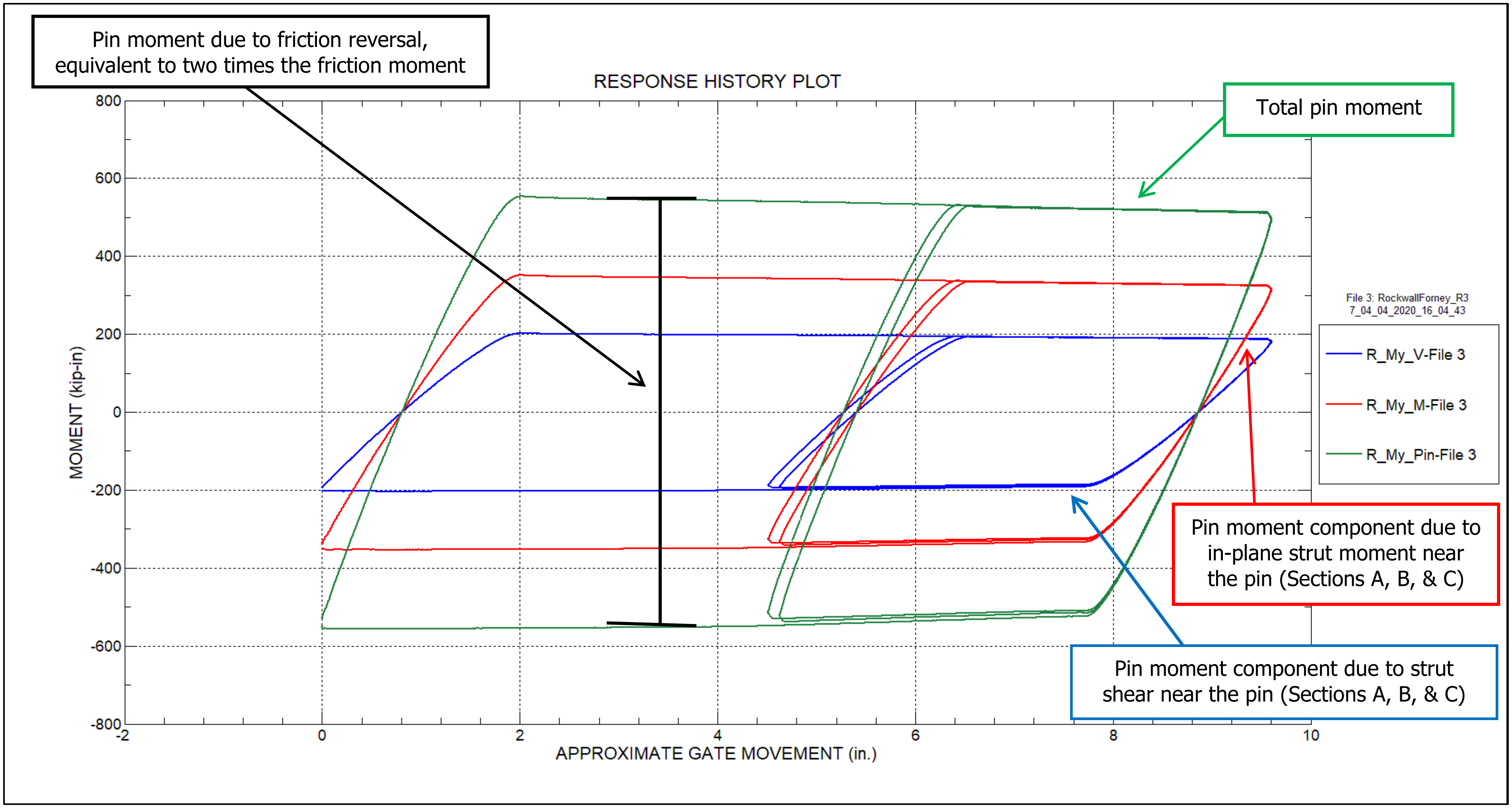

Figure 21 – Pin moment response history – Right arm

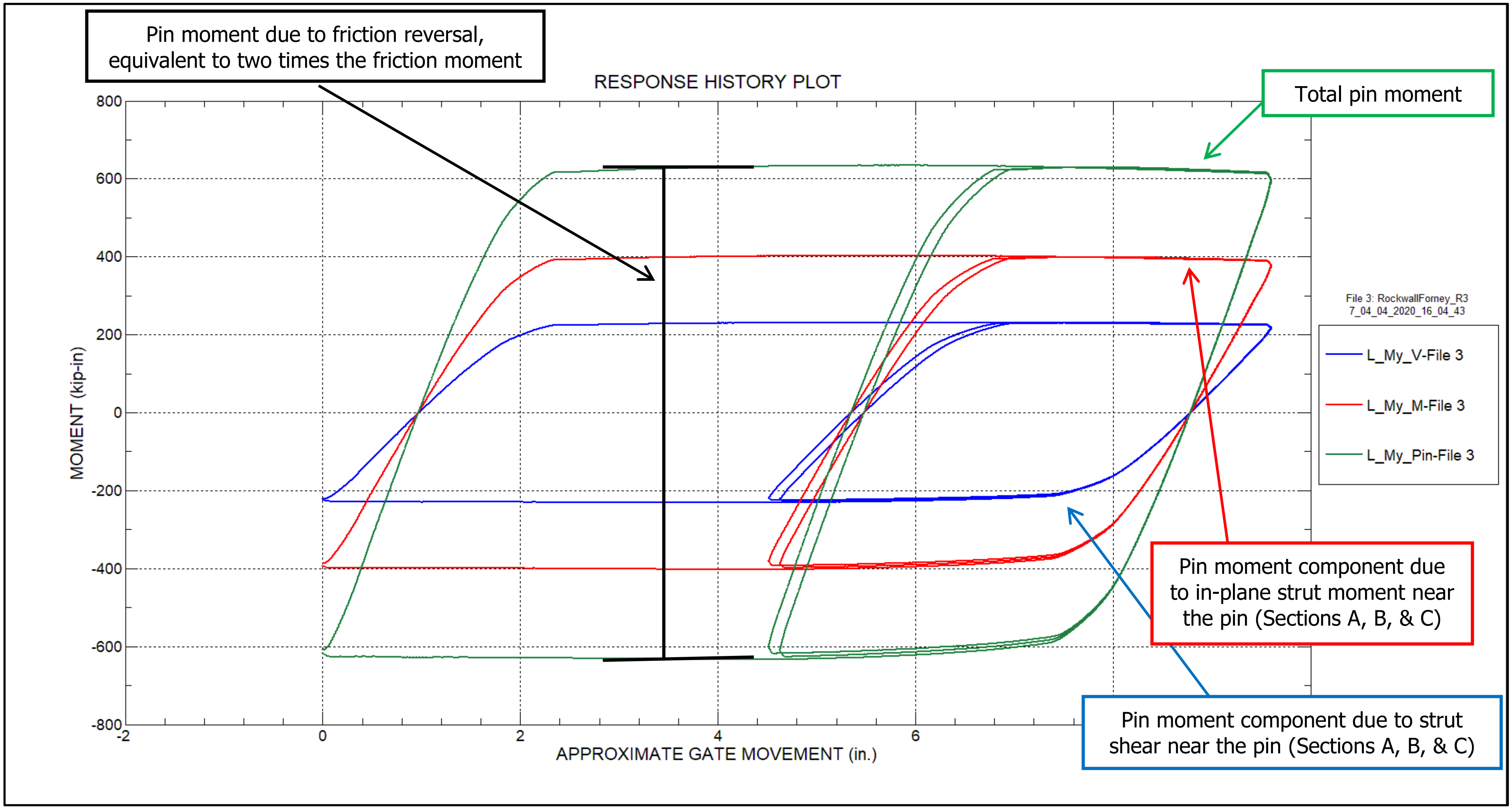

Figure 22 – Pin moment response history – Left arm

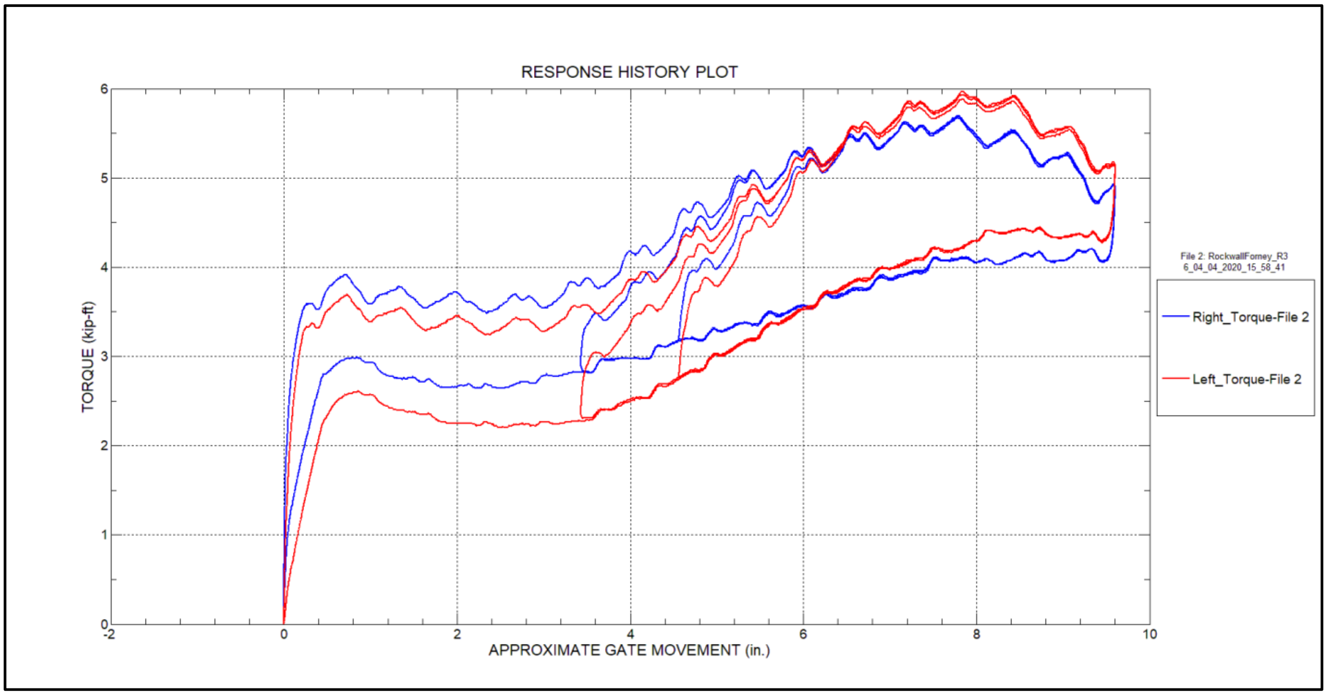

Figure 23 – Hoist torque response history – Gate 5 – Test 2

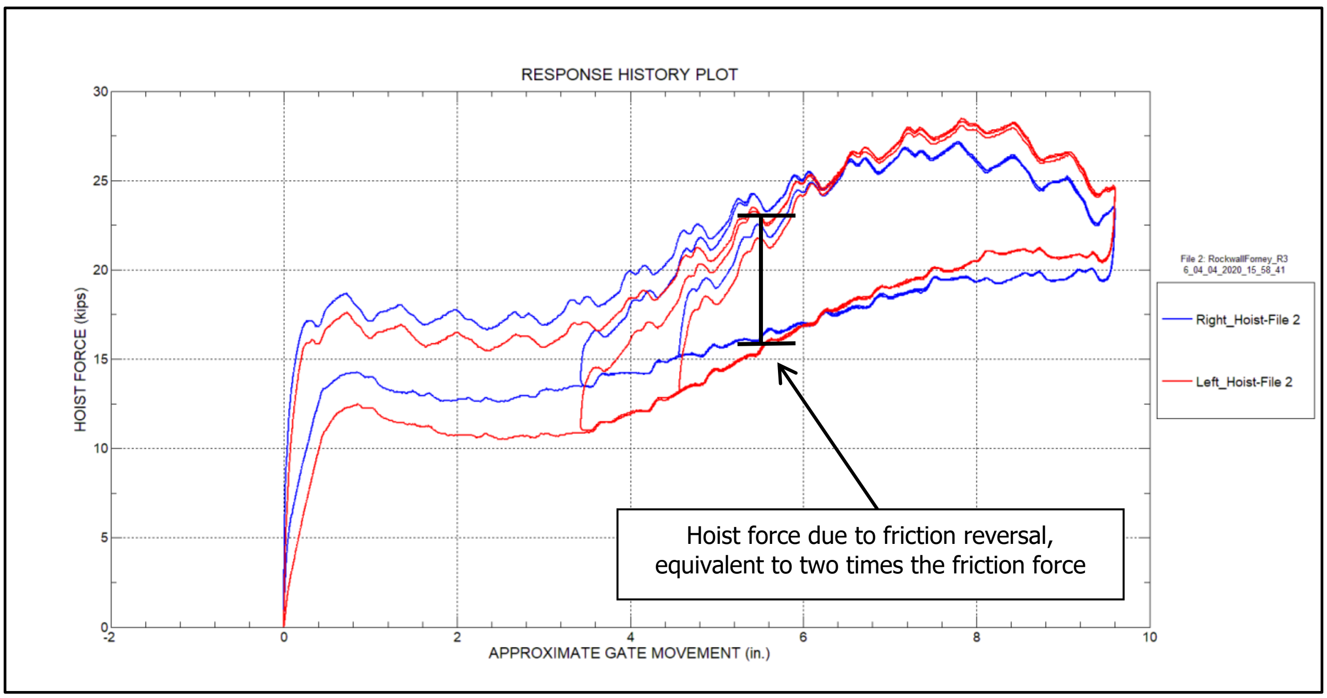

Figure 24 – Hoist force response history – Gate 5 – Test 2

Summary of Friction Results

The raw data files have been included in the submittal package for reference and were formatted as "tdms" files that can be opened in Microsoft Excel using a "tdms" reader extension.

Examination of the stress histories for each test was necessary to obtain a thorough understanding of the gate performance. The response shapes, variations in stress magnitudes, and timing sequences provided direct clues as to how the gate performed under typical service conditions. The following is a breakdown of the provided tabulated results:

+ Table 2 provides motor current ranges and maximum in-flow for lift and lower cycles for each test
+ Table 3 provides maximum hoist force as well as hoist force due to total friction for each test
+ Table 4 provides the maximum stress ranges measured at the sensor locations for each member
+ Table 5 provides maximum bending stress and moment ranges observed during the gate tests
+ Table 6 provides maximum friction bending stress and moment values at each of the instrumented strut locations
+ Table 7 provides the computed shear values in each strut due to friction
+ Table 8 provides calculated measured friction moments, calculated hydrostatic loads based on the measured water elevation, and coefficients of friction for each gate and gate arm during all three tests

The resulting pin friction moments were used to compute friction coefficients from Eq. 4, given the pin radius and the applied thrust. The thrust used in this calculation consisted of the calculated resultant hydrostatic load based on the measured water elevation and was adjusted to account for the loss of head as the gate was lifted. This thrust adjustment was based on the recorded gate movement and was performed in order to calculate more accurate friction coefficients. The water elevation during testing was nearly constant throughout each gate test and was documented during each "up-down" cycle. It should be noted that the minor thrust due to cable wrapping, which was minimal compared to hydrostatic thrust, was not included in the thrust calculation. This assumption resulted in slightly conservative friction coefficients.

$$\mu = \frac{M_F}{T * r} \qquad \text{Eq. 4}$$

where:

where:	μ	=	Friction Coefficient
	M_F	=	Friction Moment
	T	=	Thrust per Pin
	r	=	Pin Radius, 5.375"

The out-of-plane shear and moments were not considered in the pin friction calculations due to orthogonal geometry considerations (resulting pin moment associated with out-of-plane flexure being perpendicular to pin rotation).

The data was presented in a specific coordinate system applicable to both arms. Data was processed so that the positive x-axis was always pointing towards the pin and the right-hand rule applied. In-plane bending can be referred to as "bending about the horizontal or y-axis" and shows how much the beams bend up and down within the plane of the gate arms. Refer to Figure 12 above for visual reference of coordinate system and mathematical explanation of calculations. Tabulated results do not include any in-situ effects.

Table 2– Motor current summary table – Gate 5

Test Run	Current Range due to Lifting (A)	Current Range due to Lowering (A)	Max In-rush Current (A)
1	12-20	11-18	112
2	13-21	11-19	109
3	14-23	11-21	115

Table 3 – Hoist force summary table – Gate 5

Test Run	Right Arm Peak Hoist Force (kips)	Left Arm Peak Hoist Force (kips)	Right Arm Hoist Force due to Total Gate Friction (kips)	Left Arm Hoist Force due to Total Gate Friction (kips)
1	27.16	28.22	4.29	4.15
2	27.18	28.47	4.32	4.36
3	27.26	28.49	4.38	4.47

Tabulated friction force values correspond to the response induced by friction in one direction

Table 4 – Maximum measured sensor stress range

Arm Designation	Top Strut (ksi)	Middle Strut (ksi)	Bottom Strut (ksi)
Right Arm	12.02	13.08	13.19
Left Arm	12.37	14.65	13.62

Tabulated values correspond to the total measured change in response during tests

Stress values have not been extrapolated to the extreme fibers (correspond to center of gage)

Table 5 – Maximum in-plane total bending stress & moment ranges – Total

Section Label	Section Description	Right Arm Stress (ksi)	Right Arm Moment (kip-in)	Left Arm Stress (ksi)	Left Arm Moment (kip-in)
Section A	Top Strut Near Pin	10.50	117.98	12.72	142.98
Section B	Middle Strut Near Pin	13.67	316.18	14.97	346.16
Section C	Bottom Strut Near Pin	11.07	308.79	13.60	379.31
Section D	Top Strut Away from Pin	1.79	20.12	1.88	21.12
Section E	Middle Strut Away from Pin	2.17	50.15	2.50	57.91
Section F	Bottom Strut Away from Pin	1.57	43.85	1.82	50.78

Tabulated values correspond to the total measured change in response during tests

Table 6 – In-plane frictional bending stress & moment at maximum gate friction

Section Label	Section Description	Right Arm Stress (ksi)	Right Arm Moment (kip-in)	Left Arm Stress (ksi)	Left Arm Moment (kip-in)
Section A	Top Strut Near Pin	5.21	58.53	6.34	71.31
Section B	Middle Strut Near Pin	6.79	157.08	7.47	172.82
Section C	Bottom Strut Near Pin	5.52	153.87	6.79	189.30
Section D	Top Strut Away from Pin	0.87	9.76	0.90	10.16
Section E	Middle Strut Away from Pin	1.06	24.40	1.20	27.72
Section F	Bottom Strut Away from Pin	0.78	21.79	0.88	24.42

Tabulated values correspond to the response induced by friction in one direction

Table 7 – Strut shear range summary table due to friction

Arm Designation	Top Strut Shear (kip)	Middle Strut Shear (kip)	Bottom Strut Shear (kip)
Right Arm	0.71	1.89	1.82
Left Arm	0.84	2.08	2.21

Tabulated values correspond to the response induced by friction in one direction

Table 8 – Pin friction summary table

Test Run	Average Water Elevation during testing (ft)	Approximate Thrust at time of Testing (kips per arm)	Gate/Member Designation	Pin Friction Moment (kip-in)	Friction Coefficient
1	435.67	492.80	Right Pin	551.70	0.21
			Left Pin	648.60	0.24
2	435.67	492.80	Right Pin	550.00	0.21
			Left Pin	635.80	0.24
3	435.67	492.80	Right Pin	554.40	0.21
			Left Pin	633.20	0.24

Tabulated values correspond to the response induced by friction in one direction

APPENDIX A – GATE 5 TORQUE AND HOIST FORCE PLOTS

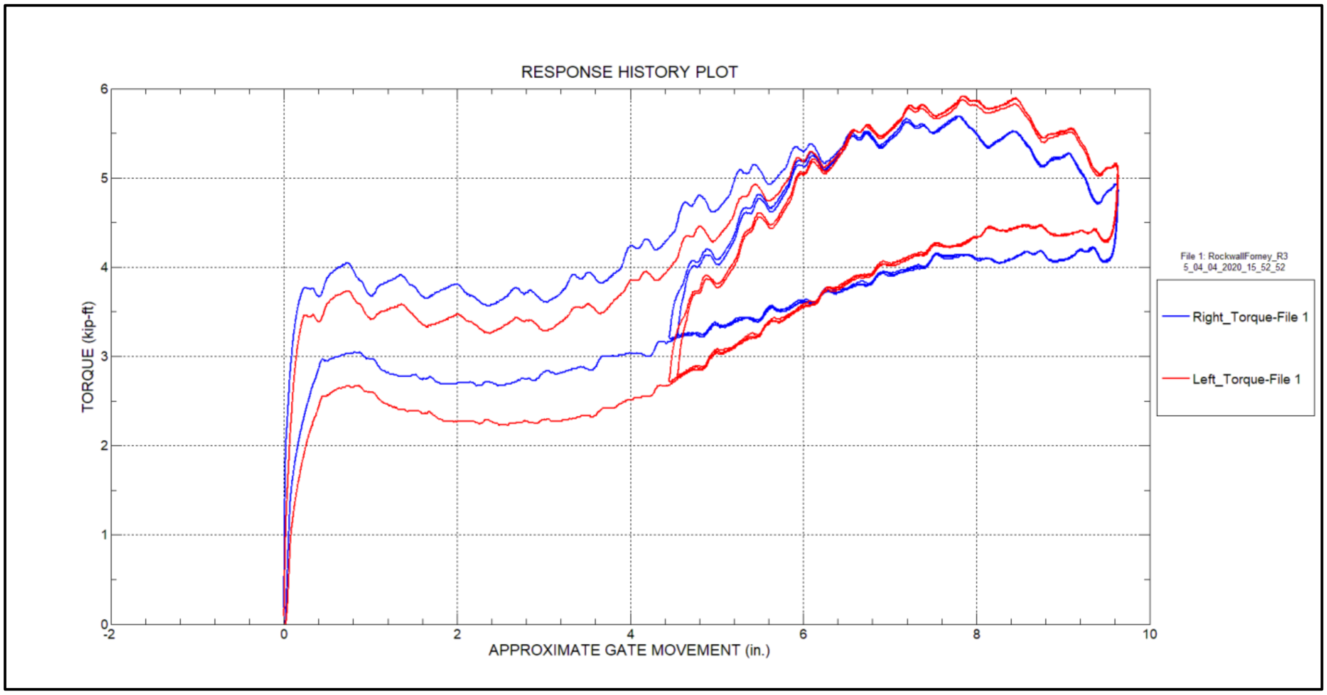

Figure 25 – Hoist torque response history – Gate 5 – Test 1

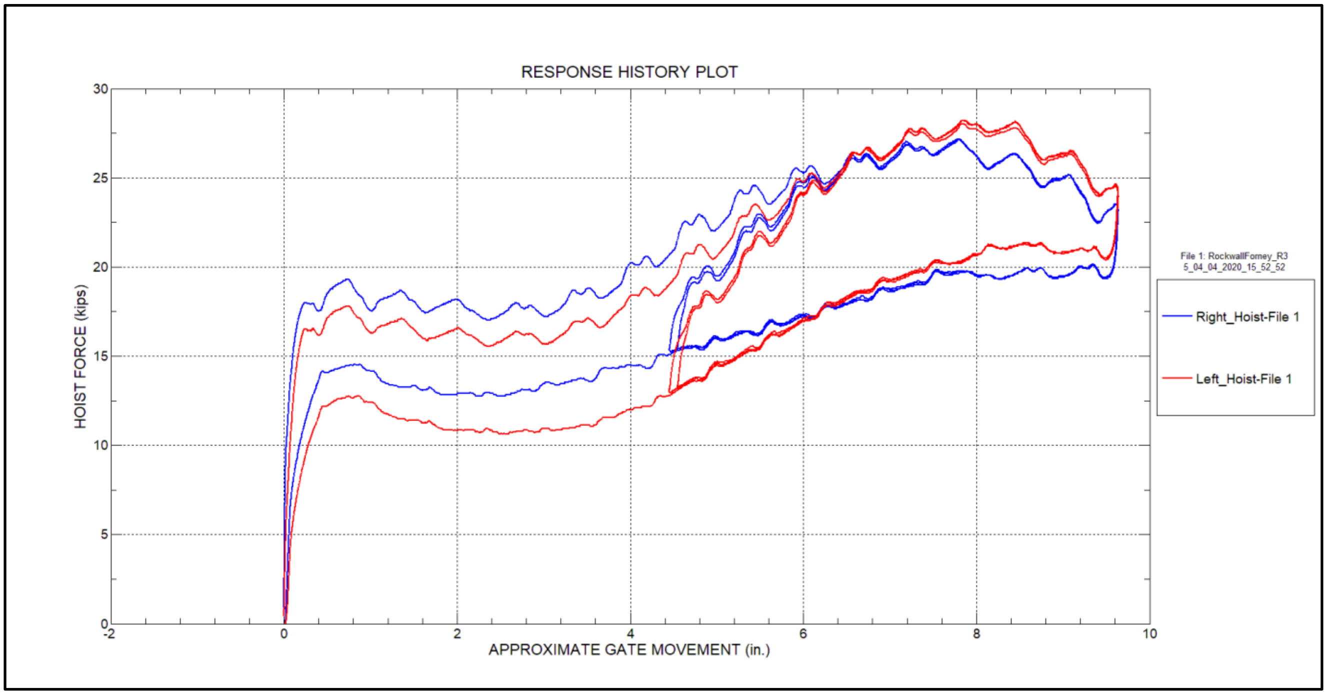

Figure 26 – Hoist force response history – Gate 5 – Test 1

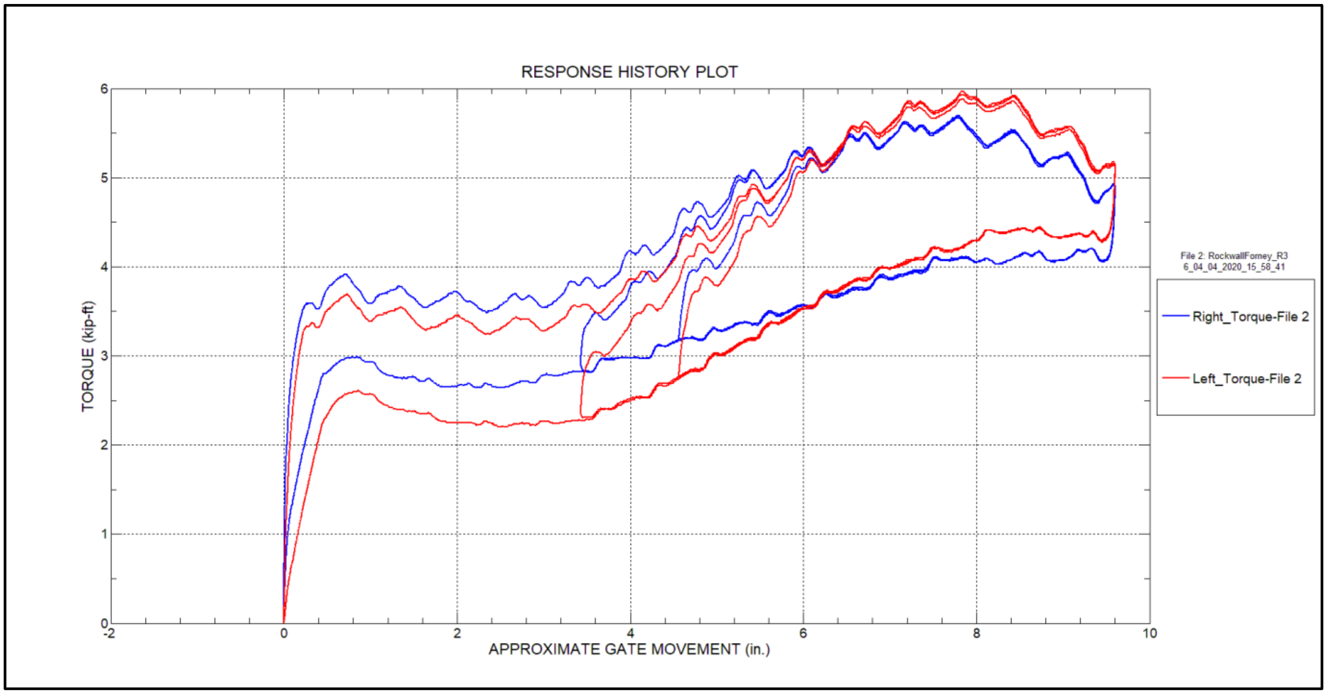

Figure 27 – Hoist torque response history – Gate 5 – Test 2

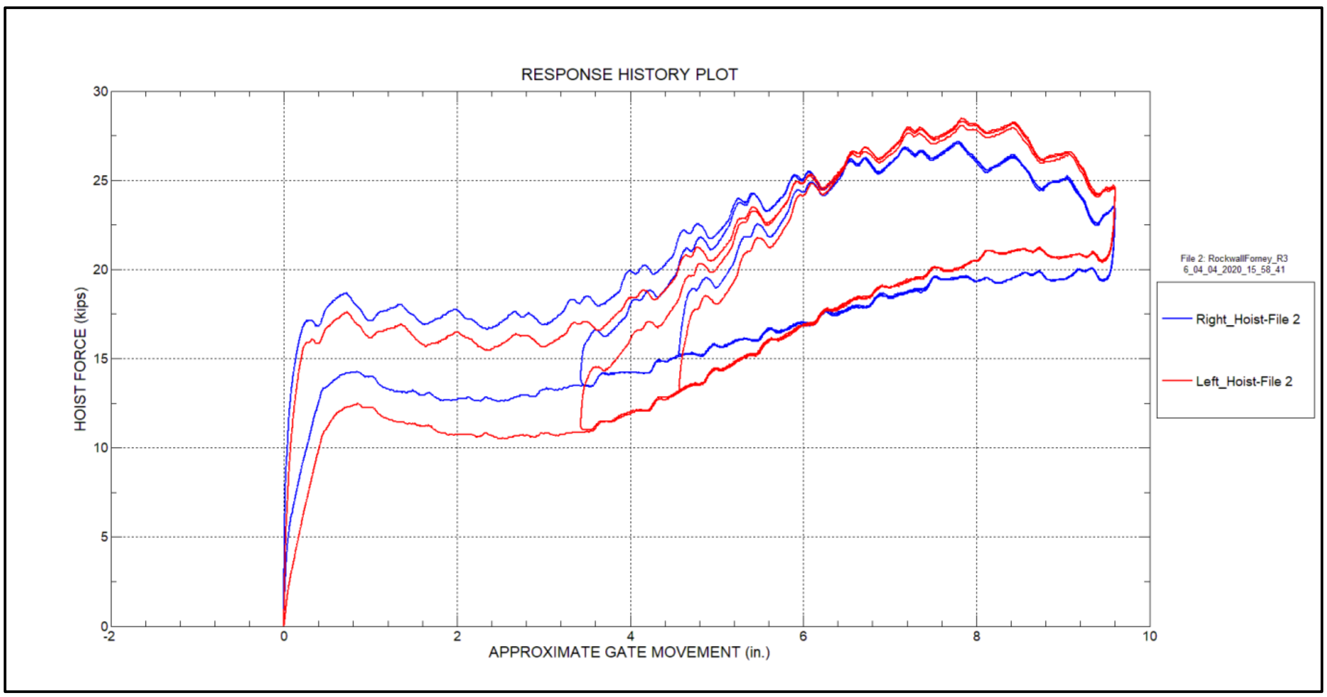

Figure 28 – Hoist force response history – Gate 5 – Test 2

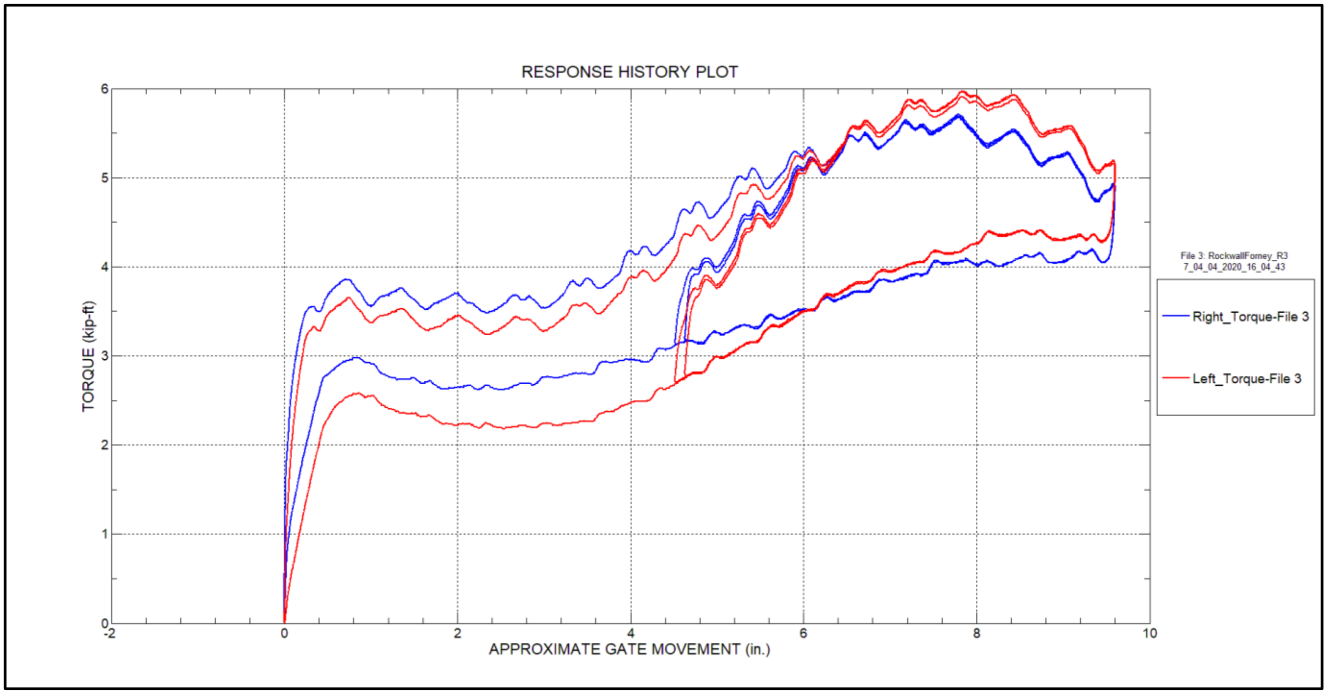

Figure 29 – Hoist torque response history – Gate 5 – Test 3

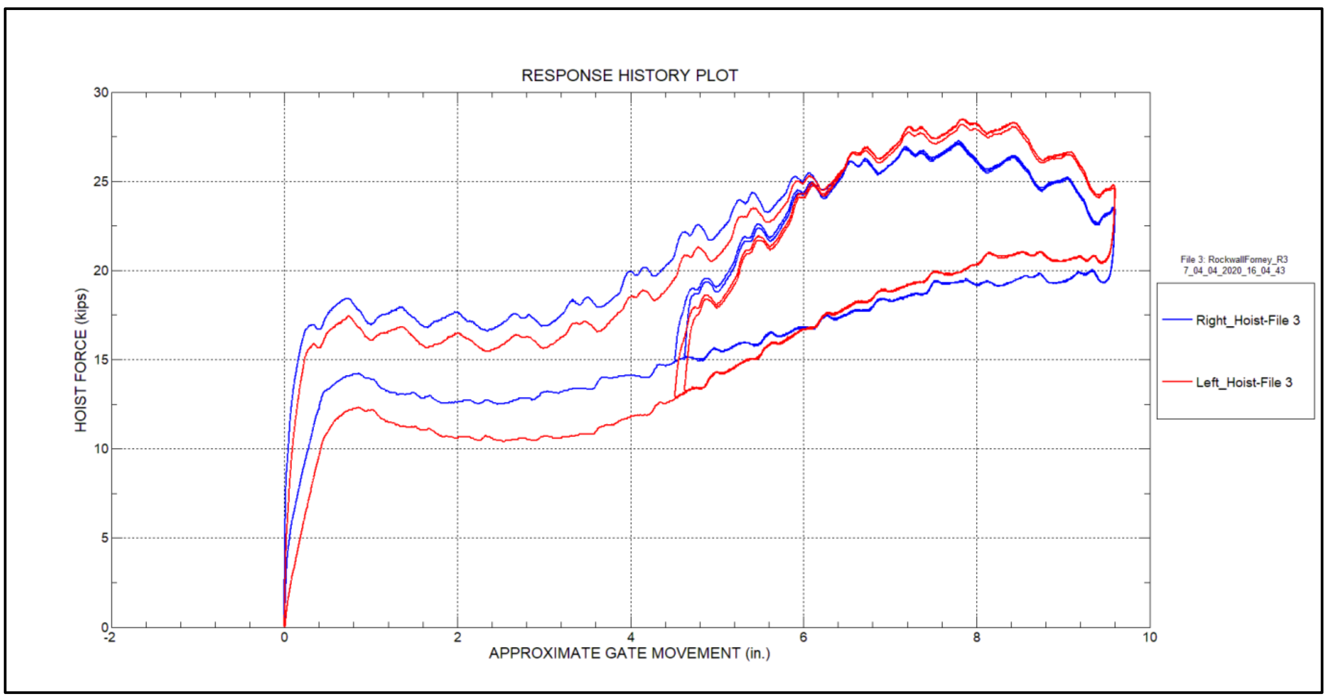

Figure 30 – Hoist force response history – Gate 5 – Test 3

APPENDIX B – GATE 5 PIN MOMENT COMPONENT PLOTS

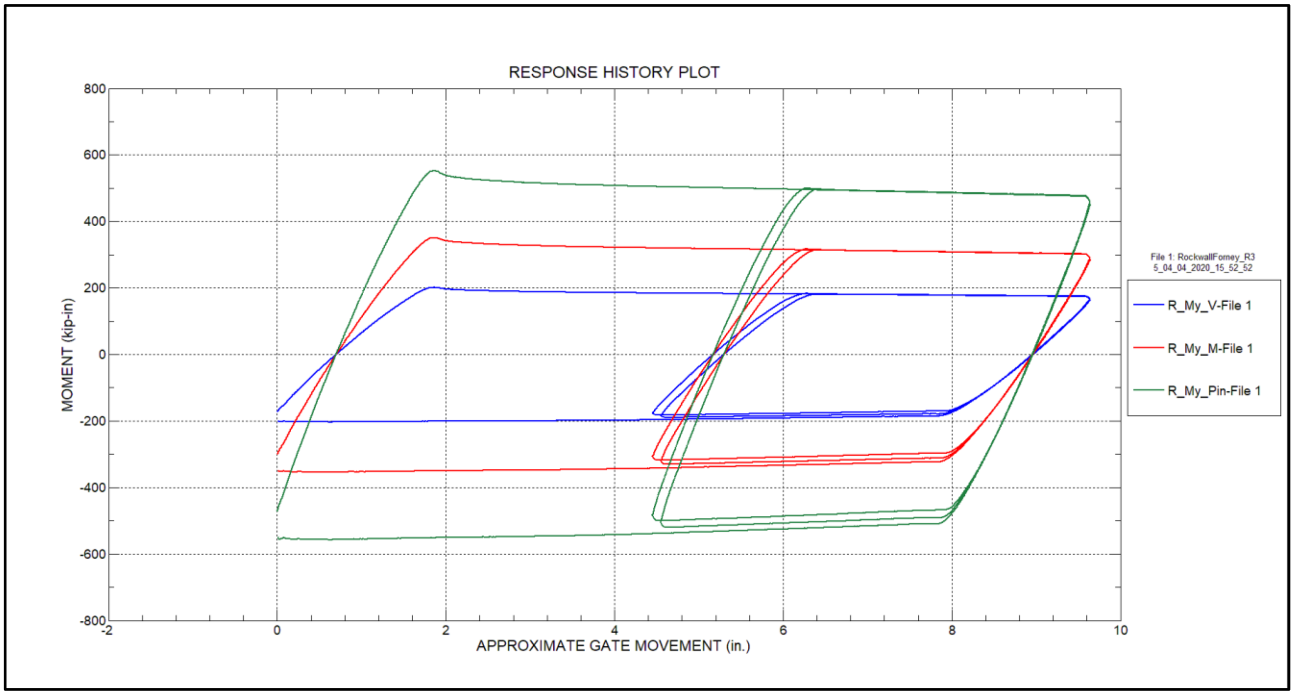

Figure 31 – Pin moment response history – Right arm – Test run 1

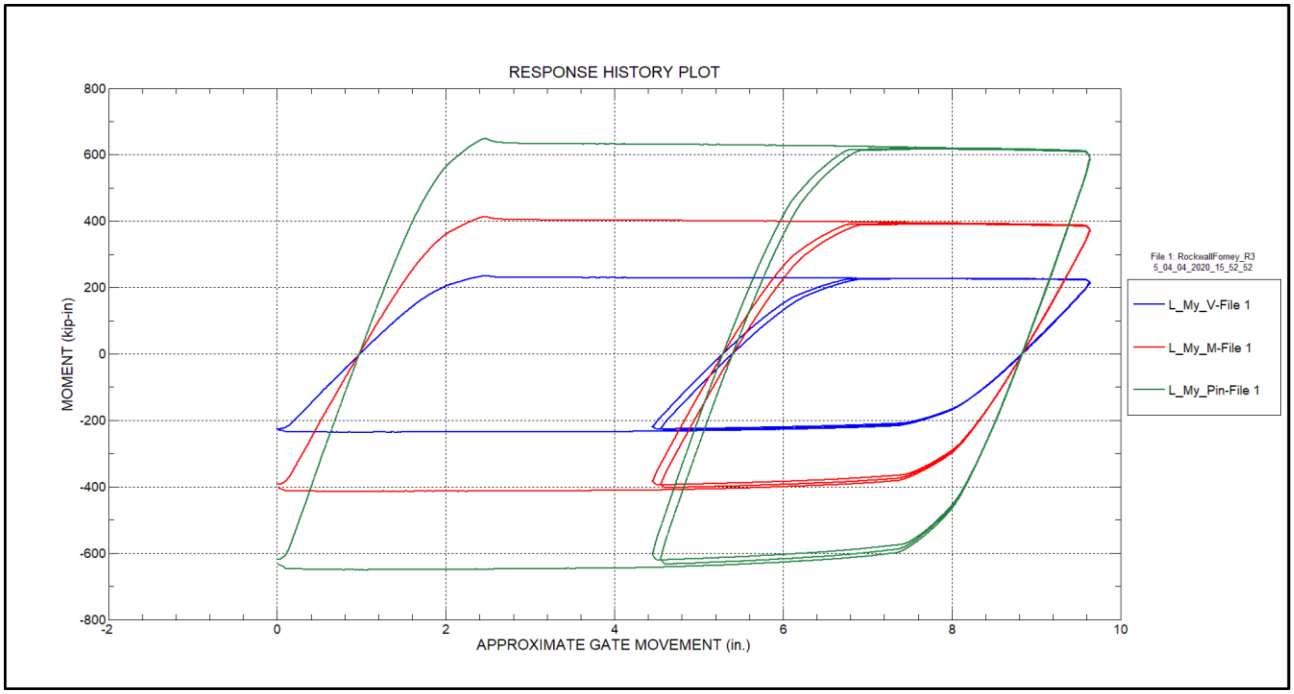

Figure 32 – Pin moment response history – Left arm – Test run 1

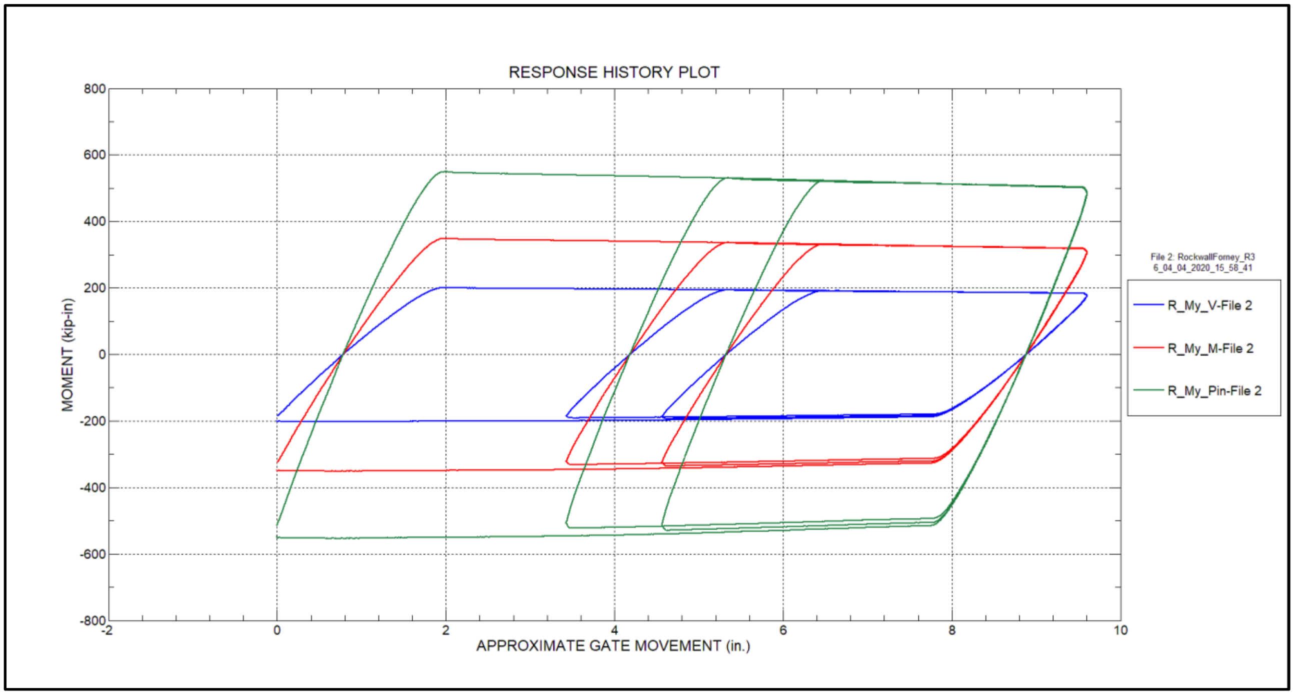

Figure 33 – Pin moment response history – Right arm – Test run 2

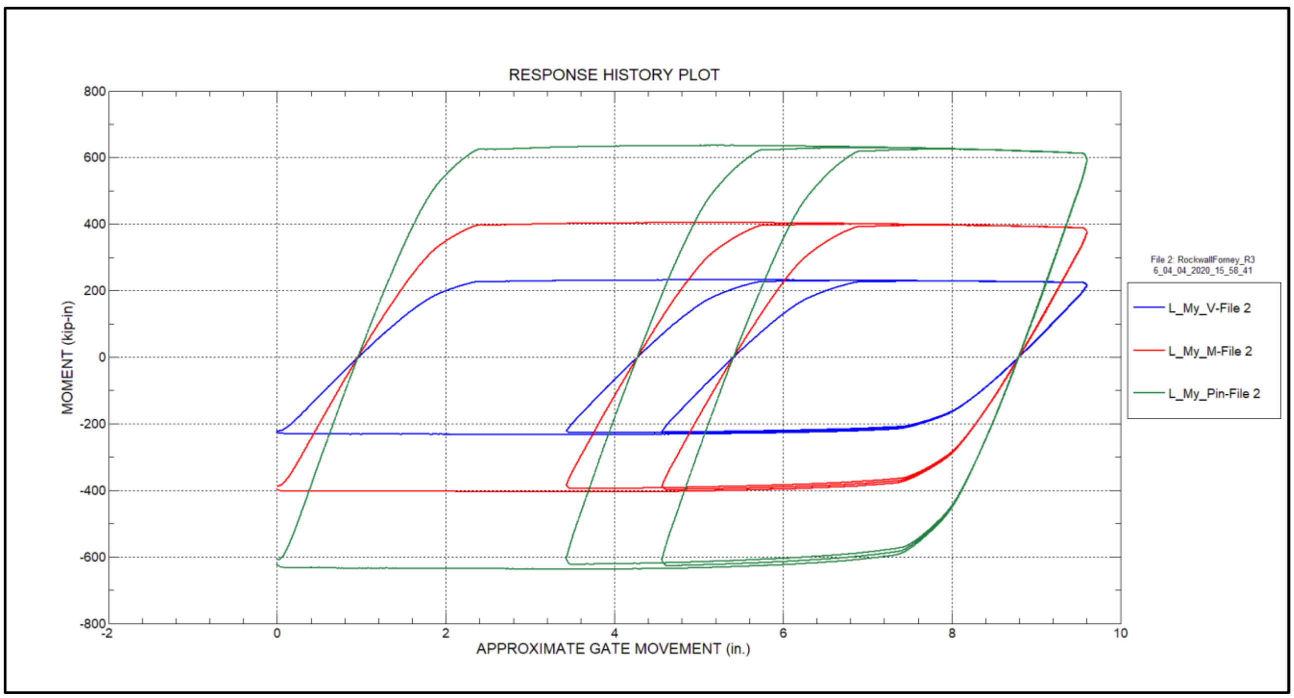

Figure 34 – Pin moment response history – Left arm – Test run 2

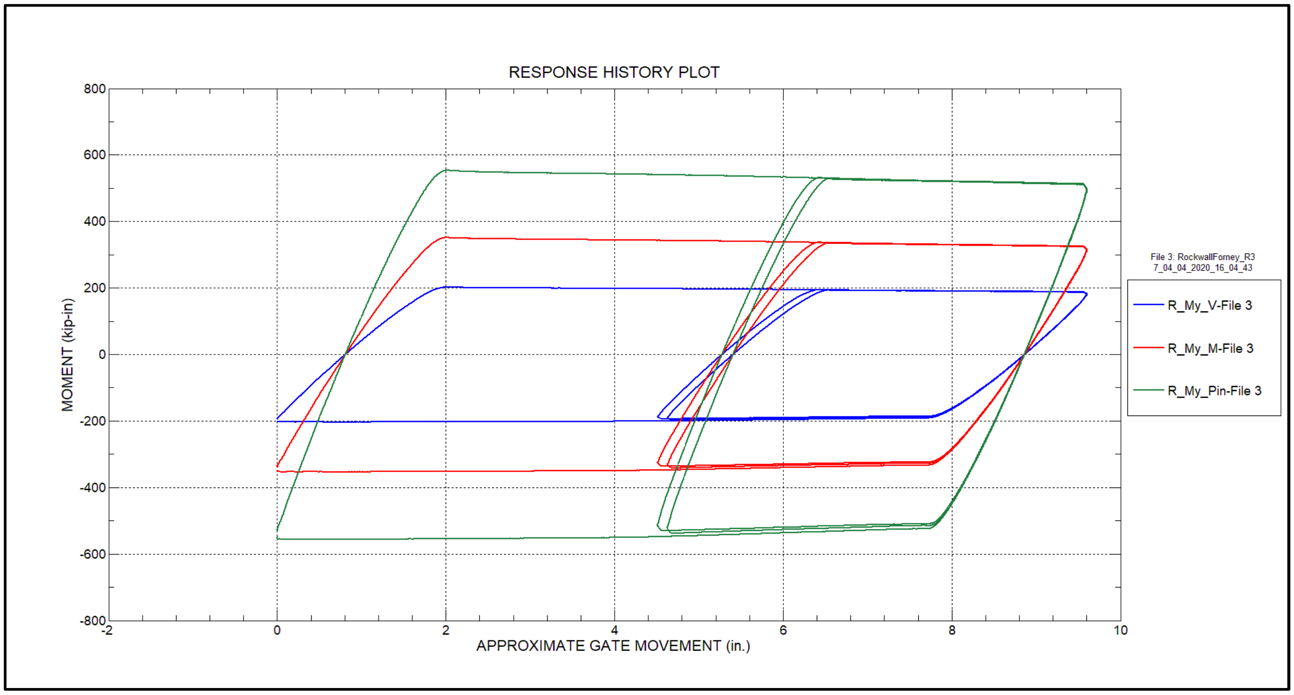

Figure 35 – Pin moment response history – Right arm – Test run 3

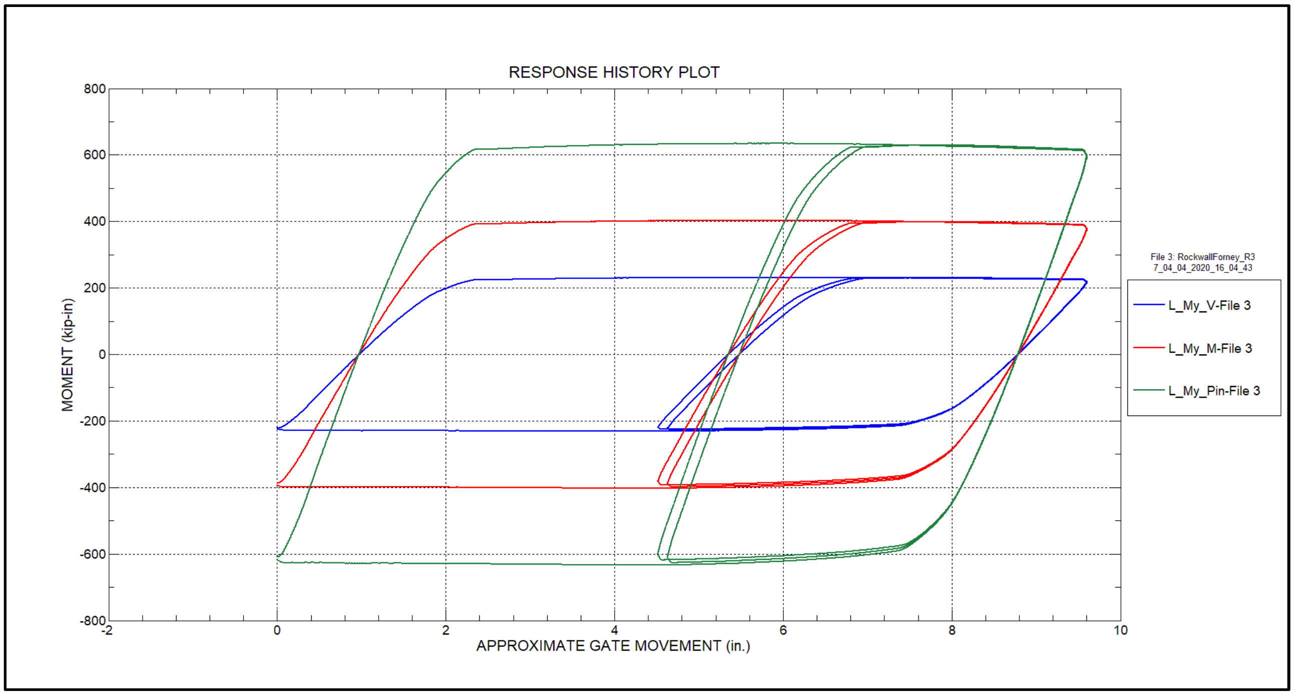

Figure 36 – Pin moment response history – Left arm – Test run 3

APPENDIX C – INSTRUMENTATION PLANS

RAW DATA. REFINED RESULTS.

SCHNABEL ENGINEERING
ROCKWALL FORNEY DAM
LIVE LOAD TESTING

RAW DATA. REFINED RESULTS.
740 S PIERCE AVE, SUITE 15
LOUISVILLE, CO 80027
303.494.3230
WWW.BDITEST.COM

ISSUE

CLIENT

SCHABEL ENGINEERING
16000 CHRISTENSEN RD, STE 101
SEATTLE, WA 98188

PROJECT NAME

SCHNABEL ENGINEERING
ROCKWALL FORNEY DAM
LIVE LOAD TESTING

Drawn By:	KNR
Checked By:	JDS
Date:	05/27/2020
Client No.:	
BDI No.:	190701-TX
SCALE:	NTS

COVER PAGE

LLT-00

The user acknowledges that these documents are instruments of professional service, and are protected by Copyright. This document and the information contained in this document are the property of Bridge Diagnostics, Inc., and shall not be reused, copied, disseminated, modified, amended or altered in any way. It is issued for information purposes only. The user agrees to hold harmless, indemnify and defend Bridge Diagnostics, Inc. against any and all damages, claims and losses, including defense costs, arising out of any use, reuse or copying of this document.

PLOT TIME: 6/12/2020 3:22 PM
FILEPATH: C:\Users\colemand\BDI\Services - Documents\Server_Remote\190701-TX_Schnabel_RockwallForneyDam\7. Instrumentation Plans\BDI_ROCKWALLFORNEY_01_GENERAL.dwg
© YYYY BRIDGE DIAGNOSTICS INC.

The user acknowledges that these documents are instruments of professional service, and are protected by Copyright. This document and the information contained in this document are the property of Bridge Diagnostics, Inc., and shall not be reused, copied, disseminated, modified, amended or altered in any way. It is issued for information purposes only. The user agrees to hold harmless, indemnify and defend Bridge Diagnostics, Inc. against any and all damages, claims and losses, including defense costs, arising out of any use, reuse or copying of this document.

GAGE LEGEND & SPECIFICATION

SYMBOL	TYPE	BRAND	MODEL	NOTES
	STRAIN TRANSDUCER	BDI	ST350	
	TILTMETER (UNI-AXIAL)	BDI	T500-030	
	TORQUE SENSOR	HPI	-	HBWS-35-125-6-0.5VR-FB
	AMP SENSOR	CR MAGNETICS	CR42105-200	

GENERAL NOTES

- INSTRUMENTATION SHALL BEGIN ON APRIL 1ST, 2020.
- GATES 1 THRU 14 SHALL BE ACCESSED USING SPRAT ROPE ACCESS TECHNIQUES.
- BDI WILL PERFORM ALL SURFACE PREPARATION, SENSOR INSTALLATION, AND EQUIPMENT INSTALLATION.
- SEE LLT-31 FOR SENSOR INSTALLATION DETAILS.
- TWO PAIRS OF TORQUE GAGES WILL BE INSTALLED ON THE GATE MOTORS' PINION SHAFTS BETWEEN THE MOTORS AND THE HOISTS.
  - GAGE PAIRS WILL BE INSTALLED 180° APART FROM EACH OTHER.
  - EXACT POSITIONS OF THE GAGE PAIRS ON THE PINION SHAFT WILL BE DETERMINED IN THE FIELD.
- THREE PHASE AMPERAGE GAGES WILL BE INSTALLED ON THE MOTOR CONTROLS BY A QUALIFIED ELECTRICIAN PROVIDED BY GARVER.

TESTING PROCEDURE:

- TESTING SHALL BE STARTED WITH THE GATE IN THE CLOSED POSITION.
- ONCE DATA COLLECTION BEGINS, THE GATE SHALL BE RAISED TO TWO OR THREE TIMES THE HEIGHT NECESSARY FOR TRUNNION FRICTION TO BE OVERCOME, H1 (TYPICALLY 6"-12"), AND HELD THERE UNTIL DATA STABILIZES.
- THE GATE SHALL BE LOWERED APPROXIMATELY TWICE THE DISTANCE TO OVERCOME TRUNNION FRICTION, H2, AND HELD THERE UNTIL DATA STABILIZES.
- THE GATE SHALL BE RAISED TO H1 AND HELD THERE UNTIL DATA STABILIZES.
- THE GATE SHALL BE LOWERED TO H2 AND HELD THERE UNTIL DATA STABILIZES.
- THE GATE SHALL BE RAISED TO H1 AND HELD THERE UNTIL DATA STABILIZES.
- THE GATE WAS LOWERED BACK TO CLOSED POSITION AND DATA COLLECTION STOPPED.
- A MINIMUM OF 3 TESTS SHALL BE PERFORMED PER GATE.

GAGE COUNT PER GATE

SENSOR LEGEND	SENSOR COUNT	CHANNEL COUNT
STRAIN TRANSDUCER	(48)	(48)
TILTMETER (UNI-AXIAL)	(4)	(4)
TORQUE SENSOR	(4)	(4)
AMP SENSOR	(3)	(3)
TOTAL	(59)	(59)

LOCATION KEY

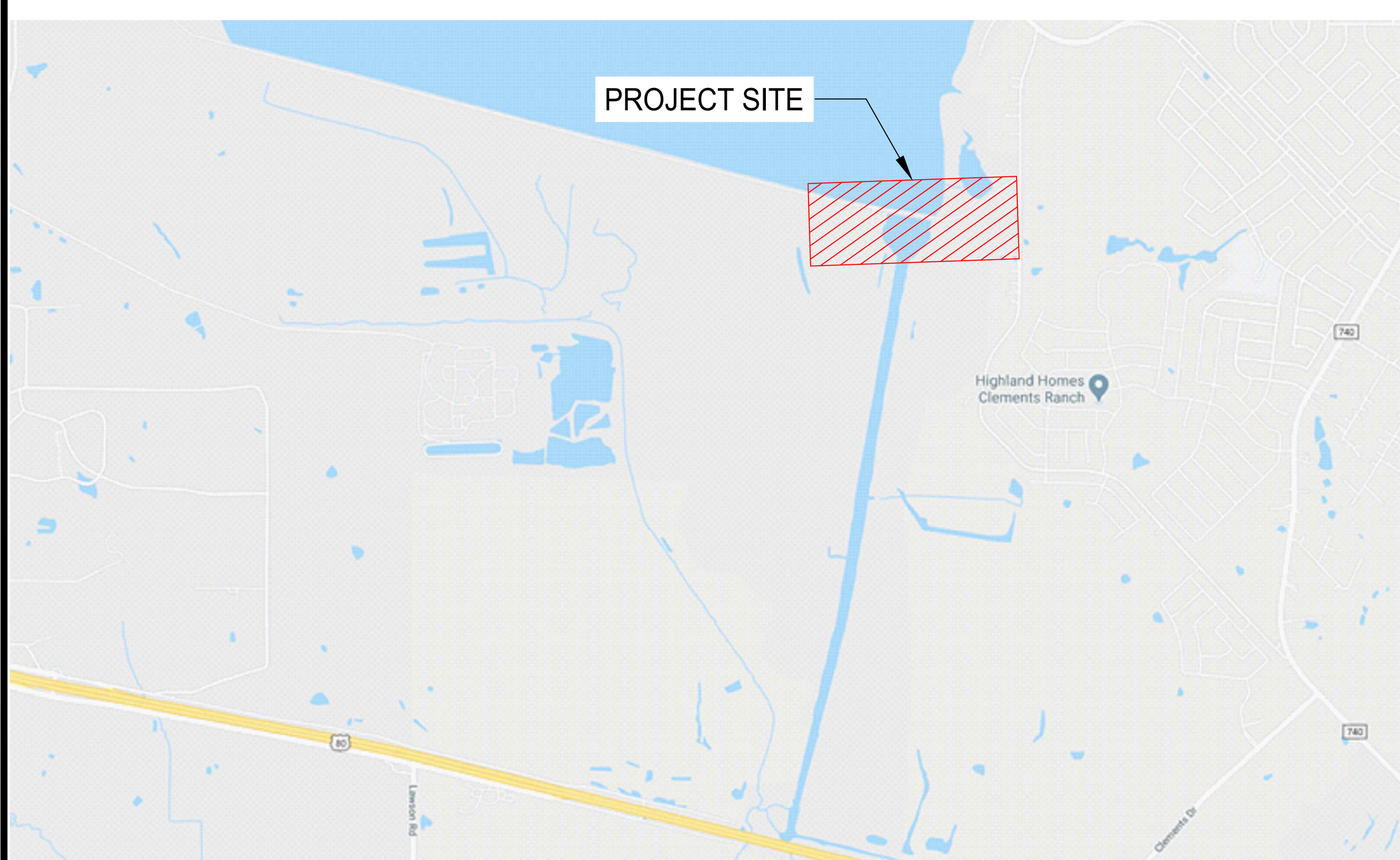

INDEX OF SHEETS

INDEX OF ISSUE

NO.	DATE	REVISION DESCRIPTION
1	3/20/2020	LIVE LOAD TESTING (LLT) INSTRUMENTATION PLAN (FOR APPROVAL)
2	5/27/2020	LIVE LOAD TESTING (LLT) INSTRUMENTATION PLAN AS BUILTS
BDI REFERENCE NUMBER: 190701-TX		

BDI
RAW DATA. REFINED RESULTS.
740 S PIERCE AVE, SUITE 15
LOUISVILLE, CO 80027
303.494.3230
WWW.BDITEST.COM

ISSUE

CLIENT

SCHABEL ENGINEERING
16000 CHRISTENSEN RD, STE 101
SEATTLE, WA 98188

PROJECT NAME

SCHABEL ENGINEERING
ROCKWALL FORNEY DAM
LIVE LOAD TESTING

Drawn By:	KNR
Checked By:	JDS
Date:	05/27/2020
Client No.:	
BDI No.:	190701-TX
SCALE:	NTS

OVERALL LEGEND

LLT-01

PLOT TIME: 6/12/2020 3:22 PM
FILEPATH: C:\Users\colemand\BDI\Services - Documents\Server_Remote\190701-TX_Schnabel_RockwallForneyDam\7. Instrumentation Plans\BDI_ROCKWALLFORNEY_01_GENERAL.dwg
© YYYY BRIDGE DIAGNOSTICS INC.

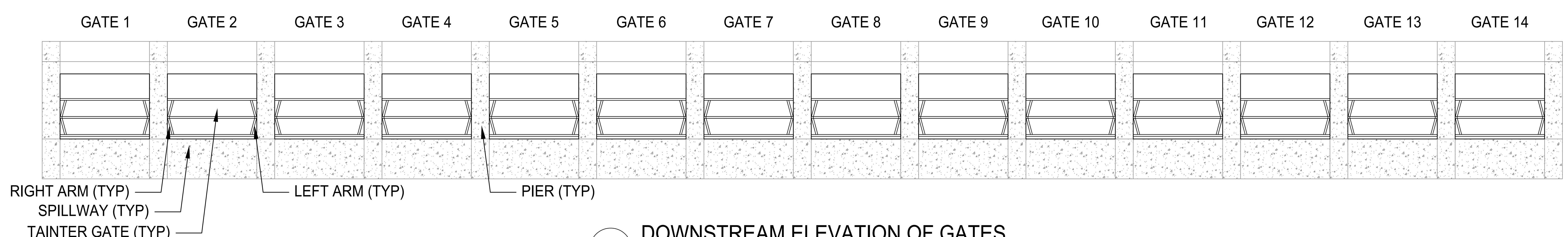

1 DOWNSTREAM ELEVATION OF GATES
LOOKING NORTH (UPSTREAM)

The user acknowledges that these documents are instruments of professional service, and are protected by Copyright. This document and the information contained in this document are the property of Bridge Diagnostics, Inc., and shall not be reused, copied, disseminated, modified, amended or altered in any way. It is issued for information purposes only. The user agrees to hold harmless, indemnify and defend Bridge Diagnostics, Inc. against any and all damages, claims and losses, including defense costs, arising out of any use, reuse or copying of this document.

PLOT TIME: 6/12/2020 3:22 PM
FILEPATH: C:\Users\colemand\BDI\Services - Documents\Server_Remote\190701-TX_Schabel_RockwallForneyDam\7. Instrumentation Plans\BDI_ROCKWALLFORNEY_01_GENERAL.dwg
© YYYY BRIDGE DIAGNOSTICS INC.

RAW DATA. REFINED RESULTS.
740 S PIERCE AVE, SUITE 15
LOUISVILLE, CO 80027
303.494.3230
WWW.BDITEST.COM

ISSUE

CLIENT

SCHABEL ENGINEERING
16000 CHRISTENSEN RD, STE 101
SEATTLE, WA 98188

PROJECT NAME

SCHNABEL ENGINEERING
ROCKWALL FORNEY DAM
LIVE LOAD TESTING

Drawn By:	KNR
Checked By:	JDS
Date:	05/27/2020
Client No.:	
BDI No.:	190701-TX
SCALE:	NTS

OVERALL STRUCTURE
LAYOUT
LLT-02

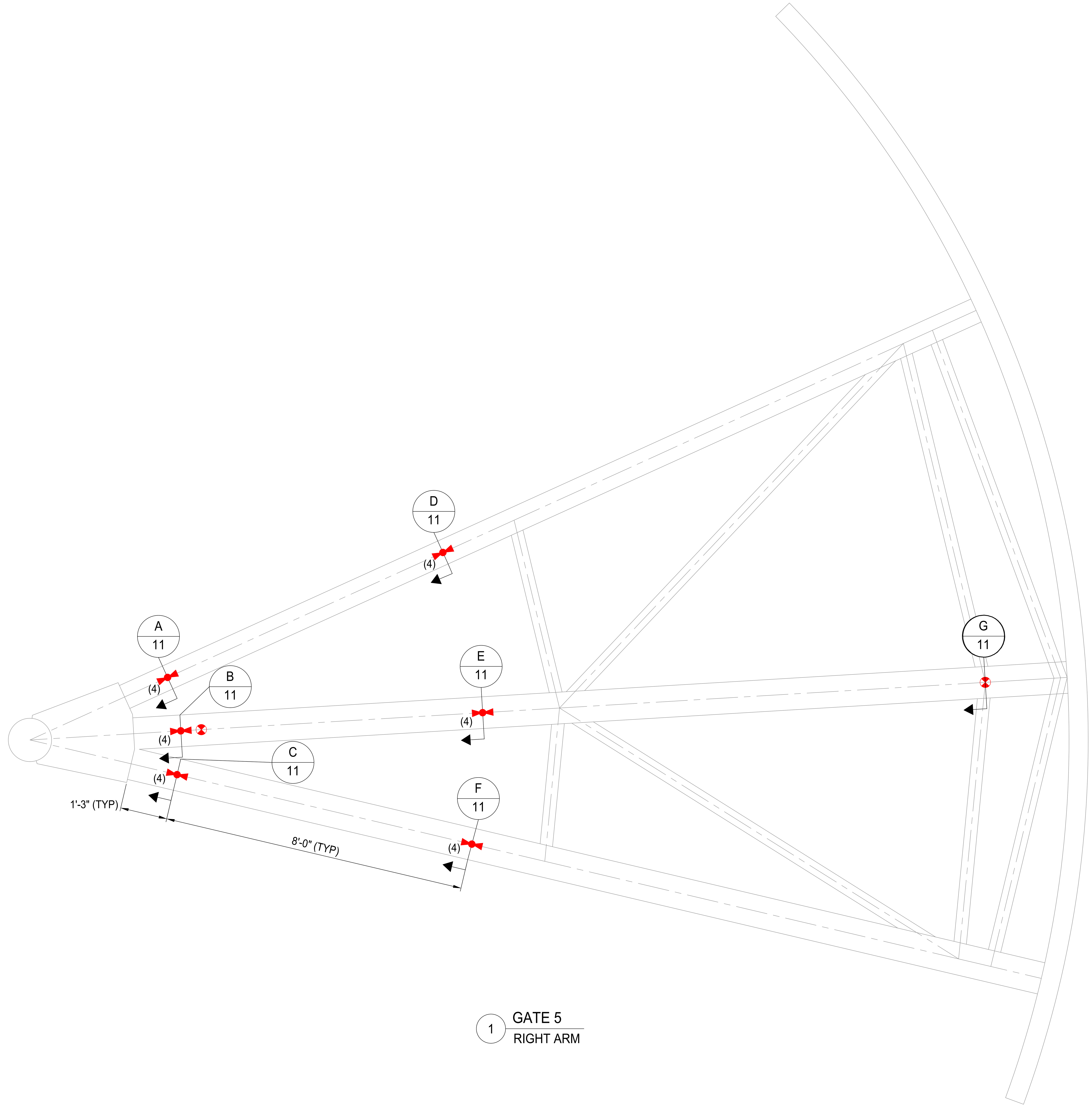

GATE 5
RIGHT ARM

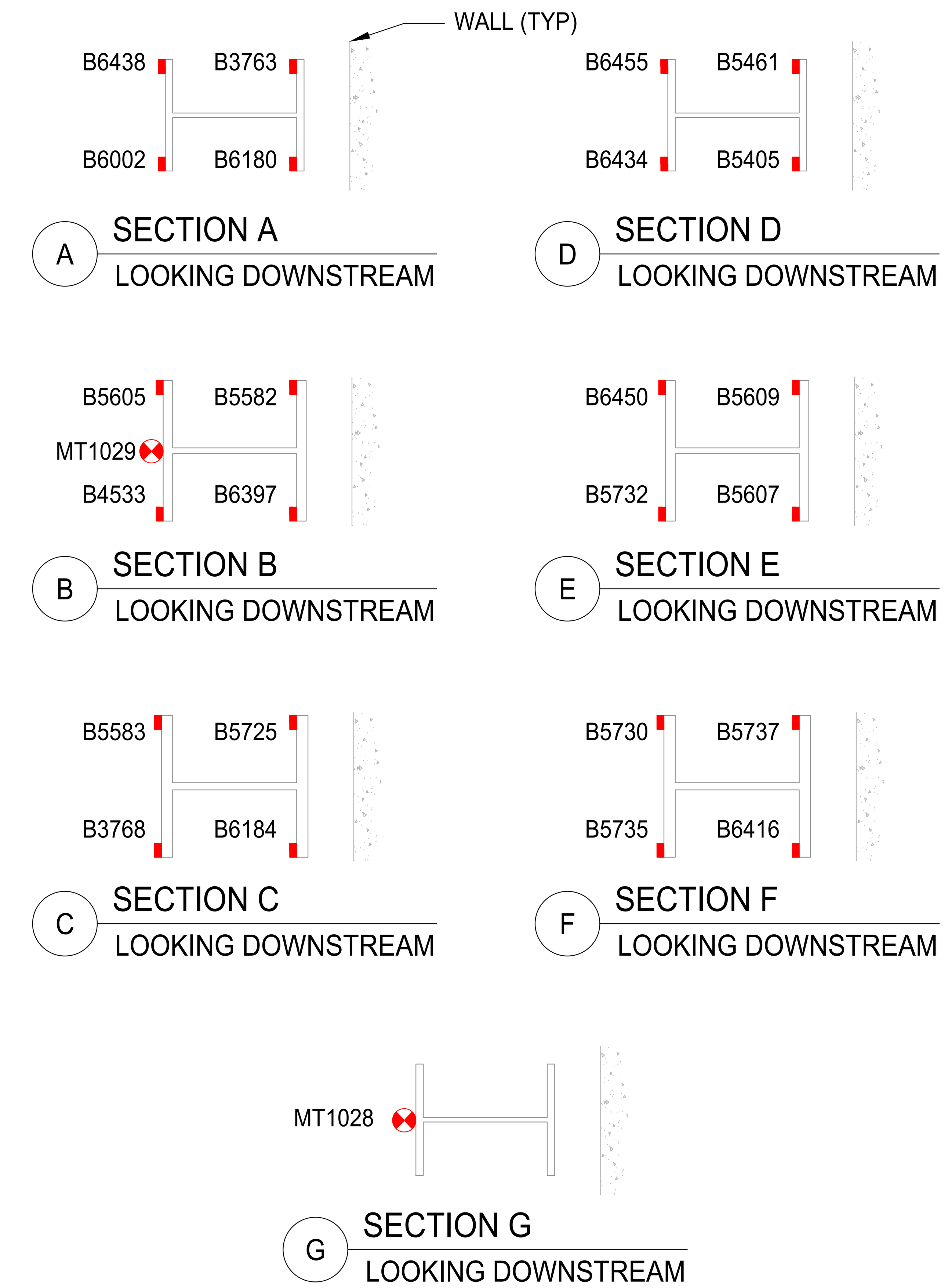

UNIT ID
TT-3

TORQUE GAGES
RIGHT ARM

NOTES:

1. SECTIONS A, B, & C SHALL BE INSTALLED 15 INCHES AWAY FROM TRUNNION PLATE.
2. TILTMETERS SHALL BE INSTALLED CENTERED ON THE MIDDLE STRUT FLANGE.
3. SECTION G'S TILTMETER SHALL BE INSTALLED AS CLOSE TO THE SKINPLATE AS POSSIBLE.

SENSOR LEGEND
- STRAIN TRANSDUCER
- TILTMETER (UNI-AXIAL)
- TORQUE SENSOR

BDI
RAW DATA. REFINED RESULTS.
740 S PIERCE AVE, SUITE 15
LOUISVILLE, CO 80027
303.494.3230
WWW.BDITEST.COM

ISSUE

CLIENT

SCHABEL ENGINEERING
16000 CHRISTENSEN RD, STE 101
SEATTLE, WA 98188

PROJECT NAME

SCHABEL ENGINEERING
ROCKWALL FORNEY DAM
LIVE LOAD TESTING

Drawn By:	KNR
Checked By:	JDS
Date:	05/27/2020
Client No.:	
BDI No.:	190701-TX
SCALE:	NTS

GATE 5 - RIGHT ARM
ELEVATION
LLT-11

The user acknowledges that these documents are instruments of professional service, and are protected by Copyright. This document and the information contained in this document are the property of Bridge Diagnostics, Inc., and shall not be reused, copied, disseminated, modified, amended or altered in any way. It is issued for information purposes only. The user agrees to hold harmless, indemnify and defend Bridge Diagnostics, Inc. against any and all damages, claims and losses, including defense costs, arising out of any use, reuse or copying of this document.

PLOT TIME: 6/12/2020 3:23 PM
FILEPATH: C:\Users\colemand\BDI\Services - Documents\Server_Remote\190701-TX_Schabel_RockwallForneyDam\7. Instrumentation Plans\BDI_ROCKWALLFORNEY_01_GENERAL.dwg

© YYYY BRIDGE DIAGNOSTICS INC.

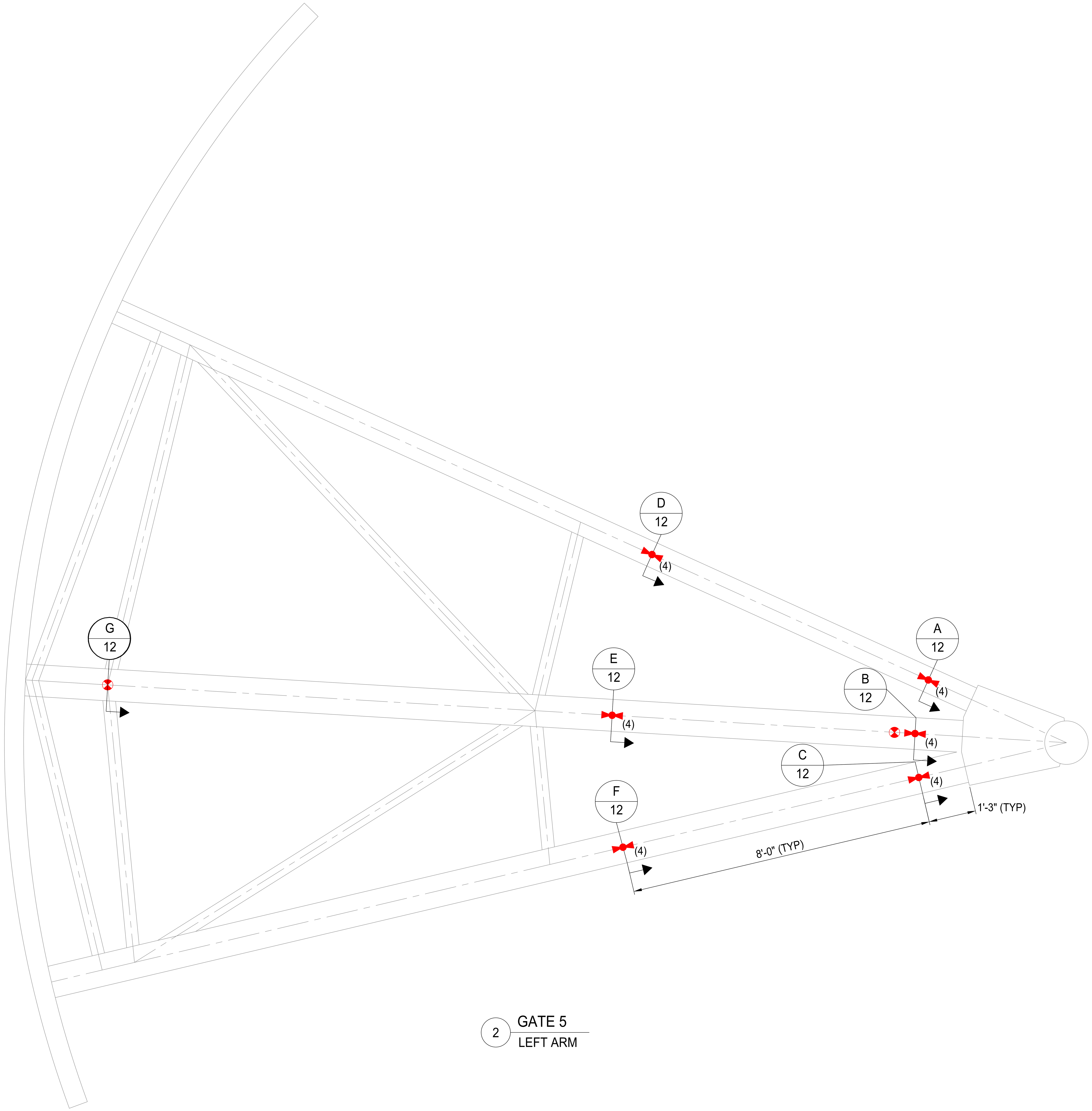

2 GATE 5
LEFT ARM

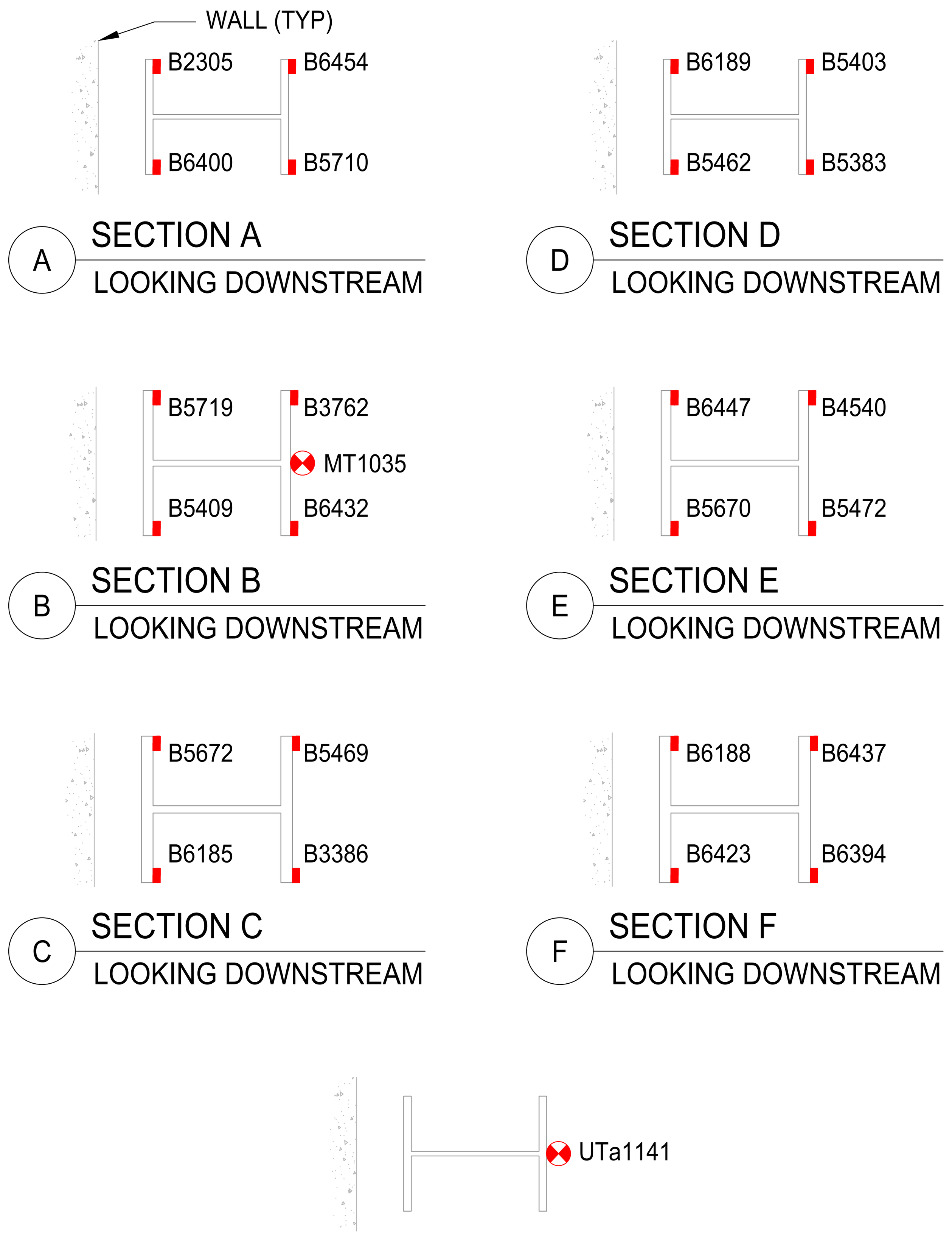

A SECTION A
LOOKING DOWNSTREAM

D SECTION D
LOOKING DOWNSTREAM

B SECTION B
LOOKING DOWNSTREAM

E SECTION E
LOOKING DOWNSTREAM

C SECTION C
LOOKING DOWNSTREAM

F SECTION F
LOOKING DOWNSTREAM

G SECTION G
LOOKING DOWNSTREAM

UNIT ID
TT-4

TORQUE GAGES
LEFT ARM

NOTES:

1. SECTIONS A, B, & C SHALL BE INSTALLED 15 INCHES AWAY FROM TRUNNION PLATE.
2. TILTMETERS SHALL BE INSTALLED CENTERED ON THE MIDDLE STRUT FLANGE.
3. SECTION G'S TILTMETER SHALL BE INSTALLED AS CLOSE TO THE SKINPLATE AS POSSIBLE.

SENSOR LEGEND

- STRAIN TRANSDUCER
- TILTMETER (UNI-AXIAL)
- TORQUE SENSOR

RAW DATA. REFINED RESULTS.
740 S PIERCE AVE, SUITE 15
LOUISVILLE, CO 80027
303.494.3230
WWW.BDITEST.COM

ISSUE

CLIENT

SCHABEL ENGINEERING
16000 CHRISTENSEN RD, STE 101
SEATTLE, WA 98188

PROJECT NAME

SCHABEL ENGINEERING
ROCKWALL FORNEY DAM
LIVE LOAD TESTING

Drawn By:	KNR
Checked By:	JDS
Date:	05/27/2020
Client No.:	
BDI No.:	190701-TX
SCALE:	NTS

GATE 5 - LEFT ARM
ELEVATION
LLT-12

The user acknowledges that these documents are instruments of professional service, and are protected by Copyright. This document and the information contained in this document are the property of Bridge Diagnostics, Inc., and shall not be reused, copied, disseminated, modified, amended or altered in any way. It is issued for information purposes only. The user agrees to hold harmless, indemnify and defend Bridge Diagnostics, Inc. against any and all damages, claims and losses, including defense costs, arising out of any use, reuse or copying of this document.

PLOT TIME: 6/12/2020 3:23 PM
FILEPATH: C:\Users\colemand\BDI\Services - Documents\Server_Remote\190701-TX_Schabel_RockwallForneyDam\7. Instrumentation Plans\BDI_ROCKWALLFORNEY_01_GENERAL.dwg
© YYYY BRIDGE DIAGNOSTICS INC.

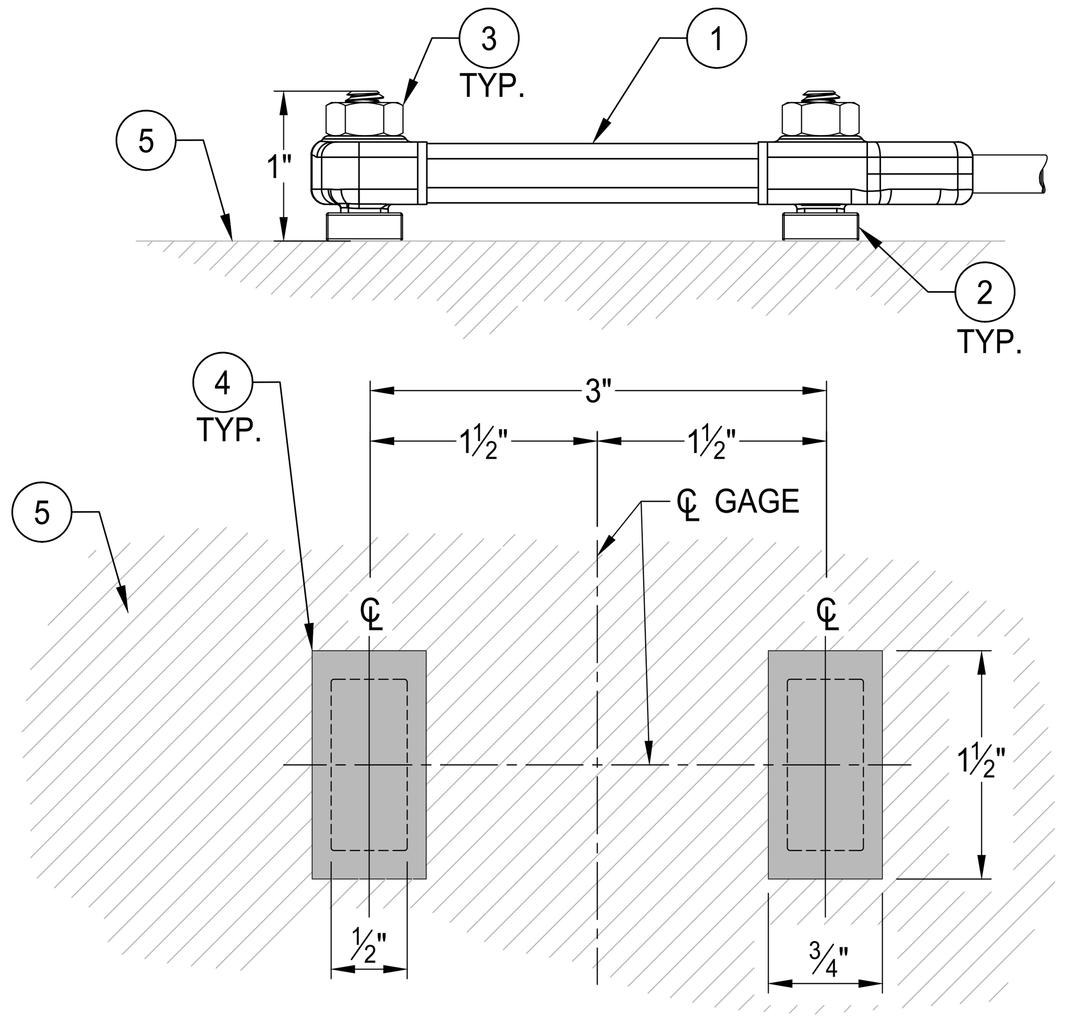

COMPONENT DESCRIPTION

1. ST350 STRAIN GAGE
2. 1/4"-20 THREADED MOUNTING TAB
3. 1/4"-20 STAINLESS STEEL NUT
4. TYPICAL SURFACE PREP REQUIRED TO MOUNT STRAIN GAGES
5. TYPICAL MOUNTING SURFACE

FOOTNOTES - INSTANT ADHESIVE
1. STRAIN GAGES SHALL BE MOUNTED WITH LOCTITE 410 INSTANT ADHESIVE AND LOCTITE 7452 ACCELERANT 2. DURING SURFACE PREP ALL PAINT AND SURFACE DEFORMATIONS MUST BE REMOVED. 3. SURFACE PREP IS REQUIRED JUST PRIOR TO GAGE INSTALLATION AS TO NOT ALLOW SURFACE CONTAMINANTS TO ACCUMULATE.

1 TYPICAL ST350 STRAIN GAGE INSTALLATION

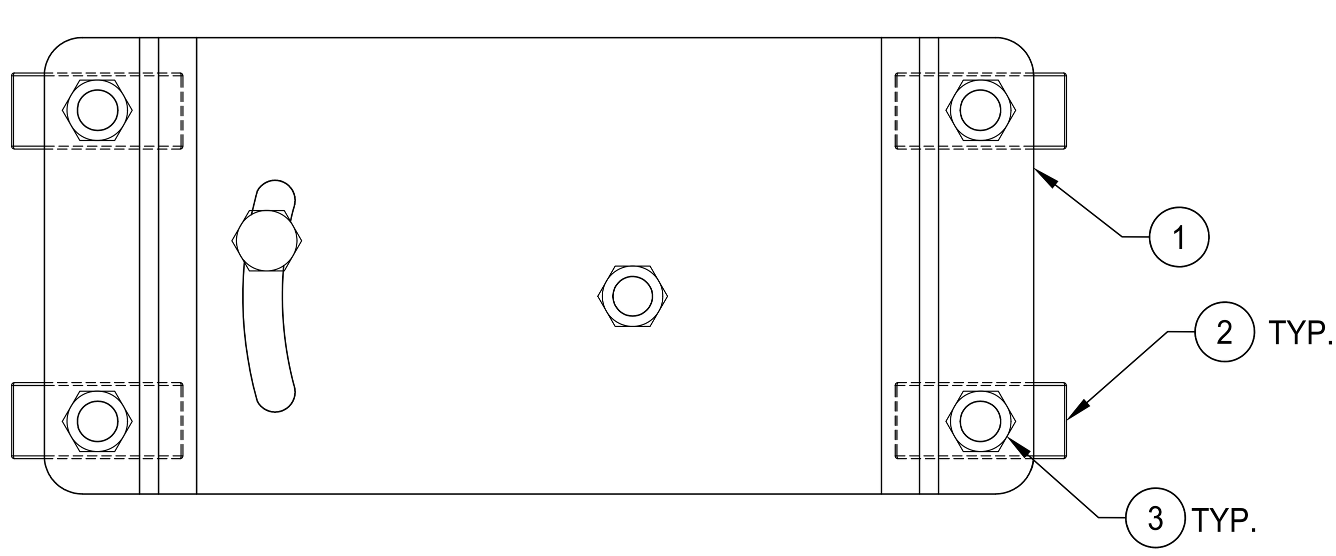

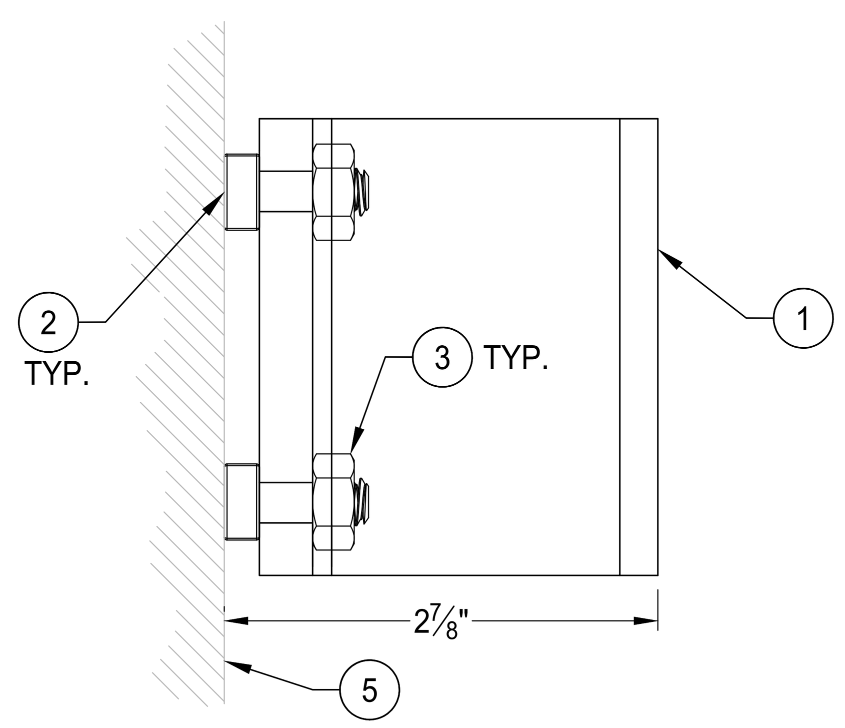

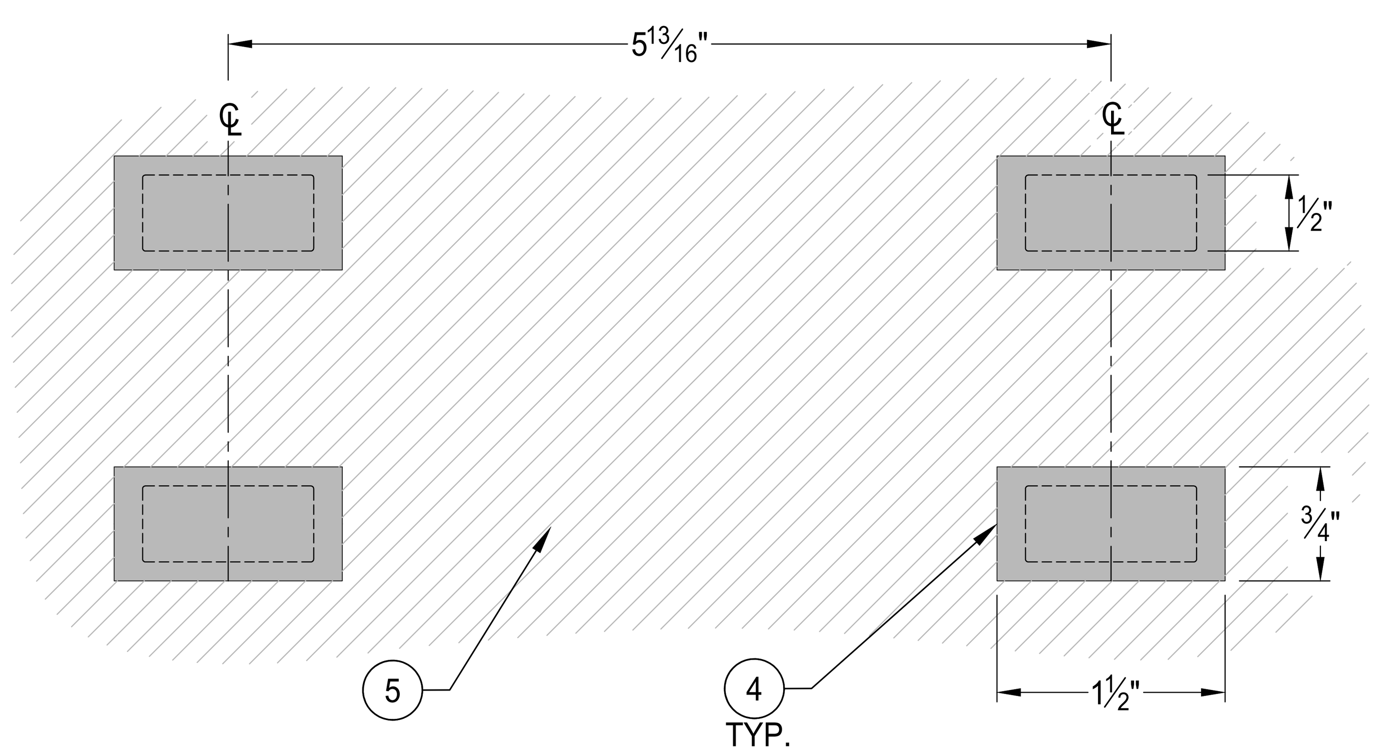

COMPONENT DESCRIPTION

1. BDI +/- 15 DEGREE TILTMETER WITH COVER AND ADJUSTMENT BOLTS
2. 1/4"-20 THREADED MOUNTING TAB
3. 1/4"-20 STAINLESS STEEL NUT
4. TYPICAL SURFACE PREP REQUIRED TO MOUNT TILTMETERS
5. TYPICAL MOUNTING SURFACE

FOOTNOTES - INSTANT ADHESIVE
1. TILTMETERS SHALL BE MOUNTED WITH LOCTITE 410 INSTANT ADHESIVE AND LOCTITE 7452 ACCELERANT 2. DURING SURFACE PREP ALL PAINT AND SURFACE DEFORMATIONS MUST BE REMOVED. 3. SURFACE PREP IS REQUIRED JUST PRIOR TO GAGE INSTALLATION AS TO NOT ALLOW SURFACE CONTAMINANTS TO ACCUMULATE.

2 TYPICAL BDI TILTMETER INSTALLATION

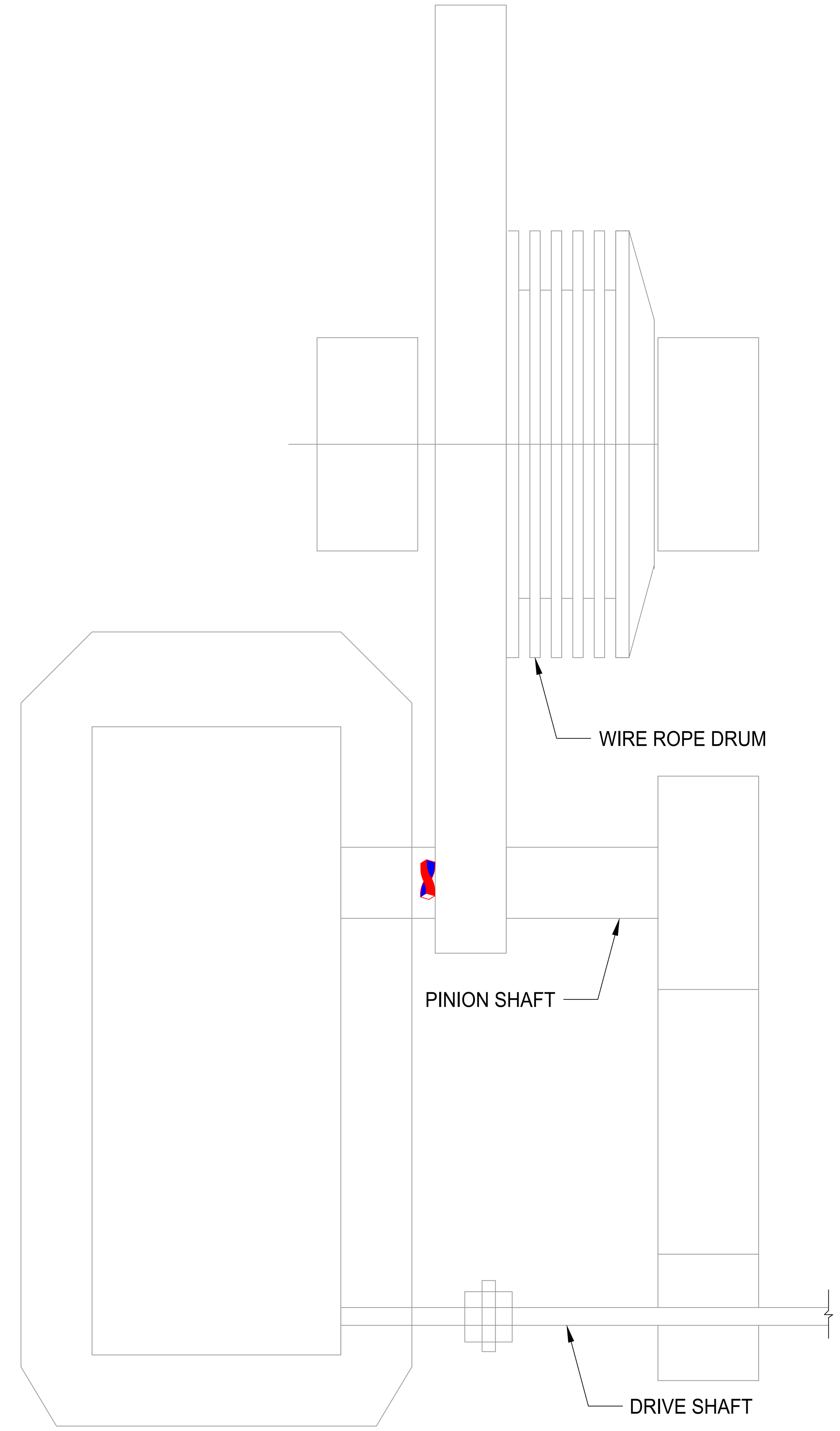

3 TYPICAL HOIST INSTRUMENTATION

TORQUE SENSOR INSTALLATION NOTES:

- TORQUE GAGES WILL BE INSTALLED ON THE PINION SHAFT ON EITHER HOIST MOTOR BETWEEN THE MOTOR AND THE HOIST DRUM
- EXACT POSITIONS OF THE GAGE PAIRS ON THE PINION SHAFT WILL BE DETERMINED IN THE FIELD

SENSOR LEGEND

TORQUE SENSOR

BDI
RAW DATA. REFINED RESULTS.
740 S PIERCE AVE, SUITE 15
LOUISVILLE, CO 80027
303.494.3230
WWW.BDITEST.COM

ISSUE

CLIENT

SCHABEL ENGINEERING
16000 CHRISTENSEN RD, STE 101
SEATTLE, WA 98188

PROJECT NAME

SCHNABEL ENGINEERING
ROCKWALL FORNEY DAM
LIVE LOAD TESTING

Drawn By:	KNR
Checked By:	JDS
Date:	05/27/2020
Client No.:	
BDI No.:	190701-TX
SCALE:	NTS

SENSOR INSTALLATION DETAILS

LLT-31

The user acknowledges that these documents are instruments of professional service, and are protected by Copyright. This document and the information contained in this document are the property of Bridge Diagnostics, Inc., and shall not be reused, copied, disseminated, modified, amended or altered in any way. It is issued for information purposes only. The user agrees to hold harmless, indemnify and defend Bridge Diagnostics, Inc. against any and all damages, claims and losses, including defense costs, arising out of any use, reuse or copying of this document.

PLOT TIME: 6/12/2020 3:24 PM
FILEPATH: C:\Users\colemand\BDI\Services - Documents\Server_Remote\190701-TX_Schnabel_RockwallForneyDam\7. Instrumentation Plans\BDI_ROCKWALLFORNEY_01_GENERAL.dwg

© YYYY BRIDGE DIAGNOSTICS INC.

SCHNABEL ENGINEERING

GATE OPERATION DATA REPORT

ROCKWALL FORNEY DAM – GATE 6
FORNEY, TX

SUBMITTED TO:

SCHNABEL ENGINEERING
16000 CHRISTENSEN RD, SUITE 101
SEATTLE, WA 98188

SUBMITTED BY:

BDI – CO
740 SOUTH PIERCE AVE, UNIT 15
LOUISVILLE, CO 80027

BDI Project No.: **190701-TX**
Report Version: **V1**
Version Submitted: **August 31, 2020**

RAW DATA. REFINED RESULTS.

This document contains Confidential Information and is submitted in confidence to the customer. The submission of the information contained herein shall not be deemed to constitute public disclosure or authorization for disclosure to other parties. BDI's information and name may not be used in advertising or for promotional purposes without BDI's written consent.

TABLE OF CONTENTS

LIST OF FIGURES

LIST OF TABLES

EXECUTIVE SUMMARY

Schnabel Engineering contracted BDI to provide instrumentation and testing services on Gates 1-14 on the Rockwall Forney Dam near Dallas, Texas. The goal of these tests was to record each gate's structural responses during a series of spill tests and use the data to compute accurate coefficients of friction for each trunnion pin, cable lift force, total gate friction, and motor amperage. Typical spill tests were not conducted on Gate 6 due to concerns about the gate's structural condition. During a recent inspection, a crack was found in the left gate arm's top strut flange-web interface during a recent inspection. Instead, response data was recorded while the gate was dewatered and then operated in a dry state during exploratory gate operations. As a result, friction results (coefficients of friction, total gate friction, etc.) were not calculated for this gate. This report provides details and observations for the data collected on Gate 6.

Instrumentation and data collection were performed on Gate 6 at the Rockwall Forney Dam on April 3rd, 2020. The gate arms were instrumented with strain and rotation sensors. The hoist's pinion shafts were instrumented with torque sensors and the hoist motor controls were instrumented with amperage sensors. Following the instrumentation, the structural responses were measured while the gate was dewatered (i.e. while the interstitial space between a bulkhead and the skin plate was drained) and during gate operation in the dry condition. During gate operation it was discovered that a log had been lodged under the right side of the skin plate. The log was removed prior to the final closing of the gate. All instrumentation setup and removal were performed using BDI's rope access team.

Following demobilization from the field, the data was examined for quality and then further processed to evaluate the gate's performance. Strain measurements were converted into strut axial forces and bending moments to better evaluate the observed behavior. The following is a summary of observations:

+ Summary tables for computed strut actions (forces and moments) and hoist forces and motor currents have been provided in Table 1 through Table 9. In general, responses from the right and left arms varied throughout both the dewatering and the dry gate operations. These tables can be utilized to further evaluate the gates condition and operational state.
+ Prior to removal of the discovered log, the gate was lowered back onto the log resulting in a spike in out-of-plane flexure in the left arm. This captured behavior is likely related to the observed issues.
+ The hoist force data showed similar behavior to Gate 1, which likely indicated minor racking or hoist system misalignment. Due to loss of the left hoist data due to wet conditions and wireless connectivity issues, further investigation would be required to confirm this observation in Gate 6. Overall, no major signs of distress from the hoist system (seizing, etc) were observed.
+ Strut responses collected during the gate dewatering can be used to observe the gate's performance under the change in hydrostatic load. Measured changes in strut axial force and bending moments can be directly compared to results generated by a finite element model of the gate.
+ Computed strut moments showed a much higher level of bending in the left arm compared to the right during dry gate operation. Bending behavior also showed a friction-like rotational resistance, as shown in Figure 10, despite no hydrostatic load being present during gate operation. This behavior may be related to the observed issues in the gate and should be further investigated.

Amperage responses were collected as verification that the motor performance was not causing unexpected gate responses. These responses indicated the motor was functioning in a stable manner and should be reviewed by a licensed electrician to further evaluate the motor's performance.

All results and recommendations provided in this report were based on the structure in its current condition; therefore, any significant changes in condition must be noted as they may alter their validity. Questions regarding this report and/or data should be directed to Kyle Ramer (kyler@bditest.com) at BDI. For further information on BDI's equipment, services, and analysis methods please visit www.bditest.com

INSTRUMENTATION AND LOAD TESTING PROCEDURE

GATE INSTRUMENTATION SUMMARY

Instrumentation and data collection were performed on Gate 6 at the Rockwall Forney Dam on April 3rd, 2020. Instrumentation plans have been provided along with this report in Appendix A and include the following number of instrumented locations and sensor types:

+ **REUSABLE SURFACE MOUNTED STRAIN TRANSDUCERS:** Each gate arm was instrumented with a total of 24 strain transducers at 6 locations on each of the gate arms (48 strain sensors total). A typical strain gage installation is shown in Figure 1. Note these sensors were installed with the mounting tabs on the extreme fiber of the strut flanges, which puts the center of the gage approximately 0.66″ from the extreme fiber.
+ **TILTMETER ROTATION SENSORS:** MEMS style rotation sensors were located on the middle strut of the gate arm near the skin plate and near the trunnion hub (4 rotation sensors total). The rotation responses were used to calculate vertical skin plate movement and measure pin rotation relative to skin plate rotation. Typical tiltmeter installations are shown in Figure 1 and Figure 2.
+ **TORQUE SENSORS:** Two total torque sensors were installed on the hoist's pinion shafts (QTY1 on each hoist pinion shaft) near the cable hoist motor to measure direct torque and in turn lift force (See Figure 3).
+ **AMPERAGE SENSORS:** 3 Hall-Effect amperage transducers were clamped over each phase of the hoist motor to measure the motor's current draw (See Figure 4). The purpose of these sensors was to provide additional data in case there were any issues with the hoist systems and to verify any data issues related to lifting and lowering the gates.
+ **BDI'S STS-4 WIRELESS DATA ACQUISITION SYSTEM:** BDI's STS-4 wireless data acquisition (DAQ) was used to collect and record data during testing. A group of sensors were wired to each nodal DAQ which then communicated wirelessly back to the wireless base station and was controlled by BDI's STS-Live testing software.

Complete specifications are available upon request and can be found at http://www.bditest.com.

SENSOR INSTALLATION

BDI strain transducers were installed by first sanding paint off the struts to expose bare metal at two small locations (1″x2″ areas) for the sensor's mounting tabs. Each transducer was then attached using a combination of fast-setting adhesive and accelerator and applying pressure until the adhesive was fully cured. Each strain transducer took approximately five minutes to attach.

Tiltmeters were installed using the same adhesive process as the strain transducers. However, no surface preparation was necessary.

Torque sensors were installed on the pinion shafts by capacitive discharge bonding. Properly bonding to the shaft required sanding the surface to a smooth finish, clean of any paint or grease. Responses from these gages were measured using Binsfeld Torque Trak 10k wireless transmitters.

A typical installation has been shown in Figure 1 through Figure 4. Access to all the sensor locations was provided by BDI's own SPRAT certified rope access technicians and engineers as shown in Figure 5.

Once data collection was completed, sensors were removed, and exposed steel areas were covered using cold galvanizing compound.

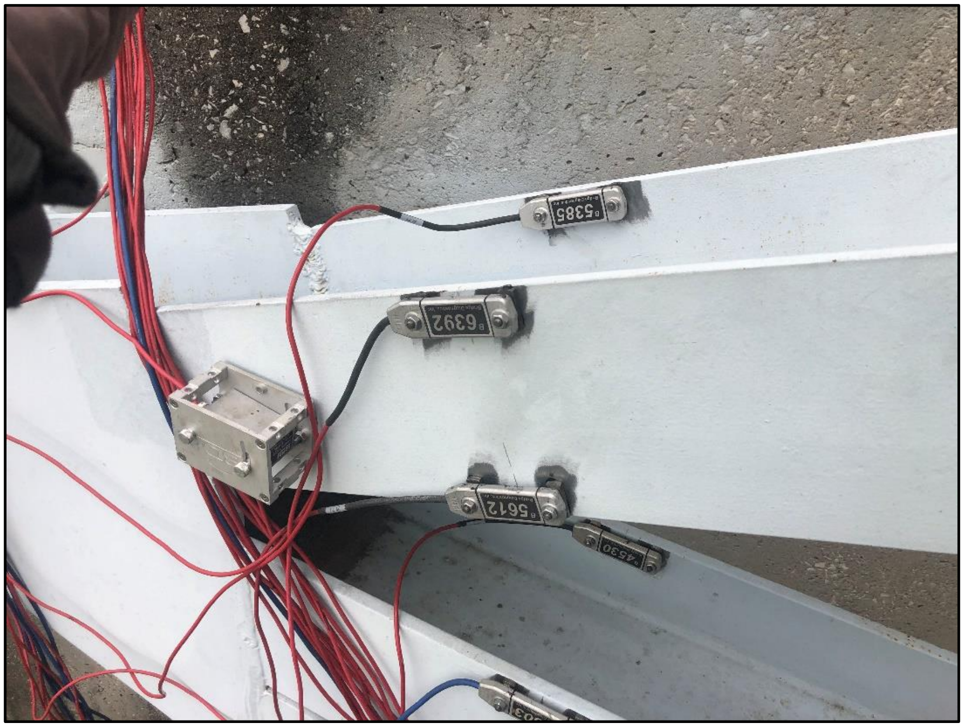

Figure 1 – BDI tiltmeter rotation sensor and reusable strain transducers installed near trunnion hub (Typical)

Figure 2 – BDI tiltmeter rotation sensor installed near skin plate (Typical)

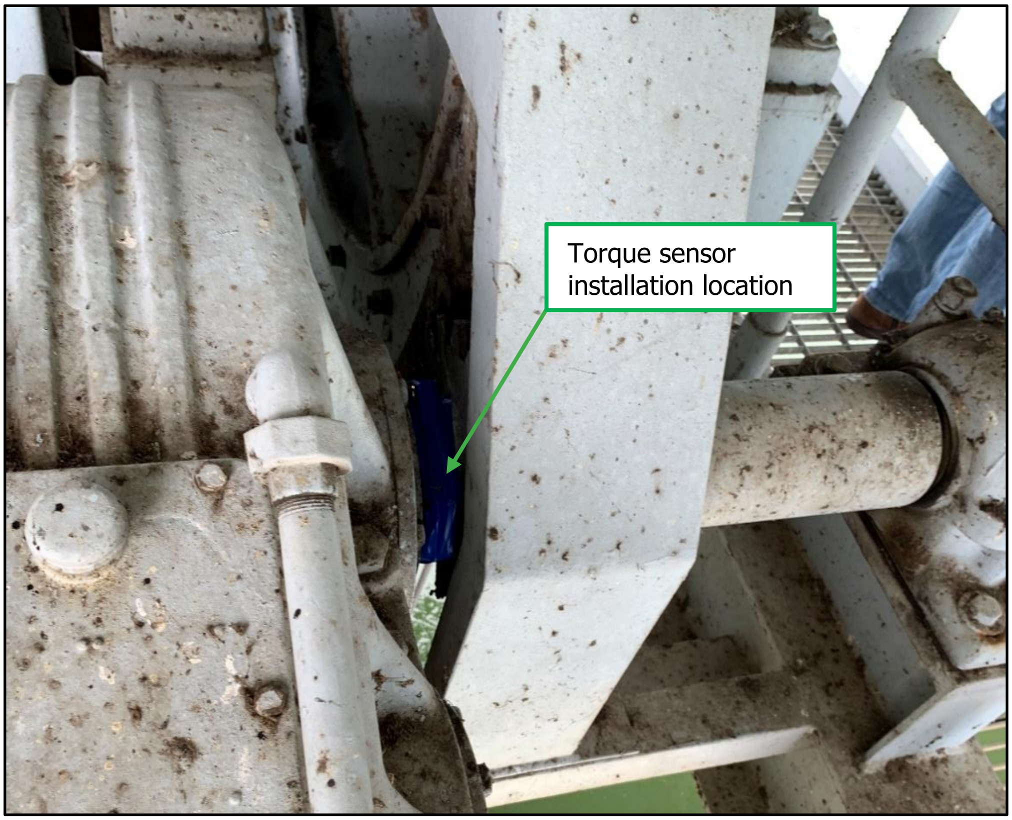

Figure 3 – Torque sensor installation on hoist pinion shaft (Typical)

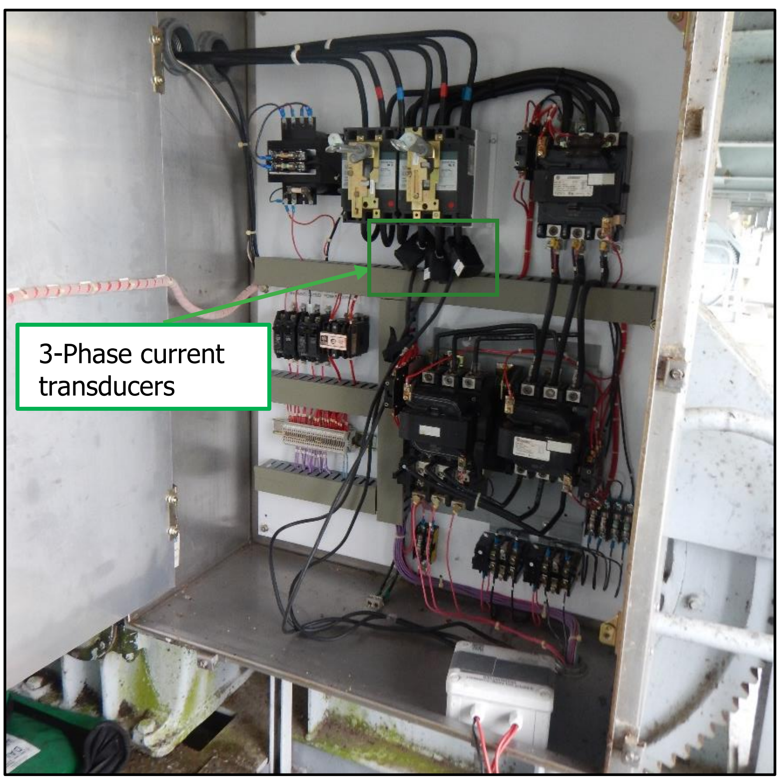

Figure 4 – Current transducers installed on hoist motor controls (Typical)

Figure 5 – BDI personnel installing instrumentation on the gate arm

TESTING PROCEDURES

Structural response data was recorded on all sensors at 10Hz while the gate was dewatered. Once the hydrostatic load was removed from the gate, structural response data was recorded at 50Hz as the gate was lifted and lowered to investigate any alignment or operational issues. During gate operation, it was discovered that a log had been lodged under the right side of the skin plate. The log was removed prior to the final closing of the gate.

Normal trunnion friction test operations were not performed on Gate 6 due to the ongoing investigation of the gate condition and the removal of the log. Without the specific operation with direction reversals, structural responses as a function of friction could not be isolated. At the time of the test, pin friction on this gate was not the primary concern in the field.

Results Summary

General Discussions Based on Structural Responses

The following outline contains general discussion points and observations that were made during the data review process. Note: Strain measurements were converted to stress for all subsequent analysis by multiplying the strain values by a steel elastic modulus of 29,000 ksi.

- **DESCRIPTIONS OF RESPONSE MEASUREMENTS:** All sensor readings were zeroed at the beginning of each data collection period so that each measurement corresponded to response change relative to the initial gate position. Stresses observed during dewatering are changes in stress due to the gradual loss of hydrostatic load on the gate where zero stress corresponds to the reservoir water level at 435.6 ft. ***It is important to note that the recorded measurements were changes in structural response due to gate movement, and do not include the in-situ stresses due to the dead load and cable wrap prior to testing.***
- **QUALITATIVE DATA REVIEW:** Review of the response data indicated good data quality. During the dewatering of the gate, responses along the gate arms were recorded (no hoist operation performed). Dewatering stress magnitudes observed in the left and right arms followed similar response shapes as shown in Figure 6. In this figure, the observed increase in stress during dewatering corresponded to a release of compression on the gate arms. During the gate operation in the dry-state, motor amperage and hoist force measurements were recorded in addition to the gate arm stresses. Gate operation did not follow BDI's typical lift and lower cycles, so response reproducibility could not be verified directly. Instead, data quality was assessed by comparing response shapes and magnitudes between the exploratory tests. During gate operation, stress magnitudes reached similar peak values as shown in Figure 7. All recorded response data was found to be valid and of good quality for use in strut force and moment calculations.
- **MOTOR PERFORMANCE:** Current measurements taken at the hoist motor indicated relatively stable current draws during the lifting and lowering portions of gate operation. However, some anomalies were observed in the current data during both operational tests, including high levels of noise and response spikes. It should be noted that wet site conditions likely played a part in the anomalies observed during response collection. An example plot of current draw and gate position is provided in Figure 8.

  Current draw ranges during lifting were higher than the ranges during lowering, which is common due to gravity/dead load. Note that the sample rates used during testing were set for collecting gate responses and may not have been appropriate to fully capture the in-rush current. The readings should be evaluated by a licensed electrician with knowledge of the operating parameters.
- **TORQUE AND HOIST FORCE:** Torque measurements taken at the hoist pinion shafts, and the derived hoist forces, indicate a shifting/force reversal between the left and right hoists, as shown in Figure 17. This observed behavior indicates possible minor racking or hoist system misalignment in the gate as it was operated. Note that issues with the wireless transmitter connected to the left gate hoist gages caused total loss of data from the left hoist. This connectivity issue is likely related to the wet site conditions encountered during testing.

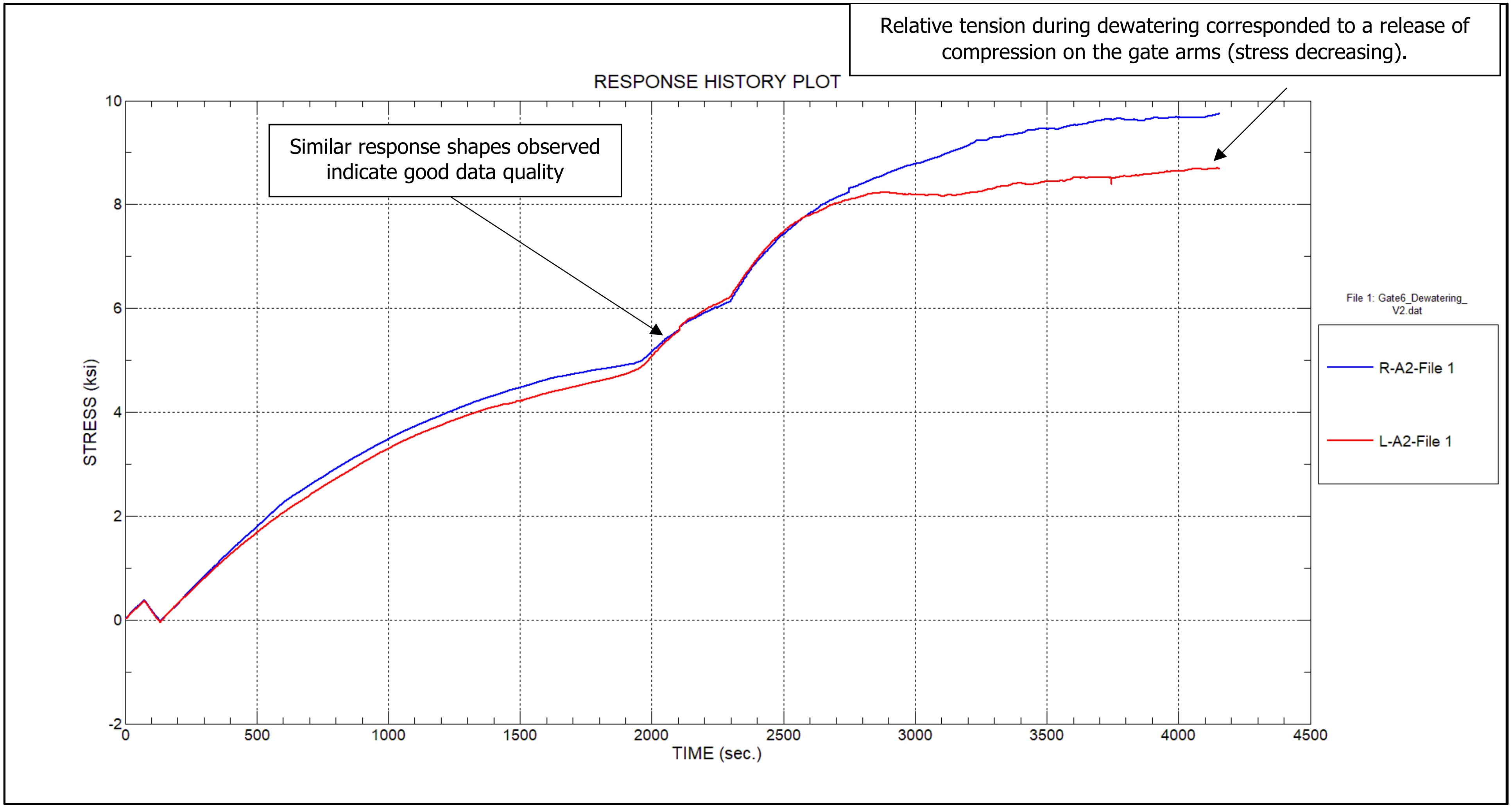

Figure 6 – Stress response history during dewatering – Right and left arms – Gage A2 – Time based
(Section A along top strut near pin – Sensor location 2 along bottom of flange)

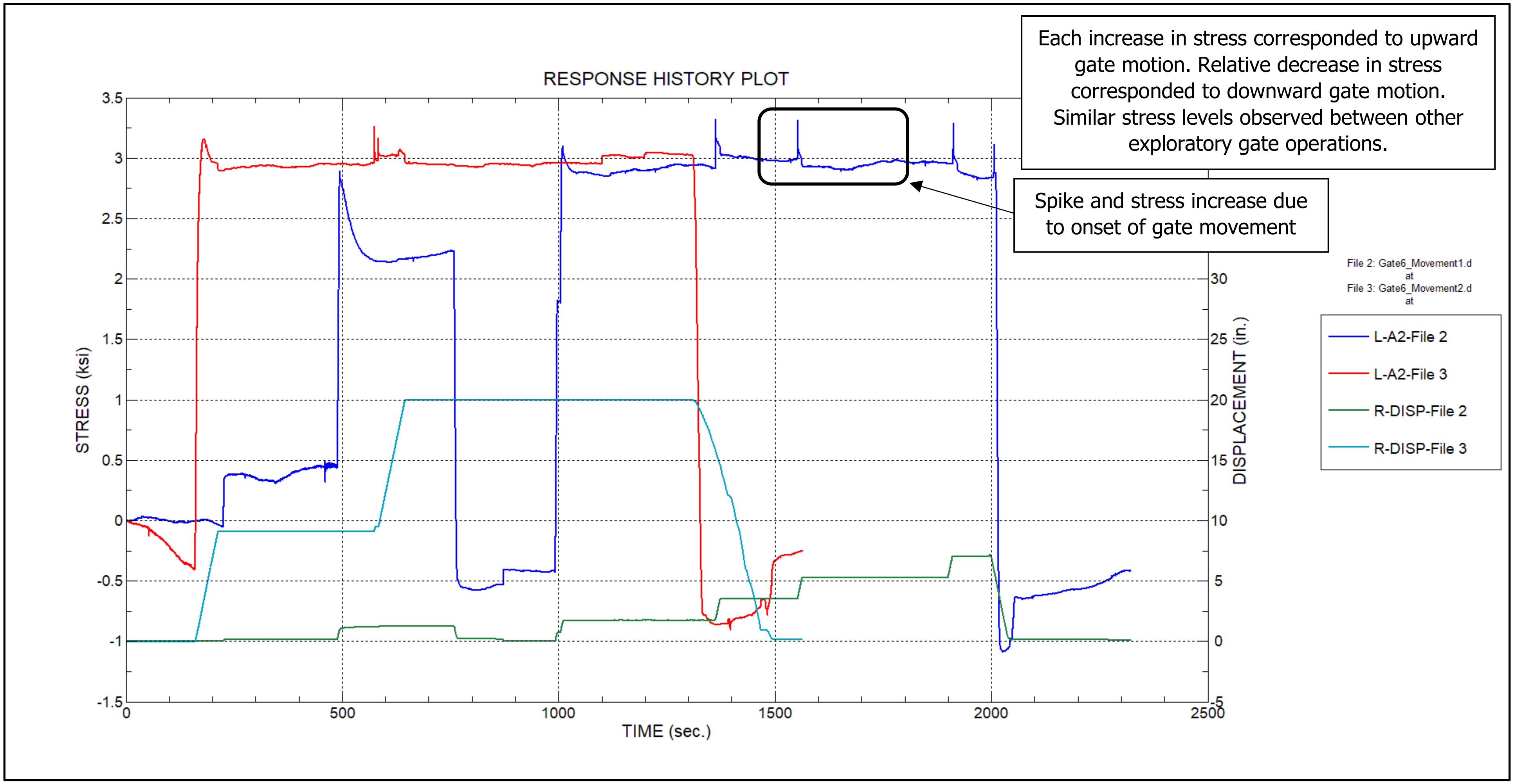

Figure 7 – Stress and displacement response history during gate operation – Left arm – Gage A2 – Time based
File 1 = Gate operation prior to log removal , File 2 = Gate operation during removal of log
(Section A along top strut near pin – Sensor location 2 along bottom of inner flange)

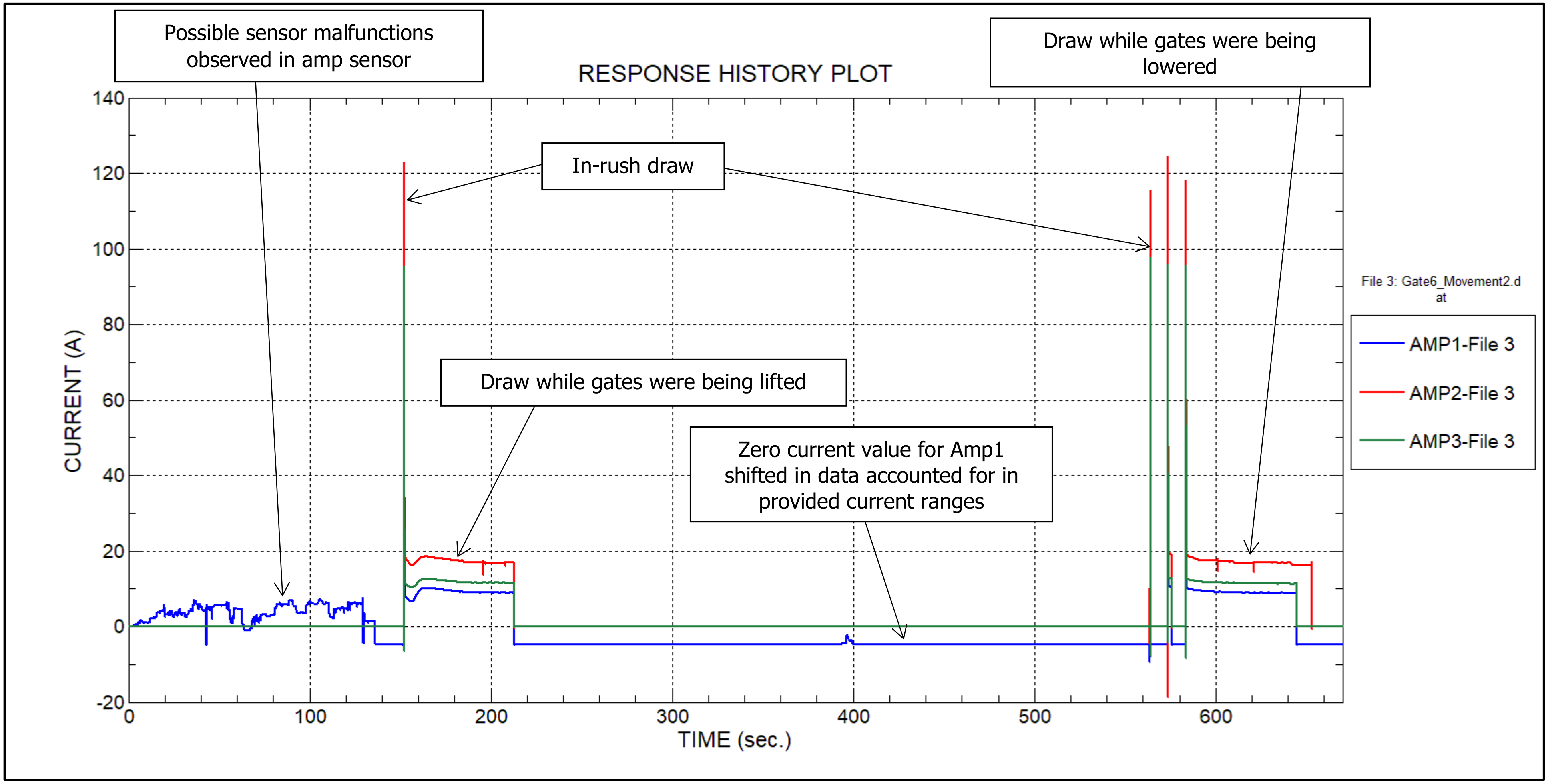

Figure 8 – Motor current & gate movement response history – Highlighting motor draw during lift and lower cycles

Methodology and Findings of The Strut Force and Moment Calculations During Dry-State Gate Operation

The following outline provides the methodology used to calculate the required member forces and moments.

- **CHANGE IN STRESS DUE TO GATE OPERATION:** Strain data can be viewed as a function of time starting when the gate was in the down position and was then lifted off the sill. When examining data in this manner, it is easy to see how stresses ramped up as the gate began to move and then changed slope once the rotational resistance was overcome. It should be noted that this friction response appears very similar to a release of pin friction; however, because no hydrostatic load was present, it is difficult to conclude the exact cause of the rotational resistance. One possibility is that the resistance is related to a gate arm misalignment with respect to the pins. The first point in time where the rotational resistance was overcome (both lifting and lowering) has been highlighted in the stress histories shown in Figure 10. These stress histories show the response of all four sensors along the top strut of the left arm near the pin (Section A). ***It is important to note that the recorded measurements were changes in structural response due to gate movement, and do not include the in-situ stresses due to the dead load and cable wrap present prior to testing.***

- **CALCULATION OF STRUT CROSS-SECTIONAL FORCES MOMENTS:** The use of symmetric strain transducer configurations (four strain gages per strut cross-section) allowed accurate in-plane and out-of-plane flexural bending moments, and axial forces to be computed from the recorded strain measurements. These forces and moments were computed for every cross-section in each gate arm using the basic mechanics equations provided in Figure 9.

  In-plane or weak-axis flexure refers to bending about a given strut's web. This designation is consistent with typical nomenclature. In-plane bending can be observed visually from the strain response histories as a difference between the top and bottom stresses, whereas out-of-plane or strong-axis bending is visualized as the difference in stress from side to side. Figure 11 provides a visual reference for both types of strut flexure.

- **OBSERVED FLEXURAL BEHAVIOR:** Example plots of strut in-plane and out-of-plane moments for instrumented sections near the pin (Sections A, B, and C) for both left and right arms have been provided in Figure 12 through Figure 15. Again, the gate was operated without any hydrostatic load applied; therefore, normal pin friction was not likely the cause of the observed rotational resistance. The presence of moment resistance without thrust likely indicate the trunnion bearing was binding, likely due to misalignment between the pin and hub.

  In general, the computed left arm struts' in-plane moments were significantly larger than the in-plane moments in the right arm struts. Additionally, the left and right arms were observed to bend out-of-plane in the same direction, towards the right wall. This behavior also indicates some level of misalignment in the gate due to the observed flexure imbalance.

  During the data review, an unusual response was also found in the left arm. During gate operation it was discovered that a log had been lodged under the right side of the skin plate. Before the log was removed, the gate was lowered back on to the log, causing a spike in out-of-plane moment primarily in the left arm. An example plot of this response has been provided in Figure 15.

+ **SHAFT TORQUE & HOIST FORCE:** Torque measurements were taken on the pinion shafts near the hoist motor during testing, with single torque gages installed on the left and right hoist pinion shaft. Responses were recorded in units of micro-strain and converted to torque in units of kip-ft using Equation 1 thru Equation 3 and the following shaft properties, as provided by Schnabel.

$$d_O = 5.5\ inches, \qquad d_I = 0\ inches, \qquad E = 29000\ ksi, \qquad \nu = 0.3$$

$$G = \frac{E}{2(1+\nu)}$$

Equation 1

$$J = \frac{\pi\left({d_O}^4 - {d_I}^4\right)}{32}$$

Equation 2

$$\tau = \varepsilon * \frac{2GJ}{\frac{d_O}{2} * 1000000 * 12}$$

Equation 3

Figure 16 shows example torque measurements, recorded on the Gate 6 torque shafts. Best practices for torque measurements is to measure torque on opposite sides of the shaft so that any bending in the shaft can be removed by averaging the two responses. Due to access limitations, only one gage at each location could be installed. Therefore, any bending in the shaft may be reflected in the torque measurements and may be related to the peaks and valleys observed in the torque responses.

Torque values were converted to force in the hoist cables per gate arm using the gear ratio and drum radius, as shown in Figure 17. The gear ratio and drum radius were 5.182 and 1.086 feet respectively, as defined in the provided as-built shop drawings. The hoist force calculated may be smaller than the actual hoist force applied, due to the limit switch engaging the brake before the hoist cable was fully slacked, resulting in an initial force in the cable.

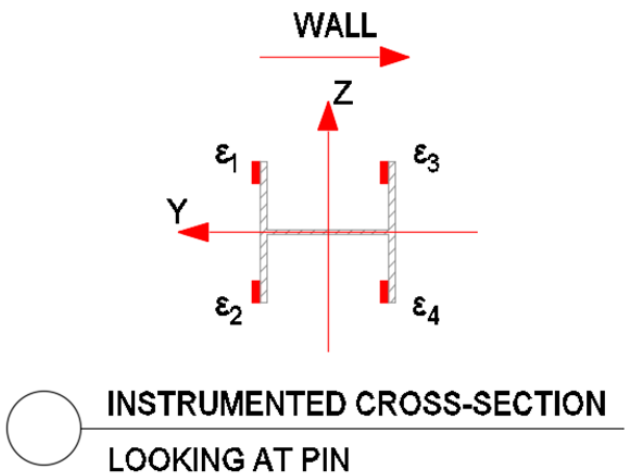

Calculation of Weak-axis (In-plane) bending

$$M_Y = \frac{E\left[\frac{(\varepsilon_2 + \varepsilon_4)}{2} - \frac{(\varepsilon_1 + \varepsilon_3)}{2}\right] S_{Y(gage)}}{2}$$

Calculation of Strong-axis (Out-of-plane) bending

$$M_Z = \frac{E\left[\frac{(\varepsilon_1 + \varepsilon_2)}{2} - \frac{(\varepsilon_3 + \varepsilon_4)}{2}\right] S_{Z(gage)}}{2}$$

Calculation of Axial force

$$F_{axial} = E\left[\frac{(\varepsilon_1 + \varepsilon_2 + \varepsilon_3 + \varepsilon_4)}{4}\right] A_{Strut}$$

Sy(gage)/ Sz(gage) = Section modulus to the center of gages (not extreme fiber of flanges)

A_{strut} = Area of strut

(locations of gages were accounted for in moment computation)

Figure 9 – Basic mechanic equation used to calculate moment and axial force

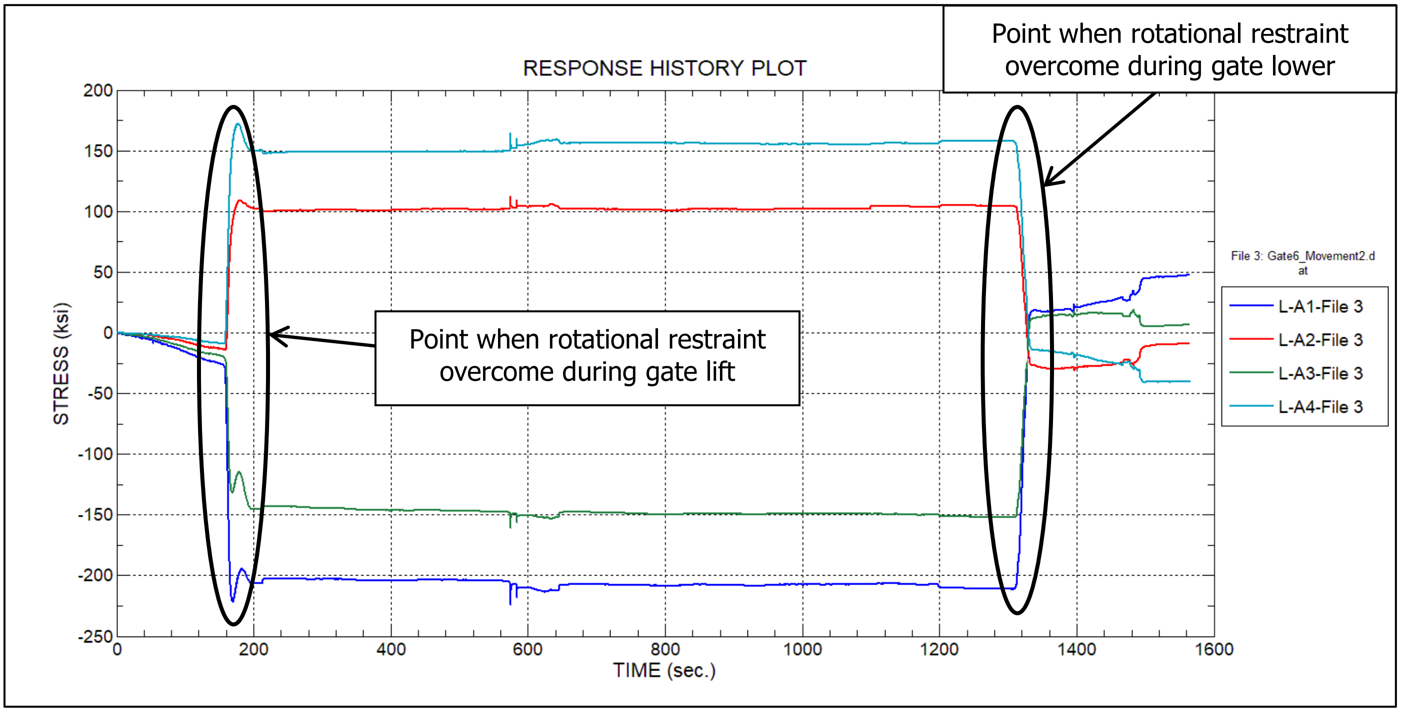

Figure 10 – Stress response history – Left arm – Section A

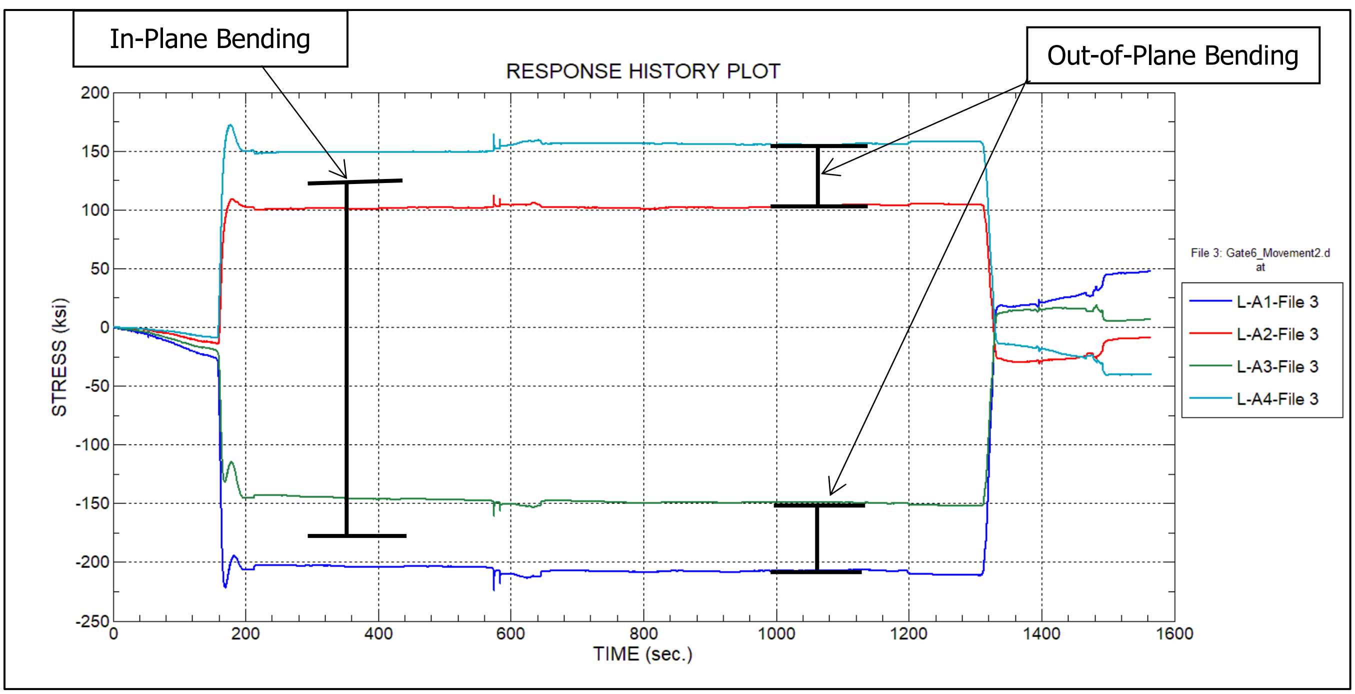

Figure 11 – Stress response history – Left arm – Section A – Bending components

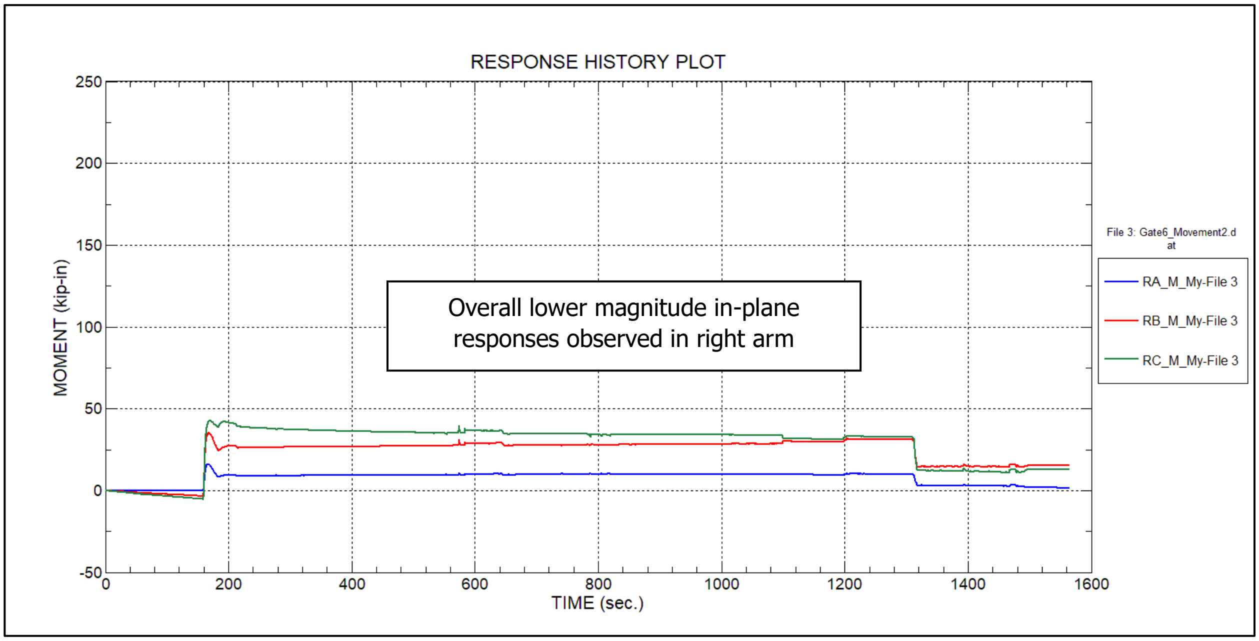

Figure 12 – Moment response history – Right arm – In-plane bending – Gate operation during log removal

(RA = Right Arm Top Strut, RB = Right Arm Middle Strut, RC = Right Arm Bottom Strut)

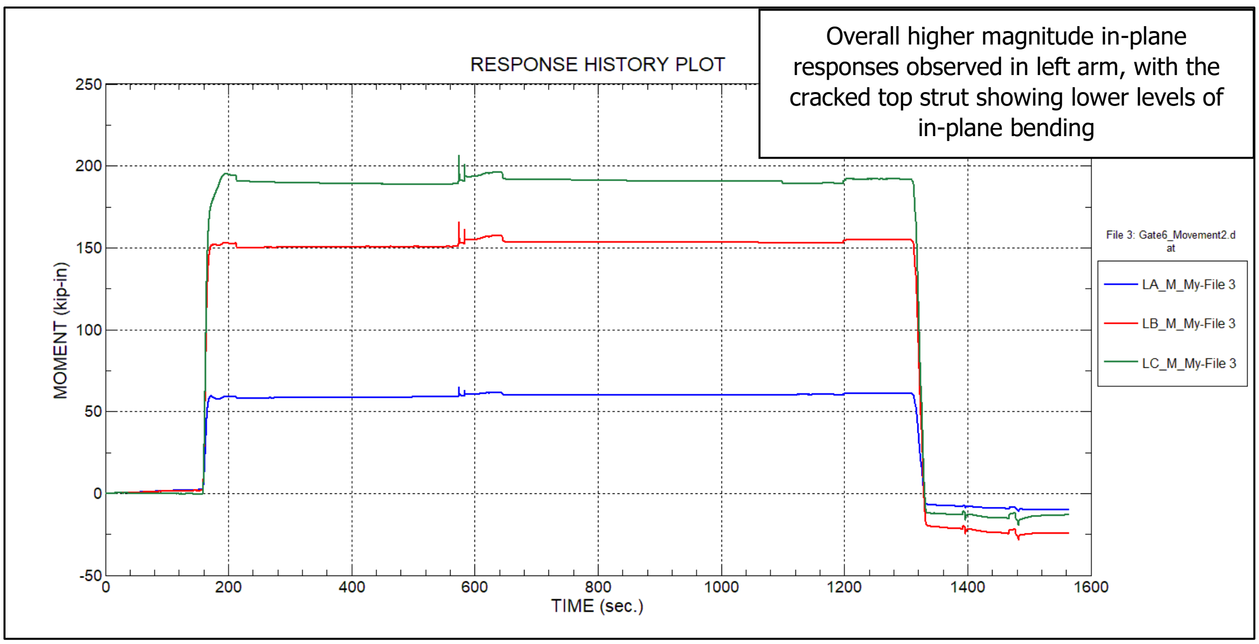

Figure 13 – Moment response history – Left arm – In-plane bending – Gate operation during log removal

(LA = Left Arm Top Strut, LB = Left Arm Middle Strut, LC = Left Arm Bottom Strut)

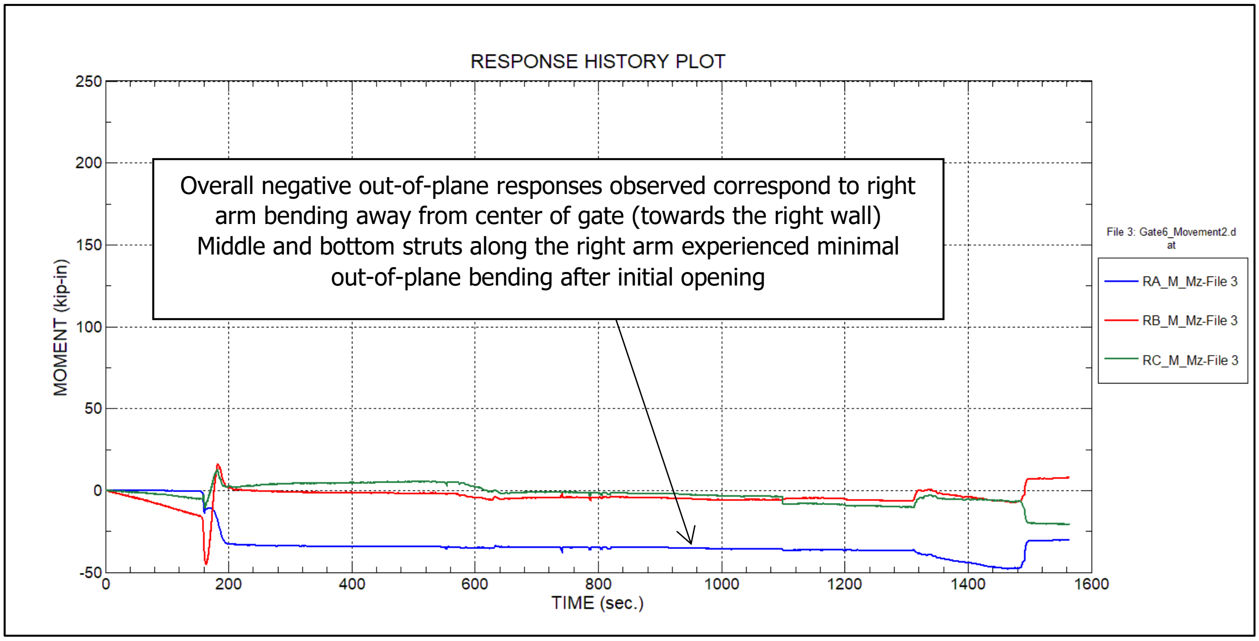

Figure 14 – Moment response history – Right arm – Out-of-plane bending – Gate operation during log removal

(RA = Right Arm Top Strut, RB = Right Arm Middle Strut, RC = Right Arm Bottom Strut)

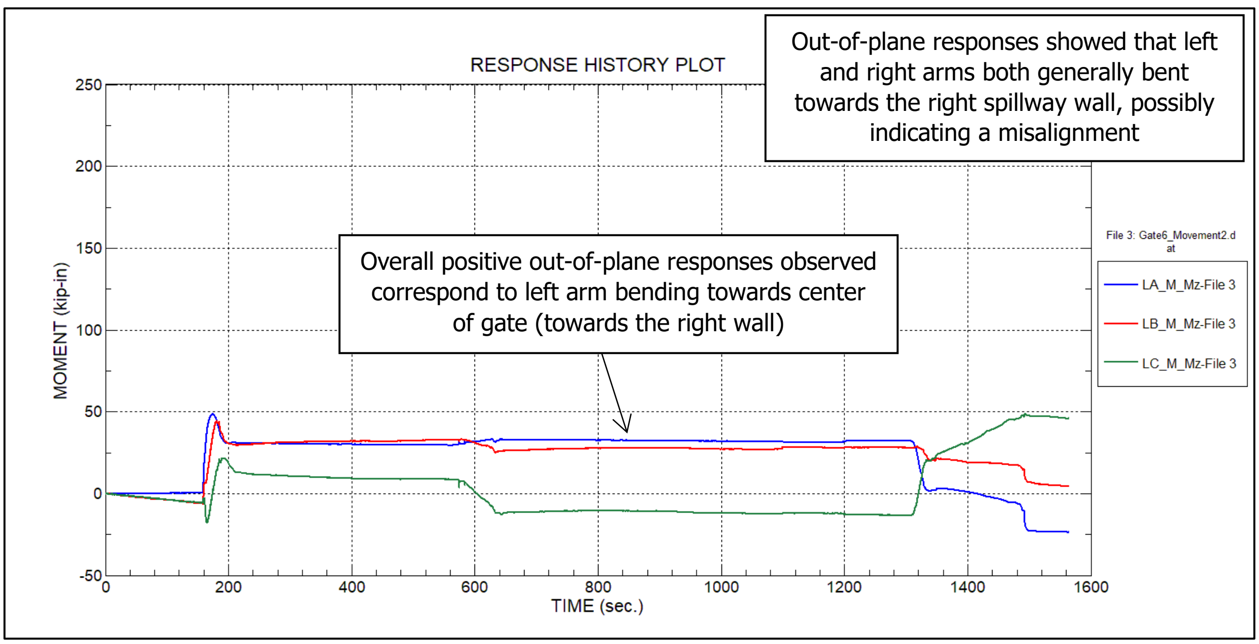

Figure 15 – Moment response history – Left arm – Out-of-plane bending – Gate operation during log removal

(LA = Left Arm Top Strut, LB = Left Arm Middle Strut, LC = Left Arm Bottom Strut)

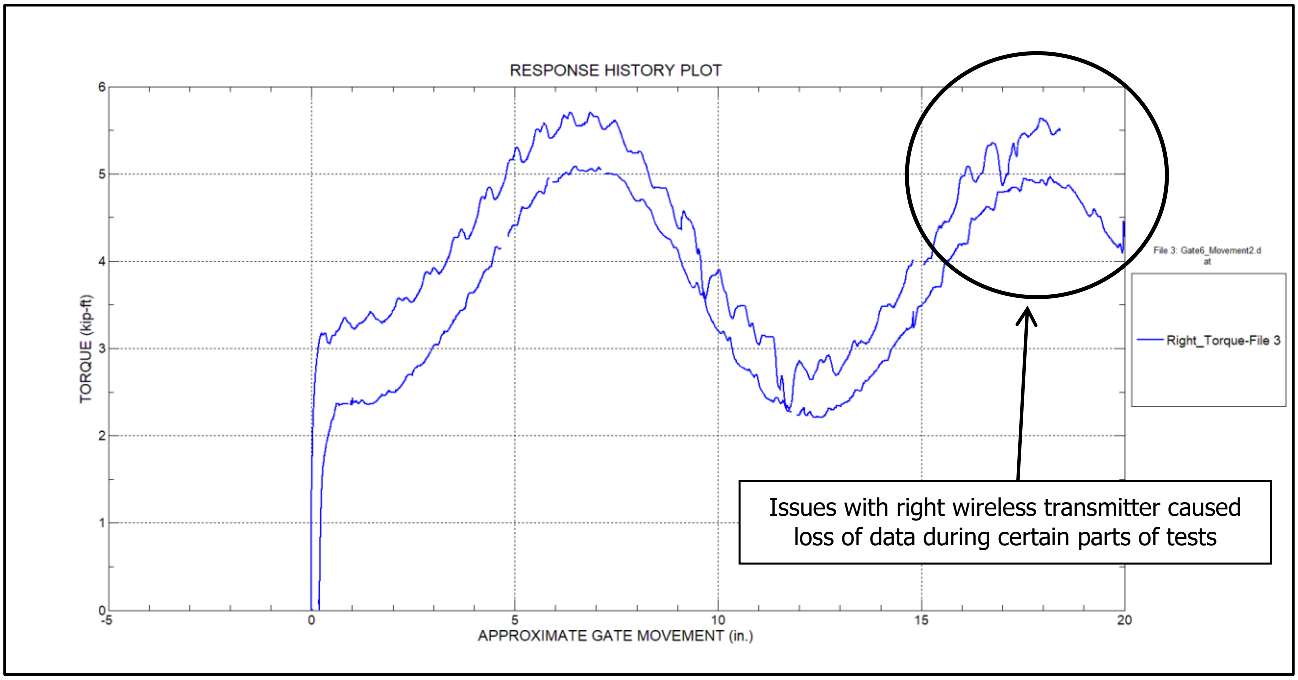

Figure 16 – Hoist torque response history – Gate 6
Note: left hoist data was not collected due to wireless connectivity issues

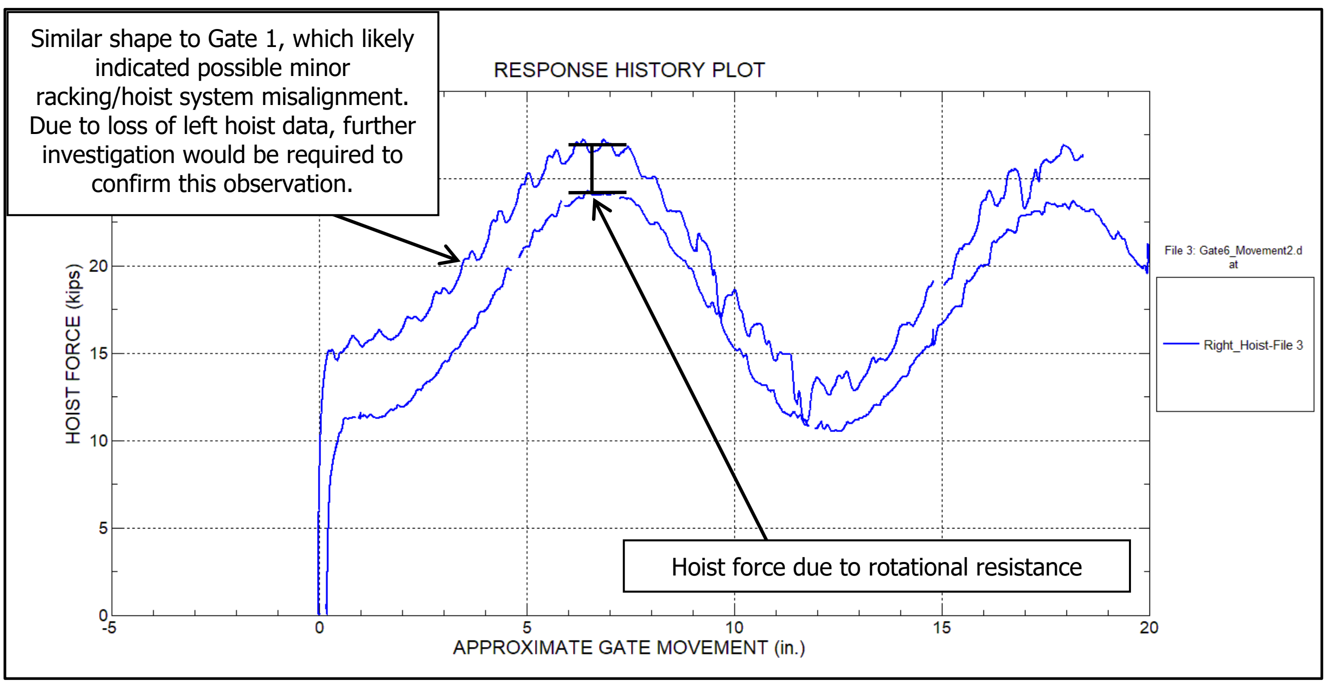

Figure 17 – Hoist force response history – Gate 6
Note: left hoist data was not collected due to wireless connectivity issues

SUMMARY OF RESULTS

The raw data files have been included in the submittal package for reference and were formatted as "tdms" files that can be opened in Microsoft Excel using a "tdms" reader extension.

Examination of the stress histories for each test was necessary to obtain a thorough understanding of the gate performance. The response shapes, variations in stress magnitudes, and timing sequences provided direct clues as to how the gate performed during dewatering and gate operations. The following is a breakdown of the provided tabulated results:

+ Table 1 provides motor current ranges and maximum in-rush for lift and lower cycles for each test
+ Table 2 provides maximum hoist force for each test
+ Table 3 and Table 4 provide the maximum stress ranges measured at the sensor locations for each member during dewatering and gate operation respectively
+ Table 5 provides the maximum axial stress and force ranges measured observed during dewatering
+ Table 6 and Table 7 provide the maximum in-plane and out-of-plane bending stresses and moment ranges observed during dewatering respectively
+ Table 8 and Table 9 provide the maximum in-plane and out-of-plane bending stresses and moment ranges observed during gate operation respectively

The data was presented in a specific coordinate system applicable to both arms. Data was processed so that the positive x-axis was always pointing towards the pin and the right-hand rule applied. In-plane bending can be referred to as "bending about the horizontal or y-axis" and shows how much the beams bend up and down within the plane of the gate arms. Refer to Figure 9 above for visual reference of coordinate system and mathematical explanation of calculations. Out-of-plane bending used a coordinate system which references bending of the strut arms towards the middle of the gate as positive, i.e. bending away from the walls for both gates. Tabulated results do not include any in-situ effects.

Table 1 – Motor current summary table – Gate 6

Test Description	Current Range due to Lifting (A)	Current Range due to Lowering (A)	Max In-rush Current (A)
Gate Operation Before Log Removal	12-20	9-16	124
Gate Operation During Log Removal	11-19	N/A	124

Table 2 – Hoist force summary table – Gate 6

Test Description	Right Arm Peak Hoist Force (kips)
Gate Operation Before Log Removal	28.12
Gate Operation During Log Removal	27.22

Table 3 – Maximum measured sensor stress range during dewatering

ARM DESIGNATION	Top Strut (ksi)	Middle Strut (ksi)	Bottom Strut (ksi)
RIGHT ARM	9.77	15.30	10.33
LEFT ARM	9.44	14.77	12.80

Tabulated values correspond to the total measured change in response during data collection

Stress values have not been extrapolated to the extreme fibers (correspond to center of gage)

Table 4 – Maximum measured sensor stress range during gate operation

ARM DESIGNATION	Top Strut (ksi)	Middle Strut (ksi)	Bottom Strut (ksi)
RIGHT ARM	2.89	7.45	9.56
LEFT ARM	8.39	12.74	14.93

No hydrostatic load was present

Tabulated values correspond to the total measured change in response during operation

Stress values have not been extrapolated to the extreme fibers (values provided correspond to center of gage)

Table 5 – Maximum axial stress & force range during dewatering

SECTION LABEL	Section Description	Right Arm Stress (ksi)	Right Arm Force (kip)	Left Arm Stress (ksi)	Left Arm Force (kip)
SECTION A	Top Strut Near Pin	8.00	91.86	8.42	96.70
SECTION B	Middle Strut Near Pin	11.18	197.44	13.17	232.51
SECTION C	Bottom Strut Near Pin	8.22	174.16	10.16	215.22
SECTION D	Top Strut Away from Pin	7.12	81.75	8.06	92.51
SECTION E	Middle Strut Away from Pin	10.26	181.23	12.86	227.05
SECTION F	Bottom Strut Away from Pin	6.89	146.02	10.56	223.68

Tabulated values correspond to the total measured change in response during data collection

Table 6 – Maximum in-plane bending stress & moment range during dewatering

SECTION LABEL	Section Description	Right Arm Stress (ksi)	Right Arm Moment (kip-in)	Left Arm Stress (ksi)	Left Arm Moment (kip-in)
SECTION A	Top Strut Near Pin	1.35	15.19	0.62	6.97
SECTION B	Middle Strut Near Pin	1.45	33.49	0.82	18.99
SECTION C	Bottom Strut Near Pin	2.02	56.34	1.78	49.71
SECTION D	Top Strut Away from Pin	0.93	10.41	0.31	3.48
SECTION E	Middle Strut Away from Pin	0.60	13.91	1.11	25.77
SECTION F	Bottom Strut Away from Pin	1.76	49.05	0.70	19.55

Tabulated values correspond to the total measured change in response during data collection

Table 7 – Maximum in-plane bending stress & moment range during operation

SECTION LABEL	Section Description	Right Arm Stress (ksi)	Right Arm Moment (kip-in)	Left Arm Stress (ksi)	Left Arm Moment (kip-in)
SECTION A	Top Strut Near Pin	1.44	16.19	7.10	79.85
SECTION B	Middle Strut Near Pin	3.13	72.43	8.79	203.34
SECTION C	Bottom Strut Near Pin	1.73	48.25	8.48	236.46
SECTION D	Top Strut Away from Pin	0.95	10.63	1.60	17.96
SECTION E	Middle Strut Away from Pin	1.03	23.90	1.88	43.53
SECTION F	Bottom Strut Away from Pin	1.34	37.37	1.84	51.20

Tabulated values correspond to the total measured change in response during operation

Table 8 – Maximum out-of-plane bending stress & moment range during dewatering

SECTION LABEL	Section Description	Right Arm Stress (ksi)	Right Arm Moment (kip-in)	Left Arm Stress (ksi)	Left Arm Moment (kip-in)
SECTION A	Top Strut Near Pin	0.65	27.38	0.99	41.70
SECTION B	Middle Strut Near Pin	1.45	33.49	1.30	87.10
SECTION C	Bottom Strut Near Pin	2.02	56.34	0.99	79.55
SECTION D	Top Strut Away from Pin	0.75	31.72	1.12	47.31
SECTION E	Middle Strut Away from Pin	0.82	55.13	1.91	127.77
SECTION F	Bottom Strut Away from Pin	2.91	233.10	1.42	114.01

Tabulated values correspond to the total measured change in response during data collection

Table 9 – Maximum out-of-plane bending stress & moment range during operation

SECTION LABEL	Section Description	Right Arm Stress (ksi)	Right Arm Moment (kip-in)	Left Arm Stress (ksi)	Left Arm Moment (kip-in)
SECTION A	Top Strut Near Pin	1.25	52.59	1.92	81.09
SECTION B	Middle Strut Near Pin	1.61	107.84	2.69	180.48
SECTION C	Bottom Strut Near Pin	0.42	33.73	2.42	193.76
SECTION D	Top Strut Away from Pin	0.87	36.58	0.42	17.57
SECTION E	Middle Strut Away from Pin	0.45	30.04	0.66	44.28
SECTION F	Bottom Strut Away from Pin	2.22	177.78	1.20	96.31

Tabulated values correspond to the total measured change in response during operation

APPENDIX A – INSTRUMENTATION PLANS

The user acknowledges that these documents are instruments of professional service, and are protected by Copyright. This document and the information contained in this document are the property of Bridge Diagnostics, Inc., and shall not be reused, copied, disseminated, modified, amended or altered in any way. It is issued for information purposes only. The user agrees to hold harmless, indemnify and defend Bridge Diagnostics, Inc. against any and all damages, claims and losses, including defense costs, arising out of any use, reuse or copying of this document.

GAGE LEGEND & SPECIFICATION

SYMBOL	TYPE	BRAND	MODEL	NOTES
	STRAIN TRANSDUCER	BDI	ST350	
	TILTMETER (UNI-AXIAL)	BDI	T500-030	
	TORQUE SENSOR	HPI	-	HBWS-35-125-6-0.5VR-FB
	AMP SENSOR	CR MAGNETICS	CR42105-200	

GENERAL NOTES

- INSTRUMENTATION SHALL BEGIN ON APRIL 1ST, 2020.
- GATES 1 THRU 14 SHALL BE ACCESSED USING SPRAT ROPE ACCESS TECHNIQUES.
- BDI WILL PERFORM ALL SURFACE PREPARATION, SENSOR INSTALLATION, AND EQUIPMENT INSTALLATION.
- SEE LLT-31 FOR SENSOR INSTALLATION DETAILS.
- TWO PAIRS OF TORQUE GAGES WILL BE INSTALLED ON THE GATE MOTORS' PINION SHAFTS BETWEEN THE MOTORS AND THE HOISTS.
  - GAGE PAIRS WILL BE INSTALLED 180° APART FROM EACH OTHER.
  - EXACT POSITIONS OF THE GAGE PAIRS ON THE PINION SHAFT WILL BE DETERMINED IN THE FIELD.
- THREE PHASE AMPERAGE GAGES WILL BE INSTALLED ON THE MOTOR CONTROLS BY A QUALIFIED ELECTRICIAN PROVIDED BY GARVER.

TESTING PROCEDURE:

- TESTING SHALL BE STARTED WITH THE GATE IN THE CLOSED POSITION.
- ONCE DATA COLLECTION BEGINS, THE GATE SHALL BE RAISED TO TWO OR THREE TIMES THE HEIGHT NECESSARY FOR TRUNNION FRICTION TO BE OVERCOME, H1 (TYPICALLY 6"-12"), AND HELD THERE UNTIL DATA STABILIZES.
- THE GATE SHALL BE LOWERED APPROXIMATELY TWICE THE DISTANCE TO OVERCOME TRUNNION FRICTION, H2, AND HELD THERE UNTIL DATA STABILIZES.
- THE GATE SHALL BE RAISED TO H1 AND HELD THERE UNTIL DATA STABILIZES.
- THE GATE SHALL BE LOWERED TO H2 AND HELD THERE UNTIL DATA STABILIZES.
- THE GATE SHALL BE RAISED TO H1 AND HELD THERE UNTIL DATA STABILIZES.
- THE GATE WAS LOWERED BACK TO CLOSED POSITION AND DATA COLLECTION STOPPED.
- A MINIMUM OF 3 TESTS SHALL BE PERFORMED PER GATE.

GAGE COUNT PER GATE

SENSOR LEGEND	SENSOR COUNT	CHANNEL COUNT
STRAIN TRANSDUCER	(48)	(48)
TILTMETER (UNI-AXIAL)	(4)	(4)
TORQUE SENSOR	(4)	(4)
AMP SENSOR	(3)	(3)
TOTAL	(59)	(59)

LOCATION KEY

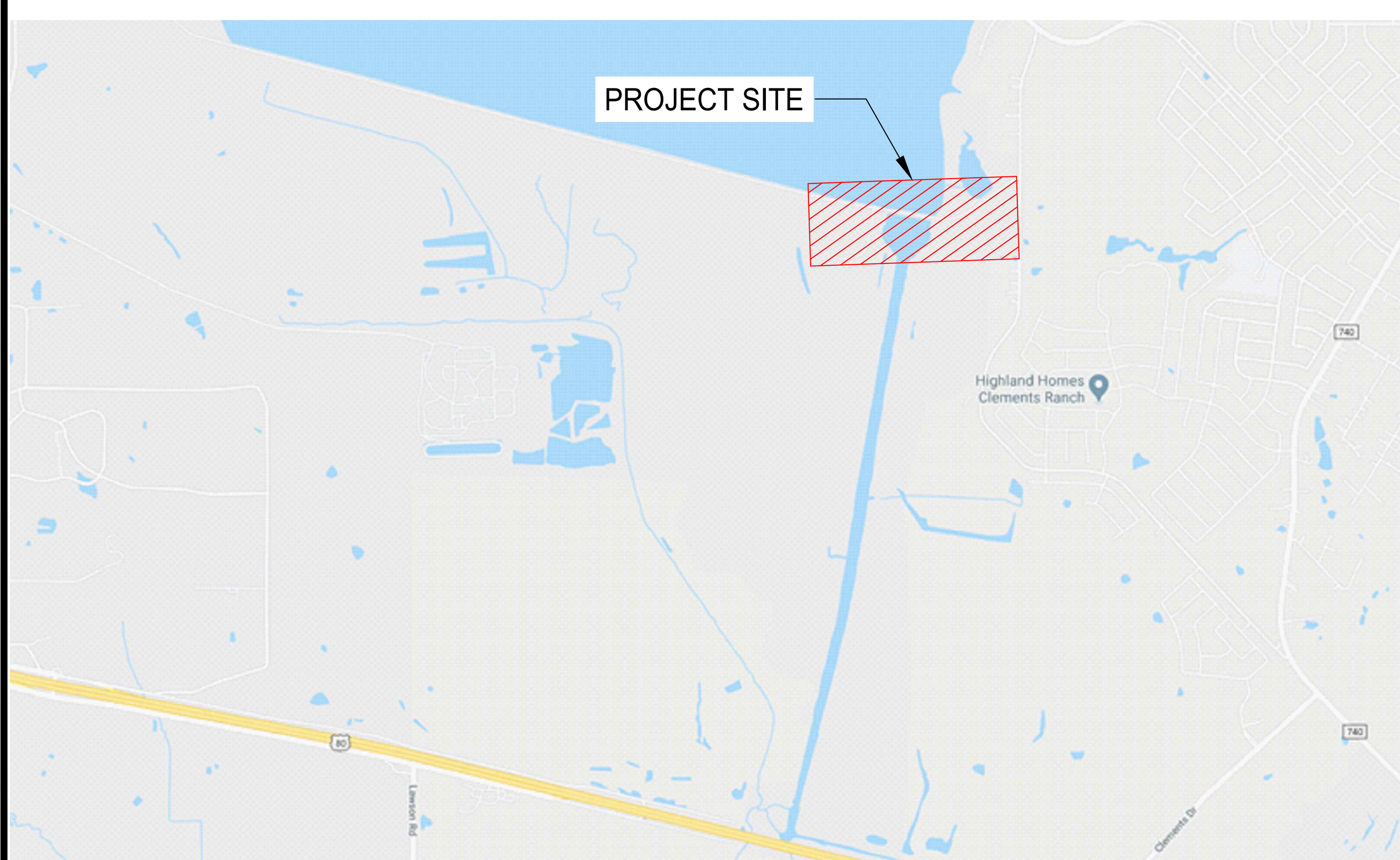

INDEX OF SHEETS

INDEX OF ISSUE

NO.	DATE	REVISION DESCRIPTION
1	3/20/2020	LIVE LOAD TESTING (LLT) INSTRUMENTATION PLAN (FOR APPROVAL)
2	5/27/2020	LIVE LOAD TESTING (LLT) INSTRUMENTATION PLAN AS BUILTS

BDI REFERENCE NUMBER: 190701-TX

BDI
RAW DATA. REFINED RESULTS.
740 S PIERCE AVE, SUITE 15
LOUISVILLE, CO 80027
303.494.3230
WWW.BDITEST.COM

ISSUE

CLIENT

SCHABEL ENGINEERING
16000 CHRISTENSEN RD, STE 101
SEATTLE, WA 98188

PROJECT NAME

SCHNABEL ENGINEERING
ROCKWALL FORNEY DAM
LIVE LOAD TESTING

Drawn By:	KNR
Checked By:	JDS
Date:	05/27/2020
Client No.:	
BDI No.:	190701-TX
SCALE:	NTS

OVERALL LEGEND

LLT-01

PLOT TIME: 6/12/2020 3:22 PM
FILEPATH: C:\Users\coleman\BDI\Services - Documents\Server_Remote\190701-TX_Schnabel_RockwallForneyDam\7. Instrumentation Plans\BDI_ROCKWALLFORNEY_01_GENERAL.dwg
© YYYY BRIDGE DIAGNOSTICS INC.

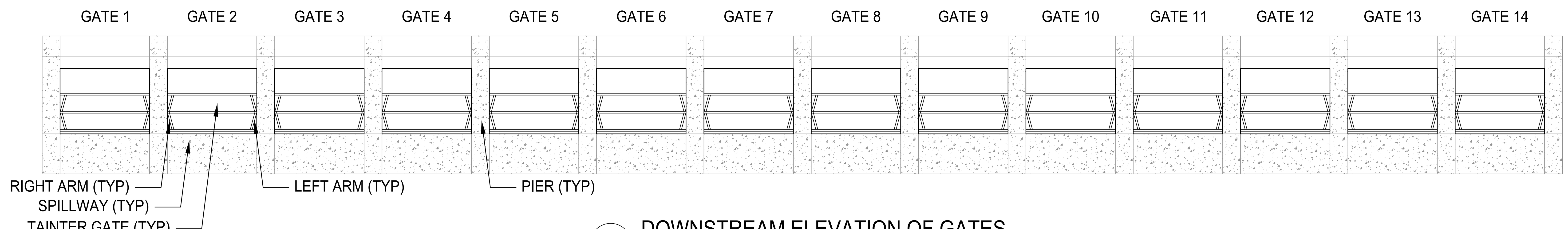

1 DOWNSTREAM ELEVATION OF GATES

LOOKING NORTH (UPSTREAM)

RAW DATA. REFINED RESULTS.
740 S PIERCE AVE, SUITE 15
LOUISVILLE, CO 80027
303.494.3230
WWW.BDITEST.COM

ISSUE

CLIENT

SCHABEL ENGINEERING
16000 CHRISTENSEN RD, STE 101
SEATTLE, WA 98188

PROJECT NAME

SCHNABEL ENGINEERING
ROCKWALL FORNEY DAM
LIVE LOAD TESTING

Drawn By:	KNR
Checked By:	JDS
Date:	05/27/2020
Client No.:	
BDI No.:	190701-TX
SCALE:	NTS

OVERALL STRUCTURE LAYOUT

LLT-02

The user acknowledges that these documents are instruments of professional service, and are protected by Copyright. This document and the information contained in this document are the property of Bridge Diagnostics, Inc., and shall not be reused, copied, disseminated, modified, amended or altered in any way. It is issued for information purposes only. The user agrees to hold harmless, indemnify and defend Bridge Diagnostics, Inc. against any and all damages, claims and losses, including defense costs, arising out of any use, reuse or copying of this document.

PLOT TIME: 6/12/2020 3:22 PM
FILEPATH: C:\Users\colemand\BDI\Services - Documents\Server_Remote\190701-TX_Schnabel_RockwallForneyDam\7. Instrumentation Plans\BDI_ROCKWALLFORNEY_01_GENERAL.dwg
© YYYY BRIDGE DIAGNOSTICS INC.

The user acknowledges that these documents are instruments of professional service, and are protected by Copyright. This document and the information contained in this document are the property of Bridge Diagnostics, Inc., and shall not be reused, copied, disseminated, modified, amended or altered in any way. It is issued for information purposes only. The user agrees to hold harmless, indemnify and defend Bridge Diagnostics, Inc. against any and all damages, claims and losses, including defense costs, arising out of any use, reuse or copying of this document.

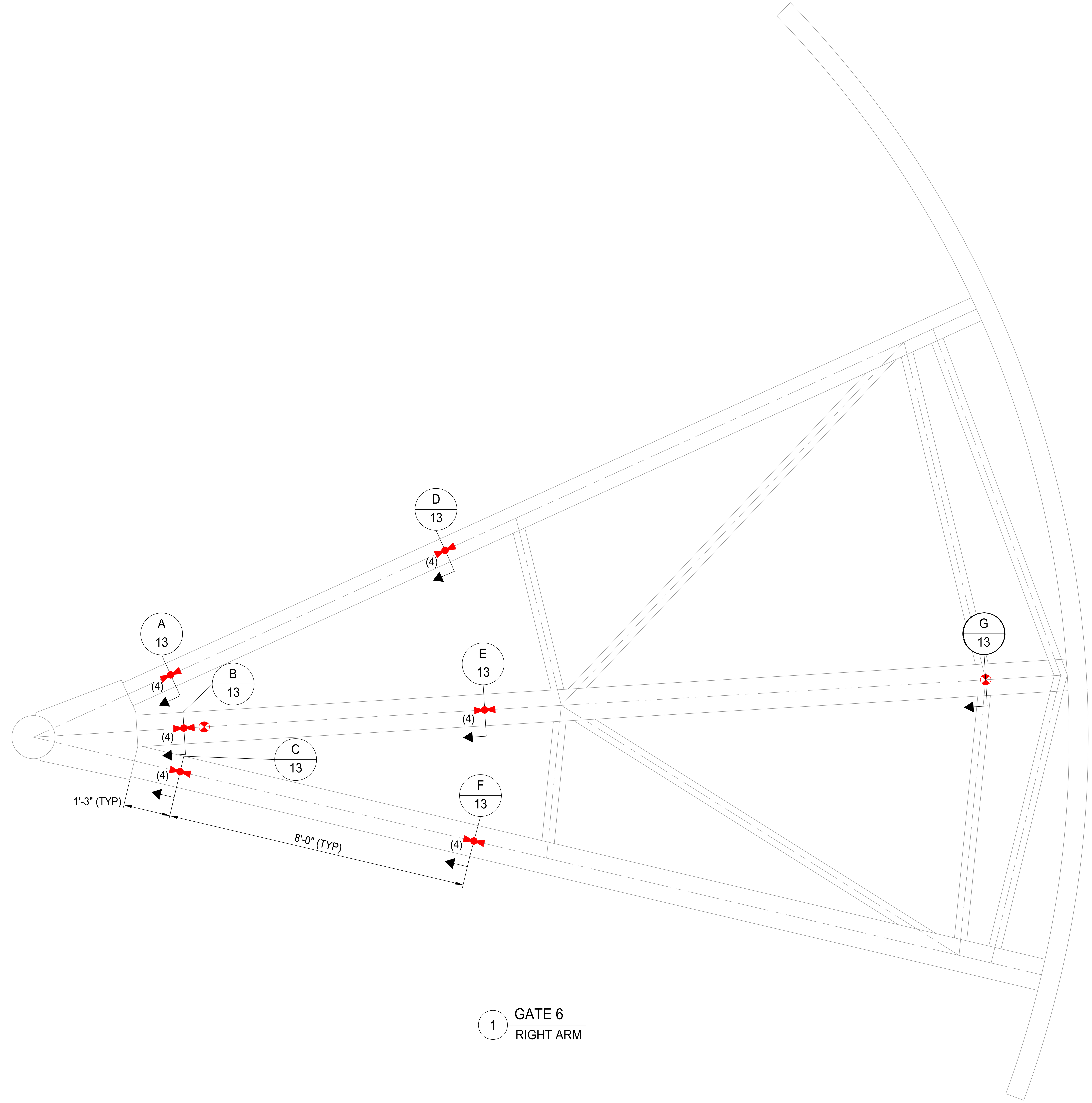

1 GATE 6
RIGHT ARM

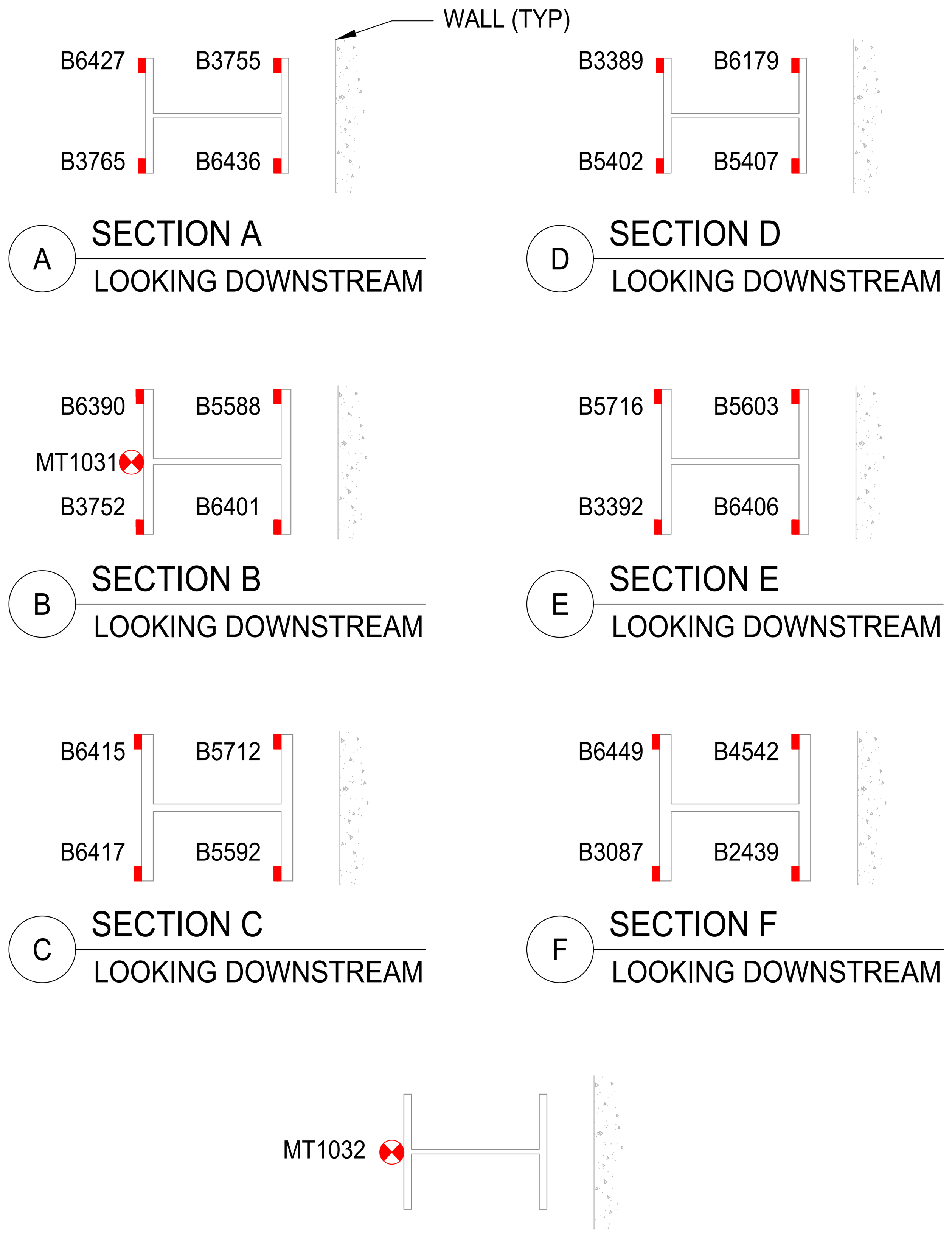

A SECTION A
LOOKING DOWNSTREAM

D SECTION D
LOOKING DOWNSTREAM

B SECTION B
LOOKING DOWNSTREAM

E SECTION E
LOOKING DOWNSTREAM

C SECTION C
LOOKING DOWNSTREAM

F SECTION F
LOOKING DOWNSTREAM

G SECTION G
LOOKING DOWNSTREAM

UNIT ID
TT-3

TORQUE GAGES
RIGHT ARM

NOTES:
1. SECTIONS A, B, & C SHALL BE INSTALLED 15 INCHES AWAY FROM TRUNNION PLATE.
2. TILTMETERS SHALL BE INSTALLED CENTERED ON THE MIDDLE STRUT FLANGE.
3. SECTION G'S TILTMETER SHALL BE INSTALLED AS CLOSE TO THE SKINPLATE AS POSSIBLE.

SENSOR LEGEND
STRAIN TRANSDUCER
TILTMETER (UNI-AXIAL)
TORQUE SENSOR

RAW DATA. REFINED RESULTS.
740 S PIERCE AVE, SUITE 15
LOUISVILLE, CO 80027
303.494.3230
WWW.BDITEST.COM

ISSUE

CLIENT
SCHABEL ENGINEERING
16000 CHRISTENSEN RD, STE 101
SEATTLE, WA 98188

PROJECT NAME
SCHABEL ENGINEERING
ROCKWALL FORNEY DAM
LIVE LOAD TESTING

Drawn By:	KNR
Checked By:	JDS
Date:	05/27/2020
Client No.:	
BDI No.:	190701-TX
SCALE:	NTS

GATE 6 - RIGHT ARM
ELEVATION
LLT-13

PLOT TIME: 6/12/2020 3:23 PM
FILEPATH: C:\Users\colemand\BDI\Services - Documents\Server_Remote\190701-TX_Schabel_RockwallForneyDam\7. Instrumentation Plans\BDI_ROCKWALLFORNEY_01_GENERAL.dwg
© YYYY BRIDGE DIAGNOSTICS INC.

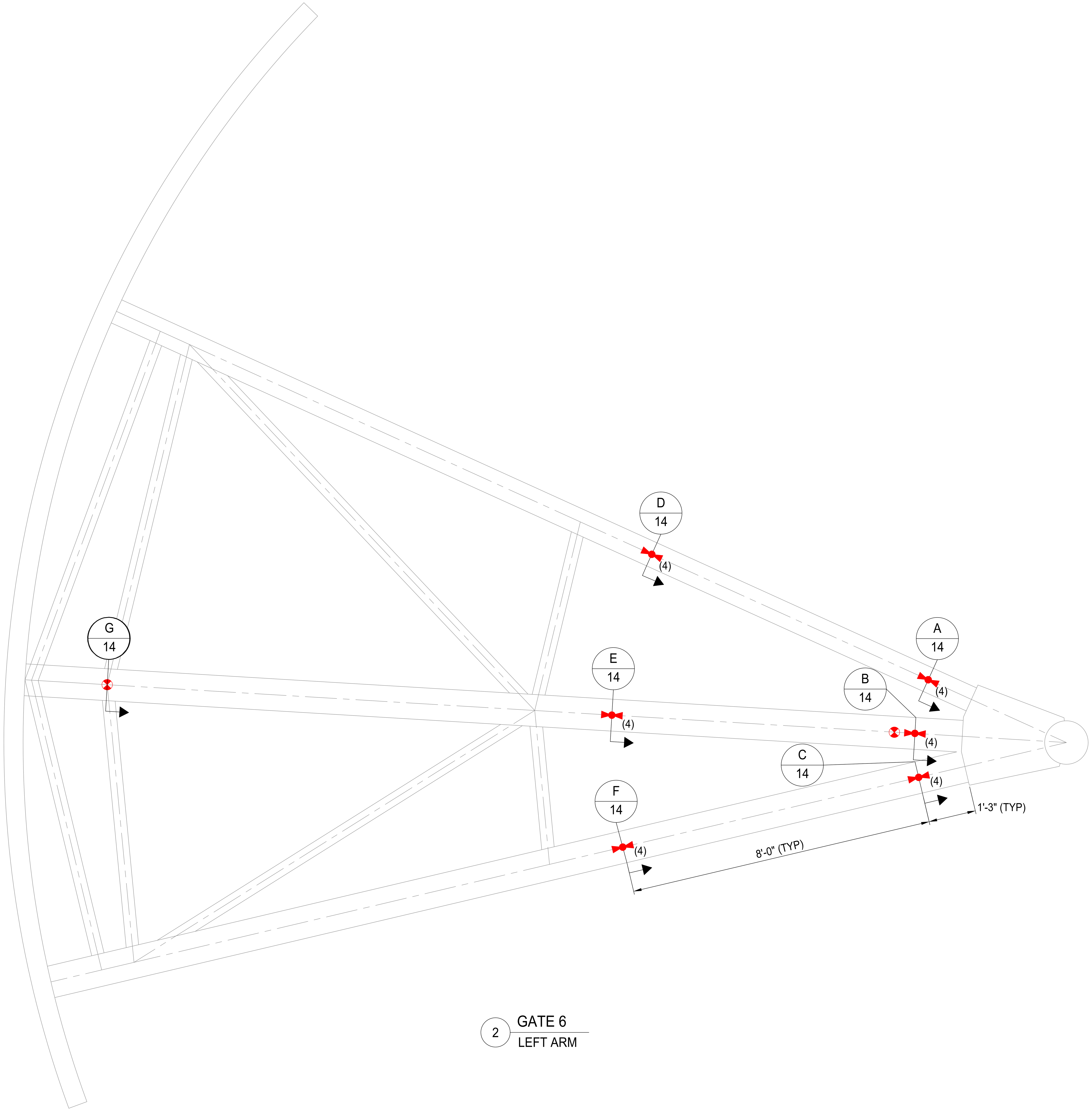

2 GATE 6
LEFT ARM

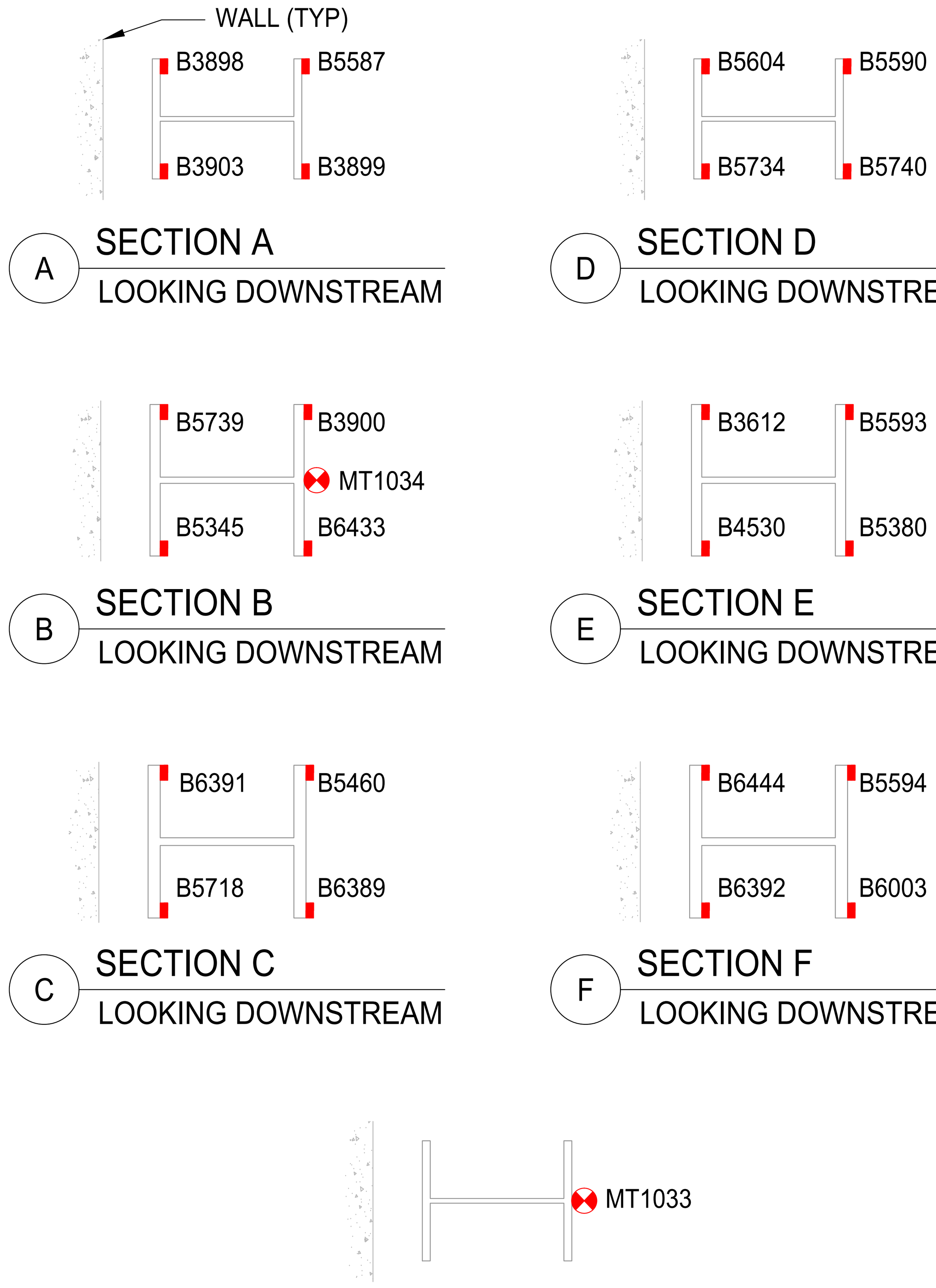

A SECTION A
LOOKING DOWNSTREAM

D SECTION D
LOOKING DOWNSTREAM

B SECTION B
LOOKING DOWNSTREAM

E SECTION E
LOOKING DOWNSTREAM

C SECTION C
LOOKING DOWNSTREAM

F SECTION F
LOOKING DOWNSTREAM

G SECTION G
LOOKING DOWNSTREAM

UNIT ID
TT-2

TORQUE GAGES
LEFT ARM

NOTES:
1. SECTIONS A, B, & C SHALL BE INSTALLED 15 INCHES AWAY FROM TRUNNION PLATE.
2. TILTMETERS SHALL BE INSTALLED CENTERED ON THE MIDDLE STRUT FLANGE.
3. SECTION G'S TILTMETER SHALL BE INSTALLED AS CLOSE TO THE SKINPLATE AS POSSIBLE.

SENSOR LEGEND
STRAIN TRANSDUCER
TILTMETER (UNI-AXIAL)
TORQUE SENSOR

RAW DATA. REFINED RESULTS.
740 S PIERCE AVE, SUITE 15
LOUISVILLE, CO 80027
303.494.3230
WWW.BDITEST.COM

ISSUE

CLIENT
SCHABEL ENGINEERING
16000 CHRISTENSEN RD, STE 101
SEATTLE, WA 98188

PROJECT NAME
SCHNABEL ENGINEERING
ROCKWALL FORNEY DAM
LIVE LOAD TESTING

Drawn By:	KNR
Checked By:	JDS
Date:	05/27/2020
Client No.:	
BDI No.:	190701-TX
SCALE:	NTS

GATE 6 - LEFT ARM
ELEVATION
LLT-14

The user acknowledges that these documents are instruments of professional service, and are protected by Copyright. This document and the information contained in this document are the property of Bridge Diagnostics, Inc., and shall not be reused, copied, disseminated, modified, amended or altered in any way. It is issued for information purposes only. The user agrees to hold harmless, indemnify and defend Bridge Diagnostics, Inc. against any and all damages, claims and losses, including defense costs, arising out of any use, reuse or copying of this document.

PLOT TIME: 6/12/2020 3:23 PM
FILEPATH: C:\Users\coleman\BDI\Services - Documents\Server_Remote\190701-TX_Schnabel_RockwallForneyDam\7. Instrumentation Plans\BDI_ROCKWALLFORNEY_01_GENERAL.dwg
© YYYY BRIDGE DIAGNOSTICS INC.

The user acknowledges that these documents are instruments of professional service, and are protected by Copyright. This document and the information contained in this document are the property of Bridge Diagnostics, Inc., and shall not be reused, copied, disseminated, modified, amended or altered in any way. It is issued for information purposes only. The user agrees to hold harmless, indemnify and defend Bridge Diagnostics, Inc. against any and all damages, claims and losses, including defense costs, arising out of any use, reuse or copying of this document.

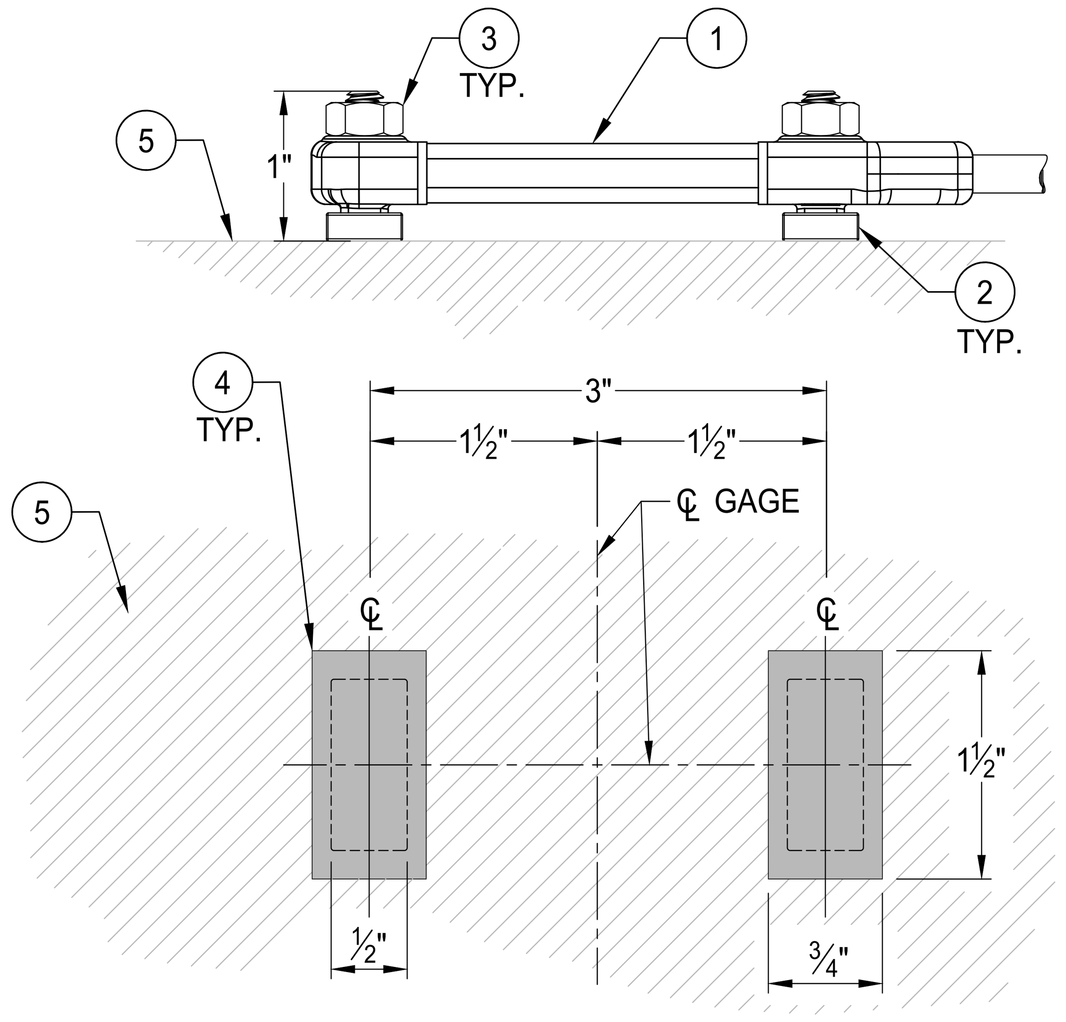

COMPONENT DESCRIPTION

1. ST350 STRAIN GAGE
2. 1/4"-20 THREADED MOUNTING TAB
3. 1/4"-20 STAINLESS STEEL NUT
4. TYPICAL SURFACE PREP REQUIRED TO MOUNT STRAIN GAGES
5. TYPICAL MOUNTING SURFACE

FOOTNOTES - INSTANT ADHESIVE
1. STRAIN GAGES SHALL BE MOUNTED WITH LOCTITE 410 INSTANT ADHESIVE AND LOCTITE 7452 ACCELERANT 2. DURING SURFACE PREP ALL PAINT AND SURFACE DEFORMATIONS MUST BE REMOVED. 3. SURFACE PREP IS REQUIRED JUST PRIOR TO GAGE INSTALLATION AS TO NOT ALLOW SURFACE CONTAMINANTS TO ACCUMULATE.

1 TYPICAL ST350 STRAIN GAGE INSTALLATION

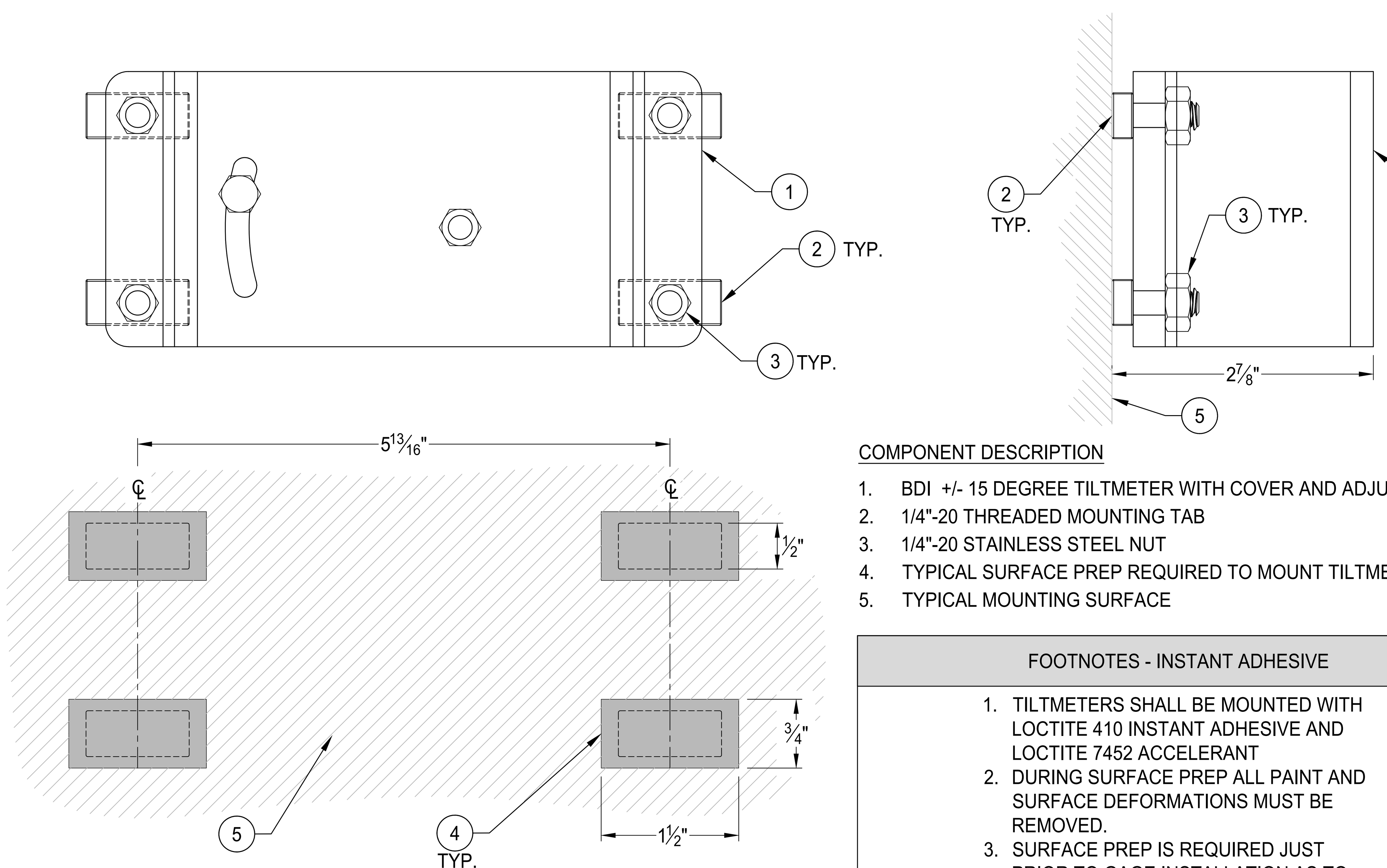

COMPONENT DESCRIPTION

1. BDI +/- 15 DEGREE TILTMETER WITH COVER AND ADJUSTMENT BOLTS
2. 1/4"-20 THREADED MOUNTING TAB
3. 1/4"-20 STAINLESS STEEL NUT
4. TYPICAL SURFACE PREP REQUIRED TO MOUNT TILTMETERS
5. TYPICAL MOUNTING SURFACE

FOOTNOTES - INSTANT ADHESIVE
1. TILTMETERS SHALL BE MOUNTED WITH LOCTITE 410 INSTANT ADHESIVE AND LOCTITE 7452 ACCELERANT 2. DURING SURFACE PREP ALL PAINT AND SURFACE DEFORMATIONS MUST BE REMOVED. 3. SURFACE PREP IS REQUIRED JUST PRIOR TO GAGE INSTALLATION AS TO NOT ALLOW SURFACE CONTAMINANTS TO ACCUMULATE.

2 TYPICAL BDI TILTMETER INSTALLATION

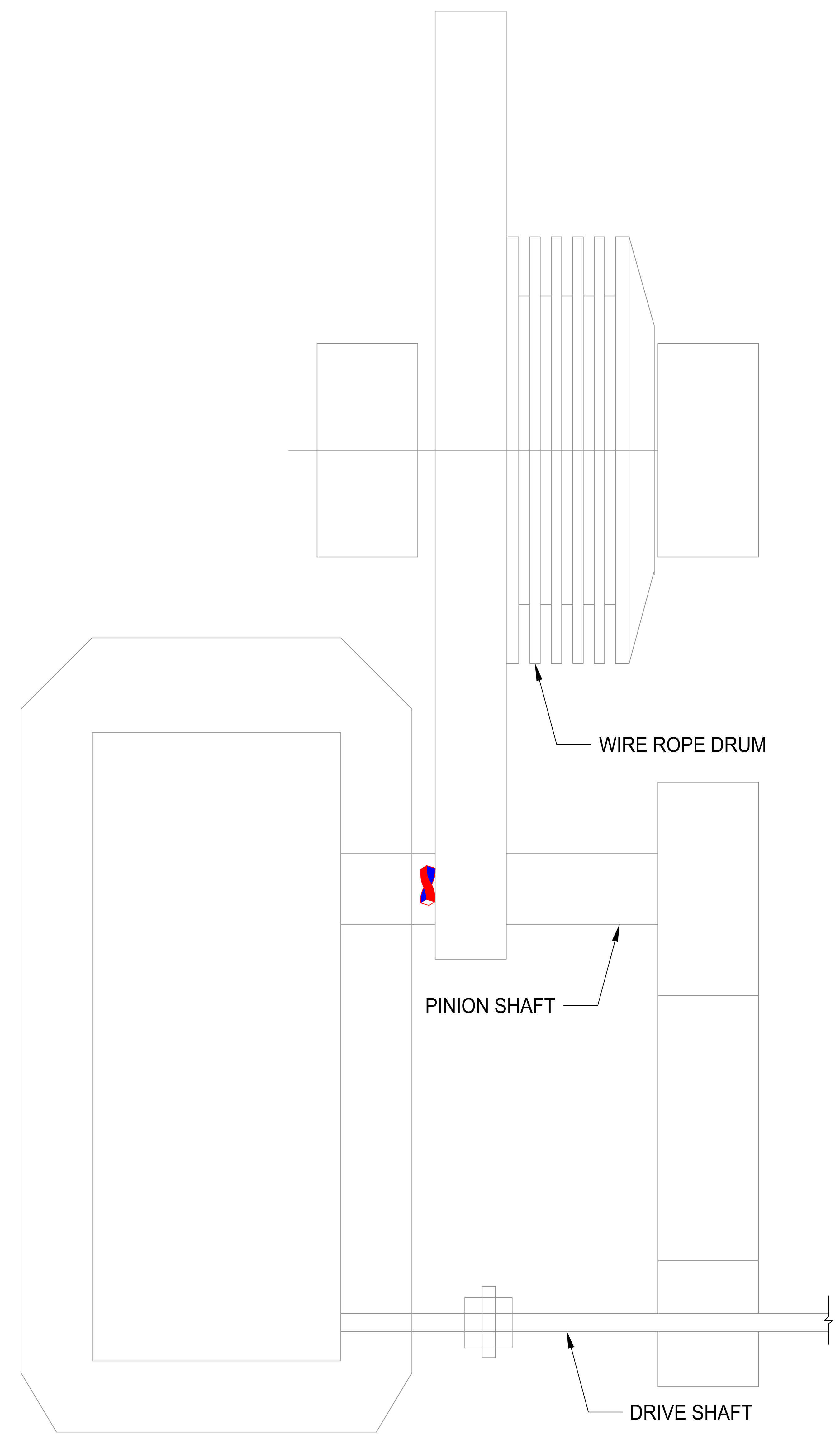

3 TYPICAL HOIST INSTRUMENTATION

TORQUE SENSOR INSTALLATION NOTES:

- TORQUE GAGES WILL BE INSTALLED ON THE PINION SHAFT ON EITHER HOIST MOTOR BETWEEN THE MOTOR AND THE HOIST DRUM
- EXACT POSITIONS OF THE GAGE PAIRS ON THE PINION SHAFT WILL BE DETERMINED IN THE FIELD

SENSOR LEGEND

TORQUE SENSOR

BDI
RAW DATA. REFINED RESULTS.
740 S PIERCE AVE, SUITE 15
LOUISVILLE, CO 80027
303.494.3230
WWW.BDITEST.COM

ISSUE

CLIENT

SCHABEL ENGINEERING
16000 CHRISTENSEN RD, STE 101
SEATTLE, WA 98188

PROJECT NAME

SCHNABEL ENGINEERING
ROCKWALL FORNEY DAM
LIVE LOAD TESTING

Drawn By:	KNR
Checked By:	JDS
Date:	05/27/2020
Client No.:	
BDI No.:	190701-TX
SCALE:	NTS

SENSOR INSTALLATION DETAILS

LLT-31

PLOT TIME: 6/12/2020 3:24 PM
FILEPATH: C:\Users\colemand\BDI\Services - Documents\Server_Remote\190701-TX_Schnabel_RockwallForneyDam\7. Instrumentation Plans\BDI_ROCKWALLFORNEY_01_GENERAL.dwg
© YYYY BRIDGE DIAGNOSTICS INC.

SCHNABEL ENGINEERING

TRUNNION PIN FRICTION TESTING REPORT

ROCKWALL FORNEY DAM – GATE 7
FORNEY, TX

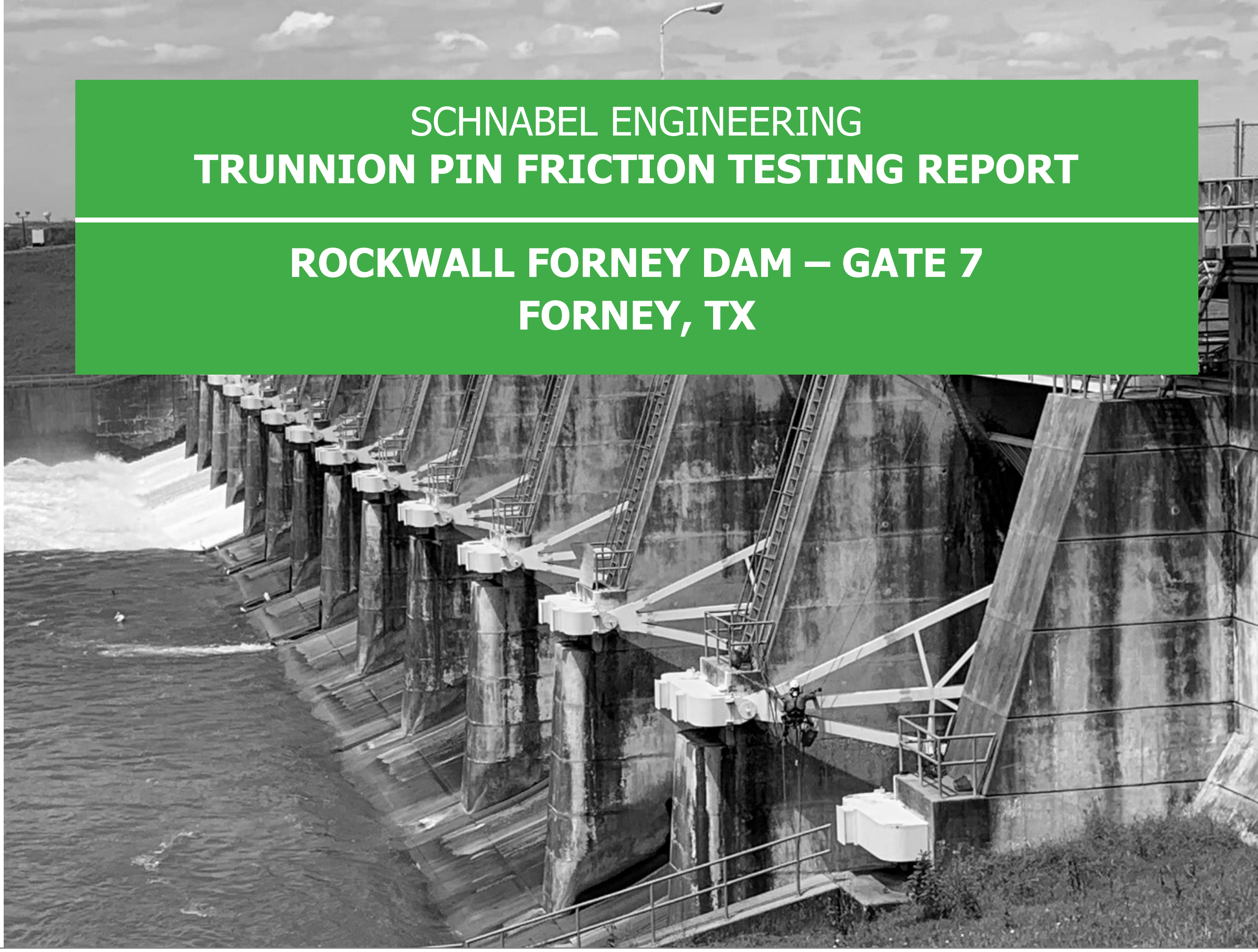

SUBMITTED TO:
SCHNABEL ENGINEERING
16000 CHRISTENSEN RD, SUITE 101
SEATTLE, WA 98188

SUBMITTED BY:
BDI – CO
740 SOUTH PIERCE AVE, UNIT 15
LOUISVILLE, CO 80027

BDI Project No.: **190701-TX**
Report Version: **V1**
Version Submitted: **August 26, 2020**

RAW DATA. REFINED RESULTS.

This document contains Confidential Information and is submitted in confidence to the customer. The submission of the information contained herein shall not be deemed to constitute public disclosure or authorization for disclosure to other parties. BDI's information and name may not be used in advertising or for promotional purposes without BDI's written consent.

TABLE OF CONTENTS

LIST OF FIGURES

LIST OF TABLES

EXECUTIVE SUMMARY

Schnabel Engineering contracted BDI to provide instrumentation and testing services on Gates 1-14 on the Rockwall Forney Dam near Dallas, Texas. The goal of these tests was to record each gate's structural responses during a series of spill tests and use the data to compute accurate coefficients of friction for each trunnion pin, cable lift force, total gate friction, and motor amperage. This report provides details on the work performed on Gate 7.

Instrumentation and testing were performed on Gate 7 at the Rockwall Forney Dam on April 6th, 2020. The gate arms were instrumented with strain and rotation sensors. The hoist motors' pinion shafts were instrumented with torque sensors and the hoist motor controls were instrumented with amperage sensors. Following the instrumentation, a series of spill tests were performed to measure the structural responses resulting from trunnion pin friction. All instrumentation setup and removal were performed using BDI's rope access team.

Following demobilization from the field, the test data was examined for quality and then further processed to evaluate the gate's performance. Strain measurements were converted into bending forces which were then applied to pin-strut free-body diagrams. By summing forces at each pin, friction induced moments could be computed, allowing accurate friction coefficients to be determined. Generally, the observed gate behavior showed that Gate 7 was operating as expected with no major signs of distress.

The resulting maximum trunnion friction coefficients and corresponding hoist forces are shown in Table 1.

Table 1 – Gate 7 performance summary

Pin Designation	Maximum Friction Coefficient	Maximum Pin Moment due to Pin Friction (kip-In)	Maximum Hoist Force (kips)	Maximum Hoist Force due to Total Gate Friction (kips)
Right Pin	0.23	606.4	24.89	4.55
Left Pin	0.33	869.3	24.91	4.49

Note: Pin designations are in reference to looking downstream

Lower maximum hoist forces were collected in Gate 7 when compared to other gates. Due to restrictions caused by the hoist limit switches, the hoist cables could not always be fully slacked at the beginning and end of the performed tests. Throughout testing of the Rockwell Forney gates, it was found that this limit switch restriction varied gate to gate and arm to arm. Therefore, it is not recommended to use the collected hoist force data to quantify overall hoist forces during gate operation. Rather, this hoist data can be better utilized to evaluate total friction behavior.

Amperage responses were not used to compute friction results and were collected as verification that the motor performance was not causing unexpected gate responses. These responses indicated the motor was functioning in a stable manner and should be reviewed by a licensed electrician to further evaluate the motor's performance.

All results and recommendations provided in this report were based on the structure in its current condition; therefore, any significant changes in condition must be noted as they may alter their validity. Questions regarding this report and/or data should be directed to Kyle Ramer (kyler@bditest.com) at BDI. For further information on BDI's equipment, services, and analysis methods please visit www.bditest.com

Instrumentation and Load Testing Procedure

Gate Instrumentation Summary

Instrumentation and testing were performed on Gate 7 at the Rockwall Forney Dam on April 6th, 2020. Instrumentation plans have been provided along with this report and include the following number of instrumented locations and sensor types:

+ **REUSABLE SURFACE MOUNTED STRAIN TRANSDUCERS:** Each gate arm was instrumented with a total of 24 strain transducers at 6 locations on each of the gate arms (48 strain sensors total). A typical strain gage installation is shown in Figure 1. Note these sensors were installed with the mounting tabs on the extreme fiber of the strut flanges, which puts the center of the gage approximately 0.66” from the extreme fiber.
+ **TILTMETER ROTATION SENSORS:** MEMS style rotation sensors were located on the middle strut of the gate arm near the skin plate and near the trunnion hub (4 rotation sensors total). The rotation responses were used to calculate vertical skin plate movement and measure pin rotation relative to skin plate rotation. Typical tiltmeter installations are shown in Figure 1 and Figure 2.
+ **TORQUE SENSORS:** Two total torque sensors were installed on the hoist’s pinion shafts (QTY1 on each hoist pinion shaft) near the cable hoist motor to measure direct torque and in turn lift force (See Figure 3).
+ **AMPERAGE SENSORS:** 3 Hall-Effect amperage transducers were clamped over each phase of the hoist motor to measure the motor's current draw (See Figure 4). The purpose of these sensors was to provide additional data in case there were any issues with the hoist systems and to verify any data issues related to lifting and lowering the gates.
+ **BDI'S STS-4 WIRELESS DATA ACQUISITION SYSTEM:** BDI's STS-4 wireless data acquisition (DAQ) was used to collect and record data during testing. A group of sensors were wired to each nodal DAQ which then communicated wirelessly back to the wireless base station and was controlled by BDI's STS-Live testing software.

Complete specifications are available upon request and can be found at http://www.bditest.com.

Sensor Installation

BDI strain transducers were installed by first sanding paint off the struts to expose bare metal at two small locations (1”x2” areas) for the sensor’s mounting tabs. Each transducer was then attached using a combination of fast-setting adhesive and accelerator and applying pressure until the adhesive was fully cured. Each strain transducer took approximately five minutes to attach.

Tiltmeters were installed using the same adhesive process as the strain transducers. However, no surface preparation was necessary.

Torque sensors were installed on the pinion shafts by capacitive discharge bonding. Properly bonding to the shaft required sanding the surface to a smooth finish, clean of any paint or grease. Responses from these gages were measured using Binsfeld Torque Trak 10k wireless transmitters.

A typical installation has been shown in Figure 1 through Figure 4. Access to all the sensor locations was provided by BDI’s own SPRAT certified rope access technicians and engineers as shown in Figure 5.

Once testing was completed, sensors were removed, and exposed steel areas were covered using cold galvanizing compound.

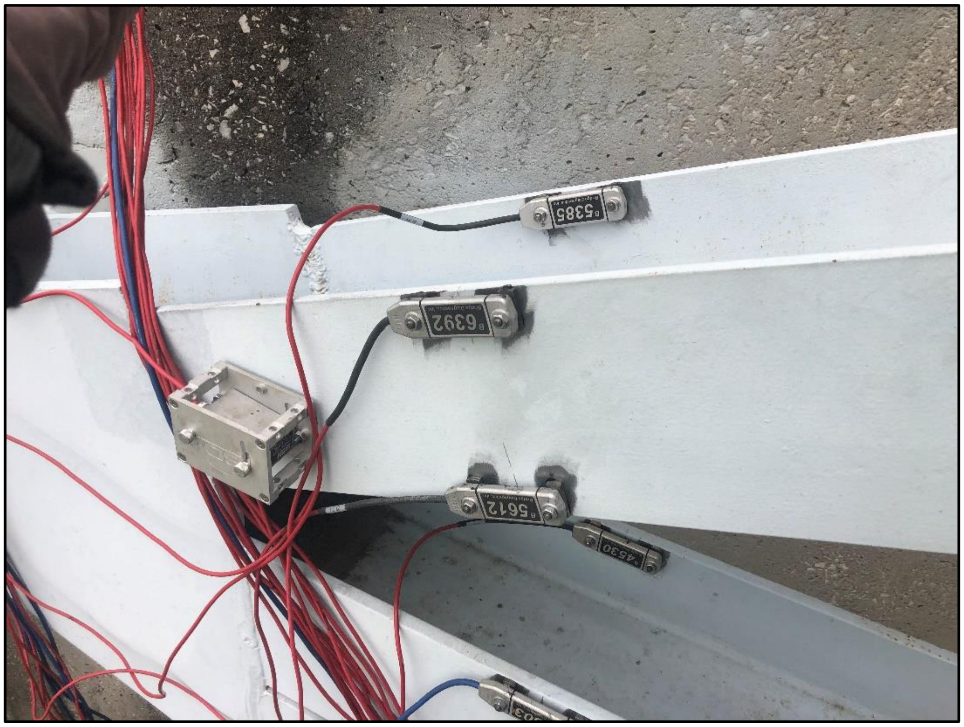

Figure 1 – BDI tiltmeter rotation sensor and reusable strain transducers installed near trunnion hub (Typical)

Figure 2 – BDI tiltmeter rotation sensor installed near skin plate (Typical)

Figure 3 – Torque sensor installation on hoist pinion shaft (Typical)

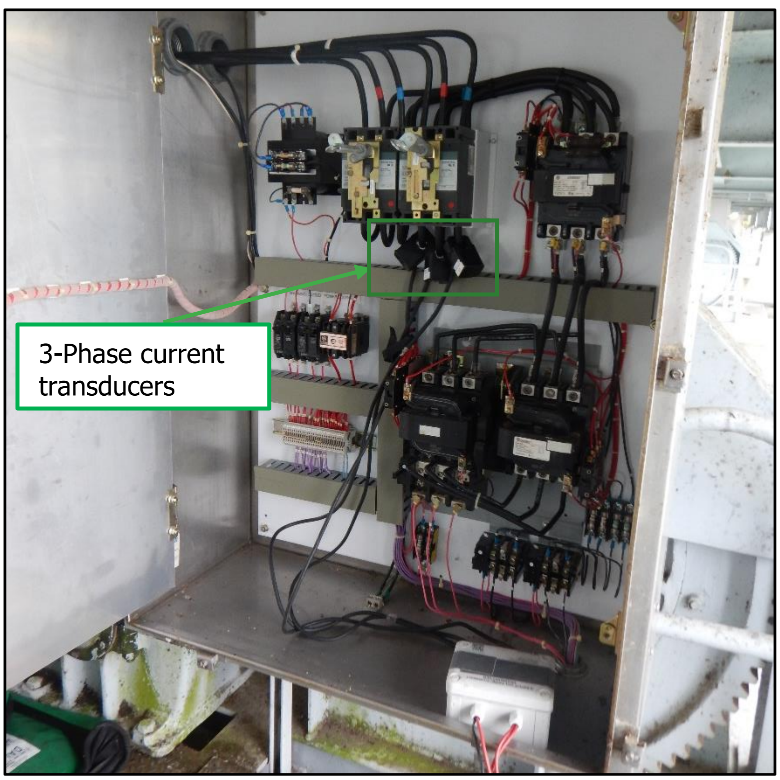

Figure 4 – Current transducers installed on hoist motor controls (Typical)

Figure 5 – BDI personnel installing instrumentation on the gate arm

TESTING PROCEDURES

Structural response data was recorded on all sensors at 50Hz while the gate was run through three spill tests. Each test consisted of three "up-down" cycles (direction reversals) without lowering the gate back to the sill. Each direction reversal consisted of lifting the gate approximately 6-12", pausing for a few seconds, and lowering the gate approximately 6", and repeating until all reversals had been completed.

RESULTS SUMMARY

GENERAL DISCUSSIONS BASED ON STRUCTURAL RESPONSES

The following outline contains general discussion points and observations that were made during the data review process. Note: Strain measurements were converted to stress for all subsequent analysis by multiplying the strain values by a steel elastic modulus of 29,000 ksi.

+ **DESCRIPTIONS OF RESPONSE MEASUREMENTS:** All sensor readings were zeroed at the end of each test (which consisted of three cycles of direction reversals) so that each measurement corresponded to response change relative to the final gate position as shown in Figure 6 (gates in the downward "closed" position with the hoist cables slacked as much as possible). It is also worth noting that the stresses did not always start and end at the same levels between tests. This variation in behavior is due to small changes in the flexed gate condition between the start and end of tests. It is common for the flex in the gate, caused by pin friction, to slowly release as it rests on the sill. The purpose of the three up-down cycles per test, prior to sitting the gate back onto the sill, is to ensure that these changes in boundary conditions, including gate flexure due to friction, did not affect BDI's trunnion friction results. ***It is important to note that the recorded measurements were changes in structural response due to gate movement, and do not include the in-situ stresses due to the dead load, cable wrap, and hydrostatic loads present prior to testing.***
+ **QUALITATIVE DATA REVIEW:** Review of the response data indicated a good level of reproducibility between the three tests. For reference, Figure 6 and Figure 7 show stress responses measured along Gate 7's right arm top strut for all three tests (Test #1-3). The data in these plots have been provided as both a function of time and the gate position as determined by the skin plate tilt sensor. Structural response behavior slightly varied during the first test's first cycle compared to subsequent lift/lower cycles and tests, with the first cycle having a slightly smaller change in stress due to pin friction. The observed variation was likely caused by a larger release of built-up pin friction as the gate rested on the sill for a longer period of time.
+ **DIRECTION/FRICTION REVERSAL IN RESPONSES:** The difference in stress during gate opening and closing for a given position is shown in Figure 8. The stress variation at any given gate position was a result of direction reversal and in turn due to trunnion friction reversal. This statement is true since all other loads such as dead-load and hydrostatic pressure were essentially constant barring small changes in hydrostatic pressure due to slight changes in head. This direction/friction reversal is depicted in Figure 9, with deflected shape renderings from a gate arm finite element model under lifting and lowering loads. Note that this figure shows an arm configuration that does not match this gate, but the concept of the direction/friction reversal still applies.
+ **MOTOR PERFORMANCE:** Current measurements taken at the hoist motor indicated steady and stable current draws during the lifting and lowering portions. An example plot of current draw and gate position is provided in Figure 10. Current draw ranges during lifting were higher than the ranges during lowering, which is common due to gravity/dead load. These results are summarized along with recorded peak in-rush current in Table 2. Note that the sample rates used during testing were set for collecting gate responses and may not have been appropriate to fully capture the in-rush current. The readings should be evaluated by a licensed electrician with knowledge of the operating parameters.
+ **TORQUE AND HOIST FORCE:** Due to restrictions caused by the hoist limit switches, the hoist cables could not always be fully slacked at the beginning and end of the performed tests. Throughout testing of the Rockwell Forney gates, it was found that this limit switch restriction varied gate to gate and arm to arm. Therefore, it is not recommended to use the collected torque and hoist force data to quantify overall hoist forces. Rather, this data was utilized to evaluate total friction behavior, which is observed as half the difference between the lifting and lowering torque/force (friction reversal).

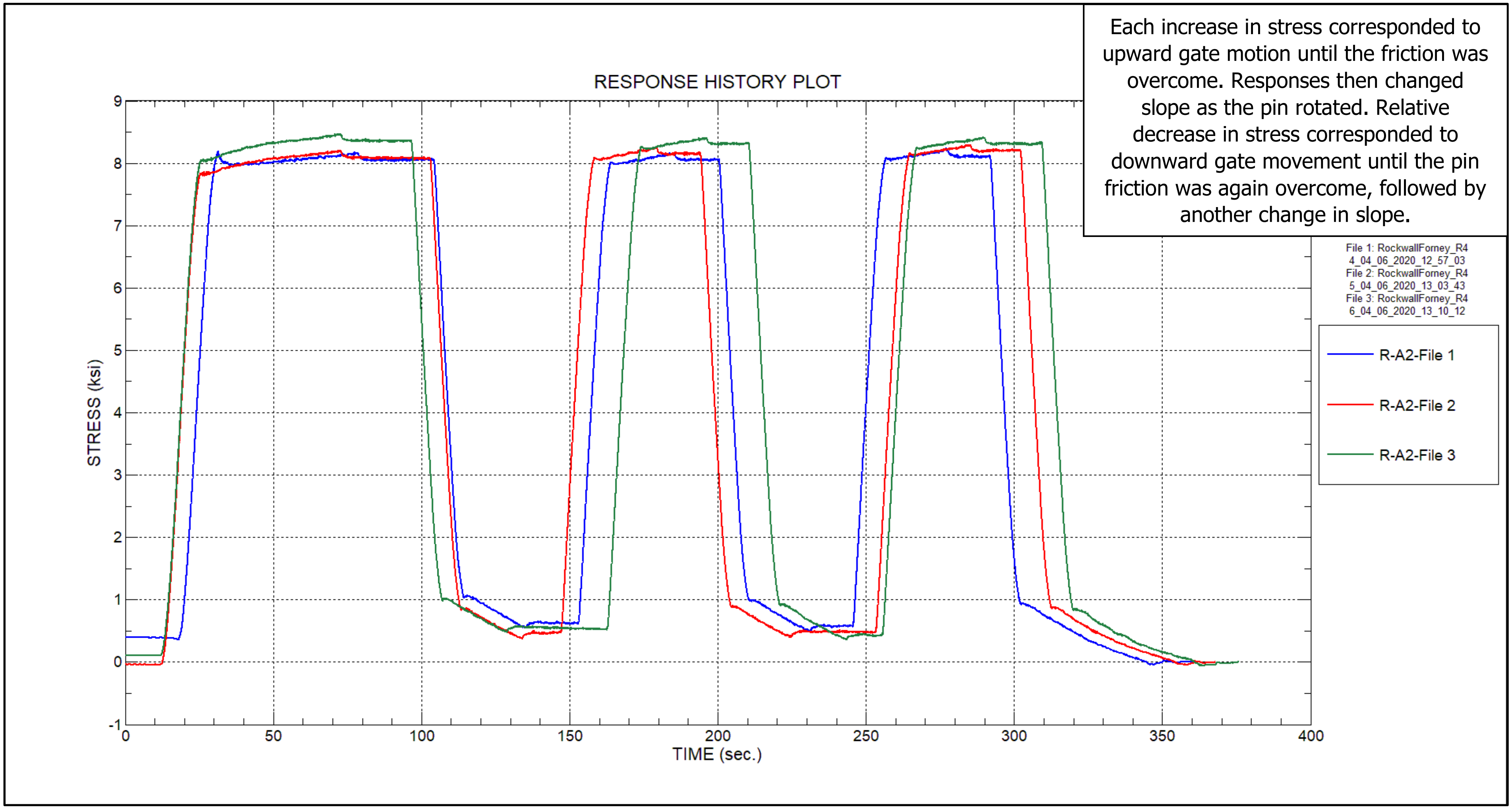

Figure 6 – Stress response history – Right arm – Gage A2 – Time based
File 1 = test run 1, File 2 = test run 2, File 3 = test run 3

(Section A along top strut near pin – Sensor location 2 along bottom of inner flange)

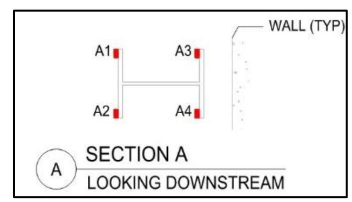

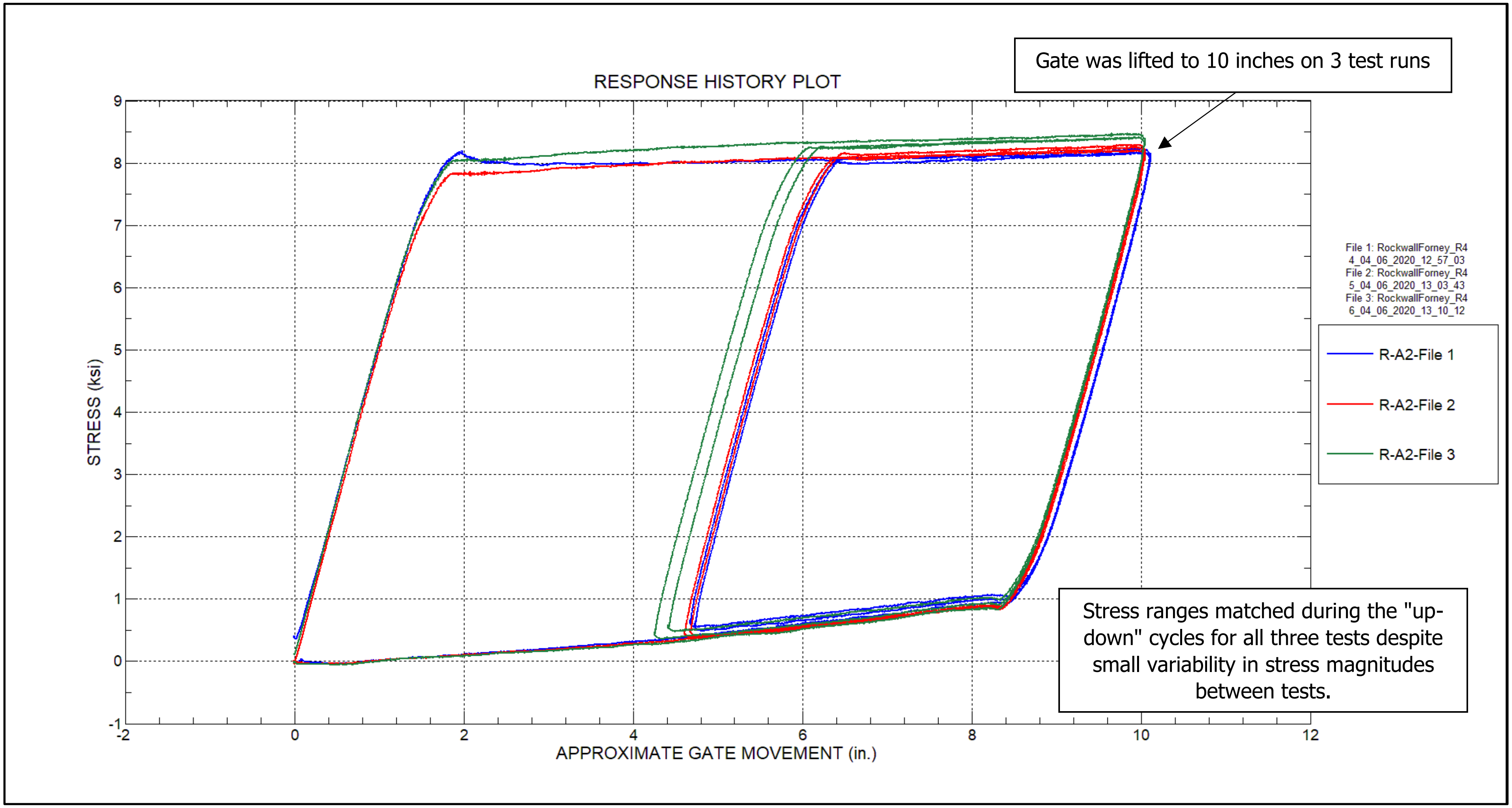

Figure 7 – Stress response history – Right arm – Gage A2 – Function of gate movement
File 1 = test run 1, File 2 = test run 2, File 3 = test run 3

(Section A along top strut near pin – Sensor location 2 along bottom of inner flange)

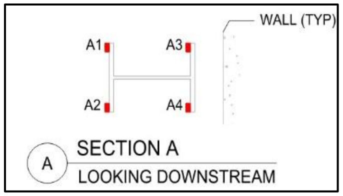

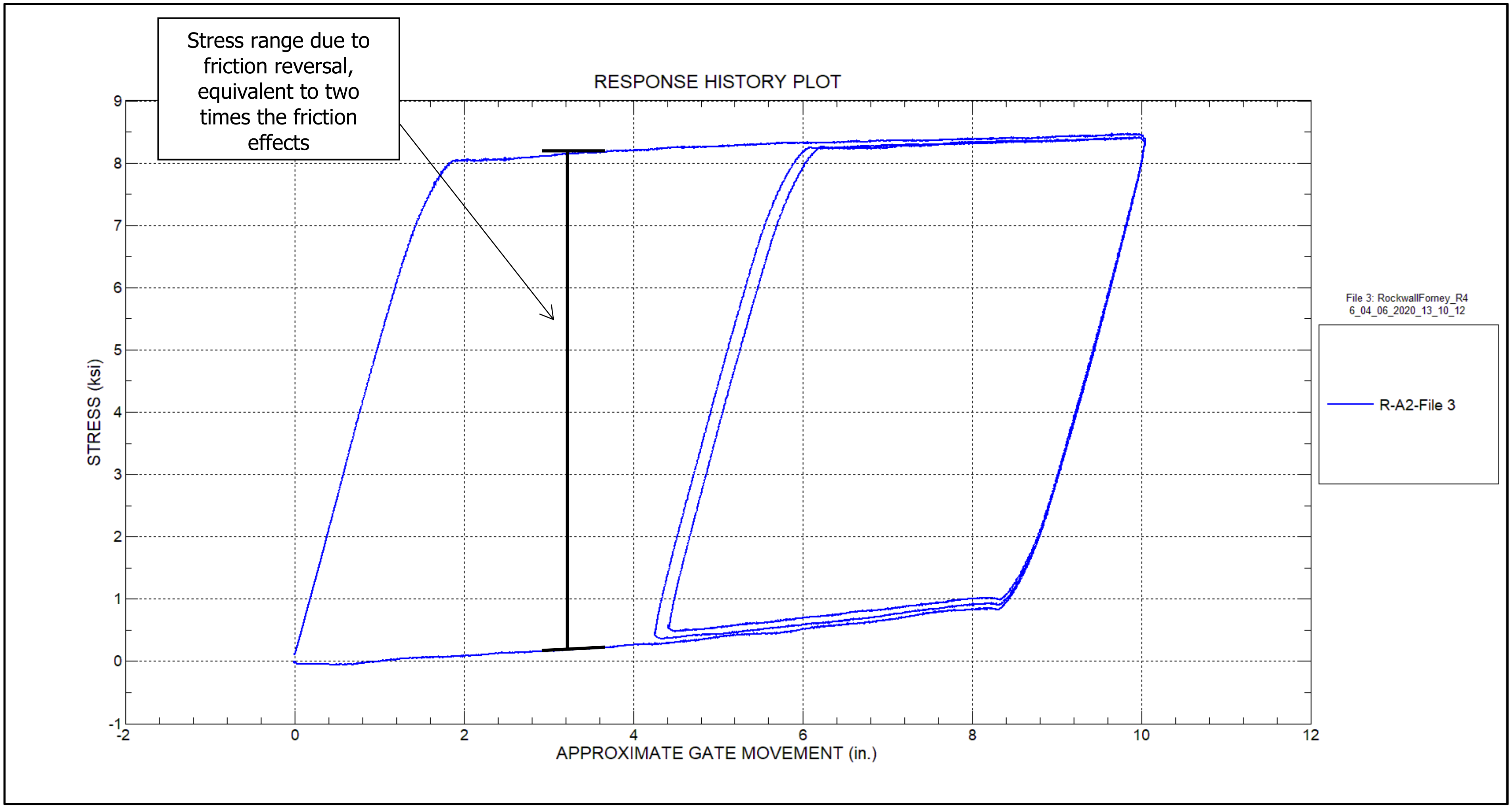

Figure 8 – Stress response history – Right arm – Gage A2 – Friction effect in stress responses

(Section A along top strut near pin – Sensor location 2 along bottom of inner flange)

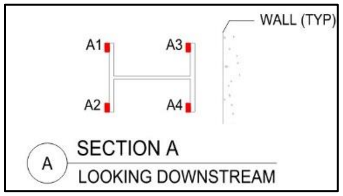

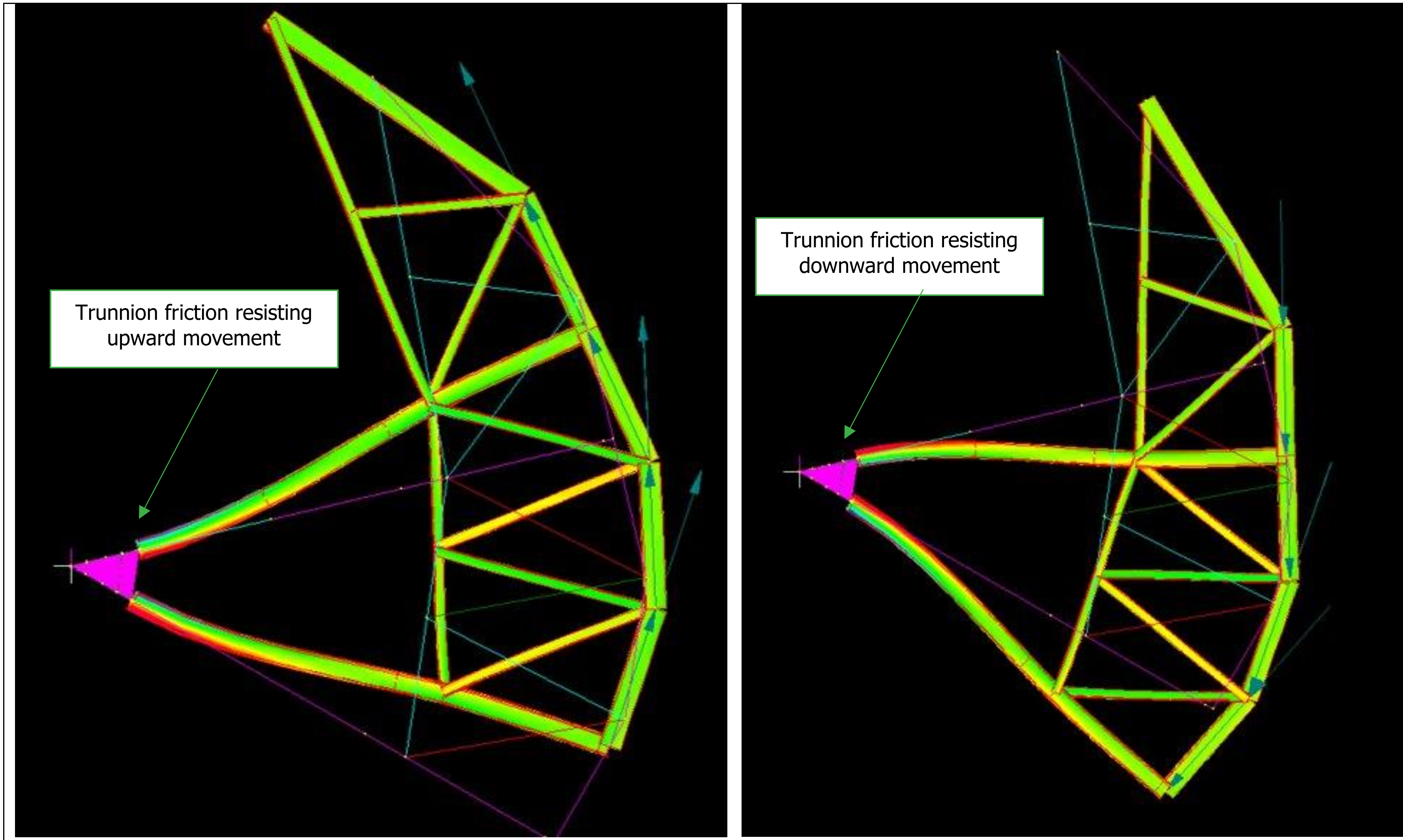

Gate traveling upward | **Gate traveling downward**

Figure 9 – Deflected shapes during lifting and lowering of Gate – Visualization of direction/friction reversals

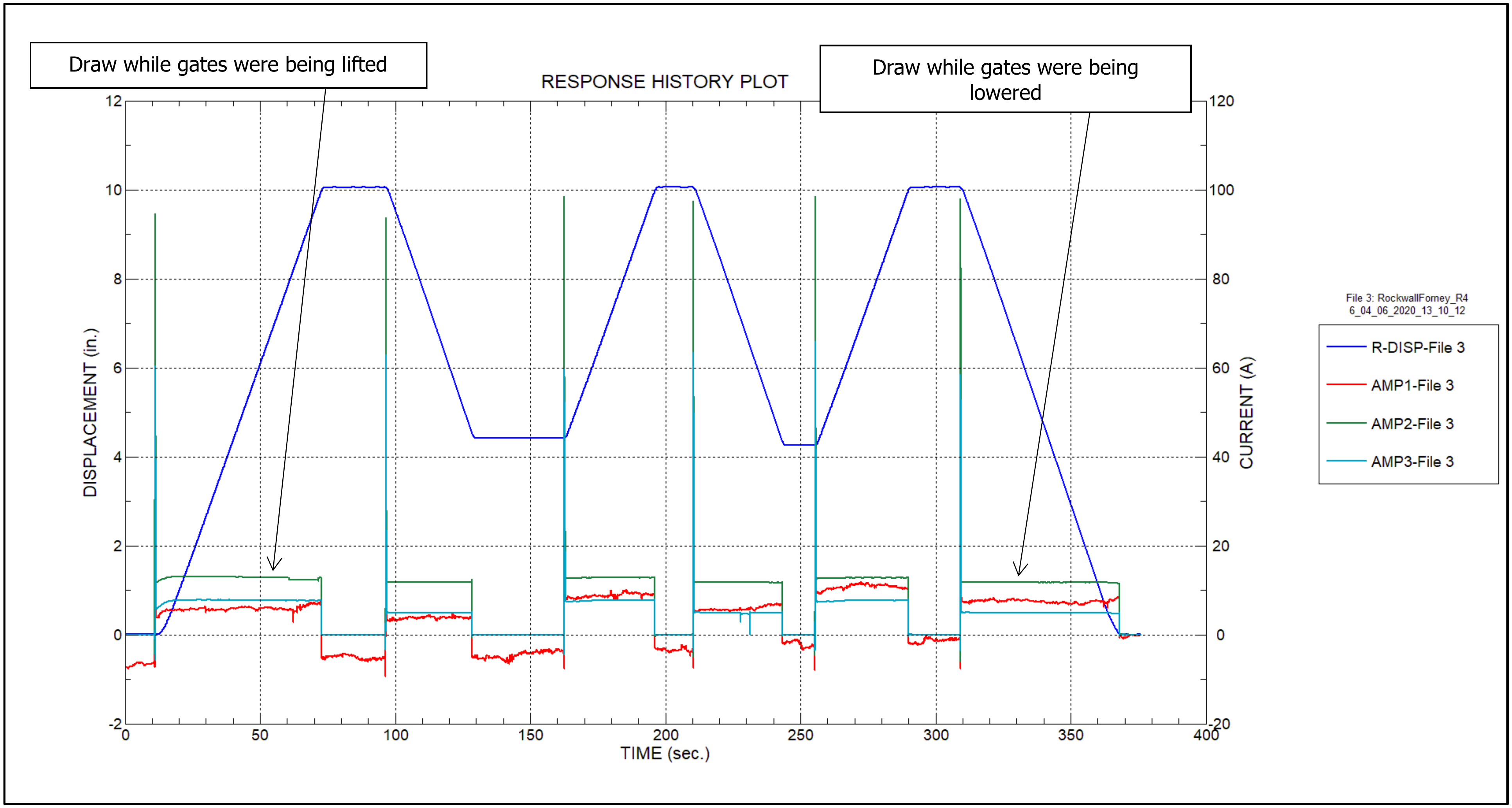

Figure 10 – Motor current & gate movement response history – Lift motor – Highlighting motor draw during lift and lower cycles

METHODOLOGY AND FINDINGS OF THE STRUT FORCE AND MOMENT CALCULATIONS

The following outline provides the methodology used to calculate the required member forces and moments.

- **CHANGE IN STRESS DUE TO GATE OPERATION:** Strain data can be viewed as a function of time starting when the gate was in the down position and was then lifted off the sill. When examining data in this manner, it is easy to see how stresses ramped up as the gate began to move and then changed slope once pin friction was overcome and the trunnion hub began to rotate with the gate. The first point in time where the friction was overcome (both lifting and lowering) has been highlighted in the stress histories shown in Figure 11. These stress histories show the response of all four sensors along the top strut of the right arm (Section A). ***It is important to note that the recorded measurements were changes in structural response due to gate movement, and do not include the in-situ stresses due to the dead load, cable wrap, and hydrostatic loads present prior to testing.***
- **CALCULATION OF STRUT CROSS-SECTIONAL MOMENTS:** The use of four strain gages per strut cross-section allowed accurate in-plane flexural bending moments to be computed from the recorded strain measurements. These moments were computed for every cross-section in each gate arm using the basic mechanics equation provided in Figure 12.

  In-plane or weak-axis flexure refers to bending about a given strut's web. This designation is consistent with typical nomenclature. In-plane bending can be observed visually from the strain response histories as a difference between the top and bottom stresses, whereas out-of-plane or strong-axis bending is visualized as the difference in stress from side to side. Figure 13 provides a visual reference for both types of strut flexure.
- **EXAMINATION OF RESPONSES AS A FUNCTION OF GATE POSITION:** Changes in cross-sectional moment related to friction becomes clearer when the responses are plotted as a function of gate position. Because the gate was operated with several up and down movements, the effects of friction associated with each direction reversal can be viewed for all measured and calculated responses. Figure 14 through Figure 17 show all cross-sectional flexural moment plots for both trunnion arms. The responses in these plots have been centered about the stress state corresponding to a zero-moment, unflexed condition. The zero-moment offset was estimated as the average moment values between up and downward movement (i.e. half the moment difference) at the gate position with the greatest pin friction moment difference (greatest difference between lifting and lowering).
- **TRUNNION FREE-BODY-DIAGRAM & PIN MOMENT CALCULATION:** Figure 18 shows the instrumented member cross-sections and shows how the measured cross-sectional flexural responses were used to compute pin moment. The in-plane moment values used in these calculations were determined directly from the strain measurements at each cross-section using the provided mechanics equations. It should be noted that the out-of-plane moments were not considered in the calculation of pin moment since they were orthogonal to the axis of the pin rotation. Total pin moment was then determined by summing all the moment components about the pin, which included the in-plane moment and the shear components at the strut cross-sections nearest the pin.
- **STRUT SHEAR CALCULATION:** From the examination of the trunnion free-body-diagram described above, the shear vectors at the three struts were a primary component in the pin moment calculation. For this type of structural element, shear vectors were calculated using the moment differential between the two cross sections along each strut. It is important to recognize that shear was constant between the two instrumented cross-sections and the applied shear was a function of the recorded change in moment ($V = dM/dX$). Subsequently, the shear vectors were calculated by dividing the difference in moment by the distance between the two instrumented cross-sections. Shear values for each strut have been plotted as a function of gate position in Figure 19 and Figure 20.

+ **CALCULATION OF PIN MOMENT DUE TO FRICTION:** Once all the trunnion arm force vectors were calculated, the equations shown in the free-body-diagram were applied to compute pin moment as a function of gate position. It is important to note that because the calculated pin moment range corresponds to a direction reversal, a reversal in friction also occurred. The effect of direction reversal on pin moment due to friction is best conceptualized by centering the moment response plots about the zero-moment axis. The moment due to lifting and the moment due to lowering can then be visualized as a change from this new zero point corresponding to the gate in an unflexed condition. Therefore, the total moment differential between lifting and lowering was twice the moment due to friction acting in a single direction. Pin-moment plots have been provided in Figure 21 and Figure 22. From these plots, it is apparent that pin moment due to friction remained relatively constant throughout the gate operation tests, with a slight decrease in pin friction moment as the gate continued to be lifted. This slight decrease in pin friction moment most likely corresponded to the change in hydrostatic load as the gate position changed. Pin-moment plots for all tests on Gate 7 are also provided for reference in Appendix B – Gate 7 Pin Moment Component Plots.
+ **SHAFT TORQUE & HOIST FORCE:** Torque measurements were taken on the pinion shafts near the hoist motor during testing, with single torque gages installed on the left and right hoist pinion shaft. Responses were recorded in units of micro-strain and converted to torque in units of kip-ft using Equation 1 thru Equation 3 and the following shaft properties.

$$d_O = 5.5\ inches, \qquad d_I = 0\ inches, \qquad E = 29000\ ksi, \qquad \nu = 0.3$$

$$G = \frac{E}{2(1+\nu)}$$

Equation 1

$$J = \frac{\pi\left(d_O{}^4 - d_I{}^4\right)}{32}$$

Equation 2

$$\tau = \varepsilon * \frac{2GJ}{\frac{d_O}{2} * 1000000 * 12}$$

Equation 3

Figure 23 shows example torque measurements, recorded on the Gate 7 torque shafts. Best practices for torque measurements is to measure torque on opposite sides of the shaft so that any bending in the shaft can be removed by averaging the two responses. Due to access limitations, only one gage at each location could be installed. Therefore, any bending in the shaft may be reflected in the torque measurements and may be related to the peaks and valleys observed in the torque responses.

Torque values were converted to force in the hoist cables per gate arm using the gear ratio and drum radius, as shown in Figure 24. The gear ratio and drum radius were 5.182 and 1.086 feet respectively, as defined in the provided as-built shop drawings. It should be noted that the hoist force calculated may be smaller than the actual hoist force applied. This difference is due to the limit switch engaging the brake before the hoist cable was fully slacked, resulting in an initial force in the cable. A hoist force due to total gate friction was then calculated. This friction hoist force was equal to half the differential in force measured during the lifting and lowering of the gate (similar to the pin friction calculations). As shown in Table 3, the change in cable force due to friction was generally consistent between tests. Note that the total hoist force was due to the total friction effects, including side seal, hoist bearings, trunnion friction effects, etc. It is difficult to determine the exact proportion and composition of the total friction sources. Additional torque and hoist force plots for all collected data files are provided in Appendix A – Gate 7 Torque and Hoist Force Plots.

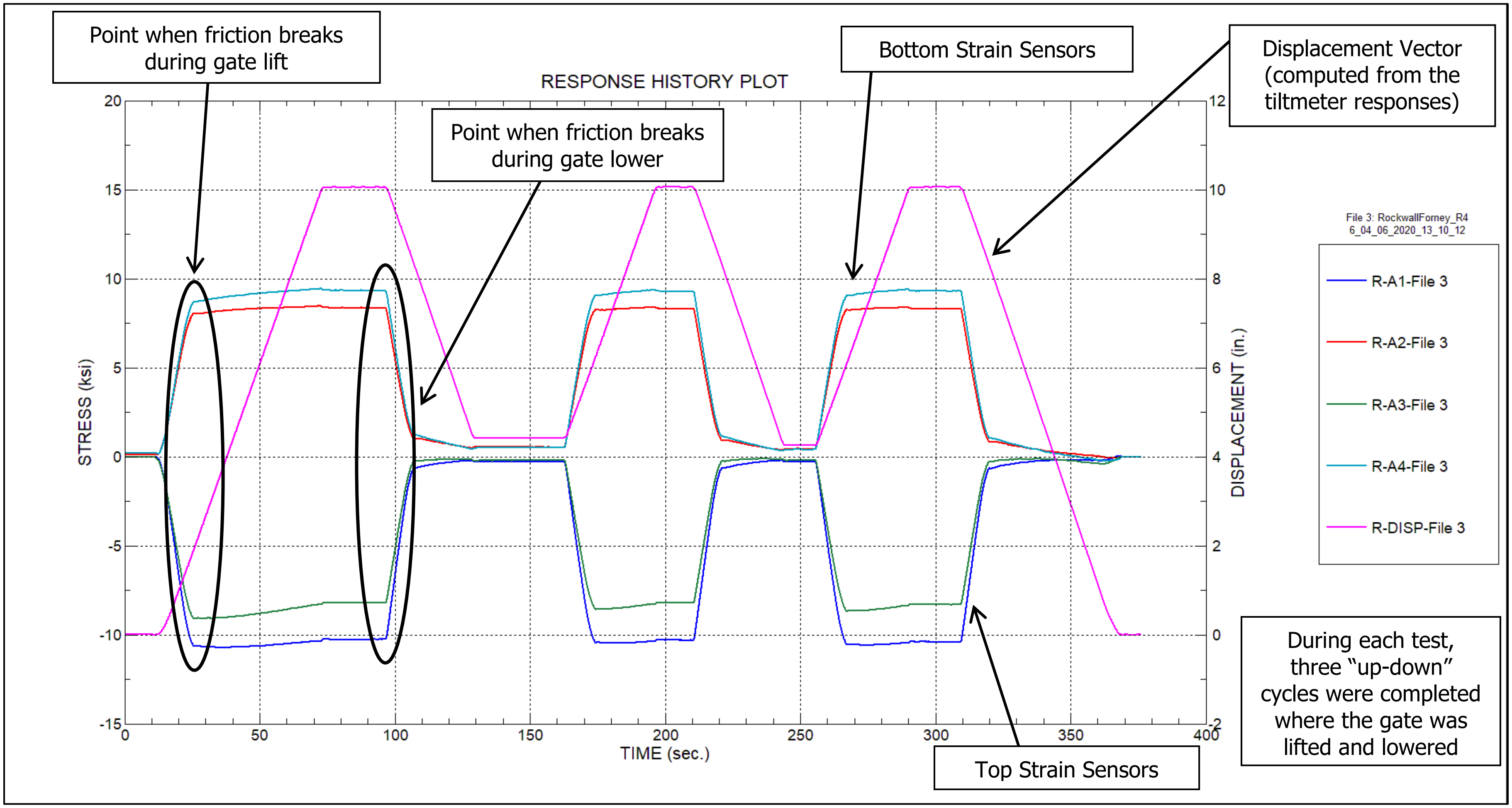

Figure 11 – Stress response & gate movement history – Right arm – Section A - Highlighting friction behavior
(Section A along top strut near pin)

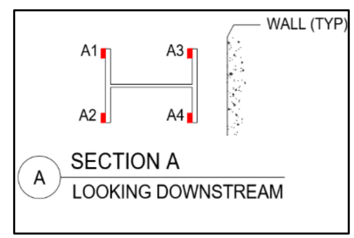

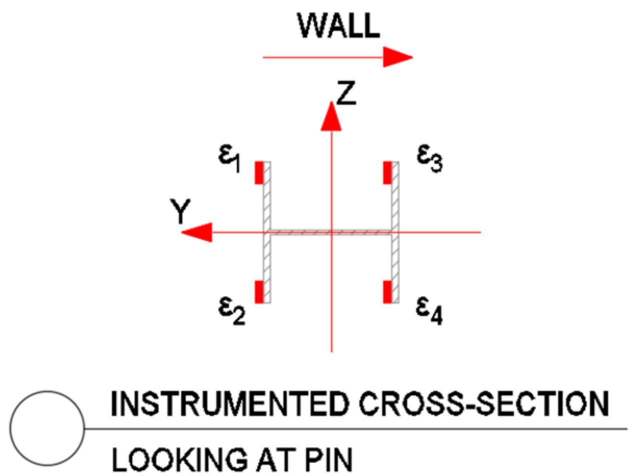

Calculation of Weak-axis (In-plane) bending

$$M_Y = \frac{E\left[\frac{\varepsilon_2 + \varepsilon_4}{2} - \frac{\varepsilon_1 + \varepsilon_3}{2}\right] S_{Y(gage)}}{2}$$

Sy(gage) = Section modulus to the center of gages (not extreme fiber of flanges)
(locations of gages were accounted for in moment computation)

Figure 12 – Basic mechanic equation used to calculate moment

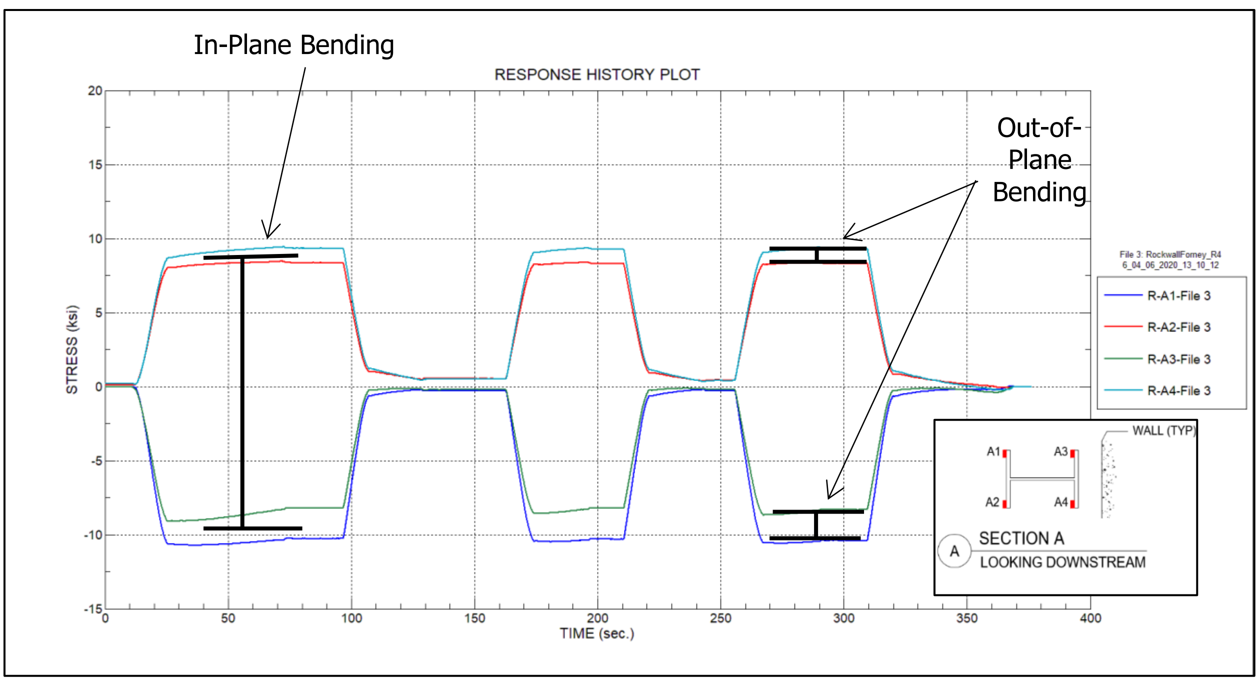

Figure 13 – Stress response history – Right arm – Section A – Bending components
(Section A along top strut near pin)

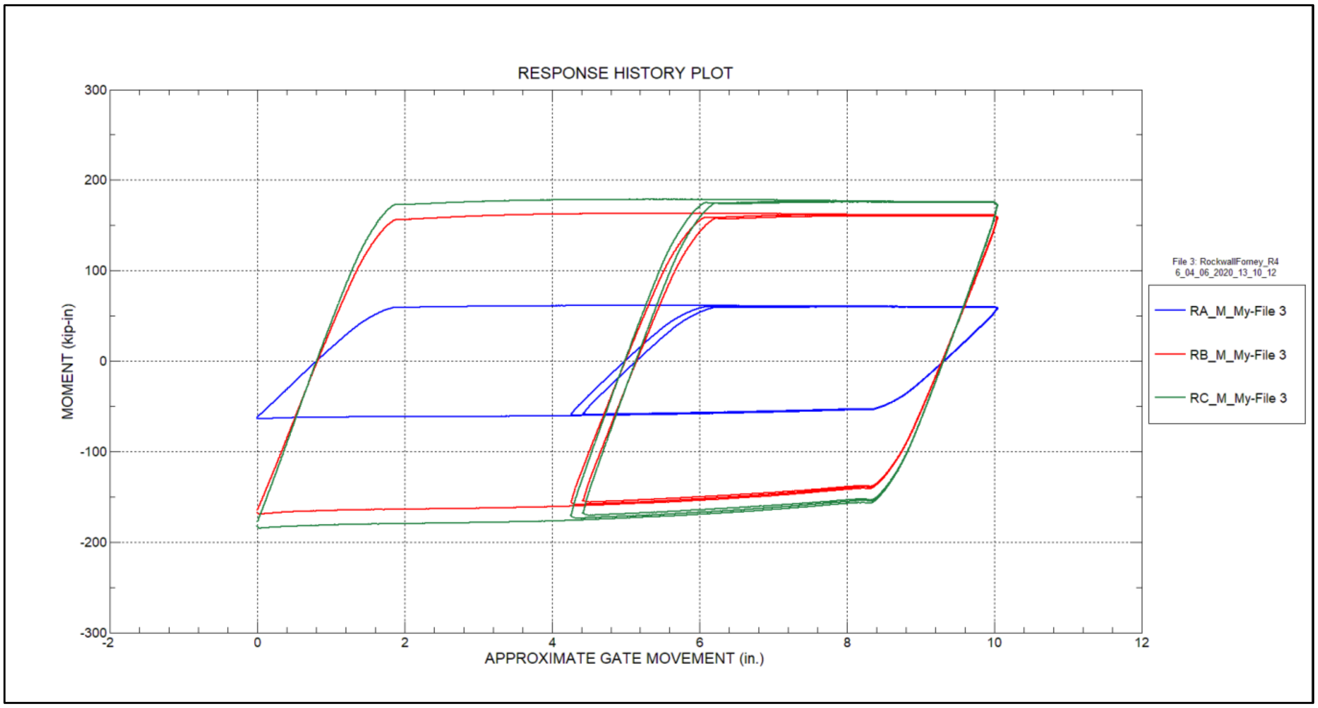

Figure 14 – In-plane moment response history – Right arm – Sections near pin

(RA = Right Arm Top Strut, RB = Right Arm Middle Strut, RC = Right Arm Bottom Strut)

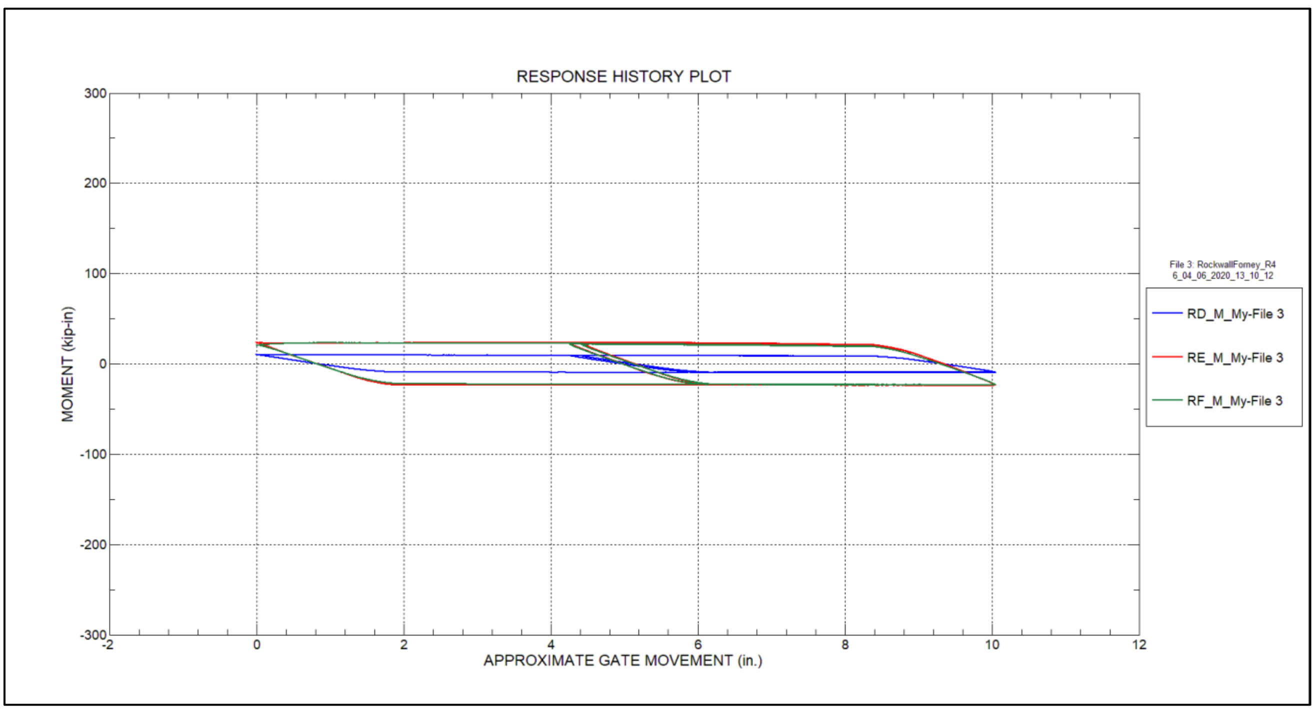

Figure 15 – In-plane moment response history – Right arm – Sections away from pin

(RD = Right Arm Top Strut, RE = Right Arm Middle Strut, RF = Right Arm Bottom Strut)

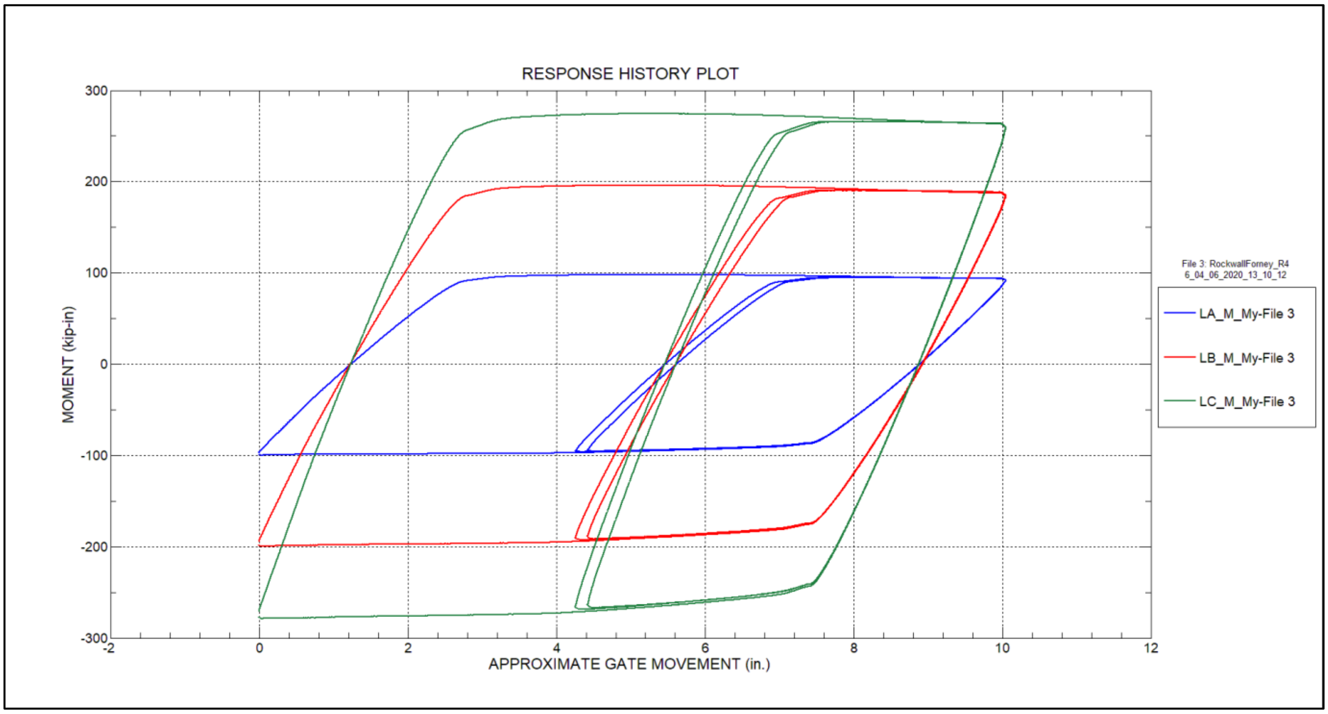

Figure 16 – In-plane moment response history – Left arm – Sections near pin

(LA = Left Arm Top Strut, LB = Left Arm Middle Strut, LC = Left Arm Bottom Strut)

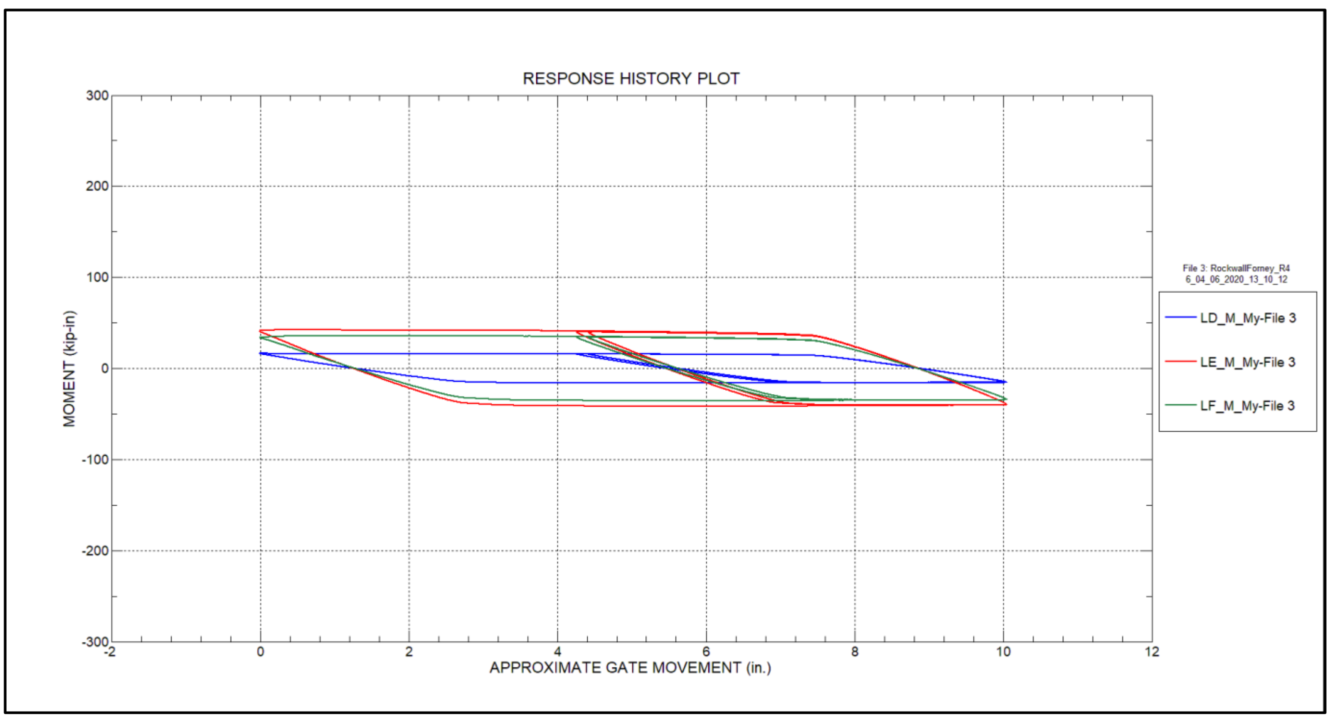

Figure 17 - In-plane moment response history – Left arm – Sections away from pin

(LD = Left Arm Top Strut, LE = Left Arm Middle Strut, LF = Left Arm Bottom Strut)

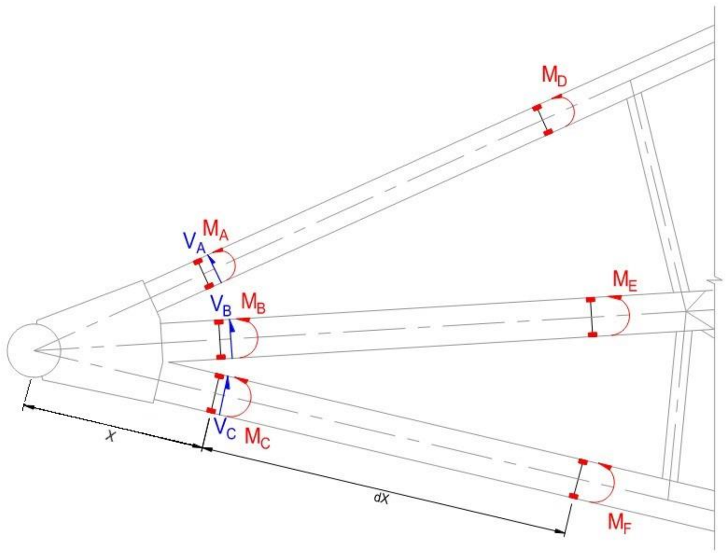

Elevation View of Gate Arm

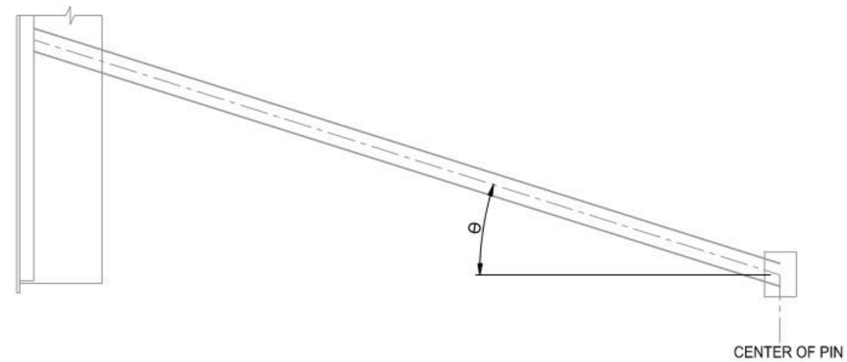

Plan View of Gate Arm

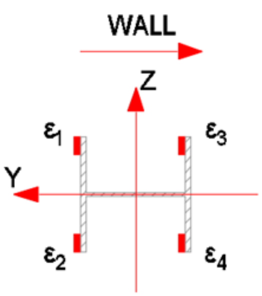

$$M_Y(M_A, M_B, M_C, M_D, M_E, M_F) = \frac{E\left[\frac{\varepsilon_2 + \varepsilon_4}{2} - \frac{\varepsilon_1 + \varepsilon_3}{2}\right] S_{Y(gage)}}{2}$$

$$V_A = \frac{M_A - M_D}{dX}$$

$$V_B = \frac{M_B - M_E}{dX}$$

$$V_C = \frac{M_C - M_F}{dX}$$

$$\sum M_o = 0$$

$$M_{PIN} = [X(V_A + V_B + V_C) + M_A + M_B + M_C]\cos\theta$$

Figure 18 – Direct calculation of pin moment from strain measurements

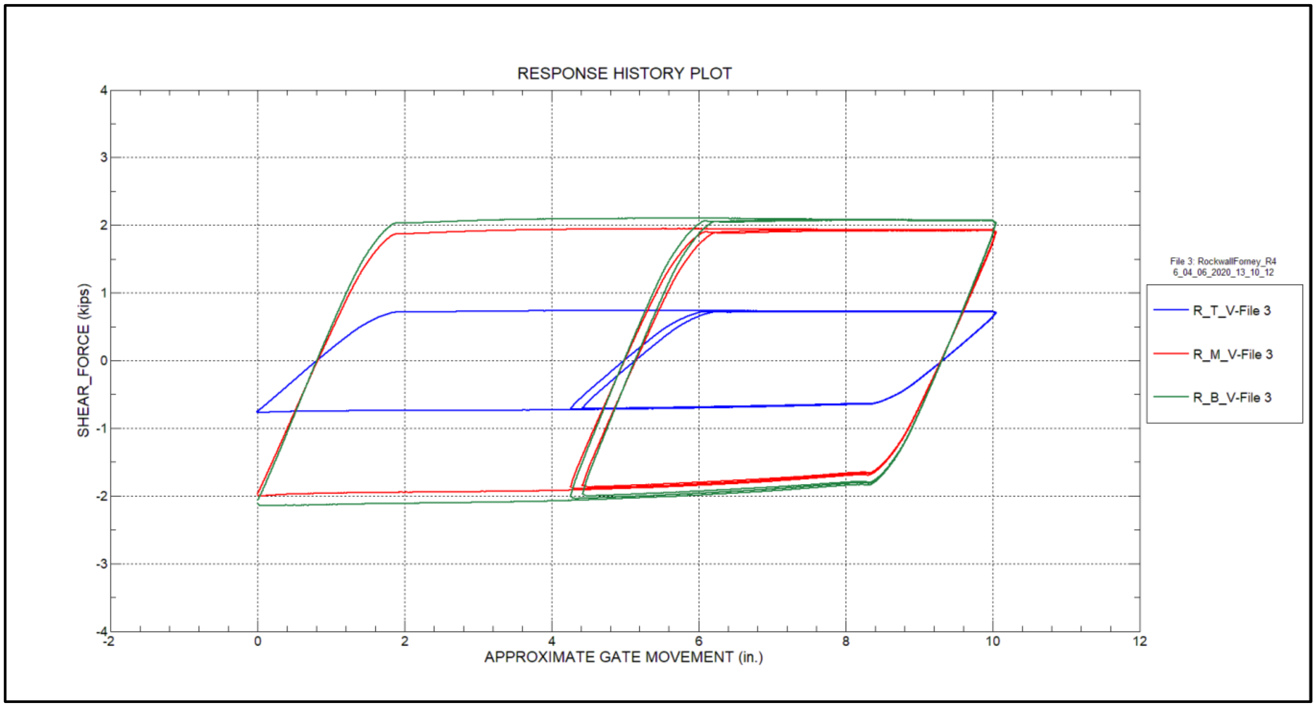

Figure 19 – Strut shear response history – Right arm

(R_T = Right Arm Top Strut, R_M = Right Arm Middle Strut, R_B = Right Arm Bottom Strut)

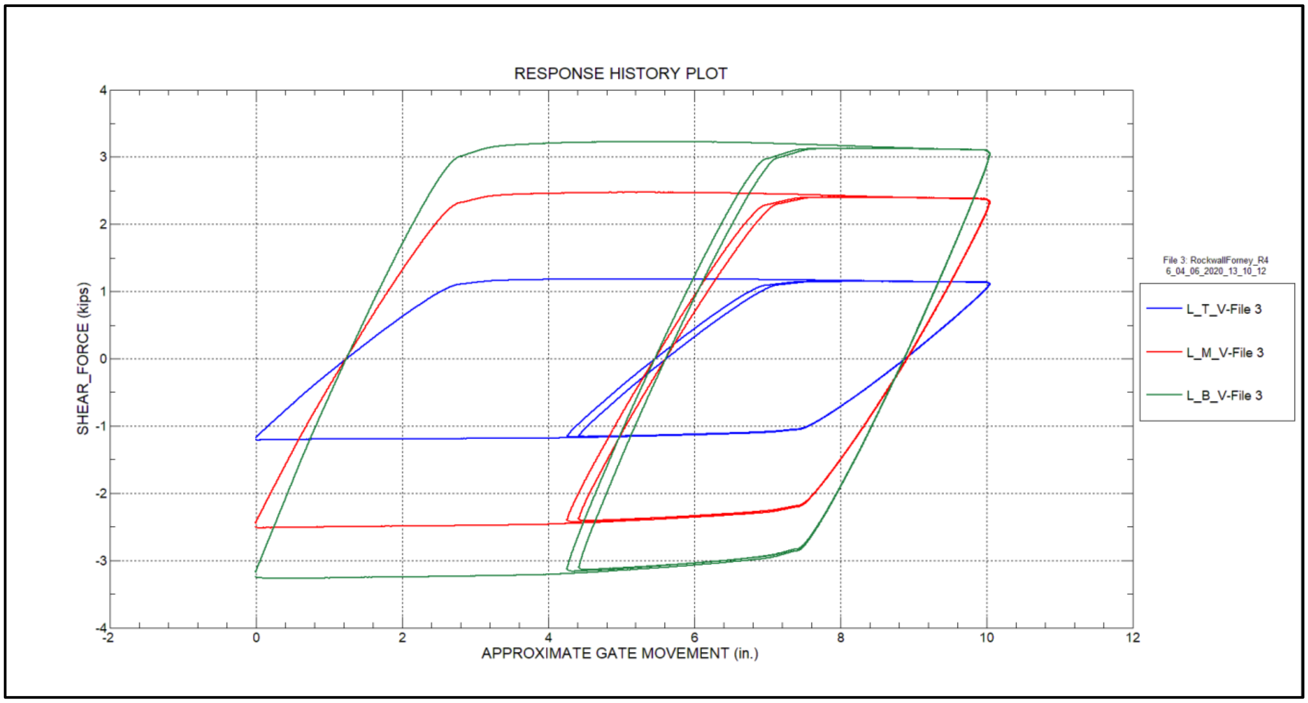

Figure 20 – Strut shear response history – Left arm

(L_T = Left Arm Top Strut, L_M = Left Arm Middle Strut, L_B = Left Arm Bottom Strut)

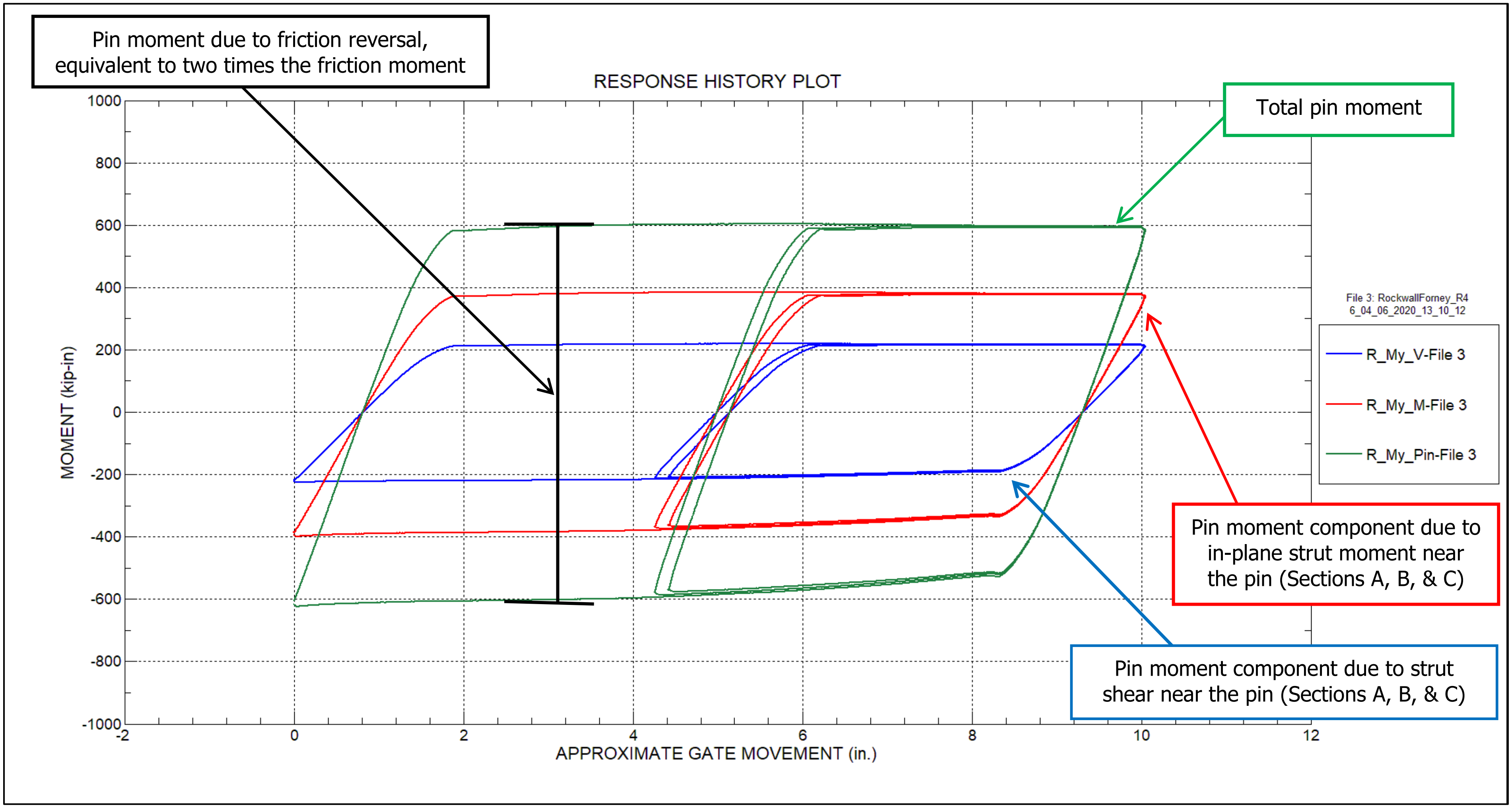

Figure 21 – Pin moment response history – Right arm

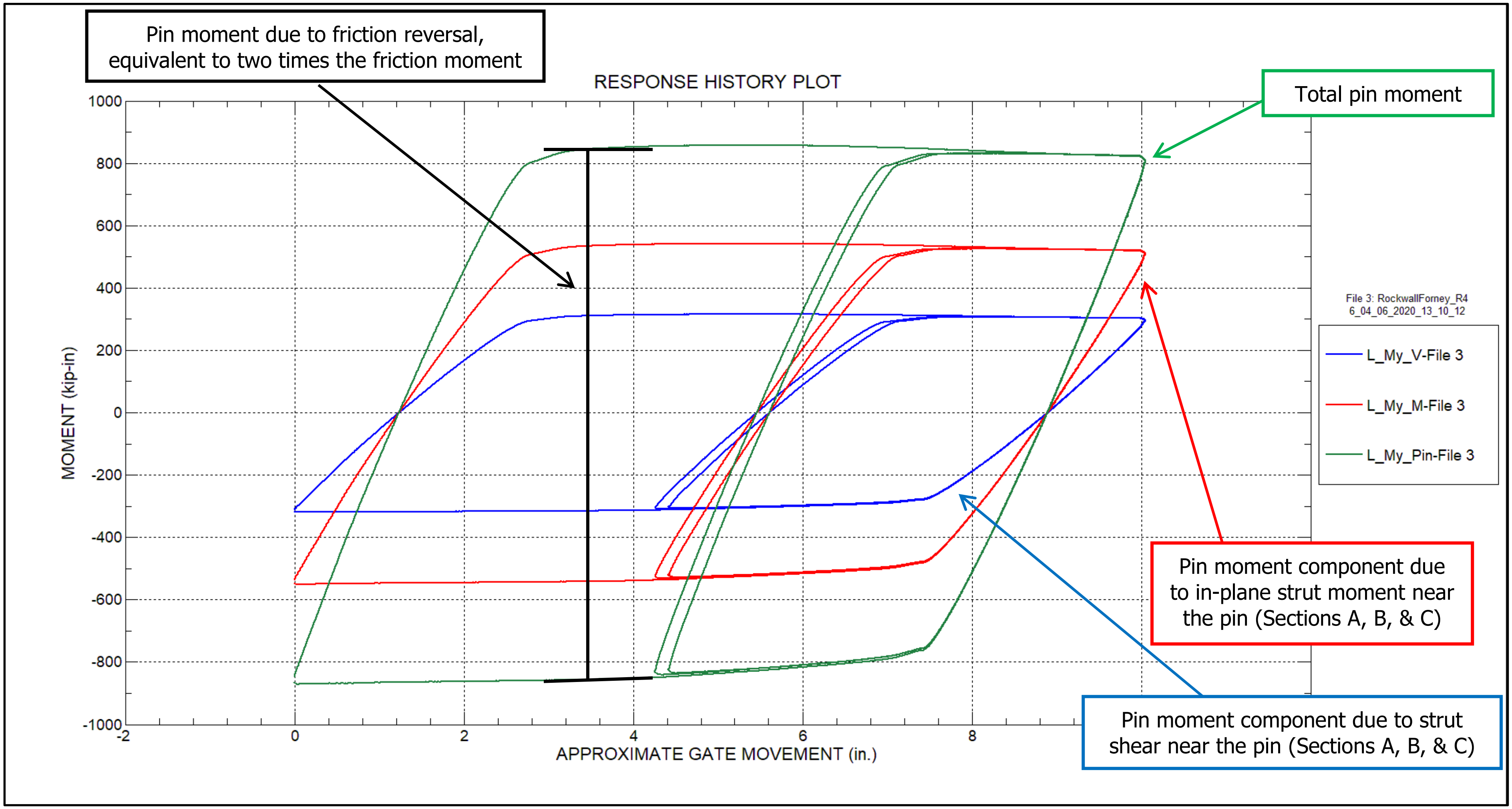

Figure 22 – Pin moment response history – Left arm

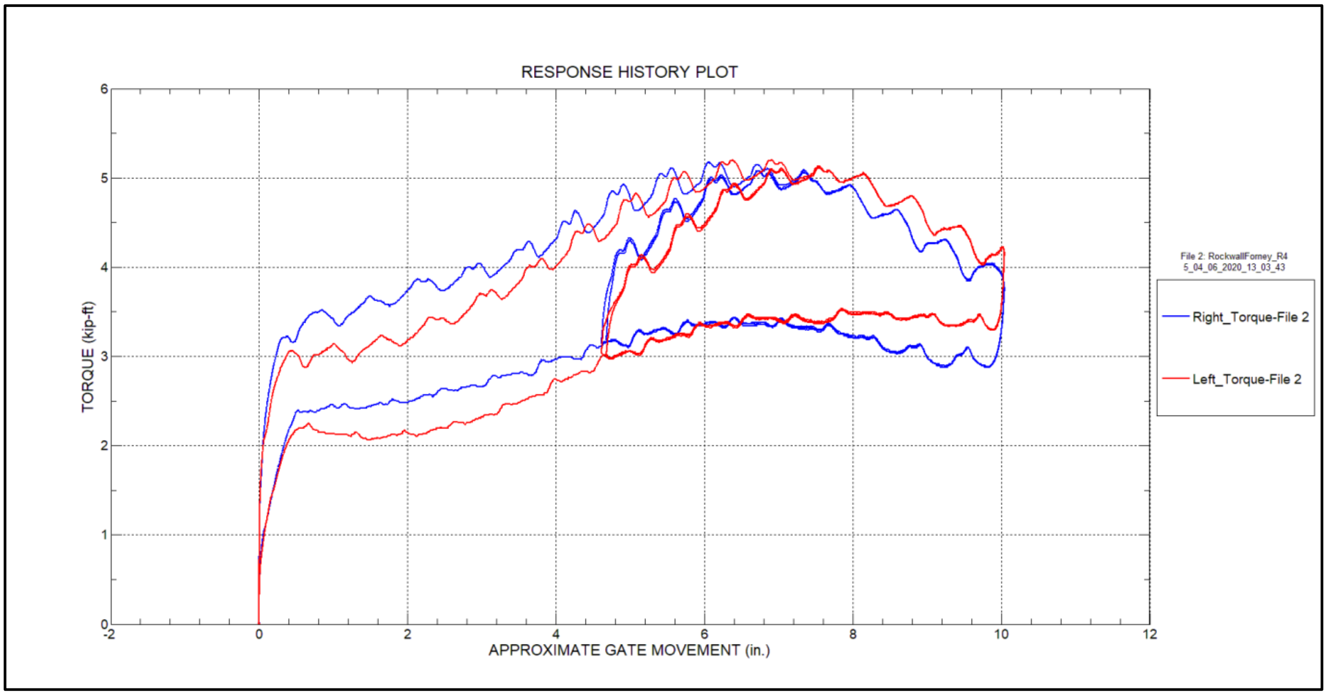

Figure 23 – Hoist torque response history – Gate 7 – Test 2

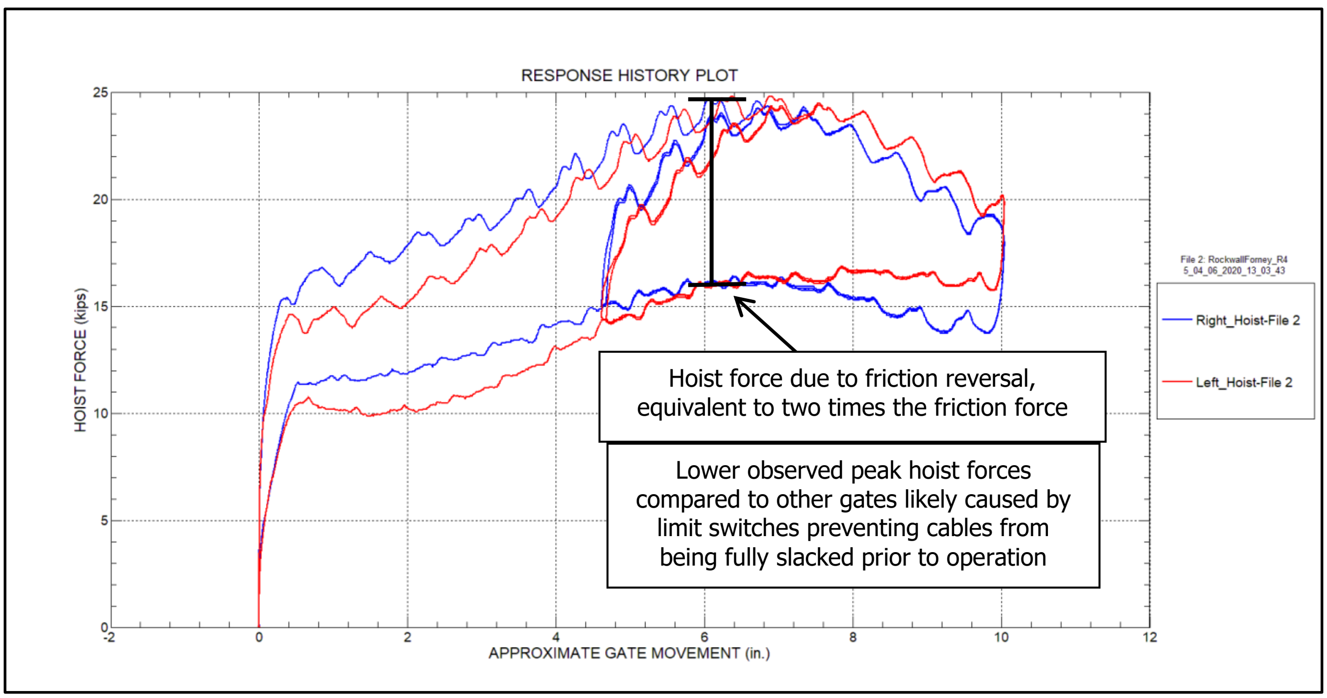

Figure 24 – Hoist force response history – Gate 7 – Test 2

SUMMARY OF FRICTION RESULTS

The raw data files have been included in the submittal package for reference and were formatted as "tdms" files that can be opened in Microsoft Excel using a "tdms" reader extension.

Examination of the stress histories for each test was necessary to obtain a thorough understanding of the gate performance. The response shapes, variations in stress magnitudes, and timing sequences provided direct clues as to how the gate performed under typical service conditions. The following is a breakdown of the provided tabulated results:

+ Table 2 provides motor current ranges and maximum in-flow for lift and lower cycles for each test
+ Table 3 provides maximum hoist force as well as hoist force due to total friction for each test
+ Table 4 provides the maximum stress ranges measured at the sensor locations for each member
+ Table 5 provides maximum bending stress and moment ranges observed during the gate tests
+ Table 6 provides maximum friction bending stress and moment values at each of the instrumented strut locations
+ Table 7 provides the computed shear values in each strut due to friction
+ Table 8 provides calculated measured friction moments, calculated hydrostatic loads based on the measured water elevation, and coefficients of friction for each gate and gate arm during all three tests

The resulting pin friction moments were used to compute friction coefficients from Eq. 4, given the pin radius and the applied thrust. The thrust used in this calculation consisted of the calculated resultant hydrostatic load based on the measured water elevation and was adjusted to account for the loss of head as the gate was lifted. This thrust adjustment was based on the recorded gate movement and was performed in order to calculate more accurate friction coefficients. The water elevation during testing was nearly constant throughout each gate test and was documented during each "up-down" cycle. It should be noted that the minor thrust due to cable wrapping, which was minimal compared to hydrostatic thrust, was not included in the thrust calculation. This assumption resulted in slightly conservative friction coefficients.

$$\mu = \frac{M_F}{T * r} \qquad \text{Eq. 4}$$

where:

where:	μ	=	Friction Coefficient
	M_F	=	Friction Moment
	T	=	Thrust per Pin
	r	=	Pin Radius, 5.375"

The out-of-plane shear and moments were not considered in the pin friction calculations due to orthogonal geometry considerations (resulting pin moment associated with out-of-plane flexure being perpendicular to pin rotation).

The data was presented in a specific coordinate system applicable to both arms. Data was processed so that the positive x-axis was always pointing towards the pin and the right-hand rule applied. In-plane bending can be referred to as "bending about the horizontal or y-axis" and shows how much the beams bend up and down within the plane of the gate arms. Refer to Figure 12 above for visual reference of coordinate system and mathematical explanation of calculations. Tabulated results do not include any in-situ effects.

Table 2– Motor current summary table – Gate 7

Test Run	Current Range due to Lifting (A)	Current Range due to Lowering (A)	Max In-rush Current (A)
1	7-13	4-13	98
2	4-13	3-13	99
3	5-13	3-12	99

Table 3 – Hoist force summary table – Gate 7

Test Run	Right Arm Peak Hoist Force (kips)	Left Arm Peak Hoist Force (kips)	Right Arm Hoist Force due to Total Gate Friction (kips)	Left Arm Hoist Force due to Total Gate Friction (kips)
1	24.89	24.88	4.36	4.40
2	24.74	24.81	4.44	4.42
3	24.72	24.91	4.55	4.49

Tabulated friction force values correspond to the response induced by friction in one direction

Table 4 – Maximum measured sensor stress range

Arm Designation	Top Strut (ksi)	Middle Strut (ksi)	Bottom Strut (ksi)
Right Arm	10.84	13.70	12.95
Left Arm	17.82	19.75	19.14

Tabulated values correspond to the total measured change in response during tests

Stress values have not been extrapolated to the extreme fibers (correspond to center of gage)

Table 5 – Maximum in-plane total bending stress & moment ranges – Total

Section Label	Section Description	Right Arm Stress (ksi)	Right Arm Moment (kip-in)	Left Arm Stress (ksi)	Left Arm Moment (kip-in)
Section A	Top Strut Near Pin	11.17	125.57	17.62	198.00
Section B	Middle Strut Near Pin	14.40	332.95	17.90	414.08
Section C	Bottom Strut Near Pin	13.15	366.77	19.95	556.32
Section D	Top Strut Away from Pin	1.78	20.04	2.89	32.46
Section E	Middle Strut Away from Pin	2.33	53.78	3.63	84.00
Section F	Bottom Strut Away from Pin	1.68	46.74	2.57	71.60

Tabulated values correspond to the total measured change in response during tests

Table 6 – In-plane frictional bending stress & moment at maximum gate friction

Section Label	Section Description	Right Arm Stress (ksi)	Right Arm Moment (kip-in)	Left Arm Stress (ksi)	Left Arm Moment (kip-in)
Section A	Top Strut Near Pin	5.49	61.65	8.68	97.55
Section B	Middle Strut Near Pin	7.03	162.55	8.87	205.17
Section C	Bottom Strut Near Pin	6.49	180.89	9.85	274.70
Section D	Top Strut Away from Pin	0.84	9.46	1.42	15.95
Section E	Middle Strut Away from Pin	1.09	25.16	1.78	41.19
Section F	Bottom Strut Away from Pin	0.81	22.72	1.26	35.16

Tabulated values correspond to the response induced by friction in one direction

Table 7 – Strut shear range summary table due to friction

Arm Designation	Top Strut Shear (kip)	Middle Strut Shear (kip)	Bottom Strut Shear (kip)
Right Arm	0.74	1.96	2.12
Left Arm	1.18	2.56	3.22

Tabulated values correspond to the response induced by friction in one direction

Table 8 – Pin friction summary table

Test Run	Average Water Elevation during testing (ft)	Approximate Thrust at time of Testing (kips per arm)	Gate/Member Designation	Pin Friction Moment (kip-in)	Friction Coefficient
1	435.67	492.80	Right Pin	606.40	0.23
			Left Pin	869.30	0.33
2	435.67	492.80	Right Pin	592.80	0.22
			Left Pin	849.20	0.32
3	435.67	492.80	Right Pin	599.60	0.23
			Left Pin	852.90	0.32

Tabulated values correspond to the response induced by friction in one direction

Appendix A – Gate 7 Torque and Hoist Force Plots

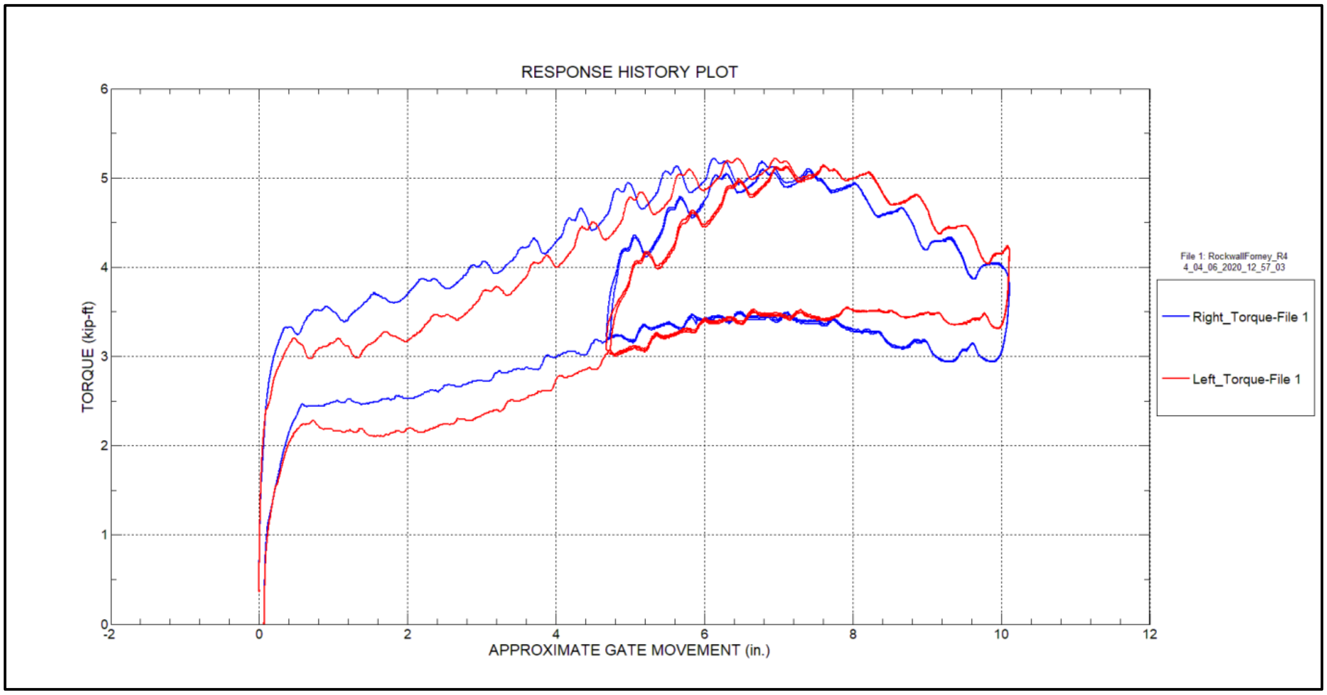

Figure 25 – Hoist torque response history – Gate 7 – Test 1

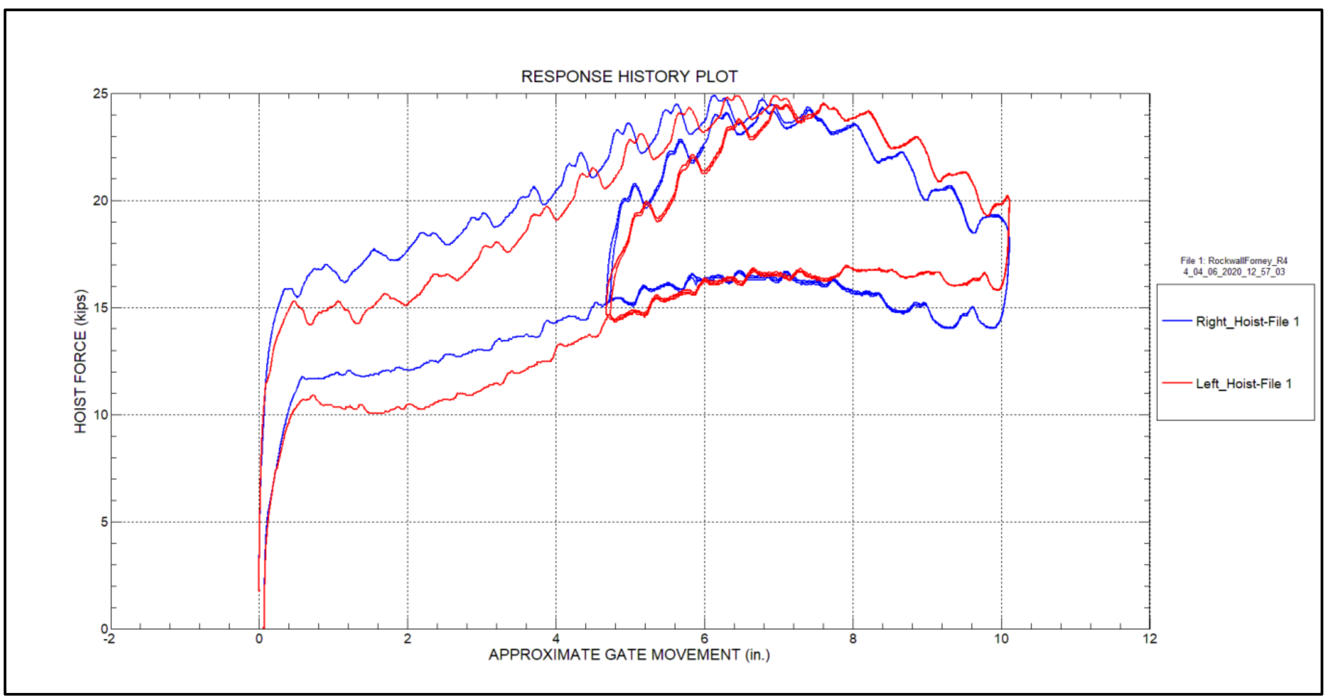

Figure 26 – Hoist force response history – Gate 7 – Test 1

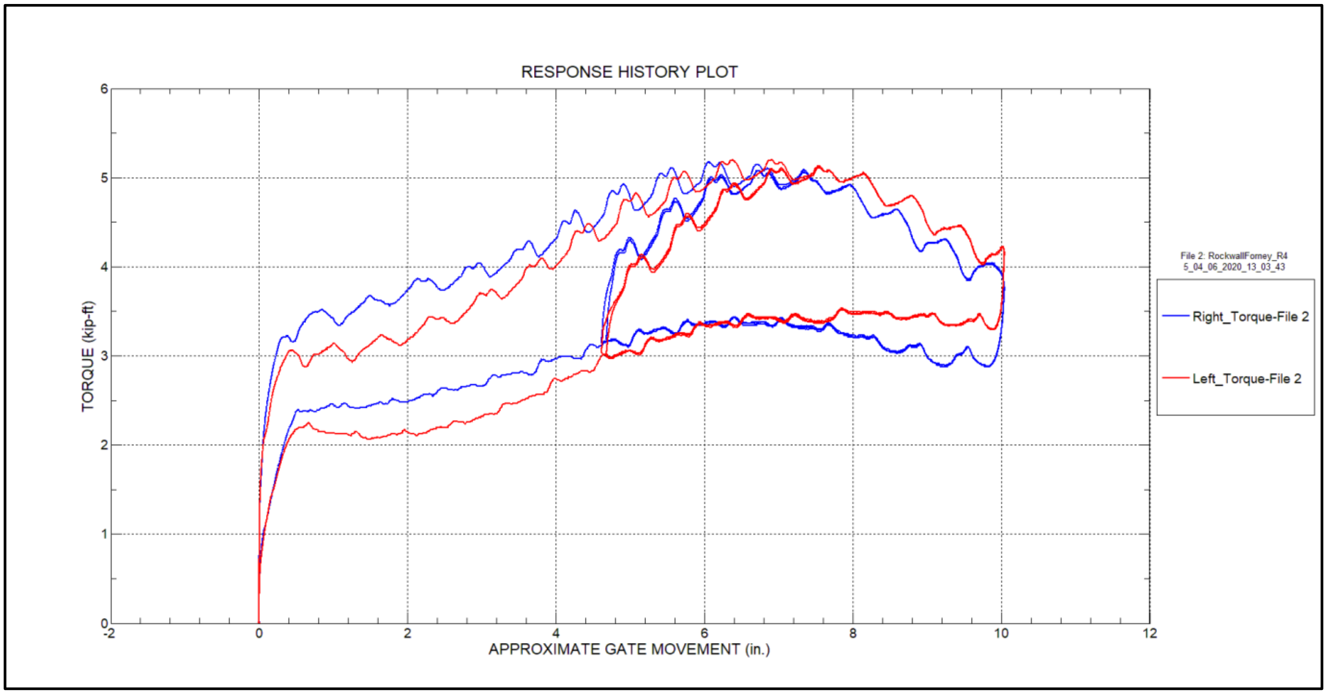

Figure 27 – Hoist torque response history – Gate 7 – Test 2

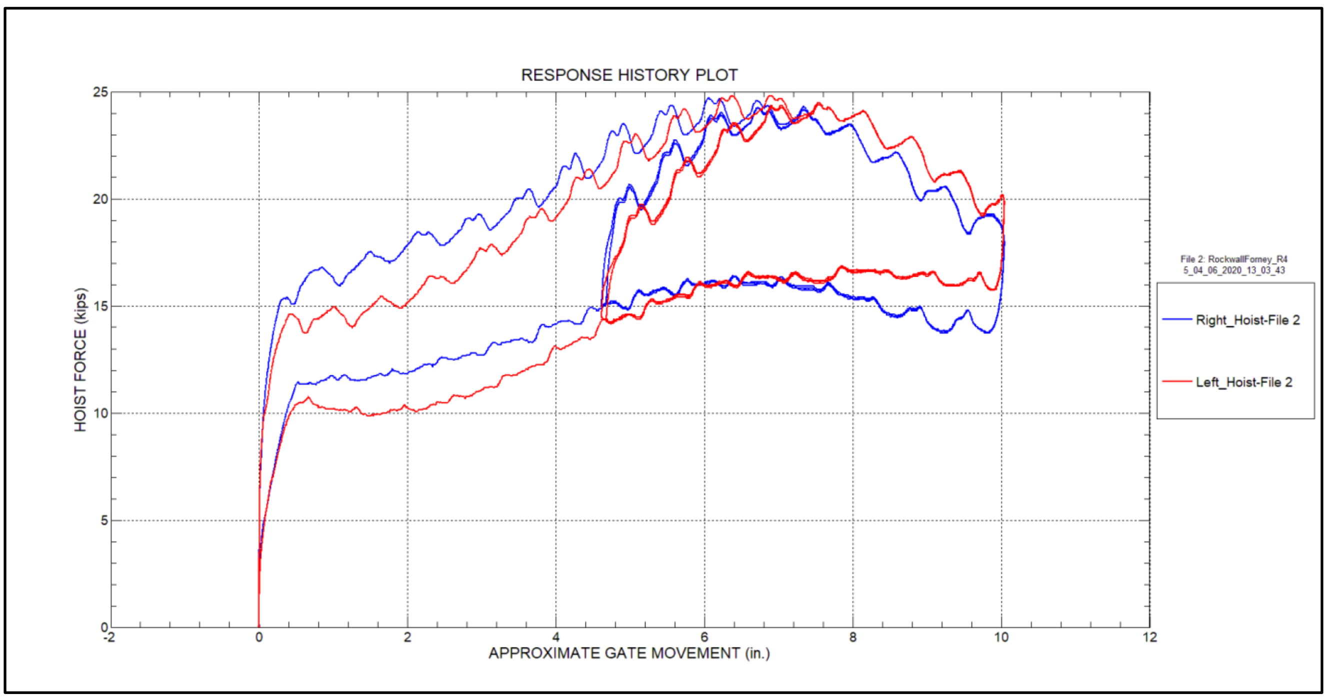

Figure 28 – Hoist force response history – Gate 7 – Test 2

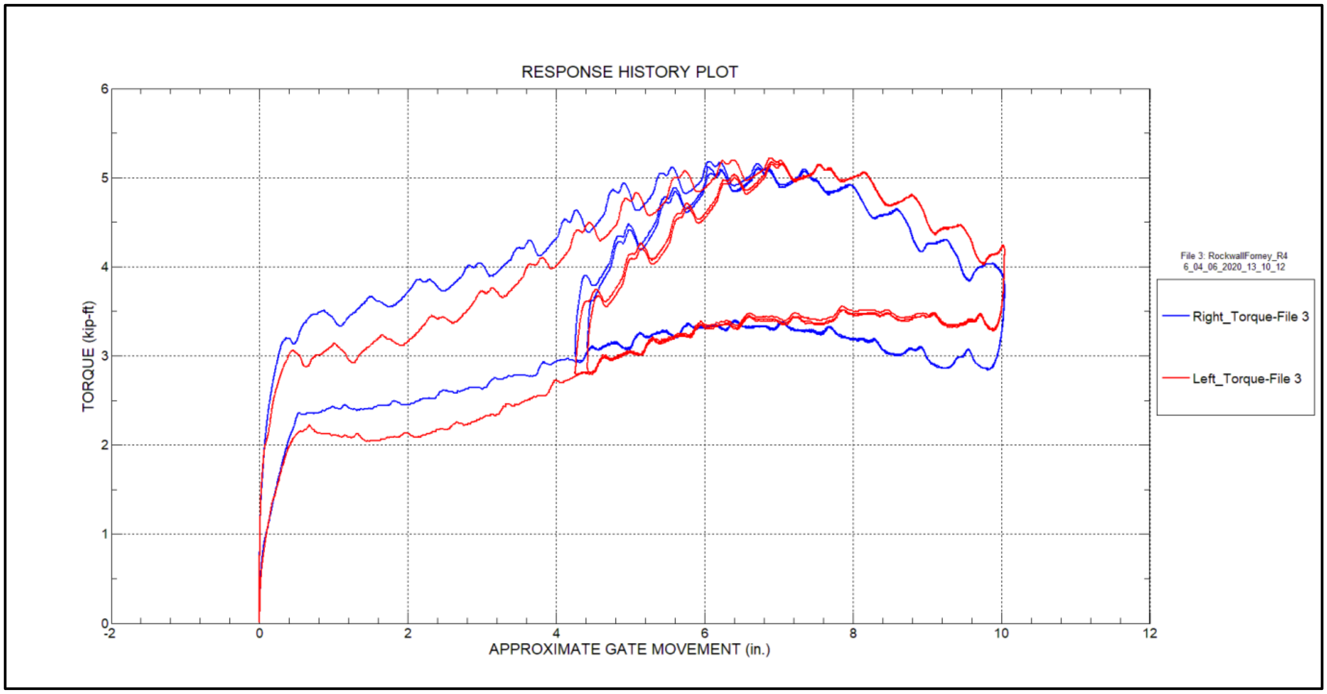

Figure 29 – Hoist torque response history – Gate 7 – Test 3

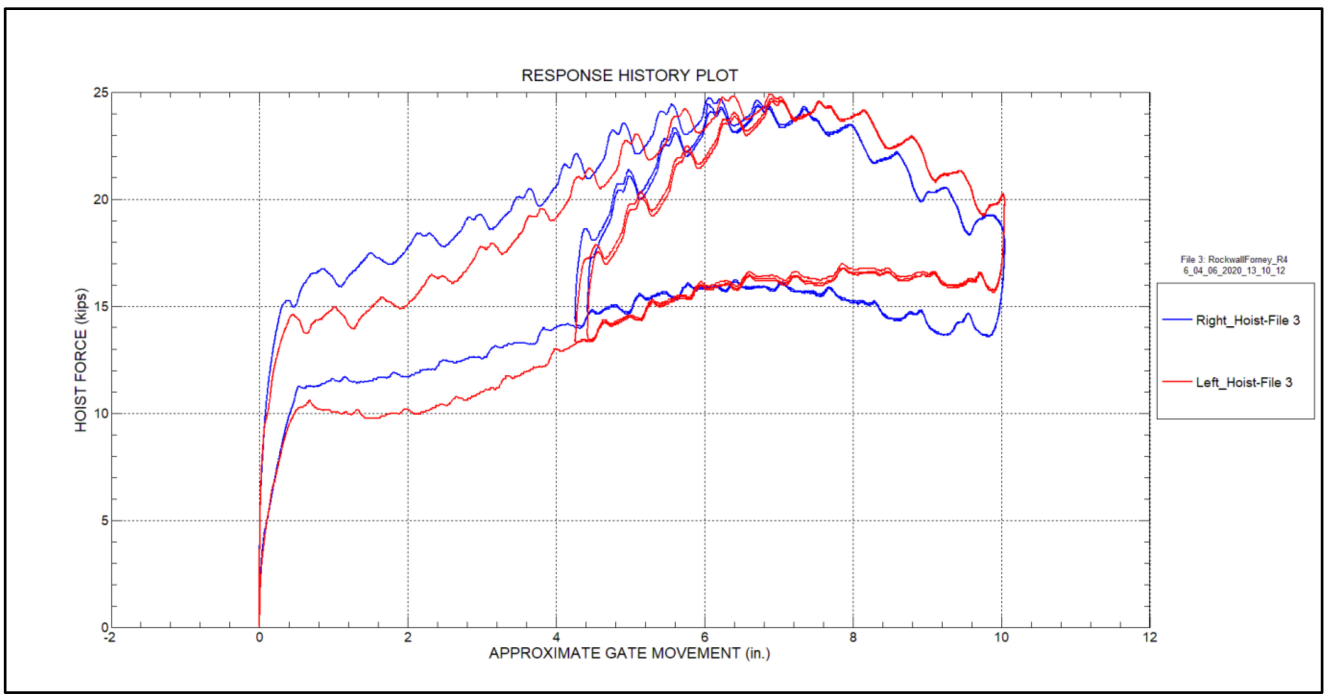

Figure 30 – Hoist force response history – Gate 7 – Test 3

Appendix B – Gate 7 Pin Moment Component Plots

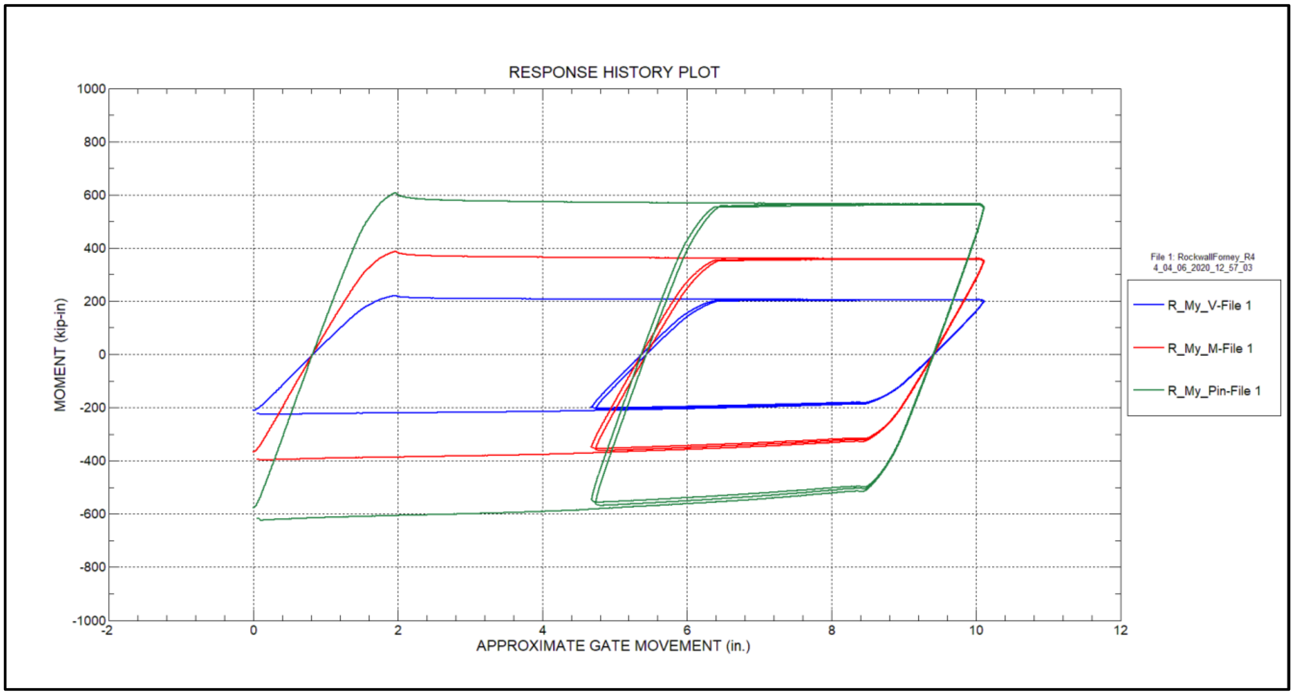

Figure 31 – Pin moment response history – Right arm – Test run 1

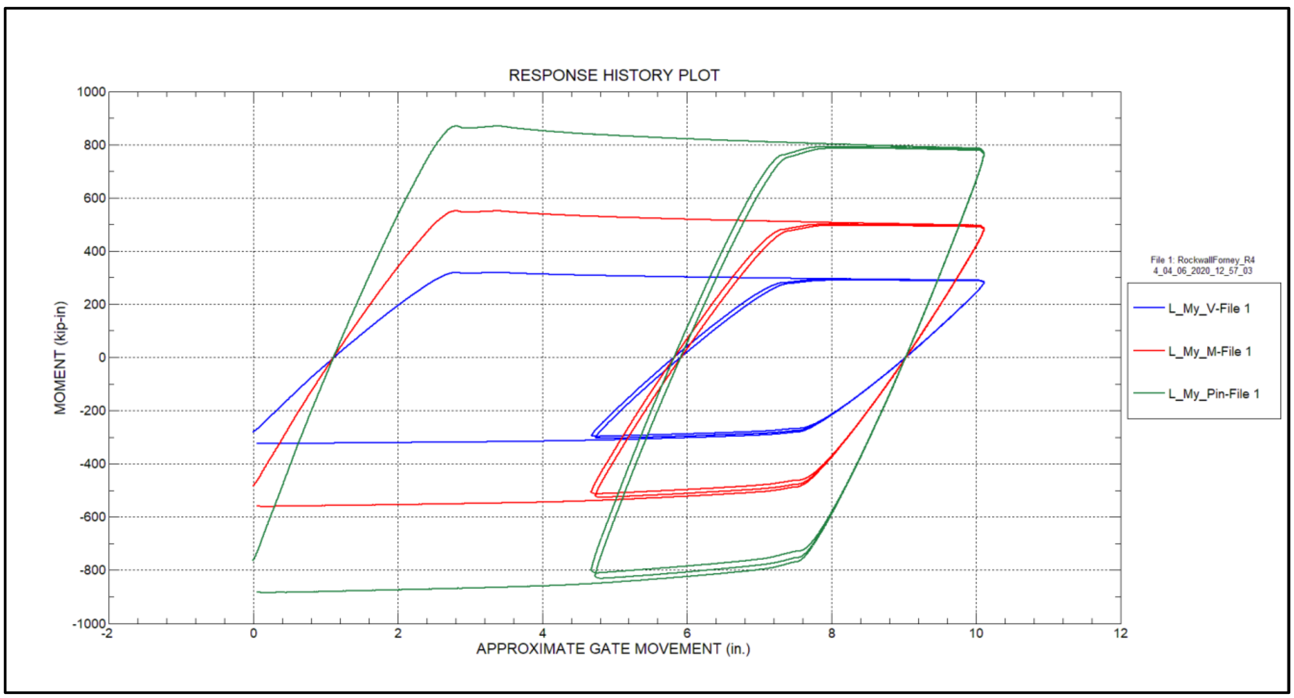

Figure 32 – Pin moment response history – Left arm – Test run 1

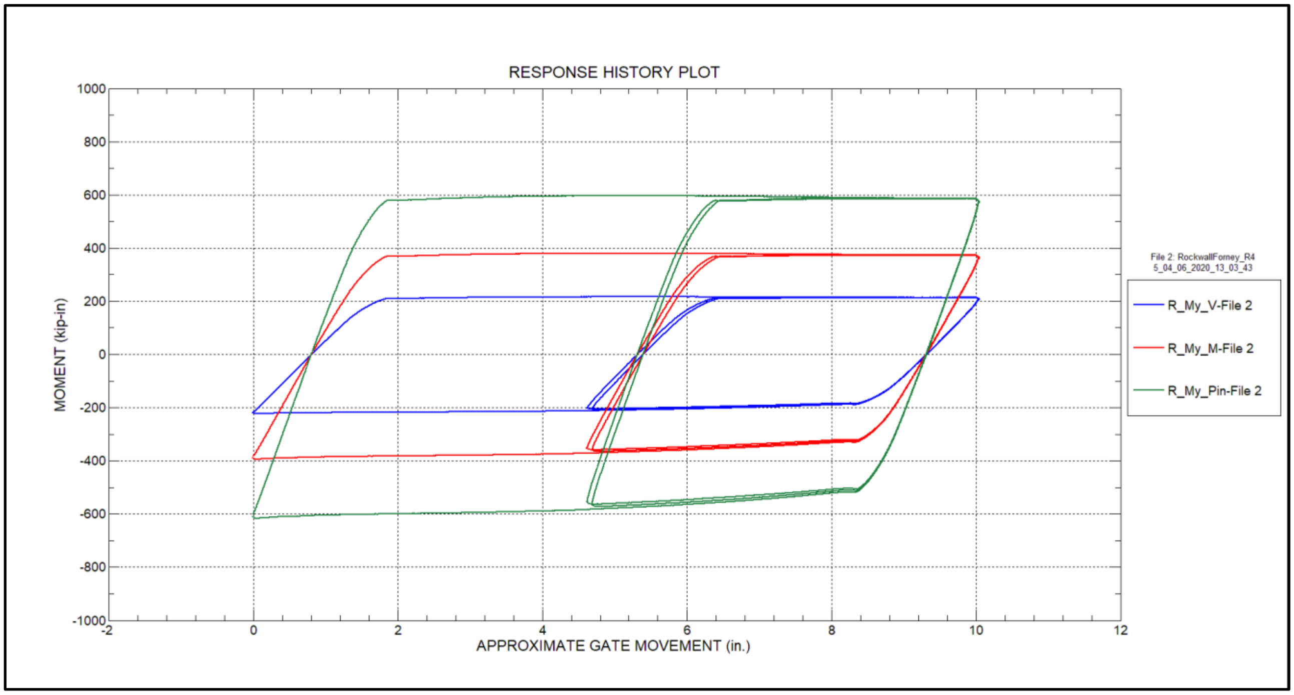

Figure 33 – Pin moment response history – Right arm – Test run 2

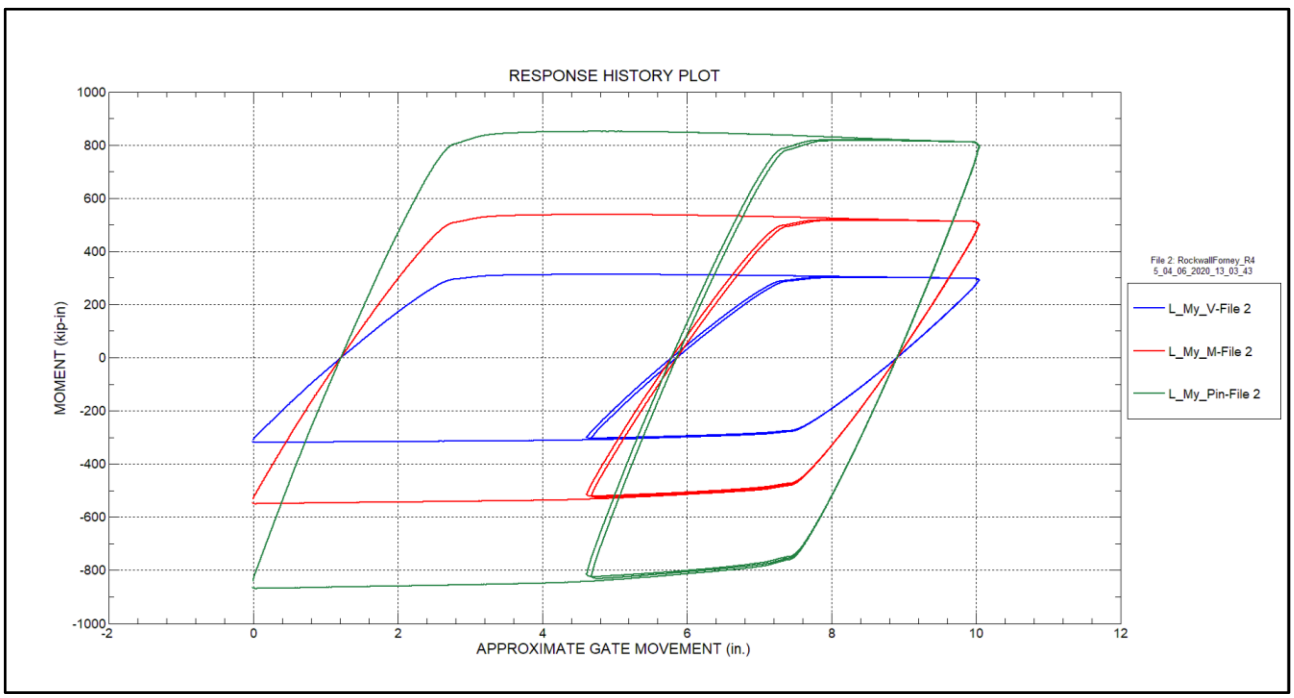

Figure 34 – Pin moment response history – Left arm – Test run 2

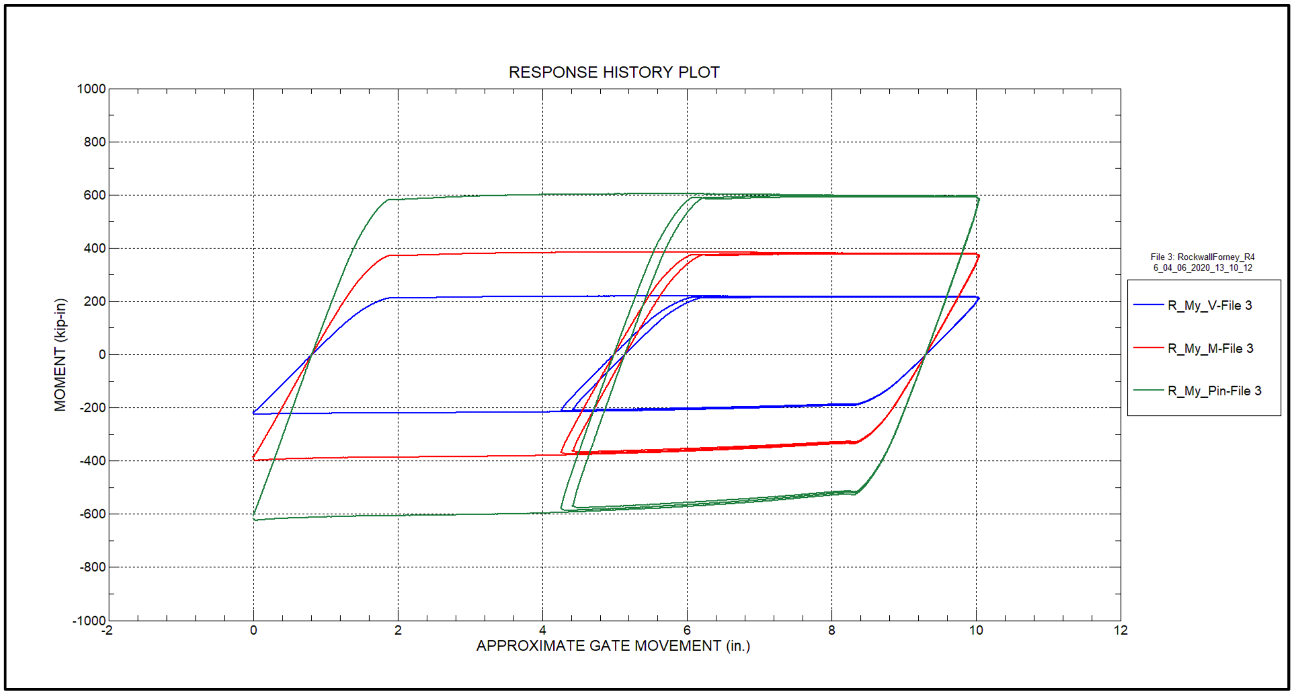

Figure 35 – Pin moment response history – Right arm – Test run 3

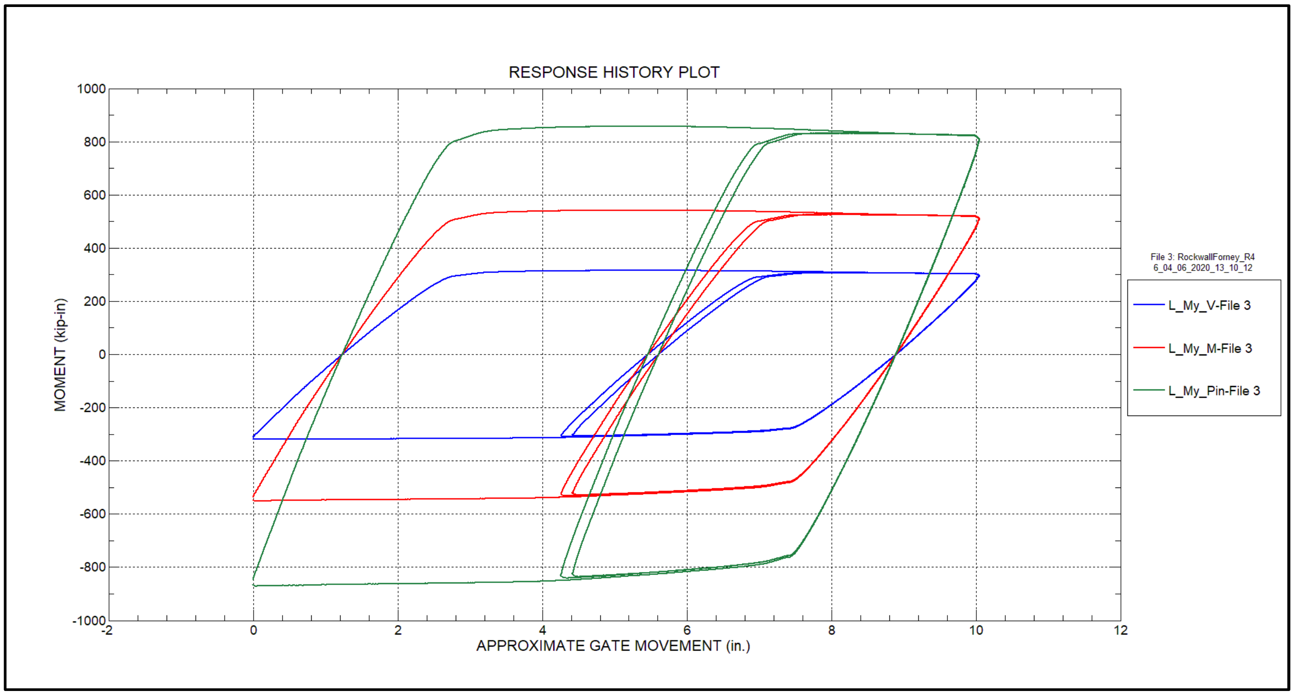

Figure 36 – Pin moment response history – Left arm – Test run 3

Appendix C – Instrumentation Plans

RAW DATA. REFINED RESULTS.

SCHNABEL ENGINEERING
ROCKWALL FORNEY DAM
LIVE LOAD TESTING

RAW DATA. REFINED RESULTS.
740 S PIERCE AVE, SUITE 15
LOUISVILLE, CO 80027
303.494.3230
WWW.BDITEST.COM

ISSUE

CLIENT

SCHABEL ENGINEERING
16000 CHRISTENSEN RD, STE 101
SEATTLE, WA 98188

PROJECT NAME

SCHNABEL ENGINEERING
ROCKWALL FORNEY DAM
LIVE LOAD TESTING

Drawn By:	KNR
Checked By:	JDS
Date:	05/27/2020
Client No.:	
BDI No.:	190701-TX
SCALE:	NTS

COVER PAGE

LLT-00

The user acknowledges that these documents are instruments of professional service, and are protected by Copyright. This document and the information contained in this document are the property of Bridge Diagnostics, Inc., and shall not be reused, copied, disseminated, modified, amended or altered in any way. It is issued for information purposes only. The user agrees to hold harmless, indemnify and defend Bridge Diagnostics, Inc. against any and all damages, claims and losses, including defense costs, arising out of any use, reuse or copying of this document.

PLOT TIME: 6/12/2020 3:22 PM
FILEPATH: C:\Users\colemand\BDI\Services - Documents\Server_Remote\190701-TX_Schnabel_RockwallForneyDam\7. Instrumentation Plans\BDI_ROCKWALLFORNEY_01_GENERAL.dwg
© YYYY BRIDGE DIAGNOSTICS INC.

The user acknowledges that these documents are instruments of professional service, and are protected by Copyright. This document and the information contained in this document are the property of Bridge Diagnostics, Inc., and shall not be reused, copied, disseminated, modified, amended or altered in any way. It is issued for information purposes only. The user agrees to hold harmless, indemnify and defend Bridge Diagnostics, Inc. against any and all damages, claims and losses, including defense costs, arising out of any use, reuse or copying of this document.

GAGE LEGEND & SPECIFICATION

SYMBOL	TYPE	BRAND	MODEL	NOTES
	STRAIN TRANSDUCER	BDI	ST350	
	TILTMETER (UNI-AXIAL)	BDI	T500-030	
	TORQUE SENSOR	HPI	-	HBWS-35-125-6-0.5VR-FB
	AMP SENSOR	CR MAGNETICS	CR42105-200	

GENERAL NOTES

- INSTRUMENTATION SHALL BEGIN ON APRIL 1ST, 2020.
- GATES 1 THRU 14 SHALL BE ACCESSED USING SPRAT ROPE ACCESS TECHNIQUES.
- BDI WILL PERFORM ALL SURFACE PREPARATION, SENSOR INSTALLATION, AND EQUIPMENT INSTALLATION.
- SEE LLT-31 FOR SENSOR INSTALLATION DETAILS.
- TWO PAIRS OF TORQUE GAGES WILL BE INSTALLED ON THE GATE MOTORS' PINION SHAFTS BETWEEN THE MOTORS AND THE HOISTS.
  - GAGE PAIRS WILL BE INSTALLED 180° APART FROM EACH OTHER.
  - EXACT POSITIONS OF THE GAGE PAIRS ON THE PINION SHAFT WILL BE DETERMINED IN THE FIELD.
- THREE PHASE AMPERAGE GAGES WILL BE INSTALLED ON THE MOTOR CONTROLS BY A QUALIFIED ELECTRICIAN PROVIDED BY GARVER.

TESTING PROCEDURE:

- TESTING SHALL BE STARTED WITH THE GATE IN THE CLOSED POSITION.
- ONCE DATA COLLECTION BEGINS, THE GATE SHALL BE RAISED TO TWO OR THREE TIMES THE HEIGHT NECESSARY FOR TRUNNION FRICTION TO BE OVERCOME, H1 (TYPICALLY 6"-12"), AND HELD THERE UNTIL DATA STABILIZES.
- THE GATE SHALL BE LOWERED APPROXIMATELY TWICE THE DISTANCE TO OVERCOME TRUNNION FRICTION, H2, AND HELD THERE UNTIL DATA STABILIZES.
- THE GATE SHALL BE RAISED TO H1 AND HELD THERE UNTIL DATA STABILIZES.
- THE GATE SHALL BE LOWERED TO H2 AND HELD THERE UNTIL DATA STABILIZES.
- THE GATE SHALL BE RAISED TO H1 AND HELD THERE UNTIL DATA STABILIZES.
- THE GATE WAS LOWERED BACK TO CLOSED POSITION AND DATA COLLECTION STOPPED.
- A MINIMUM OF 3 TESTS SHALL BE PERFORMED PER GATE.

GAGE COUNT PER GATE

SENSOR LEGEND	SENSOR COUNT	CHANNEL COUNT
STRAIN TRANSDUCER	(48)	(48)
TILTMETER (UNI-AXIAL)	(4)	(4)
TORQUE SENSOR	(4)	(4)
AMP SENSOR	(3)	(3)
TOTAL	(59)	(59)

LOCATION KEY

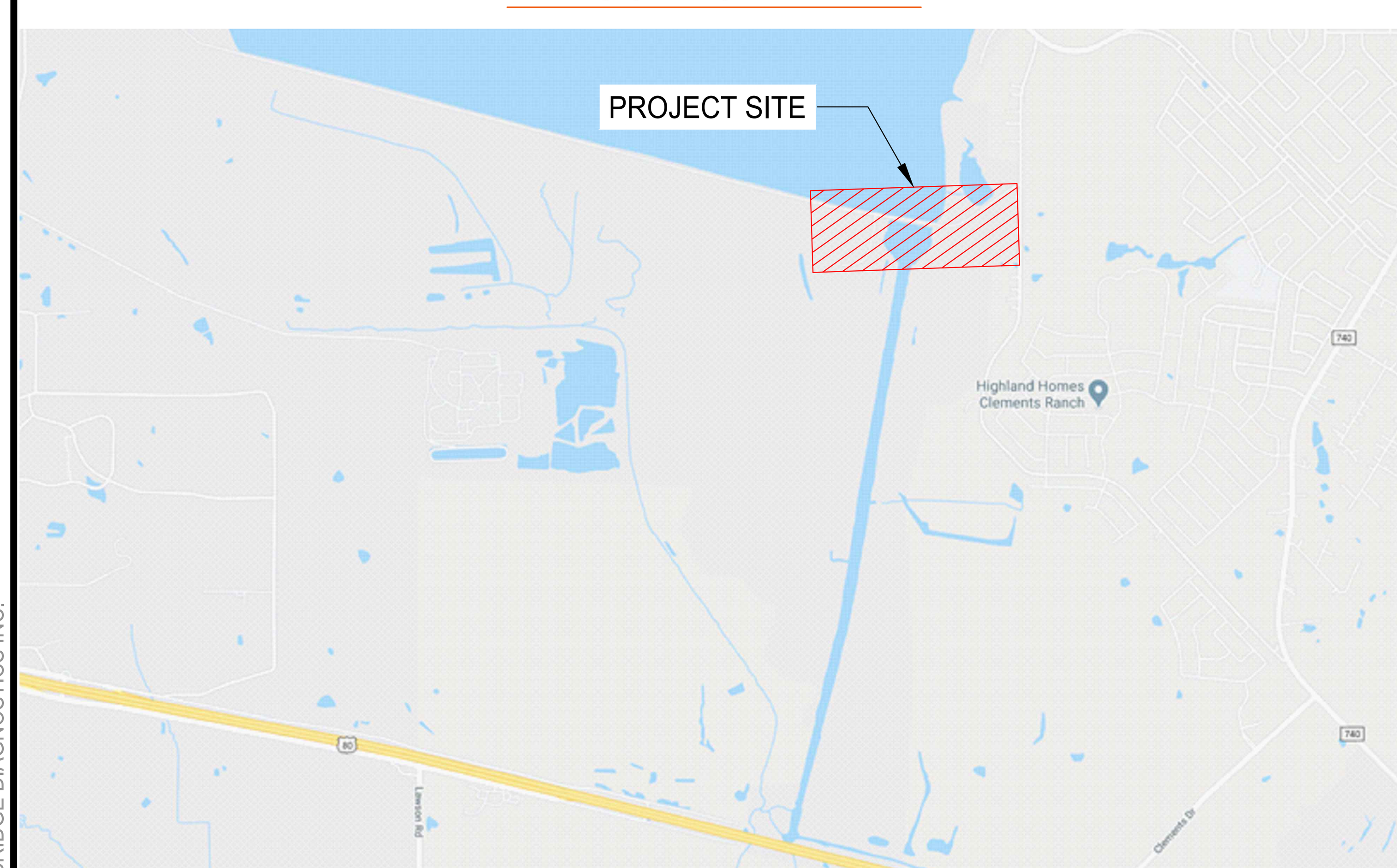

INDEX OF SHEETS

INDEX OF ISSUE

NO.	DATE	REVISION DESCRIPTION
1	3/20/2020	LIVE LOAD TESTING (LLT) INSTRUMENTATION PLAN (FOR APPROVAL)
2	5/27/2020	LIVE LOAD TESTING (LLT) INSTRUMENTATION PLAN AS BUILTS

BDI REFERENCE NUMBER: 190701-TX

RAW DATA. REFINED RESULTS.
740 S PIERCE AVE, SUITE 15
LOUISVILLE, CO 80027
303.494.3230
WWW.BDITEST.COM

ISSUE

CLIENT

SCHABEL ENGINEERING
16000 CHRISTENSEN RD, STE 101
SEATTLE, WA 98188

PROJECT NAME

SCHABEL ENGINEERING
ROCKWALL FORNEY DAM
LIVE LOAD TESTING

Drawn By:	KNR
Checked By:	JDS
Date:	05/27/2020
Client No.:	
BDI No.:	190701-TX
SCALE:	NTS

OVERALL LEGEND

LLT-01

PLOT TIME: 6/12/2020 3:22 PM
FILEPATH: C:\Users\colemand\BDI\Services - Documents\Server_Remote\190701-TX_Schnabel_RockwallForneyDam\7. Instrumentation Plans\BDI_ROCKWALLFORNEY_01_GENERAL.dwg
©YYYY BRIDGE DIAGNOSTICS INC.

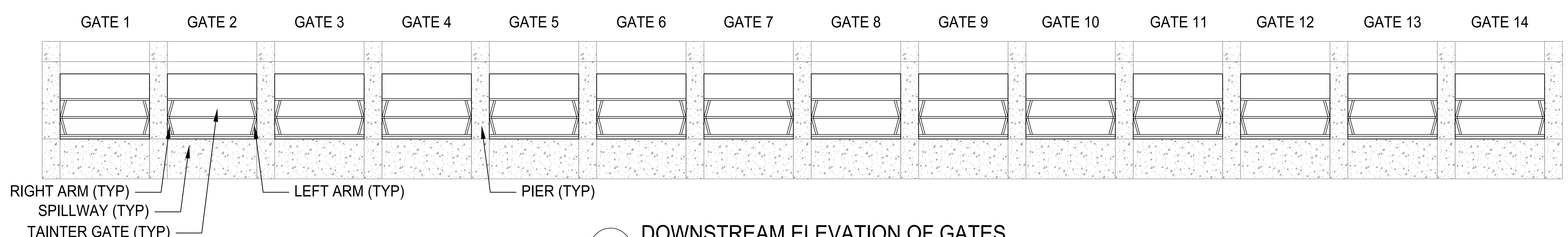

1 DOWNSTREAM ELEVATION OF GATES
LOOKING NORTH (UPSTREAM)

RAW DATA. REFINED RESULTS.
740 S PIERCE AVE, SUITE 15
LOUISVILLE, CO 80027
303.494.3230
WWW.BDITEST.COM

ISSUE

CLIENT

SCHABEL ENGINEERING
16000 CHRISTENSEN RD, STE 101
SEATTLE, WA 98188

PROJECT NAME

SCHNABEL ENGINEERING
ROCKWALL FORNEY DAM
LIVE LOAD TESTING

Drawn By:	KNR
Checked By:	JDS
Date:	05/27/2020
Client No.:	
BDI No.:	190701-TX
SCALE:	NTS

OVERALL STRUCTURE LAYOUT
LLT-02

The user acknowledges that these documents are instruments of professional service, and are protected by Copyright. This document and the information contained in this document are the property of Bridge Diagnostics, Inc., and shall not be reused, copied, disseminated, modified, amended or altered in any way. It is issued for information purposes only. The user agrees to hold harmless, indemnify and defend Bridge Diagnostics, Inc. against any and all damages, claims and losses, including defense costs, arising out of any use, reuse or copying of this document.

PLOT TIME: 6/12/2020 3:22 PM
FILEPATH: C:\Users\colemand\BDI\Services - Documents\Server_Remote\190701-TX_Schnabel_RockwallForneyDam\7. Instrumentation Plans\BDI_ROCKWALLFORNEY_01_GENERAL.dwg
© YYYY BRIDGE DIAGNOSTICS INC.

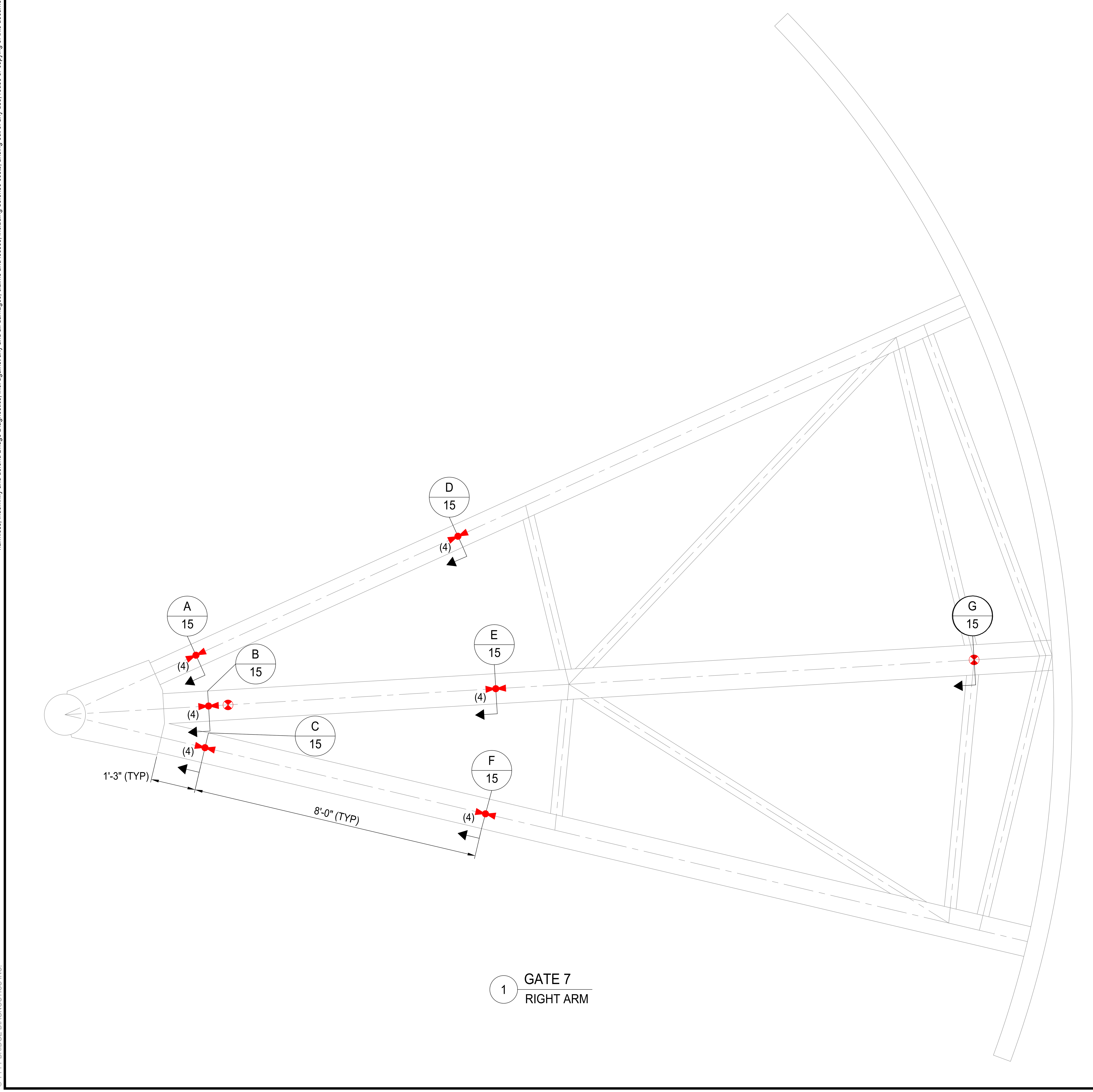

GATE 7
RIGHT ARM

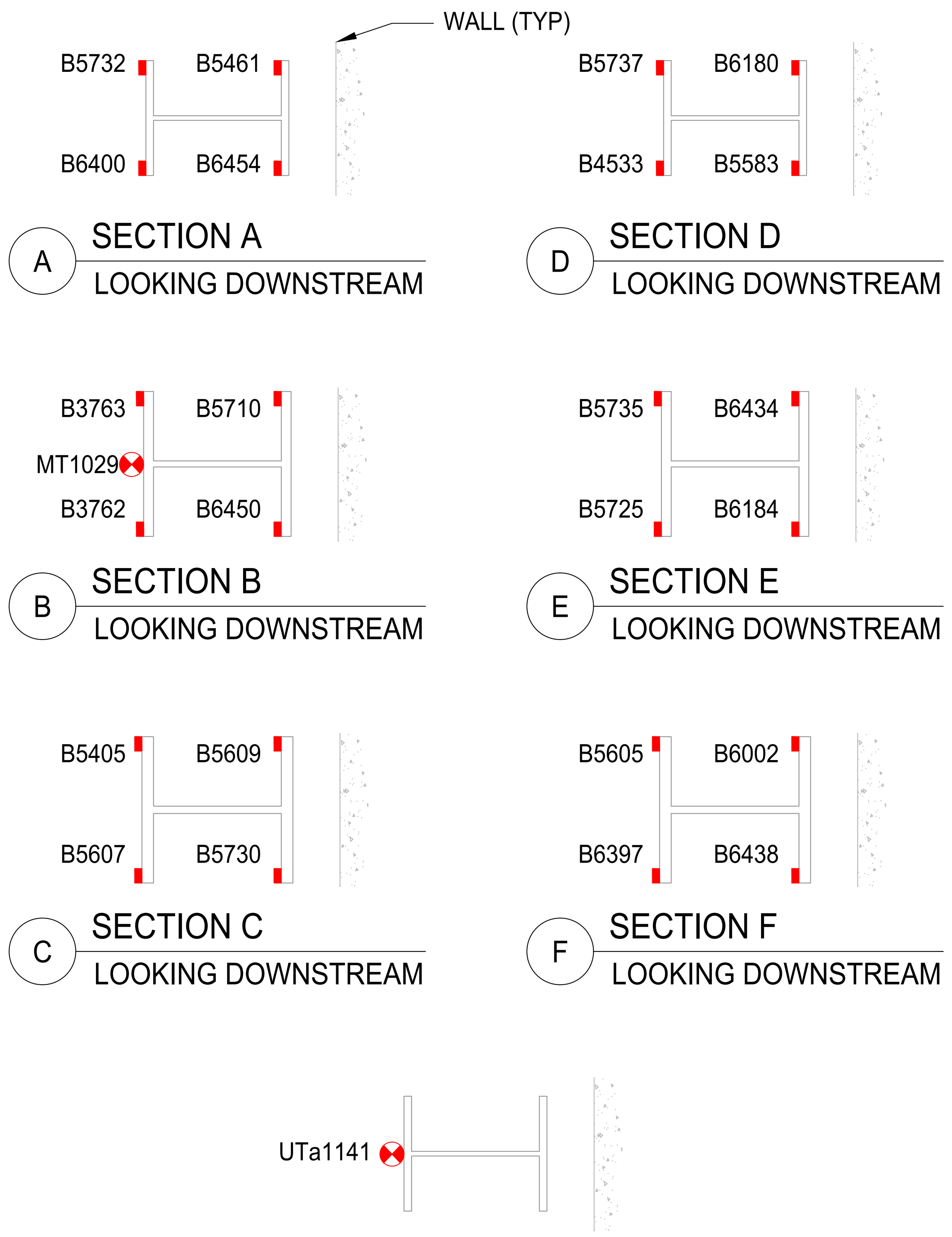

A SECTION A
LOOKING DOWNSTREAM

D SECTION D
LOOKING DOWNSTREAM

B SECTION B
LOOKING DOWNSTREAM

E SECTION E
LOOKING DOWNSTREAM

C SECTION C
LOOKING DOWNSTREAM

F SECTION F
LOOKING DOWNSTREAM

G SECTION G
LOOKING DOWNSTREAM

UNIT ID
TT-3

TORQUE GAGES
RIGHT ARM

NOTES:
1. SECTIONS A, B, & C SHALL BE INSTALLED 15 INCHES AWAY FROM TRUNNION PLATE.
2. TILTMETERS SHALL BE INSTALLED CENTERED ON THE MIDDLE STRUT FLANGE.
3. SECTION G'S TILTMETER SHALL BE INSTALLED AS CLOSE TO THE SKINPLATE AS POSSIBLE.

SENSOR LEGEND
- STRAIN TRANSDUCER
- TILTMETER (UNI-AXIAL)
- TORQUE SENSOR

BDI
RAW DATA. REFINED RESULTS.
740 S PIERCE AVE, SUITE 15
LOUISVILLE, CO 80027
303.494.3230
WWW.BDITEST.COM

ISSUE

CLIENT
SCHABEL ENGINEERING
16000 CHRISTENSEN RD, STE 101
SEATTLE, WA 98188

PROJECT NAME
SCHABEL ENGINEERING
ROCKWALL FORNEY DAM
LIVE LOAD TESTING

Drawn By:	KNR
Checked By:	JDS
Date:	05/27/2020
Client No.:	
BDI No.:	190701-TX
SCALE:	NTS

GATE 7 - RIGHT ARM
ELEVATION
LLT-15

The user acknowledges that these documents are instruments of professional service, and are protected by Copyright. This document and the information contained in this document are the property of Bridge Diagnostics, Inc., and shall not be reused, copied, disseminated, modified, amended or altered in any way. It is issued for information purposes only. The user agrees to hold harmless, indemnify and defend Bridge Diagnostics, Inc. against any and all damages, claims and losses, including defense costs, arising out of any use, reuse or copying of this document.

PLOT TIME: 6/12/2020 3:23 PM
FILEPATH: C:\Users\colemand\BDI\Services - Documents\Server_Remote\190701-TX_Schabel_RockwallForneyDam\7. Instrumentation Plans\BDI_ROCKWALLFORNEY_01_GENERAL.dwg
© YYYY BRIDGE DIAGNOSTICS INC.

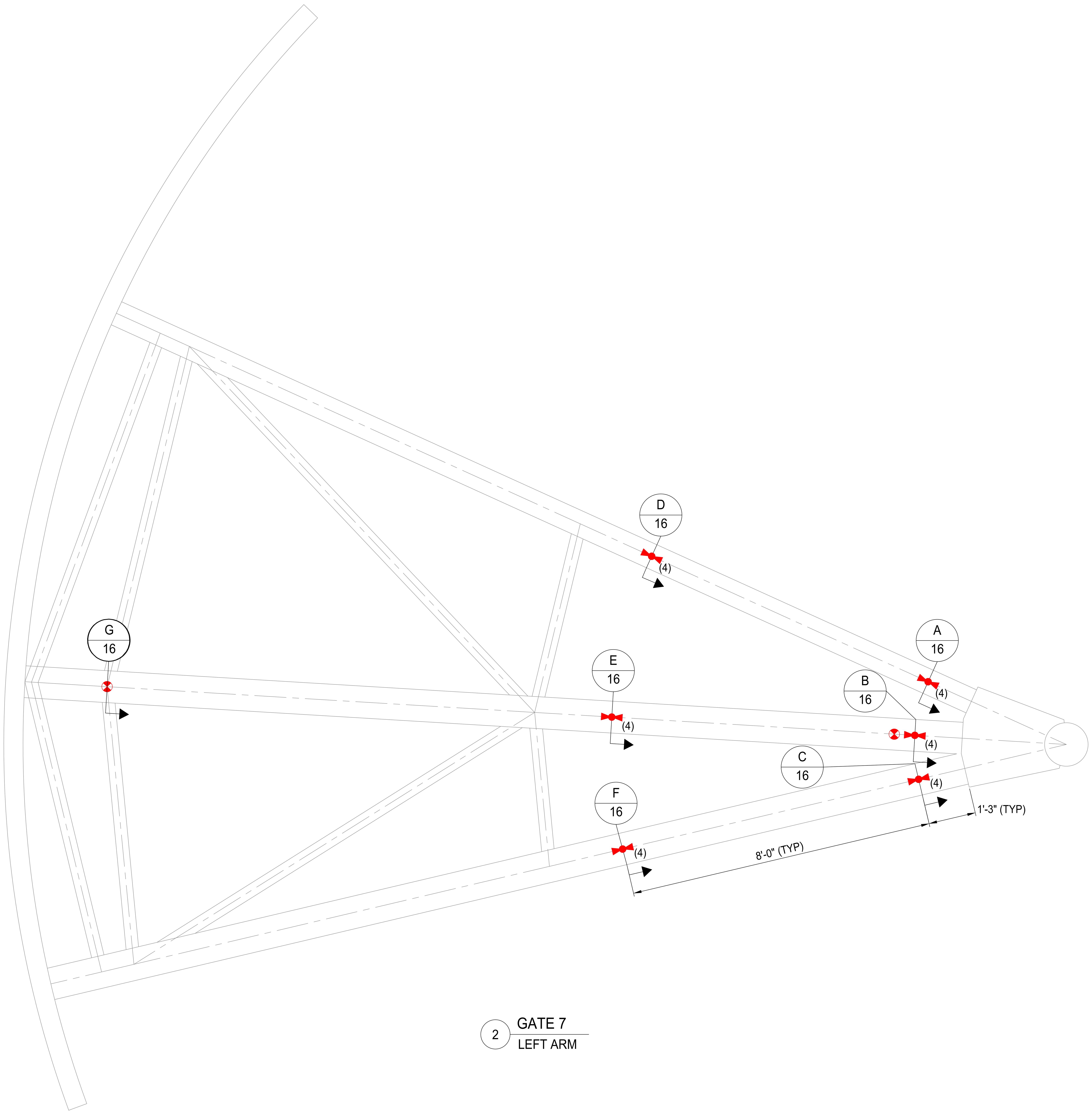

2 GATE 7
LEFT ARM

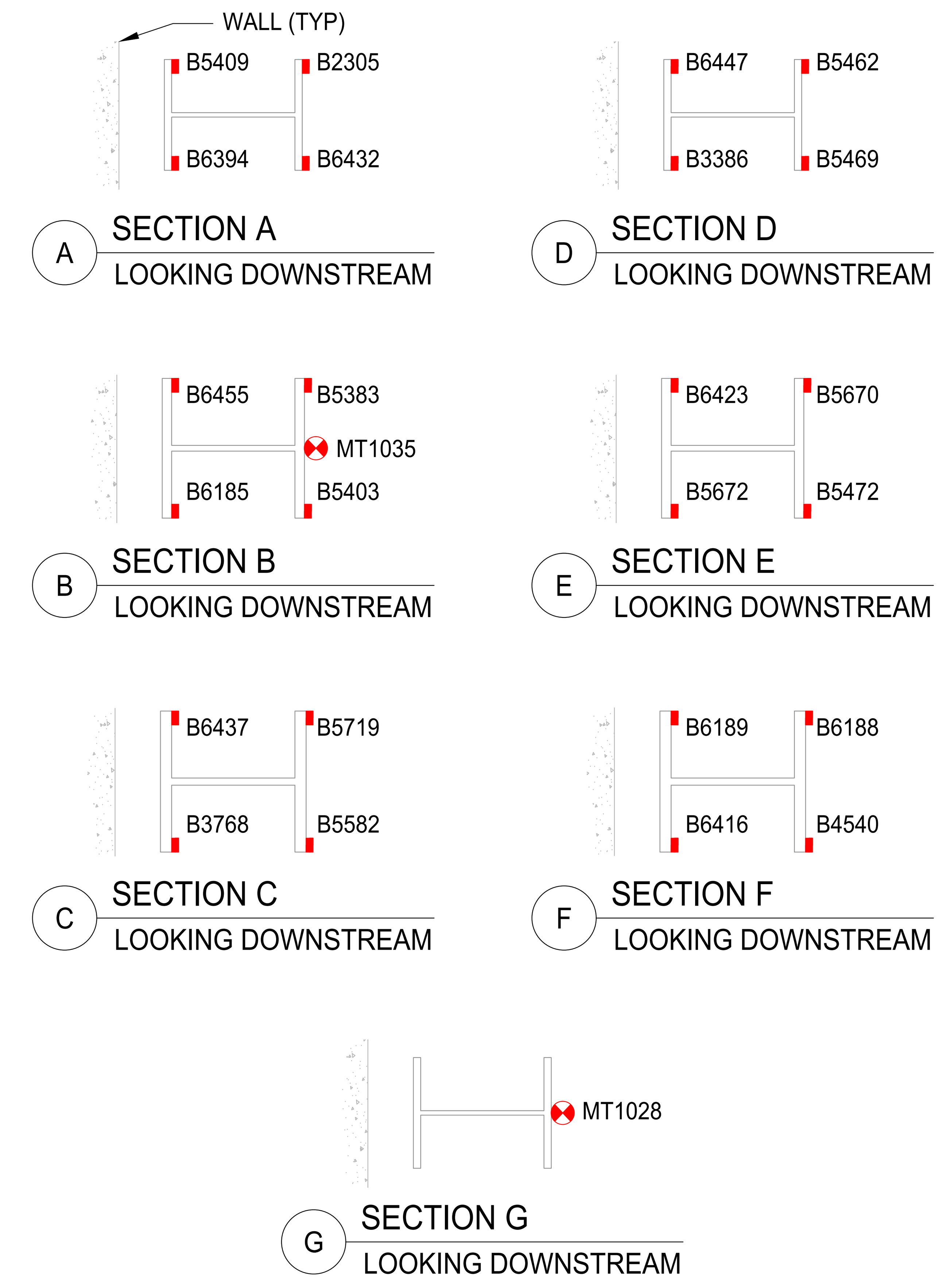

UNIT ID
TT-4

TORQUE GAGES
LEFT ARM

NOTES:

1. SECTIONS A, B, & C SHALL BE INSTALLED 15 INCHES AWAY FROM TRUNNION PLATE.
2. TILTMETERS SHALL BE INSTALLED CENTERED ON THE MIDDLE STRUT FLANGE.
3. SECTION G'S TILTMETER SHALL BE INSTALLED AS CLOSE TO THE SKINPLATE AS POSSIBLE.

SENSOR LEGEND

- STRAIN TRANSDUCER
- TILTMETER (UNI-AXIAL)
- TORQUE SENSOR

BDI
RAW DATA. REFINED RESULTS.
740 S PIERCE AVE, SUITE 15
LOUISVILLE, CO 80027
303.494.3230
WWW.BDITEST.COM

ISSUE

CLIENT

SCHABEL ENGINEERING
16000 CHRISTENSEN RD, STE 101
SEATTLE, WA 98188

PROJECT NAME

SCHABEL ENGINEERING
ROCKWALL FORNEY DAM
LIVE LOAD TESTING

Drawn By:	KNR
Checked By:	JDS
Date:	05/27/2020
Client No.:	
BDI No.:	190701-TX
SCALE:	NTS

GATE 7 - LEFT ARM
ELEVATION
LLT-16

The user acknowledges that these documents are instruments of professional service, and are protected by Copyright. This document and the information contained in this document are the property of Bridge Diagnostics, Inc., and shall not be reused, copied, disseminated, modified, amended or altered in any way. It is issued for information purposes only. The user agrees to hold harmless, indemnify and defend Bridge Diagnostics, Inc. against any and all damages, claims and losses, including defense costs, arising out of any use, reuse or copying of this document.

PLOT TIME: 6/12/2020 3:23 PM
FILEPATH: C:\Users\colemand\BDI\Services - Documents\Server_Remote\190701-TX_Schabel_RockwallForneyDam\7. Instrumentation Plans\BDI_ROCKWALLFORNEY_01_GENERAL.dwg
© YYYY BRIDGE DIAGNOSTICS INC.

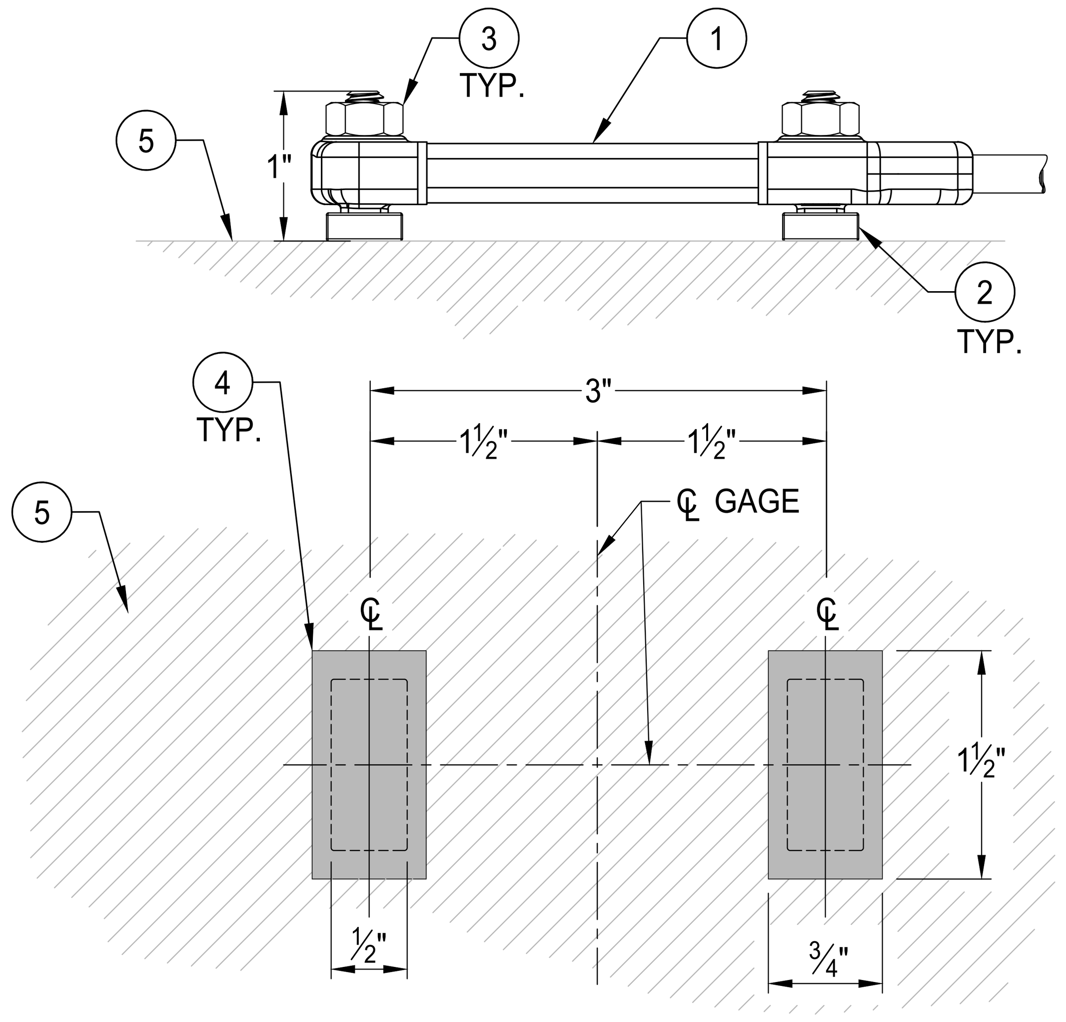

COMPONENT DESCRIPTION

1. ST350 STRAIN GAGE
2. 1/4"-20 THREADED MOUNTING TAB
3. 1/4"-20 STAINLESS STEEL NUT
4. TYPICAL SURFACE PREP REQUIRED TO MOUNT STRAIN GAGES
5. TYPICAL MOUNTING SURFACE

FOOTNOTES - INSTANT ADHESIVE
1. STRAIN GAGES SHALL BE MOUNTED WITH LOCTITE 410 INSTANT ADHESIVE AND LOCTITE 7452 ACCELERANT 2. DURING SURFACE PREP ALL PAINT AND SURFACE DEFORMATIONS MUST BE REMOVED. 3. SURFACE PREP IS REQUIRED JUST PRIOR TO GAGE INSTALLATION AS TO NOT ALLOW SURFACE CONTAMINANTS TO ACCUMULATE.

1 TYPICAL ST350 STRAIN GAGE INSTALLATION

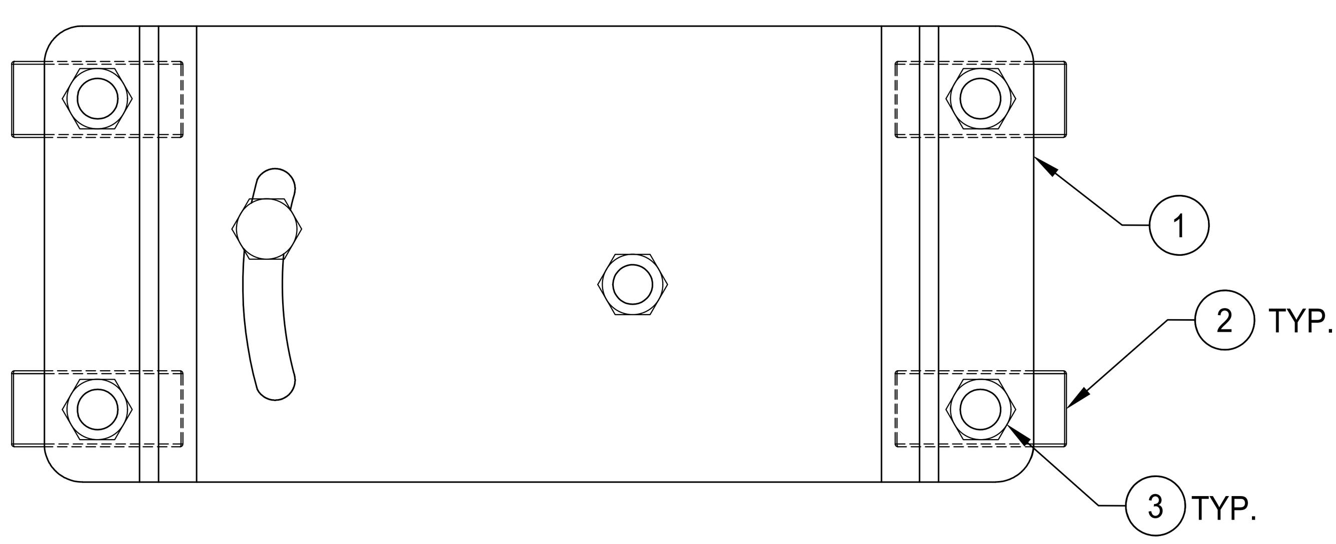

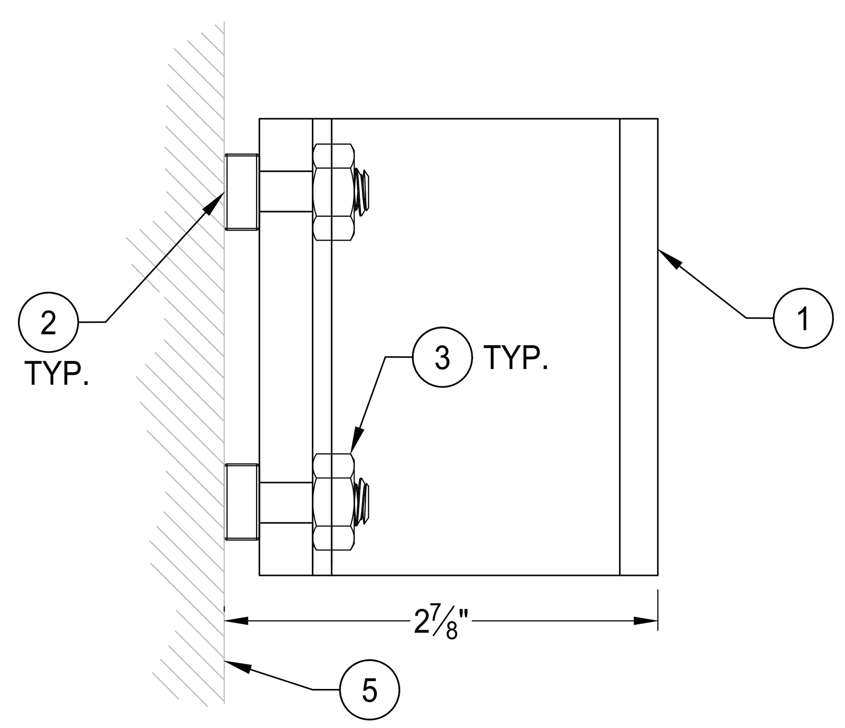

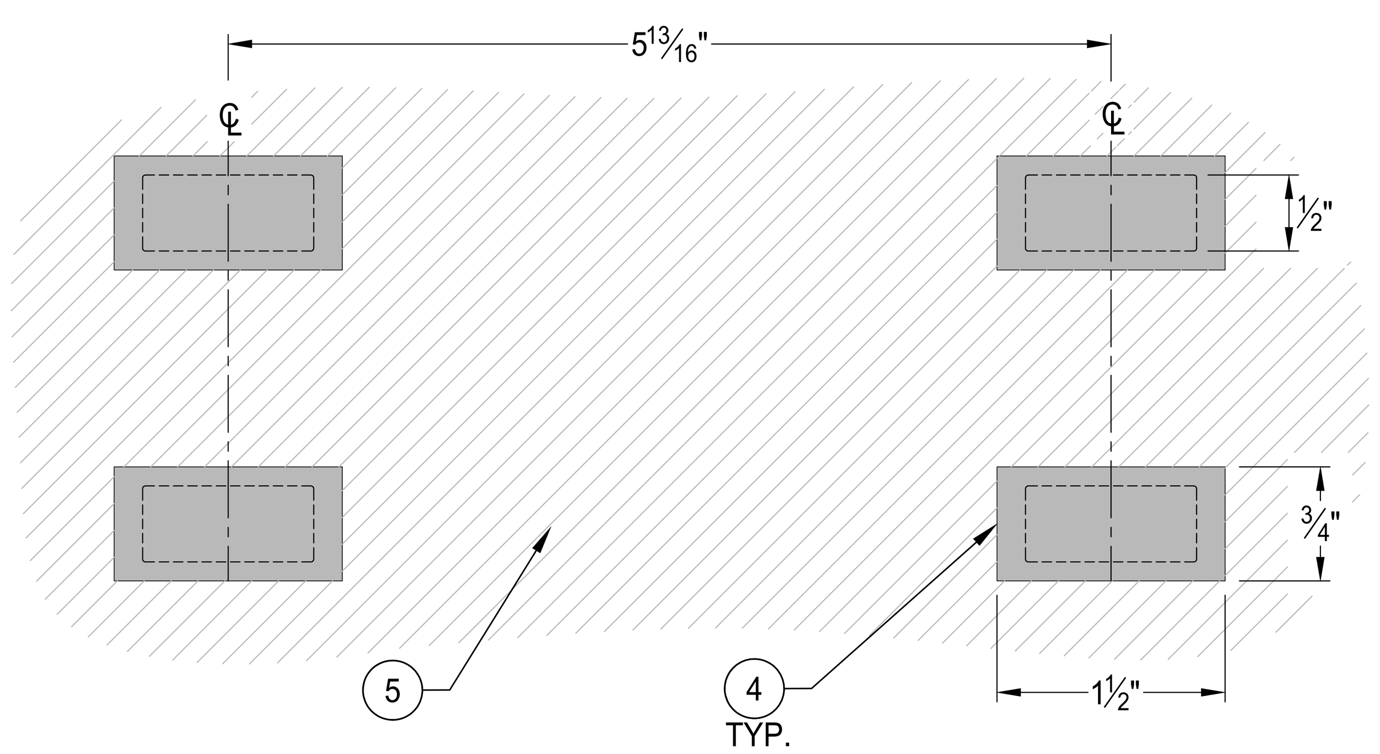

COMPONENT DESCRIPTION

1. BDI +/- 15 DEGREE TILTMETER WITH COVER AND ADJUSTMENT BOLTS
2. 1/4"-20 THREADED MOUNTING TAB
3. 1/4"-20 STAINLESS STEEL NUT
4. TYPICAL SURFACE PREP REQUIRED TO MOUNT TILTMETERS
5. TYPICAL MOUNTING SURFACE

FOOTNOTES - INSTANT ADHESIVE
1. TILTMETERS SHALL BE MOUNTED WITH LOCTITE 410 INSTANT ADHESIVE AND LOCTITE 7452 ACCELERANT 2. DURING SURFACE PREP ALL PAINT AND SURFACE DEFORMATIONS MUST BE REMOVED. 3. SURFACE PREP IS REQUIRED JUST PRIOR TO GAGE INSTALLATION AS TO NOT ALLOW SURFACE CONTAMINANTS TO ACCUMULATE.

2 TYPICAL BDI TILTMETER INSTALLATION

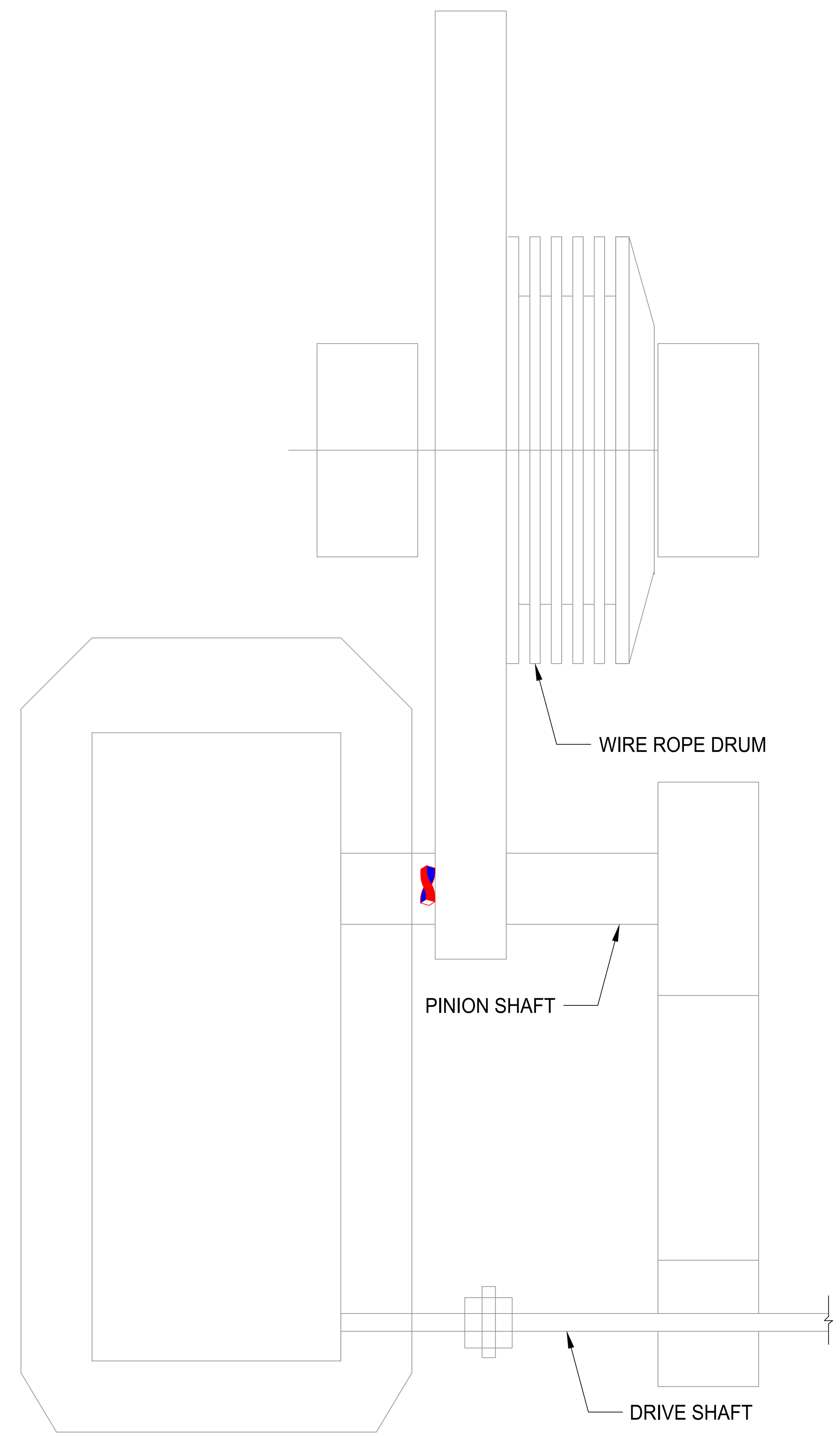

3 TYPICAL HOIST INSTRUMENTATION

TORQUE SENSOR INSTALLATION NOTES:

- TORQUE GAGES WILL BE INSTALLED ON THE PINION SHAFT ON EITHER HOIST MOTOR BETWEEN THE MOTOR AND THE HOIST DRUM
- EXACT POSITIONS OF THE GAGE PAIRS ON THE PINION SHAFT WILL BE DETERMINED IN THE FIELD

SENSOR LEGEND

TORQUE SENSOR

BDI
RAW DATA. REFINED RESULTS.
740 S PIERCE AVE, SUITE 15
LOUISVILLE, CO 80027
303.494.3230
WWW.BDITEST.COM

ISSUE

CLIENT

SCHABEL ENGINEERING
16000 CHRISTENSEN RD, STE 101
SEATTLE, WA 98188

PROJECT NAME

SCHNABEL ENGINEERING
ROCKWALL FORNEY DAM
LIVE LOAD TESTING

Drawn By:	KNR
Checked By:	JDS
Date:	05/27/2020
Client No.:	
BDI No.:	190701-TX
SCALE:	NTS

SENSOR INSTALLATION DETAILS

LLT-31

The user acknowledges that these documents are instruments of professional service, and are protected by Copyright. This document and the information contained in this document are the property of Bridge Diagnostics, Inc., and shall not be reused, copied, disseminated, modified, amended or altered in any way. It is issued for information purposes only. The user agrees to hold harmless, indemnify and defend Bridge Diagnostics, Inc. against any and all damages, claims and losses, including defense costs, arising out of any use, reuse or copying of this document.

PLOT TIME: 6/12/2020 3:24 PM
FILEPATH: C:\Users\colemand\BDI\Services - Documents\Server_Remote\190701-TX_Schnabel_RockwallForneyDam\7. Instrumentation Plans\BDI_ROCKWALLFORNEY_01_GENERAL.dwg
© YYYY BRIDGE DIAGNOSTICS INC.

SCHNABEL ENGINEERING

TRUNNION PIN FRICTION TESTING REPORT

ROCKWALL FORNEY DAM – GATE 8
FORNEY, TX

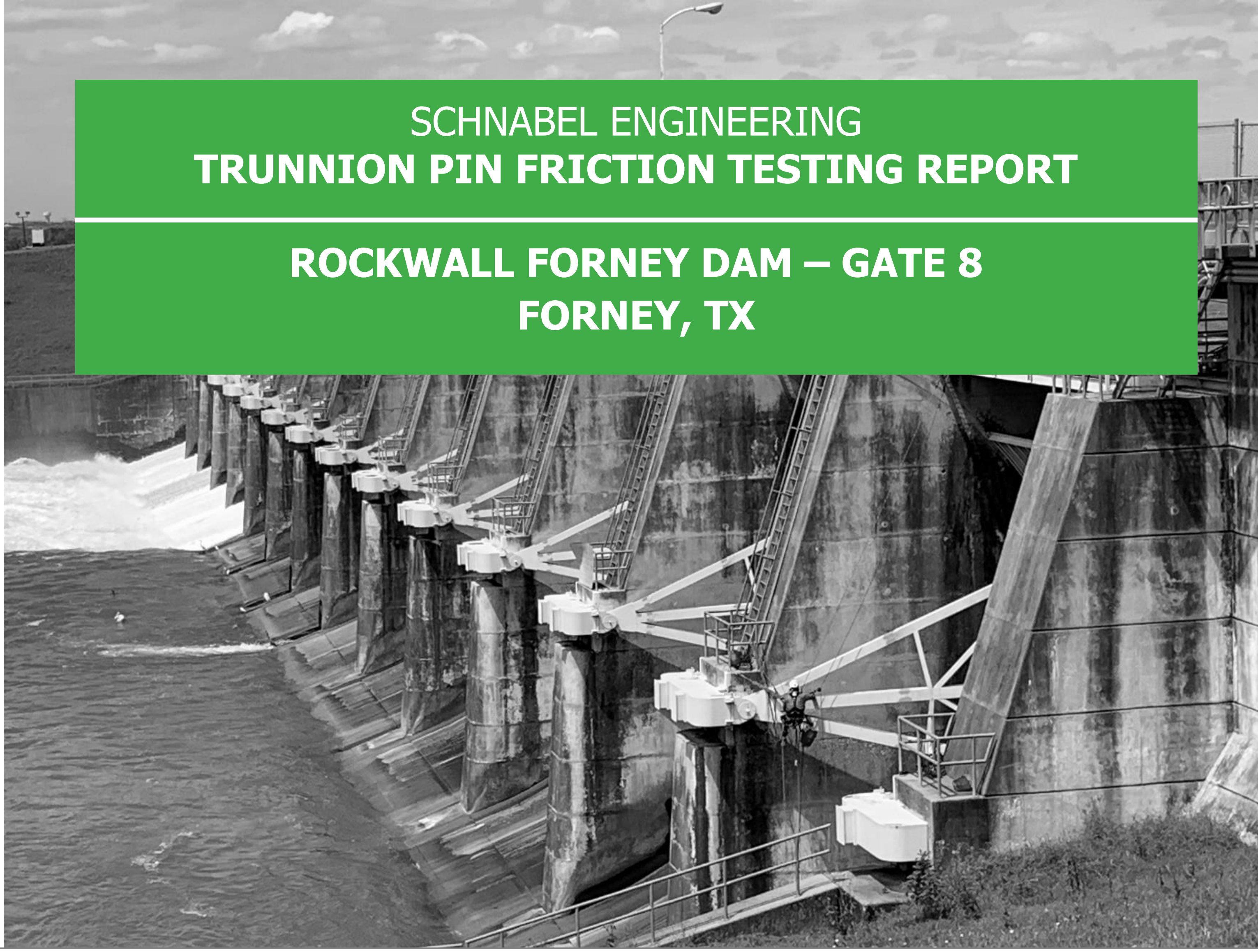

SUBMITTED TO:
SCHNABEL ENGINEERING
16000 CHRISTENSEN RD, SUITE 101
SEATTLE, WA 98188

SUBMITTED BY:
BDI – CO
740 SOUTH PIERCE AVE, UNIT 15
LOUISVILLE, CO 80027

BDI Project No.: **190701-TX**
Report Version: **V1**
Version Submitted: **August 26, 2020**

RAW DATA. REFINED RESULTS.

This document contains Confidential Information and is submitted in confidence to the customer. The submission of the information contained herein shall not be deemed to constitute public disclosure or authorization for disclosure to other parties. BDI's information and name may not be used in advertising or for promotional purposes without BDI's written consent.

TABLE OF CONTENTS

LIST OF FIGURES

LIST OF TABLES

Executive Summary

Schnabel Engineering contracted BDI to provide instrumentation and testing services on Gates 1-14 on the Rockwall Forney Dam near Dallas, Texas. The goal of these tests was to record each gate's structural responses during a series of spill tests and use the data to compute accurate coefficients of friction for each trunnion pin, cable lift force, total gate friction, and motor amperage. This report provides details on the work performed on Gate 8.

Instrumentation and testing were performed on Gate 8 at the Rockwall Forney Dam on April 7th, 2020. The gate arms were instrumented with strain and rotation sensors. The hoist motors' pinion shafts were instrumented with torque sensors and the hoist motor controls were instrumented with amperage sensors. Following the instrumentation, a series of spill tests were performed to measure the structural responses resulting from trunnion pin friction. All instrumentation setup and removal were performed using BDI's rope access team.

Following demobilization from the field, the test data was examined for quality and then further processed to evaluate the gate's performance. Strain measurements were converted into bending forces which were then applied to pin-strut free-body diagrams. By summing forces at each pin, friction induced moments could be computed, allowing accurate friction coefficients to be determined. Generally, the observed gate behavior showed that Gate 8 was operating as expected with no major signs of distress.

The resulting maximum trunnion friction coefficients and corresponding hoist forces are shown in Table 1.

Table 1 – Gate 8 performance summary

Pin Designation	Maximum Friction Coefficient	Maximum Pin Moment due to Pin Friction (kip-In)	Maximum Hoist Force (kips)	Maximum Hoist Force due to Total Gate Friction (kips)
Right Pin	0.18	486.3	32.96	4.57
Left Pin	0.28	749.9	28.07	3.89

Note: Pin designations are in reference to looking downstream

Due to restrictions caused by the hoist limit switches, the hoist cables could not always be fully slacked at the beginning and end of the performed tests. Throughout testing of the Rockwell Forney gates, it was found that this limit switch restriction varied gate to gate and arm to arm. Therefore, it is not recommended to use the collected hoist force data to quantify overall hoist forces during gate operation. Rather, this hoist data can be better utilized to evaluate total friction behavior.

Amperage responses were not used to compute friction results and were collected as verification that the motor performance was not causing unexpected gate responses. These responses indicated the motor was functioning in a stable manner and should be reviewed by a licensed electrician to further evaluate the motor's performance.

All results and recommendations provided in this report were based on the structure in its current condition; therefore, any significant changes in condition must be noted as they may alter their validity. Questions regarding this report and/or data should be directed to Kyle Ramer (kyler@bditest.com) at BDI. For further information on BDI's equipment, services, and analysis methods please visit www.bditest.com

Instrumentation and Load Testing Procedure

Gate Instrumentation Summary

Instrumentation and testing were performed on Gate 8 at the Rockwall Forney Dam on April 7th, 2020. Instrumentation plans have been provided along with this report and include the following number of instrumented locations and sensor types:

+ **REUSABLE SURFACE MOUNTED STRAIN TRANSDUCERS:** Each gate arm was instrumented with a total of 24 strain transducers at 6 locations on each of the gate arms (48 strain sensors total). A typical strain gage installation is shown in Figure 1. Note these sensors were installed with the mounting tabs on the extreme fiber of the strut flanges, which puts the center of the gage approximately 0.66″ from the extreme fiber.
+ **TILTMETER ROTATION SENSORS:** MEMS style rotation sensors were located on the middle strut of the gate arm near the skin plate and near the trunnion hub (4 rotation sensors total). The rotation responses were used to calculate vertical skin plate movement and measure pin rotation relative to skin plate rotation. Typical tiltmeter installations are shown in Figure 1 and Figure 2.
+ **TORQUE SENSORS:** Two total torque sensors were installed on the hoist's pinion shafts (QTY1 on each hoist pinion shaft) near the cable hoist motor to measure direct torque and in turn lift force (See Figure 3).
+ **AMPERAGE SENSORS:** 3 Hall-Effect amperage transducers were clamped over each phase of the hoist motor to measure the motor's current draw (See Figure 4). The purpose of these sensors was to provide additional data in case there were any issues with the hoist systems and to verify any data issues related to lifting and lowering the gates.
+ **BDI'S STS-4 WIRELESS DATA ACQUISITION SYSTEM:** BDI's STS-4 wireless data acquisition (DAQ) was used to collect and record data during testing. A group of sensors were wired to each nodal DAQ which then communicated wirelessly back to the wireless base station and was controlled by BDI's STS-Live testing software.

Complete specifications are available upon request and can be found at http://www.bditest.com.

Sensor Installation

BDI strain transducers were installed by first sanding paint off the struts to expose bare metal at two small locations (1″x2″ areas) for the sensor's mounting tabs. Each transducer was then attached using a combination of fast-setting adhesive and accelerator and applying pressure until the adhesive was fully cured. Each strain transducer took approximately five minutes to attach.

Tiltmeters were installed using the same adhesive process as the strain transducers. However, no surface preparation was necessary.

Torque sensors were installed on the pinion shafts by capacitive discharge bonding. Properly bonding to the shaft required sanding the surface to a smooth finish, clean of any paint or grease. Responses from these gages were measured using Binsfeld Torque Trak 10k wireless transmitters.

A typical installation has been shown in Figure 1 through Figure 4. Access to all the sensor locations was provided by BDI's own SPRAT certified rope access technicians and engineers as shown in Figure 5.

Once testing was completed, sensors were removed, and exposed steel areas were covered using cold galvanizing compound.

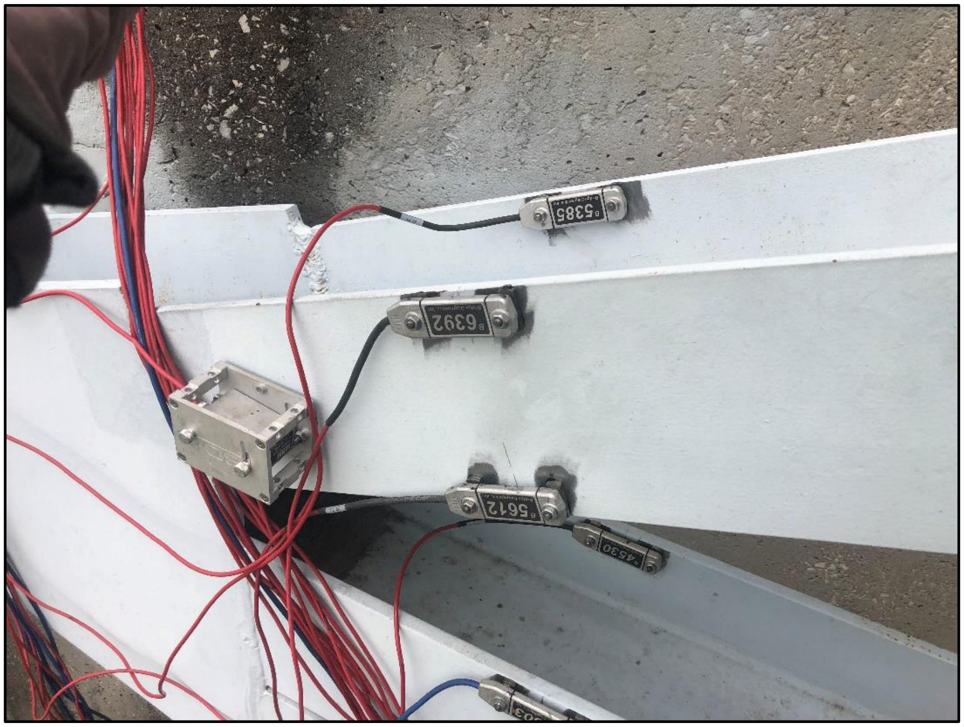

Figure 1 – BDI tiltmeter rotation sensor and reusable strain transducers installed near trunnion hub (Typical)

Figure 2 – BDI tiltmeter rotation sensor installed near skin plate (Typical)

Figure 3 – Torque sensor installation on hoist pinion shaft (Typical)

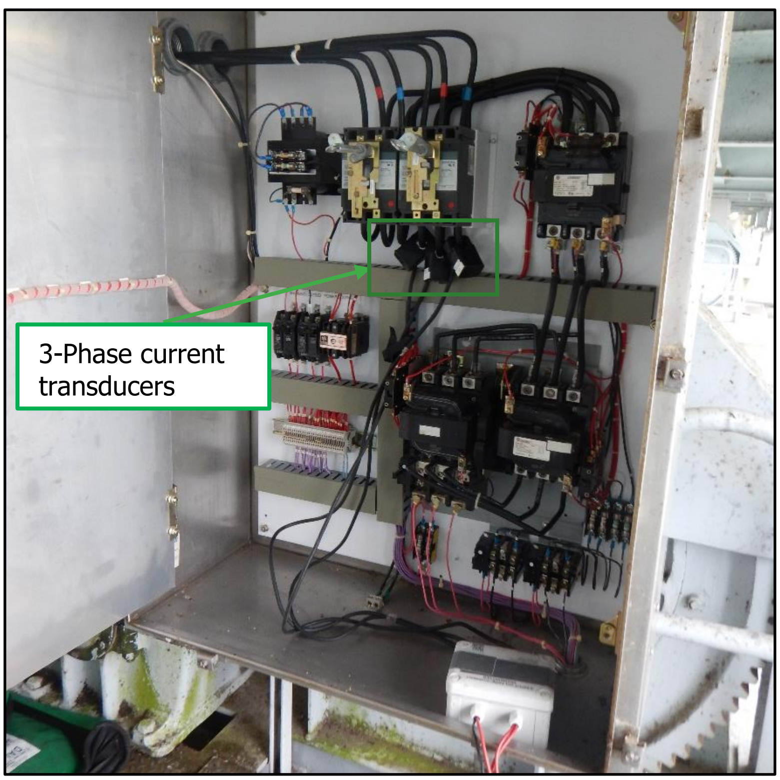

Figure 4 – Current transducers installed on hoist motor controls (Typical)

Figure 5 – BDI personnel installing instrumentation on the gate arm

TESTING PROCEDURES

Structural response data was recorded on all sensors at 50Hz while the gate was run through three spill tests. Each test consisted of three "up-down" cycles (direction reversals) without lowering the gate back to the sill. Each direction reversal consisted of lifting the gate approximately 6-12", pausing for a few seconds, and lowering the gate approximately 6", and repeating until all reversals had been completed.

Results Summary

General Discussions Based on Structural Responses

The following outline contains general discussion points and observations that were made during the data review process. Note: Strain measurements were converted to stress for all subsequent analysis by multiplying the strain values by a steel elastic modulus of 29,000 ksi.

+ **DESCRIPTIONS OF RESPONSE MEASUREMENTS:** All sensor readings were zeroed at the end of each test (which consisted of three cycles of direction reversals) so that each measurement corresponded to response change relative to the final gate position as shown in Figure 6 (gates in the downward "closed" position with the hoist cables slacked as much as possible). It is also worth noting that the stresses did not always start and end at the same levels between tests. This variation in behavior is due to small changes in the flexed gate condition between the start and end of tests. It is common for the flex in the gate, caused by pin friction, to slowly release as it rests on the sill. The purpose of the three up-down cycles per test, prior to sitting the gate back onto the sill, is to ensure that these changes in boundary conditions, including gate flexure due to friction, did not affect BDI's trunnion friction results. ***It is important to note that the recorded measurements were changes in structural response due to gate movement, and do not include the in-situ stresses due to the dead load, cable wrap, and hydrostatic loads present prior to testing.***
+ **QUALITATIVE DATA REVIEW:** Review of the response data indicated a good level of reproducibility between the three tests. For reference, Figure 6 and Figure 7 show stress responses measured along Gate 8's right arm top strut for all three tests (Test #1-3). The data in these plots have been provided as both a function of time and the gate position as determined by the skin plate tilt sensor. Structural response behavior slightly varied during the first test's first cycle compared to subsequent lift/lower cycles and tests, with the first cycle having a slightly smaller change in stress due to pin friction. The observed variation was likely caused by a larger release of built-up pin friction as the gate rested on the sill for a longer period of time.
+ **DIRECTION/FRICTION REVERSAL IN RESPONSES:** The difference in stress during gate opening and closing for a given position is shown in Figure 8. The stress variation at any given gate position was a result of direction reversal and in turn due to trunnion friction reversal. This statement is true since all other loads such as dead-load and hydrostatic pressure were essentially constant barring small changes in hydrostatic pressure due to slight changes in head. This direction/friction reversal is depicted in Figure 9, with deflected shape renderings from a gate arm finite element model under lifting and lowering loads. Note that this figure shows an arm configuration that does not match this gate, but the concept of the direction/friction reversal still applies.
+ **MOTOR PERFORMANCE:** Current measurements taken at the hoist motor indicated steady and stable current draws during the lifting and lowering portions. An example plot of current draw and gate position is provided in Figure 10. Current draw ranges during lifting were higher than the ranges during lowering, which is common due to gravity/dead load. These results are summarized along with recorded peak in-rush current in Table 2. Note that the sample rates used during testing were set for collecting gate responses and may not have been appropriate to fully capture the in-rush current. The readings should be evaluated by a licensed electrician with knowledge of the operating parameters.
+ **TORQUE AND HOIST FORCE:** Due to restrictions caused by the hoist limit switches, the hoist cables could not always be fully slacked at the beginning and end of the performed tests. Throughout testing of the Rockwell Forney gates, it was found that this limit switch restriction varied gate to gate and arm to arm. Therefore, it is not recommended to use the collected torque and hoist force data to quantify overall hoist forces. Rather, this data was utilized to evaluate total friction behavior, which is observed as half the difference between the lifting and lowering torque/force (friction reversal).

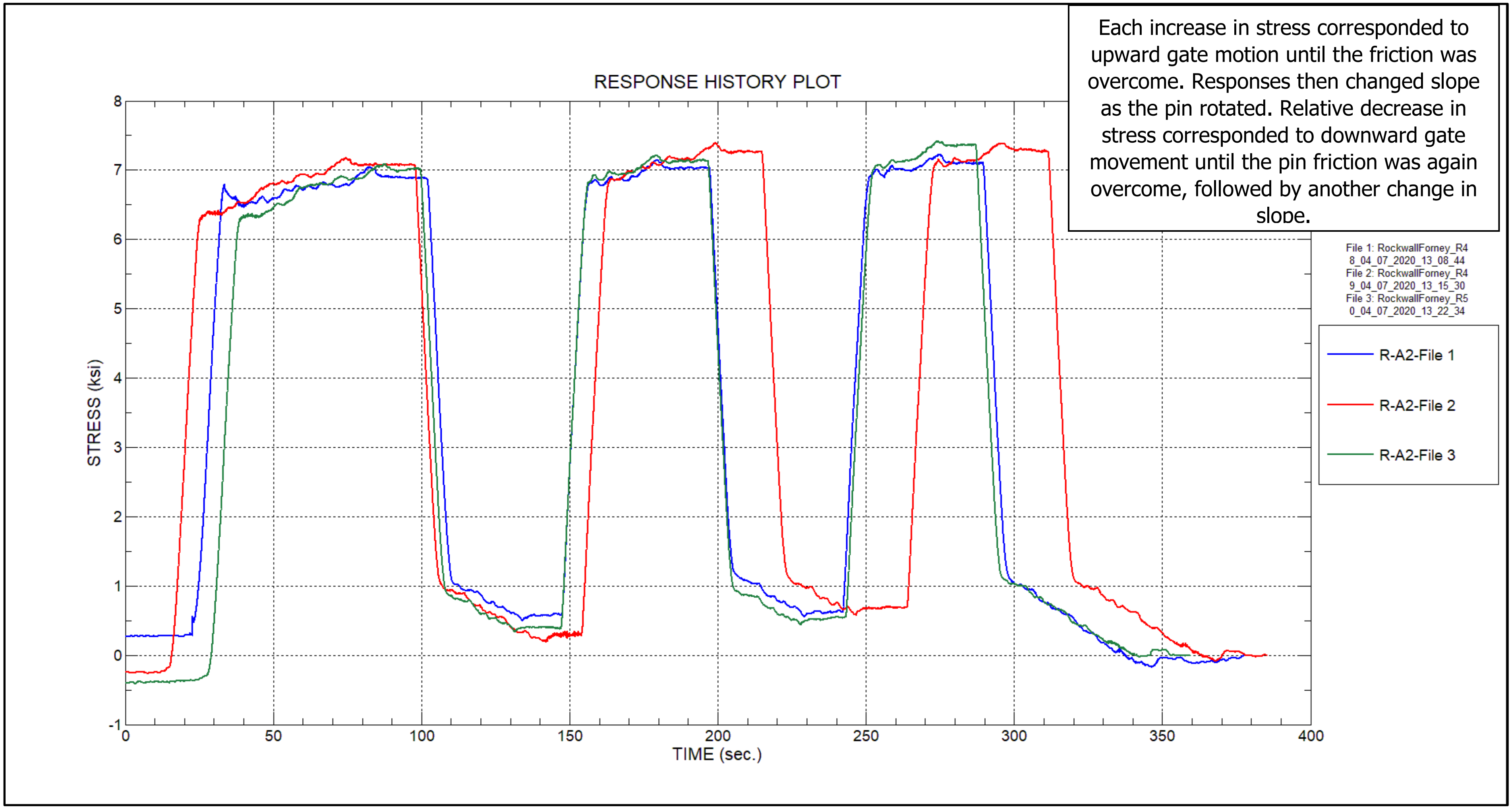

Figure 6 – Stress response history – Right arm – Gage A2 – Time based
File 1 = test run 1, File 2 = test run 2, File 3 = test run 3

(Section A along top strut near pin – Sensor location 2 along bottom of inner flange)

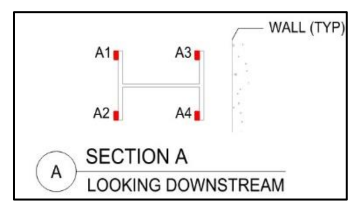

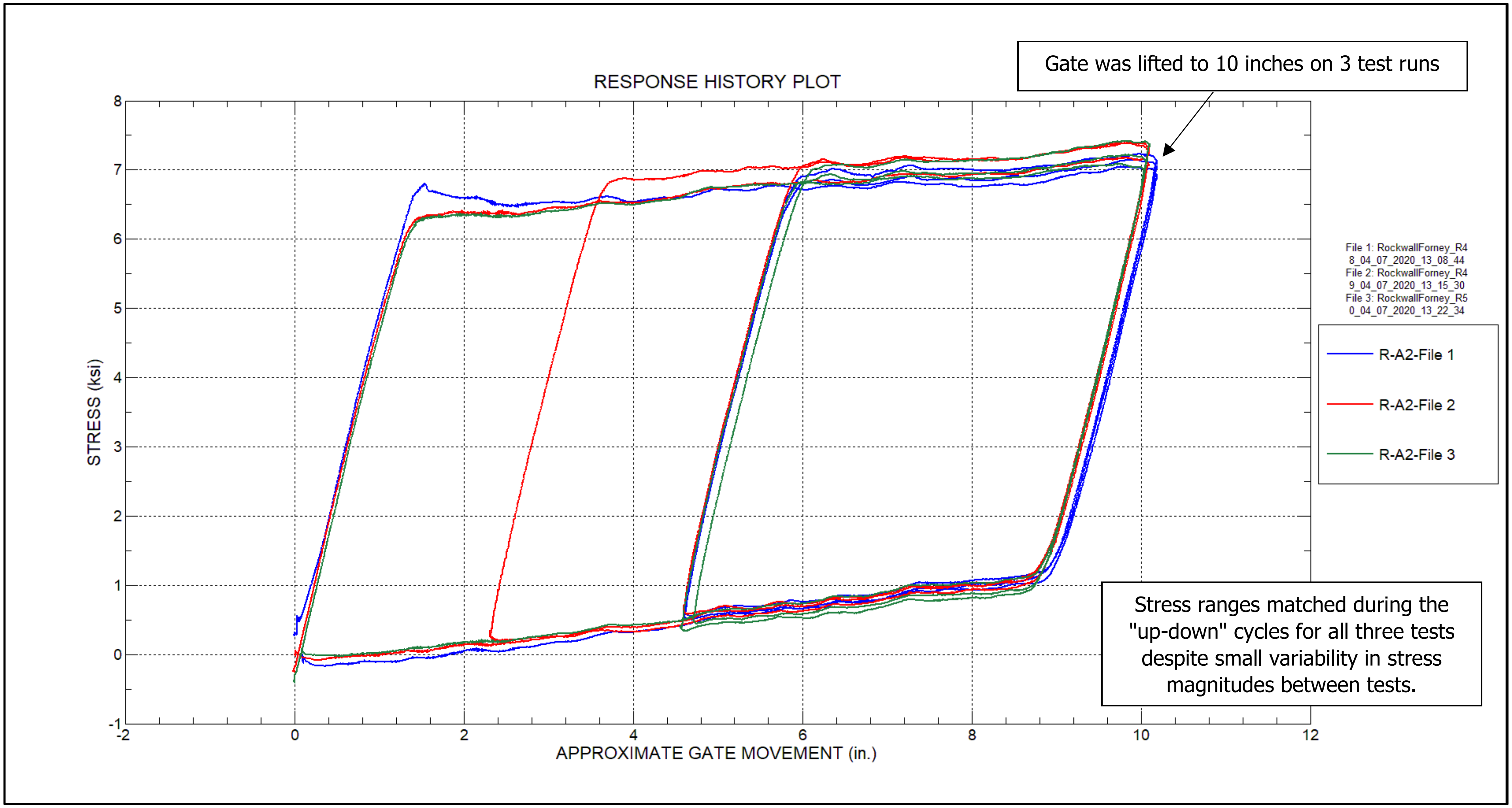

Figure 7 – Stress response history – Right arm – Gage A2 – Function of gate movement
File 1 = test run 1, File 2 = test run 2, File 3 = test run 3

(Section A along top strut near pin – Sensor location 2 along bottom of inner flange)

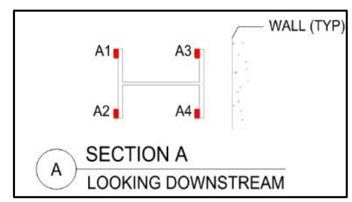

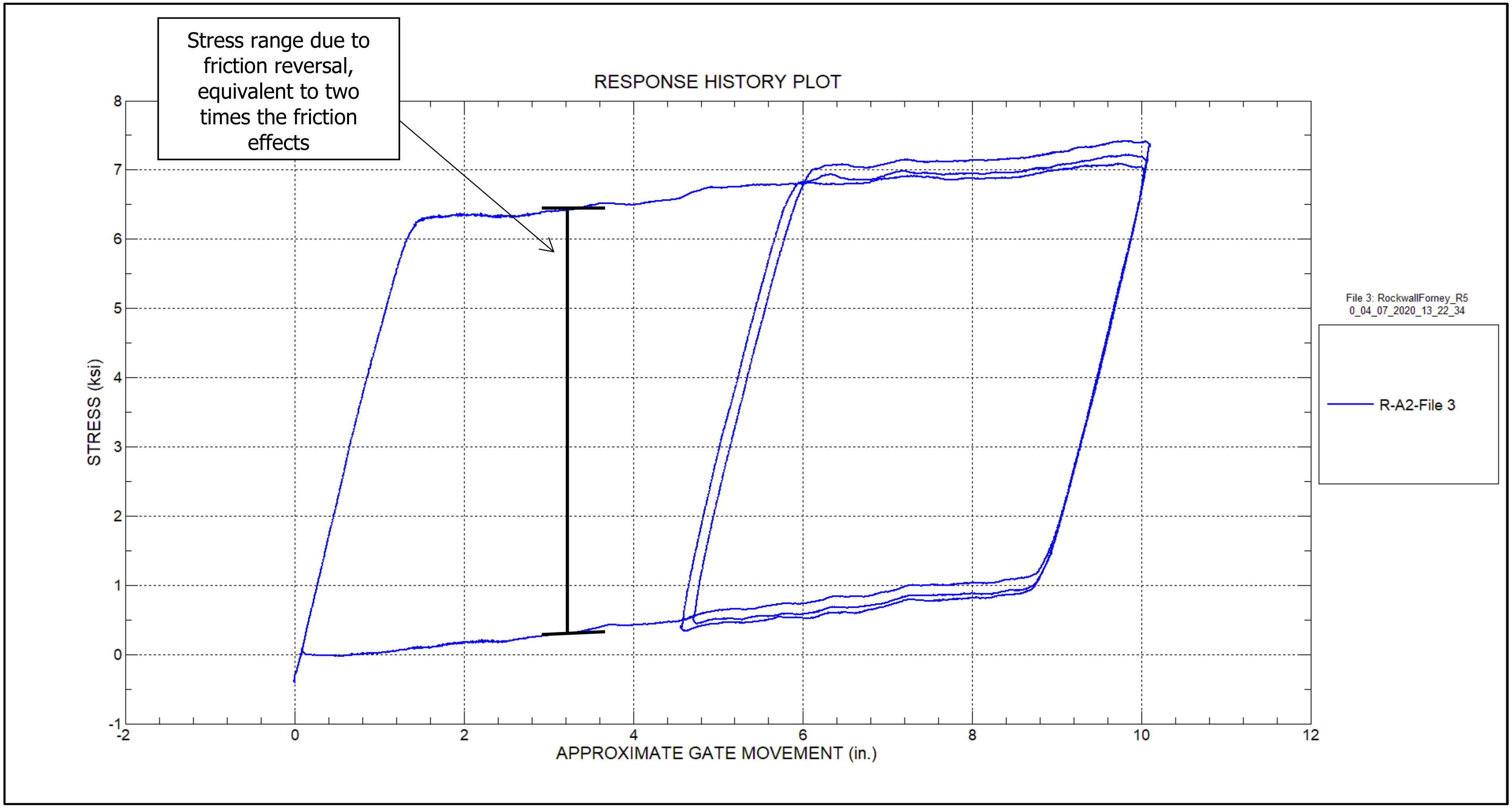

Figure 8 – Stress response history – Right arm – Gage A2 – Friction effect in stress responses

(Section A along top strut near pin – Sensor location 2 along bottom of inner flange)

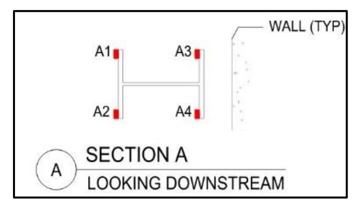

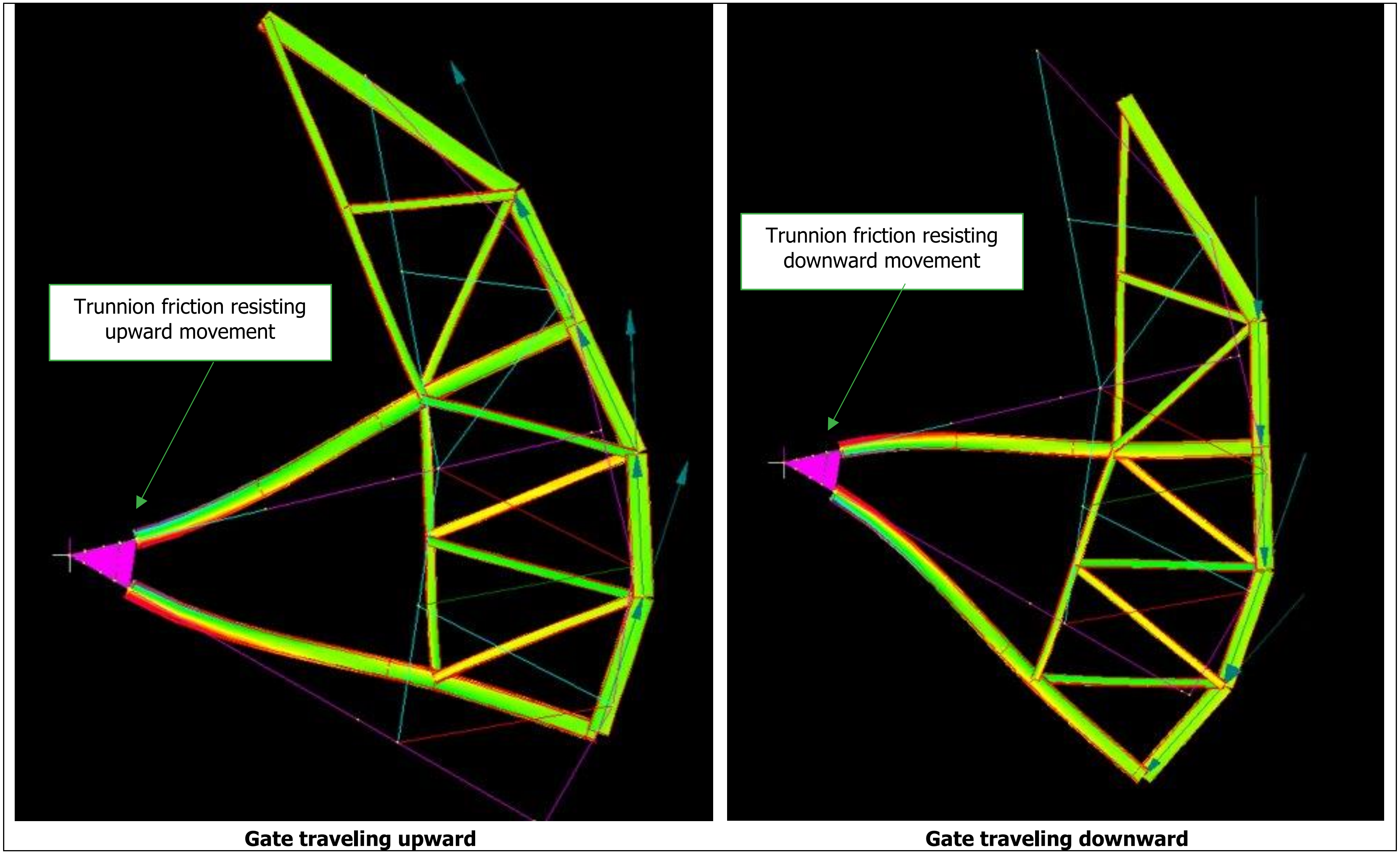

Figure 9 – Deflected shapes during lifting and lowering of Gate – Visualization of direction/friction reversals

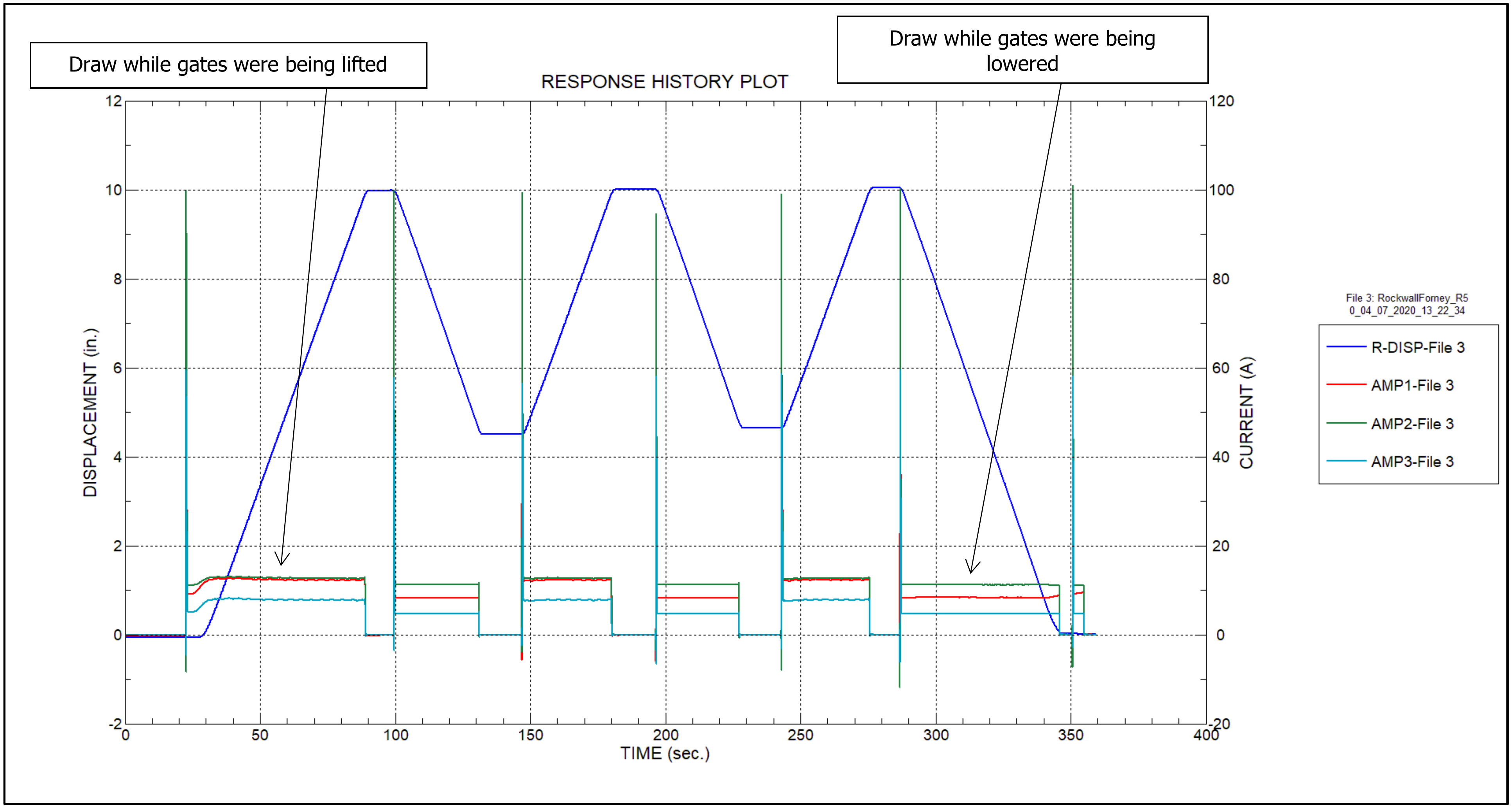

Figure 10 – Motor current & gate movement response history – Lift motor – Highlighting motor draw during lift and lower cycles

Methodology and Findings of The Strut Force and Moment Calculations

The following outline provides the methodology used to calculate the required member forces and moments.

+ **CHANGE IN STRESS DUE TO GATE OPERATION:** Strain data can be viewed as a function of time starting when the gate was in the down position and was then lifted off the sill. When examining data in this manner, it is easy to see how stresses ramped up as the gate began to move and then changed slope once pin friction was overcome and the trunnion hub began to rotate with the gate. The first point in time where the friction was overcome (both lifting and lowering) has been highlighted in the stress histories shown in Figure 11. These stress histories show the response of all four sensors along the top strut of the right arm (Section A). ***It is important to note that the recorded measurements were changes in structural response due to gate movement, and do not include the in-situ stresses due to the dead load, cable wrap, and hydrostatic loads present prior to testing.***
+ **CALCULATION OF STRUT CROSS-SECTIONAL MOMENTS:** The use of four strain gages per strut cross-section allowed accurate in-plane flexural bending moments to be computed from the recorded strain measurements. These moments were computed for every cross-section in each gate arm using the basic mechanics equation provided in Figure 12.

  In-plane or weak-axis flexure refers to bending about a given strut's web. This designation is consistent with typical nomenclature. In-plane bending can be observed visually from the strain response histories as a difference between the top and bottom stresses, whereas out-of-plane or strong-axis bending is visualized as the difference in stress from side to side. Figure 13 provides a visual reference for both types of strut flexure.
+ **EXAMINATION OF RESPONSES AS A FUNCTION OF GATE POSITION:** Changes in cross-sectional moment related to friction becomes clearer when the responses are plotted as a function of gate position. Because the gate was operated with several up and down movements, the effects of friction associated with each direction reversal can be viewed for all measured and calculated responses. Figure 14 through Figure 17 show all cross-sectional flexural moment plots for both trunnion arms. The responses in these plots have been centered about the stress state corresponding to a zero-moment, unflexed condition. The zero-moment offset was estimated as the average moment values between up and downward movement (i.e. half the moment difference) at the gate position with the greatest pin friction moment difference (greatest difference between lifting and lowering).
+ **TRUNNION FREE-BODY-DIAGRAM & PIN MOMENT CALCULATION:** Figure 18 shows the instrumented member cross-sections and shows how the measured cross-sectional flexural responses were used to compute pin moment. The in-plane moment values used in these calculations were determined directly from the strain measurements at each cross-section using the provided mechanics equations. It should be noted that the out-of-plane moments were not considered in the calculation of pin moment since they were orthogonal to the axis of the pin rotation. Total pin moment was then determined by summing all the moment components about the pin, which included the in-plane moment and the shear components at the strut cross-sections nearest the pin.
+ **STRUT SHEAR CALCULATION:** From the examination of the trunnion free-body-diagram described above, the shear vectors at the three struts were a primary component in the pin moment calculation. For this type of structural element, shear vectors were calculated using the moment differential between the two cross sections along each strut. It is important to recognize that shear was constant between the two instrumented cross-sections and the applied shear was a function of the recorded change in moment ($V = dM/dX$). Subsequently, the shear vectors were calculated by dividing the difference in moment by the distance between the two instrumented cross-sections. Shear values for each strut have been plotted as a function of gate position in Figure 19 and Figure 20.

- **CALCULATION OF PIN MOMENT DUE TO FRICTION:** Once all the trunnion arm force vectors were calculated, the equations shown in the free-body-diagram were applied to compute pin moment as a function of gate position. It is important to note that because the calculated pin moment range corresponds to a direction reversal, a reversal in friction also occurred. The effect of direction reversal on pin moment due to friction is best conceptualized by centering the moment response plots about the zero-moment axis. The moment due to lifting and the moment due to lowering can then be visualized as a change from this new zero point corresponding to the gate in an unflexed condition. Therefore, the total moment differential between lifting and lowering was twice the moment due to friction acting in a single direction. Pin-moment plots have been provided in Figure 21 and Figure 22. From these plots, it is apparent that pin moment due to friction remained relatively constant throughout the gate operation tests, with a slight decrease in pin friction moment as the gate continued to be lifted. This slight decrease in pin friction moment most likely corresponded to the change in hydrostatic load as the gate position changed. Pin-moment plots for all tests on Gate 8 are also provided for reference in Appendix B – Gate 8 Pin Moment Component Plots.
- **SHAFT TORQUE & HOIST FORCE:** Torque measurements were taken on the pinion shafts near the hoist motor during testing, with single torque gages installed on the left and right hoist pinion shaft. Responses were recorded in units of micro-strain and converted to torque in units of kip-ft using Equation 1 thru Equation 3 and the following shaft properties.

$$d_O = 5.5\ inches, \qquad d_I = 0\ inches, \qquad E = 29000\ ksi, \qquad \nu = 0.3$$

$$G = \frac{E}{2(1+\nu)}$$

Equation 1

$$J = \frac{\pi\left({d_O}^4 - {d_I}^4\right)}{32}$$

Equation 2

$$\tau = \varepsilon * \frac{2GJ}{\frac{d_O}{2} * 1000000 * 12}$$

Equation 3

Figure 23 shows example torque measurements, recorded on the Gate 8 torque shafts. Best practices for torque measurements is to measure torque on opposite sides of the shaft so that any bending in the shaft can be removed by averaging the two responses. Due to access limitations, only one gage at each location could be installed. Therefore, any bending in the shaft may be reflected in the torque measurements and may be related to the peaks and valleys observed in the torque responses.

Torque values were converted to force in the hoist cables per gate arm using the gear ratio and drum radius, as shown in Figure 24. The gear ratio and drum radius were 5.182 and 1.086 feet respectively, as defined in the provided as-built shop drawings. It should be noted that the hoist force calculated may be smaller than the actual hoist force applied. This difference is due to the limit switch engaging the brake before the hoist cable was fully slacked, resulting in an initial force in the cable. A hoist force due to total gate friction was then calculated. This friction hoist force was equal to half the differential in force measured during the lifting and lowering of the gate (similar to the pin friction calculations). As shown in Table 3, the change in cable force due to friction was generally consistent between tests. Note that the total hoist force was due to the total friction effects, including side seal, hoist bearings, trunnion friction effects, etc. It is difficult to determine the exact proportion and composition of the total friction sources. Additional torque and hoist force plots for all collected data files are provided in Appendix A – Gate 8 Torque and Hoist Force Plots.

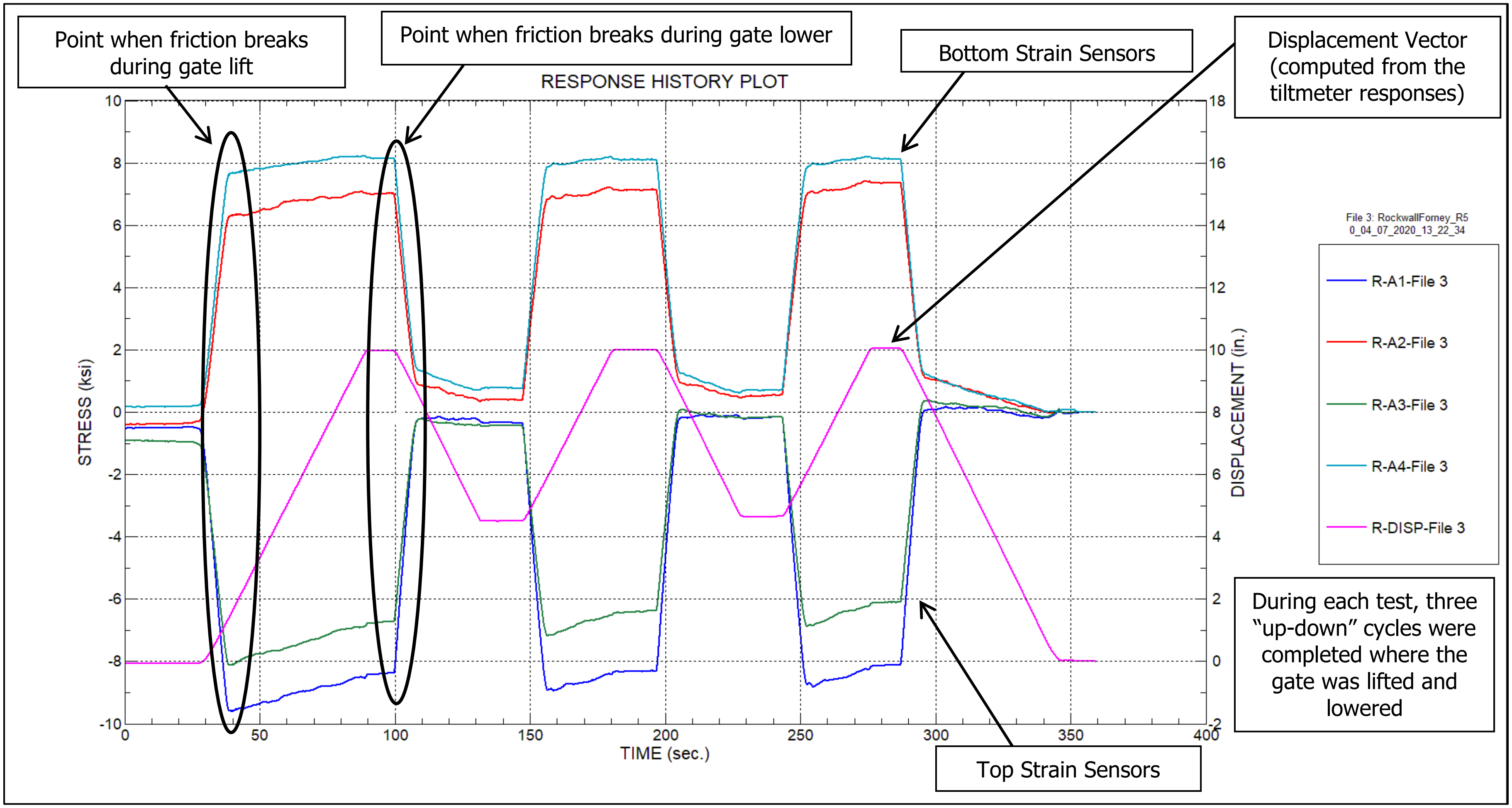

Figure 11 – Stress response & gate movement history – Right arm – Section A - Highlighting friction behavior (Section A along top strut near pin)

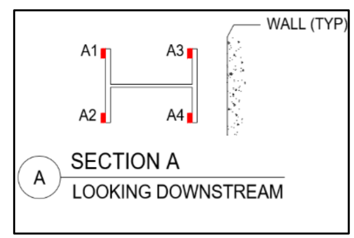

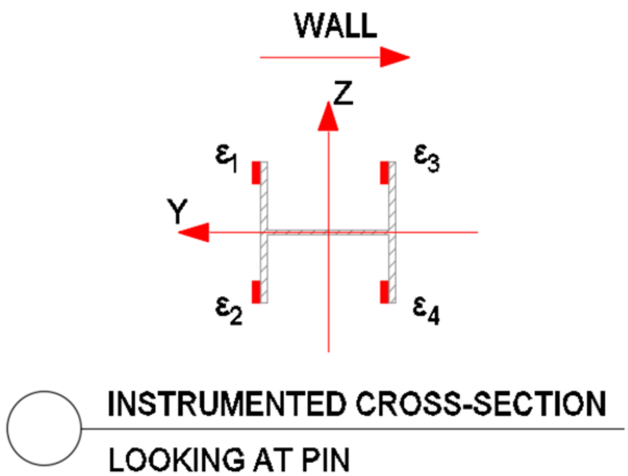

Calculation of Weak-axis (In-plane) bending

$$M_Y = \frac{E\left[\frac{\varepsilon_2 + \varepsilon_4}{2} - \frac{\varepsilon_1 + \varepsilon_3}{2}\right] S_{Y(gage)}}{2}$$

Sy(gage) = Section modulus to the center of gages (not extreme fiber of flanges)
(locations of gages were accounted for in moment computation)

Figure 12 – Basic mechanic equation used to calculate moment

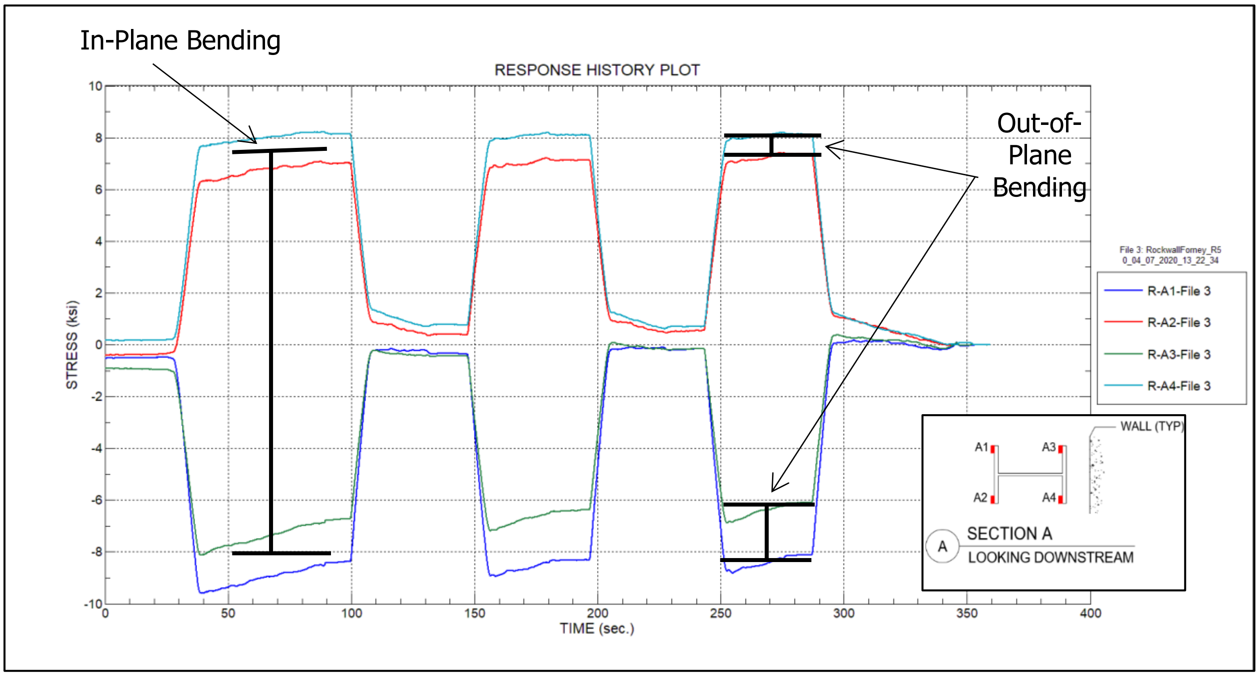

Figure 13 – Stress response history – Right arm – Section A – Bending components
(Section A along top strut near pin)

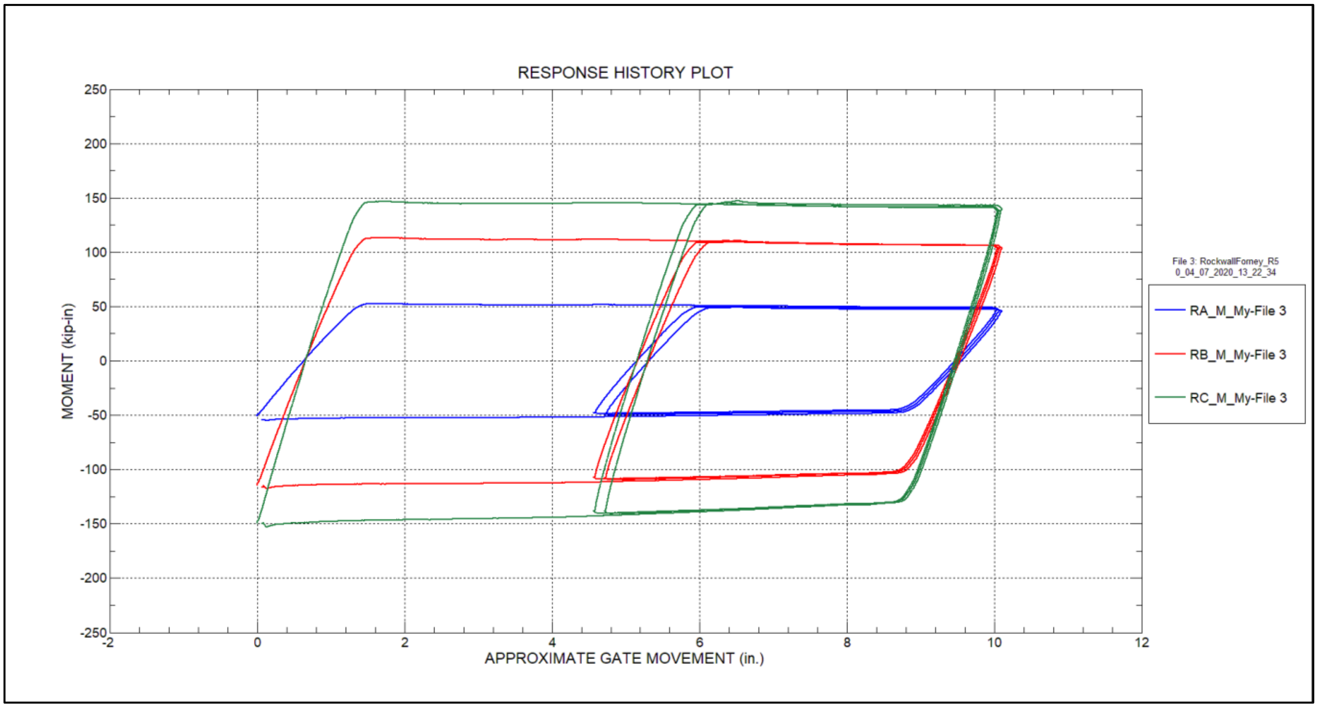

Figure 14 – In-plane moment response history – Right arm – Sections near pin

(RA = Right Arm Top Strut, RB = Right Arm Middle Strut, RC = Right Arm Bottom Strut)

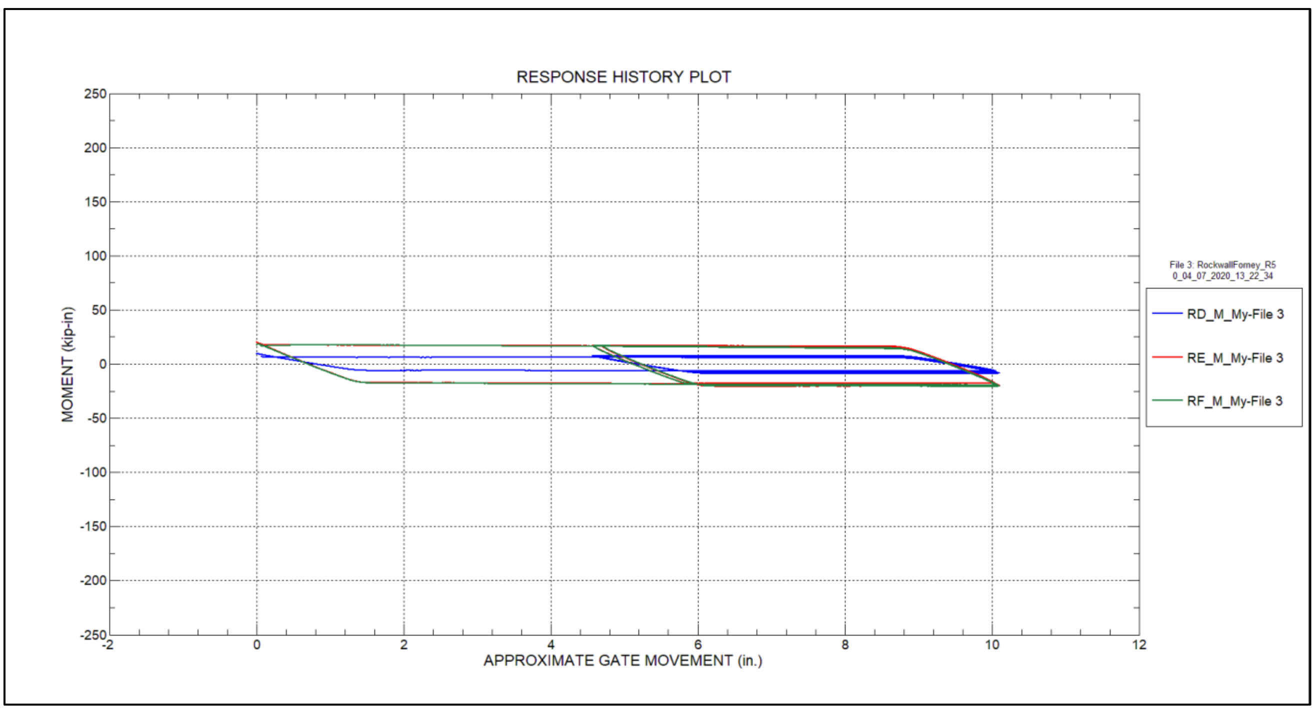

Figure 15 – In-plane moment response history – Right arm – Sections away from pin

(RD = Right Arm Top Strut, RE = Right Arm Middle Strut, RF = Right Arm Bottom Strut)

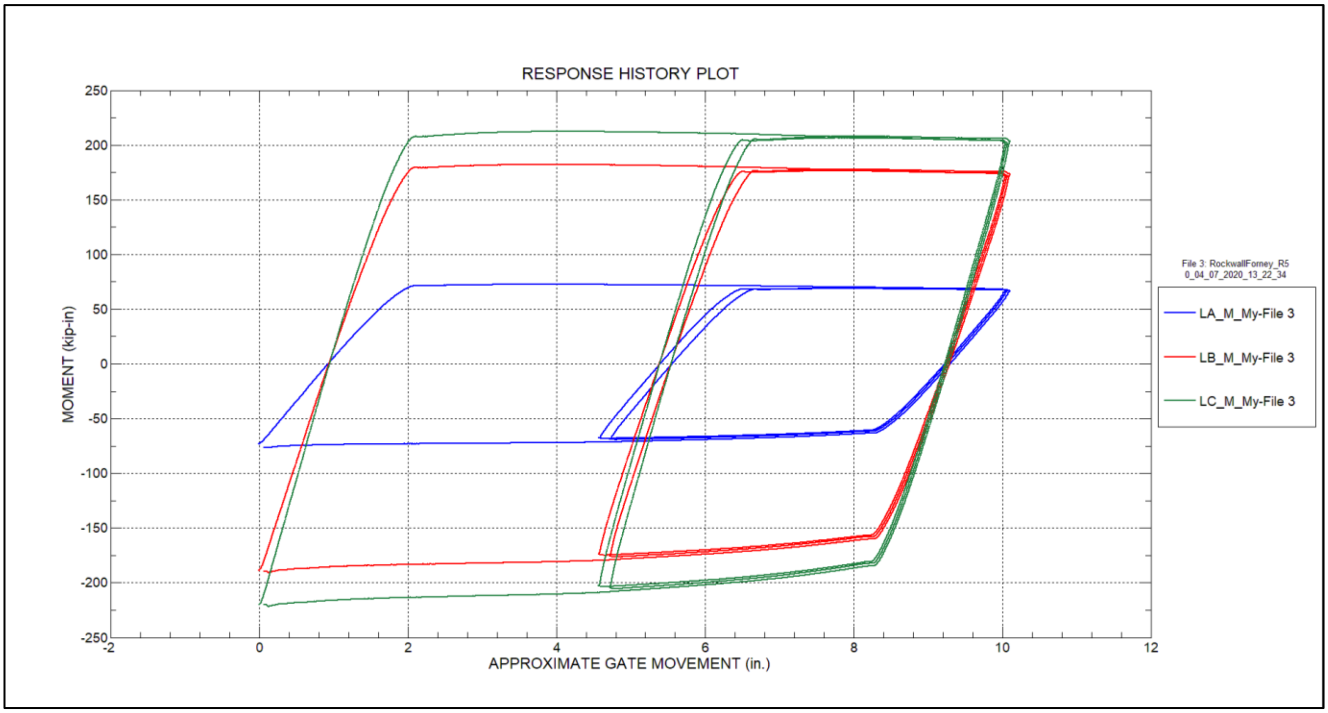

Figure 16 – In-plane moment response history – Left arm – Sections near pin

(LA = Left Arm Top Strut, LB = Left Arm Middle Strut, LC = Left Arm Bottom Strut)

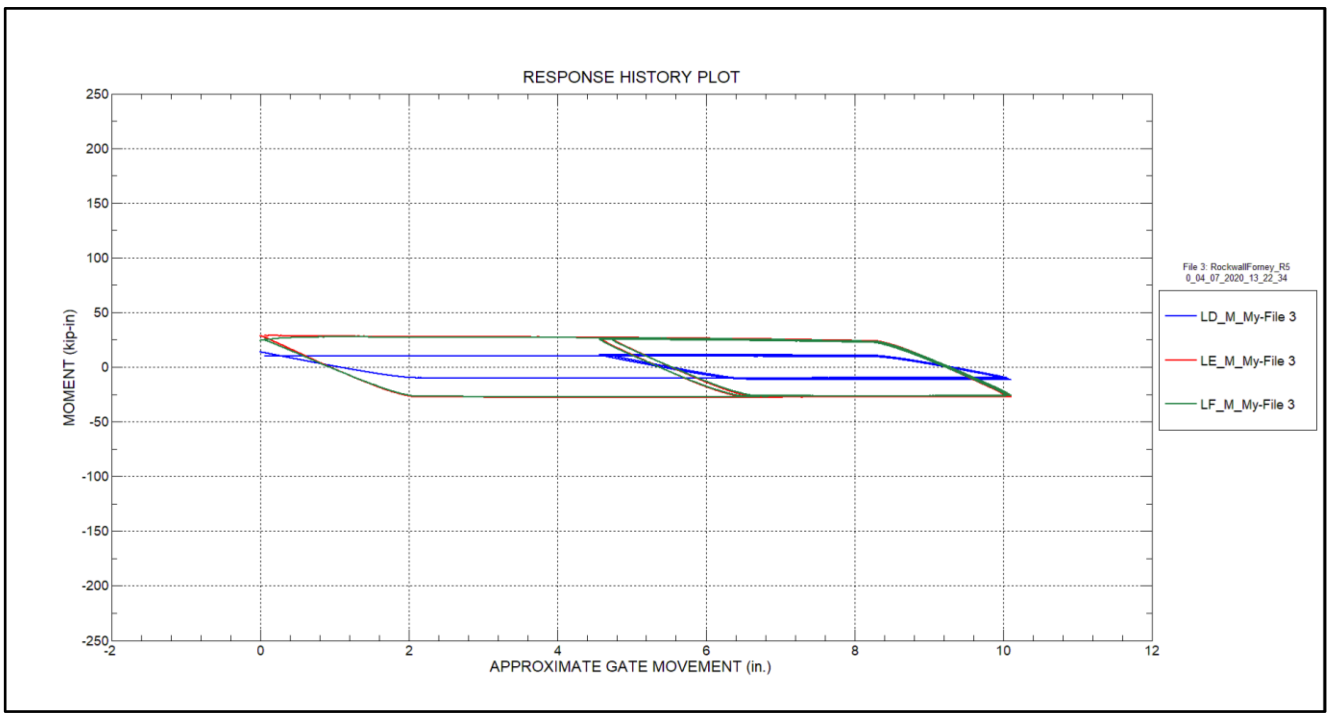

Figure 17 - In-plane moment response history – Left arm – Sections away from pin

(LD = Left Arm Top Strut, LE = Left Arm Middle Strut, LF = Left Arm Bottom Strut)

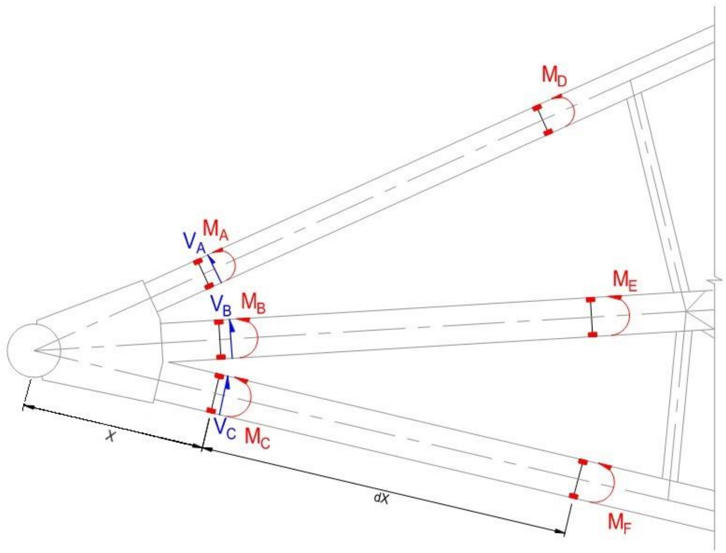

Elevation View of Gate Arm

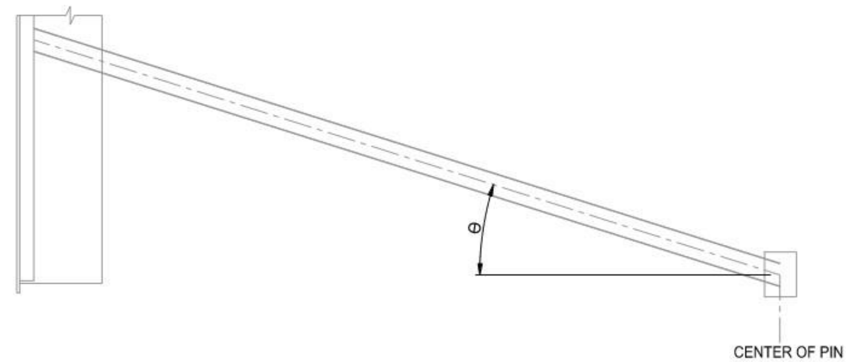

Plan View of Gate Arm

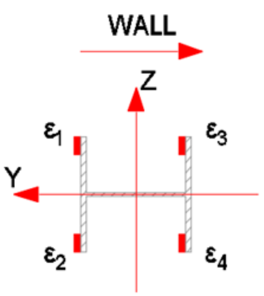

$$M_Y(M_A, M_B, M_C, M_D, M_E, M_F) = \frac{E\left[\frac{\varepsilon_2 + \varepsilon_4}{2} - \frac{\varepsilon_1 + \varepsilon_3}{2}\right] S_{Y(gage)}}{2}$$

$$V_A = \frac{M_A - M_D}{dX}$$

$$V_B = \frac{M_B - M_E}{dX}$$

$$V_C = \frac{M_C - M_F}{dX}$$

$$\sum M_o = 0$$

$$M_{PIN} = [X(V_A + V_B + V_C) + M_A + M_B + M_C] \cos\theta$$

Figure 18 – Direct calculation of pin moment from strain measurements

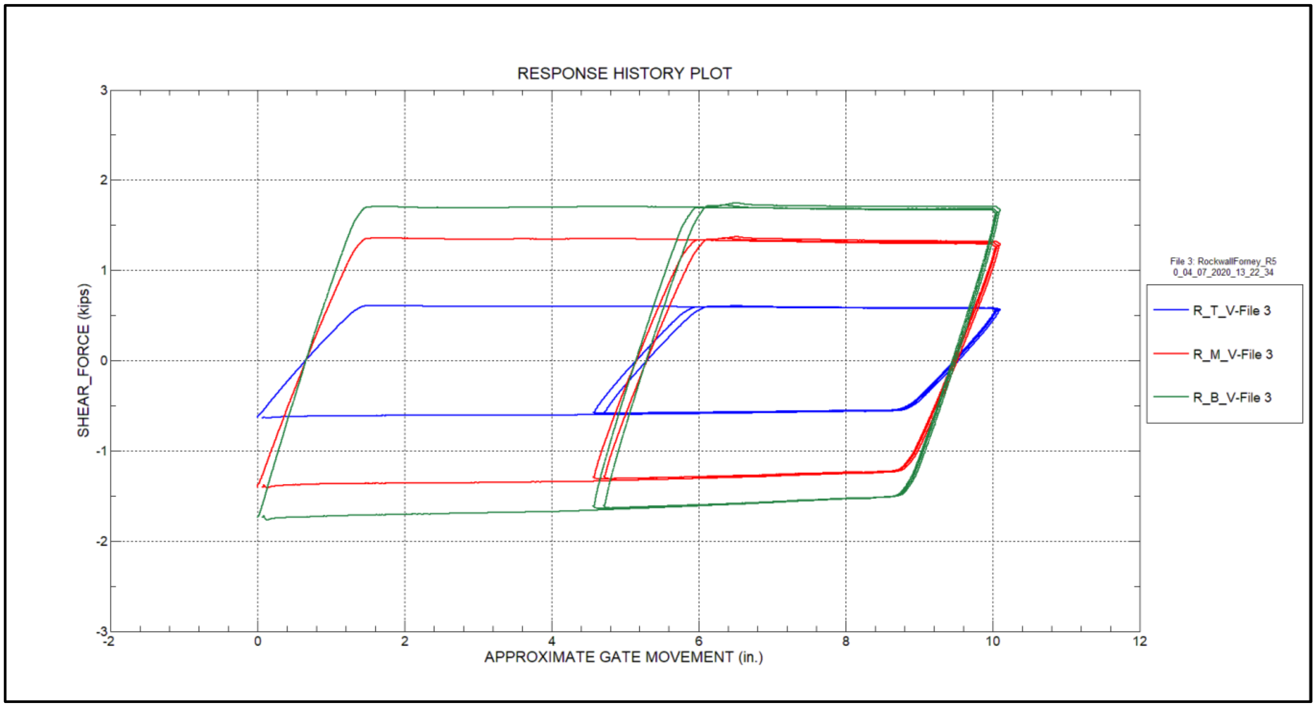

Figure 19 – Strut shear response history – Right arm

(R_T = Right Arm Top Strut, R_M = Right Arm Middle Strut, R_B = Right Arm Bottom Strut)

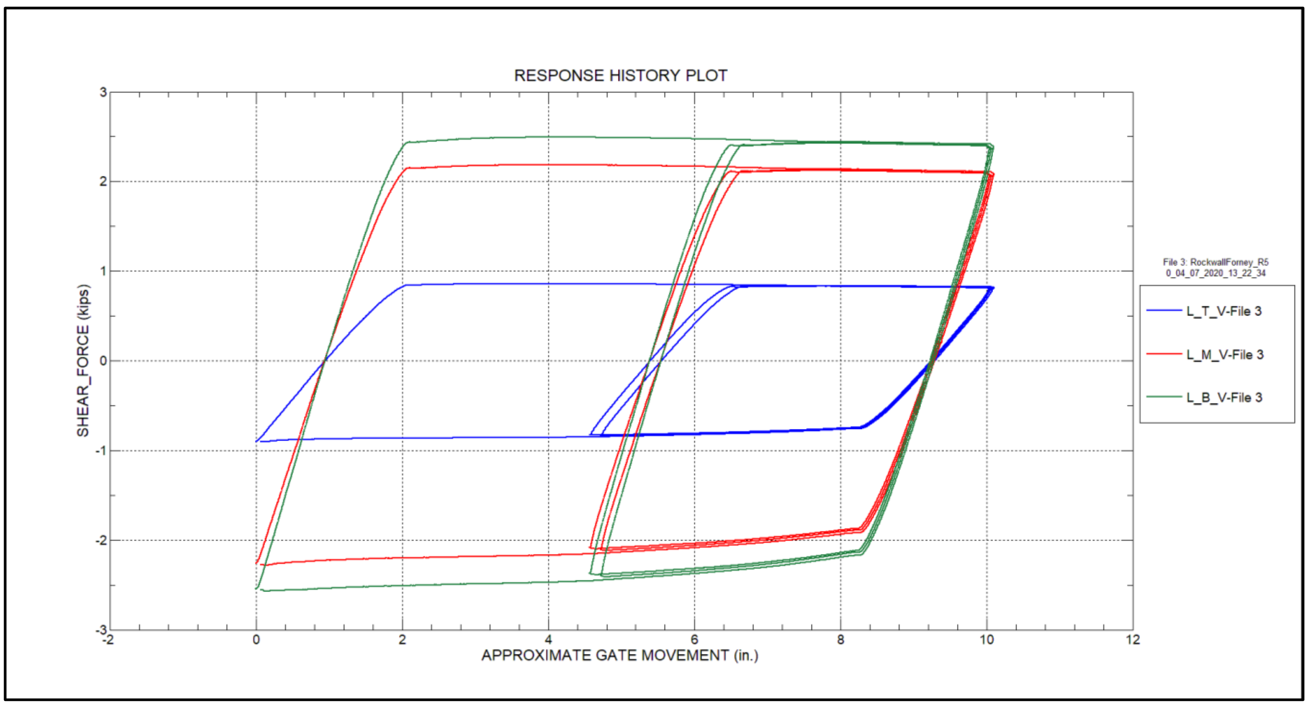

Figure 20 – Strut shear response history – Left arm

(L_T = Left Arm Top Strut, L_M = Left Arm Middle Strut, L_B = Left Arm Bottom Strut)

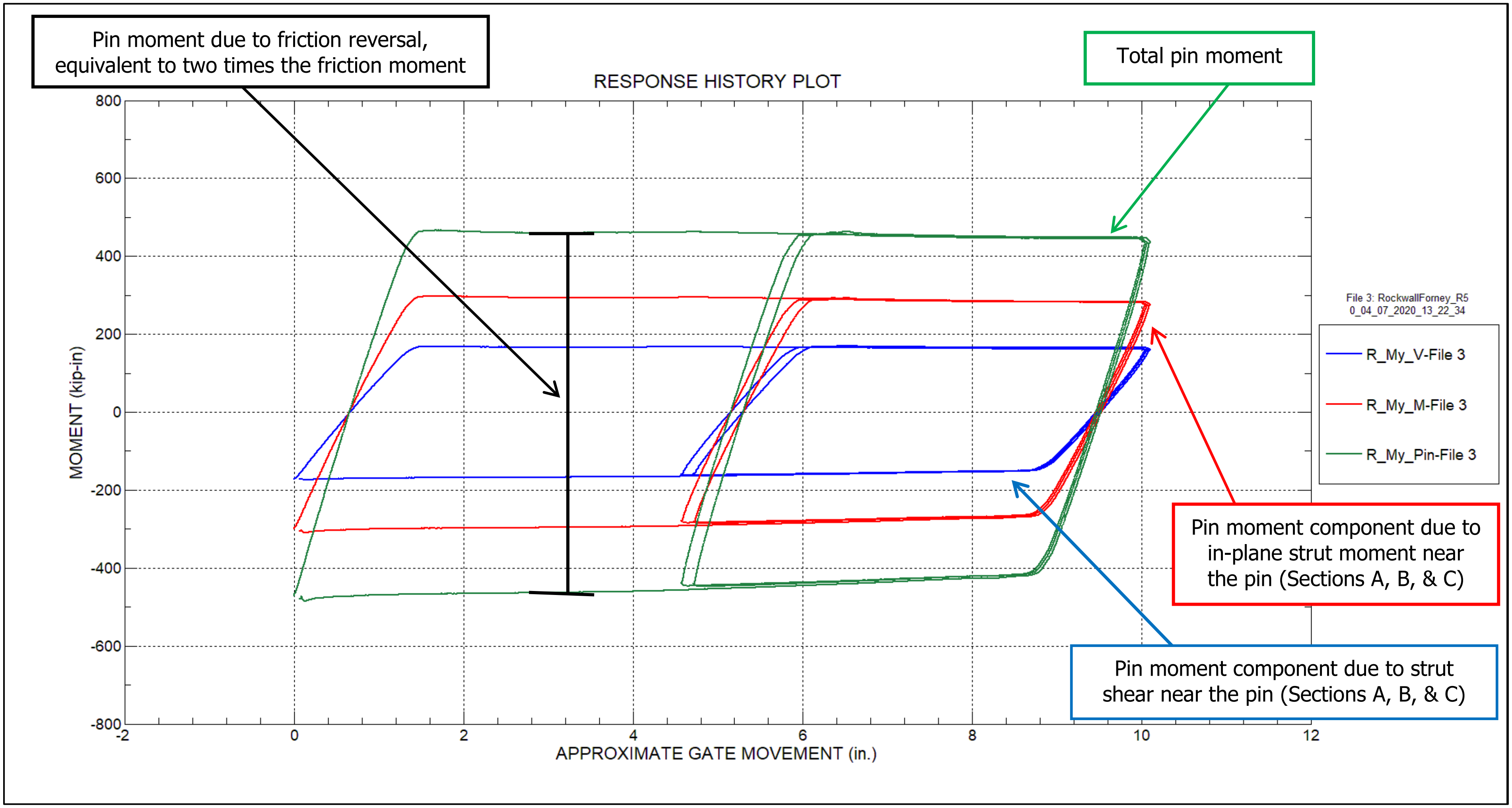

Figure 21 – Pin moment response history – Right arm

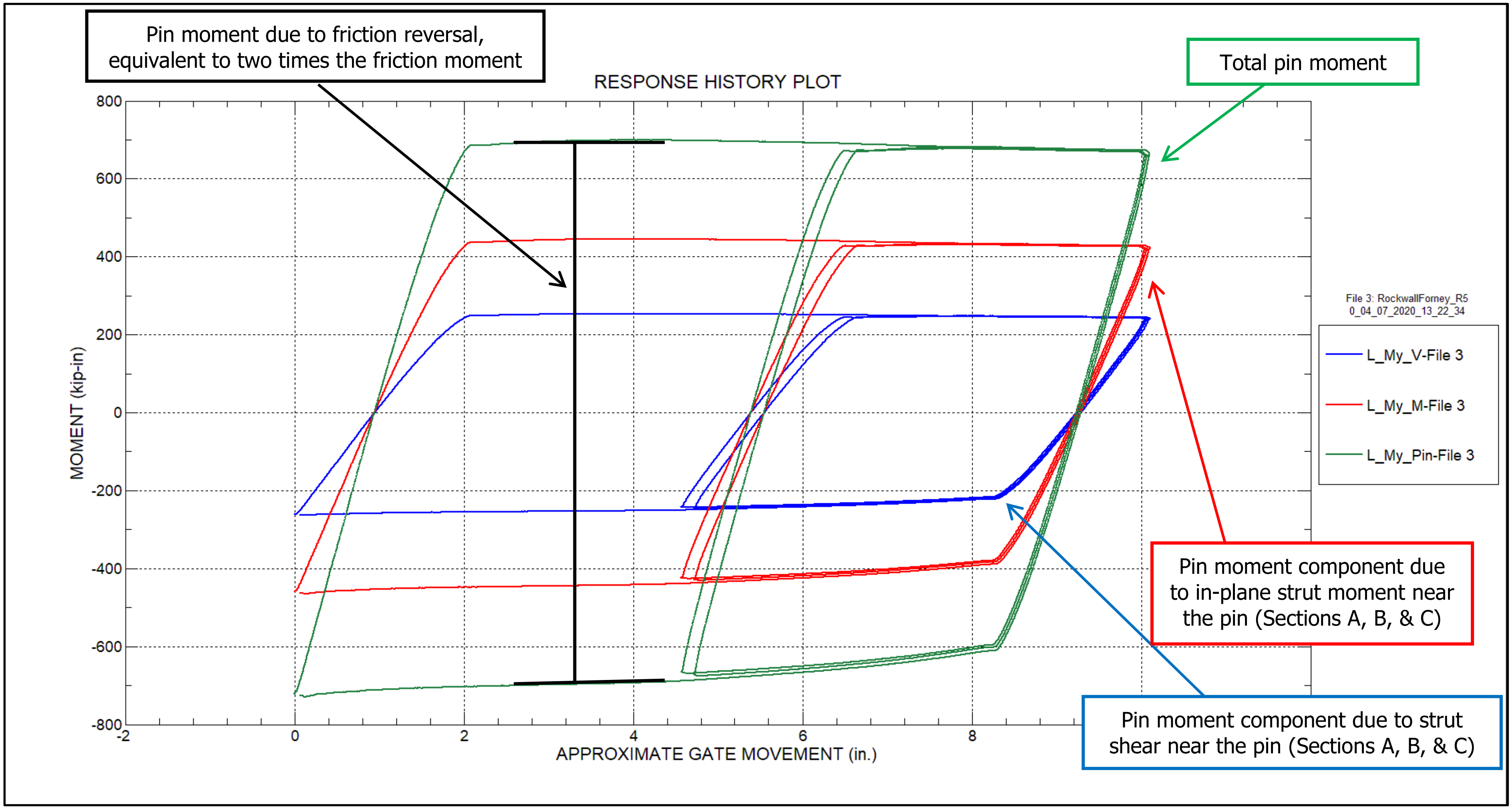

Figure 22 – Pin moment response history – Left arm

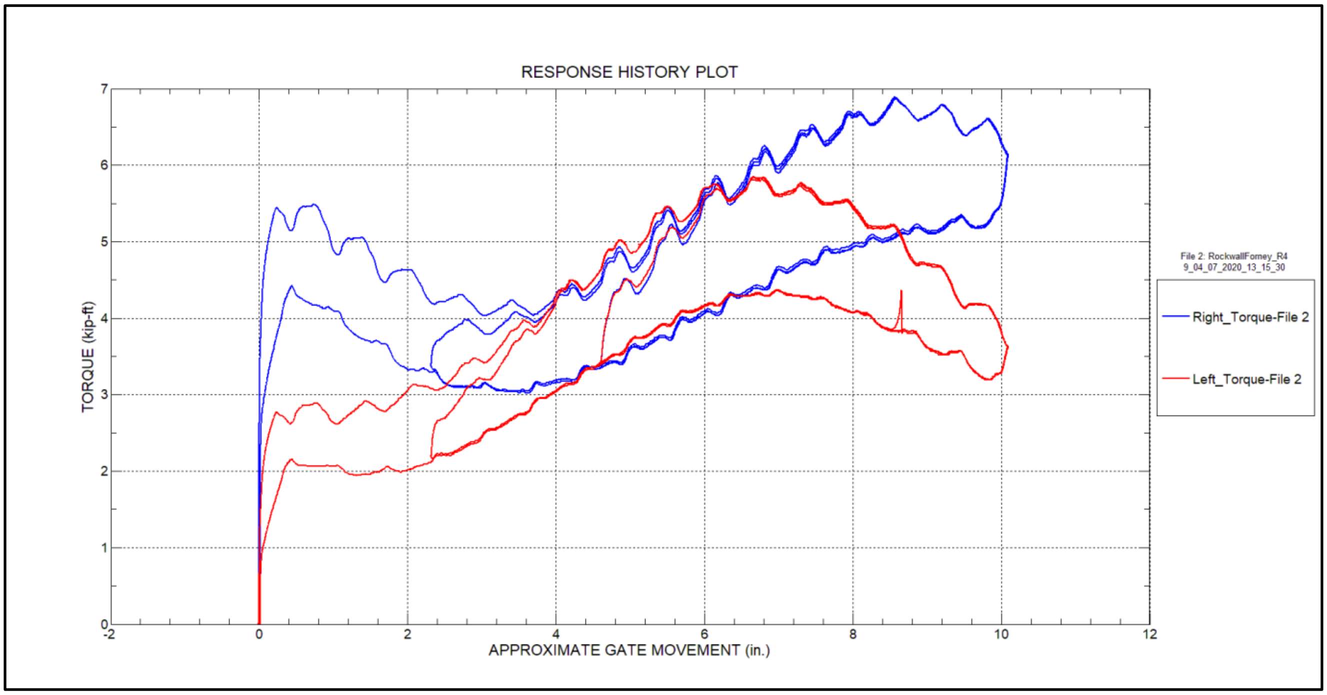

Figure 23 – Hoist torque response history – Gate 8 – Test 2

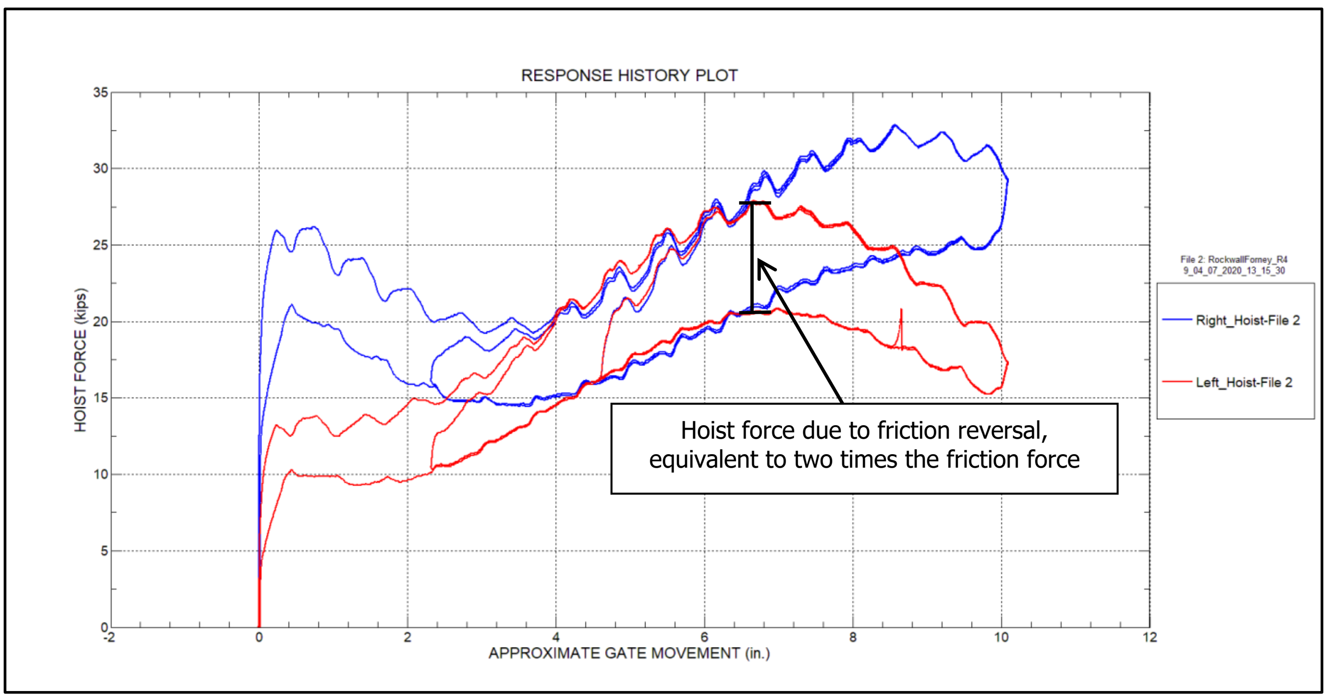

Figure 24 – Hoist force response history – Gate 8 – Test 2

SUMMARY OF FRICTION RESULTS

The raw data files have been included in the submittal package for reference and were formatted as “tdms” files that can be opened in Microsoft Excel using a "tdms" reader extension.

Examination of the stress histories for each test was necessary to obtain a thorough understanding of the gate performance. The response shapes, variations in stress magnitudes, and timing sequences provided direct clues as to how the gate performed under typical service conditions. The following is a breakdown of the provided tabulated results:

+ Table 2 provides motor current ranges and maximum in-flow for lift and lower cycles for each test
+ Table 3 provides maximum hoist force as well as hoist force due to total friction for each test
+ Table 4 provides the maximum stress ranges measured at the sensor locations for each member
+ Table 5 provides maximum bending stress and moment ranges observed during the gate tests
+ Table 6 provides maximum friction bending stress and moment values at each of the instrumented strut locations
+ Table 7 provides the computed shear values in each strut due to friction
+ Table 8 provides calculated measured friction moments, calculated hydrostatic loads based on the measured water elevation, and coefficients of friction for each gate and gate arm during all three tests

The resulting pin friction moments were used to compute friction coefficients from Eq. 4, given the pin radius and the applied thrust. The thrust used in this calculation consisted of the calculated resultant hydrostatic load based on the measured water elevation and was adjusted to account for the loss of head as the gate was lifted. This thrust adjustment was based on the recorded gate movement and was performed in order to calculate more accurate friction coefficients. The water elevation during testing was nearly constant throughout each gate test and was documented during each “up-down” cycle. It should be noted that the minor thrust due to cable wrapping, which was minimal compared to hydrostatic thrust, was not included in the thrust calculation. This assumption resulted in slightly conservative friction coefficients.

$$\mu = \frac{M_F}{T * r} \qquad \text{Eq. 4}$$

where:

μ	=	Friction Coefficient
M_F	=	Friction Moment
T	=	Thrust per Pin
r	=	Pin Radius, 5.375”

The out-of-plane shear and moments were not considered in the pin friction calculations due to orthogonal geometry considerations (resulting pin moment associated with out-of-plane flexure being perpendicular to pin rotation).

The data was presented in a specific coordinate system applicable to both arms. Data was processed so that the positive x-axis was always pointing towards the pin and the right-hand rule applied. In-plane bending can be referred to as “bending about the horizontal or y-axis” and shows how much the beams bend up and down within the plane of the gate arms. Refer to Figure 12 above for visual reference of coordinate system and mathematical explanation of calculations. Tabulated results do not include any in-situ effects.

Table 2– Motor current summary table – Gate 8

Test Run	Current Range due to Lifting (A)	Current Range due to Lowering (A)	Max In-rush Current (A)
1	8-13	5-11	102
2	8-13	5-11	100
3	8-13	5-11	100

Table 3 – Hoist force summary table – Gate 8

Test Run	Right Arm Peak Hoist Force (kips)	Left Arm Peak Hoist Force (kips)	Right Arm Hoist Force due to Total Gate Friction (kips)	Left Arm Hoist Force due to Total Gate Friction (kips)
1	32.96	27.86	4.46	3.78
2	32.90	27.93	4.52	3.81
3	32.94	28.07	4.57	3.89

Tabulated friction force values correspond to the response induced by friction in one direction

Table 4 – Maximum measured sensor stress range

Arm Designation	Top Strut (ksi)	Middle Strut (ksi)	Bottom Strut (ksi)
Right Arm	9.77	10.87	12.51
Left Arm	13.48	16.11	16.52

Tabulated values correspond to the total measured change in response during tests

Stress values have not been extrapolated to the extreme fibers (correspond to center of gage)

Table 5 – Maximum in-plane total bending stress & moment ranges – Total

Section Label	Section Description	Right Arm Stress (ksi)	Right Arm Moment (kip-in)	Left Arm Stress (ksi)	Left Arm Moment (kip-in)
Section A	Top Strut Near Pin	9.75	109.54	13.92	156.41
Section B	Middle Strut Near Pin	10.38	239.94	17.38	401.93
Section C	Bottom Strut Near Pin	11.30	315.04	16.75	467.09
Section D	Top Strut Away from Pin	1.68	18.88	2.28	25.63
Section E	Middle Strut Away from Pin	1.84	42.61	2.50	57.76
Section F	Bottom Strut Away from Pin	1.62	45.08	1.97	54.96

Tabulated values correspond to the total measured change in response during tests

Table 6 – In-plane frictional bending stress & moment at maximum gate friction

Section Label	Section Description	Right Arm Stress (ksi)	Right Arm Moment (kip-in)	Left Arm Stress (ksi)	Left Arm Moment (kip-in)
Section A	Top Strut Near Pin	4.80	53.93	6.81	76.55
Section B	Middle Strut Near Pin	5.12	118.47	8.52	196.99
Section C	Bottom Strut Near Pin	5.57	155.32	8.21	228.91
Section D	Top Strut Away from Pin	0.65	7.31	1.05	11.84
Section E	Middle Strut Away from Pin	0.75	17.36	1.22	28.11
Section F	Bottom Strut Away from Pin	0.63	17.54	0.97	27.11

Tabulated values correspond to the response induced by friction in one direction

Table 7 – Strut shear range summary table due to friction

Arm Designation	Top Strut Shear (kip)	Middle Strut Shear (kip)	Bottom Strut Shear (kip)
Right Arm	0.61	1.36	1.71
Left Arm	0.89	2.26	2.56

Tabulated values correspond to the response induced by friction in one direction

Table 8 – Pin friction summary table

Test Run	Average Water Elevation during testing (ft)	Approximate Thrust at time of Testing (kips per arm)	Gate/Member Designation	Pin Friction Moment (kip-in)	Friction Coefficient
1	435.59	489.60	Right Pin	486.30	0.18
			Left Pin	749.90	0.28
2	435.59	489.60	Right Pin	461.20	0.18
			Left Pin	700.00	0.27
3	435.59	489.60	Right Pin	467.10	0.18
			Left Pin	697.50	0.27

Tabulated values correspond to the response induced by friction in one direction

APPENDIX A – GATE 8 TORQUE AND HOIST FORCE PLOTS

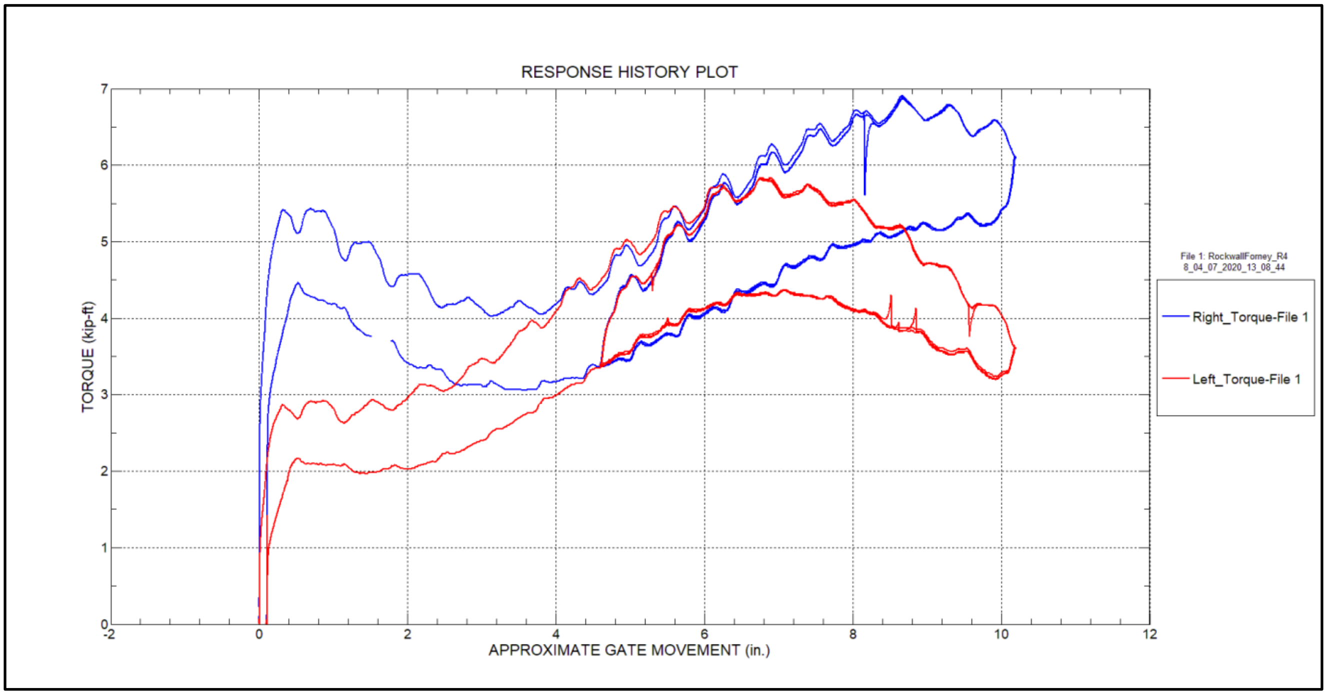

Figure 25 – Hoist torque response history – Gate 8 – Test 1

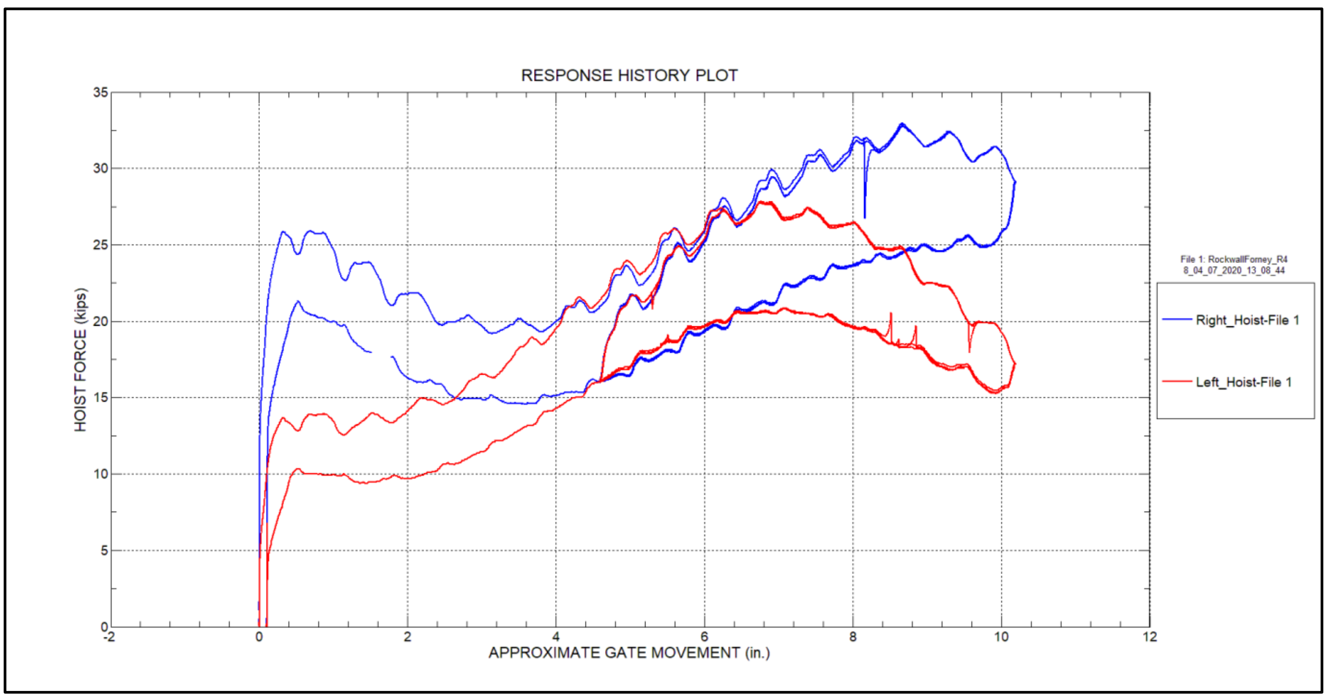

Figure 26 – Hoist force response history – Gate 8 – Test 1

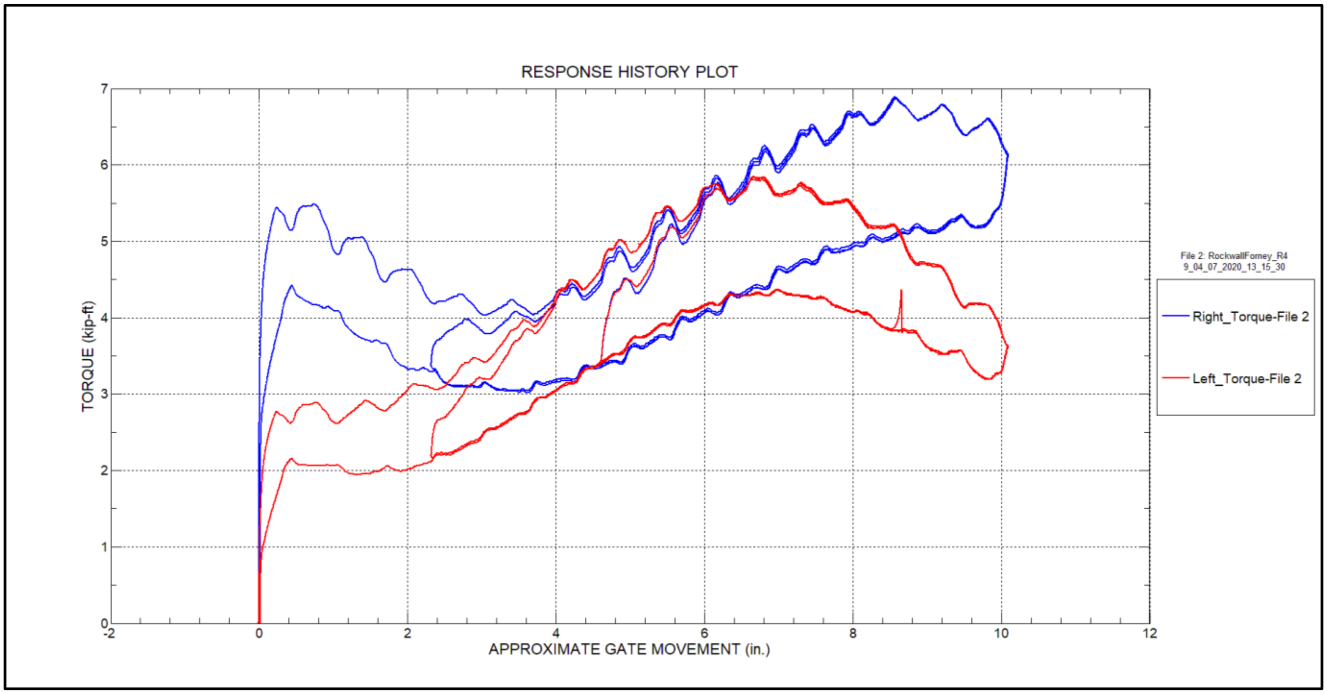

Figure 27 – Hoist torque response history – Gate 8 – Test 2

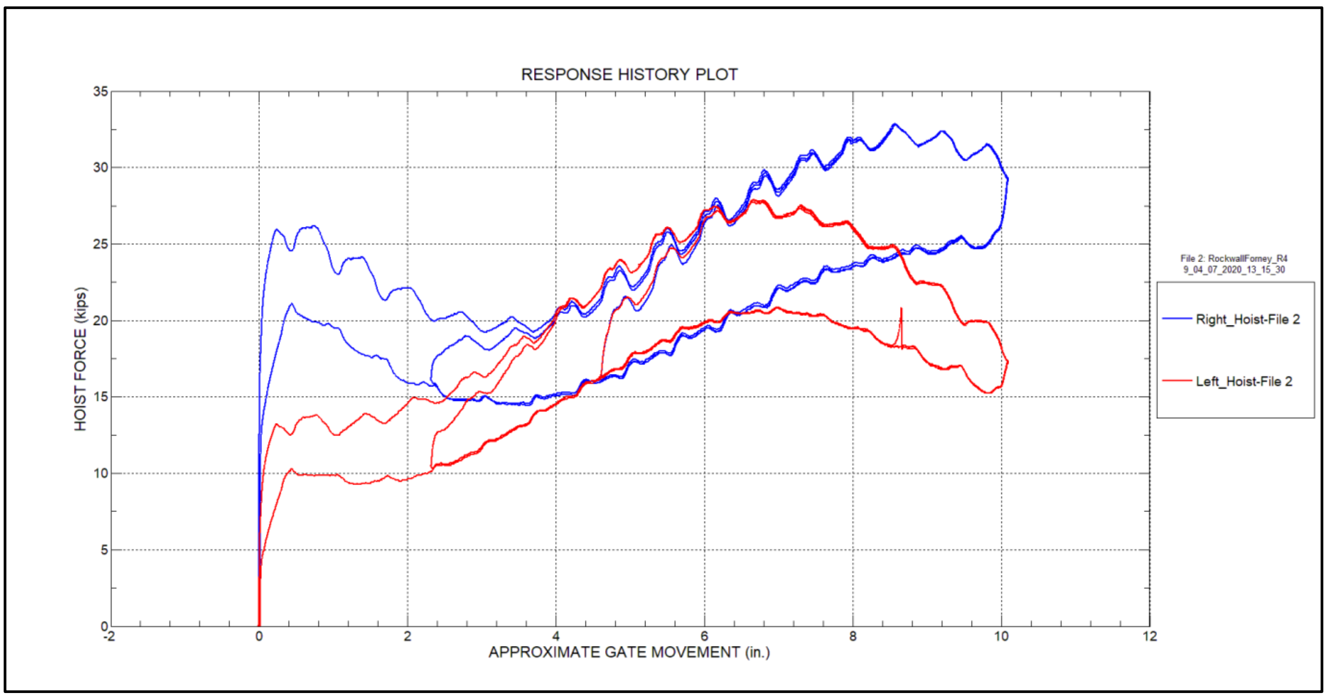

Figure 28 – Hoist force response history – Gate 8 – Test 2

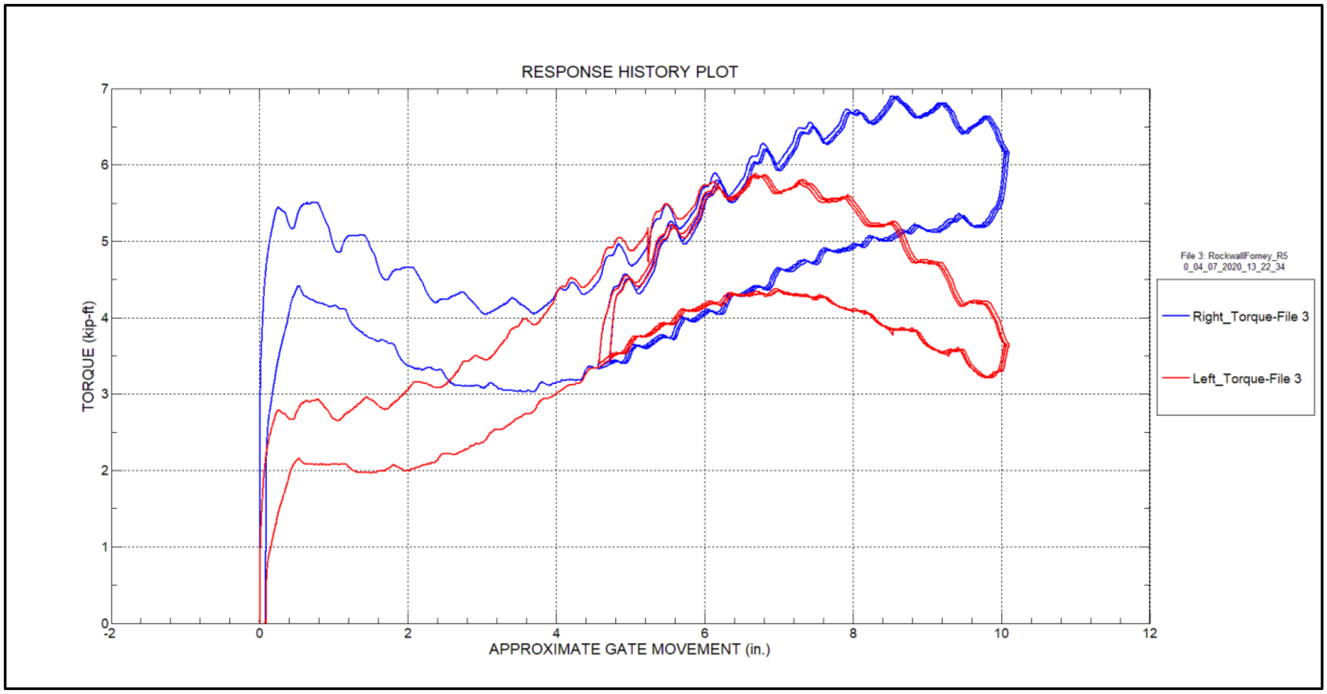

Figure 29 – Hoist torque response history – Gate 8 – Test 3

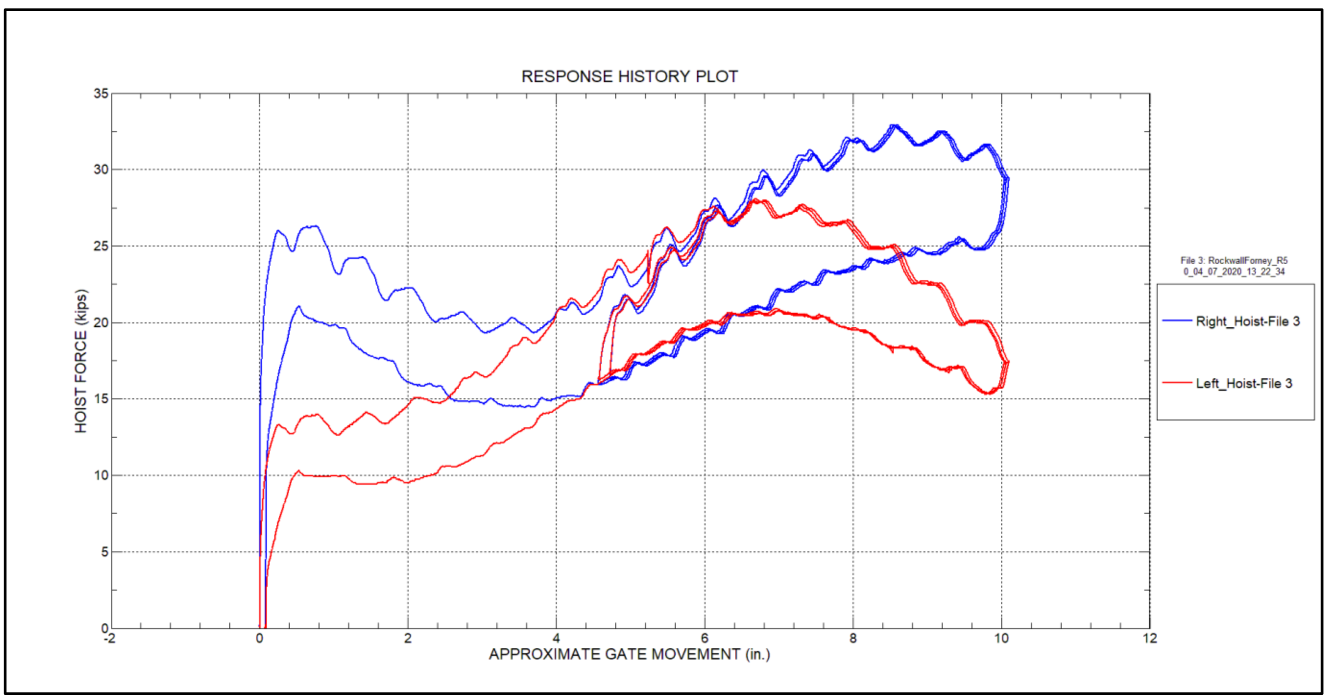

Figure 30 – Hoist force response history – Gate 8 – Test 3

APPENDIX B – GATE 8 PIN MOMENT COMPONENT PLOTS

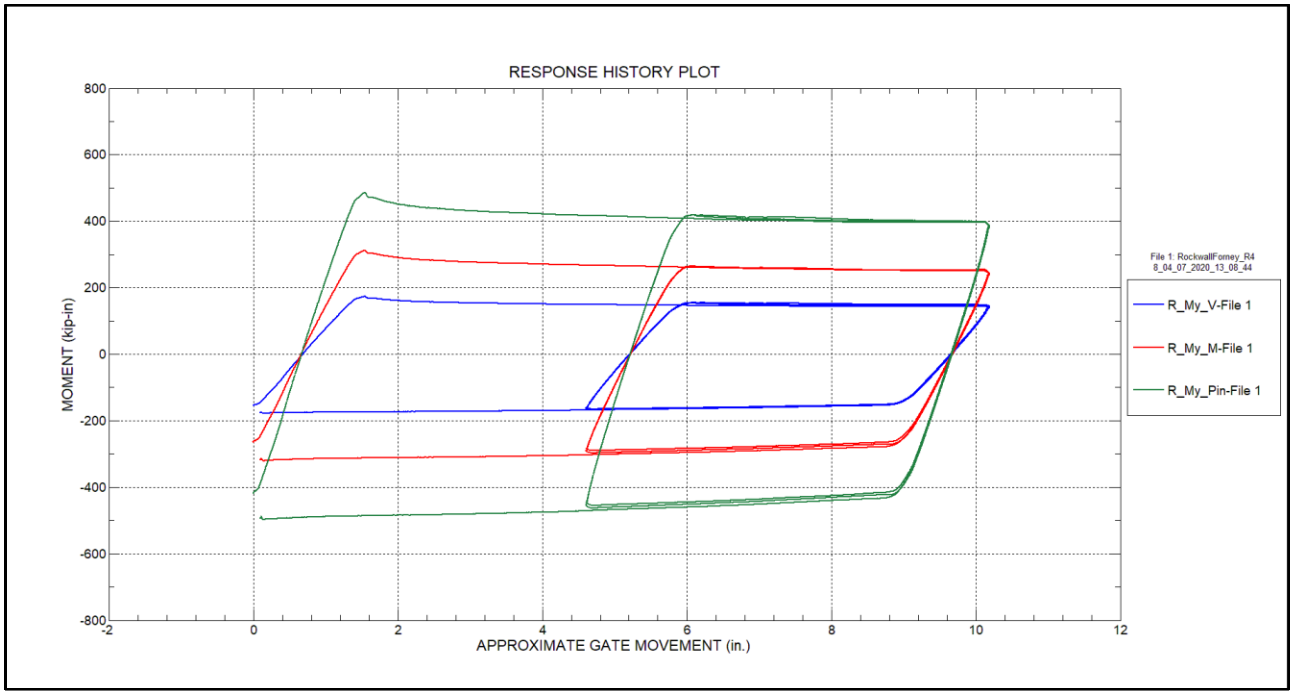

Figure 31 – Pin moment response history – Right arm – Test run 1

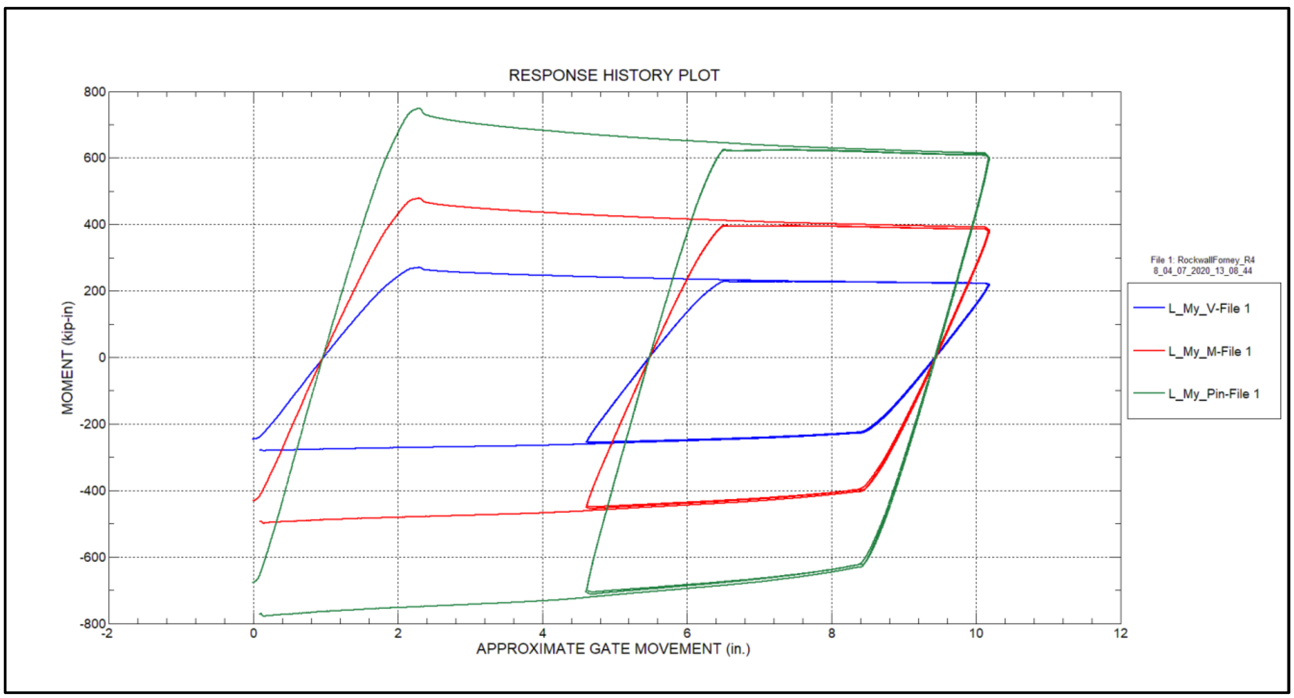

Figure 32 – Pin moment response history – Left arm – Test run 1

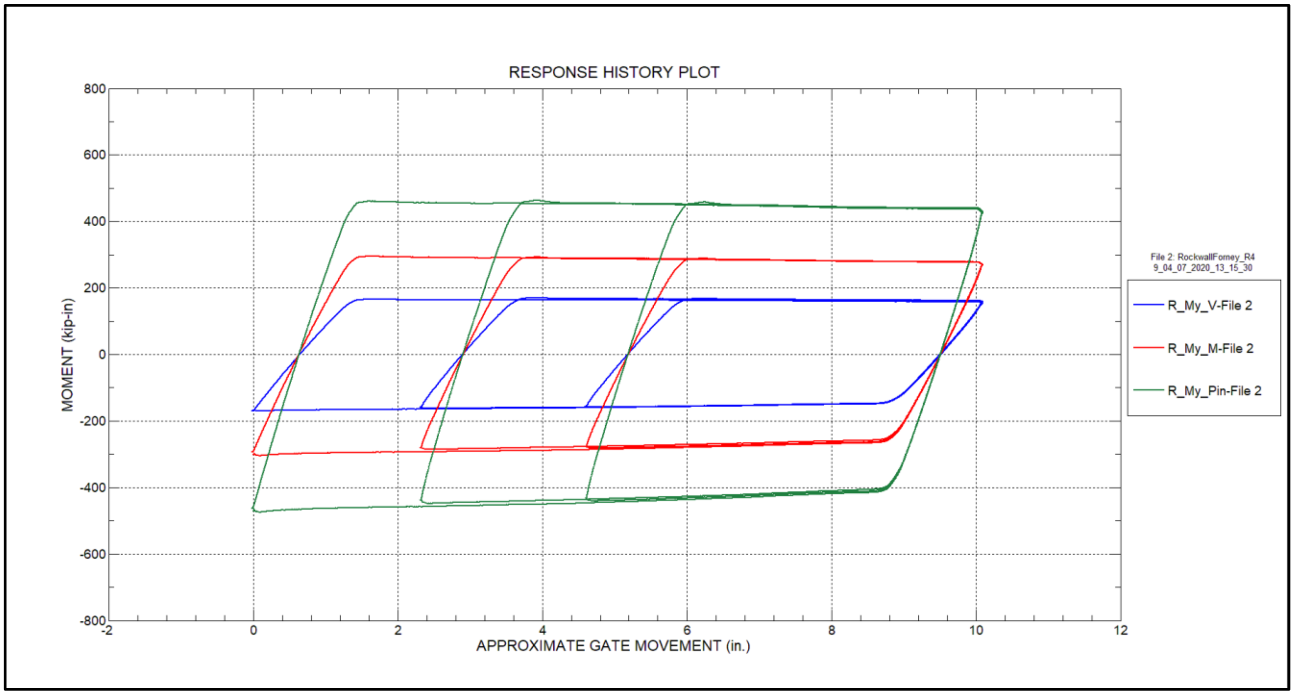

Figure 33 – Pin moment response history – Right arm – Test run 2

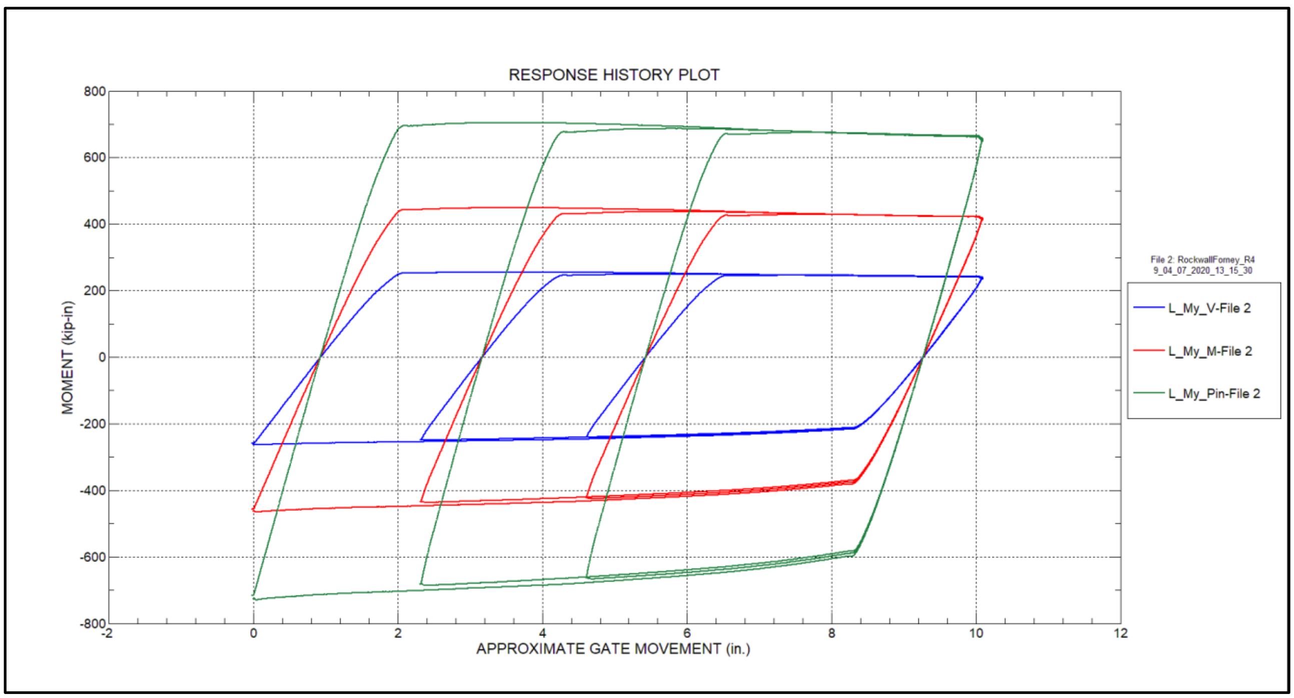

Figure 34 – Pin moment response history – Left arm – Test run 2

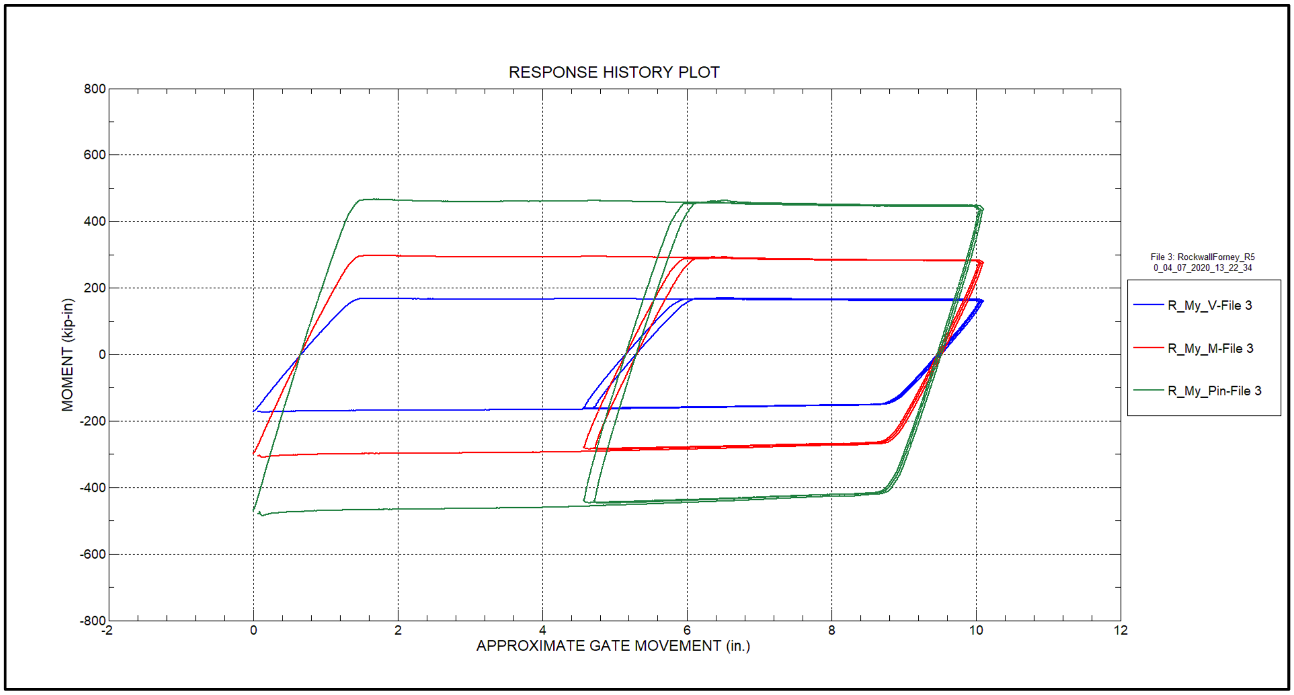

Figure 35 – Pin moment response history – Right arm – Test run 3

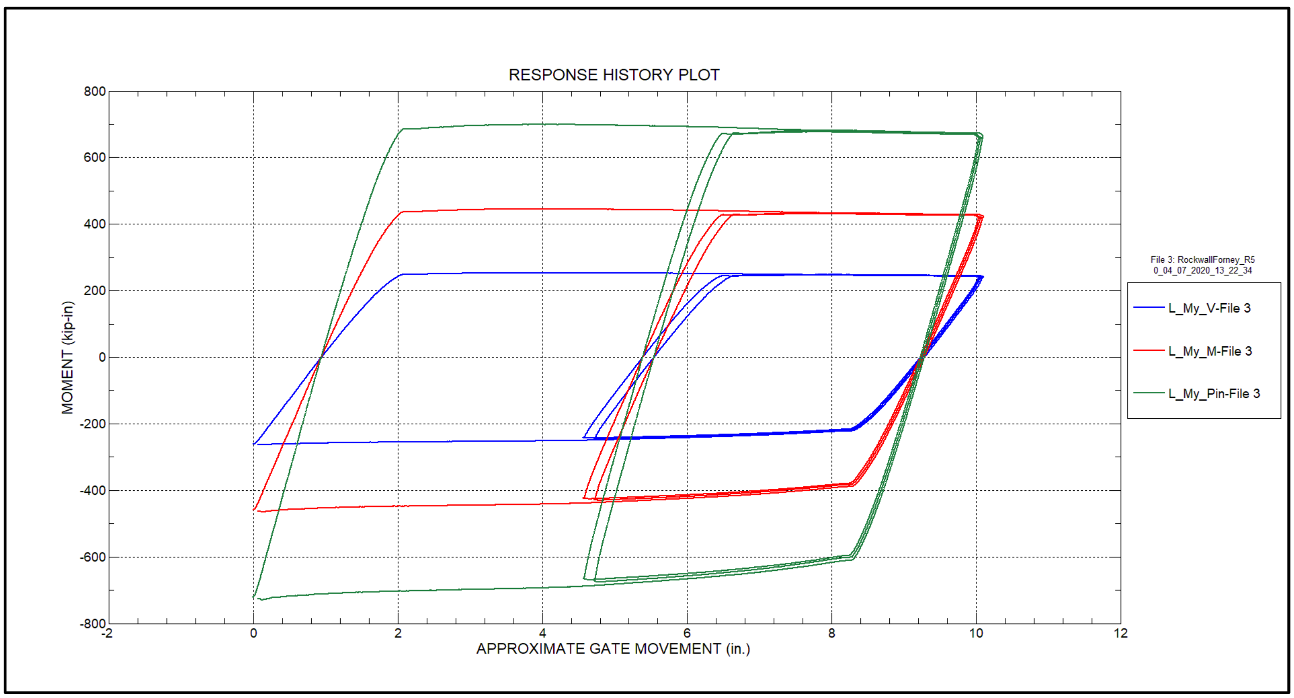

Figure 36 – Pin moment response history – Left arm – Test run 3

APPENDIX C – INSTRUMENTATION PLANS

RAW DATA. REFINED RESULTS.

SCHNABEL ENGINEERING
ROCKWALL FORNEY DAM
LIVE LOAD TESTING

RAW DATA. REFINED RESULTS.
740 S PIERCE AVE, SUITE 15
LOUISVILLE, CO 80027
303.494.3230
WWW.BDITEST.COM

ISSUE

CLIENT

SCHABEL ENGINEERING
16000 CHRISTENSEN RD, STE 101
SEATTLE, WA 98188

PROJECT NAME

SCHNABEL ENGINEERING
ROCKWALL FORNEY DAM
LIVE LOAD TESTING

Drawn By:	KNR
Checked By:	JDS
Date:	05/27/2020
Client No.:	
BDI No.:	190701-TX
SCALE:	NTS

COVER PAGE

LLT-00

The user acknowledges that these documents are instruments of professional service, and are protected by Copyright. This document and the information contained in this document are the property of Bridge Diagnostics, Inc., and shall not be reused, copied, disseminated, modified, amended or altered in any way. It is issued for information purposes only. The user agrees to hold harmless, indemnify and defend Bridge Diagnostics, Inc. against any and all damages, claims and losses, including defense costs, arising out of any use, reuse or copying of this document.

PLOT TIME: 6/12/2020 3:22 PM
FILEPATH: C:\Users\colemand\BDI\Services - Documents\Server_Remote\190701-TX_Schnabel_RockwallForneyDam\7. Instrumentation Plans\BDI_ROCKWALLFORNEY_01_GENERAL.dwg
© YYYY BRIDGE DIAGNOSTICS INC.

GAGE LEGEND & SPECIFICATION

SYMBOL	TYPE	BRAND	MODEL	NOTES
(strain transducer symbol)	STRAIN TRANSDUCER	BDI	ST350	
(tiltmeter symbol)	TILTMETER (UNI-AXIAL)	BDI	T500-030	
(torque sensor symbol)	TORQUE SENSOR	HPI	-	HBWS-35-125-6-0.5VR-FB
(amp sensor symbol)	AMP SENSOR	CR MAGNETICS	CR42105-200	

GENERAL NOTES

- INSTRUMENTATION SHALL BEGIN ON APRIL 1ST, 2020.
- GATES 1 THRU 14 SHALL BE ACCESSED USING SPRAT ROPE ACCESS TECHNIQUES.
- BDI WILL PERFORM ALL SURFACE PREPARATION, SENSOR INSTALLATION, AND EQUIPMENT INSTALLATION.
- SEE LLT-31 FOR SENSOR INSTALLATION DETAILS.
- TWO PAIRS OF TORQUE GAGES WILL BE INSTALLED ON THE GATE MOTORS' PINION SHAFTS BETWEEN THE MOTORS AND THE HOISTS.
  - GAGE PAIRS WILL BE INSTALLED 180° APART FROM EACH OTHER.
  - EXACT POSITIONS OF THE GAGE PAIRS ON THE PINION SHAFT WILL BE DETERMINED IN THE FIELD.
- THREE PHASE AMPERAGE GAGES WILL BE INSTALLED ON THE MOTOR CONTROLS BY A QUALIFIED ELECTRICIAN PROVIDED BY GARVER.

TESTING PROCEDURE:

- TESTING SHALL BE STARTED WITH THE GATE IN THE CLOSED POSITION.
- ONCE DATA COLLECTION BEGINS, THE GATE SHALL BE RAISED TO TWO OR THREE TIMES THE HEIGHT NECESSARY FOR TRUNNION FRICTION TO BE OVERCOME, H1 (TYPICALLY 6"-12"), AND HELD THERE UNTIL DATA STABILIZES.
- THE GATE SHALL BE LOWERED APPROXIMATELY TWICE THE DISTANCE TO OVERCOME TRUNNION FRICTION, H2, AND HELD THERE UNTIL DATA STABILIZES.
- THE GATE SHALL BE RAISED TO H1 AND HELD THERE UNTIL DATA STABILIZES.
- THE GATE SHALL BE LOWERED TO H2 AND HELD THERE UNTIL DATA STABILIZES.
- THE GATE SHALL BE RAISED TO H1 AND HELD THERE UNTIL DATA STABILIZES.
- THE GATE WAS LOWERED BACK TO CLOSED POSITION AND DATA COLLECTION STOPPED.
- A MINIMUM OF 3 TESTS SHALL BE PERFORMED PER GATE.

GAGE COUNT PER GATE

SENSOR LEGEND	SENSOR COUNT	CHANNEL COUNT
STRAIN TRANSDUCER	(48)	(48)
TILTMETER (UNI-AXIAL)	(4)	(4)
TORQUE SENSOR	(4)	(4)
AMP SENSOR	(3)	(3)
TOTAL	(59)	(59)

LOCATION KEY

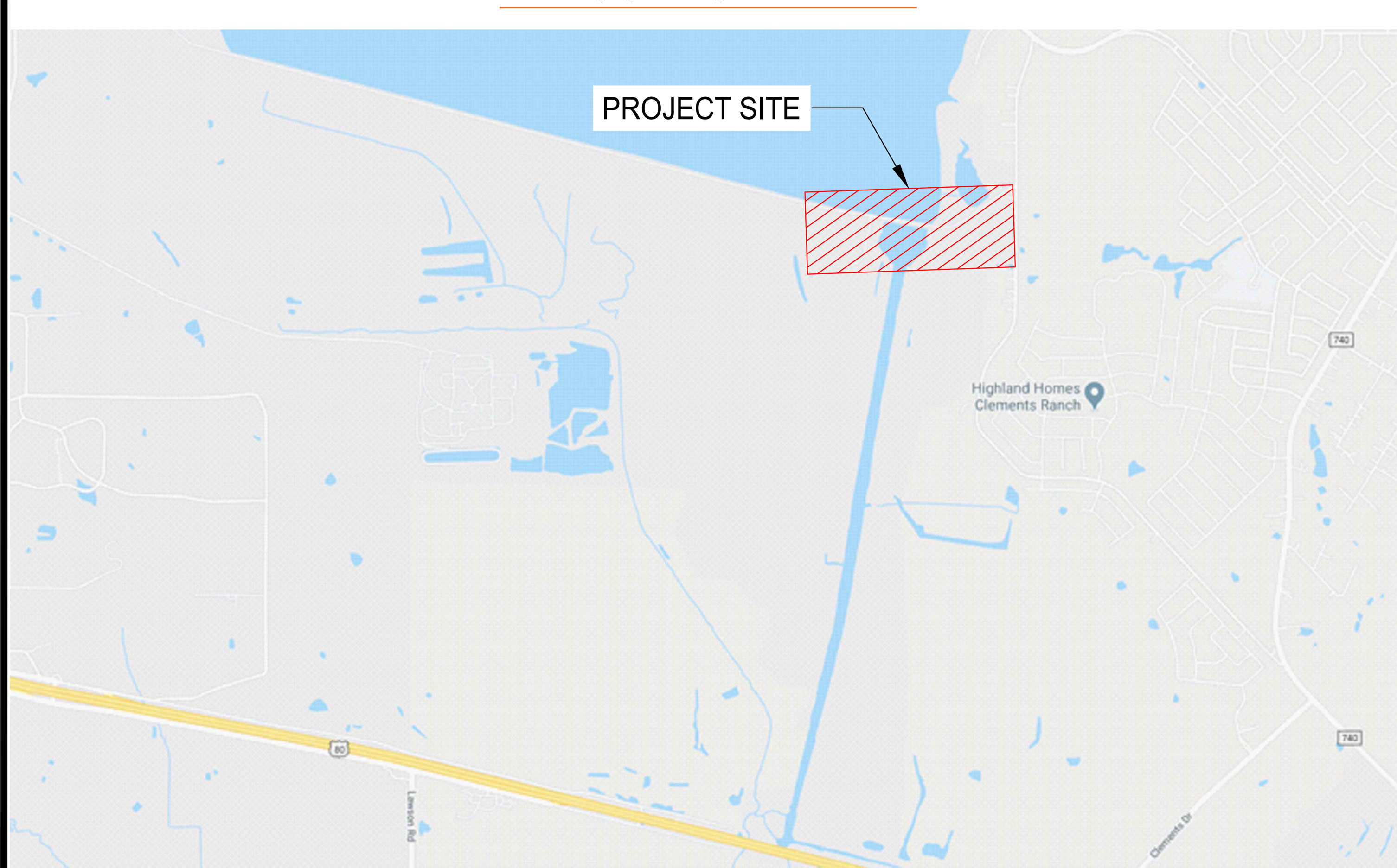

INDEX OF SHEETS

INDEX OF ISSUE

NO.	DATE	REVISION DESCRIPTION
1	3/20/2020	LIVE LOAD TESTING (LLT) INSTRUMENTATION PLAN (FOR APPROVAL)
2	5/27/2020	LIVE LOAD TESTING (LLT) INSTRUMENTATION PLAN AS BUILTS
BDI REFERENCE NUMBER: 190701-TX		

BDI
RAW DATA. REFINED RESULTS.
740 S PIERCE AVE, SUITE 15
LOUISVILLE, CO 80027
303.494.3230
WWW.BDITEST.COM

ISSUE

CLIENT

SCHABEL ENGINEERING
16000 CHRISTENSEN RD, STE 101
SEATTLE, WA 98188

PROJECT NAME

SCHNABEL ENGINEERING
ROCKWALL FORNEY DAM
LIVE LOAD TESTING

Drawn By:	KNR
Checked By:	JDS
Date:	05/27/2020
Client No.:	
BDI No.:	190701-TX
SCALE:	NTS

OVERALL LEGEND

LLT-01

The user acknowledges that these documents are instruments of professional service, and are protected by Copyright. This document and the information contained in this document are the property of Bridge Diagnostics, Inc., and shall not be reused, copied, disseminated, modified, amended or altered in any way. It is issued for information purposes only. The user agrees to hold harmless, indemnify and defend Bridge Diagnostics, Inc. against any and all damages, claims and losses, including defense costs, arising out of any use, reuse or copying of this document.

PLOT TIME: 6/12/2020 3:22 PM
FILEPATH: C:\Users\colemand\BDI\Services - Documents\Server_Remote\190701-TX_Schnabel_RockwallForneyDam\7. Instrumentation Plans\BDI_ROCKWALLFORNEY_01_GENERAL.dwg
© YYYY BRIDGE DIAGNOSTICS INC.

The user acknowledges that these documents are instruments of professional service, and are protected by Copyright. This document and the information contained in this document are the property of Bridge Diagnostics, Inc., and shall not be reused, copied, disseminated, modified, amended or altered in any way. It is issued for information purposes only. The user agrees to hold harmless, indemnify and defend Bridge Diagnostics, Inc. against any and all damages, claims and losses, including defense costs, arising out of any use, reuse or copying of this document.

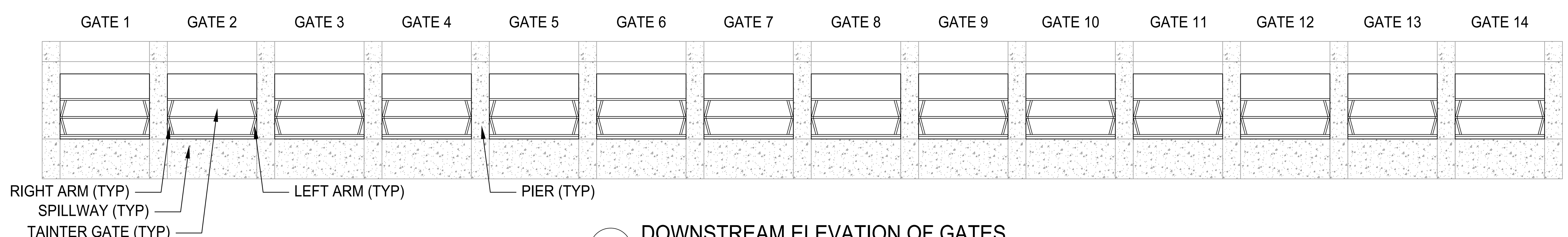

1 DOWNSTREAM ELEVATION OF GATES
LOOKING NORTH (UPSTREAM)

RAW DATA. REFINED RESULTS.
740 S PIERCE AVE, SUITE 15
LOUISVILLE, CO 80027
303.494.3230
WWW.BDITEST.COM

ISSUE

CLIENT

SCHABEL ENGINEERING
16000 CHRISTENSEN RD, STE 101
SEATTLE, WA 98188

PROJECT NAME

SCHNABEL ENGINEERING
ROCKWALL FORNEY DAM
LIVE LOAD TESTING

Drawn By:	KNR
Checked By:	JDS
Date:	05/27/2020
Client No.:	
BDI No.:	190701-TX
SCALE:	NTS

OVERALL STRUCTURE LAYOUT
LLT-02

PLOT TIME: 6/12/2020 3:22 PM
FILEPATH: C:\Users\colemand\BDI\Services - Documents\Server_Remote\190701-TX_Schnabel_RockwallForneyDam\7. Instrumentation Plans\BDI_ROCKWALLFORNEY_01_GENERAL.dwg
© YYYY BRIDGE DIAGNOSTICS INC.

The user acknowledges that these documents are instruments of professional service, and are protected by Copyright. This document and the information contained in this document are the property of Bridge Diagnostics, Inc., and shall not be reused, copied, disseminated, modified, amended or altered in any way. It is issued for information purposes only. The user agrees to hold harmless, indemnify and defend Bridge Diagnostics, Inc. against any and all damages, claims and losses, including defense costs, arising out of any use, reuse or copying of this document.

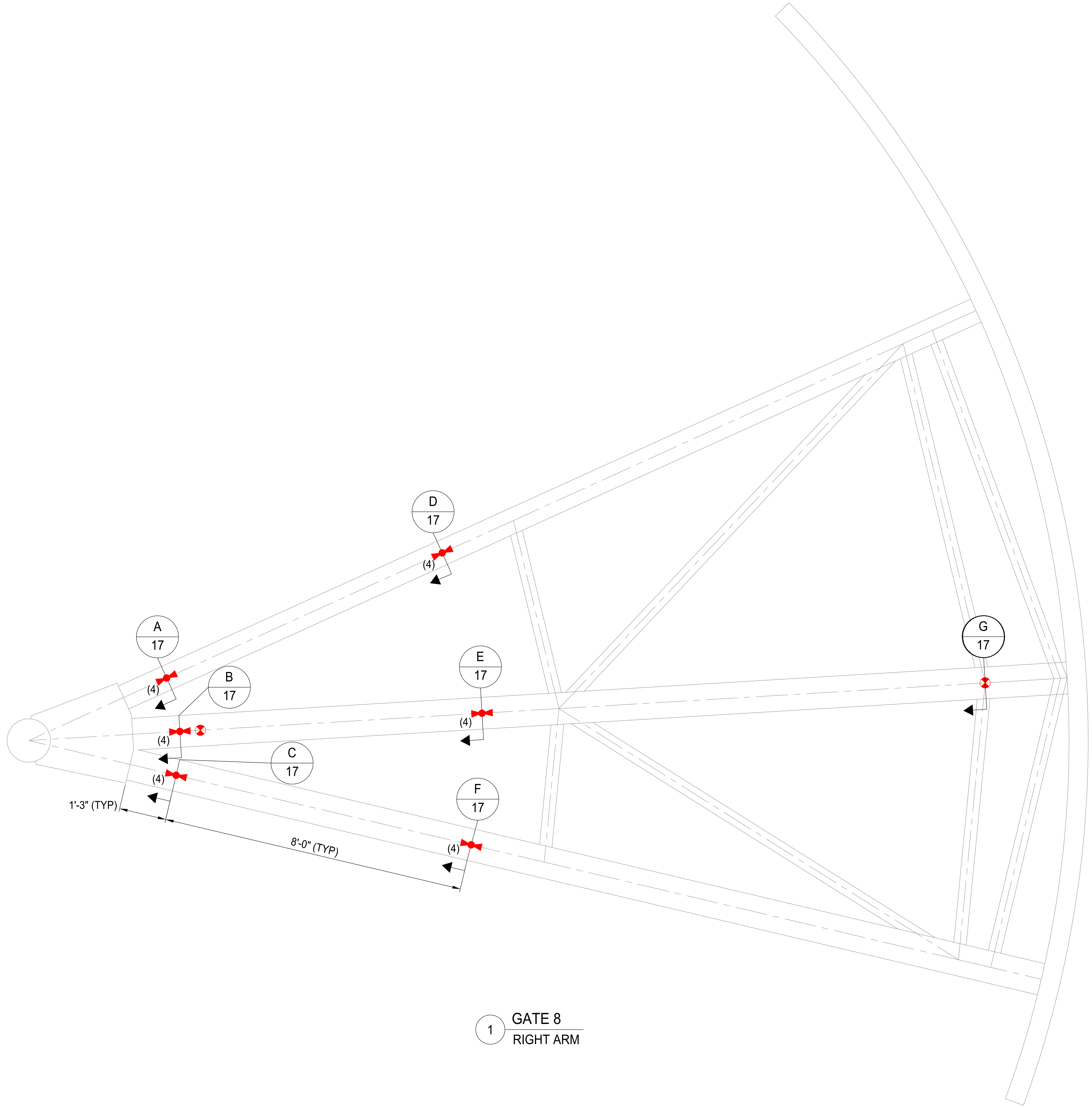

1 GATE 8
RIGHT ARM

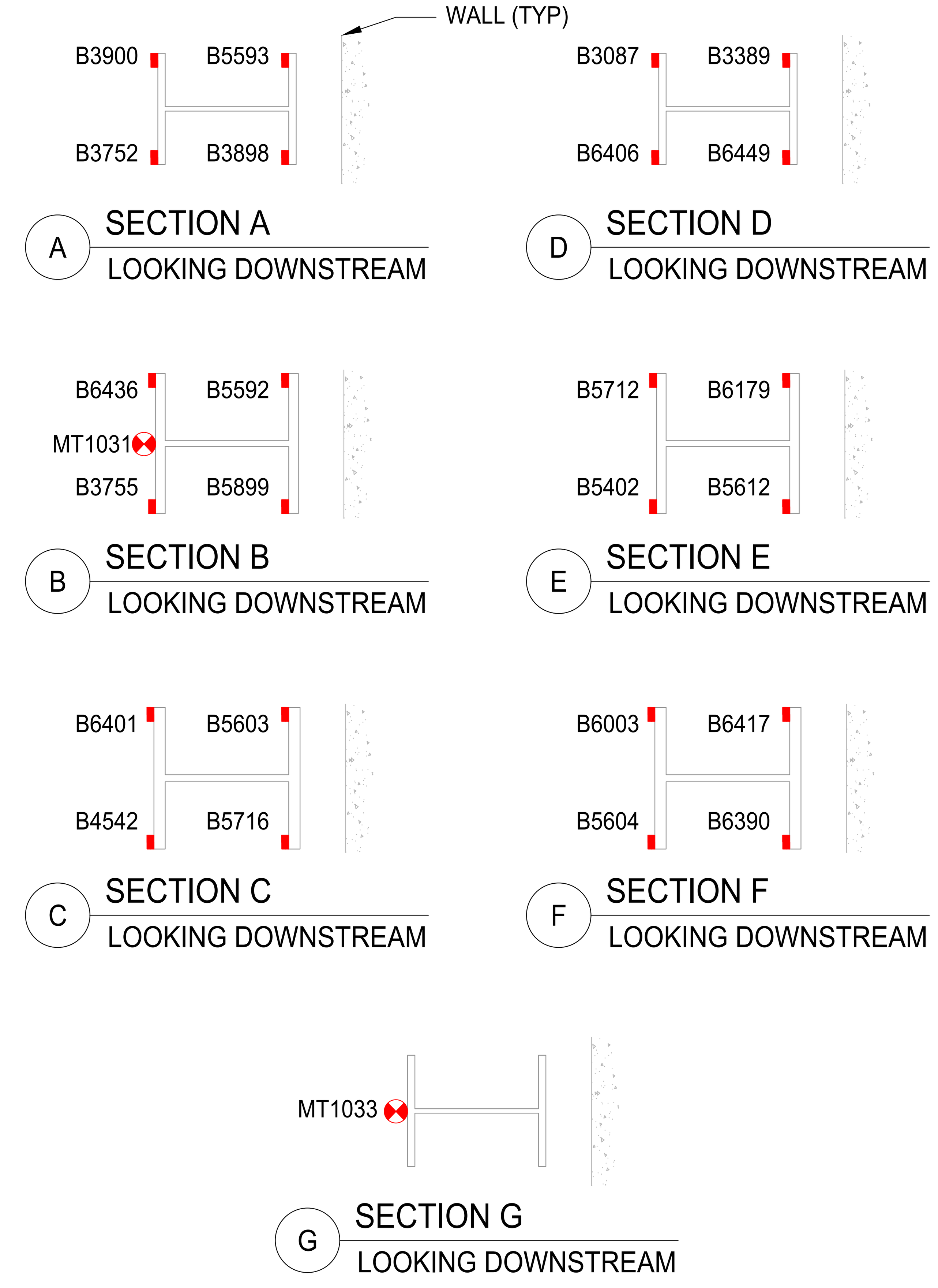

UNIT ID
TT-3

TORQUE GAGES
RIGHT ARM

NOTES:

1. SECTIONS A, B, & C SHALL BE INSTALLED 15 INCHES AWAY FROM TRUNNION PLATE.
2. TILTMETERS SHALL BE INSTALLED CENTERED ON THE MIDDLE STRUT FLANGE.
3. SECTION G'S TILTMETER SHALL BE INSTALLED AS CLOSE TO THE SKINPLATE AS POSSIBLE.

SENSOR LEGEND

- STRAIN TRANSDUCER
- TILTMETER (UNI-AXIAL)
- TORQUE SENSOR

BDI
RAW DATA. REFINED RESULTS.
740 S PIERCE AVE, SUITE 15
LOUISVILLE, CO 80027
303.494.3230
WWW.BDITEST.COM

ISSUE

CLIENT

SCHABEL ENGINEERING
16000 CHRISTENSEN RD, STE 101
SEATTLE, WA 98188

PROJECT NAME

SCHABEL ENGINEERING
ROCKWALL FORNEY DAM
LIVE LOAD TESTING

Drawn By:	KNR
Checked By:	JDS
Date:	05/27/2020
Client No.:	
BDI No.:	190701-TX
SCALE:	NTS

GATE 8 - RIGHT ARM
ELEVATION
LLT-17

PLOT TIME: 6/12/2020 3:23 PM
FILEPATH: C:\Users\colemand\BDI\Services - Documents\Server_Remote\190701-TX_Schnabel_RockwallForneyDam\7. Instrumentation Plans\BDI_ROCKWALLFORNEY_01_GENERAL.dwg
© YYYY BRIDGE DIAGNOSTICS INC.

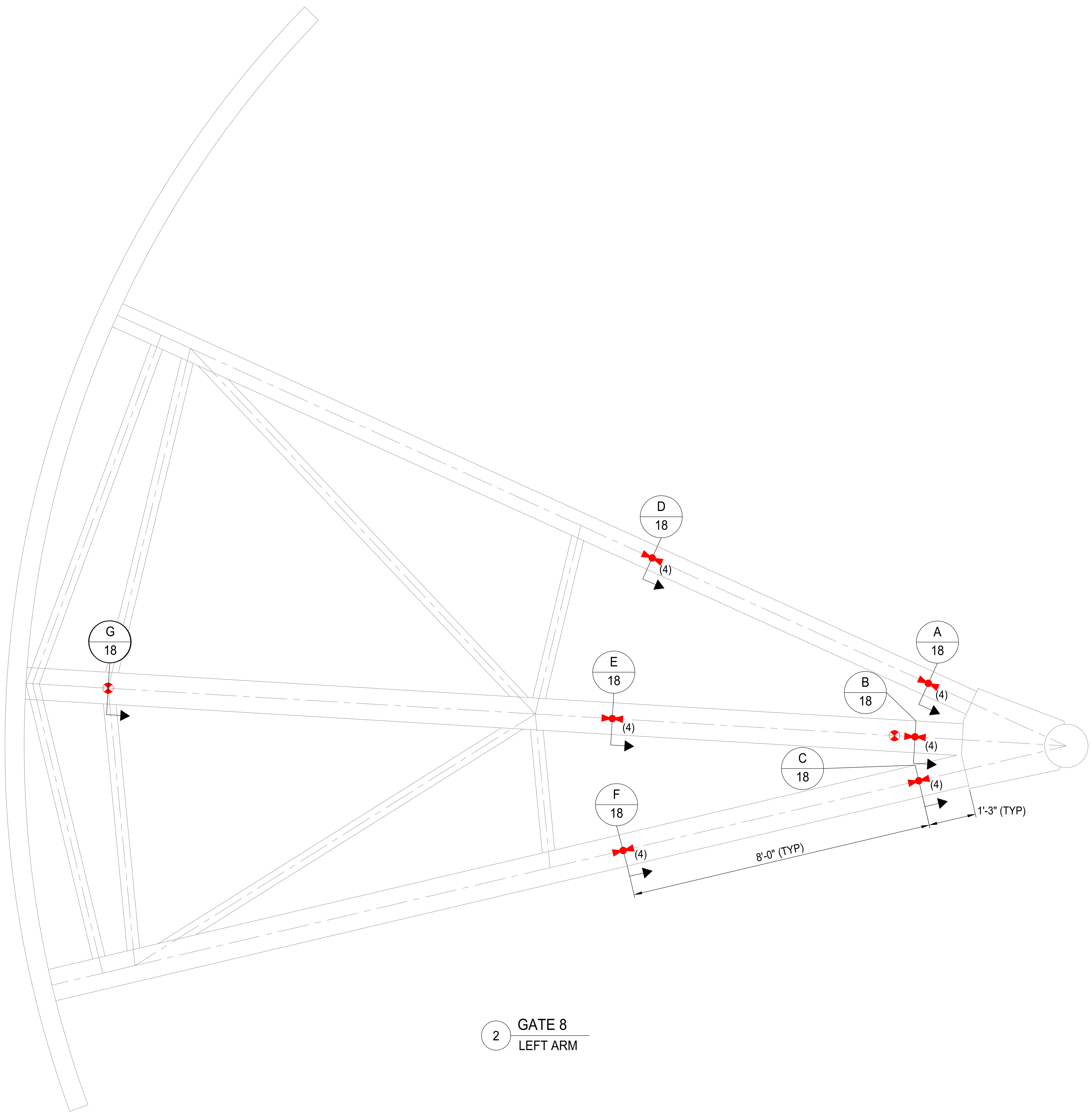

2 GATE 8
LEFT ARM

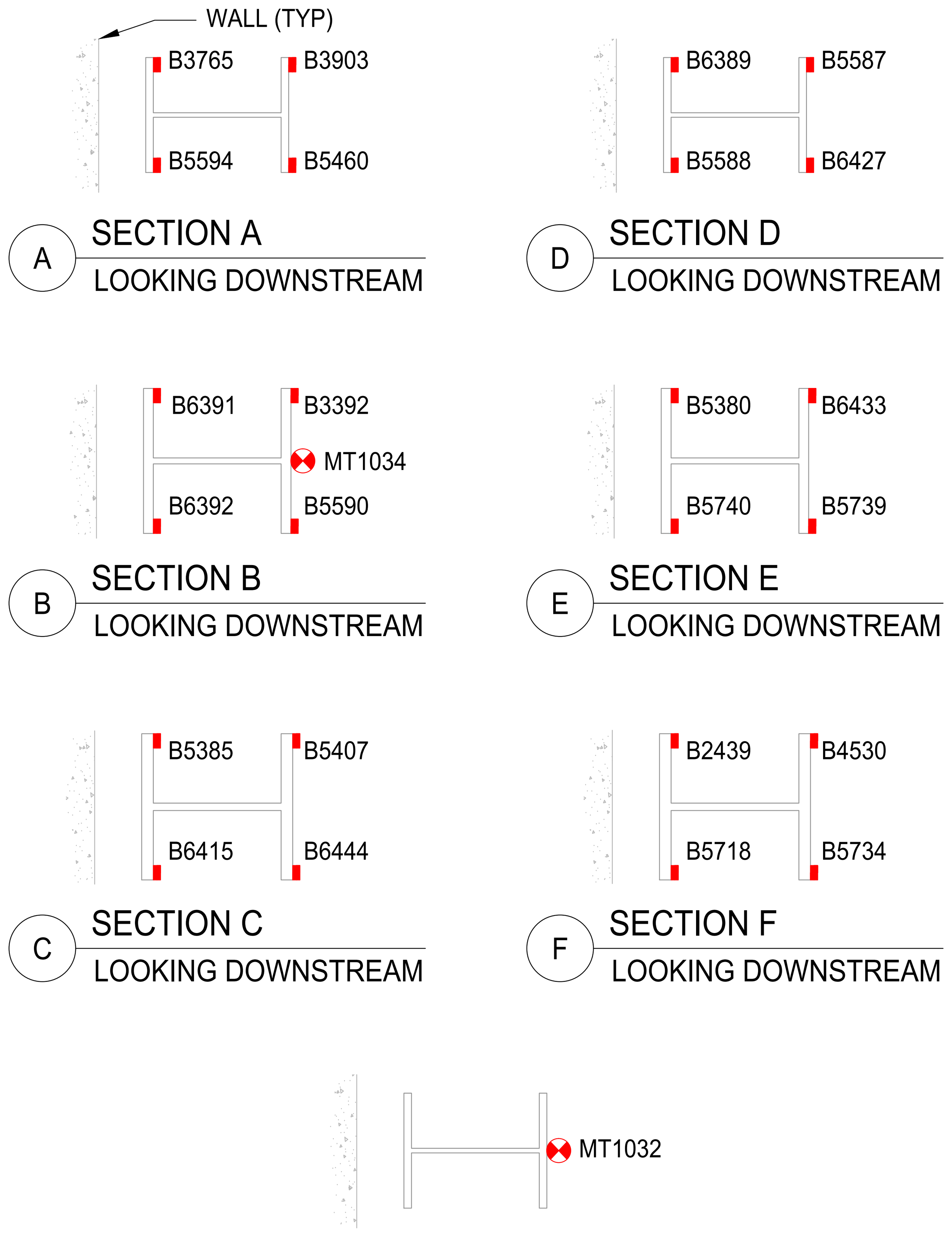

A SECTION A
LOOKING DOWNSTREAM

D SECTION D
LOOKING DOWNSTREAM

B SECTION B
LOOKING DOWNSTREAM

E SECTION E
LOOKING DOWNSTREAM

C SECTION C
LOOKING DOWNSTREAM

F SECTION F
LOOKING DOWNSTREAM

G SECTION G
LOOKING DOWNSTREAM

UNIT ID
TT-4

TORQUE GAGES
LEFT ARM

NOTES:

1. SECTIONS A, B, & C SHALL BE INSTALLED 15 INCHES AWAY FROM TRUNNION PLATE.
2. TILTMETERS SHALL BE INSTALLED CENTERED ON THE MIDDLE STRUT FLANGE.
3. SECTION G'S TILTMETER SHALL BE INSTALLED AS CLOSE TO THE SKINPLATE AS POSSIBLE.

SENSOR LEGEND

- STRAIN TRANSDUCER
- TILTMETER (UNI-AXIAL)
- TORQUE SENSOR

The user acknowledges that these documents are instruments of professional service, and are protected by Copyright. This document and the information contained in this document are the property of Bridge Diagnostics, Inc., and shall not be reused, copied, disseminated, modified, amended or altered in any way. It is issued for information purposes only. The user agrees to hold harmless, indemnify and defend Bridge Diagnostics, Inc. against any and all damages, claims and losses, including defense costs, arising out of any use, reuse or copying of this document.

BDI
RAW DATA. REFINED RESULTS.
740 S PIERCE AVE, SUITE 15
LOUISVILLE, CO 80027
303.494.3230
WWW.BDITEST.COM

ISSUE

CLIENT

SCHABEL ENGINEERING
16000 CHRISTENSEN RD, STE 101
SEATTLE, WA 98188

PROJECT NAME

SCHNABEL ENGINEERING ROCKWALL FORNEY DAM LIVE LOAD TESTING

Drawn By:	KNR
Checked By:	JDS
Date:	05/27/2020
Client No.:	
BDI No.:	190701-TX
SCALE:	NTS

GATE 8 - LEFT ARM
ELEVATION
LLT-18

PLOT TIME: 6/12/2020 3:23 PM
FILEPATH: C:\Users\colemand\BDI\Services - Documents\Server_Remote\190701-TX_Schnabel_RockwallForneyDam\7. Instrumentation Plans\BDI_ROCKWALLFORNEY_01_GENERAL.dwg
© YYYY BRIDGE DIAGNOSTICS INC.

The user acknowledges that these documents are instruments of professional service, and are protected by Copyright. This document and the information contained in this document are the property of Bridge Diagnostics, Inc., and shall not be reused, copied, disseminated, modified, amended or altered in any way. It is issued for information purposes only. The user agrees to hold harmless, indemnify and defend Bridge Diagnostics, Inc. against any and all damages, claims and losses, including defense costs, arising out of any use, reuse or copying of this document.

PLOT TIME: 6/12/2020 3:24 PM
FILEPATH: C:\Users\colemand\BDI\Services - Documents\Server_Remote\190701-TX_Schnabel_RockwallForneyDam\7. Instrumentation Plans\BDI_ROCKWALLFORNEY_01_GENERAL.dwg
© YYYY BRIDGE DIAGNOSTICS INC.

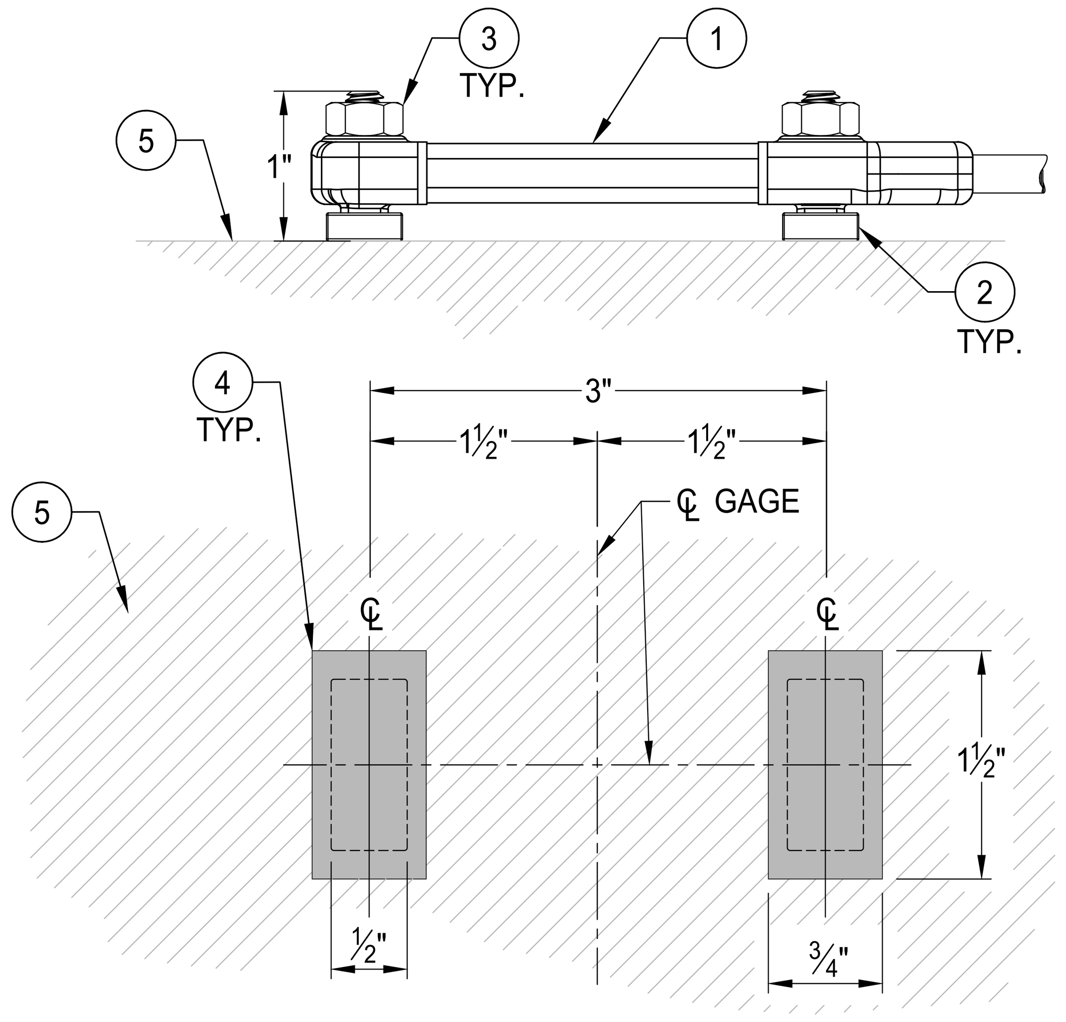

COMPONENT DESCRIPTION

1. ST350 STRAIN GAGE
2. 1/4"-20 THREADED MOUNTING TAB
3. 1/4"-20 STAINLESS STEEL NUT
4. TYPICAL SURFACE PREP REQUIRED TO MOUNT STRAIN GAGES
5. TYPICAL MOUNTING SURFACE

FOOTNOTES - INSTANT ADHESIVE
1. STRAIN GAGES SHALL BE MOUNTED WITH LOCTITE 410 INSTANT ADHESIVE AND LOCTITE 7452 ACCELERANT 2. DURING SURFACE PREP ALL PAINT AND SURFACE DEFORMATIONS MUST BE REMOVED. 3. SURFACE PREP IS REQUIRED JUST PRIOR TO GAGE INSTALLATION AS TO NOT ALLOW SURFACE CONTAMINANTS TO ACCUMULATE.

1 TYPICAL ST350 STRAIN GAGE INSTALLATION

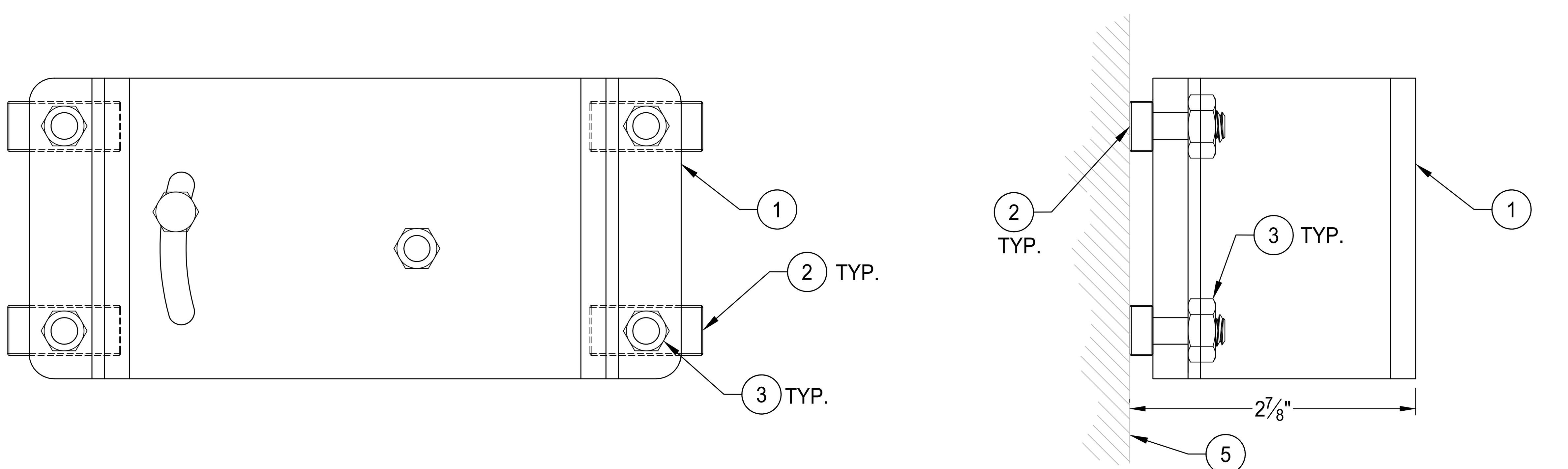

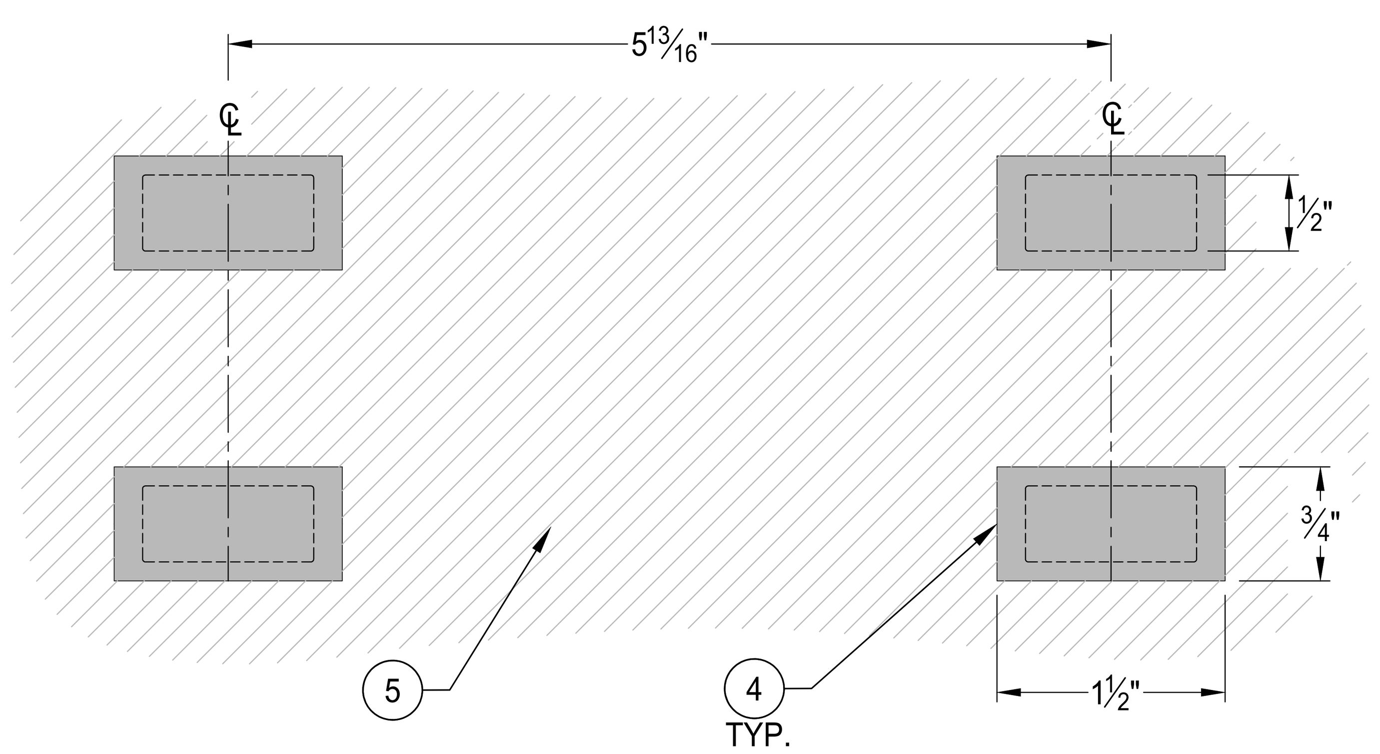

COMPONENT DESCRIPTION

1. BDI +/- 15 DEGREE TILTMETER WITH COVER AND ADJUSTMENT BOLTS
2. 1/4"-20 THREADED MOUNTING TAB
3. 1/4"-20 STAINLESS STEEL NUT
4. TYPICAL SURFACE PREP REQUIRED TO MOUNT TILTMETERS
5. TYPICAL MOUNTING SURFACE

FOOTNOTES - INSTANT ADHESIVE
1. TILTMETERS SHALL BE MOUNTED WITH LOCTITE 410 INSTANT ADHESIVE AND LOCTITE 7452 ACCELERANT 2. DURING SURFACE PREP ALL PAINT AND SURFACE DEFORMATIONS MUST BE REMOVED. 3. SURFACE PREP IS REQUIRED JUST PRIOR TO GAGE INSTALLATION AS TO NOT ALLOW SURFACE CONTAMINANTS TO ACCUMULATE.

2 TYPICAL BDI TILTMETER INSTALLATION

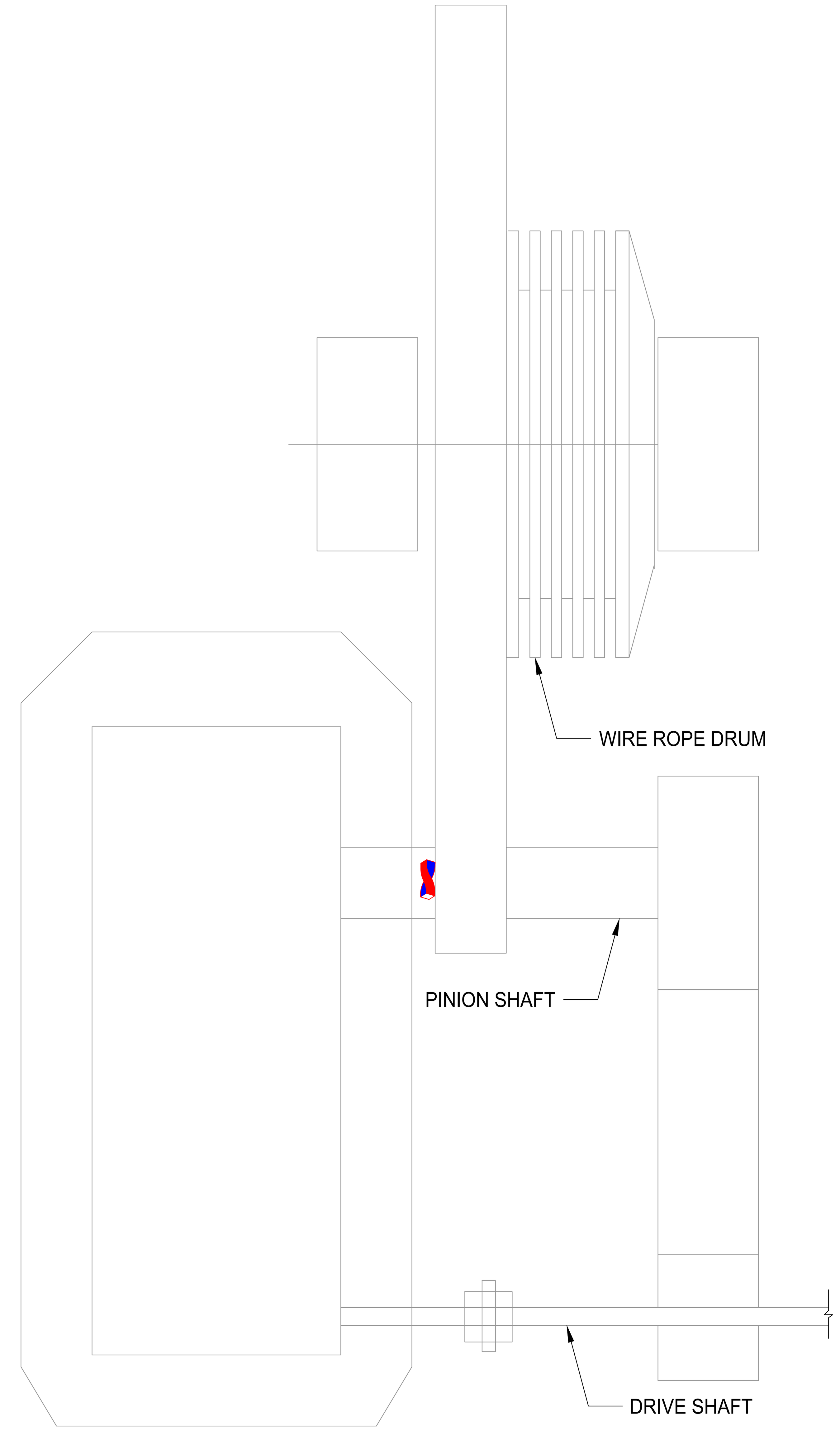

3 TYPICAL HOIST INSTRUMENTATION

TORQUE SENSOR INSTALLATION NOTES:
- TORQUE GAGES WILL BE INSTALLED ON THE PINION SHAFT ON EITHER HOIST MOTOR BETWEEN THE MOTOR AND THE HOIST DRUM
- EXACT POSITIONS OF THE GAGE PAIRS ON THE PINION SHAFT WILL BE DETERMINED IN THE FIELD

SENSOR LEGEND

TORQUE SENSOR

BDI
RAW DATA. REFINED RESULTS.
740 S PIERCE AVE, SUITE 15
LOUISVILLE, CO 80027
303.494.3230
WWW.BDITEST.COM

ISSUE

CLIENT

SCHABEL ENGINEERING
16000 CHRISTENSEN RD, STE 101
SEATTLE, WA 98188

PROJECT NAME

SCHNABEL ENGINEERING
ROCKWALL FORNEY DAM
LIVE LOAD TESTING

Drawn By:	KNR
Checked By:	JDS
Date:	05/27/2020
Client No.:	
BDI No.:	190701-TX
SCALE:	NTS

SENSOR INSTALLATION DETAILS

LLT-31

SCHNABEL ENGINEERING

TRUNNION PIN FRICTION TESTING REPORT

ROCKWALL FORNEY DAM – GATE 9
FORNEY, TX

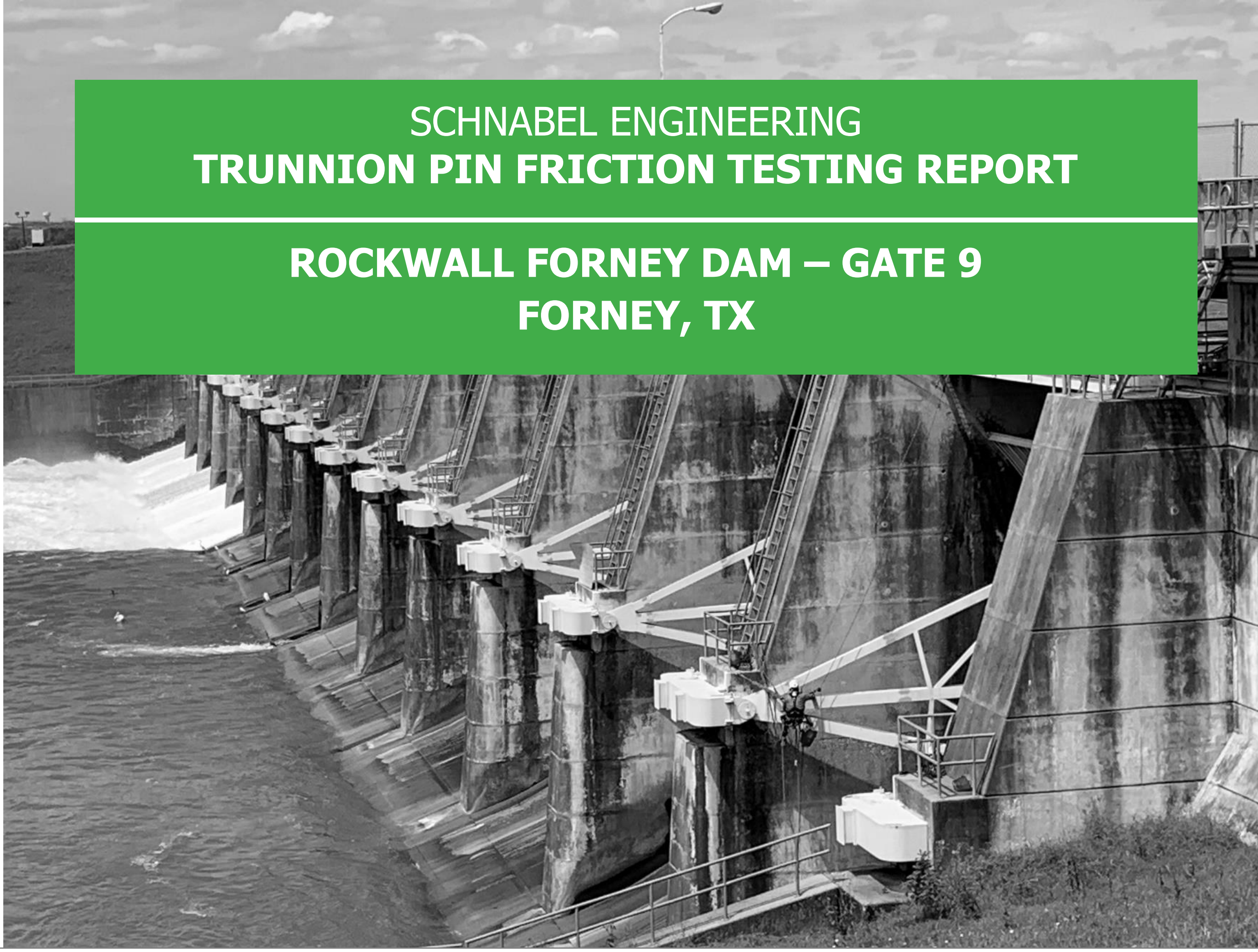

SUBMITTED TO:
SCHNABEL ENGINEERING
16000 CHRISTENSEN RD, SUITE 101
SEATTLE, WA 98188

SUBMITTED BY:
BDI – CO
740 SOUTH PIERCE AVE, UNIT 15
LOUISVILLE, CO 80027

BDI Project No.: **190701-TX**
Report Version: **V1**
Version Submitted: **August 26, 2020**

RAW DATA. REFINED RESULTS.

This document contains Confidential Information and is submitted in confidence to the customer. The submission of the information contained herein shall not be deemed to constitute public disclosure or authorization for disclosure to other parties. BDI's information and name may not be used in advertising or for promotional purposes without BDI's written consent.

TABLE OF CONTENTS

LIST OF FIGURES

LIST OF TABLES

EXECUTIVE SUMMARY

Schnabel Engineering contracted BDI to provide instrumentation and testing services on Gates 1-14 on the Rockwall Forney Dam near Dallas, Texas. The goal of these tests was to record each gate's structural responses during a series of spill tests and use the data to compute accurate coefficients of friction for each trunnion pin, cable lift force, total gate friction, and motor amperage. This report provides details on the work performed on Gate 9.

Instrumentation and testing were performed on Gate 9 at the Rockwall Forney Dam on April 8th, 2020. The gate arms were instrumented with strain and rotation sensors. The hoist motors' pinion shafts were instrumented with torque sensors and the hoist motor controls were instrumented with amperage sensors. Following the instrumentation, a series of spill tests were performed to measure the structural responses resulting from trunnion pin friction. All instrumentation setup and removal were performed using BDI's rope access team.

Following demobilization from the field, the test data was examined for quality and then further processed to evaluate the gate's performance. Strain measurements were converted into bending forces which were then applied to pin-strut free-body diagrams. By summing forces at each pin, friction induced moments could be computed, allowing accurate friction coefficients to be determined. Generally, the observed gate behavior showed that Gate 9 was operating as expected with no major signs of distress.

The resulting maximum trunnion friction coefficients and corresponding hoist forces are shown in Table 1.

Table 1 – Gate 9 performance summary

Pin Designation	Maximum Friction Coefficient	Maximum Pin Moment due to Pin Friction (kip-In)	Maximum Hoist Force (kips)	Maximum Hoist Force due to Total Gate Friction (kips)
Right Pin	0.17	443.0	31.09	4.19
Left Pin	0.20	522.7	23.34	3.05

Note: Pin designations are in reference to looking downstream

Due to restrictions caused by the hoist limit switches, the hoist cables could not always be fully slacked at the beginning and end of the performed tests. Throughout testing of the Rockwell Forney gates, it was found that this limit switch restriction varied gate to gate and arm to arm. Therefore, it is not recommended to use the collected hoist force data to quantify overall hoist forces during gate operation. Rather, this hoist data can be better utilized to evaluate total friction behavior.

Amperage responses were not used to compute friction results and were collected as verification that the motor performance was not causing unexpected gate responses. These responses indicated the motor was functioning in a stable manner and should be reviewed by a licensed electrician to further evaluate the motor's performance.

All results and recommendations provided in this report were based on the structure in its current condition; therefore, any significant changes in condition must be noted as they may alter their validity. Questions regarding this report and/or data should be directed to Kyle Ramer (kyler@bditest.com) at BDI. For further information on BDI's equipment, services, and analysis methods please visit www.bditest.com

INSTRUMENTATION AND LOAD TESTING PROCEDURE

GATE INSTRUMENTATION SUMMARY

Instrumentation and testing were performed on Gate 9 at the Rockwall Forney Dam on April 8th, 2020. Instrumentation plans have been provided along with this report and include the following number of instrumented locations and sensor types:

+ **REUSABLE SURFACE MOUNTED STRAIN TRANSDUCERS:** Each gate arm was instrumented with a total of 24 strain transducers at 6 locations on each of the gate arms (48 strain sensors total). A typical strain gage installation is shown in Figure 1. Note these sensors were installed with the mounting tabs on the extreme fiber of the strut flanges, which puts the center of the gage approximately 0.66" from the extreme fiber.
+ **TILTMETER ROTATION SENSORS:** MEMS style rotation sensors were located on the middle strut of the gate arm near the skin plate and near the trunnion hub (4 rotation sensors total). The rotation responses were used to calculate vertical skin plate movement and measure pin rotation relative to skin plate rotation. Typical tiltmeter installations are shown in Figure 1 and Figure 2.
+ **TORQUE SENSORS:** Two total torque sensors were installed on the hoist's pinion shafts (QTY1 on each hoist pinion shaft) near the cable hoist motor to measure direct torque and in turn lift force (See Figure 3).
+ **AMPERAGE SENSORS:** 3 Hall-Effect amperage transducers were clamped over each phase of the hoist motor to measure the motor's current draw (See Figure 4). The purpose of these sensors was to provide additional data in case there were any issues with the hoist systems and to verify any data issues related to lifting and lowering the gates.
+ **BDI'S STS-4 WIRELESS DATA ACQUISITION SYSTEM:** BDI's STS-4 wireless data acquisition (DAQ) was used to collect and record data during testing. A group of sensors were wired to each nodal DAQ which then communicated wirelessly back to the wireless base station and was controlled by BDI's STS-Live testing software.

Complete specifications are available upon request and can be found at http://www.bditest.com.

SENSOR INSTALLATION

BDI strain transducers were installed by first sanding paint off the struts to expose bare metal at two small locations (1"x2" areas) for the sensor's mounting tabs. Each transducer was then attached using a combination of fast-setting adhesive and accelerator and applying pressure until the adhesive was fully cured. Each strain transducer took approximately five minutes to attach.

Tiltmeters were installed using the same adhesive process as the strain transducers. However, no surface preparation was necessary.

Torque sensors were installed on the pinion shafts by capacitive discharge bonding. Properly bonding to the shaft required sanding the surface to a smooth finish, clean of any paint or grease. Responses from these gages were measured using Binsfeld Torque Trak 10k wireless transmitters.

A typical installation has been shown in Figure 1 through Figure 4. Access to all the sensor locations was provided by BDI's own SPRAT certified rope access technicians and engineers as shown in Figure 5.

Once testing was completed, sensors were removed, and exposed steel areas were covered using cold galvanizing compound.

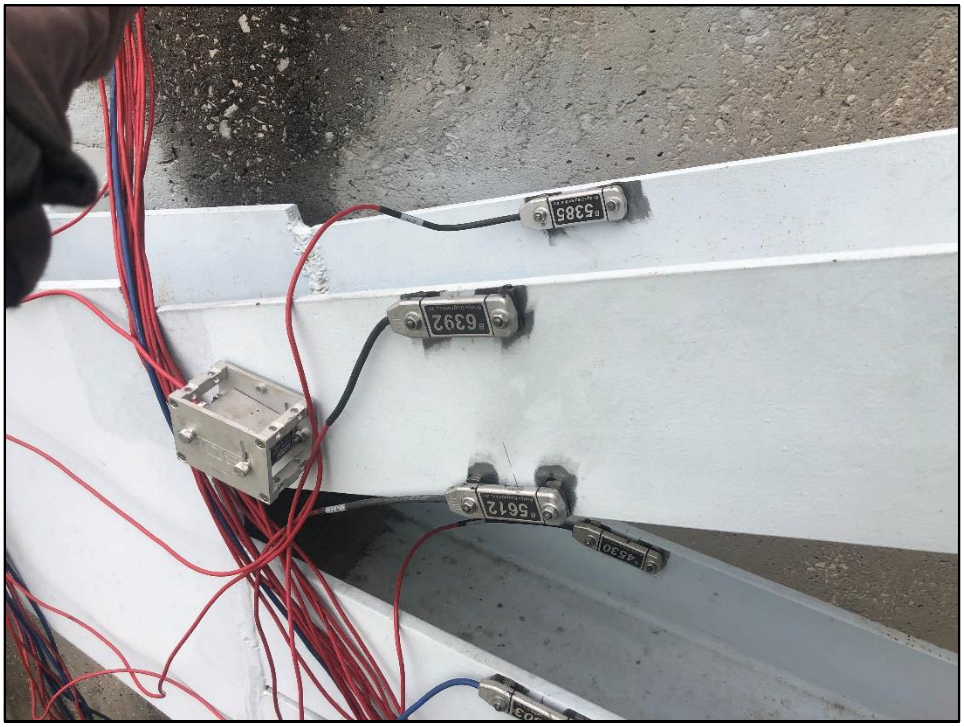

Figure 1 – BDI tiltmeter rotation sensor and reusable strain transducers installed near trunnion hub (Typical)

Figure 2 – BDI tiltmeter rotation sensor installed near skin plate (Typical)

Figure 3 – Torque sensor installation on hoist pinion shaft (Typical)

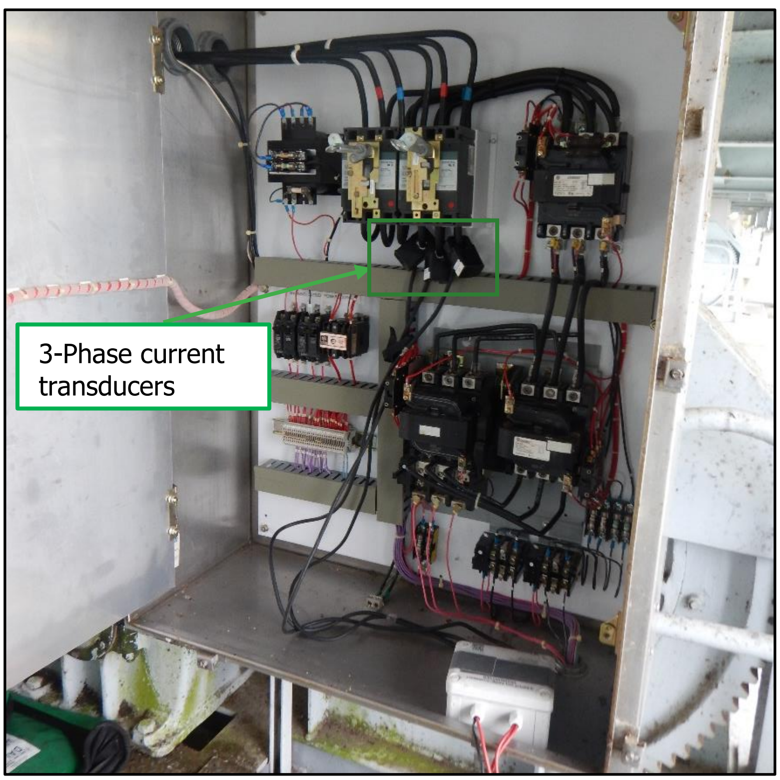

Figure 4 – Current transducers installed on hoist motor controls (Typical)

Figure 5 – BDI personnel installing instrumentation on the gate arm

Testing Procedures

Structural response data was recorded on all sensors at 50Hz while the gate was run through three spill tests. Each test consisted of three "up-down" cycles (direction reversals) without lowering the gate back to the sill. Each direction reversal consisted of lifting the gate approximately 6-12", pausing for a few seconds, and lowering the gate approximately 6", and repeating until all reversals had been completed.

RESULTS SUMMARY

GENERAL DISCUSSIONS BASED ON STRUCTURAL RESPONSES

The following outline contains general discussion points and observations that were made during the data review process. Note: Strain measurements were converted to stress for all subsequent analysis by multiplying the strain values by a steel elastic modulus of 29,000 ksi.

+ **DESCRIPTIONS OF RESPONSE MEASUREMENTS:** All sensor readings were zeroed at the end of each test (which consisted of three cycles of direction reversals) so that each measurement corresponded to response change relative to the final gate position as shown in Figure 6 (gates in the downward "closed" position with the hoist cables slacked as much as possible). It is also worth noting that the stresses did not always start and end at the same levels between tests. This variation in behavior is due to small changes in the flexed gate condition between the start and end of tests. It is common for the flex in the gate, caused by pin friction, to slowly release as it rests on the sill. The purpose of the three up-down cycles per test, prior to sitting the gate back onto the sill, is to ensure that these changes in boundary conditions, including gate flexure due to friction, did not affect BDI's trunnion friction results. ***It is important to note that the recorded measurements were changes in structural response due to gate movement, and do not include the in-situ stresses due to the dead load, cable wrap, and hydrostatic loads present prior to testing.***
+ **QUALITATIVE DATA REVIEW:** Review of the response data indicated a good level of reproducibility between the three tests. For reference, Figure 6 and Figure 7 show stress responses measured along Gate 9's right arm top strut for all three tests (Test #1-3). The data in these plots have been provided as both a function of time and the gate position as determined by the skin plate tilt sensor. Structural response behavior slightly varied during the first test's first cycle compared to subsequent lift/lower cycles and tests, with the first cycle having a slightly smaller change in stress due to pin friction. The observed variation was likely caused by a larger release of built-up pin friction as the gate rested on the sill for a longer period of time.
+ **DIRECTION/FRICTION REVERSAL IN RESPONSES:** The difference in stress during gate opening and closing for a given position is shown in Figure 8. The stress variation at any given gate position was a result of direction reversal and in turn due to trunnion friction reversal. This statement is true since all other loads such as dead-load and hydrostatic pressure were essentially constant barring small changes in hydrostatic pressure due to slight changes in head. This direction/friction reversal is depicted in Figure 9, with deflected shape renderings from a gate arm finite element model under lifting and lowering loads. Note that this figure shows an arm configuration that does not match this gate, but the concept of the direction/friction reversal still applies.
+ **MOTOR PERFORMANCE:** Current measurements taken at the hoist motor indicated steady and stable current draws during the lifting and lowering portions. An example plot of current draw and gate position is provided in Figure 10. Current draw ranges during lifting were higher than the ranges during lowering, which is common due to gravity/dead load. These results are summarized along with recorded peak in-rush current in Table 2. Note that the sample rates used during testing were set for collecting gate responses and may not have been appropriate to fully capture the in-rush current. The readings should be evaluated by a licensed electrician with knowledge of the operating parameters. Note: Test 1 amperage data did not match the other two tests, with lower amperage levels and noisy responses from the Phase 2 sensor while the gate was lowered. Given the amperage responses from tests 2 & 3 were reproducible, it is possible that the unexpected responses from test 1 were due to an issue with the amperage sensors.
+ **TORQUE AND HOIST FORCE:** Due to restrictions caused by the hoist limit switches, the hoist cables could not always be fully slacked at the beginning and end of the performed tests. Throughout testing of the Rockwell Forney gates, it was found that this limit switch restriction varied gate to gate and arm to arm. Therefore, it is not recommended to use the collected torque and hoist force data to quantify overall hoist forces. Rather, this data was utilized to evaluate total friction behavior, which is observed as half the difference between the lifting and lowering torque/force (friction reversal).

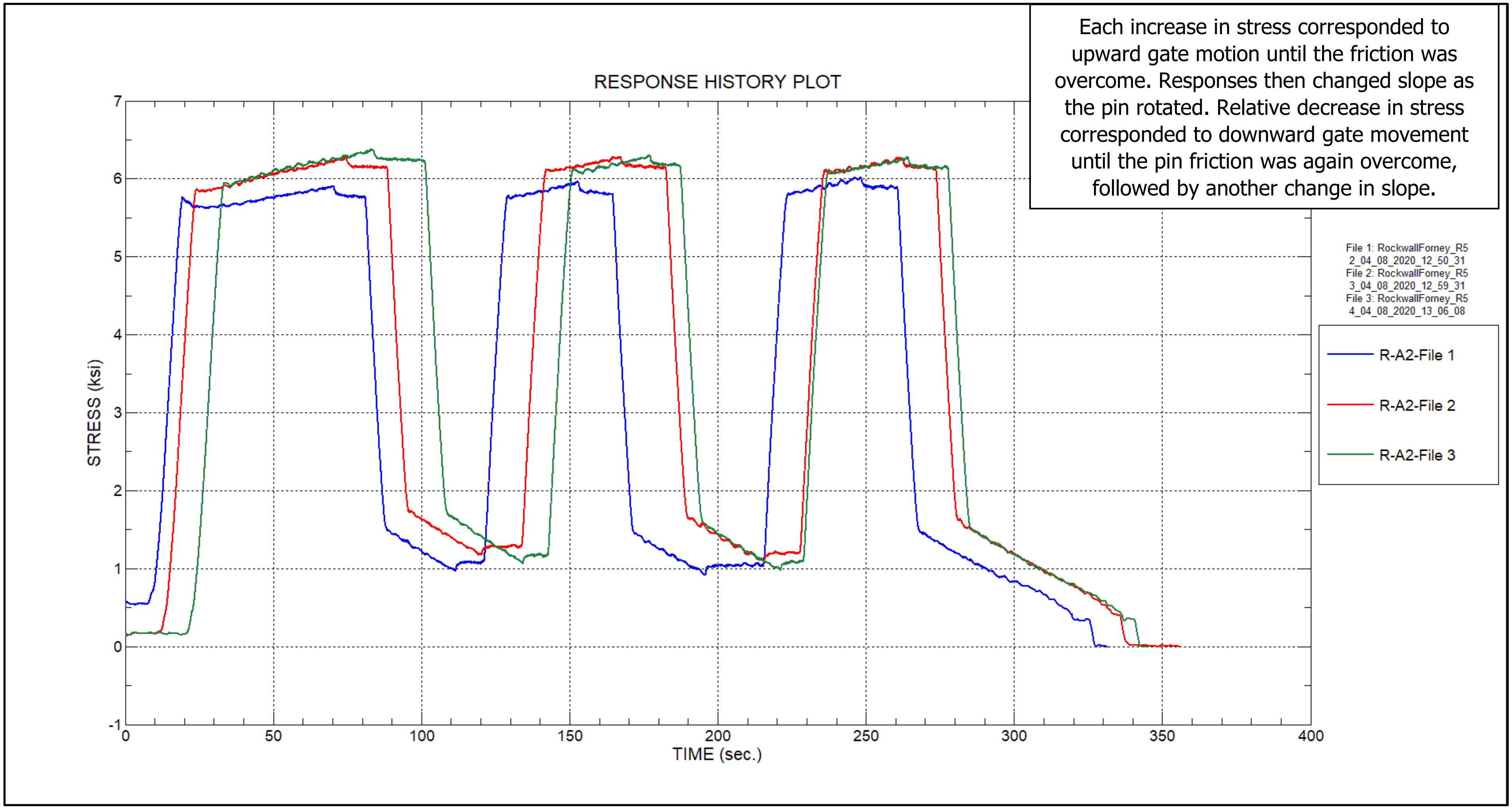

Figure 6 – Stress response history – Right arm – Gage A2 – Time based
File 1 = test run 1, File 2 = test run 2, File 3 = test run 3

(Section A along top strut near pin – Sensor location 2 along bottom of inner flange)

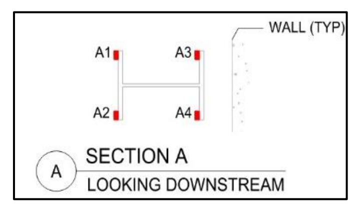

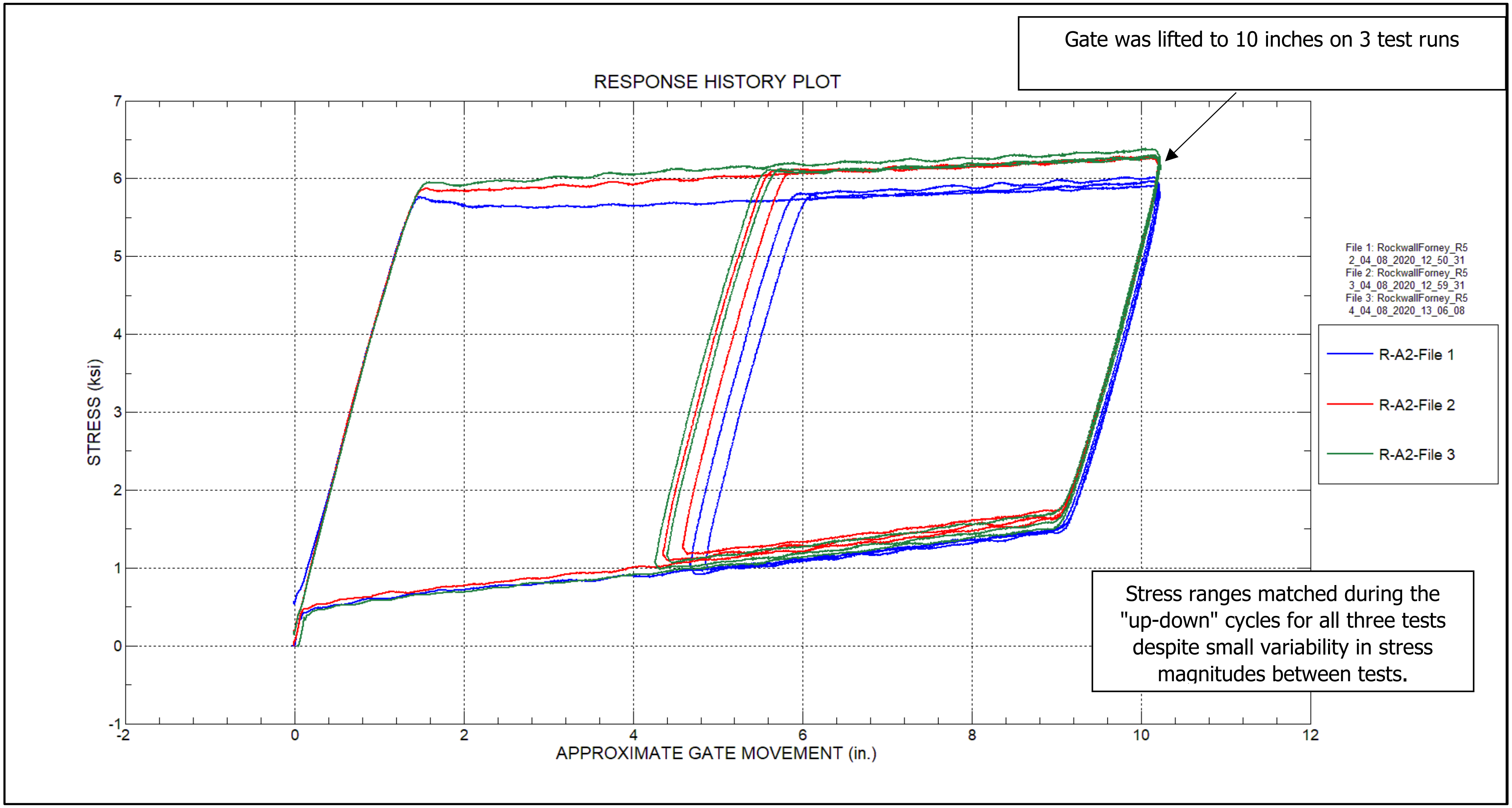

Figure 7 – Stress response history – Right arm – Gage A2 – Function of gate movement
File 1 = test run 1, File 2 = test run 2, File 3 = test run 3

(Section A along top strut near pin – Sensor location 2 along bottom of inner flange)

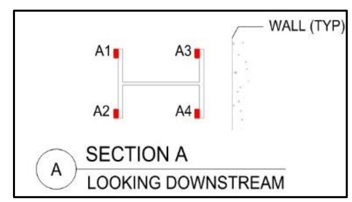

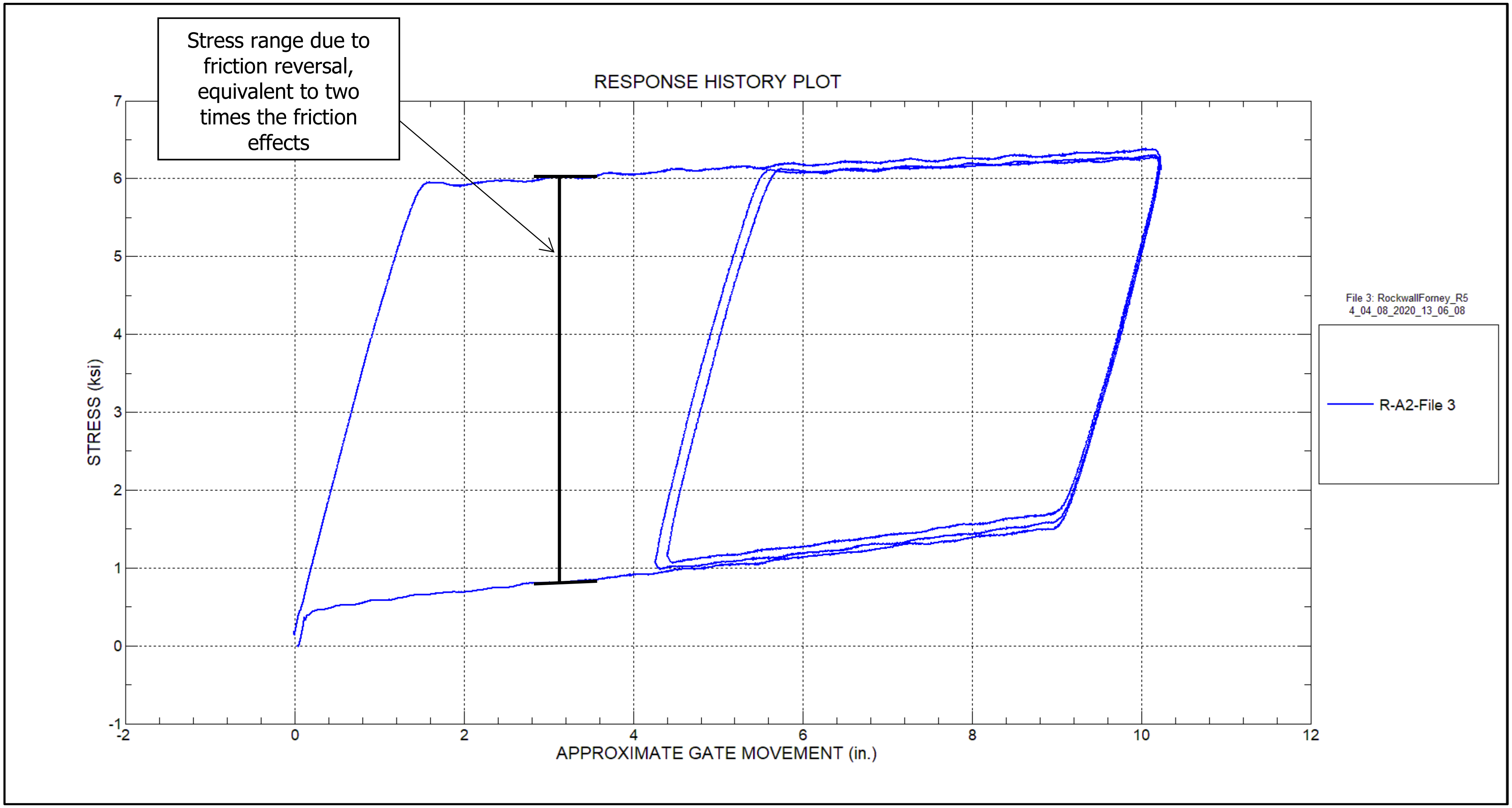

Figure 8 – Stress response history – Right arm – Gage A2 – Friction effect in stress responses

(Section A along top strut near pin – Sensor location 2 along bottom of inner flange)

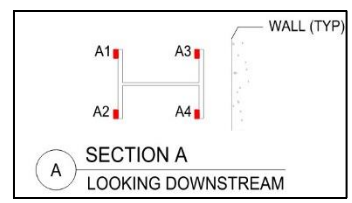

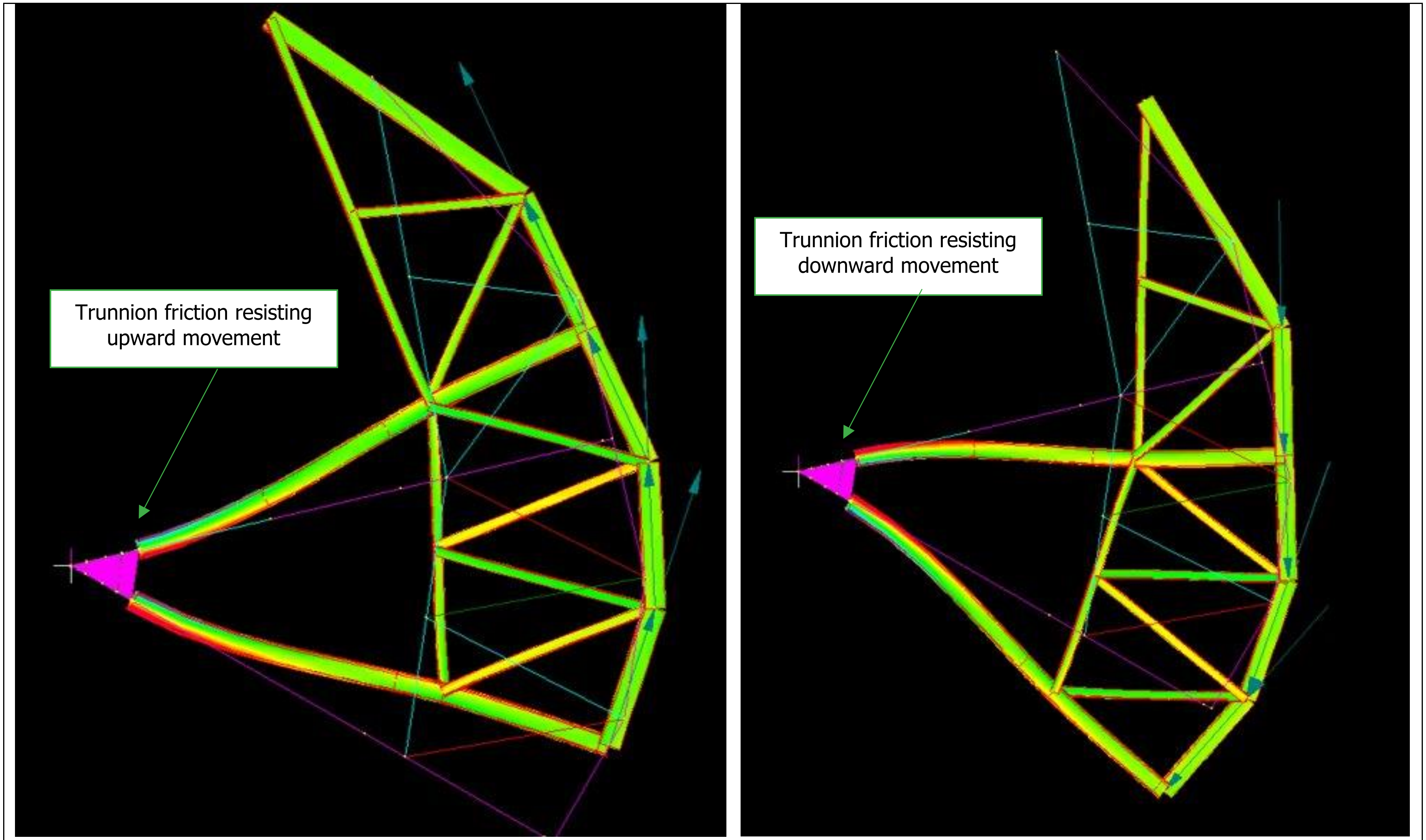

Gate traveling upward **Gate traveling downward**

Figure 9 – Deflected shapes during lifting and lowering of Gate – Visualization of direction/friction reversals

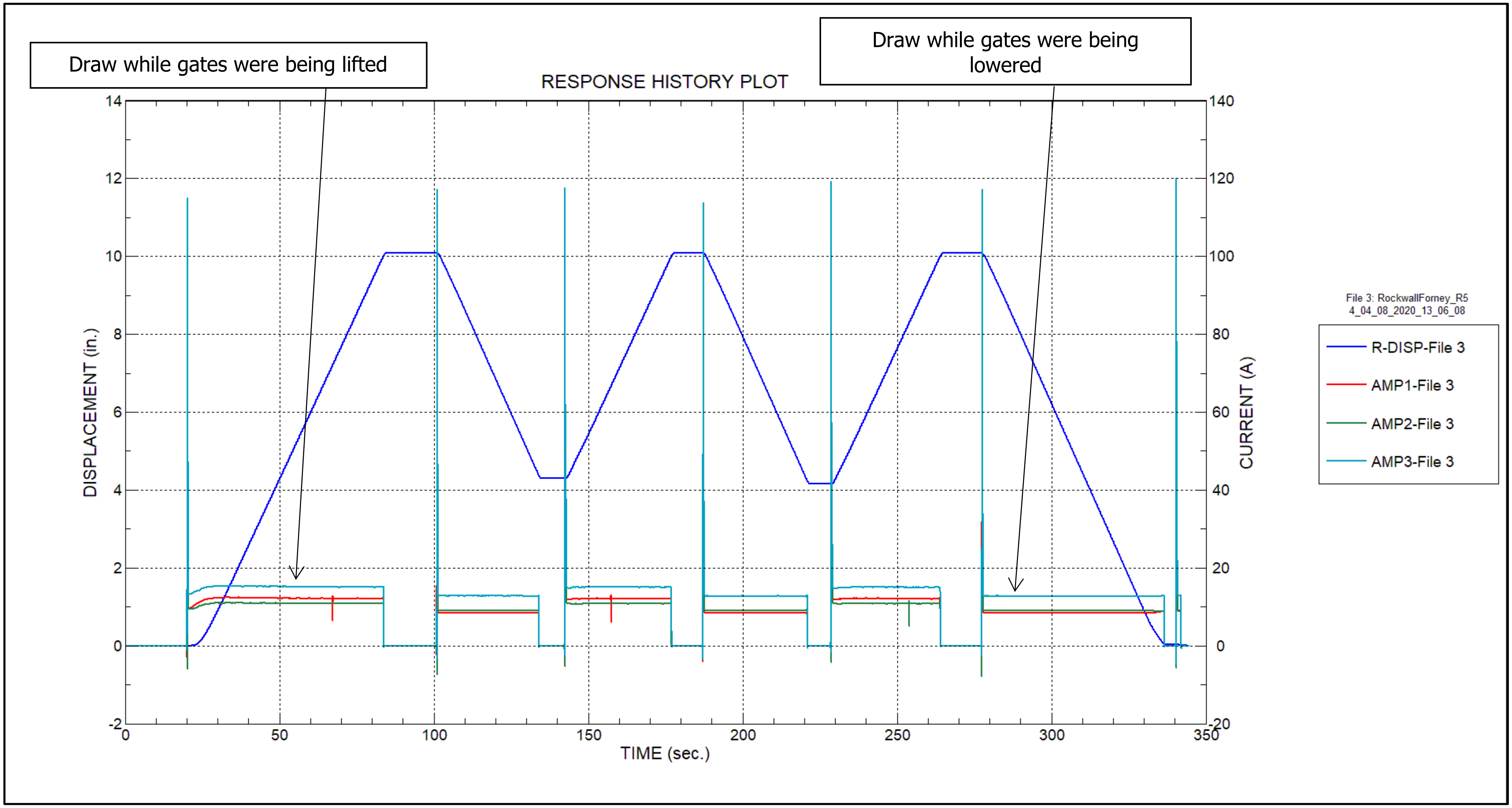

Figure 10 – Motor current & gate movement response history – Lift motor – Highlighting motor draw during lift and lower cycles

Methodology and Findings of The Strut Force and Moment Calculations

The following outline provides the methodology used to calculate the required member forces and moments.

- **CHANGE IN STRESS DUE TO GATE OPERATION:** Strain data can be viewed as a function of time starting when the gate was in the down position and was then lifted off the sill. When examining data in this manner, it is easy to see how stresses ramped up as the gate began to move and then changed slope once pin friction was overcome and the trunnion hub began to rotate with the gate. The first point in time where the friction was overcome (both lifting and lowering) has been highlighted in the stress histories shown in Figure 11. These stress histories show the response of all four sensors along the top strut of the right arm (Section A). ***It is important to note that the recorded measurements were changes in structural response due to gate movement, and do not include the in-situ stresses due to the dead load, cable wrap, and hydrostatic loads present prior to testing.***
- **CALCULATION OF STRUT CROSS-SECTIONAL MOMENTS:** The use of four strain gages per strut cross-section allowed accurate in-plane flexural bending moments to be computed from the recorded strain measurements. These moments were computed for every cross-section in each gate arm using the basic mechanics equation provided in Figure 12.

  In-plane or weak-axis flexure refers to bending about a given strut's web. This designation is consistent with typical nomenclature. In-plane bending can be observed visually from the strain response histories as a difference between the top and bottom stresses, whereas out-of-plane or strong-axis bending is visualized as the difference in stress from side to side. Figure 13 provides a visual reference for both types of strut flexure.
- **EXAMINATION OF RESPONSES AS A FUNCTION OF GATE POSITION:** Changes in cross-sectional moment related to friction becomes clearer when the responses are plotted as a function of gate position. Because the gate was operated with several up and down movements, the effects of friction associated with each direction reversal can be viewed for all measured and calculated responses. Figure 14 through Figure 17 show all cross-sectional flexural moment plots for both trunnion arms. The responses in these plots have been centered about the stress state corresponding to a zero-moment, unflexed condition. The zero-moment offset was estimated as the average moment values between up and downward movement (i.e. half the moment difference) at the gate position with the greatest pin friction moment difference (greatest difference between lifting and lowering).
- **TRUNNION FREE-BODY-DIAGRAM & PIN MOMENT CALCULATION:** Figure 18 shows the instrumented member cross-sections and shows how the measured cross-sectional flexural responses were used to compute pin moment. The in-plane moment values used in these calculations were determined directly from the strain measurements at each cross-section using the provided mechanics equations. It should be noted that the out-of-plane moments were not considered in the calculation of pin moment since they were orthogonal to the axis of the pin rotation. Total pin moment was then determined by summing all the moment components about the pin, which included the in-plane moment and the shear components at the strut cross-sections nearest the pin.
- **STRUT SHEAR CALCULATION:** From the examination of the trunnion free-body-diagram described above, the shear vectors at the three struts were a primary component in the pin moment calculation. For this type of structural element, shear vectors were calculated using the moment differential between the two cross sections along each strut. It is important to recognize that shear was constant between the two instrumented cross-sections and the applied shear was a function of the recorded change in moment ($V = dM/dX$). Subsequently, the shear vectors were calculated by dividing the difference in moment by the distance between the two instrumented cross-sections. Shear values for each strut have been plotted as a function of gate position in Figure 19 and Figure 20.

+ **CALCULATION OF PIN MOMENT DUE TO FRICTION:** Once all the trunnion arm force vectors were calculated, the equations shown in the free-body-diagram were applied to compute pin moment as a function of gate position. It is important to note that because the calculated pin moment range corresponds to a direction reversal, a reversal in friction also occurred. The effect of direction reversal on pin moment due to friction is best conceptualized by centering the moment response plots about the zero-moment axis. The moment due to lifting and the moment due to lowering can then be visualized as a change from this new zero point corresponding to the gate in an unflexed condition. Therefore, the total moment differential between lifting and lowering was twice the moment due to friction acting in a single direction. Pin-moment plots have been provided in Figure 21 and Figure 22. From these plots, it is apparent that pin moment due to friction remained relatively constant throughout the gate operation tests, with a slight decrease in pin friction moment as the gate continued to be lifted. This slight decrease in pin friction moment most likely corresponded to the change in hydrostatic load as the gate position changed. Pin-moment plots for all tests on Gate 9 are also provided for reference in Appendix B – Gate 9 Pin Moment Component Plots.

+ **SHAFT TORQUE & HOIST FORCE:** Torque measurements were taken on the pinion shafts near the hoist motor during testing, with single torque gages installed on the left and right hoist pinion shaft. Responses were recorded in units of micro-strain and converted to torque in units of kip-ft using Equation 1 thru Equation 3 and the following shaft properties.

$$d_O = 5.5\ inches, \qquad d_I = 0\ inches, \qquad E = 29000\ ksi, \qquad \nu = 0.3$$

$$G = \frac{E}{2(1+\nu)}$$

Equation 1

$$J = \frac{\pi\left(d_O{}^4 - d_I{}^4\right)}{32}$$

Equation 2

$$\tau = \varepsilon * \frac{2GJ}{\frac{d_O}{2} * 1000000 * 12}$$

Equation 3

Figure 23 shows example torque measurements, recorded on the Gate 9 torque shafts. Best practices for torque measurements is to measure torque on opposite sides of the shaft so that any bending in the shaft can be removed by averaging the two responses. Due to access limitations, only one gage at each location could be installed. Therefore, any bending in the shaft may be reflected in the torque measurements and may be related to the peaks and valleys observed in the torque responses.

Torque values were converted to force in the hoist cables per gate arm using the gear ratio and drum radius, as shown in Figure 24. The gear ratio and drum radius were 5.182 and 1.086 feet respectively, as defined in the provided as-built shop drawings. It should be noted that the hoist force calculated may be smaller than the actual hoist force applied. This difference is due to the limit switch engaging the brake before the hoist cable was fully slacked, resulting in an initial force in the cable. A hoist force due to total gate friction was then calculated. This friction hoist force was equal to half the differential in force measured during the lifting and lowering of the gate (similar to the pin friction calculations). As shown in Table 3, the change in cable force due to friction was generally consistent between tests. Note that the total hoist force was due to the total friction effects, including side seal, hoist bearings, trunnion friction effects, etc. It is difficult to determine the exact proportion and composition of the total friction sources. Additional torque and hoist force plots for all collected data files are provided in Appendix A – Gate 9 Torque and Hoist Force Plots.

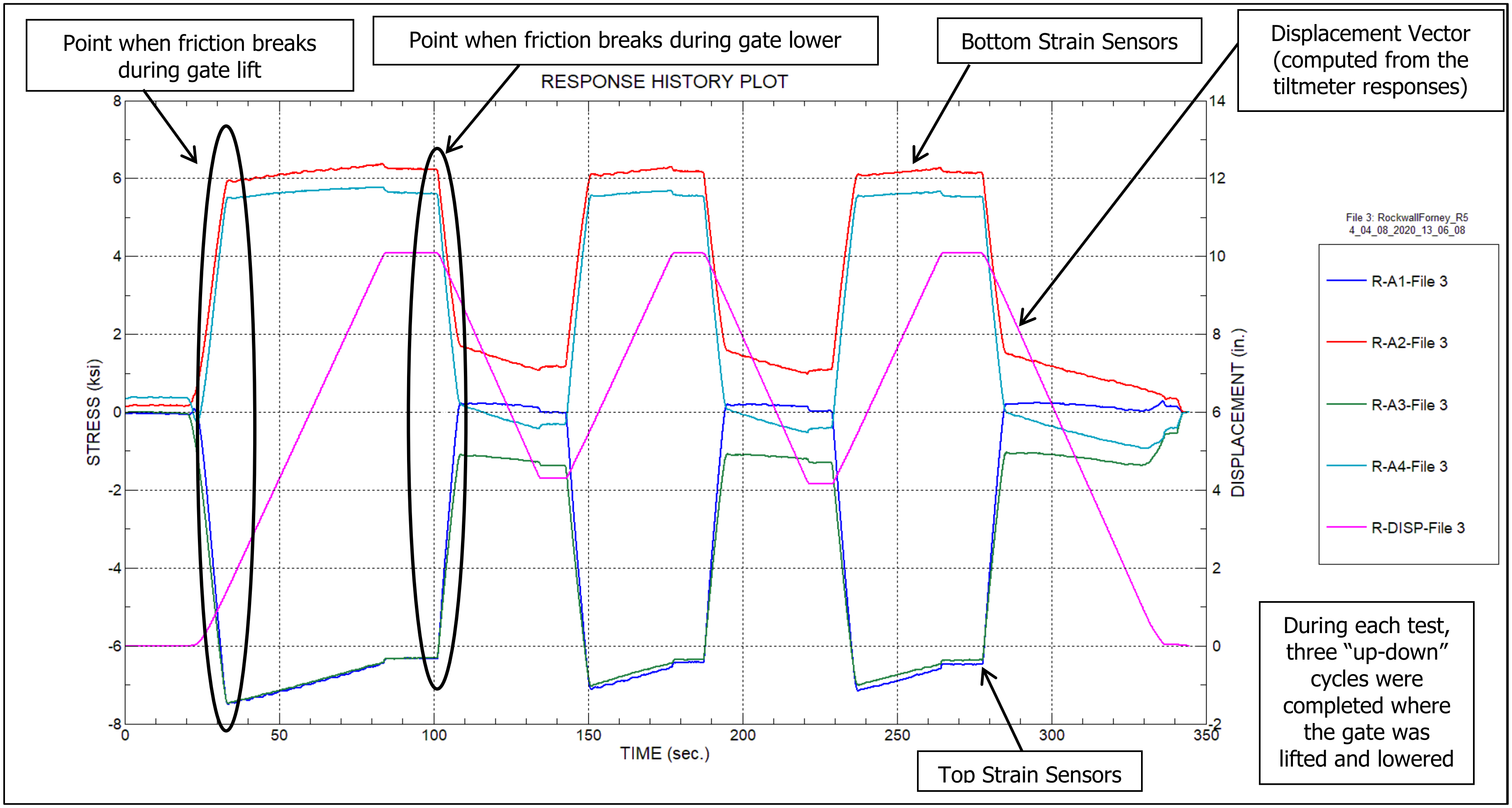

Figure 11 – Stress response & gate movement history – Right arm – Section A - Highlighting friction behavior
(Section A along top strut near pin)

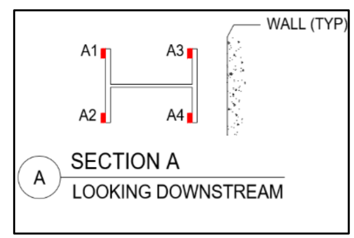

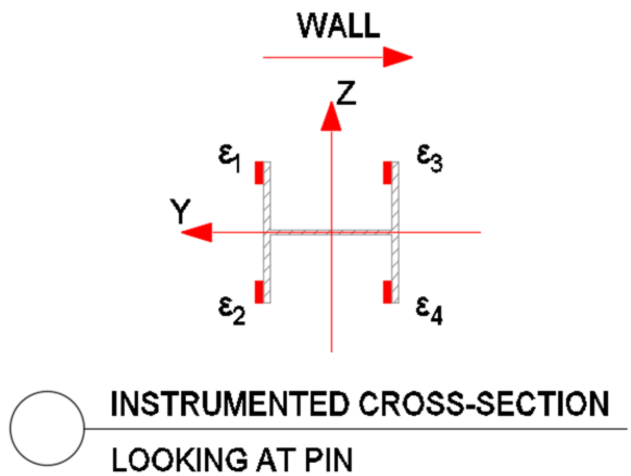

Calculation of Weak-axis (In-plane) bending

$$M_Y = \frac{E\left[\frac{\varepsilon_2 + \varepsilon_4}{2} - \frac{\varepsilon_1 + \varepsilon_3}{2}\right] S_{Y(gage)}}{2}$$

Sy(gage) = Section modulus to the center of gages (not extreme fiber of flanges)
(locations of gages were accounted for in moment computation)

Figure 12 – Basic mechanic equation used to calculate moment

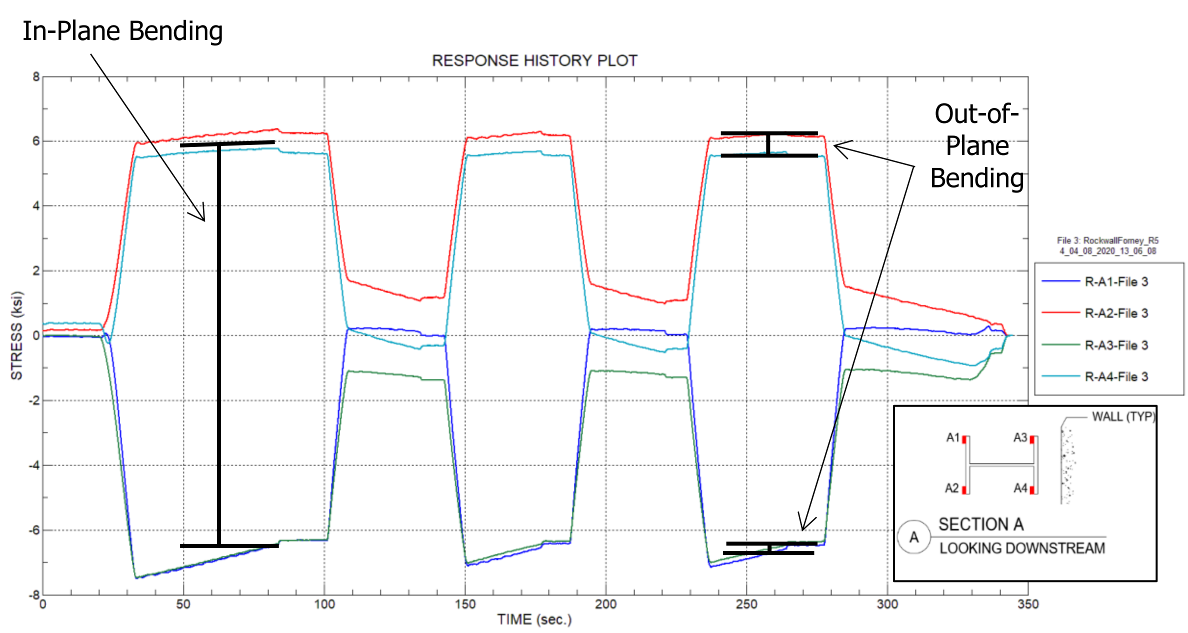

Figure 13 – Stress response history – Right arm – Section A – Bending components
(Section A along top strut near pin)

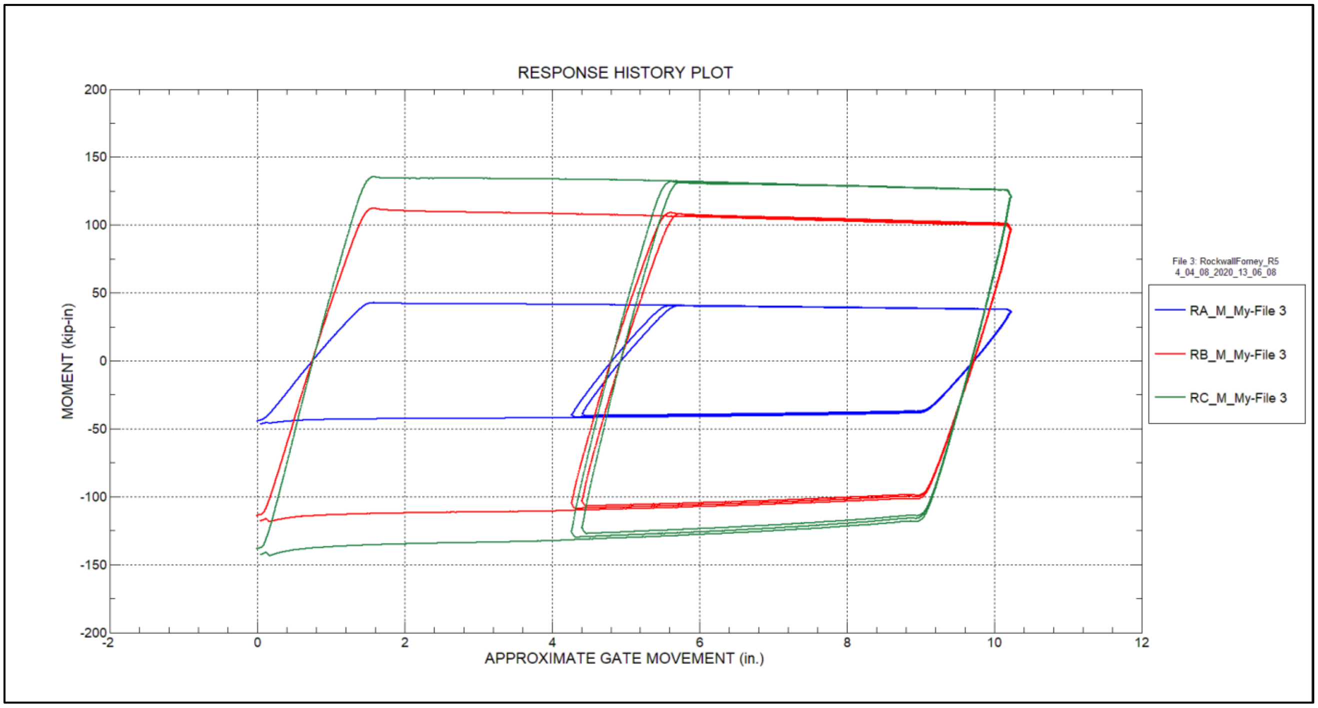

Figure 14 – In-plane moment response history – Right arm – Sections near pin

(RA = Right Arm Top Strut, RB = Right Arm Middle Strut, RC = Right Arm Bottom Strut)

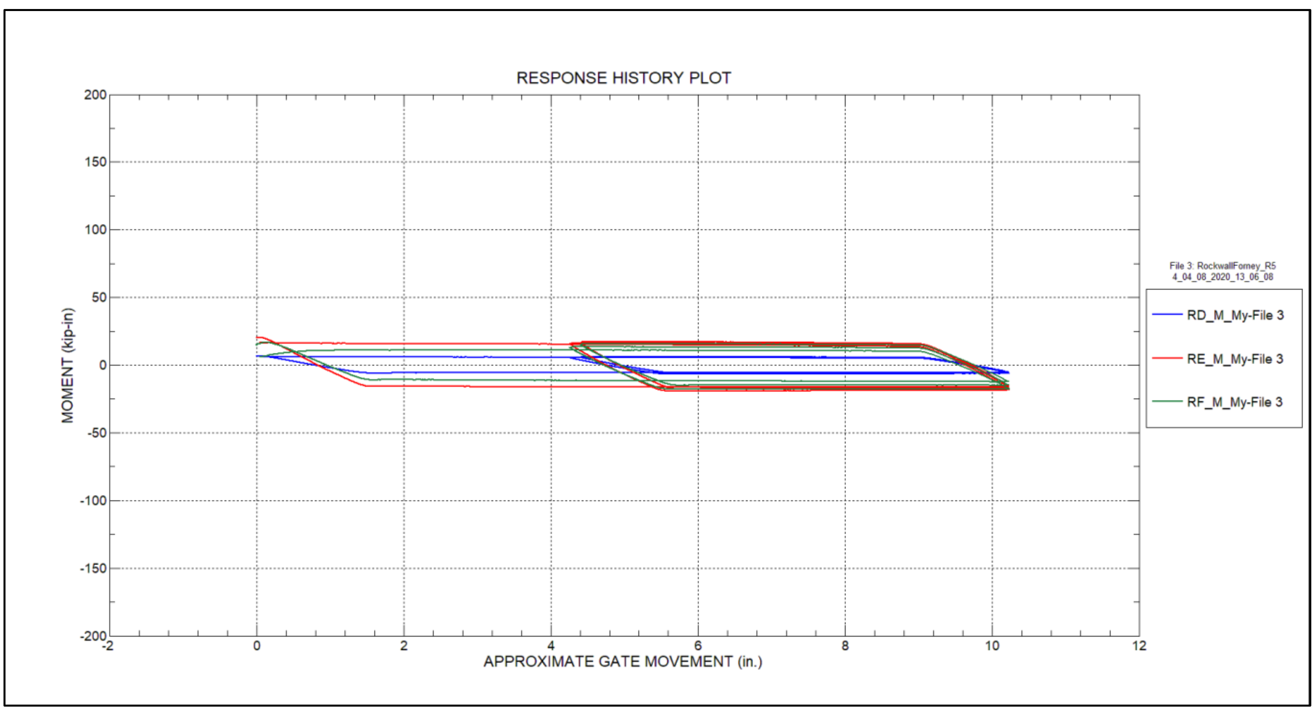

Figure 15 – In-plane moment response history – Right arm – Sections away from pin

(RD = Right Arm Top Strut, RE = Right Arm Middle Strut, RF = Right Arm Bottom Strut)

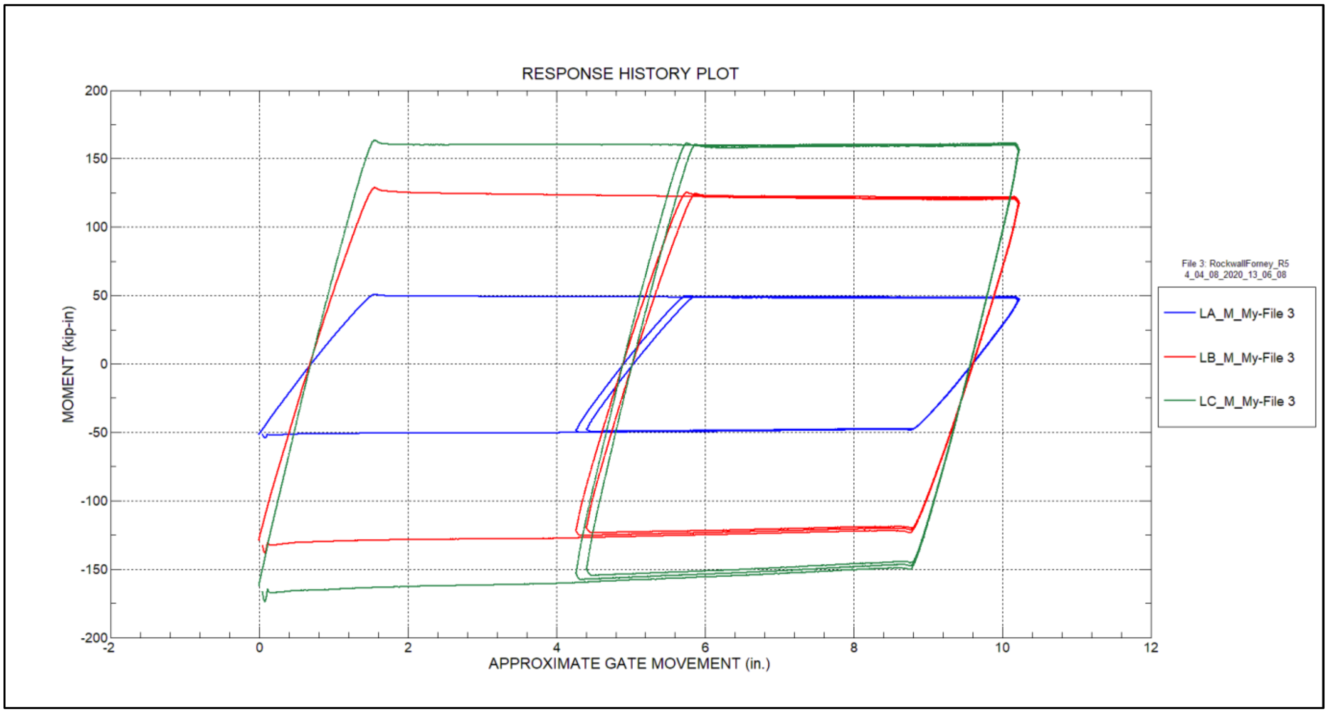

Figure 16 – In-plane moment response history – Left arm – Sections near pin

(LA = Left Arm Top Strut, LB = Left Arm Middle Strut, LC = Left Arm Bottom Strut)

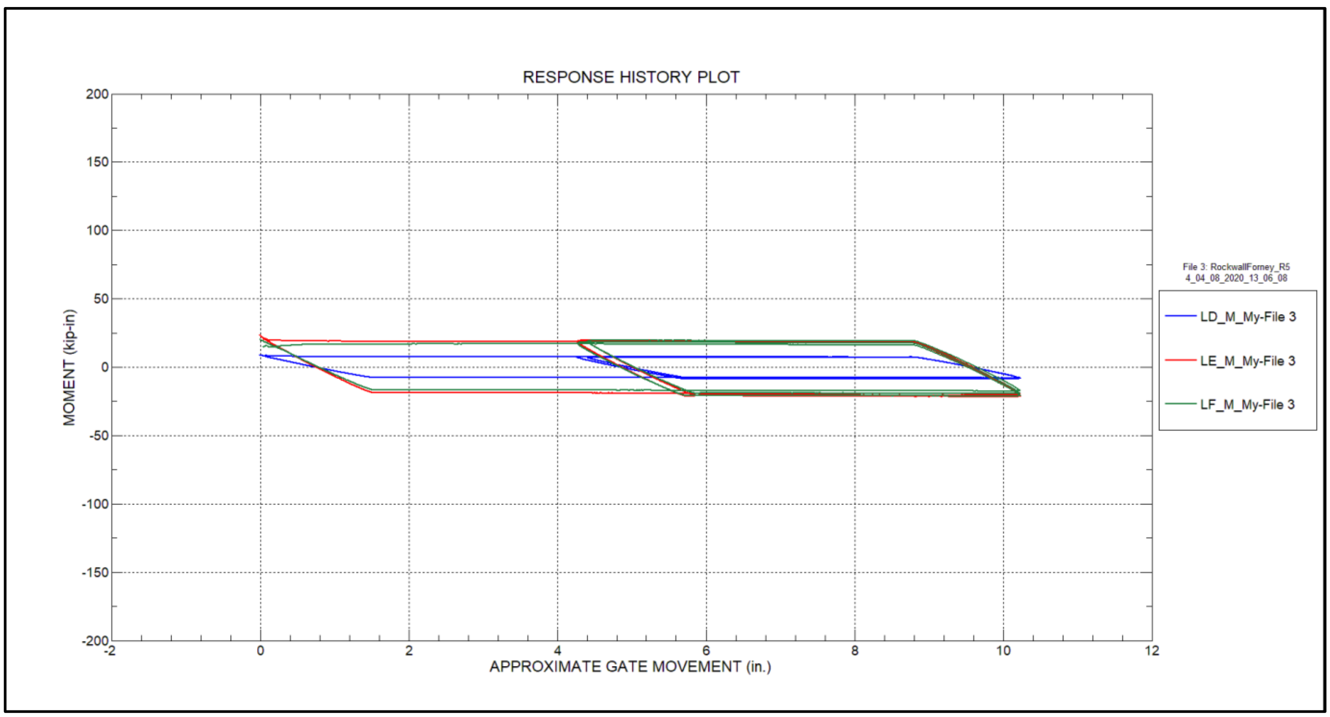

Figure 17 - In-plane moment response history – Left arm – Sections away from pin

(LD = Left Arm Top Strut, LE = Left Arm Middle Strut, LF = Left Arm Bottom Strut)

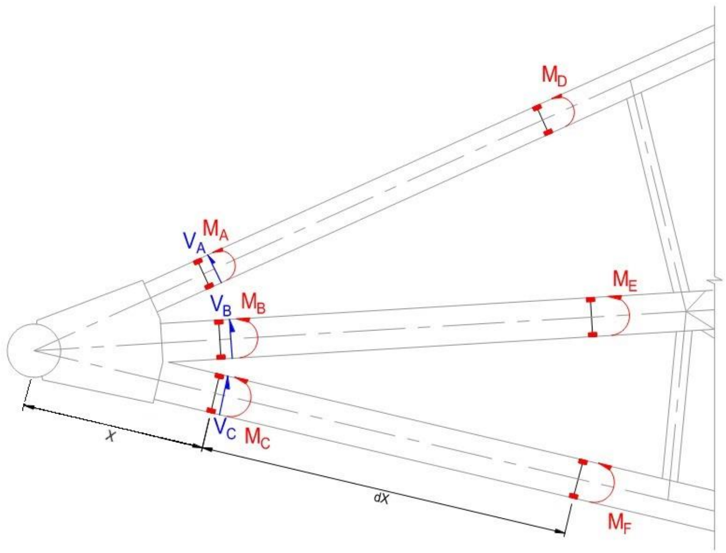

Elevation View of Gate Arm

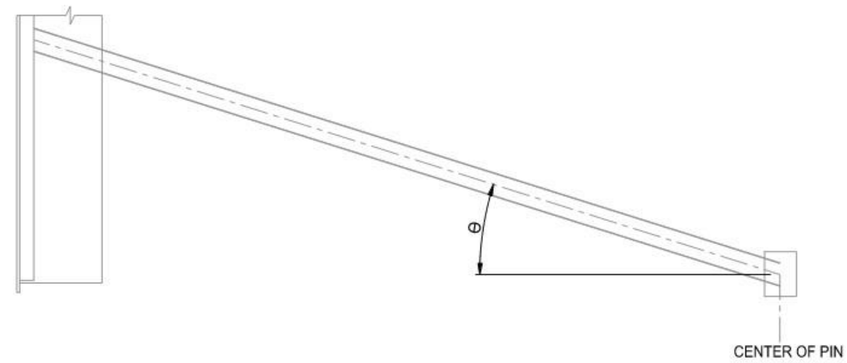

Plan View of Gate Arm

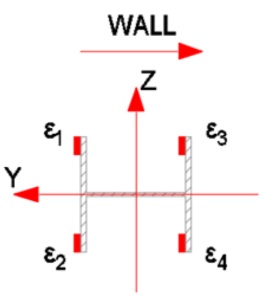

$$M_Y(M_A, M_B, M_C, M_D, M_E, M_F) = \frac{E\left[\frac{\varepsilon_2 + \varepsilon_4}{2} - \frac{\varepsilon_1 + \varepsilon_3}{2}\right] S_{Y(gage)}}{2}$$

$$V_A = \frac{M_A - M_D}{dX}$$

$$V_B = \frac{M_B - M_E}{dX}$$

$$V_C = \frac{M_C - M_F}{dX}$$

$$\sum M_o = 0$$

$$M_{PIN} = [X(V_A + V_B + V_C) + M_A + M_B + M_C]\cos\theta$$

Figure 18 – Direct calculation of pin moment from strain measurements

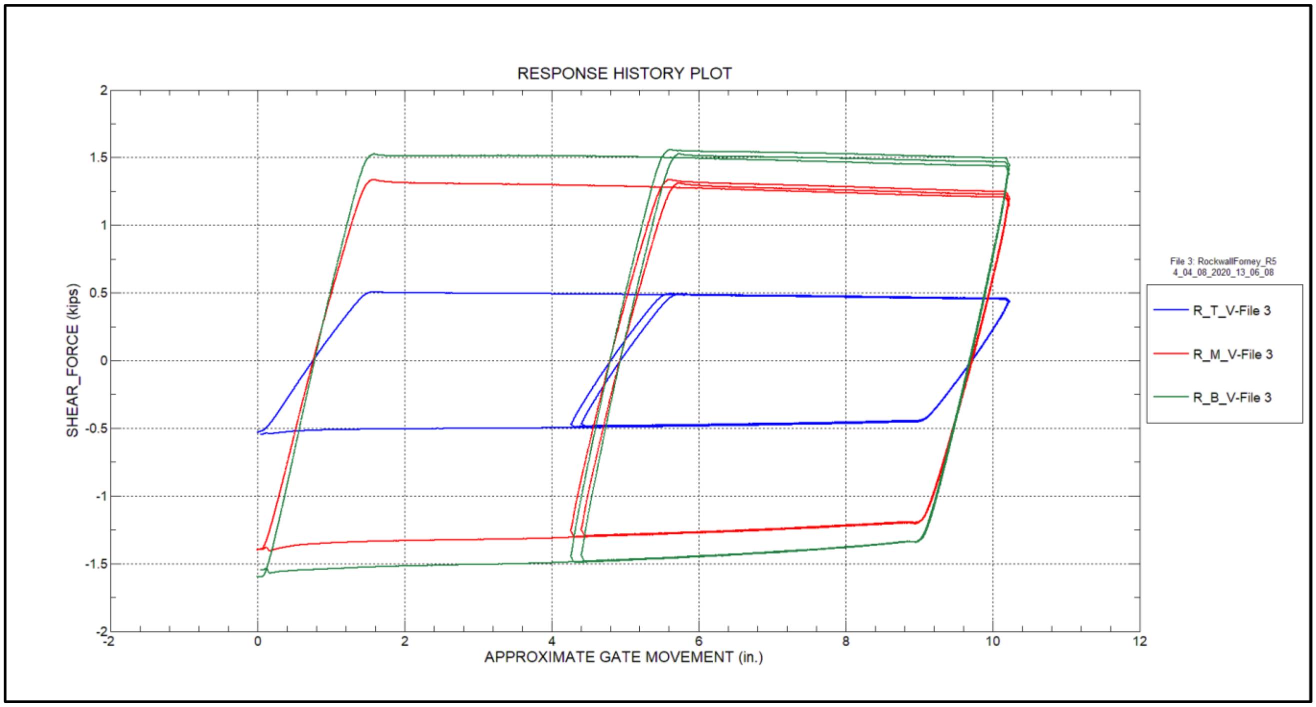

Figure 19 – Strut shear response history – Right arm

(R_T = Right Arm Top Strut, R_M = Right Arm Middle Strut, R_B = Right Arm Bottom Strut)

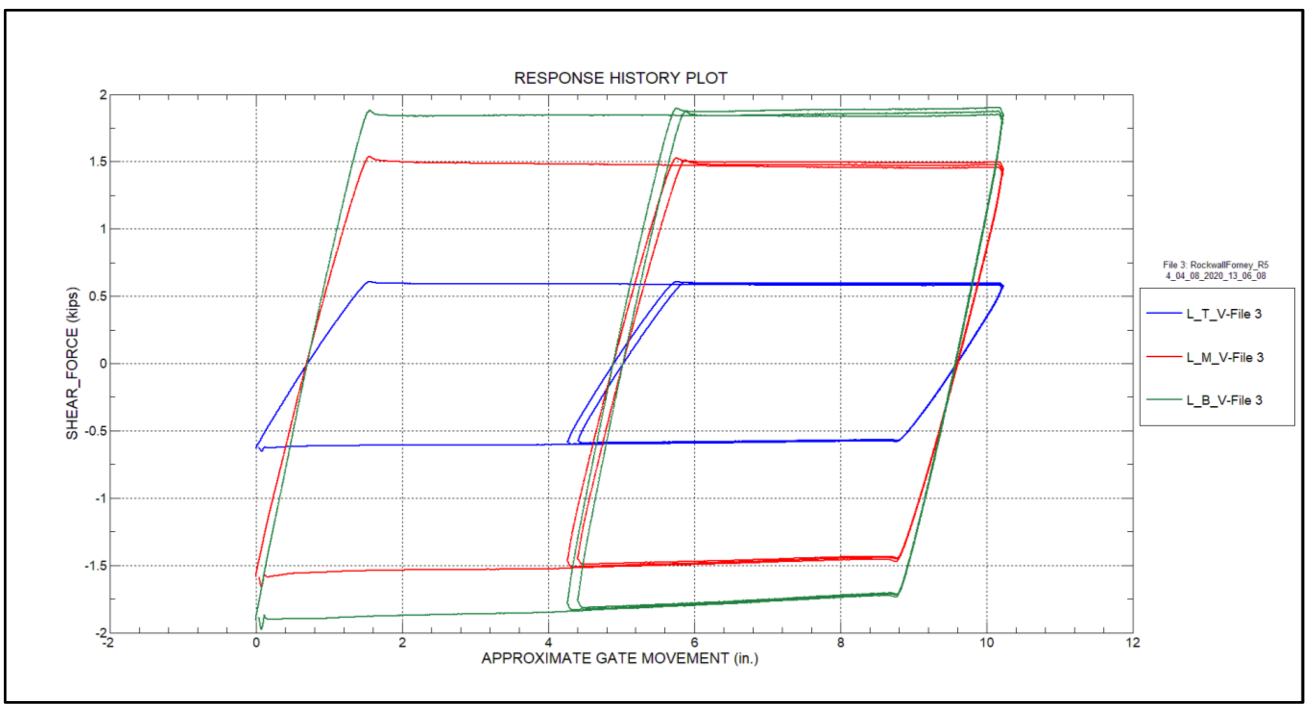

Figure 20 – Strut shear response history – Left arm

(L_T = Left Arm Top Strut, L_M = Left Arm Middle Strut, L_B = Left Arm Bottom Strut)

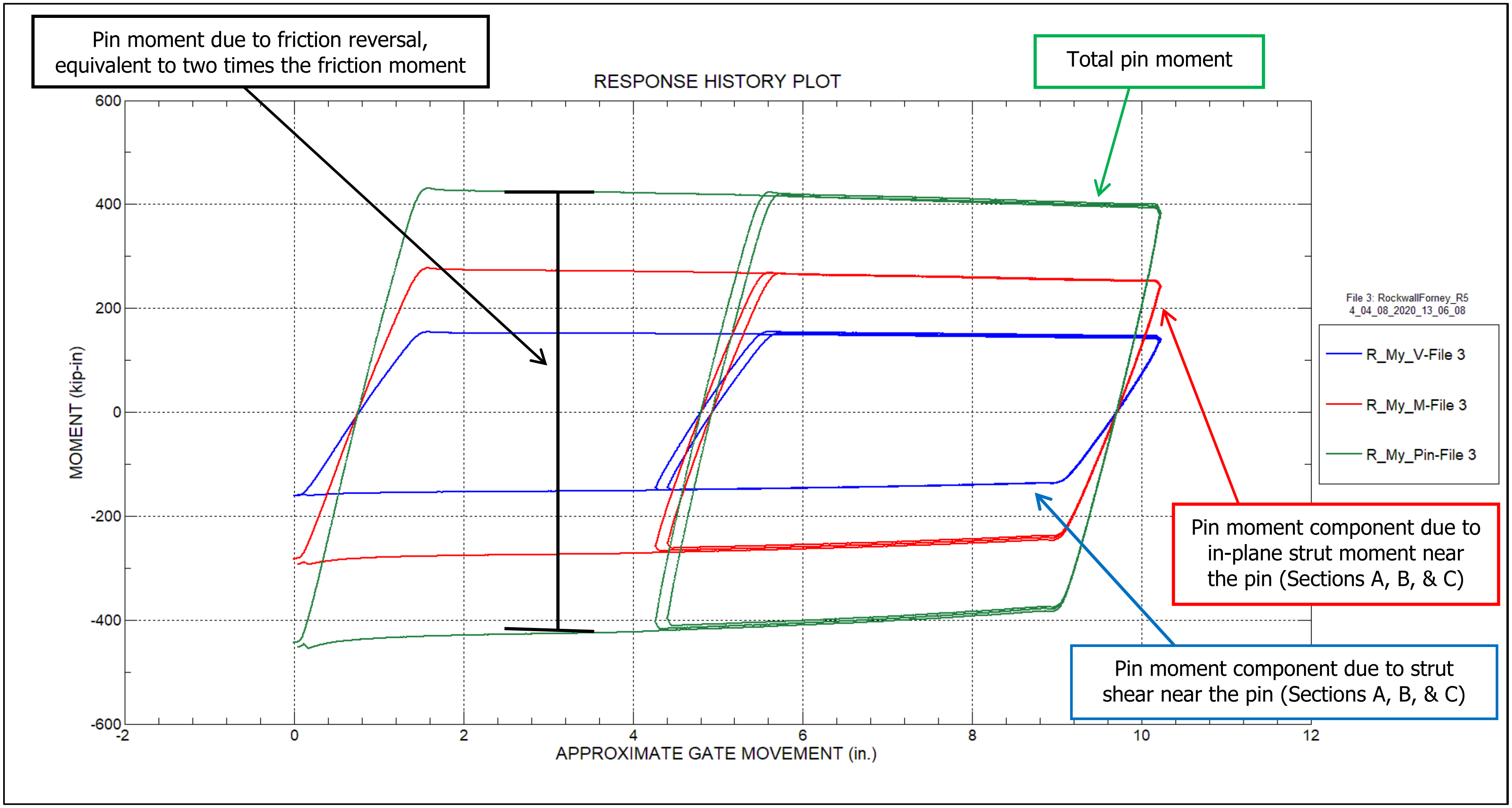

Figure 21 – Pin moment response history – Right arm

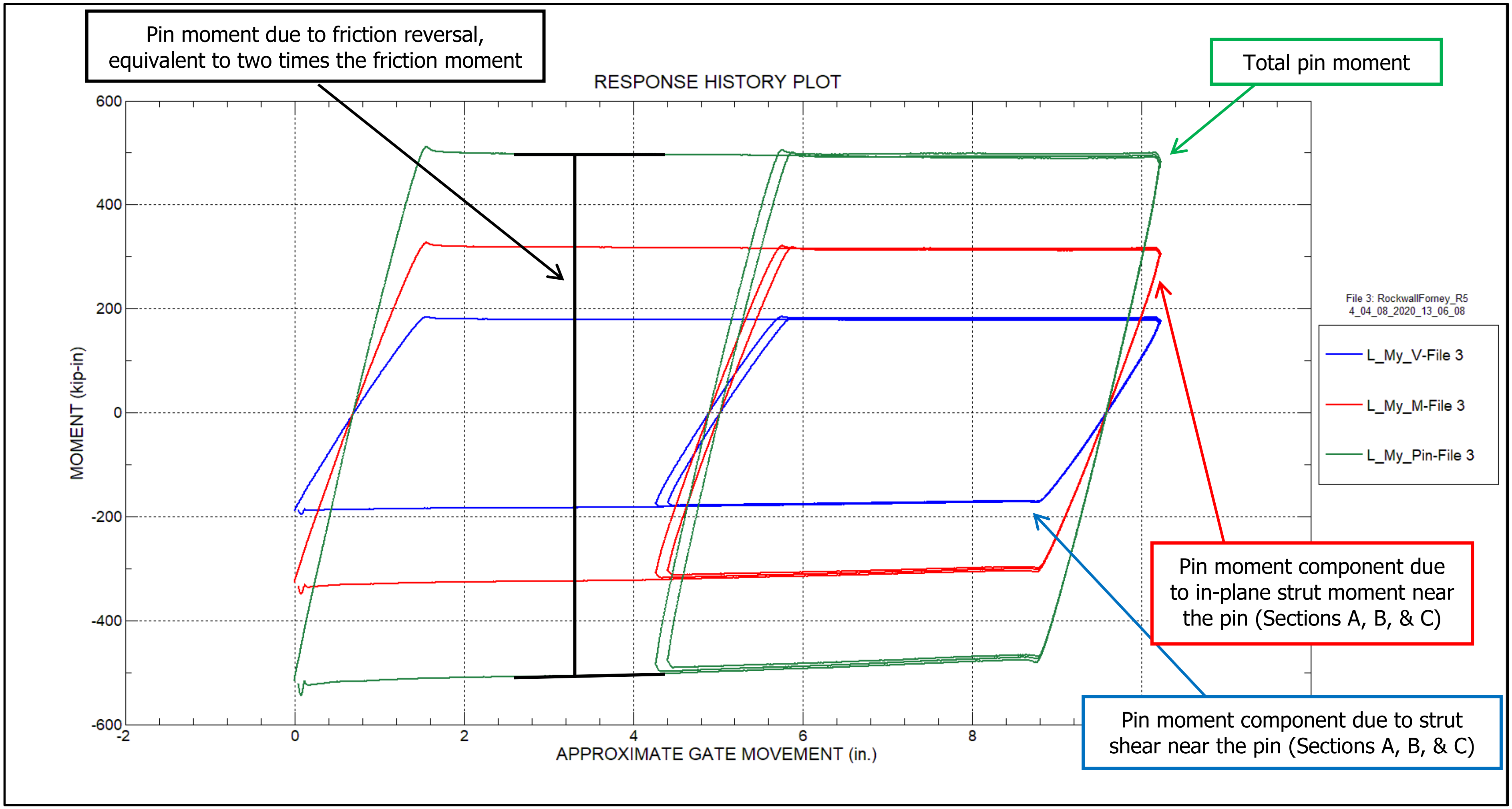

Figure 22 – Pin moment response history – Left arm

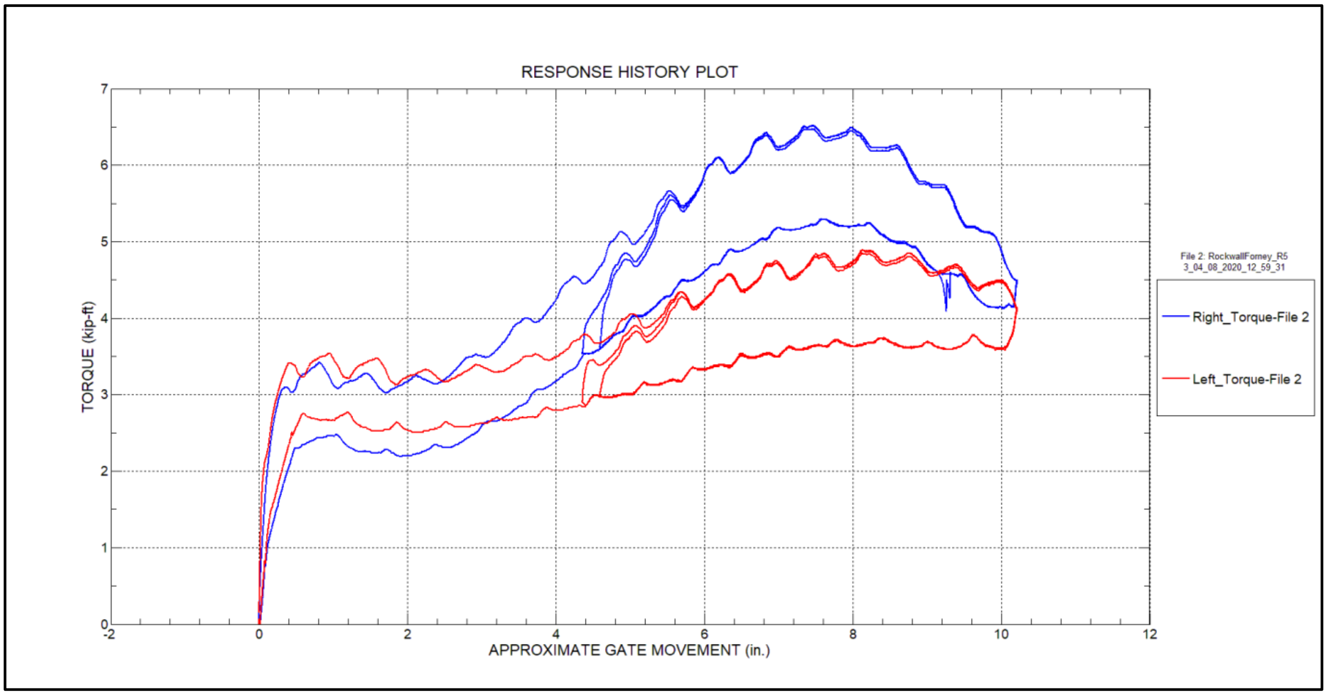

Figure 23 – Hoist torque response history – Gate 9 – Test 2

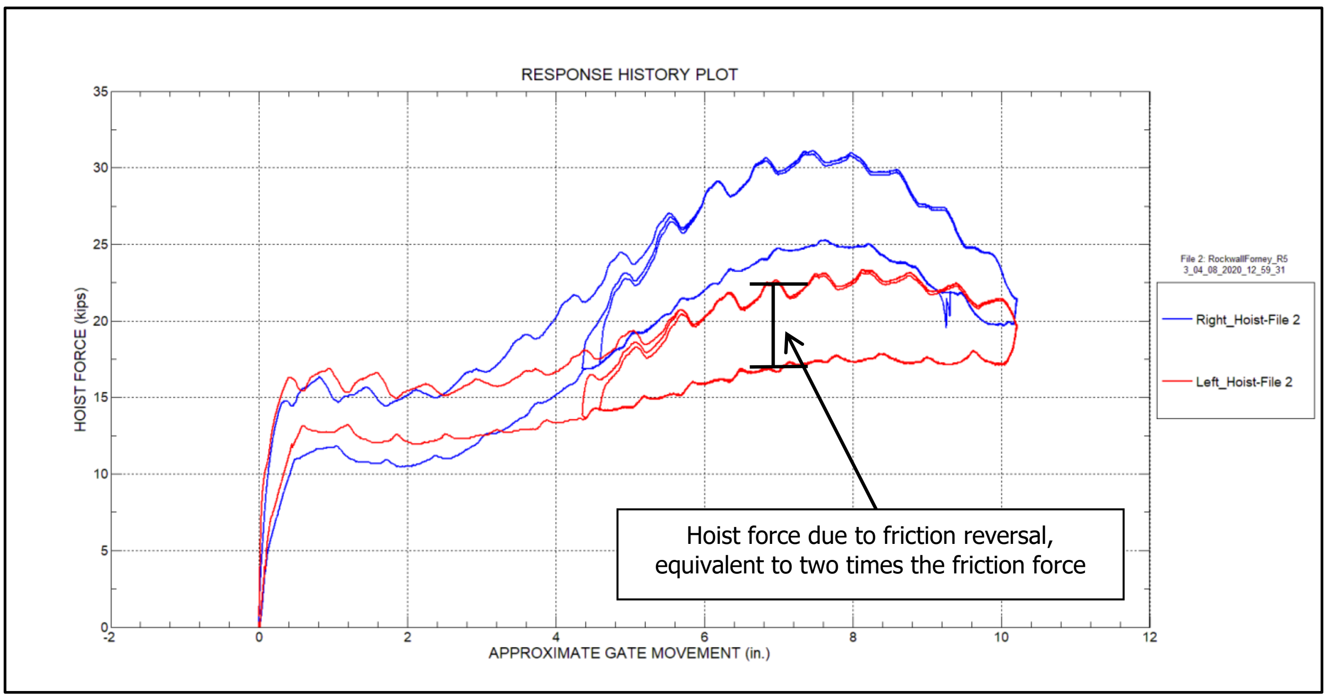

Figure 24 – Hoist force response history – Gate 9 – Test 2

Summary of Friction Results

The raw data files have been included in the submittal package for reference and were formatted as "tdms" files that can be opened in Microsoft Excel using a "tdms" reader extension.

Examination of the stress histories for each test was necessary to obtain a thorough understanding of the gate performance. The response shapes, variations in stress magnitudes, and timing sequences provided direct clues as to how the gate performed under typical service conditions. The following is a breakdown of the provided tabulated results:

+ Table 2 provides motor current ranges and maximum in-flow for lift and lower cycles for each test
+ Table 3 provides maximum hoist force as well as hoist force due to total friction for each test
+ Table 4 provides the maximum stress ranges measured at the sensor locations for each member
+ Table 5 provides maximum bending stress and moment ranges observed during the gate tests
+ Table 6 provides maximum friction bending stress and moment values at each of the instrumented strut locations
+ Table 7 provides the computed shear values in each strut due to friction
+ Table 8 provides calculated measured friction moments, calculated hydrostatic loads based on the measured water elevation, and coefficients of friction for each gate and gate arm during all three tests

The resulting pin friction moments were used to compute friction coefficients from Eq. 4, given the pin radius and the applied thrust. The thrust used in this calculation consisted of the calculated resultant hydrostatic load based on the measured water elevation and was adjusted to account for the loss of head as the gate was lifted. This thrust adjustment was based on the recorded gate movement and was performed in order to calculate more accurate friction coefficients. The water elevation during testing was nearly constant throughout each gate test and was documented during each "up-down" cycle. It should be noted that the minor thrust due to cable wrapping, which was minimal compared to hydrostatic thrust, was not included in the thrust calculation. This assumption resulted in slightly conservative friction coefficients.

$$\mu = \frac{M_F}{T * r} \qquad \text{Eq. 4}$$

where:

μ	=	Friction Coefficient
M_F	=	Friction Moment
T	=	Thrust per Pin
r	=	Pin Radius, 5.375"

The out-of-plane shear and moments were not considered in the pin friction calculations due to orthogonal geometry considerations (resulting pin moment associated with out-of-plane flexure being perpendicular to pin rotation).

The data was presented in a specific coordinate system applicable to both arms. Data was processed so that the positive x-axis was always pointing towards the pin and the right-hand rule applied. In-plane bending can be referred to as "bending about the horizontal or y-axis" and shows how much the beams bend up and down within the plane of the gate arms. Refer to Figure 12 above for visual reference of coordinate system and mathematical explanation of calculations. Tabulated results do not include any in-situ effects.

Table 2– Motor current summary table – Gate 9

Test Run	Current Range due to Lifting (A)	Current Range due to Lowering (A)	Max In-rush Current (A)
1	6-8*	4-4.5*	60*
2	11-15	8-13	120
3	11-15	8-13	119

* - Test 1 amperage data did not match the other tests, possible issues with amperage sensors

Table 3 – Hoist force summary table – Gate 9

Test Run	Right Arm Peak Hoist Force (kips)	Left Arm Peak Hoist Force (kips)	Right Arm Hoist Force due to Total Gate Friction (kips)	Left Arm Hoist Force due to Total Gate Friction (kips)
1	30.89	23.03	4.19	3.01
2	31.09	23.34	3.91	3.00
3	31.08	23.13	3.41	3.05

Tabulated values correspond to the response induced by friction in one direction

Table 4 – Maximum measured sensor stress range

Arm Designation	Top Strut (ksi)	Middle Strut (ksi)	Bottom Strut (ksi)
Right Arm	8.26	9.74	10.77
Left Arm	9.89	11.44	12.21

Tabulated values correspond to the total measured change in response during tests

Stress values have not been extrapolated to the extreme fibers (correspond to center of gage)

Table 5 – Maximum in-plane total bending stress & moment ranges – Total

Section Label	Section Description	Right Arm Stress (ksi)	Right Arm Moment (kip-in)	Left Arm Stress (ksi)	Left Arm Moment (kip-in)
Section A	Top Strut Near Pin	8.17	91.80	9.61	107.96
Section B	Middle Strut Near Pin	10.28	237.79	11.83	273.60
Section C	Bottom Strut Near Pin	10.22	284.93	12.25	341.74
Section D	Top Strut Away from Pin	1.19	13.38	1.58	17.79
Section E	Middle Strut Away from Pin	1.74	40.18	1.96	45.26
Section F	Bottom Strut Away from Pin	1.25	34.74	1.50	41.75

Tabulated values correspond to the total measured change in response during tests

Table 6 – In-plane frictional bending stress & moment at maximum gate friction

Section Label	Section Description	Right Arm Stress (ksi)	Right Arm Moment (kip-in)	Left Arm Stress (ksi)	Left Arm Moment (kip-in)
Section A	Top Strut Near Pin	3.93	44.19	4.65	52.25
Section B	Middle Strut Near Pin	5.01	115.93	5.70	131.91
Section C	Bottom Strut Near Pin	4.97	138.56	5.93	165.47
Section D	Top Strut Away from Pin	0.53	5.94	0.69	7.73
Section E	Middle Strut Away from Pin	0.69	15.89	0.89	20.53
Section F	Bottom Strut Away from Pin	0.45	12.56	0.70	19.61

Tabulated values correspond to the response induced by friction in one direction

Table 7 – Strut shear range summary table due to friction

Arm Designation	Top Strut Shear (kip)	Middle Strut Shear (kip)	Bottom Strut Shear (kip)
Right Arm	0.52	1.36	1.57
Left Arm	0.62	1.59	1.93

Tabulated values correspond to the response induced by friction in one direction

Table 8 – Pin friction summary table

Test Run	Average Water Elevation during testing (ft)	Approximate Thrust at time of Testing (kips per arm)	Gate/Member Designation	Pin Friction Moment (kip-in)	Friction Coefficient
1	435.56	488.50	Right Pin	443.00	0.17
			Left Pin	522.70	0.20
2	435.56	488.50	Right Pin	428.60	0.16
			Left Pin	507.00	0.19
3	435.56	488.50	Right Pin	431.70	0.16
			Left Pin	511.70	0.19

Tabulated values correspond to the response induced by friction in one direction

Appendix A – Gate 9 Torque and Hoist Force Plots

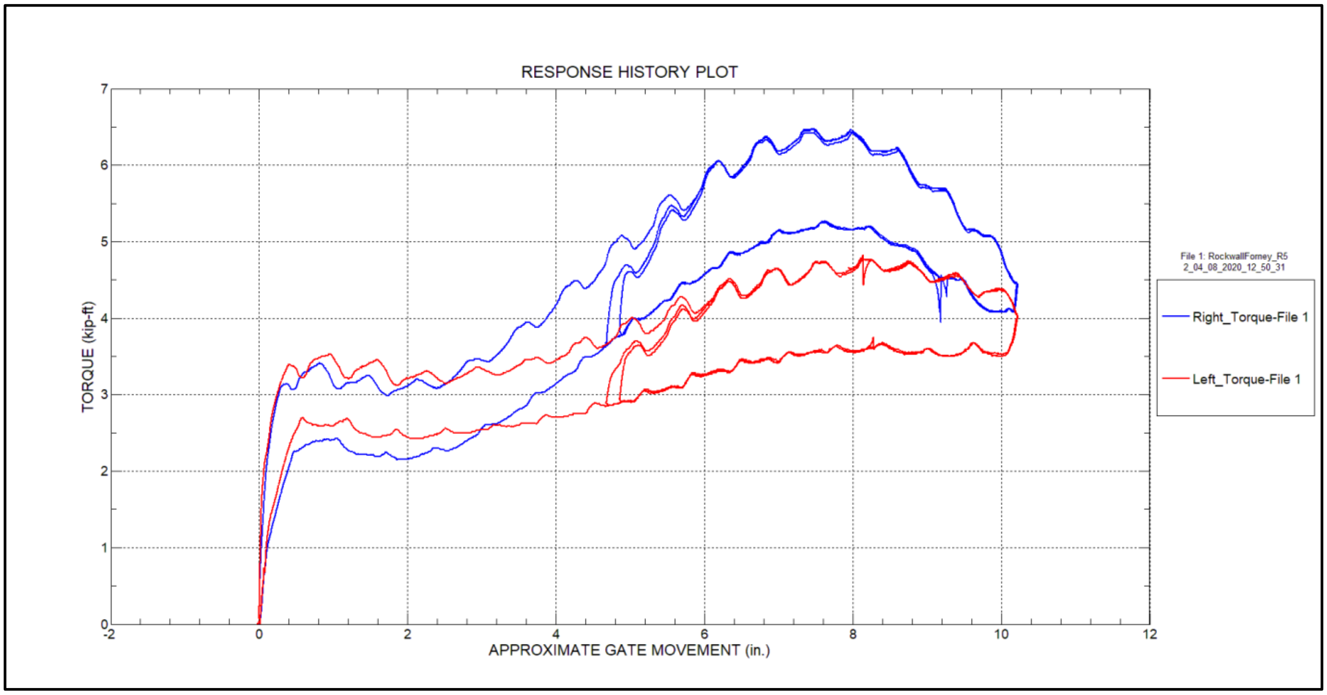

Figure 25 – Hoist torque response history – Gate 9 – Test 1

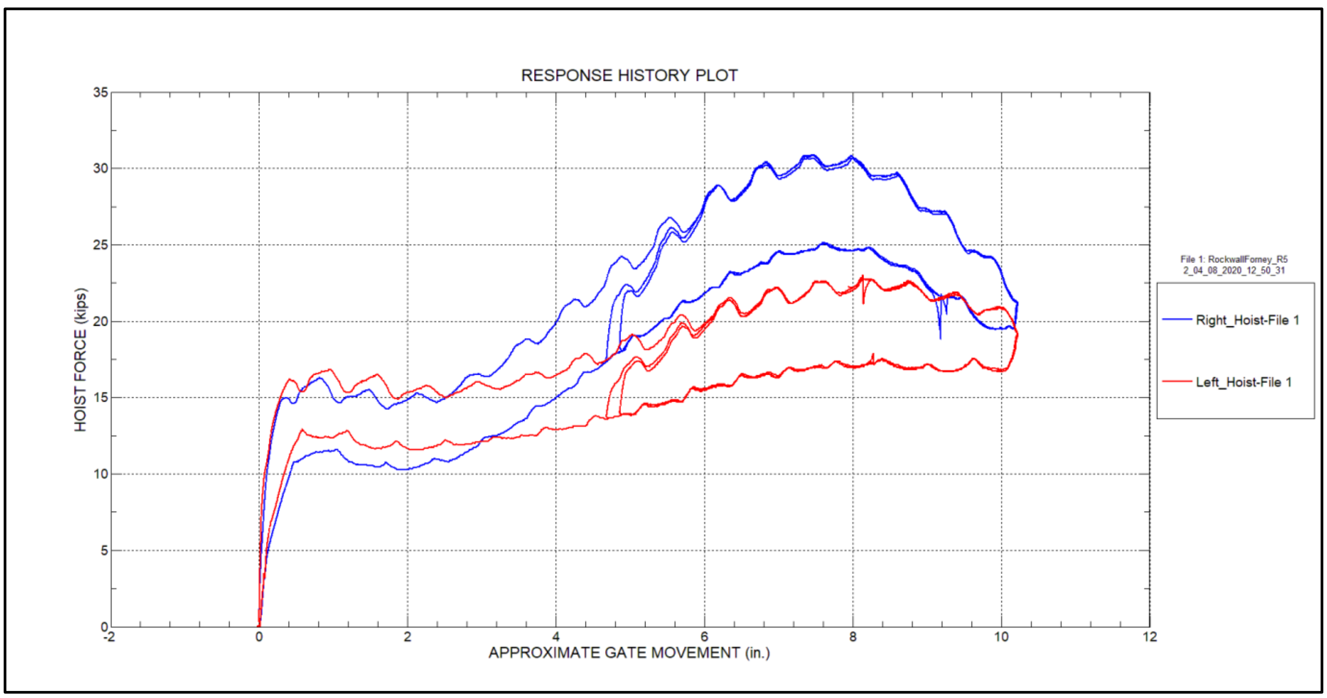

Figure 26 – Hoist force response history – Gate 9 – Test 1

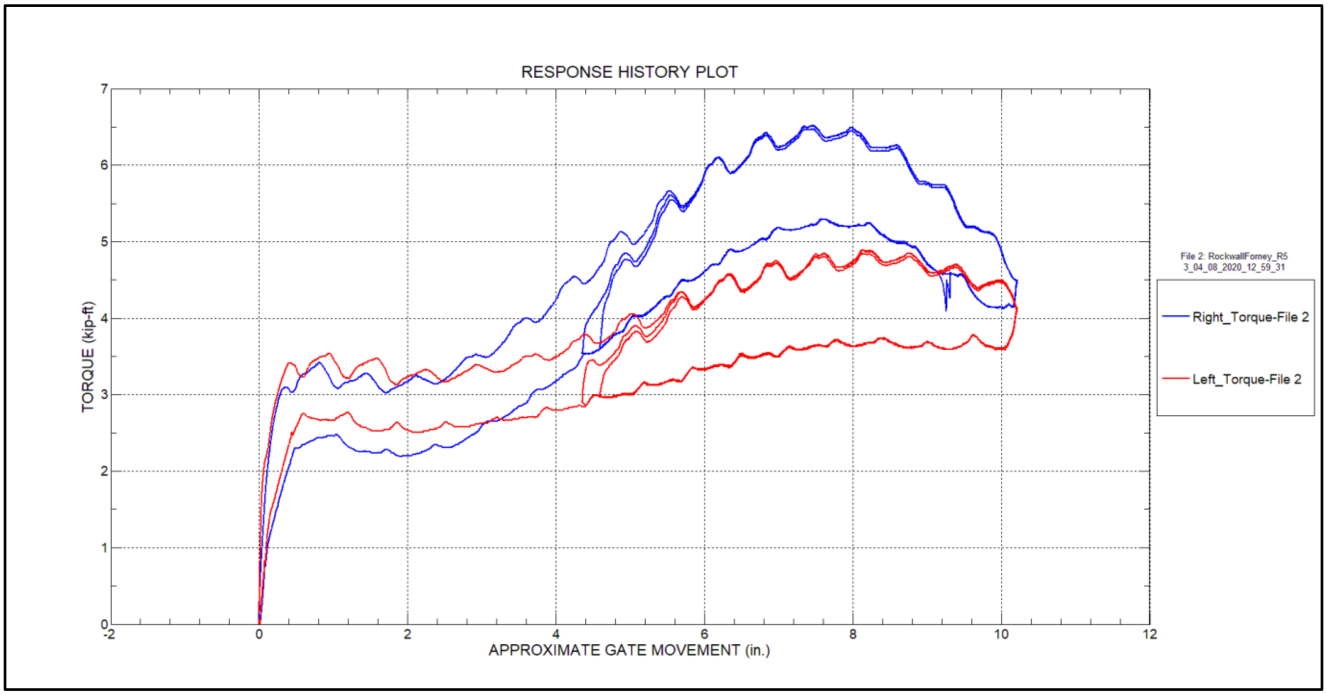

Figure 27 – Hoist torque response history – Gate 9 – Test 2

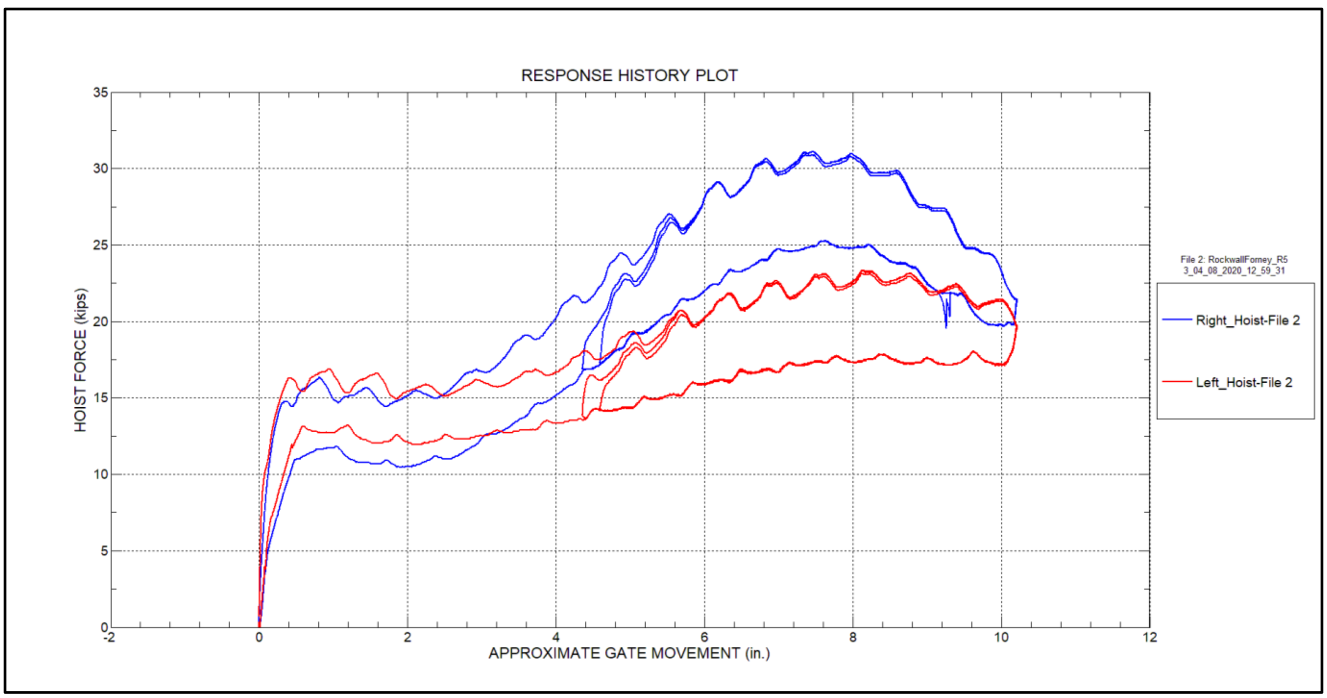

Figure 28 – Hoist force response history – Gate 9 – Test 2

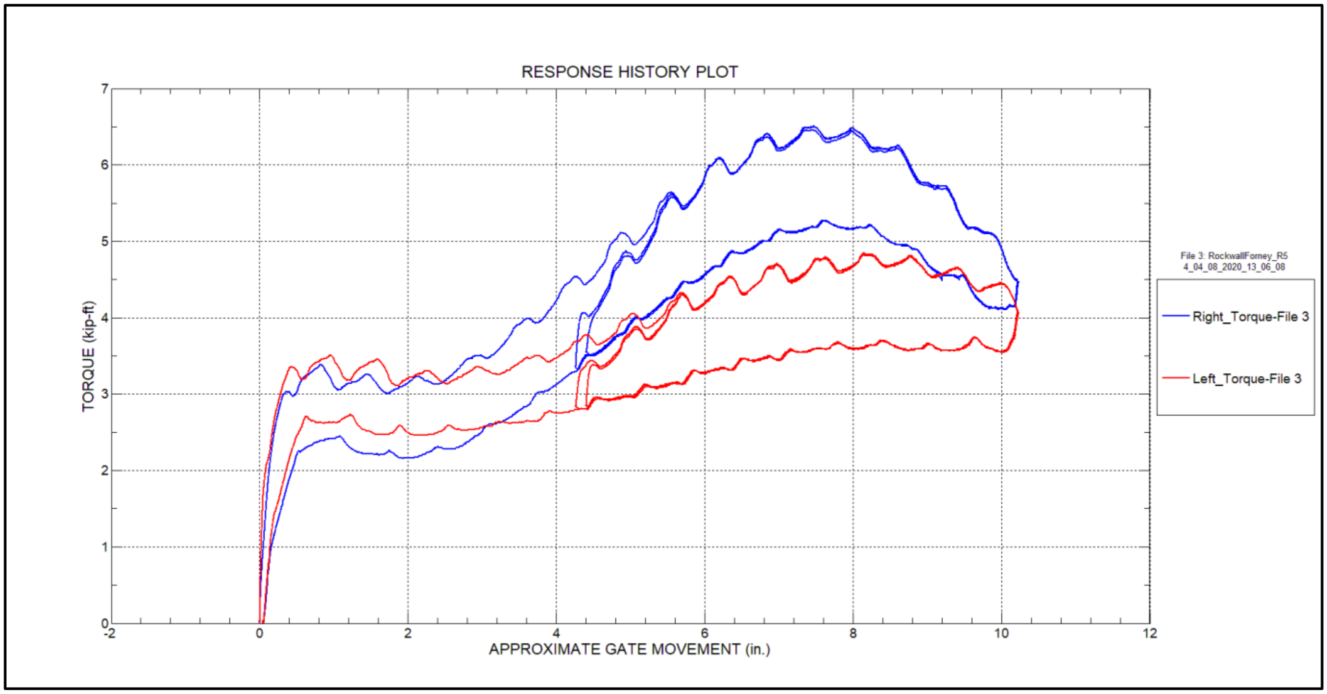

Figure 29 – Hoist torque response history – Gate 9 – Test 3

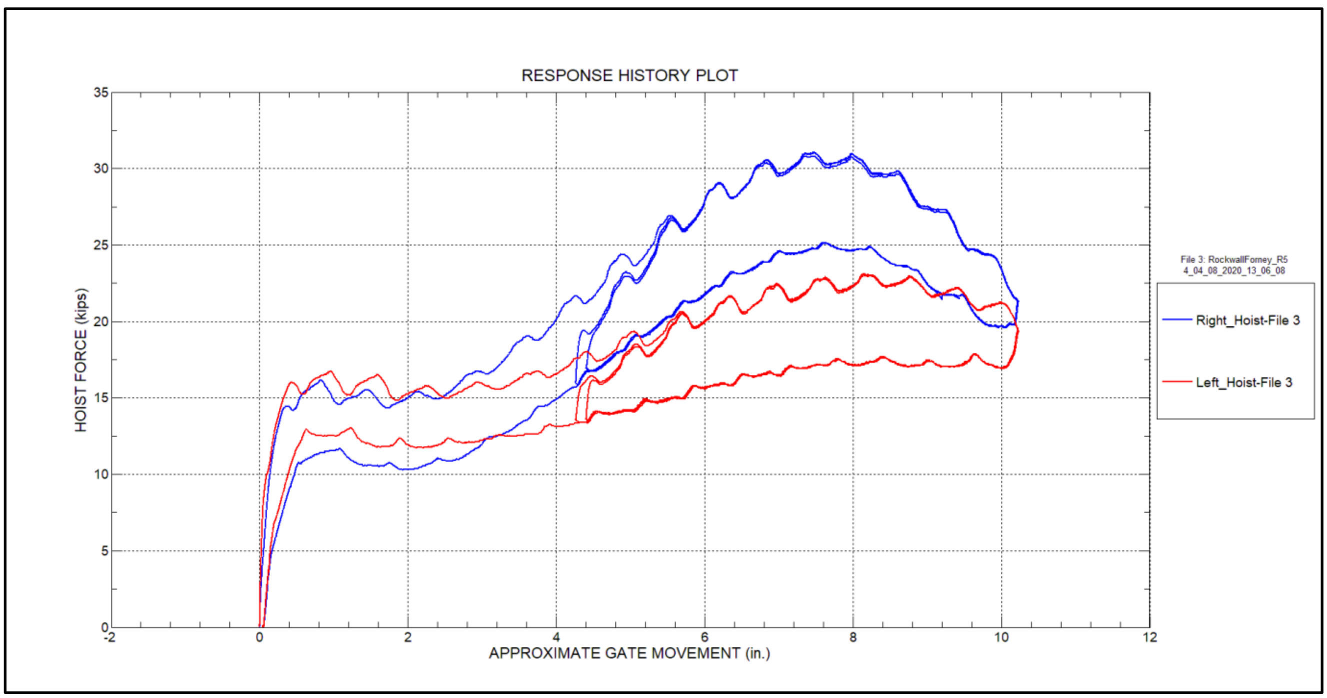

Figure 30 – Hoist force response history – Gate 9 – Test 3

APPENDIX B – GATE 9 PIN MOMENT COMPONENT PLOTS

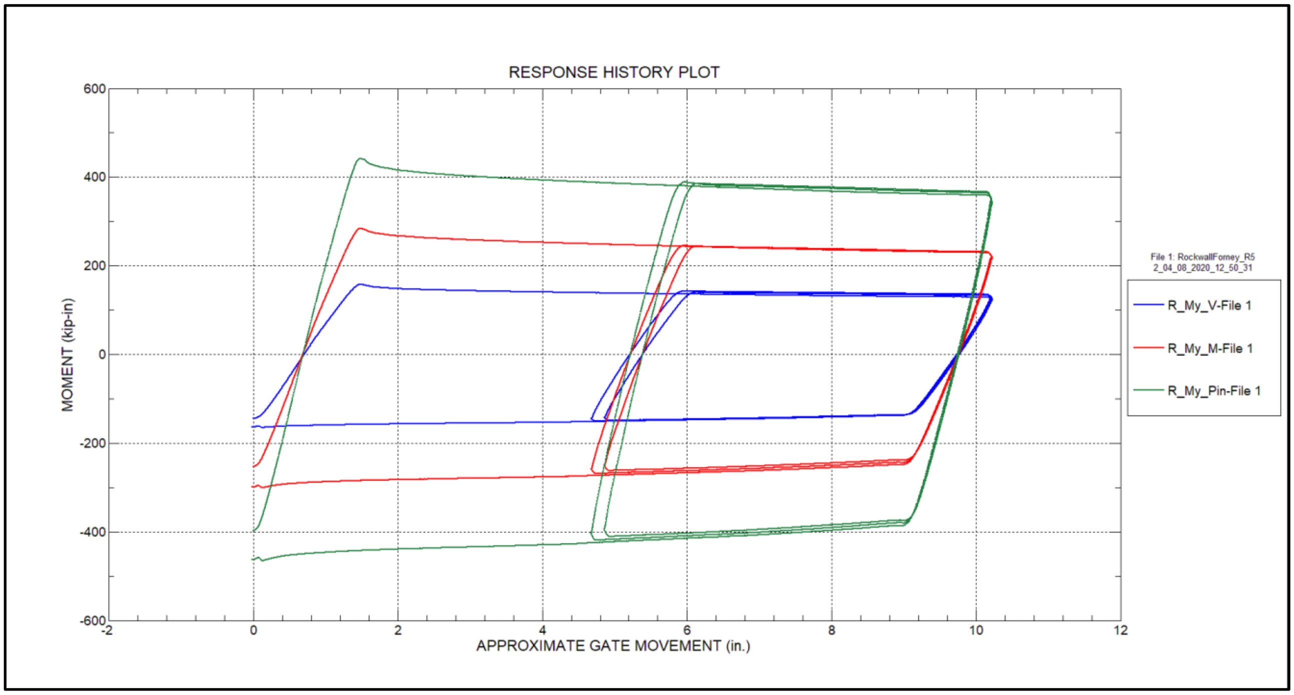

Figure 31 – Pin moment response history – Right arm – Test run 1

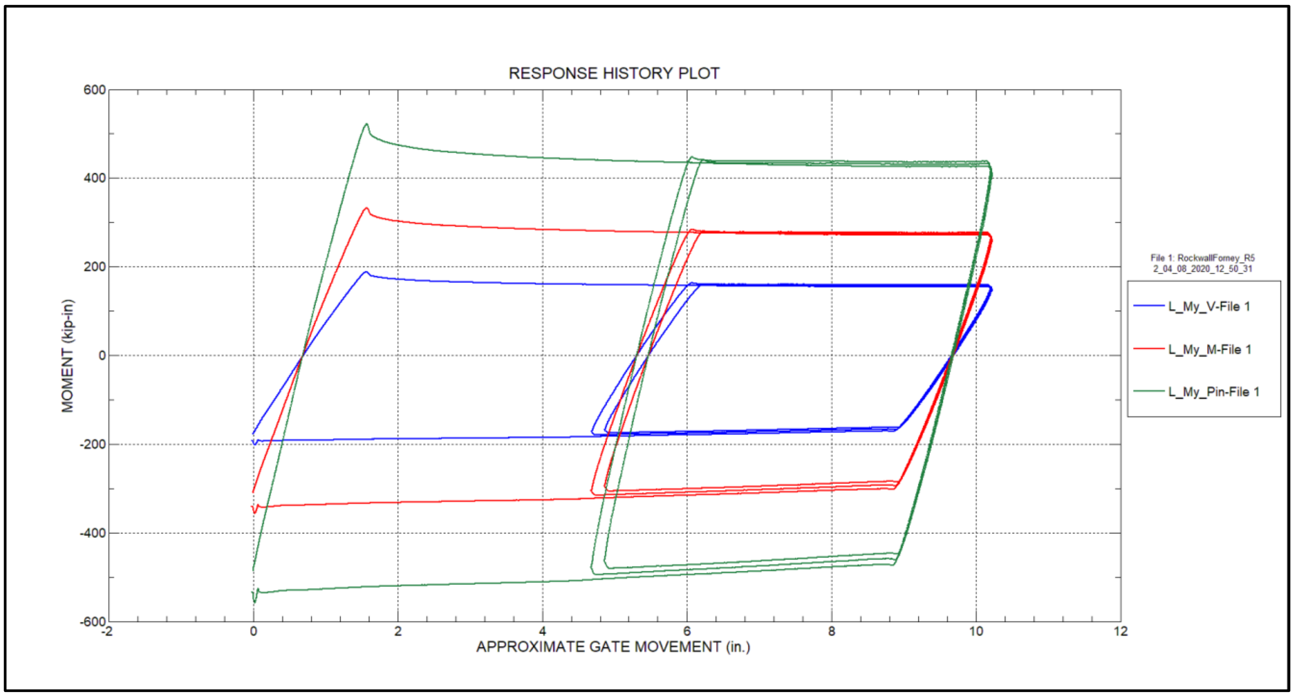

Figure 32 – Pin moment response history – Left arm – Test run 1

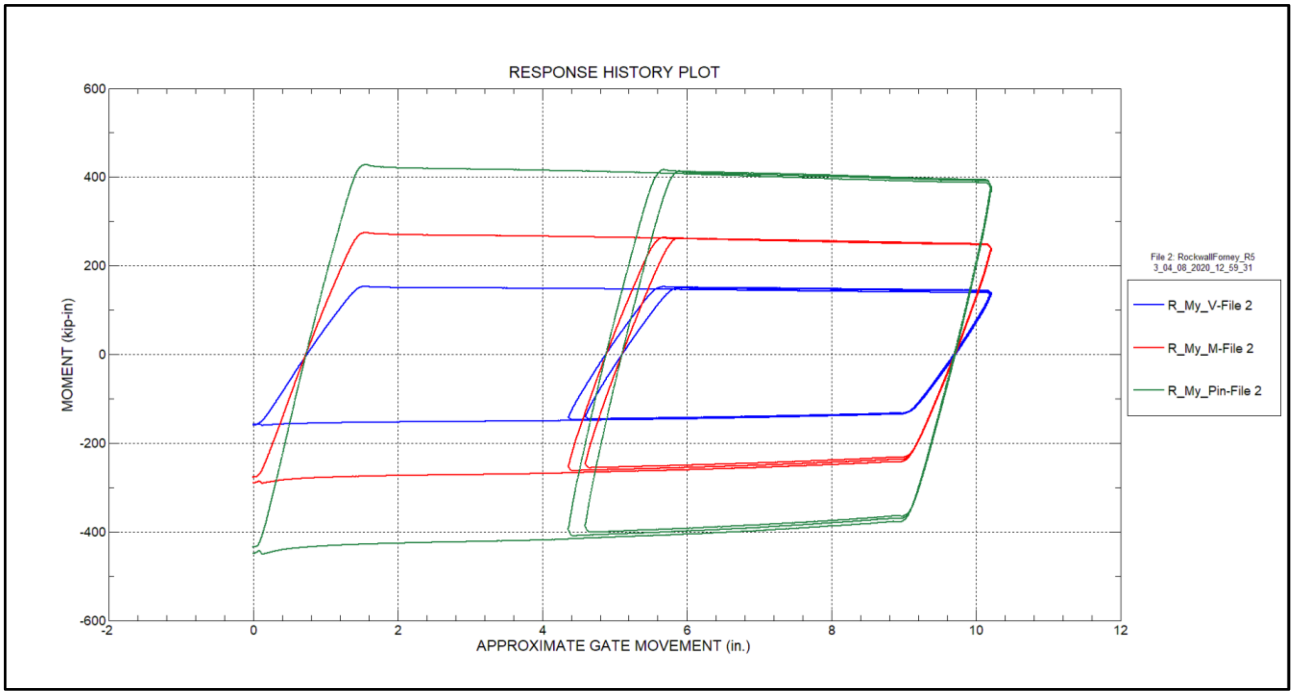

Figure 33 – Pin moment response history – Right arm – Test run 2

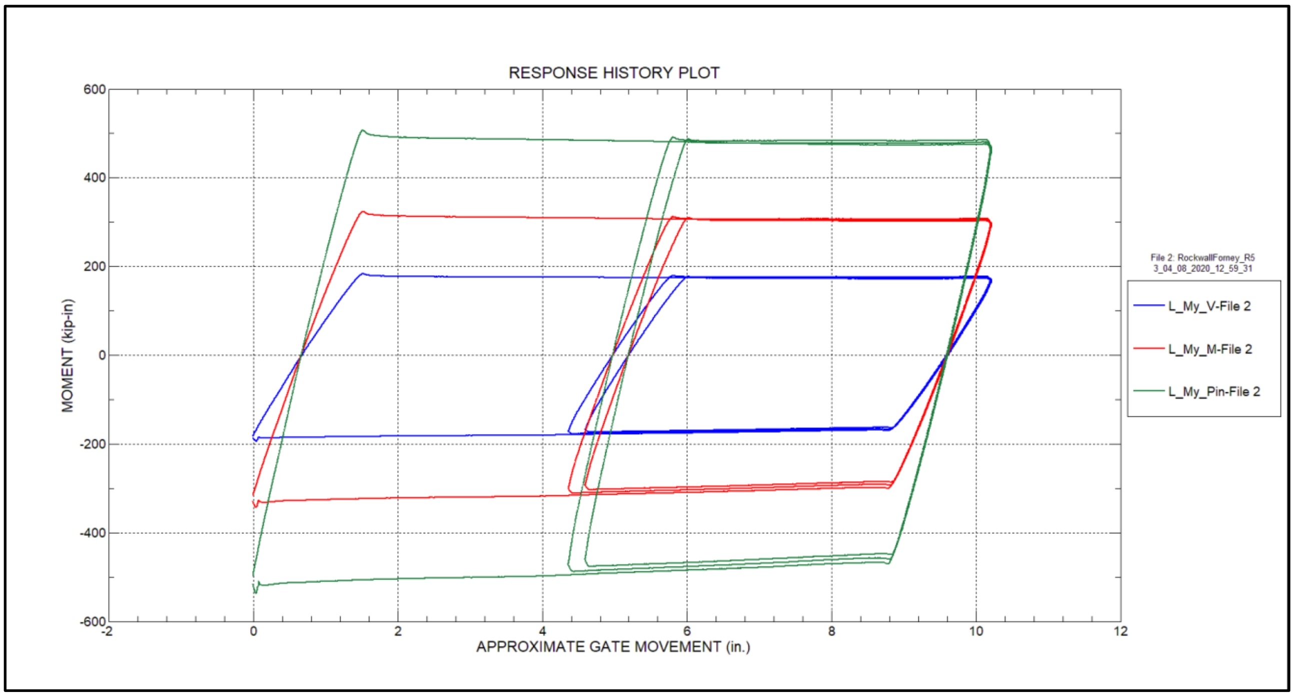

Figure 34 – Pin moment response history – Left arm – Test run 2

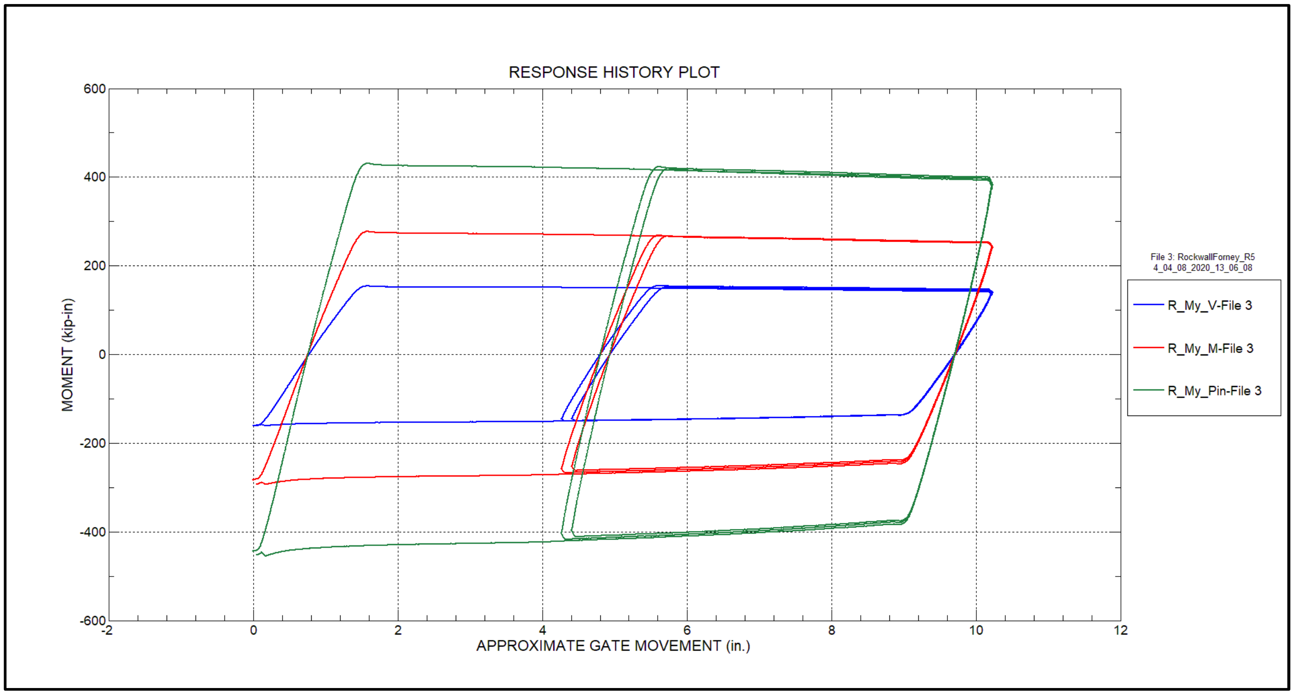

Figure 35 – Pin moment response history – Right arm – Test run 3

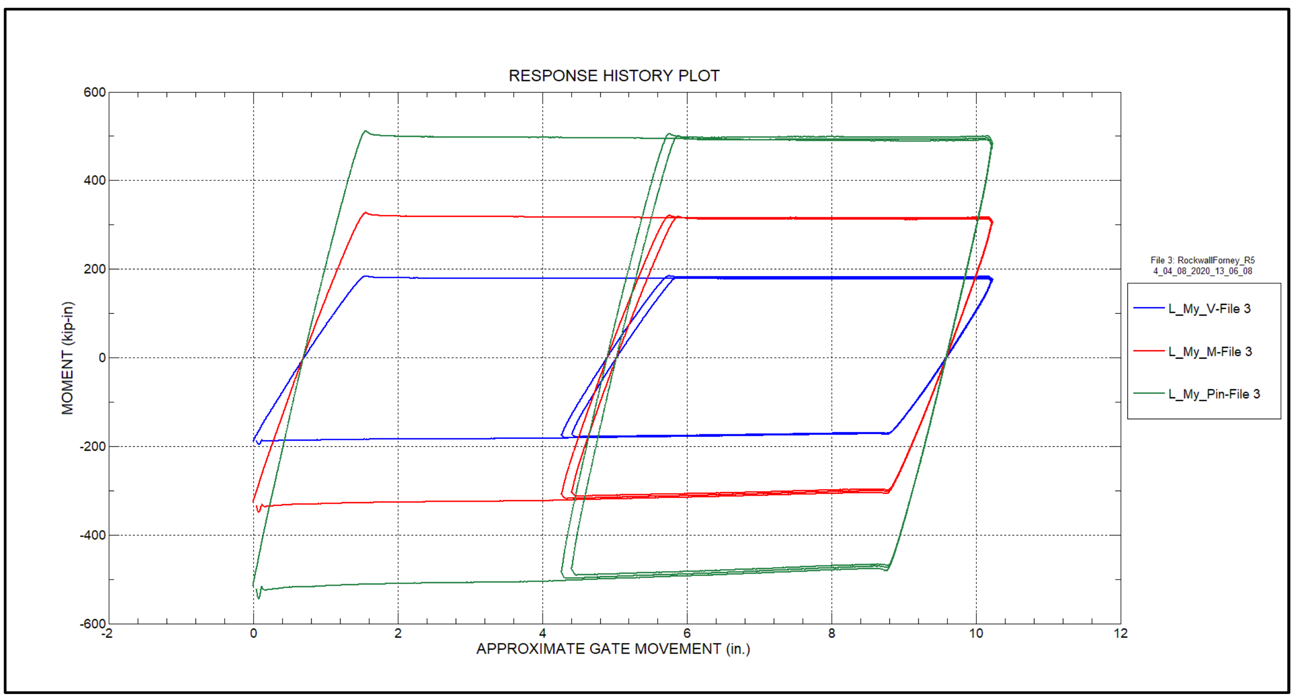

Figure 36 – Pin moment response history – Left arm – Test run 3

APPENDIX C – INSTRUMENTATION PLANS

RAW DATA. REFINED RESULTS.

SCHNABEL ENGINEERING
ROCKWALL FORNEY DAM
LIVE LOAD TESTING

RAW DATA. REFINED RESULTS.
740 S PIERCE AVE, SUITE 15
LOUISVILLE, CO 80027
303.494.3230
WWW.BDITEST.COM

ISSUE

CLIENT

SCHABEL ENGINEERING
16000 CHRISTENSEN RD, STE 101
SEATTLE, WA 98188

PROJECT NAME

SCHNABEL ENGINEERING
ROCKWALL FORNEY DAM
LIVE LOAD TESTING

Drawn By:	KNR
Checked By:	JDS
Date:	05/27/2020
Client No.:	
BDI No.:	190701-TX
SCALE:	NTS

COVER PAGE

LLT-00

The user acknowledges that these documents are instruments of professional service, and are protected by Copyright. This document and the information contained in this document are the property of Bridge Diagnostics, Inc., and shall not be reused, copied, disseminated, modified, amended or altered in any way. It is issued for information purposes only. The user agrees to hold harmless, indemnify and defend Bridge Diagnostics, Inc. against any and all damages, claims and losses, including defense costs, arising out of any use, reuse or copying of this document.

PLOT TIME: 6/12/2020 3:22 PM
FILEPATH: C:\Users\colemand\BDI\Services - Documents\Server_Remote\190701-TX_Schnabel_RockwallForneyDam\7. Instrumentation Plans\BDI_ROCKWALLFORNEY_01_GENERAL.dwg
© YYYY BRIDGE DIAGNOSTICS INC.

The user acknowledges that these documents are instruments of professional service, and are protected by Copyright. This document and the information contained in this document are the property of Bridge Diagnostics, Inc., and shall not be reused, copied, disseminated, modified, amended or altered in any way. It is issued for information purposes only. The user agrees to hold harmless, indemnify and defend Bridge Diagnostics, Inc. against any and all damages, claims and losses, including defense costs, arising out of any use, reuse or copying of this document.

GAGE LEGEND & SPECIFICATION

SYMBOL	TYPE	BRAND	MODEL	NOTES
	STRAIN TRANSDUCER	BDI	ST350	
	TILTMETER (UNI-AXIAL)	BDI	T500-030	
	TORQUE SENSOR	HPI	-	HBWS-35-125-6-0.5VR-FB
	AMP SENSOR	CR MAGNETICS	CR42105-200	

GENERAL NOTES

- INSTRUMENTATION SHALL BEGIN ON APRIL 1ST, 2020.
- GATES 1 THRU 14 SHALL BE ACCESSED USING SPRAT ROPE ACCESS TECHNIQUES.
- BDI WILL PERFORM ALL SURFACE PREPARATION, SENSOR INSTALLATION, AND EQUIPMENT INSTALLATION.
- SEE LLT-31 FOR SENSOR INSTALLATION DETAILS.
- TWO PAIRS OF TORQUE GAGES WILL BE INSTALLED ON THE GATE MOTORS' PINION SHAFTS BETWEEN THE MOTORS AND THE HOISTS.
  - GAGE PAIRS WILL BE INSTALLED 180° APART FROM EACH OTHER.
  - EXACT POSITIONS OF THE GAGE PAIRS ON THE PINION SHAFT WILL BE DETERMINED IN THE FIELD.
- THREE PHASE AMPERAGE GAGES WILL BE INSTALLED ON THE MOTOR CONTROLS BY A QUALIFIED ELECTRICIAN PROVIDED BY GARVER.

TESTING PROCEDURE:

- TESTING SHALL BE STARTED WITH THE GATE IN THE CLOSED POSITION.
- ONCE DATA COLLECTION BEGINS, THE GATE SHALL BE RAISED TO TWO OR THREE TIMES THE HEIGHT NECESSARY FOR TRUNNION FRICTION TO BE OVERCOME, H1 (TYPICALLY 6"-12"), AND HELD THERE UNTIL DATA STABILIZES.
- THE GATE SHALL BE LOWERED APPROXIMATELY TWICE THE DISTANCE TO OVERCOME TRUNNION FRICTION, H2, AND HELD THERE UNTIL DATA STABILIZES.
- THE GATE SHALL BE RAISED TO H1 AND HELD THERE UNTIL DATA STABILIZES.
- THE GATE SHALL BE LOWERED TO H2 AND HELD THERE UNTIL DATA STABILIZES.
- THE GATE SHALL BE RAISED TO H1 AND HELD THERE UNTIL DATA STABILIZES.
- THE GATE WAS LOWERED BACK TO CLOSED POSITION AND DATA COLLECTION STOPPED.
- A MINIMUM OF 3 TESTS SHALL BE PERFORMED PER GATE.

LOCATION KEY

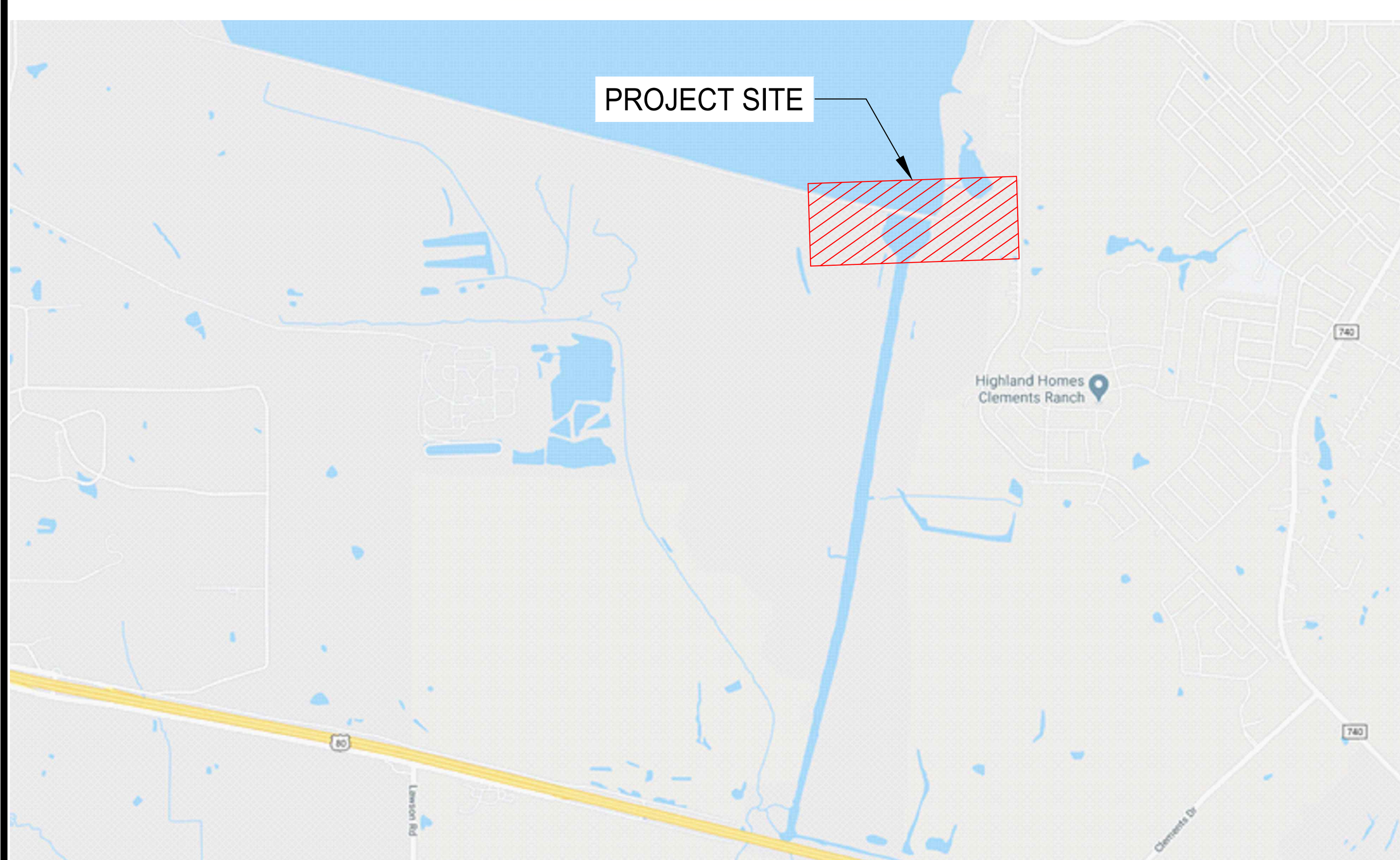

GAGE COUNT PER GATE

SENSOR LEGEND	SENSOR COUNT	CHANNEL COUNT
STRAIN TRANSDUCER	(48)	(48)
TILTMETER (UNI-AXIAL)	(4)	(4)
TORQUE SENSOR	(4)	(4)
AMP SENSOR	(3)	(3)
TOTAL	(59)	(59)

INDEX OF SHEETS

INDEX OF ISSUE

NO.	DATE	REVISION DESCRIPTION
1	3/20/2020	LIVE LOAD TESTING (LLT) INSTRUMENTATION PLAN (FOR APPROVAL)
2	5/27/2020	LIVE LOAD TESTING (LLT) INSTRUMENTATION PLAN AS BUILTS

BDI REFERENCE NUMBER: 190701-TX

RAW DATA. REFINED RESULTS.
740 S PIERCE AVE, SUITE 15
LOUISVILLE, CO 80027
303.494.3230
WWW.BDITEST.COM

ISSUE

CLIENT

SCHABEL ENGINEERING
16000 CHRISTENSEN RD, STE 101
SEATTLE, WA 98188

PROJECT NAME

SCHNABEL ENGINEERING
ROCKWALL FORNEY DAM
LIVE LOAD TESTING

Drawn By:	KNR
Checked By:	JDS
Date:	05/27/2020
Client No.:	
BDI No.:	190701-TX
SCALE:	NTS

OVERALL LEGEND

LLT-01

PLOT TIME: 6/12/2020 3:22 PM
FILEPATH: C:\Users\coleman\BDI\Services - Documents\Server_Remote\190701-TX_Schnabel_RockwallForneyDam\7. Instrumentation Plans\BDI_ROCKWALLFORNEY_01_GENERAL.dwg
© YYYY BRIDGE DIAGNOSTICS INC.

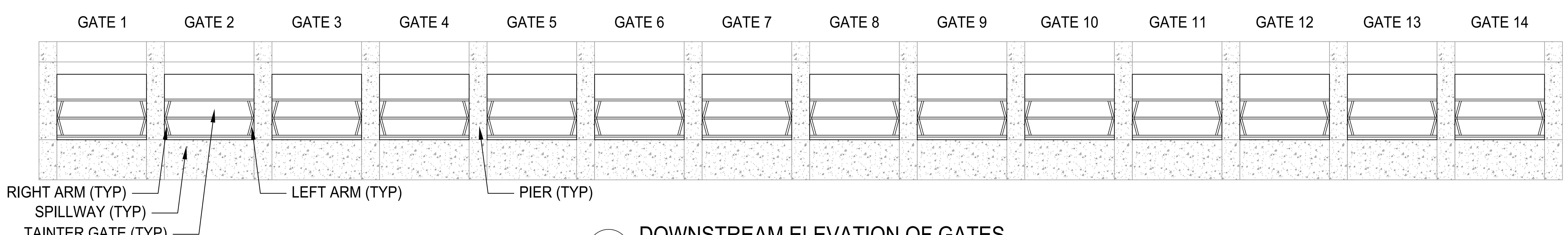

1 DOWNSTREAM ELEVATION OF GATES
LOOKING NORTH (UPSTREAM)

The user acknowledges that these documents are instruments of professional service, and are protected by Copyright. This document and the information contained in this document are the property of Bridge Diagnostics, Inc., and shall not be reused, copied, disseminated, modified, amended or altered in any way. It is issued for information purposes only. The user agrees to hold harmless, indemnify and defend Bridge Diagnostics, Inc. against any and all damages, claims and losses, including defense costs, arising out of any use, reuse or copying of this document.

PLOT TIME: 6/12/2020 3:22 PM
FILEPATH: C:\Users\colemand\BDI\Services - Documents\Server_Remote\190701-TX_Schabel_RockwallForneyDam\7. Instrumentation Plans\BDI_ROCKWALLFORNEY_01_GENERAL.dwg
© YYYY BRIDGE DIAGNOSTICS INC.

RAW DATA. REFINED RESULTS.
740 S PIERCE AVE, SUITE 15
LOUISVILLE, CO 80027
303.494.3230
WWW.BDITEST.COM

ISSUE

CLIENT

SCHABEL ENGINEERING
16000 CHRISTENSEN RD, STE 101
SEATTLE, WA 98188

PROJECT NAME

SCHNABEL ENGINEERING
ROCKWALL FORNEY DAM
LIVE LOAD TESTING

Drawn By:	KNR
Checked By:	JDS
Date:	05/27/2020
Client No.:	
BDI No.:	190701-TX
SCALE:	NTS

OVERALL STRUCTURE LAYOUT

LLT-02

The user acknowledges that these documents are instruments of professional service, and are protected by Copyright. This document and the information contained in this document are the property of Bridge Diagnostics, Inc., and shall not be reused, copied, disseminated, modified, amended or altered in any way. It is issued for information purposes only. The user agrees to hold harmless, indemnify and defend Bridge Diagnostics, Inc. against any and all damages, claims and losses, including defense costs, arising out of any use, reuse or copying of this document.

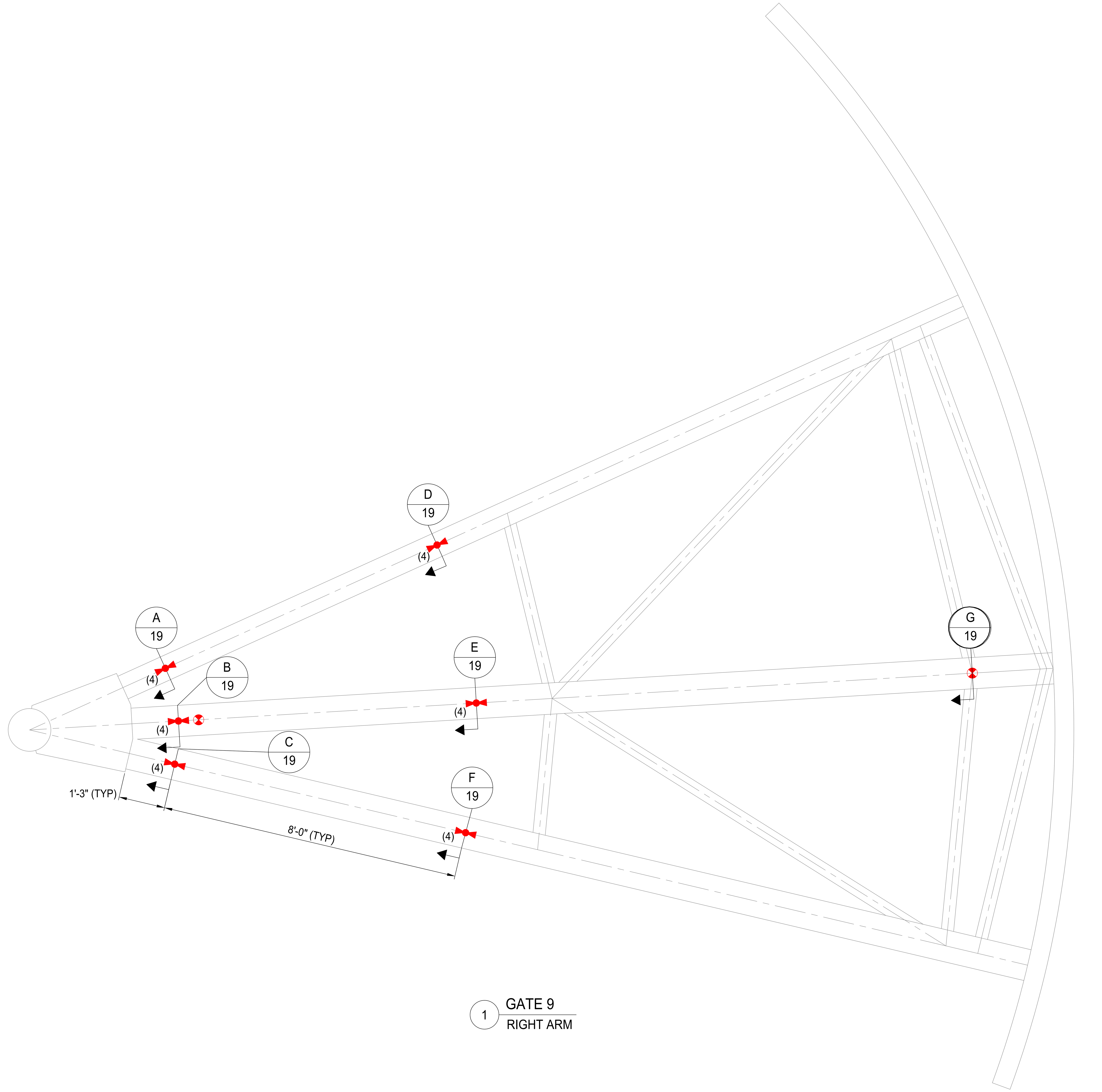

1 GATE 9
RIGHT ARM

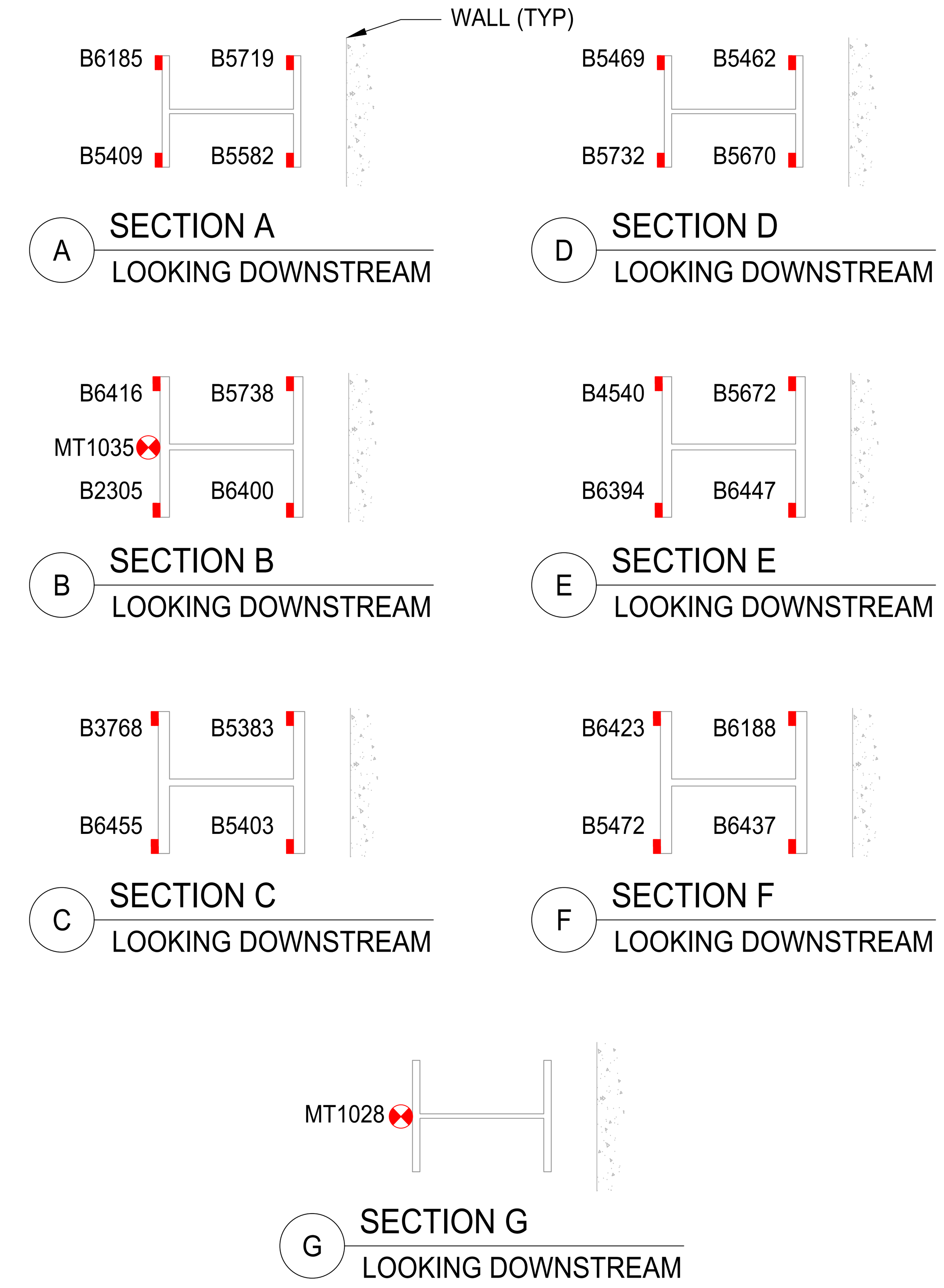

UNIT ID
TT-3

TORQUE GAGES
RIGHT ARM

NOTES:

1. SECTIONS A, B, & C SHALL BE INSTALLED 15 INCHES AWAY FROM TRUNNION PLATE.
2. TILTMETERS SHALL BE INSTALLED CENTERED ON THE MIDDLE STRUT FLANGE.
3. SECTION G'S TILTMETER SHALL BE INSTALLED AS CLOSE TO THE SKINPLATE AS POSSIBLE.

SENSOR LEGEND

- STRAIN TRANSDUCER
- TILTMETER (UNI-AXIAL)
- TORQUE SENSOR

BDI
RAW DATA. REFINED RESULTS.

740 S PIERCE AVE, SUITE 15
LOUISVILLE, CO 80027
303.494.3230
WWW.BDITEST.COM

ISSUE

CLIENT

SCHABEL ENGINEERING
16000 CHRISTENSEN RD, STE 101
SEATTLE, WA 98188

PROJECT NAME

SCHABEL ENGINEERING
ROCKWALL FORNEY DAM
LIVE LOAD TESTING

Drawn By:	KNR
Checked By:	JDS
Date:	05/27/2020
Client No.:	
BDI No.:	190701-TX
SCALE:	NTS

GATE 9 - RIGHT ARM
ELEVATION
LLT-19

PLOT TIME: 6/12/2020 3:23 PM
FILEPATH: C:\Users\colemand\BDI\Services - Documents\Server_Remote\190701-TX_Schabel_RockwallForneyDam\7. Instrumentation Plans\BDI_ROCKWALLFORNEY_01_GENERAL.dwg
© YYYY BRIDGE DIAGNOSTICS INC.

The user acknowledges that these documents are instruments of professional service, and are protected by Copyright. This document and the information contained in this document are the property of Bridge Diagnostics, Inc., and shall not be reused, copied, disseminated, modified, amended or altered in any way. It is issued for information purposes only. The user agrees to hold harmless, indemnify and defend Bridge Diagnostics, Inc. against any and all damages, claims and losses, including defense costs, arising out of any use, reuse or copying of this document.

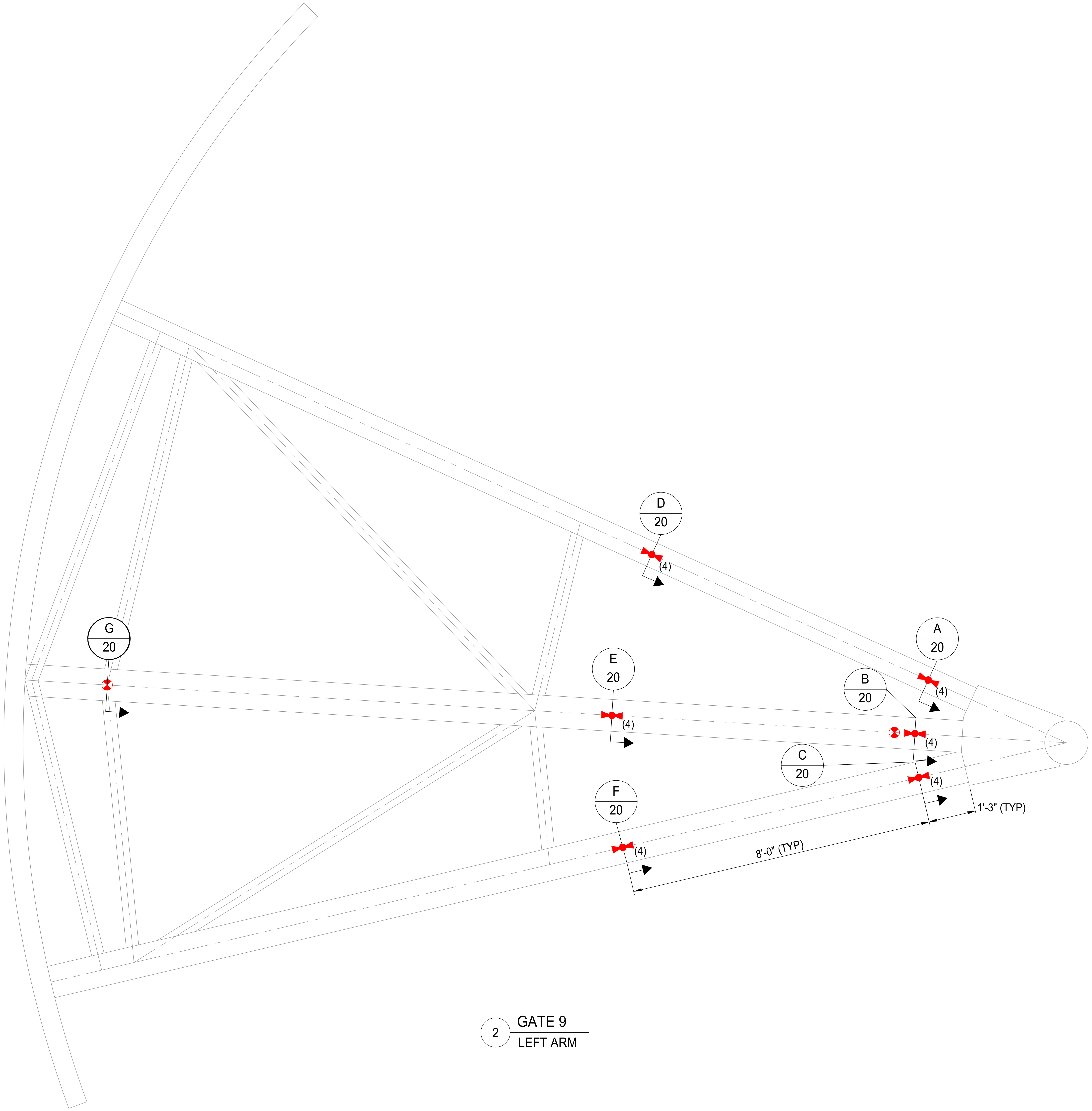

2 GATE 9
LEFT ARM

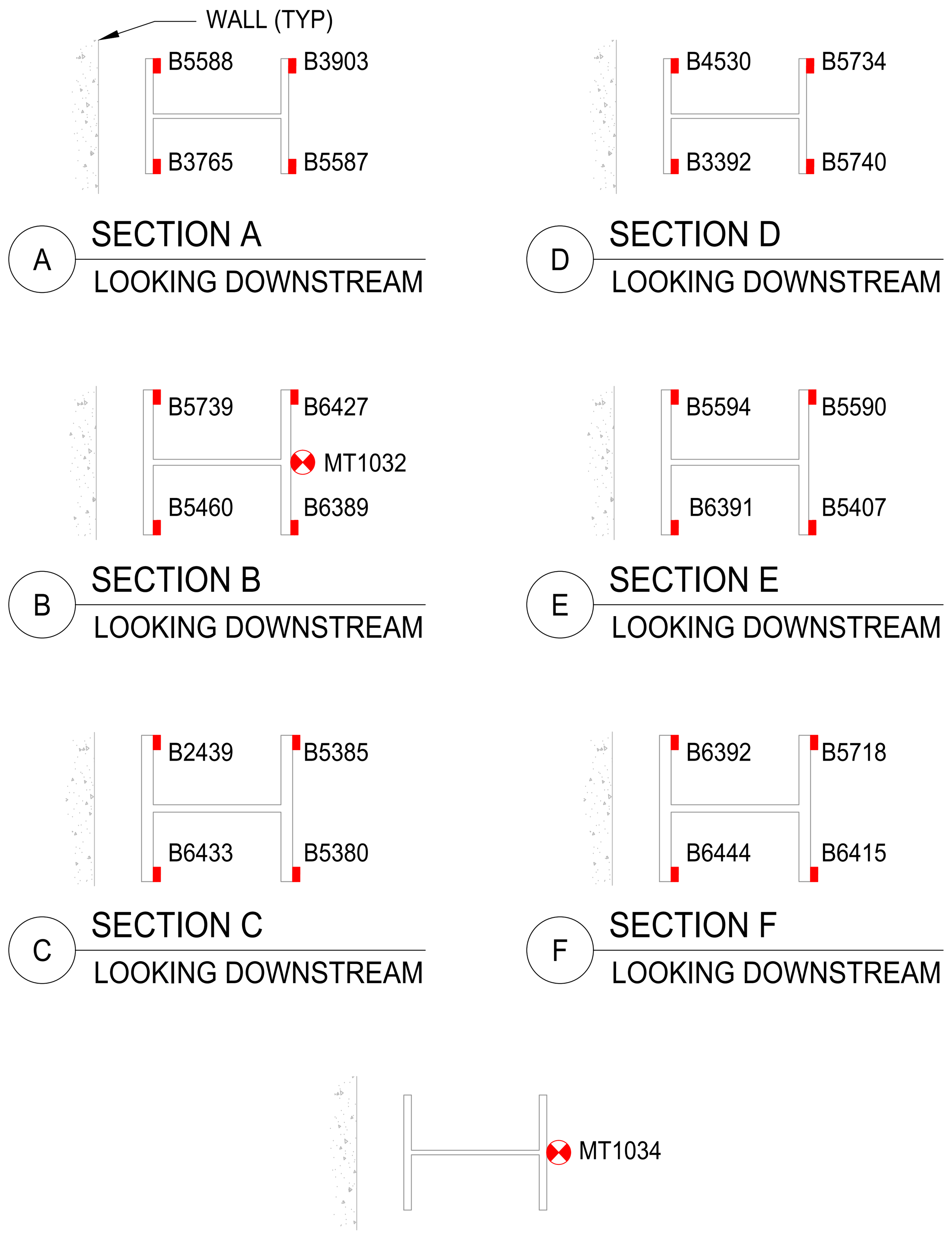

A SECTION A
LOOKING DOWNSTREAM

D SECTION D
LOOKING DOWNSTREAM

B SECTION B
LOOKING DOWNSTREAM

E SECTION E
LOOKING DOWNSTREAM

C SECTION C
LOOKING DOWNSTREAM

F SECTION F
LOOKING DOWNSTREAM

G SECTION G
LOOKING DOWNSTREAM

UNIT ID
TT-4

TORQUE GAGES
LEFT ARM

NOTES:

1. SECTIONS A, B, & C SHALL BE INSTALLED 15 INCHES AWAY FROM TRUNNION PLATE.
2. TILTMETERS SHALL BE INSTALLED CENTERED ON THE MIDDLE STRUT FLANGE.
3. SECTION G'S TILTMETER SHALL BE INSTALLED AS CLOSE TO THE SKINPLATE AS POSSIBLE.

SENSOR LEGEND

- STRAIN TRANSDUCER
- TILTMETER (UNI-AXIAL)
- TORQUE SENSOR

BDI
RAW DATA. REFINED RESULTS.
740 S PIERCE AVE, SUITE 15
LOUISVILLE, CO 80027
303.494.3230
WWW.BDITEST.COM

ISSUE

CLIENT

SCHABEL ENGINEERING
16000 CHRISTENSEN RD, STE 101
SEATTLE, WA 98188

PROJECT NAME

SCHABEL ENGINEERING
ROCKWALL FORNEY DAM
LIVE LOAD TESTING

Drawn By:	KNR
Checked By:	JDS
Date:	05/27/2020
Client No.:	
BDI No.:	190701-TX
SCALE:	NTS

GATE 9 - LEFT ARM
ELEVATION
LLT-20

PLOT TIME: 6/12/2020 3:23 PM
FILEPATH: C:\Users\colemand\BDI\Services - Documents\Server_Remote\190701-TX_Schabel_RockwallForneyDam\7. Instrumentation Plans\BDI_ROCKWALLFORNEY_01_GENERAL.dwg
© YYYY BRIDGE DIAGNOSTICS INC.

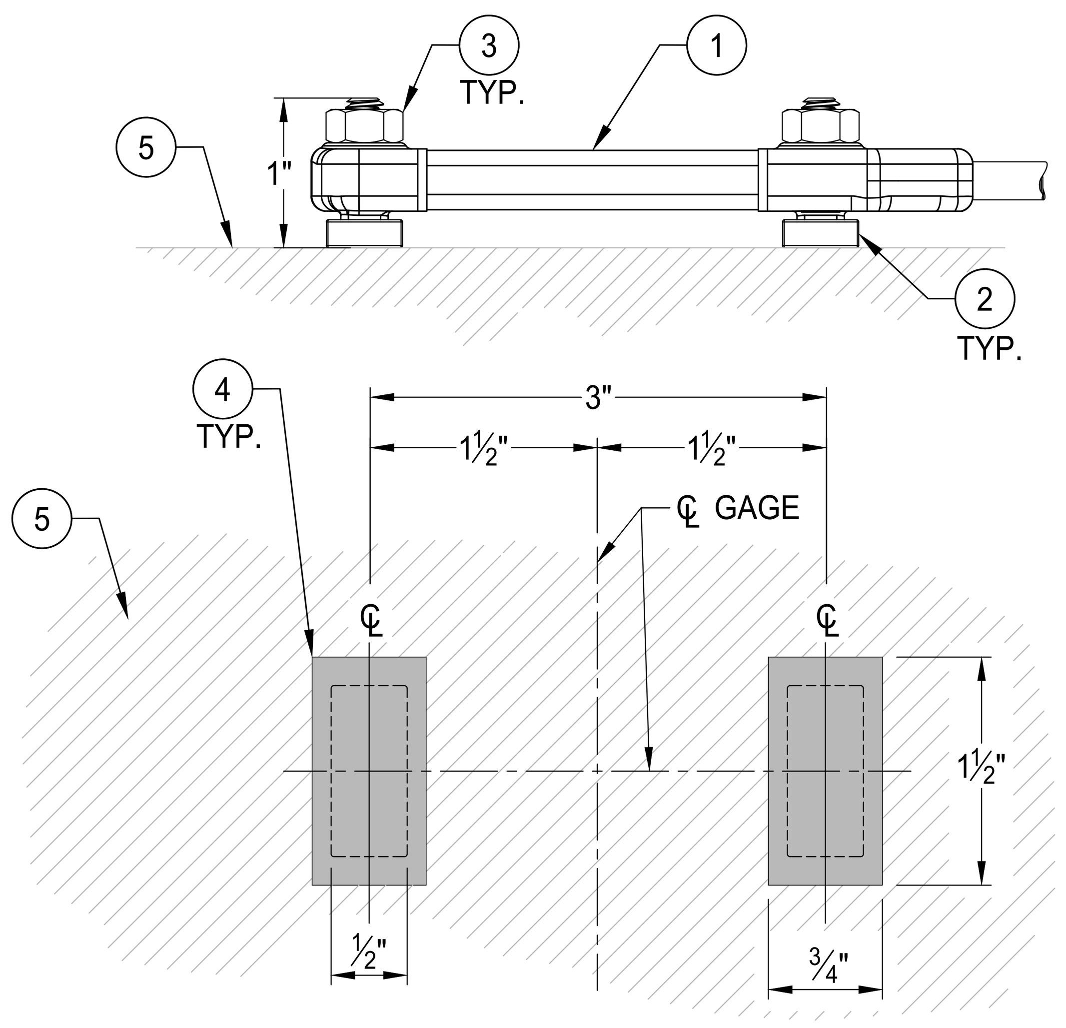

COMPONENT DESCRIPTION

1. ST350 STRAIN GAGE
2. 1/4"-20 THREADED MOUNTING TAB
3. 1/4"-20 STAINLESS STEEL NUT
4. TYPICAL SURFACE PREP REQUIRED TO MOUNT STRAIN GAGES
5. TYPICAL MOUNTING SURFACE

FOOTNOTES - INSTANT ADHESIVE
1. STRAIN GAGES SHALL BE MOUNTED WITH LOCTITE 410 INSTANT ADHESIVE AND LOCTITE 7452 ACCELERANT 2. DURING SURFACE PREP ALL PAINT AND SURFACE DEFORMATIONS MUST BE REMOVED. 3. SURFACE PREP IS REQUIRED JUST PRIOR TO GAGE INSTALLATION AS TO NOT ALLOW SURFACE CONTAMINANTS TO ACCUMULATE.

1 TYPICAL ST350 STRAIN GAGE INSTALLATION

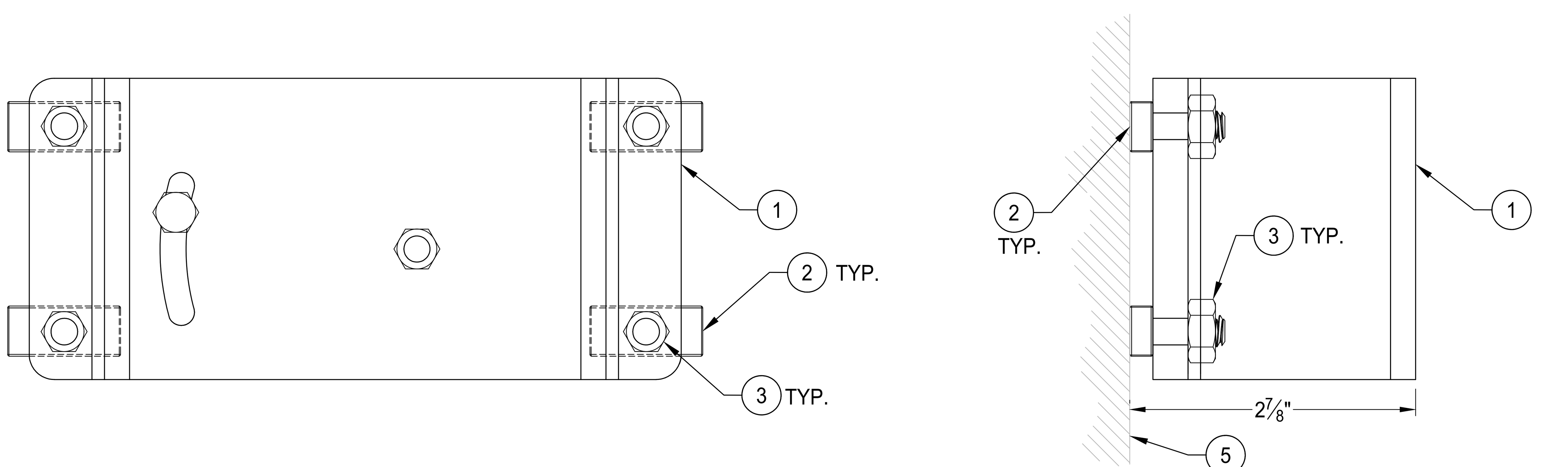

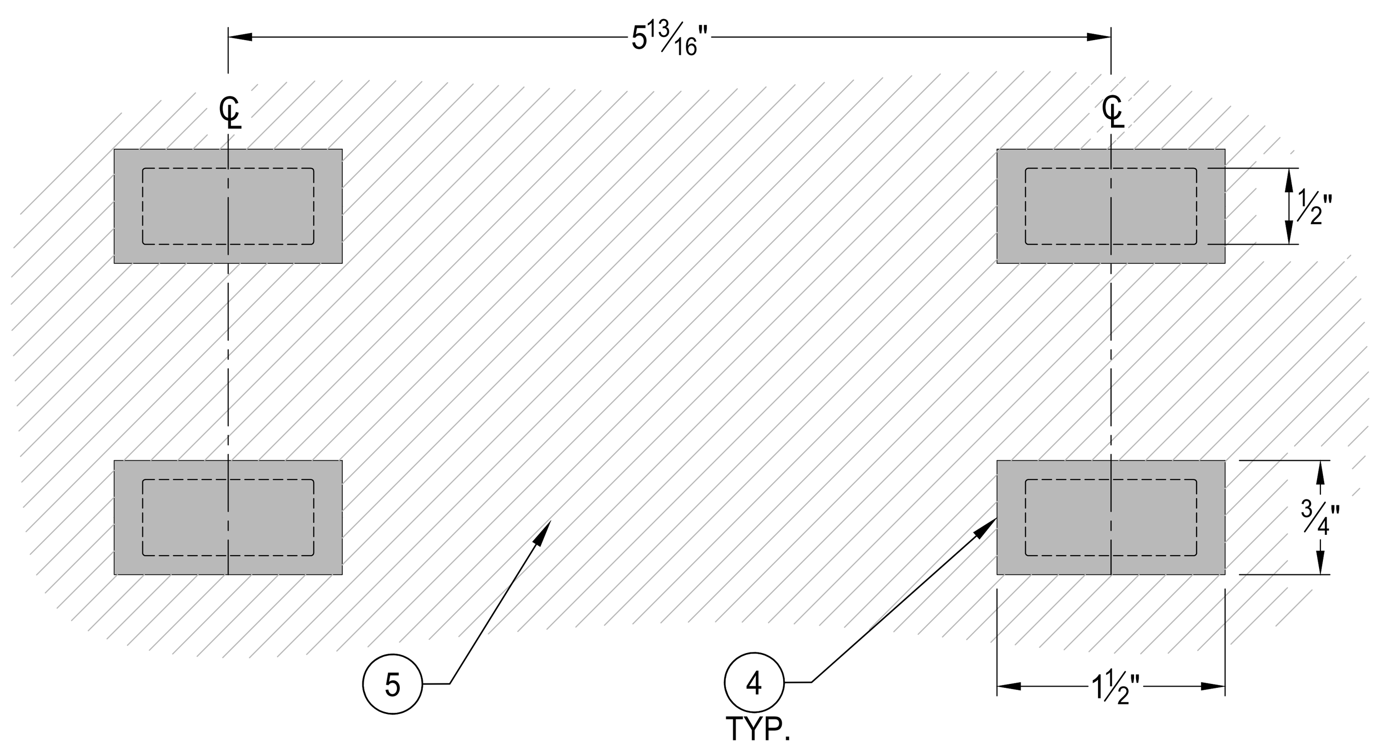

COMPONENT DESCRIPTION

1. BDI +/- 15 DEGREE TILTMETER WITH COVER AND ADJUSTMENT BOLTS
2. 1/4"-20 THREADED MOUNTING TAB
3. 1/4"-20 STAINLESS STEEL NUT
4. TYPICAL SURFACE PREP REQUIRED TO MOUNT TILTMETERS
5. TYPICAL MOUNTING SURFACE

FOOTNOTES - INSTANT ADHESIVE
1. TILTMETERS SHALL BE MOUNTED WITH LOCTITE 410 INSTANT ADHESIVE AND LOCTITE 7452 ACCELERANT 2. DURING SURFACE PREP ALL PAINT AND SURFACE DEFORMATIONS MUST BE REMOVED. 3. SURFACE PREP IS REQUIRED JUST PRIOR TO GAGE INSTALLATION AS TO NOT ALLOW SURFACE CONTAMINANTS TO ACCUMULATE.

2 TYPICAL BDI TILTMETER INSTALLATION

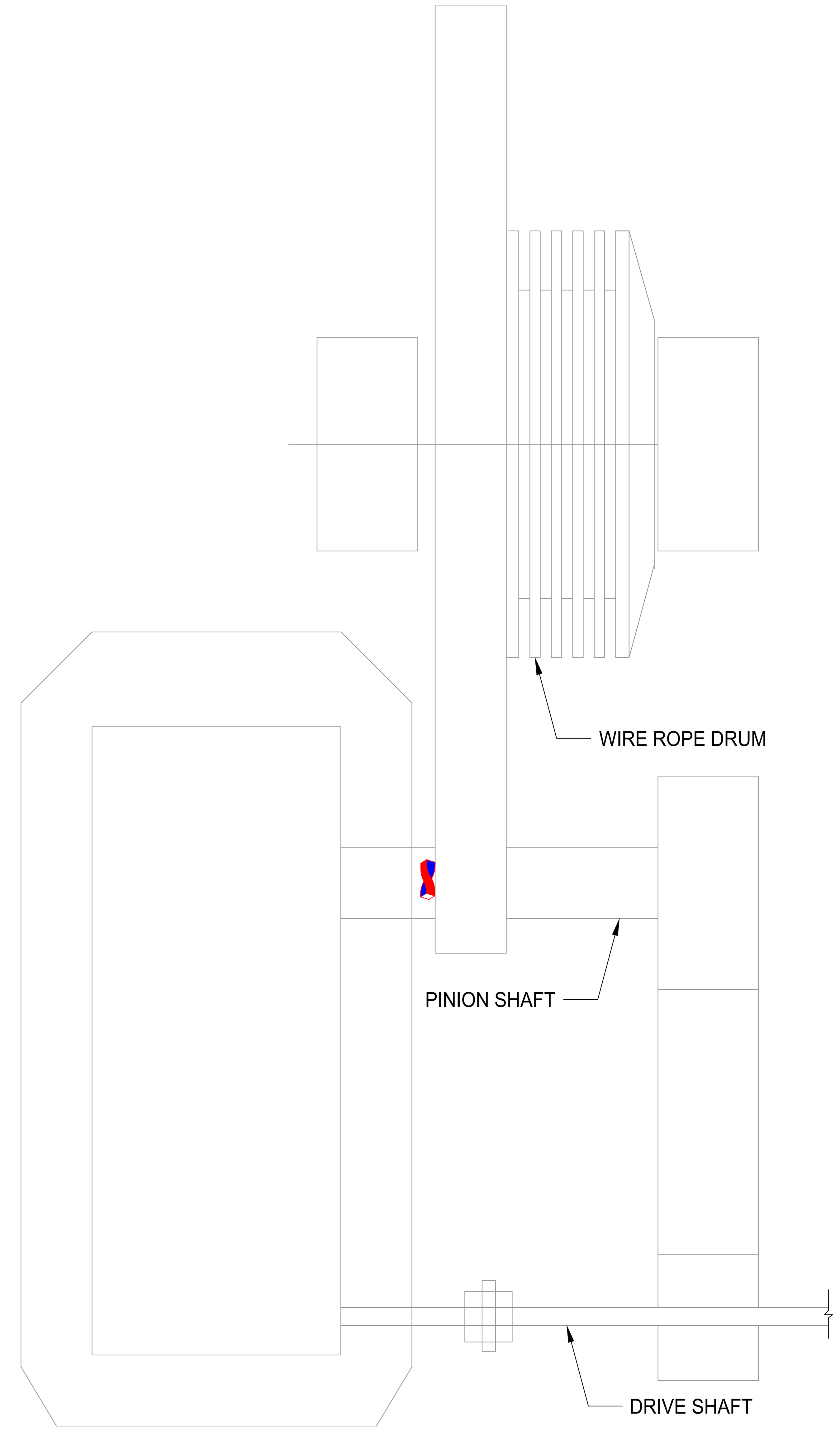

3 TYPICAL HOIST INSTRUMENTATION

TORQUE SENSOR INSTALLATION NOTES:

- TORQUE GAGES WILL BE INSTALLED ON THE PINION SHAFT ON EITHER HOIST MOTOR BETWEEN THE MOTOR AND THE HOIST DRUM
- EXACT POSITIONS OF THE GAGE PAIRS ON THE PINION SHAFT WILL BE DETERMINED IN THE FIELD

SENSOR LEGEND

TORQUE SENSOR

BDI
RAW DATA. REFINED RESULTS.
740 S PIERCE AVE, SUITE 15
LOUISVILLE, CO 80027
303.494.3230
WWW.BDITEST.COM

ISSUE

CLIENT

SCHABEL ENGINEERING
16000 CHRISTENSEN RD, STE 101
SEATTLE, WA 98188

PROJECT NAME

SCHNABEL ENGINEERING ROCKWALL FORNEY DAM LIVE LOAD TESTING

Drawn By:	KNR
Checked By:	JDS
Date:	05/27/2020
Client No.:	
BDI No.:	190701-TX
SCALE:	NTS

SENSOR INSTALLATION DETAILS

LLT-31

The user acknowledges that these documents are instruments of professional service, and are protected by Copyright. This document and the information contained in this document are the property of Bridge Diagnostics, Inc., and shall not be reused, copied, disseminated, modified, amended or altered in any way. It is issued for information purposes only. The user agrees to hold harmless, indemnify and defend Bridge Diagnostics, Inc. against any and all damages, claims and losses, including defense costs, arising out of any use, reuse or copying of this document.

PLOT TIME: 6/12/2020 3:24 PM
FILEPATH: C:\Users\colemand\BDI\Services - Documents\Server_Remote\190701-TX_Schnabel_RockwallForneyDam\7. Instrumentation Plans\BDI_ROCKWALLFORNEY_01_GENERAL.dwg
© YYYY BRIDGE DIAGNOSTICS INC.

SCHNABEL ENGINEERING
TRUNNION PIN FRICTION TESTING REPORT

ROCKWALL FORNEY DAM – GATE 10
FORNEY, TX

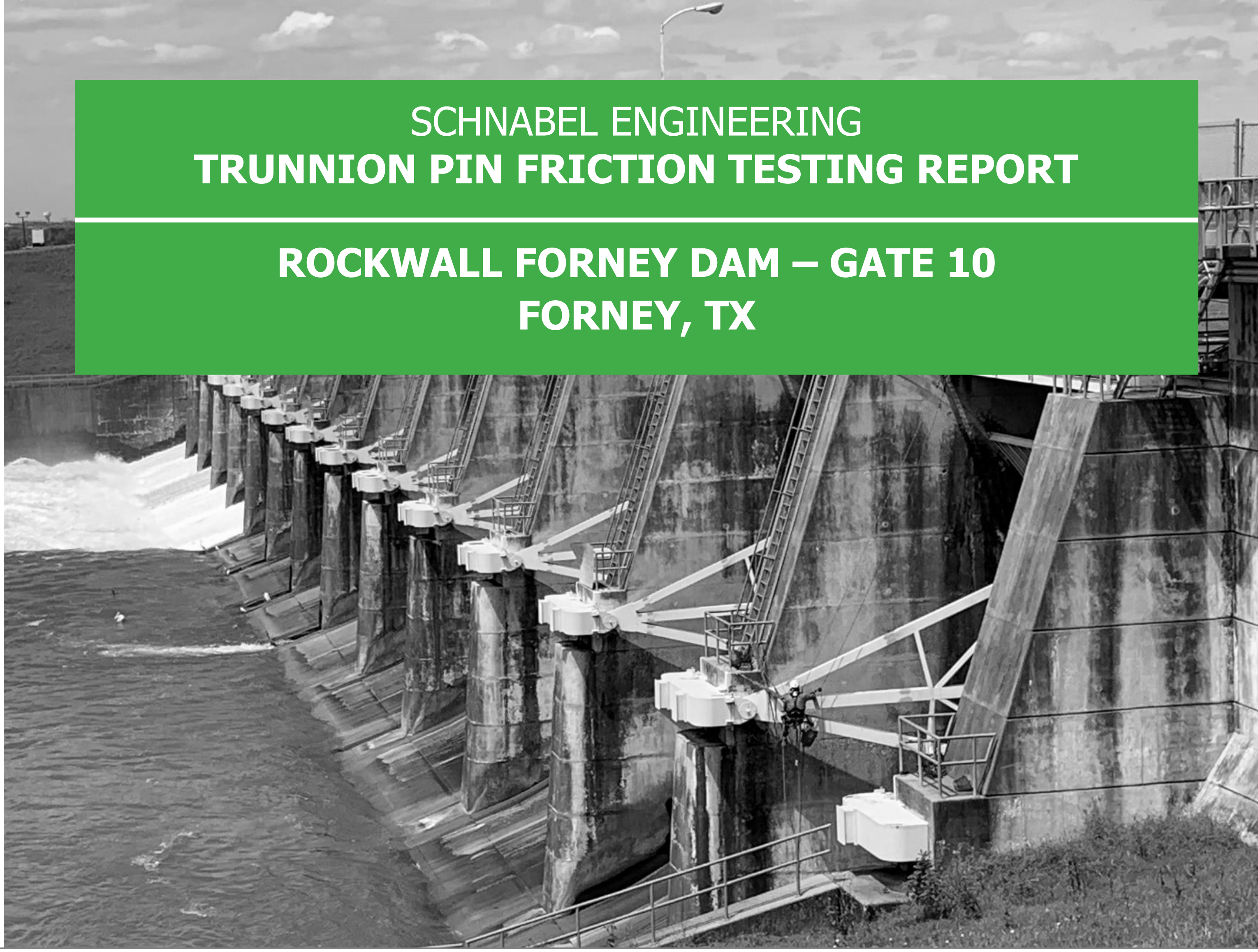

SUBMITTED TO:
SCHNABEL ENGINEERING
16000 CHRISTENSEN RD, SUITE 101
SEATTLE, WA 98188

SUBMITTED BY:
BDI – CO
740 SOUTH PIERCE AVE, UNIT 15
LOUISVILLE, CO 80027

BDI Project No.: **190701-TX**
Report Version: **V1**
Version Submitted: **August 26, 2020**

RAW DATA. REFINED RESULTS.

This document contains Confidential Information and is submitted in confidence to the customer. The submission of the information contained herein shall not be deemed to constitute public disclosure or authorization for disclosure to other parties. BDI's information and name may not be used in advertising or for promotional purposes without BDI's written consent.

TABLE OF CONTENTS

LIST OF FIGURES

LIST OF TABLES

Executive Summary

Schnabel Engineering contracted BDI to provide instrumentation and testing services on Gates 1-14 on the Rockwall Forney Dam near Dallas, Texas. The goal of these tests was to record each gate's structural responses during a series of spill tests and use the data to compute accurate coefficients of friction for each trunnion pin, cable lift force, total gate friction, and motor amperage. This report provides details on the work performed on Gate 10.

Instrumentation and testing were performed on Gate 10 at the Rockwall Forney Dam on April 9th, 2020. The gate arms were instrumented with strain and rotation sensors. The hoist motors' pinion shafts were instrumented with torque sensors and the hoist motor controls were instrumented with amperage sensors. Following the instrumentation, a series of spill tests were performed to measure the structural responses resulting from trunnion pin friction. All instrumentation setup and removal were performed using BDI's rope access team.

Following demobilization from the field, the test data was examined for quality and then further processed to evaluate the gate's performance. Strain measurements were converted into bending forces which were then applied to pin-strut free-body diagrams. By summing forces at each pin, friction induced moments could be computed, allowing accurate friction coefficients to be determined. Generally, the observed gate behavior showed that Gate 10 was operating as expected with no major signs of distress.

The resulting maximum trunnion friction coefficients and corresponding hoist forces are shown in Table 1.

Table 1 – Gate 10 performance summary

Pin Designation	Maximum Friction Coefficient	Maximum Pin Moment due to Pin Friction (kip-In)	Maximum Hoist Force (kips)	Maximum Hoist Force due to Total Gate Friction (kips)
Right Pin	0.15	397.4	29.08	3.71
Left Pin	0.20	512.3	27.57	3.60

Note: Pin designations are in reference to looking downstream

Due to restrictions caused by the hoist limit switches, the hoist cables could not always be fully slacked at the beginning and end of the performed tests. Throughout testing of the Rockwell Forney gates, it was found that this limit switch restriction varied gate to gate and arm to arm. Therefore, it is not recommended to use the collected hoist force data to quantify overall hoist forces during gate operation. Rather, this hoist data can be better utilized to evaluate total friction behavior.

Amperage responses were not used to compute friction results and were collected as verification that the motor performance was not causing unexpected gate responses. These responses indicated the motor was functioning in a stable manner and should be reviewed by a licensed electrician to further evaluate the motor's performance.

All results and recommendations provided in this report were based on the structure in its current condition; therefore, any significant changes in condition must be noted as they may alter their validity. Questions regarding this report and/or data should be directed to Kyle Ramer (kyler@bditest.com) at BDI. For further information on BDI's equipment, services, and analysis methods please visit www.bditest.com

Instrumentation and Load Testing Procedure

Gate Instrumentation Summary

Instrumentation and testing were performed on Gate 10 at the Rockwall Forney Dam on April 9th, 2020. Instrumentation plans have been provided along with this report and include the following number of instrumented locations and sensor types:

+ **REUSABLE SURFACE MOUNTED STRAIN TRANSDUCERS:** Each gate arm was instrumented with a total of 24 strain transducers at 6 locations on each of the gate arms (48 strain sensors total). A typical strain gage installation is shown in Figure 1. Note these sensors were installed with the mounting tabs on the extreme fiber of the strut flanges, which puts the center of the gage approximately 0.66" from the extreme fiber.
+ **TILTMETER ROTATION SENSORS:** MEMS style rotation sensors were located on the middle strut of the gate arm near the skin plate and near the trunnion hub (4 rotation sensors total). The rotation responses were used to calculate vertical skin plate movement and measure pin rotation relative to skin plate rotation. Typical tiltmeter installations are shown in Figure 1 and Figure 2.
+ **TORQUE SENSORS:** Two total torque sensors were installed on the hoist's pinion shafts (QTY1 on each hoist pinion shaft) near the cable hoist motor to measure direct torque and in turn lift force (See Figure 3).
+ **AMPERAGE SENSORS:** 3 Hall-Effect amperage transducers were clamped over each phase of the hoist motor to measure the motor's current draw (See Figure 4). The purpose of these sensors was to provide additional data in case there were any issues with the hoist systems and to verify any data issues related to lifting and lowering the gates.
+ **BDI'S STS-4 WIRELESS DATA ACQUISITION SYSTEM:** BDI's STS-4 wireless data acquisition (DAQ) was used to collect and record data during testing. A group of sensors were wired to each nodal DAQ which then communicated wirelessly back to the wireless base station and was controlled by BDI's STS-Live testing software.

Complete specifications are available upon request and can be found at http://www.bditest.com.

Sensor Installation

BDI strain transducers were installed by first sanding paint off the struts to expose bare metal at two small locations (1"x2" areas) for the sensor's mounting tabs. Each transducer was then attached using a combination of fast-setting adhesive and accelerator and applying pressure until the adhesive was fully cured. Each strain transducer took approximately five minutes to attach.

Tiltmeters were installed using the same adhesive process as the strain transducers. However, no surface preparation was necessary.

Torque sensors were installed on the pinion shafts by capacitive discharge bonding. Properly bonding to the shaft required sanding the surface to a smooth finish, clean of any paint or grease. Responses from these gages were measured using Binsfeld Torque Trak 10k wireless transmitters.

A typical installation has been shown in Figure 1 through Figure 4. Access to all the sensor locations was provided by BDI's own SPRAT certified rope access technicians and engineers as shown in Figure 5. Once testing was completed, sensors were removed, and exposed steel areas were covered using cold galvanizing compound.

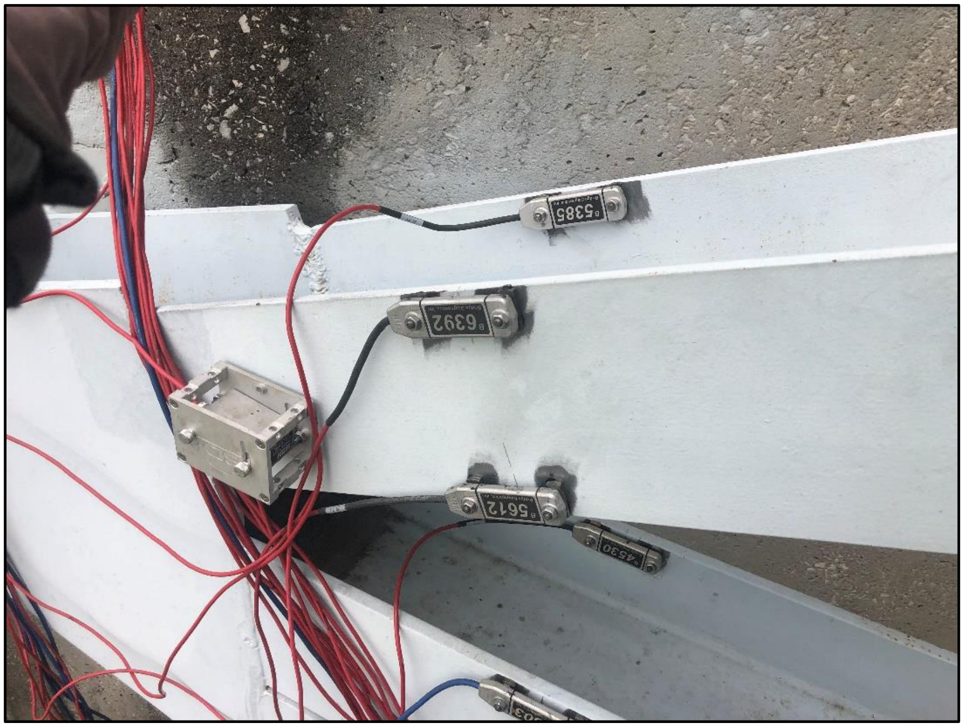

Figure 1 – BDI tiltmeter rotation sensor and reusable strain transducers installed near trunnion hub (Typical)

Figure 2 – BDI tiltmeter rotation sensor installed near skin plate (Typical)

Figure 3 – Torque sensor installation on hoist pinion shaft (Typical)

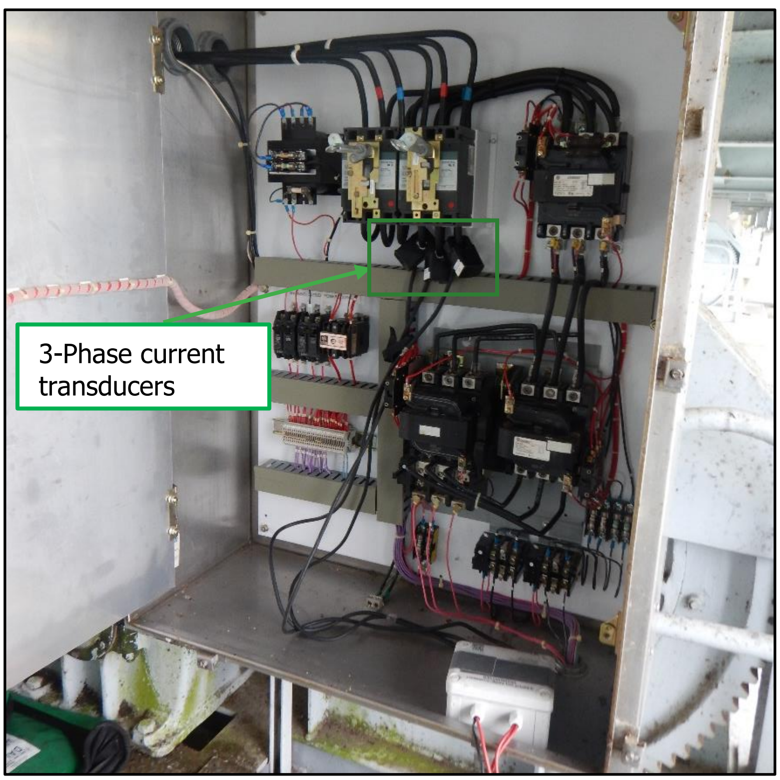

Figure 4 – Current transducers installed on hoist motor controls (Typical)

Figure 5 – BDI personnel installing instrumentation on the gate arm

TESTING PROCEDURES

Structural response data was recorded on all sensors at 50Hz while the gate was run through three spill tests. Each test consisted of three "up-down" cycles (direction reversals) without lowering the gate back to the sill. Each direction reversal consisted of lifting the gate approximately 6-12", pausing for a few seconds, and lowering the gate approximately 6", and repeating until all reversals had been completed.

Results Summary

General Discussions Based on Structural Responses

The following outline contains general discussion points and observations that were made during the data review process. Note: Strain measurements were converted to stress for all subsequent analysis by multiplying the strain values by a steel elastic modulus of 29,000 ksi.

+ **DESCRIPTIONS OF RESPONSE MEASUREMENTS:** All sensor readings were zeroed at the end of each test (which consisted of three cycles of direction reversals) so that each measurement corresponded to response change relative to the final gate position as shown in Figure 6 (gates in the downward "closed" position with the hoist cables slacked as much as possible). It is also worth noting that the stresses did not always start and end at the same levels between tests. This variation in behavior is due to small changes in the flexed gate condition between the start and end of tests. It is common for the flex in the gate, caused by pin friction, to slowly release as it rests on the sill. The purpose of the three up-down cycles per test, prior to sitting the gate back onto the sill, is to ensure that these changes in boundary conditions, including gate flexure due to friction, did not affect BDI's trunnion friction results. ***It is important to note that the recorded measurements were changes in structural response due to gate movement, and do not include the in-situ stresses due to the dead load, cable wrap, and hydrostatic loads present prior to testing.***
+ **QUALITATIVE DATA REVIEW:** Review of the response data indicated a good level of reproducibility between the three tests. For reference, Figure 6 and Figure 7 show stress responses measured along Gate 10's right arm top strut for all three tests (Test #1-3). The data in these plots have been provided as both a function of time and the gate position as determined by the skin plate tilt sensor.
+ **DIRECTION/FRICTION REVERSAL IN RESPONSES:** The difference in stress during gate opening and closing for a given position is shown in Figure 8. The stress variation at any given gate position was a result of direction reversal and in turn due to trunnion friction reversal. This statement is true since all other loads such as dead-load and hydrostatic pressure were essentially constant barring small changes in hydrostatic pressure due to slight changes in head. This direction/friction reversal is depicted in Figure 9, with deflected shape renderings from a gate arm finite element model under lifting and lowering loads. Note that this figure shows an arm configuration that does not match this gate, but the concept of the direction/friction reversal still applies.
+ **MOTOR PERFORMANCE:** Current measurements taken at the hoist motor indicated steady and stable current draws during the lifting and lowering portions. An example plot of current draw and gate position is provided in Figure 10. Current draw ranges during lifting were higher than the ranges during lowering, which is common due to gravity/dead load. These results are summarized along with recorded peak in-rush current in Table 2. Note that the sample rates used during testing were set for collecting gate responses and may not have been appropriate to fully capture the in-rush current. The readings should be evaluated by a licensed electrician with knowledge of the operating parameters.
+ **TORQUE AND HOIST FORCE:** Due to restrictions caused by the hoist limit switches, the hoist cables could not always be fully slacked at the beginning and end of the performed tests. Throughout testing of the Rockwell Forney gates, it was found that this limit switch restriction varied gate to gate and arm to arm. Therefore, it is not recommended to use the collected torque and hoist force data to quantify overall hoist forces. Rather, this data was utilized to evaluate total friction behavior, which is observed as half the difference between the lifting and lowering torque/force (friction reversal).

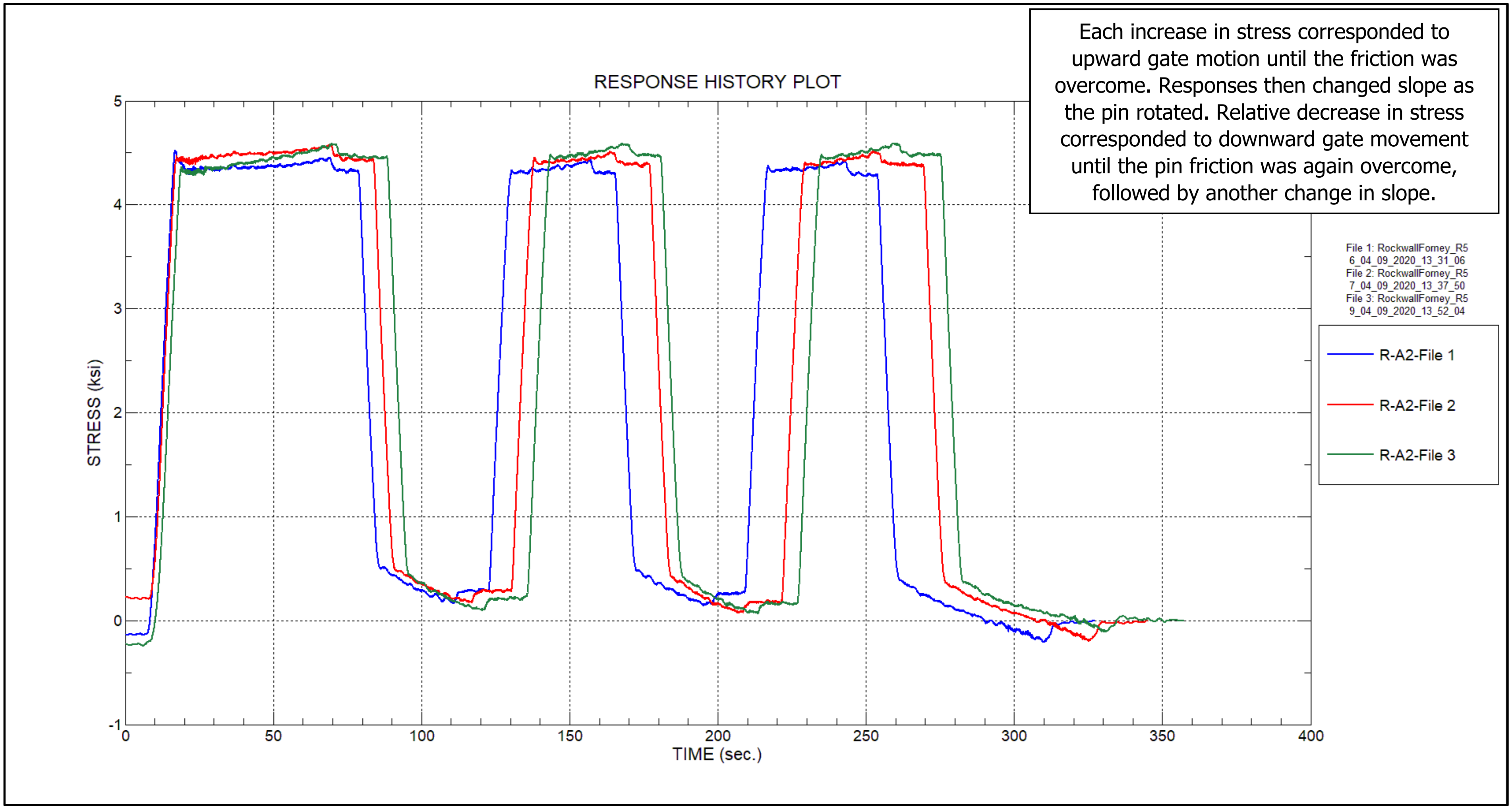

Figure 6 – Stress response history – Right arm – Gage A2 – Time based
File 1 = test run 1, File 2 = test run 2, File 3 = test run 3

(Section A along top strut near pin – Sensor location 2 along bottom of inner flange)

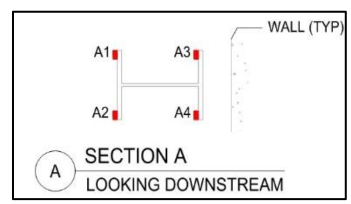

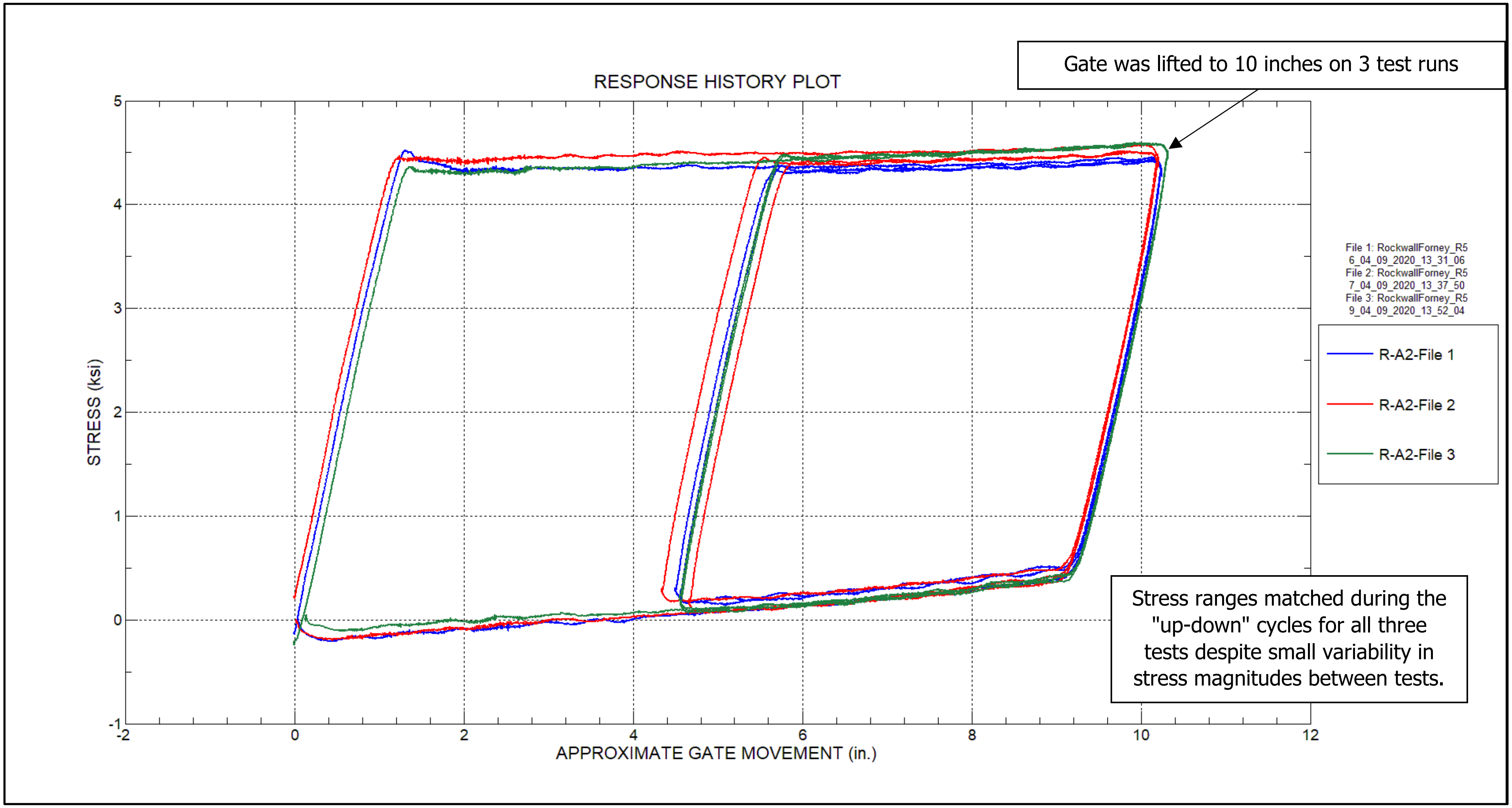

Figure 7 – Stress response history – Right arm – Gage A2 – Function of gate movement
File 1 = test run 1, File 2 = test run 2, File 3 = test run 3

(Section A along top strut near pin – Sensor location 2 along bottom of inner flange)

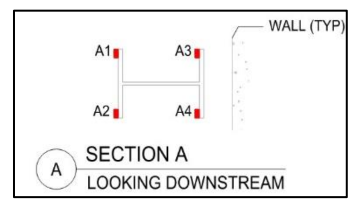

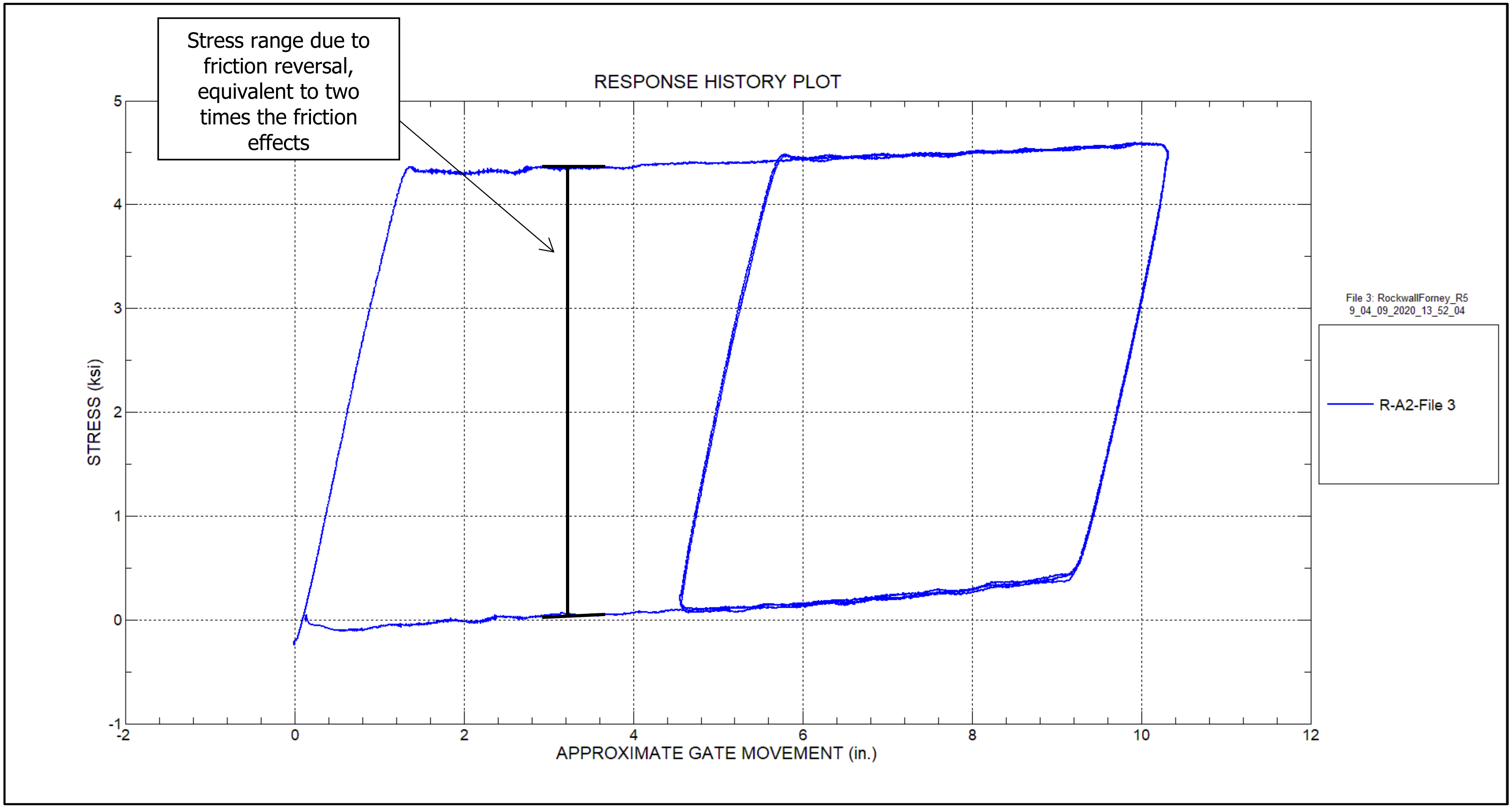

Figure 8 – Stress response history – Right arm – Gage A2 – Friction effect in stress responses

(Section A along top strut near pin – Sensor location 2 along bottom of inner flange)

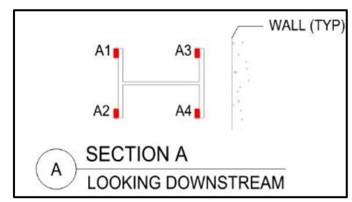

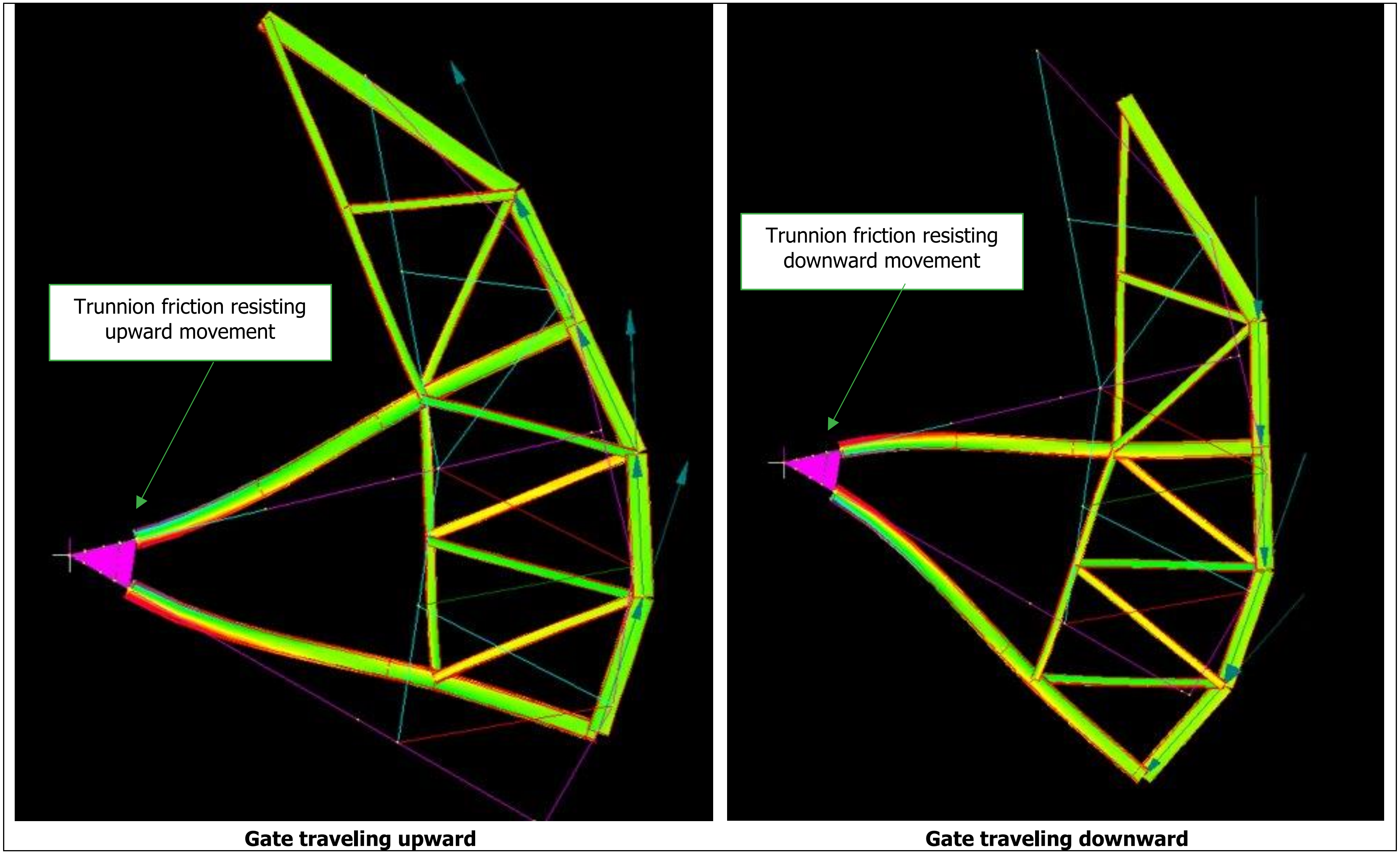

Figure 9 – Deflected shapes during lifting and lowering of Gate – Visualization of direction/friction reversals

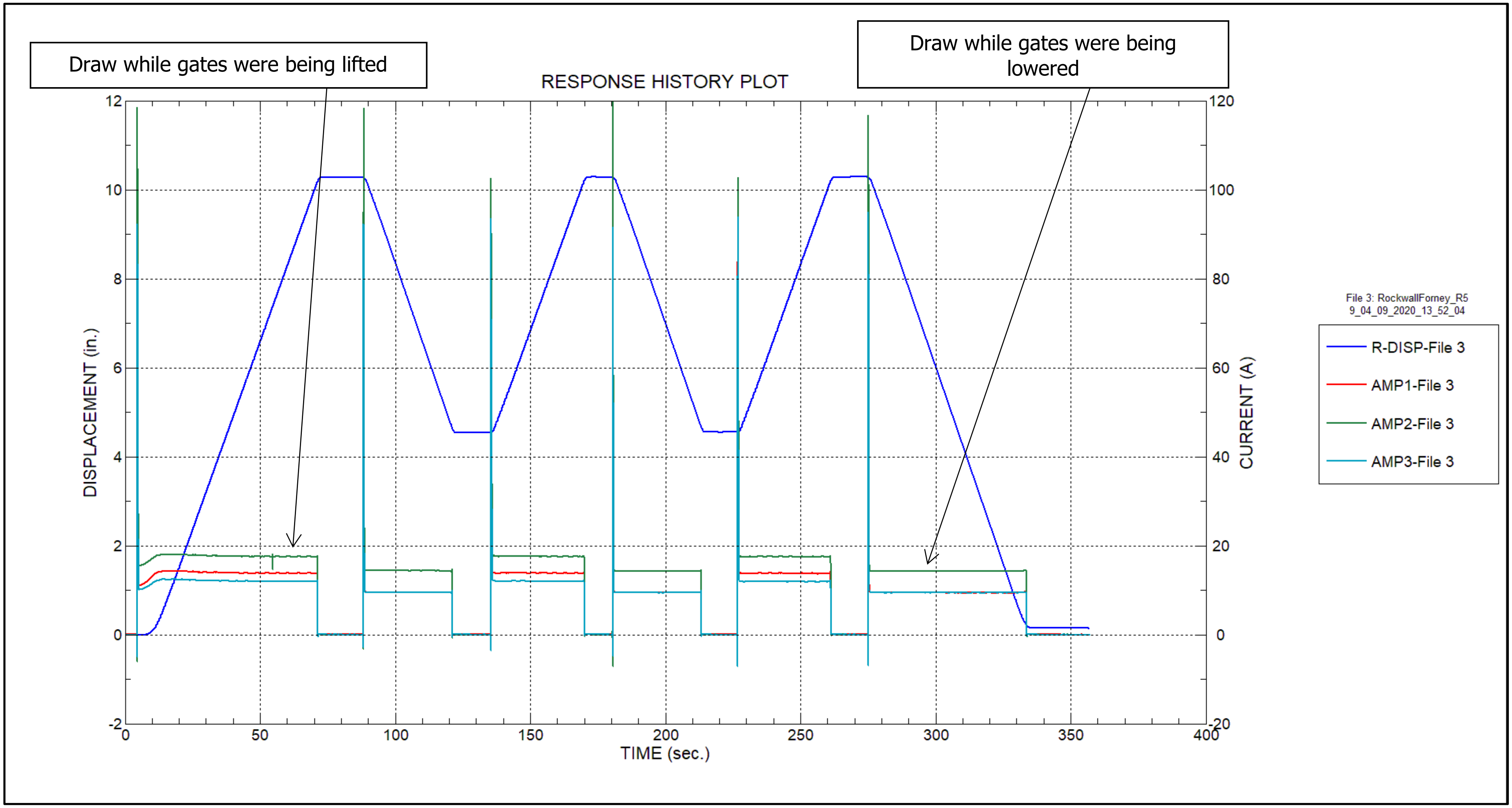

Figure 10 – Motor current & gate movement response history – Lift motor – Highlighting motor draw during lift and lower cycles

METHODOLOGY AND FINDINGS OF THE STRUT FORCE AND MOMENT CALCULATIONS

The following outline provides the methodology used to calculate the required member forces and moments.

- **CHANGE IN STRESS DUE TO GATE OPERATION:** Strain data can be viewed as a function of time starting when the gate was in the down position and was then lifted off the sill. When examining data in this manner, it is easy to see how stresses ramped up as the gate began to move and then changed slope once pin friction was overcome and the trunnion hub began to rotate with the gate. The first point in time where the friction was overcome (both lifting and lowering) has been highlighted in the stress histories shown in Figure 11. These stress histories show the response of all four sensors along the top strut of the right arm (Section A). ***It is important to note that the recorded measurements were changes in structural response due to gate movement, and do not include the in-situ stresses due to the dead load, cable wrap, and hydrostatic loads present prior to testing.***
- **CALCULATION OF STRUT CROSS-SECTIONAL MOMENTS:** The use of four strain gages per strut cross-section allowed accurate in-plane flexural bending moments to be computed from the recorded strain measurements. These moments were computed for every cross-section in each gate arm using the basic mechanics equation provided in Figure 12.

  In-plane or weak-axis flexure refers to bending about a given strut's web. This designation is consistent with typical nomenclature. In-plane bending can be observed visually from the strain response histories as a difference between the top and bottom stresses, whereas out-of-plane or strong-axis bending is visualized as the difference in stress from side to side. Figure 13 provides a visual reference for both types of strut flexure.
- **EXAMINATION OF RESPONSES AS A FUNCTION OF GATE POSITION:** Changes in cross-sectional moment related to friction becomes clearer when the responses are plotted as a function of gate position. Because the gate was operated with several up and down movements, the effects of friction associated with each direction reversal can be viewed for all measured and calculated responses. Figure 14 through Figure 17 show all cross-sectional flexural moment plots for both trunnion arms. The responses in these plots have been centered about the stress state corresponding to a zero-moment, unflexed condition. The zero-moment offset was estimated as the average moment values between up and downward movement (i.e. half the moment difference) at the gate position with the greatest pin friction moment difference (greatest difference between lifting and lowering).
- **TRUNNION FREE-BODY-DIAGRAM & PIN MOMENT CALCULATION:** Figure 18 shows the instrumented member cross-sections and shows how the measured cross-sectional flexural responses were used to compute pin moment. The in-plane moment values used in these calculations were determined directly from the strain measurements at each cross-section using the provided mechanics equations. It should be noted that the out-of-plane moments were not considered in the calculation of pin moment since they were orthogonal to the axis of the pin rotation. Total pin moment was then determined by summing all the moment components about the pin, which included the in-plane moment and the shear components at the strut cross-sections nearest the pin.
- **STRUT SHEAR CALCULATION:** From the examination of the trunnion free-body-diagram described above, the shear vectors at the three struts were a primary component in the pin moment calculation. For this type of structural element, shear vectors were calculated using the moment differential between the two cross sections along each strut. It is important to recognize that shear was constant between the two instrumented cross-sections and the applied shear was a function of the recorded change in moment ($V = dM/dX$). Subsequently, the shear vectors were calculated by dividing the difference in moment by the distance between the two instrumented cross-sections. Shear values for each strut have been plotted as a function of gate position in Figure 19 and Figure 20.

- **CALCULATION OF PIN MOMENT DUE TO FRICTION:** Once all the trunnion arm force vectors were calculated, the equations shown in the free-body-diagram were applied to compute pin moment as a function of gate position. It is important to note that because the calculated pin moment range corresponds to a direction reversal, a reversal in friction also occurred. The effect of direction reversal on pin moment due to friction is best conceptualized by centering the moment response plots about the zero-moment axis. The moment due to lifting and the moment due to lowering can then be visualized as a change from this new zero point corresponding to the gate in an unflexed condition. Therefore, the total moment differential between lifting and lowering was twice the moment due to friction acting in a single direction. Pin-moment plots have been provided in Figure 21 and Figure 22. From these plots, it is apparent that pin moment due to friction remained relatively constant throughout the gate operation tests, with a slight decrease in pin friction moment as the gate continued to be lifted. This slight decrease in pin friction moment most likely corresponded to the change in hydrostatic load as the gate position changed. Pin-moment plots for all tests on Gate 10 are also provided for reference in Appendix B – Gate 10 Pin Moment Component Plots.
- **SHAFT TORQUE & HOIST FORCE:** Torque measurements were taken on the pinion shafts near the hoist motor during testing, with single torque gages installed on the left and right hoist pinion shaft. Responses were recorded in units of micro-strain and converted to torque in units of kip-ft using Equation 1 thru Equation 3 and the following shaft properties.

$$d_O = 5.5\ inches, \qquad d_I = 0\ inches, \qquad E = 29000\ ksi, \qquad \nu = 0.3$$

$$G = \frac{E}{2(1+\nu)}$$

Equation 1

$$J = \frac{\pi\left({d_O}^4 - {d_I}^4\right)}{32}$$

Equation 2

$$\tau = \varepsilon * \frac{2GJ}{\frac{d_O}{2} * 1000000 * 12}$$

Equation 3

Figure 23 shows example torque measurements, recorded on the Gate 10 torque shafts. Best practices for torque measurements is to measure torque on opposite sides of the shaft so that any bending in the shaft can be removed by averaging the two responses. Due to access limitations, only one gage at each location could be installed. Therefore, any bending in the shaft may be reflected in the torque measurements and may be related to the peaks and valleys observed in the torque responses.

Torque values were converted to force in the hoist cables per gate arm using the gear ratio and drum radius, as shown in Figure 24. The gear ratio and drum radius were 5.182 and 1.086 feet respectively, as defined in the provided as-built shop drawings. It should be noted that the hoist force calculated may be smaller than the actual hoist force applied. This difference is due to the limit switch engaging the brake before the hoist cable was fully slacked, resulting in an initial force in the cable. A hoist force due to total gate friction was then calculated. This friction hoist force was equal to half the differential in force measured during the lifting and lowering of the gate (similar to the pin friction calculations). As shown in Table 3, the change in cable force due to friction was generally consistent between tests. Note that the total hoist force was due to the total friction effects, including side seal, hoist bearings, trunnion friction effects, etc. It is difficult to determine the exact proportion and composition of the total friction sources. Additional torque and hoist force plots for all collected data files are provided in Appendix A – Gate 10 Torque and Hoist Force Plots.

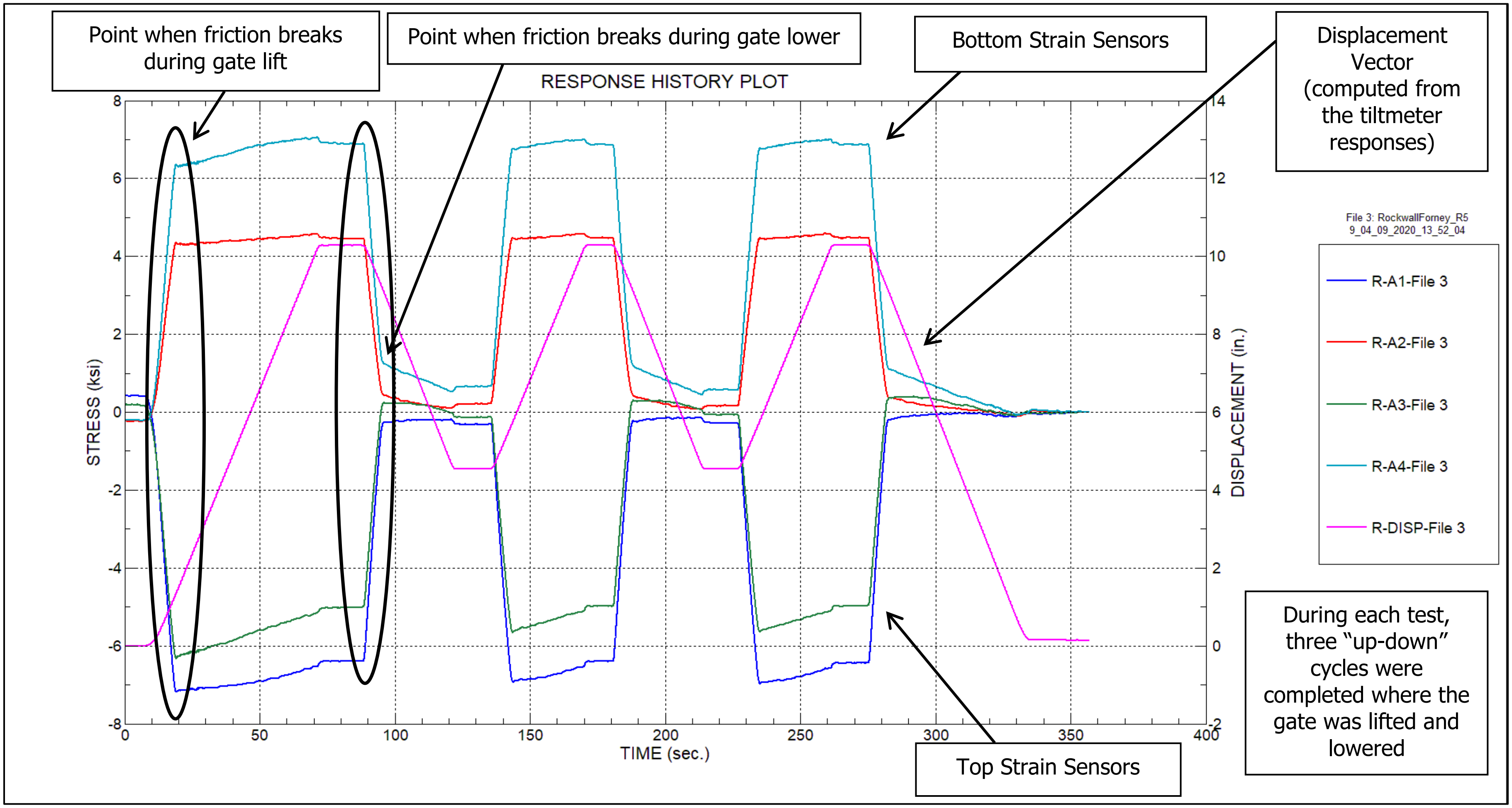

Figure 11 – Stress response & gate movement history – Right arm – Section A - Highlighting friction behavior
(Section A along top strut near pin)

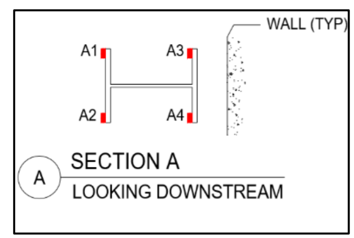

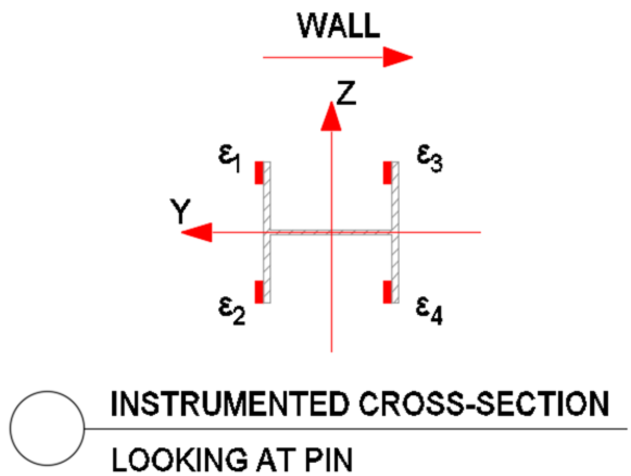

Calculation of Weak-axis (In-plane) bending

$$M_Y = \frac{E[\frac{\varepsilon_2 + \varepsilon_4}{2} - \frac{\varepsilon_1 + \varepsilon_3}{2}]S_{Y(gage)}}{2}$$

Sy(gage) = Section modulus to the center of gages (not extreme fiber of flanges)
(locations of gages were accounted for in moment computation)

Figure 12 – Basic mechanic equation used to calculate moment

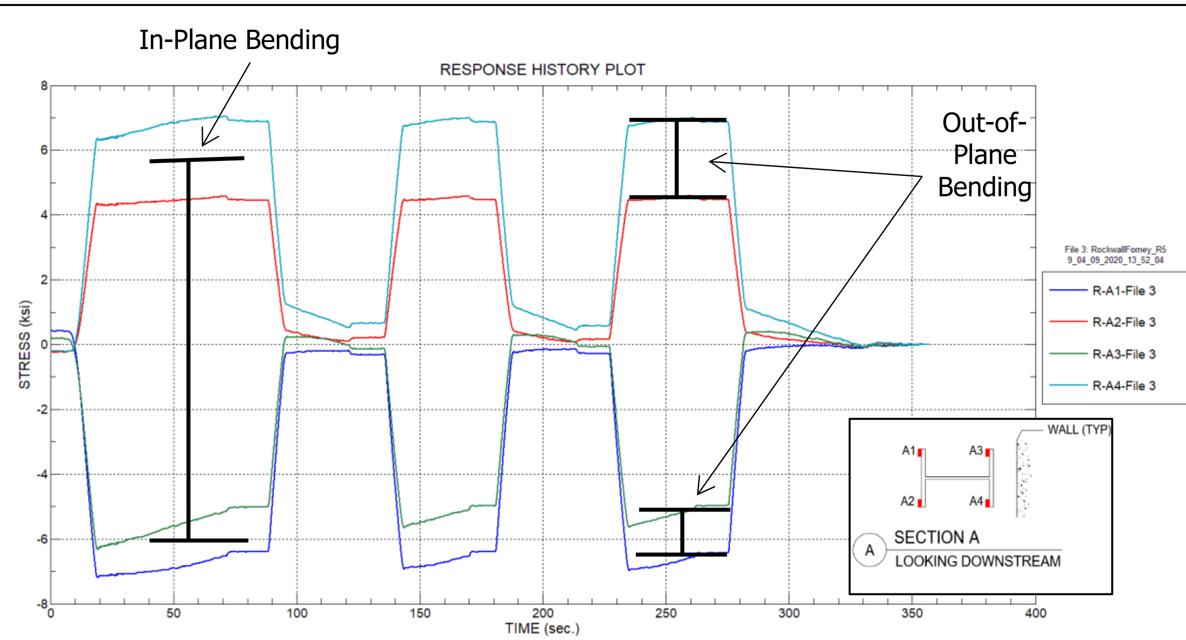

Figure 13 – Stress response history – Right arm – Section A – Bending components
(Section A along top strut near pin)

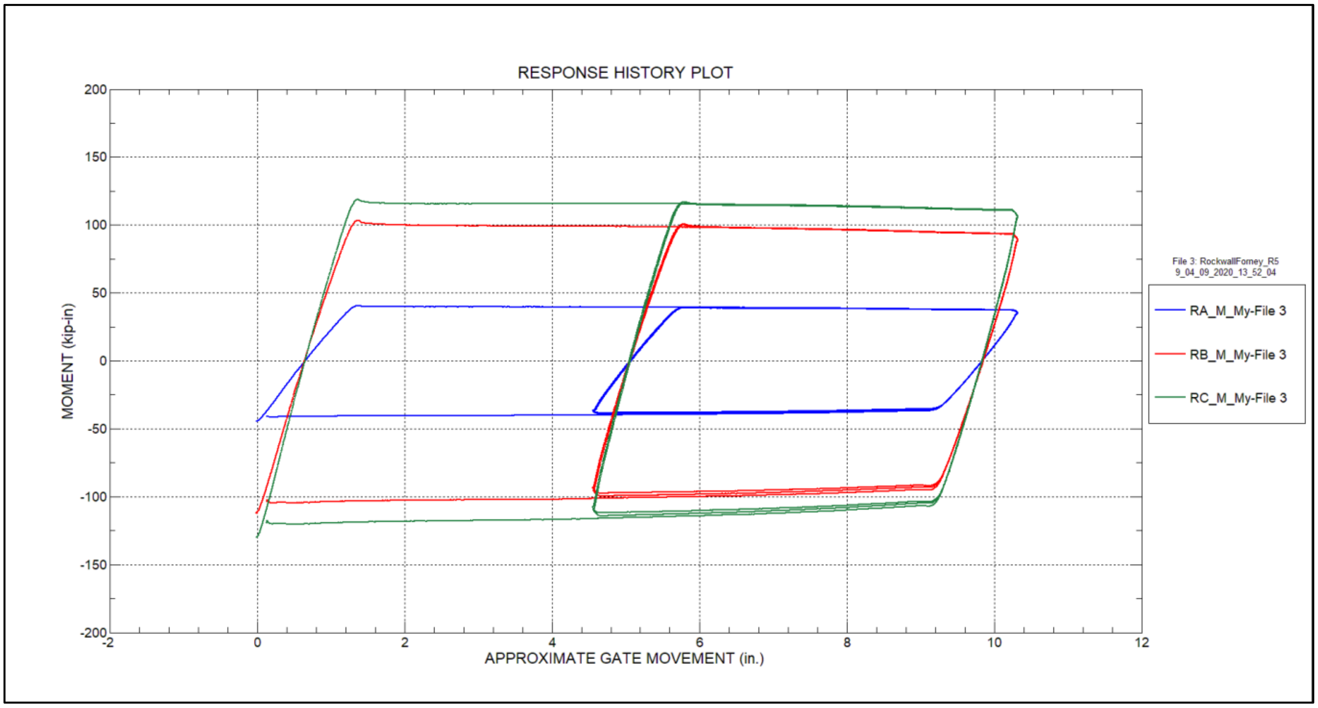

Figure 14 – In-plane moment response history – Right arm – Sections near pin

(RA = Right Arm Top Strut, RB = Right Arm Middle Strut, RC = Right Arm Bottom Strut)

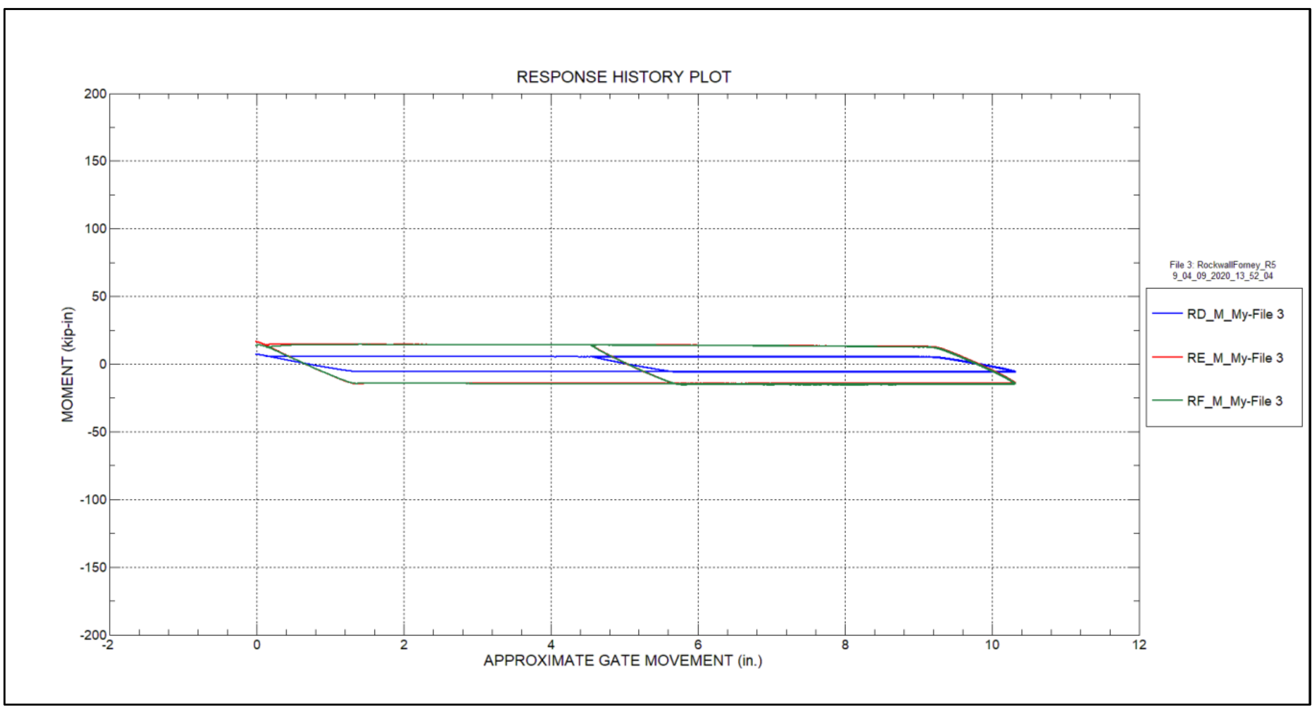

Figure 15 – In-plane moment response history – Right arm – Sections away from pin

(RD = Right Arm Top Strut, RE = Right Arm Middle Strut, RF = Right Arm Bottom Strut)

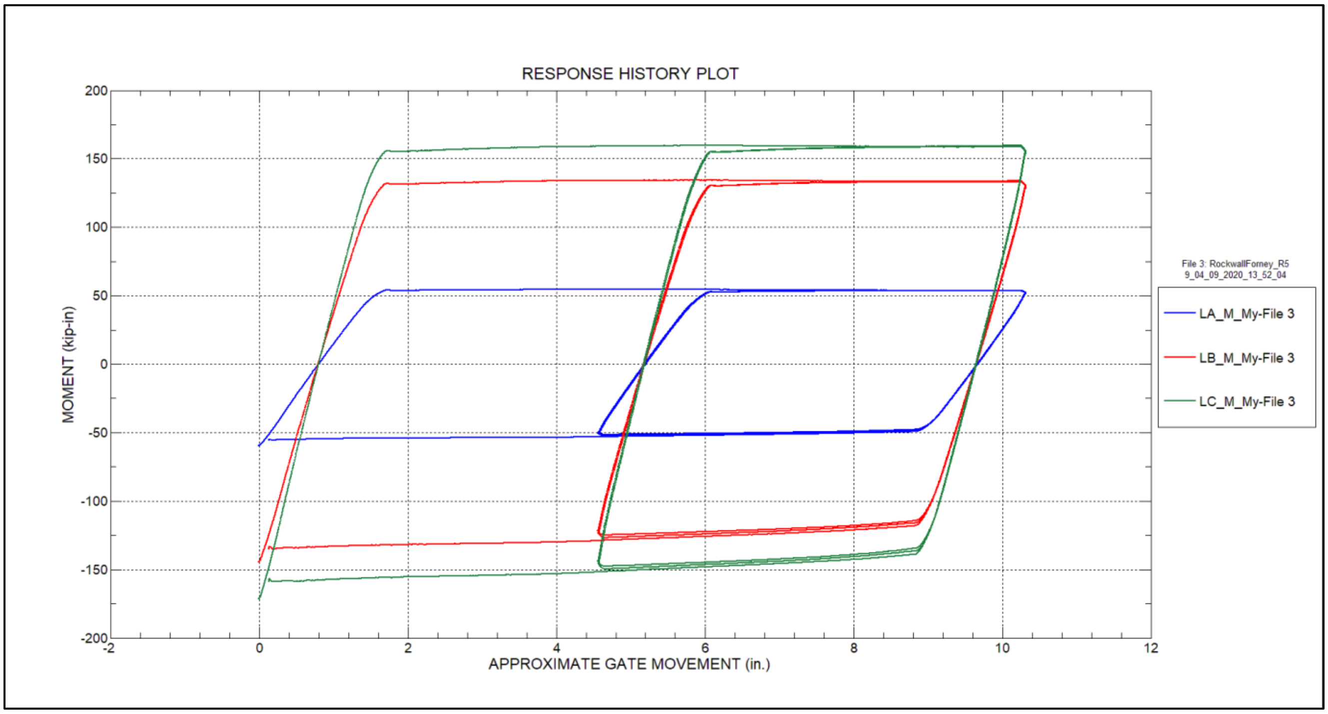

Figure 16 – In-plane moment response history – Left arm – Sections near pin

(LA = Left Arm Top Strut, LB = Left Arm Middle Strut, LC = Left Arm Bottom Strut)

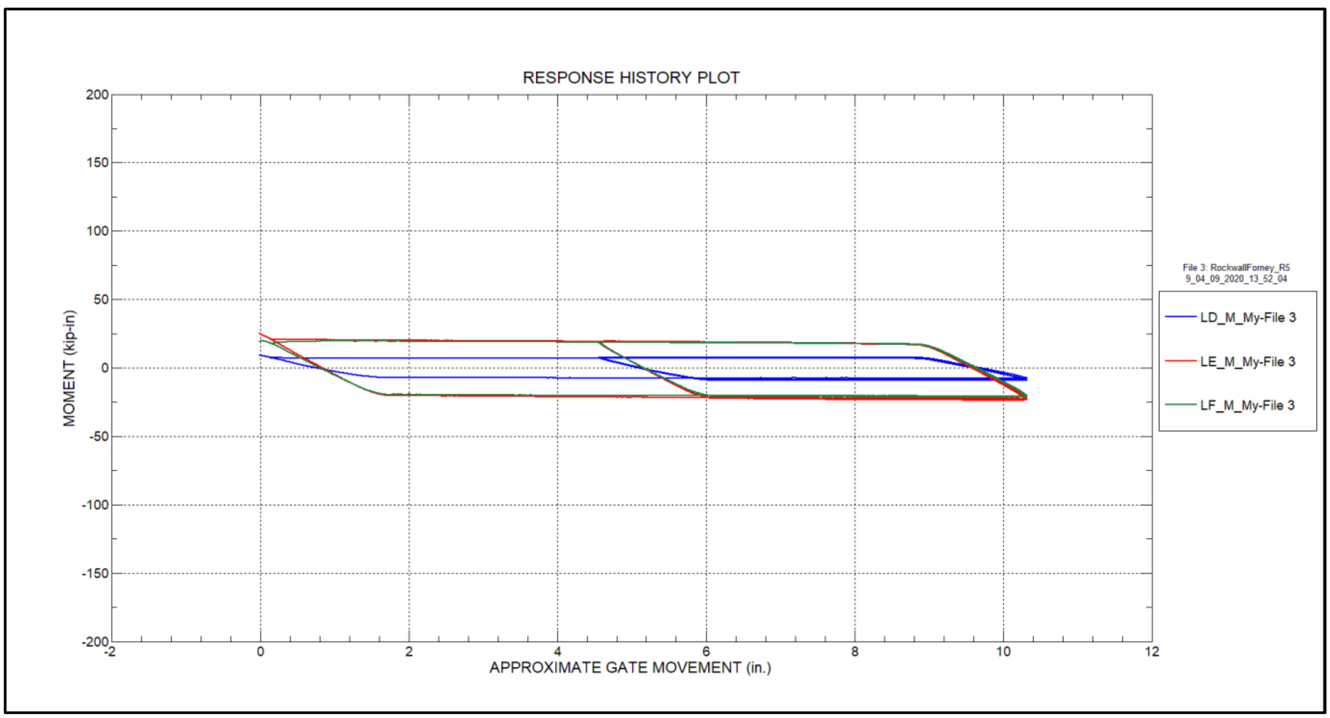

Figure 17 - In-plane moment response history – Left arm – Sections away from pin

(LD = Left Arm Top Strut, LE = Left Arm Middle Strut, LF = Left Arm Bottom Strut)

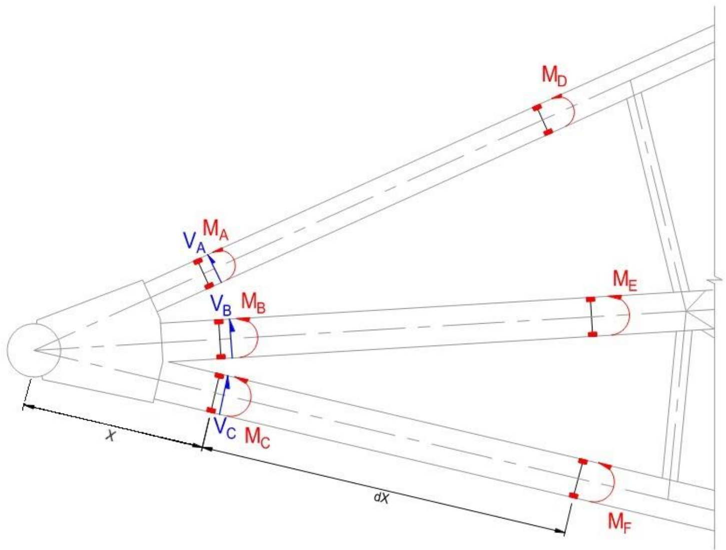

Elevation View of Gate Arm

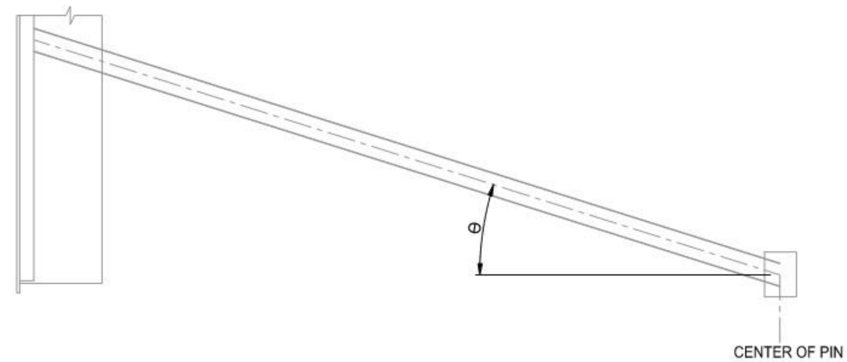

Plan View of Gate Arm

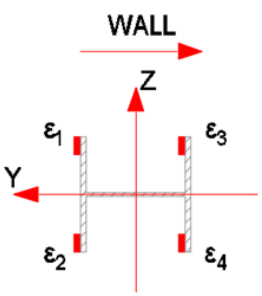

$$M_Y(M_A, M_B, M_C, M_D, M_E, M_F) = \frac{E\left[\frac{\varepsilon_2+\varepsilon_4}{2} - \frac{\varepsilon_1+\varepsilon_3}{2}\right] S_{Y(gage)}}{2}$$

$$V_A = \frac{M_A - M_D}{dX}$$

$$V_B = \frac{M_B - M_E}{dX}$$

$$V_C = \frac{M_C - M_F}{dX}$$

$$\sum M_o = 0$$

$$M_{PIN} = [X(V_A + V_B + V_C) + M_A + M_B + M_C]\cos\theta$$

Figure 18 – Direct calculation of pin moment from strain measurements

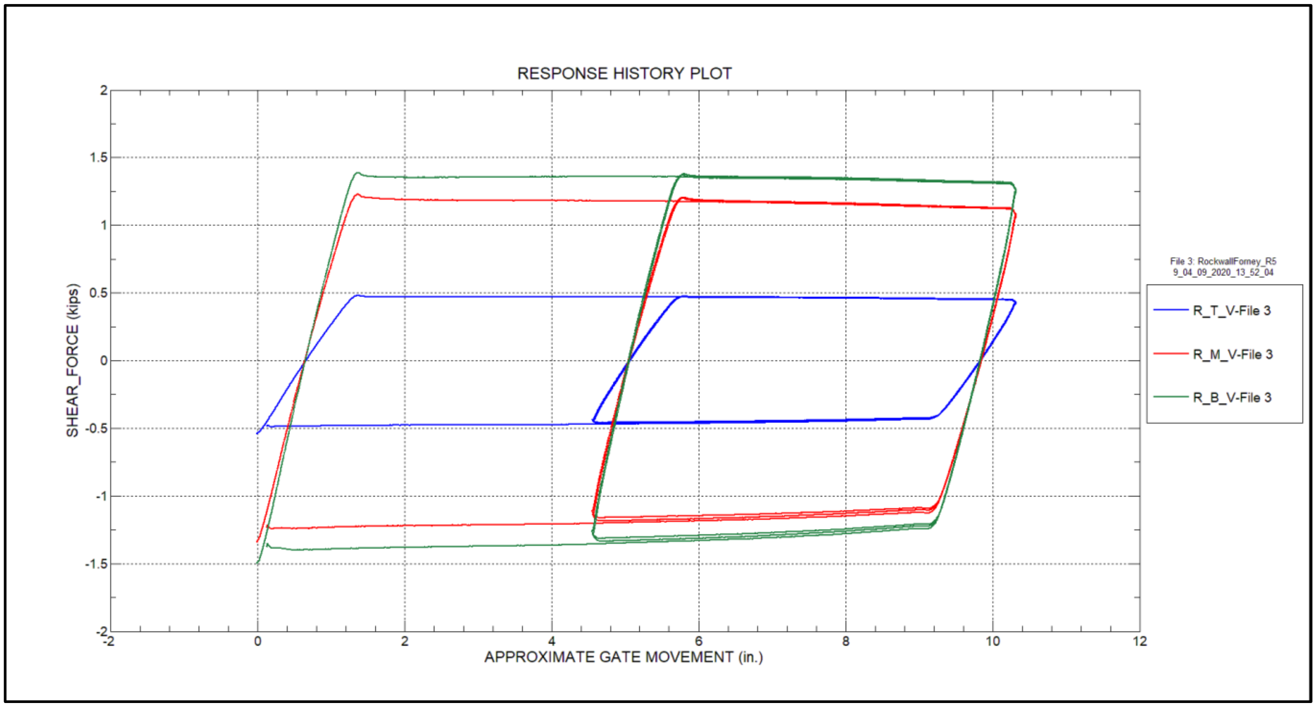

Figure 19 – Strut shear response history – Right arm

(R_T = Right Arm Top Strut, R_M = Right Arm Middle Strut, R_B = Right Arm Bottom Strut)

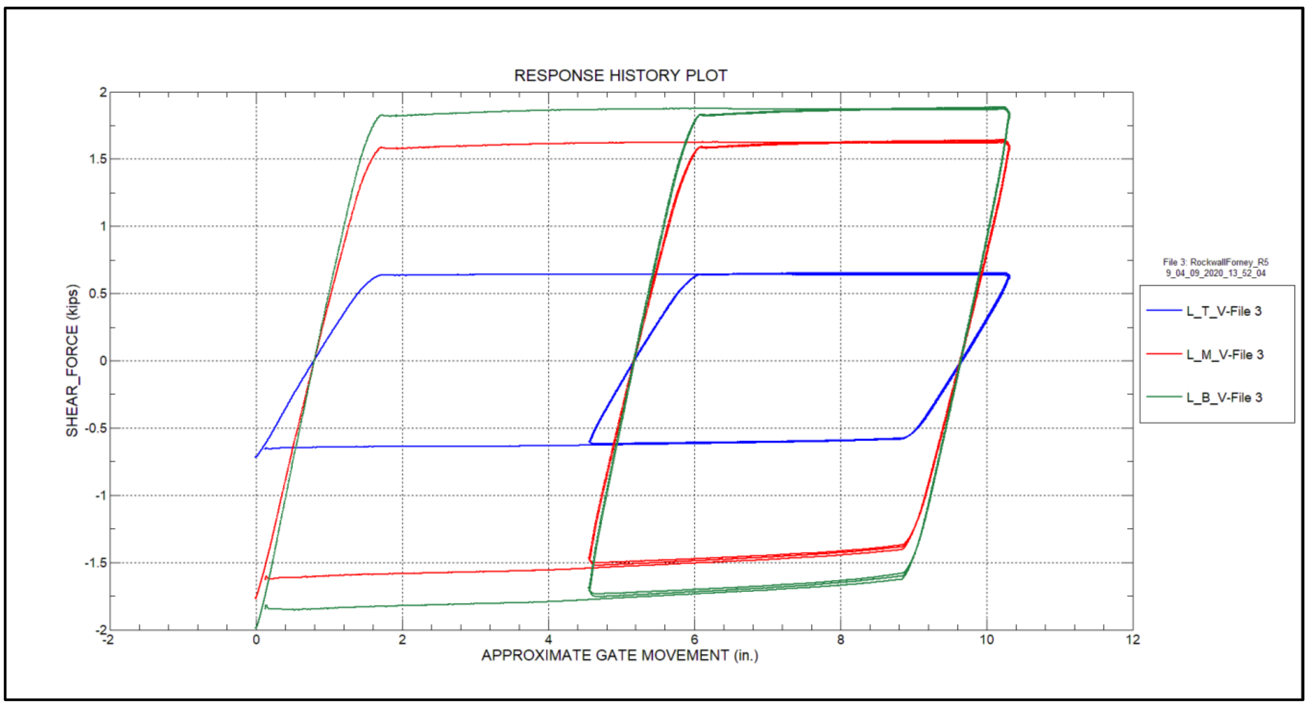

Figure 20 – Strut shear response history – Left arm

(L_T = Left Arm Top Strut, L_M = Left Arm Middle Strut, L_B = Left Arm Bottom Strut)

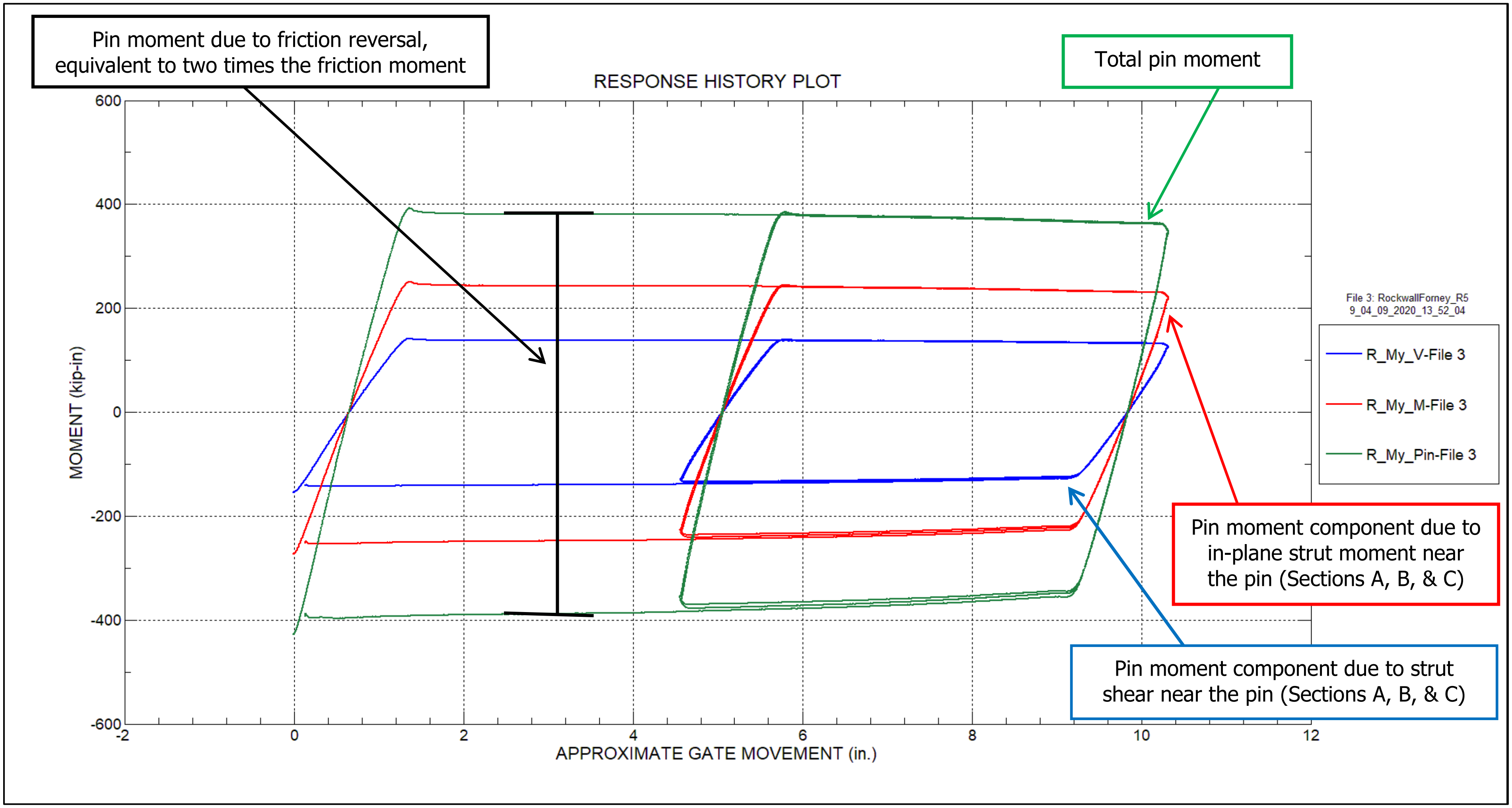

Figure 21 – Pin moment response history – Right arm

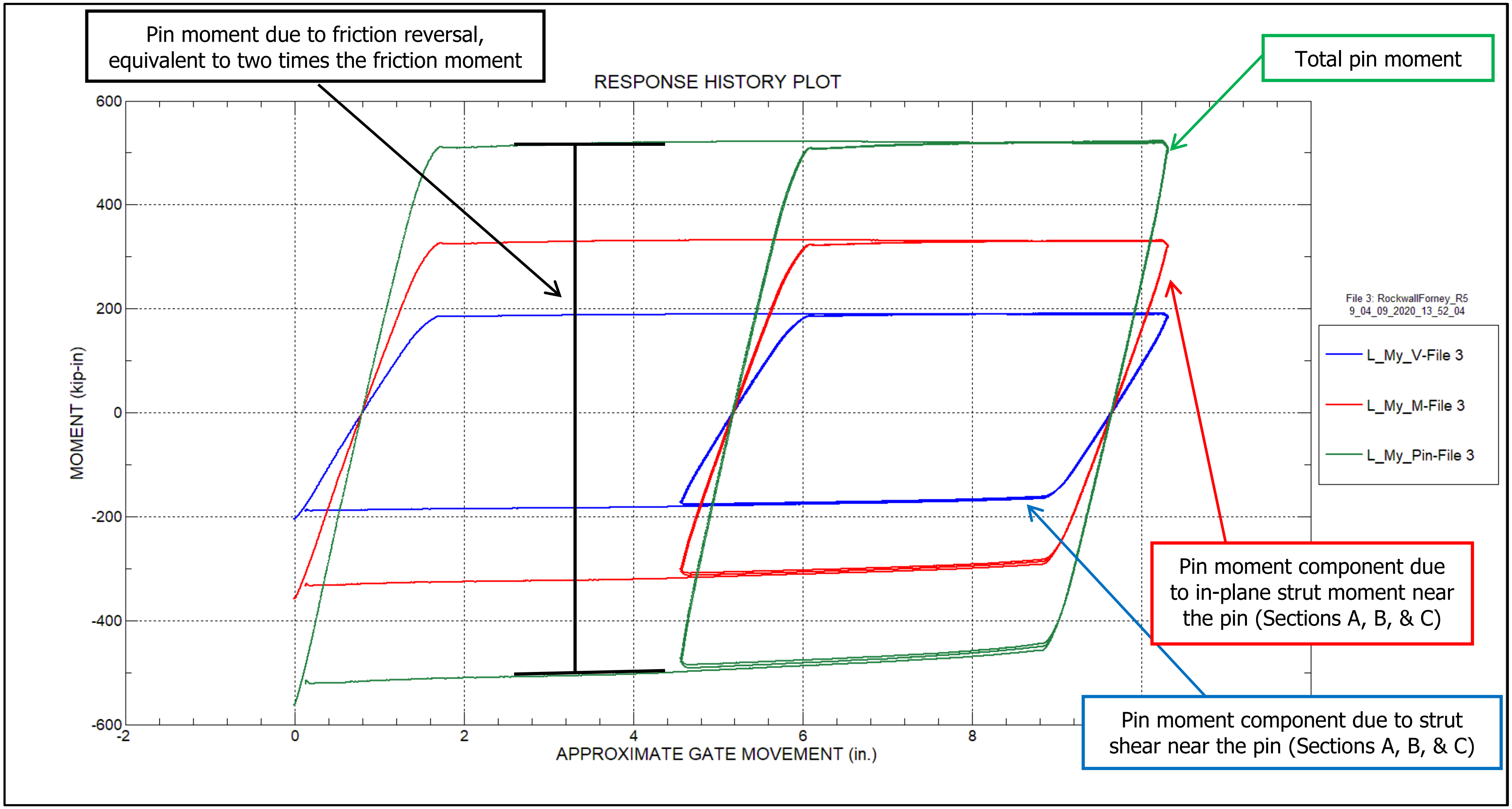

Figure 22 – Pin moment response history – Left arm

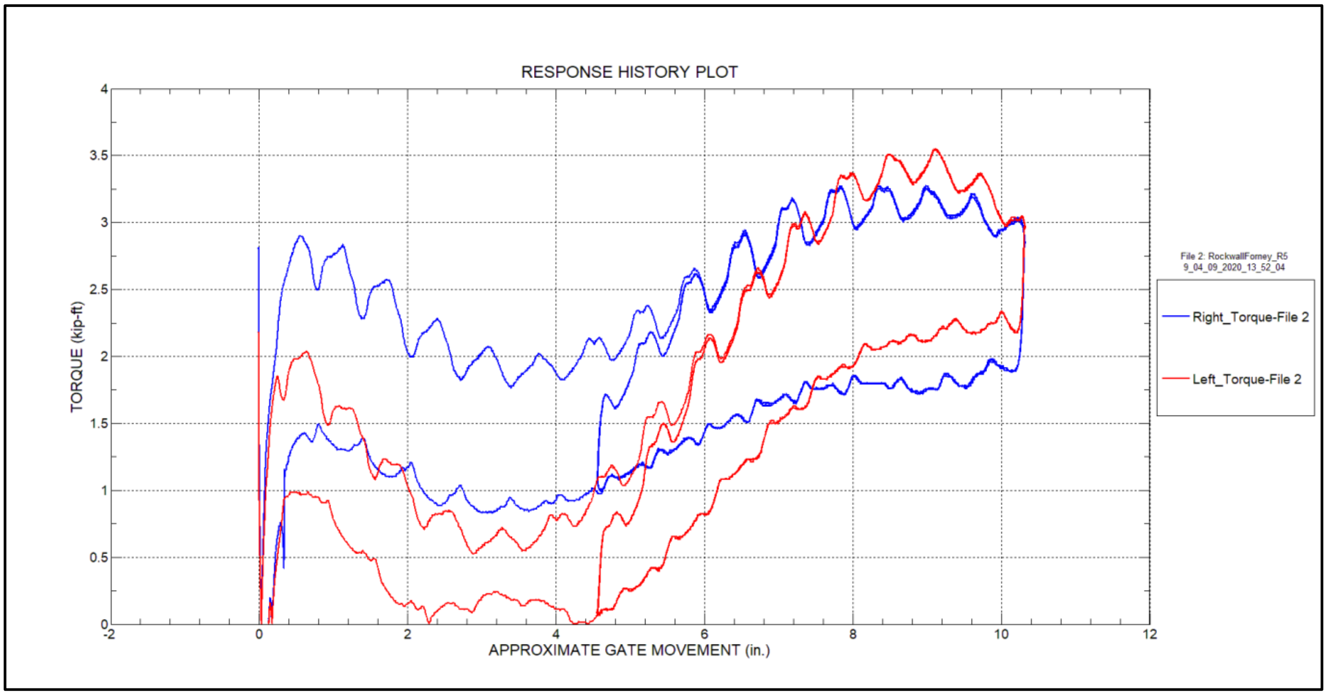

Figure 23 – Hoist torque response history – Gate 10 – Test 2

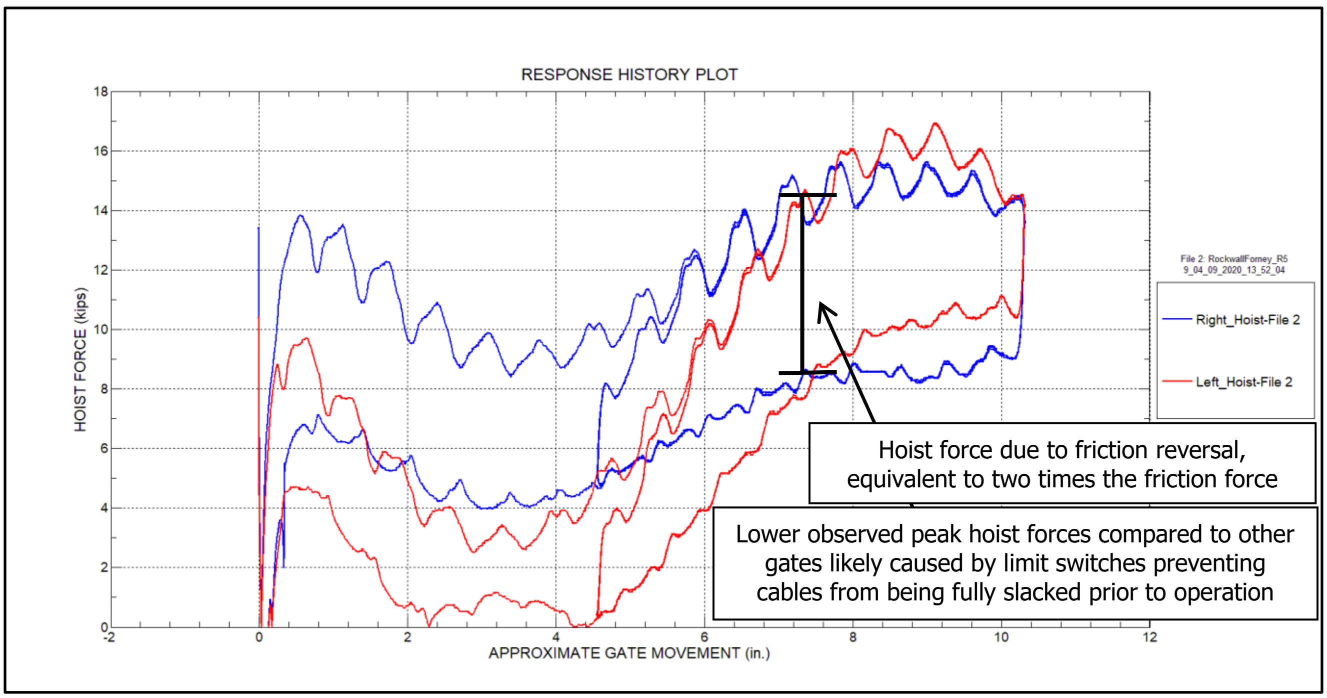

Figure 24 – Hoist force response history – Gate 10 – Test 2

Summary of Friction Results

The raw data files have been included in the submittal package for reference and were formatted as "tdms" files that can be opened in Microsoft Excel using a "tdms" reader extension.

Examination of the stress histories for each test was necessary to obtain a thorough understanding of the gate performance. The response shapes, variations in stress magnitudes, and timing sequences provided direct clues as to how the gate performed under typical service conditions. The following is a breakdown of the provided tabulated results:

+ Table 2 provides motor current ranges and maximum in-flow for lift and lower cycles for each test
+ Table 3 provides maximum hoist force as well as hoist force due to total friction for each test
+ Table 4 provides the maximum stress ranges measured at the sensor locations for each member
+ Table 5 provides maximum bending stress and moment ranges observed during the gate tests
+ Table 6 provides maximum friction bending stress and moment values at each of the instrumented strut locations
+ Table 7 provides the computed shear values in each strut due to friction
+ Table 8 provides calculated measured friction moments, calculated hydrostatic loads based on the measured water elevation, and coefficients of friction for each gate and gate arm during all three tests

The resulting pin friction moments were used to compute friction coefficients from Eq. 4, given the pin radius and the applied thrust. The thrust used in this calculation consisted of the calculated resultant hydrostatic load based on the measured water elevation and was adjusted to account for the loss of head as the gate was lifted. This thrust adjustment was based on the recorded gate movement and was performed in order to calculate more accurate friction coefficients. The water elevation during testing was nearly constant throughout each gate test and was documented during each "up-down" cycle. It should be noted that the minor thrust due to cable wrapping, which was minimal compared to hydrostatic thrust, was not included in the thrust calculation. This assumption resulted in slightly conservative friction coefficients.

$$\mu = \frac{M_F}{T * r} \qquad \text{Eq. 4}$$

where:

μ = Friction Coefficient

M_F = Friction Moment

T = Thrust per Pin

r = Pin Radius, 5.375"

The out-of-plane shear and moments were not considered in the pin friction calculations due to orthogonal geometry considerations (resulting pin moment associated with out-of-plane flexure being perpendicular to pin rotation).

The data was presented in a specific coordinate system applicable to both arms. Data was processed so that the positive x-axis was always pointing towards the pin and the right-hand rule applied. In-plane bending can be referred to as "bending about the horizontal or y-axis" and shows how much the beams bend up and down within the plane of the gate arms. Refer to Figure 12 above for visual reference of coordinate system and mathematical explanation of calculations. Tabulated results do not include any in-situ effects.

Table 2 – Motor current summary table – Gate 10

Test Run	Current Range due to Lifting (A)	Current Range due to Lowering (A)	Max In-rush Current (A)
1	12-19	9-14	118
2	12-18	9-15	125
3	12-18	9-15	120

Table 3 – Hoist force summary table – Gate 10

Test Run	Right Arm Peak Hoist Force (kips)	Left Arm Peak Hoist Force (kips)	Right Arm Hoist Force due to Total Gate Friction (kips)	Left Arm Hoist Force due to Total Gate Friction (kips)
1	17.16	17.99	2.64	1.95
2	15.64	16.94	2.77	2.39
3	16.29	17.38	2.21	2.41

Tabulated friction force values correspond to the response induced by friction in one direction

Table 4 – Maximum measured sensor stress range

Arm Designation	Top Strut (ksi)	Middle Strut (ksi)	Bottom Strut (ksi)
Right Arm	7.64	9.01	8.93
Left Arm	10.63	12.56	12.48

Tabulated values correspond to the total measured change in response during tests

Stress values have not been extrapolated to the extreme fibers (correspond to center of gage)

Table 5 – Maximum in-plane total bending stress & moment ranges – Total

Section Label	Section Description	Right Arm Stress (ksi)	Right Arm Moment (kip-in)	Left Arm Stress (ksi)	Left Arm Moment (kip-in)
Section A	Top Strut Near Pin	7.59	85.26	10.16	114.17
Section B	Middle Strut Near Pin	9.32	215.57	12.06	278.95
Section C	Bottom Strut Near Pin	8.92	248.87	11.88	331.36
Section D	Top Strut Away from Pin	1.24	13.95	1.65	18.51
Section E	Middle Strut Away from Pin	1.39	32.04	2.12	48.93
Section F	Bottom Strut Away from Pin	1.08	29.99	1.48	41.19

Tabulated values correspond to the total measured change in response during tests

Table 6 – In-plane frictional bending stress & moment at maximum gate friction

Section Label	Section Description	Right Arm Stress (ksi)	Right Arm Moment (kip-in)	Left Arm Stress (ksi)	Left Arm Moment (kip-in)
Section A	Top Strut Near Pin	3.73	41.91	4.82	54.14
Section B	Middle Strut Near Pin	4.49	103.86	5.72	132.26
Section C	Bottom Strut Near Pin	4.34	120.96	5.60	156.05
Section D	Top Strut Away from Pin	0.50	5.57	0.65	7.28
Section E	Middle Strut Away from Pin	0.63	14.62	0.88	20.27
Section F	Bottom Strut Away from Pin	0.52	14.45	0.70	19.60

Tabulated values correspond to the response induced by friction in one direction

Table 7 – Strut shear range summary table due to friction

Arm Designation	Top Strut Shear (kip)	Middle Strut Shear (kip)	Bottom Strut Shear (kip)
Right Arm	0.49	1.23	1.41
Left Arm	0.64	1.59	1.83

Tabulated values correspond to the response induced by friction in one direction

Table 8 – Pin friction summary table

Test Run	Average Water Elevation during testing (ft)	Approximate Thrust at time of Testing (kips per arm)	Gate/Member Designation	Pin Friction Moment (kip-in)	Friction Coefficient
1	435.56	488.50	Right Pin	384.60	0.15
			Left Pin	505.70	0.19
2	435.56	488.50	Right Pin	392.70	0.15
			Left Pin	512.30	0.20
3	435.56	488.50	Right Pin	397.40	0.15
			Left Pin	506.70	0.19

Tabulated values correspond to the response induced by friction in one direction

APPENDIX A – GATE 10 TORQUE AND HOIST FORCE PLOTS

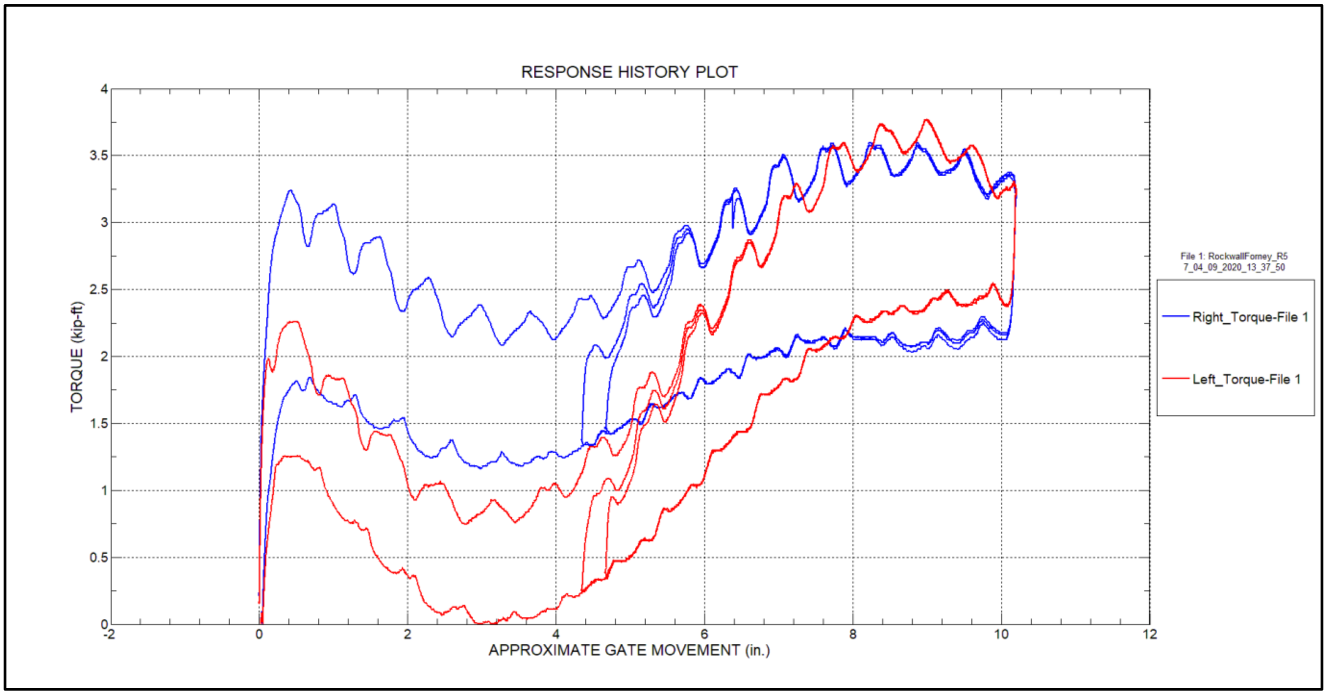

Figure 25 – Hoist torque response history – Gate 10 – Test 1

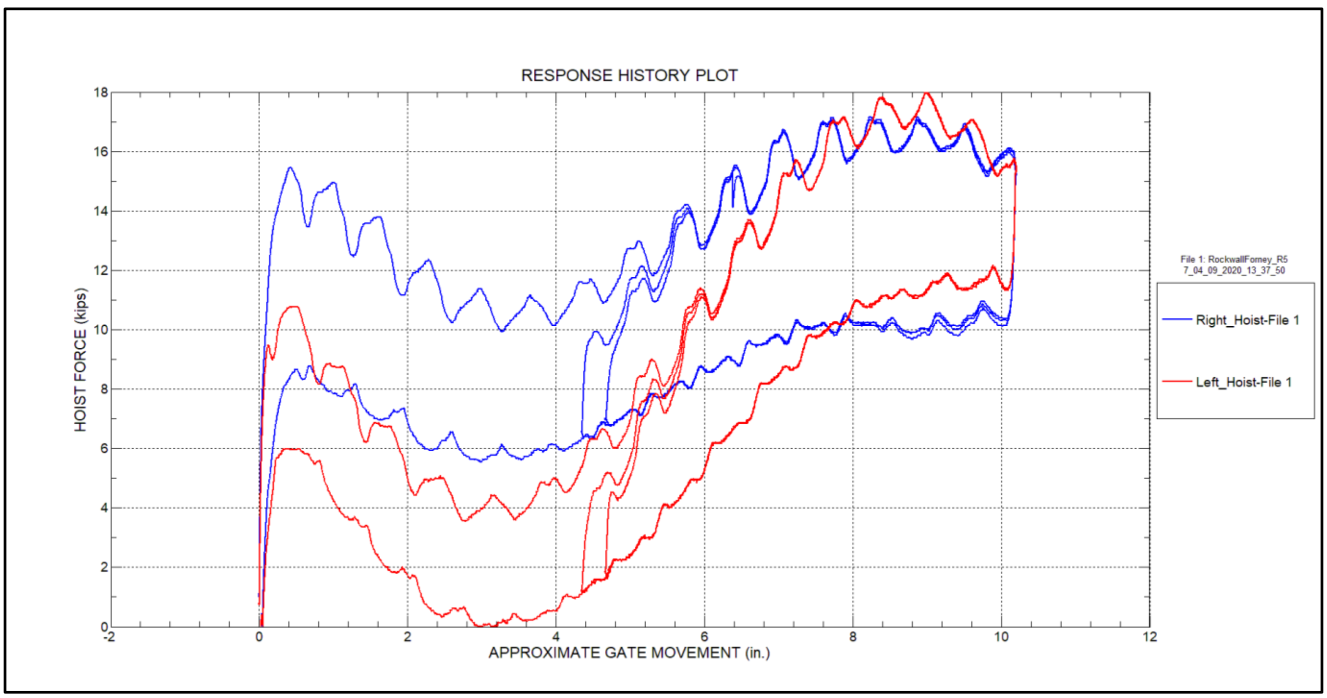

Figure 26 – Hoist force response history – Gate 10 – Test 1

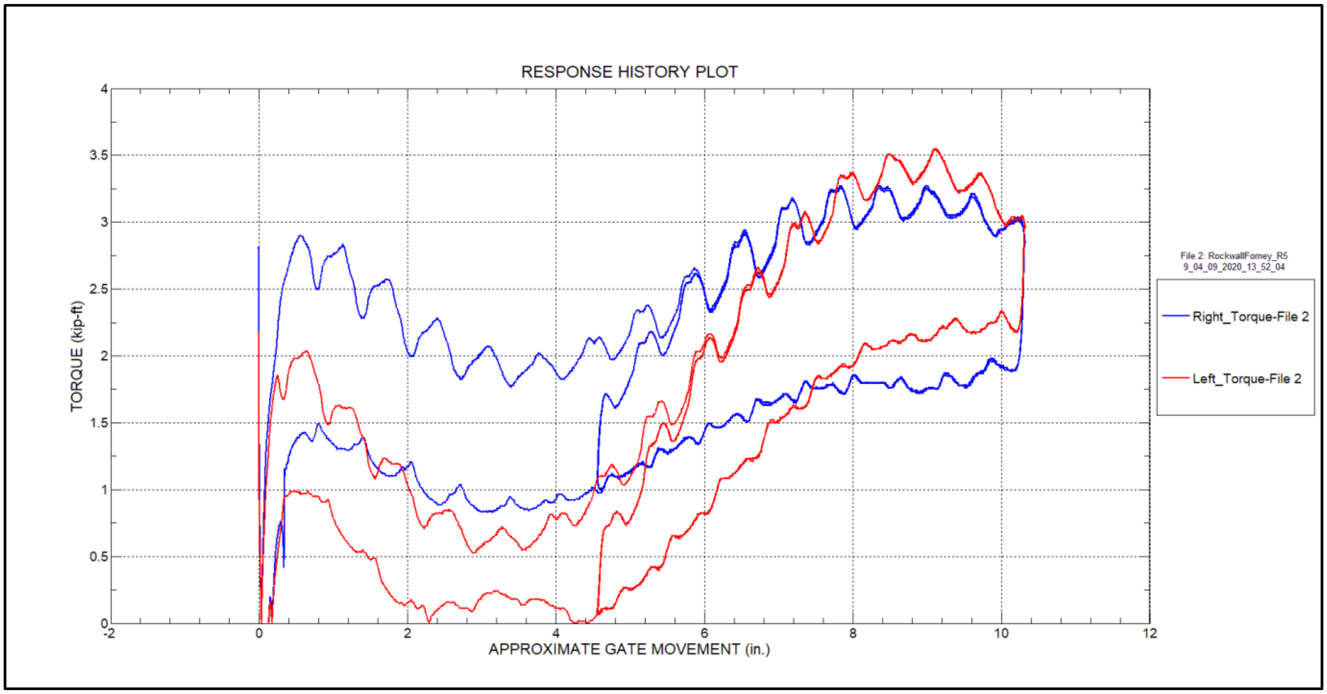

Figure 27 – Hoist torque response history – Gate 10 – Test 2

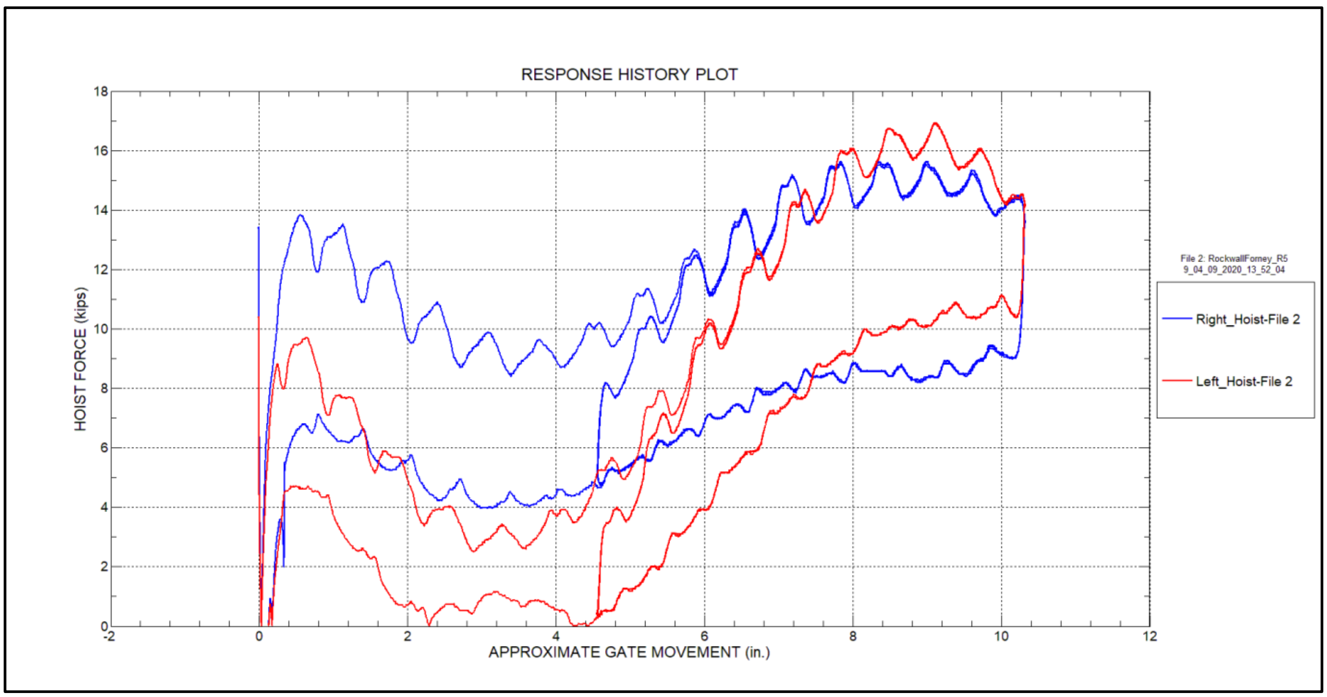

Figure 28 – Hoist force response history – Gate 10 – Test 2

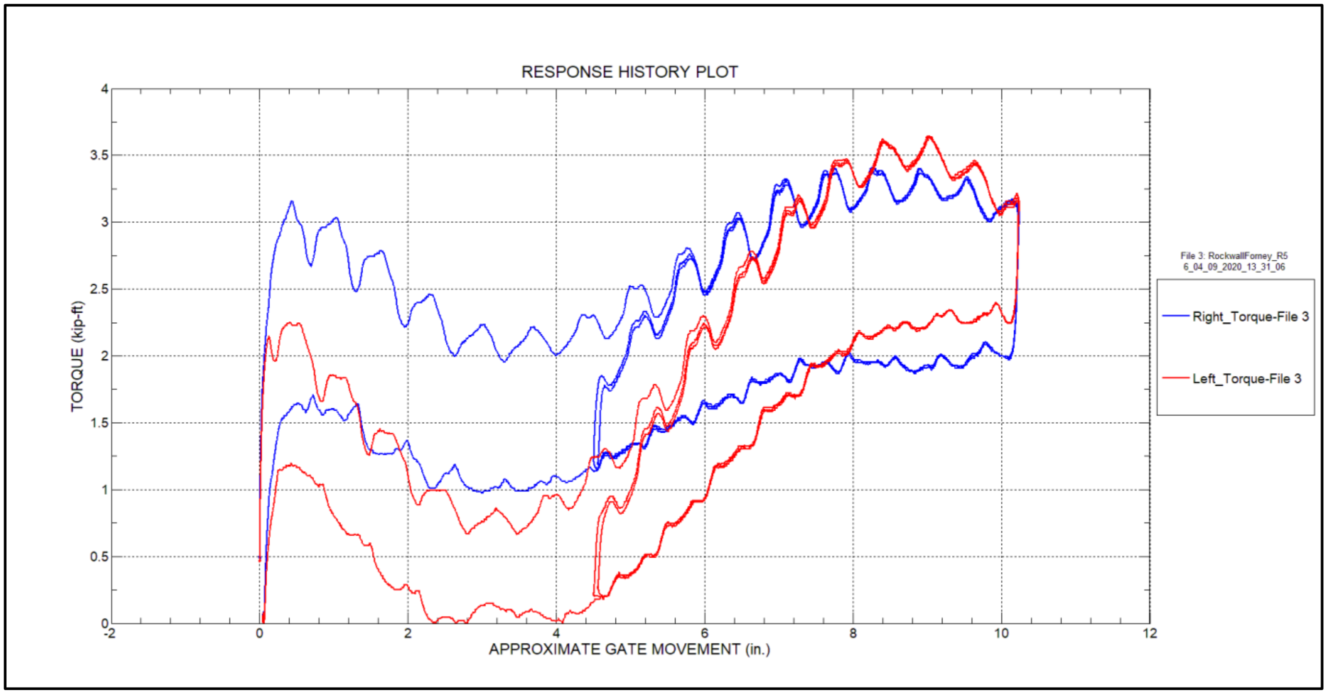

Figure 29 – Hoist torque response history – Gate 10 – Test 3

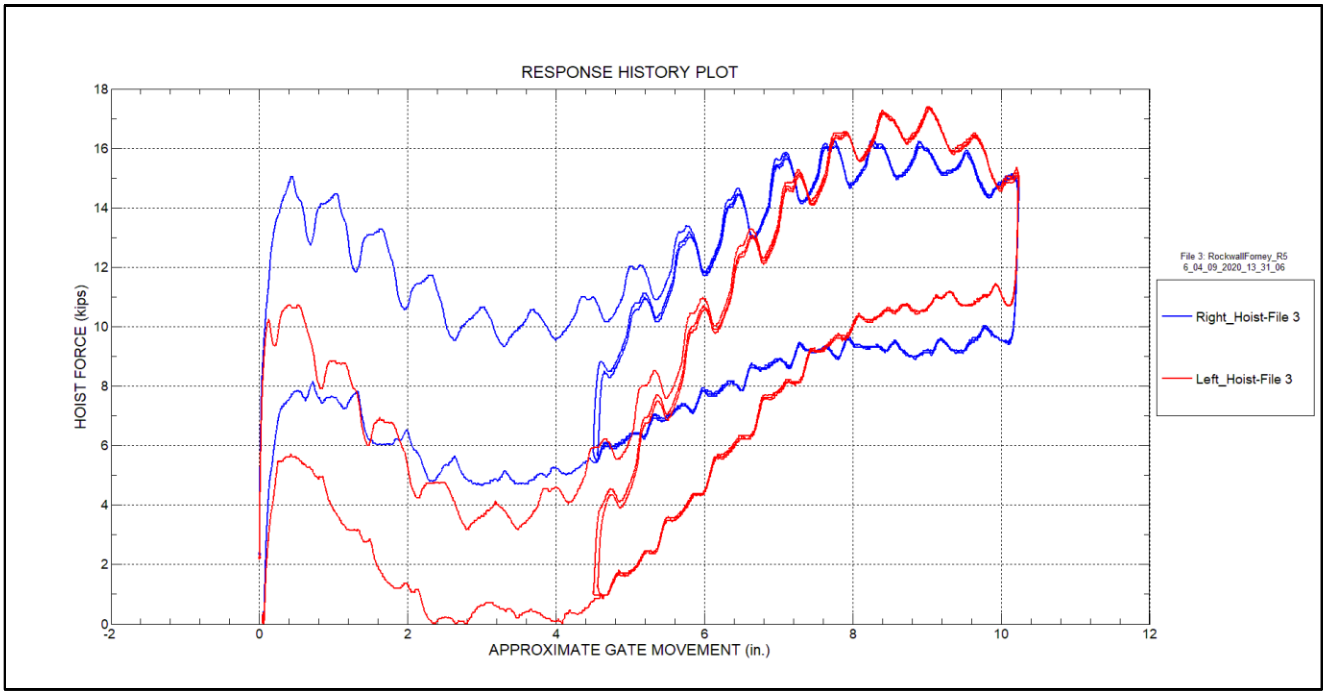

Figure 30 – Hoist force response history – Gate 10 – Test 3

APPENDIX B – GATE 10 PIN MOMENT COMPONENT PLOTS

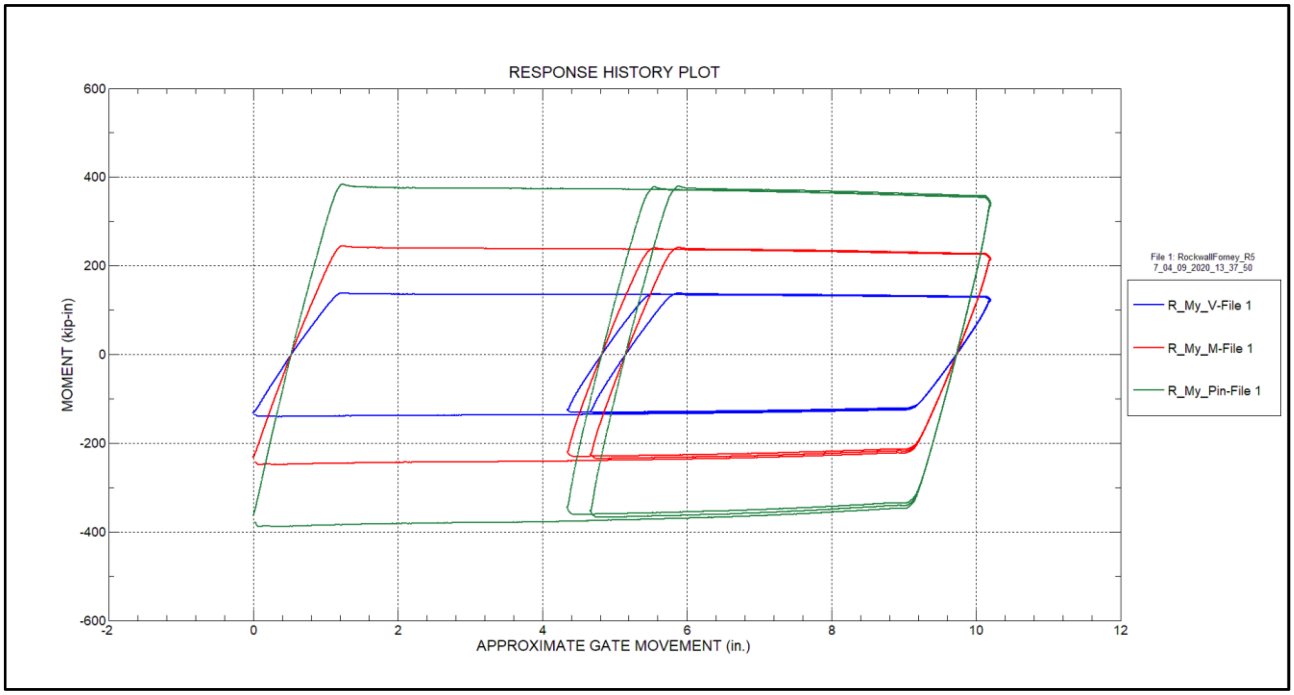

Figure 31 – Pin moment response history – Right arm – Test run 1

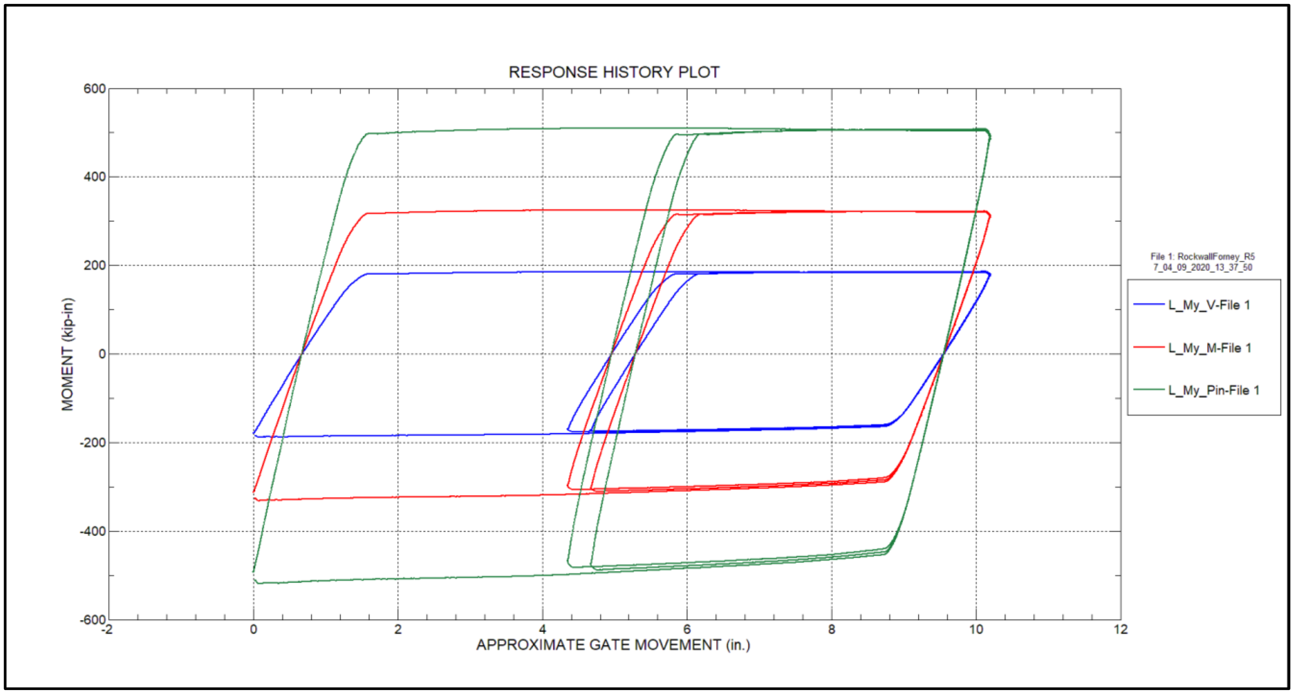

Figure 32 – Pin moment response history – Left arm – Test run 1

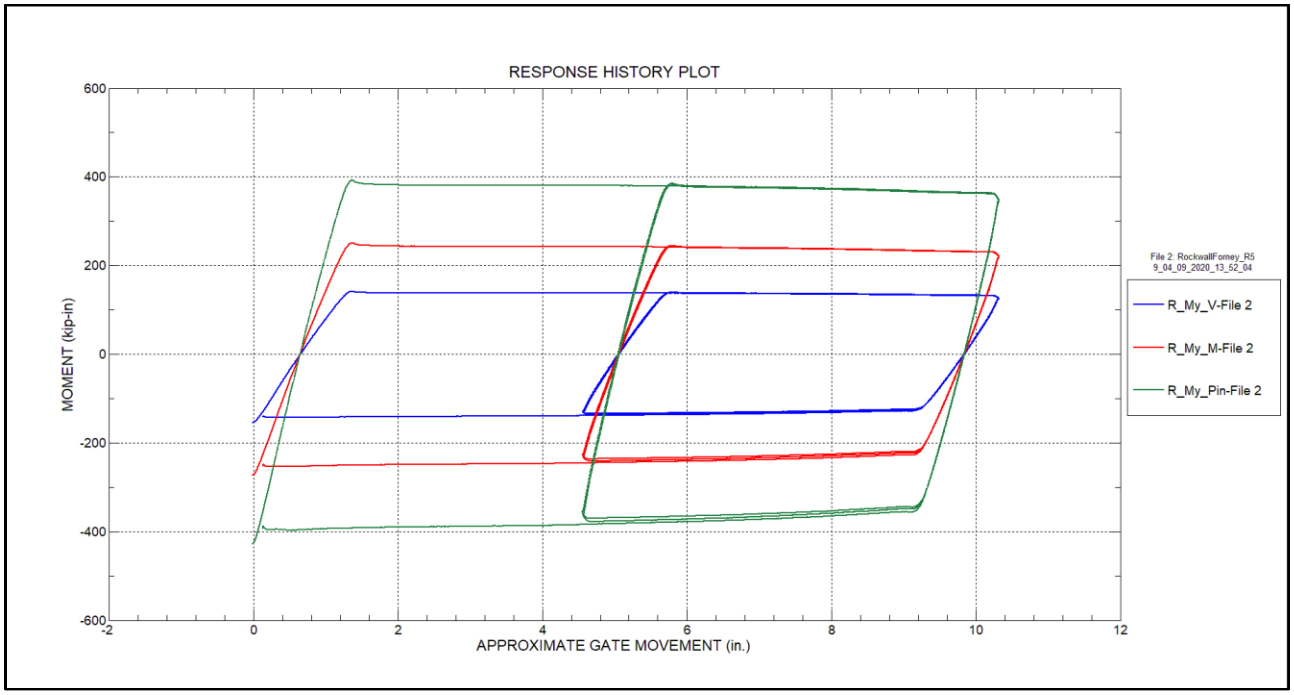

Figure 33 – Pin moment response history – Right arm – Test run 2

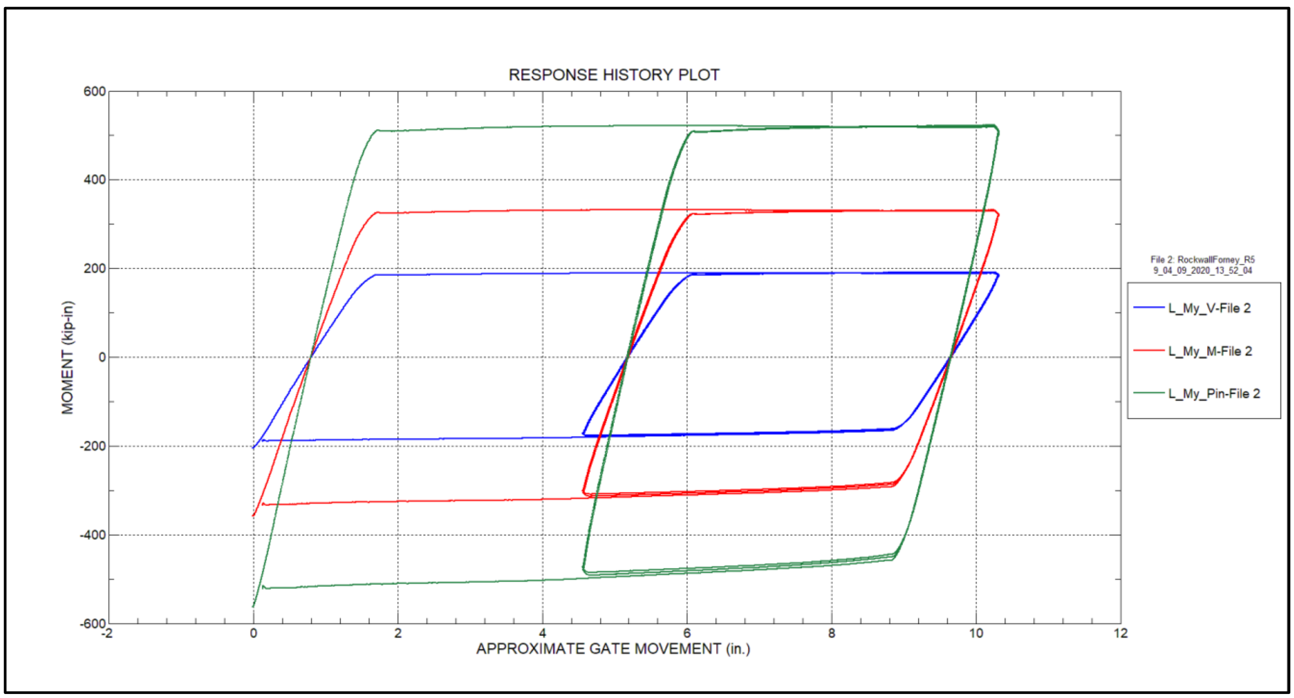

Figure 34 – Pin moment response history – Left arm – Test run 2

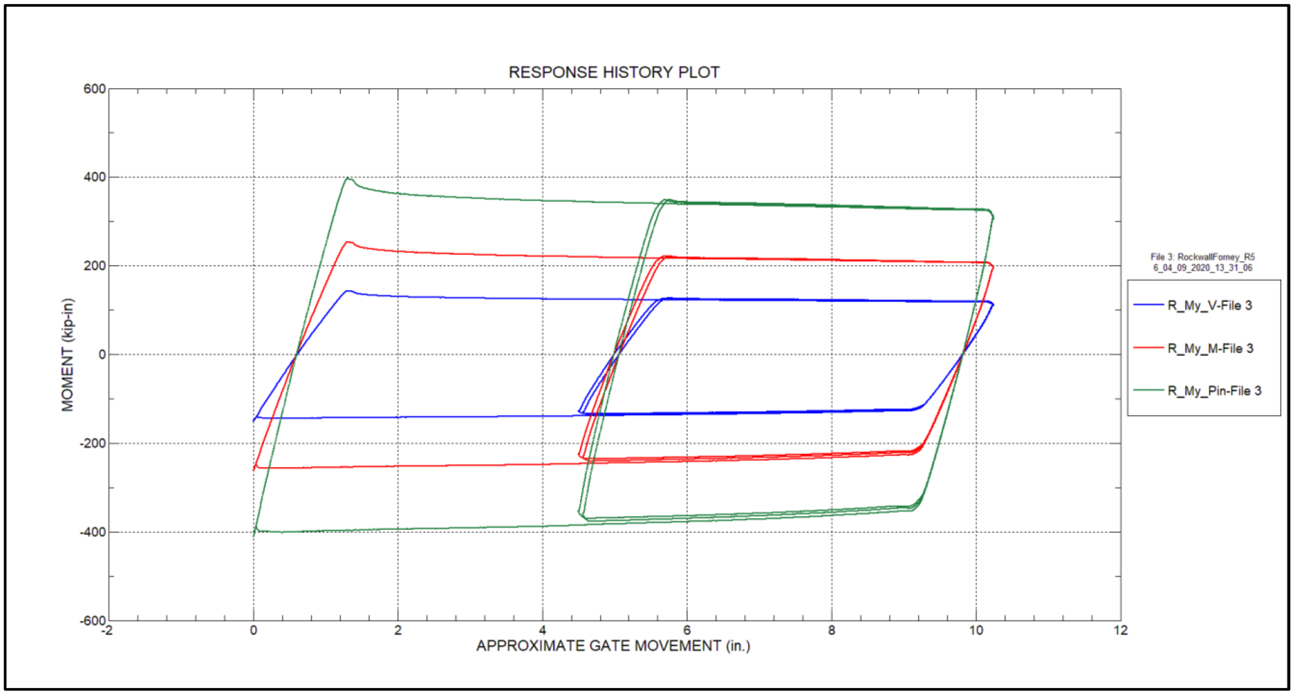

Figure 35 – Pin moment response history – Right arm – Test run 3

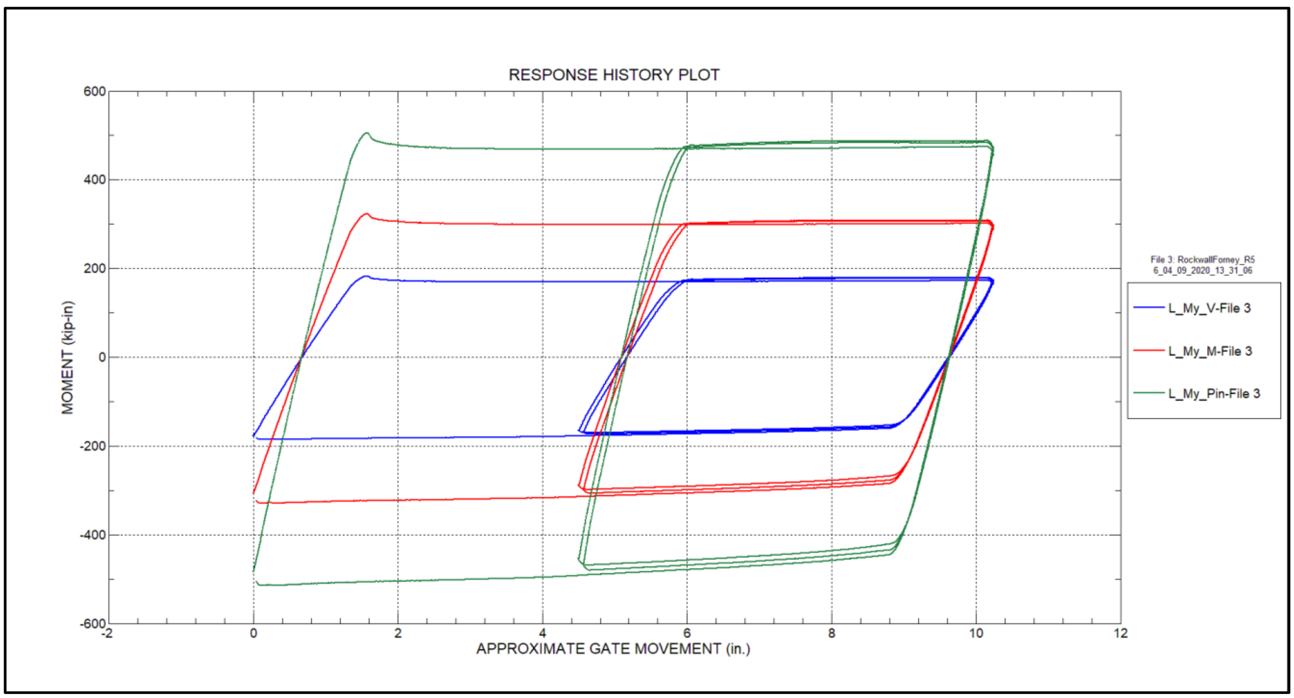

Figure 36 – Pin moment response history – Left arm – Test run 3

APPENDIX C – INSTRUMENTATION PLANS

RAW DATA. REFINED RESULTS.

SCHNABEL ENGINEERING
ROCKWALL FORNEY DAM
LIVE LOAD TESTING

The user acknowledges that these documents are instruments of professional service, and are protected by Copyright. This document and the information contained in this document are the property of Bridge Diagnostics, Inc., and shall not be reused, copied, disseminated, modified, amended or altered in any way. It is issued for information purposes only. The user agrees to hold harmless, indemnify and defend Bridge Diagnostics, Inc. against any and all damages, claims and losses, including defense costs, arising out of any use, reuse or copying of this document.

PLOT TIME: 6/12/2020 3:22 PM
FILEPATH: C:\Users\colemand\BDI\Services - Documents\Server_Remote\190701-TX_Schnabel_RockwallForneyDam\7. Instrumentation Plans\BDI_ROCKWALLFORNEY_01_GENERAL.dwg
© YYYY BRIDGE DIAGNOSTICS INC.

RAW DATA. REFINED RESULTS.
740 S PIERCE AVE, SUITE 15
LOUISVILLE, CO 80027
303.494.3230
WWW.BDITEST.COM

ISSUE

CLIENT

SCHABEL ENGINEERING
16000 CHRISTENSEN RD, STE 101
SEATTLE, WA 98188

PROJECT NAME

SCHNABEL ENGINEERING
ROCKWALL FORNEY DAM
LIVE LOAD TESTING

Drawn By:	KNR
Checked By:	JDS
Date:	05/27/2020
Client No.:	
BDI No.:	190701-TX
SCALE:	NTS

COVER PAGE

LLT-00

GAGE LEGEND & SPECIFICATION

SYMBOL	TYPE	BRAND	MODEL	NOTES
	STRAIN TRANSDUCER	BDI	ST350	
	TILTMETER (UNI-AXIAL)	BDI	T500-030	
	TORQUE SENSOR	HPI	-	HBWS-35-125-6-0.5VR-FB
	AMP SENSOR	CR MAGNETICS	CR42105-200	

GENERAL NOTES

- INSTRUMENTATION SHALL BEGIN ON APRIL 1ST, 2020.
- GATES 1 THRU 14 SHALL BE ACCESSED USING SPRAT ROPE ACCESS TECHNIQUES.
- BDI WILL PERFORM ALL SURFACE PREPARATION, SENSOR INSTALLATION, AND EQUIPMENT INSTALLATION.
- SEE LLT-31 FOR SENSOR INSTALLATION DETAILS.
- TWO PAIRS OF TORQUE GAGES WILL BE INSTALLED ON THE GATE MOTORS' PINION SHAFTS BETWEEN THE MOTORS AND THE HOISTS.
  - GAGE PAIRS WILL BE INSTALLED 180° APART FROM EACH OTHER.
  - EXACT POSITIONS OF THE GAGE PAIRS ON THE PINION SHAFT WILL BE DETERMINED IN THE FIELD.
- THREE PHASE AMPERAGE GAGES WILL BE INSTALLED ON THE MOTOR CONTROLS BY A QUALIFIED ELECTRICIAN PROVIDED BY GARVER.

TESTING PROCEDURE:

- TESTING SHALL BE STARTED WITH THE GATE IN THE CLOSED POSITION.
- ONCE DATA COLLECTION BEGINS, THE GATE SHALL BE RAISED TO TWO OR THREE TIMES THE HEIGHT NECESSARY FOR TRUNNION FRICTION TO BE OVERCOME, H1 (TYPICALLY 6"-12"), AND HELD THERE UNTIL DATA STABILIZES.
- THE GATE SHALL BE LOWERED APPROXIMATELY TWICE THE DISTANCE TO OVERCOME TRUNNION FRICTION, H2, AND HELD THERE UNTIL DATA STABILIZES.
- THE GATE SHALL BE RAISED TO H1 AND HELD THERE UNTIL DATA STABILIZES.
- THE GATE SHALL BE LOWERED TO H2 AND HELD THERE UNTIL DATA STABILIZES.
- THE GATE SHALL BE RAISED TO H1 AND HELD THERE UNTIL DATA STABILIZES.
- THE GATE WAS LOWERED BACK TO CLOSED POSITION AND DATA COLLECTION STOPPED.
- A MINIMUM OF 3 TESTS SHALL BE PERFORMED PER GATE.

GAGE COUNT PER GATE

SENSOR LEGEND	SENSOR COUNT	CHANNEL COUNT
STRAIN TRANSDUCER	(48)	(48)
TILTMETER (UNI-AXIAL)	(4)	(4)
TORQUE SENSOR	(4)	(4)
AMP SENSOR	(3)	(3)
TOTAL	(59)	(59)

LOCATION KEY

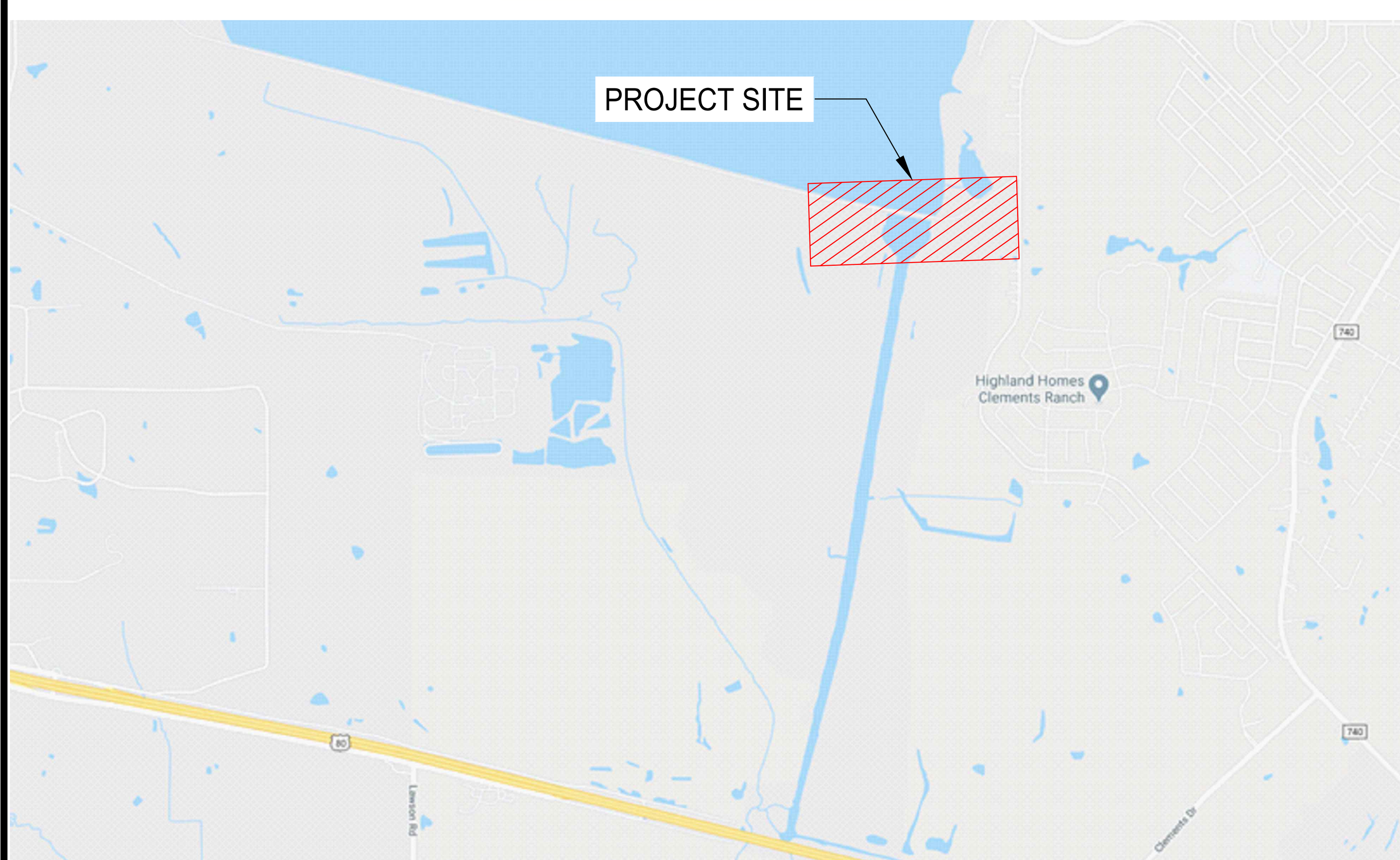

INDEX OF SHEETS

INDEX OF ISSUE

NO.	DATE	REVISION DESCRIPTION
1	3/20/2020	LIVE LOAD TESTING (LLT) INSTRUMENTATION PLAN (FOR APPROVAL)
2	5/27/2020	LIVE LOAD TESTING (LLT) INSTRUMENTATION PLAN AS BUILTS
BDI REFERENCE NUMBER: 190701-TX		

RAW DATA. REFINED RESULTS.
740 S PIERCE AVE, SUITE 15
LOUISVILLE, CO 80027
303.494.3230
WWW.BDITEST.COM

ISSUE

CLIENT

SCHABEL ENGINEERING
16000 CHRISTENSEN RD, STE 101
SEATTLE, WA 98188

PROJECT NAME

SCHABEL ENGINEERING
ROCKWALL FORNEY DAM
LIVE LOAD TESTING

Drawn By:	KNR
Checked By:	JDS
Date:	05/27/2020
Client No.:	
BDI No.:	190701-TX
SCALE:	NTS

OVERALL LEGEND

LLT-01

The user acknowledges that these documents are instruments of professional service, and are protected by Copyright. This document and the information contained in this document are the property of Bridge Diagnostics, Inc., and shall not be reused, copied, disseminated, modified, amended or altered in any way. It is issued for information purposes only. The user agrees to hold harmless, indemnify and defend Bridge Diagnostics, Inc. against any and all damages, claims and losses, including defense costs, arising out of any use, reuse or copying of this document.

PLOT TIME: 6/12/2020 3:22 PM
FILEPATH: C:\Users\colemand\BDI\Services - Documents\Server_Remote\190701-TX_Schnabel_RockwallForneyDam\7. Instrumentation Plans\BDI_ROCKWALLFORNEY_01_GENERAL.dwg
© YYYY BRIDGE DIAGNOSTICS INC.

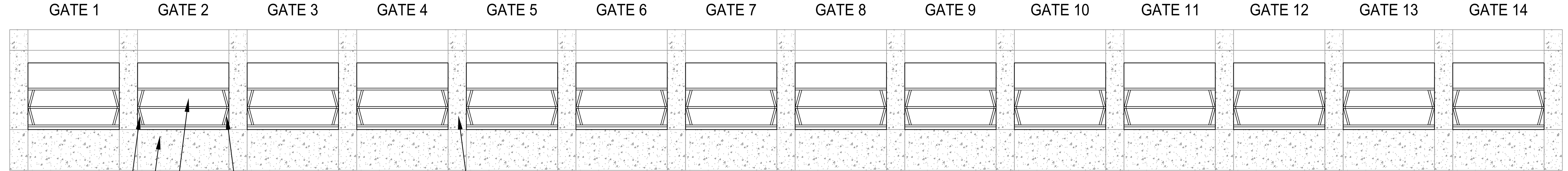

1 DOWNSTREAM ELEVATION OF GATES
LOOKING NORTH (UPSTREAM)

RAW DATA. REFINED RESULTS.
740 S PIERCE AVE, SUITE 15
LOUISVILLE, CO 80027
303.494.3230
WWW.BDITEST.COM

ISSUE

CLIENT

SCHABEL ENGINEERING
16000 CHRISTENSEN RD, STE 101
SEATTLE, WA 98188

PROJECT NAME

SCHNABEL ENGINEERING
ROCKWALL FORNEY DAM
LIVE LOAD TESTING

Drawn By:	KNR
Checked By:	JDS
Date:	05/27/2020
Client No.:	
BDI No.:	190701-TX
SCALE:	NTS

OVERALL STRUCTURE LAYOUT
LLT-02

The user acknowledges that these documents are instruments of professional service, and are protected by Copyright. This document and the information contained in this document are the property of Bridge Diagnostics, Inc., and shall not be reused, copied, disseminated, modified, amended or altered in any way. It is issued for information purposes only. The user agrees to hold harmless, indemnify and defend Bridge Diagnostics, Inc. against any and all damages, claims and losses, including defense costs, arising out of any use, reuse or copying of this document.

PLOT TIME: 6/12/2020 3:22 PM
FILEPATH: C:\Users\colemand\BDI\Services - Documents\Server_Remote\190701-TX_Schnabel_RockwallForneyDam\7. Instrumentation Plans\BDI_ROCKWALLFORNEY_01_GENERAL.dwg
© YYYY BRIDGE DIAGNOSTICS INC.

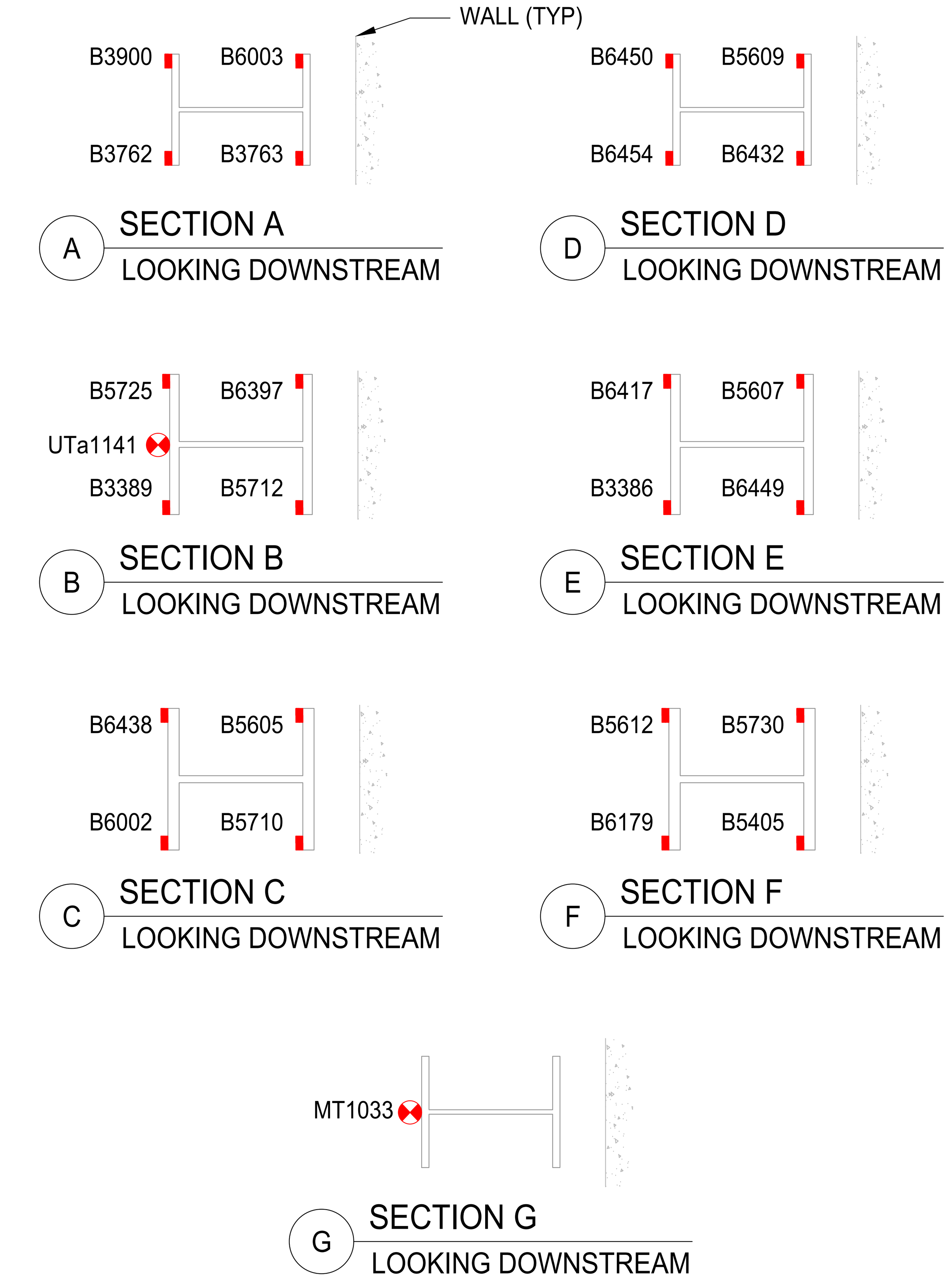

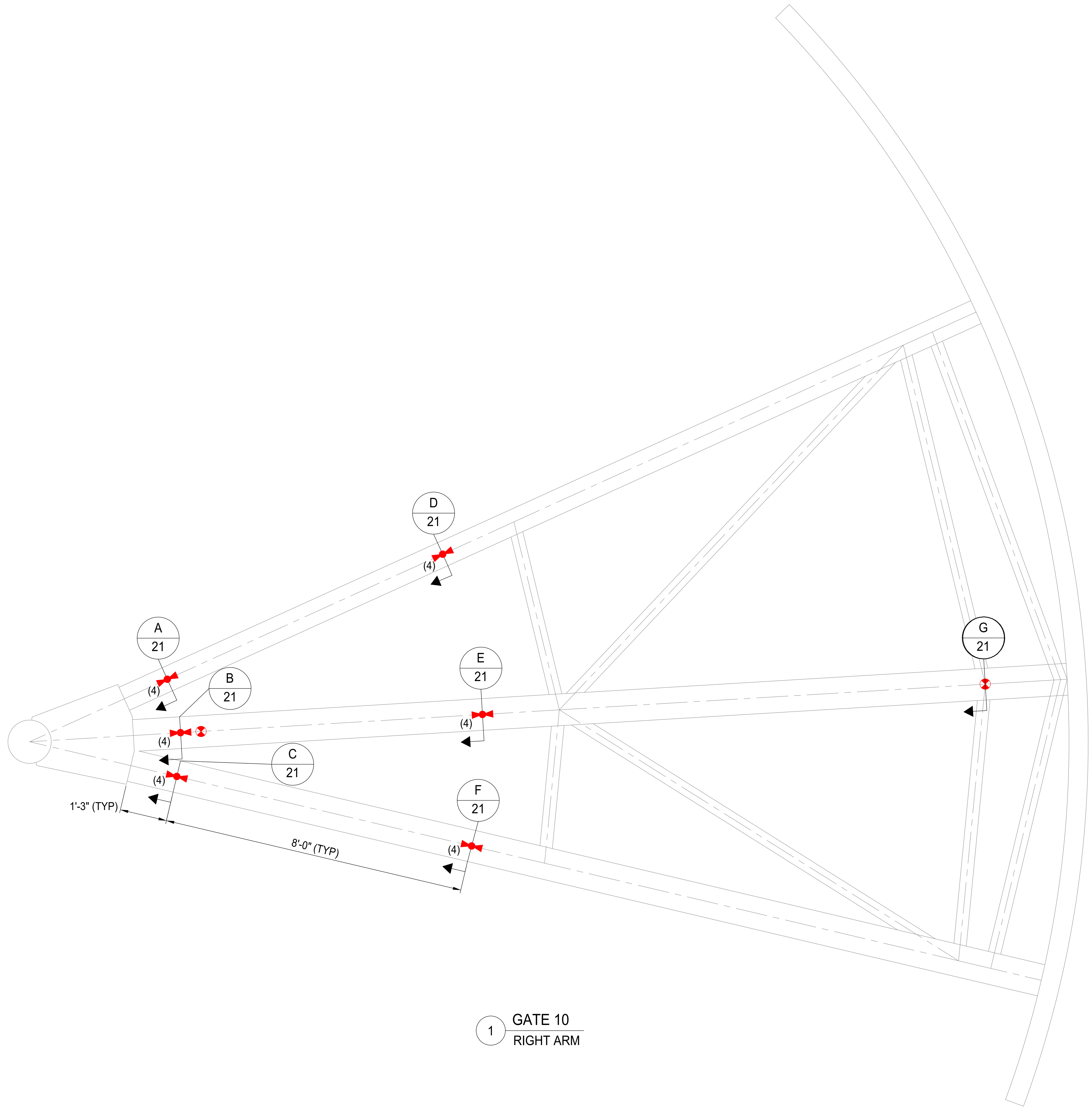

1 GATE 10
RIGHT ARM

UNIT ID
TT-3

TORQUE GAGES
RIGHT ARM

NOTES:

1. SECTIONS A, B, & C SHALL BE INSTALLED 15 INCHES AWAY FROM TRUNNION PLATE.
2. TILTMETERS SHALL BE INSTALLED CENTERED ON THE MIDDLE STRUT FLANGE.
3. SECTION G'S TILTMETER SHALL BE INSTALLED AS CLOSE TO THE SKINPLATE AS POSSIBLE.

SENSOR LEGEND

- STRAIN TRANSDUCER
- TILTMETER (UNI-AXIAL)
- TORQUE SENSOR

BDI
RAW DATA. REFINED RESULTS.
740 S PIERCE AVE, SUITE 15
LOUISVILLE, CO 80027
303.494.3230
WWW.BDITEST.COM

ISSUE

CLIENT

SCHABEL ENGINEERING
16000 CHRISTENSEN RD, STE 101
SEATTLE, WA 98188

PROJECT NAME

SCHABEL ENGINEERING ROCKWALL FORNEY DAM LIVE LOAD TESTING

Drawn By:	KNR
Checked By:	JDS
Date:	05/27/2020
Client No.:	
BDI No.:	190701-TX
SCALE:	NTS

GATE 10 - RIGHT ARM
ELEVATION

LLT-21

The user acknowledges that these documents are instruments of professional service, and are protected by Copyright. This document and the information contained in this document are the property of Bridge Diagnostics, Inc., and shall not be reused, copied, disseminated, modified, amended or altered in any way. It is issued for information purposes only. The user agrees to hold harmless, indemnify and defend Bridge Diagnostics, Inc. against any and all damages, claims and losses, including defense costs, arising out of any use, reuse or copying of this document.

PLOT TIME: 6/12/2020 3:23 PM
FILEPATH: C:\Users\colemand\BDI\Services - Documents\Server_Remote\190701-TX_Schabel_RockwallForneyDam\7. Instrumentation Plans\BDI_ROCKWALLFORNEY_01_GENERAL.dwg
© YYYY BRIDGE DIAGNOSTICS INC.

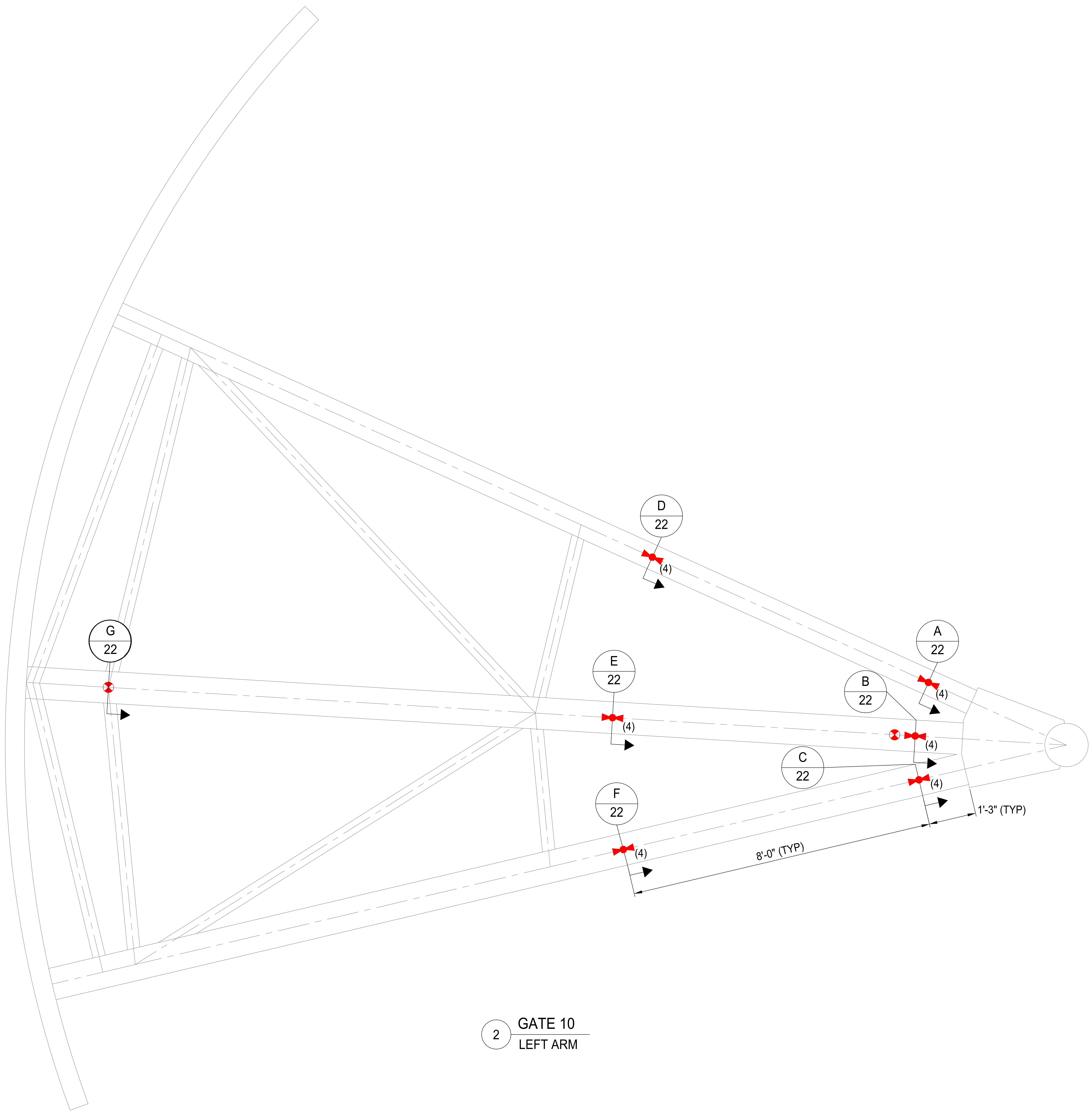

2 GATE 10
LEFT ARM

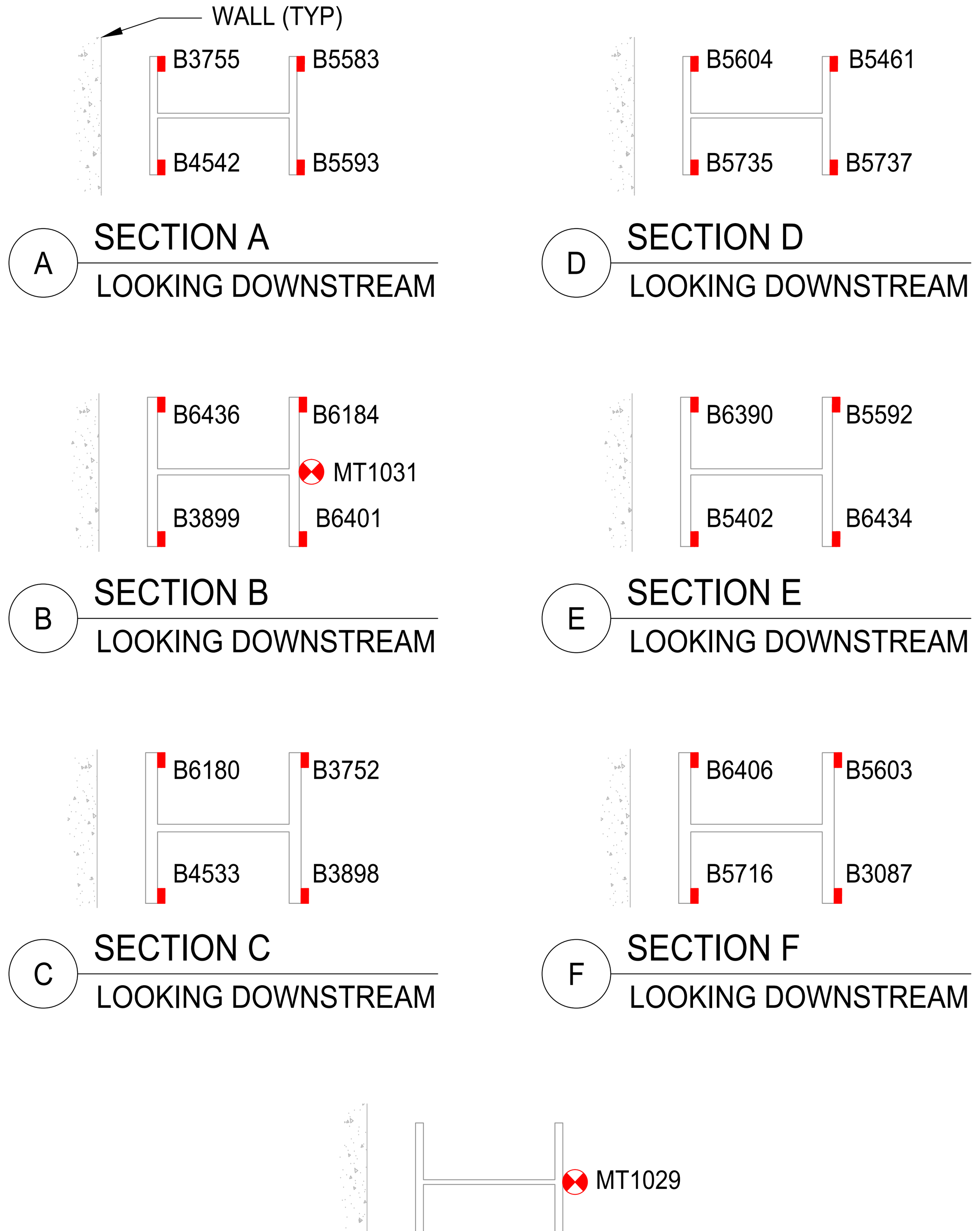

A SECTION A
LOOKING DOWNSTREAM

D SECTION D
LOOKING DOWNSTREAM

B SECTION B
LOOKING DOWNSTREAM

E SECTION E
LOOKING DOWNSTREAM

C SECTION C
LOOKING DOWNSTREAM

F SECTION F
LOOKING DOWNSTREAM

G SECTION G
LOOKING DOWNSTREAM

UNIT ID
TT-4

TORQUE GAGES
LEFT ARM

NOTES:
1. SECTIONS A, B, & C SHALL BE INSTALLED 15 INCHES AWAY FROM TRUNNION PLATE.
2. TILTMETERS SHALL BE INSTALLED CENTERED ON THE MIDDLE STRUT FLANGE.
3. SECTION G'S TILTMETER SHALL BE INSTALLED AS CLOSE TO THE SKINPLATE AS POSSIBLE.

SENSOR LEGEND
- STRAIN TRANSDUCER
- TILTMETER (UNI-AXIAL)
- TORQUE SENSOR

BDI
RAW DATA. REFINED RESULTS.
740 S PIERCE AVE, SUITE 15
LOUISVILLE, CO 80027
303.494.3230
WWW.BDITEST.COM

ISSUE

CLIENT
SCHABEL ENGINEERING
16000 CHRISTENSEN RD, STE 101
SEATTLE, WA 98188

PROJECT NAME
SCHNABEL ENGINEERING
ROCKWALL FORNEY DAM
LIVE LOAD TESTING

Drawn By:	KNR
Checked By:	JDS
Date:	05/27/2020
Client No.:	
BDI No.:	190701-TX
SCALE:	NTS

GATE 10 - LEFT ARM
ELEVATION
LLT-22

The user acknowledges that these documents are instruments of professional service, and are protected by Copyright. This document and the information contained in this document are the property of Bridge Diagnostics, Inc., and shall not be reused, copied, disseminated, modified, amended or altered in any way. It is issued for information purposes only. The user agrees to hold harmless, indemnify and defend Bridge Diagnostics, Inc. against any and all damages, claims and losses, including defense costs, arising out of any use, reuse or copying of this document.
PLOT TIME: 6/12/2020 3:23 PM
FILEPATH: C:\Users\colemand\BDI\Services - Documents\Server_Remote\190701-TX_Schnabel_RockwallForneyDam\7. Instrumentation Plans\BDI_ROCKWALLFORNEY_01_GENERAL.dwg
© YYYY BRIDGE DIAGNOSTICS INC.

The user acknowledges that these documents are instruments of professional service, and are protected by Copyright. This document and the information contained in this document are the property of Bridge Diagnostics, Inc., and shall not be reused, copied, disseminated, modified, amended or altered in any way. It is issued for information purposes only. The user agrees to hold harmless, indemnify and defend Bridge Diagnostics, Inc. against any and all damages, claims and losses, including defense costs, arising out of any use, reuse or copying of this document.

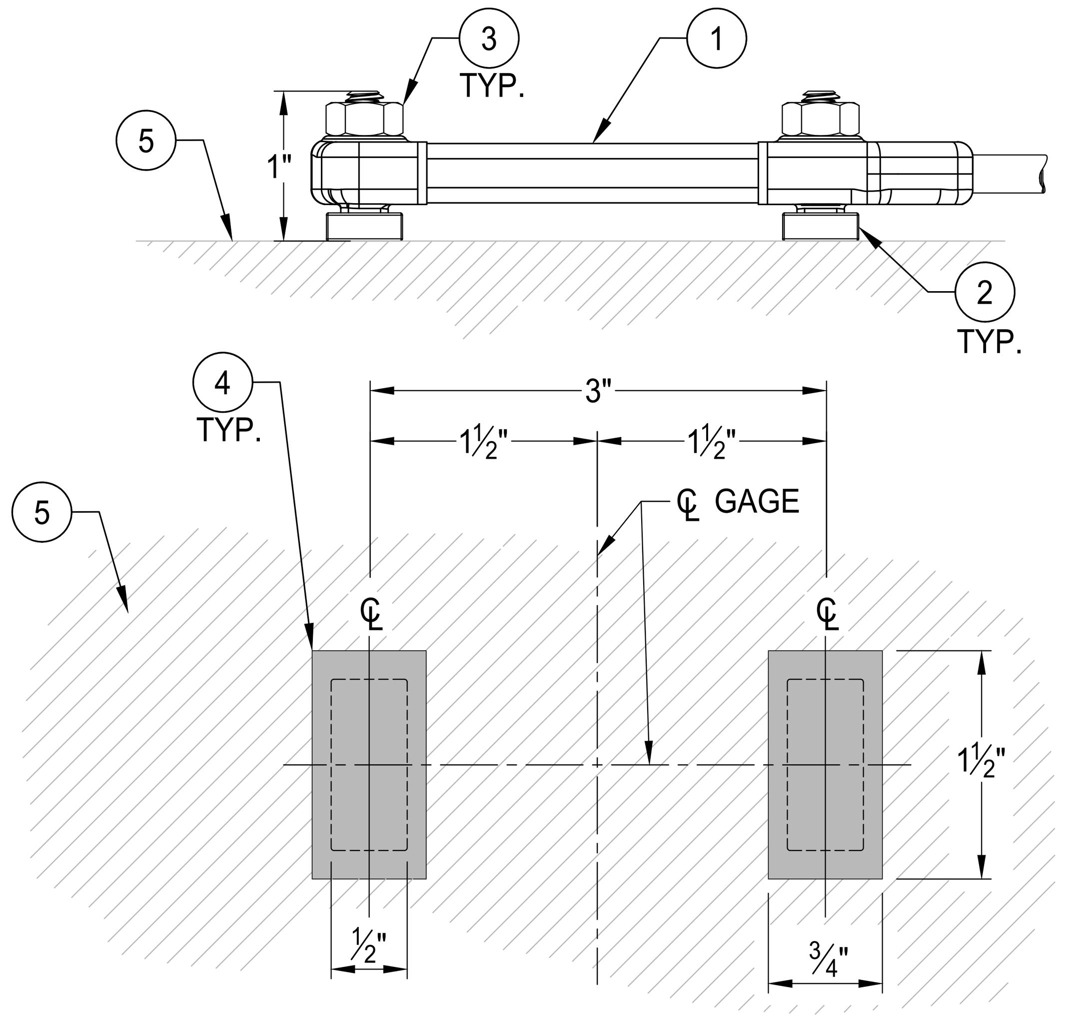

COMPONENT DESCRIPTION

1. ST350 STRAIN GAGE
2. 1/4"-20 THREADED MOUNTING TAB
3. 1/4"-20 STAINLESS STEEL NUT
4. TYPICAL SURFACE PREP REQUIRED TO MOUNT STRAIN GAGES
5. TYPICAL MOUNTING SURFACE

FOOTNOTES - INSTANT ADHESIVE
1. STRAIN GAGES SHALL BE MOUNTED WITH LOCTITE 410 INSTANT ADHESIVE AND LOCTITE 7452 ACCELERANT 2. DURING SURFACE PREP ALL PAINT AND SURFACE DEFORMATIONS MUST BE REMOVED. 3. SURFACE PREP IS REQUIRED JUST PRIOR TO GAGE INSTALLATION AS TO NOT ALLOW SURFACE CONTAMINANTS TO ACCUMULATE.

1 TYPICAL ST350 STRAIN GAGE INSTALLATION

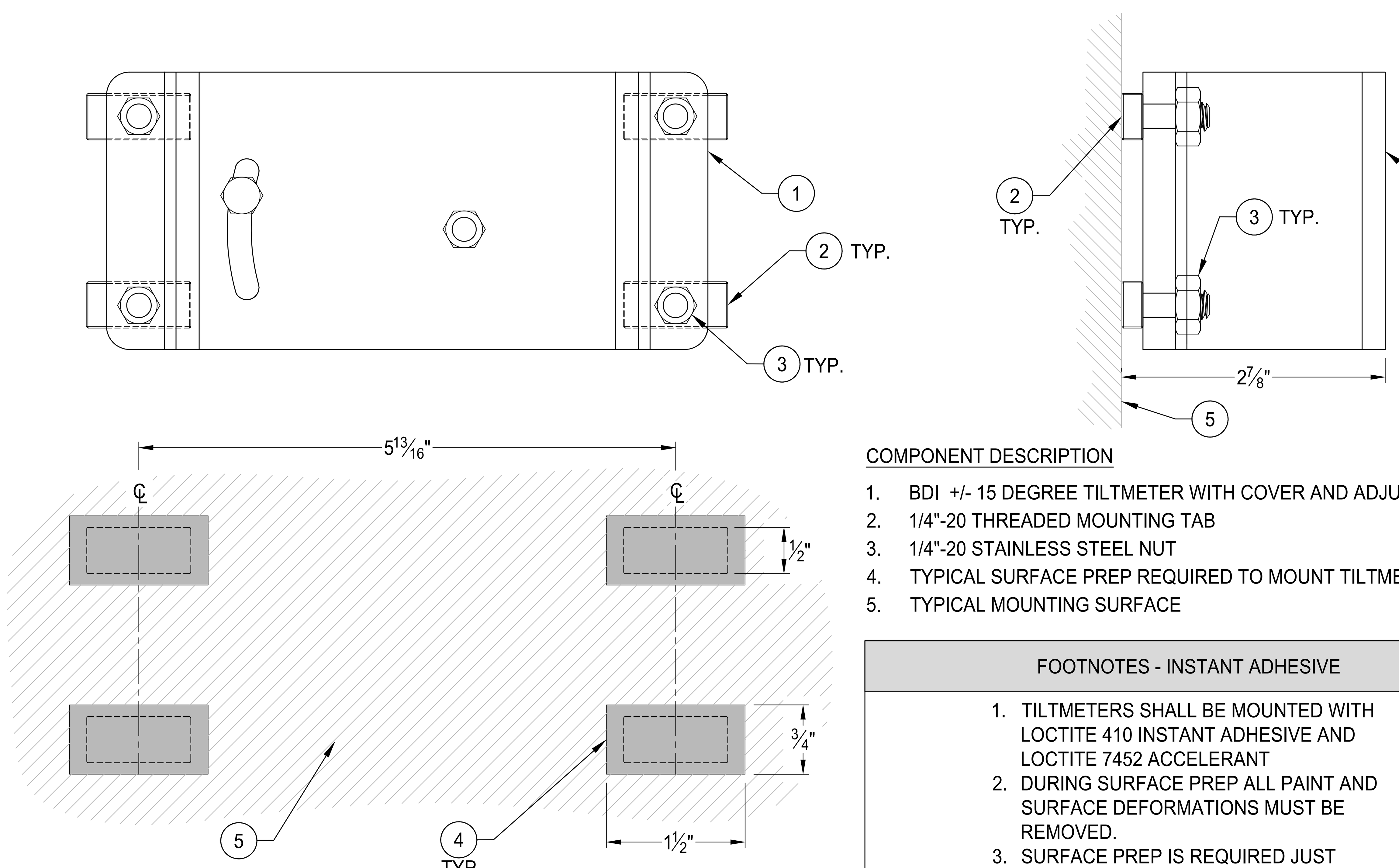

COMPONENT DESCRIPTION

1. BDI +/- 15 DEGREE TILTMETER WITH COVER AND ADJUSTMENT BOLTS
2. 1/4"-20 THREADED MOUNTING TAB
3. 1/4"-20 STAINLESS STEEL NUT
4. TYPICAL SURFACE PREP REQUIRED TO MOUNT TILTMETERS
5. TYPICAL MOUNTING SURFACE

FOOTNOTES - INSTANT ADHESIVE
1. TILTMETERS SHALL BE MOUNTED WITH LOCTITE 410 INSTANT ADHESIVE AND LOCTITE 7452 ACCELERANT 2. DURING SURFACE PREP ALL PAINT AND SURFACE DEFORMATIONS MUST BE REMOVED. 3. SURFACE PREP IS REQUIRED JUST PRIOR TO GAGE INSTALLATION AS TO NOT ALLOW SURFACE CONTAMINANTS TO ACCUMULATE.

2 TYPICAL BDI TILTMETER INSTALLATION

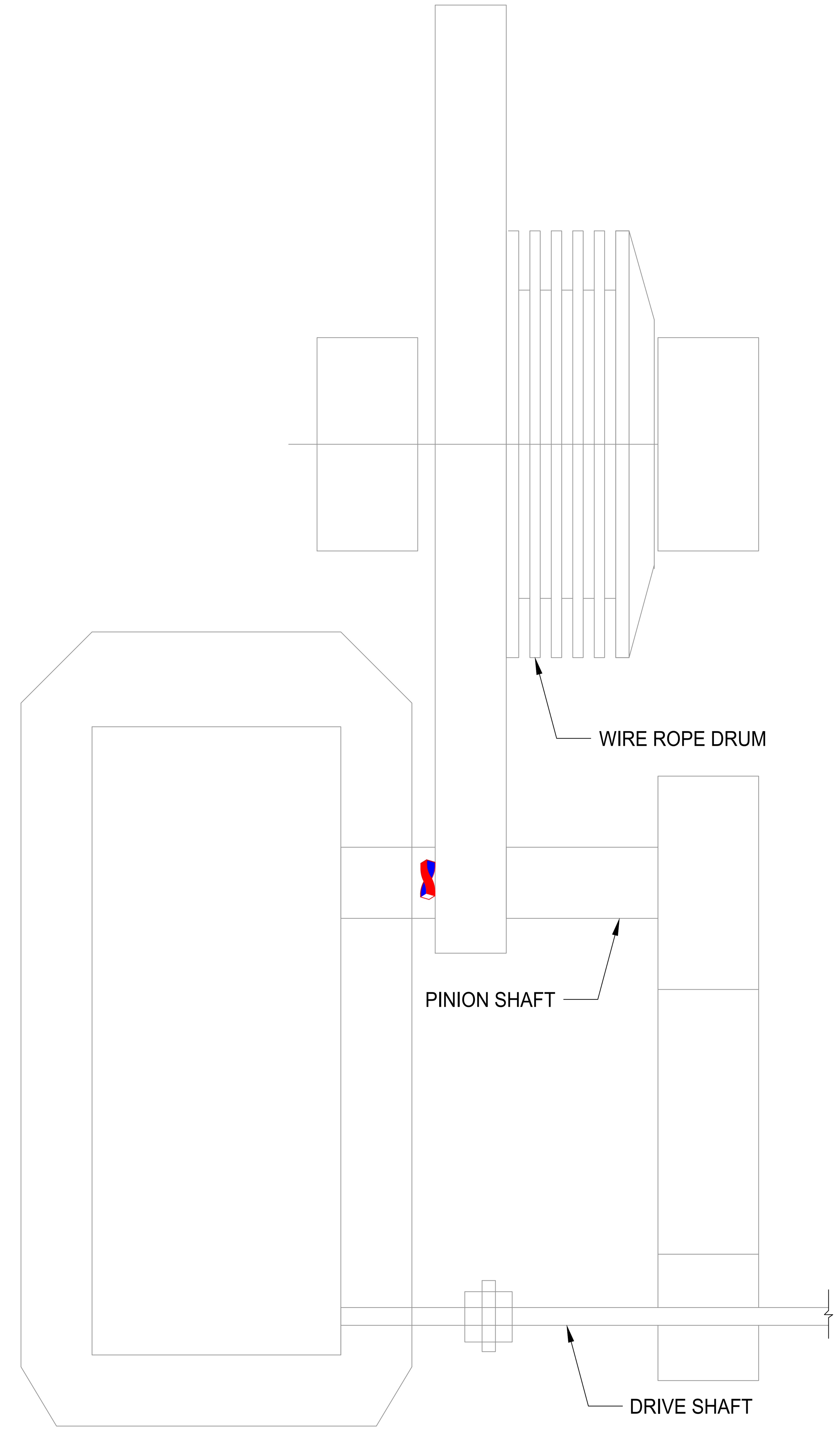

3 TYPICAL HOIST INSTRUMENTATION

TORQUE SENSOR INSTALLATION NOTES:

- TORQUE GAGES WILL BE INSTALLED ON THE PINION SHAFT ON EITHER HOIST MOTOR BETWEEN THE MOTOR AND THE HOIST DRUM
- EXACT POSITIONS OF THE GAGE PAIRS ON THE PINION SHAFT WILL BE DETERMINED IN THE FIELD

SENSOR LEGEND

TORQUE SENSOR

BDI
RAW DATA. REFINED RESULTS.
740 S PIERCE AVE, SUITE 15
LOUISVILLE, CO 80027
303.494.3230
WWW.BDITEST.COM

ISSUE

CLIENT

SCHABEL ENGINEERING
16000 CHRISTENSEN RD, STE 101
SEATTLE, WA 98188

PROJECT NAME

SCHNABEL ENGINEERING
ROCKWALL FORNEY DAM
LIVE LOAD TESTING

Drawn By:	KNR
Checked By:	JDS
Date:	05/27/2020
Client No.:	
BDI No.:	190701-TX
SCALE:	NTS

SENSOR INSTALLATION DETAILS

LLT-31

PLOT TIME: 6/12/2020 3:24 PM
FILEPATH: C:\Users\colemand\BDI\Services - Documents\Server_Remote\190701-TX_Schnabel_RockwallForneyDam\7. Instrumentation Plans\BDI_ROCKWALLFORNEY_01_GENERAL.dwg
© YYYY BRIDGE DIAGNOSTICS INC.

SCHNABEL ENGINEERING

TRUNNION PIN FRICTION TESTING REPORT

ROCKWALL FORNEY DAM – GATE 11
FORNEY, TX

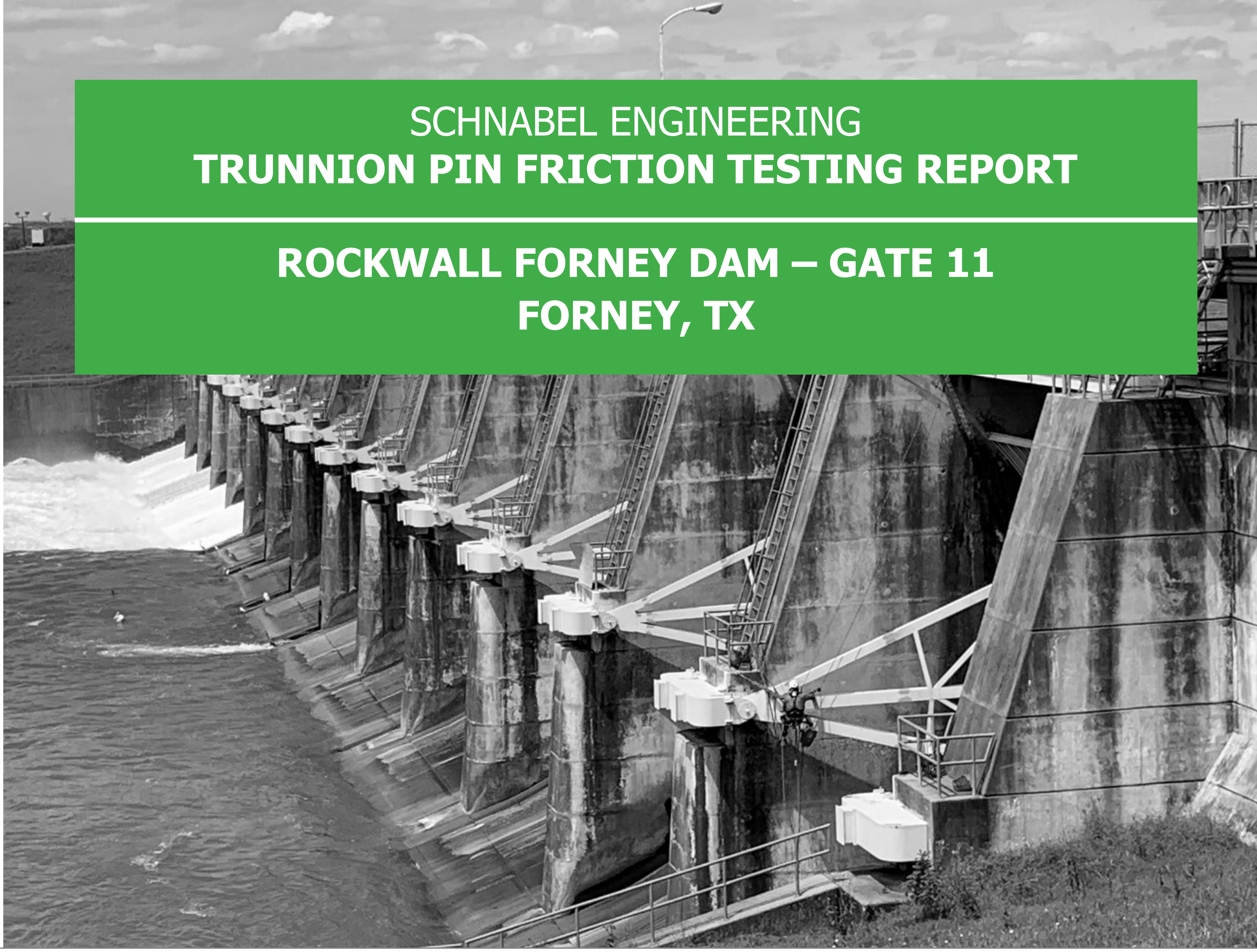

SUBMITTED TO:
SCHNABEL ENGINEERING
16000 CHRISTENSEN RD, SUITE 101
SEATTLE, WA 98188

SUBMITTED BY:
BDI – CO
740 SOUTH PIERCE AVE, UNIT 15
LOUISVILLE, CO 80027

BDI Project No.: **190701-TX**
Report Version: **V1**
Version Submitted: **August 26, 2020**

RAW DATA. REFINED RESULTS.

This document contains Confidential Information and is submitted in confidence to the customer. The submission of the information contained herein shall not be deemed to constitute public disclosure or authorization for disclosure to other parties. BDI's information and name may not be used in advertising or for promotional purposes without BDI's written consent.

TABLE OF CONTENTS

LIST OF FIGURES

LIST OF TABLES

Executive Summary

Schnabel Engineering contracted BDI to provide instrumentation and testing services on Gates 1-14 on the Rockwall Forney Dam near Dallas, Texas. The goal of these tests was to record each gate's structural responses during a series of spill tests and use the data to compute accurate coefficients of friction for each trunnion pin, cable lift force, total gate friction, and motor amperage. This report provides details on the work performed on Gate 11.

Instrumentation and testing were performed on Gate 11 at the Rockwall Forney Dam on April 10th, 2020. The gate arms were instrumented with strain and rotation sensors. The hoist motors' pinion shafts were instrumented with torque sensors and the hoist motor controls were instrumented with amperage sensors. Following the instrumentation, a series of spill tests were performed to measure the structural responses resulting from trunnion pin friction. All instrumentation setup and removal were performed using BDI's rope access team.

Following demobilization from the field, the test data was examined for quality and then further processed to evaluate the gate's performance. Strain measurements were converted into bending forces which were then applied to pin-strut free-body diagrams. By summing forces at each pin, friction induced moments could be computed, allowing accurate friction coefficients to be determined. Generally, the observed gate behavior showed that Gate 11 was operating as expected with no major signs of distress.

The resulting maximum trunnion friction coefficients and corresponding hoist forces are shown in Table 1.

Table 1 – Gate 11 performance summary

Pin Designation	Maximum Friction Coefficient	Maximum Pin Moment due to Pin Friction (kip-In)	Maximum Hoist Force (kips)	Maximum Hoist Force due to Total Gate Friction (kips)
Right Pin	0.23	604.9	35.18	4.63
Left Pin	0.20	513.7	21.35	3.11

Note: Pin designations are in reference to looking downstream

Due to restrictions caused by the hoist limit switches, the hoist cables could not always be fully slacked at the beginning and end of the performed tests. Throughout testing of the Rockwell Forney gates, it was found that this limit switch restriction varied gate to gate and arm to arm. Therefore, it is not recommended to use the collected hoist force data to quantify overall hoist forces during gate operation. Rather, this hoist data can be better utilized to evaluate total friction behavior.

Amperage responses were not used to compute friction results and were collected as verification that the motor performance was not causing unexpected gate responses. These responses indicated the motor was functioning in a stable manner and should be reviewed by a licensed electrician to further evaluate the motor's performance.

All results and recommendations provided in this report were based on the structure in its current condition; therefore, any significant changes in condition must be noted as they may alter their validity. Questions regarding this report and/or data should be directed to Kyle Ramer (kyler@bditest.com) at BDI. For further information on BDI's equipment, services, and analysis methods please visit www.bditest.com

Instrumentation and Load Testing Procedure

Gate Instrumentation Summary

Instrumentation and testing were performed on Gate 11 at the Rockwall Forney Dam on April 10th, 2020. Instrumentation plans have been provided along with this report and include the following number of instrumented locations and sensor types:

+ **REUSABLE SURFACE MOUNTED STRAIN TRANSDUCERS:** Each gate arm was instrumented with a total of 24 strain transducers at 6 locations on each of the gate arms (48 strain sensors total). A typical strain gage installation is shown in Figure 1. Note these sensors were installed with the mounting tabs on the extreme fiber of the strut flanges, which puts the center of the gage approximately 0.66" from the extreme fiber.
+ **TILTMETER ROTATION SENSORS:** MEMS style rotation sensors were located on the middle strut of the gate arm near the skin plate and near the trunnion hub (4 rotation sensors total). The rotation responses were used to calculate vertical skin plate movement and measure pin rotation relative to skin plate rotation. Typical tiltmeter installations are shown in Figure 1 and Figure 2.
+ **TORQUE SENSORS:** Two total torque sensors were installed on the hoist's pinion shafts (QTY1 on each hoist pinion shaft) near the cable hoist motor to measure direct torque and in turn lift force (See Figure 3).
+ **AMPERAGE SENSORS:** 3 Hall-Effect amperage transducers were clamped over each phase of the hoist motor to measure the motor's current draw (See Figure 4). The purpose of these sensors was to provide additional data in case there were any issues with the hoist systems and to verify any data issues related to lifting and lowering the gates.
+ **BDI'S STS-4 WIRELESS DATA ACQUISITION SYSTEM:** BDI's STS-4 wireless data acquisition (DAQ) was used to collect and record data during testing. A group of sensors were wired to each nodal DAQ which then communicated wirelessly back to the wireless base station and was controlled by BDI's STS-Live testing software.

Complete specifications are available upon request and can be found at http://www.bditest.com.

Sensor Installation

BDI strain transducers were installed by first sanding paint off the struts to expose bare metal at two small locations (1"x2" areas) for the sensor's mounting tabs. Each transducer was then attached using a combination of fast-setting adhesive and accelerator and applying pressure until the adhesive was fully cured. Each strain transducer took approximately five minutes to attach.

Tiltmeters were installed using the same adhesive process as the strain transducers. However, no surface preparation was necessary.

Torque sensors were installed on the pinion shafts by capacitive discharge bonding. Properly bonding to the shaft required sanding the surface to a smooth finish, clean of any paint or grease. Responses from these gages were measured using Binsfeld Torque Trak 10k wireless transmitters.

A typical installation has been shown in Figure 1 through Figure 4. Access to all the sensor locations was provided by BDI's own SPRAT certified rope access technicians and engineers as shown in Figure 5.

Once testing was completed, sensors were removed, and exposed steel areas were covered using cold galvanizing compound.

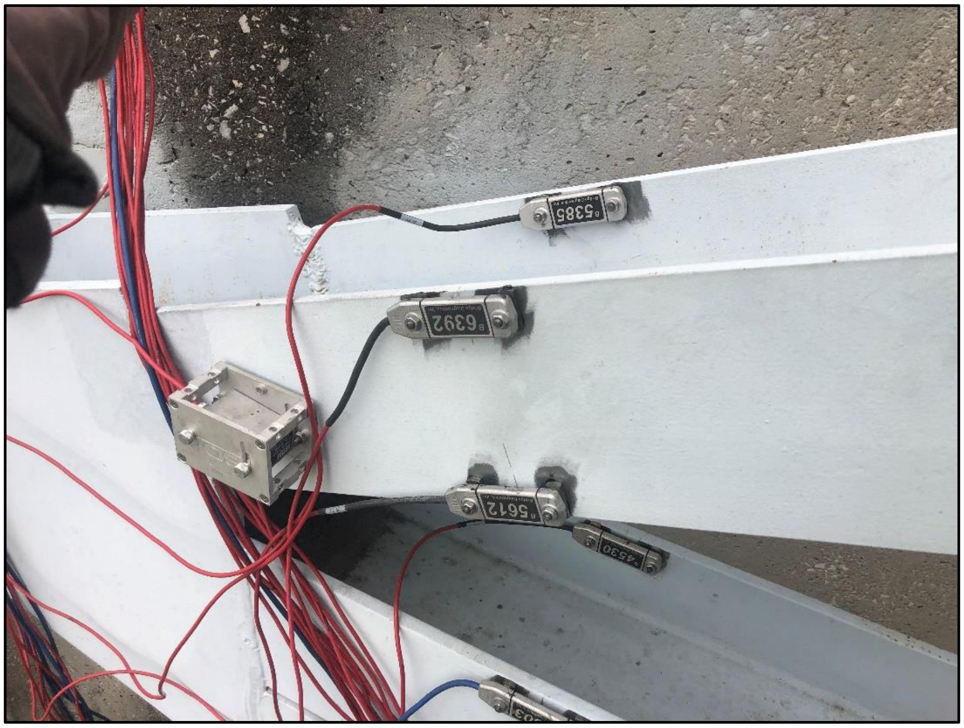

Figure 1 – BDI tiltmeter rotation sensor and reusable strain transducers installed near trunnion hub (Typical)

Figure 2 – BDI tiltmeter rotation sensor installed near skin plate (Typical)

Figure 3 – Torque sensor installation on hoist pinion shaft (Typical)

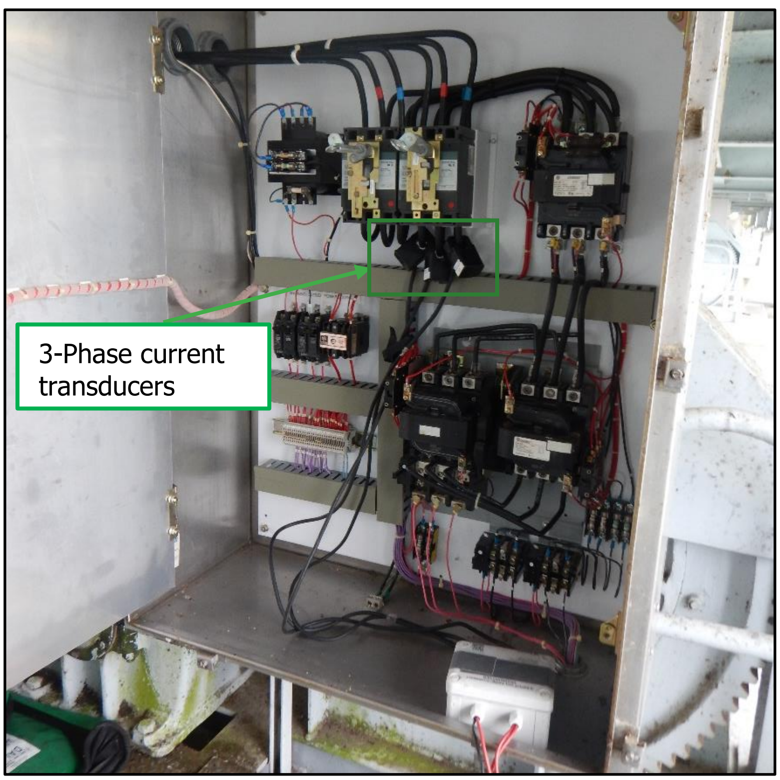

Figure 4 – Current transducers installed on hoist motor controls (Typical)

Figure 5 – BDI personnel installing instrumentation on the gate arm

TESTING PROCEDURES

Structural response data was recorded on all sensors at 50Hz while the gate was run through three spill tests. Each test consisted of three "up-down" cycles (direction reversals) without lowering the gate back to the sill. Each direction reversal consisted of lifting the gate approximately 6-12", pausing for a few seconds, and lowering the gate approximately 6", and repeating until all reversals had been completed.

Results Summary

General Discussions Based on Structural Responses

The following outline contains general discussion points and observations that were made during the data review process. Note: Strain measurements were converted to stress for all subsequent analysis by multiplying the strain values by a steel elastic modulus of 29,000 ksi.

+ **DESCRIPTIONS OF RESPONSE MEASUREMENTS:** All sensor readings were zeroed at the end of each test (which consisted of three cycles of direction reversals) so that each measurement corresponded to response change relative to the final gate position as shown in Figure 6 (gates in the downward "closed" position with the hoist cables slacked as much as possible). It is also worth noting that the stresses did not always start and end at the same levels between tests. This variation in behavior is due to small changes in the flexed gate condition between the start and end of tests. It is common for the flex in the gate, caused by pin friction, to slowly release as it rests on the sill. The purpose of the three up-down cycles per test, prior to sitting the gate back onto the sill, is to ensure that these changes in boundary conditions, including gate flexure due to friction, did not affect BDI's trunnion friction results. ***It is important to note that the recorded measurements were changes in structural response due to gate movement, and do not include the in-situ stresses due to the dead load, cable wrap, and hydrostatic loads present prior to testing.***
+ **QUALITATIVE DATA REVIEW:** Review of the response data indicated a good level of reproducibility between the three tests. For reference, Figure 6 and Figure 7 show stress responses measured along Gate 11's right arm top strut for all three tests (Test #1-3). The data in these plots have been provided as both a function of time and the gate position as determined by the skin plate tilt sensor. Structural response behavior slightly varied during the first test's first cycle compared to subsequent lift/lower cycles and tests, with the first cycle having a slightly smaller change in stress due to pin friction. The observed variation was likely caused by a larger release of built-up pin friction as the gate rested on the sill for a longer period of time.
+ **DIRECTION/FRICTION REVERSAL IN RESPONSES:** The difference in stress during gate opening and closing for a given position is shown in Figure 8. The stress variation at any given gate position was a result of direction reversal and in turn due to trunnion friction reversal. This statement is true since all other loads such as dead-load and hydrostatic pressure were essentially constant barring small changes in hydrostatic pressure due to slight changes in head. This direction/friction reversal is depicted in Figure 9, with deflected shape renderings from a gate arm finite element model under lifting and lowering loads. Note that this figure shows an arm configuration that does not match this gate, but the concept of the direction/friction reversal still applies.
+ **MOTOR PERFORMANCE:** Current measurements taken at the hoist motor indicated steady and stable current draws during the lifting and lowering portions. An example plot of current draw and gate position is provided in Figure 10. Current draw ranges during lifting were higher than the ranges during lowering, which is common due to gravity/dead load. These results are summarized along with recorded peak in-rush current in Table 2. Note that the sample rates used during testing were set for collecting gate responses and may not have been appropriate to fully capture the in-rush current. The readings should be evaluated by a licensed electrician with knowledge of the operating parameters.
+ **TORQUE AND HOIST FORCE:** Due to restrictions caused by the hoist limit switches, the hoist cables could not always be fully slacked at the beginning and end of the performed tests. Throughout testing of the Rockwell Forney gates, it was found that this limit switch restriction varied gate to gate and arm to arm. Therefore, it is not recommended to use the collected torque and hoist force data to quantify overall hoist forces. Rather, this data was utilized to evaluate total friction behavior, which is observed as half the difference between the lifting and lowering torque/force (friction reversal).

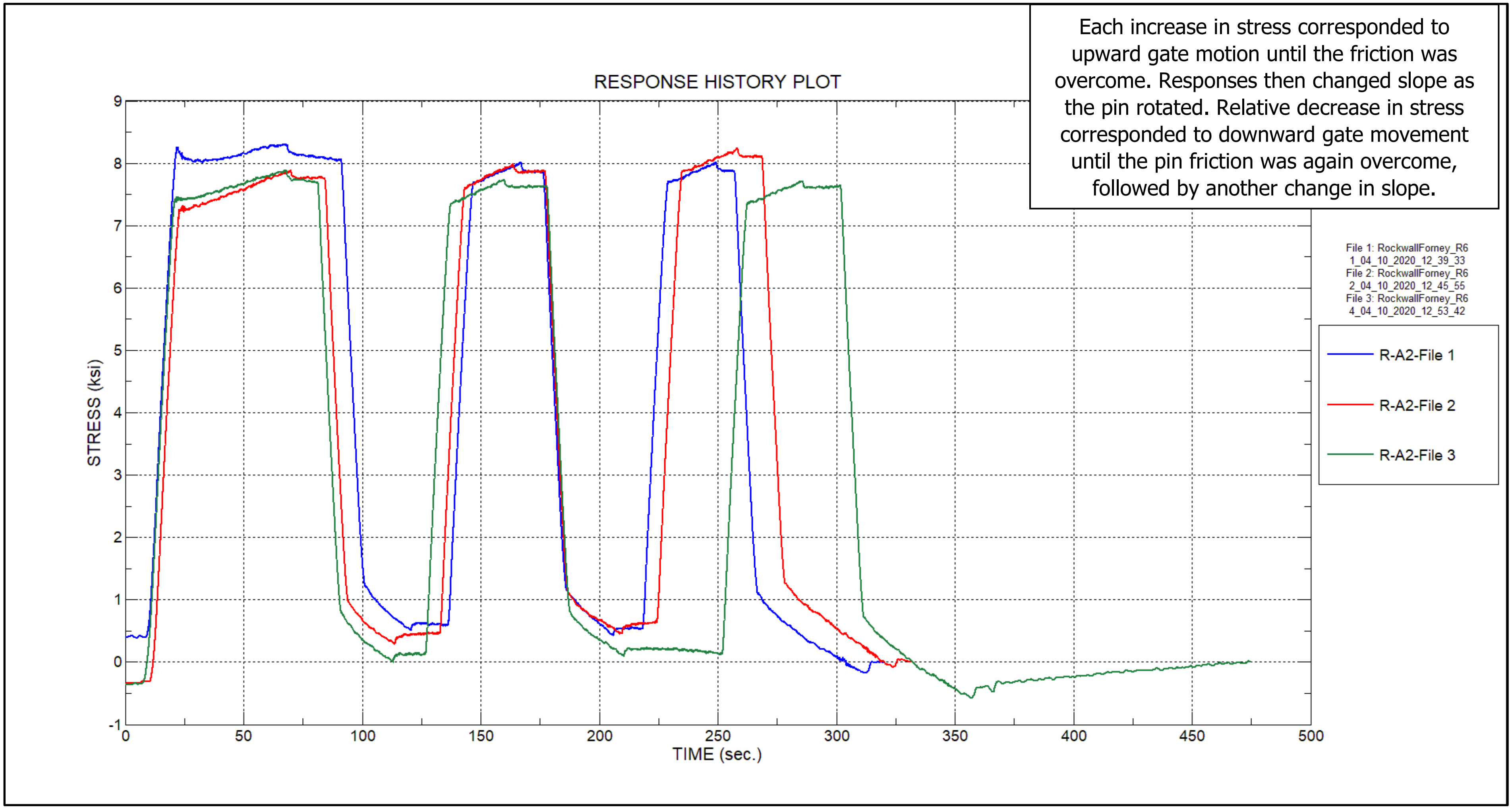

Figure 6 – Stress response history – Right arm – Gage A2 – Time based
File 1 = test run 1, File 2 = test run 2, File 3 = test run 3

(Section A along top strut near pin – Sensor location 2 along bottom of inner flange)

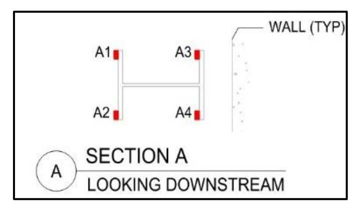

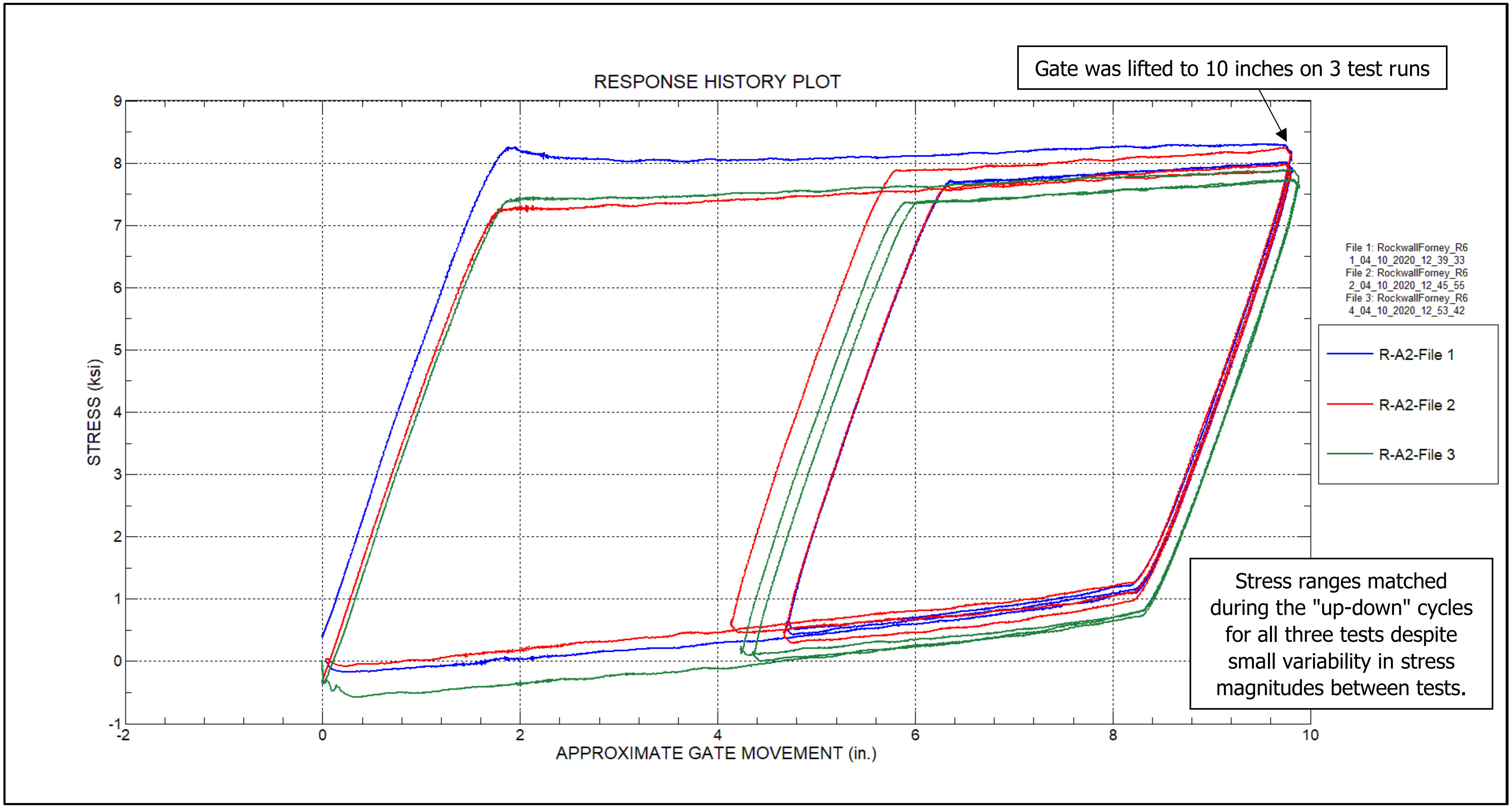

Figure 7 – Stress response history – Right arm – Gage A2 – Function of gate movement
File 1 = test run 1, File 2 = test run 2, File 3 = test run 3

(Section A along top strut near pin – Sensor location 2 along bottom of inner flange)

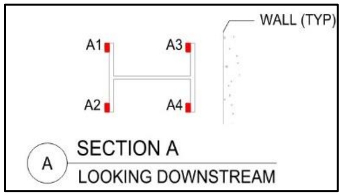

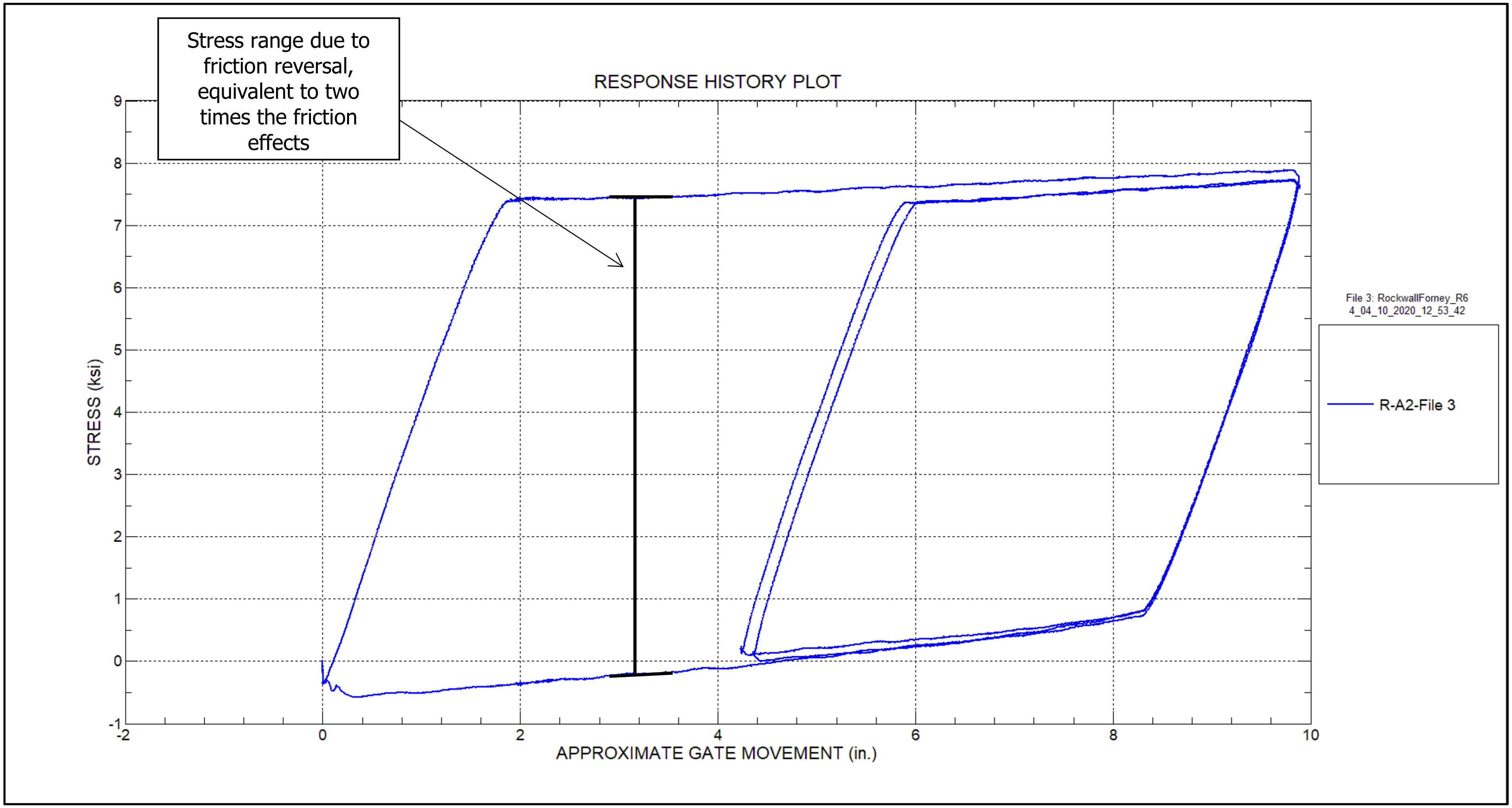

Figure 8 – Stress response history – Right arm – Gage A2 – Friction effect in stress responses

(Section A along top strut near pin – Sensor location 2 along bottom of inner flange)

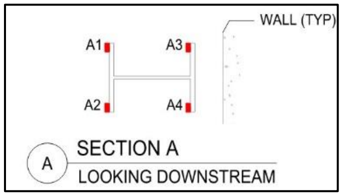

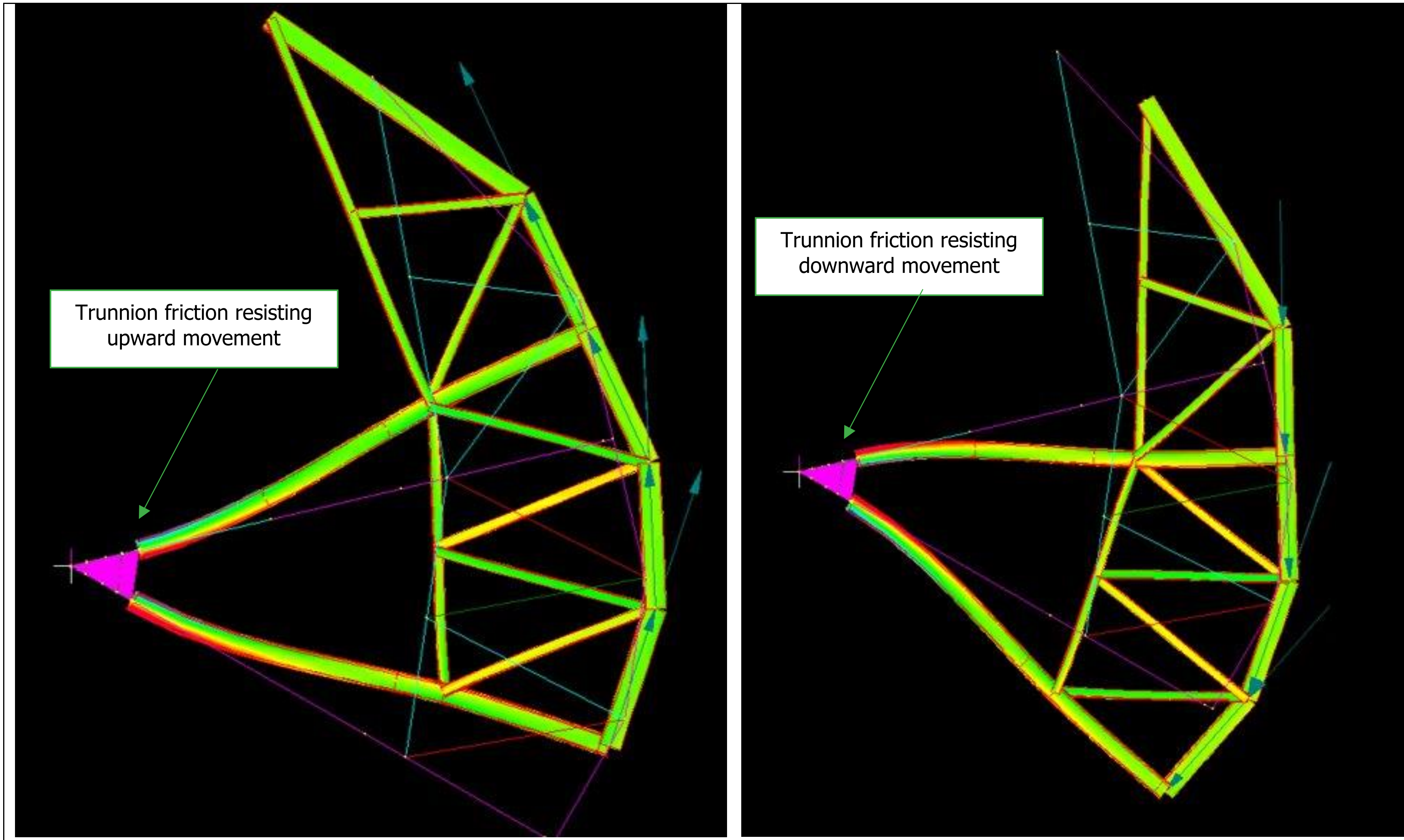

Gate traveling upward **Gate traveling downward**

Figure 9 – Deflected shapes during lifting and lowering of Gate – Visualization of direction/friction reversals

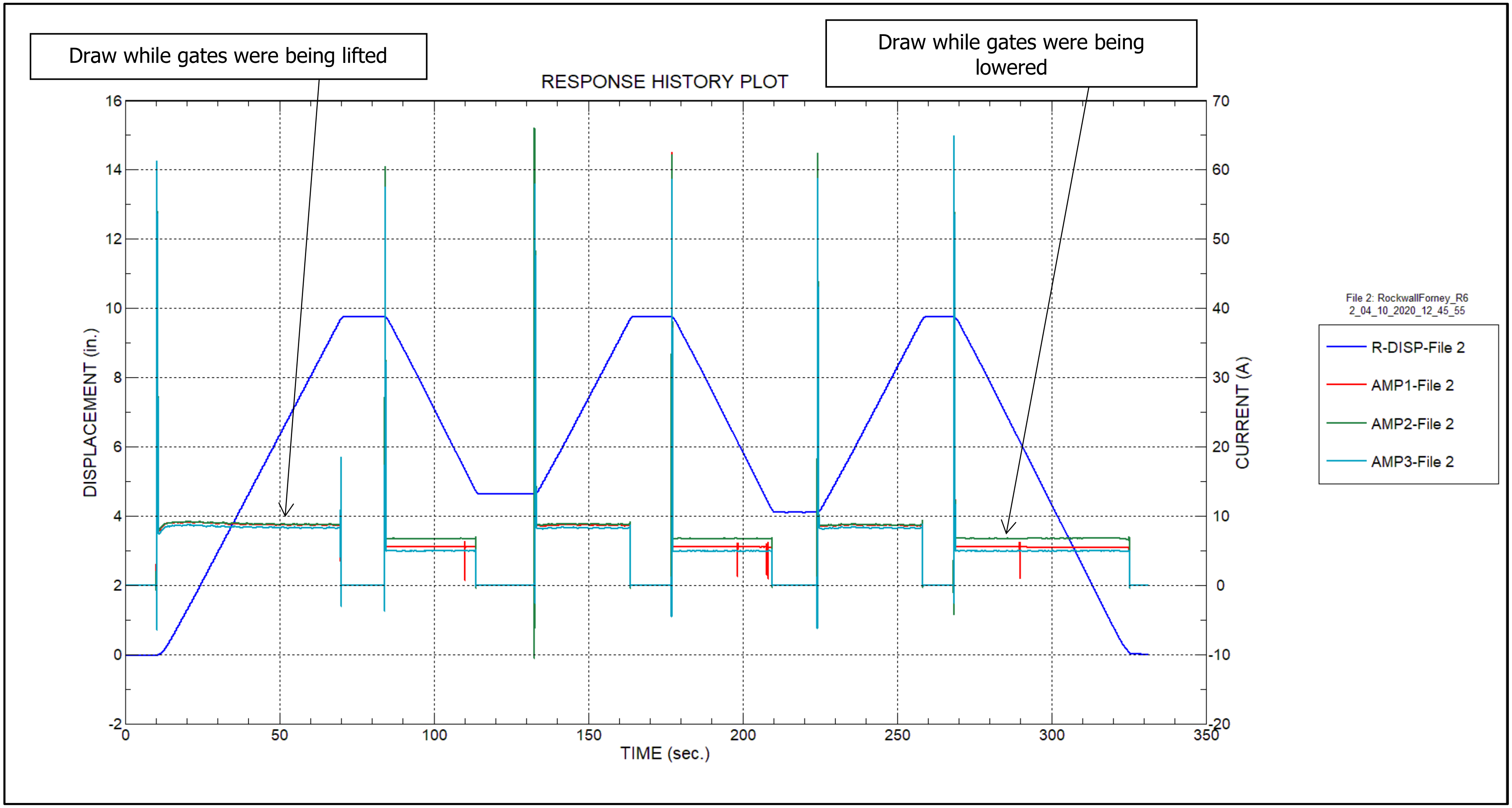

Figure 10 – Motor current & gate movement response history – Lift motor – Highlighting motor draw during lift and lower cycles

Methodology and Findings of The Strut Force and Moment Calculations

The following outline provides the methodology used to calculate the required member forces and moments.

- **CHANGE IN STRESS DUE TO GATE OPERATION:** Strain data can be viewed as a function of time starting when the gate was in the down position and was then lifted off the sill. When examining data in this manner, it is easy to see how stresses ramped up as the gate began to move and then changed slope once pin friction was overcome and the trunnion hub began to rotate with the gate. The first point in time where the friction was overcome (both lifting and lowering) has been highlighted in the stress histories shown in Figure 11. These stress histories show the response of all four sensors along the top strut of the right arm (Section A). ***It is important to note that the recorded measurements were changes in structural response due to gate movement, and do not include the in-situ stresses due to the dead load, cable wrap, and hydrostatic loads present prior to testing.***
- **CALCULATION OF STRUT CROSS-SECTIONAL MOMENTS:** The use of four strain gages per strut cross-section allowed accurate in-plane flexural bending moments to be computed from the recorded strain measurements. These moments were computed for every cross-section in each gate arm using the basic mechanics equation provided in Figure 12.

  In-plane or weak-axis flexure refers to bending about a given strut's web. This designation is consistent with typical nomenclature. In-plane bending can be observed visually from the strain response histories as a difference between the top and bottom stresses, whereas out-of-plane or strong-axis bending is visualized as the difference in stress from side to side. Figure 13 provides a visual reference for both types of strut flexure.
- **EXAMINATION OF RESPONSES AS A FUNCTION OF GATE POSITION:** Changes in cross-sectional moment related to friction becomes clearer when the responses are plotted as a function of gate position. Because the gate was operated with several up and down movements, the effects of friction associated with each direction reversal can be viewed for all measured and calculated responses. Figure 14 through Figure 17 show all cross-sectional flexural moment plots for both trunnion arms. The responses in these plots have been centered about the stress state corresponding to a zero-moment, unflexed condition. The zero-moment offset was estimated as the average moment values between up and downward movement (i.e. half the moment difference) at the gate position with the greatest pin friction moment difference (greatest difference between lifting and lowering).
- **TRUNNION FREE-BODY-DIAGRAM & PIN MOMENT CALCULATION:** Figure 18 shows the instrumented member cross-sections and shows how the measured cross-sectional flexural responses were used to compute pin moment. The in-plane moment values used in these calculations were determined directly from the strain measurements at each cross-section using the provided mechanics equations. It should be noted that the out-of-plane moments were not considered in the calculation of pin moment since they were orthogonal to the axis of the pin rotation. Total pin moment was then determined by summing all the moment components about the pin, which included the in-plane moment and the shear components at the strut cross-sections nearest the pin.
- **STRUT SHEAR CALCULATION:** From the examination of the trunnion free-body-diagram described above, the shear vectors at the three struts were a primary component in the pin moment calculation. For this type of structural element, shear vectors were calculated using the moment differential between the two cross sections along each strut. It is important to recognize that shear was constant between the two instrumented cross-sections and the applied shear was a function of the recorded change in moment ($V = dM/dX$). Subsequently, the shear vectors were calculated by dividing the difference in moment by the distance between the two instrumented cross-sections. Shear values for each strut have been plotted as a function of gate position in Figure 19 and Figure 20.

- **CALCULATION OF PIN MOMENT DUE TO FRICTION:** Once all the trunnion arm force vectors were calculated, the equations shown in the free-body-diagram were applied to compute pin moment as a function of gate position. It is important to note that because the calculated pin moment range corresponds to a direction reversal, a reversal in friction also occurred. The effect of direction reversal on pin moment due to friction is best conceptualized by centering the moment response plots about the zero-moment axis. The moment due to lifting and the moment due to lowering can then be visualized as a change from this new zero point corresponding to the gate in an unflexed condition. Therefore, the total moment differential between lifting and lowering was twice the moment due to friction acting in a single direction. Pin-moment plots have been provided in Figure 21 and Figure 22. From these plots, it is apparent that pin moment due to friction remained relatively constant throughout the gate operation tests, with a slight decrease in pin friction moment as the gate continued to be lifted. This slight decrease in pin friction moment most likely corresponded to the change in hydrostatic load as the gate position changed. Pin-moment plots for all tests on Gate 11 are also provided for reference in Appendix B – Gate 11 Pin Moment Component Plots.
- **SHAFT TORQUE & HOIST FORCE:** Torque measurements were taken on the pinion shafts near the hoist motor during testing, with single torque gages installed on the left and right hoist pinion shaft. Responses were recorded in units of micro-strain and converted to torque in units of kip-ft using Equation 1 thru Equation 3 and the following shaft properties.

$$d_O = 5.5\ inches, \qquad d_I = 0\ inches, \qquad E = 29000\ ksi, \qquad \nu = 0.3$$

$$G = \frac{E}{2(1+\nu)}$$

Equation 1

$$J = \frac{\pi\left({d_O}^4 - {d_I}^4\right)}{32}$$

Equation 2

$$\tau = \varepsilon * \frac{2GJ}{\frac{d_O}{2} * 1000000 * 12}$$

Equation 3

Figure 23 shows example torque measurements, recorded on the Gate 11 torque shafts. Best practices for torque measurements is to measure torque on opposite sides of the shaft so that any bending in the shaft can be removed by averaging the two responses. Due to access limitations, only one gage at each location could be installed. Therefore, any bending in the shaft may be reflected in the torque measurements and may be related to the peaks and valleys observed in the torque responses.

Torque values were converted to force in the hoist cables per gate arm using the gear ratio and drum radius, as shown in Figure 24. The gear ratio and drum radius were 5.182 and 1.086 feet respectively, as defined in the provided as-built shop drawings. It should be noted that the hoist force calculated may be smaller than the actual hoist force applied. This difference is due to the limit switch engaging the brake before the hoist cable was fully slacked, resulting in an initial force in the cable. A hoist force due to total gate friction was then calculated. This friction hoist force was equal to half the differential in force measured during the lifting and lowering of the gate (similar to the pin friction calculations). As shown in Table 3, the change in cable force due to friction was generally consistent between tests. Note that the total hoist force was due to the total friction effects, including side seal, hoist bearings, trunnion friction effects, etc. It is difficult to determine the exact proportion and composition of the total friction sources. Additional torque and hoist force plots for all collected data files are provided in Appendix A – Gate 11 Torque and Hoist Force Plots.

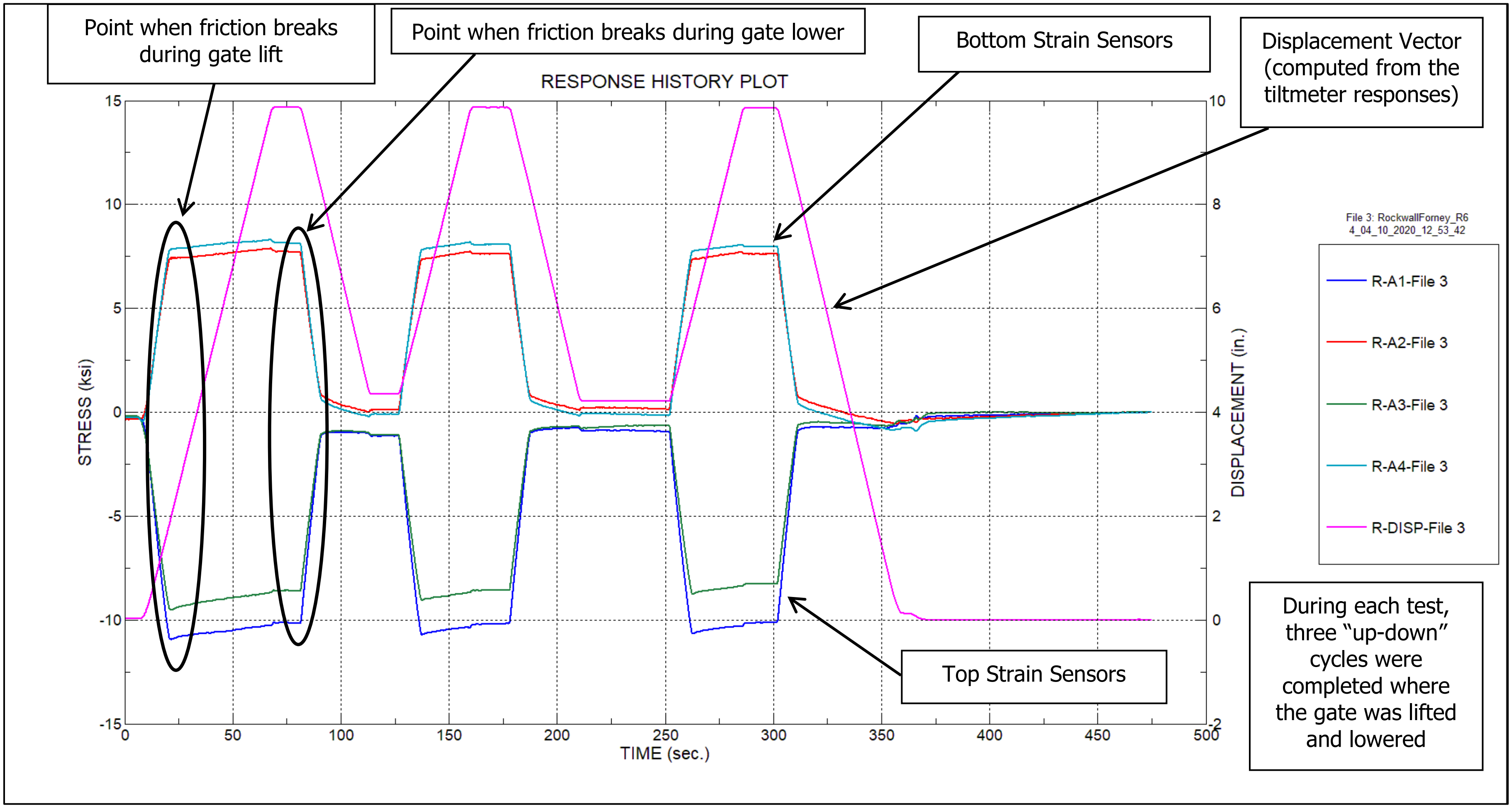

Figure 11 – Stress response & gate movement history – Right arm – Section A - Highlighting friction behavior
(Section A along top strut near pin)

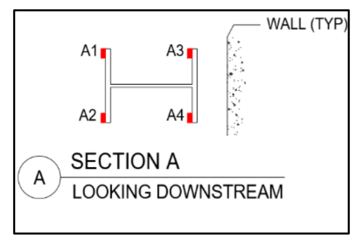

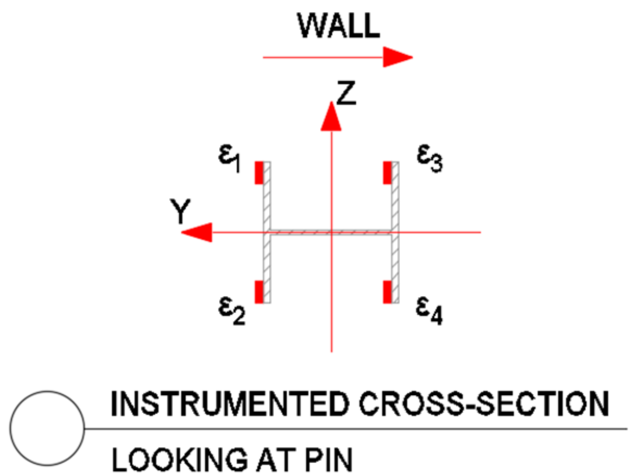

Calculation of Weak-axis (In-plane) bending

$$M_Y = \frac{E\left[\frac{\varepsilon_2 + \varepsilon_4}{2} - \frac{\varepsilon_1 + \varepsilon_3}{2}\right] S_{Y(gage)}}{2}$$

Sy(gage) = Section modulus to the center of gages (not extreme fiber of flanges)
(locations of gages were accounted for in moment computation)

Figure 12 – Basic mechanic equation used to calculate moment

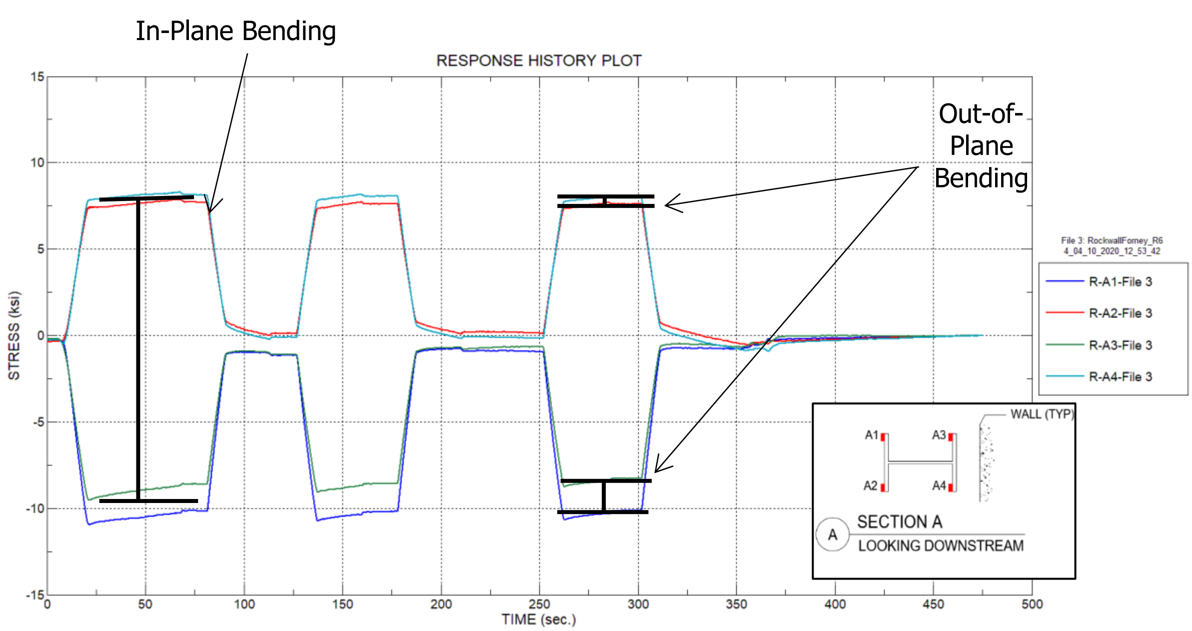

Figure 13 – Stress response history – Right arm – Section A – Bending components
(Section A along top strut near pin)

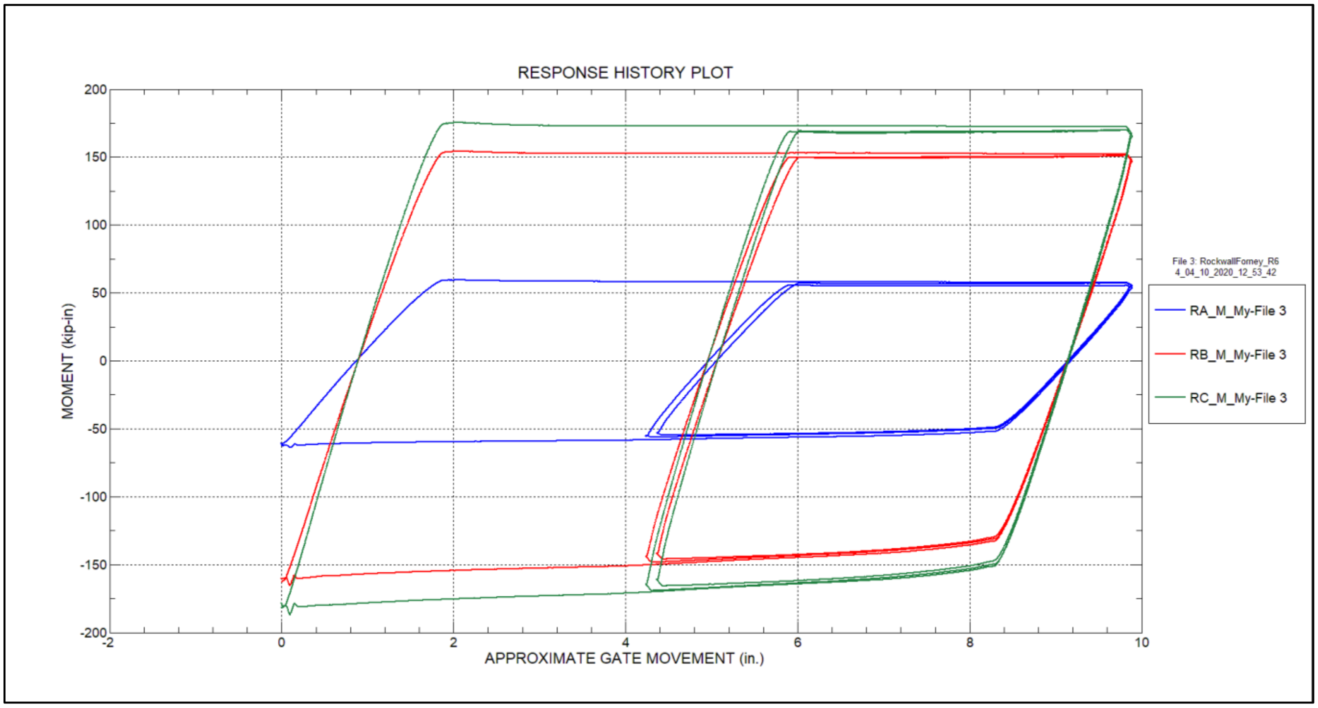

Figure 14 – In-plane moment response history – Right arm – Sections near pin

(RA = Right Arm Top Strut, RB = Right Arm Middle Strut, RC = Right Arm Bottom Strut)

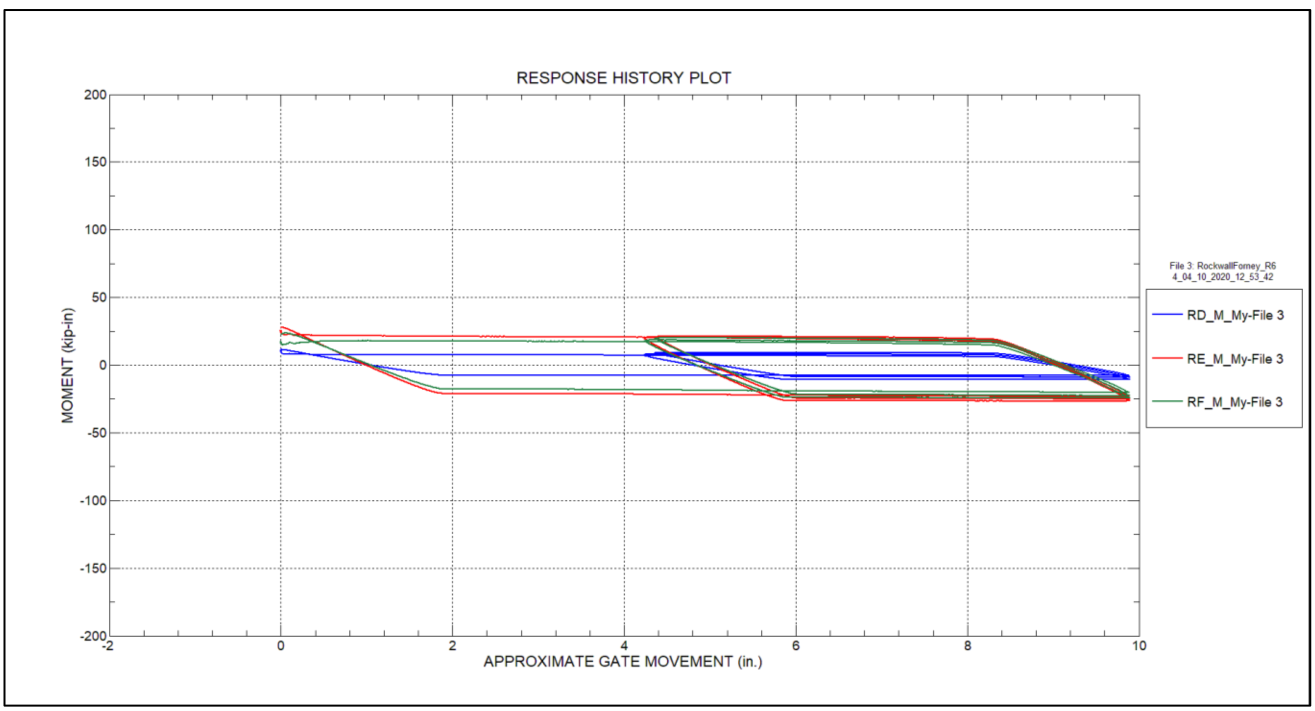

Figure 15 – In-plane moment response history – Right arm – Sections away from pin

(RD = Right Arm Top Strut, RE = Right Arm Middle Strut, RF = Right Arm Bottom Strut)

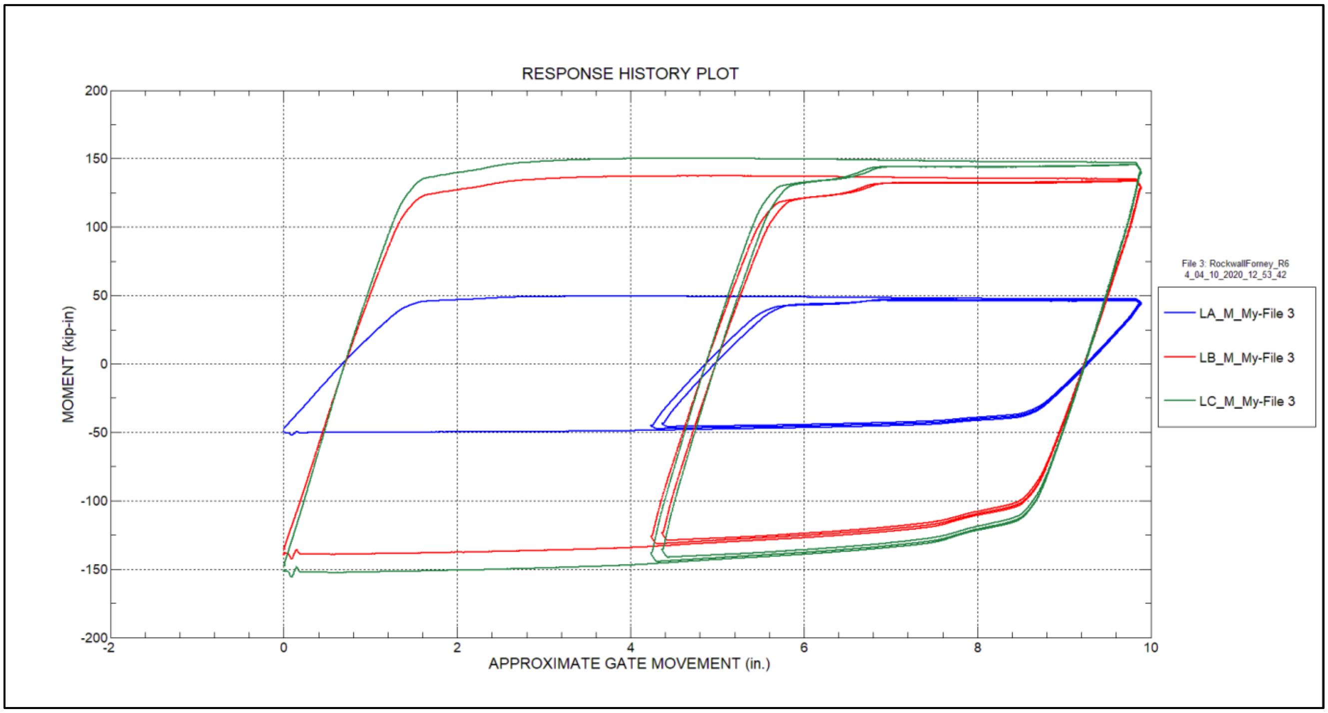

Figure 16 – In-plane moment response history – Left arm – Sections near pin

(LA = Left Arm Top Strut, LB = Left Arm Middle Strut, LC = Left Arm Bottom Strut)

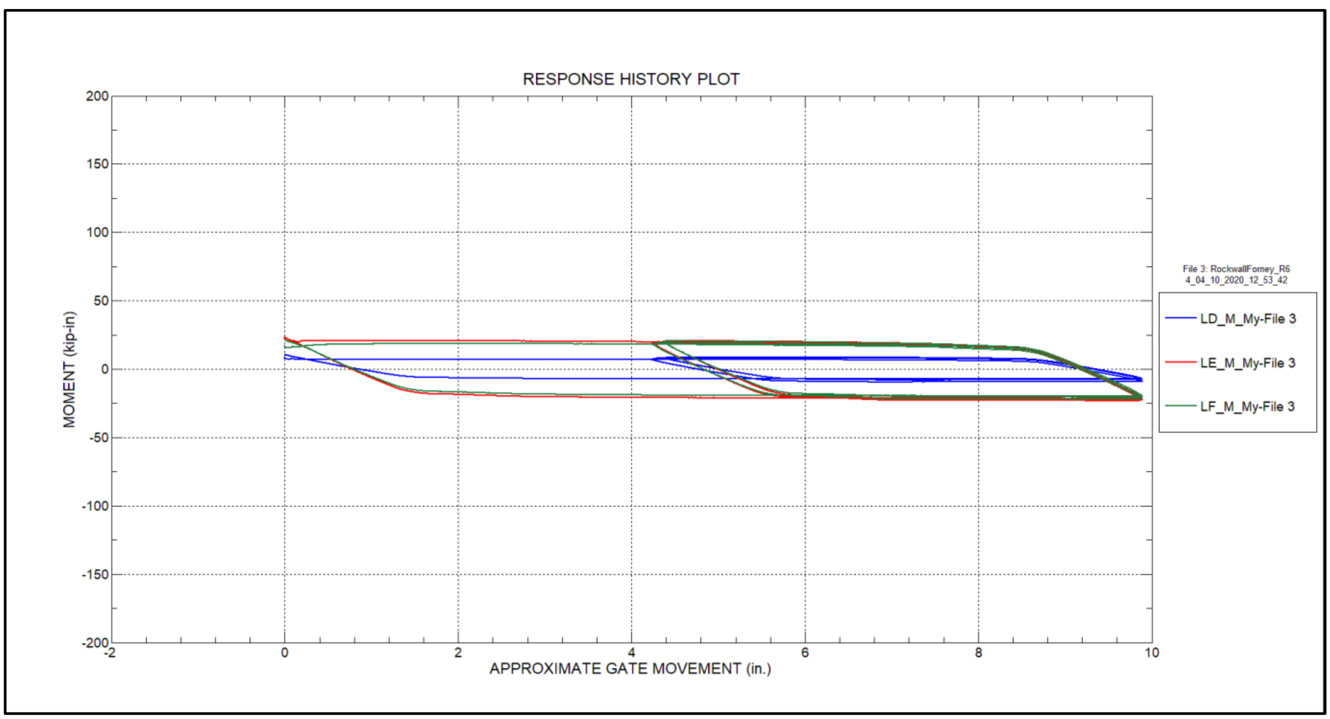

Figure 17 - In-plane moment response history – Left arm – Sections away from pin

(LD = Left Arm Top Strut, LE = Left Arm Middle Strut, LF = Left Arm Bottom Strut)

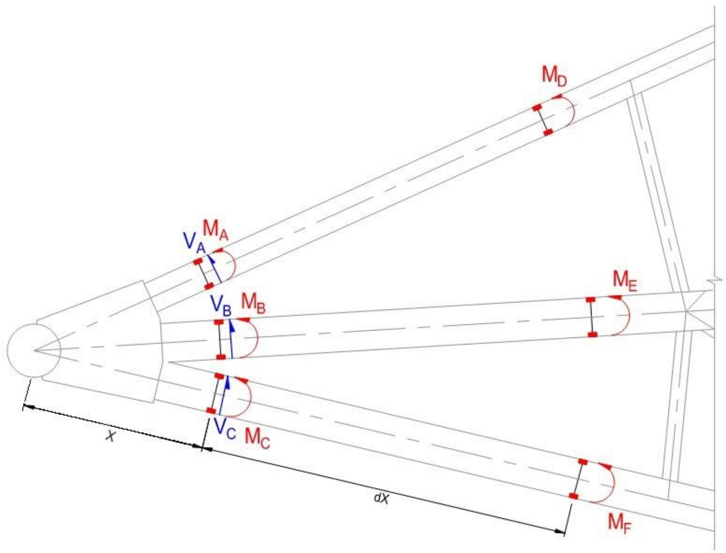

Elevation View of Gate Arm

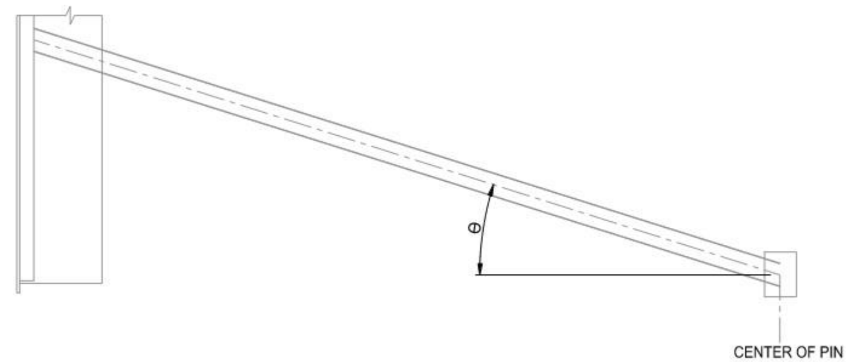

Plan View of Gate Arm

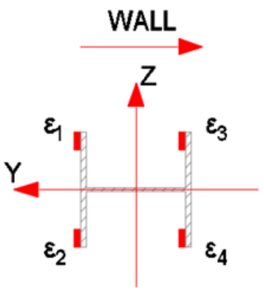

$$M_Y(M_A, M_B, M_C, M_D, M_E, M_F) = \frac{E\left[\frac{\varepsilon_2+\varepsilon_4}{2} - \frac{\varepsilon_1+\varepsilon_3}{2}\right] S_{Y(gage)}}{2}$$

$$V_A = \frac{M_A - M_D}{dX}$$

$$V_B = \frac{M_B - M_E}{dX}$$

$$V_C = \frac{M_C - M_F}{dX}$$

$$\sum M_o = 0$$

$$M_{PIN} = [X(V_A + V_B + V_C) + M_A + M_B + M_C]\cos\theta$$

Figure 18 – Direct calculation of pin moment from strain measurements

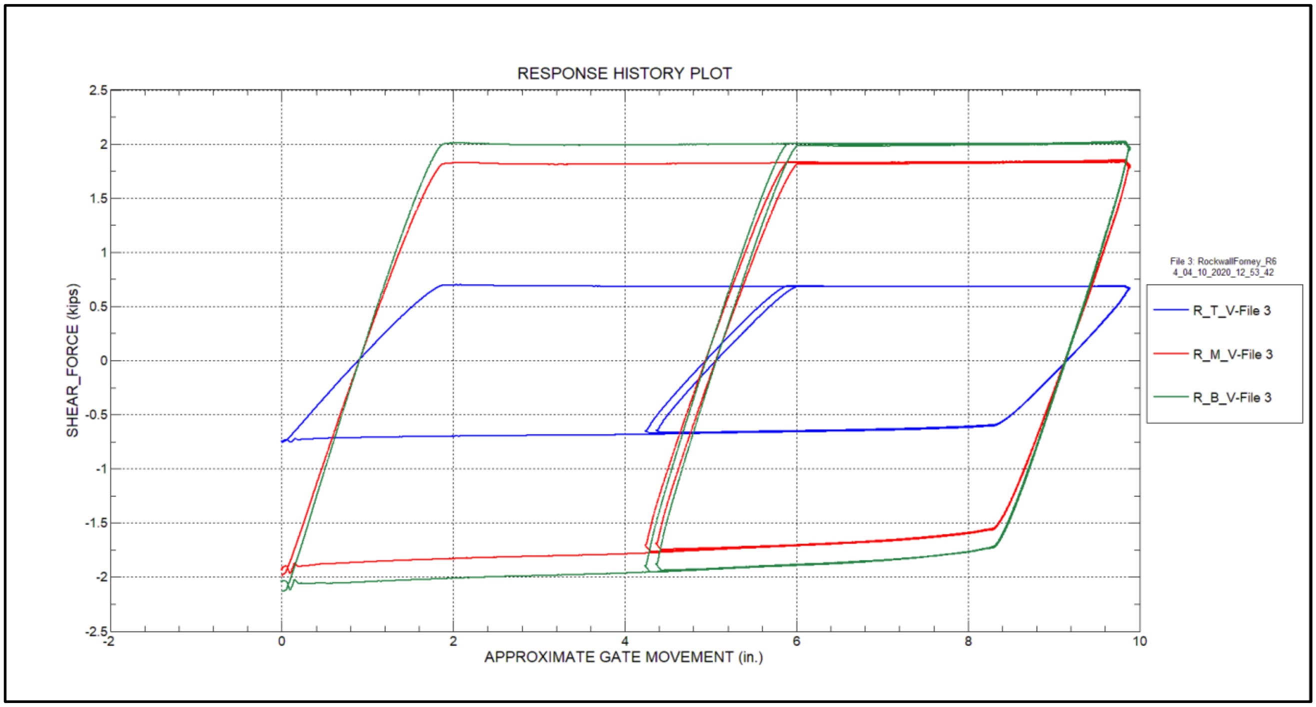

Figure 19 – Strut shear response history – Right arm

(R_T = Right Arm Top Strut, R_M = Right Arm Middle Strut, R_B = Right Arm Bottom Strut)

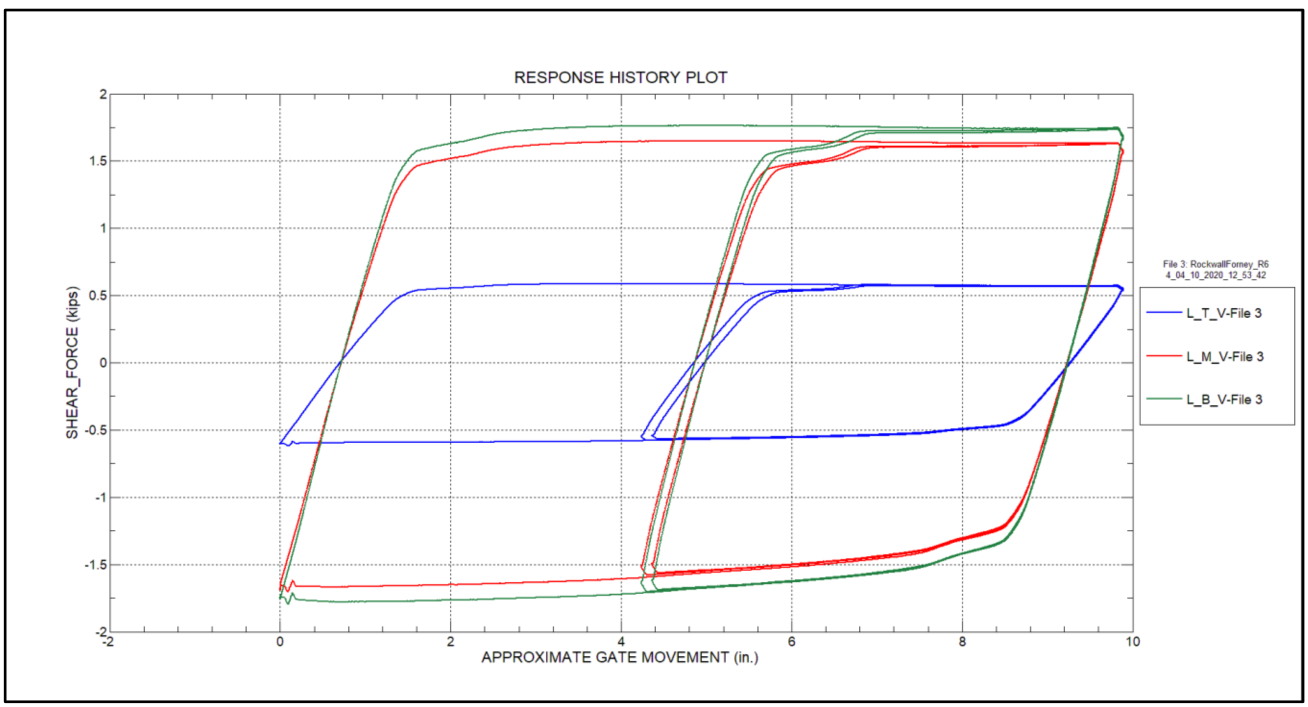

Figure 20 – Strut shear response history – Left arm

(L_T = Left Arm Top Strut, L_M = Left Arm Middle Strut, L_B = Left Arm Bottom Strut)

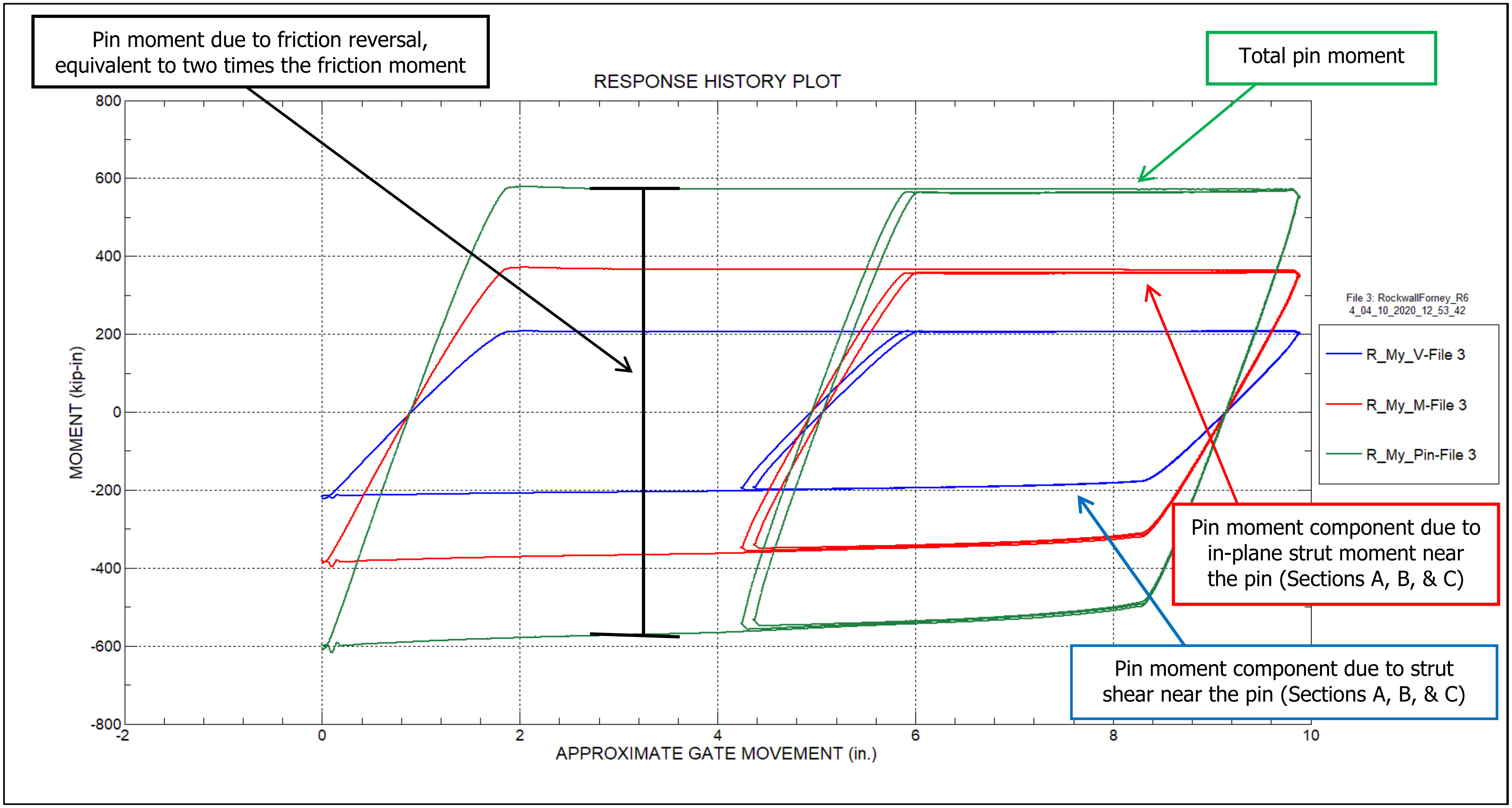

Figure 21 – Pin moment response history – Right arm

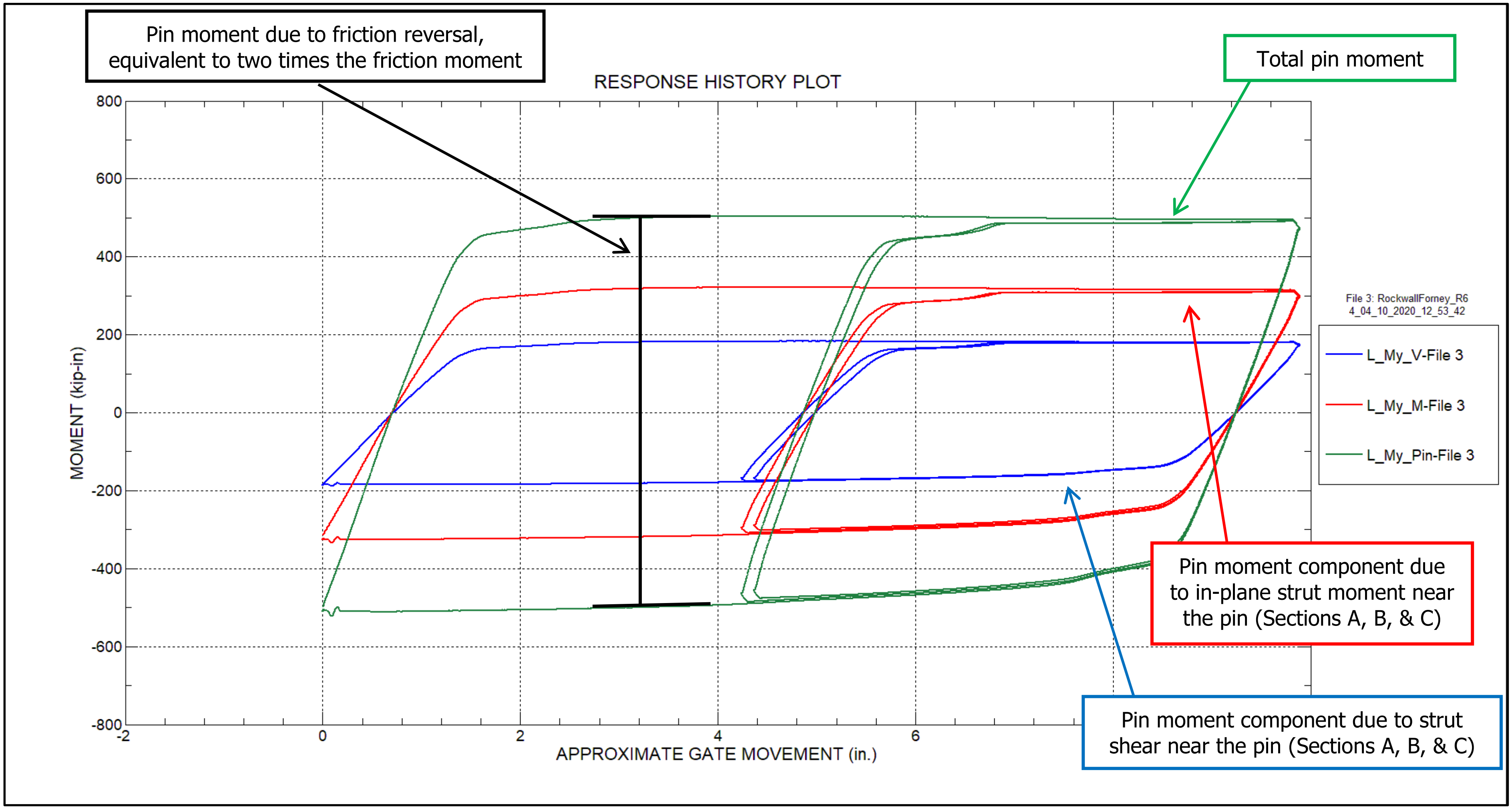

Figure 22 – Pin moment response history – Left arm

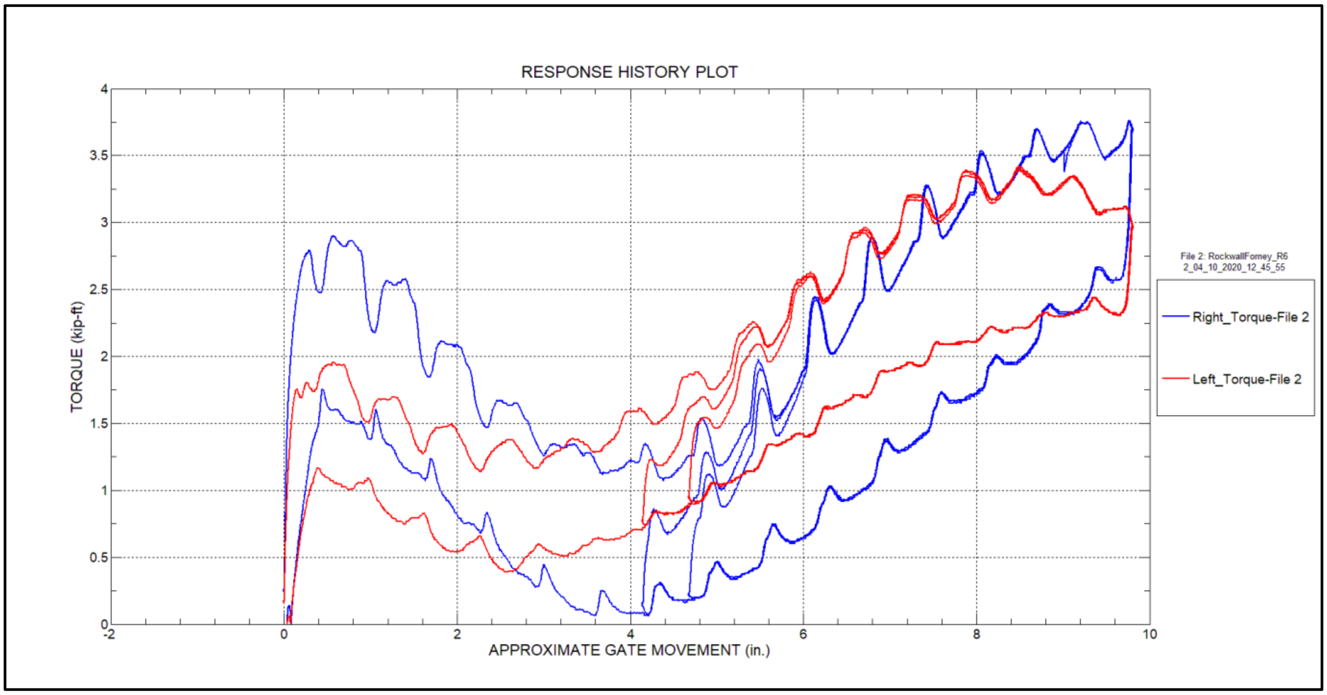

Figure 23 – Hoist torque response history – Gate 11 – Test 2

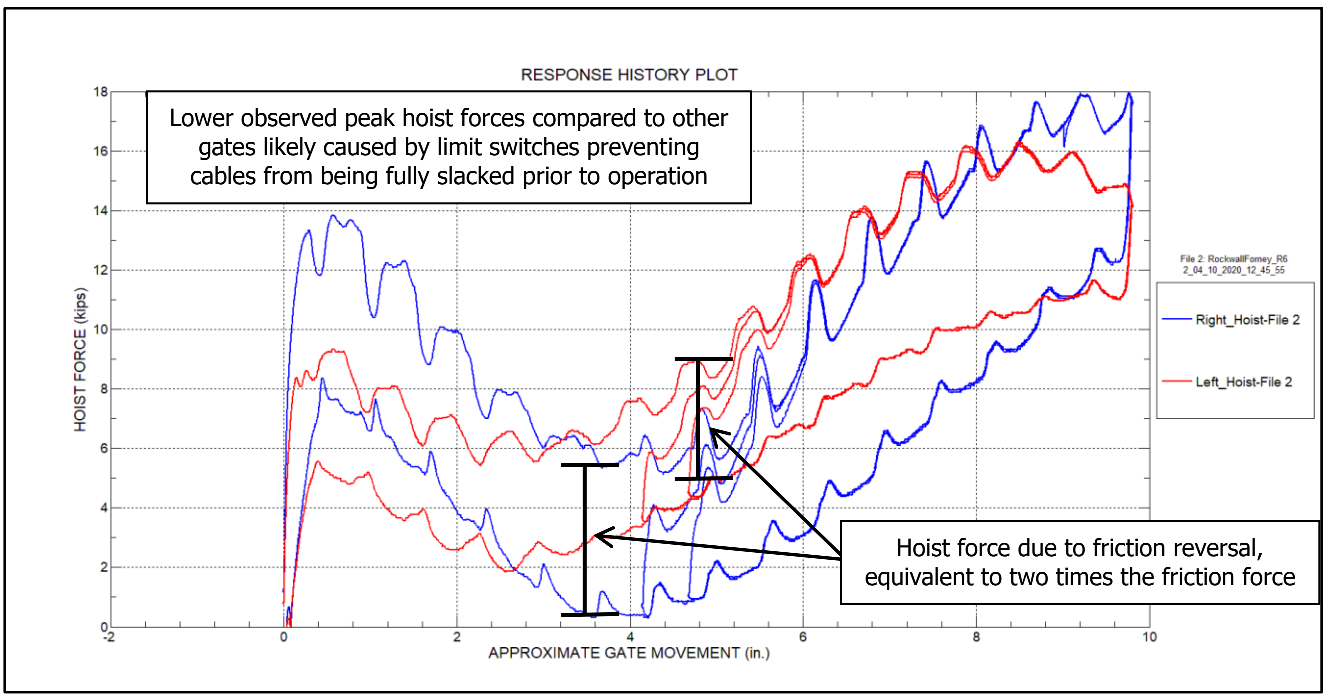

Figure 24 – Hoist force response history – Gate 11 – Test 2

SUMMARY OF FRICTION RESULTS

The raw data files have been included in the submittal package for reference and were formatted as "tdms" files that can be opened in Microsoft Excel using a "tdms" reader extension.

Examination of the stress histories for each test was necessary to obtain a thorough understanding of the gate performance. The response shapes, variations in stress magnitudes, and timing sequences provided direct clues as to how the gate performed under typical service conditions. The following is a breakdown of the provided tabulated results:

+ Table 2 provides motor current ranges and maximum in-flow for lift and lower cycles for each test
+ Table 3 provides maximum hoist force as well as hoist force due to total friction for each test
+ Table 4 provides the maximum stress ranges measured at the sensor locations for each member
+ Table 5 provides maximum bending stress and moment ranges observed during the gate tests
+ Table 6 provides maximum friction bending stress and moment values at each of the instrumented strut locations
+ Table 7 provides the computed shear values in each strut due to friction
+ Table 8 provides calculated measured friction moments, calculated hydrostatic loads based on the measured water elevation, and coefficients of friction for each gate and gate arm during all three tests

The resulting pin friction moments were used to compute friction coefficients from Eq. 4, given the pin radius and the applied thrust. The thrust used in this calculation consisted of the calculated resultant hydrostatic load based on the measured water elevation and was adjusted to account for the loss of head as the gate was lifted. This thrust adjustment was based on the recorded gate movement and was performed in order to calculate more accurate friction coefficients. The water elevation during testing was nearly constant throughout each gate test and was documented during each "up-down" cycle. It should be noted that the minor thrust due to cable wrapping, which was minimal compared to hydrostatic thrust, was not included in the thrust calculation. This assumption resulted in slightly conservative friction coefficients.

$$\mu = \frac{M_F}{T * r} \qquad \text{Eq. 4}$$

where: μ = Friction Coefficient

M_F = Friction Moment

T = Thrust per Pin

r = Pin Radius, 5.375"

The out-of-plane shear and moments were not considered in the pin friction calculations due to orthogonal geometry considerations (resulting pin moment associated with out-of-plane flexure being perpendicular to pin rotation).

The data was presented in a specific coordinate system applicable to both arms. Data was processed so that the positive x-axis was always pointing towards the pin and the right-hand rule applied. In-plane bending can be referred to as "bending about the horizontal or y-axis" and shows how much the beams bend up and down within the plane of the gate arms. Refer to Figure 12 above for visual reference of coordinate system and mathematical explanation of calculations. Tabulated results do not include any in-situ effects.

Table 2 – Motor current summary table – Gate 11

Test Run	Current Range due to Lifting (A)	Current Range due to Lowering (A)	Max In-rush Current (A)
1	8-10	5-7	67
2	8-9	5-7	66
3	8-9	5-7	66

Table 3 – Hoist force summary table – Gate 11

Test Run	Right Arm Peak Hoist Force (kips)	Left Arm Peak Hoist Force (kips)	Right Arm Hoist Force due to Total Gate Friction (kips)	Left Arm Hoist Force due to Total Gate Friction (kips)
1	17.45	15.86	4.63	3.06
2	17.95	16.34	4.47	3.07
3	35.18	21.35	4.43	3.11

Tabulated friction force values correspond to the response induced by friction in one direction

Table 4 – Maximum measured sensor stress range

Arm Designation	Top Strut (ksi)	Middle Strut (ksi)	Bottom Strut (ksi)
Right Arm	10.96	12.83	13.02
Left Arm	9.25	12.02	11.92

Tabulated values correspond to the total measured change in response during tests

Stress values have not been extrapolated to the extreme fibers (correspond to center of gage)

Table 5 – Maximum in-plane total bending stress & moment ranges – Total

Section Label	Section Description	Right Arm Stress (ksi)	Right Arm Moment (kip-in)	Left Arm Stress (ksi)	Left Arm Moment (kip-in)
Section A	Top Strut Near Pin	11.19	125.72	9.02	101.38
Section B	Middle Strut Near Pin	14.16	327.52	12.12	280.27
Section C	Bottom Strut Near Pin	13.35	372.29	11.09	309.26
Section D	Top Strut Away from Pin	1.99	22.34	1.77	19.87
Section E	Middle Strut Away from Pin	2.38	54.97	2.00	46.36
Section F	Bottom Strut Away from Pin	1.74	48.56	1.66	46.25

Tabulated values correspond to the total measured change in response during tests

Table 6 – In-plane frictional bending stress & moment at maximum gate friction

Section Label	Section Description	Right Arm Stress (ksi)	Right Arm Moment (kip-in)	Left Arm Stress (ksi)	Left Arm Moment (kip-in)
Section A	Top Strut Near Pin	5.49	61.73	4.46	50.15
Section B	Middle Strut Near Pin	6.97	161.30	5.98	138.35
Section C	Bottom Strut Near Pin	6.59	183.80	5.49	153.10
Section D	Top Strut Away from Pin	0.74	8.30	0.70	7.90
Section E	Middle Strut Away from Pin	0.98	22.77	0.96	22.25
Section F	Bottom Strut Away from Pin	0.74	20.59	0.81	22.58

Tabulated values correspond to the response induced by friction in one direction

Table 7 – Strut shear range summary table due to friction

Arm Designation	Top Strut Shear (kip)	Middle Strut Shear (kip)	Bottom Strut Shear (kip)
Right Arm	0.73	1.91	2.11
Left Arm	0.60	1.67	1.83

Tabulated values correspond to the response induced by friction in one direction

Table 8 – Pin friction summary table

Test Run	Average Water Elevation during testing (ft)	Approximate Thrust at time of Testing (kips per arm)	Gate/Member Designation	Pin Friction Moment (kip-in)	Friction Coefficient
1	435.54	487.70	Right Pin	604.90	0.23
			Left Pin	513.70	0.20
2	435.54	487.70	Right Pin	577.00	0.22
			Left Pin	502.10	0.19
3	435.54	487.70	Right Pin	579.60	0.22
			Left Pin	500.30	0.19

Tabulated values correspond to the response induced by friction in one direction

APPENDIX A – GATE 11 TORQUE AND HOIST FORCE PLOTS

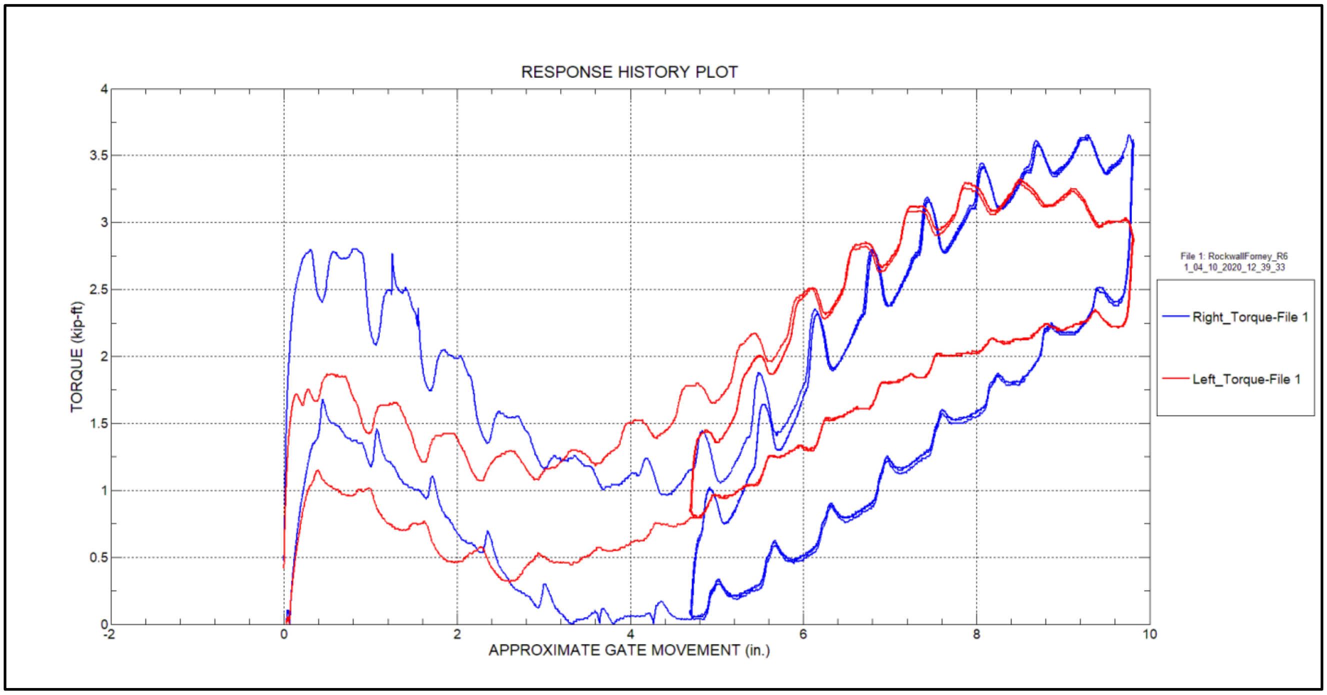

Figure 25 – Hoist torque response history – Gate 11 – Test 1

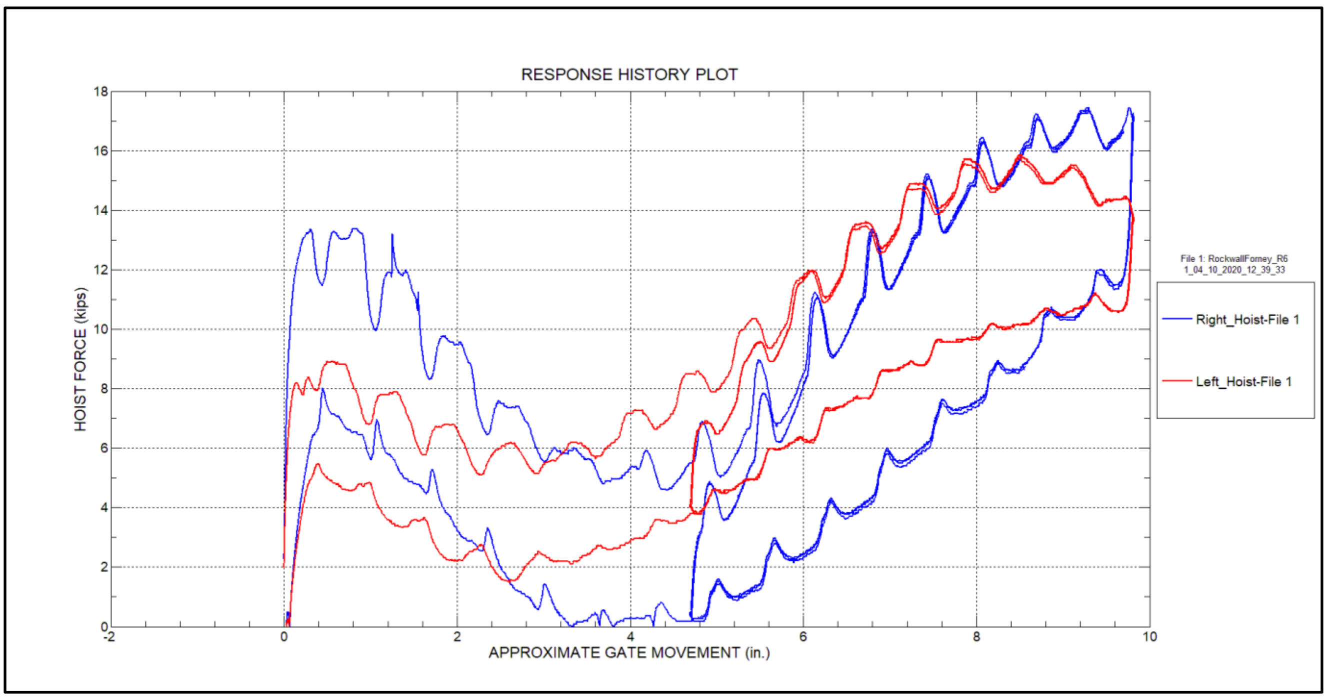

Figure 26 – Hoist force response history – Gate 11 – Test 1

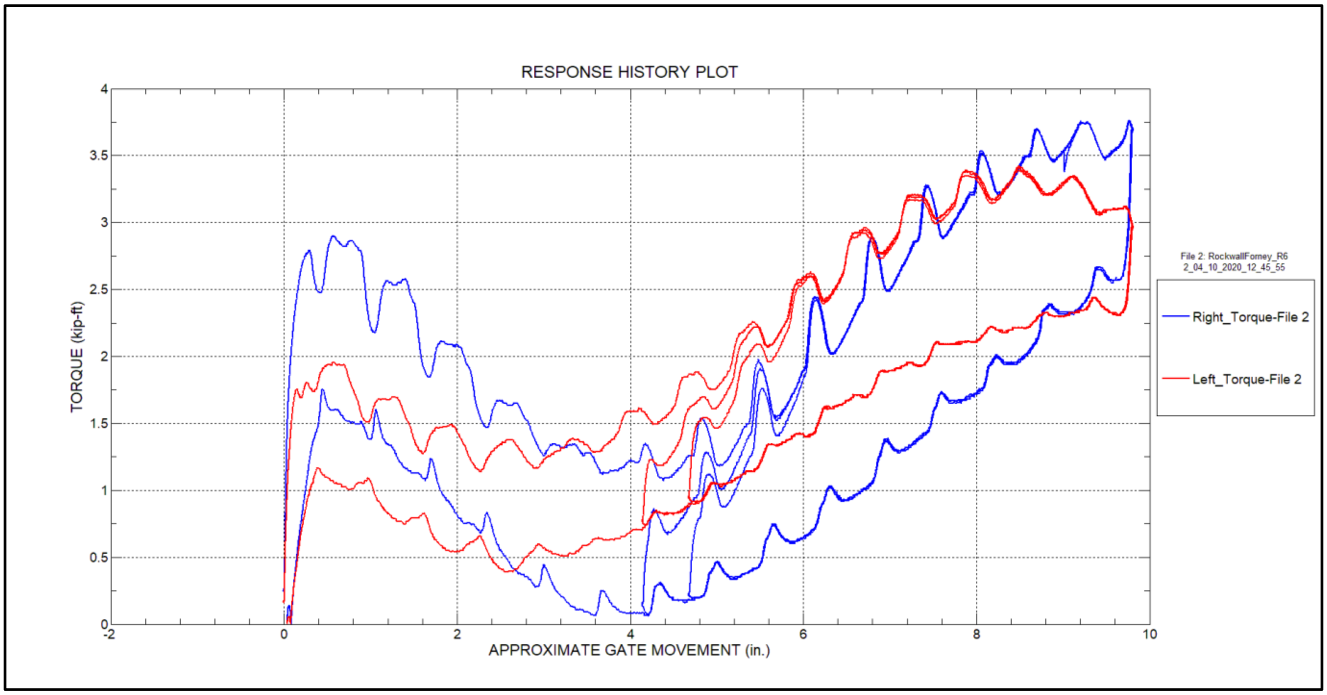

Figure 27 – Hoist torque response history – Gate 11 – Test 2

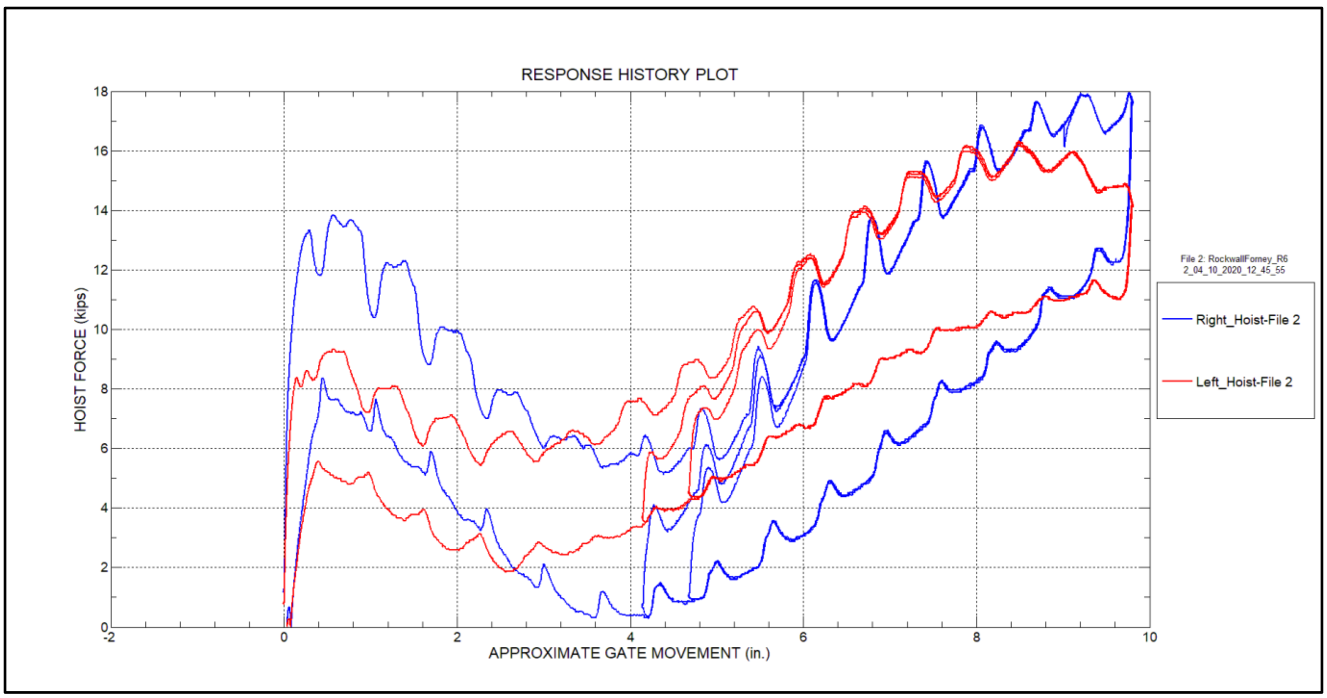

Figure 28 – Hoist force response history – Gate 11 – Test 2

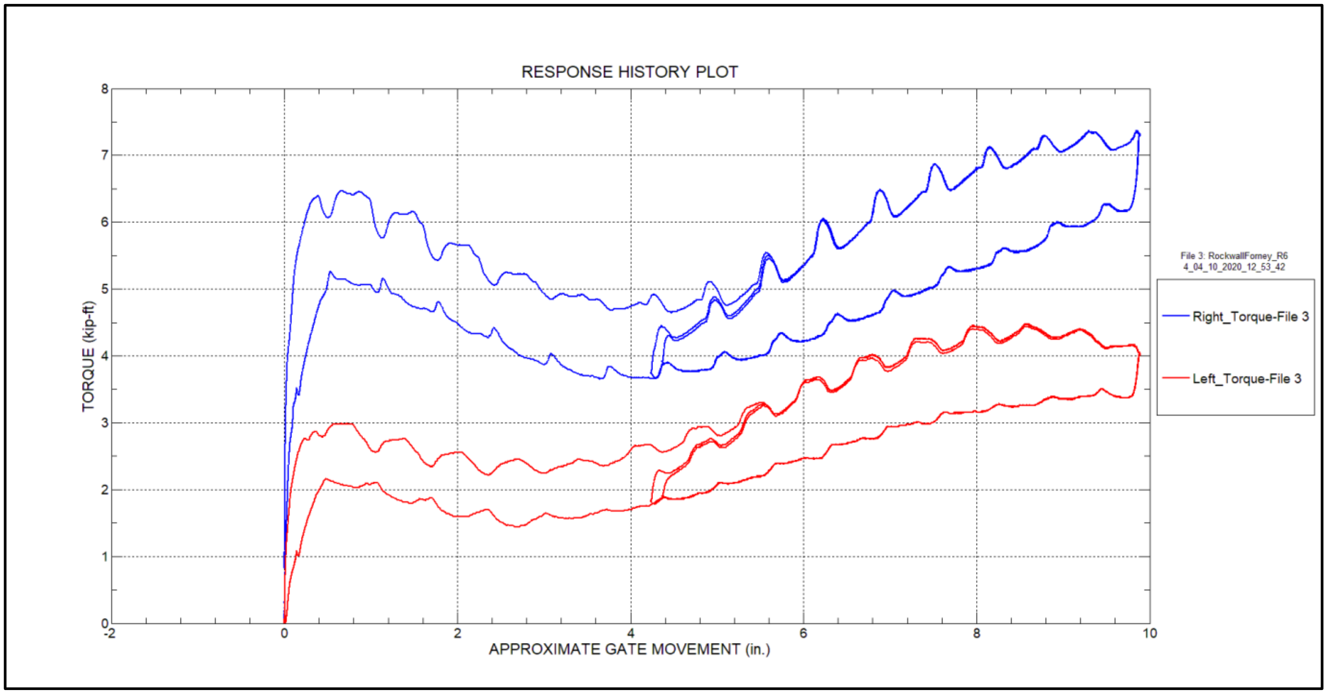

Figure 29 – Hoist torque response history – Gate 11 – Test 3

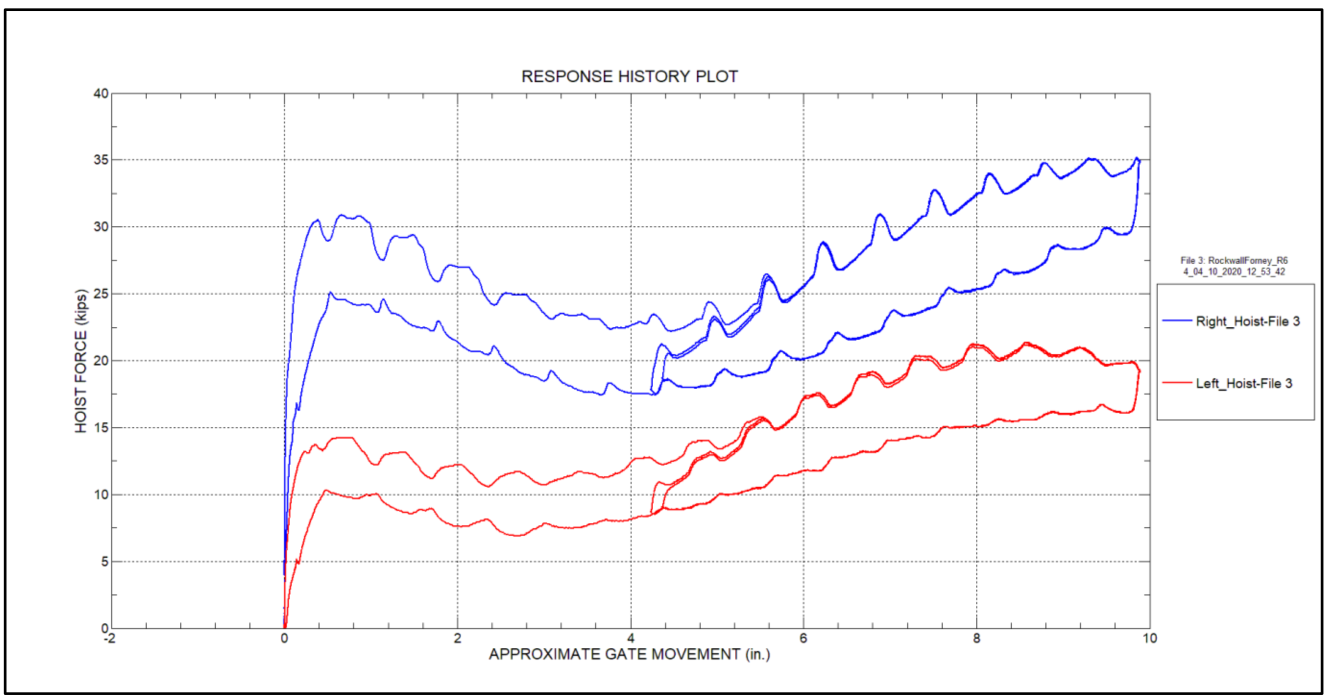

Figure 30 – Hoist force response history – Gate 11 – Test 3

APPENDIX B – GATE 11 PIN MOMENT COMPONENT PLOTS

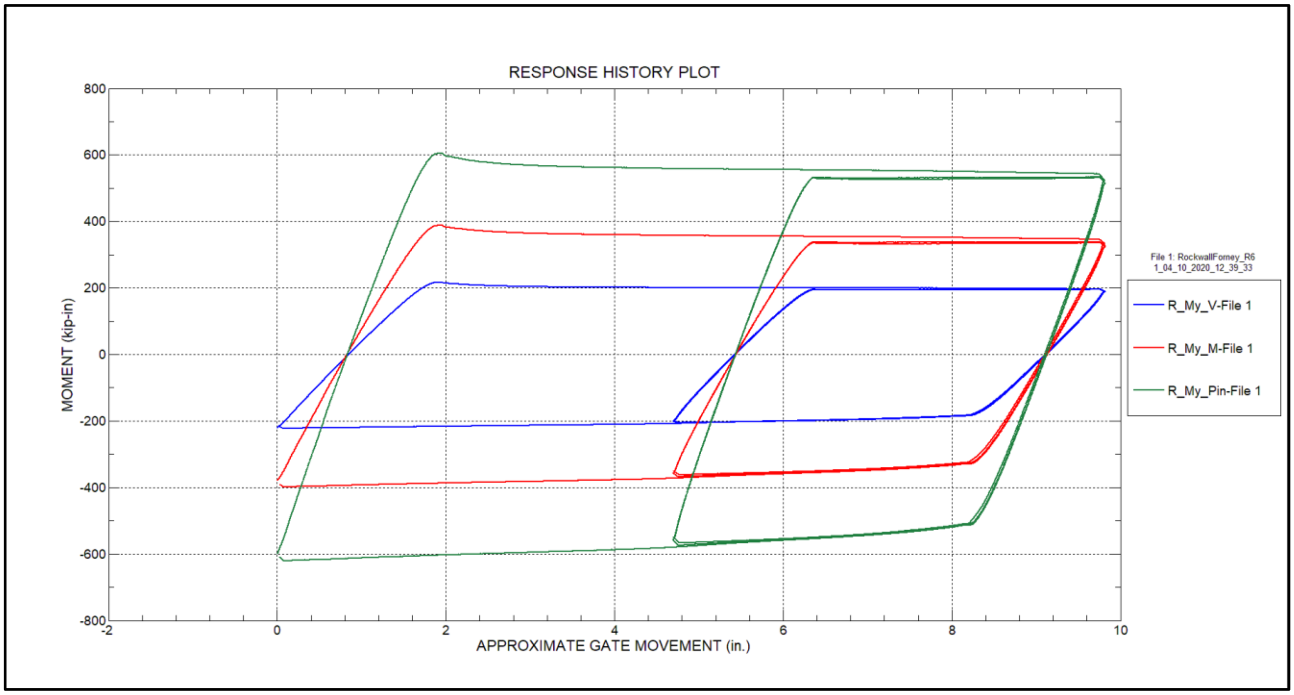

Figure 31 – Pin moment response history – Right arm – Test run 1

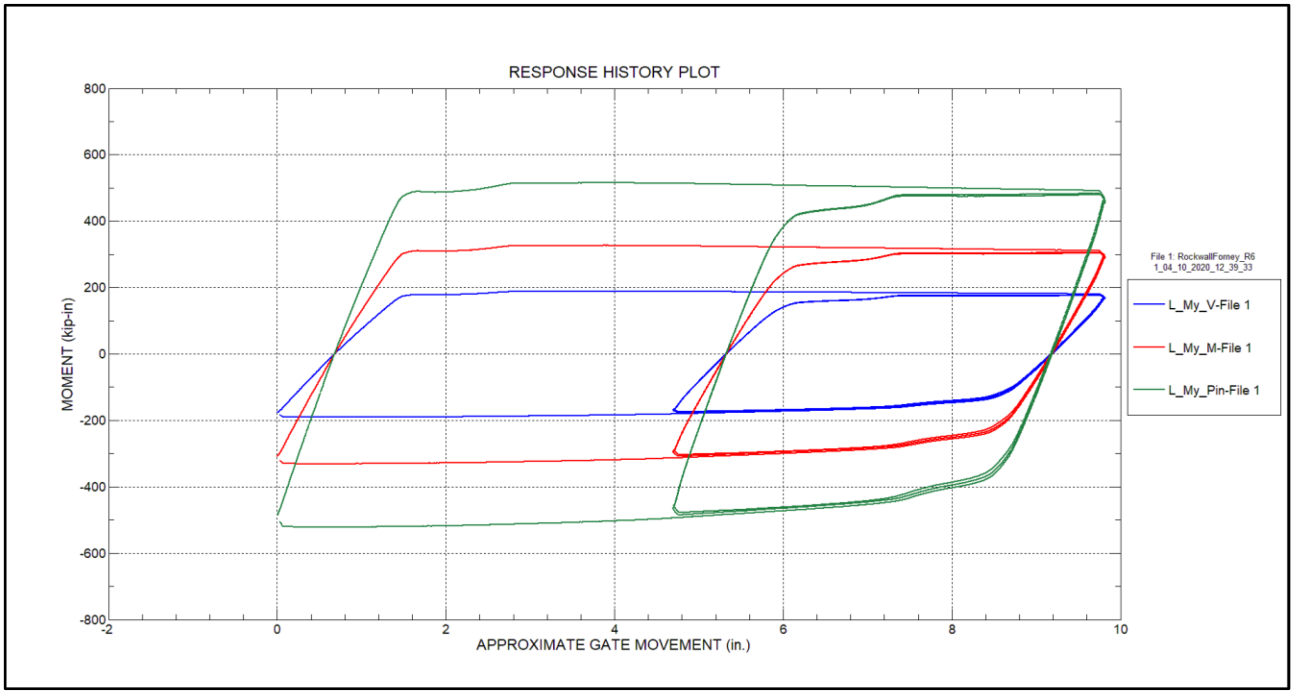

Figure 32 – Pin moment response history – Left arm – Test run 1

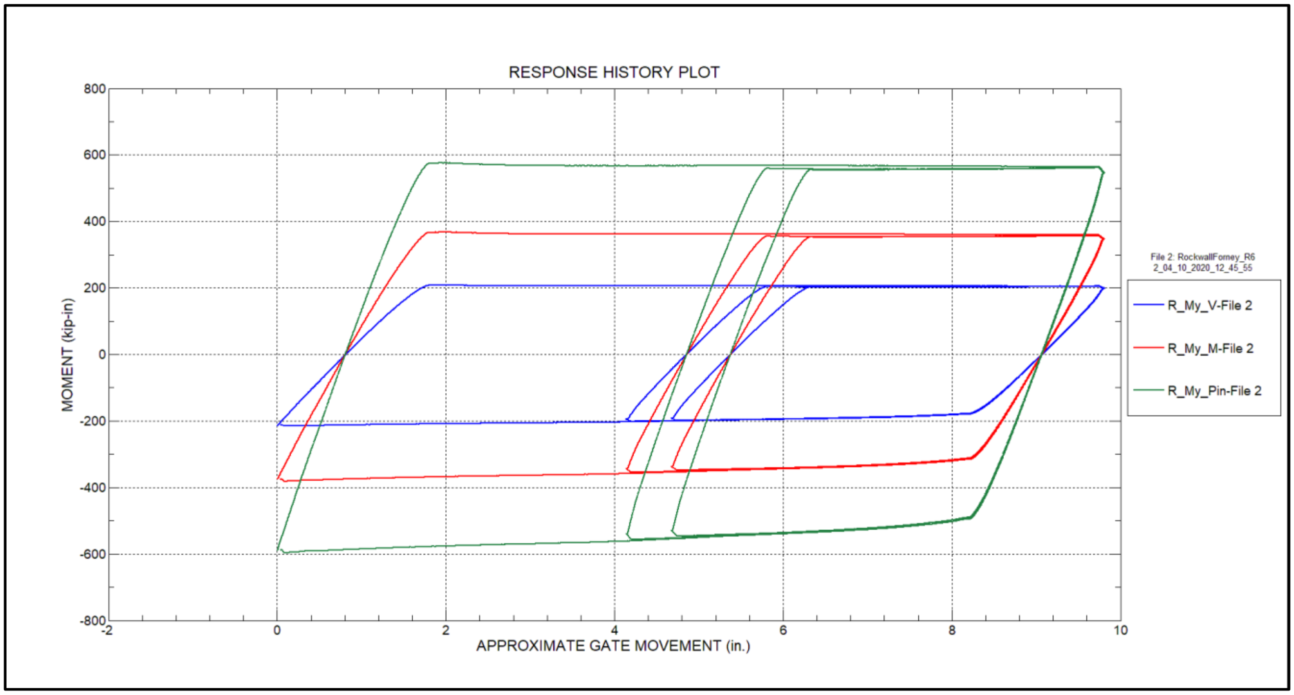

Figure 33 – Pin moment response history – Right arm – Test run 2

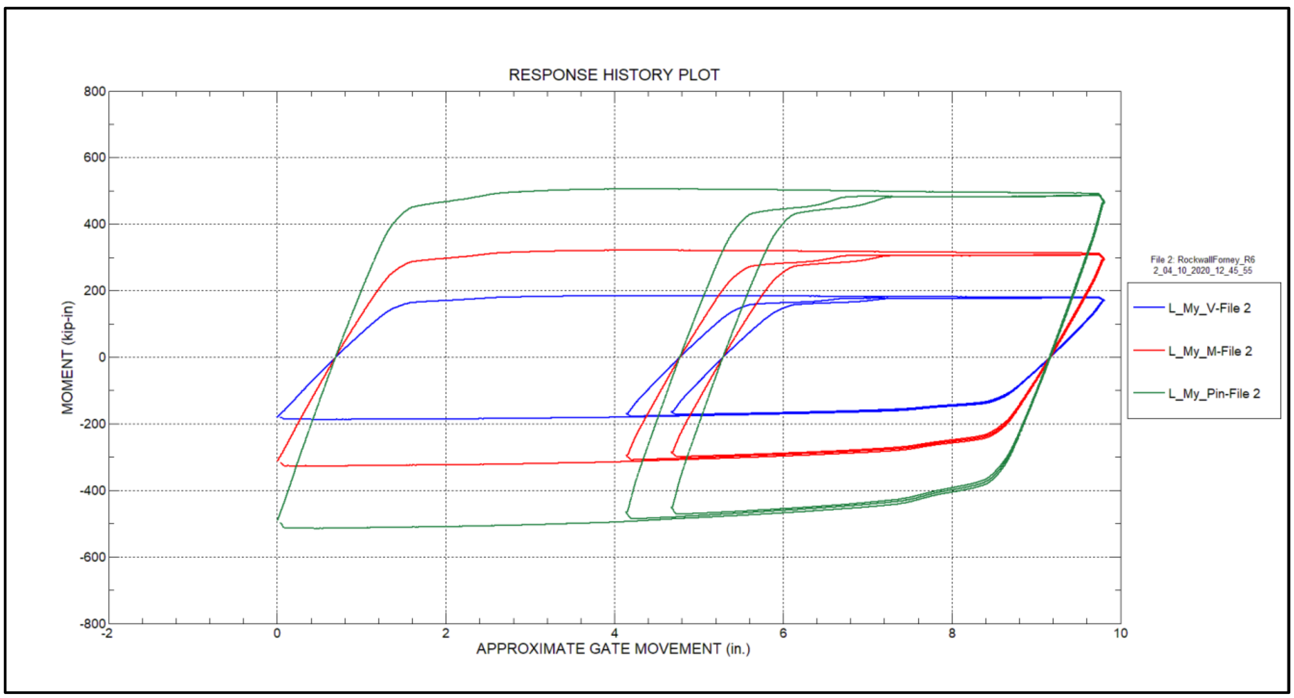

Figure 34 – Pin moment response history – Left arm – Test run 2

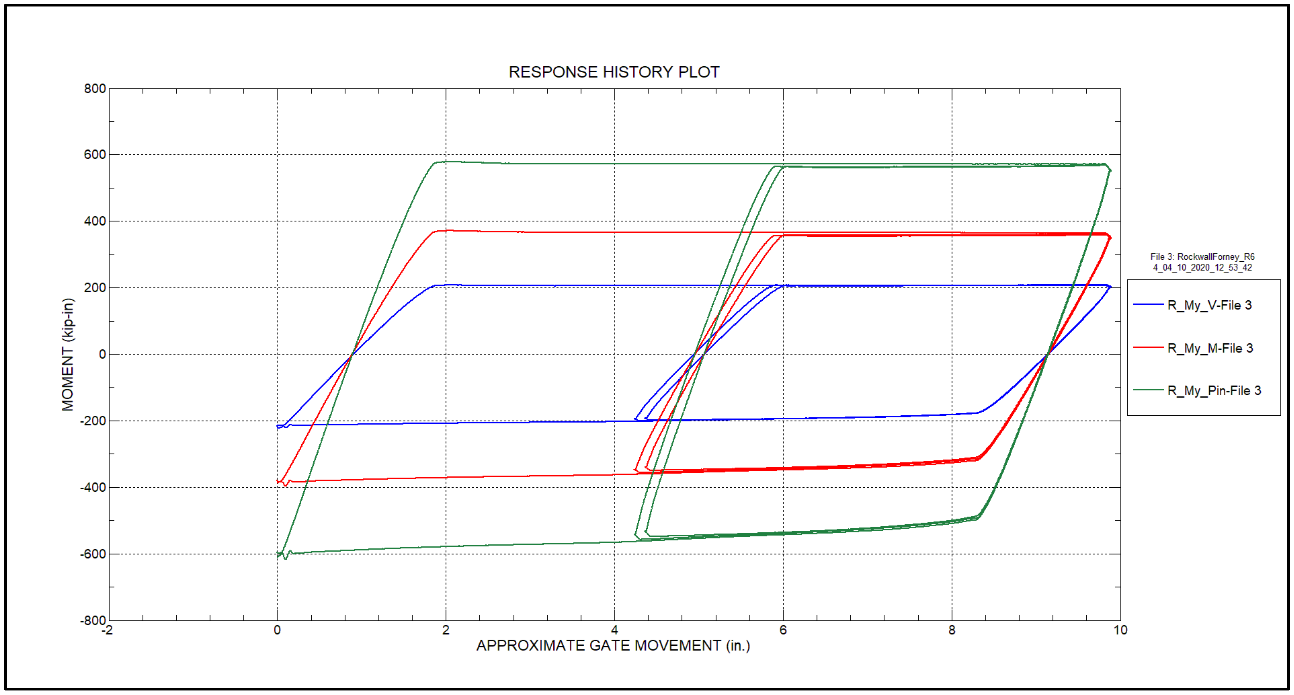

Figure 35 – Pin moment response history – Right arm – Test run 3

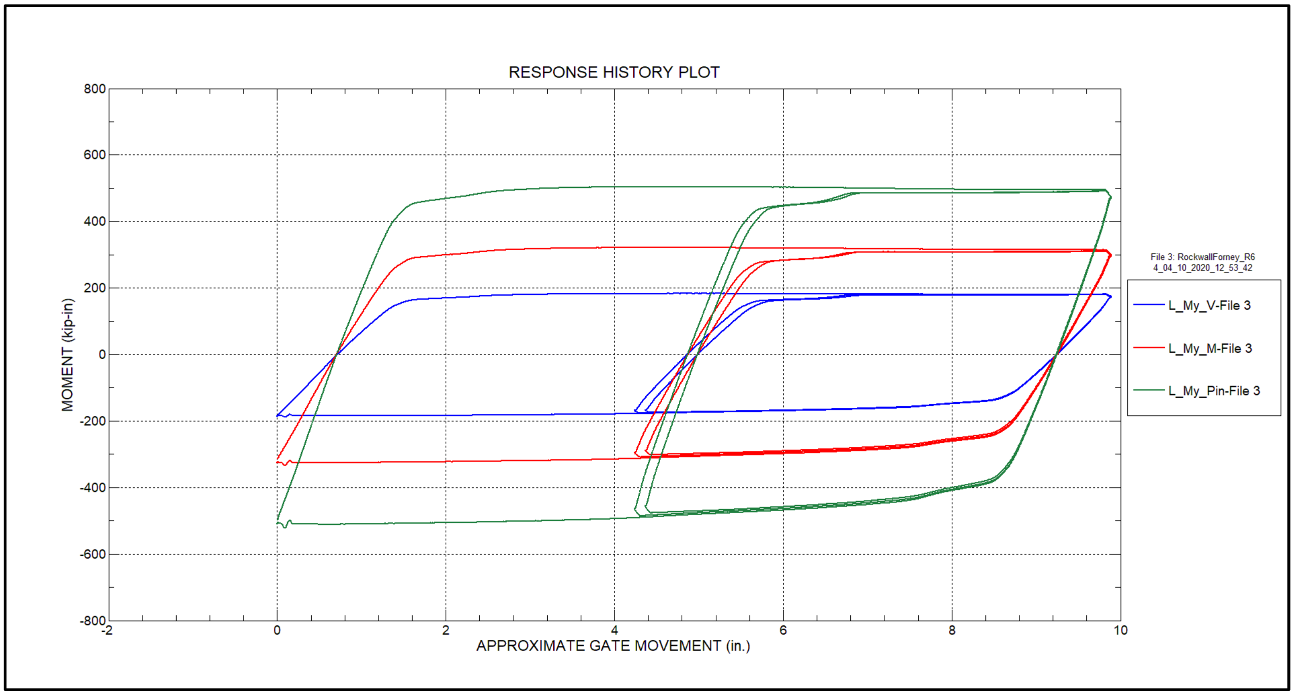

Figure 36 – Pin moment response history – Left arm – Test run 3

Appendix C – Instrumentation Plans

BDI

RAW DATA. REFINED RESULTS.

SCHNABEL ENGINEERING
ROCKWALL FORNEY DAM
LIVE LOAD TESTING

BDI
RAW DATA. REFINED RESULTS.
740 S PIERCE AVE, SUITE 15
LOUISVILLE, CO 80027
303.494.3230
WWW.BDITEST.COM

ISSUE

CLIENT

SCHABEL ENGINEERING
16000 CHRISTENSEN RD, STE 101
SEATTLE, WA 98188

PROJECT NAME

SCHNABEL ENGINEERING
ROCKWALL FORNEY DAM
LIVE LOAD TESTING

Drawn By:	KNR
Checked By:	JDS
Date:	05/27/2020
Client No.:	
BDI No.:	190701-TX
SCALE:	NTS

COVER PAGE

LLT-00

The user acknowledges that these documents are instruments of professional service, and are protected by Copyright. This document and the information contained in this document are the property of Bridge Diagnostics, Inc., and shall not be reused, copied, disseminated, modified, amended or altered in any way. It is issued for information purposes only. The user agrees to hold harmless, indemnify and defend Bridge Diagnostics, Inc. against any and all damages, claims and losses, including defense costs, arising out of any use, reuse or copying of this document.

PLOT TIME: 6/12/2020 3:22 PM
FILEPATH: C:\Users\colemand\BDI\Services - Documents\Server_Remote\190701-TX_Schnabel_RockwallForneyDam\7. Instrumentation Plans\BDI_ROCKWALLFORNEY_01_GENERAL.dwg
© YYYY BRIDGE DIAGNOSTICS INC.

The user acknowledges that these documents are instruments of professional service, and are protected by Copyright. This document and the information contained in this document are the property of Bridge Diagnostics, Inc., and shall not be reused, copied, disseminated, modified, amended or altered in any way. It is issued for information purposes only. The user agrees to hold harmless, indemnify and defend Bridge Diagnostics, Inc. against any and all damages, claims and losses, including defense costs, arising out of any use, reuse or copying of this document.

GAGE LEGEND & SPECIFICATION

SYMBOL	TYPE	BRAND	MODEL	NOTES
	STRAIN TRANSDUCER	BDI	ST350	
	TILTMETER (UNI-AXIAL)	BDI	T500-030	
	TORQUE SENSOR	HPI	-	HBWS-35-125-6-0.5VR-FB
	AMP SENSOR	CR MAGNETICS	CR42105-200	

GENERAL NOTES

- INSTRUMENTATION SHALL BEGIN ON APRIL 1ST, 2020.
- GATES 1 THRU 14 SHALL BE ACCESSED USING SPRAT ROPE ACCESS TECHNIQUES.
- BDI WILL PERFORM ALL SURFACE PREPARATION, SENSOR INSTALLATION, AND EQUIPMENT INSTALLATION.
- SEE LLT-31 FOR SENSOR INSTALLATION DETAILS.
- TWO PAIRS OF TORQUE GAGES WILL BE INSTALLED ON THE GATE MOTORS' PINION SHAFTS BETWEEN THE MOTORS AND THE HOISTS.
  - GAGE PAIRS WILL BE INSTALLED 180° APART FROM EACH OTHER.
  - EXACT POSITIONS OF THE GAGE PAIRS ON THE PINION SHAFT WILL BE DETERMINED IN THE FIELD.
- THREE PHASE AMPERAGE GAGES WILL BE INSTALLED ON THE MOTOR CONTROLS BY A QUALIFIED ELECTRICIAN PROVIDED BY GARVER.

TESTING PROCEDURE:

- TESTING SHALL BE STARTED WITH THE GATE IN THE CLOSED POSITION.
- ONCE DATA COLLECTION BEGINS, THE GATE SHALL BE RAISED TO TWO OR THREE TIMES THE HEIGHT NECESSARY FOR TRUNNION FRICTION TO BE OVERCOME, H1 (TYPICALLY 6"-12"), AND HELD THERE UNTIL DATA STABILIZES.
- THE GATE SHALL BE LOWERED APPROXIMATELY TWICE THE DISTANCE TO OVERCOME TRUNNION FRICTION, H2, AND HELD THERE UNTIL DATA STABILIZES.
- THE GATE SHALL BE RAISED TO H1 AND HELD THERE UNTIL DATA STABILIZES.
- THE GATE SHALL BE LOWERED TO H2 AND HELD THERE UNTIL DATA STABILIZES.
- THE GATE SHALL BE RAISED TO H1 AND HELD THERE UNTIL DATA STABILIZES.
- THE GATE WAS LOWERED BACK TO CLOSED POSITION AND DATA COLLECTION STOPPED.
- A MINIMUM OF 3 TESTS SHALL BE PERFORMED PER GATE.

GAGE COUNT PER GATE

SENSOR LEGEND	SENSOR COUNT	CHANNEL COUNT
STRAIN TRANSDUCER	(48)	(48)
TILTMETER (UNI-AXIAL)	(4)	(4)
TORQUE SENSOR	(4)	(4)
AMP SENSOR	(3)	(3)
TOTAL	(59)	(59)

LOCATION KEY

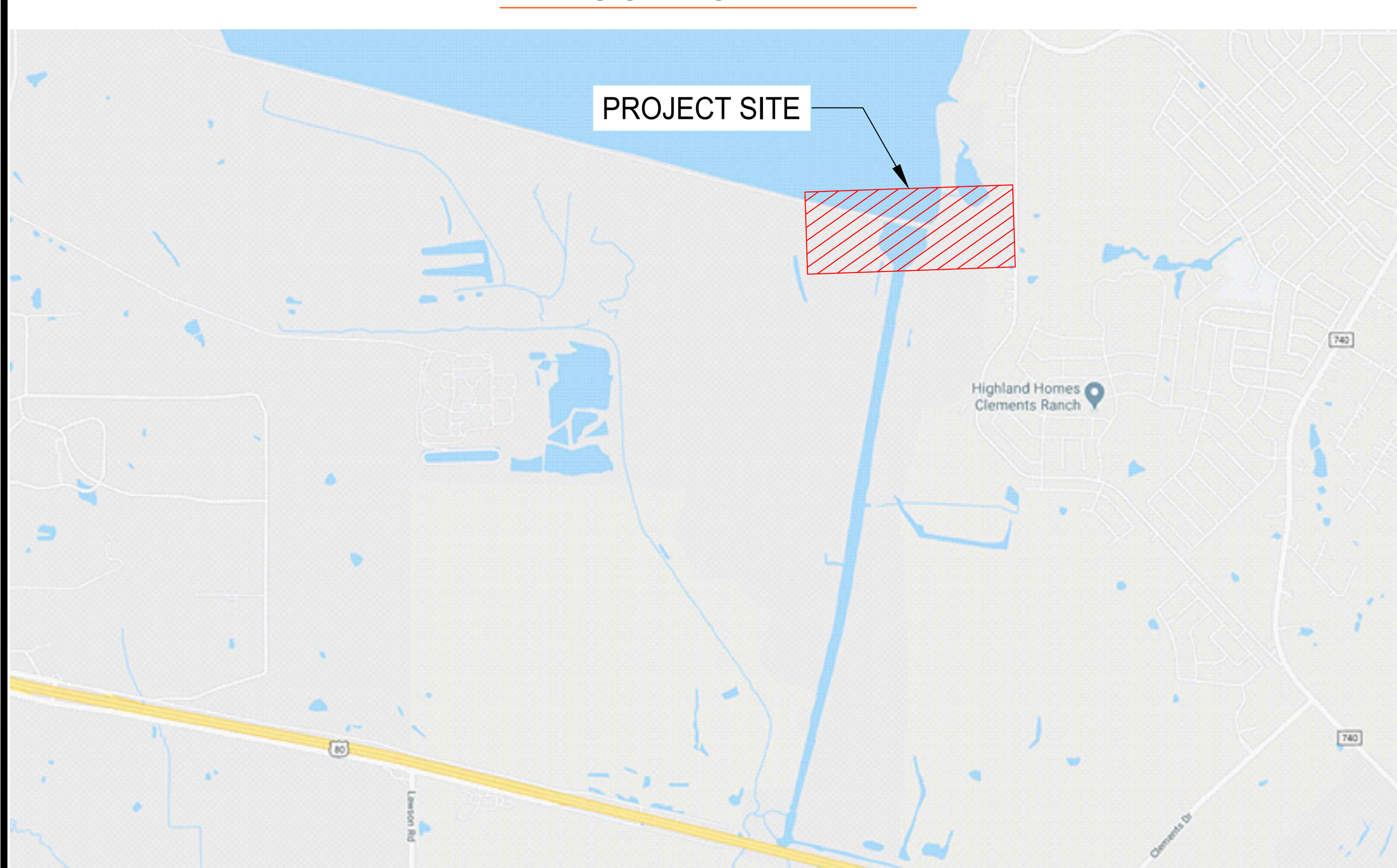

INDEX OF SHEETS

INDEX OF ISSUE

NO.	DATE	REVISION DESCRIPTION
1	3/20/2020	LIVE LOAD TESTING (LLT) INSTRUMENTATION PLAN (FOR APPROVAL)
2	5/27/2020	LIVE LOAD TESTING (LLT) INSTRUMENTATION PLAN AS BUILTS
BDI REFERENCE NUMBER: 190701-TX		

RAW DATA. REFINED RESULTS.
740 S PIERCE AVE, SUITE 15
LOUISVILLE, CO 80027
303.494.3230
WWW.BDITEST.COM

ISSUE

CLIENT

SCHABEL ENGINEERING
16000 CHRISTENSEN RD, STE 101
SEATTLE, WA 98188

PROJECT NAME

SCHABEL ENGINEERING
ROCKWALL FORNEY DAM
LIVE LOAD TESTING

Drawn By: KNR
Checked By: JDS
Date: 05/27/2020
Client No.:
BDI No.: 190701-TX
SCALE: NTS

OVERALL LEGEND

LLT-01

PLOT TIME: 6/12/2020 3:22 PM
FILEPATH: C:\Users\colemand\BDI\Services - Documents\Server_Remote\190701-TX_Schnabel_RockwallForneyDam\7. Instrumentation Plans\BDI_ROCKWALLFORNEY_01_GENERAL.dwg
© YYYY BRIDGE DIAGNOSTICS INC.

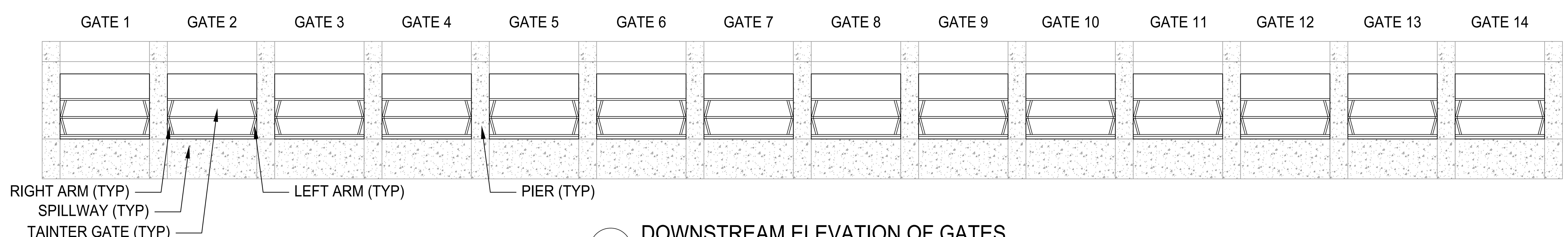

1 DOWNSTREAM ELEVATION OF GATES
LOOKING NORTH (UPSTREAM)

RAW DATA. REFINED RESULTS.
740 S PIERCE AVE, SUITE 15
LOUISVILLE, CO 80027
303.494.3230
WWW.BDITEST.COM

ISSUE

CLIENT

SCHABEL ENGINEERING
16000 CHRISTENSEN RD, STE 101
SEATTLE, WA 98188

PROJECT NAME

SCHNABEL ENGINEERING
ROCKWALL FORNEY DAM
LIVE LOAD TESTING

Drawn By:	KNR
Checked By:	JDS
Date:	05/27/2020
Client No.:	
BDI No.:	190701-TX
SCALE:	NTS

OVERALL STRUCTURE LAYOUT
LLT-02

The user acknowledges that these documents are instruments of professional service, and are protected by Copyright. This document and the information contained in this document are the property of Bridge Diagnostics, Inc., and shall not be reused, copied, disseminated, modified, amended or altered in any way. It is issued for information purposes only. The user agrees to hold harmless, indemnify and defend Bridge Diagnostics, Inc. against any and all damages, claims and losses, including defense costs, arising out of any use, reuse or copying of this document.

PLOT TIME: 6/12/2020 3:22 PM
FILEPATH: C:\Users\colemand\BDI\Services - Documents\Server_Remote\190701-TX_Schnabel_RockwallForneyDam\7. Instrumentation Plans\BDI_ROCKWALLFORNEY_01_GENERAL.dwg
© YYYY BRIDGE DIAGNOSTICS INC.

The user acknowledges that these documents are instruments of professional service, and are protected by Copyright. This document and the information contained in this document are the property of Bridge Diagnostics, Inc., and shall not be reused, copied, disseminated, modified, amended or altered in any way. It is issued for information purposes only. The user agrees to hold harmless, indemnify and defend Bridge Diagnostics, Inc. against any and all damages, claims and losses, including defense costs, arising out of any use, reuse or copying of this document.

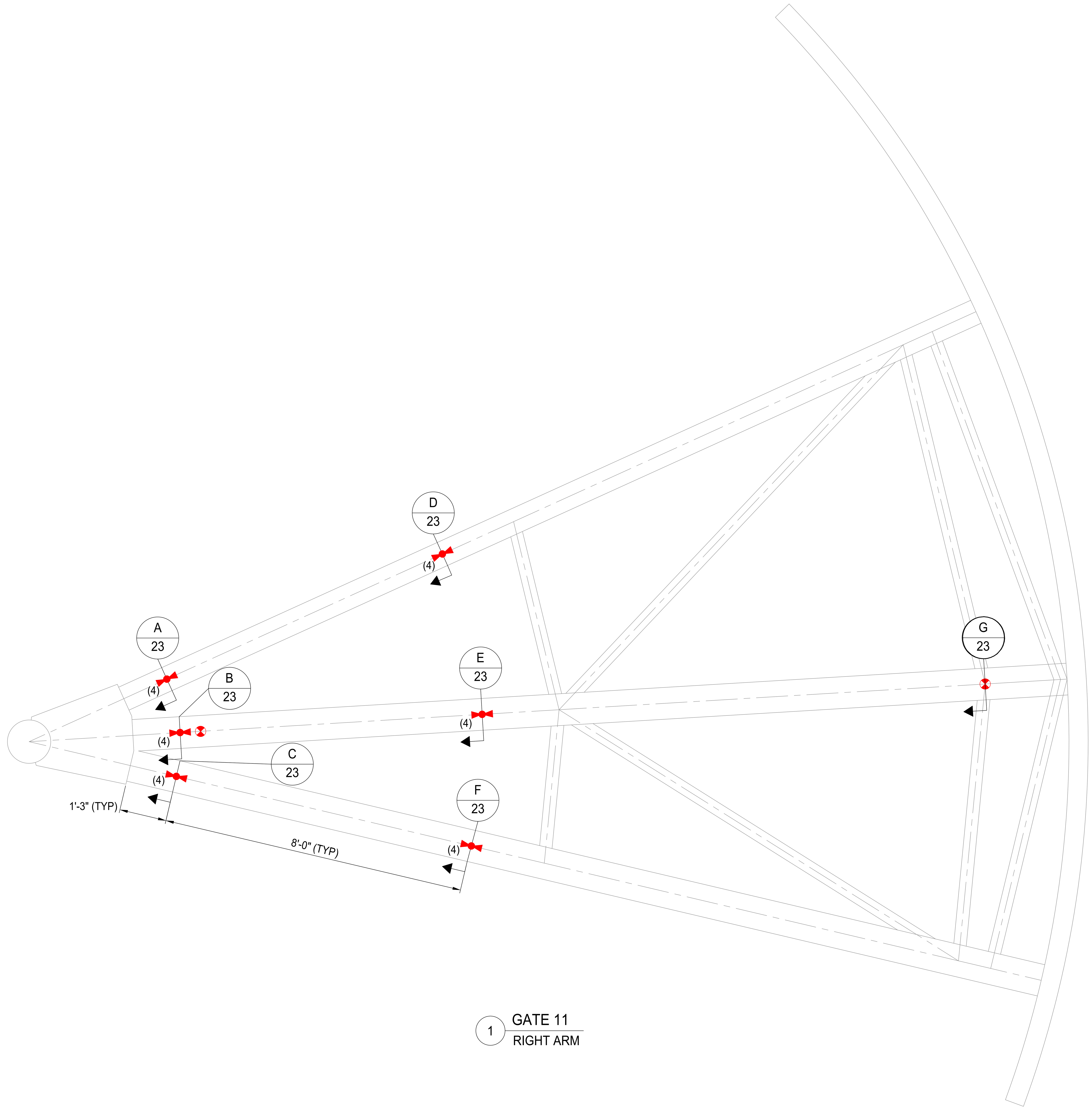

1 GATE 11
RIGHT ARM

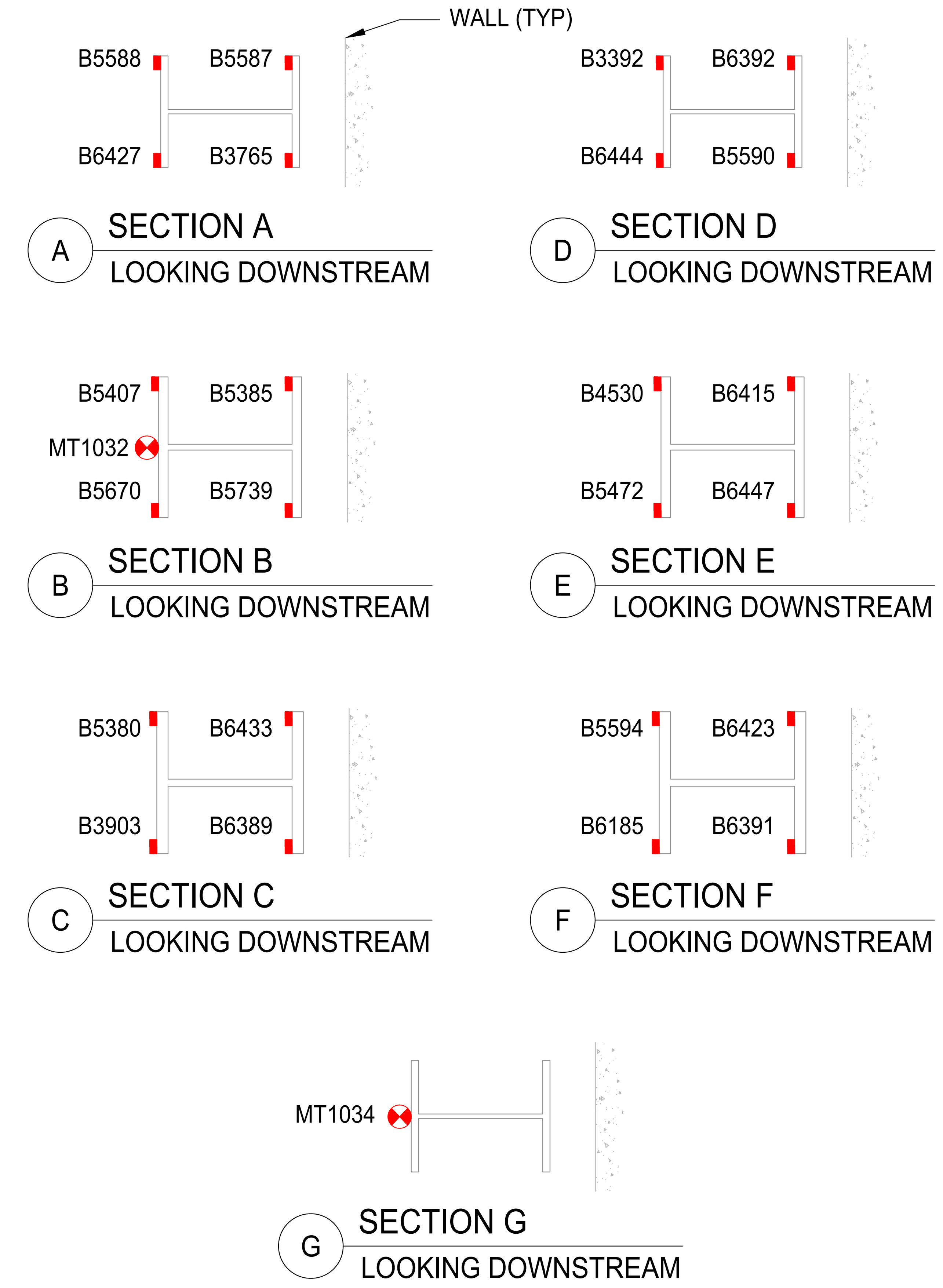

UNIT ID
TT-3

TORQUE GAGES
RIGHT ARM

NOTES:

1. SECTIONS A, B, & C SHALL BE INSTALLED 15 INCHES AWAY FROM TRUNNION PLATE.
2. TILTMETERS SHALL BE INSTALLED CENTERED ON THE MIDDLE STRUT FLANGE.
3. SECTION G'S TILTMETER SHALL BE INSTALLED AS CLOSE TO THE SKINPLATE AS POSSIBLE.

SENSOR LEGEND

- STRAIN TRANSDUCER
- TILTMETER (UNI-AXIAL)
- TORQUE SENSOR

RAW DATA. REFINED RESULTS.
740 S PIERCE AVE, SUITE 15
LOUISVILLE, CO 80027
303.494.3230
WWW.BDITEST.COM

ISSUE

CLIENT

SCHABEL ENGINEERING
16000 CHRISTENSEN RD, STE 101
SEATTLE, WA 98188

PROJECT NAME

SCHABEL ENGINEERING
ROCKWALL FORNEY DAM
LIVE LOAD TESTING

Drawn By:	KNR
Checked By:	JDS
Date:	05/27/2020
Client No.:	
BDI No.:	190701-TX
SCALE:	NTS

GATE 11 - RIGHT ARM
ELEVATION

LLT-23

PLOT TIME: 6/12/2020 3:24 PM
FILEPATH: C:\Users\colemand\BDI\Services - Documents\Server_Remote\190701-TX_Schabel_RockwallForneyDam\7. Instrumentation Plans\BDI_ROCKWALLFORNEY_01_GENERAL.dwg
© YYYY BRIDGE DIAGNOSTICS INC.

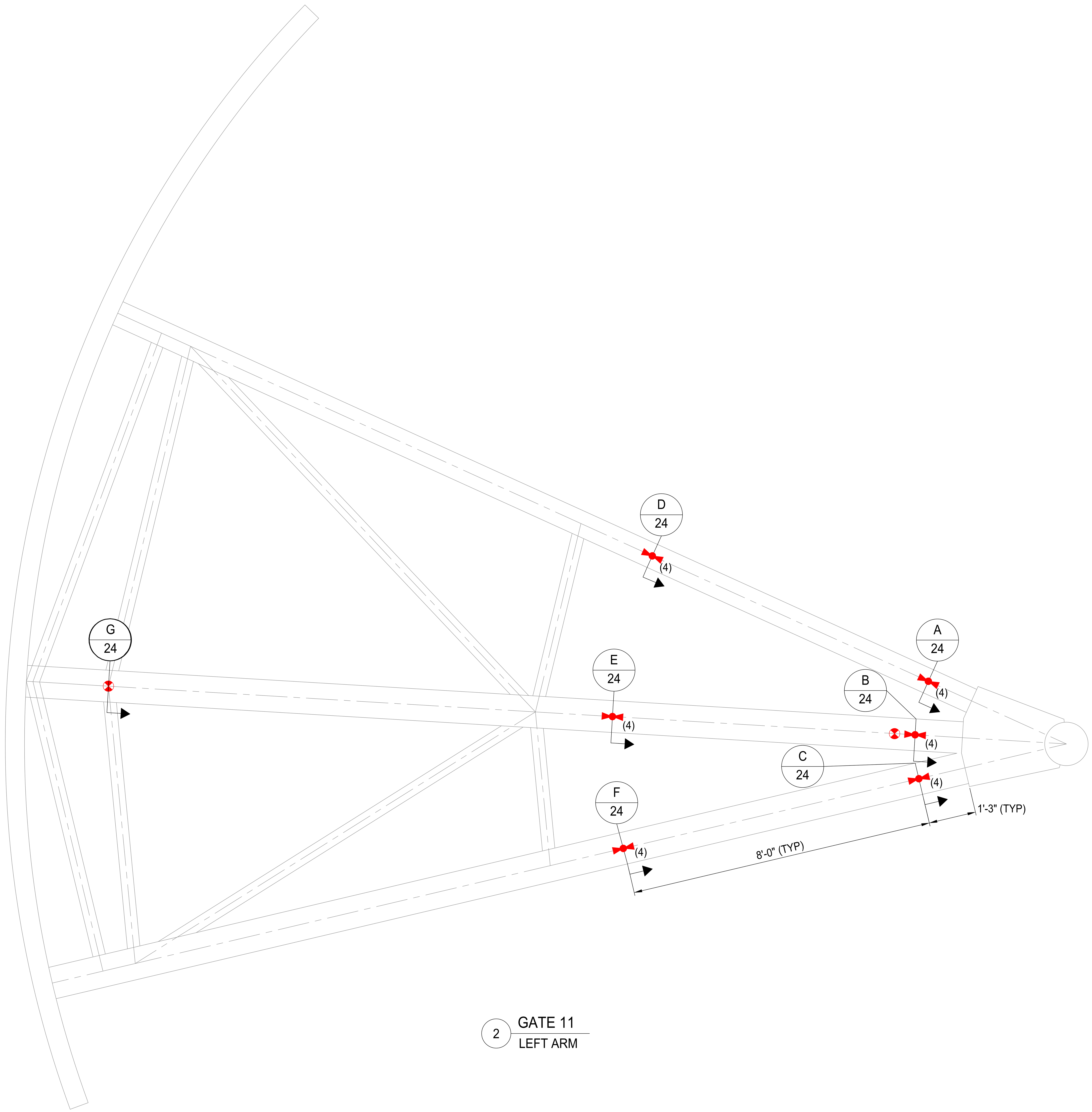

2 GATE 11
LEFT ARM

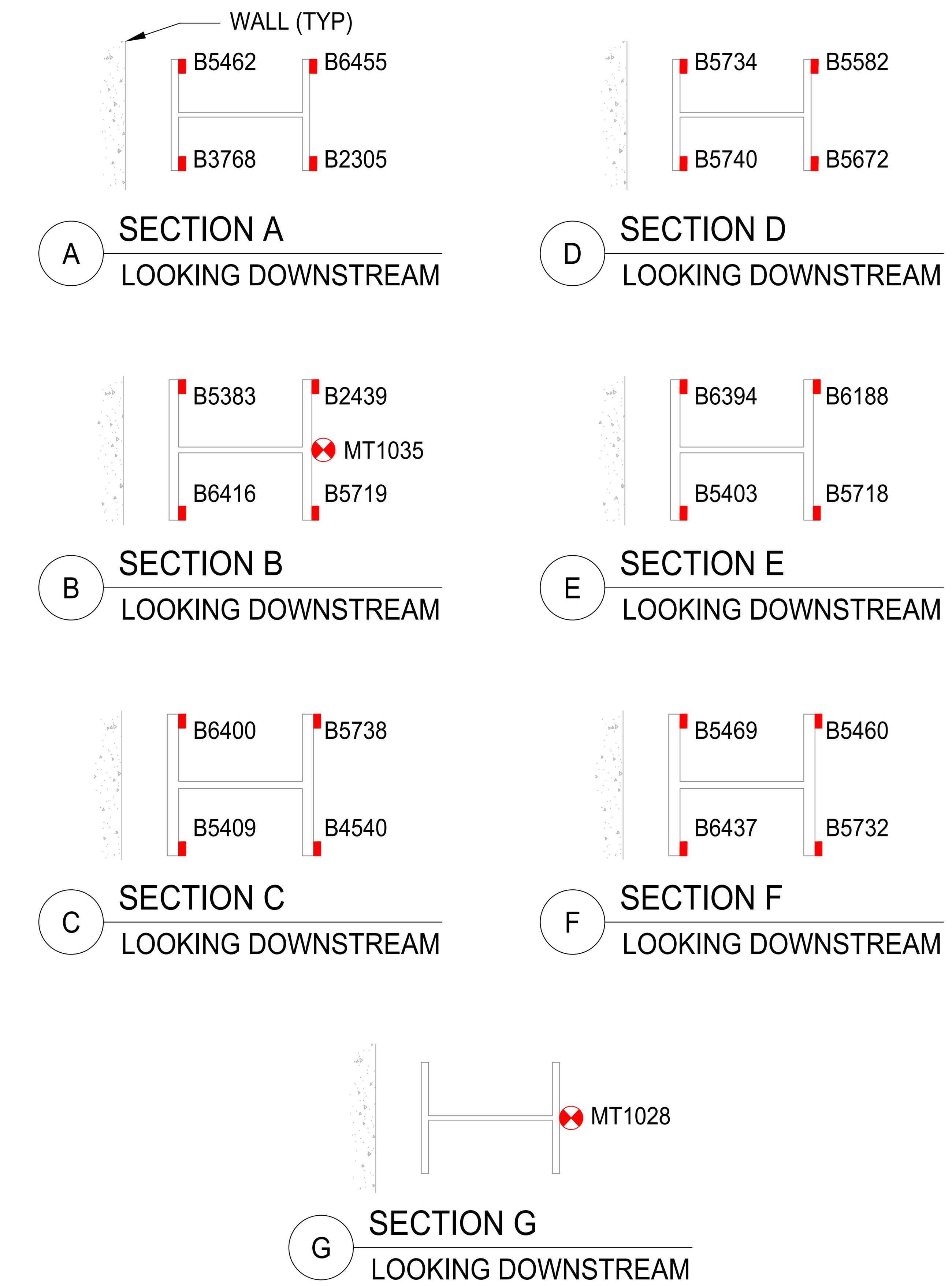

UNIT ID
TT-4

TORQUE GAGES
LEFT ARM

NOTES:

1. SECTIONS A, B, & C SHALL BE INSTALLED 15 INCHES AWAY FROM TRUNNION PLATE.
2. TILTMETERS SHALL BE INSTALLED CENTERED ON THE MIDDLE STRUT FLANGE.
3. SECTION G'S TILTMETER SHALL BE INSTALLED AS CLOSE TO THE SKINPLATE AS POSSIBLE.

SENSOR LEGEND

- STRAIN TRANSDUCER
- TILTMETER (UNI-AXIAL)
- TORQUE SENSOR

BDI
RAW DATA. REFINED RESULTS.
740 S PIERCE AVE, SUITE 15
LOUISVILLE, CO 80027
303.494.3230
WWW.BDITEST.COM

ISSUE

CLIENT

SCHABEL ENGINEERING
16000 CHRISTENSEN RD, STE 101
SEATTLE, WA 98188

PROJECT NAME

SCHABEL ENGINEERING ROCKWALL FORNEY DAM LIVE LOAD TESTING

Drawn By:	KNR
Checked By:	JDS
Date:	05/27/2020
Client No.:	
BDI No.:	190701-TX
SCALE:	NTS

GATE 11 - LEFT ARM
ELEVATION

LLT-24

The user acknowledges that these documents are instruments of professional service, and are protected by Copyright. This document and the information contained in this document are the property of Bridge Diagnostics, Inc., and shall not be reused, copied, disseminated, modified, amended or altered in any way. It is issued for information purposes only. The user agrees to hold harmless, indemnify and defend Bridge Diagnostics, Inc. against any and all damages, claims and losses, including defense costs, arising out of any use, reuse or copying of this document.

PLOT TIME: 6/12/2020 3:24 PM
FILEPATH: C:\Users\colemand\BDI\Services - Documents\Server_Remote\190701-TX_Schabel_RockwallForneyDam\7. Instrumentation Plans\BDI_ROCKWALLFORNEY_01_GENERAL.dwg

© YYYY BRIDGE DIAGNOSTICS INC.

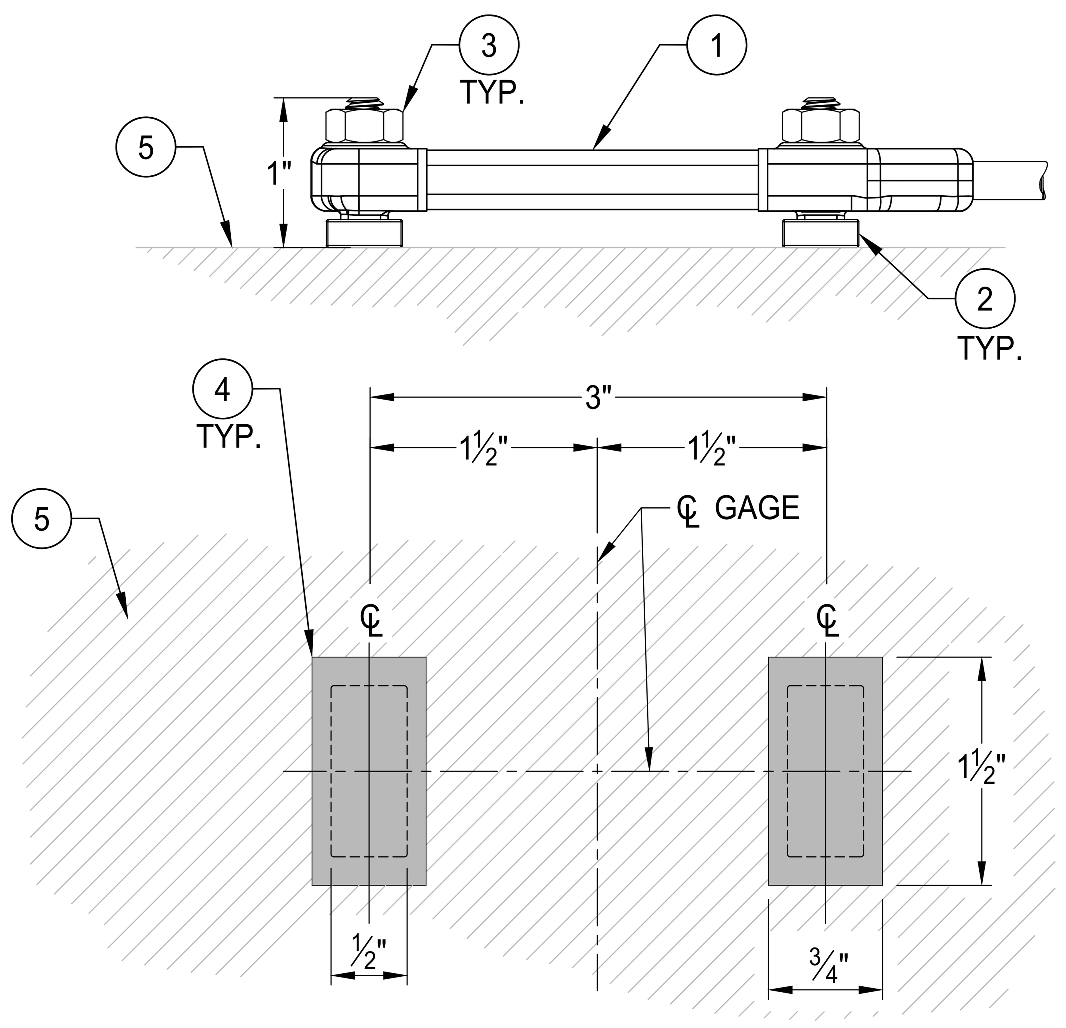

COMPONENT DESCRIPTION

1. ST350 STRAIN GAGE
2. 1/4"-20 THREADED MOUNTING TAB
3. 1/4"-20 STAINLESS STEEL NUT
4. TYPICAL SURFACE PREP REQUIRED TO MOUNT STRAIN GAGES
5. TYPICAL MOUNTING SURFACE

FOOTNOTES - INSTANT ADHESIVE
1. STRAIN GAGES SHALL BE MOUNTED WITH LOCTITE 410 INSTANT ADHESIVE AND LOCTITE 7452 ACCELERANT 2. DURING SURFACE PREP ALL PAINT AND SURFACE DEFORMATIONS MUST BE REMOVED. 3. SURFACE PREP IS REQUIRED JUST PRIOR TO GAGE INSTALLATION AS TO NOT ALLOW SURFACE CONTAMINANTS TO ACCUMULATE.

1 TYPICAL ST350 STRAIN GAGE INSTALLATION

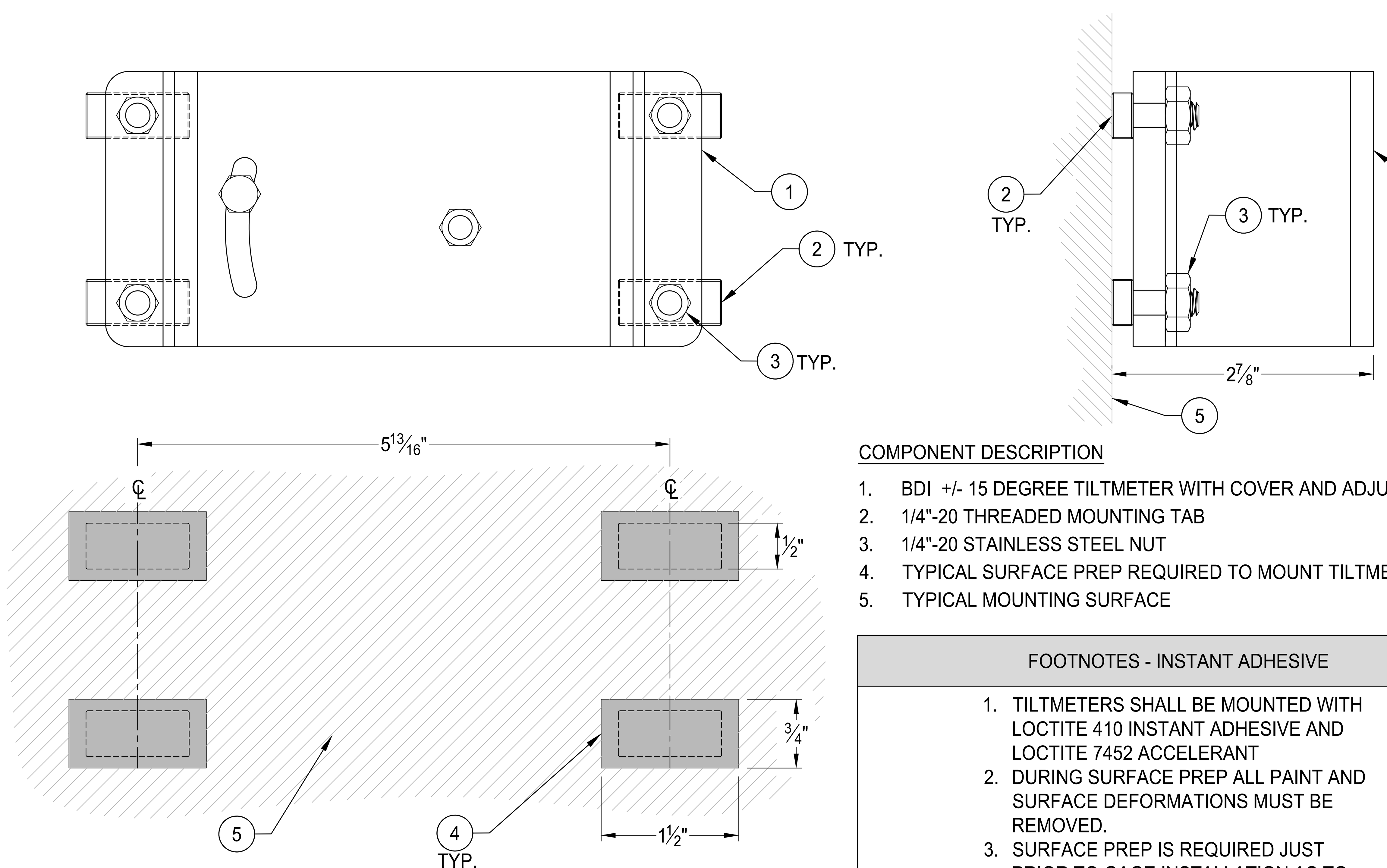

COMPONENT DESCRIPTION

1. BDI +/- 15 DEGREE TILTMETER WITH COVER AND ADJUSTMENT BOLTS
2. 1/4"-20 THREADED MOUNTING TAB
3. 1/4"-20 STAINLESS STEEL NUT
4. TYPICAL SURFACE PREP REQUIRED TO MOUNT TILTMETERS
5. TYPICAL MOUNTING SURFACE

FOOTNOTES - INSTANT ADHESIVE
1. TILTMETERS SHALL BE MOUNTED WITH LOCTITE 410 INSTANT ADHESIVE AND LOCTITE 7452 ACCELERANT 2. DURING SURFACE PREP ALL PAINT AND SURFACE DEFORMATIONS MUST BE REMOVED. 3. SURFACE PREP IS REQUIRED JUST PRIOR TO GAGE INSTALLATION AS TO NOT ALLOW SURFACE CONTAMINANTS TO ACCUMULATE.

2 TYPICAL BDI TILTMETER INSTALLATION

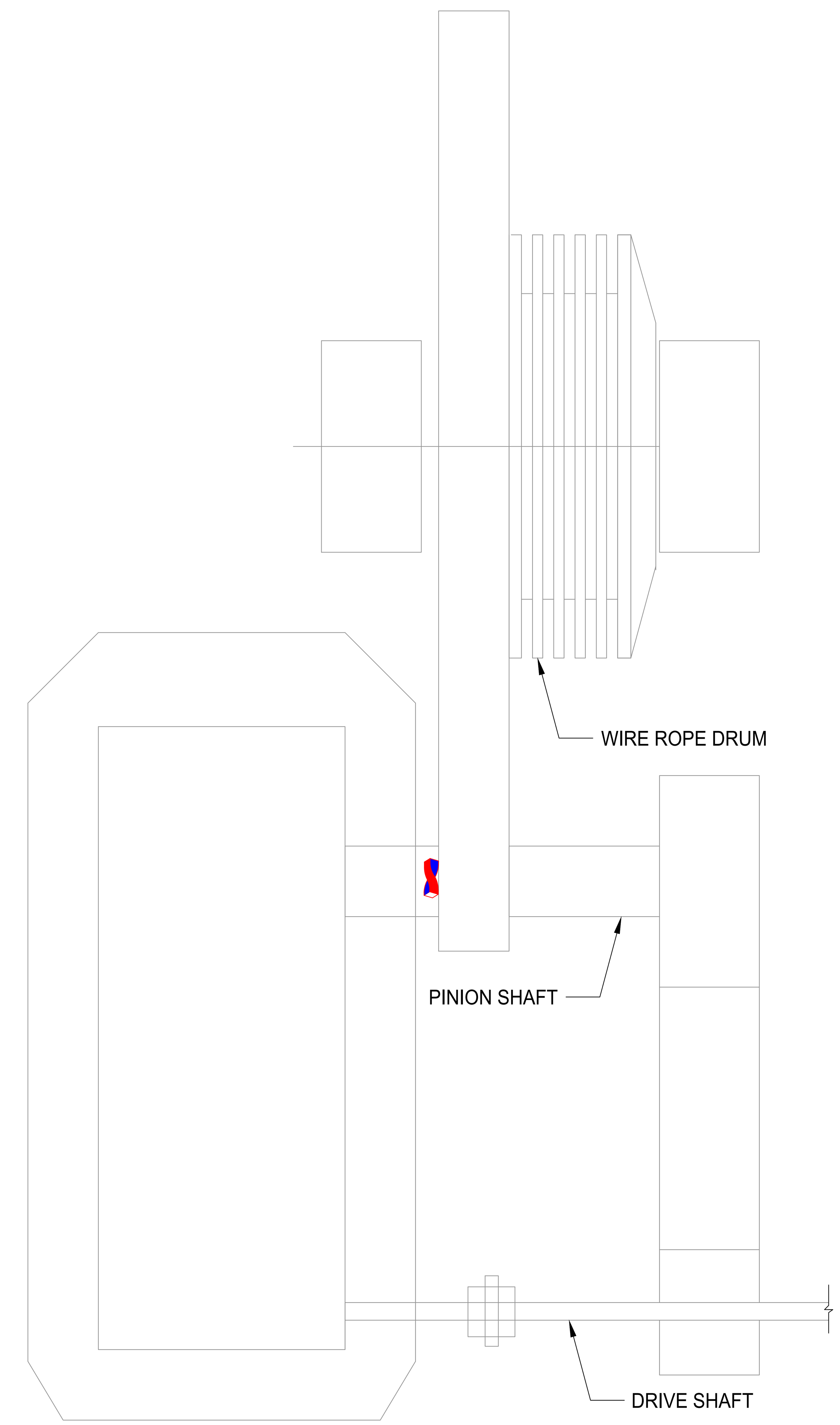

3 TYPICAL HOIST INSTRUMENTATION

TORQUE SENSOR INSTALLATION NOTES:

- TORQUE GAGES WILL BE INSTALLED ON THE PINION SHAFT ON EITHER HOIST MOTOR BETWEEN THE MOTOR AND THE HOIST DRUM
- EXACT POSITIONS OF THE GAGE PAIRS ON THE PINION SHAFT WILL BE DETERMINED IN THE FIELD

SENSOR LEGEND

TORQUE SENSOR

BDI
RAW DATA. REFINED RESULTS.
740 S PIERCE AVE, SUITE 15
LOUISVILLE, CO 80027
303.494.3230
WWW.BDITEST.COM

ISSUE

CLIENT

SCHABEL ENGINEERING
16000 CHRISTENSEN RD, STE 101
SEATTLE, WA 98188

PROJECT NAME

SCHABEL ENGINEERING
ROCKWALL FORNEY DAM
LIVE LOAD TESTING

Drawn By:	KNR
Checked By:	JDS
Date:	05/27/2020
Client No.:	
BDI No.:	190701-TX
SCALE:	NTS

SENSOR INSTALLATION DETAILS

LLT-31

The user acknowledges that these documents are instruments of professional service, and are protected by Copyright. This document and the information contained in this document are the property of Bridge Diagnostics, Inc., and shall not be reused, copied, disseminated, modified, amended or altered in any way. It is issued for information purposes only. The user agrees to hold harmless, indemnify and defend Bridge Diagnostics, Inc. against any and all damages, claims and losses, including defense costs, arising out of any use, reuse or copying of this document.

PLOT TIME: 6/12/2020 3:24 PM
FILEPATH: C:\Users\colemand\BDI\Services - Documents\Server_Remote\190701-TX_Schabel_RockwallForneyDam\7. Instrumentation Plans\BDI_ROCKWALLFORNEY_01_GENERAL.dwg
© YYYY BRIDGE DIAGNOSTICS INC.

SCHNABEL ENGINEERING
TRUNNION PIN FRICTION TESTING REPORT

ROCKWALL FORNEY DAM – GATE 12
FORNEY, TX

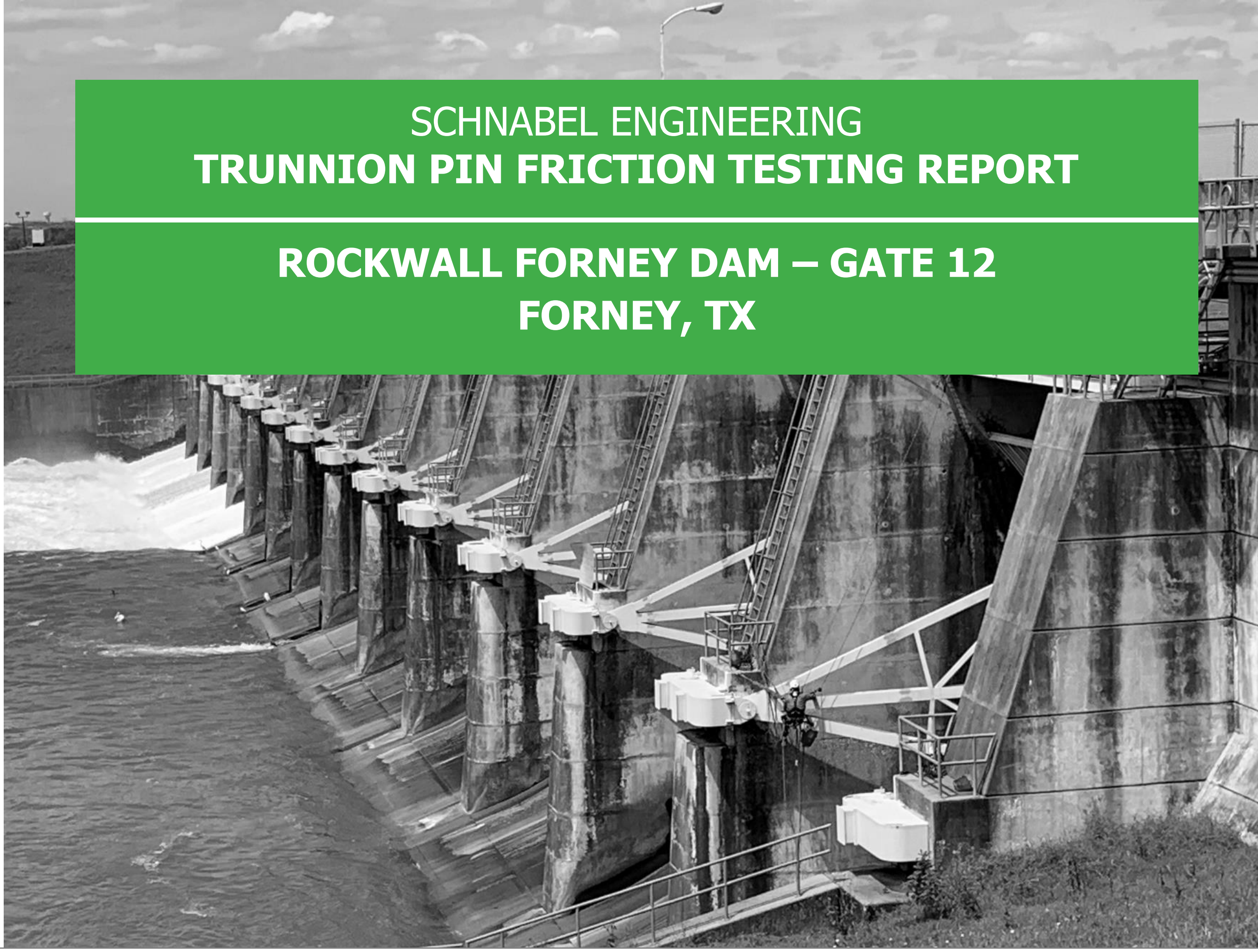

SUBMITTED TO:
SCHNABEL ENGINEERING
16000 CHRISTENSEN RD, SUITE 101
SEATTLE, WA 98188

SUBMITTED BY:
BDI – CO
740 SOUTH PIERCE AVE, UNIT 15
LOUISVILLE, CO 80027

BDI Project No.: **190701-TX**
Report Version: **V1**
Version Submitted: **August 26, 2020**

RAW DATA. REFINED RESULTS.

This document contains Confidential Information and is submitted in confidence to the customer. The submission of the information contained herein shall not be deemed to constitute public disclosure or authorization for disclosure to other parties. BDI's information and name may not be used in advertising or for promotional purposes without BDI's written consent.

RAW DATA. REFINED RESULTS.

TABLE OF CONTENTS

LIST OF FIGURES

LIST OF TABLES

Executive Summary

Schnabel Engineering contracted BDI to provide instrumentation and testing services on Gates 1-14 on the Rockwall Forney Dam near Dallas, Texas. The goal of these tests was to record each gate's structural responses during a series of spill tests and use the data to compute accurate coefficients of friction for each trunnion pin, cable lift force, total gate friction, and motor amperage. This report provides details on the work performed on Gate 12.

Instrumentation and testing were performed on Gate 12 at the Rockwall Forney Dam on April 13th, 2020. The gate arms were instrumented with strain and rotation sensors. The hoist motors' pinion shafts were instrumented with torque sensors and the hoist motor controls were instrumented with amperage sensors. Following the instrumentation, a series of spill tests were performed to measure the structural responses resulting from trunnion pin friction. All instrumentation setup and removal were performed using BDI's rope access team.

Following demobilization from the field, the test data was examined for quality and then further processed to evaluate the gate's performance. Strain measurements were converted into bending forces which were then applied to pin-strut free-body diagrams. By summing forces at each pin, friction induced moments could be computed, allowing accurate friction coefficients to be determined. Generally, the observed gate behavior showed that Gate 12 was operating as expected with no major signs of distress.

The resulting maximum trunnion friction coefficients and corresponding hoist forces are shown in Table 1.

Table 1 – Gate 12 performance summary

Pin Designation	Maximum Friction Coefficient	Maximum Pin Moment due to Pin Friction (kip-In)	Maximum Hoist Force (kips)	Maximum Hoist Force due to Total Gate Friction (kips)
Right Pin	0.13	335.0	28.51	4.02
Left Pin	0.20	530.7	28.45	3.77

Note: Pin designations are in reference to looking downstream

Due to restrictions caused by the hoist limit switches, the hoist cables could not always be fully slacked at the beginning and end of the performed tests. Throughout testing of the Rockwell Forney gates, it was found that this limit switch restriction varied gate to gate and arm to arm. Therefore, it is not recommended to use the collected hoist force data to quantify overall hoist forces during gate operation. Rather, this hoist data can be better utilized to evaluate total friction behavior.

Amperage responses were not used to compute friction results and were collected as verification that the motor performance was not causing unexpected gate responses. These responses indicated the motor was functioning in a stable manner and should be reviewed by a licensed electrician to further evaluate the motor's performance.

All results and recommendations provided in this report were based on the structure in its current condition; therefore, any significant changes in condition must be noted as they may alter their validity. Questions regarding this report and/or data should be directed to Kyle Ramer (kyler@bditest.com) at BDI. For further information on BDI's equipment, services, and analysis methods please visit www.bditest.com

Instrumentation and Load Testing Procedure

Gate Instrumentation Summary

Instrumentation and testing were performed on Gate 12 at the Rockwall Forney Dam on April 13th, 2020. Instrumentation plans have been provided along with this report and include the following number of instrumented locations and sensor types:

+ **REUSABLE SURFACE MOUNTED STRAIN TRANSDUCERS:** Each gate arm was instrumented with a total of 24 strain transducers at 6 locations on each of the gate arms (48 strain sensors total). A typical strain gage installation is shown in Figure 1. Note these sensors were installed with the mounting tabs on the extreme fiber of the strut flanges, which puts the center of the gage approximately 0.66″ from the extreme fiber.
+ **TILTMETER ROTATION SENSORS:** MEMS style rotation sensors were located on the middle strut of the gate arm near the skin plate and near the trunnion hub (4 rotation sensors total). The rotation responses were used to calculate vertical skin plate movement and measure pin rotation relative to skin plate rotation. Typical tiltmeter installations are shown in Figure 1 and Figure 2.
+ **TORQUE SENSORS:** Two total torque sensors were installed on the hoist's pinion shafts (QTY1 on each hoist pinion shaft) near the cable hoist motor to measure direct torque and in turn lift force (See Figure 3).
+ **AMPERAGE SENSORS:** 3 Hall-Effect amperage transducers were clamped over each phase of the hoist motor to measure the motor's current draw (See Figure 4). The purpose of these sensors was to provide additional data in case there were any issues with the hoist systems and to verify any data issues related to lifting and lowering the gates.
+ **BDI'S STS-4 WIRELESS DATA ACQUISITION SYSTEM:** BDI's STS-4 wireless data acquisition (DAQ) was used to collect and record data during testing. A group of sensors were wired to each nodal DAQ which then communicated wirelessly back to the wireless base station and was controlled by BDI's STS-Live testing software.

Complete specifications are available upon request and can be found at http://www.bditest.com.

Sensor Installation

BDI strain transducers were installed by first sanding paint off the struts to expose bare metal at two small locations (1″x2″ areas) for the sensor's mounting tabs. Each transducer was then attached using a combination of fast-setting adhesive and accelerator and applying pressure until the adhesive was fully cured. Each strain transducer took approximately five minutes to attach.

Tiltmeters were installed using the same adhesive process as the strain transducers. However, no surface preparation was necessary.

Torque sensors were installed on the pinion shafts by capacitive discharge bonding. Properly bonding to the shaft required sanding the surface to a smooth finish, clean of any paint or grease. Responses from these gages were measured using Binsfeld Torque Trak 10k wireless transmitters.

A typical installation has been shown in Figure 1 through Figure 4. Access to all the sensor locations was provided by BDI's own SPRAT certified rope access technicians and engineers as shown in Figure 5.

Once testing was completed, sensors were removed, and exposed steel areas were covered using cold galvanizing compound.

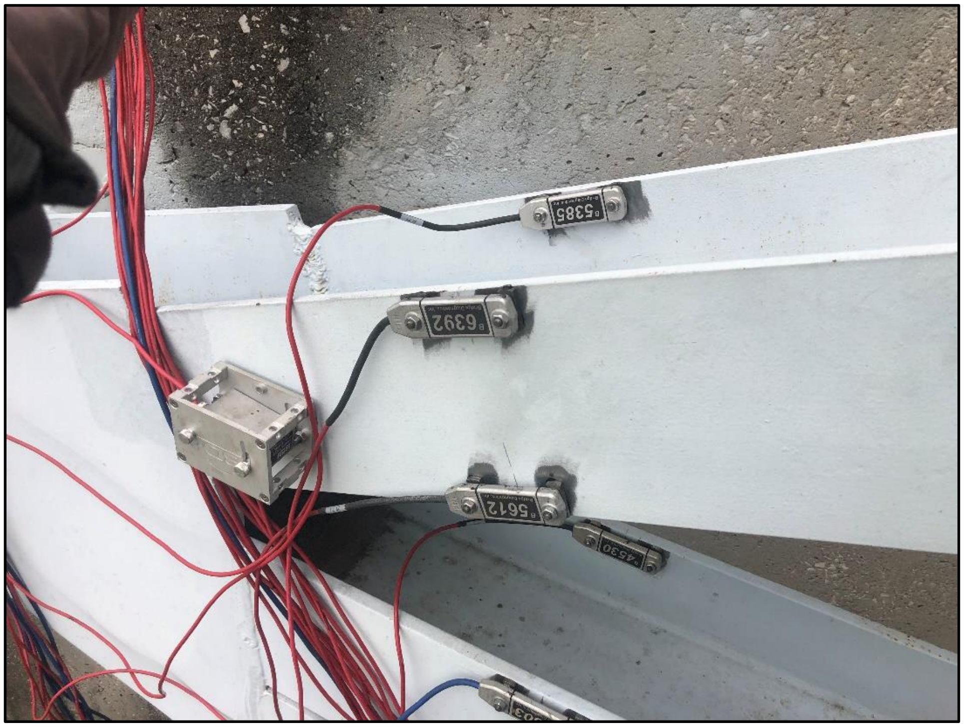

Figure 1 – BDI tiltmeter rotation sensor and reusable strain transducers installed near trunnion hub (Typical)

Figure 2 – BDI tiltmeter rotation sensor installed near skin plate (Typical)

Figure 3 – Torque sensor installation on hoist pinion shaft (Typical)

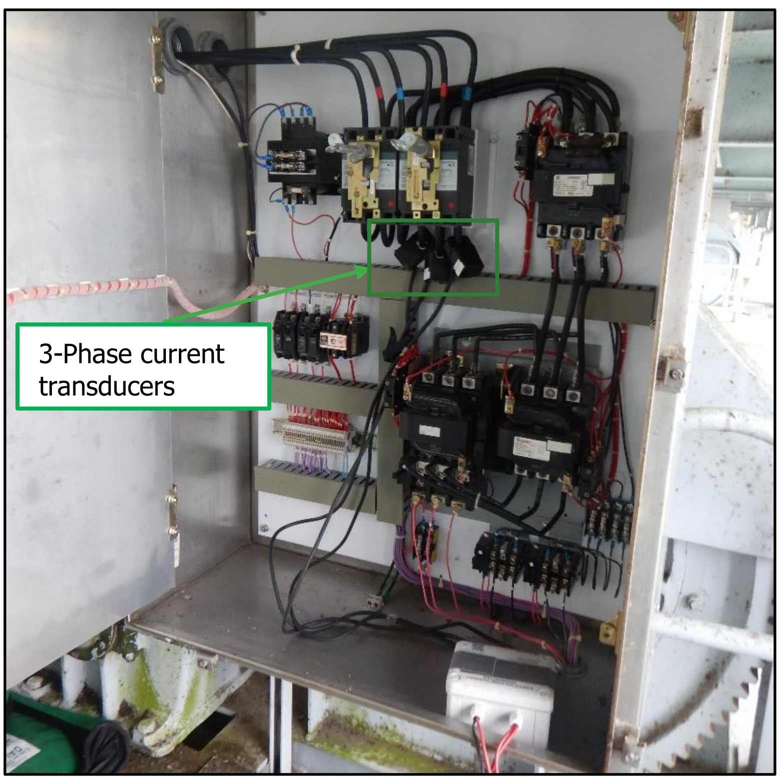

Figure 4 – Current transducers installed on hoist motor controls (Typical)

Figure 5 – BDI personnel installing instrumentation on the gate arm

Testing Procedures

Structural response data was recorded on all sensors at 50Hz while the gate was run through three spill tests. Each test consisted of three "up-down" cycles (direction reversals) without lowering the gate back to the sill. Each direction reversal consisted of lifting the gate approximately 6-12", pausing for a few seconds, and lowering the gate approximately 6", and repeating until all reversals had been completed.

RESULTS SUMMARY

GENERAL DISCUSSIONS BASED ON STRUCTURAL RESPONSES

The following outline contains general discussion points and observations that were made during the data review process. Note: Strain measurements were converted to stress for all subsequent analysis by multiplying the strain values by a steel elastic modulus of 29,000 ksi.

+ **DESCRIPTIONS OF RESPONSE MEASUREMENTS:** All sensor readings were zeroed at the end of each test (which consisted of three cycles of direction reversals) so that each measurement corresponded to response change relative to the final gate position as shown in Figure 6 (gates in the downward "closed" position with the hoist cables slacked as much as possible). It is also worth noting that the stresses did not always start and end at the same levels between tests. This variation in behavior is due to small changes in the flexed gate condition between the start and end of tests. It is common for the flex in the gate, caused by pin friction, to slowly release as it rests on the sill. The purpose of the three up-down cycles per test, prior to sitting the gate back onto the sill, is to ensure that these changes in boundary conditions, including gate flexure due to friction, did not affect BDI's trunnion friction results. ***It is important to note that the recorded measurements were changes in structural response due to gate movement, and do not include the in-situ stresses due to the dead load, cable wrap, and hydrostatic loads present prior to testing.***
+ **QUALITATIVE DATA REVIEW:** Review of the response data indicated a good level of reproducibility between the three tests. For reference, Figure 6 and Figure 7 show stress responses measured along Gate 12's right arm top strut for all three tests (Test #1-3). The data in these plots have been provided as both a function of time and the gate position as determined by the skin plate tilt sensor. Structural response behavior slightly varied during the first test's first cycle compared to subsequent lift/lower cycles and tests, with the first cycle having a slightly smaller change in stress due to pin friction. The observed variation was likely caused by a larger release of built-up pin friction as the gate rested on the sill for a longer period of time. Additionally, dynamic behavior was observed in the strut responses indicating vibration in the gate during testing.
+ **DIRECTION/FRICTION REVERSAL IN RESPONSES:** The difference in stress during gate opening and closing for a given position is shown in Figure 8. The stress variation at any given gate position was a result of direction reversal and in turn due to trunnion friction reversal. This statement is true since all other loads such as dead-load and hydrostatic pressure were essentially constant barring small changes in hydrostatic pressure due to slight changes in head. This direction/friction reversal is depicted in Figure 9, with deflected shape renderings from a gate arm finite element model under lifting and lowering loads. Note that this figure shows an arm configuration that does not match this gate, but the concept of the direction/friction reversal still applies.
+ **MOTOR PERFORMANCE:** Current measurements taken at the hoist motor indicated steady and stable current draws during the lifting and lowering portions. An example plot of current draw and gate position is provided in Figure 10. Current draw ranges during lifting were higher than the ranges during lowering, which is common due to gravity/dead load. These results are summarized along with recorded peak in-rush current in Table 2. Note that the sample rates used during testing were set for collecting gate responses and may not have been appropriate to fully capture the in-rush current. The readings should be evaluated by a licensed electrician with knowledge of the operating parameters.

TORQUE AND HOIST FORCE: Due to restrictions caused by the hoist limit switches, the hoist cables could not always be fully slacked at the beginning and end of the performed tests. Throughout testing of the Rockwell Forney gates, it was found that this limit switch restriction varied gate to gate and arm to arm. Therefore, it is not recommended to use the collected torque and hoist force data to quantify overall hoist forces. Rather, this data was utilized to evaluate total friction behavior, which is observed as half the difference between the lifting and lowering torque/force (friction reversal). Note that issues with the wireless transmitter connected to the left gate hoist gages caused loss of all data for test runs 1 and 2 and partial loss of data for test run 3. While not optimal, this data loss did not significantly affect the hoist results summarized in this report.

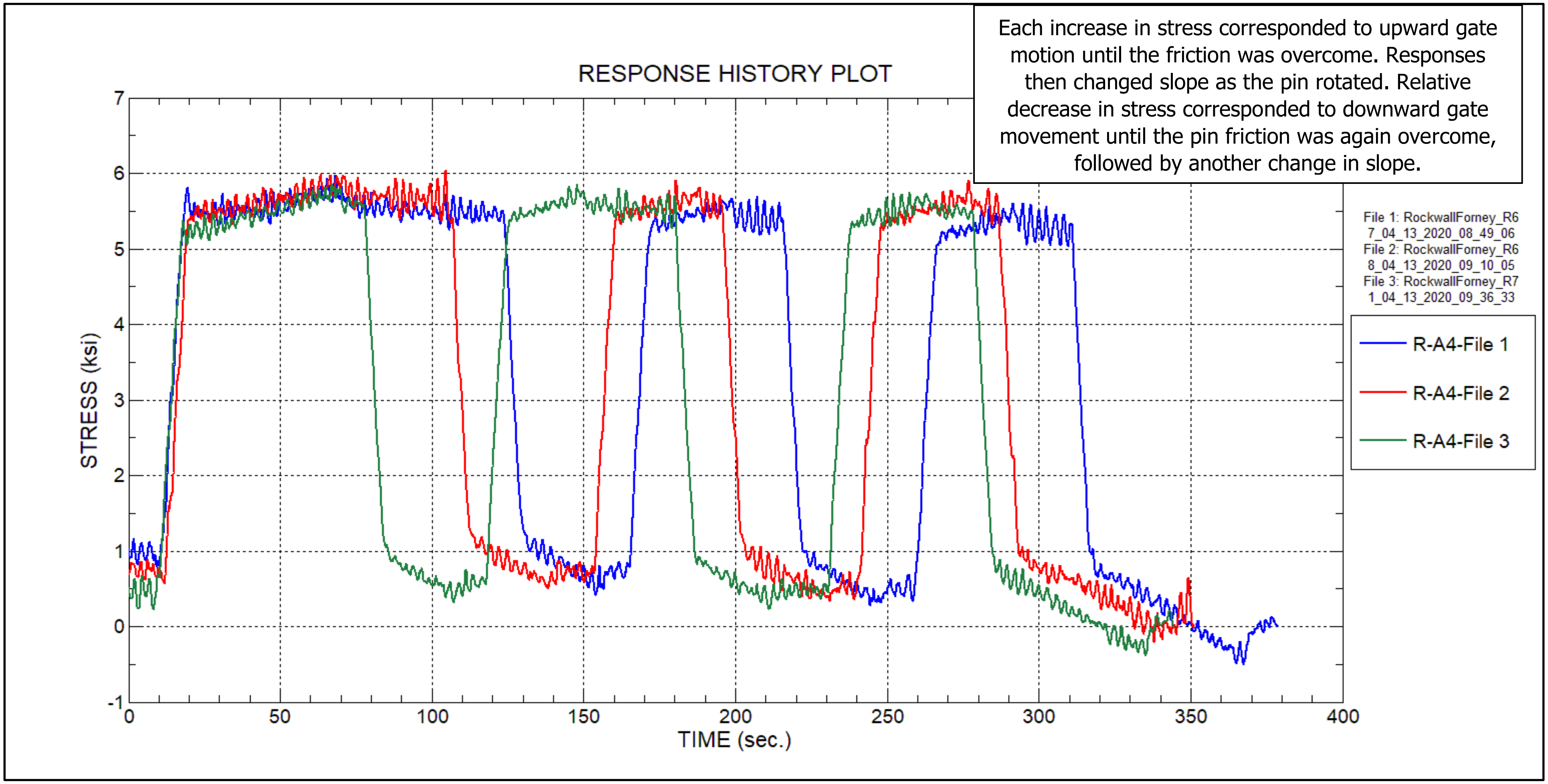

Figure 6 – Stress response history – Right arm – Gage A4 – Time based
File 1 = test run 1, File 2 = test run 2, File 3 = test run 3

(Section A along top strut near pin – Sensor location 4 along bottom of outer flange)

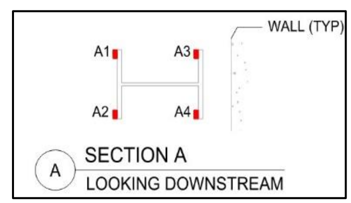

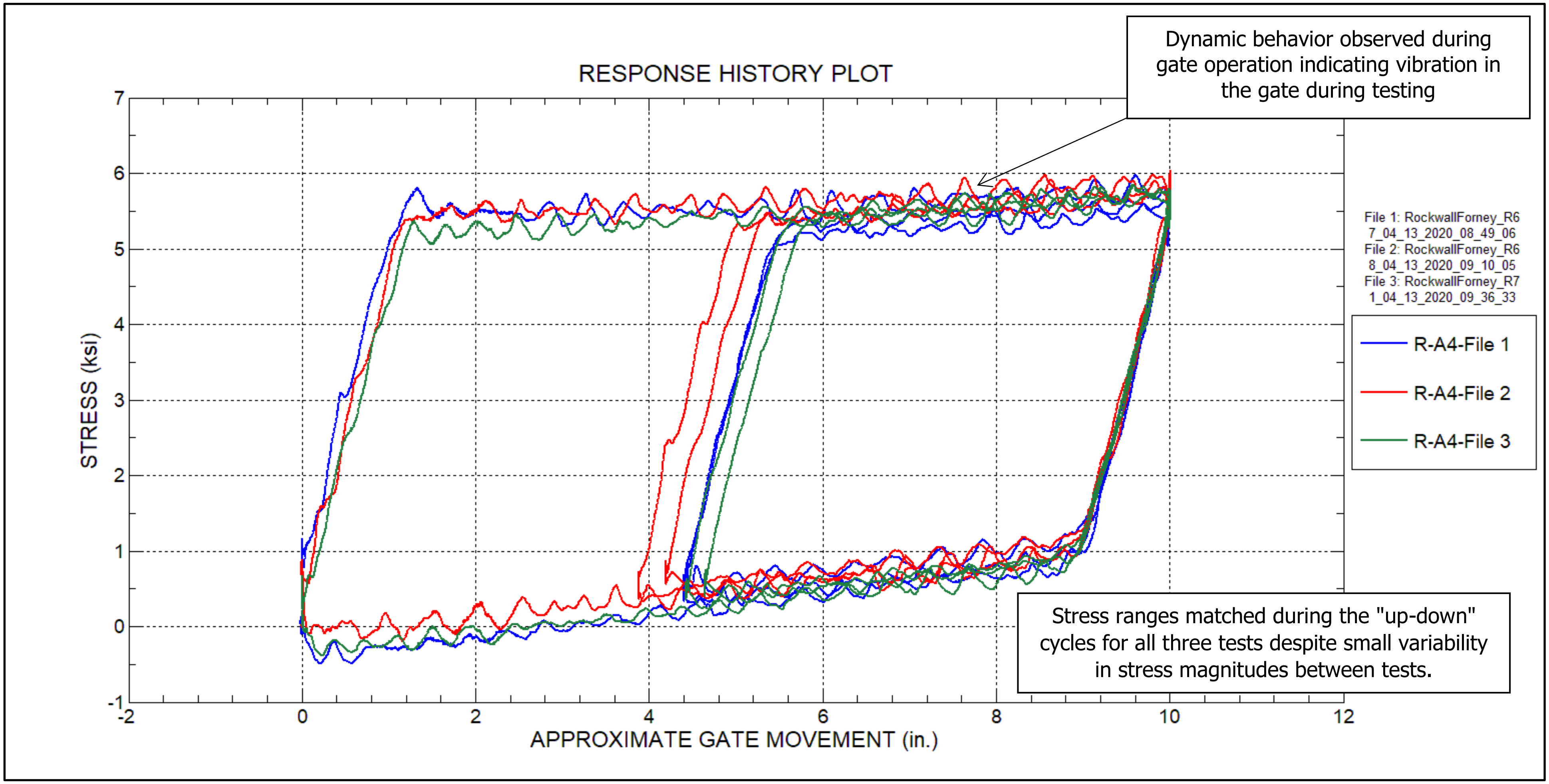

Figure 7 – Stress response history – Right arm – Gage A4 – Function of gate movement
File 1 = test run 1, File 2 = test run 2, File 3 = test run 3

(Section A along top strut near pin – Sensor location 4 along bottom of outer flange)

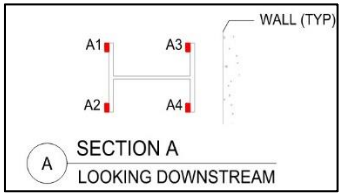

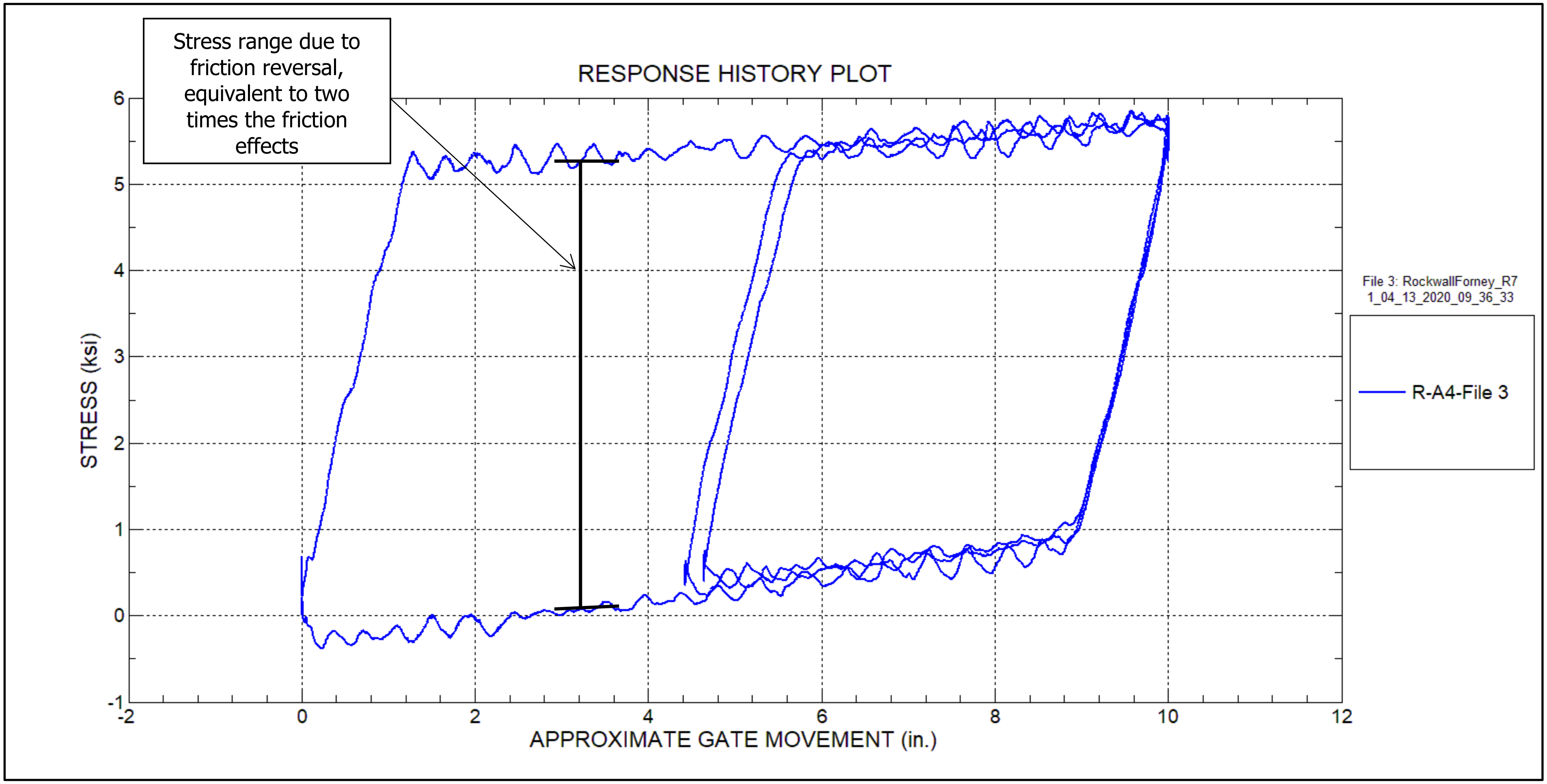

Figure 8 – Stress response history – Right arm – Gage A4 – Friction effect in stress responses

(Section A along top strut near pin – Sensor location 4 along bottom of outer flange)

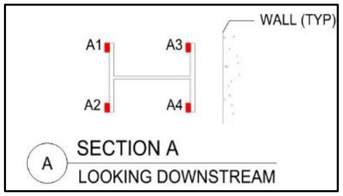

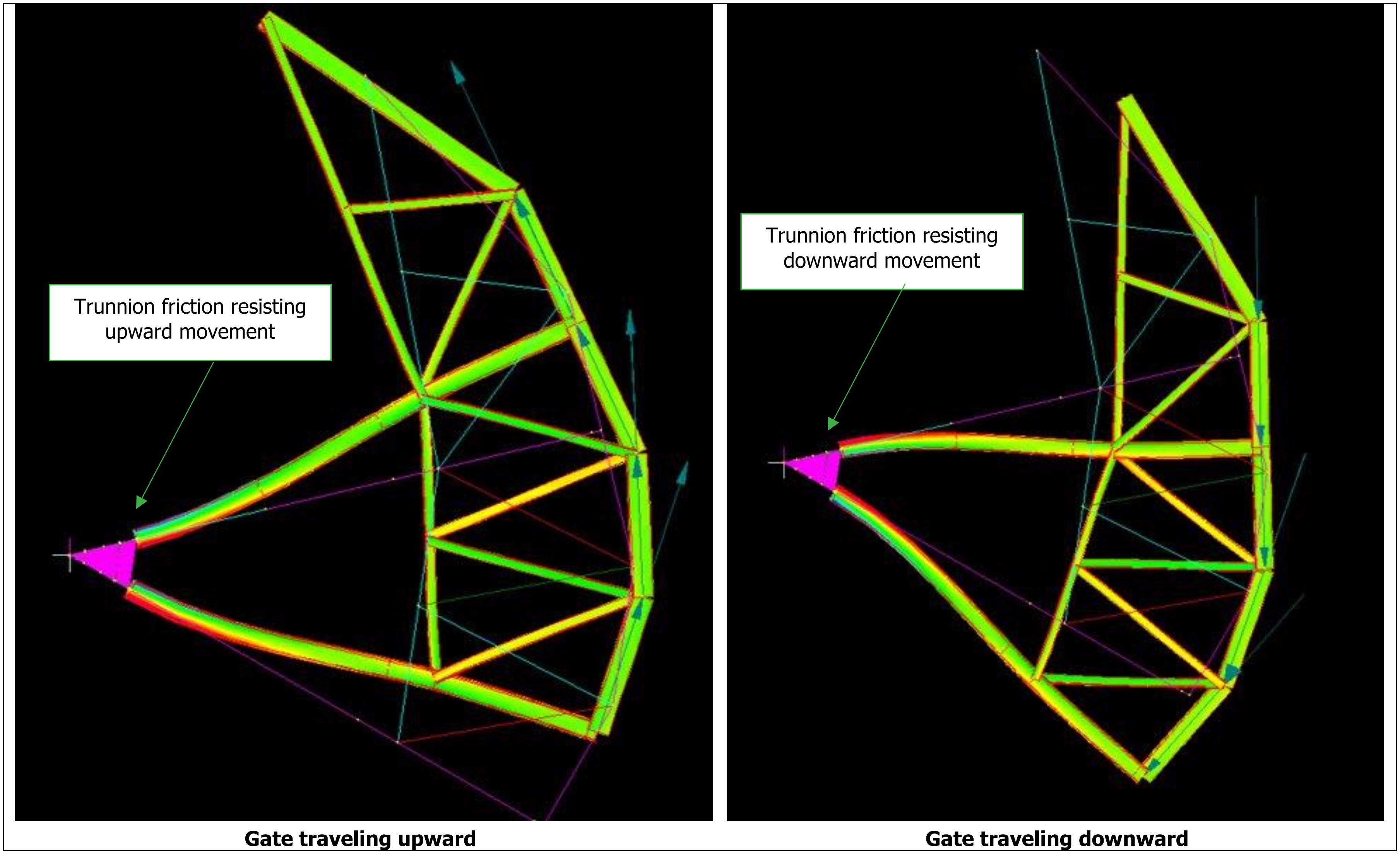

Figure 9 – Deflected shapes during lifting and lowering of Gate – Visualization of direction/friction reversals

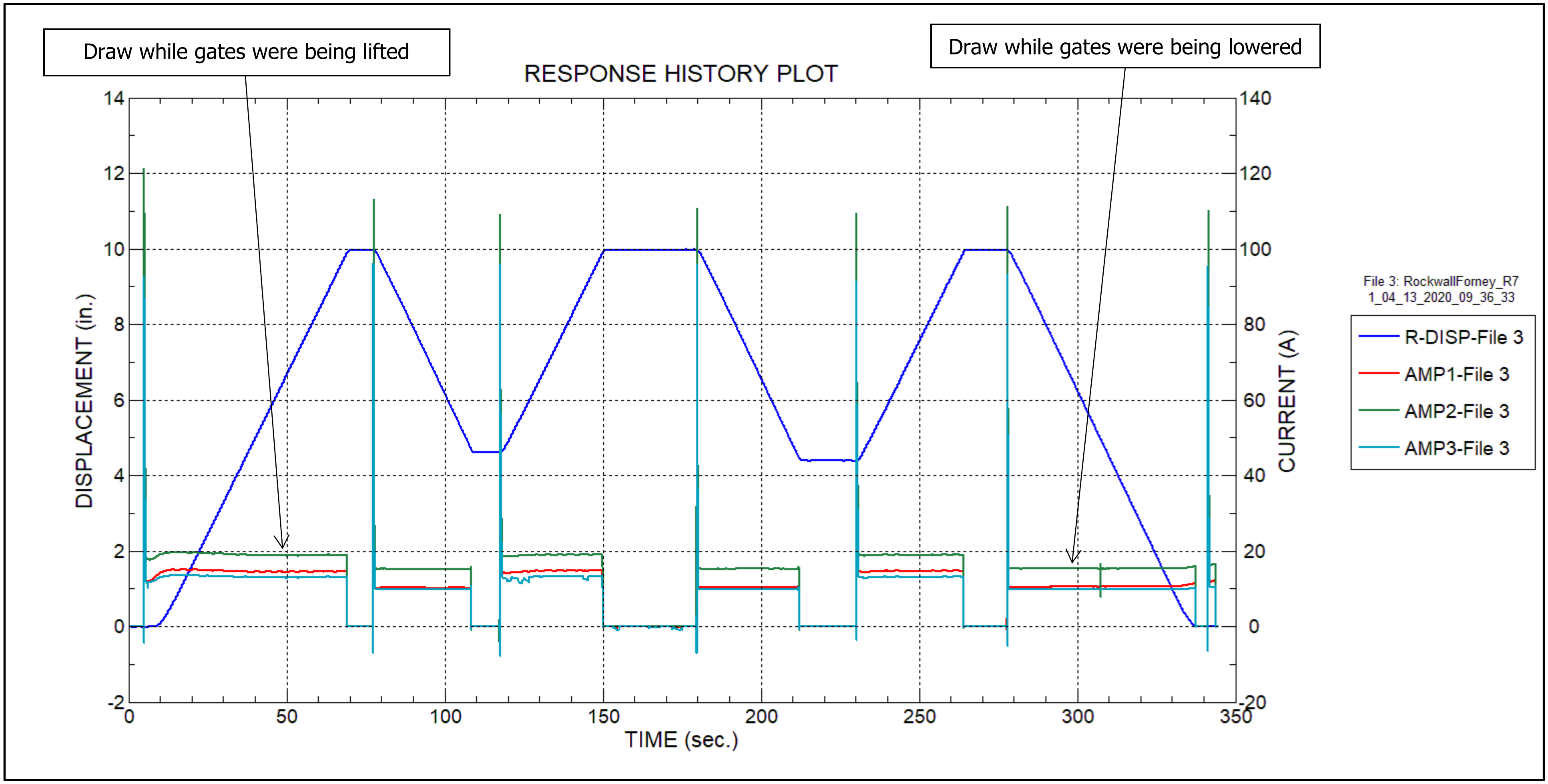

Figure 10 – Motor current & gate movement response history – Lift motor – Highlighting motor draw during lift and lower cycles

METHODOLOGY AND FINDINGS OF THE STRUT FORCE AND MOMENT CALCULATIONS

The following outline provides the methodology used to calculate the required member forces and moments.

- **CHANGE IN STRESS DUE TO GATE OPERATION:** Strain data can be viewed as a function of time starting when the gate was in the down position and was then lifted off the sill. When examining data in this manner, it is easy to see how stresses ramped up as the gate began to move and then changed slope once pin friction was overcome and the trunnion hub began to rotate with the gate. The first point in time where the friction was overcome (both lifting and lowering) has been highlighted in the stress histories shown in Figure 11. These stress histories show the response of all four sensors along the top strut of the right arm (Section A). ***It is important to note that the recorded measurements were changes in structural response due to gate movement, and do not include the in-situ stresses due to the dead load, cable wrap, and hydrostatic loads present prior to testing.***
- **CALCULATION OF STRUT CROSS-SECTIONAL MOMENTS:** The use of four strain gages per strut cross-section allowed accurate in-plane flexural bending moments to be computed from the recorded strain measurements. These moments were computed for every cross-section in each gate arm using the basic mechanics equation provided in Figure 12.

  In-plane or weak-axis flexure refers to bending about a given strut's web. This designation is consistent with typical nomenclature. In-plane bending can be observed visually from the strain response histories as a difference between the top and bottom stresses, whereas out-of-plane or strong-axis bending is visualized as the difference in stress from side to side. Figure 13 provides a visual reference for both types of strut flexure.
- **EXAMINATION OF RESPONSES AS A FUNCTION OF GATE POSITION:** Changes in cross-sectional moment related to friction becomes clearer when the responses are plotted as a function of gate position. Because the gate was operated with several up and down movements, the effects of friction associated with each direction reversal can be viewed for all measured and calculated responses. Figure 14 through Figure 17 show all cross-sectional flexural moment plots for both trunnion arms. The responses in these plots have been centered about the stress state corresponding to a zero-moment, unflexed condition. The zero-moment offset was estimated as the average moment values between up and downward movement (i.e. half the moment difference) at the gate position with the greatest pin friction moment difference (greatest difference between lifting and lowering).
- **TRUNNION FREE-BODY-DIAGRAM & PIN MOMENT CALCULATION:** Figure 18 shows the instrumented member cross-sections and shows how the measured cross-sectional flexural responses were used to compute pin moment. The in-plane moment values used in these calculations were determined directly from the strain measurements at each cross-section using the provided mechanics equations. It should be noted that the out-of-plane moments were not considered in the calculation of pin moment since they were orthogonal to the axis of the pin rotation. Total pin moment was then determined by summing all the moment components about the pin, which included the in-plane moment and the shear components at the strut cross-sections nearest the pin.
- **STRUT SHEAR CALCULATION:** From the examination of the trunnion free-body-diagram described above, the shear vectors at the three struts were a primary component in the pin moment calculation. For this type of structural element, shear vectors were calculated using the moment differential between the two cross sections along each strut. It is important to recognize that shear was constant between the two instrumented cross-sections and the applied shear was a function of the recorded change in moment ($V = dM/dX$). Subsequently, the shear vectors were calculated by dividing the difference in moment by the distance between the two instrumented cross-sections. Shear values for each strut have been plotted as a function of gate position in Figure 19 and Figure 20.

- **CALCULATION OF PIN MOMENT DUE TO FRICTION:** Once all the trunnion arm force vectors were calculated, the equations shown in the free-body-diagram were applied to compute pin moment as a function of gate position. It is important to note that because the calculated pin moment range corresponds to a direction reversal, a reversal in friction also occurred. The effect of direction reversal on pin moment due to friction is best conceptualized by centering the moment response plots about the zero-moment axis. The moment due to lifting and the moment due to lowering can then be visualized as a change from this new zero point corresponding to the gate in an unflexed condition. Therefore, the total moment differential between lifting and lowering was twice the moment due to friction acting in a single direction. Pin-moment plots have been provided in Figure 21 and Figure 22. From these plots, it is apparent that pin moment due to friction remained relatively constant throughout the gate operation tests, with a slight decrease in pin friction moment as the gate continued to be lifted. This slight decrease in pin friction moment most likely corresponded to the change in hydrostatic load as the gate position changed. Pin-moment plots for all tests on Gate 12 are also provided for reference in Appendix B – Gate 12 Pin Moment Component Plots.
- **SHAFT TORQUE & HOIST FORCE:** Torque measurements were taken on the pinion shafts near the hoist motor during testing, with single torque gages installed on the left and right hoist pinion shaft. Responses were recorded in units of micro-strain and converted to torque in units of kip-ft using Equation 1 thru Equation 3 and the following shaft properties.

$$d_O = 5.5\,inches, \qquad d_I = 0\,inches, \qquad E = 29000\,ksi, \qquad \nu = 0.3$$

$$G = \frac{E}{2(1+\nu)}$$

Equation 1

$$J = \frac{\pi\left({d_O}^4 - {d_I}^4\right)}{32}$$

Equation 2

$$\tau = \varepsilon * \frac{2GJ}{\frac{d_O}{2} * 1000000 * 12}$$

Equation 3

Figure 23 shows example torque measurements, recorded on the Gate 12 torque shafts. Best practices for torque measurements is to measure torque on opposite sides of the shaft so that any bending in the shaft can be removed by averaging the two responses. Due to access limitations, only one gage at each location could be installed. Therefore, any bending in the shaft may be reflected in the torque measurements and may be related to the peaks and valleys observed in the torque responses.

Torque values were converted to force in the hoist cables per gate arm using the gear ratio and drum radius, as shown in Figure 24. The gear ratio and drum radius were 5.182 and 1.086 feet respectively, as defined in the provided as-built shop drawings. It should be noted that the hoist force calculated may be smaller than the actual hoist force applied. This difference is due to the limit switch engaging the brake before the hoist cable was fully slacked, resulting in an initial force in the cable. A hoist force due to total gate friction was then calculated. This friction hoist force was equal to half the differential in force measured during the lifting and lowering of the gate (similar to the pin friction calculations). As shown in Table 3, the change in cable force due to friction was generally consistent between tests. Note that the total hoist force was due to the total friction effects, including side seal, hoist bearings, trunnion friction effects, etc . It is difficult to determine the exact proportion and composition of the total friction sources. Additional torque and hoist force plots for all collected data files are provided in Appendix A – Gate 12 Torque and Hoist Force Plots.

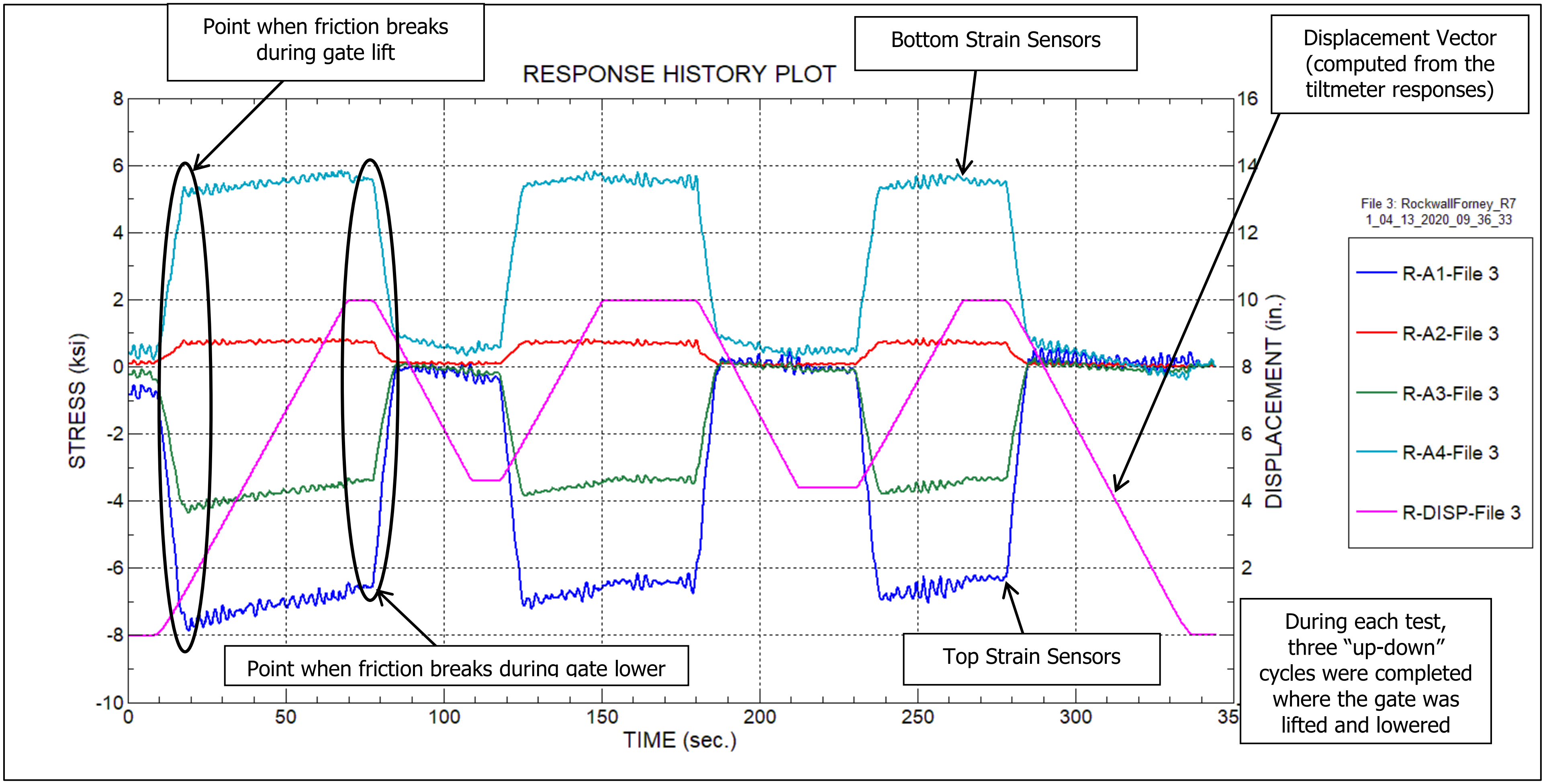

Figure 11 – Stress response & gate movement history – Right arm – Section A - Highlighting friction behavior
(Section A along top strut near pin)

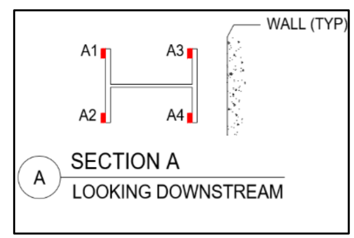

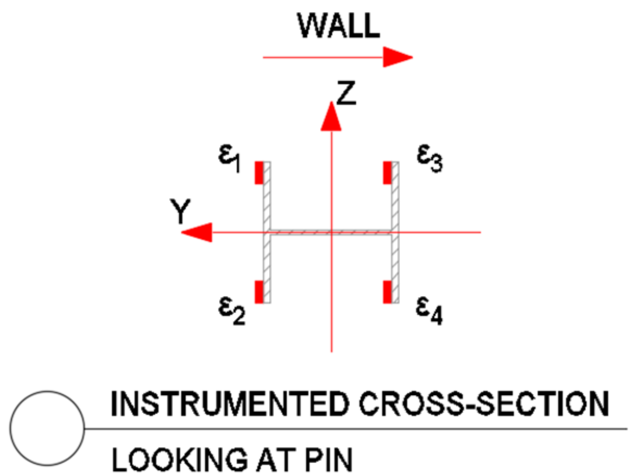

Calculation of Weak-axis (In-plane) bending

$$M_Y = \frac{E\left[\frac{\varepsilon_2 + \varepsilon_4}{2} - \frac{\varepsilon_1 + \varepsilon_3}{2}\right] S_{Y(gage)}}{2}$$

Sy(gage) = Section modulus to the center of gages (not extreme fiber of flanges)
(locations of gages were accounted for in moment computation)

Figure 12 – Basic mechanic equation used to calculate moment

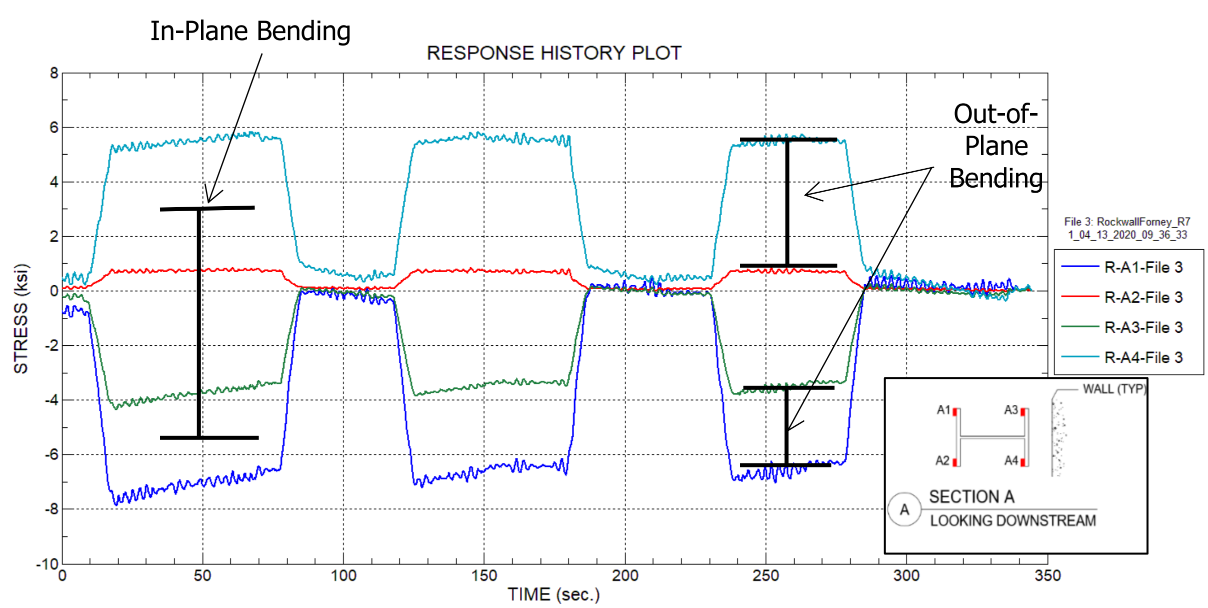

Figure 13 – Stress response history – Right arm – Section A – Bending components
(Section A along top strut near pin)

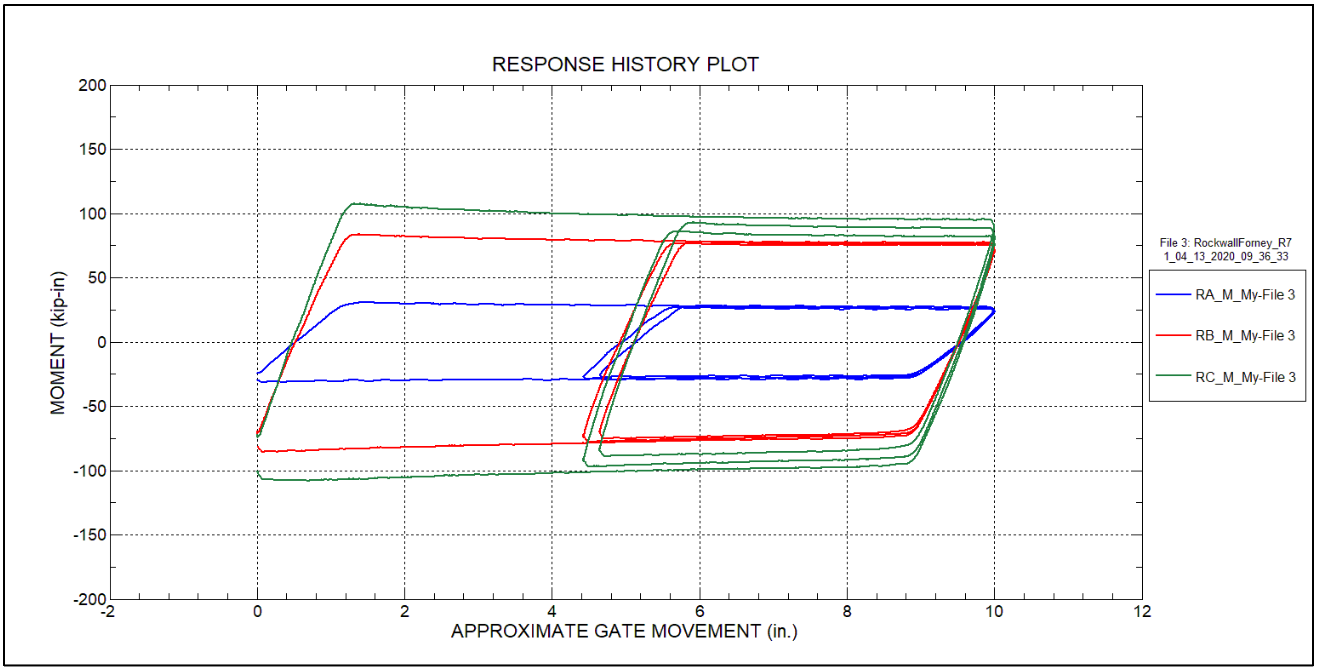

Figure 14 – In-plane moment response history – Right arm – Sections near pin

(RA = Right Arm Top Strut, RB = Right Arm Middle Strut, RC = Right Arm Bottom Strut)

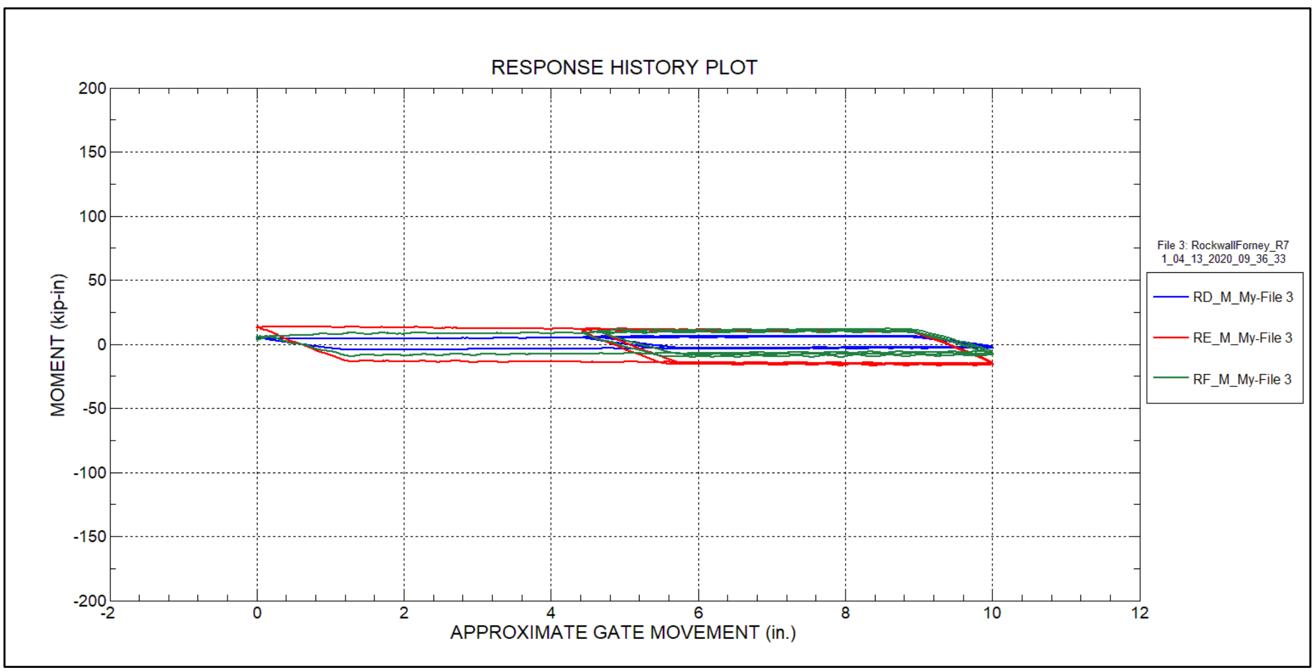

Figure 15 – In-plane moment response history – Right arm – Sections away from pin

(RD = Right Arm Top Strut, RE = Right Arm Middle Strut, RF = Right Arm Bottom Strut)

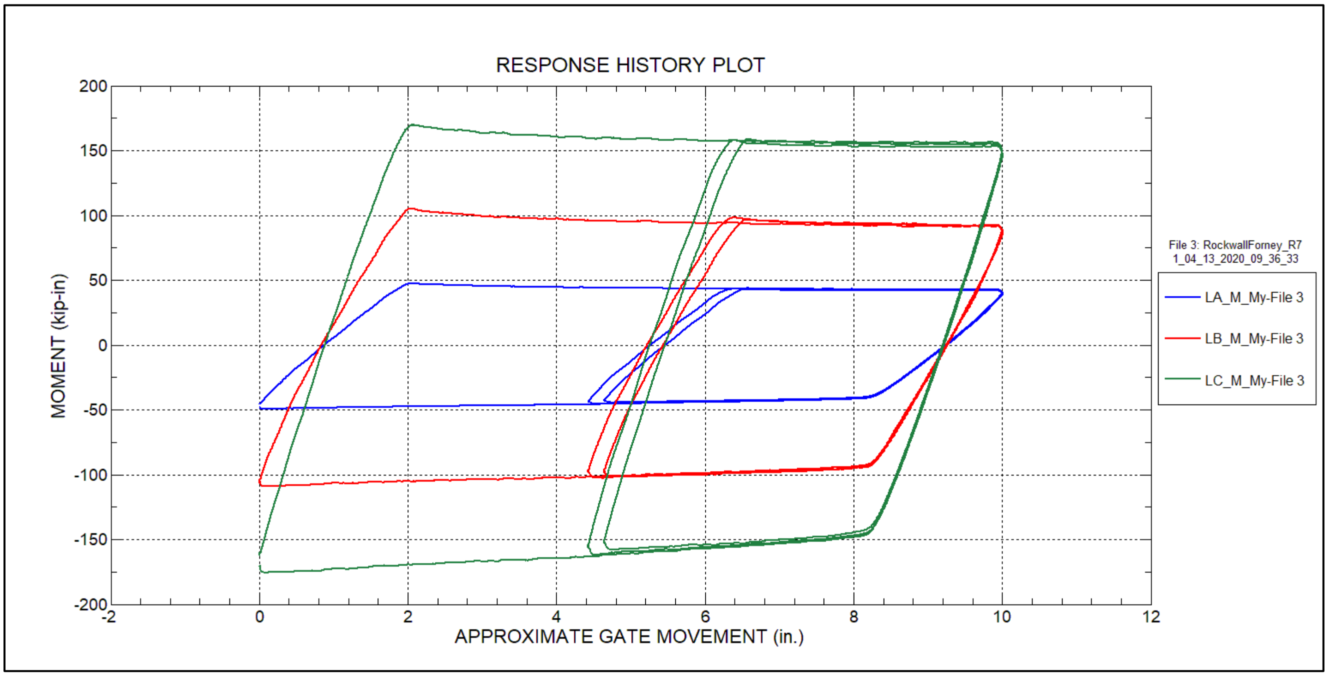

Figure 16 – In-plane moment response history – Left arm – Sections near pin

(LA = Left Arm Top Strut, LB = Left Arm Middle Strut, LC = Left Arm Bottom Strut)

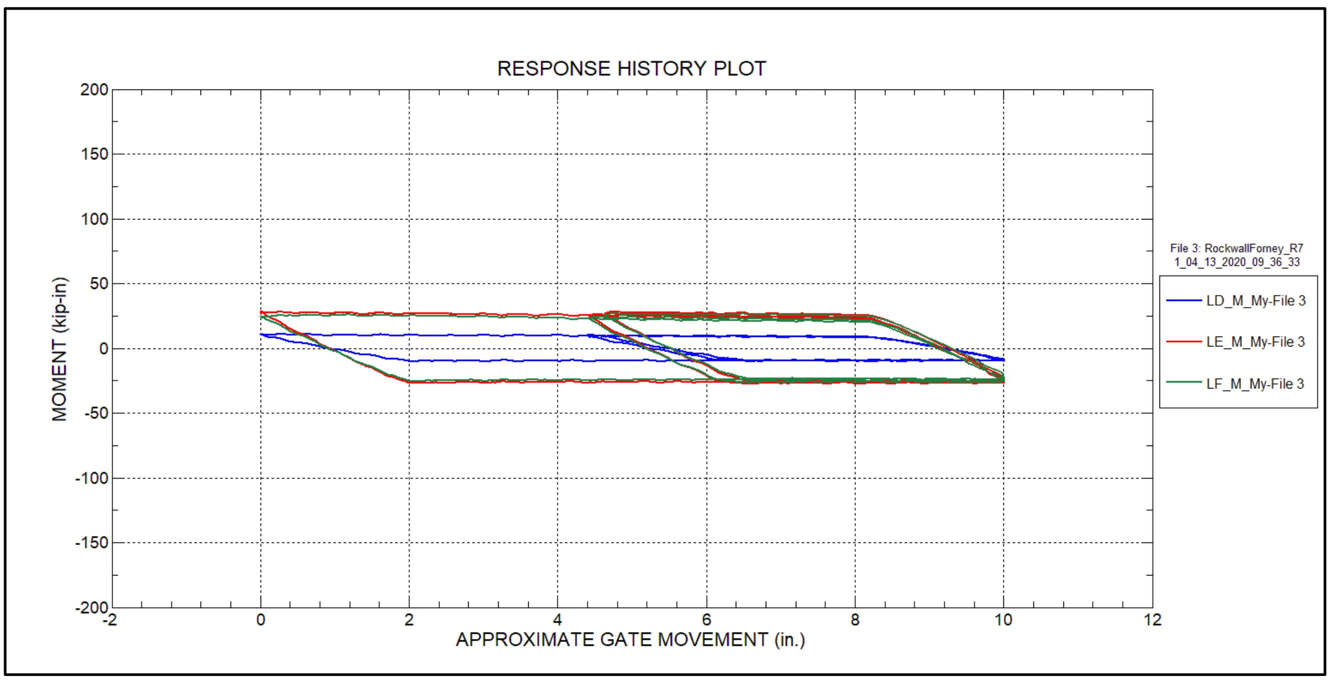

Figure 17 - In-plane moment response history – Left arm – Sections away from pin

(LD = Left Arm Top Strut, LE = Left Arm Middle Strut, LF = Left Arm Bottom Strut)

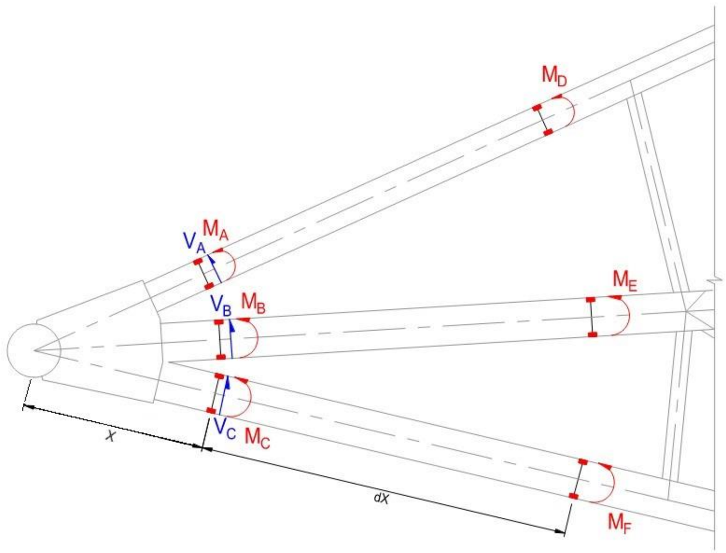

Elevation View of Gate Arm

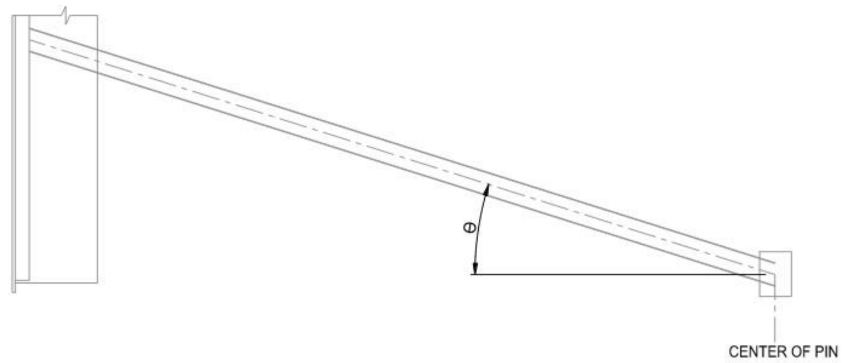

Plan View of Gate Arm

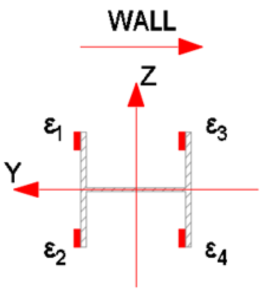

$$M_Y(M_A, M_B, M_C, M_D, M_E, M_F) = \frac{E\left[\frac{\varepsilon_2 + \varepsilon_4}{2} - \frac{\varepsilon_1 + \varepsilon_3}{2}\right] S_{Y(gage)}}{2}$$

$$V_A = \frac{M_A - M_D}{dX}$$

$$V_B = \frac{M_B - M_E}{dX}$$

$$V_C = \frac{M_C - M_F}{dX}$$

$$\sum M_o = 0$$

$$M_{PIN} = [X(V_A + V_B + V_C) + M_A + M_B + M_C]\cos\theta$$

Figure 18 – Direct calculation of pin moment from strain measurements

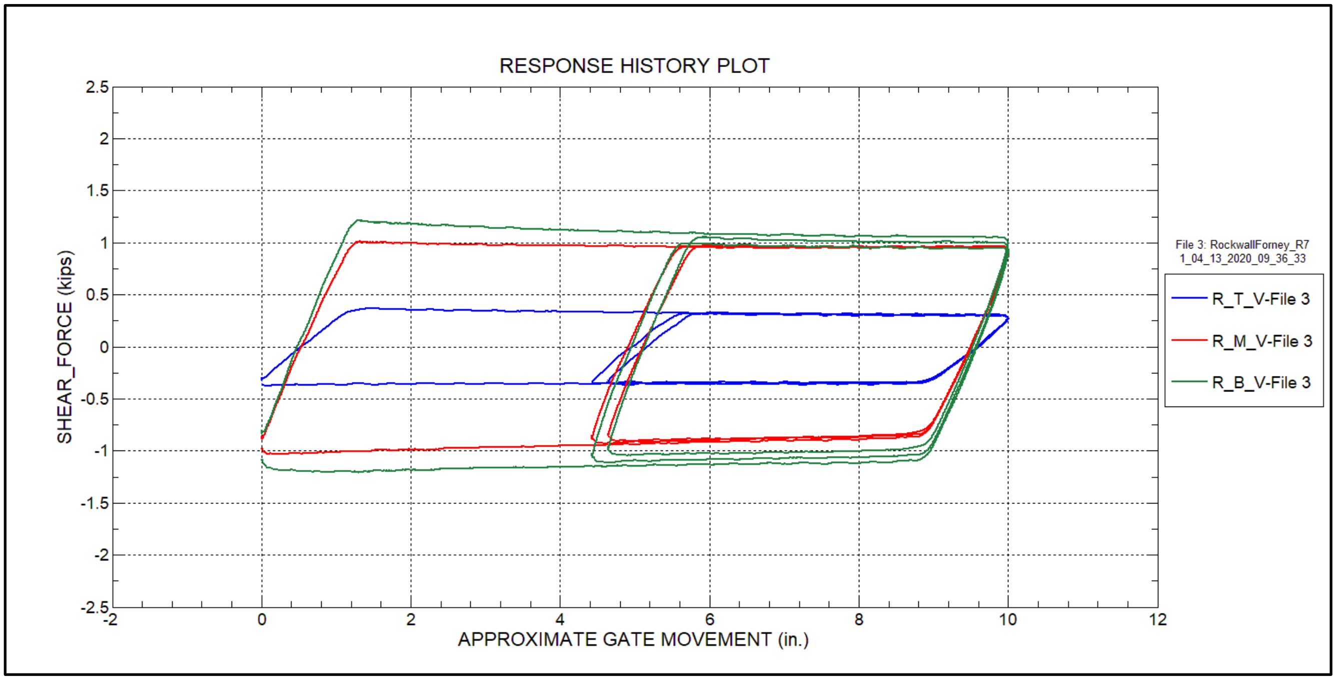

Figure 19 – Strut shear response history – Right arm

(R_T = Right Arm Top Strut, R_M = Right Arm Middle Strut, R_B = Right Arm Bottom Strut)

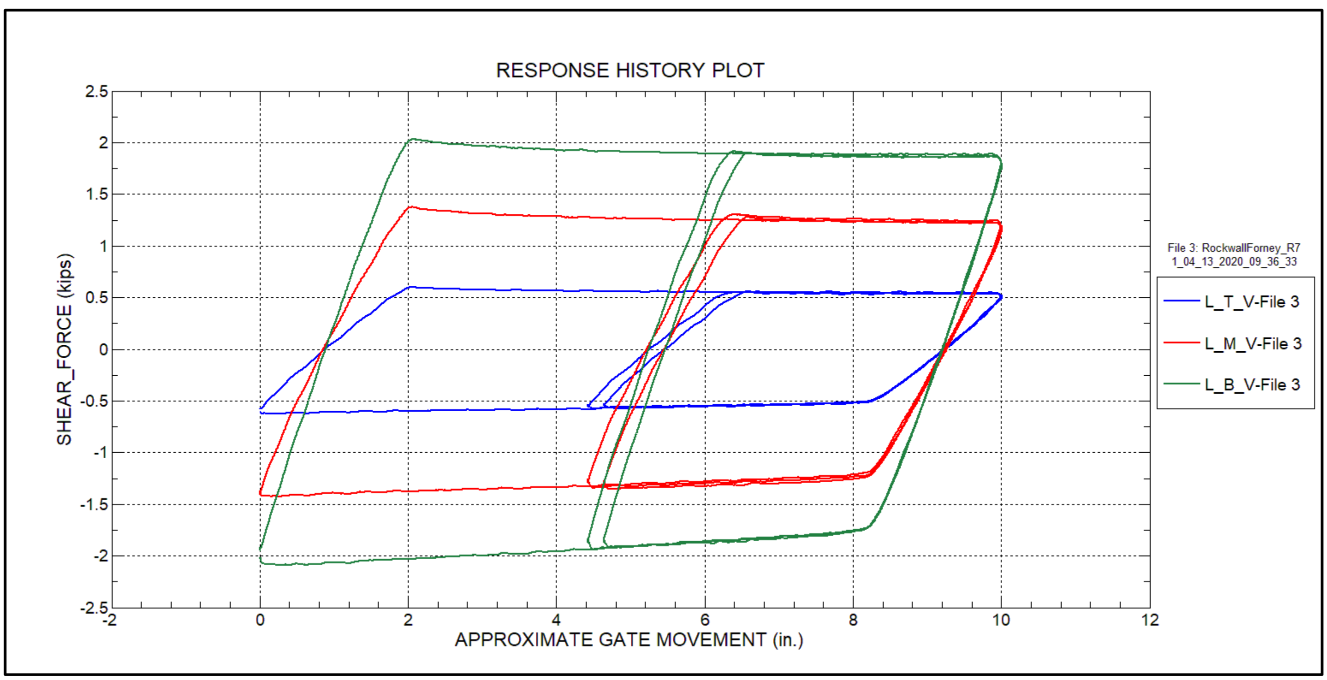

Figure 20 – Strut shear response history – Left arm

(L_T = Left Arm Top Strut, L_M = Left Arm Middle Strut, L_B = Left Arm Bottom Strut)

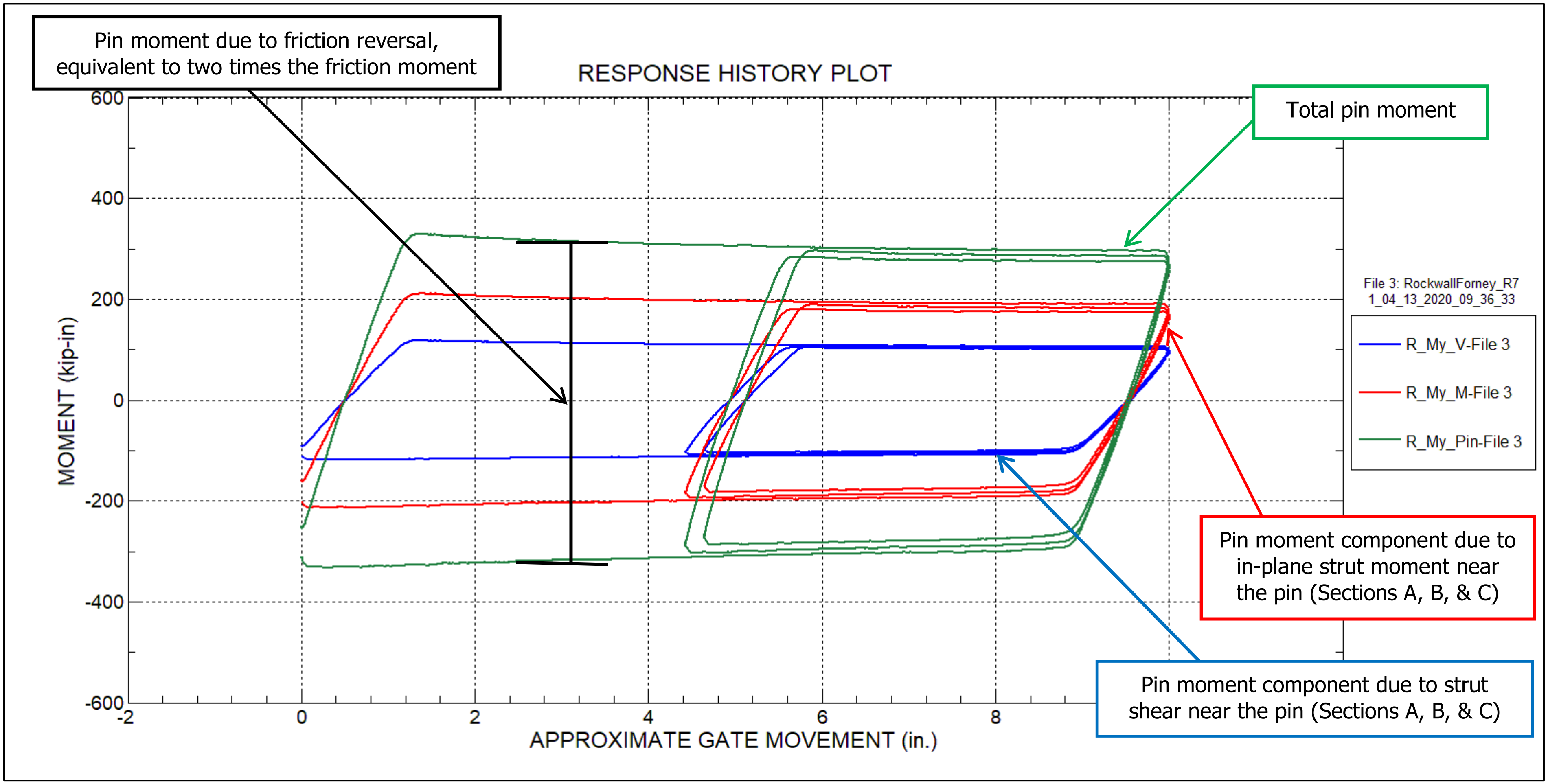

Figure 21 – Pin moment response history – Right arm

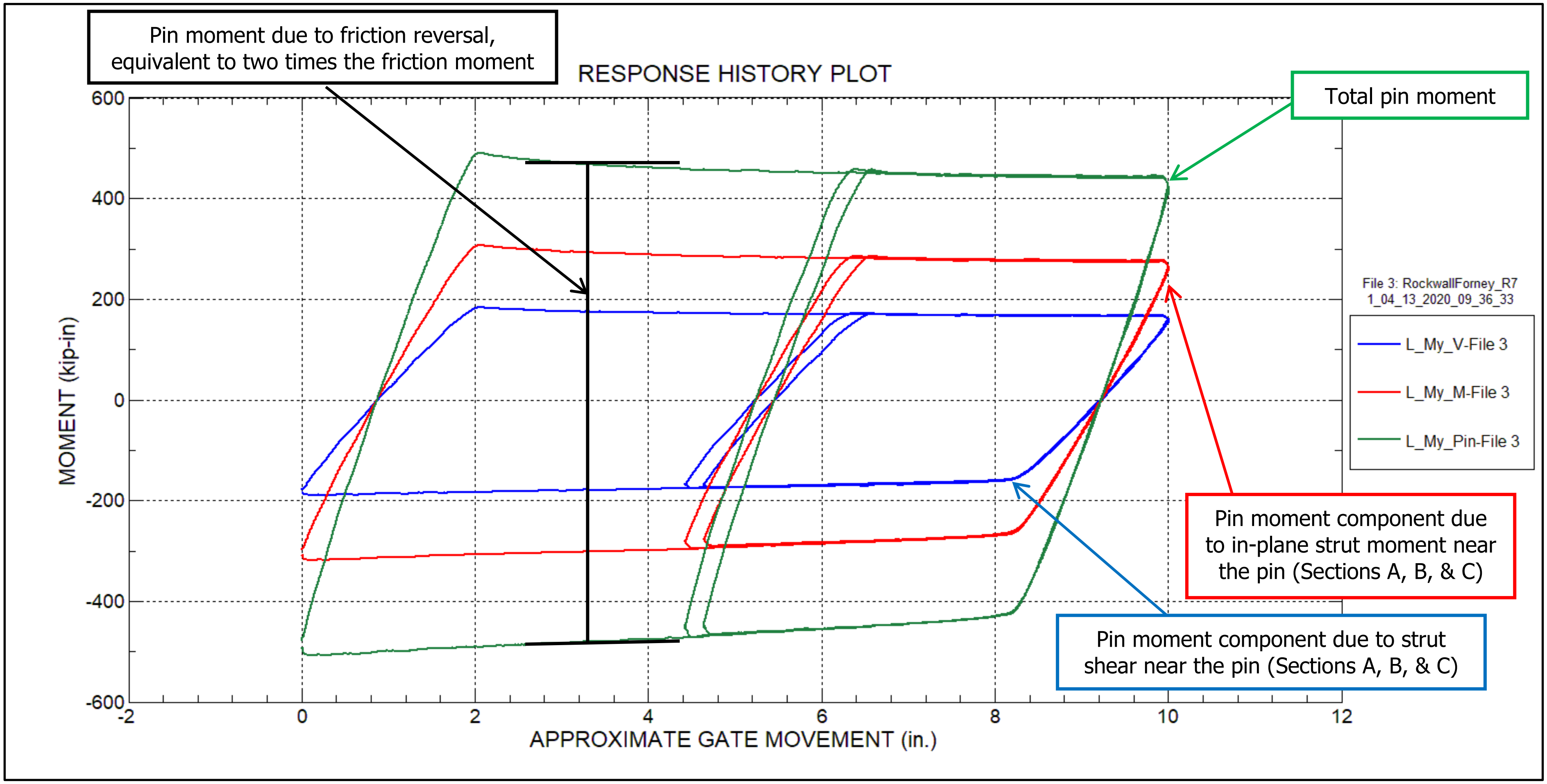

Figure 22 – Pin moment response history – Left arm

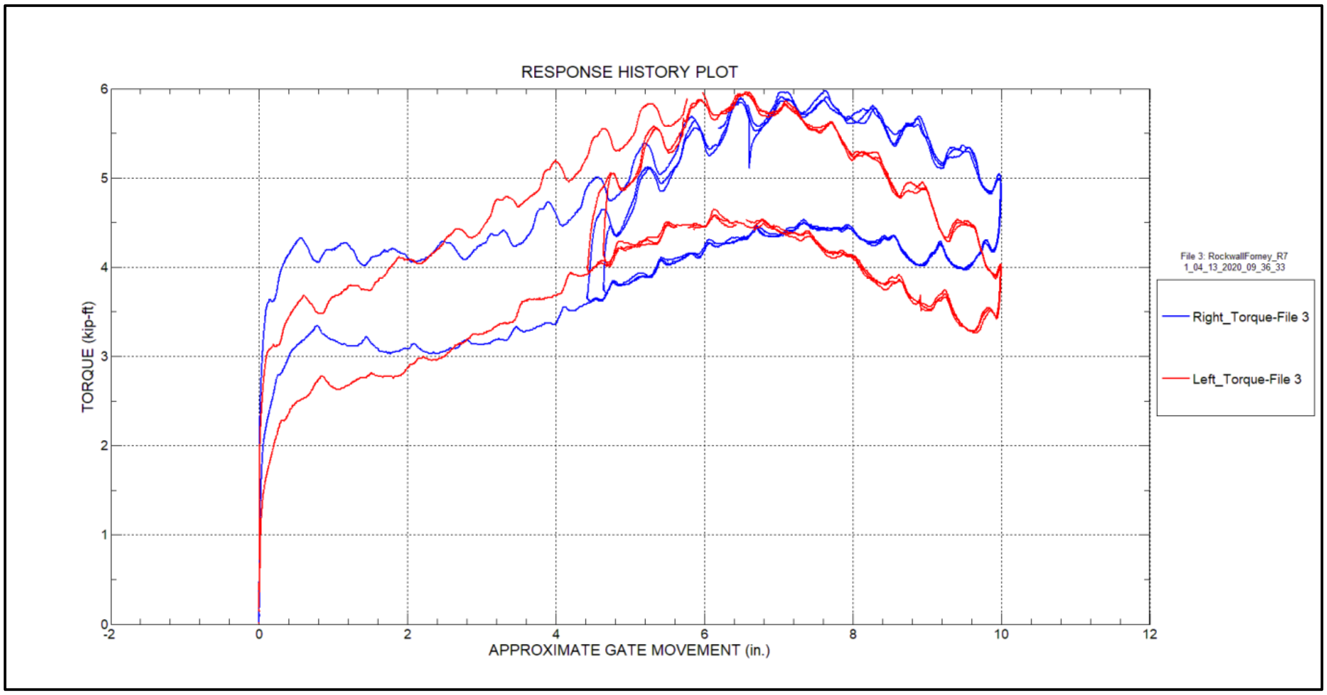

Figure 23 – Hoist torque response history – Gate 12 – Test 2
Note: missing data due to wireless connectivity issues as the sensor rotates with the pinion shaft

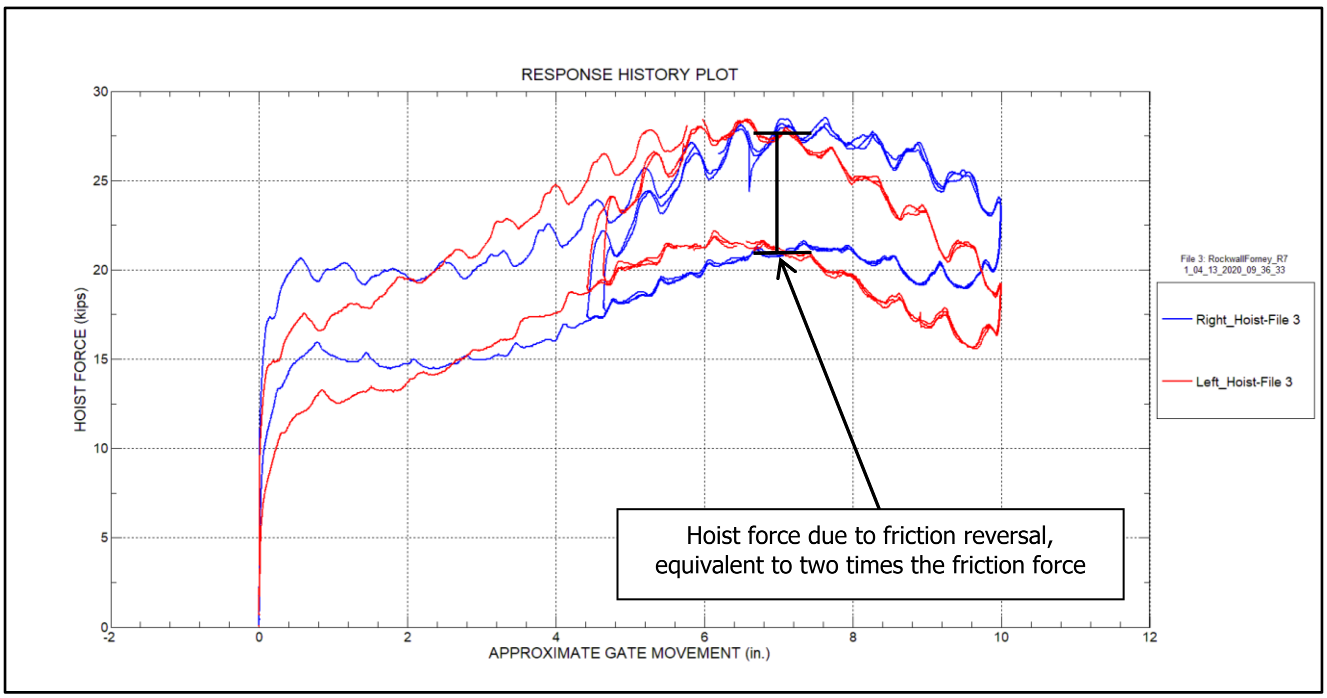

Figure 24 – Hoist force response history – Gate 12 – Test 2
Note: missing data due to wireless connectivity issues as the sensor rotated with the pinion shaft

Summary of Friction Results

The raw data files have been included in the submittal package for reference and were formatted as "tdms" files that can be opened in Microsoft Excel using a "tdms" reader extension.

Examination of the stress histories for each test was necessary to obtain a thorough understanding of the gate performance. The response shapes, variations in stress magnitudes, and timing sequences provided direct clues as to how the gate performed under typical service conditions. The following is a breakdown of the provided tabulated results:

+ Table 2 provides motor current ranges and maximum in-flow for lift and lower cycles for each test
+ Table 3 provides maximum hoist force as well as hoist force due to total friction for each test
+ Table 4 provides the maximum stress ranges measured at the sensor locations for each member
+ Table 5 provides maximum bending stress and moment ranges observed during the gate tests
+ Table 6 provides maximum friction bending stress and moment values at each of the instrumented strut locations
+ Table 7 provides the computed shear values in each strut due to friction
+ Table 8 provides calculated measured friction moments, calculated hydrostatic loads based on the measured water elevation, and coefficients of friction for each gate and gate arm during all three tests

The resulting pin friction moments were used to compute friction coefficients from Eq. 4, given the pin radius and the applied thrust. The thrust used in this calculation consisted of the calculated resultant hydrostatic load based on the measured water elevation and was adjusted to account for the loss of head as the gate was lifted. This thrust adjustment was based on the recorded gate movement and was performed in order to calculate more accurate friction coefficients. The water elevation during testing was nearly constant throughout each gate test and was documented during each "up-down" cycle. It should be noted that the minor thrust due to cable wrapping, which was minimal compared to hydrostatic thrust, was not included in the thrust calculation. This assumption resulted in slightly conservative friction coefficients.

$$\mu = \frac{M_F}{T * r} \qquad \text{Eq. 4}$$

where:

μ	=	Friction Coefficient
M_F	=	Friction Moment
T	=	Thrust per Pin
r	=	Pin Radius, 5.375"

The out-of-plane shear and moments were not considered in the pin friction calculations due to orthogonal geometry considerations (resulting pin moment associated with out-of-plane flexure being perpendicular to pin rotation).

The data was presented in a specific coordinate system applicable to both arms. Data was processed so that the positive x-axis was always pointing towards the pin and the right-hand rule applied. In-plane bending can be referred to as "bending about the horizontal or y-axis" and shows how much the beams bend up and down within the plane of the gate arms. Refer to Figure 12 above for visual reference of coordinate system and mathematical explanation of calculations. Tabulated results do not include any in-situ effects.

Table 2 – Motor current summary table – Gate 12

Test Run	Current Range due to Lifting (A)	Current Range due to Lowering (A)	Max In-rush Current (A)
1	14-20	10-15	121
2	14-19	10-15	124
3	14-19	10-15	123

Table 3 – Hoist force summary table – Gate 12

Test Run	Right Arm Peak Hoist Force (kips)	Left Arm Peak Hoist Force (kips)	Right Arm Hoist Force due to Total Gate Friction (kips)	Left Arm Hoist Force due to Total Gate Friction (kips)
1	28.17	N/A	4.02	N/A
2	27.88	26.90	4.01	N/A
3	28.51	28.45	3.99	3.77

Tabulated friction force values correspond to the response induced by friction in one direction

Table 4 – Maximum measured sensor stress range

ARM DESIGNATION	Top Strut (ksi)	Middle Strut (ksi)	Bottom Strut (ksi)
RIGHT ARM	8.43	9.11	9.39
LEFT ARM	10.93	12.66	13.38

Tabulated values correspond to the total measured change in response during tests

Stress values have not been extrapolated to the extreme fibers (correspond to center of gage)

Table 5 – Maximum in-plane total bending stress & moment ranges – Total

SECTION LABEL	Section Description	Right Arm Stress (ksi)	Right Arm Moment (kip-in)	Left Arm Stress (ksi)	Left Arm Moment (kip-in)
SECTION A	Top Strut Near Pin	5.67	63.76	9.74	109.50
SECTION B	Middle Strut Near Pin	7.88	182.14	10.39	240.40
SECTION C	Bottom Strut Near Pin	7.74	215.79	13.12	365.75
SECTION D	Top Strut Away from Pin	1.00	11.18	2.18	24.52
SECTION E	Middle Strut Away from Pin	1.37	31.75	2.54	58.69
SECTION F	Bottom Strut Away from Pin	0.80	22.22	1.92	53.42

Tabulated values correspond to the total measured change in response during tests

Table 6 – In-plane frictional bending stress & moment at maximum gate friction

SECTION LABEL	Section Description	Right Arm Stress (ksi)	Right Arm Moment (kip-in)	Left Arm Stress (ksi)	Left Arm Moment (kip-in)
SECTION A	Top Strut Near Pin	2.78	31.23	4.78	53.76
SECTION B	Middle Strut Near Pin	3.88	89.72	5.11	118.20
SECTION C	Bottom Strut Near Pin	3.84	107.21	6.45	179.81
SECTION D	Top Strut Away from Pin	0.44	4.92	0.91	10.21
SECTION E	Middle Strut Away from Pin	0.61	14.13	1.17	27.10
SECTION F	Bottom Strut Away from Pin	0.31	8.63	0.92	25.53

Tabulated values correspond to the response induced by friction in one direction

Table 7 – Strut shear range summary table due to friction

ARM DESIGNATION	Top Strut Shear (kip)	Middle Strut Shear (kip)	Bottom Strut Shear (kip)
RIGHT ARM	0.37	1.07	1.20
LEFT ARM	0.64	1.51	2.12

Tabulated values correspond to the response induced by friction in one direction

Table 8 – Pin friction summary table

TEST RUN	Average Water Elevation during testing (ft)	Approximate Thrust at time of Testing (kips per arm)	Gate/Member Designation	Pin Friction Moment (kip-in)	Friction Coefficient
1	435.71	494.40	Right Pin	335.0	0.13
			Left Pin	530.7	0.2
2	435.71	494.40	Right Pin	324.6	0.12
			Left Pin	503.7	0.19
3	435.71	494.40	Right Pin	328.7	0.12
			Left Pin	491.3	0.18

Tabulated values correspond to the response induced by friction in one direction

APPENDIX A – GATE 12 TORQUE AND HOIST FORCE PLOTS

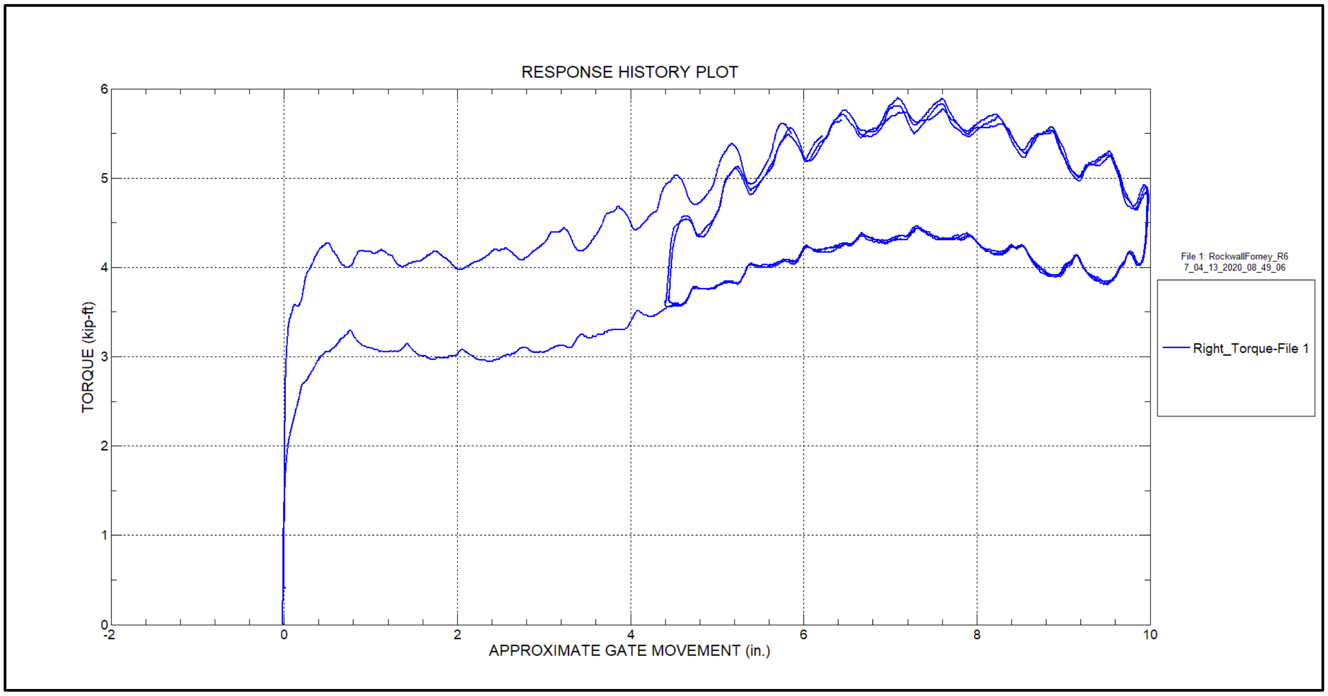

Figure 25 – Hoist torque response history – Gate 12 – Test 1

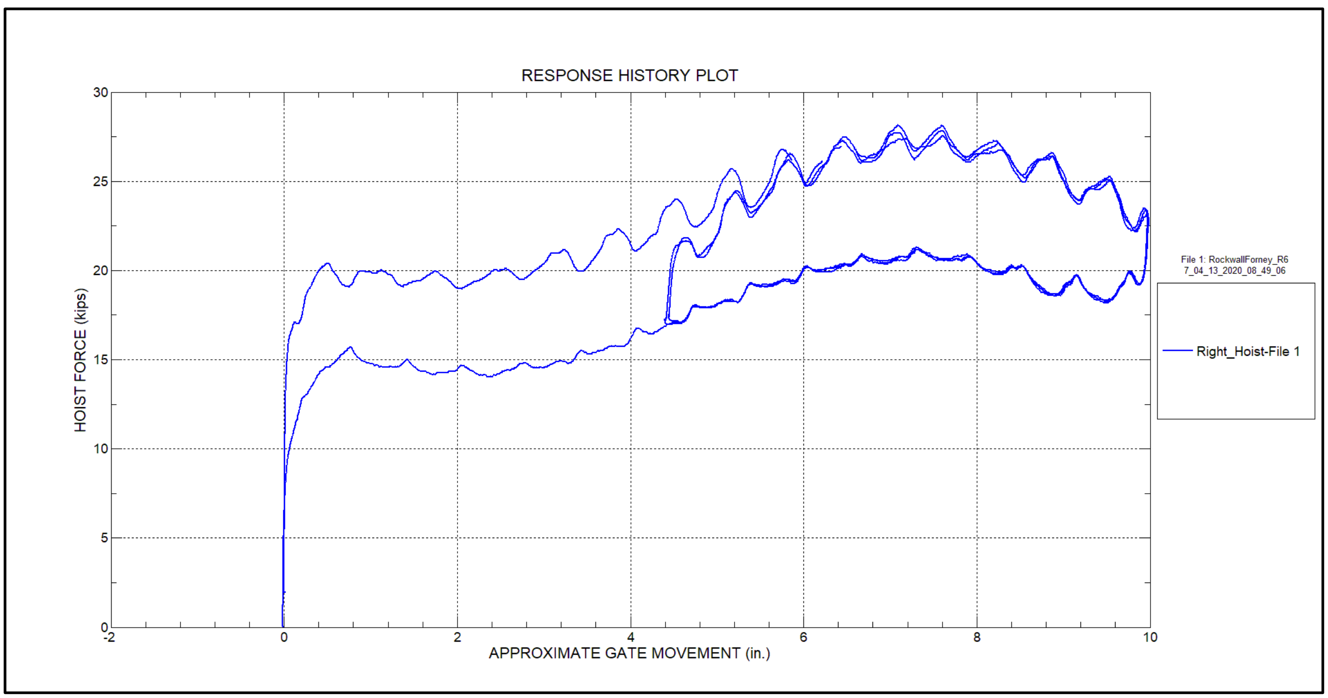

Figure 26 – Hoist force response history – Gate 12 – Test 1

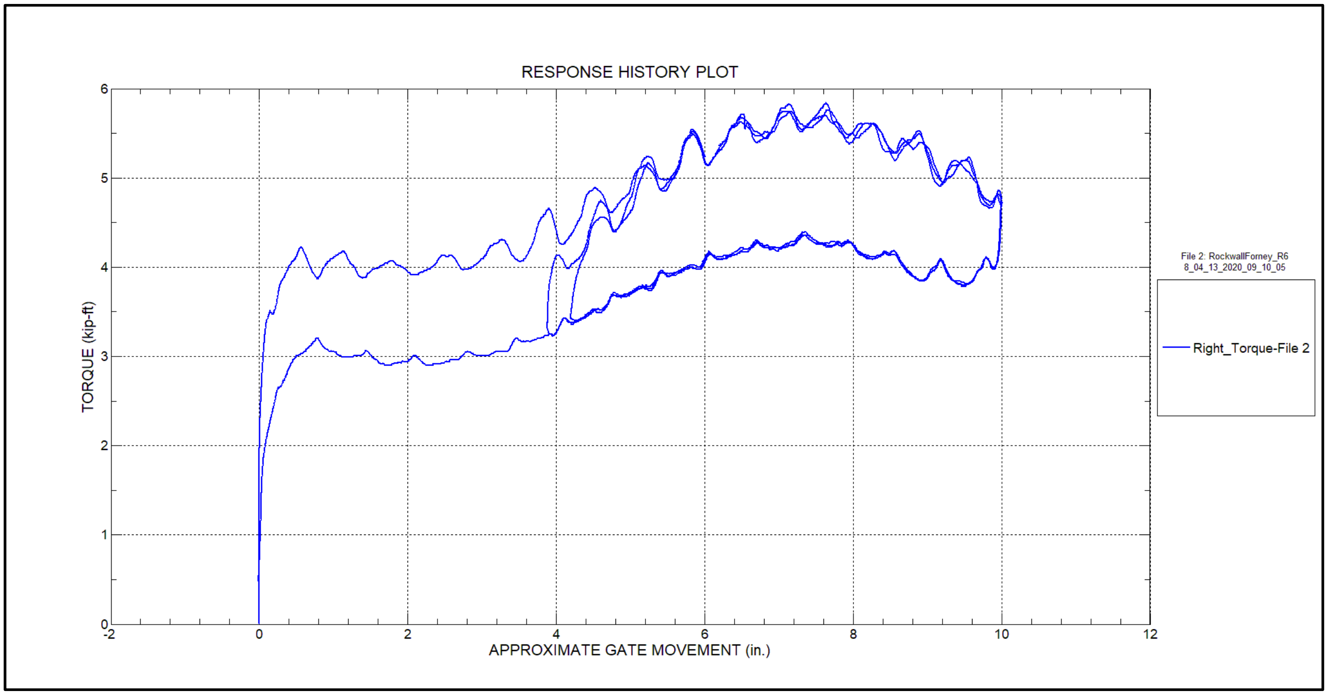

Figure 27 – Hoist torque response history – Gate 12 – Test 2

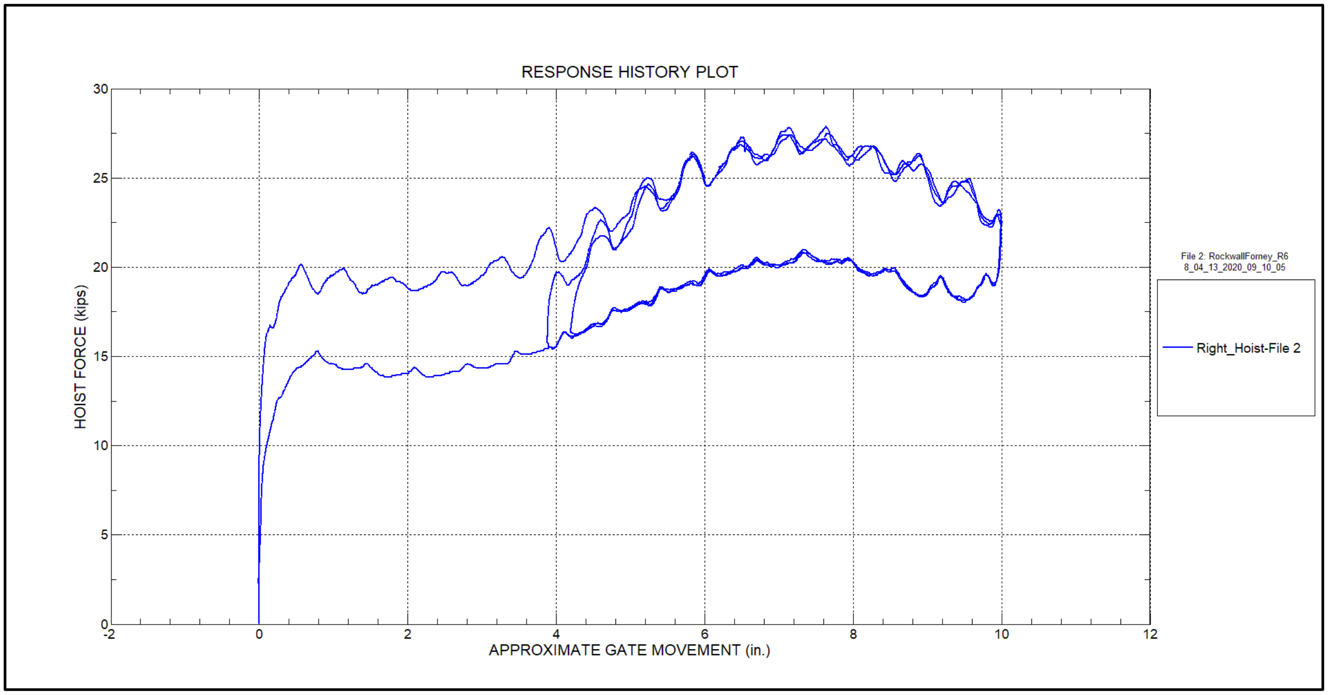

Figure 28 – Hoist force response history – Gate 12 – Test 2

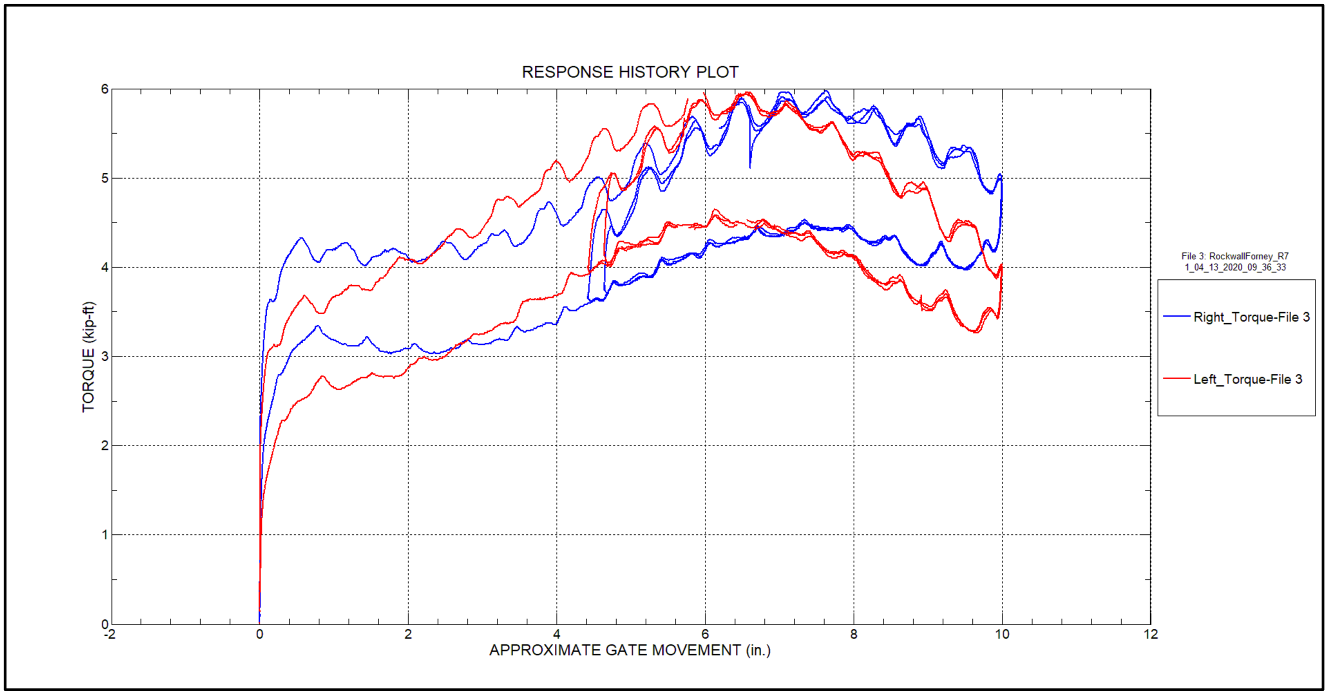

Figure 29 – Hoist torque response history – Gate 12 – Test 3

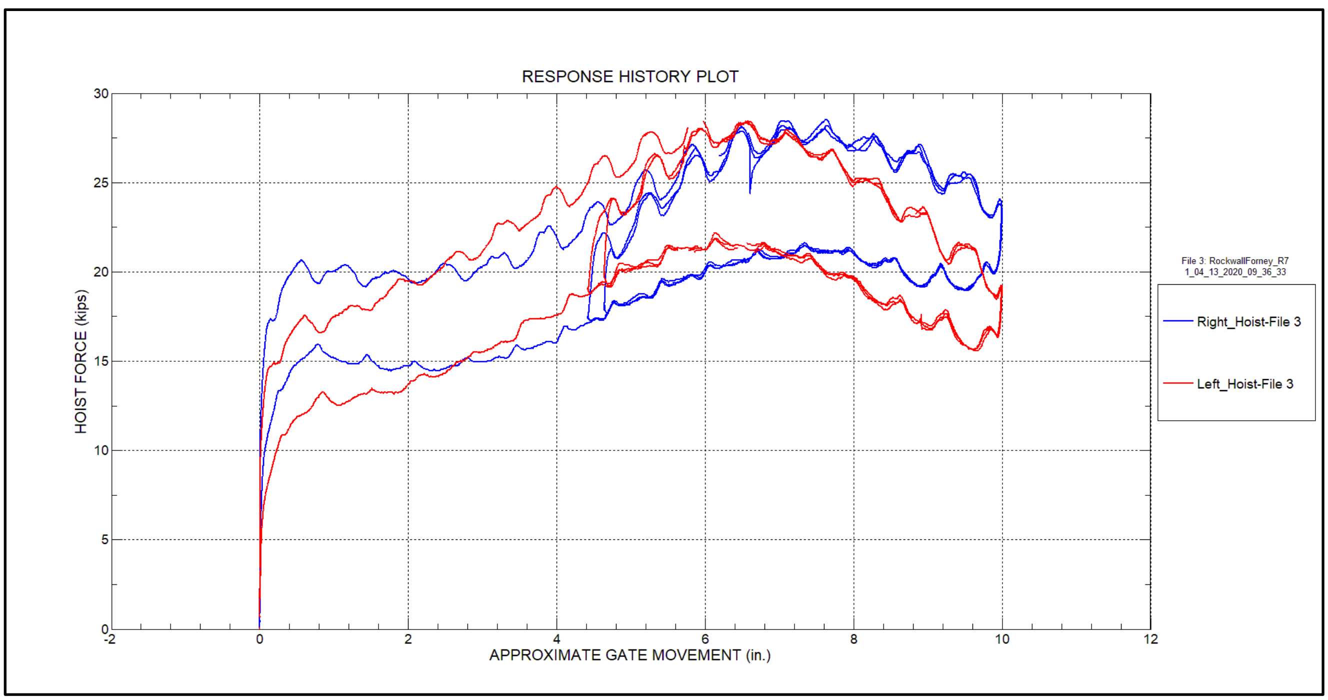

Figure 30 – Hoist force response history – Gate 12 – Test 3

Appendix B – Gate 12 Pin Moment Component Plots

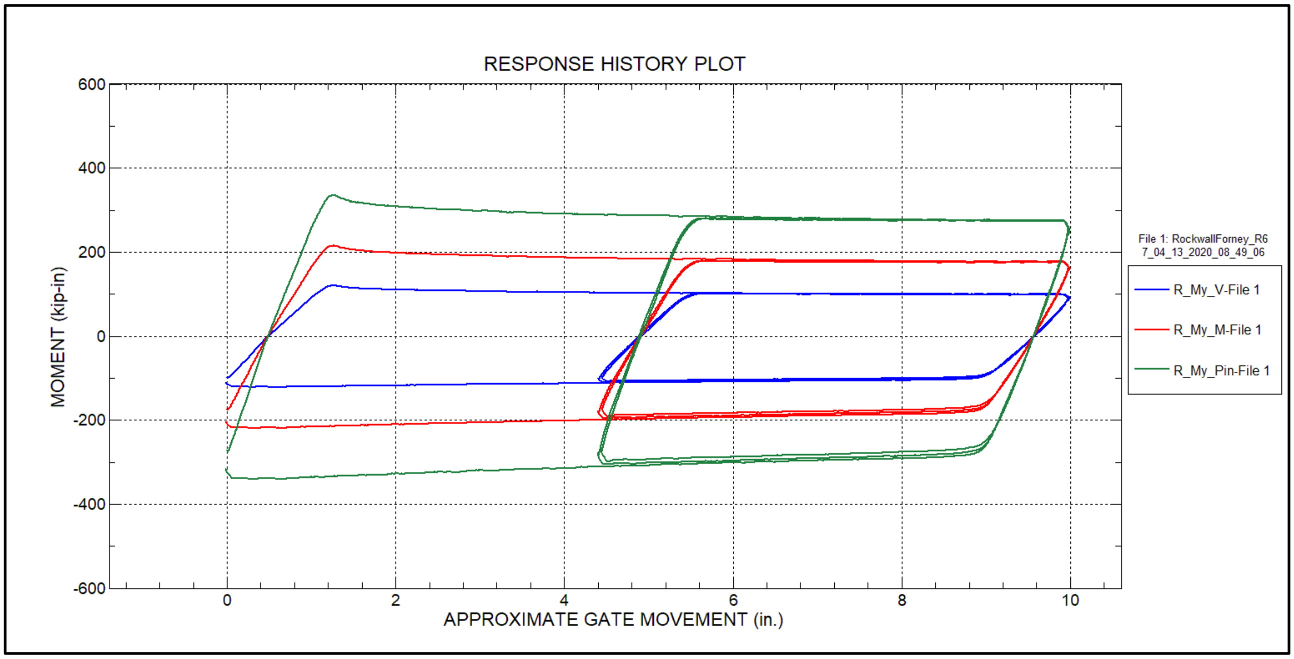

Figure 31 – Pin moment response history – Right arm – Test run 1

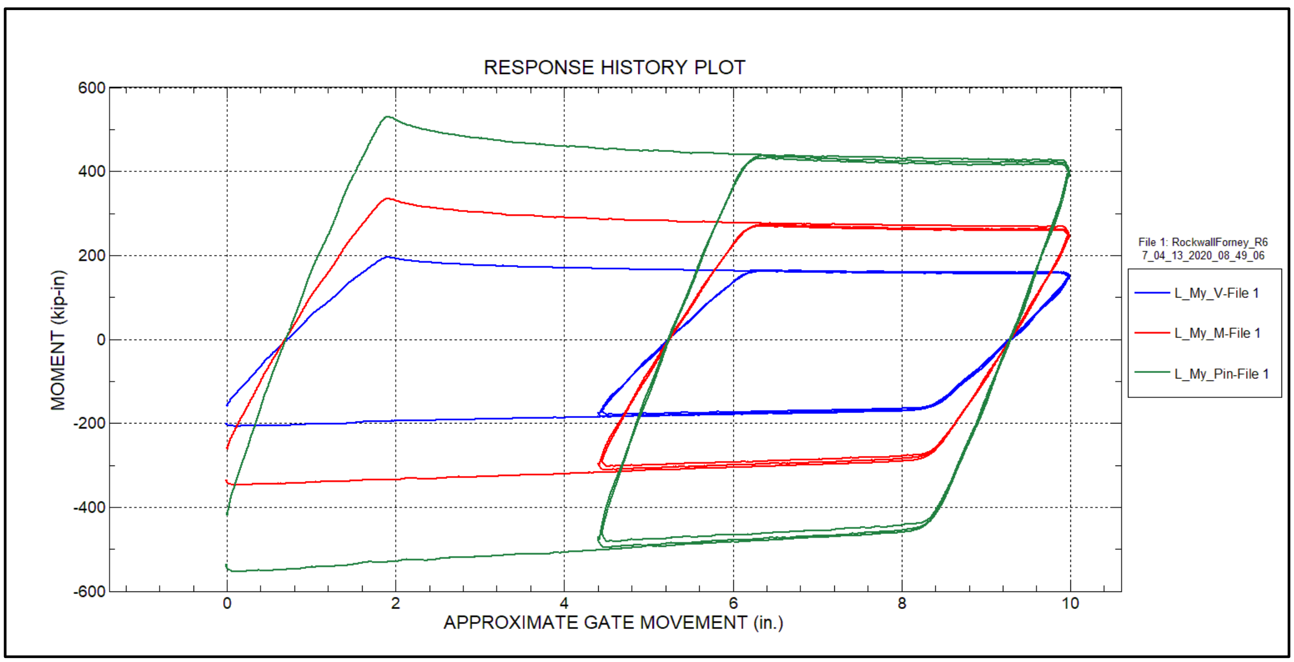

Figure 32 – Pin moment response history – Left arm – Test run 1

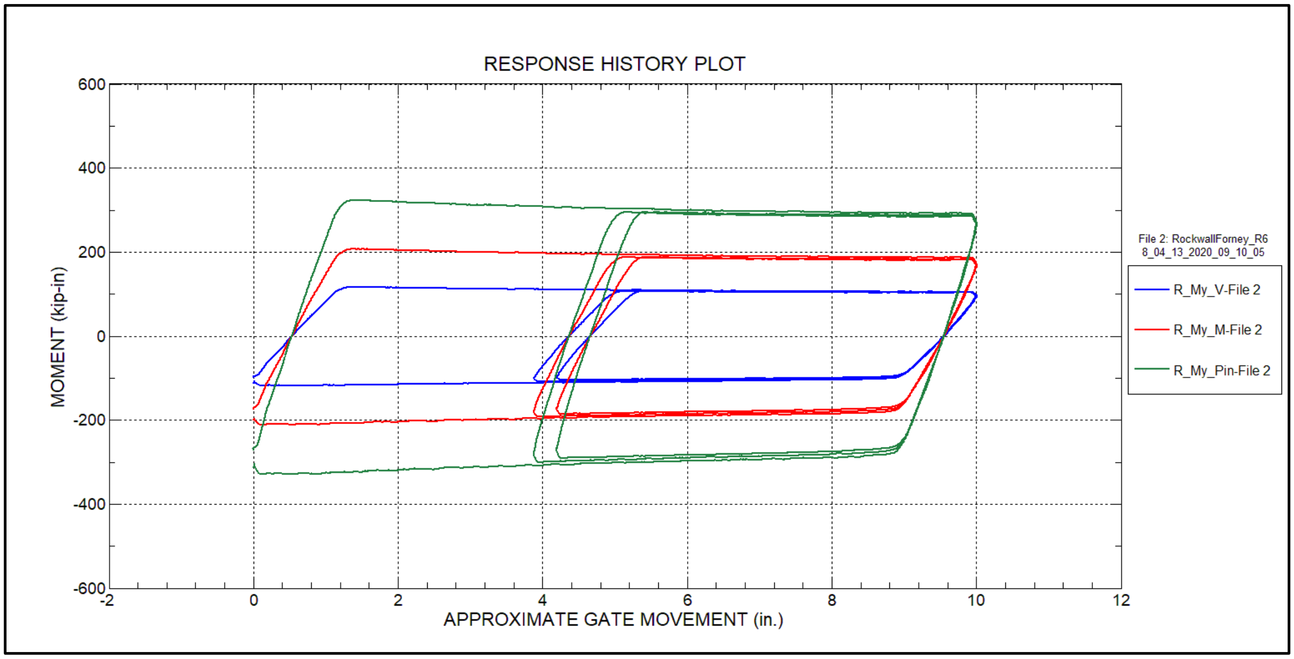

Figure 33 – Pin moment response history – Right arm – Test run 2

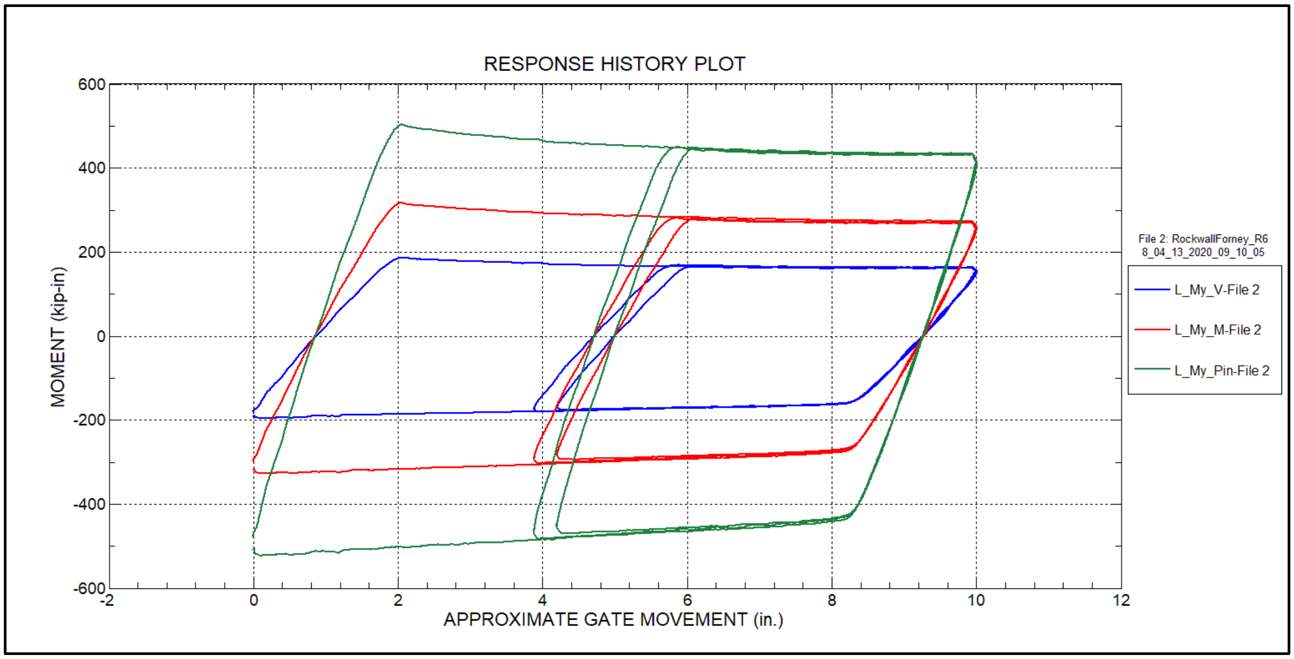

Figure 34 – Pin moment response history – Left arm – Test run 2

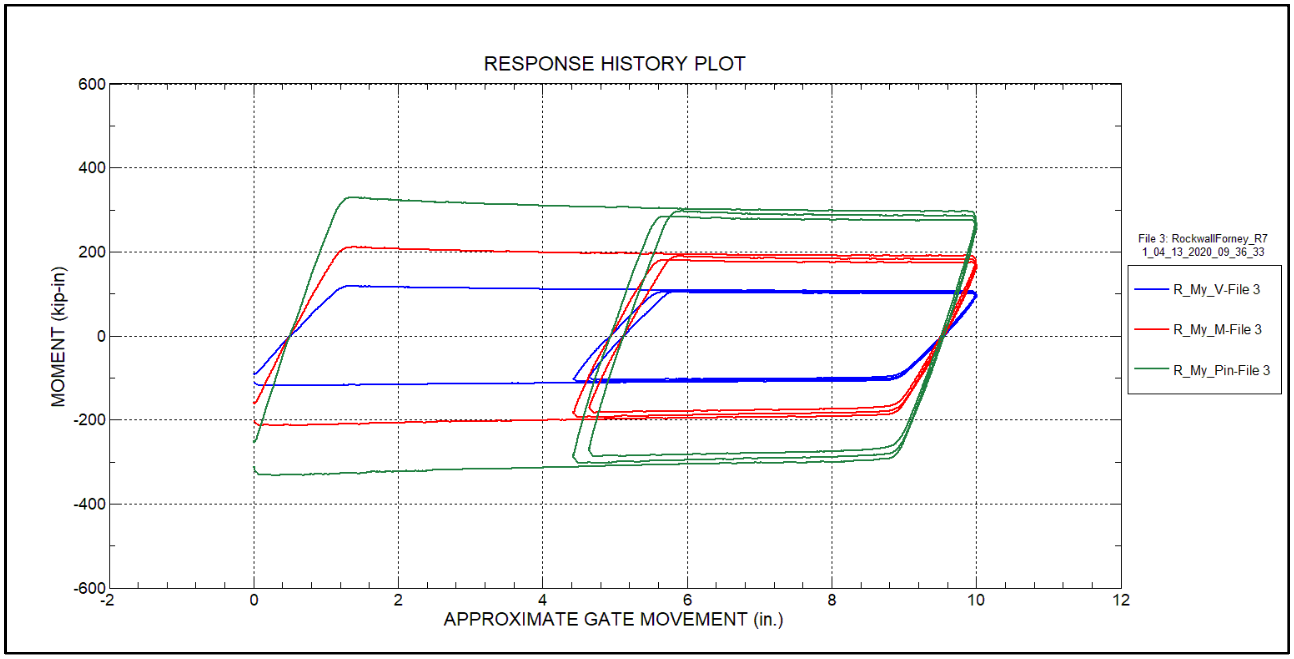

Figure 35 – Pin moment response history – Right arm – Test run 3

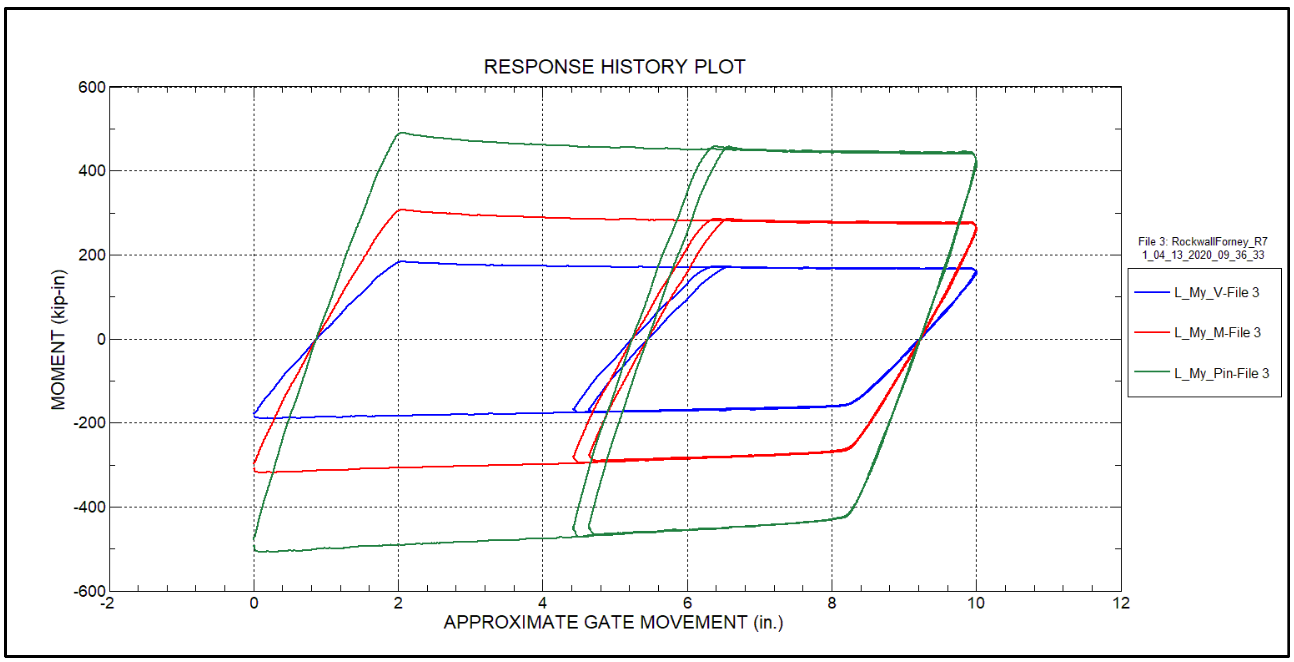

Figure 36 – Pin moment response history – Left arm – Test run 3

APPENDIX C – INSTRUMENTATION PLANS

RAW DATA. REFINED RESULTS.

SCHNABEL ENGINEERING
ROCKWALL FORNEY DAM
LIVE LOAD TESTING

The user acknowledges that these documents are instruments of professional service, and are protected by Copyright. This document and the information contained in this document are the property of Bridge Diagnostics, Inc., and shall not be reused, copied, disseminated, modified, amended or altered in any way. It is issued for information purposes only. The user agrees to hold harmless, indemnify and defend Bridge Diagnostics, Inc. against any and all damages, claims and losses, including defense costs, arising out of any use, reuse or copying of this document.

PLOT TIME: 6/12/2020 3:22 PM
FILEPATH: C:\Users\colemand\BDI\Services - Documents\Server_Remote\190701-TX_Schnabel_RockwallForneyDam\7. Instrumentation Plans\BDI_ROCKWALLFORNEY_01_GENERAL.dwg
© YYYY BRIDGE DIAGNOSTICS INC.

RAW DATA. REFINED RESULTS.
740 S PIERCE AVE, SUITE 15
LOUISVILLE, CO 80027
303.494.3230
WWW.BDITEST.COM

ISSUE

CLIENT

SCHABEL ENGINEERING
16000 CHRISTENSEN RD, STE 101
SEATTLE, WA 98188

PROJECT NAME

SCHNABEL ENGINEERING
ROCKWALL FORNEY DAM
LIVE LOAD TESTING

Drawn By:	KNR
Checked By:	JDS
Date:	05/27/2020
Client No.:	
BDI No.:	190701-TX
SCALE:	NTS

COVER PAGE

LLT-00

The user acknowledges that these documents are instruments of professional service, and are protected by Copyright. This document and the information contained in this document are the property of Bridge Diagnostics, Inc., and shall not be reused, copied, disseminated, modified, amended or altered in any way. It is issued for information purposes only. The user agrees to hold harmless, indemnify and defend Bridge Diagnostics, Inc. against any and all damages, claims and losses, including defense costs, arising out of any use, reuse or copying of this document.

GAGE LEGEND & SPECIFICATION

SYMBOL	TYPE	BRAND	MODEL	NOTES
	STRAIN TRANSDUCER	BDI	ST350	
	TILTMETER (UNI-AXIAL)	BDI	T500-030	
	TORQUE SENSOR	HPI	-	HBWS-35-125-6-0.5VR-FB
	AMP SENSOR	CR MAGNETICS	CR42105-200	

GENERAL NOTES

- INSTRUMENTATION SHALL BEGIN ON APRIL 1ST, 2020.
- GATES 1 THRU 14 SHALL BE ACCESSED USING SPRAT ROPE ACCESS TECHNIQUES.
- BDI WILL PERFORM ALL SURFACE PREPARATION, SENSOR INSTALLATION, AND EQUIPMENT INSTALLATION.
- SEE LLT-31 FOR SENSOR INSTALLATION DETAILS.
- TWO PAIRS OF TORQUE GAGES WILL BE INSTALLED ON THE GATE MOTORS' PINION SHAFTS BETWEEN THE MOTORS AND THE HOISTS.
  - GAGE PAIRS WILL BE INSTALLED 180° APART FROM EACH OTHER.
  - EXACT POSITIONS OF THE GAGE PAIRS ON THE PINION SHAFT WILL BE DETERMINED IN THE FIELD.
- THREE PHASE AMPERAGE GAGES WILL BE INSTALLED ON THE MOTOR CONTROLS BY A QUALIFIED ELECTRICIAN PROVIDED BY GARVER.

TESTING PROCEDURE:

- TESTING SHALL BE STARTED WITH THE GATE IN THE CLOSED POSITION.
- ONCE DATA COLLECTION BEGINS, THE GATE SHALL BE RAISED TO TWO OR THREE TIMES THE HEIGHT NECESSARY FOR TRUNNION FRICTION TO BE OVERCOME, H1 (TYPICALLY 6"-12"), AND HELD THERE UNTIL DATA STABILIZES.
- THE GATE SHALL BE LOWERED APPROXIMATELY TWICE THE DISTANCE TO OVERCOME TRUNNION FRICTION, H2, AND HELD THERE UNTIL DATA STABILIZES.
- THE GATE SHALL BE RAISED TO H1 AND HELD THERE UNTIL DATA STABILIZES.
- THE GATE SHALL BE LOWERED TO H2 AND HELD THERE UNTIL DATA STABILIZES.
- THE GATE SHALL BE RAISED TO H1 AND HELD THERE UNTIL DATA STABILIZES.
- THE GATE WAS LOWERED BACK TO CLOSED POSITION AND DATA COLLECTION STOPPED.
- A MINIMUM OF 3 TESTS SHALL BE PERFORMED PER GATE.

GAGE COUNT PER GATE

SENSOR LEGEND	SENSOR COUNT	CHANNEL COUNT
STRAIN TRANSDUCER	(48)	(48)
TILTMETER (UNI-AXIAL)	(4)	(4)
TORQUE SENSOR	(4)	(4)
AMP SENSOR	(3)	(3)
TOTAL	(59)	(59)

LOCATION KEY

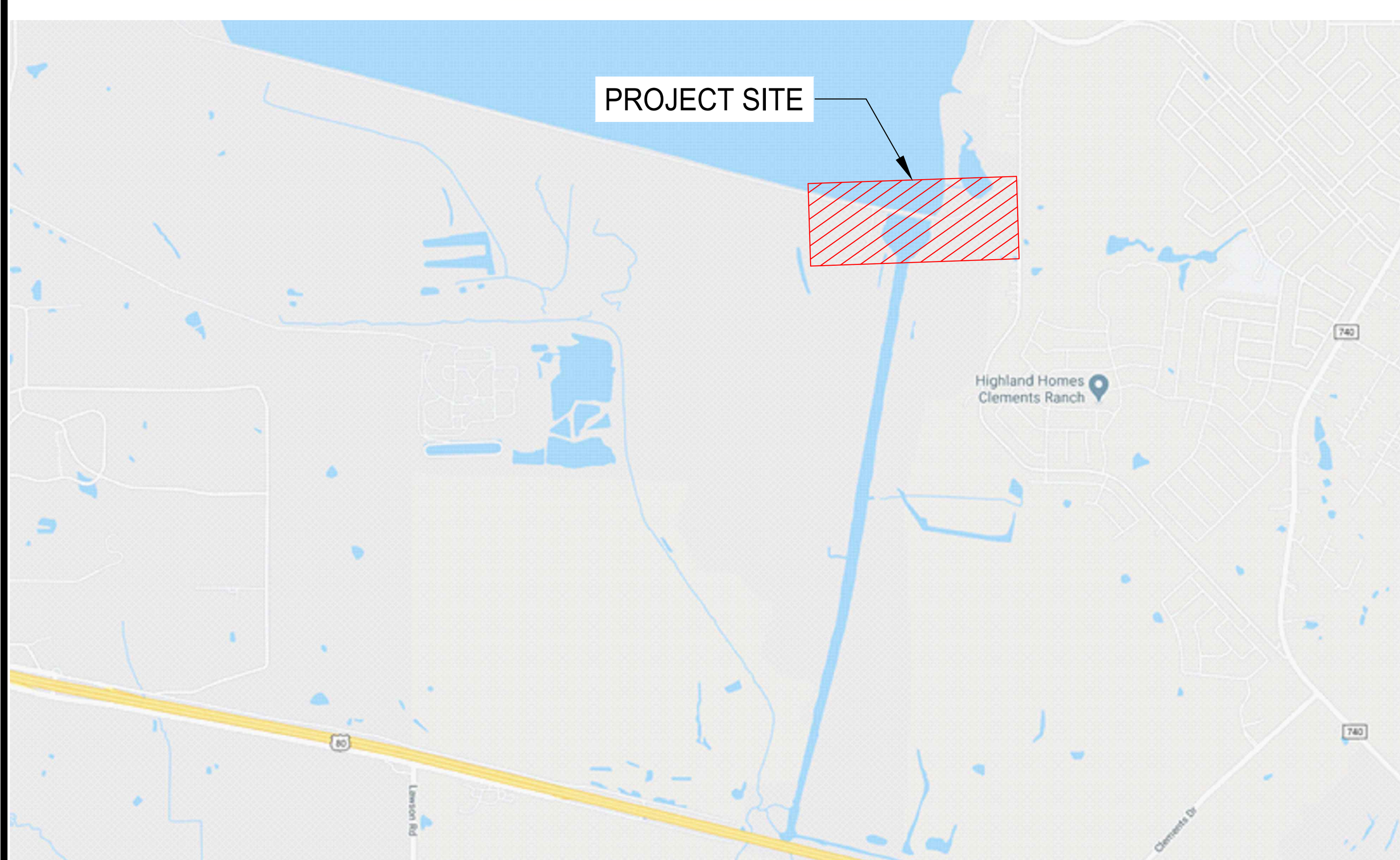

INDEX OF SHEETS

INDEX OF ISSUE

NO.	DATE	REVISION DESCRIPTION
1	3/20/2020	LIVE LOAD TESTING (LLT) INSTRUMENTATION PLAN (FOR APPROVAL)
2	5/27/2020	LIVE LOAD TESTING (LLT) INSTRUMENTATION PLAN AS BUILTS
BDI REFERENCE NUMBER: 190701-TX		

BDI
RAW DATA. REFINED RESULTS.
740 S PIERCE AVE, SUITE 15
LOUISVILLE, CO 80027
303.494.3230
WWW.BDITEST.COM

ISSUE

CLIENT

SCHABEL ENGINEERING
16000 CHRISTENSEN RD, STE 101
SEATTLE, WA 98188

PROJECT NAME

SCHNABEL ENGINEERING
ROCKWALL FORNEY DAM
LIVE LOAD TESTING

Drawn By:	KNR
Checked By:	JDS
Date:	05/27/2020
Client No.:	
BDI No.:	190701-TX
SCALE:	NTS

OVERALL LEGEND

LLT-01

PLOT TIME: 6/12/2020 3:22 PM
FILEPATH: C:\Users\colemand\BDI\Services - Documents\Server_Remote\190701-TX_Schabel_RockwallForneyDam\7. Instrumentation Plans\BDI_ROCKWALLFORNEY_01_GENERAL.dwg
© YYYY BRIDGE DIAGNOSTICS INC.

The user acknowledges that these documents are instruments of professional service, and are protected by Copyright. This document and the information contained in this document are the property of Bridge Diagnostics, Inc., and shall not be reused, copied, disseminated, modified, amended or altered in any way. It is issued for information purposes only. The user agrees to hold harmless, indemnify and defend Bridge Diagnostics, Inc. against any and all damages, claims and losses, including defense costs, arising out of any use, reuse or copying of this document.

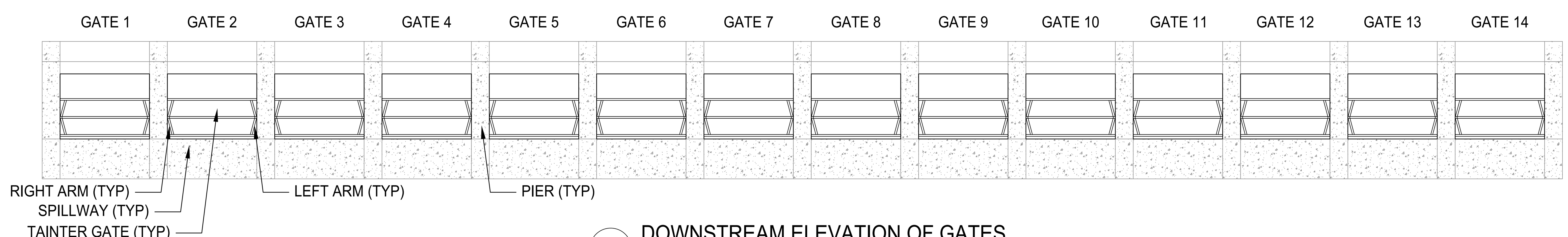

1 DOWNSTREAM ELEVATION OF GATES
LOOKING NORTH (UPSTREAM)

RAW DATA. REFINED RESULTS.
740 S PIERCE AVE, SUITE 15
LOUISVILLE, CO 80027
303.494.3230
WWW.BDITEST.COM

ISSUE

CLIENT

SCHABEL ENGINEERING
16000 CHRISTENSEN RD, STE 101
SEATTLE, WA 98188

PROJECT NAME

SCHNABEL ENGINEERING
ROCKWALL FORNEY DAM
LIVE LOAD TESTING

Drawn By:	KNR
Checked By:	JDS
Date:	05/27/2020
Client No.:	
BDI No.:	190701-TX
SCALE:	NTS

OVERALL STRUCTURE LAYOUT
LLT-02

PLOT TIME: 6/12/2020 3:22 PM
FILEPATH: C:\Users\colemand\BDI\Services - Documents\Server_Remote\190701-TX_Schnabel_RockwallForneyDam\7. Instrumentation Plans\BDI_ROCKWALLFORNEY_01_GENERAL.dwg
© YYYY BRIDGE DIAGNOSTICS INC.

The user acknowledges that these documents are instruments of professional service, and are protected by Copyright. This document and the information contained in this document are the property of Bridge Diagnostics, Inc., and shall not be reused, copied, disseminated, modified, amended or altered in any way. It is issued for information purposes only. The user agrees to hold harmless, indemnify and defend Bridge Diagnostics, Inc. against any and all damages, claims and losses, including defense costs, arising out of any use, reuse or copying of this document.

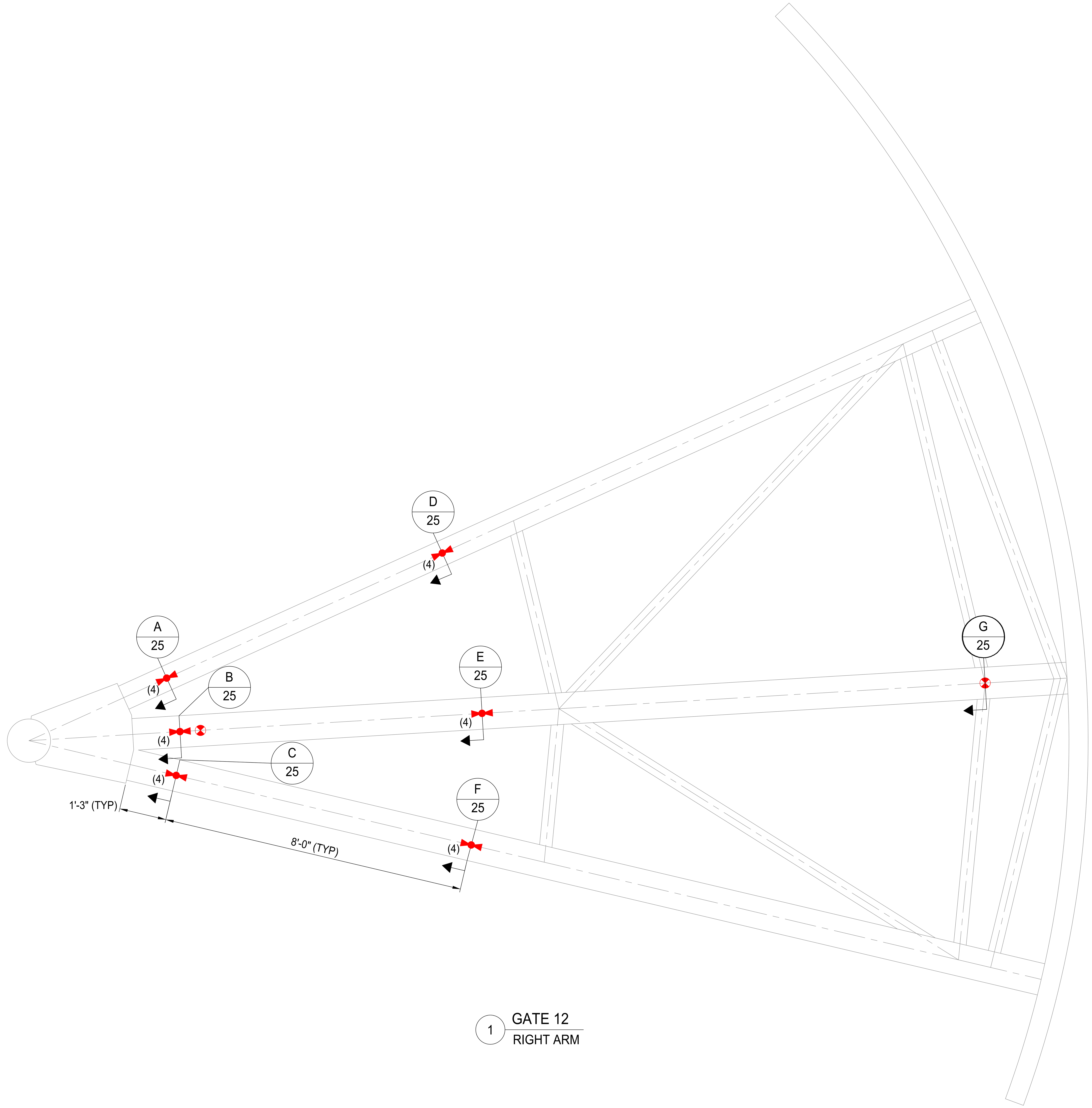

1 GATE 12
RIGHT ARM

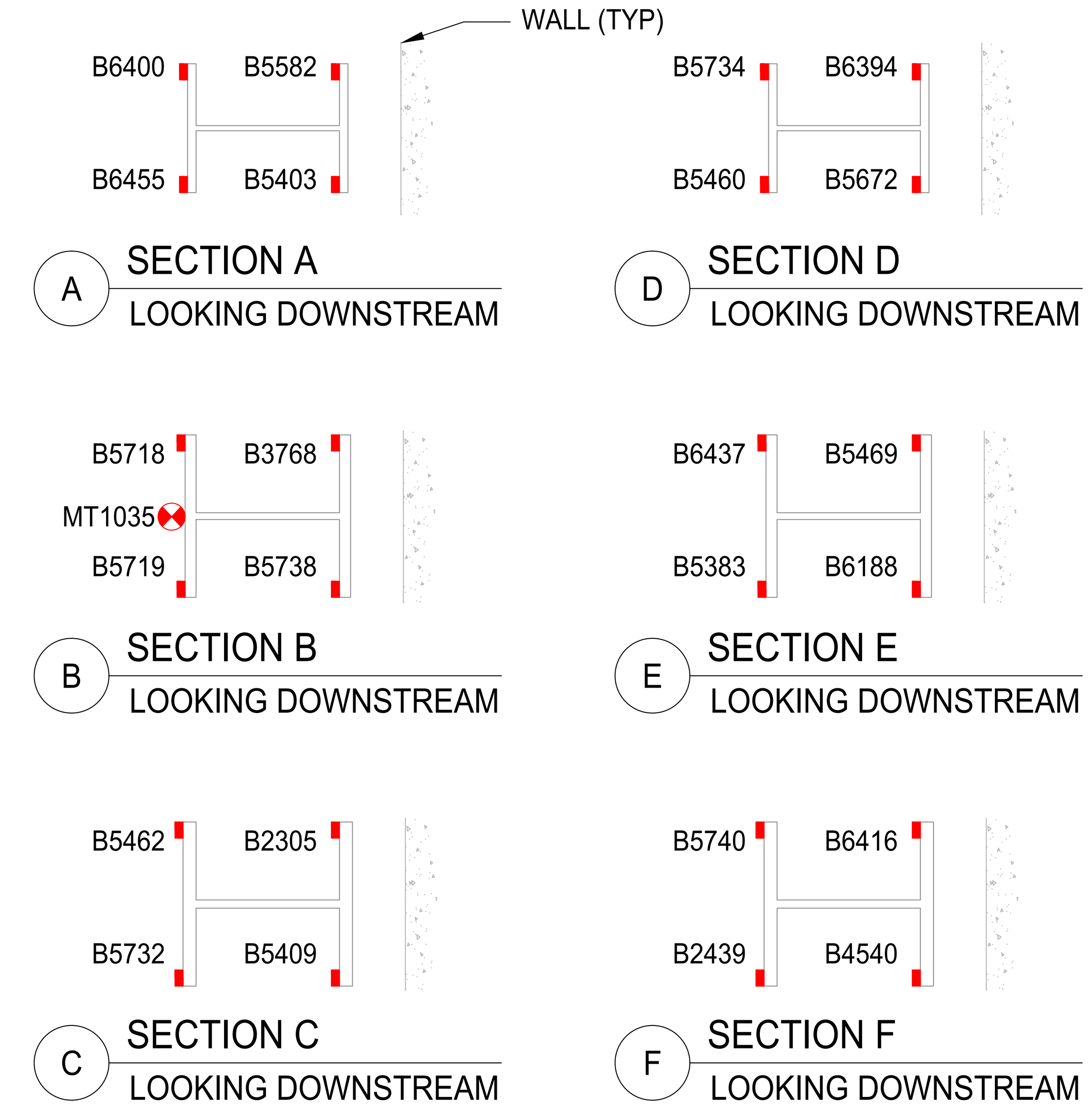

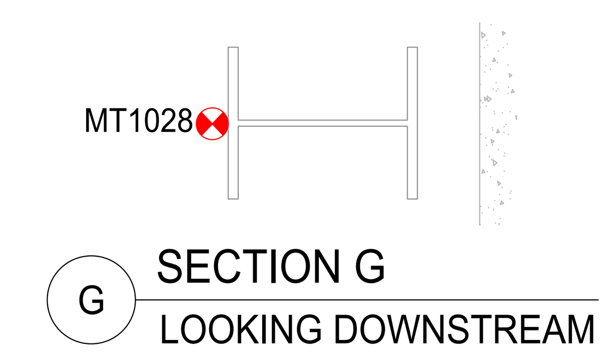

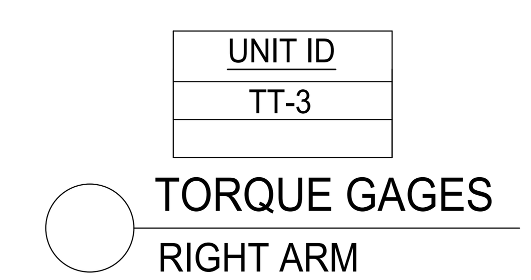

NOTES:

1. SECTIONS A, B, & C SHALL BE INSTALLED 15 INCHES AWAY FROM TRUNNION PLATE.
2. TILTMETERS SHALL BE INSTALLED CENTERED ON THE MIDDLE STRUT FLANGE.
3. SECTION G'S TILTMETER SHALL BE INSTALLED AS CLOSE TO THE SKINPLATE AS POSSIBLE.

SENSOR LEGEND

- STRAIN TRANSDUCER
- TILTMETER (UNI-AXIAL)
- TORQUE SENSOR

BDI
RAW DATA. REFINED RESULTS.
740 S PIERCE AVE, SUITE 15
LOUISVILLE, CO 80027
303.494.3230
WWW.BDITEST.COM

ISSUE

CLIENT

SCHABEL ENGINEERING
16000 CHRISTENSEN RD, STE 101
SEATTLE, WA 98188

PROJECT NAME

SCHABEL ENGINEERING
ROCKWALL FORNEY DAM
LIVE LOAD TESTING

Drawn By:	KNR
Checked By:	JDS
Date:	05/27/2020
Client No.:	
BDI No.:	190701-TX
SCALE:	NTS

GATE 12 - RIGHT ARM
ELEVATION

LLT-25

PLOT TIME: 6/12/2020 3:24 PM
FILEPATH: C:\Users\colemand\BDI\Services - Documents\Server_Remote\190701-TX_Schabel_RockwallForneyDam\7. Instrumentation Plans\BDI_ROCKWALLFORNEY_01_GENERAL.dwg
© YYYY BRIDGE DIAGNOSTICS INC.

The user acknowledges that these documents are instruments of professional service, and are protected by Copyright. This document and the information contained in this document are the property of Bridge Diagnostics, Inc., and shall not be reused, copied, disseminated, modified, amended or altered in any way. It is issued for information purposes only. The user agrees to hold harmless, indemnify and defend Bridge Diagnostics, Inc. against any and all damages, claims and losses, including defense costs, arising out of any use, reuse or copying of this document.

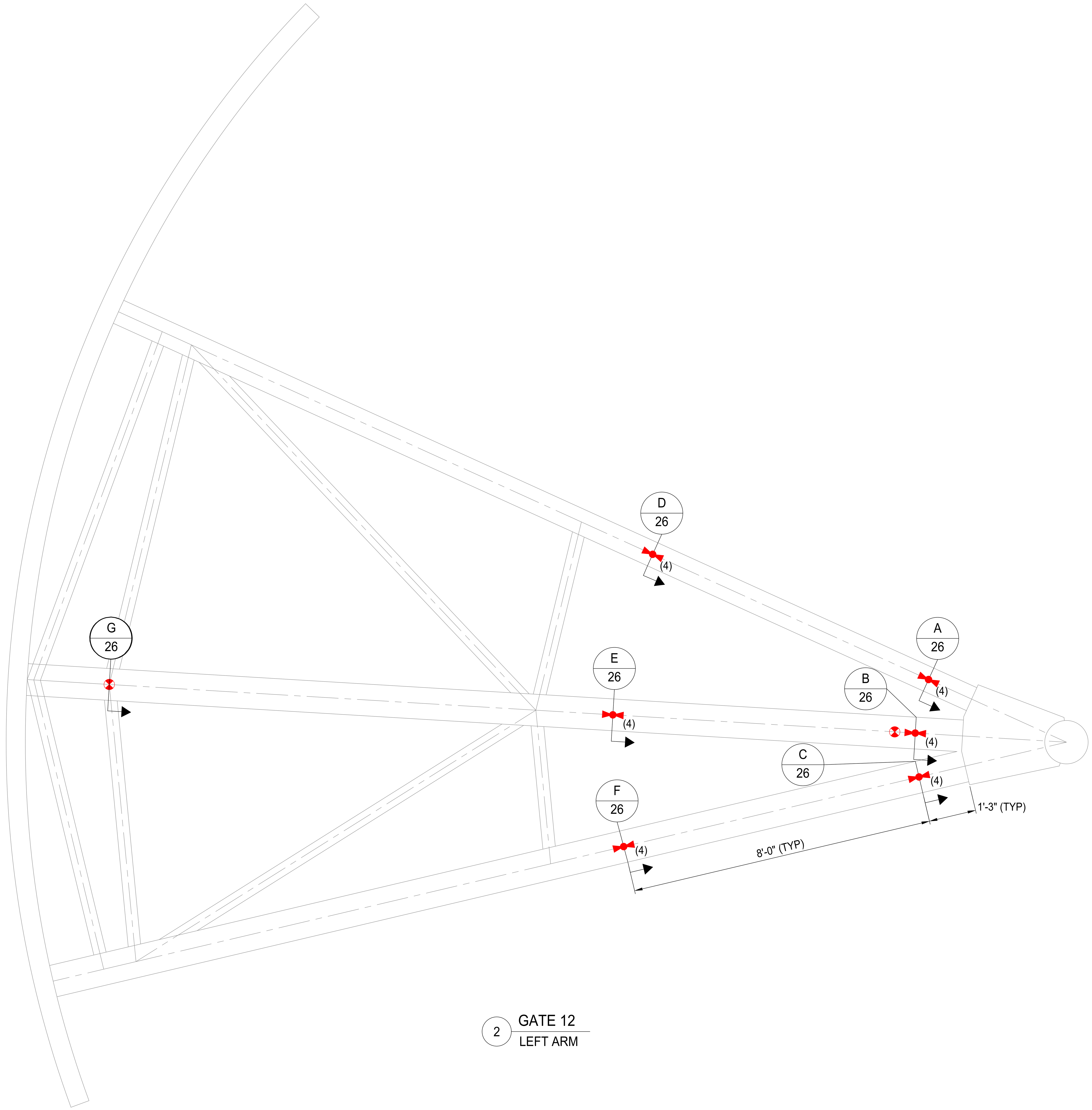

2 GATE 12
LEFT ARM

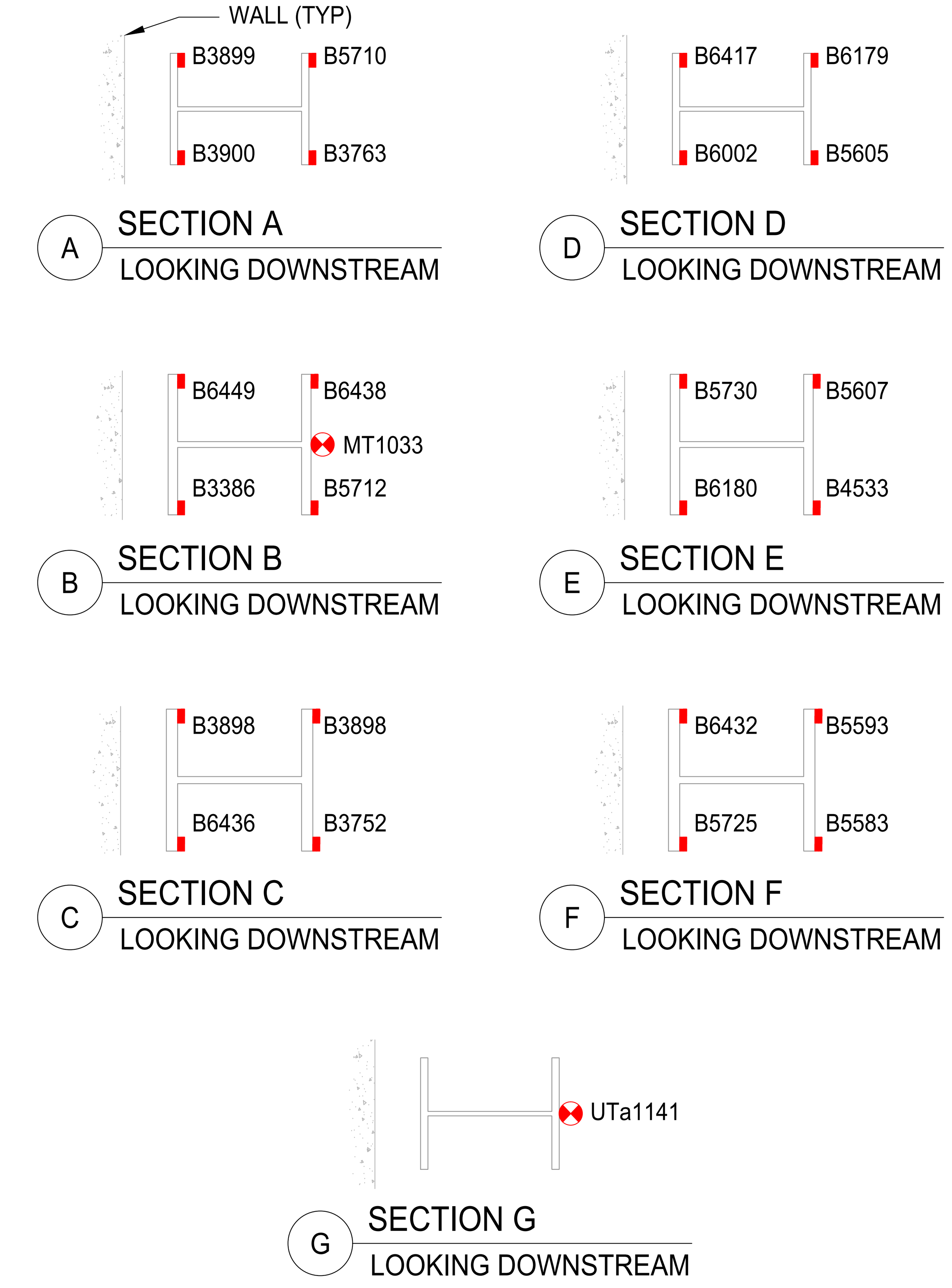

UNIT ID
TT-4

TORQUE GAGES
LEFT ARM

NOTES:

1. SECTIONS A, B, & C SHALL BE INSTALLED 15 INCHES AWAY FROM TRUNNION PLATE.
2. TILTMETERS SHALL BE INSTALLED CENTERED ON THE MIDDLE STRUT FLANGE.
3. SECTION G'S TILTMETER SHALL BE INSTALLED AS CLOSE TO THE SKINPLATE AS POSSIBLE.

SENSOR LEGEND

- STRAIN TRANSDUCER
- TILTMETER (UNI-AXIAL)
- TORQUE SENSOR

BDI
RAW DATA. REFINED RESULTS.
740 S PIERCE AVE, SUITE 15
LOUISVILLE, CO 80027
303.494.3230
WWW.BDITEST.COM

ISSUE

CLIENT

SCHABEL ENGINEERING
16000 CHRISTENSEN RD, STE 101
SEATTLE, WA 98188

PROJECT NAME

SCHABEL ENGINEERING
ROCKWALL FORNEY DAM
LIVE LOAD TESTING

Drawn By:	KNR
Checked By:	JDS
Date:	05/27/2020
Client No.:	
BDI No.:	190701-TX
SCALE:	NTS

GATE 12 - LEFT ARM
ELEVATION
LLT-26

PLOT TIME: 6/12/2020 3:24 PM
FILEPATH: C:\Users\colemand\BDI\Services - Documents\Server_Remote\190701-TX_Schabel_RockwallForneyDam\7. Instrumentation Plans\BDI_ROCKWALLFORNEY_01_GENERAL.dwg
© YYYY BRIDGE DIAGNOSTICS INC.

The user acknowledges that these documents are instruments of professional service, and are protected by Copyright. This document and the information contained in this document are the property of Bridge Diagnostics, Inc., and shall not be reused, copied, disseminated, modified, amended or altered in any way. It is issued for information purposes only. The user agrees to hold harmless, indemnify and defend Bridge Diagnostics, Inc. against any and all damages, claims and losses, including defense costs, arising out of any use, reuse or copying of this document.

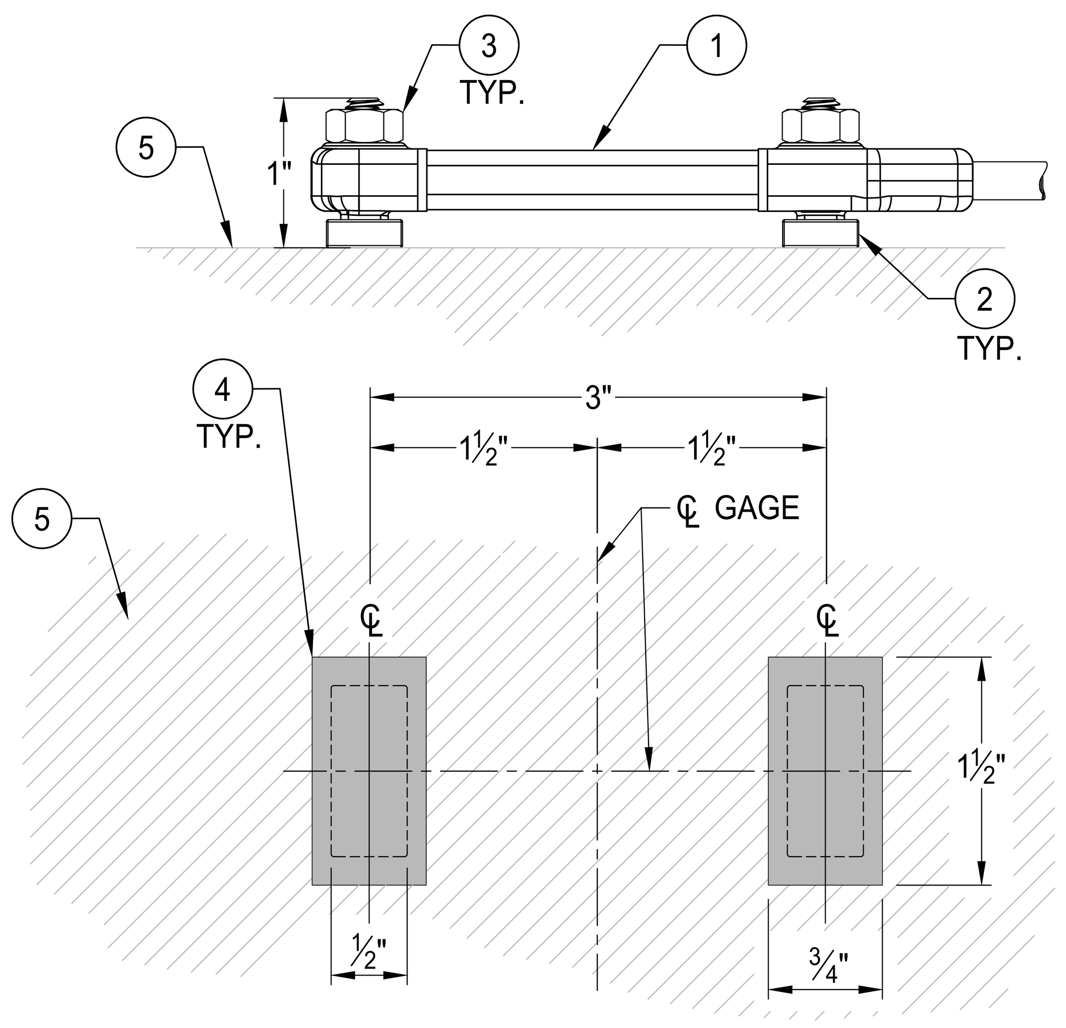

COMPONENT DESCRIPTION

1. ST350 STRAIN GAGE
2. 1/4"-20 THREADED MOUNTING TAB
3. 1/4"-20 STAINLESS STEEL NUT
4. TYPICAL SURFACE PREP REQUIRED TO MOUNT STRAIN GAGES
5. TYPICAL MOUNTING SURFACE

FOOTNOTES - INSTANT ADHESIVE
1. STRAIN GAGES SHALL BE MOUNTED WITH LOCTITE 410 INSTANT ADHESIVE AND LOCTITE 7452 ACCELERANT 2. DURING SURFACE PREP ALL PAINT AND SURFACE DEFORMATIONS MUST BE REMOVED. 3. SURFACE PREP IS REQUIRED JUST PRIOR TO GAGE INSTALLATION AS TO NOT ALLOW SURFACE CONTAMINANTS TO ACCUMULATE.

1 TYPICAL ST350 STRAIN GAGE INSTALLATION

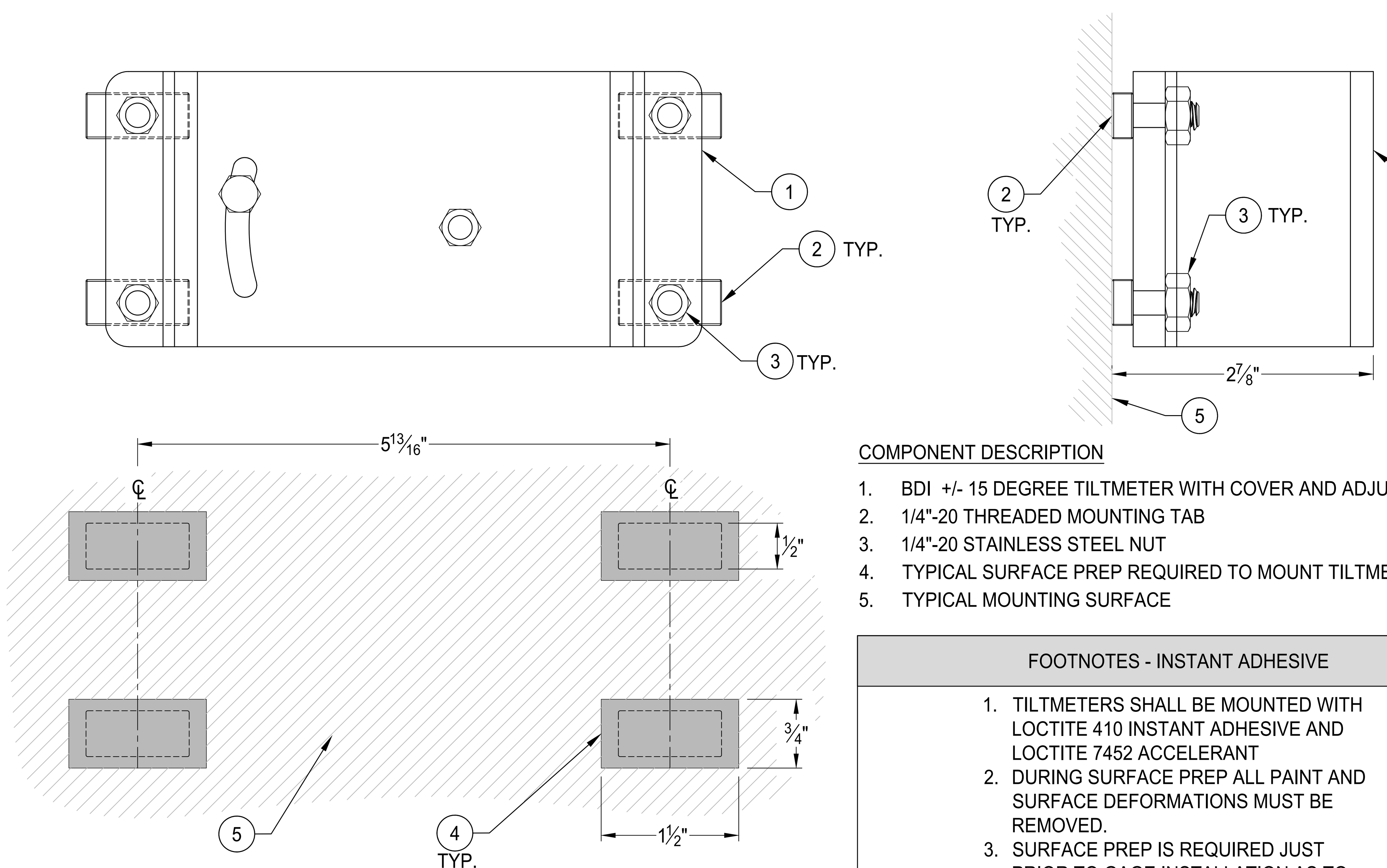

COMPONENT DESCRIPTION

1. BDI +/- 15 DEGREE TILTMETER WITH COVER AND ADJUSTMENT BOLTS
2. 1/4"-20 THREADED MOUNTING TAB
3. 1/4"-20 STAINLESS STEEL NUT
4. TYPICAL SURFACE PREP REQUIRED TO MOUNT TILTMETERS
5. TYPICAL MOUNTING SURFACE

FOOTNOTES - INSTANT ADHESIVE
1. TILTMETERS SHALL BE MOUNTED WITH LOCTITE 410 INSTANT ADHESIVE AND LOCTITE 7452 ACCELERANT 2. DURING SURFACE PREP ALL PAINT AND SURFACE DEFORMATIONS MUST BE REMOVED. 3. SURFACE PREP IS REQUIRED JUST PRIOR TO GAGE INSTALLATION AS TO NOT ALLOW SURFACE CONTAMINANTS TO ACCUMULATE.

2 TYPICAL BDI TILTMETER INSTALLATION

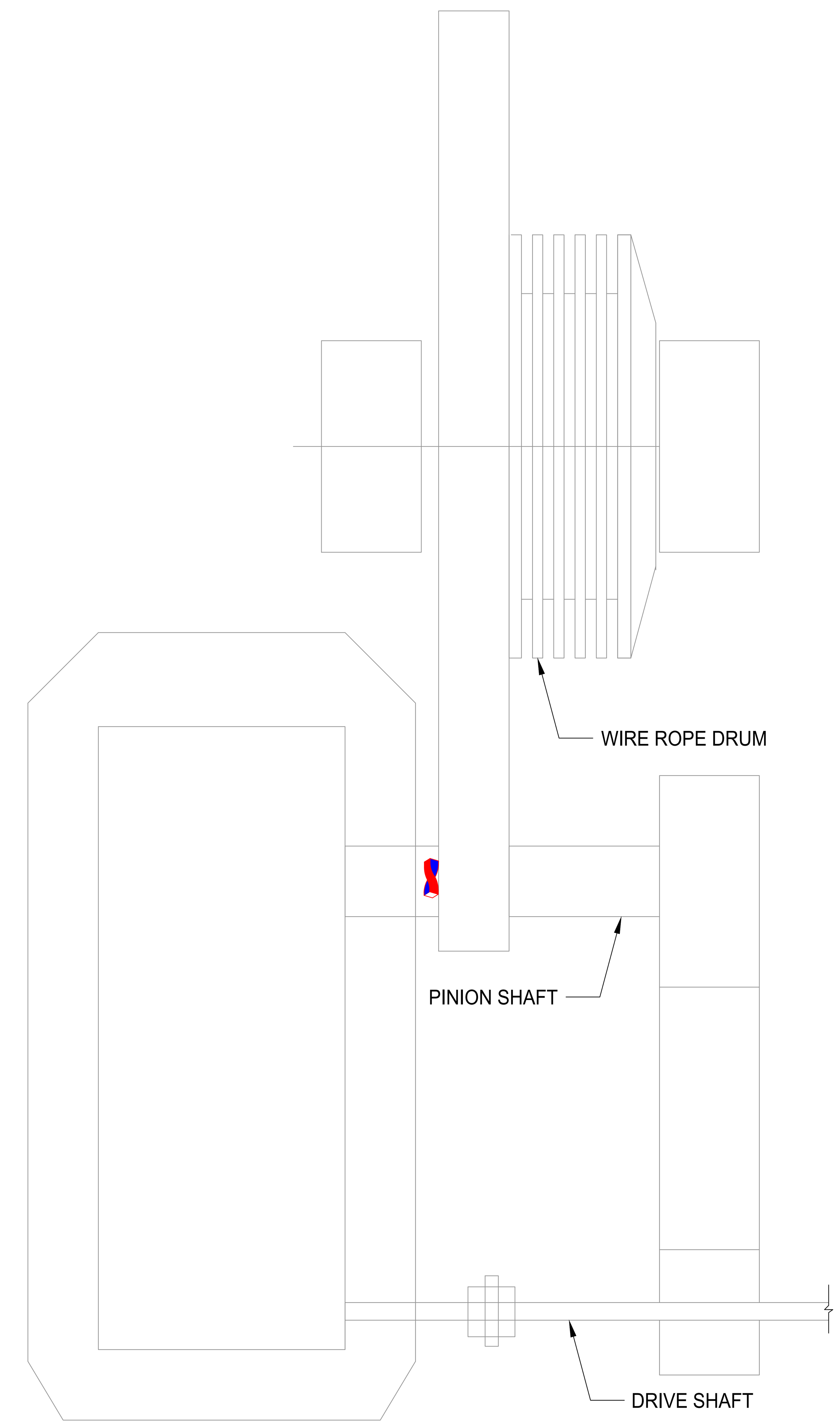

3 TYPICAL HOIST INSTRUMENTATION

TORQUE SENSOR INSTALLATION NOTES:

- TORQUE GAGES WILL BE INSTALLED ON THE PINION SHAFT ON EITHER HOIST MOTOR BETWEEN THE MOTOR AND THE HOIST DRUM
- EXACT POSITIONS OF THE GAGE PAIRS ON THE PINION SHAFT WILL BE DETERMINED IN THE FIELD

SENSOR LEGEND

TORQUE SENSOR

BDI
RAW DATA. REFINED RESULTS.

740 S PIERCE AVE, SUITE 15
LOUISVILLE, CO 80027
303.494.3230
WWW.BDITEST.COM

ISSUE

CLIENT

SCHABEL ENGINEERING
16000 CHRISTENSEN RD, STE 101
SEATTLE, WA 98188

PROJECT NAME

SCHNABEL ENGINEERING
ROCKWALL FORNEY DAM
LIVE LOAD TESTING

Drawn By:	KNR
Checked By:	JDS
Date:	05/27/2020
Client No.:	
BDI No.:	190701-TX
SCALE:	NTS

SENSOR INSTALLATION DETAILS

LLT-31

PLOT TIME: 6/12/2020 3:24 PM
FILEPATH: C:\Users\colemand\BDI\Services - Documents\Server_Remote\190701-TX_Schnabel_RockwallForneyDam\7. Instrumentation Plans\BDI_ROCKWALLFORNEY_01_GENERAL.dwg
© YYYY BRIDGE DIAGNOSTICS INC.

SCHNABEL ENGINEERING

TRUNNION PIN FRICTION TESTING REPORT

ROCKWALL FORNEY DAM – GATE 13
FORNEY, TX

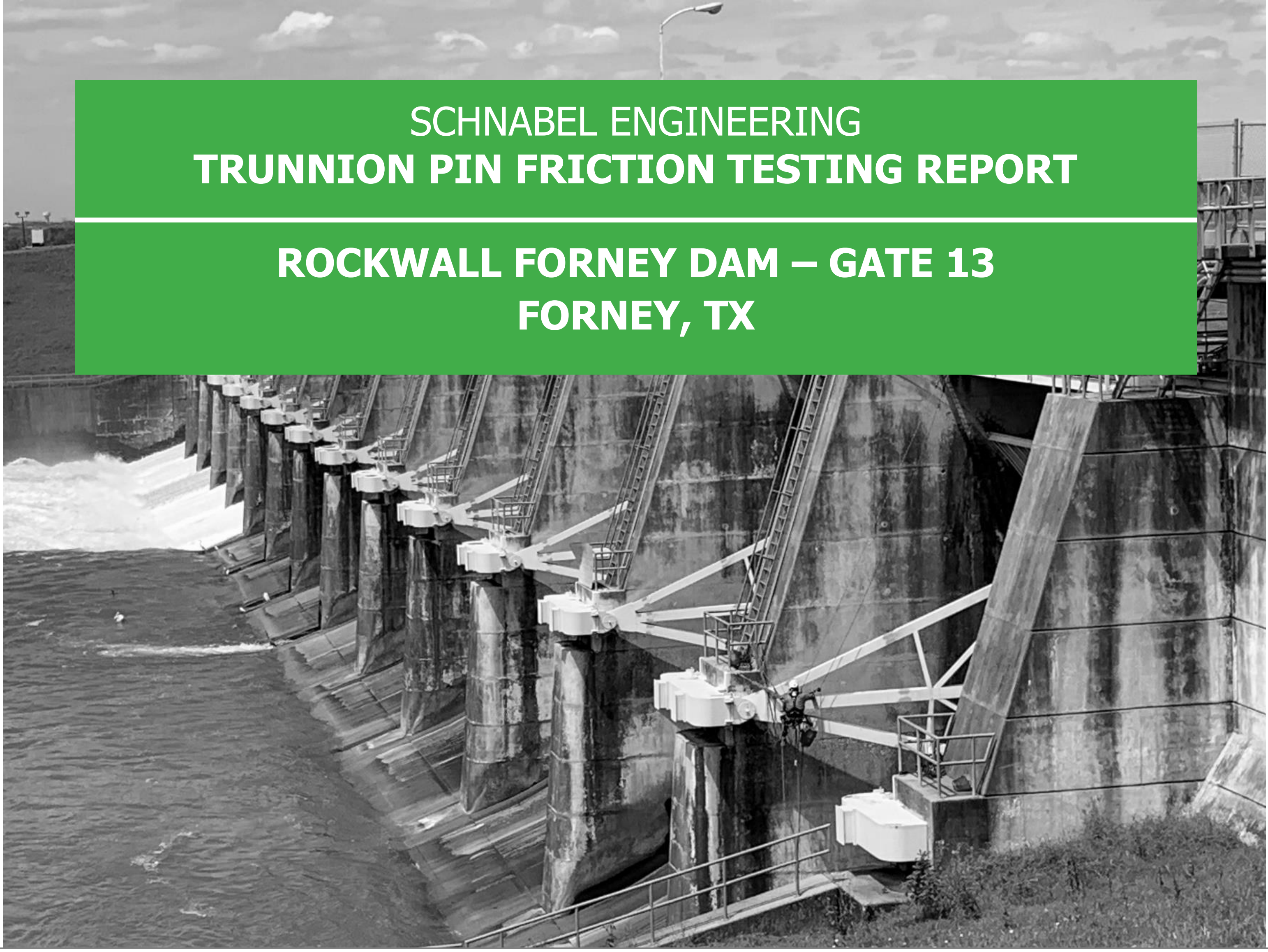

SUBMITTED TO:

SCHNABEL ENGINEERING
16000 CHRISTENSEN RD, SUITE 101
SEATTLE, WA 98188

SUBMITTED BY:

BDI – CO
740 SOUTH PIERCE AVE, UNIT 15
LOUISVILLE, CO 80027

BDI Project No.: **190701-TX**
Report Version: **V1**
Version Submitted: **August 26, 2020**

RAW DATA. REFINED RESULTS.

This document contains Confidential Information and is submitted in confidence to the customer. The submission of the information contained herein shall not be deemed to constitute public disclosure or authorization for disclosure to other parties. BDI's information and name may not be used in advertising or for promotional purposes without BDI's written consent.

TABLE OF CONTENTS

LIST OF FIGURES

LIST OF TABLES

EXECUTIVE SUMMARY

Schnabel Engineering contracted BDI to provide instrumentation and testing services on Gates 1-14 on the Rockwall Forney Dam near Dallas, Texas. The goal of these tests was to record each gate's structural responses during a series of spill tests and use the data to compute accurate coefficients of friction for each trunnion pin, cable lift force, total gate friction, and motor amperage. This report provides details on the work performed on Gate 13.

Instrumentation and testing were performed on Gate 13 at the Rockwall Forney Dam on April 13th, 2020. The gate arms were instrumented with strain and rotation sensors. The hoist motors' pinion shafts were instrumented with torque sensors and the hoist motor controls were instrumented with amperage sensors. Following the instrumentation, a series of spill tests were performed to measure the structural responses resulting from trunnion pin friction. All instrumentation setup and removal were performed using BDI's rope access team.

Following demobilization from the field, the test data was examined for quality and then further processed to evaluate the gate's performance. Strain measurements were converted into bending forces which were then applied to pin-strut free-body diagrams. By summing forces at each pin, friction induced moments could be computed, allowing accurate friction coefficients to be determined. Generally, the observed gate behavior showed that Gate 13 was operating as expected and in a symmetric manner.

The resulting maximum trunnion friction coefficients and corresponding hoist forces are shown in Table 1.

Table 1 – Gate 13 performance summary

Pin Designation	Maximum Friction Coefficient	Maximum Pin Moment due to Pin Friction (kip-In)	Maximum Hoist Force (kips)	Maximum Hoist Force due to Total Gate Friction (kips)
Right Pin	0.16	427.0	29.07	4.16
Left Pin	0.16	432.6	28.63	3.96

Note: Pin designations are in reference to looking downstream

Due to restrictions caused by the hoist limit switches, the hoist cables could not always be fully slacked at the beginning and end of the performed tests. Throughout testing of the Rockwell Forney gates, it was found that this limit switch restriction varied gate to gate and arm to arm. Therefore, it is not recommended to use the collected hoist force data to quantify overall hoist forces during gate operation. Rather, this hoist data can be better utilized to evaluate total friction behavior.

Amperage responses were not used to compute friction results and were collected as verification that the motor performance was not causing unexpected gate responses. These responses indicated the motor was functioning in a stable manner and should be reviewed by a licensed electrician to further evaluate the motor's performance.

All results and recommendations provided in this report were based on the structure in its current condition; therefore, any significant changes in condition must be noted as they may alter their validity. Questions regarding this report and/or data should be directed to Kyle Ramer (kyler@bditest.com) at BDI. For further information on BDI's equipment, services, and analysis methods please visit www.bditest.com

INSTRUMENTATION AND LOAD TESTING PROCEDURE

GATE INSTRUMENTATION SUMMARY

Instrumentation and testing were performed on Gate 13 at the Rockwall Forney Dam on April 13th, 2020. Instrumentation plans have been provided along with this report and include the following number of instrumented locations and sensor types:

+ **REUSABLE SURFACE MOUNTED STRAIN TRANSDUCERS:** Each gate arm was instrumented with a total of 24 strain transducers at 6 locations on each of the gate arms (48 strain sensors total). A typical strain gage installation is shown in Figure 1. Note these sensors were installed with the mounting tabs on the extreme fiber of the strut flanges, which puts the center of the gage approximately 0.66" from the extreme fiber.
+ **TILTMETER ROTATION SENSORS:** MEMS style rotation sensors were located on the middle strut of the gate arm near the skin plate and near the trunnion hub (4 rotation sensors total). The rotation responses were used to calculate vertical skin plate movement and measure pin rotation relative to skin plate rotation. Typical tiltmeter installations are shown in Figure 1 and Figure 2.
+ **TORQUE SENSORS:** Two total torque sensors were installed on the hoist's pinion shafts (QTY1 on each hoist pinion shaft) near the cable hoist motor to measure direct torque and in turn lift force (See Figure 3).
+ **AMPERAGE SENSORS:** 3 Hall-Effect amperage transducers were clamped over each phase of the hoist motor to measure the motor's current draw (See Figure 4). The purpose of these sensors was to provide additional data in case there were any issues with the hoist systems and to verify any data issues related to lifting and lowering the gates.
+ **BDI'S STS-4 WIRELESS DATA ACQUISITION SYSTEM:** BDI's STS-4 wireless data acquisition (DAQ) was used to collect and record data during testing. A group of sensors were wired to each nodal DAQ which then communicated wirelessly back to the wireless base station and was controlled by BDI's STS-Live testing software.

Complete specifications are available upon request and can be found at http://www.bditest.com.

SENSOR INSTALLATION

BDI strain transducers were installed by first sanding paint off the struts to expose bare metal at two small locations (1"x2" areas) for the sensor's mounting tabs. Each transducer was then attached using a combination of fast-setting adhesive and accelerator and applying pressure until the adhesive was fully cured. Each strain transducer took approximately five minutes to attach.

Tiltmeters were installed using the same adhesive process as the strain transducers. However, no surface preparation was necessary.

Torque sensors were installed on the pinion shafts by capacitive discharge bonding. Properly bonding to the shaft required sanding the surface to a smooth finish, clean of any paint or grease. Responses from these gages were measured using Binsfeld Torque Trak 10k wireless transmitters.

A typical installation has been shown in Figure 1 through Figure 4. Access to all the sensor locations was provided by BDI's own SPRAT certified rope access technicians and engineers as shown in Figure 5.

Once testing was completed, sensors were removed, and exposed steel areas were covered using cold galvanizing compound.

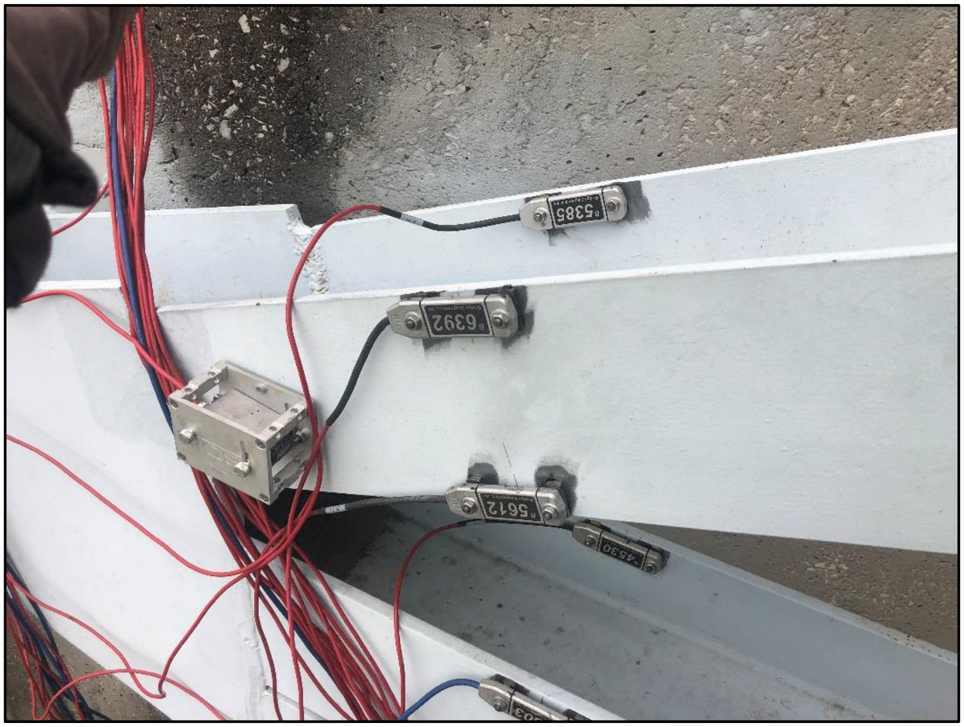

Figure 1 – BDI tiltmeter rotation sensor and reusable strain transducers installed near trunnion hub (Typical)

Figure 2 – BDI tiltmeter rotation sensor installed near skin plate (Typical)

Figure 3 – Torque sensor installation on hoist pinion shaft (Typical)

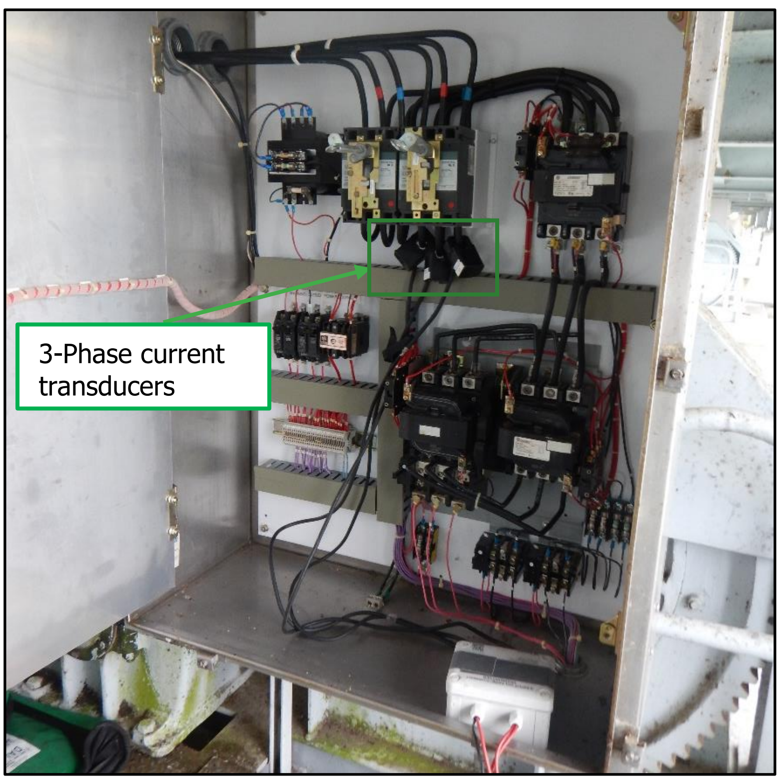

Figure 4 – Current transducers installed on hoist motor controls (Typical)

Figure 5 – BDI personnel installing instrumentation on the gate arm

TESTING PROCEDURES

Structural response data was recorded on all sensors at 50Hz while the gate was run through three spill tests. Each test consisted of three "up-down" cycles (direction reversals) without lowering the gate back to the sill. Each direction reversal consisted of lifting the gate approximately 6-12", pausing for a few seconds, and lowering the gate approximately 6", and repeating until all reversals had been completed.

RESULTS SUMMARY

GENERAL DISCUSSIONS BASED ON STRUCTURAL RESPONSES

The following outline contains general discussion points and observations that were made during the data review process. Note: Strain measurements were converted to stress for all subsequent analysis by multiplying the strain values by a steel elastic modulus of 29,000 ksi.

+ **DESCRIPTIONS OF RESPONSE MEASUREMENTS:** All sensor readings were zeroed at the end of each test (which consisted of three cycles of direction reversals) so that each measurement corresponded to response change relative to the final gate position as shown in Figure 6 (gates in the downward "closed" position with the hoist cables slacked as much as possible). It is also worth noting that the stresses did not always start and end at the same levels between tests. This variation in behavior is due to small changes in the flexed gate condition between the start and end of tests. It is common for the flex in the gate, caused by pin friction, to slowly release as it rests on the sill. The purpose of the three up-down cycles per test, prior to sitting the gate back onto the sill, is to ensure that these changes in boundary conditions, including gate flexure due to friction, did not affect BDI's trunnion friction results. ***It is important to note that the recorded measurements were changes in structural response due to gate movement, and do not include the in-situ stresses due to the dead load, cable wrap, and hydrostatic loads present prior to testing.***
+ **QUALITATIVE DATA REVIEW:** Review of the response data indicated a good level of reproducibility between the three tests. For reference, Figure 6 and Figure 7 show stress responses measured along Gate 13's right arm top strut for all three tests (Test #1-3). The data in these plots have been provided as both a function of time and the gate position as determined by the skin plate tilt sensor. Structural response behavior slightly varied during the first test's first cycle compared to subsequent lift/lower cycles and tests, with the first cycle having a slightly smaller change in stress due to pin friction. The observed variation was likely caused by a larger release of built-up pin friction as the gate rested on the sill for a longer period of time.
+ **DIRECTION/FRICTION REVERSAL IN RESPONSES:** The difference in stress during gate opening and closing for a given position is shown in Figure 8. The stress variation at any given gate position was a result of direction reversal and in turn due to trunnion friction reversal. This statement is true since all other loads such as dead-load and hydrostatic pressure were essentially constant barring small changes in hydrostatic pressure due to slight changes in head. This direction/friction reversal is depicted in Figure 9, with deflected shape renderings from a gate arm finite element model under lifting and lowering loads. Note that this figure shows an arm configuration that does not match this gate, but the concept of the direction/friction reversal still applies.
+ **MOTOR PERFORMANCE:** Current measurements taken at the hoist motor indicated steady and stable current draws during the lifting and lowering portions. An example plot of current draw and gate position is provided in Figure 10. Current draw ranges during lifting were higher than the ranges during lowering, which is common due to gravity/dead load. These results are summarized along with recorded peak in-rush current in Table 2. Note that the sample rates used during testing were set for collecting gate responses and may not have been appropriate to fully capture the in-rush current. The readings should be evaluated by a licensed electrician with knowledge of the operating parameters.
+ **TORQUE AND HOIST FORCE:** Due to restrictions caused by the hoist limit switches, the hoist cables could not always be fully slacked at the beginning and end of the performed tests. Throughout testing of the Rockwell Forney gates, it was found that this limit switch restriction varied gate to gate and arm to arm. Therefore, it is not recommended to use the collected torque and hoist force data to quantify overall hoist forces. Rather, this data was utilized to evaluate total friction behavior, which is observed as half the difference between the lifting and lowering torque/force (friction reversal).

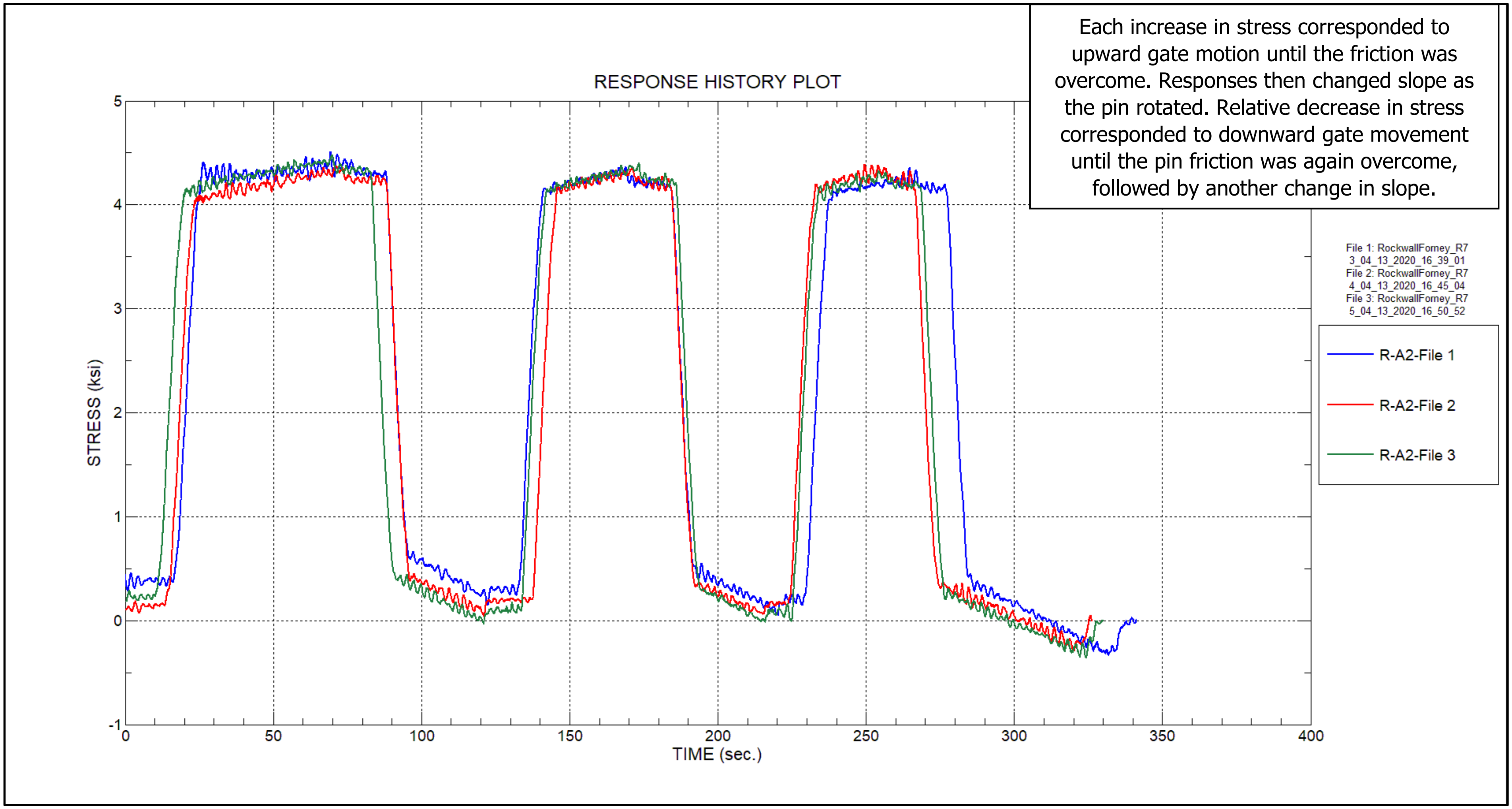

Figure 6 – Stress response history – Right arm – Gage A2 – Time based
File 1 = test run 1, File 2 = test run 2, File 3 = test run 3

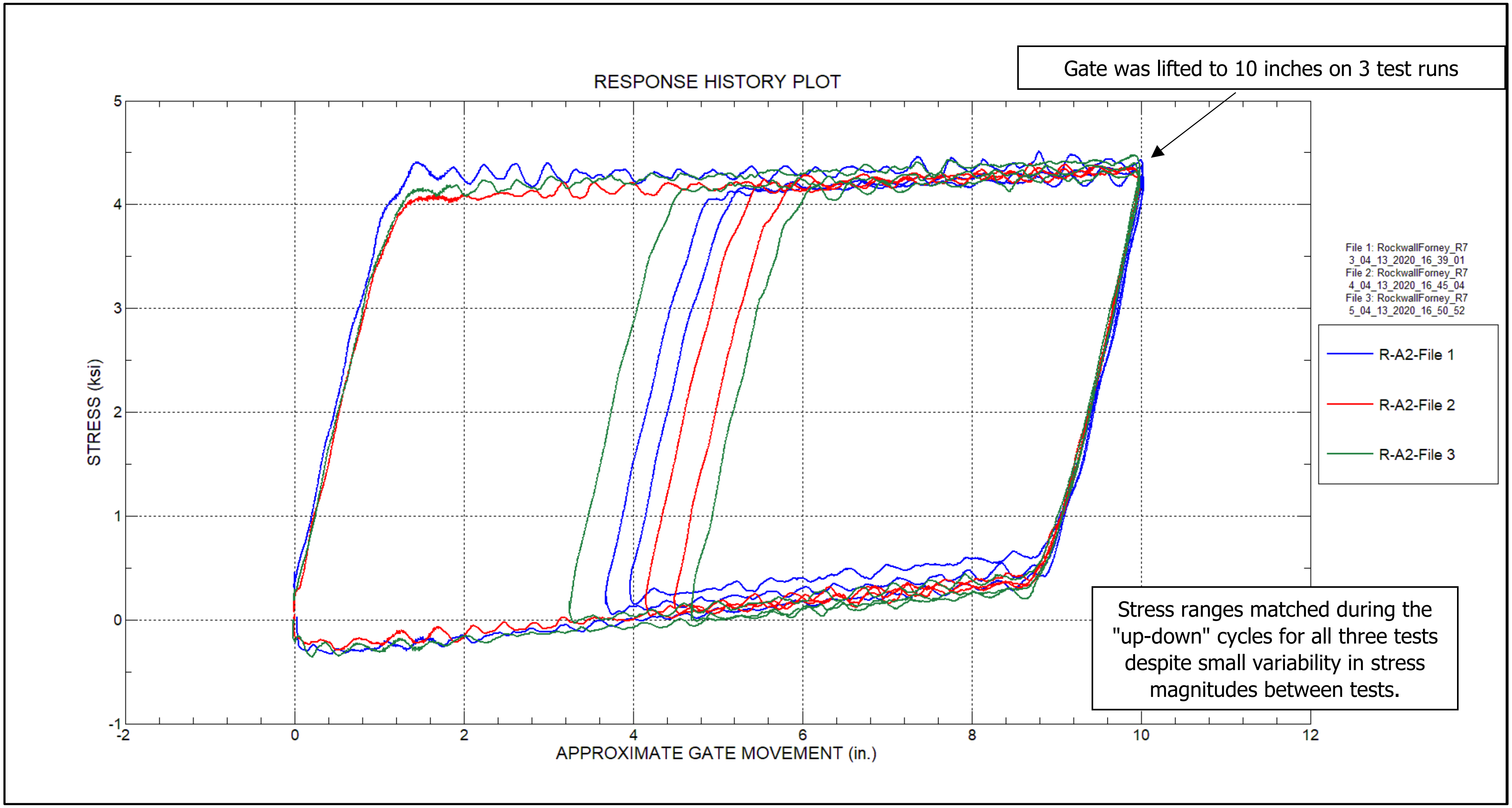

Figure 7 – Stress response history – Right arm – Gage A2 – Function of gate movement
File 1 = test run 1, File 2 = test run 2, File 3 = test run 3

(Section A along top strut near pin – Sensor location 2 along bottom of inner flange)

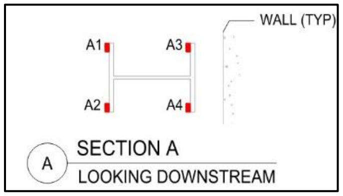

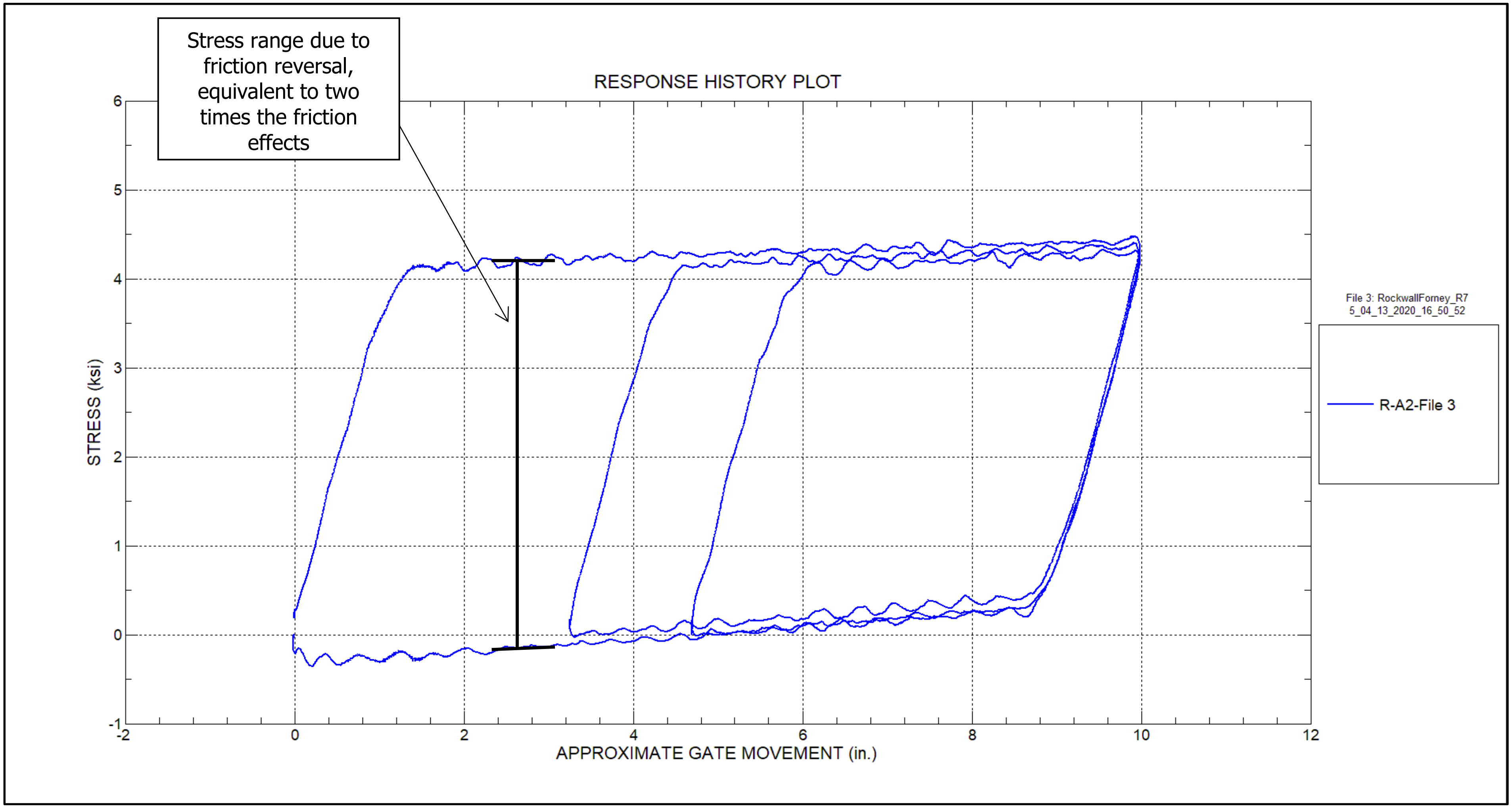

Figure 8 – Stress response history – Right arm – Gage A2 – Friction effect in stress responses

(Section A along top strut near pin – Sensor location 2 along bottom of inner flange)

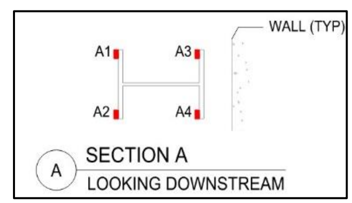

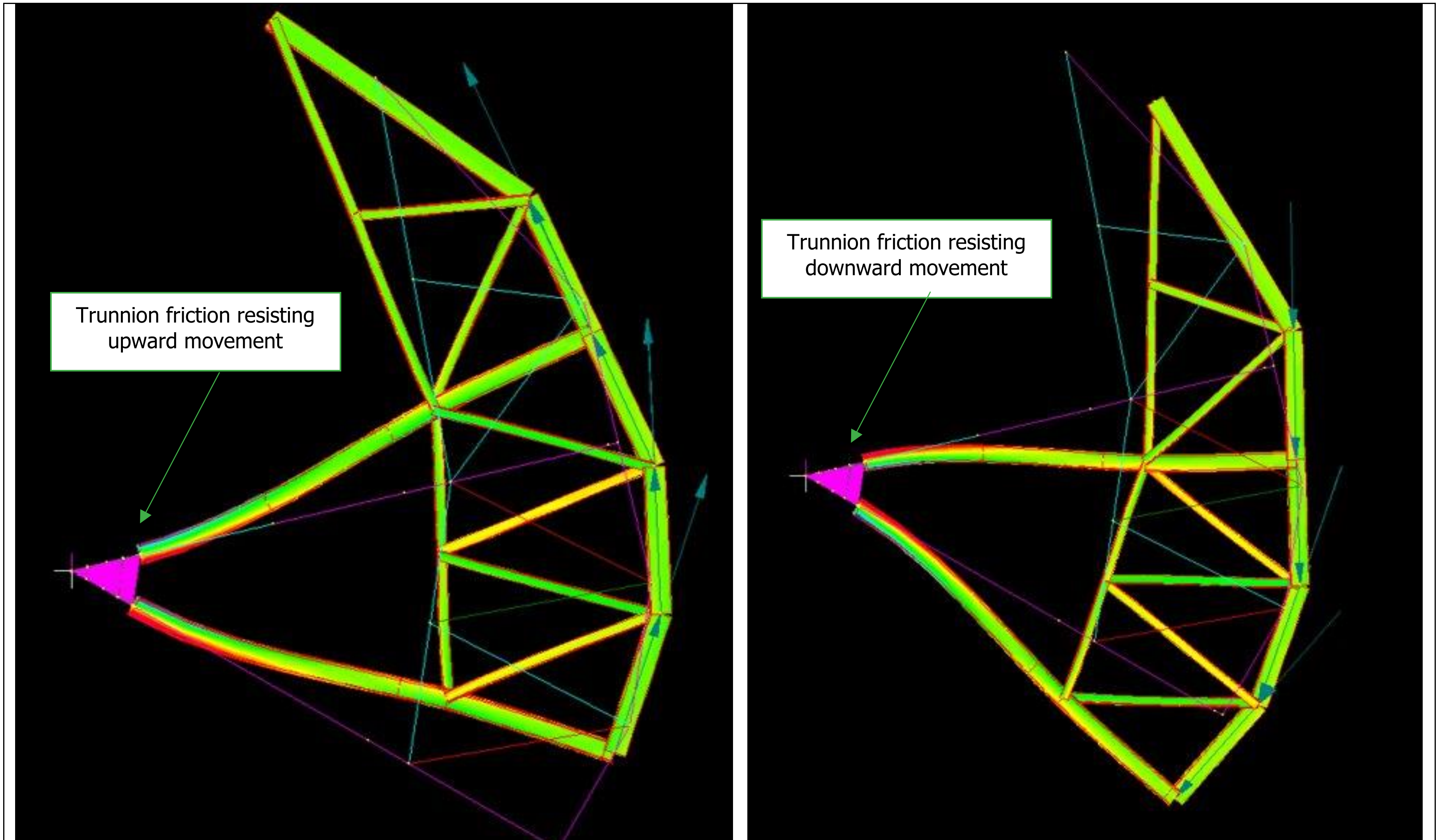

Gate traveling upward **Gate traveling downward**

Figure 9 – Deflected shapes during lifting and lowering of Gate – Visualization of direction/friction reversals

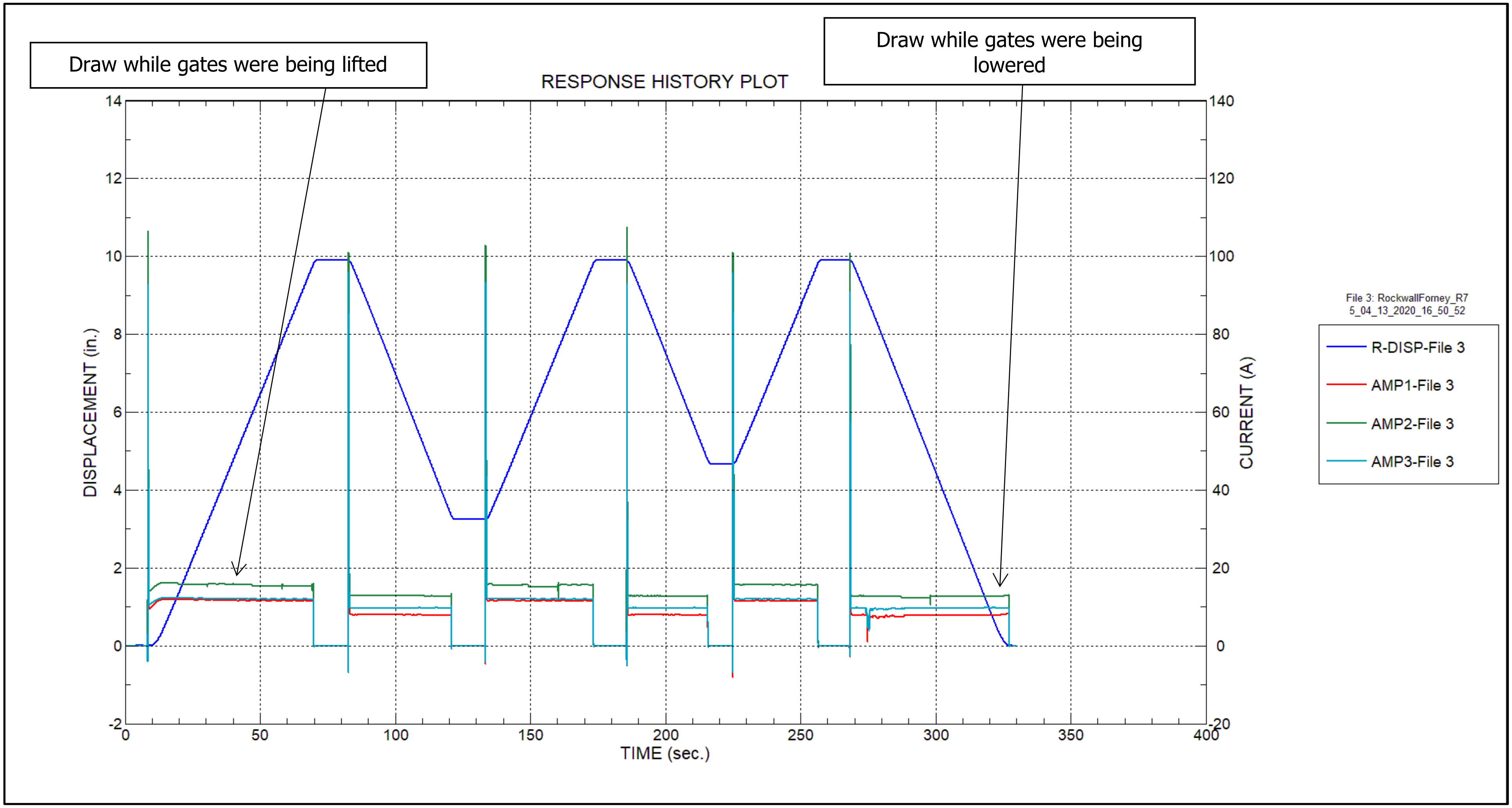

Figure 10 – Motor current & gate movement response history – Lift motor – Highlighting motor draw during lift and lower cycles

Methodology and Findings of The Strut Force and Moment Calculations

The following outline provides the methodology used to calculate the required member forces and moments.

- **CHANGE IN STRESS DUE TO GATE OPERATION:** Strain data can be viewed as a function of time starting when the gate was in the down position and was then lifted off the sill. When examining data in this manner, it is easy to see how stresses ramped up as the gate began to move and then changed slope once pin friction was overcome and the trunnion hub began to rotate with the gate. The first point in time where the friction was overcome (both lifting and lowering) has been highlighted in the stress histories shown in Figure 11. These stress histories show the response of all four sensors along the top strut of the right arm (Section A). ***It is important to note that the recorded measurements were changes in structural response due to gate movement, and do not include the in-situ stresses due to the dead load, cable wrap, and hydrostatic loads present prior to testing.***
- **CALCULATION OF STRUT CROSS-SECTIONAL MOMENTS:** The use of four strain gages per strut cross-section allowed accurate in-plane flexural bending moments to be computed from the recorded strain measurements. These moments were computed for every cross-section in each gate arm using the basic mechanics equation provided in Figure 12.

  In-plane or weak-axis flexure refers to bending about a given strut's web. This designation is consistent with typical nomenclature. In-plane bending can be observed visually from the strain response histories as a difference between the top and bottom stresses, whereas out-of-plane or strong-axis bending is visualized as the difference in stress from side to side. Figure 13 provides a visual reference for both types of strut flexure.
- **EXAMINATION OF RESPONSES AS A FUNCTION OF GATE POSITION:** Changes in cross-sectional moment related to friction becomes clearer when the responses are plotted as a function of gate position. Because the gate was operated with several up and down movements, the effects of friction associated with each direction reversal can be viewed for all measured and calculated responses. Figure 14 through Figure 17 show all cross-sectional flexural moment plots for both trunnion arms. The responses in these plots have been centered about the stress state corresponding to a zero-moment, unflexed condition. The zero-moment offset was estimated as the average moment values between up and downward movement (i.e. half the moment difference) at the gate position with the greatest pin friction moment difference (greatest difference between lifting and lowering).
- **TRUNNION FREE-BODY-DIAGRAM & PIN MOMENT CALCULATION:** Figure 18 shows the instrumented member cross-sections and shows how the measured cross-sectional flexural responses were used to compute pin moment. The in-plane moment values used in these calculations were determined directly from the strain measurements at each cross-section using the provided mechanics equations. It should be noted that the out-of-plane moments were not considered in the calculation of pin moment since they were orthogonal to the axis of the pin rotation. Total pin moment was then determined by summing all the moment components about the pin, which included the in-plane moment and the shear components at the strut cross-sections nearest the pin.
- **STRUT SHEAR CALCULATION:** From the examination of the trunnion free-body-diagram described above, the shear vectors at the three struts were a primary component in the pin moment calculation. For this type of structural element, shear vectors were calculated using the moment differential between the two cross sections along each strut. It is important to recognize that shear was constant between the two instrumented cross-sections and the applied shear was a function of the recorded change in moment ($V = dM/dX$). Subsequently, the shear vectors were calculated by dividing the difference in moment by the distance between the two instrumented cross-sections. Shear values for each strut have been plotted as a function of gate position in Figure 19 and Figure 20.

- **CALCULATION OF PIN MOMENT DUE TO FRICTION:** Once all the trunnion arm force vectors were calculated, the equations shown in the free-body-diagram were applied to compute pin moment as a function of gate position. It is important to note that because the calculated pin moment range corresponds to a direction reversal, a reversal in friction also occurred. The effect of direction reversal on pin moment due to friction is best conceptualized by centering the moment response plots about the zero-moment axis. The moment due to lifting and the moment due to lowering can then be visualized as a change from this new zero point corresponding to the gate in an unflexed condition. Therefore, the total moment differential between lifting and lowering was twice the moment due to friction acting in a single direction. Pin-moment plots have been provided in Figure 21 and Figure 22. From these plots, it is apparent that pin moment due to friction remained relatively constant throughout the gate operation tests, with a slight decrease in pin friction moment as the gate continued to be lifted. This slight decrease in pin friction moment most likely corresponded to the change in hydrostatic load as the gate position changed. Pin-moment plots for all tests on Gate 13 are also provided for reference in Appendix B – Gate 13 Pin Moment Component Plots.
- **SHAFT TORQUE & HOIST FORCE:** Torque measurements were taken on the pinion shafts near the hoist motor during testing, with single torque gages installed on the left and right hoist pinion shaft. Responses were recorded in units of micro-strain and converted to torque in units of kip-ft using Equation 1 thru Equation 3 and the following shaft properties.

$$d_O = 5.5\ inches, \qquad d_I = 0\ inches, \qquad E = 29000\ ksi, \qquad \nu = 0.3$$

$$G = \frac{E}{2(1+\nu)}$$

Equation 1

$$J = \frac{\pi\left(d_O{}^4 - d_I{}^4\right)}{32}$$

Equation 2

$$\tau = \varepsilon * \frac{2GJ}{\frac{d_O}{2} * 1000000 * 12}$$

Equation 3

Figure 23 shows example torque measurements, recorded on the Gate 13 torque shafts. Best practices for torque measurements is to measure torque on opposite sides of the shaft so that any bending in the shaft can be removed by averaging the two responses. Due to access limitations, only one gage at each location could be installed. Therefore, any bending in the shaft may be reflected in the torque measurements and may be related to the peaks and valleys observed in the torque responses.

Torque values were converted to force in the hoist cables per gate arm using the gear ratio and drum radius, as shown in Figure 24. The gear ratio and drum radius were 5.182 and 1.086 feet respectively, as defined in the provided as-built shop drawings. It should be noted that the hoist force calculated may be smaller than the actual hoist force applied. This difference is due to the limit switch engaging the brake before the hoist cable was fully slacked, resulting in an initial force in the cable. A hoist force due to total gate friction was then calculated. This friction hoist force was equal to half the differential in force measured during the lifting and lowering of the gate (similar to the pin friction calculations). As shown in Table 3, the change in cable force due to friction was generally consistent between tests. Note that the total hoist force was due to the total friction effects, including side seal, hoist bearings, trunnion friction effects, etc. It is difficult to determine the exact proportion and composition of the total friction sources. Additional torque and hoist force plots for all collected data files are provided in Appendix A – Gate 13 Torque and Hoist Force Plots.

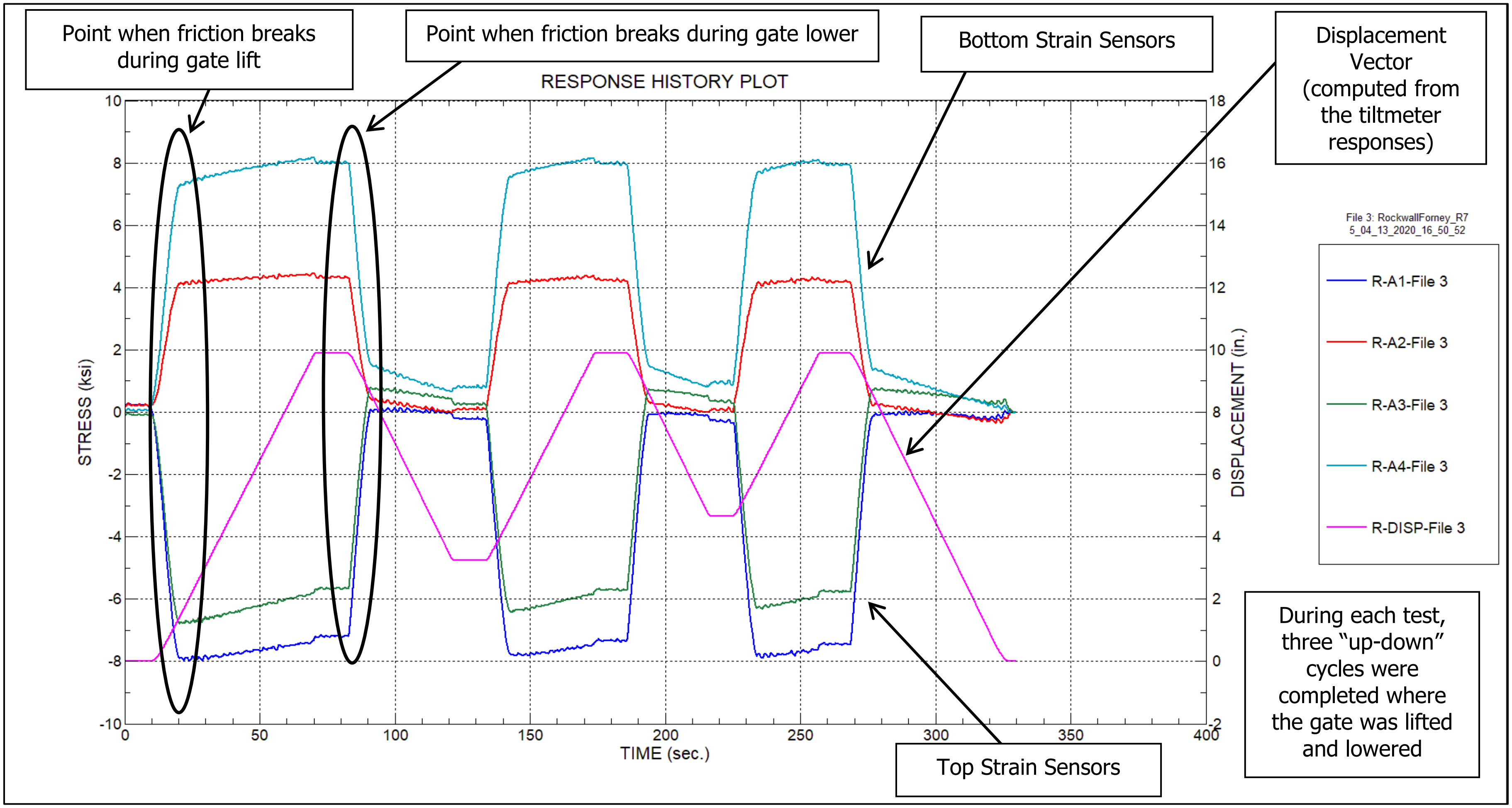

Figure 11 – Stress response & gate movement history – Right arm – Section A - Highlighting friction behavior (Section A along top strut near pin)

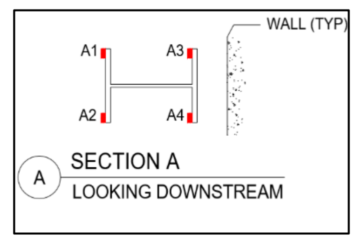

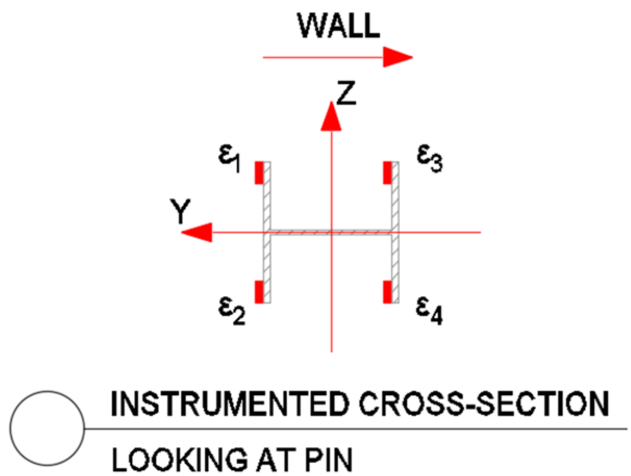

Calculation of Weak-axis (In-plane) bending

$$M_Y = \frac{E[\frac{\varepsilon_2 + \varepsilon_4}{2} - \frac{\varepsilon_1 + \varepsilon_3}{2}]S_{Y(gage)}}{2}$$

Sy(gage) = Section modulus to the center of gages (not extreme fiber of flanges)
(locations of gages were accounted for in moment computation)

Figure 12 – Basic mechanic equation used to calculate moment

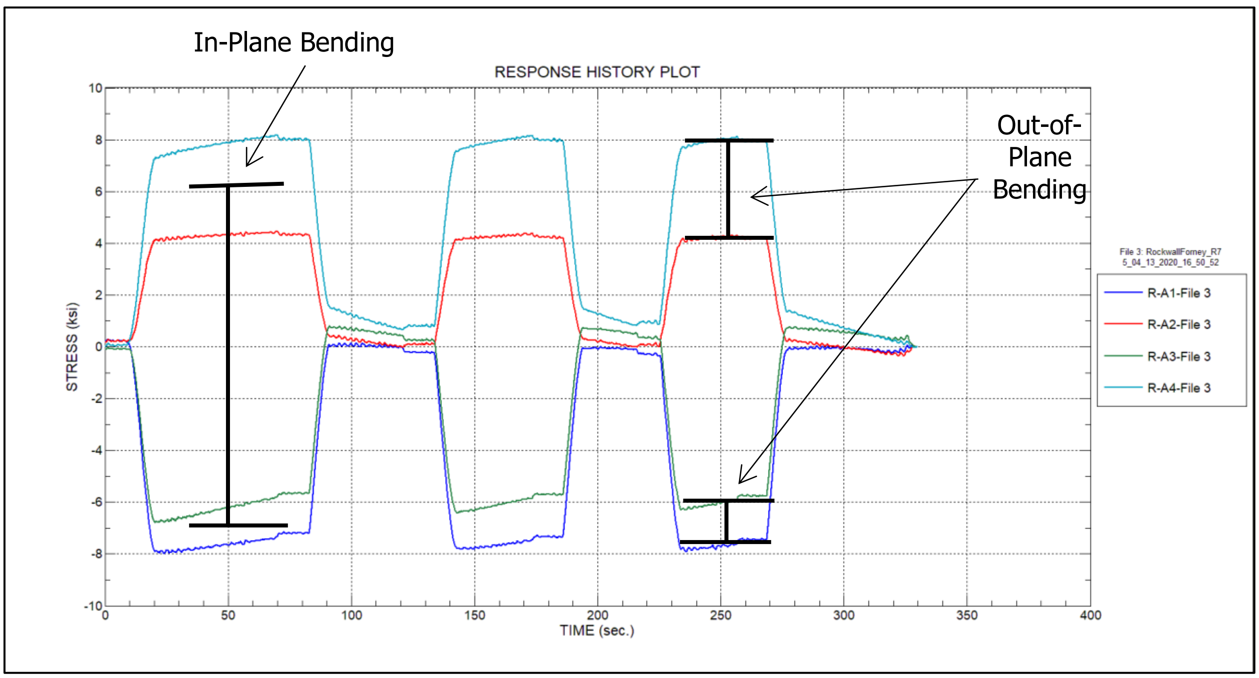

Figure 13 – Stress response history – Right arm – Section A – Bending components
(Section A along top strut near pin)

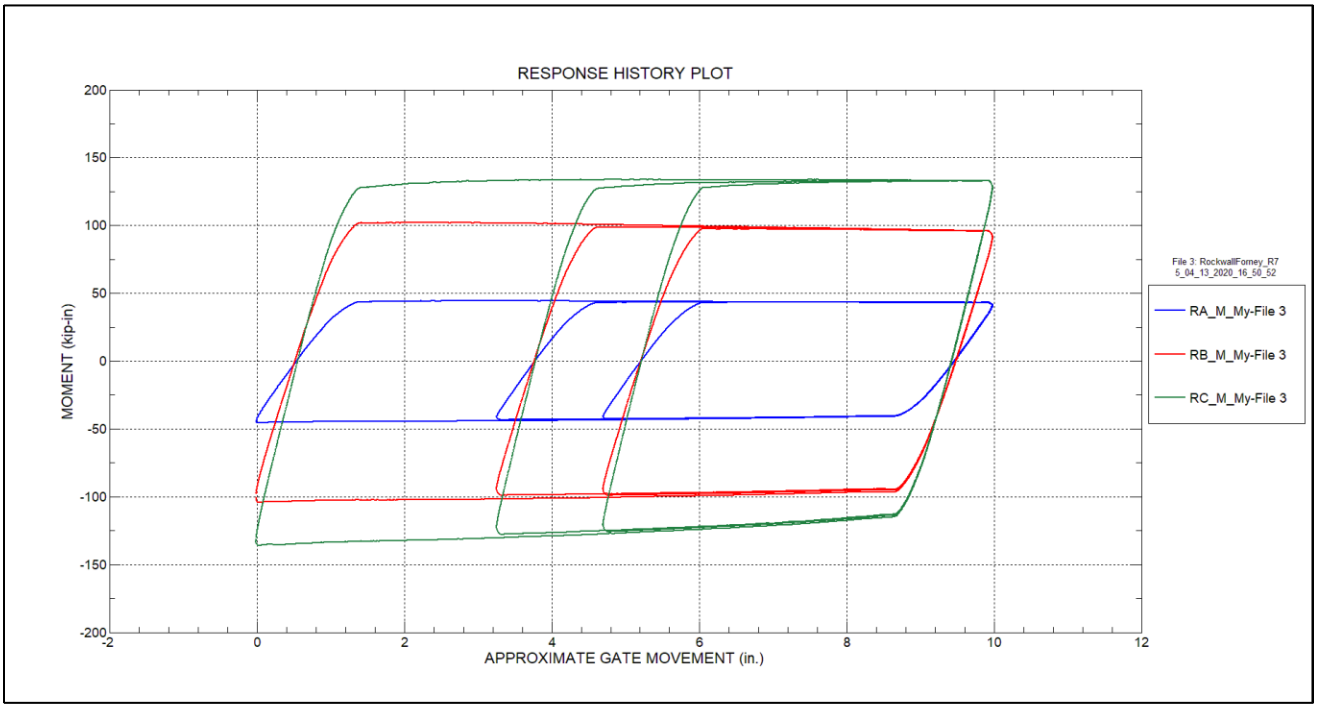

Figure 14 – In-plane moment response history – Right arm – Sections near pin

(RA = Right Arm Top Strut, RB = Right Arm Middle Strut, RC = Right Arm Bottom Strut)

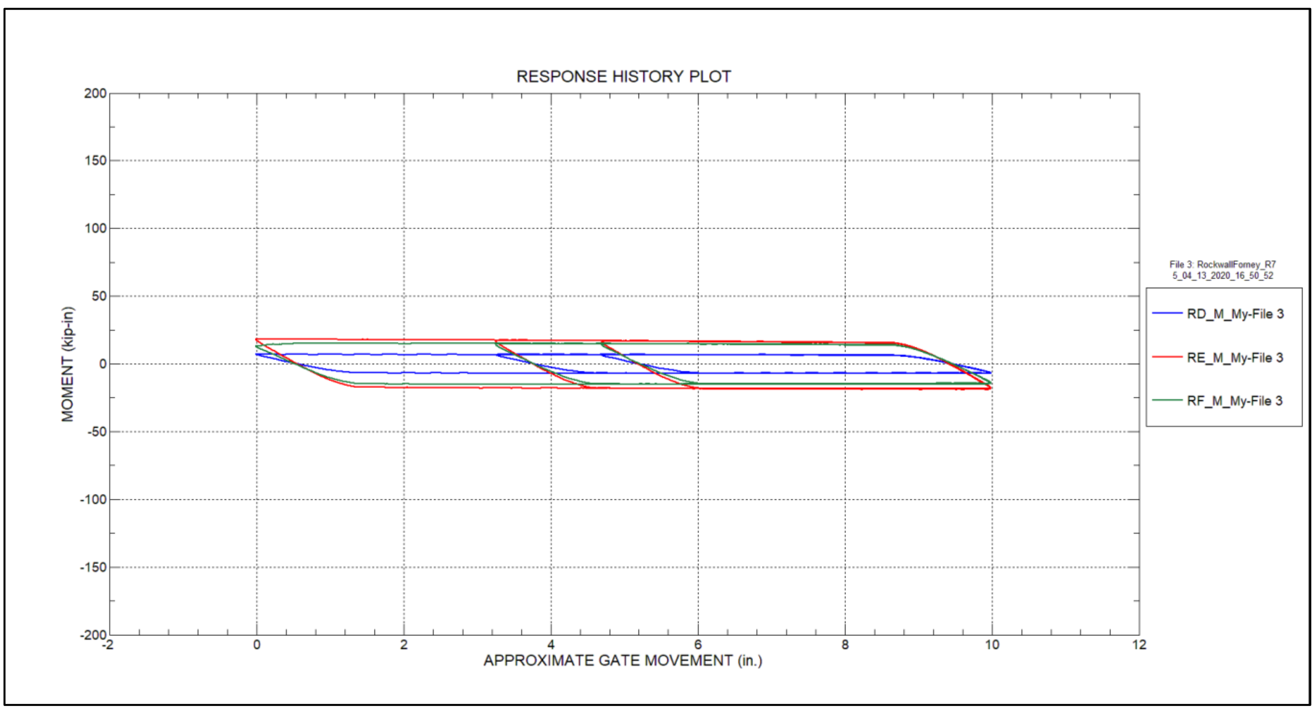

Figure 15 – In-plane moment response history – Right arm – Sections away from pin

(RD = Right Arm Top Strut, RE = Right Arm Middle Strut, RF = Right Arm Bottom Strut)

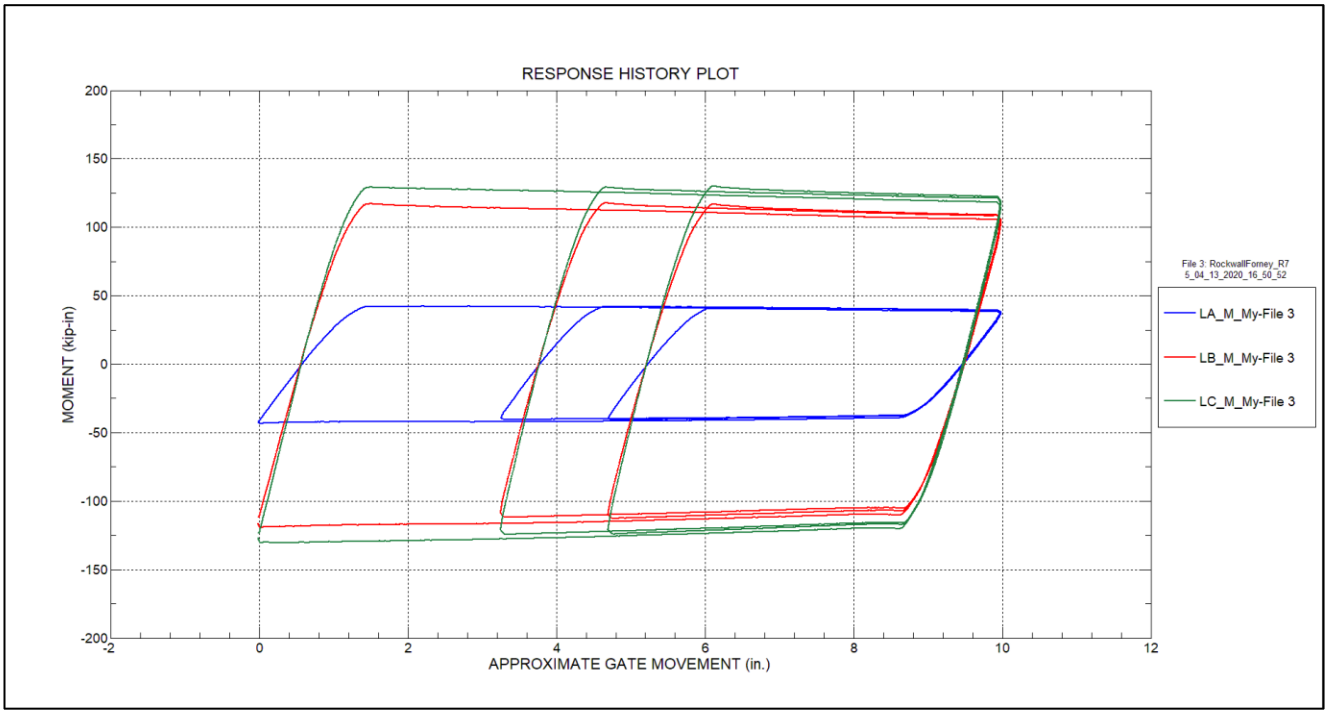

Figure 16 – In-plane moment response history – Left arm – Sections near pin

(LA = Left Arm Top Strut, LB = Left Arm Middle Strut, LC = Left Arm Bottom Strut)

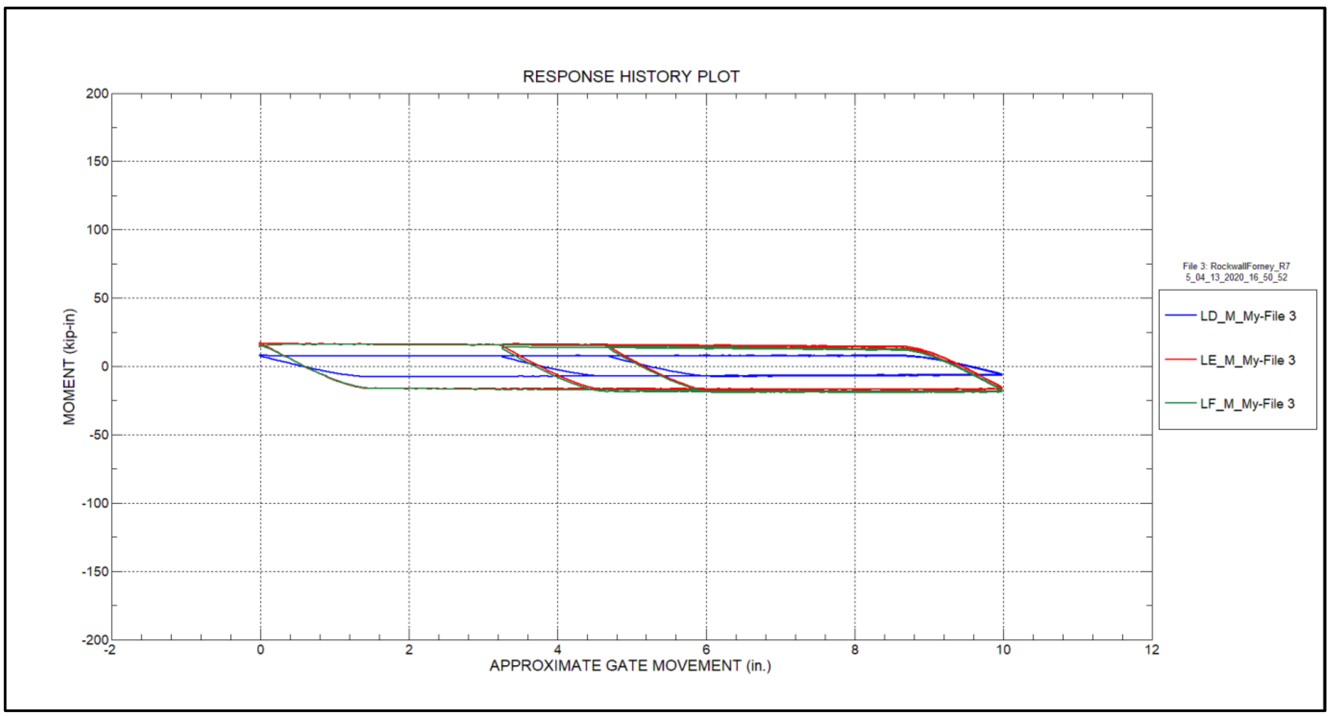

Figure 17 - In-plane moment response history – Left arm – Sections away from pin

(LD = Left Arm Top Strut, LE = Left Arm Middle Strut, LF = Left Arm Bottom Strut)

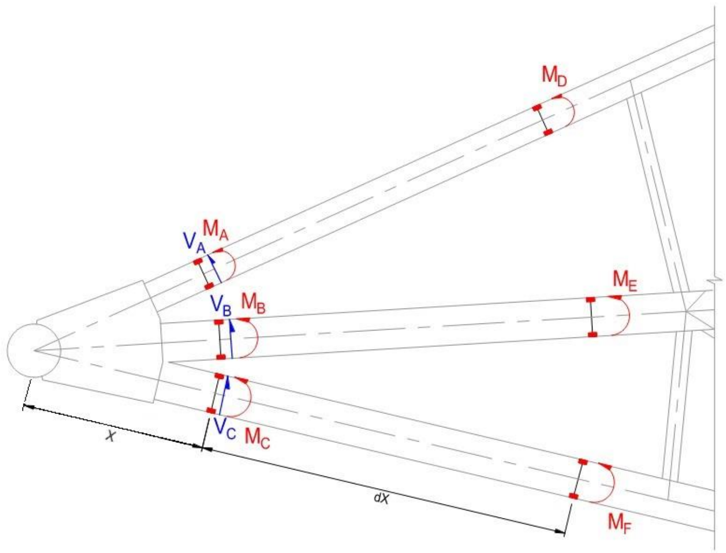

Elevation View of Gate Arm

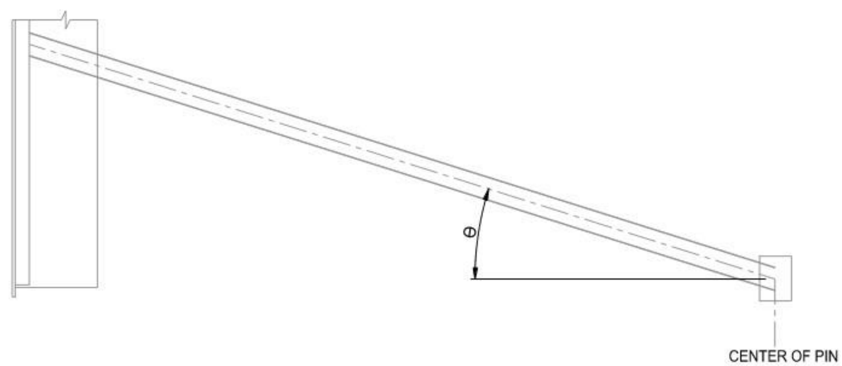

Plan View of Gate Arm

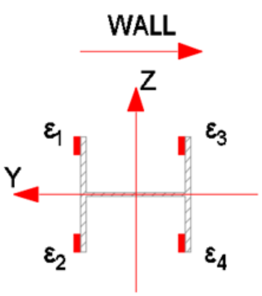

$$M_Y(M_A, M_B, M_C, M_D, M_E, M_F) = \frac{E\left[\frac{\varepsilon_2+\varepsilon_4}{2} - \frac{\varepsilon_1+\varepsilon_3}{2}\right] S_{Y(gage)}}{2}$$

$$V_A = \frac{M_A - M_D}{dX}$$

$$V_B = \frac{M_B - M_E}{dX}$$

$$V_C = \frac{M_C - M_F}{dX}$$

$$\sum M_o = 0$$

$$M_{PIN} = [X(V_A + V_B + V_C) + M_A + M_B + M_C]\cos\theta$$

Figure 18 – Direct calculation of pin moment from strain measurements

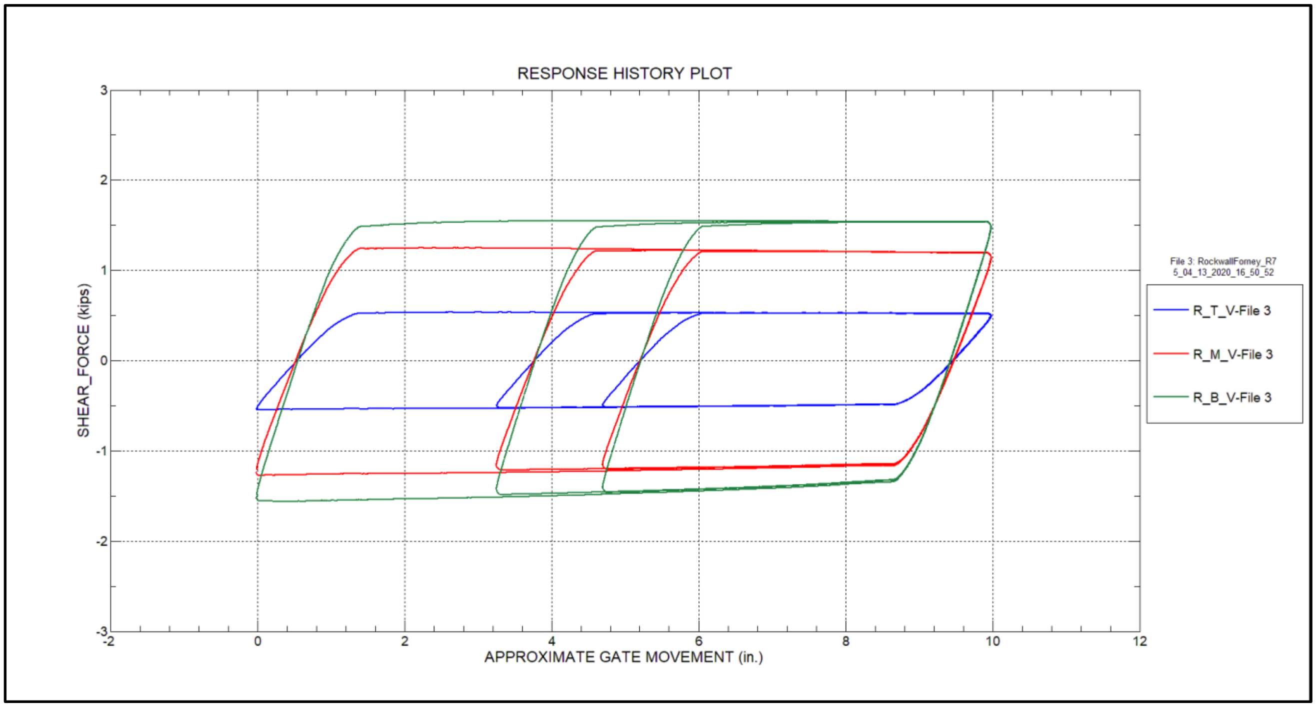

Figure 19 – Strut shear response history – Right arm

(R_T = Right Arm Top Strut, R_M = Right Arm Middle Strut, R_B = Right Arm Bottom Strut)

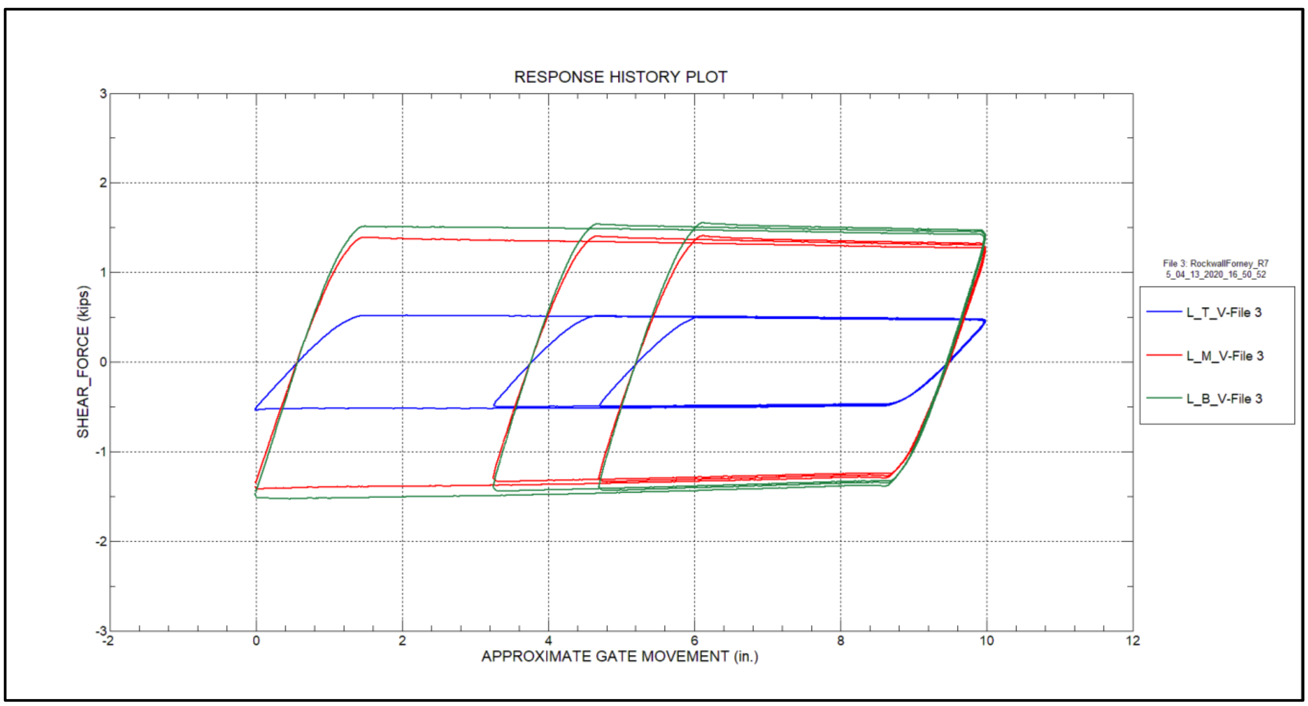

Figure 20 – Strut shear response history – Left arm

(L_T = Left Arm Top Strut, L_M = Left Arm Middle Strut, L_B = Left Arm Bottom Strut)

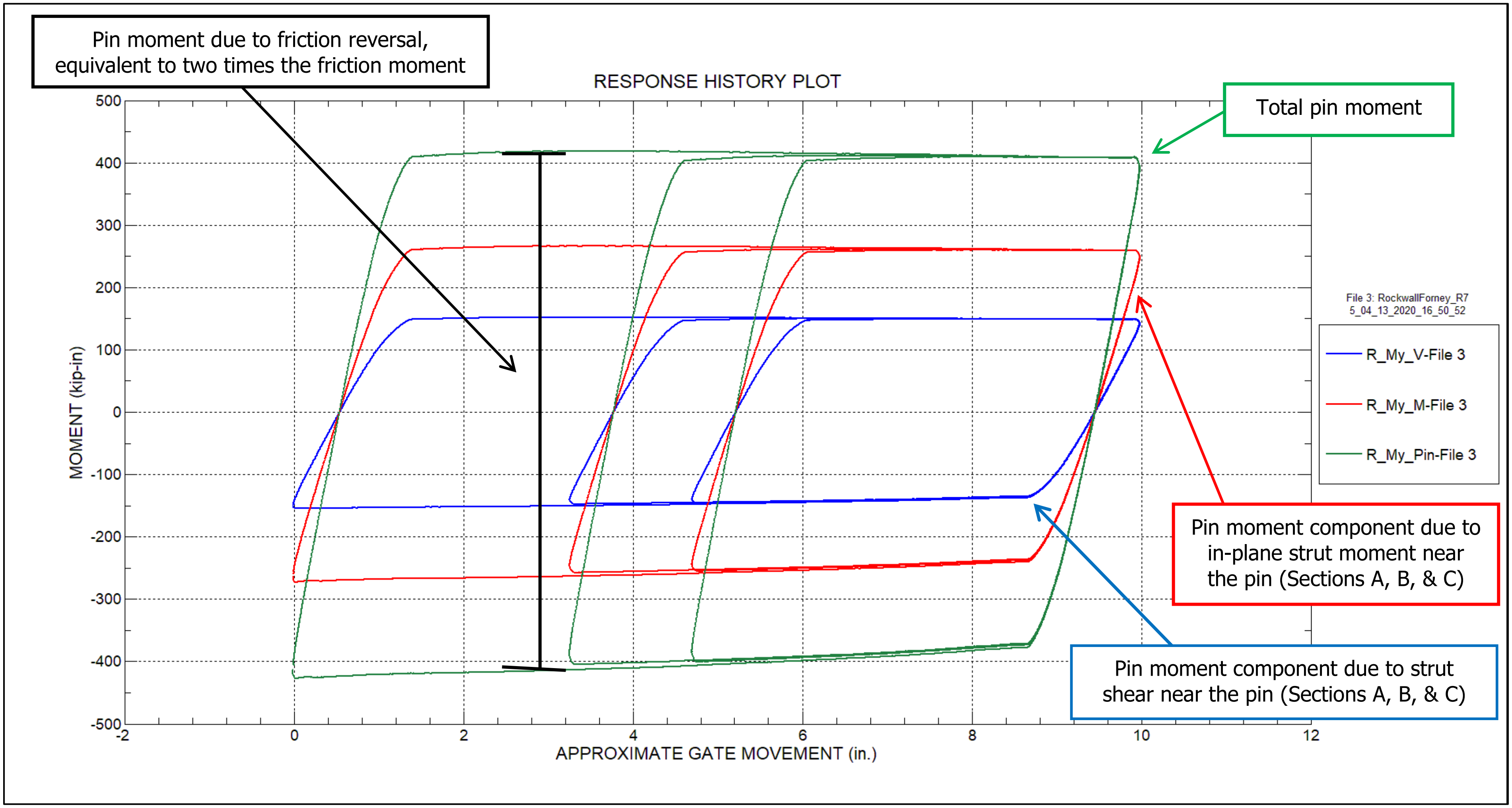

Figure 21 – Pin moment response history – Right arm

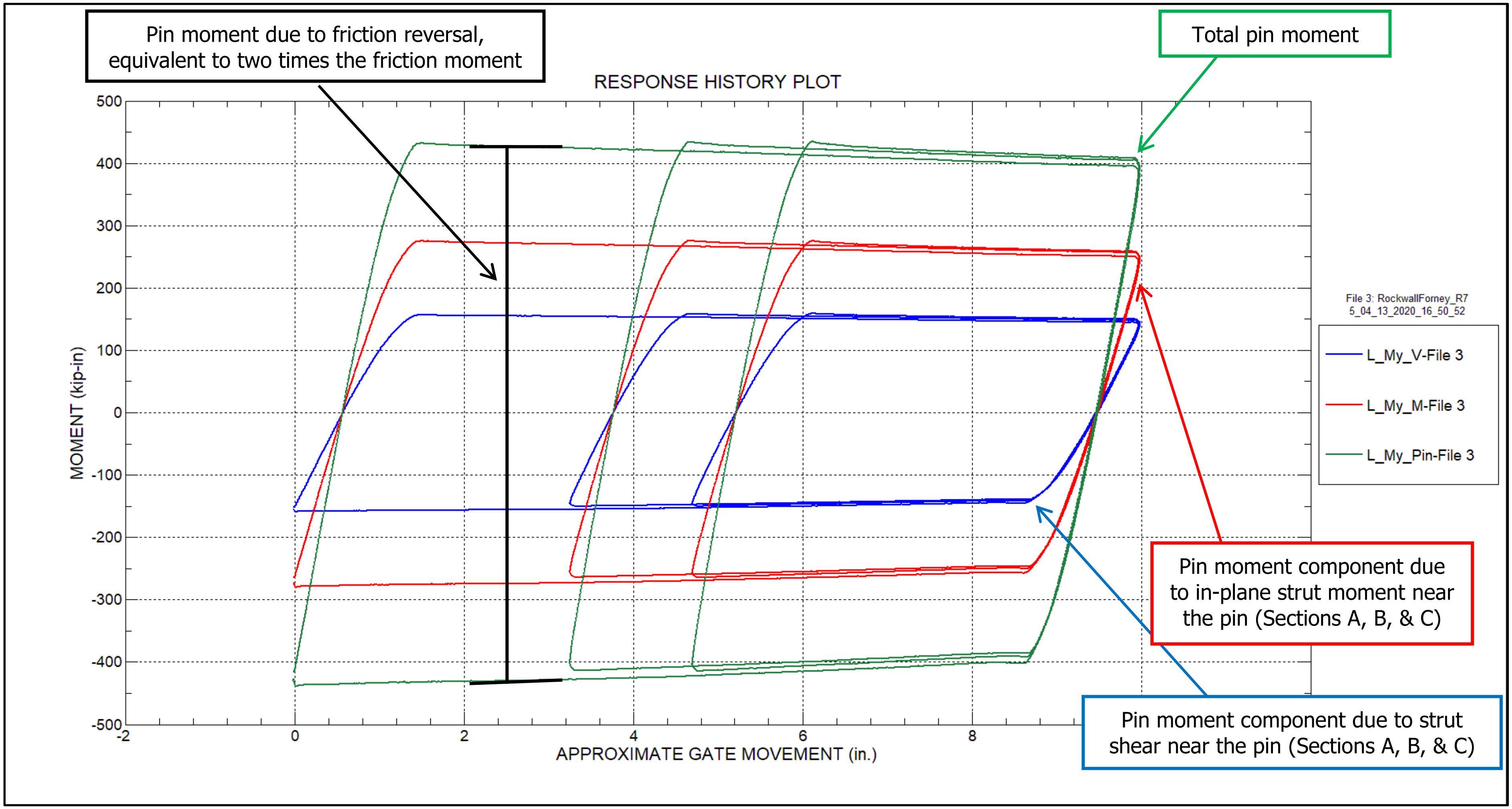

Figure 22 – Pin moment response history – Left arm

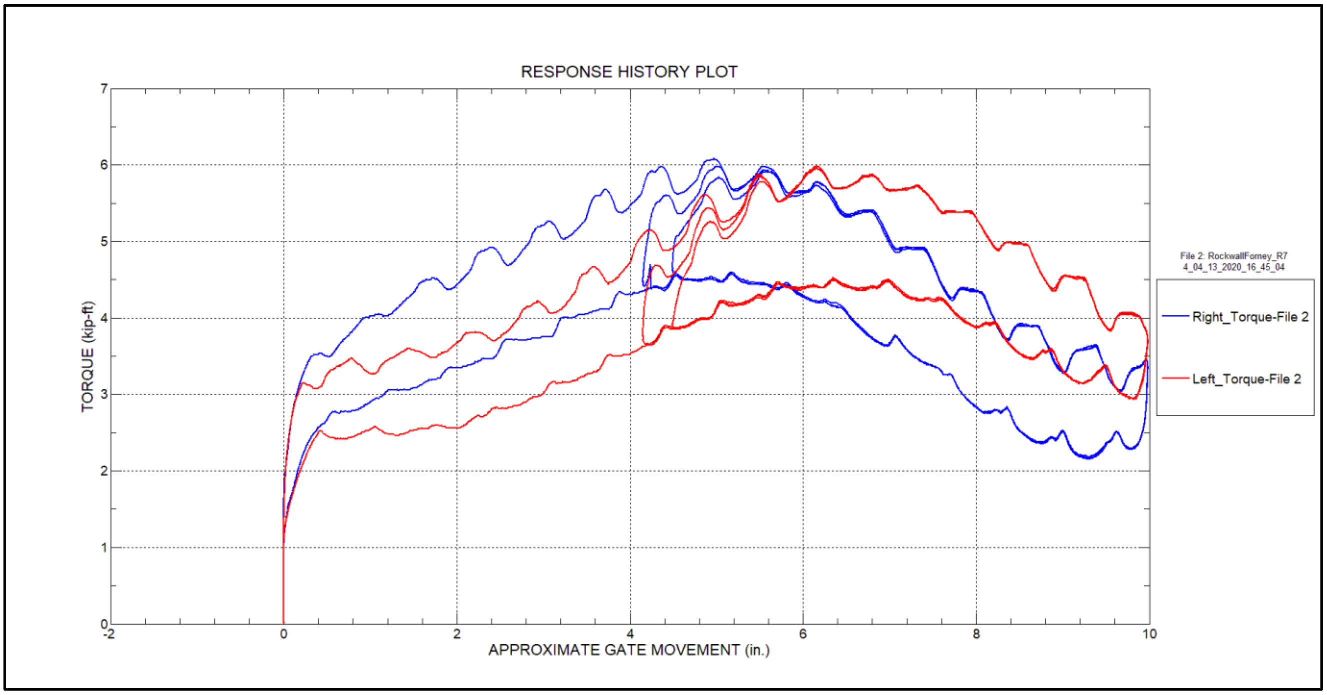

Figure 23 – Hoist torque response history – Gate 13 – Test 2

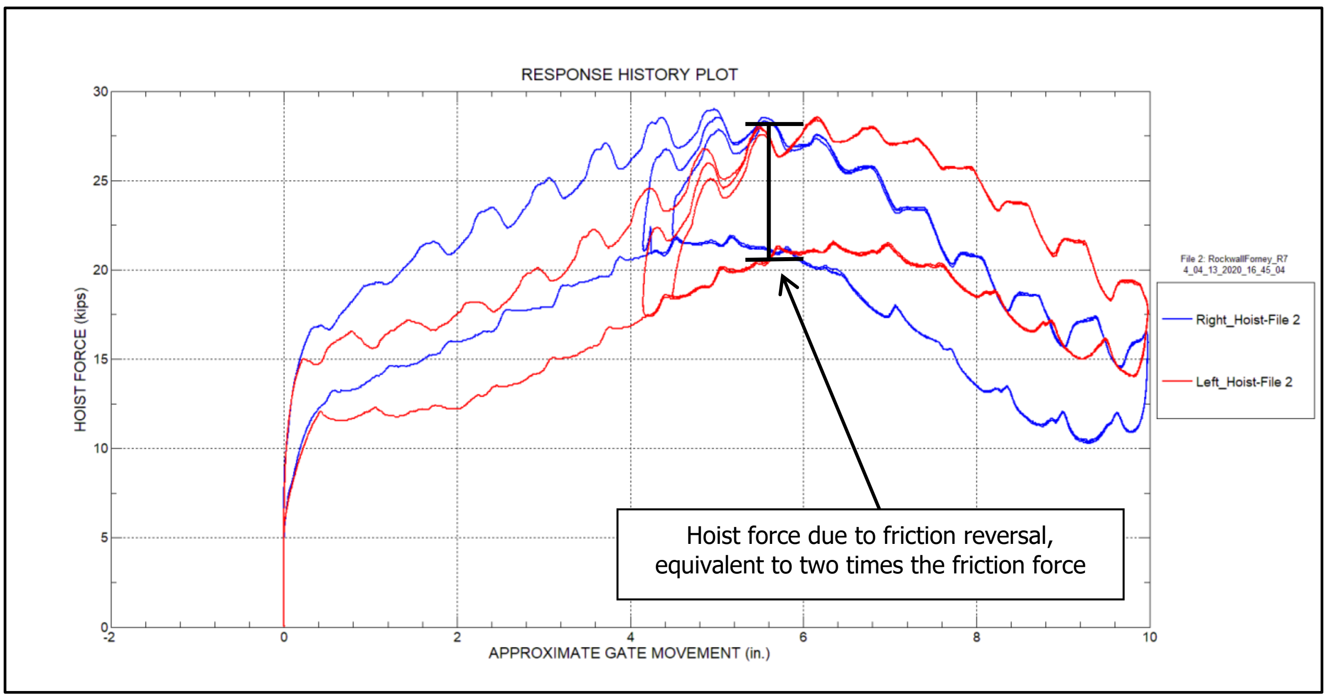

Figure 24 – Hoist force response history – Gate 13 – Test 2

SUMMARY OF FRICTION RESULTS

The raw data files have been included in the submittal package for reference and were formatted as "tdms" files that can be opened in Microsoft Excel using a "tdms" reader extension.

Examination of the stress histories for each test was necessary to obtain a thorough understanding of the gate performance. The response shapes, variations in stress magnitudes, and timing sequences provided direct clues as to how the gate performed under typical service conditions. The following is a breakdown of the provided tabulated results:

+ Table 2 provides motor current ranges and maximum in-flow for lift and lower cycles for each test
+ Table 3 provides maximum hoist force as well as hoist force due to total friction for each test
+ Table 4 provides the maximum stress ranges measured at the sensor locations for each member
+ Table 5 provides maximum bending stress and moment ranges observed during the gate tests
+ Table 6 provides maximum friction bending stress and moment values at each of the instrumented strut locations
+ Table 7 provides the computed shear values in each strut due to friction
+ Table 8 provides calculated measured friction moments, calculated hydrostatic loads based on the measured water elevation, and coefficients of friction for each gate and gate arm during all three tests

The resulting pin friction moments were used to compute friction coefficients from Eq. 4, given the pin radius and the applied thrust. The thrust used in this calculation consisted of the calculated resultant hydrostatic load based on the measured water elevation and was adjusted to account for the loss of head as the gate was lifted. This thrust adjustment was based on the recorded gate movement and was performed in order to calculate more accurate friction coefficients. The water elevation during testing was nearly constant throughout each gate test and was documented during each "up-down" cycle. It should be noted that the minor thrust due to cable wrapping, which was minimal compared to hydrostatic thrust, was not included in the thrust calculation. This assumption resulted in slightly conservative friction coefficients.

$$\mu = \frac{M_F}{T * r} \qquad \text{Eq. 4}$$

where:

μ = Friction Coefficient

M_F = Friction Moment

T = Thrust per Pin

r = Pin Radius, 5.375"

The out-of-plane shear and moments were not considered in the pin friction calculations due to orthogonal geometry considerations (resulting pin moment associated with out-of-plane flexure being perpendicular to pin rotation).

The data was presented in a specific coordinate system applicable to both arms. Data was processed so that the positive x-axis was always pointing towards the pin and the right-hand rule applied. In-plane bending can be referred to as "bending about the horizontal or y-axis" and shows how much the beams bend up and down within the plane of the gate arms. Refer to Figure 12 above for visual reference of coordinate system and mathematical explanation of calculations. Tabulated results do not include any in-situ effects.

Table 2 – Motor current summary table – Gate 13

Test Run	Current Range due to Lifting (A)	Current Range due to Lowering (A)	Max In-rush Current (A)
1	12-18	8-13	107
2	12-16	8-13	107
3	11-16	7-13	108

Table 3 – Hoist force summary table – Gate 13

Test Run	Right Arm Peak Hoist Force (kips)	Left Arm Peak Hoist Force (kips)	Right Arm Hoist Force due to Total Gate Friction (kips)	Left Arm Hoist Force due to Total Gate Friction (kips)
1	28.88	28.33	3.95	3.71
2	29.03	28.57	4.07	3.89
3	29.07	28.63	4.16	3.96

Tabulated friction force values correspond to the response induced by friction in one direction

Table 4 – Maximum measured sensor stress range

Arm Designation	Top Strut (ksi)	Middle Strut (ksi)	Bottom Strut (ksi)
Right Arm	8.44	9.06	10.28
Left Arm	8.27	10.43	9.20

Tabulated values correspond to the total measured change in response during tests

Stress values have not been extrapolated to the extreme fibers (correspond to center of gage)

Table 5 – Maximum in-plane total bending stress & moment ranges – Total

Section Label	Section Description	Right Arm Stress (ksi)	Right Arm Moment (kip-in)	Left Arm Stress (ksi)	Left Arm Moment (kip-in)
Section A	Top Strut Near Pin	8.26	92.87	7.64	85.83
Section B	Middle Strut Near Pin	9.30	215.18	10.27	237.40
Section C	Bottom Strut Near Pin	9.68	269.83	9.36	261.08
Section D	Top Strut Away from Pin	1.31	14.73	1.43	16.02
Section E	Middle Strut Away from Pin	1.64	38.03	1.55	35.74
Section F	Bottom Strut Away from Pin	1.10	30.80	1.28	35.56

Tabulated values correspond to the total measured change in response during tests

RAW DATA.
REFINED RESULTS.

Table 6 – In-plane frictional bending stress & moment at maximum gate friction

Section Label	Section Description	Right Arm Stress (ksi)	Right Arm Moment (kip-in)	Left Arm Stress (ksi)	Left Arm Moment (kip-in)
Section A	Top Strut Near Pin	4.08	45.84	3.75	42.16
Section B	Middle Strut Near Pin	4.61	106.73	5.08	117.44
Section C	Bottom Strut Near Pin	4.78	133.38	4.65	129.65
Section D	Top Strut Away from Pin	0.61	6.84	0.68	7.69
Section E	Middle Strut Away from Pin	0.77	17.71	0.71	16.39
Section F	Bottom Strut Away from Pin	0.54	15.05	0.58	16.30

Tabulated values correspond to the response induced by friction in one direction

Table 7 – Strut shear range summary table due to friction

Arm Designation	Top Strut Shear (kip)	Middle Strut Shear (kip)	Bottom Strut Shear (kip)
Right Arm	0.55	1.29	1.54
Left Arm	0.52	1.39	1.52

Tabulated values correspond to the response induced by friction in one direction

Table 8 – Pin friction summary table

Test Run	Average Water Elevation during testing (ft)	Approximate Thrust at time of Testing (kips per arm)	Gate/Member Designation	Pin Friction Moment (kip-in)	Friction Coefficient
1	435.67	492.80	Right Pin	427.00	0.16
			Left Pin	430.70	0.16
2	435.67	492.80	Right Pin	414.00	0.16
			Left Pin	422.40	0.16
3	435.67	492.80	Right Pin	417.00	0.16
			Left Pin	432.60	0.16

Tabulated values correspond to the response induced by friction in one direction

Appendix A – Gate 13 Torque and Hoist Force Plots

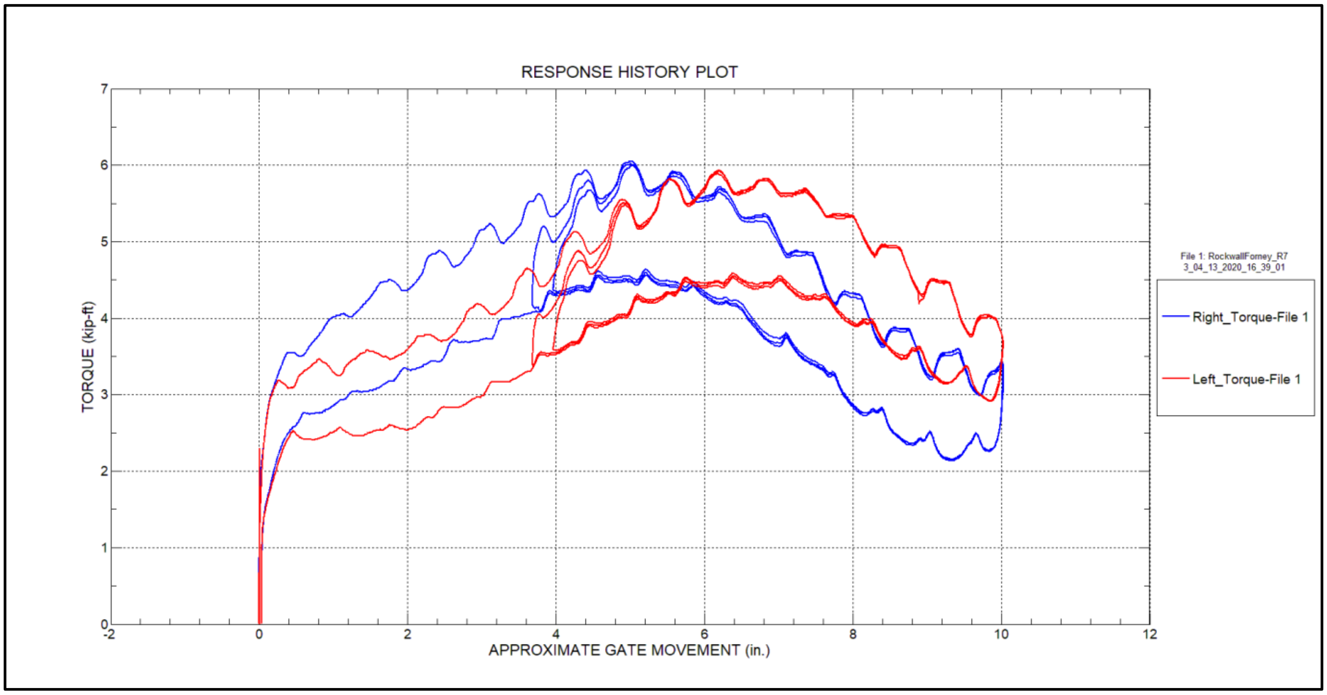

Figure 25 – Hoist torque response history – Gate 13 – Test 1

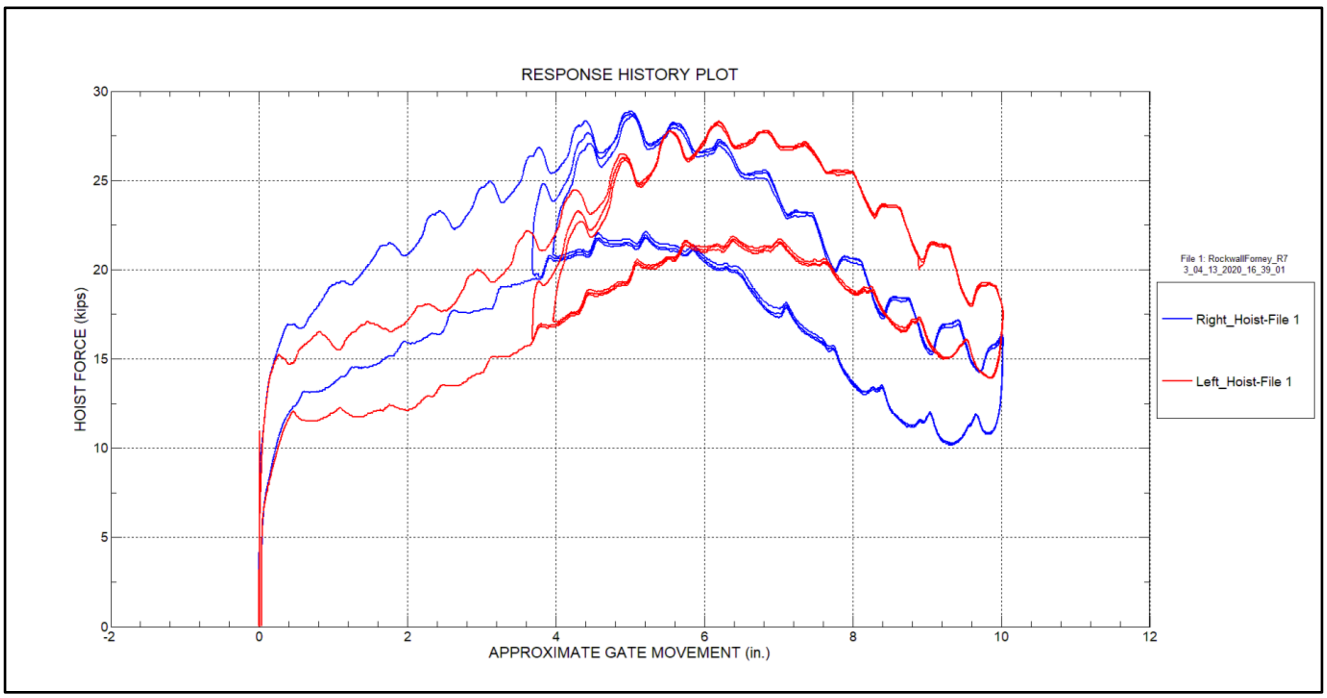

Figure 26 – Hoist force response history – Gate 13 – Test 1

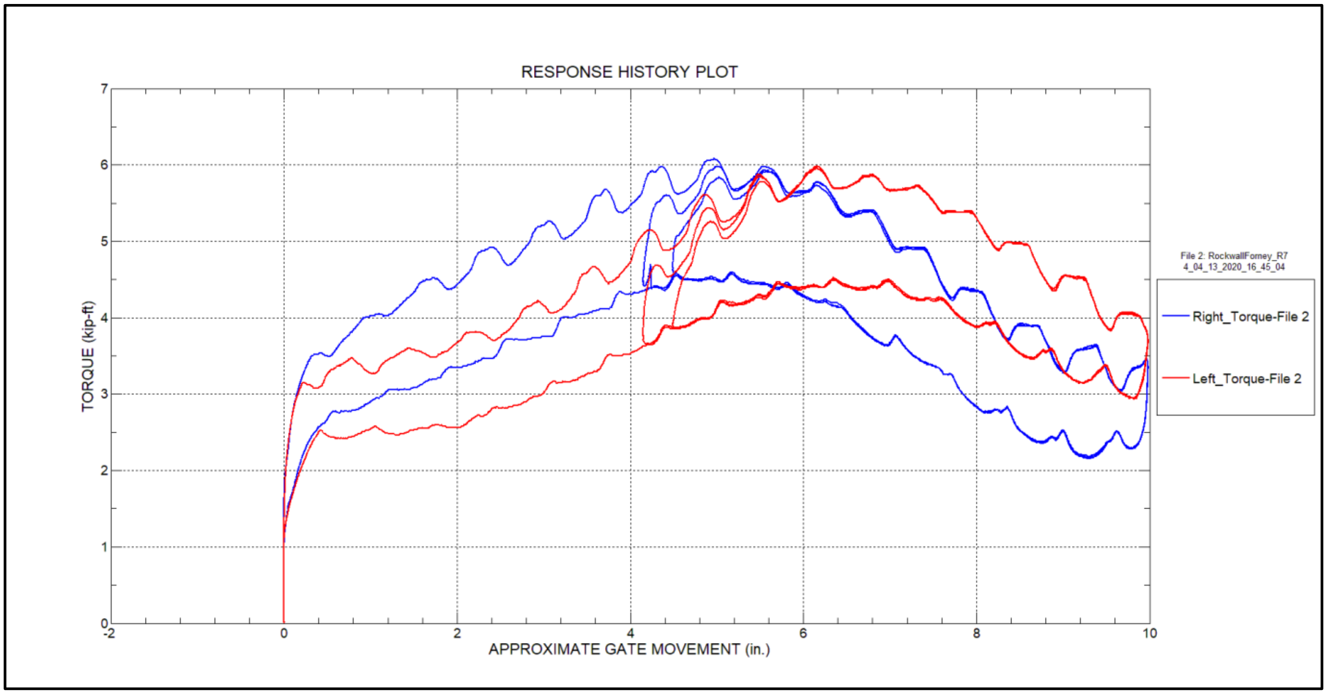

Figure 27 – Hoist torque response history – Gate 13 – Test 2

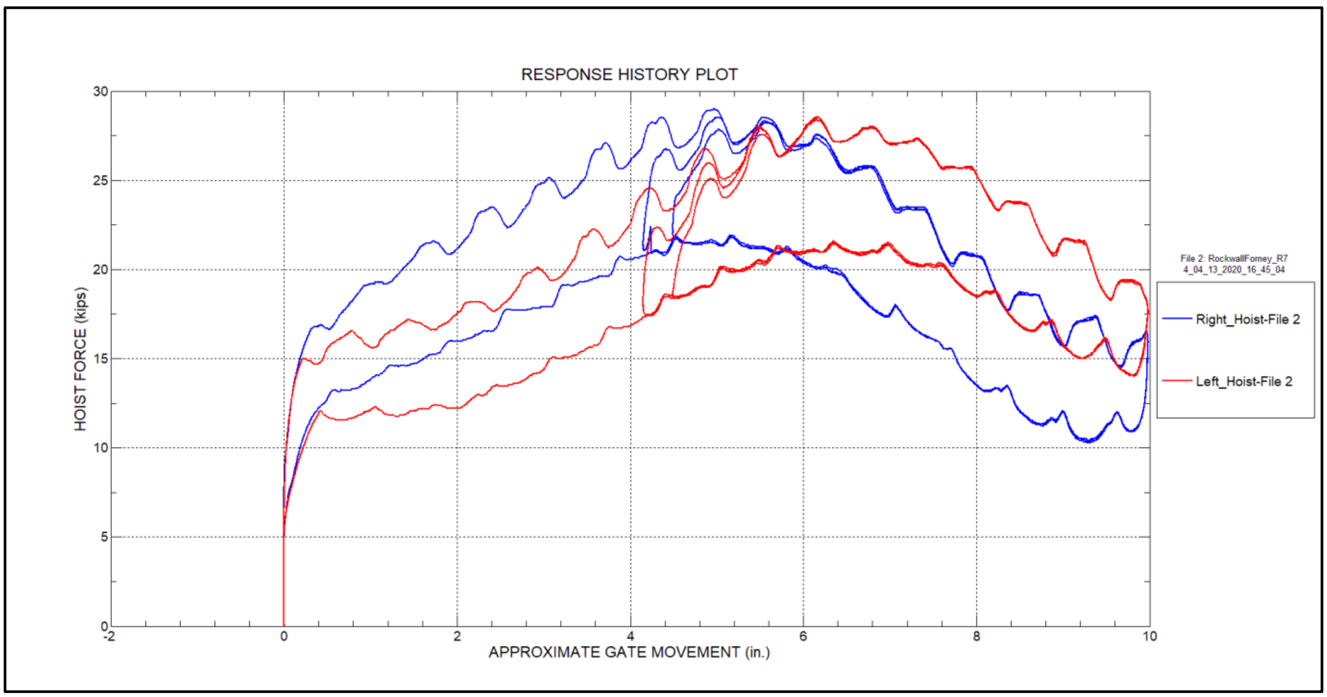

Figure 28 – Hoist force response history – Gate 13 – Test 2

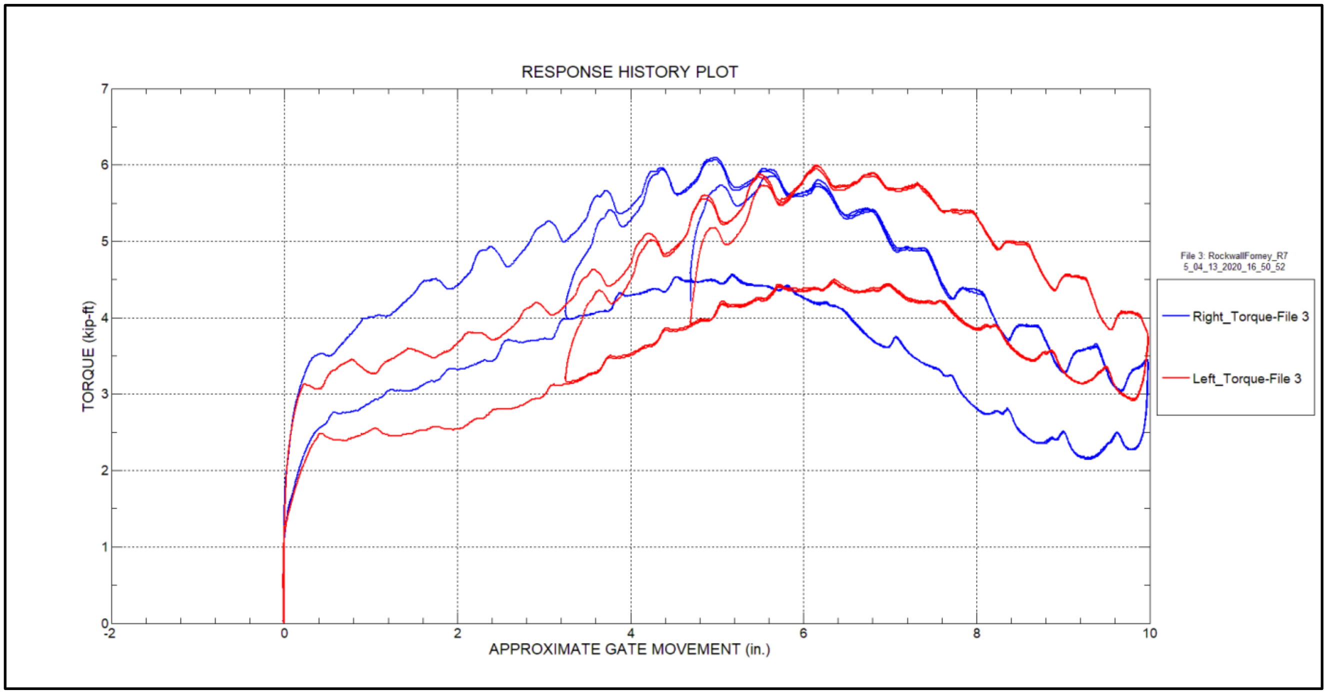

Figure 29 – Hoist torque response history – Gate 13 – Test 3

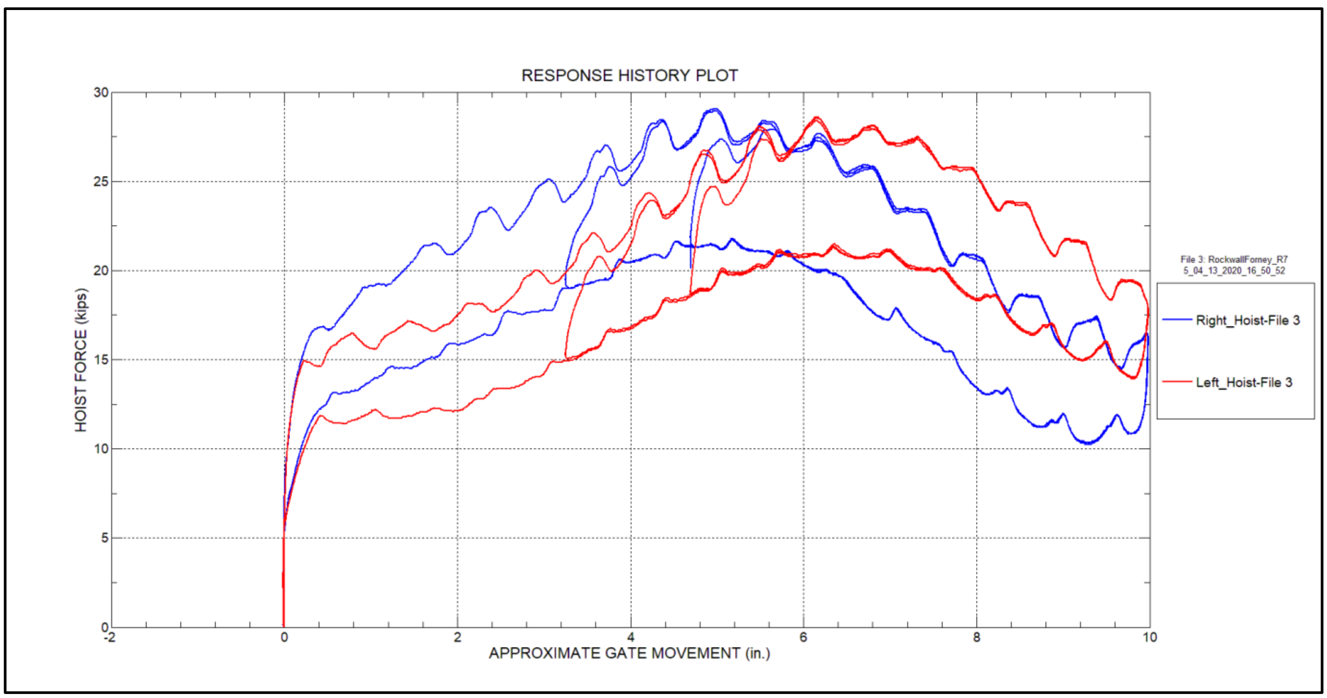

Figure 30 – Hoist force response history – Gate 13 – Test 3

APPENDIX B – GATE 13 PIN MOMENT COMPONENT PLOTS

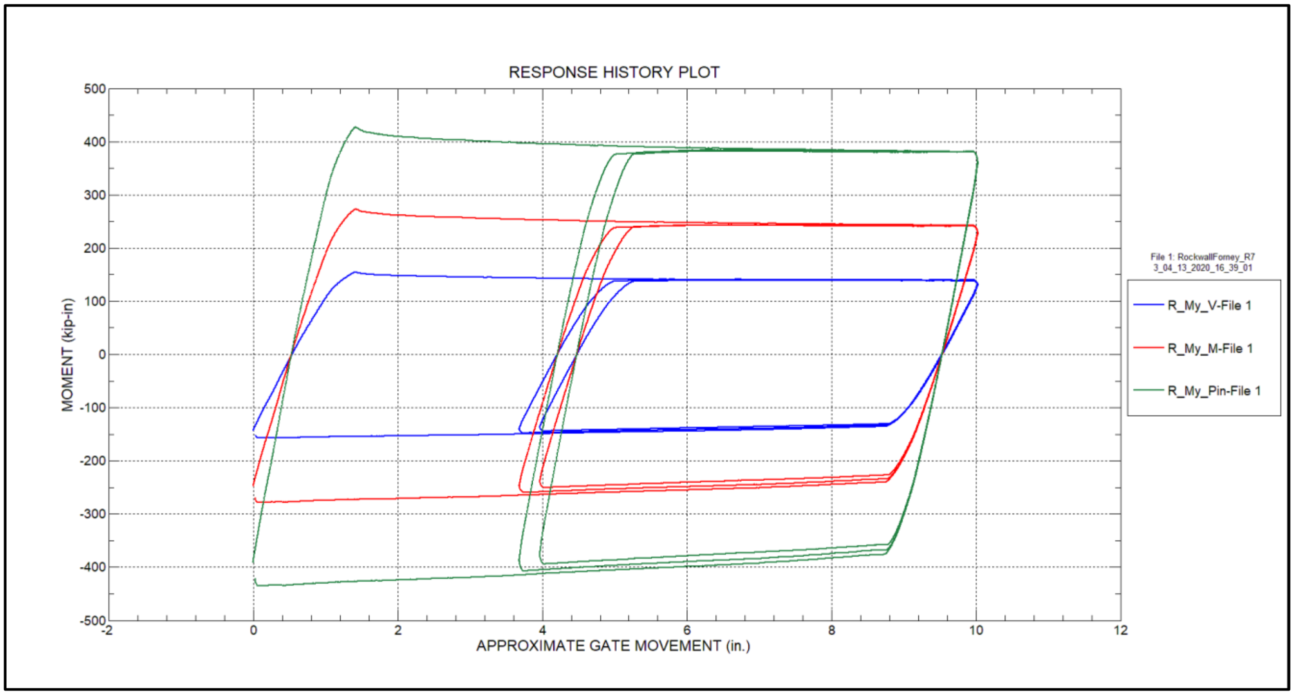

Figure 31 – Pin moment response history – Right arm – Test run 1

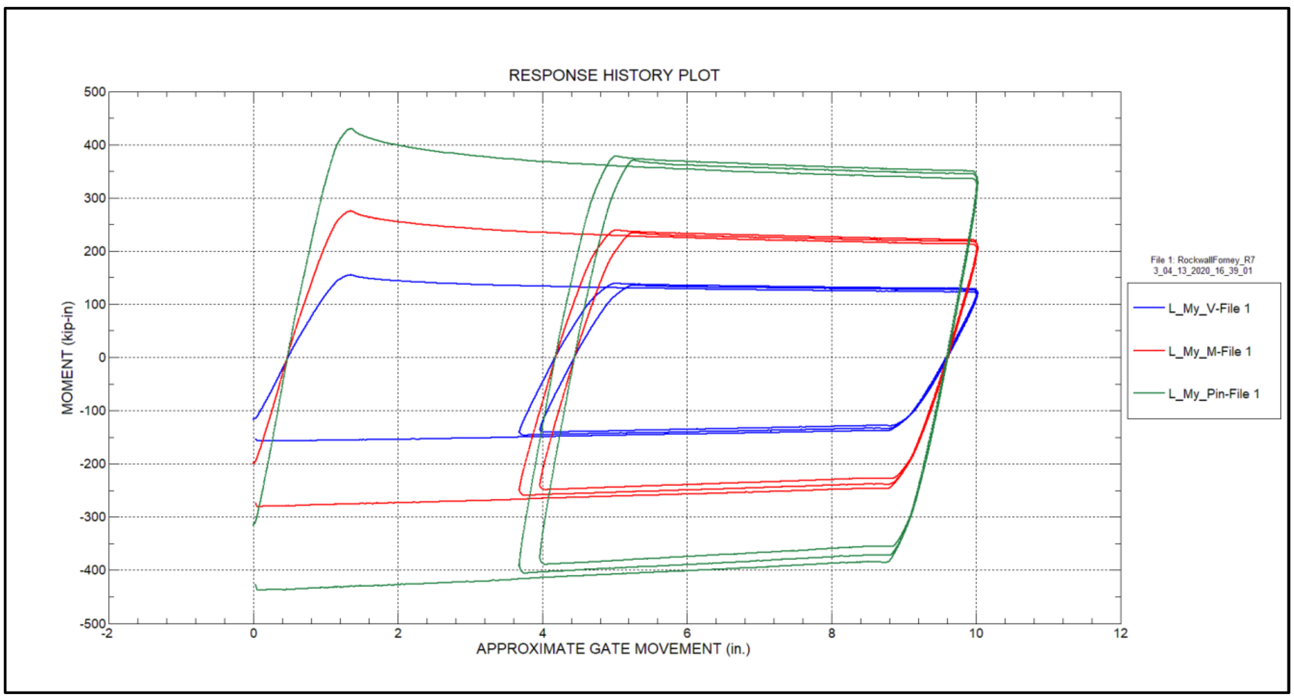

Figure 32 – Pin moment response history – Left arm – Test run 1

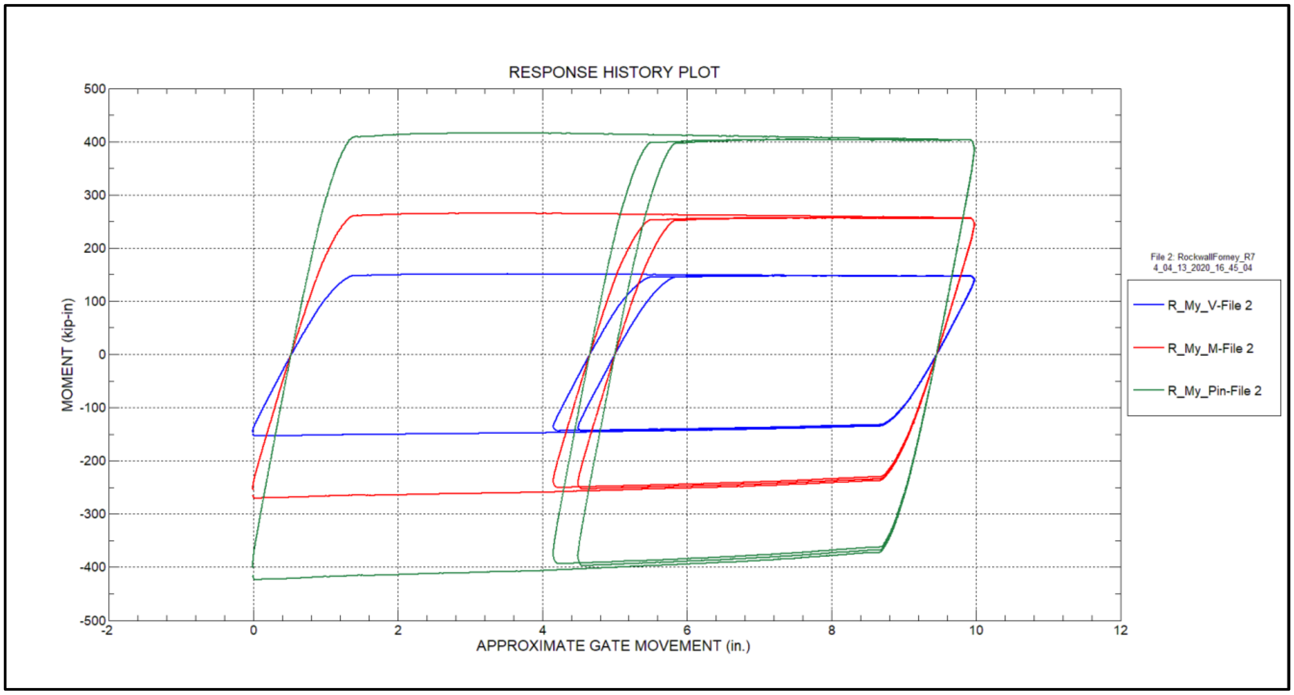

Figure 33 – Pin moment response history – Right arm – Test run 2

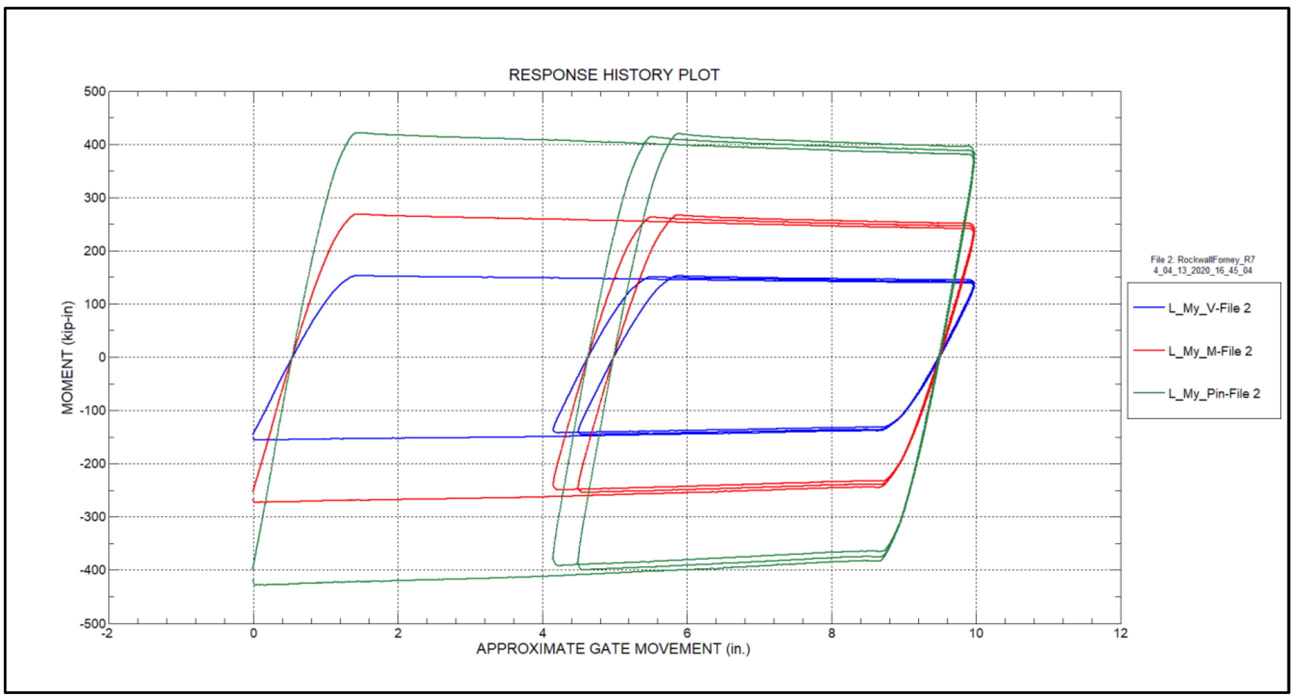

Figure 34 – Pin moment response history – Left arm – Test run 2

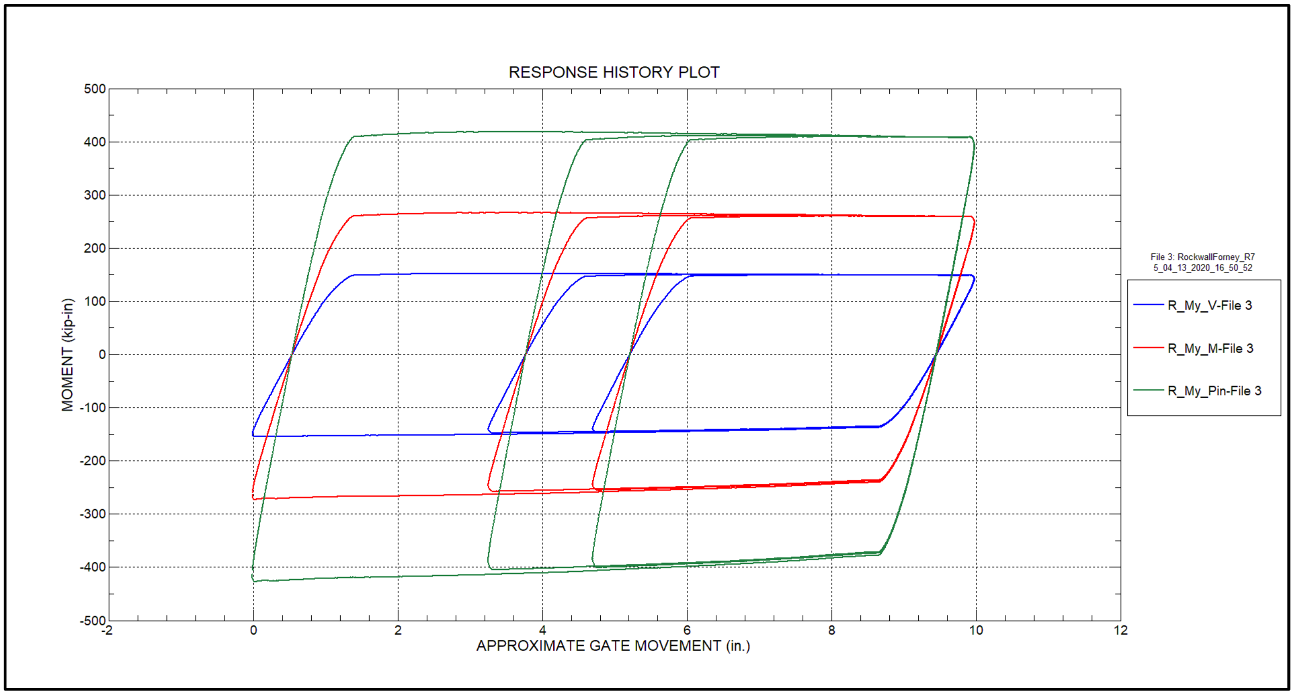

Figure 35 – Pin moment response history – Right arm – Test run 3

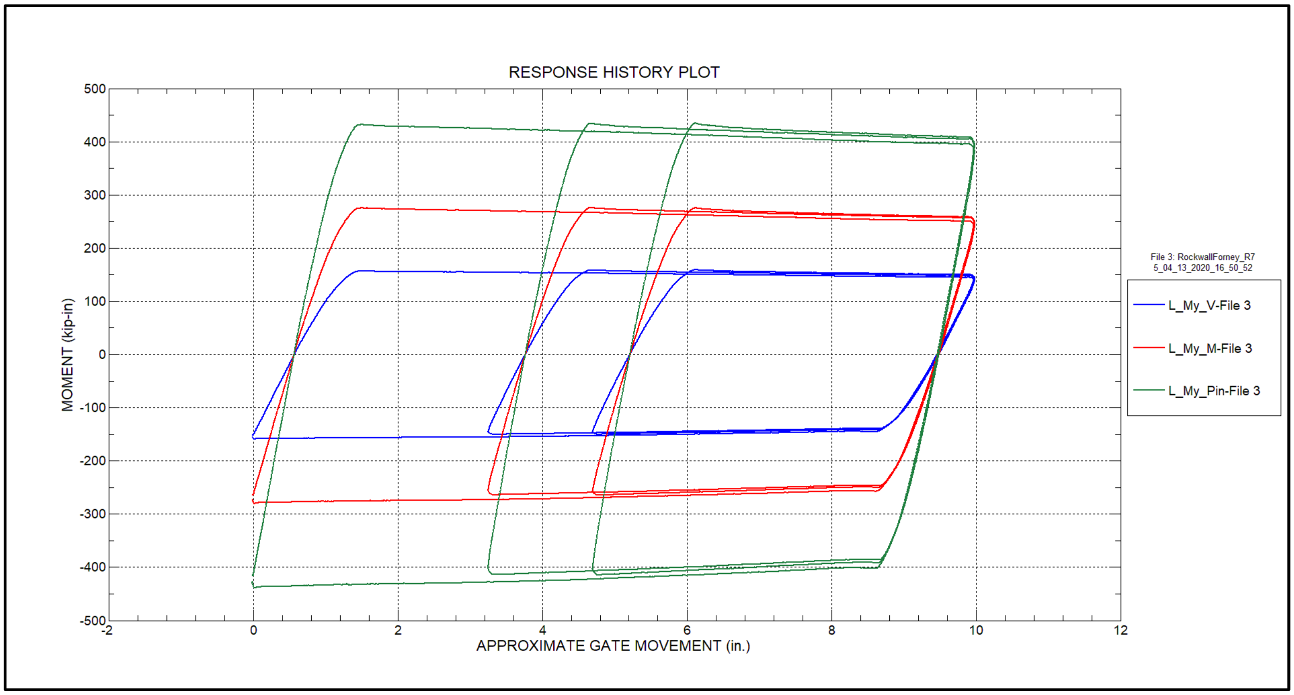

Figure 36 – Pin moment response history – Left arm – Test run 3

APPENDIX C – INSTRUMENTATION PLANS

SCHNABEL ENGINEERING
ROCKWALL FORNEY DAM
LIVE LOAD TESTING

RAW DATA. REFINED RESULTS.
740 S PIERCE AVE, SUITE 15
LOUISVILLE, CO 80027
303.494.3230
WWW.BDITEST.COM

ISSUE

CLIENT

SCHABEL ENGINEERING
16000 CHRISTENSEN RD, STE 101
SEATTLE, WA 98188

PROJECT NAME

SCHNABEL ENGINEERING
ROCKWALL FORNEY DAM
LIVE LOAD TESTING

Drawn By:	KNR
Checked By:	JDS
Date:	05/27/2020
Client No.:	
BDI No.:	190701-TX
SCALE:	NTS

COVER PAGE

LLT-00

The user acknowledges that these documents are instruments of professional service, and are protected by Copyright. This document and the information contained in this document are the property of Bridge Diagnostics, Inc., and shall not be reused, copied, disseminated, modified, amended or altered in any way. It is issued for information purposes only. The user agrees to hold harmless, indemnify and defend Bridge Diagnostics, Inc. against any and all damages, claims and losses, including defense costs, arising out of any use, reuse or copying of this document.

PLOT TIME: 6/12/2020 3:22 PM
FILEPATH: C:\Users\colemand\BDI\Services - Documents\Server_Remote\190701-TX_Schnabel_RockwallForneyDam\7. Instrumentation Plans\BDI_ROCKWALLFORNEY_01_GENERAL.dwg
© YYYY BRIDGE DIAGNOSTICS INC.

GAGE LEGEND & SPECIFICATION

SYMBOL	TYPE	BRAND	MODEL	NOTES
	STRAIN TRANSDUCER	BDI	ST350	
	TILTMETER (UNI-AXIAL)	BDI	T500-030	
	TORQUE SENSOR	HPI	-	HBWS-35-125-6-0.5VR-FB
	AMP SENSOR	CR MAGNETICS	CR42105-200	

GENERAL NOTES

- INSTRUMENTATION SHALL BEGIN ON APRIL 1ST, 2020.
- GATES 1 THRU 14 SHALL BE ACCESSED USING SPRAT ROPE ACCESS TECHNIQUES.
- BDI WILL PERFORM ALL SURFACE PREPARATION, SENSOR INSTALLATION, AND EQUIPMENT INSTALLATION.
- SEE LLT-31 FOR SENSOR INSTALLATION DETAILS.
- TWO PAIRS OF TORQUE GAGES WILL BE INSTALLED ON THE GATE MOTORS' PINION SHAFTS BETWEEN THE MOTORS AND THE HOISTS.
  - GAGE PAIRS WILL BE INSTALLED 180° APART FROM EACH OTHER.
  - EXACT POSITIONS OF THE GAGE PAIRS ON THE PINION SHAFT WILL BE DETERMINED IN THE FIELD.
- THREE PHASE AMPERAGE GAGES WILL BE INSTALLED ON THE MOTOR CONTROLS BY A QUALIFIED ELECTRICIAN PROVIDED BY GARVER.

TESTING PROCEDURE:

- TESTING SHALL BE STARTED WITH THE GATE IN THE CLOSED POSITION.
- ONCE DATA COLLECTION BEGINS, THE GATE SHALL BE RAISED TO TWO OR THREE TIMES THE HEIGHT NECESSARY FOR TRUNNION FRICTION TO BE OVERCOME, H1 (TYPICALLY 6"-12"), AND HELD THERE UNTIL DATA STABILIZES.
- THE GATE SHALL BE LOWERED APPROXIMATELY TWICE THE DISTANCE TO OVERCOME TRUNNION FRICTION, H2, AND HELD THERE UNTIL DATA STABILIZES.
- THE GATE SHALL BE RAISED TO H1 AND HELD THERE UNTIL DATA STABILIZES.
- THE GATE SHALL BE LOWERED TO H2 AND HELD THERE UNTIL DATA STABILIZES.
- THE GATE SHALL BE RAISED TO H1 AND HELD THERE UNTIL DATA STABILIZES.
- THE GATE WAS LOWERED BACK TO CLOSED POSITION AND DATA COLLECTION STOPPED.
- A MINIMUM OF 3 TESTS SHALL BE PERFORMED PER GATE.

LOCATION KEY

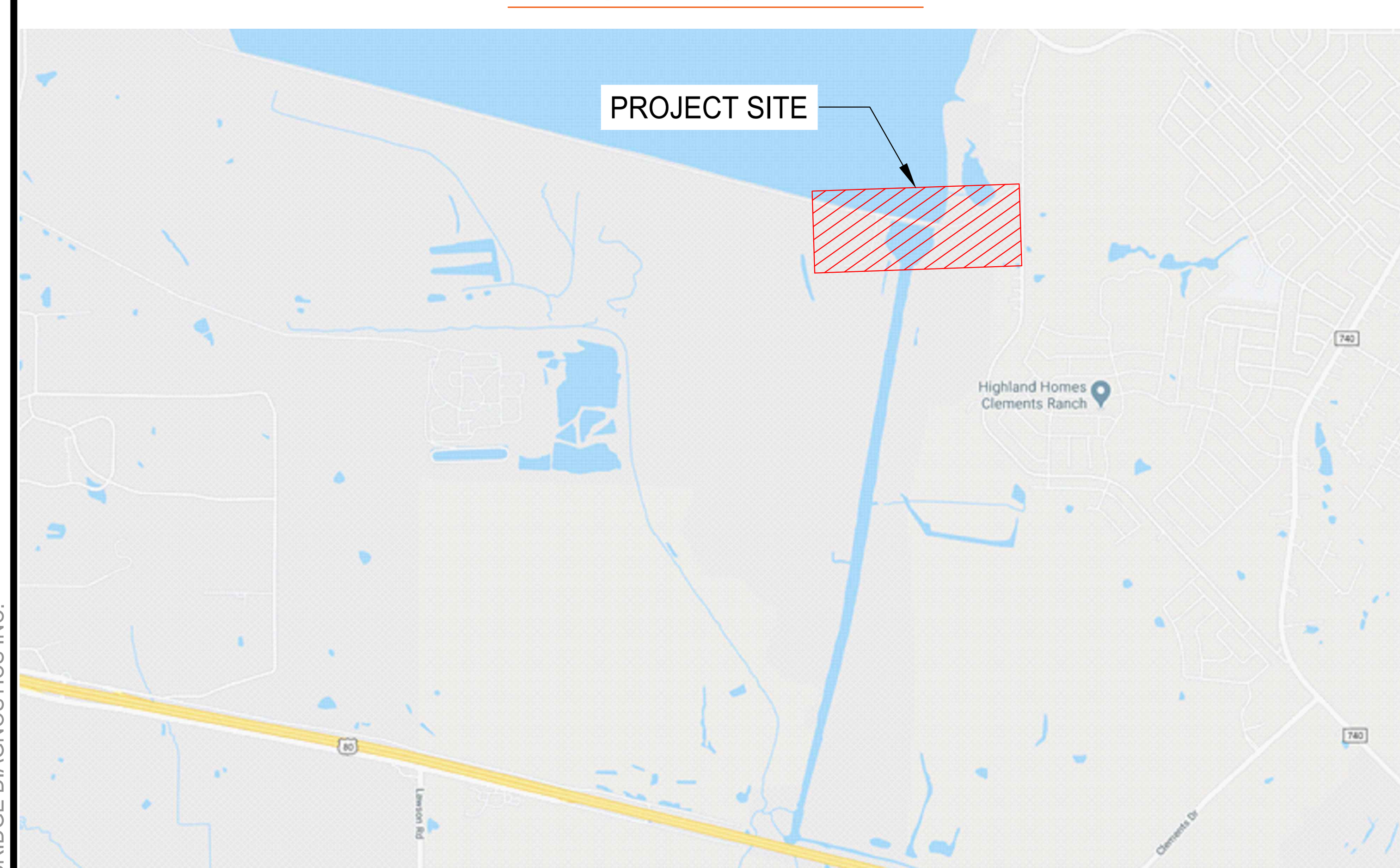

GAGE COUNT PER GATE

SENSOR LEGEND	SENSOR COUNT	CHANNEL COUNT
STRAIN TRANSDUCER	(48)	(48)
TILTMETER (UNI-AXIAL)	(4)	(4)
TORQUE SENSOR	(4)	(4)
AMP SENSOR	(3)	(3)
TOTAL	(59)	(59)

INDEX OF SHEETS

INDEX OF ISSUE

NO.	DATE	REVISION DESCRIPTION
1	3/20/2020	LIVE LOAD TESTING (LLT) INSTRUMENTATION PLAN (FOR APPROVAL)
2	5/27/2020	LIVE LOAD TESTING (LLT) INSTRUMENTATION PLAN AS BUILTS

BDI REFERENCE NUMBER: 190701-TX

RAW DATA. REFINED RESULTS.
740 S PIERCE AVE, SUITE 15
LOUISVILLE, CO 80027
303.494.3230
WWW.BDITEST.COM

ISSUE

CLIENT

SCHABEL ENGINEERING
16000 CHRISTENSEN RD, STE 101
SEATTLE, WA 98188

PROJECT NAME

SCHNABEL ENGINEERING
ROCKWALL FORNEY DAM
LIVE LOAD TESTING

Drawn By: KNR
Checked By: JDS
Date: 05/27/2020
Client No.:
BDI No.: 190701-TX
SCALE: NTS

OVERALL LEGEND

LLT-01

The user acknowledges that these documents are instruments of professional service, and are protected by Copyright. This document and the information contained in this document are the property of Bridge Diagnostics, Inc., and shall not be reused, copied, disseminated, modified, amended or altered in any way. It is issued for information purposes only. The user agrees to hold harmless, indemnify and defend Bridge Diagnostics, Inc. against any and all damages, claims and losses, including defense costs, arising out of any use, reuse or copying of this document.

PLOT TIME: 6/12/2020 3:22 PM
FILEPATH: C:\Users\colemand\BDI\Services - Documents\Server_Remote\190701-TX_Schnabel_RockwallForneyDam\7. Instrumentation Plans\BDI_ROCKWALLFORNEY_01_GENERAL.dwg
© YYYY BRIDGE DIAGNOSTICS INC.

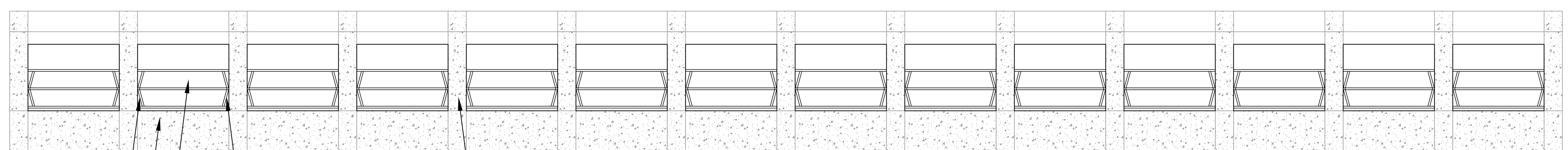

1 DOWNSTREAM ELEVATION OF GATES
LOOKING NORTH (UPSTREAM)

The user acknowledges that these documents are instruments of professional service, and are protected by Copyright. This document and the information contained in this document are the property of Bridge Diagnostics, Inc., and shall not be reused, copied, disseminated, modified, amended or altered in any way. It is issued for information purposes only. The user agrees to hold harmless, indemnify and defend Bridge Diagnostics, Inc. against any and all damages, claims and losses, including defense costs, arising out of any use, reuse or copying of this document.

PLOT TIME: 6/12/2020 3:22 PM
FILEPATH: C:\Users\colemand\BDI\Services - Documents\Server_Remote\190701-TX_Schnabel_RockwallForneyDam\7. Instrumentation Plans\BDI_ROCKWALLFORNEY_01_GENERAL.dwg
© YYYY BRIDGE DIAGNOSTICS INC.

RAW DATA. REFINED RESULTS.
740 S PIERCE AVE, SUITE 15
LOUISVILLE, CO 80027
303.494.3230
WWW.BDITEST.COM

ISSUE

CLIENT

SCHABEL ENGINEERING
16000 CHRISTENSEN RD, STE 101
SEATTLE, WA 98188

PROJECT NAME

SCHNABEL ENGINEERING
ROCKWALL FORNEY DAM
LIVE LOAD TESTING

Drawn By:	KNR
Checked By:	JDS
Date:	05/27/2020
Client No.:	
BDI No.:	190701-TX
SCALE:	NTS

OVERALL STRUCTURE LAYOUT
LLT-02

The user acknowledges that these documents are instruments of professional service, and are protected by Copyright. This document and the information contained in this document are the property of Bridge Diagnostics, Inc., and shall not be reused, copied, disseminated, modified, amended or altered in any way. It is issued for information purposes only. The user agrees to hold harmless, indemnify and defend Bridge Diagnostics, Inc. against any and all damages, claims and losses, including defense costs, arising out of any use, reuse or copying of this document.

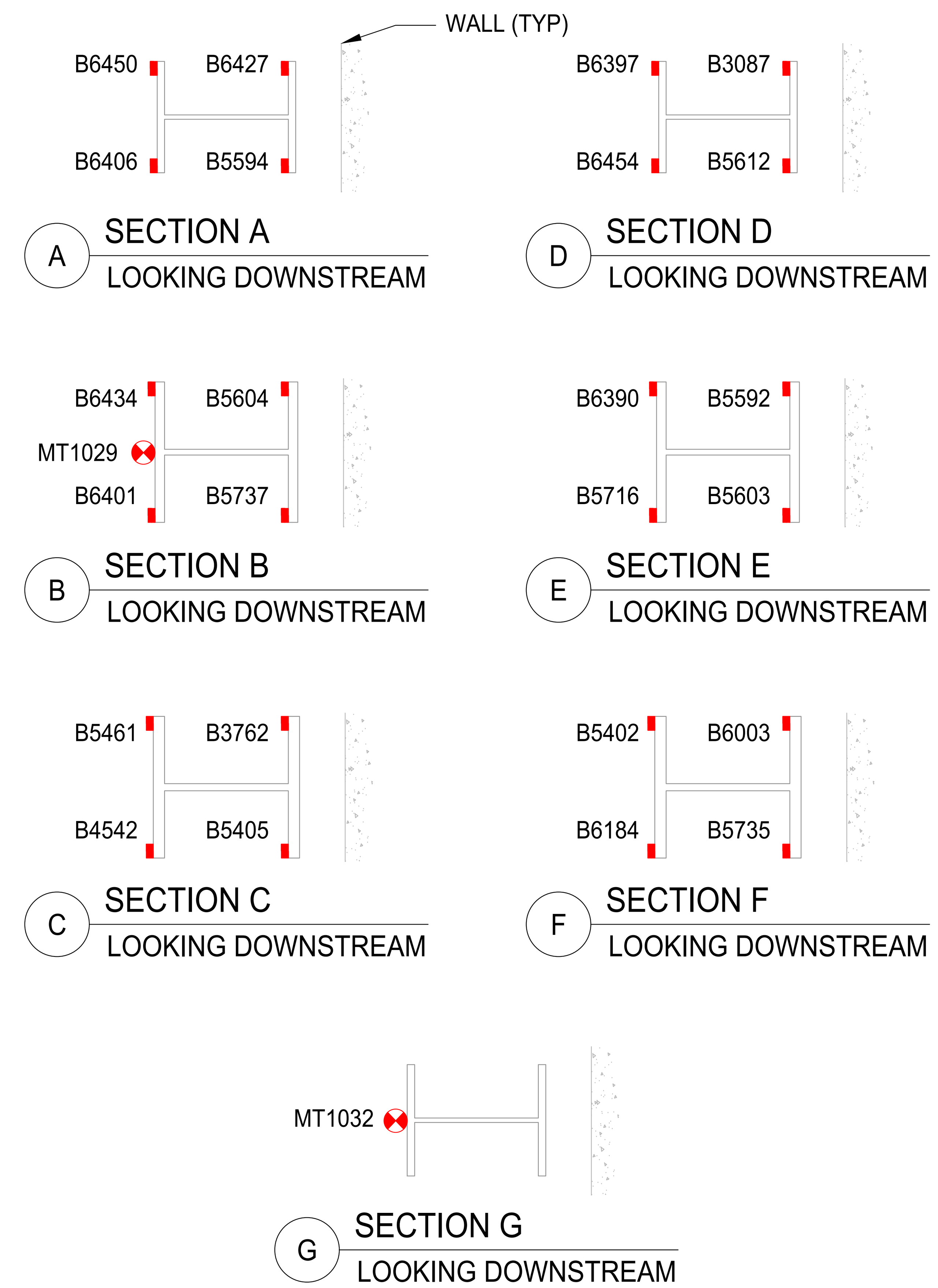

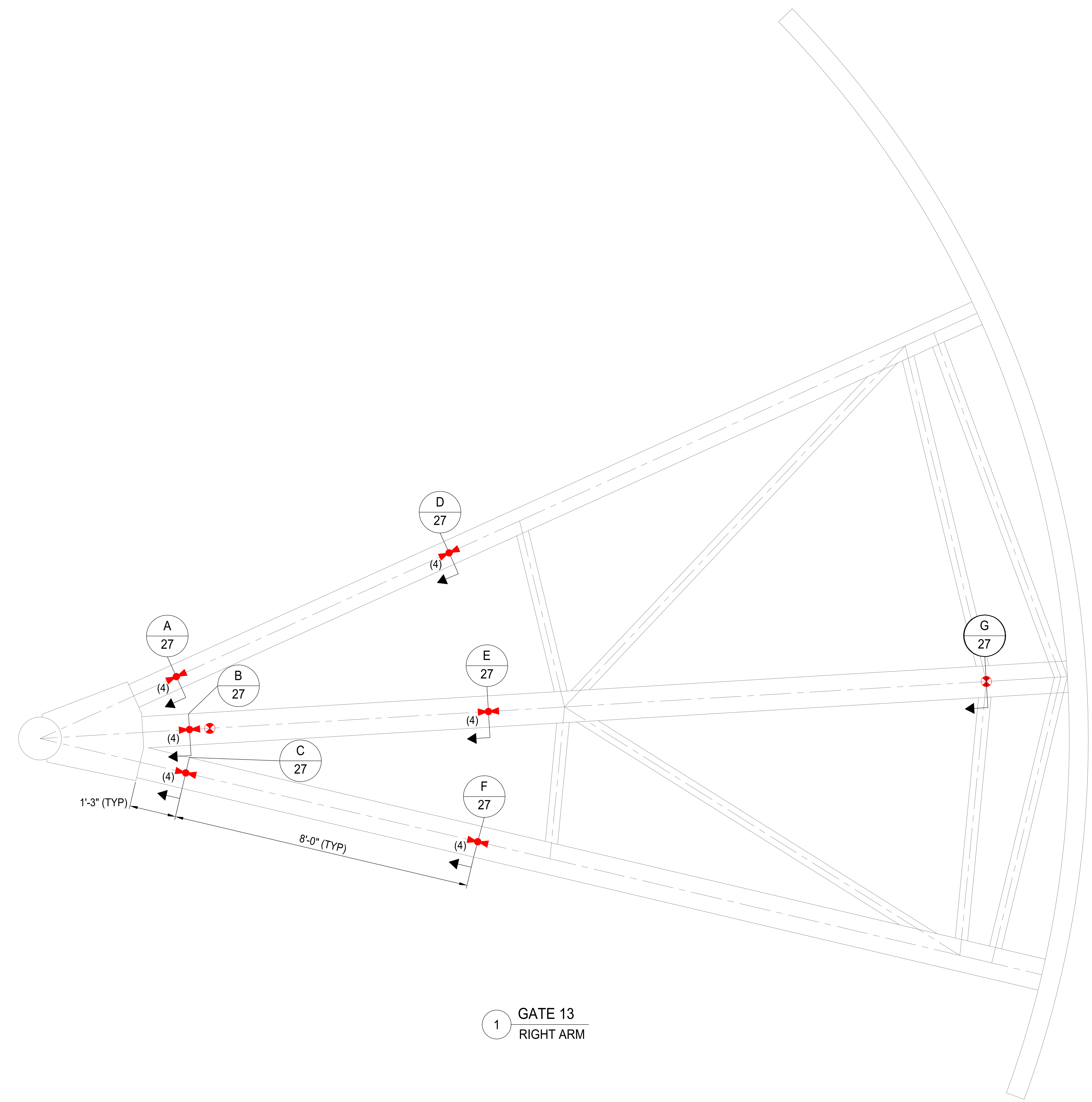

UNIT ID
TT-3

TORQUE GAGES
RIGHT ARM

NOTES:

1. SECTIONS A, B, & C SHALL BE INSTALLED 15 INCHES AWAY FROM TRUNNION PLATE.
2. TILTMETERS SHALL BE INSTALLED CENTERED ON THE MIDDLE STRUT FLANGE.
3. SECTION G'S TILTMETER SHALL BE INSTALLED AS CLOSE TO THE SKINPLATE AS POSSIBLE.

SENSOR LEGEND

- STRAIN TRANSDUCER
- TILTMETER (UNI-AXIAL)
- TORQUE SENSOR

BDI
RAW DATA. REFINED RESULTS.
740 S PIERCE AVE, SUITE 15
LOUISVILLE, CO 80027
303.494.3230
WWW.BDITEST.COM

ISSUE

CLIENT

SCHABEL ENGINEERING
16000 CHRISTENSEN RD, STE 101
SEATTLE, WA 98188

PROJECT NAME

SCHNABEL ENGINEERING ROCKWALL FORNEY DAM LIVE LOAD TESTING

Drawn By:	KNR
Checked By:	JDS
Date:	05/27/2020
Client No.:	
BDI No.:	190701-TX
SCALE:	NTS

GATE 13 - RIGHT ARM
ELEVATION

LLT-27

PLOT TIME: 6/12/2020 3:24 PM
FILEPATH: C:\Users\colemand\BDI\Services - Documents\Server_Remote\190701-TX_Schnabel_RockwallForneyDam\7. Instrumentation Plans\BDI_ROCKWALLFORNEY_01_GENERAL.dwg
© YYYY BRIDGE DIAGNOSTICS INC.

The user acknowledges that these documents are instruments of professional service, and are protected by Copyright. This document and the information contained in this document are the property of Bridge Diagnostics, Inc., and shall not be reused, copied, disseminated, modified, amended or altered in any way. It is issued for information purposes only. The user agrees to hold harmless, indemnify and defend Bridge Diagnostics, Inc. against any and all damages, claims and losses, including defense costs, arising out of any use, reuse or copying of this document.

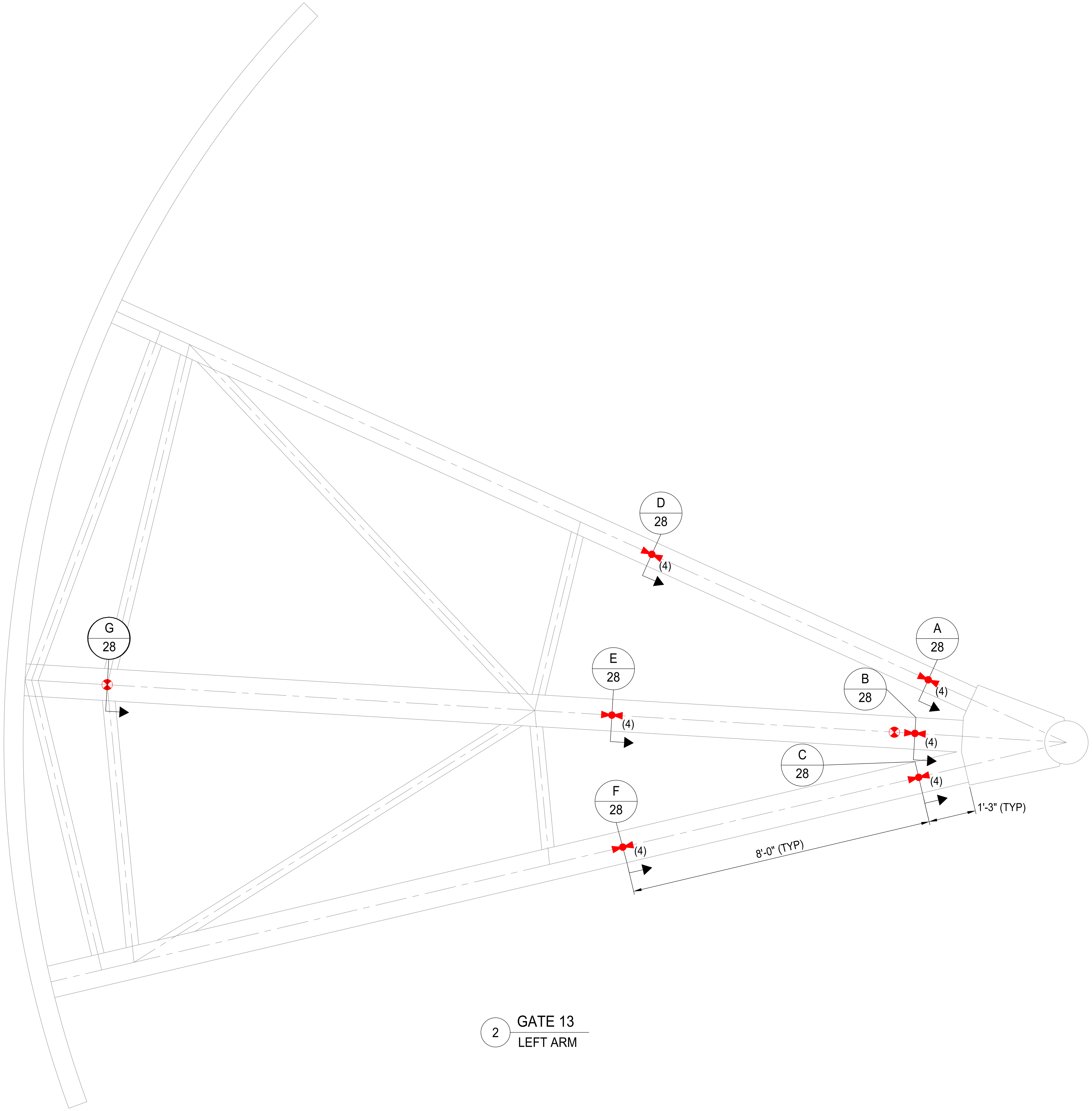

2 GATE 13
LEFT ARM

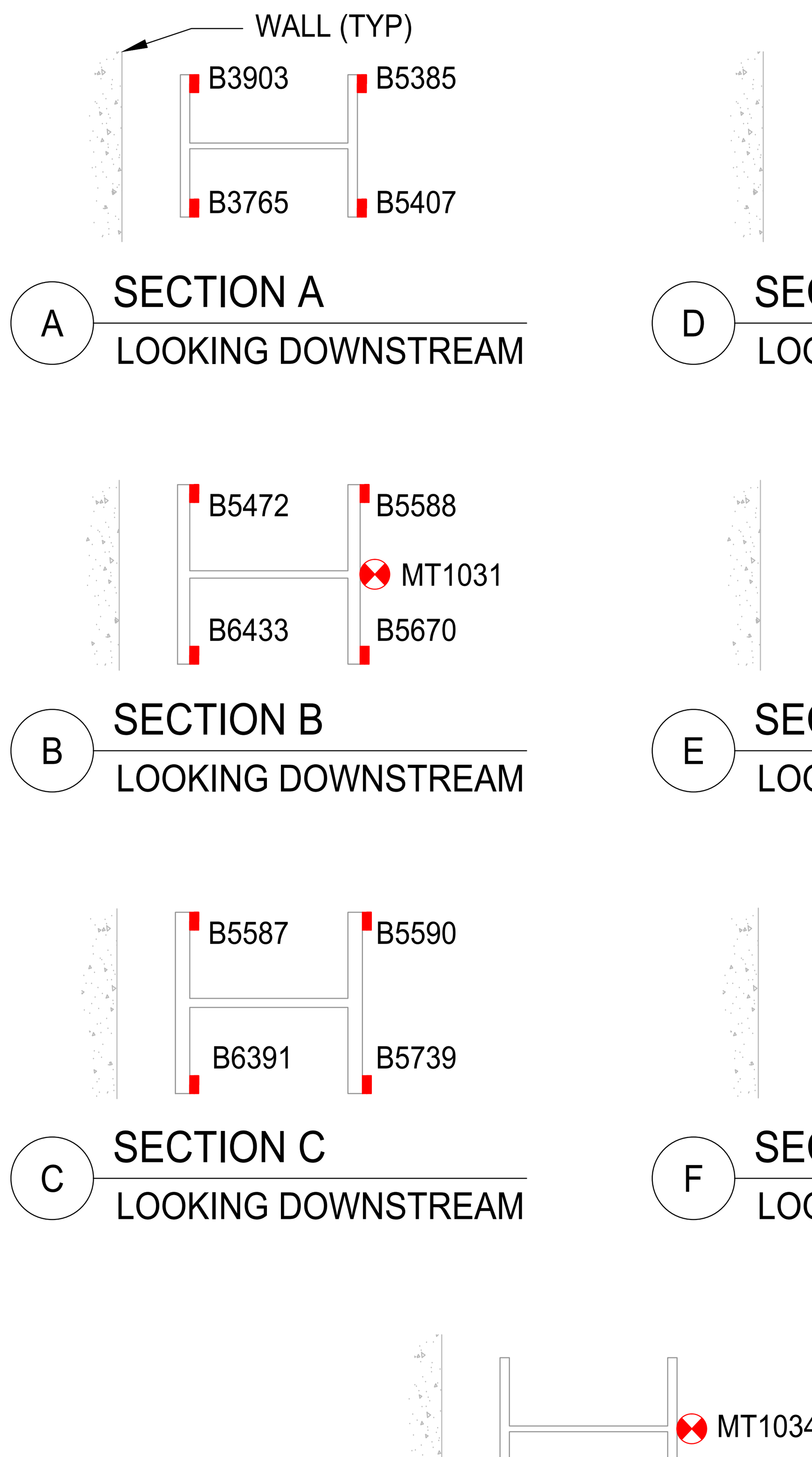

A SECTION A
LOOKING DOWNSTREAM

D SECTION D
LOOKING DOWNSTREAM

B SECTION B
LOOKING DOWNSTREAM

E SECTION E
LOOKING DOWNSTREAM

C SECTION C
LOOKING DOWNSTREAM

F SECTION F
LOOKING DOWNSTREAM

G SECTION G
LOOKING DOWNSTREAM

UNIT ID
TT-4

TORQUE GAGES
LEFT ARM

NOTES:
1. SECTIONS A, B, & C SHALL BE INSTALLED 15 INCHES AWAY FROM TRUNNION PLATE.
2. TILTMETERS SHALL BE INSTALLED CENTERED ON THE MIDDLE STRUT FLANGE.
3. SECTION G'S TILTMETER SHALL BE INSTALLED AS CLOSE TO THE SKINPLATE AS POSSIBLE.

SENSOR LEGEND
- STRAIN TRANSDUCER
- TILTMETER (UNI-AXIAL)
- TORQUE SENSOR

BDI
RAW DATA. REFINED RESULTS.
740 S PIERCE AVE, SUITE 15
LOUISVILLE, CO 80027
303.494.3230
WWW.BDITEST.COM

ISSUE

CLIENT
SCHABEL ENGINEERING
16000 CHRISTENSEN RD, STE 101
SEATTLE, WA 98188

PROJECT NAME
SCHNABEL ENGINEERING
ROCKWALL FORNEY DAM
LIVE LOAD TESTING

Drawn By:	KNR
Checked By:	JDS
Date:	05/27/2020
Client No.:	
BDI No.:	190701-TX
SCALE:	NTS

GATE 13 - LEFT ARM
ELEVATION
LLT-28

PLOT TIME: 6/12/2020 3:24 PM
FILEPATH: C:\Users\colemand\BDI\Services - Documents\Server_Remote\190701-TX_Schnabel_RockwallForneyDam\7. Instrumentation Plans\BDI_ROCKWALLFORNEY_01_GENERAL.dwg
© YYYY BRIDGE DIAGNOSTICS INC.

The user acknowledges that these documents are instruments of professional service, and are protected by Copyright. This document and the information contained in this document are the property of Bridge Diagnostics, Inc., and shall not be reused, copied, disseminated, modified, amended or altered in any way. It is issued for information purposes only. The user agrees to hold harmless, indemnify and defend Bridge Diagnostics, Inc. against any and all damages, claims and losses, including defense costs, arising out of any use, reuse or copying of this document.

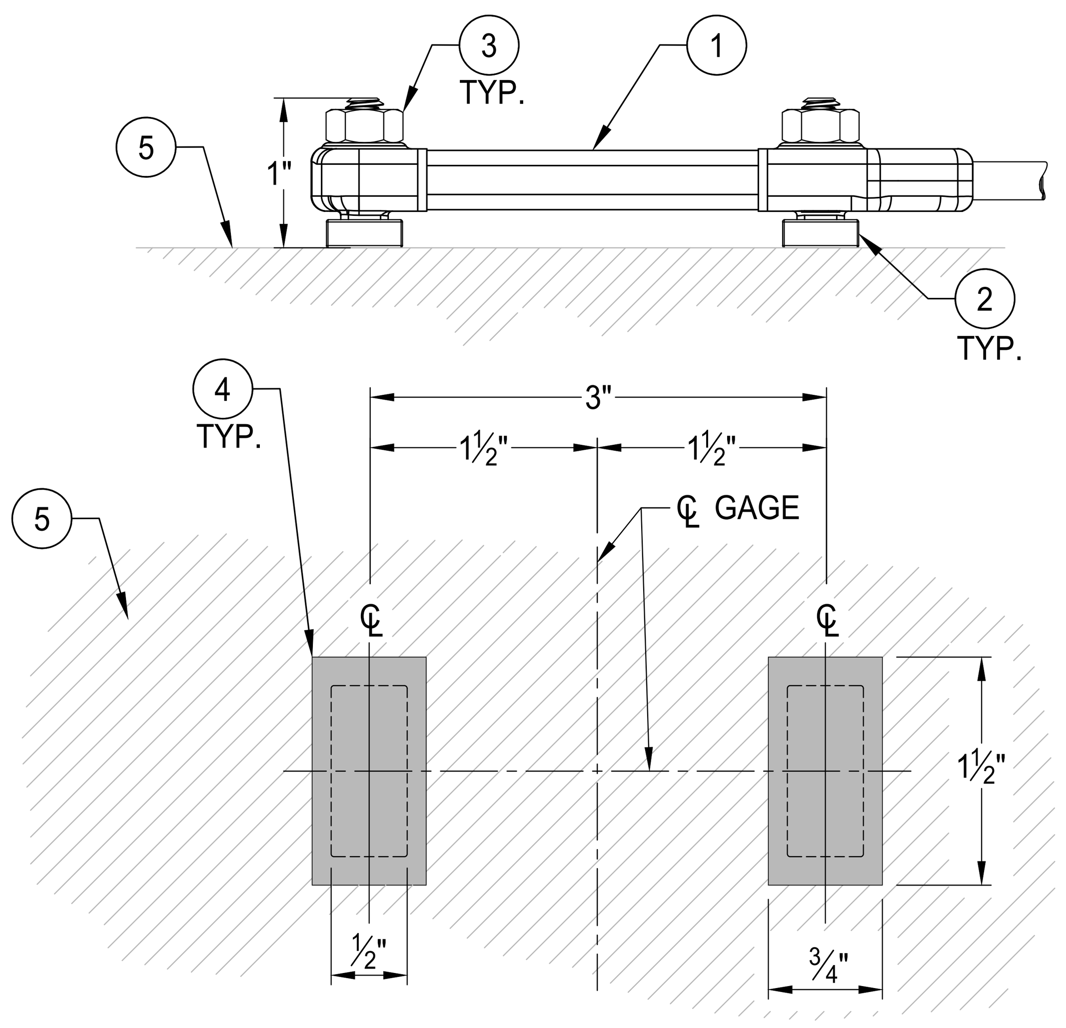

COMPONENT DESCRIPTION

1. ST350 STRAIN GAGE
2. 1/4"-20 THREADED MOUNTING TAB
3. 1/4"-20 STAINLESS STEEL NUT
4. TYPICAL SURFACE PREP REQUIRED TO MOUNT STRAIN GAGES
5. TYPICAL MOUNTING SURFACE

FOOTNOTES - INSTANT ADHESIVE
1. STRAIN GAGES SHALL BE MOUNTED WITH LOCTITE 410 INSTANT ADHESIVE AND LOCTITE 7452 ACCELERANT 2. DURING SURFACE PREP ALL PAINT AND SURFACE DEFORMATIONS MUST BE REMOVED. 3. SURFACE PREP IS REQUIRED JUST PRIOR TO GAGE INSTALLATION AS TO NOT ALLOW SURFACE CONTAMINANTS TO ACCUMULATE.

1 TYPICAL ST350 STRAIN GAGE INSTALLATION

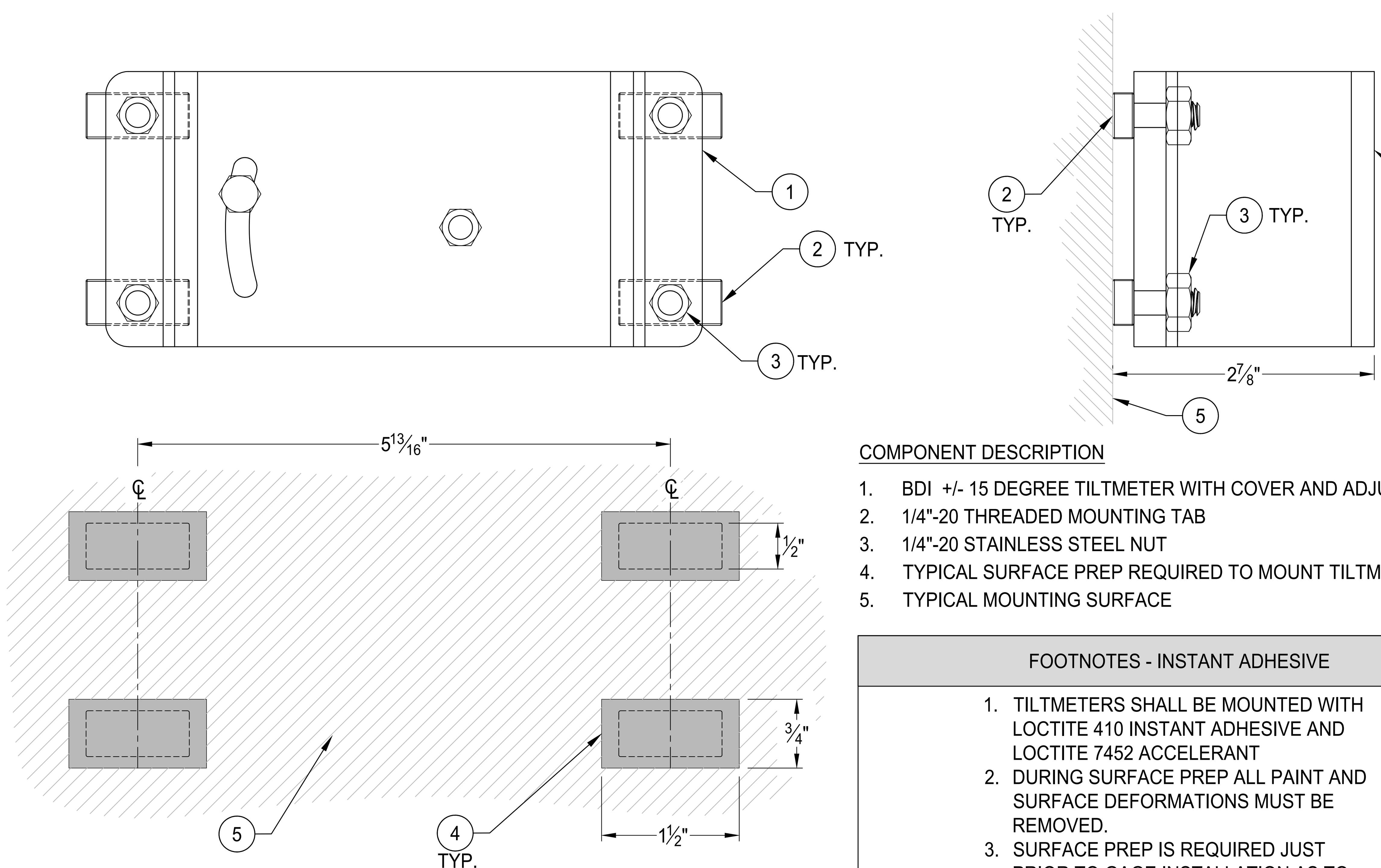

COMPONENT DESCRIPTION

1. BDI +/- 15 DEGREE TILTMETER WITH COVER AND ADJUSTMENT BOLTS
2. 1/4"-20 THREADED MOUNTING TAB
3. 1/4"-20 STAINLESS STEEL NUT
4. TYPICAL SURFACE PREP REQUIRED TO MOUNT TILTMETERS
5. TYPICAL MOUNTING SURFACE

FOOTNOTES - INSTANT ADHESIVE
1. TILTMETERS SHALL BE MOUNTED WITH LOCTITE 410 INSTANT ADHESIVE AND LOCTITE 7452 ACCELERANT 2. DURING SURFACE PREP ALL PAINT AND SURFACE DEFORMATIONS MUST BE REMOVED. 3. SURFACE PREP IS REQUIRED JUST PRIOR TO GAGE INSTALLATION AS TO NOT ALLOW SURFACE CONTAMINANTS TO ACCUMULATE.

2 TYPICAL BDI TILTMETER INSTALLATION

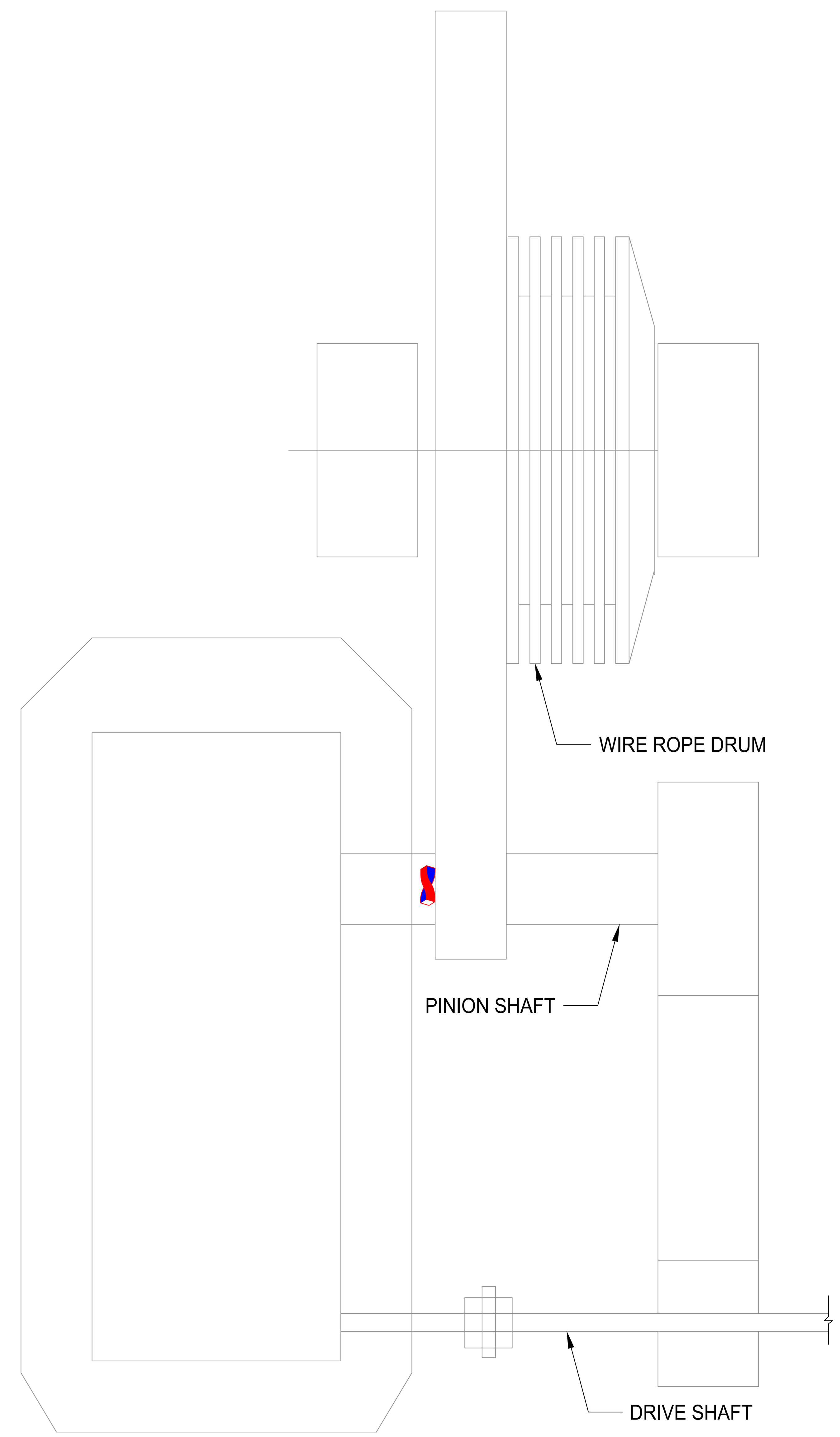

3 TYPICAL HOIST INSTRUMENTATION

TORQUE SENSOR INSTALLATION NOTES:

- TORQUE GAGES WILL BE INSTALLED ON THE PINION SHAFT ON EITHER HOIST MOTOR BETWEEN THE MOTOR AND THE HOIST DRUM
- EXACT POSITIONS OF THE GAGE PAIRS ON THE PINION SHAFT WILL BE DETERMINED IN THE FIELD

SENSOR LEGEND

TORQUE SENSOR

RAW DATA. REFINED RESULTS.
740 S PIERCE AVE, SUITE 15
LOUISVILLE, CO 80027
303.494.3230
WWW.BDITEST.COM

ISSUE

CLIENT

SCHABEL ENGINEERING
16000 CHRISTENSEN RD, STE 101
SEATTLE, WA 98188

PROJECT NAME

SCHNABEL ENGINEERING
ROCKWALL FORNEY DAM
LIVE LOAD TESTING

Drawn By:	KNR
Checked By:	JDS
Date:	05/27/2020
Client No.:	
BDI No.:	190701-TX
SCALE:	NTS

SENSOR INSTALLATION DETAILS

LLT-31

PLOT TIME: 6/12/2020 3:24 PM
FILEPATH: C:\Users\colemand\BDI\Services - Documents\Server_Remote\190701-TX_Schnabel_RockwallForneyDam\7. Instrumentation Plans\BDI_ROCKWALLFORNEY_01_GENERAL.dwg
© YYYY BRIDGE DIAGNOSTICS INC.

SCHNABEL ENGINEERING
TRUNNION PIN FRICTION TESTING REPORT

ROCKWALL FORNEY DAM – GATE 14
FORNEY, TX

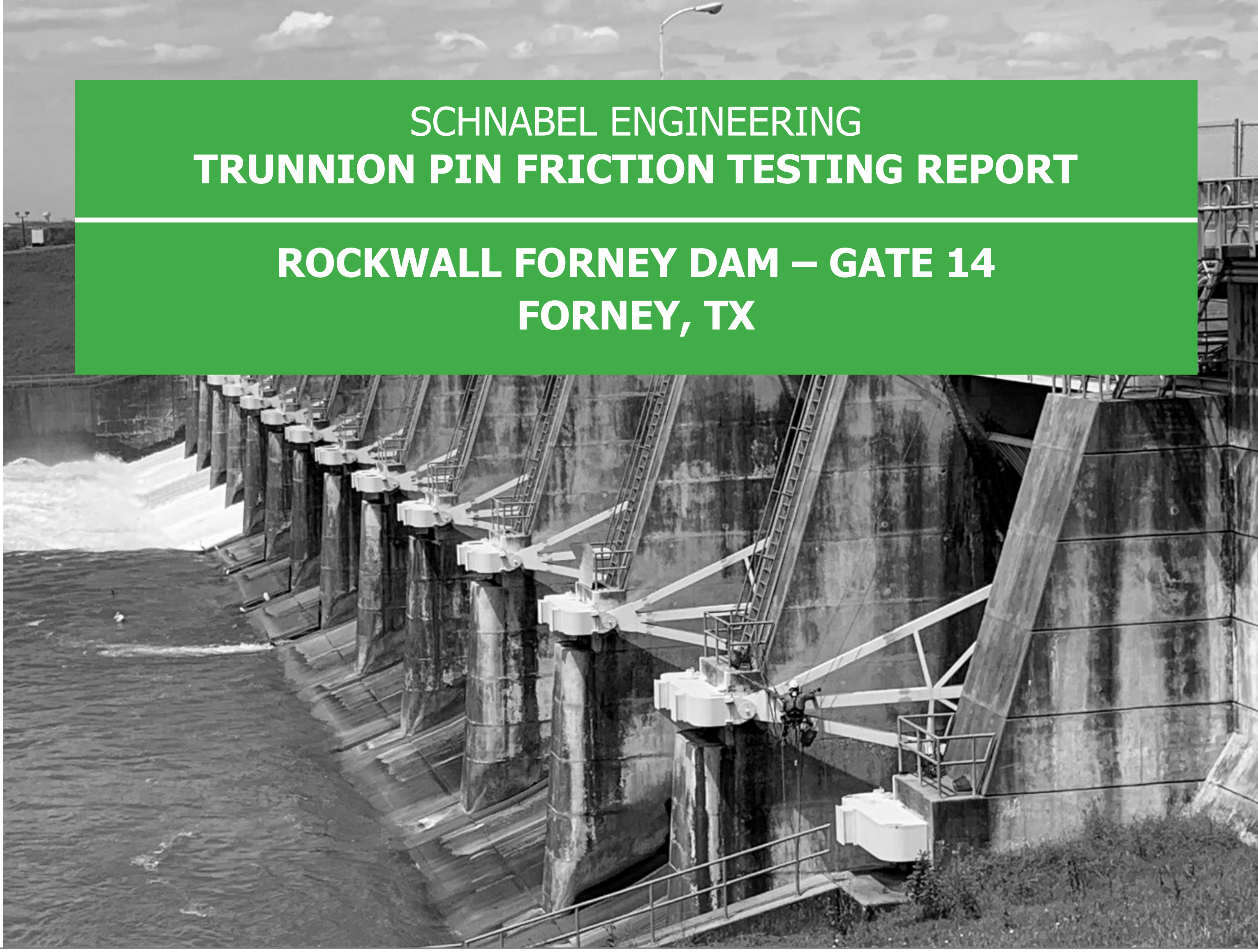

SUBMITTED TO:
SCHNABEL ENGINEERING
16000 CHRISTENSEN RD, SUITE 101
SEATTLE, WA 98188

SUBMITTED BY:
BDI – CO
740 SOUTH PIERCE AVE, UNIT 15
LOUISVILLE, CO 80027

BDI Project No.: **190701-TX**
Report Version: **V1**
Version Submitted: **August 26, 2020**

BDI
RAW DATA. REFINED RESULTS.

This document contains Confidential Information and is submitted in confidence to the customer. The submission of the information contained herein shall not be deemed to constitute public disclosure or authorization for disclosure to other parties. BDI's information and name may not be used in advertising or for promotional purposes without BDI's written consent.

TABLE OF CONTENTS

LIST OF FIGURES

LIST OF TABLES

EXECUTIVE SUMMARY

Schnabel Engineering contracted BDI to provide instrumentation and testing services on Gates 1-14 on the Rockwall Forney Dam near Dallas, Texas. The goal of these tests was to record each gate's structural responses during a series of spill tests and use the data to compute accurate coefficients of friction for each trunnion pin, cable lift force, total gate friction, and motor amperage. This report provides details on the work performed on Gate 14.

Instrumentation and testing were performed on Gate 14 at the Rockwall Forney Dam on April 14th, 2020. The gate arms were instrumented with strain and rotation sensors. The hoist motors' pinion shafts were instrumented with torque sensors and the hoist motor controls were instrumented with amperage sensors. Following the instrumentation, a series of spill tests were performed to measure the structural responses resulting from trunnion pin friction. All instrumentation setup and removal were performed using BDI's rope access team.

Following demobilization from the field, the test data was examined for quality and then further processed to evaluate the gate's performance. Strain measurements were converted into bending forces which were then applied to pin-strut free-body diagrams. By summing forces at each pin, friction induced moments could be computed, allowing accurate friction coefficients to be determined. Generally, the observed gate behavior showed that Gate 14 was operating as expected and in a symmetric manner. Gate 14 pins have been replaced, with the computed friction coefficients for this gate being the lowest of all tested gates.

The resulting maximum trunnion friction coefficients and corresponding hoist forces are shown in Table 1.

Table 1 – Gate 14 performance summary

Pin Designation	Maximum Friction Coefficient	Maximum Pin Moment due to Pin Friction (kip-In)	Maximum Hoist Force (kips)	Maximum Hoist Force due to Total Gate Friction (kips)
Right Pin	0.09	238.3	20.05	3.61
Left Pin	0.08	219.5	32.06	4.90

Note: Pin designations are in reference to looking downstream

Due to restrictions caused by the hoist limit switches, the hoist cables could not always be fully slacked at the beginning and end of the performed tests. Throughout testing of the Rockwell Forney gates, it was found that this limit switch restriction varied gate to gate and arm to arm. Therefore, it is not recommended to use the collected hoist force data to quantify overall hoist forces during gate operation. Rather, this hoist data can be better utilized to evaluate total friction behavior.

Amperage responses were not used to compute friction results and were collected as verification that the motor performance was not causing unexpected gate responses. These responses indicated the motor was functioning in a stable manner and should be reviewed by a licensed electrician to further evaluate the motor's performance.

All results and recommendations provided in this report were based on the structure in its current condition; therefore, any significant changes in condition must be noted as they may alter their validity. Questions regarding this report and/or data should be directed to Kyle Ramer (kyler@bditest.com) at BDI. For further information on BDI's equipment, services, and analysis methods please visit www.bditest.com

INSTRUMENTATION AND LOAD TESTING PROCEDURE

GATE INSTRUMENTATION SUMMARY

Instrumentation and testing were performed on Gate 14 at the Rockwall Forney Dam on April 14th, 2020. Instrumentation plans have been provided along with this report and include the following number of instrumented locations and sensor types:

+ **REUSABLE SURFACE MOUNTED STRAIN TRANSDUCERS:** Each gate arm was instrumented with a total of 24 strain transducers at 6 locations on each of the gate arms (48 strain sensors total). A typical strain gage installation is shown in Figure 1. Note these sensors were installed with the mounting tabs on the extreme fiber of the strut flanges, which puts the center of the gage approximately 0.66″ from the extreme fiber.
+ **TILTMETER ROTATION SENSORS:** MEMS style rotation sensors were located on the middle strut of the gate arm near the skin plate and near the trunnion hub (4 rotation sensors total). The rotation responses were used to calculate vertical skin plate movement and measure pin rotation relative to skin plate rotation. Typical tiltmeter installations are shown in Figure 1 and Figure 2.
+ **TORQUE SENSORS:** Two total torque sensors were installed on the hoist's pinion shafts (QTY1 on each hoist pinion shaft) near the cable hoist motor to measure direct torque and in turn lift force (See Figure 3).
+ **AMPERAGE SENSORS:** 3 Hall-Effect amperage transducers were clamped over each phase of the hoist motor to measure the motor's current draw (See Figure 4). The purpose of these sensors was to provide additional data in case there were any issues with the hoist systems and to verify any data issues related to lifting and lowering the gates.
+ **BDI'S STS-4 WIRELESS DATA ACQUISITION SYSTEM:** BDI's STS-4 wireless data acquisition (DAQ) was used to collect and record data during testing. A group of sensors were wired to each nodal DAQ which then communicated wirelessly back to the wireless base station and was controlled by BDI's STS-Live testing software.

Complete specifications are available upon request and can be found at http://www.bditest.com.

SENSOR INSTALLATION

BDI strain transducers were installed by first sanding paint off the struts to expose bare metal at two small locations (1″x2″ areas) for the sensor's mounting tabs. Each transducer was then attached using a combination of fast-setting adhesive and accelerator and applying pressure until the adhesive was fully cured. Each strain transducer took approximately five minutes to attach.

Tiltmeters were installed using the same adhesive process as the strain transducers. However, no surface preparation was necessary.

Torque sensors were installed on the pinion shafts by capacitive discharge bonding. Properly bonding to the shaft required sanding the surface to a smooth finish, clean of any paint or grease. Responses from these gages were measured using Binsfeld Torque Trak 10k wireless transmitters.

A typical installation has been shown in Figure 1 through Figure 4. Access to all the sensor locations was provided by BDI's own SPRAT certified rope access technicians and engineers as shown in Figure 5.

Once testing was completed, sensors were removed, and exposed steel areas were covered using cold galvanizing compound.

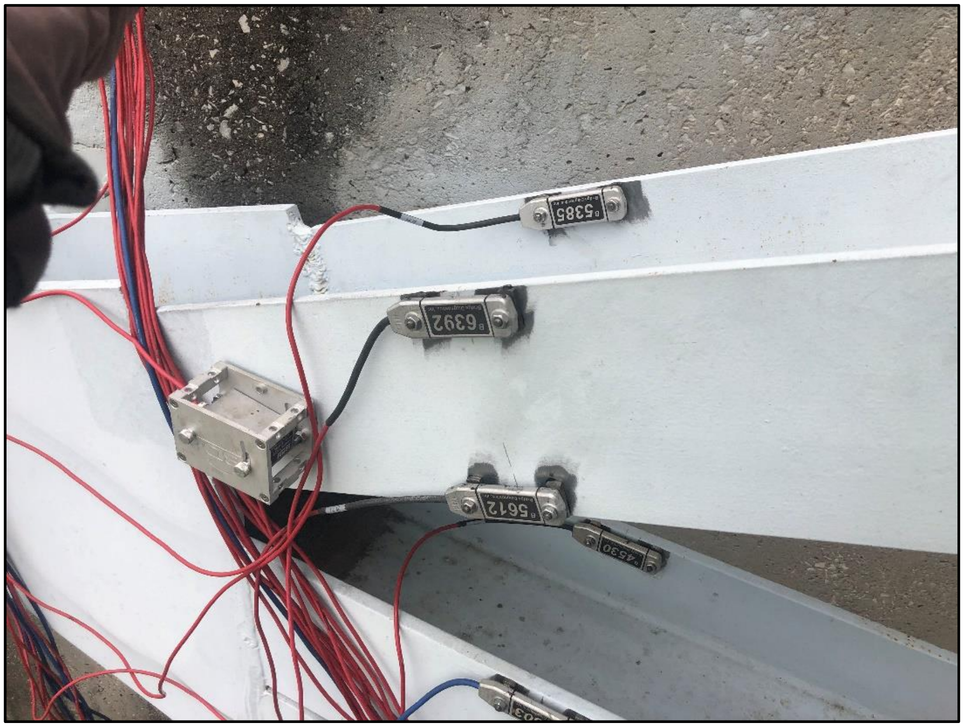

Figure 1 – BDI tiltmeter rotation sensor and reusable strain transducers installed near trunnion hub (Typical)

Figure 2 – BDI tiltmeter rotation sensor installed near skin plate (Typical)

Figure 3 – Torque sensor installation on hoist pinion shaft (Typical)

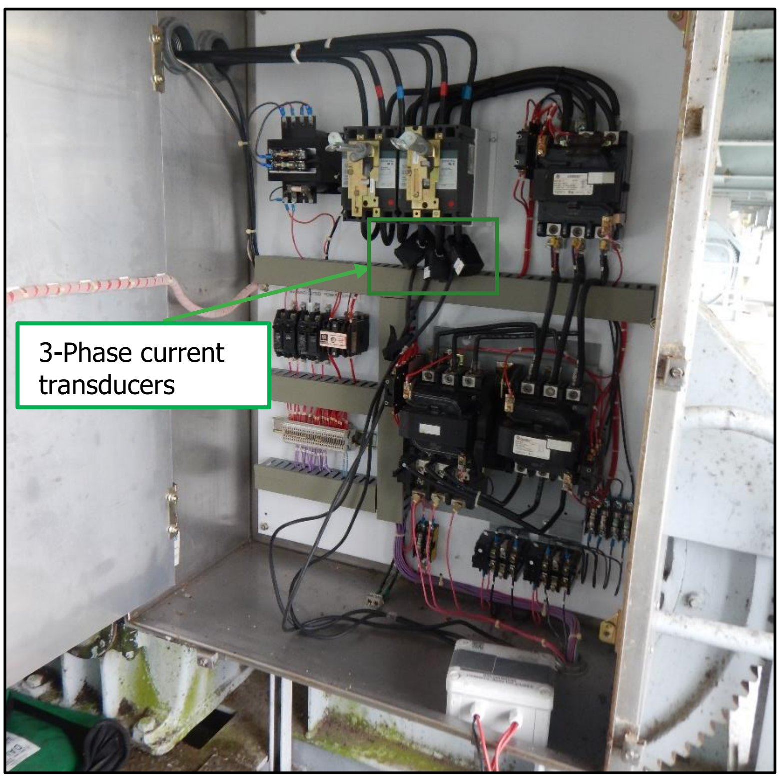

Figure 4 – Current transducers installed on hoist motor controls (Typical)

Figure 5 – BDI personnel installing instrumentation on the gate arm

TESTING PROCEDURES

Structural response data was recorded on all sensors at 50Hz while the gate was run through three spill tests. Each test consisted of three "up-down" cycles (direction reversals) without lowering the gate back to the sill. Each direction reversal consisted of lifting the gate approximately 6-12", pausing for a few seconds, and lowering the gate approximately 6", and repeating until all reversals had been completed.

Results Summary

General Discussions Based on Structural Responses

The following outline contains general discussion points and observations that were made during the data review process. Note: Strain measurements were converted to stress for all subsequent analysis by multiplying the strain values by a steel elastic modulus of 29,000 ksi.

- **DESCRIPTIONS OF RESPONSE MEASUREMENTS:** All sensor readings were zeroed at the end of each test (which consisted of three cycles of direction reversals) so that each measurement corresponded to response change relative to the final gate position as shown in Figure 6 (gates in the downward "closed" position with the hoist cables slacked as much as possible). It is also worth noting that the stresses did not always start and end at the same levels between tests. This variation in behavior is due to small changes in the flexed gate condition between the start and end of tests. It is common for the flex in the gate, caused by pin friction, to slowly release as it rests on the sill. The purpose of the three up-down cycles per test, prior to sitting the gate back onto the sill, is to ensure that these changes in boundary conditions, including gate flexure due to friction, did not affect BDI's trunnion friction results. ***It is important to note that the recorded measurements were changes in structural response due to gate movement, and do not include the in-situ stresses due to the dead load, cable wrap, and hydrostatic loads present prior to testing.***
- **QUALITATIVE DATA REVIEW:** Review of the response data indicated a good level of reproducibility between the three tests. For reference, Figure 6 and Figure 7 show stress responses measured along Gate 14's right arm top strut for all three tests (Test #1-3). The data in these plots have been provided as both a function of time and the gate position as determined by the skin plate tilt sensor. Structural response behavior slightly varied during the first test's first cycle compared to subsequent lift/lower cycles and tests, with the first cycle having a slightly smaller change in stress due to pin friction. The observed variation was likely caused by a larger release of built-up pin friction as the gate rested on the sill for a longer period of time.
- **DIRECTION/FRICTION REVERSAL IN RESPONSES:** The difference in stress during gate opening and closing for a given position is shown in Figure 8. The stress variation at any given gate position was a result of direction reversal and in turn due to trunnion friction reversal. This statement is true since all other loads such as dead-load and hydrostatic pressure were essentially constant barring small changes in hydrostatic pressure due to slight changes in head. This direction/friction reversal is depicted in Figure 9, with deflected shape renderings from a gate arm finite element model under lifting and lowering loads. Note that this figure shows an arm configuration that does not match this gate, but the concept of the direction/friction reversal still applies.
- **MOTOR PERFORMANCE:** Current measurements taken at the hoist motor indicated steady and stable current draws during the lifting and lowering portions. An example plot of current draw and gate position is provided in Figure 10. Current draw ranges during lifting were higher than the ranges during lowering, which is common due to gravity/dead load. These results are summarized along with recorded peak in-rush current in Table 2. Note that the sample rates used during testing were set for collecting gate responses and may not have been appropriate to fully capture the in-rush current. The readings should be evaluated by a licensed electrician with knowledge of the operating parameters.
- **TORQUE AND HOIST FORCE:** Due to restrictions caused by the hoist limit switches, the hoist cables could not always be fully slacked at the beginning and end of the performed tests. Throughout testing of the Rockwell Forney gates, it was found that this limit switch restriction varied gate to gate and arm to arm. Therefore, it is not recommended to use the collected torque and hoist force data to quantify overall hoist forces. Rather, this data was utilized to evaluate total friction behavior, which is observed as half the difference between the lifting and lowering torque/force (friction reversal).

Each increase in stress corresponded to upward gate motion until the friction was overcome. Responses then changed slope as the pin rotated. Relative decrease in stress corresponded to downward gate movement until the pin friction was again overcome, followed by another change in slope.

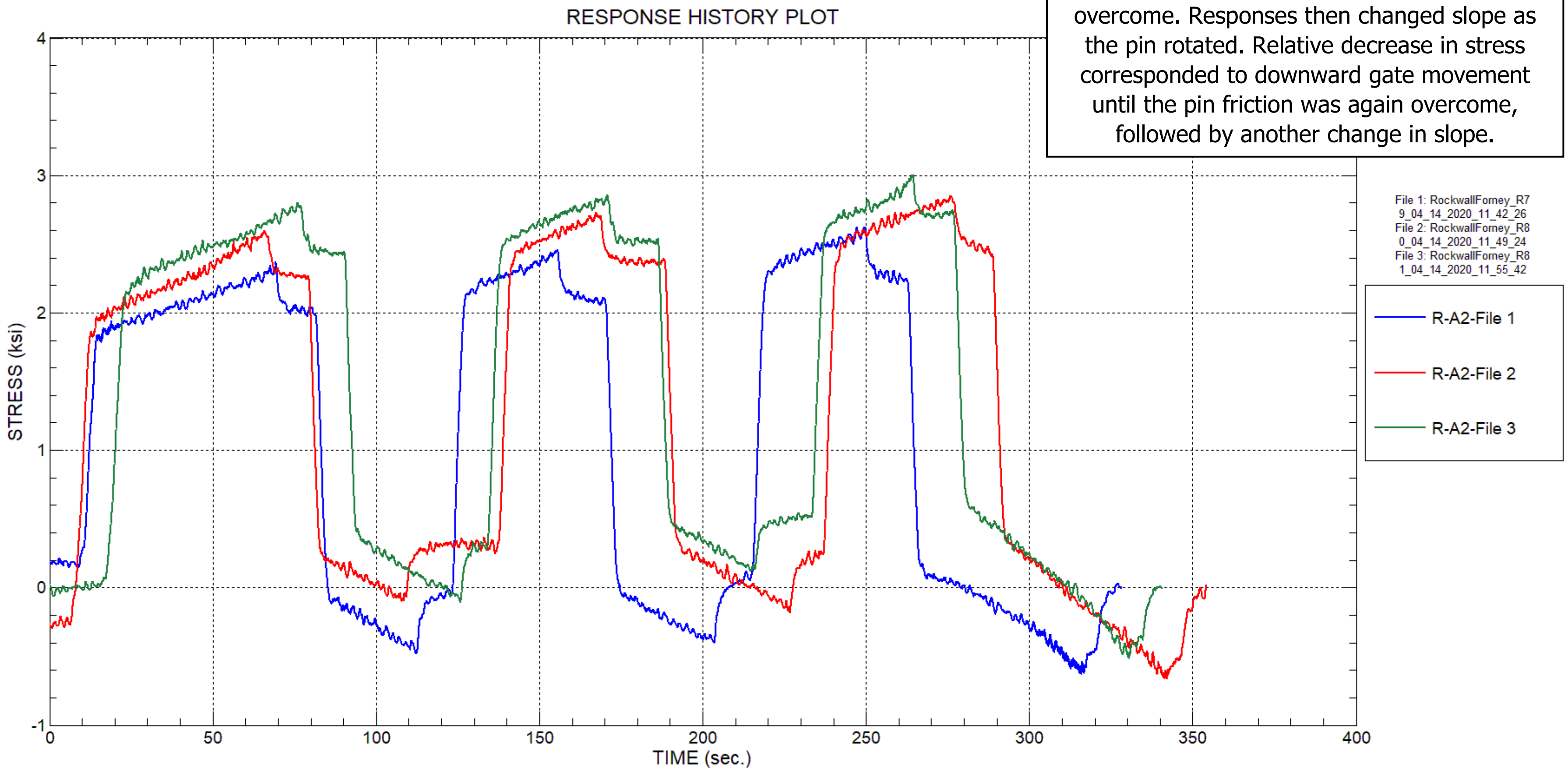

Figure 6 – Stress response history – Right arm – Gage A2 – Time based
File 1 = test run 1, File 2 = test run 2, File 3 = test run 3

(Section A along top strut near pin – Sensor location 2 along bottom of inner flange)

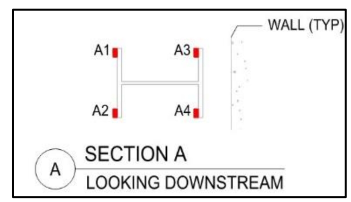

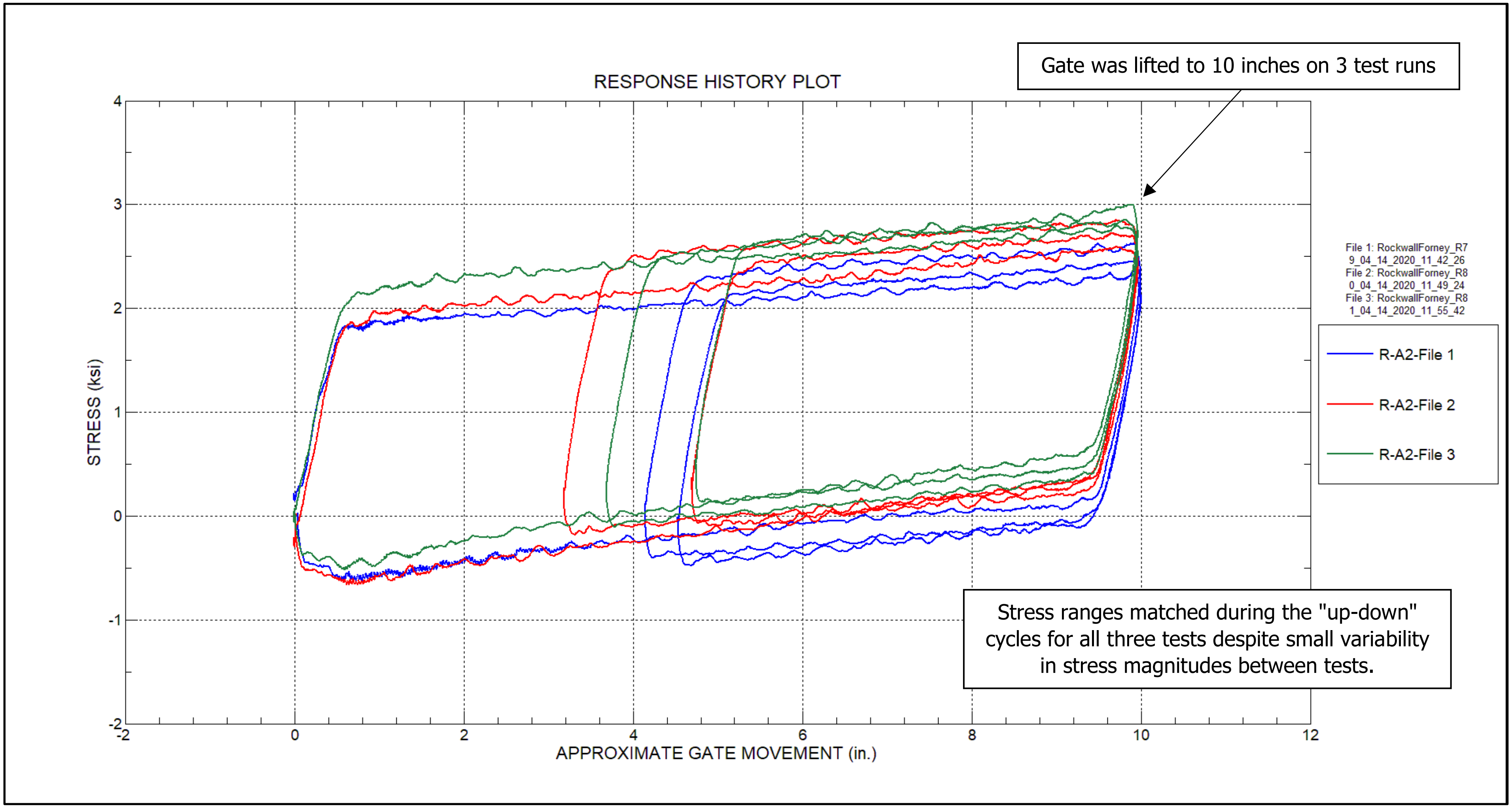

Figure 7 – Stress response history – Right arm – Gage A2 – Function of gate movement
File 1 = test run 1, File 2 = test run 2, File 3 = test run 3

(Section A along top strut near pin – Sensor location 2 along bottom of inner flange)

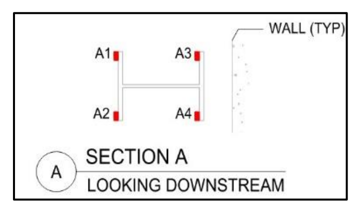

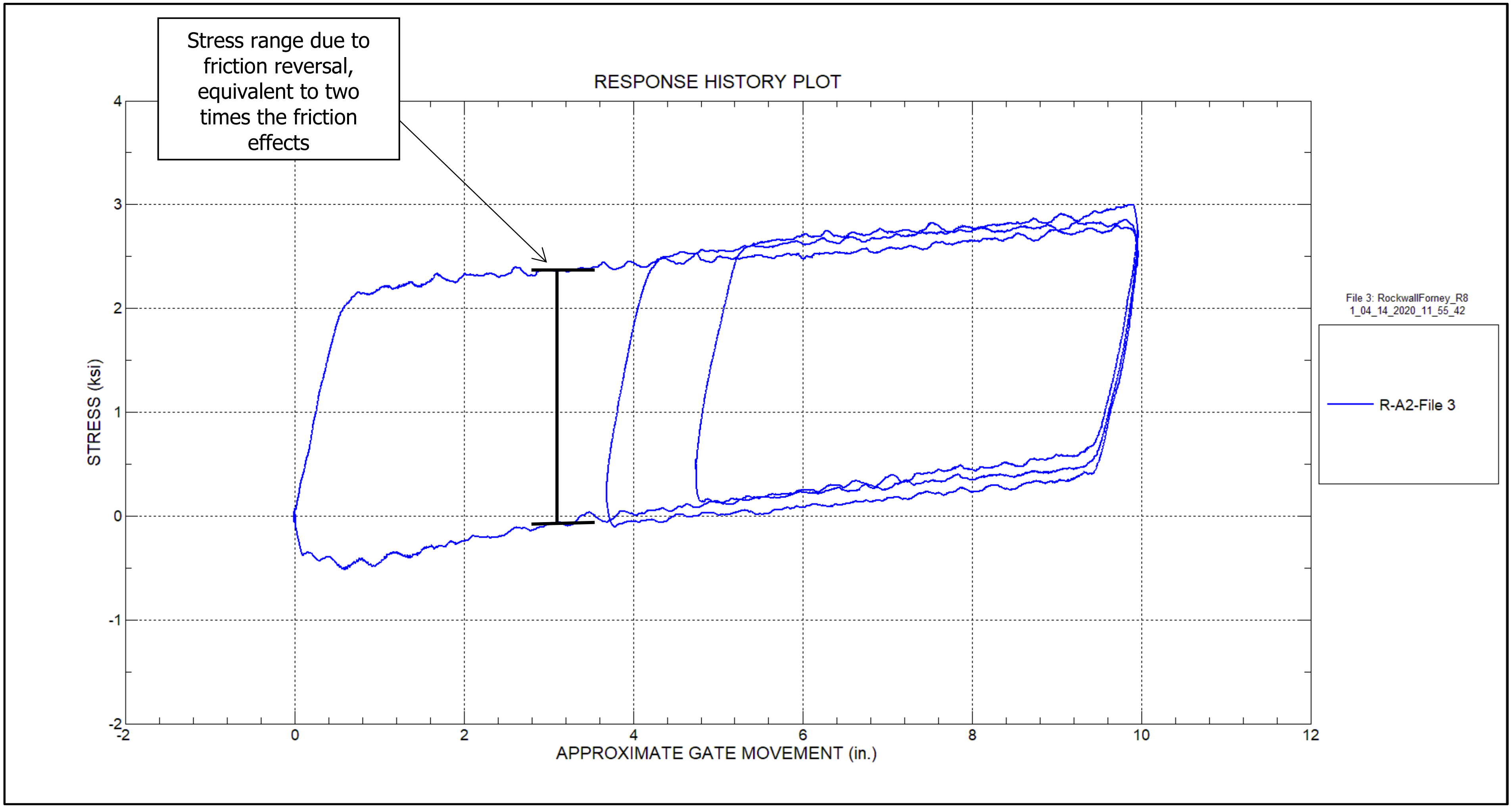

Figure 8 – Stress response history – Right arm – Gage A2 – Friction effect in stress responses

(Section A along top strut near pin – Sensor location 2 along bottom of inner flange)

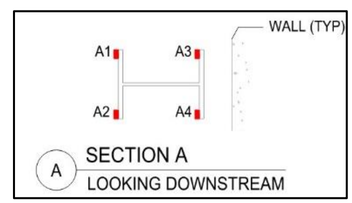

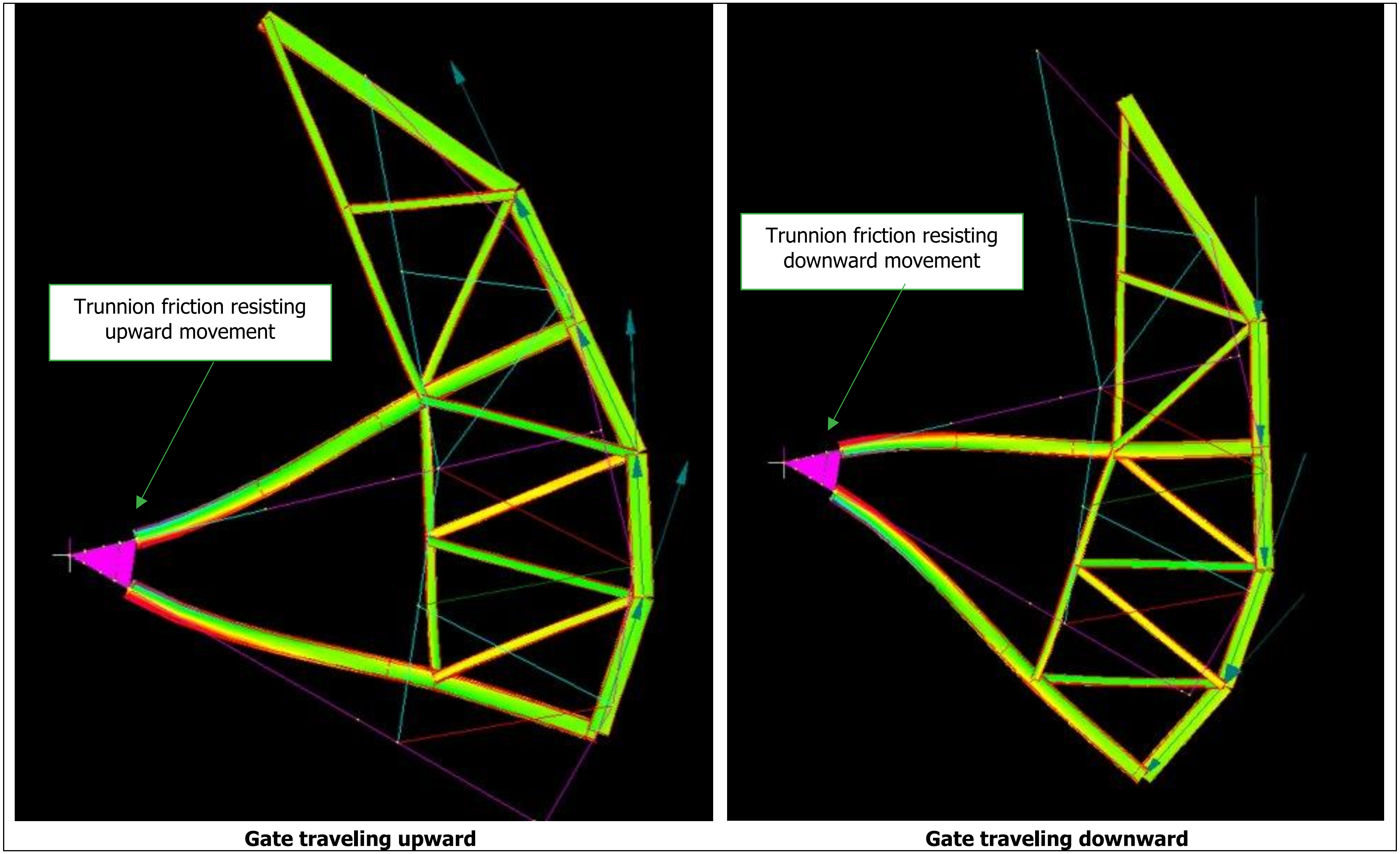

Figure 9 – Deflected shapes during lifting and lowering of Gate – Visualization of direction/friction reversals

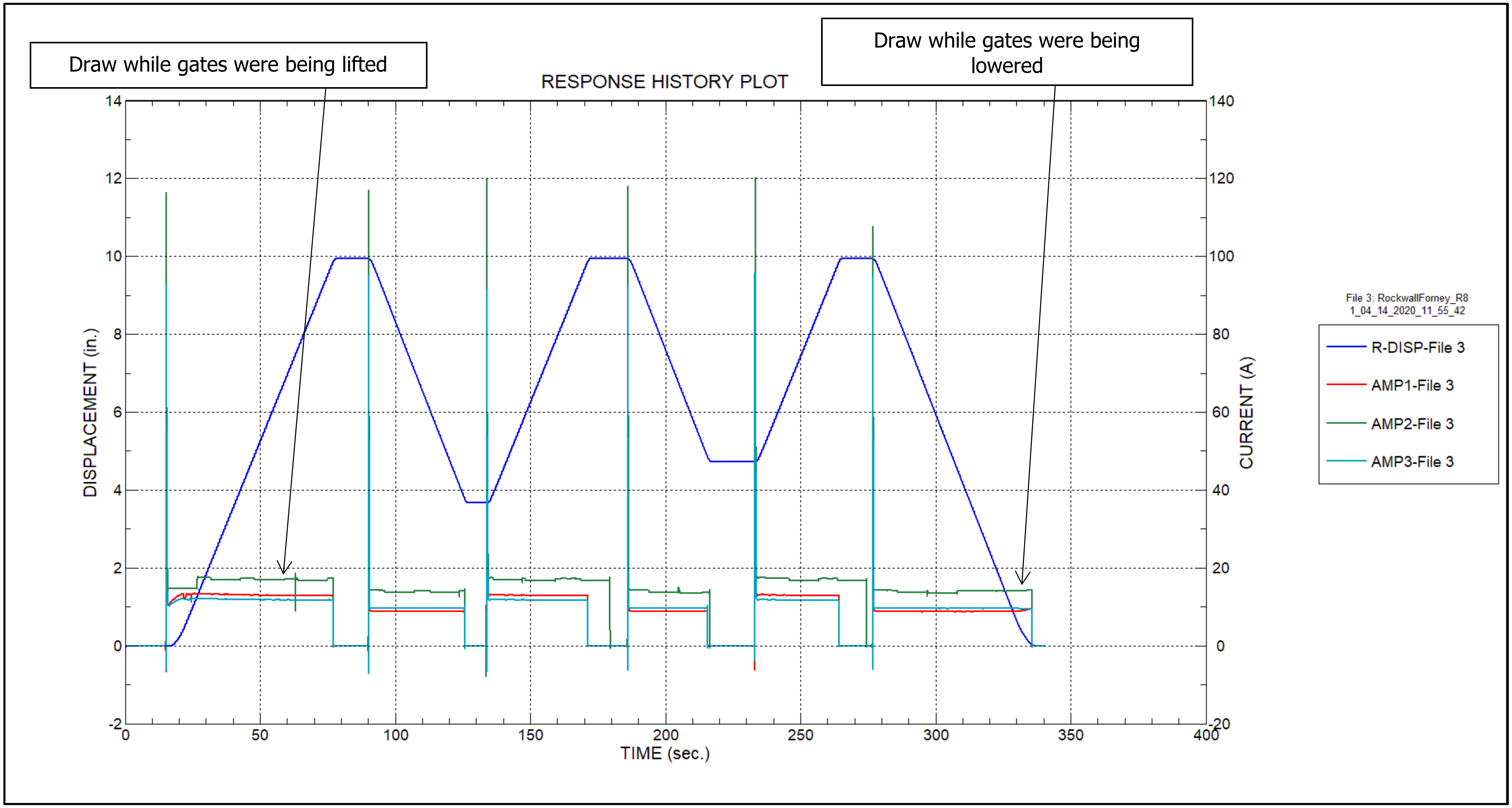

Figure 10 – Motor current & gate movement response history – Lift motor – Highlighting motor draw during lift and lower cycles

Methodology and Findings of The Strut Force and Moment Calculations

The following outline provides the methodology used to calculate the required member forces and moments.

+ **CHANGE IN STRESS DUE TO GATE OPERATION:** Strain data can be viewed as a function of time starting when the gate was in the down position and was then lifted off the sill. When examining data in this manner, it is easy to see how stresses ramped up as the gate began to move and then changed slope once pin friction was overcome and the trunnion hub began to rotate with the gate. The first point in time where the friction was overcome (both lifting and lowering) has been highlighted in the stress histories shown in Figure 11. These stress histories show the response of all four sensors along the top strut of the right arm (Section A). ***It is important to note that the recorded measurements were changes in structural response due to gate movement, and do not include the in-situ stresses due to the dead load, cable wrap, and hydrostatic loads present prior to testing.***
+ **CALCULATION OF STRUT CROSS-SECTIONAL MOMENTS:** The use of four strain gages per strut cross-section allowed accurate in-plane flexural bending moments to be computed from the recorded strain measurements. These moments were computed for every cross-section in each gate arm using the basic mechanics equation provided in Figure 12.

  In-plane or weak-axis flexure refers to bending about a given strut's web. This designation is consistent with typical nomenclature. In-plane bending can be observed visually from the strain response histories as a difference between the top and bottom stresses, whereas out-of-plane or strong-axis bending is visualized as the difference in stress from side to side. Figure 13 provides a visual reference for both types of strut flexure.
+ **EXAMINATION OF RESPONSES AS A FUNCTION OF GATE POSITION:** Changes in cross-sectional moment related to friction becomes clearer when the responses are plotted as a function of gate position. Because the gate was operated with several up and down movements, the effects of friction associated with each direction reversal can be viewed for all measured and calculated responses. Figure 14 through Figure 17 show all cross-sectional flexural moment plots for both trunnion arms. The responses in these plots have been centered about the stress state corresponding to a zero-moment, unflexed condition. The zero-moment offset was estimated as the average moment values between up and downward movement (i.e. half the moment difference) at the gate position with the greatest pin friction moment difference (greatest difference between lifting and lowering).
+ **TRUNNION FREE-BODY-DIAGRAM & PIN MOMENT CALCULATION:** Figure 18 shows the instrumented member cross-sections and shows how the measured cross-sectional flexural responses were used to compute pin moment. The in-plane moment values used in these calculations were determined directly from the strain measurements at each cross-section using the provided mechanics equations. It should be noted that the out-of-plane moments were not considered in the calculation of pin moment since they were orthogonal to the axis of the pin rotation. Total pin moment was then determined by summing all the moment components about the pin, which included the in-plane moment and the shear components at the strut cross-sections nearest the pin.
+ **STRUT SHEAR CALCULATION:** From the examination of the trunnion free-body-diagram described above, the shear vectors at the three struts were a primary component in the pin moment calculation. For this type of structural element, shear vectors were calculated using the moment differential between the two cross sections along each strut. It is important to recognize that shear was constant between the two instrumented cross-sections and the applied shear was a function of the recorded change in moment ($V = dM/dX$). Subsequently, the shear vectors were calculated by dividing the difference in moment by the distance between the two instrumented cross-sections. Shear values for each strut have been plotted as a function of gate position in Figure 19 and Figure 20.

- **CALCULATION OF PIN MOMENT DUE TO FRICTION:** Once all the trunnion arm force vectors were calculated, the equations shown in the free-body-diagram were applied to compute pin moment as a function of gate position. It is important to note that because the calculated pin moment range corresponds to a direction reversal, a reversal in friction also occurred. The effect of direction reversal on pin moment due to friction is best conceptualized by centering the moment response plots about the zero-moment axis. The moment due to lifting and the moment due to lowering can then be visualized as a change from this new zero point corresponding to the gate in an unflexed condition. Therefore, the total moment differential between lifting and lowering was twice the moment due to friction acting in a single direction. Pin-moment plots have been provided in Figure 21 and Figure 22. From these plots, it is apparent that pin moment due to friction remained relatively constant throughout the gate operation tests, with a slight decrease in pin friction moment as the gate continued to be lifted. This slight decrease in pin friction moment most likely corresponded to the change in hydrostatic load as the gate position changed. Pin-moment plots for all tests on Gate 14 are also provided for reference in Appendix B – Gate 14 Pin Moment Component Plots.
- **SHAFT TORQUE & HOIST FORCE:** Torque measurements were taken on the pinion shafts near the hoist motor during testing, with single torque gages installed on the left and right hoist pinion shaft. Responses were recorded in units of micro-strain and converted to torque in units of kip-ft using Equation 1 thru Equation 3 and the following shaft properties.

$$d_O = 5.5\ inches, \qquad d_I = 0\ inches, \qquad E = 29000\ ksi, \qquad \nu = 0.3$$

$$G = \frac{E}{2(1+\nu)}$$

Equation 1

$$J = \frac{\pi\left({d_O}^4 - {d_I}^4\right)}{32}$$

Equation 2

$$\tau = \varepsilon * \frac{2GJ}{\frac{d_O}{2} * 1000000 * 12}$$

Equation 3

Figure 23 shows example torque measurements, recorded on the Gate 14 torque shafts. Best practices for torque measurements is to measure torque on opposite sides of the shaft so that any bending in the shaft can be removed by averaging the two responses. Due to access limitations, only one gage at each location could be installed. Therefore, any bending in the shaft may be reflected in the torque measurements and may be related to the peaks and valleys observed in the torque responses.

Torque values were converted to force in the hoist cables per gate arm using the gear ratio and drum radius, as shown in Figure 24. The gear ratio and drum radius were 5.182 and 1.086 feet respectively, as defined in the provided as-built shop drawings. It should be noted that the hoist force calculated may be smaller than the actual hoist force applied. This difference is due to the limit switch engaging the brake before the hoist cable was fully slacked, resulting in an initial force in the cable. A hoist force due to total gate friction was then calculated. This friction hoist force was equal to half the differential in force measured during the lifting and lowering of the gate (similar to the pin friction calculations). As shown in Table 3, the change in cable force due to friction was generally consistent between tests. Note that the total hoist force was due to the total friction effects, including side seal, hoist bearings, trunnion friction effects, etc. It is difficult to determine the exact proportion and composition of the total friction sources. Additional torque and hoist force plots for all collected data files are provided in Appendix A – Gate 14 Torque and Hoist Force Plots.

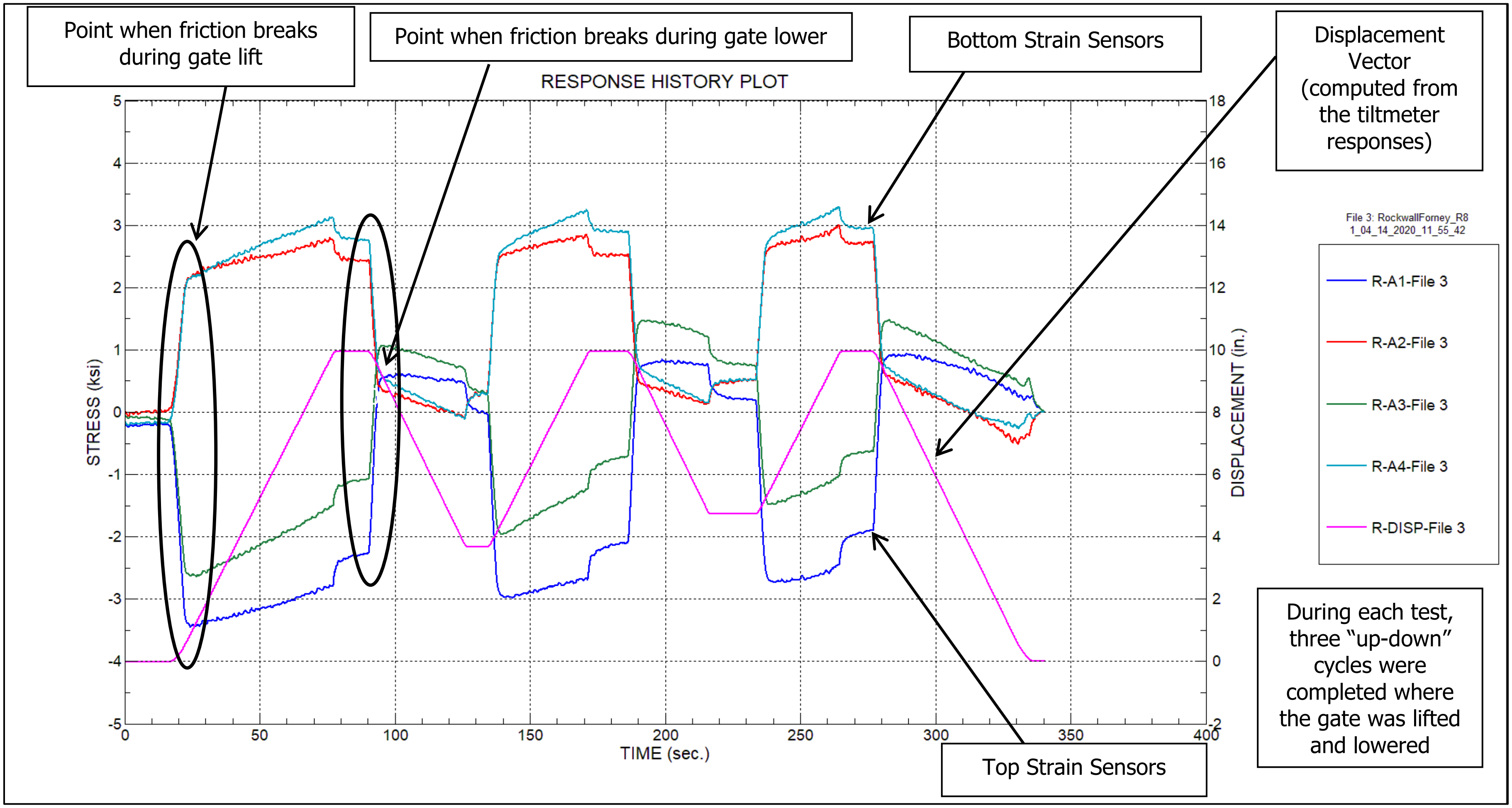

Figure 11 – Stress response & gate movement history – Right arm – Section A - Highlighting friction behavior (Section A along top strut near pin)

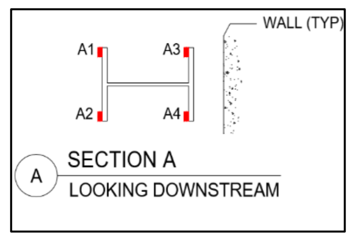

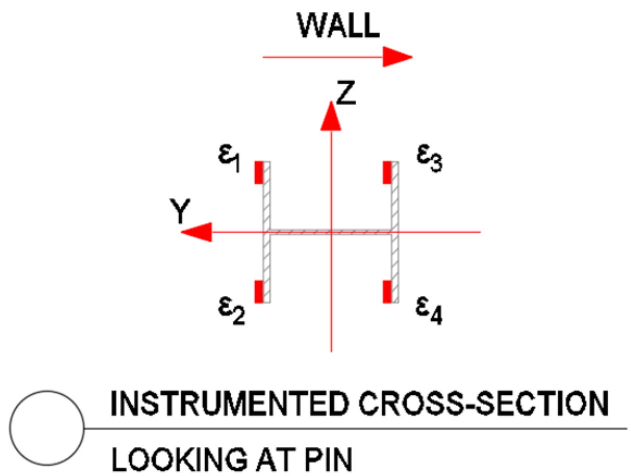

Calculation of Weak-axis (In-plane) bending

$$M_Y = \frac{E[\frac{\varepsilon_2 + \varepsilon_4}{2} - \frac{\varepsilon_1 + \varepsilon_3}{2}]S_{Y(gage)}}{2}$$

Sy(gage) = Section modulus to the center of gages (not extreme fiber of flanges)
(locations of gages were accounted for in moment computation)

Figure 12 – Basic mechanic equation used to calculate moment

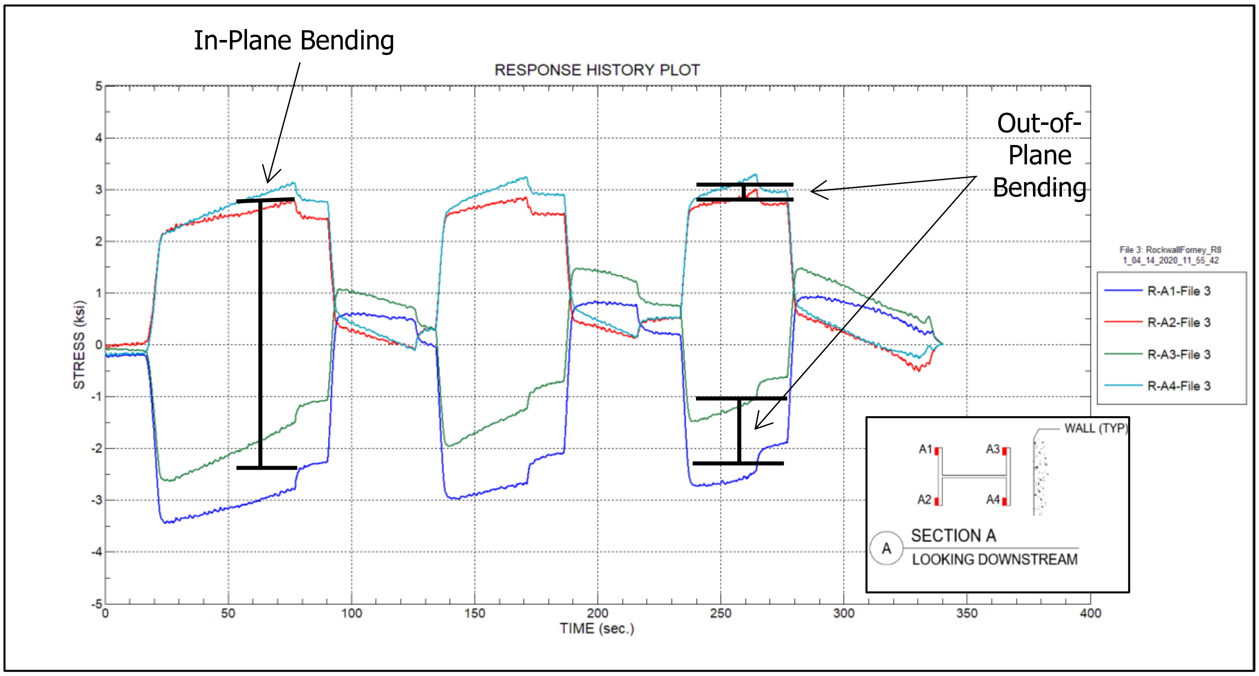

Figure 13 – Stress response history – Right arm – Section A – Bending components
(Section A along top strut near pin)

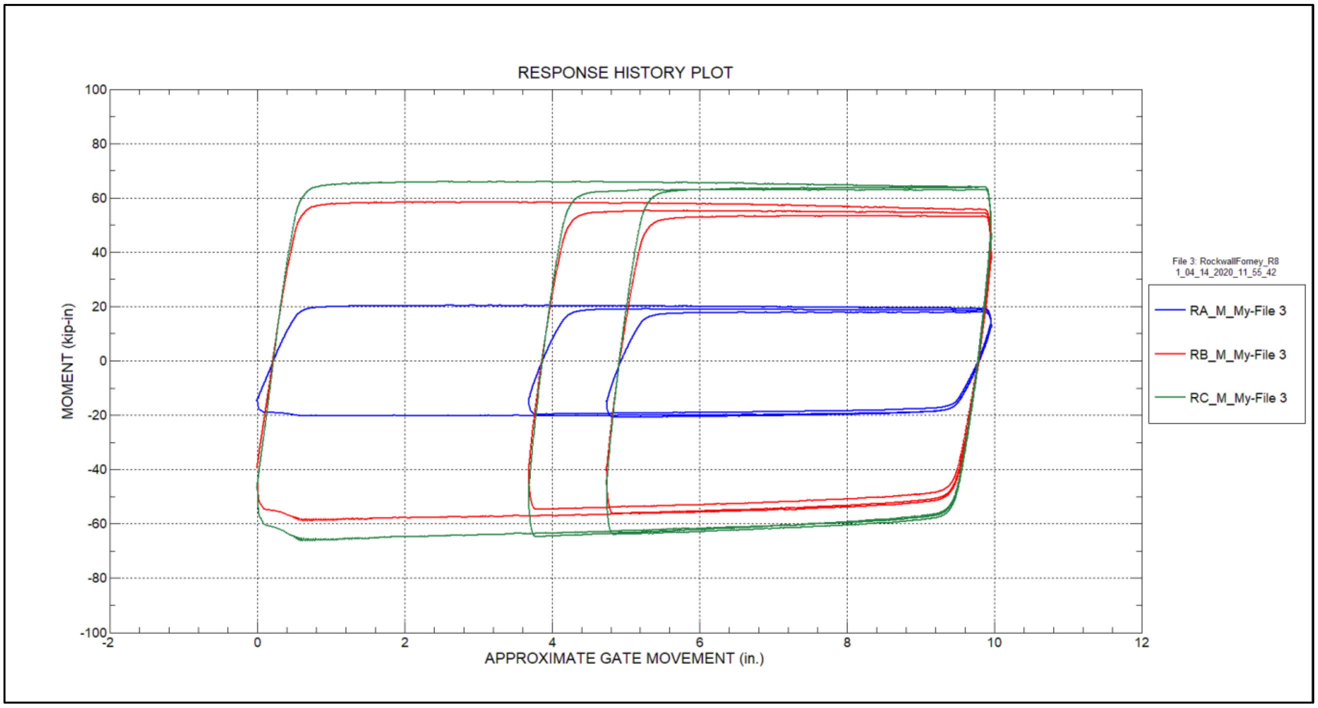

Figure 14 – In-plane moment response history – Right arm – Sections near pin

(RA = Right Arm Top Strut, RB = Right Arm Middle Strut, RC = Right Arm Bottom Strut)

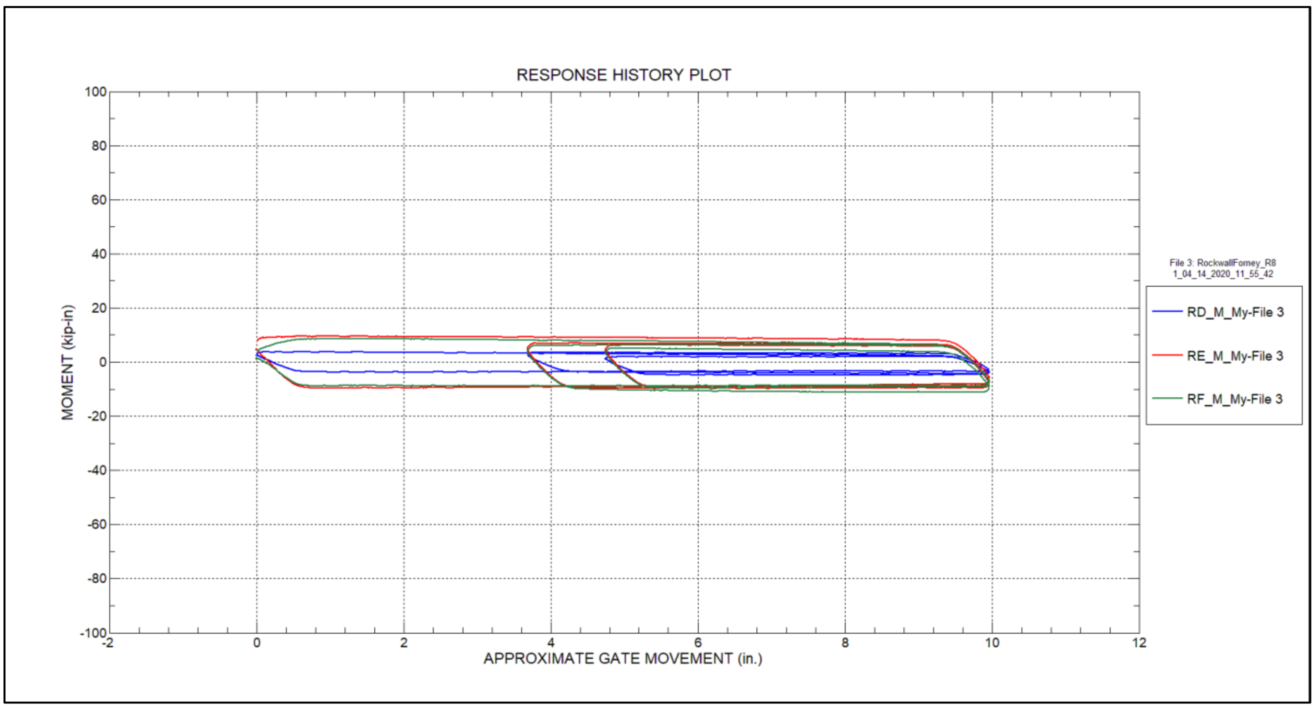

Figure 15 – In-plane moment response history – Right arm – Sections away from pin

(RD = Right Arm Top Strut, RE = Right Arm Middle Strut, RF = Right Arm Bottom Strut)

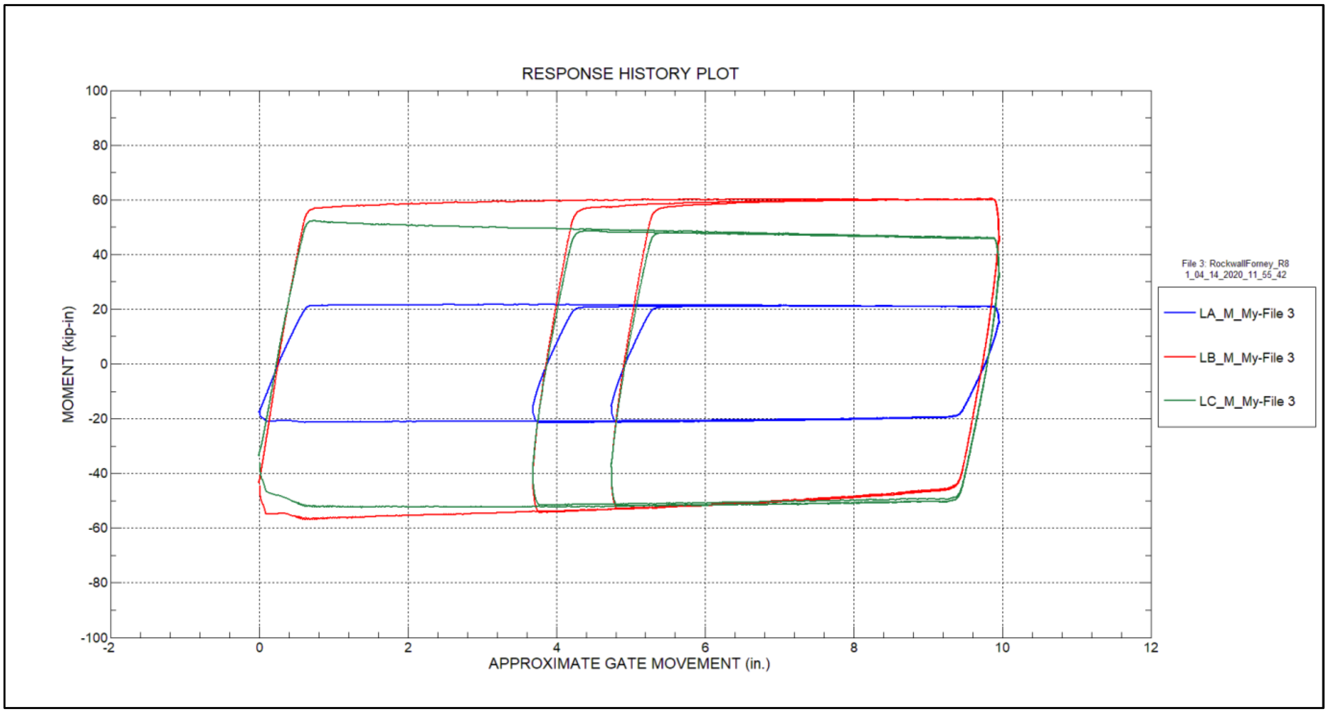

Figure 16 – In-plane moment response history – Left arm – Sections near pin

(LA = Left Arm Top Strut, LB = Left Arm Middle Strut, LC = Left Arm Bottom Strut)

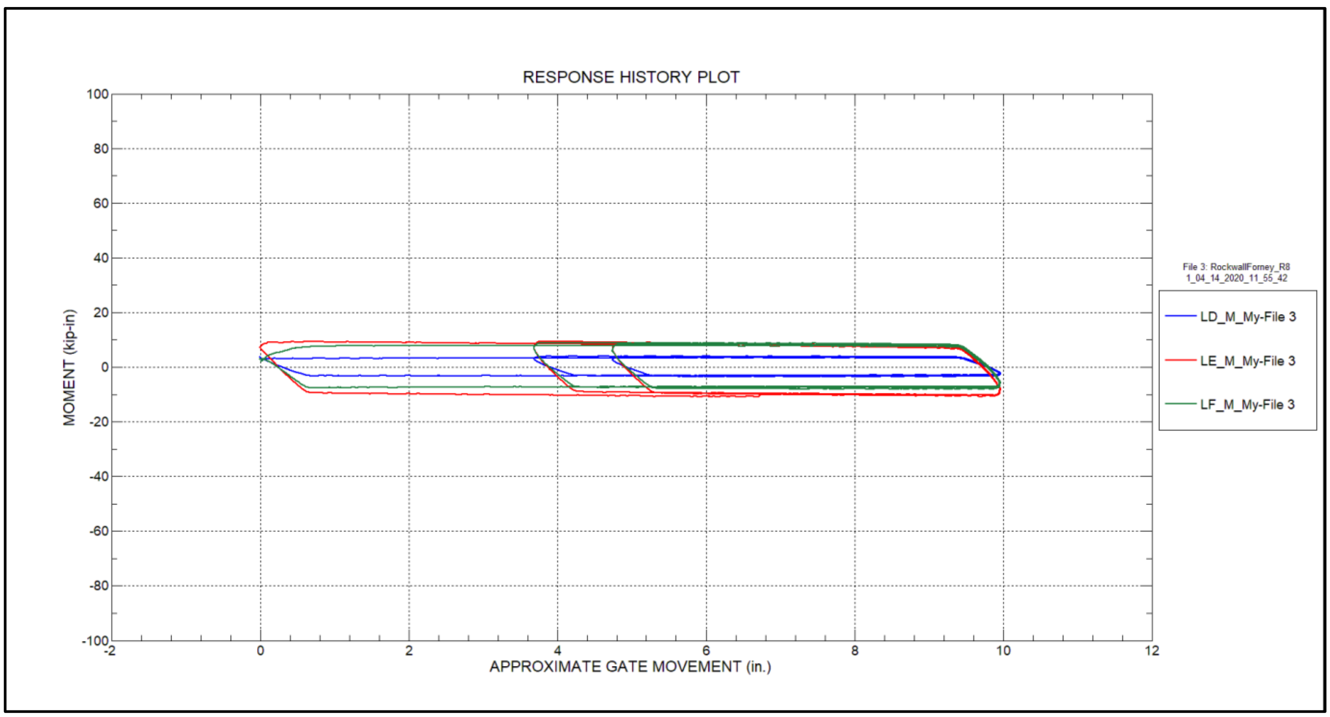

Figure 17 - In-plane moment response history – Left arm – Sections away from pin

(LD = Left Arm Top Strut, LE = Left Arm Middle Strut, LF = Left Arm Bottom Strut)

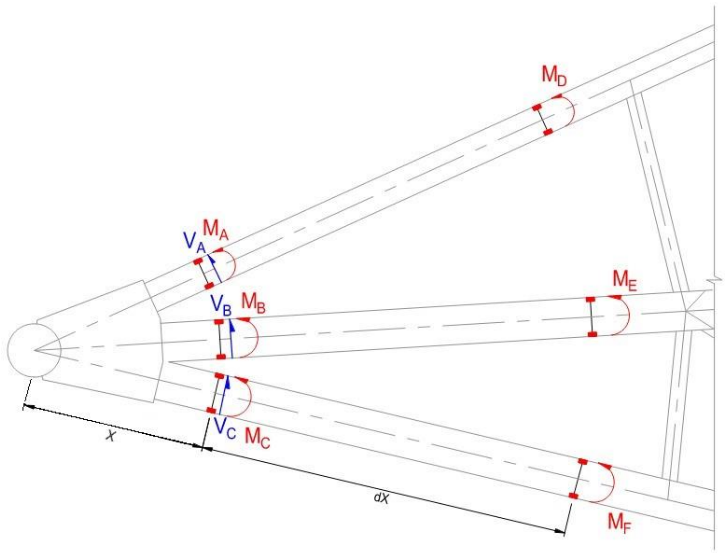

Elevation View of Gate Arm

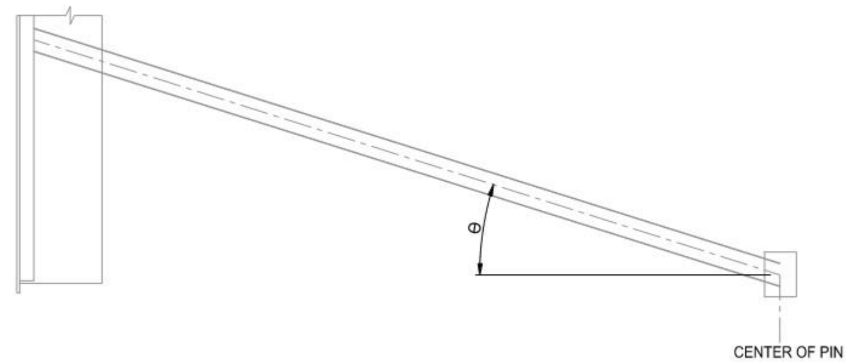

Plan View of Gate Arm

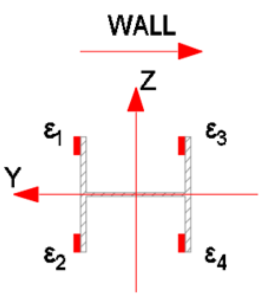

$$M_Y(M_A, M_B, M_C, M_D, M_E, M_F) = \frac{E\left[\frac{\varepsilon_2 + \varepsilon_4}{2} - \frac{\varepsilon_1 + \varepsilon_3}{2}\right] S_{Y(gage)}}{2}$$

$$V_A = \frac{M_A - M_D}{dX}$$

$$V_B = \frac{M_B - M_E}{dX}$$

$$V_C = \frac{M_C - M_F}{dX}$$

$$\sum M_o = 0$$

$$M_{PIN} = [X(V_A + V_B + V_C) + M_A + M_B + M_C]\cos\theta$$

Figure 18 – Direct calculation of pin moment from strain measurements

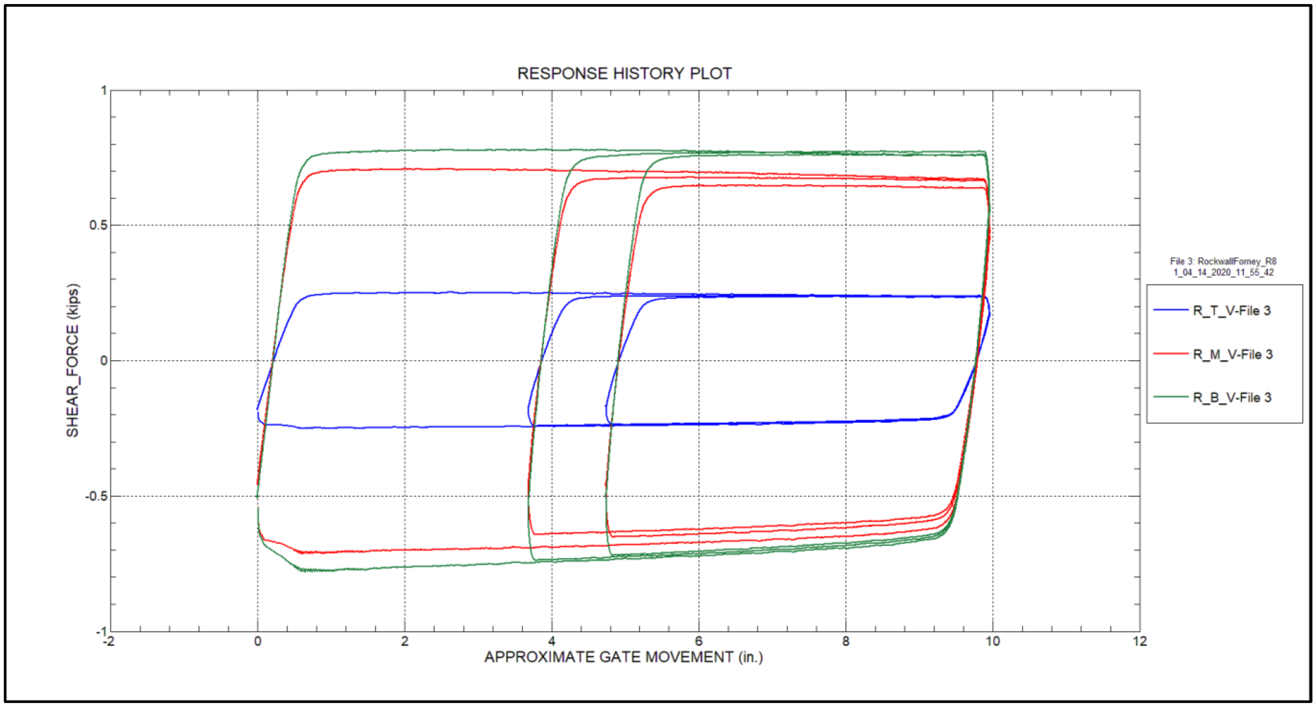

Figure 19 – Strut shear response history – Right arm

(R_T = Right Arm Top Strut, R_M = Right Arm Middle Strut, R_B = Right Arm Bottom Strut)

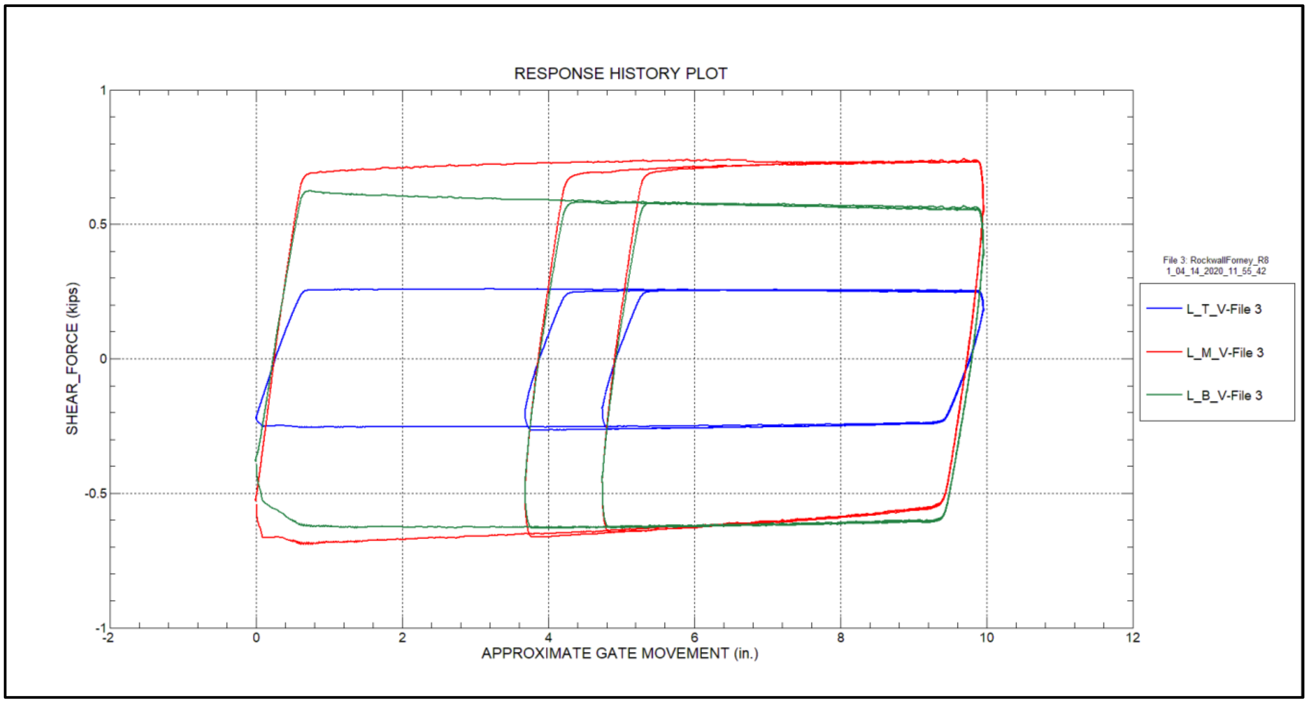

Figure 20 – Strut shear response history – Left arm

(L_T = Left Arm Top Strut, L_M = Left Arm Middle Strut, L_B = Left Arm Bottom Strut)

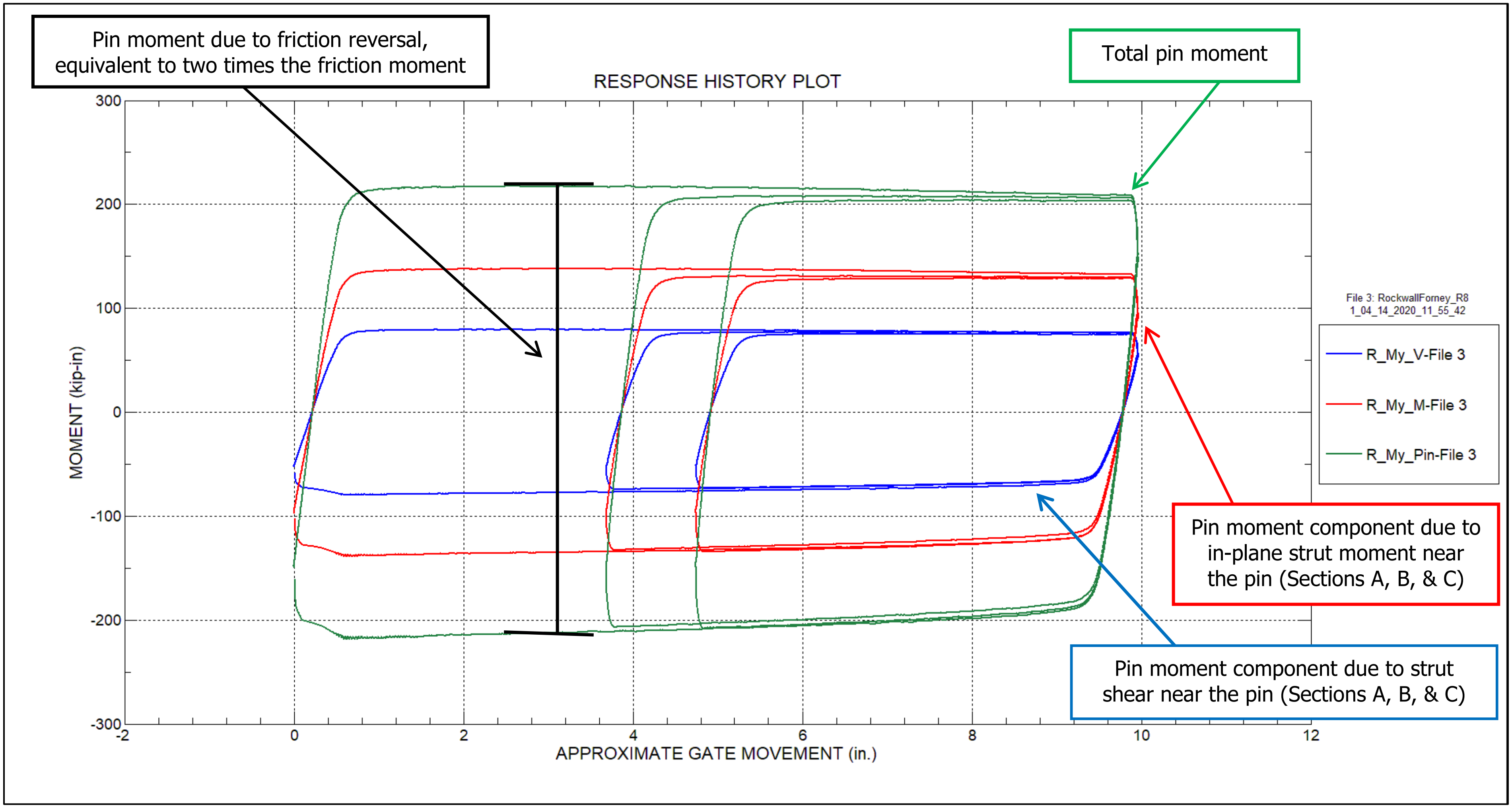

Figure 21 – Pin moment response history – Right arm

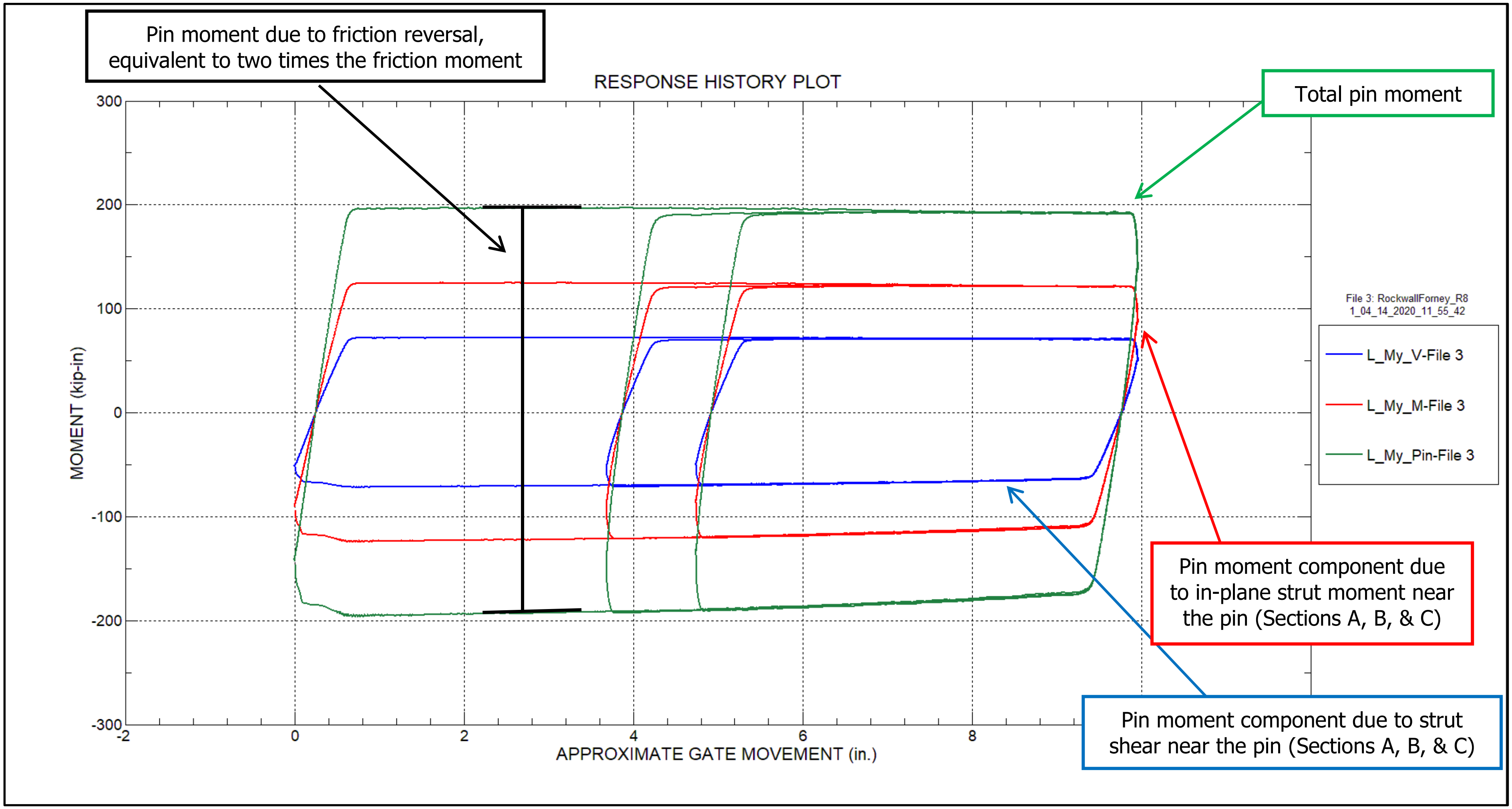

Figure 22 – Pin moment response history – Left arm

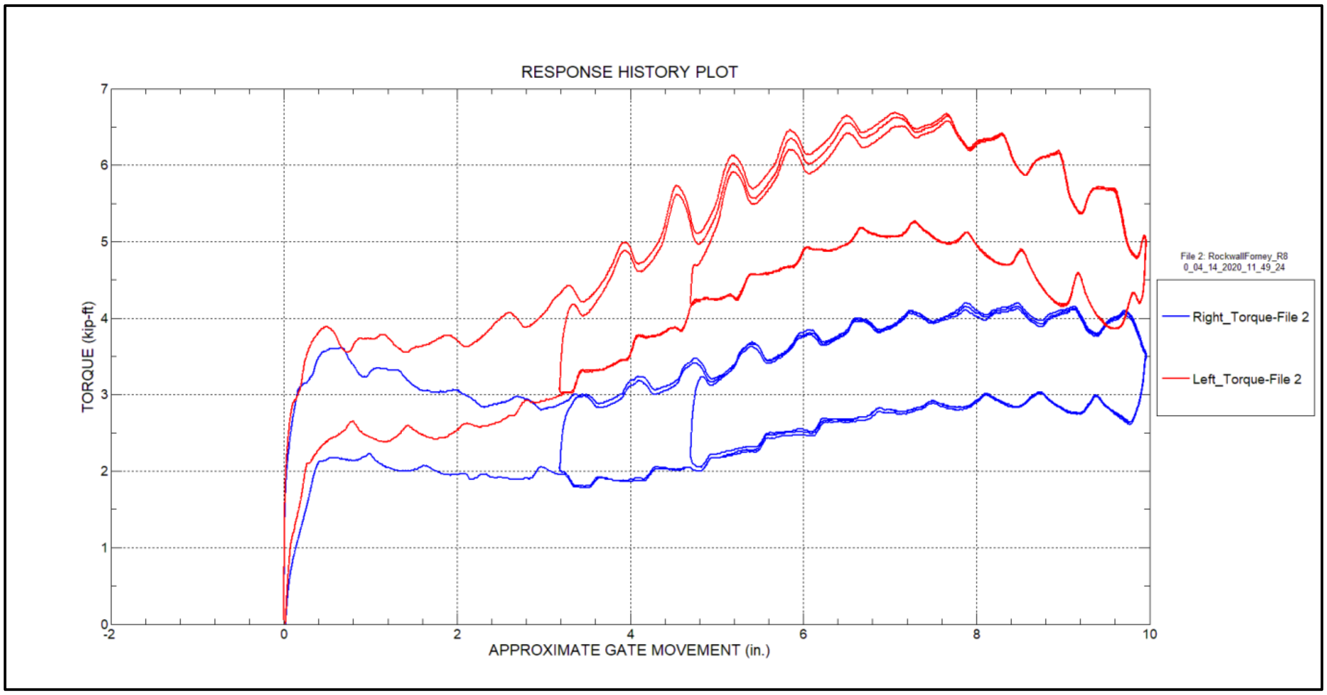

Figure 23 – Hoist torque response history – Gate 14 – Test 2

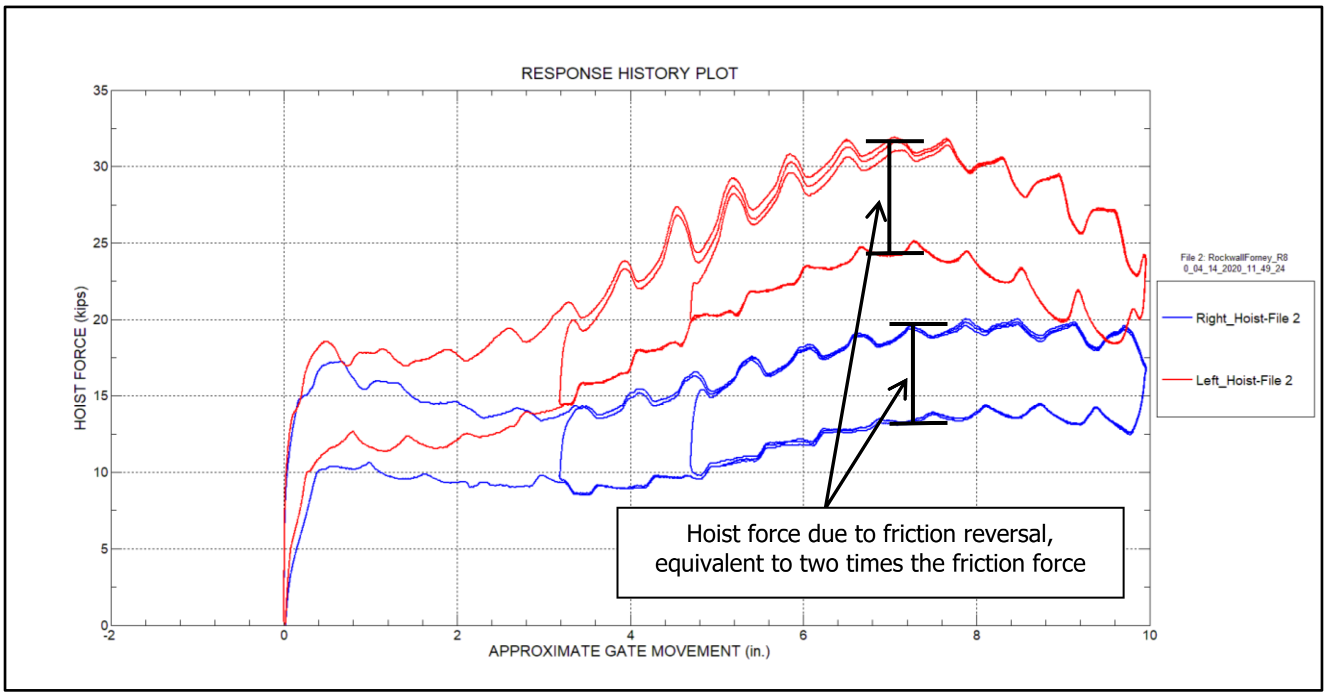

Figure 24 – Hoist force response history – Gate 14 – Test 2

Summary of Friction Results

The raw data files have been included in the submittal package for reference and were formatted as “tdms” files that can be opened in Microsoft Excel using a "tdms" reader extension.

Examination of the stress histories for each test was necessary to obtain a thorough understanding of the gate performance. The response shapes, variations in stress magnitudes, and timing sequences provided direct clues as to how the gate performed under typical service conditions. The following is a breakdown of the provided tabulated results:

+ Table 2 provides motor current ranges and maximum in-flow for lift and lower cycles for each test
+ Table 3 provides maximum hoist force as well as hoist force due to total friction for each test
+ Table 4 provides the maximum stress ranges measured at the sensor locations for each member
+ Table 5 provides maximum bending stress and moment ranges observed during the gate tests
+ Table 6 provides maximum friction bending stress and moment values at each of the instrumented strut locations
+ Table 7 provides the computed shear values in each strut due to friction
+ Table 8 provides calculated measured friction moments, calculated hydrostatic loads based on the measured water elevation, and coefficients of friction for each gate and gate arm during all three tests

The resulting pin friction moments were used to compute friction coefficients from Eq. 4, given the pin radius and the applied thrust. The thrust used in this calculation consisted of the calculated resultant hydrostatic load based on the measured water elevation and was adjusted to account for the loss of head as the gate was lifted. This thrust adjustment was based on the recorded gate movement and was performed in order to calculate more accurate friction coefficients. The water elevation during testing was nearly constant throughout each gate test and was documented during each “up-down” cycle. It should be noted that the minor thrust due to cable wrapping, which was minimal compared to hydrostatic thrust, was not included in the thrust calculation. This assumption resulted in slightly conservative friction coefficients.

$$\mu = \frac{M_F}{T * r} \qquad \text{Eq. 4}$$

where:

μ	=	Friction Coefficient
M_F	=	Friction Moment
T	=	Thrust per Pin
r	=	Pin Radius, 5.375”

The out-of-plane shear and moments were not considered in the pin friction calculations due to orthogonal geometry considerations (resulting pin moment associated with out-of-plane flexure being perpendicular to pin rotation).

The data was presented in a specific coordinate system applicable to both arms. Data was processed so that the positive x-axis was always pointing towards the pin and the right-hand rule applied. In-plane bending can be referred to as “bending about the horizontal or y-axis” and shows how much the beams bend up and down within the plane of the gate arms. Refer to Figure 12 above for visual reference of coordinate system and mathematical explanation of calculations. Tabulated results do not include any in-situ effects.

Table 2 – Motor current summary table – Gate 14

Test Run	Current Range due to Lifting (A)	Current Range due to Lowering (A)	Max In-rush Current (A)
1	12-20	9-14	121
2	12-18	9-14	123
3	11-18	9-14	120

Table 3 – Hoist force summary table – Gate 14

Test Run	Right Arm Peak Hoist Force (kips)	Left Arm Peak Hoist Force (kips)	Right Arm Hoist Force due to Total Gate Friction (kips)	Left Arm Hoist Force due to Total Gate Friction (kips)
1	19.64	31.35	3.33	4.59
2	20.05	31.97	3.51	4.85
3	29.71	19.88	3.61	4.90

Tabulated friction force values correspond to the response induced by friction in one direction

Table 4 – Maximum measured sensor stress range

Arm Designation	Top Strut (ksi)	Middle Strut (ksi)	Bottom Strut (ksi)
Right Arm	4.91	6.03	5.54
Left Arm	4.76	5.32	4.58

Tabulated values correspond to the total measured change in response during tests

Stress values have not been extrapolated to the extreme fibers (correspond to center of gage)

Table 5 – Maximum in-plane total bending stress & moment ranges – Total

Section Label	Section Description	Right Arm Stress (ksi)	Right Arm moment (kip-in)	Left Arm Stress (ksi)	Left Arm moment (kip-in)
Section A	Top Strut Near Pin	4.28	48.11	4.38	49.26
Section B	Middle Strut Near Pin	5.64	130.50	5.63	130.26
Section C	Bottom Strut Near Pin	5.30	147.76	4.16	115.94
Section D	Top Strut Away from Pin	0.89	9.98	0.81	9.06
Section E	Middle Strut Away from Pin	0.86	19.97	0.94	21.81
Section F	Bottom Strut Away from Pin	0.79	22.06	0.66	18.53

Tabulated values correspond to the total measured change in response during tests

Table 6 – In-plane frictional bending stress & moment at maximum gate friction

Section Label	Section Description	Right Arm Stress (ksi)	Right Arm moment (kip-in)	Left Arm Stress (ksi)	Left Arm moment (kip-in)
Section A	Top Strut Near Pin	2.13	23.99	2.17	24.38
Section B	Middle Strut Near Pin	2.82	65.19	2.78	64.34
Section C	Bottom Strut Near Pin	2.65	73.82	2.04	56.75
Section D	Top Strut Away from Pin	0.33	3.75	0.40	4.48
Section E	Middle Strut Away from Pin	0.42	9.62	0.46	10.74
Section F	Bottom Strut Away from Pin	0.31	8.77	0.31	8.75

Tabulated values correspond to the response induced by friction in one direction

Table 7 – Strut shear range summary table due to friction

Arm Designation	Top Strut Shear (kip)	Middle Strut Shear (kip)	Bottom Strut Shear (kip)
Right Arm	0.27	0.73	0.81
Left Arm	0.30	0.78	0.68

Tabulated values correspond to the response induced by friction in one direction

Table 8 – Pin friction summary table

Test Run	Average Water Elevation during testing (ft)	Approximate Thrust at time of Testing (kips per arm)	Gate/Member Designation	Pin Friction Moment (kip-in)	Friction Coefficient
1	435.59	489.60	Right Pin	238.30	0.09
			Left Pin	219.50	0.08
2	435.59	489.60	Right Pin	223.00	0.08
			Left Pin	199.90	0.08
3	435.59	489.60	Right Pin	216.60	0.08
			Left Pin	196.40	0.07

Tabulated values correspond to the response induced by friction in one direction

APPENDIX A – GATE 14 TORQUE AND HOIST FORCE PLOTS

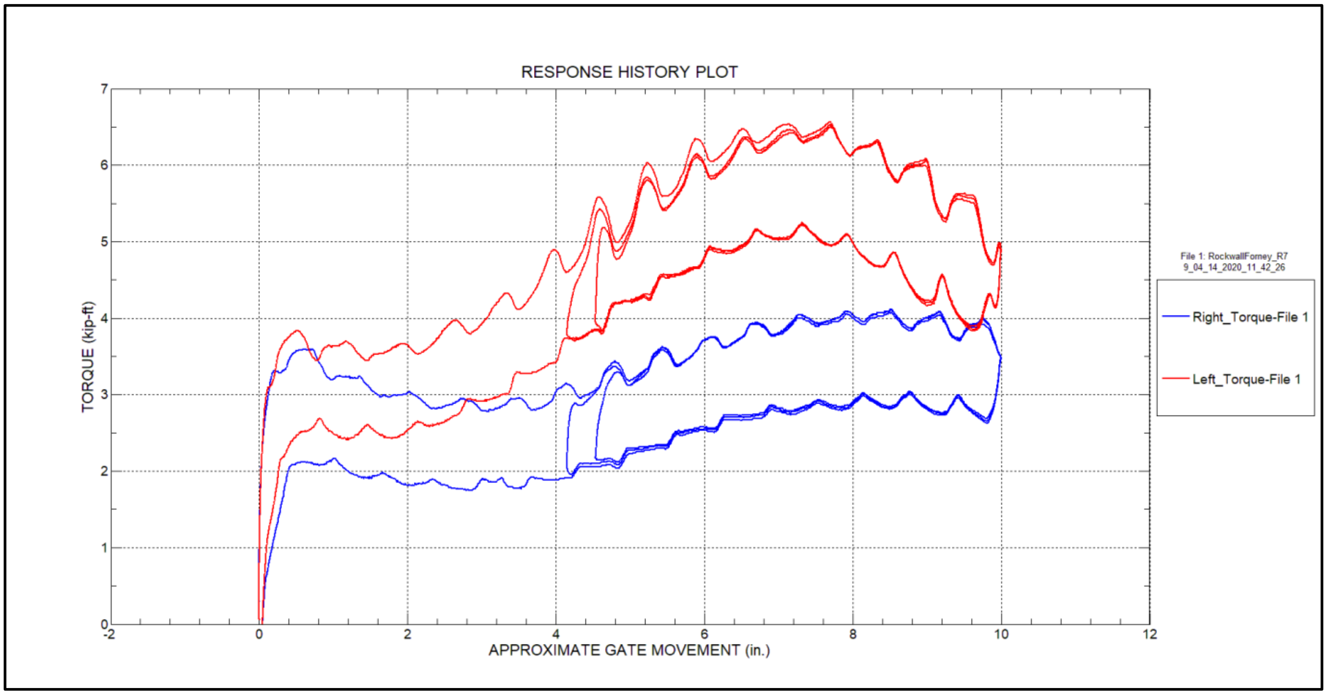

Figure 25 – Hoist torque response history – Gate 14 – Test 1

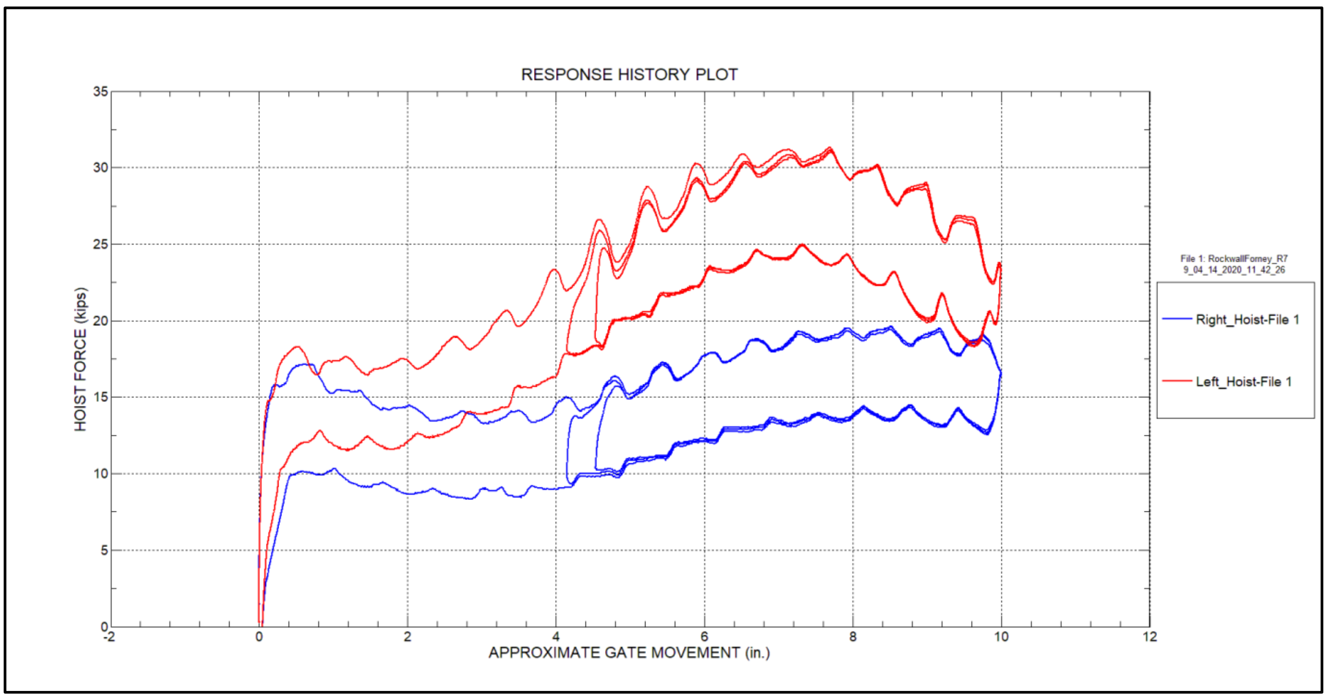

Figure 26 – Hoist force response history – Gate 14 – Test 1

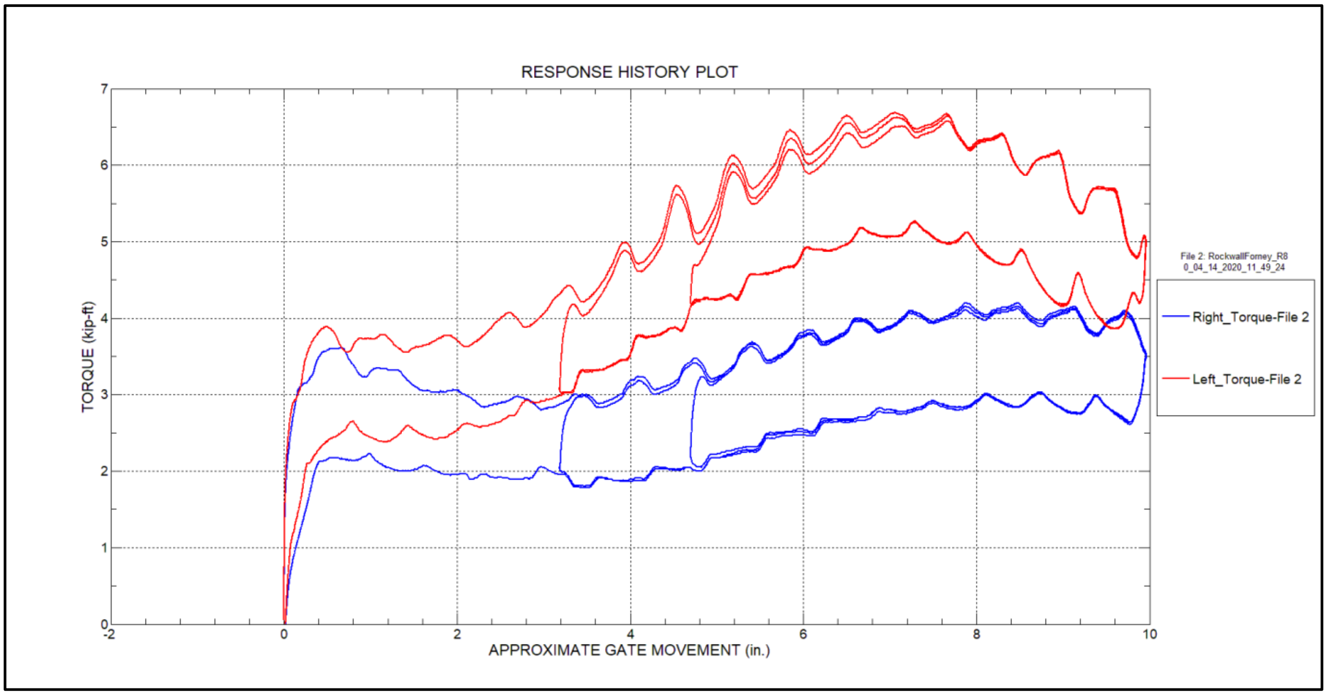

Figure 27 – Hoist torque response history – Gate 14 – Test 2

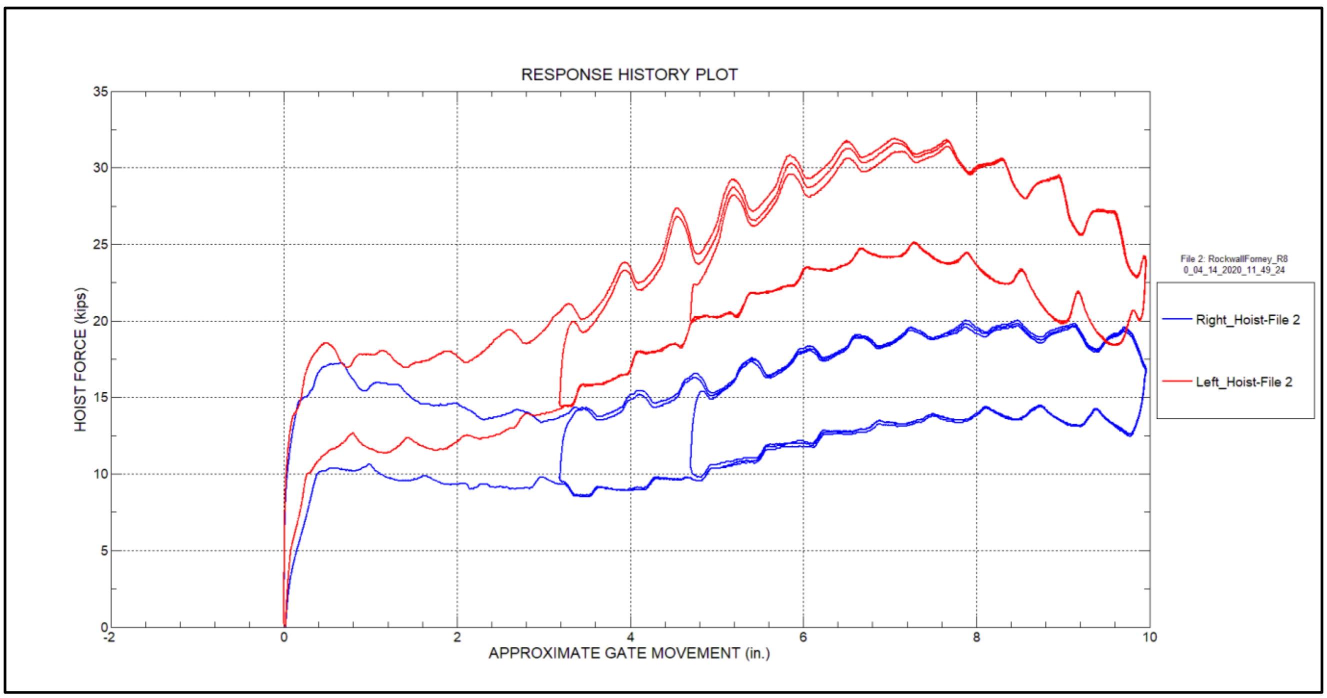

Figure 28 – Hoist force response history – Gate 14 – Test 2

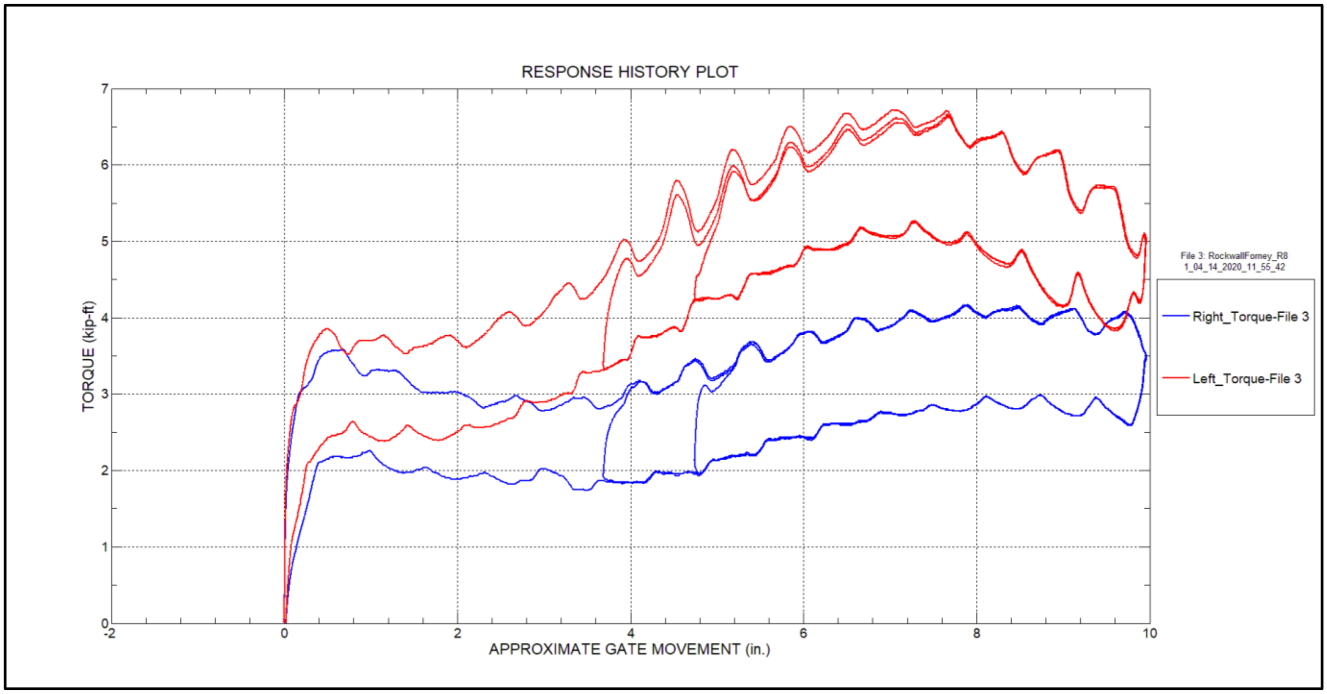

Figure 29 – Hoist torque response history – Gate 14 – Test 3

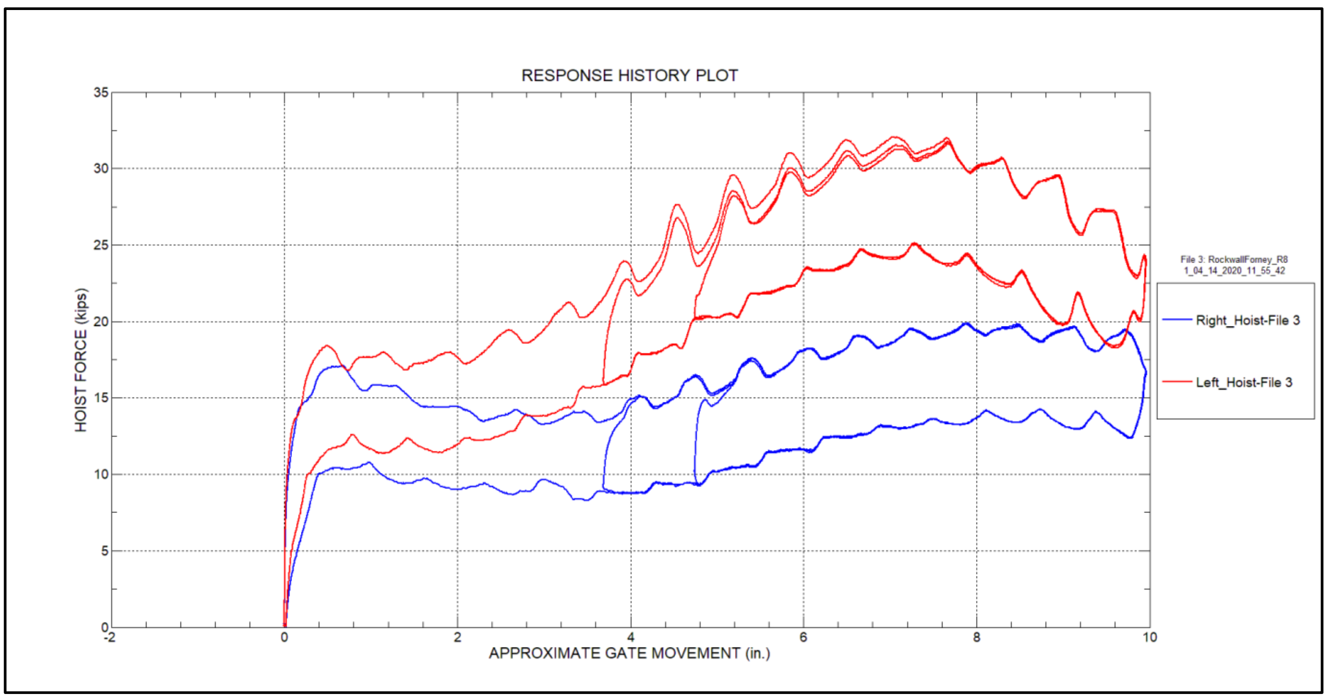

Figure 30 – Hoist force response history – Gate 14 – Test 3

Appendix B – Gate 14 Pin Moment Component Plots

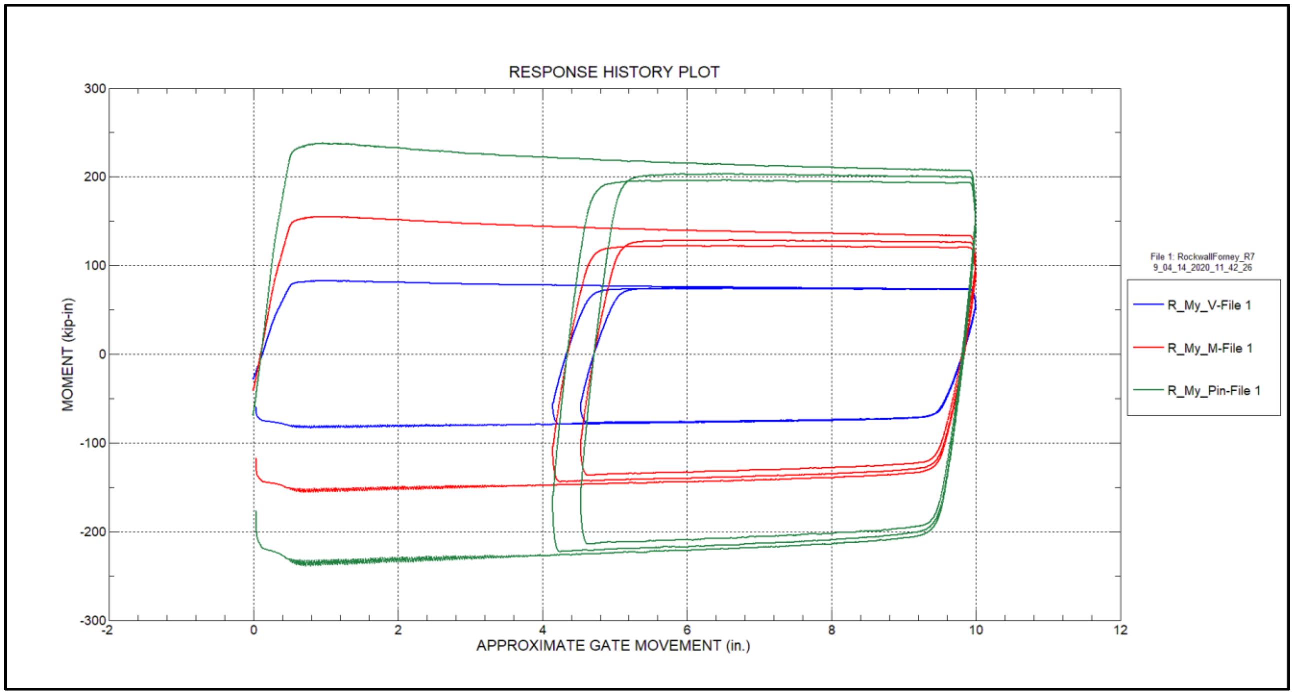

Figure 31 – Pin moment response history – Right arm – Test run 1

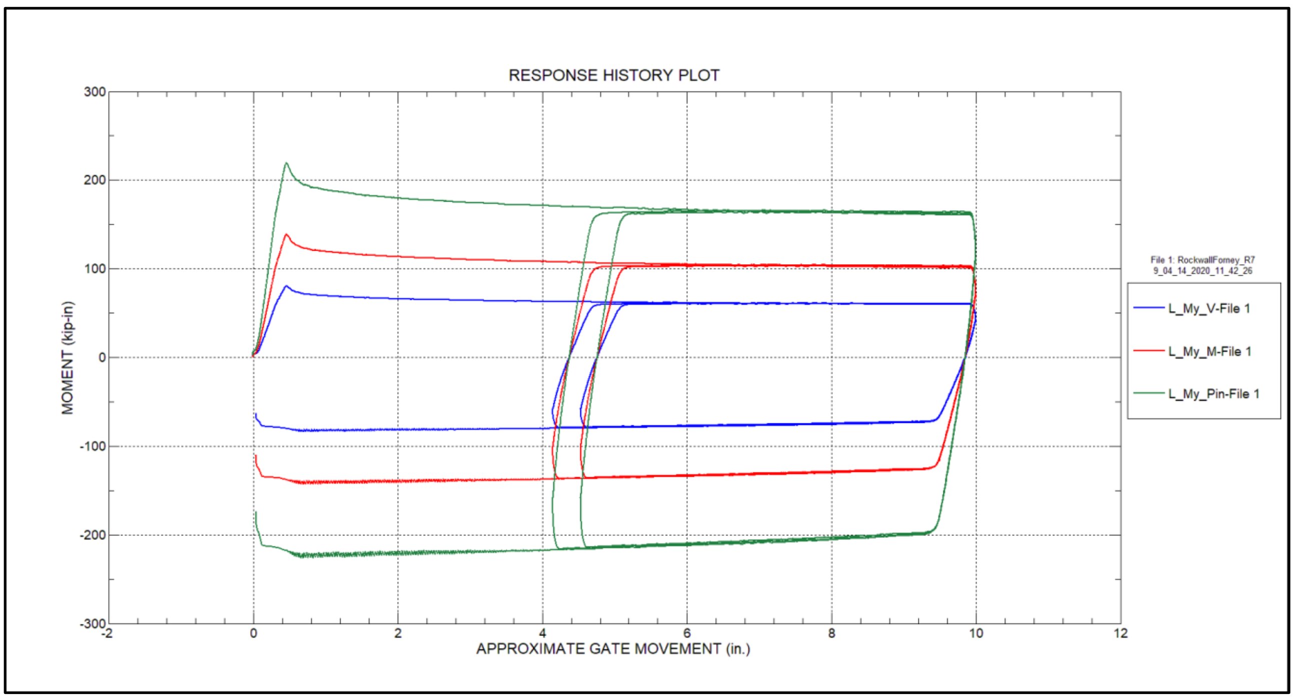

Figure 32 – Pin moment response history – Left arm – Test run 1

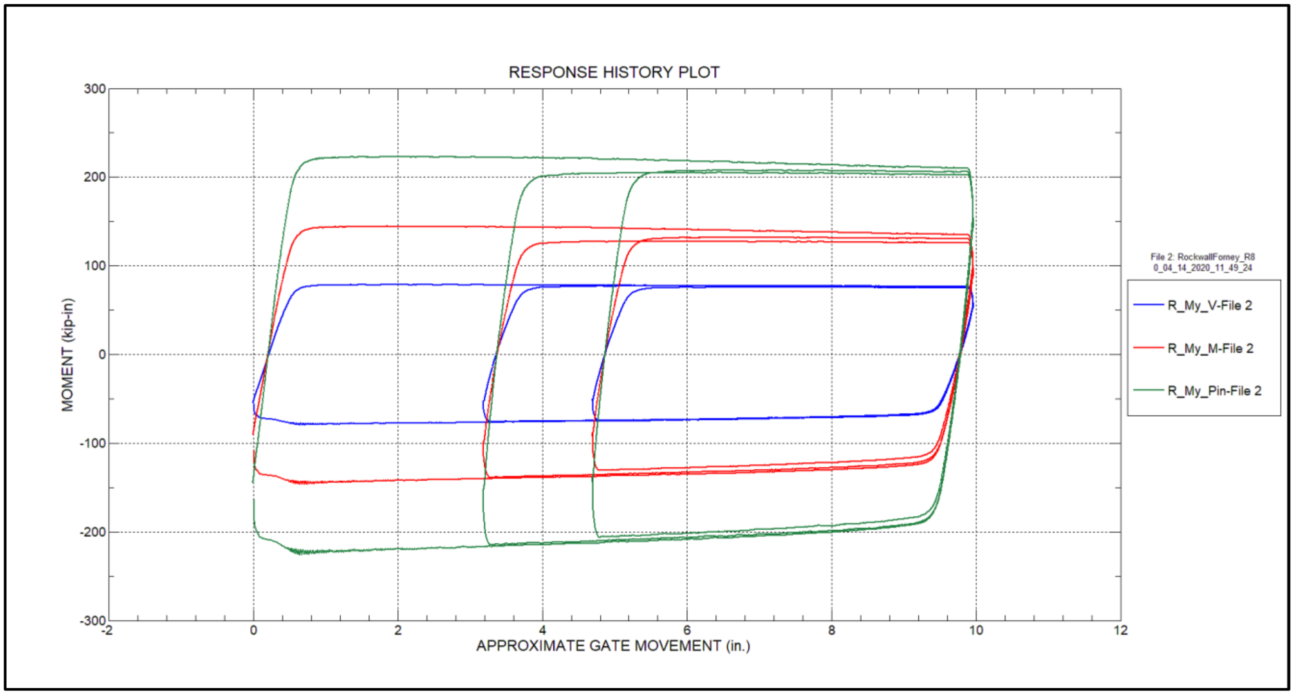

Figure 33 – Pin moment response history – Right arm – Test run 2

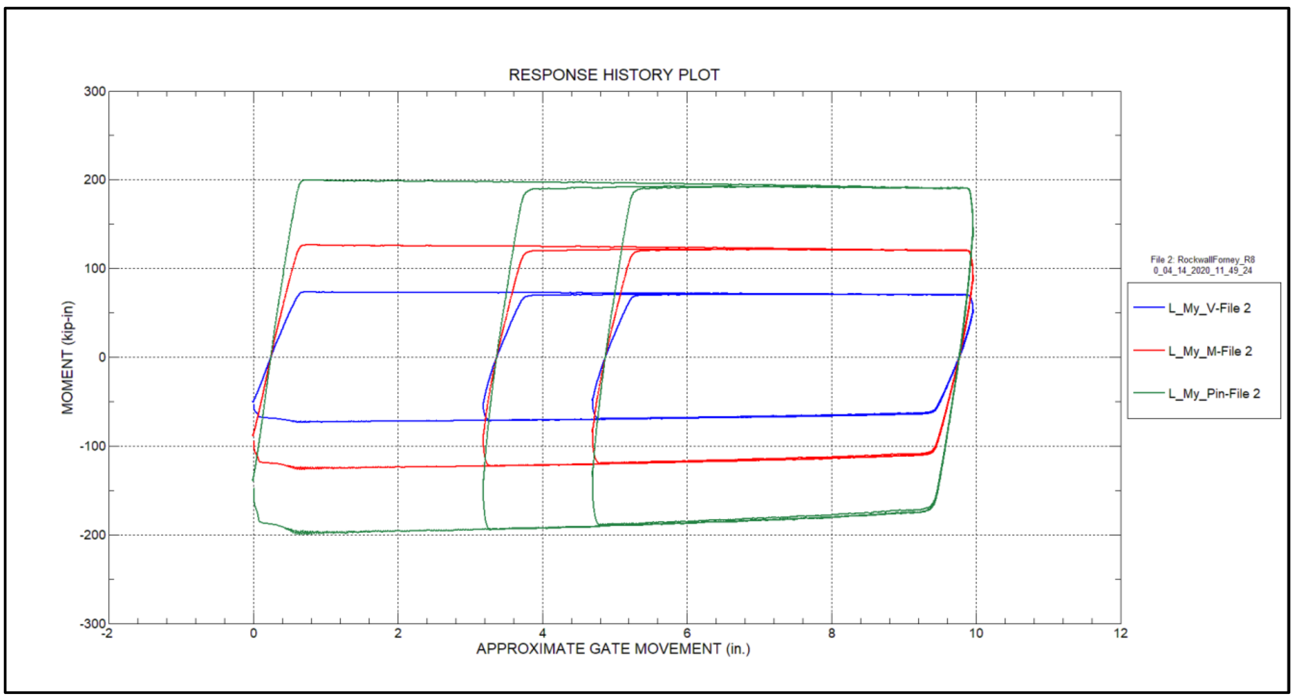

Figure 34 – Pin moment response history – Left arm – Test run 2

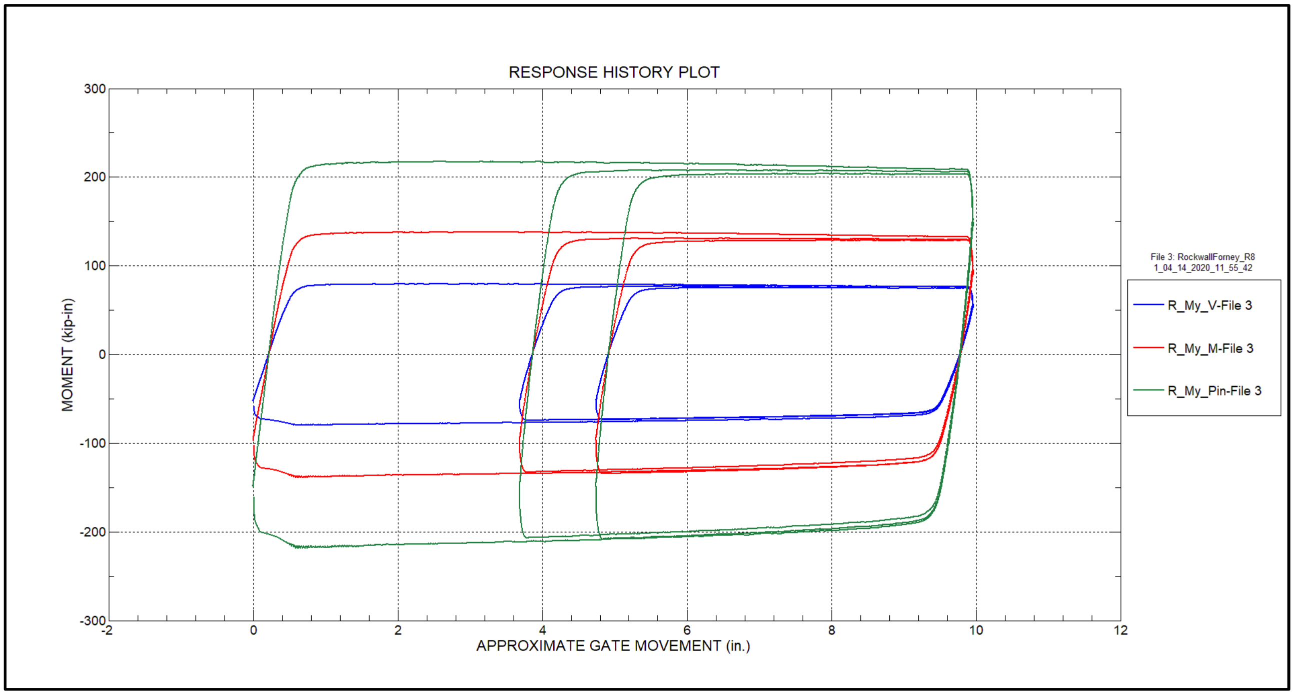

Figure 35 – Pin moment response history – Right arm – Test run 3

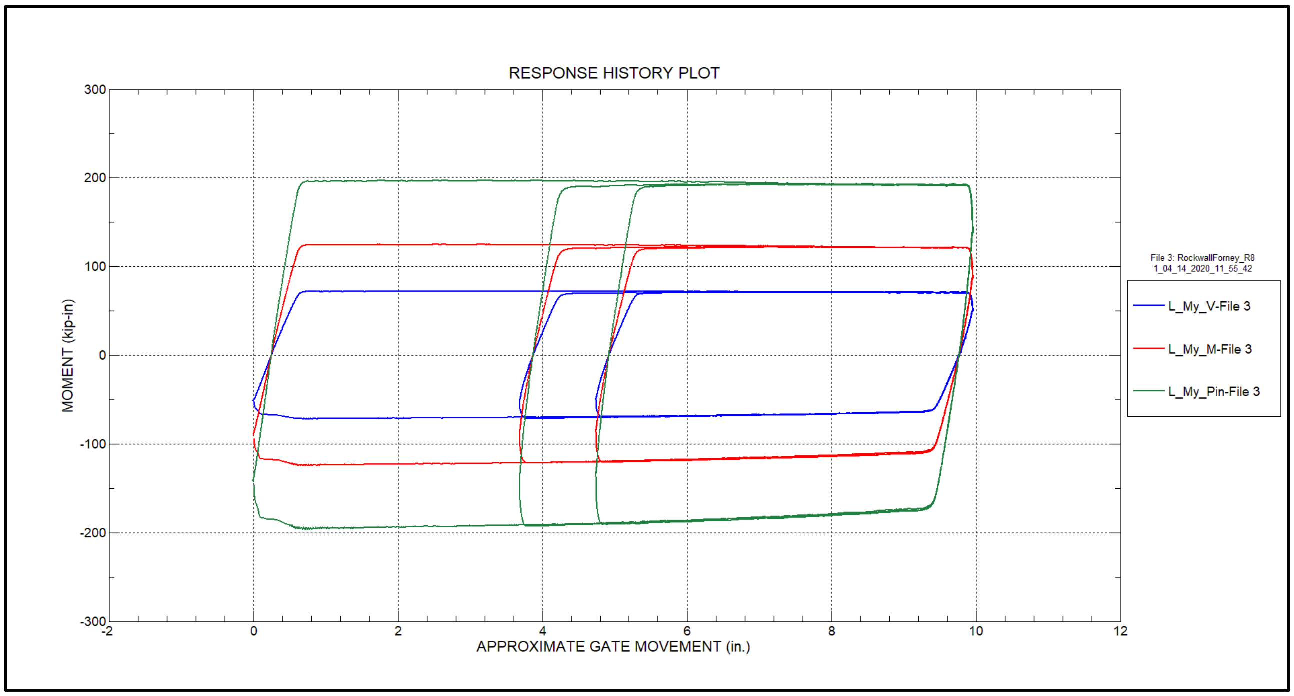

Figure 36 – Pin moment response history – Left arm – Test run 3

APPENDIX C – INSTRUMENTATION PLANS

RAW DATA. REFINED RESULTS.

SCHNABEL ENGINEERING
ROCKWALL FORNEY DAM
LIVE LOAD TESTING

BDI
RAW DATA. REFINED RESULTS.
740 S PIERCE AVE, SUITE 15
LOUISVILLE, CO 80027
303.494.3230
WWW.BDITEST.COM

ISSUE

CLIENT

SCHABEL ENGINEERING
16000 CHRISTENSEN RD, STE 101
SEATTLE, WA 98188

PROJECT NAME

SCHNABEL ENGINEERING
ROCKWALL FORNEY DAM
LIVE LOAD TESTING

Drawn By:	KNR
Checked By:	JDS
Date:	05/27/2020
Client No.:	
BDI No.:	190701-TX
SCALE:	NTS

COVER PAGE

LLT-00

The user acknowledges that these documents are instruments of professional service, and are protected by Copyright. This document and the information contained in this document are the property of Bridge Diagnostics, Inc., and shall not be reused, copied, disseminated, modified, amended or altered in any way. It is issued for information purposes only. The user agrees to hold harmless, indemnify and defend Bridge Diagnostics, Inc. against any and all damages, claims and losses, including defense costs, arising out of any use, reuse or copying of this document.

PLOT TIME: 6/12/2020 3:22 PM
FILEPATH: C:\Users\colemand\BDI\Services - Documents\Server_Remote\190701-TX_Schnabel_RockwallForneyDam\7. Instrumentation Plans\BDI_ROCKWALLFORNEY_01_GENERAL.dwg

© YYYY BRIDGE DIAGNOSTICS INC.

The user acknowledges that these documents are instruments of professional service, and are protected by Copyright. This document and the information contained in this document are the property of Bridge Diagnostics, Inc., and shall not be reused, copied, disseminated, modified, amended or altered in any way. It is issued for information purposes only. The user agrees to hold harmless, indemnify and defend Bridge Diagnostics, Inc. against any and all damages, claims and losses, including defense costs, arising out of any use, reuse or copying of this document.

GAGE LEGEND & SPECIFICATION

SYMBOL	TYPE	BRAND	MODEL	NOTES
	STRAIN TRANSDUCER	BDI	ST350	
	TILTMETER (UNI-AXIAL)	BDI	T500-030	
	TORQUE SENSOR	HPI	-	HBWS-35-125-6-0.5VR-FB
	AMP SENSOR	CR MAGNETICS	CR42105-200	

GENERAL NOTES

- INSTRUMENTATION SHALL BEGIN ON APRIL 1ST, 2020.
- GATES 1 THRU 14 SHALL BE ACCESSED USING SPRAT ROPE ACCESS TECHNIQUES.
- BDI WILL PERFORM ALL SURFACE PREPARATION, SENSOR INSTALLATION, AND EQUIPMENT INSTALLATION.
- SEE LLT-31 FOR SENSOR INSTALLATION DETAILS.
- TWO PAIRS OF TORQUE GAGES WILL BE INSTALLED ON THE GATE MOTORS' PINION SHAFTS BETWEEN THE MOTORS AND THE HOISTS.
  - GAGE PAIRS WILL BE INSTALLED 180° APART FROM EACH OTHER.
  - EXACT POSITIONS OF THE GAGE PAIRS ON THE PINION SHAFT WILL BE DETERMINED IN THE FIELD.
- THREE PHASE AMPERAGE GAGES WILL BE INSTALLED ON THE MOTOR CONTROLS BY A QUALIFIED ELECTRICIAN PROVIDED BY GARVER.

TESTING PROCEDURE:

- TESTING SHALL BE STARTED WITH THE GATE IN THE CLOSED POSITION.
- ONCE DATA COLLECTION BEGINS, THE GATE SHALL BE RAISED TO TWO OR THREE TIMES THE HEIGHT NECESSARY FOR TRUNNION FRICTION TO BE OVERCOME, H1 (TYPICALLY 6"-12"), AND HELD THERE UNTIL DATA STABILIZES.
- THE GATE SHALL BE LOWERED APPROXIMATELY TWICE THE DISTANCE TO OVERCOME TRUNNION FRICTION, H2, AND HELD THERE UNTIL DATA STABILIZES.
- THE GATE SHALL BE RAISED TO H1 AND HELD THERE UNTIL DATA STABILIZES.
- THE GATE SHALL BE LOWERED TO H2 AND HELD THERE UNTIL DATA STABILIZES.
- THE GATE SHALL BE RAISED TO H1 AND HELD THERE UNTIL DATA STABILIZES.
- THE GATE WAS LOWERED BACK TO CLOSED POSITION AND DATA COLLECTION STOPPED.
- A MINIMUM OF 3 TESTS SHALL BE PERFORMED PER GATE.

GAGE COUNT PER GATE

SENSOR LEGEND	SENSOR COUNT	CHANNEL COUNT
STRAIN TRANSDUCER	(48)	(48)
TILTMETER (UNI-AXIAL)	(4)	(4)
TORQUE SENSOR	(4)	(4)
AMP SENSOR	(3)	(3)
TOTAL	(59)	(59)

LOCATION KEY

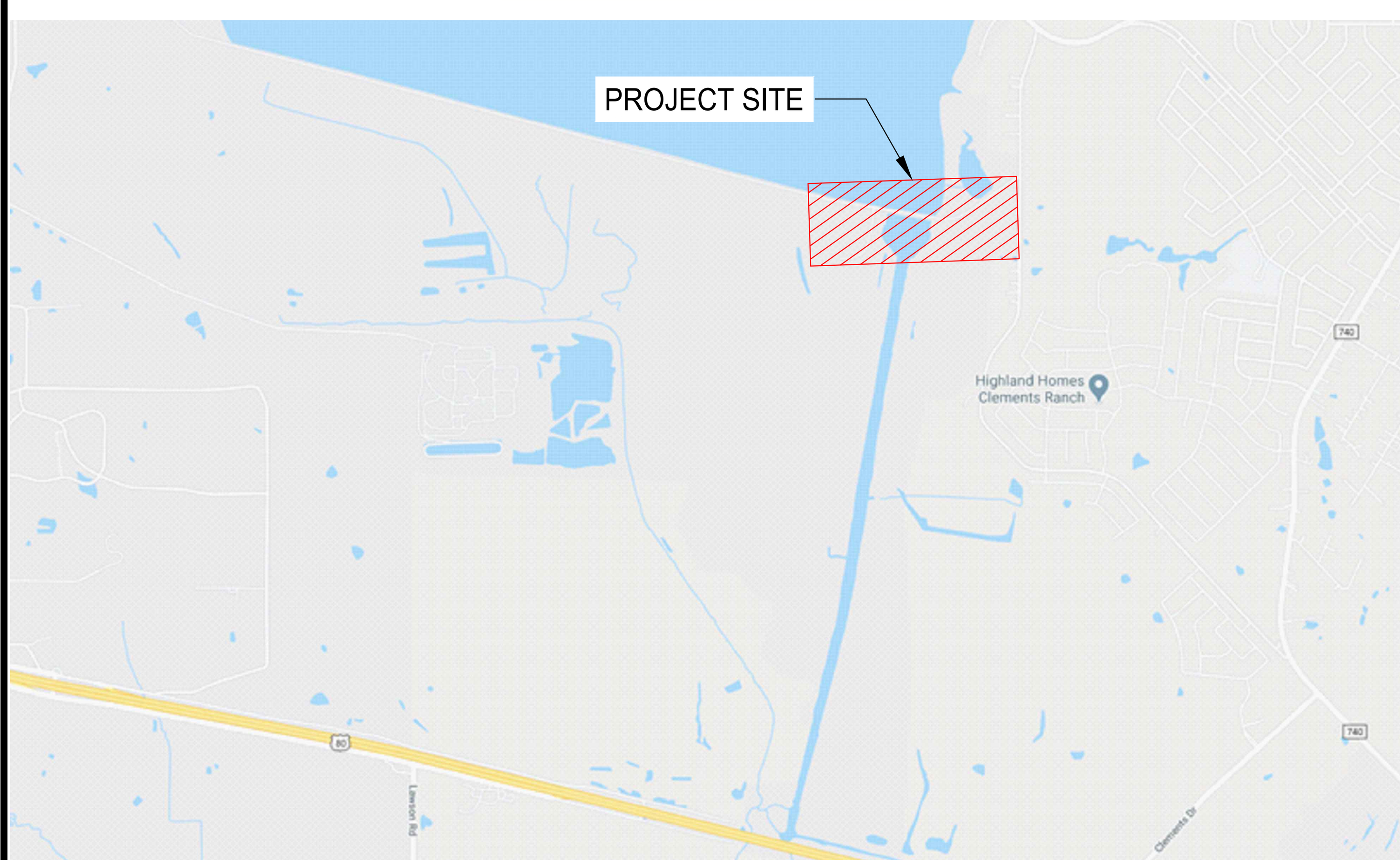

INDEX OF SHEETS

INDEX OF ISSUE

NO.	DATE	REVISION DESCRIPTION
1	3/20/2020	LIVE LOAD TESTING (LLT) INSTRUMENTATION PLAN (FOR APPROVAL)
2	5/27/2020	LIVE LOAD TESTING (LLT) INSTRUMENTATION PLAN AS BUILTS

BDI REFERENCE NUMBER: 190701-TX

BDI
RAW DATA. REFINED RESULTS.
740 S PIERCE AVE, SUITE 15
LOUISVILLE, CO 80027
303.494.3230
WWW.BDITEST.COM

ISSUE

CLIENT

SCHABEL ENGINEERING
16000 CHRISTENSEN RD, STE 101
SEATTLE, WA 98188

PROJECT NAME

SCHNABEL ENGINEERING
ROCKWALL FORNEY DAM
LIVE LOAD TESTING

Drawn By:	KNR
Checked By:	JDS
Date:	05/27/2020
Client No.:	
BDI No.:	190701-TX
SCALE:	NTS

OVERALL LEGEND

LLT-01

PLOT TIME: 6/12/2020 3:22 PM
FILEPATH: C:\Users\colemand\BDI\Services - Documents\Server_Remote\190701-TX_Schnabel_RockwallForneyDam\7. Instrumentation Plans\BDI_ROCKWALLFORNEY_01_GENERAL.dwg
© YYYY BRIDGE DIAGNOSTICS INC.

The user acknowledges that these documents are instruments of professional service, and are protected by Copyright. This document and the information contained in this document are the property of Bridge Diagnostics, Inc., and shall not be reused, copied, disseminated, modified, amended or altered in any way. It is issued for information purposes only. The user agrees to hold harmless, indemnify and defend Bridge Diagnostics, Inc. against any and all damages, claims and losses, including defense costs, arising out of any use, reuse or copying of this document.

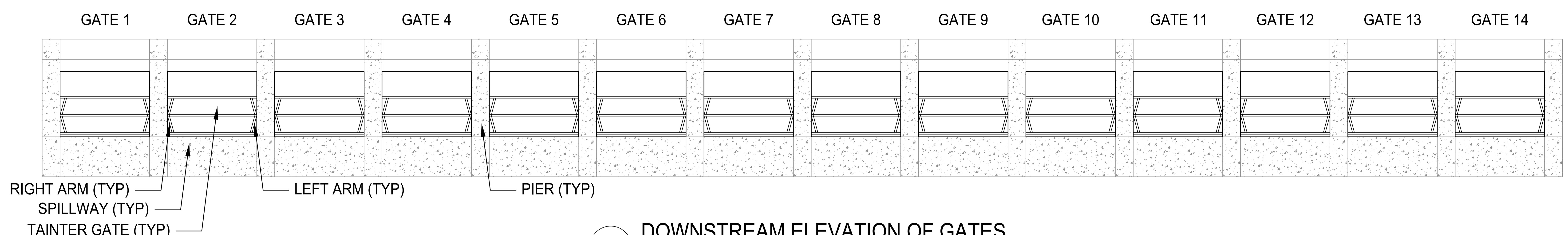

1 DOWNSTREAM ELEVATION OF GATES
LOOKING NORTH (UPSTREAM)

BDI
RAW DATA. REFINED RESULTS.
740 S PIERCE AVE, SUITE 15
LOUISVILLE, CO 80027
303.494.3230
WWW.BDITEST.COM

ISSUE

CLIENT

SCHABEL ENGINEERING
16000 CHRISTENSEN RD, STE 101
SEATTLE, WA 98188

PROJECT NAME

SCHNABEL ENGINEERING
ROCKWALL FORNEY DAM
LIVE LOAD TESTING

Drawn By:	KNR
Checked By:	JDS
Date:	05/27/2020
Client No.:	
BDI No.:	190701-TX
SCALE:	NTS

OVERALL STRUCTURE LAYOUT

LLT-02

PLOT TIME: 6/12/2020 3:22 PM
FILEPATH: C:\Users\colemand\BDI\Services - Documents\Server_Remote\190701-TX_Schnabel_RockwallForneyDam\7. Instrumentation Plans\BDI_ROCKWALLFORNEY_01_GENERAL.dwg
© YYYY BRIDGE DIAGNOSTICS INC.

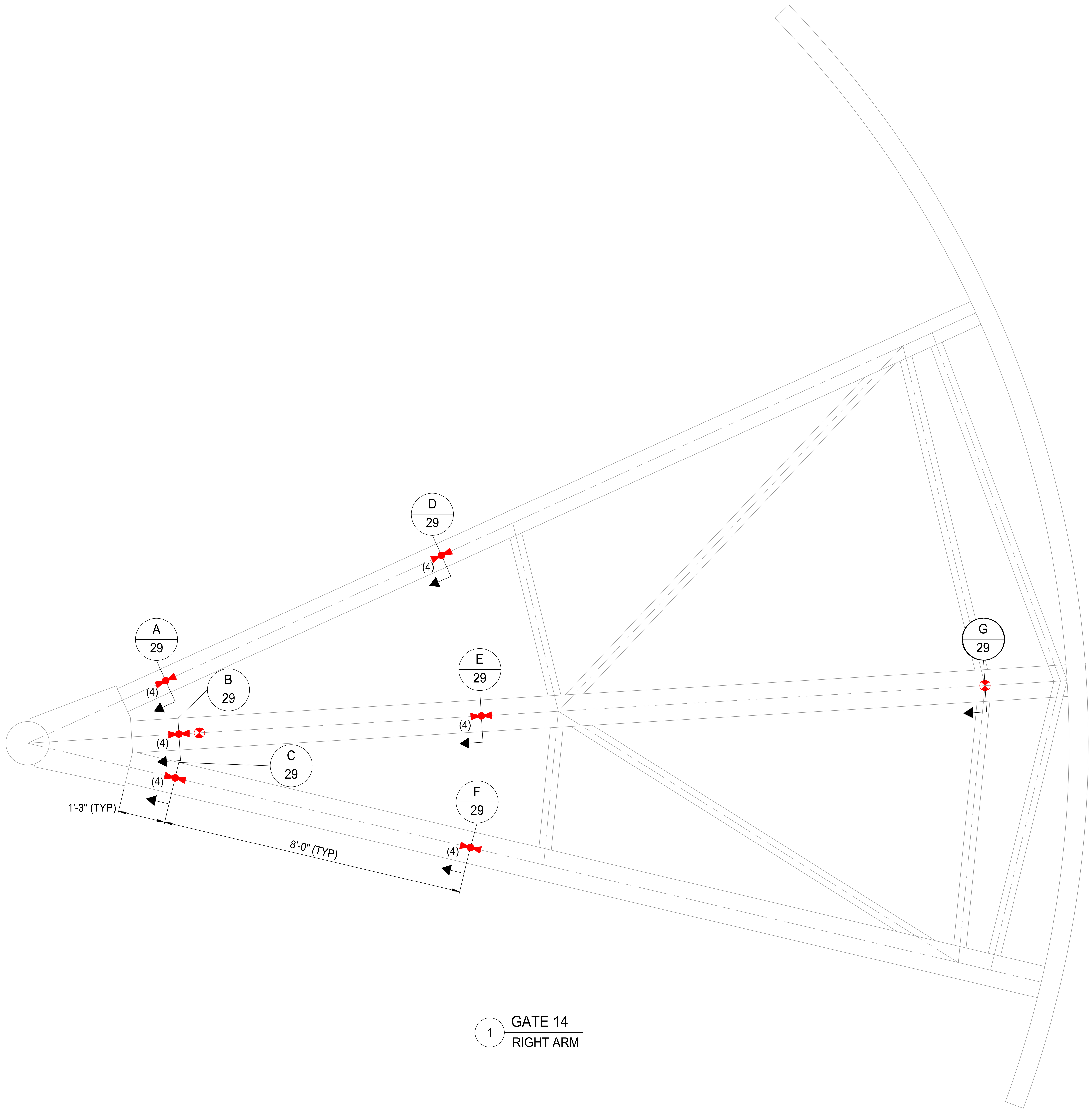

1 GATE 14
RIGHT ARM

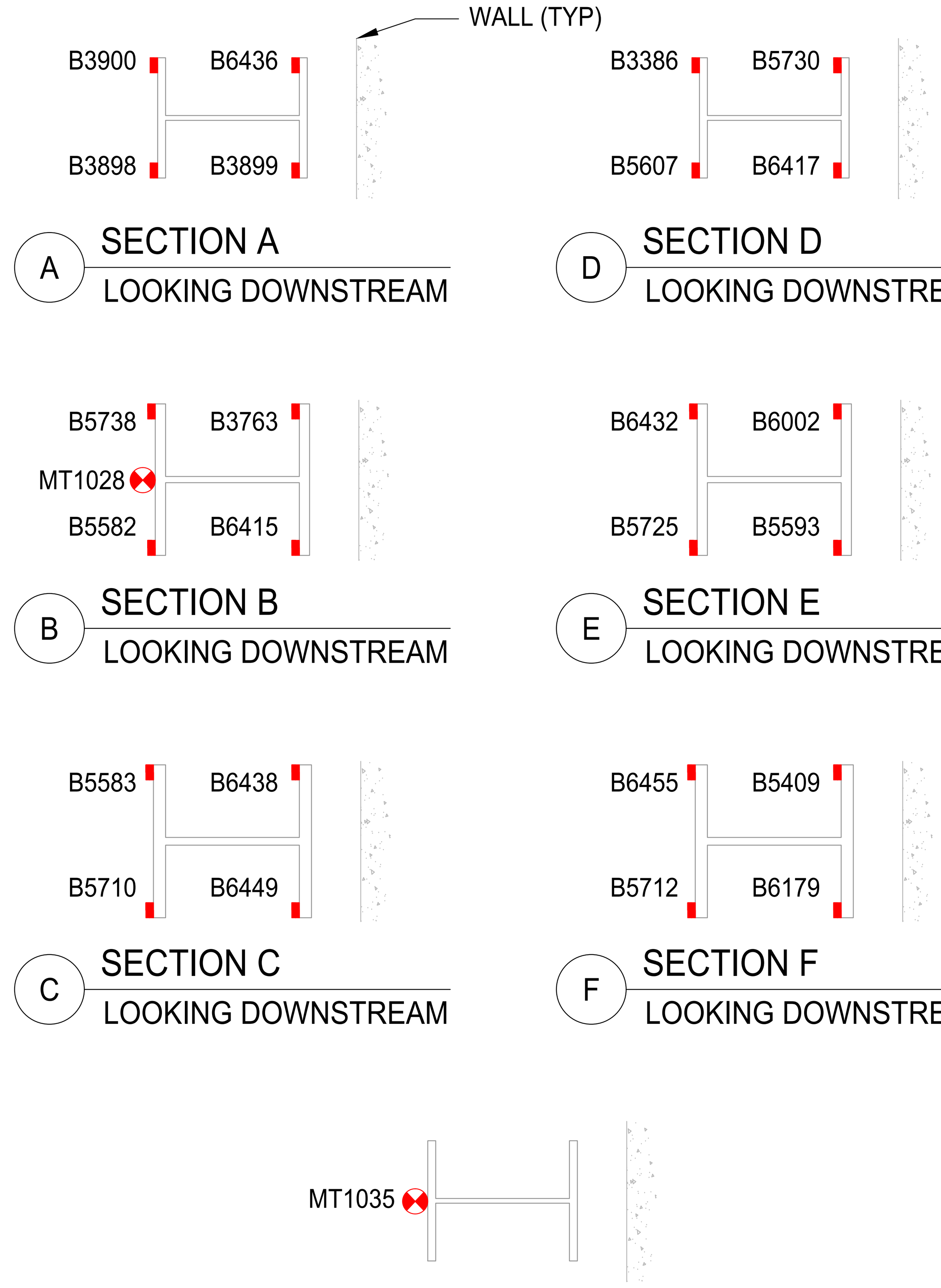

A SECTION A
LOOKING DOWNSTREAM

D SECTION D
LOOKING DOWNSTREAM

B SECTION B
LOOKING DOWNSTREAM

E SECTION E
LOOKING DOWNSTREAM

C SECTION C
LOOKING DOWNSTREAM

F SECTION F
LOOKING DOWNSTREAM

G SECTION G
LOOKING DOWNSTREAM

UNIT ID
TT-3

TORQUE GAGES
RIGHT ARM

NOTES:
1. SECTIONS A, B, & C SHALL BE INSTALLED 15 INCHES AWAY FROM TRUNNION PLATE.
2. TILTMETERS SHALL BE INSTALLED CENTERED ON THE MIDDLE STRUT FLANGE.
3. SECTION G'S TILTMETER SHALL BE INSTALLED AS CLOSE TO THE SKINPLATE AS POSSIBLE.

SENSOR LEGEND
- STRAIN TRANSDUCER
- TILTMETER (UNI-AXIAL)
- TORQUE SENSOR

BDI
RAW DATA. REFINED RESULTS.
740 S PIERCE AVE, SUITE 15
LOUISVILLE, CO 80027
303.494.3230
WWW.BDITEST.COM

ISSUE

CLIENT
SCHABEL ENGINEERING
16000 CHRISTENSEN RD, STE 101
SEATTLE, WA 98188

PROJECT NAME
SCHABEL ENGINEERING
ROCKWALL FORNEY DAM
LIVE LOAD TESTING

Drawn By:	KNR
Checked By:	JDS
Date:	05/27/2020
Client No.:	
BDI No.:	190701-TX
SCALE:	NTS

GATE 14 - RIGHT ARM
ELEVATION
LLT-29

The user acknowledges that these documents are instruments of professional service, and are protected by Copyright. This document and the information contained in this document are the property of Bridge Diagnostics, Inc., and shall not be reused, copied, disseminated, modified, amended or altered in any way. It is issued for information purposes only. The user agrees to hold harmless, indemnify and defend Bridge Diagnostics, Inc. against any and all damages, claims and losses, including defense costs, arising out of any use, reuse or copying of this document.

PLOT TIME: 6/12/2020 3:24 PM
FILEPATH: C:\Users\colemand\BDI\Services - Documents\Server_Remote\190701-TX_Schabel_RockwallForneyDam\7. Instrumentation Plans\BDI_ROCKWALLFORNEY_01_GENERAL.dwg
© YYYY BRIDGE DIAGNOSTICS INC.

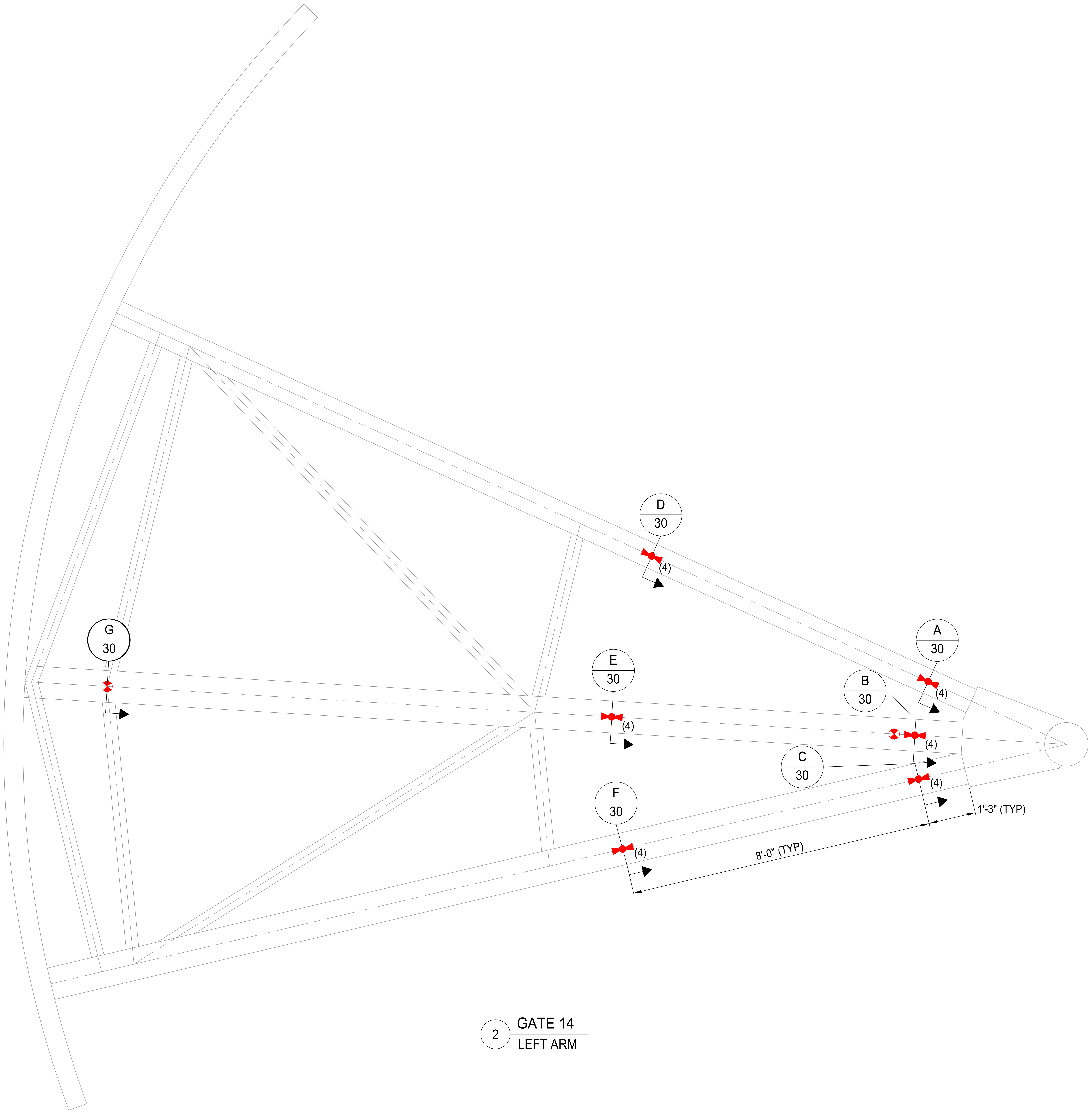

2 GATE 14
LEFT ARM

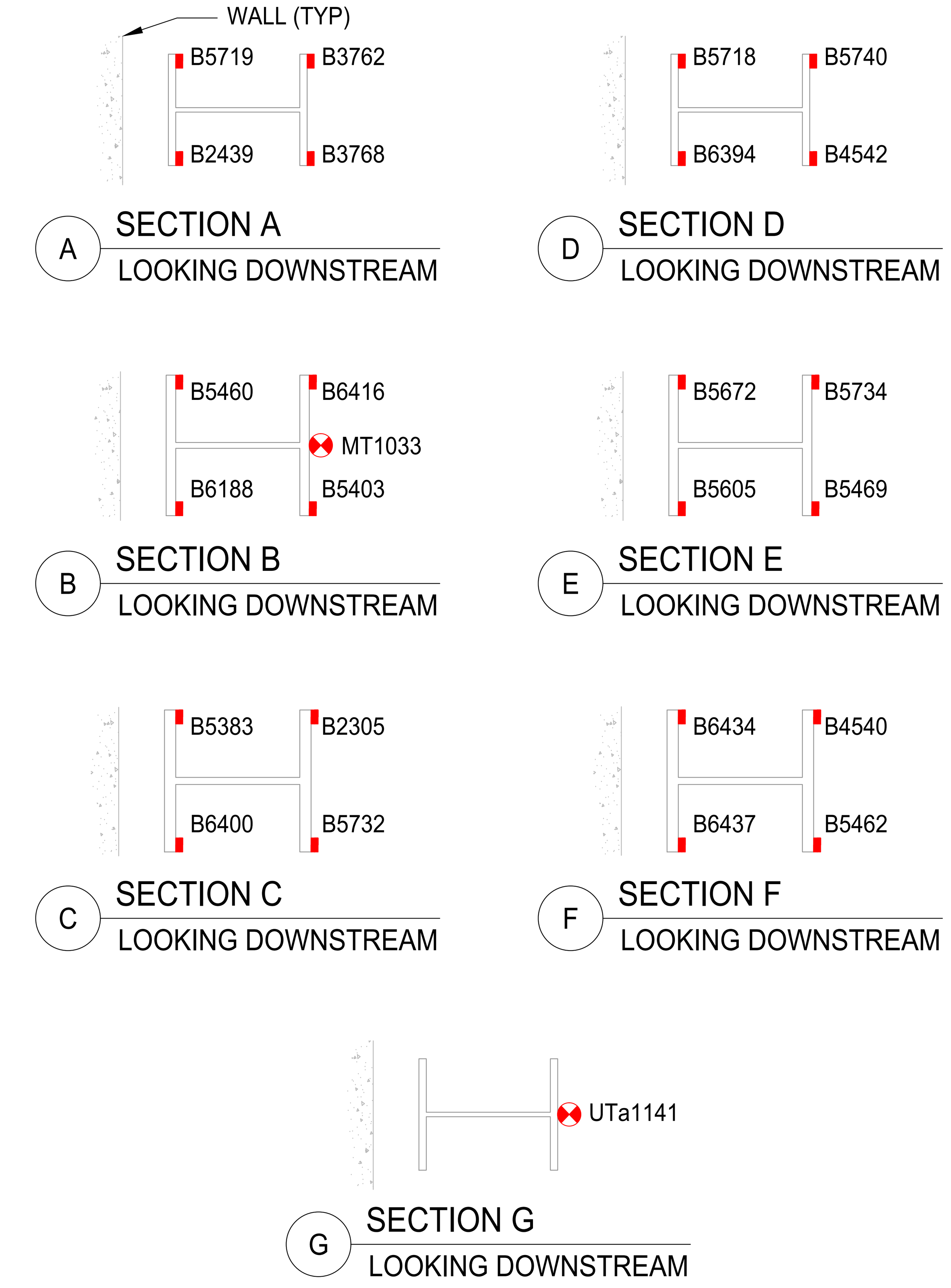

UNIT ID
TT-4

TORQUE GAGES
LEFT ARM

NOTES:

1. SECTIONS A, B, & C SHALL BE INSTALLED 15 INCHES AWAY FROM TRUNNION PLATE.
2. TILTMETERS SHALL BE INSTALLED CENTERED ON THE MIDDLE STRUT FLANGE.
3. SECTION G'S TILTMETER SHALL BE INSTALLED AS CLOSE TO THE SKINPLATE AS POSSIBLE.

SENSOR LEGEND

- STRAIN TRANSDUCER
- TILTMETER (UNI-AXIAL)
- TORQUE SENSOR

BDI
RAW DATA. REFINED RESULTS.
740 S PIERCE AVE, SUITE 15
LOUISVILLE, CO 80027
303.494.3230
WWW.BDITEST.COM

ISSUE

CLIENT

SCHABEL ENGINEERING
16000 CHRISTENSEN RD, STE 101
SEATTLE, WA 98188

PROJECT NAME

SCHABEL ENGINEERING
ROCKWALL FORNEY DAM
LIVE LOAD TESTING

Drawn By:	KNR
Checked By:	JDS
Date:	05/27/2020
Client No.:	
BDI No.:	190701-TX
SCALE:	NTS

GATE 14 - LEFT ARM
ELEVATION

LLT-30

The user acknowledges that these documents are instruments of professional service, and are protected by Copyright. This document and the information contained in this document are the property of Bridge Diagnostics, Inc., and shall not be reused, copied, disseminated, modified, amended or altered in any way. It is issued for information purposes only. The user agrees to hold harmless, indemnify and defend Bridge Diagnostics, Inc. against any and all damages, claims and losses, including defense costs, arising out of any use, reuse or copying of this document.

PLOT TIME: 6/12/2020 3:24 PM
FILEPATH: C:\Users\colemand\BDI\Services - Documents\Server_Remote\190701-TX_Schabel_RockwallForneyDam\7. Instrumentation Plans\BDI_ROCKWALLFORNEY_01_GENERAL.dwg
© YYYY BRIDGE DIAGNOSTICS INC.

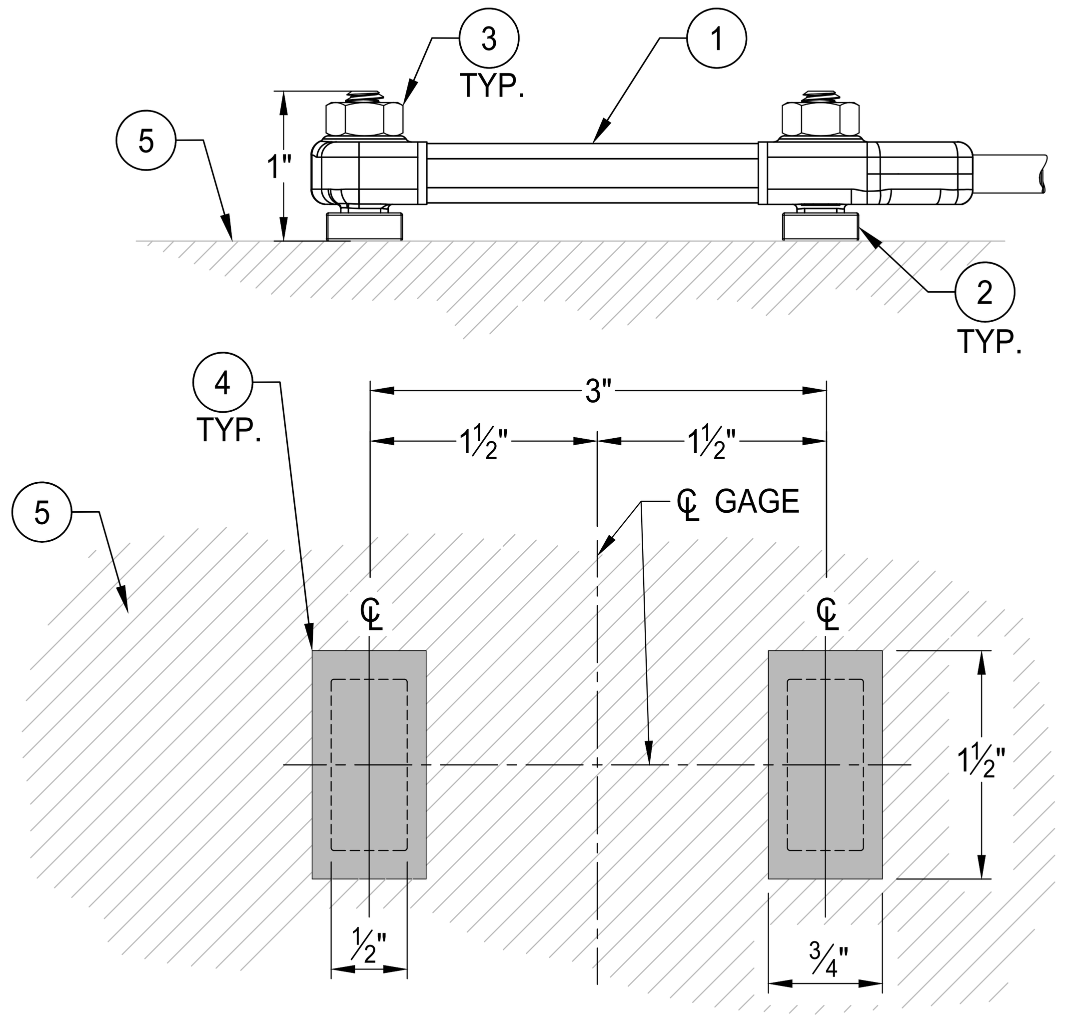

COMPONENT DESCRIPTION

1. ST350 STRAIN GAGE
2. 1/4"-20 THREADED MOUNTING TAB
3. 1/4"-20 STAINLESS STEEL NUT
4. TYPICAL SURFACE PREP REQUIRED TO MOUNT STRAIN GAGES
5. TYPICAL MOUNTING SURFACE

FOOTNOTES - INSTANT ADHESIVE
1. STRAIN GAGES SHALL BE MOUNTED WITH LOCTITE 410 INSTANT ADHESIVE AND LOCTITE 7452 ACCELERANT 2. DURING SURFACE PREP ALL PAINT AND SURFACE DEFORMATIONS MUST BE REMOVED. 3. SURFACE PREP IS REQUIRED JUST PRIOR TO GAGE INSTALLATION AS TO NOT ALLOW SURFACE CONTAMINANTS TO ACCUMULATE.

1 TYPICAL ST350 STRAIN GAGE INSTALLATION

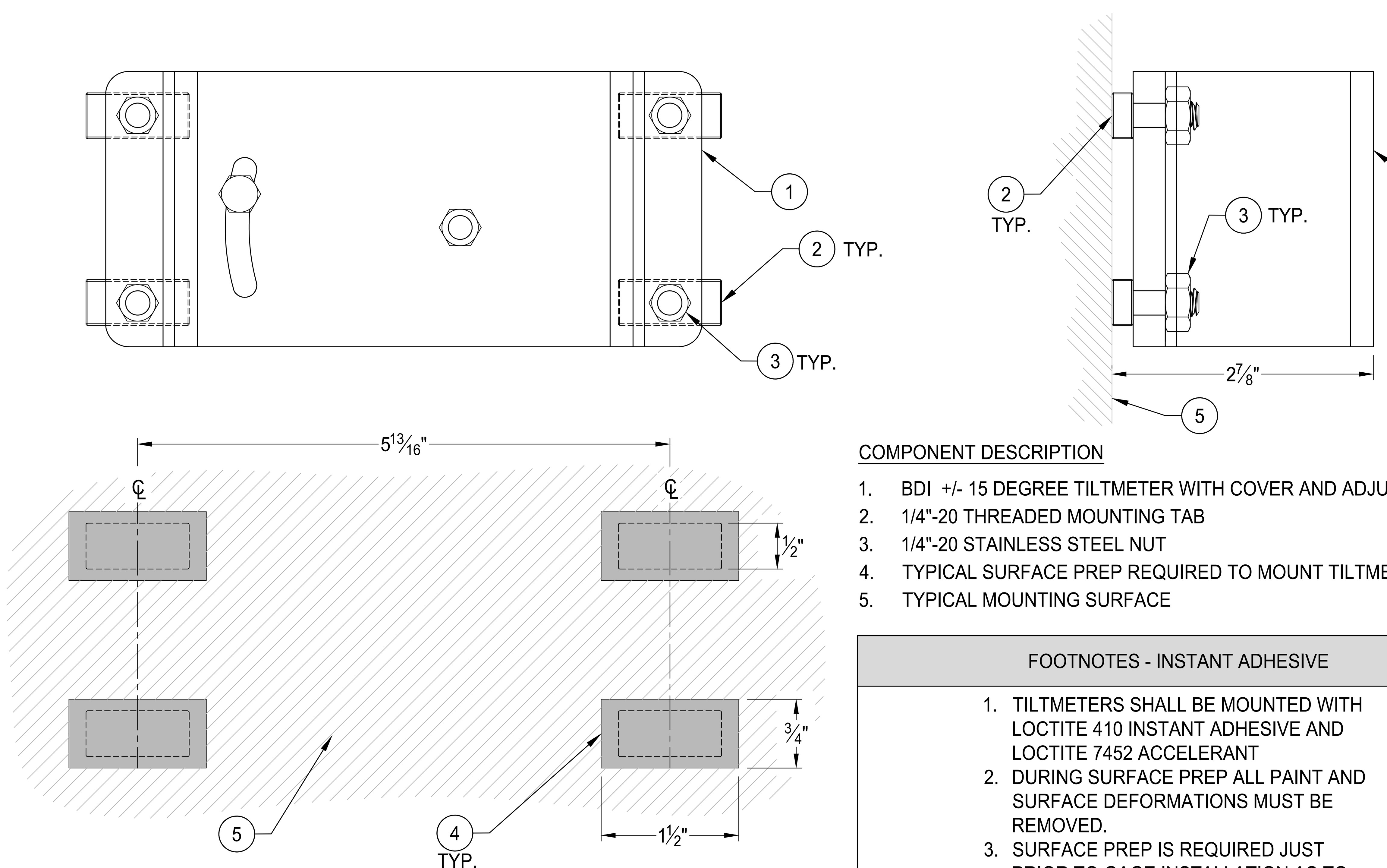

COMPONENT DESCRIPTION

1. BDI +/- 15 DEGREE TILTMETER WITH COVER AND ADJUSTMENT BOLTS
2. 1/4"-20 THREADED MOUNTING TAB
3. 1/4"-20 STAINLESS STEEL NUT
4. TYPICAL SURFACE PREP REQUIRED TO MOUNT TILTMETERS
5. TYPICAL MOUNTING SURFACE

FOOTNOTES - INSTANT ADHESIVE
1. TILTMETERS SHALL BE MOUNTED WITH LOCTITE 410 INSTANT ADHESIVE AND LOCTITE 7452 ACCELERANT 2. DURING SURFACE PREP ALL PAINT AND SURFACE DEFORMATIONS MUST BE REMOVED. 3. SURFACE PREP IS REQUIRED JUST PRIOR TO GAGE INSTALLATION AS TO NOT ALLOW SURFACE CONTAMINANTS TO ACCUMULATE.

2 TYPICAL BDI TILTMETER INSTALLATION

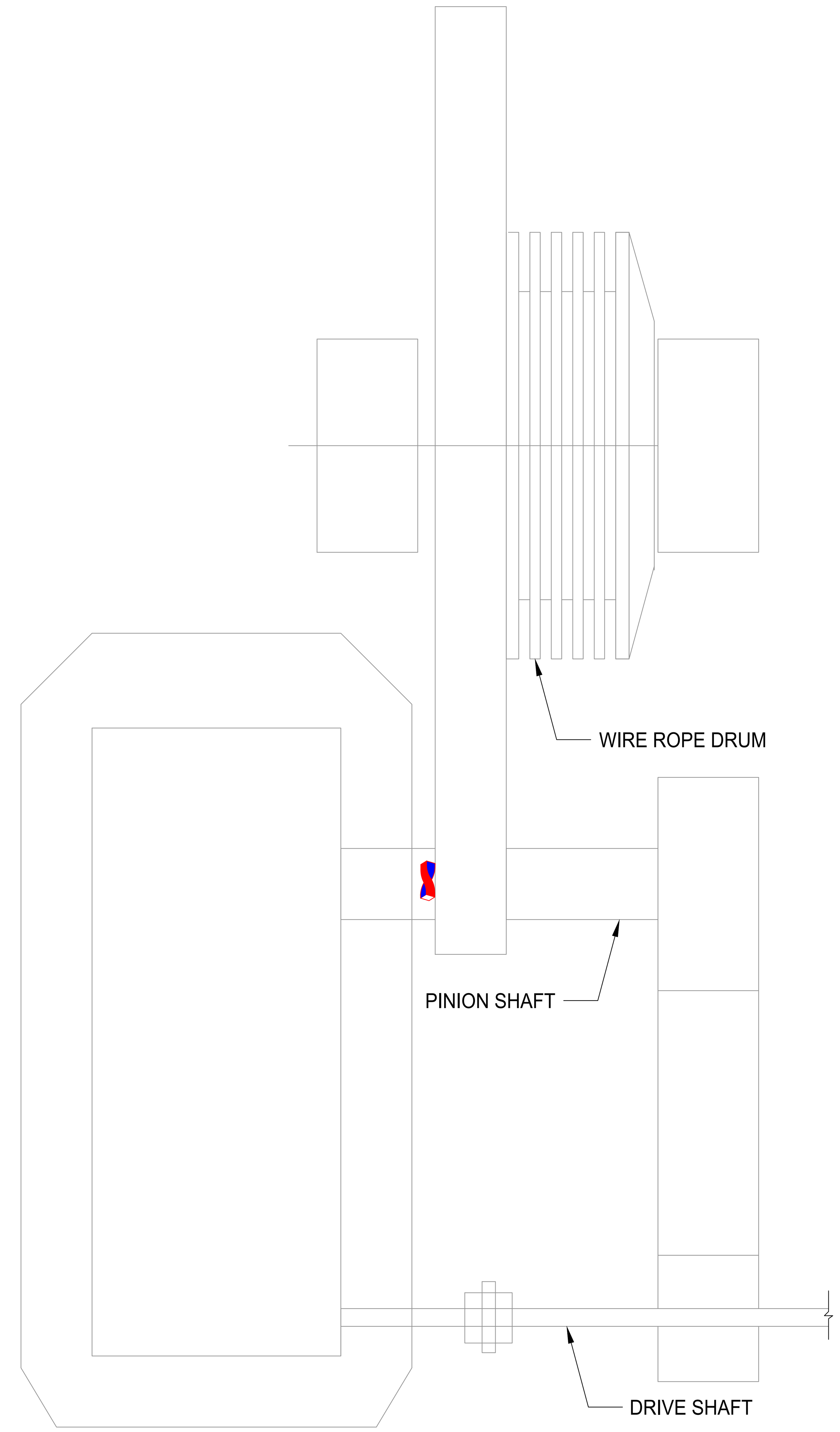

3 TYPICAL HOIST INSTRUMENTATION

TORQUE SENSOR INSTALLATION NOTES:

- TORQUE GAGES WILL BE INSTALLED ON THE PINION SHAFT ON EITHER HOIST MOTOR BETWEEN THE MOTOR AND THE HOIST DRUM
- EXACT POSITIONS OF THE GAGE PAIRS ON THE PINION SHAFT WILL BE DETERMINED IN THE FIELD

SENSOR LEGEND

TORQUE SENSOR

BDI
RAW DATA. REFINED RESULTS.
740 S PIERCE AVE, SUITE 15
LOUISVILLE, CO 80027
303.494.3230
WWW.BDITEST.COM

ISSUE

CLIENT

SCHABEL ENGINEERING
16000 CHRISTENSEN RD, STE 101
SEATTLE, WA 98188

PROJECT NAME

SCHNABEL ENGINEERING
ROCKWALL FORNEY DAM
LIVE LOAD TESTING

Drawn By:	KNR
Checked By:	JDS
Date:	05/27/2020
Client No.:	
BDI No.:	190701-TX
SCALE:	NTS

SENSOR INSTALLATION DETAILS

LLT-31

The user acknowledges that these documents are instruments of professional service, and are protected by Copyright. This document and the information contained in this document are the property of Bridge Diagnostics, Inc., and shall not be reused, copied, disseminated, modified, amended or altered in any way. It is issued for information purposes only. The user agrees to hold harmless, indemnify and defend Bridge Diagnostics, Inc. against any and all damages, claims and losses, including defense costs, arising out of any use, reuse or copying of this document.

PLOT TIME: 6/12/2020 3:24 PM
FILEPATH: C:\Users\colemand\BDI\Services - Documents\Server_Remote\190701-TX_Schnabel_RockwallForneyDam\7. Instrumentation Plans\BDI_ROCKWALLFORNEY_01_GENERAL.dwg

© YYYY BRIDGE DIAGNOSTICS INC.

APPENDIX F

FLOOD OPERATION PROCEDURES EVALUATION

Review of Flood Operation Procedures, Rockwall-Forney Dam

©2021 All Rights Reserved

Schnabel ENGINEERING

T 770.781.8008 / F 770.781.8003
6445 Shiloh Road, Suite A / Alpharetta, GA 30005 schnabel-eng.com

July 26, 2021

Randall G. McIntyre, PE
Vice President
Garver, LLC
14160 N. Dallas Parkway, Suite 850
Dallas, TX 75254

Subject: **Review of Flood Operation Procedures, Rockwall-Forney Dam, Dallas/Kaufman Counties, Texas (Schnabel Reference 20C22001.00)**

Dear Mr. McIntyre:

SCHNABEL ENGINEERING, LLC (Schnabel) has completed the review of current flood operation procedures for Lake Ray Hubbard and the Rockwall-Forney Dam (Forney Dam). This letter discusses our understanding of current procedures, describes the evaluation performed by Schnabel, outlines the observations and opinions reached based upon the evaluation, and presents recommendations for future work.

1974 OPERATION AND MAINTENANCE MANUAL REVIEW

The general plan for reservoir and flood release operations is contained in the original Operations and Maintenance (O&M) Manual for the Forney Dam and Reservoir dated 1974. In the manual, the five (5) basic policy concepts outlined which affect the operation of the reservoir, in order of priority, are as follows:

1. The reservoir storage must be regulated such that the dam and spillway will not be subjected to a more critical loading condition than that for which they were designed.
2. The reservoir must be operated in accordance with the original permit issued by the Texas Water Rights Commission.
3. The reservoir should be operated with the most cost-effective utilization of the storage capabilities, subject to policies and requirements.
4. The operation of the reservoir should not subject downstream areas to greater floods than would have occurred without the project.
5. To the extent feasible, the reservoir should be regulated to minimize the downstream flood damage, bearing in mind that premature releases or unduly prolonged releases may be a basis for damages.

As indicated in the O&M Manual, the key factor in normal operations is the water surface elevation. When the water surface is at elevation 434.5 feet or lower, the objective of reservoir operations personnel will be to generally store water as it becomes available, either through uncontrolled runoff or releases from the upstream Lake Lavon, and in keeping with the terms of the Texas Water Rights Commission permit. Under this policy, elevation 435.5 feet is the maximum storage level authorized. The O&M Manual further indicates that adjustments of low-flow gate openings will most frequently be between elevation ranges of 434.5 feet to 435.5 feet, while at the same time the Texas Water Rights Commission has authority to order releases from Lake Ray Hubbard to satisfy the rights of prior downstream appropriations.

The O&M Manual also contains information as to quantities of water which can be released with various gate settings. Under normal operating conditions, when the water surface elevation exceeds the specified target operating level, the water level must be lowered by opening one or more Tainter gates, or by the water intake through the raw water pump station in quantities as directed until the target level has again been reached. Under higher flow conditions, a reasonably accurate estimate of the reservoir inflow is necessary for the proper operation of the spillway gates. The O&M Manual indicates estimates of inflow are to be accomplished by communication with the U.S. Army Corps of Engineers (ACOE) regarding releases from Lake Lavon, as well as local inflow gauge readings and estimates of local inflow where gauge readings are not available. Close cooperation and coordination with the ACOE is necessary to obtain the most suitable water level of Lake Ray Hubbard such that the possibility of downstream damages are mitigated. Detailed gate operating procedures are included in the O&M Manual that includes appropriate gate settings for the various reservoir levels and estimated inflow conditions.

CURRENT OPERATING PROCEDURES

In 2005, a more detailed plan of operations for Lake Ray Hubbard was developed for use during flood operations. This plan considered more information that would be available in real-time and an increased number of significant factors since the more general operations provided for in the 1974 O&M plans. This plan included updated procedures for lake releases, a method for estimating lake inflows, the lake stage-elevation data, flood release settings, and gate closing procedures.

The procedures for establishing flood releases from Forney Dam require an evaluation of the hydrologic conditions throughout the course of a storm. Without prior authorization, the DWU reservoir supervisor is authorized to release up to 2,000 cubic feet per second (cfs). For releases between 2,001 to 5,000 cfs, coordination with the Reservoir Manager is required. Releases between 5,001 to 8,000 cfs require authorization from the Purification East Division Manager. Releases greater than 8,000 cfs require authorization from the Assistant Director of Water Operations. In the event that higher authority cannot be contacted for authorization, and the rising water levels could jeopardize the safety of Forney Dam, the reservoir supervisor should make the required release.

Once lake inflows have been reasonably estimated, the appropriate release rates are determined from the release tables in the 2005 operating procedures. Gate settings to achieve the desired release must consider the physical aspects of the gates and structures. At the conservation pool elevation of 435.5 feet, there is two feet of freeboard to the top the gates. As the lake level rises, freeboard is reduced unless the gates are raised. The operating procedures stipulate that freeboard should not be allowed to become less than one foot on any of the gates; thus, all of the gates must be raised by the time the lake rises to elevation 436.5 feet. During large storms, the release procedures are designed to allow for lake levels to rise. Small releases can be made using one or more of the 14 Tainter gates.

Once the maximum release has been reached during a storm event, that release is maintained until the lake level has begun to drop. Once the lake level begins to drop, the releases are decreased to 80% of the previous release and continued until the release reaches 5,000 cfs. A release of 5,000 cfs is maintained until the lake reaches normal pool elevation of 435.5 feet, and the gates are closed. If Lake Lavon has flood water stored, Lake Ray Hubbard should be returned to its normal operating level as quickly as possible. Once Lake Ray Hubbard reaches the normal operating elevation of 435.5 feet, the ACOE will begin to release water from Lake Lavon into Lake Ray Hubbard. That release is passed through Hubbard without regulation.

In the event Lake Lavon runs out of flood storage, the ACOE operation is very similar to that at Lake Ray Hubbard. In 1990, large amounts of runoff required the release of 54,000 cfs from Lake Lavon into Lake Ray Hubbard after the flood pool had filled. The release was passed through Lake Ray Hubbard without any regulation.

KEY ELEMENTS OF CURRENT OPERATIONS

As previously described, numerous measurements are taken into account for estimating inflows to Lake Ray Hubbard, as well as coordinated efforts with the ACOE in their operation of Lake Lavon. The key measurements involve USGS stream gauge data, rainfall amounts and intensity measurements throughout the watershed, stillwell water level measurements at the dam, and wind direction and velocity also measured at the dam. All of these components are required to make a reasonable estimate of inflows to the lake such that the five basic policies are adhered to for the dam and lake operations outlined in the O&M manual. These key items are discussed in the following sections.

Lake Inflow Calculations

A critical aspect of establishing the required flood release is the determination of lake inflows. In general, a reasonable estimate of inflow can normally be based on the change in lake storage over time together with reservoir releases over the same period. The 2005 operating procedures recommend that inflows be calculated based on changes in lake storage over a two hour period to account for wind effects. A continuous calculation of inflows based on lake storage is recommended throughout the course of a storm event to reduce the potential error induced by lake stage measuring inaccuracies. During periods of high rainfall, the 2005 operating procedures recommend calculations be made for each fifteen-minute interval.

In addition, the United States Geological Survey (USGS) stream gauge on Rowlett Creek at U.S. Highway 78 is a critical tool for estimating inflows. This gauge measures discharges from about 40 percent of the uncontrolled watershed of Lake Ray Hubbard downstream of Lake Lavon. During an area-wide storm event, one which rainfall is approximately uniform throughout the watershed, the 2005 operating procedures estimate the total inflow to the lake to be approximately 2.5 times the total flow at the Rowlett gauge. However, the time of travel from the gauge to the lake must be considered, and gauge discharges should not be used to estimate instantaneous inflows. In general, the Rowlett gauge can be utilized as an estimate of inflows over a period of several hours, as well as whether runoff has peaked.

Numerous other USGS stream gauges are located throughout region for measuring discharges and rainfall during a storm event. Included are four gauges that measure flows into Lake Lavon, a gauge immediately downstream from Lake Lavon measuring discharges into Lake Ray Hubbard, four gauges measuring local inflows to Lake Ray Hubbard, and three gauges downstream from Lake Ray Hubbard measuring discharges from Forney Dam, as well as runoff from the downstream area. Table 1 provides a summary of the USGS gauges within the basin.

Table 1 – USGS Stream Gauge Summary

USGS Gauge Number	Gauge Name	Approximate Basin Area (square miles)
Stream Gauges Above Lake Lavon Measuring Inflows to the Lake		
08059000	East Fork Trinity River near McKinney, TX	190
08059350	Indian Creek at SH 78 near Farmersville, TX	104
08059400	Sister Grove Creek near Blue Ridge, TX	83.1
08059590	Wilson Creek Downstream of Hwy 75 at McKinney, TX	51.1
Stream Gauges Below Lake Lavon Measuring Inflows to Lake Ray Hubbard		
08061000	East Fork Trinity River near Lavon, TX (Just Below Lake Lavon)	773
08061480	Squabble Creek at Shores Blvd near Rockwall, TX	6.70
08061540	Rowlett Creek near Sachse, TX	120
08061548	Muddy Creek at Creek Crossing Ln near Sachse, TX	28.3
Stream Gauges Downstream of Forney Dam		
08061551	East Fork Trinity River below Lake Ray Hubbard near Forney, TX	1,071
08061750	East Fork Trinity River near Forney, TX	1,118
08062000	East Fork Trinity River near Crandall, TX	1,256

Figure 1 shows the approximate Forney Dam watershed and the location of the USGS gauges within the basin.

Figure 1 – East Fork Trinity River USGS Gauge Locations

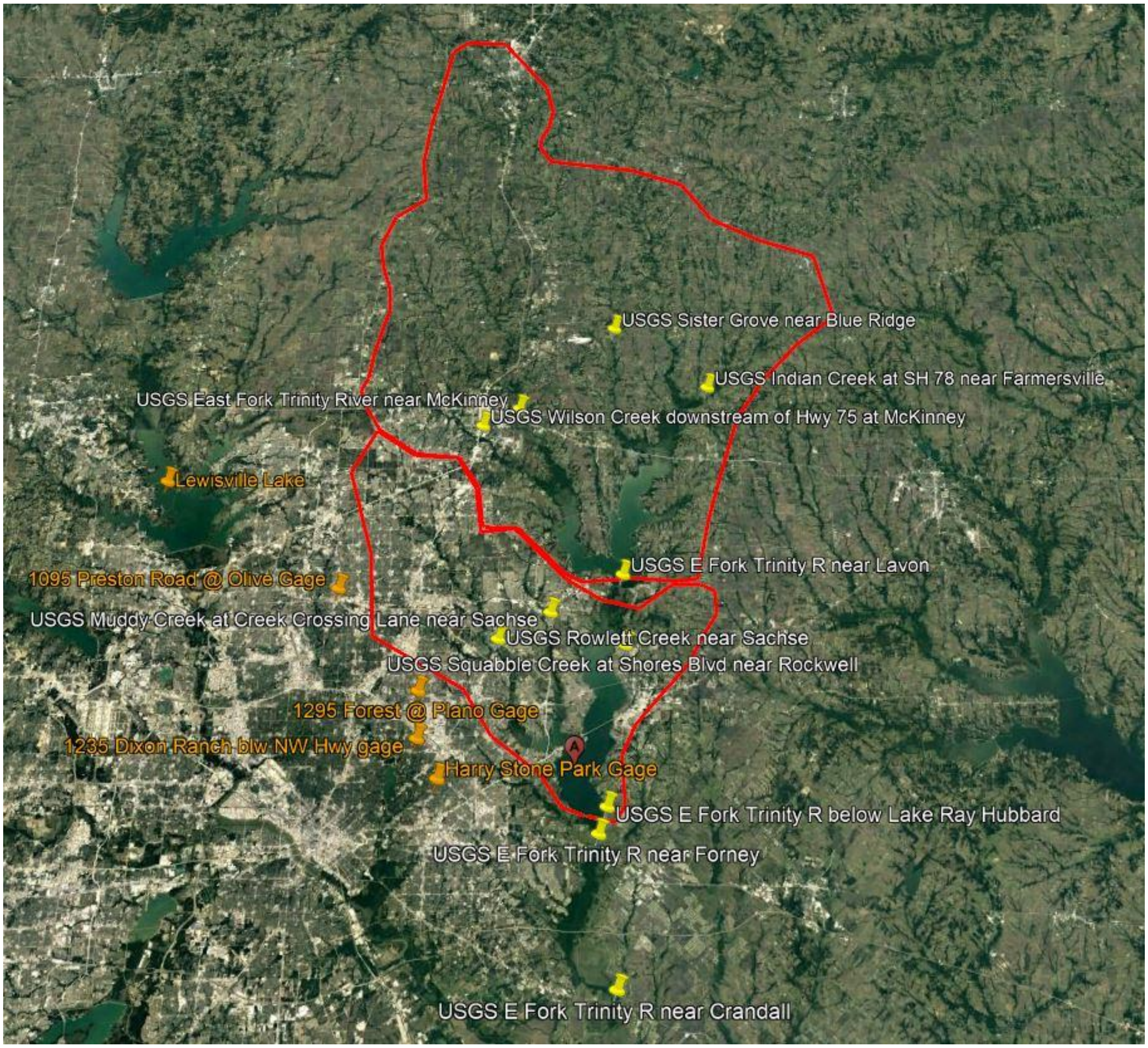

Gauges shown in orange on Figure 1 are part of the Hydrolynx network operated by the Trinity River Flood Control District, with several on the periphery of the Lake Ray Hubbard drainage basin.

Lake Ray Hubbard Water Elevation

Lake Ray Hubbard levels are normally obtained by use of supervisory control and data acquisition (SCADA) software, referred to as the Flood Alert System. The gauge at the control room in Forney Dam uses a float level and a pressure transducer to record the instantaneous water level every fifteen minutes. Data is transmitted to the base station computer at the east office.

Wind Velocity and Direction

The water level in the stillwell where the measurements are taken can fluctuate as the wind speed and direction change. Wind stack, a phenomenon where wind blows over the surface of the lake and the frictional force between the water and air pushes the water downwind, can result in a water level rise in the downwind end of the lake. The water level rises until the resisting gravitational force, equals the frictional force caused by the wind.

Often wind shifts associated with frontal passages accompany rainstorms. A wind shift from a southerly direction to a northerly direction can cause a large rise in the level gauge. According to the 2005 operating procedures, the apparent lake level can fluctuate by as much as 4 inches during high winds, resulting in inaccurate inflow calculations. Therefore, the establishment of a trend in lake levels is necessary to determine if a rise is actually occurring or is simply the result of wind-induced fluctuations. A weather station is located at Forney Dam for purposes of monitoring the wind speed and direction. This data is available to the operation center at the dam for use in the lake inflow calculations.

CURRENT STATUS OF OPERATIONS

Based on the existing documentation and procedures, the overall approach in operations is comprehensive and should provide reasonable responses to varying weather conditions, particularly during larger rain events. However, the operations are dependent on the ability to obtain all the required data in a timely manner. Based on discussions with DWU personnel, there are concerns about the timeliness of obtaining the data under current conditions.

Flood Alert System

The Flood Alert System was installed in the late 90’s in order to provide real-time data to DWU personnel for use in estimating inflows. Included in the system is the Rowlett Creek gauge and the Forney Dam gauge. Based on discussions with DWU personnel, the system has received relatively little maintenance or upgrades since installation. Although the Rowlett Creek gauge is currently operational, the equipment utilized to transmit the relevant flood data has been in place since the initial installation and has likely exceeded its life expectancy.

Although no formal plans have been made, additional rain gauge locations have been suggest by DWU personnel near Wylie, Texas, and the Camp Creek area immediately north of Rockwall, Texas. Wylie has been suggested as this is the approximate location of the Probable Maximum Flood (PMF) centroid where the highest rainfall intensity could occur. A Camp Creek gauge would be beneficial as rainfall from that area could be used to better assess appropriate gate discharge settings during rainfall events.

The existing gaging system is heavily weighted to the western side of the local drainage basin to Lake Ray Hubbard, particularly with the heavily weighted USGS Rowlett Creek stream gauge. Figure 2 depicts the basin and shows the Camp Creek area in relation to the overall basin. In localized rainfall conditions, whereby the rain falls disproportionally to the east or west side of the basin, current procedures for estimating inflows could result in less accurate estimates.

Figure 2

USGS Stream Gauges

As it measures flows from 120 square miles, or roughly 40% of the local drainage to Lake Ray Hubbard, the USGS gauge on Rowlett Creek has significant influence on estimated inflows to Lake Ray Hubbard. Historically, this gauge data has been transmitted to the Forney Dam operations center on a real-time basis for use in inflow estimates. Based on conversations with DWU personnel, a new electrical substation has resulted in the interference of the radio transmission signals, thus eliminating the collection of this real-time data.

Currently, the operations center staff must obtain Rowlett Creek stream flow data from the USGS website, which is updated hourly. As previously discussed, timely data is critical in developing inflow estimates, particularly given the significant portion of the local basin measure by this gauge. Under various storm conditions, flows can change very rapidly. This is emphasized in current operation procedures recommending estimates of inflows be computed as often as every 15 minutes during significant storm events.

Lake Ray Hubbard Water Elevation and Wind Data Instruments

A stillwell is provided toward the eastern side of the dam and provides real time water elevation data that is transmitted to the operations center via the Flood Alert System. Similarly, a weather station that provides wind speeds and direction is also located at the dam which transmits data to the operations center. The data from each instrument is provided on a real-time basis. As outlined in the current operation procedures, the measured water levels at the stillwell are adjusted based on wind conditions in an effort to obtain a more realistic overall lake elevation. Inherently, the resulting calculations of the overall lake elevation and corresponding inflows will always contain some degree of error. As such, a water level gauge farther north in the lake would be beneficial in establishing a lake level and thus provide a greater degree of confidence in the overall estimate of inflows.

CHANGES IN BASIN, OPERATIONS, OR DOWNSTREAM CONDITIONS

Basin Conditions

The hydrology for the dam, and the basis of the design, was initially performed and described in Design Memorandum No. 1 dated 1960. The design storm utilized has a duration of 60-hours and a rainfall depth of 24.8 inches over the entire 1,074 square mile drainage basin. An initial loss of 0.50 inches was assumed, as was an infiltration rate of 0.05 inches per hour thereafter. The associated volume of inflow over the period corresponded to 22.4 inches over the basin, or 1,287,250 acre-feet. Routing of the storm event resulted in a peak inflow of 445,000 cfs, a peak discharge of 375,000 cfs, and a peak flood elevation of 440.5 feet. Lake Lavon was completed in 1953 and was thus accounted for in the design of Forney Dam.

Although other hydrologic analyses have been performed in the past, the most recent hydrologic and hydraulic analysis of the PMF event was performed in May of 2014 in support of the development of an Emergency Action Plan (EAP). The results of that study indicated a peak inflow of approximately 395,000 cfs, a peak outflow of approximately 303,500 cfs, and a peak water surface elevation of 440.5 feet.

Based on discussions with DWU personnel, recent physical changes have occurred within the basin. A specific change is significant development near Rockwall, Texas on the northwest side of the lake since the late 1980’s, which was when the previous hydrology and hydraulics analysis was performed. This development results in a larger portion of impervious surface within the watershed, which causes the lake to rise more quickly than the previous flood release studies anticipated. DWU personnel indicate that annual releases of approximately 10,000 to 12,000 cfs have become commonplace in recent years, whereas releases of this amount were rare in previous decades.

Operational Conditions

The overall operation procedures are largely unchanged from those contained within the original O&M manual, with exceptions to updated procedures accounting for the use of the Flood Alert System and updated release tables based on new data obtained in 1989. Coordination with the ACOE regarding releases is made to the extent possible. Discharges from Lake Lavon are limited, when possible, or passed through Lake Ray Hubbard without attenuation. During flood events, DWU operations at Forney Dam do not include coordination with the other reservoirs within the Trinity River basin.

With respect to operation procedures, the release tables developed in 1989 are currently used and are based on the estimated elevation versus storage within Lake Ray Hubbard. The original stage-storage relationships were developed in 1968 as part of the design of Forney Dam. These stage-storage relationships were revised based on a volumetric survey in 1989 and again in May 2005. However, the revised stage-storage information only includes updated data obtained below the normal operating water surface, or elevation 435.5 feet. Stage-storage information above the normal operating level are based on the original 1968 design, which was developed using USGS topographic maps available at the time. Due to development which has taken place over the years, as well as the scale at which the USGS topographic maps are displayed, actual stage-storage information can vary significantly from the current data.

Downstream Conditions

Based on conversations with DWU personnel, significant damages to areas downstream of Forney Dam have occurred before levee improvement were made when East Fork Trinity River flows exceeded approximately 21,000 cfs. Currently, significant damages resulting from the overtopping of downstream levees are anticipated to occur when flows exceed approximately 28,000 cfs. No information regarding levee improvements was available for review.

In addition, DWU personnel indicated that other minor problems have developed over time as a result of higher release rates. For example, the Starr Turf farm, which is protected by a levee system, is located downstream on the west bank of the East Fork of the Trinity River immediately south of Highway 80. DWU personnel indicated that the turf farm drainage system, which discharges into the river, is not functional when Lake Ray Hubbard discharges exceed 3,000 cfs.

HISTORIC HYDROLOGIC DATA REVIEW

USGS Gauge Data and Flood Conditions

Discharges from Lake Lavon were recorded immediately downstream from the lake at the USGS gauge 08061000 near Lake Lavon Dam from 1954 through 1989, and resumed again in 2018. The USGS gauge 08061540 at Rowlett Creek has been recording peak flows since 1969. Peak flows have been recorded downstream from Lake Ray Hubbard since 1974 at the USGS gauge 08061551.

For the period of record described above for the USGS gauge immediately downstream of Lake Lavon, the largest recorded discharges occurred on May 26, 1957, with a peak flow of 39,000 cfs, and June 14, 1989, with a peak flow of 16,100 cfs. For the 51-year period of record for the USGS gauge at Rowlett Creek, the largest recorded flows have occurred more recently. The largest recorded discharges, in order of magnitude, occurred on September 22, 2018, with a peak flow of 57,600 cfs; May 29, 2015, with a peak flow of 47,900 cfs; November 27, 2015, with a flow of 36,200 cfs; and June 5, 1998 with a peak flow of 32,200 cfs.

As previously mentioned, the Rowlett Creek gauge represents about 40% of the Lake Ray Hubbard local drainage basin (i.e. downstream of Lake Lavon Dam), and current operation procedures estimate that inflows to Lake Ray Hubbard could be as high as 2.5 times the recorded flow at Rowlett Creek. Figure 3 depicts the recorded peak flows during the period of record for the Rowlett Creek gauge.

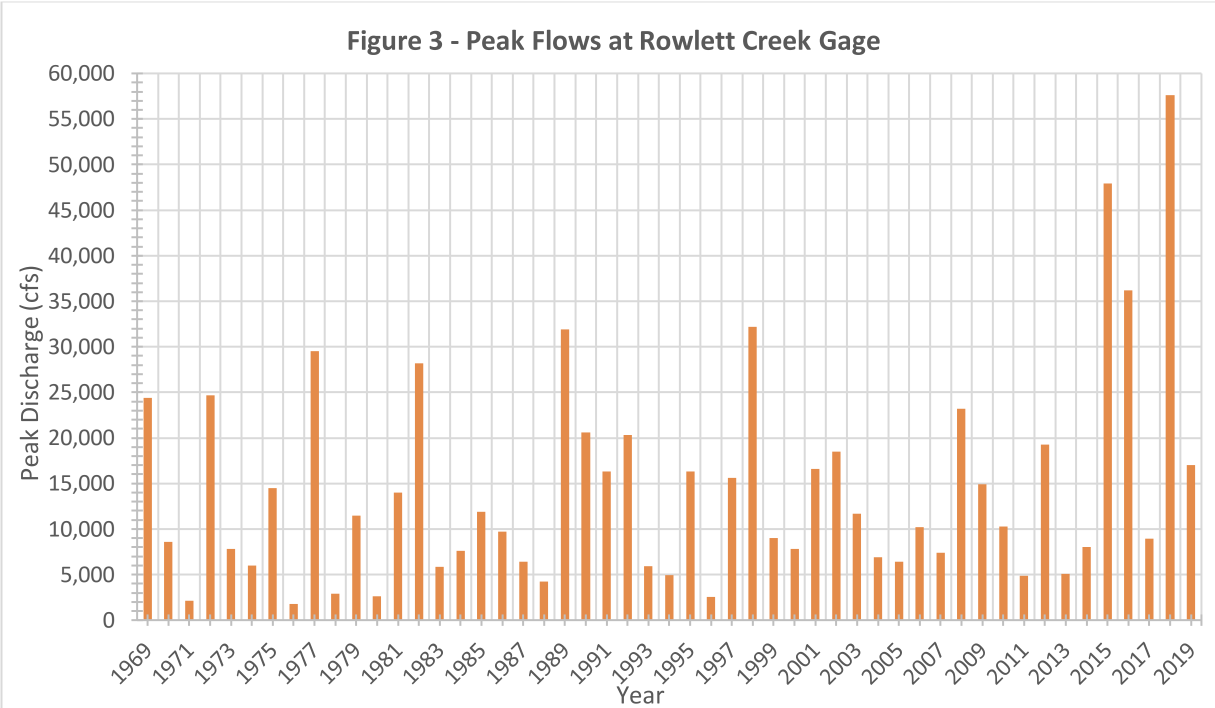

Figure 4 depicts the maximum, minimum, and mean daily discharges at the Rowlett Creek gauge over the 5-day period of September 20, 2018 through September 24, 2018, when the largest recorded flow occurred. The figure illustrates the wide variance between the maximum and minimum flows throughout the days, and further illustrates the importance of timely gauge information.

Figure 4 – Record Peak Flow at Rowlett Gauge in 2018

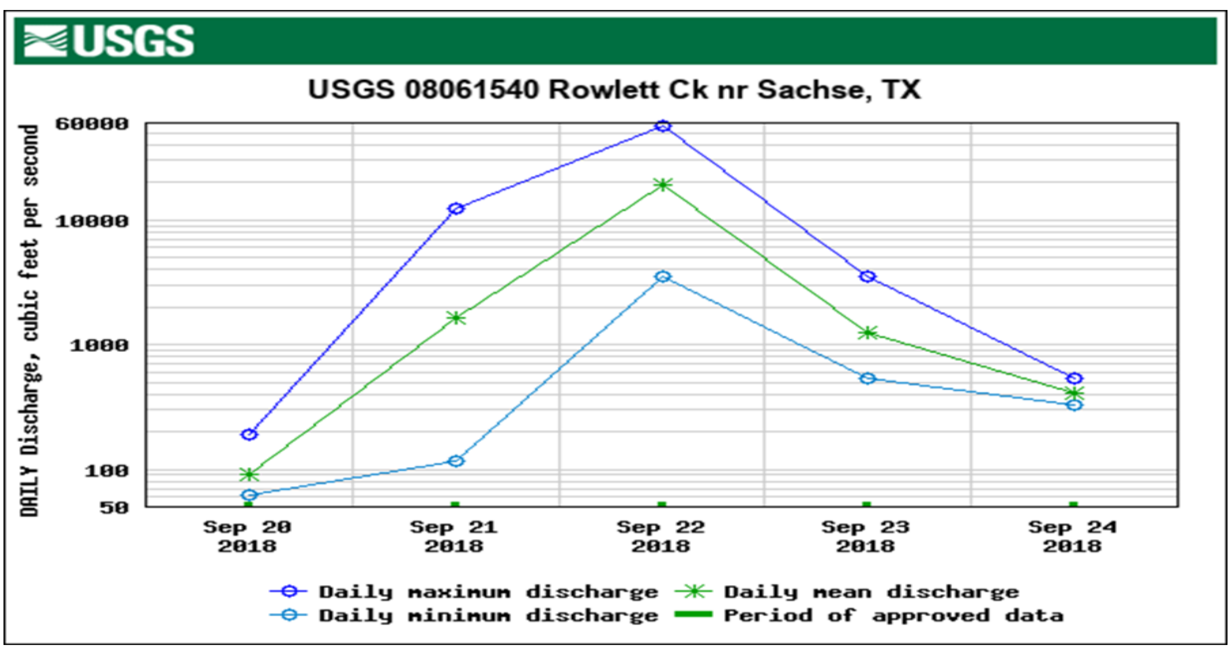

For the gauge immediately downstream of Lake Ray Hubbard, the largest recorded discharges, in order of magnitude, occurred on May 3, 1990, with a peak flow of 53,000 cfs; May 30, 2015, with a peak flow of 43,900 cfs; May 17 1989, with a peak flow of 42,700 cfs; April 13, 1991, with a peak flow of 38,200 cfs; and November 28, 2015, with a peak flow of 37,600 cfs. These flows represent discharges from Forney Dam plus any local inflows from the intervening area between Forney Dam and the gauge. Based on discussions with DWU personnel, these discharge amounts would result in damages to downstream areas.

DWU personnel specifically indicated two high flow periods in 1989 and 1991 where multiple flood releases from Lake Ray Hubbard were required. In May of 1989, releases of up to 54,000 cfs were made while in May of 1991, releases of up to 40,000 cfs were made. Table 2 provides a summary of peak flows during these two periods.

Table 2 – Recorded Peak Flows of 1989 and 1991

	USGS 08061000 East Fork Trinity near Lavon (Lavon Dam)		USGS 08061540 Rowlett Creek near Sachse		USGS 08061551 East Fork Trinity River near Forney (Forney Dam)	
Year	Date	Flow (cfs)	Date	Flow (cfs)	Date	Flow (cfs)
1989	Jun. 14, 1989	16,100	May 17, 1989	31,900	May 17 1989	42,700
1991	NA	NA	Apr. 12, 1991	16,300	Apr. 13, 1991	38,200

In May of 1989, the recorded discharges at the Rowlett Creek gauge indicate high local inflows to Lake Ray Hubbard, as well as similar corresponding discharges downstream of Forney Dam. Based on USGS data, the peak discharge from Lake Lavon Dam was nearly a month later, indicating the ACOE was able to control or limit discharges during the flood event to some extent.

In April of 1991, the USGS gauge downstream from Lake Lavon Dam was not in operation. However, based on the measured flows at Rowlett Creek and assuming potentially two and a half times the gauge flow as local inflow to Lake Ray Hubbard, Lake Lavon Dam discharges were likely minimal during this period as well.

Rain Gauge Data and Flood Conditions

Rainfall data from the National Weather Service (NWS) station at Fort Worth/Dallas, TX was obtained for periods of high flow recorded at the Rowlett Creek gauge. For the period of September 20, 2018 to September 22, 2018, the precipitation totals were 0.18, 5.85, and 2.21 inches per day, respectively. The day of the recorded peak flow at the Rowlett Creek gauge had minimal precipitation.

The second highest recorded flow occurred on May 29, 2015 with a peak flow of 47,900 cfs. For the period of May 21, 2015 to May 26, 2015, the precipitation totals were 0.57, 0.55, 0.73, 3.30, 0.42, and 0.43 inches per day, respectively. Trace amounts of rainfall were recorded on May 27, 2015, followed by daily precipitation totals of 1.56, 2.20, and 0.89 inches for May 28, 2015 through May 30, 2015. Figure 5 shows the streamflow response for this period.

Figure 5 – Rowlett Creek Response to May 2015 Storm

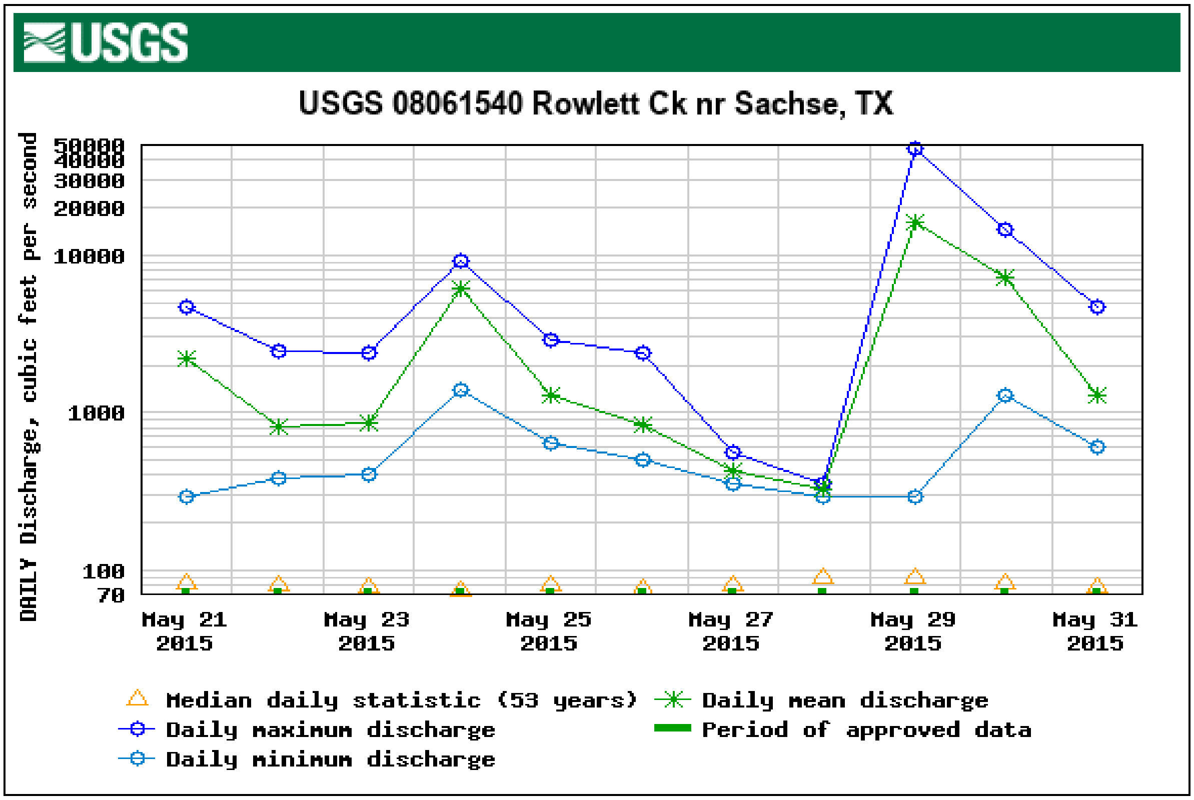

The relative streamflow response can be seen on May 24, 2015, with a rainfall total of 3.30 inches throughout the day and a corresponding increase in flow on the same day. A similar sharp increase in flow can be seen on May 29, 2015 when the daily total rainfall was 2.20 inches. While these correlations use daily, rather than hourly, data, the rapid variance in flow during relatively short periods can be seen from the graph.

The third highest recorded flow occurred on November 27, 2015 with a peak flow of 36,200 cfs. About a week preceded this flood event without any rainfall. The initial recorded daily precipitation was 2.71 inches on November 26, 2015, followed by 3.45 inches on the November 27, 2015. The following two days had rainfall totals of 0.99 and 0.88 inches per day. Figure 6 shows the streamflow response for this period.

Figure 6 – Rowlett Creek Response to May 2015 Storm

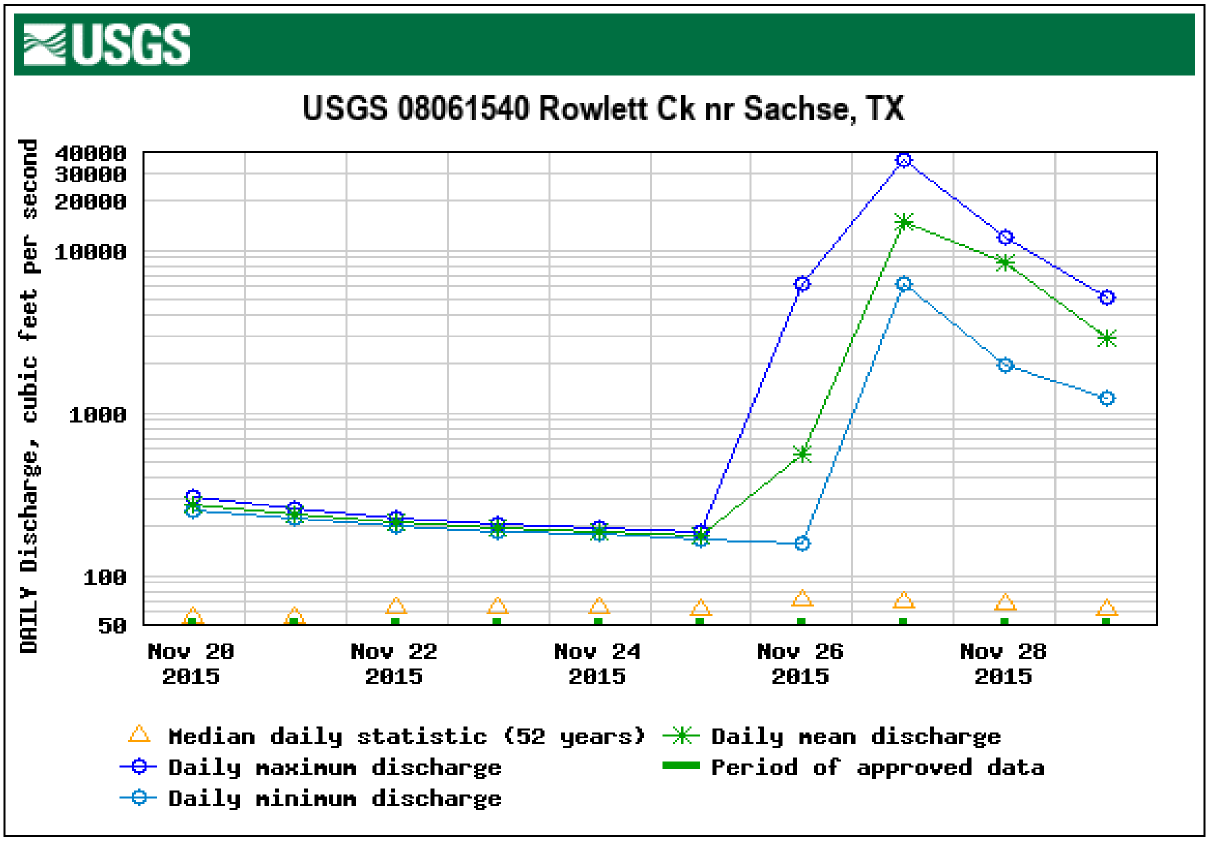

As with the previous storm, the rapid response to the rainfall is apparent. Again, the correlation is only an approximation as daily totals may not reflect the timing of high intensity rainfall or any localized discrepancy between rainfall at the NWS Fort Worth/Dallas, TX station and the actual site conditions.

Rainfall Amounts and Frequencies

The 1-, 2-, and 3-day totals for the storm events described in Section 6.2 are summarized in Table 3.

Table 3 – Cumulative Precipitation for Select Storm Events

	Cumulative Precipitation (inches)		
Storm Event	1 day	2 day	3 day
May 2015	3.30	4.03	4.58
November 2015	3.45	6.16	7.15
September 2018	5.85	8.16	8.34

The National Oceanic and Atmospheric Administration (NOAA) Atlas 14 estimates point precipitation frequencies for Texas and can be used to identify the frequency storm event for the periods described above. Table 4 shows the point rainfall frequencies from NOAA Atlas 14 at the Lavon Dam gauge.

Table 4 – Point Rainfall Frequencies from NOAA Atlas 14

Station Name: LAVON DAM										
	PRECIPITATION FREQUENCY ESTIMATES (%)									
Duration	1	2	5	10	25	50	100	200	500	1000
5-min:	0.435	0.499	0.605	0.692	0.81	0.898	0.986	1.08	1.2	1.29
10-min:	0.695	0.798	0.97	1.11	1.3	1.44	1.58	1.72	1.9	2.03
15-min:	0.868	0.995	1.21	1.38	1.61	1.78	1.96	2.13	2.37	2.54
30-min:	1.21	1.38	1.67	1.91	2.23	2.46	2.7	2.94	3.28	3.53
60-min:	1.58	1.81	2.19	2.51	2.94	3.25	3.58	3.92	4.39	4.76
2-hr:	1.93	2.24	2.76	3.19	3.78	4.24	4.71	5.21	5.91	6.47
3-hr:	2.13	2.51	3.11	3.62	4.33	4.89	5.47	6.09	6.97	7.66
6-hr:	2.51	2.99	3.74	4.39	5.31	6.04	6.8	7.64	8.81	9.75
12-hr:	2.96	3.54	4.44	5.22	6.33	7.21	8.14	9.16	10.6	11.8
24-hr:	3.46	4.14	5.2	6.11	7.41	8.43	9.52	10.7	12.5	13.9
2-day:	4.03	4.8	6.01	7.05	8.52	9.66	10.9	12.3	14.2	15.9
3-day:	4.4	5.23	6.54	7.66	9.24	10.5	11.8	13.3	15.4	17.2
4-day:	4.67	5.54	6.93	8.12	9.79	11.1	12.5	14.1	16.4	18.2
7-day:	5.22	6.21	7.75	9.09	11	12.5	14.1	15.9	18.5	20.5
	PRECIPITATION FREQUENCY ESTIMATES AT UPPER BOUND OF 90% CONFIDENCE INTERVAL									
Duration	1	2	5	10	25	50	100	200	500	1000
5-min:	0.574	0.656	0.797	0.921	1.1	1.25	1.41	1.57	1.79	1.97
10-min:	0.918	1.05	1.28	1.48	1.77	2.01	2.26	2.51	2.84	3.1
15-min:	1.15	1.31	1.59	1.83	2.19	2.48	2.79	3.1	3.54	3.89
30-min:	1.6	1.82	2.2	2.54	3.03	3.42	3.84	4.28	4.91	5.4
60-min:	2.08	2.38	2.89	3.34	3.99	4.53	5.09	5.71	6.58	7.28
2-hr:	2.51	2.9	3.58	4.19	5.08	5.82	6.62	7.49	8.74	9.75
3-hr:	2.76	3.21	4.01	4.72	5.78	6.67	7.63	8.68	10.2	11.5
6-hr:	3.22	3.78	4.77	5.66	7.01	8.14	9.37	10.7	12.7	14.4
12-hr:	3.75	4.41	5.59	6.65	8.25	9.59	11.1	12.7	15.1	17.1
24-hr:	4.33	5.1	6.47	7.7	9.53	11.1	12.8	14.7	17.5	19.9
2-day:	4.98	5.85	7.39	8.77	10.8	12.5	14.4	16.5	19.7	22.4
3-day:	5.4	6.34	7.99	9.46	11.6	13.4	15.4	17.7	21.1	24
4-day:	5.7	6.68	8.42	9.97	12.3	14.2	16.3	18.7	22.3	25.3
7-day:	6.31	7.39	9.32	11.1	13.6	15.8	18.2	20.9	24.9	28.2

The single day rainfall totals indicate a precipitation frequency ranging from the 1-year to 10-year storm event. The two- and three-day rainfall totals indicate a frequency ranging from the 1-year to 20-year storm event. Based on the precipitation frequencies provided in NOAA Atlas 14, the rainfall occurring during the periods reviewed are not extreme storm events and should be expected to occur on a fairly regular basis. As a comparison, the PMF, which was developed for use in preparation of the EAP in 2014, has 1-day precipitation amounts ranging from 8.34 to 28.72 inches, 2-day amounts ranging from 10.17 to 33.24 inches, and 3-day amounts ranging from 11.23 to 35.85 inches.

CONCLUSIONS

Based on Schnabel's review of the existing flood operation procedures, the overall approach is well presented and provides reasonable responses to varying weather conditions, particularly during larger storm events. However, the procedures are dependent on the ability to obtain all the required data in a timely manner. This data includes stream flow from various gauges, lake water levels, wind and direction measurements, precipitation amounts from the Flood Alert System, as well as forecasts or radar maps from the NWS.

DWU personnel have identified concerns related to obtaining this data in a timely manner, as well as the general age of the Flood Alert System. Additional concerns have been identified related to the release tables, which are based on outdated stage-storage estimates of the lake above the normal level, the accurate estimation of inflow rates from stream gauges, and the inherent error associated with estimating the lake level during storm events with relatively high winds.

RECOMMENDATIONS

Based on discussions with DWU personnel, as well as Schnabel's review of available documentation the following recommendations are provided:

- Evaluate a replacement SCADA system for the existing Flood Alert System which would report all relevant data to a centralized monitoring center. This system should incorporate stream gauges, rain gauges, lake level gauge(s), weather stations, and piezometer readings associated with Forney Dam.
- Install an additional lake level gauge within Lake Ray Hubbard located farther north that would assist in estimating the overall lake levels during storm events with high winds. A second lake level gauge would provide a greater degree of confidence in the overall estimate of inflows to Lake Ray Hubbard. Specific locations have not been researched as part of this review.
- Install additional gauges near Wylie and the Camp Creek area north of Rockwall. The Camp Creek gauge should be capable of measuring precipitation, as well as stream flow.
- Update the elevation-area-storage tables in the Flood Operations Manual for Lake Ray Hubbard based on the 2015 volumetric survey performed by the Texas Water Development Board. This involves extending the volumetric survey estimates above the normal pool using LiDAR-derived topographic data.
- Perform a revised hydrologic and hydraulic analysis to determine if the timing of runoff and peak inflows have changed with the additional development that has occurred since the last analysis was performed. Update the Flood Operations Manual based on the results of this study.

We appreciate the opportunity to continue to be of service for this project. Please contact the undersigned if clarification is needed for any aspect of this report.

Sincerely,

SCHNABEL ENGINEERING, LLC

William Shaffer, PE
Senior Consultant

Brett W. Dodd, PE
Project Engineer

Joseph S. Monroe
Principal

WS:BWD:JSM

APPENDIX G

SITE SAFETY AND HEALTH PLAN FOR DRAINAGE GALLERY INSPECTIONS

Site Safety and Health Plan, Rockwall-Forney Dam Adit Investigation

©2021 All Rights Reserved

Site Safety and Health Plan

Rockwall - Forney Dam
Adit Investigation

Lake Ray Hubbard
Forney, TX 75120

Table of Contents

<u>APPENDIX</u>

1.0 INTRODUCTION

This Site Safety and Health Plan (SSHP) has been formulated for Dallas Water Utilities (DWU) to establish safety and health procedures to eliminate, mitigate or limit potential risks to personnel involved with engineering and inspection of the Drainage and Inspection Gallery at the Rockwall-Forney Dam located near Forney, Texas. The safety and health of each project team member is of paramount concern. Each employee is entitled to safe working conditions. All reasonable effort shall be made in the interest of accident-injury-illness-incident prevention, and health preservation. Employees will not be expected to perform any work known to be unsafe as characterized by any applicable regulatory agency. Continual improvement of safety and health performance is expected, with periodic assessments to monitor efficacy.

DWU is committed to safety in all of its actions while focusing on employees, planning and performance to ensure the wellbeing of staff, fellow site workers, and the general public, as well as the maintaining the quality of workmanship. The Leadership Team, executives, managers and supervisors shall proactively and visibly demonstrate their commitment to safety by ensuring the specific planning and performance goals are being met. Each individual employee must take accountability for following policies, procedures, laws, regulations and other requirements to successfully and safety accomplish their tasks. Employees shall be confident in their responsibilities, as well as applicable safety requirements. Each team member shall review the job task and plan prior to mobilization and at the start of each day's work. Ensure each team has familiarity with the guidelines, safety procedures, potential hazards as well as emergency actions.

1.1 Zero Goals

The ultimate goal for this project, as well all other DWU projects, is zero incidents, zero accidents, zero injuries. Each employee shall be given the resources, training, equipment and PPE to help accomplish this goal.

1.2 Stop Work Authority

All employees are granted ***Stop Work Authority***. The health and safety of DWU employees and all fellow workers on site will take precedence over cost and schedule of the project. Employees can stop work if they see a potential or actual hazard that may threaten the safety of people or the environment. Upon stopping work, all designated personnel must be immediately notified and provided details regarding the situation. Every effort shall be made to eliminate or mitigate the hazard. Once concerns are resolved to the satisfaction of all involved, work can proceed.

The procedures in this SSHP have been developed based on site history, previous site investigations and the need to perform routine inspections of the gallery. This SSHP is not intended for work other than inspections of the gallery. Every effort has been made to address the chemical, biological and physical hazards that may be encountered during the implementation of the proposed investigative activities. However, unanticipated site-specific conditions or situations may occur during the implementation of this project. This SSHP must be considered a working document that is subject to change to meet the needs of this dynamic project. DWU and their selected contractors will complete a Job Hazard Analysis (JHA) when new tasks or different investigative techniques not addressed in the SSHP are proposed. The use of new techniques will be reviewed and if new hazards are associated with the proposed changes, they will be documented on the JHA form. An effective control measure must also be identified for each new hazard. JHA forms will be reviewed by the Site Safety and Health Officer (SSHO) prior to being implemented. Once approved, the completed forms will be reviewed with all field staff during mobilization safety meetings.

2.0 SITE DESCRIPTION AND SCOPE OF WORK

The Rockwall-Forney Dam is located on the East Fork Trinity River, downstream of the Lavon Lake Dam which is owned and operated by the U.S. Army Corps of Engineers (USACE), and about 1-¾ miles upstream from U.S. Highway 80 in Dallas and Kaufman Counties, Texas. Construction was completed circa 1967 with the full pool first attained in 1969. The dam was constructed to provide a sustainable supply of water for Dallas and surrounding communities.

The Rockwell-Forney Dam, with a height on the order of 68 feet and a crest length of about 12,000 feet, is a combination earthen embankment and concrete gravity structure. A drainage gallery exists within the concrete spillway and non-overflow sections. The gallery is 4-½ feet wide and 7 feet tall, and has a gutter along the upstream side to collect water from the foundation drains. These drains are inclined upstream 40 degrees from horizontal and extend through the concrete into the shale foundation. A 4-inch diameter steel pipe is used to convey flows from the foundation through the concrete. The drains penetrate the upstream wall of the gallery a few inches above the gallery floor. The gallery is parallel to the concrete dam axis and maintains a floor elevation of 392 feet for most of the length. The access shaft to the gallery is located in the right non-overflow section and contains a spiral staircase that leads to the gallery entrance. The crest elevation of the right non-overflow section is 452 feet. The stairs have 12 treads per circle with 8-¾ inch risers.

3.0 RISK EXPOSURE ASSESSMENT

Based on scope of work, known site conditions, applicable work and site safety plans, and anticipation of hazards that may arise, the following table identifies the likely potential safety and health hazards associated with field work:

Task	Hazard
Site/Gallery entry	Exposure to airborne dust / Inhalation
Site/Gallery entry	Heat stress
Gallery entry	Mining/Underground hazards
Site/Gallery entry	Worker fatigue
Gallery entry	Carbon Monoxide / Atmospheric conditions
Site Access / Inspection	Biological exposure (flora, fauna, insects, animals)
Site Access / Inspection	Physical hazards (struck by, construction vehicles, slips/trips/falls, traffic)

Engineering controls, administrative work practices, personal protective equipment (PPE) or a combination of all these shall be implemented to eliminate or mitigate employee exposure to these hazards. Continual assessments of site conditions shall be conducted to discern additional hazards that may arise on this dynamic work site. Field staff shall remain vigilant for changing conditions, including unusual odors, burning/stinging eyes nose throat, skin irritation, or physical symptoms like lethargy, drowsiness, or mood changes. Hazard control and mitigation techniques discussed herein.

4.0 CHEMICAL EXPOSURE AND CONTROL

The drainage and inspection gallery has been designated as a non-permit confined space, however, as work tasks or unforeseeable conditions could alter the designation. Due to low air movement, and the potential malfunctioning of the ventilation fans, atmospheric conditions could be unfavorable. Continual assessment of these conditions must be conducted. Recent inspection reports indicated the gallery was clean; however, DWU field engineers shall be prepared to encounter contamination during the investigation and, as such, utilize engineering and administrative controls and appropriate PPE to manage this potential exposure. The routes of entry for contaminant exposure will most likely be primarily inhalation and dermal. Other possible exposure routes through the eyes and mucous membranes, and ingestion are possible.

Direct-reading air monitoring instrumentation 4 gas meters will be used to determine the concentration of volatile organic compounds (VOC) vapors that may be present in the work area and in the employee's breathing zone during intrusive site activities. Although unlikely, exposure to all of the contaminants of concern may occur via ingestion (hand-to-mouth transfer). Proper work and personal hygiene and decontamination procedures can limit the potential for contaminant ingestion.

4.1 Physical Hazards and Controls

The general safety procedures in this SSHP have been developed to address the potential physical hazards associated with this site visit and investigation:

4.1.2 Slips/Trips/Falls

As in any work area, it is expected that the ground may be uneven, the surface may be unreliable due to surface unevenness, debris may be present, work is being performed on poly sheeting, and wet or muddy areas may exist. Therefore, the potential for slips, trips and falls is present. Tools, equipment and supplies must be stored in a suitable location at the site so they can be safely accessed. All work areas shall be reasonably clear of obstructions, grease, mud or any other materials likely to cause a slip, trip or fall. Special care must be taken around areas of water. A clearly designated area or zone of concern should be established around water hazards. Staff shall watch for hazards while they are walking and not carry objects that obstruct their vision. Staff shall practice proper housekeeping to keep areas free of obstacles which can cause slips and trips in work and walking areas. These areas should never be obstructed by objects of any kind. Walking and working surfaces greater than 4 feet in height must have standard guardrails for protection. When accessing ladders or equipment, always face and maintain 3 points of contact at all times. Keep ladders and equipment free of debris by cleaning boots of mud or dirt when accessing.

4.1.3 Housekeeping

Maintaining a work environment that is free from accumulated debris is key to preventing slip, trip and fall hazards at work sites. Essential elements of good housekeeping include orderly placement of materials, tools and equipment; placing trash receptacles at appropriate locations for the disposal of miscellaneous rubbish; prompt removal and secure storage of items that are not needed to perform the immediate task at hand; and awareness on the part of all employees to walk around, not over or on, equipment that may be stored in the work area. Routine inspections should be conducted regularly to ensure the work area is being maintained and that materials are being stored in dedicated areas so that tripping hazards are minimized.

4.1.4 Working around Machinery

While not applicable to routine inspection, there could be other contractors on site or other work underway. Maintain situational awareness. Heavy equipment, including bobcats/excavators/push blades/haulers, could be in use. The use of such equipment poses a potential hazard to the support crew working around the equipment. Use of heavy equipment at the site requires all employees working in the exclusion zone to wear proper PPE and ANSI-approved reflective gear. When working around heavy equipment, employees must ensure that the operator is aware of proximity and nearby activities; remain in the operator's sight; confirm hand signals to facilitate communication with the operator; if necessary approach areas where equipment is operating from a direction visible to the operator; stay out of the boom and swing radius of the excavator; do not walk or work underneath loads handled by digging equipment; stand away from spoil piles.

4.1.5 Noise Exposure

The use of equipment on site may expose the field team to noise levels that exceed the Occupational Safety and Health Administration (OSHA) Permissible Exposure Limits (PEL) of 90 decibels for an 8-hour day. Exposure to noise can result in the following:

- Temporary hearing losses where normal hearing returns after a rest period;
- Interference with speech communication and the perception of auditory signals;
- Interference with the performance of complicated tasks; and,
- Permanent hearing loss due to repeated exposure resulting in nerve destruction in the hearing organ.

Since personal noise monitoring will not be conducted during the proposed activities, employees must follow this general rule of thumb: If the noise levels are such that you must shout at someone 5 feet away from you, you need to be wearing hearing protection. Employees can wear either disposable earplugs or earmuffs but all hearing protection must have a minimum noise reduction rating (NRR) of 27 decibels.

4.2 Material Handling

Equipment may be used on site, some of which possibly bulky or awkward to maneuver. Failure to follow proper lifting techniques can result in injury. All staff will evaluate equipment before lifting or moving to determine safe methods and plan a safe and secure route. Team-lift items over 50 pounds, awkward or utilize mechanical lift methods. If mechanical devices are not available, ask for assistance. Bend at the knees, not at the waist. Use legs to lift and not the back. Do not twist, turn or pivot while lifting. Position the load as close to the body as possible before lifting. Ensure a clear path free of obstruction, slip, trip and fall hazards.

4.3 Thermal Stress

Heat related problems include heat rash, fainting, heat cramps, heat exhaustion and heat stroke. Heat rash can occur when sweat isn't allowed to evaporate, leaving the skin wet most of the time and making it subject to irritation. Fainting may occur when blood pools to lower parts of the body and as a result, does not return to the heart to be pumped to the brain. Heat related fainting often occurs during activities that require standing erect and immobile in the heat for long periods of time. Heat cramps are painful spasms of the muscles due to excessive salt loss associated with profuse sweating. Heat exhaustion results from the loss of large amounts of fluid and excessive loss of salt from profuse sweating. The skin will be clammy and moist and the affected individual may exhibit giddiness, nausea and headache.

Heat stroke occurs when the body's temperature regulatory system has failed. The skin is hot, dry, red and spotted. The affected person may be mentally confused and delirious. Early recognition and treatment is paramount. A person exhibiting signs of heat stroke should be removed from the work area to a shaded area. The person should be soaked with water to promote evaporation. Fan the person's body to increase cooling.

Early Symptoms of Heat-Related Health Problems	
Decline in performance	Excessive fatigue
Un-coordination	Reduced vigilance
Decline in alertness	Dizziness
Unsteady walk	Muscle cramps
Susceptibility to Heat Stress Increases Due To:	
Lack of physical fitness	Obesity
Lack of acclimation	Drug or alcohol use
Increased age	Sunburn
Dehydration	Infection

People unaccustomed to heat are particularly susceptible to heat fatigue. Rookie employees in PPE need to gradually adjust to the heat. PPE can have an effect on heat related illness. Sweating normally cools the body as moisture removed from the skin by evaporation. However, wearing certain PPE, particularly coveralls, reduces the body’s ability to evaporate sweat and thereby regulate heat buildup. The body’s efforts to maintain an acceptable temperature can therefore become significantly impaired by wearing PPE. To avoid heat stress: establish work-rest cycles; identify a shaded and cool rest area; rotate personnel and alternate job functions; ensure sufficient water intake and drink before feeling thirsty; eat lightly and avoid salts and alcohol; avoid double shifts or overtime.

Site personnel should regularly monitor their heart rate, and know and look for symptoms of heat related illness. Pay close attention to colleagues for these signs in colleagues as well.

4.4 Environmental Hazards and Control

The location of the project is such that environmental, or biological, hazards may be encountered. Environmental hazards that may be present include, but are not limited to ticks and insects, and small animals and snakes, especially near standing water. All employees with the potential to contact the flora and fauna indicated above should be cautious when working in areas that may support these types of hazards. The SSHO will assess suspect areas and warn workers when there is a possibility of contact with these items. Insect repellent should be worn if allowed per project, either lotion or spray, and permethrin can be used on clothes and gear prior to mobilization. All staff shall dress in light colored clothing and tape seams in heavily infested areas. A thorough post-job inspection should be conducted. It is recommended that personnel frequently check themselves when in areas that could harbor ticks, wear light color clothing and visually check when coming from wooded or vegetated areas. The tick can be removed by pulling gently at the head with tweezers. The affected area should then be disinfected with an antiseptic wipe. The employee shall notify the SSHO after a bite, and closely monitor for any signs or symptoms of tick-borne illnesses. Insects for which precautionary measures should be taken include: mosquitoes (potential carriers of disease aside from dermatitis), black flies, wasps, bees, ticks, and fire ants. Wasps and bees will cause a painful sting to anyone if they are harassed. They are of most concern for individuals with allergic reactions who can go into anaphylactic shock. Also instances where an individual is exposed to multiple stings can cause a serious health concern for anyone. These insects are most likely to sting when their hive or nest is threatened.

Snakes could be present near waterways and streams, rip rap, brush and mobilization areas. Wear heavy gloves. If spotted, step back and allow the snake to proceed. Wear boots at least 10 inches high. Watch for snakes sunning on fallen trees, limbs or other debris. A snake's striking distance is about 1/2 the total length of the snake. If bitten, note the color and shape of the snake's head to help with treatment. Keep bite victims still and calm to slow the spread of venom in case the snake is poisonous. Seek medical attention as soon as possible. Do not cut the wound or attempt to suck out the venom. Apply first aid by laying the person down so that the bite is below the level of the heart, and cover the bite with a clean, dry dressing. Seven species of venomous snakes occur in the Dallas Fort Worth area:

- Copperhead (Agkistrodon contortrix)
- Cottonmouth (Agkistrodon piscivorous)
- Western Diamondback Rattlesnake (Crotalus atrox)
- Timber Rattlesnake (Crotalus horridus)
- Massasagua (Sisturus catenatus)
- Pigmy Rattlesnake (Sisturus miliarius)
- Texas Coral Snake (Micrurus tener)

5.0 PERSONAL PROTECTIVE EQUIPMENT

The purpose of PPE is to provide a barrier, which will shield or isolate individuals from the physical hazards that may be encountered during work activities. The minimum level of PPE to be worn for this project and work task is Level D. The safety equipment shall be used for employee protection and must be regularly inspected before use. Manufacturers' procedures for donning and removing PPE will be followed in order to ensure its integrity and reduce or eliminate contamination of equipment or work zones. Employees are responsible for inspecting PPE prior to use and after work. All equipment showing signs of wear, fatigue or damage shall be removed from service and discarded. The SSHO, along with consultation from site managers and on-scene safety officers will determine appropriate levels of protective gear to be worn in the event additional hazardous materials are encountered.

High Visibility Gear: ANSI-approved Class II gear is suitable for routine construction and field activities away from DOT roadways and vehicular traffic.

Hand Protection: Various types of protective gloves are available and should be selected based on the task at hand. For routine visual inspection, gloves may not be necessary, but should be made available. Cut level gloves can be used to provide protection from slivers and abrasions. Leather gloves provide protection from sparks, some heat and from rough materials. Rubber gloves provide protection from water, solvents and various chemicals. During specimen collection, cuffed nitrile or rubber gloves can be worn to prevent dermal hazards. With each type of hand protection there are limitations that should be understood. Individual preference of size and style must be considered, but the selection of the most appropriate type of gloves shall be completed for each job performed. There are limitations to consider, including gloves with large cuffs or material that could become caught near rotating or pinching equipment. All gloves should fit appropriately and should be easily removed.

Protective Footwear: ANSI Z 41.1 approved safety boots are required for all employees on site. Boots must have steel-toes or caps, and must have soles that will prevent slipping on wet, loose or smooth surfaces. Soles should also prevent penetration by sharp objects

Head Protection: Hard hats that meet ANSI Z 89.1 standards are required and must be worn appropriately on site. Nothing should come between the user's head and the hard hat's cradle/harness (such as a ball cap). Hard hats should be regularly assessed for efficiency, and discarded if cracked, split, or any other way compromised, including the cradle/harness. Western style hardhats, aluminum hardhats, baseball caps under the hardhats, and bump caps are prohibited on the project site. The brim/bill must always face forward.

Protective Eyewear: Eye protection is required at all times. Safety glasses must meet ANSI Z 87.1 requirements. Safety glasses must fit the user snugly and not interfere with movements of the user, be durable, capable of being disinfected and easily cleaned, and should be kept in good condition. Arrangements shall be made prior to commencement of work for field staff that use corrective lenses or contact lenses.

Hearing Protection: Hearing protection is required whenever ambient noise levels equal or exceed 85 decibels (dBs). For instance, staff working with or around equipment like drilling rigs, motorized construction vehicles, or pneumatic/hydraulic tools should don hearing protection. All protective devices shall have a noise reduction rating. Noise blocking earmuffs, attached to hard hats, are the recommended method of hearing protection while working in high noise areas. Disposable or multi-use earplugs can be worn in areas when communication between staff is necessary or frequent. Administratively, if possible, reduce or rotate the exposure to noise, shut down noisy equipment when not needed, and maintain all equipment for optimal efficiency. As the use of hearing protection may decrease communication, effective hand signaling should be established prior to work activities.

Slope Work / Working Near or Over Water: Employees working over or near water where the possibility of drowning exists shall be provided with a U.S. Coast Guard approved life jacket or buoyant work vest when the danger of drowning exists. If the work area is not equipped with an OSHA-compliant railing system, employees walking or working on the apron must wear a U.S. Coast Guard approved life jacket or buoyant work vest, also called a life preserver or personal flotation device (PFD). These PFDs should be fully buckled, snapped, or zipped whenever there is a hazard of falling into the water, regardless of the size of the barge. Each employee should have a PFD accessible to them at all times. This safety precaution will allow employees the opportunity to don a PFD in a reasonable amount of time during an emergency rescue situation. Should the conditions warrant, Personal Fall Limiters (PFL) and full body fall protection harnesses can be provided on site to employees. The PFL's are designed to retract into the unit when not in use, reducing tripping hazards during operations. When wearing a harness and properly anchored PFL, the employee is 100% tied-off and can move freely within the PFL's allowable range.

5.1 PPE Inspections

PPE clothing ensembles designated for use during site activities shall be selected to provide protection against known or anticipated hazards. However, no protective garment, glove or boot is entirely chemical-resistant, nor does any PPE provide protection against all types of hazards. To obtain optimum performance from PPE, site personnel shall be trained in the proper use and inspection of PPE. Inspect PPE before and during use for imperfect seams, non-uniform coatings, tears, poorly functioning closures or other defects. Disposable PPE should not be reused after breaks unless it has been properly decontaminated.

6.0 AIR MONITORING

Air monitoring will be routinely performed while on the project site to ensure proper atmospheric conditions. Whenever possible air monitoring should be conducted upwind. An initial vapor measurement survey should be conducted to detect "hot spots" if contaminated soil is exposed at the surface. Vapor measurement surveys of the workspace should be conducted at least hourly or more often if persistent petroleum-related odors are detected.

Atmospheric monitoring will be conducted on site using the most practical equipment, based on known and suspected hazards present in work areas. A 4 gas meter will be carried on person while on the site. The 4 gas meters provide detection of combustible atmospheres, explosive gases, detect combustible organic vapors, as well as oxygen and carbon monoxide. The 4 gas meters will check oxygen levels for deficiency or enrichment, test for levels of flammable or explosive gases, monitor for hydrogen sulfide (H2S) and carbon monoxide (CO). The monitors will provide an alarm at real-time concentration, short-term exposure limit (STEL) or time-weighted average (TWA) for these monitored substances.

If conditions are **not** met, entry is prohibited. If occupied, the space must be immediately evacuated.

Potential Contaminant	Exposure Limits
Oxygen	Minimum 19.5% and Maximum 23.5%
Flammable gases	No greater than 10% LFL
Hydrogen sulfide	No greater than 10 ppm
Carbon monoxide	No greater than 50 ppm

When primary action levels are exceeded, one or more of the following mitigating steps must be taken to reduce exposures:

- Move the work area to another location where action levels are not exceeded
- Provide positive ventilation for the workspace through the use of fans or blowers

If action levels continue to be exceeded, the following mitigating steps must be taken to reduce exposures:

- Stop work
- Take action to stabilize conditions, if possible, without endangering personnel
- Move to a non-contaminated area
- Notify the Project Manager and the Health and Safety Manager

7.0 SITE CONTROLS

In addition, while on site, employees will follow all established policies to maintain a safe work environment:

- Horseplay is not permitted at anytime
- Visitors are not allowed in the work areas without authorization.
- Security will be maintained at the site by closing all gates during normal work hours. Follow site protocols for security at the end of the work shift, ensure effective security before leaving the site for the day.
- Eating, drinking, or smoking is permitted only in designated areas.
- Cell phone use while operating equipment is not allowed.
- Cell phone use while operating motor vehicles is not allowed
- Fire extinguishers will be available on site and in all areas with increased fire danger.
- A minimum of two personnel will always be on site.
- Only necessary personnel need to be on or around heavy equipment.

- Employees will not interfere with or tamper in any way with air monitoring equipment.

8.0 ADIT / GALLERY CONFINED SPACE ENTRY

For routine inspection of the drainage and inspection gallery, the following procedures are the minimum requirements for safe entry into this adit on site. The plan follows guidance from OSHA 29 CFR 1926 Subpart AA - Confined Spaces in Construction, 1926.800 promulgating underground construction, and MSHA regulations.

8.1 Definitions

Acceptable Entry Conditions – the conditions that exist in a permit-required space to allow safe entry and work within the space.

Adit – An entrance to an underground mine which is horizontal or nearly horizontal, by which the mine can be entered, drained of water, ventilated, and minerals extracted at the lowest convenient level

Attendant (Spotter) – person stationed outside one or more permit spaces who monitors the authorized employees and performs attendant's duties assigned in this policy.

Authorized Entrant/Employee – person who has received documented confined space entry training as an entrant/supervisor.

Cardiopulmonary Resuscitation (CPR) – a combination of rescue breathing and chest compressions delivered to victims thought to be in cardiac arrest.

Combustible Gas – airborne concentration of gas or vapor which may present the risk of fire or explosion if an ignition source of sufficient energy is introduced. This term is synonymous with "flammable vapor" and "explosive gas."

Confined Space – a space that meets **all** of the following criteria:

- Is large enough and so configured that an employee can bodily enter and perform assigned work;
- Has limited or restricted means for entry and exit, e.g., tanks, tunnels, vessels, silos, storage bins, hoppers, vaults, and pits; and
- Is not designed for continuous employee occupancy.

Engulfment – the surrounding or capture of a person by a liquid or finely divided (flowable) solid substance that can cause asphyxiation, drowning, or can exert enough force on the body to cause death by strangulation, constriction or crushing.

Entry – means the action by which a person passes through an opening into a permit-required confined space. Entry includes ensuing work activities in that space and is considered to have occurred as soon as any part of the entrant's body breaks the plane of an opening into the space.

Entry Permit – written authorization for entry into a permit-required confined space.

Entry Supervisor – first-line foreman or designated lead person, responsible for: determining if acceptable entry conditions have been verified and documented at a permit-required confined space where entry is planned; authorizing entry; overseeing entry operations; and terminating entry.

General Entry Permit – type of entry permit used to enter a confined space when all atmospheric and safety hazards have been controlled or eliminated. The General Permit is used to verify and document that all hazards have been controlled or eliminated. If an entry is needed to evaluate, control or eliminate the hazardous conditions in the space, then a Hazardous Permit will be needed for this portion of the entry.

Hazardous Atmosphere – an atmosphere that may expose employees to the risk of death, incapacitation, impairment of ability to self rescue, injury, or acute illness from one or more of the following causes:

- Flammable gas, vapor, or mist in excess of 10% of its lower flammable limit (LFL).
- Airborne combustible dust that is at or approaching its LFL. This concentration may be approximated as a condition in which the dust obscures vision at a distance of 5 feet or less.
- Atmospheric oxygen concentration below 19.5% or above 23.5%.
- Any chemical or substance present which may be at concentrations capable of causing death, incapacitation, impairment of ability to self-rescue, injury, or acute illness due to its health effects and is above the regulatory limit.
- Any other atmospheric condition that is immediately dangerous to life or health (IDLH).

Hazardous Permit – the type of permit used to enter a confined space when either a hazardous atmosphere and/or a safety hazard has not been completely controlled or eliminated.

Hot Work Operations – cutting, welding, brazing, torch soldering, high speed metal grinding, or use of an open flame.

Hot Work Permit – the type of permit used to enter a confined space when hot work operations will be performed in the space.

Immediately Dangerous to Life or Health (IDLH) – means any condition that poses an immediate or delayed threat to life or that would cause irreversible adverse health effects or that would interfere with an individual's ability to escape unaided from a permit space.

Intrinsically Safe (Equipment) – is defined as equipment and wiring which is incapable of releasing sufficient electrical or thermal energy under normal or abnormal conditions to cause ignition of a specific hazardous atmospheric mixture in its most easily ignited concentration. (ANSI/ISA RP12.06.01-1995 (R2002))
Lockout/Tagout – a procedure whereby a lock and/or tag device is used to hold an energy-isolating device (such as a switch, valve, etc) in the "off" or safe position.
Lower Explosive Limit (LEL) – lowest concentration at which a gas or vapor can ignite and can be used interchangeably with LFL. Concentrations below this level are too lean to burn.
Non-Permit Required Confined Space – confined spaces that do not contain or, have the potential to contain, any hazard capable of causing death or serious physical harm.
Oxygen Deficient Atmosphere – means an atmosphere containing less than 19.5 percent oxygen, by volume.
Permit-Required Confined Space – a confined space that has one or more of the following characteristics:

- Contains or has the potential to contain a hazardous atmosphere. When assessing the potential for a hazardous atmosphere, consideration must be given to portals of entry from other areas, such as pipes, ducts and vents.
- Contains a material that has the potential for engulfing an entrant.
- Has an internal configuration such that an entrant could be trapped or asphyxiated by inwardly converging walls or by a floor which slopes downward and tapers to a smaller cross-section.
- Contains any other recognized serious safety or health hazard that may have an immediate effect or inhibit the employee leaving the space unaided. Examples include: exposed electrical parts, extreme temperature.

Self-Contained Breathing Apparatus (SCBA) – An atmosphere-supplying respirator in which the source of air is contained with the respirator independent of any other source.
Upper Explosive Limit (UEL) – the highest concentration at which a gas or vapor can ignite and can be used interchangeably with UFL (Upper Flammable Limit). Concentrations above this level are too rich to burn.
Work Induced Hazard – hazard created due to nature of work, e.g., welding (generates fumes) and painting (generates solvents in the atmosphere).

8.2 Responsibilities

The SSHO will act as the Entry Supervisor and will ensure that the employees who are designated as entry candidates have been fully trained and are familiar with applicable standards, and ensure each entrant has the necessary equipment and PPE, and understands its proper use. The SSHO will conduct entrance assessments, and ensure that the provisions and procedures in place provide the suitable protection for employees. The assessment shall take the following into account:

- The nature of the space (e.g. temperature, humidity, lighting, presence of biological hazards, slippery surfaces, trip hazards, etc.)
- The atmospheric conditions and O2 level
- The work task and whether it will impact conditions inside
- Work being done near or around the confined space that could impact conditions inside (fumes, dust generation, noise)
- The means of entry and egress
- Personnel capabilities and characteristics (strength, stamina, acclimation, claustrophobia)

The information regarding hazards found at the adit entrance, maintenance of log in / log out sheets, knowing the signs and symptoms of exposure to potential contaminants at the scene, determining whether conditions are suitable for entry, and the authority to terminate entry in unsafe conditions occur. The Entry Supervisor will not cross the plane of entry and will monitor all employees inside and:

- Knows the hazards that may be faced during entry, including information on the signs or symptoms, and consequences of the exposure.
- Is aware of possible behavioral effects of hazard exposure in authorized Entrants.
- Continuously maintains communication and an accurate count of authorized Entrants in the adit.
- Remains outside the adit entrance during entry operations until relieved by another Supervisor.
- Entry Supervisor may enter the entrance to attempt a rescue, if they have been trained and equipped for rescue operations as required, and only when they have been relieved by another authorized Entry Supervisor
- Monitors activities inside and outside the adit entrance to determine if it is safe for Entrants to

remain in the space and orders the authorized Entrants to evacuate immediately under any of the following conditions:

- If the Entry Supervisor detects a prohibited condition;
- If the Entry Supervisor detects the behavioral effects of hazard exposure in an authorized Entrant;
- If the Entry Supervisor detects a situation outside the space that could endanger Entrants;
- If the Entry Supervisor cannot effectively and safely perform all the duties required.

- Summon rescue and other emergency services as soon as the Entry Supervisor determines that authorized Entrants may need assistance to escape from hazards.
- Takes the following actions when unauthorized persons approach or enter the adit while entry is underway:
    - Warn the unauthorized persons that they must stay away from the entrance;
    - Advise the unauthorized persons to exit immediately, if they have entered the space.
- Performs no duties that might interfere with the Entry Supervisor's primary duty to monitor and protect the authorized Entrants.

Authorized entrants are personnel who enter the adit to perform monitoring, work or rescue activities. They are responsible for complying with OSHA requirements, and for responding to instructions from the Entry Supervisor and emergency personnel.

8.3 Adit / Confined Space Entry

The Entry Supervisor, in conjunction with properly trained entrants and other key personnel, shall complete the DWU Confined Space Evaluation Form and the Confined Space Evaluation – Entry Permit System to determine the space's classification. If deemed permit –required, the Confined Space Entry Permit shall be prepared and issued by the approved Entry Supervisor. The permit shall only be issued for the duration of the shift (maximum 12 hours). Prior to signing, the Entry Supervisor must inspect the location to ensure that applicable precautions have been implemented, and all relevant information concerning the entry parameters are documented in the permit. All personnel performing works associated with the confined space entry shall be briefed in the permit requirements by the Entry Supervisor and sign the Confined Space Entry Permit. Upon completion of the work the Entry Supervisor will cancel the permit by signing and recording the date and time on the permit. Where required (e.g. closing a manhole cover or similar) the confined space will be sealed and returned to its original pre work safe condition. If the confined space cannot be closed until a later time, provisions must be maintained (barricades, warning signs) to highlight the dangers and stop unauthorized persons from entering the confined space. Completed Confined Space Entry Permits shall be maintained in the project folder for a minimum of 2 years.

8.3.1 Isolation / LOTO

Before commencing any work all hazardous services to the confined space must be isolated. If liquids, gases or vapors could enter the confined space the pipe work should be physically isolated. Where reasonably practical double isolation controls shall be implemented. Isolation, blocking or de-energizing can only be carried out by suitably trained and competent person(s). Before entry is permitted to any confined space that can move, or in which agitators, fans or other moving parts that may pose a risk to workers are present, the possibility of movement should be eliminated. If possible by design, ensure that gate valves are de-energized and locked out / tagged out to prevent flooding of the adit.

8.3.2 Atmospheric Testing

Atmospheric testing of the confined space shall be conducted by the Entry Supervisor to ensure a safe atmosphere. A safe atmosphere in a confined space is one that:

- Has a safe oxygen level (within range of 19.5%-23.5%)
- Is free of airborne contaminants or any airborne contaminants are in concentrations below their allowable exposure standard (if any).
- Any flammable gas or vapor in the atmosphere is at concentrations below 5% of its LEL.

Testing needs to be done immediately prior to entry, before an entry permit is issued, and may need to be conducted at regular intervals or continuously during the entry depending on the circumstances. Gas detectors used for atmospheric monitoring must be:

- Fully charged with replacement batteries or charger available.
- Calibrated in accordance with manufacturers specifications.
- Fresh air and bump tested against a known concentration of an applied gas mixture (usually methane). Where a gas detector fails the bump test it must be recalibrated and bump tested until it is reading the correct concentration of the applied gas mixture. If the device does not register the correct concentration at this stage works must not proceed until a replacement device is sourced and has satisfactorily completed the steps above.

Initial testing should be done from outside the confined space by inserting a sample probe and/or portable gas detection device at appropriately selected access holes, nozzles and openings. Because contaminants can settle at different levels, each part of the confined space should be tested (side to side and top to bottom). Peak readings from bump testing and all pre-entry checks are to be recorded on the entry permit. Ignition sources must not be brought into a confined space where there is a risk of fire or explosion. Intrinsically safe tools, lighting and ventilation equipment should be used within the confined space as required. A safe atmosphere can be achieved within the confined space using methods such as cleaning, purging and ventilation.

8.3.3 Respiratory Protection

Routine inspection of the adit should not require the use of respiratory protection. Should conditions change/warrant, the inspection will be halted and reevaluated. If engineering and administrative controls cannot alter the conditions suitable for entry, i.e., a safe oxygen level or safe levels of airborne contaminants, appropriate respiratory protective equipment shall be used to enter the confined space. The appropriate respiratory protective equipment should be selected based on the level and type of contaminants and work to be done. Selection, use, and maintenance of respiratory equipment must be identified in the confined space risk assessment. Note there are additional requirements around ensuring 'Fitness for Work' as per employee medical surveillance/exams for staff using respirators, as well as respiratory fit testing and training requirements.

8.3.4 Illumination

The confined space must be sufficiently lit to allow safe access/egress and work to be performed safely. Recent inspection reports indicate that the gallery is sufficiently lit with permanent light fixtures. If permanent light fixtures are inoperable, or work is to be performed in a location where permanent lighting is unavailable, temporary lighting and power equipment may be required for the work. Lighting must be intrinsically safe unless atmospheric monitoring can confirm flammable gas levels are below 5% of their LEL, before lights are switched on or off. While work is in progress, provide lighting in accordance with the current ANSI/IES RP-7, Recommended Practice for Industrial Lighting; ANSI/IES RP-1, and UL 924, Emergency Lighting and Power Equipment. Use nonmetallic light fixtures and support lighting conductors on insulators located on the side of the passageway or shaft opposite the excavation. Provide a minimum of 11 lux (1 foot candle) of illumination, measured at the floor to the means of egress. Some lighting conditions may be unknown, and as such, each entrant shall have an acceptable portable hand lamp or cap lamp for work and emergency use.

8.3.5 Ventilation

Mechanically ventilate all areas of the shaft, passageway and other underground workings with clean, breathable, non-recirculated outside air. Record documents indicate that the adit is affixed with a permanent ventilation system capable of supplying 10,500 cubic feet of air per minute. Place the ventilation system in operation before employees enter any underground workings, and keep the system in operation until all employees have been verified to have left the area serviced by the system. Verify that a minimum of 200 cubic feet of fresh air per minute is supplied for each employee underground. The air supply for the forced air ventilation shall be from a clean source and may not increase the hazards in the space. The atmosphere within the space shall be continuously tested as necessary to ensure that the continuous forced air ventilation is preventing the accumulation of a hazardous atmosphere. If a hazardous atmosphere is detected during entry, employees shall leave the space immediately. The space shall be evaluated to determine how the hazardous atmosphere developed; and measures shall be implemented to protect employees from the hazardous atmosphere before any subsequent entry takes place.

Forced air can supply the adit with adequate ventilation. The location of the stair and adit entry may necessitate the use of an air flow machine to supply adequate ventilation. The air flow machine shall be place outside the landing connection, with enough bellows to reach through the circular staircase and the entrance landing. Ensure that any exhaust generated by the air flow machine is downwind of the work space.

8.4 Emergency / Rescue Personnel

At mobilization and prior to entry, employees shall discuss rescue operations with the entry team and key personnel, including how to summon and communicate with the rescue team in an emergency situation, egress, location of muster points, etc.

9.0 EMERGENCY ACTION PLANNING

If an emergency occurs, quick and decisive action is required to help mitigate outcomes. Decisions must be made immediately and personnel must be ready to respond. Pre-emergency planning is essential and shall include: development of a plan; review and communication of the plan to affected staff and training; coordination of roles and responsibilities; maintaining response equipment; and regular evaluation of the plan including drills.

9.1 Evacuation Routes

In a severe emergency such as a large fire, explosion, or large chemical release, site evacuation may become necessary. The SSHO will be responsible for informing site personnel of the anticipated routes of evacuation during the mobilization safety briefing. The evacuation route and assembly area will correlate to the wind direction, topography, and the nature of the incident. Personnel will be advised to move to an upwind location at least 100 yards from any fires and/or releases, and will be advised to continually monitor wind direction for changes. If moving upwind is not possible without encountering the incident, personnel will be advised to move crosswind or downwind to a distance out of the path of vapor releases, smoke, odors, or spills.

9.2 Injury and Illness

In the event of any illness or injury, the following steps will be taken:

- Evaluate the extent of injuries or seriousness of illness.
- When employees require urgent medical attention, transport them to the hospital or call for emergency assistance. Initial first aid will be administered by on-site personnel trained and certified in CPR and first aid while awaiting an ambulance or paramedics. There will be at least two on-site personnel with up to date CPR and first aid training.
- While on site, if cell phone reception is problematic, site personnel will be issued a 2-way radio if available and instructed on its use to contact emergency responders. Instructions for this shall be conveyed during the safety briefing conducted before work begins.
- All vehicles used to transport injured persons to the off-site medical facility will be provided with directions and a map to the medical facility. Medical information (completed during the initial site-specific safety training) will be referenced in an emergency to assist with the treatment of the victim. The SSHO will accompany the victim to the hospital.
- For a non-critical injury/illness, provide first-aid treatment and evaluate the need for further treatment.

9.3 Emergency Contact List and Treating Facilities

The following are emergency contact numbers in case of an on-site accident:

Title	Contact	Number
DWU Project Manager		
DWU Department Director		
DWU SSHO		
Forney Dam Facilities Contact		
Fire	Mesquite Fire Dept.	911 or 972 216-6267
Police	Mesquite Police Dept.	911 or 972 285-6336
Emergency / Trauma Center	Baylor Scott & White Medical Cntr	972 892-3000
Urgent Care / Occupational Clinic	FastMed Urgent Care 12127 Lake June Rd B Balch Springs TX 75180	469 872-5393

Directions to Baylor Scott & White Medical Center (6.2 miles / 13 minutes)

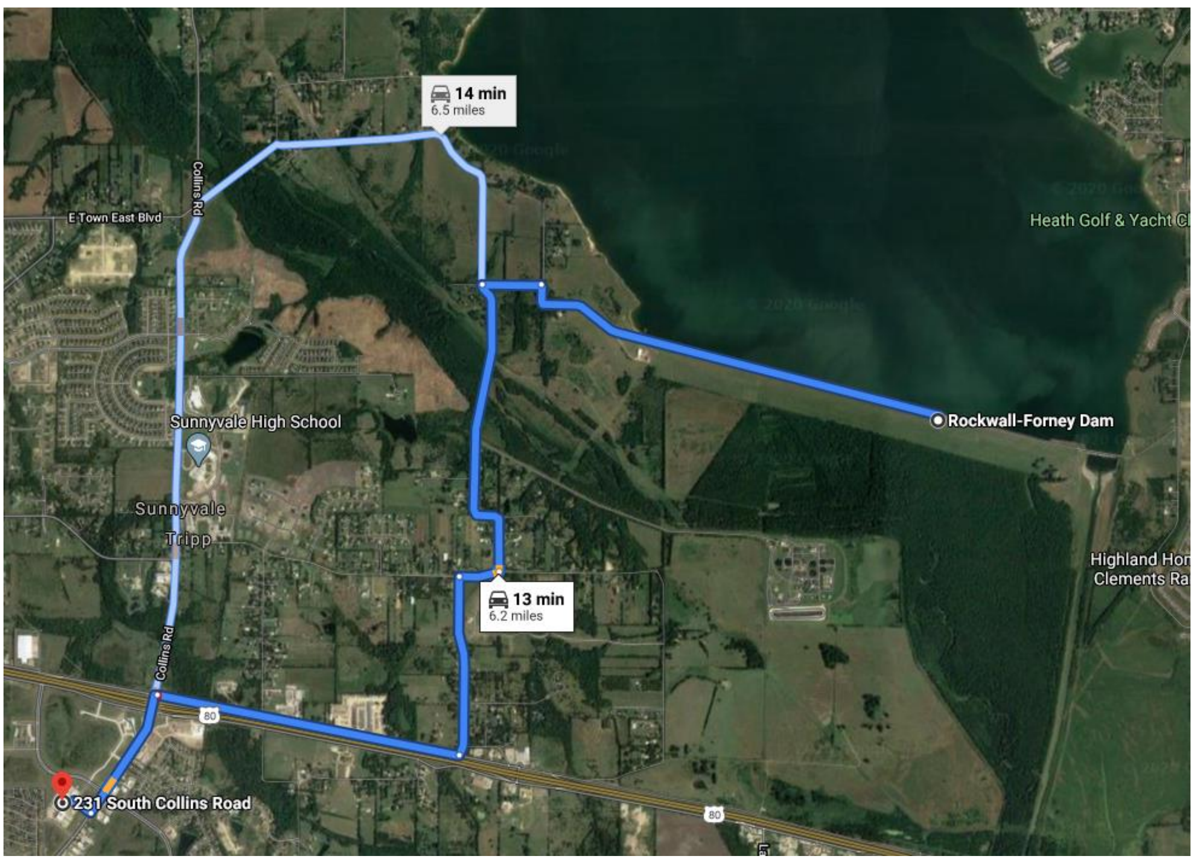

Rockwall-Forney Dam
Forney, TX 75126

Take East Fork Rd to U.S. 80 Frontage Rd in Sunnyvale

9 min (4.3 mi)

1. Head west toward Gloria Rd
   Restricted usage road
   1.8 mi
2. Turn left onto Gloria Rd W
   0.2 mi
3. Turn left at the 1st cross street onto East Fork Rd
   1.3 mi
4. Turn right onto E Tripp Rd
   0.2 mi
5. Turn left onto East Fork Rd
   0.7 mi

Drive

4 min (1.8 mi)

6. Turn right onto U.S. 80 Frontage Rd
   1.3 mi
7. Turn left onto Hwy 352 W
   0.6 mi

8. Turn right
   1 min (459 ft)

231 S Collins Rd
Sunnyvale, TX 75182

Emergency situations can be characterized as fire, explosion, environmental release, accident or injury to field personnel. The Project Manager will be notified immediately in the event of an incident. In the event of an emergency situation, all personnel will evacuate and assemble at a determined safe zone, determined and communicated at mobilization. Local emergency services shall be contacted as soon as possible. In the case of a life threatening accident, emergency first aid may be applied on site as deemed appropriate. Basic emergency and first aid equipment will be provided to staff, including first aid kits and portable fire extinguishers.

10.0 SEVERE WEATHER

When there are warnings or indications of impending severe weather (heavy rains, thunderstorms, damaging winds, tornados, hurricanes, floods, lightning, etc.), weather conditions shall be monitored using a weather station that is part of the National Oceanic and Atmospheric Administration (NOAA) weather radio, all hazards network, or similar notification system. Appropriate precautions shall be taken to protect personnel and property from the effects of the severe weather. In areas with frequent inclement weather, pre-task discussion shall include the following information specific to the particular work area:

- Severe weather alert triggers the SSHO to monitor weather conditions;
- Training on severe weather precautions, and actions;
- Identified area of retreat, preferably a substantial building

If thunder is heard, all site employees are to be alert to any visible lightning flashes. The SSHO will observe the storm front and track its direction. The SSHO will continue to observe conditions until the storm passes or until the prevailing direction is determined to be away from the site. If lightning is observed, the SSHO shall be notified. If lightning is observed by field staff, the SSSO shall be notified. When the next lightning flash is observed, a "second" count shall be initiated from the time the lightning is observed until the thunder from the strike is heard. The following action guidelines shall be implemented once the "second" count is recorded:

- "Second" count > 30, the SSHO will continually observe the storm front. If the front is moving away, work will continue. If the front is moving towards the site, the SSHO will initially place workers on alert for potential evacuation
- "Second" count ≤ 30, the SSHO will issue the evacuation command and all workers are to report to a vehicle or trailer. Work can be re-initiated once the front has passed by and thunder has not been heard for 30 minutes

Workers on open terrain / construction sites have greater risk of lightning strikes, and as such, plans should be established when the threat of lightning is forecast or occurs. When thunderstorms threaten, do not start work that cannot quickly be stopped or abandoned. Pay attention to weather forecasts and early signs, such as high winds, dark clouds, rain, or distant thunder and lightning. While on site, any worker that sees lightning or hears thunder should communicate with co-workers, supervisors and the SSHO. Depending on current conditions, a lightning warning can be issued for everyone to get to a safe location. Stay off of and away from anything tall or high, including drill rigs. Do not touch materials or surfaces that conduct electricity. If possible, get indoors.

During thunderstorms, being outside is unsafe. If thunder is heard, lightning is close enough to strike. Stop work and seek safety in a substantial building or a hard-topped metal vehicle. The best option for cover is inside a building or work trailer. The second best option is inside a car. If you cannot get indoors, position as small a target as possible. Remove tool belts and don't hold objects in hands. Stay away from water and trees. Do not lie on the ground. Do not huddle in a group.

If a co-worker is struck by lightning, remember that lightning victims do not carry an electrical charge, are safe to touch, and need urgent medical attention. Cardiac arrest is the immediate cause of death for those who die from lightning strikes. Some deaths can be prevented if the victim receives the proper first aid immediately. Call 911 and perform CPR if the person is unresponsive or not breathing. Use an Automatic External Defibrillator if one is available.

11.0 Pandemics (COVID-19)

In response to the public health emergency for the Coronavirus Disease 2019 (COVID-19) outbreak, the Federal Government and most States have declared a disaster emergency and temporarily suspended or modified laws that would prevent, hinder, or delay action necessary to cope with the disaster or emergency. The Federal Government and most States have also issued directives to allow for the expansion of certain services including those relating to emergency procurement, and to facilitate the continued work of essential businesses. As such, certain construction projects are deemed essential businesses. The purpose of this guidance is to set forth the recommended practices for contractors and consultants performing work at essential construction sites in the context of the COVID-19 health crisis. Contractors/consultants and their subcontractors must adhere to the following practices to help prevent exposure and spread of COVID-19. The following recommendations are based on what is currently known about COVID-19. Contractors/consultants and their subcontractors are advised to stay current on updates to all relevant materials and

Executive Orders and immediately implement the most current practices to protect the safety and health of your employees, clients, and the general public.

The U.S. Department of Health and Human Services' Centers for Disease Control and Prevention (CDC) provides the latest information about COVID-19 and the global outbreak. This information can be found at https://www.cdc.gov/coronavirus/2019-ncov. The OSHA COVID-19 webpage also offers information specifically for workers and employers and is located at http://www.osha.gov/covid-19.

The safety and health of each project team member (client, employee, subcontractor, or subconsultant) is of paramount concern. Every project team member is entitled to safe working conditions. All reasonable effort shall be made in the interest of accident-injury-illness-incident prevention, health and wellness preservation. Employees will not be expected to perform any work known to be unsafe as promulgated by any applicable regulatory agency. Continual improvement of safety and health performance is expected throughout the project, with periodic assessments to monitor efficacy.

11.1 About COVID-19

COVID-19 is a respiratory disease caused by the SARS-CoV-2 virus. Depending on the severity of COVID-19's impacts, outbreak conditions—including those rising to the level of a pandemic—can affect all aspects of daily life, including travel, trade, tourism, food supplies, and financial markets. To reduce the impact of COVID-19 outbreak conditions on businesses, workers, customers, and the public, it is imperative to plan now for COVID-19. The Occupational Safety and Health Administration (OSHA) has developed guidance for COVID-19 planning based on traditional infection prevention and industrial hygiene practices. It focuses on the need for employers to implement engineering, administrative, and work practice controls and personal protective equipment (PPE), as well as considerations for doing so. This addendum is intended for guidance to help identify risk levels in workplace settings and to determine any appropriate control measures to implement. Additional guidance may be needed as COVID-19 outbreak conditions change, including as new information about the virus, its transmission, and impacts, becomes available.

Symptoms of COVID-19: Infection with SARS-CoV-2, the virus that causes COVID-19, can cause illness ranging from mild to severe and, in some cases, can be fatal. Symptoms typically include fever, cough, and shortness of breath. Some people infected with the virus have reported experiencing other non-respiratory symptoms. Other people, referred to as asymptomatic cases, have experienced no symptoms at all. According to the CDC, symptoms of COVID-19 may appear in as few as 2 days or as long as 14 days after exposure.

How COVID-19 Spreads: Although the first human cases of COVID-19 likely resulted from exposure to infected animals, infected people can spread SARS-CoV-2 to other people. The virus is thought to spread mainly from person-to-person, including between people who are in close contact with one another (within about 6 feet), as well as through respiratory droplets produced when an infected person coughs or sneezes. These droplets can land in the mouths or noses of people who are nearby or possibly be inhaled into the lungs. It may be possible that a person can get COVID-19 by touching a surface or object that has SARS-CoV-2 on it and then touching their own mouth, nose, or possibly their eyes, but this is not thought to be the primary way the virus spreads. People are thought to be most contagious when they are most symptomatic (i.e., experiencing fever, cough, and/or shortness of breath). Some spread might be possible before people show symptoms and there have been reports of transmission from asymptomatic persons. Although the United States has implemented public health measures to limit the spread of the virus, some person-to-person transmission is continuing to occur in both urban and rural areas.

11.2 Responsibilities of Managers and Supervisors

All managers and supervisors must be familiar with this Plan and be ready to answer questions from employees. Managers and supervisors must set a good example by following this Plan at all times. This involves practicing good personal hygiene and jobsite safety practices to prevent the spread of the virus. Managers and supervisors must encourage this same behavior from all employees and subcontractors or subconsultants.

Title	Name	Contact
Designated Representative		
Pandemic Safety Officer		
Ops Team Leader		
Ops Team Leader		
Branch Leader		
PM		
Site Contact		

11.3 Responsibilities of Employees

Employees must be vigilant with prevention efforts while at work, including rigorous housekeeping, social distancing, and other best practices within offices and at jobsites. All employees must follow these. In addition, employees are expected to report to their managers or supervisors if they are experiencing signs or symptoms of COVID-19, as described below. If there are specific questions about this Plan or COVID-19, please consult the designated representative. OSHA and the CDC have provided the following control and preventative guidance for all workers, regardless of exposure risk:

- Frequently wash hands with soap and water for at least 20 seconds. When soap and running water are unavailable, use an alcohol-based hand rub with at least 60% alcohol. Staff should wash their hands before eating, after using the restroom, after coughing, sneezing, or blowing their noses, or any other time they are soiled.
- Avoid touching eyes, nose, or mouth.
- Follow appropriate respiratory etiquette, which includes covering for coughs and sneezes.
- Avoid close contact with people who are sick. Maintain six (6) feet separation at all times and wear a mask when six feet separation is not possible.

In addition, employees must familiarize themselves with the symptoms of COVID-19, which include the following:

- Coughing;
- Fever;
- Shortness of breath, difficulty breathing;
- Early symptoms such as chills, body aches, sore throat, headache, diarrhea, nausea/vomiting, and runny nose.

If symptomatic, **DO NOT GO TO WORK** and call your supervisor and healthcare provider right away. Likewise, if you come into close contact with someone showing these symptoms, call your supervisor and healthcare provider right away.

11.4 Jobsite Protective Measures

General Safety Policies and Rules

- Any employee/contractor/subcontractor/visitor showing symptoms of COVID-19 will be asked to leave the office or jobsite.
- Safety meetings will be by telephone, if possible. If safety meetings are conducted in-person, attendance will be collected verbally and the foreman/superintendent will sign-in each attendee. Attendance will not be tracked through passed-around sign-in sheets or mobile devices or with shared writing devises. During any in-person safety meetings, avoid gathering in groups of more than 10 people and participants must remain at least six (6) feet apart.
- Employees must avoid physical contact with others and shall direct others (coworkers/subcontractors/visitors) to maintain personal space of at least six (6) feet, where possible and wear a mask when six feet separation is not possible. Where work trailers are used, only necessary employees should enter the trailers and all employees should maintain social distancing while inside the trailers.

- All in-person meetings will be limited. To the extent possible, meetings will be conducted by telephone or other electronic medium.
- Employees/subcontractors will be encouraged to stagger breaks and lunches, if possible, to reduce the size of any group at any one time to less than ten (10) people.
- Due to the nature of the work and jobsite, access to running water for hand washing may be impractical. In these situations, utilize alcohol-based hand sanitizers and/or wipes.
- Use of co-workers' tools and equipment is prohibited.
- Employees are encouraged to limit the need for N95 respirator use, by using engineering and work practice controls to minimize dust. Such controls include the use of water delivery and dust collection systems, as well as limiting exposure time.
- Employees are encouraged to minimize ride-sharing. While in vehicles, employees must ensure adequate ventilation.
- If possible, each employee should use/drive the same truck or piece of equipment every shift. All frequently-touched surfaces of pool vehicles must be disinfected prior to, and upon completion of use.
- In lieu of using a common source of drinking water, such as a cooler, employees should use individual water bottles.

Personal Protective Equipment

In addition to regular PPE for workers engaged in various tasks (fall protection, hard hats, hearing protection), field staff shall utilize:

- Gloves: Gloves should be worn at all times while on-site. The type of glove worn should be appropriate to the task. If gloves are not typically required for the task, then any type of glove is acceptable, including latex gloves. Employees should never share gloves.
- Eye protection: Eye protection should be worn at all times while on-site.
- Masks must be worn to prevent the spread of COVID-19 when 6 feet social distancing cannot be achieved. Suitable face coverings as recommended by Federal and State Health Departments are readily available, and homemade versions have been noted as acceptable.
- The following Work Practice Controls should be followed:
    - Keep dust down by using engineering and work practice controls, specifically through the use of water delivery and dust collection systems.
    - Limit exposure time to the extent practicable.
    - Isolate workers in dusty operations by using a containment structure or distance to limit dust exposure to those employees who are conducting the tasks, thereby protecting nonessential workers and bystanders.
- Institute a rigorous housekeeping program to reduce dust levels on the jobsite.

Jobsite Cleaning and Disinfection Controls

Most field work does not involve desk/cube/job trailer locations. However, if applicable, institute regular housekeeping practices, which include cleaning and disinfecting frequently used tools and equipment, and other elements of the work environment.

- Institute a rigorous housekeeping program to reduce dust levels on the jobsite. Jobsite trailers and break/lunchroom areas will be cleaned at least once per day. Employees performing cleaning shall don required PPE, such as nitrile, latex, or vinyl gloves, as recommended by the CDC.
- Any trash collected from the jobsite must be changed frequently by someone wearing nitrile, latex, or vinyl gloves.
- Any portable jobsite toilets should be cleaned by the leasing company at least twice per week and disinfected on the inside. Frequently touched items (i.e. door pulls, toilet seats, light switches) will be disinfected frequently.
- Equipment/tools should be cleaned at least once per day and shall not be shared between employees. Frequently touched surfaces of pool vehicles shall be disinfected prior to and upon completion of use.
- OSHA has indicated that if an employee has tested positive for COVID-19, it does not typically require an employer to perform special cleaning or decontamination of work environments, unless those environments are visibly contaminated with blood or other bodily fluids. Notwithstanding this, efforts will be made to clean those

areas of the jobsite that a confirmed-positive individual may have contacted and it will do so before employees can access that work space again.

- Ensure that any disinfection shall be conducted using one of the following:
  - Common EPA-registered household disinfectant;
  - Alcohol solution with at least 60% alcohol; or
  - Diluted household bleach solutions if appropriate for the surface (15% bleach to 85% H_2O)

11.5 Jobsite Exposure Situations

There may be scenarios in which an employee is exposed to or was potentially exposed to an individual with COVID-19, either at the branch office, offsite, or outside of work. Employees should contact the Designated Representative as soon as possible for guidance and assistance with leave benefits. These conditions can vary greatly and each scenario should be urgently addressed by the Designated Representative, the Pandemic Safety Officer, and the site specific Project Managers to ensure the appropriate response:

Employee Exhibits COVID-19 Symptoms
If an employee/subconsultant/subcontractor exhibits COVID-19 symptoms, the employee must remain at home until they are symptom free for 72 hours (3 full days) without the use of fever-reducing or other symptom-altering medicines (e.g., cough suppressants). Similarly, require an employee who reports to work with symptoms to return home until they are symptom free for 72 hours (3 full days). To the extent practical, employees are required to obtain a doctor's note clearing them to return to work.

Employee Tests Positive for COVID-19
An employee who tests positive for COVID-19 will be directed to self-quarantine away from work. Employees that test positive and are symptom free may return to work when at least fourteen (14) days have passed since the date of his or her first positive test, and have not had a subsequent illness. Employees who test positive, are symptomatic, and/or have been hospitalized may return to work when directed to do so by their medical care providers. Employer will require an employee to provide documentation clearing his or her return to work.

Employee Has Close Contact with a person Who Has Tested Positive for COVID-19
Employees who have come into close contact with an individual who has tested positive for COVID-19 (co-worker or otherwise) will be directed to self-quarantine for 14 days from the last date of close contact with that individual. Close contact is defined as within six (6) feet for a prolonged period of time. If an employer learns that an employee has tested positive, the Designated Representative will conduct an investigation (using HIPAA promulgations) to determine co-workers who may have had close contact with the confirmed positive employee in the prior 14 days and direct those individuals who have had close contact with the confirmed-positive employee to self-quarantine for 14 days from the last date of close contact with that employee; or, the affected employee can return to work after a negative test result. If applicable, notify any sub-contractors, vendors/suppliers or visitors who may have had close contact with the confirmed-positive employee. If an employee learns that he or she has come into close contact with a confirmed-positive individual outside of the workplace, he/she must alert a manager or supervisor of the close contact and self-quarantine for 14 days from the last date of close contact with that individual.

Access to testing is critical. In most areas, testing criteria for COVID-19 has been expanded to include asymptomatic individuals with potential exposure to a person who has the virus or has symptoms of the virus. It also now includes those who work in a profession that puts them at high risk of exposure due to contact with the public or who works in certain industries, such as food processing. For questions or direction, contact the Pandemic Safety Officer. If needed, the nearest testing facility will be located.

11.6 Traveling

Air travel requires spending time in security lines and airport terminals, which can bring you in close contact with other people and frequently touched surfaces. Most viruses and other germs do not spread easily on flights because of how air circulates and is filtered on airplanes. However, social distancing is difficult on crowded flights, and you may have to sit near others (within 6 feet), sometimes for hours. This may increase your risk for exposure to the virus that causes COVID-19.All air travel must be approved by Branch Leaders and Ops Team. If approved:

- Clean hands often. Wash hands for 20 seconds after being in a public place. Use hand sanitizer if soap and water are not available
- Avoid touching eyes, nose and mouth
- Avoid close contact with others
- Wear a face covering in public, especially terminals
- Use wipes or disinfectant spray to clean frequently touched surfaces in rental cars and hotel rooms. Ask about cleaning procedures at purchase. Confirm that disinfection protocols are being conducted.

11.7 Confidentiality and Privacy

Except for circumstances in which the Company is legally required to report workplace occurrences of communicable disease, the confidentiality of all medical conditions will be maintained in accordance with applicable law and to the extent practical under the circumstances. When it is required, the number of persons who will be informed that an unnamed employee has tested positive will be kept to the minimum needed to comply with reporting requirements and to limit the potential for transmission to others. The Company reserves the right to inform other employees that an unnamed co-worker has been diagnosed with COVID-19 if the other employees might have been exposed to the disease so the employees may take measures to protect their own health. The Company also reserves the right to inform clients, subconsultants, subcontractors, vendors/suppliers or visitors that an unnamed employee has been diagnosed with COVID-19 if they might have been exposed to the disease so those individuals may take measures to protect their own health.

APPENDIX A

Confined Space Evaluation Form
Confined Space Entry Permit
Confined Space Pre-Entry Checklist

CONFINED SPACE EVALUATION FORM

Requestor:___________________________________ **Date:**______________________________________

Possible Space Location:____

Description of Work:____

____

____

1. Is the space large enough within to perform work? **Yes** **No**
2. Does the space have a restricted or limited means of entry and exit? **Yes** **No**
3. Is the space not designated for continuous occupancy? **Yes** **No**

If all questions answered "Yes", the space is designated as a Confined Space. Continue to answer the following questions to determine the type of Confined Space Permit required:

4. Does the space contain or have the potential to contain a hazardous atmosphere, i.e., oxygen deficiency, flammable vapors, toxic gases or dusts, etc., or pipes, ducts, vents or other entry points for potentially hazardous substances or will volatile chemicals be used, or will painting or other work that could create a breathing hazard being performed? **Yes** **No**

5. Does the space contain a material with the potential for engulfment of an entrant, e.g., grain, sand or water? **Yes** **No**

6. Does the space have an internal shape that could trap or suffocate an entrant, e.g., inwardly converging walls, floors or ceiling? **Yes** **No**

7. Does the space contain other recognized safety or health hazards such as mechanical hazards, electrical hazards, gas or chemical lines, fall or trip hazards, extreme temperatures, heat stress or noise hazards? **Yes** **No**

8. Will the work require welding, cutting, torch work, or other hot work? **Yes** **No**

"No" answers for all questions 4-8 determines the space as Non-Permit Required Confined Space.

"Yes" to question A, the space is Permit Required Confined Space, *General* or *Hazardous,* depending on the ability to adequately ventilate the space.

"Yes" for question 5, 6, or 7, the space is Permit Required Confined Space, *General* if the hazards can be controlled.

"Yes" for question 8, the space is Permit Required Confined Space, with issued Hot Work Safety Permit.

CONFINED SPACE ENTRY PERMIT

This confined space has been designated a Permit Required Confined Space. This space may only be entered by personnel who have been trained to work in a permit required confined space in accordance with Federal and State worker protection standards. Entry operations may proceed only under the direction of the entry supervisor. A specially trained attendant shall remain outside the permit required confined space for the duration of the entry operation.

1.0 Hazardous Conditions Identified During Evaluation

2.0 Atmospheric Hazards

Describe:____

Acceptable Entry Conditions:____

____

3.0 Physical Hazards

Describe:____

Acceptable Entry Conditions:____

____

4.0 Additional Personal Protective/Safety Equipment Required

Respirators:____

Equipment:____

5.0 Permit Authorization

Permit #	Entry Supervisor:
Duration of Permit	Title:
	Phone #:
	Signature:

6.0 PERMIT CANCELLATION

Date:____________ Time:___________ Cancelled by:__________________

Reason For Cancellation:

Confined Space Pre-Entry Checklist

Permit Reference:____________			Date:______________
Location and Description:			**Purpose of Entry:**
Start Time: (a.m./p.m.)		Finish Time: (a.m./p.m.)	
Employee(s) in charge of entry:			
➢ Entrants	➢ Attendants		
Pre-Entry Authorization:			

(Check those items below which are applicable to your confined space permit)

☐ Oxygen – Deficient Atmosphere ☐ Oxygen – Enriched Atmosphere ☐ Welding/Cutting	☐ Engulfment ☐ Toxic Atmosphere ☐ Flammable Atmosphere	☐ Energized Electrical Equipment ☐ Entrapment ☐ Hazardous Chemical

Safety Precautions

☐ Self-Contained Breathing Apparatus ☐ Air-Line Respirator ☐ Fire-Retardant Clothing ☐ Ventilation ☐ Protective Gloves	☐ Lifelines ☐ Respirators ☐ Lockout/Tagout ☐ Fire/Extinguishers ☐ Barricade Job Area	☐ Signs Posted ☐ Clearances Secured ☐ Lighting ☐ Ground Fault Interrupter
Remarks:		

Environmental Conditions

Initial Testing:		**Re-Testing:**	
Oxygen:_______% LEL:______% CO:______% H2S:______% Instruments Used:	Date/Time (a.m./p.m.)	Oxygen:_______% LEL:______% CO:______% H2S:______% Instruments Used:	Date/Time (a.m./p.m.)

Entry – Authorization	**Entry Cancellation**
All actions or conditions for safe entry have been performed. **Entry Supervisor (Print):**	Entry has been completed and all entrants have exited permit **Name (Print):**

APPENDIX B

Documentation of Training

DOCUMENTATION OF TRAINING

The following is a list of employees who have been equipped and trained to serve as authorized entrants or as entrants using non-permit or alternate procedures on our jobs:

Authorized Entrants(s)	Trainer	Date of Training

The following is a list of employees who have been equipped and trained to serve as attendants:

Attendant(s)	Trainer	Date of Training

The following is a list of employees who have been trained to serve as entry supervisors:

Entry Supervisor(s)	Trainer	Date of Training

The following is a list of employees who have been trained to serve as Rescue Personnel:

Rescuer(s)	Trainer	Date of Training

APPENDIX C

Decision Flow Chart

CONFINED SPACE EVALUATION--ENTRY PERMIT SYSTEM

CONFINED SPACE ENTRY DECISION FLOW CHART

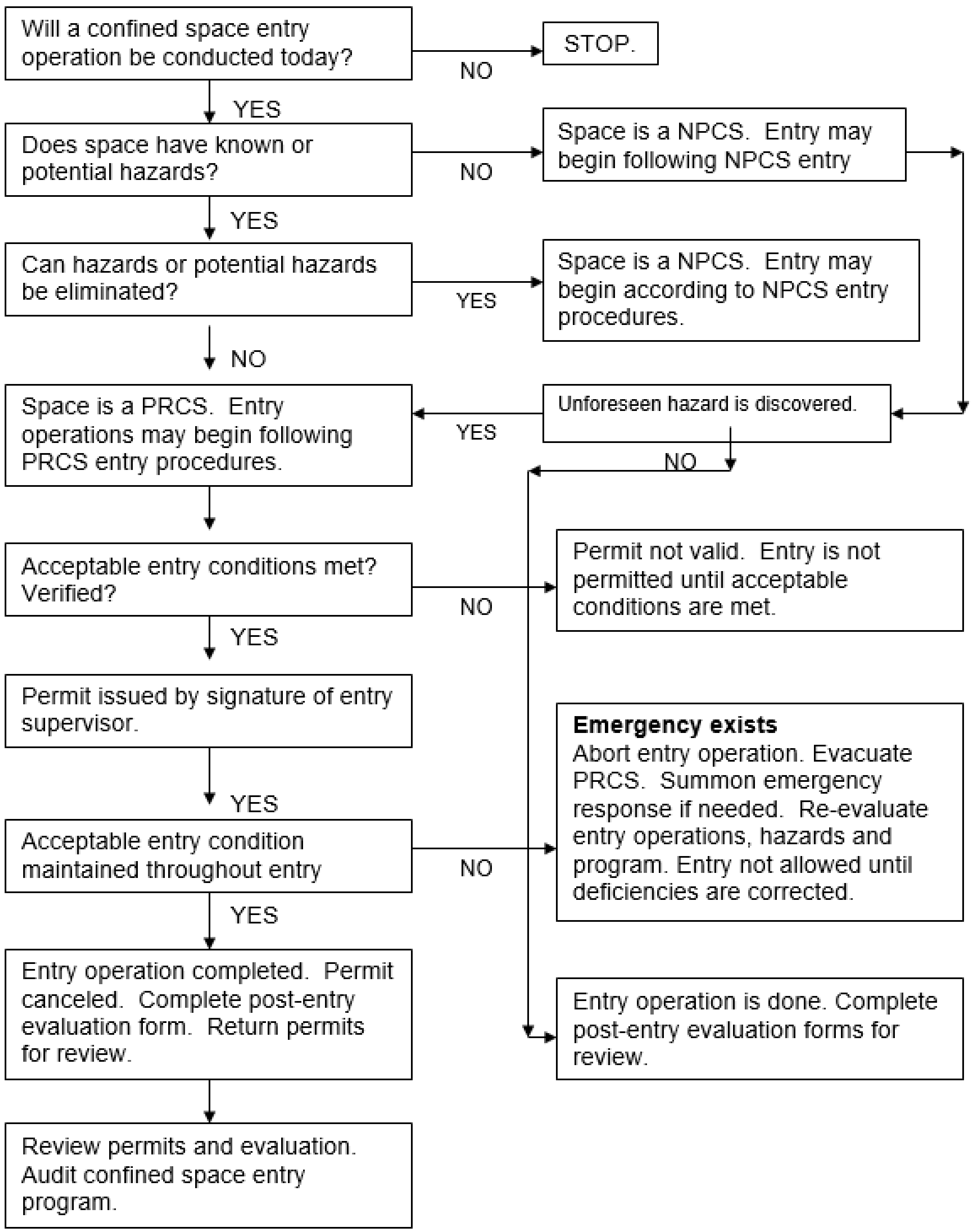

APPENDIX D

Inspection Pre-Entry Checklist

Inspection Pre-Entry Checklist

STEP #	PROCESS	COMPLETE
1.	Administrative actions	
	a. Ensure entrants have completed awareness training	
	b. Signage at site, with contact information	
	c. Site access controlled by security	
2.	Isolate the Space from hazards:	
	a. Remove unauthorized personnel from the site of entry	
	b. LOTO needed?	
	c. Block inlets and/or control water hazards	
3.	Ventilate the Space	
4.	Fill out Entry Permit to evaluate the Space	
5.	Test the atmosphere	
	a. 4 Gas meter calibrated and operational	
	b. Enter atmospheric readings on Entry Permit	
	c. O_2, CO, H_2S, LEL/UEL limits in range	
6.	Enter the Space and proceed with task:	
	a. Supervisor available and aware of entry	
	b. Attendant at entry site	
	c. Ensure proper communication method and efficacy	
	d. Required PPE in place	
	e. Observe 4 gas meter readings throughout entry	
7.	Upon completion of task and entry:	
	a. Remove all personnel, tools and debris from Space	
	b. Close the space	
	c. Cancel the permit	
8.	Review the job and retain completed form for recordkeeping	
9.	Restore and secure site	